

Abel Lajtha

Editor

Gary E. Gibson

Gerald A. Dienel

Volume Editors

SPRINGER
REFERENCE

Handbook of Neurochemistry and Molecular Neurobiology

3rd Edition

Brain Energetics. Integration of
Molecular and Cellular Processes

 Springer

Handbook of Neurochemistry and Molecular Neurobiology

Brain Energetics. Integration of Molecular and Cellular Processes

Abel Lajtha (Ed.)

Handbook of Neurochemistry and Molecular Neurobiology Brain Energetics. Integration of Molecular and Cellular Processes

Volume Editors: Gary E. Gibson and Gerald A. Dienel

With 198 Figures and 51 Tables

 Springer

Editor

Abel Lajtha
Director
Center for Neurochemistry
Nathan S. Kline Institute for Psychiatric Research
140 Old Orangeburg Road
Orangeburg
New York, 10962
USA

Volume Editors

Gary E. Gibson, Ph.D.
Professor of Neuroscience
Department of Neurology and Neuroscience
Weill Medical College of Cornell University
Burke Medical Research Institute
785 Mamaroneck Avenue
White Plains, NY 10605
USA
ggibson@med.cornell.edu

Gerald A. Dienel, Ph.D.
Professor
Dept. Neurology and Physiology & Biophysics
University Arkansas for Medical Sciences
Shorey Bldg. Room 715, Mail Slot 830
4301 W. Markham St.
Little Rock, AR 72205
USA
DienelGeraldA@uams.edu

Library of Congress Control Number: 2006922553

ISBN: 978-0-387-30366-6

Additionally, the whole set will be available upon completion under ISBN: 978-0-387-35443-9

The electronic version of the whole set will be available under ISBN: 978-0-387-30426-7

The print and electronic bundle of the whole set will be available under ISBN: 978-0-387-35478-1

© 2007 Springer Science+Business Media, LLC.

All rights reserved. This work may not be translated or copied in whole or in part without the written permission of the publisher (Springer Science+Business Media, LLC., 233 Spring Street, New York, NY 10013, USA), except for brief excerpts in connection with reviews or scholarly analysis. Use in connection with any form of information storage and retrieval, electronic adaptation, computer software, or by similar or dissimilar methodology now known or hereafter developed is forbidden.

The use in this publication of trade names, trademarks, service marks, and similar terms, even if they are not identified as such, is not to be taken as an expression of opinion as to whether or not they are subject to proprietary rights.

springer.com

Printed on acid-free paper

SPIN: 11416678 2109 - 5 4 3 2 1 0

Table of Contents

Preface	v
Contributors	xi
1 Glucose Metabolism in Brain	
1.1 Bioenergetics	3
<i>D. G. Nicholls</i>	
1.2 Glucose, Oxidative Energy Metabolism, and Neural Function in Brain Slices—Glycolysis Plays a Key Role in Neural Activity	17
<i>Y. Okada · P. Lipton</i>	
1.3 Pentose Phosphate Pathway and NADPH Metabolism	41
<i>R. Dringen · H. H. Hoepken · T. Minich · C. Ruedig</i>	
1.4 The Cerebral Tricarboxylic Acid Cycles	63
<i>T. B. Rodrigues · S. Cerdán</i>	
1.5 Electron Transport. Structure, Redox-Coupled Protonmotive Activity, and Pathological Disorders of Respiratory Chain Complexes	93
<i>S. Papa · V. Petruzzella · S. Scacco</i>	
1.6 The Mitochondrial F₁F_o ATP Synthase	119
<i>A. Gaballo · S. Papa</i>	
2 Alternative Substrates	
2.1 The Support of Energy Metabolism in the Central Nervous System with Substrates Other than Glucose	137
<i>E. L. Roberts, Jr</i>	
3 Metabolic Specialization of Brain Cell Types and Compartmentation of Function	
3.1 Anaplerosis	183
<i>B. Hassel</i>	

3.2	Glial–Neuronal Shuttle Systems	197
	<i>C. Zwingmann · D. Leibfritz</i>	
4	Molecular and Cellular Architecture Link Energy Demand with Metabolite Fluxes	
4.1	Cytoplasmic Glycolytic Enzymes. Synaptic Vesicle-Associated Glycolytic ATP-Generating Enzymes: Coupling to Neurotransmitter Accumulation	241
	<i>T. Ueda · A. Ikemoto</i>	
4.2	Mitochondrial Architecture and Heterogeneity	261
	<i>G. A. Perkins · M. H. Ellisman</i>	
4.3	Coupling of Neuronal Function to Oxygen and Glucose Metabolism Through Changes in Neurotransmitter Dynamics as Revealed with Aging, Hypoglycemia, and Hypoxia	297
	<i>J. A. Joseph · G. E. Gibson</i>	
4.4	Coupling of Brain Function and Metabolism: Endogenous Flavoprotein Fluorescence Imaging of Neural Activities by Local Changes in Energy Metabolism	321
	<i>K. Shibuki · R. Hishida · H. Kitaura · K. Takahashi · M. Tohmi</i>	
4.5	Coupling of Brain Function to Metabolism: Evaluation of Energy Requirements	343
	<i>A. Gjedde</i>	
4.6	Energy Consumption by Phospholipid Metabolism in Mammalian Brain ..	401
	<i>A. D. Purdon · S. I. Rapoport</i>	
4.7	Ion Transport and Energy Metabolism	429
	<i>O. Vergun · K. E. Dineley · I. J. Reynolds</i>	
5	Regulation of Metabolic Fluxes and Metabolic Shuttling by Neural Environment	
5.1	Acid–Base Transport and pH Regulation	469
	<i>J. W. Deitmer</i>	
5.2	Nitric Oxide in Regulation of Mitochondrial Function, Respiration, and Glycolysis	487
	<i>J. P. Bolaños · A. Almeida</i>	
5.3	Mitochondrial Production of Oxidants and Their Role in the Regulation of Cellular Processes	519
	<i>P. S. Brookes</i>	

5.4	Uncoupling Proteins	549
	<i>J. S. Kim-Han · S. S. Ali · L. L. Dugan</i>	
5.5	Actions of Toxins on Cerebral Metabolism at the Cellular Level	569
	<i>U. Sonnewald · T. Syversen · A. Schousboe · H. Waagepetersen · M. Aschner</i>	
6	Interaction of Mitochondria with Cytosol and Other Organelles	
6.1	Mitochondrial/Cytosolic Interactions via Metabolite Shuttles and Transporters	589
	<i>K. F. LaNoue · V. Carson · D. A. Berkich · S. M. Hutson</i>	
6.2	Mitochondrial-Endoplasmic Reticulum Interactions	617
	<i>G. Szabadkai · R. Rizzuto</i>	
6.3	Mitochondria-Nucleus Energetic Communication: Role for Phosphotransfer Networks in Processing Cellular Information	641
	<i>P. P. Dzeja · A. Terzic</i>	
6.4	Mitochondrial Permeability Transition in the CNS—Composition, Regulation, and Pathophysiological Relevance	667
	<i>T. Wieloch · G. Mattiasson · M. J. Hansson · E. Elmér</i>	
6.5	Mitochondrial Mechanisms of Oxidative Stress and Apoptosis	703
	<i>L. Soane · N. Solenski · G. Fiskum</i>	
7	Genes of Metabolism: Generating, Sustaining, and Modifying the Machinery of Energy Metabolism. Regulation of Gene Expression for Metabolic Enzymes	
7.1	Proteomics	737
	<i>M. H. Maurer · W. Kuschinsky</i>	
7.2	Genetics and Gene Expression of Glycolysis	771
	<i>J. C. LaManna · P. Pichiule · J. C. Chavez</i>	
7.3	Transcriptional Integration of Mitochondrial Biogenesis	789
	<i>R. C. Scarpulla</i>	
8	Metabolic Control Analysis: Modeling Local Pathway Fluxes, Control Points, System Interactions, Network Interactions	
8.1	Mechanisms and Modeling of Energy Transfer Between Intracellular Compartments	815
	<i>V. A. Saks · M. Vendelin · M. K. Aliev · T. Kekelidze · J. Engelbrecht</i>	

8.2 Modeling of Regulation of Glycolysis and Overall Energy Metabolism Under a Systems Biology Approach	861
<i>M. Cascante · L. G. Boros · J. Boren</i>	
8.3 Modeling of Electron Transport: Implications to Mitochondrial Diseases ..	877
<i>J-P. Mazat · M. Beurton-Aimar · B. Faustin · T. Letellier · M. Malgat · C. Nazaret · R. Rossignol</i>	
8.4 Metabolomics: Concepts and Potential Neuroscience Applications	889
<i>B. S. Kristal · R. Kaddurah-Daouk · M. F. Beal · W. R. Matson</i>	
Index	913

Preface

The brain depends upon a continuous supply of glucose and oxygen for normal function, and reductions in brain metabolism either cause or are associated with multiple neurodegenerative diseases and stroke. Thus, it is not surprising that energy metabolism was a central aspect of the early development of neurochemistry. Classic texts of neurochemistry, including *Chemistry of the Brain*, by I. H. Page (1937), *Neurochemistry: The Chemistry of Brain and Nerve*, edited by K. A. C. Elliott, I. H. Page, and J. H. Quastel (1962), *Biochemistry and the Central Nervous System*, by H. I. McIlwain (1971), *Brain Energy Metabolism* by B. Siesjö (1978), and *Basic Neurochemistry* (R. W. Albers et al., 1st edition, 1972; now in its 7th edition, 2005), have focused on energy metabolism. Since these texts were written, new areas of neurochemistry have been born and have grown tremendously, greatly enhancing our understanding of brain energy metabolism. During the past 50 years, our understanding of the metabolic pathways in brain, their components, regulation, cellular specialization, and cell–cell interactions has greatly expanded. As a consequence of these considerable achievements, brain energy metabolism is sometimes viewed as a mature field in which the fundamental problems have been identified and solved. However, these accomplishments have led to new and even more interesting questions.

Seamless integration of energy metabolism, neurotransmission, and signaling pathways with cellular structure and function is an implicit goal of neuroscience. Nevertheless, the interrelationships between function and metabolism are often ignored due to increasing specialization within subdisciplines of neuroscience. Thus, it is important to note that most assays of brain function are indirect, relying on measurements of changes in levels or fluxes of endogenous energy metabolites or exogenous tracers metabolized via energy-producing pathways. These processes provide signals that can be captured by different methodologies, including optical techniques with infrared and fluorescence signals, magnetic resonance spectroscopy or imaging, positron emission tomography, as well as biochemical assays. Multidisciplinary approaches are becoming increasingly necessary to probe deeper into the realm of functional and metabolic specialization of brain cells. To understand the basis of these functional metabolic signals and interpret their changes in terms of cellular and systems activities, particularly in disease states, it is essential for neuroscientists to assimilate an understanding of the complexity and heterogeneity of energy metabolism in brain.

To provide a comprehensive resource for studies of brain function and metabolism, this volume focuses on aspects of energy metabolism that are unique to the brain. The goal of each chapter is to provide a fundamental overview of each area, to define the state-of-the-art in that area as it relates to brain, and, where appropriate, describe models that portray poorly understood and apparently contradictory data sets with the goal of helping focus attention to experimental resolution of controversial issues. The contents of the chapters range from classical subjects that were covered in the early texts to areas and techniques that have not yet been applied to the brain. Our understanding of even the traditional areas of metabolism, such as glycolysis, the Krebs cycle, and electron transport chain is changing rapidly, and these new areas and ideas are driven by the innovative and powerful techniques of imaging, molecular biology, gene regulation, and mathematical analysis and modeling.

We are particularly grateful to our expert authors for their outstanding contributions to this comprehensive volume. Each chapter was exhaustively reviewed and then revised, requiring an immense amount of effort. The exceptional quality of the chapters reflects the authors' commitment to excellence to provide a resource for young and senior neuroscientists in all disciplines, and the complementary nature of their chapters make the whole greater than the sum of the parts.

We thank Dr. Abel Lajtha, Editor-In-Chief of the *Handbook of Neurochemistry and Molecular Neurobiology*, and Springer for allowing us the opportunity to edit this volume on brain energy metabolism. Their vision is to publish the third edition of the *Handbook* as a book version for easy desk reference plus a Web version that can be updated annually and easily accessed by anyone in the world. We are excited about this unique opportunity to take advantage of a great feature of twenty-first century communication by way of the Web. We anticipate that this volume on brain energy metabolism will evolve in the future as authors bring new information to their chapters and as new chapters are added to describe emerging fields of research. By this mechanism, our understanding of brain energetics from the level of genes to metabolites to cells will be integrated in terms of molecular and cellular processes that support functional systems.

Gary E. Gibson and Gerald A. Dienel

Contributors

S. S. Ali

Department of Medicine, University of California,
San Diego, CA 92093, USA

M. K. Aliev

Cardiology Research Center, Institute of Experimental
Cardiology, Laboratory of Cardiac Pathology, 121552
Moscow, Russia

A. Almeida

Universidad de Salamanca, Edificio Departamental,
Campus Miguel de Unamuno, 37007 Salamanca,
and Hospital Universitario de Salamanca, Paseo de San
Vicente 58-182, 37007 Salamanca, Spain

M. Aschner

Department of Pediatrics, B-3307 Medical Center North,
Vanderbilt University Medical Center, 1162 21st Avenue,
Nashville, TN 37232-2495, USA
Michael.aschner@vanderbilt.edu

M. F. Beal

Department of Neuroscience, Weill Medical College of
Cornell University, 525 East 68 St., NY, NY 10021, USA

D. A. Berkich

Pennsylvania State College of Medicine, Hershey,
PA 17033, USA

M. Beurton-Aimar

Inserm U688, Université Bordeaux 2, Bordeaux, France

J. P. Bolaños

Universidad de Salamanca, Edificio Departamental,
Campus Miguel de Unamuno, 37007 Salamanca, Spain
jbolanos@usal.es

J. Boren

Department of Biochemistry and Molecular Biology,
University of Barcelona, C/Martí i Franqués 1,
08028 Barcelona, Spain

L. G. Boros

UCLA School of Medicine, Division of Pediatric
Endocrinology, Los Angeles Biomedical Research
Institute at the Harbor-UCLA Medical Center,
1124 West Carson Street, RB1, Torrance,
CA 90502-2910 and SIDMAP, LLC, Los Angeles,
CA 90064, USA

P. S. Brookes

Department of Anesthesiology, Box 604, University of
Rochester Medical Center, 601 Elmwood Avenue,
Rochester, NY 14642, USA
paul_brookes@urmc.rochester.edu

V. Carson

Pennsylvania State College of Medicine, Hershey,
PA 17033, USA

M. Cascante

Department of Biochemistry and Molecular Biology,
University of Barcelona, C/Martí i Franqués 1, 08028
Barcelona, Spain
martacascante@ub.edu

S. Cerdán

Laboratory for Imaging and Spectroscopy by Magnetic
Resonance (LISMAR), Institute of Biomedical Research
"Alberto Sols" CSIC/UAM, c/ Arturo Duperier 4, E-28029
Madrid, Spain
scerdan@iib.uam.es

J. C. Chavez

Burke/Cornell Medical Research Institute, 785
Mamaroneck Ave, White Plains, NY 10605, USA

J. W. Deitmer

Abteilung für Allgemeine Zoologie, FB Biologie,
TU Kaiserslautern, P.B. 3049, D-67653 Kaiserslautern,
Germany
deitmer@rhrk.uni-kl.de

G. A. Diemel

Department of Neurology,
University of Arkansas for Medical Sciences,
4301 W. Markham St, Little Rock, AR 72205, USA
GADiemel@uams.edu

K. E. Dineley

Department of Biology, Francis Marion University,
Florence, SC 29501, USA

R. Dringen

Center for Biomolecular Interactions Bremen, University
of Bremen, P.O.B. 330 440, D-28334 Bremen,
Germany, and Department of Psychology,
Monash University, Wellington Rd., Clayton, Victoria
3800, Australia
ralf.dringen@uni-bremen.de

L. L. Dugan

Department of Medicine, University of California,
San Diego, CA 92093, USA
ladugan@ucsd.edu

P. P. Dzeja

Division of Cardiovascular Diseases, Departments of
Medicine, Molecular Pharmacology and Experimental
Therapeutics, Mayo Clinic College of Medicine,
Rochester, MN, USA
dzeja.petras@mayo.edu

M. H. Ellisman

National Center for Microscopy and Imaging Research,
Department of Neurosciences, BSB 1000, UCSD, 9500
Gilman, La Jolla, CA 92093-0608, USA

E. Elmér

Laboratory for Experimental Brain Research, Wallenberg
Neuroscience Center, Lund University, Sweden

J. Engelbrecht

Department of Mechanics and Applied Mathematics,
Institute of Cybernetics, Tallinn Technical University,
Akadeemia 21, 12618 Tallinn, Estonia

B. Faustin

Inserm U688, Université Bordeaux 2, Bordeaux, France

G. Fiskum

University of Maryland Baltimore, Department of
Anesthesiology, School of Medicine, 685 W. Baltimore St.,
Baltimore, MD 21201, USA
gfsk001@umaryland.edu

A. Gaballo

Institute of Biomembranes and Bioenergetics (IBBE),
Italian Research Council, (CNR), Bari, Italy
a.gaballo@ibbe.cnr.it

G. E. Gibson,

Weill Medical College of Cornell University, Burke
Medical Research Institute, 785 Mamaroneck Avenue,
White Plains, NY 10605, USA
ggibson@med.cornell.edu

A. Gjedde

Pathophysiological and Experimental Tomography
Center, Aarhus City Hospital, Aarhus University
Hospitals, Aarhus C, Denmark 8000
albert@pet.auh.dk

M. Hansson,

Laboratory for Experimental Brain Research,
Wallenberg Neuroscience Center, Lund University,
Sweden

B. Hassel

Norwegian Defense Research Establishment, N-2027
Kjeller, Norway
bjornar.hassel@ffi.no

R. Hishida

Department of Neurophysiology, Brain Research
Institute, Niigata University, Asahi-machi, Niigata
951-8585, Japan

H. H. Hoepken

Interfakultäres Institut für Biochemie der Universität
Tübingen, Hoppe-Seyler-Str. 4, D-72076 Tübingen,
Germany

S. M. Hutson

Wake Forest University, Winston-Salem, NC 27157, USA

A. Ikemoto

Laboratory of Nutritional Biochemistry, Department
of Family and Consumer Studies Faculty of Education
and Human Studies, Akita University, 1-1 Tegata
Gakuen-machi, Akita 010-8502, Japan
aikemoto@ed.akita-u.ac.jp

J. A. Joseph

Tufts University, Human Nutrition Research Center
on Aging, 711 Washington Street, Rm 919, Boston,
MA 02111, USA
james.joseph@tufts.edu

R. Kaddurah-Daouk

Duke University Medical Center, Department of Psychiatry, Box 3950, Durham, NC 27710, USA

T. Kekelidze

MR Center, Department of Diagnostic Imaging, Steinwiesstrasse 75, CH-8032, Zürich, Switzerland

J. S. Kim-Han

Department of Anatomy and Neurobiology, Washington University School of Medicine, St. Louis, MO 63110, USA

H. Kitaura,

Department of Neurophysiology, Brain Research Institute, Niigata University, Asahi-machi, Niigata 951-8585, Japan

B. S. Kristal

Dementia Research Service, Burke Medical Research Institute, 785 Mamaroneck Ave, White Plains, NY 10605, and Department of Neuroscience, Cornell University Medical College, 1300 York Ave, NY, NY 10021, USA
bkristal@burke.org

W. Kuschinsky

Dept. of Physiology and Pathophysiology, University of Heidelberg, Im Neuenheimer Feld 326, 69120 Heidelberg, Germany

J. C. LaManna

Department of Neurology, Case Western Reserve University School of Medicine, 10900 Euclid Avenue, Cleveland, Ohio 44106, USA
joseph.lamanna@case.edu

K. F. LaNoue

Pennsylvania State College of Medicine, Hershey, PA 17033, USA
klanoue@psu.edu

D. Leibfritz

Department of Organic Chemistry, University of Bremen, D-28359 Bremen, Germany
dieter.leibfritz@chemie.uni-bremen.de

T. Letellier

Inserm U688, Université Bordeaux 2, Bordeaux, France

P. Lipton

Department of Physiology, University of Wisconsin, 1300 University Avenue, Madison, WI 53706, USA
plipton@wisc.edu

M. Malgat

Inserm U688, Université Bordeaux 2, Bordeaux, France

W. R. Matson

Veteran's Administration, Building 70, 100 Springs Road, Bedford, MA 01486, USA

G. Mattiasson,

Laboratory for Experimental Brain Research, Wallenberg Neuroscience Center, Lund University, Sweden

M. H. Maurer

Dept. of Physiology and Pathophysiology, University of Heidelberg, Im Neuenheimer Feld 326, 69120 Heidelberg, Germany
maurer@uni-hd.de

J.-P. Mazat

Inserm U688, Université Bordeaux 2, Bordeaux, France
jpm@u-bordeaux2.fr

T. Minich

Interfakultäres Institut für Biochemie der Universität Tübingen, Hoppe-Seyler-Str. 4, D-72076 Tübingen, Germany

C. Nazaret

ESTBB, Université Bordeaux 2, Bordeaux, France

D. G. Nicholls

Buck Institute for Age Research, 8001 Redwood Boulevard, Novato, Ca 94903, USA
dnicholls@buckinstitute.org

Y. Okada

Health Science Center, Kobe Health-Life Plaza, 5-1-2-300, Hyogoku, Kobe, 652-0897 and Department of Physiology, School of Medicine, Kobe University, 7-5-1 Kusunokicho, Chuo-ku Kobe, 650-0017, Japan
life-kenkou@hyogo-yobouigaku.or.jp

S. Papa

Institute of Biomembranes and Bioenergetics (IBBE), Italian Research Council, (CNR), Bari, Italy, and Department of Medical Biochemistry, Medical Biology and Medical Physics (DIBIFIM), University of Bari, Italy
papabchm@cimedoc.uniba.it

G. A. Perkins

National Center for Microscopy and Imaging Research,
Department of Neurosciences, BSB 1000, UCSD, 9500
Gilman, La Jolla, CA 92093-0608, USA
perkins@ncmir.ucsd.edu

V. Petruzzella

Department of Medical Biochemistry, Biology and
Physics (DIBIFIM), University of Bari, Italy

P. Pichiule

Pediatric Critical Care Medicine, Morgan Stanley
Children's Hospital of New York, Columbia, and
University College of Physicians & Surgeons, 3959
Broadway, BHN 10-24, New York, NY 10032, USA

A. D. Purdon

Brain Physiology and Metabolism Section, National
Institute on Aging, National Institutes of Health,
Bethesda, Maryland 20892, USA

S. I. Rapoport

Brain Physiology and Metabolism Section, National
Institute on Aging, National Institutes of Health,
Bethesda, Maryland 0892, USA
sir@helix.nih.gov

I. J. Reynolds

Departments of Stroke & Neurodegeneration
and Ophthalmics, Merck Research Laboratories,
West Point, PA, USA
lan_reynolds@merck.com

R. Rizzuto

Department of Experimental and Diagnostic Medicine,
Section of General Pathology, Interdisciplinary Center
for the Study of Inflammation (ICSI), University of
Ferrara, Ferrara, Via Borsari 46, 44100, Italy
rzz@dns.unife.it

E. L. Roberts, Jr.

Department of Neurology, University of Miami
Leonard M. Miller School of Medicine, Miami, FL 33101,
USA
eroberts@med.miami.edu

T. B. Rodrigues

Laboratory for Imaging and Spectroscopy by Magnetic
Resonance (LISMAR), Institute of Biomedical Research
"Alberto Sols" CSIC/UAM, c/ Arturo Duperier 4, E-28029
Madrid, Spain

R. Rossignol

Inserm U688, Université Bordeaux 2, Bordeaux, France

C. Ruedig

Interfakultäres Institut für Biochemie der Universität
Tübingen, Hoppe-Seyler-Str. 4, D-72076 Tübingen,
Germany

V. A. Saks

Structural and Quantitative Bioenergetics Research
Group, Laboratory of Fundamental and Applied
Bioenergetics, INSERM E221, Joseph Fourier University
Grenoble, France, and Laboratory of Bioenergetics,
National Institute of Chemical and Biological Physics,
Tallinn, Estonia
Valdur.Saks@ujf-grenoble.fr

S. Scacco

Department of Medical Biochemistry, Biology and
Physics (DIBIFIM), University of Bari, Italy

R. C. Scarpulla

Cell and Molecular Biology, Northwestern Medical
School, 303 East Chicago Avenue, Chicago, IL 60611, USA
rsc248@northwestern.edu

A. Schousboe

Danish University of Pharmaceutical Sciences,
Department of Pharmacology, DK-2100 Copenhagen,
Denmark
as@dfuni.dk

K. Shibuki

Department of Neurophysiology, Brain Research
Institute, Niigata University, Asahi-machi, Niigata
951-8585, Japan
shibuki@bri.niigata-u.ac.jp

L. Soane

University of Maryland Baltimore, Department of
Anesthesiology, School of Medicine, 685 W. Baltimore St.,
Baltimore, MD 21201, USA

N. Solenski

Department of Neurology, University of Virginia School
of Medicine, Charlottesville, VA 22908, USA

U. Sonnewald

Department of Neuroscience, Olav Kyrres g.3,
Norwegian University of Science & Technology,
N-7489 Trondheim, Norway
ursula.sonnewald@medisin.ntnu.no

T. Syversen,

Department of Neuroscience, Olav Kyrres g.3,
Norwegian University of Science & Technology,
N-7489 Trondheim, Norway
tore.syversen@medisin.ntnu.no

G. Szabadkai

Department of Experimental and Diagnostic
Medicine, Section of General Pathology,
Interdisciplinary Center for the Study of Inflammation
(ICSI), University of Ferrara, Ferrara, Via Borsari 46,
44100, Italy

H. Takahashi

Department of Neurophysiology, Brain Research
Institute, Niigata University, Asahi-machi, Niigata
951-8585, Japan

A. Terzic

Division of Cardiovascular Diseases, Departments of
Medicine, Molecular Pharmacology and Experimental
Therapeutics, Mayo Clinic College of Medicine,
Rochester, MN, USA
terzic.andre@mayo.edu

M. Tohmi

Department of Neurophysiology, Brain Research
Institute, Niigata University, Asahi-machi, Niigata
951-8585, Japan

T. Ueda

University of Michigan Medical School, Molecular and
Behavioral Neuroscience Institute and Departments of
Pharmacology and Psychiatry, MSRB II, 1150 W. Medical
Ctr. Dr. Ann Arbor, MI 48109-0669, USA
tueda@umich.edu

M. Vendelin

Structural and Quantitative Bioenergetics Research
Group, Laboratory of Fundamental and Applied
Bioenergetics, INSERM E221, Joseph Fourier University
Grenoble, France, and Department of Mechanics and
Applied Mathematics, Institute of Cybernetics, Tallinn
Technical University Akadeemia 21, 12618 Tallinn,
Estonia

O. Vergun

Department of Neurology, University of Pittsburgh
School of Medicine, Pittsburgh PA, USA

H. Waagepetersen

Danish University of Pharmaceutical Sciences,
Department of Pharmacology, DK-2100 Copenhagen,
Denmark
hsw@dfuni.dk

T. Wieloch

Laboratory for Experimental Brain Research, Wallenberg
Neuroscience Center, Lund University, Sweden
tadeusz.wieloch@med.lu.se

C. Zwingmann

Department of Organic Chemistry, University of
Bremen, D-28359 Bremen, Germany, and Department
of Medicine, University of Montreal, Montreal H2X 1P1,
Quebec, Canada

Glucose Metabolism in Brain

1.1 Bioenergetics

D. G. Nicholls

1	<i>Introduction</i>	4
1.1	Gibbs Free Energy	4
1.2	ATP Hydrolysis	5
1.3	Creatine and Creatine Phosphate	5
1.4	Redox Potentials	5
1.5	Ion Electrochemical Potential Differences	6
2	<i>Ion Circuits</i>	6
2.1	The Mitochondrial Proton Circuit	6
2.2	The Mitochondrial Calcium and Sodium Circuits	7
3	<i>In Situ Bioenergetics</i>	9
3.1	Respiration of In Situ Mitochondria	10
3.2	Monitoring Changes in In Situ Mitochondrial Membrane Potential	10
3.3	The Integration of the Neuronal Mitochondrion with Plasma Membrane Ion Circuits	14
4	<i>Conclusion</i>	16

Abstract: This chapter reviews some of the basic thermodynamic theories required for designing and interpreting bioenergetic studies using neuronal preparations. The emphasis is on the mitochondrion, both in isolation and in situ within the intact neural cell. Methodologies for monitoring membrane potentials and respiration are described.

1 Introduction

The two dominant components of any bioenergetic investigation of a process are thermodynamic and kinetic. Thermodynamics, in its somewhat simplified “equilibrium” form employed by most nonspecialist studies, determines the displacement from equilibrium of biological reactions, ion gradients, and redox reactions. Broadly speaking, this displacement from equilibrium can be equated with the capacity of the process to do work. It must be emphasized that equilibrium thermodynamics can never say whether a process actually occurs, since this is dependent upon appropriate pathways (enzymes, ion channels, etc.), but can definitively eliminate hypothetical processes that would go against the inviolable laws of thermodynamics by producing a global decrease in entropy. As you will realize on reading this chapter, the author is a strong believer in everyday analogies; the thermodynamic displacement from equilibrium of a reaction can be likened to the height of a waterfall, or the voltage across an electrical circuit and can be called an “intensive” term.

The second class of bioenergetic functions is kinetic, and deals with the rates at which processes occur. While an overall thermodynamic disequilibrium is required to drive any process, the actual rates in the complex metabolic networks that exist in the cell can currently only be determined experimentally, although an increasingly important field is that of “control theory,” which determines the effect of a slight variation in the activity of a single step on the overall rate of a complete pathway. The realization that control of the activity of a pathway does not depend on a single “rate-limiting reaction” but is influenced by every step in the pathway is of increasing importance in interpreting the overall consequences of dysfunction of an individual process and is becoming critical for the investigation of the molecular mechanisms underlying neuronal dysfunction and neurodegenerative disease. Continuing with everyday analogies, rates are “extensive” and can be likened to the amount of water flowing over a waterfall, or the current (amps) flowing around an electrical circuit.

Extending these simplistic analogies produces two additional functions: the rate of energy transfer as the product of thermodynamic disequilibrium and flux (power or “watts” in the electrical analogy) and flux per unit driving force (equivalent to electrical conductance). As we shall see, bioenergetics can make use of each of these combinations.

The following sections provide a brief overview of some of the more salient aspects of neuronal bioenergetics. For more detailed information, the reader is referred to Nicholls and Ferguson (2002).

1.1 Gibbs Free Energy

A process can only occur if it results in an increase in the entropy of the universe. Equilibrium thermodynamics as used in most bioenergetic studies considers the experimental system (cell, mitochondrion, cuvette, etc.) to be “closed;” this means it can exchange heat, but not matter, with its surroundings. Obviously, this is a simplification, but it provides a powerful means to examine equilibria and displacement from equilibrium. Because the system is exchanging heat with the surroundings it is affecting the entropy of the latter in a way that is difficult to determine directly. The Gibbs energy change, ΔG , of the system expressed in kJ/mole takes account of this external entropy change (under conditions of constant temperature and pressure) and is the fundamental parameter used in bioenergetics. When a reaction is at equilibrium the Gibbs energy “content” G is at a minimum and the Gibbs energy “change” ΔG is zero. ΔG for a reaction that has not reached equilibrium is negative, meaning that further reaction can proceed spontaneously (if a mechanism exists). The further the displacement from equilibrium, the more negative ΔG becomes. The key equation relating ΔG to displacement from equilibrium is:

$$\Delta G \text{ (kJ/mole)} = -2.3RT \log_{10}(K/\Gamma), \quad (1)$$

where R is the gas constant, T the absolute temperature, K the equilibrium constant (equilibrium mass action ratio) for the reaction, and Γ (gamma) the actual observed mass action ratio. At 37°C, this simplifies to

$$\Delta G \text{ (kJ/mole)} = -5.9 \log_{10}(K/\Gamma). \quad (2)$$

The logarithmic relationship implies that a reaction displaced 100-fold from equilibrium will have a ΔG of -11.8 kJ/mole.

1.2 ATP Hydrolysis

The thermodynamics of the ATP–ADP pool is frequently misunderstood. ATP itself is not a “high energy compound,” rather it is the enormous displacement from equilibrium of the reaction

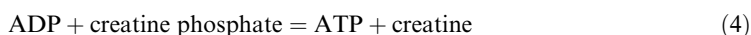


that underlies the capacity of the adenine nucleotide pool to transduce energy throughout the cell. In the cytoplasm this displacement may reach 10^{10} -fold, meaning that the turnover of 1 mole of ATP could make available almost 60 kJ of Gibbs free energy, and conversely that the regeneration of 1 mole of ATP in these circumstances would require an input of 60 kJ of free energy.

It is important to understand why it is possible to use the above “shorthand” equation for ATP hydrolysis, which ignores the involvement of water, pH, the ionization states of the nucleotides and phosphate, and chelation of divalent ions such as Mg^{2+} . As long as the equilibrium constant that is used for the reaction is obtained under exactly the same conditions for which Γ is determined, all these additional factors cancel out when the ratio K/Γ is calculated.

1.3 Creatine and Creatine Phosphate

The brain utilizes creatine phosphate as a means of buffering the ATP/ADP ratio against sudden energy demands. The apparent equilibrium constant for the reaction



catalyzed by creatine kinase is about 180, under conditions relevant to the cytoplasm (Teague and Dobson, 1992). The ratio of creatine phosphate to creatine in isolated nerve terminals is about 0.5:1 (Erecinska and Nelson, 1994). If the creatine kinase activity is sufficient for maintaining the reaction close to equilibrium then the ATP/ADP ratio should be in the region of 90. This is far higher than is measured in the same preparation by conventional extraction and enzymatic analysis, where values close to 5 are generally reported (Erecinska and Nelson, 1994). Two factors account for the discrepancy. First, whole-cell (or terminal) extracts contain adenine nucleotides from both the cytoplasm and the mitochondrial matrix. The ATP/ADP ratio in the latter compartment is considerably lower than in the cytoplasm since the export of ATP and uptake of ADP via the adenine nucleotide translocator (ANT) is not charge balanced and is driven by the membrane potential (Pfaff et al., 1969). The second reason for the discrepancy between the ATP/ADP ratios assayed and predicted from the creatine kinase equilibrium is the differential binding of ADP and ATP to cytoplasmic proteins. In fact, the calculated ATP/ADP ratio from the creatine phosphate/creatine ratio gives a more accurate estimate of the true thermodynamic cytoplasmic ATP/ADP ratio than that assayed directly.

1.4 Redox Potentials

The transfer of electrons from oxidized substrates down the respiratory chain involves the sequential reduction and reoxidation of some 20 components. The midpoint oxidoreduction (redox) potentials

($E_{m,7}$) of these reduced/oxidized couples are expressed in relation to the standard hydrogen electrode and range from -320 mV for NADH/NAD⁺ to $+820$ mV for oxygen at 1 atm in equilibrium with water. As the couple becomes more reduced, the redox potential (E_h) becomes more negative. For a $1e^-$ couple such as Fe²⁺-cyt *c*/Fe³⁺-cyt *c*, the change is -60 mV per 10-fold change in reduced/oxidized ratio while for a $2e^-$ couple (e.g., UQH₂/UQ) the change is -30 mV/decade.

The Gibbs free energy available from an electron transfer between two redox couples is proportional to the difference in their redox potentials

$$\Delta G \text{ (kJ/mole)} = -nF\Delta E_h, \quad (5)$$

where n is the number of electrons transferred, F is the Faraday constant (0.096 kJ/mole/mV) and ΔE_h is the difference in redox potential (in volts). Thus, the transfer of $2e^-$ down the respiratory chain from NADH to oxygen through a redox span of about 1,140 mV corresponds to a ΔG of -220 kJ/mole—more than sufficient for the synthesis of 3 moles of ATP.

1.5 Ion Electrochemical Potential Differences

The Gibbs free energy liberated by the transfer of 1 mole of a solute across a membrane from a concentration $[X]_A$ to a concentration $[X]_B$ and down an electrical potential gradient of $\Delta\psi$ mV is a function of both electrical and concentration gradients and is given by:

$$\Delta G \text{ (kJ/mole)} = -mF\Delta\psi + 2.3RT \log_{10}([X]_B/[X]_A), \quad (6)$$

where m is the charge on the solute. In the special case of the proton, this reduces to:

$$\Delta G \text{ (kJ/mole)} = \Delta\mu_{H^+} = -F\Delta\psi + 2.3RT\Delta pH, \quad (7)$$

where $\Delta\mu_{H^+}$ is termed the proton electrochemical potential difference. Such gradients are usually expressed in terms of voltage by dividing by the Faraday constant. For the proton, the electrochemical gradient in mV is termed the protonmotive force (pmf or Δp). At 37°C, the equation reduces to:

$$\Delta p \text{ (mV)} = \Delta\psi - 61\Delta pH. \quad (8)$$

A typical mitochondrion in State 4 (when there is no ATP synthesis) might maintain a Δp of 200 mV, with a $\Delta\psi$ of 150–170 mV and a ΔpH of -0.5 to -0.8 units (alkaline in the matrix). For an ion pump or a respiratory chain complex to pump 2 moles of protons across a membrane against a Δp of 200 mV, a Gibbs free energy change of at least -38 kJ or a redox potential drop of at least 200 mV for 2 moles of electrons is required.

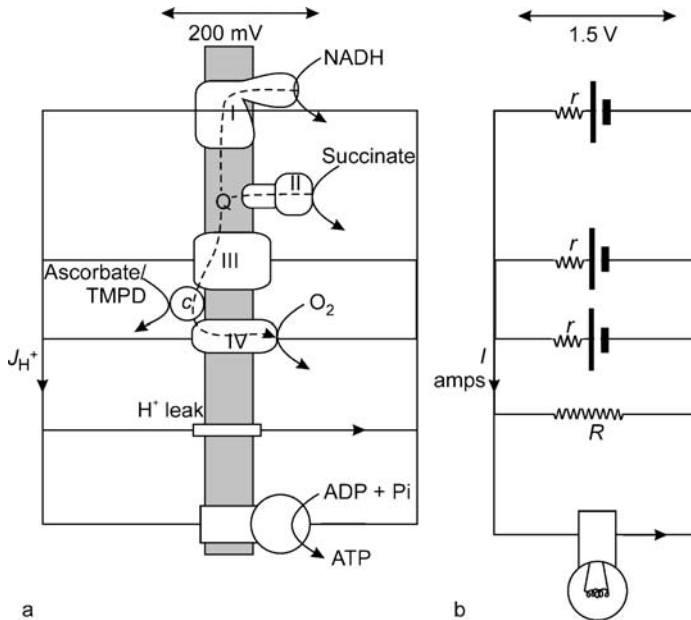
2 Ion Circuits

2.1 The Mitochondrial Proton Circuit

The simplest conceptual model for the bioenergetics of the mitochondrion is an equivalent electrical circuit (► [Figure 1.1-1](#)) where the three proton-translocating respiratory chain complexes (I, III, and IV) are visualized as three electrical cells generating a voltage of about 200 mV and arranged in parallel in a circuit completed by one or more proton reentry pathways across the inner mitochondrial membrane. The relationship between Δp , proton current, and the resistance (or conductance) of the inner membrane to proton reentry is governed by Ohm's law, an increase in inner membrane proton conductance being reflected in an increased proton current. Although proton current cannot be measured directly, the rate of proton pumping is directly proportional to the rate of electron transport down the respiratory chain, and hence to the rate of oxygen utilization. Monitoring respiration thus enables the proton current to be determined. A further analogy between the mitochondrial proton circuit and an equivalent electrical circuit is that the respiratory chain complexes (electrical cells) possess internal resistance; this means that Δp (the output voltage) drops slightly as the proton current increases.

■ Figure 1.1-1

The mitochondrial proton circuit and its electrical analog. (a) The three proton-translocating complexes of the respiratory chain (I, III, and IV) are arranged in series with respect to the electron flux and in parallel with respect to the proton circuit. Proton reentry is predominantly completed via ATP synthase with the generation of ATP, but, in addition, all mitochondria possess an endogenous proton leak that in some cases may be supplemented by an uncoupling protein. The proton current J_{H^+} flows between the generators and consumers of the proton-motive force. (b) The analogous electrical circuit has three cells arranged in parallel. Each possesses appreciable internal resistance (r) so that their output voltage decreases with increasing current. The circuit is completed by a "useful" pathway (the light bulb) and a dissipative resistive leak (R)



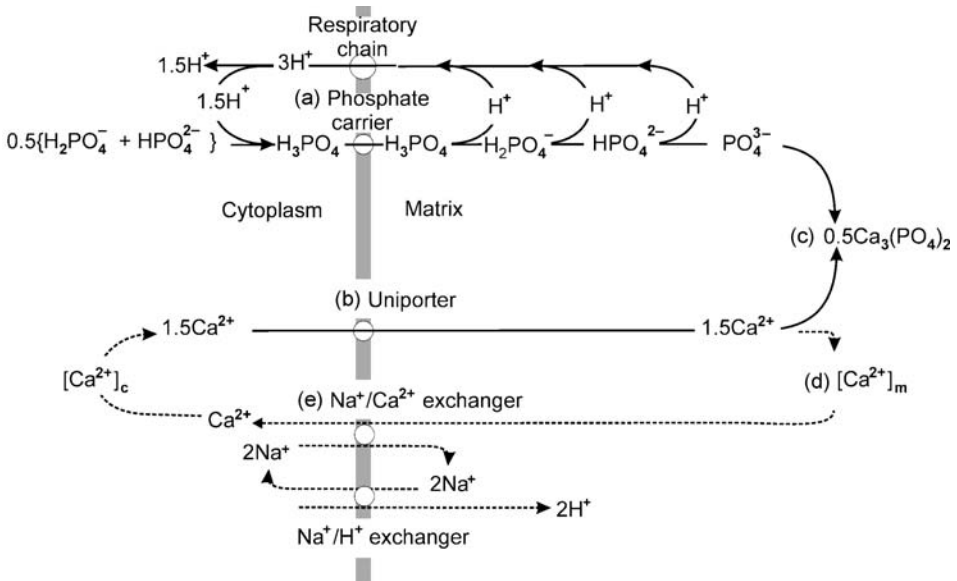
The major reentry pathway is via ATP synthase, wherein proton transfer is tightly coupled to ATP synthesis. However, in addition all mitochondria possess a constitutive inner-membrane proton leak that is responsible for the basal respiration in State 4. The activity of the proton leak is highly dependent on Δp , being active in State 4 but strongly inhibited in State 3 (the conditions of maximal ATP synthesis and turnover). The proton leak may function as a voltage-limiting device that decreases the risk of single electron leakage to oxygen in State 4 to form the superoxide anion (see below) but does not compromise ATP synthesis capacity in State 3. In addition to this endogenous proton leak, certain brain regions express uncoupling proteins that may perform a similar function of limiting superoxide formation (Brand et al., 2004) although their regulation still needs to be elucidated.

2.2 The Mitochondrial Calcium and Sodium Circuits

Brain mitochondria possess an enormous capacity to accumulate and retain calcium. The inner membrane possesses two independent Ca^{2+} transporters—a Ca^{2+} uniporter driven by the membrane potential that transports the ion with two positive charges and a 2 (or 3) Na^+/Ca^{2+} exchanger responsible for the continuous efflux of Ca^{2+} from the matrix to the cytoplasm (Nicholls and Chalmers, 2004). The two transporters allow Ca^{2+} to cycle across the inner membrane (▶ Figure 1.1-2). Ca^{2+} cycling is driven

■ Figure 1.1-2

Schematic of the ion movements involved in the net accumulation (*solid arrows*) and steady-state cycling (*dashed arrows*) of Ca^{2+} by brain mitochondria. (a) The phosphate carrier transports H_2PO_4^- in exchange for OH^- , but this is formally equivalent to the electroneutral transport of H_3PO_4 . Because three proton dissociations are required to form PO_4^{3-} , the concentration of this species is inversely proportional to the cube of the proton concentration in the matrix (Chalmers and Nicholls, 2003). (b) The uniport activity increases as the 2.5th power of cytoplasmic free Ca^{2+} concentration $[\text{Ca}^{2+}]_c$. (c) The tricalcium phosphate complex forms when its ion activity product is exceeded. Because the concentration of PO_4^{3-} increases with pH, the solubility of Ca^{2+} decreases and is about $2 \mu\text{M}$ when matrix pH is about 7.7 and external total phosphate is about 5 mM (Chalmers and Nicholls, 2003). (d) The matrix free Ca^{2+} concentration, $[\text{Ca}^{2+}]_m$, varies with total matrix Ca^{2+} until about 10 nmol/mg is accumulated and the tricalcium phosphate complex starts to form. In this initial region, matrix Ca^{2+} can regulate tricarboxylic acid enzymes. Once the complex forms, $[\text{Ca}^{2+}]_m$ is invariant with matrix Ca^{2+} load and the cytoplasmic Ca^{2+} buffering mode is seen. (e) The $\text{Na}^+/\text{Ca}^{2+}$ exchanger is controlled by $[\text{Ca}^{2+}]_m$; when the matrix is in cytoplasmic buffering mode ($>10 \text{ nmol Ca}^{2+}/\text{mg}$ accumulated), mitochondria seek to accumulate (or release) matrix Ca^{2+} to restore a set point at which the kinetics of uptake via the uniporter exactly balance efflux via the $\text{Na}^+/\text{Ca}^{2+}$ exchanger (Nicholls, 1978)



ultimately by the proton circuit, via an intermediate Na^+ cycle with the $\text{Na}^+/\text{Ca}^{2+}$ exchanger and a Na^+/H^+ exchanger. It is simpler to first discuss the ion movements occurring during net Ca^{2+} accumulation by the mitochondria. The activity of the Ca^{2+} uniporter increases as the 2.5th power of the cytoplasmic free Ca^{2+} concentration $[\text{Ca}^{2+}]_c$ (Nicholls and Chalmers, 2004). Ca^{2+} uptake is driven by $\Delta\psi_m$ and in the absence of any anion fluxes is accompanied by “net” proton extrusion by the respiratory chain. This has the effect of lowering $\Delta\psi_m$ and increasing ΔpH , so that net Ca^{2+} accumulation rapidly stops as $\Delta\psi_m$ declines. Further, net Ca^{2+} accumulation by mitochondria can occur only if accompanied by the uptake of an electroneutrally permeant anion—phosphate in the physiological context. Phosphate performs two functions:

- (1) The phosphate transporter catalyzes the exchange of H_2PO_4^- for OH^- and the efflux of the hydroxyl ion helps to neutralize the increased ΔpH resulting from the primary proton extrusion occurring in exchange for Ca^{2+} .
- (2) In the alkaline milieu of the matrix, Ca^{2+} and phosphate form an osmotically inactive tricalcium phosphate complex that limits the matrix free Ca^{2+} concentration to about $2 \mu\text{M}$ (Nicholls

and Chalmers, 2004) even though the mitochondrion can accumulate a total Ca^{2+} concentration exceeding 1 M.

The activity of the $\text{Na}^+/\text{Ca}^{2+}$ exchanger is controlled by the matrix free Ca^{2+} concentration and is thus independent of matrix Ca^{2+} load when the tricalcium phosphate complex is present. This and the 2.5th power dependency of the Ca^{2+} uniporter on cytoplasmic free Ca^{2+} means that mitochondria will only become net accumulators of cytoplasmic Ca^{2+} when the activity of the uniporter exceeds that of the $\text{Na}^+/\text{Ca}^{2+}$ exchanger. Both with isolated mitochondria and with mitochondria in situ this value is close to $0.5 \mu\text{M}$. Thus, mitochondria accumulate Ca^{2+} from the cytoplasm when $[\text{Ca}^{2+}]_c$ rises above $0.5 \mu\text{M}$ and deplete their Ca^{2+} stored when $[\text{Ca}^{2+}]_c$ is below this “set point.” Since the normal basal $[\text{Ca}^{2+}]_c$ in neurons is close to $0.1 \mu\text{M}$, this implies that the matrix Ca^{2+} is normally insufficient for the formation of the tricalcium phosphate complex. Under these conditions the matrix free Ca^{2+} roughly mirrors $[\text{Ca}^{2+}]_c$ and acts as a fine control for the activity of a number of matrix dehydrogenases including pyruvate dehydrogenase, NAD-isocitrate dehydrogenase, and α -ketoglutarate dehydrogenase (Hansford and Zorov, 1998).

Even though the capacity of mitochondria to accumulate and store Ca^{2+} is enormous, it is not infinite. With brain mitochondria under closely physiological conditions, the storage capacity is exceeded at about 800–1,500 nmol Ca^{2+}/mg protein; the inner membrane then becomes permeable to species with a molecular weight less than 1.4 kDa, resulting in a loss of Ca^{2+} , a collapse of Δp , and extensive matrix swelling resulting in rupture of the outer membrane and release of *cyt c* and other intermembrane proteins. This is the mitochondrial permeability transition (MPT) (Bernardi, 1999). The molecular nature of the pore is still debated, but the ability of adenine nucleotides and inhibitors of ANT to affect the sensitivity of mitochondria to MPT implies the involvement of the translocator. The total Ca^{2+} load at which the MPT occurs is reduced by omission of adenine nucleotides from the medium, by atractylate (which locks ANT in the cytoplasmic C conformation), and by a variety of oxidative stresses, particularly those associated with thiol or NAD(P)H oxidation. On the other hand, cyclosporine A and bongkreic acid (which locks ANT in the matrix M conformation) protect isolated mitochondria against the MPT.

3 In Situ Bioenergetics

There has been an increasing tendency in recent years to develop techniques that allow investigation of mitochondrial bioenergetics in intact cells rather than use isolated organelles. The big advantage, apart from avoiding the problem of isolation of tiny amounts of pure mitochondria from small brain areas without introducing artifacts, is that the mitochondria are studied in their physiological milieu. With fluorescence imaging techniques many mitochondrial parameters such as membrane potential can be studied at the single cell or even single organelle level. The goal in such studies is to describe the bioenergetic function of in situ mitochondria with the same precision as is possible for isolated mitochondria, including measurement of respiratory rates, the mitochondrial (and plasma) membrane potentials, Ca^{2+} accumulation, ATP synthesis rates, respiratory capacity, and mitochondrial proton leaks.

The two types of preparation that have been most intensively exploited to investigate in situ neuronal mitochondrial function are the isolated nerve terminal (or synaptosome) and primary neuronal cultures. Each has particular advantages and limitations. Isolated nerve terminals are prepared in suspension and can be investigated in fluorimeters or in conventional oxygen electrodes. They can be prepared from animals of any age, which is particularly important if age-dependent changes in presynaptic function are to be studied. The preparation contains all the machinery for the synthesis, storage, release, and reuptake of neurotransmitters, allowing the bioenergetics of presynaptic neurotransmission to be studied (Nicholls, 2003); in this context they can be induced to fire spontaneous repetitive action potentials by blocking inhibitory K^+ channels with agents such as 4-aminopyridine. On the negative side, structural information is lost by the homogenization, and all synaptosomal preparations contain mixed populations of neurotransmitters. This last problem has been resolved in a limited number of studies by the imaging of individual synaptosomes (Nayak et al., 2001), but I am aware of no mitochondrial bioenergetic studies at this level of resolution.

3.1 Respiration of In Situ Mitochondria

The synaptosome provides a simple model for investigating the bioenergetic linkages between the mitochondrion and plasma membrane ion circuits. Essentially, all synaptosomes in a preparation contain functioning mitochondria. Because synaptosomes are in suspension, their respiration may be determined using a conventional oxygen electrode. It is more meaningful to study brain mitochondrial respiration in synaptosomes, where they are surrounded by a physiologic cytoplasm and are driven by their physiologic substrate, pyruvate, than with isolated mitochondrial preparations. The basal respiration of a synaptosomal suspension is a measure of the terminals' ATP turnover and the respiration needed to counteract the inner mitochondrial membrane's inherent proton leak. Addition of the ATP synthase inhibitor oligomycin eliminates mitochondrial ATP synthesis and the resulting "State 4" respiration is a measure of this proton leak. Careful titration of synaptosomes with a protonophore such as FCCP enables the maximal respiratory capacity of the mitochondria to be determined.

Geometric considerations prevent the respiration of primary neuronal cultures cultured on coverslips from being monitored using conventional oxygen electrode chambers, although there are a limited number of studies in which cultured neurons have been resuspended from petri dishes for such studies. A recent innovation is the cell respirometer, a slowly perfused closed imaging chamber where the difference in upstream and downstream oxygen tension is measured by micro flow-through oxygen electrodes in order to quantify the population respiratory rate (Jekabsons and Nicholls, 2004). The advantages of this technique over the conventional oxygen electrode chamber are several; apart from the much greater sensitivity and the ability to retain the cells on the coverslip, the techniques allows respiration to be monitored for several hours while different agents are added and removed. At the same time, a representative field of cells is imaged to monitor morphology or the single cell fluorescence of cells loaded with any of the functional indicators of membrane potential, ion concentration, or reactive oxygen species concentration. The basic bioenergetic parameters can be quantified in a single experiment where the sequential additions of oligomycin to inhibit ATP synthase and a protonophore such as FCCP to relieve respiratory control gives precise information on the basal respiration, the ATP turnover of the cell, the native proton leak of the mitochondria, and the reserve respiratory capacity (▶ [Figure 1.1-3](#)).

3.2 Monitoring Changes in In Situ Mitochondrial Membrane Potential

Even though the oxygen electrode allows the quantification of the current flowing around the chemiosmotic proton circuit, it is important to monitor the voltage component of the circuit, namely the mitochondrial membrane potential, $\Delta\psi_m$. Strictly, the full protonmotive force, including the pH gradient across the inner membrane, is the relevant parameter, but the membrane potential is the dominant component of Δp and is usually the only parameter investigated. It needs to be emphasized at the outset that very few studies with intact cells attempt to quantify $\Delta\psi_m$. Instead, changes in potential are detected, either during the course of the experiment, or comparing two differently treated cell population.

A large majority of current investigations make use of fluorescent cations that are membrane-permeant by virtue of their extensive π -orbital systems. Three principles govern the fluorescence signal obtained from intact cells equilibrated with an "ideal" fluorescent cation.

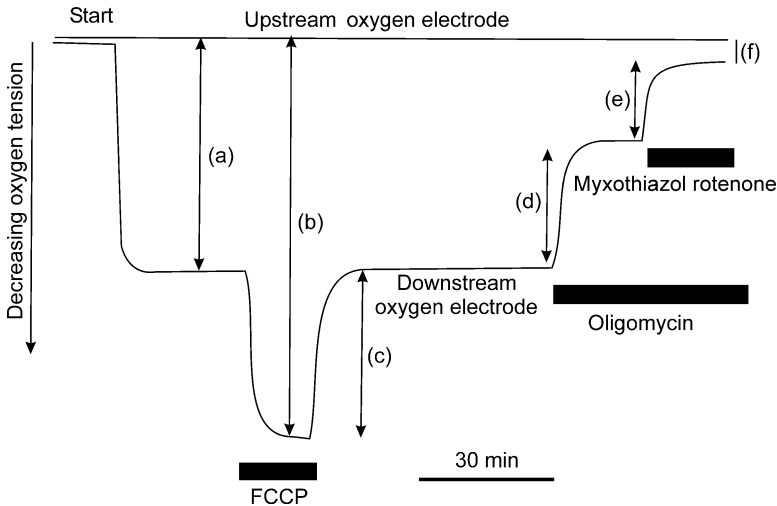
First, the probe seeks to come to a Nernst equilibrium across both the plasma and the mitochondrial membranes. The Nernst equilibrium can be thought of as the equilibrium condition for Eq. 6, i.e., when $\Delta G = 0$,

$$\Delta\psi = (2.3RT / -mF) \log_{10} ([X]_B / [X]_A). \quad (9)$$

At 37°C, this simplifies to a 10-fold gradient for each 61 mV of membrane potential. For a typical neuron equilibration with 5 nM of an indicator and with a plasma membrane potential, $\Delta\psi_p$, of -80 mV (negative in the cytoplasm) and $\Delta\psi_m$ of 150 mV (negative in the matrix relative to the cytoplasm—note the opposite sign conventions), the equilibrium probe concentration in the cytoplasm will be 100 nM and that in the matrix 30 μ M.

■ Figure 1.1-3

Schematic response quantifying the respiratory parameters of a population of coverslip-attached cultured neurons. The respirometer measured the difference in oxygen tension recorded by two flow-through oxygen electrodes placed upstream and downstream of a closed coverslip incubation chamber. The extent of the depletion is proportional to the respiratory rate of the cell population: (a) basal respiration; (b) maximal respiration in the presence of protonophore; (c) “spare” respiratory capacity; (d) respiration driving basal ATP turnover (oligomycin-sensitive); (e) basal proton leak (oligomycin-insensitive); (f) nonmitochondrial respiration (myxathiazol/rotenone insensitive). Data adapted from Jekabsons and Nicholls (2004)



Second, a consequence of the high accumulation of the cation in the matrix is that all commonly used indicators undergo aggregation above a critical concentration, typically in the 10–100 μM range. With most probes aggregation causes fluorescent quenching although with one commonly used indicator, JC-1, the aggregates show a red-shifted emission spectrum. As will be discussed later, it is of critical importance that experimental conditions clearly define whether the loading concentration is sufficient for aggregation to occur in the matrix (quench mode).

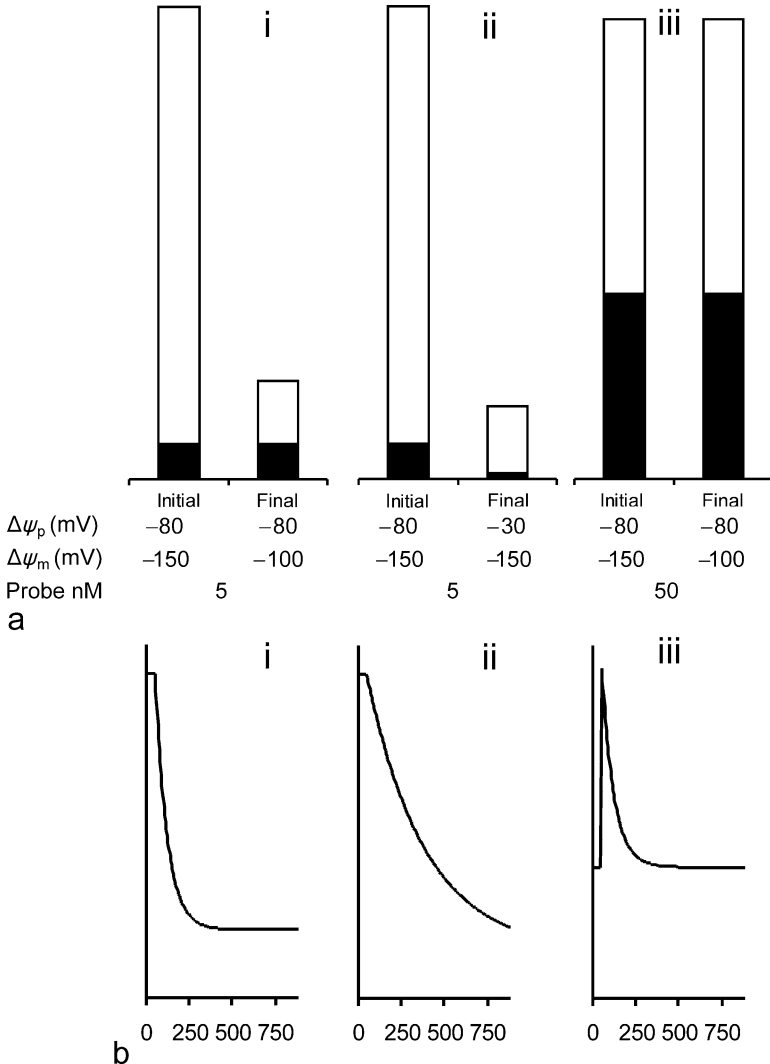
Third, the probe reequilibrates across the mitochondrial membrane in response to a transient many hundred times faster than across the plasma membrane, even though the validity of the probe depends on its nonselective permeability through lipid bilayer regions. This kinetic distinction is due to the geometry of the compartments—the relatively large, roughly spherical plasma membrane contrasted with the small, highly invaginated inner mitochondrial membrane, with the consequent vastly greater surface-to-volume ratio of the matrix.

Combining these principles allows the construction of a model (🔗 Figure 1.1-4) that explains the major features of these so-called mitochondrial membrane potential indicators (Ward et al., 2000). Two distinct types of experiments must be considered. In the first, changes in potential are monitored during the experiment while the cells are being imaged. In quench mode, a decrease in $\Delta\psi_m$ results in a release of probe from the quenched environment of the matrix into the cytoplasm, with a resultant increase in whole-cell fluorescence (🔗 Figure 1.1-5). This increase is transient since the “excess” cytoplasmic probe then leaks out of the cell until the Nernst equilibrium across the plasma membrane is restored. An important consequence of this is that the quench mode is invalid for the comparison of two populations of cells, for example, as in flow cytometry. In contrast, nonquench mode is valid both for following mitochondrial transients during the experiment and for comparing two cell populations.

The currently available indicators that have the least side effects (Scaduto and Grotyohann, 1999) are rhodamine-123 (R123) and the closely related tetramethylrhodamine methyl ester (TMRM) and

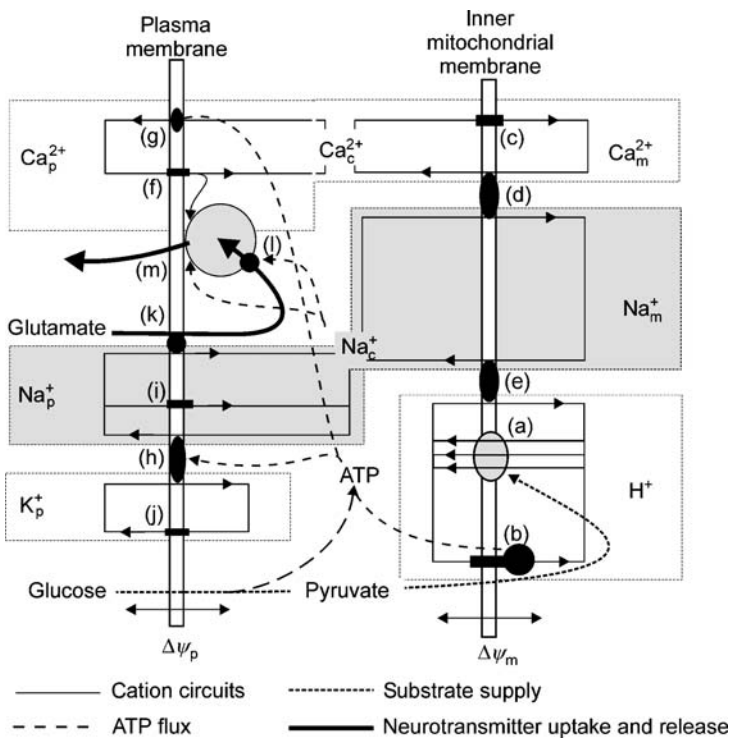
■ Figure 1.1-4

Computer simulations of whole-cell fluorescence responses for cells equilibrated with the representative “mitochondrial” membrane potential indicator TMRM⁺. The “virtual cell” computer simulation is described in Ward et al. (2000) and is available at <http://www.buckinstitute.org/nicholls.htm>. On the basis of three criteria described in the text and using the parameters—mitochondrial volume 4% of cell, plasma membrane reequilibration rate constant 0.04/s, and quench limit 40 μ M—the following simulations were performed. (A) Simulation of a “flow cytometry” type experiment comparing the fluorescence of two separate cell populations equilibrated with either (i, ii) a low (5 nM) nonquenching or (iii) a high (50 nM) quenching concentration of TMRM. Two mitochondrial membrane potentials of 150 and 100 mV (i, iii) or two plasma membrane potentials of -80 and -30 mV (ii) were simulated for the two populations. The *open bar* represents the mitochondrial fluorescence and the *closed bar* the cytoplasmic contribution. Note that the low nonquenching concentration allows the differences to be detected but distinction between the plasma and mitochondrial potentials is unclear. In contrast, the high quenching concentration obscures the major difference in $\Delta\psi_m$. (B) Simulation of whole-cell fluorescence changes in an experiment in which the same change in potentials is induced while the cells are being imaged. Note that plasma membrane depolarization in nonquench mode results in a slower reequilibration than mitochondrial depolarization, and that a transient increase in whole-cell fluorescence occurs in quench mode in response to a step mitochondrial depolarization



■ Figure 1.1-5

Simplified scheme of cation circuits operating across the neuronal plasma and inner mitochondrial membranes. The primary proton circuit (H^+) operates across the inner mitochondrial membrane, driven by the respiratory chain (a) and generating ATP via ATP synthase (b). The membrane potential generated by the respiratory chain ($\Delta\psi_m$) drives the electrophoretic accumulation of Ca^{2+} from the cytoplasm via the Ca^{2+} uniporter (c). The mitochondrial Ca^{2+} circuit (Ca_m^{2+}) is completed by the Na^+/Ca^{2+} exchanger (d). Na^+ entering in exchange for Ca^{2+} is recycled by the mitochondrial Na^+/H^+ exchanger (e) to complete the mitochondrial Na^+ circuit (Na_m^+). The plasma membrane Ca^{2+} circuit (Ca_p^{2+}) comprises a set of inward conductances (constitutive leaks and voltage-activated channels) (f) and the plasma membrane Ca^{2+} -ATPase (g) as well as the plasma membrane Na^+/Ca^{2+} exchanger (not shown). The plasma membrane Na^+ and K^+ circuits (Na_p^+ and K_p^+) are driven by Na^+/K^+ -ATPase (h) and completed, respectively, by the voltage-activated Na^+ channel (i) and a set of K^+ channels (j). The Na_p^+ circuit also drives the uptake of glutamate via the glutamate transporter (k). ATP is required for Ca^{2+} -ATPase and Na^+/K^+ -ATPase as well as for vesicular accumulation of glutamate (l) and the exocytotic process itself (m)



tetramethylrhodamine ethyl ester (TMRE). R123 is significantly more hydrophilic and hence crosses the plasma membrane more slowly. Even though JC-1 is capable of an emission shift in the aggregated form, there are artifacts in its use that preclude its use for other than crude demonstrations of depolarization.

Although these probes are described as “mitochondrial” membrane potential indicators, they also respond both in quench and in nonquench mode to changes in $\Delta\psi_p$ since this parameter defines their steady-state cytoplasmic concentration. This complication must particularly be borne in mind when it is required to monitor changes in $\Delta\psi_m$ in response to plasma membrane receptor or channel activation. In quench mode it is often possible to distinguish the responses to mitochondrial depolarization (a rapid transient increase in cell fluorescence from a plasma membrane depolarization (a slow (TMRM) or very slow (R123) decrease in fluorescence). However, in nonquench mode the whole-cell response to plasma and

mitochondrial depolarization is the same, and independent means, such as the use of anionic oxonol dyes to monitor $\Delta\psi_p$ (Wolff et al., 2003), may be required.

3.3 The Integration of the Neuronal Mitochondrion with Plasma Membrane Ion Circuits

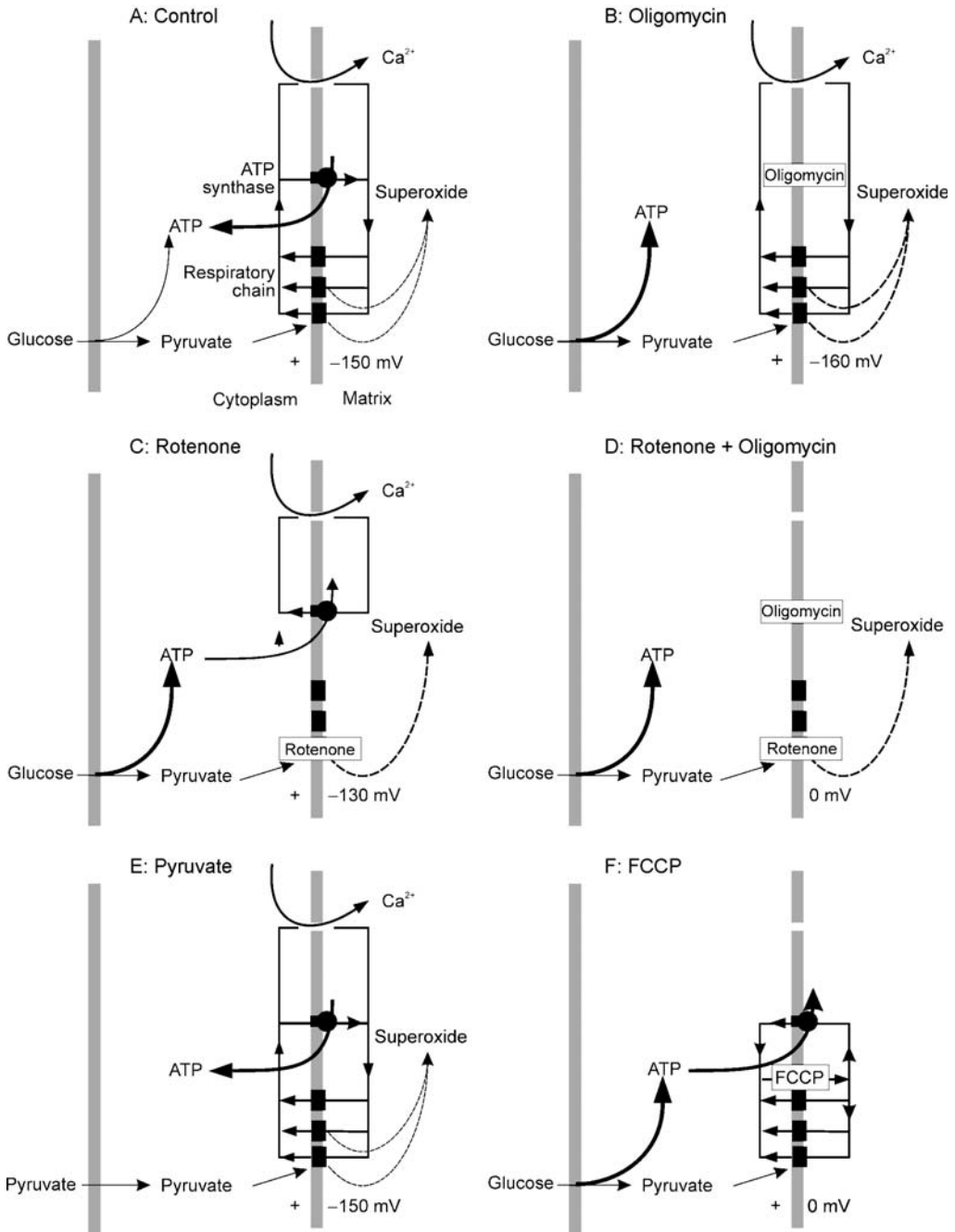
The dominant bioenergetic demands faced by the mitochondrion in situ within the terminal or neuron are associated with plasma membrane ion fluxes and the maintenance of ion gradients. Three major ion circuits operate across the plasma membrane cycling Ca^{2+} , Na^+ , and K^+ (Figure 1.1-5) while additional transporters regulate protons, Cl^- , neurotransmitters, and metabolites. The Na^+/K^+ -ATPase is potentially the largest single utilizer of ATP in the neuron; its activity in situ, however, is limited in the resting neuron by the low basal permeability of the plasma membrane to Na^+ , in contrast to the high constitutive K^+ conductance. Thus, addition of the Na^+/K^+ -ATPase inhibitor ouabain has only a slight effect on basal synaptosomal respiration. In contrast, addition of a Na^+ channel opener such as veratridine or brevetoxin results in rapid Na^+ cycling that utilizes the full capacity of the Na^+/K^+ -ATPase; this in turn requires almost the full respiratory capacity of the mitochondria (Scott and Nicholls, 1980). Thus, the mitochondrial ATP-generating capacity in the terminals appears to be well matched to the maximal ATP demand that is likely to be faced.

The use of mitochondrial substrates and inhibitors in intact cells differs in a number of respects from studies with isolated organelles (Figure 1.1-6). The first consideration is permeability across the plasma membrane. Apart from glucose, the only mitochondrial substrate that readily enters the neuron is pyruvate. Pyruvate (or lactate) can be used to supplement glucose as a fuel; this is of particular importance after ischemia when cytoplasmic ATP levels may be too low for the two ATP-requiring steps in glycolysis to function (Maus et al., 1999). Alternatively, the use of pyruvate in glucose-free media can be used to detect failures of mitochondrial ATP generation that might otherwise be masked by glycolysis. Protonophores, ionophores such as ionomycin ($\text{Ca}^{2+}/2\text{H}^+$), valinomycin (K^+), and nigericin (K^+/H^+), and hydrophobic inhibitors such as rotenone (complex I), antimycin A or myxathazol (complex III), and oligomycin (ATP synthase) readily enter neurons. However, since they distribute nonselectively into membranes their effects can be complex. Protonophores not only collapse $\Delta\psi_m$ but also cause the ATP synthase to reverse (Figure 1.1-6), depleting the cytoplasm of ATP. Unless it is actually intended that the protonophore addition should cause ATP depletion, such experiments are best performed in the presence of oligomycin, where the protonophore addition will depolarize the mitochondrion while ATP synthesis, being purely

Figure 1.1-6

Bioenergetic consequences of substrate and inhibitor additions to cultured neurons. (A) The mitochondrial proton circuit is generated by complexes I, III, and IV acting in parallel and is utilized primarily by ATP synthase to generate ATP. When cytoplasmic free Ca^{2+} exceeds a threshold, it accumulates in the matrix, driven by and utilizing the mitochondrial membrane potential. Complexes I and III contribute to superoxide ($\text{O}_2^{\bullet-}$) generation. (B) In the presence of oligomycin all ATP is produced by glycolysis, which accelerates to compensate. Mitochondrial membrane potential increases slightly, Ca^{2+} can still be accumulated and $\text{O}_2^{\bullet-}$ production continues, or is even enhanced due to the hyperpolarization. (C) Respiratory chain inhibition by rotenone requires that all ATP be generated by glycolysis; however, ATP is utilized by ATP synthase acting in reverse mode to generate a $\Delta\psi_m$ only slightly lower than in control conditions. Ca^{2+} can still be accumulated by the mitochondrion, but the increased demand on glycolytic ATP can lead to ATP depletion. Since rotenone acts downstream of the complex I $\text{O}_2^{\bullet-}$ -generating site, $\text{O}_2^{\bullet-}$ production from complex I is increased. (D) The combination of rotenone plus oligomycin allows $\Delta\psi_m$ to decay, preventing Ca^{2+} accumulation. There is no drain on glycolytic ATP, but $\text{O}_2^{\bullet-}$ is still produced. (E) Substituting pyruvate for glucose as substrate means that the cell is entirely dependent on oxidative phosphorylation. (F) Protonophores collapse $\Delta\psi_m$, but potentially deplete cytoplasmic ATP due to the rapid reversal of ATP synthase. Mitochondrial $\text{O}_2^{\bullet-}$ generation should be decreased due to the increased oxidation state of the respiratory chain

■ Figure 1.1-6 (continued)



glycolytic, will be unaffected. At the plasma membrane, even quite low protonophore concentrations acidify the cytoplasm and can result in a collapse of $\Delta\psi_p$, while collapse of the synaptic vesicle membrane potential can lead to a loss of transmitter into the cytoplasm. Ionomycin is frequently used to raise cytoplasmic free Ca^{2+} concentrations; however, when it reaches the inner mitochondrial membrane it introduces an

additional Ca^{2+} efflux pathway that leads to dissipative Ca^{2+} cycling and can effectively uncouple the mitochondria. Finally, valinomycin while hyperpolarizing the plasma membrane will collapse $\Delta\psi_m$.

An important difference between the isolated mitochondrial preparation and the intact cell is that substrate supply to in situ mitochondria is more limited. In addition, the various dehydrogenases of the citric acid cycle are interdependent since the product of one cycle enzyme is the substrate for the next. Thus, isolated mitochondria can maintain function in the presence of the complex I inhibitor rotenone by the addition of the complex II substrate succinate. However, in the intact cell the supply of succinate by the citric acid cycle is dependent on the NADH-linked dehydrogenases in the cycle and these are inhibited by rotenone.

4 Conclusion

Mitochondria occupy a central position in many areas of neuroscience. A search for “mitochondria” and “neuron or brain” produces more than 15,000 hits in PubMed. It is important that state-of-the-art techniques be employed for the continued development of this field, particularly in the more complex and demanding studies with intact cells. Using the approaches reviewed in this chapter, it is currently possible to study in situ mitochondrial bioenergetics with almost the same precision as less physiologically relevant isolated mitochondrial preparations.

References

- Bernardi P. 1999. Mitochondrial transport of cations: Channels, exchangers, and permeability transition. *Physiol Rev* 79: 1127-1155.
- Brand MD, Affourtit C, Esteves TC, Green K, Lambert AJ, et al. 2004. Mitochondrial superoxide: Production, biological effects, and activation of uncoupling proteins. *Free Radic Biol Med* 37: 755-767.
- Chalmers S, Nicholls DG. 2003. The relationship between free and total calcium concentrations in the matrix of liver and brain mitochondria. *J Biol Chem* 279: 19062-19070.
- Erecinska M, Nelson D. 1994. Effects of 3-nitropropionic acid on synaptosomal energy and transmitter metabolism: Relevance to neurodegenerative brain diseases. *J Neurochem* 63: 1033-1041.
- Hansford RG, Zorov D. 1998. Role of mitochondrial calcium transport in the control of substrate oxidation. *Mol Cell Biochem* 184: 359-369.
- Jekabsons MB, Nicholls DG. 2004. In situ respiration and bioenergetic status of mitochondria in primary cerebellar granule neuronal cultures exposed continuously to glutamate. *J Biol Chem* 279: 32989-33000.
- Maus M, Marin P, Israël M, Glowinski J, Prémont J. 1999. Pyruvate and lactate protect striatal neurons against *N*-methyl-D-aspartate-induced neurotoxicity. *Eur J Neurosci* 11: 3215-3224.
- Nayak SV, Dougherty JJ, McIntosh JM, Nichols RA. 2001. Ca^{2+} changes induced by different presynaptic nicotinic receptors in separate populations of individual striatal nerve terminals. *J Neurochem* 76: 1860-1870.
- Nicholls DG. 1978. The regulation of extra-mitochondrial free calcium by rat liver mitochondria. *Biochem J* 176: 463-474.
- Nicholls DG. 2003. Bioenergetics and transmitter release in the isolated nerve terminal. *Neurochem Res* 28: 1431-1439.
- Nicholls DG, Chalmers S. 2004. The integration of mitochondrial calcium transport and storage. *J Bioenerg Biomembr* 36: 277-281.
- Nicholls DG, Ferguson SJ. 2002. *Bioenergetics* 3, 3rd edn., London: Academic Press.
- Pfaff E, Heldt HW, Klingenberg M. 1969. Adenine nucleotide translocation of mitochondria. Kinetics of the adenine nucleotide exchange. *Eur J Biochem* 10: 484-493.
- Scaduto RCJ, Grotyohann LW. 1999. Measurement of mitochondrial membrane potential using fluorescent rhodamine derivatives. *Biophys J* 76: 469-477.
- Scott ID, Nicholls DG. 1980. Energy transduction in intact synaptosomes: Influence of plasma-membrane depolarization on the respiration and membrane potential of internal mitochondria determined in situ. *Biochem J* 186: 21-33.
- Teague WE Jr, Dobson GP. 1992. Effect of temperature on the creatine kinase equilibrium. *J Biol Chem* 267: 14084-14093.
- Ward MW, Rego AC, Freguelli BG, Nicholls DG. 2000. Mitochondrial membrane potential and glutamate excitotoxicity in cultured cerebellar granule cells. *J Neurosci* 20: 7208-7219.
- Wolff C, Fuks B, Chatelain P. 2003. Comparative study of membrane potential-sensitive fluorescent probes and their use in ion channel screening assays. *J Biomol Screen* 8: 533-543.

1.2 Glucose, Oxidative Energy Metabolism, and Neural Function in Brain Slices—Glycolysis Plays a Key Role in Neural Activity

Y. Okada · P. Lipton

1	Introduction	18
2	Plusses and Minuses of Using Brain Slices	18
3	Energy Utilization in Neocortical and Hippocampal Slices	21
3.1	Tissue from Adult Brain	21
3.2	Tissue from Developing Brain	22
4	Relationships Between Oxidative Energy Metabolism and Neural Activity	23
4.1	Principles	23
4.2	Effects of Anoxia and Ischemia on High-Energy Nucleotides and Synaptic Transmission in Adults	24
4.3	Irreversible Damage During and Following Ischemia	25
4.4	Effects of Anoxia and Ischemia on High-Energy Nucleotides and Synaptic Transmission in Developing Brain	26
5	Relationship Between Glycolytic Metabolism, Energy Levels, and Synaptic Transmission	28
5.1	Effects of Glucose Removal	28
5.2	Role of Substrates Other Than Glucose in Synaptic Transmission and ATP Maintenance	29
5.3	Role of Pathological Calcium in Removing Dependence of Transmission on Glycolysis	30
5.4	Absolute Requirement for Glucose in Synaptic Transmission	34
5.5	General Relationships Between Glucose Metabolism and Synaptic Transmission	34
5.6	Relationship of Results Described Here to Current Hypotheses on Role of Glycolysis in Neural Function	35
6	Overall Summary: Roles of Different Pathways of Energy Metabolism in Synaptic Transmission	35

Abstract: This chapter begins with a general description of the relationship between energy metabolism and brain function and then includes a discussion on the pros and cons of using brain slices for studying this phenomenon.

The major theme of the chapter is the role played by oxidative energy metabolism in synaptic transmission in rodent brain slices. In particular, it focuses on the different roles that appear to be played by the two principle components of energy production, mitochondrial oxidative metabolism and glycolysis.

Deprivation of oxygen leads to a rapid decline in synaptic transmission that, if maintained for 10 min or longer, is irreversible. This results primarily, or completely, from the resulting decline in cell ATP levels. The first measured fall in ATP precedes any measured fall in the population spike recorded from hippocampal neurons, and slowing the fall in ATP by preincubating slices in 10–20 mM creatine slows the fall in synaptic transmission.

The effects of glucose deprivation suggest that a simple fall in ATP levels does not account for the impaired transmission in this case, as quite normal levels of ATP are maintained at the time when transmission begins to fail. This is observed whether or not an alternative mitochondrial substrate such as lactate is provided. Thus, normally functioning brain slices require glycolysis for a purpose in addition to supplying substrate for the tricarboxylic acid cycle. After the slices suffer energy deprivation, or when the slices are prepared without adequate attention to speed, this requirement for glycolysis is abolished and synaptic transmission can be maintained by lactic acid and other postglycolytic substrates. This pathological transition appears to depend on an increase in intracellular calcium.

The specific role played by glycolysis in normal synaptic transmission is not known, but may be due to a requirement for a specific glycolytic intermediate or to a highly localized production of a product of glycolysis.

List of Abbreviations: GAPDH, glyceraldehyde-3-phosphate dehydrogenase; OGD, oxygen–glucose deprivation; PGK, phosphoglycerate kinase; IVI, in vitro ischemia; TIAs, transient ischemic attacks

1 Introduction

Large amounts of energy are required to maintain neural activity in the central nervous system, and deprivation of either glucose or oxygen leads to rapid failure of normal function; prolonged deprivation leads to irreversible functional failure due to cell damage (Gibbs et al., 1942; Kety, 1957; Sokoloff, 1960; Siesjo, 1978; Okada, 1988; Lipton, 1999; Tian and Baker, 2000; Dienel and Hertz, 2001).

In this chapter, we describe studies on rodent brain slices that have shed light on the role played by oxidative energy metabolism in general, and the glycolytic metabolism of glucose in particular, in generating normal neural/glial function. While some of the discussion deals with irreversible damage following energy substrate deprivation, the bulk of the chapter is devoted to the role of energy metabolism in ongoing neural activity.

2 Plusses and Minuses of Using Brain Slices

The four intact tissue preparations used for studying energy metabolism include in vivo models, brain slices, organotypic slice cultures, and cultures made from dissociated cells. The pros and cons of using these different systems to study irreversible damage have been discussed extensively elsewhere (Lipton, 1999). The major advantages to using hippocampal brain slices for acute studies are that they are far easier to prepare than in vivo models and that measurements of a wide range of variables are much easier to make than measurements in vivo. These variables include neural activity and glial activity; hippocampal slices retain some intact in vivo circuitry and both neurons and glia can be monitored with electrodes. Advantages also include relatively easy measurements of intracellular and extracellular ions and metabolites and transmitters and the posttranslational modulation of proteins, all in known cell types. Real-time measurements of cell fluorescence enables revealing measurements of many variables. In addition, the composition and temperature of the medium bathing the slices can be precisely controlled, with good temporal resolution allowing study of rapid changes (within 30 seconds to a minute) in the supply of metabolites involved in energy production. In particular, oxygen can rapidly be removed, as can glucose, and substitutions of other metabolites and drugs can be made rapidly.

The above features also apply to organotypic cell cultures, which have the benefit of durability; this allows long-term damaging effects to be measured. The main drawback of the cultures is the potential for altered gene expression. While slices and cultures have not been rigorously compared, it is clear that cultures are much more resistant to energy deprivation than are slices and *in vivo* tissue (Lipton, 1999).

Although slices have several positive features, it has become apparent that there are significant differences from *in situ* tissue. On a general level, concentrations of energy metabolites in brain slices are significantly lower than they are *in situ* suggesting that the slice is somewhat compromised, although energy charge is normal. Loss of adenylates, probably during slice preparation, is likely to be the basis for this deficit. Perhaps relatedly, Na/K ratios in slices are higher than *in situ* levels, and respiration rates are less than *in situ* (Lipton and Whittingham, 1984). Slices, which are almost always incubated in high O₂ concentrations (95% is normally used), may show elevated free-radical concentrations. Furthermore, responses to energy deprivation are incomplete compared with *in situ* preparations because there is no blood flow. Thus, several pathological changes that occur in the whole brain do not occur in slices. These include the reduced blood flow following ischemia (no-reflow) as well as the massive recruitment of white blood cells several hours after an insult (Kochanek and Hallenbeck, 1992). This inflammation is doubtless responsible for much long-term injury to neurons following many insults.

The basis for the compromised metabolism in brain slices is not known and does, in fact, remain something of a mystery. Slices that are immersed in ice-cold buffer within 30 s of decapitation, and that retain *in situ* properties in the cold, become severely compromised on initial warming and take about 45 min to recover to steady levels of high-energy metabolites (these are still well below *in situ* levels) (Feig and Lipton, 1990). Respiratory rates and rates of protein synthesis are also one-third to one-half of rates *in situ*. While it is often considered the basis, the actual ischemic insult during preparation seems far too short to be responsible; damage to brain tissue at 36°C requires at least 3 min and at low temperatures tens of minutes are required to cause permanent damage. Ischemia is extremely short during slice preparations and tissue is generally immersed in ice-cold buffers within 30 seconds to a minute of decapitation. It seems likely that the damage results from the physical trauma, due to preparation of the tissue and/or slicing. The latter puts great stress on the tissue. Various buffer compositions and conditions have been used during tissue preparation to attenuate the damage, and these are effective to different degrees. They include preincubation in buffer containing high Mg²⁺ and low Ca²⁺ (Feig and Lipton, 1990), substitution of sodium chloride by sucrose, and several other methods (Lipton et al., 1995). In no cases do they completely restore the parameters of energy metabolism.

Synaptic transmission is seemingly normal in hippocampal slices and plasticity, such as long-term potentiation (LTP) and long-term depression (LTD), is widely observed despite the metabolic abnormalities. Cells with these apparently normal electrophysiological properties are often swollen and distorted as viewed in tissue sections (Feig and Lipton, 1990). We have found, as a general rule, that slices maintained in interface chambers are morphologically more *in situ*-like than slices maintained in submerged chambers. Furthermore, slices from guinea pigs (and very probably mice) are metabolically healthier than slices from rats (P. Lipton and Feig, S.L., unpublished results).

Box 1: Terms and concepts

Population Spike

In this chapter damage to neurons is assessed as damage to neuronal transmission and effects of different energy substrates are assessed in terms of their effects on neural transmission. The response that is measured is generally the population spike. The population spike is recorded with an extracellular electrode generally placed in the target cell body layer. The recording represents the sum of action potentials generated in that layer, within about 50 μm of the recording electrode. In different experiments, the population spike is recorded from the dentate granule cell layer, the CA3 pyramidal cell layer (stratum lucidum) or the CA1 pyramidal cell layer. It can be evoked either orthodromically or antidromically.

Box 1: (continued)**Orthodromic and Antidromic Stimulation**

The orthodromic population spike is the potential change in the target cell layer following stimulation of the afferent pathway to that cell layer. It is thus a monosynaptic response. The antidromic population spike is the potential change following stimulation of the axons of the cells being recorded. It thus does not rely on synaptic transmission and measures only the ability of the particular cells to fire action potentials. The orthodromic response depends on both the firing properties of the cells and synaptic transmission. It is generally more sensitive to manipulations than the antidromic spike.

Long-Term Potentiation

This is a long term increase in the efficacy of synaptic transmission between afferent pathways and target neurons. It can be evoked by short bursts of high-frequency orthodromic stimulation of the afferent pathway and is thought to represent a long-term change in properties of the synapse. The phenomenon is thought to underlie different forms of long-term memory. The duration of LTP can vary between about 1 h and several days, depending on stimulation conditions and cell populations.

Metabolic Perturbations

Understanding how energy metabolism is coupled to function requires experimental manipulation that perturbs energy metabolism. These are used throughout the chapter and below is a short glossary of the terms as they apply to in vitro work on brain slices and cultures.

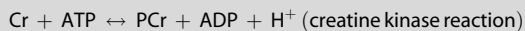
Anoxia. Perfusion of slices with buffer in which N₂ gas has been totally substituted for O₂ by equilibration for 20 min or more. In fact, complete removal is rarely attained in slice studies; oxygen levels are generally reduced to between 0.2% and 0.4%.

Hypoxia. As above except buffer is not depleted of oxygen as much as in anoxia. It is sometimes used interchangeably with anoxia, and this is the way it is used in this chapter. It is used this way to be explicit about the fact that all oxygen is probably not removed from the buffer. Basically one is hedging one's bets! In some cases specific low oxygen gas mixtures are used.

Aglycemia and hypoglycemia. These are formally similar to anoxia and hypoxia except that here glucose is removed or lowered, rather than oxygen. Here too care needs to be taken to remove all glucose to achieve true aglycemia; even very low levels of glucose (0.2 mM) can contribute to synaptic transmission. Hence, hypoglycemia is often used as a coverall term in the absence of direct measurements of medium glucose.

Ischemia. This is, strictly, reduced blood flow and is generally the origin of stroke in vivo. The condition is mimicked in vitro by a combined anoxic/aglycemic buffer. This has various designations. One is oxygen–glucose deprivation (OGD) and another is in vitro ischemia (IV). In this chapter, the term ischemia is used to denote this condition.

Phosphocreatine kinase system for maintaining ATP. Many of the studies involve investigating the specific role of ATP. To do this it is useful to be able to maintain ATP levels during energy perturbations. This can be done by equilibrating tissue for prolonged periods (usually 2 h) with creatine (Cr). This can be transported into cells at high levels and in doing so leads to the production of large amounts of phosphocreatine (PCr) via the creatine kinase enzyme, which is present in both cytosol and mitochondria.



Levels can be elevated by between two- and threefold via this reaction. In this way Cr and PCr levels are much elevated while ATP and ADP levels are maintained at normal levels via the normal mitochondrial feedback mechanisms.

During energy deprivation reversal of this reaction allows the high levels of PCr to re-supply ATP that is net broken down in the absence of normal synthesis. Thus, ATP levels can be maintained much more effectively, generally for about twice as long as normal (discussed in Lipton and Whittingham, 1982, 1984 and Whittingham and Lipton, 1982).

3 Energy Utilization in Neocortical and Hippocampal Slices

3.1 Tissue from Adult Brain

The energy metabolism of cerebral cortex slices was extensively studied in the 1950s and 1960s (McIlwain and Bachelard, 1985), and indeed it was the scholarship of Henry McIlwain, along with some others, that firmly established the usefulness of the study of brain slices in those decades. The above-referenced text contains a wealth of data on brain slice metabolism and function that were obtained prior to the introduction of the hippocampal slice preparation. Resting neocortical slices from guinea pigs and rats consume oxygen at about 10–15 $\mu\text{mol/g}$ protein/min. This is about one-third the value observed in the intact rat brain under N_2O anesthesia. When slices are strongly stimulated, at 50 Hz, the metabolic rate is approximately doubled to values that are only about 25% less than the N_2O -anesthetized brain. In the intact brain, barbiturate anesthesia decreases O_2 consumption by about 50%. Taken together, these results indicate that energy metabolism associated with neural activity may account for the difference between slice tissue and in situ tissue; however, the extent to which this is true has not been carefully determined (summarized in Lipton and Whittingham, 1984).

► *Table 1.2-1* shows oxygen consumption rates for slices taken from different regions of the guinea pig brain; measurements were taken using a microchamber with an oxygen electrode (Nishizaki and Okada, 1988; Nishizaki et al., 1988). Highest rates are in the grey matter of cerebral cortex and inferior colliculus; rates are lower in brain stem and in white matter. The basis for the lower rates in brain stem are not obvious.

■ **Table 1.2-1**

The oxygen consumption in slices from different regions of the guinea pig brain

Brain region	Oxygen consumption ($\mu\text{mol/g}$ protein/min)
Cerebral grey matter	9.69 \pm 0.25
Cerebral white matter	4.90 \pm 0.27
Hippocampus	8.43 \pm 0.21
Thalamus	8.57 \pm 0.78
Hypothalamus	6.62 \pm 0.49
Striatum	7.26 \pm 0.53
Superior colliculus	8.15 \pm 0.33
Inferior colliculus	9.46 \pm 0.38
Pons	6.53 \pm 0.49
Medulla oblongata	5.46 \pm 0.31
Medulla of the cervical spinal cord	5.55 \pm 0.25
Cerebellum	6.86 \pm 0.35

Temperature: 37°C

Number of samples assayed: Hippocampus ($n = 20$), other regions ($n = 8$) (Nishizaki et al., 1988)

Energy metabolism in subregions of hippocampus. There are expected to be significant variations in rates of energy metabolism between synaptic and nonsynaptic microregions of tissue, and these are of physiological interest. In order to determine these microregional rates the decrease of high-energy phosphate compounds during the first 1–2 min following induction of complete ischemia in an oil phase were measured in different regions of brain slices. Overall rates of high-energy phosphate utilization ($\sim\Delta P$) were then calculated from the equation

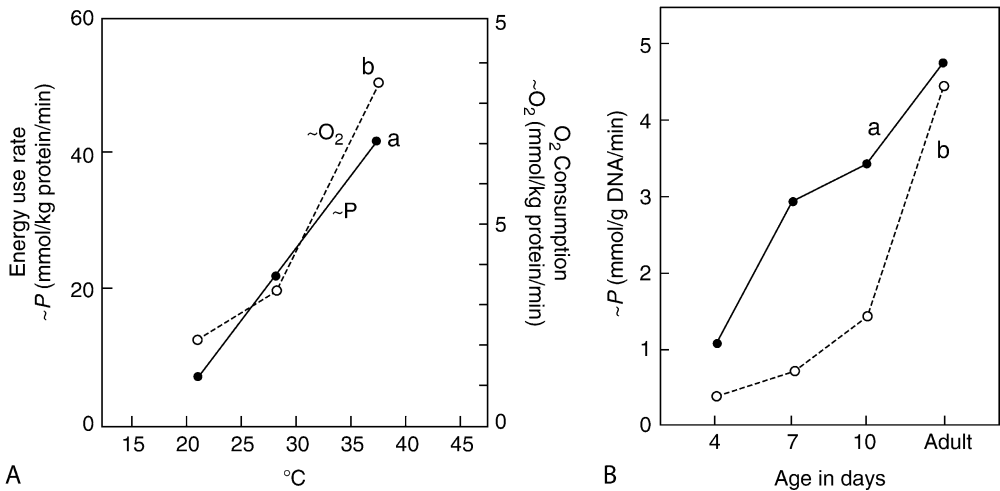
$$(\sim\Delta P) = (2 \times \Delta\text{ATP} + \Delta\text{PCr} + 1.3 \times \Delta\text{lactate}), \quad (1)$$

where 1.3 is the weighted average of 1 and 1.45, which are the net ATP production rates associated with the production of a mole of lactate from glucose and glycogen-associated glucose, respectively (Lowry et al., 1964; McDougal et al., 1968; Okada and McDougal, 1971).

This approach assumes that the rate of utilization of high-energy phosphates during early ischemia is the same as it was immediately prior to the ischemia. Empirically, it appears to be valid as judged by good agreement between this method and directly measured rates of oxygen consumption. Energy utilization of the guinea pig hippocampal slice at 37°C was calculated as 42.2 mmol $\sim P$ /kg protein/min (Tanimoto and Okada, 1987). This agrees well with the directly measured rate of oxygen consumption, 8.43 mmol O_2 /kg protein/min (Table 1.2-1), if the normal P/O ratio of 3 is assumed. (P/O_2 ratio is then 6.) The two methods are in agreement over a range of temperatures (Figure 1.2-1A).

Figure 1.2-1

(A) Effects of temperature on (a) the rate of energy utilization calculated using Eq. 1 (Tanimoto and Okada; 1987) and (b) oxygen consumption (Nishizaki et al., 1988) in hippocampal slices of adult guinea pigs. From this figure, the average calculated P/O_2 ratio is 2.97. (B) Relationship between the age of the rats and energy utilization in hippocampal slices. (a) Measured rates of energy utilization using Eq. 1. (b) Rates of energy utilization calculated from measured rates of oxygen consumption. In the 0- to 14-day-old rats, P/O_2 was taken to be 1.5 ± 0.4 (Nishizaki et al., 1988). In the adult rat it was taken to be 2.8 ± 0.3 (Holtzman and Moore, 1973). These P/O_2 ratios were used to calculate the rates of high-energy phosphate production from oxidative metabolism shown on the ordinate (Kawai et al., 1989). Taken together, these data show that there is a far higher rate of high-energy phosphate bond production from anaerobic glycolysis in young animals



Using this methodology the rate of energy utilization in the cellular and dendritic layers of the guinea pig hippocampus was determined after microdissection of cryostat sections of the freeze-dried hippocampal slice (Okada, 1990). Metabolites were measured using microassay procedures described by Lowry and Passonneau (1972) and Okada and Shimada (1976). As shown in Table 1.2-2, energy utilization in the pyramidal cell and granule cell layers is much higher than in the fimbria, which is composed of nerve fibers. The mossy fiber layer, which is rich in synapses, shows the highest rate of energy utilization.

3.2 Tissue from Developing Brain

Age-related changes in energy metabolism were studied in hippocampal slices prepared from 4-, 7-, and 10-day-old rats as well as from adult rats (Kawai et al., 1989). Rats were used for these developmental studies as they are less mature at birth than guinea pigs are. Results were calculated in terms of tissue DNA content

■ **Table 1.2-2**

Energy use rate in the layers of hippocampal slices. After removal of both oxygen and glucose from the incubation medium for 0, 1, 3, 5 min, each slice was immediately frozen on dry ice and cut into thin sections (20 μm) using the cryostat. The tissue was freeze dried overnight. The pyramidal cell layer (CA3 region), mossy fiber layer, granule cell layer (dentate gyrus), and fimbria were separately dissected out and weighed with a fish pole fiber balance. ATP, PCr, and lactate were determined in each dried sample. From the initial (1–2 min) decrease in ATP and PCr and the increase in lactate the energy use rate ($\sim\text{P}$) in each layer was calculated (Eq. 1). Each value is expressed per dry weight in the left column and per protein in the right column. The dry/protein weight ratio is approximated as 2.5 (Okada, 1990)

Layer	$\sim\text{P}$ (mmol/kg dry wt/min)	$\sim\text{P}$ (mmol/kg protein wt/min)
Whole slice	17.2	43.0
Pyramidal cell layers (CA3)	23.8	59.5
Mossy fiber layer	26.2	65.5
Granule cell layer(dentate gyrus)	21.7	54.3
Fimbria	10.9	27.3

rather than protein. This method is often used to normalize results over time for developing tissue because of changing cell numbers (Mandel and Edel-Harth, 1966). It is not entirely satisfactory because if cells get larger during development then the increasing rates per DNA measured with age may not actually represent increasing metabolic rates per tissue mass. Conversely, rates measured in this way in young animals may be artifactually small if cells are smaller than in adult tissue. However, this calculation does clearly show relative energy expenditure rates on a per cell basis. Figure 1.2-1Ba shows that the rate of high-energy phosphate utilization per DNA increased more than fourfold between 4-day-old and adult rats. The rate of oxygen utilization increased even more sharply, about sixfold over the same age span, rising from 0.13 to 0.80 mmol $\text{O}_2/\text{g DNA}/\text{min}$. Using these values, Figure 1.2-1Bb shows that the fraction of ATP turnover that can be accounted for by oxidative metabolism increases greatly during development (see legend for explanation of the calculation).

This conclusion is consistent with many *in vivo* studies showing that brains of immature animals are far more resistant to anoxia than those of mature animals (Fazekas et al., 1941; Thurston and McDougal, 1969; Duffy et al., 1975; Rice et al., 1981; Vannucci et al., 1994).

4 Relationships Between Oxidative Energy Metabolism and Neural Activity

4.1 Principles

Blockade of energy metabolism leads to inhibition of synaptic transmission and, if carried on long enough, leads to irreversible brain damage. This chapter is primarily concerned with the acute effects of inhibiting energy metabolism. This is important for two reasons. The first is that there are many pathophysiological conditions associated with transient inhibition of energy metabolism including transient ischemic attacks (TIAs) and insulin-induced hypoglycemia so that defining and understanding its effects is clinically important. Also, the way energy metabolism is coupled to synaptic transmission is a fundamental aspect of brain function and can best be understood by briefly perturbing energy metabolism.

The three major ways of inhibiting energy metabolism in brain slice tissue include (1) interfering with oxygen utilization by oxygen deprivation (hypoxia or anoxia), (2) interfering with glucose utilization by glucose deprivation (hypoglycemia or aglycemia), and (3) interfering with both these substrate supplies (oxygen–glucose deprivation or *in vitro* ischemia; note that “ischemia” will be used for “*in vitro* ischemia” or “oxygen–glucose deprivation” throughout this chapter). In many cases inhibitors of mitochondria or of glycolysis are used instead of oxygen or substrate deprivation. The short-term effects of these three treatments include both loss of ATP and failure of synaptic transmission. Long-term effects depend on

the durations of the treatments and range from complete reversibility to irreversible loss of synaptic transmission, as well as large-scale cell damage or cell death (Siesjo, 1978; Lipton, 1999).

When oxidative metabolism is blocked, by hypoxia/anoxia or ischemia, there is a rapid fall in both PCr and ATP levels and also in synaptic transmission. At 35–37°C these changes are essentially complete within 5–7 min. As far as has been studied, changes during ischemia are faster than changes during anoxia. Also, as far as can be determined, high-energy nucleotide levels fall before synaptic transmission begins to decrease. In contrast, inhibiting metabolism via the glycolytic pathway, by removal of glucose or adding inhibitors of glycolysis, leads to a far slower fall in high-energy phosphates than anoxia or ischemia does. Furthermore, synaptic transmission is abolished with little or no decrement in PCr or ATP. This suggests that glucose metabolism plays a role in synaptic transmission beyond simply fueling ATP generation. This conclusion is also supported by a large number of *in vivo* studies showing major neurological changes before any fall in high-energy phosphates during hypoglycemia (Lewis et al., 1974; Siesjo, 1978; Ratcheson et al., 1981; Ghajar et al., 1982; Siesjo, 1988). While they are qualitatively similar, all these changes are slower in brains from very young animals and are also much slowed by hypothermia.

4.2 Effects of Anoxia and Ischemia on High-Energy Nucleotides and Synaptic Transmission in Adults

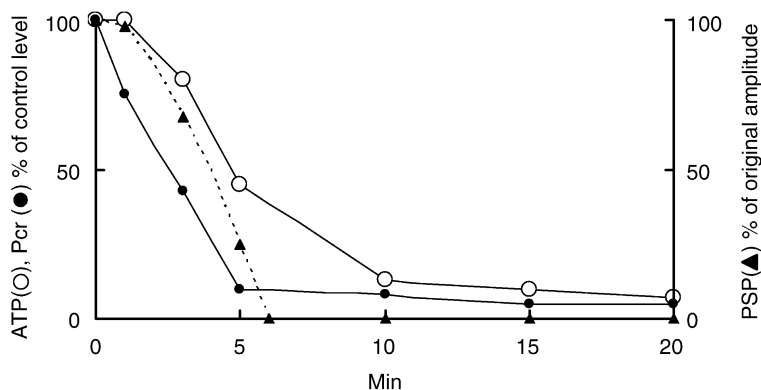
During anoxia, or ischemia, decreases in high-energy phosphates and synaptic transmission occur rapidly, with very similar time courses. While changes in these variables are slightly faster during ischemia than anoxia the changes are essentially complete within 5 min at 35–37°C. A key issue is whether the decline in high-energy phosphates is the basis for the loss of transmission. Lipton and Whittingham (1982) simultaneously determined the fall in PCr and ATP and synaptic transmission in the dentate gyrus of the guinea pig hippocampus at physiological temperatures. The earliest measured event was a fall in PCr, followed by a fall in ATP and, within seconds, the first noticeable sign of a decrease in synaptic transmission. This same sequence occurred even when the failure of transmission was greatly accelerated by incubating the slices in depolarizing buffer, containing somewhat elevated potassium. To further strengthen the conclusion that transmission failure resulted from a loss in ATP, the decay of ATP was delayed by preincubating the tissue with 25 mM creatine. In this case, the failure of transmission was also delayed (Whittingham and Lipton, 1982). These studies establish quite well that the fall in ATP is very likely the primary cause of transmission failure during anoxia.

The same rigorous test has not been applied to the ATP and synaptic transmission changes during ischemia but [Figure 1.2-2](#) shows that the two variables decay with very similar time courses. Furthermore, creatine preincubation does delay the decrease in transmission (Okada and Yoneda, 1983; Yoneda et al., 1983) suggesting that here also the fall in ATP is the primary cause of the transmission failure.

There have been many suggested explanations for the membrane changes that directly lead to the transmission failure when oxidative metabolism is blocked, and much discussion about whether the failure is primarily presynaptic, postsynaptic, or both. These issues have not been fully resolved and are outside the realm of this chapter. However, it is notable that transmission fails before the massive anoxic depolarization that occurs during these insults (Okada, 1987; Balestrino et al., 1989). Hence, the basis is more subtle than a massive depolarization-induced conduction block, though milder depolarization (Lipton and Whittingham, 1979) or hyperpolarization (LeBlond and Krnjevic, 1989) in some but not all cell types (Krnjevic and Ben-Ari, 1989) as well as extracellular adenosine buildup (Lipton and Whittingham, 1984; Fowler, 1989; Zhu and Krnjevic, 1997) are all good candidates for the causes of the earliest decrease in transmission. When CA3 cells were impaled, the order of decay of processes was inhibitory postsynaptic potential (IPSP), followed by depolarization-induced spike generation, followed by the excitatory postsynaptic potential (EPSP) (Takata and Okada, 1995). In CA1 pyramidal cells, the EPSP is invariably abolished prior to the presynaptic action potential (P. Lipton and D. Lobner, unpublished results), which survives until the anoxic depolarization. This strongly suggests that synaptic transmission failure results from failure of exocytotic and/or postsynaptic events rather than conduction in processes. Mechanisms, and thus sequences of failures, may certainly be different in different cell types.

■ Figure 1.2-2

Effects of deprivation of both oxygen and glucose on the amplitude of population spike (PS) in CA3 region elicited by stimulating the granule cell layer of dentate gyrus and on the levels of ATP and PCr in whole-hippocampal slices from adult guinea pig at 37°C. For each variable the ordinate shows the percentage of the values immediately prior to ischemia. Original levels of ATP and PCr were 15.0 ± 1.6 and 29.3 ± 2.5 mmol/kg protein, respectively. Each plot indicates mean value from eight slices. SEM was within 10% of each plotted mean value (not shown). (Modified from Okada (1988))



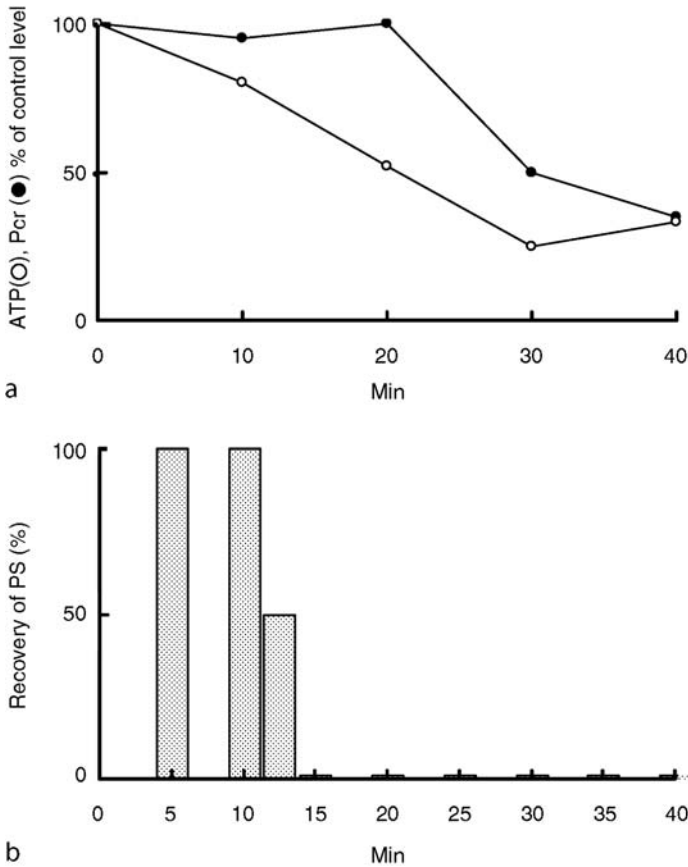
4.3 Irreversible Damage During and Following Ischemia

Irreversible damaging effects of anoxia and ischemia depend on the insult and its duration. Details of timing differ among different laboratories but results show identical trends. [▶ Figure 1.2-3a](#) shows the effects of different durations of ischemia on the recovery of PCr and ATP measured 40 min after the insult. [▶ Figure 1.2-3b](#) shows the effect of different ischemic durations on recovery of the population spike. Slice ATP and the population spike in the mossy fiber to the CA3 pyramidal cell pathway both recover by about 75% following 10 min ischemia. However, damage to the population spike increases more dramatically than failure of ATP recovery after longer ischemic durations. A similar reduction in both population spike and ATP levels occurs in the dentate gyrus of rat hippocampal slices 1 h following 10 min ischemia (Kass and Lipton, 1989). These different results raise the question as to whether failure of energy metabolism per se in the postischemic period is responsible for the long-term transmission failure. Other results make this very unlikely. In CA1 of rat hippocampal slices, ATP levels are maintained at control levels 1 h following 10 min anoxia while synaptic transmission remains abolished. Furthermore, removal of calcium during anoxia allows full recovery of synaptic transmission in both dentate gyrus and CA1, 1 h after anoxia, but has no effect on the ATP levels during this recovery period. (Kass and Lipton, 1982, 1986). Hence, postischemic changes in ATP do not appear to be directly responsible for the irreversible transmission failure.

The metabolic basis for the transition from reversible to irreversible synaptic transmission damage is not yet known despite a large number of excellent relevant studies (Lipton, 1999; Chan, 2004; Chiarugi, 2005; Moro et al., 2005; Panickar and Norenberg, 2005). As with the acute decay in transmission, the decrease in ATP is a primary factor, as irreversible damage is strongly attenuated when ATP levels are maintained by creatine incubation (Kass and Lipton, 1982). There is strong evidence implicating anoxic depolarization, which occurs during anoxia/ischemia, as the critical event in causing profound long-term transmission damage (Balestrino et al., 1989) and consistent with this conclusion, factors that change dramatically at this point, including calcium levels and arachidonic acid, seem to be critical in initiating the damage. Downstream events are much less certain, although both proteases and free radicals appear to play important roles (Lipton, 1999).

■ Figure 1.2-3

(a) Recovery of ATP and Pcr levels in the hippocampal slices from adult guinea pigs measured 20 min after ischemia. The abscissa shows the duration of ischemia prior to the 20-min reoxygenation in normal buffer. (b) Recovery of the population spike (PS) in the CA3 pyramidal cell layer in response to stimulation of the granule cell layer. Abscissa shows the duration of ischemia prior to the 20-min recovery period. In (a) each point is the average from 8–10 slices. SEM of each point was within 15%. In (b) each bar represents the percentages of the PSs that recovered to at least 80% of their original amplitude. For each bar, 8–10 slices were averaged. (Modified from Tanimoto and Okada (1987) and Okada (1988))

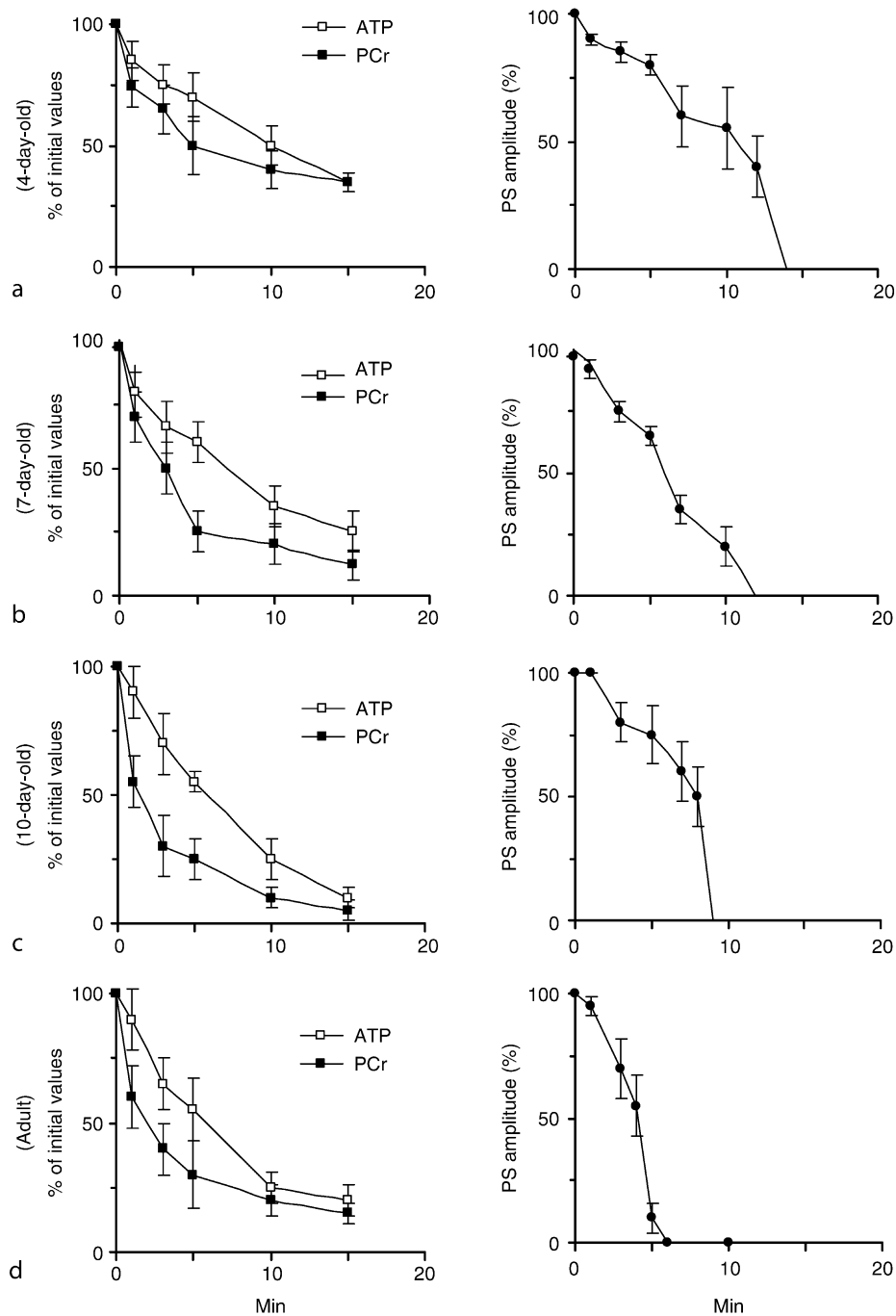


4.4 Effects of Anoxia and Ischemia on High-Energy Nucleotides and Synaptic Transmission in Developing Brain

Studies similar to the above have been carried out in developing brain to determine how age affects sensitivity to oxidative energy deprivation. Hippocampal slices from 4-, 7-, and 10-day-old rats as well as from adult rats were studied both metabolically and electrophysiologically, during ischemia (● Figure 1.2-4). The two variables show quite different patterns of change with respect to animal age. The decrease in ATP levels during ischemia is slow in the 4-day-old animal, perhaps due to decreased energy expenditure, and it essentially reaches adult levels by the time the animal is only 7-days old. On the other hand, the decay in synaptic transmission is much slower in all the developing animals than it is in the adult. This

Figure 1.2-4

Effects of ischemia on the levels of ATP and PCr (left column) and on the population spike (PS) evoked in the CA3 pyramidal cell layer in hippocampal slices from rats of the indicated ages. The abscissa is the duration of ischemia. Each point is the average value from six slices. (Modified from Nabetani et al. (1995))



suggests an enhanced, ATP-independent, sensitivity of synaptic transmission to energy deprivation in older animals. The basis for this intriguing effect is not known. Effects of age during ischemia differ from events during anoxia alone, where the enhanced anaerobic glycolysis in young animals is a major factor. During anoxia alone the decay in ATP is much slower in young rats than in the adults even out to 30 days of age (Kass and Lipton, 1989; Nabetani et al., 1995), leading to a much slower decay in synaptic transmission in all the younger rats (Nabetani et al., 1995). This slower fall in ATP is also associated with a decreased vulnerability of synaptic transmission to anoxia in hippocampal slices from younger rats (Kass and Lipton, 1989).

These results indicate that the immature rat is quite resistant to oxygen deprivation alone while the adult rat depends critically on oxygen. Anaerobic glucose metabolism plays a stronger role in younger animals, as described earlier.

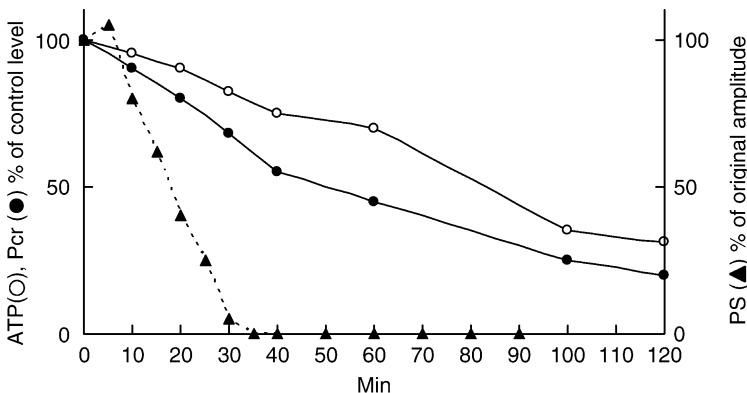
5 Relationship Between Glycolytic Metabolism, Energy Levels, and Synaptic Transmission

5.1 Effects of Glucose Removal

Events during hypoglycemia differ significantly from events during oxygen deprivation. In guinea pig hippocampal slices, ATP levels fall far more slowly following glucose deprivation than following oxygen or oxygen/glucose deprivation (ischemia). Furthermore, there is a clear dissociation between the fall in synaptic transmission and in ATP. Synaptic transmission decays well before the decline in ATP. Synaptic transmission decays to zero either minutes before there is any measurable decrease in ATP (J. Whalen and P. Lipton, unpublished results) or after ATP has fallen by only 30% or less (Figure 1.2-5) (Okada, 1988; Saitoh et al., 1994; Yamane et al., 2000). This dissociation is similar to events during insulin-induced hypoglycemia in vivo where normal electrophysiological function decays well before there is any measured cortical ATP change (Siesjo, 1978, 1988). These results suggest that glucose itself, or glycolysis, plays a critical role in the preservation of neural activity in addition to supplying reducing equivalents to mitochondria and directly synthesizing ATP.

■ Figure 1.2-5

Effects of deprivation of only glucose on the levels of ATP, PCr, and population spike (PS) in the CA3 pyramidal cell layer in hippocampal slices from adult guinea pigs at 37°C. The abscissa denotes the time after starting glucose deprivation. (Modified from Okada (1988) and Saitoh et al. (1994))



5.2 Role of Substrates Other Than Glucose in Synaptic Transmission and ATP Maintenance

The direct role of glucose has been further tested by substituting alternate substrates and then measuring ATP and synaptic transmission in the slices of olfactory cortex (Okada and Kurosawa, 1977; Okada, 1982) and hippocampus (Kanatani et al., 1995) of the adult guinea pig. These alternate substrates, including particularly lactate and pyruvate but also including mannitol, fructose, and maltose all maintained ATP and PCr at or near control levels. However, in all cases synaptic transmission rapidly and profoundly decayed often to zero levels. Taken together, these results lend strong support to the conclusion that glucose metabolism itself plays a key role in synaptic transmission. The mechanism of this effect is not known. It certainly does not appear to be due to loss of neurotransmitter glutamate pools as calcium-dependent glutamate release from the CA1 region by elevated K^+ is unaffected by aglycemia at the time that transmission is abolished in guinea pig hippocampal slices (Whalen and Lipton, unpublished results).

Further studies revealed, unexpectedly, that this specific requirement for glucose was transient. Saitoh and coworkers (1994) and Yamane and coworkers (2000) showed that longer periods of glucose deprivation combined with incubation with mannose, fructose, lactate, or pyruvate led to a recovery of neural activity in the slices after the early failure. This occurred in both dentate gyrus and in CA3 after about 30 min of the glucose deprivation (▶ [Figure 1.2-6](#)). Throughout this period ATP and PCr levels were maintained at control levels (Wada et al., 1998), showing that decreased ATP during the early glucose deprivation was not responsible for removing the glucose dependency of transmission. Also, the graph in ▶ [Figure 1.2-6D](#) strongly suggests that it is the duration of glucose deprivation rather than the alternate substrate exposure that leads to the recovery of transmission. Prolonged pre-exposure to lactate did not prevent the transient depression.

This transient dependency of transmission on glycolysis in guinea pigs differs sharply from the reported studies of others (Schurr, 1988; Fowler, 1993; Izumi et al., 1997), which show that lactate can immediately substitute for glucose in supporting synaptic transmission.

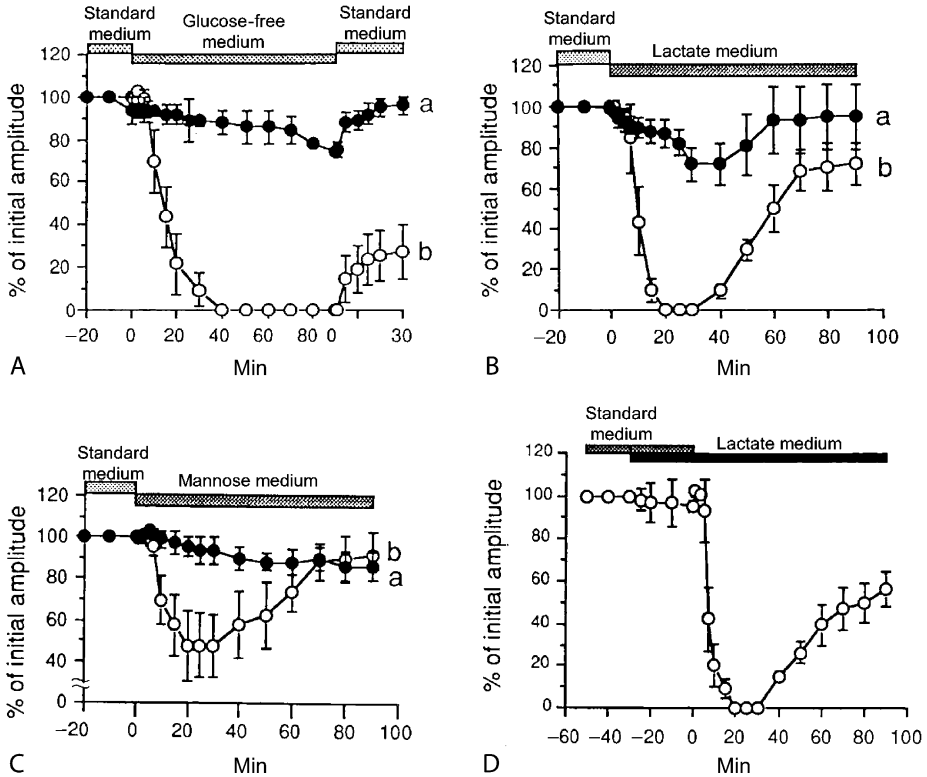
A surprising and revealing basis for this discrepancy emerged from closer examination of the procedure used to prepare the hippocampal slices (Yamane et al., 2000; Takata et al., 2001). In the studies described in this chapter, slices are normally prepared rapidly; they are cut within 1 min of removal of the hippocampus from the brain. However, when slices are cut more slowly, after incubating 5–20 min in ice-cold buffer (as occurs when mechanical methods such as tissue slicers or vibratomes are used to prepare the slices), they have different properties. ATP and PCr levels are far lower than when slices are cut within 1 min (compare ▶ [Figure 1.2-7a2](#) and ▶ [1.2-7b2](#)). Such longer procedures are generally used by other workers. Most relevant to the question of the effect of glucose depletion is that the more slowly prepared slices, with lower ATP levels, did not show the transient loss of synaptic activity after removal of glucose in the presence of lactate (▶ [Figure 1.2-7b](#)). Hence, the slower preparation removes the specific requirement of synaptic transmission for glycolysis! The data thus suggest that metabolically compromised tissue may suffer a change which allows lactate and other substrates to substitute for glucose. The tissues lose their normal dependence on glucose metabolism. ▶ [Figure 1.2-8](#) shows that when guinea pig slices prepared in the normal rapid fashion are pre-exposed to a reversible hypoglycemic/hypoxic insult, they become able to effectively utilize lactate for transmission immediately after removing glucose from the perfusate (Takata et al., 2004). This is consistent with the conclusion that healthy tissue is not able to use lactate for synaptic transmission directly after glucose removal but that compromised tissue is able to do so.

Even in the absence of a prior insult lactate immediately supports synaptic transmission in rapidly prepared guinea pig hippocampal slices when the temperature of the incubation medium is low. At 30°C, the population spike in guinea pig hippocampal slices could be supported immediately upon substitution of lactate for glucose (▶ [Figure 1.2-9](#)).

Other investigators, who reported that slices could readily substitute lactate for glucose (Fowler, 1993; Izumi et al., 1997; Schurr et al., 1997), used different preparations. These included the Schaffer collateral–CA1 synapse from rat and guinea pig hippocampal slices. In order to test directly whether the difference in preparative methodology could explain the discrepancies in results, Okada carried out sets of comparative preparative studies on rat and guinea pig hippocampal slices. The same results were

■ Figure 1.2-6

(A) Effect of deprivation of glucose on antidromic (filled circles, a) and orthodromic (open circles, b) responses to stimulation in hippocampal slices from adult guinea pigs. Recordings were made in the dentate granule cell layer after stimulation of the mossy fibers (for a) and perforant path (for b). (B) Similar to (A) except that 5 mM lactate was also added as shown. (C) Similar to (A) except that 10 mM mannose was also added as shown. (D) Similar to A except that 5 mM lactate was also added as shown. ATP and PCr were maintained at their original levels when glucose was replaced with lactate or mannose (data not shown). Each plot indicates the mean value \pm SEM from eight slices. Orthodromic and antidromic are defined in Box 1. (Modified from Saitoh et al. (1994))



obtained in all cases: the rapidly prepared slices, with high levels of ATP and PCr, showed the transient loss of synaptic activity after replacement of glucose with lactate. Slowly prepared slices did not, as reported by others.

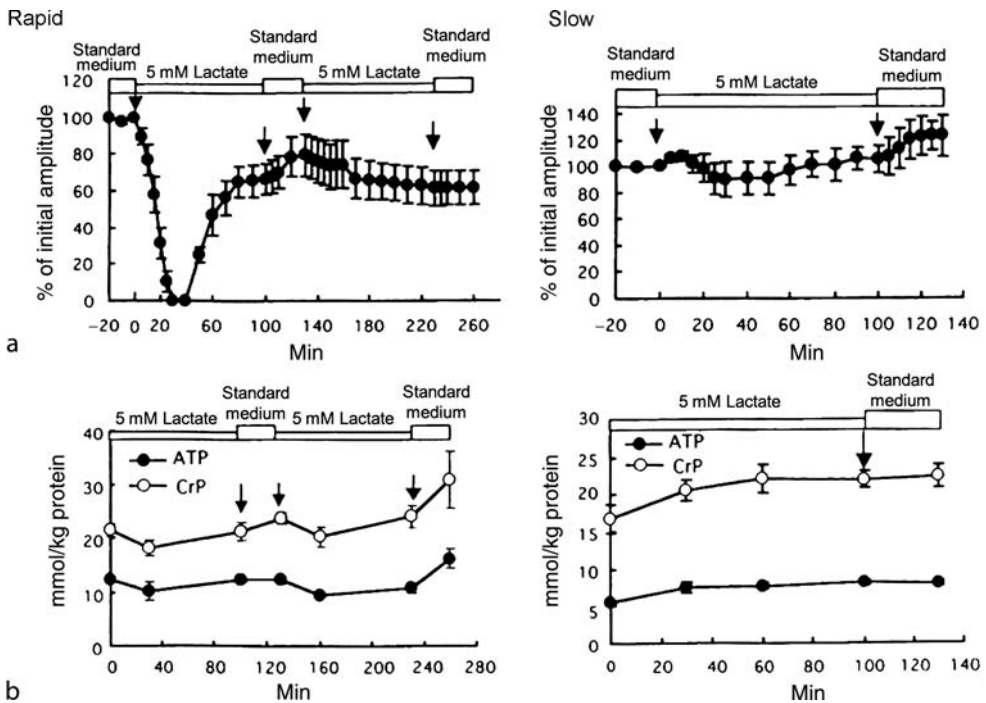
These studies all point to the very important conclusion that synaptic transmission in “healthy” slices does indeed require glucose, and that slices with some damage (or at lower temperatures) do not, and are able to utilize alternate substrates for synaptic transmission.

5.3 Role of Pathological Calcium in Removing Dependence of Transmission on Glycolysis

As described above, the requirement for glucose is removed by incubation with lactate and zero glucose. Events during this incubation period were studied to determine the basis for the transition. Substituting lactate for glucose depolarized the membrane (Takata and Okada, 1995; Allen et al., 2005) and led to both

■ Figure 1.2-7

(a) Effect of sequential exposures to zero glucose/5 mM lactate on the population spike (PS) in (1) CA3 and the levels of (2) ATP and PCr measured in guinea pig hippocampal slices that had been prepared rapidly. (b) Effect of zero glucose/5 mM lactate on PS in CA3 and ATP and PCr levels in guinea pig hippocampal slices that have been prepared slowly. Note that replacement of glucose with lactate did not cause the reduction of the PS amplitude in the slowly prepared slices and note that the second addition of lactate caused no reduction of the PS amplitude in rapidly prepared slices. Note also that in the rapidly prepared slices, the initial levels of ATP and PCr after preincubation are higher than those in slowly prepared samples. Also note that ATP and PCr levels stay constant during substitution of lactate for glucose. Thus, changes in these levels cannot account for the loss of the PS in lactate-substituted buffer. Vertical bars of each plot indicate SEM ($n = 4-6$). (Yamane et al., 2000)



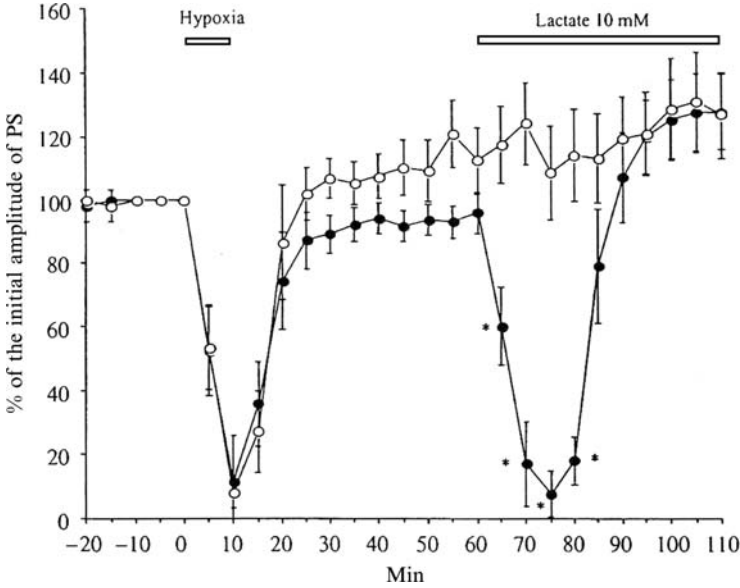
cytosolic calcium accumulation and extracellular glutamate accumulation (Takata et al., 1995, 2001). [Figure 1.2-10](#) shows there is a significant increase in cytosolic Ca during this period and that these same changes occurred in zero glucose without lactate. The time course for decay of the population spike and increase of Ca^{2+} levels during lactate replacement was similar to that during glucose deprivation.

Importantly, addition of the *N*-methyl-D-aspartate blocker (–)-D-2-amino-5-phosphonovaleric acid or the L-type calcium blocker, nimodipine, during lactate replacement, blocked the spontaneous recovery of the population spike ([Figure 1.2-11](#)), maintaining the glucose dependency of transmission. Thus, Ca entry through both *N*-methyl-D-aspartate and L-type calcium channels is what removes the dependency of synaptic transmission on glucose (Takata et al., 2001). Omission of calcium from the bathing medium during this period also prevented the recovery in lactate (Takata et al., 2004).

Although all of the measurable calcium increase during lactate perfusion is prevented by the ryanodine receptor blocker dantrolene, it does not prevent the transition from glucose dependency ([Figure 1.2-11](#)). Thus, it appears that the small pool of calcium moving across the plasmalemma during glucose deprivation is leading to a change on tissue function that is removing the dependence of transmission on glucose. There

■ Figure 1.2-8

Effect of prior exposure to hypoxia on the effect of lactate substitution for glucose on the population spike (PS) in the granule cell layer of the hippocampal slice of adult guinea pig. Hypoxia was introduced for 10 min (*open horizontal bar*) in the medium containing 5 mM (*open circle*) or 10 mM (*closed circles*) glucose. Oxygen and 10 mM glucose were reintroduced for 40 min after which glucose was replaced with 10 mM lactate. Each point is the mean value \pm SEM from five slices. *Asterisks* indicate a significant difference in amplitude between 5 and 10 mM glucose conditions (Takata et al., 2004). Note that after exposure to low glucose/hypoxic conditions transmission is maintained by lactate



■ Figure 1.2-9

Effect of hypothermia during replacement of glucose with lactate. The population spike (PS) was measured in the granule cell layer of the dentate gyrus in hippocampal slices from adult guinea pigs. Note that during mild hypothermia the PS amplitude is increased (Aihara et al., 2001) and, most importantly, that lactate supports transmission at 30°C. Each point is the mean value \pm SEM from five slices. (Figure taken from Takata et al. (2004))

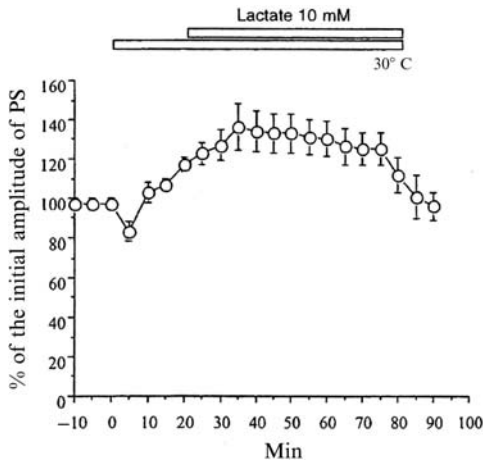


Figure 1.2-10

(a) Effects of glucose deprivation on the population spike (PS) (field potential) and relative intracellular Ca^{2+} levels in the granule cells of the adult guinea pig hippocampal slice. (b) Similar to (A) except that lactate is substituted for glucose. Amplitudes of PS before glucose deprivation correspond to 100%. Vertical bars indicate the SEM (Takata et al., 2001)

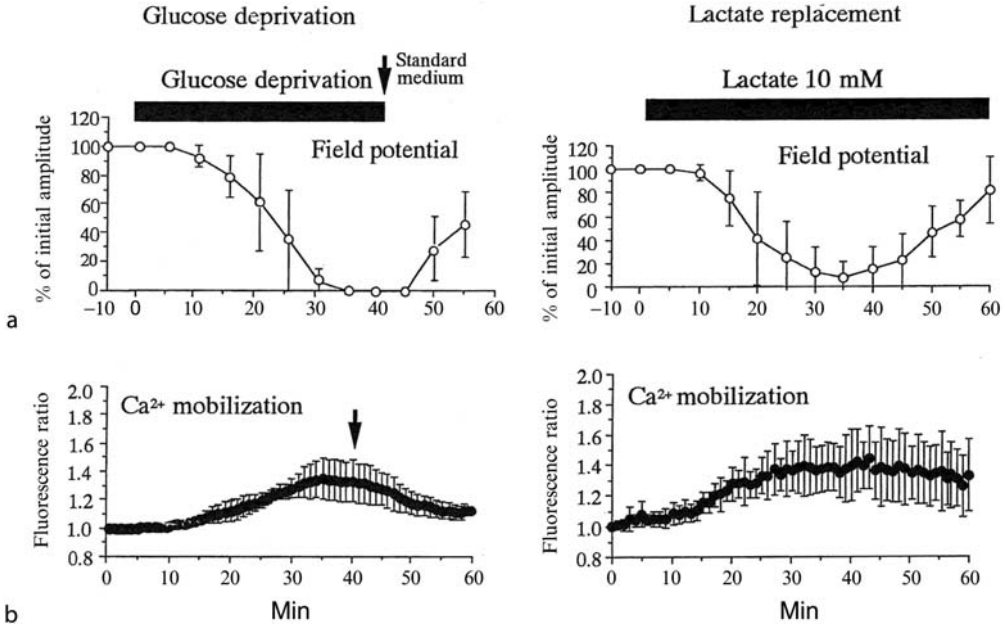
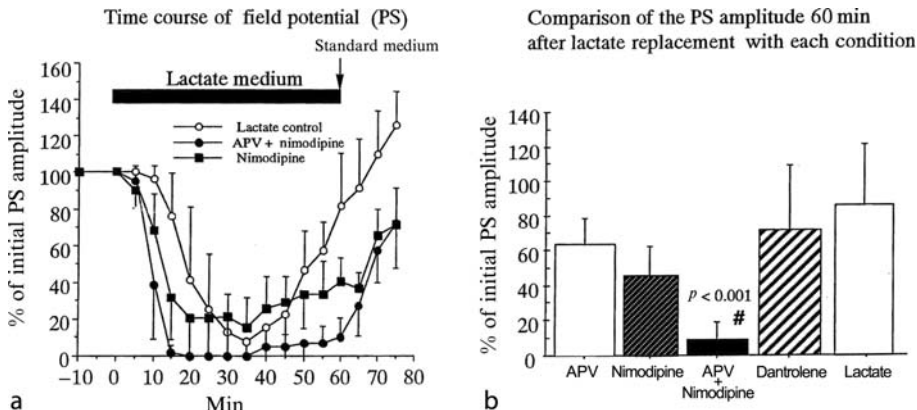


Figure 1.2-11

Effect of APV and nimodipine (50 μ M) on the recovery of the population spike (PS) in the dentate granule cell layer of the guinea pig hippocampal slice during replacement of glucose with lactate. Each plot is the average \pm SEM from seven experiments. (a) shows the time courses and (b) shows the values 60 min after replacement. Note that when both routes of calcium entry were blocked with APV and nimodipine, transmission remained dependent on glucose. It did not recover in lactate-substituted buffer for at least 60 min. $p < 0.001$ using ANOVA with posthoc test. (Takata et al., 2001)



are preliminary data showing that PKC activation may mediate this effect of Ca^{2+} influx (not shown). Hence, it appears that increased calcium in the region of the plasmalemma, possibly along with other metabolic changes, triggers a change that makes synaptic transmission no longer require glucose metabolism.

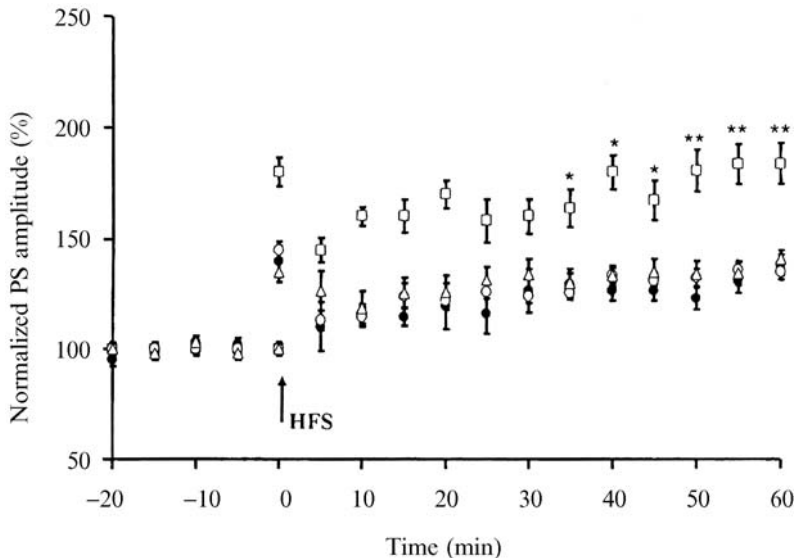
5.4 Absolute Requirement for Glucose in Synaptic Transmission

These data along with others (Whalen and Lipton, unpublished results) show that in certain cases glucose is absolutely required for synaptic transmission, and that this is not due to loss of ATP. Furthermore, the above results strongly suggest that this is a property of healthy tissue and that only when in vitro tissue becomes metabolically compromised does oxidative metabolism of lactate become sufficient to drive synaptic transmission. This appears to be the case in adult slices of both rats and guinea pigs.

Even during the period when lactate is able to support transmission there may be compromised function (Sakurai et al., 2000; Yang et al., 2003). As shown in [Figure 1.2-12](#), at least in some conditions, long-term potentiation is not as robust in lactate-supported guinea pig hippocampal slices as it is when the substrate is glucose.

Figure 1.2-12

Early long-term potentiation (e-LTP) of the population spike (PS) in dentate gyrus of adult guinea pig hippocampal slices. High-frequency stimulation of the perforant path (HFS, 500 Hz, 8 pulses, 3 trains, 10 s apart) induced robust e-LTP in normal glucose-fortified buffer (\square , $n = 8$). Similarly induced LTP was reduced in slices that were supported by 10 mM lactate (closed circle, $n = 8$) or by 10 mM pyruvate (open circle, $n = 8$). Asterisk denotes statistically significant differences from values in other groups. *, $p < 0.05$, **, $p < 0.01$ (Yang et al., 2003)



5.5 General Relationships Between Glucose Metabolism and Synaptic Transmission

Evidence from several sources supports the conclusion that glycolysis itself is important for cytosolic ion homeostasis despite the fact that ATP generated by oxidative phosphorylation in mitochondria makes up the vast majority of the total ATP in neurons (Lipton and Robacker, 1984; Xu et al., 1995;

Martinez-Zaguilan and Wesson, 1996; Silver and Erecinska, 1997). These are consistent with the studies described above showing that lactate could not sustain the resting membrane potential in hippocampal CA1 and CA3 pyramidal neurons when the slices were prepared rapidly (Takata and Okada, 1995; Allen et al., 2005). No mechanisms for these observations have been determined.

There is indirect evidence suggesting possible bases for the specific dependence of transmission on glucose. Wu and coworkers (1997) reported that glycolytic enzymes including glyceraldehyde-3-phosphate dehydrogenase (GAPDH) and phosphoglycerate kinase (PGK) were localized in the postsynaptic density and Ikemoto and coworkers (2003) reported that these two glycolytic enzymes were also present in synaptic vesicles. Furthermore, glutamate accumulation in these vesicles was iodoacetate sensitive but was not blocked by the mitochondrial inhibitor, oligomycin. These data are certainly consistent with a specific glycolytic requirement for synaptic transmission but studies have not been done to establish their involvement.

There is a strong coupling of glucose metabolism to neural activity that is shown in *in vivo* studies using PET, fMRI, and measurements of arterial–venous differences in oxygen and glucose content (Fox et al., 1988; Prichard et al., 1991; Fellows et al., 1993; Madsen et al., 1999). Use of glucose is certainly enhanced beyond the amount necessary to fuel the measured increase in oxygen consumption. Clinically, Alzheimer's disease is associated with markedly impaired glucose metabolism (Pietrini et al., 2000) and glycolytic enzyme activities are preferentially reduced in brains of Alzheimer's patients (Bigl et al., 1999). Furthermore, in Tg2546 transgenic mice, which overexpress amyloid precursor protein and accumulate amyloid plaque, there is a decreased activity of phosphofructokinase (PFK) in cortex and hippocampus, and reduced PFK-C (cortical type isozyme of PFK) expression in amyloid-associated neurons (Bigl et al., 2003). These data suggest that failure of the glycolytic pathway may underlie some of the pathology of Alzheimer's disease.

5.6 Relationship of Results Described Here to Current Hypotheses on Role of Glycolysis in Neural Function

The conclusion from these studies, that oxidative metabolism of lactate cannot support synaptic transmission in healthy hippocampal tissue, is controversial. It throws into question another strongly argued theory that lactate derived from glial metabolism drives neuronal function in the normal brain (Pellerin et al., 1998; Sibson et al., 1998; Magistretti, 2000). The applicability of this theory to the *in vivo* brain has been questioned on various bases (Chih et al., 2001). In particular, the suppressive effect of the monocarboxylate transporter inhibitor, α -cyano-4-hydroxycinnamate, on synaptic activity in glucose-supported slices has been used to support the conclusion that lactate utilization per se is necessary for synaptic transmission. However, transport of pyruvate into mitochondria is also blocked by this inhibitor (Halcistrap and Price, 1999), and so the inhibitor could be blocking the glucose-fueled energy generation. It is well established that lactate is a very effective substrate for recovery of synaptic transmission following an ischemic or hypoglycemic insult (Schurr et al., 1997; Yamane et al., 2000; Kitano et al., 2002; Sakurai et al., 2002; Carter et al., 2003; Takata et al., 2004); this is consistent with such insults removing the dependence of transmission on glucose metabolism, as described in this chapter.

6 Overall Summary: Roles of Different Pathways of Energy Metabolism in Synaptic Transmission

A major theme of this chapter has been the difference in the roles played by the two principle stages of oxidative energy metabolism.

When oxidative metabolism is blocked at the mitochondrial level there is a dramatic rapid fall in ATP that appears to be the basis for the very rapid failure of synaptic transmission. While there are a great deal of data, there is no firm conclusion as to the events between the fall in ATP and failure of transmission, and mechanisms may well be different in different cell types. These results imply that a major function of mitochondrial metabolism is to supply ATP which powers synaptic transmission.

When glucose is removed, or glycolysis is inhibited, the fall in ATP is far slower than it is when mitochondrial metabolism is blocked. Transmission failure is also slower. However, importantly, it occurs well before any significant fall in ATP and, in fact, occurs in the absence of any fall in ATP if glucose is substituted by another substrate that is capable of being metabolized by mitochondria. These results show that glucose metabolism has a crucial (and currently unknown) role in maintaining synaptic transmission that is independent of its supplying substrate to the mitochondria. Other substrates, endogenous or exogenous, which supply adequate reducing equivalents to the mitochondria to maintain cell ATP levels, do not support synaptic transmission. Thus, glucose normally has a dual role in the coupling between energy metabolism and synaptic transmission.

Very interestingly, this specific requirement for glucose metabolism is removed following 20–30 min metabolic stress, and this removal is dependent on calcium entering across the plasmalemma. Some switch occurs in the coupling of metabolism to synaptic transmission.

This dependence of synaptic transmission on glucose metabolism in healthy brain slices calls into question the astrocyte–neuron lactate shuttle hypothesis, which suggests that the lactate derived from glial cells adequately fuels normal neuronal activity.

References

- Aihara H, Okada Y, Tamaki N. 2001. The effect of cooling and re-warming on the neural activity of pyramidal neurons in guinea pig hippocampal slices. *Brain Res* 893: 36-45.
- Allen NJ, Karadottir R, Attwell D. 2005. A preferential role for glycolysis in preventing the anoxic depolarization of rat hippocampal area CA1, pyramidal cells. *J Neurosci* 26: 848-859.
- Balestrino M, Aitken PM, Somjen GG. 1989. Spreading-depression-like hypoxic depolarization in CA1 fascia dentate of hippocampal slices: Relationship to selective vulnerability. *Brain Res* 497: 102-107.
- Bigl M, Apelt J, Eschrich K, Schilebs R. 2003. Cortical glucose metabolism is altered in aged transgenic Tg2576 mice that demonstrate Alzheimer plaque pathology. *J Neural Transm* 110: 22-94.
- Bigl M, Bruckner MK, Arendt T, Bigl V, Eschrich K. 1999. Activities of key glycolytic enzymes in the brains of patients with Alzheimer's disease. *J Neural Transm* 106: 499-511.
- Carter HL, Chandratheva A, Benham CD, Morrison B, Sundstrom LE. 2003. Lactate and glucose as energy substrates during, and after, oxygen deprivation in rat hippocampal acute and cultured slices. *J Neurochem* 87: 1381-1390.
- Chan PH. 2004. Mitochondria and neuronal death/survival signaling pathways in cerebral ischemia. *Neurochem Res* 29: 1943-1949.
- Chiarugi A. 2005. Poly(ADP-ribosyl)ation and stroke. *Pharmacol Res* 52: 15-24.
- Chih C, Lipton P, Roberts EL Jr. 2001. Do active neurons really use lactate rather than glucose? *Trend Neurosci* 24: 573-578.
- Dienel GA, Hertz L. 2001. Glucose and lactate metabolism during brain activation. *J Neurosci Res* 66: 824-838.
- Duffy TE, Kohle SJ, Vannucci RC. 1975. Carbohydrate and energy metabolism in perinatal rat brain: Relation to survival in anoxia. *J Neurochem* 24: 271-276.
- Fazekas JF, Alexander FAD, Hinmich HE. 1941. Tolerance of newborn to anoxia. *Am J Physiol* 134: 281-287.
- Feig SL, Lipton P. 1990. *N*-methyl-D-aspartate receptor activation and Ca^{2+} account for poor pyramidal cell structure in hippocampal slices. *J Neurochem* 55: 473-483.
- Fellows LK, Boutelle MG, Fillenz M. 1993. Physiological stimulation increases non-oxidative glucose metabolism in the brain of the freely moving rat. *J Neurochem* 60: 1258-1263.
- Fowler JC. 1989. Adenosine antagonists delay hypoxia-induced depression of neuronal activity in hippocampal brain slice. *Brain Res* 490: 378-384.
- Fowler JC. 1993. Glucose deprivation results in a lactate preventable increase in adenosine and depression of synaptic transmission in rat hippocampal slices. *J Neurochem* 60: 572-576.
- Fox PT, Raichle ME, Minten MA, Dance C. 1988. Non-oxidative glucose consumption during focal physiologic neural activity. *Science* 241: 462-464.
- Ghajar JBG, Plum F, Duffy TE. 1982. Cerebral oxidative metabolism and blood flow during acute hypoglycemia and recovery in unanesthetized rats. *J Neurochem* 38: 397-409.
- Gibbs EL, Lennox WG, Nims LF, Gibbs FA. 1942. Arterial and cerebral venous blood: Arterial-venous differences in man. *J Biol Chem* 144: 325-332.
- Halcstrap AP, Price MT. 1999. The proton-linked monocarboxylate transport (MCT) family: Structure, function and regulation. *Biochem J* 343: 281-299.
- Ikemoto A, Bole DG, Ueda T. 2003. Glycolysis and glutamate accumulation into synaptic vesicles. Role of glyceraldehyde

- phosphate dehydrogenase and 3-phosphoglycerate kinase. *J Biol Chem* 278: 5928-5940.
- Izumi Y, Benz AM, Katuki H, Zorumski CF. 1997. Endogenous monocarboxylates sustain hippocampal synaptic function and morphological integrity during energy deprivation. *J Neurosci* 17: 9448-9457.
- Kanatani T, Mizuno K, Okada Y. 1995. Effects of glycolytic metabolites on the preservation of high-energy phosphate level and synaptic transmission in the granule cells of guinea pig hippocampal slices. *Experientia* 51: 213-216.
- Kass IS, Lipton P. 1982. Mechanisms involved in irreversible anoxic damage to the in vitro rat hippocampal slice. *J Physiol* 332: 459-472.
- Kass IS, Lipton P. 1986. Calcium and long-term transmission damage following anoxia in dentate gyrus and CA1 regions of the hippocampal slice. *J Physiol* 378: 313-334.
- Kass IS, Lipton P. 1989. Protection of hippocampal slices from young rats against anoxic transmission damage is due to better maintenance of ATP. *J Physiol* 413: 1-11.
- Kawai S, Yonetani M, Nakamura H, Okada Y. 1989. Effect of deprivation of oxygen and glucose on the neural activity and the level of high energy phosphates in the hippocampal slices of immature and adult rat. *Dev Brain Res* 48: 11-18.
- Kety SS. 1957. The general metabolism of brain in vivo. *Metabolism of the Nervous System*. Richter D, editor. London: Pergamon Press; pp. 221-237.
- Kitano T, Nishimaru N, Shibata E, Iwasaki H, Noguchi T T, et al. 2002. Lactate utilization as an energy substrate in ischemic preconditioned rat brain slices. *Life Sci* 72: 557-564.
- Kochanek PM, Hallenbeck JM. 1992. Polymorphonuclear leukocytes and monocytes/macrophages in the pathogenesis of cerebral ischemia and stroke. *Stroke* 23: 1367-1379.
- Krnjevic K, Ben-Ari Y. 1989. Anoxic changes in dentate granule cells. *Neurosci Lett* 107: 89-93.
- LeBlond J, Krnjevic K. 1989. Hypoxic changes in hippocampal neurons. *J Neurophysiol* 62: 1-14.
- Lewis LD, Ljunggren B, Ratcheson RA, Siesjo BK. 1974. Cerebral energy state in insulin-induced hypoglycemia related to blood glucose and to EEG. *J Neurochem* 23: 673-679.
- Lipton P. 1999. Ischemic cell death in brain neurons. *Physiol Rev* 79: 1431-1566.
- Lipton P, Robacker KM. 1984. Glycolysis and brain function: K^+ stimulation of protein synthesis and K^+ uptake require glycolysis. *Fed Proc* 42: 2875-2889.
- Lipton P, Whittingham TS. 1979. The effect of hypoxia on evoked potentials in the in vitro rat hippocampus. *J Physiol* 287: 427-438.
- Lipton P, Whittingham TS. 1982. Reduced ATP concentration as a basis for synaptic transmission failure during hypoxia in the in vitro guinea pig hippocampus. *J Physiol* 325: 51-65.
- Lipton P, Whittingham TS. 1984. Energy metabolism and brain slice function. *Brain Slices*. Dingledine R, editor. New York: Plenum; Chapter 5.
- Lowry OH, Passonneau JV. 1972. A flexible enzymatic analysis. Academic Press, New York, 1972.
- Lowry OH, Passonneau JV, Hasselberger FX, Schulz DW. 1964. Effect of ischemia on known substrates and co-factors of the glycolytic pathway in brain. *J Biol Chem* 239: 18-30.
- Madsen PL, Cruz NF, Sokoloff L, Dienel GA. 1999. Cerebral oxygen/glucose ratio is low during sensory stimulation and rises above normal during recovery: Excess glucose consumption during stimulation is not accounted for by lactate efflux from or accumulation in brain tissue. *J Cereb Blood Flow Metab* 19: 393-400.
- Magistretti PJ. 2000. Cellular bases of functional brain imaging: Insights from neuron-glia metabolic coupling. *Brain Res* 886: 108-112.
- Mandel P, Edel-Harth S. 1966. Free nucleotides in the rat brain during postnatal development. *J Neurochem* 13: 591-595.
- Martinez-Zaguilan R, Wesson DE. 1996. Regulation of endoplasmic reticulum- Ca^{2+} -ATPase by glycolysis in eukaryotic cells. *Miner Electrol Metab* 22: 318-335.
- McDougal DB Jr, Halowach J, Howe MC, Jones EM, Thomas CVA. 1968. *J Neurochem* 15: 577.
- McIlwain H, Bachelard HS. 1985. *Biochemistry and the Central Nervous System*. 5th edition. Edinburgh: Livingstone; pp. 54-83.
- Moro MA, Almeida A, Bolanaos JF, Lizasoain I. 2005. Mitochondrial respiratory chain and free radical generation in stroke. *Free Radic Biol Med* 39: 1291-1304.
- Nabetani M, Okada Y, Kawai S, Nakamura H. 1995. Neural activity and the levels of high energy phosphates during deprivation of oxygen and/or glucose in hippocampal slices of immature and adult rats. *Int J Dev Neuroscience* 13: 3-12.
- Nishizaki T, Okada Y. 1988. Effect of excitatory amino acids on the oxygen consumption of hippocampal slices from the guinea pig. *Brain Res* 452: 11-20.
- Nishizaki T, Yamauchi R, Tanimoto M, Okada Y. 1988. Effects of temperature on the oxygen consumption in thin slices from different brain regions. *Neurosci Lett* 86: 301-305.
- Okada Y. 1982. Ischemia and anoxia and neural activity. *Jpn J Neuropsychopharmacol* 4: 369-379.
- Okada Y. 1987. Energy metabolism and neural functions of brain slices—effects of deprivation of oxygen and/or glucose. *Jpn J Neuropsychopharmacol* 9: 757-776.
- Okada Y. 1988. Reversibility of neuronal function of hippocampal slice during deprivation of oxygen and/or glucose. *Mechanism of Cerebral Hypoxia and Stroke*. Somjen G, editor. New York: Plenum Press; pp. 191-203.

- Okada Y. 1990. Neural activity of brain slice during deprivation of oxygen and/or glucose. Protein, Nucleic Acid and Enzymes (Japanese). 35: 1137-1150.
- Okada Y, Kurosawa F. 1977. Role of glucose on the preservation of post-synaptic potential (PSP) of olfactory cortex slice from guinea pig. *J Physiol Soc (Japan)* 39: 345.
- Okada Y, McDougal DB Jr. 1971. Physiological and biochemical changes in frog sciatic nerve during anoxia and recovery. *J Neurochem* 18: 2335-2353.
- Okada Y, Shimada C. 1976. Gamma-aminobutyric acid (GABA) concentration in single neuron-localization of GABA in Deiters' neuron. *Brain Res* 107: 658-662.
- Okada Y, Yoneda K. 1983. Effect of accumulation of phosphocreatine on the survival time in thin hippocampal slices from the guinea pig during deprivation of both oxygen and glucose. *Neurosci Lett* 41: 119-124.
- Panickar KS, Norenberg MD. 2005. Astrocytes in cerebral ischemic injury: Morphological and general considerations. *Glia* 50: 287-298.
- Pellerin L, Pellegrini G, Bittar PG, Charnay Y, Bouras C, et al. 1998. Evidence supporting the existence of an activity-dependent astrocyte-neuron lactate shuttle. *Dev Neurosci* 20: 291-299.
- Pietrini P, Alexander GE, Furey ML, Hampel H, Guazzelli M. 2000. The neurometabolic landscape of cognitive decline: In vivo studies with positron emission tomography in Alzheimer's disease. *Int J Psychophysiol* 37: 87-98.
- Prichard J, Rothman D, Novotny E, Petroff O, Kuwabara T, et al. 1991. Lactate rise detected by ¹H NMR in human visual cortex during physiologic stimulation. *Proc Natl Sci USA* 88: 5829-5831.
- Ratcheson RA, Blank AC, Ferrendelli JA. 1981. Regionally selective metabolic effects of hypoglycemia in brain. *J Neurochem* 36: 1952-1958.
- Rice JE, Vannucci RC, Brierley JB. 1981. The influence of immaturity on hypoxia-ischemia brain damage in the rat. *Ann Neurol* 9: 131-141.
- Saitoh M, Okada Y, Nabetani M. 1994. Effect of mannose, fructose and lactate on the preservation of synaptic potentials in hippocampal slices. *Neurosci Lett* 171: 125-128.
- Sakurai T, Yang B, Takata T, Yokono K. 2000. Exogenous lactate sustains synaptic activity and neuronal viability but fails to induce long term potentiation. *Jpn J Geriatr* 37: 962-965.
- Sakurai T, Yang B, Takata T, Yokono K. 2002. Synaptic adaptation to repeated hypoglycemia depends on the utilization of monocarboxylates in guinea pig hippocampal slices. *Diabetes* 51: 430-438.
- Schurr A. 1988. Lactate-supported synaptic function in the rat hippocampal slice preparation. *Science* 240: 1326-1327.
- Schurr A, Payne RS, Miller JJ, Rigor BM. 1997. Brain lactate, not glucose, fuels the recovery of synaptic function from hypoxia upon reoxygenation: An in vitro study. *Brain Res* 744: 105-111.
- Sibson NR, Dhankhar A, Mason GF, Rothman DL, Behar KL, et al. 1998. Stoichiometric coupling of brain glucose metabolism and glutamatergic neuronal activity. *Proc Natl Acad Sci USA* 95: 316-321.
- Siesjo BK. 1978. *Brain Energy Metabolism*. New York: Wiley.
- Siesjo BK. 1988. Hypoglycemia, brain metabolism, and brain damage. *Diabetes/Metab Res Rev* 4: 113-144.
- Silver IA, Erecinska M. 1997. Energetic demands of the Na⁺/K⁺ ATPase in mammalian astrocytes. *Glia* 21: 35-45.
- Sokoloff L. 1960. Metabolism of the central nervous system in vivo. *Handbook of Physiology: Neurophysiology*, Vol. 3. Field J, Magoun HW, Hall VE, editors. Washington, DC: American Physiological Society; pp. 1843-1864.
- Takata T, Okada Y. 1995. Effects of deprivation of oxygen or glucose on the neural activity in the guinea pig hippocampal slice intracellular recording study of pyramidal neurons. *Brain Res* 683: 109-116.
- Takata T, Hirai H, Shigemoto T, Okada Y. 1995. The release of glutamate and accumulation of intracellular calcium in the pig hippocampal slices during glucose deprivation. *Neurosci Lett* 189: 21-24.
- Takata T, Sakurai T, Yokono K, Okada Y. 2001. Effect of lactate on the synaptic potential, energy metabolism, calcium homeostasis and extracellular glutamate concentration in the dentate gyrus of the hippocampus from guinea pig. *Neuroscience* 104: 371-378.
- Takata T, Yang B, Sakurai T, Okada Y, Yokono K. 2004. Glycolysis regulates the induction of lactate utilization for synaptic potentials after hypoxia in the granule cell of guinea pig hippocampus. *Neurosci Res* 50: 467-474.
- Tanimoto M, Okada Y. 1987. The protective effect of hypothermia on hippocampal slices from guinea pig during deprivation of oxygen and glucose. *Brain Res* 414: 239-246.
- Thurston JH, McDougal DB Jr. 1969. Effect of ischemia on metabolism of the brain of the newborn mouse. *Am J Physiol* 216: 348-352.
- Tian G-F, Baker AJ. 2000. Glycolysis prevents anoxia-induced synaptic transmission damage in rat hippocampal slices. *J Neurophysiol* 83: 1830-1839.
- Vannucci RC, Yager JY, Vannucci SJ. 1994. Cerebral glucose and energy utilization during the evolution of hypoxic-ischemic brain damage in the immature rat. *J Cereb Blood Flow Metab* 14: 279-288.
- Wada H, Okada Y, Usuo T, Nakamura H. 1998. The effects of glucose, mannose, fructose and lactate on the preservation of neural activity in the hippocampal slices from the guinea pig. *Brain Res* 788: 144-150.

- Whittingham TS, Lipton P. 1982. Cerebral transmission during anoxia is protected by creatine. *J Neurochem* 37: 1618-1621.
- Wu K, Aoki C, Elste A, Rogalski-Wilk AA, Siekevitz P. 1997. The synthesis of ATP by glycolytic enzymes in the postsynaptic density and the effect of endogenously generated nitric oxide. *Proc Natl Acad Sci USA* 94: 13273-13278.
- Xu KY, Zweier JL, Backer LC. 1995. Functional coupling between glycolysis and sarcoplasmic reticulum Ca^{2+} transport. *Circ Res* 77: 88-97.
- Yamane K, Yokono K, Okada Y. 2000. Anaerobic glycolysis is crucial for the maintenance of neural activity in guinea pig hippocampal slices. *J Neurosci Meth* 103: 163-171.
- Yang B, Sakurai T, Takata T, Yokono K. 2003. Effects of lactate/pyruvate on synaptic plasticity in the hippocampal dentate gyrus. *Neurosci Res* 46: 333-337.
- Yoneda K, Arakawa T, Asaoka Y, Fukuda Y, Kinugasa T, et al. 1983. Effect of accumulation of high-energy phosphates during anoxia and recovery in thin hippocampal slices from the guinea pig. *Exp Neurol* 82: 215-222.
- Zhu PJ, Krnjevic K. 1997. Endogenous adenosine on membrane properties of CA1 neurons in rat hippocampal slices during normoxia and hypoxia. *Neuropharmacol* 36: 169-176.

1.3 Pentose Phosphate Pathway and NADPH Metabolism

R. Dringen · H. H. Hoepken · T. Minich · C. Ruedig

1	Introduction	42
2	Enzymes of the PPP in Brain	43
2.1	Glucose-6-Phosphate Dehydrogenase	43
2.2	6-Phosphogluconolactonase	45
2.3	6-Phosphogluconate Dehydrogenase	45
2.4	Ribulose-5-Phosphate Converting Enzymes	45
2.5	Transketolase	46
2.6	Transaldolase	46
2.7	Other Enzymes	46
3	Functions of the PPP	46
4	Regulation of the PPP	47
4.1	Measuring Metabolite Fluxes Through the PPP	47
4.2	Glucose-6-Phosphate Dehydrogenase as Key Regulator	48
4.3	Activation of the PPP	48
5	NADPH Metabolism of Brain Cells	49
5.1	NADPH-Regenerating Enzymes	49
5.2	NADPH-Consuming Processes	50
5.2.1	GSSG Reduction and Peroxide Disposal	51
5.2.2	Synthesis of Fatty Acids	51
5.2.3	Synthesis of Cholesterol	52
5.2.4	NO Production by NO Synthases	52
5.2.5	Superoxide Production by NADPH Oxidase	52
5.2.6	Hydroxylation Reactions	53
5.2.7	Degradation of Heme	53
5.2.8	Polyol Metabolism	53
5.2.9	Thioredoxin System	53
6	PPP and Neurological Diseases	54
6.1	Glucose-6-Phosphate Dehydrogenase	54
6.2	Transketolase	54
6.3	Transaldolase	55
7	Conclusions	55

Abstract: The pentose phosphate pathway (PPP) is an essential metabolic pathway in the glucose metabolism of the brain. Under normal conditions, the PPP plays a minor part in total glucose consumption. However, its products NADPH and ribose-5-phosphate have important functions in brain cells as electron donor for various enzymatic reactions and as precursor for the synthesis of nucleotides, respectively. This chapter discusses properties of PPP enzymes and the regulation of the flux of metabolites through the PPP in brain and neural cells. The functions of the PPP in neural cells are described with special emphasis on the roles of cytosolic NADPH in brain cells. This reduced cofactor is highly important for the antioxidative defense of brain cells by glutathione (GSH) redox cycling. In addition, NADPH provides reduction equivalents for biosynthetic reactions as well as for the generation of nitric oxide and superoxide. Finally, evidence for a connection between human diseases and alterations in the activities of PPP enzymes in brain are presented.

1 Introduction

The pentose phosphate pathway (PPP, also called hexose monophosphate shunt) is an important metabolic pathway in cellular sugar metabolism. Presence of the PPP has been reported for bacteria, yeast, plants, and animals (Wood, 1986; Baquer et al., 1988; Kruger and von Schaewen, 2003), indicating that this pathway was developed early in evolution. Compared with the energy-producing pathways like glycolysis and citric acid cycle, the PPP is only a minor contributor to total glucose oxidation. However, the PPP products NADPH and ribose-5-phosphate are essential for cells as reduction equivalents for antioxidative and biosynthetic processes and as precursor for nucleotide synthesis, respectively. The enzymes of the PPP have been predominantly found in the cytosol, but low activities of such enzymes have also been reported for other cellular compartments of many tissues, including the brain (Vallejo et al., 1971; Bublitz and Steavenson, 1988).

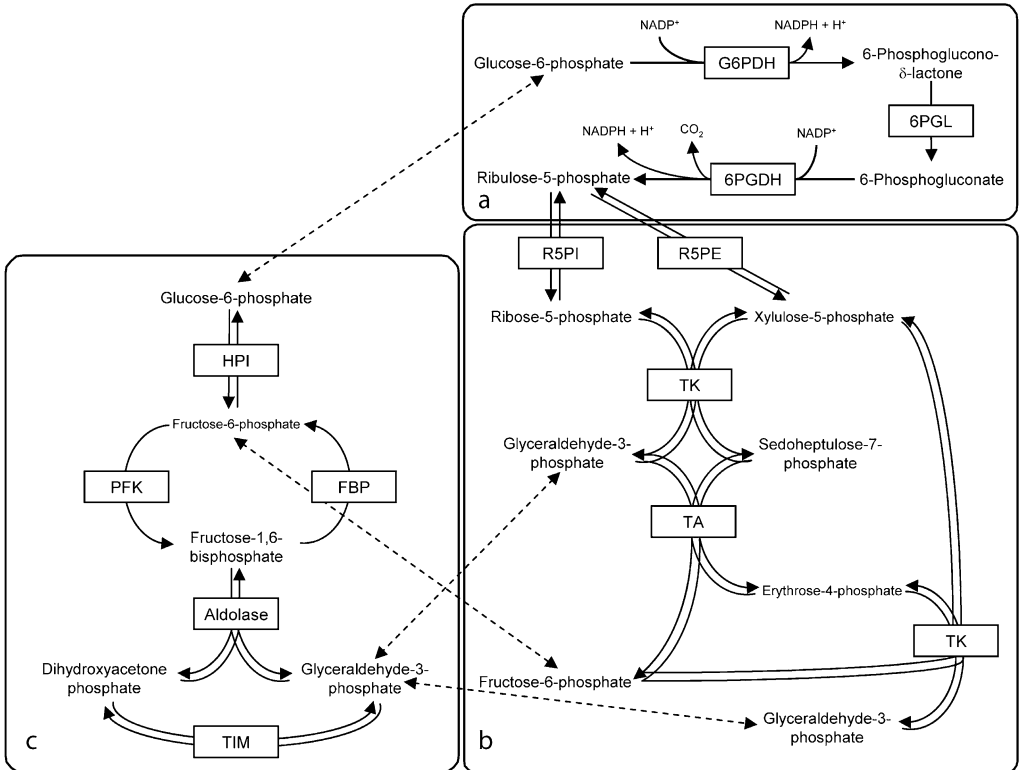
The PPP is a network of reactions of seven enzymes that interconvert sugar phosphates. It can be considered a combination of two sets of reactions, an oxidative part and a nonoxidative part. The oxidative part of the pathway consists of the reactions that are catalyzed by the enzymes glucose-6-phosphate dehydrogenase (G6PDH; EC 1.1.1.49), 6-phosphogluconolactonase (6PGL; EC 3.1.1.17), and 6-phosphogluconate dehydrogenase (6PGDH; EC 1.1.1.44). These enzymes oxidize glucose-6-phosphate to 6-phosphoglucono- δ -lactone, hydrolyze the lactone to 6-phosphogluconate, and oxidize 6-phosphogluconate to ribulose-6-phosphate, respectively (🔗 [Figure 1.3-1](#)). The overall reaction catalyzed by the oxidative part of the PPP is the oxidation of glucose-6-phosphate to ribulose-5-phosphate and CO₂. The reduction equivalents generated during this oxidation are used by the two dehydrogenases to reduce NADP⁺.

The nonoxidative part of the PPP consists of the reactions that are catalyzed by the enzymes ribulose-5-phosphate isomerase (R5PI; EC 5.3.1.6), ribulose-5-phosphate-3-epimerase (R5PE; EC 5.1.3.1), transaldolase (TA; EC 2.2.1.2), and transketolase (TK; EC 2.2.1.1). R5PI and R5PE convert ribulose-5-phosphate to ribose-5-phosphate and xylulose-5-phosphate, respectively (🔗 [Figure 1.3-1](#)). The reactions catalyzed by TA and TK interconvert a set of phosphorylated aldoses (ribose-5-phosphate, erythrose-4-phosphate, glyceraldehyde-3-phosphate) and ketoses (xylulose-5-phosphate, fructose-6-phosphate, sedoheptulose-7-phosphate). This network of phosphorylated sugars is connected to glycolysis by their common intermediates glyceraldehyde-3-phosphate and fructose-6-phosphate (🔗 [Figure 1.3-1](#)).

Depending on the metabolic status of cells, the demand for NADPH and ribose-5-phosphate may differ greatly. If large amounts of NADPH but little ribose-5-phosphate is required, the ribulose-5-phosphate that is generated in the oxidative part of the PPP is converted by the nonoxidative part of the PPP to glucose-6-phosphate. Requirement of large amounts of ribose-5-phosphate but little NADPH can be met by the nonoxidative part of the PPP using fructose-6-phosphate and glyceraldehyde-3-phosphate as substrates. Thus, depending on the cell type and its demand for either NADPH or ribose-5-phosphate the ratio of oxidative to nonoxidative part of the PPP can differ greatly. In many organs, including brain, the flux through the oxidative part of the PPP is much higher than that through the nonoxidative part and the activity of the whole pathway is determined by the activity of the nonoxidative part (Cabezas et al., 1999).

Figure 1.3-1

Reactions of the PPP and connection with glycolysis; a, oxidative part of the PPP; b, nonoxidative part of the PPP; c, connected part of glycolysis. For explanations on enzyme reactions, see text. G6PDH, glucose-6-phosphate dehydrogenase; 6PGL, 6-phosphogluconolactonase; 6PGDH, 6-phosphogluconate dehydrogenase; R5PI, ribulose-5-phosphate isomerase; R5PE, ribulose-5-phosphate epimerase; TK, transketolase; TA, transaldolase; HPI, hexosephosphate isomerase; FBP, fructose-1,6-bisphosphatase, PFK, phosphofructokinase; TIM, triosephosphate isomerase



Properties and functions of the PPP in brain have been summarized by Baquer et al. (1988). Here we give a more recent overview on the PPP enzymes as well as on the regulation and functions of the PPP in brain and in neural cells.

2 Enzymes of the PPP in Brain

2.1 Glucose-6-Phosphate Dehydrogenase

G6PDH catalyzes the NADP^+ -dependent oxidation of glucose-6-phosphate to 6-phosphogluconolactone. This enzyme is the key regulatory enzyme of the oxidative part of the PPP and controls the flux of glucose-6-phosphate through the pathway. G6PDH deficiency is the most common known enzymopathy and affects 400 million people worldwide. The most frequent clinical symptoms are hemolytic anemia and neonatal jaundice. In some cases, neonatal jaundice can cause permanent neurological damage or death (for overview see Luzzatto et al., 2001). G6PDH deficiency is genetically heterogeneous. About 400 different

variants have been reported on the basis of diverse biochemical characteristics (Luzzatto et al., 2001). In mice, moderate G6PDH deficiency in brain leads to a significant distortion of cellular redox control and to a substantial elevation of the somatic mutation rate (Felix et al., 2002). Results on embryonic stem cells with homozygous disruption of the G6PDH gene have demonstrated that the oxidative part of the PPP is dispensable for the synthesis of ribose-5-phosphate but is essential to generate NADPH that is required to protect cells against oxidative stress (Pandolfi et al., 1995; Filosa et al., 2003).

G6PDH has been intensively studied in many organs (Smith and Barker, 1974; Katsurada et al., 1989; Nasr et al., 1989; Zimmer et al., 1992), including the brain (Baquer et al., 1988). The amino acid sequences of G6PDHs are highly conserved. Human G6PDH has more than 30% amino acid identity with the enzymes of other species including prokaryotic sequences (Au et al., 1999). The conserved motif RIDHYLGK has been suggested to be important for glucose-6-phosphate binding (Bhadbhade et al., 1987; Camardella et al., 1988) whereas the arginine in the motif GxxGDLA seems to be important for NADP⁺ binding (Levy et al., 1996).

The active human enzyme purified from erythrocytes exists in a dimer–tetramer equilibrium (Cohen and Rosemeyer, 1969). Recently the crystal structure of a human G6PDH (the Canton mutant Arg459Leu) was solved with 3 Å resolution (Au et al., 2000). The enzyme contains a structural NADP⁺ molecule in all subunits, close to the dimer interface but integral to the subunit. Since the nicotinamide ring of this NADP⁺ is completely buried in the protein with no access for hydride transfer, this NADP⁺ has been suggested to be of structural importance (Au et al., 2000). Moreover, structural analysis revealed the presence of an intrasubunit disulphide bond between Cys13 and Cys446 (Au et al., 2000).

G6PDH has been purified from rat (Askar et al., 1996) and rabbit brain (Ninfali et al., 2001). The native enzyme is a dimer composed of two identical subunits of 56–62 kDa. In contrast to purified G6PDH from other tissues, the brain G6PDH may have two binding sites for glucose-6-phosphate (Askar et al., 1996). Brain G6PDH is completely inhibited by *p*-chloromercuribenzoate; this inhibition is completely reversed by dithiothreitol (Askar et al., 1996), indicating that thiol groups in the enzyme are essential for its catalytic activity. Since preincubation of the enzyme with NADP⁺, but not with glucose-6-phosphate, provided considerable protection against *p*-chloromercuribenzoate inhibition, thiol groups of G6PDH have been considered to be essential for coenzyme binding (Askar et al., 1996). G6PDH is inactivated by reactive oxygen species (ROS) and by 4-hydroxy-2-nonenal (Ninfali et al., 2001) as well as by dehydroepiandrosterone (DHEA) (Gordon et al., 1995; Tian et al., 1998; García-Nogales et al., 1999). Moreover, brain G6PDH is inhibited by aluminum (Cho and Joshi, 1989) and by fatty acids and their CoA esters (Mukhopadhyay and Mukherjea, 1994).

For the purified rat brain G6PDH two binding sites for glucose-6-phosphate have been reported with apparent K_m values of 29 and 41 μM , of which the latter may represent a regulatory substrate binding site (Askar et al., 1996). The K_m value of purified rabbit brain G6PDH for glucose-6-phosphate is 65 μM (Ninfali et al., 2001). The reported apparent K_m values for NADP⁺ of brain G6PDH are 17 and 4 μM for the enzymes from rat and rabbit brain, respectively (Askar et al., 1996; Ninfali et al., 2001). As in G6PDHs from other tissues, the activity of brain G6PDH is regulated by ATP with noncompetitive kinetics with respect to glucose-6-phosphate and NADP⁺ (Askar et al., 1996). NADPH is a strong competitive inhibitor of G6PDH. The apparent K_i for NADPH inhibition is 3.5 μM (Askar et al., 1996). Consequently, the K_i value of rat brain G6PDH for NADPH is lower than the K_m of the enzyme for NADP⁺, explaining the potent inhibition of G6PDH by NADPH.

In rat brain, there were substantial activities of G6PDH in many regions (Kauffman, 1972; Ninfali et al., 1998), the highest activity being measured in the olfactory bulb (Ninfali et al., 1997, 1998). During postnatal development, G6PDH activity increases till postnatal day 21 in several rat brain areas (Bilger and Nehlig, 1992). After that age little alteration or some increase in G6PDH activity in brain has been reported (Baquer et al., 1973, 1975; El-Hassan et al., 1981; Leong and Clark, 1984; de Almeida et al., 1989; Bilger and Nehlig, 1992). This contrasts with the situation of many tissues in which G6PDH activity was significantly reduced with age (de Almeida et al., 1989).

All brain cell types appear to contain G6PDH. At least for cultured brain cells, G6PDH activity was measured in astrocytes, oligodendrocytes, neurons, and microglial cells (Cammer and Zimmerman, 1982;

Cammer et al., 1982; Rust et al., 1991; García-Nogales et al., 2003; Kussmaul and Dringen, unpublished work). Among the different brain cell types, oligodendrocytes appear to contain high amounts of G6PDH (Friede et al., 1963; Cammer et al., 1982). This finding correlates with the observation that cultured oligodendrocytes process substantially higher amounts of glucose through the PPP than cultured astrocytes or neurons (Edmond et al., 1987).

2.2 6-Phosphogluconolactonase

6-Phosphogluconolactonase (6PGL) catalyzes the hydrolysis of 6-phosphoglucono- δ -lactone, thereby connecting the two dehydrogenases of the PPP. This reaction occurs nonenzymatically at a significant rate but is substantially accelerated by 6PGL (Miclet et al., 2001). This enzyme is specific for the phosphorylated lactone and does not hydrolyze gluconolactone (Bauer et al., 1983). Purified 6PGL from bovine erythrocytes is a monomer with a molecular mass of 30 kDa (Bauer et al., 1983). A human cDNA encoding a 6PGL with the same molecular mass and monomeric structure has been cloned (Collard et al., 1999). However, 6PGL activity has also been described as a second activity of enzymes such as mammalian hexose-6-phosphate dehydrogenases (Clarke and Mason, 2003). Sequence comparison revealed that mammalian hexose-6-phosphate dehydrogenases contain a C-terminal domain homologous to the *devB* gene of microorganisms (Mason et al., 1999), which has been reported to be homologous to human 6PGL (Collard et al., 1999). This suggests that mammalian hexose-6-phosphate dehydrogenases might be bifunctional enzymes. In contrast to the periphery, expression and functions of 6PGL in brain have not been reported so far.

2.3 6-Phosphogluconate Dehydrogenase

6PGDH catalyzes the oxidative decarboxylation of 6-phosphogluconate to ribulose-5-phosphate, NADPH, and CO_2 . 6PGDH has been purified from human and rat brain. The dimeric human and rat enzymes have molecular masses of 90 and 98 kDa, respectively (Sinicropi and Kauffman, 1979; Weisz et al., 1985). Human brain 6PGDH is inhibited by its products NADPH, ribulose-5-phosphate, and CO_2 (Weisz et al., 1985). NADPH inhibits the enzyme competitively with respect to NADP^+ , and the K_i values for this inhibition depend on the concentration of 6-phosphogluconate (Weisz et al., 1985).

6PGDH activity does not vary greatly between different brain areas in the adult brain (Kauffman, 1972). The specific activity of 6PGDH increases during gestation (Mukhopadhyay and Mukherjea, 1994) but decreases after birth (Bagdasarian and Hulanicka, 1965; Guerra et al., 1967). The activity of 6PGDH is inhibited by 6-aminonicotinamide (6AN). This substance can replace nicotinamide in the synthesis of NADP^+ and the resulting 6AN adenine dinucleotide inhibits 6PGDH 60 times stronger than G6PDH (Lange et al., 1970). In addition, fatty acids such as oleate and acyl-CoA esters such as palmitoyl-CoA inhibit 6PGDH (Mukhopadhyay and Mukherjea, 1994). Little is known about the distribution of 6PGDH in the various cell types in brain. For cultured neural cells, presence of 6PGDH has been reported for cultured astrocytes, oligodendrocytes, and neurons (Rust et al., 1991).

2.4 Ribulose-5-Phosphate Converting Enzymes

Ribulose-5-phosphate isomerase (R5PI) and ribulose-5-phosphate epimerase (R5PE) convert ribulose-5-phosphate to ribose-5-phosphate and xylulose-5-phosphate, respectively. Activities of both enzymes have been reported for several mammalian tissues including the adult human brain (Novello and McLean, 1968; Wood, 1974; Spencer and Hopkinson, 1980). R5PE has about 10-fold higher activity in mammalian tissue than does R5PI (Novello and McLean, 1968). Compared with other tissues, rat brain contains very low specific activities of R5PI but appears to have two molecular forms of the enzyme (Wood, 1974).

2.5 Transketolase

TK catalyzes the transfer of a C2 unit from xylulose-5-phosphate to ribose-5-phosphate or erythrose-4-phosphate, yielding glyceraldehyde-3-phosphate and sedoheptulose-7-phosphate or fructose-6-phosphate, respectively. The sequence of TK contains regions that are strongly conserved between species such as *Escherichia coli*, yeast, and humans (Schenk et al., 1998). The human TK is a 623-amino-acid protein with a molecular mass of 68 kDa (Schenk et al., 1998). Apparent K_m values of mouse brain TK are 330 μM for ribose-5-phosphate and 130 μM for xylulose-4-phosphate (Blass et al., 1982). Active TK is a dimer that requires thiamine pyrophosphate (TPP) and Mg^{2+} as cofactors (Massod et al., 1971). For dimer formation, a yet unknown cytosolic factor is required (Wang et al., 1997). Full activity of the holoenzyme is reached after a variable lag period after binding of TPP to the enzyme (Egan and Sable, 1981; Blass et al., 1982). Incorporation of TPP appears to be essential to maintain the activity of rat brain TK since brain apo-TK is unstable (Jeyasingham et al., 1986; Jeyasingham and Pratt, 1988). The importance of TK is clearly demonstrated by the facts that mice with homozygous disruption of the TK gene are not viable and that disruption of just one allele resulted in growth retardation and reduced fertility in female mice (Xu et al., 2002). In brain, an increase of TK activity was reported during postnatal development (Baquer et al., 1977; Iwata et al., 1988). TK is widely distributed in brain but enriched in particular neuronal perikarya in various areas of the rat brain (Calingasan et al., 1995). In addition, presence of TK was found in glial and ependymal cells (Calingasan et al., 1995).

2.6 Transaldolase

TA catalyzes the transfer of a C3 unit from sedoheptulose-7-phosphate to glyceraldehyde-3-phosphate, yielding erythrose-4-phosphate and fructose-6-phosphate. Human TA is a single-copy gene (Banki et al., 1997) encoding a 336-amino-acid protein of 38 kDa (Banki et al., 1994b). The human TA gene is located on chromosome 11 in a region that has been connected to a number of developmental disorders and tumor suppression (Banki et al., 1997). TA has been investigated in a number of species and tissues but little information is available on the distribution and functions of TA in mammalian brain. The expression of TA is regulated in a developmental (Baquer et al., 1977) and tissue-specific (Novello and McLean, 1968; Heinrich et al., 1976) manner with maximal activity at birth and early stages of embryogenesis. In brain, high activity of TA coincides with brain growth and myelination during the development of the nervous system (Banki et al., 1994a). Among the different brain cell types, oligodendrocytes have been reported to contain high levels of TA in human brain and in murine brain cell cultures (Banki et al., 1994a).

2.7 Other Enzymes

The metabolites glucose-6-phosphate and glyceraldehyde-3-phosphate interconnect the PPP with glycolysis/gluconeogenesis. Also the enzymes hexose phosphate isomerase (EC 5.3.1.9), phosphofructokinase (EC 2.7.1.11)/fructose biphosphatase (EC 3.1.3.11), and aldolase (EC 4.1.2.13) have to be considered for functional fluxes of metabolites through the nonoxidative part of the PPP. These enzymes and their functions in brain are described in more detail in Chapter 1.2 of this volume.

3 Functions of the PPP

The PPP has two major functions in cells: providing reduction equivalents in the form of NADPH and generation of ribose-5-phosphate. The importance of NADPH for various important reactions in brain cells is described in detail below. Ribose-5-phosphate is a cellular precursor for the synthesis of nucleotides. In contrast to this sugar phosphate, the other intermediates of the PPP do not seem to be used as building blocks or precursors of biosyntheses in the brain. The demand for ribose-5-phosphate in cells of the adult

brain for de novo synthesis of nucleotides appears to be rather low. Because of recycling of ribonucleotides during RNA turnover, little net synthesis of ribose-5-phosphate is required to enable RNA synthesis. In addition, DNA synthesis is of low quantitative importance in the adult brain. With the exception of processes such as DNA repair (Brooks, 2002) and proliferation of stem cells (Baizabal et al., 2003), little net synthesis of ribose-5-phosphate is required for the generation of deoxyribonucleotides. Thus, in the adult brain provision of ribose-5-phosphate for the synthesis of ribonucleotides and deoxyribonucleotides does not appear to be a major function of the PPP. However, ribose-5-phosphate generated by the PPP is likely to be of higher importance for the brain during periods of active cell proliferation, for example during brain development (Giuffrida, 1983; Bilger and Nehlig, 1992) and for the growth of brain tumors (Loreck et al., 1987; Spence et al., 1997). The view of a prominent function of the PPP during brain development for provision of both NADPH and ribose-5-phosphate is strongly supported by the increase in G6PDH activity during development in brain (Sengupta et al., 1985; Bilger and Nehlig, 1992) and by the higher flux rates of metabolites through the PPP in the developing brain than in the mature brain (Guerra et al., 1967; Baquer et al., 1977; Hothersall et al., 1979; Niedermüller, 1986).

Neurological symptoms and neural cell death have frequently been reported for animals that were treated with the 6PGDH inhibitor 6AN (Herken et al., 1969, 1976; Friede and Bischhausen, 1978; Griffiths et al., 1981; Krum, 1995), or were suffering from thiamine deficiency (Giguère and Butterworth, 1987; Pitkin and Savage, 2001). However, such observations have to be carefully considered regarding the importance of the PPP for normal brain functions. 6AN treatment strongly inhibits 6PGDH, but the accumulating 6-phosphogluconate affects also the flux of glycolysis by inhibition of hexose phosphate isomerase (Kriegstein and Stock, 1975; Tyson et al., 2000). In addition, thiamine deficiency not only affects TK but also reduces the specific activity of α -ketoglutarate dehydrogenase (EC 1.2.4.2) (Gibson et al., 1984). Thus, several mechanisms may contribute to the neurological symptoms that have been observed after 6AN treatment or during thiamine deficiency.

4 Regulation of the PPP

The PPP is responsible for a minor but important part of the glucose consumption of the brain. Under unstressed conditions, the PPP contributes to less than 5% of the total glucose consumption of brain (Hothersall et al., 1979; Gaitonde et al., 1983; Ben Yoseph et al., 1996b). However, if the demand of brain cells for PPP products is increased, the flux of metabolites through the PPP can be substantially increased.

4.1 Measuring Metabolite Fluxes Through the PPP

Information on the presence and importance of the PPP has frequently been obtained by quantifying specific activities of the PPP enzymes. However, such activity values represent maximal activities and do not reflect fluxes through the PPP. Such fluxes have been studied in brain lysates for the oxidative part of the PPP, for the nonoxidative part of the PPP, and for the total PPP by monitoring the reduction of NADP^+ after application of glucose-6-phosphate, ribose-5-phosphate, and ribose-5-phosphate plus G6PDH, respectively (Cabezas et al., 1999). In many organs, including brain, the flux through the oxidative part of the PPP (glucose-6-phosphate to ribulose-5-phosphate) is much higher than that through the nonoxidative part (ribose-5-phosphate to glucose-6-phosphate). The activity of the whole pathway (ribose-5-phosphate to ribulose-5-phosphate via G6PDH) is the same as the activity of the nonoxidative part (Cabezas et al., 1999). For brain homogenates the activity of the oxidative part of the PPP is about 14 times higher than that of the nonoxidative part (Cabezas et al., 1999). High ratios of oxidative versus nonoxidative part of the PPP have also been found for the mammary gland (33:1), adipose tissue (20:1), lung (11:1), and skeletal muscle (9:1), whereas liver (2.8:1) and kidney (1.9:1) have lesser ratios of the oxidative over the nonoxidative part of the PPP (Cabezas et al., 1999).

The traditional and well-established method to quantify the fluxes of glucose through the PPP is the comparison of the amounts of $^{14}\text{CO}_2$ that are produced from cells or cell extracts in the presence of

D-[1-¹⁴C]glucose and D-[6-¹⁴C]glucose (for overview see Baquer et al., 1988). This method allows to discriminate between the consumption of glucose-6-phosphate by glycolysis and the oxidative part of the PPP. The oxidative part of the PPP quickly releases ¹⁴CO₂ from [1-¹⁴C]glucose but not from [6-¹⁴C]glucose, whereas glycolysis converts both glucose isotopomers to pyruvate that is subsequently oxidized to CO₂ by pyruvate dehydrogenase and the citric acid cycle.

More recently, the activity of the PPP was measured in intact brain cells by using the asymmetrically substituted glucose molecule D-[1,6-¹³C₂,6,6-²H₂]glucose (Ben Yoseph et al., 1994a, b, 1995; Ross et al., 1994). This molecule is converted in cells by glycolysis to [3-¹³C]lactate plus [3-¹³C,3,3-²H₂]lactate, whereas flux through the PPP produces [3-¹³C,3,3-²H₂]lactate and unlabeled lactate. Following cellular degradation of D-[1,6-¹³C₂,6,6-²H₂]glucose, the different lactate isotopomers that have been released by the cells can be quantified by gas chromatography followed by mass spectrometry and the ratio of the lactate isotopomers can be used to determine relative activities of PPP and glycolysis. This method has been applied to measure PPP fluxes for brain cells in culture as well as for brain cells in vivo by microdialysis studies (Ben Yoseph et al., 1994a, 1995, 1996a, b).

4.2 Glucose-6-Phosphate Dehydrogenase as Key Regulator

The master regulator of the PPP is G6PDH (Kletzien et al., 1994). This enzyme controls the entry of glucose-6-phosphate into the PPP. G6PDH is considered a constitutively expressed housekeeping enzyme. In many cell types and tissues G6PDH activity is modulated by external stimuli such as hormones, nutrients, or oxidative stress (Kletzien et al., 1994). However, for brain G6PDH little is known about such regulations of the enzyme.

The activity of G6PDH depends strongly on the availability of the substrates glucose-6-phosphate and NADP⁺ and is regulated by the cellular concentration of NADPH. Since NADPH is an effective competitive inhibitor of brain G6PDH with a *K_i* value that is lower than the *K_m* value for NADP⁺ (Askar et al., 1996), the cytosolic ratio of NADP⁺ to NADPH determines the flux of metabolites through G6PDH. Unstressed cells have a high NADPH/NADP⁺ ratio (Adams et al., 2001), and the activity of G6PDH is rather low under such conditions. Consequently, under unstressed conditions the PPP contributes to only a few percent of the total glucose-6-phosphate consumption in brain (Hothersall et al., 1979; Gaitonde et al., 1983; Ben Yoseph et al., 1994a, 1996a, b).

The glucose metabolism of brain cells, including the PPP, is strongly influenced by NO and nitrosative stress (Bolaños et al., 2004). In cultured astrocytes G6PDH mRNA expression, G6PDH activity, and glucose oxidation through the PPP are increased after treatment with lipopolysaccharide (García-Nogales et al., 1999). Peroxynitrite, the reaction product of NO with superoxide, appears to be of high importance in this respect. Treatment of cultured astrocytes and neurons with peroxynitrite induced a rapid activation of the PPP that was correlated with the accumulation of NADPH and with an increase in the ratio of 6-phosphogluconate to glucose-6-phosphate (García-Nogales et al., 2003). This increase in G6PDH activity and flux through the oxidative part of the PPP was connected to a peroxynitrite-dependent release of G6PDH from intracellular structures, suggesting activation of G6PDH activity and PPP flux by trans-compartmentalization of the enzyme in brain cells (García-Nogales et al., 2003).

4.3 Activation of the PPP

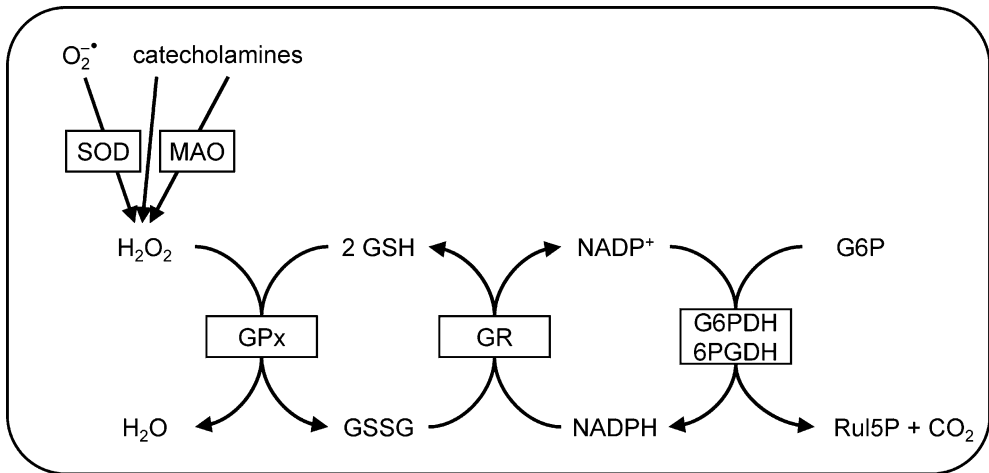
Oxidation of cellular NADPH will simultaneously decrease the concentration of the G6PDH inhibitor NADPH and increase the cellular concentration of the PPP substrate NADP⁺, resulting in elevated activity of G6PDH and consequently in an increased flux through the oxidative part of the PPP. This regulation was confirmed for brain cells by application of phenazine methosulfate (PMS), a chemical oxidant of NADPH. PMS upregulates the PPP severalfold in brain (Ben Yoseph et al., 1994a, 1995), brain slices (Hothersall et al., 1979; Domanska-Janik, 1988), and synaptosomes (Hothersall et al., 1982). In addition, treatment of mixed

cerebrocortical cultures and astrocyte cultures with PMS increased the rate of PPP to 35% and 80% of total glucose consumption, respectively (Ben Yoseph et al., 1996a).

Exposure of cells to peroxides causes a rapid oxidation of NADPH, since this cofactor provides the reduction equivalents for glutathione reductase (GR)-catalyzed regeneration of glutathione (GSH) that was oxidized during peroxide disposal (🔗 [Figure 1.3-2](#)). This scenario explains that application of catechola-

■ **Figure 1.3-2**

Peroxide and NADPH metabolism in brain cells. H_2O_2 is generated from superoxide by superoxide dismutases (SODs) or from catecholamines by autoxidation and by the monoamine oxidase (MAO)-catalyzed reaction. Glutathione peroxidases (GPx) reduce H_2O_2 to water. Glutathione (GSH), which is oxidized to glutathione disulfide (GSSG) during the GPx reaction, is regenerated by glutathione reductase (GR). NADPH that is consumed as cosubstrate in the reaction catalyzed by GR is regenerated by glucose-6-phosphate dehydrogenase (G6PDH) and 6-phosphogluconate dehydrogenase (6PGDH)



mines, which are substrates of the H_2O_2 -generating monoamine oxidases, to synaptosomes (Appel and Parrot, 1970; Baquer et al., 1977; Hothersall et al., 1982) as well as perfusion of brains of conscious rats with H_2O_2 (Ben Yoseph et al., 1994a, 1996b) enhances the flux of glucose through the PPP. Moreover, exposure of mixed cerebrocortical cultures and cultured astrocytes to H_2O_2 increased the rate of PPP from 1% to 22% (Ben Yoseph et al., 1994a, 1996a, b) and 7% to 67% (Ben Yoseph et al., 1994a, 1996a) of total glucose consumption, respectively.

5 NADPH Metabolism of Brain Cells

5.1 NADPH-Regenerating Enzymes

The two dehydrogenases of the oxidative part of the PPP, G6PDH and 6PGDH, are likely to be the most important generators of NADPH in the cytosol of brain cells. The major reason for this is the continuous generation of glucose-6-phosphate by hexokinase (EC 2.7.1.1) in brain cells and the potential of G6PDH to use this metabolite as substrate as soon as NADPH is required. In addition, in brain astrocytes and ependymal cells, glucose-6-phosphate is also available from glycogen (Rahman et al., 2000; Prothmann et al., 2001). From this endogenous glucose store glucose-6-phosphate can be generated quicker than from

exogenous glucose, if high amounts of NADPH are required due to peroxide exposure (Rahman et al., 2000). However, other enzymes, such as malic enzyme (ME; EC 1.1.1.40) and NADP⁺-dependent isocitrate dehydrogenase (ICDH; EC 1.1.1.42), can also contribute to the cytosolic NADP⁺ reduction (Winkler et al., 1986; Dringen et al., 2005). Although such enzymes are able to provide sufficient NADPH under unstressed conditions in G6PDH-deficient embryonic stem cells, they cannot supply sufficient NADPH to keep the cellular redox potential reduced during oxidative stress (Filosa et al., 2003).

MEs, ICDHs, and nicotinamide nucleotide transhydrogenase (EC 1.6.1.2) are expressed in brain cells (Bukato et al., 1995; Arkblad et al., 2002; Minich et al., 2003) and may therefore contribute to NADPH regeneration in brain. Although G6PDH and 6PGDH are found almost exclusively in the cytosol, both ME and ICDH isoforms that are localized either in the cytosol or in the mitochondria have been described (Kurz et al., 1993; Bukato et al., 1995; Vogel et al., 1998a; Minich et al., 2003). Transhydrogenase is an enzyme of the inner mitochondrial membrane of brain cells (Arkblad et al., 2002). The cytosolic ME (cME) is expressed in cultured astrocytes and oligodendrocytes (Kurz et al., 1993), whereas expression of mitochondrial ME (mME) has been reported for neurons (Vogel et al., 1998b). Since ME has been considered an anaplerotic enzyme that generates malate by reductive carboxylation of pyruvate (Hassel, 2000), in neurons the mME could bypass the missing pyruvate carboxylase (EC 6.4.1.1) reaction. In this context, it is important to mention that in its anaplerotic function ME will consume reduction equivalents in the form of NADPH.

Substantial activities of cICDH and mICDH are observed in cultures of astrocytes, neurons, oligodendrocytes, and microglial cells (Minich et al., 2003). A direct involvement of ICDHs in NADPH regeneration in the cytosol of cells is highly likely, since at least during peroxide disposal ICDHs have been reported to support the resistance of cells against oxidative stress (Jo et al., 2001; Lee et al., 2002; Maeng et al., 2004). No evidence has been presented so far about the substantial contribution of cME to cytosolic NADPH regeneration in neural cells. In contrast, a contribution of mME, as well as of mICDH and transhydrogenase, in GSSG reduction has been shown for isolated brain mitochondria (Vogel et al., 1999), demonstrating that these enzymes can provide NADPH for GSH redox cycling in brain cells.

The mitochondrial nicotinamide nucleotide transhydrogenase uses the proton gradient of the inner mitochondrial membrane to drive the transfer of electrons from NADH to NADP⁺, thereby generating NADPH from NADH. To our knowledge, such a direct link between NAD⁺/NADH and NADP⁺/NADPH pools has not been reported for the cytosol. Nevertheless, an increase in PPP activity is likely to affect the cytosolic NAD⁺/NADH at least indirectly by a lowered rate of NAD⁺ reduction in the glyceraldehydephosphate dehydrogenase (EC 1.2.1.12) reaction due to a reduced glycolysis rate. Whether the PPP and/or the cytosolic NADP⁺/NADPH ratio can influence the mitochondrial NADP⁺/NADPH ratio and whether transfer of NADPH reduction equivalents between cytosol and mitochondria of brain cells occur remains to be elucidated.

5.2 NADPH-Consuming Processes

NADPH supplies essential reduction equivalents for a variety of important metabolic pathways in brain cells. In this context it is important to consider that the demand of the various pathways for NADPH differs strongly in individual types of brain cells and depends on the functions, the localization, and the activation status of a given cell type. In addition, the quantitative importance of a given NADPH-consuming pathway in brain is likely to change with the development of the brain as well as in pathological conditions. Under some conditions, several pathways may simultaneously require NADPH in a brain cell, implicating the occurrence of competition of the NADPH-dependent enzymes for their substrate NADPH. Under such conditions, the K_m values of the NADPH-consuming enzymes for NADPH as well as local concentrations of NADPH in the cells are likely to determine the flux of electrons from NADPH into the different pathways (Dringen, 2005).

Among the various NADPH-consuming processes in the adult brain, the regeneration of the antioxidant GSH is likely to be quantitatively the most important one. The human brain consumes 20% of the

oxygen used by the body (Clarke and Sokoloff, 1999). Since oxidative metabolism is directly connected with the generation of ROS (Halliwell and Gutteridge, 1999), they are continuously generated in brain. NADPH is essential to regenerate the major antioxidant GSH, which is highly important for the detoxification of radicals and peroxides in brain cells (Dringen, 2000; Dringen and Hirrlinger, 2003; Dringen et al., 2005). Consequently, antioxidative defense is a key function for all brain cells. Other pathways that consume NADPH may be restricted to a low number of brain cells, to given areas of the brain, or to individual cell types in brain. In this context, adult brain is likely to differ strongly from developing brain. For example, enzymes that use NADPH in brain cells for reductive biosyntheses of compounds such as fatty acids and cholesterol are likely to consume substantial amounts of NADPH during brain development but are of less quantitative importance for NADPH consumption in the mature brain.

5.2.1 GSSG Reduction and Peroxide Disposal

In mammalian cells ROS such as peroxides and oxygen radicals are continuously generated during aerobic metabolism as by-products of the respiratory chain (Halliwell, 2001). In addition, ROS are produced by spontaneous (Clement et al., 2002; Hirrlinger et al., 2002) or monoamine oxidase (EC 1.4.3.4)-catalyzed (Nagatsu, 2004) oxidation of catecholamines. To avoid ROS-mediated cellular damage such as lipid peroxidation, protein inactivation, and DNA strand breaks, antioxidative mechanisms are present in cells that remove ROS or even prevent their generation. The GSH system is an important component of the antioxidative potential of brain cells (Dringen, 2000; Dringen and Hirrlinger, 2003; Dringen et al., 2005). GSH reacts directly with radicals and it is the electron donor in the reactions catalyzed by GSH peroxidases (GPx; EC 1.11.1.9). The product of the oxidation of GSH by GPx is glutathione disulfide (GSSG). Within cells GSH is regenerated from GSSG in the reaction catalyzed by GR (EC 1.6.4.2) (Figure 1.3-2) (Dringen and Gutterer, 2002), a flavoenzyme that transfers electrons from NADPH to GSSG.

The cycling of GSH in the reactions catalyzed by GPx and GR depends on the availability of reduction equivalents in the form of NADPH. Since all brain cell types contain GR (Gutterer et al., 1999; Hirrlinger et al., 2002) and are able to efficiently dispose of peroxides (Hirrlinger et al., 2002; Dringen et al., 2005), these brain cells require effective NADPH regeneration for their GSH redox cycling during peroxide clearance. Moreover, NADPH may also act directly as antioxidant that reduces ROS in an enzyme-independent reaction (Kirsch and de Groot, 2001). Whether this reaction of NADPH plays an important role in the antioxidative defense of brain cells and/or is a major consumer of NADPH in brain cells remains to be elucidated.

The importance of the PPP for neural peroxide clearance has clearly been demonstrated by the strong activation of the PPP after application of H₂O₂ to neural cells in vitro and in vivo (Ben Yoseph et al., 1994a, 1996b), by the reduction of peroxide clearance rates in cultured astrocytes after glucose deprivation (Dringen and Hamprecht, 1997; Dringen et al., 1998; Kussmaul et al., 1999) as well as by the rapid mobilization of stored glucose from glycogen after peroxide application to astrocytes (Rahman et al., 2000).

5.2.2 Synthesis of Fatty Acids

The brain is highly enriched in long-chain polyunsaturated fatty acids (PUFAs), particularly arachidonic acid and docosahexanoic acid, which play important roles in structure and functions of the brain (Qi et al., 2002; Innis, 2003). These fatty acids are accumulated during fetal and infant development or are synthesized from precursors in brain (Qi et al., 2002). Cerebral endothelial cells and astrocytes avidly elongate and desaturate precursors of PUFAs (Moore, 2001) in processes that require NADPH as electron donor (Yoshida et al., 1988). In addition, astrocytes have been reported to synthesize and release oleic acid that serves as neurotrophic factor for neurons (Medina and Taberner, 2002). Neonatal brain appears to acquire PUFAs, but not long-chain saturated or monounsaturated fatty acids, from the circulation. Ketone bodies

and ketogenic substrates such as linoleate and α -linolenate seem to be circulated for de novo lipogenesis in rat brain (Cunnane et al., 1999). The decline, from the birth to the adult stage, in the contribution of the PPP to the glucose metabolism that corresponds to the decline in lipid synthesis over the same period (Baquer et al., 1977) suggests the importance of the PPP for fatty acid synthesis in brain. Among the different types of brain cells, the myelin-forming oligodendrocytes have the highest requirements for fatty acids. At least for cultured oligodendrocytes it was demonstrated that the PPP is required to supply NADPH for synthesis of fatty acids and cholesterol (Sykes et al., 1986). Also, the strong expression of TA in oligodendrocytes (Banki et al., 1994a) and the high rate of glucose consumption by the PPP in cultured oligodendrocytes (Edmond et al., 1987) suggest the importance of the PPP for lipid synthesis in these cells.

5.2.3 Synthesis of Cholesterol

Almost all cholesterol in brain is a product of local synthesis (Björkhem and Meaney, 2004). Consequently, the enzymes required for cholesterol synthesis have to be present in brain cells. 3-Hydroxy-3-methylglutaryl (HMG) CoA reductase (EC 1.1.1.34) is the rate-limiting enzyme in cholesterol synthesis and uses NADPH as cofactor (Istvan and Deisenhofer, 2000). In addition, NADPH is required for enzymes that catalyze later reactions in cholesterol synthesis. In the brain, cholesterol synthesis appears to be a pivotal function of glial cells (Björkhem and Meaney, 2004), which supply neurons with cholesterol that is essential for synaptogenesis (Mauch et al., 2001; Slezak and Pfrieger, 2003). Cholesterol synthesis and metabolism in brain have recently become hot research topics, since amounts and distribution of cholesterol within neurons impact A β synthesis (Puglielli et al., 2003) and since statins, inhibitors of HMGCoA reductase, have been demonstrated to provide protection against neurological disorders (Björkhem and Meaney, 2004; Reiss et al., 2004). However, it should be considered that the HMGCoA reductase product mevalonate is also a precursor for the synthesis of other important cellular compounds. For example, inhibition of this enzyme may also affect the synthesis of dolichylphosphate (Schedin et al., 1998) and geranylgeranylpyrophosphate (Meske et al., 2003; Schulz et al., 2004).

5.2.4 NO Production by NO Synthases

The NO radical has been implicated in numerous biological functions in many tissues including the brain (Murphy, 2000; Wiesinger, 2001; Esplugues, 2002). NO is the product of the reaction that is catalyzed by NO synthases (NOSs) (EC 1.14.13.39). The constitutive NOS-1 and NOS-3 produce NO only for short periods, after activation by a raise in intracellular Ca²⁺ concentration. In contrast, the induction of the expression of NOS-2 (inducible NOS (iNOS)) causes a long-lasting generation of high amounts of NO (Wiesinger, 2001). All isoforms of NOS need NADPH as an electron donor to produce NO and citrulline from arginine and molecular oxygen. Since NO production and expression of constitutive or inducible NOSs have been reported for neurons and different types of glial cells (Murphy, 2000; Wiesinger, 2001; Dringen, 2005), NADPH consumption by NOSs contributes to NADPH consumption by brain cells under certain conditions.

5.2.5 Superoxide Production by NADPH Oxidase

NADPH oxidase (Nox; EC 1.6.3.1) is a multi-subunit protein complex that uses electrons derived from NADPH to reduce molecular oxygen to superoxide. Activation of cells leads to the association of cytosolic protein subunits of Nox with the membrane-associated proteins to form the active complex that produces superoxide (Bokoch and Knaus, 2003). Expression of mRNAs of all the subunits of Nox and of several Nox proteins have been reported for microglial cells (Sankarapandi et al., 1998; Green et al., 2001; Lavigne et al., 2001). In the central nervous system (CNS), Nox is expressed predominantly in microglial cells and to a lesser extent in other cell types such as neurons and astrocytes (Zekry et al., 2003). Recently six novel

ROS-generating oxidases with homology to the Nox2 of granulocytes, of which three are also expressed in brain cells, have been discovered (Zekry et al., 2003). Presence and function of Nox in brain cells has been best investigated for microglial cells (Dringen, 2005). In culture, these cells generate superoxide upon activation with phorbol esters (Colton and Gilbert, 1987; Sankarapandi et al., 1998).

5.2.6 Hydroxylation Reactions

A large number of drug-metabolizing enzymes that consist of cytochromes P450 and NADPH-cytochrome P450 reductase (EC 1.6.2.4) have been reported for brain cells (Hedlund et al., 2001; Strobel et al., 2001). These NADPH-dependent enzymes are involved in the hydroxylation of neurosteroids, the regulation of brain cholesterol homeostasis, the elimination of retinoids, and the metabolism of xenobiotics (Hedlund et al., 2001; Strobel et al., 2001). One prominent example for such an enzyme is aromatase (EC 1.14.14.1), which is involved in the production of estrogens in brain (Conley and Hinshelwood, 2001).

5.2.7 Degradation of Heme

Two enzymes in heme degradation require reduction equivalents from NADPH: heme oxygenase (HO; EC 1.14.99.3) and biliverdin reductase (EC 1.3.1.24). Several isoforms of HO are expressed in brain cells (Wagner et al., 2003). These enzymes metabolize heme to biliverdin, iron, and CO. The latter has been discussed as a neurotransmitter (Zakhary et al., 1997; Barañano and Snyder, 2001; Barañano et al., 2001). Biliverdin is reduced to bilirubin in the reaction catalyzed by biliverdin reductase. Bilirubin is toxic for the brain of newborns but NADPH-dependent recycling of bilirubin by biliverdin reductase may also be of considerable importance for the antioxidative potential of cells (Barañano et al., 2002; Sedlak and Snyder, 2004).

5.2.8 Polyol Metabolism

Aldose reductase (EC 1.1.1.200) is an enzyme involved in the polyol metabolism of cells that uses NADPH as substrate to reduce glucose to sorbitol, which subsequently is oxidized by sorbitol dehydrogenase (EC 1.1.1.14) to fructose. Both aldose reductase and sorbitol dehydrogenase are present in brain and cultured astrocytes (O'Brien and Schofield, 1980; Song et al., 1987; Wiesinger et al., 1990; Jacquín-Becker and Labourdette, 1997). Although evidence for flux through the sorbitol pathway has been presented for brain, the function of this pathway, which bypasses the glucose metabolism control point hexokinase (Jeffery and Jörnvall, 1983), remains enigmatic. However, an elevated flux through the sorbitol pathway has been reported in the brains of diabetic patients (Kwee et al., 1996). This may contribute to complications during diabetes. It has been suggested that depletion of cellular NADPH due to exaggerated flux through aldose reductase contributes to oxidative stress-mediated dysfunctions of neural cells in diabetes (Ng et al., 1998; Lee and Chung, 1999).

5.2.9 Thioredoxin System

The thioredoxin system, formed by thioredoxin and thioredoxin reductase (EC 1.8.1.9), is an important constituent of the intracellular redox environment (Gromer et al., 2004). Thioredoxin reductase is homologous to GR and depends on NADPH as electron donor. So far, the importance of the thioredoxin system for brain function has not been studied in great detail. Cytosolic thioredoxin reductase is present in cultured brain cells (Eftekharpour et al., 2000). The thioredoxin system may be of high importance for brain cells under pathological conditions. For example, the thioredoxin system can repair peroxynitrite-induced disulfides in brain tubulin (Landino et al., 2004).

6 PPP and Neurological Diseases

The enzymes G6PDH, TK, and TA have been connected with pathological and age-related neurological disorders. These connections are discussed in more detail below.

Only little is known about alterations of other PPP enzymes in neurological diseases. 6PGDH appears to be unaltered in most pathological conditions, although, compared with the activity in controls, an elevated 6PGDH activity has been reported for brains of Alzheimer's disease (AD) patients (Martins et al., 1986a; Palmer, 1999). Deficiency in R5PI leads to increased polyol levels (Huck et al., 2004). This has been suggested to contribute to the observed leukoencephalopathy and peripheral neuropathy (Huck et al., 2004).

6.1 Glucose-6-Phosphate Dehydrogenase

G6PDH deficiency is the most common human enzymopathy (see Luzzatto et al., 2001). Although such deficiencies cause severe peripheral symptoms, mostly hemolytic anemias (Au et al., 2000), none of them appear to cause severe neurological symptoms in humans. In contrast, already moderate G6PDH deficiency in mice leads to a disturbed GSSG-to-GSH ratio in brain and to an increased somatic mutation rate (Felix et al., 2002).

Alterations in G6PDH activity in brain have been reported several times for AD patients. A reduced specific G6PDH activity was found in the hippocampus of AD patients (Bigl et al., 1999), whereas increased activity of G6PDH that correlated with an increased lipid peroxidation was reported for the temporal cortex of AD patients (Palmer, 1999). Elevated neuronal G6PDH immunoreactivity in hippocampus and cerebellum (Russell et al., 1999) and increased G6PDH activity in total brain (Martins et al., 1986a; Soucek et al., 2003) were also reported for brains of AD patients, suggesting an upregulation of G6PDH to compensate the higher demand for NADPH that is needed for antioxidative defense.

Brain G6PDH has also been connected with diabetes. Rats that were treated with alloxan to induce diabetes showed increased G6PDH activity in some brain areas (Lakhman et al., 1994). This observation was confirmed in streptozotocin-induced diabetic rats (Ulusu et al., 2003), whereas another group did not observe differences in G6PDH activity between the brains from control and those from streptozotocin-induced diabetic rats (Martins et al., 1986b). The increase in G6PDH activity in diabetic rats appears to be mediated by oxidative stress, since it was at least partially prevented by application of antioxidants (Ulusu et al., 2003). An upregulation of G6PDH by oxidative stress may also explain that epileptogenic foci induced by FeCl₃ in rat brains showed an elevated G6PDH activity (Singh and Pathak, 1990) and that PPP activity is upregulated in A β -resistant cell lines and in cultured neurons that were treated with subtoxic levels of A β peptide (Soucek et al., 2003).

6.2 Transketolase

TK activity is strongly affected by thiamine deficiency that is usually associated with alcoholism or impaired nutrition. These conditions can lead to the Wernicke–Korsakoff syndrome (WKS), a severe neurological disorder (Zubaran et al., 1997). In rats, thiamine deficiency leads to a strong decrease of TK activity (Giguère and Butterworth, 1987) and TK immunoreactivity (Sheu et al., 1996) in brain and reduces TK activity in cultured cerebral granule cells (Pannunzio et al., 2000). Thiamine administration results in normalization of neurological symptoms, although TK activity is not completely recovered in all brain regions (Giguère and Butterworth, 1987).

Animal models of alcoholism lead to thiamine deficiency that is accompanied with decreased TK activity (Zimatkin and Zimatkina, 1996). The effects of thiamine deficiency and ethanol on TK activity have been proposed to be the prime reason for the brain damage that is associated with alcoholism (Heap et al., 2002). However, since activities of several important enzymes are reduced in thiamine deficiency (Gibson et al., 1984), pathways other than the PPP could also contribute to the impairments that cause the

neurological symptoms. The report of a WKS patient, who suffered from a deficiency in a cytosolic factor that is necessary for stable assembly of the TK dimer, suggests a pivotal role of TK deficiency in WKS but does not exclude other TPP-dependent enzymes, since the cytosolic factor could be required for assembly of all thiamine-dependent enzymes (Wang et al., 1997).

Evidence for a reduced TK activity in brain was also reported for AD (Gibson et al., 1988; Héroux et al., 1996). Even brain regions that did not appear to be histologically affected by AD exhibited reduced TK activity (Gibson et al., 1988). Reason for the decreased TK activity may be the reduced thiamine levels that were reported for brains of AD patients (Héroux et al., 1996). However, thiamine levels in the cerebrospinal fluid (CSF) of AD patients were not significantly reduced compared with the levels in controls (Molina et al., 2002).

6.3 Transaldolase

Human TA is considered a prime target for autoimmunity in multiple sclerosis (MS) (Banki et al., 1994a; Colombo et al., 1997). A subset of patients with MS had high-affinity autoantibodies against TA in their serum and CSF, whereas such antibodies were absent in controls (Banki et al., 1994a). Application of recombinant TA antigen stimulated lymphocyte proliferation in the sera of MS patients (Banki et al., 1994a), even stronger than myelin basic protein (Colombo et al., 1997). Since autoimmunoreactive antibodies against prominent TA epitopes crossreact with peptides from virus proteins (Banki et al., 1994a; Esposito et al., 1999), molecular mimicry between viral proteins and TA may play a role in breaking the immunological tolerance and leading to selective destruction of oligodendrocytes in MS.

7 Conclusions

Although under normal conditions the PPP plays only a minor part in the total glucose consumption in brain, its products NADPH and ribose-5-phosphate have important functions for this organ. This importance is underlined by the strong increase in flux rates through the PPP in brain cells that have elevated NADPH consumption. This upregulation demonstrates that the PPP in neural cells has a high reserve potential and provides its products depending on the demand of the cell.

For adult brain, the quantitatively most important function of the PPP appears to be the supply of sufficient reduction equivalents in the form of NADPH for the regeneration of GSH during the defense against ROS. In addition, several reductive biosyntheses require NADPH in brain cells. The strong dependence of NADPH-dependent enzymes for their cofactor suggests that cells that consume high amounts of NADPH are especially well equipped with an active PPP. For example, high G6PDH activity in neurons has been connected with the need for providing reduction equivalents required for NADPH-dependent reactions (Biagiotti et al., 2003, 2005). Further studies on the colocalization of the PPP dehydrogenases with NADPH-dependent enzymes in brain cells will demonstrate the strong functional coupling between these enzymes.

Several human neurological diseases have already been connected with altered activities of PPP enzymes. A decreased activity of the PPP in brain cells may lead to insufficient supply of NADPH that is highly important for antioxidative defense and to an impairment of various biosynthetic processes. On the other hand, elevated activities of PPP enzymes may be a consequence of an increased demand for NADPH and could serve as an indicator for increased NADPH consumption to defend oxidative stress.

Acknowledgments

Ralf Dringen is supported by NeuroSciences Victoria as a recipient of a senior research fellowship. Tobias Minich is supported by the Fortune Program of the medical faculty of the University of Tübingen (grant 1310-0-0).

References

- Adams JD Jr, Klaidman LK, Chang ML, Yang J. 2001. Brain oxidative stress—analytical chemistry and thermodynamics of glutathione and NADPH. *Curr Top Med Chem* 1: 473-482.
- Appel SH, Parrot BL. 1970. Hexose monophosphate pathway in synapses. *J Neurochem* 17: 1619-1626.
- Arklblad EL, Egorov M, Shakhparonov M, Romanova L, Polzikov M, et al. 2002. Expression of proton-pumping nicotinamide nucleotide transhydrogenase in mouse, human brain and *C. elegans*. *Comp Biochem Physiol B Biochem Mol Biol* 133: 13-21.
- Askar MA, Sumathy K, Baquer NZ. 1996. Regulation and properties of purified glucose-6-phosphate dehydrogenase from rat brain. *Indian J Biochem Biophys* 33: 512-518.
- Au SW, Gover S, Lam VM, Adams MJ. 2000. Human glucose-6-phosphate dehydrogenase: The crystal structure reveals a structural NADP(+) molecule and provides insights into enzyme deficiency. *Structure Fold Des* 8: 293-303.
- Au SW, Naylor CE, Gover S, Vandeputte-Rutten L, Scopes DA, et al. 1999. Solution of the structure of tetrameric human glucose 6-phosphate dehydrogenase by molecular replacement. *Acta Crystallogr D Biol Crystallogr (Pt 4)*: 55 826-834.
- Bagdasarian G, Hulanicka D. 1965. Changes of mitochondrial glucose-6-phosphate dehydrogenase and 6-phosphogluconate dehydrogenase during brain development. *Biochim Biophys Acta* 99: 367-369.
- Baizabal JM, Furlan-Magaril M, Santa-Olalla J, Covarrubias L. 2003. Neural stem cells in development and regenerative medicine. *Arch Med Res* 34: 572-588.
- Banki K, Colombo E, Sia F, Halladay D, Mattson DH, et al. 1994a. Oligodendrocyte-specific expression and autoantigenicity of transaldolase in multiple sclerosis. *J Exp Med* 180: 1649-1663.
- Banki K, Eddy RL, Shows TB, Halladay DL, Bullrich F, et al. 1997. The human transaldolase gene (TALDO1) is located on chromosome 11 at p15. 4-p15.5. *Genomics* 45: 233-238.
- Banki K, Halladay D, Perl A. 1994b. Cloning and expression of the human gene for transaldolase. A novel highly repetitive element constitutes an integral part of the coding sequence. *J Biol Chem* 269: 2847-2851.
- Baquer NZ, Hothersall JS, Greenbaum AL, McLean P. 1975. The modifying effect of manganese on the enzymic profiles and pathways of carbohydrate metabolism in rat liver and adipose tissue during development. *Biochem Biophys Res Commun* 62: 634-641.
- Baquer NZ, Hothersall JS, McLean P. 1988. Function and regulation of the pentose phosphate pathway in brain. *Curr Top Cell Regul* 29: 265-289.
- Baquer NZ, Hothersall JS, McLean P, Greenbaum AL. 1977. Aspects of carbohydrate metabolism in developing brain. *Dev Med Child Neurol* 19: 81-104.
- Baquer NZ, McLean P, Greenbaum AL. 1973. Enzymic differentiation in pathways of carbohydrate metabolism in developing brain. *Biochem Biophys Res Commun* 53: 1282-1288.
- Barañano DE, Ferris CD, Snyder SH. 2001. Atypical neural messengers. *Trends Neurosci* 24: 99-106.
- Barañano DE, Rao M, Ferris CD, Snyder SH. 2002. Biliverdin reductase: A major physiologic cytoprotectant. *Proc Natl Acad Sci USA* 99: 16093-16098.
- Barañano DE, Snyder SH. 2001. Neural roles for heme oxygenase: Contrasts to nitric oxide synthase. *Proc Natl Acad Sci USA* 98: 10996-11002.
- Bauer HP, Srihari T, Jochims JC, Hofer HW. 1983. 6-phosphogluconolactonase. Purification, properties and activities in various tissues. *Eur J Biochem* 133: 163-168.
- Ben Yoseph O, Boxer PA, Ross BD. 1994a. Oxidative stress in the central nervous system: Monitoring the metabolic response using the pentose phosphate pathway. *Dev Neurosci* 16: 328-336.
- Ben Yoseph O, Boxer PA, Ross BD. 1996a. Assessment of the role of the glutathione and pentose phosphate pathways in the protection of primary cerebrocortical cultures from oxidative stress. *J Neurochem* 66: 2329-2337.
- Ben Yoseph O, Boxer PA, Ross BD. 1996b. Noninvasive assessment of the relative roles of cerebral antioxidant enzymes by quantitation of pentose phosphate pathway activity. *Neurochem Res* 21: 1005-1012.
- Ben Yoseph O, Camp DM, Robinson TE, Ross BD. 1995. Dynamic measurements of cerebral pentose phosphate pathway activity in vivo using [1,6-¹³C₂,6,6-²H₂]glucose and microdialysis. *J Neurochem* 64: 1336-1342.
- Ben Yoseph O, Kingsley PB, Ross BD. 1994b. Metabolic loss of deuterium from isotopically labeled glucose. *Magn Reson Med* 32: 405-409.
- Bhadbhade MM, Adams MJ, Flynn TG, Levy HR. 1987. Sequence identity between a lysine-containing peptide from *Leuconostoc mesenteroides* glucose-6-phosphate dehydrogenase and an active site peptide from human erythrocyte glucose-6-phosphate dehydrogenase. *FEBS Lett* 211: 243-246.
- Biagiotti E, Guidi L, Del Grande P, Ninfali P. 2003. Glucose-6-phosphate dehydrogenase expression associated with NADPH-dependent reactions in cerebellar neurons. *Cerebellum* 2: 178-183.
- Biagiotti E, Ferri, P, Dringen, R, del Grande, P, Ninfali, P. 2005. NADPH-dependent reactions correlate with glucose-6-phosphate dehydrogenase in the rat olfactory bulb:

- An immunohistochemical and histochemical study. *J Neurosci Res* 80: 434-441.
- Bigl M, Bruckner MK, Arendt T, Bigl V, Eschrich K. 1999. Activities of key glycolytic enzymes in the brains of patients with Alzheimer's disease. *J Neural Transm* 106: 499-511.
- Bilger A, Nehlig A. 1992. Quantitative histochemical changes in enzymes involved in energy metabolism in the rat brain during postnatal development. II. Glucose-6-phosphate dehydrogenase and beta-hydroxybutyrate dehydrogenase. *Int J Dev Neurosci* 10: 143-152.
- Björkhem I, Meaney S. 2004. Brain cholesterol: Long secret life behind a barrier. *Arterioscler Thromb Vasc Biol* 24: 806-815.
- Blass JP, Piacentini S, Boldizar E, Baker A. 1982. Kinetic studies of mouse brain transketolase. *J Neurochem* 39: 729-733.
- Bokoch GM, Knaus UG. 2003. NADPH oxidases: Not just for leukocytes anymore! *Trends Biochem Sci* 28: 502-508.
- Bolaños JP, Ciudad P, García-Nogales P, Delgado-Esteban M, Fernández E, et al. 2004. Regulation of glucose metabolism by nitrosative stress in neural cells. *Mol Aspects Med* 25: 61-73.
- Brooks PJ. 2002. DNA repair in neural cells: Basic science and clinical implications. *Mutat Res* 509: 93-108.
- Bublitz C, Steavenson S. 1988. The pentose phosphate pathway in the endoplasmic reticulum. *J Biol Chem* 263: 12849-12853.
- Bukato G, Kochan Z, Swierczynski J. 1995. Purification and properties of cytosolic and mitochondrial malic enzyme isolated from human brain. *Int J Biochem Cell Biol* 27: 47-54.
- Cabezas H, Raposo RR, Melendez-Hevia E. 1999. Activity and metabolic roles of the pentose phosphate cycle in several rat tissues. *Mol Cell Biochem* 201: 57-63.
- Calingasan NY, Sheu KF, Baker H, Jung EH, Paoletti F, et al. 1995. Heterogeneous expression of transketolase in rat brain. *J Neurochem* 64: 1034-1044.
- Camardella L, Caruso C, Rutigliano B, Romano M, Di Prisco G, et al. 1988. Human erythrocyte glucose-6-phosphate dehydrogenase. Identification of a reactive lysyl residue labelled with pyridoxal 5'-phosphate. *Eur J Biochem* 171: 485-489.
- Cammer W, Snyder DS, Zimmerman TR Jr, Farooq M, Norton WT. 1982. Glycerol phosphate dehydrogenase, glucose-6-phosphate dehydrogenase, and lactate dehydrogenase: Activities in oligodendrocytes, neurons, astrocytes, and myelin isolated from developing rat brains. *J Neurochem* 38: 360-367.
- Cammer W, Zimmerman TR Jr. 1982. Glycerolphosphate dehydrogenase, glucose-6-phosphate dehydrogenase, lactate dehydrogenase and carbonic anhydrase activities in oligodendrocytes and myelin: Comparisons between species and CNS regions. *Brain Res* 282: 21-26.
- Cho SW, Joshi JG. 1989. Inactivation of glucose-6-phosphate dehydrogenase isozymes from human and pig brain by aluminum. *J Neurochem* 53: 616-621.
- Clarke DD, Sokoloff L. 1999. Circulation and energy metabolism of the brain. *Basic neurochemistry*. Siegel GJ, Agranoff BW, Albers RW, Fisher SK, Uhler MD, editors. New York: Lippincott Williams & Wilkins; pp. 637-669.
- Clarke JL, Mason PJ. 2003. Murine hexose-6-phosphate dehydrogenase: A bifunctional enzyme with broad substrate specificity and 6-phosphogluconolactonase activity. *Arch Biochem Biophys* 415: 229-234.
- Clement MV, Long LH, Ramalingam J, Halliwell B. 2002. The cytotoxicity of dopamine may be an artefact of cell culture. *J Neurochem* 81: 414-421.
- Cohen P, Rosemeyer MA. 1969. Subunit interactions of glucose-6-phosphate dehydrogenase from human erythrocytes. *Eur J Biochem* 8: 8-15.
- Collard F, Collet JF, Gerin I, Veiga-da-Cunha M, Van Schaftingen E. 1999. Identification of the cDNA encoding human 6-phosphogluconolactonase, the enzyme catalyzing the second step of the pentose phosphate pathway(1). *FEBS Lett* 459: 223-226.
- Colombo E, Banki K, Tatum AH, Daucher J, Ferrante P, et al. 1997. Comparative analysis of antibody and cell-mediated autoimmunity to transaldolase and myelin basic protein in patients with multiple sclerosis. *J Clin Invest* 99: 1238-1250.
- Colton CA, Gilbert DL. 1987. Production of superoxide anions by a CNS macrophage, the microglia. *FEBS Lett* 223: 284-288.
- Conley A, Hinshelwood M. 2001. Mammalian aromatases. *Reproduction* 121: 685-695.
- Cunnane SC, Menard CR, Likhodii SS, Brenna JT, Crawford MA. 1999. Carbon recycling into de novo lipogenesis is a major pathway in neonatal metabolism of linoleate and alpha-linolenate. *Prostaglandins Leukot Essent Fatty Acids* 60: 387-392.
- de Almeida AF, Curi R, Newsholme P, Newsholme EA. 1989. Maximal activities of key enzymes of glutaminolysis, glycolysis, Krebs cycle and pentose-phosphate pathway of several tissues in mature and aged rats. *Int J Biochem* 21: 937-940.
- Domanska-Janik K. 1988. Hexose monophosphate pathway activity in normal and hypoxic rat brain. *Resuscitation* 16: 79-90.
- Dringen R. 2000. Metabolism and functions of glutathione in brain. *Prog Neurobiol* 62: 649-671.
- Dringen R. 2005. Oxidative and anti-oxidative potential of brain microglial cells. *Antioxid Redox Signal* 7: 1223-1233.
- Dringen R, Gutterer JM. 2002. Glutathione reductase from bovine brain. *Methods Enzymol* 348: 281-288.
- Dringen R, Hamprecht B. 1997. Involvement of glutathione peroxidase and catalase in the disposal of exogenous

- hydrogen peroxide by cultured astroglial cells. *Brain Res* 759: 67-75.
- Dringen R, Hirrlinger J. 2003. Glutathione pathways in the brain. *Biol Chem* 384: 505-516.
- Dringen R, Kussmaul L, Hamprecht B. 1998. Rapid clearance of tertiary butyl hydroperoxide by cultured astroglial cells via oxidation of glutathione. *Glia* 23: 139-145.
- Dringen R, Pawlowski PG, Hirrlinger J. 2005. Peroxide detoxification by brain cells. *J Neurosci Res* 79: 157-165.
- Edmond J, Robbins RA, Bergstrom JD, Cole RA, de Vellis J. 1987. Capacity for substrate utilization in oxidative metabolism by neurons, astrocytes, and oligodendrocytes from developing brain in primary culture. *J Neurosci Res* 18: 551-561.
- Eftekharpour E, Holmgren A, Juurlink BH. 2000. Thioredoxin reductase and glutathione synthesis is upregulated by t-butylhydroquinone in cortical astrocytes but not in cortical neurons. *Glia* 31: 241-248.
- Egan RM, Sable HZ. 1981. Transketolase kinetics. The slow reconstitution of the holoenzyme is due to rate-limiting dimerization of the subunits. *J Biol Chem* 256: 4877-4883.
- El-Hassan A, Zubairu S, Hothersall JS, Greenbaum AL. 1981. Age-related changes in enzymes of rat brain. 1. Enzymes of glycolysis, the pentose phosphate pathway and lipogenesis. *Enzyme* 26: 107-112.
- Esplugues JV. 2002. NO as a signalling molecule in the nervous system. *Br J Pharmacol* 135: 1079-1095.
- Esposito M, Venkatesh V, Otvos L, Weng Z, Vajda S, et al. 1999. Human transaldolase and cross-reactive viral epitopes identified by autoantibodies of multiple sclerosis patients. *J Immunol* 163: 4027-4032.
- Felix K, Rockwood LD, Pretsch W, Nair J, Bartsch H, et al. 2002. Moderate G6PD deficiency increases mutation rates in the brain of mice. *Free Radic Biol Med* 32: 663-673.
- Filosa S, Fico A, Paglialonga F, Balestrieri M, Crooke A, et al. 2003. Failure to increase glucose consumption through the pentose-phosphate pathway results in the death of glucose-6-phosphate dehydrogenase gene-deleted mouse embryonic stem cells subjected to oxidative stress. *Biochem J* 370: 935-943.
- Friede RL, Bischhausen R. 1978. How do axons control myelin formation? The model of 6-aminonicotinamide neuropathy. *J Neurol Sci* 35: 341-353.
- Friede RL, Fleming LM, Knoller M. 1963. A comparative mapping of enzymes involved in hexosemonophosphate shunt and citric acid cycle in the brain. *J Neurochem* 10: 263-277.
- Gaitonde MK, Evison E, Evans GM. 1983. The rate of utilization of glucose via hexosemonophosphate shunt in brain. *J Neurochem* 41: 1253-1260.
- García-Nogales P, Almeida A, Bolaños JP. 2003. Peroxynitrite protects neurons against nitric oxide-mediated apoptosis. A key role for glucose-6-phosphate dehydrogenase activity in neuroprotection. *J Biol Chem* 278: 864-874.
- García-Nogales P, Almeida A, Fernández E, Medina JM, Bolaños JP. 1999. Induction of glucose-6-phosphate dehydrogenase by lipopolysaccharide contributes to preventing nitric oxide-mediated glutathione depletion in cultured rat astrocytes. *J Neurochem* 72: 1750-1758.
- Gibson GE, Ksiezak-Reding H, Sheu KF, Mykytyn V, Blass JP. 1984. Correlation of enzymatic, metabolic, and behavioral deficits in thiamin deficiency and its reversal. *Neurochem Res* 9: 803-814.
- Gibson GE, Sheu KF, Blass JP, Baker A, Carlson KC, et al. 1988. Reduced activities of thiamine-dependent enzymes in the brains and peripheral tissues of patients with Alzheimer's disease. *Arch Neurol* 45: 836-840.
- Giguère JF, Butterworth RF. 1987. Activities of thiamine-dependent enzymes in two experimental models of thiamine deficiency encephalopathy: 3. Transketolase. *Neurochem Res* 12: 305-310.
- Giuffrida AM. 1983. Nucleic acids in developing brain. *Handbook of neurochemistry*. Lajtha A, editor. New York: Plenum Press; pp. 227-250.
- Gordon G, Mackow MC, Levy HR. 1995. On the mechanism of interaction of steroids with human glucose 6-phosphate dehydrogenase. *Arch Biochem Biophys* 318: 25-29.
- Green SP, Cairns B, Rae J, Errett-Baroncini C, Hongo JA, et al. 2001. Induction of gp91-phox, a component of the phagocyte NADPH oxidase, in microglial cells during central nervous system inflammation. *J Cereb Blood Flow Metab* 21: 374-384.
- Griffiths IR, Kelly PA, Grome JJ. 1981. Glucose utilization in the central nervous system in the acute gliopathy due to 6-aminonicotinamide. *Lab Invest* 44: 547-552.
- Gromer S, Urig S, Becker K. 2004. The thioredoxin system—from science to clinic. *Med Res Rev* 24: 40-89.
- Guerra RM, Melgar E, Villavicencio M. 1967. Alternative pathways of glucose metabolism in fetal rat brain. *Biochim Biophys Acta* 148: 356-361.
- Gutterer JM, Dringen R, Hirrlinger J, Hamprecht B. 1999. Purification of glutathione reductase from bovine brain, generation of an antiserum, and immunocytochemical localization of the enzyme in neural cells. *J Neurochem* 73: 1422-1430.
- Halliwell B. 2001. Role of free radicals in the neurodegenerative diseases: Therapeutic implications for antioxidant treatment. *Drugs Aging* 18: 685-716.
- Halliwell B, Gutteridge JMC. 1999. *Free Radicals in Biology and Medicine*. New York: Oxford University Press.
- Hassel B. 2000. Carboxylation and anaplerosis in neurons and glia. *Mol Neurobiol* 22: 21-40.
- Heap LC, Pratt OE, Ward RJ, Waller S, Thomson AD, et al. 2002. Individual susceptibility to Wernicke-Korsakoff

- syndrome and alcoholism-induced cognitive deficit: Impaired thiamine utilization found in alcoholics and alcohol abusers. *Psychiatr Genet* 12: 217-224.
- Hedlund E, Gustafsson JA, Warner M. 2001. Cytochrome P450 in the brain; a review. *Curr Drug Metab* 2: 245-263.
- Heinrich PC, Morris HP, Weber G. 1976. Behavior of transaldolase (EC 2. 2.1.2) and transketolase (EC 2.2.1.1) activities in normal, neoplastic, differentiating, and regenerating liver. *Cancer Res* 36: 3189-3197.
- Herken H, Lange K, Kolbe H. 1969. Brain disorders induced by pharmacological blockade of the pentose phosphate pathway. *Biochem Biophys Res Commun* 36: 93-100.
- Herken H, Meyer-Estorf G, Halbhüner K, Loos D. 1976. Spastic paresis after 6-aminonicotinamide: Metabolic disorders in the spinal cord and electromyographically recorded changes in the hind limbs of rats. *Naunyn Schmiedebergs Arch Pharmacol* 293: 245-255.
- Héroux M, Raghavendra RV, Lavoie J, Richardson JS, Butterworth RF. 1996. Alterations of thiamine phosphorylation and of thiamine-dependent enzymes in Alzheimer's disease. *Metab Brain Dis* 11: 81-88.
- Hirrlinger J, Schulz JB, Dringen R. 2002. Effects of dopamine on the glutathione metabolism of cultured astroglial cells: Implications for Parkinson's disease. *J Neurochem* 82: 458-467.
- Hothersall JS, Baquer N, Greenbaum AL, McLean P. 1979. Alternative pathways of glucose utilization in brain. Changes in the pattern of glucose utilization in brain during development and the effect of phenazine methosulfate on the integration of metabolic routes. *Arch Biochem Biophys* 198: 478-492.
- Hothersall JS, Greenbaum AL, McLean P. 1982. The functional significance of the pentose phosphate pathway in synaptosomes: Protection against peroxidative damage by catecholamines and oxidants. *J Neurochem* 39: 1325-1332.
- Huck JH, Verhoeven NM, Struys EA, Salomons GS, Jakobs C, et al. 2004. Ribose-5-phosphate isomerase deficiency: New inborn error in the pentose phosphate pathway associated with a slowly progressive leukoencephalopathy. *Am J Hum Genet* 74: 745-751.
- Innis SM. 2003. Perinatal biochemistry and physiology of long-chain polyunsaturated fatty acids. *J Pediatr* 143: S1-S8.
- Istvan ES, Deisenhofer J. 2000. The structure of the catalytic portion of human HMG-CoA reductase. *Biochim Biophys Acta* 1529: 9-18.
- Iwata H, Tonomura H, Matsuda T. 1988. Transketolase and 2-oxoglutarate dehydrogenase activities in the brain and liver of the developing rat. *Experientia* 44: 780-781.
- Jacquín-Becker C, Labourdette G. 1997. Regulation of aldose reductase expression in rat astrocytes in culture. *Glia* 20: 135-144.
- Jeffery J, Jörnvall H. 1983. Enzyme relationships in a sorbitol pathway that bypasses glycolysis and pentose phosphates in glucose metabolism. *Proc Natl Acad Sci USA* 80: 901-905.
- Jeyasingham MD, Pratt OE. 1988. Rat brain apotransketolase: Activation and inactivation. *J Neurochem* 50: 1537-1541.
- Jeyasingham MD, Pratt OE, Thomson AD, Shaw GK. 1986. Reduced stability of rat brain transketolase after conversion to the apo form. *J Neurochem* 47: 278-281.
- Jo SH, Son MK, Koh HJ, Lee SM, Song IH, et al. 2001. Control of mitochondrial redox balance and cellular defense against oxidative damage by mitochondrial NADP⁺-dependent isocitrate dehydrogenase. *J Biol Chem* 276: 16168-16176.
- Katsurada A, Iritani N, Fukuda H, Matsumura Y, Noguchi T, et al. 1989. Effects of nutrients and insulin on transcriptional and post-transcriptional regulation of glucose-6-phosphate dehydrogenase synthesis in rat liver. *Biochim Biophys Acta* 1006: 104-110.
- Kauffman FC. 1972. The quantitative histochemistry of enzymes of the pentose phosphate pathway in the central nervous system of the rat. *J Neurochem* 19: 1-9.
- Kirsch M, de Groot H. 2001. NAD(P)H, a directly operating antioxidant? *FASEB J* 15: 1569-1574.
- Kletzien RF, Harris PK, Foellmi LA. 1994. Glucose-6-phosphate dehydrogenase: A "housekeeping" enzyme subject to tissue-specific regulation by hormones, nutrients, and oxidant stress. *FASEB J* 8: 174-181.
- Kriegelstein J, Stock R. 1975. Decreased glycolytic flux rate in the isolated perfused rat brain after pretreatment with 6-aminonicotinamide. *Naunyn Schmiedebergs Arch Pharmacol* 290: 323-327.
- Kruger NJ, von Schaeuwen A. 2003. The oxidative pentose phosphate pathway: Structure and organisation. *Curr Opin Plant Biol* 6: 236-246.
- Krum JM. 1995. Age-dependent susceptibility of CNS glial populations in situ to the antimetabolite 6-aminonicotinamide. *Mol Chem Neuropathol* 26: 79-94.
- Kurz GM, Wiesinger H, Hamprecht B. 1993. Purification of cytosolic malic enzyme from bovine brain, generation of monoclonal antibodies, and immunocytochemical localization of the enzyme in glial cells of neural primary cultures. *J Neurochem* 60: 1467-1474.
- Kussmaul L, Hamprecht B, Dringen R. 1999. The detoxification of cumene hydroperoxide by the glutathione system of cultured astroglial cells hinges on hexose availability for the regeneration of NADPH. *J Neurochem* 73: 1246-1253.
- Kwee IL, Igarashi H, Nakada T. 1996. Aldose reductase and sorbitol dehydrogenase activities in diabetic brain: In vivo kinetic studies using 19F 3-FDG NMR in rats. *Neuroreport* 7: 726-728.
- Lakhman SS, Sharma P, Kaur G, Kaur G. 1994. Changes in glucose metabolism from discrete regions of rat brain and

- its relationship to reproductive failure during experimental diabetes. *Mol Cell Biochem* 141: 97-102.
- Landino LM, Iwig JS, Kennett KL, Moynihan KL. 2004. Repair of peroxynitrite damage to tubulin by the thioredoxin reductase system. *Free Radic Biol Med* 36: 497-506.
- Lange K, Kolbe H, Keller K, Herken H. 1970. Der Kohlenhydratstoffwechsel des Gehirns nach Blockade des Pentose-Phosphat-Weges durch 6-Aminonicotinsäureamid. *Hoppe-Seyler's Z Physiol Chem* 351: 1241-1252.
- Lavigne MC, Malech HL, Holland SM, Leto TL. 2001. Genetic requirement of p47phox for superoxide production by murine microglia. *FASEB J* 15: 285-287.
- Lee AY, Chung SS. 1999. Contributions of polyol pathway to oxidative stress in diabetic cataract. *FASEB J* 13: 23-30.
- Lee SM, Koh HJ, Park DC, Song BJ, Huh TL, et al. 2002. Cytosolic NADP(+)-dependent isocitrate dehydrogenase status modulates oxidative damage to cells. *Free Radic Biol Med* 32: 1185-1196.
- Leong SF, Clark JB. 1984. Regional enzyme development in rat brain. Enzymes associated with glucose utilization. *Biochem J* 218: 131-138.
- Levy HR, Vought VE, Yin X, Adams MJ. 1996. Identification of an arginine residue in the dual coenzyme-specific glucose-6-phosphate dehydrogenase from *Leuconostoc mesenteroides* that plays a key role in binding NADP+ but not NAD+. *Arch Biochem Biophys* 326: 145-151.
- Loreck DJ, Galarraga J, Van der FJ, Phang JM, Smith BH, et al. 1987. Regulation of the pentose phosphate pathway in human astrocytes and gliomas. *Metab Brain Dis* 2: 31-46.
- Luzzatto L, Mehta A, Vulliamy T. 2001. Glucose 6-phosphate dehydrogenase deficiency. The metabolic & molecular base of inherited disease. Scriver CR, Beaudet AL, Sly WS, Valle D, editors. New York: McGraw-Hill; pp. 4517-4553.
- Maeng O, Kim YC, Shin HJ, Lee JO, Huh TL, et al. 2004. Cytosolic NADP(+)-dependent isocitrate dehydrogenase protects macrophages from LPS-induced nitric oxide and reactive oxygen species. *Biochem Biophys Res Commun* 317: 558-564.
- Martins RN, Harper CG, Stokes GB, Masters CL. 1986a. Increased cerebral glucose-6-phosphate dehydrogenase activity in Alzheimer's disease may reflect oxidative stress. *J Neurochem* 46: 1042-1045.
- Martins RN, Stokes GB, Masters CL. 1986b. Regulation of liver and brain hexose monophosphate dehydrogenases by insulin and dietary intake in the female rat. *Mol Cell Biochem* 70: 169-175.
- Mason PJ, Stevens D, Diez A, Knight SW, Scopes DA, et al. 1999. Human hexose-6-phosphate dehydrogenase (glucose 1-dehydrogenase) encoded at 1p36: Coding sequence and expression. *Blood Cells Mol Dis* 25: 30-37.
- Massod MF, McGuire SL, Werner KR. 1971. Analysis of blood transketolase activity. *Am J Clin Pathol* 55: 465-470.
- Mauch DH, Nägler K, Schumacher S, Göritz C, Müller EC, et al. 2001. CNS synaptogenesis promoted by glia-derived cholesterol. *Science* 294: 1354-1357.
- Medina JM, Taberero A. 2002. Astrocyte-synthesized oleic acid behaves as a neurotrophic factor for neurons. *J Physiol Paris* 96: 265-271.
- Meske V, Albert F, Richter D, Schwarze J, Ohm TG. 2003. Blockade of HMG-CoA reductase activity causes changes in microtubule-stabilizing protein tau via suppression of geranylgeranylpyrophosphate formation: Implications for Alzheimer's disease. *Eur J Neurosci* 17: 93-102.
- Miclet E, Stoven V, Michels PA, Opperdoes FR, Lallemand JY, et al. 2001. NMR spectroscopic analysis of the first two steps of the pentose-phosphate pathway elucidates the role of 6-phosphogluconolactonase. *J Biol Chem* 276: 34840-34846.
- Minich T, Yokota S, Dringen R. 2003. Cytosolic and mitochondrial isoforms of NADP+-dependent isocitrate dehydrogenases are expressed in cultured rat neurons, astrocytes, oligodendrocytes and microglial cells. *J Neurochem* 86: 605-614.
- Molina JA, Jimenez-Jimenez FJ, Hernanz A, Fernandez-Vivancos E, Medina S, et al. 2002. Cerebrospinal fluid levels of thiamine in patients with Alzheimer's disease. *J Neural Transm* 109: 1035-1044.
- Moore SA. 2001. Polyunsaturated fatty acid synthesis and release by brain-derived cells in vitro. *J Mol Neurosci* 16: 195-200.
- Mukhopadhyay D, Mukherjea M. 1994. Inhibition of two HMP shunt pathway enzymes by fatty acids and their CoA esters in developing human brain: Role of fatty acid binding protein. *Indian J Biochem Biophys* 31: 464-468.
- Murphy S. 2000. Production of nitric oxide by glial cells: Regulation and potential roles in the CNS. *Glia* 29: 1-13.
- Nagatsu T. 2004. Progress in monoamine oxidase (MAO) research in relation to genetic engineering. *Neurotoxicology* 25: 11-20.
- Nasr LB, Monet JD, Lucas P, Bader CA. 1989. Vitamin D3 and glucose-6-phosphate dehydrogenase in rat duodenal epithelial cells. *Am J Physiol* 257: G760-G765.
- Ng TF, Lee FK, Song ZT, Calcutt NA, Lee AY, et al. 1998. Effects of sorbitol dehydrogenase deficiency on nerve conduction in experimental diabetic mice. *Diabetes* 47: 961-966.
- Niedermüller H. 1986. Effects of aging on the recycling via the pentose cycle and on the kinetics of glycogen and protein metabolism in various organs of the rat. *Arch Gerontol Geriatr* 5: 305-316.
- Ninfali P, Aluigi G, Balduini W, Pompella A. 1997. Glucose-6-phosphate dehydrogenase activity is higher in the olfactory bulb than in other brain areas. *Brain Res* 744: 138-142.

- Ninfali P, Aluigi G, Pompella A. 1998. Postnatal expression of glucose-6-phosphate dehydrogenase in different brain areas. *Neurochem Res* 23: 1197-1204.
- Ninfali P, Ditroilo M, Capellacci S, Biagiotti E. 2001. Rabbit brain glucose-6-phosphate dehydrogenase: Biochemical properties and inactivation by free radicals and 4-hydroxy-2-nonenal. *Neuroreport* 12: 4149-4153.
- Novello F, McLean P. 1968. The pentose phosphate pathway of glucose metabolism. *Biochem J* 107: 775-791.
- O'Brien MM, Schofield PJ. 1980. Polyol-pathway enzymes of human brain. Partial purification and properties of aldose reductase and hexonate dehydrogenase. *Biochem J* 187: 21-30.
- Palmer AM. 1999. The activity of the pentose phosphate pathway is increased in response to oxidative stress in Alzheimer's disease. *J Neural Transm* 106: 317-328.
- Pandolfi PP, Sonati F, Rivi R, Mason P, Grosveld F, et al. 1995. Targeted disruption of the housekeeping gene encoding glucose 6-phosphate dehydrogenase (G6PD): G6PD is dispensable for pentose synthesis but essential for defense against oxidative stress. *EMBO J* 14: 5209-5215.
- Pannunzio P, Hazell AS, Pannunzio M, Rao KV, Butterworth RF. 2000. Thiamine deficiency results in metabolic acidosis and energy failure in cerebellar granule cells: An in vitro model for the study of cell death mechanisms in Wernicke's encephalopathy. *J Neurosci Res* 62: 286-292.
- Pitkin SR, Savage LM. 2001. Aging potentiates the acute and chronic neurological symptoms of pyriethamine-induced thiamine deficiency in the rodent. *Behav Brain Res* 119: 167-177.
- Prothmann C, Wellard J, Berger J, Hamprecht B, Verleysdonk S. 2001. Primary cultures as a model for studying ependymal functions: Glycogen metabolism in ependymal cells. *Brain Res* 920: 74-83.
- Puglielli L, Tanzi RE, Kovacs DM. 2003. Alzheimer's disease: The cholesterol connection. *Nat Neurosci* 6: 345-351.
- Qi K, Hall M, Deckelbaum RJ. 2002. Long-chain polyunsaturated fatty acid accretion in brain. *Curr Opin Clin Nutr Metab Care* 5: 133-138.
- Rahman B, Kussmaul L, Hamprecht B, Dringen R. 2000. Glycogen is mobilized during the disposal of peroxides by cultured astroglial cells from rat brain. *Neurosci Lett* 290: 169-172.
- Reiss AB, Siller KA, Rahman MM, Chan ES, Ghiso J, et al. 2004. Cholesterol in neurologic disorders of the elderly: Stroke and Alzheimer's disease. *Neurobiol Aging* 25: 977-989.
- Ross BD, Kingsley PB, Ben Yoseph O. 1994. Measurement of pentose phosphate-pathway activity in a single incubation with [1,6-¹³C₂,6,6-²H₂]glucose. *Biochem J* 302 (Pt 1): 31-38.
- Russell RL, Siedlak SL, Raina AK, Bautista JM, Smith MA, et al. 1999. Increased neuronal glucose-6-phosphate dehydrogenase and sulfhydryl levels indicate reductive compensation to oxidative stress in Alzheimer disease. *Arch Biochem Biophys* 370: 236-239.
- Rust RS Jr, Carter JG, Martin D, Nerbonne JM, Lampe PA, et al. 1991. Enzyme levels in cultured astrocytes, oligodendrocytes and Schwann cells, and neurons from the cerebral cortex and superior cervical ganglia of the rat. *Neurochem Res* 16: 991-999.
- Sankarapandi S, Zweier JL, Mukherjee G, Quinn MT, Huso DL. 1998. Measurement and characterization of superoxide generation in microglial cells: Evidence for an NADPH oxidase-dependent pathway. *Arch Biochem Biophys* 353: 312-321.
- Schedin S, Nilsson M, Chojnacki T, Dallner G. 1998. Alterations in the biosynthesis of cholesterol, dolichol and dolichyl-P in the genetic cholesterol homeostasis disorder, Niemann-Pick type C disease. *Biochim Biophys Acta* 1394: 177-186.
- Schenk G, Dugleby RG, Nixon PF. 1998. Heterologous expression of human transketolase. *Int J Biochem Cell Biol* 30: 369-378.
- Schulz JG, Bosel J, Stoeckel M, Megow D, Dirnagl U, et al. 2004. HMG-CoA reductase inhibition causes neurite loss by interfering with geranylgeranylpyrophosphate synthesis. *J Neurochem* 89: 24-32.
- Sedlak TW, Snyder SH. 2004. Bilirubin benefits: Cellular protection by a biliverdin reductase antioxidant cycle. *Pediatrics* 113: 1776-1782.
- Sengupta T, Datta C, Dasgupta J, De K, De S, et al. 1985. Role of hexosemonophosphate shunt pathway in glucose metabolism in developing human foetal brain. *Indian J Biochem Biophys* 22: 208-210.
- Sheu KF, Calingasan NY, Diemel GA, Baker H, Jung EH, et al. 1996. Regional reductions of transketolase in thiamine-deficient rat brain. *J Neurochem* 67: 684-691.
- Singh R, Pathak DN. 1990. Lipid peroxidation and glutathione peroxidase, glutathione reductase, superoxide dismutase, catalase, and glucose-6-phosphate dehydrogenase activities in FeCl₃-induced epileptogenic foci in the rat brain. *Epilepsia* 31: 15-26.
- Sinicropi DV, Kauffman FC. 1979. Retrograde alteration of 6-phosphogluconate dehydrogenase in axotomized superior cervical ganglia of the rat. *J Biol Chem* 254: 3011-3017.
- Slezak M, Pfrieger FW. 2003. New roles for astrocytes: Regulation of CNS synaptogenesis. *Trends Neurosci* 26: 531-535.
- Smith ER, Barker KL. 1974. Effects of estradiol and nicotinamide adenine dinucleotide phosphate on the rate of

- synthesis of uterine glucose 6-phosphate dehydrogenase. *J Biol Chem* 249: 6541-6547.
- Song HP, Das B, Srivastava SK. 1987. Microdetermination of aldose and aldehyde reductases from human tissues. *Curr Eye Res* 6: 1001-1006.
- Soucek T, Cumming R, Dargusch R, Maher P, Schubert D. 2003. The regulation of glucose metabolism by HIF-1 mediates a neuroprotective response to amyloid beta peptide. *Neuron* 39: 43-56.
- Spence AM, Graham MM, Muzi M, Freeman SD, Link JM, et al. 1997. Feasibility of imaging pentose cycle glucose metabolism in gliomas with PET: Studies in rat brain tumor models. *J Nucl Med* 38: 617-624.
- Spencer N, Hopkinson DA. 1980. Biochemical genetics of the pentose phosphate cycle: Human ribose 5-phosphate isomerase (RPI) and ribulose 5-phosphate 3-epimerase (RPE). *Ann Hum Genet* 43: 335-342.
- Strobel HW, Thompson CM, Antonovic L. 2001. Cytochromes P450 in brain: Function and significance. *Curr Drug Metab* 2: 199-214.
- Sykes JEC, Lopez-Cardozo M, van den Bergh SG. 1986. Relationship between the pentose-phosphate pathway and the de novo synthesis of fatty acids and cholesterol in oligodendrocyte-enriched glial cultures. *Neurochem Int* 8: 77-82.
- Tian WN, Braunstein LD, Pang J, Stuhlmeier KM, Xi QC, et al. 1998. Importance of glucose-6-phosphate dehydrogenase activity for cell growth. *J Biol Chem* 273: 10609-10617.
- Tyson RL, Perron J, Sutherland GR. 2000. 6-Aminonicotinamide inhibition of the pentose phosphate pathway in rat neocortex. *Neuroreport* 11: 1845-1848.
- Ulus NN, Sahilli M, Avci A, Canbolat O, Ozansoy G, et al. 2003. Pentose phosphate pathway, glutathione-dependent enzymes and antioxidant defense during oxidative stress in diabetic rodent brain and peripheral organs: Effects of stobadine and vitamin E. *Neurochem Res* 28: 815-823.
- Vallejo CG, Marco R, Sebastian J. 1971. The glucose 6-phosphate metabolic crossroads in brain. Studies at the enzyme level. *Arch Biochem Biophys* 147: 41-48.
- Vogel R, Hamprecht B, Wiesinger H. 1998a. Malic enzyme isoforms in astrocytes: Comparative study on activities in rat brain tissue and astroglia-rich primary cultures. *Neurosci Lett* 247: 123-126.
- Vogel R, Jennemann G, Seitz J, Wiesinger H, Hamprecht B. 1998b. Mitochondrial malic enzyme: Purification from bovine brain, generation of an antiserum, and immunocytochemical localization in neurons of rat brain. *J Neurochem* 71: 844-852.
- Vogel R, Wiesinger H, Hamprecht B, Dringen R. 1999. The regeneration of reduced glutathione in rat forebrain mitochondria identifies metabolic pathways providing the NADPH required. *Neurosci Lett* 275: 97-100.
- Wagner KR, Sharp FR, Ardizzone TD, Lu A, Clark JF. 2003. Heme and iron metabolism: Role in cerebral hemorrhage. *J Cereb Blood Flow Metab* 23: 629-652.
- Wang JJ, Martin PR, Singleton CK. 1997. A transketolase assembly defect in a Wernicke-Korsakoff syndrome patient. *Alcohol Clin Exp Res* 21: 576-580.
- Weisz KS, Schofield PJ, Edwards MR. 1985. Human brain 6-phosphogluconate dehydrogenase: Purification and kinetic properties. *J Neurochem* 44: 510-517.
- Wiesinger H. 2001. Arginine metabolism and the synthesis of nitric oxide in the nervous system. *Prog Neurobiol* 64: 365-391.
- Wiesinger H, Thiess U, Hamprecht B. 1990. Sorbitol pathway activity and utilization of polyols in astroglia-rich primary cultures. *Glia* 3: 277-282.
- Winkler BS, DeSantis N, Solomon F. 1986. Multiple NADPH-producing pathways control glutathione (GSH) content in retina. *Exp Eye Res* 43: 829-847.
- Wood T. 1974. The detection and occurrence of multiple forms of D-ribose 5-phosphate ketol isomerase. *Arch Biochem Biophys* 160: 40-46.
- Wood T. 1986. Physiological functions of the pentose phosphate pathway. *Cell Biochem Funct* 4: 241-247.
- Xu ZP, Wawrousek EF, Piatigorsky J. 2002. Transketolase haploinsufficiency reduces adipose tissue and female fertility in mice. *Mol Cell Biol* 22: 6142-6147.
- Yoshida S, Saitoh T, Takeshita M. 1988. Hydrogen transfer by NADPH-dependent reductases in elongation of very-long-chain saturated and polyunsaturated fatty-acyl-CoA in swine cerebral microsomes. *Biochim Biophys Acta* 958: 361-367.
- Zakhary R, Poss KD, Jaffrey SR, Ferris CD, Tonegawa S, et al. 1997. Targeted gene deletion of heme oxygenase 2 reveals neural role for carbon monoxide. *Proc Natl Acad Sci USA* 94: 14848-14853.
- Zekry D, Epperson TK, Krause KH. 2003. A role for NOX NADPH oxidases in Alzheimer's disease and other types of dementia? *IUBMB Life* 55: 307-313.
- Zimatkin SM, Zimatkina TI. 1996. Thiamine deficiency as predisposition to, and consequence of, increased alcohol consumption. *Alcohol* 31: 421-427.
- Zimmer HG, Lankat-Buttgereit B, Kolbeck-Rühmkorff C, Nagano T, Zierhut W. 1992. Effects of norepinephrine on the oxidative pentose phosphate pathway in the rat heart. *Circ Res* 71: 451-459.
- Zubaran C, Fernandes JG, Rodnight R. 1997. Wernicke-Korsakoff syndrome. *Postgrad Med J* 73: 27-31.

1.4 The Cerebral Tricarboxylic Acid Cycles

T. B. Rodrigues · S. Cerdán

1	Introduction	64
2	The Cerebral Tricarboxylic Acid Cycle	67
2.1	Regionalization and Subcellular Distribution	70
2.2	Regulation	72
3	Methodologies to Investigate Tricarboxylic Acid Cycle Activity	72
3.1	Radioactive Procedures	73
3.2	Nuclear Magnetic Resonance Methods	74
3.3	Dual Photon NADH Fluorescence Microscopy	79
4	The Cerebral Tricarboxylic Acid Cycles During Cerebral Activation	79
4.1	The Metabolic Coupling Hypothesis	79
4.2	¹³ C NMR Evidences and the Neuronal Tricarboxylic Acid Cycle	80
4.3	The Astroglial Tricarboxylic Acid Cycle	82
4.4	The Redox Switch and the Redox Coupling Hypothesis	83
4.5	NADH Balance in Neurons and Glia During Cerebral Activation	85
5	Concluding Remarks and Future Perspectives	86

Abstract: We review the operation of the cerebral tricarboxylic acid (TCA) cycles in the neuronal and glial compartments of the adult rat brain, with an emphasis on the mechanisms underlying intercellular oxidative coupling during glutamatergic neurotransmission. We begin with an update of the enzymatic properties, gene location, regulation, and regional distribution of the enzymes involved. Then, we describe the main methodologies used to investigate TCA cycle activity *in vitro* and *in vivo* such as autoradiography, positron emission tomography (PET), nuclear magnetic resonance (NMR) imaging or spectroscopy, and dual photon fluorescence microscopy. Previous interpretations conceived cerebral glucose metabolism during glutamatergic neurotransmission as a coupled process, involving exclusively anaerobic metabolism in the astrocytes and oxidative metabolism in the neurons. The glutamine cycle was proposed to be stoichiometrically coupled to astrocytic glucose uptake, glutamine synthesis being supported by astrocytic glycolysis only and glutamine being the main precursor of cerebral glutamate. Compelling evidences have accumulated since then, showing that (i) astrocytes display significant oxidative capacity *in vivo*, (ii) more than 60% of the glutamine is produced from ATP synthesized by astroglial oxidative phosphorylation, and (iii) approximately 40% of cerebral glutamate is not derived from glutamine. Together, these findings suggest that the coupling mechanisms between astrocytic and neuronal oxidative and nonoxidative metabolisms are more complex than initially envisioned. In this review, we propose a novel mechanism based on the operation of intracellular redox switches and the transcellular coupling of the NAD(P)/NAD(P)H redox states between both cell types through lactate transfers. The redox switch/redox coupling hypothesis is compatible with the simultaneous operation of glycolytic and oxidative metabolisms in both neural cell types. Transcellular redox coupling through lactate transfers mimics the intracellular coupling existing between cytosolic NADH production and mitochondrial NADH oxidation, as seen from the redox shuttles exchanging reducing equivalents through the inner mitochondrial membrane of neural cells.

List of Abbreviations: Aco, aconitase (EC 4.2.1.3); CS, citrate synthase (EC 2.3.3.1); Cr, creatine; Cho, choline; FDG, 2-fluorodeoxyglucose; fMRI, functional magnetic resonance imaging; Fum, fumarase (EC 4.2.1.2); GABA: γ -aminobutyric acid; GAPDH, glyceraldehyde-3-phosphate dehydrogenase (EC 1.2.1.12); GDH, glutamate dehydrogenase (NAD: EC 1.4.1.2, NADP: EC 1.4.1.4); ICDH, isocitrate dehydrogenase (NAD EC 1.1.1.41, NADP; EC 1.1.1.42); Ino, *myo*-inositol; α -KG, α -ketoglutarate; α -KGDH, α -ketoglutarate dehydrogenase (EC 1.2.4.2); LDH, lactate dehydrogenase (EC 1.1.1.27); MDH, malate dehydrogenase (EC 1.1.1.37); MSO, methionine sulfoximine; NMR, nuclear magnetic resonance; NAA, *N*-acetyl aspartic acid; OAA, oxalacetate; PCr, phosphocreatine; PDE, phosphodiesterases; PDHC, pyruvate dehydrogenase complex (EC 1.2.4.1); PET, positron emission tomography; P_g , cytosolic pyruvate pool derived from glucose; P_i , inorganic phosphate; PME, phosphomonoesters; P_p , cytosolic pyruvate pool derived from extracellular lactate; SDH, succinate dehydrogenase (EC 1.3.5.1); TCA, tricarboxylic acid cycle; TFA, trifluoroacetic acid; V_{cycle} , glutamine cycle flux; V_{TCAg} , astroglial tricarboxylic acid cycle; V_{TCAn} , neuronal tricarboxylic acid cycle; V_x , global α -ketoglutarate/glutamate exchange

Everything should be made as simple as possible, but not simpler.

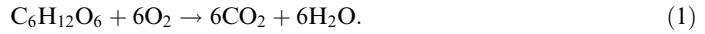
Albert Einstein

1 Introduction

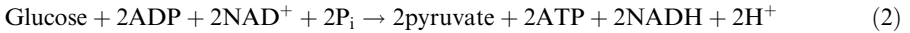
The tricarboxylic acid (TCA) cycle plays a central role in cerebral metabolism, providing the main pathway where carbohydrates, fats, and amino acids are oxidized to obtain the energy needed to maintain cerebral functions (Dienel, 2002; Hertz and Dienel, 2002). It also fulfills a fundamental role, providing intermediates for many cerebral biosynthetic processes and neurotransmitters such as glutamate and γ -aminobutyric acid (GABA) (Gruetter, 2002; Owen et al., 2002). Pioneering work, performed shortly after its discovery in 1937, allowed the understanding of the basic enzymology of the cycle and the principles of its metabolic regulation (Krebs and Johnson, 1937; Krebs, 1964, 1970). Later progress has led to the purification of all the enzymes involved and the elucidation of their primary amino acid sequence and 3D structure. Recently, the sequencing of the mouse and human genomes has allowed the localization of the corresponding genes in specific chromosomes (Consortium, 2001, 2002). Despite these impressive developments, many aspects

of the integrated operation of the TCA cycles in the different cellular environments of the *in vivo* brain and their coordinated response to fundamental physiological processes such as cerebral activation remain incompletely understood.

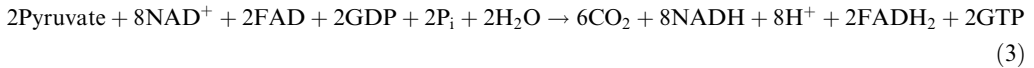
It is well established that plasma glucose is the main substrate for the adult mammalian brain (Sokoloff, 1989, 1992). Under normoxic conditions, glucose is completely oxidized to six molecules of CO₂ and water, as shown in the equation



This process involves a complex sequence of reactions starting with transport of glucose to the intracellular milieu and the glycolytic pathway that generates two pyruvate molecules in the cytosol of neural cells.



Cytosolic pyruvate may then be transported to the mitochondrial matrix where it is first decarboxylated to acetyl-CoA and later completely oxidized in the TCA cycle with production of CO₂ and reducing equivalents (see Eq. 3) (Dienel, 2002; Hertz and Dienel, 2002).



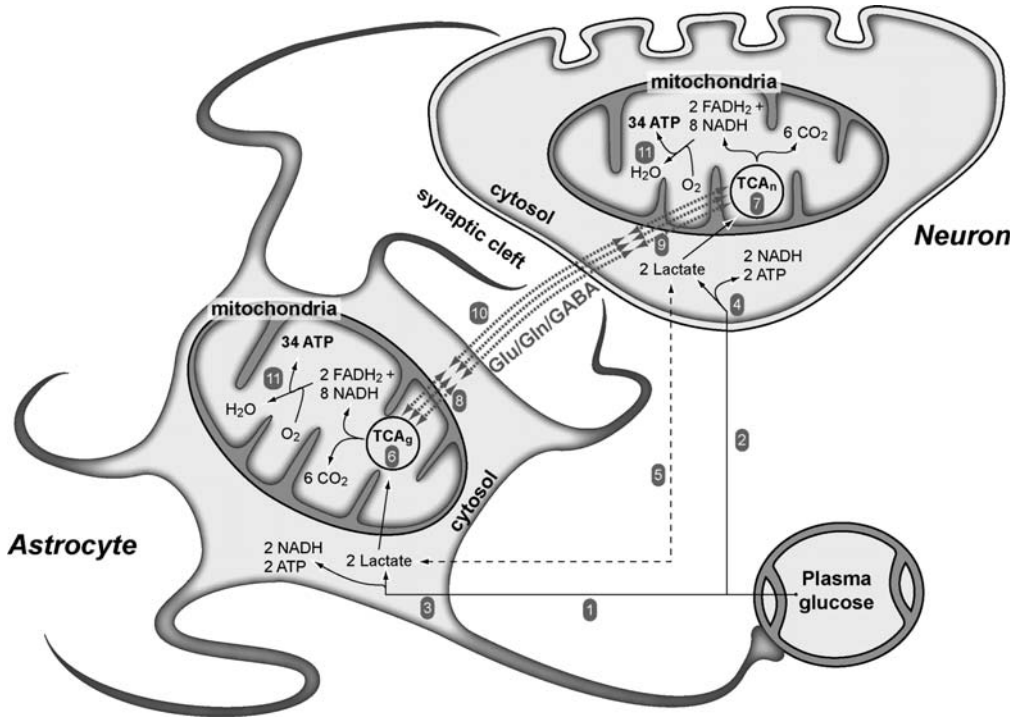
The mitochondrial respiratory chain is strictly coupled to TCA cycle activity, oxidizing the reducing equivalents produced therein to obtain ATP through oxidative phosphorylation (Almeida and Medina, 1997). Since every FADH₂ or NADH molecule oxidized in the respiratory chain produces essentially two or three molecules of ATP, respectively, the complete oxidation of one glucose molecule in a neural cell generates up to 34 ATP molecules. This represents a vast improvement over the two ATP molecules produced by anaerobic metabolism in glycolysis, a circumstance that makes the TCA cycle the most efficient cerebral bioenergetic process under aerobic conditions (Smith and Morowitz, 2004).

A brief historical background will help to gain a more defined perspective over the plurality of TCA cycles in brain and the evolution of the classical concepts toward our more recent interpretations. Initial evidences supporting the existence of two kinetically different TCA cycles in brain were obtained in the 1960s (▶ [Figure 1.4-1](#)). Soon after the intracerebral administration of ¹⁴C acetate, authors measured higher specific radioactivity in glutamine than in its precursor glutamate (Berl, 1965; Berl et al., 1968, 1970). A similar situation was found with ¹⁴CO₃H⁻ and butyrate, but not with glucose or glycerol. These findings could only be explained through the existence of two slowly exchanging pools of glutamate, denoted then as “large” and “small,” which exchanged radioactivity with “small” and “large” glutamine pools, respectively. Soon, the “large” and “small” glutamate and glutamine pools were associated with the operation of the “energy” and “synthetic” TCA cycles, proposed to represent the neuronal and glial compartments, respectively (Van den Berg et al., 1966, 1969). Subsequently, both cycles were connected by vectorial transfers of glutamate from the neuronal to the glial cycle, and glutamine in the opposite direction. The “glutamate–glutamine cycle” was conceived only as a mechanism to replenish small glutamate losses in the neurons during neurotransmission (Garfinkel, 1966; van den Berg and Garfinkel, 1971).

▶ [Figure 1.4-2](#) illustrates the current status of these concepts, emphasizing the aspects that remain incompletely understood. Plasma glucose is taken up by neural cells from the capillaries, mainly by the astrocytic end feet (process 1) and possibly also to some extent by the neurons (process 2). Both neurons and astrocytes contain mitochondria equipped with the enzymatic machinery required for glycolytic (processes 3 and 4) and oxidative glucose metabolism (processes 6 and 7). However, the quantitative contribution of neuronal and glial metabolisms to overall cerebral glycolysis or oxidation *in vivo* remains imprecise. Similarly, it has not been possible to quantify unambiguously the relative proportions of glucose or lactate used to support neuronal oxidative metabolism *in vivo* (process 5). Finally, the operation of the TCA cycle in neural cells demands the transfer of reducing equivalents from cytosol to mitochondria as well as the exchange of TCA cycle intermediates between these subcellular compartments (processes 8 and 9). The rate at which these processes occur *in vivo* and how subcellular transport may modulate TCA cycle activity in neurons and astrocytes constitute important challenges of modern neurochemistry.

■ Figure 1.4-2

Metabolic interactions between oxidative and nonoxidative metabolisms in neurons and glia. (1) Glucose uptake by the astrocyte, (2) glucose uptake by the neuron, (3) astroglial glycolysis, (4) neuronal glycolysis, (5) exchange of lactate between the neurons and glia, (6) astroglial TCA cycle, (7) neuronal TCA cycle, (8) and (9) astrocytic and neuronal mitochondrial transporters allowing exchange of reducing equivalents between mitochondria and cytosol, (10) intercellular exchange of glutamate, glutamine, and GABA, (11) astrocytic and neuronal respiratory chain



2 The Cerebral Tricarboxylic Acid Cycle

◆ Figure 1.4-3 and ◆ Table 1.4-1 summarize the individual reactions of the TCA cycle and the main properties of the enzymes involved, respectively. Mitochondrial pyruvate oxidation begins with its decarboxylation to acetyl-CoA by pyruvate dehydrogenase. The pyruvate dehydrogenase complex (PDHC, EC 1.2.4.1) plays a key role in the oxidative metabolism of pyruvate and its regulation, catalyzing the irreversible decarboxylation of pyruvate to CO_2 , acetyl-CoA, and NADH (Patel and Korotchkina, 2001).

The TCA cycle starts by the irreversible condensation of oxaloacetate (OAA) and acetyl-CoA to produce citryl-CoA, which is then hydrolyzed to citrate and CoA. This reaction is catalyzed by citrate synthase (CS) (EC 2.3.3.1), a homodimer of 52-kDa subunits coded in humans by the CS gene, the enzyme being found in the mitochondrial matrix of all cells capable of oxidative metabolism (Goldenthal et al., 1998). The synthesis of citrate is a crucial control point of the TCA cycle. Citrate synthase is allosterically inhibited by ATP, through an increase in the K_m for acetyl-CoA. This inhibition is easily reversed by an increase in the ADP concentration, which induces an allosteric stimulation. Concomitantly, high concentrations of NADH and succinyl-CoA also retroinhibit this enzyme (Matsuoka and Srere, 1973).

The next step is catalyzed by the 85-kDa monomeric mitochondrial aconitase (Aco) (EC 4.2.1.3). It is a sequential reaction comprising dehydration and hydration processes. Citrate is isomerized to isocitrate via

■ Figure 1.4-3

The turnover of carbon and hydrogen in the tricarboxylic acid cycle. Using (1,2-¹³C₂)acetyl-CoA as substrate, ¹³C is incorporated successively in (4,5-¹³C₂)citrate (citrate synthase), (4,5-¹³C₂)*cis*-aconitate (aconitase), (4,5-¹³C₂)isocitrate (aconitase), and (4,5-¹³C₂)α-ketoglutarate (NAD-isocitrate dehydrogenase). α-ketoglutarate dehydrogenase produces (3,4-¹³C₂)succinyl-CoA and an equimolar mixture of (1,2-¹³C₂) and (3,4-¹³C₂)succinate (succinyl CoA synthetase), followed by the production of (1,2-¹³C₂) or (3,4-¹³C₂)fumarate (succinate dehydrogenase) and (1,2-¹³C₂) or (3,4-¹³C₂)malate or oxaloacetate. Hydrogens from water incorporate in the H₃_{proR} and H₃_{proS} of isocitrate, α-ketoglutarate and glutamate, the H₂ (or H₃) of succinate and fumarate, and the H₃ of oxalacetate and malate. ¹³C atoms are indicated in red or green (lost by decarboxylation). Hydrogen exchange is considered to start from fumarate on, being indicated in cyan and light blue (H₃ and H_{3'} hydrogens of α-ketoglutarate) or white contour (H₃ malate or oxalacetate). The same color is maintained in the different intermediates to follow the metabolic history of every carbon or hydrogen

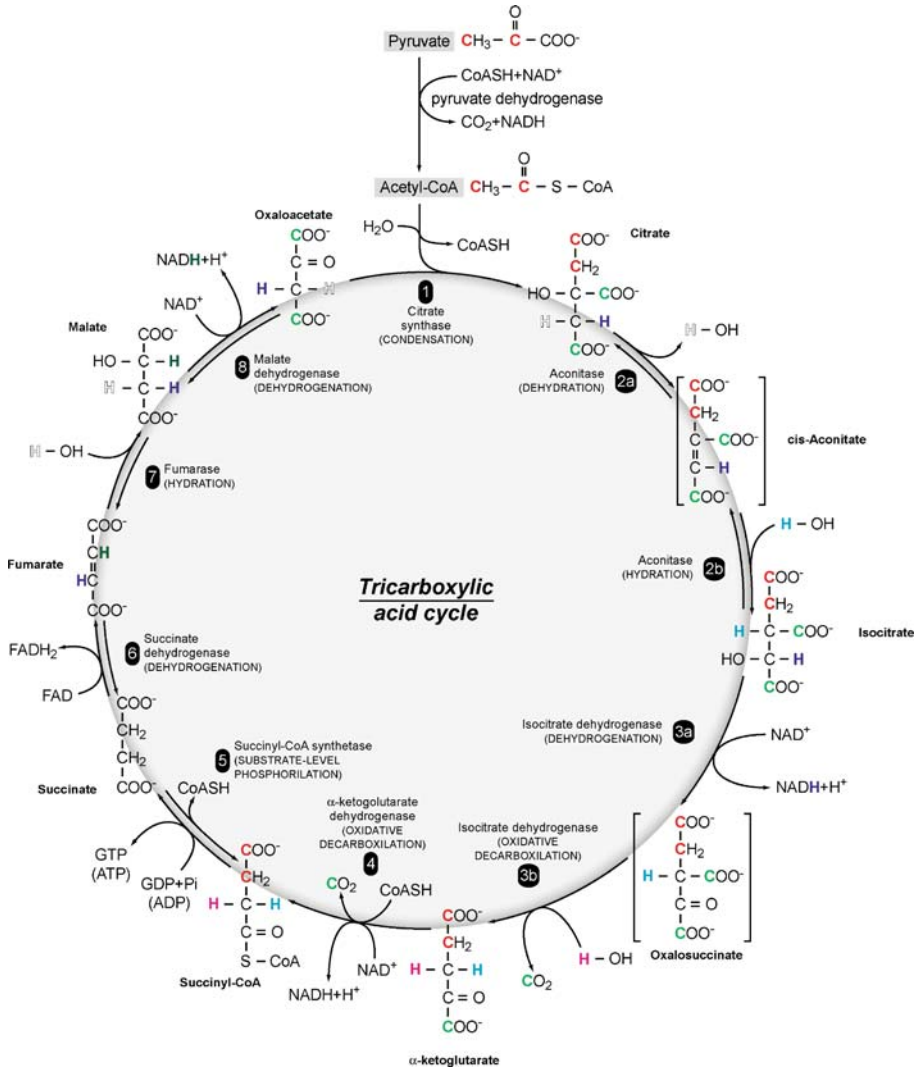


Table 1.4-1
Structural and genomic properties of the tricarboxylic acid cycle enzymes

Enzyme (EC number)	Substrates	Products	Prosthetic group	MW/structure	Genetic sequence/cloned
Citrate synthase (EC: 2.3.3.1)	Oxaloacetate acetyl-CoA	Citrate		52 kDa, homodimer (by similarity)	CS
Aconitase (EC: 4.2.1.3)	Citrate	Isocitrate	Fe-S	85 kDa, monomer (by similarity)	ACO2
NAD ⁺ -dependent isocitrate dehydrogenase (EC: 1.1.1.41)	Isocitrate	α -Ketoglutarate		Heterooligomer of subunits α (40 kDa), β (42 kDa), and γ (43 kDa) in the apparent ratio of 2:1:1 (by similarity)	IDH3A (α), IDH3B (β), IDH3G(γ)
α -Ketoglutarate dehydrogenase complex	α -Ketoglutarate	Succinyl-CoA	Lipoic acid, FAD, TPP	Three enzymatic components: α -ketoglutarate dehydrogenase (E1, EC: 1.2.4.2, 113 kDa), transsuccinylase (E2, EC: 2.3.1.61, 49 kDa), and dihydrolipoyl dehydrogenase (E3, EC: 1.8.1.4, 54 kDa)	OGDH (E1), DLST (E2), DLD (E3)
Succinyl-CoA synthetase (EC: 6.2.1.4)	Succinyl-CoA	Succinate		Heterodimer of an α (35 kDa) and a β chain (41 kDa) (by similarity)	SUCLG1(α) SUCLG2 (β)
Succinate dehydrogenase (EC: 1.3.5.1)	Succinate	Fumarate	FAD, Fe-S	Three enzymatic components: a flavoprotein (fp, 70 kDa), an iron protein (ip, 27 kDa), and a cytochrome <i>b</i> composed of two integral membrane proteins	SDHA (fp), SDHB (ip), and SDHC and SDHB (integral membrane proteins)
Fumarase (EC: 4.2.1.2)	Fumarate	Malate		55 kDa, homotetramer	FH
Malate dehydrogenase (EC: 1.1.1.37)	Malate	Oxaloacetate		36 kDa, homodimer	MDH2

cis-aconitate. Aconitase is an iron–sulfur protein encoded by the ACO2 gene containing a 4Fe–4S cluster to which the substrate binds (Mirel et al., 1998).

The mitochondrial NAD⁺-dependent isocitrate dehydrogenase (EC 1.1.1.41) catalyzes an ordered reaction consisting of the initial oxidation of isocitrate to the unstable β-keto acid oxalosuccinate, followed by decarboxylation to α-ketoglutarate (α-KG). This constitutes the second rate-limiting step of the TCA cycle, being allosterically activated by increasing intramitochondrial ADP/ATP ratios and Ca²⁺. There are additional cytosolic and mitochondrial NADP⁺-dependent isoenzymes that contribute actively to the NADP/NADPH-dependent detoxification reactions and fatty acid synthesis (Sazanov and Jackson, 1994; Minich et al., 2003). Both isoenzymes are heterotetramers of two 40-kDa α subunits (coded by the IDH3A gene), one 42-kDa β subunit (IDH3B), and one 43-kDa γ subunit (IDH3G) (Kim et al., 1995, 1999; Brenner et al., 1997). It is possible that the fate of cytosolic and mitochondrial isocitrate through the NAD⁺ and NADP⁺ isoenzymes is determined by the availability of NAD⁺ and NADP⁺, respectively.

The reaction mechanism of the mitochondrial α-ketoglutarate dehydrogenase (α-KGDH) complex is analogous to the conversion of pyruvate to acetyl-CoA by PDHC, since both complexes are structurally very similar (Sheu and Blass, 1999). The assembly contains multiple copies of three enzymatic components: α-ketoglutarate dehydrogenase (E1, EC 1.2.4.2, encoded by the OGDH gene, 113 kDa), transsuccinylase (E2, EC 2.3.1.61, encoded by the DLST gene, 49 kDa), and dihydrolipoyl dehydrogenase (E3, EC 1.8.1.4, encoded by the DLD gene, 54 kDa) (Feigenbaum and Robinson, 1993; Ali et al., 1994; Szabo et al., 1994). The α-ketoglutarate dehydrogenase complex requires several cofactors including lipoamide, thiamine pyrophosphate, CoA, FAD, and NAD⁺. Succinyl-CoA and NADH inhibit the reaction, providing the third control point of the TCA cycle flux, after citrate synthase and isocitrate dehydrogenase (NAD).

Succinyl-CoA synthetase (EC 6.2.1.4) is a mitochondrial enzyme that performs the only substrate-level phosphorylation of the TCA cycle, converting succinyl-CoA into succinate. GDP is phosphorylated to GTP, which then goes on to phosphorylate ADP, producing only one ATP molecule directly by the TCA cycle. It is a heterodimer of an α (35 kDa) and a β chain (41 kDa), encoded by SUCLG1 and SUCLG2 genes, respectively (James et al., 1997; Johnson et al., 1998).

The succinate dehydrogenase (SDH) complex (EC 1.3.5.1) oxidizes succinate to fumarate. It comprises a 70-kDa flavoprotein (fp), a 27-kDa iron–sulfur protein (ip), and a cytochrome *b* composed of two integral membrane proteins, encoded by SDHA, SDHB, SDHC, and SDHD genes, respectively (Morris et al., 1994; Au et al., 1995; Elbehti-Green et al., 1998; Hirawake et al., 1999). The SDH complex is the only enzyme of the TCA cycle to be imbedded in the inner mitochondrial membrane. Because free-energy change for this oxidation is not sufficient to reduce NAD⁺, FAD is used as the hydrogen acceptor of this reaction (de Gomez-Puyou et al., 1972).

The next step is the hydration of fumarate to form L-malate. This stereospecific trans addition of H and OH is catalyzed by 55-kDa fumarase (Fum) (EC 4.2.1.2), a homotetramer that exists both in the mitochondrial and in the cytosolic compartments of the intact brain and is encoded by the FH gene (Akiba et al., 1984; Kinsella and Doonan, 1986).

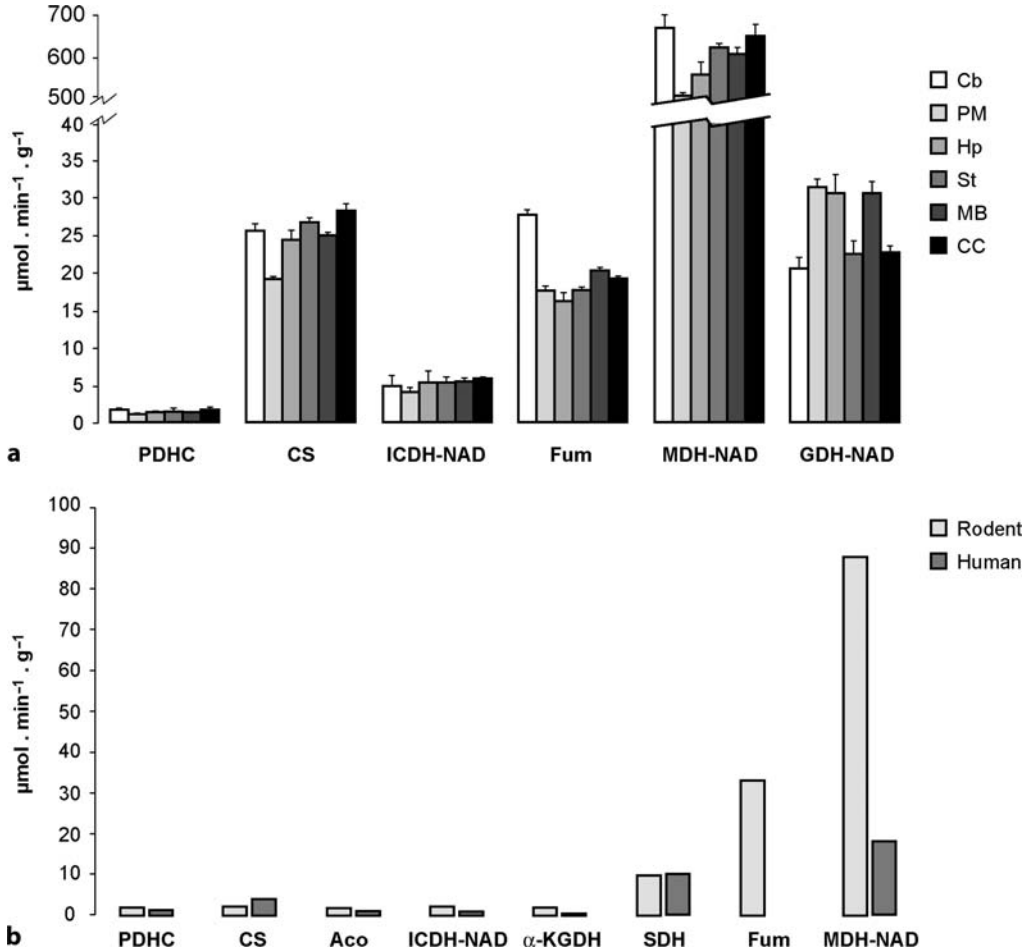
Finally, malate dehydrogenase (MDH) (EC 1.1.1.37) catalyzes the reversible oxidation of L-malate to oxaloacetate. This 36-kDa homodimer is located in the mitochondrial matrix, and uses the NAD/NADH cofactor system. The enzyme is encoded by the MDH2 gene (Benn et al., 1977). In addition, malate dehydrogenase plays a crucial role in the redox coupling between the mitochondrial and the cytosolic compartments, through the malate–aspartate shuttle (Malik et al., 1993).

2.1 Regionalization and Subcellular Distribution

Classical studies determined the maximal activities of TCA cycle enzymes in whole brain and in different cerebral regions. ▶ *Figure 1.4-4* shows the maximal activities of TCA cycle enzymes in human and rodent brain (▶ *Figure 1.4-4a*) and their regional variation within different cerebral structures (◉ *Figure 1.4-4b*) (Clark and Lai, 1989; Diemel, 2002). Maximal activities of TCA cycle enzymes were in most cases higher in rodent than in human brain and higher in the cerebral cortex than in the midbrain, basal ganglia, and cerebellum, a finding consistent with the higher oxidative capacity of the cortex.

■ Figure 1.4-4

Distribution of maximal activities of tricarboxylic acid cycle enzymes within different brain regions of young male rats (a) and relative activities in rodent and human brain (b). Cb, cerebellum; PM, pons/medulla; Hp, hippocampus; St, striatum; MB, midbrain; CC, cerebral cortex; Aco, aconitase; PDHC, pyruvate dehydrogenase complex; CS, citrate synthase; ICDH-NAD, isocitrate dehydrogenase (NAD); α -KGDH, α -ketoglutarate dehydrogenase; SDH, succinate dehydrogenase; Fum, fumarase; MDH-NAD, malate dehydrogenase (NAD); GDH-NAD, glutamate dehydrogenase (NAD). Results are expressed in $\mu\text{mol min}^{-1} \text{g}^{-1}$. (a) Adapted from Clark and Lai (1989) with permission of the publisher. (b) Adapted from Dienel (2002) with permission of the publisher



As far as cellular distribution is concerned, both neurons and astrocytes in primary culture show TCA cycle activity and therefore contain its complete enzymatic machinery. However, the specific activity of TCA cycle enzymes is much higher in cultures of neurons than in cultures of astrocytes, in agreement with the higher oxidative capacity of the former (Stewart et al., 1998; Hertz and Hertz, 2003; Hertz, 2004). At the subcellular level, the TCA cycle occurs exclusively in the mitochondria. Consistent with this localization, pyruvate dehydrogenase, citrate synthase, and succinyl-CoA synthetase activities are found only in the mitochondrial fractions (Lai and Clark, 1989; Almeida and Medina, 1997, 1998). However, many of the remaining enzymes are found also in the cytosol of both neurons and astrocytes. This is the case with aconitase, isocitrate dehydrogenase, and malate dehydrogenase. Interestingly enough, cytosolic fumarase

has been reported to be lacking in the brain (Akiba et al., 1984). Various reports have proposed the functional organization of Krebs cycle enzymes in mitochondrial supramolecular complexes (Robinson and Srere, 1985a, b).

2.2 Regulation

The regulation of the TCA cycle demands a close integration with the activities of the upstream glycolytic pathway and the downstream mitochondrial respiratory chain. To this end, the TCA cycle flux is inhibited by NADH and ATP as its products, or activated by NAD and ADP as its substrates (Krebs, 1970; Bachelard et al., 1974; McIlwain and Bachelard, 1985; Clarke et al., 1989; Sokoloff, 1989). Control by these allosteric effectors occurs mainly at the first irreversible step of pyruvate dehydrogenase, with additional modulations at the citrate synthase, isocitrate dehydrogenase (NAD), and α -ketoglutarate dehydrogenase steps (Gibson et al., 2000; Patel and Korotchkina, 2001). These relatively simple substrate activation or product inhibition mechanisms allow for an effective increase in TCA cycle activity under circumstances of augmented energy demand, or for a decrease in TCA cycle flux when overproduction of NADH or ATP occurs.

The integrated regulation of glycolysis and the TCA cycle activity plays a central role in cerebral energetics (Bachelard et al., 1974; Siesjo, 1982; McIlwain and Bachelard, 1985; Clarke et al., 1989). This process involves a series of highly sophisticated redox and energetic signaling processes that communicate with the mitochondrial and cytosolic environments. Under physiological circumstances, tight coupling between the TCA cycle and glycolysis relies on the fast exchange between the mitochondrial and cytosolic ATP/ADP and NAD/NADH ratios. This occurs through the ATP/ADP exchanger and the various transporters involved in the transfer of reducing equivalents in the inner mitochondrial membrane (Palmieri et al., 1996, 2001; Palmieri, 2004). In this way, mitochondrial perturbations in ATP/ADP or NAD/NADH ratios should appear reflected in the corresponding cytosolic ratios and vice versa.

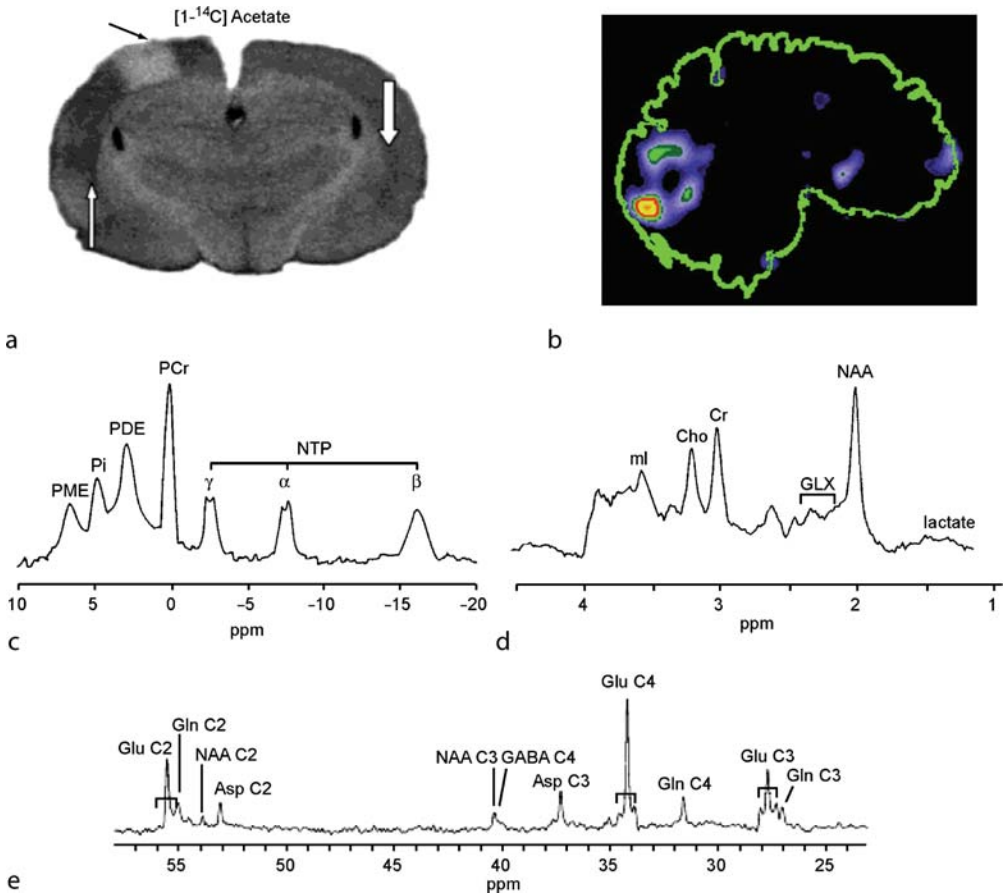
The glycolytic pathway is classically known to be modulated in the brain, mainly at the phosphofructokinase step, through the balance of positive and negative effectors (Passonneau and Lowry, 1964; Sacktor et al., 1966). ATP and NADH inhibit phosphofructokinase activity, while citrate, ADP, NAD^+ , and NH_4^+ increase it. Under hypoxic conditions, oxygen limitations make the reoxidation of mitochondrial NADH difficult, resulting in a more reduced intramitochondrial NAD/NADH ratio that inhibits the TCA cycle flux. As a consequence, the mitochondrial and cytosolic ATP/ADP ratios decrease, activating glycolytic flux and net lactate production because cytosolic NADH cannot be completely reoxidized by the respiratory chain. This situation is reversible upon return to physiological oxygen tensions, which normalize intracellular ATP/ADP and NAD/NADH ratios, restoring the coupling between glycolysis and the TCA cycle flux (Almeida et al., 2004). Finally, it should be mentioned here that even though the general properties of the integration between glycolysis and the TCA cycle are sufficiently understood, many aspects concerning the subcellular redox and energetic coupling mechanisms as well as the mitochondrial transporters and shuttles involved in neurons and glia remain to be quantitatively and kinetically characterized.

3 Methodologies to Investigate Tricarboxylic Acid Cycle Activity

Experimental procedures to investigate the activity of the TCA cycle *in vitro* have traditionally involved polarographic measurements of oxygen consumption in suspensions of isolated synaptic or nonsynaptic mitochondria from brain (🔗 [Figure 1.4-5](#)). The approach required the preparation of mitochondrial suspensions and the determination of oxygen consumption and ATP/ADP cycling, under different substrate conditions (Rossignol et al. 2000; Barrientos, 2002). Despite the important information obtained on the mechanisms of oxidative phosphorylation using these methods, this *in vitro* approach did not allow the investigation of the more complex aspects of TCA cycle regulation and intercellular coupling between astrocytic and neuronal environments, as they occur in the *in vivo* brain. Basically, four different methods

■ Figure 1.4-5

Different approaches to measure oxidative capacity in the brain. (a) Autoradiography after ($1\text{-}^{14}\text{C}$) acetate reflects glial TCA cycle activity during spreading cortical depression (Dienel et al., 2001). (b) A PET scan during the paradigm of "reading words" detects increased ^{18}F FDG accumulation in the visual cortex (Mintun et al., 2004). (c) Localized ^{31}P NMR spectra in vivo depict resonances from α , β , and γ phosphates of nucleotide triphosphates NTP (mainly MgATP), PCr, PDE, inorganic phosphate (P_i), and phosphomonoesters (PME) (Ross and Sachdev, 2004). (d) Localized ^1H NMR spectrum in vivo showing resonances from *N*-acetyl aspartic acid (NAA), glutamate and glutamine (Glx), creatine and PCr, choline derivatives (Cho) and *myo*-inositol (ml) (Ross and Sachdev, 2004). (e) Localized ^{13}C NMR spectroscopy during ($1\text{-}^{13}\text{C}$)glucose infusion shows resonances from the C3, C4, and C2 carbons of glutamate (GLU) and glutamine (GLN) and the C3 and C2 carbons of aspartate (Asp) and *N*-acetyl aspartate (NAA) (Gruetter et al., 2003). Reproduced with permission of the publisher



have been implemented to address these aspects: autoradiography, PET, NMR, and dual photon fluorescence confocal microscopy. The following sections describe these in more detail.

3.1 Radioactive Procedures

Autoradiography and PET methods are normally based on the measurement of regional cerebral glucose consumption, after the administration of 2-deoxyglucose labeled either with ^{14}C or with ^{18}F (Sokoloff,

1981a,b, 1983a,b; Wienhard, 2002; Herholz and Heiss, 2004). These methodologies determine the regional accumulation of 2- $(^{14}\text{C}$ or $^{18}\text{F})$ deoxyglucose-6-phosphate, a virtually unmetabolizable analog of glucose-6-phosphate. Autoradiography was one of the first methods to be proposed. It provided ex vivo images of the regional accumulation of radioactive 2-deoxyglucose (or other radioactive substrates such as acetate and butyrate), as reflected in photographic plates obtained from sections of fixed brain tissue. PET yielded in vivo images of the regional uptake of (^{18}F) 2-deoxyglucose (FDG), or other positron emitters in different brain sections, as resolved tomographically by a coronal arrangement of positron-selective gamma cameras. Both methods allow the determination of cerebral metabolic rates for glucose (CMR_{glc}) in different brain regions after appropriate modeling of the underlying tracer kinetics (Price, 2003). In addition, the use of $^{15}\text{O}_2$ as an inspired gas or of $^{15}\text{OH}_2$ as a freely diffusible tracer allows the measurement of regional oxygen consumption, cerebral blood volume, and blood flow by using PET (Hatazawa et al., 1995). Both radioactive approaches are limited in resolution and chemical specificity, which do not make it possible to image single neural cells in the examined area, or to investigate the downstream metabolism of glucose below the phosphofructokinase step.

3.2 Nuclear Magnetic Resonance Methods

Pioneering NMR approaches to cerebral energetics began most probably with the application of ^{31}P NMR (Moore et al., 1999; Ross and Sachdev, 2004). ^{31}P NMR spectra from rodent, cat, dog, or human brain depicted resonances from ATP, phosphocreatine (PCr), inorganic phosphate (P_i), phosphomonoesters (PME, mainly phosphorylethanolamine), and phosphodiesteres (PDE, glycerolphosphorylcholine) (Hilberman et al., 1984; Gyulai et al., 1987; Komatsumoto et al., 1987; Nioka et al., 1991). It was possible to follow noninvasively the rates of PCr breakdown and recovery after hypoxic and ischemic episodes. In general, PCr decrease was the first phenomenon observed, with ATP concentrations initially remaining relatively constant and decreasing eventually after PCr stores had been depleted. The recovery rates of PCr after restoring normal oxygen delivery conditions reflected directly oxidative phosphorylation and TCA cycle activity in vivo. Under these circumstances, the P_i resonance increased and shifted to a more acidic pH. PME increased in the late phases of hypoxia/ischemia, in agreement with increased phospholipase activation and intracellular Ca^{2+} rises due to membrane depolarization.

Today, ^1H NMR approaches to cerebral competence are probably the widely used in clinics (Burtscher and Holtas, 2001). ^1H NMR spectra from human or rodent brain show resonances from the methyl group of *N*-acetyl aspartic acid (NAA), the methyl groups of creatine (Cr) and PCr, the trimethylammonium groups of choline (Cho)-containing compounds, and the *myo*-inositol (Ino) resonances. NAA and Ino are thought to represent the neuronal and glial contributions, respectively, to the observed voxel. Notably, the methyl group of lactate becomes readily observable under hypoxic or ischemic conditions, providing an unambiguous proof of increased net glycolytic flux under hypoxic or ischemic situations.

^{13}C NMR approaches constitute probably the most elaborate, chemically specific tool to trace the metabolic fate of ^{13}C -labeled glucose or acetate in the brain, both in vivo and in vitro (Cruz and Cerdan, 1999; Cerdan, 2003; de Graaf et al., 2003; Gruetter et al., 2003; Garcia-Espinosa et al., 2004). The ^{13}C NMR approach is useful because it is possible to investigate the activities of the neuronal and glial TCA cycles in vivo and in vitro, providing direct insight into cerebral metabolic compartmentation. Traditionally, either (^{13}C) glucose, a universal substrate for neurons or glial cells, or (^{13}C) acetate, an exclusive substrate for the glia, has been used (Badar-Goffer et al., 1990; Cerdan et al., 1990; Fitzpatrick et al., 1990; Mason et al., 1992b). $(1\text{-}^{13}\text{C})$ glucose is metabolized to $(3\text{-}^{13}\text{C})$ pyruvate, which eventually labels $(4\text{-}^{13}\text{C})$ glutamate and $(4\text{-}^{13}\text{C})$ glutamine. Similarly, $(2\text{-}^{13}\text{C})$ and $(1,2\text{-}^{13}\text{C}_2)$ acetate produce $(4\text{-}^{13}\text{C})$ and $(4,5\text{-}^{13}\text{C}_2)$ glutamate and glutamine, respectively (see [Figure 1.4-3](#)). Consequently, dynamic or steady-state measurements of the turnover and fractional ^{13}C enrichments of glutamate C4 and glutamine C4, as labeled from (^{13}C) glucose or (^{13}C) acetate precursors, have often been interpreted to reflect the neuronal ($V_{\text{TCA}n}$) and glial ($V_{\text{TCA}g}$) TCA cycle fluxes, respectively. These interpretations, however, rely on the assumption that exchange of α -ketoglutarate and glutamate through the cytosolic and mitochondrial aspartate aminotransferases and through the inner mitochondrial membrane (V_x) of both neurons and astrocytes is faster than

the TCA cycle rate. This assumption allows considering a single cerebral glutamate pool in both neural cell types and approximating the neuronal and glial TCA cycles by the kinetics (or steady-state values) of ^{13}C enrichment in glutamate C4 and glutamine C4, respectively.

• **Table 1.4-2** summarizes the values for the TCA cycle flux obtained using different in vivo and in vitro ^{13}C NMR approaches, as compared with earlier radioactive isotope methods and more recent ^{13}C isotopomer approaches. In general, TCA cycle fluxes calculated for the normoxic adult rat or human brain were in the range 0.5–1.4 $\mu\text{mol}/\text{min}/\text{g}$. More accurate measurements taken recently provide values for the neuronal TCA cycle flux in the vicinity of 0.5 $\mu\text{mol}/\text{min}/\text{g}$. This value may decrease to virtually undetectable levels with increasing states of anesthesia (Sibson et al., 1998b) or increase by 25–50% with different cerebral activation protocols (Hyder et al., 1996, 1997; Chhina et al., 2001). TCA cycle fluxes in the glial compartment of rodent or human brain are in the range of 0.4–0.14 $\mu\text{mol}/\text{min}/\text{g}$, representing approximately 20% of the total cerebral TCA cycle activity. • **Table 1.4-2** also shows sizes and turnover rates of the glutamate compartments associated to the “large” and “small” glutamate pools. To our knowledge no direct measurements of these pool sizes exist. The values shown are based on the assumption that the small glutamate pool accounts for approximately 10% of total cerebral glutamate during ($1\text{-}^{13}\text{C}$)glucose metabolism. Recently, it has been possible to determine simultaneously the relative labeling of the large and small glutamate pools ex vivo using ($1\text{-}^{13}\text{C}$)glucose and ($2\text{-}^{13}\text{C}$, $2\text{-}^2\text{H}_3$)acetate as substrates (Chapa et al., 2000).

Although there is strong evidence supporting fast α -ketoglutarate/glutamate exchange in the cytosolic and mitochondrial aminotransferases (Erecinska and Silver, 1990), there is less information concerning the in situ activity of the neuronal or glial dicarboxylate carrier and the glutamate/aspartate exchanger, which are responsible for α -ketoglutarate/glutamate exchange between mitochondria and cytosol in these cells. However, experiments with purified mitochondrial preparations from brain incubated with ($\text{U}\text{-}^{14}\text{C}$)glutamate have revealed that the exchange of α -ketoglutarate/glutamate is slower than the TCA cycle flux in vitro (Berkich et al., 2005). Moreover, hydrogen turnover experiments, as monitored by (^{13}C , ^2H) NMR, have recently revealed the existence of more than one glutamate pool in the neuronal and glial compartments of the adult rat brain ex vivo (Sierra et al., 2004). Taken together, these results suggest that α -ketoglutarate/glutamate exchange through the mitochondrial membrane of neural cells is of the same order of magnitude or slightly slower than the TCA cycle flux. The influence of these findings on previous ^{13}C NMR modeling results, which assumed fast α -ketoglutarate/glutamate exchange, remains to be analyzed.

The main advantage of hydrogen turnover experiments over the classical ^{13}C turnover approach is that hydrogen exchange occurs in a much faster time scale than ^{13}C exchange (Garcia-Martin et al., 2002). Using (^{13}C , ^2H) NMR it is possible to monitor fast processes, which could not be monitored previously with ^{13}C NMR (García-Martín et al., 2001). The exchange of the different hydrogens of glutamate and glutamine molecules by deuterons from heavy water is stereospecific (Cerdan et al., 2003). The H2 hydrogen of glutamate is exchanged mainly by aspartate aminotransferase, while the H3_{proR} and H3_{proS} hydrogens are exchanged by aconitase and isocitrate dehydrogenase, respectively. The H4 hydrogens of glutamate are derived from the methyl group of acetyl-CoA and one of them is exchanged during the citrate synthase reaction. This stereospecific exchange is conveniently illustrated by the sequence of exchange of the H3_{proR} and H3_{proS} hydrogens of ($2\text{-}^{13}\text{C}$)glutamate by deuterons from the solvent (• **Figure 1.4-6**).

High-resolution ^{13}C NMR makes it possible to distinguish between perprotonated, monodeuterated, and doubly deuterated ^{13}C -labeled glutamate and glutamine isotopomers. This is possible because deuterium substitutions induce readily observable, additive, isotopic shifts in ^{13}C NMR resonances. It has been possible to show, in the perfused liver, that exchange of the H3 hydrogens can be resolved in two different kinetic components (Garcia-Martin et al., 2002). A fast exchange of either H3_{proR} or H3_{proS} hydrogens occurs first on preexisting ($2\text{-}^{13}\text{C}$)glutamate or glutamine molecules. This fast process substitutes only one of the H3 hydrogens, in a way that substitution of H3_{proR} precludes substitution of the H3_{proS} and vice versa. The fast process may be catalyzed by either cytosolic aconitase or isocitrate dehydrogenases (NADP). A slower double deuteration of the H3_{proR} and H3_{proS} occurs later, but is only possible on the ($2\text{-}^{13}\text{C}$)glutamate molecules newly synthesized during TCA cycle activity. Similar kinetics that are occurring in brain have been reported recently (Sierra et al., 2005). Thus, the (^{13}C , ^2H) NMR approach allows resolving the fast turnover of cytosolic ($2\text{-}^{13}\text{C}$, $3\text{-}^2\text{H}$)glutamate and the slower turnover of ($2\text{-}^{13}\text{C}$, $3,3'\text{-}^2\text{H}_2$)glutamate produced in the TCA cycle. The fact that the fast and slow components of H3 exchange can be resolved by

Table 1.4-2 Tricarboxylic acid cycle and glutamate/glutamine exchange between the neuronal and glial compartments of the adult mammalian brain as calculated with different models and methodologies

Process/model	Garfinkel ^a	Van den Berg and Garfinkel ^b	Kunnecke et al. ^c Preece and Cerdan ^d	Mason et al. ^e Sibson et al. ^{f,g} Shen et al. ^h Lebon et al. ⁱ	Gruetter et al. ^j	Bluml et al. ^k
Total cerebral TCA cycle flux (μmol/min/g)	1.05	1.5	1.4	1.6 or 0.7, ^e 0.6, ^f 1.0–0.2, ^g 0.8 ^h	0.6	0.84
Neuronal TCA cycle flux (μmol/min/g)	0.40	1.2	1.0	1.6, ^e 0.6, ^f 1.0–0.2, ^g 0.8 ^h	0.6	0.70
Glial TCA cycle flux (μmol/min/g)	0.65	0.3	0.4	0.14 ⁱ		0.14
Size (μmol/g)/turnover (per min) of large glutamate pool	8.8/21.7	7.0/5.7	5.8/5.8	n.a.		n.a.
Size (μmol/g)/turnover (per min) of small glutamate pool	1.7/2.6	1.25/4.16	0.5/1.25	n.d./7.7 ⁱ		n.a.
Net transfer of neuronal glutamate to glial compartment (μmol/min/g)	0.08 ^m	0.14	0.1	0.21, ^f 0.40–0.0, ^g 0.32, ^h 0.3 ⁱ	0.3 (0.2) ⁿ	n.a.
Net transfer of glial glutamine to neuronal compartment (μmol/min/g)	0.45	n.a	0.1	0.21, ^f 0.40–0.0, ^g 0.32, ^h 0.3 ⁱ	0.3 (0.2) ^{kn}	n.a.

^aCalculated from specific radioactivity measurements in brain extracts obtained after intracranial injections of various radioactive precursors including (U-¹⁴C)glutamate, (U-¹⁴C) aspartate, ¹⁴CO₃H⁻, and ¹⁵NH₄ acetate (Garfinkel, 1966)

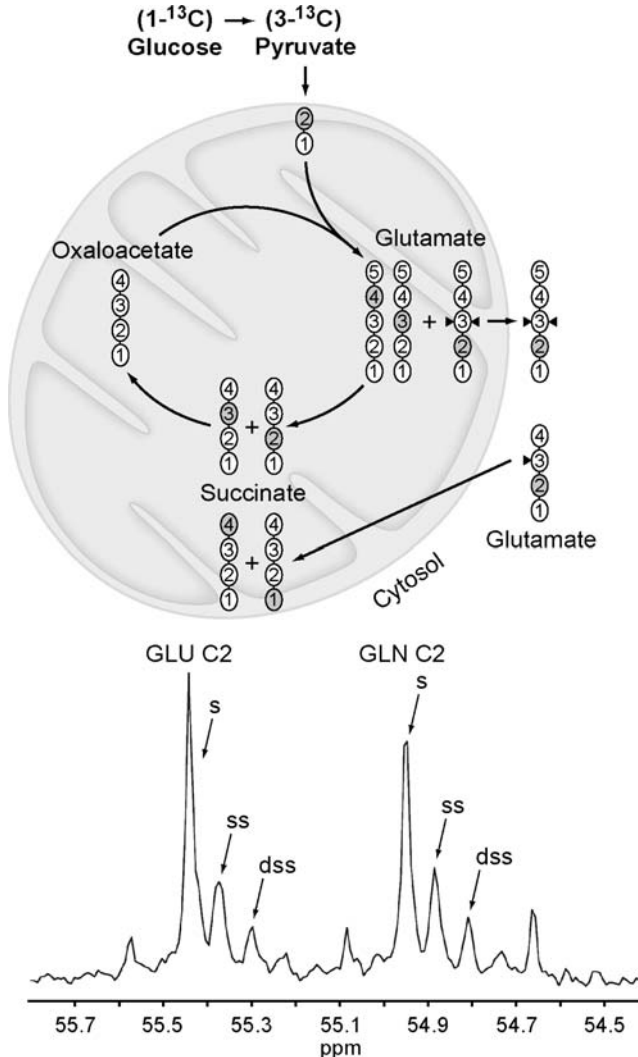
^bCalculated from specific radioactivity measurements in glutamate, glutamine, and aspartate from mouse brain extracts prepared after intraperitoneal injections of ¹⁴C-labeled glucose and acetate (van den Berg and Garfinkel, 1971)

- ^cRelative flux values were calculated as described in (Kunnecke et al., 1993) and from the relative ¹³C isotopomer populations in glutamate, glutamine, and GABA measured by high-resolution ¹³C NMR in rat brain extracts after infusion of (1,2-¹³C₂) acetate (Chapa et al., 1995)
- ^dAbsolute flux values were determined from the relative values described in note c by measuring the absolute rate of GABA accumulation induced by vigabatrin, a selective inhibitor of GABA transaminase (Preece and Cerdan, 1996)
- ^eDetermined in vivo from the kinetics of ¹³C enrichment in glutamate and glutamine C4 carbons from rat or human brain during infusion of (1-¹³C) glucose, respectively (Mason et al., 1992a; Mason et al., 1995)
- ^fDetermined in vivo from the kinetics of ¹³C labeling in glutamate and glutamine C4 (Sibson et al., 1997)
- ^gDetermined in vivo from the kinetics of ¹³C enrichment in glutamate and glutamine C4, under different conditions of morphine, α -chloralose, and pentobarbital anesthesia (Sibson et al., 1998a)
- ^hDetermined in the human brain in vivo during (1-¹³C) glucose infusion. Glutamate/Glutamine exchange concluded to be stoichiometric 1:1 with CMRglc (Shen et al., 1999)
- ⁱDetermined in the human brain during metabolism of (2-¹³C) acetate (Lebon et al., 2002)
- ^jDetermined in the human brain during (1-¹³C) glucose infusion with a different model than that used in f-i (Gruetter et al., 2001)
- ^kDetermined in the human brain during (1-¹³C) acetate metabolism (Bluml et al., 2002)
- ^lDetermined in vivo as the inverse of the rate constant of ¹³C labeling in cerebral glutamate C4 during (1-¹³C) glucose infusions (Mason et al., 1992b)
- ^mOriginally proposed as an α -ketoglutarate exchange between the large and small compartments (Garfinkel, 1966)
- ⁿOnly a fraction of glutamine synthesis considered to be derived from neurotransmitter glutamate. Glutamate/glutamine exchange concluded nonstoichiometric with CMRglc, approaching 0.4 rather than the value of 1 concluded in f-i (Gruetter et al., 2001)

n.a; not applicable, n.d; not detectable. Adapted from Cruz and Cerdan (1999). Reproduced with permission of the publisher

■ Figure 1.4-6

The turnover of the H3 hydrogens of cerebral glutamate and glutamine reveals subcellular compartmentation in the neuronal and glial compartments of rat brain. A fast deuterium exchange occurs during the metabolism of (1-¹³C)glucose on the H_{3_{proR}} and H_{3_{proS}} hydrogens of preexisting molecules of (2-¹³C)glutamate, catalyzed by cytosolic isocitrate dehydrogenase (NADP) and aconitase, respectively. A slower double exchange of the H_{3_{proR}} and H_{3_{proS}} occurs only in newly formed (2-¹³C)glutamate molecules in the TCA cycle (*upper panel*). Additive isotopic shifts make it possible to distinguish between perprotonated (2-¹³C)glutamate (GLU C2) and glutamine (GLN C2) (singlets, *s*), (2-¹³C, ²H)glutamate and glutamine (shifted singlets, *ss*), and (2-¹³C, 3,3'-²H₂) glutamate and glutamine (doubly shifted singlet, *dss*) by high-resolution ¹³C NMR (*lower panel*). Deuterons are indicated by black triangles. ¹³C atoms are shown as dark gray circles



(¹³C, ²H) NMR indicates that the exchange of glutamate across the inner mitochondrial membrane is slow in the H3 hydrogen exchange time scale.

Finally, despite their enormous potential in the evaluation of metabolic pathways *in vivo* and *in vitro*, ¹³C NMR procedures (and to a smaller extent ³¹P NMR or ¹H NMR) are limited by their low sensitivity and

spatial resolution. Unfortunately, *in vivo* and *in vitro* ^{13}C NMR spectra are often obtained from relatively large voxels (up to approximately 50 ml in humans) or extracts prepared from sufficiently large tissue biopsies. These frequently include the weighted contributions from gray and white matter, as well as from smaller cerebral structures, making it impossible to resolve the metabolism of individual neurons and astrocytes.

3.3 Dual Photon NADH Fluorescence Microscopy

Dual photon fluorescence microscopy is able to provide cellular resolution of fluorescent indicators at moderate tissue depths lower than 0.5 mm (Gratton et al., 2001; Kim and Schwille, 2003). The technique is based on classical approaches used previously to measure surface fluorescence (single photon) of NADH (Chance, 2004). Dual photon fluorescence microscopy uses pulsed laser excitation with two photons, the emission being detected with confocal optics. Advantages of the technique over classical single photon fluorescence include deeper penetration (because of the lower wavelength of the excitation pulses), lower “bleaching,” and the possibility of using longer examination times because of the lower energy involved. NADH fluorescence is particularly attractive from the point of view of TCA cycle activity measurements. A net increase in glycolytic activity is revealed by increased NADH fluorescence and a net increase in TCA cycle activity is associated to a decrease in NADH fluorescence. Notably, the important limitation of dual photon NADH fluorescence stems from the fact that only net increases or decreases in NADH can be measured. This reveals only the net metabolic balance between NADH-producing and -consuming pathways, and not the individual activities of glycolysis or the TCA cycle. Thus, it is not appropriate to interpret net NADH changes as revealing exclusively glycolytic or TCA cycle activity, since they could contain opposite contributions from either or both processes.

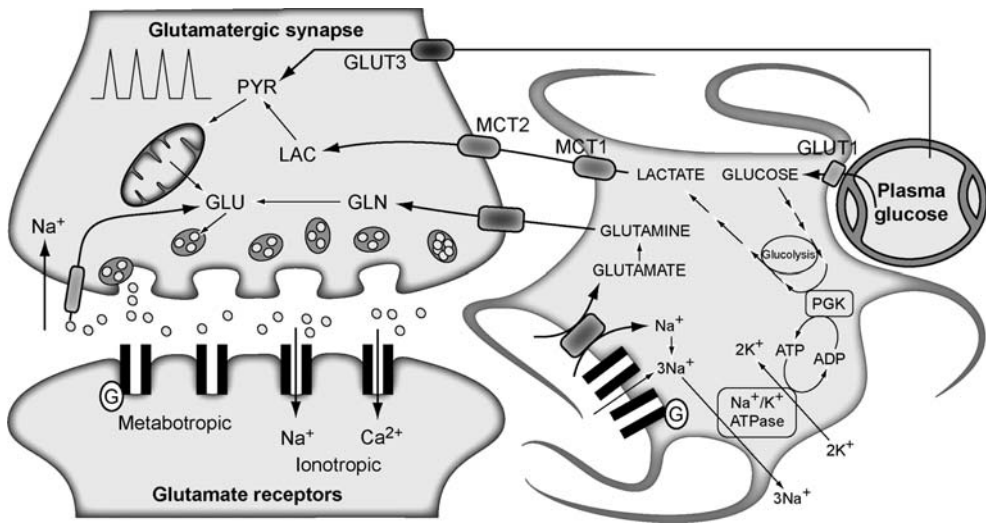
4 The Cerebral Tricarboxylic Acid Cycles During Cerebral Activation

4.1 The Metabolic Coupling Hypothesis

◆ *Figure 1.4-7* summarizes the main aspects of the metabolic coupling hypothesis in neurons and glia during glutamatergic neurotransmission, according to the early formulations of Tsacopoulos and Magistretti (1996). Their interpretation was based on pioneering experiments on the retina of honeybee drone, demonstrating that these Muller cells released alanine to the medium during photostimulation (Tsacopoulos et al., 1994). These results were soon confirmed with preparations of brain astrocytes, showing that these cells liberated lactate (instead of alanine) to the incubation medium after a glutamate challenge (Pellerin and Magistretti, 1994). These findings matched earlier evidences of cerebral activation *in vivo* as obtained from autoradiography, PET, functional magnetic resonance imaging (fMRI), and magnetic resonance spectroscopy (Magistretti and Pellerin, 1999, 2000). Most of the glutamate released to the synaptic cleft after the presynaptic action potential is recaptured by the surrounding astrocytes. Presynaptic glutamate release largely exceeds the amount needed for neurotransmission, causing a transient increase in extracellular glutamate levels from approximately 4–5 μM in the resting state to well over 100 μM just after its release from presynaptic vesicles. These high glutamate concentrations could preclude further neurotransmission events or even become neurotoxic, unless rapidly cleared from the synapses. This vital task is performed by the astrocytes surrounding the synapses, which are able to remove the large excess of synaptic glutamate through their highly efficient glutamate transporters. Glutamate is cotransported to the astrocyte together with three Na^+ ions, which need to be returned to the extracellular medium to restore the membrane potential. This is thought to involve the activity of the Na^+/K^+ -ATPase, at the expense of one ATP molecule. Once in the astrocyte, glutamate is amidated to glutamine by glutamine synthase, an exclusively astrocytic enzyme, consuming one additional ATP molecule. Thus, complete transformation of astrocytic glutamate in glutamine demands two ATP molecules, which were originally proposed to be derived exclusively from the anaerobic metabolism of glucose. According to this proposal, astrocytes would

■ Figure 1.4-7

The metabolic coupling hypothesis in neurons and glial cells during glutamatergic neurotransmission as formulated originally. Glutamate released to the synaptic cleft during glutamatergic neurotransmission is cotransported with Na^+ to the astrocytes. Astroglial Na^+ is exchanged by extracellular K^+ through the Na^+/K^+ -ATPase, consuming one ATP molecule. Astrocytic glutamate produces glutamine through glutamine synthase, consuming one additional ATP molecule. Lactate produced in astroglial glycolysis to support these energy demands is extruded to the extracellular medium, taken up by the surrounding neurons, and oxidized as their main metabolic fuel. Note the apparent stoichiometric coupling between glutamate–glutamine cycling and glucose uptake as well as the exclusive glycolytic or oxidative metabolisms in astrocytes and neurons, respectively. MCT1 and MCT2, monocarboxylate transporters 1 and 2; GLUT 1 and GLUT 3, glucose transporters 1 and 3. Adapted with permission from Tscopoulos and Magistretti (1996)



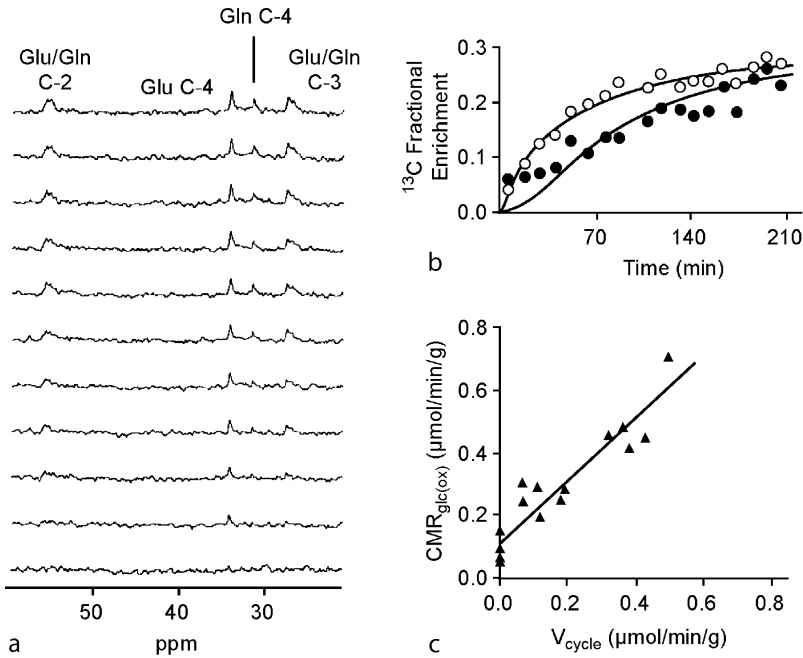
only need the anaerobic degradation of one glucose molecule taken from nearby capillaries to transform one glutamate molecule into glutamine, in a process producing two lactate molecules. Glutamine and lactate released from astrocytes would be taken up by the neurons, to regenerate neurotransmitter glutamate and become oxidized in the neuronal TCA cycle to maintain neuronal energetics, respectively. On these grounds, glutamatergic neurotransmission was proposed to be stoichiometrically coupled to astrocytic glucose uptake and lactate production, the latter becoming the main oxidative fuel for neurons (Magistretti et al., 1999; Rothman et al., 1999; Shulman et al., 2004).

4.2 ^{13}C NMR Evidences and the Neuronal Tricarboxylic Acid Cycle

Early *in vivo* ^{13}C NMR experiments supported this hypothesis (Sibson et al., 1997, 1998a). Authors infused ($1\text{-}^{13}\text{C}$)glucose and followed its metabolism in the *in vivo* brain using ^{13}C NMR. It was possible to observe the accumulation of ^{13}C label in the C4 carbons of glutamate and glutamine (Figure 1.4-8a and Figure 1.4-8b). The turnover of the C4 carbon of glutamate was considered to reflect the activity of the neuronal TCA cycle (V_{TCAAn}) while the turnover of the glutamine C4 carbon was thought to indicate the turnover of the glutamate–glutamine cycle (V_{cycle}). The results obtained confirmed earlier measurements of the cerebral TCA cycle flux *in vivo* ($V_{\text{TCAAn}} = 0.5\text{--}0.6 \mu\text{mol}/\text{min}/\text{g}$), assuming its predominant neuronal location under these conditions. It was also possible to calculate the flux through glutamine synthase ($0.2 \mu\text{mol}/\text{min}/\text{g}$), assuming that it accounted for a major part of glutamate turnover in the brain. These *in*

■ Figure 1.4-8

The cerebral tricarboxylic acid cycle and glutamatergic neurotransmission as detected by in vivo ^{13}C NMR. (a) Consecutive ^{13}C NMR spectra of rat brain during ($1\text{-}^{13}\text{C}$)glucose infusion (Sibson et al., 1997). (b) In vivo kinetics of ^{13}C enrichment in cerebral glutamate C4 and glutamine C4 during ($1\text{-}^{13}\text{C}$)glucose infusion, thought to represent the neuronal TCA cycle and the glutamine cycle, respectively (Sibson et al., 1997). (c) Apparent stoichiometric relationship between the cerebral metabolic rate for glucose oxidation (CMR_{glc}) and the glutamine cycle flux (V_{cycle}), during the metabolism of ($1\text{-}^{13}\text{C}$)glucose in the brain of rats subjected to increasing degrees of anesthesia (Sibson et al., 1998a). Reproduced with permission of the publisher



vivo results were consistent with the stoichiometric coupling of glucose metabolism and glutamate–glutamine cycling. Further experiments monitored dynamically the cerebral metabolism of ($1\text{-}^{13}\text{C}$) glucose in rats subjected to increasing degrees of anesthesia, as obtained with α -chloralose, morphine, or pentobarbital (Figure 1.4-8). Quantitative analysis of the time courses of ^{13}C enrichments in glutamate and glutamine C4, with the help of a minimal mathematical model of the neuronal TCA cycle and the glial glutamine synthase, revealed that the glutamate–glutamine cycle is a major pathway of cerebral metabolism accounting for up to 80% of the energy derived from glucose oxidation in the brain (Rothman et al., 2003).

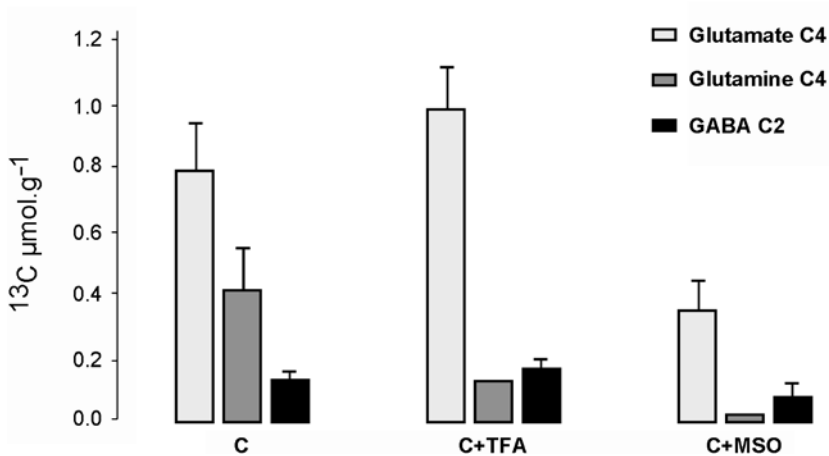
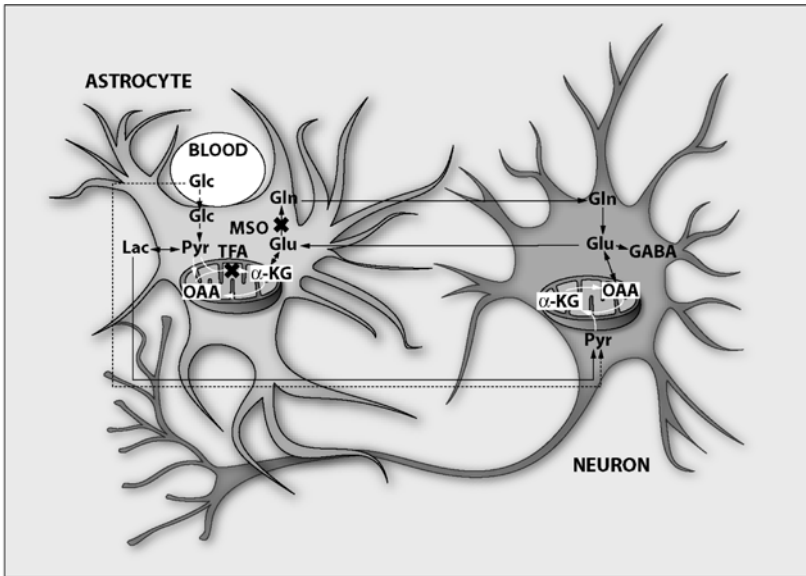
An important aspect of these studies concerned the energetics of glutamatergic neurotransmission. For a TCA cycle flux of $0.6 \mu\text{mol/min/g}$ and a glutamine cycle flux of $0.2 \mu\text{mol/min/g}$, the cerebral oxidative ATP production capacity approaches $20.4 \mu\text{mol/min/g}$ while the ATP demand for glutamine synthesis is $0.4 \mu\text{mol/min/g}$. Thus, glutamine production and the glutamine cycle account for approximately 2% of the energy produced during glucose oxidation, the rest being invested in the maintenance of presynaptic and postsynaptic resting and action potentials and other processes associated with neurotransmission. This balance corresponds to the calculations of Attwell and Iadecola (2002), who proposed an energy budget to interpret the energetics of cerebral activation as observed in fMRI experiments. Their conclusions indicated that in rodents 2% of cerebral energy is dedicated to maintaining the glutamine cycle, the remaining being invested in maintaining the resting membrane potential or presynaptic and postsynaptic action potentials.

4.3 The Astroglial Tricarboxylic Acid Cycle

An important limitation of these interpretations is the neglected role of the astroglial TCA cycle during glutamine synthesis and under conditions of cerebral activation. To address this aspect more specifically, authors infused ($1\text{-}^{13}\text{C}$)glucose in the presence and in the absence of trifluoroacetic acid (TFA), a selective inhibitor of the astroglial TCA cycle or methionine sulfoximine (MSO), a selective inhibitor of glutamine synthase (● [Figure 1.4-9a](#)) (Garcia-Espinosa et al., 2003). TFA inhibited approximately 60% of glutamine

■ Figure 1.4-9

Role of the astroglial tricarboxylic acid cycle supporting glutamatergic neurotransmission. (a) Trifluoroacetic acid (TFA) and methionine sulfoximine (MSO) strategies to inhibit the astroglial TCA cycle and glutamine synthase, respectively. (b) Effects of TFA or MSO on the steady-state labeling of ($4\text{-}^{13}\text{C}$)glutamate, ($4\text{-}^{13}\text{C}$)glutamine, and ($2\text{-}^{13}\text{C}$)GABA after ($1\text{-}^{13}\text{C}$)glucose infusions. (c) Control. Reproduced from Garcia-Espinosa et al. (2004) with permission of the publisher



synthesis, revealing a predominant contribution of the glial TCA cycle to the energy used in glutamine synthesis (▶ [Figure 1.4-9b](#)). This finding introduced an important modification over preexisting concepts that considered glutamine synthesis to be exclusively dependent on glycolytic ATP production (Garcia-Espinosa et al., 2004). These results also showed that complete inhibition of glutamine synthesis with MSO did not abort glutamate turnover, as would be expected for a precise stoichiometric coupling of the glutamate–glutamine cycle. In contrast, the experiments showed that approximately 40% of cerebral glutamate was not derived from astroglial glutamine, suggesting that additional neuronal precursors such as glucose or lactate play an important role in its synthesis.

Notably, nonstoichiometric coupling of the glutamine cycle with glucose uptake has also been found during ($1\text{-}^{13}\text{C}$)glucose metabolism, with very similar data and with a different model of cerebral metabolism (Gruetter et al., 2001). Taken together, these studies disclosed an important role for the astroglial TCA cycle supporting astrocytic energetics and glutamine synthesis, revealing that the coupling mechanisms between neurons and glial cells during glutamatergic neurotransmission were more complex than those initially envisioned.

4.4 The Redox Switch and the Redox Coupling Hypothesis

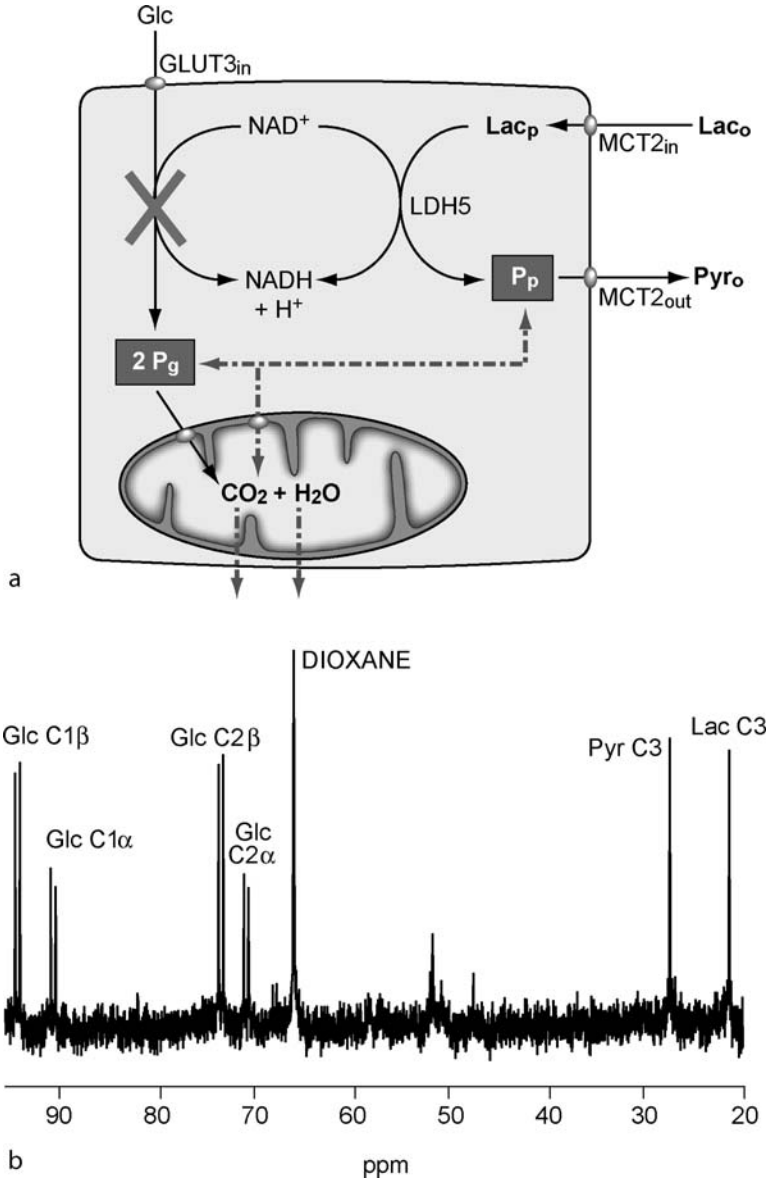
An interesting aspect of the original metabolic coupling hypothesis is that it confined anaerobic metabolism of glucose to astrocytes and lactate oxidation to neurons, suggesting that lactate produced in the astrocytes became the main fuel for the neurons (Tsacopoulos and Magistretti, 1996; Magistretti et al., 1999). However, glucose was known to be present in the extracellular space in similar concentrations as lactate, and neurons were known to be equipped with adequate glucose transporters and glycolytic machinery. Therefore, extracellular glucose could also become an important substrate for neuronal cells *in vivo*. An attractive proposal integrating the glucose/lactate competition as neuronal substrates has been put forward recently (Cruz et al., 2001).

To address this point, the authors investigated the competitive metabolism of ($1,2\text{-}^{13}\text{C}_2$)glucose and ($3\text{-}^{13}\text{C}$)pyruvate in primary cultures of cortical neurons. It was shown that even though both lactate precursors were simultaneously available to the neurons, the ($3\text{-}^{13}\text{C}$)lactate released into the incubation medium was derived only from ($3\text{-}^{13}\text{C}$)pyruvate (▶ [Figure 1.4-10b](#)). This implied that cytosolic pyruvate in the neurons was compartmentalized in two kinetically different pools (▶ [Figure 1.4-10a](#)), one being derived from extracellular three-carbon precursors such as pyruvate or lactate (P_p pool) and the other arising from the glycolytic metabolism of glucose (P_g pool). It was proposed that increased extracellular pyruvate or lactate concentrations drastically modified the neuronal cytosolic NAD^+/NADH redox state, modulating glycolytic flux at the glyceraldehyde-3-phosphate dehydrogenase (GAPDH) step and acting eventually as a redox switch. It followed that high extracellular lactate concentrations, such as those produced during neuronal activation, would inhibit neuronal GAPDH by significantly decreasing cytosolic NAD^+ availability. This would concomitantly decrease the formation of neuronal pyruvate from glucose and favor the oxidation of the pyruvate pool derived from extracellular three-carbon precursors. From this point of view, kinetic compartmentation of the intracellular pyruvate pool in the neurons was considered to be due to the faster time scales of lactate transport and lactate dehydrogenase (LDH) activity, as compared with the slower glycolytic flux, rather than due to any intracellular organization of the different lactate dehydrogenase isozymes (Bittar et al., 1996; Laughton et al., 2000). It should also be mentioned at this point that pyruvate compartmentation was almost simultaneously demonstrated in primary cultures of astrocytes (Zwingmann et al., 2001).

These findings contain important implications for the traditional conceptions of metabolic coupling between neurons and glial cells. First, it was shown that oxidative metabolism in the neurons could switch between glucose or lactate as alternative substrates, depending mainly on the cytosolic NAD/NADH redox state. Second, the neuronal cytosolic redox state was shown to be determined by the extracellular NAD/NADH redox balance, depending on the relative concentrations of extracellular pyruvate or lactate.

■ Figure 1.4-10

The redox switch. (a) Neurons are known to contain two kinetically different pools of pyruvate, a P_p pool with fast turnover derived from extracellular lactate, and a P_g pool with slower turnover derived from glucose. Extracellular lactate (Lac_o) enters the neuron, being instantly oxidized by LDH to pyruvate, which then enters the TCA cycle. Since NAD^+ has been used fast and completely to oxidize the intracellular lactate pool, the glycolytic flux is decreased or even stopped by the resulting NAD^+ limitation, and pyruvate derived from glucose (P_g) is not appreciably oxidized under these conditions. (b) ^{13}C NMR spectra of the incubation medium of neurons incubated with 1 mM ($1,2-^{13}C_2$)glucose and 1 mM ($3-^{13}C$)pyruvate. Note that only the ($3-^{13}C$)lactate singlet derived from pyruvate is detected. Adapted from Cruz et al. (2001). Reproduced with permission of the publisher



Finally, the extracellular NAD/NADH redox state could be modulated by changes in astrocytic lactate (and pyruvate) production, a process known to increase after glutamatergic neurotransmission. Together, these evidences disclosed that intracellular pyruvate compartmentation in the neurons and the redox switch could play a fundamental role in the metabolic coupling between oxidative and nonoxidative metabolisms of neurons and glia during glutamatergic neurotransmission.

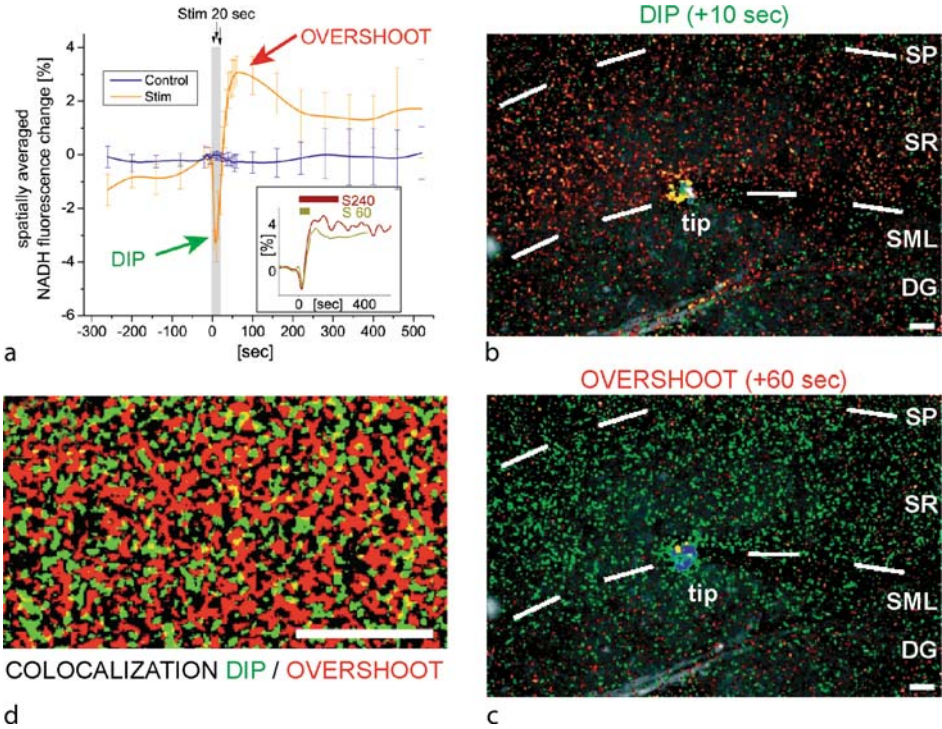
The redox coupling hypothesis supports the following sequence of events. Following presynaptic glutamate release, astrocytic transporters incorporate glutamate and three Na^+ ions to the astrocytic cytosol, Na^+ ions being removed later through the plasma membrane Na^+/K^+ -ATPase. This results in decreased astrocytic ATP/ADP concentrations, which stimulates both glycolysis and the astroglial TCA cycle (see *Sect. 3.2*). Both astrocytic glycolysis and the TCA cycle contribute the energy required by glutamine synthase, with a predominant contribution from the oxidative metabolism. However, the energy demands during glutamatergic neurotransmission exceed the reduced capacity of the astrocytic TCA cycle, resulting in a net activation of the glycolic flux and a net production of lactate, which is rapidly extruded to the extracellular space. Extracellular lactate is taken up by neurons, their cytosolic redox being reduced to a point where glycolysis is inhibited at the GAPDH step. Under these conditions, extracellular lactate is mainly consumed during oxidation in the neurons, and also in the astrocytes, until its extracellular concentration decreases to preactivation levels, setting up the stage for a new glutamatergic event. Interestingly, this proposal is consistent with the simultaneous operation of both the neuronal and the glial TCA cycles, making this intercellular coupling similar to the intracellular redox coupling by transfer of reducing equivalents from cytosol to mitochondria in individual neural cells. Intracellular compartmentation of pyruvate in neurons and astrocytes allows both cells to switch between glucose and lactate as their main oxidative substrates during resting and stimulated conditions, respectively. Our proposal is consistent with the well-known capacity of neurons and astrocytes to use glucose or lactate as energy fuels, allowing neurons to maintain a predominant oxidative role and astrocytes a predominant glycolytic role. This interpretation is also consistent with the predominant location of the glutamate–aspartate exchanger in neurons (Ramos et al., 2003) and the successive oxidative and glycolytic NADH balances in neurons and astrocytes, following electrical simulation, as indicated below.

4.5 NADH Balance in Neurons and Glia During Cerebral Activation

Recently, dual photon NADH fluorescence confocal microscopy has been able to resolve in time the NADH balances occurring in neurons and astrocytes during glutamatergic activation (Kasischke et al., 2004; Pellerin and Magistretti, 2004; [Figure 1.4-11](#)). Using cerebral cortex slices stimulated electrically, the authors first found a transient decrease in NADH fluorescence colocalized with neuronal markers and sensitive to postsynaptic receptor inhibitors. After the fast neuronal NADH depression, a sustained and more pronounced increase in NADH fluorescence was observed, which colocalized with astrocytic markers. The transient decrease of neuronal NADH fluorescence could be due to net aerobic oxidation of glucose in the neuronal respiratory chain, while the increase in astrocytic NADH fluorescence could be attributed to anaerobic net lactate production in the astrocytes. These interesting observations are consistent with our redox switch and redox coupling hypothesis, as well as with earlier PET/FDG, ^1H NMR, and ^{13}C NMR results (Prichard et al., 1991; Hyder et al., 1996; Raichle, 1998; Mintun et al., 2001). In particular, NADH fluorescence results suggest that the FDG accumulation observed during cerebral activation occurs in the astrocytes, rather than in the neurons, as was originally thought. However, it should be emphasized here that the measured fluorescence increases or decreases represent only the net balance between NADH production and consumption processes in neurons and astrocytes, rather than their absolute oxidative or glycolytic capacities. These results are therefore in agreement with the significant oxidative capacity proposed for the astrocytes as well as with the considerable glycolytic capacity known to be available to neurons, as long as the net balance between both processes favors neuronal oxidation and astrocytic glycolysis in the early and late phases of cerebral activation, respectively.

■ Figure 1.4-11

Confocal dual photon NADH fluorescence of neurons and glial cells *ex vivo* during electrical stimulation of cerebral cortex slices. (a) Biphasic response after activation of the Schaffer collateral pathway (orange) as compared with resting state (blue). Note the NADH fluorescence dip followed by NADH fluorescence overshoot (orange). (b) The NADH dip colocalizes with neurons (green). (c) The NADH overshoot colocalizes with astrocytes (red). (d) Binary image of NADH dip and NADH overshoot shows that both phases are anticolocalized. Reproduced from Kasischke et al. (2004) with permission of the publisher



5 Concluding Remarks and Future Perspectives

In summary, we provide an update on the operation of the TCA cycles in the neuronal and glial compartments of the adult mammalian brain and the methodologies used to investigate them. Present results reveal that cerebral activation increases the activity of both neuronal and glial TCA cycles. These changes result in important redox shifts in astrocytes and neurons, connected through the vectorial transfer of lactate-reducing equivalents. We propose here that redox coupling, redox switching, and intracellular pyruvate compartmentation provide the necessary coupling between oxidative and glycolytic metabolisms of neurons and glia. Intercellular redox coupling is proposed to operate in a manner similar to the intracellular coupling between cytosolic and mitochondrial NAD(P)/NAD(P)H redox states in individual neural cells, involving transcellular lactate transfers rather than intracellular mitochondrial shuttles.

Finally, our understanding of the coupling mechanisms between glucose oxidation and glycolysis in the neuronal and glial compartments of the adult brain, or their relationship to glutamatergic neurotransmission, is far from complete. More quantitative information is needed on the redox dependence of glycolysis and respiration in astrocytes and neurons and on how these processes are integrated in the *in vivo* brain. To progress in this direction, we need faster measurements of cerebral metabolite turnover at the cellular and subcellular levels and experimental approaches providing increased sensitivity and resolution.

Acknowledgments

This work was supported in part by grants SAF 2001-224, SAF 2004-03197, FISss C03/08, G03/155, C03/10 and PI051530 to S.C. JUSTESA IMAGEN S.A. provided the core support of LISMAR during this work. T.B. R was supported by a fellowship from Fundação para a Ciência e Tecnologia, Portugal (SFRH/BD/5407/2001). The authors are indebted to Mr. Javier Pérez for careful drafting of the illustrations.

References

- Akiba T, Hiraga K, Tuboi S. 1984. Intracellular distribution of fumarate in various animals. *J Biochem (Tokyo)* 96: 189-195.
- Ali G, Wasco W, Cai X, Szabo P, Sheu KF, et al. 1994. Isolation, characterization, and mapping of gene encoding dihydrolypoyl succinyltransferase (E2k) of human alpha-ketoglutarate dehydrogenase complex. *Somat Cell Mol Genet* 20: 99-105.
- Almeida A, Medina JM. 1997. Isolation and characterization of tightly coupled mitochondria from neurons and astrocytes in primary culture. *Brain Res* 764: 167-172.
- Almeida A, Medina JM. 1998. A rapid method for the isolation of metabolically active mitochondria from rat neurons and astrocytes in primary culture. *Brain Res Brain Res Protoc* 2: 209-214.
- Almeida A, Moncada S, Bolanos JP. 2004. No glial cell with NO. *Nat Cell Biol* 6(1): 17-18.
- Attwell D, Iadecola C. 2002. The neural basis of functional brain imaging signals. *Trends Neurosci* 25: 621-625.
- Au HC, Ream-Robinson D, Bellew LA, Broomfield PL, Saghbini M, et al. 1995. Structural organization of the gene encoding the human iron-sulfur subunit of succinate dehydrogenase. *Gene* 159: 249-253.
- Bachelard HS, Lewis LD, Ponten U, Siesjo BK. 1974. Mechanisms activating glycolysis in the brain in arterial hypoxia. *J Neurochem* 22: 395-401.
- Badar-Goffer RS, Bachelard HS, Morris PG. 1990. Cerebral metabolism of acetate and glucose studied by ^{13}C -n.m.r. spectroscopy. A technique for investigating metabolic compartmentation in the brain. *Biochem J* 266: 133-139.
- Barrientos A. 2002. In vivo and in organello assessment of OXPHOS activities. *Methods* 26: 307-316.
- Benn P, Chern CJ, Bruns G, Craig IW, Croce CM. 1977. Assignment of the genes for human beta-glucuronidase and mitochondrial malate dehydrogenase to the region pter leads to q22 of chromosome 7. *Cytogenet Cell Genet* 19: 273-280.
- Berkich DA, Xu Y, Lanoue KF, Gruetter R, Hutson SM. 2005. Evaluation of brain mitochondrial glutamate and alpha-ketoglutarate transport under physiologic conditions. *J Neurosci Res* 79: 106-113.
- Berl S. 1965. Compartmentation of glutamic acid metabolism in developing cerebral cortex. *J Biol Chem* 240: 2047-2054.
- Berl S, Clarke DD. 1969. Compartmentation of amino acid metabolism. Lajtha AL, editor. *Handbook of neurochemistry*. Plenum Press; editor. New York; pp. 447-472.
- Berl S, Nicklas WJ, Clarke DD. 1968. Compartmentation of glutamic acid metabolism in brain slices. *J Neurochem* 15: 131-140.
- Berl S, Nicklas WJ, Clarke DD. 1970. Compartmentation of citric acid cycle metabolism in brain: Labelling of glutamate, glutamine, aspartate and gaba by several radioactive tracer metabolites. *J Neurochem* 17: 1009-1015.
- Bittar PG, Charnay Y, Pellerin L, Bouras C, Magistretti PJ. 1996. Selective distribution of lactate dehydrogenase isoenzymes in neurons and astrocytes of human brain. *J Cereb Blood Flow Metab* 16: 1079-1089.
- Bluml S, Moreno-Torres A, Shic F, Nguy CH, Ross BD. 2002. Tricarboxylic acid cycle of glia in the in vivo human brain. *NMR Biomed* 15: 1-5.
- Brenner V, Nyakatura G, Rosenthal A, Platzer M. 1997. Genomic organization of two novel genes on human Xq28: Compact head to head arrangement of IDH gamma and TRAP delta is conserved in rat and mouse. *Genomics* 44: 8-14.
- Burtscher IM, Holtas S. 2001. Proton MR spectroscopy in clinical routine. *J Magn Reson Imaging* 13: 560-567.
- Cerdan S. 2003. ^{13}C NMR and cerebral biochemistry. *NMR Biomed* 16: 301-302.
- Cerdan S, Kunnecke B, Seelig J. 1990. Cerebral metabolism of [1,2- $^{13}\text{C}_2$]acetate as detected by in vivo and in vitro ^{13}C NMR. *J Biol Chem* 265: 12916-12926.
- Cerdan S, Rodrigues TB, Ballesteros P, Lopez P, Perez-Mayoral E. 2003. *The subcellular metabolism of water and its implications for magnetic resonance image contrast*. Magnetic resonance in food science. Belton PS, Gil AM, Webb GA, Rutledge D, editors. Oxford: Royal Society of Chemistry; pp. 121-135.
- Chance B. 2004. Mitochondrial NADH redox state, monitoring discovery and deployment in tissue. *Methods Enzymol* 385: 361-370.
- Chapa F, Cruz F, Garcia-Martin ML, Garcia-Espinosa MA, Cerdan S. 2000. Metabolism of (1- ^{13}C) glucose and (2- ^{13}C , 2- $^2\text{H}_3$) acetate in the neuronal and glial compartments of the adult rat brain as detected by [^{13}C , ^2H] NMR spectroscopy. *Neurochem Int* 37: 217-228.

- Chapa F, Kunnecke B, Calvo R, Escobar del Rey F, Morreale de Escobar G, et al. 1995. Adult-onset hypothyroidism and the cerebral metabolism of (1,2-¹³C₂) acetate as detected by ¹³C nuclear magnetic resonance. *Endocrinology* 136: 296-305.
- Chhina N, Kuestermann E, Halliday J, Simpson LJ, Macdonald IA, et al. 2001. Measurement of human tricarboxylic acid cycle rates during visual activation by ¹³C magnetic resonance spectroscopy. *J Neurosci Res* 66: 737-746.
- Clark JB, Lai JCK. 1989. *Glycolytic, tricarboxylic acid cycle and related enzymes in brain*. Carbohydrates and energy metabolism. Boulton AA, Baker GB, Butterworth RF, editors. Clifton, NJ: Humana Press; pp. 233-281.
- Clarke DD, Lajtha AL, Maker HS. 1989. *Intermediary metabolism*. Basic neurochemistry. Siegel G, Agranoff B, Albers RW, Molinoff P, editors. New York: Raven Press; pp. 541-564.
- Consortium IHGS. 2001. Initial sequencing and analysis of the human genome. *Nature* 409: 860-921.
- Consortium MGS. 2002. Initial sequencing and comparative analysis of the mouse genome. *Nature* 420: 520-562.
- Cruz F, Cerdan S. 1999. Quantitative ¹³C NMR studies of metabolic compartmentation in the adult mammalian brain. *NMR Biomed* 12: 451-462.
- Cruz F, Villalba M, Garcia-Espinosa MA, Ballesteros P, Bogonez E, et al. 2001. Intracellular compartmentation of pyruvate in primary cultures of cortical neurons as detected by ¹³C NMR spectroscopy with multiple ¹³C labels. *J Neurosci Res* 66: 771-781.
- De Gomez-Puyou MT, Chavez E, Freitas D, Gomez-Puyou A. 1972. On the regulation of succinate dehydrogenase in brain mitochondria. *FEBS Lett* 22: 57-60.
- De Graaf RA, Mason GF, Patel AB, Behar KL, Rothman DL. 2003. In vivo ¹H-¹³C-NMR spectroscopy of cerebral metabolism. *NMR Biomed* 16: 339-357.
- Dienel GA. 2002. Energy generation in the central nervous system. Edvinsson L, Krause DN, editors. *Cerebral blood flow and metabolism*. Philadelphia: Lippincott Williams & Wilkins; pp. 141-171.
- Dienel GA, Liu K, Cruz NF. 2001. Local uptake of ¹⁴C-labeled acetate and butyrate in rat brain in vivo during spreading cortical depression. *J Neurosci Res* 66: 812-820.
- Elbehti-Green A, Au HC, Mascarello JT, Ream-Robinson D, Scheffler IE. 1998. Characterization of the human SDHC gene encoding of the integral membrane proteins of succinate-quinone oxidoreductase in mitochondria. *Gene* 213: 133-140.
- Erecinska M, Silver IA. 1990. Metabolism and role of glutamate in mammalian brain. *Prog Neurobiol* 35: 245-296.
- Feigenbaum AS, Robinson BH. 1993. The structure of the human dihydrolipoamide dehydrogenase gene (DLD) and its upstream elements. *Genomics* 17: 376-381.
- Fitzpatrick SM, Hetherington HP, Behar KL, Shulman RG. 1990. The flux from glucose to glutamate in the rat brain in vivo as determined by ¹H-observed, ¹³C-edited NMR spectroscopy. *J Cereb Blood Flow Metab* 10: 170-179.
- Garcia-Espinosa MA, Garcia-Martin ML, Cerdan S. 2003. Role of glial metabolism in diabetic encephalopathy as detected by high resolution ¹³C NMR. *NMR Biomed* 16: 440-449.
- Garcia-Espinosa MA, Rodrigues TB, Sierra A, Benito M, Fonseca C, et al. 2004. Cerebral glucose metabolism and the glutamine cycle as detected by in vivo and in vitro ¹³C NMR spectroscopy. *Neurochem Int* 45: 297-303.
- García-Martín ML, Ballesteros P, Cerdan S. 2001. The metabolism of water in cells and tissues as detected by NMR methods. *Prog Nucl Magn Reson Spectrosc* 39: 41-77.
- Garcia-Martin ML, Garcia-Espinosa MA, Ballesteros P, Bruix M, Cerdan S. 2002. Hydrogen turnover and subcellular compartmentation of hepatic [2-¹³C]glutamate and [3-¹³C]aspartate as detected by ¹³C NMR. *J Biol Chem* 277: 7799-7807.
- Garfinkel D. 1966. A simulation study of the metabolism and compartmentation in brain of glutamate, aspartate, the Krebs cycle, and related metabolites. *J Biol Chem* 241: 3918-3929.
- Gibson GE, Park LC, Sheu KF, Blass JP, Calingasan NY. 2000. The alpha-ketoglutarate dehydrogenase complex in neurodegeneration. *Neurochem Int* 36: 97-112.
- Goldenthal MJ, Marin-Garcia J, Ananthkrishnan R. 1998. Cloning and molecular analysis of the human citrate synthase gene. *Genome* 41: 733-738.
- Gratton E, Barry NP, Beretta S, Celli A. 2001. Multiphoton fluorescence microscopy. *Methods* 25: 103-110.
- Gruetter R. 2002. In vivo ¹³C NMR studies of compartmentalized cerebral carbohydrate metabolism. *Neurochem Int* 41: 143-154.
- Gruetter R, Adriany G, Choi IY, Henry PG, Lei H, et al. 2003. Localized in vivo ¹³C NMR spectroscopy of the brain. *NMR Biomed* 16: 313-338.
- Gruetter R, Seaquist ER, Ugurbil K. 2001. A mathematical model of compartmentalized neurotransmitter metabolism in the human brain. *Am J Physiol Endocrinol Metab* 281: E100-E112.
- Gyulai L, Schnall M, McLaughlin AC, Leigh Jr, JS Chance B. 1987. Simultaneous ³¹P- and ¹H-nuclear magnetic resonance studies of hypoxia and ischemia in the cat brain. *J Cereb Blood Flow Metab* 7: 543-551.
- Hatazawa J, Fujita H, Kanno I, Satoh T, Iida H, et al. 1995. Regional cerebral blood flow, blood volume, oxygen extraction fraction, and oxygen utilization rate in normal volunteers measured by the autoradiographic technique and the single breath inhalation method. *Ann Nucl Med* 9: 15-21.

- Herholz K, Heiss WD. 2004. Positron emission tomography in clinical neurology. *Mol Imaging Biol* 6: 239-269.
- Hertz L. 2004. Intercellular metabolic compartmentation in the brain: Past, present and future. *Neurochem Int* 45: 285-296.
- Hertz L, Dienel GA. 2002. Energy metabolism in the brain. *Int Rev Neurobiol* 51: 1-102.
- Hertz L, Hertz E. 2003. Cataplerotic TCA cycle flux determined as glutamate-sustained oxygen consumption in primary cultures of astrocytes. *Neurochem Int* 43: 355-361.
- Hilberman M, Subramanian VH, Haselgrove J, Cone JB, Egan JW, et al. 1984. In vivo time-resolved brain phosphorus nuclear magnetic resonance. *J Cereb Blood Flow Metab* 4: 334-342.
- Hirawake H, Taniwaki M, Tamura A, Amino H, Tomitsuka E, et al. 1999. Characterization of the human SDHD gene encoding the small subunit of cytochrome *b* (cybS) in mitochondrial succinate-ubiquinone oxidoreductase. *Biochim Biophys Acta* 1412: 295-300.
- Hyder F, Chase JR, Behar KL, Mason GF, Siddeek M, et al. 1996. Increased tricarboxylic acid cycle flux in rat brain during forepaw stimulation detected with $^1\text{H}[^{13}\text{C}]$ NMR. *Proc Natl Acad Sci USA* 93: 7612-7617.
- Hyder F, Rothman DL, Mason GF, Rangarajan A, Behar KL, et al. 1997. Oxidative glucose metabolism in rat brain during single forepaw stimulation: A spatially localized $^1\text{H}[^{13}\text{C}]$ nuclear magnetic resonance study. *J Cereb Blood Flow Metab* 17: 1040-1047.
- James M, Man NT, Edwards YH, Morris GE. 1997. The molecular basis for cross-reaction of an anti-dystrophin antibody with alpha-actinin. *Biochim Biophys Acta* 1360: 169-176.
- Johnson JD, Mehus JG, Tews K, Milavetz BI, Lambeth DO. 1998. Genetic evidence for the expression of ATP- and GTP-specific succinyl-CoA synthetases in multicellular eucaryotes. *J Biol Chem* 273: 27580-27586.
- Kasischke KA, Vishwasrao HD, Fisher PJ, Zipfel WR, Webb WW. 2004. Neural activity triggers neuronal oxidative metabolism followed by astrocytic glycolysis. *Science* 305: 99-103.
- Kim SA, Schwille P. 2003. Intracellular applications of fluorescence correlation spectroscopy: Prospects for neuroscience. *Curr Opin Neurobiol* 13: 583-590.
- Kim YO, Oh IU, Park HS, Jeng J, Song BJ, et al. 1995. Characterization of a cDNA clone for human NAD^+ -specific isocitrate dehydrogenase alpha-subunit and structural comparison with its isoenzymes from different species. *Biochem J* 308 (Pt 1): 63-68.
- Kim YO, Park SH, Kang YJ, Koh HJ, Kim SH, et al. 1999. Assignment of mitochondrial NAD^+ -specific isocitrate dehydrogenase beta subunit gene (IDH3B) to human chromosome band 20p13 by in situ hybridization and radiation hybrid mapping. *Cytogenet Cell Genet* 86: 240-241.
- Kinsella BT, Doonan S. 1986. Nucleotide sequence of a cDNA coding for mitochondrial fumarase from human liver. *Biosci Rep* 6: 921-929.
- Komatsuoto S, Nioka S, Greenberg JH, Yoshizaki K, Subramanian VH, et al. 1987. Cerebral energy metabolism measured in vivo by ^31P -NMR in middle cerebral artery occlusion in the cat—relation to severity of stroke. *J Cereb Blood Flow Metab* 7: 557-562.
- Krebs HA. 1964. *The citric acid cycle*. Nobel lectures, physiology or medicine 1942-1962. Amsterdam: Elsevier; pp. 399-410.
- Krebs HA. 1970. Rate control of the tricarboxylic acid cycle. *Adv Enzyme Regul* 8: 335-353.
- Krebs HA, Johnson WA. 1937. Metabolism of ketonic acids in animal tissues. *Biochem J* 31: 645-660.
- Kunnecke B, Cerdan S, Seelig J. 1993. Cerebral metabolism of $[1,2-^{13}\text{C}]$ glucose and $[\text{U}-^{13}\text{C}]3$ -hydroxybutyrate in rat brain as detected by ^{13}C NMR spectroscopy. *NMR Biomed* 6: 264-277.
- Lai CK, Clark JB. 1989. Isolation and characterization of synaptic and nonsynaptic mitochondria from mammalian brain. Boulton AA, Baker GB, Butterworth RF, editors. *Carbohydrates and energy metabolism*. Clifton, NJ: Humana Press; pp. 43-98.
- Laughton JD, Charnay Y, Belloir B, Pellerin L, Magistretti PJ, et al. 2000. Differential messenger RNA distribution of lactate dehydrogenase LDH-1 and LDH-5 isoforms in the rat brain. *Neuroscience* 96: 619-625.
- Lebon V, Petersen KF, Cline GW, Shen J, Mason GF, et al. 2002. Astroglial contribution to brain energy metabolism in humans revealed by ^{13}C nuclear magnetic resonance spectroscopy: Elucidation of the dominant pathway for neurotransmitter glutamate repletion and measurement of astrocytic oxidative metabolism. *J Neurosci* 22: 1523-1531.
- Magistretti PJ, Pellerin L. 1999. Cellular mechanisms of brain energy metabolism and their relevance to functional brain imaging. *Philos Trans R Soc Lond B Biol Sci* 354: 1155-1163.
- Magistretti PJ, Pellerin L. 2000. The astrocyte-mediated coupling between synaptic activity and energy metabolism operates through volume transmission. *Prog Brain Res* 125: 229-240.
- Magistretti PJ, Pellerin L, Rothman DL, Shulman RG. 1999. Energy on demand. *Science* 283: 496-497.
- Malik P, McKenna MC, Tildon JT. 1993. Regulation of malate dehydrogenases from neonatal, adolescent, and mature rat brain. *Neurochem Res* 18: 247-257.
- Mason GF, Behar KL, Rothman DL, Shulman RG. 1992a. NMR determination of intracerebral glucose concentration and transport kinetics in rat brain. *J Cereb Blood Flow Metab* 12: 448-455.

- Mason GF, Gruetter R, Rothman DL, Behar KL, Shulman RG, et al. 1995. Simultaneous determination of the rates of the TCA cycle, glucose utilization, alpha-ketoglutarate/glutamate exchange, and glutamine synthesis in human brain by NMR. *J Cereb Blood Flow Metab* 15: 12-25.
- Mason GF, Rothman DL, Behar KL, Shulman RG. 1992b. NMR determination of the TCA cycle rate and alpha-ketoglutarate/glutamate exchange rate in rat brain. *J Cereb Blood Flow Metab* 12: 434-447.
- Matsuoka Y, Srere PA. 1973. Kinetic studies of citrate synthase from rat kidney and rat brain. *J Biol Chem* 248: 8022-8030.
- McIlwain H, Bachelard HS. 1985. *Biochemistry and the central nervous system*. London: Churchill-Livingstone.
- Minich T, Yokota S, Dringen R. 2003. Cytosolic and mitochondrial isoforms of NADP⁺-dependent isocitrate dehydrogenases are expressed in cultured rat neurons, astrocytes, oligodendrocytes and microglial cells. *J Neurochem* 86: 605-614.
- Mintun MA, Lundstrom BN, Snyder AZ, Vlassenko AG., Shulman GL, et al. 2001. Blood flow and oxygen delivery to human brain during functional activity: Theoretical modeling and experimental data. *Proc Natl Acad Sci USA* 98: 6859-6864.
- Mintun MA, Vlassenko AG, Rundle MM, Raichle ME. 2004. Increased lactate/pyruvate ratio augments blood flow in physiologically activated human brain. *Proc Natl Acad Sci USA* 101: 659-664.
- Mirel DB, Marder K, Graziano J, Freyer G, Zhao Q, et al. 1998. Characterization of the human mitochondrial aconitase gene (ACO2). *Gene* 213: 205-218.
- Moore CM, Frederick BB, Renshaw PF. 1999. Brain biochemistry using magnetic resonance spectroscopy: Relevance to psychiatric illness in the elderly. *J Geriatr Psychiatry Neurol* 12: 107-117.
- Morris AA, Farnsworth L, Ackrell BA, Turnbull DM, Birch-Machin MA. 1994. The cDNA sequence of the flavoprotein subunit of human heart succinate dehydrogenase. *Biochim Biophys Acta* 1185: 125-128.
- Nioka S, Zaman A, Yoshioka H, Masumura M, Miyake H, et al. 1991. ³¹P magnetic resonance spectroscopy study of cerebral metabolism in developing dog brain and its relationship to neuronal function. *Dev Neurosci* 13: 61-68.
- Owen OE, Kalhan SC, Hanson RW. 2002. The key role of anaplerosis and cataplerosis for citric acid cycle function. *J Biol Chem* 277: 30409-30412.
- Palmieri F. 2004. The mitochondrial transporter family (SLC25): Physiological and pathological implications. *Pflugers Arch* 447: 689-709.
- Palmieri F, Bisaccia F, Capobianco L, Dolce V, Fiermonte G, et al. 1996. Mitochondrial metabolite transporters. *Biochim Biophys Acta* 1275: 127-132.
- Palmieri L, Pardo B, Lasorsa FM, del Arco A, Kobayashi K, et al. 2001. Citrin and aralar1 are Ca²⁺-stimulated aspartate/glutamate transporters in mitochondria. *EMBO J* 20: 5060-5069.
- Passonneau JV, Lowry OH. 1964. The role of phosphofructokinase in metabolic regulation. *Adv Enzyme Regul* 2: 265-274.
- Patel MS, Korotchkina LG. 2001. Regulation of mammalian pyruvate dehydrogenase complex by phosphorylation: Complexity of multiple phosphorylation sites and kinases. *Exp Mol Med* 33: 191-197.
- Pellerin L, Magistretti PJ. 1994. Glutamate uptake into astrocytes stimulates aerobic glycolysis: A mechanism coupling neuronal activity to glucose utilization. *Proc Natl Acad Sci USA* 91: 10625-10629.
- Pellerin L, Magistretti PJ. 2004. Neuroscience. Let there be (NADH) light. *Science* 305: 50-52.
- Preece NE, Cerdan S. 1996. Metabolic precursors and compartmentation of cerebral GABA in vigabatrin-treated rats. *J Neurochem* 67: 1718-1725.
- Price JC. 2003. Principles of tracer kinetic analysis. *Neuroimaging Clin N Am* 13: 689-704.
- Prichard J, Rothman D, Novotny E, Petroff O, Kuwabara T, et al. 1991. Lactate rise detected by ¹H NMR in human visual cortex during physiologic stimulation. *Proc Natl Acad Sci USA* 88: 5829-5831.
- Raichle ME. 1998. Imaging the mind. *Semin Nucl Med* 28: 278-289.
- Ramos M, del Arco A, Pardo B, Martinez-Serrano A, Martinez-Morales JR, et al. 2003. Developmental changes in the Ca²⁺-regulated mitochondrial aspartate-glutamate carrier aralar1 in brain and prominent expression in the spinal cord. *Brain Res Dev Brain Res* 143: 33-46.
- Robinson Jr, JB Srere PA. 1985a. Organization of Krebs tricarboxylic acid cycle enzymes. *Biochem Med* 33: 149-157.
- Robinson Jr, JB Srere PA. 1985b. Organization of Krebs tricarboxylic acid cycle enzymes in mitochondria. *J Biol Chem* 260: 10800-10805.
- Ross AJ, Sachdev PS. 2004. Magnetic resonance spectroscopy in cognitive research. *Brain Res Brain Res Rev* 44: 83-102.
- Rossignol R, Letellier T, Malgat M, Rocher C, Mazat JP. 2000. Tissue variation in the control of oxidative phosphorylation: Implication for mitochondrial diseases. *Biochem J* 347 Pt 1: 45-53.
- Rothman DL, Behar KL, Hyder F, Shulman RG. 2003. In vivo NMR studies of the glutamate neurotransmitter flux and neuroenergetics: Implications for brain function. *Annu Rev Physiol* 65: 401-427.
- Rothman DL, Sibson NR, Hyder F, Shen J, Behar KL, et al. 1999. In vivo nuclear magnetic resonance spectroscopy studies of the relationship between the glutamate-glutamine

- neurotransmitter cycle and functional neuroenergetics. *Philos Trans R Soc Lond B Biol Sci* 354: 1165-1177.
- Sacktor B, Wilson JE, Tiekert CG. 1966. Regulation of glycolysis in brain, in situ, during convulsions. *J Biol Chem* 241: 5071-5075.
- Sazanov LA, Jackson JB. 1994. Proton-translocating transhydrogenase and NAD- and NADP-linked isocitrate dehydrogenases operate in a substrate cycle which contributes to fine regulation of the tricarboxylic acid cycle activity in mitochondria. *FEBS Lett* 344: 109-116.
- Shen J, Petersen KF, Behar KL, Brown P, Nixon TW, et al. 1999. Determination of the rate of the glutamate/glutamine cycle in the human brain by in vivo ^{13}C NMR. *Proc Natl Acad Sci USA* 96: 8235-8240.
- Sheu KF, Blass JP. 1999. The alpha-ketoglutarate dehydrogenase complex. *Ann N Y Acad Sci* 893: 61-78.
- Shulman RG, Rothman DL, Behar KL, Hyder F. 2004. Energetic basis of brain activity: Implications for neuroimaging. *Trends Neurosci* 27: 489-495.
- Sibson NR, Dhankhar A, Mason GF, Behar KL, Rothman DL, et al. 1997. In vivo ^{13}C NMR measurements of cerebral glutamine synthesis as evidence for glutamate-glutamine cycling. *Proc Natl Acad Sci USA* 94: 2699-2704.
- Sibson NR, Dhankhar A, Mason GF, Rothman DL, Behar KL, et al. 1998a. Stoichiometric coupling of brain glucose metabolism and glutamatergic neuronal activity. *Proc Natl Acad Sci USA* 95: 316-321.
- Sibson NR, Shen J, Mason GF, Rothman DL, Behar KL, et al. 1998b. Functional energy metabolism: In vivo ^{13}C -NMR spectroscopy evidence for coupling of cerebral glucose consumption and glutamatergic neuronal activity. *Dev Neurosci* 20: 321-330.
- Sierra A, Lopes da Fonseca L, Ballesteros P, Cerdan S. 2004. Quantitative modelling of H3 hydrogen turnover in ($2\text{-}^{13}\text{C}$) glutamate and ($2\text{-}^{13}\text{C}$) glutamine during ($2\text{-}^{13}\text{C}$) acetate metabolism in the adult rat brain; Copenhagen. p. 36.
- Siesjo BK. 1982. Lactic acidosis in the brain: Occurrence, triggering mechanisms and pathophysiological importance. *Ciba Found Symp* 87: 77-100.
- Smith E, Morowitz HJ. 2004. Universality in intermediary metabolism. *Proc Natl Acad Sci USA* 101: 13168-13173.
- Sokoloff L. 1981a. The deoxyglucose method for the measurement of local glucose utilization and the mapping of local functional activity in the central nervous system. *Int Rev Neurobiol* 22: 287-333.
- Sokoloff L. 1981b. Localization of functional activity in the central nervous system by measurement of glucose utilization with radioactive deoxyglucose. *J Cereb Blood Flow Metab* 1: 7-36.
- Sokoloff L. 1983a. Mapping local functional activity by measurement of local cerebral glucose utilization in the central nervous system of animals and man. *Harvey Lect* 79: 77-143.
- Sokoloff L. 1983b. Measurement of local glucose utilization and its use in localization of functional activity in the central nervous system of animals and man. *Recent Prog Horm Res* 39: 75-126.
- Sokoloff L. 1989. Circulation and energy metabolism of the brain. Siegel G, Agranoff B, Albers RW, Molinoff P, editors. *Basic neurochemistry*. New York: Raven Press; pp. 565-590.
- Sokoloff L. 1992. The brain as a chemical machine. *Prog Brain Res* 94: 19-33.
- Stewart VC, Land JM, Clark JB, Heales SJ. 1998. Comparison of mitochondrial respiratory chain enzyme activities in rodent astrocytes and neurones and a human astrocytoma cell line. *Neurosci Lett* 247: 201-203.
- Szabo P, Cai X, Ali G, Blass JP. 1994. Localization of the gene (OGDH) coding for the E1k component of the alpha-ketoglutarate dehydrogenase complex to chromosome 7p13-p11.2. *Genomics* 20: 324-326.
- Tsacopoulos M, Magistretti PJ. 1996. Metabolic coupling between glia and neurons. *J Neurosci* 16: 877-885.
- Tsacopoulos M, Veuthey AL, Saravelos SG, Perrotet P, Tsoupras G. 1994. Glial cells transform glucose to alanine, which fuels the neurons in the honeybee retina. *J Neurosci* 14: 1339-1351.
- Van den Berg CJ, Garfinkel D. 1971. A stimulation study of brain compartments. Metabolism of glutamate and related substances in mouse brain. *Biochem J* 123: 211-218.
- Van den Berg CJ, Krzalic L, Mela P, Waelsch H. 1969. Compartmentation of glutamate metabolism in brain. Evidence for the existence of two different tricarboxylic acid cycles in brain. *Biochem J* 113: 281-290.
- Van den Berg CJ, Mela P, Waelsch H. 1966. On the contribution of the tricarboxylic acid cycle to the synthesis of glutamate, glutamine and aspartate in brain. *Biochem Biophys Res Commun* 23: 479-484.
- Wienhard K. 2002. Measurement of glucose consumption using ^{18}F fluorodeoxyglucose. *Methods* 27: 218-225.
- Zwingmann C, Richter-Landsberg C, Leibfritz D. 2001. ^{13}C isotopomer analysis of glucose and alanine metabolism reveals cytosolic pyruvate compartmentation as part of energy metabolism in astrocytes. *Glia* 34: 200-212.

1.5 Electron Transport. Structure, Redox-Coupled Protonmotive Activity, and Pathological Disorders of Respiratory Chain Complexes

S. Papa · V. Petruzzella · S. Scacco

1	<i>Introduction</i>	94
2	<i>The Electron Transfer Centers of the Respiratory Chain</i>	94
3	<i>The Protein Structure of the Respiratory Chain Complexes</i>	97
3.1	Complex I	97
3.2	Complex II	99
3.3	Electron-Transferring Flavoprotein and ETFDH	99
3.4	Complex III	100
3.5	Complex IV	102
4	<i>The Mechanism of Protonmotive Energy Transfer in the Respiratory Chain</i>	102
5	<i>Biogenesis of Respiratory Chain Complexes</i>	107
6	<i>Genetic Disorders of the Respiratory Chain in Human Pathology</i>	109
6.1	Defects of Complex I	109
6.2	Defects of Complex II	110
6.3	Defects of Coenzyme Q	110
6.4	Defects of Complex III	110
6.5	Defects of Complex IV	110
6.6	Multiple Respiratory Chain Defects	111

Abstract: This chapter is intended to provide an overview of mitochondrial respiratory chain complexes from protein structure and functional mechanisms to their biogenesis and genetic disorders in neurological and other diseases. The general features and the electron transfer centers of the protonmotive respiratory chain is first dealt with. This section is followed by a description of the protein structure of the four redox complexes of the chain. A section is devoted to mechanism of the proton pump of complexes I, III and IV with particular emphasis to complex IV. The last two sections cover aspects of the biogenesis of the redox complexes and their genetic disorders in human pathology respectively.

1 Introduction

In mammals, oxidative phosphorylation (OXPHOS) in mitochondria under normal conditions can supply more than 80% of the cellular energy need. An adult human with a daily energy expenditure of approximately 2,500 kcal produces and consumes 250–300 moles (125–150 kg) of ATP. The brain is the organ with the highest demand for respiratory ATP. With a mass of only 2% of the total body weight, the brain consumes, under standard conditions around 300 l of O₂ per day, which amounts to 20% of all the atmospheric oxygen we breathe (Erecinska and Silver, 1989). Thus serious brain injuries can result from limited oxygen. On the other hand, the brain, dealing with so much oxygen, is extremely susceptible to oxidative damage caused by production of oxygen-free radicals (Langley and Ratan, 2004). Expression and functional activity of respiratory chain complexes and ATP synthase in mitochondria play a key role in cell development (Bates et al., 1994; Papa, 1996; Papa et al., 2004a) and apoptosis (Kuznetsov et al., 2004). Genetic disorders of the mitochondrial respiratory chain are primarily associated with human encephalopathies (DiMauro, 2004). Dysfunction of the respiratory chain is also observed in various neurodegenerative diseases (Orth and Schapira, 2001).

The respiratory chain of mitochondria is made up of four-redox-enzyme complexes. These are organized in the inner mitochondrial membrane so that reduced nicotinamide nucleotides and flavin coenzymes can be oxidized by oxygen in a stepwise controlled process, with conservation of up to 50% of the free energy thus made available as ATP (Papa, 1976; Papa et al., 1995; Saraste, 1999; Gnaiger et al., 2000) (▶ *Figure 1.5-1*). A key feature of cellular respiration is represented by regulation of the functional capacity of respiratory chain complexes at the level of gene expression (Scarpulla, 2005), posttranslational processing (Käser and Langer, 2000), membrane traffic (Wiedemann et al., 2004), membrane assembly (Koelher, 2004), and flux control processes (D. Nicholls, this volume). Protein kinases and phosphatases are present in mammalian mitochondria (cAMP-dependent protein kinase, casein kinases, protein kinase C, etc.) (Papa et al., 1999b; Thomson, 2002; Wong and Scott, 2004; Horbinski and Chu, 2005). Protein kinases and their substrates can provide mitochondrial extension of cellular signaling cascades, which may have an impact on mitochondrial functions and biogenesis.

The availability of the human genome sequence and the exponential development of functional genomics and proteomics offer new opportunities to decipher functional features and pathological disorders of the respiratory chain at the molecular level.

This chapter deals with the following aspects of the respiratory chain in mammalian mitochondria:

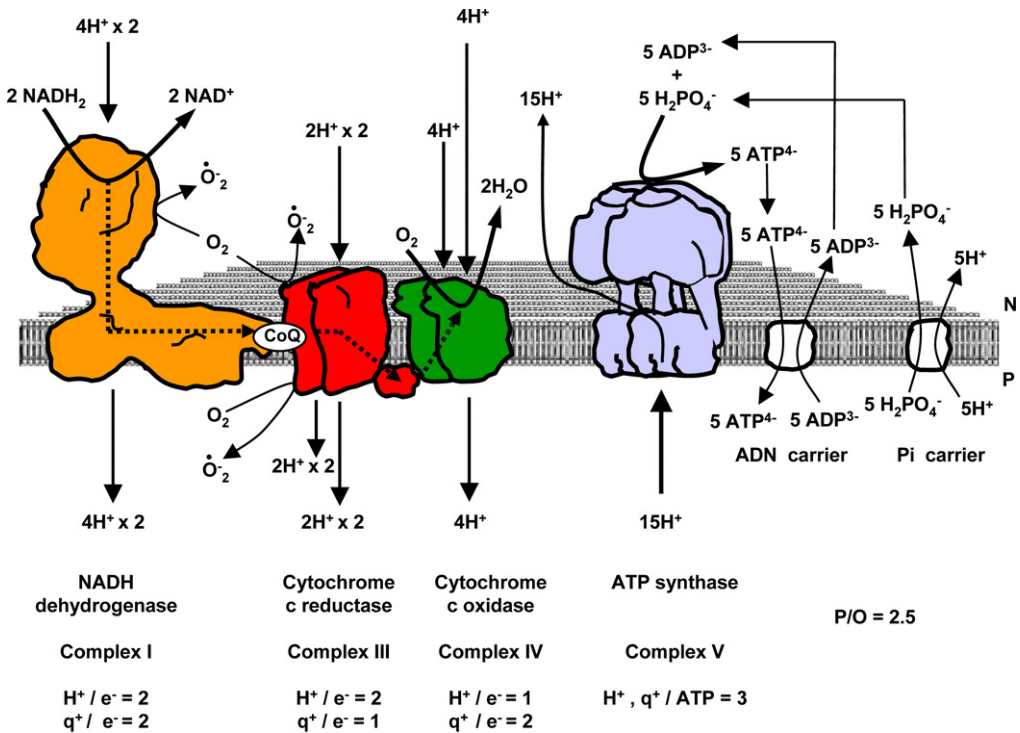
1. The electron transfer centers
2. The protein structure of the redox complexes
3. The mechanism of protonmotive energy transfer
4. The biogenesis of respiratory chain complexes
5. The genetic disorders of the respiratory chain

2 The Electron Transfer Centers of the Respiratory Chain

The concept of the respiratory chain was developed in 1920–1930 by D. Keilin and associates with the identification of cytochromes *a*, *b*, and *c* as universal redox carriers in aerobic organisms, acting in series to transfer electrons from reduced coenzymes to oxygen (Keilin, 1966). Keilin thus solved the

Figure 1.5-1

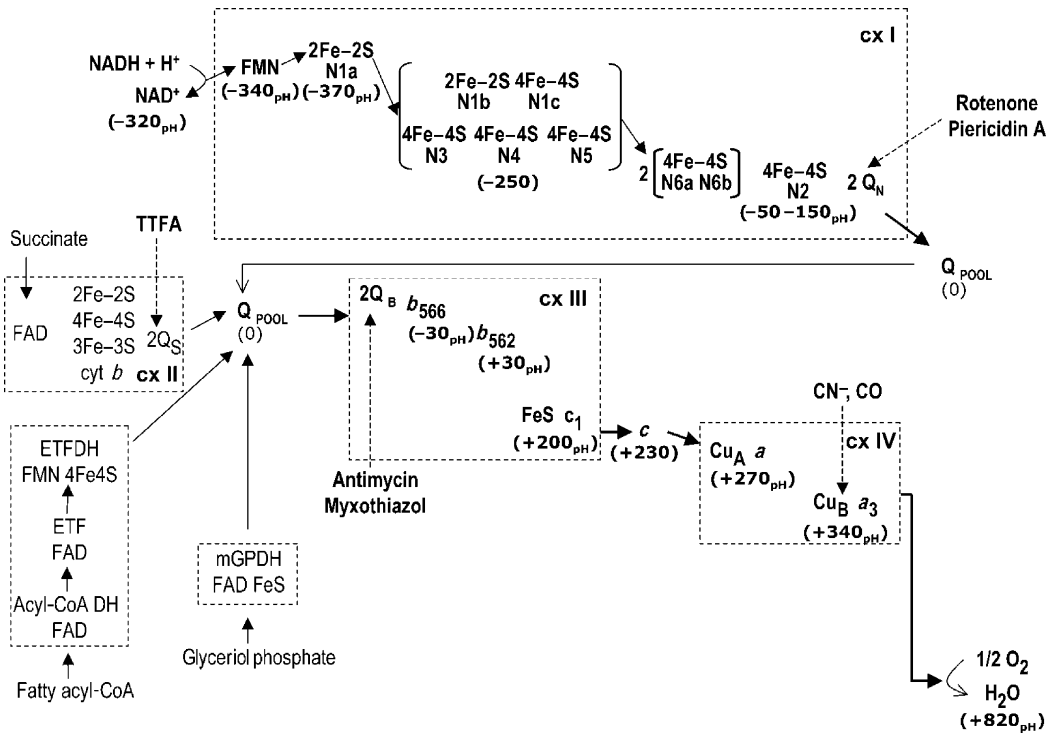
Respiratory complexes, ATP synthase, and protonic coupling of oxidative phosphorylation in the inner mitochondrial membrane. The shape of complex I is obtained from high-resolution electron microscopy image reconstitution (Friedrich and Bottcher, 2004), those of complex III (Xia et al., 1997, Hunte et al., 2000) and complex IV (Tsukihara et al., 1996) from X-ray crystallographic structures of the bovine heart enzymes. The shape of complex V results from X-ray (Abrahams et al., 1994; Stock et al., 1999) and electron microscopy structure reconstruction (Rubinstein et al., 2003). Complex III, IV, and V are shown in the dimeric state as they appear in the structural analysis. Complex II (succinate dehydrogenase), ETF dehydrogenase, and glycerolphosphate dehydrogenase, which feed reducing equivalents into the ubiquinone pool, are not shown in the scheme (however, see, Figure 1.5-2) and Sect. 3). The NADH₂ protons are released in the outer space upon oxidation of ubiquinone in complex III. The dotted line traversing the complexes represents the flow of reducing equivalents from NADH₂ to O₂. The maximal H⁺/e⁻ (proton release per e⁻ transfer) and q⁺/e⁻ (outward transfer of positive charges per e⁻ transfer) ratios attainable for the three redox complexes and the H⁺/ATP ratio for the ATP synthase are given at the bottom of the scheme. Proton and charge translocation for the import of H₂PO₄⁻ and ADP³⁻ with export of ATP⁴⁻ is also shown. The overall balance of oxidative phosphorylation results in the production of five ATP molecules in the oxidation of two molecules of NADH₂ by one molecule of O₂. The P/O of 2.5 represents the maximal attainable efficiency of oxidative phosphorylation. Under certain physiological conditions the efficiency of oxidative phosphorylation can decrease because of slips in the redox proton pumps (Canton et al., 1995; Lorusso et al., 1995; Papa et al., 1995; Capitanio et al., 1996) and proton backflow by leaks, or mediated by the uncoupler protein (Ricquier et al., 2000). Oxygen-free radical production at complexes I and III is also shown. N side, matrix space; P side, cytosolic side



Wieland–Warburg debate by linking cytochromes with the hydrogen-activating dehydrogenase of Wieland and with the oxygen-activating enzyme of Warburg. Keilin and associates showed that cytochrome *a* contains two hemes “*a*” and “*a*₃”, the latter reacting directly with CO and CN⁻ (Figure 1.5-2), the inhibitors used by Warburg to characterize the oxygen-activating enzyme. In the years that followed, the

Figure 1.5-2

Electron transfer centers of the respiratory chain in mammalian mitochondria. The centers are schematically shown with their midpoint potentials under standard conditions (25°C and pH 7.0). Where indicated by a suffix, electron transfer by cytochromes and iron–sulfur clusters exhibits pH dependence; this reflects cooperative H^+/e^- linkage at the center (redox Bohr effect Papa, 1976; Papa and Capitanio, 1998). Dotted boxes circumscribe the enzyme complexes (see Sect. 3) to which the redox centers are associated. Two specific ubiquinone binding sites are present in complexes I, II, and III (Meinhardt et al., 1987; Ohnishi, 1998). Q_{POOL} : ubiquinone of the pool Q_B : protein-bound ubiquinone. Specific inhibitor sites are also shown. Rotenone, antimycin, and myxothiazol exert their inhibitory effect by interacting specifically with only one of the two ubiquinone sites present in complex I (QN, QNf) and complex III (Qi and Qo), respectively. For more information see Beinert (1986), Brandt (1997), and Ohnishi (1998)



number of cytochromes identified in the eukaryotic respiratory chain increased to seven, and two copper atoms were found to be present in aa_3 cytochrome *c* oxidase (Nicholls, 1999). As additional components of the respiratory chain ubiquinone (Crane et al., 1957), in its free state in the membrane and protein-bound specific forms (Meinhardt et al., 1987; Ohnishi, 1998), riboflavin prosthetic groups and Fe–S centers (Beinert, 1986), the latter being more numerous than hemes, were identified and characterized (Figure 1.5-2).

In the years 1950–1960, two important breakthroughs shed new light on the structure/function of the respiratory chain. The first was the isolation of the four enzyme complexes I, II, III, and IV from bovine heart mitochondria, each catalyzing a separate redox step of the chain, which could be combined, in the presence of cytochrome *c*, to reconstitute the entire respiratory chain (Hatefi, 1999). The other development was the chemiosmotic hypothesis of oxidative and photosynthetic phosphorylation proposed by Mitchell (1961, 1966). Mitchell postulated that the respiratory chain, due to its anisotropic arrangement in the coupling membrane, directly converts redox free energy into a transmembrane electrochemical proton gradient ($\Delta\mu H$, protonmotive force, PMF), in turn utilized to phosphorylate ADP to ATP by the ATP synthase in the membrane.

▶ *Figure 1.5-2* provides a picture of the redox centers in the respiratory chain of mammalian mitochondria. Reducing equivalents donated by NADH/NAD at -320 mV are accepted by FMN in complex I and passed to Fe-S centers and protein-bound ubiquinone; they leave the last Fe-S center (N2) at an E_m of -50 to 150 mV (▶ *Figure 1.5-2*). Electrons from complex I, succinate dehydrogenase, acyl-CoA:Fp dehydrogenases, ETF, ETF dehydrogenase, and glycerolphosphate dehydrogenase converge into the ubiquinone pool (Q_p) at an E_m around zero (▶ *Figure 1.5-2*). Ubiquinone transfers electrons to *b* cytochromes in complex III. In this complex, electrons move down the Fe-S center and cytochrome c_1 , with the involvement of protein-bound quinone(s) (Meinhardt et al., 1987), and are passed to cytochrome c ($E_m = 230$ mv). Ferrocycytochrome c is oxidized during the reduction of molecular oxygen to H_2O by aa_3 cytochrome c oxidase. Enough redox energy is made available in electron flow from NADH to Q_p , Q_p to cytochrome c , and cytochrome c to O_2 to drive the ATP synthesis coupled to protonmotive electron flow in these three spans of the respiratory chain.

3 The Protein Structure of the Respiratory Chain Complexes

The four redox complexes that are part of the respiratory chain can be isolated by conventional salting in/out or affinity chromatography procedures in the pure, active enzyme state. The features of the enzyme catalytic activity, sensitivity to specific inhibitors, identification of redox components, and phospholipid requirement can be analyzed in these preparations (Hatefi, 1999). The purified soluble enzymes can be incorporated in well-characterized phospholipid vesicles (Papa et al., 1996a) or planar phospholipid membranes (Bamberg et al., 1993), in which the protonmotive energy transfer can be studied. In this way it was shown that complexes I, III, and IV can each, separately, function as a redox-driven proton pump. The subunit composition of the four complexes has been determined for the purified enzymes. By direct protein analysis and extensive cDNA (complementary DNA) sequencing, the primary structures of all the subunits of the complexes have been determined. Nowadays proteomic analysis is providing additional important information on the translational products of these proteins and their posttranslational modifications (Taylor et al., 2003). The overall subunit pattern of the complexes and their assembly status in the membrane can be easily obtained by two-dimensional nondenaturing blue native electrophoresis/SDS-PAGE (Schagger, 2001). This procedure is now largely used to simultaneously screen a subunit assembly of the complexes, in particular in mitochondrial diseases (see *Sect. 5* and *6*). It has also provided evidence indicating that the human respiratory complexes can be assembled into supramolecular structures in the inner mitochondrial membrane. Complexes I, III, and IV can apparently associate to form a structure-denominated “respirasome” (Schagger, 2002). The possible functional implication of the dimeric form of complexes III, IV, and V and of the association of complexes I, III, and IV in the respirasome is under investigation in various laboratories.

3.1 Complex I

By means of high-resolution electron microscopy and by studying two-dimensional projection maps and three-dimensional structures of prokaryotic and eukaryotic proton pumping, the structure of complex I (NADH ubiquinone oxidoreductase, EC 1.6.5.3) has been determined (Guenebaut et al., 1998; Grigorieff, 1999; Friedrich and Bottcher, 2004). The complex appears to have an L-shaped structure with two arms, the membrane-integral sector and the peripheral-catalytic moiety protruding in the matrix, perpendicular to each other (see ▶ *Figure 1.5-1*). Fourteen subunits of complex I are conserved in all the species from prokaryotes to eukaryotes so far analyzed (Carroll et al., 2003; Yagi and Matsuno-Yagi, 2003). These subunits contain all the known redox cofactors of the complex (Brandt, 1997; Vinogradov, 2001; Albracht et al., 2003), seven of them are hydrophobic and have putative membrane-spanning α -helices, and are considered to constitute the minimal functional core of the complex. In mammals, these subunits are encoded by the mitochondrial DNA (mtDNA). Mammalian complex I contains 39 additional subunits all encoded by nuclear genes (Hirst et al., 2003; Papa et al., 2004a) (▶ *Table 1.5-1*). The function of the

■ Table 1.5-1

Gene nomenclature, protein denomination, and functions of subunits of mammalian mitochondrial respiratory complex I. For details see text. ACP, acyl-carrier protein

Gene	Protein denomination	MW (kDa)	Redox centers	Biochemical features
<i>Nuclear</i>				
NDUFA1	MWFE, NIMM	8.1		Phosphorylation
NDUFA2	B8, NI8M	11.0		
NDUFA3	B9, NI9M	9.2		
NDUFA4	MLRQ, NUML	9.3		
NDUFA5	B13, NUFM	13.2		
NDUFA6	B14, NB4M	15.0		
NDUFA7	B14.5a, N4AM	12.6		Ubiquinone binding?
NDUFA8	PGIV, NUPM	20.0		
NDUFA9/ NDUFSL2	39 kDa, NUEM	39.1		NAD(P)H binding
NDUFA10	42 kDa, NUDM	36.7		
NDUFAB1	SDAP, ACPM	10.1		Binds phosphopantothenine, ACP
NDUFB1	MNLL, NINM	7.0		
NDUFB2	AGGG, NIGM	8.5		
NDUFB3	B12, NB2M	11.0		
NDUFB4	B15, NB5M	15.1		
NDUFB5	SGDH, NISM	16.7		
NDUFB6	B17, NB7M	15.4		
NDUFB7	B18, NB8M	16.5		
NDUFB8	ASHI, NIAM	18.7		
NDUFB9	B22, NI2M	21.7		
NDUFB10	PDSW, NIDM	20.8		
NDUFC1	KFYI, NIKM	5.8		
NDUFC2	B14.5b, N4BM	14.1		
NDUFS1	75 kDa, NUAM	77.0	3(4Fe-4S): N1c,N4,N5; (2Fe-2S): N1b	Electron transfer
NDUFS2	49 kDa, NUCM	49.2		UQ binding?
NDUFS3	30 kDa, NUGM	26.4		
NDUFS4	18 kDa (AQDQ), NUYM	15.3		Phosphorylation
NDUFS5	15 kDa, NIPM	12.5		
NDUFS6	13 kDa, NUMM	10.5		
NDUFS7	20 kDa (PSST), NUKM	20.1	(4Fe-4S): N2	Electron transfer
NDUFS8	23 kDa (TYKY), NUIM	20.2	2(4Fe-4S): N6a,N6b	Electron transfer, complex assembly stability
NDUFV1	51 kDa, NUBM	48.4	FMN; (4Fe-4S): N3	NADH binding, electron transfer
NDUFV2	24 kDa, NUHM	23.8	(2Fe-2S): N1a	Electron transfer
NDUFV3	10 kDa, NUOM	8.4		
–	B17.2	17.2		
NDUFB11	ESSS	13		Phosphorylation assembly
–	B14.7	14.7		
–	B16.6	16.6		Homologous to GRIM-19, apoptosis?
–	10.566	10.5		

■ **Table 1.5-1 Continued**

Gene	Protein denomination	MW (kDa)	Redox centers	Biochemical features
<i>Mitochondrial</i>				
ND1	NU1M	36.0		
ND2	NU2M	39.0		
ND3	NU3M	13.0		
ND4	NU4M	52.0		
ND5	NU5M	67.0		
ND6	NU6M	19.0		Assembly
ND4L	NULM	11.0		

supernumerary subunits is not yet understood. Some of them exhibit particular features. The NDUFB1 (10-kDa subunit) has been found to be an acyl carrier protein with a phosphopantothen prosthetic group (Hirst et al., 2003). The NDUFA9 (39-kDa subunit) binds NADH and NADPH. Sequence comparison suggests that it is related to short-chain dehydrogenase/reductase (Schulte et al., 1999). Subunit B16.6 is highly homologous to human GRIM-19 (a retinoic binding factor involved in cell death factor) (Fearnley et al., 2001). There is evidence showing that subunits NDUFS4 (18-kDa subunit) (Papa et al., 1996b; Technikova-Dobrova et al., 2001), NDUFB11 (ESSS subunit), and NDUFA1 (MWFE subunit) (Chen et al., 2004) are phosphorylated by cAMP-dependent protein kinase. These subunits have a serine phosphorylation consensus site in the mature sequence and in the presequence (▶ [Figure 1.5-3](#)). The phosphorylation state of these subunits “in vivo” and the possible impact of phosphorylation on protein stability, import/assembly, and functional activity of the complex are under investigation (Papa, 2002; Pasdois et al., 2003; Maj et al., 2004; Scheffler et al., 2004). Cellular/biochemical studies on cell lines from patients with mutations in nuclear genes of complex I have shown that some of the structural subunits are involved in the assembly of the complex in the membrane (see [Sect. 5](#)).

3.2 Complex II

Complex II (succinate ubiquinone oxidoreductase, SQR, EC 1.3.5.1) is bound to the inner mitochondrial membrane and participates in the citric acid cycle and in the respiratory chain. SQR is very similar to the bacterial quinol/fumarate oxidoreductase (QFR) (Lancaster and Kröger, 2000; Lancaster, 2001) (▶ [Table 1.5-2](#)). SQRs generally contain four subunits, referred to as A, B, C, and D. Subunits A and B are hydrophilic, whereas subunits C and D are integral membrane proteins. SQRs contain three iron–sulfur centers that are exclusively bound by the B subunit. The larger hydrophilic subunit A carries covalently bound flavin adenine dinucleotide (Thorpe, 1991) (▶ [Table 1.5-2](#)).

3.3 Electron-Transferring Flavoprotein and ETFDH

The mitochondrial matrix electron-transferring flavoprotein (ETF) accepts electrons from different substrate dehydrogenases (acyl-CoA dehydrogenases and others) and transfers them to the inner-membrane-bound ETF ubiquinone oxidoreductase (ETF dehydrogenase, EC 1.5.5.1) (▶ [Table 1.5-2](#)) (Thorpe, 1991). ETF is a heterodimeric complex, consisting of two subunits, α and β , both nuclear encoded, which folds into three distinct domains. Each heterodimer binds a FAD coenzyme. ETF partitions the functions of partner binding and electron transfer between the recognition loop, which acts as a static anchor at the ETF/acyl-CoA dehydrogenase interface and the highly mobile redox active FAD domain compatible with fast interprotein electron transfer. The crystal structure of the human ETF–MCAD (medium-chain acyl-CoA dehydrogenase) complex reveals a single ETF molecule interacting with a MCAD homotetramer (Colombo et al., 1994; White et al., 1996; Toogood et al., 2004). ETFDH (ETF-QO, ETF ubiquinone oxidoreductase)

■ Figure 1.5-3

Sequence comparison analysis of human and bovine complex I subunits NDUFB11 (gi: 1471504, human; 23954189, bovine), NDUF54 (gi: 3287881, human; 400578, bovine), and NDUF11 (gi: 2274974, human; 28461217, bovine). The cleaved mitochondrial import presequences are *underlined*. Putative cAMP-dependent protein kinase consensus site are *boxed*. For details see text

NDUFB11 (ESSS)		
Human	<u>MAAGLFGLSARRLLAAATRGLPAARV</u> <u>RWESS</u> SSFSRTVVAPSAVAGKRPPE	50
Bovine	----- <u>LPAARV</u> <u>RWESS</u> SSSRAVIAPSTLAG <u>KR</u> <u>PSE</u>	29
Human	PTTPWQEDPEPEDENLYEKNPDSHGVD-KDPVLDVWNMRLVFFFGVSIIL	99
Bovine	PTLRWQEDPEPEDENLYEKNPDSHGVD-KDPAVDIWNMRVVFVFFGFSSIVL	78
Human	VLGSTFVAYLPDYRCTGCPRAWDMKEWSRREAERLVKYREANGLPIMES	149
Bovine	VLGSTFVAYLPDYR-----MQEWARREAERLVKYREAHGLPIMES	118
Human	NCFDPSKIQLPEDE-----	163
Bovine	NCFDPSKIQLPEDED-----	133
NDUF54 (AQDQ)		
Human	----- <u>MAAVSMSV</u> <u>VLRLQTLWRRRAVAVAAALS</u> <u>SVSRV</u>	30
Bovine	----- <u>MAAVSMSVALRQALWGRRVATVA</u> <u>AVSVSKV</u>	30
Human	----- <u>P</u> <u>T</u> <u>R</u> <u>S</u> <u>L</u> <u>E</u> <u>T</u> <u>S</u> <u>T</u> <u>W</u> <u>R</u> <u>L</u> <u>A</u> <u>Q</u> <u>D</u> <u>Q</u> <u>T</u> <u>Q</u> -----DTQLITVDEKLDITT	63
Bovine	----- <u>S</u> <u>T</u> <u>R</u> <u>S</u> <u>L</u> <u>S</u> <u>T</u> <u>S</u> <u>T</u> <u>W</u> <u>R</u> <u>L</u> <u>A</u> <u>Q</u> <u>D</u> <u>Q</u> <u>T</u> <u>R</u> -----DTQLITVDEKLDITT	63
Human	LTGVP--EEHIKTRKVRIFVPPARNNMQSGVNNTKKWKMEFDTRER--WE	108
Bovine	ITGVP--EEHIKTRKARIFVPPARNNMQSGVNNTKKWKMEFDTRER--WE	108
Human	NPLMGWASTADPLSNMVLTFSTKEDAVSFAEKNWGSYDIEERKVPK-PKS	157
Bovine	NPLMGWASTADPLSNLVLTFSTKEDAVAFAEKNWGSYDVEERKVPK-PKS	157
Human	KSYGANFSWNKR <u>TRV</u> <u>STK</u>	175
Bovine	KSYGANFSWNKR <u>TRV</u> <u>STK</u>	175
NDUF11 (MWFE)		
Human	MWFEILPGLSVMGVCLLIPGLATAYIHRFTNGGKEKRVVAHFGYHWSLMER	50
Bovine	MWFEVLPGLAVMGVCLFIPGMATARI <u>HRFS</u> NGGKEKRVVAHYPYQWYLMER	50
Human	<u>DRRIS</u> GVDRYYVSKGLENID	70
Bovine	<u>DRRVS</u> GVNRSYVSKGLENID	70

mediates electron transfer between ETF and ubiquinone. It is an integral membrane protein (≈ 64 kDa) containing one equivalent of FAD and a [4Fe-4S] cluster, and is one of the simplest quinone oxidoreductases in the respiratory chain (Frerman, 1988).

Mitochondrial glycerol-3-phosphate dehydrogenase (EC 1.1.99.5) is located on the outer surface of the inner mitochondrial membrane (Cole et al., 1978). It catalyzes the conversion of L-glycerol-3-P to dihydroxyacetone phosphate and together with the cytoplasmic NAD-linked glycerol-3-phosphate dehydrogenase (EC 1.1.1.8) constitutes an electron shuttle between the cytosolic NAD/NADH pool and the mitochondrial electron transport chain (Hess and Pearse, 1961).

3.4 Complex III

X-ray crystallographic structures of mitochondrial complex III (bc_1 complex, ubiquinone cytochrome c oxidoreductase, EC 1.6.99.3) from bovine heart (Xia et al., 1997; Iwata et al., 1998), chicken heart (Berry et al., 2000), and *Saccharomyces cerevisiae* (Hunte et al., 2000) are available. The whole structures of the complex so far analyzed consist of a homodimer of two bc_1 complex monomers (Berry et al., 2000)

■ Table 1.5-2

Gene nomenclature, protein denomination, and functions of subunits of succinate dehydrogenase, ETF, ETF dehydrogenase, and glycerolphosphate dehydrogenase. For details see text

Gene	Protein denomination	MW (kDa)	Redox centers	Biochemical features
Succinate dehydrogenase, ETF				
Water-soluble part				
SDHA	Subunit A (Fp), SDH1	67.1	FAD	Electron transfer
SDHB	Subunit B (Ip), SDH2	28.0	(2Fe–2S); (4Fe–4S); (3Fe–4S)	Electron transfer, UQ binding
Membrane anchor proteins				
SDHC	Subunit C, SDH3	20.0	Cyt b_{560} -heme	Membrane anchor for SDH1; electron transfer
SDHD	Subunit D, SDH4	16.6		Membrane anchor for SDH2
ETF and ETF dehydrogenase				
Etfa	α ETF	32	FAD	Electron transfer from substrate dehydrogenases to ETFDH
Etfb	β ETF	27		
Etfdh	ETF-DH, ETF-QO	64	FAD; 4Fe–4S	Integral membrane protein, transfers electrons from ETF to ubiquinone
FAD-dependent glycerolphosphate dehydrogenase				
GPD-2	mGPDH	75	FAD; Fe–S	Cytosol/mitochondrial NADH shuttle

■ Table 1.5-3

Gene nomenclature, protein denomination, and functions of subunits of mammalian mitochondrial respiratory complex III. For details see text

Gene	Protein denomination	MW (kDa)	Redox centers	Biochemical features
Complex III sub I	Core I	53.6		Metallo endopeptidase (MPP)
Complex III sub II	Core II	46.5		
CYTB (mt)	Cytochrome <i>b</i>	42.6	Heme b_H (b_{562}), Heme b_L (b_{566})	Electron transfer, E_m pH dependent
Complex III sub IV	Cytochrome c_1	27.3	Heme c_1	Electron donor to cytochrome <i>c</i>
Complex III sub V	Rieske ISP	21.6	2Fe–2S	Electron donor to cytochrome c_1
Complex III sub. VI	Subunit VI	13.3		
Complex III sub VII	Subunit VII	9.5		
Complex III sub VIII	Subunit VIII	9.2		Hinge protein (interacts with c_1)
Complex III sub IX	Subunit IX	8.0		
Complex III sub X	Subunit X	7.2		
Complex III sub XI	Subunit XI	6.4		
CYCS	Cytochrome <i>c</i>	12	Heme <i>c</i>	Electron transfer, apoptosis

(► [Figure 1.5-1](#)). There is enough interdigitation between the monomers, suggesting that dissociation of the monomer is unlikely to occur in the native state in the membrane. The mammalian bc_1 complex is composed of 11 subunits (► [Table 1.5-3](#)). Cytochrome *b* is encoded by the mitochondrial genome, all the other subunits by nuclear genes. Cytochrome *b*, cytochrome c_1 , and the Rieske iron–sulfur protein are evolutionary conserved in all the prokaryotic and eukaryotic species analyzed and contribute the minimal

functional core of the protonmotive complex (Berry et al., 2000). Each monomer of the dimer consists of a central core of 12 transmembrane helices: eight transmembrane helices of cytochrome *b*, one membrane-anchoring helix each of the Rieske protein and cytochrome *c*₁, as well as a single transmembrane helix each of subunits 8 and 9 (Berry et al., 2000).

The two large so-called core proteins are extramembranous subunits attached to the membrane domains and protrude into the matrix. Sequence comparisons indicate that core proteins belong to the pitrilysin family, a group of Zn²⁺-dependent metalloendopeptidases (Deng et al., 2001). They are closely related by sequence homology to the matrix processing peptidases (MPP), which are also members of this family. MPPs are soluble heterodimeric proteins that are located in the mitochondrial matrix and cleave precursor proteins after their import into mitochondria (Gakh et al., 2002).

3.5 Complex IV

X-ray crystallographic structures of complex IV (cytochrome *aa*₃, cytochrome *c* oxidase, EC 1.9.3.1) from bovine heart mitochondria (Tsukihara et al., 1996), *P. denitrificans* (Iwata et al., 1995), *Thermus thermophilus* (Souliname et al., 2000), and *Rhodobacter sphaeroides* (Svensson-Ek et al., 2002) are available. These show a similar atomic three-dimensional structure of three conserved subunits I, II, and III representing the minimal core of the enzyme. The bovine heart cytochrome *c* oxidase crystallizes as a dimer (Tsukihara et al., 1996) (🔵 [Figure 1.5-1](#)). The middle part of the crystal structure is a large transmembrane bundle of 28 α -helices; *aa*₃ cytochrome *c* oxidase has four redox centers: a binuclear Cu_A center, titrating as one electron redox entity, bound to subunit II, heme *a*, heme *a*₃ and Cu_B, all bound to subunit I (Fergusson-Miller and Babcock, 1996). Cytochrome *c* delivers electrons to Cu_A; heme *a*₃ and Cu_B constitute the binuclear center where O₂ is reduced to H₂O. Heme *a* mediates electron transfer from Cu_A to the binuclear center (🔵 [Figure 1.5-4](#)). The mammalian *aa*₃ cytochrome *c* oxidase has in addition to three conserved subunits, encoded by mtDNA, ten nuclear-encoded subunits (🔵 [Table 1.5-4](#)), some of which present tissue-specific isoforms (Kadenbach et al., 2000). The supernumerary subunits contribute Zn (Richter and Ludwig, 2003) and ADP/ATP-binding sites, which might have a regulatory role (Kadenbach et al., 2000). The supernumerary subunits surround the central core structure of subunits I, II, and III. Subunits IV, VIa, VIc, VIIa, VIIb, VIIc, and VIII each traverse the membrane in a single helical arrangement, whereas Va and Vb (Zn binding) face the matrix side and VIb is oriented toward the intermembrane space (Tsukihara et al., 1996). Both subunits VIa and VIb are mainly responsible for the contacts between monomers in the dimer (Tsukihara et al., 1996; Yoshikawa, 2002). The bovine heart structure also shows a total of eight well-defined phospholipid molecules. The space between the two monomers is large enough for placing two cardiolipins and two cholate moieties, one of them possibly accounting for the nucleotide binding site with steric requirements similar to an ADP group (Bender and Kadenbach, 2000; Yoshikawa, 2002).

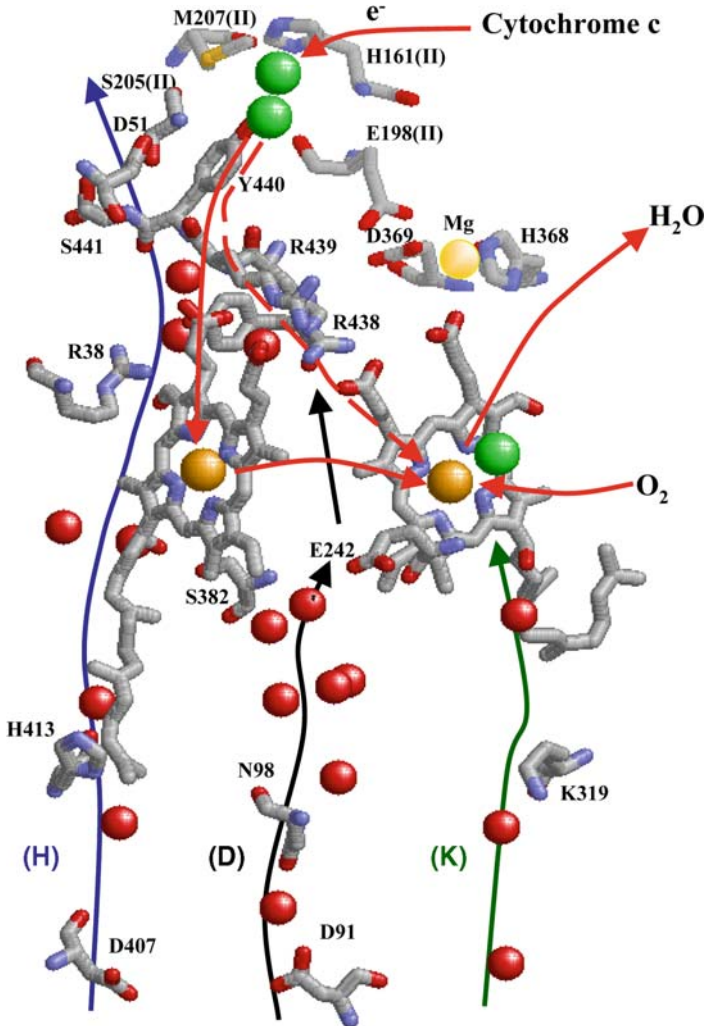
4 The Mechanism of Protonmotive Energy Transfer in the Respiratory Chain

During the years 1960–1970, chemiosmotic hypothesis, although it was fiercely opposed by proponents of chemical and conformational hypothesis, promoted an enormous amount of work in different laboratories, which resulted in experimental verification of its general postulates and its acceptance (Mitchell, 1979).

Each of the respiratory complexes I, III, and IV is plugged through the osmotic barrier of the inner mitochondrial membrane and converts chemical redox energy into PMF. It is today accepted that oxidative phosphorylation is mediated by cyclic proton flow between redox PMF generators and reversible protonmotive F₀F₁ ATP synthase (🔵 [Figure 1.5-1](#)) (Papa et al., 1999a). However, to what extent protonic coupling involves only bulk-phase to bulk-phase transmembrane PMF without some more direct protonic coupling of the redox and synthase complexes through localized proton gradient in membrane micro-environments is still questionable (Williams, 2002). Considering that the protonmotive activity of redox complexes and ATP synthase involves conformational changes in these complexes, and OHPHOS

■ Figure 1.5-4

A parallel view of the membrane showing the location of acid/base residues contributing to proton-conducting pathways in subunit I of cytochrome *c* oxidase. The structure was drawn with Rasmol 2.7 from the PDB coordinates of the crystal structure of the fully oxidized bovine heart enzyme (1.8 Å resolution, file 1V54) (Tsukihara et al., 1996, 2003). The red spheres show the position of water molecules intercalating protolytic residues along channels "H" (blue arrow), "D" (black arrows), and "K" (green arrow). The coupled electron transfer pathway is shown by solid red arrows. Uncoupled electron transfer from Cu_A to the a₃-Cu_B binuclear center is shown by a dashed red arrow. For other details see text and Papa et al. (2004b)



complexes can also be associated in supercomplexes (Schagger, 2002), some promiscuity of the chemiosmotic hypothesis and the original conformational hypothesis can be envisaged here.

The remarkable advancement in X-ray analysis of the protein structure of respiratory complexes as well as in spectrometric and electrometric analysis of catalytic intermediates at the redox centers is today providing new possibilities of deciphering the mechanism of protonmotive energy transfer at a molecular/atomic level. Mitchell (1961, 1966) originally proposed the protonmotive activity of redox complexes to

■ **Table 1.5-4**

Gene nomenclature, protein denomination, and functions of subunits of mammalian mitochondrial respiratory complex IV. Some of the nuclear-encoded subunits present tissue-specific isoforms. For more details see text

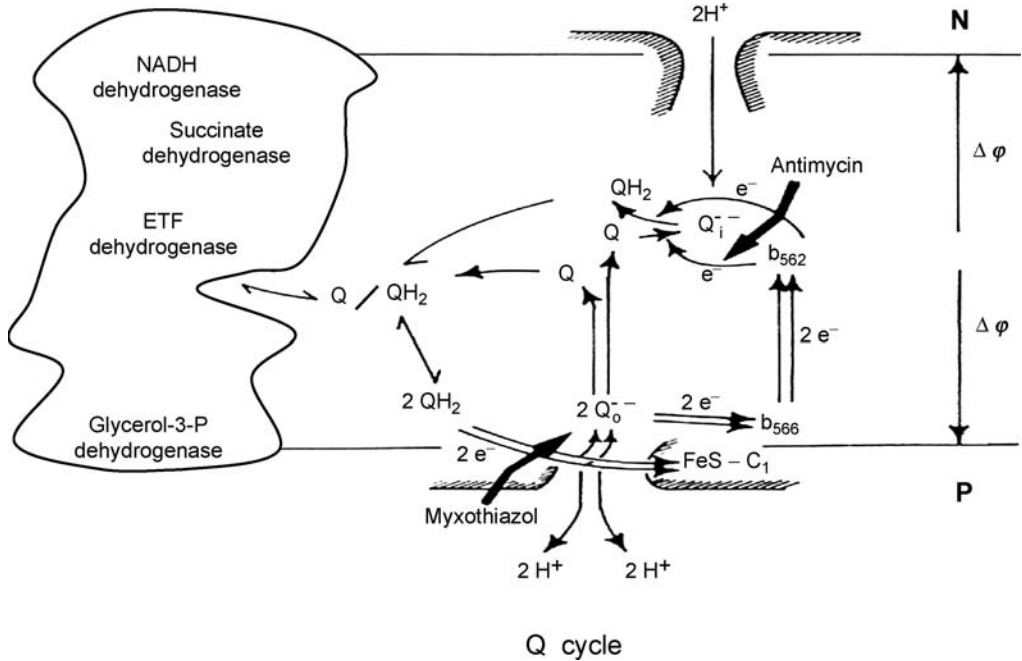
Gene	Protein denomination	MW (kDa)	Redox centers	Biochemical features
Cox1 (mt)	COX-I	53.6	Heme <i>a</i> , heme a_3 -Cu _B	Electron transfer, oxygen reduction
Cox2 (mt)	COX-II	26.0	Cu _A -Cu _A	Cytochrome <i>c</i> binding site, electron transfer
Cox3 (mt)	COX-III	29.9		
Cox4 (1,2)	COX-IV 1,2	17.1		Ubiquitous (ATP binding), lung isoforms
Cox5a	COX-Va	12.4		Thyroid hormone, T2 binding
Cox5b	COX-Vb	10.6		Zn binding
Cox6a (1,2)	COX-VIa H/L	9.4		Heart, liver isoforms
Cox6b (1,2)	COX-VIb 1,2	9.4		Ubiquitous, testis isoforms
Cox6c	COX-VIc	8.4		
Cox7a (1,2)	COX-VIIa H/L	6.2		Heart, liver isoforms
Cox7b	COX-VIIb	6.0		
Cox7c	COX-VIIc	5.4		
Cox8 (1,2,3)	COX-VIII H/L/3	4.9		Heart, liver, ubiquitous isoforms

be a direct consequence of hydrogen conduction in one direction from the inner (N) to the outer space (P) and electron transfer in the opposite direction across the membrane by the redox prosthetic groups (protonmotive redox loops). Mitchell (1976) formulated the ubiquinone cycle to explain proton translocation in complex III (▶ [Figure 1.5-5](#)) based on the oxidant-induced reduction of *b* cytochromes (Wikstrom and Berden, 1972) and on the direct measurement of proton pumping associated to electron flow from quinol to cytochrome *c*, which showed H^+/e^- ratios higher than those predicted by linear redox loops (Lawford and Garland, 1972; Papa et al., 1974) Although this mechanism rationalizes a body of experimental observations and is largely accepted (Trumpower, 1999), alternative mechanisms that can equally well explain the protonmotive activity of complex III in a manner consistent with experimental phenomena have been proposed (Papa et al., 1990; Matsuno-Yagi and Hatefi, 2001). For a detailed discussion of the relative merits of the ubiquinone cycle and alternative mechanisms, see Rieske (1986), Papa et al. (1990), and Matsuno-Yagi and Hatefi (2001).

Generation of PMF by cytochrome *c* oxidase and by other members of the heme-copper oxidase family (Pereira et al., 2001) results from the consumption of protons from the inner (N) space due to the reduction of O_2 to H_2O by ferrocycytochrome *c* located at the outer (P) side of the membrane (Papa, 1976), as originally postulated by Mitchell (1966). In addition to this, the oxidase displays a net proton-pumping activity from the N to the P space, coupled to electron flow from ferrocycytochrome *c* to O_2 (Wikstrom et al., 1981). Although the proton-pumping activity of heme-copper oxidases is being investigated in several laboratories, its detailed molecular mechanism is not fully understood as yet. Studies on the mechanism of proton pumping have resulted, from time to time, in proposals that this process is coupled to oxidoreduction of Cu_A or heme *a*, or to the binuclear center (Gelles and Chan, 1985; Ferguson-Miller and Babcock, 1996; Papa et al., 1998; Michel, 1999; Brezinsky and Larsson, 2003; Tsukihara et al., 2003; Wikstrom, 2004). Proton transfer promoted by redox events at the catalytic centers, which are buried in the protein at discrete distances from the surface exposed to the water bulk phases, has to extend to the N and P phase through proton input and proton output pathways. Intraprotein proton pathways in heme-copper oxidases have been identified by X-ray crystallographic analysis (Iwata et al., 1995; Tsukihara et al., 1996; Soulimane et al., 2000; Svensson-Ek et al., 2002). The crystal structures of bovine and prokaryotic cytochrome *c* oxidase reveal possible proton-conducting pathways in subunit I that start at the N side of the membrane

■ Figure 1.5-5

Ubiquinone cycle model of electron transfer and proton translocation in complex III (bc_1 complex). QH_2 (ubiquinol of the membrane pool) is oxidized at the P side, one electron is transferred to the Fe-S cluster \rightarrow cyt c_1 \rightarrow cyt c , two H^+ are released in the P space, the electron of $Q_0^{\bullet-}$ is transferred back to cyt b_{566} , cyt b_{562} , and rereduces Q , which diffuses to the N side, to $Q_0^{\bullet-}$. The cycle is completed by the oxidation of a second molecule of QH_2 . Another two H^+ are released in the P space; one electron is transferred to FeS \rightarrow c_1 \rightarrow c , the electron of $Q_0^{\bullet-}$ cycles back via cyt b_{566} \rightarrow cyt b_{562} and reduces $Q_0^{\bullet-}$, transiently bound at the N side, to QH_2 . The overall cycle, which involves two turnovers of the bc_1 complex, results in the net oxidation of one QH_2 reduction of two molecules of cyt c , the release of $4H^+$ in the P space. Two of these are substrate protons, two are electrogenically pumped from the N to the P space (Mitchell, 1976; Trumpower, 1999)



⦿ Figure 1.5-4). Two of these, denominated D and K pathways, can apparently conduct H^+ from the aqueous space N to the binuclear heme a_3 - Cu_B center, located in the protein 30 \AA away from the N surface. It can be noted that E242 in the inner part of the D pathway is symmetrically located with respect to hemes a and a_3 . In *P. denitrificans* oxidase, the closest carboxyl oxygen of this residue is 12.3 \AA away from the heme a_3 iron and 12.8 \AA from the heme a iron (Michel, 1998; see also Papa et al., 1998) (⦿ Figure 1.5-4). A third proton pathway (H pathway), initially identified in the bovine enzyme (Tsukihara et al., 1996), can conduct H^+ from the N space to heme a , also located 30 \AA away from the N surface. Amino acid sequence comparison and structural alignment of a large number of heme-copper oxidases as well as site-directed mutagenesis studies, however, show that some of the protonable residues, thought to be critical for H^+ conduction in the D, K, and H pathways, are not conserved in some heme-copper oxidases that are fully functional (Pereira et al., 2001). On the other hand, cavities are seen in these proton pathways, which can be occupied by water molecules. This water, bound to hydrophilic residues or peptide backbone amide/carboxyl groups, can contribute efficient H^+ transfer. Proton conduction pathways might, in fact, require a less stringent amino acid specificity than electron transfer pathways, and a search for critical protonable residues by sequence comparison and/or site-directed mutagenesis could sometimes turn out to be useless if not misleading.

Figure 1.5-6

Protonmotive catalytic cycle in cytochrome *c* oxidase (a) Overall reaction scheme and location of redox centers. *Black arrows* show the redox reaction and its orientation with respect to the membrane. *Gray arrows* depict proton translocation coupled to the redox reaction. The heme groups and Cu_B lie within the membrane at a relative dielectric depth (d) from the positively charged P surface. Electron transfer across d , proton consumption across $1-d$, and proton pumping across the entire membrane contribute to the generation of electric membrane potential. (b) Protonmotive catalytic cycle. *Gray squares* depict the main cycle. *White squares* show a side path initiated by decay of the metastable O_H intermediate to O . *Gray arrows* indicate proton translocation, and *black arrows* show uptake of substrate protons. R, fully reduced oxidase; A, fully reduced oxidase with bound O_2 ; P_M , peroxy compound; F, ferryl compound; O_H , metastable oxidized compound; E_H , one electron reduced binuclear center; O, oxidized ground state. Reproduced from Bloch et al. (2004). For further specification of these intermediates see Bloch et al. (2004)

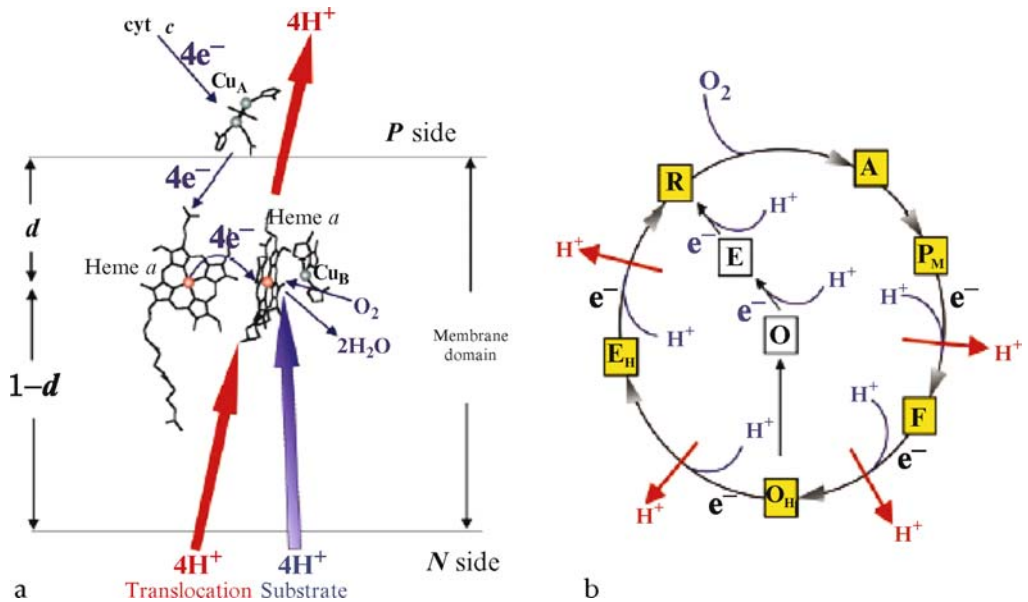


Figure 1.5-6 depicts a model in which proton pumping is conceived to be directly coupled to intermediate steps in the oxygen reduction chemistry at the heme a_3 - Cu_B binuclear center, where protons are also consumed in the protonation of intermediates in the oxygen reduction to H_2O (Bloch et al., 2004). Special devices have to be assumed here to prevent annihilation of the pumped protons in the reduction of O_2 to H_2O .

Proton-pumping models involving coupling at heme a and/or Cu_A , which are at a distance from the a_3 - Cu_B binuclear center and not involved in oxygen binding and reduction, require indirect, cooperative linkage between oxidoreduction of these centers and proton transfer by acid-base groups in the enzyme. On the basis of the principles of cooperative linkage of solute binding at separate sites in allosteric proteins (Monod et al., 1965), in particular hemoglobin (Perutz, 1976), Papa et al. (1973) proposed in the 1970s a general model based on cooperative redox-linked pK shifts in electron transfer proteins (redox Bohr effect) for proton pumping in the respiratory chain (vectorial Bohr mechanism). Reduction of the metal prosthetic center in a redox enzyme in the membrane was proposed to result in the pK increase of a residue in the protein, in protonic connection with the inner (N) side of the membrane and with proton uptake from this space; on the other hand, oxidation of the metal was proposed to result in the decrease of the pK of this or

another group in protonic connection with the first, with proton release in the outer (P) space (Papa, 1976; Papa and Capitanio, 1998).

This principle now seems to be widely incorporated in recent models of redox-linked proton translocation (Papa et al., 1998; Michel, 1999; Brezinsky and Larsson, 2003; Tsukihara et al., 2003; Papa, 2005).

It has been shown experimentally that heme *a* and Cu_A share H⁺/e⁻ cooperative coupling with a common acid/base cluster, which results in vectorial translocation of around 1 H⁺ equivalent per mole of the enzyme undergoing oxidoreduction (Capitanio et al., 2000a, b). This interactive cooperative coupling of heme *a* and Cu_A causes a decrease of the E_m of both centers by about -20 mV per pH unit increase. With interactive coupling, while one electron reduction of heme *a*/Cu_A is sufficient to produce maximal protonation of the cluster, release of the proton bound to the cluster will take place only when both heme *a* and Cu_A are oxidized. The consequence is that at the steady state one electron at a time has to pass through Cu_A and heme *a* so as to result in the translocation of 1 H⁺ per electron. This restriction of one electron at a time might represent one of the causes of slips in the proton pump as observed at high electron pressure imposed on the oxidase (Capitanio et al., 1996; Papa et al., 2004b). A proton pump model of cytochrome *c* oxidase has been proposed based on these observations, in which two acid/base clusters, A1 and A2, cooperatively linked to heme *a*/Cu_A and heme *a*₃/Cu_B, respectively, operating in close sequence, constitute together the gate of the proton pump of the oxidase (Papa, 2005).

It can be noted that the other two protonmotive complexes of the respiratory chain have components that exhibit redox Bohr effects, N1a and N2 in complex I (Brandt, 1997; Ohnishi, 1998) and cytochrome *b* (Urban and Klingenberg, 1969; Papa et al., 1986) and Fe-S Rieske center in complex III (Brandt et al., 1997). In these complexes cooperative H⁺/e⁻ coupling at the electron transfer centers can be involved, in association with protonmotive activity of protein-bound quinone species, in proton pumping. This is, for example, illustrated by the Q-gated pump model of complex III (Papa et al., 1990). On the same grounds, various versions of proton-pumping models in complex I have been proposed, all of which are speculative (Brandt, 1997; Papa et al., 1999a). In complex I extended conformational changes could also be involved in proton pumping (Mamedova et al., 2004).

Clearly, more work is necessary for a full understanding of the mechanism of redox proton pumping in the respiratory chain.

5 Biogenesis of Respiratory Chain Complexes

Biogenesis of respiratory chain complexes is controlled by a framework of cellular signaling (Nisoli, et al., 2004) that culminates in the coordinated expression of two genomes: the mtDNA and the nuclear DNA (nDNA) (see R. Scarpulla, this volume). The mitochondrial genome encodes most of the core subunits of the respiratory chain complexes but hundreds of nuclear-encoded proteins involved in respiration must be synthesized in the rough endoplasmic reticulum and imported into mitochondria. The mitochondrial membranes contain specific systems for recognition, translocation, and membrane insertion of nuclear-encoded proteins (Neupert and Brunner, 2002). These can be divided into two main classes. The first is made of precursor proteins with N-terminal cleavable presequences targeted to the mitochondrial matrix, as well as to the inner membrane and intermembrane space. The positively charged presequences function as targeting signals that interact with the mitochondrial import receptors and direct the preproteins across both outer and inner membranes. Precursors of the second class, without cleavable presequences, carry various internal targeting signals and include outer membrane proteins and many intermembrane and inner membrane proteins. The translocase of the outer mitochondrial membrane (TOM complex) represents the main entry for practically all nuclear-encoded mitochondrial proteins and consists of several preprotein receptors and a general import pore (Wiedemann et al., 2004). Most of the mitochondrial precursor proteins are imported after cytosolic translation (posttranslational import) and are likely guided to the mitochondria by cytosolic chaperones, including the classical heat shock proteins (Young et al., 2003) and additional cytosolic factors recently identified (Komiya et al., 1998; Yano et al., 2003). It has been found

that in some cases, however, the presequence is inserted into the TOM machinery while a C-terminal portion is still undergoing synthesis on the ribosome (cotranslational import) (Knox et al., 1998). Nuclear-encoded precursor subunits of respiratory chain complexes, after passing through the TOM complex, are brought in contact with the translocase system of the inner mitochondrial membrane (TIM). The TIM23 complex mediates the transport of presequence-containing proteins across and into the inner membrane and requires the PAM complex (presequence-translocase-associated motor complex) and a membrane potential ($\Delta\psi$) (Wiedemann et al., 2004). The TIM22 complex (a twin-pore carrier translocase) catalyzes the insertion of multispanning proteins that have internal targeting signals into the inner membrane and uses $\Delta\psi$ as an external driving force (Rehling et al., 2004). Subunits without a presequence and precursor subunits, the latter after cleavage of the presequence by the mitochondrial processing peptidase (MPP), are finally assembled into the respiratory complexes (Koehler et al., 2004). The quality control of mitochondrial proteins and the essential steps in mitochondrial biogenesis are ensured by conserved ATP-dependent proteases that degrade nonassembled mitochondria-encoded proteins to peptides and amino acids, which are released from mitochondria (Augustin et al., 2005).

Little is known of how the 46 subunits of complex I are assembled in the active complex, which factors are involved in this process, and how it is controlled. Most of what is known of the assembly of complex I comes from studies carried out in *Neurospora crassa*. The 35 subunits of this complex I (Videira and Duarte, 2001) form independently the membrane part and the protruding arm also in the absence of mitochondria-encoded subunits (Tuschen et al., 1990; Duarte et al., 1995). Two proteins, the complex I intermediate associated proteins, CIA30 and CIA84, have been shown to associate with intermediates of the assembly process (Kuffner et al., 1998). A human homolog has been found for CIA30 (Janssen et al., 2002). To date, it is unclear whether complex I assembly in mammalian cells is comparable with that in *N. crassa*. Studies on the patterns of partially assembled complexes in complex I-deficient patients, harboring mutations in either mtDNA or nDNA, have allowed the construction of two different models for the complex I assembly. The first one suggests no separate formation of the peripheral and membrane arms (Antonicka et al., 2003b). In an alternative model, the complex I assembly is a semisequential process where preassembled subcomplexes are joined to form holocomplex I (Ugalde et al., 2004).

The precursor forms of complex IV subunits must be guided into the mitochondrial inner membrane to be assembled, along with two heme a groups, three coppers, one zinc, and one magnesium ion, into a functional complex. The assembly pathway of complex IV is believed to be a sequential process in which pools of unassembled subunits exist and at least two assembly intermediates are formed (Wielburski and Nelson, 1983; Nijtmans et al., 1998). The findings of these assembly intermediates led to the proposal of a model for the oxidase assembly (Nijtmans et al., 1998), which is consistent with the published three-dimensional structure of bovine heart cytochrome *c* oxidase (Tsukihara et al., 1996). In the first step, a subcomplex S1 containing COX-I, possibly with associated heme groups, is formed. In the next step, COX-IV is added and subcomplex S2 is formed. COX-II and COX-III are then incorporated into this subcomplex together with COX-Va,b, COX-VIb,c, COX-VIIa or b, COX VIIc, and COX-VIII, to obtain S3. Finally, COX-VIa and COX-VIIa or VIIb are added to complete S4, the holoCOX, and subsequently the dimer is formed (Nijtmans et al., 1998). A large number of proteins that regulate this process to ensure the proper assembly and functioning of the enzyme have been identified. They include proteins involved in the processing and translation of mitochondria-encoded mRNAs, in the insertion of newly synthesized polypeptides into the inner membrane, and in the addition of cofactors. In humans, mutations have been found that affect the stability and incorporation of COX subunits into the assembled complex, associated with different phenotypical presentations of COX deficiency (see below).

In yeast, several genes have been shown to be involved in the assembly of complex III such as *cbp3* (Wu and Tzagoloff, 1989), *cbp4* (Crivellone, 1994), *bcs1* (Nobrega et al., 1992), and *abc1* (Bousquet et al., 1991). So far only one such gene, *BCS1L*, has been identified in humans (Petruzzella et al., 1998). The loss of complex III prevents “respirasome” formation (Schagger, 2002) and leads to a secondary significant reduction of complex I. This has been shown in skeletal muscle (Schagger et al., 2004) and in a reproduced combined complex I+III defect in mouse and human cultured cell models harboring mutations in cytochrome *b* gene (Acin-Perez et al., 2004).

6 Genetic Disorders of the Respiratory Chain in Human Pathology

Epidemiological studies of mitochondrial diseases have estimated that the minimum prevalence of OXPHOS diseases is 1:8,500 in a Caucasian population in Northern England (Chinnery et al., 2000). Very recent studies reveal, however, that mitochondrial diseases are far more common than was previously estimated, amounting to a minimum prevalence of at least 1 in 5,000 and could be much higher (Schaefer et al., 2004). Two categories of mitochondrial encephalomyopathies with deficiency of the respiratory chain have been identified: one due to defects in mtDNA, the other to defects in nDNA. Generally, nDNA abnormalities appear in childhood whereas mtDNA abnormalities, which can be either primary or secondary to an nDNA defect, appear in late childhood or adult life.

Mitochondrial DNA encodes for 11 structural subunits of the OXPHOS system. Seven subunits of NADH dehydrogenase are encoded by *ND1–6* and *ND4L* genes. One subunit of complex III, cytochrome *b*, is encoded by the *CYTB* gene. Subunits I, II, and III of cytochrome *c* oxidase are encoded by *COXI*, *COXII*, and *COXIII* genes. The F_0 portion of ATP synthase has two mitochondria-encoded subunits, *ATP6* and *ATP8* (also called A6 and A8). Most information is encoded on the H strand, with 2 rRNAs, 14 tRNAs, and 12 polypeptides. The L strand encodes for eight tRNAs and a single polypeptide, namely ND6 (Attardi and Schatz, 1988; Wallace et al., 1988). Multiple copies of the mtDNA genome are found in individual mitochondria in somatic cells (2–10 copies) and only a single copy is found in those of the oocyte (Jansen and de Boer, 1998). Normally, cells have a single mtDNA sequence variant, a condition known as “homoplasmy.” At fertilization, although sperm mitochondria contribute little to the zygote, they are selectively eliminated through the ubiquitin-targeting degradation mechanism (Sutovsky et al., 2004). This pattern of transmission is called “maternal inheritance.” When a mutation occurs in an mtDNA molecule it can result in “heteroplasmy,” with mutant and wild-type populations of mtDNA coexisting within the same cell. Upon mitosis, because of the random way in which mitochondria segregate in dividing cells, wild-type and mutant mtDNA coexist in variable proportions in any given cell. In nondividing cells, such as myocytes and neurons, this proportion is relatively stable. In dividing cells, it may shift rapidly so that, after several cell cycles, a given cell may come to contain mostly mutant mtDNA (replicative segregation).

Alterations in some tRNA genes and in protein-coding genes may present biochemically as an isolated respiratory complex deficiency. Conversely, large-scale rearrangements of mtDNA may occur with combined and multiple respiratory complex deficiencies. Point mutations, including substitution of single bases or microinsertions/microdeletions in the mtDNA molecule, may equally affect tRNA, rRNA, or mRNA genes. mtDNA point mutations are maternally transmitted; they are often, but not always, heteroplasmic. Although more than 100 point mutations have been associated with an extremely wide spectrum of clinical entities, only a few of them are frequent and associated with well-defined clinical syndromes (DiMauro, 2001).

The second group of disorders is caused by mutations in “nuclear genes” encoding proteins, which directly or indirectly affect OXPHOS complexes. These proteins include structural components of the respiratory chain, factors controlling OXPHOS complexes, factors needed for the intramitochondrial protein synthesis, proteins that control the integrity and replication of mtDNA, and proteins indirectly correlated to OXPHOS (metabolism of the lipid bilayer of mitochondrial membrane, import, proteins for fusion and fission of mitochondria) (DiMauro, 2004).

6.1 Defects of Complex I

Deficiency in complex I is now emerging as one of the most common OXPHOS-related pathologies. Complex I deficiency starts mostly at birth or early childhood, and in general complex I failure results in multisystem disorders with a fatal outcome (Robinson, 1998; Kirby et al., 1999; Loeffen et al., 2000). The most affected tissues are usually those requiring high energy production, like brain, heart, kidney, and skeletal muscle. Leigh syndrome (LS, early-onset fatal neurodegenerative disorder) (Leigh, 1951) or Leigh-like disease are the most common phenotypes associated with an isolated complex I deficiency, representing up to 50% of total cases (Rahman et al., 1996; Robinson, 1998; Loeffen et al., 2000; Janssen et al., 2004).

In addition to LS, isolated complex I deficiency is associated with progressive leukoencephalopathy, neonatal cardiomyopathy, severe infantile lactic acidosis, and a miscellaneous group of unspecified encephalomyopathies.

The genetic basis of complex I deficiency is found in nucleotide alterations in structural subunits of complex I encoded by mtDNA or nDNA. It has been estimated that in about 40% of the cases clinically relevant complex I deficiencies can be attributed to mutations in the seven mitochondria-encoded and in seven of the thirty-nine nuclear-encoded complex I subunits (Benit et al, 2003). However, an ever-expanding number of mutations in both mitochondrial *ND* genes and nuclear *NDUF* genes has been reported (Bugiani et al., 2004).

The pathogenic mechanism of the mutations in complex I genes has been clarified for three different mutations in the *NDUFS4* gene, showing that alteration in this structural nDNA-encoded subunit of the complex may prevent its normal assembly (Petruzzella and Papa, 2002; Scacco et al., 2003). However, the genetic basis for complex I deficiency could not be found in a large number of the patients, suggesting that mutations in other genetic factors probably involved in the assembly or maintenance of the complex, and as yet unknown in humans, are frequent in these disorders.

6.2 Defects of Complex II

Isolated complex II deficiency was associated with mutations in the *SDHA* gene in two families with autosomal recessive LS (Bourgeron et al., 1995; Parfait, et al., 2000) and in a family with late-onset neurodegenerative disease (Birch-Machin et al., 2000). The gene encodes the flavoprotein, one of the four subunits of complex II (see [Table 1.5-2](#)). Two other mutations in both *SDHC* and *SDHD* have been reported in families with autosomal dominant hereditary paraganglioma (PGL), a disorder characterized by the presence of benign tumors of parasympathetic ganglia (Baysal et al., 2000; Niemann and Muller, 2000). Germline mutations in *SDHB* and *SDHD* have also been reported in patients with familial pheochromocytoma, chromaffin cell tumors that usually arise in the adrenal medulla (Niemann and Muller, 2000). These studies clearly implicate genes encoding structural subunits of complex II as tumor suppressors, but the molecular basis for these effects remains undetermined.

6.3 Defects of Coenzyme Q

Recently, syndromes due to ubiquinone ten (CoQ10) deficiency have been reported (Rotig et al., 2000). They can occur with three major forms: a predominant myopathic disorder, a predominant encephalopathic disorder with ataxia and cerebellar atrophy, and a generalized neurodegenerative form. The molecular basis is not known but these presentations are most likely due to mutations in different biosynthetic enzymes (Lamperti et al., 2003).

6.4 Defects of Complex III

A number of mutations have been reported in *CYTB* in patients with myopathy, with or without myoglobinuria (Andreu et al., 1999). So far, no mutations have been reported in the nuclear-encoded structural subunits. *BCS1L* belongs to the AAA-ATPase family and in yeast is believed to act as a chaperone for the Rieske Fe-S subunit of complex III. Mutations in *BCS1L* have been associated with Leigh disease (de Lonlay et al., 2001) and with a fatal infantile multisystemic disease (Visaapa et al., 2002).

6.5 Defects of Complex IV

In complex I, all pathogenic mutations have, so far, been found in structural subunits, whereas in complex IV none has been identified in any of the 10 nuclear-encoded structural subunits in patients. In isolated

complex IV deficiency, mtDNA mutations, 15-bp microdeletion (Keightley et al., 1996), and point mutations in the *COXIII* gene (Manfredi et al., 1995; Santorelli et al., 1997; Pulkes et al., 1999; Tiranti et al., 2000) and in the *COXI* gene (Comi et al., 1998; Karadimas et al., 2000) have been identified separately in patients with various clinical phenotypes. On the whole, however, the defects of mtDNA origin in cytochrome *c* oxidase are outnumbered by genetic defects in proteins needed for the biogenesis of the enzyme. Their identification was greatly aided by studies of yeast *pet* mutants, i.e., strains defective for the assembly (Tzagoloff and Dieckmann, 1990). The first human orthologs of these genes have been identified while searching for candidate genes of human pathologies (Petruzzella et al., 1998). Mutations in the *SURF1* gene cause typical LS (Tiranti et al., 1998; Zhu et al., 1998). Less frequent are mutations in other assembly genes that seem to affect additional organs besides the brain (Papadopoulou et al., 1999; Valnot et al., 2000; Antonicka et al., 2003a). Recently mutations in the *LRPPRC* gene (which encodes an mRNA-binding protein) have been described in patients with oxidase-deficient LS, French Canadian type (LSFC) (Mootha et al., 2003).

6.6 Multiple Respiratory Chain Defects

Heteroplasmic large-scale rearrangements of mtDNA can be either partial deletions or, less frequently, partial duplications of mtDNA. About 40% of the patients harbor a single deletion of about 5.0 kb, the so-called common deletion (Holt et al., 1988). mtDNA deletions are less abundant in leukocytes and other tissues than in skeletal muscle. Single deletions of mtDNA have been associated with three usually sporadic conditions: Kearns–Sayre syndrome (KSS) (MIM 530000), progressive external ophthalmoplegia (PEO), and Pearson’s syndrome (MIM 557000) (DiMauro, 2004). Duplications of mtDNA can occur in isolation or with deletions and have been seen in patients with KSS or diabetes mellitus and deafness. The result of gross deletions in the mtDNA is the complete or partial removal of the sequences of structural genes of respiratory complexes and one or more tRNAs. All this leads to impairment of intramitochondrial protein synthesis and multiple deficiencies of respiratory complexes.

Intramitochondrial translation requires ribosomal proteins and tRNA synthetases. In general, approximately 100 different proteins are involved in the translation of the 13 proteins encoded by the mitochondrial genome, emphasizing the considerable investment required to maintain the mitochondrial genetic system. In this respect, a new class of disorders gathers mutations in nuclear-encoded components of the mitochondrial translation apparatus (Coenen et al., 2004; Miller et al., 2004).

Acknowledgments

This work was supported by grants from the National Project on Bioenergetics: functional genetics, functional mechanisms, and physiopathological aspects, 2003, MIUR, Italy, and the Center of Excellence on Comparative Genomics, University of Bari.

References

- Abrahams JP, Leslie AG, Lutter R, Walker JE. 1994. Structure at 2.8 Å resolution of F₁-ATPase from bovine heart mitochondria. *Nature* 370: 621-628.
- Acin-Perez R, Bayona-Bafaluy MP, Fernandez-Silva P, Moreno-Loshuertos R, Perez-Martos A, et al. 2004. Respiratory complex III is required to maintain complex I in mammalian mitochondria. *Mol Cell* 13: 805-815.
- Albracht SPJ, van der Linden E, Faber BW. 2003. Quantitative amino acid analysis of bovine NADH: Ubiquinone oxidoreductase (complex I) and related enzymes. Consequence for the number of prosthetic groups. *Biochim Biophys Acta* 1557: 41-49.
- Andreu AL, Hanna MG, Reichmann H, Bruno C, Penn AS, et al. 1999. Exercise intolerance due to mutations in the cytochrome *b* gene of mitochondrial DNA. *N Engl J Med* 341: 1037-1044.
- Antonicka H, Mattman A, Carlson CG, Glerum DM, Hoffbuhr KC, et al. 2003a. Mutations in COX15 produce a

- defect in the mitochondrial heme biosynthetic pathway, causing early-onset fatal hypertrophic cardiomyopathy. *Am J Hum Genet* 72: 101-114.
- Antonicka H, Ogilvie I, Taivassalo T, Anitori RP, Haller RG, et al. 2003b. Identification and characterization of a common set of complex I assembly intermediates in mitochondria from patients with complex I deficiency. *J Biol Chem* 278: 43081-43088.
- Attardi G, Schatz G. 1988. Biogenesis of mitochondria. *Annu Rev Cell Biol* 4: 289-333.
- Augustin S, Nolden M, Muller S, Hardt O, Arnold I, et al. 2005. Characterisation of peptides released from mitochondria: Evidence for constant proteolysis and peptide efflux. *J Biol Chem* 280: 2691-2699.
- Bamberg E, Butt H-J, Eisenrauch A, Fendler K. 1993. Charge transport of ion pumps on lipid bilayer membranes. *Q Rev Biophys* 26: 1-25.
- Bates TE, Almeida A, Heales SJ, Clark JB. 1994. Postnatal development of the complexes of the electron transport chain in isolated rat brain mitochondria. *Dev Neurosci* 16: 321-327.
- Baysal BE, Ferrell RE, Willett-Brozick JE, Lawrence EC, Myssiorek D, et al. 2000. Mutations in SDHD, a mitochondrial complex II gene, in hereditary paraganglioma. *Science* 287: 848-851.
- Beinert H. 1986. Iron-sulphur clusters: Agents of electron transfer and storage, and direct participants in enzymic reactions. Tenth Keilin memorial lecture. *Biochem Soc Trans* 14: 527-533.
- Bender E, Kadenbach B. 2000. The allosteric ATP-inhibition of cytochrome *c* oxidase activity is reversibly switched on by cAMP-dependent phosphorylation. *FEBS Lett* 466: 130-134.
- Benit P, Beugnot R, Chretien D, Giurgea I, De Lonlay-Debeney P, et al. 2003. Mutant NDUFB2 subunit of mitochondrial complex I causes early onset hypertrophic cardiomyopathy and encephalopathy. *Hum Mutat* 21: 582-586.
- Berry EA, Guergova-Kuras M, Huang LS, Crofts AR. 2000. Structure and function of cytochrome *bc* complexes. *Annu Rev Biochem* 69:1005-1075.
- Birch-Machin MA, Taylor RW, Cochran B, Ackrell BA, Turnbull DM. 2000. Late-onset optic atrophy, ataxia, and myopathy associated with a mutation of a complex II gene. *Ann Neurol* 48: 330-335.
- Bloch D, Belevich I, Jasaitis A, Ribacka C, Puustinen A, et al. 2004. The catalytic cycle of cytochrome *c* oxidase is not the sum of its two halves. *Proc Natl Acad Sci USA* 101: 529-533.
- Bourgeron T, Rustin P, Chretien D, Birch-Machin M, Bourgeois M, et al. 1995. Mutation of a nuclear succinate dehydrogenase gene results in mitochondrial respiratory chain efficiency. *Nat Genet* 11: 144-149.
- Bousquet I, Dujardin G, Slonimski PP. 1991. ABC1, a novel yeast nuclear gene has a dual function in mitochondria: It suppresses a cytochrome *b* mRNA translation defect and is essential for the electron transfer in the bc₁ complex. *EMBO J* 10: 2023-2031.
- Brandt U. 1997. Proton-translocation by membrane-bound NADH: Ubiquinone-oxidoreductase (complex I) through redox-gated ligand conduction. *Biochim Biophys Acta* 1318: 79-91.
- Brandt U, Djafarzadeh-Andabili R. 1997. Binding of MOA-stilbene to the mitochondrial cytochrome *bc*₁ complex is affected by the protonation state of a redox-Bohr group of the 'Rieske' iron-sulfur protein. *Biochim Biophys Acta* 1321: 238-242.
- Brzezinski P, Larsson G. 2003. Redox-driven proton pumping by heme-copper oxidases. *Biochim Biophys Acta* 1605: 1-13.
- Bugiani M, Invernizzi F, Alberio S, Briem E, Lamantea E, et al. 2004. Clinical and molecular findings in children with complex I deficiency. *Biochim Biophys Acta* 1659: 136-147.
- Canton M, Luvisetto S, Schmehl I, Azione GF. 1995. The nature of mitochondrial respiration and discrimination between membrane and pump properties. *Biochem J* 310: 477-481.
- Capitanio N, Capitanio G, Boffoli D, Papa S. 2000a. The proton/electron coupling ratio at heme *a* and Cu(A) in bovine heart cytochrome *c* oxidase. *Biochemistry* 39: 15454-15461.
- Capitanio N, Capitanio G, Demarinis DA, De Nitto E, Massari S, et al. 1996. Factors affecting the H⁺/e⁻ stoichiometry in mitochondrial cytochrome *c* oxidase: Influence of the rate of electron flow and transmembrane delta pH. *Biochemistry* 35: 10800-10806.
- Capitanio N, Capitanio G, Minuto M, De Nitto E, Palese LL, et al. 2000b. Coupling of electron transfer with proton transfer at heme *a* and Cu(A) (redox Bohr effects) in cytochrome *c* oxidase. Studies with the carbon monoxide inhibited enzyme. *Biochemistry* 39: 6373-6379.
- Carroll J, Fearnley IM, Shannon RJ, Hirst J, Walker JE. 2003. Analysis of the subunit composition of complex I from bovine heart mitochondria. *Mol Cell Proteomics* 2: 117-126.
- Chen C, Ko Y, Delannoy M, Ludtke SJ, Chiu W, et al. 2004. Mitochondrial ATP synthasome. *J Biol Chem* 279: 31761-31768.
- Chen R, Fearnley IM, Peak-Chew SY, Walker JE. 2004. The phosphorylation of subunits of complex I from bovine heart mitochondria. *J Biol Chem* 279: 26036-26045.

- Chinnery PF, Johnson MA, Wardell TM, Singh-Kler R, Hayes C, et al. 2000. The epidemiology of pathogenic mitochondrial DNA mutations. *Ann Neurol* 48: 188-193.
- Coenen MJ, Antonicka H, Ugalde C, Sasarman F, Rossi R, et al. 2004. Mutant mitochondrial elongation factor G1 and combined oxidative phosphorylation deficiency. *N Engl J Med* 351: 2080-2086.
- Cole ES, Lepp CA, Holohan PD, Fondy TP. 1978. Isolation and characterization of flavin-linked glycerol-S-phosphate dehydrogenase from rabbit skeletal muscle mitochondria and comparison with the enzyme from rabbit brain. *J Biol Chem* 253: 7952-7959.
- Colombo I, Finocchiaro G, Garavaglia B, Garbuglio N, Yamaguchi S, et al. 1994. Mutations and polymorphisms of the gene encoding the beta-subunit of the electron transfer flavoprotein in three patients with glutaric acidemia type II. *Hum Mol Genet* 3: 429-435.
- Comi GP, Bordoni A, Salani S, Franceschina L, Sciacco M, et al. 1998. Cytochrome *c* oxidase subunit I microdeletion in a patient with motor neuron disease. *Ann Neurol* 43: 110-116.
- Crane FL, Hatefi Y, Lester RL, Widmer C. 1957. Isolation of a quinone from beef heart mitochondria. *Biochim Biophys Acta* 25: 220-221.
- Crivellone MD. 1994. Characterization of CBP4, a new gene essential for the expression of ubiquinol-cytochrome *c* reductase in *Saccharomyces cerevisiae*. *J Biol Chem* 269: 21284-21292.
- De Lonlay P, Valnot I, Barrientos A, Gorbatyuk M, Tzagoloff A, et al. 2001. A mutant mitochondrial respiratory chain assembly protein causes complex III deficiency in patients with tubulopathy, encephalopathy and liver failure. *Nat Genet* 29: 57-60.
- Deng K, Shenoy SK, Tso SC, Yu L, Yu CA. 2001. Reconstitution of mitochondrial processing peptidase from the core proteins (subunits I and II) of bovine heart mitochondrial cytochrome *bc*(1) complex. *J Biol Chem* 276: 6499-6505.
- DiMauro S. 2001. Lessons from mitochondrial DNA mutations. *Semin Cell Dev Biol* 12: 397-405.
- DiMauro S. 2004. *Mitochondrial medicine*. *Biochim Biophys Acta* 1659: 107-114.
- Duarte M, Sousa R, Videira A. 1995. Inactivation of genes encoding subunits of the peripheral and membrane arms of *Neurospora* mitochondrial complex I and effects on enzyme assembly. *Genetics* 139: 1211-1221.
- Erecinska M, Silver IA. 1989. ATP and brain function. *J Cereb Blood Flow Metab* 9: 2-19.
- Fearnley IM, Carroll J, Shannon RJ, Runswick MJ, Walker JE, et al. 2001. GRIM-19, a cell death regulatory gene product, is a subunit of bovine mitochondrial NADH: Ubiquinone oxidoreductase (complex I). *J Biol Chem* 276: 38345-38348.
- Ferguson-Miller S, Babcock GT. 1996. Heme/copper terminal oxidases. *Chem Rev* 96: 2889-2908.
- Frerman FE. 1988. Acyl-CoA dehydrogenases, electron transfer flavoprotein and electron transfer flavoprotein dehydrogenase. *Biochem Soc Trans* 16: 416-418.
- Friedrich T, Bottcher B. 2004. The gross structure of the respiratory complex I: A Lego system. *Biochim Biophys Acta* 1608: 1-9.
- Gakh O, Cavadini P, Isaya G. 2002. Mitochondrial processing peptidases. *Biochim Biophys Acta* 1592: 63-77.
- Gelles J, Chan SI. 1985. Chemical modification of the CuA center in cytochrome *c* oxidase by sodium p-(hydroxymethyl)benzoate. *Biochemistry* 24: 3963-3972.
- Gnaiger E, Mendez G, Hand SC. 2000. High phosphorylation efficiency and depression of uncoupled respiration in mitochondria under hypoxia. *Proc Natl Acad Sci USA* 97: 11080-11085.
- Grigorieff N. 1999. Structure of the respiratory NADH: Ubiquinone oxidoreductase (complex I). *Curr Opin Struct Biol* 9: 476-483.
- Guenebaut V, Schlitt A, Weiss H, Leonard K, Friedrich T. 1998. Consistent structure between bacterial and mitochondrial NADH: Ubiquinone oxidoreductase (complex I). *J Mol Biol* 276: 105-112.
- Hatefi Y. 1999. The mitochondrial enzymes of oxidative phosphorylation. Papa S, Guerrieri F, Tager JM, editors. *Frontiers of cellular bioenergetics: Molecular biology, biochemistry and physiopathology*. New York: Kluwer Academy/Plenum Publishers; pp. 23-47.
- Hess R, Pearse AG. 1961. Histochemical and homogenization studies of mitochondrial alpha-glycerophosphate dehydrogenase in the nervous system. *Nature* 191: 718-719.
- Hirst J, Carroll J, Fearnley IM, Shannon RJ, Walker JE. 2003. The nuclear encoded subunits of complex I from bovine heart mitochondria. *Biochim Biophys Acta* 1604: 135-150.
- Holt IJ, Harding AE, Morgan-Hughes JA. 1988. Deletions of muscle mitochondrial DNA in patients with mitochondrial myopathies. *Nature* 331: 717-719.
- Horbinski C, Chu CT. 2005. Kinase signaling cascades in the mitochondrion: A matter of life or death. *Free Radic Biol Med* 38: 2-11.
- Hunte C, Koepke J, Lange C, Rossmann T, Michel H. 2000. Structure at 2.3 Å resolution of the cytochrome *bc*(1) complex from the yeast *Saccharomyces cerevisiae* co-crystallized with an antibody Fv fragment. *Structure Fold Des* 8: 669-684.
- Iwata S, Lee JW, Okada K, Lee JK, Iwata M, et al. 1998. Complete structure of the 11-subunit bovine mitochondrial cytochrome *bc*₁ complex. *Science* 281: 64-71.

- Iwata S, Ostermeier C, Ludwig B, Michel H. 1995. Structure at 2.8 Å resolution of cytochrome *c* oxidase from *Paracoccus denitrificans*. *Nature* 376: 660-669.
- Jansen RP, de Boer K. 1998. The bottleneck: Mitochondrial imperatives in oogenesis and ovarian follicular fate. *Mol Cell Endocrinol* 145: 81-88.
- Janssen R, Smeitink J, Smeets R, van den Heuvel L. 2002. CIA30 complex I assembly factor: A candidate for human complex I deficiency? *Hum Genet* 110: 264-270.
- Janssen RJ, van den Heuvel LP, Smeitink JA. 2004. Genetic defects in the oxidative phosphorylation (OXPHOS) system. *Expert Rev Mol Diagn* 4: 143-156.
- Kadenbach B, Huttemann M, Arnold S, Lee I, Bender E. 2000. Mitochondrial energy metabolism is regulated via nuclear-coded subunits of cytochrome *c* oxidase. *Free Radic Biol Med* 29: 211-221.
- Karadimas CL, Greenstein P, Sue CM, Joseph JT, Tanji K, et al. 2000. Recurrent myoglobinuria due to a nonsense mutation in the COX I gene of mitochondrial DNA. *Neurology* 55: 644-649.
- Kaser M, Langer T. 2000. Protein degradation in mitochondria. *Semin Cell Dev Biol* 11: 181-190.
- Keightley JA, Hoffbuhr KC, Burton MD, Salas VM, Johnston WS, et al. 1996. A microdeletion in cytochrome *c* oxidase (COX) subunit III associated with COX deficiency and recurrent myoglobinuria. *Nat Genet* 12: 410-416.
- Keilin D. 1966. *The history of cell respiration and cytochromes*. Keilin J, editor. Oxford, UK: Oxford University Press.
- Kirby DM, Crawford M, Cleary MA, Dahl HH, Dennett X, et al. 1999. Respiratory chain complex I deficiency: An underdiagnosed energy generation disorder. *Neurology* 52: 1255-1264.
- Knox C, Sass E, Neupert W, Pines O. 1998. Import into mitochondria, folding and retrograde movement of fumarase in yeast. *J Biol Chem* 273: 25587-25593.
- Koehler CM. 2004. New developments in mitochondrial assembly. *Annu Rev Cell Dev Biol* 20: 309-335.
- Komiya T, Rospert S, Koehler C, Looser R, Schatz G, et al. 1998. Interaction of mitochondrial targeting signals with acidic receptor domains along the protein import pathway: Evidence for the 'acid chain' hypothesis. *EMBO J* 17: 3886-3898.
- Kuffner R, Rohr A, Schmiede A, Krull C, Schulte U. 1998. Involvement of two novel chaperones in the assembly of mitochondrial NADH: Ubiquinone oxidoreductase (complex I). *J Mol Biol* 283: 409-417.
- Kuznetsov AV, Janakiraman M, Margreiter R, Troppmair J. 2004. Regulating cell survival by controlling cellular energy production: Novel functions for ancient signaling pathways? *FEBS Lett* 577: 1-4.
- Lamperti C, Naini A, Hirano M, De Vivo DC, Bertini E, et al. 2003. Cerebellar ataxia and coenzyme Q10 deficiency. *Neurology* 60: 1206-1208.
- Lancaster CR, Kröger A. 2000. Succinate: Quinone oxidoreductases: New insights from X-ray crystal structures. *Biochim Biophys Acta* 1459: 422-431.
- Lancaster CRD. 2001. *Handbook of metalloproteins*. Messerschmidt A, et al., editors. Chichester, UK: John Wiley and Sons; pp. 379-395.
- Langley B, Ratan RR. 2004. Oxidative stress-induced death in the nervous system: Cell cycle dependent or independent? *J Neurosci Res* 77: 621-629.
- Lawford HG, Garland PB. 1972. Proton translocation coupled to quinone reduction by reduced nicotinamide—adenine dinucleotide in rat liver and ox heart mitochondria. *Biochem J* 130: 1029-1044.
- Leigh D. 1951. Subacute necrotizing encephalomyelopathy in an infant. *J Neurochem* 14: 216-221.
- Loeffen JL, Smeitink JA, Trijbels JM, Janssen AJ, Triepels RH, et al. 2000. Isolated complex I deficiency in children: Clinical, biochemical and genetic aspects. *Hum Mutat* 15: 123-134.
- Lorusso M, Cocco T, Minuto M, Capitanio N, Papa S. 1995. Proton/electron stoichiometry of mitochondrial bc1 complex. Influence of pH and transmembrane delta pH. *J Bioenerg Biomembr* 27: 101-118.
- Maj MC, Raha S, Myint T, Robinson BH. 2004. Regulation of NADH/CoQ oxidoreductase: Do phosphorylation events affect activity? *Protein J* 23: 25-32.
- Mamedova AA, Holt PJ, Carroll J, Sazanov LA. 2004. Substrate-induced conformational change in bacterial complex I. *J Biol Chem* 279: 23830-23836.
- Manfredi G, Schon EA, Moraes CT, Bonilla E, Berry GT, et al. 1995. A new mutation associated with MELAS is located in a mitochondrial DNA polypeptide-coding gene. *Neuromuscul Disord* 5: 391-398.
- Matsuno-Yagi A, Hatefi Y. 2001. Ubiquinol: Cytochrome *c* oxidoreductase (complex III). Effect of inhibitors on cytochrome *b* reduction in submitochondrial particles and the role of ubiquinone in complex III. *J Biol Chem* 276: 19006-19011.
- Meinhardt SW, Yang XH, Trumpower BL, Ohnishi T. 1987. Identification of a stable ubisemiquinone and characterization of the effects of ubiquinone oxidation—reduction status on the Rieske iron—sulfur protein in the three-subunit ubiquinol—cytochrome *c* oxidoreductase complex of *Paracoccus denitrificans*. *J Biol Chem* 262: 8702-8706.
- Michel H. 1998. The mechanism of proton pumping by cytochrome *c* oxidase. *Proc Natl Acad Sci USA* 95: 12819-12824.
- Michel H. 1999. Cytochrome *c* oxidase: Catalytic cycle and mechanisms of proton pumping—a discussion. *Biochemistry* 38: 15129-15140.
- Miller C, Saada A, Shaul N, Shabtai N, Ben-Shalom E, et al. 2004. Defective mitochondrial translation caused by a

- ribosomal protein (MRPS16) mutation. *Ann Neurol* 56: 734-738.
- Mitchell P. 1961. Coupling of phosphorylation to electron and hydrogen transfer by a chemi-osmotic type of mechanism. *Nature* 191: 144-148.
- Mitchell P. 1966. Chemiosmotic coupling in oxidative and photosynthetic phosphorylation. *Biol Rev Camb Philos Soc* 41: 445-502.
- Mitchell P. 1976. Possible molecular mechanisms of the protonmotive function of cytochrome systems. *J Theor Biol* 62: 327-367.
- Mitchell P. 1979. Keilin's respiratory chain concept and its chemiosmotic consequences *Science* 206: 1148-1159.
- Monod J, Wyman J, Changeux JP. 1965. On the nature of allosteric transitions: A plausible model. *J Mol Biol* 12: 88-118.
- Mootha VK, Lepage P, Miller K, Bunkenborg J, Reich M, et al. 2003. Identification of a gene causing human cytochrome *c* oxidase deficiency by integrative genomics. *Proc Natl Acad Sci USA* 100: 605-610.
- Neupert W, Brunner M. 2002. The protein import motor of mitochondria. *Nat Rev Mol Cell Biol* 3: 555-565.
- Nicholls P. 1999. The mitochondrial and bacterial respiratory chains from MacMunn and Keilin to current concepts. *Frontiers of cellular bioenergetics: Molecular biology, biochemistry and physiopathology*. Papa S, Guerrieri F, Tager JM, editors. New York: Kluwer Academy/Plenum Publishers; pp. 1-22.
- Niemann S, Muller U. 2000. Mutations in SDHC cause autosomal dominant paraganglioma, type 3. *Nat Genet* 26: 268-270.
- Nijtmans LG, Taanman JW, Muijsers AO, Speijer D, Van den Bogert C. 1998. Assembly of cytochrome-*c* oxidase in cultured human cells. *Eur J Biochem* 254: 389-394.
- Nisoli E, Clementic E, Moncada S, Carruba MO. 2004. Mitochondrial biogenesis as a cellular signaling framework. *Biochem Pharmacol* 67: 1-15.
- Nobrega FG, Nobrega MP, Tzagoloff A. 1992. BCS1, a novel gene required for the expression of functional Rieske iron-sulfur protein in *Saccharomyces cerevisiae*. *EMBO J* 11: 3821-3829.
- Ohnishi T. 1998. Iron-sulfur clusters/semiquinones in complex I. *Biochim Biophys Acta* 1364: 186-206.
- Orth M, Schapira AH. 2001. Mitochondria and degenerative disorders. *Am J Med Genet* 106: 27-36.
- Papa S. 1976. Proton translocation reactions in the respiratory chains. *Biochim Biophys Acta* 456: 39-84.
- Papa S. 1996. Mitochondrial oxidative phosphorylation changes in the life span. Molecular aspects and physiopathological implications. *Biochim Biophys Acta* 1276: 87-105.
- Papa S. 2002. The NDUFS4 nuclear gene of complex I of mitochondria and the cAMP cascade. *Biochim Biophys Acta* 1555: 147-153.
- Papa S. 2005. Role of cooperative H⁺/e⁻ linkage (redox Bohr effect) at heme *a*/Cu_A and heme *a₃*/Cu_B in the proton pump of cytochrome *c* oxidase. *Biochemistry (Mosc)* 70: 178-186.
- Papa S, Capitanio N. 1998. Redox Bohr effects (cooperative coupling) and the role of heme *a* in the proton pump of cytochrome *c* oxidase. *J Bioenerg Biomembr* 30: 109-119.
- Papa S, Capitanio N, Capitanio G, Palese LL. 2004b. Protonmotive cooperativity in cytochrome *c* oxidase. *Biochim Biophys Acta* 1658: 95-105.
- Papa S, Capitanio N, Villani G. 1998. A cooperative model for protonmotive heme-copper oxidases. The role of heme *a* in the proton pump of cytochrome *c* oxidase. *FEBS Letters* 439: 1-8.
- Papa S, Capitanio N, Villani G. 1999a. Proton pumps of respiratory chain enzymes. *Frontiers of cellular bioenergetics. Molecular biology, biochemistry and physiopathology*. Papa S, Guerrieri F, Tager JM, editors. New York: Kluwer Academy/Plenum Publishers; pp. 49-87.
- Papa S, Guerrieri F, Izzo G. 1986. Cooperative proton-transfer reactions in the respiratory chain: Redox Bohr effects. *Methods Enzymol* 126: 331-343.
- Papa S, Guerrieri F, Lorusso M. 1974. Mechanism of respiration-driven proton translocation in the inner mitochondrial membrane. Analysis of proton translocation associated to oxido-reductions of the oxygen-terminal respiratory carriers. *Biochim Biophys Acta* 357: 181-92.
- Papa S, Guerrieri F, Lorusso M, Simone S. 1973. Proton translocation and energy transduction in mitochondria. *Biochimie* 55: 703-716.
- Papa S, Lorusso M, Capitanio N. 1995. On the mechanism of proton pumps in respiratory chains. *Biochemistry of cell membranes*. Papa S, Tager JM, editors. Switzerland: Birkhäuser Verlag Basel; pp. 151-166.
- Papa S, Lorusso M, Capitanio N, Zanotti F. 1996a. Liposomes in reconstitution of proton-motive proteins. *Handbook of nonmedical applications of liposomes*, vol II. Barenholtz Y, Lasic DD, editors. Boca Raton, FL: CRC Press; pp. 245-259.
- Papa S, Lorusso M, Cocco T, Boffoli D, Lombardo M. 1990. Protonmotive ubiquinol-cytochrome *c* oxidoreductase of mitochondria. A possible example of co-operative anisotropy of protolytic redox catalysis. Lenaz G, Barnabei O, Rabbi A, Battino M. editors. London, New York, Philadelphia: Highlights in ubiquinone research. Taylor & Francis; pp. 122-135.
- Papa S, Petruzzella V, Scacco S, Vergari R, Panelli D, et al. 2004a. Respiratory complex I in brain development and genetic disease. *Neurochem Res* 29: 547-560.
- Papa S, Sardanelli AM, Cocco T, Speranza F, Scacco SC, et al. 1996b. The nuclear-encoded 18 kDa (IP) AQDQ subunit of bovine heart complex I is phosphorylated by the

- mitochondrial cAMP-dependent protein kinase. *FEBS Lett* 379: 299-301.
- Papa S, Sardanelli AM, Scacco S, Technikova-Dobrova Z. 1999b. cAMP-dependent protein kinase and phosphoproteins in mammalian mitochondria. An extension of the cAMP-mediated intracellular signal transduction. *FEBS Lett* 444: 245-249.
- Papadopoulou LC, Sue CM, Davidson MM, Tanji K, Nishino I, et al. 1999. Fatal infantile cardioencephalomyopathy with COX deficiency and mutations in SCO2, a COX assembly gene. *Nat Genet* 23: 333-337.
- Parfait B, Chretien D, Rötig A, Marsac C, Munnich A, et al. 2000. Compound heterozygous mutations in the flavoprotein gene of the respiratory chain complex II in a patient with Leigh syndrome. *Hum Genet* 106: 236-243.
- Pasdois P, Deveaud C, Voisin P, Bouchaud V, Rigoulet M, et al. 2003. Contribution of the phosphorylatable complex I in the growth phase-dependent respiration of C6 glioma cells in vitro. *J Bioenerg Biomembr* 35: 439-450.
- Pereira MM, Santana M, Teixeira M. 2001. A novel scenario for the evolution of haem-copper oxygen reductases. *Biochim Biophys Acta* 1505: 185-208.
- Perutz MF. 1976. Haemoglobin: Structure, function and synthesis. *Br Med Bull* 32: 193-194.
- Petruzzella V, Papa S. 2002. Mutations in nuclear genes encoding for subunits of mitochondrial respiratory complex I: The NDUF54 gene. *Gene* 286: 149-154.
- Petruzzella V, Tiranti V, Fernandez P, Ianna P, Carrozzo R, et al. 1998. Identification and characterization of human cDNAs specific to BCS1, PET112, SCO1, COX15, and COX11, five genes involved in the formation and function of the mitochondrial respiratory chain. *Genomics* 54: 494-504.
- Pulkes T, Eunson L, Patterson V, Siddiqui A, Wood NW, et al. 1999. The mitochondrial DNA G13513A transition in ND5 is associated with a LHON/MELAS overlap syndrome and may be a frequent cause of MELAS. *Ann Neurol* 46: 916-919.
- Rahman S, Blok RB, Dahl HH, Danks DM, Kirby DM, et al. 1996. Leigh syndrome: Clinical features and biochemical and DNA abnormalities. *Ann Neurol* 39: 343-351.
- Rehling P, Brandner K, Pfanner N. 2004. Mitochondrial import and the twin-pore translocase. *Nat Rev Mol Cell Biol* 5: 519-530.
- Richter OM, Ludwig B. 2003. Cytochrome *c* oxidase—structure, function, and physiology of a redox-driven molecular machine. *Rev Physiol Biochem Pharmacol* 147: 47-74.
- Ricquier D, Bouillaud F. 2000. The uncoupling protein homologues: UCP1, UCP2, UCP3, StUCP and AtUCP. *Biochem J* 345: 161-179.
- Rieske JS. 1986. Experimental observations on the structure and function of mitochondrial complex III that are unresolved by the protonmotive ubiquinone-cycle hypothesis. *J Bioenerg Biomembr* 18: 235-257.
- Robinson BH. 1998. Human complex I deficiency: Clinical spectrum and involvement of oxygen free radicals in the pathogenicity of the defect. *Biochim Biophys Acta* 1364: 271-286.
- Rotig A, Appelkvist EL, Geromel V, Chretien D, Kadhon N, et al. 2000. Quinone-responsive multiple respiratory-chain dysfunction due to widespread coenzyme Q10 deficiency. *Lancet* 356: 391-395.
- Rubinstein JL, Walker JE, Henderson R. 2003. Structure of the mitochondrial ATP synthase by electron cryomicroscopy. *EMBO J* 22: 6182-6192.
- Santorelli FM, Tanji K, Kulikova R, Shanske S, Vilarinho L, et al. 1997. Identification of a novel mutation in the mtDNA ND5 gene associated with MELAS. *Biochem Biophys Res Commun* 238:326-328.
- Saraste M. 1999. Oxidative phosphorylation at the fin de siècle. *Science* 283: 1488-1493.
- Scacco S, Petruzzella V, Budde S, Vergari R, Tamborra R, et al. 2003. Pathological mutations of the human NDUF54 gene of the 18-kDa (AQDQ) subunit of complex I affect the expression of the protein and the assembly and function of the complex. *J Biol Chem* 278: 44161-44167.
- Schaefer AM, Taylor RW, Turnbull DM, Chinnery PF. 2004. The epidemiology of mitochondrial disorders—past, present and future. *Biochim Biophys Acta* 1659: 115-120.
- Schagger H. 2001. Blue-native gels to isolate protein complexes from mitochondria. *Meth Cell Biol* 65:231-244.
- Schagger H. 2002. Respiratory chain supercomplexes of mitochondria and bacteria. *Biochim Biophys Acta* 1555: 154-159.
- Schagger H, de Coo R, Bauer MF, Hofmann S, Godinot C, et al. 2004. Significance of respirasomes for the assembly/stability of human respiratory chain complex I. *J Biol Chem* 279: 36349-36353.
- Scheffler IE, Yadava N, Potluri P. 2004. *Molecular genetics of complex I-deficient Chinese hamster cell lines*. *Biochim Biophys Acta* 1659: 160-171.
- Schulte U, Haupt V, Abelmann A, Fecke W, Brors B, et al. 1999. A reductase/isomerase subunit of mitochondrial NADH: Ubiquinone oxidoreductase (complex I) carries an NADPH and is involved in the biogenesis of the complex. *J Mol Biol* 292: 569-580.
- Soulimane T, Buse G, Bourenkov GP, Bartunik HD, Huber R, et al. 2000. Structure and mechanism of the aberrant ba(3)-cytochrome *c* oxidase from *Thermus thermophilus*. *EMBO J* 19: 1766-1776.
- Stock D, Leslie AG, Walker JE. 1999. Molecular architecture of the rotary motor in ATP synthase. *Science* 286: 1700-1705.
- Sutovsky P, Van Leyen K, McCauley T, Day BN, Sutovsky M. 2004. Degradation of paternal mitochondria after fertilization: Implications for heteroplasmy, assisted reproductive

- technologies and mtDNA inheritance. *Reprod Biomed Online* 8: 24-33.
- Svensson-Ek M, Abramson J, Larsson G, Tornroth S, Brzezinski P, et al. 2002. The X-ray crystal structures of wild-type and EQ(I-286) mutant cytochrome *c* oxidases from *Rhodobacter sphaeroides*. *J Mol Biol* 321: 329-339.
- Taylor SW, Fahy E, Zhang B, Glenn GM, Warnock DE, et al. 2003. Characterization of the human heart mitochondrial proteome. *Nat Biotechnol* 21: 281-286.
- Technikova-Dobrova Z, Sardanelli AM, Speranza F, Scacco S, Signorile A, et al. 2001. Cyclic adenosine monophosphate-dependent phosphorylation of mammalian mitochondrial proteins: Enzyme and substrate characterization and functional role. *Biochemistry* 40: 13941-13947.
- Thomson M. 2002. Evidence of undiscovered cell regulatory mechanisms: Phosphoproteins and protein kinases in mitochondria. *Cell Mol Life Sci* 59: 213-219.
- Thorpe C. 1991. *Chemistry and biochemistry of flavoenzymes*. Muller F, editor. vol II., Boca Raton, FL: CRC Press; pp. 471-486.
- Tiranti V, Corona P, Greco M, Taanman JW, Carrara F, et al. 2000. A novel frameshift mutation of the mtDNA COXIII gene leads to impaired assembly of cytochrome *c* oxidase in a patient affected by Leigh-like syndrome. *Hum Mol Genet* 9: 2733-2742.
- Tiranti V, Hoertnagel K, Carrozzo R, Galimberti C, Munaro M, et al. 1998. Mutations of SURF-1 in Leigh disease associated with cytochrome *c* oxidase deficiency. *Am J Hum Genet* 63: 1609-1621.
- Toogood HS, van A, Thiel J, Basran Sutcliffe MJ, Scrutton NS, et al. 2004 Extensive domain motion and electron transfer in the human electron transferring flavoprotein-medium chain Acyl-CoA dehydrogenase complex. *J Biol Chem* 279: 32904-32912.
- Trumpower BL. 1999. Energy transduction in mitochondrial respiration by the proton-motive Q-cycle mechanism of the cytochrome *bc₁* complex. *Frontiers of cellular bioenergetics. Molecular biology, biochemistry, and physiopathology*. Papa S, Guerrieri F, Tager JM, editors. New York: Kluwer Academic/Plenum Publishers; pp. 233-261.
- Tsukihara T, Aoyama H, Yamashita E, Tomizaki T, Yamaguchi H, et al. 1996. The whole structure of the 13-subunit oxidized cytochrome *c* oxidase at 2.8 Å. *Science* 272: 1136-1144.
- Tsukihara T, Shimokata K, Katayama Y, Shimada H, Muramoto K, et al. 2003. The low-spin heme of cytochrome *c* oxidase as the driving element of the proton-pumping process. *Proc Natl Acad Sci U S A* 100: 15304-15309.
- Tuschen G, Sackmann U, Nehls U, Haiker H, Buse G, et al. 1990 Assembly of NADH-ubiquinone reductase (complex I) in *Neurospora* mitochondria. Independent pathways of nuclear-encoded and mitochondrially encoded subunits. *J Mol Biol* 213: 845-857.
- Tzagoloff A, Dieckmann CL. 1990. PET genes of *Saccharomyces cerevisiae*. *Microbiol Rev* 54: 211-225.
- Ugalde C, Vogel R, Huijbens R, Van Den Heuvel B, Smeitink J, et al. 2004. Human mitochondrial complex I assembles through the combination of evolutionary conserved modules: A framework to interpret complex I deficiencies. *Hum Mol Genet* 13: 2461-2472.
- Urban PF, Klingenberg M. 1969. On the redox potentials of ubiquinone and cytochrome *b* in the respiratory chain. *Eur J Biochem* 9: 519-525.
- Valnot I, Osmond S, Gigarel N, Mehaye B, Amiel J, et al. 2000. Mutations of the SCO1 gene in mitochondrial cytochrome *c* oxidase deficiency with neonatal-onset hepatic failure and encephalopathy. *Am J Hum Genet* 67: 1104-1109.
- Videira A, Duarte M. 2001. On complex I and other NADH: Ubiquinone reductases of *Neurospora crassa* mitochondria. *J Bioenerg Biomembr* 33: 197-203.
- Vinogradov AD. 2001. Respiratory complex I: Structure, redox components, and possible mechanisms of energy transduction. *Biochemistry (Mosc)* 66: 1086-1097.
- Visapaa I, Fellman V, Vesa J, Dasvarma A, Hutton JL, et al. 2002. GRACILE syndrome, a lethal metabolic disorder with iron overload, is caused by a point mutation in BCS1L. *Am J Hum Genet* 71: 863-876.
- Wallace DC, Singh G, Lott MT, Hodge JA, Schurr TG, et al. 1988. Mitochondrial DNA mutation associated with Leber's hereditary optic neuropathy. *Science* 242: 1427-1430.
- White RA, Dowler LL, Angeloni SV, Koeller DM. 1996. Assignment of Etfhd, Etfb, and Etfα to chromosomes 3, 7, and 13: The mouse homologs of genes responsible for glutaric acidemia Type II in human. *Genomics* 33: 131-134.
- Wiedemann N, Frazier AE, Pfanner N. 2004. The protein import machinery of mitochondria. *J Biol Chem* 279: 14473-14476.
- Wielburski A, Nelson BD. 1983. Evidence for the sequential assembly of cytochrome oxidase subunits in rat liver mitochondria. *Biochem J* 212: 829-834.
- Wikstrom M. 2004. Cytochrome *c* oxidase: 25 years of the elusive proton pump. *Biochim Biophys Acta* 1655: 241-247.
- Wikstrom M, Krab K, Saraste M. 1981. Proton-translocating cytochrome complexes. *Annu Rev Biochem* 50: 623-655.
- Wikstrom MK, Berden JA. 1972. Oxidoreduction of cytochrome *b* in the presence of antimycin. *Biochim Biophys Acta* 283: 403-420.
- Williams RJ. 2002. The problem of proton transfer in membranes. *J Theor Biol* 219: 389-396.
- Wong W, Scott J.D. 2004. AKAP signalling complexes: Focal points in space and time. *Nat Rev Mol Cell Biol* 5: 959-970.
- Wu M, Tzagoloff A. 1989. Identification and characterization of a new gene (CBP3) required for the expression of yeast coenzyme QH₂-cytochrome *c* reductase. *J Biol Chem* 264: 11122-11130.

- Xia D, Yu CA, Kim H, Xia JZ, Kachurin AM, et al. 1997. Crystal structure of the cytochrome *bc₁* complex from bovine heart mitochondria. *Science* 277: 60-66.
- Yagi T, Matsuno-Yagi A. 2003. The proton-translocating NADH-quinone oxidoreductase in the respiratory chain: The secret unlocked. *Biochemistry* 42: 2266-2274.
- Yano M, Terada K, Mori M. 2003. AIP is a mitochondrial import mediator that binds to both import receptor Tom20 and preproteins. *J Cell Biol* 163: 45-56.
- Young JC, Hoogenraad NJ, Hartl FU. 2003. Molecular chaperones Hsp90 and Hsp70 deliver preproteins to the mitochondrial import receptor Tom70. *Cell* 112: 41-50.
- Yoshikawa S. 2002. Cytochrome *c* oxidase. *Adv Protein Chem* 60: 341-395.
- Zhu Z, Yao J, Johns T, Fu K, De Bie I, et al. 1998. SURF1, encoding a factor involved in the biogenesis of cytochrome *c* oxidase, is mutated in Leigh syndrome. *Nat Genet* 20: 337-343.

1.6 The Mitochondrial F_1F_o ATP Synthase

A. Gaballo · S. Papa

1	<i>Introduction</i>	120
2	<i>F₁: X-ray Crystallographic Studies and Catalysis</i>	122
3	<i>Structure and Functional Mechanism of the F_1F_o Complex</i>	124
4	<i>The Inhibitor Protein: Structure and Physiopathological Role</i>	127
5	<i>ATP Synthase and Human Diseases</i>	128

1 Introduction

Adenosine triphosphate (ATP) is the general energy currency of living organisms from simple prokaryotes to the more complex eukaryotes. It is continually produced at the expense of nutrients and utilized by endergonic biological processes in large amounts that usually exceed the weight of the organism. In aerobic prokaryotic and eukaryotic cells, although some ATP is produced by soluble enzymes, the largest proportion comes from oxidative phosphorylation of coupling membranes. Oxidative phosphorylation is an integrated process in which the free energy, made available by downhill electron flow in the respiratory chain as a transmembrane electrochemical gradient of protons ($\Delta\mu H^+$, or protonmotive force (PMF)), is utilized by the F_1F_0 ATP synthase complex to make ATP from ADP (adenosine diphosphate) and P_i (inorganic phosphate). The F_1F_0 ATP synthase, also known as complex V, is a proton pump that converts the PMF into mechanochemical energy to drive ATP synthesis. When the PMF becomes limiting, as in extremely hypoxic conditions, the ATP synthase is reversed and it hydrolyzes ATP produced essentially by glycolysis until the PMF is reestablished.

Research on the structural organization and the catalytic mechanism of the ATP synthase began in the 1960s and evolved contextually to Peter Mitchell's chemiosmotic hypothesis. In 1962, ATP synthase was directly observed, for the first time, by electron microscopy. Many spherical "bead-like structures" were visible at the surface of the inner mitochondrial membrane (Fernandez-Moran, 1962). The spheres appeared to be connected to the membrane by a thin stalk. A pioneer in this field was E. Racker who succeeded in isolating the hydrosoluble "factor" (F_1) from the mitochondrial inner membrane. F_1 could be reconstituted with the stalk moiety in the membrane in the presence of the "oligomycin sensitivity conferring protein" (OSCP), a protein required for the sensitivity of complex V to the antibiotic oligomycin (Kagawa and Racker, 1966). Oligomycin sensitivity is a feature of mitochondrial F_1F_0 ATP synthase and is used to distinguish it from the other two major types of ion-motive ATPases (P-type and V-type ATPases). Since then many significant advances in understanding the structural organization and the catalytic mechanism of F_1F_0 ATP synthase have been made, culminating in the X-ray crystallographic analysis of the three-dimensional structure of the F_1 catalytic moiety from bovine heart (Abrahams et al., 1994) and other sources (Shirakihara et al., 1997; Bianchet et al., 1998; Hausrath et al., 1999; Groth and Pohl, 2001). The resolution at 2.8 Å of the atomic structure of bovine heart F_1 (Abrahams et al., 1994) provided the structural basis for the development of the rotary model of the F_1F_0 ATP synthase. This was further supported by the demonstration of ATP-driven rotation of the γ subunit of F_1 (Noji et al., 1997).

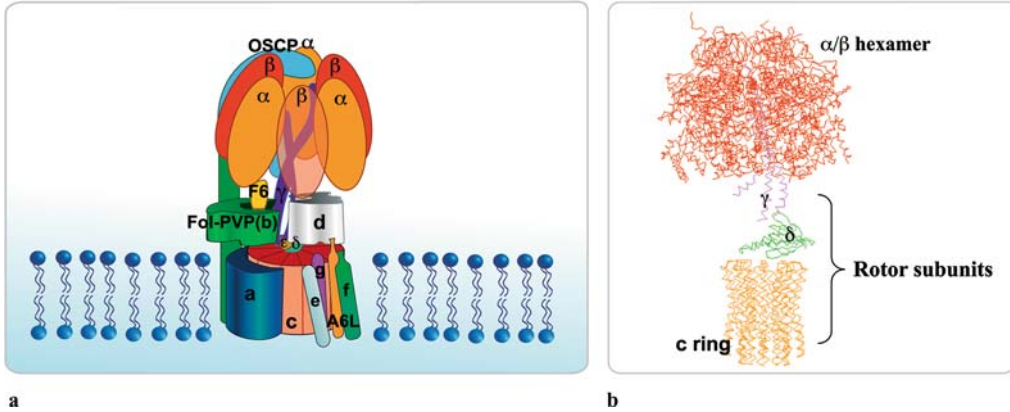
F_1F_0 ATP synthase is a large oligomeric complex whose general structure is highly conserved among bacteria, chloroplasts, and mitochondria. Very recently, the presence of a F_1F_0 ATP synthase complex has been demonstrated in the plasma membrane of human endothelial cells (HUVEC) where it produces extracellular ATP, which is involved in angiogenesis, and appears to be the angiotensin receptor (Moser et al., 1999, 2001; Arakaki et al., 2003; Burwick et al., 2004).

In mammalian mitochondria, the F_1F_0 ATP synthase is composed of 16 subunits (only eight in bacteria), with an overall molecular weight of about 550 kDa. In mitochondria, but not in chloroplasts and bacteria, the F_1F_0 complex has been shown to exist as a dimer (Arnold et al., 1998; Schagger and Pfeiffer, 2000) or even as an oligomer (Krause et al., 2005). In yeast mitochondria, the ATP synthase oligomer is thought to have a role in modulating the morphology of the mitochondrial inner membrane (Gavin et al., 2004). Furthermore, a recent report has indicated the presence of an ATP supercomplex containing F_1F_0 , adenine nucleotide, and P_i carriers (Chen et al., 2004).

The monomeric ATP synthase complex consists of two major domains, a large globular catalytic moiety known as F_1 that consists of an assembly of five subunits with the stoichiometry of $\alpha_3\beta_3\gamma\delta\epsilon$, protruding into the mitochondrial matrix, and a membrane-embedded domain known as F_0 , involved in transmembrane proton translocation coupled to enzyme catalysis (● [Figure 1.6-1a](#)). The F_0 domain has a variable number of different subunits depending on the species. In mammals, there are 11 subunits, including the IF_1 inhibitor protein, which plays a key role in ATP hydrolase regulation. Subunits a, b, and c, represent the conserved core of F_0 with the stoichiometry 1:1:10–12. In the mammalian F_0F_1 complex, all the subunits are

■ Figure 1.6-1

Model of the mitochondrial ATP synthase. (a) Subunit arrangement of the mitochondrial ATP synthase. The model is based on electron microscopic (EM) images, crystal structures, and on other biochemical and reconstitution studies reviewed in the text. (b) Electron density map of the F₁-c₁₀ subcomplex obtained from *Saccharomyces cerevisiae* at 3.9 Å resolution (Stock et al., 1999) (PDB = 1Q01). The subunits that constitute the rotor, except subunit ε which is not resolved in the crystal structure, are shown. Molecular graphics by RasMol 2.6



nuclear encoded except two, subunits a (mt gene ATP6) and A6L (mt gene ATP8), which are encoded by the mitochondrial DNA (mt DNA) (Table 1.6-1) (Papa et al., 2000).

The F₁ and F_o moieties are structurally and functionally connected by two stalks: a central stalk, which constitutes the rotor and a peripheral stalk referred to as the stator of the rotary-motor model of the ATP synthase (Collinson et al., 1996; Ogilvie et al., 1997).

■ Table 1.6-1

The mitochondrial F₁F_o ATP synthase subunits

Subunits	ncopies	Location	Mass (Da)	Gene
F ₁				
α	3	External hexagon	55164	Nuclear
β	3	External hexagon	51595	Nuclear
γ	1	Internal cavity and stalk	30141	Nuclear
δ	1	Stalk	15065	Nuclear
ε	1	Stalk	5652	Nuclear
IF1	1	Surface	9582	Nuclear
F _o				
F _{ol} -PVP(b)	1	Stalk membrane	24670	Nuclear
ATP6(a)	1	Transmembrane	24815	Mitochondrial
OSCP	1	Surface F ₁ and stalk	20968	Nuclear
d	1	Stalk membrane	18603	Nuclear
g	1	Transmembrane	11328	Nuclear
f	1	Transmembrane	10209	Nuclear
F ₆	1	Stalk membrane	8958	Nuclear
e	1–2	Transmembrane	8189	Nuclear
c	10–12	Transmembrane	7608	Nuclear
A6L	1	Transmembrane	7964	Mitochondrial

This chapter deals with the following aspects of the F_1F_0 ATP synthase in mammalian mitochondria:

1. F_1 : X-ray crystallographic studies and catalysis
2. Structure and functional mechanism of the F_1F_0 complex
3. The inhibitor protein: structure and physiopathological role
4. ATP synthase and human diseases

2 F_1 : X-ray Crystallographic Studies and Catalysis

In 1994, Walker's group in Cambridge published the first high-resolution structure of $F_1\alpha_3\beta_3\gamma$ subcomplex at 2.8 Å resolution (Abrahams et al., 1994). This structure, prepared in the presence of the inhibitory ATP analog AMP-PNP, shows that the α and β subunits are alternatively arranged to form a spherical hexamer. The β subunits appear different in terms of nucleotide binding states; the first β binds Mg-AMP-PNP, the second Mg-ADP, and the third is empty (no bound nucleotide). These sites are termed β_{TP} , β_{DP} , and β_E and correspond to "tight," "loose," and "open" conformations, respectively (🔗 [Figure 1.6-2a](#)). All three α subunits bind the ATP analog AMP-PNP. Only the coiled coil C and N termini regions of the γ subunit that penetrate the α/β spherical hexamer are visible, the rest of the protein not being ordered in the crystal (🔗 [Figure 1.6-2a](#)). The empty conformation of β_E appears to be induced by the γ subunit, which seems to prevent the rotation of the β lower C-terminal part by pushing it toward the central axis (🔗 [Figure 1.6-2a](#)). The asymmetry of β subunits is the most important feature of this F_1 crystal structure (Abrahams et al., 1994). Similar asymmetric β structure has also been observed in subsequent crystal structures analyzed by Walker and coworkers (Abrahams et al., 1996; van Raaij et al., 1996a; Orriss et al., 1998; Braig et al., 2000; Gibbons et al., 2000), except for a structure obtained in the presence of MgADP and an excess of aluminum fluoride (Menz et al., 2001). In this structure all the catalytic sites are filled (closed conformation) and the β subunit, corresponding to the former β_E (open conformation), appears in a "half closed" conformation. This partial closure of the β C-terminal region, apparently induced by binding and hydrolysis of ATP, is thought to result from a 20° rotation of the γ subunit, which presents a different feature with respect to all the other crystals examined. The β subunit, in a half-closed conformation, binds ADP and sulfate, the latter mimicking P_i , so that this structure represents a posthydrolysis intermediate with β_{ADP+P_i} ready to pass to the "open conformation" and release the products (Menz et al., 2001).

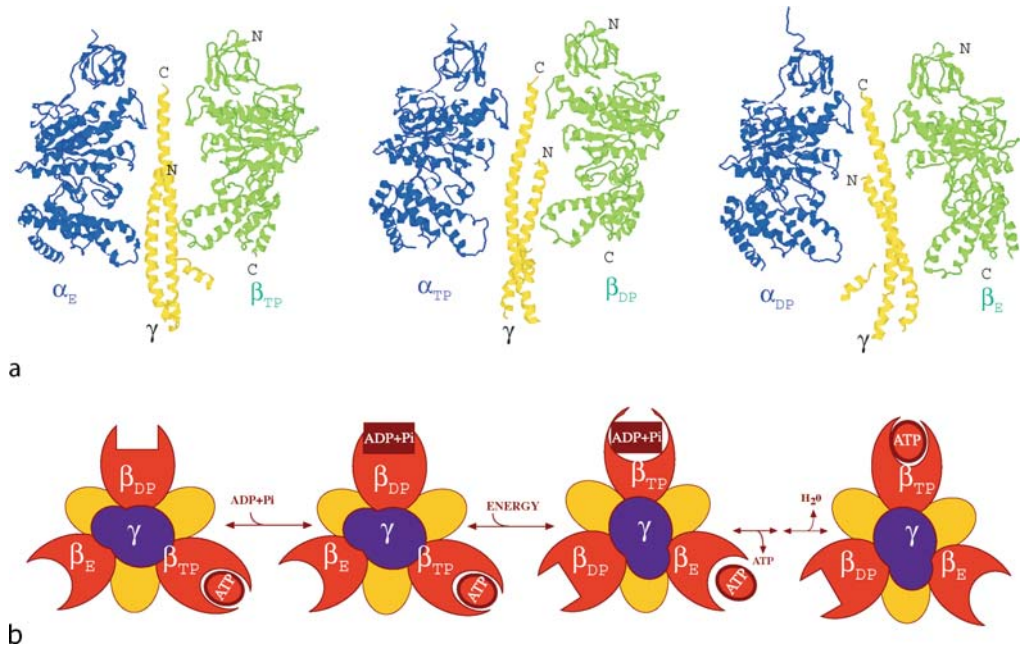
The structural data described have been of high impact and are generally considered to be illustrative of the reaction mechanism of the enzyme. They all appeared to be consistent with what Boyer's "binding change mechanism" predicts (🔗 [Figure 1.6-2b](#)) (Boyer, 1993, 1997). During catalysis, the three catalytic sites pass sequentially through three different nucleotide conformations, namely "tight," "loose," and "open," and cooperative interconversion of the states is associated with a rotation of the γ subunit (🔗 [Figure 1.6-2b](#)) (Boyer, 1993, 1997). The γ rotation, driven by transmembrane proton translocation through the complex, results in a decrease in the affinity of F_1 for ATP (and probably increases the affinity for ADP and P_i) with ATP release in the medium (🔗 [Figure 1.6-2b](#)). ATP formation at one catalytic site would take place after binding of ADP and P_i without energy expenditure.

Kinetic data have, in fact, shown that ATP synthase catalysis can occur involving only one catalytic site (unisite catalysis), two catalytic sites (bisite catalysis) (🔗 [Figure 1.6-2b](#)), or all the three catalytic sites (trisite catalysis). Unisite catalysis, measured only for ATP hydrolysis, can take place at very low ATP concentrations (ATP: F_1 ratio of 1:3). In these conditions, the rate of ATP hydrolysis is much lower (10^{-5} to 10^{-6}) than that measured during steady-state (multisite) catalysis; the release of products P_i and ADP is also very slow. Thus, when only one catalytic site is filled with the substrate, the substrate is tightly bound and the reaction proceeds slowly. The successive binding of the substrate dramatically enhances ATP hydrolysis (or synthesis) and product release. Whether two catalytic sites (bisite catalysis) or three catalytic sites (trisite catalysis) have to be filled in order to achieve a significant rate of hydrolysis is still a matter of debate (see below).

The "binding change mechanism" postulates that the catalytic sites on β subunits are in three different states during catalysis, this being due to the physical rotation of the γ subunit in the internal cavity of the $\alpha_3\beta_3$ hexamer. Cross and coworkers performed experiments in which a labeled β subunit was reversibly cross-linked with the γ subunit. They observed that the addition of ATP after cleavage and before

■ Figure 1.6-2

(a) Different structural conformations of F₁ α , β , and γ subunits as observed in the F₁ crystal structure inhibited by AMP-PNP. Longitudinal sections of F₁ moiety, each showing partially resolved subunit γ with facing α and β subunits, are depicted. The three different conformations adopted by the three β subunits are visible: β_{TP} , which corresponds to the tight state with high affinity for substrate and catalytically active β_{DP} , which corresponds to the loose state with low affinity for substrate and catalytically inactive; and β_E , which corresponds to the open state with very low affinity for substrates and catalytically inactive. Structural data are from bovine heart mitochondrial F₁ crystal structure (Abrahams et al., 1994) (PDB ID = 1 bmf). Molecular graphics by RasMol 2.6. (b) The binding change mechanism. Bisite catalysis scheme in which only two catalytic sites in the β subunits are occupied by adenine nucleotides (ATP and ADP + P_i) during steady-state catalysis. From left to right (ATP synthesis), an ATP molecule can be seen bound at the high-affinity site (β_{TP}); the binding of ADP and P_i at the loose site (β_{DP}); and interconversion of the catalytic sites in association with rotation of the γ subunit. In the last step ATP is released from the open site (β_E). The feature of this model is that the energy-requiring steps are substrate binding and product release (see Abrahams et al., 1994)



reinduction of cross-linking caused the γ subunit to be cross-linked to a β subunit different from the one initially labeled (Duncan et al., 1995). Junge's group employed the technique of "polarized absorption recovery after photobleaching" (PARAP) of a probe labeled to γ subunit, which allowed observation of rotation of this subunit during ATP hydrolysis (Sabbert et al., 1996). Finally, rotation of γ subunit induced by ATP hydrolysis was directly observed by optical microscopy with attachment of fluorescent actin filaments to γ or ϵ subunits in a $\alpha 3\beta 3\gamma \epsilon$ subcomplex, (Noji et al., 1997; Kato-Yamada et al., 1998). Seen from the F_o side, the γ subunit rotated anticlockwise, proceeding by a 120° step upon hydrolysis of one ATP molecule. This fact indicated that the γ subunit rotates, interacting with all the three β subunits. Later, better resolution experiments showed that the 120° step could be divided into two substeps (Yasuda et al., 2001; Shimabukuro et al., 2003; Nishizaka et al., 2004). These were proposed to correspond to ATP binding and ADP release, respectively. Thus, according to these "mechanical" data, rotation of the γ subunit is driven solely by ATP binding and not by its hydrolysis. On the other hand, other models based on kinetic data support the proposal that the initial rotation substep involves not only nucleotide binding but also

both binding and hydrolysis of MgATP (Senior et al., 2002; Weber and Senior, 2003). This is one of the aspects of the ATP synthase mechanism that is still a matter of debate.

Subunit γ protrudes out of the $\alpha_3\beta_3$ hexamer (Abrahams et al., 1994; Stock et al., 1999), extends throughout the stalk, and contacts the polar inner loop of membrane-embedded c subunits (Watts et al., 1995; Fillingame, 1997). Mutational analysis, cross-linking experiments, and X-ray crystallography (Aggeler et al., 1997; Stock et al., 1999) have shown that the γ subunit, together with the ϵ subunit in *Escherichia coli* and the δ subunit in the mitochondrial ATP synthase (Karrash and Walker, 1999), constitutes the central stalk. A crystallographic analysis at 2.4 Å resolution of bovine F_1 provided additional insight into the nature of the F_1 protruding central stalk (Gibbons et al., 2000). This X-ray structure revealed a new domain in the γ subunit, containing a Rossman fold, which together with subunits δ and ϵ , forms a foot-like structure in contact with the F_0 subunit c (▶ [Figure 1.6-1b](#)) (Stock et al., 1999). F_1 δ subunit, as it appears in this structure (homolog to the bacterial ϵ subunit), consists of two domains—an N-terminal β sandwich and a C-terminal α -helical hairpin—while the mitochondrial ϵ subunit, which has no counterpart in prokaryotes or chloroplasts, has a helix–loop–helix structure. This subunit appears to stabilize the foot of the central stalk, where γ , δ , and ϵ subunits may interact with the c-ring and couple the transmembrane protonmotive force to catalysis in the $\alpha_3\beta_3$ domain (Gibbons et al., 2000). More recently a key role of the δ subunit in the mechanical coupling of the c-ring with subunit γ has been proposed (Duvezin-Caubert et al., 2003).

Despite all this work, there is no consensus as yet on the mechanism by which the ATP synthase operates. The reasons for this controversy are both structural and kinetic. From a structural point of view, the strong asymmetry of the β subunits detected in the crystal structures described (Abrahams et al., 1994, 1996; van Raaij et al., 1996a; Orriss et al., 1998; Gibbons et al., 2000) is not observed in other X-ray studies where a more symmetric situation of β subunits is apparent (Shirakihara et al., 1997; Bianchet et al., 1998; Groth and Pohl, 2001; Menz et al., 2001; Groth, 2002). Such a difference could essentially be due to the different crystallization conditions.

Another controversial aspect is related to the number of catalytic sites that must be filled for efficient steady-state catalysis (bisite or trisite catalysis). A steady-state mechanism in which all three catalytic sites are filled (three-site catalysis) appears to gain more acceptance with respect to bisite catalysis (Boyer, 2000, 2002). The three-site catalysis, initially based on results of tryptophan fluorescence experiments (Weber and Senior, 2000), is also supported by data from single-molecule experiments (Nishizaka et al., 2004).

Two possible reaction schemes for ATP hydrolysis, both supporting trisite catalysis, have recently been proposed based on various structural data obtained and by integrating these with tryptophan fluorescence measurements (Weber and Senior, 2000) and mechanics of rotation (Noji et al., 1997; Nishizaka et al., 2004). The two mechanisms differ essentially in the assignment of the β subunit (β_{DP} or β_{TP}) where ATP hydrolysis occurs (for details see Kagawa et al., 2004).

3 Structure and Functional Mechanism of the F_1F_0 Complex

Although many attempts have been made, a three-dimensional structure has not been obtained for the complete F_1F_0 enzyme purified from various sources. The first model proposed, for the *E. coli* F_0 , consisted of a structure in which the a and b subunits were surrounded by a ring of c subunits. With reference to the flagellar motor, it was postulated that rotation of subunits b, inside the c-ring together with F_1 $\gamma\delta\epsilon$ subunits, would drive ATP synthesis (Cox et al., 1984, 1986). Later, different experimental approaches (Schneider and Altendorf, 1987) showed that the a and b subunits are located on one side of the ring of c subunits. It was then proposed that the c-ring is made to rotate, by transmembrane proton translocation, relative to the a and b subunits. Images obtained by electron microscopy (Birkenhager et al., 1995) and atomic force microscopy (Singh et al., 1996; Takeyasu et al., 1996) confirmed the asymmetric organization of the F_0 subunits, showing that two b subunits are anchored to the membrane at one side of the c-ring by the N terminus hydrophobic segment, while the C terminus protrudes toward the F_1 moiety.

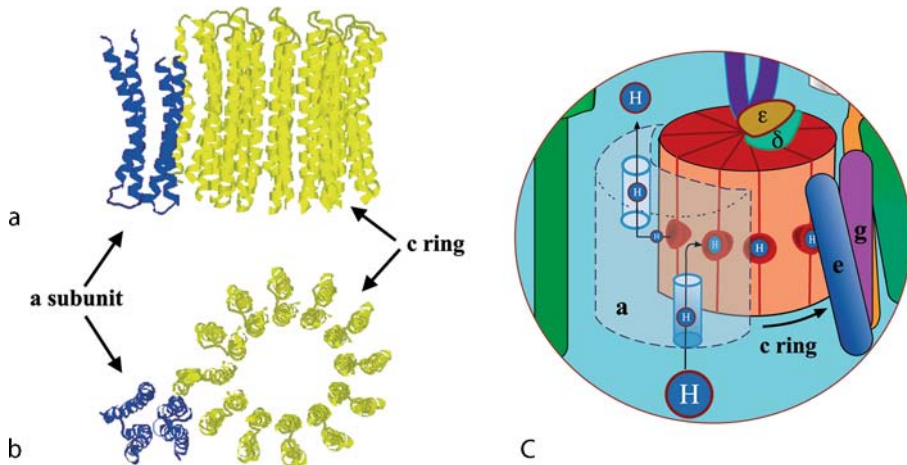
In the late 1990s, contrary to the general view (Gogol et al., 1987; Capaldi et al., 1994; Walker and Collinson, 1994), according to which the stalk subunits were assembled in a single central structure

connecting F₁ and F_o moieties, cross-linking results (Ogilvie et al., 1997; Wilkens et al., 1997) and better resolved electron microscopy images (Bottcher et al., 1998; Wilkens and Capaldi, 1998; Karrash and Walker, 1999) showed that, in addition to a central stalk, there exists a second lateral stalk connecting the periphery of F₁ and F_o (▶ [Figure 1.6-1a](#)). This observation came concomitantly with the first single-molecule experiment showing directly subunit γ rotation in the F₁ moiety (Noji et al., 1997). The lateral moiety was thus conceived to function as a static element (stator) of the ATP synthase rotary motor, holding the $\alpha_3\beta_3$ hexamer relative to the central rotor. It was proposed that the latter involves the membrane-embedded subunit c-ring (▶ [Figure 1.6-1b](#)), in addition to γ , δ , and ϵ F₁ subunits (γ and ϵ in prokaryotes).

Subunit c has been studied extensively. Cross-linking experiments and NMR structural analysis of the *E. coli* protein have shown that this highly hydrophobic subunit folds in the membrane as a hairpin with two membrane-spanning α -helices connected by a polar loop region that comes in contact with the F₁ sector on the matrix side (Girvin et al., 1998; Dmitriev et al., 1999) (▶ [Figure 1.6-3a–c](#)). There are several

■ Figure 1.6-3

Structure of the c subunit ring and model of the rotational movement of the two half-channels in the F_o rotary motor. (a) Side view of the NMR model for the ac₁₂ subcomplex, which includes four of the five transmembrane helices of subunit a (Rastogi and Girvin, 1999) (PDB = 1c17). The c subunits are arranged in a ring with subunit a on one side. (b) Top view of the ac₁₂ subcomplex. (c) The interaction between the a subunit and the c ring is shown. Proton flow (toward the F₁ region) through the two half-channels in the a subunit is allowed by the c oligomer stepwise rotation. In each step a different c subunit comes into contact with the a subunit, thus allowing proton translocation across the membrane. Molecular graphic by RasMol 2.6



copies of the c subunit organized in an oligomer with a ring-like shape (▶ [Figure 1.6-3a, b](#)). Each copy has the N-terminal transmembrane helix on the inside of the c-ring and the C-terminal helix on the outside. Evidence obtained shows that the number of c-subunit copies range from 10 to 14 in bacteria, chloroplasts, and mitochondria (Stock et al., 1999; Seelert et al., 2000; Jiang et al., 2001; Vonck et al., 2002). In bacteria, the c-subunit stoichiometry may vary depending upon metabolic conditions (Schemidt et al., 1998; Tomashek and Brusilow, 2000).

In the middle of the C-terminal helix of subunit c, there is a highly conserved residue (D61 in *E. coli*; E65 in mitochondria) essential for proton translocation through F_o (Miller et al., 1990). A low-resolution electron density map of the *Saccharomyces cerevisiae* F₁ATPase connected with the membrane-embedded c subunits has been obtained (Stock et al., 1999) (▶ [Figure 1.6-1b](#)). This structure shows an oligomer of 10 c subunits and confirms the structural data obtained from the *E. coli* enzyme. It also shows that the

central stalk, and in particular subunits γ and δ of F_1 , makes extensive contacts by “sitting” asymmetrically on the polar loop regions of six c subunits (▶ [Figure 1.6-1b](#)).

Subunit a of F_o is located at one side of the c -subunit ring (Fillingame et al., 2000). It is encoded by mtDNA and consists of five membrane-spanning helices (Long et al., 1998; Wada et al., 1999; Dmitriev et al., 2004). Arg210 in the fourth transmembrane helix of subunit a interacts with D61 in subunit c . These two residues, together with other neighboring polar residues, are directly involved in proton translocation through the complex (Valiyaveetil and Fillingame, 1997; Jiang and Fillingame, 1998; Cain, 2000; Fillingame et al., 2002a, b). Different models have been proposed to explain how protons are transferred through F_o and how this passage causes the rotation of subunits. In the “two half channel” model (▶ [Figure 1.6-3c](#)), subunit a , located at one side of the subunit c -ring, contributes two half channels providing a gate for protons toward or from subunit c carboxylate (D61 in *E. coli*; E65 in mitochondria) (Vik and Antonio, 1994). The sequential protonation and deprotonation of subunit c carboxylate would be coupled to a stepwise movement of the c -subunit ring. Another elegant model, derived from NMR studies of subunit c at two different pHs (Rastogi and Girvin, 1999), proposed that deprotonation of D61 (*E. coli* residue) causes structural changes leading to a 140° rotation of subunit c C-terminal helix, with respect to the N-terminal helix, followed by the movement of the c -ring. Recently, it has been proposed that in addition to subunit c , the fourth transmembrane helix of subunit a also rotates to alternately expose the two half-channels to D61 of subunit c during the proton transport cycle. Thus, subunits a and c would both rotate in a concerted mode, and this motion would generate the mechanical force necessary to drive the rotation of all the c -oligomers (Fillingame et al., 2003).

Direct evidence of ATP driven subunit c rotation from different experimental approaches has confirmed that the c -subunit oligomer functions as the main rotor element of the F_1F_o ATP synthase motor (Sambongi et al., 1999; Panke et al., 2000; Tsunoda et al., 2001; Nishio et al., 2002). Single-molecule experiments have shown that, upon ATP hydrolysis, the oligomer rotates counterclockwise when viewed from the membrane side (Sambongi et al., 1999; Panke et al., 2000; Nishio et al., 2002). Proton-driven rotation of the F_1F_o complex has also been observed and the direction is opposite to that generated by ATP hydrolysis (Diez et al., 2004). The rotational properties of the intact F_1F_o complex have been shown to be the same as those of the F_1 subcomplex, indicating negligible drag due to the F_o moiety (Ueno et al., 2005). All these data show that the c -subunit oligomer is part of the rotor element of the ATP synthase motor; it can rotate either clockwise or anticlockwise depending on the direction of the proton flow. This rotation is in both cases strictly related to the rotation of the central stalk, allowing the transfer of mechanical energy from or to the catalytic sites.

The lateral stalk, also known as stator, is the other critical part of the ATP synthase molecular machinery. In the *E. coli* enzyme, as well as in other bacteria and chloroplasts, the lateral stalk is made up of the membrane-embedded a subunit and two neighboring copies of b subunits, which arises from the membrane, extends till the $\alpha\beta$ hexamer, and comes into contact with one of the α/β interface region (Weber et al., 2004b) and with the δ subunit (Ogilvie et al., 1997). The δ subunit sits with its C-terminal domain on the C-terminal domain of b subunits while its N-terminal domain is connected to the top of the F_1 moiety where it contacts the N-terminal domain of the α subunit (Ogilvie et al., 1997; McLachlin et al., 1998; Wilkens and Capaldi, 1998; Weber et al., 2004a). It has recently been shown that a correct interaction between α and δ subunits is essential for the membrane assembly of ATP synthase (Weber et al., 2004a).

The lateral stalk in the mitochondrial F_1F_o ATP synthase appears to be more complex than in prokaryotes. The lateral stalk of the bovine enzyme has been studied extensively with different approaches such as limited proteolysis of subunits, cross-linking analysis, in vitro assembly of stalk complexes, and immunodecoration by subunit-specific antibodies. It is made up of single copies of subunits a , OSCP, d , e , F_6 , FoI-PVP(b), A6L, f , and g (▶ [Figure 1.6-1a](#)) (Zanotti et al., 1988, 1994; Collinson et al., 1994, 1996; Papa et al., 1999, 2000). By employing subunit-specific antibodies in mitoplasts and in inner membrane inside-out vesicles, it has been shown that FoI-PVP(b), d , F_6 , and OSCP subunits are exposed at the matrix, but not at the cytosolic side of the inner mitochondrial membrane, while subunits c and a are shielded to their antibodies on both sides (Hekman et al., 1991). Subunit A6L, which is encoded by mtDNA, has a membrane-embedded N terminus while the C terminus protrudes into the matrix side. Subunits f and g both have the N terminus at the matrix side of the membrane, while the e subunit appears to be essentially

exposed at the cytosolic side (Belogradov et al., 1996). Subunit e has been shown to exist as a dimer in yeast (Arnold et al., 1998; Shagger and Pfeiffer, 2000) and in rat liver mitochondrial ATP synthase (Arakaki et al., 2001). It has also been shown that this subunit plays a central role in the dimerization process, in the stabilization of dimer-specific F_o subunits, subunits g and k, in the modulation of the mitochondrial morphology of yeast ATP synthase (Arnold et al., 1998; Everard-Gigot et al., 2005), as well as in the Ca²⁺-dependent regulation of H⁺ ATP synthase activity (Arakaki et al., 2001).

FoI-PVP(b) subunit contributes to the functional coupling of F₁ and F_o and is located externally, at one side of the ring of c subunits (▶ [Figure 1.6-1a](#)), like the *E. coli* subunit b (Zanotti et al., 1988). As in *E. coli*, the FoI-PVP(b) N-terminal region folds in the inner mitochondrial membrane, while the hydrophilic part (residues 79–214) protrudes toward the $\alpha\beta\beta_3$ hexamer. Oligomycin sensitivity of ATP hydrolysis appears to be strictly dependent on the correct assembly of the hydrophilic portion of FoI-PVP(b), OSCP, and F6 subunits (Guerrieri et al., 1991).

Cross-linking studies in submitochondrial particles have shown that, in the absence of a transmembrane electrochemical proton gradient, FoI-PVP(b) C-terminal segment is in close contact with the γ subunit. The cross-linking between FoI-PVP(b) and γ subunits is completely prevented by the presence of a transmembrane electrochemical proton gradient, which, probably causing conformational changes, places the two subunits in a position that prevents their cross-linking (Gaballo et al., 1998). It must be recalled that mutational deletions in the *E. coli* b subunit indicate that this protein has a flexible structure (Sorgen et al., 1998, 1999). Furthermore, the elasticity of subunit b has been postulated to allow reorientations of the stator for rotation in opposite directions (clockwise and anticlockwise) during either ATP synthesis or ATP hydrolysis (Grabar and Cain, 2003).

Limited cleavage experiments have shown that OSCP, like subunit δ of the *E. coli* enzyme, sits on the C-terminal region of subunit FoI-PVP(b) and extends toward the top of F₁, where it interacts with the N terminus of the α subunit (▶ [Figure 1.6-1a](#)) (Xu et al., 2000; Rubinstein and Walker, 2002, 2003).

4 The Inhibitor Protein: Structure and Physiopathological Role

In mitochondria, the F₁F_o complex functions essentially as an ATP synthase. In conditions of anoxia or ischemia, the enzyme can alternatively hydrolyze ATP, pumping protons in the reverse direction with respect to that in ATP synthesis. In vivo, regulation of the ATP synthase involves ADP, pH, membrane potential, and a natural protein inhibitor, IF₁ (Pullman and Monroy, 1963; Harris and Das, 1991; Lebowitz and Pedersen, 1993). IF₁ was first isolated from bovine heart mitochondria in 1963 (Pullman and Monroy, 1963). It is absent in bacteria and chloroplasts where an analogous counterpart is thought to be represented by the ϵ subunit of the F₁ moiety (Pullman and Monroy, 1963). The inhibitor protein acts by binding reversibly to the F₁F_o ATP synthase and selectively inhibiting ATP hydrolysis, but has no effect on ATP synthesis (Panchenko and Vinogradov, 1985; Harris and Das, 1991). The respiratory protonmotive force ($\Delta\mu\text{H}^+$) across the mitochondrial inner membrane displaces IF₁ from its binding site in the ATP synthase complex (Harris and Das, 1991). The ΔpH component of the $\Delta\mu\text{H}^+$ and in particular the pH of the matrix side, where IF₁ binds to the complex, is the critical factor that modulates binding and inhibitory activity. IF₁ exerts a low inhibitory capacity at alkaline pH, becoming very active at a pH around 6.5.

IF₁ is a small basic protein of 10 kDa. Its primary sequence is significantly conserved among species, presenting a 75% identity between bovines and humans. The binding and inhibitory activity of IF₁ appears to be associated with its central segment (van Raaij et al., 1996b). By using synthetic peptides it has been found that the segment from Leu 42 to Lys 58 is as active as the intact bovine IF₁ (Papa et al., 1996), displaying the same kinetic, temperature, and pH dependence as the native IF₁ (Zanotti et al., 2000). The pH dependence is an essential feature of IF₁ and appears to be related to the presence of His49 in the central segment. Three other histidine residues are also present in the primary sequence of the protein (positions 48, 55, 56), which are likely to increase the stability of the interaction between the inhibitor and the ATP synthase complex.

In yeast mitochondria, the binding site of IF₁ to the F₁F_o complex has been shown to involve both α and β subunits (Mimura et al., 1993), probably including the DELSEED sequence of the β subunit, which, on

the other hand, contacts the γ subunit during catalysis (Abrahams et al., 1994). A bovine IF_1 three-dimensional structure has been obtained at 2.2 Å resolution (Cabezon et al., 2001). It shows that the purified bovine inhibitor protein (IF_1) exists in vitro at pH 6.7 as a dimer made up of two monomers that associate through an antiparallel α -helical coiled coil in the C-terminal region, leaving the N termini protruding in opposite directions (Cabezon et al., 2001).

More recently, the structure of crystal bovine IF_1 - F_1 complex has also been solved (Cabezon et al., 2003). It shows that an IF_1 -active dimer associates with two F_1 regions supposed to belong to an ATP synthase dimer. In particular, each of the two N termini of the IF_1 dimer, located between two F_1 moieties, interacts with the 4–40 and 4–47 residues respectively, and also with the α/β interface of one of the two F_1 regions in the ATP synthase dimer. Contribution of IF_1 to the ATP synthase dimerization is still a matter of debate. Evidence obtained shows that the ATP synthase dimerization occurs in the membrane independently of the binding of the inhibitor protein IF_1 (Tomasetig et al., 2002). Recently, Zanotti et al. have shown that the binding of IF_1 with the α/β subunits is pH dependent and involves, in particular, the Leu42–Lys58 inhibitory segment. In addition, evidence has been obtained indicating that the C-terminal region of IF_1 interacts with the OSCP subunit of the F_0 moiety in a pH-independent process (Zanotti et al., 2004). This pH-independent binding of IF_1 to OSCP in the lateral stalk could be relevant at alkaline pH of the matrix when the inhibitory segment is detached from the $\alpha\beta$ subunits, keeping the inhibitor protein (IF_1) attached to the complex.

The role of IF_1 in pathophysiology has been essentially investigated in the context of ischemia and tumor cell growth. In the absence of oxygen, the electrochemical gradient vanishes and glycolysis becomes the only cellular source of ATP. Under these conditions, ATP can be rapidly hydrolyzed by F_1F_0 ATP synthase, causing rapid cellular energy depletion. The inhibitory action of IF_1 , by preventing dissipative hydrolysis of glycolytic ATP, can contribute to prevent ischemic cell injuries. The protective role of IF_1 can be especially relevant for cardiac muscle tissue and other tissues with a high oxidative metabolism (Rouslin, 1991; Rouslin and Broge, 1996).

Also, IF_1 has been found to be overexpressed in murine and human neoplastic cells, whose rapid growth is essentially supported by increased glycolytic production of ATP (Luciakova and Kuzela, 1984; Chernyak et al., 1994; Capuano et al., 1997). These observations have very recently been confirmed by cross-linking studies and kinetic data from rat hepatoma cells. These studies showed that neoplastic cells overexpress the IF_1 inhibitor protein that binds with high efficiency to the ATP synthase complex, thus preventing energy dissipation (Bravo et al., 2004).

The IF_1 ATPase inhibitor appears to be missing in Luft's disease, a mitochondrial myopathy. Oxidative phosphorylation in mitochondria isolated from skeletal muscle of patients suffering from Luft's disease is loosely coupled with abnormally low P/O ratios (Yamada and Huzel, 1992).

5 ATP Synthase and Human Diseases

Among the mitochondrial pathologies, those associated with a defect in the F_1F_0 ATP synthase complex are very severe and primarily involve the pediatric population (Houstek et al., 2004). The symptoms of these disorders include muscle weakness or exercise intolerance, heart failure or rhythm disturbances, dementia, movement disorders, stroke-like episodes, deafness, blindness, limited mobility of the eyes, vomiting, and seizures. The prognosis for these disorders ranges in severity from progressive weakness to death.

In mammals, all the ATP synthase subunits, except two mitochondrial-encoded subunits (ATP6 and A6L), are nuclear encoded. The presence of proteins encoded by two separate genomes in different cellular compartments makes the biogenesis and assembly of eukaryotic complex V a complex process. Furthermore, additional nuclear factors are needed for the assembly of the enzyme. The biogenesis of complex V is a poorly understood multistep process with several assembly intermediates. Five assembly factors have been identified in yeast mitochondria. Two of them, Atp10p and Atp22p, mediate F_0 assembly (Ackerman and Tzagoloff, 1990a; Helfenbein et al., 2003) while the other three, Atp11p, Atp12p, and Fmc1p, have been found to be involved in F_1 assembly. Only two human orthologs of Atp11p and Atp12p have been identified (Ackerman and Tzagoloff, 1990b; Lefebvre-Legendre et al., 2001).

Genetic defects in mitochondrial ATP synthase appear to involve either mtDNA mutations in the ATP6 gene, encoding the F_o a subunit, or nuclear mutation in genes that encode specific assembly proteins or biosynthetic factors. No pathogenic mutations involving nuclear-encoded structural subunits of ATP synthase have yet been reported.

The neurogenic muscle weakness, ataxia, and retinitis pigmentosa (NARP) syndrome and the maternally inherited Leigh's syndrome (MILS) are two maternally inherited primary ATPase defects associated with mutations in the mitochondrial ATP6 gene (subunit a). The ATP synthase H⁺ channel of these patients displays an impairment that is often, but not always, related to decreased ATP production. No mutation has so far been described for the mitochondrial ATP 8 gene (Houstek et al., 2004).

Some other ATP synthase defects of nuclear origin have been identified by complementation analysis (Houstek et al., 1999; De Meirleir et al., 2004; Mayr et al., 2004). Usually, these patients have a selective decrease of the complex V content, caused by a diminished biogenesis of the ATPase complex. Complete loss of the ATP synthase enzyme is probably incompatible with life. However, partial loss of the complex has been associated with human diseases (Houstek et al., 2004). ATP synthase is also involved in some brain degenerative processes. Some of these display an accumulation of complex V subunits in cellular compartments other than mitochondria, while others show a decreased ATP synthase activity (Das, 2003).

Recently, evidence has been obtained for the implication of the α subunit of the ATP synthase in neurofibrillary degeneration of Alzheimer's disease. The α subunit accumulates in the cytosol of degenerating neurons in Alzheimer's disease and could have a role in the neurodegenerative process (Sergeant et al., 2003).

Some forms of neuronal ceroid lipofuscinosis (Batten disease in man), a neurodegenerative lysosomal storage disease, are characterized by structurally altered mitochondria and by an altered cellular handling of the F_o subunit c (Palmer et al., 1992). This protein appears to accumulate in lysosomes and constitutes more than 50% of the fluorescent storage bodies associated with most forms of this pathology. The relationship between subunit c accumulation and neuronal degeneration is still unknown. The occurrence of subunit c homologs on the plasma membrane of neurons, where it assembles to form high-conductance ion pores, has led to the hypothesis that subunit c accumulation in Batten disease can result in altered cation permeability due to an increased number of subunit c pores in the plasma membrane (McGeoch and Palmer, 1999). Reduced ATP levels have been observed in fibroblasts from patients with early infantile, infantile, and juvenile neuronal ceroid lipofuscinosis (CLN1, CLN2, and CLN3, respectively) (Das and Kohlschutter, 1996; Das et al., 1999).

A significant inhibition of the ATP synthase complex activity has been observed in cultures of mixed cortex cells from rat brain incubated with 3-hydroxyglutarate (Ullrich et al., 1999). 3-hydroxyglutarate contributes to neurodegeneration (Flott-Rahmel et al., 1997) and accumulates, together with glutaconic acid, in the brain and cerebrospinal fluid of patients with glutaconic aciduria, an organic aciduria due to inborn deficiency of glutaryl-CoA dehydrogenase (Hoffmann and Zschocke, 1999). The neurodegenerative process appears to be related to disturbed energy supply, which causes a "slow onset excitotoxicity" comprising membrane depolarization and successive alteration in homeostasis of calcium and other ions due to the opening of N-methyl-D-aspartate receptor ion channels (Beal, 1992, 1995).

References

- Abrahams JP, Leslie AGW, Lutter R, Walker JE. 1994. Structure at 2.8 Å resolution of F₁-ATPase from bovine heart mitochondria. *Nature* 370: 621-628.
- Abrahams JP, Buchanan SK, Van Raaij MJ, Fearnley IM, Leslie AG, et al. 1996. The structure of bovine F₁-ATPase complexed with the peptide antibiotic efrapeptin. *Proc Natl Acad Sci USA* 93: 9420-9424.
- Ackerman SH, Tzagoloff A. 1990a. ATP 10, a yeast nuclear gene required for the assembly of the mitochondrial F₁-F_o complex. *J Biol Chem* 265: 9952-9959.
- Ackerman SH, Tzagoloff A. 1990b. Identification of two nuclear genes (ATP11, ATP12) required for assembly of the yeast F₁-ATPase. *Proc Natl Acad Sci USA* 87: 4986-4990.
- Aggeler R, Ogilvie I, Capaldi RA. 1997. Rotation of a gamma-epsilon subunit domain in the *Escherichia coli* F₁F_o-ATP synthase complex. The gamma-epsilon subunits are essentially randomly distributed relative to the alpha3beta3delta domain in the intact complex. *J Biol Chem* 272: 19621-19624.

- Arakaki N, Nagao T, Niki R, Toyofuku A, Tanaka H, et al. 2003. Possible role of cell surface H⁺-ATP synthase in the extracellular ATP synthesis and proliferation of human umbilical vein endothelial cells. *Mol Cancer Res* 1: 931-939.
- Arakaki N, Ueyama Y, Hirose M, Himeda T, Shibata H, et al. 2001. Stoichiometry of subunit e in rat liver mitochondrial H(+)-ATP synthase and membrane topology of its putative Ca(2+)-dependent regulatory region. *Biochim Biophys Acta* 1504: 220-228.
- Arnold I, Pfeiffer K, Neupert W, Stuart RA, Schagger H. 1998. Yeast mitochondrial F₁F₀-ATP synthase exists as a dimer: Identification of three dimer-specific subunits. *EMBO J* 17: 7170-7178.
- Beal MF. 1992. Does impairment of energy metabolism result in excitotoxic neuronal death in neurodegenerative illnesses? *Ann Neurol* 31: 119-130.
- Beal MF. 1995. Aging, energy, and oxidative stress in neurodegenerative diseases. *Ann Neurol* 38: 357-366.
- Belogradov GI, Tomich JM, Hatefi Y. 1996. Membrane topography and near-neighbor relationships of the mitochondrial ATP synthase subunits e, f, and g. *J Biol Chem* 271: 20340-20345.
- Bianchet MA, Hüllihen J, Pedersen PL, Amzel LM. 1998. The 2.8-Å structure of rat liver F₁-ATPase: Configuration of a critical intermediate in ATP synthesis/hydrolysis. *Proc Natl Acad Sci* 95: 11065-11070.
- Birkenhager R, Hoppert M, Deckers-Hebestreit G, Mayer F, Altendorf K. 1995. The F₀ complex of the *Escherichia coli* ATP synthase. Investigation by electron spectroscopic imaging and immunoelectron microscopy. *Eur J Biochem* 230: 58-67.
- Bottcher B, Schwarz L, Graber P. 1998. Direct indication for the existence of a double stalk in CF₀F₁. *J Mol Biol* 281: 757-762.
- Boyer PD. 1993. The binding change mechanism for ATP synthase—some probabilities and possibilities. *Biochim Biophys Acta* 1140: 215-250.
- Boyer PD. 1997. The ATP synthase—a splendid molecular machine. *Annu Rev Biochem* 66: 717-749.
- Boyer PD. 2000. Catalytic site forms and controls in ATP synthase catalysis. *Biochim Biophys Acta* 1458: 252-262.
- Boyer PD. 2002. Catalytic site occupancy during ATP synthase catalysis. *FEBS Lett* 512: 29-32.
- Braig K, Menz RI, Montgomery MG, Leslie AG, Walker JE. 2000. Structure of bovine mitochondrial F(1)-ATPase inhibited by Mg(2+) ADP and aluminium fluoride. *Structure*. 8: 567-573.
- Bravo C, Minauro-Sanmiguel F, Morales-Rios E, Rodriguez-Zavala JS, Garcia, JJ. 2004. Overexpression of the inhibitor protein IF(1) in AS-30D hepatoma produces a higher association with mitochondrial F(1)F(0) ATP synthase compared to normal rat liver: Functional and cross-linking studies. *J Bioenerg Biomembr* 36: 257-264.
- Burwick NR, Wahl ML, Fang J, Zhong Z, Moser TL, et al. 2004. An inhibitor of the F₁ subunit of ATP synthase (IF₁) modulates the activity of angiostatin on the endothelial cell surface. *J Biol Chem* 280: 1740-1745.
- Cabezon E, Montgomery MG, Leslie AG, Walker JE. 2003. The structure of bovine F₁-ATPase in complex with its regulatory protein IF₁. *Nat Struct Biol* 10: 744-750.
- Cabezon E, Runswick MJ, Leslie AG, Walker JE. 2001. The structure of bovine IF(1), the regulatory subunit of mitochondrial F-ATPase. *EMBO J* 20: 6990-6996.
- Cain BD. 2000. Mutagenic analysis of the F₀ stator subunits. *J Bioenerg Biomembr* 32: 365-371.
- Capaldi RA, Aggeler R, Turina P, Wilkens S. 1994. Coupling between catalytic sites and the proton channel in F₁F₀-type ATPases. *Trends Biochem Sci* 19: 284-289.
- Capuano F, Guerrieri F, Papa S. 1997. Oxidative phosphorylation enzymes in normal and neoplastic cell growth. *J Bioenerg Biomembr* 29: 379-384.
- Chen C, Ko Y, Delannoy M, Ludtke SJ, Chiu W, et al. 2004. Mitochondrial ATP synthasome: Three-dimensional structure by electron microscopy of the ATP synthase in complex formation with carriers for P_i and ADP/ATP. *J Biol Chem* 279: 31761-31768.
- Chernyak BV, Dedov VN, Gabai VL. 1994. Mitochondrial ATP hydrolysis and ATP depletion in thymocytes and Ehrlich ascites carcinoma cells. *FEBS Lett* 337: 56-59.
- Collinson IR, Fearnley IM, Skehel JM, Runswick MJ, Walker JE. 1994. ATP synthase from bovine heart mitochondria: Identification by proteolysis of sites in F₀ exposed by removal of F₁ and the oligomycin-sensitivity conferral protein. *Biochem J* 303: 639-645.
- Collinson IR, Skehel JM, Fearnley IM, Runswick MJ, Walker JE. 1996. The F₁F₀-ATPase complex from bovine heart mitochondria: The molar ratio of the subunits in the stalk region linking the F₁ and F₀ domains. *Biochemistry* 35: 12640-12646.
- Cox GB, Fimmel AL, Gibson F, Hatch L. 1986. The mechanism of ATP synthase: A reassessment of the functions of the b and a subunits. *Biochim Biophys Acta* 849: 62-69.
- Cox GB, Jans DA, Fimmel AL, Gibson F, Hatch L. 1984. Hypothesis. The mechanism of ATP synthase. Conformational change by rotation of the beta-subunit. *Biochim Biophys Acta* 768: 201-208.
- Das AM. 2003. Regulation of the mitochondrial ATP-synthase in health and disease. *Mol Genet Metab* 79: 71-82.
- Das AM, Jolly RD, Kohlschütter A. 1999. Anomalies of mitochondrial ATP synthase regulation in four different types of neuronal ceroid lipofuscinosis. *Mol Genet Metab* 66: 349-355.

- Das AM, Kohlschutter A. 1996. Decreased activity of the mitochondrial ATP-synthase in fibroblasts from children with late-infantile and juvenile neuronal ceroid lipofuscinosis. *J Inherit Metab Dis* 19: 130-132.
- De Meirleir L, Seneca S, Lissens W, De Clercq I, Eyskens F, et al. 2004. Respiratory chain complex V deficiency due to a mutation in the assembly gene ATP12. *J Med Genet* 41: 120-124.
- Diez M, Zimmermann B, Borsch M, König M, Schweinberger E, et al. 2004. Proton-powered subunit rotation in single membrane-bound F₀F₁-ATP synthase. *Nat Struct Mol Biol* 11: 135-141.
- Dmitriev OY, Altendorf K, Fillingame RH. 2004. Subunit A of the *E. coli* ATP synthase: Reconstitution and high resolution NMR with protein purified in a mixed polarity solvent. *FEBS Lett* 556: 35-38.
- Dmitriev OY, Jones PC, Fillingame RH. 1999. Structure of the subunit c oligomer in the F₁F₀ ATP synthase: Model derived from solution structure of the monomer and cross-linking in the native enzyme. *Proc Natl Acad Sci USA* 96: 7785-7790.
- Duncan TM, Bulygin VV, Zhou Y, Hutcheon ML, Cross RL. 1995. Rotation of subunits during catalysis by *Escherichia coli* F₁-ATPase. *Proc Natl Acad Sci USA* 92: 10964-10968.
- Duvezin-Caubet S, Caron M, Giraud MF, Velours J, di Rago JP. 2003. The two rotor components of yeast mitochondrial ATP synthase are mechanically coupled by subunit delta. *Proc Natl Acad Sci USA* 100: 13235-13240.
- Everard-Gigot V, Dunn CD, Dolan BM, Brunner S, Jensen RE, et al. 2005. Functional Analysis of Subunit e of the F₁F₀-ATP Synthase of the Yeast *Saccharomyces cerevisiae*: Importance of the N-terminal membrane anchor region. *Eukaryot Cell* 4: 346-355.
- Fernandez-Moran H. 1962. Cell-membrane ultrastructure. Low-temperature electron microscopy and x-ray diffraction studies of lipoprotein components in lamellar systems. *Circulation* 26: 1039-1065.
- Fillingame RH. 1997. Coupling H⁺ transport and ATP synthesis in F₁F₀-ATP synthases: Glimpses of interacting parts in a dynamic molecular machine. *J Exp Biol* 200: 217-224.
- Fillingame RH, Angevine CM, Dmitriev OY. 2002a. Coupling proton movements to c-ring rotation in F(1)F(0) ATP synthase: Aqueous access channels and helix rotations at the a-c interface. *Biochim Biophys Acta* 1555: 29-36.
- Fillingame RH, Angevine CM, Dmitriev OY. 2003. Mechanics of coupling proton movements to c-ring rotation in ATP synthase. *FEBS Lett* 555: 29-34.
- Fillingame RH, Dmitriev OY. 2002b. Structural model of the transmembrane F₀ rotary sector of H⁺-transporting ATP synthase derived by solution NMR and intersubunit cross-linking in situ. *Biochim Biophys Acta* 1565: 232-245.
- Fillingame RH, Jiang W, Dmitriev OY. 2000. The oligomeric subunit C rotor in the F₀ sector of ATP synthase: Unresolved questions in our understanding of function. *J Bioenerg Biomembr* 32: 433-439.
- Flott-Rahmel B, Falter C, Schluff P, Fingerhut R, Christensen E, et al. 1997. Nerve cell lesions caused by 3-hydroxyglutaric acid: A possible mechanism for neurodegeneration in glutaric acidemia I. *J Inherit Metab Dis* 20: 387-390.
- Gaballo A, Zanotti F, Solimeo A, Papa S. 1998. Topological and functional relationship of subunits F₁-gamma and F₀-PVP(b) in the mitochondrial H⁺-ATP synthase. *Biochemistry* 37: 17519-17526.
- Gavin PD, Prescott M, Luff SE, Devenish RJ. 2004. Cross-linking ATP synthase complexes in vivo eliminates mitochondrial cristae. *J Cell Sci* 117: 2333-2343.
- Gibbons C, Montgomery MG, Leslie AGW, Walker JE. 2000. The structure of the central stalk in bovine F(1)-ATPase at 2.4 Å resolution. *Nat Struct Biol* 7: 1055-1061.
- Girvin ME, Rastogi VK, Abildgaard F, Markley JL, Fillingame RH. 1998. Solution structure of the transmembrane H⁺-transporting subunit c of the F₁F₀ATP synthase. *Biochemistry* 37: 8817-8824.
- Gogol EP, Lucken U, Capaldi RA. 1987. The stalk connecting the F₁ and F₀ domains of ATP synthase visualized by electron microscopy of unstained specimens. *FEBS Lett* 219: 274-278.
- Grabar TB, Cain BD. 2003. Integration of b subunits of unequal lengths into F₁F₀-ATP synthase. *J Biol Chem* 278: 34751-34756.
- Groth G. 2002. Structure of spinach chloroplast F₁-ATPase complexed with the phytopathogenic inhibitor tentoxin. *Proc Natl Acad Sci USA* 99: 3464-3468.
- Groth G, Pohl E. 2001. The structure of the chloroplast F₁-ATPase at 3.2 Å resolution. *J Biol Chem* 276: 1345-1352.
- Guerrieri F, Zanotti F, Capozza G, Colaianni G, Ronchi S, et al. 1991. Structural and functional characterization of subunits of the F₀ sector of the mitochondrial F₀F₁-ATP synthase. *Biochim Biophys Acta* 1059: 348-354.
- Harris DA, Das AM. 1991. Control of mitochondrial ATP synthesis in the heart. *Biochem J* 280: 561-573.
- Hausrath AC, Gruber G, Matthews BW, Capaldi RA. 1999. Structural features of the gamma subunit of the *Escherichia coli* F(1) ATPase revealed by a 4.4-Å resolution map obtained by x-ray crystallography. *Proc Natl Acad Sci USA* 96: 13697-13702.
- Hekman C, Tomich JM, Hatefi Y. 1991. Mitochondrial ATP synthase complex. Membrane topography and stoichiometry of the F₀ subunits. *J Biol Chem* 266: 13564-13571.
- Helpfenbein KG, Ellis TP, Dieckmann CL, Tzagoloff A. 2003. ATP22, a nuclear gene required for expression of the F₀ sector of mitochondrial ATPase in *Saccharomyces cerevisiae*. *J Biol Chem* 278: 19751-19756.

- Hoffmann GF, Zschocke J. 1999. Glutaric aciduria type I: From clinical, biochemical and molecular diversity to successful therapy. *J Inher Metab Dis* 22: 381-391.
- Houstek J, Klement P, Floryk D, Antonicka H, Hermanska J, et al. 1999. A novel deficiency of mitochondrial ATPase of nuclear origin. *Hum Mol Genet* 8: 1967-1974.
- Houstek J, Mracek T, Vojtiskova A, Zeman J. 2004. Mitochondrial diseases and ATPase defects of nuclear origin. *Biochim Biophys Acta* 1658: 115-121.
- Jiang W, Fillingame RH. 1998. Interacting helical faces of subunits a and c in the F₁F₀ ATP synthase of *Escherichia coli* defined by disulfide cross-linking. *Proc Natl Acad Sci USA* 95: 6607-6612.
- Jiang W, Hermolin J, Fillingame RH. 2001. The preferred stoichiometry of c subunits in the rotary motor sector of *Escherichia coli* ATP synthase is 10. *Proc Natl Acad Sci USA* 98: 4966-4971.
- Kagawa R, Montgomery MG, Braig K, Leslie AG, Walker JE. 2004. The structure of bovine F(1)-ATPase inhibited by ADP and beryllium fluoride. *EMBO J* 23: 2734-2744.
- Kagawa Y, Racker E. 1966. Partial resolution of the enzymes catalyzing oxidative phosphorylation. IX. Reconstruction of oligomycin-sensitive adenosine triphosphatase. *J Biol Chem* 241: 2467-2474.
- Karrasch S, Walker JE. 1999. Novel features in the structure of bovine ATP synthase. *J Mol Biol* 290: 379-384.
- Kato-Yamada Y, Noji H, Yasuda R, Kinoshita Jr, K Yoshida M. 1998. Direct observation of the rotation of epsilon subunit in F₁-ATPase. *J Biol Chem* 273: 19375-19377.
- Krause F, Reifschneider NH, Goto S, Dencher NA. 2005. Active oligomeric ATP synthases in mammalian mitochondria. *Biochem Biophys Res Commun* 329: 583-590.
- Lebowitz MS, Pedersen PL. 1993. Regulation of the mitochondrial ATP synthase/ATPase complex: cDNA cloning, sequence, overexpression, and secondary structural characterization of a functional protein inhibitor. *Arch Biochem Biophys* 301: 64-70.
- Lefebvre-Legendre L, Vaillier J, Benabdelhak H, Velours J, Slonimski PP, et al. 2001. Identification of a nuclear gene (FMC1) required for the assembly/stability of yeast mitochondrial F(1)-ATPase in heat stress conditions. *J Biol Chem* 276: 6789-6796.
- Long JC, Wang S, Vik SB. 1998. Membrane topology of subunit a of the F₁F₀ ATP synthase as determined by labeling of unique cysteine residues. *J Biol Chem* 273: 16235-16240.
- Luciakova K, Kuzela S. 1984. Increased content of natural ATPase inhibitor in tumor mitochondria. *FEBS Lett* 177: 85-88.
- Mayr JA, Paul J, Pecina P, Kurnik P, Forster H, et al. 2004. Reduced respiratory control with ADP and changed pattern of respiratory chain enzymes as a result of selective deficiency of the mitochondrial ATP synthase. *Pediatr Res* 55: 988-994.
- McGeoch JE, Palmer DN. 1999. Ion pores made of mitochondrial ATP synthase subunit c in the neuronal plasma membrane and Batten disease. *Mol Genet Metab* 66: 387-392.
- McLachlin DT, Bestard JA, Dunn SD. 1998. The b and delta subunits of the *Escherichia coli* ATP synthase interact via residues in their C-terminal regions. *J Biol Chem* 273: 15162-15168.
- Menz RI, Walker JE, Leslie AG. 2001. Structure of bovine mitochondrial F(1)-ATPase with nucleotide bound to all three catalytic sites: Implications for the mechanism of rotary catalysis. *Cell* 106: 331-341.
- Miller MJ, Oldenburg M, Fillingame RH. 1990. The essential carboxyl group in subunit c of the F₁F₀ ATP synthase can be moved and H(+)-translocating function retained. *Proc Natl Acad Sci* 87: 4900-4904.
- Mimura H, Hashimoto T, Yoshida Y, Ichikawa N, Tagawa K. 1993. Binding of an intrinsic ATPase inhibitor to the interface between alpha- and beta-subunits of F₁F₀ATPase upon de-energization of mitochondria. *J Biochem* 113: 350-354.
- Moser TL, Kenan DJ, Ashley TA, Roy JA, Goodman MD, et al. 2001. Endothelial cell surface F₁-F₀ ATP synthase is active in ATP synthesis and is inhibited by angiotatin. *Proc Natl Acad Sci USA* 98: 6656-6661.
- Moser TL, Stack MS, Asplin I, Enghild JJ, Hojrup P, et al. 1999. Angiotatin binds ATP synthase on the surface of human endothelial cells. *Proc Natl Acad Sci USA* 96: 2811-2816.
- Nishio K, Iwamoto-Kihara A, Yamamoto A, Wada Y, Futai M. 2002. Subunit rotation of ATP synthase embedded in membranes: A or beta subunit rotation relative to the c subunit ring. *Proc Natl Acad Sci USA* 99: 13448-13452.
- Nishizaka T, Oiwa K, Noji H, Kimura S, Muneyuki E, et al. 2004. Chemomechanical coupling in F₁-ATPase revealed by simultaneous observation of nucleotide kinetics and rotation. *Nat Struct Mol Biol* 11: 142-148.
- Noji H, Yasuda R, Yoshida M, Kinoshita K. 1997. Direct observation of the rotation of F₁-ATPase. *Nature* 386: 299-302.
- Ogilvie I, Aggeler R, Capaldi RA. 1997. Cross-linking of the delta subunit to one of the three alpha subunits has no effect on functioning, as expected if delta is a part of the stator that links the F₁ and F₀ parts of the *Escherichia coli* ATP synthase. *J Biol Chem* 272: 16652-16656.
- Orriss GL, Leslie AG, Braig K, Walker JE. 1998. Bovine F₁-ATPase covalently inhibited with 4-chloro-7-nitrobenzofurazan: The structure provides further support for a rotary catalytic mechanism. *Structure* 6: 831-837.
- Palmer DN, Fearnley IM, Walker JE, Hall NA, Lake BD, et al. 1992. Mitochondrial ATP synthase subunit c storage in the ceroid-lipofuscinoses (Batten disease). *Am J Med Genet* 42: 561-567.

- Panchenko MV, Vinogradov AD. 1985. Interaction between the mitochondrial ATP synthetase and ATPase inhibitor protein. Active/inactive slow pH-dependent transitions of the inhibitor protein. *FEBS Lett* 184: 226-230.
- Panke O, Gumbiowski K, Junge W, Engelbrecht S. 2000. F-ATPase: specific observation of the rotating c subunit oligomer of EF(o) EF(1). *FEBS Lett* 472: 34-38.
- Papa S, Xu T, Gaballo A, Zanotti F. 1999. Frontiers of cellular bioenergetics: Molecular biology, biochemistry and physiopathology. Papa S, Guerrieri E, Tager JM, editors. London, New York: Plenum Press; pp. 459-487.
- Papa S, Zanotti F, Cocco T, Perrucci C, Candita C, et al. 1996. Identification of functional domains and critical residues in the adenosinetriphosphatase inhibitor protein of mitochondrial F₀F₁ ATP synthase. *Eur J Biochem* 240: 461-467.
- Papa S, Zanotti F, Gaballo A. 2000. The structural and functional connection between the catalytic and proton translocating sectors of the mitochondrial F₁F₀-ATP synthase. *J Bioenerg Biomembr* 32: 401-411.
- Pullman ME, Monroy GC. 1963. A naturally occurring inhibitor of mitochondrial adenosine triphosphatase. *J Biol Chem* 238: 3762-3769.
- Rastogi VK, Girvin ME. 1999. Structural changes linked to proton translocation by subunit c of the ATP synthase. *Nature* 402: 263-268.
- Rouslin W. 1991. Regulation of the mitochondrial ATPase in situ in cardiac muscle: Role of the inhibitor subunit. *J Bioenerg Biomembr* 23: 873-888.
- Rouslin W, Broge CW. 1996. IF₁ function in situ in uncoupler-challenged ischemic rabbit, rat, and pigeon hearts. *J Biol Chem* 271: 23638-23641.
- Rubinstein J, Walker J. 2002. ATP synthase from *Saccharomyces cerevisiae*: Location of the OSCP subunit in the peripheral stalk region. *J Mol Biol* 321: 613-619.
- Rubinstein JL, Walker JE, Henderson R. 2003. Structure of the mitochondrial ATP synthase by electron cryomicroscopy. *EMBO J* 22: 6182-6192.
- Sabbert D, Engelbrecht S, Junge W. 1996. Intersubunit rotation in active F-ATPase. *Nature* 381: 623-625.
- Sambongi Y, Iko Y, Tanabe M, Omote H, Iwamoto-Kihara A, et al. 1999. Mechanical rotation of the c subunit oligomer in ATP synthase (F₀F₁): Direct observation. *Science* 286: 1722-1724.
- Schagger H, Pfeiffer K. 2000. Supercomplexes in the respiratory chains of yeast and mammalian mitochondria. *EMBO J* 19: 1777-17783.
- Schmidt RA, Qu J, Williams JR, Brusilow WS. 1998. Effects of carbon source on expression of F₀ genes and on the stoichiometry of the c subunit in the F₁F₀ ATPase of *Escherichia coli*. *J Bacteriol* 180: 3205-3208.
- Schneider E, Altendorf K. 1987. Bacterial adenosine 5'-triphosphate synthase (F₁F₀): Purification and reconstitution of F₀ complexes and biochemical and functional characterization of their subunits. *Microbiol Rev* 51: 477-497.
- Seelert H, Poetsch A, Dencher NA, Engel A, Stahlberg H, et al. 2000. Structural biology. Proton-powered turbine of a plant motor. *Nature* 405: 418-419.
- Senior AE, Nadanaciva S, Weber J. 2002. The molecular mechanism of ATP synthesis by F₁F₀-ATP synthase. *Biochim Biophys Acta* 1553: 188-211.
- Sergeant N, Watzek A, Galvan-valencia M, Ghestem A, David JB, et al. 2003. Association of ATP synthase alpha-chain with neurofibrillary degeneration in Alzheimer's disease. *Neuroscience* 117: 293-303.
- Shimabukuro K, Yasuda R, Muneyuki E, Hara KY, Kinoshita K Jr, et al. 2003. Catalysis and rotation of F₁ motor: Cleavage of ATP at the catalytic site occurs in 1 ms before 40 degree substep rotation. *Proc Natl Acad Sci USA* 100: 14731-14736.
- Shirakihara Y, Leslie AG, Abrahams JP, Walker JE, Ueda T, et al. 1997. The crystal structure of the nucleotide-free alpha 3 beta 3 subcomplex of F₁-ATPase from the thermophilic *Bacillus PS3* is a symmetric trimer. *Structure* 5: 825-836.
- Singh S, Turina P, Bustamante CJ, Keller DJ, Capaldi R. 1996. Topographical structure of membrane-bound *Escherichia coli* F₁F₀ ATP synthase in aqueous buffer. *FEBS Lett* 397: 30-34.
- Sorgen PL, Bubb MR, Cain BD. 1999. Lengthening the second stalk of F(1)F(0) ATP synthase in *Escherichia coli*. *J Biol Chem* 274: 36261-36266.
- Sorgen PL, Caviston TL, Perry RC, Cain BD. 1998. Deletions in the second stalk of F₁F₀-ATP synthase in *Escherichia coli*. *J Biol Chem* 273: 27873-27878.
- Stock D, Leslie AGW, Walker JE. 1999. Molecular architecture of the rotary motor in ATP synthase. *Science* 286: 1700-1705.
- Takeyasu K, Omote H, Nettikadan S, Tokumasu F, Iwamoto-Kihara A, et al. 1996. Molecular imaging of *Escherichia coli* F₀F₁-ATPase in reconstituted membranes using atomic force microscopy. *FEBS Lett* 392: 110-113.
- Tomasetig L, Di Pancrazio F, Harris DA, Mavelli I, Lippe G. 2002. Dimerization of F₀F₁ATP synthase from bovine heart is independent from the binding of the inhibitor protein IF₁. *Biochim Biophys Acta* 1556: 133-141.
- Tomashuk JJ, Brusilow WS. 2000. Stoichiometry of energy coupling by proton-translocating ATPases: A history of variability. *J Bioenerg Biomembr* 32: 493-500.
- Tsunoda SP, Aggeler R, Yoshida M, Capaldi RA. 2001. Rotation of the c subunit oligomer in fully functional F₁F₀ ATP synthase. *Proc Natl Acad Sci USA* 98: 898-902.
- Ueno H, Suzuki T, Kinoshita K Jr, Yoshida M. 2005. ATP-driven stepwise rotation of F₀F₁-ATP synthase. *Proc Natl Acad Sci USA* 102: 1333-1338.

- Ullrich K, Flott-Rahmel B, Schluff P, Musshoff U, Das A, et al. 1999. Glutaric aciduria type I: Pathomechanisms of neurodegeneration. *J Inher Metab Dis* 22: 392-403.
- Valiyaveetil FI, Fillingame RH. 1997. On the role of Arg-210 and Glu-219 of subunit a in proton translocation by the *Escherichia coli* F₀F₁-ATP synthase. *J Biol Chem* 272: 32635-32641.
- van Raaij MJ, Abrahams JP, Leslie AG, Walker JE. 1996a. The structure of bovine F₁-ATPase complexed with the antibiotic inhibitor aurovertin B. *Proc Natl Acad Sci USA* 93: 6913-6917.
- van Raaij MJ, Orriss GL, Montgomery MG, Runswick MJ, Fearnley IM, et al. 1996b. The ATPase inhibitor protein from bovine heart mitochondria: The minimal inhibitory sequence. *Biochemistry* 35: 15618-15625.
- Vik SB, Antonio BJ. 1994. A mechanism of proton translocation by F₁F₀ ATP synthases suggested by double mutant of the a subunit. *J Biol Chem* 269: 30364-30369.
- Vonck J, von Nidda TK, Meier T, Matthey U, Mills DJ, et al. 2002. Molecular architecture of the undecameric rotor of a bacterial Na⁺-ATP synthase. *J Mol Biol* 321: 307-316.
- Wada T, Long JC, Zhang D, Vik SB. 1999. A novel labeling approach supports the five-transmembrane model of subunit a of the *Escherichia coli* ATP synthase. *J Biol Chem* 274: 17353-17357.
- Walker JE, Collinson IR. 1994. The role of the stalk in the coupling mechanism of F₁F₀-ATPases. *FEBS Lett* 346: 39-43.
- Watts SD, Zhang Y, Fillingame RH, Capaldi RA. 1995. The gamma subunit in the *Escherichia coli* ATP synthase complex (ECF₁F₀) extends through the stalk and contacts the c subunits of the F₀ part. *FEBS Lett* 368: 235-238.
- Weber J, Senior AE. 2000. ATP synthase: What we know about ATP hydrolysis and what we do not know about ATP synthesis. *Biochim Biophys Acta* 1458: 300-309.
- Weber J, Senior AE. 2003. ATP synthesis driven by proton transport in F₁F₀-ATP synthase. *FEBS Lett* 545: 61-70.
- Weber J, Muharemagic A, Wilke-Mounts S, Senior AE. 2004a. Analysis of sequence determinants of F₁F₀-ATP synthase in the N-terminal region of alpha subunit for binding of delta subunit. *J Biol Chem* 279: 25673-25679.
- Weber J, Wilke-Mounts S, Nadanaciva S, Senior AE. 2004b. Quantitative determination of direct binding of b subunit to F₁ in *Escherichia coli* F₁F₀-ATP synthase. *J Biol Chem* 279: 11253-11258.
- Wilkens S, Capaldi RA. 1998. ATP synthase's second stalk comes into focus. *Nature* 393: 429.
- Wilkens S, Dunn SD, Chandler J, Dahlquist FW, Capaldi RA. 1997. Solution structure of the N-terminal domain of the delta subunit of the *E. coli* ATP synthase. *Nat Struct Biol* 4: 198-201.
- Xu T, Zanotti F, Gaballo A, Raho G, Papa S. 2000. F₁ and F₀ connections in the bovine mitochondrial ATP synthase: The role of the alpha subunit N-terminus, oligomycin-sensitivity conferring protein (OCSF) and subunit d. *Eur J Biochem* 267: 4445-4455.
- Yamada EW, Huzel NJ. 1992. Distribution of the ATPase inhibitor proteins of mitochondria in mammalian tissues including fibroblasts from a patient with Luft's disease. *Biochim Biophys Acta* 1139: 143-147.
- Yasuda R, Noji H, Yoshida M, Kinoshita K Jr, Itoh H. 2001. Resolution of distinct rotational substeps by submillisecond kinetic analysis of F₁-ATPase. *Nature* 410: 898-904.
- Zanotti F, Guerrieri F, Capozza G, Houstek J, Ronchi S, et al. 1988. Identification of nucleus-encoded F₀I protein of bovine heart mitochondrial H⁺-ATPase as a functional part of the F₀ moiety. *FEBS Lett* 237: 9-14.
- Zanotti F, Guerrieri F, Deckers-Hebestreit G, Fiermonte M, Altendorf K, et al. 1994. Cross-reconstitution studies with polypeptides of *Escherichia coli* and bovine heart mitochondrial F₀F₁ ATP synthase. *Eur J Biochem* 222: 733-741.
- Zanotti F, Raho G, Gaballo A, Papa S. 2004. Inhibitory and anchoring domains in the ATPase inhibitor protein IF₁ of bovine heart mitochondrial ATP synthase. *J Bioenerg Biomembr* 36: 447-457.
- Zanotti F, Raho G, Vuolo R, Gaballo A, Papa S, et al. 2000. Functional domains of the ATPase inhibitor protein from bovine heart mitochondria. *FEBS Lett* 482: 163-166.

Alternative Substrates

2.1 The Support of Energy Metabolism in the Central Nervous System with Substrates Other than Glucose

E. L. Roberts, Jr

1	Introduction	139
2	Alternative Energy Substrates: Glycolytic Intermediates	142
2.1	Lactate	142
2.1.1	Lactate Metabolism	142
2.1.2	Lactate Dehydrogenase	143
2.1.3	Lactate Transport	144
2.1.4	The Ability of Lactate to Support Brain Function In Vitro	145
2.1.5	Utilization of Exogenous Lactate Extracted from the Bloodstream	146
2.1.6	Production and Utilization of Endogenous Lactate in the Intact Brain	148
2.1.7	Conventional Hypothesis of Glucose and Lactate Utilization	148
2.1.8	Early Version of the Astrocyte-Neuron Lactate Shuttle Hypothesis (ANLSH)	149
2.1.9	Current Version of the ANLSH	149
2.1.10	Is Lactate Released from Astrocytes Used by Active Neurons?	150
2.1.11	Is Lactate Produced During Neural Activity Eventually Oxidized by Neurons?	151
2.1.12	Lactate Use by the Developing Brain	154
2.1.13	Lactate Use During Hypoglycemia	154
2.2	Pyruvate	155
2.3	Fructose-1,6-bisphosphate	156
3	Alternative Energy Substrates: Glycogen	156
3.1	Glycogen Storage	156
3.2	Glycogenolysis	157
3.3	Release of Glucose or Lactate from Astrocytes as a Result of Glycogenolysis	158
3.4	Glycogen Synthesis	159
4	Alternative Energy Substrates: Fructose and Mannose	160
5	Alternative Energy Substrates: Amino Acids and TCA Cycle Intermediates	160
5.1	Amino Acids	160
5.1.1	Glutamate	161
5.1.2	Glutamine	161
5.1.3	Alanine	162
5.2	TCA Cycle Intermediates	162
6	Alternative Energy Substrates: Ketone Bodies	162
6.1	Ketone Body Metabolism	162
6.1.1	Metabolic Pathway	162

6.1.2	Glucose-Sparing Effect of Ketone Bodies	163
6.2	Transport of Ketone Bodies	164
6.3	Use of Ketone Bodies as Energy Substrates In Vitro	164
6.4	Utilization of Ketone Bodies in the Developing Brain	165
6.4.1	Enzyme Activities in the Developing Brain	165
6.4.2	Ketone Body Concentrations in the Blood During Development	166
6.4.3	Expression of MCT1 in the Blood-Brain Barrier (BBB) During Development	166
6.5	Ketone Bodies in Fasting and Starvation	166
6.6	Use of Ketone Bodies Produced Within the Brain	168
7	Summary	168

1 Introduction

The brain is extremely active metabolically, with its local energy demands fluctuating rapidly between high and low activity states. However, the brain's endogenous energy stores are small. Consequently, normal brain function requires a continuous supply of exogenous substrates obtained via the bloodstream. Under normal physiological conditions, glucose is the dominant exogenous energy substrate in the adult brain (Clarke and Sokoloff, 1999). Glucose is transported into the brain via glucose transporters located in the endothelial cells of the blood–brain barrier (BBB) (Clarke and Sokoloff, 1999). A favorable concentration gradient drives this transport given that blood glucose is about 5–7 mM (Ruderman et al., 1974; Hasselbalch et al., 1994) and glucose in the extracellular space of the brain is about 1–2 mM (Silver and Erecinska, 1994; Pfeuffer et al., 2000) (see [Table 2.1-1](#)). An ample supply of glucose and tight regulation of glycolysis by the prevailing cellular energy status allows brain cells to respond quickly to fluctuations in energy demands (Chih and Roberts, 2003). However, other exogenous or endogenous energy substrates can serve as alternatives to glucose under certain physiological or pathological conditions.

In vitro studies have shown that cultured brain cells or isolated brain tissue can oxidize a variety of substrates. These substrates include glycolytic intermediates such as pyruvate (Peng et al., 1994b) and lactate (McKenna, 1993; Itoh, 2003), tricarboxylic acid (TCA) cycle intermediates such as α -ketoglutarate and citrate (Westergaard et al., 1994; Hodgkins and Schwarcz, 1998), amino acids such as glutamate and glutamine (Hertz and Hertz, 2003), and ketone bodies (Tildon et al., 1983; Lopes-Cardozo et al., 1986). These substrates can either partially or fully maintain high-energy phosphate levels or neural function in isolated brain tissue (e.g., see Schurr et al., 1988; Roberts, 1993; Kanatani et al., 1995; Roberts et al., 1997; Wada et al., 1997; Yamane et al., 2000; Brown et al., 2001; Massieu et al., 2003; Bui et al., 2004). However, the ability of isolated brain tissue to metabolize these substrates does not necessarily mean that they are used to sustain neural function in situ. One major reason for the limited use of most of these alternative substrates by the adult brain is the low permeability of the BBB to them, and the lack of efficient transport systems to move them into the brain (Cremer et al., 1976; Sacks et al., 1982; Pardridge, 1983, 1991).

The most widely studied alternative energy substrates used by the brain are lactate and ketone bodies (β -hydroxybutyrate and acetoacetate; the small contributions of acetone are not included in this review). Lactate is the primary energy substrate in rats after birth and up to the onset of suckling (Medina and Taberner, 2005), which usually occurs within 12–16 h of birth (Nehlig and Pereira de Vasconcelos, 1993). During the suckling period, ketone bodies become the major exogenous substrates for human and rat brains because of the metabolism of fat from maternal milk (Nehlig and Pereira de Vasconcelos, 1993). The ability of the developing brain to use alternative energy substrates contributes to its tolerance of hypoglycemia and other metabolic stresses. Although glucose is the primary substrate for the adult brain, ketone bodies may become important energy substrates for the brain during prolonged starvation (Owen et al., 1967) and induced hypoglycemia (Ruderman et al., 1974). Ketone bodies are also important substrates for the brains of individuals on a ketogenic diet (Klepper et al., 2004).

Besides exogenous energy substrates, some endogenous energy substrates produced within the brain may serve as energy sources. For example, glycogen, which can be synthesized from various precursors, such as glucose, alanine, and lactate, may be used by brain cells during neural activity (Wender et al., 2000; Brown et al., 2004), especially in areas where mitochondria are rare (Chih and Roberts, 2003; Dienel and Cruz, 2003; Hertz et al., 2004). Also, some brain cells have low glycolytic capacity and must use other endogenous substrates instead of glucose. For example, oligodendrocytes, microglia, and Purkinje neurons have little glycolytic capacity and may use other endogenous substrates such as lactate (Dringen et al., 1993). Some energy substrates generated within the brain, such as glutamate, may be used as energy sources (Hertz and Hertz, 2003) to prevent the buildup of these substrates in the brain. The use of alternative endogenous substrates by brain cells may also depend on the prevailing energy demands of these cells. Cellular glycolytic rates are tightly regulated by the cellular energy status to accommodate the rapid fluctuations in the energy demands of brain cells (Clarke and Sokoloff, 1999). Increased rates of glycolysis during heightened energy demand may prevent the use of other oxidative substrates, such as lactate, even though brain tissue can use lactate in vitro when glucose is not present (Chih et al., 2001b; Chih and Roberts, 2003).

Table 2.1-1
Distributions and arteriovenous differences for metabolic substrates in the normoglycemic brain

Substrate	Subjects	Blood/ plasma (mM)	CSF/ECF (mM)	Brain ($\mu\text{mol/g}$)	A–V difference ^a (mM)	References
Glucose	Adult rat	6.34		1.21	0.51	Hawkins et al. (1971)
		6.13			0.55	Leegsma-Vogt et al. (2003)
		7.46		2.9	0.48	Ruderman et al. (1974)
	Human	7.11		2.13	0.83	Dahlquist and Persson (1976)
		5.41			0.54	DeVivo et al. (1978)
		4.90			0.52	Hasselbalch et al. (1994)
Lactate	Adult rat	7.6	2.4 (ECF)			Wahren et al. (1999)
		5.5	2.6 (ECF)			Silver and Erecinska (1994)
			0.82 (brain dialysate)			Hu and Wilson (1997b)
	Human	1.1		1.89	–0.04	Abi-Saab et al. (2002)
		0.42			–0.29	Hawkins et al. (1971)
		1.03			–0.02	Leegsma-Vogt et al. (2003)
	0.85		1.56	–0.16	Ruderman et al. (1974)	
					Dahlquist and Persson (1976)	
					DeVivo et al. (1978)	
					Hasselbalch et al. (1994)	
					Wahren et al. (1999)	
					Pan et al. (2000)	
					Hanstock et al. (1988)	
					Prichard et al. (1991)	
					Abi-Saad et al. (2002)	
			1.38 (brain dialysate)	0.69	–0.13	
				0.50	–0.06	
				0.71		

Pyruvate	Adult rat	0.14		0.08	-0.003	Hawkins et al. (1971)
	Human	0.07		0.11	-0.04	DeVivo et al. (1978)
		0.09			-0.009	Hasselbalch et al. (1994)
		0.09		0.09	0.004	Wahren et al. (1999)
		0.06			0.008	Hawkins et al. (1971)
		0.12			0.053	Ruderman et al. (1974)
						Dahlquist and Persson (1976)
β -Hydroxybutyrate	Adult rat			0.01		DeVivo et al. (1978)
		0.23			0.02	Hasselbalch et al. (1994)
	Human	0.04			0.002	Wahren et al. (1999)
		0.03		0.05		Pan et al. (2000)
Acetoacetate	Adult rat	0.13		0.04	0.022	Hawkins et al. (1971)
		0.09			0.014	Ruderman et al. (1974)
	Human	0.05			0.01	Hasselbalch et al. (1994)
Glutamate	Human	0.09	0.003 (CSF)			O'Kane and Hawkins (2003)
				11.27		DeVivo et al. (1978)
Glutamine	Human	0.67	0.55 (CSF)			O'Kane and Hawkins (2003)
		0.6			-0.003	Wahren et al. (1999)
				4.87		DeVivo et al. (1978)
Alanine	Human	0.24	0.02 (CSF)			O'Kane and Hawkins (2003)
		0.3			-0.003	Wahren et al. (1999)
				0.68		DeVivo et al. (1978)

^aPositive numbers represent brain uptake; negative numbers represent brain release

A—V arteriovenous, CSF cerebrospinal fluid, ECF, extracellular fluid

Note: This table provides the control values for Tables 2.1-2 and 2.1-3

In this chapter, how brain cells use alternative substrates under various *in vivo* and *in vitro* conditions is discussed. This discussion includes an examination of the ability of brain cells, particularly neurons and astrocytes, to oxidize alternative substrates and to use them to support brain function.

2 Alternative Energy Substrates: Glycolytic Intermediates

2.1 Lactate

Unlike extraction of glucose, extraction of lactate from the circulation is normally limited due to the slow transport of lactate across the BBB and the lack of a large concentration gradient for lactate across the BBB (Hawkins et al., 1971; Cremer et al., 1976; Dienel and Hertz, 2001; Abi-Saab et al., 2002) (🔗 [Table 2.1-1](#)). However, the brain can take up appreciable quantities of lactate when blood lactate increases sharply, such as during exercise (Ide et al., 2000). Also, the brain can produce lactate during neural activity (Fellows et al., 1993; Fray et al., 1996; Hu and Wilson, 1997a) through glycogenolysis or anaerobic glycolysis. Because the transport of lactate across the BBB is relatively slow under normal physiological conditions, the brain might metabolize some of this lactate to prevent it from reaching excessively high levels within the brain (see 🔗 [Sects. 2.1.6](#) and 🔗 [2.1.10](#) for a detailed discussion). In addition, lactate is a major metabolic fuel for the brains of rat pups immediately after their birth (Arizmendi and Medina; 1983). Moreover, lactate has been used as an alternative substrate to treat diabetic patients during hypoglycemia (Maran et al., 2000). For these reasons, lactate is perhaps the most widely studied of the alternative substrates for the brain.

2.1.1 Lactate Metabolism

The first step in lactate metabolism is the conversion of lactate to pyruvate (lactate dehydrogenation). This reaction is catalyzed by lactate dehydrogenase (LDH), which is present at high levels of activity in the brain (McIlwain and Bachelard, 1985). Pyruvate derived from lactate can have many different fates. Reactions pertinent to energy metabolism are considered here. In one pathway, pyruvate is converted into acetyl-CoA via the pyruvate dehydrogenase complex (PDHC). Acetyl-CoA can then enter the TCA cycle for further oxidation. Another possible pathway is the conversion of pyruvate to oxaloacetate via pyruvate carboxylase. Oxaloacetate generated from pyruvate can either replenish TCA cycle intermediates or be converted to phosphoenolpyruvate (PEP). PEP serves as a substrate for gluconeogenesis and for glycogen synthesis. Complete oxidation of one molecule of lactate can produce 18 molecules of adenosine triphosphate (ATP). This amount of ATP is only slightly lower than the ATP produced by an equivalent amount of glucose. However, the lack of glycolytic ATP production when lactate is the energy substrate may have important functional consequences since glycolytic ATPs may be linked to ion transport and are essential for providing energy for synaptic function in those areas of the synapse where mitochondria are rare (see 🔗 [Sect. 2.1.4](#)).

Although brain cells can use lactate as an energy substrate in the absence of glucose (Schurr et al., 1988; Walz and Mukerji, 1988; Roberts, 1993; Peng et al., 1994b), whether brain cells use lactate in the presence of glucose is controversial (see 🔗 [Sects. 2.1.5–2.1.11](#)). Unlike the key enzymes of the glycolytic pathway, which are tightly regulated by energy demand, LDH is not regulated by energy status. Instead, the rate and direction of the reaction it catalyzes are mainly controlled by changes in the concentrations of the reaction's substrates and products. When both glucose and lactate are available as energy substrates in the brain, oxidation of lactate is mainly determined by the prevailing glycolytic rate. In the resting (unstimulated) brain, the resting levels of pyruvate, lactate, and H^+ , and the $NADH/NAD^+$ ratio, drive the LDH reaction toward lactate formation (Clarke et al., 1989), leading to a net efflux of lactate from the brain to the bloodstream (Owen et al., 1967; Hawkins et al., 1971; Ruderman et al., 1974; Hasselbalch et al., 1994; Wahren et al., 1999; Leegsma-Vogt et al., 2003) (see 🔗 [Table 2.1-1](#)). When glycolytic rates increase in the brain, such as during neural activation, pyruvate levels, H^+ levels, and the $NADH/NAD^+$ ratio increase (Goldberg et al., 1966; Ferrendelli and McDougal, 1971; Hochachka and Mommsen; 1983; Clarke et al., 1989). These increases make the thermodynamics of the LDH reaction even more favorable for lactate

production. Thus, for lactate to be used as an energy substrate in the brain at rest or during neural activity, lactate levels in brain cells must be high enough so that the thermodynamics of the LDH reaction favor pyruvate production rather than lactate production. In vitro studies have shown that achieving such high concentrations may be difficult since, in the presence of glucose, unstimulated neural cells continued to produce lactate when lactate concentrations in culture media ranged from 1 mM to as high as 10–11 mM (Waagepetersen et al., 2000; Bouzier-Sore et al., 2003; Winkler et al., 2004). Also, moderate hypoglycemia (3–4 mM glucose in the plasma) induced by prolonged starvation leads to increased lactate release from the adult brain (Hawkins et al., 1971; Ruderman et al., 1974) (see [Table 2.1-3](#); also see [Sect. 2.1.13](#)) rather than lactate uptake by the brain, which would be expected if the brain were metabolizing lactate. In addition, during insulin-induced hypoglycemia, the lactate efflux is unchanged (Wahren et al., 1999) ([Table 2.1-2](#)). Thus, the adult brain does not utilize lactate as an energy substrate even when its glucose supply is limited.

Another complication in many in vivo and in vitro studies where both glucose and lactate were available as substrates has been the reversible exchange of lactate with pyruvate via the LDH reaction (for a detailed

Table 2.1-2

Effects of short-term (24 h), insulin-induced hypoglycemia in healthy human subjects on the distributions and arteriovenous differences of metabolic substrates in the brain

Substrate	Plasma (mM)	CSF/ECF (mM)	A–V difference (mM)	References
Glucose	2.42	0.27 (brain dialysate)	0.41	Wahren et al. (1999)
	3.00			Abi-Saad et al. (2002)
Lactate	0.85	1.64 (brain dialysate)	–0.01	Wahren et al. (1999)
	1.36			Abi-Saad et al. (2002)
Pyruvate	0.123		0.002	Wahren et al. (1999)
β -Hydroxybutyrate	0.007		0	Wahren et al. (1999)

discussion see [Sect. 2.1.11](#)). Because of this “reversible equilibrium,” labeled lactate carbons from extracellular lactate can show up in the intermediates or end products of many cellular metabolic pathways, even when the net direction of the LDH reaction in cells is toward lactate formation. This problem has complicated the interpretation of data from many experiments in which radiolabeled lactate and glucose were used to determine the contributions of lactate to energy production in neural tissue (e.g., Poirity-Yamate et al., 1995; Waagepetersen et al., 2000; Bouzier-Sore, 2003; Itoh et al., 2003; also see discussion in [Sect. 2.1.11](#)) since the net direction of the LDH reaction was not determined in these studies. Thus, the lactate levels required to reverse the direction of the LDH reaction in the presence of glucose in vivo and in vitro remain unclear.

2.1.2 Lactate Dehydrogenase

Although LDH is generally present at high concentrations in the brain (McIlwain and Bachelard, 1985), the distribution of LDH varies within the brain (Friede and Fleming, 1963; Borowsky and Collins, 1989). Maps of the LDH distribution have been used as indicators of the glycolytic capacity of various brain regions (Friede and Fleming, 1963; Borowsky and Collins, 1989). In some brain regions, such as the hippocampus, olfactory cortex, and olfactory bulb, there are reciprocal distributions of LDH and cytochrome oxidase, suggesting that oxidative and glycolytic metabolism may be partially segregated anatomically in certain regions of the brain (Borowsky and Collins, 1989).

LDH isozymes are distributed differently among the different types of brain cells. LDH-1 is found in both neurons and astrocytes (Tholey, 1981; Bittar et al., 1996), while LDH-5 is found mainly in astrocytes (Tholey, 1981; Bittar et al., 1996). The kinetic properties of the two isozymes are different in that LDH-1 has a lower K_m for both lactate and pyruvate than does LDH-5, while LDH-5 has a higher V_{max} than does

LDH-1 (Battellino and Blanco, 1970; Everse and Kaplan, 1973). In vitro studies have shown that LDH-1 catalyzes a lower rate of lactate production than LDH-5 (Pesce et al., 1967; Nitisewojo and Hultin, 1976). Also, LDH-1 is more easily inhibited than LDH-5 by its substrate and product. For example, the K_i for pyruvate product inhibition is 0.18 mM for LDH-1 and 0.28 mM for LDH-5 (Stambaugh and Post, 1966). Since the resting pyruvate level in the brain is around 0.1–0.2 mM (McIlwain and Bachelard, 1985), LDH-1 is more easily inhibited whenever the pyruvate level increases as a result of an increase in the glycolytic rate. Consequently, pyruvate derived from glucose is directed toward oxidation rather than toward reduction to lactate. This means that there is a greater tendency for glucose to be fully oxidized in neurons than in astrocytes. This also means that the dominant presence of LDH-1 in neurons may make neurons less able than astrocytes to use lactate as an oxidative substrate when the glycolytic rate is increased.

The differences in the kinetic characteristics of the two LDH isozymes are in general agreement with their distributions in different tissues. For example, in cells or tissues where large amounts of lactate are produced and utilized, such as skeletal muscle, LDH-5 is the dominant isoform. In contrast, in cells or tissues where glucose tends to be more fully oxidized, such as cardiac muscle cells or neurons, LDH-1 is the dominant isoform (Cahn et al., 1962; Dawson et al., 1964).

2.1.3 Lactate Transport

Diffusion of lactate down its concentration gradient across the BBB is facilitated by monocarboxylate transporters (MCTs). MCTs also transport ketone bodies (see [Sect. 6.2](#)). MCTs are found in endothelial cells forming the BBB (Gerhart et al., 1997; Enerson and Drewes, 2003; Vannucci and Simpson, 2003) and in intraparenchymal brain cells (Gerhart et al., 1999; Leino et al., 1999; Debernardi et al., 2003; Vannucci and Simpson, 2003; Pellerin et al., 2005). Transport of lactate across the BBB is slow during resting conditions due in part to the lack of large concentration gradients for lactate across the BBB (Hasselbalch et al., 1994; Wahren et al., 1999) (see [Table 2.1-1](#)). However, significant lactate influxes into, or effluxes out of, the brain can take place under those circumstances where a large concentration gradient for lactate exists. For example, a significant influx of lactate from the blood to the brain can occur after exercise-induced increases in blood lactate levels (Ide, 2000). Also, a significant lactate efflux from the brain is often seen in association with elevated lactate levels in the brain occurring with spreading depression, intense seizures, and hyperammonemia (Hawkins et al., 1973; Calabrese et al., 1991).

The three major MCT isoforms (MCT1, MCT2, and MCT4) have different distributions in the brain. The functional significance of their heterogeneous distributions is not entirely clear. MCT1 is the major lactate transporter of the BBB (Gerhart et al., 1997; Leino et al., 1999; Enerson and Drewes, 2003; Vannucci and Simpson, 2003) and is also found in significant quantities in astrocytes (Broer et al., 1997; Leino et al., 1999; Debernardi et al., 2003; Vannucci and Simpson, 2003; Pellerin et al., 2005). MCT2 is the major monocarboxylate transporter isoform in neurons (Broer et al., 1997, 1999; Debernardi et al., 2003). MCT4 is found mainly in astrocytes (Pellerin et al., 2005) and has not been reported in neurons. MCT2 has a lower K_m (0.7 mM) for lactate than MCT1 (3–5 mM) and MCT4 (15–34 mM) do (Broer et al., 1997, 1999; Dimmer et al., 2000). This means that MCT2 is more saturated than the other two isoforms when lactate is at its resting level (approximately 1 mM; [Table 2.1-1](#)). These differences in affinity may influence the degree to which lactate transport increases during rapid rises in lactate levels. Because MCT2 is more saturated at rest (about 60%, Hertz and Dienel, 2004), it cannot increase its rate of lactate transport as much as the other MCT isoforms when lactate levels increase above 1 mM (Hertz and Dienel, 2004). Thus, when lactate goes up in neurons during heightened glycolysis, the rate at which this lactate is transported out of neurons may increase less than what might be seen in other cell types such as astrocytes. Therefore, the dominant presence of LDH1 (the more easily inhibited LDH isoform) and MCT2 (the high-affinity MCT isoform) in neurons may work together to minimize the amount of pyruvate reduced to lactate, which is released from cells when the glycolytic rate increases. Instead, pyruvate may be driven toward oxidation, which ensures the full oxidation of glucose taken up by neurons. Also, neurons may be more limited in their ability to use lactate as a substrate even when the dehydrogenation of lactate to pyruvate is thermodynamically feasible. This is due to the limitations placed on lactate transport by the K_m of MCT2.

It should be noted that the different LDH and MCT isoforms can only influence the rate of lactate flux, not the direction. Lactate can only be used as a substrate when the concentration gradient between the extracellular space and cytoplasm favors lactate influx and when the cytoplasmic lactate/pyruvate and NADH/NAD⁺ ratios favor pyruvate production.

Upregulation of monocarboxylate transport often occurs with changes in the concentrations of lactate or ketone bodies in the brain or circulation. For example, MCT1 mRNA expression increases in the BBB of rat brains in response to elevated lactate levels following the induction of permanent focal ischemia (Zhang et al., 2005). In this case, MCT1 is thought to be expressed to eliminate excess lactate from the brain (Zhang et al., 2005). Also, expression of MCT1 in the developing brain follows changes in the concentration of blood-borne ketone bodies; so expression peaks in the suckling period and gradually declines by adulthood (Vannucci and Simpson, 2003). In addition, the increased expression of MCT1 during development coincides with the elevated output of lactate from the developing brain, which exceeds the lactate output of the adult brain (Hawkins et al., 1971; Dahlquist and Persson, 1976). Moreover, the expression of MCTs in the BBB goes up in the brains of adult rats fed a high-fat (ketogenic) diet (Leino et al., 2001). Finally, upregulation of the MCT occurs in the brain after two or more days of starvation or fasting (Gjedde and Crone, 1975; Pan et al., 2000; Pan, 2001). Thus, upregulation of MCTs in the BBB may be in response to the brain's need to eliminate excess lactate from the brain, or to take up ketone bodies as metabolic substrates.

2.1.4 The Ability of Lactate to Support Brain Function In Vitro

The role of lactate as an energy substrate has been studied at the cellular level in isolated brain cell preparations and in cultured cells. Both neurons and astrocytes can oxidize lactate (Ito et al., 1986; McKenna et al., 1993; Vicario et al., 1993; Peng et al., 1994b). Also, cultured human Müller cells can maintain their ATP levels in the presence of lactate (Winkler et al., 2000). In stimulated brain slices, sufficient concentrations of lactate can support the same rates of oxygen consumption as seen with glucose (McIlwain and Bachelard, 1985). In addition, when substituted for glucose, lactate maintains the same levels of high-energy phosphates in hippocampal slices (Roberts and Chih, 1995; Roberts et al., 1997; Takata et al., 2001) and in the superfused retina preparation (Winkler, 1981) as seen with glucose.

Some in vitro studies (Schurr et al., 1988; Izumi et al., 1994; Takata et al., 2001) have shown that lactate can support synaptic transmission in brain slices in the absence of glucose. However, in other studies, a depression or loss of synaptic transmission can occur in hippocampal slices during the first 20–30 min of exposure to physiological solutions in which lactate, and not glucose, is the energy substrate (Kanatani et al., 1995; Takata and Okada, 1995; Wada et al., 1997, 1998). This initial depression though has not been observed by all investigators (e.g., see Fowler, 1993). When synaptic transmission fails during exposure to lactate-containing solutions, its failure resembles that seen in hippocampal slices exposed to glucose-free conditions (energy substrate absent) (e.g., Schurr et al., 1988; Izumi et al., 1994; Takata and Okada, 1995; Wada et al., 1997, 1998; Yamane et al., 2000). If the exposure of hippocampal slices to lactate-containing solutions continues beyond this initial 20- to 30-min period, synaptic transmission recovers incompletely (Yamane et al., 2000).

The effects of lactate on synaptic plasticity have also been examined. Lactate supported paired-pulse facilitation as well as glucose in the dentate region of the guinea pig hippocampal slices (Yang et al., 2003). However, lactate was less effective than glucose in supporting the induction of long-term potentiation in hippocampal slices (Yang et al., 2003).

Lactate does not match the ability of glucose to support recovery of synaptic transmission from some metabolic insults. For example, synaptic transmission recovered less from anoxic and NMDA insults in hippocampal slices exposed to lactate than in slices exposed to glucose (Roberts, 1993; Roberts et al., 1998; Chih et al., 2001a).

Lactate also supports axonal excitability. This ability was shown in rat (Brown et al., 2001) and mouse (Brown, 2003) optic nerves, where lactate as well as glucose supported generation of the compound action potential (CAP).

The ability of lactate to provide metabolic energy for maintenance of ion homeostasis in brain slices also varied in different studies. Although lactate can maintain K^+ and H^+ homeostasis in resting conditions (Roberts, 1993; Roberts et al., 1998), intracellular Ca^{2+} ($[Ca^{2+}]_i$) increased in slices exposed to lactate (Takata and Okada, 1995; Takata et al., 2001). This rise in $[Ca^{2+}]_i$ was due to release of Ca^{2+} from intracellular stores since the rise was blocked by sodium dantrolene (Takata et al., 2001). In addition, clearance of K^+ from the extracellular space of hippocampal slices following high-frequency stimulation was slower when lactate was the metabolic substrate instead of glucose (Roberts, 1993). The latter result indicates that lactate is less suitable than glucose as a substrate when energy demands are high.

The fact that lactate cannot fully replace glucose as a substrate, particularly during high-frequency stimulation (Roberts, 1993), is not unexpected. As mentioned in [Sect. 2.1.1](#), LDH is not regulated by energy status, so the rate of lactate oxidation may not respond to heightened energy demands for ion pumping. For example, cultured cerebellar granule cells exposed to high K^+ concentrations doubled their rates of glucose and pyruvate oxidation but experienced no statistically significant changes in lactate oxidation when all substrate levels remained unchanged (Peng et al., 1994b). This lack of coupling of LDH to energy demand represents a major problem in using lactate as an alternative energy substrate. Also, glycolytic ATP and ion transport may be linked (Proverbio and Hoffman, 1977; Paul et al., 1979). In addition, glycolytic ATP may be needed in localized areas where mitochondria are rare or absent, or TCA cycle enzyme activities are low. For example, dendritic spines and peripheral processes of astrocytes near the synapse are equipped with glycolytic enzymes, but rarely have mitochondria (Wu et al., 1997; Diemel and Cruz, 2003). In such localized areas or brain regions, glycolysis or glycogenolysis may assume great importance for energy production. Thus, lactate may not fully support all aspects of synaptic function as glucose does.

2.1.5 Utilization of Exogenous Lactate Extracted from the Bloodstream

As mentioned earlier, transport of lactate across the BBB is slow, and lactate usually shows a small net efflux out of the brain under normal resting conditions (Clarke et al., 1989; Hasselbalch et al., 1994; Wahren et al., 1999) ([Table 2.1-1](#)). The slow transport of lactate across the BBB suggests that the adult brain does not normally use exogenous lactate as an energy substrate. In addition, the brain does not appear to use exogenous lactate as an energy source even when the supply of glucose declines. For example, lactate release by the brain either was unchanged (Owen et al., 1967; Hasselbalch et al., 1994; Wahren et al., 1999) or increased (Hawkins et al., 1971; Ruderman et al., 1974; Dahlquist and Persson, 1976) ([Tables 2.1-2](#) and [2.1-3](#)) during insulin- or starvation-induced hypoglycemia.

Extraction of lactate from the blood by the brain can be significant when blood lactate levels increase due to lactate infusion or other physiological conditions, such as exercise (Ide et al., 2000; Leegsma-Vogt et al., 2001). In humans, the blood lactate concentration can increase 400–600% during exercise (Ide et al., 2000). However, increases in extracellular lactate in the brain during exercise are only moderate. For example, while extracellular lactate in rat muscles increases about 900% during exercise, extracellular lactate in the rat hippocampus and striatum increases only about 40% (Korf, 1996). Whether lactate taken up by the brain during infusion or exercise is metabolized remains unclear. For example, Leegsma-Vogt et al. (2003) reported a lactate influx during 80 min of lactate infusion, but a lactate efflux in the 60 min immediately after lactate infusion, in the brains of anesthetized rats. In this study, most (89%) of the lactate taken up by the brain was later released to the circulation and not used as an energy substrate by the brain (Leegsma-Vogt et al., 2003). Leegsma-Vogt et al. (2003) also found that glucose uptake did not decrease during lactate infusion. This lends support to the idea that lactate taken up by the brain during infusion did not replace glucose as an energy substrate. In contrast, Ide et al. (2000) reported a lactate influx during exercise and 30 min after exercise in humans. However, glucose uptake by the human brain did not change during exercise and in fact significantly increased after exercise in the study by Ide et al. (2000). Therefore, in this study, whether lactate taken up by the brain was actually metabolized remains questionable. As mentioned previously, the thermodynamics of the LDH reaction in the resting brain favors lactate production. Indeed, the resting brain has a small lactate efflux (Clarke et al., 1989; Hasselbalch et al., 1994; Wahren et al., 1999). For lactate to be oxidized in brain cells, lactate must increase to levels high

■ **Table 2.1-3**

Effects of long-term (2 days) starvation/fasting-induced hypoglycemia on the distributions and arteriovenous differences of metabolic substrates in the brain

Substrate	Subjects/duration	Plasma (mM)	Brain (mM)	A–V difference (mM)	References
Glucose	Adult rat/3 days	4.36		0.46	Hawkins et al. (1971)
	Adult rat/2 days	4.77	2.4	0.40	Ruderman et al. (1974)
	Adult rat/2 days	7.60		0.86	Dahlquist and Persson (1976)
	Human/3.5 days	3.45		0.40	Hasselbach et al. (1994)
	Human/38–41 days	4.49		0.26	Owen et al. (1967)
	Adult rat/3 days	0.36		–0.14	Hawkins et al. (1971)
	Adult rat/2 days	0.70		–0.18	Ruderman et al. (1974)
	Adult rat/2 days	1.51		–0.56	Dahlquist and Persson (1976)
Lactate	Human/3.5 days	0.48		–0.1	Hasselbach et al. (1994)
	Human/3 days		1.47		Pan et al. (2000)
	Human/38–41 days	0.53		–0.2	Owen et al. (1967)
Pyruvate	Adult rat/3 days	0.06		–0.009	Hawkins et al. (1971)
	Human/3.5 days	0.07		–0.02	Hasselbach et al. (1994)
	Human/38–41 days	0.054		–0.029	Owen et al. (1967)
	Adult rat/3 days	2.12		0.05	Hawkins et al. (1971)
β-Hydroxybutyrate	Adult rat/2 days	2.05	0.32	0.09	Ruderman et al. (1974)
	Human/3.5 days	2.94		0.26	Hasselbach et al. (1994)
	Human/3 days	3.15	0.98		Pan et al. (2000)
Acetoacetate	Human/38–41 days	6.67		0.34	Owen et al. (1967)
	Adult rat/3 days	0.91		0.08	Hawkins et al. (1971)
	Adult rat/2 days	0.53		0.06	Ruderman et al. (1974)
	Human/3.5 days	0.28		0.08	Hasselbach et al. (1994)
	Human/38–41 days	1.18		0.06	Owen et al. (1967)

enough that the thermodynamics of the LDH reaction favor pyruvate production. This level may be very high, since in vitro neural cells exposed to glucose export lactate to the medium even when as much as 10–11 mM lactate has been added to the medium (Bouzier-Sore et al., 2003; Winkler et al., 2004) (also see [● Sect. 2.1.11](#)). How high lactate levels have to be in the brain so that the LDH reaction shifts from lactate production to pyruvate production remains undetermined.

Two in vivo studies (Bouzier et al., 2000; Hassel and Bråthe, 2000) have been cited in the literature as evidence that infused lactate is taken up and metabolized by the brain. In these two studies, ^{13}C from 3- ^{13}C -lactate, which was infused into rats (Bouzier et al., 2000) or mice (Hassel and Bråthe, 2000), was incorporated into brain amino acids. However, because LDH catalyzes a reversible reaction, and the activity of LDH is high in the brain, rapid random exchanges between lactate and pyruvate can occur irrespective of the direction of the LDH reaction (Wolfe et al., 1988; Wolfe, 1990) (see [● Sect. 2.1.11](#) for more discussion and examples). Also, because the intracellular lactate concentration is much higher than the intracellular pyruvate concentration ([● Table 2.1-1](#)), labeling of pyruvate from labeled lactate through this reversible equilibrium can be very fast and significant even when the direction of the LDH reaction is toward lactate formation (Wolfe et al., 1988; Wolfe, 1990). This means that when both glucose and lactate are present, ^{13}C from 3- ^{13}C -lactate can be incorporated into metabolic intermediates or CO_2 even when the brain is not using lactate as an energy substrate. Thus, interpreting the metabolism of labeled lactate is difficult when both glucose and lactate are present as substrates.

In the above-mentioned in vivo study of Bouzier et al. (2000), the radioactive enrichment of lactate in the brain decreased from 45% to 26% during a 60-min 3- ^{13}C -lactate infusion, indicating that the radioactivity of lactate was diluted due to the endogenous production of unlabeled lactate from glucose. Thus, the

brain apparently produces substantial amounts of lactate despite a significant increase in brain lactate levels due to lactate infusion. As has been emphasized in this chapter, the prevailing glycolytic rate is the principal factor governing lactate utilization in the brain. Increases in lactate levels alone do not necessarily drive the reaction catalyzed by LDH toward pyruvate formation. Therefore, whether the labeling of amino acids from $3\text{-}^{13}\text{C}$ -lactate represents real lactate metabolism or simply the reversible equilibrium of lactate and pyruvate remains unclear in this study and that of Hassel and Bråthe (2000).

Despite the controversies regarding the utilization of exogenous lactate in the normoglycemic brain, exogenous lactate is used as an alternative substrate in the developing brain (Nehlig and Pereira de Vasconcelos, 1993) (also see [Sect. 2.1.12](#)). Also, exogenous lactate may be used under certain pathological conditions (see [Sect. 2.1.13](#)).

2.1.6 Production and Utilization of Endogenous Lactate in the Intact Brain

Although exogenous lactate cannot easily cross the BBB, endogenous lactate can be produced by brain cells during neural activation. During such activation in the rat brain *in vivo*, extracellular lactate increases between 0% and 135% (Kuhr and Korf, 1988; Fellows et al., 1993; Fray et al., 1996; Hu and Wilson, 1997a). Most of such increases occur toward the end of activation or after the termination of neural activity. The rate of efflux of lactate from the brain during functional activation is low (Madsen et al., 1999). Thus, the possibility exists that some lactate produced during neural activity is used as an energy substrate by neighboring inactive brain cells (Cruz et al., 1999; Dienel and Hertz, 2001; Hertz and Dienel, 2002, 2004; Dienel and Cruz, 2003;) or by brain cells in general during the subsequent recovery period (Chih and Roberts, 2003), particularly by brain cells with little glycolytic capacity (Dringen et al., 1993).

The role that lactate plays as an endogenous brain substrate has attracted much recent attention because of the proposal of what has become known as the astrocyte–neuron lactate shuttle hypothesis (ANLSH) (Tsacopoulos and Magistretti, 1996; Magistretti, 1999, 2000). The ANLSH represents a major departure from the conventional view of how glucose is metabolized at the cellular level in the brain. Given the central role of glucose utilization in brain energy metabolism and the widespread confusion about the ANLSH in the extant literature, a review regarding the development of, and changes in, the ANLSH is needed. [Sects. 2.1.7–2.1.9](#) briefly discuss the theoretical background and some of the experimental evidence used to support either the conventional view of glucose and lactate utilization in the brain or the ANLSH.

2.1.7 Conventional Hypothesis of Glucose and Lactate Utilization

The conventional hypothesis of glucose metabolism views glucose as the principal substrate for oxidative metabolism in both neurons and astrocytes. During neural activity, activation of glycolysis leads to production of lactate by both neurons and astrocytes. The possible causes of lactate production include faster activation of glycolysis compared with oxidative metabolism, inefficient operation of NADH shuttle or shuttles (Clarke, 1989), and the lack of colocalization of glycolytic enzymes and mitochondria in some brain regions (Wu et al., 1997; Shepherd and Harris, 1998; Sorra and Harris, 2000). The lactate produced during activity requires removal to avoid a buildup of lactate, which can inhibit glycolysis in both neurons and astrocytes. The conventional hypothesis contends that lactate produced by both neurons and astrocytes in active brain areas either diffuses to inactive areas (Cruz et al., 1999; Dienel and Hertz, 2001; Hertz and Dienel, 2002, 2004; Dienel and Cruz, 2003) or is removed via the circulation (Cruz et al., 1999; Dienel and Hertz, 2001; Dienel and Cruz, 2003; Hertz and Dienel, 2004). However, because of the slow transport of lactate across the BBB, some lactate produced by brain cells may be utilized in the brain. The conventional hypothesis asserts that both neurons and astrocytes may metabolize lactate when the prevailing glycolytic rate is low and brain lactate levels are high enough to drive the LDH reaction toward pyruvate production. However, the conventional hypothesis does not presuppose the proportion of lactate used by inactive neurons or astrocytes or specify the direction of the lactate flux (from neurons to astrocytes or vice versa). The conventional hypothesis does acknowledge the structural and biochemical heterogeneity of brain cells.

It does not exclude the use of lactate by those brain cells that have a low glycolytic capacity (e.g., oligodendrocytes (Kao-Jen and Wilson, 1980; Snyder and Wilson, 1983) and Purkinje neurons (Kao-Jen and Wilson, 1980; Simurda and Wilson, 1980; Katoh-Semba et al., 1988)), or the use of lactate in localized areas where glucose may be temporarily in short supply.

2.1.8 Early Version of the Astrocyte-Neuron Lactate Shuttle Hypothesis (ANLSH)

The ANLSH was first formally stated in the mid-1990s (Pellerin and Magistretti, 1994; Tsacopoulos and Magistretti, 1996; Sibson et al., 1998; Magistretti et al., 1999, 2000). Briefly, the hypothesis postulated that neural activation increases extracellular glutamate, which is taken up by astrocytes via Na^+ -dependent transporters. Increases in glutamate and Na^+ in astrocytes activate Na^+/K^+ -ATPase and lead to the activation of glycolysis (Pellerin and Magistretti, 1994). The lactate resulting from glycolysis is transported out of astrocytes and into active neurons where it fuels the activity-related energy needs of neurons (Magistretti et al., 1999). The major assertions of the ANLSH stated in the literature include (quotations come directly from the cited references):

- (1) that “the increase in glucose uptake during activation can be ascribed predominantly, if not exclusively, to astrocytes . . .” (Magistretti, 1999, p. 403),
- (2) that “energy substrates must be released by astrocytes to meet the energy demands of neurons” (Magistretti, 1999, p. 403), and
- (3) that “glucose is processed glycolytically [in astrocytes], resulting in the release of lactate as an energy substrate for neurons” (Magistretti et al., 1999, p. 497).

The primary experimental evidence used to support the early version of the ANLSH included (1) a putative 1:1 ratio between oxidative glucose consumption and astrocytic glutamate cycling in the rat brain (Sibson et al., 1998), which was used as evidence that lactate released from astrocytes paces neuronal oxidative metabolism during neural activity (Rothman et al., 1999); (2) the release of lactate by cultured astrocytes exposed to glutamate (Pellerin and Magistretti, 1994), which was used as evidence that glucose taken up during neural activity is processed glycolytically in astrocytes (Magistretti et al., 1999); (3) the predominant presence of LDH-1 in neurons (Bittar et al., 1996); and (4) the putative consumption by photoreceptor cells of lactate released by Müller cells, and in an isolated retina preparation containing both of these cell types (Poitry-Yamate et al., 1995). Studies by Bittar et al. (1996) and Poitry-Yamate et al. (1995) were used as evidence that neurons preferred lactate to glucose as an energy substrate (Magistretti et al., 1999, 2000). However, careful examination of the preceding evidence led several reviewers (e.g., Chih et al., 2001b; Dienel and Hertz, 2001; Chih and Roberts, 2003; Dienel and Cruz, 2003, 2004; Roberts and Chih, 2004), including the present one, to conclude that the evidence provided little support for this earlier version of the ANLSH.

2.1.9 Current Version of the ANLSH

In response to these critical reviews, proponents of the ANLSH revised the lactate shuttle hypothesis (Pellerin and Magistretti, 2003). The current version of the ANLSH now has only two components. These include (quotations come directly from the cited reference):

- (1) that “an enhancement of aerobic glycolysis, defined as preferential glucose use and lactate production despite sufficient oxygen levels to support oxidative phosphorylation, occurs in astrocytes in response to neuronal activation at glutamatergic synapses” (Pellerin and Magistretti, 2003, p. 1283), and
- (2) that “lactate produced by both neurons and astrocytes is eventually oxidized by neurons” (Pellerin and Magistretti, 2003, p. 1285).

The current ANLSH does not exclude the activation of glycolysis and production of lactate in active neurons. Also, it no longer requires a direct coupling between astrocytic lactate release and neuronal lactate

oxidation. Instead, the current ANLSH proposes that lactate produced by active neurons and astrocytes is released into an extracellular lactate pool, and that this lactate is eventually used by neurons either at rest or during activity.

As it now stands, the key points of contention between the current version of the ANLSH and the conventional hypothesis are (1) whether lactate released by astrocytes during neural activation is used by active neurons, and (2) whether lactate produced by both neurons and astrocytes during neural activation is eventually oxidized by neurons only. The first point of contention concerns the functional significance of the hypothesized lactate shuttle. If astrocyte-released lactate is not used by active neurons, or represents only an insignificant amount of energy substrate used by active neurons, then the hypothesized lactate shuttle would have little functional significance, even if it exists. The second point of contention concerns the validity of the shuttle. If lactate produced by neurons and astrocytes during neural activity is not predominantly used by neurons, then there is little reason to suggest the existence of an astrocyte–neuron lactate shuttle.

The current version of the ANLSH has been critically reviewed by Hertz (2004). [▶ Sects. 2.1.10](#) and [▶ 2.1.11](#) discuss the two key points of contention between the conventional hypothesis and the current ANLSH.

2.1.10 Is Lactate Released from Astrocytes Used by Active Neurons?

Any argument about whether lactate is an energy substrate for the brain needs to take into account that lactate cannot supplement the use of glucose as an energy substrate. This is because both glycolysis and dehydrogenation of lactate require NAD^+ . What makes this important is that NAD^+ regeneration is a limiting factor for glycolysis both at rest and during activation (Clarke, 1989). This is seen in the production of lactate by brain cells both at rest (Clarke, 1989) and during activation (Kuhr and Korf, 1988; Fellows et al., 1993; Fray et al., 1996; Hu and Wilson, 1997a). Thus, any use of lactate would be at the expense of glucose. Since glucose is readily available to neurons, lactate must compete successfully with glucose for lactate to become a significant source of energy for active neurons.

The conventional hypothesis contends that lactate cannot compete with glucose as a substrate for active neurons for several reasons. First, glycolytic enzymes can be rapidly activated by increased energy demand (Clarke et al., 1989). Also, neurons are replete with glycolytic enzymes (Kao-Jen and Wilson, 1980; Harris et al., 2001) and glucose transporters (McCall et al., 1994; Leino et al., 1997) that allow them to increase glucose utilization in response to heightened energy demands. This point has been demonstrated in vitro in studies showing that neuronal glycolytic rates increase dramatically as energy demand increases (Walz and Mukerji, 1988; Peng et al., 1994b). In contrast, LDH is not regulated by energy status, so any changes in the flux through the LDH reaction depend upon changes in the levels of the substrate and products of this reaction. Second, the rapid increases in glycolytic rates during neuronal activity will raise both pyruvate and H^+ levels, and increase the cytoplasmic NADH/NAD^+ ratio (Goldberg et al., 1966; Ferrendelli and McDougal, 1971; Hochachka and Mommsen, 1983; Clarke et al., 1989). All of these changes drive the LDH reaction toward lactate formation. Also, the intracellular acidification resulting from heightened glycolysis would favor lactate efflux from neurons since each molecule of lactate is cotransported with a proton (Bevensee and Boron, 1998). Third, for lactate to replace glucose as energy substrate during heightened glycolysis, extracellular lactate concentrations must increase greatly to change the direction of the LDH reaction from lactate formation to pyruvate formation. For example, cultured, unstimulated neurons and cultured astrocytes exposed to glucose and 10–11 mM extracellular lactate still produced lactate from glucose (Bouzier-Sore et al., 2003; Winkler et al., 2004) (see [▶ Sect. 2.1.11](#)). Since lactate is produced by the resting brain (Owen et al., 1967; Hawkins et al., 1971; Ruderman et al., 1974; Hasselbalch et al., 1994; Wahren et al., 1999; Leegsma-Vogt et al., 2003), and since glycolytic rates increase greatly during increased energy demand (Clarke et al., 1989), the lactate level required to reverse the direction of the LDH reaction from lactate production to pyruvate production during neural activity may be very high. However, during neural activity, increases in extracellular lactate from its resting level are slow and moderate (0–135%) in magnitude (Kuhr and Korf, 1988; Fellows et al., 1993; Fray et al., 1996; Hu and

Wilson, 1997a). Also, most of these increases occur after neural activation has ended (Fellows et al., 1993; Fray et al., 1996; Hu and Wilson, 1997a). Thus, the observed moderate increases in extracellular lactate probably do not reverse the direction of the LDH-catalyzed reaction during neural activity. Fourth, the dominant presence of LDH-1 in neurons (Tholey et al., 1981; Bittar et al., 1996), which is easily inhibited by increased pyruvate levels (Stambaugh and Post, 1966) (see [▶ Sect. 2.1.2](#)), does not favor the utilization of lactate in active neurons in which the glycolytic flux increases. Fifth, conversion of glucose to pyruvate, which produces two net ATPs and two NADHs, is thermodynamically more favorable than the conversion of lactate to pyruvate, which produces NADH but no ATP. Finally, glucose consumption is increased significantly in the active brain (Fox et al., 1988; Madsen et al., 1999), while no evidence exists that lactate is used by active neurons when glucose is readily available. All of these considerations support the conventional view that glucose is the predominant energy substrate for active neurons.

Many studies have tried to compare glucose and lactate as energy substrates, but interpreting the results from a large number of these studies has been complicated by several issues (see Chih and Roberts (2003) for a discussion of individual studies). First, most studies regarding substrate preference have been done in unstimulated brain cell or tissue preparations. However, glucose metabolism is tightly regulated by energy demand, and lactate utilization is inhibited during heightened glycolysis. Thus, comparisons of how glucose and lactate are utilized by active neurons must use stimulated brain cells or tissues. Second, many *in vitro* studies comparing glucose and lactate as energy substrates used neurons and astrocytes cultured from immature brains, which have a greater capacity to utilize lactate than adult brains (see [▶ Sect. 2.1.12](#)). Third, in studies where radiolabeled substrates were used, the fact that the LDH reaction is reversible would allow radioactive carbon from radiolabeled lactate to be incorporated into metabolic intermediates or end products without the use of lactate as an energy substrate (see [▶ Sect. 2.1.11](#) for detailed discussion). Failure to consider the reversibility of the LDH reaction has led to misinterpretations concerning lactate utilization in many *in vivo* and *in vitro* studies where radiolabeled substrates were used. Finally, the impact of cellular compartmentation on glucose and lactate utilization is difficult to assess. Some evidence (Cruz et al., 2001; Waagepetersen et al., 2001; Zwingmann et al., 2001) suggests that multiple compartments for both pyruvate and lactate metabolism exist in the brain cells. However, local fluctuations in substrate concentrations and in the catalytic direction or activity of enzymes are currently difficult, if not impossible, to predict.

So far, no convincing *in vitro* or *in vivo* evidence has been presented for the use of lactate by active neurons when both glucose and lactate were present at physiologically relevant concentrations. If lactate is not used by active neurons *in situ*, then any use of lactate accumulated during activity by inactive brain cells would be mainly for removing excess lactate. This would leave little functional significance for a presumptive lactate shuttle, even if it did exist.

2.1.11 Is Lactate Produced During Neural Activity Eventually Oxidized by Neurons?

The current ANLSH requires that neurons eventually oxidize the lactate produced during neural activity. Despite much evidence showing that lactate can be oxidized by both neurons and astrocytes *in vitro* (McKenna et al., 1993; Peng et al., 1994b), proponents of the ANLSH argue that lactate is a preferred substrate for neurons, but not for astrocytes (Pellerin and Magistretti, 2003). Two studies (Bouzier-Sore et al., 2003; Itoh et al., 2003) are used as evidence for this proposition. These two studies are discussed in greater detail here because they reflect some of the confusion that can arise in interpreting the results from experiments with radiolabeled substrates when both glucose and lactate are present (e.g., Waagepetersen et al., 2000; Itoh et al., 2003; Bouzier-Sore et al., 2003 (also see the discussion by Winkler et al. (2004) concerning these interpretational difficulties)). In the study by Itoh et al., addition of unlabeled lactate to the culture medium significantly reduced $^{14}\text{CO}_2$ production from radiolabeled glucose in both neurons and astrocytes (about 78% and 48% reduction in neurons and astrocytes, respectively, when 2.5 mM glucose and 2 mM lactate were used; estimated from Figure 1 of Itoh et al., 2003). In contrast, adding unlabeled glucose to the medium reduced $^{14}\text{CO}_2$ production from labeled lactate in astrocytes (about 20% when 2.5 mM glucose and 2 mM lactate were used; estimated from Figure 1 of Itoh et al., 2003), but not in neurons.

Proponents of the ANLSH have argued that these results show “that lactate is a preferential oxidative substrate for neurons, but not for astrocytes . . .” (Pellerin and Magistretti, 2003, p. 1284). However, the results from the study by Itoh et al. are complicated by the rapid reversible equilibrium between lactate and pyruvate mentioned previously (➤ Sect. 2.1.5). In a reversible reaction, reactants and products undergo constant interconversion. The net direction of such a reaction is determined by the relative rates of the forward and reverse reactions (Lehninger et al., 1993). Because LDH catalyzes a reversible reaction and because LDH is present at high activities in brain cells (McIlwain and Bachelard, 1985), a rapid exchange between lactate and pyruvate must exist regardless of the net direction of the LDH reaction (Wolfe et al., 1988; Wolfe, 1990). Also, because of the high lactate/pyruvate ratio in the cytoplasm (about 10:1), a large portion of the pyruvate pool in the cytoplasm can exchange with lactate in a short time. Thus, when both glucose and lactate are added to a cell culture, large quantities of carbon from lactate can appear in the intermediates or end products in the metabolic pathway due to this rapid interconversion of lactate with pyruvate, even when the net direction of the reaction catalyzed by LDH is toward lactate formation (i.e., lactate is not used as an energy substrate). Therefore, the net changes in lactate levels in the culture medium must be measured to determine whether lactate has been utilized or produced by brain cells.

Examples of the reversible equilibrium of the LDH reaction at work can be seen in some *in vitro* studies. For example, Waagepetersen et al. (2000) reported that when both glucose (2.5 mM) and labeled lactate (1 mM) were added to neuronal cultures, labeled lactate decreased in the culture medium while total lactate in the medium increased significantly. In another study in which primary neuronal cultures were incubated with both glucose (5.5 mM) and lactate (1.1, 5.5, or 11 mM) (Bouzier-Sore et al., 2003), carbon from lactate in the medium was incorporated into glutamate while lactate produced from glucose was released to the medium. It should be noted that the authors of these two studies (Waagepetersen et al., 2000; Bouzier-Sore et al., 2003) did not take into account the reversible equilibrium of LDH reaction in their interpretation of their experimental results (see Chih and Roberts (2003) for more discussion of the Waagepetersen et al. (2000) study).

How the reversible equilibrium of the LDH reaction affects the results of the Itoh et al. study can be seen by comparing the data from this study with the data from the aforementioned study of Waagepetersen et al. (2000). In the study by Itoh et al., addition of 0.5 mM unlabeled lactate reduced $^{14}\text{CO}_2$ production from labeled glucose (2.5 mM) about 40% in neuronal cultures and about 24% in astrocyte cultures (estimated from Figure 1 of Itoh et al., 2003). However, in the Waagepetersen et al. study, when neurons or astrocytes were incubated in 2.5 mM glucose and 1 mM lactate, media lactate concentrations increased in both neuronal cultures (from 1 mM to 1.4 or 1.9 mM, depending on the volume of the incubation medium) and astrocyte cultures (from 1 mM to 2.1 or 3.2 mM, depending on the volume of the incubation medium) (both estimated from Table 1 of Waagepetersen et al., 2000). Thus, the net direction of the LDH reaction in the Itoh et al. study was most likely toward lactate formation. Also, the reduction in $^{14}\text{CO}_2$ production from labeled glucose observed when unlabeled lactate was added was most likely due to the reversible equilibrium of the LDH reaction. Specifically, when unlabeled lactate is added to labeled glucose in the culture medium, the specific activity of the pyruvate derived from labeled glucose is diluted due to the exchange of labeled pyruvate with unlabeled lactate. This would occur even when the net direction of the LDH reaction is toward lactate formation. Also, as incubation continues, the labeled lactate produced from labeled glucose would mix with the unlabeled lactate in the medium. This would reduce the diluting effect of unlabeled lactate on $^{14}\text{CO}_2$ production from labeled glucose. Because cultured astrocytes have a much stronger tendency to produce lactate than cultured neurons (Walz and Mukerji, 1988; Schousboe et al., 1997; Waagepetersen et al., 2000), at the end of an experiment, the diluting effect of unlabeled lactate on $^{14}\text{CO}_2$ production would be less in cultured astrocytes than in cultured neurons. Thus, in the Itoh et al. study, the reason why the level of $^{14}\text{CO}_2$ from labeled glucose goes down less following unlabeled lactate addition in astrocyte cultures than in neuronal cultures is that there is probably a greater release of labeled lactate from labeled glucose to the medium in astrocyte cultures.

Why adding unlabeled glucose dilutes $^{14}\text{CO}_2$ production from labeled lactate less in neurons than in astrocytes has an explanation similar to that made above. It should be noted that the reduction of $^{14}\text{CO}_2$ production caused by adding unlabeled glucose to labeled lactate will be much less than the reduction of $^{14}\text{CO}_2$ caused by adding unlabeled lactate to labeled glucose. This is because of the high lactate to pyruvate

ratio (about 10:1) in brain cells. Thus, even when brain cells derive 100% of their energy from unlabeled glucose, most unlabeled pyruvate from unlabeled glucose will rapidly exchange with labeled lactate via the reversible equilibrium of the LDH reaction. Consequently, most CO₂ produced by the brain will still be labeled even though lactate was not used as an energy substrate. Thus, without knowing how lactate levels in the culture medium changed in the Itoh et al. study, one cannot determine whether lactate was actually used as an oxidative substrate (also see discussion in Winkler, 2004). Since cultured neurons can produce lactate from glucose when the culture medium contains lactate at concentrations as high as 10–11 mM (Bouzier-Sore et al., 2003; Winkler et al., 2004), it is likely that, in the Itoh et al. study, the net direction of the LDH reaction was toward lactate formation, and glucose was the only energy substrate used by neurons and astrocytes. Because lactate levels in solutions were not measured in the Itoh et al. study, no conclusions can be drawn from this study regarding the preferential use of lactate by these brain cells.

Other evidence used to support the proposition of the ANLSH that neurons prefer to use lactate instead of glucose is the above-mentioned study of Bouzier-Sore et al. (2003). In this study, labeling of glutamate was used to measure oxidative metabolism in primary neuronal cultures. Like the study by Itoh et al., this study showed that more carbon from lactate than from glucose was incorporated into glutamate when both glucose and lactate were added to the medium. However, lactate produced from glucose was released into the incubation medium while carbon from lactate was incorporated into glutamate. Thus, whether there was actually a net consumption of lactate by neurons remains unclear in this study. Although the incorporation of carbon from lactate into glutamate can be explained by the reversible equilibrium of the LDH reaction, Bouzier-Sore et al. (2003) proposed that the presumptive concomitant production and utilization of lactate were due to the compartmentation of glycolysis and TCA cycle activity inside neurons. According to their proposal, neurons convert glucose to lactate via glycolysis. This lactate is released into the medium, and then is reused as an oxidative substrate. However, there is no experimental evidence or theoretical basis for this proposition. As explained above, the net change of lactate in the medium must be measured to determine whether neurons actually use lactate as a substrate in the presence of glucose. Since this study did not demonstrate a net consumption of lactate by neurons, no conclusions regarding the preferential use of lactate can be drawn.

Thus, the results from studies by Itoh et al. and Bouzier et al. provide little support for the idea that lactate is used preferentially by neurons and not by astrocytes. Other studies used to support this idea have been critically reviewed elsewhere (e.g., Chih and Roberts, 2003; Hertz and Dienel, 2004), so the reader is directed to these reviews should further information be desired. ANLSH proponents have argued that if neurons prefer lactate to glucose (and since resting extracellular lactate levels are similar to resting extracellular glucose levels), then lactate should provide a substantial portion of neuronal energy needs (Pellerin and Magistretti, 2003, p. 1284). However, as has been pointed out, when neurons are incubated in media containing glucose and lactate at concentrations similar to those observed in the intact brain, they produce, instead of utilize, lactate (see Waagepetersen et al., 2000). Also, lactate is released by the resting brain (Hawkins et al., 1971; Ruderman et al., 1974; Hasselbalch et al., 1994; Wahren, 1999; Leegsma-Vogt et al., 2003) (🔗 [Table 2.1-1](#)), and the amount released increases during starvation-induced hypoglycemia in the adult brain (Hawkins, 1971; Ruderman, 1974; Dahlquist and Persson, 1976). These findings indicate that neurons do not prefer lactate to glucose. So far, ANLSH proponents have not yet provided any experimental evidence to support their proposition that most or all lactate produced during neural activity is eventually oxidized by neurons. Therefore, there is little reason to speculate that a lactate shuttle from astrocytes to neurons exists.

In conclusion, the existing evidence and theoretical considerations suggest that glucose is the predominant substrate for both neurons and astrocytes at rest or during neural activity. Furthermore, lactate produced during neural activity by both neurons and astrocytes most likely diffuses to neighboring, inactive areas, where it is either used by inactive brain cells, particularly those possessing little glycolytic capacity, or released into the circulation. Also, since both neurons and astrocytes can produce and use lactate, the lactate flux in the brain could be in any direction between astrocytes and neurons, and would be controlled by local fluctuations in lactate concentrations and by the prevailing glycolytic rate. So far, little evidence exists to support the propositions of the current ANLSH (1) that lactate released from astrocytes serves as an energy source for active neurons, and (2) that lactate

produced during neural activity is eventually oxidized by neurons. Thus, the validity and functional significance of the current ANLSH remain questionable.

2.1.12 Lactate Use by the Developing Brain

Lactate is used by the brain during the early neonatal period in several species (Nehlig and Pereira de Vasconcelos, 1993). Before rats start suckling, which usually occurs within 12–16 h of birth (Nehlig and Pereira de Vasconcelos, 1993), brain glucose supplies are insufficient due to the low rate of hepatic glycogenolysis and gluconeogenesis in newborn rats (Cuezva et al., 1980; Fernandez et al., 1983). Also, newborn rats lack white adipose tissue (Girard and Ferre, 1982), which is needed for ketogenesis (Nehlig and Pereira de Vasconcelos, 1993). In contrast, blood lactate concentrations are high due in part to the accumulation of lactate in fetal blood during late gestation (Cuezva et al., 1980; Girard and Ferre, 1982) and to the hypoxic stress of vaginal birth (Vannucci and Duffy, 1974). Consequently, exogenous lactate is a major metabolic fuel for the rat brain in the early perinatal period before suckling begins (Nehlig and Pereira de Vasconcelos, 1993).

During the suckling stage, ketone bodies became an important energy substrate for the brains of mammals because of the high fat content of maternal milk. Also, during suckling, the brain produces lactate that it releases to the venous circulation in quantities larger than those seen in the adult brain (Hawkins et al., 1971; Dahlquist and Persson, 1976) (🔗 [Table 2.1-4](#)). This lactate production is possibly due to the

■ **Table 2.1-4**

The effects of starvation on the circulating levels and on the arteriovenous differences of metabolic substrates in the developing rat brain (from Hawkins et al.)

Substrate	Age/status	Blood/plasma (mM)	A–V difference (mM)
Glucose	16 days/fed	6.97	0.58
	17 days/starved 24 h	5.02	0.22
Lactate	16 days/fed	1.07	–0.54
	17 days/starved 24 h	1.02	–0.27
Pyruvate	16 days/fed	0.12	–0.11
	17 days/starved 24 h	0.09	–0.05
β-Hydroxybutyrate	16 days/fed	1.25	0.20
	17 days/starved 24 h	2.30	0.20
Acetoacetate	16 days/fed	0.30	0.12
	17 days/starved 24 h	0.53	0.13

delayed development of PDHC in relation to enzymes of the TCA cycle (Nehlig and Pereira de Vasconcelos, 1993). However, the neonatal brain can still use exogenous lactate when blood lactate levels increase (Nehlig and Pereira de Vasconcelos, 1993), or when glucose levels decrease (Nehlig and Pereira de Vasconcelos, 1993). After weaning, glucose becomes the major oxidative substrate, and the ability to use exogenous lactate decreases as the expression of MCT1 declines following the suckling period (Vannucci and Simpson, 2003).

2.1.13 Lactate Use During Hypoglycemia

Lactate infusion has been used to alleviate autonomic and neuroglycopenic symptoms and cognitive dysfunction caused by acute insulin-induced hypoglycemia, both in normal human subjects (King et al., 1997; Maran et al., 2000) and in diabetic patients (King et al., 1998; Maran et al., 2000). In insulin-treated streptozotocin-diabetic dogs, lactate release from the brain during euglycemia increases significantly, and

lactate uptake from the blood during insulin-induced hypoglycemia also increases (Avogaro et al., 1990). These results suggest that the capacity of the BBB to transport lactate may be modified by diabetes. However, without lactate infusion, the normal adult brain does not appear to utilize lactate even when blood glucose is sharply decreased. For example, during hypoglycemia induced by starvation of 2–4 days, lactate released from the brain increased, and glucose remained the major substrate for cerebral metabolism (Ruderman et al., 1974; Dahlquist and Persson, 1976; Hasselbalch et al., 1994) (🔗 [Table 2.1-1](#)). In fact, release of lactate by the rat brain increased ninefold after 48 h of fasting-induced hypoglycemia (Ruderman et al., 1974). Also, during acute insulin-induced hypoglycemia in healthy human subjects, lactate efflux from the brain did not change despite a more than 50% decrease in the glucose concentration of the plasma (Wahren et al., 1999) (🔗 [Table 2.1-2](#)). These studies suggest that lactate is not used as an energy substrate in the normal adult brain even under hypoglycemic conditions. However, in the developing brain, where the glycolytic capacity is not fully developed (Nehlig and Pereira de Vasconcelos, 1993), lactate may be an important oxidative substrate during hypoglycemia (Nehlig and Pereira de Vasconcelos, 1993).

2.2 Pyruvate

Pyruvate represents a branch point in glucose metabolism. As a product of glycolysis in the cytoplasm, pyruvate can be transported into mitochondria for further oxidation, or converted to lactate to balance the NADH/NAD⁺ ratio. In mitochondria, pyruvate can be oxidized to acetyl-CoA through the action of PDHC or converted to oxaloacetate by the action of pyruvate carboxylase. The latter process is essential for the replenishment of TCA intermediates removed to serve as biosynthetic precursors. In the brain, most pyruvate carboxylation takes place in glial cells (Yu et al., 1983; Shank et al., 1985; Waagepetersen et al., 2001), although pyruvate carboxylation has been reported to occur in neurons (Hassel et al., 2001). Many exogenously supplied energy substrates, such as lactate and alanine, enter the oxidative metabolic pathway via pyruvate.

Pyruvate levels are tightly controlled in the brain. The resting level of pyruvate in the brain is about 0.1–0.2 mM (McIlwain and Bachelard, 1985). Changes in the pyruvate concentration influence many key enzymes that regulate different metabolic pathways. For example, increases in pyruvate levels augment the activity of PDHC (Lehninger et al., 1993), the key regulatory enzyme complex of oxidative metabolism, and enhance the activity of pyruvate carboxylase (Lehninger et al., 1993), a key regulatory enzyme for gluconeogenesis and anaplerosis. During accelerated glycolysis, rapid increases in pyruvate and NADH levels drive the LDH-catalyzed reaction toward lactate production, and lead to the release of lactate to the extracellular space (Clarke et al., 1989).

Pyruvate can be used in vitro to support oxidative energy metabolism in brain cells. For example, pyruvate can be oxidized by cultured neurons and astrocytes (Peng et al., 1994b). In addition to glucose, it is also a required component for culturing many types of neurons and glia (e.g., Facci et al., 1985; Selak et al., 1985), both as an energy source and as a carbon skeleton for biosynthesis. Unstimulated cerebellar granule cells and astrocytes oxidize pyruvate at approximately the same rate, which is the same as the rate at which they oxidize glucose (Peng et al., 1994b). Pyruvate is also an effective substrate for maintaining membrane potentials and ion homeostasis in cultured astrocytes, but it is less effective in cultured neurons (Silver et al., 1997). In hippocampal slices, pyruvate is as effective as glucose in maintaining high-energy phosphate levels (Kanatani et al., 1995; Yamane et al., 2000). In addition, pyruvate completely blocks histological damage in hippocampal slices exposed to the glycolytic blocker iodoacetate (IAA), while lactate is only partially effective in preventing damage (Izumi et al., 1994).

Pyruvate can be used in vitro to support electrophysiological activity in various isolated brain tissue preparations. For example, pyruvate fully supports the generation of orthodromic population spikes and field excitatory postsynaptic potentials (f-EPSPs) in hippocampal slices when the slices are exposed to pyruvate for a sufficient duration (>30 min) (Izumi et al., 2003). Also, pyruvate fully restores f-EPSPs in hippocampal slices deprived of glucose for 60 min (Izumi et al., 1994). In addition, pyruvate is as effective as glucose in supporting induction of LTP in the CA1 region of hippocampal slices (Izumi et al., 1997).

Moreover, pyruvate is used as an energy substrate by the rat optic nerve, where it supports generation of the compound action potential (CAP) as well as glucose does (Brown et al., 2001).

Although pyruvate can be used as energy substrate *in vitro*, it does not easily cross the BBB. Like lactate, pyruvate is transported across the BBB by MCTs (Oldendorf, 1973; Cremer et al., 1979, 1982; Pardridge, 1983). Pyruvate moves across the mitochondrial inner membrane by means of the pyruvate carrier (Berg et al., 2002). The concentration of pyruvate in the blood (0.07–0.09 mM (Hasselbalch et al., 1994; Wahren et al., 1999) (see [Table 2.1-1](#))) is in the same range as pyruvate levels in the brain. In fact, the normoglycemic human brain has a small net efflux of pyruvate into the blood (Hasselbalch et al., 1994; Wahren et al., 1999). During starvation- or insulin-induced hypoglycemia, pyruvate efflux from the brain changes little (Owen et al., 1967; Hasselbalch et al., 1994; Wahren et al., 1999). Also, earlier studies showed that infusion of pyruvate during hypoglycemic coma only caused a small increase in the uptake of oxygen and no improvement in the recovery of the brain (Goldfarb and Wortis, 1941). Thus, exogenous pyruvate is probably not used as an energy substrate *in vivo*.

2.3 Fructose-1,6-bisphosphate

Fructose-1,6-bisphosphate (FBP) is a glycolytic intermediate that has been used as an intervention for various hypoxic and ischemic conditions for two decades. The mechanism of its neuroprotective effect remains unclear, but initial studies suggested that FBP protected cells in the brain, at least in part, through its action as a substrate for anaerobic glycolysis (Markov, 1986). Although the highly charged FBP does diffuse through cell membranes in a dose-dependent manner (Ehringer et al., 2000), NMR studies have shown that FBP was not metabolized by either brain slices or astrocytes (Donohoe et al., 2001). Also, added FBP had little effect on oxidative CO₂ production and lactate production from glycolysis, and production of CO₂ and lactate from labeled FBP was minimal in cultured astrocytes (Kelleher et al., 1995). In addition, FBP in the absence of glucose did not preserve ATP levels, synaptic excitability, or neuronal morphology in rat hippocampal slices (Izumi et al., 2003). These studies suggested that the neuroprotective effect of FBP may be due to mechanisms other than an increase in energy production.

Possible mechanisms by which infused FBP protects the brain in cerebral hypoxia/ischemia include blocking catastrophic increases in intracellular Ca²⁺ (Kelleher et al., 1995), limiting superoxide and H₂O₂ production by activated neutrophils (Markov, 1986), and preserving reduced glutathione by increasing levels of glutathione reductase (Vexler et al., 2003). More recent research has shown that FBP protects neurons by activating phospholipase C and mitogen/extracellular signaling pathways that modulate intracellular Ca²⁺ homeostasis, as opposed to Ca²⁺ chelation or glutamate receptor inhibition (Donohoe et al., 2001; Fahlman et al., 2002).

3 Alternative Energy Substrates: Glycogen

3.1 Glycogen Storage

Glycogen is the largest reservoir of glucose in the brain, where its concentration, when all glucosyl residues are taken into account, exceeds that of glucose (Gruetter, 2003). Reports concerning its locations and concentrations in the brain show high variability (e.g., Cruz and Diemel, 2002; Choi et al., 2003; Gruetter, 2003). The major reason for this variability in glycogen content is that glycogenolysis can occur very quickly during experimental procedures and during tissue sampling and extraction (Ibrahim, 1975; Cruz and Diemel, 2002). Also, the rate of glycogenolysis may vary at different sites during experimental procedures, depending on the blood supply and mitochondrial density. In addition, glycogen may exist in a form that is too dispersed in some areas to permit its identification in the granular form (Guth and Watson, 1968). All of these factors influence the interpretation of the distribution and levels of glycogen in the brain.

Glycogen is found throughout the brain at levels that vary by cellular location and brain region. At the cellular level, glycogen granules are frequently seen in astrocytic perikarya and processes, especially the

perivascular end feet (Shimizu and Kumamoto, 1952; Koizumi and Shiraishi, 1970). Also, large quantities of glycogen have been found in the large neurons of the basal ganglia, brain stem, and spinal cord (Ibrahim, 1975). Other than these large neurons, glycogen was localizable but generally more difficult to find in neuronal perikarya and in pre- and postsynaptic sites (Shimizu and Kumamoto, 1952; Koizumi and Shiraishi, 1970). Recent studies have also shown that glycogen is found in localized areas of neurons, such as synaptic boutons and dendritic spines (Fiala et al., 2003), where mitochondria are relatively scarce (Wu et al., 1997; Shepherd and Harris, 1998; Sorra and Harris, 2000).

Reported brain glycogen levels range from 3.3 $\mu\text{mol/g}$ (Choi et al., 2003) to 12 $\mu\text{mol/g}$ (Cruz and Dienel, 2002). The glycogen content is lower in the brain than in muscle and liver, but it has been suggested that glycogen can make up for deficits in the brain's glucose supply during hypoglycemic episodes lasting more than 100 min (Gruetter, 2003). Indeed, glycogen content decreases during neural activity (Swanson, 1992; Swanson and Choi, 1993; Wender et al., 2000; Brown et al., 2004), hypoglycemia (Choi et al., 2003), hypoxia (Ibrahim, 1975; Kintner et al., 1983), and ischemia (Wagner and Lanier, 1994), indicating that glycogen plays an important role in meeting energy demands during both normoxia and hypoxia.

3.2 Glycogenolysis

Glycogenolysis may occur during neural stimulation (Swanson, 1992; Swanson and Choi, 1993; Wender et al., 2000; Brown et al., 2004), seizures (Harik et al., 1982), hypoglycemia (Choi et al., 2003), hypoxia (Breckenridge and Norman, 1962, 1965; Kogure et al., 1977), or ischemia (Harik et al., 1982; Wagner and Lanier, 1994). Initial histological studies showed that phosphorylase (the key enzyme controlling the rate of glycogenolysis), glycogen branching enzyme, and glycogen generally shared similar distributions, and that phosphorylase was present in both neurons and astrocytes (Ibrahim, 1975). However, recent studies with immunocytochemical methods have shown that phosphorylase is abundant in astrocytes and frequently observed in astrocytic processes adjacent to synaptic structures (Richter et al., 1996), but that phosphorylase is not found in neurons (Pfeiffer et al., 1992; Richter et al., 1996). Why the results differ between histochemical and immunocytochemical methods is unclear.

Phosphorylase exists in active (phosphorylase *a*) and inactive (phosphorylase *b*) forms. Under resting conditions, most phosphorylase in the brain is in the inactive form (Breckenridge and Norman, 1965). Conversion of phosphorylase *b* to phosphorylase *a* is catalyzed by phosphorylase *b* kinase, which may be activated by a cAMP-dependent protein kinase or by an increase in intracellular Ca^{2+} (Hertz and Dienel, 2002). Activities of both phosphorylase *a* and phosphorylase *b* are also regulated allosterically by changes in AMP levels, which directly link glycogenolysis to changes in energy demand (Ibrahim, 1975).

The existing evidence supports two roles for glycogen as an energy substrate. One role is to supply energy for regular neural activity (Wender et al., 2000; Cruz and Dienel, 2002; Brown et al., 2004). The other role is to provide glucose equivalents when glucose or oxygen is in short supply, such as during hypoglycemia or ischemia/hypoxia (Gruetter, 2003; Choi et al., 2003). Several studies have suggested that glycogenolysis takes place under normoglycemic conditions during neural activity (Swanson, 1992; Swanson and Choi, 1993; Wender et al., 2000; Dienel et al., 2002; Dienel and Cruz, 2003; Brown et al., 2004). The fact that the glycogen content of the brain decreases during sleep deprivation (Kong et al., 2002) and increases during sleep and anesthesia (Nelson et al., 1968; Karnovsky et al., 1980, 1983; Benington and Heller, 1995) also implies that glycogen may be used to maintain normal neural activity. However, the exact mechanism that activates glycogenolysis during neural stimulation has not been established. Phosphorylase *b* may be activated by neurotransmitters via cAMP- or Ca^{2+} -dependent mechanisms (see Hertz and Dienel, 2002). Also, active neurons can undergo increases in intracellular Ca^{2+} (Kandel et al., 2000) and AMP levels (e.g., Clarke and Sokoloff, 1999).

Glycogen may play an important role in providing energy substrates for neural activity in localized cellular areas where mitochondria are absent or rare. For example, glycogen granules are found frequently in astrocytic processes that interdigitate between axons and dendrites (Fiala et al., 2003). These astrocytic processes are most likely too narrow for mitochondria to occupy (Dienel and Cruz, 2003; Hertz et al., 2004). Glycogen granules have also been found in synaptic boutons and occasionally in dendritic spines

(Fiala et al., 2003), where mitochondria are relatively rare (Wu et al., 1997; Shepherd and Harris, 1998). Energy supplies in these areas may depend heavily on glycolytic ATP due to the low mitochondrial density. Since anaerobic energy metabolism is much less efficient with regard to ATP production than oxidative energy metabolism, large quantities of glucose or glucose equivalents may be needed in these localized areas when energy demands increase rapidly. Glycogen can then serve as an additional source of glucose equivalents (glucose-1-phosphate) for anaerobic ATP production. Also, conversion of glycogen to pyruvate produces one more ATP molecule than conversion of glucose to pyruvate, which may be an important factor when mitochondrial ATP production is not available. In addition, glycogenolysis may be activated faster than glycolysis. Glycogenolysis may be initiated by neurotransmitters or increases in intracellular Ca^{2+} , and may take place before ATP or AMP levels show any significant decreases (Ibrahim, 1975). Thus, glycogen may be strategically located to support metabolic activity in those areas of neurons and astrocytes that have elevated energy needs but have little support from mitochondria to meet those needs. Lactate produced in these localized areas is most likely transported to nonactivated areas or to the bloodstream (see [Sect. 2.1.6](#)).

Glycogen may also serve as an endogenous glucose reservoir to protect the brain against severe hypoglycemia or hypoxia/ischemia. During hypoxia, the inactive phosphorylase *b* can be converted to active phosphorylase *a* through cAMP activation of phosphorylase *b* kinase (Breckenridge and Norman, 1962) within seconds of the onset of hypoxia, even while ATP levels are still normal (Ibrahim, 1975). This activation could be due to a rise in catecholamine levels resulting from the stress of the procedures used to induce hypoxia (Ibrahim, 1975). During severe hypoxia/ischemia, increases in AMP levels or intracellular Ca^{2+} levels resulting from energy depletion may further activate phosphorylase. For example, all the glycogen in the neurons and astrocytes of hippocampal slices is depleted within 6 min after decapitation of the rat from which the slices were removed (Fiala, 2003). During acute insulin-induced hypoglycemia, glycogen content also declines in response to glucose depletion (Gruetter, 2003). Thus, glycogen mobilization can occur during energy depletion. The fact that glycogen content recovers within 2–3 h from hypoxia or hypoglycemia, and even overshoots its initial values during recovery (Gruetter, 2003), also implies that glycogen resynthesis after injury may act as a defensive mechanism to protect against possible further damage.

3.3 Release of Glucose or Lactate from Astrocytes as a Result of Glycogenolysis

The fact that glycogen is more frequently seen in astrocytes has led some investigators to suggest that glucose is released to neighboring neurons by astrocytes. This suggestion has caused controversy since other investigators have argued that glucose-6-phosphatase, the enzyme catalyzing the conversion of glucose-6-phosphate to glucose, is not present in large enough quantities to be physiologically relevant. For example, some investigators have reported that glucose-6-phosphatase is either absent (Nelson et al., 1985; Dienel et al., 1988) or present in negligible quantities (Gotoh et al., 2000) in the brain and astrocytes. Other investigators have found glucose-6-phosphatase in astrocytes (Forsyth et al., 1993) and goat brain slices (Bhattacharya and Datta, 1993), and reported the possible conversion of glycogen to glucose in the brain (Fray et al., 1996), although some of these findings have been disputed (Dienel et al., 1988; Gotoh et al., 2000). One problem is that brain glucose-6 phosphatase appears to have a very high K_m for glucose-6-phosphate in vitro, which is well above the physiological range of glucose-6-phosphate (Forsyth et al., 1996; Fray et al., 1996). Recently, an active glucose-6-phosphatase complex consisting of glucose-6-phosphatase and the glucose-6-phosphate transporter has been identified in astrocytes (Ghosh et al., 2005). Ghosh et al. (2005) suggest that the presence of this complex in astrocytes may mean that astrocytes serve as endogenous providers of glucose for the brain. The validity of this suggestion will most likely be tested in the near future.

Astrocytic glycogenolysis can potentially lead to release of glucose or lactate. However, no clear evidence exists that either glucose or lactate is released by astrocytes because of glycogenolysis during neural activity. Although an in vivo microdialysis study (Fray et al., 1996) has shown that dialysate glucose increased about

5% after physiological stimulation, and that this increase was blocked by the β -adrenoceptor antagonist propranolol, this study provides only indirect evidence of glucose release from astrocytes. Results from two other studies (Wender et al., 2000; Brown et al., 2004) have been used as evidence that stimulus-induced glycogenolysis in astrocytes during glucose deprivation may lead to release of lactate that could be used by neurons to support neural function. However, as mentioned previously (▶ Sects. 2.1.1, ▶ 2.1.10, and ▶ 2.1.11), in the presence of glucose, lactate may not be used as an energy substrate unless it is present at high concentrations. Thus, the results from experiments on preparations exposed to aglycemic conditions may not apply to normoglycemic conditions. Also, the results from these two studies are not conclusive. In these studies, failure of the optic nerve CAP during aglycemia was accelerated by the MCT blocker 4-CIN (Wender et al., 2000; Brown et al., 2004) or D-lactate (Brown et al., 2004), both of which were used to block lactate transport. The authors suggested that CAP failure was due to blockade of lactate transport from astrocytes to neurons. However, since 4-CIN may block entry of pyruvate into mitochondria (Halestrap and Denton, 1974), addition of 4-CIN may inhibit oxidative metabolism in both neurons and astrocytes, and impair neural function (Chih et al., 2001b). Also, a high concentration of D-lactate in the medium may block L-lactate efflux, inhibit glycogenolysis and glycolysis in both astrocyte and neurons, and inhibit energy generation pathways. Thus, the addition of 4-CIN and D-lactate may influence neural function by directly blocking energy production in neurons and not by blocking the presumptive transport of lactate from astrocytes to neurons. Therefore, no definite conclusions can be drawn from these experiments. As mentioned earlier, in localized areas where mitochondria are rare, lactate may be produced from both glycolysis and glycogenolysis in neurons and astrocytes. Except for these localized areas, the end product of glycogenolysis during neural activity remains unclear.

Astrocytic glycogenolysis might also lead to release of glucose or lactate from astrocytes during hypoglycemia or hypoxia/ischemia. Dringen et al. (1993) showed that astrocytes incubated in glucose-free medium release lactate and not glucose. This study has been used as evidence that glycogenolysis in astrocytes releases lactate instead of glucose. However, since astrocytes need to metabolize glycogen to meet their own energy needs during glucose deprivation, and since cultured astrocytes tend to metabolize glucose anaerobically (Fray et al., 1996; Forsyth et al., 1996), the results from cultured astrocytes do not necessarily apply to the intact brain. In addition, during hypoxia or ischemia, the release of lactate will not benefit neighboring neurons.

3.4 Glycogen Synthesis

Glycogen represents an energy reservoir through which alternative substrates may be channeled. For example, alanine, aspartate, glutamate, lactate, and mannose can serve as precursors, in addition to glucose, for the production of glycogen in astrocytes or brain tissue (Ide et al., 1969; Hevor et al., 1986; Dringen et al., 1993, 1994; Huang et al., 1994; Schmoll et al., 1995). The proportional contribution of these precursors and glucose to glycogen synthesis *in situ* is unknown. These precursors need to be converted to glucose-6-phosphate via gluconeogenesis before glycogen synthesis can occur. Some of the key enzymes of gluconeogenesis, such as pyruvate carboxylase, are found mainly in astrocytes (Yu et al., 1983; Shank, 1985). Also, fructose-1,6-bisphosphatase, which converts fructose-1,6-bisphosphate to fructose-6-phosphate, is thought to be found almost exclusively in astrocytes (see Hevor et al., 1986). However, fructose-1,6-bisphosphatase mRNA is found in both astrocytes and neurons (Loffler et al., 2001).

The key enzyme in glycogen synthesis, glycogen synthase, has generally the same distribution as glycogen and phosphorylase (Ibrahim, 1975). Glycogen synthase has been found in neuronal perikarya and processes, the neuropil, and astrocytes. Like phosphorylase, glycogen synthase exists in inactive (glycogen synthase *b*) and active (glycogen synthase *a*) forms. Glycogen synthase *b* can be converted to glycogen synthase *a* by phosphoprotein phosphatase. Inactivation of glycogen synthase *a* to glycogen synthase *b* is stimulated by cAMP. Thus, phosphorylase and glycogen synthase are reciprocally regulated by a phosphorylation–dephosphorylation cycle. Glycogen synthase activity is also inhibited by glycogen and increased by glucose.

Glycogen synthesis can take place during recovery from heightened energy demand, hypoglycemia, hypoxia, or ischemia, although the speed of resynthesis is slow compared with the recovery of other metabolites (Fiala et al., 2003; Gruetter, 2003). Pathological conditions also can lead to glycogen accumulation in the brain. For example, glycogen deposits are found in the human brain in association with conditions such as diabetic coma, tuberous sclerosis, and uremia (Ibrahim, 1975). Why glycogen is deposited in conjunction with these disorders is unclear.

4 Alternative Energy Substrates: Fructose and Mannose

The brain can use the sugars fructose and mannose as energy substrates. Fructose and mannose can both be obtained from the diet, but the concentrations of these sugars in the bloodstream are typically low (Panneerselvam and Freeze, 1996; Hawkins et al., 2002). Mannose enters the brain via glucose transporters, while fructose most likely enters the brain via diffusion (Bergbauer et al., 1996; Maher et al., 1996; Wiesinger et al., 1997). Both fructose and mannose are phosphorylated by hexokinase to fructose-6-phosphate and mannose-6-phosphate, respectively (Dringen et al., 1994; Bergbauer et al., 1996). Brain hexokinase phosphorylates fructose and mannose at rates much slower than that for glucose (Sols and Crane, 1954). Mannose-6-phosphate is converted to fructose-6-phosphate by mannose-6-phosphate isomerase, which is active in brain tissue. Fructose-6-phosphate is then metabolized via the glycolytic pathway. In addition to being oxidizable substrates, both mannose and fructose can be used as substrates for glycogen synthesis in astrocytes (Dringen et al., 1994; Bergbauer et al., 1996).

In vitro, fructose (Bergbauer et al., 1996; Wiesinger et al., 1997) and mannose (Dringen et al., 1994; Wiesinger et al., 1997) are used as energy substrates by cultured astrocytes and brain slices (McIlwain, 1953). Also, mannose can replace glucose as a metabolic substrate in the perfused, isolated rat brain (Sloviter, 1982). Sufficient concentrations of mannose and fructose kept the ATP and creatine phosphate levels in hippocampal slices at or near those seen with glucose (Bachelard et al., 1984; Wada et al., 1998; Yamane et al., 2000). However, fructose and mannose may not support synaptic function as well as glucose. For example, transient (<30 min) depression or loss of postsynaptic excitability usually occurred when hippocampal slices were transferred from media containing glucose to media containing one of these sugars (Bachelard et al., 1984; Kanatani et al., 1995; Wada et al., 1998; Yamane et al., 2000), although synaptic excitability may recover to 70–80% of that seen in glucose. In the rat optic nerve, fructose and mannose fully support the generation of CAPs in the absence of glucose (Brown et al., 2001).

Fructose has been used as an alternative substrate in patients with ischemic brain injury to avoid the adverse effects of glucose infusion after this type of injury (Cherian et al., 1994). However, infusion of fructose in vivo to treat experimental spinal cord ischemia in rabbits increased blood glucose and lactate concentrations, and resulted in a significantly poorer recovery of the spinal somatosensory-evoked potential (Cherian et al., 1994).

5 Alternative Energy Substrates: Amino Acids and TCA Cycle Intermediates

Several studies have shown that brain cells or brain slices can use exogenously supplied amino acids and TCA cycle intermediates as alternative energy substrates (see below). Also, brain cells may use amino acids and TCA cycle intermediates generated within the brain (Hertz et al., 2000; Hertz and Hertz, 2003).

5.1 Amino Acids

The concentrations of all amino acids except glutamine are much higher in the blood than in the cerebrospinal fluid (CSF) (Kruse et al., 1985). The concentration gradients for amino acids are maintained in part by the poor permeability of the BBB to many amino acids (O’Kane and Hawkins, 2003), and in part

by Na^+ -dependent active transport systems in the BBB, which export many amino acids from the brain to the blood (Lee et al., 1998; O'Kane and Hawkins, 2003). Under most physiological conditions, the arteriovenous differences for most amino acids are small (Felig et al., 1973; Drewes et al., 1977). During insulin-induced hypoglycemia, uptake of amino acids by the brain did not increase even with intravenous infusion of amino acids (Wahren et al., 1999). These studies suggest that exogenous amino acids may not be a significant energy source for the brain. However, endogenous amino acids can be used as energy substrates. For example, during severe insulin-induced hypoglycemia, available amino acids were consumed within 5 min (Agardh et al., 1981).

5.1.1 Glutamate

Several studies have shown that glutamate can be used as an energy substrate by the brain. In brain cells, glutamate is converted to α -ketoglutarate, and then enters the TCA cycle for further oxidation. Cultured astrocytes and neurons can metabolize glutamate (Erecinska et al., 1988; Schousboe et al., 1993, 1997). Also, infused glutamate may be oxidized by the brain *in vivo* (Zielke et al., 1988). The extent to which glutamate is metabolized via the TCA cycle in astrocytes appears to be concentration-dependent (Hertz et al., 1998; Hertz and Hertz, 2003).

Although brain cells can take up and utilize glutamate *in vitro*, the poor permeability of the BBB to glutamate essentially precludes the use of exogenous glutamate as an alternative substrate in the brain. Also, because glutamate is the chief excitatory neurotransmitter in the brain, glutamate levels in the extracellular space of the brain are normally kept in the range of 3–4 μM to allow glutamate to function as a neurotransmitter and to avoid excitotoxicity (Danbolt, 2001). Most of neurotransmitter glutamate released by neurons during neural activity is taken up by astrocytes (Hertz et al., 1999). Conversion of glutamate to glutamine in astrocytes and the subsequent release of glutamine by astrocytes can replenish neurotransmitter glutamate in neurons via the glutamate–glutamine cycle (for a review of the glutamate–glutamine cycle, see Danbolt (2001) and Hertz and Dienel (2004)). Some glutamate enters the circulation via Na^+ -dependent transporters in the BBB (Lee et al., 1998; O'Kane and Hawkins, 2003). A significant portion of the glutamate released by neurons and taken up by astrocytes during neural activation may enter the astrocytic TCA cycle, where it is used as an oxidative energy substrate (Hertz et al., 1998, 2000; Hertz and Hertz, 2003).

5.1.2 Glutamine

Several studies have shown that the brain can use glutamine as an energy substrate. In brain cells, glutamine is converted to glutamate and NH_4 by phosphate-dependent glutaminase. The resulting glutamate is then converted to α -ketoglutarate, which enters the TCA cycle. Glutamine can be oxidized by dissociated brain cells (Roeder et al., 1984a; Vicario et al., 1991), by cultured neurons (Vicario et al., 1993), by isolated synaptosomes (McKenna et al., 1993, 1994), by cultured astrocytes (McKenna et al., 1993; Vicario et al., 1993; Huang and Hertz, 1995), and in the brain *in vivo* (Zielke et al., 1998). Also, exogenously supplied glutamine can partially support CAP in the absence of glucose in the rat optic nerve preparation (Brown et al., 2001).

Glutamine is normally the most abundant amino acid in the plasma (Lee et al., 1998). Influxes of exogenous glutamine, like those of glutamate, are greatly restricted across the BBB (Eberling et al., 1995; O'Kane and Hawkins, 2003). However, astrocytes can synthesize glutamine from glutamate and NH_4 via glutamine synthetase. Glutamine released from astrocytes is taken up by neurons and converted to glutamate (the glutamate–glutamine cycle). Also, generation of glutamine in astrocytes and the subsequent transport of glutamine into endothelial cells in the BBB, possibly by Na^+ -dependent carriers (Lee et al., 1998; O'Kane and Hawkins, 2003), represents a major mechanism for ammonia detoxification in the rat brain (Farrow et al., 1990; Suarez et al., 2002). Although glutamine can be oxidized *in vitro* and *in vivo*, high extracellular glutamine concentrations may adversely affect brain cells (Farrow et al., 1990; Rama Rao, 2005). For

example, exposure to high glutamine concentrations can cause induction of the mitochondrial permeability transition in cultured astrocytes, possibly through generation of ammonia in astrocytes (Rama Rao et al., 2005). The ability of the brain cells to utilize glutamine and glutamate may serve as an additional control in the regulation of glutamate and glutamine levels in the brain (Hertz et al., 2000; Daikhin and Yudkoff, 2000).

5.1.3 Alanine

Alanine is another amino acid whose putative role as an energy substrate has been examined. Alanine does not easily cross the BBB (Farrow et al., 1990), but is formed within the brain, particularly in astrocytes (Westergaard et al., 1993), from the transamination of pyruvate by alanine aminotransferase (Hertz et al., 2000). Alanine can serve as a substrate for oxidative metabolism in cultured neurons (Westergaard et al., 1993; Peng et al., 1994b) and cultured astrocytes (Westergaard et al., 1993). In addition, alanine, like glutamate and glutamine, can be used as a substrate for gluconeogenesis and glycogen synthesis in cultured astrocytes (Schmoll et al., 1995) and brain slices (Bhattacharya and Datta, 1993). Glycogen derived from these glucogenic amino acids can then be used as an energy substrate. Unlike glutamine, exogenously supplied alanine cannot support generation of CAP in the rat optic nerve preparation (Brown et al., 2001).

Concentrations of alanine in the brain and the CSF are usually low (McIlwain and Bachelard, 1985; Clarke and Sokoloff, 1999). Infusion of alanine *in vivo* may cause an increase in the cerebral ammonia concentration (Farrow et al., 1990), which may be detrimental to brain function. For example, alanine infusion inhibits the mitochondrial respiratory chain in the rat brain (Rech et al., 2002). However, alanine infusion during hypoglycemia was found to support cognitive performance partially in human subjects (Evans et al., 2004). How alanine might function as an energy substrate *in vivo* needs further study.

5.2 TCA Cycle Intermediates

Several TCA cycle intermediates have been examined as alternative energy substrates *in vitro*. For example, both cultured neurons and astrocytes can oxidize citrate (Westergaard et al., 1994) and malate (Hertz et al., 1992; McKenna et al., 1993). In astrocyte cultures, citrate added to the culture medium reduces hypoxia-induced injury (Kelleher et al., 1996). In brain slices, high-energy phosphate levels are either partially or fully restored by citrate or oxaloacetate in the absence of glucose (Kanatani et al., 1995; Hodgkins and Schwarcz, 1998). Also, α -ketoglutarate and oxaloacetate can replace pyruvate as a required component needed in addition to glucose for culturing neurons and astrocytes (Facci et al., 1985). Both α -ketoglutarate and succinate have some ability to support excitability in neural tissue, as seen in their partial support of b-waves noted in electroretinograms recorded from rat retinas (Bui et al., 2004).

6 Alternative Energy Substrates: Ketone Bodies

The brains of many mammals can use the ketone bodies D- β -hydroxybutyrate (D-3-hydroxybutyrate) and acetoacetate as metabolic substrates. The use of ketone bodies as substrates occurs mainly during development and when glucose availability is limited, such as during long-term starvation or fasting, and in individuals on a ketogenic diet (see later).

6.1 Ketone Body Metabolism

6.1.1 Metabolic Pathway

Ketone bodies are oxidized in the mitochondria of brain cells. The first step in the metabolism of D- β -hydroxybutyrate involves its conversion into acetoacetate in a reaction catalyzed by β -hydroxybutyrate

dehydrogenase (Krebs et al., 1971; Nehlig and Pereira de Vasconcelos, 1993). Acetoacetate is converted into acetoacetyl coenzyme A (acetoacetyl-CoA) via 3-ketoacid-CoA transferase. Acetoacetyl-CoA is cleaved into two acetyl-CoAs in a reaction catalyzed by acetoacetyl-CoA thiolase (Krebs et al., 1971; Nehlig and Pereira de Vasconcelos, 1993). Acetyl-CoA can then enter the TCA cycle and be oxidized into CO₂ (Krebs et al., 1971; Nehlig and Pereira de Vasconcelos, 1993). All of the preceding reactions are near equilibrium (Krebs et al., 1971).

Production of ketone bodies by the liver is linked to changes in the blood glucose concentration, which is under tight hormonal regulation (Lehninger et al., 1993). Decreases in the blood glucose concentration stimulate the secretion of glucagon, which activates glycogenolysis and gluconeogenesis in the liver (Lehninger et al., 1993). Increased gluconeogenesis in the liver reduces its TCA cycle intermediates, which leads to the accumulation of acetyl-CoA (Pogozelski et al., 2005). At the same time, glucagon mobilizes triacylglycerols that are metabolized into free fatty acids (FFA) (Berg et al., 2002), which become the main fuel for the liver (Cahill, 1970). Oxidation of fatty acids in the liver also leads to accumulation of acetyl-CoA (Berg et al., 2002). The reduced levels of TCA intermediates and increased acetyl-CoA levels in liver mitochondria then drive acetyl-CoA toward the synthesis of ketone bodies (Berg et al., 2002). Since the liver does not have the enzymes to utilize ketone bodies (Krebs et al., 1971), ketone bodies are released by the liver to the bloodstream. From the bloodstream, they are taken up and utilized by various tissues and organs, including the brain, as energy substrates. Thus, the concentration of ketone bodies in the blood is heavily influenced by blood glucose levels.

Utilization of ketone bodies by the brain is concentration-dependent (Hawkins et al., 1971; Krebs et al., 1971; Page et al., 1971; Ruderman et al., 1974; Nehlig and Pereira de Vasconcelos, 1993). Blood or plasma concentrations of ketone bodies are nearly directly proportional to the rate of utilization of ketone bodies in brain tissue (Hawkins et al., 1971; Krebs et al., 1971; Blomqvist et al., 2002). Under normoglycemic conditions, the concentrations of ketone bodies in the blood and brain (see [Table 2.1-1](#)) are low. In humans subjected to starvation, the concentration of ketone bodies in the bloodstream can increase from close to zero to more than 5 mM after a week of fasting (see [Sect. 6.5](#)). Influxes of ketone bodies increase sharply as the concentrations of ketone bodies in the blood increase during starvation (Owen et al., 1967; Hasselbalch et al., 1994) ([Table 2.1-3](#)), and may even exceed the rate of glucose influx after 38–41 days of starvation (Owen et al., 1967). Increases in the utilization of ketone bodies during prolonged fasting reflect the glucose-sparing effect of ketone bodies. As in glucose, a large concentration gradient for ketone bodies is present across the BBB in the ketogenic brain, with ketone body concentrations much lower in the brain than in the blood (Pan et al., 2000, 2001) ([Table 2.1-3](#)). This is in contrast to the lack of an appreciable concentration gradient across the BBB for lactate (Hasselbalch et al., 1994; Wahren et al., 1999) ([Table 2.1-1](#)). Lactate is normally released, rather than used, by the brain during normoglycemia (Clarke and Sokoloff, 1999; Wahren et al., 1999; Leegsma et al., 2003) and hypoglycemia (Owen et al., 1967; Hawkins et al., 1971; Ruderman et al., 1974) ([Tables 2.1-2](#) and [2.1-3](#)).

6.1.2 Glucose-Sparing Effect of Ketone Bodies

During prolonged fasting, ketone bodies become a significant substrate for oxidative metabolism (Owen et al., 1967; Ruderman et al., 1974; Hasselbalch et al., 1994) ([Table 2.1-3](#)), thus sparing some glucose for other uses. Ketone bodies have glucose-sparing actions because they can inhibit glucose oxidation. This action most likely occurs through inhibition of PDHC, which catalyzes the conversion of pyruvate to acetyl-CoA. For example, β -hydroxybutyrate can stimulate PDH kinase activity. PDH kinase phosphorylates PDHC, which inactivates PDHC (Randle, 1981; Reed, 1981; Patel and Korotchkina, 2003). Also, acetyl-CoA and NADH (the products of β -hydroxybutyrate metabolism) inhibit the activity of PDHC (Randle, 1981; Reed, 1981; Patel and Korotchkina, 2003) (also see Lai and Sheu, 1987). Inhibition of PDHC by ketone bodies leads to an increase in brain pyruvate levels (DeVivo et al., 1975), and to increases in the production and release of lactate by the brain (Ruderman et al., 1974; DeVivo et al., 1978; Pan et al., 2000). Besides inhibiting PDHC, ketone bodies may also affect the activities of glycolytic enzymes. For example, phosphofructokinase may be inhibited in the ketogenic brain (Ruderman et al., 1974; DeVivo et al., 1978).

One possible explanation for this inhibition is an increase in citrate (Ruderman et al., 1974), which is a potent inhibitor of phosphofructokinase (Ruderman et al., 1974). Citrate goes up in brain cells as a result of the increased supply of acetyl-CoA in the ketogenic brain (Miller et al., 1982). In addition, β -hydroxybutyrate might also indirectly affect pyruvate utilization by competing with pyruvate for entry into mitochondria (Patel and Owen, 1977; Booth and Clark, 1981).

However, inhibition of glucose oxidation by ketone bodies can be counteracted by changes in energy status. As has been mentioned, decreases in ATP can activate glycolysis through activation of hexokinase and phosphofructokinase (Clarke and Sokoloff, 1999). Also, decreases in ATP increase the activity of PDHC (Lehninger et al., 1993) and limit the action of PDH kinase (Randle, 1981; Reed, 1981; Patel and Korotchkina, 2003). In addition, increases in the glycolytic rate lead to increased pyruvate levels (Goldberg et al., 1966; Ferrendelli and McDougal, 1971). A large enough increase in pyruvate can in turn inhibit PDH kinase activity and activate PDHC by increasing the percentage of active PDHC (Randle, 1981; Reed, 1981; Patel and Korotchkina, 2003). Thus, when there is a large increase in energy demand, such as during neural activation, the resulting decrease in ATP will counteract the inhibition of ketone bodies on glucose utilization.

This sparing effect of ketone bodies is important in preserving glucose during prolonged fasting when glucose supplies are limited. The brain uses ketone bodies to supplement energy production so that glucose is available as needed for the production of glycolytic ATP, or for biosynthetic pathways that require glucose or glycolytic intermediates. It should be noted that ketone bodies cannot be used to generate pyruvate or to replenish TCA cycle intermediates through anaplerotic pathways. Thus, ketone bodies can supplement, but not totally replace, glucose as an energy substrate. Also, although ketone bodies can spare the use of glucose as an energy substrate during hypoglycemia, ketone bodies do not interfere with glucose metabolism during normoglycemia. This is because they are kept at extremely low levels when glucose concentrations are normal (see [Table 2.1-1](#)).

6.2 Transport of Ketone Bodies

Ketone bodies may cross the BBB via simple diffusion (Gjedde and Crone, 1975; Cremer et al., 1982; Hasselbalch et al., 1995) and by the MCT (Gjedde and Crone, 1975; Cremer et al., 1976, 1982; Moore et al., 1976; Pardridge, 1991). Of the three different forms of MCTs found in the brain so far (MCT1, MCT2, and MCT4) only MCT1 has been found with great frequency in capillary endothelial cells of the BBB (Gerhart, 1997; Enerson and Drewes, 2003; Vannucci and Simpson, 2003). At the cellular level, MCT1, MCT2, and MCT4 are found in astrocytes (Leino et al., 1999; Debernardi et al., 2003; Vannucci and Simpson, 2003; Pellerin et al., 2005), while MCT1 and MCT2 are found in neurons (Debernardi et al., 2003; Vannucci and Simpson, 2003; Pellerin et al., 2005), with MCT2 being the dominant isoform (Debernardi et al., 2003). Movement of ketone bodies into mitochondria occurs via the pyruvate carrier (Papa and Paradies, 1974; Halestrap, 1975; Paradies and Papa, 1977).

As mentioned previously, expression of MCTs in the BBB may be upregulated when ketone bodies are used as energy substrates. For example, MCT expression in the BBB increases in suckling rats (Vannucci and Simpson, 2003) when ketone bodies are major energy sources and in adult rats fed a ketogenic diet (Leino et al., 2001). Also, upregulation of the MCT occurs during starvation (Gjedde and Crone, 1975; Hasselbalch et al., 1995), when there is a significant increase in the utilization of ketone bodies in the brain (Hawkins et al., 1971; Krebs et al., 1971; Ruderman et al., 1974; Hasselbalch et al., 1994).

6.3 Use of Ketone Bodies as Energy Substrates In Vitro

Ketone bodies have been used as energy substrates for in vitro nervous system preparations. For example, ketone bodies can be oxidized by brain homogenates (Lopes-Cardozo and Klein, 1982; Roeder et al., 1984b), dissociated brain cells (Roeder et al., 1984a), cultured neurons and astrocytes (Lopes-Cardozo et al., 1986; Edmond et al., 1987; McKenna et al., 1987), isolated synaptic terminals

(McKenna et al., 1994), oligodendrocytes (Lopes-Cardozo et al., 1986; Edmond et al., 1987), and brain slices (Patel, 1977; Swiatek et al., 1984). Rates of respiration of ketone bodies were greater in brain preparations from young rats than from adult rats (Patel, 1977; Roeder et al., 1984a, b; McKenna et al., 1994).

When provided as the only energy substrate, ketone bodies can maintain high-energy phosphates in some *in vitro* preparations. For example, β -hydroxybutyrate maintained ATP and phosphocreatine (PCr) levels in rat hippocampal slices (Wada et al., 1997). Also, DL- β -hydroxybutyrate maintained PCr levels in cortical brain slices from neonatal rats (Brooks et al., 1998). However, in guinea pig hippocampal slices exposed to solutions containing DL- β -hydroxybutyrate, ATP levels were maintained, but PCr levels decreased about 40% (Arakawa et al., 1991). PCr levels also dropped in the presence of DL- β -hydroxybutyrate in cortical slices from adult rats (Brooks et al., 1998). In cultured hippocampal neurons, added acetoacetate preserved ATP concentrations and improved cell viability when glycolysis was blocked with IAA (Massieu et al., 2003).

The ability of D- β -hydroxybutyrate to support nerve excitability has also been examined. Postsynaptic excitability decreased or disappeared as the time of exposure to β -hydroxybutyrate increased in hippocampal slices from both guinea pigs (Arakawa et al., 1991) and rats of different ages (Wada et al., 1997). Also, postsynaptic excitability declined faster in hippocampal slices from adult rats than in slices from younger rats (Wada et al., 1997). In addition, DL- β -hydroxybutyrate did not support recovery of synaptic transmission from glucose deprivation in hippocampal slices from postnatal day 30 rats or adult rats (Izumi et al., 1998). However, it did support recovery in hippocampal slices from postnatal day 15 rats (Izumi et al., 1998). Finally, optic nerves from 50- to 80-day-old rats exposed to D- β -hydroxybutyrate lost excitability, as seen in the disappearance of the stimulus-evoked CAP (Brown et al., 2001). These results show that D- β -hydroxybutyrate by itself cannot support neural function in adult brain tissue even though ATP levels are maintained for as long as 2 h (Arakawa et al., 1991).

The inability of ketone bodies to support fully neural excitability in the adult brain is not unexpected. As noted previously (*Sect. 6.1.2*), pyruvate cannot be synthesized from ketone bodies. As a consequence, TCA cycle intermediates, which are constantly removed to serve as precursors for many biosynthetic pathways, cannot be replenished via the anaplerotic pathway. Thus, when ketone bodies are provided as the only substrates, many biosynthetic pathways, including the synthesis of many neurotransmitters, may be inhibited. As a result, synaptic function can be compromised. Also, as mentioned in *Sect. 2.1.4*, glycolytic ATP may be essential for full functionality in localized synaptic areas, such as dendritic spine heads and synaptic boutons, where mitochondria are rare. Thus, ketone bodies alone cannot fully support neural function.

6.4 Utilization of Ketone Bodies in the Developing Brain

Many mammals, including humans (Hambraeus, 1977) and rats (Nehlig and Pereira de Vasconcelos, 1993), derive much of their metabolic energy from fats in milk during the early postnatal stage. Milk fat is metabolized into ketone bodies in the liver (Nehlig and Pereira de Vasconcelos, 1993). These ketone bodies are released into the circulation and can be used for energy production in the brain. In suckling rats, the influx of β -hydroxybutyrate into the brain can become more than 50 times the influx into the adult rat brain (Hawkins et al., 1971) (🔗 *Table 2.1-4*). Also, during the suckling stage, the rat brain meets as much as 30–70% of its energetic needs with ketone bodies derived from fat (Nehlig and Pereira de Vasconcelos, 1993). Several changes occur in the developing mammalian brain that enhance its use of ketone bodies as energy substrates, including (1) increases in the activities of enzymes involved in the metabolism of ketone bodies, (2) increases in the concentrations of ketone bodies in the circulation, and (3) increases in the density of ketone body transporters in the BBB.

6.4.1 Enzyme Activities in the Developing Brain

The developing brain undergoes large-scale changes in enzyme activities to keep up with the increasing blood concentrations of ketone bodies seen after birth. The activities of both β -hydroxybutyrate

dehydrogenase and 3-ketoacid-CoA transferase rise throughout the suckling period of the rat, peaking around the time of weaning (Krebs et al., 1971; Page et al., 1971; Booth et al., 1980; Nehlig and Pereira de Vasconcelos, 1993). Mitochondrial acetoacetyl-CoA thiolase also follows a similar pattern of increase as the preceding enzymes (Middleton, 1973; Booth et al., 1980). After rat pups are weaned, the levels of β -hydroxybutyrate dehydrogenase, 3-ketoacid-CoA transferase, and mitochondrial acetoacetyl-CoA thiolase in their brains decline toward adult values (Krebs et al., 1971; Dienel et al., 1977; Booth et al., 1980). The mitochondrial enzymes of ketone body metabolism continue to decrease in activity during aging, at least in rats (Patel, 1977; Leong et al., 1981).

The heightened activity of brain mitochondrial enzymes for ketone metabolism in suckling rats helps explain the greater ability of brain preparations from such rats to utilize ketone bodies for energy production. For example, rat brain homogenates from suckling-stage rat pups oxidize ketone bodies much faster than homogenates from adult rats (Tildon et al., 1983; Roeder et al., 1984a). Also, synaptosomes obtained from 17- to 18-day-old rats oxidize D- β -hydroxy[3- 14 C]butyrate to 14 CO $_2$ three times faster than synaptosomes from 7- to 8-week-old rats (McKenna et al., 1994).

6.4.2 Ketone Body Concentrations in the Blood During Development

The increased concentration of ketone bodies in the blood is the principal factor driving utilization of ketone bodies in the developing brain. At birth, the total concentration of ketone bodies in the blood of rat pups is around 0.1–0.4 mM (Girard et al., 1973, Yeh and Zee, 1976). Shortly after birth, circulating levels of ketone bodies in rat pups decline to values as low as 0.02 mM, then start increasing sharply, between 12 and 16 h postparturition (Ferre et al., 1978; Nehlig and Pereira de Vasconcelos, 1993). By 24 h postparturition, circulating ketone body concentrations in rat pups reach levels approximately four times greater than those seen at birth (Nehlig and Pereira de Vasconcelos, 1993). Circulating levels of ketone bodies in the developing rat remain high for 2–3 weeks after birth (Hawkins et al., 1971; Krebs et al., 1971; Pereira de Vasconcelos, 1987; Nehlig and Pereira de Vasconcelos, 1993; Vannucci and Simpson, 2003), usually at a combined concentration of 1–2 mM (Nehlig and Pereira de Vasconcelos, 1993). After weaning, the concentrations of ketone bodies in the blood decline to adult levels (for examples of adult levels, see [Table 2.1-3](#)).

6.4.3 Expression of MCT1 in the Blood-Brain Barrier (BBB) During Development

Expression of MCT1 in the BBB of the rat brain tends to run parallel to the changes in the circulating concentrations of ketone bodies seen during development (Vannucci and Simpson, 2003). Expression of mRNA and protein for MCT1 is readily apparent in the endothelium of the BBB at around 1 or 2 weeks after birth, and is greater than that found in adults (Gerhart et al., 1997; Vannucci and Simpson, 2003). At about 3 weeks after birth, the label for MCT1 in brain endothelial cells of suckling rats is 25 times greater than that in brain endothelial cells of adult rats (Leino et al., 1999). The expression of mRNA and protein for MCT1 in the BBB declines after weaning and reaches levels much lower than at earlier stages of development (Vannucci and Simpson, 2003). While one report suggested that endothelial cells in the brains of mice no longer express MCT1 by adulthood (Pellerin et al., 1998), many others have found that MCT1 is present in endothelial cells of adult rats (Gerhart et al., 1997; Leino et al., 1999; Enerson and Drewes, 2003; Vannucci and Simpson, 2003).

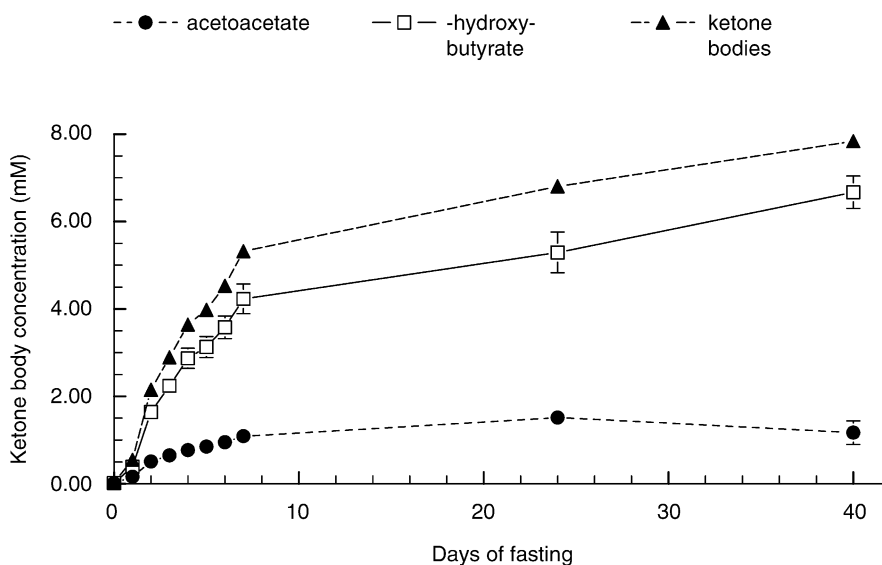
6.5 Ketone Bodies in Fasting and Starvation

Ketone bodies do not contribute much to energy metabolism in the adult brain when circulating levels of glucose are normal or near normal, as seen after feeding or short-term fasting. However, the importance of ketone bodies as energy substrates for the brain increases during long-term fasting or starvation.

After about 24–48 h of fasting or starvation in humans and rats, blood glucose levels drop (Cahill et al., 1966; Hawkins et al., 1971; Krebs et al., 1971). Decreases in blood glucose stimulate the secretion of glucagon, which mobilizes triacylglycerols and stimulates glycogenolysis and gluconeogenesis in the liver. The liver also increases its production and release of ketone bodies (see *Sect. 6.1.1*). At the same time, PDHC is downregulated in the cells of many organs and tissues throughout the body such as the liver, kidney, skeletal muscle, heart, and lactating mammary gland (Wieland et al., 1971; Wu et al., 2000; Patel and Korotchkina, 2003; Huang et al., 2003). However, downregulation of PDHC does not occur in the brain during the early stages of fasting. As a result, glucose oxidation is inhibited in most locations in the body except the brain, and instead other substrates such as fatty acids or ketone bodies are used in those locations as oxidative substrates. The inactivation of PDHC in these nonbrain organs is probably mediated by increases in the activity of PDH kinase (see *Sect. 6.1.2*) and by decreases in the activity of PDH phosphorylase, which activates PDHC by dephosphorylating it (Randle, 1981; Reed, 1981; Patel and Korotchkina, 2003). In contrast, PDHC activity in the brain is basically unaltered during the first 2 days of starvation (Patel and Korotchkina, 2003). Also, the levels of ketone bodies in the blood increase only moderately (about 0.55 mM (Cahill et al., 1966) during the first 24–36 h of fasting; [Figure 2.1-1](#); all data from Cahill

■ **Figure 2.1-1**

Changes in plasma concentrations of ketone bodies during fasting in humans. Data from Cahill et al. (1966) (days 0 to 7), Owen and Reichard (1971) (day 24), and Owen et al. (1967) (day 40 (38–41 days of fasting)). Error bars are standard errors of the mean



et al., 1966; Owen et al., 1967; Owen and Reichard, 1971). Consequently, glucose is still the principal energy substrate used by the brain in the early stages of fasting or starvation (Patel and Korotchkina, 2003). As fasting in humans continues for a week, the circulating levels of ketone bodies increase steeply ([Figure 2.1-1](#)). The blood concentrations of ketone bodies continue to rise as fasting continues beyond 1 week, but not as steeply ([Figure 2.1-1](#)). These increases in blood ketone body concentrations lead to large increases in the concentration gradient for ketone bodies across the BBB (see [Table 2.1-3](#)). These concentration gradient changes, coupled with upregulation of the MCT (Gjedde and Crone, 1975; Hasselbalch et al., 1995) and of at least one enzyme in the metabolic pathway of ketone bodies (e.g., Bässler et al., 1973), promote utilization of ketone bodies by the brain (Hawkins et al., 1971; Krebs et al., 1971; Ruderman et al., 1974;

Hasselbalch et al., 1994). Meanwhile, increasingly higher β -hydroxybutyrate levels in the brain during prolonged fasting may inhibit PDHC through phosphorylation or by increasing the levels of acetyl-CoA or NADH. The inhibition of PDHC leads to increases in pyruvate (DeVivo et al., 1975) and lactate levels (Ruderman et al., 1974; DeVivo et al., 1978; Pan et al., 2000) in the brain and to increased release of lactate (Ruderman et al., 1974) by the brain. Also, higher β -hydroxybutyrate levels may inhibit glycolysis by inhibiting PFK (Ruderman et al., 1974; DeVivo et al., 1978). As a result, glucose oxidation is slowed, and ketone bodies become important energy substrates as fasting becomes prolonged. Indeed, after 3.5 days of fasting, ketone bodies are responsible for about 25% of the oxygen consumption in the brain (Hasselbalch et al., 1994). During prolonged fasting (5–6 weeks), ketone body consumption accounts for up to 60% of the oxygen consumption in the human brain (Owen et al., 1967). As noted earlier (*Sect. 6.3*), because pyruvate and TCA cycle intermediates cannot be derived from ketone bodies, glucose is always needed for the brain's survival and functionality.

6.6 Use of Ketone Bodies Produced Within the Brain

Although the concentrations of ketone bodies are very low in the blood and brain of mature mammals during normoglycemia, some investigators have proposed that ketone bodies produced within the brain by astrocytes may be used by other brain cells. Auestad et al. (1991) found that cultured astrocytes produce ketone bodies from fatty acids, and suggested that astrocytes in the developing brain might produce ketone bodies that neurons and oligodendrocytes utilize to meet some of their energy needs. Guzman and Blazquez (2001) have further suggested that ketone bodies produced by astrocytes in the brain may serve as energy substrates for neurons during neural activity. In their model, which is similar to the ANLSH, Guzman and Blazquez propose that glutamate released by neurons during heightened synaptic activity is taken up by astrocytes and triggers the breakdown of fatty acids in astrocytes. Astrocytes then release the ketone bodies produced by fatty acid breakdown, which are taken up by active neurons and used as energy substrates. However, key elements of this hypothesis are yet to be supported by experimental evidence. Also, no evidence exists that astrocytes release ketone bodies during heightened neural activity, nor is there any proven mechanism that might activate ketone body synthesis in astrocytes during such activity. Although Guzman and Blazquez have claimed that glutamate enhances ketogenesis in cultured astrocytes, they have provided no data to support their claim. Also, no evidence can be found that ketone body concentrations increase during neural activity. Since utilization of ketone bodies is concentration-dependent (see *Sect. 6.4.2*), the lack of evidence for an increase in ketone bodies during neural activity represents a major drawback for this ketone body shuttle hypothesis.

Second, the source of substrates for ketone body synthesis in astrocytes during neural activity is questionable. Although cultured astrocytes can generate ketone bodies in the presence of high concentrations of fatty acids (Auestad et al., 1991), fatty acids are not readily available to astrocytes *in vivo* (see Pardridge, 1983, 1991). Only a small quantity of free fatty acids (FFAs) in the bloodstream normally passes through brain capillaries (Pardridge, 1991). The fact that the arteriovenous difference for FFAs in the adult human brain is extremely small, even after 5–6 weeks of fasting in humans (Owen et al., 1967), suggests that net utilization of FFAs from exogenous sources in the adult brain is minimal. The brain does have a requirement for certain essential polyunsaturated fatty acids (PUFAs) that can be obtained only from exogenous sources (Agranoff et al., 1999; Rapoport, 2003), and these must cross the BBB successfully. However, most of these exogenous FFAs are incorporated into brain lipids that are structural or are involved in signal transduction (Rapoport, 2003). Therefore, it would appear highly unlikely that ketone bodies are produced by astrocytes from FFAs to meet the needs of heightened synaptic activity in active neurons.

7 Summary

Glucose is the predominant oxidative energy substrate used by the adult brain, but other substrates can be used by the developing brain or by the adult brain under certain physiological and pathological conditions.

Many substrates, including glycolytic intermediates, amino acids, TCA cycle intermediates, and ketone bodies, can be used by brain cells when these substrates are supplied in large quantities either *in vitro* or *in vivo*. However, the use of these substrates *in situ* is often limited by their low permeability to the BBB.

Lactate and ketone bodies are important energy sources for the immature rat brain, which does not have a fully developed capacity to use glucose. Lactate is used by the rat brain in the early neonatal period before suckling begins because of the limited supply of glucose and ketone bodies, and because of the accumulation of lactate in fetal blood during late gestation. After suckling begins, ketone bodies become major energy substrates, and a large increase in lactate release from the rat brain occurs. Utilization of ketone bodies by the brain is associated with high blood ketone body concentrations, increased expression of MCTs in the BBB, and enhanced activities of enzymes in the metabolic pathways that convert ketone bodies to acetyl-CoA.

The mature brain uses ketone bodies when glucose is in short supply, such as during prolonged starvation. Ketone bodies are also used in the brains of individuals on a ketogenic diet. Increased ketone body concentrations may slow glucose oxidation by inhibiting PDHC, thus sparing the use of glucose as an energy substrate. However, the inhibitory effects of ketone bodies on glucose utilization may be offset by rapid increases in energy demand. Increased use of ketone bodies in the adult brain is also associated with rising blood ketone body concentrations and greater expression of MCTs in the BBB. Although increased MCTs during prolonged hypoglycemia can potentially augment the transport of both ketone bodies and lactate, lactate utilization by the brain does not increase during hypoglycemia. In fact, lactate release from the brain increases during hypoglycemia, indicating that lactate does not have the glucose-sparing effect that ketone bodies have.

In addition to exogenous energy substrates, some substrates produced within the brain can be used as energy sources. For example, glycogen, which is synthesized from a variety of precursors in the brain, becomes an energy source during neural activity and hypoglycemia. Glycogen may be particularly important in providing energy for neural activation in localized areas where mitochondria are rare, such as synaptic boutons, dendritic spines, and fine peripheral astrocytic processes. Also, it has been proposed that lactate and ketone bodies may be produced by astrocytes during neural activity and shuttled to neurons to be used as energy substrates. The experimental evidence and theoretical background for these two hypothesized shuttles are discussed in this chapter to explain why these hypothesized shuttles most likely have no role in the intact brain.

Acknowledgment

This work was supported by an award from the American Heart Association, Florida/Puerto Rico Affiliate.

References

- Abi-Saab WM, Maggs DG, Jones T, Jacob R, Srihari V, et al. 2002. Striking differences in glucose and lactate levels between brain extracellular fluid and plasma in conscious human subjects: Effects of hyperglycemia and hypoglycemia. *J Cereb Blood Flow Metab* 22(3): 271-279.
- Agarth CD, Chapman AG, Nilsson B, Siesjo BK. 1981. Endogenous substrates utilized by rat brain in severe insulin-induced hypoglycemia. *J Neurochem* 36(2): 490-500.
- Agranoff BW, Benjamins JA, Hajra AK. 1999. Lipids. Basic neurochemistry. Molecular, cellular and medical aspects. Siegel GJ, Agranoff BW, Albers RW, Fisher SK, Uhler MD, editors. Philadelphia: Lippincott-Raven Publishers; chap. 3, pp. 47-67.
- Arakawa T, Goto T, Okada Y. 1991. Effect of ketone body (D-3-hydroxybutyrate) on neural activity and energy metabolism in hippocampal slices of the adult guinea pig. *Neurosci Lett* 130(1): 53-56.
- Arizmendi C, Medina JM. 1983. Lactate as an oxidizable substrate for rat brain *in vitro* during the perinatal period. *Biochem J* 214(2): 633-635.
- Auestad N, Korsak RA, Morrow JW, Edmond J. 1991. Fatty acid oxidation and ketogenesis by astrocytes in primary culture. *J Neurochem* 56(4): 1376-1386.
- Avogaro A, Nosadini R, Doria A, Tremolada C, Baccaglioni U, et al. 1990. Substrate availability other than glucose in the brain during euglycemia and insulin-induced hypoglycemia in dogs. *Metabolism* 39(1): 46-50.

- Bachelard HS, Cox DW, Drower J. 1984. Sensitivity of guinea-pig hippocampal granule cell field potentials to hexoses in vitro: An effect on cell excitability? *J Physiol (Lond)* 352: 91-102.
- Bässler KH, Ackermann RH, Wagner K, Schönstedt B. 1973. Enzymatic changes associated with ketosis in long standing diabetes and prolonged starvation of rats. *Hoppe Seylers Z Physiol Chem* 354(1): 48-52.
- Battellino L, Blanco A. 1970. Catalytic properties of the lactate dehydrogenase isozyme X from mouse tissue. *J Exp Zool* 174: 173-186.
- Benington JH, Heller HC. 1995. Restoration of brain energy metabolism as the function of sleep. *Prog Neurobiol* 45(4): 347-360.
- Berg JM, Tymoczko JL, Stryer L, Clarke ND. 2002. Biochemistry. New York: WH Freeman and Company.
- Bergbauer K, Dringen R, Verleysdonk S, Gebhardt R, Hamprecht B, et al. 1996. Studies on fructose metabolism in cultured astroglial cells and control hepatocytes: Lack of fructokinase activity and immunoreactivity in astrocytes. *Dev Neurosci* 18(5-6): 371-379.
- Bevensee MO, Boron WF. 1998. pH regulation in mammalian neurons. pH and brain function. Kaila K, Ransom BR, editors. New York: Wiley-Liss; chap. 12, pp. 211-231.
- Bhattacharya SB, Datta AG. 1993. Is brain a gluconeogenic organ? *Mol Cell Biochem* 125(1): 51-57.
- Bittar PG, Charnay Y, Pellerin L, Bouras C, Magistretti PJ. 1996. Selective distribution of lactate dehydrogenase isoenzymes in neurons and astrocytes of human brain. *J Cereb Blood Flow Metab* 16(6): 1079-1089.
- Blomqvist G, Alvarsson M, Grill V, Heijne G, Ingvar M, et al. 2002. Effect of acute hyperketonemia on the cerebral uptake of ketone bodies in nondiabetic subjects and IDDM patients. *Am J Physiol Endocrinol Metab* 283(1): E20-E28.
- Booth RF, Clark JB. 1981. Energy metabolism in rat brain: Inhibition of pyruvate decarboxylation by 3-hydroxybutyrate in neonatal mitochondria. *J Neurochem* 37(1): 179-185.
- Booth RF, Patel TB, Clark JB. 1980. The development of enzymes of energy metabolism in the brain of a precocial (guinea pig) and non-precocial (rat) species. *J Neurochem* 34(1): 17-25.
- Borowsky, IW, Collins RC. 1989. Metabolic anatomy of brain: A comparison of regional capillary density, glucose metabolism, and enzyme activities. *J Comp Neurol* 288(3): 401-413.
- Bouzier A-K, Thiaudiere E, Biran M, Rouland R, Canioni P, Merle M. 2000. The metabolism of [$3\text{-}^{13}\text{C}$]lactate in the rat brain is specific of a pyruvate carboxylase-deprived compartment. *J Neurochem* 75(2): 480-486.
- Bouzier-Sore A-K, Voisin P, Canioni P, Magistretti PJ, Pellerin L. 2003. Lactate is a preferential oxidative energy substrate over glucose for neurons in culture. *J Cereb Blood Flow Metab* 23(11): 1298-1306.
- Breckenridge BM, Norman JH. 1962. Glycogen phosphorylase in brain. *J Neurochem* 9: 383-392.
- Breckenridge BM, Norman JH. 1965. The conversion of phosphorylase b to phosphorylase a in brain. *J Neurochem* 12: 51-57.
- Broer A, Brookes N, Ganapathy V, Dimmer KS, Wagner CA, et al. 1999. The astroglial ASCT2 amino acid transporter as a mediator of glutamine efflux. *J Neurochem* 73(5): 2184-2194.
- Broer S, Rahman B, Pellegrini G, Pellerin L, Martin JL, et al. 1997. Comparison of lactate transport in astroglial cells and monocarboxylate transporter 1 (MCT 1) expressing *Xenopus laevis* oocytes. Expression of two different monocarboxylate transporters in astroglial cells and neurons. *J Biol Chem* 272(48): 30096-30102.
- Brooks KJ, Clark JB, Bates TE. 1998. 3-Hydroxybutyrate aids the recovery of the energy state from aglycaemic hypoxia of adult but not neonatal rat brain slices. *J Neurochem* 70(5): 1986-1990.
- Brown AM, Baltan Tekkok S, Ransom BR. 2004. Energy transfer from astrocytes to axons: The role of CNS glycogen. *Neurochem Int* 45(4): 529-536.
- Brown AM, Tekkok SB, Ransom BR. 2003. Glycogen regulation and functional role in mouse white matter. *J Physiol (Lond)* 549(2): 501-512.
- Brown AM, Wender R, Ransom BR. 2001. Metabolic substrates other than glucose support axon function in central white matter. *J Neurosci Res* 66(5): 839-843.
- Bui BV, Kalloniatis M, Vingrys AJ. 2004. Retinal function loss after monocarboxylate transport inhibition. *Invest Ophthalmol Vis Sci* 45(2): 584-593.
- Cahill GF Jr, 1970. Starvation in man. *N Engl J Med* 282(12): 668-675.
- Cahill GF Jr, Herrera MG, Morgan AP, Soeldner JS, Steinke J, et al. 1966. Hormone-fuel interrelationships during fasting. *J Clin Invest* 45(11): 1751-1769.
- Cahn RD, Kaplan NO, Levine L, Zwilling LE. 1962. Nature and development of lactic dehydrogenases. *Science* 136: 962-969.
- Calabrese VP, Gruemer HD, James K, Hranowsky N, DeLorenzo RJ. 1991. Cerebrospinal fluid lactate levels and prognosis in status epilepticus. *Epilepsia* 32(6): 816-821.
- Cherian L, Peek K, Robertson CS, Goodman JC, Grossman RG. 1994. Calorie sources and recovery from central nervous system ischemia. *Crit Care Med* 22(11): 1841-1850.
- Chih CP, He J, Sly TS, Roberts EL Jr. 2001. Comparison of glucose and lactate as substrates during NMDA-induced activation of hippocampal slices. *Brain Res* 893(1-2): 143-154.

- Chih CP, Lipton P, Roberts EL Jr. 2001. Do active cerebral neurons really use lactate rather than glucose? *Trends Neurosci* 24(10): 573-578.
- Chih C-P, Roberts EL Jr. 2003. Energy substrates for neurons during neural activity: A critical review of the astrocyte–neuron lactate shuttle hypothesis. *J Cereb Blood Flow Metab* 23(11): 1263-1281.
- Choi IY, Seaquist ER, Gruetter R. 2003. Effect of hypoglycemia on brain glycogen metabolism in vivo. *J Neurosci Res* 72(1): 25-32.
- Clarke DD, Lajtha AL, Maker HS. 1989. Intermediary metabolism. *Basic neurochemistry*. New York: Raven Press; pp. 542-550.
- Clarke DD, Sokoloff L. 1999. Circulation and energy metabolism of the brain. *Basic neurochemistry*. Siegel GJ, Agranoff BW, Albers RW, Fisher SK, Uhler MD, editors. New York: Lippincott-Raven; chap. 31, pp. 637-669.
- Cremer JE, Braun LD, Oldendorf WH. 1976. Changes during development in transport processes of the blood–brain barrier. *Biochim Biophys Acta* 448(4): 633-637.
- Cremer JE, Cunningham VJ, Pardridge WM, Braun LD, Oldendorf WH. 1979. Kinetics of blood–brain barrier transport of pyruvate lactate and glucose in suckling, weanling and adult rats. *J Neurochem* 33: 439-445.
- Cremer JE, Teal HM, Cunningham VJ. 1982. Inhibition, by 2-oxo acids that accumulate in maple-syrup-urine disease, of lactate, pyruvate, and 3-hydroxybutyrate transport across the blood-brain barrier. *J Neurochem* 39(3): 674-677.
- Cruz F, Villalba M, García-Espinosa MA, Ballesteros P, Bogón E, et al. 2001. Intracellular compartmentation of pyruvate in primary cultures of cortical neurons as detected by ^{13}C NMR spectroscopy with multiple ^{13}C labels. *J Neurosci Res* 66(5): 771-781.
- Cruz NF, Adachi K, Dienel GA. 1999. Rapid efflux of lactate from cerebral cortex during K^+ -induced spreading cortical depression. *J Cereb Blood Flow Metab* 19(4): 380-392.
- Cruz NF, Dienel GA. 2002. High glycogen levels in brains of rats with minimal environmental stimuli: Implications for metabolic contributions of working astrocytes. *J Cereb Blood Flow Metab* 22(12): 1476-1489.
- Cuevas JM, Moreno FJ, Medina JM, Mayor F. 1980. Prematurity in the rat. I. Fuels and gluconeogenic enzymes. *Biol Neonate* 37(1-2): 88-95.
- Dahlquist G, Persson B. 1976. The rate of cerebral utilization of glucose, ketone bodies, and oxygen: A comparative in vivo study of infant and adult rats. *Pediatr Res* 10(11): 910-917.
- Daikhin Y, Yudkoff M. 2000. Compartmentation of brain glutamate metabolism in neurons and glia. *J Nutr* 130 (Suppl 4S): 1026S-1031S.
- Danbolt NC. 2001. Glutamate uptake. *Prog Neurobiol* 65(1): 1-105.
- Dawson DM, Goodfriend TL, Kaplan NO. 1964. Lactic dehydrogenases: Function of the two types. *Science* 143: 929-933.
- Debernardi R, Pierre K, Lengacher S, Magistretti PJ, Pellerin L. 2003. Cell-specific expression pattern of monocarboxylate transporters in astrocytes and neurons observed in different mouse brain cortical cell cultures. *J Neurosci Res* 73(2): 141-155.
- DeVivo DC, Leckie MP, Ferrendelli JS, McDougal DB Jr. 1978. Chronic ketosis and cerebral metabolism. *Ann Neurol* 3(4): 331-337.
- DeVivo DC, Malas KL, Leckie MP. 1975. Starvation and seizures. Observation on the electroconvulsive threshold and cerebral metabolism of the starved adult rat. *Arch Neurol* 32(11): 755-760.
- Dienel G, Ryder E, Greengard O. 1977. Distribution of mitochondrial enzymes between the perikaryal and synaptic fractions of immature and adult rat brain. *Biochim Biophys Acta* 496(2): 484-494.
- Dienel GA, Cruz NF. 2003. Neighborly interactions of metabolically-activated astrocytes in vivo. *Neurochem Int* 43(4-5): 339-354.
- Dienel GA, Cruz NF. 2004. Nutrition during brain activation: Does cell-to-cell lactate shuttling contribute significantly to sweet and sour food for thought? *Neurochem Int* 45(2-3): 321-351.
- Dienel GA, Hertz L. 2001. Glucose and lactate metabolism during brain activation. *J Neurosci Res* 66(5): 824-838.
- Dienel GA, Nelson T, Cruz NF, Jay T, Crane AM, et al. 1988. Over-estimation of glucose-6-phosphatase activity in brain in vivo. Apparent difference in rates of [$^2\text{-}^3\text{H}$]glucose and [$\text{U-}^{14}\text{C}$]glucose utilization is due to contamination of precursor pool with ^{14}C -labeled products and incomplete recovery of ^{14}C -labeled metabolites. *J Biol Chem* 263(36): 19697-19708.
- Dienel GA, Wang RY, Cruz NF. 2002. Generalized sensory stimulation of conscious rats increases labeling of oxidative pathways of glucose metabolism when the brain glucose–oxygen uptake ratio rises. *J Cereb Blood Flow Metab* 22(12): 1490-1502.
- Dimmer KS, Friedrich B, Lang F, Deitmer JW, Broer S. 2000. The low-affinity monocarboxylate transporter MCT4 is adapted to the export of lactate in highly glycolytic cells. *Biochem J* 350 (Pt 1): 219-227.
- Donohoe PH, Fahlman CS, Bickler PE, Vexler ZS, Gregory GA. 2001. Neuroprotection and intracellular Ca^{2+} modulation with fructose-1,6-bisphosphate during in vitro hypoxia–ischemia involves phospholipase C-dependent signaling. *Brain Res* 917(2): 158-166.
- Drewes LR, Conway WP, Gilboe DD. 1977. Net amino acid transport between plasma and erythrocytes and perfused dog brain. *Am J Physiol* 233(4): E320-E325.

- Dringen R, Bergbauer K, Wiesinger H, Hamprecht B. 1994. Utilization of mannose by astroglial cells. *Neurochem Res* 19(1): 23-30.
- Dringen R, Gebhardt R, Hamprecht B. 1993. Glycogen in astrocytes: Possible function as lactate supply for neighboring cells. *Brain Res* 623(2): 208-214.
- Dringen R, Schmoll D, Cesar M, Hamprecht B. 1993. Incorporation of radioactivity from [¹⁴C]lactate into the glycogen of cultured mouse astroglial cells: Evidence for gluconeogenesis in brain cells. *Biol Chem* 374(5): 343-347.
- Eberling JL, Roberts JA, Demanincor DJ, Brennan KM, Hanrahan SM, et al. 1995. PET studies of cerebral glucose metabolism in conscious rhesus macaques. *Neurobiol Aging* 16(5): 825-832.
- Edmond J, Robbins RA, Bergstrom JD, Cole RA, de Vellis J. 1987. Capacity for substrate utilization in oxidative metabolism by neurons, astrocytes, and oligodendrocytes from developing brain in primary culture. *J Neurosci Res* 18(4): 551-561.
- Ehringer WD, Niu W, Chiang B, Wang OL, Gordon L, et al. 2000. Membrane permeability of fructose-1,6-diphosphate in lipid vesicles and endothelial cells. *Mol Cell Biochem* 210(1-2): 35-45.
- Enerson BE, Drewes LR. 2003. Molecular features, regulation, and function of monocarboxylate transporters: Implications for drug delivery. *J Pharm Sci* 92(8): 1531-1544.
- Erecinska M, Zaleska MM, Nissim I, Nelson D, Dagani F, et al. 1988. Glucose and synaptosomal glutamate metabolism: Studies with [¹⁵N]glutamate. *J Neurochem* 51(3): 892-902.
- Evans ML, Hopkins D, Macdonald IA, Amiel SA. 2004. Alanine infusion during hypoglycaemia partly supports cognitive performance in healthy human subjects. *Diabet Med* 21(5): 440-446.
- Everse J, Kaplan NO. 1973. Lactate dehydrogenases: Structure and function. *Adv Enzymol* 37: 61-133.
- Facci L, Skaper SD, Varon S. 1985. Specific replacements of pyruvate for trophic support of central and peripheral nervous system neurons. *J Neurochem* 45(3): 926-934.
- Fahlman CS, Bickler PE, Sullivan B, Gregory GA. 2002. Activation of the neuroprotective ERK signaling pathway by fructose-1,6-bisphosphate during hypoxia involves intracellular Ca²⁺ and phospholipase C. *Brain Res* 958(1): 43-51.
- Farrow NA, Kanamori K, Ross BD, Parivar F. 1990. A ¹⁵N-n.m.r. study of cerebral, hepatic and renal nitrogen metabolism in hyperammonaemic rats. *Biochem J* 270(2): 473-481.
- Felig P, Wahren J, Ahlborg G. 1973. Uptake of individual amino acids by the human brain. *Proc Soc Exp Biol Med* 142(1): 230-231.
- Fellows LK, Boutelle MG, Fillenz M. 1993. Physiological stimulation increases nonoxidative glucose metabolism in the brain of the freely moving rat. *J Neurochem* 60(4): 1258-1263.
- Fernandez E, Valcarce C, Cuezva JM, Medina JM. 1983. Postnatal hypoglycaemia and gluconeogenesis in the newborn rat. Delayed onset of gluconeogenesis in prematurely delivered newborns. *Biochem J* 214(2): 525-532.
- Ferre P, Pegorier JP, Williamson DH, Girard JR. 1978. The development of ketogenesis at birth in the rat. *Biochem J* 176(3): 759-765.
- Ferrendelli JA, McDougal DB Jr. 1971. The effect of audiogenic seizures on regional CNS energy reserves, glycolysis and citric acid cycle flux. *J Neurochem* 18: 1207-1220.
- Fiala JC, Kirov SA, Feinberg MD, Petrak LJ, George P, et al. 2003. Timing of neuronal and glial ultrastructure disruption during brain slice preparation and recovery in vitro. *J Comp Neurol* 465(1): 90-103.
- Forsyth R, Fray A, Boutelle M, Fillenz M, Middleditch C, et al. 1996. A role for astrocytes in glucose delivery to neurons. *Dev Neurosci* 18: 360-370.
- Forsyth RJ, Bartlett K, Burchell A, Scott HM, Eyre JA. 1993. Astrocytic glucose-6-phosphatase and the permeability of brain microsomes to glucose 6-phosphate. *Biochem J* 294 (Part 1): 145-151.
- Fowler JC. 1993. Glucose deprivation results in a lactate preventable increase in adenosine and depression of synaptic transmission in rat hippocampal slices. *J Neurochem* 60(2): 572-576.
- Fox PT, Raichle ME, Mintun MA, Dence C. 1988. Nonoxidative glucose consumption during focal physiologic neural activity. *Science* 241: 462-464.
- Fray AE, Forsyth RJ, Boutelle MG, Fillenz M. 1996. The mechanisms controlling physiologically stimulated changes in rat brain glucose and lactate: A microdialysis study. *J Physiol (Lond)* 496(1): 49-57.
- Friede RL, Fleming LM. 1963. A mapping of the distribution of lactic dehydrogenase in the brain of the rhesus monkey. *Am J Anat* 113: 215-234.
- Gerhart DZ, Enerson BE, Zhdankina OY, Leino RL, Drewes LR. 1997. Expression of monocarboxylate transporter MCT1 by brain endothelium and glia in adult and suckling rats. *Am J Physiol* 273(1 Pt 1): E207-E213.
- Gerhart DZ, Leino RL, Drewes LR. 1999. Distribution of monocarboxylate transporters MCT1 and MCT2 in rat retina. *Neuroscience* 92(1): 367-375.
- Ghosh A, CheungYY, Mansfield BC, Chou JY. 2005. Brain contains a functional glucose-6-phosphatase complex capable of endogenous glucose production. *J Biol Chem* 280 (12): 11114-11119.
- Girard J, Ferre P. 1982. Metabolic and hormonal changes around birth. *Biochemical development of the fetus and the neonate*. Jones CT, editor. Elsevier; Amsterdam: pp. 517-551.

- Girard JR, Cuendet GS, Marliiss EB, Kervran A, Rieutort M, et al. 1973. Fuels, hormones, and liver metabolism at term and during the early postnatal period in the rat. *J Clin Invest* 52(12): 3190-3200.
- Gjedde A, Crone C. 1975. Induction processes in blood-brain transfer of ketone bodies during starvation. *Am J Physiol* 229(5): 1165-1169.
- Goldberg ND, Passonneau JV, Lowry OH. 1966. Effects of changes in brain metabolism on the levels of citric acid cycle intermediates. *J Biol Chem* 241(17): 3997-4003.
- Goldfarb W, Wortis J. 1941. Availability of sodium pyruvate for human brain oxidations. *Proc Soc Exp Biol Med* 46: 121-123.
- Gotoh J, Itoh Y, Kuang TY, Cook M, Law MJ, et al. 2000. Negligible glucose-6-phosphatase activity in cultured astroglia. *J Neurochem* 74(4): 1400-1408.
- Gruetter R. 2003. Glycogen: The forgotten cerebral energy store. *J Neurosci Res* 74(2): 179-183.
- Guth L, Watson PK. 1968. A correlated histochemical and quantitative study on cerebral glycogen after brain injury in the rat. *Exp Neurol* 22(4): 590-602.
- Guzman M, Blazquez C. 2001. Is there an astrocyte-neuron ketone body shuttle? *Trends Endocrinol Metab* 12(4): 169-173.
- Halestrap AP. 1975. The mitochondrial pyruvate carrier. Kinetics and specificity for substrates and inhibitors. *Biochem J* 148: 85-96.
- Halestrap AP, Denton RM. 1974. Specific inhibition of pyruvate transport in rat liver mitochondria and human erythrocytes by cyano-4-hydroxycinnamate. *Biochem J* 138: 313-316.
- Hambraeus L. 1977. Proprietary milk versus human breast milk in infant feeding. A critical appraisal from the nutritional point of view. *Pediatr Clin North Am* 24(1): 17-36.
- Hanstock CC, Rothman DL, Prichard JW, Jue T, Shulman RG. 1988. Spatially localized ¹H NMR spectra of metabolites in the human brain. *Proc Natl Acad Sci USA* 85(6): 1821-1825.
- Harik SI, Busto R, Martinez E. 1982. Norepinephrine regulation of cerebral glycogen utilization during seizures and ischemia. *J Neurosci* 2(4): 409-414.
- Harris RA, Huang B, Wu P. 2001. Control of pyruvate dehydrogenase kinase gene expression. *Adv Enzyme Regul* 41: 269-288.
- Hassel B. 2001. Pyruvate carboxylation in neurons. *J Neurosci Res* 66(5): 755-762.
- Hassel B, Bråthe A. 2000. Cerebral metabolism of lactate in vivo: Evidence for neuronal pyruvate carboxylation. *J Cereb Blood Flow Metab* 20(2): 327-336.
- Hasselbalch SG, Knudsen GM, Jakobsen J, Hageman LP, Holm S, et al. 1994. Brain metabolism during short-term starvation in humans. *J Cereb Blood Flow Metab* 14(1): 125-131.
- Hasselbalch SG, Knudsen GM, Jakobsen J, Hageman LP, Holm S, et al. 1995. Blood-brain barrier permeability of glucose and ketone bodies during short-term starvation in humans. *Am J Physiol* 268(6 Pt 1): E1161-E1166.
- Hawkins M, Gabriely I, Wozniak R, Vilcu C, Shamoon H, et al. 2002. Fructose improves the ability of hyperglycemia per se to regulate glucose production in type 2 diabetes. *Diabetes* 51(3): 606-614.
- Hawkins RA, Miller AL, Nielsen RC, Veech RL. 1973. The acute action of ammonia on rat brain metabolism in vivo. *Biochem J* 134(4): 1001-1008.
- Hawkins RA, Williamson DH, Krebs HA. 1971. Ketone-body utilization by adult and suckling rat brain in vivo. *Biochem J* 122(1): 13-18.
- Hertz L. 2004. The astrocyte-neuron lactate shuttle: A challenge of a challenge. *J Cereb Blood Flow Metab* 24(11): 1241-1248.
- Hertz L, Dienel GA. 2002. Energy metabolism in the brain. *Int Rev Neurobiol* 51: 1-102.
- Hertz L, Dienel GA. 2004. Lactate transport and transporters: General principles and functional roles in brain cells. *J Neurosci Res* 79(1-2): 11-18.
- Hertz L, Dringen R, Schousboe A, Robinson SR. 1999. Astrocytes: Glutamate producers for neurons. 1999. *J Neurosci Res* 57(4): 417-428.
- Hertz L, Hertz E. 2003. Cataplerotic TCA cycle flux determined as glutamate-sustained oxygen consumption in primary cultures of astrocytes. *Neurochem Int* 43(4-5): 355-361.
- Hertz L, Peng L, Kjeldsen CC, O'Dowd BS, Dienel GA. 2004. Ion, transmitter and drug effects on energy metabolism in astrocytes. *Advances in molecular and cell biology: Non-neuronal cells of the nervous system: Function and dysfunction*. Hertz L, editor. New York: Elsevier; Vol 31-II, pp. 435-460.
- Hertz L, Peng L, Lai JC. 1998. Functional studies in cultured astrocytes. *Methods* 16(3): 293-310.
- Hertz L, Yu AC, Kala G, Schousboe A. 2000. Neuronal-astrocytic and cytosolic-mitochondrial metabolite trafficking during brain activation, hyperammonemia and energy deprivation. *Neurochem Int* 37(2-3): 83-102.
- Hertz L, Yu AC, Schousboe A. 1992. Uptake and metabolism of malate in neurons and astrocytes in primary cultures. *J Neurosci Res* 33(2): 289-296.
- Hevor TK, Delorme P, Beauvillain JC. 1986. Glycogen synthesis and immunocytochemical study of fructose-1,6-bisphosphatase in methionine sulfoximine epileptogenic rodent brain. *J Cereb Blood Flow Metab* 6(3): 292-297.
- Hochachka PW, Mommsen TP. 1983. Protons and anaerobiosis. *Science* 219: 1391-1397.

- Hodgkins PS, Schwarcz R. 1998. Interference with cellular energy metabolism reduces kynurenic acid formation in rat brain slices: Reversal by lactate and pyruvate. *Eur J Neurosci* 10(6): 1986-1994.
- Hu YB, Wilson GS. 1997a. A temporary local energy pool coupled to neuronal activity: Fluctuations of extracellular lactate levels in rat brain monitored with rapid-response enzyme-based sensor. *J Neurochem* 69(4): 1484-1490.
- Hu YB, Wilson GS. 1997b. Rapid changes in local extracellular rat brain glucose observed with an in vivo glucose sensor. *J Neurochem* 68(4): 1745-1752.
- Huang B, Wu P, Popov KM, Harris RA. 2003. Starvation and diabetes reduce the amount of pyruvate dehydrogenase phosphatase in rat heart and kidney. *Diabetes* 52(6): 1371-1376.
- Huang R, Hertz L. 1995. Noradrenaline-induced stimulation of glutamine metabolism in primary cultures of astrocytes. *J Neurosci Res* 41(5): 677-683.
- Huang R, Peng L, Chen Y, Hajek I, Zhao Z, et al. 1994. Signalling effect of elevated potassium concentrations and monoamines on brain energy metabolism at the cellular level. *Dev Neurosci* 16(5-6): 337-351.
- Ibrahim MZ. 1975. Glycogen and its related enzymes of metabolism in the central nervous system. *Adv Anat Embryol Cell Biol* 52: 3-89.
- Ide K, Schmalruch IK, Quistorff B, Horn A, Secher NH. 2000. Lactate, glucose and O₂ uptake in human brain during recovery from maximal exercise. *J Physiol (Lond)* 522: 159-164.
- Ide T, Steinke J, Cahill GF Jr. 1969. Metabolic interactions of glucose, lactate, and beta-hydroxybutyrate in rat brain slices. *Am J Physiol* 217(3): 784-792.
- Ito M, Fukui T, Saito T, Tomita K. 1986. Acetoacetyl-CoA synthetase specific activity and concentration in rat tissues. *Biochim Biophys Acta* 876(2): 280-287.
- Itoh Y, Esaki T, Shimoji K, Cook M, Law MJ, et al. 2003. Dichloroacetate effects on glucose and lactate oxidation by neurons and astroglia in vitro and on glucose utilization by brain in vivo. *Proc Natl Acad Sci USA* 100(8): 4879-4884.
- Izumi Y, Benz AM, Katsuki H, Matsukawa M, Clifford DB, et al. 2003. Effects of fructose-1,6-bisphosphate on morphological and functional neuronal integrity in rat hippocampal slices during energy deprivation. *Neuroscience* 116(2): 465-475.
- Izumi Y, Benz AM, Zorumski CF, Olney JW. 1994. Effects of lactate and pyruvate on glucose deprivation in rat hippocampal slices. *Neuroreport* 5(5): 617-620.
- Izumi Y, Ishii K, Katsuki H, Benz AM, Zorumski CF. 1998. β -Hydroxybutyrate fuels synaptic function during development. Histological and physiological evidence in rat hippocampal slices. *J Clin Invest* 101(5): 1121-1132.
- Izumi Y, Katsuki H, Zorumski CF. 1997. Monocarboxylates (pyruvate and lactate) as alternative energy substrates for the induction of long-term potentiation in rat hippocampal slices. *Neurosci Lett* 232(1): 17-20.
- Kanatani T, Mizuno K, Okada Y. 1995. Effects of glycolytic metabolites on preservation of high energy phosphate level and synaptic transmission in the granule cells of guinea pig hippocampal slices. *Experientia* 51(3): 213-216.
- Kandel ER, Schwartz JH, Jessell TM, editors. 2000. Principles of neural science. New York: McGraw-Hill.
- Kao-Jen J, Wilson JE. 1980. Localization of hexokinase in neural tissue: Electron microscopic studies of rat cerebellar cortex. *J Neurochem* 35(3): 667-678.
- Karnovsky ML, Burrows BL, Zoccoli MA. 1980. Cerebral glucose-6-phosphatase and the movement of 2-deoxyglucose during slow wave sleep. Cerebral metabolism and neural function. Passonneau JV, Hawkins RA, Lust WD, Welsh FA, editors. Baltimore: Williams & Wilkins; chap. 39, pp. 359-366.
- Karnovsky ML, Reich P, Anchors JM, Burrows BL. 1983. Changes in brain glycogen during slow-wave sleep in the rat. *J Neurochem* 41(5): 1498-1501.
- Katoh-Semba R, Keino H, Kashiwamata S. 1988. A possible contribution by glial cells to neuronal energy production: Enzyme-histochemical studies in the developing rat cerebellum. *Cell Tissue Res* 252(1): 133-139.
- Kelleher JA, Chan PH, Chan TYY, Gregory GA. 1995. Energy metabolism in hypoxic astrocytes: Protective mechanism of fructose-1,6-bisphosphate. *Neurochem Res* 20(7): 785-792.
- Kelleher JA, Chan TYY, Chan PH, Gregory GA. 1996. Protection of astrocytes by fructose 1,6-bisphosphate and citrate ameliorates neuronal injury under hypoxic conditions. *Brain Res* 726(1-2): 167-173.
- King P, Kong MF, Parkin H, Macdonald IA, Barber C, et al. 1998. Intravenous lactate prevents cerebral dysfunction during hypoglycaemia in insulin-dependent diabetes mellitus. *Clin Sci* 94(2): 157-163.
- King P, Parkin H, Macdonald IA, Barber C, Tattersall, RB. 1997. The effect of intravenous lactate on cerebral function during hypoglycaemia. *Diabet Med* 14(1): 19-28.
- Kintner D, Fitzpatrick JH Jr, Louie JA, Gilboe DD. 1983. Cerebral glucose metabolism during 30 minutes of moderate hypoxia and reoxygenation. *Am J Physiol* 245(4): E365-E372.
- Klepper J, Diefenbach S, Kohlschutter A, Voit T. 2004. Effects of the ketogenic diet in the glucose transporter 1 deficiency syndrome. *Prostaglandins Leukot Essent Fatty Acids* 70(3): 321-327.
- Kogure K, Scheinberg P, Utsunomiya Y, Kishikawa H, Busto R. 1977. Sequential cerebral biochemical and physiological events in controlled hypoxemia. *Ann Neurol* 2(4): 304-310.

- Koizumi J, Shiraishi H. 1970. Ultrastructural appearance of glycogen in the hypothalamus of the rabbit following chlorpromazine administration. *Exp Brain Res* 10(3): 276-282.
- Kong J, Shepel PN, Holden CP, Mackiewicz M, Pack AI, et al. 2002. Brain glycogen decreases with increased periods of wakefulness: Implications for homeostatic drive to sleep. *J Neurosci* 22(13): 5581-5587.
- Korf J. 1996. Intracerebral trafficking of lactate in vivo during stress, exercise, electroconvulsive shock and ischemia as studied with microdialysis. *Dev Neurosci* 18(5-6): 405-414.
- Krebs HA, Williamson DH, Bates MW, Page MA, Hawkins RA. 1971. The role of ketone bodies in caloric homeostasis. *Adv Enzyme Regul* 9: 387-409.
- Kruse T, Reiber H, Neuhoff V. 1985. Amino acid transport across the human blood-CSF barrier. An evaluation graph for amino acid concentrations in cerebrospinal fluid. *J Neurol Sci* 70(2): 129-138.
- Kuhr WG, Korf J. 1988. Extracellular lactic acid as an indicator of brain metabolism: Continuous on-line measurement in conscious, freely moving rats with intrastriatal dialysis. *J Cereb Blood Flow Metab* 8(1): 130-137.
- Lai JC, Sheu KF. 1987. The effect of 2-oxoglutarate or 3-hydroxybutyrate on pyruvate dehydrogenase complex in isolated cerebocortical mitochondria. *Neurochem Res* 12(8): 715-722.
- Lee WJ, Hawkins RA, Vina JR, Peterson DR. 1998. Glutamine transport by the blood-brain barrier: A possible mechanism for nitrogen removal. *Am J Physiol* 274(4 Pt 1): C1101-C11107.
- Leegsma-Vogt G, Venema K, Korf J. 2003. Evidence for a lactate pool in the rat brain that is not used as an energy supply under normoglycemic conditions. *J Cereb Blood Flow Metab* 23(8): 933-941.
- Leegsma-Vogt G, Venema K, Postema F, Korf J. 2001. Monitoring arterio-venous differences of glucose and lactate in the anesthetized rat with or without brain damage with ultrafiltration and biosensor technology. *J Neurosci Res* 66(5): 795-802.
- Lehninger AL, Nelson DL, Cox MM. 1993. Principles of biochemistry. New York: Worth Publishers.
- Leino RL, Gerhart DZ, Drewes LR. 1999. Monocarboxylate transporter (MCT1) abundance in brains of suckling and adult rats: A quantitative electron microscopic immunogold study. *Brain Res Dev Brain Res* 113(1-2): 47-54.
- Leino RL, Gerhart DZ, Duelli R, Enerson BE, Drewes LR. 2001. Diet-induced ketosis increases monocarboxylate transporter (MCT1) levels in rat brain. *Neurochem Int* 38(6): 519-527.
- Leino RL, Gerhart DZ, Van Bueren AM, McCall AL, Drewes LR. 1997. Ultrastructural localization of GLUT 1 and GLUT 3 glucose transporters in rat brain. *J Neurosci Res* 49(5): 617-626.
- Leong SF, Lai JC, Lim L, Clark JB. 1981. Energy-metabolising enzymes in brain regions of adult and aging rats. *J Neurochem* 37(6): 1548-1556.
- Löffler T, Al-Robaiy S, Bigl M, Eschrich K, Schliebs R. 2001. Expression of fructose-1,6-bisphosphatase mRNA isoforms in normal and basal forebrain cholinergic lesioned rat brain. *Int J Dev Neurosci* 19(3): 279-285.
- Lopes-Cardozo M, Klein W. 1982. Ketone-body utilization by homogenates of adult rat brain. *Neurochem Res* 7(6): 687-703.
- Lopes-Cardozo M, Larsson OM, Schousboe A. 1986. Acetoacetate and glucose as lipid precursors and energy substrates in primary cultures of astrocytes and neurons from mouse cerebral cortex. *J Neurochem* 46(3): 773-778.
- Madsen PL, Cruz NF, Sokoloff L, Dienel GA. 1999. Cerebral oxygen/glucose ratio is low during sensory stimulation and rises above normal during recovery: Excess glucose consumption during stimulation is not accounted for by lactate efflux from or accumulation in brain tissue. *J Cereb Blood Flow Metab* 19(4): 393-400.
- Magistretti PJ. 1999. Brain energy metabolism. Fundamental neuroscience. Zigmond MJ, Bloom FE, Landis SC, Roberts JL, Squire LR, editors. New York: Academic Press; chap. 14, pp. 389-413.
- Magistretti PJ. 2000. Cellular bases of functional brain imaging: Insights from neuron-glia metabolic coupling. *Brain Res* 886(1-2): 108-112.
- Magistretti PJ, Pellerin L, Rothman DL, Shulman, RG. 1999. Energy on demand. *Science* 283(5401): 496-497.
- Maher F, Davies-Hill TM, Simpson IA. 1996. Substrate specificity and kinetic parameters of GLUT3 in rat cerebellar granule neurons. *Biochem J* 315(Part 3): 827-831.
- Maran A, Crepaldi C, Trupiani S, Lucca T, Jori E, et al. 2000. Brain function rescue effect of lactate following hypoglycaemia is not an adaptation process in both normal and type I diabetic subjects. *Diabetologia* 43(6): 733-741.
- Markov AK. 1986. Hemodynamics and metabolic effects of fructose 1-6 diphosphate in ischemia and shock—experimental and clinical observations. *Ann Emerg Med* 15(12): 1470-1477.
- Massieu L, Haces ML, Montiel T, Hernandez-Fonseca K. 2003. Acetoacetate protects hippocampal neurons against glutamate-mediated neuronal damage during glycolysis inhibition. *Neuroscience* 120(2): 365-378.
- McCall AL, Van Bueren AM, Moholt-Siebert M, Cherry NJ, Woodward WR. 1994. Immunohistochemical localization of the neuron-specific glucose transporter (GLUT3) to neuropil in adult rat brain. *Brain Res* 659(1-2): 292-297.
- McIlwain H. 1953. Glucose level, metabolism, and response to electrical impulses in cerebral tissues from man and laboratory animals. *Biochem J* 55: 618-624.

- McIlwain H, Bachelard HS. 1985. *Biochemistry and the central nervous system*. New York: Churchill Livingstone.
- McKenna MC, Tildon JT, Stevenson JH, Boatright R, Huang S. 1993. Regulation of energy metabolism in synaptic terminals and cultured rat brain astrocytes: Differences revealed using aminooxyacetate. *Dev Neurosci* 15(3–5): 320-329.
- McKenna MC, Tildon JT, Stevenson JH, Hopkins IB. 1994. Energy metabolism in cortical synaptic terminals from weanling and mature rat brain: Evidence for multiple compartments of tricarboxylic acid cycle activity. *Dev Neurosci* 16(5–6): 291-300.
- Medina JM, Taberero A. 2005. Lactate utilization by brain cells and its role in CNS development. *J Neurosci Res* 79(1–2): 2-10.
- Middleton B. 1973. The acetoacetyl-coenzyme A thiolases of rat brain and their relative activities during postnatal development. *Biochem J* 132(4): 731-737.
- Miller AL, Kiney CA, Corddry DH, Staton DM. 1982. Interactions between glucose and ketone body use by developing brain. *Brain Res* 256(4): 443-450.
- Moore TJ, Lione AP, Sugden MC, Regen DM. 1976. Beta-hydroxybutyrate transport in rat brain: Developmental and dietary modulations. *Am J Physiol* 230(3): 619-630.
- Nehlig A, Pereira A, de Vasconcelos. 1993. Glucose and ketone body utilization by the brain of neonatal rats. *Prog Neurobiol* 40(2): 163-221.
- Nelson SR, Schulz DW, Passonneau JV, Lowry OH. 1968. Control of glycogen levels in brain. *J Neurochem* 15(11): 1271-1279.
- Nelson T, Lucignani G, Atlas S, Crane AM, Dienel GA, et al. 1985. Reexamination of glucose-6-phosphatase activity in the brain in vivo: No evidence for a futile cycle. *Science* 229(4708): 60-62.
- Nitisewojo P, Hultin HO. 1976. A comparison of some kinetic properties of soluble and bound lactate dehydrogenase isoenzymes at different temperatures. *Eur J Biochem* 67: 87-94.
- O’Kane RL, Hawkins RA. 2003. Na⁺-dependent transport of large neutral amino acids occurs at the abluminal membrane of the blood–brain barrier. *Am J Physiol Endocrinol Metab* 285(6): E1167-E1173.
- Oldendorf WH. 1973. Carrier-mediated blood–brain barrier transport of short-chain monocarboxylic organic acids. *Am J Physiol* 224(6): 1450-1453.
- Owen OE, Morgan AP, Kemp HG, Sullivan JM, Herrera MG, et al. 1967. Brain metabolism during fasting. *J Clin Invest* 46(10): 1589-1595.
- Owen OE, Reichard GA Jr. 1971. Human forearm metabolism during progressive starvation. *J Clin Invest* 50(7): 1536-1545.
- Page MA, Krebs HA, Williamson DH. 1971. Activities of enzymes of ketone-body utilization in brain and other tissues of suckling rats. *Biochem J* 121(1): 49-53.
- Pan JW, Rothman TL, Behar KL, Stein DT, Hetherington HP. 2000. Human brain beta-hydroxybutyrate and lactate increase in fasting-induced ketosis. *J Cereb Blood Flow Metab* 20(10): 1502-1507.
- Pan JW, Telang FW, Lee JH, de Graaf RA, Rothman DL, et al. 2001. Measurement of beta-hydroxybutyrate in acute hyperketonemia in human brain. *J Neurochem* 79(3): 539-544.
- Panneerselvam K, Freeze HH. 1996. Mannose enters mammalian cells using a specific transporter that is insensitive to glucose. *J Biol Chem* 271(16): 9417-9421.
- Papa S, Paradies G. 1974. On the mechanism of translocation of pyruvate and other monocarboxylic acids in rat-liver mitochondria. *Eur J Biochem* 49(1): 265-274.
- Paradies G, Papa S. 1977. On the kinetics and substrate specificity of the pyruvate translocator in rat liver mitochondria. *Biochim Biophys Acta* 462(2): 333-346.
- Pardridge WM. 1983. Brain metabolism: A perspective from the blood–brain barrier. *Physiol Rev* 63(4): 1481-1535.
- Pardridge WM. 1991. Blood–brain barrier transport of glucose, free fatty acids, and ketone bodies. *Adv Exp Med Biol* 291: 43-53.
- Patel MS. 1977. Age-dependent changes in the oxidative metabolism in rat brain. *J Gerontol* 32(6): 643-646.
- Patel MS, Korotchikina LG. 2003. The biochemistry of the pyruvate dehydrogenase complex. *Biochem Mol Biol Edu, Miniseries: Modern Metabolic Concepts* 31(1): 5-15.
- Patel MS, Owen OE. 1977. Development and regulation of lipid synthesis from ketone bodies by rat brain. *J Neurochem* 28(1): 109-114.
- Paul RJ, Bauer M, Pease W. 1979. Vascular smooth muscle: Aerobic glycolysis linked to sodium and potassium transport processes. *Science* 206(4425): 1414-1416.
- Pellerin L, Halestrap AP, Pierre K. 2005. Cellular and subcellular distribution of monocarboxylate transporters in cultured brain cells and in the adult brain. *J Neurosci Res* 79(1–2): 55-64.
- Pellerin L, Magistretti PJ. 1994. Glutamate uptake into astrocytes stimulates aerobic glycolysis: A mechanism coupling neuronal activity to glucose utilization. *Proc Natl Acad Sci USA* 91(22): 10625-10629.
- Pellerin L, Magistretti PJ. 2003. Food for thought: Challenging the dogmas. *J Cereb Blood Flow Metab* 23(11): 1282-1286.
- Pellerin L, Pellegrini G, Martin JL, Magistretti PJ. 1998. Expression of monocarboxylate transporter mRNAs in mouse brain: Support for a distinct role of lactate as an energy substrate for the neonatal vs. Adult brain. *Proc Natl Acad Sci USA* 95(7): 3990-3995.

- Peng L, Zhang X, Hertz L. 1994a. Alteration in oxidative metabolism of alanine in cerebellar granule cell cultures as a consequence of the development of the ability to utilize alanine as an amino group donor for synthesis of transmitter glutamate. *Brain Res Dev Brain Res* 79(1): 128-131.
- Peng L, Zhang X, Hertz L. 1994b. High extracellular potassium concentrations stimulate oxidative metabolism in a glutamatergic neuronal culture and glycolysis in cultured astrocytes but have no stimulatory effect in a GABAergic neuronal culture. *Brain Res* 663(1): 168-172.
- Pereira de Vasconcelos A, Schroeder H, Nehlig A. 1987. Effects of early chronic phenobarbital treatment on the maturation of energy metabolism in the developing rat brain. II. Incorporation of beta-hydroxybutyrate into amino acids. *Brain Res* 433(2): 231-236.
- Pesce A, Fondt TP, Stolzenbach F, Castillo F, Kaplan NO. 1967. The comparative enzymology of lactic dehydrogenases. *J Biol Chem* 242(9): 2151-2167.
- Pfeiffer B, Meyermann R, Hamprecht B. 1992. Immunohistochemical co-localization of glycogen phosphorylase with the astroglial markers glial fibrillary acidic protein and S-100 protein in rat brain sections. *Histochemistry* 97(5): 405-412.
- Pfeuffer J, Tkac I, Gruetter R. 2000. Extracellular-intracellular distribution of glucose and lactate in the rat brain assessed noninvasively by diffusion-weighted ^1H nuclear magnetic resonance spectroscopy in vivo. *J Cereb Blood Flow Metab* 20(4): 736-746.
- Pogozelski W, Arpaia N, Priore S. 2005. The metabolic effects of low-carbohydrate diets and incorporation into a biochemistry course. *Biochem Mol Biol Edu* 33(2): 91-100.
- Poity-Yamate CL, Poity S, Tsacopoulos M. 1995. Lactate released by Muller glial cells is metabolized by photoreceptors from mammalian retina. *J Neurosci* 15(7 Part 2): 5179-5191.
- Pritchard J, Rothman D, Novotny E, Petroff O, Kuwabara T, et al. 1991. Lactate rise detected by ^1H NMR in human visual cortex during physiologic stimulation. *Proc Natl Acad Sci USA* 88(13): 5829-5831.
- Proverbio F, Hoffman JF. 1977. Membrane compartmentalized ATP and its preferential use by Na, K-ATPase of human red cell ghosts. *J Gen Physiol* 69: 605-632.
- Rama Rao KV, Jayakumar AR, Norenberg MD. 2005. Differential response of glutamine in cultured neurons and astrocytes. *J Neurosci Res* 79(1-2): 193-199.
- Randle PJ. 1981. Phosphorylation-dephosphorylation cycles and the regulation of fuel selection in mammals. *Curr Top Cell Regul* 18: 107-129.
- Rapoport SI. 2003. In vivo approaches to quantifying and imaging brain arachidonic and docosahexaenoic acid metabolism. *J Pediatr* 143(4 Suppl): S26-S34.
- Rech VC, Feksa LR, Dutra-Filho CS, Wyse ATS, Wajner M, et al. 2002. Inhibition of the mitochondrial respiratory chain by alanine in rat cerebral cortex. *Metab Brain Dis* 17(3): 123-130.
- Reed LJ. 1981. Regulation of mammalian pyruvate dehydrogenase complex by a phosphorylation-dephosphorylation cycle. *Curr Top Cell Regul* 18: 95-106.
- Richter K, Hamprecht B, Scheich H. 1996. Ultrastructural localization of glycogen phosphorylase predominantly in astrocytes of the gerbil brain. *Glia* 17(4): 263-273.
- Roberts EL Jr. 1993. Glycolysis and recovery of potassium ion homeostasis and synaptic transmission in hippocampal slices after anoxia or stimulated potassium release. *Brain Res* 620(2): 251-258.
- Roberts EL Jr, Chih CP, Rosenthal M. 1997. Age-related changes in brain metabolism and vulnerability to anoxia. *Adv Exp Med Biol* 411: 83-89.
- Roberts EL Jr, Chih CP. 1995. Age-related alterations in energy metabolism contribute to the increased vulnerability of the aging brain to anoxic damage. *Brain Res* 678(1-2): 83-90.
- Roberts EL Jr, Chih C-P. 2004. A role for lactate released from astrocytes in energy production during neural activity? *Advances in molecular and cell biology: Non-neuronal cells of the nervous system: Function and dysfunction. Part II: Biochemistry, physiology and pharmacology.* Hertz L, editor. New York: Elsevier; vol. 31: chap. 17, pp. 391-407.
- Roberts EL Jr, He J, Chih CP. 1998. The influence of glucose on intracellular and extracellular pH in rat hippocampal slices during and after anoxia. *Brain Res* 783(1): 44-50.
- Roeder LM, Tildon JT, Holman DC. 1984a. Competition among oxidizable substrates in brains of young and adult rats. *Dissociated cells. Biochem J* 219(1): 131-135.
- Roeder LM, Tildon JT, Stevenson JH Jr. 1984b. Competition among oxidizable substrates in brains of young and adult rats. *Whole homogenates. Biochem J* 219(1): 125-130.
- Rothman DL, Sibson NR, Hyder F, Shen J, Behar KL, et al. 1999. In vivo nuclear magnetic resonance spectroscopy studies of the relationship between the glutamate-glutamine neurotransmitter cycle and functional neuroenergetics. *Philos Trans R Soc Lond B Biol Sci* 354(1387): 1165-1177.
- Ruderman NB, Ross PS, Berger M, Goodman MN. 1974. Regulation of glucose and ketone-body metabolism in brain of anaesthetized rats. *Biochem J* 138(1): 1-10.
- Sacks W, Sacks S, Brebbia DR, Fleischer A. 1982. Cerebral uptake of amino acids in human subjects and rhesus monkeys in vivo. *J Neurosci Res* 7(4): 431-436.
- Schmoll D, Fuhrmann E, Gebhardt R, Hamprecht B. 1995. Significant amounts of glycogen are synthesized from 3-carbon compounds in astroglial primary cultures from

- mice with participation of the mitochondrial phosphoenolpyruvate carboxykinase isoenzyme. *Eur J Biochem* 227(1–2): 308–315.
- Schousboe A, Westergaard N, Sonnewald U, Petersen SB, Huang R, et al. 1993. Glutamate and glutamine metabolism and compartmentation in astrocytes. *Dev Neurosci* 15(3–5): 359–366.
- Schousboe A, Westergaard N, Waagepetersen HS, Larsson OM, Bakken IJ, et al. 1997. Trafficking between glia and neurons of TCA cycle intermediates and related metabolites. *Glia* 21(1): 99–105.
- Schurr A, West CA, Rigor BM. 1988. Lactate-supported synaptic function in the rat hippocampal slice preparation. *Science* 240(4857): 1326–1328.
- Selak I, Skaper SD, Varon S. 1985. Pyruvate participation in the low molecular weight trophic activity for central nervous system neurons in glia-conditioned media. *J Neurosci* 5(1): 23–28.
- Shank RP, Bennett GS, Freytag SO, Campbell GL. 1985. Pyruvate carboxylase: An astrocyte-specific enzyme implicated in the replenishment of amino acid neurotransmitter pools. *Brain Res* 329(1–2): 364–367.
- Shepherd GMG, Harris KM. 1998. Three-dimensional structure and composition of CA3-CA1 axons in rat hippocampal slices: Implications for presynaptic connectivity and compartmentalization. *J Neurosci* 18(20): 8300–8310.
- Shimizu N, Kumamoto T. 1952. Histochemical studies on the glycogen of the mammalian brain. *Anat Rec* 114(3): 479–497.
- Sibson NR, Dhankhar A, Mason GF, Rothman DL, Behar KL, et al. 1998. Stoichiometric coupling of brain glucose metabolism and glutamatergic neuronal activity. *Proc Natl Acad Sci USA* 95(1): 316–321.
- Silver IA, Deas J, Erecinska M. 1997. Ion homeostasis in brain cells: Differences in intracellular ion responses to energy limitation between cultured neurons and glial cells. *Neuroscience* 78(2): 589–601.
- Silver IA, Erecinska M. 1994. Extracellular glucose concentration in mammalian brain: Continuous monitoring of changes during increased neuronal activity and upon limitation in oxygen supply in normo-, hypo-, and hyperglycemic animals. *J Neurosci* 14(8): 5068–5076.
- Simurda M, Wilson JE. 1980. Localization of hexokinase in neural tissue: Immunofluorescence studies on the developing cerebellum and retina of the rat. *J Neurochem* 35(1): 58–66.
- Sloviter HA. 1982. Metabolic studies with an isolated, perfused rat brain preparation. *Isr J Med Sci* 18(1): 59–66.
- Snyder CD, Wilson JE. 1983. Relative levels of hexokinase in isolated neuronal, astrocytic, and oligodendroglial fractions from rat brain. *J Neurochem* 40(4): 1178–1181.
- Sols A, Crane RK. 1954. Substrate specificity of brain hexokinase. *J Biol Chem* 210(2): 581–595.
- Sorra KE, Harris KM. 2000. Overview on the structure, composition, function, development, and plasticity of thippocampal dendritic spines. *Hippocampus* 10(5): 501–511.
- Stambaugh R, Post D. 1966. Substrate and product inhibition of rabbit muscle lactic dehydrogenase heart (H₄) and muscle (M₄) isozymes. *J Biol Chem* 241(7): 1462–1467.
- Suarez I, Bodega G, Fernandez B. 2002. Glutamine synthetase in brain: Effect of ammonia. *Neurochem Int* 41(2–3): 123–142.
- Swanson RA. 1992. Physiologic coupling of glial glycogen metabolism to neuronal activity in brain *Can J Physiol Pharmacol* 70(Suppl): S138–S144.
- Swanson RA, Choi DW. 1993. Glial glycogen stores affect neuronal survival during glucose deprivation in vitro. *J Cereb Blood Flow Metab* 13(1): 162–169.
- Swiatek KR, Dombrowski GJ Jr, Chao KL. 1984. The metabolism of D- and L-3-hydroxybutyrate in developing rat brain. *Biochem Med* 31(3): 332–346.
- Takata T, Okada Y. 1995. Effects of deprivation of oxygen or glucose on the neural activity in the guinea pig hippocampal slice—intracellular recording study of pyramidal neurons. *Brain Res* 683(1): 109–116.
- Takata T, Sakurai T, Yang B, Yokono K, Okada Y. 2001. Effect of lactate on the synaptic potential, energy metabolism, calcium homeostasis and extracellular glutamate concentration in the dentate gyrus of the hippocampus from guinea-pig. *Neuroscience* 104(2): 371–378.
- Tholey G, Roth-Schechter BF, Mandel P. 1981. Activity and isoenzyme pattern of lactate dehydrogenase in neurons and astroblasts cultured from brains of chick embryos. *J Neurochem* 36(1): 77–81.
- Tildon JT, Merrill S, Roeder LM. 1983. Differential substrate oxidation by dissociated brain cells and homogenates during development. *Biochem J* 216(1): 21–25.
- Tsacopoulos M, Magistretti PJ. 1996. Metabolic coupling between glia and neurons. *J Neurosci* 16(3): 877–885.
- Vannucci RC, Duffy TE. 1974. Influence of birth on carbohydrate and energy metabolism in rat brain. *Am J Physiol* 226(4): 933–940.
- Vannucci SJ, Simpson IA. 2003. Developmental switch in brain nutrient transporter expression in the rat. *Am J Physiol Endocrinol Metab* 285(5): E1127–E1134.
- Vexler ZS, Wong A, Francisco C, Manabat C, Christen S, et al. 2003. Fructose-1,6-bisphosphate preserves intracellular glutathione and protects cortical neurons against oxidative stress. *Brain Res* 960(1–2): 90–98.
- Vicario C, Arizmendi C, Malloch G, Clark JB, Medina JM. 1991. Lactate utilization by isolated cells from early neonatal rat brain. *J Neurochem* 57(5): 1700–1707.

- Vicario C, Taberero A, Medina JM. 1993. Regulation of lactate metabolism by albumin in rat neurons and astrocytes from primary culture. *Pediatr Res* 34(6): 709-715.
- Waagepetersen HS, Qu H, Schousboe A, Sonnewald U. 2001. Elucidation of the quantitative significance of pyruvate carboxylation in cultured cerebellar neurons and astrocytes. *J Neurosci Res* 66(5): 763-770.
- Waagepetersen HS, Sonnewald U, Larsson OM, Schousboe A. 2000. A possible role of alanine for ammonia transfer between astrocytes and glutamatergic neurons. *J Neurochem* 75(2): 471-479.
- Waagepetersen HS, Sonnewald U, Larsson OM, Schousboe A. 2001. Multiple compartments with different metabolic characteristics are involved in biosynthesis of intracellular and released glutamine and citrate in astrocytes. *Glia* 35(3): 246-252.
- Wada H, Okada Y, Nabetani M, Nakamura H. 1997. The effects of lactate and β -hydroxybutyrate on the energy metabolism and neural activity of hippocampal slices from adult and immature rat. *Dev Brain Res* 101(1-2): 1-7.
- Wada H, Okada Y, Uzuo T, Nakamura H. 1998. The effects of glucose, mannose, fructose and lactate on the preservation of neural activity in the hippocampal slices from the guinea pig. *Brain Res* 788(1-2): 144-150.
- Wagner SR, Lanier WL. 1994. Metabolism of glucose, glycogen, and high-energy phosphates during complete cerebral ischemia: A comparison of normoglycemic, chronically hyperglycemic diabetic, and acutely hyperglycemic nondiabetic rats. *Anesthesiology* 81(6): 1516-1526.
- Wahren J, Ekberg K, Fernqvist-Forbes E, Nair S. 1999. Brain substrate utilisation during acute hypoglycaemia. *Diabetologia* 42(7): 812-818.
- Walz W, Mukerji S. 1988. Lactate release from cultured astrocytes and neurons: A comparison. *Glia* 1: 366-370.
- Wender R, Brown AM, Fern R, Swanson RA, Farrell K, et al. 2000. Astrocytic glycogen influences axon function and survival during glucose deprivation in central white matter. *J Neurosci* 20(18): 6804-6810.
- Westergaard N, Sonnewald U, Unsgard G, Peng L, Hertz L, et al. 1994. Uptake, release, and metabolism of citrate in neurons and astrocytes in primary cultures. *J Neurochem* 62(5): 1727-1733.
- Westergaard N, Varming T, Peng L, Sonnewald U, Hertz L, et al. 1993. Uptake, release, and metabolism of alanine in neurons and astrocytes in primary cultures. *J Neurosci Res* 35(5): 540-545.
- Wieland O, Siess E, Schulze-Wethmar FH, von Funcke HG, Winton B. 1971. Active and inactive forms of pyruvate dehydrogenase in rat heart and kidney: Effect of diabetes, fasting, and refeeding on pyruvate dehydrogenase interconversion. *Arch Biochem Biophys* 143(2): 593-601.
- Wiesinger H, Hamprecht B, Dringen R. 1997. Metabolic pathways for glucose in astrocytes. *Glia* 21(1): 22-34.
- Winkler BS. 1981. Glycolysis and oxidative metabolism in relation to retinal function. *J Gen Physiol* 77: 667-692.
- Winkler BS, Arnold MJ, Brassell MA, Puro DG. 2000. Energy metabolism in human retinal Müller cells. *Invest Ophthalmol Vis Sci* 41(10): 3183-3190.
- Winkler BS, Starnes CA, Sauer MW, Firouzgan Z, S-C. Chen. 2004. Cultured retinal neuronal cells and Müller cells both show net production of lactate. *Neurochem Int* 45(2-3): 311-320.
- Wolfe RR. 1990. Isotopic measurement of glucose and lactate kinetics. *Ann Med* 22(3): 163-170.
- Wolfe RR, Jahoor F, Miyoshi H. 1988. Evaluation of the isotopic equilibration between lactate and pyruvate. *Am J Physiol* 254(4 Pt 1): E532-E535.
- Wu K, Aoki C, Elste A, Rogalski-Wilk AA, Siekevitz P. 1997. The synthesis of ATP by glycolytic enzymes in the postsynaptic density and the effect of endogenously generated nitric oxide. *Proc Natl Acad Sci USA* 94(24): 13273-13278.
- Wu P, Blair P, Sato VJ, Jaskiewicz J, Popov KM, et al. 2000. Starvation increases the amount of pyruvate dehydrogenase kinase in several mammalian tissues. *Arch Biochem Biophys* 381(1): 1-7.
- Yamane K, Yokono K, Okada Y. 2000. Anaerobic glycolysis is crucial for the maintenance of neural activity in guinea pig hippocampal slices. *J Neurosci Methods* 103(2): 163-171.
- Yang B, Sakurai T, Takata T, Yokono K. 2003. Effects of lactate/pyruvate on synaptic plasticity in the hippocampal dentate gyrus. *Neurosci Res* 46(3): 333-337.
- Yeh YY, Zee P. 1976. Insulin, a possible regulator of ketosis in newborn and suckling rats. *Pediatr Res* 10(3): 192-197.
- Yu AC, Drejer J, Hertz L, Schousboe A. 1983. Pyruvate carboxylase activity in primary cultures of astrocytes and neurons. *J Neurochem* 41(5): 1484-1487.
- Zhang F, Vannucci SJ, Philp NJ, Simpson IA. 2005. Monocarboxylate transporter expression in the spontaneous hypertensive rat: Effect of stroke. *J Neurosci Res* 79(1-2): 139-145.
- Zielke HR, Collins RM, Jr, Baab PJ, Y, Huang Zielke CL, et al. 1998. Compartmentation of [^{14}C]glutamate and [^{14}C]glutamine oxidative metabolism in the rat hippocampus as determined by microdialysis. *J Neurochem* 71(3): 1315-1320.
- Zwingmann C, Richter-Landsberg C, Leibfritz D. 2001. ^{13}C isotopomer analysis of glucose and alanine metabolism reveals cytosolic pyruvate compartmentation as part of energy metabolism in astrocytes. *Glia* 34(3): 200-212.

Metabolic Specialization of Brain Cell Types and Compartmentation of Function

3.1 Anaplerosis

B. Hassel

1	<i>Definition and Function of Anaplerosis</i>	184
2	<i>Anaplerotic Carboxylation Reactions</i>	186
3	<i>Amino Acids as a Source of TCA Cycle Intermediates In Vivo and In Vitro</i>	187
4	<i>Is Anaplerosis Confined to a Specific Cell Type?</i>	188
5	<i>Cataplerotic Decarboxylation: Glial or Neuronal? Pyruvate Recycling</i>	189
6	<i>Estimates of Pyruvate Carboxylation in the Brain</i>	189
7	<i>Mechanisms that Counteract Loss of TCA Cycle Intermediates in Glutamatergic and GABAergic Neurotransmission: Reuptake and the Glutamine Cycle</i>	190
8	<i>The Lack of Data on the Ultrastructural Localization of Anaplerotic Enzymes</i>	191
9	<i>Clinical Aspects of Anaplerosis: Deficiency of Anaplerotic Enzymes</i>	191
10	<i>Anaplerosis and Brain Tumors</i>	192

Abstract: Several biochemical reactions in the brain, such as the formation of glutamine or transmitter glutamate and GABA, imply that the tricarboxylic acid (TCA) cycle is drained of intermediates, especially α -ketoglutarate. Anaplerosis, which compensates for this drain, is the formation of TCA cycle intermediates from precursors that are not TCA cycle intermediates themselves. In the brain, anaplerosis occurs through two types of reactions: In the first, pyruvate reacts with CO_2 or HCO_3^- to form TCA cycle intermediates malate or oxaloacetate, so-called pyruvate carboxylation; in the second type of reaction, TCA cycle intermediates are formed from amino acids. Because there is no net fixation of CO_2 in the brain and because the export of derivatives of TCA cycle intermediates from the brain to the circulation is very small, it follows that anaplerosis must be balanced by cataplerosis, such as decarboxylation of malate or oxaloacetate. Different cell types may differ in their anaplerotic and cataplerotic reactions. Anaplerosis is important for cerebral energy production, NH_3 removal, and glutamatergic and GABAergic neurotransmission.

List of Abbreviations: NMRS, nuclear magnetic resonance spectroscopy; PEPCK, phosphoenolpyruvate carboxykinase; TCA cycle, tricarboxylic acid cycle

1 Definition and Function of Anaplerosis

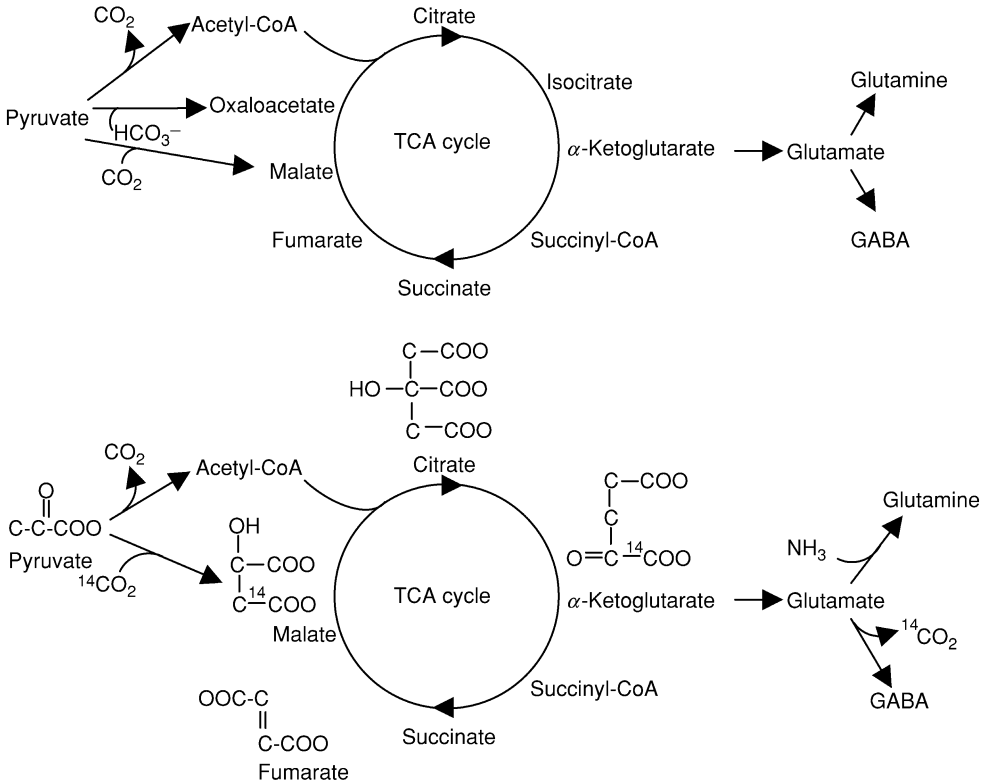
Anaplerosis is the synthesis of tricarboxylic acid (TCA) cycle intermediates from precursors that are not TCA cycle intermediates themselves; this is also termed “de novo” synthesis of TCA cycle intermediates. Anaplerosis (from Greek *αναπληρωσις*: “upfilling”) “fills up” the TCA cycle with intermediates. Anaplerotic reactions fall into two categories: carboxylation reactions and amino acid-metabolizing reactions. In the former, pyruvate or its derivative phosphoenolpyruvate reacts with CO_2 or HCO_3^- to form malate or oxaloacetate (▶ *Figure 3.1-1*). In the amino acid-metabolizing reactions, glucogenic amino acids (see below) are converted into TCA cycle intermediates (▶ *Figure 3.1-2*). Cellular uptake of TCA cycle intermediates from the extracellular fluid or from the circulation could also replenish the TCA cycle with intermediates; such uptake does not constitute synthesis, but may nevertheless be considered anaplerotic.

Anaplerotic reactions compensate for the loss of TCA cycle intermediates that occurs when such intermediates are diverted to cellular functions other than energy production. Loss of TCA cycle intermediates occurs when α -ketoglutarate is converted into glutamate and hence into GABA and used in neurotransmission or when glutamate in glial cells is converted into glutamine in the glutamine synthetase reaction. The latter reaction detoxifies free ammonia in the brain, and it forms part of the inactivation mechanism for transmitter glutamate. A small efflux of glutamine from the brain to the circulation has been documented (~ 10 nmol/g/min; Grill et al., 1992). The TCA cycle may lose citrate through the export of citrate to the extracellular fluid; this appears to occur primarily in astrocytes (Sonnewald et al., 1991). The TCA cycle loses malate through the malic enzyme reaction, which generates NADPH from the decarboxylation of malate to pyruvate, and it loses oxaloacetate and α -ketoglutarate, respectively, when aspartate and glutamate (or their derivatives) are consumed in the synthesis of peptides (e.g., glutathione: γ -glutamyl-cysteinyl-glycine) and proteins. The transmitter status of aspartate is uncertain, since it does not appear to be concentrated in synaptic vesicles; aspartate may, however, act as an excitatory neurotransmitter by leaving neurons from the cytosol through amino acid transporters or exchangers; such a release of aspartate would constitute a drain of oxaloacetate from the TCA cycle. Oxaloacetate is also lost through its decarboxylation to phosphoenolpyruvate in gluconeogenesis, which has been shown in astrocytes (Schmoll et al., 1995). A loss of oxaloacetate may be expected through its reaction with H_2O_2 , which leads to nonenzymatic decarboxylation and formation of malonate, CO_2 , and water (Desagher et al., 1997). Loss of intermediates from the TCA cycle may be called cataplerosis, although the strict meaning of this term (downfilling) seems to contradict itself.

The cyclic nature of the TCA cycle means that loss of an intermediate leads to the subsequent loss, not only of its downstream product but also of its precursor. If the loss of α -ketoglutarate inherent in glutamatergic neurotransmission is not compensated, there will be less succinyl-CoA, succinate, fumarate, etc., and eventually less isocitrate and α -ketoglutarate. An increase in the flux of acetyl-CoA into the cycle through pyruvate dehydrogenase will not replenish the pool of TCA cycle intermediates,

■ Figure 3.1-1

The relationship between the flux of pyruvate into the TCA cycle and efflux of α -ketoglutarate as glutamate, glutamine, or GABA. *Upper panel* shows decarboxylation of pyruvate to acetyl-CoA (by pyruvate dehydrogenase) and the carboxylation of pyruvate with HCO_3^- to oxaloacetate (by pyruvate carboxylase in astrocytes) and with CO_2 to malate (by malic enzyme). *Lower panel* shows the fate of $^{14}\text{CO}_2$ fixed in the malic enzyme reaction. Note that the label is lost when glutamate is decarboxylated to GABA (by glutamic acid decarboxylase). Note also that if malate equilibrates with the symmetrical fumarate, half the label will be transferred to the first carbon position in malate and subsequently to the sixth position in citrate, which is subsequently lost in the decarboxylation of isocitrate to α -ketoglutarate



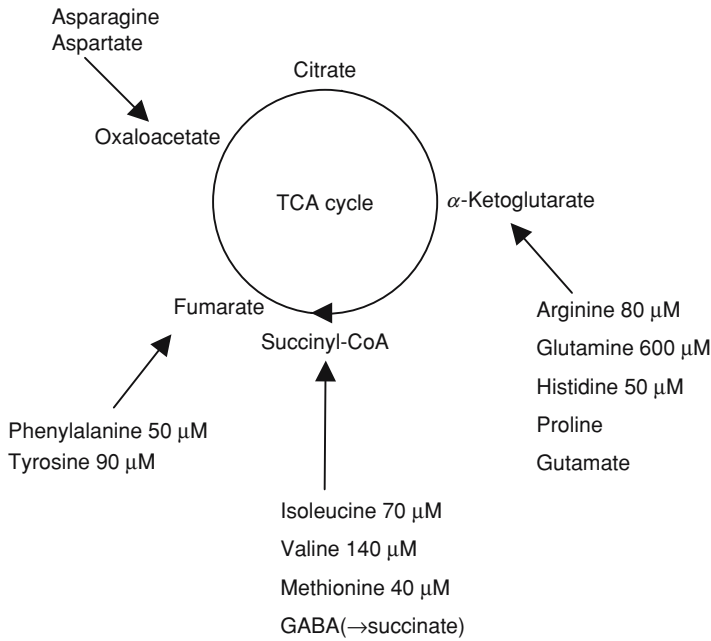
because acetyl-CoA needs to react with oxaloacetate, a downstream product of α -ketoglutarate, to form citrate (▶ *Figure 3.1-1*). However, anaplerosis does not necessarily mean the de novo formation of the same TCA cycle intermediate that is being lost; another intermediate may be the product. For instance, formation of malate or oxaloacetate through pyruvate carboxylation may compensate for the loss of α -ketoglutarate.

The TCA cycle also loses citrate through the citrate lyase reaction, which supplies cytosolic acetyl-CoA for the synthesis of fatty acids and acetylcholine; however, in this reaction, oxaloacetate is regenerated and may reenter mitochondria after conversion into malate. The citrate lyase reaction, therefore, does not necessarily require anaplerosis.

From the above it seems probable that diversion of intermediates from the TCA cycle to other cellular functions, such as synthesis of proteins and neurotransmitters, cannot occur without anaplerosis. Further, because TCA cycle activity is the major pathway for the generation of $\text{NADH} + \text{H}^+$ and FADH_2 , which form the basis for ATP production, anaplerosis is crucial for maintaining mitochondrial energy production during cataplerosis. We have to assume, however, that the concentration of TCA cycle intermediates in

■ Figure 3.1-2

Amino acids that may be metabolized into TCA cycle intermediates. Values are concentrations in plasma (Pardridge, 1983)



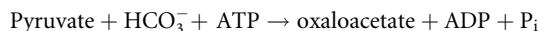
brain mitochondria is constant over time, so that anaplerosis equals cataplerosis. There is, for instance, no net CO_2 fixation in the brain; the O_2 consumption/ CO_2 production ratio is 1 (Sokoloff, 1989).

2 Anaplerotic Carboxylation Reactions

The principal anaplerotic carboxylation reactions in the brain are probably those that catalyze carboxylation of pyruvate to malate or oxaloacetate (► *Figure 3.1-1*). Carboxylation of phosphoenolpyruvate to oxaloacetate could also contribute to anaplerosis. In addition, carboxylation of propionyl-CoA is a step in the formation of the TCA cycle intermediate succinyl-CoA from isoleucine, valine, and methionine. Several nonanaplerotic carboxylation reactions also take place in the brain (see Hassel, 2000, for review).

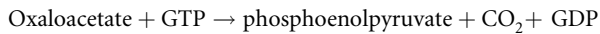
The three enzymes that have received most interest as anaplerotic carboxylating enzymes are pyruvate carboxylase, phosphoenolpyruvate carboxykinase (PEPCK), and malic enzyme (Salganicoff and Koeppe, 1968; Patel, 1974).

Pyruvate carboxylase, a mitochondrial enzyme, catalyzes the formation of oxaloacetate from pyruvate and HCO_3^- ; it depends on ATP, Mn^{2+} , and biotin for activity, and requires acetyl-CoA as a positive modulator:



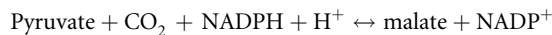
The reaction is physiologically unidirectional, because of the low tissue concentration of oxaloacetate in the brain ($<10 \mu\text{M}$; Siesjö, 1978). Pyruvate carboxylase has been shown by both biochemical and immunocytochemical methods to be expressed by cultured astrocytes, but not by cultured neurons (Shank et al., 1981, 1985; Yu et al., 1983; Cesar and Hamprecht, 1995). So far, its cellular expression has not been determined in the brain.

PEPCK, a predominantly mitochondrial enzyme, at least in rats, normally acts to decarboxylate oxaloacetate to phosphoenolpyruvate. In conjunction with pyruvate carboxylase, it participates in the formation of phosphoenolpyruvate from pyruvate, an important step in gluconeogenesis. PEPCK depends on GTP (or ITP) as a phosphate donor:



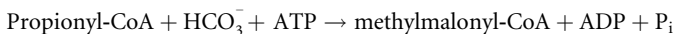
The enzyme's low affinity for CO_2 drives the reaction in the decarboxylating direction, but fixation of radiolabeled CO_2 through PEPCK activity has been shown in liver cells (Rognstad, 1982). Whether this fixation represents a net synthesis of oxaloacetate or merely an exchange of unlabeled carboxylic groups for $^{14}\text{CO}_2$ (see below) is not clear. PEPCK has been detected in cultured astrocytes and neurons and in the adult brain (Cheng and Cheng, 1972; Patel, 1974; Cruz et al., 1998). B. Hamprecht and coworkers found evidence of PEPCK-dependent gluconeogenesis and glycogen formation in cultured astrocytes (Schmoll et al., 1995). However, compared with the activity in other tissues the brain activity of PEPCK is apparently very low (Wiese et al., 1991).

Malic enzyme, which exists in a cytosolic and a mitochondrial form, catalyzes the reversible formation of malate from pyruvate and CO_2 . The reaction depends on NADPH and Mg^{2+} or Mn^{2+} :



Both the cytosolic and mitochondrial isoforms of malic enzyme have been detected in astrocytes and neurons (Kurz et al., 1993; McKenna et al., 1995, 2000; Vogel et al., 1998; Hassel and Bråthe, 2000a). Malic enzyme has traditionally been thought of as an anaplerotic enzyme in the liver (Lehninger, 1978), and it is assumed to act in the carboxylating direction in the heart (Russell and Taegtmeier, 1991). However, it has generally been considered to be a decarboxylating enzyme in the brain (Vogel et al., 1998; Hertz et al., 1999; McKenna et al., 2000). Nevertheless, there is evidence for a pyruvate-carboxylating action in cultured neurons (Hassel and Bråthe, 2000a) and in the adult mouse brain (Hassel and Bråthe, 2000b). In fact, it is not clear from experimental evidence whether pyruvate carboxylase or malic enzyme performs the pyruvate carboxylation that can be demonstrated in cultured astrocytes.

Propionyl-CoA carboxylase catalyzes the reaction



It is a biotin-dependent enzyme and is linked to anaplerosis, since its product, methylmalonyl-CoA, may be converted into the TCA cycle intermediate succinyl-CoA through methylmalonyl-CoA racemase and methylmalonyl-CoA mutase. The substrate of propionyl-CoA carboxylase, propionyl-CoA, is an intermediate in the catabolism of valine, isoleucine, methionine (see below), and propionate.

3 Amino Acids as a Source of TCA Cycle Intermediates In Vivo and In Vitro

Amino acids that can be converted into TCA cycle intermediates are called glucogenic, because they eventually give rise to oxaloacetate, which is an early step in gluconeogenesis (see above: PEPCK). Amino acids first that give rise to α -ketoglutarate are glutamate, glutamine, arginine, histidine, and proline; amino acids that give rise to succinyl-CoA are isoleucine, valine, threonine, and methionine; GABA yields succinate; amino acids that give rise to fumarate are phenylalanine and tyrosine; amino acids that give rise to oxaloacetate are aspartate and asparagine (🔗 [Figure 3.1-2](#)). Glucogenic amino acids also comprise those that are converted into pyruvate (alanine, cysteine, glycine, serine), but they will not be considered here as their anaplerotic conversion into TCA cycle intermediates depends on pyruvate carboxylation, which is described above.

Metabolism of methionine, asparagine, isoleucine, and valine, amino acids that cross the blood-brain barrier (Oldendorf and Szabo, 1976; Miller et al., 1985), has been demonstrated in brain tissue in vitro or in vivo (Gaitonde, 1976; Reubi et al., 1980; Murthy and Hertz, 1987). The influx of amino acids across the blood-brain barrier is restricted; however, the uptake into rat brain of large neutral amino acids that may enter anaplerotic pathways is approximately 28 nmol/g tissue per min (Miller et al., 1985) or 3% of the

cerebral uptake of glucose in the same animal model (Braun et al., 1985). When compared with the calculated value for cerebral CO₂ fixation (~10% of metabolic rate for glucose, see below), the contribution of blood-borne glucogenic amino acids to cerebral anaplerosis may be quite significant. In contrast, transfer of TCA cycle intermediates themselves across the blood–brain barrier seems to be so limited that it probably does not contribute much to replenishment of the cerebral TCA cycle (Hassel et al., 2002).

Glucogenic amino acids may be an even greater source of anaplerotic substrates in cultured cells than in the intact brain, since the concentration of glucogenic amino acids in the culture medium is much higher than in serum (for review, see Hassel, 2000).

4 Is Anaplerosis Confined to a Specific Cell Type?

When radiolabeled HCO₃⁻ is infused intravenously into rats, the specific activity of glutamine becomes greater than that of glutamate (Berl et al., 1962; Waelsch et al., 1964; Xu et al., 2004). (The specific activity is the amount of radioactivity in the amino acid divided by the total amount of amino acid.) Such a labeling pattern has been interpreted to mean that the carboxylation reaction takes place in glial cells, which express glutamine synthetase (Martinez-Hernandez et al., 1977; Tansey et al., 1991). If a radiolabeled substrate is metabolized primarily in glia, it will label the glial pool of glutamate, which is the precursor pool for glutamine (Figure 3.1-1). The large neuronal pool of glutamate will remain unlabeled. When the tissue is homogenized and amino acids are extracted, the unlabeled neuronal pool of glutamate will dilute the labeled glial glutamate pool, and the specific activity will become low. Radiolabeled glutamine, which is not diluted similarly, will therefore achieve a higher specific activity than glutamate. If a radiolabeled substrate is metabolized primarily in neurons, the specific activity of glutamate becomes greater than that of glutamine, since the large neuronal pool of glutamate becomes labeled, while (glial) glutamine does not. The finding of a higher specific activity for glutamine than for glutamate after intravenous infusion of H¹⁴CO₃ (Berl et al., 1962; Waelsch et al., 1964) suggested glial ¹⁴CO₂ fixation, and it agreed well with the subsequent finding that pyruvate carboxylase was expressed in cultured astrocytes but not in cultured neurons (Shank et al., 1981, 1985; Yu et al., 1983; Cesar and Hamprecht, 1995).

While it is clear that glial cells constitute an important compartment for CO₂ fixation, the specific activities of glutamate and glutamine cannot be used to attribute pyruvate carboxylation exclusively to glia. As long as the pyruvate-carboxylating activity of glial cells is greater than that of neurons (expressed as pyruvate carboxylation/pyruvate dehydrogenase activity), the specific activity of glutamine will exceed that of glutamate. Neuronal pyruvate carboxylation becomes evident when pyruvate radiolabeled in the carboxylic group, [1-¹⁴C]pyruvate, is used. If metabolized through pyruvate dehydrogenase [1-¹⁴C]pyruvate loses its radiolabeled carboxylic group as ¹⁴CO₂. However, if it is carboxylated, the radiolabel will be retained in [1-¹⁴C]malate or [1-¹⁴C]oxaloacetate. If [1-¹⁴C]malate equilibrates with the symmetrical fumarate so that [4-¹⁴C]malate is formed, then α-ketoglutarate, glutamate, and glutamine may become labeled in the first carbon atom. (When [1-¹⁴C]malate is metabolized through the TCA cycle without equilibration with fumarate, the sixth carbon position of citrate and isocitrate becomes labeled; this carbon is lost as CO₂ in the isocitrate dehydrogenase reaction.) Intracerebral injection of [1-¹⁴C]pyruvate leads to a higher specific activity of glutamate than of glutamine (Hassel and Bråthe, 2000a); incubation of brain slices with [1-¹⁴C]pyruvate produces the same labeling pattern (Cheng and Nakamura, 1972), indicating that pyruvate carboxylation also takes place in cells that do not form glutamine, i.e., neurons. Neuronal pyruvate carboxylation has since been demonstrated in cultured cerebellar granule neurons, malic enzyme being the likely responsible enzyme (Hassel and Bråthe, 2000a).

Pyruvate enters neurons rather than glial cells (O'Neal and Koeppe, 1966; Hassel and Bråthe, 2000a; Gonzalez et al., 2005), so [1-¹⁴C]pyruvate cannot be used to estimate the neuronal versus the glial contribution to cerebral pyruvate carboxylation. Glucose, on the other hand, is a substrate for all brain cells, and glucose radiolabeled in the third and fourth carbon positions, [3,4-¹⁴C]glucose, yields [1-¹⁴C]pyruvate after glycolytic metabolism. [3,4-¹⁴C]Glucose yields a higher specific activity of glutamate than of glutamine in the brain after intraperitoneal injection in mice (Van den Berg, 1973) or injection into the dorsal root ganglion of anesthetized cats (Johnson, 1976). These findings point to neurons as an important

pyruvate-carboxylating compartment. Again, it is unknown, however, whether the labeling obtained with [1-¹⁴C]pyruvate or [3,4-¹⁴C]glucose represents net synthesis or exchange of unlabeled carbon chains for [1-¹⁴C]pyruvate. Also, it is possible that the equilibration of oxaloacetate and malate with fumarate is less extensive in glial cells than in neurons (Merle et al., 1996), in which case glial pyruvate carboxylation is underestimated with the use of [3,4-¹⁴C]glucose, since the radiolabeled carboxylic group would be lost in the isocitrate step of the TCA cycle (see above).

The quantitative importance of glucogenic amino acids for anaplerosis in glia and neurons is largely uninvestigated, but several of these amino acids are present in blood (for values, see Figure 3.1-2), and some cross the blood–brain barrier. Further, since cultured neural cells metabolize isoleucine and valine to CO₂ and water (Murthy and Hertz, 1987), a certain formation of TCA cycle intermediates from these amino acids may be expected in the intact brain.

5 Cataplerotic Decarboxylation: Glial or Neuronal? Pyruvate Recycling

Because there is no net fixation of CO₂ in the brain, the CO₂ fixation that occurs in carboxylating reactions must be balanced by a similar decarboxylating cataplerotic activity. Evidence of malate decarboxylation in astrocytes has been found in vitro (Sonnewald et al., 1993; Hassel et al., 1994; McKenna et al., 1996; Bakken et al., 1997a, b) and in vivo (Hassel and Sonnewald, 1995; Hassel et al., 2002). An oxaloacetate-decarboxylating activity of PEPCK has been documented in cultured astrocytes (Schmoll et al., 1995).

If astrocytes carboxylate pyruvate to oxaloacetate through pyruvate carboxylase and then decarboxylate malate through malic enzyme, this may seem like a futile cycle. However, at this stage we do not know whether the enzymes are localized together or in different compartments in the astrocytes. If the two reactions take place in different cellular compartments (e.g., cell bodies and processes) they may serve different cellular functions; if they take place in the same compartment, pyruvate carboxylation followed by malate decarboxylation would yield NADPH at the expense of ATP.

The neuronal expression of malic enzyme (McKenna et al., 1995, 2000; Vogel et al., 1998; Hassel and Bråthe, 2000a) confirms the capacity of neurons to decarboxylate malate.

Formation of pyruvate from malate and its subsequent metabolism through pyruvate dehydrogenase is called pyruvate recycling; it has been visualized in rat brain with the use of doubly ¹³C-labeled acetate, [1,2-¹³C]acetate, in conjunction with ¹³C NMRS (Cerdan et al., 1990; Cruz et al., 1998). [1,2-¹³C]Acetate initially leads to formation of [4,5-¹³C]glutamate and [4,5-¹³C]glutamine, but with time [4-¹³C]glutamate is formed, reflecting the decarboxylation of [2,3-¹³C]malate to monolabeled [3-¹³C]pyruvate, which after metabolism through pyruvate dehydrogenase and the first part of the TCA cycle yields [4-¹³C]α-ketoglutarate and [4-¹³C]glutamate. Because formation of [4-¹³C]glutamate predominated over formation of [4-¹³C]glutamine, the authors concluded that pyruvate recycling occurred in neurons. Whether this process also takes place in glia in vivo is not known, but it has been identified in cultured astrocytes (Sonnewald et al., 1996; Waagepetersen et al., 2002). The ¹³C NMRS studies on in vivo brain metabolism of ¹³C-labeled acetate (Cerdan et al., 1990; Hassel and Sonnewald, 1995; Cruz et al., 1998) suggest a glial–neuronal interaction with respect to cataplerosis and pyruvate recycling, namely decarboxylation of malate to pyruvate in astrocytes and transfer of pyruvate (or lactate) to neurons with subsequent metabolism.

6 Estimates of Pyruvate Carboxylation in the Brain

Estimates of cerebral CO₂ fixation have been based on the isotopic labeling of glutamate and glutamine after intravenous administration of isotopically labeled HCO₃⁻ or glucose into experimental animals. Both approaches pose interesting problems. Estimates based on the infusion of radiolabeled HCO₃⁻ yield values of approximately 10% of the cerebral metabolic rate for glucose (Van den Berg, 1973; Xu et al., 2004). Some important factors may influence results. First, it is not known whether the infused H¹⁴CO₃⁻ equilibrates fully with cytosolic and mitochondrial CO₂. Second, it is not known whether the labeling of cerebral metabolites with H¹⁴CO₃⁻ represents the net synthesis of TCA cycle intermediates rather than exchange of unlabeled carboxylic groups for H¹⁴CO₃⁻. Both malic enzyme and PEPCK are reversible

enzymes that may cause radiolabeling of their products through exchange. Third, loss of the fixed $\text{H}^{14}\text{CO}_3^-$ may occur if the labeled $[4\text{-}^{14}\text{C}]\text{oxaloacetate}$ or $[4\text{-}^{14}\text{C}]\text{malate}$ equilibrates with the symmetrical fumarate, so that $[1\text{-}^{14}\text{C}]\text{oxaloacetate}$ or $[1\text{-}^{14}\text{C}]\text{malate}$ is formed. The first carbon of oxaloacetate and malate is lost as $^{14}\text{CO}_2$ in the isocitrate dehydrogenase reaction, i.e., before the label reaches glutamate and glutamine. Xu et al. (2004) took all of these factors into consideration, and so their value of 10% for pyruvate carboxylation is probably as close as one gets with this approach, which assesses global cerebral pyruvate carboxylation in awake rats. In a similar study, Öz et al. (2004) demonstrated that cerebral CO_2 fixation was reduced by anesthesia, which they reasonably assumed to reflect the reduced importance of pyruvate carboxylation in glutamine formation during anesthesia-induced neuronal inactivity.

^{13}C -labeled glucose in conjunction with NMRS of brain extracts has also been used to quantify cerebral pyruvate carboxylation. After administration of $[1\text{-}^{13}\text{C}]\text{glucose}$ (glucose that carries a ^{13}C in its first carbon position), $[3\text{-}^{13}\text{C}]\text{pyruvate}$ and hence $[2\text{-}^{13}\text{C}]\text{acetyl-CoA}$ become labeled when the ^{13}C has passed through glycolysis and the pyruvate dehydrogenase reaction. When the label enters the TCA cycle the fourth carbon of $\alpha\text{-ketoglutarate}$ and hence glutamate and glutamine (and the corresponding second carbon of GABA) become labeled. When the label makes one full turn in the TCA cycle, it becomes scrambled between the second and third carbons of $\alpha\text{-ketoglutarate}$ and hence glutamate and glutamine become labeled. Instead of the expected equal labeling of the second and third carbons of glutamate and glutamine, several groups have reported that the second carbon of glutamine achieves a better labeling than the third (Shank et al., 1993; Lapidot and Gopher, 1994; Hassel et al., 1995; Aureli et al., 1997). This finding has been assumed to reflect carboxylation of $[3\text{-}^{13}\text{C}]\text{pyruvate}$ by pyruvate carboxylase in astrocytes. The carboxylation product of $[3\text{-}^{13}\text{C}]\text{pyruvate}$ would be $[3\text{-}^{13}\text{C}]\text{oxaloacetate}$, which eventually yields $[2\text{-}^{13}\text{C}]\alpha\text{-ketoglutarate}$, glutamate, and glutamine. On the basis of the labeling inequality of the second and third carbons of glutamine the flux of pyruvate through the glia carboxylation pathways has been estimated at 25–60% of the flux through the glial pyruvate dehydrogenase reaction (Shank et al., 1993; Lapidot and Gopher, 1994; Hassel et al., 1995; Aureli et al., 1997). In these calculations, it has been assumed that no labeled oxaloacetate or malate labeled in the third carbon through pyruvate carboxylation would equilibrate with the symmetrical fumarate. Such equilibration, which has been documented in cultured astrocytes and neurons (Merle et al., 1996), would scramble the label between the second and third carbons, and the above values for glial pyruvate carboxylation would be underestimates. However, Merle et al. (2002) have shown that the relative difference in the labeling of the second and third carbons of glutamine is reduced as a function of the duration of exposure of the brain to $[1\text{-}^{13}\text{C}]\text{glucose}$.

Pyruvate carboxylation in neurons is difficult to quantify with $[1\text{-}^{13}\text{C}]\text{glucose}$ and NMRS, because equilibration of oxaloacetate and malate with fumarate is probably extensive in neurons (Merle et al., 1996, 2002), resulting in scrambling of label and equal labeling of the second and third carbons of glutamate. In cultured, glutamatergic, cerebellar granule cells the flux through the pyruvate carboxylating pathway, as determined with $[1\text{-}^{14}\text{C}]\text{pyruvate}$, was approximately 30% of that through pyruvate dehydrogenase, as determined with $[3\text{-}^{14}\text{C}]\text{pyruvate}$ (Hassel and Bräthe, 2000b). This high value may have been caused by the absence of glutamine or other glucogenic amino acids in the incubation medium, which could have made the cells especially dependent on pyruvate carboxylation for anaplerosis.

Taken together, the values for cerebral pyruvate carboxylation obtained with $\text{H}^{14}\text{CO}_3^-$ and $[1\text{-}^{13}\text{C}]\text{glucose}$ may seem to be at odds with one another. However, both methods have been used to assess global pyruvate-carboxylating activity in the brain. More research is required to quantify the pyruvate-carboxylating activity in brain and to determine whether brain regions or subcellular specializations differ with respect to pyruvate-carboxylating activity.

7 Mechanisms that Counteract Loss of TCA Cycle Intermediates in Glutamatergic and GABAergic Neurotransmission: Reuptake and the Glutamine Cycle

When glutamate or GABA is released to the extracellular fluid, the neuronal TCA cycle is drained of $\alpha\text{-ketoglutarate}$. In this respect, glutamatergic and GABAergic neurotransmission pose a challenge to the

energy production in neurons, since loss of α -ketoglutarate will endanger ATP production. At least two mechanisms other than anaplerosis counteract the loss of TCA cycle intermediates inherent in glutamatergic and GABAergic neurotransmission. First, transmitters are taken back up into the nerve terminals by specific transporters. The glutamate transporter EAAT2 (GLT in the rat) has been found to be expressed in nerve terminals as well as in astrocytes (Chen et al., 2002, 2004; Chen and Swanson, 2003; Suchak et al., 2003); the same is true for GABA transporters (Radian et al., 1990). Second, glutamate and GABA may be taken up by astrocytes, which, in exchange, may return glutamine to the extracellular fluid, from which neurons accumulate it. The latter mechanism, called the “glutamine cycle” (see Chapter 5), was proposed to explain the fluxes of amino acids between neurons and glia (e.g., Van den Berg and Garfinkel, 1971). Current evidence suggests that the flux of glutamate from neurons to glia is large, maybe 40–50% of the metabolic rate for glucose (Hassel et al., 1997; Broman et al., 2000; Xu et al., 2004). It has not been shown, however, that all this glutamate is transmitter glutamate in the sense that it is of vesicular origin. The transfer of glutamine to neurons has been calculated to be of a similar magnitude (Lebon et al., 2002). The astrocytic uptake of GABA has not been estimated, but could vary considerably between brain regions, as suggested by the variation in neuronal GABA transporter expression (Radian et al., 1990). Accordingly, there may be differences in the transmitter-inactivating role of astrocytes between brain regions. Balázs et al. (1970) found evidence of active astrocytic uptake of radiolabeled GABA in slices from cerebral cortex, as could be seen from the high specific activity of glutamine (glutamine synthetase being a glia-specific enzyme in the brain; Martinez-Hernandez et al., 1977), whereas the weaker labeling of glutamine than of glutamate after injection of radiolabeled GABA into rat striatum suggested a predominantly neuronal uptake in this structure (Hassel et al., 1992).

The exchange of glutamine for glutamate and GABA can only be compensatory if the neurons that take up glutamine express glutaminase, which deamidates glutamine to glutamate. From immunocytochemical and *in situ* hybridization studies, it appears that not all glutamatergic or GABAergic neurons express this enzyme (Najlerahim et al., 1990; Kaneko and Mizuni, 1994; Laake et al., 1999). These neurons would be expected to rely on neuronal pyruvate carboxylation or metabolism of glucogenic amino acids to counteract loss of TCA cycle intermediates. Even nerve terminals that do express glutaminase may have anaplerotic capacity, just as they may have transporters for reuptake of glutamate or GABA.

8 The Lack of Data on the Ultrastructural Localization of Anaplerotic Enzymes

The idea of the glutamine cycle as a mechanism for the inactivation and recycling of transmitter glutamate and GABA was strengthened by (1) the finding of transporter proteins for glutamate, GABA, and glutamine in astrocytic processes that surround the synapse (Radian et al., 1990; Danbolt, 2001; Boulland et al., 2002), (2) the finding of glutamine synthetase in astrocytic processes (Derouiche and Frotscher, 1991), (3) the demonstration that nerve terminals take up glutamine (Bradford et al., 1978), and (4) the fact that many glutamatergic nerve terminals contain phosphate-activated glutaminase (Laake et al., 1999). Although pyruvate carboxylase has been thought to support synthesis and export of glutamine as a precursor for transmitter glutamate (e.g., Shank et al., 1985), and although malic enzyme has been suggested to support formation of transmitter glutamate in neurons (Hassel and Bråthe, 2000a), the ultrastructural localization of these enzymes in the brain has not been determined. Therefore, the role of pyruvate-carboxylating enzymes in glutamatergic and GABAergic neurotransmission remains somewhat uncertain. The same is true for the role of glucogenic amino acids as anaplerotic substrates that could support synthesis of transmitter glutamate and GABA; it is not known whether the enzymes responsible for the metabolism of glucogenic amino acids are located at or near glutamatergic or GABAergic synapses. Therefore, studies on the ultrastructural localization of anaplerotic enzymes are clearly needed.

9 Clinical Aspects of Anaplerosis: Deficiency of Anaplerotic Enzymes

Loss of pyruvate carboxylase activity may be seen as a rare genetic disorder that affects the expression of the enzyme, and it may be seen in biotin deficiency. In the former instance, severe lactic acidosis,

hyperammonemia, and brain pathology ensue; this condition is often fatal. Treatment with high doses of citrate and aspartate has been reported to correct blood chemistry, but not brain chemistry, as evidenced by subnormal levels of glutamine in the cerebrospinal fluid (CSF) (Ahmad et al., 1999). Biotin deficiency affects all biotin-dependent carboxylases. It may cause various central nervous symptoms, such as mental retardation, ataxia, and seizures. Biotin deficiency may be seen after prolonged formula feeding without biotin supplementation or in biotinidase deficiency. Biotinidase, a hydrolase, recycles biotin from its peptide-bound forms to free biotin, which may be reused by biotin-dependent enzymes (carboxylases). A defect of holocarboxylase, the enzyme that causes biotin to bind to biotin-dependent carboxylases, is a cause of functional biotin deficiency.

Recently, idiopathic generalized epilepsies (absence epilepsy, juvenile myoclonic epilepsy, generalized tonic-clonic epilepsy) were shown to be associated with mutations of the mitochondrial malic enzyme (Greenberg et al., 2005). The functional consequences of these mutations have not been established. However, it is interesting that fairly wide areas surrounding epileptic foci are hypometabolic (for review, see Duncan, 1997), suggesting a widespread reduction in energy production, the molecular basis of which is not known, but which could involve malic enzyme deficiency.

Propionyl-CoA carboxylase deficiency leads to propionic acidemia and a variety of neurological symptoms, to some extent correlated with the degree of acidosis (Surtees et al., 1992; Yorifuji et al., 2002). The cerebral symptoms and neurological sequelae may, however, be a combination of systemic consequences of the disease (acidosis) and specific effects of propionyl-CoA carboxylase deficiency on the brain.

10 Anaplerosis and Brain Tumors

Malignant cells avidly consume extracellular glutamine as an energy substrate (for review, see Medina, 2001). Glutaminase activity is high in tumor cells (Perez-Gomez et al., 2005) and appears to correlate with tumor aggressiveness (Lobo et al., 2000). In the brain, this high glutaminase activity may have several consequences. First, a brain tumor, be it a primary brain tumor or a metastasis, may increase the anaplerotic demand on neighboring glutamine-producing glial cells. Second, uptake and metabolism of extracellular glutamine by the tumor may affect neuronal energy metabolism through the consumption of the anaplerotic substrate of glutamatergic and GABAergic neurons. Third, metabolism of glutamine may lead to release of glutamate from the tumor. *In vitro* studies have shown that gliomas release glutamate and produce toxic concentrations of glutamate in the extracellular fluid (Ye and Sontheimer, 1999). In this way, brain tumors may cause excessive activation of glutamate receptors, leading to neuronal death. Excessive activation of glutamate receptors may also be the cause of peritumoral epileptic activity, which entails an even greater metabolic demand on the peritumoral tissue (for review, see Sontheimer, 2004). Thus, an important aspect of brain tumor biology may be a disturbance of the anaplerotic–cataplerotic balance in the brain, with consequences for both energy metabolism and neurotransmission.

References

- Ahmad A, Kahler SG, Kishnani PS, Artigas-Lopez M, Pappu AS, et al. 1999. Treatment of pyruvate carboxylase deficiency with high doses of citrate and aspartate. *Am J Med Genet* 87: 331-338.
- Aureli T, Di Cocco ME, Calvani M, Conti F. 1997. The entry of [^{13}C]glucose into biochemical pathways reveals a complex compartmentation and metabolite trafficking between glia and neurons: A study by ^{13}C -NMR spectroscopy. *Brain Res* 765: 218-227.
- Bakken IJ, Sonnewald U, Clark JB, Bates TE. 1997a. [^{13}C] glutamate metabolism in rat brain mitochondria reveals malic enzyme activity. *Neuroreport* 8: 1567-1570.
- Bakken IJ, White LR, Aasly J, Unsgard G, Sonnewald U. 1997b. Lactate formation from [^{13}C]aspartate in cultured astrocytes: Compartmentation of pyruvate metabolism. *Neurosci Lett* 237: 117-120.
- Balázs R, Machiyama Y, Hammond BJ, Julian T, Richter D. 1970. The operation of the gamma-aminobutyrate bypath

- of the tricarboxylic acid cycle in brain tissue in vitro. *Biochem J* 116: 445-461.
- Berl S, Takagaki G, Clarke DD, Waelsch H. 1962. Carbon dioxide fixation in the brain. *J Biol Chem* 237: 2570-2573.
- Boulland JL, Osen KK, Levy LM, Danbolt NC, Edwards RH, et al. 2002. Cell-specific expression of the glutamine transporter SN1 suggests differences in dependence on the glutamine cycle. *Eur J Neurosci* 15: 1615-1631.
- Bradford HF, Ward HK, Thomas AJ. 1978. Glutamine—a major substrate for nerve endings. *J Neurochem* 30: 1453-1460.
- Braun LD, Miller LP, Pardridge WM, Oldendorf WH. 1985. Kinetics of regional blood-brain barrier glucose transport and cerebral blood flow determined with the carotid injection technique in conscious rats. *J Neurochem* 44: 911-915.
- Broman J, Hassel B, Rinvik E, Ottersen OP. 2000. Biochemistry and anatomy of transmitter glutamate. *Handbook of chemical neuroanatomy*, vol. 18. Ottersen OP, Storm-Mathisen, editors. Amsterdam: Elsevier; pp. 1-44.
- Cerdan S, Kunnecke B, Seelig J. 1990. Cerebral metabolism of [1,2-¹³C₂]acetate as detected by in vivo and in vitro ¹³C NMR. *J Biol Chem* 265: 12916-12926.
- Cesar M, Hamprecht B. 1995. Immunocytochemical examination of neural rat and mouse primary cultures using monoclonal antibodies raised against pyruvate carboxylase. *J Neurochem* 64: 2312-2318.
- Chen W, Aoki C, Mahadomrongkul V, Gruber CE, Wang GJ, et al. 2002. Expression of a variant form of the glutamate transporter GLT1 in neuronal cultures and in neurons and astrocytes in the rat brain. *J Neurosci* 22: 2142-2152.
- Chen W, Mahadomrongkul V, Berger UV, Bassan M, DeSilva T, et al. 2004. The glutamate transporter GLT1a is expressed in excitatory axon terminals of mature hippocampal neurons. *J Neurosci* 24: 1136-1148.
- Chen Y, Swanson RA. 2003. The glutamate transporters EAAT2 and EAAT3 mediate cysteine uptake in cortical neuron cultures. *J Neurochem* 84: 1332-1339.
- Cheng SC, Cheng RH. 1972. A mitochondrial phosphoenolpyruvate carboxykinase from rat brain. *Arch Biochem Biophys* 151: 501-511.
- Cheng SC, Nakamura R. 1972. Metabolism related to the tricarboxylic acid cycle in rat brain slices. Observations on CO₂ fixation and metabolic compartmentation. *Brain Res* 38: 355-370.
- Cruz F, Scott SR, Barroso I, Santisteban P, Cerdan S. 1998. Ontogeny and cellular localization of the pyruvate recycling system in rat brain. *J Neurochem* 70: 2613-2619.
- Danbolt NC. 2001. Glutamate uptake. *Prog Neurobiol* 65: 1-105.
- Derouiche A, Frotscher M. 1991. Astroglial processes around identified glutamatergic synapses contain glutamine synthetase: Evidence for transmitter degradation. *Brain Res* 552: 346-350.
- Desagher S, Glowinski J, Premont J. 1997. Pyruvate protects neurons against hydrogen peroxide-induced toxicity. *J Neurosci* 17: 9060-9067.
- Duncan JS. 1997. Imaging and epilepsy. *Brain* 120: 339-377.
- Gaitonde MK. 1976. Conversion of [U-¹⁴C]threonine into ¹⁴C-labelled amino acids in the brain of thiamin-deficient rats. *Biochem J* 150: 285-295.
- Gonzalez SV, Nguyen NH, Rise F, Hassel B. 2005. Brain metabolism of exogenous pyruvate. *J Neurochem* 95: 284-293.
- Greenberg DA, Cayanis E, Strug L, Marathe S, Durner M, et al. 2005. Malic enzyme 2 may underlie susceptibility to adolescent-onset idiopathic generalized epilepsy. *Am J Hum Genet* 76: 139-146.
- Grill V, Bjorkman O, Gutniak M, Lindqvist M. 1992. Brain uptake and release of amino acids in nondiabetic and insulin-dependent diabetic subjects: Important role of glutamine release for nitrogen balance. *Metabolism* 41: 28-32.
- Hassel B. 2000. Carboxylation and anaplerosis in neurons and glia. *Mol Neurobiol* 22: 21-40.
- Hassel B, Bachelard HS, Jones P, Fonnum F, Sonnewald U. 1997. Trafficking of amino acids between neurons and glia in vivo. Effects of inhibition of glial metabolism by fluorooacetate. *J Cereb Blood Flow Metab* 17: 1230-1238.
- Hassel B, Bråthe A. 2000a. Neuronal pyruvate carboxylation supports formation of transmitter glutamate. *J Neurosci* 20: 1342-1347.
- Hassel B, Bråthe A. 2000b. Cerebral metabolism of lactate in vivo. Evidence for neuronal pyruvate carboxylation. *J Cereb Blood Flow Metab* 20: 327-336.
- Hassel B, Bråthe A, Petersen D. 2002. Cerebral dicarboxylate transport and metabolism studied with isotopically labelled fumarate, malate and malonate. *J Neurochem* 82: 410-419.
- Hassel B, Paulsen RE, Johnsen A, Fonnum F. 1992. Selective inhibition of glial cell metabolism in vivo by fluorocitrate. *Brain Res* 576: 120-124.
- Hassel B, Sonnewald U. 1995. Glial formation of pyruvate and lactate from TCA cycle intermediates. Implications for the inactivation of transmitter amino acids? *J Neurochem* 65: 2227-2234.
- Hassel B, Sonnewald U, Fonnum F. 1995. Glial-neuronal interactions as studied by cerebral metabolism of [2-¹³C]acetate and [1-¹³C]glucose: An ex vivo ¹³C NMR spectroscopic study. *J Neurochem* 64: 2773-2782.
- Hassel B, Sonnewald U, Unsgård G, Fonnum F. 1994. NMR spectroscopy of cultured astrocytes: Effects of glutamine and the gliotoxin fluorocitrate. *J Neurochem* 62: 2187-2194.
- Hertz L, Dringen R, Schousboe A, Robinson SR. 1999. Astrocytes: Glutamate producers for neurons *J Neurosci Res* 57: 417-428.

- Johnson JL. 1976. A comparative analysis of compartmentation of metabolism in the dorsal root ganglion and ventral spinal cord gray using [U - ^{14}C]glucose, [2 - ^{14}C]glucose, [6 - ^{14}C]glucose, [$3,4$ - ^{14}C]glucose, $NaH^{14}CO_3$, and [2 - ^{14}C]pyruvate. *Brain Res* 101: 523-532.
- Kaneko T, Mizuno N. 1994. Glutamate-synthesizing enzymes in GABAergic neurons of the neocortex: A double immunofluorescence study in the rat. *Neuroscience* 61: 839-849.
- Kurz GM, Wiesinger H, Hamprecht B. 1993. Purification of cytosolic malic enzyme from bovine brain, generation of monoclonal antibodies, and immunocytochemical localization of the enzyme in glial cells of neural primary cultures. *J Neurochem* 60: 1467-1474.
- Laake JH, Takumi Y, Eidet J, Torgner IA, Roberg B, et al. 1999. Postembedding immunogold labelling reveals subcellular localization and pathway-specific enrichment of phosphate activated glutaminase in rat cerebellum. *Neuroscience* 88: 1137-1151.
- Lapidot A, Gopher A. 1994. Cerebral metabolic compartmentation. Estimation of glucose flux via pyruvate carboxylase/pyruvate dehydrogenase by ^{13}C NMR isotopomer analysis of D-[U - ^{13}C]glucose metabolites. *J Biol Chem* 269: 27198-27208.
- Lebon V, Petersen KF, Cline GW, Shen J, Mason GF, et al. 2002. Astroglial contribution to brain energy metabolism in humans revealed by ^{13}C nuclear magnetic resonance spectroscopy: Elucidation of the dominant pathway for neurotransmitter glutamate repletion and measurement of astrocytic oxidative metabolism. *J Neurosci* 22: 1523-1531.
- Lehninger AL. 1978. *Biochemistry*. New York: Worth.
- Lobo C, Ruiz-Bellido MA, Aledo JC, Marquez J, Nunez De Castro I, et al. 2000. Inhibition of glutaminase expression by antisense mRNA decreases growth and tumourigenicity of tumour cells. *Biochem J* 348: 257-261.
- Martinez-Hernandez A, Bell KP, Norenberg MD. 1977. Glutamine synthetase: Glial localization in brain. *Science* 195: 1356-1358.
- McKenna MC, Sonnewald U, Huang X, Stevenson J, Zielke HR. 1996. Exogenous glutamate concentration regulates the metabolic fate of glutamate in astrocytes. *J Neurochem* 66: 386-393.
- McKenna MC, Stevenson JH, Huang X, Tildon JT, Zielke CL, et al. 2000. Mitochondrial malic enzyme activity is much higher in mitochondria from cortical synaptic terminals compared with mitochondria from primary cultures of cortical neurons or cerebellar granule cells. *Neurochem Int* 36: 451-459.
- McKenna MC, Tildon JT, Stevenson JH, Huang X, Kingwell KG. 1995. Regulation of mitochondrial and cytosolic malic enzymes from cultured rat brain astrocytes. *Neurochem Res* 12: 1491-1501.
- Medina MA. 2001. Glutamine and cancer. *J Nutr* 131: 2539S-2542S.
- Merle M, Bouzier-Sore AK, Canioni P. 2002. Time-dependence of the contribution of pyruvate carboxylase versus pyruvate dehydrogenase to rat brain glutamine labelling from [1 - ^{13}C]glucose metabolism. *J Neurochem* 82: 47-57.
- Merle M, Martin M, Villegier A, Canioni P. 1996. [1 - ^{13}C]glucose metabolism in brain cells: Isotopomer analysis of glutamine from cerebellar astrocytes and glutamate from granule cells. *Dev Neurosci* 18: 460-468.
- Miller LP, Pardridge WM, Braun LD, Oldendorf WH. 1985. Kinetic constants for blood-brain barrier amino acid transport in conscious rats. *J Neurochem* 45: 1427-1432.
- Murthy CR, Hertz L. 1987. Acute effect of ammonia on branched-chain amino acid oxidation and incorporation into proteins in astrocytes and in neurons in primary cultures. *J Neurochem* 49: 735-741.
- Najlerahim A, Harrison PJ, Barton AJ, Heffernan J, Pearson RC. 1990. Distribution of messenger RNAs encoding the enzymes glutaminase, aspartate aminotransferase and glutamic acid decarboxylase in rat brain. *Brain Res Mol Brain Res* 7: 317-333.
- Oldendorf WH, Szabo J. 1976. Amino acid assignment to one of three blood-brain barrier amino acid carriers. *Am J Physiol* 230: 94-98.
- O'Neal RM, Koeppe RE. 1966. Precursors in vivo of glutamate, aspartate and their derivatives of rat brain. *J Neurochem* 13: 835-847.
- Öz G, Berkich DA, Henry PG, Xu Y, La Noue K, et al. 2004. Neuroglial metabolism in the awake rat brain: CO_2 fixation increases with brain activity. *J Neurosci* 24: 11273-11279.
- Pardridge WM. 1983. Brain metabolism: A perspective from the blood-brain barrier. *Physiol Rev* 63: 1481-1535.
- Patel MS. 1974. The relative significance of CO_2 -fixing enzymes in the metabolism of rat brain. *J Neurochem* 22: 717-724.
- Perez-Gomez C, Campos-Sandoval JA, Alonso FJ, Segura JA, Manzanares E, et al. 2005. Co-expression of glutaminase K and L isoenzymes in human tumour cells. *Biochem J* 386: 535-542.
- Radian R, Ottersen OP, Storm-Mathisen J, Castel M, Kanner BI. 1990. Immunocytochemical localization of the GABA transporter in rat brain. *J Neurosci* 10: 1319-1330.
- Reubi JC, Toggenburger G, Cuenod M. 1980. Asparagine as precursor for transmitter aspartate in corticostriatal fibres. *J Neurochem* 35: 1015-1017.
- Rognstad R. 1982. $^{14}CO_2$ fixation by phosphoenolpyruvate carboxykinase during gluconeogenesis in the intact rat liver cell. *J Biol Chem* 257: 11486-11488.
- Russell RR 3rd, Taegtmeier H. 1991. Pyruvate carboxylation prevents the decline in contractile function of rat hearts oxidizing acetoacetate. *Am J Physiol* 261: H1756-H1762.

- Salganicoff L, Koeppe RE. 1968. Subcellular distribution of pyruvate carboxylase, diphosphopyridine nucleotide and triphosphopyridine nucleotide isocitrate dehydrogenases, and malate enzyme in rat brain. *J Biol Chem* 243: 3416-3420.
- Schmoll D, Fuhrmann E, Gebhardt R, Hamprecht B. 1995. Significant amounts of glycogen are synthesized from 3-carbon compounds in astroglial primary cultures from mice with participation of the mitochondrial phosphoenolpyruvate carboxykinase isoenzyme. *Eur J Biochem* 227: 308-315.
- Shank RP, Bennett GS, Freytag SO, Campbell GL. 1985. Pyruvate carboxylase: An astrocyte-specific enzyme implicated in the replenishment of amino acid neurotransmitter pools. *Brain Res* 329: 364-367.
- Shank RP, Campbell GL, Freytag SO, Utter MF. 1981. Evidence that pyruvate carboxylase is an astrocyte specific enzyme in CNS tissues. *Abstr Soc Neurosci* 7: 936.
- Shank RP, Leo GC, Zielke HR. 1993. Cerebral metabolic compartmentation as revealed by nuclear magnetic resonance analysis of D-[1-¹³C]glucose metabolism. *J Neurochem* 61: 315-323.
- Siesjö BK. 1978. Brain energy metabolism. New York: John Wiley and Sons.
- Sokoloff L. 1989. Circulation and energy metabolism of the brain. Basic neurochemistry 4th Edition. Siegel G, Agranoff B, Albers RW, Molinoff P, editors. New York: Raven Press; pp. 565-590.
- Sonnenwald U, Westergaard N, Jones P, Taylor A, Bachelard HS, et al. 1996. Metabolism of [U-¹³C₅] glutamine in cultured astrocytes studied by NMR spectroscopy: First evidence of astrocytic pyruvate recycling. *J Neurochem* 67: 2566-2572.
- Sonnenwald U, Westergaard N, Krane J, Unsgard G, Petersen SB, et al. 1991. First direct demonstration of preferential release of citrate from astrocytes using [¹³C]NMR spectroscopy of cultured neurons and astrocytes. *Neurosci Lett* 128: 235-239.
- Sonnenwald U, Westergaard N, Petersen SB, Unsgard G, Schousboe A. 1993. Metabolism of [U-¹³C]glutamate in astrocytes studied by ¹³C NMR spectroscopy: Incorporation of more label into lactate than into glutamine demonstrates the importance of the tricarboxylic acid cycle. *J Neurochem* 61: 1179-1182.
- Sontheimer H. 2004. Ion channels and amino acid transporters support the growth and invasion of primary brain tumors. *Mol Neurobiol* 29: 61-71.
- Suchak SK, Baloyianni NV, Perkinton MS, Williams RJ, Meldrum BS, et al. 2003. The "glial" glutamate transporter, EAAT2 (Glt-1) accounts for high affinity glutamate uptake into adult rodent nerve endings. *J Neurochem* 84: 522-532.
- Surtees RA, Matthews EE, Leonard JV. 1992. Neurologic outcome of propionic acidemia. *Pediatr Neurol* 8: 333-337.
- Tansey FA, Farooq M, Cammer W. 1991. Glutamine synthetase in oligodendrocytes and astrocytes: New biochemical and immunocytochemical evidence. *J Neurochem* 56: 266-272.
- Van den Berg CJ. 1973. A model of compartmentation in mouse brain based on glucose and acetate metabolism. Metabolic compartmentation in the brain. Balazs R, Cremer JE, editors. London: MacMillan; pp. 137-166.
- Van den Berg CJ, Garfinkel D. 1971. A simulation study of brain compartments. Metabolism of glutamate and related substances in mouse brain. *Biochem J* 123: 211-218.
- Vogel R, Jennemann G, Seitz J, Wiesinger H, Hamprecht B. 1998. Mitochondrial malic enzyme: Purification from bovine brain, generation of an antiserum, and immunocytochemical localization in neurons of rat brain. *J Neurochem* 71: 844-852.
- Waagepetersen HS, Qu H, Hertz L, Sonnewald U, Schousboe A. 2002. Demonstration of pyruvate recycling in primary cultures of neocortical astrocytes but not in neurons. *Neurochem Res* 27: 1431-1437.
- Walsch H, Berl S, Rossi CA, Clarke DD, Purpura DP. 1964. Quantitative aspects of CO₂ fixation in mammalian brain in vivo. *J Neurochem* 11: 717-728.
- Wiese TJ, Lambeth DO, Ray PD. 1991. The intracellular distribution and activities of phosphoenolpyruvate carboxykinase isozymes in various tissues of several mammals and birds. *Comp Biochem Physiol B* 100: 297-302.
- Xu Y, Öz G, La Noue KF, Keiger CF, Berkich DA, et al. 2004. Whole-brain glutamate metabolism evaluated by steady-state kinetics using a double-isotope procedure: Effects of gabapentin. *J Neurochem* 90: 1104-1116.
- Ye ZC, Sontheimer H. 1999. Glioma cells release excitotoxic concentrations of glutamate. *Cancer Res* 59: 4383-4391.
- Yorifuji T, Kawai M, Muroi J, Mamada M, Kurokawa K, et al. 2002. Unexpectedly high prevalence of the mild form of propionic acidemia in Japan: Presence of a common mutation and possible clinical implications. *Hum Genet* 111: 161-165.
- Yu ACH, Drejer J, Hertz L, Schousboe A. 1983. Pyruvate carboxylase activity in primary cultures of astrocytes and neurons. *J Neurochem* 41: 1484-1487.

3.2 Glial–Neuronal Shuttle Systems

C. Zwingmann · D. Leibfritz

1	Introduction	199
2	Cerebral Glucose Metabolism	201
2.1	Introduction	201
2.2	Overview	202
2.3	NMR Analysis of the Metabolic Fate of ¹³ C-Labeled Glucose	203
2.4	Cell-Specific Glucose Metabolism in Astrocytes and Neurons	204
2.5	Glucose Metabolism Through Glycolysis	206
2.6	Glucose Oxidation Through the TCA Cycle	207
2.7	Glucose Metabolism via Anaplerosis	208
2.8	Ratio of Anaplerotic/Oxidative Glucose Metabolism	209
3	Cerebral Acetate Metabolism	211
3.1	Introduction	211
3.2	Overview: Acetate as a Glial Reporter Molecule?	211
3.3	Experimental Evidence for Glial-Specific Acetate Metabolism	212
3.4	Use of Acetate as Cerebral Substrate to Investigate Glial–Neuronal Interactions	213
4	Cerebral Glutamine Metabolism	213
4.1	Introduction	213
4.2	Glutamine versus Glucose as Neuronal TCA Cycle Substrate and Glutamate Precursor	213
5	Pyruvate Recycling in the Brain	216
5.1	Introduction	216
5.2	Overview	216
5.3	Cellular Localization of the Pyruvate Recycling Pathway in the Brain	217
5.4	Cellular Evidence for the Pyruvate Recycling Pathway	218
5.5	Cerebral Capacity of TCA Cycle Metabolism Through Pyruvate Recycling	219
5.6	Flux Through Mitochondrial and Cytosolic Malic Enzyme	221
5.7	Flux Through Phosphoenolpyruvate Carboxykinase	221
5.8	Importance of the Pyruvate Recycling Pathway in the Brain	222
6	Intercellular Transfer of Nitrogen to Operate the Glutamine–Glutamate Cycle	222
6.1	Introduction: Cellular Nitrogen Transfer as NH ₃ or NH ₄ ⁺	222
6.2	Overview: Cellular Nitrogen Transfer as Amino Acids	223
6.3	Ammonia Cycling via the Alanine–Lactate Shuttle	223
6.3.1	Alanine Synthesis in Neurons	223
6.3.2	Metabolism of Alanine in Astrocytes	225
6.4	Nitrogen Cycling via the Leucine/α-Ketoisocaproate Shuttle	225
6.5	Cycling of Nitrogen Through Aspartate Synthesis	226
6.6	Significance of Metabolic Shuttles Complementary to the Glutamine–Glutamate Cycle	227

7	<i>Regulatory Metabolic Mechanisms via Intracellular Compartmentation</i>	228
7.1	Cytosolic Pyruvate Compartmentation	228
7.2	Mitochondrial Heterogeneity	230
8	<i>Concluding Remarks</i>	231

Abstract: The glutamine–glutamate cycle between astrocytes and neurons is an essential part of neuronal function and activity. However, this cycle is not stoichiometric and is modulated by different regulatory mechanisms. By this means, in particular, the astrocytes are flexible in their intracellular regulation of metabolism and their ability to support the neurons in form of energy substrates and precursors for the neurotransmitter glutamate. Among conventional biochemical and molecular studies, *ex vivo* and *in vitro* ^{13}C -NMR spectroscopy has been used to monitor neural function, tissue metabolism, and neuronal–glial metabolic interactions. Special emphasis has been given to the metabolic specialization of astrocytes and its enzymatic regulation. For this purpose primary cell cultures are useful tools to study neuronal–glial metabolic relationships as the extracellular fluid can be investigated and manipulated by various stimuli. In cultured astrocytes, glucose is utilized predominantly anaerobically. Glycolysis is interrelated to the astrocytic tricarboxylic acid (TCA) cycle via bidirectional signals and metabolic exchange processes between astrocytes and neurons. Besides glucose oxidation, neuronally released glutamate is metabolized through the glial TCA cycle, while astrocyte-derived glutamine is used by the neurons as an energy substrate and glutamate precursor. The flexibility of glutamate- and glutamine metabolism depends on ammonia- and energy homeostasis, and the pyruvate recycling pathway in astrocytes modulates the glutamine–glutamate cycle. ^{13}C -NMR studies have further extended the concept of the “nonstoichiometric” glutamine–glutamate cycle between neurons and astrocytes by the alanine/lactate as well as leucine/ α -ketoisocaproate (α -KIC) shuttles between neurons and astrocytes. These shuttles contribute to nitrogen transfer from neurons to astrocytes and recycling of energy substrates for neurons, thereby promoting intercellular glutamine–glutamate cycling. The provision of neuronal energy substrates is further regulated by intracytosolic pyruvate compartmentation in astrocytes. In essence, the metabolic flexibility and compartmentalized enzymatic specialization of astrocytes buffers the brain tissue against metabolic impairments and excitotoxicity in response to extracellular stimuli. The knowledge about these mechanisms is important for the understanding of the physiological and pathophysiological regulation of neural metabolism and general brain function.

List of Abbreviations: ALAT, alanine aminotransferase; BBB, blood–brain barrier; BCAA, branched-chain amino acid; cME, cytoplasmic malic enzyme; GABA, γ -aminobutyric acid; GDH, glutamate dehydrogenase; GS, glutamine synthetase; HE, hepatic encephalopathy; α -KIC, α -ketoisocaproate; LDH, lactate dehydrogenase; ME, malic enzyme; mME, mitochondrial malic enzyme; MSO, methionine–sulfoximine; PAG, phosphate-activated glutaminase; PC, pyruvate carboxylase; PDH, pyruvate dehydrogenase; 3-NPA, 3-nitropropionic acid; PEPCK, phosphoenolpyruvate carboxykinase; PK, pyruvate kinase; PEP, phosphoenolpyruvate; TBOA, D,L-threo- β -benzyloxyaspartate; TCA, tricarboxylic acid cycle

1 Introduction

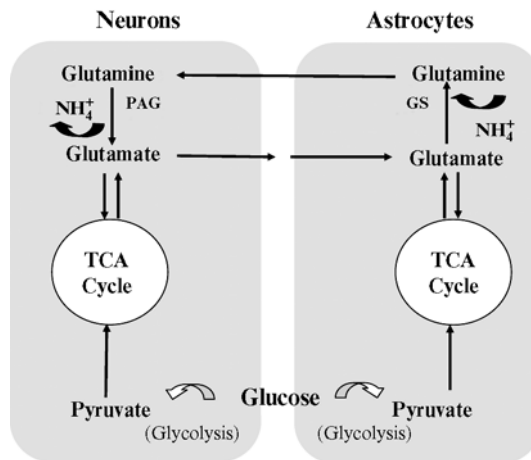
Brain energy metabolism depends mainly on the provision of glucose (Sokoloff, 1992; Gjedde and Marrett, 2001). Although the weight of the mature brain is only 2%–3% of the total body weight, it consumes up to one-fourth of the body’s glucose supply (Sokoloff, 1983–84). With regard to brain glucose metabolism, it has to be considered that the brain is a metabolically heterogeneous system containing distinct metabolic compartments (Berl and Clarke, 1969, 1983), associated with at least two kinetically different tricarboxylic acid (TCA) cycles, i.e., neuronal and glial compartments. Glial cells outnumber the neurons by more than tenfold. However, glial cells were long suggested to be a sort of glue holding the neurons together, and we have started to understand their active role only recently (Vesce et al., 2001). Attention has been given to a particular glial cell type—the astrocyte as a dynamic and the metabolically most active glial cell in the brain. To date, it is known that astrocytes actively participate in several processes crucial to brain function and neuronal activity, such as provision of energy, nutrients, and neurotransmitter precursors to neurons, scavenging of free radicals, as well as uptake and recycling of neurotransmitters.

To ensure normal brain function, neurotransmitters released from the neurons into the extracellular space have to be removed rapidly from the synaptic cleft. In particular, efficient mechanisms are needed to maintain a very high ratio of intracellular/extracellular glutamate. High-affinity glutamate transporters

exist on neurons and astrocytes. However, it has been demonstrated *in vivo* and *in vitro* that the majority of functional glutamate uptake is carried out by glial glutamate transporters, and astrocytic glutamate transporters are expressed mainly in those brain regions with the most extensive glutamate neurotransmission (Rothstein et al., 1996). After uptake of glutamate into the astrocytes, glutamate is converted to glutamine. Glutamine is synthesized through amidation of glutamate via glutamine synthetase (GS), a gliaspecific reaction (Martinez-Hernandez et al., 1977; Tansey et al., 1991). Glutamine is transferred back to the neuron to be hydrolyzed by phosphate-activated glutaminase (PAG) to glutamate, and to close the so-called “glutamine–glutamate cycle” in the brain. This cycle is tightly coupled to the metabolism of glucose, which is converted to pyruvate via TCA cycle activity (Figure 3.2-1). However, the precise nature of this cycle in relation to cerebral glucose metabolism remains not clearly resolved.

■ **Figure 3.2-1**

The glutamine–glutamate cycle between astrocytes and neurons. Glucose is degraded to pyruvate, which enters the mitochondrial TCA cycle of both astrocytes and neurons to synthesize glutamate via α -ketoglutarate. Glutamate is released by the neurons as a neurotransmitter. Astrocytic glutamate transporters remove neuronal-released glutamate from the synaptic cleft. GS, which converts glutamate to glutamine, is localized selectively in astrocytes. Glutamine is transported back to the neurons and converted to glutamate by PAG. GS, glutamine synthetase; PAG, phosphate-activated glutaminase



To date, ambiguity still exists regarding the cellular localization of glucose utilization in the brain. Glucose has been thought for long time to be metabolized mainly in the neuronal TCA cycle (Minchin and Beart, 1975). The assumption was mainly based on the results of the authors indicating that [^{14}C]glucose was incorporated into a large pool of glutamate, but that this glutamate pool did not synthesize glutamine or GABA to any great extent. [^{14}C]Acetate, on the other hand, which is an astrocyte-specific substrate (see Sect. 3), was incorporated into a small glutamate pool which was readily converted to glutamine. Furthermore, the high rates of cerebral oxygen consumption and glucose utilization measured *in vivo* in the brain have been suggested to be devoted to neuronal signaling (Attwell and Laughlin, 2001), and therefore to be dependent on the metabolic demands of the neurons. In addition, the relative energy requirements of neurons and glial cells (see the review of Magistretti et al., 1993) led to the conclusion that no more than 5% of energy usage can be attributed to glial function (see Pellerin and Magistretti, 2003 and references therein). However, this conclusion is only one hypothesis, which is discussed controversially. It also does not imply necessarily that the majority of glucose is taken up by neurons, and evidence was provided that astrocytes could be the primary site of glucose uptake during neuronal activity (for review see Magistretti et al., 1993). Glucose can be transported within the brain through several ways. After crossing the blood–brain

barrier (BBB), glucose (1) may enter both astrocytes and neurons through the intercellular space or (2) may be transported into neurons after passing the endothelial cells and astrocytes or (3) enter the astrocytes and may be metabolized to other substrates, which are subsequently supplied to neurons. In general, glucose largely passes through the astrocytes, whose endfeet are located on blood vessels and neuronal processes. Unmetabolized glucose is not transmitted from astrocytes to neurons; glucose entering the astrocytes may be metabolized to other substrates, which are supplied to neurons. However, controversy exists about the relative contribution of released astrocytic metabolites and neuronal glucose uptake to neuronal metabolic activity and energy production (Gjedde and Marrett, 2001).

It is clear that the fluxes, distribution, and interconversion of glutamate and glutamine between neurons and astrocytes must be flexible to changes in neuronal activity. A variety of mechanisms may contribute to such homeostasis. In particular, astrocytes and neurons interact metabolically in other processes involving intercellular metabolite transfer of several other substances derived from glucose metabolism (Hertz et al., 2000; Dienel and Cruz, 2003). One hypothesis, for example, suggests that oxidative metabolism of glutamate in astrocytes provides the energy required for its uptake and conversion to glutamine (Peng et al., 2001). In addition, astrocyte-derived glutamine is not only a precursor for transmitter amino acids but is also an energy substrate for neurons *in vivo* (Bradford et al., 1978; Hassel et al., 1995a; Zielke et al., 1998). This indicates a remarkably compartmentalized regulation of the neuronal–astrocytic homeostasis, and modulation of astrocytic intracellular metabolism may be an integral component of the glutamate–glutamine cycle.

Metabolic compartmentation in the brain has been studied traditionally using different tracer substrates which label either a large pool of glutamate (in neurons) with a low turnover or a small glial glutamate pool with a high turnover rate (Berl and Clarke, 1969; Balazs et al., 1970; Berl et al., 1970; Minchin and Beart, 1975; Shank and Campbell, 1983; Hassel et al., 1992). ^{13}C -NMR spectroscopic studies, though being less sensitive than other tracer methods, have the advantage of being noninvasive and nondestructive, and do not require metabolite isolation. In particular, the high chemical specificity of ^{13}C -NMR permits the identification of the ^{13}C -label in specific positions of given compounds (isotopomers) and allows the calculation of various metabolic fluxes and substrate concentrations simultaneously. In addition, NMR can reveal unexpected metabolic features that may not be observed using other methods focused on a particular enzymatic pathway.

One problem in studies using the intact brain is that the tissue consists of metabolically different brain regions and cell types. In addition, investigations of uptake and release of substances are restricted by the BBB permeability. Therefore, primary cultures of brain cells are extensively used to study neuronal–glial metabolic interactions. The present chapter discusses how metabolic interactions between astrocytes and neurons can be regulated through inter- and intracellular metabolic mechanisms.

2 Cerebral Glucose Metabolism

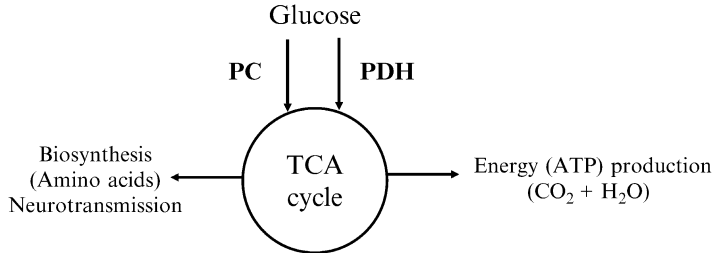
2.1 Introduction

Glucose is the major metabolic substrate for the brain, and normal brain function is dependent on the supply of both glucose and oxygen by the blood. In the brain, glucose serves as (1) a substrate for the biosynthesis of amino acids, proteins etc., and (2) as mitochondrial TCA-cycle substrate to maintain the energy needs of brain cells. Among the amino acids being produced from the carbons in glucose, glutamate and γ -aminobutyric acid (GABA) are regarded as the most important excitatory and inhibitory neurotransmitter amino acids, respectively. Only a small portion of glucose in the brain is used for biosynthesis; its majority is completely oxidized to CO_2 and H_2O in the TCA cycle (Sokoloff, 1977) (Figure 3.2-2).

There are different methods to study glucose metabolism and the relative contributions of amino acid biosynthesis and glucose oxidation in the brain. The use of radiolabeled (^{14}C) glucose allows to analyze its incorporation into amino acids and CO_2 . However, this method requires derivatization and isolation processes. Moreover, there are different pathways, such as pyruvate dehydrogenase (PDH) and pyruvate carboxylase (PC) (Figure 3.2-1), by which glucose can enter the Krebs cycle, and which contribute differentially to biosynthesis and brain energy production.

■ **Figure 3.2-2**

Basic glucose metabolism in the brain. The carbons in glucose can enter the Krebs cycle via PC or PDH, which are transformed to TCA cycle intermediates and subsequently to amino acids including those required for neurotransmission. On the other hand, glucose can be oxidized in the TCA cycle, which produces CO_2 and H_2O , and, subsequently, ATP in the oxidative phosphorylation process



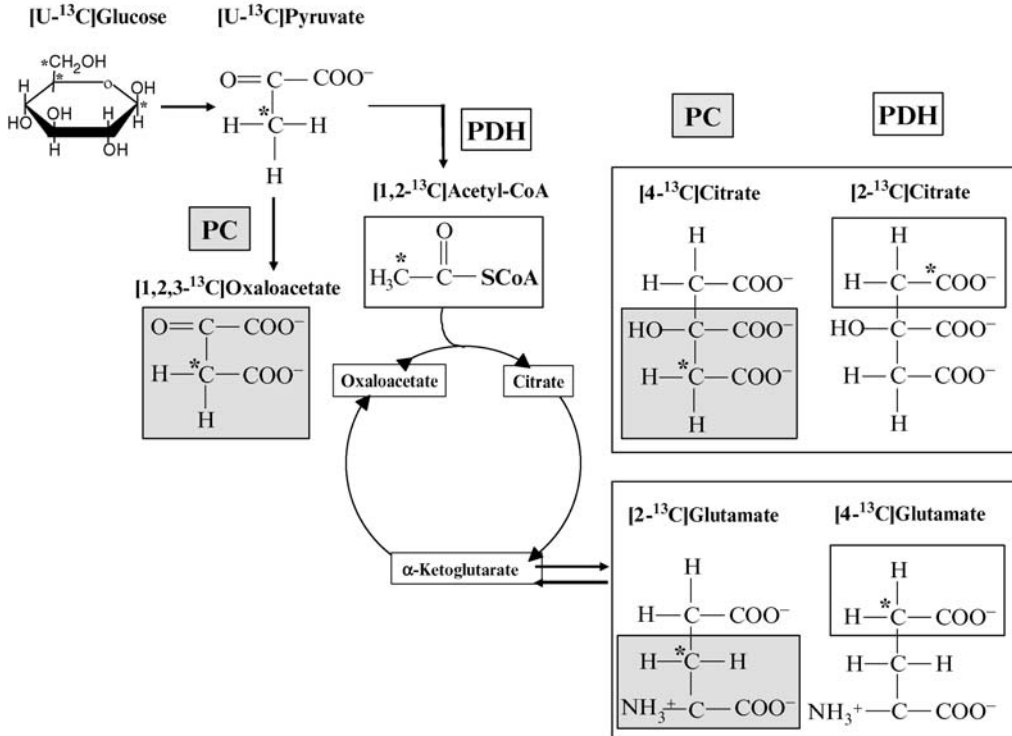
In particular ^{13}C -NMR spectroscopy is a method to follow up the fate of the carbons in metabolites derived via different metabolic pathways without transformation or isolation processes. Therefore, glucose labeled with the magnetic active isotope ^{13}C is well suited to follow cellular metabolism using NMR spectroscopy as all ^{13}C -labeled metabolites derived from ^{13}C -labeled glucose are detected in a single ^{13}C -NMR spectrum. In addition, the localization of a ^{13}C -isotope in a specific carbon position of a given metabolite and the fine structure of each signal (^{13}C is attached to another ^{13}C or a ^{12}C) allow for differentiation of metabolic pathways in one step. In vivo, ex vivo, and in vitro ^{13}C -NMR spectroscopic methods have been applied for many years to study the metabolism of glucose and metabolic interactions between neurons and astrocytes in the brain.

2.2 Overview

^{13}C -NMR investigations of glucose metabolism is a major topic of this chapter to discuss glial–neuronal shuttle systems involved in brain glucose metabolism. Therefore, first a short introduction is given on how the metabolism of ^{13}C -labeled glucose is analyzed using NMR. In the brain, glucose is metabolized by both astrocytes and neurons. However, different hypotheses exist to which relative extent glucose is metabolized by these two cell types. Major hypotheses favor a predominantly neuronal glucose consumption with respect to the functional activities in the brain. Also, on the other hand, a predominantly astrocytic conversion of glucose to other substrates, such as lactate, which are subsequently provided to the neurons, is an important hypothesis (i.e., Magistretti’s hypothesis). The major literature on data discussing different hypotheses of cellular glucose consumption are presented for both in vivo and in vitro investigations. Furthermore, glucose can be converted by different pathways, such as glycolysis and subsequently the TCA cycle, whereby PDH and PC are the major pathways, by which the carbons originating from glucose enter the TCA cycle. All these pathways are expressed differentially in neurons and astrocytes. For example, the anaplerotic enzyme PC, which is needed to replenish TCA cycle intermediates in both astrocytes and neurons, is selectively expressed in astrocytes. Astrocytes are also considered to be “glycolytic” cells and are suggested to be able to produce more ATP in the cytosol than neurons during pathological conditions. However, major controversy still exists about the relative contribution of astrocytes to mitochondrial glucose oxidation and ATP production. Indeed, glucose oxidation via the TCA cycle maintains the high energy need of neurons. However, astrocytic functions also require energy in the form of ATP, and the anaplerotic flux through PC, which is also needed to synthesize metabolic precursors for the neuronal TCA cycle, cannot be maintained without concomitant fluxes through PDH in these cells (see [Figure 3.2-3](#)). The controversial hypotheses about the relative glucose oxidation via the neuronal or the astrocytic TCA cycle are mostly due to the lack of appropriate techniques to analyze cell-specific metabolism within the intact brain. ^{13}C -NMR spectroscopy remains the most appropriate technique to analyze cell-specific

■ Figure 3.2-3


Label distribution (*stars*) during $[1-^{13}\text{C}_1]\text{glucose}$ metabolism through the Krebs cycle after glycolytic formation to $[3-^{13}\text{C}_1]\text{pyruvate}$, which is converted via PDH and PC to $[2-^{13}\text{C}_1]\text{acetyl-CoA}$ and $[3-^{13}\text{C}_1]\text{oxaloacetate}$, respectively. The fluxes through PDH and PC lead to a different ^{13}C -labeling pattern in the Krebs cycle intermediate citrate and are finally measured by the isotopomer pattern of glutamate in ^{13}C -NMR spectra. The same isotopomer pattern as in glutamate is seen in glutamine. PC, pyruvate carboxylase; PDH, pyruvate dehydrogenase




metabolism, and this chapter outlines some of the major literature on data obtained on both the intact brain *in vivo* and on primary cells in culture *in vitro*. While all these data are consistent with the localization of PC in astrocytes and their important “nutritional role,” the relative cellular distribution of PDH and the ratio of PC/PDH in the astrocytes seem to depend on physiological and pathophysiological situations as well as experimental conditions both *in vivo* and *in vitro*.

2.3 NMR Analysis of the Metabolic Fate of ^{13}C -Labeled Glucose

The oxidation of glucose occurs in the mitochondrial TCA cycle after the PDH-mediated conversion of pyruvate to acetyl-CoA. However, as shown in [Figure 3.2-3](#), this process provides only two carbons into the TCA cycle. Since these two carbons are oxidized to two molecules of CO_2 , PDH alone cannot sustain net biosynthesis of amino acids. In fact, the continuous drain of TCA cycle intermediates due to biosynthetic processes must be complemented by a mechanism that replenishes TCA cycle intermediates (so-called “anaplerosis”). The principal anaplerotic enzyme in the brain is PC (Patel, 1974), which is, like GS, selectively localized in astrocytes, while PDH is expressed in both astrocytes and neurons. Therefore, astrocytes play a “nutritional” role by delivering energy substrates to neurons, and glial pyruvate

carboxylation and glutamine synthesis have been shown to be prerequisites for the replenishment of neuronal glutamate (Gruetter, 2002).  *Figure 3.2-3* shows how the fluxes through PDH and PC can be differentiated using NMR spectroscopy. Briefly, via glycolysis, one molecule of $[1-^{13}\text{C}_1]$ glucose is transformed into two molecules of $[3-^{13}\text{C}_1]$ pyruvate. $[3-^{13}\text{C}_1]$ pyruvate is transformed via PDH to $[2-^{13}\text{C}_1]$ acetyl-CoA or is carboxylated via PC to $[3-^{13}\text{C}_1]$ oxaloacetate, which condenses with acetyl-CoA to citrate. Glucose flux through these two pathways can be quantified from ^{13}C -NMR spectra from the ^{13}C -labeling pattern in glutamate synthesized from the TCA cycle intermediate α -ketoglutarate (Zwingmann and Leibfritz, 2003). Glutamate is subsequently transformed to glutamine or GABA. De novo synthesis of metabolites and associated metabolic pathways can be differentiated in a single ^{13}C -NMR spectrum.

A detailed description of the isotopomers arising via the main pathways of the most commonly used glucose isotopomers, i.e., of $[1-^{13}\text{C}_1]$ -, $[2-^{13}\text{C}_1]$ -, and $[U-^{13}\text{C}_6]$ glucose, is given in Zwingmann and Leibfritz (2003). The metabolites in the brain/brain cells are multiple labeled with ^{13}C in specific carbon positions, depending on the enzymatic pathway. As an example,  *Figure 3.2-4* shows the isotopomers of glutamate and glutamine, formed from $[1-^{13}\text{C}_1]$ glucose via the first passage through PC or via the first and second turn through PDH. Briefly, $[1-^{13}\text{C}_1]$ glucose is transformed via the glycolytic pathway to $[3-^{13}\text{C}_1]$ pyruvate (and subsequently to $[3-^{13}\text{C}_1]$ alanine via alanine aminotransferase (ALAT; EC 2.6.1.2)) and to $[3-^{13}\text{C}_1]$ lactate via lactate dehydrogenase (LDH; EC 1.1.1.27). Then $[3-^{13}\text{C}_1]$ pyruvate enters the TCA cycle via the anaplerotic pathway (PC; EC 6.4.1.1) (or malic enzyme (ME; EC 1.1.1.40); not shown) or the oxidative pathway (PDH; EC 1.2.4.1). After carboxylation of pyruvate via PC or ME, the ^{13}C -labeled intermediates leaving the TCA cycle are indistinguishable. In the anaplerotic and oxidative pathway, $[2-^{13}\text{C}_1]$ - or $[3-^{13}\text{C}_1]$ - and $[4-^{13}\text{C}_1]$ glutamate will be formed, respectively, during the first TCA cycle turn. After the second turn via PDH, $[3,4-^{13}\text{C}_2]$ - and $[2,4-^{13}\text{C}_2]$ glutamate will be formed, if $[2-^{13}\text{C}_1]$ acetyl-CoA enters the TCA cycle. Different isotopomers are formed during subsequent TCA cycle turns. The same isotopomer pattern as in glutamate is seen in glutamine. For a more detailed isotopomer analysis and the isotopomer pattern in GABA, see Zwingmann and Leibfritz (2003). The mono- and double labeled isotopomers are observed in ^{13}C -NMR spectra as singlet- and doublet (i.e., two adjacent carbon positions are labeled) signals, respectively.

However, the precise nature of cerebral glucose metabolism remains not clearly resolved, since astrocytes and neurons interact metabolically in processes involving intercellular metabolite transfer of several compounds derived from glucose metabolism.

2.4 Cell-Specific Glucose Metabolism in Astrocytes and Neurons

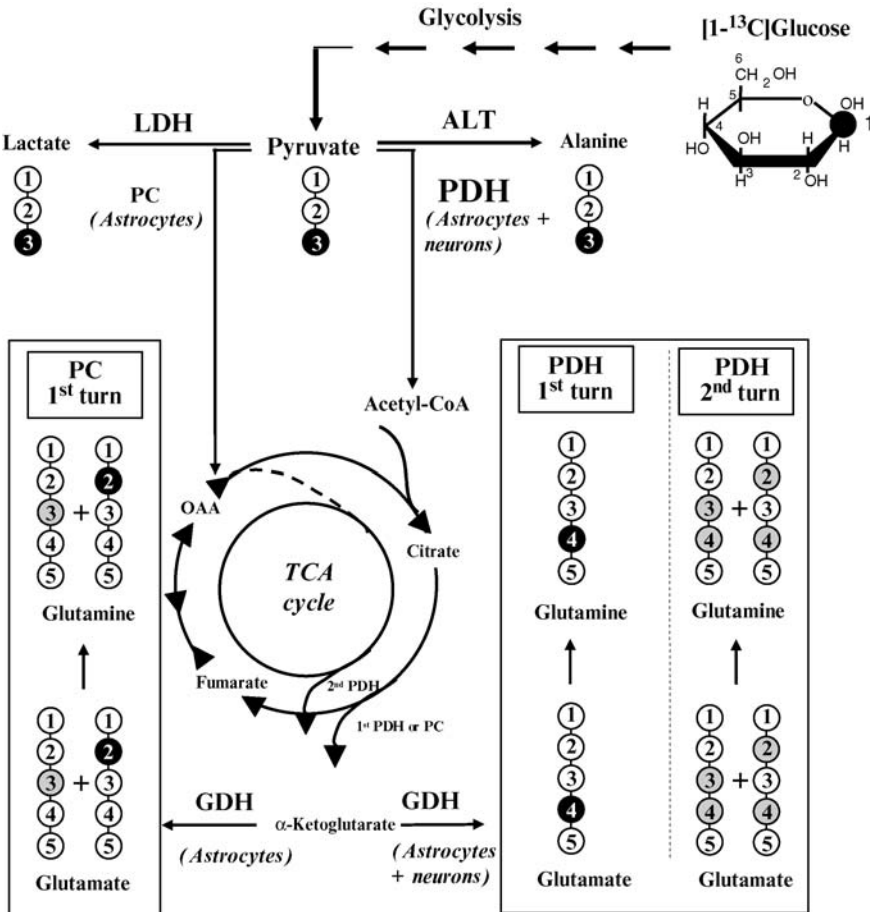
Glucose has long been thought to be metabolized mainly in the neuronal TCA cycle (see *Sect. 1*). However, it also has been hypothesized that glucose is a predominantly astrocytic substrate. Magistretti and colleagues proposed in 1994 a mechanism whereby lactate is produced glycolytically by astrocytes and supplied to the neurons as an energy substrate (Pellerin and Magistretti, 1994, 2003; Magistretti et al., 1999; Magistretti and Pellerin, 1999). This implies that (1) about 85% of glucose consumption during brain activation is initiated by aerobic glycolysis in astrocytes, triggered by the demand for glycolytically derived energy for Na^+ -dependent accumulation of transmitter glutamate and its amidation to glutamine, and that (2) the generated lactate is transferred to neurons for oxidative degradation. However, this is a highly controversial issue not directly confirmed by some others (see Dienel and Hertz, 2001 and references therein), discussed in more detail below.

Consistent with Magistretti's hypothesis, astrocytes have the capacity to release large amounts of lactate (Walz and Mukerji, 1998), which is thought to be an important fuel for neurons (Magistretti et al., 1999). Similarly, also Tsacopoulos and colleagues demonstrated in retinal (Mueller) cells a stimulatory effect of glutamate and ammonia on glial glycolysis (Tsacopoulos et al., 1997; Tsacopoulos, 2002). It has been proposed that net production and release of lactate (and alanine) by Mueller cells serves to maintain their stimulated glycolysis and to fuel mitochondrial oxidative metabolism and glutamate resynthesis in photoreceptors. However, controversy still exists about the extent of this mechanism (Hertz et al., 1999).

Both astrocytes and neurons are potentially capable of oxidizing glucose completely to CO_2 and H_2O , and glucose transporters are present on both cell types (Vannucci et al., 1997). Studies in cell culture have

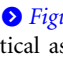
Figure 3.2-4

Catabolites of $[1-^{13}\text{C}_1]\text{glucose}$ are labeled in different carbon positions, depending upon the involved enzymatic pathways. Briefly, $[3-^{13}\text{C}_1]\text{pyruvate}$, $[3-^{13}\text{C}_1]\text{alanine}$, and $[3-^{13}\text{C}_1]\text{lactate}$ are formed via glycolysis. $[3-^{13}\text{C}_1]\text{pyruvate}$ enters the TCA cycle via PC as $[3-^{13}\text{C}_1]\text{OAA}$ or via the oxidative pathway (PDH) as $[2-^{13}\text{C}_1]\text{acetyl-CoA}$. These pathways are reflected by the isotopomer pattern in $\alpha\text{-ketoglutarate}$ (and subsequently glutamate and glutamine) (left and right hand side): During the first PC turn an unlabeled molecule of acetyl-CoA condenses with $[3-^{13}\text{C}_1]\text{OAA}$, and $\alpha\text{-ketoglutarate}$ (and subsequently glutamate and glutamine) is mono labeled at C2 (black circles) (or at C3 after equilibration of OAA with the symmetrical fumarate; grey circles). During the first PDH turn an unlabeled molecule of OAA reacts with $[2-^{13}\text{C}_1]\text{acetyl-CoA}$ to form $\alpha\text{-ketoglutarate}$ mono labeled at C4 (black circles). During the second PDH turn, doubly labeled $\alpha\text{-ketoglutarate}$ is synthesized (grey circles). After TCA cycle entry of $[3-^{13}\text{C}_1]\text{pyruvate}$ as $[3-^{13}\text{C}_1]\text{OAA}$, as well as during the first turn via PDH, $[3-^{13}\text{C}_1]\text{aspartate}$ (and $[3-^{13}\text{C}_1]\text{aspartate}$ after equilibration of OAA with fumarate) can be formed via Aspartate aminotransferase (not shown in figure), whereby glutamate is transaminated to $\alpha\text{-ketoglutarate}$. Note: The reaction is reversible, and $\alpha\text{-ketoglutarate}$ can serve as precursor for glutamate by transamination with aspartate. ALAT, alanine aminotransferase; GS, glutamine synthetase; GDH, glutamate dehydrogenase; LDH, lactate dehydrogenase; OAA, oxaloacetate; PC, pyruvate carboxylase; PDH, pyruvate dehydrogenase



measured the rates of glucose consumption in cultured neurons and astrocytes. Values for glucose uptake by cultured astrocytes obtained by the 2-DG method range between 100 and 250 nmol/h/mg of cell protein and are almost one-half in cultured neurons (Peng et al., 1994, 2001; Hamai et al., 1999; Marris and Juurlink, 1999). Vega and coworkers (2003) studied the uptake and distribution of locally applied 2-DG, glucose, or lactate in a rat vagus nerve preparation and showed that approximately 80% of the labeled 2-DG (and by extension of glucose utilization) occurs in Schwann cells, the counterparts of astrocytes in the peripheral nervous system. Consistent with the anatomical localization of astrocytes, all these studies indicate active glucose metabolism in astrocytes, and it is evident that the export of metabolic intermediates is associated with astrocytic glucose uptake (see Tsacopoulos et al., 1988, 1994; Dringen et al., 1993; Tsacopoulos and Magistretti, 1996; Tsacopoulos, 2002). In addition, astrocytic, but not neuronal, uptake of glucose has been shown to respond to manipulations of the extracellular milieu, such as in the concentration of potassium (Peng et al., 1994).

2.5 Glucose Metabolism Through Glycolysis

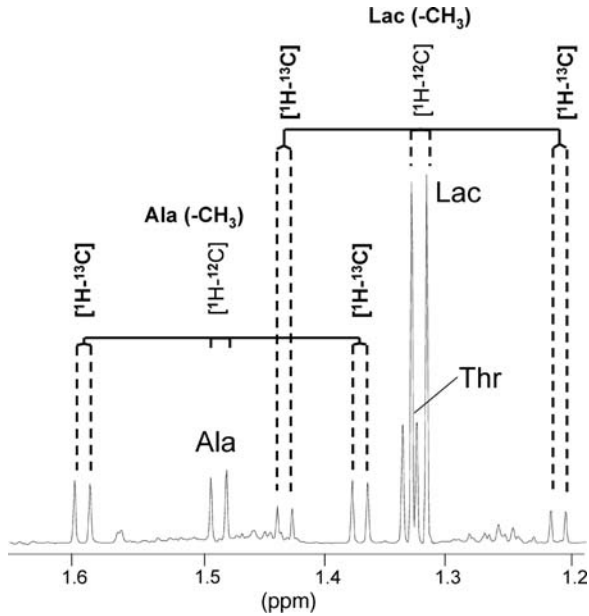
The rate of glycolysis can be estimated by the rate of lactate formation. It should be mentioned that total amounts of lactate do not accurately reflect glycolytic activity. Pyruvate and subsequently lactate may be produced from other (unlabeled or labeled) precursors such as lipids and fatty acids, ketone bodies, as well as amino acids present in the medium, or produced by catabolism of cellular proteins. In contrast to biochemical methods, the use of ^{13}C -labeled glucose allows to measure the rate of lactate synthesis from glucose. In particular, the heteronuclear spin pattern of lactate in the high-field region of ^1H -NMR spectra allows to distinguish between lactate synthesized after glycolytic transformation of ^{13}C -labeled glucose (^{13}C -labeled lactate shows an additional doublet splitting due to ^1H - ^{13}C coupling ($J = 128$ Hz)) and the unlabeled isotopomer ($[^{12}\text{C}]$ lactate) synthesized from unlabeled pyruvate, which has been formed from substrates other than ^{13}C -labeled glucose.  *Figure 3.2-5* shows representative segments of ^1H -NMR spectra of extracts obtained from cultured cortical astrocytes incubated for 24 h with 2.5 mM $[1-^{13}\text{C}_1]$ glucose.

Because of different experimental conditions and cell types used in cell culture studies, the values for the uptake of glucose and release of lactate for the individual cell types vary over a wide range (Zwingmann and Leibfritz, 2003). These values are on average only slightly higher than those of glucose uptake in the intact rat brain of approximately $0.42 \mu\text{mol/h/mg}$ (Sokoloff, 1983–84), and consistently demonstrate much higher glucose utilization and lactate production rates by astrocytes compared with cultured neurons. The wide range of values may be due also to cellular reuptake of extracellular lactate. Cellular lactate uptake occurs by carrier-mediated diffusion, which is determined to a large extent by the ratio of intra/extracellular lactate and lactate utilization (Dienel and Hertz, 2001). As reported by Dienel and Hertz (2001), both in cultured astrocytes and in glutamatergic neurons the ratio of lactate uptake/glucose oxidation is approximately 1/4. In cortical neurons (GABAergic), for example, the amount of extracellular administered $[\text{U-}^{13}\text{C}_3]$ lactate (1 mM) in the medium did not change during 4 h incubation, indicating a balance between consumption and production (Waagepetersen et al., 1998a). In cocultures of astrocytes and neurons, the ratio of glucose consumption/lactate production was approximately intermediate (0.75–1) between those in individual astrocytes (1.2–1.3) and neurons (0.3–0.35) (Schousboe et al., 1997; Zwingmann et al., 2000). Interestingly, cultured cerebellar neurons (glutamatergic) have a much higher capacity for lactate production than cortical neurons (GABAergic neurons) (Hassel et al., 1995b) and are able to respond to hypoxia with a switch to anaerobic glycolysis (Sonnewald et al., 1994). This difference may be due to the presence of low amounts of the H_4 -LDH isoenzyme in cortical, but not in cerebellar neurons (Schousboe et al., 1993a).

Consistent with the NMR data, astrocytes are considered to be “glycolytic” cells, as astrocytes, unlike neurons, can maintain ATP levels and cellular function by glycolytic metabolism alone (Kauppinen et al., 1988; Yu et al., 1989). The high dependence of astrocytic energy production on glycolysis was shown by significantly decreased ATP production under glucose deprivation (Mertens-Strijthagen et al., 1996). In addition, mitochondrial toxins and hypoxia strongly stimulate glucose metabolism through the glycolytic

■ Figure 3.2-5

Segments of $^1\text{H-NMR}$ extract spectra obtained from cultured cortical astrocytes incubated for 24 h with 2.5 mM [$1\text{-}^{13}\text{C}_1$]glucose. The use of ^{13}C -labeled glucose allows to measure the rate of lactate synthesis from glucose. In particular, the heteronuclear spin pattern of lactate in the high-field region of $^1\text{H-NMR}$ spectra distinguishes between lactate synthesized via glycolytic degradation of ^{13}C -labeled glucose (^{13}C -labeled lactate shows an additional doublet splitting due to $^1\text{H}\text{-}^{13}\text{C}$ coupling ($J = 128\text{ Hz}$)) and the unlabeled isotopomer ($[^{12}\text{C}]$ lactate) synthesized from unlabeled pyruvate, which has been formed from substrates other than ^{13}C -labeled glucose. The ratio between ^{13}C -labeled and -unlabeled lactate, therefore, reflects the relative glycolytic flux of ^{13}C -labeled glucose. The doublet downfield of lactate represents the methyl group protons of unlabeled Thr. Ala, alanine; Lac, lactate; Thr, threonine



pathway in astrocytes, whereas neurons are unable to utilize glycolysis as the unique source of ATP (see Taylor et al., 1996). The amount of glucose in the blood is five times higher than is the availability of oxygen for the oxidative metabolism of glucose (Huang et al., 1997), and astrocytes seem to survive hypoxia as long as there is a supply of glucose for anaerobic glycolysis, provided that the pH does not drop below 6.5 due to lactic acidosis (Swanson et al., 1997; Marrif and Juurlink, 1999). On the other hand, astrocytes appear to be responsible for the release of lactate into the extracellular space as demonstrated in cultured astrocytes as well as in the brain under conditions of perturbed brain energy metabolism, such as hypoxia or hypoglycemia (Walz and Mukerji, 1998; Korf, 1996), and their ability to upregulate glycolysis therefore may be important for their neuroprotective functions.

2.6 Glucose Oxidation Through the TCA Cycle

The functional activities in the brain require glucose metabolism through both glycolysis and the TCA cycle, and most of the energy necessary for brain function is derived from the full oxidation of glucose in the TCA cycle. An important question in terms of cellular energy metabolism concerns the relative ATP productions in neurons and astrocytes.

PDH, leading to acetyl-CoA entering the TCA cycle, is the key enzyme for oxidative and energy metabolism in the brain. Magistretti's hypothesis implies that glycolytic consumption of glucose by

astrocytes provides maximum 2 molecules of ATP in these cells and 36 molecules of ATP in neurons per mole of oxidized glucose. This would mean that approximately 5% of the ATP is produced in the glial cell while the rest would be generated from lactate in the neurons (Pellerin and Magistretti, 2003). These values for ATP would corroborate with relative energy production under the assumption that approximately 95% of glucose is taken up and metabolized by neurons (Pellerin and Magistretti, 2003). However, these assumptions are, also considering the difficulties of measuring cellular ATP production in the whole brain, speculative and can just serve as one hypothesis.

Indeed, there is no doubt that glutamate uptake in astrocytes drives their metabolism toward ATP production, but the necessary energy may be fueled either by glycolysis or by glucose oxidation in these cells. Considering glutamate uptake rates by astrocytes and the cotransport of two or three Na^+ ions per molecule glutamate, which have to be removed via the Na^+/K^+ -ATPase (Silver and Erecinska, 1997), it was calculated that astrocytic glutamate transport will consume 40 nmol ATP/min/mg protein (Yager et al., 1994; Marrif and Juurlink, 1999). Assuming a maximal glycolytic rate of 15 nmol of glucose utilized/min/mg, at least 10 nmol of glucose utilized/min/mg must be provided by oxidative metabolism (Dienel and Hertz, 2001). Data obtained on this issue are controversial. While Magistretti's model (1994) states that uptake of glutamate mainly stimulates aerobic glycolysis and lactate production, Peng and coworkers (2001) provided evidence that the energy demand for the uptake of glutamate is fueled by its own oxidation via the TCA cycle. A further study showed that glucose deprivation in cultured astrocytes alone had little effect on removal of glutamate from the culture medium and was only partially reduced during exposure to combined hypoglycemia/hypoxia, but the presence of iodoacetate (a glycolysis inhibitor) or incubation in a low-oxygen atmosphere decreased glutamate clearance by 50% (Bakken et al., 1998a). In addition, the TCA cycle inhibitors fluorocitrate (Swanson and Graham, 1994) and 3-nitropropionic acid (3-NPA) (Bakken et al., 1997a) caused only minor decreases in $[\text{U-}^{13}\text{C}_5]$ glutamate uptake in cultured astrocytes, supporting the view that glycolytic metabolism is of major importance for the ability of astrocytes to take up glutamate, or for compensation if oxidation is impaired.

2.7 Glucose Metabolism via Anaplerosis

Nonoxidized glucose, not used for mitochondrial energy metabolism, is mainly used for biosynthetic processes. However, neurons are continuously drained as a result of neurotransmitter synthesis and release, but cannot sustain their TCA cycle intermediates by providing oxaloacetate as substrate for the citrate synthase reaction. In particular, neurons depend on the metabolic support from astrocytes (Shank et al., 1985; Kaufman and Driscoll, 1993), as the loss of neuronal α -ketoglutarate stores has to be replenished by an anaplerotic mechanism, i.e., by carboxylation of pyruvate to oxaloacetate. In addition, glutamate (and GABA) is not completely recycled by glutamine formation in astrocytes, i.e., via the glutamate (GABA)–glutamine cycle, but also catabolized in both the neuronal and the astrocytic TCA cycles, and used for synthesis of other compounds, such as glutathione, cellular proteins, etc. In astrocytes, on the other hand, formation of glutamine, which is supplied to neurons, and its continuous release from the brain (with a rate of approximately 10 nmol/g tissue/min) (Grill et al., 1992), leads to a loss of TCA cycle intermediates in these cells.

Net production of α -ketoglutarate (and subsequently glutamate and glutamine) from glucose requires (1) synthesis of oxaloacetate (or malate) from pyruvate and CO_2 (Patel, 1974), (2) formation of acetyl-CoA, which enters the TCA cycle through condensation with oxaloacetate, and (3) decarboxylation of citrate (via isocitrate) to α -ketoglutarate. Note that there is still a controversy as to the specific roles and relative importance as well as cellular distribution of certain enzymes involved in glutamate and glutamine metabolism in both neurons and astrocytes, such as aminotransferases interconverting α -ketoglutarate and glutamate via glutamate dehydrogenase (GDH), which can contribute significantly to the compartmentation of metabolism, as reviewed by McKenna et al. (2000a).

Pyruvate carboxylation in the brain depends mainly on the activity of PC but is mediated also via ME, though to a much lower extent (Patel, 1974). While the exact inter- and intracellular localizations of ME and phosphoenolpyruvate carboxykinase (PEPCK) are not fully elucidated, and both were found

in neurons and astrocytes, PC activity has been demonstrated to be glial both *in vivo* and *in vitro* (Shank et al., 1993, 1985; Yu et al., 1983; Kaufman and Driscoll, 1993), which was confirmed using immunocytochemistry by Cesar and Hamprecht (1995).

The association of the astrocytic TCA cycle with PC confirms the early notion of pyruvate carboxylation as an important prerequisite for glutamine formation (Waelsch et al., 1964; Gruetter, 2002). Consistent with a strong association of glutamine synthesis with PC, pyruvate carboxylation supports glial formation and export of glutamine both *in vivo* and *in vitro* (Shank et al., 1985; Martin et al., 1995, 1997; Gamberino et al., 1997; Lieth et al., 2001; Hassel, 2002; Oz et al., 2004). The essential role of glutamine synthesis for brain function is evident also from the stimulated glutamine synthesis as well as glutamine release into the medium in cerebellar and cortical astrocytes between 15 and 35 days in culture (Martin et al., 1995, 1997). This observation is in agreement with indications from Caldani et al. (1982) that the increase in GS activity in cultured astrocytes is closely correlated with the *in vivo* increase in the activity of this enzyme in the developing brain.

Previous studies measuring the rate of $^{14}\text{CO}_2$ fixation relative to glucose oxidation to CO_2 in the rat brain (Naruse et al., 1966a, b) reveal an approximately 10% contribution of the anaplerotic pathway to the total glucose metabolism. Later metabolic studies using ^{14}C -labeled glucose and pyruvate confirmed this 10% value (Shank and Aprison, 1981). However, in measurements based on CO_2 fixation or production alone (without considering the metabolic intermediates), it should be kept in mind that CO_2 can be fixed also nonanaplerotically through several reactions, such as by formation of malonyl-CoA from acetyl-CoA during fatty acid synthesis, by purine and pyrimidine syntheses, through carboxylation of glutamyl residues in proteins, etc. By using ^{13}C -NMR spectroscopy in the intact brain and brain cells in primary cultures, metabolic fluxes through acetyl-CoA and pyruvate carboxylation can be investigated separately, because the labeling pattern of the citrate molecule, and thus of α -ketoglutarate and subsequently glutamate, glutamine, and GABA, differs according to the relative operation of both pathways. After systemic administration of ^{13}C -labeled glucose the flux of carbon through PC for net formation of glutamate, glutamine, and GABA in brain *in situ* corresponds to approximately 10% and 20% of the total turnover in the TCA cycle in rats and humans, respectively (Aureli et al., 1997; Cruz and Cerdan, 1999; Hertz et al., 1999; Gruetter et al., 2001). The astrocytic-selective metabolism of ^{13}C -labeled acetate in human *in vivo* (Bluml et al., 2002; Lebon et al., 2002) revealed that the astrocytic TCA cycle contributes to 15%–20% of total brain oxidative metabolism, and that up to 30% of the glutamine transferred to the neurons by the cycle may be derived from astrocytic anaplerosis, supporting an active role of astrocytes for neurotransmitter activity. This reflects somewhat the four times higher rate of glutamine formation compared to pyruvate carboxylation measured by *in vivo* ^{13}C -MRS in the resting human brain (Gruetter et al., 1998).

The rate of TCA cycle turnover amounts to 6 nmol/min/mg protein in human brains and 14 nmol/min/mg in rat brains under normal, resting conditions (Hertz and Dienel, 2002 and references therein). Considering the relative contribution of pyruvate carboxylation to the TCA cycle flux, the rate of pyruvate carboxylation amounts to approximately 1–1.5 nmol/min/mg protein. Under the assumption of neuronal and glial TCA cycle of approximately 13 and 3 nmol/min/mg, respectively, reported in mouse brain *in vivo* (van den Berg and Garfinkel, 1971), approximately 1/3 to 1/2 of astrocytic metabolism may account for pyruvate carboxylation. As astrocytes constitute 20%–30% of total brain volume (Hertz and Dienel, 2002 and references therein), a value of approximately 5 nmol/min/mg of astrocytic protein is very similar to the rate of pyruvate carboxylation in cultured astrocytes (4 nmol/min/mg protein) (Yu et al., 1983).

2.8 Ratio of Anaplerotic/Oxidative Glucose Metabolism

Most *ex vivo* and *in vitro* estimations of the contribution of flux through PC compared with PDH are based on the labeling pattern of amino acids derived from the metabolism of [$^{13}\text{C}_1$]glucose isotopomers (see Zwingmann and Leibfritz, 2003). However, accurate estimations of PC/PDH ratios after [$1\text{-}^{13}\text{C}_1$]glucose metabolism are limited by the appearance of same isotopomers arising from different metabolic pathways. Therefore, the range of values for the relative contributions of PC and PDH to amino acid labeling is rather large. For example, the PC/PDH ratio reflected in glutamine isotopomers (labeled from intraperitoneally

injected [$1\text{-}^{13}\text{C}_1$]glucose in rats) was 33%, 36%, and 9.8% after 15, 30, or 45 min, respectively (Shank et al., 1993). On the other hand, after intravenous [$1\text{-}^{13}\text{C}_1$]glucose injection in mice the PC/PDH values were 58%, 41%, and 0 at 5, 15, 30 min, respectively (Hassel et al., 1995a). The results for glutamate (and GABA) vary even more.

However, these values were obtained using different formula. Furthermore, the label in α -ketoglutarate at C-2 and C-3 (C-4 and C-3 of GABA) may arise both via PC- and ME- mediated entry of pyruvate into the TCA cycle as well as during the second turn via PDH, whereas [$4\text{-}^{13}\text{C}_1$] α -ketoglutarate and [$2\text{-}^{13}\text{C}_1$]GABA are generated exclusively by the activity of PDH. For example, the accurate use of the formula C2+C3/C4 as a reflection of the ratio of PC/PDH must assume that these isotopomers arise only via the first PC and PDH turns, which is not true in most studies lasting long enough to allow for further TCA cycle turns. The same consideration has to be taken when estimating the PC/PDH ratio by the ratio of C-2/C-4 in α -ketoglutarate.

In several studies, where the C-2 position of glutamine and glutamate is labeled to a higher degree than the C-3 position, the formula (C2–C3)/C4 has been used to calculate the ratio of PC/PDH glucose (Merle et al., 1996a, b). These calculations assume an absent equilibration of malate with fumarate. Also the consistently higher label enrichment in C-3 than in C-2 of aspartate suggests a noncomplete equilibration of oxaloacetate with fumarate. However, the aspartate aminotransferase reaction, catalyzing the interconversion of aspartate and glutamate (alanine) to oxaloacetate and α -ketoglutarate (pyruvate), proceeds very fast, and an extensive equilibration of oxaloacetate (or malate) with fumarate has been observed consistently *in vivo* and *in vitro*. For example, a 39% cycling between oxaloacetate and fumarate was deduced from labeling of glutamine from [$1\text{-}^{13}\text{C}_1$]glucose (Merle et al., 1996a, b). This mechanism also becomes more important with the time duration of the experiment (Waelsch et al., 1964). Using this formula, the anaplerotic pathway contributed only little (not more than 3%) to glutamate synthesis. The possibility that glutamate is metabolically not very active in these cells is not likely, because label must have passed through glutamate prior to accumulating in glutamine. Therefore, the content of glutamate in astrocytes may be so small that the enrichment in C-2 relative to C-3 in these cells was nearly obscured by the much larger amount of glutamate labeled via the oxidative pathway in neurons. However, the relative neuronal and astrocytic pools of glutamate in the brain are approximately 10 mM and 1–2 mM, which is consistent with a 9% contribution of the glial glutamate pool to total cerebral glutamate, as also demonstrated by analysis of isotopomer pattern in these amino acids after [$1\text{-}^{13}\text{C}_1$]glucose and [$2\text{-}^{13}\text{C}_1$, $2\text{-}^2\text{H}_3$]acetate metabolism in rat brains (Chapa et al., 2000). Therefore, the low values estimated for the contribution of PC to glutamate synthesis likely are an underestimation because of neglecting the label equilibration.

It is difficult to measure the equilibration between oxaloacetate and fumarate in studies in the intact brain, as it may be different in astrocytes and neurons. In *in vitro* studies, it occurs either in neurons (Brand et al., 1992, 1993; Martin et al., 1993; Merle et al., 1996a, b) or in astrocytes (Brand et al., 1992, 1993; Martin et al., 1993, 1997; Zwingmann et al., 1998). In addition, the extent of equilibration even varied between different types of astrocytes in primary cultures (Martin et al., 1995). Consistent with an important contribution of the equilibration of label in oxaloacetate, the values for PC/PDH obtained using the formula (C2–C3)/C4 show not only large variations, but also in some cases even a negative value for the PC/PDH contribution to glutamine and glutamate formation (Zwingmann and Leibfritz, 2003).

An unequivocal means of assessing relative PC/PDH fluxes comes from the use of [$2\text{-}^{13}\text{C}_1$]pyruvate (Brand et al., 1992, 1993) or [$2\text{-}^{13}\text{C}_1$]glucose (Badar-Goffer et al., 1990; Kanamatsu and Tsukada, 1999; Sibson et al., 2001). In contrast to metabolism of [$1\text{-}^{13}\text{C}_1$]glucose or [$3\text{-}^{13}\text{C}_1$]pyruvate, α -ketoglutarate (and subsequently glutamate and glutamine), labeled in C-3 or C-2 (C-2 only through equilibration of label in oxaloacetate) from [$2\text{-}^{13}\text{C}_1$]pyruvate (C-3 and C-4 in GABA), can be synthesized only via the anaplerotic pathway, whereas the label at C-5 in α -ketoglutarate (C-1 in GABA) results only through PDH activity. In addition, as the label in C-3 arises only through equilibration of oxaloacetate with fumarate, the contribution of this pathway can be included into the calculation. Furthermore, the calculations can be extended to the relative contribution of PC and PDH to aspartate synthesis, as labeling of this amino acid in C-2 and C-3 is possible only through pyruvate carboxylation. The PC/PDH ratio is calculated by the ratio of C-3/C-5 in glutamate and glutamine and C-4/C-1 in GABA. Studies of cortical brain slices using [$2\text{-}^{13}\text{C}_1$]glucose revealed PC/PDH ratios of 5.6, 13.5, and 10 for glutamate, glutamine, and GABA, respectively (Taylor et al., 1996), demonstrating a significant contribution of flux through PC for glutamate synthesis. Another means

for the determination of PC/PDH ratios is to use doubly labeled $[1,2-^{13}\text{C}_2]$ glucose as substrate *in vivo* as well as *ex vivo* (Kunnecke et al., 1993). The PC pathway produces $[2,3-^{13}\text{C}_2]$ oxaloacetate and, in the first turn of the TCA cycle, also $[2,3-^{13}\text{C}_2]$ glutamate and -glutamine. After $[1,2-^{13}\text{C}_2]$ glucose infusion in rats, 38% of the total flux through the glial TCA cycle is derived from the contribution of PC, estimated from the isotopomer distributions in glutamate and glutamine.

Even more information on the PC/PDH ratio may be obtained by using $[\text{U}-^{13}\text{C}_6]$ glucose, which has the advantage of unambiguous detection of incorporation of label into metabolites due to ^{13}C – ^{13}C spin–spin coupling patterns. The higher labeling of $[2,3-^{13}\text{C}_2]$ - and $[2,3,4,5-^{13}\text{C}_4]$ glutamate formed after PC-mediated entry of pyruvate into the TCA cycle and condensation of oxaloacetate with ^{13}C -labeled or unlabeled acetyl-CoA, respectively, versus $[1,2,3-^{13}\text{C}_3]$ - and $[\text{U}-^{13}\text{C}_5]$ glutamate, formed in the third TCA cycle turn via PDH, in astrocytes compared to the converse ratio in neurons confirmed the astrocyte-specific pyruvate carboxylation (Waagepetersen et al., 2001). However, the relative contribution of PC may be overestimated, as $[2,3,4,5-^{13}\text{C}_4]$ glutamate is synthesized also in the third turn via PC, but only if oxaloacetate condenses for two turns with PDH-derived acetyl-CoA, and $[2,3,4,5-^{13}\text{C}_4]$ glutamate is formed in the third PDH turn without contribution of PC as well. Furthermore, $[2,3-^{13}\text{C}_2]$ glutamate is formed also during the third PDH turn after condensation of oxaloacetate with unlabeled acetyl-CoA, and $[4,5-^{13}\text{C}_2]$ glutamate is synthesized also during the second PC turn after condensation of labeled acetyl-CoA. This may influence the relative PC/PDH ratios in astrocytes and neurons, in particular, if these cell types display different relative TCA cycling ratios. In the study conducted by Lapidot and Gopher (1994) using $[\text{U}-^{13}\text{C}_6]$ glucose (as well as that of Kunnecke et al. (1993) using $[1,2-^{13}\text{C}_2]$ glucose), the ratio of PC/PDH was estimated assuming total cycling of oxaloacetate to fumarate, which means that the relative contribution of PC may be overestimated.

3 Cerebral Acetate Metabolism

3.1 Introduction

The dependence of brain function on glucose as metabolic fuel does not exclude the possibility that other substrates may be used as metabolic fuels by brain cells. Energy substrates other than glucose can enter the TCA cycle and replenish TCA cycle intermediates. These include fatty acids and ketone bodies (Edmond, 1992), as well as several amino acids that cross the BBB (Oldendorf and Szabo, 1976; Kruse et al., 1985). These substrates may be used by the astrocytic or the neuronal compartments differently. Special emphasis in this chapter, however, is given to the metabolism of acetate in the brain. Acetate can be transformed to acetyl-CoA (🔗 [Figure 3.2-6](#)) via acetyl-CoA synthetase (EC 6.2.1.1 acetate: acetyl-CoA ligase). This reaction takes place in the cytosol.

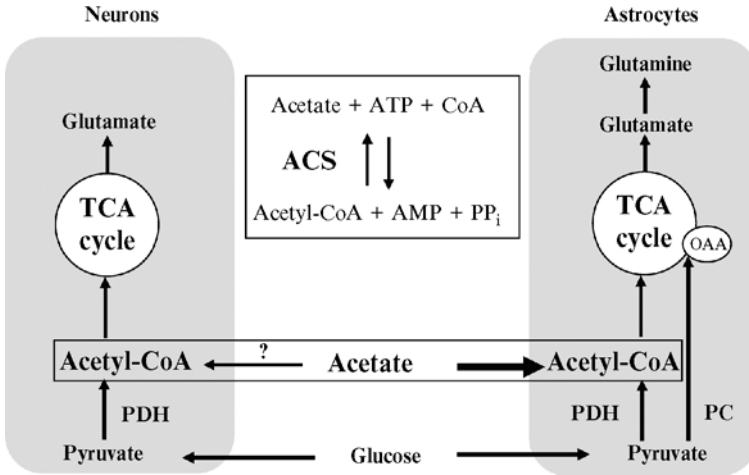
3.2 Overview: Acetate as a Glial Reporter Molecule?

Acetate is considered to be a glia-specific substrate and has been taken as a glial reporter molecule to study astrocytic metabolism and neuronal–astrocytic interactions. Although the activity of acetyl-CoA synthetase was observed to be greater in synaptosomes (neuron-rich homogenates) than in astrocytes (Waniewski and Martin, 1998); the production of $^{14}\text{CO}_2$ due to Krebs cycle metabolism of acetate was 18 times faster in astrocytes compared with synaptosomes. Transport studies showed that this glial-specific metabolism of acetate was attributed to the presence of a specific acetate-uptake mechanism in astrocytes (Waniewski and Martin, 1998). However, controversy exists about this selectivity, and acetate has been shown to be metabolized also in the TCA cycle of primary neurons obtained from rat brains (Brand et al., 1997). Whether this is a phenomenon observed in only cultured juvenile neurons *in vitro* is uncertain. However, it demonstrates the potential capability of neurons also to take up and metabolize acetate.

Nonetheless, a number of *ex vivo* studies using ^{13}C -labeled acetate as substrate provided convincing evidence for the preferential metabolism of acetate in glial cells *in vivo* (see Sonnewald and Kondziella, 2003; Zwingmann and Leibfritz, 2003). Acetate isotopomers used in metabolic NMR studies include

■ Figure 3.2-6

In addition to the transformation of pyruvate to acetyl-CoA via PDH (see also [Figure 2](#)), the carbon skeleton of acetate may react with CoA catalyzed by acetyl-CoA synthetase (ACS) to form acetyl-CoA. This reaction occurs in the cytosol after uptake of acetate through the cellular membrane



[1-¹³C₁]-, [2-¹³C₁]-, and [1,2-¹³C₂]acetate. In addition, the use of acetate simultaneously enriched with ¹³C and ²H (i.e., [2-¹³C₁, 2-²H₃]acetate) uncovered some of the previously unknown aspects of cellular substrate selection in brain energy metabolism (Chapa et al., 2000). As acetate is a very poor substrate for the brain, it is generally administered in the presence of another substrate, i.e., of glucose, which is metabolized by both neurons and astrocytes (Badar-Goffer et al., 1990; Haberg et al., 1998a, b; Chateil et al., 2001; Rae et al., 2003, see Zwingmann and Leibfritz, 2003). Studies using ¹³C-labeled acetate provided some important features of astrocytic and neuronal intermediary metabolism and intercellular trafficking of metabolites in the brain under physiological and pathological conditions. Strong evidence for selective glial metabolism of acetate from all these studies came from comparison of the glutamine/glutamate isotopomer pattern. For example, glutamine can be synthesized from acetate only in the astrocytes, which contain GS activity. Furthermore, the relative contributions of neurons and glial cells to the synthesis of glutamate, glutamine, and GABA under physiological and pathological conditions can be estimated by this approach, i.e., by the administration of labeled glucose (metabolized by astrocytes and neurons) and/or acetate (metabolized by astrocytes).

3.3 Experimental Evidence for Glial-Specific Acetate Metabolism

The cerebral metabolism of acetate takes place in glia as does the formation of glutamine (Martinez-Hernandez et al., 1977), while glutamate de novo synthesis from pyruvate occurs in both glia and neurons. Because of the localization of glutamine synthesis in astrocytes and the much larger pool of glutamate in the neurons, the ratio of glutamine/glutamate synthesized through PDH becomes less than one with [1-¹³C₁] glucose and greater than one with [2-¹³C₁]acetate. The metabolites arising from [2-¹³C₁]acetate metabolism are labeled equally to those after [1-¹³C₁]glucose metabolism through PDH (see [Figure 3.2-2](#)), confirming the supposition that [1-¹³C₁]glucose is primarily metabolized by neurons, whereas [2-¹³C₁]acetate is metabolized by the small compartment that corresponds to glia (Chateil et al., 2001). This fits to anatomical data using autoradiographic methods in brain and retina, demonstrating that [³H]acetate as well as [³H] fluoroacetate may be markers of nonneuronal metabolism (Muir et al., 1986).

3.4 Use of Acetate as Cerebral Substrate to Investigate Glial–Neuronal Interactions

Combined glucose and acetate administration may be used to develop procedures that will provide complementary and extended data to that obtained with 2-DG on regional metabolism in the brain. Using this approach, numerous NMR studies in experimental animal models, perfused brain slices, and primary brain cells in cultures provided an enormous amount of information about the role of astrocytes and neuronal–astrocytic metabolism under physiological conditions, in experimental ischemia, hypoxia, and hyperglycemia, during development of experimental hydrocephalus, limbic seizures, and adult-onset hypothyroidism, in experimental chronic hepatic encephalopathy, and under conditions of (neuronal) metabolic perturbations on the level of TCA cycle metabolism (for reviews see Sonnewald and Kondziella, 2003; Zwingmann and Leibfritz, 2003). Finally, these studies were able to recognize the pyruvate-recycling pathway in astrocytes and suggested mitochondrial heterogeneity in these cells (discussed later). Recently, infusion of ^{13}C -labeled acetate has been applied also in the *in vivo* human brain to investigate the role of glial metabolism, i.e., the astrocytic TCA cycle, brain oxidative metabolism, and the glutamine–glutamate cycle (Bluml et al., 2002; Lebon et al., 2002). These studies indicated that the mean rate of acetate oxidation in fasted normal subjects was approximately 20% of the total cerebral TCA cycle rate (Bluml et al., 2002). Furthermore, the glutamate–glutamine neurotransmitter cycle between astroglia and neurons seems to be the major pathway for neuronal glutamate repletion, whereby the astroglial TCA cycle flux accounts for approximately 14% of brain oxygen consumption, and up to 30% of the glutamine transferred to the neurons by the cycle may be derived from the replacement of oxidized glutamate by anaplerosis (Lebon et al., 2002). However, it should be kept in mind that interpretations based on acetate metabolism are limited and valid only for relatively short time periods owing to intercellular exchange of metabolites and dilution of the ^{13}C -label coming from acetate by the metabolism of glucose (Taylor et al., 1996).

4 Cerebral Glutamine Metabolism

4.1 Introduction

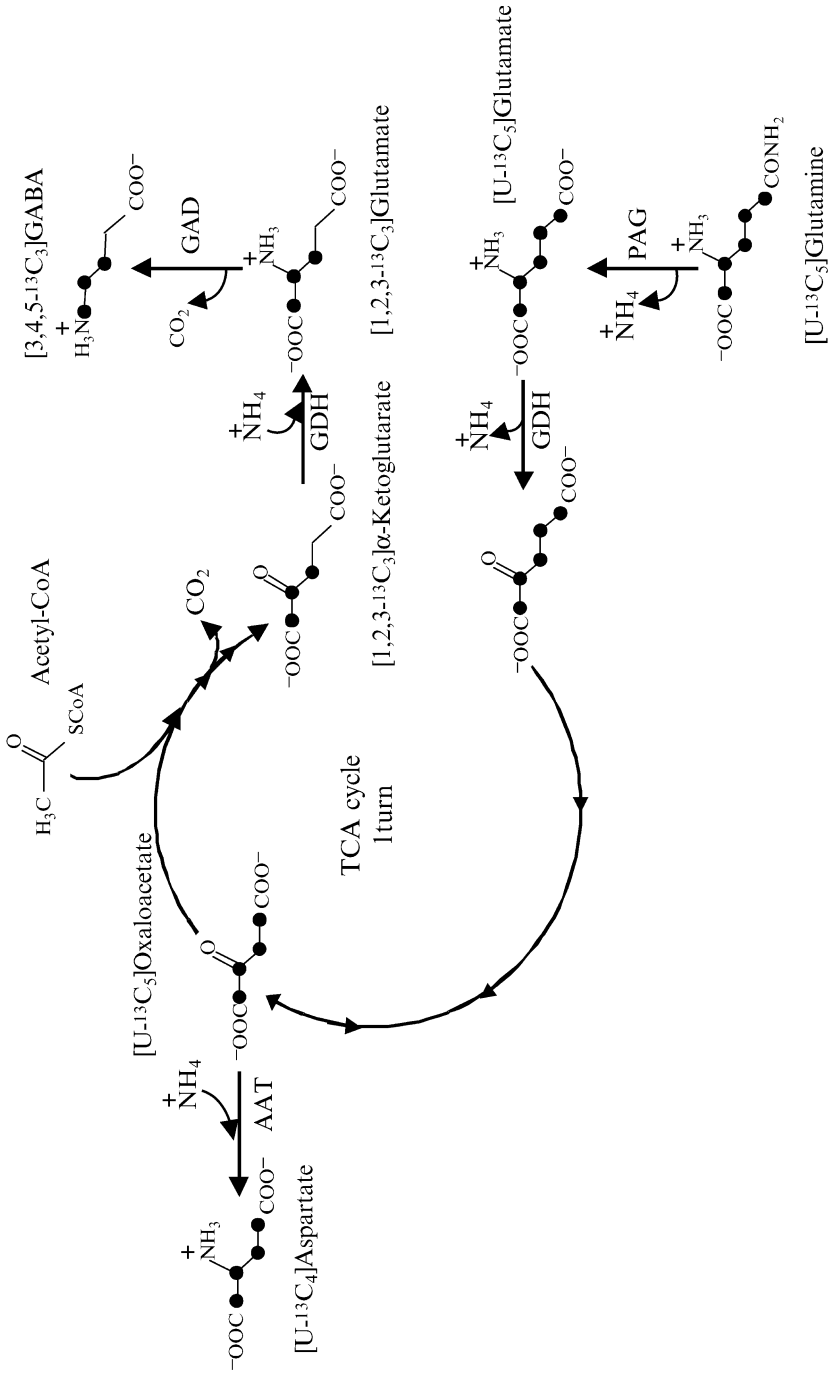
For the synthesis of neurotransmitter glutamate as well as net biosynthesis, neurons rely on carbon supply for mitochondrial energy metabolism. Since adult neurons lack the astrocyte-specific PC, other anaplerotic mechanisms must take place to replenish neuronal TCA cycle intermediates. Glutamine is an amino acid, which is released by the astrocytes and taken up by neurons (see [▶ Figure 3.2-1](#)). In neurons, glutamine is first hydrolyzed by PAG to glutamate ([▶ Figure 3.2-1](#)). However, several studies using different paradigms demonstrated that astrocyte-derived glutamine is not used exclusively for immediate glutamate synthesis, but may also enter the neuronal TCA cycle (Bradford et al., 1978; Hassel et al., 1995a; Zielke et al., 1998) ([▶ Figure 3.2-7](#)). During the transformation of glutamine into the four-carbon intermediate oxaloacetate, one molecule of CO_2 is released from the TCA cycle. Furthermore, the provision of oxaloacetate allows its condensation with acetyl-CoA to the six-carbon intermediate citrate. During the transformation of citrate to α -ketoglutarate, one more molecule of CO_2 is released from the TCA cycle. Furthermore, α -ketoglutarate can be transformed to glutamate. Thus, glutamine acts (1) as an anaplerotic substrate by provision of the four-carbon unit oxaloacetate, which is a substrate for the additional entry of two carbons in the form of acetyl-CoA into the TCA cycle, and (2) as a mitochondrial energy substrate producing two molecules of CO_2 .

4.2 Glutamine versus Glucose as Neuronal TCA Cycle Substrate and Glutamate Precursor

Still controversial are (1) the relative roles of glutamine as direct precursor for glutamate versus its use as substrate for the TCA cycle and (2) the relative contributions of (astrocyte-derived) glutamine and glucose

Figure 3.2-7

Metabolic fate of $[U-^{13}C_5]$ glutamine through the TCA cycle. In neurons, $[U-^{13}C_5]$ glutamine is transformed to $[U-^{13}C_5]$ glutamate via PAG. $[U-^{13}C_5]$ glutamate is converted via GDH to the TCA cycle intermediate $[U-^{13}C_4]$ α -ketoglutarate, which is transformed via TCA cycle activity to $[U-^{13}C_4]$ oxaloacetate. The labeling pattern in oxaloacetate is detected in aspartate. $[U-^{13}C_4]$ oxaloacetate can condense with acetyl-CoA, which can be provided from unlabeled glucose, to citrate. After one TCA cycle turn, $[1,2,3-^{13}C_3]$ α -ketoglutarate is formed, which can be transformed to $[1,2,3-^{13}C_3]$ glutamate and subsequently to $[3,4,5-^{13}C_3]$ GABA. AAT, aspartate aminotransferase; GDH, glutamate dehydrogenase; PAG, phosphate-activated glutaminase

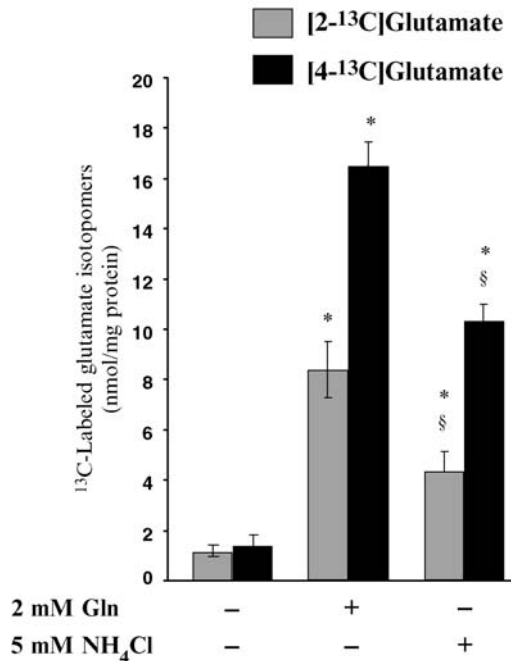


to neuronal metabolism. Recent studies by Shokati and coworkers (2005) showed that intracellular glutamate concentrations in cultured cortical neurons were indeed twofold higher when the cells were incubated in a medium containing 2 mM glutamine compared with glutamine-free medium. However, compared to the total concentrations of glutamate, the increase in percent ^{13}C enrichment in glutamate after incubation with $[1-^{13}\text{C}_1]\text{glucose}$ was much higher using the glutamine-containing medium. In particular, the four carbons derived from exogenous glutamine are metabolized in the TCA cycle to replenish the oxaloacetate pool, allowing the entry of $[2-^{13}\text{C}_1]\text{acetyl-CoA}$ from $[1-^{13}\text{C}_1]\text{glucose}$. This means that glutamate was mainly synthesized after TCA cycle metabolism of $[1-^{13}\text{C}]\text{glutamate}$, which was increased by the presence of unlabeled glutamine. This observation is consistent with data obtained from C6 glioma cells (Portais et al., 1996) and primary astrocytes (Martin et al., 1995), demonstrating an “isotopic-exchange process” between unlabeled glutamine and $[1-^{13}\text{C}_1]\text{glucose}$.

An important question remains: whether the amide group in glutamine, which is set free as ammonia via the neuronal PAG, mediates secondarily the entry of the carbon skeleton from glucose into the TCA cycle. Increased metabolic activity through the TCA cycle contributing to neuronal glutamate synthesis was observed also in ammonia-exposed cultured granule cells (Chan et al., 2003) and cortical neurons (Shokati et al., 2005). However, the addition of 5 mM ammonia to a glutamine-free medium did not have such a major effect on stimulating the synthesis of glutamate from $[1-^{13}\text{C}_1]\text{glucose}$ as did the addition of 2 mM glutamine (▶ *Figure 3.2-4*) (Shokati et al., 2005). This clearly confirmed utilization of extracellular glutamine as the neuronal substrate for the TCA cycle (▶ *Figure 3.2-8*).

■ **Figure 3.2-8**

Concentrations of glutamate isotopomers synthesized from $[1-^{13}\text{C}_1]\text{glucose}$ (nmol/mg protein). The C-4 isotopomer arises from the first PDH turn, and the C-2 isotopomer arises from the second TCA cycle turn. The values were obtained from ^{13}C -NMR spectra of cell extracts from cortical neurons after 24 h incubation in the absence or presence of 2 mM glutamine or 5 mM NH_4Cl (Shokati et al., 2005). The data are expressed as means \pm SD. * $p < 0.05$ versus incubation in glutamine- and NH_4Cl -free media; § < 0.05 compared to glutamine-containing medium without NH_4Cl



In a recent study, Waagepetersen and coworkers (2005) used [U - $^{13}C_6$]glucose and [U - $^{13}C_5$]glutamine as labeled precursors in cultured cerebellar granule cells as a model system for glutamatergic neurons. On the basis of ^{13}C labeling patterns of glutamate, the biosynthesis of the intracellular pool of glutamate from glutamine was found to involve the TCA cycle to a considerable extent (approximately 50%). After inhibiting neuronal glutamate uptake by D,L-threo- β -benzyloxyaspartate (TBOA), the difference between the intracellular and the vesicular pools with regard to the extent of involvement of the TCA cycle in glutamate synthesis from glutamine was eliminated. After repetitive release of glutamate from the vesicular pool in the presence of TBOA, the intracellular pool of glutamate decreased, indicating not only that neuronal reuptake of released glutamate is involved in the maintenance of the neurotransmitter pool but also that 0.5 mM exogenous glutamine is inadequate to sustain this pool (Waagepetersen et al., 2005).

In this context experiments on cortical tissue slices are of interest, wherein glutamine mainly entered a large, slow turnover pool (likely located in neurons), which did not interact with the glutamate/glutamine neurotransmitter cycle (Rae et al., 2003). Furthermore, a limitation of neuronal glutamine supply could not be adequately compensated by increased *de novo* synthesis from glucose (Rae et al., 2003). Thus, glutamine is not only a complementary fuel to glucose, but its catabolism can stimulate the entry of acetyl-CoA into the TCA cycle. All these observations provide further evidence that the glutamine–glutamate cycle is far from stoichiometric equilibrium, since large amounts of glutamine enter the TCA cycle rather than being converted quantitatively to neuronal glutamate stores.

5 Pyruvate Recycling in the Brain

5.1 Introduction

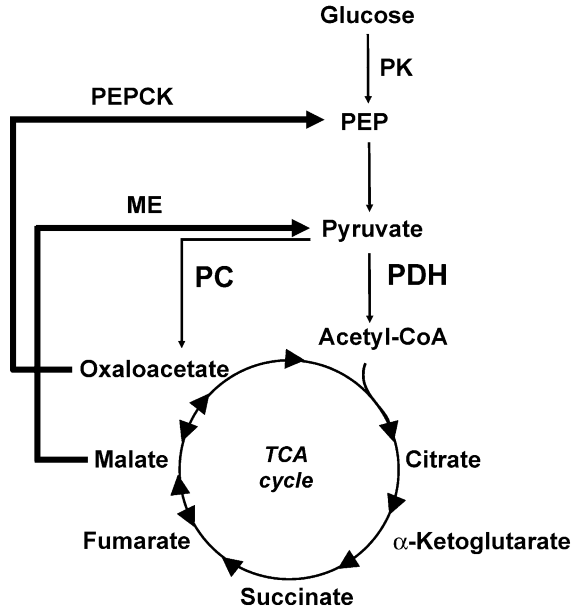
The synthesis of pyruvate from TCA cycle intermediates was first described in the perfused liver (Friedman et al., 1971) and termed “pyruvate recycling” (Hue, 1982). There are two general pathways that mediate the degradation of TCA cycle intermediates: (1) NADP-linked ME, which converts malate to pyruvate and (2) the combined activities of PEPCK (EC 4.1.1.32) and pyruvate kinase (PK; EC 2.7.1.40) converting oxaloacetate to phosphoenolpyruvate (PEP) and to pyruvate (▶ [Figure 3.2-9](#)). Pyruvate can then reenter the TCA cycle. The presence of the required enzymes was demonstrated in rat brains (Cerdan et al., 1990; Chapa et al., 1995).

5.2 Overview

Since the first discovery of the pyruvate recycling pathway in the brain (Cerdan et al., 1990), hypotheses on the cellular dispersal in the brain have been controversial. It was previously suggested that this pathway is predominantly neuronal. However, studies using acetate as the astrocytic substrate have challenged this view, and today, most literature confirm a predominantly astrocytic expression of this pathway. Estimations show that up to 20% of astrocytic lactate is derived from pyruvate recycling. Nevertheless, the different steps involved in the pyruvate recycling pathways are not always or only in part detected both *in vivo* and in cultured astrocytes. In this regard, TCA cycle intermediates such as malate showed at least the first steps of pyruvate recycling in these cells, and amino acids entering the TCA cycle, such as aspartate and glutamate, further confirmed also the reentry of recycled pyruvate into the TCA cycle. The enzymatic machinery involved in the pyruvate recycling pathway, the metabolic capacity of the brain, and its individual cell types, as well as their cellular and subcellular localization might explain the lack of evidence for neuronal pyruvate recycling *in vitro*. However, the final result when comparing all available literature, as well as the ontogenesis of the associated pathways *in vivo*, is that, although most experimental evidence points to a predominant astrocytic pyruvate recycling, a neuronal pyruvate recycling pathway cannot be excluded. For example, the mitochondrial isozyme of ME (mME) has been found to be expressed in neurons (McKenna et al., 2000b). Whether pyruvate recycling plays an essential role for cerebral metabolism is not completely

■ Figure 3.2-9

Pyruvate recycling is mediated via: (1) ME, converting malate to pyruvate, and (2) the combined activities of PEPCK, converting oxaloacetate to PEP, and PK, converting PEP to pyruvate. Pyruvate can reenter the TCA cycle via PDH or PC. ME, malic enzyme; PEP, phosphoenolpyruvate; PEPCK, phosphoenolpyruvate carboxykinase; PC, pyruvate carboxylase; PDH, pyruvate dehydrogenase; PK, pyruvate kinase



clear, but it may provide at least some metabolic flexibility to buffer different metabolic impairments in both astrocytes and neurons.

5.3 Cellular Localization of the Pyruvate Recycling Pathway in the Brain

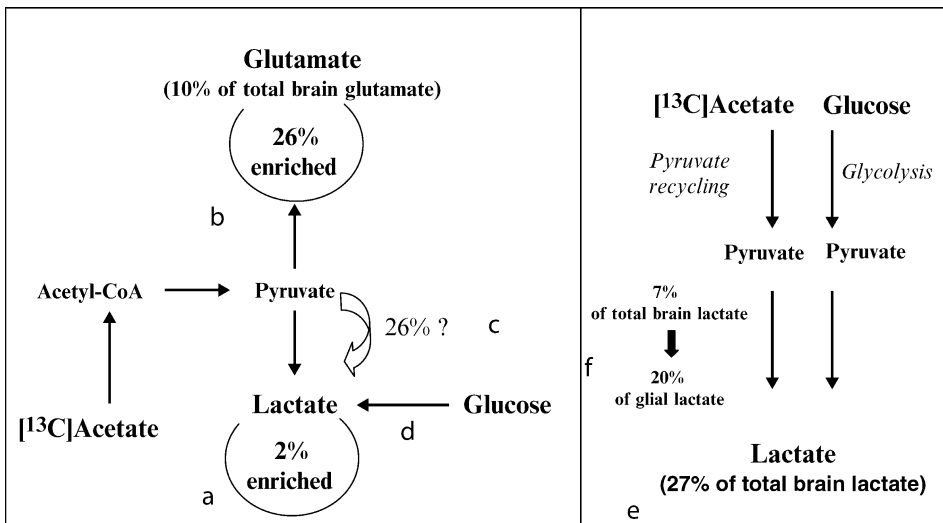
Ex vivo studies using [1,2- $^{13}\text{C}_2$]acetate and subsequent ^{13}C -NMR tissue analysis showed for the first time directly the pyruvate recycling in rat brain (Cerdan et al., 1990; Cruz et al., 1998; Haberg et al., 1998b; Nishina et al., 2004), where approximately 30% of the acetyl-CoA molecules entering the TCA cycle were derived from pyruvate recycled via this pathway. Although acetate is an astrocyte-specific substrate, it was suggested that the pyruvate recycling pathway was predominantly neuronal. This conclusion was based on the observation that the glutamate isotopomers, synthesized from pyruvate formed after metabolism of acetate through the TCA cycle, were not correspondingly reflected in glutamine. Likely, pyruvate formed through astrocytic pyruvate recycling might be converted to lactate (or other metabolites), which is subsequently transferred to neurons and metabolized to glutamate. In addition, the glutamate pool is much smaller in the astrocytes compared to neurons, which might underestimate the glial contribution to pyruvate recycling.

Former studies using [U- $^{13}\text{C}_6$]-, [1- $^{13}\text{C}_1$]-, or [1,2- $^{13}\text{C}_2$]glucose as substrates did not observe cerebral pyruvate recycling in rabbits, mice, and rats (Shank et al., 1985; Lapidot and Gopher, 1994; Hassel and Sonnewald, 1995a, b). However, Aureli and coworkers (1997) identified subsequently pyruvate recycling and reentry of acetyl-CoA into the TCA cycle by the appearance of [5- $^{13}\text{C}_1$]glutamate after [1- $^{13}\text{C}_1$]glucose infusion in rats (0–60 min). Further studies investigating the metabolism of ^{13}C -labeled acetate and/or

^{13}C -labeled glucose in animal models (Hassel and Sonnewald, 1995a; Haberg et al., 1998b and references therein) and in primary astrocyte cultures (Sonnewald et al., 1993b; Hassel et al., 1994) showed that up to 20% of the newly synthesized lactate was derived after recycling of pyruvate from TCA cycle intermediates, and suggested that this occurred in astrocytes. This calculation, which based on many assumptions (Hassel and Sonnewald, 1995a), is explained in [▶ Figure 3.2-10](#). However, also, further *ex vivo* studies using acetate

■ Figure 3.2-10

Estimation of the pyruvate recycling pathway in rat brain using acetate as substrate (Hassel and Sonnewald, 1995a). Left hand side: astrocytic compartment with the assumption that (1) acetate metabolism occurs in astrocytes and (2) that glial glutamate accounts for 10% of total brain glutamate. Right hand side: astrocytic compartment with the assumption that 30% of total brain glucose consumption occurs in the glia, and therefore 30% of glycolytic lactate is glial, which is 27% of the total lactate. Calculation: (a) The percentage ^{13}C -enrichment in lactate C-2 and C-3 derived from $[2-^{13}\text{C}_1]$ acetate was approximately 2%. The percentage $^{13}\text{C}_1$ -enrichment of total brain glutamate C-3 and C-4 was 2.6%. (b) Since only glial glutamate is enriched from $[2-^{13}\text{C}_1]$ acetate, the glial glutamate pool is 26% enriched with ^{13}C label. (c) It was assumed that the enrichment in glutamate is equal to that of α -ketoglutarate, and if lactate is formed from the same precursor as α -ketoglutarate, i.e., from recycled pyruvate, its enrichment should also be 26%. (d) Thus, the enrichment in lactate of 2% means that glycolytic lactate (formed from unlabelled glucose) has diluted the enrichment in lactate by 1:13, and 7%–8% of lactate may be synthesized through the pyruvate recycling pathway. (e) It was assumed that 30% of total brain glucose consumption occurs in the glia, and therefore 30% of glycolytic lactate is glial, which is 27% of the total lactate. (f) The lactate formed through pyruvate recycling (approximately 7% of total lactate) could therefore account for 20% of the total glial pool of lactate

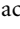


labeled twice with ^{13}C and ^2H confirmed a significant contribution of glial pyruvate recycling as seen by the appearance of glutamate isotopomers after entry of $[2-^{13}\text{C}_1]$ - and $[2-^{13}\text{C}_1, ^2\text{H}_3]$ acetyl-CoA into the glial TCA cycle (Chapa et al., 2000).

5.4 Cellular Evidence for the Pyruvate Recycling Pathway

Subsequent NMR studies using different ^{13}C -labeled substrates provided evidences for a predominant glial localization of pyruvate recycling. In cultured astrocytes, it has been demonstrated that pyruvate is

formed from TCA cycle intermediates, which is the first part of this cycle. This was evident by the appearance of the ^{13}C label in the C-2 position of lactate after incubation with $[1\text{-}^{13}\text{C}_1]\text{glucose}$ or $[3\text{-}^{13}\text{C}_1]\text{pyruvate}$, while the direct pathway without pyruvate recycling leads to the synthesis of the C-3 labeled lactate isotopomer (Leo et al., 1993; Sonnewald et al., 1993b; Hassel et al., 1994; Alves et al., 1995; Sonnewald et al., 1995, 1996a).

The first direct evidence of pyruvate recycling involving the subsequent reintroducing of acetyl-CoA into the TCA cycle on the cellular level was obtained by the use of pyruvate labeled with ^{13}C at the C-2 position, which led to the C-4-labeled glutamate isotopomer (Brand et al., 1992). In a further study pyruvate recycling was detected in primary cultures of astrocytes because of the formation of isotopomers from $[\text{U-}^{13}\text{C}_5]\text{glutamine}$ (Sonnewald et al., 1996b). In this study, the concomitant incubation with $[\text{U-}^{13}\text{C}_5]\text{glutamine}$ and unlabeled glutamate allowed for differentiation between glutamate formed from oxaloacetate directly derived from glutamine (uniformly labeled) and glutamate formed after condensation of oxaloacetate with labeled acetyl-CoA.  *Figure 3.2-11* shows the isotopomers of glutamate formed after direct conversion of $[\text{U-}^{13}\text{C}_5]\text{glutamine}$ via PAG or after recycling of pyruvate from $[\text{U-}^{13}\text{C}_5]\text{glutamine}$. In particular, the synthesis of $[4,5\text{-}^{13}\text{C}_2]\text{glutamate}$ could occur only if unlabeled oxaloacetate reacts with $[1,2\text{-}^{13}\text{C}_2]\text{acetyl-CoA}$, which is formed from $[\text{U-}^{13}\text{C}_5]\text{glutamine}$ through recycling of pyruvate.

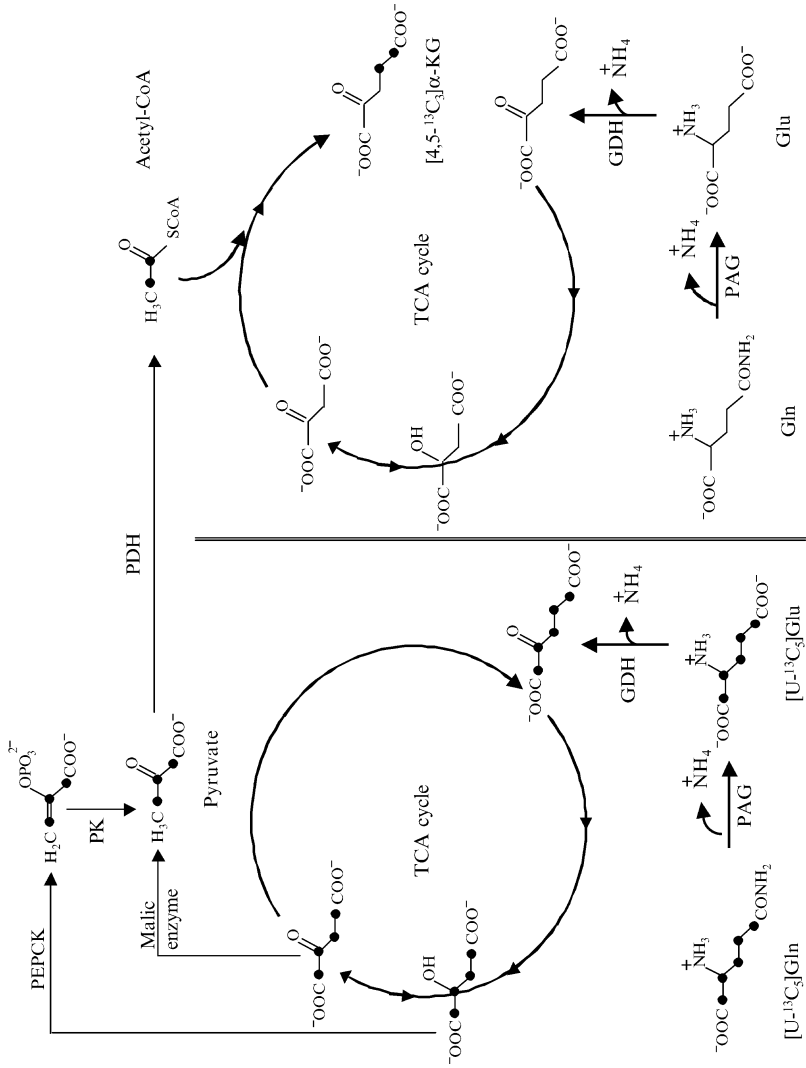
NMR studies using $[3\text{-}^{13}\text{C}_1]\text{-}$ or $[\text{U-}^{13}\text{C}_5]\text{glutamate}$ provided extended information on the regulation of pyruvate recycling in primary cultures of astrocytes and neurons (Haberg et al., 1998b; Waagepetersen et al., 2002). While mitochondrial metabolism of ^{13}C -labeled glutamate via α -ketoglutarate occurred in astrocytes and in neurons, the first steps of the pyruvate recycling pathway was dominant in astrocytes, as evident by the appearance of labeled intra- and extracellular lactate in these cells. These studies showed that ^{13}C -labeled glutamate can generate labeled lactate at a rate of approximately 1 nmol/min/mg protein. In addition, considerably higher percentage ^{13}C -enrichments in lactate (> 80% in C-3) than in glutamine carbons (10–15%) from $[\text{U-}^{13}\text{C}_5]\text{glutamate}$ demonstrate the importance of the TCA cycle for glutamate degradation, which has been observed also in brain slices (Taylor et al., 1996). In cultured neurons, on the other hand, pyruvate recycling was not detected after incubation with $[\text{U-}^{13}\text{C}_5]\text{glutamate}$ or $[\text{U-}^{13}\text{C}_5]\text{glutamine}$ (Westergaard et al., 1995; Sonnewald et al., 1996c; Haberg et al., 1998b; Qu et al., 2001; Waagepetersen et al., 2002). Also $[\text{U-}^{13}\text{C}_4]\text{aspartate}$ is metabolized in the TCA cycle in both astrocytes and neurons after conversion to $[\text{U-}^{13}\text{C}_4]\text{oxaloacetate}$, as shown by the labeling patterns of lactate, aspartate, glutamate, and, in astrocytes, of glutamine (Bakken et al., 1997b, 1998b). However, only in astrocytes the isotopomers $[1,3,4\text{-}^{13}\text{C}_3]\text{aspartate}$ and $[1,2,4\text{-}^{13}\text{C}_3]\text{aspartate}$ were detected, which are synthesized from recycled pyruvate in a subsequent TCA cycle turn. This observation was confirmed using $[3\text{-}^{13}\text{C}_1]\text{malate}$ under normoglycemic or hypoglycemic conditions, which supported pyruvate recycling in astrocytes (Alves et al., 2000).

5.5 Cerebral Capacity of TCA Cycle Metabolism Through Pyruvate Recycling

From the ^{13}C -NMR studies discussed above, pyruvate recycling seems to be a predominantly glial pathway. However, as TCA cycle intermediates are not ^{13}C -NMR visible, data obtained by these metabolic flux analyses should be compared with the enzymatic machinery and the metabolic capacity of the brain and its individual cell types. Considering a relative flux of the TCA cycle through pyruvate recycling of 30% (Cruz et al., 1998) and cerebral TCA cycle rates of approximately 15 nmol/min/mg protein (van den Berg and Garfinkel, 1971; Mason et al., 1992; Preece and Cerdan, 1996), approximately 5 nmol/min/mg of the TCA cycle flux may be mediated by pyruvate recycling. The lower in vitro TCA cycle rates in astrocytes and neurons (8–12 nmol/min/mg protein) (Cruz et al., 1998) compared with the in vivo brain suggested approximately 3.3 mol/min/mg protein of pyruvate recycling to the TCA cycle flux. The measured maximal activities of ME and PEPCK in the brain are higher than this estimated value (7.6 and 1.6 nmol/min/mg protein, respectively) (Cruz et al., 1998), suggesting that the capacity of these enzymes possibly will not limit the recycling rates in the brain in vivo. However, the capacity of pyruvate recycling may be restricted by the cellular and subcellular localization of ME and PEPCK, which may also explain the lack of evidence for neuronal pyruvate recycling in vitro: While the activities of ME and PEPCK are very low in neurons (below

Figure 3.2-11

Metabolic fate of [U - ^{13}C]glutamine after recycling of pyruvate. [U - $^{13}C_5$]glutamine (left) enters the TCA cycle and is converted into [U - $^{13}C_4$]malate and [U - $^{13}C_4$]oxaloacetate, which can leave the TCA cycle via phosphoenolpyruvate carboxykinase (PEPCK) or malic enzyme. [U - $^{13}C_3$]pyruvate can reenter the TCA cycle (right) via pyruvate dehydrogenase (PDH) and condense with unlabeled oxaloacetate. Then, [$4,5$ - $^{13}C_2$]glutamate is formed, which will be detected only after recycling of pyruvate from [U - $^{13}C_5$]glutamine. Gln, glutamine; Glu, glutamate; Asp, aspartate; α -KG, α -ketoglutarate; ML, malate; OXAC, oxaloacetate



0.3 nmol/min/mg and not detectable, respectively), they are much higher in astrocytes (approximately 2.1 and 0.5 nmol/min/mg of protein, respectively) (Cruz et al., 1998). Furthermore, ME activity and the flux of [1,2- $^{13}\text{C}_2$]acetate through the cerebral pyruvate recycling system increase accordingly with the developmental stage of the rat brain, which further explains the lack of this pathway in cultures of neurons obtained from neonatal brain (Cruz et al., 1998).

5.6 Flux Through Mitochondrial and Cytosolic Malic Enzyme

Three isoforms of ME have been described in mammalian tissues: a cytosolic NADP⁺-dependent enzyme, a NADP⁺-dependent mitochondrial isoform, and a mitochondrial isozyme that can use both NAD⁺ and NADP⁺ but is more effective with NAD⁺ (Bukato et al., 1995). Another aspect concerning pyruvate recycling through ME is whether flux occurs through the mitochondrial (mME) or through the cytosolic (cME) isozyme.

In brain homogenates, the relative enzyme activities of mME and cME are 55% and 45%, respectively (Vogel et al., 1998). While cME preferentially, if not exclusively, is a glial enzyme (McKenna et al., 2000b), the mitochondrial isozyme is expressed in neurons (McKenna et al., 2000b). cME accounts for as much as 95% of total ME activity in astrocytes (McKenna et al., 2000b). This enzyme is potentially reversible, but at physiological concentrations of malate and pyruvate, more than 95% of malate is transferred to pyruvate (Kimmich et al., 2002).

Though cME is a predominant glial enzyme, neurons *in vivo* express mME through which pyruvate recycling can occur (Cruz et al., 1998). Therefore, the lack of pyruvate recycling in cultured neurons may be a cell culture effect. In addition, the activity of neuronal mME develops mainly after synaptogenesis *in vivo* (Cruz et al., 1998), whereas neurons at the time of their preparation from neonatal brain are in a still immature stage. In addition to ME activity, also the metabolic flux through the pyruvate recycling pathway increases with the developmental stage of the liver as demonstrated in a NMR study using [1,2- $^{13}\text{C}_2$]acetate (Cruz et al., 1998, 2001). Therefore, a neuronal pyruvate recycling pathway cannot be excluded based on the current data, since the ontogenesis of the associated pathway has to be considered when comparing *in vitro* and *in vivo* experiments.

5.7 Flux Through Phosphoenolpyruvate Carboxykinase

Pyruvate can be recycled also via flux through PEPCK, which was demonstrated in studies investigating [U- $^{13}\text{C}_4$]aspartate metabolism in cultured astrocytes (Bakken et al., 1997b, 1998b). If pyruvate recycling from aspartate is prevented by inhibition of ME and PEPCK by hydroxymalonate and 3-mercaptopycolinic acid, respectively, the formation of [U- $^{13}\text{C}_3$]lactate fails, while the inhibition of PEPCK (either in the absence or in the presence of hydroxymalonate) impaired the incorporation of ^{13}C -labeled acetyl-CoA into TCA cycle intermediates. These effects might be due to the expression of ME and PEPCK in different compartments. It has been shown that PEPCK is selectively localized in mitochondria of astrocytes (Schmoll et al., 1995), indicating an important role of this enzyme for recycling of pyruvate.

PEPCK is also the first in the conversion of oxaloacetate to glucose (and glycogen) through gluconeogenesis. Glial cells are potentially able to perform at least the first steps of gluconeogenesis as observed by analysis of [2- $^{13}\text{C}_1$]pyruvate metabolism (Brand et al., 1992, 1993). Further support for PEPCK activity in astrocytes was demonstrated by the formation of glycogen from mitochondrial precursors (Schmoll et al., 1995). Under hypoglycemic conditions, which depletes glycogen stores (Dringen and Hamprecht, 1992), the glycolytic flux of [1- $^{13}\text{C}_1$]glucose to [3- $^{13}\text{C}_1$]lactate was not affected, while the recycling of pyruvate, leading to the [2- $^{13}\text{C}_1$]lactate isotopomer, decreased under these conditions (Alves et al., 1995). Furthermore, when cultured astrocytes were treated with IGF-1 and insulin, known to stimulate glycogen formation, the formation of [2- $^{13}\text{C}_1$]lactate from [1- $^{13}\text{C}_1$]glucose decreased by 43% (Sonnewald et al., 1996a; Cruz et al., 2001).

5.8 Importance of the Pyruvate Recycling Pathway in the Brain

It is not clear to date whether the pyruvate recycling pathway plays an essential role for cerebral metabolism. However, the enzymatic capacity of this pathway (Cruz et al., 1998) is much higher than the measured metabolic fluxes *in vivo*. This suggests that the associated enzymes might be upregulated under pathological conditions, which provides metabolic flexibility to buffer metabolic impairments. One might suggest that this pathway might be activated under conditions leading to decreased acetyl-CoA levels. However, in cultured astrocytes, glucose deprivation or the addition of iodoacetate, which inhibits glycolysis, did not lead to an increased flux of [U - $^{13}C_5$]glutamate through pyruvate recycling (Bakken et al., 1998a).

In vivo, this process might also contribute to the maintenance of the extracellular glutamate homeostasis to avoid excitotoxic levels of glutamate. In fact, astrocytes convert glutamate to glutamine. However, it has been shown that the extracellular concentration of glutamate determines its metabolic fate in astrocytes, e.g., the conversion of glutamate to glutamine via GS versus its consumption via TCA cycle activity (McKenna et al., 1996): the amount of glutamate metabolized via the TCA cycle progressively increased as the extracellular glutamate concentration increased. In this regard, it is interesting that approximately 70% of glutamate entering the TCA cycle of cultured astrocytes is recycled to pyruvate (Sonnewald et al., 1993a), which might contribute not only to the removal of extracellular glutamate but also to the lactate supply to neurons.

Considering the presence of gluconeogenic enzymes in astrocytes (Schmoll et al., 1995; Bernard-Helary et al., 2002), the degradation of TCA cycle intermediates to PEP might also contribute to glucose and glycogen formation (Schmoll et al., 1995), which may regulate the continuous turnover of glycogen during neuronal activation (Gruetter, 2002). On the other hand, astrocytic pyruvate recycling might be important to supply the neurons with pyruvate (in the form of lactate), which is either reduced to acetyl-CoA or carboxylated even to malate by mME. It has been shown that pyruvate and malate are beneficial for cortical neurons during glutamate excitotoxicity (Ruiz et al., 1998).

An important question remains: whether and to what extent recycled pyruvate reenters the TCA cycle via PC. The relative contribution of PC to the pyruvate recycling pathway is difficult to assess by NMR, as pyruvate recycling would lead to identical ^{13}C -labeled metabolites as flux through PC. By this means, the estimated values for the relative contribution of pyruvate recycling to the TCA cycle flux might be even underestimated. The elucidation of the relative role of pyruvate recycling for complete astrocytic substrate oxidation and energy production versus anaplerosis should require future research, considering the important role of anaplerosis in astrocytes for the replenishment of TCA cycle intermediates and subsequent transfer to neurons.

6 Intercellular Transfer of Nitrogen to Operate the Glutamine–Glutamate Cycle

6.1 Introduction: Cellular Nitrogen Transfer as NH_3 or NH_4^+

The glutamine–glutamate cycle has been proven not to be stoichiometric (Shank and Aprison, 1988), which is further indicated by the oxidative degradation of substrates including glutamate and glutamine (Shank and Aprison, 1988). In addition, the consumption of ammonia in this cycle by GS in astrocytes and its release by neuronal glutaminase requires a net transfer of ammonia from astrocytes to neurons (see [Figure 3.2-1](#)). Benjamin and Quastel proposed in 1975 a flux of ammonium from glutamatergic neurons to glial cells (Benjamin and Quastel, 1975). The transport of ammonia occurs either by diffusion of NH_3 or by any transport system for NH_4^+ . More than 98% of ammonia exists as NH_4^+ under physiological conditions, which can be transported via ion channels (K^+ -selective) and membrane transporters. Transmembrane diffusion of NH_3 has been generally suggested to be substantially fast (see Cooper et al., 1979; Cooper and Plum, 1987). As critically discussed recently by Ott and Larsen (2004), a substantial uptake of NH_4^+ should be considered. For example, in isolated astrocytes, a transport protein-mediated translocation of NH_4^+ is predominant (Nagaraja and Brookes, 1998). Diffusion of NH_3 into the cells was most effective immediately

after incubation of astrocytes with ammonia, but within less than a minute translocation of NH_4^+ predominated (Nagaraja and Brookes, 1998), whereby 80% of the NH_4^+ flux was mediated by the K^+ channel. Furthermore, NH_4^+ is transported not only via K^+ channels (Raichle and Larson, 1981; Cooper and Plum, 1987), but also via specific transporters that may be present (see Ott and Larsen, 2004). These considerations of a significant contribution of astrocytic uptake of NH_4^+ versus NH_3 are important considering physiological consequences. For example, while the transport of the undissociated, neutral form (NH_3) would result in transient intracellular pH imbalances, the uptake of NH_4^+ via K^+ -channels may depolarize the cells. Furthermore, astrocytic uptake of NH_4^+ is associated with increased extracellular K^+ , which is a potent cerebral vasodilator, and thereby might be implicated in diseases where an increased cerebral blood flow is a critical pathogenetic factor, such as in acute hepatic encephalopathy (HE) (Ott and Larsen, 2004).

6.2 Overview: Cellular Nitrogen Transfer as Amino Acids

The operation of the glutamine–glutamate cycle between astrocytes and neurons requires mechanisms for the transfer of nitrogen between these cells. Molecules carrying nitrogen are amino acids. Besides α -ketoglutarate and oxaloacetate, which are transaminated to glutamate and aspartate, respectively, other α -keto acids such as pyruvate or α -ketoisocaproate (α -KIC) may be transaminated in neurons to the corresponding amino acids alanine and leucine. Subsequently, they are transported to the astrocytes. ^{13}C -NMR spectroscopic studies using cortical and cerebellar astrocytes and neurons as well their co-cultures demonstrated in a comprehensive manner that a complementary lactate (pyruvate)–alanine cycle accounts for the nitrogen exchange required in the glutamine–glutamate cycle (▶ [Figure 3.2-12](#)) (Waagepetersen et al., 2000; Zwingmann et al., 2000).

However, the contribution of this cycle to supplement the glutamine–glutamate cycle in vivo still remains open for further studies. Furthermore, still controversial is the relative contribution of astrocytes and neurons for both synthesis and uptake of alanine. Evidence is also given for leucine to enable the transfer of nitrogen from neurons to astrocytes (Yudkoff et al., 1993, 1994; McKenna et al., 1998; Bixel et al., 2004), whereby the astrocytes transaminate leucine to the ketoacid α -KIC (▶ [Figure 3.2-13](#)). However, direct in vivo evidence for a leucine/ α -KIC cycle needs to be confirmed. Much less discussed is a possible cycling of nitrogen through aspartate synthesis, but, like for the alanine–lactate shuttle, its contribution is disputed. Although further in vitro and in vivo experimental approaches need to be performed to elucidate the functional significance of these shuttles complementary to the glutamine–glutamate cycle in vivo, the feasibility of these mechanisms contributing to the nitrogen transport from neurons to astrocytes has been proven and is discussed in detail below.

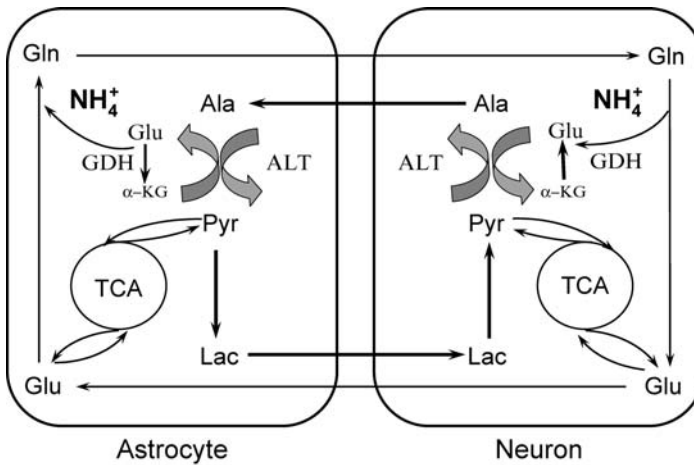
6.3 Ammonia Cycling via the Alanine–Lactate Shuttle

6.3.1 Alanine Synthesis in Neurons

Both cortical and cerebellar neurons show several-fold higher de novo synthesis and release of alanine from either glucose and lactate compared with the corresponding astrocyte cultures (Waagepetersen et al., 2000; Zwingmann et al., 2000), confirming neuronal binding of nitrogen. Also, astrocytes synthesize preferentially lactate from glucose and minimum amounts of alanine, while the opposite is found in cultured neurons (see Zwingmann and Leibfritz, 2003). Using $[3\text{-}^{13}\text{C}_1]$ pyruvate as the direct precursor for alanine, cortical neurons show an approximately four-times higher de novo synthesis of alanine than cortical astrocytes (Brand et al., 1992). It is interesting to compare the substrate selection for alanine synthesis in different in vitro systems. For example, in cortical brain slices, alanine synthesis is also almost four-times higher using 2 mM $[3\text{-}^{13}\text{C}_1]$ pyruvate compared to that using 5 mM $[3\text{-}^{13}\text{C}_1]$ lactate as the substrate (Rae et al., 2003). On the other hand, in cortical neurons, ^{13}C -labeled pyruvate contributes only one-half to alanine synthesis compared with ^{13}C -labeled glucose (Cruz et al., 2001). Furthermore, a close correlation of alanine C-3

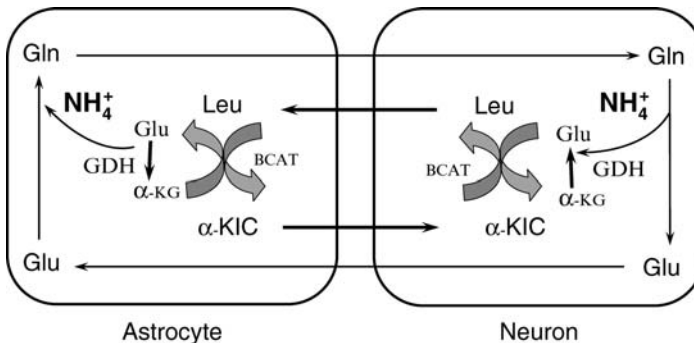
■ Figure 3.2-12

Glutamine–glutamate cycle in the brain complemented by an alanine–lactate shuttle between neurons and astrocytes. Ammonia is fixed by glutamine synthesis in astrocytes. Astrocytic glutamine is transferred to the neurons, and converted to glutamate; in the PAG reaction ammonia is set free. In addition to glutamine, glycolytically formed lactate is transported from astrocytes and neurons. Lactate is converted to pyruvate, which may enter the TCA cycle or is transaminated to alanine, whereby part of the glutamate can also be regenerated through the neuronal TCA cycle. The shuttle is complemented by the transport of alanine to astrocytes where it is converted into pyruvate and subsequently lactate. Note: the conversion of alanine to pyruvate as well as of pyruvate to alanine proceeds through the combined action of alanine aminotransferase and glutamate dehydrogenase. Ammonia is consumed again by glutamine synthesis. Ala, alanine; ALT, alanine aminotransferase; GDH, glutamate dehydrogenase; Gln, glutamine; Glu, glutamate; α -KG, α -ketoglutarate; Lac, lactate; Pyr, pyruvate



■ Figure 3.2-13

Similar to the alanine–lactate shuttle (Figure 3.2-12), a cycle utilizing glutamate, α -ketoglutarate, and α -KIC may contribute to the transfer of ammonia through leucine between neurons and astrocytes. In this cycle, leucine is transaminated with α -KG to glutamate and α -KIC. After regeneration of α -KG from glutamate through GDH, ammonia is set free and used for synthesis of glutamine. Note: the conversion of leucine to α -KIC as well as of α -KIC to leucine proceeds through the combined action of branched-chain aminotransferase and glutamate dehydrogenase. α -KIC is transported from astrocytes to neurons and converted to leucine. BCAT, branched-chain aminotransferase; GDH, glutamate dehydrogenase; Gln, glutamine; Glu, glutamate; Leu, leucine; α -KG, α -ketoglutarate; α -KIC, α -ketoisocaproate



labeling with that of glutamate C-4 in these neurons (31% versus 37%) as well as in cortical brain slices incubated with [$1\text{-}^{13}\text{C}_1$]glucose during inhibition of cellular glutamine transport (Rae et al., 2003) reinforce the notion that these isotopomers are generated in the same cellular, i.e., the neuronal, compartment. Although direct *in vivo* evidence for preferential neuronal alanine synthesis is not yet given, a substantial ^{13}C -label incorporation into cerebral alanine (approximately 20%) was observed after injection of rats with ^{13}C -labeled lactate (Bouzier et al., 2000).

6.3.2 Metabolism of Alanine in Astrocytes

Further, direct evidence that astrocytes preferentially transform also exogenous alanine to lactate was given by ^{13}C -isotopomer analysis of cell extracts and incubation media obtained from cortical astrocytes neurons and their co-cultures. In particular, approximately 90% of exogenous [$3\text{-}^{13}\text{C}_1$]alanine taken up from the medium within 24 h was released as [$3\text{-}^{13}\text{C}_1$]lactate from astrocytes, while only 12.5% and 30% of the consumed [$3\text{-}^{13}\text{C}_1$]alanine was found in [$3\text{-}^{13}\text{C}_1$]lactate of neurons and co-cultures, respectively (Zwingmann et al., 2000). Furthermore, [$3\text{-}^{13}\text{C}_1$]alanine was much less incorporated into other astrocytic metabolites than lactate (Zwingmann et al., 2000), and lactate formation from [$1\text{-}^{13}\text{C}_1$]glucose was much lower than from [$3\text{-}^{13}\text{C}_1$]alanine (Zwingmann et al., 2001). Interestingly, high amounts of [$3\text{-}^{13}\text{C}_1$]alanine were converted to both glutamine and glutamate when astrocytes were co-cultured with neurons, while this was not observed in pure astrocyte cultures (Zwingmann et al., 2000, 2001). A similar extent of label incorporation from either [$\text{U}\text{-}^{13}\text{C}_3$]alanine or [^{15}N]alanine into glutamine and glutamate was observed in co-cultures (Waagepetersen et al., 2000). These studies support the notion that synthesis and release of alanine from neurons contribute to nitrogen transfer to astrocytes, which may promote, in return, the operation of the glutamine–glutamate cycle between these both cell types (▶ [Figure 3.2-12](#)).

The nonstoichiometry of the glutamine–glutamate cycle and its complementation by nitrogen transfer through intercellular alanine–lactate shuttling was suggested also in experiments using exogenous glutamine for cultured brain cells and cortical brain slices (Rae et al., 2003). In particular, the inhibition of the glutamine transport system N by histidine decreases glutamate and GABA concentrations in cortical brain slices, which cannot adequately be compensated by increased neuronal *de novo* synthesis from [$1\text{-}^{13}\text{C}_1$]glucose. Under hypoglycemic conditions (0.2 mM glucose), the presence of exogenous glutamine leads to an increased synthesis of alanine from [$3\text{-}^{13}\text{C}_1$]pyruvate, an inhibition of alanine uptake to 63% and 45% by glutamine and histidine, respectively, as well as an impaired alanine synthesis from [$3\text{-}^{13}\text{C}_1$]lactate after inhibition of the neuronal system A glutamine transport by MeAIB. These results also suggest that glutamine is metabolized in the neuronal TCA cycle supporting alanine synthesis and subsequent transfer to astrocytes. The inhibition of alanine uptake by glutamine is consistent with data demonstrating that glutamine in nerve terminals is preferentially transported by the L-alanine preferring carrier and to a lesser extent by the carrier for large neutral amino acids (Shank and Campbell, 1982). Further data from Westergaard et al. (1993) showed an IC_{50} value of around 3 mM for this effect. Furthermore, a recent study by Shokati and coworkers (2005) clearly confirmed that glutamine enters the neuronal TCA cycle, and added further hints into the issue of neuronal ammonia binding by alanine formation in demonstrating increased alanine formation from [$1\text{-}^{13}\text{C}_1$]glucose in the presence of exogenous glutamine (Shokati et al., 2005).

Altogether, these *in vitro* studies suggest nitrogen cycling via an alanine–lactate shuttle between neurons and astrocytes. However, the *in vivo* contribution of this cycle relative to the glutamine–glutamate cycle still remains open for further studies. Furthermore, apart from intercellular alanine–lactate shuttling, several other mechanisms may operate *in vivo* to support the transfer of nitrogen needed for the operation of the glutamine–glutamate cycle.

6.4 Nitrogen Cycling via the Leucine/ α -Ketoisocaproate Shuttle

Besides alanine, the branched-chain amino acid (BCAA) leucine also carries nitrogen. Since leucine is rapidly degraded by brain slices (Sadasivudu and Lajtha, 1970) as well as cultured astrocytes (Yudkoff et al., 1996),

this amino acid can take part in cerebral nitrogen turnover. BCAAs easily cross the BBB (Oldendorf, 1971), whereby leucine is known to be transported much faster than other BCAAs in exchange for glutamine (Cangiano et al., 1983). But leucine can be synthesized also de novo from α -KIC. A leucine/ α -KIC cycle was proposed to operate in the brain (for review see Cooper and Plum, 1987; Yudkoff, 1997) proposed a leucine/ α -KIC cycle in the brain (▶ [Figure 3.2-13](#)).

In this cycle, metabolic interactions among glutamate, leucine, α -ketoglutarate, and α -KIC contribute to the intercellular transfer of nitrogen. It has been shown that leucine contributes its amino group for glutamate and glutamine synthesis in cultured astrocytes (Cooper and Plum, 1987; Yudkoff et al., 1993, 1994), and studies with ^{15}N -labeled BCAAs indicate that 25% of the amino groups of brain glutamate are derived from leucine (Yudkoff, 1997). After transamination of leucine and glutamate or glutamine syntheses, astrocytes release α -KIC to the extracellular fluid, as demonstrated using $[4,5\text{-}^3\text{H}]$ leucine (Bixel and Hamprecht, 1995). After transport of α -KIC to the neurons, these cells can convert α -KIC back to leucine, which will be transported to the astrocytes to close the cycle. Yudkoff et al. and coworkers (2005) suggested that this process, which consumes an equimolar amount of glutamate, may provide a mechanism for “buffering” of brain glutamate, if levels of this excitatory neurotransmitter become elevated to excitotoxic levels. Recent ^{13}C -NMR studies have been shown to be particularly useful to obtain more information about the regulation of this cycle through glial metabolism (Bixel et al., 2004). In these experiments, cultured astrocytes released the label from $[\text{U-}^{13}\text{C}_6]$ leucine in the form of not only α -KIC and ketone bodies but also ^{13}C -labeled alanine, citrate, glutamine, lactate, and succinate, which were identified. Their detailed isotopomer analyses proved that $[\text{U-}^{13}\text{C}_6]$ leucine is converted to ^{13}C -labeled acetyl-CoA, which enters the astrocytic TCA cycle. It has been observed previously that up to one-third of the amino groups of leucine appear in glutamine in astrocyte cultures demonstrating that leucine is a major source of amine nitrogen for glutamine (Yudkoff et al., 1994). The ^{13}C -NMR studies by Bixel and coworkers (2004) add further hints to the potential involvement of leucine metabolism in the glutamine–glutamate cycle between neurons and astrocytes. Furthermore, the released α -KIC might be transported to the neurons, and at least some neurons are equipped with the enzymes required for keto acid catabolism (Bixel et al., 1997). Thus, though direct in vivo evidence has yet to be demonstrated, a leucine/ α -KIC cycle most likely contributes to the complementation of the glutamine–glutamate cycle in the brain.

6.5 Cycling of Nitrogen Through Aspartate Synthesis

While exogenous alanine was not able to stimulate glutamine synthesis from glucose in cultured astrocytes (Zwingmann et al., 2000), it increases intracellular aspartate more than threefold (Waagepetersen et al., 2000). This effect was not observed in neurons or co-cultures. Evidence that aspartate might, like alanine and leucine, be involved in intercellular carbon and nitrogen transfer was given by the observation that superfused cerebral brain slices take up and metabolize alanine in the astrocytic compartment and export large amounts of aspartate (Griffin et al., 1998). It has further been shown that production of aspartate from $[2\text{-}^{13}\text{C}_1, ^{15}\text{N}]$ alanine occurs via PC (Griffin et al., 2003). However, it was impossible to distinguish whether this is caused by the complete ^{15}N and ^{13}C labeling at the C-2 position of the glial aspartate pool, occurring in a compartment with a small glutamate pool that becomes rapidly labeled by ^{15}N , or if, alternatively, $[2\text{-}^{13}\text{C}_1\text{-}^{15}\text{N}]$ aspartate was produced via a “metabolon” arrangement, whereby the products of the enzymes ALAT, PC, and AAT are channeled into each other sequentially, i.e., by which ^{15}N glutamate formed by ALAT from $[2\text{-}^{13}\text{C}_1, ^{15}\text{N}]$ alanine is channeled directly to AAT to form $[2\text{-}^{13}\text{C}_1, ^{15}\text{N}]$ aspartate. Aspartate synthesis takes place in both astrocytes and neurons. For example, in synaptosomes, α -ketoglutarate and malate are metabolized rapidly to glutamate and aspartate, consistent with neuronal synthesis of aspartate, an intermediate in the malate–aspartate shuttle, which is very active in neurons (Shank and Campbell, 1983).

Data regarding the cellular localization of aspartate are controversial, so are those on the cellular localization of alanine. However, astrocytes obviously possess a pool of metabolically active aspartate as demonstrated by the incorporation of ^{13}C -label from glucose and glutamate into aspartate of cultured astrocytes (Aureli et al., 1997; McKenna and Sonnewald, 2005). Furthermore, the presence of extracellular alanine increased the total pool size of aspartate from 0.43 $\mu\text{mol}/100$ mg protein to 1.45 $\mu\text{mol}/100$ mg of

protein (Waagepetersen et al., 2000). Ex vivo studies using intraperitoneal injection of [$1\text{-}^{13}\text{C}_1$]glucose in rats additionally demonstrated a higher contribution of the astrocytic anaplerotic pathway to aspartate synthesis than to that of glutamate (Shank et al., 1993). This indicates a comparatively higher aspartate concentration in astrocytes or the fact that aspartate is metabolically more active in astrocytes than in neurons.

Interestingly, exogenous glutamate (0.5 mM) increases intracellular aspartate concentrations fivefold, and tenfold after concomitant incubation with glutamine, and also, exogenous glutamine stimulates aspartate synthesis from [$\text{U-}^{13}\text{C}_6$]glucose (Sonnewald et al., 1997). It is obvious that there is carbon and nitrogen channeling between the amino groups in aspartate, glutamate, and alanine in astrocytes, which express high activities of ALAT (Zwingmann et al., 2000) and of AAT (Hertz and Schousboe, 1986; Westergaard et al., 1993), with the latter exceeding GS activity (Hertz and Schousboe, 1986). In favor of a role of aspartate synthesis in astrocytes, the de novo synthesis of aspartate was stimulated by 115%–130% and 158%–165% of control after 3 h incubation of astrocytes with pathological concentrations of ammonia and inhibition of GS with methionine–sulfoximine (MSO), respectively, with an additive effect (increase to 200%–290%) after concomitant administration of ammonia and MSO (Zwingmann et al., 1998). Similarly, also in brain slices, the MSO-induced inhibition of GS results in aspartate accumulation (Nicklas, 1987).

Much evidence supports the notion that aspartate synthesis occurs in both astrocytes and neurons, whereby the relative in vivo contribution of both cell types is not clear. Nevertheless, in favor of a role of aspartate similar to that of alanine in the alanine–lactate shuttle between neurons and astrocytes, aspartate synthesis from [$\text{U-}^{13}\text{C}_6$]glucose can be stimulated by exogenous glutamine in cortical neurons (Waagepetersen et al., 1998a, b), and the nitrogen in aspartate can be transferred to alanine in astrocytes (Yudkoff et al., 1987). However, many details of the metabolic fate of aspartate in astrocytes are still undefined. If aspartate synthesis is involved in the intercellular transfer of nitrogen, the nitrogen group has, in return, to be released via transamination. Consistent with this possibility, ^{14}C - and ^{13}C -studies demonstrated that aspartate carbon enters the TCA cycle of both cultured neurons and astrocytes (Bakken et al., 1997b). In this regard, astrocytes might play an important role for the clearance of exogenous aspartate (Gundersen et al., 1991). This is further indicated by the uptake and metabolism of aspartate from the incubation medium of cultured astrocytes, which are both as rapid as that of glutamate and faster than the utilization of other amino acids (Yudkoff et al., 1987).

6.6 Significance of Metabolic Shuttles Complementary to the Glutamine–Glutamate Cycle

It is difficult to estimate the in vivo proportion of alanine as a carrier of nitrogen from neurons to astrocytes and its participation in the glutamine–glutamate cycle. However, present evidence suggests that the alanine–lactate shuttle accounts for at least part of the intercellular nitrogen flux between neurons and astrocytes. If the alanine–lactate shuttle is functionally integrated into the glutamine–glutamate cycle, this shuttle may act as a mechanism through which the cycle can be regulated. Considering the association of alanine uptake and metabolism with several enzymes involved in astrocytic energy metabolism, the alanine–lactate shuttle may also link the operation of the glutamine–glutamate cycle to cerebral energy metabolism. For example, similar to Tsacopoulos' hypothesis in the model system of the honeybee retina (Tsacopoulos et al., 1997; Tsacopoulos, 2002), neuronal release of neurotransmitter glutamate may stimulate astrocytic glutamine synthesis and release by an activity-dependent signal, which in turn may after transport to the neurons activate neuronal alanine synthesis. Contradicting a functional integration of the alanine–lactate shuttle into the glutamine–glutamate cycle, recent in vitro studies by Bak and coworkers (2005) using cultured astrocytes, glutamatergic neurons, and co-cultures could not provide evidence for an activity-dependent coupling of both cycles. In particular, labeling from [^{15}N]alanine in glutamine, aspartate, and glutamate in cerebellar co-cultures was independent of depolarization of neurons, while an activity-dependent increase in the labeling of both glutamate and aspartate (but not alanine) was observed in cerebellar neurons. Although these experiments further support the existence of an alanine–lactate shuttle between neurons and astrocytes, only the glutamine–glutamate cycle seems to be activity dependent.

It must also be considered that like the glutamine–glutamate cycle, the alanine–lactate and the leucine/ α -KIC shuttles are not stoichiometric, and basically any other pair of amino acid and its α -keto acid analogue could fulfill the function as a nitrogen carrier as well. In addition, there must be a net consumption of cerebral ammonia, considering high uptake rates for ammonia at the BBB (Cooper et al., 1979), while very little ammonia diffuses out of the brain. In contrast to ammonia itself, the amino acid glutamine easily leaves the brain via BBB. Further quantitative experiments using *in vitro* and *in vivo* experimental approaches need to be performed to elucidate the functional significance of these shuttles complementary to the glutamine–glutamate cycle *in vivo*.

7 Regulatory Metabolic Mechanisms via Intracellular Compartmentation

This section discusses the possible mechanisms by which astrocytes, in particular, manage the operation of metabolic cycles between astrocytes and neurons complementary to the glutamine–glutamate cycle. Special emphasis is given to intracellular pyruvate compartmentation as well as to the compartmentation and heterogeneity of mitochondria.

7.1 Cytosolic Pyruvate Compartmentation

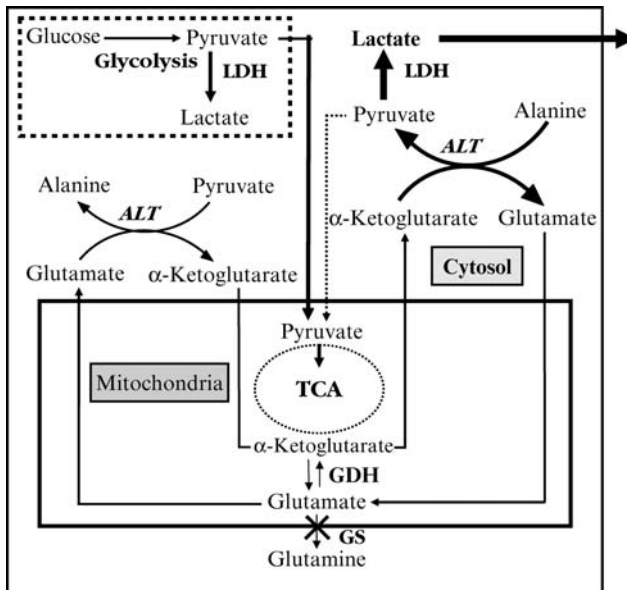
As discussed above, the enzymes involved in pyruvate recycling in astrocytes, ME and PEPCK, are compartmentalized in the cytosol and mitochondria, respectively. Therefore, the metabolism of TCA cycle intermediates and their release in the form of lactate might involve mitochondrial–cytosolic regulation of pyruvate metabolism. In addition, it is interesting that there was no detectable incorporation of ^{13}C from glutamate into alanine in cultured astrocytes, not even in the presence of α -KIC, which increased formation of lactate from glutamate twofold (McKenna et al., 1998). This observation is consistent with a compartmentation of cytosolic pyruvate. In particular, pyruvate from mitochondrial glutamate metabolism is the precursor for lactate and does not mix with glycolytically synthesized pyruvate, which is the precursor for alanine. Furthermore, studies using $[\text{U-}^{13}\text{C}_5]$ glutamine indicate an incomplete equilibration between the cytosolic and mitochondrial pools of pyruvate in astrocytes by the differential labeling patterns in alanine and lactate (Sonnewald et al., 1996b). In particular, while lactate was uniformly labeled, the presence of only monolabeled alanine indicated that alanine is derived from a TCA cycle associated with PC and/or a cycle in which α -ketoglutarate remains for more than one turn. Similarly, labeling of lactate from $[\text{U-}^{13}\text{C}_6]$ glucose exceeded that of alanine, while the opposite was observed in cultured neurons (Waagepetersen et al., 2000). The equal ^{13}C enrichments in alanine and lactate in co-cultures incubated either with $[\text{U-}^{13}\text{C}_6]$ glucose plus lactate (41% and 49%) or with $[\text{U-}^{13}\text{C}_3]$ lactate plus glucose (17% and 19%), but not with $[3\text{-}^{13}\text{C}_1]$ alanine plus glucose (or with $[1\text{-}^{13}\text{C}_1]$ glucose plus alanine (24% and 21%)) (Waagepetersen et al., 2000), indicate a functional importance of this intracellular compartmentation for the exchange of these metabolites between astrocytes and neurons.

In both cultured glia and neurons, it has been confirmed that cytosolic pyruvate is compartmentalized in two intracellular pools (Bouzier et al., 1998; Waagepetersen et al., 2000; Cruz et al., 2001; Zwingmann et al., 2001). These, at least two pools of pyruvate are consistent with one pool converting pyruvate into acetyl-CoA, and the other pool converting pyruvate into lactate. For example, in astrocytes incubated with $[1\text{-}^{13}\text{C}_1]$ glucose, the presence of unlabeled alanine did not affect the amount of extracellular $[3\text{-}^{13}\text{C}_1]$ lactate, synthesized via glycolysis, while $[3\text{-}^{13}\text{C}_1]$ alanine appeared in the medium only in the presence of unlabeled alanine (Zwingmann et al., 2001). In contrast to unchanged $[3\text{-}^{13}\text{C}_1]$ lactate, unlabeled lactate was synthesized from unlabeled alanine. A more detailed isotopomer analysis of intra- and extracellular alanine and lactate in this study, as well as studies in cultured astrocytes using ^{13}C -labeled alanine (Zwingmann et al., 2000) suggested that pyruvate, synthesized from alanine by cytosolic ALAT, is preferentially converted into the releasable pool of lactate. Together with data on the uptake and release rates of glucose, as well as of the enzyme activities of LDH, ALAT, PK, and GDH in cell homogenates and mitochondrial fractions of astrocytes, these results were consistent with the presence of two cytosolic pyruvate pools in cultured

astrocytes (● Figure 3.2-14). The pool, which is preferred for synthesis of releasable lactate, exchanges with extracellular alanine (upper right of ● Figure 3.2-14).

■ Figure 3.2-14

Cytosolic pyruvate compartmentation in astrocytes. Glucose is metabolized glycolytically to pyruvate, which is reduced to lactate in the cytosol. The majority of alanine is transaminated to pyruvate by ALT and reduced to a different pool of pyruvate in the cytosol. A minor part of unlabeled pyruvate is metabolized via TCA cycle activity. Oxidative metabolism of glycolytic pyruvate provides α -ketoglutarate, which is needed for the operation of cytosolic ALT toward alanine consumption. Glutamate, formed either by transamination of alanine in the cytosol or by mitochondrial GDH activity, is used in part by cytosolic ALT toward alanine synthesis from glycolytic pyruvate and is accumulated in astrocytes without additional glutamine synthesis. Glutamate and α -ketoglutarate are channeled between the cytosol and the mitochondria to allow the operation of cytosolic ALT and mitochondrial GDH. ALT, alanine aminotransferase; GDH, glutamate dehydrogenase; GS, glutamine synthetase; LDH, lactate dehydrogenase



The second pool is related more closely to the mitochondrial TCA cycle and is synthesized glycolytically from glucose (left side). Glycolytic pyruvate is used for synthesis of α -ketoglutarate, which is needed for cytosolic ALAT in the direction of alanine consumption. The stimulation of glutamate de novo synthesis from [1- $^{13}\text{C}_1$]glucose in the presence of unlabeled alanine, which was not correspondingly found in glutamine, provides evidence for a mitochondrial–cytosolic exchange. The reason for the apparent increase of ^{13}C -labeled glutamate is presumably channeling of glutamate between mitochondrial and cytosolic ALAT, mediated by intracellular pyruvate compartmentation.

Cytosolic synthesis of alanine was also concluded from observations by McKenna and coworkers (1996), in which cytosolic pyruvate, which is transaminated to alanine, did not exchange with mitochondrial pyruvate after entry of ^{13}C -labeled glutamate into the TCA cycle of astrocytes. The existence of two metabolically compartmentalized pools of intracellular lactate were also observed in C6 glioma cells (Bouzier et al., 1998), in which the pool related to glycolysis was metabolically disconnected from oxidative metabolism, but preferentially reduced to lactate. A similar conclusion was drawn from a study on the metabolism of [3- $^{13}\text{C}_1$]pyruvate in rabbit heart (Lewandowski, 1992). In addition, Peuhkurinen and

coworkers (1983) confirmed two functional cytosolic pyruvate pools in rat heart with radiolabeled substrates, one pool closely related to glycolysis and the other in equilibrium both with extracellular lactate and with mitochondrial pyruvate. Thus, data obtained with astrocytes differ from observations in C6 cells and rat heart, indicating different methods of metabolic regulation.

The relationship between alanine and glutamate formation from the same pyruvate pool in astrocytes may be found in the redox potential of the involved metabolites (Zwingmann et al., 2001). After incubation with alanine, glycolytic activity increases, which requires the supply of NAD^+ for the glyceraldehyde-3-phosphate dehydrogenase (GAPDH) reaction. NAD^+ can be regenerated by the reduction of pyruvate to lactate. In addition to the high synthesis of lactate by LDH in astrocytes in the presence of alanine, the transamination of pyruvate to alanine maintains the redox potential to enable a high glycolytic flux, as NAD^+ is regenerated by amination of α -ketoglutarate to glutamate through GDH, whose activity in the mitochondria was increased by approximately 80% in the presence of exogenous alanine (Zwingmann et al., 2001).

Intracellular cytosolic compartmentation of pyruvate is not specific for the astrocytes and has been demonstrated also in cultured cortical neurons (Cruz et al., 2001). In their study, the pool of pyruvate derived from extracellular pyruvate was mainly used for lactate and alanine production, while that derived from glucose was primarily used for subsequent oxidation in the TCA cycle. The underlying mechanism evidenced and outlined by Cruz and coworkers (2001) is convincing. The authors proposed, on the basis of the redox potential of the involved metabolites, that a redox switch using the cytosolic NAD^+/NADH ratio modulates the glycolytic flux. This switch controls which one of the two pyruvate pools is metabolized in the TCA cycle when substrates with a different redox potential than that of glucose are present. In particular, when both pyruvate and glucose were present in the medium, extracellular pyruvate has been shown to be the unique precursor for lactate, while pyruvate produced from glucose is used predominantly for oxidative metabolism. In contrast, when lactate and glucose are present in the medium, the reduced cytosolic redox state (increased NADH/NAD^+ ratio) would inhibit glycolysis at the GAPDH step, leading to preferential mitochondrial oxidation of pyruvate derived from lactate.

All together, these data give further insights into intracellular mechanisms in astrocytes supporting the lactate supply to neurons. In particular, extracellular alanine is used for regulated synthesis and release of lactate, which is mediated by intracytosolic pyruvate compartmentation, and may represent one regulatory mechanisms contributing to the recycling of energy substrates for use by neurons.

7.2 Mitochondrial Heterogeneity

In addition to cytosolic pyruvate compartmentation there is also evidence arising from ^{13}C -NMR studies using experimental animal models and primary cell cultures that mitochondrial metabolism of either astrocytes and neurons may be compartmentalized, i.e., differentially regulated intermediary metabolism through two different TCA cycles (Sonnewald et al., 1993b; see Sonnewald et al., 1998).

Mitochondrial heterogeneity in astrocytes was suggested, for example, by the observation that ^{14}C label from glutamine was incorporated to a higher extent in intracellular glutamate than glutamine, and from the different aspartate labeling pattern using glutamate or glutamine as substrates (Schousboe et al., 1993b). Furthermore, the observation of a conversion of ^{13}C -labeled glucose to glutamine, but not to citrate, while ^{13}C -label from acetate was found in both glutamine and citrate, led to the conclusion that glutamine precursors and citrate are either produced in different types of astrocytes or in different TCA cycles, located in functionally different mitochondria in the same cell (Sonnewald et al., 1993b). In addition, the pyruvate recycling pathway in astrocytes using $[\text{U-}^{13}\text{C}_5]\text{glutamine}$ (Sonnewald et al., 1996b) or $[1,2\text{-}^{13}\text{C}_2]\text{acetate}$ was reflected by the isotopomers of glutamate, but not of glutamine (Leo et al., 1993). Evidence for the operation of two TCA cycle in astrocytes (and in neurons) is discussed in Sonnewald et al. (1998) in light of mitochondrial location, ultrastructure, and development. It should be noted that although there is an enormous amount of evidence supporting mitochondrial heterogeneity in astrocyte cultures, this is not necessarily because of different TCA cycles within a single cell, but may be due to as yet unidentified

different types of astrocytes showing the same morphology. Further experiments are needed to obtain clarification as the presence of different mitochondrial compartments would represent a highly regulated system, for example when different compartments are used for energy production and amino acid *de novo* biosynthesis.

8 Concluding Remarks

Glial cells play a crucial role in maintaining neuronal function. Despite striking experimental progress, the detailed mechanisms on how glial metabolism modulates neuronal activity remains not completely resolved. This chapter describes aspects of neural metabolism and intercellular metabolic interactions contributing to normal brain function. Special emphasis is given to the metabolic regulation in astrocytes.

^{13}C -NMR spectroscopy is a powerful tool to assess cerebral metabolism by following the metabolic fate of various ^{13}C -labeled substrates. *In vivo* and *ex vivo* ^{13}C -NMR studies have confirmed the concept of metabolic compartmentation of two kinetically different glutamate pools, as well as the existence of the glutamine–glutamate cycle between astrocytes and neurons. Additional features of this cycle have also been elucidated, in particular, its tight coupling with other nitrogen-carrying systems confirmed that the glutamine–glutamate cycle between astrocytes and neurons is by no means stoichiometric, and that the modulation of astrocytic intracellular metabolism is an integral component of the glutamine–glutamate cycle.

A regulated interplay between oxidative metabolism, glycolysis, and the pyruvate recycling pathway in astrocytes contributes to the uptake of glutamate from the synaptic cleft and thereby substantiates the neuroprotective function of astrocytes. Nonetheless, the detailed mechanisms by which glial metabolism modulates neuronal activity are not yet completely resolved. It should be mentioned that astrocytes also express a repertoire of neurotransmitter receptors, reflecting those of neighboring synapses. It has been demonstrated that energy deficits or membrane depolarization evokes reversed electrogenic glutamate uptake in astrocytes (Szatkowski et al., 1990), while glutamate may be stored also in vesicles in astrocytes and released through an exocytotic pathway (Araque et al., 2000). An alanine–lactate shuttle between neurons and astrocytes provides nitrogen transfer from neurons to astrocytes, recycles energy substrates for neurons, and promotes in return intercellular glutamine–glutamate cycling. The conversion of alanine to lactate in astrocytes is regulated by cytosolic pyruvate compartmentation. Also, mitochondrial heterogeneity has been observed in astrocytes.

Experiments using primary astrocytes, neurons, and their co-cultures exposed to various pathological conditions have further emphasized the role of astrocytes as essential metabolic partners of neurons, thus providing a better understanding of pathological events contributing to neuronal dysfunction. It is noteworthy that the implications of these *in vitro* findings in astrocytes cannot necessarily be transferred to the *in vivo* situation in the brain without restrictions. Further quantitative experiments using *in vivo* and *in vitro* approaches need to be performed to link these phenomena on a cellular level to the functional significance *in vivo*. However, because of limitations set by the permeability of the BBB, the cellular and structural heterogeneity of the brain, and the inaccessibility of the extracellular fluid, it is almost impossible to confirm results obtained from *in vitro* studies by *in vivo* studies. Therefore, NMR studies on primary cell cultures are an alternative way to investigate numerous features of metabolic regulation, and to discover yet unknown metabolic control points. Ultimately, data from *in vitro* studies could serve as a basis for the formation of new hypotheses and concepts concerning the particular role of astrocytic metabolic control points, which appear to be highly flexible and regulated through neuronal function and neurotransmitter homeostasis.

References

- Alves PM, McKenna MC, Sonnewald U. 1995. Lactate metabolism in mouse brain astrocytes studied by ^{13}C -NMR spectroscopy. *Neuroreport* 6: 2201–2204.
- Alves PM, Nunes R, Zhang C, Maycock CD, Sonnewald U, et al. 2000. Metabolism of $[3-^{13}\text{C}]$ malate in primary cultures of mouse astrocytes. *Dev Neurosci* 22: 456–462.

- Araque A, Li N, Doyle RT, Haydon PG. 2000. SNARE protein-dependent glutamate release from astrocytes. *J Neurosci* 20: 666-673.
- Attwell D, Laughlin SB. 2001. An energy budget for signaling in the grey matter of the brain. *J Cereb Blood Flow Metab* 21: 1133-1145.
- Aureli T, Di Cocco ME, Calvani M, Conti F. 1997. The entry of [^{13}C]glucose into biochemical pathways reveals a complex compartmentation and metabolite trafficking between glia and neurons: A study by ^{13}C -NMR spectroscopy. *Brain Res* 765: 218-227.
- Badar-Goffer RS, Bachelard HS, Morris PG. 1990. Cerebral metabolism of acetate and glucose studied by ^{13}C NMR spectroscopy. A technique for investigating metabolic compartmentation in the brain. *Biochem J* 266: 133-139.
- Bak LK, Sickmann HM, Schousboe A, Waagepetersen HS. 2005. Activity of the lactate-alanine shuttle is independent of glutamate-glutamine cycle activity in cerebellar neuronal-astrocytic cultures. *J Neurosci Res* 79: 88-96.
- Bakken IJ, Johnsen SF, White LR, Unsgard G, Aasly J, et al. 1997a. NMR spectroscopy study of the effect of 3-nitropropionic acid on glutamate metabolism in cultured astrocytes. *J Neurosci Res* 47: 642-649.
- Bakken IJ, White LR, Aasly J, Unsgard G, Sonnewald U. 1997b. Lactate formation from [^{13}C]aspartate in cultured astrocytes: Compartmentation of pyruvate metabolism. *Neurosci Lett* 237: 117-120.
- Bakken IJ, White LR, Unsgard G, Aasly J, Sonnewald U. 1998a. [^{13}C]glutamate metabolism in astrocytes during hypoglycemia and hypoxia. *J Neurosci Res* 51: 636-645.
- Bakken IJ, White LR, Aasly J, Unsgard G, Sonnewald U. 1998b. [^{13}C] aspartate metabolism in cultured cortical astrocytes and cerebellar granule neurons studied by NMR spectroscopy. *Glia* 23: 271-277.
- Balazs R, Machiyama Y, Hammond BJ, Julian T, Richter D. 1970. The operation of the γ -aminobutyrate bypath of the tricarboxylic acid cycle in brain tissue in vitro. *Biochem J* 116: 445-461.
- Benjamin AM, Quastel JH. 1975. Metabolism of amino acids and ammonia in rat brain cortex slices in vitro: A possible role of ammonia in brain function. *J Neurochem* 25: 197-206.
- Berl S, Clarke DD. 1969. Compartmentation of amino acid metabolism. In *Handbook of Neurochemistry*, Vol. 2. Lajtha A, editor. New York: Plenum Press; pp. 447-472.
- Berl S, Clarke DD. 1983. The metabolic compartmentation concept. In *Glutamine, Glutamate and GABA in the CNS*. Hertz L, Kvamme E, McGeer EG, Schousboe A, editors. New York: Alan R. Liss; pp. 205-217.
- Berl S, Nicklas WJ, Clarke DD. 1970. Compartmentation of citric acid cycle metabolism in brain: Labelling of glutamate, glutamine, aspartate and GABA by several radioactive tracer metabolites. *J Neurochem* 17: 1009-1015.
- Bernard-Helary K, Ardourel M, Magistretti P, Hevor T, Cloix JF. 2002. Stable transfection of cDNAs targeting specific steps of glycogen metabolism supports the existence of active gluconeogenesis in mouse cultured astrocytes. *Glia* 37: 379-382.
- Bixel MG, Hamprecht B. 1995. Generation of ketone bodies from leucine by cultured astroglial cells. *J Neurochem* 65: 2450-2461.
- Bixel MG, Engelmann J, Willker W, Hamprecht B, Leibfritz D. 2004. Metabolism of [^{13}C]leucine in cultured astroglial cells. *Neurochem Res* 29: 2057-2067.
- Bixel MG, Hutson SM, Hamprecht B. 1997. Cellular distribution of branched-chain amino acid aminotransferase isoenzymes among rat brain glial cells in culture. *J Histochem Cytochem* 45: 685-694.
- Bluml S, Moreno-Torres A, Shic F, Nguy CH, Ross BD. 2002. Tricarboxylic acid cycle of glia in the in vivo human brain. *NMR Biomed* 15: 1-5.
- Bouzier AK, Thiaudiere E, Biran M, Rouland R, Canioni P, et al. 2000. The metabolism of [^{13}C]lactate in the rat brain is specific of a pyruvate carboxylase-deprived compartment. *J Neurochem* 75: 480-486.
- Bouzier AK, Voisin P, Goodwin R, Canioni P, Merle M. 1998. Glucose and lactate metabolism in C6 glioma cells: Evidence for the preferential utilization of lactate for cell oxidative metabolism. *Dev Neurosci* 20: 331-338.
- Bradford HF, Ward HK, Thomas AJ. 1978. Glutamine—a major substrate for nerve endings. *J Neurochem* 30: 1453-1459.
- Brand A, Engelmann J, Leibfritz D. 1992. A ^{13}C NMR study on fluxes into the TCA cycle of neuronal and glial tumor cell lines and primary cells. *Biochimie* 74: 941-948.
- Brand A, Richter-Landsberg C, Leibfritz D. 1993. Multinuclear NMR studies on the energy metabolism of glial and neuronal cells. *Dev Neurosci* 15: 289-298.
- Brand A, Richter-Landsberg C, Leibfritz D. 1997. Metabolism of acetate in rat brain neurons, astrocytes and cocultures: Metabolic interactions between neurons and glia cells, monitored by NMR spectroscopy. *Cell Mol Biol (Noisy-le-grand)* 43: 645-657.
- Bukato G, Kochan Z, Swierczynski J. 1995. Purification and properties of cytosolic and mitochondrial malic enzyme isolated from human brain. *Int J Biochem Cell Biol* 27: 47-54.
- Caldani M, Rolland B, Fages C, Tardy M. 1982. Glutamine synthetase activity during mouse brain development. *Experientia* 38: 1199-1202.
- Cangiano C, Cardelli-Cangiano P, James JH, Rossi-Fanelli F, Patrizi MA, et al. 1983. Brain microvessels take up large neutral amino acids in exchange for glutamine. Cooperative role of Na^+ -dependent and Na^+ -independent systems. *J Biol Chem* 258: 8949-9054.

- Cerdan S, Kunnecke B, Seelig J. 1990. Cerebral metabolism of [1,2-¹³C₂]acetate as detected by in vivo and in vitro ¹³C NMR. *J Biol Chem* 265: 12916-12926.
- Cesar M, Hamprecht B. 1995. Immunocytochemical examination of neural rat and mouse primary cultures using monoclonal antibodies raised against pyruvate carboxylase. *J Neurochem* 64: 2312-2318.
- Chan H, Zwingmann C, Pannunzio M, Butterworth RF. 2003. Effects of ammonia on high affinity glutamate uptake and glutamate transporter EAAT3 expression in cultured rat cerebellar granule cells. *Neurochem Int* 43: 137-146.
- Chapa F, Cruz F, Garcia-Martin ML, Garcia-Espinosa MA, Cerdan S. 2000. Metabolism of (1-¹³C) glucose and (2-¹³C, 2-²H₃) acetate in the neuronal and glial compartments of the adult rat brain as detected by [¹³C, ²H] NMR spectroscopy. *Neurochem Int* 37: 217-228.
- Chapa F, Künnecke B, Clavo R, Escobar del Rey F, Morreale de Escobar G. et al. 1995. Adult onset hypothyroidism and the cerebral metabolism of (1,2-¹³C₂)acetate. *Endocrinology* 136: 296-305.
- Chateil J, Biran M, Thiaudiere E, Canioni P, Merle M. 2001. Metabolism of [1-¹³C]glucose and [2-¹³C]acetate in the hypoxic rat brain. *Neurochem Int* 38: 399-407.
- Cooper AJ, Plum F. 1987. Biochemistry and physiology of brain ammonia. *Physiol Rev* 67: 440-519.
- Cooper AJ, McDonald JM, Gelbard AS, Gledhill RF, Duffy TE. 1979. The metabolic fate of ¹³N-labeled ammonia in rat brain. *J Biol Chem* 254: 4982-4992.
- Cooper AJ, Nieves E, Coleman AE, Filc-DeRicco S, Gelbard AS. 1979. Short-term metabolic fate of [¹³N]ammonia in rat liver in vivo. *J Biol Chem* 262: 1073-1080.
- Cruz F, Cerdan S. 1999. Quantitative ¹³C NMR studies of metabolic compartmentation in the adult mammalian brain. *NMR Biomed* 12: 451-462.
- Cruz F, Scott SR, Barroso I, Santisteban P, Cerdan S. 1998. Ontogeny and cellular localization of the pyruvate recycling system in rat brain. *J Neurochem* 70: 2613-2619.
- Cruz F, Villalba M, Garcia-Espinosa MA, Ballesteros P, Bogonez E, et al. 2001. Intracellular compartmentation of pyruvate in primary cultures of cortical neurons as detected by ¹³C NMR spectroscopy with multiple ¹³C labels. *J Neurosci Res* 66: 771-781.
- Dienel GA, Cruz NF. 2003. Neighborly interactions of metabolically activated astrocytes in vivo. *Neurochem Int* 43: 339-354.
- Dienel GA, Hertz L. 2001. Glucose and lactate metabolism during brain activation. *J Neurosci Res* 66: 824-838.
- Dringen R, Hamprecht B. 1992. Glucose, insulin, and insulin-like growth factor I regulate the glycogen content of astroglia-rich primary cultures. *J Neurochem* 58: 511-517.
- Dringen R, Gebhardt R, Hamprecht B. 1993. Glycogen in astrocytes: Possible function as lactate supply for neighboring cells. *Brain Res* 623: 208-214.
- Edmond J. 1992. Energy metabolism in developing brain cells. *Can J Physiol Pharmacol* 70 (Suppl): S118-S129.
- Friedman B, Goodman EH, Saunders HL, Kostos C, Weinhouse S. 1971. Estimation of pyruvate recycling during gluconeogenesis in perfused rat liver. *Metabolism* 20: 2-12.
- Gamberino WC, Berkich DA, Lynch CJ, Xu B, LaNoue KF. 1997. Role of pyruvate carboxylase in facilitation of synthesis of glutamate and glutamine in cultured astrocytes. *J Neurochem* 69: 2312-2325.
- Gjedde A, Marrett S. 2001. Glycolysis in neurons, not astrocytes, delays oxidative metabolism of human visual cortex during sustained checkerboard stimulation in vivo. *J Cereb Blood Flow Metab* 21: 1384-1392.
- Griffin JL, Keun H, Richter C, Moskau D, Rae C. et al. 2003. Compartmentation of metabolism probed by [2-¹³C]alanine: Improved ¹³C NMR sensitivity using a CryoProbe detects evidence of a glial metabolon. *Neurochem Int* 42: 93-99.
- Griffin JL, Rae C, Dixon RM, Radda GK, Matthews PM. 1998. Excitatory amino acid synthesis in hypoxic brain slices: Does alanine act as a substrate for glutamate production in hypoxia? *J Neurochem* 71: 2477-2486.
- Grill V, Bjorkman O, Gutniak M, Lindqvist M. 1992. Brain uptake and release of amino acids in nondiabetic and insulin-dependent diabetic subjects: Important role of glutamine release for nitrogen balance. *Metabolism* 41: 28-32.
- Gruetter R. 2002. In vivo ¹³C NMR studies of compartmentalized cerebral carbohydrate metabolism. *Neurochem Int* 41: 143-154.
- Gruetter R, Seaquist ER, Kim S, Ugurbil K. 1998. Localized in vivo ¹³C-NMR of glutamate metabolism in the human brain: Initial results at 4 Tesla. *Dev Neurosci* 20: 380-388.
- Gruetter R, Seaquist ER, Ugurbil K. 2001. A mathematical model of compartmentalized neurotransmitter metabolism in the human brain. *Am J Physiol Endocrinol Metab* 281: E100-E112.
- Gundersen V, Ottersen OP, Storm-Mathisen J. 1991. Aspartate- and glutamate-like immunoreactivities in rat hippocampal slices: Depolarization-induced redistribution and effects of precursors. *Eur J Neurosci* 3: 1281-1299.
- Haberg A, Qu H, Haraldseth O, Unsgard G, Sonnewald U. 1998a. In vivo injection of [1-¹³C]glucose and [1,2-¹³C]acetate combined with ex vivo ¹³C nuclear magnetic resonance spectroscopy: A novel approach to the study of middle cerebral artery occlusion in the rat. *J Cereb Blood Flow Metab* 18: 1223-1232.
- Haberg A, Qu H, Bakken IJ, Sande LM, White LR, et al. 1998b. In vitro and ex vivo ¹³C-NMR spectroscopy studies of pyruvate recycling in brain. *Dev Neurosci* 20: 389-398.

- Hamai M, Minokoshi Y, Shimazu T. 1999. L-Glutamate and insulin enhance glycogen synthesis in cultured astrocytes from the rat brain through different intracellular mechanisms. *J Neurochem* 73: 400-407.
- Hassel B. 2002. Carboxylation and anaplerosis in neurons and glia. *Mol Neurobiol* 22: 21-40.
- Hassel B, Sonnewald U. 1995a. Glial formation of pyruvate and lactate from TCA cycle intermediates: Implications for the inactivation of transmitter amino acids? *J Neurochem* 65: 2227-2234.
- Hassel B, Sonnewald U. 1995b. Selective inhibition of the tricarboxylic acid cycle of GABAergic neurons with 3-nitropropionic acid in vivo. *J Neurochem* 65: 1184-1191.
- Hassel B, Paulsen RE, Johnsen A, Fonnum F. 1992. Selective inhibition of glial cell metabolism in vivo by fluorocitrate. *Brain Res* 576: 120-124.
- Hassel B, Sonnewald U, Fonnum F. 1995a. Glial–neuronal interactions as studied by cerebral metabolism of [2-¹³C] acetate and [1-¹³C]glucose: An ex vivo ¹³C NMR spectroscopic study. *J Neurochem* 64: 2773-2782.
- Hassel B, Westergaard N, Schousboe A, Fonnum F. 1995b. Metabolic differences between primary cultures of astrocytes and neurons from cerebellum and cerebral cortex. Effects of fluorocitrate. *Neurochem Res* 20: 413-420.
- Hassel B, Sonnewald U, Unsgard G, Fonnum F. 1994. NMR spectroscopy of cultured astrocytes: Effects of glutamine and the gliotoxin fluorocitrate. *J Neurochem* 62: 2187-2194.
- Hertz L, Dienel GA. 2002. Energy metabolism in the brain. *Int Rev Neurobiol* 51: 1-102.
- Hertz L, Schousboe A. 1986. Role of astrocytes in compartmentation of amino acid and energy metabolism. In *Astrocytes*, Vol. 2. Federoff S, Vernadakis A, editors. Academic Press; pp. 179-208.
- Hertz L, Dringen R, Schousboe A, Robinson SR. 1999. Astrocytes: Glutamate producers for neurons. *J Neurosci Res* 57: 417-428.
- Hertz L, Yu AC, Kala G, Schousboe A. 2000. Neuronal–astrocytic and cytosolic–mitochondrial metabolite trafficking during brain activation, hyperammonemia, and energy deprivation. *Neurochem Int* 37: 83-102.
- Huang NC, Yongbi MN, Helpert JA. 1997. The influence of preischemic hyperglycemia on acute changes in the apparent diffusion coefficient of brain water following global ischemia in rats. *Brain Res* 757: 139-145.
- Hue L. 1982. Futile cycles and regulation of metabolism. In *Metabolic Compartmentation*. Sies H, editor. New York: Academic Press; pp. 71-97.
- Kanamatsu T, Tsukada Y. 1999. Effects of ammonia on the anaplerotic pathway and amino acid metabolism in the brain: An ex vivo ¹³C NMR spectroscopic study of rats after administering [2-¹³C]glucose with or without ammonium acetate. *Brain Res* 841: 11-19.
- Kaufman EE, Driscoll BF. 1993. Evidence for cooperativity between neurons and astroglia in the regulation of CO₂ fixation in vitro. *Dev Neurosci* 15: 299-305.
- Kauppinen RA, Enkvist K, Holopainen I, Akerman KE. 1988. Glucose deprivation depolarizes plasma membrane of cultured astrocytes and collapses transmembrane potassium and glutamate gradients. *Neuroscience* 26: 283-289.
- Kimmich GA, Roussie JA, Randles J. 2002. Aspartate aminotransferase isotope exchange reactions: Implications for glutamate/glutamine shuttle hypothesis. *Am J Physiol Cell Physiol* 282: C1404-C1413.
- Korf J. 1996. Intracerebral trafficking of lactate in vivo during stress, exercise, electroconvulsive shock, and ischemia as studied with microdialysis. *Dev Neurosci* 18: 405-414.
- Kruse T, Reiber H, Neuhoff V. 1985. Amino acid transport across the human blood–CSF barrier. An evaluation graph for amino acid concentrations in cerebrospinal fluid. *J Neurol Sci* 70: 129-138.
- Kunnecke B, Cerdan S, Seelig J. 1993. Cerebral metabolism of [1,2-¹³C₂]glucose and [U-¹³C₄]3-hydroxybutyrate in rat brain as detected by ¹³C NMR spectroscopy. *NMR Biomed* 6: 264-277.
- Lapidot A, Gopher A. 1994. Cerebral metabolic compartmentation. Estimation of glucose flux via pyruvate carboxylase/pyruvate dehydrogenase by ¹³C NMR in isotopomer analysis of D-(U-¹³C) glucose metabolism. *J Biol Chem* 269: 27198-27208.
- Lebon V, Petersen KF, Cline GW, Shen J, Mason GF, et al. 2002. Astroglial contribution to brain energy metabolism in humans revealed by ¹³C nuclear magnetic resonance spectroscopy: Elucidation of the dominant pathway for neurotransmitter glutamate repletion and measurement of astrocytic oxidative metabolism. *J Neurosci* 22: 1523-1531.
- Leo GC, Driscoll BF, Shank RP, Kaufman E. 1993. Analysis of [1-¹³C]D-glucose metabolism in cultured astrocytes and neurons using nuclear magnetic resonance spectroscopy. *Dev Neurosci* 15: 282-288.
- Lewandowski ED. 1992. Metabolic heterogeneity of carbon substrate utilization in mammalian heart: NMR determinations of mitochondrial versus cytosolic compartmentation. *Biochemistry* 31: 8916-8923.
- Lieth E, LaNoue KF, Berkich DA, Xu B, Ratz M, et al. 2001. Nitrogen shuttling between neurons and glial cells during glutamate synthesis. *J Neurochem* 76: 1712-1723.
- Magistretti PJ, Pellerin L. 1999. Cellular mechanisms of brain energy metabolism and their relevance to functional brain imaging. *Philos Trans R Soc Lond B Biol Sci* 354: 1155-1163.

- Magistretti PJ, Pellerin L, Rothman DL, Shulman RG. 1999. Energy on demand. *Science* 283: 496-497.
- Magistretti PJ, Sorg O, Yu N, Martin JL, Pellerin L. 1993. Neurotransmitters regulate energy metabolism in astrocytes: Implications for the metabolic trafficking between neural cells. *Dev Neurosci* 15: 306-312.
- Marrif H, Juurlink BH. 1999. Astrocytes respond to hypoxia by increasing glycolytic capacity. *J Neurosci Res* 57: 255-260.
- Martin M, Canioni P, Merle M. 1997. Analysis of carbon metabolism in cultured cerebellar and cortical astrocytes. *Cell Mol Biol (Noisy-le-grand)* 43: 631-643.
- Martin M, Portais JC, Labouesse J, Canioni P, Merle M. 1993. [^{13}C]glucose metabolism in rat cerebellar granule cells and astrocytes in primary culture. Evaluation of flux parameters by ^{13}C - and ^1H -NMR spectroscopy. *Eur J Biochem* 217: 617-625.
- Martin M, Portais JC, Voisin P, Rousse N, Canioni P, et al. 1995. Comparative analysis of ^{13}C -enriched metabolites released in the medium of cerebellar and cortical astrocytes incubated with [^{13}C]glucose. *Eur J Biochem* 231: 697-703.
- Martinez-Hernandez A, Bell KP, Norenberg MD. 1977. Glutamine synthetase: Glial localization in brain. *Science* 195: 1356-1358.
- Mason GF, Rothman DL, Behar KL, Shulman RG. 1992. NMR determination of the TCA cycle rate and α -ketoglutarate/glutamate exchange rate in rat brain. *J Cereb Blood Flow Metab* 12: 434-447.
- McKenna MC, Sonnewald U. 2005. GABA alters the metabolic fate of [^{13}C]glutamate in cultured cortical astrocytes. *J Neurosci Res* 79: 81-87.
- McKenna MC, Sonnewald U, Huang X, Stevenson J, Johnsen SF, et al. 1998. α -ketoisocaproate alters the production of both lactate and aspartate from [^{13}C]glutamate in astrocytes: A ^{13}C NMR study. *J Neurochem* 70: 1001-1008.
- McKenna MC, Sonnewald U, Huang X, Stevenson J, Zielke HR. 1996. Exogenous glutamate concentration regulates the metabolic fate of glutamate in astrocytes. *J Neurochem* 66: 386-393.
- McKenna MC, Stevenson JH, Huang X, Hopkins IB. 2000a. Differential distribution of the enzymes glutamate dehydrogenase and aspartate aminotransferase in cortical synaptic mitochondria contributes to metabolic compartmentation in cortical synaptic terminals. *Neurochem Int* 37: 229-241.
- McKenna MC, Stevenson JH, Huang X, Tildon JT, Zielke CL, et al. 2000b. Mitochondrial malic enzyme activity is much higher in mitochondria from cortical synaptic terminals compared with mitochondria from primary cultures of cortical neurons or cerebellar granule cells. *Neurochem Int* 36: 451-459.
- Merle M, Martin M, Villegier A, Canioni P. 1996a. Mathematical modelling of the citric acid cycle for the analysis of glutamine isotopomers from cerebellar astrocytes incubated with [^{13}C]glucose. *Eur J Biochem* 239: 742-751.
- Merle M, Martin M, Villegier A, Canioni P. 1996b. [^{13}C]glucose metabolism in brain cells: Isotopomer analysis of glutamine from cerebellar astrocytes and glutamate from granule cells. *Dev Neurosci* 18: 460-468.
- Mertens-Strijthagen J, Lacreman-Pirsoul J, Baudoux G. 1996. Recovery potential in glucose-deprived astrocytes. *Neurosci Res* 26: 133-139.
- Minchin MC, Beart PM. 1975. Compartmentation of amino acid metabolism in the rat dorsal root ganglion: A metabolic and autoradiographic study. *Brain Res* 83: 437-449.
- Muir D, Berl S, Clarke DD. 1986. Acetate and fluoroacetate as possible markers for glial metabolism in vivo. *Brain Res* 380: 336-340.
- Nagaraja TN, Brookes N. 1998. Intracellular acidification induced by passive and active transport of ammonium ions in astrocytes. *Am J Physiol* 274: C883-C891.
- Naruse H, Cheng SC, Waelsch H. 1966a. CO_2 fixation in the nervous system. V. CO_2 fixation and citrate metabolism in rabbit nerve. *Exp Brain Res* 1: 291-298 contd.
- Naruse H, Cheng SC, Waelsch H. 1966b. CO_2 fixation in the nervous tissue. IV. CO_2 fixation and citrate metabolism in lobster nerve. *Exp Brain Res* 1: 284-90 contd.
- Nicklas WJ, Zeevalk G, Hyndman A. 1987. Interactions between neurons and glia in glutamate/glutamine compartmentation. *Biochem Soc Trans* 15: 208-210.
- Nishina M, Suzuki M, Matsushita K. 2004. *Trichinella spiralis*: Activity of the cerebral pyruvate recycling pathway of the host (mouse) in hypoglycemia induced by the infection. *Exp Parasitol* 106: 62-65.
- Oldendorf WH. 1971. Brain uptake of radiolabeled amino acids, amines, and hexoses after arterial injection. *Am J Physiol* 221: 1629-1639.
- Oldendorf WH, Szabo J. 1976. Amino acid assignment to one of three blood-brain barrier amino acid carriers. *Am J Physiol* 230: 94-98.
- Ott P, Larsen FS. 2004. Blood-brain barrier permeability to ammonia in liver failure: A critical reappraisal. *Neurochem Int* 44: 185-198.
- Oz G, Berkich DA, Henry PG, Xu Y, LaNoue K, et al. 2004. Neuroglial metabolism in the awake rat brain: CO_2 fixation increases with brain activity. *J Neurosci* 24: 11273-22379.
- Patel MS. 1974. The relative significance of CO_2 -fixing enzymes in the metabolism of rat brain. *J Neurochem* 22: 717-724.
- Pellerin L, Magistretti PJ. 1994. Glutamate uptake into astrocytes stimulates aerobic glycolysis: A mechanism coupling

- neuronal activity to glucose utilization. *Proc Natl Acad Sci USA* 91: 10625-10629.
- Pellerin L, Magistretti PJ. 2003. How to balance the brain energy budget while spending glucose differently. *J Physiol* 546: 325.
- Peng L, Swanson RA, Hertz L. 2001. Effects of L-glutamate, D-aspartate, and monensin on glycolytic and oxidative glucose metabolism in mouse astrocyte cultures: Further evidence that glutamate uptake is metabolically driven by oxidative metabolism. *Neurochem Int* 38: 437-443.
- Peng L, Zhang X, Hertz L. 1994. High extracellular potassium concentrations stimulate oxidative metabolism in a glutamatergic neuronal culture and glycolysis in cultured astrocytes but have no stimulatory effect in a GABAergic neuronal culture. *Brain Res* 663: 168-172.
- Peuhkurinen KJ, Hiltunen JK, Hassinen IE. 1983. Metabolic compartmentation of pyruvate in the isolated perfused rat heart. *Biochem J* 210: 193-198.
- Portais JC, Voisin P, Merle M, Canioni P. 1996. Glucose and glutamine metabolism in C6 glioma cells studied by carbon ¹³C NMR. *Biochimie* 78: 155-164.
- Preece NC, Cerdan S. 1996. Metabolic precursors and compartmentation of cerebral GABA in vigabratin-treated rats. *J Neurochem* 67: 1718-1725.
- Qu H, Konradsen JR, van Hengel M, Wolt S, Sonnewald U. 2001. Effect of glutamine and GABA on [U-¹³C]glutamate metabolism in cerebellar astrocytes and granule neurons. *J Neurosci Res* 66: 885-890.
- Rae C, Hare N, Bubbs WA, McEwan SR, Broer A, et al. 2003. Inhibition of glutamine transport depletes glutamate and GABA neurotransmitter pools: Further evidence for metabolic compartmentation. *J Neurochem* 85: 503-514.
- Raichle ME, Larson KB. 1981. The significance of the NH₃-NH₄⁺ equilibrium on the passage of ¹³N-ammonia from blood to brain. A new regional residue detection model. *Circ Res* 48: 913-937.
- Rothstein JD, Dykes-Hoberg M, Pardo CA, Bristol LA, Jin L, et al. 1996. Knockout of glutamate transporters reveals a major role for astroglial transport in excitotoxicity and clearance of glutamate. *Neuron* 16: 675-686.
- Ruiz F, Alvarez G, Pereira R, Hernandez M, Villalba M, et al. 1998. Protection by pyruvate and malate against glutamate-mediated neurotoxicity. *Neuroreport* 9: 1277-12782.
- Sadasivudu B, Lajtha A. 1970. Metabolism of amino acids in incubated slices of mouse brain. *J Neurochem* 17: 1299-1311.
- Schmoll D, Fuhrmann E, Gebhardt R, Hamprecht B. 1995. Significant amounts of glycogen are synthesized from 3-carbon compounds in astroglial primary cultures from mice with participation of the mitochondrial phosphoenolpyruvate carboxykinase isoenzyme. *Eur J Biochem* 227: 308-315.
- Schousboe A, Westergaard N, Waagepetersen HS, Larsson OM, Bakken IJ, et al. 1997. Trafficking between glia and neurons of TCA cycle intermediates and related metabolites. *Glia* 21: 99-105.
- Schousboe I, Tonder N, Zimmer J, Schousboe A. 1993a. A developmental study of lactate dehydrogenase isozyme and aspartate aminotransferase activity in organotypic rat hippocampal slice cultures and primary cultures of mouse neocortical and cerebellar neurons. *Int J Dev Neurosci* 11: 765-772.
- Schousboe A, Westergaard N, Sonnewald U, Petersen SB, Huang R, et al. 1993b. Glutamate and glutamine metabolism and compartmentation in astrocytes. *Dev Neurosci* 15: 359-366.
- Shank RP, Aprison M. 1988. Glutamate as a neurotransmitter. In *Glutamate and Glutamine in Mammals*, Vol. 2. Kvamme E, editor. Florida: CRC Press, Boca Raton; pp. 3-20.
- Shank RP, Aprison MH. 1981. The present status and significance of the glutamine cycle in neuronal tissues. *Life Sci* 28: 837-842.
- Shank RP, Campbell GL. 1982. Glutamine and α -ketoglutarate uptake and metabolism by nerve terminal enriched material from mouse cerebellum. *Neurochem Res* 7: 601-616.
- Shank RP, Campbell GL. 1983. Glutamate in the CNS. In *Handbook of Neurochemistry*, Vol. 3. Lajtha A, editor. New York: Plenum Press; pp. 381-404.
- Shank RP, Bennett GS, Freytag SO, Campbell GL. 1985. Pyruvate carboxylase: An astrocyte-specific enzyme implicated in the replenishment of amino acid neurotransmitter pools. *Brain Res* 329: 364-367.
- Shank RP, Leo GC, Zielke HR. 1993. Cerebral metabolic compartmentation as revealed by nuclear magnetic resonance analysis of D-[¹³C]glucose metabolism. *J Neurochem* 61: 315-323.
- Shokati T, Zwingmann C, Leibfritz D. 2005. Glutamine as an anaplerotic substrate of primary cultured neurons: A re-evaluation by multinuclear NMR spectroscopy. *Neurochem Res* 30: 1269-1281.
- Sibson NR, Mason GF, Shen J, Cline GW, Herskovits AZ, et al. 2001. In vivo ¹³C NMR measurement of neurotransmitter glutamate cycling, anaplerosis, and TCA cycle flux in rat brain during [2-¹³C] glucose infusion. *J Neurochem* 76: 975-989.
- Silver IA, Erecinska M. 1997. Energetic demands of the Na⁺/K⁺-ATPase in mammalian astrocytes. *Glia* 21: 35-45.
- Sokoloff L. 1977. Relation between physiological function and energy metabolism in the central nervous system. *J Neurochem* 29: 13-26.
- Sokoloff L. 1983-84. Mapping local functional activity by measurement of local cerebral glucose utilization in the central nervous system of animals and man. *Harvey Lect* 79: 77-143.
- Sokoloff L. 1992. The brain as a chemical machine. *Progr Brain Res* 94: 19-33.

- Sonnenwald U, Kondziella D. 2003. Neuronal-glial interaction in different neurological diseases studied by ex vivo ^{13}C NMR spectroscopy. *NMR Biomed* 16: 424-429.
- Sonnenwald U, Hertz L, Schousboe A. 1998. Mitochondrial heterogeneity in the brain at the cellular level. *J Cereb Blood Flow Metab* 18: 231-237.
- Sonnenwald U, Muller TB, Westergaard N, Unsgard G, Petersen SB, et al. 1994. NMR spectroscopic study of cell cultures of astrocytes and neurons exposed to hypoxia: Compartmentation of astrocyte metabolism. *Neurochem Int* 24: 473-483.
- Sonnenwald U, Wang AY, Petersen SB, Westergaard N, Schousboe A, et al. 1995. ^{13}C NMR study of IGF-I- and insulin-effects on mitochondrial function in cultured brain cells. *Neuroreport* 6: 878-880.
- Sonnenwald U, Wang AY, Schousboe A, Erikson R, Skottner A. 1996a. New aspects of lactate metabolism: IGF-1 and insulin regulate mitochondrial function in cultured brain cells during normoxia and hypoxia. *Dev Neurosci* 18: 443-448.
- Sonnenwald U, Westergaard N, Jones P, Taylor A, Bachelard HS, et al. 1996b. Metabolism of $[\text{U-}^{13}\text{C}_5]\text{glutamine}$ in cultured astrocytes studied by NMR spectroscopy: First evidence of astrocytic pyruvate recycling. *J Neurochem* 67: 2566-2572.
- Sonnenwald U, White LR, Odegard E, Westergaard N, Bakken IJ, et al. 1996c. MRS study of glutamate metabolism in cultured neurons/glia. *Neurochem Res* 21: 987-993.
- Sonnenwald U, Westergaard N, Petersen SB, Unsgard G, Schousboe A. 1993a. Metabolism of $[\text{U-}^{13}\text{C}]\text{glutamate}$ in astrocytes studied by ^{13}C NMR spectroscopy: Incorporation of more label into lactate than into glutamine demonstrates the importance of the tricarboxylic acid cycle. *J Neurochem* 61: 1179-1182.
- Sonnenwald U, Westergaard N, Hassel B, Muller TB, Unsgard G, et al. 1993b. NMR spectroscopic studies of ^{13}C acetate and ^{13}C glucose metabolism in neocortical astrocytes: Evidence for mitochondrial heterogeneity. *Dev Neurosci* 15: 351-358.
- Sonnenwald U, Westergaard N, Schousboe A. 1997. Glutamate transport and metabolism in astrocytes. *Glia* 21: 56-63.
- Swanson RA, Graham SH. 1994. Fluorocitrate and fluoroacetate effects on astrocyte metabolism in vitro. *Brain Res* 664: 94-100.
- Swanson RA, Farrell K, Stein BA. 1997. Astrocyte energetics, function, and death under conditions of incomplete ischemia: A mechanism of glial death in the penumbra. *Glia* 21: 142-153.
- Szatkowski M, Barbour B, Attwell D. 1990. Nonvesicular release of glutamate from glial cells by reversed electrogenic glutamate uptake. *Nature* 348: 443-446.
- Tansey FA, Farooq M, Cammer W. 1991. Glutamine synthetase in oligodendrocytes and astrocytes: New biochemical and immunocytochemical evidence. *J Neurochem* 56: 266-272.
- Taylor A, McLean M, Morris P, Bachelard H. 1996. Approaches to studies of neuronal/glial relationships by ^{13}C MRS analysis. *Dev Neurosci* 18: 434-442.
- Tsacopoulos M. 2002. Metabolic signaling between neurons and glial cells: A short review. *J Physiol Paris* 96: 283-288.
- Tsacopoulos M, Magistretti PJ. 1996. Metabolic coupling between glia and neurons. *J Neurosci* 16: 877-885.
- Tsacopoulos M, Evequoz-Mercier V, Perrottet P, Buchner E. 1988. Honeybee retinal glial cells transform glucose and supply the neurons with metabolic substrate. *Proc Natl Acad Sci USA* 85: 8727-8731.
- Tsacopoulos M, Poitry-Yamate CL, Poitry S, Perrottet P, Veuthey AL. 1997. The nutritive function of glia is regulated by signals released by neurons. *Glia* 2: 84-91.
- Tsacopoulos M, Veuthey AL, Saravelos SG, Perrottet P, Tsoupras G. 1994. Glial cells transform glucose to alanine, which fuels the neurons in the honeybee retina. *J Neurosci* 14: 1339-1351.
- van den Berg CJ, Garfinkel D. 1971. A stimulation study of brain compartments. Metabolism of glutamate and related substances in mouse brain. *Biochem J* 123: 211-218.
- Vannucci SJ, Maher F, Simpson IA. 1997. Glucose transporter proteins in brain: Delivery of glucose to neurons and glia. *Glia* 21: 2-21.
- Vega C, Martiel JL, Drouhault D, Burckhart MF, Coles JA. 2003. Uptake of locally applied deoxyglucose, glucose, and lactate by axons and Schwann cells of rat vagus nerve. *J Physiol* 546: 551-564.
- Vesce S, Bezzi P, Volterra A. 2001. Synaptic transmission with the glia. *News Physiol Sci* 16: 178-184.
- Vogel R, Hamprecht B, Wiesinger H. 1998. Malic enzyme isoforms in astrocytes: Comparative study on activities in rat brain tissue and astroglia-rich primary cultures. *Neurosci Lett* 247: 123-126.
- Waagepetersen HS, Bakken IJ, Larsson OM, Sonnewald U, Schousboe A. 1998a. Comparison of lactate and glucose metabolism in cultured neocortical neurons and astrocytes using ^{13}C -NMR spectroscopy. *Dev Neurosci* 20: 310-320.
- Waagepetersen HS, Bakken IJ, Larsson OM, Sonnewald U, Schousboe A. 1998b. Metabolism of lactate in cultured GABAergic neurons studied by ^{13}C nuclear magnetic resonance spectroscopy. *J Cereb Blood Flow Metab* 18: 109-117.
- Waagepetersen HS, Qu H, Hertz L, Sonnewald U, Schousboe A. 2002. Demonstration of pyruvate recycling in primary cultures of neocortical astrocytes but not in neurons. *Neurochem Res* 27: 1431-1437.
- Waagepetersen HS, Qu H, Schousboe A, Sonnewald U. 2001. Elucidation of the quantitative significance of pyruvate carboxylation in cultured cerebellar neurons and astrocytes. *J Neurosci Res* 66: 763-770.

- Waagepetersen HS, Qu H, Sonnewald U, Shimamoto K, Schousboe A. 2005. Role of glutamine and neuronal glutamate uptake in glutamate homeostasis and synthesis during vesicular release in cultured glutamatergic neurons. *Neurochem Int* 24; [Epub ahead of print]
- Waagepetersen HS, Sonnewald U, Larsson OM, Schousboe A. 2000. A possible role of alanine for ammonia transfer between astrocytes and glutamatergic neurons. *J Neurochem* 75: 471-479.
- Waelch H, Berl HW, Rossi CA, Clarke DD, Purpura DP. 1964. Quantitative aspects of CO₂ fixation in mammalian brain in vivo. *J Neurochem* 11: 717-728.
- Walz W, Mukerji S. 1998. Lactate release from cultured astrocytes and neurons: A comparison. *Glia* 1: 366-370.
- Waniewski RA, Martin DL. 1998. Preferential utilization of acetate by astrocytes is attributable to transport. *J Neurosci* 18: 5225-5233.
- Westergaard N, Sonnewald U, Schousboe A. 1995. Metabolic trafficking between neurons and astrocytes: The glutamate/glutamine cycle revisited. *Dev Neurosci* 17: 203-211.
- Westergaard N, Varming T, Peng L, Sonnewald U, Hertz L, et al. 1993. Uptake, release, and metabolism of alanine in neurons and astrocytes in primary cultures. *J Neurosci Res* 35: 540-545.
- Yager JY, Kala G, Hertz L, Juurlink BH. 1994. Correlation between content of high-energy phosphates and hypoxic-ischemic damage in immature and mature astrocytes. *Brain Res Dev Brain Res* 82: 62-68.
- Yu AC, Drejer J, Hertz L, Schousboe A. 1983. Pyruvate carboxylase activity in primary cultures of astrocytes and neurons. *J Neurochem* 41: 1484-1487.
- Yu AC, Gregory GA, Chan PH. 1989. Hypoxia-induced dysfunctions and injury of astrocytes in primary cell cultures. *J Cereb Blood Flow Metab* 9: 20-28.
- Yudkoff M. 1997. Brain metabolism of branched-chain amino acids. *Glia* 21: 92-98.
- Yudkoff M, Daikhin Y, Grunstein L, Nissim I, Stern J, et al. 1996. Astrocyte leucine metabolism: Significance of branched-chain amino acid transamination. *J Neurochem* 66: 378-385.
- Yudkoff M, Daikhin Y, Lin ZP, Nissim I, Stern J, et al. 1994. Interrelationships of leucine and glutamate metabolism in cultured astrocytes. *J Neurochem* 62: 1192-1202.
- Yudkoff M, Daikhin Y, Nissim I, Horyn O, Luhovyy B, et al. 2005. Brain amino acid requirements and toxicity: The example of leucine. *J Nutr* 135: 1531S-1538S.
- Yudkoff M, Nissim I, Daikhin Y, Lin ZP, Nelson D, et al. 1993. Brain glutamate metabolism: Neuronal–astroglial relationships. *Dev Neurosci* 15: 343-350.
- Yudkoff M, Nissim I, Pleasure D. 1987. [¹⁵N]aspartate metabolism in cultured astrocytes. Studies with gas chromatography–mass spectrometry. *Biochem J* 24: 193-201.
- Zielke HR, Collins RM Jr, Baab PJ, Huang Y, Zielke CL, et al. 1998. Compartmentation of [¹⁴C]glutamate and [¹⁴C]glutamine oxidative metabolism in the rat hippocampus as determined by microdialysis. *J Neurochem* 71: 1315-1320.
- Zwingmann C, Leibfritz D. 2003. Regulation of glial metabolism studied by ¹³C-NMR. *NMR Biomed* 16: 370-399.
- Zwingmann C, Brand A, Richter-Landsberg C, Leibfritz D. 1998. Multinuclear NMR spectroscopy studies on NH₄Cl-induced metabolic alterations and detoxification processes in primary astrocytes and glioma cells. *Dev Neurosci* 20: 417-426.
- Zwingmann C, Richter-Landsberg C, Brand A, Leibfritz D. 2000. NMR spectroscopic study on the metabolic fate of [3-¹³C]alanine in astrocytes, neurons, and cocultures: Implications for glia–neuron interactions in neurotransmitter metabolism. *Glia* 32: 286-303.
- Zwingmann C, Richter-Landsberg C, Leibfritz D. 2001. ¹³C isotopomer analysis of glucose and alanine metabolism reveals cytosolic pyruvate compartmentation as part of energy metabolism in astrocytes. *Glia* 34: 200-212.

Molecular and Cellular Architecture Link Energy Demand with Metabolite Fluxes

4.1 Cytoplasmic Glycolytic Enzymes. Synaptic Vesicle-Associated Glycolytic ATP-Generating Enzymes: Coupling to Neurotransmitter Accumulation

T. Ueda · A. Ikemoto

1	<i>Introduction</i>	242
2	<i>Methods</i>	243
3	<i>Complex Formation of GAPDH and 3-PGK on Synaptic Vesicles</i>	245
4	<i>Vesicular GAPDH/3-PGK-Coupled Glutamate Uptake</i>	245
5	<i>Other Roles of GAPDH/3-PGK in Synaptic Function</i>	247
6	<i>Coupling of Glycolysis to Proton Pump ATPase, Other Cation Pump ATPases, and Ion Channels</i>	248
7	<i>Physiological Relevance</i>	250
8	<i>Pathophysiological Implications</i>	252
9	<i>Concluding Remarks</i>	253

Abstract: Glucose metabolism is of paramount importance in synaptic transmission and brain function, providing the major cerebral energy source. Yet, under hypoglycemic conditions in which abnormal synaptic transmission and pathophysiological behavior are observed, averaged cellular ATP levels are barely altered. Investigations into this apparent paradox led to the discovery in synaptic vesicles of the glycolytic ATP-generating enzymes glyceraldehyde phosphate dehydrogenase and 3-phosphoglycerate kinase; these enzymes, when activated, are capable of supporting uptake into synaptic vesicles of the major excitatory neurotransmitter glutamate. This represents the first evidence for coupling between glycolysis and neurotransmitter transport into synaptic vesicles. Further studies have shown that glycolytically produced ATP, rather than ATP synthesized in mitochondria, plays a major role in accumulating glutamate within synaptic vesicles in synaptosomes (pinched-off nerve ending preparation). These lines of evidence could provide fresh insight into the essential nature of glycolysis in synaptic transmission. It is argued that the locally produced ATP on the surface of synaptic vesicles by glycolytic enzymes is preferentially harnessed to rapidly refill emptied synaptic vesicles with neurotransmitters. A variety of evidence is briefly reviewed, which indicates that glycolysis is also coupled to the transport of other cations, namely Na^+ , K^+ and Ca^{2+} . It is proposed that subcellular local glycolytic synthesis of ATP plays a crucial role in meeting rapid energy demand for various speedy cellular processes.

List of Abbreviations: 4-AP, 4-aminopyridine; 1,3-BPG, 1,3-bisphosphoglycerate; GAP, glyceraldehyde-3-phosphate; 3-PG, 3-phosphoglycerate; GABA, γ -aminobutyric acid; GAPDH, glyceraldehyde-3-phosphate dehydrogenase; 3-PGK, 3-phosphoglycerate kinase; PK, pyruvate kinase; VGLUT, vesicular glutamate transporter; PSD, postsynaptic density

1 Introduction

Normal brain function and synaptic transmission require glucose metabolism (Sokoloff, 1977). Under normal conditions, glucose serves as the major substrate for cerebral energy (Siesjo, 1978). This glucose requirement has been ascribed to production of ATP required for normal synaptic transmission. There is recent evidence demonstrating the correlation between glucose utilization and cognitive function as well as physiologic neural activity (Fox et al., 1988; McNay et al., 2000). Hypoglycemia results in impairment of memory function (Sommerfield et al., 2003), and in various pathophysiological states and abnormal electrophysiological activity; however, this occurs long before significant alteration in tissue ATP levels is detected (Lewis et al., 1974; Dirks et al., 1980; Ghajar et al., 1982; Bachelard et al., 1984; Fleck et al., 1993). The glycolytic downstream product pyruvate does not support, in the absence of glucose, normal evoked neuronal activity, even when tissue ATP levels return to normal (Cox and Bachelard, 1982; Cox et al., 1983; Kanatani et al., 1995). Abnormal synaptic transmission caused by hypoglycemia involves, at least in part, a presynaptic mechanism (Spuler et al., 1988; Shoji, 1992; Fleck et al., 1993). Substantial reduction of extracellular glucose results in a decrease in stimulus-evoked glutamate release, with no apparent changes in ATP levels (Fleck et al., 1993). Together, these lines of evidence indicate that glycolysis or glycolytic intermediate(s), or appropriate concentrations of subcellularly localized ATP, are necessary for normal synaptic transmission independent of global cellular ATP levels.

Glycolytic enzymes were initially regarded as components of the cytoplasm. However, different kinds of evidence now indicate that the glycolytic pathway is compartmentalized in various tissues. In skeletal muscle, glycolytic enzymes are bound to F-actin and associated protein (Knull, 1990; Masters, 1996). In the brain, five glycolytic enzymes, glyceraldehyde phosphate isomerase, glyceraldehyde phosphate dehydrogenase (GAPDH), aldolase, pyruvate kinase (PK), and lactate dehydrogenase, are associated with the synaptic plasma membrane via actin (Knull, 1980), which allows glycolysis to occur efficiently at high-energy-requiring presynaptic membrane sites. The postsynaptic density (PSD) has also been found associated with GAPDH and 3-phosphoglycerate kinase (3-PGK), which are capable of glycolytically generating ATP (Wu et al., 1977). Moreover, GAPDH was shown to be enriched in synaptosomes and synaptic vesicles (Schlaefter et al., 1994; Rogalski-Wilk and Cohen, 1997; Ikemoto et al., 2003). Synaptic vesicles were also found to be enriched in 3-PGK that occurs in a complex with GAPDH, endowing synaptic vesicles with the capacity to

synthesize ATP locally (Ikemoto et al., 2003). This glycolytically generated ATP is sufficient to support vesicular glutamate uptake (Ikemoto et al., 2003). Glutamate is responsible, as the major excitatory neurotransmitter, for triggering neuronal firing in the vertebrate central nervous system (Cotman, et al., 1981, 1988; Watkins and Evans, 1981; Fonnum, 1984; Ueda, 1986; Collingridge and Bliss, 1987; Nicholls, 1989; Maycox et al., 1990; Ozkan and Ueda, 1998). As such, proper glutamate synaptic transmission is involved in learning and memory formation (Collingridge and Bliss, 1987; Cotman et al., 1988) and is essential for basic neuronal communication. Active glutamate transport into synaptic vesicles in the nerve terminal is an initial crucial step in glutamate transmission (Ueda, 1986; Maycox et al., 1990; Ozkan and Ueda, 1998; Takamori et al., 2000; Otis, 2001; Reimer et al., 2001). This process requires ATP to generate an electrochemical gradient, which serves as the direct driving force for glutamate uptake into synaptic vesicles (Naito and Ueda, 1983, 1985; Maycox et al., 1988; Hell et al., 1990; Tabb and Ueda, 1991; Tabb et al., 1992; Wolosker et al., 1996; Bellocchio et al., 2000).

Recent evidence indicates that glycolytically produced ATP, in particular that produced by GAPDH and 3-PGK, not mitochondria-derived ATP, is harnessed for transport of glutamate into synaptic vesicles within the synaptosome (Ikemoto et al., 2003). Glutamate accumulated in synaptic vesicles in this manner represents a release-competent pool of glutamate. Reduction of GAPDH activity by a glycolysis inhibitor diminishes vesicular glutamate content, resulting in decreased glutamate release. These observations could provide new insight into glycemia-induced aberrant synaptic transmission and into the essential nature of glycolysis in normal synaptic transmission. We describe here briefly the evidence suggesting coupling between the glycolytic enzymes GAPDH/3-PGK and vesicle-bound proton pump ATPase, required for vesicular accumulation of glutamate, an essential step prior to its exocytotic release to the synaptic cleft.

This is the first study suggesting a linkage of GAPDH/3-PGK to the H⁺ pump ATPase. However, there is a great deal of evidence for coupling of GAPDH/3-PGK to other cation pump ATPases, such as the Na⁺/K⁺ pump ATPase and the Ca²⁺ pump ATPase. This evidence will also be briefly reviewed as well as evidence suggesting other roles of GAPDH/3-PGK in synaptic function without involving cation pump ATPases. The possibility is thus raised that coupling of membrane-bound GAPDH/3-PGK to cation pumps may represent a common feature in biological cells, playing various fundamentally important roles in physiological cell function.

2 Methods

Preparation of Subcellular Fractions. Synaptic vesicles were prepared from bovine cerebrum through the discontinuous sucrose gradient procedure as described elsewhere (Kish and Ueda, 1989). The subcellular fractions of bovine cerebrum were prepared as described elsewhere (Ueda et al., 1979). Synaptosomes were prepared from cerebra of male Sprague–Dawley rats (150–200 g) and purified through the Percoll gradient centrifugation step, as described by Dunkley et al. (1988).

Immunoprecipitation. Antibodies (10 µg) were absorbed onto immobilized protein G (0.1 ml as 50% slurry) and chemically cross-linked, using the Seize X mammalian immunoprecipitation kit (Pierce, Rockford, IL). The synaptic vesicle fraction (50 µg protein) was stirred in 0.2 ml of buffer containing 0.32 M sucrose, 4 mM Tris-maleate (pH 7.4), and 0.2 M NaCl for 5 min at 4°C and centrifuged at 200,000g_{max} for 1 h at 4°C. The supernatant (180 µl) was subjected to immunoprecipitation with immobilized antibody, according to the manufacturer's protocol. Aliquots (20 µl) were subjected to SDS-PAGE (sample boiling was omitted), according to Laemmli (1970), followed by Western blot analysis or autoradiography, as appropriate.

Western Blot Analysis. For analysis of subcellular fractions, 30 µg of protein was subjected to standard SDS-PAGE (Laemmli, 1970). In NaCl solubilization experiments, the synaptic vesicle fraction (50 µg protein) was stirred in 0.2 ml of buffer containing 0.32 M sucrose, 4 mM Tris-maleate (pH 7.4), and various concentrations of NaCl for 5 min at 4°C, then centrifuged at 200,000g_{max} for 1 h. The pellet was dissolved in 30 µl of SDS sample buffer. The protein in the supernatant (180 µl) was precipitated with 15% trichloroacetic acid and dissolved in 30 µl of SDS sample buffer. Aliquots (25 µl) of the centrifuged (at 200,000g_{max}) pellet and supernatant fractions were subjected to standard SDS-PAGE. For the analysis of

GAPDH and 3-PGK binding to synaptic vesicles, synaptic vesicles (1 mg protein) were washed twice with 20 ml of buffer containing 0.32 M sucrose, 4 mM Tris-maleate (pH 7.4), and 0.8 M NaCl; bound NaCl was then removed by washing twice with 20 ml of the same buffer without NaCl. The washed synaptic vesicles (40 µg protein) were incubated at 37°C for 10 min in 0.1 ml of buffer in the absence or presence of 2 µg of purified GAPDH or 3-PGK. The synaptic vesicles were pelleted by centrifugation at 200,000g_{max} for 1 h at 4°C and washed twice with the buffer. The pellet was suspended in 80 µl of SDS sample buffer and an aliquot (25 µl) subjected to standard SDS-PAGE. Proteins were electrotransferred onto the Immobilon-P PVDF membrane (Millipore, MA) using a semidry transfer apparatus (Bio-Rad Trans-Blot SD). The membrane was treated with 5% nonfat dry milk in a solution containing 50 mM Tris-HCl (pH 7.4), 0.5 M NaCl, and 0.1% Tween-20 (TBS-T) for 1 h, then incubated for 2 h at room temperature with anti-GAPDH monoclonal antibody at a 1:50 dilution or with anti-3-PGK polyclonal antibodies at 1:500 dilution, followed by incubation with alkaline phosphatase-conjugated goat antimouse IgG or antirabbit IgG, at room temperature for 1.5 h. Unbound antibodies were washed out with TBS-T. 5-Bromo-4-chloro-3-indolyl phosphate and nitro blue tetrazolium (Bio-Rad, CA) were used as substrates for color development, and the resulting color was analyzed using an image analyzer (Bio-Rad Gel Doc 2000).

Glutamate Uptake into Synaptic Vesicles. Vesicular glutamate uptake was measured by the filtration-based assay using Whatman GF/C filters as described elsewhere (Naito and Ueda, 1983; Kish and Ueda, 1989), with minor modifications. In the standard assay, aliquots (10 µg protein) of bovine synaptic vesicles were incubated at 30°C for 10 min with 100 µM [³H]glutamate (a specific activity of 7.4 GBq/mmol was obtained by addition of unlabeled glutamate to [³H]glutamate) in 0.1 ml of an incubation medium (pH 7.4) containing 20 mM Hepes-KOH, 0.25 M sucrose, 4 mM MgSO₄, 4 mM KCl, and 2 mM L-aspartate in the absence or presence of 2 mM ATP (pH adjusted to 7.4 by addition of Tris-base). Prior to incubation, preincubation without ATP and [³H]glutamate was carried out for 1 min at 30°C. When inhibitor effect was tested, test agents were added at the start of the preincubation period. In experiments measuring GAPDH/3-PGK-dependent glutamate uptake, ATP was replaced with a mixture of 2 mM GAP (glyceraldehyde-3-phosphate), 2 mM P_i, 2 mM NAD, and 0.1 mM ADP (pH adjusted to 7.4 by addition of Tris-base) as a source of the glutamate uptake activator.

Glutamate Content in Synaptic Vesicles within Synaptosomes. [³H]glutamate content in synaptic vesicles within the synaptosome was assayed as described elsewhere (Ogita et al., 2001; Bole et al., 2002), with minor modifications. Synaptosomes (100 µg protein) were suspended in 0.1 ml of oxygenated (95% O₂/5% CO₂) Krebs-Ringer buffer (KRB) containing 150 mM NaCl, 2.4 mM KCl, 1.2 mM Na₂HPO₄, 1.2 mM CaCl₂, 1.2 mM MgSO₄, 5 mM Hepes-Tris (pH 7.4), and 10 mM glutamate, and preincubated at 37°C for 10 min in the absence or presence of iodoacetate, oligomycin (Calbiochem, San Diego, CA), and pyruvate at indicated concentrations. After 3 µCi of [³H]glutamate (42.0 Ci/mmol) was added to the medium, synaptosomes were incubated for an additional 10 min. Aliquots (10 µl) were removed and filtered on Whatman GF/C filters to determine the total amount of [³H]glutamate taken up by the synaptosomes, and the rest immediately frozen on dry ice. For the determination of vesicular [³H]glutamate, the frozen synaptosomes (90 µl) were thawed by adding 1.5 ml of ice-cold hypotonic solution containing 6 mM Tris-maleate (pH 8.1) and 2 mM aspartate, and incubated for 20 min at 4°C. Aliquots (1 ml) were filtered on Whatman GF/C filters, and radioactivity retained on filters determined in a Beckman LS 6500 scintillation spectrophotometer.

Glutamate Release from Synaptosomes. Glutamate release from synaptosomes was assayed using the superfusion technique described elsewhere (Ogita et al., 2001), with minor modifications. Synaptosomes (200 µg protein) were suspended in 1.5 ml of oxygenated (95% O₂/5% CO₂) artificial cerebrospinal fluid (ACSF) containing 124 mM NaCl, 5 mM KCl, 2 mM MgSO₄, 1.25 mM NaH₂PO₄, 22 mM NaHCO₃, and 10 mM D-glutamate, and preincubated with or without 300 µM iodoacetate or 2 µM oligomycin at 37°C for 10 min. After 3.5 µCi of [³H]glutamate (42.0 Ci/mmol) was added to the medium, synaptosomes were incubated for an additional 10 min. An aliquot (1.0 ml) of [³H]glutamate-loaded synaptosomal suspension was layered onto a cellulose acetate membrane filter (pore size 0.45 µm) placed in a superfusion chamber. The synaptosomes were superfused (0.5 ml/min) with ACSF for 60 min before application of 50 µM 4-aminopyridine (4-AP) and 2 mM CaCl₂ to trigger depolarization of the synaptosomal membrane. In some control experiments, synaptosomes were superfused with ACSF containing 300 µM iodoacetate or

2 μM oligomycin for the first 20 min of the superfusion period. This period was the same as the sum of the synaptosomal preincubation and [^3H]glutamate-loading periods. All these procedures were carried out at 37°C. Fractions were collected every 10 s for 3 min starting from 30 s prior to 4-AP application. The amount of [^3H]glutamate released into each fraction was expressed as a percentage of the total [^3H]glutamate taken up by synaptosomes at the end of 10 min of [^3H]glutamate loading. The total [^3H]glutamate loaded into synaptosomes was calculated from the amount of [^3H]glutamate present in 0.1 ml of loaded synaptosomes, determined by the same filtration method used for the vesicular glutamate uptake assay.

Other Biochemical Analyses. GAPDH activity was measured using 20 μg of protein from synaptic vesicles in a reaction mixture (1 ml) containing 0.1 M Tris-HCl (pH 8.5), 1.7 mM sodium arsenate, 20 mM sodium fluoride, 1 mM NAD, 1 mM GAP, and 5 mM KH_2PO_4 (Berenski, 1990). Activity was calculated from the rate of increase in NADH formation by monitoring absorbance at 340 nm at 25°C. ATP levels in the synaptic vesicle and synaptosome suspensions were determined under the same conditions described for vesicular glutamate uptake and vesicular glutamate content assays, respectively, by the luciferin/luciferase method, using an ATP bioluminescent assay kit (Sigma-Aldrich, St. Louis, MO), according to the manufacturer's protocol.

3 Complex Formation of GAPDH and 3-PGK on Synaptic Vesicles

The analysis of subcellular fractions using SDS-PAGE/Western blotting has indicated that GAPDH is enriched in the synaptic vesicle fraction (🔗 [Figure 4.1-1a](#)). The GAPDH concentration is higher in this vesicle fraction than in any other fraction tested. At the physiological ionic strength, GAPDH is largely associated with synaptic vesicle membranes, although it is almost entirely dissociated with high salt concentrations (0.8 M NaCl) (Ikemoto et al., 2003). GAPDH has also been found in synaptic vesicles purified from the electric organ of an electric ray (Schlaefer et al., 1994). In this study, it was suggested that GAPDH serves as a nucleotide translocator, catalyzing ATP transport into vesicles. We have proposed that ATP produced by vesicle-bound GAPDH in conjunction with 3-PGK is harnessed to support glutamate uptake into synaptic vesicles via the vesicular H^+ pump ATPase (Ikemoto et al., 2003). Consistent with this hypothesis, the specific content of 3-PGK has been found to be significantly greater in the synaptic vesicle fraction than in all the other subcellular fractions examined (🔗 [Figure 4.1-1](#)). This is the first evidence supporting that this glycolytic ATP-generating enzyme system is enriched in synaptic vesicles. Further studies have demonstrated that 3-PGK forms a complex with GAPDH and that this complex is associated with synaptic vesicles in large part via GAPDH (🔗 [Figure 4.1-1](#)). The experiments shown in this figure indicate that GAPDH binds to synaptic vesicles in the absence of 3-PGK, whereas 3-PGK binding to vesicles essentially requires the presence of GAPDH in the reconstitution medium. These observations suggest that synaptic vesicles have the capacity to generate ATP when substrates for GAPDH and 3-PGK are supplied. Indeed, synaptic vesicles have been shown to produce ATP in the presence of their substrates, with the expected sensitivity to the GAPDH inhibitor iodoacetate (Ikemoto et al., 2003).

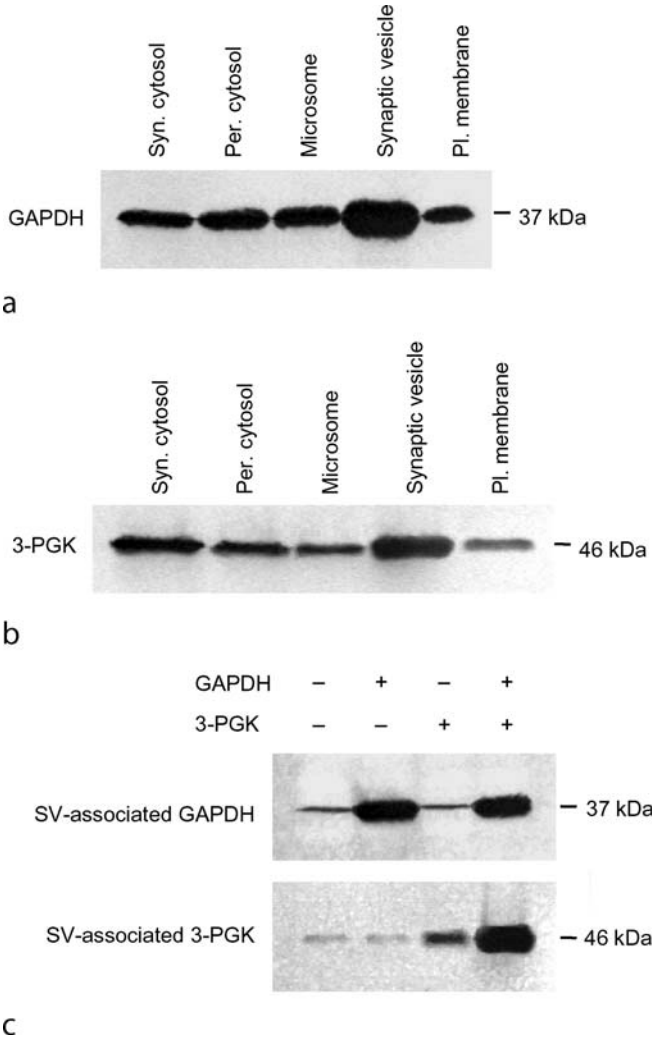
In muscle, there is good evidence that GAPDH and 3-PGK exist in a complex and are capable of synthesizing ATP at the expense of their substrates (Weber and Bernhard, 1982; Srivastava and Bernhard, 1986). Heilmeyer et al. (1990) have shown that the muscle “junctional triad,” where excitation–contraction coupling takes place, contains GAPDH as one of the major components and has the capacity to generate ATP from GAPDH/3-PGK substrates. This demonstrates that glycolytic ATP is locally produced at the site where energy demand must be met in a timely fashion.

4 Vesicular GAPDH/3-PGK-Coupled Glutamate Uptake

In an effort to provide supporting evidence for the notion that local synthesis of glycolytic ATP on the surface of synaptic vesicles is utilized to fuel ATP-dependent glutamate uptake into vesicles via the vesicular H^+ pump ATPase, we have measured vesicular glutamate uptake in the presence of GAPDH/3-PGK substrates. In fact, the evidence indicates that glutamate transport into synaptic vesicles does occur under these conditions, but not when any of these components is omitted (🔗 [Figure 4.1-2](#)). This figure

■ **Figure 4.1-1**

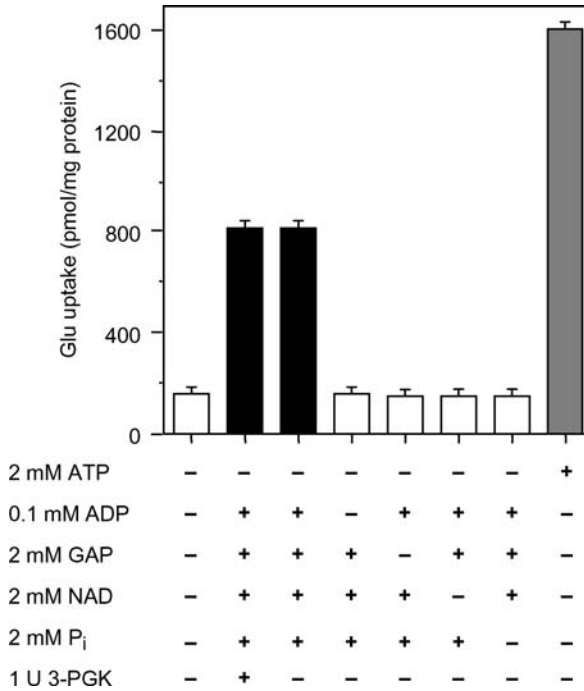
Vesicle-bound GAPDH and 3-PGK. Various subcellular fractions analyzed for (a) GAPDH and (b) 3-PGK by SDS-PAGE/Western blot. (c) Reconstitution of association of GAPDH and 3-PGK with synaptic vesicles. Synaptic vesicles were washed twice with 0.8 M NaCl and incubated in the absence or presence of GAPDH, each with or without 3-PGK at 37°C for 10 min, followed by two additional washings with low-salt buffer. The synaptic vesicle pellets were then analyzed for GAPDH and 3-PGK by SDS-PAGE/Western blot. The data shown are representative of results obtained from three separate experiments. Syn. cytosol, synaptosomal cytosol; Per. cytosol, pericaryal cytosol; Pl. membrane, plasma membrane. (With permission from Ikemoto et al., 2003)



also shows that isolated vesicles are saturated with 3-PGK in their capacity to support vesicular glutamate uptake. This glutamate uptake, as well as ATP production, is sensitive to the GAPDH inhibitor iodoacetate (Ikemoto et al., 2003). Other evidence suggests that glycolytically produced ATP by vesicle-bound GAPDH/3-PGK is more efficiently harnessed than exogenous ATP to fuel the H^+ pump ATPase coupled to glutamate transport (Ikemoto et al., 2003). Moreover, the observation that a combination of GAPDH substrates stimulates exogenous ATP-dependent vesicular glutamate uptake, which is observed in the presence of low

■ Figure 4.1-2

GAPDH and 3-PGK substrate requirement for vesicular Glu uptake. Glu uptake into synaptic vesicles was measured at 30°C after 10-min incubation in the absence or presence of various combinations of 2 mM ATP, 0.1 mM ADP, 2 mM GAP, 2 mM NAD, 2 mM inorganic phosphate (P_i), and exogenous 3-PGK (1 U). (With permission from Ikemoto et al., 2003)



ATP concentrations, suggests that ADP produced by the vesicular H⁺ pump ATPase is recycled back to ATP by vesicular 3-PGK when GAPDH is in operation (Ikemoto et al., 2003). These studies represent the first evidence supporting the concept that active glutamate transport into synaptic vesicles is efficiently achieved at the expense of endogenously produced ATP by vesicle-bound glycolytic enzymes.

Additional studies have revealed that this uptake system exhibits a peculiar biphasic response to varying ADP concentrations (Ikemoto et al., 2003). Maximal uptake activity is at around 0.1 mM of ADP, a physiologically relevant concentration. Higher concentrations are inhibitory; however, this ADP inhibition may not occur under normal physiological conditions *in vivo*. The ADP inhibition also occurs even when exogenous ATP is used as the energy source (Ikemoto et al., 2003). The mechanism of ADP inhibition is yet to be elucidated. The inhibition is not due to competition with ATP or glutamate for their binding sites (Ikemoto et al., 2003). ADP can dissipate ATP-induced membrane potential, with potency lower than that observed for glutamate uptake (Ikemoto et al., 2003). Another demonstration awaited is the direct physical interaction between 3-PGK and the H⁺ pump ATPase. Despite these remaining issues, it is clear that the vesicle-bound GAPDH/3-PGK complex can function as a local glycolytic ATP generator to support active glutamate transport into synaptic vesicles.

5 Other Roles of GAPDH/3-PGK in Synaptic Function

The GAPDH/3-PGK complex has been shown to occur in the isolated PSD (Wu et al., 1977). Their enzyme substrates GAP, NAD, inorganic phosphate, and ADP can generate ATP capable of Ca²⁺-calmodulin kinase-mediated protein phosphorylation in the PSD, including major PSD protein phosphorylation.

Recently, the γ -aminobutyric acid (GABA) receptor $\alpha 1$ subunit has been shown to be associated with GAPDH (Laschet et al., 2004). Evidence indicates that GAPDH not only serves as a glycolytic enzyme, but also functions as the receptor kinase, phosphorylating the intracellular loop of the $\alpha 1$ subunit (at Ser/Thr residues of the NXXS(T)K motif). In a cerebral cortex plasma membrane preparation, this phosphorylation occurs in the presence of GAPDH/3-PGK substrates. This glycolytically produced ATP-supported phosphorylation prevents the rundown of the GABA receptor, which is attributed to vanadate-sensitive dephosphorylation.

Another line of evidence, obtained using a 3-PGK mutant *Drosophila*, suggests that 3-PGK-generated ATP is critical for endocytosis (Wang et al., 2004). It has been proposed that the defect in endocytosis induced by the lack of this glycolytic ATP-generating system could account for the loss of activity-dependent synaptic transmission and abnormal motor behavior.

More recently, Allen et al. (2005) have provided evidence in neurons that glycolysis-derived ATP, as opposed to ATP synthesized in mitochondria, is preferentially used to maintain membrane potential via Na^+/K^+ -ATPase under anoxic conditions. Anoxia-induced depolarization in the hippocampus is prevented far more effectively by glucose superfusion than by allowing mitochondria to be functional. Lactate is ineffective in this regard, suggesting that ATP produced from glial lactate may contribute little to the energy pool for neuronal Na^+/K^+ -ATPase in conditions of energy deprivation.

6 Coupling of Glycolysis to Proton Pump ATPase, Other Cation Pump ATPases, and Ion Channels

The observation that activation of vesicle-bound GAPDH/3-PGK leads to glutamate uptake into synaptic vesicles suggests that 3-PGK is coupled to the H^+ pump ATPase in the vesicle. The vesicular GAPDH/3-PGK complex is indeed capable of producing ATP, and ATP generated in this manner supports vesicular glutamate uptake (Ikemoto et al., 2003). This represents the first evidence pointing to the functional coupling of glycolytically generated ATP to the V-type H^+ pump ATPase. Recent studies indicate that activation of vesicle-associated PK, another glycolytic ATP generator, can also fuel glutamate transport into a subpopulation of vesicles (Ishida et al., 2005). Moreover, vesicular transport of GABA, serotonin, and dopamine is also achieved by activation of vesicle-bound PK as well as by activation of GAPDH/3-PGK (Ishida, Bole, and Ueda, unpublished data). These observations suggest that PK as well as the GAPDH/3-PGK complex may be linked to the vesicular H^+ pump ATPase. Observations made by utilizing cross-linking agents are consistent with a physically close association between the vesicle-bound PK and the ATP-hydrolyzing subunit of the vesicular H^+ pump ATPase (Ishida, Bole, and Ueda, unpublished observations). These results support the notion that ATP produced by vesicle-bound glycolytic enzymes is preferentially utilized by the vesicular H^+ pump ATPase.

Despite initial skepticism about the role of membrane-associated glycolytic enzymes, there is growing evidence that glycolytically produced energy is coupled to cation pump ATPases. Schrier (1966) provided evidence that a significant portion of the glycolytic enzyme 3-PGK is closely associated with the red-cell ghost membranes, and suggested that ATP produced by the membrane-bound 3-PGK is transferred to the cation pump Na^+/K^+ -ATPase. Parker and Hoffman (1967) demonstrated that the activity of the Na^+/K^+ pump ATPase controls the rate of glycolysis by influencing membrane-bound 3-PGK in red cells. They proposed that ADP produced in the microenvironment by the cation pump ATPase serves as a substrate for the membrane-bound 3-PGK. Conversely, evidence was also presented suggesting that ATP produced by membrane-bound 3-PGK is utilized by Na^+/K^+ -ATPase (Proverbio and Hoffman, 1977). These studies have pointed to the occurrence of coupling between these enzymes. Consistent with this view, Okonkwo et al. (1975) have also provided evidence suggesting that the product of each of these enzymes serves as the immediate substrate for the other. Mercer and Dunham (1981) demonstrated that the GAPDH/3-PGK substrates support Na^+ transport into inside-out plasma vesicles from isolated red cells, suggesting that ATP produced in a microenvironment by membrane-bound 3-PGK is harnessed by Na^+/K^+ -ATPase. This further supports the notion that glycolysis is coupled to cation ion transport via membrane-bound 3-PGK.

There are different kinds of evidence in other cells indicating that glycolysis is linked to ion transport. In the vascular smooth muscle, Paul et al. (1979) and Campbell and Paul (1992) have presented evidence that glycolysis is coupled to the Na^+/K^+ transport process, and suggested that glycolytically synthesized ATP is utilized for ion transport and mitochondrially synthesized ATP for contractile force. The coupling of glycolysis and Na^+/K^+ -ATPase has also been observed in transformed cells and tumor cells (Balaban and Bader, 1984). It has been suggested that glycolysis is more effective than mitochondrial oxidative phosphorylation in providing ATP to the Na^+/K^+ pump ATPase in these cultured cells. Evidence obtained using cultured epithelium cells indicates that glucose-induced enhancement of Na^+/K^+ -ATPase pump activity is due to an increase in the maximal capacity (V_{max}) of the enzyme, and is not related to changes in cytosolic ATP concentrations (Lynch and Balaban, 1987). It has been suggested that this increase occurs through specific coupling between glycolysis and the Na^+/K^+ -ATPase. Thus, this coupling confers kinetic advantage on the pump activity. The preferential usage of glycolytically produced ATP to fuel Na^+/K^+ -ATPase has also been observed in cardiac Purkinje cells (Glitsch and Tappe, 1993). More recently, evidence linking Na^+/K^+ -ATPase to glycolysis has also been presented for skeletal muscle (James et al., 1996; Levy et al., 2005). In the nervous system, much evidence indicates that glycolytically produced ATP is preferentially utilized by Na^+/K^+ -ATPase (Lipton and Robacker, 1983; Raffin et al., 1988; Roberts, 1993; Silva et al., 1997; Allen et al., 2005).

Glycolysis has also been shown to be coupled to Ca^{2+} pump ATPase. Paul et al. (1989) have demonstrated that plasmalemmal vesicles prepared from stomach smooth muscle cells are associated with most glycolytic enzymes, and that their substrates support calcium uptake into these associated plasma membrane vesicles. Evidence provided by Hardin et al. (1992) indicates that ATP generated by membrane-bound glycolytic enzymes, as opposed to exogenously added ATP, is preferentially utilized to fuel calcium uptake. These studies support the notion that glycolysis is coupled to active calcium transport across the plasma membrane.

Roe et al. (1994) have presented evidence that in pancreatic β cells glycolysis leads to a reduction in cytosolic calcium concentration; this effect is blocked by thapsigargin, an inhibitor of sarcoplasmic reticulum Ca^{2+} -ATPase. Stimulation of pancreatic islets of Langerhans with glucose and D-glyceraldehyde, but not by deoxyglucose, resulted in decreased cytosolic Ca^{2+} concentration. Glucose-induced reduction in intracellular Ca^{2+} was not mimicked by (a) pyruvate, the final glycolytic product fed into mitochondria to produce ATP, (b) azide, a blocker of mitochondrial ATP production, or (c) calmidazolium, an inhibitor of calmodulin-sensitive plasma membrane Ca^{2+} -ATPase. These observations suggest that glycolysis induces calcium uptake, which is blocked by the inhibitor, into the endoplasmic reticulum. Consistent with this notion, Xu et al. (1995) provided evidence in cardiac and skeletal muscle that glycolytic enzymes associated with isolated sarcoplasmic reticulum vesicles are functionally coupled to the Ca^{2+} pump ATPase. These lines of evidence indicate that membrane-bound glycolytic enzymes could play a functional role in calcium homeostasis in the cell.

All the evidence mentioned above points to a common theme—membrane-associated glycolytic ATP generating systems are coupled to cation (including proton) pumps, as summarized in [Table 4.1-1](#). The specific cellular physiological functions that they subserve depend upon the subcellular location of each cation pump in a given cell. It remains to be seen whether such a coupling to the H^+ pump ATPase occurs in coated vesicles, lysosomes, endosomes, the endoplasmic reticulum, and the Golgi apparatus.

Bernhard and coworker(s) have shown in skeletal muscle that the GAPDH product 1,3-bisphosphoglycerate (1,3-BPG) is directly transferred to 3-PGK (Weber and Bernhard, 1982; Srivastava and Bernhard, 1986). There is some evidence suggesting that ATP synthesized by the membrane-bound 3-PGK is transferred with a minimal diffusion to Na^+/K^+ -ATPase (Mercer and Dunham, 1981) and Ca^{2+} -ATPase (Paul et al., 1989; Hardin et al., 1992). However, it remains to be determined whether ATP transfer from vesicle-bound 3-PGK to the v-type H^+ pump ATPase occurs in a similar manner.

In addition to the important role in cation transport, there is some evidence that glycolytic ATP modulates certain ion channels. In cardiac myocytes, Weiss and Lamps (1987) provided evidence that ATP generated during glycolysis is preferentially utilized to prevent ATP-sensitive K^+ channels from opening, thereby maintaining cellular membrane potential. Opening this channel results in shortening of the action potential (Deutsch et al., 1991; Weiss et al., 1992), which ultimately leads to reduction of

■ **Table 4.1-1**

Cation pumps fueled by ATP produced by the membrane-bound glycolytic enzymes GAPDH/3-PGK and/or PK

Membrane-bound glycolytic ATP generator	Cation pump	Function	References
GAPDH/3-PGK	Na ⁺ /K ⁺ -ATPase (PM)	Na ⁺ , K ⁺ homeostasis	Schrier (1966), Parker and Hoffman (1967), Proverbio and Hoffman (1977), Okonkwo et al. (1975), Mercer and Dunham (1981)
GAPDH/3-PGK, PK	Ca ²⁺ -ATPase (PM)	Ca ²⁺ homeostasis	Paul et al. (1989), Hardin et al. (1992)
GAPDH/3-PGK, PK	Ca ²⁺ -ATPase (SR, ER)	Ca ²⁺ homeostasis	Xu et al. (1995)
GAPDH/3-PGK, PK	H ⁺ -ATPase (SV)	NT refill	Ikemoto et al. (2003), Ishida et al. (2005)

PK, pyruvate kinase; PM, plasma membrane; SR, sarcoplasmic reticulum; ER, endoplasmic reticulum; SV, synaptic vesicle; NT, neurotransmitter

contractility. In smooth muscle, Lorenz and Paul (1997) presented evidence suggesting that glycolysis-derived ATP is required to prevent the rundown of a calcium channel. In cardiomyocytes, the L-type Ca²⁺ channel whose opening prolongs action potential is allosterically modulated by glycolytic ATP, devoid of phosphorylation (Losito et al., 1998).

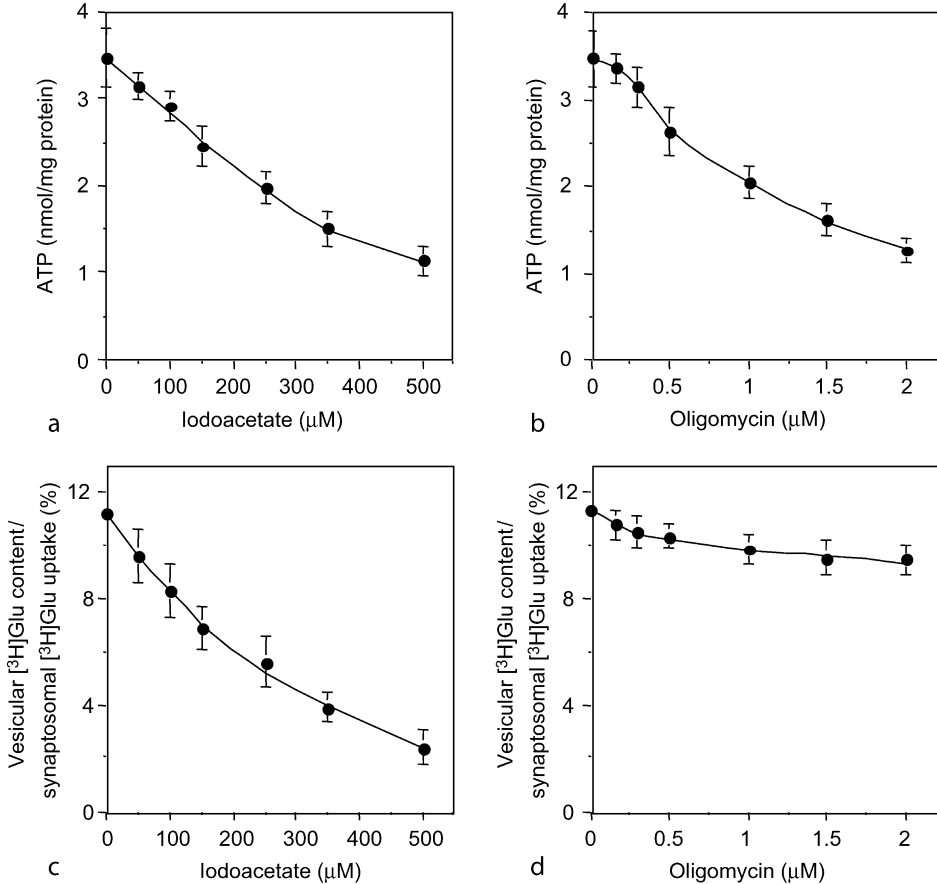
7 Physiological Relevance

The observation that ATP generated by synaptic vesicle-associated GAPDH/3-PGK is sufficient in supporting glutamate loading into synaptic vesicles suggests that vesicular accumulation of glutamate in the nerve ending may occur at the expense of glycolytically produced ATP, as opposed to ATP synthesized in mitochondria. The GAPDH inhibitor iodoacetate and the mitochondrial ATP synthase inhibitor oligomycin serve as useful agents to distinguish between the two sources of ATP. Iodoacetate is known to block glycolysis, resulting in reduction of pyruvate as well as of ATP produced during glycolysis; limiting pyruvate supply will lead to a decrease in ATP formation in mitochondria as well. Oligomycin, on the other hand, inhibits the mitochondrial synthesis of ATP without affecting glycolytic ATP production. Indeed, both agents have been shown to reduce ATP content in synaptosomes to a similar extent. However, iodoacetate led to a much larger reduction (80%) in vesicular glutamate content in synaptosomes than did oligomycin (15%) (● [Figure 4.1-3](#)). Moreover, substitution of pyruvate for glucose, which can cause an increase in total ATP levels in the synaptosome, fails to enhance vesicular glutamate content (Ikemoto et al., 2003). These lines of evidence are consistent with the notion that vesicular glutamate refilling in the nerve terminal is supported in large part by locally produced glycolytic ATP, in particular by GAPDH/3-PGK bound to synaptic vesicles. This pool of glutamate stored in synaptic vesicles at the expense of glycolytic ATP is releasable upon depolarization in the presence of calcium (● [Figure 4.1-4](#)); 4-AP does not induce the release of [³H]glutamate in the absence of calcium (Ogita et al., 2001).

Thus, glycolytically synthesized ATP at the surface of synaptic vesicles may play a pivotal role in enabling rapid glutamate refilling of release-competent synaptic vesicles in neurons. Mitochondria alone may not be entirely able to meet the ATP requirement for sustaining normal synaptic transmission, an extremely rapid cellular process. After releasing their contents, synaptic vesicles must be rapidly refilled in order to continuously support normal neurotransmission (Pyle et al., 2000). The energy demanded for vesicular transmitter uptake would be dynamic and reflect nerve activity. The synaptic vesicle's function of transmitter refilling would be more efficient if ATP were generated "locally" by vesicle-bound GAPDH/3-PGK, especially if the neurotransmitters in question were involved in fast synaptic transmission, as in the case of glutamate. In isolated synaptic vesicles, GAPDH/3-PGK-generated ATP appears to be more effective than exogenous ATP in supporting vesicular glutamate uptake (see [Fig. 4](#)) from Ikemoto et al., 2003). In neurons, mitochondria located in the nerve ending do not appear close enough to synaptic vesicles in order

■ Figure 4.1-3

Iodoacetate reduces vesicular [^3H]Glu content in synaptosomes more effectively than oligomycin, whereas both agents have similar effects on synaptosomal ATP levels. Synaptosomes were preincubated at 37°C for 10 min in the presence of various concentrations of (a, c) iodoacetate and (b, d) oligomycin, followed by addition of [^3H]Glu; (a, b) ATP level and (c, d) vesicular [^3H]Glu content were determined at 37°C after 10 min, as described in Sect. 2. Vesicular [^3H]Glu content was expressed as percentage of total synaptosomal [^3H]Glu uptake. (With permission from Ikemoto et al., 2003)



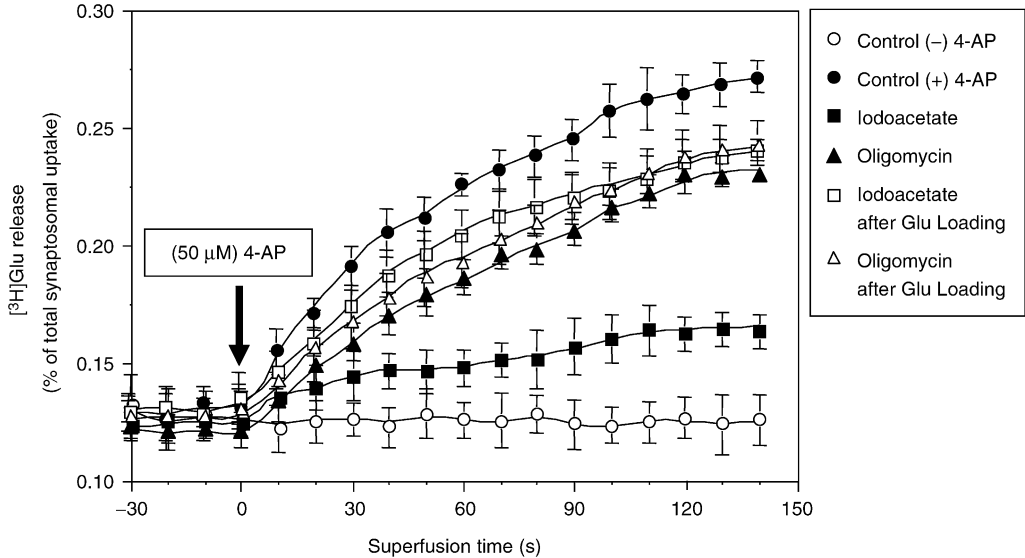
to provide sufficient ATP in a timely fashion for sustaining adequate transmitter accumulation. Moreover, ATP synthesis in mitochondria occurs after ATP formation during glycolysis. Thus, the glycolytic ATP-generating system on synaptic vesicles, GAPDH/3-PGK, in its prompt response to energy demand for transmitter refill, would have spatial and temporal advantages over mitochondrial ATP synthase in ATP delivery to the site of consumption, i.e., the H^+ pump ATPase in the vesicle.

The importance of glycolytically generated ATP in presynaptic function is also supported by electron micrographic evidence showing that half the nerve terminals are devoid of mitochondria (Shepherd and Harris, 1998). This finding does suggest that nerve endings, in large part, are likely to rely heavily on glycolytically produced ATP to fuel normal presynaptic function. This evidence is consistent with the notion that glycolysis-generated ATP, specifically via vesicle-bound enzymes, plays a physiologically vital role in rapid vesicular neurotransmitter refill for the sustenance of normal synaptic transmission.

Disruption of this supply of ATP to the H^+ pump ATPase coupled with the vesicular glutamate transporter (VGLUT) results in a reduction of releasable vesicular glutamate content (Ikemoto et al.,

■ Figure 4.1-4

Treatment of synaptosomes with iodoacetate prior to and during the [^3H]Glu-loading period reduces [^3H]Glu release. Synaptosomes were preincubated at 37°C for 10 min in the absence (○, ●, □, and △) and presence of 300 μM iodoacetate (■) and in the presence of 2 μM oligomycin (▲); [^3H]Glu was loaded into the synaptosome at 37°C and incubated for 10 min. The [^3H]Glu-loaded synaptosomes were layered onto the membrane in the superfusion chamber and superfused at 37°C for 20 min with artificial cerebrospinal fluid (ACSF) in the absence (○, ●, ■, and ▲) and presence of 300 μM iodoacetate (□) and in the presence of 2 μM oligomycin (△). After further superfusion with ACSF at 37°C for 40 min, synaptosomes were subjected to depolarization with and without 50 μM 4-aminopyridine (4-AP; ●, ■, ▲, □, and ○). (With permission from Ikemoto et al., 2003)



2003), and thereby would impair synaptic transmission. This tight coupling between the glycolytic supply of ATP by vesicle-bound enzymes and vesicular glutamate accumulation could provide an explanation for hypoglycemia-induced abnormal synaptic activity and shed new light on the essential nature of glucose metabolism in normal synaptic transmission and brain function, including learning and memory formation.

Glycolytic ATP-fueled Na^+/K^+ -ATPase and Ca^{2+} -ATPase would have fundamentally important roles in maintaining membrane potential and Ca^{2+} homeostasis, respectively. Proper membrane potential controls membrane excitability and the Na^+ gradient is essential for neurotransmitter reuptake. In cardiac myocytes, glycolytic ATP plays a role in maintaining membrane potential by keeping ATP-sensitive K^+ channels in a closed state (Weiss and Lamps, 1987). In skeletal muscle, glycolytic enzymes are substantially enriched in the white vastus, compared with the soleus where mitochondria are abundant, and glycolytically produced ATP is thought to be harnessed for the function of fast twitch fibers (Baldwin et al., 1973; Holloszy and Booth, 1976). The junctional triad is capable of generating ATP at the expense of GAPDH/3-PGK substrates, indicating that localized synthesis of glycolytic ATP can occur at the site of immediate energy demand (Heilmeyer et al., 1990). All the evidence and considerations mentioned above support the concept that rapid, energy-consuming cellular processes rely on locally produced glycolytic ATP.

8 Pathophysiological Implications

Severe hypoglycemia causes lethargy prior to coma. Hypoglycemia could result in rapid functional decoupling of the vesicular 3-PGK from the H^+ pump ATPase, slowing down or diminishing the vesicular refilling process. This could initially lead to subdued excitatory neurotransmission and thereby contribute

to the lethargic state manifested during hypoglycemia. Prolonged hypoglycemia could result in obliteration of vesicular glutamate content, due to continuous inactivity of vesicular 3-PGK coupled to the H^+ pump ATPase–VGLUT system. This would lead to complete cessation of excitatory neurotransmission. Thus, the possibility is raised that this mechanism might be involved in ischemia-induced coma.

Studies by Allen et al. (2005) indicate that deficient coupling between glycolysis and Na^+/K^+ -ATPase results in the loss of the maintenance of membrane potential. This causes glutamate efflux by reversing the physiological function of the Na^+ -dependent plasma membrane transporter (Rossi et al., 2000). Aberrant excessive glutamate efflux to the synaptic cleft is attributable to excitotoxicity underlying neuronal ischemia-induced neuronal death (Choi and Rothman, 1990). These lines of evidence suggest that functional decoupling of vesicle-bound and plasma membrane-bound 3-PGK from cation pumps (H^+ -ATPase and Na^+/K^+ -ATPase) could play a pivotal role in initiating hypoglycemia-induced brain pathophysiology.

Recently, Sommerfield et al. (2003) have demonstrated that moderate hypoglycemia impairs multiple cognitive functions, in particular working memory. Acute hypoglycemia would lead to reduced functional coupling of vesicular 3-PGK to the H^+ pump ATPase–VGLUT system. The resulting decrease in vesicular glutamate content could cause weakening of excitatory synaptic transmission. Since normal glutamate transmission as well as undisrupted glucose metabolism is thought to be required for adequate memory function, it is feasible that moderate hypoglycemia-induced loss of memory function might involve functional decoupling of 3-PGK from the VGLUT-linked H^+ pump ATPase.

Hypoglycemic conditions induce depression of synaptic transmission (Cox and Bachelard, 1982; Bachelard et al., 1984; Fleck et al., 1993; Fowler, 1993a, b). Fowler (1993a, b) provided evidence that this synaptic depression is mediated by the release of adenosine. Adenosine inhibits glutamate release by acting on the presynaptic A_1 receptor, whose activation leads to inactivation of a G-protein-regulated calcium channel (Dolphin and Archer, 1983; Dolphin and Prestwick, 1985; Yawo and Chuhma, 1993; Wu and Saggan, 1994). Adenosine can also inhibit quantal neurotransmitter release via activation of a G protein, independently of calcium influx inhibition (Scholz and Miller, 1992). The depressive effect of adenosine on synaptic transmission could also be achieved by postsynaptic mechanisms. Adenosine can hyperpolarize postsynaptic neurons via activation of a potassium channel or voltage-dependent chloride channel (Siggins and Schubert, 1981; Mager et al., 1990; Segal, 1992). The concerted action of these mechanisms results in reduction of glutamate receptor-mediated ion channel activities (Fleck et al., 1993; De Mendonca et al., 1995).

Growing evidence implicates energy deficits due to mitochondrial dysfunction in the pathogenesis of various neurodegenerative diseases including Parkinson's and Alzheimer's diseases (Nicklas et al., 1987; Schapira et al., 1990; Mizuno et al., 1995; Gibson et al., 2000, 2003; Dauer and Przedborski, 2003; Jenner, 2003; Beal, 2004; Emerit et al., 2004). In Parkinson's disease, recent evidence suggests that cytosolic dopamine or its metabolite plays a pivotal role in selective degeneration of dopaminergic neurons (Lotharius and O'Malley, 2000; Sulzer, 2001; Lotharius et al., 2002; Ben-Shachar et al., 2004; Sidhu et al., 2004). An aberrant increase in cytosolic dopamine concentration could result from impaired dopamine uptake into synaptic vesicles.

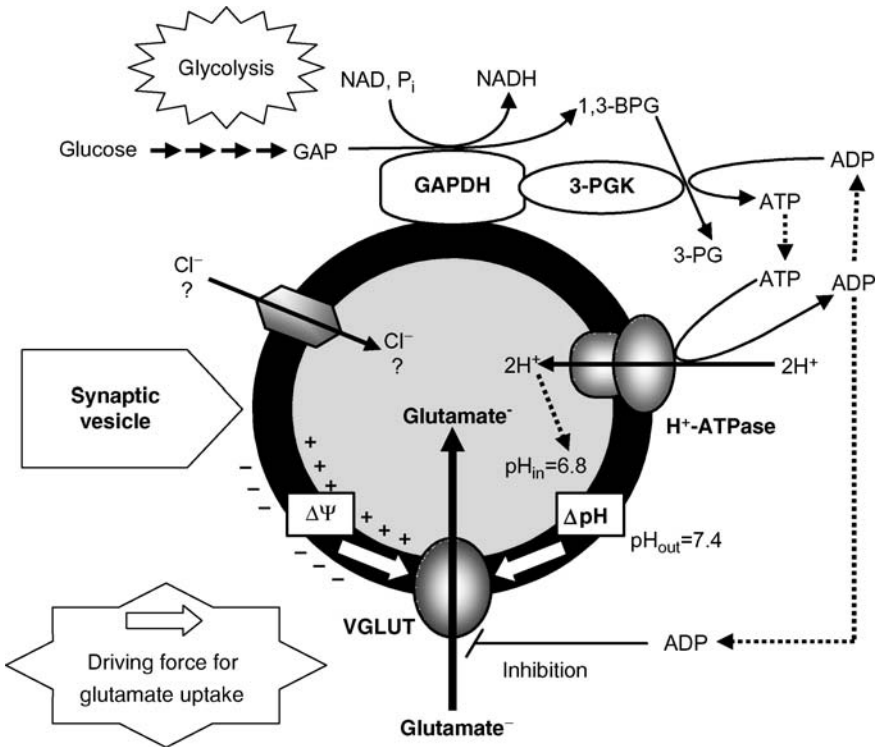
This impairment could occur due to deficits in energy supply from dysfunctional mitochondria. Alternatively, mitochondrial dysfunction can induce augmentation of glycolysis in an effort to compensate for energy deficits (Christians et al., 2004). Globally enhanced glycolysis achieved in this manner might result in a decrease in glycolytic substrates available for local glycolytic ATP production. Thus, the reduction in local ATP synthesis induced by deficits in mitochondrial enzymes might contribute to the impaired dopamine accumulation in synaptic vesicles, leading to elevation of extravesicular cytosolic dopamine.

9 Concluding Remarks

It is proposed here that the pool of ATP produced by vesicle-bound GAPDH and 3-PGK plays a crucial role in swiftly refilling presynaptic nerve terminal vesicles with the major excitatory neurotransmitter glutamate. This could apply to other neurotransmitters as well. According to the model presented in [Figure 4.1-5](#), the glycolytic intermediate GAP is converted to the high-energy intermediate 1,3-BPG at the expense of NAD and P_i by synaptic vesicle-bound GAPDH; GAPDH-bound 3-PGK transfers the 1,3-BPG high-energy

■ Figure 4.1-5

Proposed role of GAPDH and 3-PGK in vesicular glutamate uptake. Synaptic vesicle-associated GAPDH catalyzes the conversion of the glycolytic intermediate GAP to the high-energy mixed-acid anhydride 1,3-BPG in the presence of NAD and P_i . GAPDH-associated 3-PGK transfers the high-energy phosphate of 1,3-BPG to ADP, forming ATP and 3-PG. ATP thus produced is efficiently consumed by vesicular H^+ -ATPase that generates an electrochemical proton gradient in the presence of chloride. This provides the driving force for glutamate uptake, the process catalyzed by the vesicular glutamate transporter (VGLUT). ADP generated by vesicular H^+ -ATPase is efficiently converted to ATP by 3-PGK in the presence of glycolysis. When ADP is accumulated, glutamate uptake into synaptic vesicles would be inhibited. $\Delta\Psi$, membrane potential; ΔpH , pH gradient



phosphate to ADP, forming ATP at the vesicle surface. This pool of ATP is utilized by the vesicular H^+ pump ATPase to generate an electrochemical proton gradient across the vesicle membrane, providing the driving force for glutamate transport into synaptic vesicles. ADP produced by ATPase would be rapidly recycled to ATP by the GAPDH/3-PGK system in the presence of glycolysis, eliminating its potential inhibitory effect on glutamate uptake. Acute depletion of glucose could lead to a reduction of ATP produced via glycolysis within the microenvironment of the presynaptic nerve terminal. This would diminish glutamate transport into the vesicle, resulting in a decreased amount of released glutamate, thereby reducing glutamate-mediated synaptic transmission. Moreover, when a state of limited glycolysis is prolonged by hypoglycemia, excess ADP would be accumulated, impairing the ATP-dependent vesicular uptake system, and further contributing to reduction in vesicular glutamate content and release. The mechanism outlined above could offer fresh insight into the mechanism underlying hypoglycemia-induced abnormal electrophysiological activity and resulting clinical symptoms, as well as into the essential requirement for glucose metabolism in normal synaptic transmission.

The recent demonstration of the coupling of vesicle-bound GAPDH/3-PGK to the H^+ pump ATPase supporting glutamate uptake represents the first evidence for functional coupling of membrane-bound

glycolytic ATP-generating enzymes to the H^+ pump ATPase. Such a relationship will likely be observed to occur in other intracellular organelles, where such a coupled system may be linked to transport of chloride and other anions. In contrast, there is already evidence for functional linkage of membrane-bound glycolytic ATP-producing enzymes to other ion pumps, namely, Na^+/K^+ -ATPase and Ca^{2+} -ATPase. Coupling between membrane-bound ATP-producing glycolytic enzymes and a cation pump ATPase may represent a common feature in biological cells, subserving various cellular functions.

Membrane-bound GAPDH/3-PGK + cation pump ATPase \rightarrow various cellular functions

(glycolytic ATP-producing enzymes)

This endows cells with an efficient energy delivery mechanism from production site to consumption site. This type of localized, fast energy delivery system would be essential for rapid, energy-consuming cellular processes, especially those involved in synaptic transmission and fast muscle fiber twitching. Decoupling of membrane-bound ATP-generating enzymes from cation pump ATPases could result in various pathophysiological states and deficits in cognitive function.

Acknowledgments

This work was supported by National Institutes of Health Grant NS 42200 (TU). We thank Mary Roth and Judy Ueda for excellent assistance in preparation of the manuscript.

References

- Allen NJ, Káradóttir R, Attwell D. 2005. A preferential role for glycolysis in preventing the anoxic depolarization of rat hippocampal area CA1 pyramidal cells. *J Neurosci* 25: 848-859.
- Bachelard HS, Cox DWG, Drower J. 1984. Sensitivity of guinea-pig hippocampal granule cell field potentials to hexoses in vitro: An effect on cell excitability? *J Physiol* 352: 91-102.
- Balaban RS, Bader JP. 1984. Studies on the relationship between glycolysis and $(Na^+ + K^+)$ -ATPase in cultured cells. *Biochim Biophys Acta* 804: 419-426.
- Baldwin KM, Winder WW, Terjung RL, Holloszy JO. 1973. Glycolytic enzymes in different types of skeletal muscle: Adaptation to exercise. *Am J Physiol* 225: 962-966.
- Beal MF. 2004. Mitochondrial dysfunction and oxidative damage in Alzheimer's and Parkinson's diseases and coenzyme Q10 as a potential treatment. *J Bioenerg Biomembr* 36: 381-386.
- Bellocchio EE, Reimer RJ, Fremereau RT Jr, Edwards RH. 2000. Uptake of glutamate into synaptic vesicles by an inorganic phosphate transporter. *Science* 289: 957-960.
- Ben-Shachar D, Zuk R, Gazawi H, Ljubuncic P. 2004. Dopamine toxicity involves mitochondrial complex I inhibition: Implications to dopamine-related neuropsychiatric disorders. *Biochem Pharmacol* 67: 1965-1974.
- Berenski LM, Kim CJ, Jung CY. 1990. An ATP-modulated specific association of glyceraldehyde-3-phosphate dehydrogenase with human erythrocyte glucose transporter. *J Biol Chem* 265: 15449-15454.
- Bole DG, Hirata K, Ueda T. 2002. Prolonged depolarization of rat cerebral synaptosomes leads to an increase in vesicular glutamate content. *Neurosci Lett* 322: 17-20.
- Campbell JD, Paul RJ. 1992. The nature of fuel provision for the Na^+,K^+ -ATPase in porcine vascular smooth muscle. *J Physiol* 447: 67-82.
- Choi DW, Rothman SM. 1990. The role of glutamate neurotoxicity in hypoxic-ischemic neuronal death. *Annu Rev Neurosci* 13: 171-182.
- Christians U, Gottschalk S, Miljus J, Heinz C, Benet LZ, et al. 2004. Alterations in glucose metabolism by cyclosporine in rat brain slices link to oxidative stress: Interactions with mTOR inhibitors. *Br J Pharmacol* 143: 38.
- Collingridge GL, Bliss TVP. 1987. NMDA receptors: Their role in long-term potentiation. *Trends Neurosci* 10: 288-293.
- Cotman CW, Foster A, Lanthorn T. 1981. Glutamate as a neurotransmitter. DiChiara G, Gessa GL, editors. New York: Raven Press; pp. 1-27.
- Cotman CW, Monaghan DT, Ganong AH. 1988. Excitatory amino acid neurotransmission: NMDA receptors and Hebb-type synaptic plasticity. *Annu Rev Neurosci* 11: 61-80.
- Cox DWG, Bachelard HS. 1982. Attenuation of evoked field potentials from dentate granule cells by low glucose,

- pyruvate +; malate, and sodium fluoride. *Brain Res* 239: 527-534.
- Cox DWG, Morris PG, Feeney J, Bachelard HS. 1983. ³¹P-n.m.r. studies on cerebral energy metabolism under conditions of hypoglycaemia and hypoxia in vitro. *Biochem J* 212: 365-370.
- Dauer W, Przedborski S. 2003. Parkinson's disease: Mechanisms and models. *Neuron* 39: 889-909.
- De Mendonca A, Sebastiao AM, Ribeiro AJ. 1995. Inhibition of NMDA receptor-mediated currents in isolated rat hippocampal neurons by adenosine A1 receptor activation. *Neuroreport* 6: 1097-1100.
- Deutsch N, Klitzner TS, Lamp ST, Weiss JN. 1991. Activation of cardiac ATP-sensitive K⁺ current during hypoxia: Correlation with tissue ATP levels. *Am J Physiol* 261: H671-H676.
- Dirks B, Hanke J, Kriegstein J, Stock R, Wickop G. 1980. Studies on the linkage of energy metabolism and neuronal activity in the isolated perfused rat brain. *J Neurochem* 35: 311-317.
- Dolphin AC, Archer ER. 1983. An adenosine agonist inhibits and a cyclic AMP analogue enhances the release of glutamate but not GABA from slices of rat dentate gyrus. *Neurosci Lett* 43: 49-54.
- Dolphin AC, Prestwick SA. 1985. Pertussis toxin reverses adenosine inhibition of neuronal glutamate release. *Nature* 316: 148-150.
- Dunkley PR, Heath JW, Harrison SM, Jarvie PE, Glenfield PJ, et al. 1988. A rapid Percoll gradient procedure for isolation of synaptosomes directly from an S1 fraction: Homogeneity and morphology of subcellular fractions. *Brain Res* 441: 59-71.
- Emerit J, Edeas M, Bricaire F. 2004. Neurodegenerative diseases and oxidative stress. *Biomed Pharmacother* 58: 39-46.
- Fleck MW, Henze DA, Barrionuevo G, Palmer AM. 1993. Aspartate and glutamate mediate excitatory synaptic transmission in area CA1 of the hippocampus. *J Neurosci* 13: 3944-3955.
- Fonnum F. 1984. Glutamate: A neurotransmitter in mammalian brain. *J Neurochem* 42: 1-11.
- Fowler JC. 1993a. Purine release and inhibition of synaptic transmission during hypoxia and hypoglycemia in rat hippocampal slices. *Neurosci Lett* 157: 83-86.
- Fowler JC. 1993b. Glucose deprivation results in a lactate preventable increase in adenosine and depression of synaptic transmission in rat hippocampal slices. *J Neurochem* 60: 572-576.
- Fox PT, Raichle ME, Mintun MA, Dence C. 1988. Nonoxidative glucose consumption during focal physiological neural activity. *Science* 241: 462-464.
- Ghajar JBG, Plum F, Duffy TE. 1982. Cerebral oxidative metabolism and blood flow during acute hypoglycemia and recovery in unanesthetized rats. *J Neurochem* 38: 397-409.
- Gibson GE, Kingsbury AE, Xu H, Lindsay JG, Daniels S, et al. 2003. Deficits in a tricarboxylic acid cycle enzyme in brains from patients with Parkinson's disease. *Neurochem Int* 43: 129-135.
- Gibson GE, Park LCH, Sheu K-FR, Blass JP, Calingasan NY. 2000. The alpha-ketoglutarate dehydrogenase complex in neurodegeneration. *Neurochem Int* 36: 97-112.
- Glitsch HG, Tappe A. 1993. The Na⁺/K⁺ pump of cardiac Purkinje cells is preferentially fuelled by glycolytic ATP production. *Pflugers Arch* 422: 380-385.
- Hardin CD, Raeymaekers L, Paul RJ. 1992. Comparison of endogenous and exogenous sources of ATP in fueling Ca²⁺ uptake in smooth muscle plasma membrane vesicles. *J Gen Physiol* 99: 21-40.
- Heilmeyer Jr, LMG Han JW, Thieleczek R, Varsanyi M, Mayr GW. 1990. Relation of phosphatidylinositol metabolism to glycolytic pathway in skeletal muscle membranes. *Mol Cell Biochem* 99: 111-116.
- Hell JW, Maycox PR, Jahn R. 1990. Energy dependence and functional reconstitution of the γ -aminobutyric acid carrier from synaptic vesicles. *J Biol Chem* 265: 2111-2117.
- Holloszy JO, Booth FW. 1976. Biochemical adaptations to endurance exercise in muscle. *Annu Rev Physiol* 38: 273-291.
- Ikemoto A, Bole DG, Ueda T. 2003. Glycolysis and glutamate accumulation into synaptic vesicles. Role of glyceraldehyde phosphate dehydrogenase and 3-phosphoglycerate kinase. *J Biol Chem* 278: 5929-5940.
- Ishida A, Noda Y, Bole DG, Ueda T. 2005. Phosphoenolpyruvate-ADP-dependent incorporation of [³H]glutamate into isolated synaptic vesicles. *Soc Neurosci Annu Meeting Abstr*.
- James JH, Fang C-H, Schrantz SJ, Hasselgren P-O, Paul R, et al. 1996. Linkage of aerobic glycolysis to sodium-potassium transport in rat skeletal muscle. Implications for increased muscle lactate production in sepsis. *J Clin Invest* 98: 2388-2397.
- Jenner P. 2003. Oxidative stress in Parkinson's disease. *Ann Neurol* 53: S26-S36.
- Kanatani T, Mizuno K, Okada Y. 1995. Effects of glycolytic metabolites on preservation of high energy phosphate level and synaptic transmission in the granule cells of guinea pig hippocampal slices. *Experientia* 51: 213-216.
- Kish PE, Ueda T. Glutamate accumulation into synaptic vesicles. 1989. *Meth Enzymol* 174: 9-25.
- Knoll HR. 1980. Compartmentation of glycolytic enzymes in nerve endings as determined by glutaraldehyde fixation. *J Biol Chem* 255: 6439-6444.

- Knull HR. 1990. Structural and organizational aspects of metabolic regulation. Seve PA, Jones ME, Mathews CK, editors. New York: Wiley-Liss; pp. 215-228.
- Laemmli UK. 1970. Cleavage of structural proteins during the assembly of the head of bacteriophage T4. *Nature* 227: 680-685.
- Laschet JJ, Minier F, Kurcewicz I, Bureau MH, Trottier S, et al. 2004. Glyceraldehyde-3-phosphate dehydrogenase is a GABAA receptor kinase linking glycolysis to neuronal inhibition. *J Neurosci* 24: 7614-7622.
- Levy B, Gibot S, Franck P, Cravoisy A, Bollaert P-E. 2005. Relation between muscle Na^+K^+ ATPase activity and raised lactate concentrations in septic shock: A prospective study. *Lancet* 365: 871-875.
- Lewis LD, Ljunggren B, Ratcheson RA, Siesjo BK. 1974. Cerebral energy state in insulin-induced hypoglycemia, related to blood glucose and to EEG. *J Neurochem* 23: 673-679.
- Lipton P, Robacker K. 1983. Glycolysis and brain function: $[\text{K}^+]_o$ stimulation of protein synthesis and K^+ uptake require glycolysis. *Fed Proc* 42: 2875-2880.
- Lorenz JN, Paul RJ. 1997. Dependence of Ca^{2+} channel currents on endogenous and exogenous sources of ATP in portal vein smooth muscle. *Am J Physiol* 252: H987-994.
- Losito VA, Tsushima RG, Diaz RJ, Wilson GJ, Backx PH. 1998. Preferential regulation of rabbit cardiac L-type Ca^{2+} current by glycolytic derived ATP via a direct allosteric pathway. *J Physiol* 511(pt 1): 67-78.
- Lotharius J, Barg S, Wiekop B, Lundberg C, Raymon HK, et al. 2002. Effect of mutant α -synuclein on dopamine homeostasis in a new human mesencephalic cell line. *J Biol Chem* 277: 38884-38894.
- Lotharius J, O'Malley K. 2000. The Parkinsonism-inducing drug 1-methyl-4-phenylpyridinium triggers intracellular dopamine oxidation. A novel mechanism of toxicity. *J Biol Chem* 275: 38581-38588.
- Lynch RM, Balaban RS. 1987. Coupling of aerobic glycolysis and Na^+K^+ -ATPase in renal cell line MDCK. *Am J Physiol* 253: C269-C276.
- Mager R, Ferroni S, Schubert P. 1990. Adenosine modulates a voltage-dependent chloride conductance in cultured hippocampal neurons. *Brain Res* 532: 58-62.
- Masters C. 1996. The cytoskeleton, vol 2. Role in cell physiology. Hesketh JE, Pryme IF, editors. London: JAI; pp. 1-30.
- Maycox PR, Deckwerth T, Hell JW, Jahn R. 1988. Glutamate uptake by brain synaptic vesicles. Energy dependence of transport and functional reconstitution in proteoliposomes. *J Biol Chem* 263: 15423-15428.
- Maycox PR, Hell JW, Jahn R. 1990. Amino acid neurotransmission: Spotlight on synaptic vesicles. *Trends Neurosci* 13: 83-87.
- McNay EC, Fries TM, Gold PE. 2000. Decreases in rat extracellular hippocampal glucose concentration associated with cognitive demand during a spatial task. *Proc Natl Acad Sci USA* 97: 2881-2885.
- Mercer RW, Dunham PB. 1981. Membrane-bound ATP fuels the Na/K pump. Studies on membrane-bound glycolytic enzymes on inside-out vesicles from human red cell membranes. *J Gen Physiol* 78: 547-568.
- Mizuno Y, Ikebe S, Hattori N, Nakagawa-Hattori Y, Michizuki H, et al. 1995. Role of mitochondria in the etiology and pathogenesis of Parkinson's disease. *Biochim Biophys Acta* 1271: 265-274.
- Naito S, Ueda T. 1983. Adenosine triphosphate-dependent uptake of glutamate into protein I-associated synaptic vesicles. *J Biol Chem* 258: 696-699.
- Naito S, Ueda T. 1985. Characterization of glutamate uptake into synaptic vesicles. *J Neurochem* 44: 99-109.
- Nicholls DG. 1989. Release of glutamate, aspartate, and γ -aminobutyric acid from isolated nerve terminals. *J Neurochem* 52: 331-341.
- Nicklas WJ, Youngster SK, Kindt MV, Heikkila RE. 1987. MPTP, MPP+ and mitochondrial function. *Life Sci* 40: 721-729.
- Ogita K, Hirata K, Bole DG, Yoshida S, Tamura Y, et al. 2001. Inhibition of vesicular glutamate storage and exocytotic release by Rose Bengal. *J Neurochem* 77: 34-42.
- Okonkwo PO, Longenecker G, Askari A. 1975. Studies on the mechanism of inhibition of the red cell metabolism by cardiac glycosides. *J Pharmacol Exp Ther* 194: 244-254.
- Otis TS. 2001. Vesicular glutamate transporters in cognition. *Neuron* 29: 11-14.
- Ozkan ED, Ueda T. 1998. Glutamate transport and storage in synaptic vesicles. *Jpn J Pharmacol* 77: 1-10.
- Parker JC, Hoffman JF. 1967. The role of membrane phosphoglycerate kinase in the control of glycolytic rate by active cation transport in human red blood cells. *J Gen Physiol* 50: 893-916.
- Paul RJ, Bauer M, Pease W. 1979. Vascular smooth muscle: Aerobic glycolysis linked to sodium and potassium transport processes. *Science* 206: 1414-1416.
- Paul RJ, Hardin CD, Raeymaekers L, Wuytack F, Casteels R. 1989. Preferential support of Ca^{2+} uptake in smooth muscle plasma membrane vesicles by an endogenous glycolytic cascade. *FASEB J* 3: 2298-2301.
- Proverbio F, Hoffman JF. 1977. Membrane compartmentalized ATP and its preferential use by the Na,K-ATPase of human red cell ghosts. *J Gen Physiol* 69: 605-632.
- Pyle JL, Kavalali ET, Piedras-Renteria ES, Tsien RW. 2000. Rapid reuse of readily releasable pool vesicles at hippocampal synapses. *Neuron* 28: 221-231.

- Raffin CN, Sick T, Rosenthal M. 1988. Inhibition of glycolysis alters potassium ion transport and mitochondrial redox activity in rat brain. *J Cereb Blood Flow Metab* 8: 857-865.
- Reimer RJ, Fremerey RT Jr, Bellocchio EE, Edwards RH. 2001. The essence of excitation. *Curr Opin Cell Biol* 13: 417-421.
- Roberts EL Jr. 1993. Glycolysis and recovery of potassium ion homeostasis and synaptic transmission in hippocampal slices after anoxia or stimulated potassium release. *Brain Res* 620: 251-258.
- Roe MW, Mertz RJ, Lancaster ME, Worley III, JF Duke ID. 1994. Thapsigargin inhibits the glucose-induced decrease of intracellular Ca^{2+} in mouse islets of Langerhans. *Am J Physiol* 266(6 pt 1): E852-E862.76.
- Rogalski-Wilk AA, Cohen RS. 1997. Glyceraldehyde-3-phosphate dehydrogenase activity and F-actin associations in synaptosomes and postsynaptic densities of porcine cerebral cortex. *Cell Mol Neurobiol* 17: 51-70.
- Rossi DJ, Oshima T, Attwell D. 2000. Glutamate release in severe brain ischaemia is mainly by reversed uptake. *Nature* 403: 316-321.
- Schapira AH, Cooper JM, Dexter D, Clark JB, Jenner P, et al. 1990. Mitochondrial complex I deficiency in Parkinson's disease. *J Neurochem* 54: 823-827.
- Schlaefter M, Volknaendt W, Zimmermann H. 1994. Putative synaptic vesicle nucleotide transporter identified as glyceraldehyde-3-phosphate dehydrogenase. *J Neurochem* 63: 1924-1931.
- Scholz KP, Miller R. 1992. Inhibition of quantal transmitter release in the absence of calcium influx by a G protein-linked adenosine receptor at hippocampal synapses. *Neuron* 8: 1139-1150.
- Schrier SL. 1966. Organization of enzymes in human erythrocyte membranes. *Am J Physiol* 210: 139-145.
- Segal M. 1982. Intracellular analysis of a postsynaptic action of adenosine in the rat hippocampus. *Europ J Pharmacol* 79: 193-199.
- Shepherd GM, Harris KM. 1998. Three-dimensional structure and composition of CA3→CA1 axons in rat hippocampal slices: Implications for presynaptic connectivity and compartmentalization. *J Neurosci* 18: 8300-8310.
- Shoji S. 1992. Glucose regulation of synaptic transmission in the dorsolateral septal nucleus of the rat. *Synapse* 12: 322-332.
- Sidhu A, Wersinger C, Vernier P. 2004. α -synuclein regulation of the dopaminergic transporter: A possible role in the pathogenesis of Parkinson's disease. *FEBS Lett* 565: 1-5.
- Siesjo BK. 1978. Brain energy metabolism. New York: John Wiley & Sons; pp. 101-130.
- Siggins GR, Schubert P. 1981. Adenosine depression of hippocampal neurons in vitro: An intracellular study of dose-dependent actions on synaptic and membrane potentials. *Neurosci Lett* 23: 55-60.
- Silver IA, Deas J, Erecinska M. 1997. Ion homeostasis in brain cells: Differences in intracellular ion responses to energy limitation between cultured neurons and glial cells. *Neurosci* 78: 589-601.
- Sokoloff L. 1977. Relation between physiological function and energy metabolism in the central nervous system. *J Neurochem* 29: 13-26.
- Sommerfield AJ, Deary IJ, McAulay V, Frier BM. 2003. Moderate hypoglycemia impairs multiple memory functions in healthy adults. *Neuropsychology* 17: 125-132.
- Spuler A, Endres W, Grafe P. 1988. Glucose depletion hyperpolarizes guinea pig hippocampal neurons by an increase in potassium conductance. *Exp Neurol* 100: 248-252.
- Srivastava DK, Bernhard SA. 1986. Enzyme-enzyme interactions and the regulation of metabolic reaction pathways. *Curr Top Cell Reg* 28: 1-68.
- Sulzer D. 2001. α -synuclein and cytosolic dopamine: Stabilizing a bad situation. *Nat Med* 7: 1280-1282.
- Tabb JS, Kish PE, Van Dyke R, Ueda T. 1992. Glutamate transport into synaptic vesicles. Roles of membrane potential, pH gradient, and intravesicular pH. *J Biol Chem* 267: 15412-15418.
- Tabb JS, Ueda T. 1991. Phylogenetic studies on the synaptic vesicle glutamate transport system. *J Neurosci* 11: 1822-1828.
- Takamori S, Rhee JS, Rosenmund C, Jahn R. 2000. Identification of a vesicular glutamate transporter that defines a glutamatergic phenotype in neurons. *Nature* 407: 189-194.
- Ueda T. 1986. Excitatory amino acids. Roberts PJ, Storm-Mathisen J, Bradford HF, editors. London: Macmillan; pp. 173-195.
- Ueda T, Greengard P, Berzins K, Cohen RS, Blomberg F, et al. 1979. Subcellular distribution in cerebral cortex of two proteins phosphorylated by a cAMP-dependent protein kinase. *J Cell Biol* 83: 308-319.
- Wang P, Saraswati S, Guan Z, Watkins CJ, Wurtman RJ, et al. 2004. A Drosophila temperature-sensitive seizure mutant in phosphoglycerate kinase disrupts ATP generation and alters synaptic function. *J Neurosci* 24: 4518-4529.
- Watkins JC, Evans RH. 1981. Excitatory amino acid transmitters. *Annu Rev Pharmacol Toxicol* 21: 165-204.
- Weber JB, Bernhard SA. 1982. Transfer of 1,3-diphosphoglycerate between glyceraldehyde-3-phosphate dehydrogenase and 3-phosphoglycerate kinase via an enzyme-substrate-enzyme complex. *Biochemistry* 21: 4184-4194.

- Weiss JN, Lamps SJ. 1987. Glycolysis preferentially inhibits ATP-sensitive K^+ channels in isolated guinea pig cardiac myocytes. *Science* 238: 67-69.
- Weiss JN, Venkatesh N, Lamp ST. 1992. ATP-sensitive K^+ channels and cellular K^+ loss in hypoxic and ischaemic mammalian ventricle. *J Physiol* 447: 649-673.
- Wolosker H, Reis M, Assreuy J, de Meis L. 1996. Inhibition of glutamate uptake and proton pumping in synaptic vesicles by S-nitrosylation. *J Neurochem* 66: 1943-1948.
- Wu K, Aoki C, Elste A, Rogalski-Wilk AA, Siekevitz P. 1977. The synthesis of ATP by glycolytic enzymes in the postsynaptic density and the effect of endogenously generated nitric oxide. *Proc Natl Acad Sci USA* 94: 13273-13278.
- Wu L-G, Saggau P. 1994. Adenosine inhibits evoked synaptic transmission primarily by reducing presynaptic calcium influx in area CA1 of hippocampus. *Neuron* 12: 1139-1148.
- Xu KY, Zweier JL, Becker LC. 1995. Functional coupling between glycolysis and sarcoplasmic reticulum Ca^{2+} transport. *Circ Res* 77: 88-97.
- Yawo H, Chuhma N. 1993. Preferential inhibition of omega-conotoxin-sensitive presynaptic Ca^{2+} channels by adenosine autoreceptors. *Nature* 365: 256-258.

4.2 Mitochondrial Architecture and Heterogeneity

G. A. Perkins · M. H. Ellisman

1	Introduction	262
2	The Architecture of Neuronal Mitochondria	263
2.1	The Crista Junction	264
2.2	Two Hypotheses	265
2.3	Contact Sites	267
2.4	Mitochondrial Network	268
2.5	Mitochondrial Motility in Neurons	268
2.6	Mitochondrial Turnover	269
2.7	Mitochondrial Fission and Fusion	270
3	Heterogeneity of Mitochondrial Structure and Function in Brain Regions	270
3.1	Mitochondrial Enzymes	270
4	How Do Neuronal and Glial Mitochondria Differ?	274
4.1	Mitochondrial Localization	274
4.2	Mitochondrial Structure	274
4.3	Compartmentation of the TCA Cycle	275
4.4	Mitochondrial Enzymes	275
5	Heterogeneity of Mitochondria in Neuronal Compartments	276
5.1	Mitochondrial Structure and Translocation	276
5.2	Mitochondria-Associated Adherens Complex	278
5.3	Dendritic Mitochondria	279
5.4	Axonal Mitochondria	279
5.5	Mitochondrial Enzymes	280
5.6	Mitochondrial Compartmentation	281
6	Mitochondria in the Aging Brain	281
6.1	Mitochondrial Structural Damage	282
6.2	Decline in Mitochondrial Function	282
6.3	mtDNA	283
6.4	Mitochondrial Enzymes	283
6.5	Antioxidants	284
6.6	Delaying Mitochondrial Decline	284
7	Mitochondria in the Developing Brain	285
7.1	Mitochondrial Proliferation	285
7.2	Apoptosis	286
7.3	Mitochondrial Enzymes	286
8	Summations, Challenging Problems, and Future Avenues	287
8.1	Biological Avenues	287
8.2	Technological Avenues	288

Abstract: Brain mitochondria are heterogeneous in structure, enzyme complement, energy metabolism, motility, and compartmentation. In recent years, the detailed three-dimensional structure of these organelles has been provided by electron tomography, which has generated new paradigms of mitochondrial architecture. Consistent variations are found in mitochondrial structure or enzyme content among various neuronal and neuroglial cell types suggesting differences in functional capacities. Brain energy metabolism depends largely on aerobic glycolysis and displays marked regional differences reflecting differential expression or regulation of mitochondrial enzymes, including within the four major compartments of neurons—axon, dendrite, soma, and synapse. Evidence is building that the functional decline in the aging brain is related to a decrease in mitochondrial viability. On the other side of lifespan, the developing brain uses a proliferation of mitochondria to establish the onset of aerobic metabolism and uses mitochondrial components for programmed cell death crucial for proper development. Mitochondrial heterogeneity has only recently been addressed to understand the dynamics of energy signatures of neuronal cell types, including the actions of signaling molecules targeted to mitochondria. Tools on the horizon should prove useful for probing local control of mitochondrial functioning and the dynamics of signaling, both to and from this organelle.

List of Abbreviations: 2D, two dimensional; 3D, three dimensional; ADP, adenosine diphosphate; ANT, adenine nucleotide transporter; ATP, adenosine triphosphate; Bax, BCL2-associated X protein; Bid, BH3 interacting domain death agonist; CALI, chromophore-assisted light inactivation; CAT, computer-aided tomography; DAB, diaminobenzidine; DCIP, dichloroindophenol; Drp1, dynamin-related protein-1; EELS, electron energy loss spectroscopy; FRET, fluorescence resonance energy transfer; GABA, γ -amino butyric acid; GFP, green fluorescent protein; KAT, kynurenine aminotransferase; MAC, mitochondrial-associated adherens complex; MRI, magnetic resonance imaging; mt, mitochondrial; NAD, nicotinamide adenine dinucleotide; NADH, reduced form of nicotinamide adenine dinucleotide; NADP, nicotinamide adenine dinucleotide phosphate; NGF, nerve growth factor; NMDA, *N*-methyl *D*-aspartate; NMR, nuclear magnetic resonance; OPA1, optic atrophy 1; PTP, permeability transition pore; QD, quantum dot; TCA, tricarboxylic acid cycle; TIM, translocase inner membrane; TOM, translocase outer membrane; VDAC, voltage-dependent anion channel

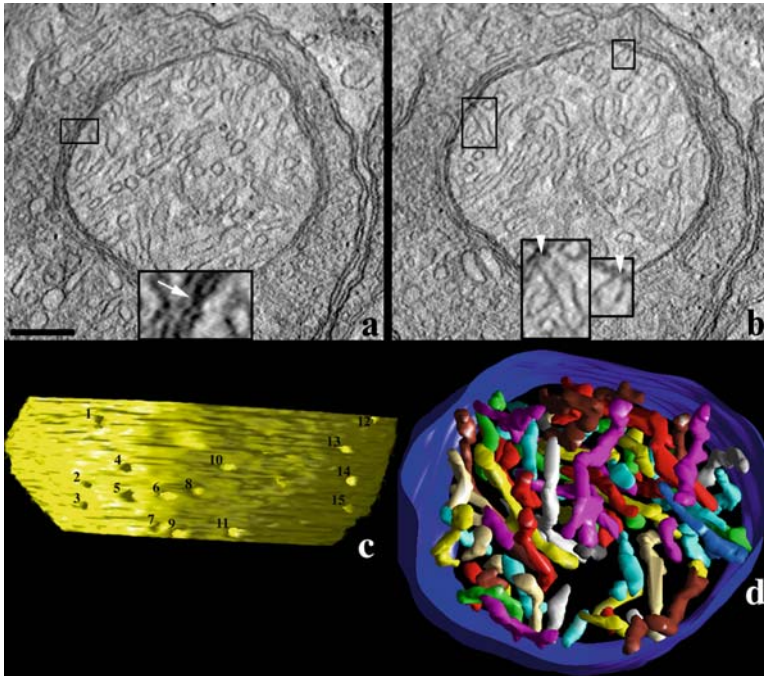
1 Introduction

The elucidation of the structure, function, and design of mitochondria in the brain is an active area of research for interested neurochemists and neurobiologists. Much progress has been made regarding the unifying features and functions of normal, i.e., nondiseased or nonperturbed, mitochondria. However, less is known about mitochondrial heterogeneity, especially in the brain. The goal of this chapter is to review the literature that describes the extent of heterogeneity in brain mitochondria that is not due to a disease state or perturbations, e.g., apoptosis—literature too vast to cover in a single chapter. (Although, see Chapters Wieloch Elmer & Hansson, and Solenski & Fiskum in this volume.) Striking heterogeneity in form (see *Figures* [4.2-1](#), [4.2-2](#), [4.2-3](#), and [4.2-4](#)), metabolic function, and enzyme and substrate concentrations in mitochondrial populations exists not only among the various brain regions but also between neurons and glia. In addition, within the four major compartments of neurons—axons, cell bodies (soma, perikarya), dendrites, and synapses—there exists notable compartmentation of mitochondrial properties that likely reflects the specific designs of these neuronal regions. Along the way, the new paradigm of mitochondrial membrane structure is reviewed, with functional implications. [Sects. 6](#) and [7](#) describe what is currently known about mitochondria in the aging brain and the developing brain—growing fields of research.

Observations of heterogeneous mitochondrial appearance preceded reports of heterogeneous function. The first indication that mitochondria are not homogeneous organelles was provided by light microscopy. Scheffler (1999) pointed out that more than 100 years ago, through the use of selective stains, light microscopists described “mito” (filaments) and “chondria” (grains). However, it took the advent of the electron microscope to provide the details of mitochondrial structural heterogeneity. Compare, for example, the varied appearances, membrane topology, and compartment sizes of the neuronal mitochondria in

■ **Figure 4.2-1**

Typical mitochondrial architecture found in neurons. (a) Slice through a tomographic volume of a rod terminal showing a large mitochondrion with many cristae. Contact sites (where outer and inner membrane come together), which are punctate in nature, are randomly distributed on the mitochondrial periphery. An example is shown boxed with an *inset* showing the contact site (*arrow*) expanded 3× displayed at the bottom. Scale bar = 200 nm. (b) Another slice through the volume showing two crista junctions (*boxed*) that are tubular openings connecting the cristae with the intermembrane space. The *inset* at the bottom shows the openings (*arrowheads*) of the two crista junctions expanded 2×. (c) Side view of the inner membrane of the segmented volume displayed with left lighting. The crista junction openings, invariably narrow and tubular and remarkably uniform in diameter (about 30 nm across), are numbered. Fifteen such junctions are observed in this view. (d) Top view of the segmented volume showing the outer membrane and a subset of cristae. Most of the cristae are tubular. Yet, a subset of cristae possesses lamellar compartments that connect to the periphery via tubes. By segmenting the volume in this way, complex membrane topologies can be analyzed, spatial relationships between compartments discovered, and governing architectures proposed. In collaboration with Don Fox, University of Houston, USA



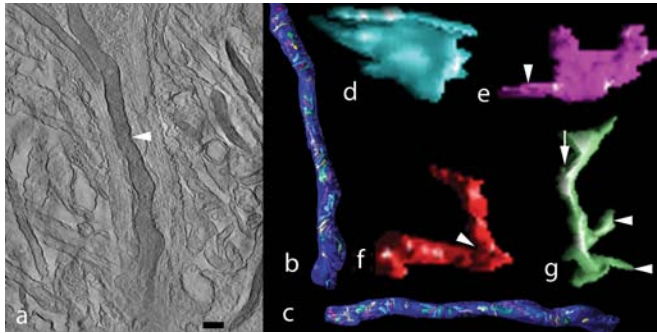
Figures 4.2-1, 4.2-2, 4.2-3, and 4.2-4. The dissection of this organelle, biochemically as well as structurally, has been one of the more exciting chapters in the history of cell biology. As early as 1963, evidence started to accumulate that mitochondria are biochemically different in distinct regions of the brain (Tolani and Talwar, 1963). To this day, studies on brain mitochondria have not been exhausted because of the rich diversity of the central nervous system in its regional, cellular, and subcellular complexities.

2 The Architecture of Neuronal Mitochondria

In recent years, electron tomography has provided detailed three-dimensional (3D) reconstructions of neuronal mitochondria that have helped to redefine our concept of mitochondrial architecture, and in

Figure 4.2-2

Mitochondria in dendritic processes are often elongated with transverse cristae. (a) Slice through a tomographic volume showing a long mitochondrion (*arrowhead*) in a dendritic process and portions of four other mitochondria. The length of the marked mitochondrion captured in this reconstruction is more than $5\ \mu\text{m}$ and extends beyond the top of the panel. Scale bar = 400 nm. (b) Top view and (c) side view of the segmented volume of the mitochondrion marked in (a). The volume was segmented along the outer and inner membranes. There are 37 cristae in this length of mitochondrion (d, e, f, and g). (d) Lamellar crista. (e) Mostly lamellar crista but with a long tubular extension (*arrowhead*) ending in a crista junction that connects the intracristal space to the intermembrane space. (f) Crista with more-or-less tubular segments that connect at a roughly 90° joint (*arrowhead*). (g) Crista with a long tubular shaft (*arrow*) that has extensions ending in crista junctions (*arrowheads*). In collaboration with Ella Bossy-Wetzels, the Burnham Institute, USA



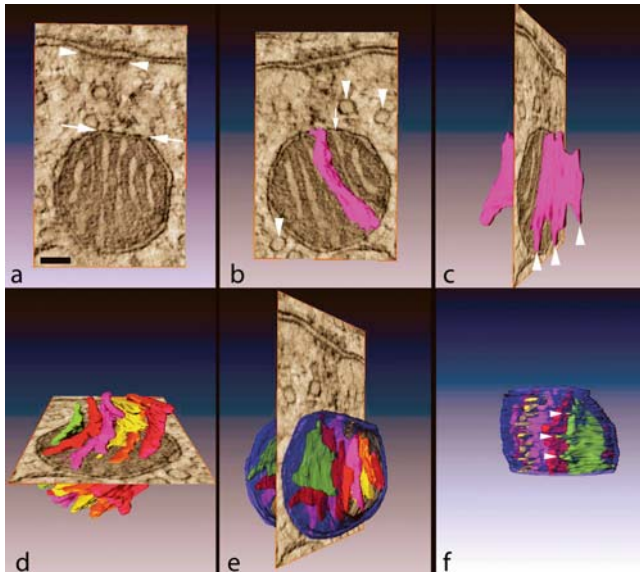
particular introduced the crista junction paradigm (Perkins et al., 1997, 2001a; Perkins and Frey, 2000; Frey et al., 2002). Electron tomography is a powerful technique that is closely related to computerized axial tomography used by computer-aided tomography (CAT) or magnetic resonance imaging (MRI) scanners in radiological imaging, in that computational methods are used to calculate a 3D structure from many two-dimensional (2D) images or projections recorded over a wide range of tilt angles. The typical membrane architecture seen in neuronal mitochondria and cultured cells of neurons (Barsoum et al., 2005) consists of an inner membrane divided into two components, the inner-boundary membrane closely apposed to the outer membrane and the cristae membranes that project into the matrix compartment. The basic architecture of neuronal mitochondria is the same in all regions of the brain studied to date. These mitochondria have the majority of cristae composed of both tubular and lamellar segments with the tubes generally arranged more peripherally and the lamellae usually more centrally located. Cristae that are entirely tubular are commonly seen and those that are entirely lamellar (with no tubular segments connecting to the periphery) are rare, except within a mitochondrial-associated adherens complex (MAC) (see [Sect. 2.1](#)). A structurally distinct type of contact site was revealed in neuronal mitochondria, namely the bridge contact site. It was proposed that these bridges play a role in the structural integrity of the outer- and inner-boundary membranes by holding the two together, which is likely important for protein import and energy transduction (Perkins et al., 2001a). All these studies have involved neurons, yet no glia. Do the same architectural principles hold with mitochondria in neuroglia?

2.1 The Crista Junction

The two inner-membrane components are connected by tubular structures of relatively uniform size called crista junctions whose diameters are distributed over a relatively narrow range around a mean of 28 nm ([Figure 4.2-1](#)). These structures are probably dynamic, with crista junctions forming and disappearing

■ **Figure 4.2-3**

The mitochondrion-associated adherens complex (MAC) commonly found in the calyx of Held. (a) Slice through a tomographic volume. The flattened face of the mitochondrion is indicated by *arrows*. Density at the presynaptic face is marked by *arrowheads*. Notice that the cristae are oriented roughly perpendicular to the synaptic membranes. Scale bar = 100 nm. (b) A segmented crista superimposed on a slice through the volume different from the one shown in (a). A crista junction is indicated by an *arrow*. Synaptic vesicles near to the mitochondrion are marked with *arrowheads*. (c) A mostly side view of this lamellar crista that has three finger-like extensions that end in crista junctions (*arrowheads*). (d) View showing all six cristae in this MAC mitochondrion. Notice that all are lamellar, which is highly unusual for brain mitochondria, and appears to be a distinctive feature of MAC mitochondria. (e) A different view of the segmented volume, now showing the outer membrane, made transparent to better visualize the cristae. (f) Another view of the segmented volume without the slice through the reconstruction. As with the crista shown in (c), the end crista has three finger-like extensions that end in crista junctions (*arrowheads*). In collaboration with George Spirou, West Virginia University, USA



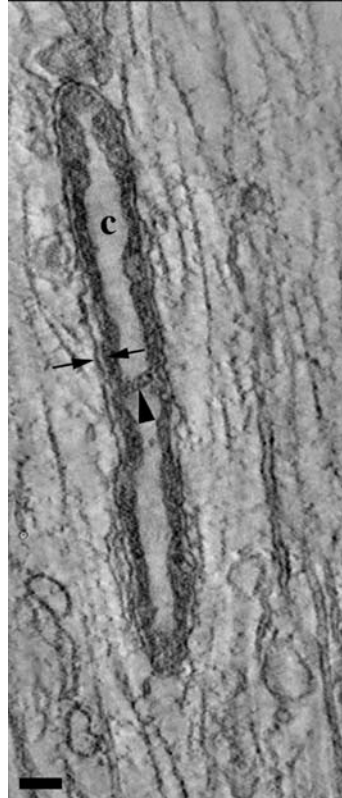
in response to changes in environment, mitochondrial shape, inner-membrane surface area, etc. The crista junction model has stimulated a reexamination of long-held paradigms of mitochondrial structures. One reexamination concerns the relationship between crista curvature and membrane bilayer energetics (Renken et al., 2002; Gilkerson et al., 2003; Perkins et al., 2004); another concerns mitochondrial fission in neuronal cells (Bossy-Wetzel et al., 2004; Perkins et al., 2004); a third concerns a mitochondrial network or reticulum in neurons (Muller et al., 2005).

2.2 Two Hypotheses

How are crista junctions formed and maintained? Two hypotheses have been proposed. One hypothesis requires a physical mechanism to initiate the tubular shape and subsequently constrain its diameter (Griparic and van der Bliik, 2001). Paumard et al. (2002) discuss the possibility that ATP synthase dimers stabilize crista junctions because the dimer approximates a truncated cone in overall shape. Thus, a rigid arc might be formed by linear association of adjacent dimers. An implication of a rigid proteinaceous arc is that diffusion of complexes between the inner boundary and the cristae membrane may be restricted once the

■ Figure 4.2-4

A slice through the tomographic volume of a mitochondrion with few longitudinally oriented cristae in the axoplasm of a spinal root neuron. The mitochondrion shown is 1.4 μm long. The mitochondria in the axonal shafts of spinal root are elongated and typically condensed. The condensation of the matrix and hence expansion of the intracristal space (c) is typically not seen in brain mitochondria in situ. Because of the condensed nature of these mitochondria, matrix bridges are observed (*arrowhead*). The condensed spinal root mitochondria differ from isolated mitochondria in that the inner-boundary membrane is not pulled away from the outer membrane (*arrows*). This feature could be due to homeostatic properties in tissues not present in vitro. Scale bar = 100 nm. In collaboration with George Spirou, West Virginia University, USA



arc is completed. This restriction is consistent with the finding that the cristae membranes, as opposed to the inner-boundary membrane, are the principal sites for oxidative phosphorylation (Frey et al., 2002; Gilkerson et al., 2003). Also, in the rat brain, it was discovered that the inner-boundary membrane contains the adenine nucleotide transporters (ANTs) ANT-1 and ANT-2, whereas the cristae membranes contain only ANT-2. This differential distribution of the two ANT isotypes suggests specific functional compartmentation of the boundary and cristae parts of the inner membrane (Vyssokikh et al., 2001). It has also been proposed that Mgm1, a dynamin-like GTPase involved with mitochondrial fusion and localized to the mitochondrial periphery, mediates and stabilizes crista formation at crista junctions (Wong et al., 2000; Polyakov et al., 2003). It is unknown if Mgm1's counterpart involved in mitochondrial fission (division), Dnm1, has a role in crista cleavage. An alternative hypothesis for the crista junction architecture uses a thermodynamic model (Renken et al., 2002). The distribution of crista junction sizes and shapes is predicted by a thermodynamic model based on the energy of membrane bending and influenced by the relative volume of the matrix. In this model, the circular crista junction is a thermodynamically stable

structure, yet can be readily deformed, and the distribution of crista junction size is a thermal fluctuation about a shape and size of minimal energy.

The crista junction does not appear to be a permanent structure (Renken et al., 2002). If the first hypothesis that they are formed by some kind of protein architecture is true, the junction must be able to disassemble when fewer junctions are needed. If the second hypothesis is true, the junction forms and disappears spontaneously as a response to changes in the inner-membrane surface area and matrix volume. Consistent with this hypothesis is the finding that the distribution of crista junction diameters for swollen mitochondria (sometimes observed in aged brain; see [▶ Sect. 6](#)) is 4 nm smaller than for normal mitochondria, as would be predicted by a thermodynamic control of diameter responding to increased matrix pressure (Frey et al., 2002). With isolated mitochondria, as the matrix condenses, crista junctions increase in diameter to the point that they are no longer discrete structures, and the inner-boundary membrane is pulled away from the outer membrane except at contact sites.

The discovery that crista junctions are much smaller than the broad folds described in the baffle model raises the question of what role they play in mitochondrial function. The size of these junctions might constitute a barrier to the diffusion of molecules such as adenosine triphosphate (ATP) or adenosine diphosphate (ADP) from the intracristal compartments to the intermembrane space, and simulations give credence to this possibility (Mannella et al., 2001). OPA-1 (optic atrophy 1) may play a role in controlling the structure and dynamics of crista junctions (reviewed by Bossy-Wetzel et al., 2003). In particular, the opening of the narrow crista junctions, proposed by Scorrano et al. (2002) to allow for the release of sequestered cytochrome *c*, might require inactivation of OPA-1. It is still speculative whether Bid or Bax aids in the opening of crista junctions (Bossy-Wetzel et al., 2003). However, another role for these junctions in the normal functioning of mitochondria could be to separate two inner-membrane compartments with differing membrane protein compositions. An efficient division of inner-membrane function might result if the boundary membrane were enriched with ion and metabolite transport proteins, facilitating their movement between the cytosol and the matrix. The electron transport proteins, on the other hand, have no particular need to communicate directly with the cytosol and would function efficiently within the cristae membrane (Gilkerson et al., 2003). Such compartmentation might be controlled by chaperones or could result passively if the ion and metabolite proteins were drawn to the periphery by interactions with outer-membrane proteins forming complexes. A definitive answer to this question might be afforded by new methods for labeling specific proteins for visualization by electron tomography. (See [▶ Sect. 8](#)).

2.3 Contact Sites

Mitochondrial contact sites play a role in energy metabolism, protein import, and apoptosis (Bernardi, 1999; Doran and Halestrap, 2000; Lutter et al., 2001; Crompton et al., 2002; Reichert and Neupert, 2002; Vyssokikh and Brdiczka, 2004). These sites were first defined structurally as foci where the inner and outer membranes pinch together ([▶ Figure 4.2-1](#)). They are nearly always punctate and in neuronal mitochondria are about 14 nm in diameter (Perkins et al., 1997, 2001a). Their function and protein composition are still being defined because purification schemes based on assumptions about what contact sites should contain vary in the number and identity of the purported constituents (100 proteins). Moreover, there may be functionally different types of contact sites, which may not be structurally distinguishable. There may be stable and labile contact sites, or otherwise “dynamic” and “static” contacts (van der Klei et al., 1994). Contact sites may be held together by creatine kinase octomers (Vyssokikh and Brdiczka, 2004) that reside in the intermembrane space and by the protein translocases, translocase outer membrane (TOM) and translocase inner membrane (TIM) (Bauer and Neupert, 2001); as yet, little is known about the cooperation of the respective translocases across outer and inner membranes. There are “translocation” contact sites involved with protein import into mitochondria (Chacinska et al., 2003). There are contact sites that house the permeability transition pore (PTP) (Halestrap and Brennerb, 2003), structural contact sites that may hold the outer- and inner-boundary membranes close to each other (Perkins et al., 2001a), and contact sites likely involved in energy transduction (Bernardi, 1999). Are these functional units necessarily at different sites, or could more than one functional unit share the same punctate site? Are they spatially segregated or

randomly dispersed on the mitochondrial periphery? Measurements on tomographic volumes indicated that contact sites are randomly located with respect to crista junctions (Perkins et al., 1997). Incubation of brain mitochondria in buffers with elevated calcium concentration increases the formation (number) of contact sites (Sandri et al., 1988). The minimal protein composition of the PTP is a voltage-dependent anion channel (VDAC), ANT, and cyclophilin D (Halestrap and Brennerb, 2003). VDAC is an outer-membrane pore and binds to the outer face of the ANT (an inner-membrane transporter) at contact sites; cyclophilin D binds from the matrix side to the inner face of the ANT and regulates the PTP. Cytochrome *c*, glycerol kinase, and hexokinase might be invited guests of the PTP (Vyssokikh and Brdiczka, 2004). In this model, hexokinase can occupy a VDAC-binding site to impede Bax binding to the contact site and to inhibit the permeability transition. Contact sites are purported to have a unique lipid environment that is rich in cardiolipin. The need for cardiolipin has been implicated in the function of several mitochondrial proteins including complexes I and III of the electron transport chain, the ANT, TOM, and TIM proteins, and in the localization of mitochondrial creatine kinase (Muller et al., 1985; Hoffmann et al., 1994; Chen et al., 1995; Weiss et al., 1999). The interaction of the proapoptotic protein, Bid, with cardiolipin at contact sites enhances its function (Kim et al., 2004). Mgm1 is localized to both outer- and inner-boundary membranes and may reside at contact sites (Sesaki and Jensen, 2004).

2.4 Mitochondrial Network

Ever since mitochondria have been labeled with fluorescence markers in cultured cells and structural networks of this organelle observed using the 3D capability of confocal microscopy, there has been a debate concerning whether mitochondria also exist as a network or reticulum in tissues, including brain tissue. In neurons cultured from mouse respiratory center, the mitochondria form functionally coupled, dynamically organized aggregates such as chains and clusters, while single mitochondrion are rarely seen (Muller et al., 2005). The chain structures predominate in dendrites, whereas the clusters are mostly found in the soma. In brain tissue, however, structural mitochondrial networks have not been observed (Peters et al., 1976; Perkins et al., 1997, 2001a). How have cultured cells been perturbed so that discrete mitochondria form networks, and from a functional standpoint, how is mitochondrial function affected by the networking?

2.5 Mitochondrial Motility in Neurons

Mitochondria in both axons and dendrites of cultured neurons are highly motile (Ligon and Steward, 2000a) and show assisted movement by microtubules and actin microfilaments with different patterns of transport, but no transport by neurofilaments (Morris and Hollenbeck, 1995; Ligon and Steward, 2000b). Transport is thought to reflect local energy needs. For example, moving mitochondria became persistently stationary in active growth cones, but regained their motility when growth cone activity was halted (Morris and Hollenbeck, 1993). Mitochondrial transport in axons is influenced by action potentials (Vanden Berghe et al., 2004). When the sodium channel is blocked, mitochondrial mobility is impeded. In contrast, when actin is stabilized, mitochondrial velocity increases. In addition, calcium stores are necessary for efficient transport. Mitochondria transported in opposite directions do not necessarily impede each others' mobility (Vanden Berghe et al., 2004). Mitochondria in astrocytes also show motility (Funk et al., 1999). However, a quantitative analysis has yet to be performed in these cells.

Transport of mitochondria in neuronal processes occurs bidirectionally along both microtubules and actin microfilaments, with a broad range of velocities and net movement (Morris and Hollenbeck, 1993, 1995). Using cultured cells treated so that either only microtubules or only actin microfilaments were present (with exception of the control, which had the normal complement of tubules and filaments), the authors of this study found four principal differences between microtubule and microfilament transport of mitochondria. One, the mean velocity of mitochondria on microtubules ($\sim 0.6 \mu\text{m/s}$) was about three times greater than the mean velocity on microfilaments ($\sim 0.2 \mu\text{m/s}$). Two, although mitochondria had a slower mean velocity when transported on microfilaments, the net transport velocity was about 11 times higher (microfilaments: $1.52 \mu\text{m/min}$, microtubules: $0.14 \mu\text{m/min}$) because of prolonged retrograde movement.

Three, net transport on microtubules was anterograde, but retrograde on microfilaments. Four, the maximum distance traveled by mitochondria in control cells was significantly greater (25 μm anterograde, 15 μm retrograde) than those transported on microfilaments alone (1.1 μm anterograde, 5.3 μm retrograde), consistent with known greater lengths of axonal microtubules compared with microfilaments. Because the mean velocity of mitochondrial transport for the control ($\sim 0.35 \mu\text{m/s}$) is between the mean velocities for microfilament-only and microtubule-only transport, an interpretation of these measurements might be that mitochondrial transport is simply a weighted mean of the microtubule- and microfilament-based carriers. Yet, because microfilament transport of mitochondria is predominantly retrograde, it is unlikely to contribute substantially to net anterograde movement. Furthermore, microtubule-based transport alone has been demonstrated to be effective for both anterograde and retrograde transport of mitochondria within axons; so why a second transport mechanism? Morris and Hollenbeck (1995) suggest that transport along microfilaments provide a local transport system that might (1) cluster mitochondria in a particular region or (2) move mitochondria that have become dissociated from microtubules back onto the microtubular track for continued transport in either direction. (For example, a mitochondrion might be required to become stationary because of local energy needs; an everyday analogy would be workers getting off a subway when they reach their place of work and getting back on at the end of the workday.)

More recently, Chada and Hollenbeck (2004) showed that nerve growth factor (NGF) causes mitochondria to accumulate in sensory neurons where focal stimulation occurs. An analysis using light microscopy showed that this accumulation results from increased mitochondrial transport into regions of focal stimulation followed by inhibition of transport out of these regions. Interestingly, in axons made devoid of F-actin, bidirectional transport of mitochondria continues, but there is no longer accumulation in the region of NGF stimulation, thus providing further support for local control of transportation by microfilaments. A second transport mechanism would substitute in regions of the axon where microtubules are few or absent as in branch points or growth cones. Another use for microfilament tracks might be to return mitochondria to microtubules after having become mistakenly dissociated, because the capacity of mitochondria to diffuse within the axoplasm is limited, or to assist the organelle to “jump” to an adjacent microtubule from the end of a currently traveled microtubule because a single microtubule does not traverse the entire length of the longer axons (like making a subway connection to a different line). A local transport mechanism for mitochondria might reduce unwanted “layover” time. These studies suggest a complex system for mitochondrial transport in neuronal processes involving multiple motors, each with its own intrinsic properties (Scheffler, 1999). More work needs to be done, however, to understand the purposes of the various motors that exist presumably for fine-tuning mitochondrial trafficking.

There are both similarities and differences between axonal and dendritic mitochondrial transport. Ligon and Steward (2000a) used cultured hippocampal neurons to observe that in both axons and dendrites, roughly one-third of the mitochondria were in motion at a given time. About 70% of the mitochondria moved in the anterograde direction, whereas the remainder followed a retrograde movement. The velocity of mitochondria in each direction in each compartment ranged from 0.1 $\mu\text{m/s}$ to 2 $\mu\text{m/s}$ with similar means and distributions. Two differences were found. One, mitochondria in axons moved with a higher velocity than those in dendrites. Two, axonal mitochondria traveled farther distances than dendritic mitochondria. Why these differences exist has yet to be elucidated.

2.6 Mitochondrial Turnover

Mitochondrial turnover occurs in the brain at a significantly slower rate than in other organs. In an early study, the half-life of brain mitochondria was measured to be 16.4 days (Khan and Wilson, 1965). Later, Menzies and Gold (1971) measured the turnover rate in brain mitochondria to be 24.4 days, longer than the 17.5, 12.6, and 9.3 days for heart, testes, and liver, respectively. Mitochondrial half-lives for lung, small intestine, and kidney were even shorter. Mitochondrial proteins generally have a different range of half-lives than do mitochondrial lipids (Munn, 1974). Phosphatidylcholine has a long half-life in rat brain (48.7 days) and cardiolipin even longer (424 days). By comparison, in liver and kidney, the half-lives of the mitochondrial phospholipids measured were found in the range of 9–12 days (Munn, 1974).

2.7 Mitochondrial Fission and Fusion

Just as cells arise from preexisting cells, mitochondria arise from preexisting mitochondria. The mechanism by which this occurs is fission. The role of fusion is more speculative. Fusion of mitochondria is thought to mix content and thus make the population of mitochondria more homogeneous, which might be important for maintenance and inheritance, might counteract mitochondrial DNA (mtDNA)-linked diseases, and also might serve as a defense against the accumulation of oxidative damage during aging (Westermann, 2002). The fission and fusion of mitochondria is regulated by large GTPases of the dynamin family. Dynamin-related protein-1 (Drp1) is a fission protein that associates on the outer surface of mitochondria at fission sites (Smirnova et al., 2001), and optic atrophy 1 (OPA1) is a fusion protein with extensive brain expression (Misaka et al., 2002) located inside mitochondria (Olichon et al., 2002). Fis1 is another mitochondrial fission protein (Suzuki et al., 2003) and Fzo, Mgm1, Ugo1 (Sesaki and Jensen, 2004) and Mitofusin1 and 2 are mitochondrial fusion proteins (Ishihara et al., 2004) that have yet to be shown to act in neurons or glia. As with energy profiles in neurons, it appears that neuronal activity regulates the fusion/fission balance, the distribution of mitochondria particularly in dendrites, and the motility of these organelles and not vice versa (Li et al., 2004). This group provided evidence that Drp1 is critical for the distribution of mitochondria to dendrites, likely facilitated by mitochondrial fission in the neuronal soma; in other words, fission might be the signal for the transport of mitochondria from the soma to dendrites. The signal might also depend on calcium influx through L-type voltage-gated calcium channels and NMDA receptors. The balance of mitochondrial fusion/fission was found to shift toward fusion in neurons silenced by tetrodotoxin and toward fission in neurons undergoing potassium depolarization. It was found that mitochondrial fusion requires an inner-membrane potential but is independent of mitochondrial attachment to microtubules or actin (Mattenberger et al., 2003). Finally, as might seem logical, it was shown in the same study that mitochondrial fusion is independent of fission.

3 Heterogeneity of Mitochondrial Structure and Function in Brain Regions

The mammalian brain is the organ with the highest demand for aerobic ATP production, accounting for roughly 20% of total oxygen consumption at rest (Papa, 1996). It also produces ATP at a faster rate than other organs except the heart (Kwong and Sohal, 2000). Brain energy metabolism largely depends on aerobic glycolysis and displays marked regional differences (Clark and Sokoloff, 1999) with neurons, differing in metabolic rates from glia (see [▶ Sect. 4](#)). In 1970, it was already recognized that many populations of mitochondria, each with its own enzyme complement, exist in the brain (Blokhuys and Veldstra, 1970). This was because different preparations of brain mitochondria were enriched with some enzymes and were deficient in others. In addition to differential enzyme complement, in Chapter by Saks and coworkers of this volume, Saks and coworkers report that rates of aerobic glycolysis differ in gray and white matter. In cerebral gray matter, aerobic glycolysis is high and fluctuates rapidly in correlation with neuronal activity. In contrast, aerobic glycolysis is lower and more stable in white matter. A key feature pertains to creatine kinase activity. This activity differs in defined patterns between white matter and gray matter, reflecting a heterogeneity in ATP utilization. In the cerebellum, ubiquitous brain-type mitochondrial creatine kinase was found mainly in the glomeruli structures of the granule layer. To a lesser extent, this kinase was found in Bergmann glial cells (Kaldis et al., 1996).

3.1 Mitochondrial Enzymes

An extensive body of literature provides evidence that mitochondrial enzymes are differentially expressed and regulated in the brain. In 1963, evidence that brain mitochondria may be heterogeneous in their enzyme content was first reported (Tolani and Talwar, 1963). A few years later, the hypothesis was made for the existence of mitochondria with specialized functions within brain cells (Neidle et al., 1969). Since then, this hypothesis has been supported by many studies and [▶ Table 4.2-1](#) documents the reports of heterogeneous enzyme expression in the various brain regions studied. By comparing the activity of NADP-linked

■ Table 4.2-1

Heterogeneity of mitochondrial enzyme expression as a function of brain region

Mitochondrial enzyme	Brain regions or fractions that differ in enzyme content	References
ATP synthase	Nucleus basalis of Meynert, substantia nigra, locus coeruleus, hippocampus, cerebral cortex	Takase et al. (1996)
Citrate synthase	Cortex, striatum, pons, and medulla oblongata Hippocampus Cholinergic cerebellar synapse Fractions from whole-brain homogenate	Leong et al. (1984b) Villa et al. (1989) Wilkin et al. (1979) Blokhuis and Veldstra (1970)
Creatine kinase	White versus grey matter Cerebellum, hippocampus Cortex, striatum, pons, and medulla oblongata	Holtzman et al. (1998) Kaldis et al. (1996) Leong et al. (1984b)
Cytochrome c	Cortex, striatum, hippocampus	Battino et al. (1991)
Cytochrome oxidase	Pontine nuclei, supraoptic nucleus, cerebellum, striatum Hippocampus Striatum Striatum Cortex, hippocampus Cortex, striatum, hippocampus Cortex, striatum, hippocampus	McEnery et al. (1993) Villa et al. (1989) Gimenez-Amaya (1991) Difiglia et al. (1987) Davey et al., (1997) Battino et al. (1991) Gorini et al. (1989)
Dihydroipoamide acetyltransferase	Nucleus basalis of Meynert, substantia nigra, locus coeruleus, hippocampus, cerebral cortex	Takase et al. (1996)
Dihydroipoamide succinyl transferase	Nucleus basalis of Meynert, substantia nigra, locus coeruleus, hippocampus, cerebral cortex	Takase et al. (1996)
Fumarase	Cortex, striatum, pons, and medulla oblongata Cholinergic cerebellar synapse	Leong et al. (1984b) Wilkin et al. (1979)
GABA-aminotransferase	Cholinergic cerebellar synapse	Wilkin et al. (1979)
Glutamate dehydrogenase	Heterogeneous in glia Glia from neurons, several forebrain regions Medulla oblongata and pons, hypothalamus, cerebellum, striatum, cortex Pontine nuclei, supraoptic nucleus, cerebellum, striatum Hippocampus Cholinergic cerebellar synapse Fractions from whole-brain homogenate	Aoki et al. (1987) Aoki et al. (1987b) Leong and Clark (1984) McEnery et al. (1993) Villa et al. (1989) Wilkin et al. (1979) Blokhuis and Veldstra (1970)
Glutaminase	Purkinje, Golgi cells, mossy, parallel, and climbing fibers Cortex, striatum, accumbens nuclei Fractions from whole-brain homogenate	Laake et al. (1999) Aoki et al. (1991) Blokhuis and Veldstra (1970)
Hexokinase	Cortex, striatum, pons, and medulla oblongata	Leong et al. (1984b)
Hydroxybutyrate dehydrogenase	Cortex, striatum, pons, and medulla oblongata	Leong et al. (1984b)
Isocitrate dehydrogenase-NAD	Fractions from whole-brain homogenate	Blokhuis and Veldstra (1970)
Isocitrate dehydrogenase-NADP	Fractions from whole-brain homogenate	Blokhuis and Veldstra (1970)

■ **Table 4.2-1 (continued)**

Mitochondrial enzyme	Brain regions or fractions that differ in enzyme content	References
Kynurenine aminotransferase	9 brain regions including olfactory bulb and cerebellum	Okuno et al. (1991)
Malate dehydrogenase	Hippocampus	Villa et al. (1989)
Malic enzyme	Cortical synaptic terminals, cultured cortical neurons, cerebellar granule cells, astrocytes	McKenna et al. (2000)
	Pons, substantia alba, frontal cortex, cerebellum, striatum, Corpus callosum	Bukato et al. (1994)
MnSOD	Many brain regions	Zhang et al. (1994)
Monoamine oxidase	Cortex, striatum, pons, and medulla	Lai et al. (1994)
	Fractions from whole-brain homogenate	Blokhuys and Veldstra (1970)
	Fractions from whole-brain homogenate	Owen et al. (1977)
	Cholinergic cerebellar synapse	Wilkin et al. (1979)
Monoamine oxidase type B	Dorsal raphe nucleus, suprachiasmatic nucleus	Arai et al. (2002)
NADH-cytochrome c reductase	Cortex, striatum, hippocampus	Battino et al. (1991)
NAD-linked isocitrate dehydrogenase	Hippocampus	Villa et al. (1989)
NAD-linked isocitrate dehydrogenase	Cortex, striatum, pons, and medulla oblongata	Leong et al. (1984b)
NAD-linked malate dehydrogenase	Cortex, striatum, pons, and medulla oblongata	Leong et al. (1984b)
NADP-linked isocitrate dehydrogenase	Cortex, striatum, pons, and medulla oblongata	Leong et al. (1984b)
Pyruvate dehydrogenase	Neurons versus astrocytes	Lai (1992)
	Cortex, striatum, pons, and medulla oblongata	Leong et al. (1984b)
	Many brain regions	Milner et al. (1987)
Succinate-cytochrome c reductase	Cortex, striatum, hippocampus	Battino et al. (1991)
Succinate-DCIP	Cortex, striatum, hippocampus	Battino et al. (1991)
Succinate dehydrogenase	Cholinergic cerebellar synapse	Wilkin et al. (1979)
Ubiquinol2-cytochrome c reductase	Cortex, striatum, hippocampus	Battino et al. (1991)
VDAC	Pontine nuclei, supraoptic nucleus, cerebellum, striatum	McEnery et al. (1993)

malic enzymes in mitochondria isolated from striatum, cerebellum, cortex, pons, substantia alba, and corpus callosum, Bukato et al. (1994) found the activity highest in mitochondria from the striatum and lowest in the corpus callosum. This finding is interesting because of the report that the corpus callosum is predominated by glial cells (Tolani and Talwar, 1963). In [Sect. 4](#), evidence is presented showing that mitochondrial activity in glial cells is reduced in comparison with that in neurons. The biosynthetic enzyme, kynurenine aminotransferase (KAT), found in mitochondria, is distributed heterogeneously between nine brain regions, with the KAT-rich olfactory bulb having about five times higher activity than the cerebellum, the region with lowest KAT activity (Okuno et al., 1991). In preparations from rat cerebellum, Wilkin et al. (1979) examined the profiles of six mitochondrial enzymes, finding notable differences in the fractions of predominantly neuronal origin, thus providing further evidence that the enzyme composition of cerebellar mitochondria is not uniform. A mitochondrial porin, VDAC, that is ubiquitous, nevertheless has pronounced regional variations in the rat brain, with the pontine nuclei, the

supraoptic nucleus, the Purkinje cells of the cerebellum, and the caudate putamen evidencing the highest density of this outer membrane protein (McEnery et al., 1993).

In the hippocampus, there is highly diversified expression of citrate synthase, malate dehydrogenase, NADH-cytochrome *c* reductase, and cytochrome oxidase (enzymes involved in energy transduction), and glutamate dehydrogenase (enzyme involved in amino acid metabolism) (Villa et al., 1989). In the nucleus basalis of Meynert, substantia nigra, locus coeruleus, cortex, and especially in the hippocampus, dihydro-lipoamide acetyltransferase was strongly labeled in comparison with dihydro-lipoamide succinyltransferase and ATP synthase (Takase et al., 1996). In the CA3 region of the hippocampus and in the brain stem auditory relay nuclei, both regions exhibiting high levels of spontaneous and synaptic activities, cytochrome oxidase is richly expressed (Wong-Riley, 1989). Mitochondrial creatine kinase is localized to the granule and pyramidal cells of the hippocampus (Kaldis et al., 1996). The epithelial cells of the choroid plexus are also highly enriched in this kinase.

In the striatum, cytochrome oxidase has regional differences in distribution. Interestingly, regions with high concentration of this electron transport complex matched regions in which acetylcholine esterase was high as well (Gimenez-Amaya, 1991). It may be that this correlation reflects the coupling of mitochondrial activity with transmitter turnover. However, later work by the same investigator (Gimenez-Amaya, 1992) seems to refute this by purporting that in the globus pallidus, the distribution of cytochrome oxidase was opposite to that found for acetylcholine esterase. The activities of several electron transport complexes such as succinate-cytochrome *c* reductase, NADH-cytochrome *c* reductase, succinate-dichloroindophenol (DCIP), ubiquinol2-cytochrome *c* reductase, and cytochrome oxidase are lower in mitochondria in the striatum and hippocampus than in the cortex (Battino et al., 1991). In addition, the temperature dependence of the activities of these mitochondria displayed significant differences. Could this effect be due to the different properties of the lipids surrounding these enzymes (Toescu et al., 2000)? This brain region difference is consistent with the finding that the hippocampal CA1 region possesses a lower mitochondrial respiratory capability and cytochrome oxidase activity than does the cortex (Davey et al., 1997). In contrast, in the study by Battino and coworkers, it was reported that the activity of cytochrome *c* was significantly higher (about 50%) in the hippocampus and striatum than in the cortex. Why two enzymes coupled in the electron transport chain, cytochrome oxidase and cytochrome *c*, should have opposite levels of activities in the three brain regions examined is a mystery. Could an explanation be found in the additional role that cytochrome *c* has in apoptosis? Monoamine oxidase, involved with amine metabolism, has marked activity differences between striatum, cortex, pons and medulla (Lai et al., 1994). Pyruvate dehydrogenase is intensely labeled not only in the striatum, but also in the medial septal nuclei, the nuclei of the diagonal band, the nuclei basalis, the entorhinal cortex, the supraoptic hypothalamic nuclei, reticular thalamic nuclei, lateral substantia nigra, most of the tegmental nuclei, lateral nuclei of the trapezoid body, raphe pontis and obscuris, and the caudal part of the lateral reticular nuclei (Milner et al., 1987). In addition, many of the motor nuclei of the cranial nerves were intensely labeled. However, and intriguingly, the intensity of labeling was significantly greater in the regions containing cholinergic neurons as opposed to regions dominant in catecholaminergic neurons. The significance of this difference among nerve types is unknown.

In the cortex, glutaminase-immunoreactive perikarya were numerous but sparse within striatal perikarya and accumbens nuclei, regions recognized to contain high densities of glutamatergic terminals but few, if any, glutamatergic perikarya (Aoki et al., 1991). Tolani and Talwar (1963) reported that the corpus callosum, populated with only glial cells, has cytochrome oxidase activity significantly lower than that in the cortex or cerebellum, with the highest activity seen in layers II, III and IV of human cerebral cortex. On observing postmortem human brains, Zhang et al. (1994) found a heterogeneous distribution of manganese-dependent superoxide dismutase in the seven layers of the cortex. Regional variations were also observed in the cerebellum, hippocampus, striatum, many nuclei regions of the brain stem, and forebrain regions. The suggestion was made that the heterogeneous, but not ubiquitous, distribution of cells expressing this superoxide dismutase indicates that not all regions in the human brain are protected to the same extent against the effects of superoxide. In summary, these reports (see additional literature referenced in [Table 4.2-1](#)) show that many mitochondrial enzymes are not expressed synchronously in the various regions of the brain, suggesting the differential regulation of mitochondrial enzymes and the governing principle of mitochondrial heterogeneity.

4 How Do Neuronal and Glial Mitochondria Differ?

4.1 Mitochondrial Localization

What has aided the pursuit of this question is the capability of distinguishing between mitochondria derived from neuronal and glial cells and synaptic and nonsynaptic mitochondria (Owen and Bourne, 1977). Consistent variations are found in mitochondrial structure or content among different neurons and neuroglia, suggesting that differences exist in their capacities (Pysh and Khan, 1972). What dictates the distribution of mitochondria in neurons and glial cells? In 1958, it was reported that the density of mitochondria in most neurons and their larger processes is higher than in oligodendroglia or astrocytes (Windle et al., 1958). It is generally accepted that mitochondria are distributed to regions requiring a high (or at least steady) supply of ATP (Scheffler, 1999), and in normal neuronal function mitochondria produce nearly 90% of the ATP (Toescu et al., 2000). However, the distribution might be dependent on more than energy designations. As pointed out by Saks and coworkers, the cytoplasm of brain cells appears to be highly organized and macromolecules and organelles, including mitochondria, are involved in multiple structural and functional interactions. These interactions are aided by their precise localization. One example is the sequestration and release of calcium and molecules involved in apoptosis (see the Chapters by Wieloch and coworkers, and Solenski & Fiskum in this volume). Mitochondrial position seems to be governed by cytoskeletal elements, such as microtubules and neurofilaments.

4.2 Mitochondrial Structure

Within a small field containing both neurons and glia, mitochondria are really quite variable in size, shape, and cristae packing (Peters et al., 1976). The cristal volume fraction of mitochondria (cristal packing density) is higher in neurons than in astrocytes and oligodendrocytes. Mitochondrial volume fractions (concentration) vary markedly among different neuronal and neuroglial somata (Pysh and Khan, 1972). It is likely that differences in mitochondrial volume fractions coupled with differences in cristal packing density reflect considerable variation in the capacity for oxidative metabolism. In nearly all brain regions, some of the mitochondria are globular and of various sizes; others are sausage-shaped organelles 0.5 μm or more in width and still others are elongated threads that can be as thin as 0.1 μm in diameter and usually several microns long (▶ [Figure 4.2-2](#)). (Mitochondria as long as 25 μm have been reported.) Branching forms are not uncommon in axons, dendrites, and cell soma, although rarely seen in axon terminals. “Y-shaped” branching occurs in astrocytes. In the narrower processes of both neurons and astrocytes, the mitochondria tend to be of simpler form, usually unbranched rodlets about 0.1 μm across and 1 μm or more long. Sometimes, unusual structural variations exist in a neuronal bundle. For example, in the spinal ganglion cells of the slow loris, nearly all the light cells contain filamentous mitochondria, whereas only 35% of the dark cells contain filamentous mitochondria, the other 65% displaying uncommonly seen vacuolated mitochondria (Ahmed and Kanagasuntheram, 1976). A peculiarity of neuronal mitochondria is that they contain few dense matrix granules, in contrast to liver mitochondria replete with such granules. These granules are deposits of hydroxyapatite sequestered by the oxidative activity of the mitochondrion in the presence of calcium. It is speculated that the paucity of neuronal mitochondrial granules is correlated to the high requirements for glucose and oxygen and low reserves of ATP that are characteristic of neurons (Peters et al., 1976).

In glial cells, there exists almost as much variation in mitochondrial size and form as in neurons (Peters et al., 1976). For example, in satellite cells, rounded mitochondria are prominent and are clustered in the perinuclear zone. The form of mitochondria in Schwann cells is similar to those in satellite cells. However, instead of clustering perinuclearly, they cluster in the outer cytoplasm of paranodes. In general, within the perikaryon of astrocytes, the mitochondria can be either globular or elongated and are randomly dispersed. In the processes, they are most often rod-like and almost always oriented parallel to the long axes of the processes and, consequently, parallel to the microtubules and filaments. However, note that the mitochondria of the fibrous astrocytes (found in white matter) are predominantly elongated. As in neuronal

processes, some branch so that they have the form of a letter “Y.” The protoplasmic astrocytes (found in gray matter) have large, elongated mitochondria. Mitochondria occur in the larger processes of these astrocytes, but in the smaller processes, mitochondria are usually and mysteriously absent. In oligodendrocytes, because of the density of the cytoplasm, the mitochondria are often inconspicuous. Most of them are rather small, with cristae arranged transversely. In ependymal cells, the mitochondria generally have an elongated form resembling those of astrocytes. However, they cluster at the apical poles of the cells.

4.3 Compartmentation of the TCA Cycle

A characteristic feature of both neurons and astrocytes that may have ramifications for the specific activities of these cells is that metabolism seems to be compartmentalized. This compartmentation has been studied most thoroughly by Sonnewald, Schousboe, and their collaborators and is best explained by postulating that more than one type of tricarboxylic acid (TCA) cycle exists that very likely relates to individual cells containing mitochondrial populations having different metabolic roles. Evidence for the different types of TCA cycle is obtained from cycles with different properties regarding cycling rates and ratio as well as from the differential coupling to amino acid biosynthesis, predominantly involving glutamate and aspartate (Sonnewald et al., 1998) and also pyruvate and citrate (Sonnewald et al., 1993). Using monotypic cultured astrocytes and neurons, Waagepetersen et al. (1999a, b, 2000, 2003) found the role of the TCA cycle in the biosynthetic machinery responsible for formation of γ -amino butyric acid (GABA) from glutamine to be greater than hitherto anticipated. Observed glutamate gradients may depend on the anchoring of distinctive populations of mitochondria in different parts of the cell (Sonnewald et al., 2004), and these mitochondria may reside where they do because they have different enzyme compositions and substrate concentrations. However, functionally different mitochondria in the same astrocyte or neuron needs to be experimentally verified.

4.4 Mitochondrial Enzymes

In glia, so far documented, there are only a few mitochondrial enzymes that show a difference from those in neurons (🔗 [Table 4.2-2](#)). However, one suspects that further studies would uncover additional heterogeneity. The sarcomeric muscle-type mitochondrial creatine kinase was localized in the Purkinje neurons but

■ **Table 4.2-2**
Mitochondrial heterogeneity between neurons and glia

Enzyme	Difference between neurons and glia	References
Creatine kinase	Purkinje neurons, but not glia of cerebellum	Kaldis et al. (1996)
Cytochrome oxidase	Lower activity in glia	Tolani and Talwar (1963); Difiglia et al. (1987); Wong-Riley (1989)
Glutamate dehydrogenase	Enriched in glia	Aoki et al. (1987b)
Glutaminase	Noncompartmentalized labeling in glia	Aoki et al. (1991); Laake et al. (1999)
Mn-superoxide dismutase	Limited distribution in glia	Zhang et al. (1994)
Other Differences		References
Glia depend more on anaerobic glycolysis rather than oxidative phosphorylation		Wong-Riley (1989)
Glia have a lower density of mitochondria		Tolani and Talwar (1963)
Packing density of cristae lowest in glia		Pysh and Khan (1972)
Glia exhibit different compartmentation of glutamate metabolism from neurons		Waagepetersen et al. (2003)

not in other neurons or glia of the cerebellum (Kaldis et al., 1996). It was hypothesized that the partition of this kinase reflects the specific energy requirements associated with calcium spiking in these specialized neurons. Also, in the hippocampus, the ubiquitous isotype of mitochondrial creatine kinase was found in the granule and pyramidal neurons, but not in the surrounding glia. Although not detected in all neurons, the distribution of Mn superoxide dismutase was greater in neurons, being found in more brain regions, than in glia (Zhang et al., 1994). It was discovered that glutamate dehydrogenase exists in neuroglial cells (Aoki et al., 1987b). Moreover, glial mitochondria are heterogeneous with respect to the presence of this enzyme, being enriched in areas displaying chronically active glutamatergic transmission (Aoki et al., 1987a). Whereas the perikarya and dendrites of neurons were labeled for glutaminase, whereas glial cell mitochondria were devoid of specific labeling of this not-exclusively-mitochondrial enzyme (Aoki et al., 1991; Laake et al., 1999). With cytochrome oxidase, glia are much lighter stained than are neurons, in agreement with the observation that glia depend more on anaerobic glycolysis than on oxidative metabolism (Tolani and Talwar, 1963; Difiglia et al., 1987; Wong-Riley, 1989). However, an anomaly was reported with astrocytes from primary culture. In contrast to brain tissue, these showed higher rates of oxidative phosphorylation than did primary cultured neurons (Jameson et al., 1984). Caution is needed though in interpreting these results because a recent report demonstrated that with primary cultured neurons, large variations in mean mitochondrial membrane potential can exist among cells of the same type within a single culture dish (Huang et al., 2004).

5 Heterogeneity of Mitochondria in Neuronal Compartments

5.1 Mitochondrial Structure and Translocation

Even though the membrane architecture of neuronal mitochondria is similar to that of mitochondria in other vertebrate cells (Perkins et al., 1997, 2001a; Frey and Mannella, 2000), the variation in their sizes and shapes is greater (see [Table 4.2-3](#)), no doubt reflecting the different roles of neuronal compartments. The mitochondria of dendrites can be quite long ([Figure 4.2-2](#)) and Y-shaped or branched (Peters et al., 1976). Small and rounded forms also occur and are often in close proximity to the endoplasmic reticulum, as in the cell body (see Chapter by Rizzuto and Szabadkai in this volume). Alnaes and Rahamimoff (1975) proposed that presynaptic mitochondria help to regulate the release of transmitter from nerve terminals by participating in the regulation of intracellular free calcium (see Chapters in this volume by Gibson and Joseph; Reynolds and Vergun; Rizzuto and Szabadkai; Wieloch, Elmer, and Hansson; Solenski and Fiskum). In larger dendrites, the mitochondria are clustered toward the peripheral cytoplasm, leaving the core to other organelles, principally the endoplasmic reticulum, and to fibers involved in transport such as microtubules and neurofilaments. As successive bifurcations reduce the width of the dendritic processes, the mitochondria are pushed into the center and appear to be wrapped in a basket of parallel-oriented microtubules or filaments. The number of mitochondrial profiles per unit cross-sectional area increases in the smaller dendritic branches so that the mitochondria appear more numerous in small dendrites than in large ones (Peters et al., 1976). An exception to this is found in the lateral vestibular nucleus of mature rats where some of the dendrites are enlarged to form varicosities filled with mitochondria. These varicosities vary from 1 to 3 μm in diameter, and the mitochondria within them are long and slender and either are arranged parallel to the long axis of the dendrite or form gently swirling figures around the long axis. Movies of neural tissues in culture chambers show that the mitochondria of neurons change their shape, size, and position in the cell (reviewed in Peters et al., 1976). Mitochondria migrate at variable rates from the perikaryon into one process or another and back again. Elongated mitochondria traverse relatively long distances in axonal shafts. Often, they migrate within spatially confined highways marked by tubules and filaments. Not surprisingly, because the microtubules and neurofilaments in the dendritic stems pass by the stalks of the spines and do not enter them, mitochondria are only rarely observed in the spinal cytoplasm; at least this is true in the adult brain. A more recent study examined mitochondrial motility in cultured mouse brainstem neurons (Muller et al., 2005). Two types of mitochondrial associations (network or reticulum) were observed. The mitochondria that network in chains predominate in dendrites, whereas

■ **Table 4.2-3**
Heterogeneity of mitochondria in neuronal compartments

Enzyme	Somatic, axonal, dendritic, or synaptic regions that differ in enzyme content	References
Aspartate aminotransferase	Synaptic versus nonsynaptic	McKenna et al. (2000b)
Citrate synthase	Synaptic versus nonsynaptic	Lai and Clark (1976); Leong et al. (1984)
Citrate synthase	Soma versus synaptic	Villa et al. (1989)
Creatine kinase	Synaptic versus nonsynaptic	Leong et al. (1984)
Cytochrome oxidase	Soma versus axon versus dendrite	Difiglia et al. (1987)
Cytochrome oxidase	Synaptic versus nonsynaptic	Gorini et al. (1989)
Cytochrome oxidase	Soma versus synaptic	Villa et al. (1989)
Cytochrome oxidase	Soma versus axon versus dendrite versus axon terminals	Wong-Riley (1989)
Fumarase	Synaptic versus nonsynaptic	Leong et al. (1984)
Glutamate dehydrogenase	Soma versus synaptosomes	Dienel et al. (1977)
Glutamate dehydrogenase	Synaptic versus nonsynaptic	Lai and Clark (1976); McKenna et al. (2000b)
Glutamate dehydrogenase	Soma versus synaptic	Villa et al. (1989)
Glutaminase	Axon terminal versus soma	Aoki et al. (1991)
Glutaminase	Soma versus synaptosomes	Dienel et al. (1977)
Glutamine transporter	Synaptic versus nonsynaptic	Kvamme et al. (2000)
Hexokinase	Soma versus synaptosomes	Dienel et al. (1977)
Hexokinase	Synaptic versus nonsynaptic	Leong et al. (1984)
Hydroxybutyrate dehydrogenase	Soma versus synaptosomes	Dienel et al. (1977)
Hydroxybutyrate dehydrogenase	Synaptic versus nonsynaptic	Leong et al. (1984)
Isocitrate dehydrogenase	Synaptic versus nonsynaptic	Lai and Clark (1976)
Malate dehydrogenase	Synaptic versus nonsynaptic	Lai and Clark (1976)
Malate dehydrogenase	Soma versus synaptic	Villa et al. (1989)
Malate NADP dehydrogenase	Soma versus synaptosomes	Dienel et al. (1977)
Monoamine oxidase	Soma versus axon versus dendrite versus axon terminals	Arai et al. (2002)
Monoamine oxidase	Synaptic versus nonsynaptic	Lai et al. (1994)
NADH-cytochrome c reductase	Soma versus synaptic	Villa et al. (1989)
NADH dehydrogenase	Synaptic versus nonsynaptic	Davey et al. (1997)

■ **Table 4.2-3 (continued)**

Enzyme	Somatic, axonal, dendritic, or synaptic regions that differ in enzyme content	References
NAD-linked isocitrate dehydrogenase	Synaptic versus nonsynaptic	Leong et al. (1984)
NAD-linked malate dehydrogenase	Synaptic versus nonsynaptic	Leong et al. (1984)
NADP-linked isocitrate dehydrogenase	Synaptic versus nonsynaptic	Leong et al. (1984)
Pyruvate dehydrogenase	Synaptic versus nonsynaptic	Lai and Clark (1976); Lai (1992); Leong et al. (1984)
Succinate dehydrogenase	Soma versus synaptosomes	Dienel et al. (1977)
Neuronal compartment		
Differences in Mitochondrial Structure		
References		
Axon	Long, slender mitochondria predominate with one or a small number of longitudinal cristae	Peters et al. (1976)
Axon terminal	Small, globular mitochondria with lamellar cristae are common	Peters et al. (1976); Perkins et al. (2001)
Dendrite	Small to large rounded mitochondria, Y-shaped or branched configurations not infrequent, elongated mitochondria in processes, mitochondria rare in spines, densely packed transverse cristae with both tubular and lamellar forms	Peters et al. (1976); Perkins et al. (2001)
Soma	small to large, rounded to elongated mitochondria with transverse cristae	Peters et al. (1976); Perkins et al. (2001)

mitochondria associated in clusters are found mostly in the soma. Both types of associations displayed Brownian (chaotic) movement. In addition, the mitochondrial chains revealed salutatory motion that could be disrupted by colchicine or nocodazole indicating transport along microtubules, in agreement with earlier findings that mitochondria often travel along microtubular highways. Movement was also arrested upon mitochondrial depolarization or blockade of mitochondrial ATP synthesis. The discovery that protein phosphorylation seems to control both mitochondrial transport and organization suggests a role for the cell's often-used signaling pathway in the close interaction of mitochondria and cytoskeletal elements. Might phosphorylation/dephosphorylation signaling regulate the positioning of mitochondria at energetic "hot spots"?

5.2 Mitochondria-Associated Adherens Complex

A unique composite structure with a prominent mitochondrion was discovered in large synaptic terminals in the calyx of Held, an auditory region of the brain (Spirou et al., 1998). The calyx of Held is characterized by fast glutamatergic neurotransmission with high rates and low temporal jitter. This composite assembly, called a mitochondria-associated adherens complex (MAC), consists of an adherens plaque attached by filamentous strands to a mitochondrion that is unusual in that the peripheral membranes are flattened facing the plaque (but not anywhere else), which is closer to the presynaptic membrane (▶ [Figure 4.2-3](#)); the plaque runs parallel to the presynaptic membrane. Other than the flattened face, the globular shape and smallish size of the MAC mitochondrion make its appearance similar to typical presynaptic mitochondria.

Although small in size, mitochondria that are part of a MAC have a high density of cristae membranes that are all lamellar (and this differs from typical mitochondria in the axon terminal that have both tubular and lamellar crista segments; Perkins et al., 2001a) and hence have a greater surface area. Another unusual feature is that the lamellae are always oriented perpendicular to the plaque (and hence perpendicular to the presynaptic membrane). Could this distinguishing orientation have a functional ramification? Other fibers connect the plaque to the synaptic membrane, and coated and uncoated vesicles are seen associated with these fibers, and are therefore called the vesicular chain. Another distinguishing feature is the consistent distance of 180 nm between the plaque and the presynaptic membrane. Could the fibers connecting the synaptic membrane to the plaque and the mitochondrion have a scaffolding role in addition to their apparent role in synaptic vesicle transport and organization? Synaptic vesicle endocytotic regions close to MACs were identified (Rowland et al., 2000). It was hypothesized that because large terminals of the lower auditory system exhibit high activity rates, the MAC may function to tether mitochondria to synapses that generate high rates of synaptic vesicle recycling.

5.3 Dendritic Mitochondria

Direct evidence in support of the hypothesis that the proper dendritic distribution of mitochondria is critical for normal physiology is now available. Li et al. (2004) showed that the movement of mitochondria into protrusions growing from the dendritic shaft of hippocampal neurons correlates with the development and the structural plasticity of spines. First, the role for this movement is speculated to be a response to the activity of ATP-driven pumps required for the large ionic load associated with the opening of neurotransmitter and voltage-gated channels. Second, mitochondria resident in protrusions may buffer the calcium integral to NMDA receptor activity and to voltage-gated calcium channels. Third, these mitochondria might be mobilized to fuel the local protein synthesis or degradation essential for synaptic plasticity (Steward and Schuman, 2003). Something similar might be involved with the local synthesis of nuclear-encoded mitochondrial proteins in nerve terminals (Kaplan et al., 2004). Fourth, the recruitment of mitochondria to spine necks might be a means to fuel glutamate receptor trafficking.

5.4 Axonal Mitochondria

In axons, slender mitochondria predominate except in the synaptic terminals, where small globular mitochondria are the norm (*Table 4.2-3*). An exception is the tenuous preterminal axons where extremely long and slender mitochondria are most often seen. In such terminals, some as long as 20 μm have been observed (Peters et al., 1976). Also, in intraventricular nerve endings, which appear to form synapse-like contacts with ependymal cells, there are large numbers of long and thin mitochondria that are unusual in that each has a single crista oriented parallel to the length of the mitochondrion (Leonhardt, 1976). This crista architecture is also observed with axonal mitochondria in the peripheral saphenous and spinal root nerves, although with some, more than one longitudinal crista is noted (🔗 *Figure 4.2-4*). The condensed configuration of these elongated mitochondria is unusual when compared with that in brain mitochondria. The condensation of the matrix differs from that seen typically in isolated mitochondria in that the inner-boundary membrane is not pulled away from the outer membrane (Cortese et al., 1992). Could this feature be due to homeostatic properties in tissues not present *in vitro*? The condensed and orthodox configurations reflect the energetic state of isolated mitochondria, with the rate of ATP production higher in the typical condensed state (Hackenbrock, 1968). Could it be that because of the length of the axonal shafts in saphenous and spinal roots, there are relatively fewer mitochondria to provide for the energetic demands and hence each mitochondrion is required to work harder to produce ATP and this aspect accounts for the unusual condensed mitochondrial configuration? In axonal shafts, mitochondria have to be translocated and distributed, often along considerable lengths. Scheffler (1999) describes both retrograde and anterograde movement of mitochondria in intact axons as well as in extruded axoplasm. A characteristic aspect of such movements is their salutatory property suggesting a motor-driven mechanism on

cytoskeletal elements. The work of Chada and Hollenbeck (2003) suggests that mitochondrial movement in axons is a complex process involving several motors that are presumably able to fine-tune mitochondrial distributions for purposes that require further study.

5.5 Mitochondrial Enzymes

Evidence is mounting that mitochondria with different enzyme complements exist within the four compartments of neurons—axon, dendrite, soma, and synapse. Results from several enzyme activity measurements strongly support the hypothesis that mitochondria in synaptic or nonsynaptic populations derived from either the same or another brain region are heterogeneous (Lai, 1992). Wong-Riley (1989) reviewed the evidence showing that the entire neuron is often metabolically heterogeneous, as supported by differential cytochrome oxidase activity. The neuronal soma can have low, moderate, or high levels of cytochrome oxidase activity, whereas its dendrites are almost always intensely active. Activity levels within axon shafts are often low, whereas levels in axon terminals may be low or high. Differences in cytochrome oxidase levels exist not only between the soma and its dendrites, but also between segments of the same dendritic arbor. This supports the underlying hypothesis of local control of oxidative capacity for use with active ion transport (repolarization) and other neuronal demands.

With respect to additional differences between mitochondrial enzymes of neuronal soma, dendrites, and axon terminals, Arai et al. (2002) discovered that there exist two kinds of mitochondria in serotonergic neuronal cell soma and dendrites. One contains monoamine oxidase type B, an outer membrane enzyme, and the other lacks this enzyme but instead has type A monoamine oxidase. However, mitochondria in serotonergic axon terminals do not possess monoamine oxidase type B. So, it was hypothesized that only mitochondria lacking monoamine oxidase type B are transported to axon terminals in serotonergic neurons. It cannot be ruled out, though, that mitochondria containing monoamine oxidase type B are transported along the axons, but that this enzyme undergoes a change, for example, conformational change, decomposition, or removal from the membranes, before it reaches the terminal. Cytochrome oxidase has the highest activity in the dendrites of spiny neurons (Difiglia et al., 1987). Many axon terminals were also highly reactive. In contrast, mitochondria in neuronal soma and primary dendrites exhibited relatively little activity of this electron transport protein. Diemel et al. (1977) found a difference in enzyme expression between soma and synaptosomes for six mitochondrial enzymes: glutamate dehydrogenase, succinate dehydrogenase, hexokinase, glutaminase, malate NADP dehydrogenase, and β -hydroxybutyrate dehydrogenase (🔗 [Table 4.2-3](#)).

Most of the enzyme differences have been documented between synaptosomal and nonsynaptosomal mitochondria because techniques have been available for a long time to separate these fractions (Lai and Clark, 1976). These differences are not surprising because in the same study, different protein compositions and densities in synaptic and nonsynaptic mitochondria were indicated by rate-zonal separation, with the nonsynaptic mitochondria having higher buoyant density. Could this mean less oxidative capacity in nonsynaptic mitochondria? Synaptic and nonsynaptic mitochondria from adult rat brain exhibit pronounced differences in the activity of a number of TCA cycle enzymes (Lai et al., 1977). Pyruvate dehydrogenase, citrate synthase, NAD-linked isocitrate dehydrogenase, NADP-linked isocitrate dehydrogenase, fumarase, NAD-linked malate dehydrogenase, D-3-hydroxybutyrate dehydrogenase, mitochondria-bound hexokinase, monoamine oxidase, glutamate dehydrogenase, and creatine kinase (Leong et al., 1984; Lai et al., 1994) are some of these enzymes displaying different activities in synaptic and nonsynaptic fractions (🔗 [Table 4.2-3](#)). The activities of aspartate aminotransferase and glutamate dehydrogenase in mitochondrial subfractions from cortical synaptic terminals showed different levels in the different synaptic fractions (McKenna et al., 2000b). This differential distribution suggests compartmentation of metabolism. Malic enzyme activity is higher in mitochondria from cortical synaptic terminals than in mitochondria from primary cultures of cortical neurons (McKenna et al., 2000a). The high activity of malic enzyme in synaptic mitochondria is consistent with a role for maintaining intramitochondria-reduced glutathione in terminals and for the functioning of this enzyme in the pyruvate recycling pathway, although the latter role is controversial. Glutamine uptake is significantly higher in synaptic mitochondria than in nonsynaptic

mitochondria, suggesting that it may be controlled by different isotypes that may be situated on distinct mitochondria in heterogeneous populations (Kvamme et al., 2000). Of the substrates studied, pyruvate and malate were oxidized most rapidly by both synaptic and nonsynaptic mitochondrial populations (Lai and Clark, 1976). However, the nonsynaptic mitochondria oxidized glutamate and malate almost twice as rapidly as did the synaptic mitochondria. NADH dehydrogenase is the only electron transport complex that has different activities in synaptic and nonsynaptic mitochondria (Davey et al., 1997). In mitochondria of synaptic origin, but not of nonsynaptic origin, a threshold of only 25% inhibition of NADH dehydrogenase severely impairs energy metabolism, resulting in reduced ATP synthesis (Davey et al., 1998).

In a show of consistency, when different research groups, sometimes spanning many years, examined the distributions and activities of the same mitochondrial enzyme in brain regions ([Table 4.2-1](#)) or between neurons and glia ([Table 4.2-2](#)) or even neuronal compartments ([Table 4.2-3](#)), few discrepancies surfaced. Among the many reports, only two discrepancies were found: when citrate synthase and glutamate dehydrogenase activities were measured in synaptic versus nonsynaptic mitochondrial fractions. With citrate synthase, Lai and Clark (1976) reported that activities were similar in both synaptic and nonsynaptic fractions, whereas Leong et al. (1984) reported that nonsynaptic mitochondria showed higher enzyme specific activity. With glutamate dehydrogenase, Lai and Clark (1976) reported that the activity in nonsynaptic mitochondria was lower than that in synaptic mitochondria, whereas Diemel et al. (1977) reported that the synaptic fraction contained very little glutamate dehydrogenase, with the concentration ratio between nonsynaptic and synaptic mitochondria being 7.5. In the first instance, the discrepancy might be explained by the use of selected brain regions (Leong et al., 1984) instead of whole brain homogenate (Lai and Clark, 1976). In the second instance, the discrepancy might be explained by a difference between activity (Lai and Clark, 1976) and concentration (Diemel et al., 1977) measurements.

5.6 Mitochondrial Compartmentation

The accumulated evidence of heterogeneity in neuronal mitochondrial size, shape, cristae packing, volume packing, position and translocation, local protein synthesis, buoyant density, and enzyme content provides strong support for the hypothesis of mitochondrial compartmentation. By using ^{13}C NMR spectroscopy on primary cultures of mouse cerebral cortical neurons, it was found that the appearance of ^{12}C incorporation in aspartate was not identical when $[\text{U-}^{13}\text{C}]\text{glutamate}$ and $[\text{U-}^{13}\text{C}]\text{glutamine}$ were used as substrates (Westergaard et al., 1995). Because glutamine must be converted to glutamate before it can enter the TCA cycle as 2-oxoglutarate, incorporation would have been expected to be identical. However, this was not observed and so supports the concept of compartmentation of mitochondrial glutamate metabolism. On the basis of this hypothesis and fueled by the proposal for the existence of multiple TCA cycles with different turnover rates, Waagepetersen et al. (2000) suggested that mitochondria associated with neurotransmitter synthesis are distinct from those aimed at energy production. These researchers also believe that mitochondrial compartmentation is further supported by the finding that the total percent labeling of fumarate and aspartate with ^{13}C , again detected by NMR spectroscopy, differs significantly from each other.

6 Mitochondria in the Aging Brain

With aging, there is a progressive decline in an organism's ability to respond to stresses applied by the environment. Cognition and ambulatory capability decline with age. The mechanism that causes losses in the efficiency of normal cellular functions during aging has not been completely elucidated. It is hypothesized, though, that the functional decline in the aged brain is related to a decrease in mitochondrial viability. A decline in mitochondrial viability might be caused by (1) structural abnormalities that increase with age, (2) uncorrected mtDNA mutations and deletions, (3) oxidative damage to mitochondrial proteins and lipids, or (4) changes in the concentrations or activities of mitochondrial enzymes. What might be the

manifestations of these causative factors? In old rats, compared with young rats, the following functional markers are lower: mitochondrial membrane potential, cardiolipin level, respiratory control ratio, and cellular oxygen uptake; whereas the following decay markers are higher: oxidants produced per oxygen consumed, neuronal RNA oxidation, and levels of mutagenic aldehydes from lipid peroxidation (Ames, 2004).

6.1 Mitochondrial Structural Damage

With respect to structural damage in aged mitochondria, Frolkis et al. (1984) found destructive changes like destruction of mitochondrial cristae, formation of autophagosomes, and residual bodies in old molluscan neurons (22–24 months). In addition, they observed the appearance of an adaptive mechanism—hypertrophy of mitochondria—that might counteract the loss of viable mitochondria. However, with human aging, this hypertrophy might instead be defective mitochondrial turnover that results in the accumulation of defective mitochondrial constituents (Lee and Wei, 1997). When examining the mitochondria of neuronal perikarya in the spinal ganglia of 12-, 42-, and 79-month-old rabbits, it was found that the mean percentage of perikaryal volume occupied by mitochondria decreased with age (Ledda et al., 2001). The mitochondrial structure did not change. However, mitochondrial size increased with age, indicating that there were fewer mitochondria in the aged perikarya. These observations are consistent with the finding of a 10% decrease in the fractional volume of mitochondria in aged rat brains (24–28 months) (Vidal et al., 2004). An increase in the size of mitochondria with age (28 months) was also observed in the endothelial cells of the dorsal lateral geniculate nucleus in rats (Alba et al., 2004) and may have implications for blood and brain cell regulation, perhaps contributing to the development of degenerative alterations in aging neurons. Could it be that the rate of mitochondrial fission has been reduced, or alternatively, the rate of fusion increased? In a comparison study, in the satellite cell sheaths that envelope the spinal ganglion neurons, in parallel with the observation in neurons, the mean percentage of cytoplasmic volume occupied by mitochondria decreased with age. This decrease was principally due to a reduction in mitochondrial mass. As with neurons, mitochondrial structure did not change, whereas mitochondrial size increased with age in satellite cells. The comparison also found that: (1) the mean percentage of cytoplasmic volume occupied by mitochondria was greater in neuronal perikarya than in satellite cell sheaths and the ratio between these two percentages remained constant with advancing age, (2) mitochondrial mass was greater in neuronal perikarya than in the sheaths of satellite cells; the ratio between these two values increased with advancing age, and (3) the increase in mitochondrial size with age was similar in neuronal perikarya and satellite sheaths. Taken altogether, these results indicate that in addition to the documented increase in size, even though the number of mitochondria in both neurons and satellite cell sheaths were decreased, there was a more pronounced mitochondrial mass loss in the sheaths. This suggests that the decreased ability of sensory neurons in old animals to meet high-energy demands may be partly due to the even greater impairment of their associated satellite cell sheaths. After examining the quantitative activity of cytochrome oxidase in synaptic mitochondria of the cerebellum of 24- to 26-month-old rats, Bertoni-Freddari et al. (2004b, 2005) provided evidence for a decline in metabolic competence and for a number of small- and medium-sized (but not large-sized) mitochondria. In contrast, in hippocampal dentate gyrus, it was found that the number of synaptic mitochondria, their volume fraction, and their metabolic competence did not change significantly with aging (Bertoni-Freddari et al., 2004a). Obviously, other brain regions need to be examined and a more detailed analysis of the mitochondrial inner membrane needs to be performed, perhaps using a 3D structural approach, before anything definitive can be stated with regard to the finer structural alterations to mitochondria during aging.

6.2 Decline in Mitochondrial Function

Essentially, any dysfunction of mitochondria may pose a threat for cellular health and this is especially true for postmitotic brain cells (Bertoni-Freddari et al., 2004c). Evidence for the age-related decline in brain

mitochondrial function at the bioenergetic, enzymatic, and even genetic levels is reviewed by Toescu et al. (2000). As opposed to pathological cell demise, e.g., Alzheimer's disease, normal aging is not accompanied by significant neuronal loss. With respect to diminished functioning of mitochondria in aged brain, autoradiography of young and senescent (30-month-old) rat brain sections showed a reduction of oxygen consumption with aging in the cerebrum, with the senescent consumption being only 77.4% of that of the young animal (Sasaki et al., 1999). In a follow-up study, evidence for diminished electron transport and glutathione concentration in the senescent rat was presented (Sasaki et al., 2001). During long-term (>3 weeks) culture of primary cerebellar granule neurons, there was a gradual and time-dependent depolarization of mitochondria (Xiong et al., 2004). There was also a significantly longer repolarization period in older neurons. In these older neurons (DIV 22), the threshold calcium level required for the initiation of mitochondrial depolarization was increased by 50% compared with young (DIV 10) neurons. Stimulation via KCl-evoked depolarization induced a mitochondrial depolarization caused by entry of cytosolic calcium into mitochondria. In young cultures, the mitochondrial membrane potential had a larger amplitude change and a lower threshold for initiation, and recovered fully much more quickly than did old cultures. Thus, neuronal aging manifests a mitochondrial response both in resting conditions and during stimulation. This response might be due to changes in the homeostasis of calcium that occur during brain aging (reviewed in Toescu and Verkhratsky, 2003). In particular, there appears to be a decrease of calcium homeostatic reserve so that the capacity to respond effectively to stressors is reduced. However, this perturbation of calcium homeostasis usually does not reach the trigger required to induce neuronal death. With advancing age (18- to 27-month-old rats), the decline in mitochondrial ATP synthesis promotes GABA synthesis, which then blocks the calcium-dependent exocytotic release of all transmitter modulators (Marczynski, 1998). This leads to dystrophy of chronically depolarized axon terminals and blocks the retrograde transport of target-produced trophins, causing "starvation" and death of neurons. In the forebrain, there is observed dystrophic axonal varicosities, loss of transmitter vesicles, and swollen mitochondria.

6.3 mtDNA

The accumulation of mutations, and in particular large deletions in mitochondrial DNA (mtDNA), has been gaining increasing attention because of their potential role in normal aging via increased impairment of mitochondrial functioning (Chomyn and Attardi, 2003). Briefly, deletions of mtDNA have been shown to accumulate with age in a variety of species (mice and humans in particular; human samples divided into >50 years and <50 years populations) regardless of mean or maximal life span (Melov et al., 1999). Further, small sequence rearrangements, which have been observed in unicircular dimers of mouse and human mtDNA, occur also in monomeric mtDNA from normal tissues and accumulate with aging (28- to 29-month-old mice) (Piko et al., 1988). For more details, refer to Chapters in this volume by Gibson & Joseph, and Scarpulla.

6.4 Mitochondrial Enzymes

We can now start to frame the picture of how mitochondrial enzymes, nucleic acids, and membranes are affected by aging with the few studies that have been published; however, more studies need to be performed to get a clearer picture. The hypothesis that has received the most attention is that with age, increased oxidative damage to proteins, nucleic acids, and lipids, particularly in mitochondria, causes a deformation of enzyme and nucleic acid structures and decreased membrane fluidity, with a consequent decrease of enzyme activity, substrate binding affinity, transcription and translation, and membrane integrity. Heavy synaptic mitochondria, thought to be the oldest population, possess the highest levels of hydroperoxides (Battino et al., 2000). The fatty acid modifications displayed by these mitochondria altered their protein/lipid ratio. The mitochondrial inner-membrane lipid, cardiolipin, is involved in the optimal activity of certain inner-membrane proteins like NADH dehydrogenase, cytochrome *bc1*, ATP synthase,

cytochrome oxidase, adenine nucleotide translocase, and the phosphate carrier (Hoch, 1992). Brain mitochondria contain lower amounts of cardiolipin compared with liver or heart. Another feature of cardiolipin is that, again compared with heart and liver, the brain isotype has lower amounts of saturated fatty acyls and a higher content of polyunsaturated fatty acyls. Because of this higher concentration of polyunsaturated fatty acyls, these cardiolipins are more susceptible to oxidation by free radicals (Toescu et al., 2000). Alterations in the protein–lipid interaction is hypothesized to affect the performance of the mitochondrial phosphate carrier during aging (28-month-old rats), because its maximal velocity was significantly decreased even though its affinity remained about the same upon aging (Paradies and Ruggiero, 1991). This study was conducted with liver mitochondria. How might the performance of the phosphate carrier be affected by aging in the brain with its different inner-membrane lipid composition? It is hypothesized that another mitochondrial transporter, the glutamate/OH-antiporter, experiences an age-dependent reduction in function because of age-related changes in lipid composition (Toescu et al., 2000). This is because in aging brain mitochondria, there is a sharp reduction of glutamate uptake resulting in a decrease in the utilization of glutamate/malate, but not succinate.

Mitochondrial enzyme activities behave as markers of brain aging. The activity of NADH dehydrogenase and its rotenone sensitivity showed a decrease in nonsynaptic mitochondria from the cortex of old rats (Lenaz et al., 1998). There was also a 5-kb mtDNA deletion found only in the old animals. The specific activity of cytochrome oxidase is significantly lower in heavy synaptic mitochondria than in the light ones at all the ages examined (4, 8, 12, 16, 20, and 24 months) (Gorini et al., 1989). The activity of this enzyme in light mitochondria from hippocampus and striatum increased during aging, but remained unchanged in this fraction from the cerebral cortex. Could the half-life of mitochondria be different in these different brain regions? The activity of cytochrome oxidase has been followed in brain homogenates from birth to death and was found to be low at birth, to peak during the period of most rapid growth and maturation of the brain (adolescence), and to decline significantly by old age (Wong-Riley, 1989). The decrease in activity of cytochrome oxidase, NADH dehydrogenase, and mitochondrial nitric oxide synthase was directly related to the appearance of reactive oxygen species and to the loss of neurological function in aged mice (Navarro, 2004). Could these enzymes be used as indicators of the effectiveness of antiaging treatments?

6.5 Antioxidants

Can antioxidants slow the decline in mitochondrial functioning during aging? The abundance of the antioxidant, vitamin E, increases with age in nonsynaptic and light synaptic mitochondria, but remains constant in heavy synaptic mitochondria (Battino et al., 2001). Does this mean that the longest-lived mitochondria are not as protected against oxidative damage? Ingestion of the mitochondrial metabolites acetylcarnitine and lipoic acid and the mitochondrial antioxidants α -phenyl-*N*-*t*-butyl nitron and *N*-*t*-butyl hydroxylamine partially restores mitochondrial structure and function and improves the age-associated decline of ambulatory activity and memory (Liu et al., 2002). Treatment of senescent rats (28 months) with acetylcarnitine restored the activity of adenine nucleotide translocase and cytochrome oxidase to the level seen in young rats (Paradies et al., 1994). It was hypothesized that the salubrious effect of this compound was through the action on mitochondrial cardiolipin synthase. This study was performed in rat hearts. Might acetylcarnitine treatment have the same effect in the brain? In the aged brain (>24 months), glutamate dehydrogenase activity was found to be significantly lower in the medulla oblongata and pons regions but not in other regions, when compared with the activity in 90-day-old adults (Leong and Clark, 1984) suggesting that changes in mitochondrial functioning with age are brain region dependent.

6.6 Delaying Mitochondrial Decline

Ames (2004) reviews the recent progress made in delaying mitochondrial decline during aging. Most of the progress involves reversing deficiencies in micronutrients. In particular, deficiencies in the diet of the

micronutrients iron, zinc, biotin, vitamin B6, pantothenate, and copper can accelerate neurodegeneration through a decline in mitochondrial function. Using neuroblastomas, astrocytomas, and rat primary hippocampal neurons, it was found that heme deficiency decreases cytochrome oxidase activity, activates nitric oxide synthase (nitric oxide is involved in apoptosis and implicated with neuronal cell death; Bossy-Wetzel et al., 2004.), alters the performance of amyloid precursor protein, disrupts iron and zinc homeostasis, and produces metabolic consequences similar to those seen in dysfunctional neurons in patients with Alzheimer's disease (Ames, 2004).

Toescu et al. (2000) speculate that mitochondrial heterogeneity in aging brain cells suggests the existence of mechanisms by which these cells can compensate for the loss of functional mitochondria. An obvious mechanism would be to increase the workload of the remaining viable mitochondria; this hypothesis is testable in one aspect— measurement of the inner-membrane potential. Another mechanism would be to increase the mtDNA copy number in aging tissue; again, this is testable. A third mechanism, most likely in conjunction with the last, would be to increase the expression of nuclear-encoded mitochondrial proteins. A feedback mechanism would be possible with all three scenarios that would allow the cell to monitor overall mitochondrial function and restore mitochondrial function at the cellular level, designed to overcome a localized drop in mitochondrial viability. These compensatory mechanisms, though, while masking localized deficiencies in mitochondrial function, would increase the cell's energy expenditure. In the long term, would this increased energy expenditure overtax the cell and contribute to a decline leading to senescence? In summary, when metabolic events in the brain are studied in the aging process, the heterogeneity of its mitochondria must be considered.

7 Mitochondria in the Developing Brain

Mitochondria appear to play just as important a role in brain development as they play in brain aging. Yet, few studies have been conducted with the former in mind. Perhaps this is due to the sentiment that therapeutics might and should be developed to reduce the deterioration caused by aging, whereas brain development is best not tampered with and should be left to proceed by its own volition.

7.1 Mitochondrial Proliferation

The onset of aerobic metabolism within maturing regions of a newborn's developing brain increases the proliferation of mitochondria (Harold, 1986). Higher levels of energy are then available for the increasing demands of biosynthesis, apoptosis, and the transport of materials to their final destination. With this aerobic onset, neurons increase their synaptic connectivity and new adaptive brain structures are organized (Schore, 1997). As neurons mature, they have greater energy-consuming demands than do immature neurons. Part of the energy consumption is by mitochondria themselves for fueling their rapid growth and the replication of their genome and for a concomitant elevation of environmentally regulated mitochondrial protein synthesis, including an increase in cytochrome oxidase levels (Pysh, 1970; Mjaatvedt and Wong-Riley, 1988). The result is an augmentation of brain energy metabolism.

In postnatal development, mitochondria proliferate in both presynaptic and postsynaptic processes. Infant animals exposed to social experiences have greater numbers of mitochondria in the dendritic volumes of developing cortical areas (Sirevaag and Greenough, 1987). The transient increase in the fission and growth of new mitochondria peaks as dendrites experience their greatest growth in response to synaptogenesis (Mjaatvedt and Wong-Riley, 1988). During these same time periods, catecholamines cause dynamic changes in the shape and branching patterns of dendrites and induce the growth of dendritic spines by initiating the maturation of energy generation in mitochondria (Schore, 1997). These spines modulate rapid changes in the brain throughout the course of its development by acting as potential sites of synaptic contact. As such, they have the greatest energy requirements in the brain. Wong-Riley (1979) found that excitatory sensory input, including visual input, is required for increasing cytochrome oxidase activity in spines of growing dendrites of the developing cortex. Again using cytochrome oxidase as a marker for oxidative metabolism,

Purves and LaMantia (1990) showed that cytochrome oxidase-rich zones in the cortex increase in number during development. It is no surprise, then, that the proliferation of mitochondria is as high as it is in the dendritic shafts where spines are forming. During fetal and perinatal development, the glycogen content of axonal terminals is much greater than is seen in adults (Vaughn and Grieshaber, 1972; Peters et al., 1976). Upon the progressive addition of aerobic pathways to anaerobic ones postnatally, glycogen content diminishes and mitochondria occupy a proportionally greater volume of terminals.

7.2 Apoptosis

The apoptotic pathway needed for the construction, maintenance, and repair of the developing brain goes through mitochondria. Embryogenic apoptosis uses mitochondrial components, including cytochrome *c*, to combine with Apaf1 in the apoptosome (Ceconi and Gruss, 2001). These researchers found that Apaf1 is the death regulator of the neuronal founder cells. Greater detail of apoptosis in the brain can be found in Chapters by Wieloch, Elmer & Hansson, and Solenski & Fiskum in this volume.

7.3 Mitochondrial Enzymes

The patterns of activities of mitochondrial enzymes differ during brain development. Dienel et al. (1977) found that brains of young rats had concentrations of the mitochondrial enzymes, glutamate dehydrogenase, succinate dehydrogenase, glutaminase, hexokinase, malate NADP dehydrogenase, and β -hydroxybutyrate dehydrogenase, that were different to the concentrations in the adult rat brain, with the first three showing the greatest concentration changes. These results extend mitochondrial enzyme heterogeneity to the immature brain (previously heterogeneity was noted only in the adult brain), in agreement with a study of mitochondrial enzyme activities in rat hippocampus during development (Villa et al., 1989). In the hippocampus, a developmental stage-dependent expression of mitochondrial creatine kinase was noted (Kaldis et al., 1996). In a study on development, it was suggested that the distribution and activity of glutamate dehydrogenase in astrocytes activates amino acid neurotransmitters in the neurons of the hippocampus (Kugler, 1993). As previously noted, the activity of cytochrome oxidase recorded in brain mitochondrial fractions is low at birth and peaks during the period of most rapid growth and maturation of the developing brain (Wong-Riley, 1989). This researcher postulates that the level of cytochrome oxidase activity within brain cells should correlate positively with their functional level of activity. Support for this postulate comes from observations of a parallel increase in mitochondrial numerical density, percentage mitochondrial volume fraction, and cristae volume fraction from birth to adulthood. Interestingly, these structural changes in mitochondria correlate better with synaptogenesis than with nerve growth and myelination. Finally, the neonatal brain is the principal site of ketone body utilization, as an oxidative fuel for mitochondria to spare glucose overconsumption (Williamson, 1985). Once oxidative metabolism is at full capacity in the adult brain, ketone body use is diminished. At the onset of oxidative metabolism, however, oligodendrocytes may be vulnerable to oxidative stress because of their active acquisition of iron for differentiation, at a time of relative delay in the development of certain key antioxidant defenses in the brain (Buonocore et al., 2001).

During development of the rat cortex, the activities of succinate reductase and NADH reductase were low at 0–5 days of age, increased until 15 days, and decreased significantly in adult mitochondria (Sato et al., 2000). These functional measurements were correlated with morphological measurements showing that the mitochondrial cross-sectional area per cell increased gradually until 21 days, but decreased significantly in the adult. Likewise, the number of mitochondria per cell was low at 0–5 days, but much higher between 10 and 21 days. It was proposed that these results indicate that the rate of mitochondrial division is maximal between 5 and 10 days postnatal. Small and underdeveloped mitochondria were observed at day 0, with mitochondrial growth and cristae proliferation accelerating from day 5 to day 21. This study supports the hypothesis that increased activities of mitochondrial respiratory enzymes parallel the structural maturation of mitochondria.

8 Summations, Challenging Problems, and Future Avenues

8.1 Biological Avenues

It appears that a governing principle in the mammalian brain is that neuronal activity controls energy expenditure, and not vice versa. The differences in energy expenditure between neurons and glia are starting to be teased out based on mitochondrial shape, size, inner-membrane abundance, position, aggregation, membrane potential, and enzyme complement. However, more work needs to be done, especially with neuroglia, in order to better understand the dynamics of the energy signature of each cell type, in particular the flux of ions and other signaling molecules. Quantitative studies of mitochondrial motility in neuroglia, similar to the many already published for neurons, still need to be performed in relation to energy signature and growth dynamics. Those studies published with neurons investigated *in vitro* systems or cultured cells; yet, the results might differ in significant but unknown ways in nervous tissue, especially due to interactions of neurons with their surrounding neuroglia and extracellular matrix. One burgeoning area of interest is how cell–cell signaling and intracellular signaling might regulate the positioning of mitochondria at energetic “hot spots.” Protein kinases may be one signaling pathway (Perkins et al., 2001b; Chada and Hollenbeck, 2004). Further avenues to investigate other signaling pathways targeted to mitochondria now exist.

Sorting out local control of oxidative capacity is a challenging problem that may require new tools. The proper distribution of mitochondria is critical for normal physiology in dendrites (Li et al., 2004). While this concept is assumed to hold for other regions of the neuron, and by extension neuroglia, direct evidence is yet to be produced. The exciting underlying hypothesis of this concept is the local control of oxidative capacity. For a neuron, this means that the axon terminal controls the number, aggregation, and activity of its mitochondria, including recruiting additional organelles as needed. The same would hold true for dendrites, somata, and axonal shafts, including the node of Ranvier that might have a different oxidative signature than the myelinated axoplasm between each node. The oxidative signature would reflect the level of such activities as active ion transport, repolarization, and in general wherever there is exchange of ATP currency. In support of the hypothesis of local control of mitochondrial capacity is the documentation that the brain has greater variety of mitochondrial structures than any other organ. However, structural considerations only give a hint that local control might be true. The proof must come from functional assays, including probing microdomains.

Compartmentation of mitochondrial function is an avenue for future discovery. A current avenue that has lead to unexpected destinations is the working model for compartmentation of the TCA cycle that seems to adequately explain heterogeneity in amino acid metabolism (see the many papers on this subject by Sonnewald, Schousboe, and coworkers). It is known that the mitochondrial outer and inner membranes display important differences in structure, protein and lipid compositions, and function (Scheffler, 1999). We are starting to gain insight into how the enzyme and lipid compositions differ in brain regions, in neurons and neuroglia, and within neurons. However, the distribution and compartmentation of only a relatively few mitochondrial proteins have been reported, and are documented in [▶ Tables 4.2-1](#), [▶ 4.2-2](#), and [▶ 4.2-3](#). Just as mapping the entire gene and protein complements of a given organism is the goal of genomics and proteomics, respectively, the goal of mitochondriomics should be to map all of the components of this organelle. The currently reviewed heterogeneity in brain mitochondria is likely just the tip of the iceberg. It is anticipated that a component map of mitochondria from different brain regions and between neurons and glia would uncover additional heterogeneity that might aid research into energy-driven functional boundaries, e.g., rate of ion transport, including performance boundaries in certain neurodiseases and aging.

A substantial amount of 3D information has been accumulated on neuronal mitochondria using the high-resolution approach of electron tomography (Perkins et al., 1997, 2001a; Frey et al., 2002; Renken et al., 2002). However, no tomographic work has been done on astrocytic or oligodendrocytic mitochondria. This begs the question: do the same architectural principles, found with 3D methods, hold with mitochondria in neuroglia? Related unanswered questions of general import are: how are crista junctions formed and maintained and why do cultured cells form mitochondrial networks, but are much less prevalent in neuronal tissues?

A few of the purposeful avenues that researchers are taking to investigate mitochondria in aging have been mapped out. With only a few examples to date, it seems that mitochondrial enzyme activities can behave as markers of brain aging. Because of the growing belief that the functional decline in the aging brain is related to a decrease in mitochondrial viability, mapping additional mitochondrial aging markers would be an avenue worth following. Already, researchers are marching down the avenues of antioxidants and micronutrients, especially as they relate to delaying mitochondrial functional decline (Ames, 2004). However, much more mechanistic work needs to be done in order to grasp how these might keep mitochondria viable for longer periods, or increase turnover of the damaged organelles.

8.2 Technological Avenues

There seems to be a steady advance in technology that can be productively applied to issues related to brain mitochondria. This section describes those technological avenues that have to do with advances in light and electron microscopy and the novel labeling techniques being developed for them. Just as the new technology of electron tomography revealed structural aspects of brain mitochondria long hidden, advancements in microscopy have the potential to address current challenging problems in brain mitochondria research.

A novel approach for labeling recombinant proteins uses biarsenical fluorophores. This method relies on the high-affinity covalent bonding of paired arsenic atoms for a unique tetracysteine domain that is genetically engineered into the target protein of interest (Gaietta et al., 2002). This approach is a landmark in that it represents the first successful solution to the problem of specifically attaching small synthetic organic molecules to a short peptide motif of natural, genetically encodable amino acids within recombinant proteins in living cells. The fluorescent biarsenical ligands exhibit diverse spectral characteristics, including the capability of photooxidizing diaminobenzidine for correlated light and electron microscopy. A further aspect is the combination of green fluorescent protein (GFP) and biarsenical fluorophores for enhanced signaling and detection of low-abundance targets. One projected use for tetracysteine technology is to follow the targeting and insertion of nuclear-encoded proteins into the mitochondrial inner membrane and to find if they disperse to the cristae membranes or remain in the inner-boundary membrane. One could follow the assembly of electron transport complexes, such as complex I, which must be assembled from many subunits (Yadava et al., 2004) and perform the pulse-chase experiments pioneered by Gaietta et al. (2002). One could also probe for the occurrence of microdomains of enrichment of specific proteins that would answer questions of mitochondrial compartmentation.

Another novel labeling approach uses fluorescent nanocrystal quantum dots (QDs). Hoshino et al. (2004) showed that QDs conjugated with a mitochondrial signal peptide are transported to the mitochondria in live cells. What makes QDs powerful is that they can be easily seen with the electron microscope. This aspect makes it possible to correlate live-cell imaging using confocal and two-photon microscopy with high-resolution 3D imaging using electron tomography. QDs, then, provide an avenue to reveal the transduction of proteins through the cytoplasm, across the outer- (and inner-) mitochondrial membrane and into specific submitochondrial compartments as a tool for investigating import, assembly, and compartmentation *in vivo* and *in situ*.

There are new imaging modalities that could be brought to bear on research questions pertaining to brain mitochondria. Fluorescence photooxidation utilizing fluorescent resonance energy transfer (FRET) can probe the distance-dependent interaction between two molecules (Zhang et al., 2002). FRET could be used to investigate the coupling of the five complexes in the electron transport chain, for example, and for determining signaling pathways targeted to mitochondria. Chromophore assisted light inactivation (CALI) is a powerful technique that allows for highly selective, temporal, and localized acute inactivation of target proteins in living cells in order to assess specific protein function (Rajfur et al., 2002). It may be that CALI can be combined with tetracysteine–biarsenical labeling for correlated light and electron microscopy. High-speed multiphoton microscopes are now being used to monitor physiological events down to the organellar levels of resolution ($\sim 0.5\mu\text{m}$) and to image living systems at video rates or faster (>30 frames/s) (Helmchen

and Denk, 2002). It would be possible to record 3D volumes quickly and follow the mitochondrially labeled proteins in 3D over long periods of time (4D) (Bestvater et al., 2002).

New avenues available in electron tomography will contribute to an accurate, high-resolution, three-dimensional understanding of components in mitochondria. With energy filtering, high-resolution images of thick samples can be produced. This would be the best way to investigate mitochondrial networks at high spatial resolution. In addition, with electron energy loss spectroscopy (EELS), this microscopy can image and differentiate metals at high resolution (Leapman, 2003). By applying this technique to mitochondria, one can produce a 3D map of proteins containing metallic chromophores (usually iron), such as are found in the electron transport chain complexes. Three-dimensional supramolecular imaging is now becoming available with electron tomography. One approach would be to use template matching pioneered by Baumeister's group (Baumeister, 2004) to find the 3D distribution of mitochondrial proteins in situ that are large enough to be resolved with this technique (about 3-nm resolution). Another approach would be to photoconvert tetracysteine constructs in the presence of diaminobenzidine (DAB) to produce a DAB polymer that is osmiophilic, yielding a highly localized deposition of osmium that is fixable by electron microscopy. This presents the possibility of localizing specific mitochondrial proteins in 3D maps generated by electron tomography.

Acknowledgments

Samples for figures were provided by Don Fox, Ella Bossy-Wetzel, and George Spirou. Andrew White and Joshua Brown helped with tomography. Arrowsmith was used for literature searches. This work was supported by NIH grants P41RR04050 and R01 NS14718.

References

- Ahmed MM, Kanagasuntheram R. 1976. Mitochondrial variations in the spinal ganglion cells of the slow loris: An electron microscopic study. *J Anat* 121: 223-230.
- Alba C, Vidal L, Diaz F, Villena A, de Vargas IP. 2004. Ultrastructural and quantitative age-related changes in capillaries of the dorsal lateral geniculate nucleus. *Brain Res Bull* 64: 145-153.
- Alnaes E, Rahamimoff R. 1975. On the role of mitochondria in transmitter release from motor nerve terminals. *J Physiol* 248: 285-306.
- Ames BN. 2004. Delaying the mitochondrial decay of aging. *Ann N Y Acad Sci* 1019: 406-411.
- Aoki C, Kaneko T, Starr A, Pickel VM. 1991. Identification of mitochondrial and non-mitochondrial glutaminase within select neurons and glia of rat forebrain by electron microscopic immunocytochemistry. *J Neurosci Res* 28: 531-548.
- Aoki C, Milner TA, Berger SB, Sheu KF, Blass JP, et al. 1987a. Glial glutamate dehydrogenase: Ultrastructural localization and regional distribution in relation to the mitochondrial enzyme, cytochrome oxidase. *J Neurosci Res* 18: 305-318.
- Aoki C, Milner TA, Sheu KF, Blass JP, Pickel VM. 1987b. Regional distribution of astrocytes with intense immunoreactivity for glutamate dehydrogenase in rat brain: Implications for neuron-glia interactions in glutamate transmission. *J Neurosci* 7: 2214-2231.
- Arai R, Karasawa N, Kurokawa K, Kanai H, Horiike K, et al. 2002. Differential subcellular location of mitochondria in rat serotonergic neurons depends on the presence and the absence of monoamine oxidase type B. *Neuroscience* 114: 825-835.
- Barsoum MJ, Yuan H, Lee WD, Liot G, Kushnareva Y, et al. 2005. Mitochondrial fission is a unifying early event in neurodegeneration. *Science*.
- Battino M, Bertoli E, Formiggini G, Sassi S, Gorini A, et al. 1991. Structural and functional aspects of the respiratory chain of synaptic and nonsynaptic mitochondria derived from selected brain regions. *J Bioenerg Biomembr* 23: 345-363.
- Battino M, Bompadre S, Leone L, Villa RF, Gorini A. 2001. Coenzymes Q9 and Q10, vitamin E and peroxidation in rat synaptic and non-synaptic occipital cerebral cortex mitochondria during ageing. *Biol Chem* 382: 925-931.
- Battino M, Quiles JL, Huertas JR, Mataix JF, Villa RF, et al. 2000. Cerebral cortex synaptic heavy mitochondria may represent the oldest synaptic mitochondrial population: Biochemical heterogeneity and effects of L-acetylcarnitine. *J Bioenerg Biomembr* 32: 163-173.

- Bauer MF, Neupert W. 2001. Import of proteins into mitochondria: A novel pathomechanism for progressive neurodegeneration. *J Inher Metab Dis* 24: 166-180.
- Baumeister W. 2004. Mapping molecular landscapes inside cells. *Biol Chem* 385: 865-872.
- Bernardi P. 1999. Mitochondrial transport of cations: Channels, exchangers, and permeability transition. *Physiol Rev* 79: 1127-1155.
- Bertoni-Freddari C, Fattoretti P, Giorgetti B, Solazzi M, Baliotti M, et al. 2004a. Cytochrome oxidase activity in hippocampal synaptic mitochondria during aging: A quantitative cytochemical investigation. *Ann N Y Acad Sci* 1019: 33-36.
- Bertoni-Freddari C, Fattoretti P, Giorgetti B, Solazzi M, Baliotti M, et al. 2004b. Decay of mitochondrial metabolic competence in the aging cerebellum. *Ann N Y Acad Sci* 1019: 29-32.
- Bertoni-Freddari C, Fattoretti P, Giorgetti B, Solazzi M, Baliotti M, et al. 2004c. Role of mitochondrial deterioration in physiological and pathological brain aging. *Gerontology* 50: 187-192.
- Bertoni-Freddari C, Fattoretti P, Giorgetti B, Spazzafumo, L, Solazzi, M, et al. 2005. Age-related decline in metabolic competence of small and medium-sized synaptic mitochondria. *Naturwissenschaften* 92: 82-85.
- Bestvater F, Spiess E, Stobrawa G, Hacker M, Feurer T, et al. 2002. Two-photon fluorescence absorption and emission spectra of dyes relevant for cell imaging. *J Microsc* 208: 108-115.
- Blokhuys GG, Veldstra H. 1970. Heterogeneity of mitochondria in rat brain. *FEBS Lett* 11: 197-199.
- Bossy-Wetzel E, Barsoum MJ, Godzik A, Schwarzenbacher R, Lipton SA. 2003. Mitochondrial fission in apoptosis, neurodegeneration and aging. *Curr Opin Cell Biol* 15: 706-716.
- Bossy-Wetzel E, Talantova MV, Lee WD, Scholzke MN, Harrop A, et al. 2004. Crosstalk between nitric oxide and zinc pathways to neuronal cell death involving mitochondrial dysfunction and p38-activated K⁺ channels. *Neuron* 41: 351-365.
- Bukato G, Kochan Z, Swierczynski J. 1994. Subregional and intracellular distribution of NADP-linked malic enzyme in human brain. *Biochem Med Metab Biol* 51: 43-50.
- Buonocore G, Perrone S, Bracci R. 2001. Free radicals and brain damage in the newborn. *Biol Neonate* 79: 180-186.
- Cecconi F, Gruss P. 2001. Apaf1 in developmental apoptosis and cancer: How many ways to die? *Cell Mol Life Sci* 58: 1688-1697.
- Chacinska A, Rehling P, Guiard B, Frazier AE, Schulze-Specking A, et al. 2003. Mitochondrial translocation contact sites: Separation of dynamic and stabilizing elements in formation of a TOM-TIM-preprotein supercomplex. *EMBO J* 22: 5370-5381.
- Chada SR, Hollenbeck PJ. 2003. Mitochondrial movement and positioning in axons: The role of growth factor signaling. *J Exp Biol* 206: 1985-1992.
- Chada SR, Hollenbeck PJ. 2004. Nerve growth factor signaling regulates motility and docking of axonal mitochondria. *Curr Biol* 14: 1272-1276.
- Chen JJ, Bertrand H, Yu BP. 1995. Inhibition of adenine nucleotide translocator by lipid peroxidation products. *Free Radic Biol Med* 19: 583-590.
- Chomyn A, Attardi G. 2003. MtDNA mutations in aging and apoptosis. *Biochem Biophys Res Commun* 304: 519-529.
- Clark D, Sokoloff L. 1999. Circulation and energy metabolism in brain. *Basic neurochemistry*. Siegel GJ, Agranoff BW, Albers RW, Fisher SK, Uhler MD, editors. New York: Raven Press; pp. 645-681.
- Cortese JD, Vogliano AL, Hackenbrock CR. 1992. The ionic strength of the intermembrane space of intact mitochondria is not affected by the pH or volume of the intermembrane space. *Biochim Biophys Acta* 1100: 189-197.
- Crompton M, Barksby E, Johnson N, Capano M. 2002. Mitochondrial intermembrane junctional complexes and their involvement in cell death. *Biochimie* 84: 143-152.
- Davey GP, Canevari L, Clark JB. 1997. Threshold effects in synaptosomal and nonsynaptic mitochondria from hippocampal CA1 and paramedian neocortex brain regions. *J Neurochem* 69: 2564-2570.
- Davey GP, Peuchen S, Clark JB. 1998. Energy thresholds in brain mitochondria. Potential involvement in neurodegeneration. *J Biol Chem* 273: 12753-12757.
- Dienel G, Ryder E, Greengard O. 1977. Distribution of mitochondrial enzymes between the perikaryal and synaptic fractions of immature and adult rat brain. *Biochim Biophys Acta* 496: 484-494.
- Difiglia M, Graveland GA, Schiff L. 1987. Cytochrome oxidase activity in the rat caudate nucleus: Light and electron microscopic observations. *J Comp Neurol* 255: 137-145.
- Doran E, Halestrap AP. 2000. Cytochrome *c* release from isolated rat liver mitochondria can occur independently of outer-membrane rupture: Possible role of contact sites. *Biochem J* 348 Pt 2: 343-350.
- Frey TG, Mannella CA. 2000. The internal structure of mitochondria. *Trends Biochem Sci* 25: 319-324.
- Frey TG, Renken CW, Perkins GA. 2002. Insight into mitochondrial structure and function from electron tomography. *Biochim Biophys Acta* 1555: 196-203.
- Frolkis VV, Stupina AS, Martinenko OA, Toth S, Timchenko AI. 1984. Aging of neurons in the mollusc *Lymnaea stagnalis*. Structure, function and sensitivity to transmitters. *Mech Ageing Dev* 25: 91-102.
- Funk RH, Nagel F, Wonka F, Krinke HE, Golfert F, et al. 1999. Effects of heat shock on the functional morphology of cell

- organelles observed by video-enhanced microscopy. *Anat Rec* 255: 458-464.
- Gaietta G, Deerinck TJ, Adams SR, Bouwer J, Tour O, et al. 2002. Multicolor and electron microscopic imaging of connexin trafficking. *Science* 296: 503-507.
- Gilkerson RW, Selker JM, Capaldi RA. 2003. The cristal membrane of mitochondria is the principal site of oxidative phosphorylation. *FEBS Lett* 546: 355-358.
- Gimenez-Amaya JM. 1991. A note upon the striatal distribution of cytochrome oxidase activity in the rat and in the cat. *Acta Anat (Basel)* 142: 158-164.
- Gimenez-Amaya JM. 1992. Some observations upon the distribution of cytochrome oxidase activity in the globus pallidus of the rat. *Acta Anat (Basel)* 143: 246-252.
- Gorini A, Arnaboldi R, Ghigini B, Villa RF. 1989. Brain cytochrome oxidase activity of synaptic and nonsynaptic mitochondria during aging. *Basic Appl Histochem* 33: 139-145.
- Gripacic L, Blik van der AM. 2001. The many shapes of mitochondrial membranes. *Traffic* 2: 235-244.
- Hackenbrock CR. 1968. Ultrastructural bases for metabolically linked mechanical activity in mitochondria. II. Electron transport-linked ultrastructural transformations in mitochondria. *J Cell Biol* 37: 345-369.
- Halestrap AP, Brennerb C. 2003. The adenine nucleotide translocase: A central component of the mitochondrial permeability transition pore and key player in cell death. *Curr Med Chem* 10: 1507-1525.
- Harold FM. 1986. *The vital force: A study of bioenergetics*. W. H. Freeman, New York.
- Harold FM. 1986. *The vital force: A study of bioenergetics*. W.H. Freeman, New York.
- Helmchen F, Denk W. 2002. New developments in multiphoton microscopy. *Curr Opin Neurobiol* 12: 593-601.
- Hoch FL. 1992. Cardiolipins and biomembrane function. *Biochim Biophys Acta* 1113: 71-133.
- Hoffmann B, Stockl A, Schlame M, Beyer K, Klingenberg M. 1994. The reconstituted ADP/ATP carrier activity has an absolute requirement for cardiolipin as shown in cysteine mutants. *J Biol Chem* 269: 1940-1944.
- Hoshino A, Fujioka K, Oku T, Nakamura S, Suga M, et al. 2004. Quantum dots targeted to the assigned organelle in living cells. *Microbiol Immunol* 48: 985-994.
- Huang HM, Fowler C, Zhang H, Gibson GE. 2004. Mitochondrial heterogeneity within and between different cell types. *Neurochem Res* 29: 651-658.
- Ishihara N, Eura Y, Mihara K. 2004. Mitofusin 1 and 2 play distinct roles in mitochondrial fusion reactions via GTPase activity. *J Cell Sci* 117: 6535-6546.
- Jameson, N, Olson, J, Nguyen, H, Holtzman D. 1984. Respiration in primary cultured cerebellar granule neurons and cerebral cortical neurons. *J Neurochem* 42: 470-474.
- Kaldis P, Hemmer W, Zanolta E, Holtzman D, Wallimann T. 1996. 'Hot spots' of creatine kinase localization in brain: Cerebellum, hippocampus and choroid plexus. *Dev Neurosci* 18: 542-554.
- Kaplan BB, Lavina ZS, Gioio AE. 2004. Subcellular compartmentation of neuronal protein synthesis: New insights into the biology of the neuron. *Ann N Y Acad Sci* 1018: 244-254.
- Khan AA, Wilson JE. 1965. Studies of turnover in mammalian subcellular particles: Brain nuclei, mitochondria and microsomes. *J Neurochem* 12: 81-86.
- Kim TH, Zhao Y, Ding WX, Shin JN, He X, et al. 2004. Bid-cardiolipin interaction at mitochondrial contact site contributes to mitochondrial cristae reorganization and cytochrome *c* release. *Mol Biol Cell* 15: 3061-3072.
- Kugler P. 1993. In situ measurements of enzyme activities in the brain. *Histochem J* 25: 329-338.
- Kvamme E, Roberg B, Torgner IA. 2000. Glutamine transport in brain mitochondria. *Neurochem Int* 37: 131-138.
- Kwong LK, Sohal RS. 2000. Age-related changes in activities of mitochondrial electron transport complexes in various tissues of the mouse. *Arch Biochem Biophys* 373: 16-22.
- Laake JH, Takumi Y, Eidet J, Torgner IA, Roberg B, et al. 1999. Postembedding immunogold labelling reveals subcellular localization and pathway-specific enrichment of phosphate activated glutaminase in rat cerebellum. *Neuroscience* 88: 1137-1151.
- Lai JC. 1992. Oxidative metabolism in neuronal and non-neuronal mitochondria. *Can J Physiol Pharmacol* 70 (Suppl): S130-S137.
- Lai JC, Clark JB. 1976. Preparation and properties of mitochondria derived from synaptosomes. *Biochem J* 154: 423-432.
- Lai JC, Leung TK, Lim L. 1994. Heterogeneity of monoamine oxidase activities in synaptic and non-synaptic mitochondria derived from three brain regions: Some functional implications. *Metab Brain Dis* 9: 53-66.
- Lai JC, Walsh JM, Dennis SC, Clark JB. 1977. Synaptic and non-synaptic mitochondria from rat brain: Isolation and characterization. *J Neurochem* 28: 625-631.
- Leapman RD. 2003. Detecting single atoms of calcium and iron in biological structures by electron energy-loss spectrum-imaging. *J Microsc* 210: 5-15.
- Ledda M, Martinelli C, Pannese E. 2001. Quantitative changes in mitochondria of spinal ganglion neurons in aged rabbits. *Brain Res Bull* 54: 455-459.
- Lee HC, Wei YH. 1997. Mutation and oxidative damage of mitochondrial DNA and defective turnover of mitochondria in human aging. *J Formos Med Assoc* 96: 770-778.
- Lenaz G, Cavazzoni M, Genova ML, D'Aurelio M, Merlo Pich M, et al. 1998. Oxidative stress, antioxidant defences and aging. *Biofactors* 8: 195-204.
- Leong SF, Clark JB. 1984. Regional development of glutamate dehydrogenase in the rat brain. *J Neurochem* 43: 106-111.

- Leong SF, Lai JC, Lim L, Clark JB. 1984. The activities of some energy-metabolising enzymes in nonsynaptic (free) and synaptic mitochondria derived from selected brain regions. *J Neurochem* 42: 1306-1312.
- Leonhardt H. 1976. "Axonal spheroids" in the spinal cord of normal rabbits. *Cell Tissue Res* 174: 99-108.
- Li Z, Okamoto K, Hayashi Y, Sheng M. 2004. The importance of dendritic mitochondria in the morphogenesis and plasticity of spines and synapses. *Cell* 119: 873-887.
- Ligon LA, Steward O. 2000a. Movement of mitochondria in the axons and dendrites of cultured hippocampal neurons. *J Comp Neurol* 427: 340-350.
- Ligon LA, Steward O. 2000b. Role of microtubules and actin filaments in the movement of mitochondria in the axons and dendrites of cultured hippocampal neurons. *J Comp Neurol* 427: 351-361.
- Liu J, Atamna H, Kuratsune H, Ames BN. 2002. Delaying brain mitochondrial decay and aging with mitochondrial antioxidants and metabolites. *Ann N Y Acad Sci* 959: 133-166.
- Lutter M, Perkins GA, Wang X. 2001. The pro-apoptotic Bcl-2 family member tBid localizes to mitochondrial contact sites. *BMC Cell Biol* 2: 22.
- Mannella CA, Pfeiffer DR, Bradshaw PC, Moraru II, Slepchenko B, et al. 2001. Topology of the mitochondrial inner membrane: Dynamics and bioenergetic implications. *IUBMB Life* 52: 93-100.
- Marczynski TJ. 1998. GABAergic deafferentation hypothesis of brain aging and Alzheimer's disease revisited. *Brain Res Bull* 45: 341-379.
- Mattenberger Y, James DI, Martinou JC. 2003. Fusion of mitochondria in mammalian cells is dependent on the mitochondrial inner membrane potential and independent of microtubules or actin. *FEBS Lett* 538: 53-59.
- McEnery MW, Dawson TM, Verma A, Gurley D, Colombini M, et al. 1993. Mitochondrial voltage-dependent anion channel. Immunohistochemical and immunohistochemical characterization in rat brain. *J Biol Chem* 268: 23289-23296.
- McKenna MC, Stevenson JH, Huang X, Hopkins IB. 2000b. Differential distribution of the enzymes glutamate dehydrogenase and aspartate aminotransferase in cortical synaptic mitochondria contributes to metabolic compartmentation in cortical synaptic terminals. *Neurochem Int* 37: 229-241.
- McKenna MC, Stevenson JH, Huang X, Tildon JT, Zielke CL, et al. 2000a. Mitochondrial malic enzyme activity is much higher in mitochondria from cortical synaptic terminals compared with mitochondria from primary cultures of cortical neurons or cerebellar granule cells. *Neurochem Int* 36: 451-459.
- Melov S, Schneider JA, Coskun PE, Bennett DA, Wallace DC. 1999. Mitochondrial DNA rearrangements in aging human brain and in situ PCR of mtDNA. *Neurobiol Aging* 20: 565-571.
- Menzies RA, Gold PH. 1971. The turnover of mitochondria in a variety of tissues of young adult and aged rats. *J Biol Chem* 246: 2425-2429.
- Milner TA, Aoki C, Sheu KF, Blass JB, Pickel VM. 1987. Light microscopic immunocytochemical localization of pyruvate dehydrogenase complex in rat brain: Topographical distribution and relation to cholinergic and catecholaminergic nuclei. *J Neurosci* 7: 3171-3190.
- Misaka T, Miyashita T, Kubo Y. 2002. Primary structure of a dynamin-related mouse mitochondrial GTPase and its distribution in brain, subcellular localization, and effect on mitochondrial morphology. *J Biol Chem* 277: 15834-15842.
- Mjaatvedt AE, Wong-Riley MT. 1988. Relationship between synaptogenesis and cytochrome oxidase activity in Purkinje cells of the developing rat cerebellum. *J Comp Neurol* 277: 155-182.
- Morris RL, Hollenbeck PJ. 1993. The regulation of bidirectional mitochondrial transport is coordinated with axonal outgrowth. *J Cell Sci* 104 (Pt 3): 917-927.
- Morris RL, Hollenbeck PJ. 1995. Axonal transport of mitochondria along microtubules and F-actin in living vertebrate neurons. *J Cell Biol* 131: 1315-1326.
- Muller M, Mironov SL, Ivannikov MV, Schmidt J, Richter DW. 2005. Mitochondrial organization and motility probed by two-photon microscopy in cultured mouse brainstem neurons. *Exp Cell Res* 303: 114-127.
- Muller M, Moser R, Cheneval D, Carafoli E. 1985. Cardiolipin is the membrane receptor for mitochondrial creatine phosphokinase. *J Biol Chem* 260: 3839-3843.
- Munn EA. 1974. The structure of mitochondria. New York: Academic Press; p. 465.
- Navarro A. 2004. Mitochondrial enzyme activities as biochemical markers of aging. *Mol Aspects Med* 25: 37-48.
- Neidle A, van den Berg CJ, Grynbau A. 1969. The heterogeneity of rat brain mitochondria isolated on continuous sucrose gradients. *J Neurochem* 16: 225-234.
- Okuno E, Schmidt W, Parks DA, Nakamura M, Schwarcz R. 1991. Measurement of rat brain kynurenine aminotransferase at physiological kynurenine concentrations. *J Neurochem* 57: 533-540.
- Olichon A, Emorine LJ, Descoins E, Pelloquin L, Bricchese L, et al. 2002. The human dynamin-related protein OPA1 is anchored to the mitochondrial inner membrane facing the inter-membrane space. *FEBS Lett* 523: 171-176.
- Owen F, Bourne R. 1977. The heterogeneity of monoamine oxidase in distinct populations of rat brain mitochondria. *Biochem Pharmacol* 26: 289-292.

- Papa S. 1996. Mitochondrial oxidative phosphorylation changes in the life span. Molecular aspects and physiopathological implications. *Biochim Biophys Acta* 1276: 87-105.
- Paradies G, Ruggiero FM. 1991. Effect of aging on the activity of the phosphate carrier and on the lipid composition in rat liver mitochondria. *Arch Biochem Biophys* 284: 332-337.
- Paradies G, Ruggiero FM, Petrosillo G, Gadaleta MN, Quagliariello E. 1994. Effect of aging and acetyl-L-carnitine on the activity of cytochrome oxidase and adenine nucleotide translocase in rat heart mitochondria. *FEBS Lett* 350: 213-215.
- Paumard P, Vaillier J, Couлары B, Schaeffer J, Soubannier V, et al. 2002. The ATP synthase is involved in generating mitochondrial cristae morphology. *EMBO J* 21: 221-230.
- Perkins G, Renken C, Martone ME, Young SJ, Ellisman M, et al. 1997. Electron tomography of neuronal mitochondria: Three-dimensional structure and organization of cristae and membrane contacts. *J Struct Biol* 119: 260-272.
- Perkins GA, Ellisman MH, Fox DA. 2004. The structure-function correlates of mammalian rod and cone photoreceptors: Observations and unanswered questions. *Mitochondrion* 4: 695-703.
- Perkins GA, Frey TG. 2000. Recent structural insight into mitochondria gained by microscopy. *Micron* 31: 97-111.
- Perkins GA, Renken CW, Frey TG, Ellisman MH. 2001a. Membrane architecture of mitochondria in neurons of the central nervous system. *J Neurosci Res* 66: 857-865.
- Perkins GA, Wang L, Huang LJ, Humphries K, Yao VJ, et al. 2001b. PKA, PKC, and AKAP localization in and around the neuromuscular junction. *BMC Neurosci* 2: 17.
- Peters A, Palay SL, Webster HD. 1976. The fine structure of the nervous system: The neurons and supporting cells. Philadelphia: Saunders; p. 406.
- Piko L, Hougham AJ, Bulpitt KJ. 1988. Studies of sequence heterogeneity of mitochondrial DNA from rat and mouse tissues: Evidence for an increased frequency of deletions/additions with aging. *Mech Ageing Dev* 43: 279-293.
- Polyakov VY, Soukhom linova MY, Fais D. 2003. *Biochemistry (Mosc)*. 68: 838-849.
- Purves D, La Mantia AS. 1990. Numbers of "blobs" in the primary visual cortex of neonatal and adult monkeys. *Proc Natl Acad Sci USA* 87: 5764-5767.
- Pysh JJ. 1970. Mitochondrial changes in rat inferior colliculus during postnatal development: An electron microscopic study. *Brain Res* 18: 325-342.
- Pysh JJ, Khan T. 1972. Variations in mitochondrial structure and content of neurons and neuroglia in rat brain: An electron microscopic study. *Brain Res* 36: 1-18.
- Rajfur Z, Roy P, Otey C, Romer L, Jacobson K. 2002. Dissecting the link between stress fibres and focal adhesions by CALI with EGFP fusion proteins. *Nat Cell Biol* 4: 286-293.
- Reichert AS, Neupert W. 2002. Contact sites between the outer and inner membrane of mitochondria—role in protein transport. *Biochim Biophys Acta* 1592: 41-49.
- Renken C, Siragusa G, Perkins G, Washington L, Nulton J, et al. 2002. A thermodynamic model describing the nature of the crista junction: A structural motif in the mitochondrion. *J Struct Biol* 138: 137-144.
- Rowland KC, Irby NK, Spirou GA. 2000. Specialized synapse-associated structures within the calyx of Held. *J Neurosci* 20: 9135-9144.
- Sandri G, Siagri M, Panfilì E. 1988. Influence of Ca²⁺ on the isolation from rat brain mitochondria of a fraction enriched of boundary membrane contact sites. *Cell Calcium* 9: 159-165.
- Sasaki T, Senda M, Kim S, Kojima S, Kubodera A. 2001. Age-related changes of glutathione content, glucose transport and metabolism, and mitochondrial electron transfer function in mouse brain. *Nucl Med Biol* 28: 25-31.
- Sasaki T, Soga S, Ishii S, Kobayashi T, Nagai H, Senda M. 1999. Visualization of mitochondrial oxygen fixation in brain slices by gas-tissue autoradiography. *Brain Res* 831: 263-272.
- Sato I, Konishi K, Mikami A, Sato T. 2000. Developmental changes in enzyme activities and in morphology of rat cortex mitochondria. *Okajimas Folia Anat Jpn* 76: 353-361.
- Scheffler IE. 1999. *Mitochondria*. New York: Wiley-Liss; p. 367.
- Schore AN. 1997. Early organization of the nonlinear right brain and development of a predisposition to psychiatric disorders. *Dev Psychopathol* 9: 595-631.
- Scorrano L, Ashiya M, Buttle K, Weiler S, Oakes SA, et al. 2002. A distinct pathway remodels mitochondrial cristae and mobilizes cytochrome *c* during apoptosis. *Dev Cell* 2: 55-67.
- Sesaki H, Jensen RE. 2004. Ugo1p links the Fzo1p and Mgm1p GTPases for mitochondrial fusion. *J Biol Chem* 279: 28298-28303.
- Sirevaag AM, Greenough WT. 1987. Differential rearing effects on rat visual cortex synapses. III. Neuronal and glial nuclei, boutons, dendrites, and capillaries. *Brain Res* 424: 320-332.
- Smirnova E, Griparic L, Shurland DL, Blik van der AM. 2001. Dynamin-related protein Drp1 is required for mitochondrial division in mammalian cells. *Mol Biol Cell* 12: 2245-2256.
- Sonnenwald U, Hertz L, Schousboe A. 1998. Mitochondrial heterogeneity in the brain at the cellular level. *J Cereb Blood Flow Metab* 18: 231-237.

- Sonnwald U, Schousboe A, Qu H, Waagepetersen HS. 2004. Intracellular metabolic compartmentation assessed by ¹³C magnetic resonance spectroscopy. *Neurochem Int* 45: 305-310.
- Sonnwald U, Westergaard N, Hassel B, Muller TB, Unsgard G, et al. 1993. NMR spectroscopic studies of ¹³C acetate and ¹³C glucose metabolism in neocortical astrocytes: Evidence for mitochondrial heterogeneity. *Dev Neurosci* 15: 351-358.
- Spirou GA, Rowland KC, Berrebi AS. 1998. Ultrastructure of neurons and large synaptic terminals in the lateral nucleus of the trapezoid body of the cat. *J Comp Neurol* 398: 257-272.
- Steward O, Schuman EM. 2003. Compartmentalized synthesis and degradation of proteins in neurons. *Neuron* 40: 347-359.
- Suzuki M, Jeong SY, Karbowski M, Youle RJ, Tjandra N. 2003. The solution structure of human mitochondria fission protein Fis1 reveals a novel TPR-like helix bundle. *J Mol Biol* 334: 445-458.
- Takase C, Nakano K, Ohta S, Nakagawa S, Matuda SY. 1996. Different distribution of dihydrolipoamide succinyltransferase, dihydrolipoamide acetyltransferase and ATP synthase beta-subunit in monkey brain. *In Vivo* 10: 495-501.
- Toescu EC, Myronova N, Verkhratsky A. 2000. Age-related structural and functional changes of brain mitochondria. *Cell Calcium* 28: 329-338.
- Toescu EC, Verkhratsky A. 2003. Neuronal ageing from an intraneuronal perspective: Roles of endoplasmic reticulum and mitochondria. *Cell Calcium* 34: 311-323.
- Tolani AJ, Talwar GP. 1963. Differential metabolism of various brain regions. *Biochemical heterogeneity of mitochondria*. *Biochem J* 88: 357-362.
- van der Klei IJ, Veenhuis M, Neupert W. 1994. A morphological view on mitochondrial protein targeting. *Microsc Res Tech* 27: 284-293.
- Vanden Berghe P, Hennig GW, Smith TK. 2004. Characteristics of intermittent mitochondrial transport in guinea pig enteric nerve fibers. *Am J Physiol Gastrointest Liver Physiol* 286: G671-G682.
- Vaughn JE, Grieshaber JA. 1972. An electron microscopic investigation of glycogen and mitochondria in developing and adult rat spinal motor neuropil. *J Neurocytol* 1: 397-412.
- Vidal L, Ruiz C, Villena A, Diaz F, Perez de Vargas I. 2004. Quantitative age-related changes in dorsal lateral geniculate nucleus relay neurons of the rat. *Neurosci Res* 48: 387-396.
- Villa RF, Gorini A, Geroldi D, Lo Faro A, Dell'Orbo C. 1989. Enzyme activities in perikaryal and synaptic mitochondrial fractions from rat hippocampus during development. *Mech Ageing Dev* 49: 211-225.
- Vysokikh M, Brdiczka D. 2000. VDAC and peripheral channeling complexes in health and disease. *Mol Cell Biochem* 256/257: 117-126.
- Vysokikh MY, Katz A, Rueck A, Wuensch C, Dorner A, et al. 2001. Adenine nucleotide translocator isoforms 1 and 2 are differently distributed in the mitochondrial inner membrane and have distinct affinities to cyclophilin D. *Biochem J* 358: 349-358.
- Waagepetersen HS, Sonnwald U, Larsson OM, Schousboe A. 2000. Compartmentation of TCA cycle metabolism in cultured neocortical neurons revealed by ¹³C MR spectroscopy. *Neurochem Int* 36: 349-358.
- Waagepetersen HS, Sonnwald U, Qu H, Schousboe A. 1999b. Mitochondrial compartmentation at the cellular level: Astrocytes and neurons. *Ann N Y Acad Sci* 893: 421-425.
- Waagepetersen HS, Sonnwald U, Schousboe A. 1999a. The GABA paradox: Multiple roles as metabolite, neurotransmitter, and neurodifferentiative agent. *J Neurochem* 73: 1335-1342.
- Waagepetersen HS, Sonnwald U, Schousboe A. 2003. Compartmentation of glutamine, glutamate, and GABA metabolism in neurons and astrocytes: Functional implications. *Neuroscientist* 9: 398-403.
- Weiss C, Oppliger W, Vergeres G, Demel R, Jenö P, et al. 1999. Domain structure and lipid interaction of recombinant yeast Tim44. *Proc Natl Acad Sci USA* 96: 8890-8894.
- Westergaard N, Sonnwald U, Petersen SB, Schousboe A. 1995. Glutamate and glutamine metabolism in cultured GABAergic neurons studied by ¹³C NMR spectroscopy may indicate compartmentation and mitochondrial heterogeneity. *Neurosci Lett* 185: 24-28.
- Westermann B. 2002. Merging mitochondria matters: Cellular role and molecular machinery of mitochondrial fusion. *EMBO Rep* 3: 527-531.
- Wilkin GP, Reijnierse GL, Johnson AL, Balazs R. 1979. Subcellular fractionation of rat cerebellum: Separation of synaptosomal populations and heterogeneity of mitochondria. *Brain Res* 164: 153-163.
- Williamson DH. 1985. Ketone body metabolism during development. *Fed Proc* 44: 2342-2346.
- Windle WF, Smart JO, Beers JJ. 1958. Residual function after subtotal spinal cord transection in adult cats. *Neurology* 8: 518-521.
- Wong ED, Wagner JA, Gorsich SW, McCaffery JM, Shaw JM, Nunnari J. 2000. *J Cell Biol* 151: 341-352.
- Wong-Riley M. 1979. Changes in the visual system of monocularly sutured or enucleated cats demonstrable with cytochrome oxidase histochemistry. *Brain Res* 171: 11-28.

- Wong-Riley MT. 1989. Cytochrome oxidase: An endogenous metabolic marker for neuronal activity. *Trends Neurosci* 12: 94-101.
- Xiong J, Camello PJ, Verkhatsky A, Toescu EC. 2004. Mitochondrial polarisation status and $[Ca^{2+}]_i$ signalling in rat cerebellar granule neurones aged in vitro. *Neurobiol Aging* 25: 349-359.
- Yadava N, Houchens T, Potluri P, Scheffler IE. 2004. Development and characterization of a conditional mitochondrial complex I assembly system. *J Biol Chem* 279: 12406-12413.
- Zhang J, Campbell RE, Ting AY, Tsien RY. 2002. Creating new fluorescent probes for cell biology. *Nat Rev Mol Cell Biol* 3: 906-918.
- Zhang P, Anglade P, Hirsch EC, Javoy-Agid F, Agid Y. 1994. Distribution of manganese-dependent superoxide dismutase in the human brain. *Neuroscience* 61: 317-330.

4.3 Coupling of Neuronal Function to Oxygen and Glucose Metabolism Through Changes in Neurotransmitter Dynamics as Revealed with Aging, Hypoglycemia, and Hypoxia

J. A. Joseph · G. E. Gibson

1	Introduction	298
2	Brain Function and Metabolism	298
2.1	Hypoxia Is a Classical Model of Impaired Metabolism Leading to Diminished Brain Function that Mimics Aging	298
2.2	Oxidative Stress	300
3	Linkage of Metabolic Pathways, Oxygen, and Neurotransmitter Synthesis	300
3.1	Relationship Between Acetylcholine and Metabolism as Revealed by Manipulation of Metabolism and Aging	301
3.2	Acetylcholine and Metabolism in Disease	302
3.3	Connection of DA to Metabolism	304
3.4	Association of Metabolism and DA in Aging and Disease	305
4	The Dependence of Neurotransmitters on Calcium may Account for Age and Metabolic Induced Changes	306
4.1	Changes in Neurotransmitters Mediated by Calcium with Alterations in Metabolism	306
4.2	Interaction of Calcium and Age-Related Deficits	307
5	Free Radicals may Account for Many Changes Associated with Aging or Altered Metabolism	307
5.1	Production of Free Radicals	307
5.2	Free Radicals in Aging	307
5.3	Free Radicals and Regulation of Release	308
5.4	Free Radicals and the DA Transporter	308
5.5	Regulation of Receptor Subtypes and Oxidative Stress (OS)	309
5.6	Regulation of Muscarinic Receptors	309
6	Reversal of the Effects of Oxidative Stress (OS) on Calcium Buffering with Antioxidants	313
7	Changes in Lipids May Alter the Interactions of Oxidative Stress (OS), Calcium, and Neurotransmitters	314
8	Conclusions	315

Abstract: Normal brain function is tightly linked to adequate glucose and oxygen availability and to energy metabolism. This close coupling of metabolism to function is mediated, in part, through regulation of neurotransmitter dynamics. Metabolism may regulate neurotransmission by controlling synthesis and release of neurotransmitters or receptor interactions. Many of the effects of altered metabolism on neurotransmission are mediated by reactive oxygen species (ROS) and calcium and are modified by lipids. The coupling is difficult to demonstrate under normal conditions. However, the importance of the tight link between metabolism neurotransmitter dynamics and neural function can be readily demonstrated with conditions that alter metabolism (e.g., hypoglycemia or hypoxia) or by normal aging. An understanding of these interactions will help our understanding of normal brain function as well as lead to the development of treatments for age-related neurodegenerative diseases.

List of Abbreviations: ACh, acetylcholine; AD, Alzheimer's disease; APP, amyloid precursor protein; A β , amyloid- β peptide; BB, blueberry extract; BSO, buthionine sulfoximine; CHL, cholesterol; DA, dopamine; GABA, γ -amino butyric acid; OS, oxidative stress; PL, phospholipids; ROS, reactive oxygen species; SPH, sphingomyelin

1 Introduction

Metabolism and brain function (including motor and cognitive processes) are intimately linked to each other. This chapter emphasizes that the interaction of metabolism with multiple aspects of neurotransmitter dynamics underlies the close link between brain function and metabolism. The coupling of metabolism to brain function is difficult to demonstrate under resting conditions, so the effects must be shown by either inhibiting or stimulating metabolic pathways and determining the effects on neurotransmitters and brain function. Diminishing metabolism (e.g., hypoxia or hypoglycemia) reduces brain function and alters normal neurotransmission. Stimulation of glucose metabolism by hyperglycemia can enhance neurotransmitter metabolism and improve brain function. The linkage of metabolism with neurotransmitters may be direct (e.g., availability of oxygen or carbon sources for synthesis), through the production of free radicals (i.e., oxidative stress) that modify essential aspects of neurotransmitter dynamics (e.g., receptors), or by alterations in calcium within the cells (🔗 [Figure 4.3-1](#)). Many of the same cognitive or neuronal changes that have been observed with mild interruption of metabolism also occur with normal aging, which suggests they may interact with the same fundamental mechanisms. Thus, the relation of age-related changes in brain function to altered coupling of metabolism to neurotransmitters through oxidative stress (OS) and calcium dysregulation will also be described.

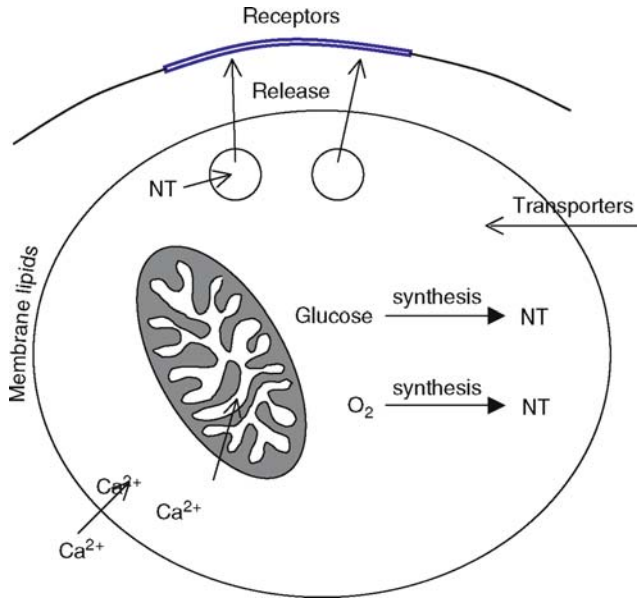
Further, OS (a normal product of metabolism that is damaging when exaggerated) and alterations in metabolism can exaggerate other age-related changes and promote abnormal processing of proteins (e.g., amyloid precursor protein (APP) processing) or phosphorylation of proteins (e.g., tau) that lead to the changes in age-related diseases such as Alzheimer's disease (AD) (Gibson et al., 2005). However, this chapter focuses on how changes in metabolism and aging reveal the interaction of neurotransmitter dynamics with metabolism, calcium, and OS. Although many neurotransmitters are likely important in these interactions, this chapter focuses on the interaction of metabolism and aging with acetylcholine (ACh) and dopamine (DA). Metabolism provides the acetyl group for ACh synthesis and oxygen is required for DA synthesis. Release, reuptake, and interactions of these neurotransmitters with their receptors are sensitive to perturbations in calcium and in metabolism including OS.

2 Brain Function and Metabolism

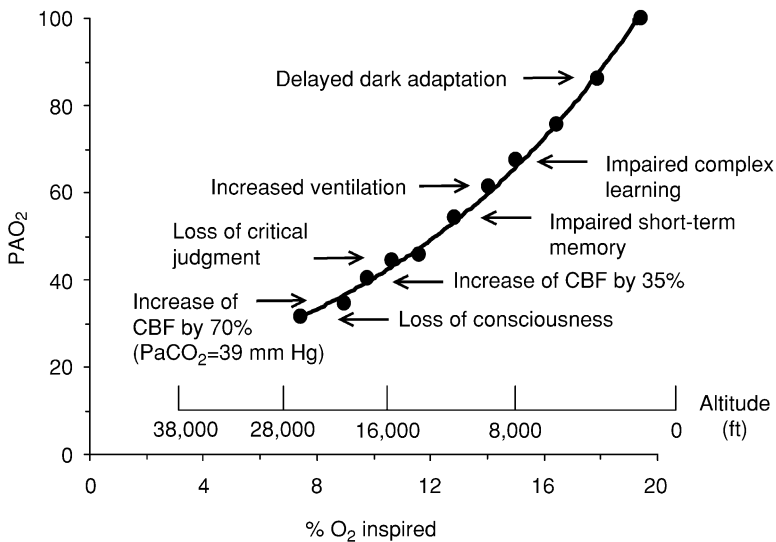
2.1 Hypoxia Is a Classical Model of Impaired Metabolism Leading to Diminished Brain Function that Mimics Aging

Even slight reductions in the oxygen or glucose available to the brain diminish brain function. These have been best documented for decline in oxygen availability. Changes with hypoxia reveal the tight coupling of

■ **Figure 4.3-1**
Sites of interaction of metabolism with neurotransmitter function



■ **Figure 4.3-2**
Hypoxia impairs mental function in a manner that resembles the changes with aging. The data are from McFarland (1963) as compiled by Plum and Posner (1980). The vertical axis is alveolar oxygen tensions



brain function to metabolism (▶ [Figure 4.3-2](#)). Even slight reductions of atmospheric oxygen (from 20% to 16%) impair short-term memory and judgment, delay dark adaptation, diminish visual acuity, alter light sensitivity and concentration span, and reduce complex mental function (McFarland, 1963). Reductions in inspired air of this magnitude are too small to diminish ATP concentrations (Gibson and Blass, 1976).

As described below, many of these hypoxia-induced changes in behavior can be attributed to alterations in neurotransmitters dynamics mediated by ROS or calcium.

Studies beginning in the 1920s suggest that hypoxia and hypoglycemia as well as normal aging diminish brain function by acting on the same fundamental mechanisms. In a series of studies between 1929 and 1963, McFarland demonstrated in humans that many of the earliest behavioral changes that are observed in normal aging also accompany mild acute hypoxia or hypoglycemia. Similar changes occur in delayed dark adaptation, visual acuity, light sensitivity, impaired short-term memory, span of concentration, and complex mental functions (McFarland, 1963). In this respect, aging can be defined as a condition where stressors such as “oxidative stress” or “inflammation” that are not counteracted by protective functions or repair mechanisms lead to a dysregulation. These changes can be translated into decrements in neuronal function accompanied by behavioral declines (decreases in motor and cognitive performance) in both humans and animals. Age-related deficits include both cognitive (Bartus, 1990) and motor (Joseph et al., 1983; Kluger et al., 1997) behaviors. Cognitive declines in aging include decrements in spatial learning and memory (Bartus, 1990; Ingram et al., 1994; West, 1996; Muir, 1997; Shukitt-Hale et al., 1998). Deficits in motor function include decreases in balance, muscle strength, and coordination (Joseph et al., 1983, which are thought to be the result of age-related alterations in the striatal DA system (Joseph, 1992) or in cerebellar noradrenergic function. (Bickford et al., 1992; Bickford, 1993).

2.2 Oxidative Stress

Similarities of changes with conditions that promote OS and normal aging have also been documented in animals. Young animals exposed to oxidative stressors exhibit neuronal and behavioral changes similar to those seen in aging. For example, exposing young rats to particles of high energy and to charged (HZE particles) particle radiation, which increases oxidative and inflammatory stressors, produces behavioral deficits that parallel those observed in aging (Joseph et al., 1998a, b, c, 2000; Shukitt-Hale et al., 2000). HZE particles also disrupt the functioning of the dopaminergic system and DA-mediated behaviors, such as motor behavior (Joseph et al., 1992), spatial learning and memory performance (Shukitt-Hale et al., 2000), and amphetamine-induced conditioned taste aversion (Rabin et al., 1998). These conclusions are supported by additional studies that show a normobaric hyperoxia environment of 100% oxygen produces deficits in motor behavioral performance similar to that seen in aging (Bickford et al., 1999).

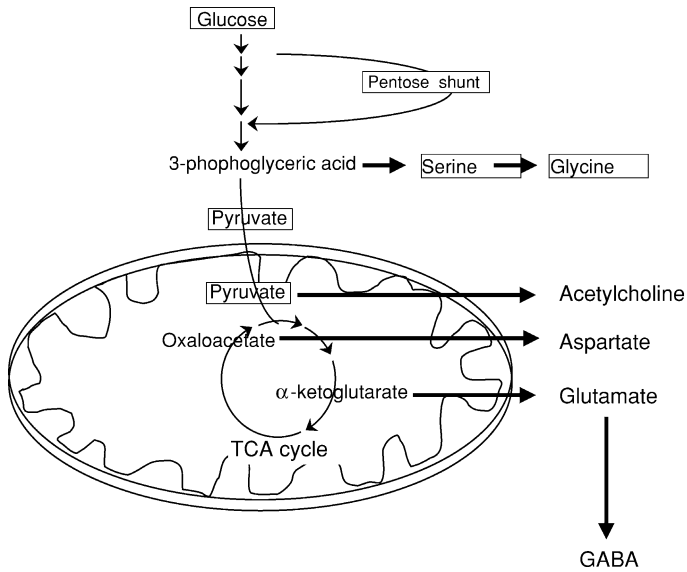
Induction of OS by reducing the levels of the endogenous antioxidant glutathione with buthionine sulfoximine (BSO), followed by central DA administration to create conditions similar to those seen in aging, also produced decrements in both cognitive and motor performance. BSO given prior to DA administration selectively impaired psychomotor (Shukitt-Hale et al., 1997) and cognitive performance (Shukitt-Hale et al., 1998). Neither BSO alone nor DA alone had detrimental effects on behavior. The finding that OS under reduced antioxidant protection enhances effects on these parameters is particularly important, since the CNS is particularly vulnerable to OS and this vulnerability may increase during aging. While the mechanisms underlying age-related changes in motor and cognitive deficits in aging remain to be discerned, the effects of OS may be a critical factor, or they may affect similar underlying mechanisms.

3 Linkage of Metabolic Pathways, Oxygen, and Neurotransmitter Synthesis

The basic pathways of energy metabolism are linked to the synthesis of multiple neurotransmitters. At least six neurotransmitters derive their carbon skeleton from glycolysis and the tricarboxylic acid cycle: ACh, γ -amino butyric acid (GABA), glutamate, aspartate, glycine, and serine (▶ [Figure 4.3-3](#)). This link to basic pathways of energy metabolism provides a direct connection between brain metabolism and neurotransmitters, and thus to brain function. When radioactive glucose is provided to the brain in vivo or in vitro, a large portion is very rapidly incorporated into these compounds. Surprisingly, the pathways that connect the neurotransmitters to metabolism are not entirely known. For example, the pathway for the production of the acetyl group for ACh synthesis is not known (Cooper, 1994). The dual role of many of these compounds as neurotransmitters and metabolites of common metabolic pathways makes it difficult to

■ **Figure 4.3-3**

Relationship of neurotransmitter synthesis to pathways of energy metabolism



discern precise changes in neurotransmitter pools. For example, the relationship of the neurotransmitter pool of glutamate to the metabolic pool of glutamate is controversial.

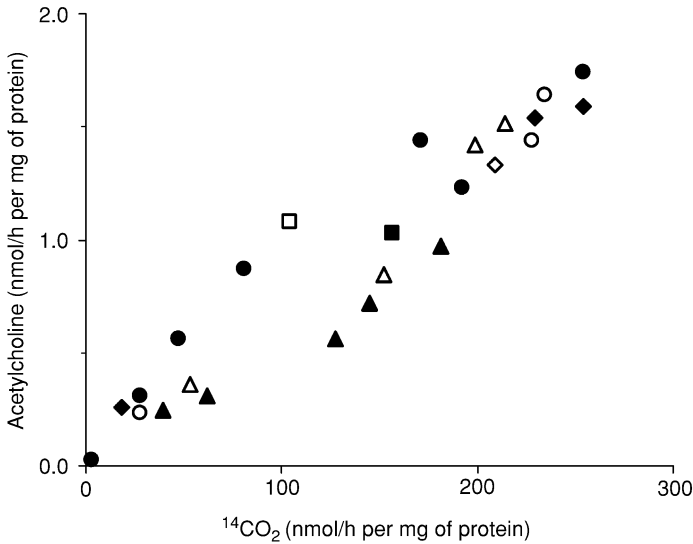
The synthesis of other neurotransmitters depends upon oxygen. The availability of molecular oxygen has a critical role in the biosynthesis of the neurotransmitters DA, norepinephrine, and serotonin. Oxygen is required in the rate-limiting steps of their synthesis (dopamine- β -hydroxylase, tyrosine hydroxylase, and tryptophan hydroxylase, respectively). Since the K_m for oxygen (7 mm Hg = 12 μ M) (Fisher and Kaufman, 1972) is approximately the same as normal brain oxygen tensions (Lubbers, 1968), biosynthesis is one possible site of interaction with metabolism. However, metabolism, oxygen, and neurotransmitters can be linked in multiple ways, in addition to being linked by synthesis. This includes the ability to load neurotransmitter into vesicles, release and reuptake mechanisms, and interaction with receptors. All of these can be modified by interactions with metabolism, including OS to modify brain function (▶ [Figure 4.3-1](#)).

3.1 Relationship Between Acetylcholine and Metabolism as Revealed by Manipulation of Metabolism and Aging

Any interruption in brain metabolism due to either hypoxia or hypoglycemia leads to diminished synthesis of ACh. This is true even though only a small fraction of metabolized glucose (<1%) is used in the formation of ACh. For example, less than 0.1% of pyruvate oxidized goes to ACh, but any inhibition of oxidation leads to diminished ACh synthesis (▶ [Figure 4.3-4](#)). This coupling appears to be physiologically relevant. In rats that are made slightly hypoglycemic there is a decline in ACh synthesis (Ghajar et al., 1985). The *in vivo* extracellular release of ACh from the striatum of rats was measured by intracerebral microdialysis. During hypoxia, the ACh levels decline to 62% and 44% of the control value with 10% and 5% oxygen, respectively, which supports the suggestion of a high sensitivity of the striatal cholinergic system to hypoxia (Chleide and Ishikawa, 1990). Indeed, there seems to be little safety factor for ACh release; diminished oxygen reduces ACh metabolism (Park et al., 1987). In addition, hypoxia-induced deficits in behavior can be treated with acetylcholinesterase inhibitors (Gibson et al., 1983). Diminished synthesis of ACh is also observed with normal aging (Gibson et al., 1981). Age-related changes in ACh parallel those

■ Figure 4.3-4

Relation of acetylcholine (ACh) synthesis to oxidative metabolism as revealed by $^{14}\text{CO}_2$ production. Even slight reductions in metabolism impair ACh synthesis even though less than 1% of the metabolized carbohydrate goes to ACh (data from Gibson et al., 1975). The inhibitors are as follows: (\diamond) leucine, (\square) 2-oxo-3-methylpentanoic acid, (\blacksquare) 2-oxo-3-methylbutanoate, (\circ) pentobarbital, (\triangle) 2-oxo-4-methylpentanoate, (\bullet) bromopyruvate, (\blacktriangle) 2-oxobutyrate, (\blacklozenge) amobarbital



related to hypoxia-induced changes. With aging, ACh synthesis and release decline in parallel with the performance on behavioral tasks (🔗 Figure 4.3-5).

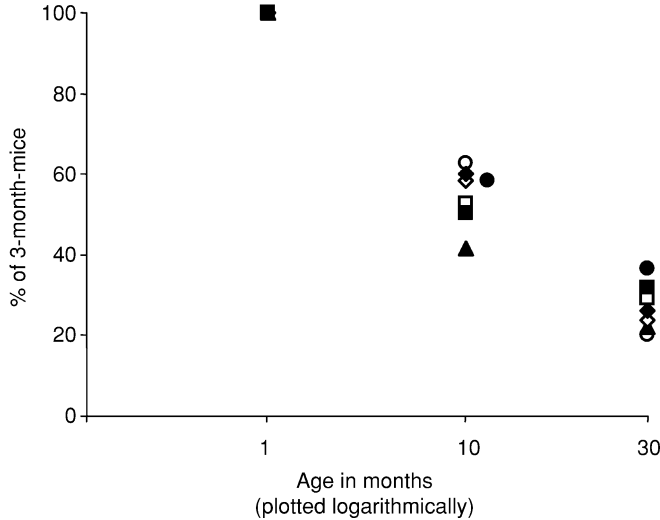
3.2 Acetylcholine and Metabolism in Disease

ACh production can be stimulated by promoting metabolism, and the enhancement appears to be clinically relevant. Relatively modest increases in circulating glucose concentrations enhance ACh production (🔗 Figure 4.3-6). The increase appears to be physiologically relevant in animals and humans. In rats, systemic injections of glucose enhance learning and memory under many conditions. When microinjected into specific brain sites, glucose has selective behavioral and pharmacological effects. Glucose increases spontaneous alternation scores (69.5%) and ACh output (121.5% versus baseline) compared with alternation scores (44.7%) and ACh output (58.9% versus baseline) of saline controls. The glucose-induced increase in alternation scores and ACh output is not secondary to changes in locomotor activity. These findings suggest that glucose enhances memory by directly or indirectly increasing the release of ACh. The results also indicate that hippocampal ACh release is increased in rats performing a spatial task. Moreover, because glucose enhances ACh output only during behavioral testing, circulating glucose may modulate ACh release only under conditions in which cholinergic cells are activated (Ragozzino et al., 1996, 1998).

The relative safety of glucose has permitted tests of glucose effects on cognitive functions in humans. Glucose enhances learning and memory in healthy aged humans and enhances several other cognitive functions in subjects with severe cognitive pathologies, including individuals with Alzheimer's disease and Down's syndrome. The increases in circulating glucose concentrations have robust and broad influences on brain functions that span many neural and behavioral measures, in all species tested. (🔗 Figure 4.3-7) (Hall et al., 1989; Gold, 1995). The positive effects of glucose on cognition in AD patients has been reviewed recently (Watson and Craft, 2004). Thus, the coupling of metabolism and ACh appears to be clinically relevant.

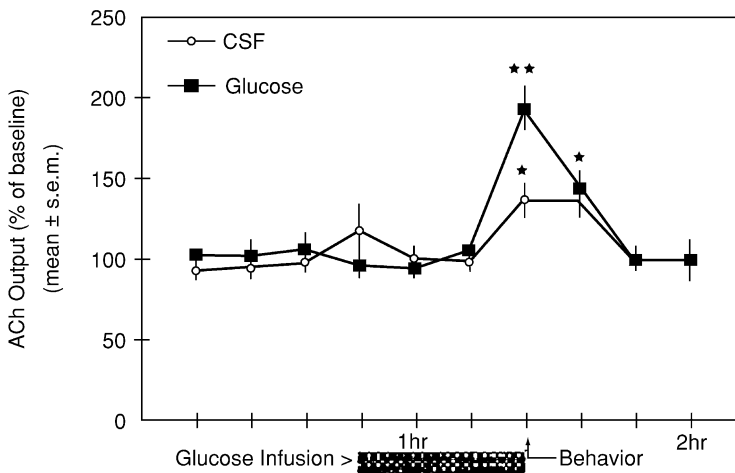
■ Figure 4.3-5

The correlation of changes in acetylcholine (ACh) synthesis with decrements in behavioral performance. (Figure is from Gibson and Peterson, 1982). The conditions that are compared are as follows: (○) in vitro ACh RELEASE Balb/c, (●) in vivo ACh synthesis Balb/c, (□) in vitro ACh release C57Bl, (■) in vivo ACh synthesis C57Bl, (▲) tight rope performance Balb/c, (◆) tight rope performance C57Bl, (◇) passive avoidance latency C57Bl



■ Figure 4.3-6

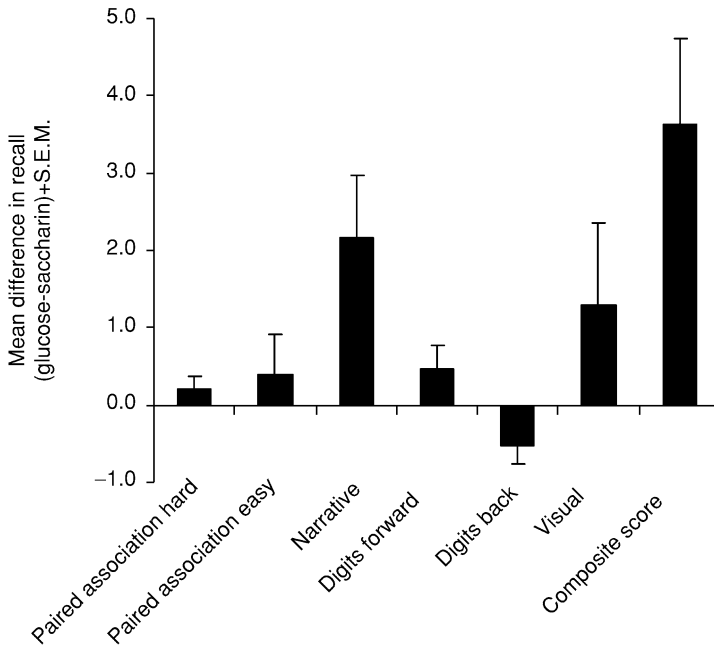
Effect of unilateral infusions of glucose on hippocampal extracellular acetylcholine (ACh). (From Ragozzino et al., 1998)



Insensitivity to insulin, which diminishes glucose entry into tissue, also diminishes cognition. This may be important in type 2 diabetes. Some of the glucose effects on memory appear to be modulated by insulin sensitivity. The acute effects of glucose administration should be distinguished from the effects of chronic hyperglycemia (diabetes), which has been associated with cognitive impairments, at least in older adults. In healthy adults and patients with Alzheimer's disease, raising plasma insulin levels while maintaining euglycemia

■ Figure 4.3-7

Glucose enhancement of memory in elderly subjects (data from Hall et al., 1989). The bars represent differences in scores after glucose and saccharin administration. Glucose ingestion improved on the logical memory (narrative prose passage as well as the overall composite score)



can improve memory; however, raising plasma glucose while suppressing endogenous insulin secretion may not improve memory, suggesting that adequate levels of insulin and glucose are necessary for memory facilitation. Clinical studies have corroborated findings that patients with Alzheimer's disease are more likely to have reduced insulin sensitivity than healthy older adults. Together, these findings support an association among cognition, impaired glucose metabolism, and reduced insulin sensitivity (Watson and Craft, 2004).

Although glucose is the brain's principal energy substrate, alternative substrates can substitute to maintain brain function and this appears to be at least in part by maintaining neurotransmitter function. A reduction in glucose available to brain slices diminishes ACh synthesis. Ketone bodies can serve as alternative substrates to maintain brain function. This is at least in part by maintaining neurotransmitter levels. β -Hydroxybutyrate can maintain synthesis of ACh in the presence of low glucose concentrations (Gibson and Blass, 1979; Tomaszewicz et al., 1997). These interactions have been used clinically to treat children with a reduced ability to use glucose (Falk et al., 1976) and can also be used to treat patients with AD who appear to have a pathological decrease in the brain's ability to use glucose. Elevation of plasma ketone body levels through an oral dose of medium-chain triglycerides may improve cognitive functioning in older adults with memory disorders. Treatment with medium-chain triglycerides facilitates performance on the Alzheimer's disease assessment scale-cognitive subscale. Higher ketone values are associated with greater improvement in paragraph recall with medium-chain triglyceride treatment relative to placebo (Reger et al., 2004).

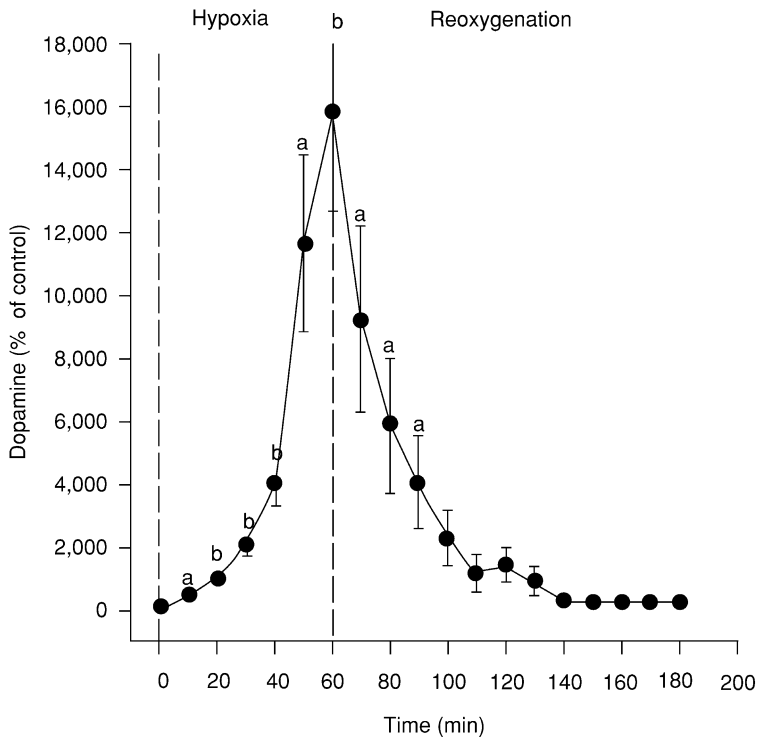
3.3 Connection of DA to Metabolism

DA synthesis depends directly on molecular oxygen. DA, like ACh, is very sensitive to hypoxia, but the responses are very different. Hypoxia decreases DA synthesis in vivo (Freeman et al., 1986). However, in vitro

reductions in oxygen increase DA concentrations in the extracellular space (Freeman and Gibson, 1986). In vivo, even slight reductions in the inspired air increase extracellular DA. Decreasing the oxygen fraction in the inspired gas from 21% to 14%, 11%, and 9% reduces cortical oxygen pressure from 31–35 Torr to about 24 Torr, 15 Torr, and 4 Torr, respectively. The stepwise decrease in the cortical oxygen pressure increases extracellular DA by about 80%, 200%, and 550% respectively, as measured by microdialysis. After restoring inspired air to control values (i.e., 21%), the cortical oxygen pressure rapidly increases to above normal, and then returns to control values. Dopamine levels return to normal more slowly (▶ Figure 4.3-8). Thus, there

■ Figure 4.3-8

The effect of 7% hypoxia on the extracellular concentrations of dopamine (DA) in striatum. (Graph is from Olano et al., 1995). A microdialysis probe was in the striatum



is no “oxygen reserve” to protect DA release and metabolism from decreases in oxygen pressure (Pastuszko et al., 1993; Huang et al., 1994; Olano et al., 1995). The increase in extracellular levels may be due to neuronal depolarization and inhibition of reuptake systems or some combination of increased release and decreased uptake. In vitro studies suggest that hypoxia-induced increase in extracellular levels is related to an increase in the release of DA (Freeman and Gibson, 1986). Increased extracellular levels may also impair further synthesis (Freeman and Gibson, 1986). These results indicate that multiple factors regulate extracellular DA levels and DA synthesis in response to metabolic perturbation.

3.4 Association of Metabolism and DA in Aging and Disease

Aging also alters the dopaminergic system. Results indicate that while aging increases the basal release of DA from striatal slices (Freeman and Gibson, 1987), no alterations are seen in K^+ - or amphetamine-induced

DA release (Thompson et al., 1981; Freeman and Gibson, 1987). However, oxotremorine-enhanced K^+ -evoked DA release ($K(+)$ -ERDA) from superfused striatal slices declines as a function of age (Joseph et al., 1996). Thus, the underlying mechanisms inducing presynaptic changes in both aging and hypoxia interact with multiple aspects of DA release.

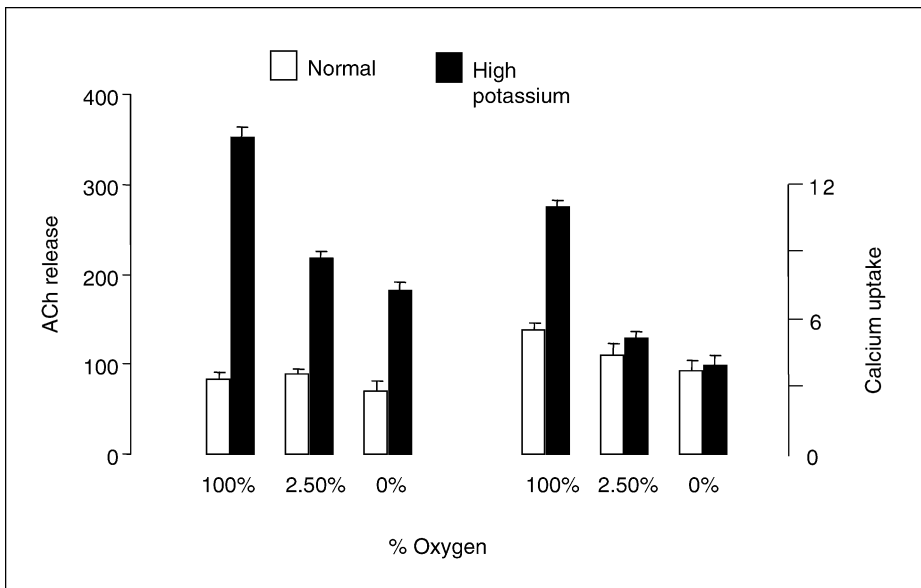
4 The Dependence of Neurotransmitters on Calcium may Account for Age and Metabolic Induced Changes

4.1 Changes in Neurotransmitters Mediated by Calcium with Alterations in Metabolism

Calcium is critical to neurotransmitter dynamics, especially release, and is regulated by energy metabolism (see *Chapter 4.6*). Calcium in the terminal can be regulated by the mitochondrial calcium uptake, the Na/Ca exchanger, the endoplasmic reticulum, and by multiple receptor-mediated processes. Hypoxia increases resting calcium in cells and exaggerates the response of calcium to depolarizing concentrations of K^+ . Calcium uptake into the isolated nerve terminal is diminished by hypoxia (Peterson and Gibson, 1984; Peterson et al., 1985a). The decline in calcium uptake into the presynaptic terminal parallels the decline in ACh release in both hypoxia and aging (Peterson and Gibson, 1982) (Figure 4.3-9). These are surprisingly complex changes that are not fully understood. The increases vary between different parts of the cells. In the cell bodies of differentiated PC12 cells, the increase in calcium is blocked by L-channel blockers, whereas in the nerve terminal (growth cone), the increase is blocked by N-channel calcium channel blockers (Gibson et al., 1997). Hypoxic-induced changes in calcium can also be blocked by antibodies to amyloid- β -peptide (A β) (Green and Peers, 2001), a toxic peptide that is increased in AD.

■ Figure 4.3-9

Hypoxia causes similar changes in acetylcholine (ACh) release and calcium uptake (Figure is from Gibson and Peterson, 1982)



4.2 Interaction of Calcium and Age-Related Deficits

There is a long history of studies showing the presence of elevated intracellular calcium during normal aging and age-related neurodegenerative disease (e.g., see Gibson and Peterson, 1987; Landfield and Eldridge, 1994; Herman et al., 1998; Joseph et al., 1999; Toescu and Verkhatsky, 2000). Calcium uptake into the isolated nerve terminal is diminished during aging (Peterson and Gibson, 1983). The decline in calcium uptake into the presynaptic terminal parallels the decline in ACh release in aging (Peterson and Gibson, 1983) (🔗 [Figure 4.3-9](#)). Normal aging reduces the ability of nerve terminal calcium to recover from depolarization (Giovannelli and Pepeu, 1989). This could be due to an inability of mitochondria to take up calcium. Calcium uptake into mitochondria within isolated nerve endings is diminished by aging (Peterson et al., 1985b). Thus, the nerve is exposed to prolonged elevated calcium following depolarization (Villaba et al., 1995) that may result from alterations in mitochondria. In addition, decrements in calcium buffering may reduce the effectiveness of endogenous antioxidants in the aged organism (Joseph et al., 1998a, b, c, d, 2001).

5 Free Radicals may Account for Many Changes Associated with Aging or Altered Metabolism

5.1 Production of Free Radicals

In addition to regulating neurotransmitter precursor availability and calcium levels, metabolism and oxygen interact with neurotransmitters through OS, mediated by ROS (i.e., free radicals). Free radicals are a part of normal metabolism that are exaggerated by numerous conditions and these ROS modulate many other pathways (see Chapters by Paul Brookes and Juan Bolanos) including multiple aspects of neurotransmitter metabolism such as synthesis, release, and the interaction of the neurotransmitter with the receptors.

Excessive free radicals are produced by many perturbations of metabolism. If the electron transport chain is interrupted, the reducing equivalents “back up” and the number of free radicals is amplified (see Chapter by Paul Brookes). Although in isolated mitochondria, hypoxia does not elevate ROS, in cell systems hypoxia does elevate ROS production (Chandel et al., 1998; Duranteau et al., 1998; Huang et al., 2004). For example, if mixed neuronal cultures are incubated without added glucose or oxygen, ROS production increases (🔗 [Figure 4.3-10](#)). The increase is likely related to the increase in reducing equivalents that are produced by glycolysis. Studies on the heart show that hypoxia can induce similar changes in regulation of mitochondrial function as induced by H_2O_2 —a common method of inducing OS (Duranteau et al., 1998).

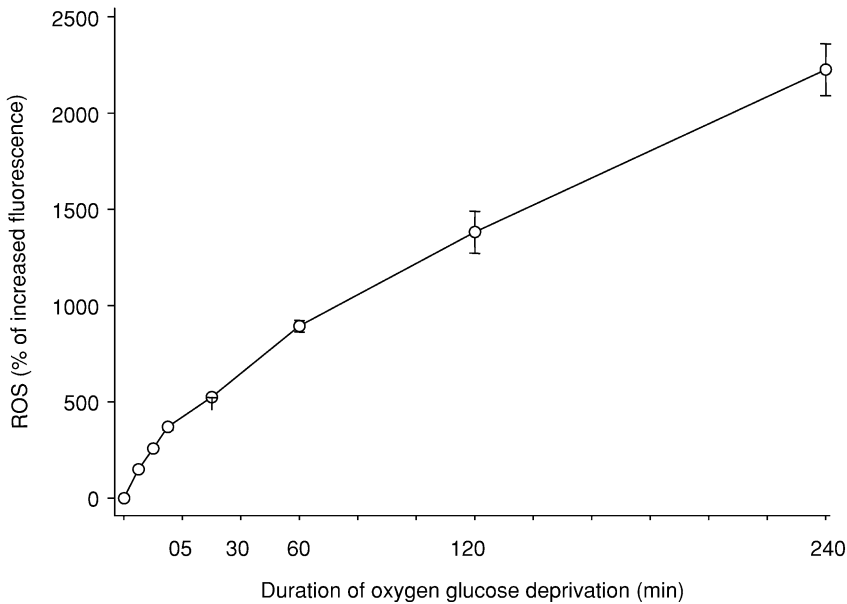
5.2 Free Radicals in Aging

An increase in free radicals occurs in aging, and evidence of damage from increased OS with aging is strong. Data are accumulating that suggest that one of the most important factors mediating the deleterious effects of aging on behavior and neuronal function is decreases in the balance between antioxidant activity and OS (see Floyd, 1999, for review). Indicators of OS in the aged brain include increases in the ratio of oxidized to total glutathione (Olanow, 1992), membrane lipid peroxidation (Yu, 1994; Denisova et al., 1998), elevated bcl-2 (an antioxidant that shows higher levels during OS, Sadoul, 1998), lipofuscin accumulation (Gilissen et al., 1999), decreases in glutamine synthetase (Carney et al., 1994), reductions in redox active iron (Gilissen et al., 1999; Savory et al., 1999), changes in the microvasculature (Floyd and Hensley, 2002), and increases in oxidized proteins and lipids (Floyd and Hensley, 2002).

Furthermore, the aged brain is more sensitive to oxidative stressors such as DA. Data show that senescent rats exhibit significantly greater motor behavioral deficits and decreases in tyrosine hydroxylase immunoreactivity (in the pars compacta) than do young rats following intranigral applications of DA (Cantuti-Castelvetri et al., 2003).

■ Figure 4.3-10

Production of reactive oxygen species (ROS) in mixed neuronal cultures after exposure to hypoxia and glucose deprivation. Data are from Huang et al. (2004)



5.3 Free Radicals and Regulation of Release

Free radicals may regulate neurotransmitter release. Addition of exogenous H_2O_2 increases intracellular ROS and diminishes release of DA (Chen et al., 2001) and glutamate (Gilman et al., 1992; Zoccarato et al., 1995). Glutamate-dependent inhibition of DA release in striatum is mediated by H_2O_2 (Avshalumov et al., 2003). H_2O_2 can reversibly depress evoked population spikes in hippocampal slices (Pellmar, 1986, 1995). Membrane peroxidation of synaptosomes from 2-month-old rats diminished the release of ACh to levels seen in old rats (Meyer et al., 1994). The site of reactive oxygen appears to be presynaptic. However, the precise site of action is unclear. Many calcium-dependent steps including oxidative modification of the intracellular proteins that are involved in vesicular loading and release are sensitive to OS. For example, oxidants can modify calcium-dependent SNARE-binding interactions involving redox-sensitive amino acids like cysteine or alterations in the balance of kinases and phosphatases (Distasi et al., 2002). Oxidants may also modify the clearance of released neurotransmitters. For example, 4-hydroxy-2-nonenal modifies glial glutamate transporter (Lauderback et al., 2001).

The vulnerability of the release process to OS in the CNS increases during aging (see Joseph et al., 2001, for review). Age-related differences in oxotremorine-induced K^+ -evoked DA (K^+ -ERDA) release from perfused striatal slices provide one example of these changes (Joseph et al., 1996). Greater decrements in K^+ -ERDA occur in the striata from old rats than in those from young rats. The age-related differences are further increased when the tissue is preincubated with various concentrations of H_2O_2 .

5.4 Free Radicals and the DA Transporter

The DA transporter is one of the proteins at risk for oxidant modification, because it has a high affinity for DA and contains several cysteinyl residues. Uptake of DA is inhibited by ascorbate and this inhibition is prevented by an iron chelator, suggesting that ascorbate acts as a prooxidant in the presence of iron.

Preincubation with xanthine/xanthine oxidase also reduces DA uptake. These findings suggest that ROS can modify DA transport function (Berman et al., 1996). Hypoxia also diminishes DA uptake (Freeman and Gibson, 1986).

5.5 Regulation of Receptor Subtypes and Oxidative Stress (OS)

OS may selectively modify various neurotransmitter receptor subtypes (Joseph et al., 1998a, b, c, d). Exposure of brain slices to DA induces OS in striatal slices from both young and old rats. The selective response to OS can be determined by applying D_1 or D_2 agonists and assessing differences in D_1 - or D_2 carbachol-stimulated GTPase activity. DA significantly reduces GTPase activity in both age groups and through both D_1 and D_2 receptors. DA is more effective in reducing D_1 receptor carbachol-stimulated GTPase activity in the striata from the old animals. The DA effect can be effectively antagonized with the antioxidant α -phenyl-*n*-tert-butyl nitron. These results demonstrate that there is differential vulnerability to OS among various receptor subtypes, and this may be one factor mediating overall sensitivity to OS under normal conditions and especially during aging.

5.6 Regulation of Muscarinic Receptors

Muscarinic receptors (MACHRs) are selectively sensitive to oxidants and to aging. Strong evidence suggests that MACHRs may modulate excitatory hippocampal synaptic transmission (Marino et al., 1998), and that MACHR activation provides protection against possible OS and subsequent apoptosis (De Sarno et al., 2003). MACHRs are intimately involved in various aspects of both neuronal (e.g., APP processing, Rossner et al., 1998) and vascular functions (Elhousseiny et al., 1999) that have been associated with diseases. The MACHR/vascular interaction is important, since vascular disease and AD can occur in concert in aging and vascular disease may exacerbate cognitive dysfunction in AD (Morris, 2000; Deschamps et al., 2001). Data suggest that there are complex interactions between vascular dementia and AD (Morris, 2000; Deschamps et al., 2001). Thus, any OS-induced alteration in MACHR responsiveness, or sensitivity to OS in aging or AD, could have multiple consequences. Considerable evidence indicates a loss of responsiveness in MACHRs with AD, as well as with aging (Cutler et al., 1994; Flynn et al., 1995; Ferrari-DiLeo et al., 1995; Claus, et al., 1997; Ladner and Lee, 1999; Muma et al., 2003; see Joseph et al., 2001, for review). The decline in MACHR function may result from alterations in receptor G protein coupling/uncoupling (e.g., Cutler et al., 1994; Muma et al., 2003), an index that has been shown to be extremely vulnerable to OS (e.g., Venters et al., 1997).

The vulnerability of different MACHRs to OS must be studied directly in cells transfected with different MACHRs, because defining sensitivity of molecules to OS is difficult with brain tissue. COS-7 cells that are transfected with five MACHR subtypes (M_1 – M_5) and exposed to DA (Joseph et al., 2002) or $A\beta$ (Joseph and Fisher, 2003) show differences in sensitivity to OS, expressed as a function of Ca^{2+} buffering assessed by examining the ability of the cell to extrude or sequester Ca^{2+} following oxotremorine-induced depolarization. COS-7 cells transfected with M_1 , M_2 , or M_4 ACh receptors are more sensitive to DA- or $A\beta$ -induced disruptions in calcium buffering than those transfected with M_3 or M_5 AChR.

The selective alteration of MACHRs in response to oxidants may begin to explain previous results that show significant differences in the rates of aging among various brain regions. Areas such as the hippocampus (Nyakas et al., 1997; Kaufmann et al., 2001), cerebellum (Hartmann et al., 1996; Kaufmann et al., 2001), and striatum (Joseph et al., 1996; Kaasinen et al., 2000) show profound alterations in morphology, electrophysiology, and receptor sensitivity with aging. These age-related changes at least partially correspond to the distribution of OS-sensitive MACHR subtypes. M_1 receptor protein is expressed in 78% of the neurons of the striatum, while M_2 receptors may be the predominant MACHR in the striatum, and M_4 receptors are localized to 44% of striatal cells (Hersch et al., 1994). In addition, a wide distribution in these receptor subtypes occurs in the dentate gyrus (Levey et al., 1996) and M_2 and M_4 MACHR protein concentrations are high in the fimbria-fornix.

The relationship between variations in sensitivity to OS among the various MACHR subtypes and their structural differences is not known. However, recent evidence indicates that this may occur through the i3 loop (Joseph et al., 2004a, b). This is an intracellular loop that emerges from the third transmembrane segment of the MACHR. Indirect evidence for the importance of i3 loop in OS sensitivity is provided by studies showing that G protein β , which interacts with the i3 loop of the MACHR, is inhibited by the G protein α subunit and is necessary for phosphorylation and subsequent signal transduction (Wu et al., 1997, 1998, 2000). The $G\beta\gamma$ subunit interacts with a plethora of potential signaling agents that involve calcium channels, G-protein-gated inwardly rectifying potassium channels, and G protein receptor kinases (Wu et al., 2000). Reduction in muscarinic signaling that involves decrements in MACHR G protein coupling/uncoupling occurs in aging and AD, and plausible mechanisms link these to OS (see Joseph et al., 2001, for review).

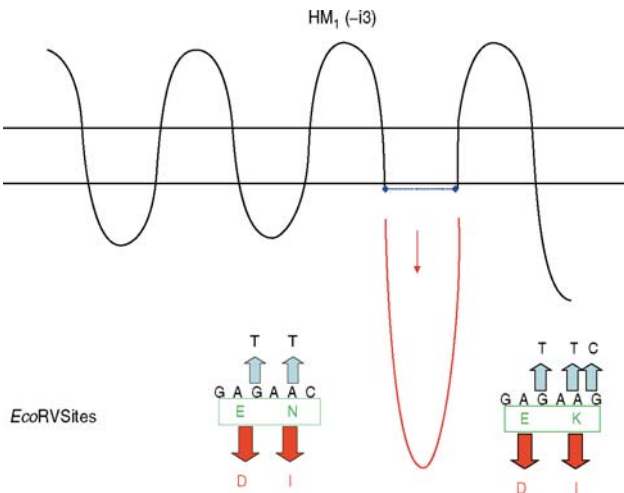
Deletion experiments provide direct evidence on the possible involvement of the i3 loop in OS. Deletion of the entire i3 loop increases DA sensitivity (a lower percentage of cells show recovery following depolarization) in both the M_1 and M_3 subtypes (Joseph et al., 2004b) (▶ [Figures 4.3-11](#) and ▶ [4.3-12](#)). Chimerics of M_1 , where the i3 loop of the M_3 AChR is switched with the i3 loop of the M_1 AChR (M_1M_3i3 ; ▶ [Figure 4.3-13](#)), show DA-induced disruptions in calcium buffering (percentage of cells showing increases in calcium clearance i.e., decreased calcium levels) following depolarization. In the M_3 chimerics containing M_1i3 (M_3M_1i3), the i3 loop (▶ [Figure 4.3-14](#)) offers no protection against DA-induced decrements in calcium buffering.

Whether the i3 loops of other OS-sensitive (M_2 and M_4) and -insensitive receptors (M_5) have properties similar to those of the M_1 and M_3 i3 loops is unknown. However, findings clearly show that if the i3 loop does not provide sufficient OS protection to the receptor, then vulnerability to OS might be increased. Thus, it may be that in addition to the numerous functions alluded to above, the i3 loop may also be responsible for providing protection against OS or perhaps, even inflammatory stressors. Damage to these loops may ultimately be expressed as decreased neuronal communication and behavioral performance.

A great deal more work is needed to determine the possible relationships among the amino acids of the i3 loops from the various MACHR subtypes and sensitivity to OS. It is possible, though, to speculate about the structural/OS vulnerability differences by examining the entire receptor. ▶ [Table 4.3-1](#) shows the

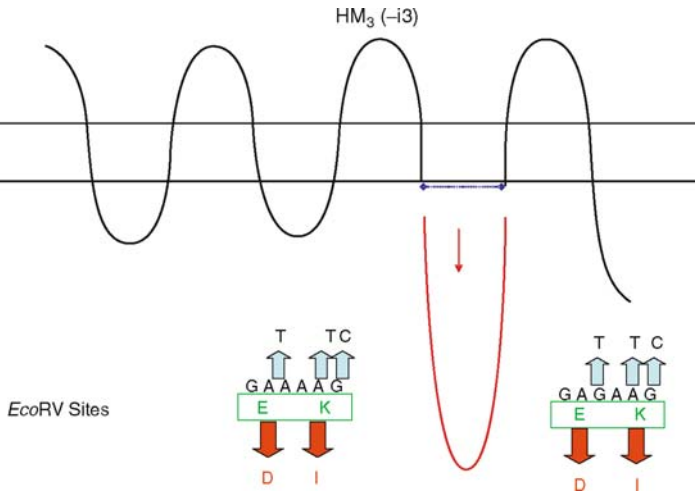
■ Figure 4.3-11

Structure of the HM_1 muscarinic receptor and the resulting chimeric made by removal of the i3 loop ($HM_1(-i3)$) and its mutation. Shown are the location of the incorporated *EcoRV* sites at the amino terminus and carboxyl terminus of the i3 loop



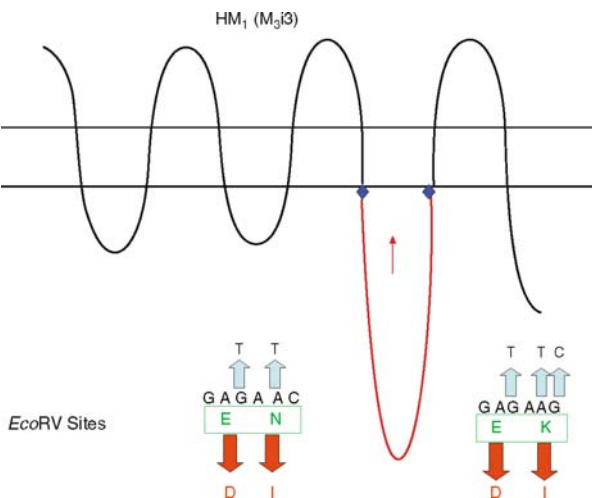
■ Figure 4.3-12

Structure of the HM_3 muscarinic receptor and the resulting chimeric made by removal of the i3 loop ($HM_3(-i3)$) and its mutation. Shown are the location of the incorporated *EcoRV* sites at the amino terminus and carboxyl terminus of the i3 loop



■ Figure 4.3-13

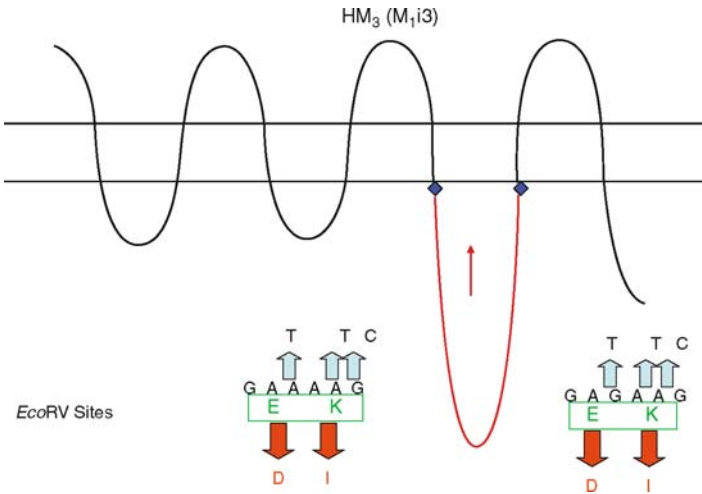
Structure of the HM_1 chimeric shown after translocation of the i3 loop ($HM_1(M_3i3)$). Shown are the location of the incorporated *EcoRV* sites at the amino terminus and carboxyl terminus of the i3 loop



distribution of three amino acids that may affect metal sequestration and their distribution among the five MACHR subtypes. Note that the highest numbers of the amino acids, His, Lys, and Tyr, are found in the MACHR that show the least vulnerability to OS. Thus, His >7, Lys >32, and Tyr >17 may enhance protection against OS through metal sequestration. M_1^- , M_2^- , and M_4^- -transfected COS-7 cells would show greater sensitivity to OS than those transfected with M_3 or M_5 receptor subtypes. For example, it has been

■ Figure 4.3-14

Structure of the HM₃ chimeric shown after translocation of the i3 loop (HM₃(m₁i3)). Shown are the location of the incorporated *EcoRV* sites at the amino terminus and carboxyl terminus of the i3 loop



■ Table 4.3-1

Amino acids, muscarinic receptor subtype, and oxidative stress

	M ₁	M ₂	M ₃	M ₄	M ₅
His	2	6	9	6	8
Lys	24	31	38	25	38
Tyr	16	16	18	15	22

shown that ZnT-1, a mammalian protein that is located in plasma membranes and increases zinc extrusion, has a histidine-rich intracellular loop (Palmiter et al., 1996).

In the same vein, the i3 loop of the M₁AChR contains 157 amino acids, while the M₃AChR i3 loop contains 240 amino acids. Thus, one factor that could be important with respect to protection may be the length of the i3 loop. Although there are a greater number of amino acids in the i3 loop, not all of the amino acids are represented. Only selected ones are found (phe, leu, ser, gln, arg, thr, lys, ala, and asp). Others are approximately the same in both i3 and i1 loops (e.g., arg, glu, and gly). Lys seems to be greater in both the whole receptor and the i3 loop of the M₃ receptor than in the M₁. Perhaps that site may be important in determining vulnerability to OS. Further research employing site-directed mutagenesis is necessary to specify additional sites that may also be important in determining differential protection against OS among these i3 loops.

However, the results thus far (Joseph et al., 2004b) suggest that the longer i3 loop of the M₃AChR may be decreasing sensitivity to OS. Investigations of specific targeting properties of various antioxidants are required. Although there are no data specifically concerned with antioxidant effects on the i3 loop, preliminary data from the MACHR-transfected COS-7 cells suggest that this loop may to some extent control the efficacy of the antioxidant treatment. As described below, preliminary studies indicate that pretreatment with blueberry extract (BB) (i.e., a broad-range antioxidant) prior to DA exposure protects calcium buffering assessed following oxotremorine-induced depolarization in the M₁- or M₃-transfected, wild-type, truncated, or chimeric COS-7 cells (Joseph et al., manuscript in preparation).

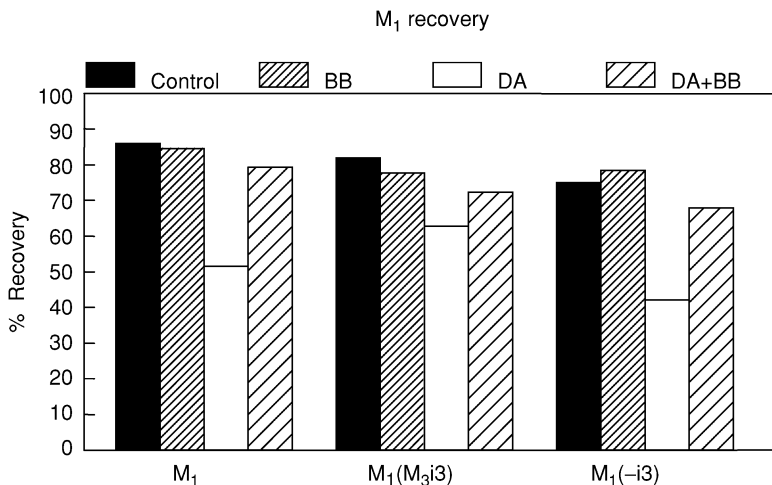
6 Reversal of the Effects of Oxidative Stress (OS) on Calcium Buffering with Antioxidants

BB extract is utilized in these studies since the secondary compounds (e.g., flavonoids such as anthocyanins, proanthocyanidins) found in blueberries and other fruits have potent antioxidant properties (see Prior et al., 2003). BBs, as well as other fruit extracts, are effective in protecting M_1 -transfected COS-7 cells from the deleterious effects of DA or $A\beta$ on calcium buffering. Following depolarization via oxotremorine, the BB-treated cells that have been exposed to DA or $A\beta$ are able to reduce intracellular levels to the same extent as that seen in control cells (Joseph et al., 2004a).

BB pretreatment is effective in protecting against the deleterious effects of DA on calcium buffering in the M_1 wild-type and in the truncated M_1 -transfected cells. Since DA does not alter the calcium buffering ability of the M_1M_3i3 chimerics, no effects are seen with respect to BB pretreatment (▶ [Figure 4.3-15](#)).

■ Figure 4.3-15

Ca^{2+} clearance (expressed as % cells showing recovery) following oxotremorine-induced depolarization in M_1 wild type, M_1M_3i3 chimerics, and truncated M_1 -transfected COS-7 control cells and those pretreated with blueberries and DA

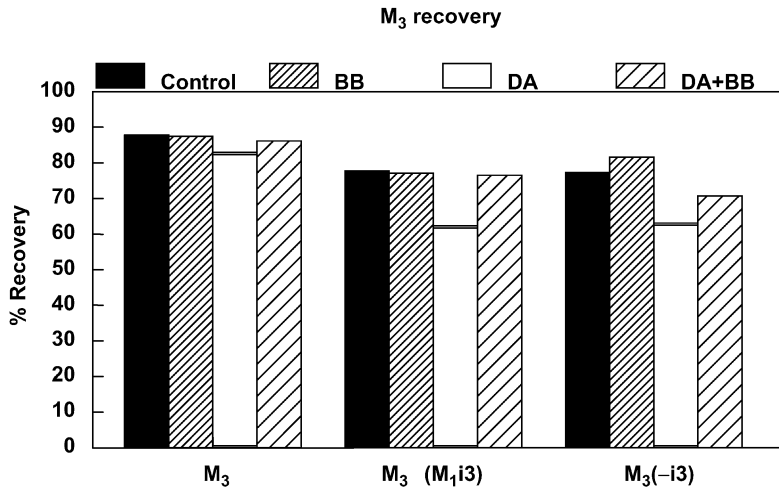


In the M_3 -transfected cells, BB pretreatment is protective against the DA effects in the cells transfected with the M_3M_3i3 chimerics but does not protect the truncated M_3 -transfected cells (▶ [Figure 4.3-16](#)). These findings, coupled with those showing that the M_3i3 loop offers some protection in the M_1M_3i3 chimerics, suggest that the M_3i3 loop may at least partially mediate the protective effects of BB in M_3 cells. This effect is normally masked in the cells transfected with the wild-type M_3AChR , since they are not normally sensitive to OS. In the case of the M_1 receptor, the $i3$ loop may be less involved in mediating the BB effects, since BB treatment is effective against the DA effects on calcium buffering in the cells transfected with the truncated M_1 receptors.

Besides the $i3$ loop, flavonoids may also act at other cellular sites that alter the interaction of neurotransmitters and metabolism. Flavonoids such as taxifolin and quercetin can protect against the onset of mitochondrial permeability transition (Santos et al., 1998; see Chapter by Wieloch), and, depending on the concentration, can interfere with mitochondrial calcium sequestration as well as the energetics of the cell and production of ROS. This would have important implications for both cell

■ Figure 4.3-16

Ca^{2+} clearance (expressed as % cells showing recovery) following oxotremorine-induced depolarization in M_1 wild type, M_3M_1i3 chimerics, and truncated M_3 -transfected COS-7 control cells and those pretreated with blueberries and DA



protection in the case of preservation of neuronal communication and behavior in aging. For example, deficits in such parameters as motor and cognitive behavior, calcium clearance, muscarinic receptor sensitivity, and neurogenesis improve in senescent animals maintained for 2 months on a diet containing 2% BB supplementation (Joseph et al., 1999; Casadesus et al., 2004).

7 Changes in Lipids May Alter the Interactions of Oxidative Stress (OS), Calcium, and Neurotransmitters

Alterations in lipid composition and metabolism in the brain may also modify calcium homeostasis and sensitivity to OS. The brain is highly enriched in lipids (cholesterol (CHL), phospholipids (PL), gangliosides, etc.) (Avrova et al., 1973; Zhang et al., 1996). Apolipoproteins play an important role in the regulation of PL and CHL content in neuronal tissue, in the formation of membranes and synapses (Krugers et al., 1997; Michikawa et al., 2000), and in the regulation of membrane molecular structures (Igbavboa, 1996).

A loss of membrane asymmetry may have important consequences for neuronal function. CHL comprises over 40 mol% of membrane lipids (Igbavboa, 1996), is associated with bulk membrane fluidity (Leibel et al., 1987), and translocates from the inner plasma membrane leaflet to the exofacial leaflet (Igbavboa et al., 1996) to significantly reduce both overall membrane fluidity and asymmetry in senescence (e.g., see Igbavboa, 1996). Importantly, CHL that is oxidized in the outer leaflet of synaptosomes induces significant reductions in the activity of the Ca^{2+} ATPase “pump” (Igbavboa, 1996) and decreases calcium buffering. For example, when the phosphatidylcholine/sphingomyelin ratio is reduced and the CHL levels are elevated in cultured myocytes (a profile seen in aged myocytes), decrements in muscarinic receptor-G protein coupling, much like that seen in aging, occur. These deficits are reduced when the lipid profile is altered with liposomes containing phosphatidylcholine (Moscona-Amir et al., 1986).

Sphingomyelin (SPH) regulates CHL trafficking (Leppimaki et al., 1998). CHL movement to the inner-membrane leaflet is directly related to increased SPH metabolic activity and metabolite formation (Slotte et al., 1988). However, SPH and its metabolites may also have more direct interactions with oxidative stressors that increase sensitivity to free radicals. For example, PC-12 cells in which SPH and CHL are increased to the levels

seen in the aging brain aging and following exposure to H_2O_2 have a reduced ability to regulate (sequester or extrude) calcium following 30 mM KCl-induced depolarization (Denisova et al., 1997). OS may enhance calcium dysfunction (Cheng et al., 1994) in cells that are already compromised, with subsequent prooxidant generation and loss of functional capacity of the cell. Of the major SPH metabolites, only sphingosine-1-phosphate added to the cells significantly increases the sensitivity to OS induced by exposure to H_2O_2 , as assessed by a loss of calcium buffering following depolarization with 30 mM KCl. A second SPH metabolite, ceramide, when added to the cells, while not affecting calcium buffering, significantly increases free radicals in PC-12 cells treated with this metabolite and exposed to H_2O_2 (Denisova et al., 1999).

Several membrane changes in aging could enhance the vulnerability to OS. These may include alterations in CHL transfer or levels, SPH regulation of CHL transfer, or SPH-induced reductions in glutathione levels. Moreover, membrane fatty-acid-binding proteins may also decrease in aging, further inhibiting normal CHL trafficking (Pu et al., 1999). The role of these lipid changes in vulnerability to OS, or to the receptor changes described above, remains to be determined.

8 Conclusions

Brain function is closely coupled to neural energy metabolism and this is not simply an effect on concentration of energy metabolites such as ATP. Many of the changes are due to a direct interaction of metabolism on specific aspects of neurotransmitter function. These interactions can be revealed by perturbing metabolism and determining the consequences, or by reversing the effects with compounds of known action. Hypoxia, hypoglycemia, and aging interfere with metabolism and alter brain function and these changes are at least in part because of the interaction of metabolism with multiple aspects of neurotransmitter function. The similarity of these diverse insults on brain function suggests that they act on similar fundamental mechanisms. Some aspects of the aging brain are similar to the hypoxic or the hypoglycemic brain in that factors such as cognition, motor behavior, cholinergic and dopaminergic function, and calcium buffering decrease under all of these conditions. One common mechanism that may be involved in these deleterious effects may be OS, since radiation produces behavioral deficits that parallel those observed in aging. Similarly, reductions in the levels of glutathione along with central DA administration also produce age-like conditions in motor and cognitive behavior. Age-related changes in lipids and decreases in endogenous antioxidant protection may increase sensitivity to OS as a function of age. Given these and other factors discussed earlier that are concerned with reducing sensitivity to OS via antioxidants, it may be that some of the deleterious effects of aging could be reduced or forestalled by dietary and other methods that increase antioxidant defenses.

References

- Avrova NF, Chenyakaeva EY, Obukhova EL. 1973. Ganglioside composition and content of rat-brain subcellular fractions. *J Neurochem* 20: 997-1004.
- Avshalumov MV, Chen BT, Marshall SP, Pena DM, Rice ME. 2003. Glutamate-dependent inhibition of dopamine release in striatum is mediated by a new diffusible messenger, H_2O_2 . *J Neurosci* 23: 2744-2750.
- Bartus RT. 1990. Drugs to treat age-related neurodegenerative problems. The final frontier of medical science? *J Am Geriatr Soc* 38: 680-695.
- Berman SB, Zigmond MJ, Hastings TG. 1996. Modification of dopamine transporter function: Effect of reactive oxygen species and dopamine. *J Neurochem* 67: 593-600.
- Bickford P. 1993. Motor learning deficits in aged rats are correlated with loss of cerebellar noradrenergic function. *Brain Res* 620: 133-138.
- Bickford P, Heron C, Young DA, Gerhardt GA, De La Garza R. 1992. Impaired acquisition of novel locomotor tasks in aged and norepinephrine-depleted F344 rats. *Neurobiol Aging* 13: 475-481.
- Bickford PC, Chadman K, Williams B, Shukitt-Hale B, Holmes D, et al. 1999. Effect of normobaric hyperoxia on two indexes of synaptic function in Fisher 344 rats. *Free Radic Biol Med* 26: 817-824.
- Cantuti-Castelvetri I, Shukitt-Hale B, Joseph JA. 2003. Dopamine neurotoxicity: Age-dependent behavioral and histological effects. *Neurobiol Aging* 24: 697-706.

- Carney JM, Smith CD, Carney AM, Butterfield DA. 1994. Aging- and oxygen-induced modifications in brain biochemistry and behavior. *Ann N Y Acad Sci* 738: 44-53.
- Casadesus G, Shukitt-Hale B, Stellwagen HM, Zhu X, Lee HG, et al. 2004. Modulation of hippocampal plasticity and cognitive behavior by short-term blueberry supplementation in aged rats. *Nutr Neurosci* 7: 309-316.
- Chandel NS, Maltepe E, Goldwasser E, Mathieu CE, Simon MC, et al. 1998. Mitochondrial reactive oxygen species trigger hypoxia-induced transcription. *Proc Natl Acad Sci USA* 95: 11715-11720.
- Chen BT, Avshalumov MV, Rice ME. 2001. H(2)O(2) is a novel endogenous modulator of synaptic dopamine release. *J Neurophysiol* 85: 2468-2476.
- Cheng Y, Wixom P, James-Kracke MR, Sun AY. 1994. Effects of extracellular ATP on Fe(2+)-induced cytotoxicity in PC-12 cells. *J Neurochem* 63: 895-902.
- Chleide E, Ishikawa K. 1990. Hypoxia-induced decrease of brain acetylcholine release detected by microdialysis. *Neuroreport* 1: 197-199.
- Claus JJ, Dubois EA, Booij J, Habraken J, de Munck JC, et al. 1997. Demonstration of a reduction in muscarinic receptor binding in early Alzheimer's disease using iodine-123 dextetimide single-photon emission tomography. *Eur J Nucl Med* 24: 602-608.
- Cooper JR. 1994. Unsolved problems in the cholinergic nervous system. *J Neurochem* 63: 395-399.
- Cutler R, Joseph JA, Yamagami K, Villalobos-Molina R, Roth GS. 1994. Area specific alterations in muscarinic stimulated low Km GTPase activity in aging and Alzheimer's disease: Implications for altered signal transduction. *Brain Res* 664: 54-60.
- Denisova NA, Erat SA, Kelly JF, Roth GS. 1998. Differential effect of aging on cholesterol modulation of carbachol-stimulated low-K(m) GTPase in striatal synaptosomes. *Exp Gerontol* 33: 249-265.
- Denisova NA, Fisher D, Provost M, Joseph JA. 1999. The role of glutathione membrane sphingomyelin and its metabolites in oxidative stress-induced calcium "dysregulation" in PC12 cells. *Free Radic Biol Med* 27: 1292-1301.
- Denisova NA, Strain JG, Joseph JA. 1997. Oxidant injury in PC12 cells—a possible model of calcium "dysregulation" in aging: II. Interactions with membrane lipids. *J Neurochem* 69: 1259-1266.
- De Sarno P, Shestopal SA, King TD, Zmijewska A, Song L, et al. 2003. Muscarinic receptor activation protects cells from apoptotic effects of DNA damage oxidative stress and mitochondrial inhibition. *J Biol Chem* 278: 11086-11093.
- Deschamps V, Barberger-Gateau P, Peuchant E, Orgogozo JM. 2001. Nutritional factors in cerebral aging and dementia: Epidemiological arguments for a role of oxidative stress. *Neuroepidemiology* 20: 7-15.
- Di Stasi AM, Mallozzi C, Macchia G, Maura G, Petrucci TC, Minetti M. 2002. Peroxynitrite affects exocytosis and SNARE complex formation and induces tyrosine nitration of synaptic proteins. *J Neurochem* 82: 420-429.
- Duranteau J, Chandel NS, Kulisz A, Shao Z, Schumacker PT. 1998. Intracellular signaling by reactive oxygen species during hypoxia in cardiomyocytes. *J Biol Chem* 273: 11619-11624.
- Elhusseiny A, Cohen Z, Olivier A, Stanimirovic DB, Hamel E. 1999. Functional acetylcholine muscarinic receptor subtypes in human brain microcirculation: Identification and cellular localization. *J Cereb Blood Flow Metab* 19: 794-802.
- Falk RE, Cederbaum SD, Blass JP, Gibson GE, Kark RA, et al. 1976. Ketonic diet in the management of pyruvate dehydrogenase deficiency. *Pediatrics* 58: 713-721.
- Ferrari-DiLeo G, Mash DC, Flynn DD. 1995. Attenuation of muscarinic receptor-G-protein interaction in Alzheimer disease. *Mol Chem Neuropathol* 24: 69-91.
- Fisher DB, Kaufman S. 1972. The inhibition of phenylalanine and tyrosine hydroxylases by high oxygen levels. *J Neurochem* 19: 1359-1365.
- Floyd RA. 1999. Antioxidants oxidative stress and degenerative neurological disorders. *Proc Soc Exp Biol Med* 222: 236-245.
- Floyd RA, Hensley K. 2002. Oxidative stress in brain aging. Implications for therapeutics of neurodegenerative diseases. *Neurobiol Aging* 23: 795-807.
- Flynn DD, Ferrari-DiLeo G, Levey AI, Mash DC. 1995. Differential alterations in muscarinic receptor subtypes in Alzheimer's disease: Implications for cholinergic-based therapies. *Life Sci* 56: 869-876.
- Freeman GB, Gibson GE. 1986. Effect of decreased oxygen on in vitro release of endogenous 34-dihydroxyphenylethylamine from mouse striatum. *J Neurochem* 47: 1924-1931.
- Freeman GB, Gibson GE. 1987. Selective alteration of mouse brain neurotransmitter release with age. *Neurobiol Aging* 8: 147-152.
- Freeman GB, Nielsen P, Gibson GE. 1986. Monoamine neurotransmitter metabolism and locomotor activity during chemical hypoxia. *J Neurochem* 46: 733-738.
- Ghajar JB, Gibson GE, Duffy TE. 1985. Regional acetylcholine metabolism in brain during acute hypoglycemia and recovery. *J Neurochem* 44: 94-98.
- Gibson G, Toral-Barza L, Zhang H. 1997. Selective changes in cell bodies and growth cones of nerve growth factor-differentiated PC12 cells induced by chemical hypoxia. *J Neurochem* 69: 603-611.
- Gibson GE, Blass JP. 1976. Impaired synthesis of acetylcholine in brain accompanying mild hypoxia and hypoglycemia. *J Neurochem* 27: 37-42.
- Gibson GE, Blass JP. 1979. Proportional inhibition of acetylcholine synthesis accompanying impairment of 3-hydroxybutyrate oxidation in rat brain slices. *Biochem Pharmacol* 28: 133-139.

- Gibson GE, Blass JP, Beal MF, Bunik V. 2005. The alpha-ketoglutarate-dehydrogenase complex: A mediator between mitochondria and oxidative stress in neurodegeneration. *Mol Neurobiol* 31: 43-64.
- Gibson GE, Jope R, Blass JP. 1975. Decreased synthesis of acetylcholine accompanying impaired oxidation of pyruvic acid in rat brain minces. *Biochem J* 148: 17-23.
- Gibson GE, Pelmas CJ, Peterson C. 1983. Cholinergic drugs and 4-aminopyridine alter hypoxic-induced behavioral deficits. *Pharmacol Biochem Behav* 18: 909-916.
- Gibson GE, Peterson C. 1982. Biochemical and behavioral parallels in aging and hypoxia. *The aging brain: Cellular and molecular mechanisms of aging in the nervous system*. New York: Raven Press; 290: 107-122.
- Gibson GE, Peterson C, Jenden DJ. 1981. Brain acetylcholine synthesis declines with senescence. *Science* 213: 674-676.
- Gibson GE, Peterson C. 1987. Calcium and the aging nervous system. *Neurobiol Aging* 8(4): 329-343.
- Gilissen EP, Jacobs RE, Allman JM. 1999. Magnetic resonance microscopy of iron in the basal forebrain cholinergic structures of the aged mouse lemur. *J Neurol Sci* 168: 21-27.
- Gilman SC, Bonner MJ, Pellmar TC. 1992. Peroxide effects on [³H] glutamate release by synaptosomes isolated from the cerebral cortex. *Neurosci Lett* 140: 157-160.
- Giovannelli L, Pepeu G. 1989. Effect of age on K⁺-induced cytosolic Ca²⁺ changes in rat cortical synaptosomes. *J Neurochem* 53: 392-398.
- Gold PE. 1995. Role of glucose in regulating the brain and cognition. *Am J Clin Nutr* 61: 987S-995S.
- Green KN, Peers C. 2001. Amyloid beta peptides mediate hypoxic augmentation of Ca(2+) channels. *J Neurochem* 77: 953-956.
- Hall JL, Gonder-Frederick LA, Chewing WW, Silveira J, Gold PE. 1989. Glucose enhancement of performance on memory tests in young and aged humans. *Neuropsychologia* 27: 1129-1138.
- Hartmann H, Velbinger K, Eckert A, Muller WE. 1996. Region-specific downregulation of free intracellular calcium in the aged rat brain. *Neurobiol Aging* 17: 557-563.
- Herman JP, Chen KC, Booze R, Landfield PW. 1998. Up-regulation of alpha1D Ca²⁺ channel subunit mRNA expression in the hippocampus of aged F344 rats. *Neurobiol Aging* 19: 581-587.
- Hersch SM, Gutekunst CA, Rees HD, Heilman CJ, Levey AL. 1994. Distribution of m1-m4 muscarinic receptor proteins in the rat striatum: Light and electron microscopic immunocytochemistry using subtype-specific antibodies. *J Neurosci* 14: 3351-3363.
- Huang CC, Lajevardi NS, Tammela O, Pastuszko A, Delivoria-Papadopoulos M, et al. 1994. Relationship of extracellular dopamine in striatum of newborn piglets to cortical oxygen pressure. *Neurochem Res* 19: 649-655.
- Huang HM, Zhang H, Ou HC, Chen HL, Gibson GE. 2004. Alpha-keto-beta-methyl-n-valeric acid diminishes reactive oxygen species and alters endoplasmic reticulum Ca(2+) stores. *Free Radic Biol Med* 37: 1779-1789.
- Igbavboa U, Avdulov NA, Schroeder F, Wood WG. 1996. Increasing age alters transbilayer fluidity and cholesterol asymmetry in synaptic plasma membranes of mice. *J Neurochem* 66: 1717-1725.
- Ingram DK, Jucker M, Spangler E. 1994. Behavioral manifestations of aging. I. Pathobiology of the aging rat, Vol. 2. Mohr U, Cungworth DL, Capen CC, editors. Washington: ILSI Press; pp. 149-170.
- Joseph JA. 1992. The putative role of free radicals in the loss of neuronal functioning in senescence. *Integr Physiol Behav Sci* 27: 216-227.
- Joseph JA, Bartus RT, Clody D, Morgan D, Finch C, et al. 1983. Psychomotor performance in the senescent rodent: Reduction of deficits via striatal dopamine receptor up-regulation. *Neurobiol Aging* 4: 313-319.
- Joseph JA, Denisova N, Fisher D, Bickford P, Prior R, et al. 1998a. Age-related neurodegeneration and oxidative stress: Putative nutritional intervention. *Neurol Clin* 16: 747-755.
- Joseph JA, Denisova N, Villalobos-Molina R, Erat S, Strain J. 1996. Oxidative stress and age-related neuronal deficits. *Mol Chem Neuropathol* 28: 35-40.
- Joseph JA, Erat S, Denisova N, Villalobos-Molina R. 1998b. Receptor- and age-selective effects of dopamine oxidation on receptor-G protein interactions in the striatum. *Free Radic Biol Med* 24: 827-834.
- Joseph JA, Fisher DR. 2003. Muscarinic receptor subtype determines vulnerability to amyloid beta toxicity in transfected cos-7 cells. *J Alzheimers Dis* 5: 197-208.
- Joseph JA, Fisher DR, Carey AN. 2004a. Fruit extracts antagonize Aβ- or DA-induced deficits in Ca²⁺ flux in M1-transfected COS-7 cells. *J Alzheimers Dis* 6: 403-411; discussion 443-449.
- Joseph JA, Fisher DR, Carey A, Szprengiel A. 2004b. The M3 muscarinic receptor i3 domain confers oxidative stress protection on calcium regulation in transfected COS-7 cells. *Aging Cell* 3: 263-271.
- Joseph JA, Fisher DR, Strain J. 2002. Muscarinic receptor subtype determines vulnerability to oxidative stress in COS-7 cells. *Free Radic Biol Med* 32: 153-161.
- Joseph JA, Hunt WA, Rabin BM, Dalton TK. 1992. Possible "accelerated striatal aging" induced by 56Fe heavy-particle irradiation: Implications for manned space flights. *Radiat Res* 130: 88-93.
- Joseph JA, Shukitt-Hale B, Denisova NA, Bielinski D, Martin A, et al. 1999. Reversals of age-related declines in neuronal signal transduction cognitive and motor behavioral deficits with blueberry spinach or strawberry dietary supplementation. *J Neurosci* 19: 8114-8121.

- Joseph JA, Shukitt Hale B, Denisova NA, Martin A, Perry G, et al. 2001. Copernicus revisited: Amyloid beta in Alzheimer's disease. *Neurobiol Aging* 22: 131-146.
- Joseph JA, Shukitt-Hale B, Denisova NA, Prior RL, Cao G, et al. 1998c. Long-term dietary strawberry spinach or vitamin E supplementation retards the onset of age-related neuronal signal-transduction and cognitive behavioral deficits. *J Neurosci* 18: 8047-8055.
- Joseph JA, Shukitt-Hale B, McEwen J, Rabin BM. 2000. CNS-induced deficits of heavy particle irradiation in space: The aging connection. *Adv Space Res* 25: 2057-2064.
- Joseph JA, Villalobos-Molina R, Denisova N, Erat S, Cutler R, et al. 1996. Age differences in sensitivity to H₂O₂- or NO-induced reductions in K(+)-evoked dopamine release from superfused striatal slices: Reversals by PBN or Trolox. *Free Radic Biol Med* 20: 821-830.
- Joseph JA, Villalobos-Molina R, Denisova N, Erat S, Jimenez N, et al. 1996. Increased sensitivity to oxidative stress and the loss of muscarinic receptor responsiveness in senescence. *Ann N Y Acad Sci* 786: 112-119.
- Kaasinen V, Vilkkman H, Hietala J, Nagren K, Helenius H, Olsson H, Farde L, Rinne J. 2000. Age-related dopamine D2/D3 receptor loss in extrastriatal regions of the human brain. *Neurobiol Aging* 21(5): 683-688.
- Kaufmann JA, Bickford PC, Tagliatalata G. 2001. Oxidative-stress-dependent upregulation of Bcl-2 expression in the central nervous system of aged Fisher-344 rats. *J Neurochem* 76(4): 1099-1108.
- Kluger A, Gianutsos JG, Golomb J, Ferris SH, George AE, et al. 1997. Patterns of motor impairment in normal aging mild cognitive decline and early Alzheimer's disease. *J Gerontol B Psychol Sci Soc Sci* 52: P28-P39.
- Krugers HJ, Mulder M, Korff J, Havekes L, de Kloet ER, et al. 1997. Altered synaptic plasticity in hippocampal CA1 area of apolipoprotein E deficient mice. *Neuroreport* 8: 2505-2510.
- Ladner CJ, Lee JM. 1999. Reduced high-affinity agonist binding at the M(1) muscarinic receptor in Alzheimer's disease brain: Differential sensitivity to agonists and divalent cations. *Exp Neurol* 158: 451-458.
- Landfield PW, Eldridge JC. 1994. The glucocorticoid hypothesis of age-related hippocampal neurodegeneration: Role of dysregulated intraneuronal calcium. *Ann N Y Acad Sci* 746: 308-321; discussion 321-326.
- Lauderback CM, Hackett JM, Huang FF, Keller JN, Szweda LI, et al. 2001. The glial glutamate transporter GLT-1 is oxidatively modified by 4-hydroxy-2-nonenal in the Alzheimer's disease brain: The role of Aβ1-42. *J Neurochem* 78: 413-416.
- Leibel WS, Firestone LL, Legler DC, Braswell LM, Miller KW. 1987. Two pools of cholesterol in acetylcholine receptor-rich membranes from Torpedo. *Biochim Biophys Acta* 897: 249-260.
- Leppimäki P, Kronqvist R, Slotte JP. 1998. The rate of sphingomyelin synthesis de novo is influenced by the level of cholesterol in cultured human skin fibroblasts. *Biochem J* 335 (Pt 2): 285-291.
- Levey AI. 1996. Muscarinic acetylcholine receptor expression in memory circuits: Implications for treatment of Alzheimer disease. *Proc Natl Acad Sci USA* 93: 13541-135456.
- Lubbers DW. 1968. Tissue hypoxia: Cellular oxygen requirements with special regard to the in vivo pO₂ of the brain. *Scand J Clin Lab Invest Suppl* 102: II: A.
- Marino MJ, Rouse ST, Levey AI, Potter LT, Conn PJ. 1998. Activation of the genetically defined m1 muscarinic receptor potentiates N-methyl-D-aspartate (NMDA) receptor currents in hippocampal pyramidal cells. *Proc Natl Acad Sci USA* 95: 11465-11470.
- McFarland RA. 1963. Experimental evidence of the relationship between ageing and oxygen want: In search of a theory of ageing. *Ergonomics Research Society*, p. 339-366.
- Meyer EM, Judkins JH, Momol AE, Hardwick EO. 1994. Effects of peroxidation and aging on rat neocortical ACh release and protein kinase C. *Neurobiol Aging* 15: 63-67.
- Michikawa M, Fan QW, Isobe I, Yanagisawa K. 2000. Apolipoprotein E exhibits isoform-specific promotion of lipid efflux from astrocytes and neurons in culture. *J Neurochem* 74: 1008-1016.
- Morris MC, Scherr PA, Hebert LE, Bennett DA, Wilson RS, et al. 2000. The cross-sectional association between blood pressure and Alzheimer's disease in a biracial community population of older persons. *J Gerontol A Biol Sci Med Sci* 55: M130-M136.
- Moscona-Amir E, Henis YI, Yechiel E, Barenholz Y, Sokolovsky M. 1986. Role of lipids in age-related changes in the properties of muscarinic receptors in cultured rat heart myocytes. *Biochemistry* 25: 8118-8124.
- Muir JL. 1997. Acetylcholine aging and Alzheimer's disease. *Pharmacol Biochem Behav* 56: 687-696.
- Muma NA, Mariyappa R, Williams K, Lee JM. 2003. Differences in regional and subcellular localization of G(q/11) and RGS4 protein levels in Alzheimer's disease: Correlation with muscarinic M1 receptor binding parameters. *Synapse* 47: 58-65.
- Nyakas C, Oosterink BJ, Keijsers J, Felszeghy K, de Jong GI, et al. 1997. Selective decline of 5-HT_{1A} receptor binding sites in rat cortex hippocampus and cholinergic basal forebrain nuclei during aging. *J Chem Neuroanat* 13: 53-61.
- Olano M, Song D, Murphy S, Wilson DF, Pastuszko A. 1995. Relationships of dopamine cortical oxygen pressure and hydroxyl radicals in brain of newborn piglets during hypoxia and posthypoxic recovery. *J Neurochem* 65: 1205-1212.

- Olanow CW. 1992. An introduction to the free radical hypothesis in Parkinson's disease. *Ann Neurol* 32(Suppl): S2-S9.
- Palmiter RD, Cole TB, Findley SD. 1996. ZnT-2 a mammalian protein that confers resistance to zinc by facilitating vesicular sequestration. *EMBO J* 15: 1784-1791.
- Park IR, Thorn MB, Bachelard HS. 1987. Threshold requirements for oxygen in the release of acetylcholine from and in the maintenance of the energy state in rat brain synaptosomes. *J Neurochem* 49: 781-788.
- Pastuszko A, Saadat-Lajevardi N, Chen J, Tammela O, Wilson DF, et al. 1993. Effects of graded levels of tissue oxygen pressure on dopamine metabolism in the striatum of newborn piglets. *J Neurochem* 60: 161-166.
- Pellmar T. 1986. Electrophysiological correlates of peroxide damage in guinea pig hippocampus in vitro. *Brain Res* 364: 377-381.
- Pellmar TC. 1995. Use of brain slices in the study of free-radical actions. *J Neurosci Methods* 59: 93-98.
- Peterson C, Gibson GE. 1982. 34-Diaminopyridine alters acetylcholine metabolism and behavior during hypoxia. *J Pharmacol Exp Ther* 222: 576-582.
- Peterson C, Gibson GE. 1983a. Aging and 34-diaminopyridine alter synaptosomal calcium uptake. *J Biol Chem* 258: 11482-11486.
- Peterson C, Gibson GE. 1983b. Amelioration of age-related neurochemical and behavioral deficits by 34-diaminopyridine. *Neurobiol Aging* 4: 25-30.
- Peterson C, Gibson GE. 1984. Synaptosomal calcium metabolism during hypoxia and 34-diaminopyridine treatment. *J Neurochem* 42: 248-253.
- Peterson C, Nicholls DG, Gibson GE. 1985a. Subsynaptosomal calcium distribution during hypoxia and 34-diaminopyridine treatment. *J Neurochem* 45: 1779-1790.
- Peterson C, Nicholls DG, Gibson GE. 1985b. Subsynaptosomal distribution of calcium during aging and 34-diaminopyridine treatment. *Neurobiol Aging* 6: 297-304.
- Plum F, Posner JB. 1980. *The diagnosis of stupor and coma*. Philadelphia, PA: F.A. Davis.
- Prior RL, Hoang H, Gu L, Wu X, Bacchiocca M, et al. 2003. Assays for hydrophilic and lipophilic antioxidant capacity (oxygen radical absorbance capacity (ORAC(FL))) of plasma and other biological and food samples. *J Agric Food Chem* 51: 3273-3279.
- Pu L, Igbaybova U, Wood WG, Roths JB, Kier AB, et al. 1999. Expression of fatty acid binding proteins is altered in aged mouse brain. *Mol Cell Biochem* 198: 69-78.
- Rabin BM, Joseph JA, Erat S. 1998. Effects of exposure to different types of radiation on behaviors mediated by peripheral or central systems. *Adv Space Res* 22: 217-225.
- Ragozzino ME, Pal SN, Unick K, Stefani MR, Gold PE. 1998. Modulation of hippocampal acetylcholine release and spontaneous alternation scores by intrahippocampal glucose injections. *J Neurosci* 18: 1595-1601.
- Ragozzino ME, Unick KE, Gold PE. 1996. Hippocampal acetylcholine release during memory testing in rats: Augmentation by glucose. *Proc Natl Acad Sci USA* 93: 4693-4698.
- Reger MA, Henderson ST, Hale C, Cholerton B, Baker LD, et al. 2004. Effects of beta-hydroxybutyrate on cognition in memory-impaired adults. *Neurobiol Aging* 25: 311-314.
- Rossner S, Ueberham U, Schliebs R, Perez-Polo JR, Bigl V. 1998. The regulation of amyloid precursor protein metabolism by cholinergic mechanisms and neurotrophin receptor signaling. *Prog Neurobiol* 56: 541-569.
- Sadoul R. 1998. Bcl-2 family members in the development and degenerative pathologies of the nervous system. *Cell Death Differ* 5: 805-815.
- Santos AC, Uyemura SA, Lopes JL, Bazon JN, Mingatto FE, et al. 1998. Effect of naturally occurring flavonoids on lipid peroxidation and membrane permeability transition in mitochondria. *Free Radic Biol Med* 24: 1455-1461.
- Savory J, Rao JK, Huang Y, Letada PR, Herman MM. 1999. Age-related hippocampal changes in Bcl-2: Bax ratio oxidative stress redox-active iron and apoptosis associated with aluminum-induced neurodegeneration: Increased susceptibility with aging. *Neurotoxicology* 20: 805-817.
- Shukitt-Hale B, Casadesus G, McEwen JJ, Rabin BM, Joseph JA. 2000. Spatial learning and memory deficits induced by exposure to iron-56-particle radiation. *Radiat Res* 154: 28-33.
- Shukitt-Hale B, Denisova NA, Strain JG, Joseph JA. 1997. Psychomotor effects of dopamine infusion under decreased glutathione conditions. *Free Radic Biol Med* 23: 412-418.
- Shukitt-Hale B, Erat SA, Joseph JA. 1998. Spatial learning and memory deficits induced by dopamine administration with decreased glutathione. *Free Radic Biol Med* 24: 1149-1158.
- Shukitt-Hale B, Mouzakis G, Joseph JA. 1998. Psychomotor and spatial memory performance in aging male Fischer 344 rats. *Exp Gerontol* 33: 615-624.
- Slotte JP, Bierman EL. 1988. Depletion of plasma-membrane sphingomyelin rapidly alters the distribution of cholesterol between plasma membranes and intracellular cholesterol pools in cultured fibroblasts. *Biochem J* 250: 653-658.
- Thompson JM, Whitaker JR, Joseph JA. 1981. [³H]dopamine accumulation and release from striatal slices in young mature and senescent rats. *Brain Res* 224: 436-440.
- Toescu EC, Verkhratsky A. 2000. Parameters of calcium homeostasis in normal neuronal ageing. *J Anat* 197(Pt 4): 563-569.
- Tomaszewicz M, Bielarczyk H, Jankowska A, Szutowicz A. 1997. Pathways of beta-hydroxybutyrate contribution to

- metabolism of acetyl-CoA and acetylcholine in rat brain nerve terminals. *Folia Neuropathol* 35: 244-246.
- Venters HD Jr, Bonilla LE, Jensen T, Garner HP, Bordayo EZ, et al. 1997. Heme from Alzheimer's brain inhibits muscarinic receptor binding via thyl radical generation. *Brain Res* 764: 93-100.
- Villalba M, Pereira R, Martinez-Serrano A, Satrustegui J. 1995. Altered cell calcium regulation in synaptosomes and brain cells of the 30-month-old rat: Prominent effects in hippocampus. *Neurobiol Aging* 16: 809-816.
- Watson GS, Craft S. 2004. Modulation of memory by insulin and glucose: Neuropsychological observations in Alzheimer's disease. *Eur J Pharmacol* 490: 97-113.
- West RL. 1996. An application of prefrontal cortex function theory to cognitive aging. *Psychol Bull* 120: 272-292.
- Wu G, Benovic JL, Hildebrandt JD, Lanier SM. 1998. Receptor docking sites for G-protein betagamma subunits. Implications for signal regulation. *J Biol Chem* 273: 7197-7200.
- Wu G, Bogatkevich GS, Mukhin YV, Benovic JL, Hildebrandt JD, et al. 2000. Identification of Gbetagamma binding sites in the third intracellular loop of the M(3)-muscarinic receptor and their role in receptor regulation. *J Biol Chem* 275: 9026-9034.
- Wu G, Krupnick JG, Benovic JL, Lanier SM. 1997. Interaction of arrestins with intracellular domains of muscarinic and alpha2-adrenergic receptors. *J Biol Chem* 272: 17836-17842.
- Yu BP. 1994. Cellular defenses against damage from reactive oxygen species. *Physiol Rev* 74: 139-162.
- Zhang Y, Appelkvist EL, Kristensson K, Dallner G. 1996. The lipid compositions of different regions of rat brain during development and aging. *Neurobiol Aging* 17: 869-875.
- Zoccarato F, Valente M, Alexandre A. 1995. Hydrogen peroxide induces a long-lasting inhibition of the Ca(2+)-dependent glutamate release in cerebrocortical synaptosomes without interfering with cytosolic Ca2+. *J Neurochem* 64: 2552-2558.

4.4 Coupling of Brain Function and Metabolism: Endogenous Flavoprotein Fluorescence Imaging of Neural Activities by Local Changes in Energy Metabolism

K. Shibuki · R. Hishida · H. Kitaura · K. Takahashi · M. Tohmi

1	<i>Introduction</i>	322
2	<i>Flavoprotein Fluorescence Imaging and Other Methods for Functional Brain Imaging</i>	322
3	<i>Flavoprotein Fluorescence Imaging In Vitro</i>	325
4	<i>Flavoprotein Fluorescence Imaging In Vivo</i>	329
5	<i>Flavoprotein Fluorescence Imaging for Investigating Neural Plasticity In Vivo</i>	332
6	<i>Transcranial Flavoprotein Fluorescence Imaging of Mouse Cortical Activities and Its Application to Future Studies</i>	334
7	<i>Conclusion</i>	339

Abstract: The close coupling of neuronal activities to glucose and oxygen metabolism is well established. The imaging of activity-dependent changes in the endogenous fluorescence of NADH and mitochondrial flavoproteins provides the basis for many experimental approaches to visualize brain activities based on local changes in cellular energy metabolism. This chapter summarizes the results of the novel experimental applications of flavoprotein fluorescence for imaging local dynamic coupling of the functional activities of brain cells and temporal linkage to different events (such as electrical activity, calcium flux, and redox changes). These points are discussed in comparison with other methods using endogenous signals (such as deoxygenation of hemoglobin or blood flow changes) and with those using exogenous probes that are sensitive to voltage, calcium, or pH. The technical merits of flavoprotein fluorescence imaging for investigating plastic changes in neural activities and visualizing mouse cortical activities through the intact skull are discussed. Flavoprotein fluorescence imaging is an excellent tool for investigating neural plasticity, and may be a complementary method of functional brain imaging that can be used to understand brain functions.

1 Introduction

The brain is composed of numerous neurons, each of which shows electrical activities such as synaptic potentials and action potentials. Therefore, to understand the function of the brain as a whole, electrophysiological recording of each neuronal component of the brain should be performed. Unfortunately, such an attempt is only partly possible using electrophysiological techniques that use multiple electrodes. An alternative way is to record the neuronal activities as two-dimensional images using optical methods (Ebner and Chen, 1995; Grinvald and Hildesheim, 2004). The latter approach is especially valid in neuronal tissues with cortical structures, because the two-dimensional images obtained from optical recording are very effective for extracting the essential aspects of neuronal functions in the two-dimensional surface of cortical structures (Grinvald et al., 1986; Frostig et al., 1990; Bonhoeffer and Grinvald, 1991). Recent advances in cameras and computers have made this approach practical. To date, numerous methods for converting electrophysiological signals to optical signals have been considered. The pioneering studies of optical recording characterized various endogenous parameters of neural tissue that are directly affected by neuronal depolarization (Cohen et al., 1968, 1978). However, such signals are only detected under specialized experimental conditions, and these are not easily applicable to functional brain imaging in whole-brain preparations. The essential requirement is a fluorophore whose properties are affected by neuronal excitation, since an efficient fluorophore can convert electrophysiological phenomena to fluorescence signals and the resulting changes can be detected optically. However, there are few endogenous fluorophores or optically measurable parameters suitable for this purpose.

Neuronal excitation triggers a number of phenomena including an intracellular Ca^{2+} increase and the subsequent enhancement of energy metabolism (Fein and Tsacopoulos, 1988; Shibuki, 1989, 1990; Vanzetta and Grinvald, 1999). An alternative way, therefore, is to use the parameters affected by the cellular processes triggered by neural activities. Green fluorescence derived from mitochondrial flavoproteins is one of these parameters applicable for optical recordings (Chance et al., 1962). Surprisingly, however, this classical knowledge has not been applied to visualization of the dynamic metabolic changes paralleling stimulus-specific neural activities *in vivo*. However, recent reevaluation of flavoprotein fluorescence has clearly indicated that activity-dependent changes in endogenous fluorescence signals are useful for functional brain imaging *in vivo* in small animals such as rats and mice (Shibuki et al., 2003; Coutinho et al., 2004; Murakami et al., 2004; Reinert et al., 2004; Weber et al., 2004).

2 Flavoprotein Fluorescence Imaging and Other Methods for Functional Brain Imaging

Flavoprotein fluorescence imaging has a number of merits. Flavoprotein fluorescence provides a quantitative signal within all cell types of the brain, bypassing the difficulties introduced by the often-inhomogeneous distribution of exogenous dyes or indicators. Another advantage of endogenous fluorescence imaging is

that cellular and subcellular resolution can be achieved (Kasischke et al., 2004). To understand this point, it may be helpful to compare it with other methods. Optical recording using voltage-sensitive dyes is a typical method for visualizing membrane depolarization caused by neuronal excitation (Lieke et al., 1989; Ebner and Chen, 1995; Grinvald and Hildesheim, 2004). The dyes used for this purpose are hydrophobic in nature and soluble in the cell membrane. Changes in neuronal membrane potentials cause conformational changes in the dye incorporated in the membrane, and such changes can be optically detectable. This method can be combined with the recently developed nonlinear microscopy (Dombeck et al., 2004). However, the problem with using voltage-sensitive dyes is that the signal obtained is usually very small (<1%). These small signals are very sensitive to various movement artifacts, such as heartbeats and breathing. Furthermore, homogeneous staining of the brain with hydrophobic dyes is very difficult. Bleaching of the dyes is inevitable during the recordings, and this makes stable recording difficult. Therefore, optical recording using voltage-sensitive dyes is a delicate technique, although it is useful for detecting fast neural events, such as action potentials or synaptic transmission.

Another approach to optically record neural activities is to measure the intracellular Ca^{2+} increase, which is almost inevitably coupled with neuronal activities and synaptic transmission. The time course of Ca^{2+} rise is sufficiently fast to faithfully reflect the original neural activities. The changes in Ca^{2+} concentration can be measured using Ca^{2+} -binding compounds with fluorophores, and Ca^{2+} imaging using these indicators is one of the most widely used and successful optical recording techniques for investigating neural activities in cultured neurons and slice preparations. However, this method also requires delivery of the Ca^{2+} indicators into the neurons, and since the indicators are membrane-impermeable, this requirement makes the application of Ca^{2+} imaging to whole-brain preparations difficult (Helmchen and Waters, 2002).

The problem of loading exogenous dyes or indicators into the brain can be avoided if an endogenous compound with an appropriate fluorophore can be used for optical recording. An intracellular Ca^{2+} increase following synaptic transmission and neuronal excitation triggers a number of phenomena, such as neurosecretion, which may be detected by changes in the light-scattering properties of the neural tissue (Salzberg et al., 1985). However, these changes are also very small and difficult to detect in whole-brain preparations. The increased intracellular Ca^{2+} is partially taken up by the mitochondria (Budd and Nicholls, 1996; Gunter et al., 1998; Rizzuto et al., 2000) and stimulates energy metabolism (McCormack et al., 1990; Hansford, 1994; Kavanagh et al., 2000; Territo et al., 2000). These results can be observed as enhanced O_2 consumption after neural activities (Fein and Tsacopoulos, 1988; Shibuki, 1989, 1990; Vanzetta and Grinvald, 1999), as discussed in other chapters in this volume. The changes in energy metabolism are sufficiently clear and rapid to influence the optical properties of a number of endogenous fluorophores in whole-brain preparations.

So-called intrinsic signal recording is a method that uses hemoglobin as the endogenous indicator (Grinvald et al., 1986; Lieke et al., 1989; Frostig et al., 1990). Enhanced energy metabolism triggered by neural activities consumes the oxygen bound to hemoglobin in the capillary blood vessels. The resulting conversion of oxyhemoglobin to deoxyhemoglobin is accompanied by changes in the light absorption spectrogram. These changes can be detected by the absorbance or reflection of red light (>600 nm) projected on to the surface of the brain. This intrinsic signal recording is one of the most successful methods for optical imaging of brain activities *in vivo* (Bonhoeffer and Grinvald, 1991; Haglund et al., 1992; Shtoyerman et al., 2000; Sato et al., 2002) and is especially useful for investigating columnar structures in the cerebral cortex (Bonhoeffer and Grinvald, 1991; Sharon and Grinvald, 2002). Intrinsic signal derived from hemoglobin is free from photobleaching, and the method is applicable for larger animals including human subjects (Haglund et al., 1992; Sato et al., 2002). However, the amplitude of intrinsic signal is small, and neural activities can only be detected within a narrow time window between the stimulus onset and the initiation of stimulus-triggered hemodynamic changes, because the amount of hemoglobin in the capillary blood vessels is strongly affected by blood flow changes, which are spread over several columns (Thompson et al., 2003). Activity-dependent hemodynamic responses (Fox and Raichle, 1986; Malonek and Grinvald, 1996; Woolsey et al., 1996; Duong et al., 2001; Erinjeri and Woolsey, 2002) are also important for monitoring human brain activities noninvasively using transcranial absorption of near-infrared light (Tamura et al., 1997) or magnetic resonance imaging (MRI) (Ogawa et al., 1990). The quantitative analysis

of the small intrinsic signal before the onset of the blood flow increase (the “initial dip”) depends on the experimental conditions and assumptions on the optical path length (Lindauer et al., 2001). Furthermore, the spatial resolution of the intrinsic signal is principally limited by the resolution of the capillary bed supplying the brain (Frostig et al., 1990; Malonek and Grinvald, 1996; Erinjeri and Woolsey, 2002).

Neuronal activities also trigger intracellular neuronal acidification. This acidification following enhanced energy metabolism is caused by the metabolic production of carbon dioxide or lactic acid. Efflux of HCO_3^- and release/influx of H^+ elicited by an intracellular Ca^{2+} rise also contribute to the acidification. The resulting changes in pH can be optically detected using pH indicators, such as neutral red (Chen et al., 1998; Gao et al., 2003). A merit of this technique is that systemic administration of the dye, which is permeable through the blood–brain barrier and cell membranes, is sufficient for loading the dye into the whole brain. Using this technique, images of large signal amplitude with good spatial resolution and modest temporal resolution are obtained.

Intracellular energy metabolism can be monitored by changes in endogenous fluorescence, since endogenous fluorescence substances are involved in oxygen metabolism (Chance et al., 1962; Benson et al., 1979). Endogenous fluorescence of neural tissue is sometimes regarded as a factor causing artifacts in specific fluorescence measurements using exogenous fluorescence dyes. However, the distribution of endogenous fluorescence in freeze-trapped samples has been measured for investigating the oxidation–reduction state in mitochondria (Chance et al., 1979). Furthermore, the dynamic aspects of endogenous fluorescence in the brain seem to be ideal for use in functional brain imaging. Pioneering studies have utilized the intimate relationship between endogenous fluorescence and oxygen metabolism for monitoring the metabolic state of the brain during anoxia (Chance et al., 1962; Tomlinson et al., 1993), spreading depression (Mayevsky and Chance, 1974; Lothman et al., 1975; Haselgrove et al., 1990; Hashimoto et al., 2000), or during direct cortical stimulation and epileptic activities (Jöbsis et al., 1971; Rosenthal and Jöbsis, 1971; O’Connor et al., 1973; Lothman et al., 1975; Lewis and Schuette, 1976). Measurement of endogenous fluorescence has also been conducted in cultured cells or brain slices using one-photon (Aubin, 1979; Duchon, 1992; Mironov and Richter, 2001; Schuchmann et al., 2001; Shuttleworth et al., 2003) and two-photon excitation microscopy (Bennet et al., 1996; Kasischke et al., 2004). However, it should be pointed that nonneuronal cells and connective tissue are a source of intrinsic fluorescence from neural tissue. Furthermore, astrocytes and possibly other nonneural cell types may exhibit activity-dependent changes in energy metabolism, with subsequent changes in their intrinsic fluorescence.

Two types of endogenous compounds, NADH and flavoproteins, are directly related to cellular energy metabolism. In mitochondria, NADH is produced from nonfluorescent NAD^+ by the Krebs-cycle dehydrogenases and subsequently oxidized by the respiratory chain. In the cytoplasm, NADH is produced from NAD^+ at the glyceraldehyde-3-phosphate dehydrogenase step of glycolysis and subsequently reoxidized by the conversion of pyruvate to lactate. NADPH is also an important source of intrinsic fluorescence in addition to NADH. NADPH is the principal electron donor in reductive biosynthesis while NADH is the principal electron donor in oxidative metabolism. However, in brain tissue, the contribution of NADPH may be minor, since analytical measurements of NADH and NADPH in rodent brain have shown that both the resting fluorescence and the fluorescence changes are dominated by NADH rather than NADPH (Merrill and Guynn, 1981; Klaidman et al., 1995).

Brain tissue contains high levels of flavin adenine nucleotide of a lipoamide dehydrogenase, which shows green fluorescence with a peak emission at approximately 520 nm when excited with blue light (Kunz and Gellerich, 1993). This flavoprotein is a major source of mitochondrial flavin fluorescence (Hassinen and Chance, 1968; Chance et al., 1979). Enhanced mitochondrial energy metabolism converts reduced flavoproteins to their oxidized forms, emitting green fluorescence (Hassinen and Chance, 1968; Ragan and Garland, 1969; Chance et al., 1979). Since only the oxidized forms of flavoproteins exhibit green fluorescence, the neural activities and resulting enhancement in mitochondrial energy metabolism should be reflected by the green fluorescence. Intracellular calcium rises triggering the fluorescence changes have important roles in neural functions, such as synaptic transmission or induction of neural plasticity. Mitochondria are widely distributed in various cellular compartments, including the presynaptic terminals (Billups and Forsythe, 2002), and the metabolic load produced by neuronal excitation and synaptic transmission is efficiently covered by the enhanced energy metabolism in mitochondria. These fluorescence

signals exhibit biphasic responses after electrical stimulation of neural tissue (Lipton, 1973; Shuttleworth et al., 2003). It has been suggested that the earlier phase corresponds to aerobic energy metabolism in neurons and the later phase reflects glycolysis (Kasischke et al., 2004).

Although the flavoprotein signal was reported to be much smaller than the NADH signal (Aubin, 1979), recent studies using advanced optical equipment have demonstrated that the flavoprotein fluorescence signal in the earlier phase is suitable for functional brain imaging in the cerebral cortex (Shibuki et al., 2003; Murakami et al., 2004; Weber et al., 2004), cerebellar cortex (Coutinho et al., 2004; Reinert et al., 2004), and hippocampal slices (Shuttleworth et al., 2003). If both the NADH and flavoprotein signals are available as choices, flavoprotein signal may be better. This is because excessive exposure to ultraviolet light required for exciting NADH signals can be detrimental, and blue light required for exciting flavoprotein signals penetrates deeper into tissue than ultraviolet light. However, two-photon fluorescence microscopy of NADH circumvents the need for ultraviolet light (Bennett et al., 1996; Kasischke et al., 2004). Two-photon imaging of flavoprotein fluorescence has also been demonstrated and might provide an alternative to one-photon imaging in the future (Huang et al., 2002). Although flavoprotein signals are reported to be much smaller than NADH signals (Aubin, 1979), flavoprotein signals as much as 30% of $\Delta F/F$ can be recorded in cerebral slices after electrical stimulation (Shibuki et al., 2003).

3 Flavoprotein Fluorescence Imaging In Vitro

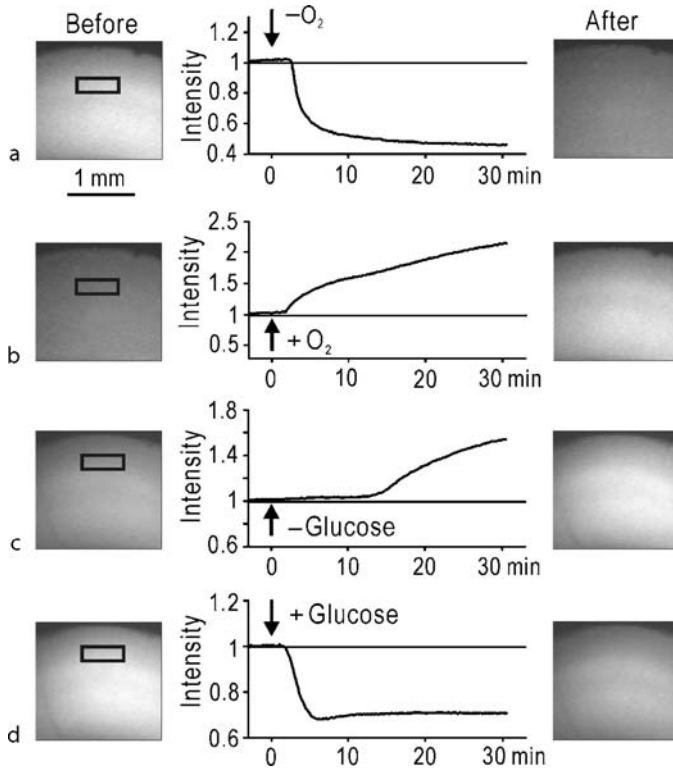
To confirm the usefulness of the flavoprotein fluorescence signal, we investigated the properties of endogenous fluorescence in cortical slices. First, the nature of the basal green fluorescence corresponding to that of flavoprotein signals was investigated (▶ [Figure 4.4-1](#)). The basal level of green fluorescence in blue light decreased by about 50% in a medium bubbled with 95% N₂ and 5% CO₂ (▶ [Figure 4.4-1a](#)). There was no bias in the distribution of the change in fluorescence over the slices, and the decrease was reversed when the slices were reincubated in normal oxygenated medium (▶ [Figure 4.4-1b](#)). In contrast, an increase in the basal fluorescence was observed when glucose was removed from the medium (▶ [Figure 4.4-1c](#)). Reincubation in normal medium containing glucose restored the basal fluorescence level (▶ [Figure 4.4-1d](#)). Mitochondrial flavoproteins are expected to be fully reduced in the absence of oxygen and fully oxidized in the absence of glucose. Therefore, these changes can be explained if approximately 50% of the green fluorescence is modulated by the presence or absence of oxygen and glucose. This proportion of the green fluorescence can be attributed to mitochondrial flavoproteins coupled with oxygen metabolism (Benson et al., 1979).

Next, we investigated the dynamic changes in the green fluorescence in the cortical slices (▶ [Figure 4.4-2](#)). Electrical stimulation at 20 Hz was applied to the slices for 1 s, and a localized increase in green fluorescence was observed at the stimulated site in layer V (▶ [Figure 4.4-2a](#)). Fluorescence changes were also observed in the supragranular layers. The peak response in the fluorescence intensity ($\Delta F/F$) was observed at about 2 s after the stimulus onset, and the amplitude was as large as $27 \pm 2\%$ (mean \pm SD, $n = 35$). Endogenous red fluorescence (>590 nm) in green light (541–551 nm) showed no apparent change (▶ [Figure 4.4-2b](#)). This spectral dependence allowed us to compare the Ca²⁺ signal and green fluorescence in the same slices ($n = 3$) using rhod-2, a Ca²⁺ indicator emitting red fluorescence in green light (Minta et al., 1989). Although the Ca²⁺ signal showed a rapid increase during repetitive stimulation at 20 Hz, the spatial distribution was essentially similar to that of the fluorescence changes (▶ [Figure 4.4-2c](#), ▶ [d](#)), suggesting the importance of the Ca²⁺ signal for triggering the mitochondrial energy metabolism and the flavoprotein fluorescence signal.

The flavoprotein fluorescence changes are assumed to be triggered by neural activities and the resulting intracellular Ca²⁺ rise. These mechanisms were confirmed by pharmacological experiments. Application of 2 μ M tetrodotoxin (TTX), which completely blocked the neural activities, also blocked the flavoprotein fluorescence responses. Ca²⁺-free medium, which suppressed the postsynaptic population spikes of field potentials, almost completely inhibited the fluorescence responses in slice preparations (▶ [Figure 4.4-2e](#)), although the suppression by Ca²⁺-free medium was less clear in anesthetized animals (Coutinho et al., 2004; Reinert et al., 2004). The effect of Ca²⁺-free medium is modest on the fluorescence responses derived

■ **Figure 4.4-1**

Changes in green autofluorescence in cortical slices. (a) Basal autofluorescence images of cortical slices before and during application of O_2 -free medium, and the time course of the relative fluorescence intensity in the window placed in layer II/III. The intensity in the time course was normalized by the value before application of the O_2 -free medium. (b) Recovery of the autofluorescence after application of normal oxygenated medium to the same slice shown in (a). (c and d) Autofluorescence changes before and during application of (c) glucose-free medium and recovery in the same slice in (d) normal glucose-containing medium. (Modified from Shibuki et al., 2003)

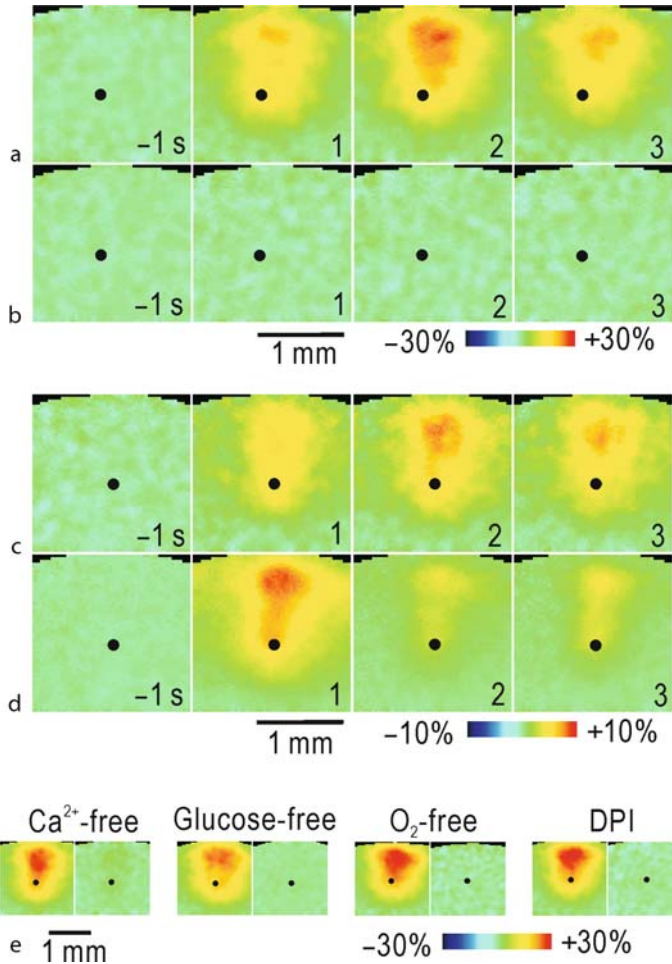


from NADH (Kann et al., 2003; Shuttleworth et al., 2003), suggesting other changes that influence ADP/ATP ratios can also affect the NADH signal. While flavoprotein fluorescence is predominately or even exclusively of mitochondrial origin, NADH is involved in both glycolytic and oxidative energy metabolism and therefore NADH fluorescence originates from both the cytoplasm and the mitochondria.

Although the postsynaptic potentials were also blocked by 10 μ M 6-cyano-7-nitroquinoxaline-2,3-dione (CNQX), an inhibitor of non-NMDA glutamate receptors, the flavoprotein fluorescence responses were only partially inhibited, indicating that the antidromic/presynaptic and postsynaptic activities contribute almost equally to the flavoprotein fluorescence responses. Removal of glucose or oxygen in the perfusion medium partially suppressed the postsynaptic field potentials, while the flavoprotein fluorescence responses were absent in these experiments (● [Figure 4.4-2e](#)). Diphenyleneiodonium (DPI, 10 μ M), which binds selectively to flavoproteins and inhibits their functions (Majander et al., 1994; Arnould et al., 1997; Ratz et al., 2000), profoundly suppressed the flavoprotein fluorescence responses (● [Figure 4.4-2e](#)). The effect of DPI might be explained by the loss of neural activities, which are dependent on mitochondrial metabolism in vivo. However, the effect in slice preparations could not be explained by this indirect mechanism, since almost normal field potentials were recorded in the slices treated with DPI (data not shown). With the exception of the suppression by DPI, all these effects were reversible (data not shown).

■ Figure 4.4-2

Activity-dependent changes for autofluorescence in slices. (a) Pseudocolor images of the changes in green autofluorescence ($\Delta F/F$) after electrical stimulation at 20 Hz for 1 s applied at layer V (black spots). The time before (negative value) or after the stimulus onset is shown in each image. (b) Red autofluorescence in the same slice shown in (a). (c) Green autofluorescence responses in a slice loaded with rhod-2. (d) Ca^{2+} signal in the same slice shown in (c). (e) Autofluorescence responses before (left) and during (right) application of Ca^{2+} -free (Ca^{2+} was replaced with Mg^{2+}) medium, glucose-free (glucose was replaced with NaCl) medium, O_2 -free medium bubbled with 95% N_2 and 5% CO_2 , and 10 μM DPI. (Modified from Shibuki et al., 2003)

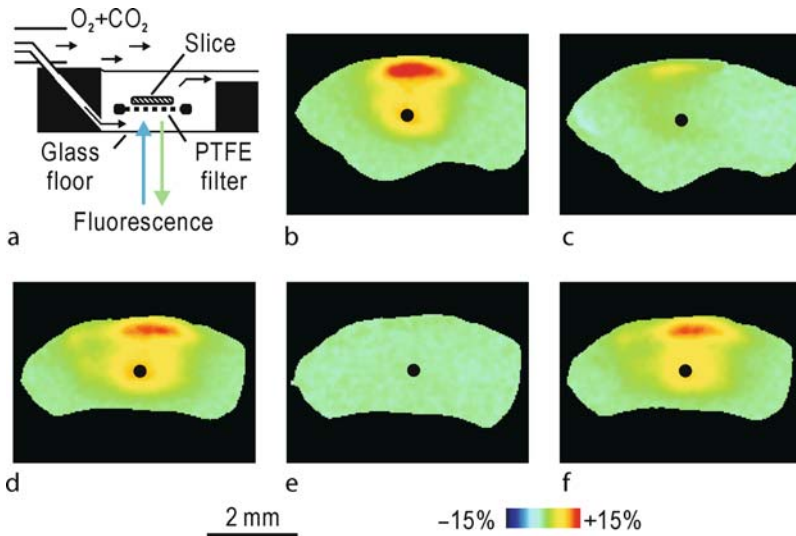


These findings can be explained by assuming that Ca^{2+} -dependent activation of aerobic metabolism and the resulting oxidation of flavoproteins underlie the recorded fluorescence responses. The flavoprotein fluorescence responses are assumed to be caused by neural activities and the resulting increase in $[\text{Ca}^{2+}]_i$. It is important to consider the contribution of glial cells to the fluorescence signal, since they also show activity-dependent $[\text{Ca}^{2+}]_i$ changes (Verkhatsky and Kettenmann, 1996) and are intimately coupled with neurons in energy metabolism (Pellerin et al., 1994; Magistretti et al., 1999; Magistretti, 2000). Indeed, a recent study using two-photon fluorescence imaging of NADH suggests that the earlier phase of the fluorescence responses corresponds to the aerobic energy metabolism in neurons while the later phase reflects glial glycolysis (Kasischke et al., 2004).

The green fluorescence changes are derived from oxidized flavoproteins, since only the oxidized forms emit green fluorescence in blue light (Chance et al., 1962; Benson et al., 1979). The flavoprotein fluorescence signal in our experiments is larger than those reported by other laboratories (Aubin, 1979). One of the important factors for determining the signal amplitude of flavoprotein fluorescence is the oxygen level in the brain tissue, especially in experiments using slices. We kept the oxygen pressure at the surface of slices emitting fluorescence as high as possible. The slices were placed on a hydrophilic polytetrafluoroethylene (PTFE) membrane filter, which was permeable to oxygenated medium (Figure 4.4-3a). This porous filter

Figure 4.4-3

Importance of O_2 in autofluorescence imaging in cortical slices. (a) Recording chamber designed for efficient O_2 supply to cortical slices. (b) Pseudocolor image of the green autofluorescence changes ($\Delta F/F$) in blue light after electrical stimulation (20 Hz for 1 s) applied at layer V (black spot). An image of the maximal fluorescence change at 2 s after the stimulus onset is shown. (c) Response of the same slice shown in (b). In this experiment, the slice was placed directly on the glass floor of the recording chamber. (d) Control autofluorescence response. In this experiment, the oxygenated medium was pumped into the recording chamber through stainless steel tubing. (e) Autofluorescence responses of the same slice shown in (d). The oxygenated medium was pumped through silicon rubber tubing. (f) Recovery of autofluorescence responses after stainless steel tubing was used again. The data in (d–f) were obtained in the same slice



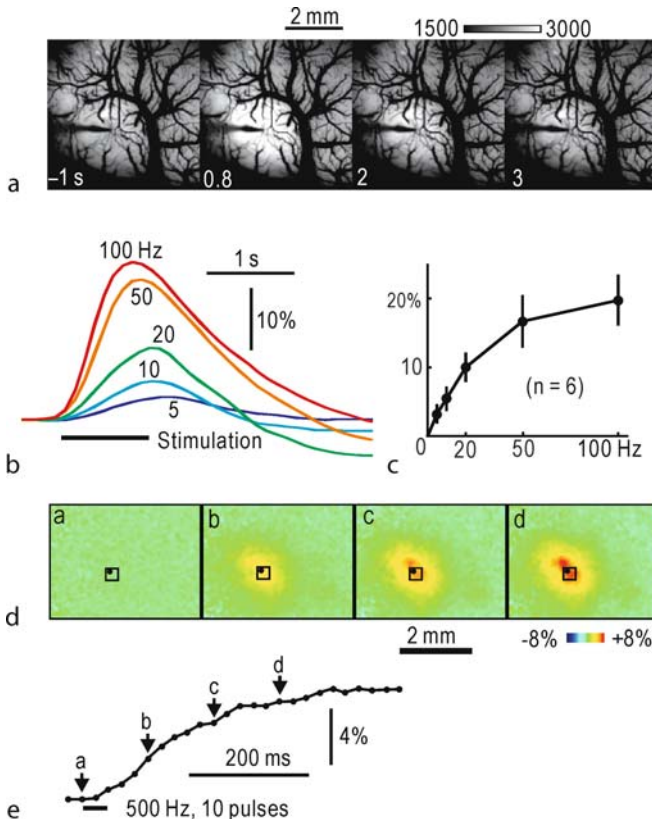
became transparent in water, because the refractive index of the constituent material was almost the same as that of water. Although flavoprotein fluorescence responses were clearly recorded in slices placed on this filter (Figure 4.4-3b), the same slices placed directly on the glass floor of the recording chamber showed only faint responses (Figure 4.4-3c). The small response that remained near the pial surface of the slices (Figure 4.4-3c) could be maintained by diffusion of oxygen from the pial surface. Moreover, it is important to note that the permeability of oxygen differs among various materials. When oxygenated medium was pumped into the recording chamber through stainless steel tubing, clear fluorescence responses were recorded in slices placed on the PTFE filter (Figure 4.4-3d, f). However, the same slices showed no response when the medium was pumped through silicone rubber tubing (Figure 4.4-3e). In this experiment, the oxygen level in the recording chamber was reduced to that present in air, because the silicon rubber tubing was permeable to oxygen. Taken together, these data indicate the importance of oxygen supply to the neural tissue for recording clear images of the flavoprotein fluorescence signal.

4 Flavoprotein Fluorescence Imaging In Vivo

The validity of the flavoprotein fluorescence signal for functional brain imaging has been tested in anesthetized animals (Shibuki et al., 2003; Coutinho et al., 2004; Murakami et al., 2004; Reinert et al., 2004; Weber et al., 2004). We anesthetized rats with urethane and directly stimulated the somatosensory cortex. Repetitive electrical stimulation at 100 Hz for 1 s was delivered via a tungsten electrode inserted into the cortex at a depth of 0.5 mm from the cortical surface. This stimulation produced a localized increase in green fluorescence recorded in blue light around the stimulated site (● [Figure 4.4-4a](#)). Since the maximal amplitude of the increase was very large ($20 \pm 4\%$, $n = 6$), the increase was recognized in the raw fluorescence images without any processing. Although the depth of the response area was not directly

■ Figure 4.4-4

Autofluorescence responses elicited by cortical stimulation in vivo. (a) Autofluorescence images of the exposed somatosensory cortex before and after electrical stimulation at 100 Hz for 1 s. The fluorescence intensities between 1,500 and 3,000 in arbitrary units were expanded on a grayscale. Note the shadow of the stimulating electrode. (b) Time course of $\Delta F/F$ in a window of 10×10 pixels. The results in (a) and (b) were obtained from the same rat. (c) Relationship between the amplitudes of $\Delta F/F$ and the stimulus frequency. The mean \pm SD are shown. (d) Autofluorescence responses elicited by high-frequency stimulation at 500 Hz with 10 pulses (*black spots*). In this experiment, images were taken at 45 frames/s. (e) Time course of the fluorescence changes in the windows shown in (d). The *arrows (a-d)* correspond to the images in (d). ((a-c) were modified from Shibuki et al., 2003)



estimated in this experiment, it was expected to be about 300 μm from the cortical surface since the neural tissue at this depth showed clear fluorescence changes in the slice experiments (e.g., [Figure 4.4-3b](#)). The time course of the increase *in vivo* was much faster than that observed in the slices, probably because the recording temperature in the slices was too low. Next, we varied the stimulus frequency from 5 to 100 Hz. The relative distribution of the flavoprotein fluorescence responses remained remarkably constant within this range. However, the amplitude increased as the stimulus frequency increased ([Figure 4.4-4b](#), [Figure 4.4-4c](#)), and the relationship between these two parameters was almost linear when the stimulus frequency was lower than 20 Hz ([Figure 4.4-4c](#)). Therefore, the amplitude of the fluorescence signal in this range is a useful parameter for quantitative analysis of neural activities. The flavoprotein fluorescence responses showed a comparable distribution to the field potentials recorded in various points of the cortex, suggesting that flavoprotein fluorescence increases are a good indicator of the neural activities. The fluorescence responses were gradually suppressed and completely inhibited within 90–120 min of covering the exposed brain surface with agar containing 100 μM DPI. The neural activities were distorted near the stimulated site when the cortex was covered with DPI. The apparent effects of DPI on the neural activities in the anesthetized rats suggest the importance of aerobic energy metabolism in whole-brain preparations kept at physiological temperature but not in slices maintained at room temperature.

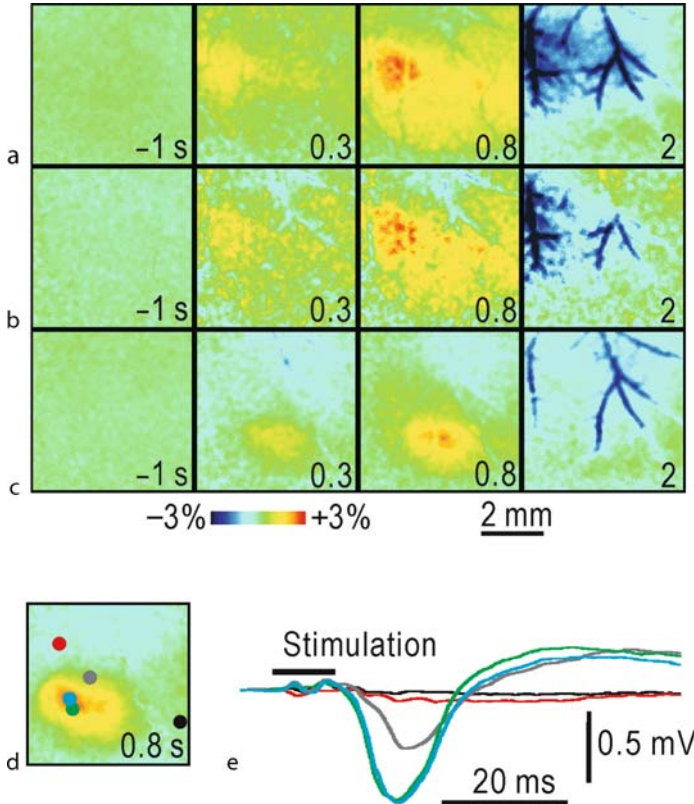
To investigate the temporal resolution of the fluorescence responses, ten electrical pulses at 500 Hz were applied to the somatosensory cortex, and the resulting increase in fluorescence was recorded at a frame rate of 45 images/s ([Figure 4.4-4d](#), [Figure 4.4-4e](#)). The fluorescence increase reached a peak at about 200 ms after the stimulus onset. Therefore, it was concluded that this value represents the upper limit of temporal resolution after the stimulus onset. However, the changes did not recover to the baseline as quickly. The slow recovery process of the fluorescence may reflect maintenance of the rise in intracellular Ca^{2+} , which is an essential factor for stimulating flavoprotein fluorescence responses in slice preparations ([Figure 4.4-2e](#)).

Although direct cortical stimulation produced very clear responses in the flavoprotein fluorescence, the validity of the fluorescence imaging needs to be tested using natural stimuli. To stimulate neural activities in the somatosensory cortex, flutter vibration (displacement: ± 1 mm, 50 Hz for 1 s) was applied to the surface of the contralateral plantar forepaw. The vibratory stimulation produced localized fluorescence responses in the primary somatosensory cortex ([Figure 4.4-5a](#)). The responses peaked at about 0.8 s after the stimulus onset and were followed by darkening of the arterial images that last for several seconds ([Figure 4.4-5](#)). These responses were even observed in a single trial, but averaging over several trials improved the quality of the images ([Figure 4.4-5b](#)). Hindpaw stimulation produced fluorescence responses at a different location in the cortex of the same rat, according to the somatotopic map of peripheral afferents in the cortex ([Figure 4.4-5c](#)). The amplitude of the peak response elicited by vibratory stimulation of the contralateral hindpaw was $2.6 \pm 0.5\%$ ($n = 33$). The flavoprotein fluorescence responses were compared with the field potentials recorded at various points of the cortex ([Figure 4.4-5d](#), [Figure 4.4-5e](#)), and a good correlation was found between the two sets of data. This good correlation indicates that the flavoprotein fluorescence increases reflect the somatosensory neural activities elicited by natural stimuli.

Neural activities trigger not only enhancement of energy metabolism but also hemodynamic responses. Localized hemodynamic responses triggered by neural activities are widely used for noninvasive functional brain imaging using near-infrared light (Tamura et al., 1997) or MRI (Ogawa et al., 1990). Therefore, it is important to investigate the relationship between the flavoprotein fluorescence responses and the subsequent hemodynamic responses. Any changes in the blood flow are also detected by flavoprotein fluorescence imaging because hemoglobin absorbs the blue or green light used for the fluorescence imaging. When the hindpaw was stimulated, the flavoprotein fluorescence responses were followed by darkening of the arterial images ([Figure 4.4-5a](#), [Figure 4.4-5c](#)). When green- or blue-light reflection was imaged in the same rat, only slow darkening of the arterial images was observed. The flavoprotein fluorescence responses recorded as increases in the light intensity, however, were more localized and faster than the hemodynamic responses observed as decreases in the light intensity ([Figure 4.4-5a](#), [Figure 4.4-5c](#)). The polarity and characteristic distribution patterns of the latter were easily distinguished from the flavoprotein fluorescence responses, which were not observed in the blood vessels. Of these two parameters, the flavoprotein fluorescence responses are clearly better indicators for the neural activities under these experimental conditions.

■ Figure 4.4-5

Autofluorescence responses elicited by natural stimulation *in vivo*. (a) Autofluorescence responses elicited by vibratory forepaw stimulation at 50 Hz for 1 s and recorded in the somatosensory cortex. (b) Responses in a single trial in (a). (c) Responses elicited by hindpaw stimulation. The results in (a–c) were obtained from the same rat. (d) Autofluorescence responses elicited by hindpaw stimulation (50 Hz, 1 s). (e) Field potentials elicited by stimulation with a single mechanical pulse (duration, 10 ms) and recorded at the spots in (d). The colors of the spots correspond to those of the traces. (Modified from Shibuki et al., 2003)



To confirm the neural origin of the flavoprotein fluorescence responses, we tried to separate the fluorescence responses from the subsequent hemodynamic responses. Since the neural activities and hemodynamic responses may be coupled with nitric oxide (Goadsby et al., 1992; Northington et al., 1992), we tried to selectively inhibit the hemodynamic responses using N^G -nitro-L-arginine, an inhibitor of nitric oxide synthase. The exposed brain was covered with agar containing 100 μM N^G -nitro-L-arginine. In these rats, very clear fluorescence responses were observed after hindpaw stimulation, while darkening of the arterial images was almost completely suppressed. These findings suggest that the hemodynamic responses following neural activities may be partly mediated by nitric oxide and that the pure fluorescence responses can be separated from the subsequent hemodynamic responses, although the role of nitric oxide in hemodynamic responses is controversial (Wang et al., 1993; Adachi et al., 1994). The difference between the present study and previous negative reports regarding the role of nitric oxide may have arisen because we applied a high dose (100 μM) of N^G -nitro-L-arginine directly onto the surface of the brain, such that any nitric oxide synthesis inside the blood–brain barrier would be completely inhibited. Nitric oxide is derived from neurons or nerve terminals inside the blood–brain barrier (Toda et al., 2000), and therefore could have important roles in the coupling between neural activities and vasodilatation.

5 Flavoprotein Fluorescence Imaging for Investigating Neural Plasticity In Vivo

Activity-dependent neural plasticity, such as long-term potentiation (LTP) or long-term depression (LTD), is a basic mechanism of higher-order brain functions, such as learning and memory (Bliss and Collingridge, 1993; Kandel, 2001). The spatial distribution of neural plasticity can be observed using Ca^{2+} imaging in cortical slices (Seki et al., 1999, 2001; Hishida et al., 2003). LTP-like potentiation has been observed in the cerebral cortex of anesthetized animals (Frégnac et al., 1992; Cruikshank and Weinberger, 1996). Therefore, optical recording of neural plasticity in vivo would provide us with important information, if an appropriate technique were available for this purpose.

For investigating neural plasticity with optical imaging, the reproducibility and stability of the obtained images are very important. The reproducibility of flavoprotein fluorescence imaging in slices and anesthetized animals are comparable with those obtained using ordinary electrophysiological recordings. This is because flavoproteins are essential components in energy metabolism and abundantly present in all regions of the brain. The stability of the flavoprotein fluorescence signal was tested in slices. The amplitude of the flavoprotein fluorescence responses was stable for at least 4 h, whereas the rhod-2 signal used for Ca^{2+} imaging in the same slice markedly reduced during the same 4 h, probably due to bleaching or leakage of the loaded rhod-2. In anesthetized rats, no apparent changes were observed between images taken at an interval of 1 h. Although bleaching of the flavoprotein fluorescence was recognized in these experiments, it recovered within a few minutes in darkness. These properties make flavoprotein fluorescence imaging suitable for investigating neural plasticity.

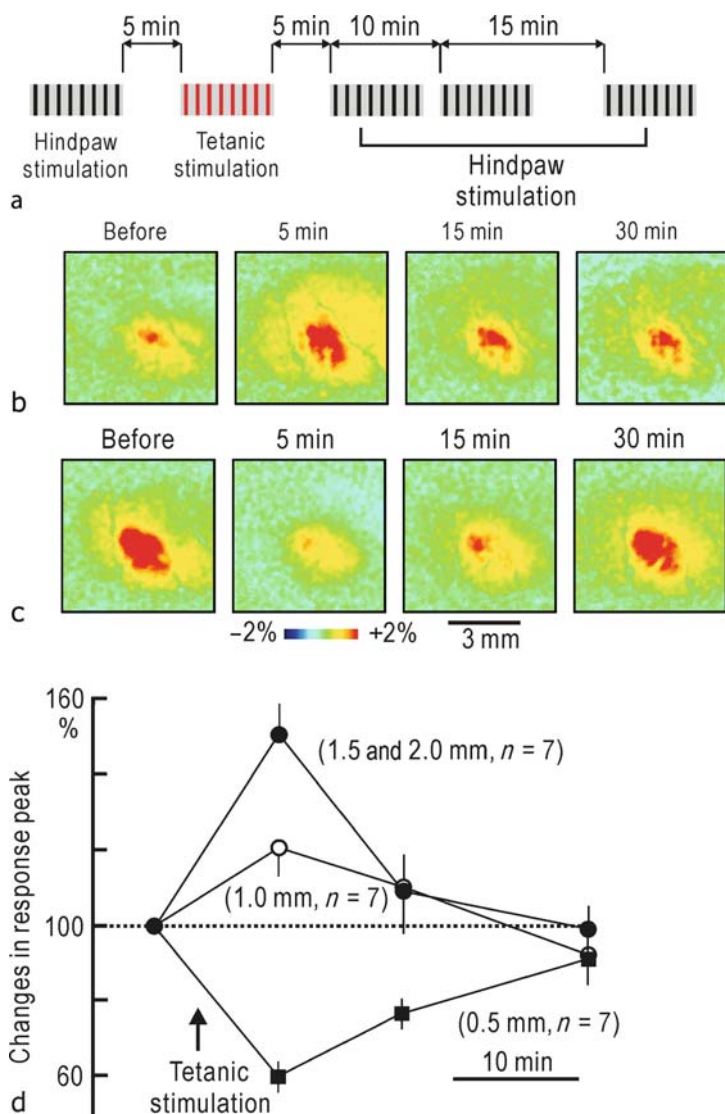
To induce neural plasticity in vivo, we used high-frequency direct cortical stimulation, because similar stimulation is widely used for inducing LTP in slice preparations (Kudoh and Shibuki, 1996, 1997). First, control images in response to vibratory skin stimulation were taken (▶ [Figure 4.4-6a](#)). Next, high-frequency tetanic stimulation (TS, 100 Hz for 1 s at 300 μA) was applied to the response center eight times at 1-min intervals. The effects of TS were evaluated by applying peripheral stimulation in recording sessions started at various times after the cessation of TS (▶ [Figure 4.4-6a](#)). When TS was applied at the depth of the infragranular layers (1.5–2.0 mm from the cortical surface), the fluorescence responses were potentiated in the recording session started at 5 min after TS (▶ [Figure 4.4-6b](#), ▶ [d](#)). The amplitude of the response peak ($\Delta F/F$) was potentiated to $150 \pm 8\%$ ($n = 7$) of the control value recorded before TS. The response area ($\Delta F/F > 1\%$) was also potentiated to $319 \pm 79\%$. However, these potentiated responses returned to the baseline level within 30 min after TS (▶ [Figure 4.4-6d](#)). When TS was applied at layer IV (1.0 mm from the cortical surface), the magnitude of the potentiation in the peak amplitude was $120 \pm 8\%$ ($n = 7$) and that in the response area ($\Delta F/F > 1\%$) was $150 \pm 30\%$. When TS was applied at a depth of 0.5 mm from the surface (▶ [Figure 4.4-6c](#)), clear depression of the responses was observed. These depth-dependent plastic changes in the optical responses were confirmed by electrophysiological recordings using slice preparations. However, the suppressed optical responses recovered to the baseline level within 30 min after TS (▶ [Figure 4.4-6c](#), ▶ [d](#)), while those in slices were maintained for at least 30 min.

We also investigated the changes in neural activities mediated by commissural fibers connected to the bilateral somatosensory cortex (Iwamura et al., 1994). As reported previously, somatosensory plasticity occurs in the neural circuits in both hemispheres (Clarey et al., 1996; Zarei and Stephenson, 2000). TS applied to the left somatosensory cortex at a depth of 2.0 mm produced flavoprotein fluorescence responses not only at the stimulated site but also at the symmetric position in the contralateral right cortex (▶ [Figure 4.4-7a](#), ▶ [b](#)). Vibratory stimuli applied to the left hindpaw produced flavoprotein fluorescence responses not only in the contralateral right cortex but also in the ipsilateral left cortex (▶ [Figure 4.4-7c](#), ▶ [e](#)), indicating functional roles for the commissural fibers in these responses. Potentiation of the fluorescence responses to peripheral stimulation was clearly observed in the ipsilateral cortex after TS was applied to the ipsilateral cortex (▶ [Figure 4.4-7d](#), ▶ [e](#)). This result suggests that TS-induced potentiation is observed not only in the responses mediated via thalamocortical fibers but also in those activated via commissural fibers.

A weak point of the investigation into neural plasticity using flavoprotein fluorescence imaging was that the plasticity was only maintained for a short period. However, this feature could be attributed to the

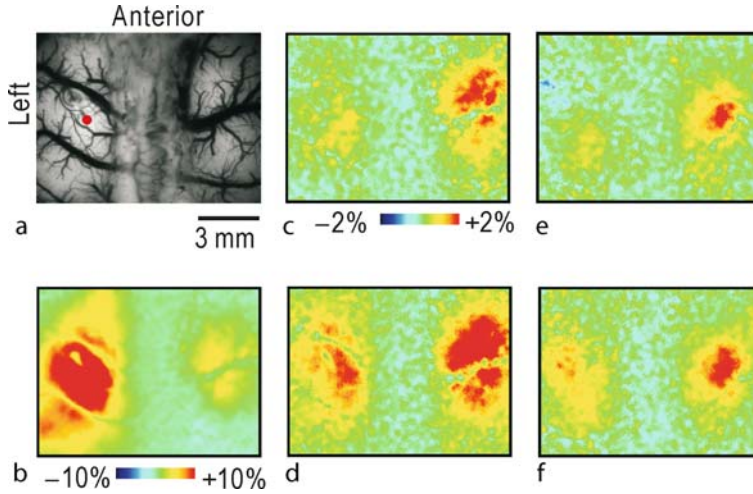
■ Figure 4.4-6

Potentiation and depression of somatosensory responses induced by cortical stimulation applied at various depths. (a) Scheme of the experiments for investigating the interaction between cortical tetanic stimulation (TS, 100 Hz for 1 s, 8 trials in 8 min) and hindpaw stimulation (50 Hz for 1 s, 8 trials in 8 min). (b) Autofluorescence responses to vibratory skin stimulation recorded before and during 5–30 min after TS applied at a depth of 1.0–2.0 mm from the cortical surface. Images of the maximal responses taken at 0.7–0.9 s after the stimulus onset are shown. (c) Autofluorescence responses to vibratory skin stimulation recorded before and during 5–30 min after TS applied at a depth of 0.5 mm. (d) Time course of the changes in the response peak ($\Delta F/F$) normalized by the values before TS. The potentiation induced by TS at depths of 1.5 and 2.0 mm ($n = 3$ and 4, respectively, ●), 1.0 mm ($n = 7$, ○), and 0.5 mm ($n = 7$, ■) from the cortical surface are shown separately. (Modified from Murakami et al., 2004)



■ **Figure 4.4-7**

Potentiation of somatosensory responses mediated by commissural fibers. (a) Original fluorescence image of the bilateral somatosensory cortex. The *red spot* shows the stimulated site. (b) Autofluorescence responses in the right cortex elicited by tetanic stimulation (TS, 100 Hz for 1 s) applied at a depth of 2.0 mm in the left somatosensory cortex (*red spot* in (a)). (c and d) Autofluorescence responses elicited by left hindpaw stimulation in the bilateral somatosensory cortices (c) before and (d) after TS. The images in (a–d) were recorded in the same rat. (e and f) Autofluorescence responses elicited by left hindpaw stimulation (e) before and (f) after TS in another rat. The pseudocolor scale in (c) is applicable to (d–f). (Modified from Murakami et al., 2004)



preparation, because similar experiments using slices showed a plasticity that lasted for at least 30 min. The rectal temperature of the anesthetized rats was maintained at 38°C, while the recording temperature in the slice experiments was about 30°C. Therefore, the temperature dependence of metabolism may be important for determining the lifetime of the plasticity. Another possibility is that the spontaneous firing of neurons observed in vivo but not usually in the slices may be important for the lifetime of the plasticity, since LTP can be reversed by applying low-frequency stimulation (Fujii et al., 1991; Jouvenceau et al., 2003), which may be mimicked by spontaneous neural firing. Such depotentiation of excitatory or inhibitory synapses might reduce the lifetime of somatosensory plasticity in vivo.

To overcome these difficulties, synaptic plasticity induced during natural training of animal behavior should be investigated using flavoprotein fluorescence imaging in animals anesthetized after the training. We have already tested such a possibility. We visualized learning-induced changes in the neural activities in the rat primary somatosensory cortex. Rats were trained to discriminate floor vibration at different frequencies. After this learning was established, the rats were anesthetized and the somatosensory responses to vibratory stimulation at the rewarded and nonrewarded frequencies were compared. The results revealed that only the unrewarded responses were inhibited after the discrimination learning (Shibuki et al., 2004). These learning-induced changes were recorded in the animals more than 6 h after cessation of the discrimination test, suggesting the usefulness of flavoprotein fluorescence imaging for investigating the mechanisms underlying learning and memory.

6 Transcranial Flavoprotein Fluorescence Imaging of Mouse Cortical Activities and Its Application to Future Studies

Recently, the importance of mice as experimental animals in neuroscience has increased, since various techniques for manipulating the mouse genome have been established and many kinds of genetically

manipulated mouse strains have been developed for experimental use. However, analysis of higher brain functions in mice is rather limited, partly because the small cerebral cortex of mice is fragile and electrophysiological analyses are difficult. As far as the optical imaging of cortical activities is concerned, mice have a great advantage since their skull is thin and sufficiently transparent to allow transcranial imaging of the cerebral neural activities using intrinsic signal recording (Schuett et al., 2002) or flavoprotein fluorescence imaging. The transparency of the skull can be maintained if drying of the skull is prevented by covering it with mineral oil during recordings. Transcranial imaging has a number of technical merits. The operations involved in exposing the cerebral surface, which require some skill in mice, can be avoided. Furthermore, brain movement caused by heartbeats or breathing can easily be inhibited by fixing the skull, since the brain is fixed inside the intact skull. Flavoprotein fluorescence imaging is suitable for small animals. We have confirmed that flavoprotein fluorescence imaging works well in rats and mice. However, good results were not obtained in preliminary experiments using cats, dogs, or human subjects during surgical operations. These results seem to suggest that the body weight of the animals or subjects used for the recording is very important. The success of flavoprotein fluorescence imaging in small animals can partly be explained by differences in the metabolic rate with respect to the body weight, since this parameter is inversely proportional to a quarter power of the body weight (Gillooly et al., 2001). Motion artifacts produced by breathing or heartbeats are more serious in large animals. The level of endogenous green fluorescence insensitive to neural activities might be increased in larger animals. Furthermore, the excitation or emission light used for fluorescence measurements can penetrate a small brain more easily. Therefore, flavoprotein fluorescence imaging in animals larger than rats may not produce good results, as found in pioneering studies of endogenous fluorescence imaging.

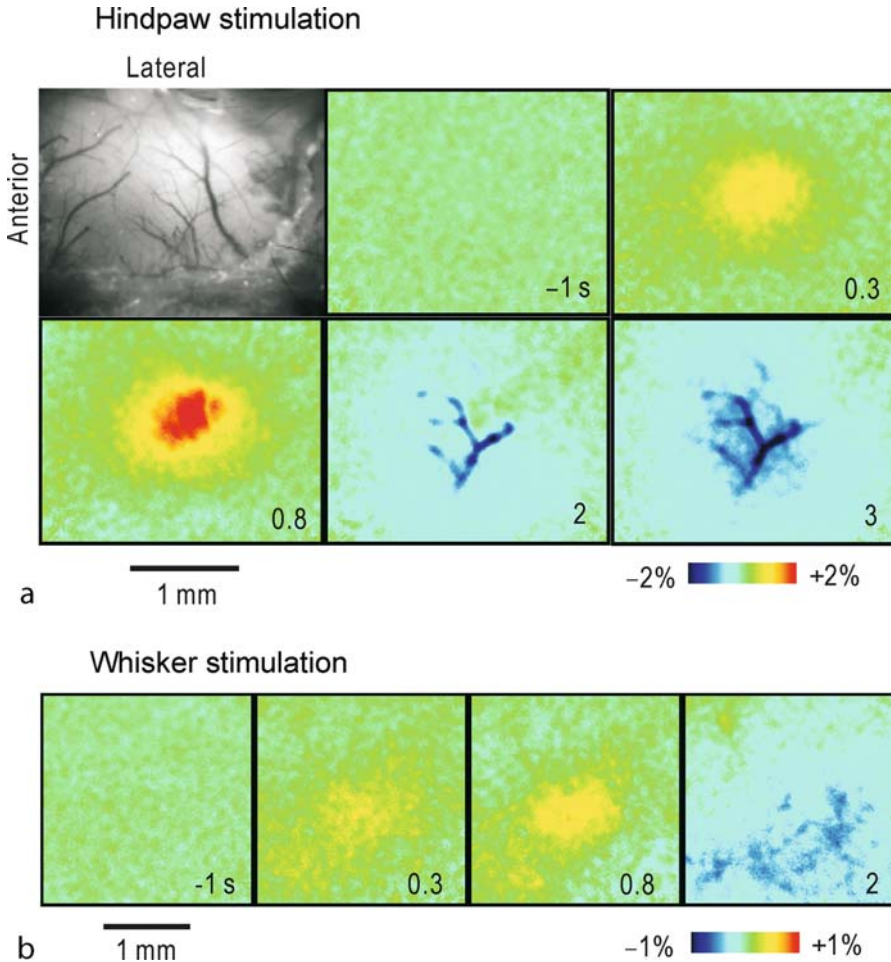
We tried to apply flavoprotein fluorescence imaging to three types of sensory cortices in mice: the somatosensory, auditory, and visual cortices. In all three areas, natural stimuli produced significant fluorescence responses of easily recognized amplitude through the intact skull. For visualizing neural activities in the somatosensory cortex, mice were anesthetized with urethane (1.6 g/kg, i.p.) and the skull was exposed. The cleaned surface of the skull was covered with a mixture of Vaseline and liquid paraffin to prevent drying (▶ [Figure 4.4-8a](#)). Vibratory stimuli applied to the surface of the contralateral hindpaw produced a fluorescence increase followed by arterial darkening (▶ [Figure 4.4-8a](#)). The time courses of these responses were quite similar to those recorded on the exposed surface of the rat somatosensory cortex (▶ [Figure 4.4-5](#)). When the stimuli were applied to a single whisker on the contralateral side, a corresponding spot appeared in the somatosensory cortex (▶ [Figure 4.4-8b](#)). Stimuli applied to the skin or whiskers produced neural activities according to the somatotopic distribution of the afferent projections from the skin. The maximal amplitude of the fluorescence responses were reduced to about 50% of that recorded in the exposed cortex of anesthetized mice (data not shown). In essence, no obvious differences were observed for the data obtained with rats and mice, although the amplitudes of the mouse responses could be underestimated by loss due to the presence of the skull.

Transcranial flavoprotein fluorescence imaging was also applied to visualize neural activities in the auditory cortex (▶ [Figure 4.4-9](#)). In these experiments, sound stimuli of various pitches were given to anesthetized mice. A clear increase in the flavoprotein fluorescence followed by hemodynamic responses was observed in the auditory cortex (▶ [Figure 4.4-9a–c](#)). Previously, it was demonstrated with optical recordings that dual tonotopic maps of neural activities are present in the anterior auditory field and primary auditory cortex (e.g., Horikawa et al., 2001). In agreement with these reports, dual tonotopic maps were observed using transcranial flavoprotein fluorescence imaging (▶ [Figure 4.4-9d](#), ▶ [e](#)).

The visual cortex is one of the most intensively investigated brain areas in the field of neuroscience. However, the number of reports investigating the mouse visual cortex is comparatively small, probably because the delicate nature of the mouse cortex requires fine techniques and skills for investigation. The neural activities elicited by visual stimuli in the visual cortex were clearly demonstrated using transcranial flavoprotein fluorescence imaging (▶ [Figure 4.4-10](#)). The neural activities in the monocular region of the visual cortex only produced flavoprotein fluorescence responses on the contralateral side (▶ [Figure 4.4-10a](#)), while the binocular region showed bilateral responses (▶ [Figure 4.4-10b](#)). The time courses of the flavoprotein fluorescence responses followed by the hemodynamic responses were essentially similar among the somatosensory, auditory, and visual cortices. The usefulness of transcranial imaging for investigating mouse

■ **Figure 4.4-8**

Transcranial autofluorescence imaging in the mouse somatosensory cortex. (a) Original fluorescence image and changes in the fluorescence elicited by hindpaw stimulation at 50 Hz for 1 s. C57BL/6 mice were anesthetized with urethane (1.6 g/kg). The skull was kept intact. (b) Autofluorescence images before and after mechanical stimulation at 10 Hz for 1 s applied to a single whisker

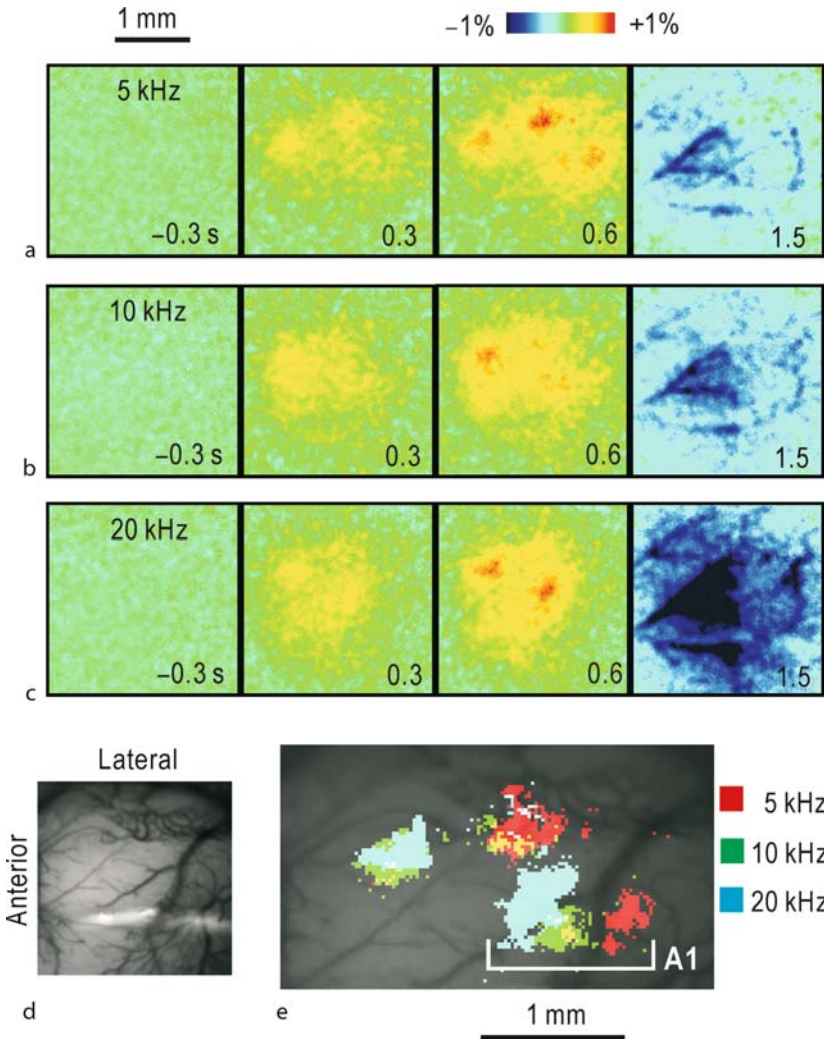


cortical functions is clearly demonstrated by these results. Furthermore, activity-dependent changes were identified in the somatosensory, auditory, and visual cortices (unpublished observations). Therefore, we expect that transcranial flavoprotein fluorescence imaging will become one of the standard methods for optical recording in the mouse cortex in the near future.

Another possibility for transcranial flavoprotein fluorescence imaging in mice is that it allows visualization of the neural activities in awake mice. If the surface of the skull is properly covered with a transparent dental resin, the skull covering the brain can be protected against infection and can maintain its transparency for several weeks after the surgical operation. Movement of the skull in awake mice is very easily suppressed by screwing a metal piece, which is attached to the skull with dental resin, on a manipulator. With this simple technique, we have already recorded dynamic images of the cortical activities in unanesthetized mice in preliminary experiments. Optical recording from awake animals is very important for investigating higher brain functions, because these functions are only active in awake animals. Therefore,

■ Figure 4.4-9

Transcranial autofluorescence imaging in the mouse auditory cortex. (a) Autofluorescence responses elicited by sound stimuli of 5 kHz for 500 ms at an intensity of 60 dB SPL. (b and c) Autofluorescence responses elicited by sound stimuli at (b) 10 kHz and (c) 20 kHz. (d) Original fluorescence image. (e) Peak responses in (a–c) superimposed on the original fluorescence image. Note the tonotopic map in the primary auditory cortex (A1).

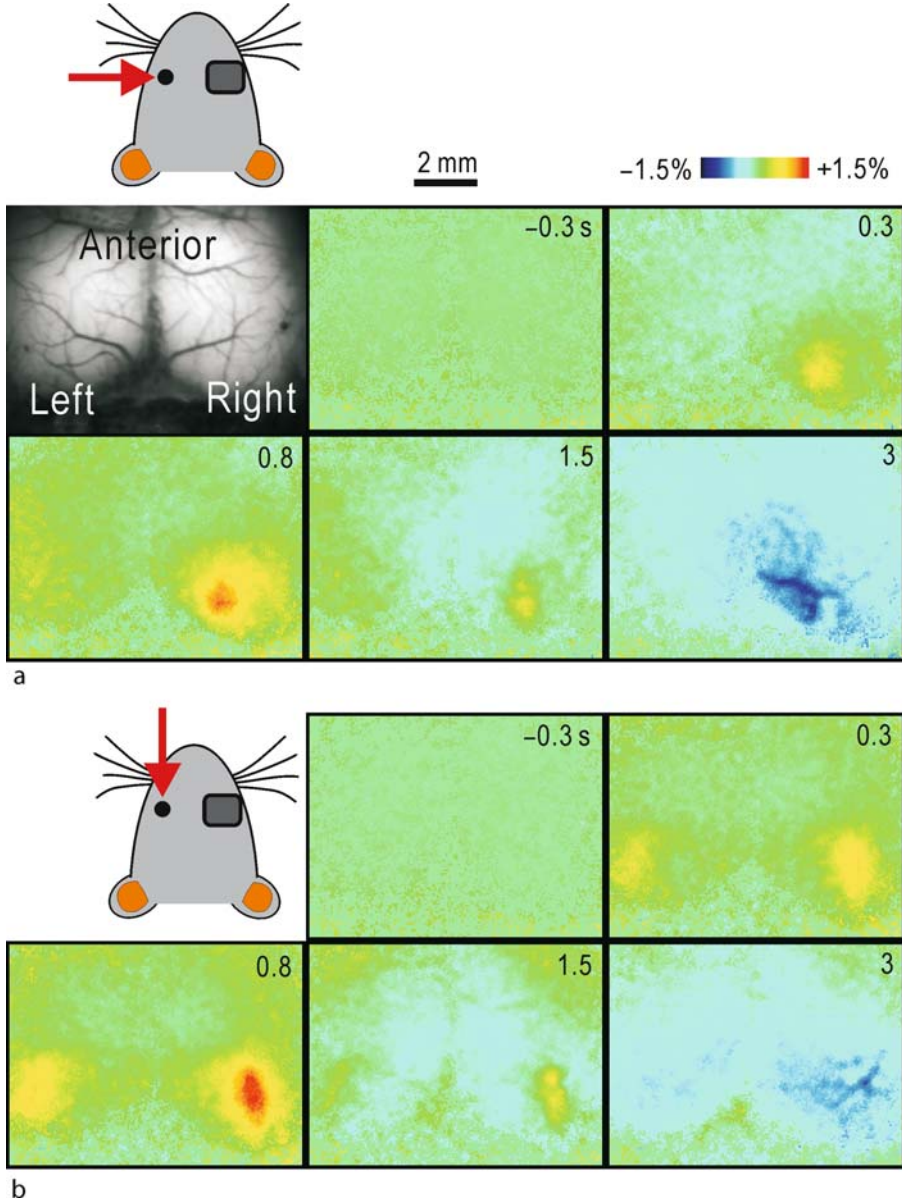


transcranial flavoprotein fluorescence imaging in awake mice with genetically manipulated genomes may allow us to investigate the molecular mechanisms of higher brain functions.

Recently, new GFP-based fluorescence probes have been developed for functional brain imaging (Miyawaki et al., 1997; Honda et al., 2001; Knöpfel et al., 2003), and these probes have been already applied for the functional imaging of the mouse brain in vivo (Bozza et al., 2004). However, the conditions required for fluorescence measurements of these GFP-based fluorescence probes are also suitable for recording the green fluorescence signals derived from endogenous flavoproteins, which are abundantly present in the brain of naive mice. Therefore, the flavoprotein fluorescence signals must be carefully distinguished from the desired signals derived from the new probes. However, if both signals are optically distinguishable,

■ Figure 4.4-10

Transcranial autofluorescence imaging in the mouse visual cortex. (a) Original fluorescence image of the bilateral visual cortex and autofluorescence responses elicited by a red LED light that was turned on for 3 s on the left side of the mouse. In this experiment, the right eye was closed. (b) Autofluorescence responses elicited by a red LED light in front of the mouse



experimental protocols using flavoprotein fluorescence imaging can also be applicable in mice along with the new probes, and the flavoprotein fluorescence signals can provide control information for whether or not the system works well.

7 Conclusion

In this chapter, the principle and history of NADH fluorescence imaging and flavoprotein fluorescence imaging were introduced. Its characteristics as a method for functional brain imaging were mainly explained using results obtained in our laboratory. Although the principle of flavoprotein fluorescence imaging has been known since 1962, its application to functional brain imaging has not been widely investigated. The intimate coupling between neural activities and energy metabolism is the underlying mechanism for intrinsic signal recording, which has been successfully and widely used in the field of neuroscience for more than 15 years. We hope that flavoprotein fluorescence imaging may also become a successful method in neuroscience, since it has a number of merits for functional brain imaging in the mouse cortex.

References

- Adachi K, Takahashi S, Melzer P, Campos KL, Nelson, T, et al. 1994. Increases in local cerebral blood flow associated with somatosensory activation are not mediated by NO. *Am J Physiol* 267: H2155-H2162.
- Arnould S, Berthon JL, Hubert C, Dias M, Cibert C, et al. 1997. Kinetics of protoporphyrinogen oxidase inhibition by diphenyleneiodonium derivatives. *Biochemistry* 36: 10178-10184.
- Aubin JE. 1979. Autofluorescence of viable cultured mammalian cells. *J Histochem Cytochem* 27: 36-43.
- Bennett BD, Jetton TL, Ying G, Magnuson MA, et al. 1996. Quantitative subcellular imaging of glucose metabolism within intact pancreatic islets. *J Biol Chem* 271: 3647-3651.
- Benson RC, Meyer RA, Zaruba ME, McKhann GM. 1979. Cellular autofluorescence—is it due to flavins? *J Histochem Cytochem* 27: 44-48.
- Billups B, Forsythe ID. 2002. Presynaptic mitochondrial calcium sequestration influences transmission at mammalian central synapses. *J Neurosci* 22: 5840-5847.
- Bliss TV, Collingridge GL. 1993. A synaptic model of memory: Long-term potentiation in the hippocampus. *Nature* 361: 31-39.
- Bonhoeffer T, Grinvald A. 1991. Iso-orientation domains in cat visual cortex are arranged in pinwheel-like patterns. *Nature* 353: 429-431.
- Bozza T, McGann JP, Mombaerts P, Wachowiak M. 2004. In vivo imaging of neuronal activity by targeted expression of a genetically encoded probe in the mouse. *Neuron* 42: 9-21.
- Budd SL, Nicholls DG. 1996. A reevaluation of the role of mitochondria in neuronal Ca^{2+} homeostasis. *J Neurochem* 66: 403-411.
- Chance B, Cohen P, Jöbsis FF, Schoener B. 1962. Intracellular oxidation–reduction states in vivo. *Science* 137: 499-508.
- Chance B, Schoener B, Oshino R, Itshak F, Nakase Y. 1979. Oxidation–reduction ratio studies of mitochondria in freeze-trapped samples. NADH and flavoprotein fluorescence signals. *J Biol Chem* 254: 4764-4771.
- Chen G, Hanson CL, Ebner TJ. 1998. Optical responses evoked by cerebellar surface stimulation in vivo using neutral red. *Neuroscience* 84: 645-668.
- Clarey JC, Tweedale R, Calford MB. 1996. Interhemispheric modulation of somatosensory receptive fields: Evidence for plasticity in primary somatosensory cortex. *Cereb Cortex* 6: 196-206.
- Cohen LB, Keynes RD, Hille B. 1968. Light scattering and birefringence changes during nerve activity. *Nature* 218: 438-441.
- Cohen LB, Salzberg BM, Grinvald A. 1978. Optical methods for monitoring neuron activity. *Annu Rev Neurosci* 1: 171-182.
- Coutinho V, Mutoh H, Knöpfel T. 2004. Functional topology of the mossy fibre–granule cell–Purkinje cell system revealed by imaging of intrinsic fluorescence in mouse cerebellum. *Eur J Neurosci* 20: 740-748.
- Cruikshank SJ, Weinberger NM. 1996. Receptive-field plasticity in the adult auditory cortex induced by Hebbian covariance. *J Neurosci* 16: 861-875.
- Dombeck DA, Blanchard-Desce M, Webb WW. 2004. Optical recording of action potentials with second-harmonic generation microscopy. *J Neurosci* 24: 999-1003.
- Duchen MR. 1992. Ca^{2+} -dependent changes in the mitochondrial energetics in single dissociated mouse sensory neurons. *Biochem J* 283: 41-50.
- Duong TQ, Kim DS, Ugurbil K, Kim SG. 2001. Localized cerebral blood flow response at submillimeter columnar resolution. *Proc Natl Acad Sci USA* 98: 10904-10909.
- Ebner TJ, Chen G. 1995. Use of voltage-sensitive dyes and optical recordings in the central nervous system. *Prog Neurobiol* 46: 463-506.
- Erinjeri JP, Woolsey TA. 2002. Spatial integration of vascular changes with neural activity in mouse cortex. *J Cereb Blood Flow Metab* 22: 353-360.

- Fein A, Tsacopoulos M. 1988. Activation of mitochondrial oxidative metabolism by calcium ions in *Limulus* ventral photoreceptor. *Nature* 331: 437-440.
- Fox PT, Raichle ME. 1986. Focal physiological uncoupling of cerebral blood flow and oxidative metabolism during somatosensory stimulation in human subjects. *Proc Natl Acad Sci USA* 83: 1140-1144.
- Frégnac Y, Shulz D, Thorpe S, Bienenstock E. 1992. Cellular analogs of visual cortical epigenesis. I. Plasticity of orientation selectivity. *J Neurosci* 12: 1280-1300.
- Frostig RD, Lieke EE, Ts'o DY, Grinvald A. 1990. Cortical functional architecture and local coupling between neuronal activity and the microcirculation revealed by in vivo high-resolution optical imaging of intrinsic signals. *Proc Natl Acad Sci USA* 87: 6082-6086.
- Fujii S, Saito K, Miyakawa H, Ito K, Kato H. 1991. Reversal of long-term potentiation (depotentiation) induced by tetanus stimulation of the input to CA1 neurons of guinea pig hippocampal slices. *Brain Res* 555: 112-122.
- Gao W, Dunbar RL, Chen G, Reinert KC, Oberdick J, et al. 2003. Optical imaging of long-term depression in the mouse cerebellar cortex in vivo. *J Neurosci* 23: 1859-1866.
- Gillooly JF, Brown JH, West, GB, Savage, VM, Charnov EL. 2001. Effects of size and temperature on metabolic rate. *Science* 293: 2248-2251.
- Goadsby PJ, Kaube H, Hoskin KL. 1992. Nitric oxide synthesis couples cerebral blood flow and metabolism. *Brain Res* 595: 167-170.
- Grinvald A, Hildesheim R. 2004. VSDI: A new era in functional imaging of cortical dynamics. *Nat Rev Neurosci* 5: 874-885.
- Grinvald A, Lieke E, Frostig RD, Gilbert CD, Wiesel TN. 1986. Functional architecture of cortex revealed by optical imaging of intrinsic signals. *Nature* 324: 361-364.
- Gunter TE, Buntinas L, Sparagna GC, Gunter KK. 1998. The Ca^{2+} transport mechanisms of mitochondria and Ca^{2+} uptake from physiological-type Ca^{2+} transients. *Biochim Biophys Acta* 1366: 5-15.
- Haglund MM, Ojemann GA, Hochman DW. 1992. Optical imaging of epileptiform and functional activity in human cerebral cortex. *Nature* 358: 668-771.
- Hansford RG. 1994. Physiological role of mitochondrial Ca^{2+} transport. *J Bioenerg Biomembr* 26: 495-508.
- Haselgrove JC, Bashford CL, Barlow CH, Quistorff B, Chance B, et al. 1990. Time resolved 3-dimensional recording of redox ratio during spreading depression in gerbil brain. *Brain Res* 506: 109-114.
- Hashimoto M, Takeda Y, Sato T, Kawahara H, Nagano O, et al. 2000. Dynamic changes of NADH fluorescence images and NADH content during spreading depression in the cerebral cortex of gerbils. *Brain Res* 872: 294-300.
- Hassinen I, Chance B. 1968. Oxidation-reduction properties of the mitochondrial flavoprotein chain. *Biochem Biophys Res Commun* 31: 895-900.
- Helmchen F, Waters J. 2002. Ca^{2+} imaging in the mammalian brain in vivo. *Eur J Pharmacol* 447: 119-129.
- Hishida R, Hoshino K, Kudoh M, Norita M, Shibuki K. 2003. Anisotropic functional connections between the auditory cortex and area 18a in rat cerebral slices. *Neurosci Res* 46: 171-182.
- Honda A, Adams SR, Sawyer CL, Lev-Ram V, Tsien RY, et al. 2001. Spatiotemporal dynamics of guanosine 3',5'-cyclic monophosphate revealed by a genetically encoded, fluorescent indicator. *Proc Natl Acad Sci USA* 98: 2437-2442.
- Horikawa J, Hess A, Nasu M, Hosokawa Y, Scheich H, et al. 2001. Optical imaging of neural activity in multiple auditory cortical fields of guinea pigs. *Neuroreport* 12: 3335-3339.
- Huang S, Heikal AA, Webb WW. 2002. Two-photon fluorescence spectroscopy and microscopy of NAD(P)H and flavoprotein. *Biophys J* 82: 2811-2825.
- Iwamura Y, Iriki A, Tanaka M. 1994. Bilateral hand representation in the postcentral somatosensory cortex. *Nature* 369: 554-556.
- Jöbsis FF, O'Connor M, Vitale A, Vreman H. 1971. Intracellular redox changes in functioning cerebral cortex. I. Metabolic effects of epileptiform activity. *J Neurophysiol* 34: 735-749.
- Jouveneau A, Billard JM, Haditsch U, Mansuy IM, Dutar P. 2003. Different phosphatase-dependent mechanisms mediate long-term depression and depotentiation of long-term potentiation in mouse hippocampal CA1 area. *Eur J Neurosci* 18: 1279-1285.
- Kandel ER. 2001. The molecular biology of memory storage: A dialogue between genes and synapses. *Science* 294: 1030-1038.
- Kann O, Schuchmann S, Buchheim K, Heinemann U. 2003. Coupling of neuronal activity and mitochondrial metabolism as revealed by NAD(P)H fluorescence signals in organotypic hippocampal slice cultures of the rat. *Neuroscience* 119: 87-100.
- Kasischke KA, Vishwasrao HD, Fisher PJ, Zipfel WR, Webb WW. 2004. Neural activity triggers neuronal oxidative metabolism followed by astrocytic glycolysis. *Science* 305: 99-103.
- Kavanagh NI, Ainscow EK, Brand, MD. 2000. Calcium regulation of oxidative phosphorylation in rat skeletal muscle mitochondria. *Biochim Biophys Acta* 1457: 57-70.
- Klaidman LK, Leung AC, Adams JD Jr. 1995. High-performance liquid chromatography analysis of oxidized and reduced pyridine dinucleotides in specific brain regions. *Anal Biochem* 228: 312-317.

- Knöpfel T, Tomita K, Shimazaki R, Sakai R. 2003. Optical recordings of membrane potential using genetically targeted voltage-sensitive fluorescent proteins. *Methods* 30: 42-48.
- Kudoh M, Shibuki K. 1996. Long-term potentiation of supra-granular pyramidal outputs in the rat auditory cortex. *Exp Brain Res* 110: 21-27.
- Kudoh M, Shibuki K. 1997. Importance of polysynaptic inputs and horizontal connectivity in the generation of tetanus-induced long-term potentiation in the rat auditory cortex. *J Neurosci* 17: 9458-9465.
- Kunz WS, Gellerich FN. 1993. Quantification of the content of fluorescent flavoproteins in mitochondria from liver, kidney cortex, skeletal muscle, and brain. *Biochem Med Metab Biol* 50: 103-110.
- Lewis DV, Schuette WH. 1976. NADH fluorescence, $[K^+]_o$, and oxygen consumption in cat cerebral cortex during direct cortical stimulation. *Brain Res* 110: 523-535.
- Lieke EE, Frostig RD, Arieli A, Ts'o DY, Hildesheim R, et al. 1989. Optical imaging of cortical activity: Real-time imaging using extrinsic dye-signals and high resolution imaging based on slow intrinsic-signals. *Annu Rev Physiol* 51: 543-559.
- Lindauer U, Royl G, Leithner C, Kuhl M, Gold L, et al. 2001. No evidence for early decrease in blood oxygenation in rat whisker cortex in response to functional activation. *Neuroimage* 6: 988-1001.
- Lipton P. 1973. Effects of membrane depolarization on nicotinamide nucleotide fluorescence in brain slices. *Biochem J* 136: 999-1009.
- Lothman E, Lamanna J, Cordingley G, Rosenthal M, Somjen G. 1975. Responses of electrical potential, potassium levels, and oxidative metabolic activity of the cerebral neocortex of cats. *Brain Res* 88: 15-36.
- Magistretti PJ. 2000. Cellular bases of functional brain imaging: Insights from neuron-glia metabolic coupling. *Brain Res* 886: 108-112.
- Magistretti PJ, Pellerin L, Rothman DL, Shulman RG. 1999. Energy on demand. *Science* 283: 496-497.
- Majander A, Finel M, Wikstrom M. 1994. Diphenyleneiodonium inhibits reduction of iron-sulfur clusters in the mitochondrial NADH-ubiquinone oxidoreductase (complex I). *J Biol Chem* 269: 21037-21042.
- Malonek D, Grinvald A. 1996. Interactions between electrical activity and cortical microcirculation revealed by imaging spectroscopy: Implications for functional brain mapping. *Science* 272: 551-554.
- Mayevsky A, Chance B. 1974. Repetitive patterns of metabolic changes during cortical spreading depression of the awake rat. *Brain Res* 65: 529-533.
- McCormack JG, Halestrap AP, Denton RM. 1990. Role of calcium ions in regulation of mammalian intramitochondrial metabolism. *Physiol Rev* 70: 391-425.
- Merrill DK, Guynn RW. 1981. The calculation of the cytoplasmic free $[NADP^+]/[NADPH]$ ratio in brain: Effect of electroconvulsive seizure. *Brain Res* 221: 307-318.
- Minta A, Kao JPY, Tsien RY. 1989. Fluorescent indicators for cytosolic calcium based on rhodamine and fluorescein chromophores. *J Biol Chem* 264: 8171-8178.
- Mironov SL, Richter DW. 2001. Oscillations and hypoxic changes of mitochondrial variables in neurons of the brainstem respiratory centre of mice. *J Physiol* 533: 227-236.
- Miyawaki A, Llopis J, Heim R, McCaffery JM, Adams JA, et al. 1997. Fluorescent indicators for Ca^{2+} based on green fluorescent proteins and calmodulin. *Nature* 388: 882-887.
- Murakami H, Kamatani D, Hishida R, Takao T, Kudoh M, et al. 2004. Short-term plasticity visualized with flavoprotein autofluorescence in the somatosensory cortex of anaesthetized rats. *Eur J Neurosci* 19: 1352-1360.
- Northington FJ, Matherne GP, Berne RM. 1992. Competitive inhibition of nitric oxide synthase prevents the cortical hyperemia associated with peripheral nerve stimulation. *Proc Natl Acad Sci USA* 89: 6649-6652.
- O'Connor MJ, Lewis DV, Herman CJ. 1973. Effects of potassium on oxidative metabolism and seizures. *Electroencephalogr Clin Neurophysiol* 35: 205-208.
- Ogawa S, Lee TM, Kay AR, Tank DW. 1990. Brain magnetic resonance imaging with contrast dependent on blood oxygenation. *Proc Natl Acad Sci USA* 87: 9868-9872.
- Pellerin L, Magistretti PJ. 1994. Glutamate uptake into astrocytes stimulates aerobic glycolysis—a mechanism coupling neuronal activity to glucose utilization. *Proc Natl Acad Sci USA* 91: 10625-10629.
- Ragan CI, Garland PB. 1969. The intra-mitochondrial localization of flavoproteins previously assigned to the respiratory chain. *Eur J Biochem* 10: 399-410.
- Ratz JD, McGuire JJ, Anderson DJ, Bennett BM. 2000. Effects of the flavoprotein inhibitor, diphenyleneiodonium sulfate, on ex vivo organic nitrate tolerance in the rat. *J Pharmacol Exp Ther* 293: 569-577.
- Reinert KC, Dunbar RL, Gao W, Chen G, Ebner TJ. 2004. Flavoprotein autofluorescence imaging of neuronal activation in the cerebellar cortex in vivo. *J Neurophysiol* 92: 199-211.
- Rizzuto R, Bernardi P, Pozzan T. 2000. Mitochondria as all-round players of the calcium game. *J Physiol (Lond)* 529: 37-47.
- Rosenthal M, Jöbsis FF. 1971. Intracellular redox changes in functioning cerebral cortex. II. Effects of direct cortical stimulation. *J Neurophysiol* 34: 750-762.
- Salzberg BM, Obaid AL, Gainer H. 1985. Large and rapid changes in light scattering accompany secretion by nerve terminals in the mammalian neurohypophysis. *J Gen Physiol* 86: 395-411.

- Sato K, Nariai T, Sasaki S, Yazawa I, Mochida H, et al. 2002. Intraoperative intrinsic optical imaging of neuronal activity from subdivisions of the human primary somatosensory cortex. *Cereb Cortex* 12: 269-280.
- Schuchmann S, Kovacs R, Kann O, Heinemann U, Buchheim K. 2001. Monitoring NAD(P)H autofluorescence to assess mitochondrial metabolic functions in rat hippocampal-entorhinal cortex slices. *Brain Res Protoc* 7: 267-276.
- Schuett S, Bonhoeffer T, Hubener M. 2002. Mapping retinotopic structure in mouse visual cortex with optical imaging. *J Neurosci* 22: 6549-6559.
- Seki K, Kudoh M, Shibuki K. 1999. Long-term potentiation of Ca^{2+} signal in the rat auditory cortex. *Neurosci Res* 34: 187-197.
- Seki K, Kudoh M, Shibuki K. 2001. Sequence dependence of post-tetanic potentiation after sequential heterosynaptic stimulation in the rat auditory cortex. *J Physiol (Lond)* 533: 503-518.
- Sharon D, Grinvald A. 2002. Dynamics and constancy in cortical spatiotemporal patterns of orientation processing. *Science* 295: 512-515.
- Shibuki K. 1989. Calcium-dependent and ouabain-resistant oxygen consumption in the rat neurohypophysis. *Brain Res* 487: 96-104.
- Shibuki K. 1990. Activation of neurohypophysial vasopressin release by Ca^{2+} influx and intracellular Ca^{2+} accumulation in the rat. *J Physiol (Lond)* 422: 321-331.
- Shibuki K, Hishida R, Murakami H, Kudoh M, Kawaguchi T, et al. 2003. Dynamic imaging of somatosensory cortical activity in the rat visualized by flavoprotein autofluorescence. *J Physiol* 549: 919-927.
- Shibuki K, Ono K, Hishida R, Kudoh M. 2004. Frequency-specific suppression of somatosensory cortical responses induced by somatosensory frequency discrimination learning in the rat. *Jpn J Physiol* 54(Suppl): S144.
- Shtoyerman E, Arieli A, Slovov H, Vanzetta I, Grinvald A. 2000. Long-term optical imaging and spectroscopy reveal mechanisms underlying the intrinsic signal and stability of cortical maps in V1 of behaving monkeys. *J Neurosci* 20: 8111-8121.
- Shuttleworth CW, Brennan AM, Connor JA. 2003. NAD(P)H fluorescence imaging of postsynaptic neuronal activation in murine hippocampal slices. *J Neurosci* 23: 3196-3208.
- Tamura M, Hoshi Y, Okada F. 1997. Localized near-infrared spectroscopy and functional optical imaging of brain activity. *Philos Trans R Soc Lond B Biol Sci* 352: 737-742.
- Territo PR, Mootha VK, French SA, Balaban RS. 2000. Ca^{2+} activation of heart mitochondrial oxidative phosphorylation: Role of the F_0/F_1 -ATPase. *Am J Physiol* 278: C423-C435.
- Thompson JK, Peterson MR, Freeman RD. 2003. Single-neuron activity and tissue oxygenation in the cerebral cortex. *Science* 299: 1070-1072.
- Toda N, Ayajiki K, Tanaka T, Okamura T. 2000. Preganglionic and postganglionic neurons responsible for cerebral vasodilation mediated by nitric oxide in anesthetized dogs. *J Cereb Blood Flow Metab* 20: 700-708.
- Tomlinson FH, Anderson RE, Meyer FB. 1993. Brain pH, cerebral blood flow, and NADH fluorescence during severe incomplete global ischemia in rabbits. *Stroke* 24: 435-443.
- Vanzetta I, Grinvald A. 1999. Increased cortical oxidative metabolism due to sensory stimulation: Implications for functional brain imaging. *Science* 286: 1555-1558.
- Verkhratsky A, Kettenmann H. 1996. Calcium signalling in glial cells. *Trends Neurosci* 19: 346-352.
- Wang Q, Kjaer T, Jorgensen MB, Paulson OB, Lassen NA, et al. 1993. Nitric oxide does not act as a mediator coupling cerebral blood flow to neural activity following somatosensory stimuli in rats. *Neurol Res* 15: 33-36.
- Weber B, Burger C, Wyss MT, von Schulthess GK, Scheffold F, et al. 2004. Optical imaging of the spatiotemporal dynamics of cerebral blood flow and oxidative metabolism in the rat barrel cortex. *Eur J Neurosci* 20: 2664-2670.
- Woolsey TA, Rovainen CM, Cox SB, Henegar MH, Liang GE, et al. 1996. Neuronal units linked to microvascular modules in cerebral cortex: Response elements for imaging the brain. *Cereb Cortex* 6: 647-660.
- Zarei M, Stephenson JD. 2000. Transhemispheric cortical reorganization in rat SmI and involvement of central noradrenergic system. *Brain Res* 870: 142-149.

4.5 Coupling of Brain Function to Metabolism: Evaluation of Energy Requirements

A. Gjedde

1	Brain Work	345
2	Ion Homeostasis	347
3	Brain Energy Metabolism	348
3.1	Definition of Brain Activity Levels	349
3.2	Stages of Brain Metabolic Activity	350
3.2.1	Baseline Metabolism (Stages 0–1)	350
3.2.2	Resting Metabolism (Stage 2)	350
3.2.3	Normal (Default) and Physiologically Elevated Metabolism (Stages 3–4)	350
4	Substrate Transport in Brain	351
4.1	Glucose Transport	352
4.2	Monocarboxylate Transport	353
4.3	Oxygen Transport	355
5	ATP Homeostasis	355
5.1	Hydrolysis of Phosphocreatine	357
5.2	Glycolysis	358
5.2.1	Hexokinase and Phosphofructokinase-1	358
5.2.2	Pyruvate and Lactate Dehydrogenases	359
5.3	Oxidative Phosphorylation	360
5.3.1	Pyruvate Dehydrogenase Complex and the Tricarboxylic Acid Cycle	361
5.3.2	Cytochrome Oxidation and the Electron Transport Chain	361
6	Metabolic Compartmentation	363
6.1	Functional Properties of Neurons and Astrocytes	363
6.2	Metabolic Properties of Neurons and Astrocytes	363
6.2.1	Oxidative and Glycolytic Capacities	364
6.2.2	Metabolite Cycling	368
7	Activation	368
7.1	Ion Homeostasis During Activation	370
7.2	Brain Energy Metabolism During Activation	371
7.2.1	Global Steady-State Changes of Energy Metabolism	371
7.2.2	Localized Changes of Energy Metabolism in Response to Stimulation	372
7.2.3	Vascular and Tissue Metabolite Changes During Activation	373
7.3	Substrate Delivery During Activation	377
7.3.1	Regulation of Microvascular Oxygen	378
7.3.2	BOLD Signal Changes During Activation	378

7.3.3	Regulation of Tissue Oxygen	380
7.4	Regulation of Blood Flow	382
7.4.1	Nitric Oxide	382
7.4.2	Prostanoids	383
7.4.3	Potassium	383
7.5	ATP Homeostasis During Activation	384
7.5.1	Hydrolysis of Phosphocreatine During Activation	384
7.5.2	Glycolysis During Activation	384
7.5.3	Reaction Potential Changes During Activation	386
7.5.4	Oxidative Phosphorylation During Activation	386
7.6	Metabolic Compartmentation During Activation	388
7.6.1	Sites of Cellular Activity During Activation	388
7.6.2	Cellular Interactions During Activation	389
8	Conclusions	391

Abstract: There is no rigid association in vivo between changes of oxygen consumption, glucose combustion, and blood flow in the human brain. The claim that cerebral blood flow rises to satisfy the demands for oxygen and glucose during neuronal excitation therefore is simplistic. Energy budget estimates indicate that most of the cerebral energy demand reflects the steady-state level of graded post-synaptic membrane depolarization, followed by action potential generation and propagation. Increased energy supply is required to maintain the depolarization of neuronal membranes when sodium and potassium conductances are increased. Glucose, pyruvate and lactate occupy single tissue compartments, but transient shifts of the relative activity of neurons and astrocytes disrupt the steady-state, and the properties of lactate dehydrogenase may vary temporally, as dictated by transient shifts of cytosolic redox potentials and pH values. Pyruvate and lactate generation invariably occurs when astrocytes are activated by glutamate release. In these cases, the increased demand for glutamate imposes a metabolic rate on astroglial cells that exceeds their modest oxidative capacity. Although the resulting pyruvate and lactate accumulation is influenced by lactate export or import across the blood-brain barrier, pyruvate and lactate accumulate in a joint pool, to which astrocytes produce more pyruvate than neurons. The blood flow increase appears to be coupled to the rate of glycolysis. There is increasing evidence that the putative mechanism underlying the flow-glycolysis couple resides in astrocytes. The evidence suggests that the increase of oxidative metabolism in neurons is coupled to a rise of pyruvate, as dictated by the degree of mitochondrial activation. Under some circumstances, regional 'peaks' of increased blood flow and increased oxygen consumption could be dissociated by the differential activation of primary and secondary neuronal networks. The activations accompanying the most complex processing of information could be those with the tightest coupling between oxygen consumption and blood flow and hence with the least generation of lactate.

List of Abbreviations: AA, arachidonic acid; ADP, adenosine diphosphate; AMP, adenosine monophosphate; A/N, astrocyte-to-neuron activation ratio, relative to baseline; ATP, adenosine triphosphate; avd, arteriovenous deficit; CBF, cerebral blood flow; CK, creatine kinase; CMR_{glc} , cerebral metabolic rate of glucose; $CMRO_2$, cerebral metabolic rate of oxygen; CO_2^{art} , arterial oxygen concentration; COX, cyclooxygenase; CYP4A, cytochrome P450 4A, enzymes; EAAT, excitatory amino acid transporter; EET, epoxyeicosatrienoate; E_{O_2} , oxygen extraction fraction; $FADH_2$, flavin adenine dinucleotide; f_{glc} , fraction of ATP, generated non-oxidatively; f_{O_2} , fraction of ATP, generated oxidatively; GLAST, glutamate astrocyte-specific transporter; glc, glucose; GLT, glutamate transporter; GLUT, glucose transporter; GTP, guanosine triphosphate; 20-HETE, 20-hydroxyeicosatetraenoate; hg, hectogram; H4 LDH, heart type; HK, hexokinase; J_{glc} , glucose metabolic rate; J_{max} , maximum metabolite flux; J_{O_2} , oxygen metabolic rate; K_M , K_m Michaelis half-saturation constant; L , oxygen conductivity of tissue; lact, lactate; LD, lactate dehydrogenase subtype; LDH, lactate dehydrogenase; LGI, lactate-glucose index; M4, LDH, muscle type; MAI, metabolite accumulation index; MCT, monocarboxylic acid transporter; MGI, metabolites-glucose index; mGluR, metabotropic glutamate receptor; Mi-CK, mitochondrial creatine kinase; mMCT, mitochondrial monocarboxylic acid transporter; mmHg, millimeter Mercury; mRNA, messenger RNA, (ribonucleic acid); MUR, metabolite uptake ratio; NAD^+ , nicotinamide adenine dinucleotide (oxidized form); NADH, nicotinamide adenine dinucleotide (reduced form); NSI, non-steady-state index; NO, nitric oxide; NOS, nitric oxide synthase; OGI, oxygen-glucose index; P_{50} , half-saturation oxygen tension; P_{50}^{cytox} , half-saturation oxygen tension of cytochrome oxidase; PCr, phosphocreatine; PDH, pyruvate dehydrogenase; PFK, phosphofructokinase; PGE2, prostaglandin E2; P_i , inorganic phosphate; P_{O_2} , oxygen partial pressure (tension); p_R , reaction potential; pyr, pyruvate; S, saturation; TCA, tricarboxylic acid; T_{max} , maximum transporter-mediated flux; V_{max} , maximum enzyme reaction velocity

1 Brain Work

Brain function and brain work are separate terms for brain activity, and a major issue concerns their relationship. Energy is the ability to do work. Rates of energy turnover in the brain are among the highest in the body, yet it is not clear how the work that this energy turnover fuels is related to brain function. Brain function, on the other hand, is a description of what the brain does. This section presents the known

correlations between information exchange and energy turnover, and between neurotransmission and energy turnover, and speculates about their causal links.

The close coupling of neuronal function to glucose and oxygen metabolism is well established. The three most important factors include the processes that consume the most energy in activated cells under different conditions, the regional and activation-dependent differences in stoichiometry of oxygen and glucose utilization, and the mechanisms that supply the energy for the work of the brain. These factors are increasingly well understood. Yet, emerging evidence has required that the energy budget available to different states of localized and general brain activity be updated in the light of this evidence.

The brain derives most of its energy from the combustion of glucose. About 90% of the glucose is metabolized to carbon dioxide, and the oxidative metabolism of glucose in turn covers 99.5% of the brain's energy budget under normal stationary circumstances, also known as the normal (default) steady state. Under special circumstances the brain covers larger fractions of its energy turnover by nonoxidative metabolism of glucose, or by oxidative metabolism of monocarboxylic acids, including lactate, β -hydroxybutyrate, acetoacetate, and acetate. The normal steady-state energy yield from these sources on the average is 10 μmol ATP (adenosine triphosphate) per minute for every gram of human cortical brain tissue (*see Box 1*).

Box 1: Human vs Rodent Brain

The present chapter is focused on the human brain but occasionally refers to results obtained in the rat brain. The rat brain is much smaller than the human brain (2 g vs 1250 g) but has a higher density of cells and microvessels, and hence higher rates of blood flow and metabolism per unit weight. Generally speaking, these rates in the rodent brain are about twice the rates in the human brain.

Although the brain accounts for only about 1%–2% of the total body mass, at rest it consumes 10% of the resting human body's glucose and oxygen supplies and receives 10% of its blood supply. It is generally assumed that these values of blood flow and energy metabolism reflect the work associated with the functions of the brain but the precise link is not well defined, nor is it known to which extent the link is crucially important to the understanding of the organization of the brain and its functions. Therefore, to clarify the mechanisms linking the signals from brain images to the brain's electrochemical work, it is important to consider:

- the kind of work carried out in the brain,
- the cells that carry out the brain's work,
- the mechanism linking the work of these cells to the relative and absolute magnitudes of oxidative and nonoxidative energy metabolism in brain tissue, and
- the mechanism relating the blood supply of the brain to the magnitudes of the brain's oxidative and nonoxidative metabolism.

The brain's work commonly is held to involve the transfer, processing, and exchange of information. The concept of information is not entirely clear, but it is generally held to be a function of the number of different states that a system can occupy. Thus, for n different states, each state is said to contain $\log_2(n)$ bits, or $\log_2(n)/8$ bytes, of information. To the extent that a synapse can be considered a simple on–off device (switch), the central nervous system in human beings may have as many as 10^{15} switches, allowing the brain to occupy at least $2^{10^{15}}$ different states, and thus to hold 10^{15} bits of information. Changes of this mass of information occur when the switches are thrown. The throwing of a switch represents a single binary operation, and the toggling incurs a cost to the system's energy supplies that qualifies as work but is probably unrelated to the actual information being exchanged.

It is believed that the energy cost of the information transfer can be calculated from the concept of entropy, according to which the information locally reduces the entropy of the system represented by the entire brain. Entropy can be reduced only by the supply of energy. Thus, the energy cost can be estimated from the combustion of fuels measured during the functional activity of the brain. According to one such

calculation, a single binary operation requires a minimum energy supply of 3×10^{-24} kJ (Morowitz, 1978). The hydrolysis of ATP yields free energy of about 3×10^{-5} kJ μmol^{-1} , and the human brain hydrolyzes $10 \mu\text{mol ATP g}^{-1} \text{min}^{-1}$. Assuming an upper limit of thermodynamic efficiency of 50%, brain tissue has the capacity to perform binary operations at the rate of no more than 10^{11} megabytes $\text{g}^{-1} \text{s}^{-1}$, or about 10^{18} operations per second per brain.

2 Ion Homeostasis

Much of the energy turnover of the brain subserves the restoration of ion gradients across leaky cell membranes. The leakiness of the cell membranes in turn is affected by the presence of neurotransmitters, inhibitory as well as excitatory, and by the magnitude of the membrane potential established by the leaky membranes. The leakier the membranes are, the more work it requires to maintain a specific membrane potential. Therefore, brain work is also an index of the leakiness of neural membranes.

Information transfer and processing in the brain occur as propagated changes of membrane potential, brought on by changes of membrane permeability to several extra- or intracellularly concentrated cations. The present section deals with the mechanisms that maintain the concentration of these ions in the face of changing membrane potentials. Neurons impose metabolic needs on the brain by being subject to excitation- and inhibition-induced changes of the membrane permeabilities to sodium, potassium, chloride, and calcium ions. Increases of the intracellular concentration of Na^+ or the extracellular concentration of K^+ stimulate the membrane Na^+/K^+ -ATPase activity. How much of the ATPase activity subserves the transfer of information, and how much is necessary to keep the cells intact, is not known with certainty. The evidence cited below suggests that the ATPase activity associated with the functional activity of information transfer varies, from a value that is twice the absolute minimum required to maintain cellular integrity, to a value that is an order of magnitude greater.

According to the “sodium theory,” (see Box 2) the conductances of sodium and potassium underlying the resting membrane potential, as well as the increased conductances associated both with excitation above

Box 2: The Sodium Theory

The “sodium theory” (Hodgkin and Huxley, 1952) is the name for the mechanism that explains the origin of the membrane potential and the graded or alternating depolarization of cells by the presence of sodium, calcium, potassium, and chloride equivalents as free ions in the intra- and extracellular spaces, and by the action on and of specific ion channels in the plasma membranes, across which the ions are exchanged. The theory ascribes the electrical properties of the membrane to diffusion potentials established by the membrane conductances controlled by these channels (Hodgkin and Huxley, 1952).

the nonexcited baseline and with excitation above the resting or “default” average, must be matched by appropriately active ion pumping to maintain constant ion concentrations. The P-type (plasma membrane-type) Na^+/K^+ -ATPase combines with ATP, Mg^{2+} , Na^+ , and K^+ to form an enzyme–substrate association during which the enzyme is phosphorylated, and Mg^{2+} and ADP are released (Skou, 1960). As the phosphorylated enzyme splits into inorganic phosphate and the original enzyme, Na^+ and K^+ ions are translocated in the appropriate directions, outward for sodium and inward for potassium. This means that the energy released by the hydrolysis of $5 \mu\text{mol g}^{-1}$ ATP every minute (half the ATP turnover) is sufficient to transport $15 \mu\text{mol Na}^+ \text{g}^{-1}$ every minute. The resulting half-life of sodium in the cells is less than a minute, and also considerably less than the 20 min half-life of sodium in stimulated squid axons (Hodgkin and Keynes, 1956).

The apparent average sodium permeability-surface area product in the steady state can be calculated from the sodium flux. With the concentrations listed in [Table 4.5-1](#), as well as assumed values of an average steady-state membrane potential and corresponding sodium flux calculated from the measured

■ **Table 4.5-1**

Ion concentrations in nerve cells

Variable	Unit	Ion				
		Sodium		Potassium		Chloride
		E&S	M	E&S	M	M
Equilibrium potential	mV	+41	+40	-84	-100	-75
Intracellular concentration	mM	27	30	80	140	8
Extracellular concentration	mM	133	150	3	3	130

From Erecinska and Silver (1989) ("E&S"); McCormick (1990) ("M")

ATP turnover, and the 3:2 ratio between the net sodium and potassium fluxes in the steady state, the permeability-surface area products of sodium and potassium of [Table 4.5-2](#) were calculated by means of Goldman's flux equation (Goldman, 1943; Hodgkin and Katz, 1949). Details of this calculation were given

■ **Table 4.5-2**

Ion movements across nerve cell membranes

Variable	Unit	Ion		
		Sodium	Potassium	Chloride
Transmembrane leakage	$\mu\text{mol g}^{-1} \text{min}^{-1}$	15	10	5
PS product at -65 mV	$\text{ml g}^{-1} \text{min}^{-1}$	0.038	0.404	0.549
PS product at -55 mV	$\text{ml g}^{-1} \text{min}^{-1}$	0.044	0.285	0.246

From Gjedde (1993b), assuming 50% of ATP turnover dedicated to ion transport, calculated from the concentrations listed in [Table 4.5-1](#) ("M"). To estimate the chloride permeability, it was necessary to use a simplified form of the equation

by Gjedde (1993a). The equation yields the membrane potential difference on the basis of the permeability-weighted individual concentrations of sodium, potassium, and chloride. In the steady state, the chloride flux matches the difference between the sodium and potassium fluxes, rendering the total ion flux electroneutral. The calculation ignores the requirements imposed by calcium ion fluxes but the calcium ion flux is a minor requirement in energetic terms, although it is now known to be of major functional significance (Lauritzen, 2005), as discussed below.

3 Brain Energy Metabolism

Neuroenergetics is the study of brain energy metabolism that deals with the energy gained from the breakdown of nutrients in brain tissue. Neuroenergetics is focused on the relationship between the biochemistry of the cells that are the sites of glucose breakdown and the use of oxygen and the functional activity that these cells participate in. The main questions include the issue of whether there is a typical rate of brain energy metabolism and how much of this rate is directly coupled to the execution of brain function. In this section, brain energy metabolism is shown to undergo characteristic stepwise changes in relation to shifts among fundamental levels of brain function.

The precise link between the work performed by brain tissue and the rate of metabolism is not known. Several possibilities have been raised, including the claim that the concept of a link itself is obsolete; the metabolism "is" the work. Of the putative links, the simplest but least plausible is feedback regulation of metabolism by the changing concentrations of metabolites such as ATP as ADP (*see Box 6*). This subsection

deals with the attempts to identify a regulatory mechanism that elicits the appropriate changes of metabolite flux in association with, rather than in response to, the changes of the work of the brain.

3.1 Definition of Brain Activity Levels

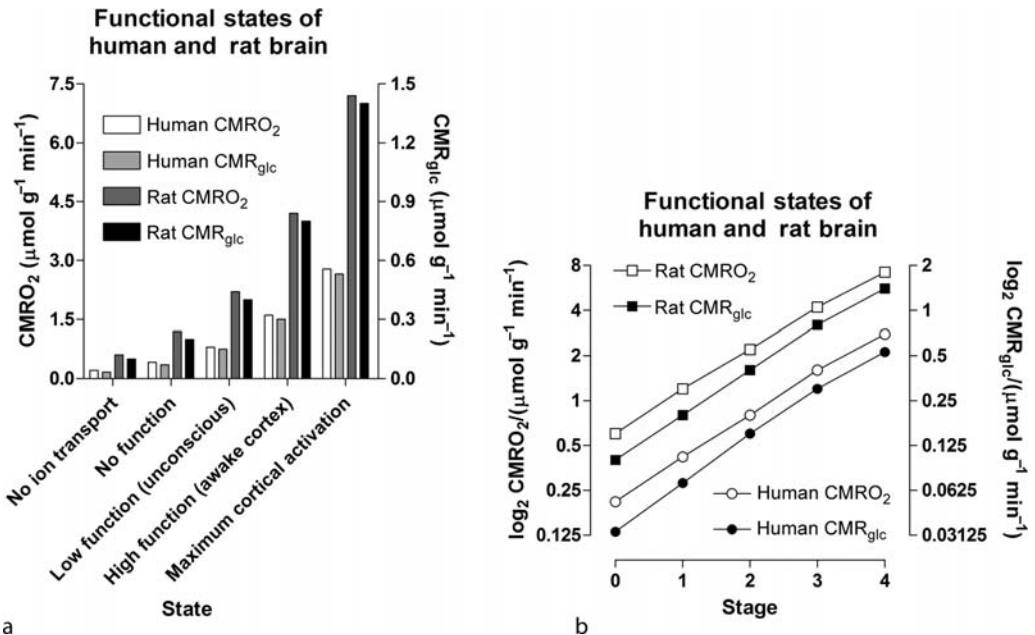
The definition of the brain's baseline activity is in dispute and the issue of the brain's normal activity is complex. Recent theories of brain functional organization distinguish between activation, default, resting, and baseline states, but the definitions of these states are not universally agreed upon.

The question of the range of work between baseline (or "household") and normal (default) activities of brain tissue hinges on the definitions of average and baseline states. In the work of Sibson et al. (1998), Shulman and Rothman (1998), and Shulman et al. (2005), functional activity is defined as the rate of metabolism that is linked to the rate of release of the excitatory neurotransmitter glutamate. Close reading of this work suggests that the maximum functional activity of both rodent and human brains is about twice the normal (default) activity, which in turn is about twice the "resting" activity measured in apparently unconscious but otherwise intact brains. This resting activity also turns out to be about twice the activity associated with a neuronally nonfunctioning baseline, which in turn is about twice the activity associated with the state of absent ion transport. The nonfunctioning baseline is a state in which cells survive but undergo no depolarizations, and hence do not communicate functionally.

This evidence suggests the rule of thumb that brain energy metabolism doubles for every standard increment of functional activity as shown in [Figure 4.5-1](#). By standard increment is meant a change from one fundamental stage of functional level to the next. These stages are illustrated in [Figure 4.5-1](#) and

■ **Figure 4.5-1**

Relationship among functional activity of mammalian brain and estimates of rates of energy metabolism of oxygen and glucose. From studies of rat and human brain summarized by Gjedde et al. (2002); Shulman et al. (2005); and Hyder et al. (2006). (a) Ordinates show oxygen (left) and glucose (right) metabolic rates for five distinct levels of functional activity. (b) Abscissa: Functional stage on a scale from 0 to 4. Ordinates: Log₂ scale of oxygen (left) and glucose (right) metabolic rates in units of $\mu\text{mol g}^{-1} \text{min}^{-1}$



include the states of no ion transport (stage 0), no functional activity (baseline stage 1), low functional activity without consciousness (baseline stage 2), high functional activity with consciousness arising from activity in the cerebral cortex (default stage 3), and elevated functional activity associated with the highest degree of physiological activation (stage 4). Activity above stage 4 can be considered pathological. Panel B shows that the metabolic or work rates associated with these stages approximately obey the simple formula

$$\text{CMR}(S) = \text{CMR}(0) 2^S, \quad (1)$$

where CMR is the cerebral metabolic rate, CMR(0) is the cerebral metabolic rate of stage 0, and S is one of the five functional stages (0–4) defined above. The equation has an interesting similarity to the formula (see above) for a system that holds S bits of information.

3.2 Stages of Brain Metabolic Activity

3.2.1 Baseline Metabolism (Stages 0–1)

It is necessary to distinguish between energetic and functional baselines. The energetic baseline is the absence of ion transport, which is not consistent with continued cellular integrity. In contrast, the functional baseline in this context is the state of absent functional activity in the form of communication among nerve cells. The rule of thumb derived above from recent experiments with living intact mammalian brains makes it a reasonable estimate that one-fourth or 25% of the normal or default energy turnover (12.5% of the maximum physiological excitation) of the human brain subserves the basic ion transport in the absence of functional activity associated with isoelectricity.

However, the maintenance of an immutable membrane potential is not the only demand made on brain energy utilization at the functional baseline, as shown by Whittam (1962) who estimated the metabolism of isolated brain tissue associated with the transport of sodium and potassium to represent 40% of the functional baseline, and 50% of the functional baseline was found to remain when ion transport in isolated nervous tissue was blocked completely by inactivation of the Na^+/K^+ -ATPase (Baker and Connelly, 1966; Ritchie, 1967; Hertz and Schousboe, 1975; Mata et al., 1980). The target of the remaining activity is not known with certainty but is assumed to be the biochemical processes that maintain the infrastructure of the cell.

3.2.2 Resting Metabolism (Stage 2)

The term “resting” state for normal brain tissue has little meaning *in vivo*, as the healthy brain never rests, but for present purposes it suffices to define rest as a state of lowered but not completely absent functional activity, in which no particular excitation is present. The energy metabolism of brain tissue in any one of a variety of conditions of absent higher cognitive activity (severed connections, coma, persistent vegetative state, anesthesia) is all about 50% of the normal default average (and hence close to 25% of the maximum physiological excitation) (McIlwain, 1951; Shalit et al., 1970, 1972; Brodersen and Jørgensen, 1974; Sokoloff et al., 1977; Levy et al., 1987; Alkire et al., 1995, 1997, 1999). These observations show that the work associated with lowered but not absent depolarization of neural membranes is about half of the work imposed by the average degree of depolarization.

3.2.3 Normal (Default) and Physiologically Elevated Metabolism (Stages 3–4)

The normal or default metabolic stage refers to the awake and normally functioning mammalian brain. As this stage has been studied more closely in awake humans than in other mammals, stage 3 metabolism may refer more accurately to the cerebral cortex, while whole-brain values may tend to represent a mixture of stage 2 and stage 3 metabolic conditions.

Using now classical neuroimaging methods, Kety (1949) and Lassen (1959) reported the average magnitudes of normal brain energy metabolism and blood flow in living human brains. More recently determined but similar steady-state values of energy metabolism and blood flow of the human brain are listed in [Table 4.5-3](#), together with the steady-state turnover rates of ATP, pyruvate, and lactate.

Table 4.5-3
Average properties of human whole brain and cerebral cortex

Variable [unit]	Whole brain	Cerebral cortex
CMR _{glc} [$\mu\text{mol g}^{-1} \text{min}^{-1}$]	0.25	0.30
CMR _{O₂} [$\mu\text{mol g}^{-1} \text{min}^{-1}$]	1.40	1.60
CBF [$\text{ml g}^{-1} \text{min}^{-1}$]	0.43	0.50
OGI [ratio]	5.6	5.3
ATP turnover [J_{ATP} , $\mu\text{mol g}^{-1} \text{min}^{-1}$]	9.4	10.2
Pyruvate turnover [J_{pyr} , $\mu\text{mol g}^{-1} \text{min}^{-1}$]	0.5	0.6
Lactate efflux [J_{lact} , $\mu\text{mol g}^{-1} \text{min}^{-1}$]	0.035	0.07
LGI [ratio]	-0.14	-0.23

Modified from Kuwabara et al. (1992), Vafaee et al. (1999), and Gjedde et al. (2005), using [Eqs. \(7-9\)](#)

The whole-brain oxygen–glucose index (OGI) is the steady-state ratio between the molar quantities of oxygen and glucose used by the brain. The index has a value close to 5.6 under normal circumstances, indicating that about 90% of the glucose is oxidatively metabolized to CO₂ (see also Himwich and Himwich (1946)). In the normal (default) state, total glucose consumption of the cerebral cortex rather than whole brain is about 30 $\mu\text{mol hg}^{-1} \text{min}^{-1}$, with an OGI of 5.3. The unit “hg” is the SI unit for 100 g (hectogram), used throughout this text. The 10% nonoxidative metabolism of glucose leads to a lactate production of about 5–7 $\mu\text{mol hg}^{-1} \text{min}^{-1}$, as well as biosyntheses of serine, alanine, glycine, acetyl coenzyme A (acetyl-CoA), lipids and amino acids derived from Krebs’ cycle, and the pentose phosphate shunt pathway (see below). The lactate flux is known to be about 25% of the maximum transport capacity (T_{max}) of the blood–brain barrier transporter of monocarboxylic acids (MCT1, see below). According to Michaelis–Menten kinetics, this is consistent with a tissue lactate concentration of about 1.5 mM, as listed in [Table 4.5-3](#). The corresponding ATP turnover calculated from [Eq. 3](#) (see *Box 3*) is 10 $\mu\text{mol g}^{-1} \text{min}^{-1}$. Altogether, the brain tissue metabolite stores, including ATP itself, represent about 1 min worth of ATP turnover ([Table 4.5-4](#)). Attwell and Laughlin (2001) reevaluated the energy turnover involved in the different processes contributing to functional activity, now known as the energy “budget” of the brain, including the energy requirements of processes such as biosynthesis, during functional activity in vivo, neurotransmitter vesicle formation, fusion, and release. According to this budget, 90% of the energy turnover is devoted to “synaptic” and hence functional activity in general in the brain, and of this turnover, 80% occurs in neurons and the remainder apparently in glial cells. The authors also conclude that almost all of the energy is spent on the restoration of ion gradients by means of the Na⁺/K⁺-ATPase.

There is early as well as more recent evidence that the oxygen consumption of the human brain may rise to as much as 300 $\mu\text{mol hg}^{-1} \text{min}^{-1}$ under some physiological circumstances, with concurrent increases of glucose consumption to as much as 50 $\mu\text{mol hg}^{-1} \text{min}^{-1}$ (Roland et al., 1987; Shulman et al., 2005), judged from magnetic resonance spectroscopic measurements of total oxidative metabolism of pyruvate which reach as high as 0.8–0.9 $\mu\text{mol g}^{-1} \text{min}^{-1}$ in normal human cerebral cortex.

4 Substrate Transport in Brain

The mechanisms of delivery of the substrates of brain metabolism are important to the understanding of regulation of blood flow and capillary density in brain tissue, the two factors that constrain the delivery

Box 3: Oxygen Tension in Capillaries, Average Brain Tissue, and Mitochondria

Calculation of the oxygen tensions in brain tissue is based on the assumption that oxygen's saturation of hemoglobin in capillaries is a simple function of the net extraction of oxygen, assuming a reasonably even distribution of the oxygen delivery along the length of all capillaries, according to the equation

$$\bar{S}_{O_2} = S_{aO_2} \left(1 - \frac{E_{O_2}}{2} \right), \quad (2)$$

where \bar{S}_{O_2} is the average capillary oxygen saturation of hemoglobin, S_{aO_2} is the arterial oxygen saturation, and E_{O_2} is the net oxygen extraction fraction, equal to the ratio $J_{O_2}/(FC_{O_2})$, in which F is the blood flow, and C_{O_2} is the arterial oxygen concentration. The mean capillary oxygen tension and hemoglobin saturation are also related by the equation for the oxygen dissociation curve

$$\bar{S}_{O_2} = \frac{1}{1 + \left[\frac{P_{50}^{hb}}{\bar{P}_{O_2}^{cap}} \right]^h}, \quad (3)$$

where P_{50}^{hb} is the hemoglobin half-saturation oxygen tension, $\bar{P}_{O_2}^{cap}$ is the average arterial oxygen tension, and h is the Hill coefficient. The resulting equation establishes the inverse correlation between the net extraction fraction and the average capillary oxygen tension

$$\bar{P}_{O_2}^{cap} = P_{50} \sqrt{\frac{h S_{aO_2} (2 - E_{O_2})}{2 - S_{aO_2} (2 - E_{O_2})}} = P_{50} \sqrt{\frac{2}{E_{O_2}} - 1} \quad \text{for } S_{aO_2} \approx 1, \quad (4)$$

where the second equality requires an arterial oxygen saturation of 100%. The maximum delivery is proportional to the mean capillary oxygen tension for a given effective capillary density associated with a particular diffusion capacity L . The average mitochondrial oxygen tension is therefore

$$\bar{P}_{O_2}^{mit} = \bar{P}_{O_2}^{cap} - \frac{J_{O_2}}{L}, \quad (5)$$

where $\bar{P}_{O_2}^{mit}$ is the maximum oxygen delivery capacity, J_{O_2} is the rate of oxygen consumption, and L is the tissue oxygen diffusion capacity for the mean distance between the capillary lumen and the mitochondria. The average tension of oxygen in brain tissue depends on the distribution of oxygen delivery and consumption sites but can be approximated by the formula

$$\bar{P}_{O_2}^{br} = \bar{P}_{O_2}^{cap} - \frac{J_{O_2}}{2L}, \quad (6)$$

where the average tissue oxygen tension is $\bar{P}_{O_2}^{br}$. The average normal tensions of oxygen in the vasculature and tissue compartments, estimated with the compartment equations above, are shown in the model illustrated in

▶ [Figure 4.5-2](#) (Gjedde, 2005).

under normal and pathological circumstances. Glucose delivery primarily depends on the glucose concentration in the circulation and the properties of glucose transporters in the membranes of brain cells, while oxygen delivery primarily depends on the binding of oxygen to hemoglobin in red blood cells, the magnitude of blood flow, and the diffusion distances in brain tissue as presented in *Box 3*.

4.1 Glucose Transport

Glucose is the source of pyruvate and enters brain tissue, both neurons and astrocytes, by means of facilitative insulin- and sodium-insensitive transport mediated by several members of the so-called GLUT family of membrane-spanning proteins (Gjedde, 1992). In brain, the important members are GLUT-1 and GLUT-3 (Drewes, 1999). The 55-kDa GLUT-1 resides in the membranes of the capillary endothelium

■ Table 4.5-4

Average metabolites in human brain

Metabolite	Cytosol		Glycolytic equivalents	
	Concentration (mM)	Content ($\mu\text{mol g}^{-1}$)	ATP ($\mu\text{mol g}^{-1}$)	Lactate ($\mu\text{mol g}^{-1}$)
PCr	5.0	4.0	4.0	
Glycogen	3.0	2.4	3.6	3.6
Glucose	1.2	1.0	2.0	2.0
ATP	2.2	1.7	1.7	
ADP	1.2×10^{-2}	1.0×10^{-2}	5.0×10^{-3}	
AMP	7.1×10^{-5}	5.6×10^{-5}		
Pyruvate	0.16	0.13		0.1
Lactate	2.9 (0.75 ^a)	2.3 (0.6 ^a)		2.3
Total			11.3	8.0

From Olesen (1970); Roth & Weiner (1991). The “glycolytic equivalent” is the ATP reserve that each metabolite would represent in case of complete depletion

^aMRS measurements generally yield lower values of lactate in vivo (0.5–1 mM) but corresponding pyruvate values are not reported and the determination is indirect (see Prichard et al. (1991); Sappey-Marini er et al. (1992))

constituting the blood–brain barrier, while a slightly modified 45-kDa GLUT-1 resides in the membranes of astrocytes and choroid plexus. The GLUT-3 protein resides in the membranes of neurons. The transport of glucose is nonlinearly proportional to the difference between blood plasma and cytoplasm concentrations, ensuring that the glucose concentration everywhere in brain tissue is the same substantial fraction of the plasma glucose (Silver and Erecinska, 1994).

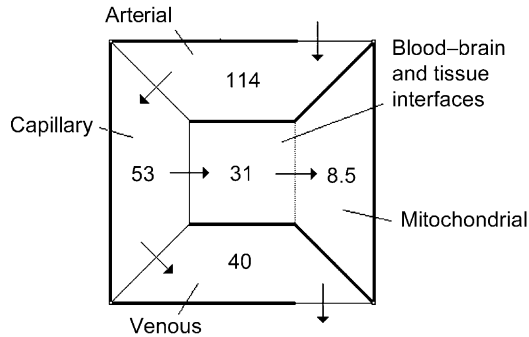
The transport capacities of GLUT-1 and GLUT-3 are known in some detail, which indicates that glucose provision itself is not rate-limiting for brain oxidative metabolism (Gjedde, 1983, 1992). For glucose, the maximum transport rate (T_{max}) of the endothelial GLUT-1 glucose transport across the blood–brain barrier is about 2–4 times the rate of unidirectional glucose transport, which in turn is about twice the net transport of glucose (see Gjedde (1992)). The magnitudes of the T_{max} of the neuronal and glial glucose transporters GLUT-3 and GLUT-1 are 5000-fold higher (Diemer et al., 1985). Thus, under normal circumstances, glucose transport is not rate limiting for glycolysis, and glucose concentrations in the different cellular compartments of brain tissue are likely to be similar. However, as blood–brain glucose transport may become rate limiting in pronounced hypoglycemia, it is possible that it could also be rate limiting under conditions of extreme glycolysis, unless blood flow changes are sufficient to continuously supply the glucose. During physiological activation of rats, Silver and Erecinska (1994) found slight decreases of the extracellular glucose concentration, determined by means of glucose-sensitive microelectrodes placed in the brain tissue.

4.2 Monocarboxylate Transport

The monocarboxylic acids, pyruvate and lactate, cross the membranes of brain tissue by means of facilitative proton-dependent transport catalyzed by the MCT family of membrane-spanning proteins (Oldendorf, 1973; Halestrap, 1975; Poole and Halestrap, 1993; Halestrap and Price, 1999). In brain tissue, the important transporters are MCT1, MCT2, and MCT4 (Drewes et al., 2002; Pierre and Pellerin, 2005). The MCT1 protein spans the membranes of the capillary endothelium and astrocytes. Gerhart et al. (1997, 1998) claimed that MCT1 resides on neurons and the MCT2 protein on astrocytes, particularly their foot processes. However, the original assignment by Broer et al. (1997) of MCT1 to astrocytes and MCT2 to neurons, particularly the glutamatergic synapses, has now been confirmed (Bergersen et al., 2005). The MCT4 protein appears to be specific for astrocytes.

■ **Figure 4.5-2**

Compartment model of oxygen tensions in brain. The compartments include arterial, capillary, venous, and mitochondrial spaces. The interface between the capillary and mitochondrial compartments is a diffusion barrier, the exact position of which is not known with certainty, although it may be dominated by the capillary endothelium. The numbers refer to normal oxygen tensions in units of mmHg, calculated from ▶ *Eq. (4)* for capillary oxygen tension and venous oxygen tensions, and from ◀ *Eq. (5)* for mitochondrial oxygen tension (see *Box 3*). The oxygen tension of the average tissue compartment or capillary–mitochondrial diffusion interface is a simple linear average. Note that the term capillary bed is used for the entire portion of the vascular bed that interacts with the tissue. This portion may include elements of arterial microvessels (Duling and Berne, 1970). From Gjedde (2006)



The transport mechanism of the MCT family is near-equilibrium proton symport and as such is influenced by the pH of the cells and declines when the pH rises. The MCT2 is of higher affinity (1 mM) toward pyruvate and lactate than the MCT1 (3–5 mM) indicating that it is saturable by lactate at normal concentrations to a greater extent than MCT1. For this reason, it is likely that preference for MCT1 over MCT2 is controlled by the lactate concentration in brain: At higher concentrations, lactate prefers MCT1. However, the lower affinity of MCT1 also means that the transporter turnover number is higher, which makes the approach to a new steady state faster, other factors being equal. Neither isoform restricts the

Box 4: Enzyme and Transporter Kinetics

In classical Michaelis–Menten kinetics (Michaelis and Menten, 1913), the reaction velocity of a process mediated by an enzyme or transporter is given by the maximum reaction velocity (V_{\max} for enzymes, T_{\max} for transporters), the affinity constant (K_m), and the substrate concentration (C), according to the Michaelis–Menten Formula

$$v = \frac{V_{\max} C}{K_m + C} \quad \text{and} \quad J = \frac{T_{\max} C}{K_m + C}$$

for the enzyme and transporter reactions, respectively. The affinity is given by the Michaelis constant, defined by the relationship $K_m = (k_{\text{in}} + k_{\text{off}})/k_{\text{on}}$ where k_{in} is the turnover number or catalysis rate, k_{off} is the rate of dissociation of the substrate from the transporter or enzyme, and k_{on} is the association constant. The higher the value of K_m , the lower is the affinity, i.e., the higher concentration at which the transporter or enzyme is half saturated. However, the reaction velocity is a function of the amount of transporter or enzyme and the magnitude of the turnover number, which is given by the relationship $v = k_{\text{in}} B$, where v is the reaction velocity and B is the amount of transporter or enzyme to which the substrate is bound at any time. As more substrate is transported or converted to product when the turnover number is higher, affinity and time to reach a new steady state often are inversely correlated.

exchange of pyruvate at the normal low concentration, but the MCT2 isoform may restrict the exchange of lactate between neurons and the extracellular space at higher concentrations.

The maximal transport capacity (T_{\max}) of the MCT1 at the blood–brain barrier is $0.2 \mu\text{mol g}^{-1} \text{min}^{-1}$ (Pardridge, 1981), with a Michaelis constant for lactate of about 5 mM (Halestrap and Price, 1999), which is substantially higher than the normal lactate content of brain (Table 4.5-3). Under normal conditions, the efflux rate across the blood–brain barrier is therefore only 25% of the T_{\max} . Since the T_{\max} and K_t of the MCT1 are about the same for pyruvate and lactate (Cremer et al., 1979), the export of pyruvate to the circulation is about one-tenth that of lactate (Himwich and Himwich, 1946). Considering the surface area of neurons and glia, it is probable that the pyruvate and lactate exchange among the compartments of the brain is near equilibrium, as it is for glucose.

As discussed below, it is possible that both pyruvate and lactate are transported into mitochondria by a specific mitochondrial monocarboxylic acid transporter (mMCT) (Brooks et al., 1999a; reviewed by Schurr (2006)). The exact nature of mMCT is not known, but the bulk of the evidence suggests that it is related to MCT2 (Halestrap and Price, 1999), the high-affinity transporter, although its identity with MCT1 has also been reported (Brooks et al., 1999a). That the mMCT is closer to the MCT2 than the MCT1 is supported by the K_t of the mMCT, which is $0.5 \mu\text{mol g}^{-1}$, i.e., somewhat higher than the cytosolic pyruvate concentration of $0.1\text{--}0.2 \mu\text{mol g}^{-1}$, with a T_{\max} of $3 \mu\text{mol g}^{-1} \text{min}^{-1}$ (LaNoue and Schoolwerth, 1979; Nalecz et al., 1992), depending on the mitochondrial density. This appears to be much higher than the average flux of pyruvate in human cerebral cortex ($0.6 \mu\text{mol g}^{-1} \text{min}^{-1}$), but differences of mitochondrial density exist among the different cellular constituents of brain tissue. Thus, it is only on average that the rate of pyruvate entry into mitochondria can rise fivefold in the absence of a change in the T_{\max} .

The possibility that the mitochondrial mMCT activity may be rate limiting for oxidative metabolism in tissue other than the brain was explored by Halestrap (1978). Halestrap and Armston (1984) concluded that this was not the case in the liver. However, Shearman and Halestrap (1984) argued that pyruvate transport is rate limiting for pyruvate oxidation in actively respiring heart mitochondria. This could be true also for the brain, although it is more commonly assumed that the mitochondrial pyruvate concentration is sufficient to saturate the pyruvate dehydrogenase (PDH) in keeping with its flux-generating role in oxidative metabolism, rendering the pyruvate flux a function of the total PDH activity in the tissue in question.

4.3 Oxygen Transport

Oxygen transport from the blood to brain tissue is significantly limited by hemoglobin binding and possibly by other factors as well, including a specific resistance at the endothelium of brain capillaries (Gjedde et al., 1991; Kassissia et al., 1995).

Simple one-dimensional models of oxygen delivery to brain tissue (Buxton and Frank, 1997; Gjedde, 1997; Vafae and Gjedde, 2000) confirm that disproportionately increased blood flow delivers more oxygen during functional activation. As described in Box 3, these models assume that the mean capillary hemoglobin saturation by oxygen is a simple function of the net extraction of oxygen. As capillaries contain more oxygen, when the extraction is lower, an inverse relation exists between the extraction and the average capillary oxygen tension. The average tension of oxygen in brain tissue depends on the delivery as well as the topography of oxygen delivery and consumption sites and is affected by the consumption of oxygen in another inverse relationship. The inverse relations of capillary and tissue oxygen tensions to oxygen consumption imply that oxygen consumption rates can rise only when blood flow rises more than the oxygen consumption. The advent of this counterintuitive insight was a major underpinning of the practice of functional magnetic resonance imaging (fMRI).

5 ATP Homeostasis

As the energy currency of brain cells, ATP is the target of processes involved in energy turnover in brain tissue. Remarkably, it appears that the ATP level is preserved so closely that no change occurs when the work

of brain function changes at a site of brain activity. It is evident that the homeostatic process goes through both glycolytic and oxidative phases, of which the oxidative metabolism is the last link in the chain of ATP-preserving processes. This section deals with the mechanisms that maintain a constant concentration of ATP, regardless of the rate of its expenditure. This homeostasis is supplemented by feed-forward adjustments of glycolysis and oxidative phosphorylation that establish advance conditions consistent with a specific functional activity, in addition to the feedback mechanisms that teleologically react to the consequences of fluctuating functional demands.

ATP is the energy “currency” of brain cells that links the energy-utilizing and energy-producing processes. Generally speaking, these processes are organized into two linked pathways, i.e., glycolysis, the breakdown of glucose to pyruvate, and oxidative phosphorylation, the breakdown of pyruvate to carbon dioxide accompanied by the reduction of oxygen to water in the tricarboxylic acid (TCA) cycle of reactions. Both processes give rise to a net gain of ATP, the sum of which can be calculated from the net rates of consumption of glucose and oxygen. At steady state, the normal stoichiometric relationships between the main substrate fluxes are given by the equations

$$J_{\text{pyr}} = 2J_{\text{glc}}, \quad (7)$$

$$J_{\text{ATP}} = J_{\text{pyr}} + 6J_{\text{O}_2}, \quad (8)$$

and

$$J_{\text{lact}} = J_{\text{pyr}} - \frac{1}{3}J_{\text{O}_2}, \quad (9)$$

where J_{ATP} is the ATP production, J_{glc} the glucose consumption, J_{pyr} the pyruvate generation rate, and J_{lact} the lactate production and efflux rate. These relationships apply only to the steady state in which there are no changes of substrate concentrations in the brain. The formulation of lactate production applies to the tissue as a whole, as pyruvate is transported between compartments by means of equilibrating transporters in the form of facilitated diffusion. Thus, the lactate production is a function of the nearly uniform pyruvate concentration and the lactate export across the blood–brain barrier. Under non-steady-state circumstances, changes of glucose, glycogen, pyruvate, and lactate concentrations contribute to the ATP turnover rates in complex ways that are explored below.

Under normal circumstances, brain energy metabolism maintains a constant concentration of ATP. Observations in heart and brain suggest that two- to tenfold variations of the rate of work can be sustained with minimal change of ATP (Matthews et al., 1981; Balaban et al., 1986; Detre et al., 1990a, 1990b; Wyss et al. 1992). Thus, the processes which maintain this metabolite are sensitive (directly or indirectly) to increased ATP utilization (feedback), or the increased ATP utilization and the increased ATP synthesis are equally sensitive to the same early control system (feed-forward) (*see Box 6*).

There are several mechanisms that could be responsible for the remarkable ability of brain tissue to vary chemical work, blood flow, and metabolism manifold with little change of the ATP concentration. Although the corresponding ADP concentration is difficult to ascertain, it is likely that it undergoes an increase during elevations of metabolism. As the functions of enzymes and transporters kinetically are similar, it is likely that both types of protein are among the non- and near-equilibrium reactions, which contribute to the maintenance of ATP levels. However, many of the conventional explanations of cellular energetics fail if the proposed mechanisms of homeostasis depend on concentrations of nucleotides or other intermediates that do not actually change.

It is necessary here to distinguish between near-equilibrium reactions on one hand and flux-generating and flux-directing reactions on the other (*see Box 5*). Near-equilibrium reactions operate in both directions of the process at almost the same velocities, such that the net reaction velocity is but a small fraction of the unidirectional velocities. The proteins mediating near-equilibrium reactions generally are not saturated, and therefore respond easily to changes of concentration but in both directions of operation. Flux-generating and -directing reactions operate in one preferred direction, and the proteins mediating the reactions tend to be saturated. For this and other reasons associated with regulation, the reaction

Box 5: Near-Equilibrium, Nonequilibrium, and Flux-Generating Reactions

Reactions in a metabolic pathway are of two general kinds, near-equilibrium and nonequilibrium reactions. Near-equilibrium reactions are near equilibrium in the sense that the fluxes are nearly the same in the two directions from substrate to product and from product to substrate, and the net flux is very small compared with the unidirectional velocities. The substrate concentration is low compared with the affinity constant (see *Box 4*) and small changes of the concentration lead to large changes of the net flux. The direction of the flux can easily change as well. A nonequilibrium reaction, on the other hand, is characterized by a substrate that nearly saturates the enzyme and hence has little influence on the actual flux. The flux in the opposite direction is low, and the net flux is therefore a large fraction of the total flux in the direction of the product. A nonequilibrium reaction is said to be flux generating if the enzyme is under the influence of regulators that change the maximum reaction velocity, and hence impose a specific flux on the reaction from substrate to product. A flux-generating enzyme can be flux directing if a substrate is subject to the catalysis of several enzymes, of which the one with the capacity to change its affinity can impose the direction of the product formation.

Box 6: Feed-Forward: The Anticipation of Perturbations

Both feedback and feed-forward control involve action on the part of a system to compensate for the effect of a fluctuation. Feed-forward control acts on the perturbation before it changes the system's variable components. This action is based on the ability of the system to anticipate the impact of perturbations on the system's outcome variables. The control system has the capacity to transmit relevant information about fluctuations in time for the system to adjust its components appropriately. The disadvantage of feedback control is that a change or deviation must occur before the system can react. Therefore, feedback control alone is asynchronous, while feed-forward control in principle, but not always in practice, may be error free.

velocities of flux-generating and -directing reactions tend to be insensitive to changes of substrate concentration. These reactions instead block changes of concentration from proceeding down a biochemical pathway.

Near-equilibrium reactions buffer minute changes of their substrates, but flux-generating and -directing nonequilibrium reactions adjust the magnitude and direction of metabolism as dictated by extrinsic regulators. The probable targets of extrinsic regulators of brain energy metabolism include the nonequilibrium hexokinase (HK) and phosphofructokinase-1 (PFK-1) reactions of glycolysis and the nonequilibrium PDH, citrate synthase, and oxoglutarate dehydrogenase reactions of the TCA-cycle and oxidative phosphorylation in mitochondria.

5.1 Hydrolysis of Phosphocreatine

Creatine kinase (CK) occupies a pivotal role in the early buffering of the ATP concentration (Wyss et al., 1992). The cytosolic enzyme has tissue-specific isoforms. The brain-predominant subtype is BB-CK. There also is a form bound to the inner mitochondrial membrane, Mi-CK. The function of CK isoforms in different compartments is subject to debate, as is the near-equilibrium status of Mi-CK. However, there is agreement that the cytosolic CK reaction is in near-equilibrium in living human brain (Roth and Weiner, 1991; Mora et al., 1992). The near-equilibrium cytosolic CK reaction transfers a high-energy phosphate bond from phosphocreatine to ADP to synthesize ATP. When the near-equilibrium of cytoplasmic CK is perturbed, the reaction buffers any increase of ADP by increased phosphorylation of ADP to ATP. Cytoplasmic phosphocreatine is replenished by mitochondrial CK, which is regenerated by hydrolysis of mitochondrially generated ATP (Fedosov, 1994). CK catalyzes the reversible reaction:

phosphocreatine + ADP + H⁺ = ATP + creatine, in which hydrogen ions are buffered when ATP is regenerated. Phosphocreatine may also be used to transport phosphate groups from one compartment of a cell to another. Phosphocreatine diffuses an order of magnitude faster than the adenine nucleotides (Wyss et al., 1992), but under conditions of high metabolic activity ATP homeostasis may not be maintained because of rate limitation of the CK-transphosphorylation reaction in the mitochondria (Fedosov, 1994).

5.2 Glycolysis

Aerobic glycolysis is the breakdown of glucose to pyruvate under normal aerobic conditions. Anaerobic glycolysis is the conversion of glucose to lactate under anaerobic conditions. As glucose is the preferred substrate for the brain, the understanding of the control of glycolysis is integral to the appreciation of how increased energy production and utilization are linked. The rate is regulated by the nonequilibrium reactions catalyzed by HK and PFK.

The main reactions and their time constants (see *Box 7*) are listed in [▶ Table 4.5-5](#), and their interactions are shown in [▶ Figure 4.5-3](#).

Box 7: Rate and Time Constants

As reciprocals of rate constants, time constants indicate how long it takes to change the concentration of specific metabolite. The former expresses the fraction of a pool that undergoes a change per unit time. Thus, a rate constant of 0.1 min⁻¹ indicates that 10% of a metabolite pool is lost and normally also replenished every minute. The corresponding time constant is 10 min, indicating that a standard fraction of the pool has undergone change every tenth minute. If the metabolite pool is not actually replenished, it may be useful to convert its time constant to a half-life, which indicates the time it takes to deplete one-half of the pool left at any one time. Mathematically, it is possible to show that the half-life is 69.3% of the time constant. Thus, the time constants express the half-times and hence the rapidity of change, i.e., the time it takes a system to reach halfway to a new steady state.

It is apparent from [▶ Table 4.5-5](#) that the conversion of pyruvate to lactate and hence anaerobic glycolysis responds to change with time-constants of the order of milliseconds, while import of pyruvate into mitochondria and subsequent oxidative metabolism only responds with time-constants of seconds or minutes. Hence, oxidative metabolism is apt to respond to any stimulus with a considerable delay, compared with the generation of lactate.

5.2.1 Hexokinase and Phosphofructokinase-1

Phosphate and citrate ions, AMP, ammonium and hydrogen ions, and glucose-6-phosphate and phosphocreatine, are among the classic regulators of one or the other of the glycolytic enzymes HK and PFK-1, which catalyze the nonequilibrium and irreversible phosphorylations of glycolytic intermediates. The classical list of extrinsic regulators of these enzymes includes Mg²⁺, the concentration of which may change when there is increased ATP turnover and increased CK activity. Although two mol ATP are consumed during the first stage of glycolysis, per mol of glucose metabolized, four mol ATP are generated during the second stage of glycolysis, for a net return of one mol ATP and two hydrogen ion equivalents per mole of pyruvate synthesized.

■ **Table 4.5-5**
Selected brain metabolic reactions and metabolite transporters

Reaction or transporter	Equilibrium status	Activity ($\mu\text{mol g}^{-1} \text{min}^{-1}$)	Substrate concentration [$\mu\text{mol g}^{-1}$]	Time constant (s)	(ms)
HK ^a	Flux generating	0.3	2	400	
PFK-1 ^b	Flux generating	0.3	0.1	20	
PDH ^c	Flux generating	0.3	0.01	2	
GLUT-1 ^d	Flux limiting	2	5	150	
MCT (BBB) ^e	Flux limiting	0.2	0.1	30	
mMCT ^f (mitochondria)	Flux limiting	3	0.1	3	
GLUT-3 ^g	Near equilibrium	1000	1		60
LDH (lactate) ^h	Near equilibrium	2000	1		30
MCT (cell membranes) ⁱ	Near equilibrium	1000	0.1		6
LDH (pyruvate) ^h	Near equilibrium	2000	0.1		3

^ahexokinase (Gjedde 1983)

^bphosphofruktokinase-1 (Gjedde 1983)

^cpyruvate dehydrogenase complex (Katayama et al. 1998)

^dglucose transporter-1 (Gjedde 1992)

^emonocarboxylic acid transporters (Cremer et al. 1979)

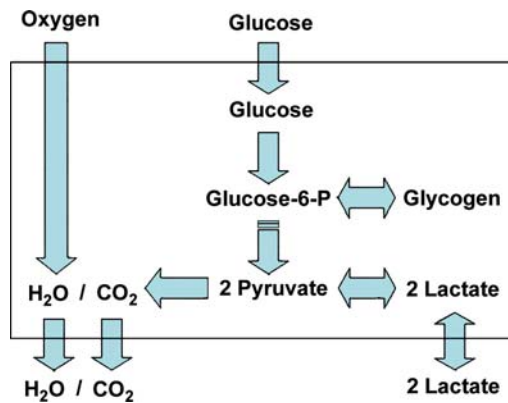
^fmitochondrial monocarboxylic acid transport (Poole et al. 1993)

^gglucose transporter-3 (Diemer et al. 1985)

^hlactate dehydrogenase (Salceda et al. 1998)

ⁱmonocarboxylic acid transporters (Desagher et al. 1997)

■ **Figure 4.5-3**
Simplified illustration of the main metabolic pathways of the mammalian brain



5.2.2 Pyruvate and Lactate Dehydrogenases

Pyruvate participates in several different reactions in brain tissue, of which the following three are the most important. It can be reduced by conversion to lactate, transported into mitochondria, or transported out of brain by the monocarboxylate transporters (MCTs) in cell membranes and the endothelium of brain capillaries. The last of these processes is minimal for pyruvate and can probably be ignored because of pyruvate's low concentration compared with lactate.

As a near-equilibrium reaction, the enzyme lactate dehydrogenase (LDH) buffers changes of the concentration of pyruvate. The near-equilibrium reaction catalyzed by LDH is bidirectional but strongly balanced toward lactate. Synthesis of one mol of lactate from one mol of pyruvate removes one cytosolic reducing equivalent, so the net yield is only two mol ATP per mole of glucose converted to lactic acid.

The brain has at least two isozymes of LDH, the “heart” isozyme H4 (LD1), to which pyruvate has a lower affinity, characteristic of oxidative tissues, and the “muscle” isozyme M4 (LD5), to which pyruvate has a higher affinity, characteristic of less oxidative tissues such as liver and some muscles (Kaplan and Everse, 1972). The measured lactate/pyruvate ratio of 10:1 suggests that the prevailing LDH isozyme pattern is closer to that of LD1 than that of LD5, because the relatively low ratio reflects a relatively low affinity toward pyruvate. The entities controlling the steady-state lactate/pyruvate ratio, in addition to the inherent affinities of the enzyme for the two substrates, which must have the same ratio for all the subtypes for thermodynamic reasons, include both pH and the NAD^+/NADH ratio

$$\frac{[\text{lact}]}{[\text{pyr}]} = K_{eq} \frac{[\text{NADH}][\text{H}^+]}{[\text{NAD}^+]},$$

where K_{eq} is the equilibrium constant of the LDH reaction. The ratio between the concentrations of lactate and pyruvate is also the apparent ratio between their affinities. At steady state, the ratio must be the same everywhere, given the near-equilibrium and facilitated diffusion nature of the proton symporters of lactate and pyruvate. The constant ratio implies that the different inherent kinetic properties of LDH exist to accommodate differences of the NAD^+/NADH ratio in different parts of the tissue (Newsholme and Crabtree, 1979).

The affinity of an enzyme for a substrate is a function of, among other factors, the turnover number of the enzyme. The turnover number is the rate constant of catalysis itself, which yields the reaction rate when it is multiplied with the amount of substrate bound to the enzyme (see *Box 4*). As the affinity constant is the sum of the dissociation rate constant and the turnover number, relative to the association constant, the velocity of the reaction is related to the affinity constant; the higher the magnitude of the affinity constant (i.e., the lower the affinity), the higher the turnover number and hence the reaction velocity, other factors being equal. The cytosolic NAD^+/NADH ratio is an indicator of the oxidation status of the tissue, which is low when the ratio is lower than normal (<1000) and high when it is higher than normal (>1000).

It is a common claim that the relatively low affinity of pyruvate for LD1 makes this enzyme particularly useful to a tissue of high oxidative capacity because it allows rapid buildup of pyruvate, while LD5 is more effective at buffering the increase of pyruvate in a tissue of lower oxidative capacity, because of the relatively high affinity toward pyruvate. Thus, there is evidence that LD1 and the mRNA for the subtype are found exclusively in neurons, while astrocytes appear to possess both LD1 and LD5 and their corresponding mRNA (Tholey et al., 1981; Bittar et al., 1996; Laughton et al., 2000). However, it is incorrect to infer a net direction of the LDH reaction simply from the presence of a specific subtype in a population of cells (Van Hall, 2000). For practical purposes, it is more useful to regard the properties of the LDH subtypes LD1 and LD5 as states of sensitivity to transient events during activation or deactivation of the tissue, explored below.

5.3 Oxidative Phosphorylation

At steady state, brain metabolism has a respiratory quotient (ratio of CO_2 production to O_2 consumption) of unity, consistent with the oxidation of glucose (Himwich and Fazekas, 1937; Gibbs et al., 1942; Himwich and Himwich, 1946) and with the integration of glycolysis and oxidative metabolism. The net effect of the metabolism of pyruvate to CO_2 is to provide the electron chain complexes with the nicotinamide (NADH) and flavin (FADH_2) adenine dinucleotides necessary for electron transport and oxygen metabolism. This subsection presents the primary regulatory steps for oxidative metabolism in the mitochondria.

5.3.1 Pyruvate Dehydrogenase Complex and the Tricarboxylic Acid Cycle

Recent evidence suggests that mitochondria may import both pyruvate and lactate (Brooks et al., 1999a; Schurr, 2006). Inside the mitochondria, the lactate is reconverted to pyruvate in another LDH-catalyzed near-equilibrium reaction (Brandt et al., 1987; Brooks et al., 1999b). Pyruvate provides the mitochondrial electron carrier complexes I and II with NADH and FADH₂, respectively. Per mol glucose, two mol NAD⁺ are reduced in glycolysis, and two mol NAD⁺ are reduced by the oxidation of pyruvate in the PDH complex. The remainder of the NAD⁺ and all of the FAD are reduced by the flux-generating TCA cycle enzymes citrate synthase and oxoglutarate dehydrogenase. Via the regeneration of guanine triphosphate (GTP), the TCA cycle leads to the nonoxidative phosphorylation of two mol ATP per mol glucose. In total, per mol glucose, 20 hydrogen ion equivalents are extruded from the mitochondrial matrix and join four hydrogen ion equivalents generated in the cytosol. The 24 hydrogen ion equivalents provide the driving force for the rephosphorylation of ADP, although part of this gradient is dissipated by so-called proton leakage (Rolfe and Brown, 1997) and possibly by entry of positive ions such as Ca⁺⁺ (Lauritzen, 2005). Thus, somewhat less than three mol ATP (approximately 80% or 2.4 mol), for each mol NADH oxidized to NAD⁺ and somewhat less than two mol ATP for each mol FADH₂, are formed from ADP and P_i by the ATP synthase.

5.3.2 Cytochrome Oxidation and the Electron Transport Chain

Respiration is defined as the oxidation of cytochrome *c* by molecular oxygen, which serves as the ultimate electron acceptor. Oxide ions are generated in this reaction catalyzed by the cytochrome *aa*₃ complex (complex IV), commonly known as cytochrome *c* oxidase. The transfer of protons into the matrix allows hydrogen and oxide ions to form water. While oxygen is provided by the circulation, reduced cytochrome *c* is regenerated by the NADH and FADH₂ adenine dinucleotides in complex near-equilibrium reactions catalyzed by proteins collectively functioning as a cytochrome reductase. In these reactions, hydrogen ions escape through complex IV to the outside of the inner membrane.

Although the mitochondrial oxygen tension is a function of the relationship between the delivery of oxygen and the rate of cytochrome *c* oxidation, its influence on oxidative metabolism *in vivo* is poorly understood. The “near-equilibrium” hypothesis of Erecinska et al. (1974) and Erecinska and Wilson (1982) assigned the flux generation to the irreversible reaction between oxygen and cytochrome *c*, catalyzed by the cytochrome oxidase (Wang and Oster, 1998; Springett et al., 2000). The near-equilibrium status refers to the entire electron transport chain with the exception of the cytochrome *c* oxidase reaction and hence also of ATP synthesis, catalyzed by the proton-driven F-type ATPase in the inner membrane of the mitochondrial cristae, named for its discoverer Ephraim (“F”) Racker (Pullman et al., 1960), and now known as ATP synthase.

Cytochrome *c* has been calculated to be 95% saturated at the oxygen tension prevailing in mitochondria in human brain *in vivo*, but the sensitivity to variations of oxygen tension is much greater than implied by this occupancy, because diffusion of oxygen from the microvessels is impaired at lower mitochondrial oxygen tensions, as discussed above. The “near-equilibrium” hypothesis therefore requires that the maximum reaction rate (V_{\max}) or apparent affinity (P_{50}), or both, of cytochrome oxidase toward oxygen be adjusted in response to the $[ADP][P_i]/[ATP]$, or energy charge, ratio in the cytosol, to allow the enzyme to maintain an adequate rate of ATP synthesis. The hypothesis predicts that increases of this ratio change the properties of cytochrome oxidase in such a way that cytochrome *c* continues to react with oxygen at the rate which matches the rate of cytosolic ATP utilization. However, as shown below, there is a theoretical limit to the efficacy of this adjustment, particularly when the cytosolic energy charge is unchanged (Gjedde et al., 2005). In reality, therefore, the near-equilibrium hypothesis assigns the ultimate maintenance of oxygen consumption to the regulation of oxygen delivery, particularly in situations in which the mitochondrial oxygen tension threatens to fall below a minimum threshold (Gjedde et al., 2005).

Using rat heart mitochondria as a model, LaNoue et al. (1986) showed that near-equilibrium of oxidative phosphorylation exists when respiration is very slow (state 4) but that mitochondrial ATP synthesis occurs far from equilibrium when respiration is active (state 3). These observations show that

the near-equilibrium of oxidative metabolism could fail in normally and rapidly respiring brain tissue. As a result of the imbalance between the delivery of oxygen and the cytochrome oxidase activity in these states, cytochrome *c* oxidase does not remain saturated when the mitochondrial P_{O_2} declines relative to the average capillary P_{O_2} , $P_{O_2}^{cap}$.

The equations governing the consumption of oxygen catalyzed by cytochrome *c* oxidase describe how the rate of oxygen consumption depends directly on the average capillary oxygen tension and that it fails to rise above a certain threshold despite increases of the cytochrome oxidase activity, unless the affinity or diffusibility of oxygen are simultaneously adjusted (see Box 8). Below this important threshold, the supply

Box 8: Delivery Limitations for Oxygen

The imbalance between the delivery of oxygen and the cytochrome oxidase activity in mitochondria, i.e., the extent to which oxygen delivery is sufficient to maintain adequate saturation of cytochrome oxidase, can be expressed as a simple Michaelis–Menten relationship between the mitochondrial oxygen tension and the kinetic properties of the cytochrome oxidase

$$J_{O_2} = V_{max} \sigma_e \sigma_o, \quad (10)$$

where J_{O_2} is the net oxygen consumption, V_{max} is the maximum cytochrome *c* oxidase activity, and σ_e and σ_o are the cytochrome *c* oxidase saturation fractions for electrons and oxygen, respectively. The oxygen tension in mitochondria ($P_{O_2}^{mit}$) is the tension consistent with the observed oxygen consumption rate, given the magnitude of the apparent affinity or half-saturation constant (P_{50}^{cytox}) of the enzyme

$$P_{O_2}^{mit} = \frac{P_{50}^{cytox} J_{O_2}}{J_{max} - J_{O_2}}, \quad (11)$$

where J_{max} is the product of V_{max} and σ_e . It follows from equations in Box 3, that the corresponding average capillary oxygen tension ($P_{O_2}^{cap}$) required to drive the delivery is given by

$$\bar{P}_{O_2}^{cap} = \frac{J_{O_2}}{L} \left[1 + \frac{LP_{50}^{cytox}}{J_{max} - J_{O_2}} \right], \quad (12)$$

where L is the oxygen diffusion capacity. This relationship describes the minimum oxygen tension in brain capillaries compatible with a given oxygen consumption (J_{O_2}) when diffusion (L), enzyme activity (J_{max}), and enzyme affinity (P_{50}^{cytox}) are fixed.

of oxygen for brain energy metabolism would fail if compensatory mechanisms do not intervene. The threshold is dictated by the mitochondrial oxygen tension and is reached when the tension declines below the level associated with sufficient oxygen saturation of the cytochrome *c* oxidase enzyme. Only elevations of the oxygen diffusion capacity by some form of capillary recruitment, or the mean capillary oxygen tension by increased blood flow, allow the rate of oxygen consumption to rise above this threshold (see [Sect. 7.3: Substrate Delivery During Activation](#)).

Calcium ions play a role in the oxidation of pyruvate by activating the mitochondrial enzymes mediating the nonequilibrium and flux-generating reactions (PDH complex, citrate synthase, NAD⁺-linked isocitrate dehydrogenase, and the 2-oxoglutarate dehydrogenase complex), which supply the NADH and FADH₂ for the mitochondrial complexes I and II (Denton and McCormack, 1985). In the resting state, mitochondria contain little calcium, but calcium accumulates after excitatory agonist amino acid stimulation of postsynaptic neurons (Zonta et al., 2003; Lauritzen, 2005). The calcium entry is facilitated by the Ca²⁺ uniporter in the mitochondrial membrane and driven by the mitochondrial membrane potential established by the H⁺ extrusion mechanism. Rises in calcium concentration often occur as repeated spikes with steep up-slopes and shallower down-slopes, which reach baseline during sustained excitation (Clapham, 1995). A steady agonist level may induce pulsatile calcium release from calcium stores, and the frequency of this calcium pulsation apparently depends on the agonist concentration.

6 Metabolic Compartmentation

Compartments of many kinds exist in any tissue but the important issue is whether they play an important functional role in the regulation of brain energy metabolism. The recent resumption of discussions of this issue specifically focuses on the possible division of metabolic labor between the glial cell population of astrocytes and the neurons with which they associate. Recent evidence and an emerging consensus imply that energy metabolism is regulated differently in astrocytes and neurons because the metabolism serves different roles in the two populations of cells: Neurons maintain and adjust depolarizations used to exchange information at rates consistent with the time constants of neuro-transmission (as low as 10 ms), while astrocytes maintain the composition of the internal milieu of synapses that permits this rapid exchange of information.

Brain tissue has several populations of cells, all of which undoubtedly play important roles in brain function. This section deals with the attempts to understand the properties of neurons and astrocytes that infer important combined roles in the regulation of the metabolic responses to excitation.

6.1 Functional Properties of Neurons and Astrocytes

Classically, the compartmentation of brain metabolism distinguishes between the “large” and “small” pools of the excitatory amino acid transmitter glutamate (Cremer, 1976; Cremer et al., 1979). There is quantitative conversion of glutamine to glutamate in the large pool, catalyzed by glutaminase, while the opposite process takes place in the small pool, catalyzed by glutamine synthetase and fueled by ATP. The two pools of glutamate are now believed to largely represent neurons and astrocytes, respectively. In the mammalian cortex, the transfer of glutamate between the two pools occurs by neuronal release of glutamate during excitation and subsequent import by neurons and the glial subpopulation of astrocytes.

Astrocytes play a critical role in the import of glutamate and potassium from the interstitial space surrounding the intrasynaptic clefts. Astrocytic processes engulf the synapses and possess excitatory amino acid (glutamate) transporters (EAAT-3 in humans; Vandenberg (1998); GLAST and GLT-1 in rats; Rothstein et al. (1996)) in abundance. The transporters reside also on neurons (Vandenberg, 1998) but gene knockout studies show that the glial EAAT is indispensable for normal brain function, unlike the neuronal EAAT (Tanaka et al., 1997). One molecule of glutamate is symported from the extracellular space with three sodium ions. The transport increases the intracellular content of sodium and leads to export of sodium ions coupled to astrocytic import and accumulation of potassium ions. The result is a net increase of potassium in the astrocytes.

6.2 Metabolic Properties of Neurons and Astrocytes

The different transporter properties of neurons and astrocytes are summarized in *Sect. 4*, showing that astrocytes possess the low affinity MCT2 transporter. In addition, there are important enzymatic differences that cause the two groups of cells to react differently to changes in metabolism. The enzymatic peculiarities of astrocytes include the presence of the higher affinity LDH isozyme LD5 and the enzyme pyruvate carboxylase, which serves anaplerosis and provides an alternative pathway of oxidative metabolism. Anaplerosis is the synthesis of components of the TCA cycle that are lost to other pathways. This is true of the metabolite α -ketoglutarate, which can replenish glutamate and GABA when these transmitters exit neurons, as well as glutamine when this amino acid exits glial cells. Anaplerosis by means of pyruvate carboxylation occurs primarily in glia but anaplerotic pyruvate carboxylation recently was demonstrated also in glutamatergic neurons where it may replace glutamine as a source of glutamate and GABA (Hassel and Bråthe, 2000).

Astrocytes also have comparatively larger stores of glycogen, and they consume acetate in addition to glucose. The low affinity MCT2 transporter and the high affinity LD5 enzyme together would establish a preference for export of pyruvate rather than conversion to lactate, but the need for regeneration of NAD^+ from NADH when the oxidative capacity is low favors conversion of pyruvate to lactate. In short, it appears

that astrocytes are particularly well equipped to ensure both the generation and oxidative metabolism of pyruvate, in astrocytes, or after export as pyruvate or lactate, in other cells. The import of glutamate has been reported to stimulate ATP hydrolysis by glutamine synthetase and Na^+/K^+ -ATPase, as well as glucose utilization and lactate generation in cultured astrocytes (Pellerin and Magistretti, 1994; Magistretti et al., 1998, 1999), but these findings have not been replicated in other studies (Eriksson et al., 1995; Hertz et al., 1998; Anderson and Swanson, 2000; Peng et al., 2001; Liao and Chen, 2003; Winkler et al., 2004, reviewed by Dienel and Cruz 2006).

A novel hypothesis of the metabolic interactions among neurons and astrocytes currently is the topic of vigorous discussion. The main element of the hypothesis is: As oxidative metabolism is as much as 19-fold more productive of ATP than nonoxidative metabolism, it is of considerable interest that the fraction of total brain energy metabolism now ascribed to nonneuronal cells (15%) (Attwell and Iadecola, 2002, Shulman et al. 2004, Hyder et al. 2006) is of the same order as the fraction ascribed to nonoxidative metabolism of glucose (10%) for the tissue as a whole. In this situation, the energy derived from nonoxidative metabolism of 10% of the glucose supply would be no more than 0.5% of the total energy turnover. Thus, if neuronal metabolism is primarily nonglycolytic, the entire metabolism of glucose to pyruvate would be confined to the nonneuronal cells, while the oxidative metabolism of pyruvate would have to occur to a great extent in neurons and other cells with known oxidative potential for phosphorylation of ADP.

The question is therefore whether the known differences between neurons and astrocytes are consistent with the claim that all or most of the glucose supplied to the brain undergoes glycolysis to pyruvate and lactate in astrocytes, which in turn would supply all of the pyruvate needed in neurons that use no glucose of their own (Magistretti et al., 1999). The claim is somewhat reminiscent of an early speculation that the astrocytic processes serve to siphon glucose from the microvessels to the neuron terminals (Andriezen, 1893).

First, the logical deduction from this claim, i.e., that glucose undergoes net transport only into astrocytes, is not consistent with early electron microscopic studies by Brightman and Reese (1969) according to which the blood–brain barrier involves the endothelial cells of brain microvessels but not the foot-processes of astrocytes (Reese et al., 1971), which cannot therefore direct glucose preferentially into glial cells. Second, the claim that all glucose undergoes phosphorylation in macroglial cells is now being replaced by the claim of a more flexible sharing of joint pyruvate and lactate pools among neurons and astrocytes, which depends on a much more flexible concept of independently adjusted oxidative and glycolytic capacities of the two cell types (Gjedde et al., 2002; Hyder et al., 2006) to be discussed below.

6.2.1 Oxidative and Glycolytic Capacities

Pyruvate is oxidatively metabolized in astrocytes (Alves et al., 1995). Although increasingly it is clear that the metabolic profile of astrocytes is not only quantitatively but also qualitatively different from that of neurons, it is also becoming evident that the most important differences are in fact quantitative. Generally, it appears that astrocytes are more glycolytic than neurons, but detailed regional measurements in the mammalian brain *in vivo* are still missing. Until the advent of high field strength magnetic resonance spectroscopy (Hyder et al., 2006), isolated populations of astrocytes and neurons were studied only *in vitro*, where exchange of metabolites among different cell types is not possible. In one such study of both cell types in isolation, Itoh et al. (2003) found that both cell types release lactate, albeit to different extents. When both cell types release lactate, there is of course no net exchange of pyruvate or lactate between the two cell types. These observations apply to the *in vitro* situation characterized by two conditions, which are at variance with the situation *in vivo*. First, the cells operate at a low level of activity because they are not stimulated as they would be *in vivo*, and second, the different populations cannot interact with one another the way they would *in vivo*.

This means that it is possible that the net neuronal release of lactate *in vitro* is the result of the isolation. Cells grown in isolation provide a poor model of the potential exchanges of pyruvate and lactate under the more active conditions prevailing *in vivo*. In theory, there is no reason why neurons and astrocytes cannot release pyruvate and lactate at the lower activity *in vitro* and yet require net uptake of either of the two metabolites at the higher activity that prevails *in vivo*. The significance of this point depends crucially on the

two factors, which are still incompletely understood, i.e., (1) the individual glycolytic and oxidative capacities of the two cell types, and (2) the extent to which these capacities undergo change during functional activity *in vivo*. Attempts have been made to map the oxidative and glycolytic capacities of neurons and neuroglial cells since the 1960s but only recently a convergence of largely circumstantial evidence has tended to support the claim that the oxidative capacity of astrocytes is considerably lower than that of neurons, while the opposite appears to be case for the glycolytic capacity.

Pysh and Khan (1972) used quantitative electron microscopy to compare the structure and quantity of mitochondria in different types of neurons and neuroglial cells in rat brains. Their findings suggested that neurons generally have more mitochondrial respiratory enzymes than macroglia, which is consistent with the results of a large number of previous histochemical studies that revealed higher activity of mitochondrial oxidative enzymes in neurons than in macroglia. The study also suggested that mitochondrial volume fractions are reliable indices of the relative oxidative metabolism of different brain regions. Mitochondria subsequently have been observed to be particularly concentrated in the dendritic structures of the neuropil, particularly the proximal dendrites (Ribak, 1981; Gonzalez-Lima and Jones, 1994; Wong-Riley, 1989), which stain weakly for HK (Snyder and Wilson, 1983). Together these observations strongly suggest that the glycolytic and oxidative reactions occur in separate subcellular compartments, although the compartmentation is not complete (Aoki et al., 1987).

In a slightly different approach, Silver and Erecinska (1997) studied astrocytoma cells *in vitro* and found that 25%–32% of the ATP production in these cells is glycolytic *in vitro*. Recent indirect studies *in vivo* or *ex vivo* (Vega et al., 2003; Nehlig et al., 2004; Hyder et al., 2006) suggest that the fraction of glycolytic ATP generation in astrocytes (f_{glc}) is at least as high as 0.20 *in vivo*. A simple quantitative analysis shows that a fraction of 0.20 implies an OGI of unity in these cells (*see Box 9*).

Box 9: OGI as Function of NonOxidative ATP Production

A simple relationship relates the percentage of glycolytic ATP production to the oxygen–glucose index (OGI), assuming that 1 mol glucose metabolized to CO_2 generates 38 mol ATP at the expense of 6 mol O_2

$$\text{OGI} = \frac{6(1 - f_{\text{glc}})}{1 + 18f_{\text{glc}}}, \quad (13)$$

where f_{glc} is the fraction of glycolytic ATP production. This dependence of f_{glc} on OGI is illustrated graphically in [▶ Figure 4.5-4](#). An f_{glc} fraction of 0.20 indicates an OGI of 1. The glucose metabolic rate associated with this OGI can be calculated from the oxidative metabolism of the tissue

$$J_{\text{O}_2}^{\text{A}} = f_{\text{O}_2}^{\text{A}} J_{\text{O}_2}, \quad (14)$$

where $J_{\text{O}_2}^{\text{A}}$ is the oxygen metabolic rate of the astrocytic compartment (A), and $f_{\text{O}_2}^{\text{A}}$ is the fraction of oxidative metabolism assigned to the astrocytic compartment, and

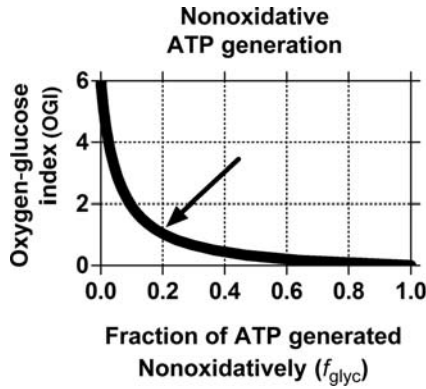
$$J_{\text{glc}}^{\text{A}} = J_{\text{O}_2}^{\text{A}} / \text{OGI}, \quad (15)$$

where $J_{\text{glc}}^{\text{A}}$ is the glucose metabolic rate. The fluxes of ATP and pyruvate and the efflux of lactate can then be computed by means of [▶ Eqs. \(2–4\)](#).

When the normal (default) energy metabolic rate of astrocytes of 15% of the total rate of brain energy metabolism (determined as the rate of ATP generation or the rate of glucose metabolized to CO_2) is combined with this estimate of the OGI of astrocytes and with the average OGI of 5.3 of cerebral cortex ([▶ Table 4.5-3](#)), the surprising conclusion is reached that neurons must have an OGI of 23. This value of course is meaningful only when neurons import the majority of the necessary pyruvate from extraneuronal sources inside or outside the brain tissue. When astrocytes or extracerebral sources of lactate supply pyruvate to a joint tissue pool, neurons then draw the required fraction of their need for oxidative substrate from this pool. Estimated values of this relationship are given in [▶ Table 4.5-6](#) and illustrated in [▶ Figure 4.5-5](#).

■ Figure 4.5-4

Illustration of behavior of f_{glyc} inverted to show f_{glyc} as function of the oxygen–glucose index (OGI). Abscissa: OGI (ratio). Ordinate: Fraction of ATP generated from that part of glycolysis that does not proceed to the tricarboxylic acid (TCA) cycle. At an OGI of 5.3 of the normal human cerebral cortex, the fraction is only 0.5%



Neurons and astrocytes occupy similar volumes of cerebral cortex (50% and 33%, respectively) (Norenberg 1994). It is noteworthy therefore that the circumstances listed in [Table 4.5-6](#) are consistent with a fourfold higher rate of production of pyruvate in astrocytes than in neurons, as shown also by Itoh et al. (2003) in vitro. This implies that the relative degrees of oxidative and glycolytic capacities are preserved over a wide range of functional activity that appears to include the in vitro situation.

■ Table 4.5-6

Average estimates of neuronal and astrocytic metabolism in human cerebral cortex

Metabolite	Flux ($\mu\text{mol g}^{-1} \text{min}^{-1}$)		
	Astrocytes	Neurons	Total
ATP	1.92	8.28	10.2
Glucose	0.24	0.06	0.30
Oxygen	0.24	1.36	1.60
OGI	1	23	5.3
Pyruvate generation	0.48	0.12	
Pyruvate consumption	0.08	0.45	
Lactate production			0.07

Conversely, calculations such as these show that the oxidative capacity of astrocytes is low, both because of an innately higher capacity for glycolysis and because of a low rate of work. Neurons are the major sites of oxidative rephosphorylation of ATP, accounting for 80% of the oxidative metabolism but only 20% of the glycolytic metabolism of brain tissue (Silver and Erecinska 1997; Shulman and Rothman, 1998; Sokoloff 1999; Hassel and Bråthe, 2000; Itoh et al., 2003; Hyder et al., 2006). The estimated distribution of glycolytic and oxidative metabolism of neurons and astrocytes are shown in [Figure 4.5-6](#).

The issue of the rates of glycolysis and oxidative phosphorylation in neurons and glial cells hinges on the mechanisms underlying the estimates of the relative glycolytic and oxidative capacities of the respective cellular compartments. The relative capacities arise from the differential activities of HK/PFK and cytochrome oxidase in the two cell groups, respectively, which in turn appear to depend on the time constants of the metabolic fluctuations as well as on the average metabolic activity. Low time constants are likely to favor glycolysis and low average oxidative rates, while high time constants favor high oxidative rates, much as in

Figure 4.5-5

Estimated glycolytic and oxidative fluxes and pools of glucose, pyruvate, lactate, CO₂, and ATP, among extracellular fluid and neuronal and astrocytic compartments in human cerebral cortex. Glucose, pyruvate, and lactate are shown as occupying single individual pools (light gray). Glucose feeds into the pyruvate pool in proportion to hexokinase (HK) capacities of the two cellular compartments, and pyruvate supplies the oxidative metabolism of the two cell types (dark gray) in proportion to their oxidative capacities

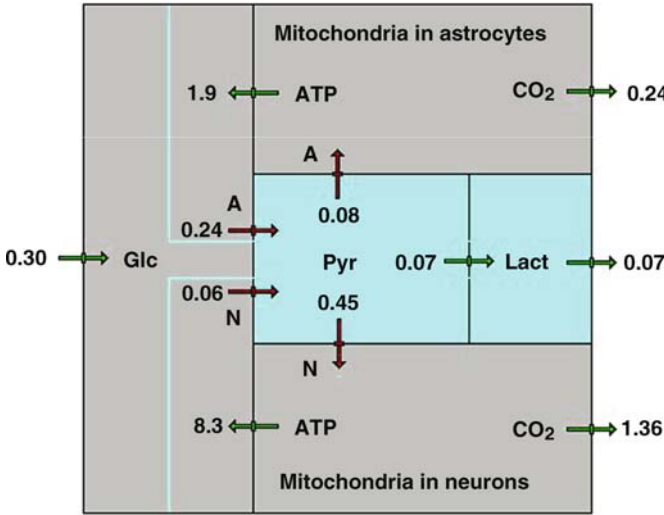
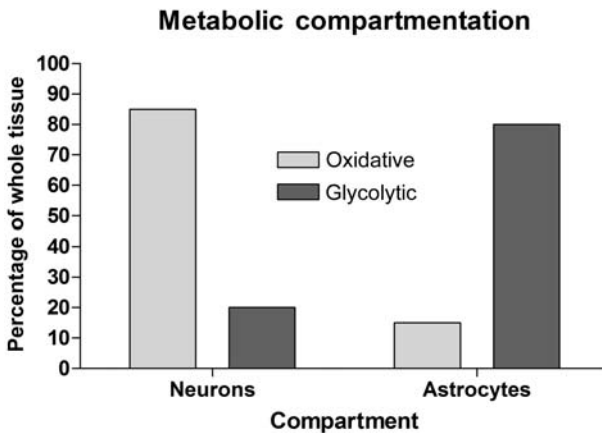


Figure 4.5-6

Metabolic compartmentation of ATP regeneration in neurons and astrocytes (modified from Silver and Erecinska (1997)). The proportions of glucose and oxygen metabolism carried out in neuronal and glial tissue compartments, respectively, are shown. The percentages were calculated from oxygen–glucose indices of glial and neuronal compartments according to Eq. (13) based on glycolytic ATP synthesis fractions reported by Silver and Erecinska (1997), Vega et al. (2003), Nehlig et al. (2004), and Hyder et al. (2006)



muscle cells (Wong-Riley, 1989). Although it has not been possible to obtain direct evidence that glutamate import actually enhances glycolysis in astrocytes *in vivo* (Hertz et al., 1998), there is increasingly suggestive evidence that glycolytic and oxidative rates of metabolism have different proportions in astrocytes and neurons under normal physiological conditions *in vivo*, such that most of the glycolytic capacity resides in astrocytes, while most of the oxidative capacity resides in neurons.

6.2.2 Metabolite Cycling

While neurons and astrocytes are strongly suspected to differ with respect to metabolite enzyme and transporter distributions, there is no evidence that the pools of glucose, pyruvate, and lactate are compartmentalized in distinct pools corresponding to the populations of neurons and neuroglia. Such separation would require an essential impermeability of cell membranes to these substrates, or active transport, which does not occur in brain tissue for these substrates. Thus, there is little direct evidence of a fundamental difference between the ability of neurons and glia to oxidize pyruvate, except for the probability of greater activity of glycolytic enzymes in glial cells, and greater density of mitochondria with the greater activity of cytochrome oxidase in neurons.

Unless pyruvate were strictly compartmentalized (which is ruled out by the abundance of MCT1 and MCT2), it is logically impossible for neurons to prefer pyruvate of nonneuronal origin, whether directly or indirectly imported, over pyruvate of neuronal origin, despite claims to the contrary (Poitry-Yamate et al., 1995). A kinetic preference must refer to the sources of pyruvate, whether pyruvate generated from glucose or pyruvate generated from lactate. Both sources are associated with generation of NADH but glycolysis is regulated while LDH operates at near-equilibrium. Thus, generation of pyruvate from lactate is likely to inhibit the generation of pyruvate from glucose. The evidence summarized above suggests that the two populations of cells contribute differentially to joint pyruvate and lactate pools when glycolysis is stimulated to a greater extent than oxidative metabolism, but the extent of the differential distribution would be a function of the degree of activation of the two cell types.

The simplified model of metabolite pathways gleaned from these considerations is shown in [Figure 4.5-7](#), in which the control points of the differential glycolytic and oxidative capacities are shown as the HK/PFK and PDH steps, respectively. The capacities of the separate PDH steps in neurons and astrocytes are most likely related to the number of calcium-stimulated mitochondria, while the capacities of the HK/PFK steps are subject to the temporal requirements of glutamate transport and metabolism in astrocytes and glycolysis in neurons (Attwell and Gibb, 2005). This consideration suggests that the functional ranges of the activities are very different in the two cell types, in keeping with the very different functional contingencies facing the two cell types in normally functioning brain tissue.

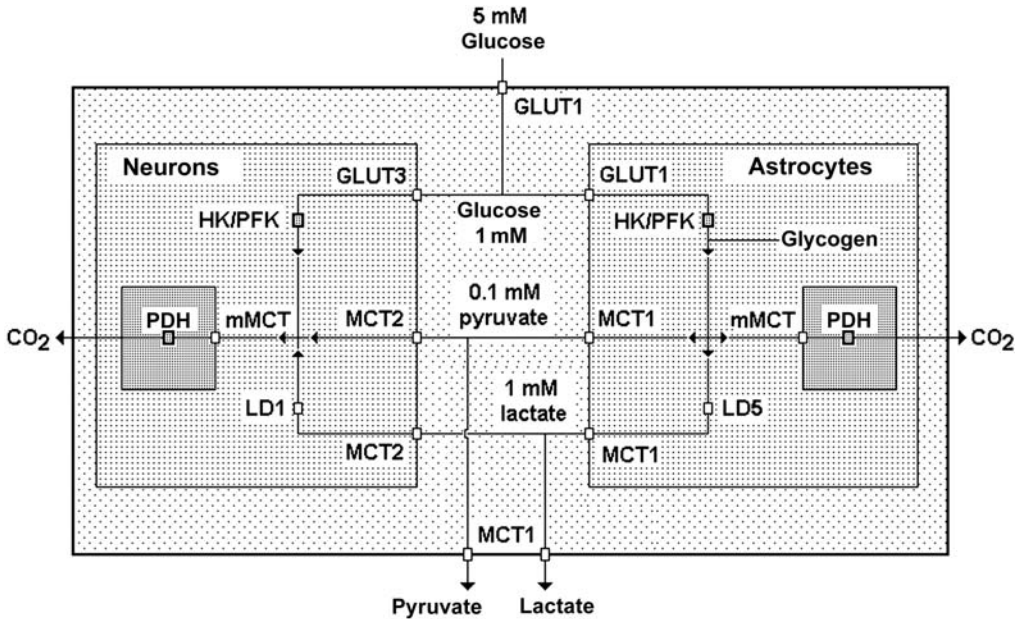
The evidence cited above shows that the glial energy metabolism in general is low compared with neuronal metabolism in cerebral cortex, where glial cells occupy 33% of the cell volume but generate only 20% of the ATP. Per unit cell volume, this amounts to a threefold difference in energy metabolism in normally functioning brains, generally consistent with the mitochondrial volume fractions published by Pysch and Khan (1972). Sustained stimulation of glial metabolism taxes the oxidative capacity of astrocytes beyond its normal limit. During some forms of excitation, for example, the neuronal firing frequency increases substantially and may require removal of excitatory neurotransmitters by glial cells at rates incompatible with the time constants of their oxidative capacity (Attwell and Gibb, 2005). By analogy, the presence of the LDH subtype LD5 in astrocytes also suggests that the average oxidative metabolic rate is low, while the glycolytic rate is subject to fluctuations in the form of brief, intense activations.

7 Activation

The responses of neurons and astrocytes to stimuli that activate brain tissue are linked closely to the peculiarities of their metabolic machinery. As flux-generating enzymes, both HK and PDH appear to operate at their maximum reaction rates. For this reason it appears logical to claim that neurons have a greater oxidative capacity than other cells because they react oxidatively to stimulation, while astrocytes have a greater

■ Figure 4.5-7

Idealized Metabolic compartmentation of control points of hexokinase (HK) and phosphofructokinase (PFK) enzymes, and pyruvate dehydrogenase (PDH) complex (dark square points), and near-equilibrium transporters and enzymes responsible for branching among pools (light square points). Metabolites linked by near-equilibrium transporter and enzyme reactions are shown with bidirectional arrows. Metabolic fates of pyruvate and lactate depend on relative preferences for each transporter or enzyme, which are regulated by affinities in relation to pyruvate and lactate concentrations



glycolytic capacity because they react glycolytically. The reason they have low glycolytic and oxidative capacities, respectively, must be because they reside in the same tissue. The key insight from this arrangement is the realization that neurons and astrocytes did not evolve separately to collaborate during activation but rather that activation became possible because of the intrinsic properties of neurons and astrocytes.

In neuroscience, activation and deactivation are conventional labels for changing brain function. Understanding brain function is the goal of the neuroscientific explorations of brain activity, but it is sometimes not clear which specific hypotheses the explorations actually test. To be sure, activation and its opposite represent a range of observations of a change of any number of different physiological measures of brain activity, such as action potential frequency, local field potentials, membrane polarity, ATP turnover, blood flow, glucose consumption, oxygen consumption, tissue oxygen tension, oxygen extraction fraction, hemoglobin saturation, absolute and relative concentrations and amounts of oxy- and deoxyhemoglobin, and blood and vascular volumes. Collectively, these measures can contribute to a comprehensive description of activity in brain tissue, but no single measure can be said to unequivocally represent activation, or even brain function, per se.

At the core of the conundrum is consciousness, of course. The emerging discipline of neuroenergetics focuses on measures of energy turnover of brain tissue as keys to the functional integrity of brain tissue, including consciousness. The insights gleaned from the accomplishments of this discipline have been limited by the convention that changes of energy turnover are a consequence of, or response to, changes of brain function, rather than the opposite (Fodor, 1983, 2000). However, it is possible that this relationship in reality could be turned around, as suggested in [Figure 4.5-1](#). It is possible that conscious brain function is a phase transition induced by sufficient energy turnover in specific populations of neurons. Much empirical evidence could be cited in favor of the theory that the unitary experience of consciousness is

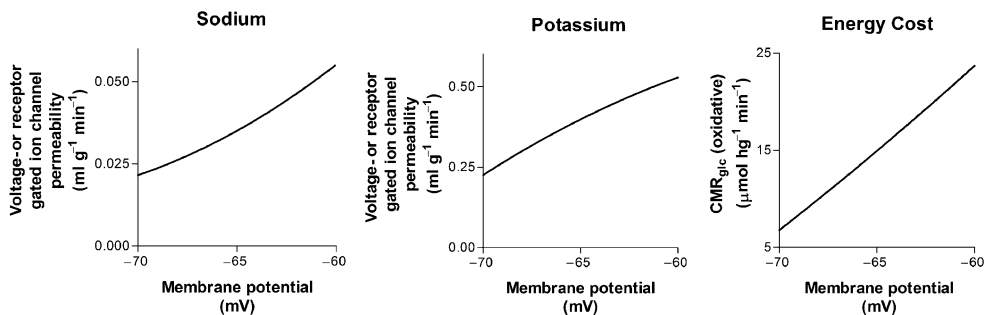
related to the global level of energy turnover in the brain rather than to activity in specific regions of the brain. Among these lines of evidence is the correlation between reported magnitudes of global brain energy metabolism and levels of consciousness (Shulman et al., 2005).

7.1 Ion Homeostasis During Activation

The sodium theory (described in *Box 4*) explains how neuronal excitation increases the work of the brain by increasing the leakage of ions across cell membranes, and how depolarization of neuronal membranes leads to increased oxygen uptake (Erecinska et al., 1991). This empirical finding is important, because cells in theory could undergo steady-state depolarization or repolarization without a change in ATP utilization when an average steady-state change of sodium conductance is paired with substantial declines of potassium and chloride conductances (Gjedde, 1993b). [▶ Table 4.5-2](#) illustrates this point by listing the identical ATP requirements at two different membrane potentials (-65 and -55 mV). The Goldman–Hodgkin–Katz constant field equation predicts the changes of the membrane potential that occur when ion permeabilities change. Using the permeabilities calculated in [▶ Table 4.5-2](#), the corresponding membrane potentials were calculated as shown in [▶ Figure 4.5-8](#).

■ Figure 4.5-8

Energy cost of depolarization, redrawn from Gjedde (1993b). Left and Center Panels: Steady-state neuronal membrane potential changes as a function of altered sodium and potassium ion membrane permeabilities at $0.549 \text{ ml g}^{-1} \text{ min}^{-1}$ constant chloride ion permeability. Ordinates: Ion permeability ($\text{ml g}^{-1} \text{ min}^{-1}$). Abscissae: Membrane potential (mV), calculated from the Goldman–Hodgkin–Katz constant field equation. Right Panel: Steady-state metabolism permitting membrane depolarization of the magnitude dictated by the increased sodium and potassium permeability. Abscissa: Membrane potential (mV), calculated from the Goldman–Hodgkin–Katz constant field equation, based on chosen changes of sodium and potassium ion permeabilities. Ordinate: Steady-state glucose consumption ($\mu\text{mol hg}^{-1} \text{ min}^{-1}$), calculated from steady-state ion flux, assuming constant chloride ion permeability. The membrane potentials reflect changes of both sodium and potassium (adjusted to preserve the 3:2 flux ratio required by the P-type Na^+/K^+ -ATPase), or chloride, permeability. The resulting Na^+/K^+ -ATPase activity was calculated as the flux required to preserve ion homeostasis. The glucose demand was in turn calculated as the nutrient delivery required to compensate for a steady-state ATPase activity of this magnitude by oxidative phosphorylation



[▶ Figure 4.5-8](#) reveals the metabolic consequence of sodium and potassium leakage: For an arbitrary depolarization from -70 to -60 mV, the ATP turnover must increase fourfold from 2.5 to $9 \mu\text{mol g}^{-1} \text{ min}^{-1}$ to preserve ion homeostasis. With a sodium-ion-transport-stimulated glucose metabolic rate of $0.15 \mu\text{mol g}^{-1} \text{ min}^{-1}$, the total glucose demand would be expected to increase from 0.2 to $0.4 \mu\text{mol g}^{-1} \text{ min}^{-1}$ to fuel this turnover of ATP. For further depolarization to a firing level of -55 mV, the glucose supply would have to increase to as much as $0.6 \mu\text{mol g}^{-1} \text{ min}^{-1}$ to fuel an ATP turnover of $20 \mu\text{mol g}^{-1} \text{ min}^{-1}$. In the

absence of oxygen (or with no increase of oxygen consumption), the glucose supply would have to increase to as much as $10 \mu\text{mol g}^{-1} \text{min}^{-1}$, a 30-fold increase, to cover the same need for ATP.

7.2 Brain Energy Metabolism During Activation

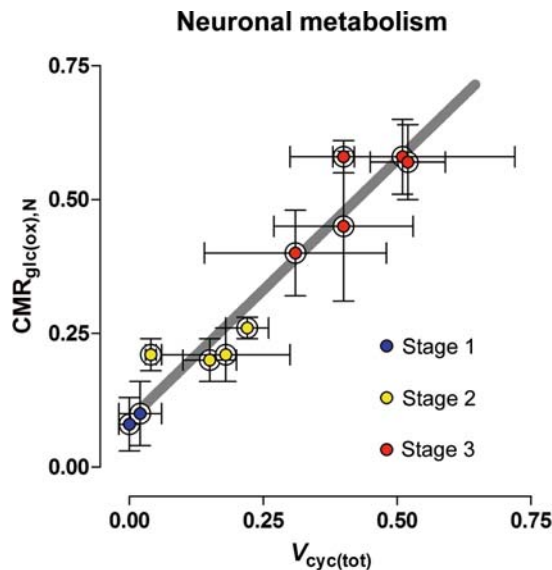
During excitation of brain tissue *in vivo*, local increases in metabolism reach 100% or more of the metabolism of the normal default state, depending on the intensity of stimulation (Bowers and Zigmond, 1979; Yarowsky and Ingvar, 1981; Kadekaro et al., 1985; Shulman and Rothman, 1998). The evidence for the increase of brain energy metabolism *in vivo* comes in three different forms, i.e., as global steady-state changes brought on by general reductions or increases of brain activity; as localized responses to specific stimulation, mostly of the cerebral cortex; and as changes of substrates and metabolites in the circulation and in brain tissue.

7.2.1 Global Steady-State Changes of Energy Metabolism

Average global steady-state changes are given in [Figure 4.5-9](#), in which recent magnetic resonance spectroscopic and allied studies in the rodent cerebral cortex show a linear relationship between calculated cycling rates of glutamate between the larger (neuronal) and smaller (neuroglial) metabolic compartments, and the calculated turnover rates of the TCA in the larger (neuronal) compartment. In [Figure 4.5-9](#), these findings were assigned to hypothetical functional stages based on the observed states of the brains of these animals.

■ Figure 4.5-9

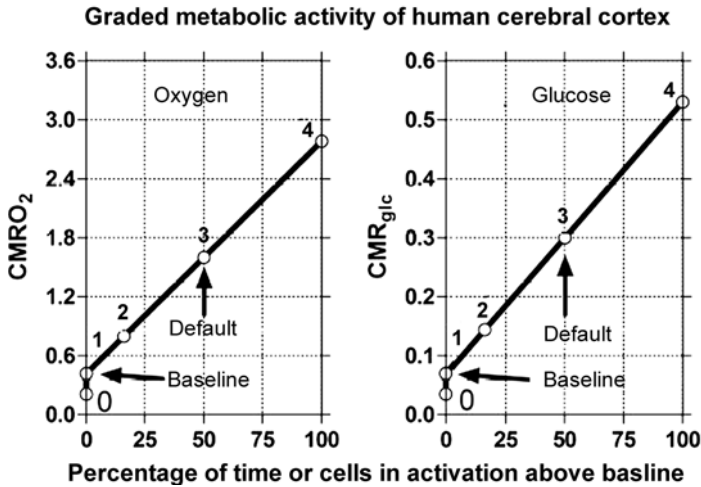
Stages of rat brain oxidative metabolism versus rate of glutamate cycling measured by Sibson et al. (1998), Choi et al. (2002), Henry et al. (2002), de Graaf et al. (2004), Patel et al. (2004), Oz et al. (2004) (modified from Hyder et al. (2006)). Abscissa: Combined neuronal and astrocytic glutamate turnover rate ($\mu\text{mol g}^{-1} \text{min}^{-1}$). Ordinate: Oxidative metabolism of glucose in neurons ($\mu\text{mol g}^{-1} \text{min}^{-1}$). Functional stages were inferred from the type and level of general anaesthesia used in each experiment. Slope of line is $0.97 + 0.09$ (unitless), and y-intercept is $0.09 + 0.03 \mu\text{mol g}^{-1} \text{min}^{-1}$



The relation between glutamate cycling and oxidative glucose metabolism shown in [Figure 4.5-9](#) is consistent with the oxidative metabolism of one mole of glucose for each mole of glutamate released and recycled. As such it combines the individual rates of oxygen consumption and the corresponding rates of glucose consumption. To show total glucose consumption (nonoxidative as well as oxidative), it is necessary to take into account the quantities of glucose converted to lactate, which is subsequently lost from brain by export across the blood–brain barrier. Overall OGI values indicate that these quantities are small. As functions of the rate of glutamate turnover, the individual rates of glucose and oxygen consumption portrayed in [Figure 4.5-9](#) must have slopes that differ in magnitude by a factor just below 6, the value of the OGI. These lines calculated for the parallel case of human cerebral cortex are predicted in [Figure 4.5-10](#), with markers indicating the average positions of the functional stages that they are likely to

Figure 4.5-10

Model of stage transitions of oxidative and glycolytic metabolism in human cerebral cortex during activation. Abscissae: Percentage of time or cells associated with activation. Ordinates: Oxygen or glucose metabolic rates in units of $\mu\text{mol g}^{-1} \text{min}^{-1}$. Left panel: Increments of oxygen consumption using the formula, $J_{\text{O}_2} = 0.42 (1-A) + 2.78 A$ ($\mu\text{mol g}^{-1} \text{min}^{-1}$). Right panel: Increments of glucose consumption according to the formula, $J_{\text{glc}} = 0.07 (1-A) + 0.53 A$ ($\mu\text{mol g}^{-1} \text{min}^{-1}$), where A is the percentage of activation



be associated with, copied from [Figure 4.5-1](#). Two plausible hypotheses claim, first, that the quantity of glutamate released and recycled is a function of nervous activity in percentage of maximum physiological activation, expressed either as a percentage of active cells or as a percentage of time engaged in activation, and, second, that the oxygen–glucose index undergoes a minor decline from 6 at stage 1 to 5.2 at stage 4. These assumptions are important foundations for a quantitative assessment of activation but they should be regarded as no more than models that at best generate testable predictions. How the underlying changes of activation are distributed among the participating cells during the period of activation is an independent topic of investigation in its own right but full elucidation is not necessary in order to use the percentage of maximum activation in quantitative correlations.

7.2.2 Localized Changes of Energy Metabolism in Response to Stimulation

While global changes of brain energy metabolism (judged as ATP turnover or oxidative glucose metabolism to CO_2) can be substantial, focal changes brought on by specific stimulation of cerebral cortex generally are small, suggesting that the energy turnover of the cerebral cortex normally operates at the same level most of

the time. Reports of substantial increases of glucose metabolism brought on by local stimulation of rat cerebral cortex are difficult to interpret because no corresponding measurements of oxygen consumption are available for technical reasons.

Localized activation responses from a number of stimulation studies of human brain are summarized in [Table 4.5-7](#) (Gjedde et al., 2002), divided into two fundamentally different types of stimulation. Simple kinds of stimulation generally show little or no change of oxygen consumption (Fox and Raichle, 1986; Fox

■ **Table 4.5-7**

Neuronal activation of brain metabolism

Stimulus	Supply			Products	
	ΔCBF	ΔJ_{glc} [%]	ΔJ_{O_2}	ΔJ_{ATP} [$\mu\text{mol g}^{-1} \text{min}^{-1}$]	ΔJ_{lact}
Primary	29	19	3.4	0.43	0.089
Secondary and motor	36	38	25	2.89	0.090

Modified from Gjedde 2001, based on studies by Fox and Raichle (1986); Seitz and Roland (1992); Fujita et al. (1999); Kuwabara et al. (1992); Ginsberg et al. (1988); Ribeiro et al. (1993); Fox et al. (1988); Marrett and Gjedde (1997); Vafae and Gjedde (2000); Katayama (1986); Roland et al. (1987); Roland et al. (1989); Raichle (1976); Iida et al. (1993); Vafae and Gjedde (2004)

et al., 1988; Seitz and Roland, 1992; Ohta et al., 1999). For example, with the single-inhalation method of measuring oxygen consumption, Fujita et al. (1999) compared changes of blood flow and oxygen consumption during 30 min of vibrotactile stimulation of the fingers of one hand. In primary sensory cortex, the blood flow change was 18% at the onset of stimulation and still 11% after 20 min of stimulation, but the oxygen consumption failed to increase for as long as 30 min. However, with more complex stimulation, significant increases of oxygen consumption are noted together with the change of blood flow (see references to [Table 4.5-7](#)).

The observation that there are two fundamental kinds of response of oxidative metabolism to brain activation is consistent with one fundamental response being a primary somatosensory response, in which the rise of oxygen consumption averages only 10% of the rise of blood flow, and another fundamental response being a motor or more complex secondary somatosensory response, in which the rise of oxygen consumption averages 75% of the rise of blood flow, both relative to their baselines. The average primary somatosensory response is a 3% increase of CMR_{O_2} for a 29% increase of CBF, while the average motor and secondary somatosensory responses average a 25% increase of CMR_{O_2} for a 36% increase of CBF, as illustrated in [Figure 4.5-11](#).

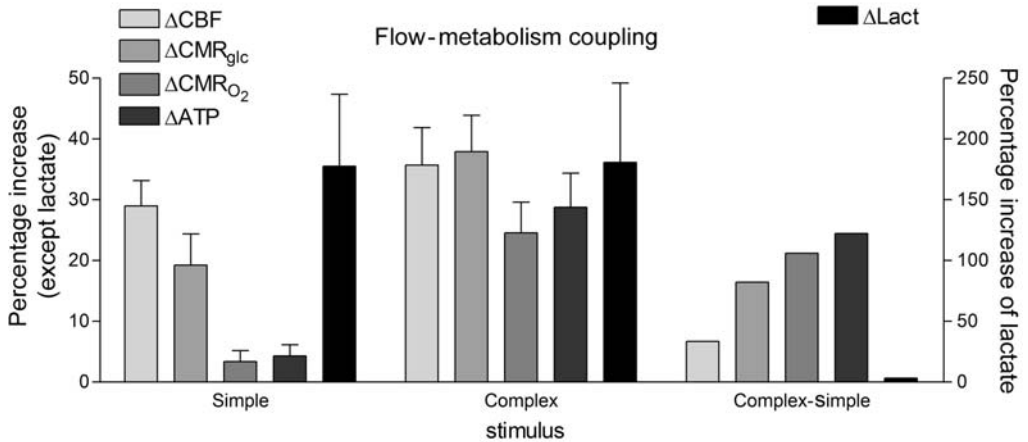
The discrepancy between the results of the two different types of stimulation listed in [Table 4.5-7](#) suggests that the ultimate increase of oxygen consumption depends significantly on the biochemical peculiarities of the neuronal pathway mediating the response to the stimulus (Borowsky and Collins, 1989). In brain as well as in muscle cells, the cytochrome oxidase activity of populations of cells is regulated by the habitual energy requirement, averaged over longer periods of time (Pette, 1985; Hevner et al., 1995). In muscle cells, neural input regulates the categorization of muscle cells into types I, IIa, or IIb. Changing the oxidative capacity requires sustained stimulation for an extended period.. Conversely, brief transient increases of energy metabolism above the habitual level of activity are not accompanied by commensurately increased oxygen consumption. In the brain, the same consideration leads to the conclusion that the two different kinds of response are related to the known differential oxidative and glycolytic responsiveness of neurons and glial cells.

7.2.3 Vascular and Tissue Metabolite Changes During Activation

It is a fundamental claim that transient changes of energy metabolism occur as changes of flux rather than concentration but the evidence is not strong for this claim. The reason is the difficulty of measuring the

■ **Figure 4.5-11**

Flow-CMR and flow-glycolysis coupling during stimulation of comparatively nonoxidative and oxidative cells. Relative increases of glycolysis, blood flow, and oxidative metabolism, estimated for two categories of response to stimulation (simple or primary somatosensory stimulation (“simple” response); and complex or secondary somatosensory and motor stimulation (“complex” response) (listed in ▶ [Table 4.5-7](#)). Note similar flow-glycolysis coupling in the two stimulations. Also shown are rates of incremental ATP and lactate production during excitation. Stimulus and/or cells fall into two metabolic categories, one with average incremental ATP/lactate ratio of less than 10 and one with average ratio of 300. Ordinates: Percentage increments of variables listed in graph (from Gjedde 2001)



changes at the same time. Flux measurements usually apply to periods of varying duration, while measurements of concentration reflect single time points. Non-steady-states, by definition, incur mismatches of the two types of measurement.

An additional complication is the fact that the mechanisms governing the transient changes of metabolite pools during activation involve a vast number of reactants. However, in terms of their importance to energy metabolism, as well as the ease of measurement, the most important concentrations traditionally have been those of glucose, glycogen in neuroglial cells, lactate, and NAD^+ and NADH . To relate the concentrations to metabolite fluxes, they must be compared to the influx and efflux of glucose, lactate, and oxygen during the activation to give an accurate view of the dynamic relations between fluxes and concentrations.

The main flux measurements of importance to the brain energy metabolism *in vivo* are the determinations of net metabolite fluxes across the blood-brain barrier, obtained by multiplying measured blood flow rates with arteriovenous deficits, which are of relevance only to the whole brain, and determination of regional net flux of glucose across the blood-brain barrier with labeled 2-deoxyglucose in animals or labeled 6-fluoro-2-deoxyglucose in humans. The blood flow measurements require only minutes, while the deoxyglucose measurements take at least 45 min.

The following two examples of the evidence of dynamic metabolite changes during brain activation illustrate the difficulty raised by attempts to make unequivocal conclusions about the changes of fluxes and concentrations in the mammalian brain, one in rodents and the other in humans. Dienel and Cruz (2003, 2004) reviewed metabolite and circulatory changes imposed on rat brain during activation by manual stroking of the rat's whiskers, head, paws, back, and tail. The measurements allowed comparisons to be made between the actually measured accumulation of the metabolites (as the metabolite accumulation index (MAI) defined in ▶ [Eq. \(16\)](#) (see [Box 10](#))) and the corresponding metabolites-glucose index (MGI). These two measurements differ only with respect to the net glucose uptake and the duration of metabolite measurement. In ▶ [Figure 4.5-12](#), the comparison reveals that both the activation period and the

Box 10: Indices of Steady or Non-Steady-State of Brain Metabolism: From OGI to NSI

Several indices have traditionally been used to evaluate dynamic changes of brain energy metabolism and metabolites in brain tissue, viewed from the perspective either of the circulation or of the tissue. The simplest index in the circulation is the oxygen–glucose index (OGI), which can be determined for whole brain from arteriovenous deficits at single time points. It fails to account for the contribution of lactate from the circulation, and it is therefore often replaced by the metabolite uptake ratio (MUR), which is defined as

$$\text{MUR} = J_{\text{O}_2} / \left(J_{\text{glc}} + \frac{1}{2} J_{\text{lact}} \right),$$

where J_{O_2} , J_{glc} , and J_{lact} are the net rates of oxygen, glucose, and lactate transport across the blood–brain barrier. These rates are obtained by multiplying the arteriovenous deficits with simultaneously determined blood flow values. It is important to note that the rates are positive when arteriovenous deficits are positive as they are when the metabolite is taken up by the brain, and negative when the metabolite is released from the brain, as lactate is under normal circumstances. The MUR is not always useful as an index of the magnitude of non-steady-state because its values are difficult to translate into changes of tissue concentrations. An alternative formulation that makes this easier is the metabolites-glucose index (MGI), which also assesses the dynamic changes of brain energy metabolism from the point of view of the circulation, but is slightly differently defined as

$$\text{MGI} = \text{OGI} - 3 \text{LGI},$$

where OGI is the oxygen–glucose index and LGI similarly is the ratio of net lactate and glucose rates of transfer across the blood–brain barrier, also known as the lactate–glucose index, calculated from arteriovenous deficits across the vasculature of the brain (negative for efflux, positive for uptake). The MGI is in essence an index of the ratio of sinks of the products of metabolism (CO_2 and lactate) to sources of the substrates of metabolism (glucose). If the value differs from 6, then sinks and sources are mismatched and a non-steady-state exists. The MGI is related to the MUR by the formula

$$\text{MUR} = \frac{6 \text{LGI}}{2 + \text{LGI}} + \frac{2}{2 + \text{LGI}} \text{MGI},$$

where the indices MGI and MUR assume the value of 6 in the steady state but have different values in the non-steady-state, depending on the magnitude of the lactate–glucose index. Thus, MUR and MGI values different from 6 both indicate non-steady-states in which metabolite concentrations have changed in brain tissue. The relationship between the metabolite measurements in circulation and those in the tissue can be assessed by a steady-state formulation that relates the changes of the main metabolites to the transport of glucose across the blood–brain barrier, the period in which the changes are followed, and the results of the glucose metabolism to CO_2 or lactate

$$\text{MAI} = \Delta[\text{glc}] + \Delta[\text{glyc}] + \frac{1}{2} \Delta[\text{lact}] = J_{\text{glc}} \left(1 - \frac{1}{6} \text{MGI} \right) \Delta T, \quad (16)$$

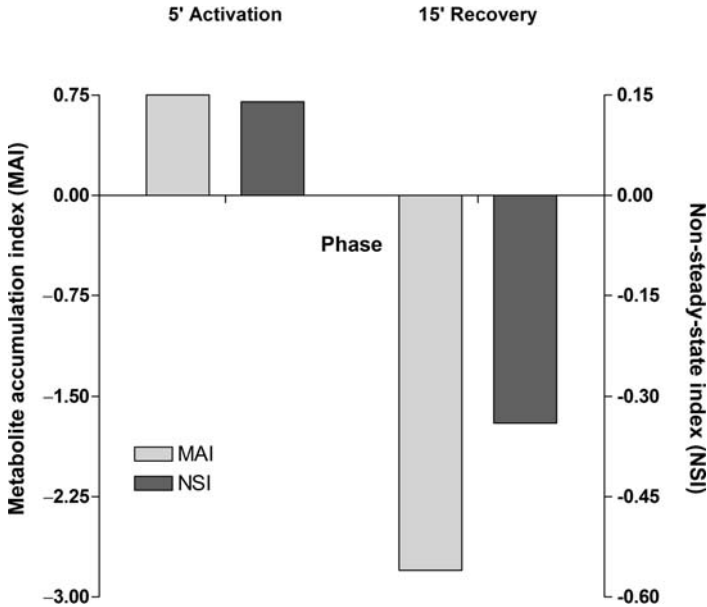
where both sides of the equation define a metabolite accumulation index (MAI), from the perspectives of the tissue (left side of equation) or the circulation (right side of equation), respectively. The terms $\Delta[\text{glc}]$, $\Delta[\text{glyc}]$, and $\Delta[\text{lact}]$ are the changes of the tissue concentrations of glucose, glycogen (in units of glucose moieties), and lactate respectively, as weighted averages over the period of observation ΔT . The value of the MAI is zero in steady states. Occasionally, it is sufficient to determine the MAI relative to the rate of net glucose transport (J_{glc}) and period of observation (ΔT), for example when arteriovenous deficits are available but no blood flow rates or tissue concentrations have been determined. This relative MAI can be said to serve as the simplest non-steady-state index (NSI)

$$\text{NSI} = \text{MAI} / (J_{\text{glc}} \Delta T) = 1 - \frac{1}{6} \text{MGI},$$

which assumes the value of zero in steady-states. Only by taking at least these factors into account can discrepancies among changes of any of these main metabolites be properly evaluated during the transient changes of an activation. The equation allows metabolite changes to be predicted from measurements in the circulation, or vice versa.

■ Figure 4.5-12

Changes of metabolite accumulation index (MAI) and non-steady-state index (NSI) during 5 min stimulation and 15 min recovery of rat brain *in vivo*, calculated from summary published by Dienel and Cruz (2003, 2004) according to [Eq. \(16\)](#) as described in *Box 10*. Left ordinate: Metabolite accumulation index (MAI) determined according to left side of [Eq. \(16\)](#) in units of $\mu\text{mol g}^{-1}$. Right ordinate: Non-steady-state index (NSI) calculated from metabolite-glucose indices of arteriovenous deficits. The graph shows, paradoxically, that a positive non-steady-state occurs and metabolites accumulate during stimulation of rat brain, while they decline during recovery, as reflected both in metabolite concentrations in brain tissue and in the arteriovenous deficits of glucose and lactate



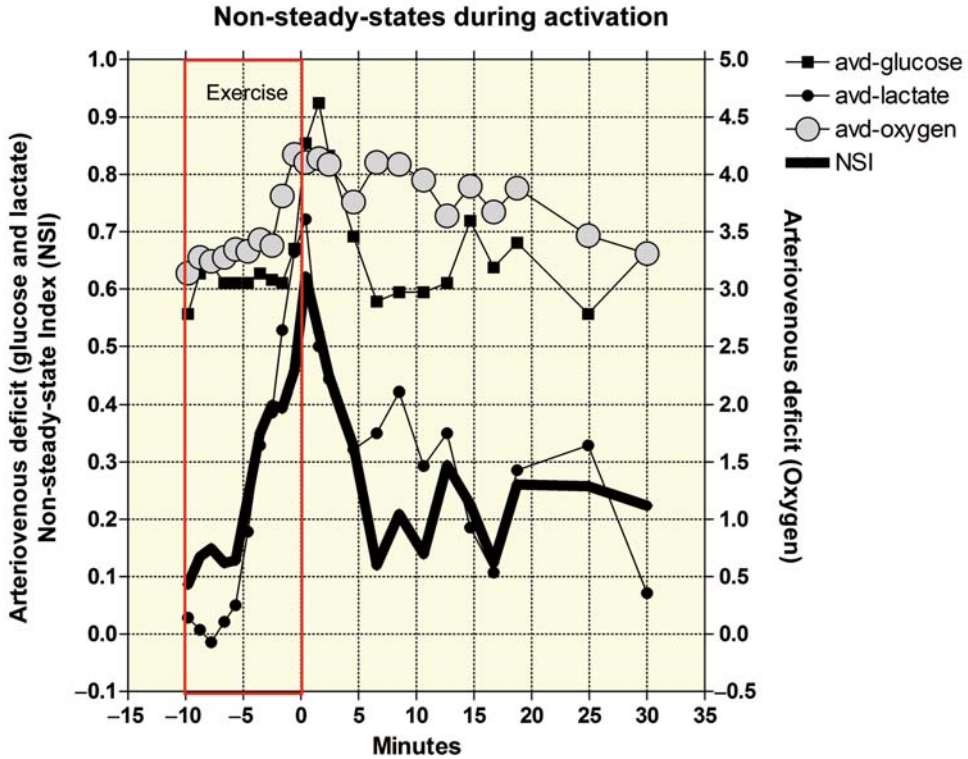
ensuing recovery period are characterized by non-steady-state consistent with changes of metabolite concentrations. The metabolites accumulate (particularly glucose and lactate) during the 5-min activation period while they decline (particularly glycogen) in the subsequent 15-min recovery period. It is evident that the OGI declines during the activation and rises above normal when the rats are again at rest. These changes can be understood only by invoking differential activation of cells with different oxidative and glycolytic capacities.

Ide et al. (2000) reported the measurements of arteriovenous differences across the brain in humans, shown in [Figure 4.5-13](#). These values can be used similarly to predict metabolite accumulation during and after exercise. The calculations confirm that the MGI rises substantially during the exercise and returns slowly toward but never reaches zero over the next half hour. The OGI declines at the end of the exercise period, only to rise above normal after the exercise.

Kasischke et al. (2004) used fluorescence imaging to determine changes of NADH in slices of hippocampus exposed to 32 Hz electrical stimuli. The NADH signal from dendritic mitochondria declined during the first 10 s of a 20 s period of stimulation, indicating conversion of NADH to NAD^+ , and then returned to baseline at the end of the 40 s recovery period. The NADH signal from astrocytic cytosol increased toward the end of the 20 s stimulus and continued to rise for the following 20 s of recovery, indicating generation of pyruvate in excess of metabolism (oxidative as well as nonoxidative) in astrocytes in this period. Above all, these findings reveal a failure of oxidative metabolism to increase in parallel with stimulation, beyond the brief initial exhaustion of the putative oxygen reserve in mitochondria, whether

■ Figure 4.5-13

Changes of non-steady-state index (NSI) calculated from measured arteriovenous deficits of oxygen, lactate, and glucose during 10 min strenuous exercise and 35 min recovery of human whole brain in vivo, calculated from results published by Ide et al. (2000) as described in *Box 10*. Right ordinate: Arteriovenous deficit of oxygen. Left ordinate: Glucose and lactate arteriovenous deficits and non-steady-state index (NSI) (see *Box 10*), calculated from the arteriovenous deficits. The graph shows that, paradoxically, non-steady-state occurs and metabolites accumulate during stimulation and that both normalize during recovery



because of limited oxygen delivery to the slice, or because of a constitutive inability of pyruvate breakdown in mitochondria to match the increased generation of pyruvate. The beginning of recovery of NADH in dendritic mitochondria in the second half of the stimulation is evidence of increased pyruvate oxidation in the neurons, but it is still unclear where this pyruvate is generated. There is no indication of the fate of lactate in the study. Together, the changes of energy metabolism and metabolites show that metabolites accumulate during stimulation and decline during recovery. This paradoxical conclusion implies that oxygen availability declines during stimulation and returns to, or exceeds, normal during recovery.

7.3 Substrate Delivery During Activation

The measurements underlying [Table 4.5-7](#) (cited in Gjedde (2001)) suggest that the relation between the changes of blood flow and the generation of additional ATP is markedly variable during activation, with ratios between the relative changes ranging from unity to 20. It is not known which specific aspect of neuronal excitation is most critically dependent on the blood flow increase but surprisingly the findings

suggest that the blood flow changes are unrelated to an immediate satisfaction of increased oxygen requirements for oxidative phosphorylation. The following section deals with the attempts to identify agents to which the blood flow responds when brain tissue undergoes activation.

7.3.1 Regulation of Microvascular Oxygen

Gjedde et al. (1991) considered whether the discrepancy between the two reactions to stimulation (blood flow and oxygen consumption) could be explained by the failure of blood flow to rise sufficiently in some circumstances to raise the oxygen delivery sufficiently. However, restricted oxygen supply is not the reason for the inappropriately named oxygen “debt” during exercise of tissues such as skeletal muscle (Connett et al., 1985; Ye et al., 1990; McCully et al., 1991; Ohira and Tabata 1992; Reeves et al., 1992). In testing this proposal in healthy volunteers, Kuwabara et al. (1992) (also see Ohta et al. (1996) and Fujita et al. (1999)) found cerebral oxygen consumption in the brain to remain unchanged during vibrotactile stimulation of the sensorimotor cortex, despite increased blood flow and increased capillary diffusion capacity. Because oxygen tension in the tissue must go up when blood flow rises if oxygen consumption does not increase as well, this experiment showed that deficient oxygen supply does not explain the limited oxygen consumption in the brain under these circumstances. However, Vafaei et al. (2000) tested two patients with mitochondrial encephalopathy and found that the muted oxygen consumption response to complex visual stimulation is associated with a similarly muted blood flow response.

Possible clues to the understanding of the discrepant changes of oxygen consumption and blood flow come from studies of the kinetics of oxygen delivery to brain cells (Gjedde, 1996, 1997, 2005). The diffusion limitation imposed by the hemoglobin binding renders oxygen transport, as reflected in the extraction fraction, somewhat insensitive to blood flow increases (Honig et al., 1992), so blood flow must increase disproportionately to raise oxygen transport. The problem is that a flow-CMR_{O₂} couple of unity means the same capillary oxygen tension profile and extraction fraction at all times and in all situations, and hence no change of the oxygen tension gradient in the tissue. The kinetic analysis of cytochrome oxidase activity shown in [Figure 4.5-14](#) reveals that increases of blood flow above the increase of oxygen consumption are necessary for the delivery of additional oxygen during excitation (*see Box 11*).

When the decline of the mitochondrial oxygen tension threatens to reduce the oxygen saturation of cytochrome oxidase, oxygen consumption becomes dependent on the mean capillary oxygen tension for a given capillary density (Gjedde et al., 1990, 2005). Brain activation above this threshold therefore demands disproportionately increased blood flow to increase the mean capillary oxygen tension.

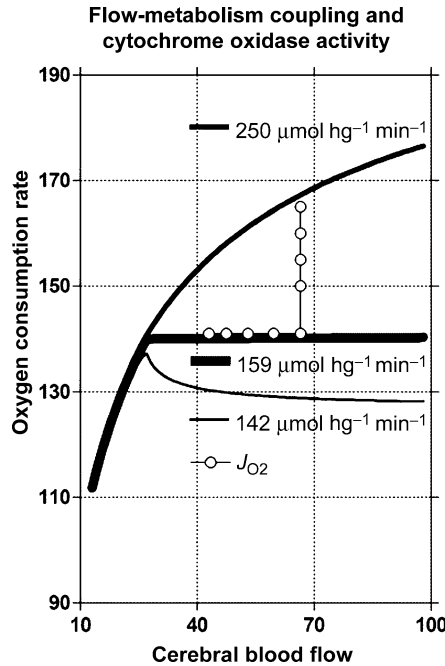
The maximum oxygen delivery capacity is the upper limit of oxygen consumption, reached when the mitochondrial oxygen tension is at the minimum level sufficient to sustain the cytochrome oxidase activity. This limit, at which the average oxygen tension of capillary blood drives most of the oxygen consumption, previously was thought to be approached only in situations of pathologically limited blood flow but may in fact be the rule rather than the exception. The effect of the blood flow increase is then to raise the maximum to which oxygen consumption can rise ($J_{O_2}^{\max}$). When more oxygen is needed and blood flow rises disproportionately to satisfy this need, the oxygen extraction paradoxically declines and raises the average capillary oxygen tension to the magnitude consistent with the pressure gradient required to drive oxygen to mitochondria (Gjedde et al., 2005).

7.3.2 BOLD Signal Changes During Activation

The blood-oxygenation-level-dependent (BOLD) magnetic resonance signal is the BOLD measure from deoxyhemoglobin in brain vasculature (*see Box 11*). It arises because deoxyhemoglobin, unlike oxyhemoglobin, is paramagnetic (Ogawa et al., 1990a, 1990b, 1993). The measure has become a very popular determination of a variable that is a good approximation of the oxygen extraction fraction because it relates to the amount of deoxyhemoglobin in the tissue, which can only arise from the removal of oxygen from

■ Figure 4.5-14

Oxygen consumption versus blood flow estimated for human whole brain according to Eq. (21) for three different cytochrome oxidase activities (J_{max}), calculated from results published by Gjedde et al. (2005) and Summarized in Box 12. Abscissa: Cerebral blood flow in units of $\text{ml hg}^{-1} \text{min}^{-1}$. Ordinate: Oxygen consumption in units of $\mu\text{mol hg}^{-1} \text{min}^{-1}$. Baseline oxygen consumption is $140 \mu\text{mol hg}^{-1} \text{min}^{-1}$, indicated by the heavy horizontal line. Cytochrome oxidase activities are given in the graph. Oxygen diffusibility (L) is $3.2 \mu\text{mol hg}^{-1} \text{min}^{-1} \text{mmHg}^{-1}$, and the arterial oxygen concentration ($C_{O_2}^{\text{art}}$) is 8.8 mM . The cytochrome oxidase affinity for oxygen (P_{50}^{cytox}) as a function of cerebral blood flow is given by Eq. (21) when other variables are kept constant. Increases of blood flow without change of oxygen consumption (white circles) cause oxygen tension to rise in the tissue. At a given blood flow rate, increases of oxygen consumption require increased cytochrome oxidase activity as shown by the white circles, which in turn cause the oxygen tension to decline, as shown in Figure 4.5-15



Box 11: Average Capillary Oxygen Tension

In the absence of proportionately increased oxygen consumption, increased blood flow leads to higher capillary oxygen tensions and lower extraction fractions and reduces the fraction of deoxygenated hemoglobin in capillary and venous blood, according to Eq. (4)

$$\bar{P}_{O_2}^{\text{cap}} = P_{50} \sqrt{\frac{2}{E_{O_2}} - 1}, \quad (17)$$

where the symbols represent the same as those in Eq. (4) (see Box 3). In Eq. (17), the extraction fraction equals the fraction of deoxyhemoglobin in venous blood. Its decline is a measure of the relative increase of oxygenation in cerebral veins when blood flow increases. As deoxyhemoglobin is paramagnetic, its relative decline gives rise to so-called BOLD magnetic resonance contrast changes associated with brain activation (Ogawa et al., 1990a, b, 1993; Kwong et al., 1992). The signal is primarily a function of the average extraction of oxygen from the vascular bed (Gjedde et al., 1999).

hemoglobin when hemoglobin is fully saturated in arterial blood, as is normally the case. When oxygen consumption often increases much less than blood flow during activation of brain regions, the BOLD measure has acquired an inaccurate but common reputation as an index of blood flow change easily determined by fMRI.

7.3.3 Regulation of Tissue Oxygen

If disproportionately greater blood flow increases are required to drive enough oxygen into brain tissue during functional activation, it is important to understand the mechanism that elicits the increase. Yet, the detailed relationships among the possible agents (glutamatergic and acetylcholinergic activity, synthesis of nitric oxide, (NO) extracellular accumulation of potassium, generation of lactic acid) and the functionally induced blood flow changes of brain tissue remain unknown. The elucidation of these relations is among the most pressing items on the neuroscientific agenda. Information concerning three important putative agents, NO, potassium, and prostanoids, is reviewed below.

Somewhat surprisingly, the mathematical treatment given in *Box 12* describes a compulsory flow limitation that dictates the oxygen consumption associated with a given blood flow rate when all other

Box 12: Coupling of Oxygen Metabolism to Blood Flow

Assuming full saturation of arterial hemoglobin and quantitatively negligible oxygen in physical solution in arterial plasma, the minimum oxygen tension in mitochondria can now be calculated as the tension commensurate with the actual delivery of oxygen, by combination of [Eqs. \(4\)](#) or [\(17\)](#) and [\(5\)](#)

$$P_{O_2}^{\text{mit}} = \left(P_{50} \sqrt{h \frac{2}{E_{O_2}} - 1} \right) - \left(\frac{J_{O_2}}{L} \right), \quad (18)$$

where $P_{O_2}^{\text{mit}}$ is the average oxygen tension in mitochondria, and L is the oxygen diffusibility, assumed to be constant in the absence of recruitment. Solving for the cerebral blood flow (F), [Eq. \(18\)](#) yields

$$F = \frac{J_{O_2}}{2C_{O_2}^{\text{art}}} \left(1 + \left[\frac{J_{O_2} + LP_{O_2}^{\text{mit}}}{LP_{50}} \right]^h \right), \quad (19)$$

where $C_{O_2}^{\text{art}}$ is the arterial oxygen concentration. The equation expresses blood flow as an apparent function of the rate of oxygen consumption and the mitochondrial oxygen tension for a given arterial oxygen concentration. In this relationship, the mitochondrial oxygen tension reflects the balance between the delivery and consumption of oxygen. The tension depends on, rather than controls, the rate of oxygen consumption, according to the simple Michaelis–Menten-type kinetics expression (Gnaiger, 1993; Gnaiger et al., 1995; Gnaiger et al., 1998)

$$P_{O_2}^{\text{mit}} = P_{50}^{\text{cytox}} \left(\frac{J_{O_2}}{J_{\text{max}} - J_{O_2}} \right), \quad (20)$$

where P_{50}^{cytox} is the apparent half-saturation constant of the oxygen reaction with cytochrome oxidase and J_{max} is the maximum reaction rate at a given cytochrome c occupancy of the enzyme. [Equation \(20\)](#) eliminates $P_{O_2}^{\text{mit}}$ from [Eq. \(19\)](#) and yields an expanded expression of the relations among the primary factors affecting oxidative metabolism

$$F = \frac{J_{O_2}}{2C_{O_2}^{\text{art}}} \left(1 + \left(\left[1 + \frac{LP_{50}^{\text{cytox}}}{J_{\text{max}} - J_{O_2}} \right] \left[\frac{J_{O_2}}{LP_{50}} \right] \right)^h \right), \quad (21)$$

where the independent variables are F , P_{50}^{cytox} , and J_{max} , and the dependent variable is J_{O_2} , when $C_{O_2}^{\text{art}}$ and L are constants and arterial blood remains fully saturated. The independent variables may be linked, of course. [Equation \(21\)](#) combines the Hill equation of the oxygen saturation of hemoglobin (Hill, 1910, 1913) and the Michaelis–Menten equation of substrate occupancy of an enzyme (Michaelis and Menten, 1913).

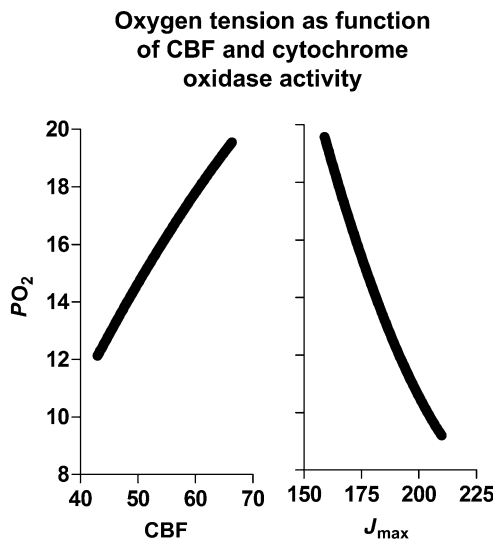
parameters are constant. A change of any of the independent variables that includes flow, arterial oxygen tension, hemoglobin affinity, oxygen diffusion coefficient, and cytochrome activity and affinity by necessity is reflected in the rate of oxygen consumption. If there is no change of the oxygen consumption after a change of any of the independent variables, it is a fair assumption that a compensatory change of at least one other independent variable has set in. Thus, invariant oxygen consumption (J_{O_2}) with variable flow (F) most probably implies compensatory change of cytochrome affinity (P_{50}^{cytox}) or activity (J_{max}) or both.

Figure 4.5-14 illustrates the analysis of the relationship (expressed in Eq. (19) in Box 12) published by Gjedde et al. (2005). Previous studies of oxygen supply and delivery suggested that the affinity of cytochrome *c* oxidase for oxygen changes inversely with the oxidative metabolism of a tissue, and thus preserves the sensitivity of the cytochrome *c* oxidase reaction to changes of the maximum velocity (see Brown (2001) for a review of these findings). Gjedde et al. (2005) hypothesized that a similar change explains the invariant cerebral oxygen consumption measured during moderate changes of blood flow to the brain, exemplified by the middle line of Figure 4.5-14. Changes of the cytochrome *c* oxidase activity (J_{max}) at a given rate of blood flow would then raise or lower oxygen consumption as shown in the upper and lower curves, of which the upper curve is the completely flow-limited extreme, above which the oxygen consumption cannot rise. The effect of the respective changes of flow (F) or cytochrome activity (J_{max}) is to raise or lower tissue and mitochondrial oxygen tensions according to Eq. (21).

Predicted changes of oxygen consumption and P_{O_2} are shown in Figures 4.5-14 and 15 in which first blood flow and then cytochrome oxidase activity rise as shown in Figure 4.5-15, causing oxygen

Figure 4.5-15

Biphasic change of mitochondrial oxygen tension in response to changes of blood flow and cytochrome oxidase activity (J_{max}) shown in Figure 4.5-14, calculated from Eqs. (20) and (21). In left panel, J_{max} equals $159 \mu\text{mol hg}^{-1} \text{min}^{-1}$; in right panel, CBF equals $65 \text{ ml hg}^{-1} \text{min}^{-1}$. Abscissae: Cerebral blood flow ($\text{ml hg}^{-1} \text{min}^{-1}$) and cytochrome oxidase activity ($\mu\text{mol hg}^{-1} \text{min}^{-1}$). Ordinates: Mitochondrial oxygen tension (mmHg). Note that oxygen tension may fall below normal when cytochrome oxidase activity rises as shown experimentally by Thompson et al. (2003)



consumption to change as shown in Figure 4.5-14. The authors also speculated that the blood flow modulator NO acts as an adjustable inhibitor of cytochrome *c* oxidase affinity that competes with oxygen's access to the enzyme. The unexpected finding that oxygen tension rises during the phase when blood flow increases and declines below normal during the phase when brain energy metabolism increases was

demonstrated by Thompson et al. (2003), who determined oxygen tensions in cat visual cortex during stimulation with stripes of varying angles. Oxygen tensions increased during the stimulation, except when the angle of the stripe elicited an activation of the monitored neuron. As predicted by the model, the oxygen tension declined when the neurons started working.

The relationship depicted in [Figure 4.5-14](#) assumes that there is no “absolute” recruitment of the capillary bed capable of increasing the diffusion capacity for oxygen by reducing the diffusion distance in the tissue, or increasing the intrinsic permeability of the capillary endothelial wall. It is the current consensus that recruitment of capillaries in brain tissue is “relative,” i.e., it occurs by reduction of capillary transit times toward greater homogeneity of transit times and a lower average transit time, rather than by an absolute increase of the number of perfused capillaries (Kuschinsky and Paulson, 1992). Because the capillary surface area remains the same, relative recruitment makes very little difference to the transport of oxygen.

7.4 Regulation of Blood Flow

The observation that oxygen consumption sometimes fails to increase, despite adequately increased blood flow (e.g., in response to vibrotactile stimulation), suggests either that additional factors prevent neurons from using the available oxygen or that additional oxygen is not needed. Increased blood flow elicits a number of changes. It delivers substrates such as glucose and amino acids and removes substances such as water, hydrogen ions, lactate, and pyruvate. Therefore, it is possible that increased oxygen delivery is not the most important effect of increased blood flow.

A consensus is emerging that the neurotransmitters glutamate and acetylcholine are the prime but indirect agents of blood flow change when they bind to their appropriate membrane receptors, which for glutamate are placed primarily on postsynaptic neurons. Among the direct blood flow stimulators, prostaglandins, epoxyeicosatrienoic acid (EET), carbon dioxide, adenosine, and potassium and hydrogen ions appear to require increased synthesis of the originally endothelium-derived relaxation factor NO by means of activation of the enzyme responsible for NO synthesis, NO synthase (NOS) (Iadecola, 1992; Fabricius and Lauritzen 1994; Iadecola et al., 1994; Villringer and Dirnagl, 1995; Lauritzen, 2005). Adenosine is a product of the hydrolysis of adenosine nucleotides, which are the key elements in energy metabolism and hence is attractive as a potential signal for blood flow change with a biochemical role similar to that of a second messenger. Compared with the mM concentration range of ATP, adenosine has a low concentration in the 10–100 nM range, which is controlled by two enzymes, adenosine deaminase and adenosine kinase, with different affinities that tend to rule out fluctuations commensurate with flow changes. Large changes of adenosine concentration, on the other hand, appear to be inhibited by the absence of ATP changes in physiologically functioning brain tissue.

7.4.1 Nitric Oxide

Computationally active neurons release glutamate. This activates Ca^{2+} influx through neuronal NMDA-type receptors/channels, which leads NOS to release NO, which then works on smooth muscle to dilate arterioles. These observations place NO in a key position as a modulator both of blood flow and of cytochrome *c* oxidase affinity for oxygen, and they raise the question of the link between the neurotransmitter-induced receptor stimulation and the activation of NOS. It now appears that a common link between the synthesis of NO and activation of oxidative metabolism can be the flux of calcium ions into cells through voltage- and receptor-gated channels and through the mitochondrial membrane (Lauritzen, 2005). NO causes vasodilatation of brain resistance vessels, in addition to other effects in glial cells and pre- and postsynaptic neurons. It is synthesized in endothelial cells and neurons in proportion to the cytosolic concentration of unbound calcium (Iadecola, 2004). The NO is generated in reactions catalyzed by the cell-specific NO synthases, which include endothelial NOS (eNOS) and neuronal NOS (nNOS), of which nNOS is by far the most abundant, as well as by the inducible NOS (iNOS). Activation of eNOS is mediated by

acetylcholine acting on the M₅ subtype muscarinic receptors (Wang et al., 1994; Elhusseiny et al., 1999; Elhusseiny and Hamel, 2000). It is not clear to which extent NOS activation is involved in functionally induced increases of cerebral blood flow. Pharmacologic blockade of the vascular receptors involved in the synthesis of NO abolishes functionally induced blood flow increases, although the specificity of the blockade is in doubt. Focal changes of cortical blood flow induced by sensory stimulation can be eliminated by blocking endothelial acetylcholine receptors (Ogawa et al., 1994), including those involved in mediating synthesis of NO, apparently without altering the underlying neuronal activation (Ogawa et al., 1994). Other evidence suggests that the cerebral vasodilatation associated with simple somatosensory stimulation in rodents is modulated rather than mediated by NO synthesized by nNOS and not by eNOS- or iNOS-stimulated NO synthesis (Ayata et al., 1996; Ma et al., 1996; Cholet et al., 1997; Lindauer et al., 1999). Reutens et al. (1997) stimulated NO synthesis with the precursor L-arginine in humans, and cerebral blood flow was found to be globally increased, but the regional blood flow increase in response to vibrotactile stimulation was unaffected, either because NO is not involved in the increase or because the increase was already maximally stimulated by NO.

7.4.2 Prostanoids

Studies of circulation in skeletal muscle studies show that a correlation exists between the increase of blood flow and the increase of lactate (Connett et al., 1985; Lupton et al., 1988), suggesting that blood flow increase may reflect a glycolytic response. In brain, astrocytes provide a link between the extracellular space close to the microvascular walls and the extracellular space close to synapses. Glutamate released into the synaptic cleft also binds to astrocyte receptors (mGluRs), which raise the calcium levels in astrocytes, where it stimulates the generation of arachidonic acid (AA) via phospholipase A2. Cyclooxygenase-generated derivatives of AA (PGE₂) dilate arterioles. Upon stimulation, astrocytic endfeet have been shown to mediate vasodilation by agents that appear to be products of the prostaglandin-synthesizing enzyme cyclooxygenase-2 (COX-2) in the brain. Products that inhibit COX-2 are known to cause reduction of cerebral blood flow (Rasmussen et al., 2003; Gjedde et al., 2005). Prostaglandins are released from astrocytes in response to intracellular calcium ion elevation when metabotropic receptors bind glutamate. The evidence suggests that the COX product prostaglandin E₂ (PGE₂) is involved in astrocyte-mediated vasodilation (Zonta et al., 2003). Mulligan and MacVicar (2004) showed that a product of the cytochrome P450 4A enzymes (CYP4A) in astrocytic endfeet, 20-hydroxyeicosatetraenoic acid (20-HETE), constricts microvessels during autoregulation. NO-mediated inhibition of the CYP4A enzymes in turn may explain part of the vasodilatory effect of NO (Gebremedhin et al., 2003; Takano et al. 2006).

7.4.3 Potassium

As a consequence of the increased potassium conductance of the cell membrane during neuronal excitation, activation raises the extracellular potassium ion concentration, which drives the potassium into astrocytes by several nonenergy-requiring routes in addition to the usual energy-dependent mechanisms, as well as in response to glutamate import. Paulson and Newman (1987) speculated that excess potassium in glial cells is released perivascularly where it may relax smooth muscle cells and dilate resistance vessels. They reasoned that the time constant of delivery of potassium to the perivascular space is much lower when the potassium is siphoned to the vessels inside the foot processes (66 ms) than when the potassium is left to diffuse through the extracellular space (2.5 s). Hypothetically, the lower time constant may assure a tighter regulation of the blood flow response. The role of potassium ions in mediating functionally induced increases of blood flow in the brain was tested by Caesar et al. (1999), who found evidence of considerable heterogeneity in responses. The relative contributions of extracellularly applied potassium ions and adenosine to the blood flow regulation in cerebellum varied among the cell populations, NO and potassium playing the greatest role in parallel fiber connections, and NO and adenosine playing the greatest role in climbing fiber connections.

7.5 ATP Homeostasis During Activation

To satisfy the need for increased energy turnover during neuronal excitation, additional nutrients must be supplied from tissue stores or from the circulation. With no additional nutrients and no net loss of ATP, the phosphocreatine (PCr), glycogen, and glucose concentrations could sustain the additional energy demands of a 100% rise of ATP turnover for less than a minute (▶ [Table 4.5-5](#)). However, available evidence, exemplified in ▶ [Figures 4.5-12](#) and ▶ [4.5-13](#), suggests that an abundance of additional sources of energy is provided at the onset of activation and that it depends on the type of activation to which extent the potential for this additional energy turnover is actually used.

7.5.1 Hydrolysis of Phosphocreatine During Activation

Hydrolysis of PCr buffers ATP concentrations at the expense of increased energy utilization. Roth and Weiner (1991) demonstrated that a substantial reduction of the concentration of PCr (5 mM) is compatible with minimal change of ATP. This decline of PCr may be as much as threefold the normal turnover of ATP in 1 min, and hence allows a threefold increase of ATP hydrolysis with little or no change of the ATP concentration during the first minute. A decrease in PCr is associated with an increase in the cytosolic free ADP concentration. Erecinska and Silver (1989) calculated that hydrolysis of 5 mM PCr may raise the pH of brain tissue by as much as 0.3 units at the prevailing buffering capacity. This finding was anticipated by Chesler and Kraig (1987, 1989) who found that astrocytes become more alkaline when depolarized during brain activation. The change is observed in several kinds of cells in which a rise in pH correlates with an increase in metabolic activity (Kraig, 1990).

7.5.2 Glycolysis During Activation

Increase in ADP concentration and alkalinization of brain tissue by hydrolysis of phosphocreatine both stimulate glycolysis at the PFK step, as in skeletal muscle (Connett, 1987). Thus, increases in the glycolytic rate by as much as 50% were measured during functional activation of human cerebral cortex (Fox et al., 1988; Ginsberg et al. 1988). When maximally stimulated, the rate of pyruvate generation can rise to 3–4 $\mu\text{mol g}^{-1} \text{min}^{-1}$ in rat brain (Robin et al., 1984; Gjedde, 1984), which is close to the calculated T_{max} (see [Box 4](#)) of the mMCT symporter. At these rates of pyruvate generation, the pyruvate concentration rises until the rate of removal by any route matches the generation. The increase benefits the net pyruvate conversion to lactate, as well as its transport into the mitochondrial matrix and export to the circulation. The lower the NAD^+/NADH ratio, and hence the greater the equilibrium lactate/pyruvate ratio, the more slowly this rise occurs.

The failure of the oxygen consumption to increase during simple stimulation is frequently held to confirm that changes of oxidative phosphorylation cannot match the sevenfold increase of pyruvate production seen under the most extreme circumstances of glycolytic stimulation of the mammalian brain (van den Berg and Bruntink, 1983). On the other hand, to increase the flux of pyruvate to mitochondria, cytosolic pyruvate must increase, or mitochondrial pyruvate must decline. Hence, insufficient accumulation of pyruvate due to conversion to lactate may prevent the activation of oxidative phosphorylation and instead stimulate oxidation of NADH to NAD^+ in the cytosol. Connett et al. (1983, 1984) found that the lactate concentration (and hence also pyruvate concentration) in working dog skeletal muscle is directly rather than inversely proportional to the rate of oxygen consumption, as expected if a sufficient pyruvate level is required to sustain a given rate of oxygen consumption.

In the absence of an increase of oxidative phosphorylation, the 50% increase of glucose phosphorylation and corresponding increase of pyruvate generation, listed in ▶ [Table 4.5-7](#), causes the pyruvate and lactate levels to rise in the tissue and in turn the lactate efflux to rise fivefold to 0.35 $\mu\text{mol g}^{-1} \text{min}^{-1}$ and the fraction of nonoxidative metabolism to rise from 10% at the default stage to as much as 40%, although the total ATP flux rises by a mere 5%. It may well be asked why the concentrations must rise if pyruvate is a

substrate of reactions that effectively remove the metabolite as rapidly as it is generated. However, the main transporters and enzymes responsible for the removal of pyruvate all display some saturability in the range of pyruvate concentrations, particularly the LDH isozyme LD5 but also LD1 and the mitochondrial pyruvate transporter mMCT. Saturability in the relevant concentration range means that concentrations must rise for the flux to increase.

When the concentration of pyruvate rises, the lactate concentration continues to rise (with the concentration of pyruvate), until pyruvate's transport into mitochondria by the mMCT and oxidation by the PDH complex, conversion to lactate, and efflux of lactate, match the rate of pyruvate's generation. The speed with which the pyruvate concentration rises depends on the turnover numbers of the enzymes and transporters removing the pyruvate and hence on the affinities of the processes toward pyruvate (see *Box 13*). Paradoxically it is the case that the lower the affinities are, the faster the rise is, other factors being equal (see *Box 4*): Enzymes of high affinity are saturated at comparatively low concentrations of the substrate, at which the flux is fixed. Enzymes of lower affinity, on the other hand, can raise the flux in proportion to the rising concentration of the substrate.

Box 13: Lactate Pool as Function of Pyruvate Flux

The change of the pool size of pyruvate induced by an increase of the rate of glycolysis can be approximated by equations for the tissue contents of pyruvate (M_{pyr}) and lactate (M_{lact}). The equations account for the three pathways available to pyruvate (export from cells, conversion to lactate, and transport into mitochondria) and the two pathways available to lactate (conversion to pyruvate and export from cells). For pyruvate, Gjedde and Marrett (2001) described the increase of pyruvate as,

$$\Delta M_{\text{pyr}}(t) = \frac{1}{(1 + \lambda)k} \Delta J_{\text{pyr}} (1 - e^{-kt}), \quad (22)$$

where λ is the steady-state ratio of the pyruvate and lactate concentrations, ΔJ_{pyr} is the incremental generation of pyruvate, and k is the rate constant of approach to a new steady state, which is a function of the kinetic properties of LDH in the presence of its substrates. The magnitude of the rate constant of approach to a new steady state, k , varies with the isozyme subtype, such that the oxidative heart form LD1 (H4) has the lower affinity (and hence the higher k) and the nonoxidative muscle and liver form LD5 (M4) the higher affinity (and hence the lower k). The magnitude of k differs between the isozymes (0.5 min^{-1} for LD1, 0.07 min^{-1} for LD5) (Gjedde and Marrett 2001). Thus, the isozyme LD1 causes pyruvate to rise quickly for a given increase of glycolysis, while LD5 causes pyruvate to rise more slowly. Essentially, k is proportional to the blood–brain barrier permeability to lactate and the oxidative capacity of the tissue. A value of 0.4 min^{-1} for average cortical tissue indicates that cells with LD1 (neurons) predominate the energy metabolism. The magnitude of λ , the ratio between the lactate and pyruvate concentrations, depends primarily on the NADH/NAD⁺ ratio and the pH but does not affect the velocity of the approach to steady state. Together λ and k determine the magnitude of the coefficient $1/[(1 + \lambda)k]$, which is about 0.1 min for the LDH isozymes in brain tissue at steady state (Gjedde and Marrett, 2001). The change of tissue content of lactate is a function of the effective ratio of the affinities of LDH toward the two substrates (Gjedde and Marrett, 2001)

$$\Delta M_{\text{lact}}(t) = \frac{\lambda}{(1 + \lambda)k} \Delta J_{\text{pyr}} (1 - e^{-kt}), \quad (23)$$

where $\Delta M_{\text{lact}}(t)$ is the accumulated lactate in the tissue. The higher LDH's apparent affinities (i.e., the lower the ratio between the Michaelis constants) are for lactate and pyruvate, the more rapid the approach to a new steady state, with a time constant of $1/k$. Plots of these relationships are shown by Gjedde and Marrett (2001).

Substantial lactate generation reflects the situation in which glutamate is released presynaptically but excitation is subliminal and postsynaptic depolarization is prevented by parallel inhibitory input. Mathiesen et al. (1998) showed that stimulation of cerebellar neurons in some cases led to increased blood flow despite inhibition of postsynaptic spiking activity by prevention of postsynaptic depolarization. Minimal postsynaptic depolarization would have two important consequences: Postsynaptic mitochondrial dehydrogenases would

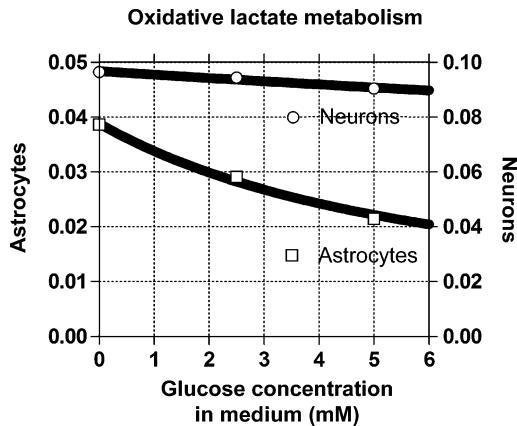
not be activated by calcium, but astrocytes nevertheless would be stimulated to remove glutamate at a rate that exceeds the oxidative capacity of the tissue, and hence to generate lactate.

7.5.3 Reaction Potential Changes During Activation

Transporters and enzymes with different affinities are affected differently when substrates rise in the tissue, because the individual saturabilities vary according to the affinity. The variable saturability of transporters and enzymes in turn influences the pathway preferences of substrates. The sensitivity of lactate's conversion to pyruvate and subsequent oxidation at increasing substrate concentrations was tested *in vitro* by Itoh et al. (2003) who fed different concentrations of ordinary glucose to cultures of astrocytes and neurons and observed the effect on the oxidative metabolism of ^{14}C -labeled lactate. The results of the ability of glucose to inhibit the metabolism of lactate are shown in [Figure 4.5-16](#). The authors found that the lactate generated

Figure 4.5-16

Sensitivity of lactate metabolism by LDH isozymes in neurons and astrocytes to substrate concentration changes *in vitro* (published by Itoh et al. (2003)). Abscissa: Glucose added to medium *in vitro* at the concentrations shown (mM). Ordinates: ^{14}C -labeled lactate oxidation rate *in vitro*, approximated from metabolism measured per mg protein ($\mu\text{mol g}^{-1}\text{min}^{-1}$). The graph shows that astrocytic LDH has 10-fold higher affinity toward the substrate than neuronal LDH. (From Itoh et al. (2003))



from the unlabeled glucose inhibits the LDH reaction in astrocytes (including LD5) much more than the LDH in neurons (LD1). This implies that lactate is more readily converted to pyruvate in neurons than in astrocytes during transient non-steady-states (see *Box 14*).

Estimates of saturability of the main transporters and enzymes of interest to pyruvate and lactate pathways are listed in [Table 4.5-8](#). The table shows that the processes most likely to be inhibited at higher substrate concentrations are MCT2 and mMCT for lactate and LD5 for both pyruvate and lactate. This inhibition is likely to direct elevated lactate toward MCT1 and LD1, a path that keeps lactate in neurons, and to direct pyruvate toward MCT1, MCT2, LD1, and mMCT, a path that leads pyruvate generated in astrocytes toward metabolism in neurons where the density of mMCT is greatest.

7.5.4 Oxidative Phosphorylation During Activation

In contrast to the results of no change of oxygen consumption upon simple primary somatosensory stimulation, both motor stimulation and more complex stimulation of visual cortex with a reversing checkerboard pattern for 5 or 10 min caused significant increases of oxygen consumption (Raichle et al., 1976;

Box 14: Reaction Potential and Transporter and Enzyme Saturability

The inhibition of a transporter or enzyme can be expressed as the relative change of a reaction potential (p_R), which is defined as the velocity/substrate ratio (v/C) (see *Box 4*) of the enzyme or transporter reaction at a given concentration C

$$v/C = p_R(C) = \frac{V_{\max}}{K_M + C} = \frac{V_{\max}/K_M}{1 + \frac{C}{K_M}} = \frac{p_R(0)}{1 + \frac{C}{K_M}}, \quad (24)$$

where v is the reaction velocity, C is a substrate or inhibitor concentration, and K_m is half-saturation or half-inhibition constant (see *Box 4*). The relative decline of the reaction potential is then a measure of the occupancy of the substrate and the saturability of the transporter or enzyme

$$S = \frac{p_R(0) - p_R(C)}{p_R(0)} = \frac{\Delta p_R}{p_R(0)} = \frac{C}{K_m + C}, \quad (25)$$

where S is the substrate's occupancy of the transporter or enzyme.

■ **Table 4.5-8**

Estimated saturability of transporters and enzymes of pyruvate and lactate

	Pyruvate			Lactate		
	K_M (mM)	S		K_M (mM)	S	
		(0.1 mM)	(0.5 mM)		(1 mM)	(5 mM)
MCT1	5	0.02	0.09	5	0.17	0.50
MCT2	1	0.09	0.33	1	0.50	0.83
LD1	0.5	0.17	0.50	5.0	0.17	0.50
mMCT	0.5	0.17	0.50	0.5	0.67	0.91
LD5	0.05	0.67	0.91	0.5	0.67	0.91

Degree of saturation of key transporters and enzymes of pyruvate and lactate calculated from values summarized above (▶ *Sect. 4*) as shown in *Box 14*

Box 15: Oxygen Consumption and Lactate Concentration

If pyruvate transport is rate limiting in activation stages 3 and 4 (Shearman and Halestrap, 1984), the consumption of oxygen must depend on the cytosolic pyruvate concentration and hence on the rate of glycolysis as described by ▶ *Eq. (22)*

$$\Delta J_{O_2}(t) = \frac{[OGI]}{2} \Delta J_{\text{pyr}}(1 - e^{-kt}), \quad (26)$$

where k is the rate constant defined in Eqs. (22) and (23). The relation between the rise of lactate and the rise of oxygen consumption similarly can be derived from the ratio between ▶ *Eqs. (22)* and (26), which eliminates the function of time

$$\Delta J_{O_2}(t) \approx k \frac{[OGI]}{2} \Delta M_{\text{lact}}(t) \quad (27)$$

in which the relationship is seen to depend both on the properties of LDH (k) and on the oxidative capacity (OGI) of the cells in which the change occurs. When other factors are constant, the change of oxygen consumption and lactate accumulation are simply proportional.

Marrett and Gjedde, 1997; Vafaee et al., 1998, 1999; Hoge et al., 1999; Vafaee and Gjedde, 2000; Mintun et al., 2002). (see Box 15).

The relative ATP and lactate changes ($\Delta J_{\text{ATP}} - \Delta J_{\text{lact}}$ ratio), listed in [Table 4.5-7](#), divide the metabolic responses to excitation into glycolytic (“simple”) and oxidative (“complex”) responses, illustrated in [Figure 4.5-11](#), of which the “simple” responses are the primary somatosensory responses and the “complex” responses are the motor and secondary somatosensory responses. The distribution of glycolytic and oxidative capacities among the two cell types suggests that neuronal metabolism is in part responsible for a “red” response ($\text{OGI} \approx 4$), while astrocytes exclusively generate a “white” response ($\text{OGI} \approx 1$).

7.6 Metabolic Compartmentation During Activation

Taken at face value, the findings discussed above indicate activation of at least two different populations of cells, one with a lower oxidative capacity and the other with a higher (see [Sect. 6.2](#)). The slow or absent rise of oxidative metabolism during primary somatosensory stimulation accompanies a slow rise of the pyruvate concentration in the presence of a substantial lactate sink. This behavior is to be expected when the bulk of the acceleration of metabolism occurs in cells of low oxidative capacity. The more substantial rise of oxygen consumption during more complex stimulation is the consequence of activation of cells with a higher oxidative capacity. These two types of responses conveniently fit the properties of the astrocytic and neuronal compartments.

7.6.1 Sites of Cellular Activity During Activation

The cellular and subcellular sites of the increases of glucose and oxygen metabolism accompanying brain activation have been the subjects of much investigation (Rose, 1975; Muir et al., 1986; Bachelard et al., 1991; Poitry-Yamate and Tsacopoulos, 1992; Magistretti et al., 1999). There is evidence that the site of increased glycolysis is the synaptic structures of the neuropil (Eisenberg et al., 1993; Sokoloff et al., 1996; Sokoloff, 1999), including astrocytic endfeet (Kasischke et al., 2004), which is also the predominant location of LDH (Borowsky and Collins, 1989).

Mitochondria, on the other hand, have been observed to be particularly concentrated in the dendritic structures of the neuropil, particularly the proximal dendrites (Ribak, 1981; Wong-Riley 1989; Gonzalez-Lima and Jones, 1994), which stain weakly for HK (Snyder and Wilson, 1983). These observations suggest that the glycolytic and oxidative reactions occur in separate cellular compartments, although the compartmentation is not complete (Aoki et al., 1987).

The removal of glutamate and the consequent hydrolysis and rephosphorylation of ATP in astrocytes must be sufficiently rapid to allow the frequent firing of excitatory neurons believed to underlie the functional integration of neurons in the cerebral cortex (Joliot et al., 1995; Pedroarena and Llinas, 1997). During nonsteady- or otherwise transiently excited states, it is possible that rapid removal of glutamate (Kojima et al., 1999) may stimulate astrocytes to generate pyruvate in excess of the average oxidative capacity and that this may explain how astrocytes react more glycolytically to stimulation than neurons.

Thus, although recent measurements of the relative contributions of oxidative phosphorylation to the energy turnover in neurons and astrocytes show that 15% of the total energy turnover (measured as ATP turnover or oxidative glucose metabolism to CO_2) in brain tissue takes place in astrocytes at normal steady state (Shulman et al., 2004; Hyder et al., 2006), the evidence summarized in [Figure 4.5-11](#) shows that the astrocytes may contribute significantly more to the increase of nonoxidative metabolism, and this is likely to be the case when concomitant excitation of dendritic structures is prevented by parallel inhibition (Gjedde et al., 2002; Lauritzen 2005).

As brain energy metabolism is predominantly oxidative (Hevner et al., 1995), the compartmentation of glycolytic and oxidative metabolism suggests that enhanced oxidative metabolism associated with brain activation occurs predominantly in the proximal dendritic structures of postsynaptic neurons. When there is little increase of the oxidative metabolism, probably because of insufficient calcium ion influx (Lauritzen,

2005), despite increased glutamate release and subsequent uptake of glutamate into astrocytes, the generated lactate is left in the tissue eventually to be metabolized or exported across the blood–brain barrier and removed by the increased blood flow. These hypothetical events are supported by the evidence of positive non-steady-state during many forms of activation, i.e., the accumulation of metabolites in brain tissue consistent with values of OGI, MUR, and MGI below 6 and values of NSI above 0 (see *Box 10*) during activation, followed by values rising toward or exceeding 6 (OGI, MUR, and MGI) and declining toward or falling below 0 (NSI) during recovery from activation. Lactate accumulation in the blood stream adds to this non-steady-state if the activation is accompanied by motor activity and physical exercise. This consideration suggests that the transport of lactate into brain tissue made possible by the emergence of lactate in the circulation is an epiphenomenon rather than a necessity, as the metabolic situation in brain tissue during cerebral activation is characterized by surplus of products of glycolysis rather than shortage. The main reason for this surplus appears to be excess activation of cellular elements of high glycolytic capacity, probably the astrocytes.

This hypothetical situation would explain the low ATP/lactate flux ratio seen when the response to activation is of the “white” (astrocytic) kind, associated with less increase of oxidative metabolism and greater increase of glycolytic metabolism. Conversely, in activations such as the one observed when the visual cortex is stimulated by a complex checkerboard pattern, the energy demand rises greatly but further lactate accumulation is kept at bay by the rise of oxygen consumption. In this case, the ATP/lactate flux ratio is in the high range. The increased oxygen supply explains the increased ATP turnover characteristic of the “red” (dendritic) response of higher oxidative capacity but lower glycolytic capacity.

7.6.2 Cellular Interactions During Activation

The following section is by necessity speculative. The main problem of assessing the distribution of metabolic activities between subpopulations of cells in brain tissue during the transient events of activation occurs because the situation *in vivo* offers a view only of the whole tissue. The distribution must be inferred from the sum of uncertain parts. It helps that some fundamental differences exist among well-defined populations of cells but we cannot be sure that the compartmentation obeys well-defined distinctions between groups of cells when transients evolve spatially as well as temporally. Transient distinctions that transcend cellular definitions include the metabolic differences among distal and proximal dendrites, neuronal cell bodies, axons, and neuronal terminals, as well as the metabolic differences among astrocytic foot processes, cell bodies, and endfeet. Glycolytic and oxidative enzyme densities and activities differ between all of these subdivisions. Thus, it is by no means certain that the coarse grouping of cells into neuronal and astrocytic populations is particularly useful to the evaluation of changes of brain energy turnover during activation. When attempts nonetheless are made to understand how these two kinds of cells react in general it can only be because it is believed that their reactions differ in such major ways that their elucidation imparts novel insights into the regulation of brain function.

One possible model of the interaction between neurons and glial cells during activation of the human cerebral cortex has its origin in the observation that the oxidative and glycolytic capacities differ *in vivo* as presented above, and that the metabolism declines to low levels *in vitro*, as also presented above. The model that derives from these fundamental observations is illustrated in [▶ Figure 4.5-17](#) in which the ranges of oxidative and glycolytic capacities of the two cellular compartments are given for the two extremes of complete rest (stage 1) and complete activation (stage 4), extracted from the sum of the two observed in human cerebral cortex *in vivo* and shown in [▶ Figure 4.5-10](#). Activation of the two cell types between these two extremes results in the metabolic changes summarized in [▶ Figure 4.5-10](#). If it is assumed that the normal (default) condition of stage 3 is characterized by activation close to 50% of the maximum activation, for example by half of the cells in each group being active at all times, or all of the cells being active half of the time, the model predicts the ranges of pyruvate and ATP production rates associated with variable activation from 0% to 100%, as shown in [▶ Figure 4.5-18](#). Depending on the relative activation of the two cell types, the model predicts the changes of lactate production or lactate uptake and the changes of OGI seen during activation of cortical brain tissue.

Figure 4.5-17

Model of ranges of oxidative and glycolytic metabolism in astrocytes (*top boxes*) and neurons (*bottom boxes*) in human cerebral cortex. The illustration shows two sets of cells, one at complete rest (stage 1), the other fully activated (stage 4). The calculation of these end points is based on the observation that the baseline (stage 1) activation is one quarter of the default (stage 3) activation, and the full activation (stage 4) is twice the default (stage 3) activation, and the assumption that the OGI is 6 in the baseline and 5.3 at stage 3. Numbers have units of $\mu\text{mol g}^{-1} \text{min}^{-1}$. Asterisks indicate main control points (HK/PFK in astrocytes, PDH in neurons), conferring specific oxidative and glycolytic capacities on the cell populations when stimulated. In the model, astrocytes and neurons can be differentially stimulated, depending on the degree of dendritic inhibition and activation. Stimulation either increases the number of cells activated or the time in which all cells are activated

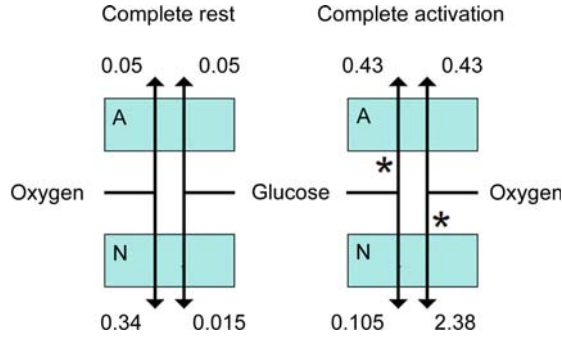


Figure 4.5-18

Rates of pyruvate and ATP generation in astrocytes and neurons, estimated from model shown in Figure 4.5-17. Abscissae: Percentage time or cells associated with activation. Ordinates: ATP and pyruvate fluxes in units of $\mu\text{mol g}^{-1} \text{min}^{-1}$, as functions of the degree of activation. For astrocytes, the lines are given by the equations $J_{\text{pyr}} = 0.105 (1-A) + 0.86 A$ and $J_{\text{ATP}} = 0.40 (1-A) + 3.44 A$ in units of $\mu\text{mol g}^{-1} \text{min}^{-1}$ where A is the fraction of full activation. For the neurons, the lines are given by $J_{\text{pyr}} = 0.03 (1-A) + 0.21 A$ and $J_{\text{ATP}} = 2.07 (1-A) + 14.49 A$, also in units of $\mu\text{mol g}^{-1} \text{min}^{-1}$ where A is again the fraction of full activation. The graph shows how astrocytes generate much pyruvate but little ATP while neurons do the opposite upon stimulation

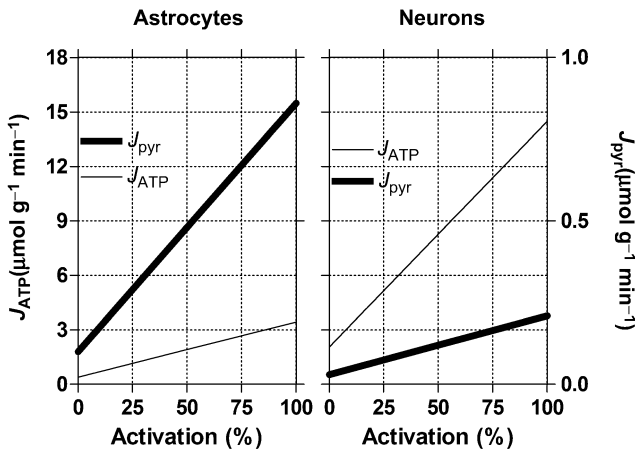
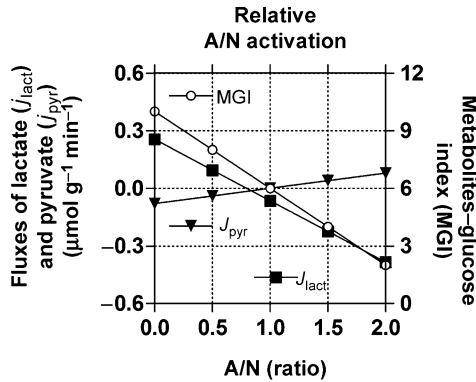


Figure 4.5-19 illustrates the predicted range of relative differential activation of glial cells and neurons, relative to the normal (default) activation of neurons: When astrocytes are more active than

Figure 4.5-19

Metabolites-glucose index (MGI) (see Box 10), available exogenous lactate flux from circulation (J_{lact}) and endogenous pyruvate flux (J_{pyr}) as functions of changing activation of astrocytes relative to neurons. MGI is an index of the ratio of sinks of pyruvate over sources of pyruvate. MGI above 6 signifies insufficient exogenous sources (glucose and lactate in circulation) leading to depletion of endogenous sources of pyruvate (glucose, glycogen, and lactate in brain). Shortage of exogenous sources of pyruvate and resulting depletion of endogenous sources of pyruvate determine the magnitude of MGI when ratio between A and N activation is shifted. If no lactate were available from circulation, MGI would rise to 23 for A/N = 0. Abscissa: Degree of astrocytic activation relative to normal (default) neuronal activation. Left ordinate: Exogenous (lactate) and endogenous (J_{pyr}) sources of pyruvate in units of flux ($\mu\text{mol g}^{-1} \text{min}^{-1}$) as exported from (negative) or imported to (positive) the tissue. Right ordinate: Metabolites-glucose index (MGI) (see Box 10) ratio. Lines are given by $J_{\text{lact}} = 0.255 - 0.32 (A/N)$, $J_{\text{pyr}} = 0.08 A/N$, and $\text{MGI} = 10 - 4 (A/N)$, relative to normal (default) neuronal activity



neurons, the OGI declines and the lactate efflux increases. On the other hand, when neurons are more active than astrocytes, the OGI increases and the lactate efflux decreases or switches to influx of lactate or depletion of glycolytic stores such as glucose, glycogen, or lactate. The evidence from Ide et al. (2000), Dienel and Cruz (2003, 2004) and other recent studies of experimental or physiological activation (Dalsgaard et al., 2004) shows that the MUR and the MGI both decline below 6 during activation, while the opposite changes occur during recovery, leading to non-steady-states of metabolite concentrations during both of these events. Any disruption of the steady-state relationship between the metabolic rates of neurons and astrocytes necessarily induces a shift of metabolites; one possible explanation of this phenomenon is an increase of the activity of astrocytes above that of neurons during the activation itself, with increase of the activity of neurons above that of astrocytes during the subsequent recovery period, possibly because the effects of excitation persist longer in the neurons than in the astrocytes after the termination of the direct activation.

8 Conclusions

Current evidence suggests that there is no rigid association in vivo among changes of oxygen consumption, glucose combustion, and blood flow in the human brain. The claim that increased blood flow must occur simply to satisfy the demands for oxygen and glucose during neuronal excitation therefore is simplistic.

Energy budget estimates indicate that most of the cerebral energy demand reflects the steady-state level of graded postsynaptic membrane depolarization, followed by action potential generation and propagation. Increased energy supply is required to maintain the graded dendritic and somatic depolarization of

neuronal membranes with increased sodium and potassium conductances. Increased energy turnover is not required to sustain hyperpolarization caused by decreased conductance of sodium or increased conductance of potassium or chloride.

Glucose, pyruvate, and lactate occupy single tissue compartments, but transient shifts of the relative activations of neurons and astrocytes may delay the establishment of new steady states. For this reason, it is improbable that the effective properties of the LDH subtypes *in vivo* differ spatially between different populations of cells, except during non-steady-states. Thus, the properties may vary temporally, as dictated by transient shifts of the cytosolic redox potentials and pH values. Excess pyruvate and lactate generation invariably occurs when glutamate release is not followed by sufficient dendritic depolarization, i.e., when astrocytes are activated more than postsynaptic neurons are. In these cases, the increased demand for glutamate imposes a metabolic rate on astroglial cells that exceeds their lower oxidative capacity. Although the resulting pyruvate and lactate accumulation is influenced by lactate export or import across the blood–brain barrier, the pyruvate and lactate thus accumulated may not be needed by the neurons. To this joint pool, astrocytes produce much more pyruvate than neurons. The evidence suggests that the rapid astrocytic (“white”) response reflects postsynaptic depolarization with glutamate release, while the bulk of the neuronal (“red”) response reflects substantial mitochondrial activation of primarily dendritic origin, induced by sufficient influx of calcium ions.

The blood flow increase appears to be coupled to the rate of glycolysis. There is increasing evidence that the putative mechanism underlying such a flow–glycolysis couple is an astrocytic function. The physiological reason for an astrocytically mediated blood flow increase is not very clear, as flow has only a moderate effect on glucose delivery when not accompanied by capillary recruitment, suggesting that increased glycolysis is a signal rather than a direct demand.

The evidence suggests that the increase of oxidative metabolism in neurons is coupled to the rise of pyruvate, as dictated by the prevailing kinetic profile of LDH and the degree of mitochondrial activation. The tissue pyruvate level at which this occurs is under the control of the LDH isozyme profile, and therefore differs for different populations of cells. Under some circumstances, regional “peaks” of increased blood flow and increased oxygen consumption could be dissociated by the differential activation of primary and secondary neuronal networks. The activations accompanying the most complex processing of information could be those with the tightest coupling between oxygen consumption and blood flow and hence with the least generation of lactate.

Acknowledgments

The author wishes to thank the Medical Research Councils of Canada and Denmark and the National Science Foundation of Denmark for support.

References

- Alkire MT, Haier RJ, Barker SJ, Shah NK, Wu JC, et al. 1995. Cerebral metabolism during propofol anesthesia in humans studied with positron emission tomography. *Anesthesiology* 82: 393-403.
- Alkire MT, Haier RJ, Shah NK, Anderson CT 1997. Positron emission tomography study of regional cerebral metabolism in humans during isoflurane anesthesia. *Anesthesiology* 86: 549-557.
- Alkire MT, Pomfrett CJ, Haier RJ, Gianzero MV, Chan CM, et al. 1999. Functional brain imaging during anesthesia in humans: Effects of halothane on global and regional cerebral glucose metabolism. *Anesthesiology* 90: 701-709.
- Alves PM, McKenna MC, Sonnewald U. 1995. Lactate metabolism in mouse brain astrocytes studied by [¹³C]NMR spectroscopy. *Neuroreport* 6: 2201-2204.
- Anderson CM, Swanson RA. 2000. Astrocyte glutamate transport: Review of properties, regulation, and physiological functions. *Glia* 32: 1-14.
- Andriezen WL. 1893. The neuroglia elements in the human brain. *Brit Med J* ii: 227-230.
- Aoki C, Milner TA, Berger SB, Sheu KF, Blass JB, et al. 1987. Glial glutamate dehydrogenase: Ultrastructural localization and regional distribution in relation to the mitochondrial enzyme, cytochrome oxidase. *J Neurosci Res* 18(2): 305-318.

- Attwell D, Gibb A. 2005. Neuroenergetics and the kinetic design of excitatory synapses. *Nat Rev Neurosci* 6: 841-849.
- Attwell D, Iadecola C. 2002. The neural basis of functional brain imaging signals. *Trends Neurosci* 25: 621-625.
- Attwell D, Laughlin SB. 2001. An energy budget for signaling in the grey matter of the brain. *J Cereb Blood Flow Metab* 21: 1133-1145.
- Ayata C, Ma J, Meng W, Huang P, Moskowitz MA. 1996. L-NA-sensitive rCBF augmentation during vibrissal stimulation in type III nitric oxide synthase mutant mice. *J Cereb Blood Flow Metab* 16: 539-541.
- Bachelard HS, Brooks KJ, Garofalo O. 1991. Studies on the compartmentation of DOG metabolism in the brain. *Neurochem Res* 16: 1025-1030.
- Baker PF, Connelly CM. 1966. Some properties of the external activation site of the sodium pump in crab nerve. *J Physiol (Lond)* 185: 270-297.
- Balaban RS, Kantor HL, Katz LA, Briggs RW. 1986. Relation between work and phosphate metabolites in the in vivo paced mammalian heart. *Science* 232: 1121-1123.
- Bergersen LH, Magistretti PJ, Pellerin L. 2005. Selective post-synaptic colocalization of MCT2 with AMPA receptor GluR2/3 subunits at excitatory synapses exhibiting AMPA receptor trafficking. *Cereb Cortex* 15: 361-370.
- Bittar PG, Charnay Y, Pellerin L, Bouras C, Magistretti PJ. 1996. Selective distribution of lactate dehydrogenase isoenzymes in neurons and astrocytes of human brain. *J Cereb Blood Flow Metab* 16: 1079-1089.
- Borowsky IW, Collins RC. 1989. Metabolic anatomy of brain: A comparison of regional capillary density, glucose metabolism, and enzyme activities. *J Comp Neurol* 288: 401-413.
- Bowers C, Zigmond R. 1979. Localization of neurons in the rat superior cervical ganglion that project into different postganglionic trunks. *J Comp Neurol* 185: 381-391.
- Brandt RB, Laux JE, Spainhour SE, Kline ES. 1987. Lactate dehydrogenase in rat mitochondria. *Arch Biochem Biophys* 259: 412-422.
- Brightman MW, Reese TS. 1969. Junctions between intimately apposed cell membranes in the vertebrate brain. *J Cell Biol* 40: 648-677.
- Brodersen P, Jørgensen EO. 1974. Cerebral blood flow and oxygen uptake, and cerebrospinal fluid biochemistry in severe coma. *J Neurol Neurosurg Psychiatry* 37: 384-391.
- Broer S, Rahman B, Pellegrini G, Pellerin L, Martin JL, et al. 1997. Comparison of lactate transport in astroglial cells and monocarboxylate transporter 1 (MCT 1) expressing *Xenopus laevis* oocytes. Expression of two different monocarboxylate transporters in astroglial cells and neurons. *J Biol Chem* 272: 30096-30102.
- Brooks GA, Brown MA, Butz CE, Sicurello JP, Dubouchaud H. 1999a. Cardiac and skeletal muscle mitochondria have a monocarboxylate transporter MCT1. *Appl Physiol* 87: 1713-1718.
- Brooks GA, Dubouchaud H, Brown M, Sicurello JP, Butz CE. 1999b. Role of mitochondrial lactate dehydrogenase and lactate oxidation in the intracellular lactate shuttle. *Proc Natl Acad Sci USA* 96: 1129-1134.
- Brown GC. 2001. Regulation of mitochondrial respiration by nitric oxide inhibition of cytochrome c oxidase. *Biochem Biophys Acta Mar* 1; 1504(1): 46-57. Review.
- Buxton R, Frank R. 1997. A model for the coupling between cerebral blood flow and oxygen consumption during neuronal stimulation. *J Cereb Blood Flow Metab* 17: 64-72.
- Caesar K, Akgoren N, Mathiesen C, Lauritzen M. 1999. Modification of activity-dependent increases in cerebellar blood flow by extracellular potassium in anaesthetized rats. *J Physiol (Lond)* 520: 281-292.
- Chesler M, Kraig RP. 1987. Intracellular pH of astrocytes increases rapidly with cortical stimulation. *Am J Physiol* 253: R666-R670.
- Chesler M, Kraig RP. 1989. Intracellular pH transients of mammalian astrocytes. *J Neurosci* 9: 2011-2019.
- Choi IY, Lei H, Gruetter R. 2002. Effect of deep pentobarbital anesthesia on neurotransmitter metabolism in vivo: On the correlation of total glucose consumption with glutamatergic action. *J Cereb Blood Flow Metab* 22: 1343-1351.
- Cholet N, Seylaz J, Lacombe P, Bonvento G. 1997. Local uncoupling of the cerebrovascular and metabolic responses to somatosensory stimulation after neuronal nitric oxide synthase inhibition. *J Cereb Blood Flow Metab* 17: 1191-1201.
- Clapham DE. 1995. Calcium signalling. *Cell* 80: 259-268.
- Connett RJ. 1987. Glycolytic regulation during aerobic rest-to-work transition in dog gracilis muscle. *J Appl Physiol* 63: 2366-2374.
- Connett RJ, Gayeski TE, Honig CR. 1983. Lactate production in a pure red muscle in absence of anoxia: Mechanisms and significance. *Adv Exp Med Biol* 159: 327-335.
- Connett RJ, Gayeski TE, Honig CR. 1984. Lactate accumulation in fully aerobic, working dog gracilis muscle. *Am J Physiol* 246: H120-H128.
- Connett RJ, Gayeski TE, Honig CR. 1985. Energy sources in fully aerobic rest-work transitions: A new role for glycolysis. *Am J Physiol* 248: H922-H929.
- Cremer JE. 1976. The influence of liver bypass on transport and compartmentation in vivo. *Adv Exp Med Biol* 69: 95-102.
- Cremer JE, Cunningham VJ, Pardridge WM, Braun LD, Oldendorf WH. 1979. Kinetics of blood-brain barrier transport of pyruvate, lactate, and glucose in suckling, weanling, and adult rats. *J Neurochem* 33: 439-446.
- Dalsgaard MK, Volianitis S, Yoshiga CC, Dawson EA, Secher NH. 2004. Cerebral metabolism during upper and lower body exercise. *J Appl Physiol Nov*; 97(5): 1733-9.

- de Graaf RA, Mason GF, Patel AB, Rothman DL, Behar KL. 2004. Regional glucose metabolism and glutamatergic neurotransmission in rat brain in vivo. *Proc Natl Acad Sci USA* 101: 12700-12705.
- Denton RM, McCormack JG. 1985. Ca transport by mammalian mitochondria and its role in hormone action. *Am J Physiol* 249: E543-E554.
- Desagher S, Glowinski J, Premont JJ. 1997. Pyruvate protects neurons against hydrogen peroxide-induced toxicity. *Neuroscience* 17: 9060-9067.
- Detre JA, Koretsky AP, Williams DS, Ho C. 1990a. Absence of pH changes during altered work in the in vivo sheep heart: A ³¹P-NMR investigation. *J Mol Cell Cardiol*. 22: 543-53
- Detre JA, Williams DS, Koretsky AP. 1990b. Nuclear magnetic resonance determination of flow, lactate, and phosphate metabolites during amphetamine stimulation of the rat brain. *NMR Biomed* 3: 272-278.
- Diemer NH, Benveniste H, Gjedde A. 1985. In vivo cell membrane permeability to deoxyglucose in rat brain. *Acta Neurol Scand* 72: 87.
- Dienel GA, Cruz NF. 2003. Neighborly interactions of metabolically activated astrocytes in vivo. *Neurochem Int* 43: 339-354.
- Dienel GA, Cruz NF. 2004. Nutrition during brain activation: Does cell-to-cell lactate shuttling contribute significantly to sweet and sour food for thought? *Neurochem Int* 45: 321-351.
- Dienel GA, Cruz NF. 2006. Astrocyte activation in working brain: Energy supplied by minor substrates. *Neurochem Int* 48: 586-595.
- Drewes L. 1999. Transport of brain fuels, glucose, and lactate. In: Paulson OB, Knudsen GM, Moos T, editors. *Brain Barrier Systems, Alfred Benzon Symposium 45*, Munksgaard, Copenhagen; pp. 285-295.
- Drewes LR. 2002. Molecular architecture of the brain microvasculature: Perspective on blood-brain transport. *J Mol Neurosci* 16: 93-98.
- Duling BR, Berne RM. 1970. Longitudinal gradients in periarteriolar oxygen tension. A possible mechanism for the participation of oxygen in local regulation of blood flow. *Circ Res* 27(5): 669-678.
- Elhousseiny A, Cohen Z, Olivier A, Stanimirovic DB, Hamel E. 1999. Functional acetylcholine muscarinic receptor subtypes in human brain microcirculation: Identification and cellular localization. *J Cereb Blood Flow Metab* 19: 794-802.
- Elhousseiny A, Hamel E. 2000. Muscarinic—but not nicotinic—acetylcholine receptors mediate a nitric oxide-dependent dilation in brain cortical arterioles: A possible role for the M₅ receptor subtype. *J Cereb Blood Flow Metab* 20: 298-305.
- Eisenberg HM, Kadekaro M, Freeman S, Terrell ML. 1993. Metabolism in the globus pallidus after fetal implants in rats with nigral lesions. *J Neurosurg* 78: 83-89.
- Erecinska M, Veech RL, Wilson DF. 1974. Thermodynamic relationships between the oxidation-reduction reactions and the ATP synthesis in suspensions of isolated pigeon heart mitochondria. *Arch Biochem Biophys* 160: 412-421.
- Erecinska M, Wilson DF. 1982. Regulation of cellular energy metabolism. *J Membr Biol* 70: 1-14.
- Erecinska M, Silver I. 1989. ATP and brain function. *J Cereb Blood Flow Metab* 9: 2-19.
- Erecinska M, Nelson D, Chance B. 1991. Depolarization-induced changes in cellular energy production. *Proc Natl Acad Sci USA* 88: 7600-7604.
- Eriksson G, Peterson A, Iverfeldt K, Walum E. 1995. Sodium-dependent glutamate uptake as an activator of oxidative metabolism in primary astrocyte cultures from newborn rat. *Glia* 15: 152-156.
- Fabricius M, Lauritzen M. 1994. Examination of the role of nitric oxide for the hypercapnic rise of cerebral blood flow in rats. *Am J Physiol* 266: H1457-1464.
- Fedosov SN. 1994. Creatine-creatine phosphate shuttle modeled as two-compartment system at different levels of creatine kinase activity. *Biochim Biophys Acta* 1208: 238-246.
- Fodor JA. 1983. *The modularity of mind*. Cambridge: The MIT Press.
- Fodor JA. 2000. *The mind doesn't work that way*. Cambridge: The MIT Press.
- Fox PT, Raichle ME. 1986. Focal physiological uncoupling of cerebral blood flow and oxidative metabolism during somatosensory stimulation in human subjects. *Proc Natl Acad Sci USA* 83: 1140-1144.
- Fox PT, Raichle ME, Mintun MA, Dence CE. 1988. Nonoxidative glucose consumption during focal physiological activity. *Science* 241: 462-464.
- Fujita H, Kuwabara H, Reutens DC, Gjedde A. 1999. Oxygen consumption of cerebral cortex fails to increase during continued vibrotactile stimulation. *J Cereb Blood Flow Metab* 19: 266-271.
- Gebremedhin D, Yamaura K, Zhang C, Bylund J, Koehler RC, et al. 2003. Metabotropic glutamate receptor activation enhances the activities of two types of Ca²⁺-activated K⁺ channels in rat hippocampal astrocytes. *J Neurosci* 23: 1678-1687.
- Gerhart DZ, Enerson BE, Zhbankina OY, Leino RL, Drewes LR. 1997. Expression of monocarboxylate transporter MCT1 by brain endothelium and glia in adult and suckling rats. *Am J Physiol* 273: E207-E213.
- Gerhart DZ, Enerson BE, Zhbankina OY, Leino RL, Drewes LR. 1998. Expression of the monocarboxylate transporter MCT2 by rat brain glia. *Glia* 22: 272-281.

- Gibbs EL, Lennox WG, Nims LF, Gibbs FA. 1942. Arterial and cerebral venous blood: Arterial-venous differences in man. *J Biol Chem* 144: 325-332.
- Ginsberg MD, Chang JY, Kelley RE, Yoshii F, Barker WW, et al. 1988. Increases in both cerebral glucose utilization and blood flow during execution of a somatosensory task. *Ann Neurol* 23: 152-160.
- Gjedde A. 1983. Modulation of substrate transport to the brain. *Acta Neurol Scand* 67: 3-25.
- Gjedde A. 1984. On the measurement of glucose in brain. *Neurochem Res* 9: 1667-1671.
- Gjedde A, Kuwabara H, Hakim AM. 1990. Reduction of functional capillary density in human brain after stroke. *J Cereb Blood Flow Metab* 10(3): 317-26.
- Gjedde A. 1992. Blood-brain glucose transfer. *Physiology and Pharmacology of the Blood-Brain Barrier*, Chapter 6a: *Handbook of Experimental Pharmacology*. Bradbury, editor. MWB Springer-Verlag, Berlin Heidelberg 1992; pp. 65-115.
- Gjedde A. 1993a. The energy cost of neuronal depolarization. Gulyas B, Ottoson D, Roland PE, editors. *Functional Organization of the Human Visual Cortex*. Pergamon Press; Oxford: pp. 291-306.
- Gjedde A. 1993b. Interpreting physiology maps of the living human brain. Uemura K, Lassen NA, Jones T, Kanno I, editors. *Quantification of Brain Function. Tracer Kinetics and Image Analysis in Brain PET*. Elsevier; Amsterdam: pp. 187-196.
- Gjedde A. 1996. PET criteria of cerebral tissue viability in ischemia. *Acta Neurol Scand (Suppl)* 166: 3-5.
- Gjedde A. 1997. The relation between brain function and cerebral blood flow and metabolism. Batjer HH, editor. *Cerebrovascular Disease*. Lippincott-Raven; New York: pp. 23-40.
- Gjedde A. 2001. Brain energy metabolism and the physiological basis of the hemodynamic response. In: Jezzard P, Matthews PM, Smith S, editors. *Functional Magnetic Resonance Imaging: Methods for Neuroscience*. Oxford University Press; Oxford: pp. 37-65.
- Gjedde A. 2005. Blood-brain transfer and metabolism of oxygen. *Blood-Brain Barriers*, Dermietzel R, Spray DC, Nedergaard M, editors. New York: Wiley-VCHO, vol. 2, chapter 22, pp. 523-549.
- Gjedde A, Marrett S. 2001. Glycolysis in neurons, not astrocytes, delays oxidative metabolism of human visual cortex during sustained checkerboard stimulation in vivo. *J Cereb Blood Flow Metab* 21: 1384-1392.
- Gjedde A, Kuwabara H, Hakim A. 1990. Reduction of functional capillary density in human brain after stroke. *J Cereb Blood Flow Metab* 10: 317-316.
- Gjedde A, Johannsen P, Cold GE, Ostergaard L. 2005. Cerebral metabolic response to low blood flow: Possible role of cytochrome oxidase inhibition. *J Cereb Blood Flow Metab* 25: 1183-1196.
- Gjedde A, Marrett S, Vafaee M. 2002. Oxidative and nonoxidative metabolism of excited neurons and astrocytes. *J Cereb Blood Flow Metab* 22:1-14. Review.
- Gjedde A, Ohta S, Kuwabara H, Meyer E. 1991. Is oxygen diffusion limiting for blood-brain transfer of oxygen? *Brain Work and Mental Activity*. Lassen NA, Ingvar DH, Raichle ME, Friberg L, editors. *Alfred Benzon Symposium 31*, Munksgaard, Copenhagen; pp. 177-184.
- Gjedde A, Poulsen PH, Østergaard L. 1999. On the oxygenation of hemoglobin in the human brain. *Adv Exp Med Biol* 471: 67-81.
- Gnaiger E. 1993. Homeostatic and microoxic regulation of respiration in transitions to anaerobic metabolism. Bicudo JEPW, editor. *The Vertebrate Gas Transport Cascade: Adaptations to Environment and Mode of Life*. CRC Press; Boca Raton: pp 358-370.
- Gnaiger E, Steinlechner-Maran R, Mendez G, Eberl T, Margreiter R. 1995. Control of mitochondrial and cellular respiration by oxygen. *J Bioenerg Biomembr* 27: 583-596.
- Gnaiger E, Lassnig B, Kuznetsov A, Rieger G, Margreiter R. 1998. Mitochondrial oxygen affinity, respiratory flux control, and excess capacity of cytochrome *c* oxidase. *J Exp Biol* 201: 1129-39.
- Goldman DE. 1943. Potential, impedance, and rectification in membranes. *J Gen Physiol* 27: 37-60.
- Gonzalez-Lima F, Jones D. 1994. Quantitative mapping of cytochrome oxidase activity in the central auditory system of the gerbil: A study with calibrated activity standards and metal-intensified histochemistry. *Brain Res* 660: 34-49.
- Halestrap AP. 1975. The mitochondrial pyruvate carrier. *Biochem J* 148: 85-96.
- Halestrap AP. 1978. Stimulation of pyruvate transport in metabolizing mitochondria through changes in the transmembrane pH gradient induced by glucagon treatment of rat. *Biochem J* 172: 389-398.
- Halestrap AP, Armston AE. 1984. A reevaluation of the role of mitochondrial pyruvate transport in the hormonal control of rat liver mitochondrial pyruvate metabolism. *Biochem J* 223: 677-685.
- Halestrap AP, Price NT. 1999. The proton-linked monocarboxylate transporter (MCT) family: Structure, function, and regulation. *Biochem J* 343: 281-299.
- Hassel B, Bråthe A. 2000. Cerebral metabolism of lactate in vivo: Evidence for neuronal pyruvate carboxylation. *J Cereb Blood Flow Metab* 20: 327-336.
- Henry PG, Lebon V, Vaufray F, Brouillet E, Hantraye P, et al. 2002. Decreased TCA cycle rate in the rat brain after acute 3-NP treatment measured by in vivo ^1H - ^{13}C NMR spectroscopy. *J Neurochem* 82: 857-866.

- Hertz L, Schousboe A. 1975. Ion and energy metabolism of the brain at the cellular level. *Int Rev Neurobiol* 18: 141-211.
- Hertz L, Swanson RA, Newman GC, Marrif H, Juurlink BH, et al. 1998. Can experimental conditions explain the discrepancy over glutamate stimulation of aerobic glycolysis? *Dev Neurosci* 20: 339-347.
- Hevner RF, Liu S, Wong-Riley MT. 1995. A metabolic map of cytochrome oxidase in the rat brain: Histochemical, densitometric, and biochemical studies. *Neuroscience* 65: 313-342.
- Hill AV. 1910. The possible effect of aggregation of the molecules of haemoglobin on its dissociation curve. *J Physiol* 40: iv-vii.
- Hill AV. 1913. The combination of haemoglobin with oxygen and with carbon monoxide. *Biochem J* 7: 471-480.
- Himwich HE, Fazekas JF. 1937. Effect of hypoglycemia on metabolism of brain. *Endocrinology* 21: 800-807.
- Himwich WA, Himwich HE. 1946. Pyruvic acid exchange of brain. *J Neurophysiol* 9: 133-136.
- Hodgkin AL, Katz B. 1949. The effect of sodium ions on the electrical activity of the giant axon of the squid. *J Physiol (Lond)* 108: 37-77.
- Hodgkin AL, Huxley 1952. A quantitative description of membrane current and its application to conductance and excitation in nerve. *J Physiol (Lond)* 117: 500-544.
- Hodgkin AL, Keynes RD. 1956. Experiments on the injection of substances into squid giant axons by means of a microsyringe. *J Physiol (Lond)* 131: 592-616.
- Hoge RD, Atkinson J, Gill B, Crelier GR, Marrett S, Pike GB. 1999. Linear coupling between cerebral blood flow and oxygen consumption in activated human cortex. *Proc Natl Acad Sci USA* Aug 3; 96(16): 9403-8.
- Honig CR, Connert RJ, Gayeski TE. 1992. O₂ transport and its interaction with metabolism; a systems view of aerobic capacity. *Med Sci Sports Exercise* 24: 47-53.
- Hyder F, Patel AB, Gjedde A, Rothman DL, Gehar KL, et al. 2006. Neuronal-glia glucose oxidation and glutamatergic-GABAergic function. *J Cereb Blood Flow Metab* 26: 865-877.
- Iadecola C. 1992. Does nitric oxide mediate the increases in cerebral blood flow elicited by hypercapnia? *Proc Natl Acad Sci USA* 89: 3913-3916.
- Iadecola C, Pelligrino DA, Moskowitz MA, Lassen NA. 1994. Nitric oxide synthase inhibition and cerebrovascular regulation. *J Cereb Blood Flow Metab* 14: 175-192.
- Iadecola C. 2004. Neurovascular regulation in the normal brain and in Alzheimer's disease. *Nat Rev Neurosci* 5: 347-360.
- Ide K, Schmalbruch IK, Quistorff B, Horn A, Secher NH. 2000. Lactate, glucose, and O₂ uptake in human brain during recovery from maximal exercise. *J Physiol* 522: 159-164.
- Iida H, Jones T, Miura S. 1993. Modeling approach to eliminate the need to separate arterial plasma in oxygen-15 inhalation positron emission tomography. *J Nucl Med* Aug; 34(8): 1333-40.
- Itoh Y, Esaki T, Shimoji K, Cook M, Law MJ, et al. 2003. Dichloroacetate effects on glucose and lactate oxidation by neurons and astroglia in vitro and on glucose utilization by brain in vivo. *Proc Natl Acad Sci USA* 100: 4879-4884.
- Joliot M, Ribary U, Llinas R. 1995. Human oscillatory brain activity near 40 Hz coexists with cognitive temporal binding. *Proc Natl Acad Sci USA* 91: 11748-11751.
- Kadekaro M, Crane AM, Sokoloff L. 1985. Differential effects of electrical stimulation of sciatic nerve on metabolic activity in spinal cord and dorsal root ganglion in the rat. *Proc Natl Acad Sci USA* 82: 6010-6013.
- Kaplan NO, Everse J. 1972. Regulatory characteristics of lactate dehydrogenases. *Adv Enzyme Regul* 10: 323-336.
- Kasischke KA, Vishwasrao HD, Fisher PJ, Zipfel WR, Webb WW. 2004. Neural activity triggers neuronal oxidative metabolism followed by astrocytic glycolysis. *Science* 305: 99-103.
- Kassissia IG, Goresky CA, Rose CP, Schwab AJ, Simard A, et al. 1995. Tracer oxygen distribution is barrier-limited in the cerebral microcirculation. *Circ Res* 77: 1201-1211.
- Katayama Y, Tsubokawa T, Hirayama T, Kido G, Tsukiyama T, et al. 1986. Response of regional cerebral blood flow and oxygen metabolism to thalamic stimulation in humans as revealed by positron emission tomography. *J Cereb Blood Flow Metab* 6: 637-634.
- Katayama Y, Fukuchi T, Mc Kee A, Terashi A. 1998. Effect of hyperglycemia on pyruvate dehydrogenase activity and energy metabolites during ischemia and reperfusion in gerbil brain. *Brain Res* 788: 302-304.
- Kety SS. 1949. The physiology of the human cerebral circulation. *Anesthesiology* 10: 610-614.
- Kojima S, Nakamura T, Nidaira T, Nakamura K, Ooashi N, et al. 1999. Optical detection of synaptically induced glutamate transport in hippocampal slices. *J Neurosci* 19: 2580-2588.
- Kraig RP. 1990. Astrocytic acid-base homeostasis in cerebral ischemia. *Cerebral Ischemia and Resuscitation*. Schurr A, Rigor BM, editors. Boca Raton: CRC Press, pp. 89-99.
- Kuschinsky W, Paulson OB. 1992. Capillary circulation in the brain. *Cerebrovasc Brain Met* 4: 261-286.
- Kuwabara H, Ohta S, Brust P, Meyer E, Gjedde A. 1992. Density of perfused capillaries in living human brain during functional activation. *Prog Brain Res* 91: 209-215.
- Kwong KK, Belliveau JW, Chesler DA, Goldberg IE, Weisskoff RM, et al. 1992. Dynamic magnetic resonance imaging of human brain activity during primary sensory stimulation. *Proc Natl Acad Sci USA* 5675-5679.

- La Noue KF, Schoolwerth AC. 1979. Metabolite transport in mitochondria. *Ann Rev Biochem* 48: 871-922.
- La Noue KF, Jeffries FM, Radda GK. 1986. Kinetic control of mitochondrial ATP synthesis. *Biochemistry* 25: 7667-7675.
- Laptook AR, Peterson J, Porter AM. 1988. Effects of lactic acid infusions and pH on cerebral blood flow and metabolism. *J Cereb Blood Flow Metab* 8: 193-200.
- Lassen NA. 1959. Cerebral blood flow and oxygen consumption in man. *Physiol Rev* 39: 183-238.
- Laughton JD, Charnay Y, Belloir B, Pellerin L, Magistretti PJ, et al. 2000. Differential messenger RNA distribution of lactate dehydrogenase LDH-1 and LDH-5 isoforms in the rat brain. *Neuroscience* 96: 619-625.
- Lauritzen M. 2005. Reading vascular changes in brain imaging: Is dendritic calcium the key? *Nat Rev Neurosci* 6: 77-85.
- Levy DE, Sidtis JJ, Rottenberg DA, Jarden JO, Strother SC, et al. 1987. Differences in cerebral blood flow and glucose utilization in vegetative versus locked-in patients. *Ann Neurol* 22: 673-682.
- Liao SL, Chen CJ. 2003. L-glutamate decreases glucose utilization by rat cortical astrocytes. *Neurosci Lett* 348: 81-84.
- Lindauer U, Megow D, Matsuda H, Dirnagl U. 1999. Nitric oxide: A modulator, but not a mediator, of neurovascular coupling in rat somatosensory cortex. *Am J Physiol* 277: H799-H811.
- Ma J, Ayata C, Huang PL, Fishman MC, Moskowitz MA. 1996. Regional cerebral blood flow response to vibrissal stimulation in mice lacking type I NOS gene expression. *Am J Physiol* 270: H1085-H1090.
- Magistretti PJ, Cardinaux JR, Martin JL. 1998. VIP and PACAP in the CNS: Regulators of glial energy metabolism and modulators of glutamatergic signaling. *Ann N Y Acad Sci* Dec 11; 865:213-25. Review.
- Magistretti PJ, Pellerin L, Rothman DL, Shulman RG. 1999. Energy on demand. *Science* 283: 496-497.
- Marrett S, Gjedde A. 1997. Changes of blood flow and oxygen consumption in visual cortex of living humans. *Adv Exp Med Biol* 413: 205-208.
- Mata M, Fink DG, Gainer H, Smith CB, Davidsen L, et al. 1980. Activity-dependent energy metabolism in rat posterior pituitary primarily reflects sodium pump activity. *J Neurochem* 34: 213-215.
- Mathiesen C, Caesar K, Akgoren N, Lauritzen M. 1998. Modification of activity-dependent increases of cerebral blood flow by excitatory synaptic activity and spikes in rat cerebellar cortex. *J Physiol (Lond)* 512: 555-566.
- Matthews PM, Bland JL, Gadian DG, Radda GK. 1981. The steady-state rate of ATP synthesis in the perfused rat heart measured by ^{31}P NMR saturation transfer. *Biochem Biophys Res Commun* 103: 1052-1059.
- McCormick DA. 1990. Membrane properties and neurotransmitter actions. *The Synaptic Organization of the Brain*, 3rd Ed. Shepherd G, editor Oxford University Press, New York, pp. 32-66.
- McCully KK, Kakihiira H, van den Borne K, Kent-Braun J. 1991. Noninvasive measurements of activity-induced changes in muscle metabolism. *J Biomech* 24: (Suppl 1): 153-161.
- McIlwain H. 1951. Metabolic response in vitro to electrical stimulation of section. *Biochem J* 49: 382-393.
- Michaelis L, Menten ML. 1913. Zur Kinetik der Invertinwirkung. *Biochem Z* 49: 333-369.
- Mintun MA, Vlassenko AG, Shulman GL, Snyder AZ. 2002. Time-related increase of oxygen utilization in continuously activated human visual cortex. *Neuroimage Jun*; 16(2): 531-7.
- Mora BN, Narasimhan PT, Ross BD. 1992. ^{31}P magnetization transfer studies in the monkey brain. *Magn Reson Med* 26: 100-115.
- Morowitz HJ. 1978. *Foundations of Bioenergetics*. New York: Academic Press.
- Muir D, Berl S, Clarke DD. 1986. Acetate and fluoroacetate as possible markers for glial metabolism in vivo. *Brain Res* 380: 336-340.
- Mulligan SJ, Mac Vicar BA. 2004. Calcium transients in astrocyte endfeet cause cerebrovascular constrictions. *Nature* 431: 195-199.
- Nalecz KA, Kaminska J, Nalecz MJ, Azzi A. 1992. The activity of pyruvate carrier in a reconstituted system: Substrate specificity and inhibitor sensitivity. *Arch Biochem Biophys* 297: 162-168.
- Nehlig A, Wittendorp-Rechenmann E, Lam CD. Selective uptake of [^{14}C]2-deoxyglucose by neurons and astrocytes: High-resolution microautoradiographic imaging by cellular ^{14}C -trajectography combined with immunohistochemistry. *J Cereb Blood Flow Metab* 24(9):1004-1014.
- Newsholme EA, Crabtree B. 1979. Theoretical principles in the approaches to control of metabolic pathways and their application to glycolysis in muscle. *J Mol Cell Cardiol* 11: 839-856.
- Norenberg MD. 1994. Astrocyte responses to CNS injury. *J Neuropathol Exp Neurol May*; 53(3):213-20. Review.
- Ogawa M, Magata Y, Ouchi Y, Fukuyama H, Yamauchi H, et al. 1994. Scopolamine abolishes cerebral blood flow response to somatosensory stimulation in anesthetized cats: PET study. *Brain Res* 650: 249-252.
- Ogawa S, Lee TM, Nayak AS, et al. 1990a. Oxygenation-sensitive contrast in magnetic resonance imaging of rodent brain at high magnetic fields. *Magn Reson Med* 14: 68-78.
- Ogawa S, Lee TM, Kay AR, Tank DW. 1990b. Brain magnetic resonance imaging with contrast dependent on blood oxygenation. *Proc Natl Acad Sci USA* 87: 9868-9872.
- Ogawa S, Menon RS, Tank DW, Kim SG, Merkle H, et al. 1993. Functional brain mapping by blood oxygenation

- level-dependent contrast magnetic resonance imaging. A comparison of signal characteristics with a biophysical model. *Biophys-J* 64: 803-812.
- Ohira Y, Tabata I. 1992. Muscle metabolism during exercise: Anaerobic threshold does not exist. *Ann Physiol Anthropol* 11: 319-323.
- Ohta S, Meyer E, Gjedde A. 1996. Cerebral [¹⁵O]water clearance in humans determined by PET. I. Theory and normal values. *J Cereb Blood Flow Metab* 16: 765-780.
- Ohta S, Reutens DC, Gjedde A. 1999. Brief vibrotactile stimulation does not increase cortical oxygen consumption when measured by single inhalation of positron emitting oxygen. *J Cereb Blood Flow Metab* 19: 260-265.
- Oldendorf WH. 1973. Carrier-mediated blood-brain barrier transport of short-chain monocarboxylic organic acids. *Am J Physiol* 224: 1450-1453.
- Olesen J. 1970. Total CO₂, lactate, and pyruvate in brain biopsies taken after freezing the tissue in situ. *Acta Neurol Scand* 46: 141-148.
- Oz G, Berkich DA, Henry PG, Xu Y, La Noue K, et al. 2004. Neuroglial metabolism in the awake rat brain: CO₂ fixation increases with brain activity. *J Neurosci*. 24: 11273-11279.
- Patel AB, de Graaf RA, Mason GF, Kanamatsu T, Rothman DL, et al. 2004. Glutamatergic neurotransmission and neuronal glucose oxidation are coupled during intense neuronal activation. *J Cereb Blood Flow Metab*. 24: 972-985.
- Pardridge WM. 1981. Transport of nutrients and hormones through the blood-brain barrier. *Diabetologia* 20: 246-254.
- Paulson OB, Newman EA. 1987. Does the release of potassium from astrocyte endfeet regulate cerebral blood flow? *Science* 237: 896-898.
- Pedroarena C, Llinas R. 1997. Dendritic calcium conductances generate high-frequency oscillation in thalamocortical neurons. *Proc Natl Acad Sci USA* 94: 724-728.
- Pellerin L, Magistretti PJ. 1994. Glutamate uptake into astrocytes stimulates aerobic glycolysis: A mechanism coupling neuronal activity to glucose utilization. *Proc Natl Acad Sci USA* 91: 10625-10629.
- Peng L, Swanson RA, Hertz L. 2001. Effects of L-glutamate, D-aspartate, and monensin on glycolytic and oxidative glucose metabolism in mouse astrocyte cultures: Further evidence that glutamate uptake is metabolically driven by oxidative metabolism. *Neurochem Int* 38: 437-443.
- Pette D. 1985. Metabolic heterogeneity of muscle fibres. *J Exp Biol* 115: 179-189.
- Pierre K, Pellerin L. 2005. Monocarboxylate transporters in the central nervous system: Distribution, regulation, and function. *J Neurochem*. 94: 1-14.
- Poitry-Yamate CL, Tsacopoulos M. 1992. Glucose metabolism in freshly isolated Muller glial cells from a mammalian retina. *J Comp Neurol* 320: 257-266.
- Poitry-Yamate CL, Poitry S, Tsacopoulos M. 1995. Lactate released by Muller glial cells is metabolized by photoreceptors from mammalian retina. *J Neurosci*. 15: 5179-5191.
- Poole RC, Halestrap AP. 1993. Transport of lactate and other monocarboxylates across mammalian plasma membranes. *Am J Physiol* 264: C761-C782.
- Prichard J, Rothman D, Novotny E, Petroff O, Kuwabara T, et al. 1991. Lactate rise detected by ¹H NMR in human visual cortex during physiological stimulation. *Proc Natl Acad Sci USA* 88: 5829-5831.
- ME; Pullman HS; Penefsky Datta A; Racker E. 1960. Partial resolution of the enzymes catalyzing oxidative phosphorylation. I. Purification and properties of soluble dinitrophenol-stimulated adenosine triphosphatase. *J Biol Chem* 235: 3322-3329.
- Pysh JJ, Khan T. 1972. Variations in mitochondrial structure and content of neurons and neuroglia in rat brain: An electron microscopic study. *Brain Res* 14: 1-18.
- Raichle ME, Grubb RL Jr, Gado MH, Eichling JO, Ter-Pogossian MM. 1976. Correlation between regional cerebral blood flow and oxidative metabolism. In vivo studies in man. *Arch Neurol*. 33: 523-526.
- Rasmussen M, Poulsen PH, Treiber A, Delahaye S, Tankisi A, et al. 2003. No influence of the endothelin receptor antagonist bosentan on basal and indomethacin-induced reduction of cerebral blood flow in pigs. *Acta Anaesthesiol Scand* 47: 200-207.
- Reese TS, Feder N, Brightman MW. 1971. Electron microscopic study of the blood-brain and blood-cerebrospinal fluid barriers with microperoxidase. *J Neuropathol Exp Neurol*. 30: 137-138.
- Reeves JT, Wolfel EE, Green HJ, Mazzeo RS, Young AJ, et al. 1992. Oxygen transport during exercise at altitude and the lactate paradox: Lessons from Operation Everest II and Pike's Peak. *Exerc Sport Sci Rev* 20: 275-296.
- Reutens DC, McHugh MD, Toussaint PJ, Evans AC, Gjedde A, et al. 1997. L-arginine infusion increases basal but not activated cerebral blood flow in humans. *J Cereb Blood Flow Metab* 17: 309-315.
- Ribak CE. 1981. The histochemical localization of cytochrome oxidase in the dentate gyrus of the rat hippocampal. *Brain Res* 212: 169-174.
- Ribeiro L, Kuwabara H, Meyer E, Fujita H, Marrett S, et al. 1993. Cerebral blood flow and metabolism during nonspecific bilateral visual stimulation in normal subjects. Quantification of Brain Function. *Tracer Kinetics and Image Analysis in Brain PET*. Uemura K, Lassen NA, Jones T, Kanno I, editors. Amsterdam: Elsevier; pp. 217-224.
- Ritchie JM. 1967. The oxygen consumption of mammalian nonmyelinated fibres at rest and during activity. *J Physiol (Lond)* 188: 309-329.

- Robin ED, Murphy BJ, Theodore J. 1984. Coordinate regulation of glycolysis by hypoxia in mammalian cells. *J Cell Physiol* 118: 287-290.
- Roland PE, Eriksson L, Stone-Elander S, Widen L. 1987. Does mental activity change the oxidative metabolism of the brain? *J Neurosci* 8: 2373-2389.
- Roland PE, Eriksson L, Widen L, Stone-Elander S. 1989. Changes in regional cerebral oxidative metabolism induced by tactile learning and recognition in man. *Eur J Neurosci* 7: 2373-2389.
- Rolfe DF, Brown GC. 1997. Cellular energy utilization and molecular origin of standard metabolic rate in mammals. *Physiol Rev* 77: 731-758.
- Rose SP. 1975. Cellular compartmentation of brain metabolism and its functional significance. *J Neurosci Res.* 1: 19-30.
- Roth K, Weiner MW. 1991. Determination of cytosolic ADP and AMP concentrations and the free energy of ATP hydrolysis in human muscle and brain tissues with ^{31}P NMR spectroscopy. *Magn Reson Med* 22: 505-511.
- Rothstein JD, Dykes HM, Pardo CA, Bristol LA, Jin L, et al. 1996. Knockout of glutamate transporters reveals a major role for astroglial transport in excitotoxicity and clearance of glutamate. *Neuron* 16: 675-686.
- Salceda R, Vilchis C, Coffe V, Hernandez-Munoz R. 1998. Changes in the redox state in the retina and brain during the onset of diabetes in rats. *Neurochem Res.* 23: 893-897.
- Sappey-Mariniere D, Calabrese G, Fein G, Hugg JW, Biggins C, et al. 1992. Effect of photic stimulation on human visual cortex lactate and phosphates using ^1H and ^{31}P magnetic resonance spectroscopy. *J Cereb Blood Flow Metab.* 12: 584-592.
- Schurr A. 2006. Lactate: The ultimate cerebral oxidative energy substrate? *J Cereb Blood Flow Metab* 26: 142-152.
- Seitz RJ, Roland PE. 1992. Vibratory stimulation increases and decreases the regional cerebral blood flow and oxidative metabolism: A positron emission tomography (PET) study. *Acta Neurol Scand* 86: 60-67.
- Shalit MN, Beller AJ, Feinsod M, Drapkin AJ, Cotev S. 1970. The blood flow and oxygen consumption of the dying brain. *Neurology* 20: 740-748.
- Shalit MN, Beller AJ, Feinsod M. 1972. Clinical equivalents of cerebral oxygen consumption in coma. *Neurology* 22: 155-160.
- Shearman MS, Halestrap AP. 1984. The concentration of the mitochondrial pyruvate carrier in rat liver and heart mitochondria determined with α -cyano- β -(1-phenylindol-3-yl) acrylate. *Biochem J* 223: 673-676.
- Shulman RG, Rothman DL. 1998. Interpreting functional imaging studies in terms of neurotransmitter cycling. *Proc Natl Acad Sci USA* 95: 11993-11998.
- Shulman RG, Rothman DL, Behar KL, Hyder F. 2005. Energetic basis of brain activity: Implications for neuroimaging. *Trends Neurosci.* 27: 489-95.
- Sibson NR, Dhankhar A, Mason GF, Rothman DL, Behar KL, et al. 1998. Stoichiometric coupling of brain glucose metabolism and glutamatergic neuronal activity. *Proc Natl Acad Sci USA* 95: 316-321.
- Silver IA, Erecinska M. 1994. Extracellular glucose concentration in mammalian brain: Continuous monitoring of changes during increased neuronal activity and upon limitation in oxygen supply in normo-, hypo-, and hyperglycemic animals. *J Neurosci* 14: 5068-5076.
- Silver IA, Erecinska M. 1997. Energetic demands of the Na^+/K^+ -ATPase in mammalian astrocytes. *Glia* 21: 35-45.
- Skou JC. 1960. Further investigations on a $\text{Mg}^{2+}/\text{Na}^+$ -activated adenosine triphosphatase, possibly related to the active, linked transport of Na^+ and K^+ across the nerve membrane. *Biochim Biophys Acta* 42: 6-23.
- Snyder CD, Wilson JE. 1983. Relative levels of hexokinase in isolated neuronal, astrocytic, and oligodendroglial fractions from rat brain. *J Neurochem* 40: 1178-1181.
- Sokoloff L, Reivich M, Kennedy C, Des Rosiers MH, Patlak CS, et al. 1977. The ^{14}C deoxyglucose method for the measurement of local cerebral glucose utilization: Theory, procedure, and normal values in the conscious and anesthetized albino rat. *J Neurochem* 28: 897-916.
- Sokoloff L, Takahashi S, Gotoh J, Driscoll BF, Law MJ. 1996. Contribution of astroglia to functionally activated energy metabolism. *Dev Neurosci* 18: 344-352.
- Sokoloff L. 1999. Energetics of functional activation in neural tissues. *Neurochem Res* 24: 321-329.
- Springett R, Wylezinska M, Cady EB, Cope M, Delpy DT. 2000. Oxygen dependency of cerebral oxidative phosphorylation in newborn piglets. *J Cereb Blood Flow Metab.* 20: 280-289.
- Takano T, Tian GF, Peng W, Lou N, Libionka W, et al. 2006. Astrocyte-mediated control of cerebral blood flow. *Nat Neurosci* 9: 260-267.
- Tanaka K, Watase K, Manabe T, Yamada K, Watanabe M, et al. 1997. Epilepsy and exacerbation of brain injury in mice lacking the glutamate transporter GLT-1. *Science* 276: 1699-1702.
- Tholey G, Roth-Schechter BF, Mandel P. 1981. Activity and isoenzyme pattern of lactate dehydrogenase in neurons and astroblasts cultured from brains of chick embryos. *J Neurochem* 36: 77-81.
- Thompson JK, Peterson MR, Freeman RD. 2003. Single-neuron activity and tissue oxygenation in the cerebral cortex. *Science.* 299: 1070-1072.
- Vafaei MS, Meyer E, Marrett S, Evans AC, Gjedde A. 1998. Increased oxygen consumption in human visual cortex:

- Respond to visual stimulation. *Acta Neurol Scand* 98: 85-89.
- Vafaee MS, Meyer E, Marrett S, Paus T, Evans AC, et al. 1999. Frequency-dependent changes in cerebral metabolic rate of oxygen during activation of human visual cortex. *J Cereb Blood Flow Metab* 19: 272-277.
- Vafaee MS, Gjedde A. 2000. Model of blood-brain transfer of oxygen explains nonlinear flow-metabolism coupling during stimulation of visual cortex. *J Cereb Blood Flow Metab* 20: 747-754.
- Vafaee MS, Gjedde A. 2004. Spatially dissociated flow-metabolism coupling in brain activation. *Neuroimage* Feb; 21(2):507-15.
- Vafaee MS, Meyer E, Gjedde A. 2000. Impaired activation of oxygen consumption and blood flow in visual cortex of patients with mitochondrial encephalomyopathy. *Ann Neurol* 48: 676-679.
- Vandenberg RJ. 1998. Molecular pharmacology and physiology of glutamate transporters in the central nervous system. *Clin Exp Pharmacol Physiol* 25: 393-400.
- Van Hall G. 2000. Lactate as a fuel for mitochondrial respiration. *Acta Physiol Scand*. 168: 643-656.
- van den Berg CJ, Bruntink R. 1983. Glucose oxidation in the brain during seizures: Experiments with labeled glucose and deoxyglucose. Glutamine, Glutamate, and GABA in the Central Nervous System. Hertz L, Kvamme E, McGeer EG, Schousboe A, editors. New York: Alan R Liss; pp. 619-624.
- Vega C, Martiel JL, Drouhault D, Burckhart MF, Coles JA. 2003. Uptake of locally applied deoxyglucose, glucose, and lactate by axons and Schwann cells of rat vagus nerve. *J Physiol*. 546: 551-564.
- Villringer A, Dirnagl U. 1995. Coupling of brain activity and cerebral blood flow: Basis of functional neuroimaging. *Cerebrovasc Brain Met* 7: 240-276.
- Wang H, Oster G. 1998. Energy transduction in the F1 motor of ATP synthase. *Nature* 396: 279-282.
- Wang SZ, Zhu SZ, el-Fakahany EE. 1994. Efficient coupling of M₅ muscarinic acetylcholine receptors to activation of nitric oxide synthase. *J Pharmacol Exp Ther* 268: 552-557.
- Whittam R. 1962. The dependence of the respiration of brain cortex on active cation transport. *Biochem J* 82: 205-212.
- Winkler BS, Sauer MW, Starnes CA. 2004. Effects of L-glutamate/D-aspartate and monensin on lactic acid production in retina and cultured retinal Muller cells. *J Neurochem* 89: 514-525.
- Wong-Riley MT. 1989. Cytochrome oxidase: An endogenous metabolic marker for neuronal activity. *Trends Neurosci* 12: 94-101.
- Wyss M, Smeitink J, Wevers RA, Wallimann T. 1992. Mitochondrial creatine kinase: A key enzyme of aerobic energy metabolism. *Biochim Biophys Acta* 1102: 119-166.
- Yarowsky PJ, Ingvar DH. 1981. Neuronal activity and energy metabolism. *Fed Proc* 40: 2353-2362.
- Ye JM, Colquhoun EQ, Hettiarachchi M, Clark MG. 1990. Flow-induced oxygen uptake by the perfused rat hindlimb is inhibited by vasodilators and augmented by norepinephrine: A possible role for the microvasculature in hindlimb thermogenesis. *Can J Physiol Pharmacol* 68: 119-125.
- Zonta M, Angulo MC, Gobbo S, Rosengarten B, Hossmann KA, et al. 2003. Neuron-to-astrocyte signaling is central to the dynamic control of brain microcirculation. *Nature Neurosci* 6: 43-50.

4.6 Energy Consumption by Phospholipid Metabolism in Mammalian Brain

A. D. Purdon · S. I. Rapoport

1	Introduction	402
2	General Compartmental Model for Calculating Half-Lives and Turnover Rates of Brain Lipids and Their Components	403
3	Net Rate of ATP Consumption by Mammalian Brain	405
4	Estimated Rates of ATP Consumption by Different Metabolic Processes Involving Phospholipids	406
5	ATP Consumption by Fatty Acid Recycling (Acylation–Deacylation) in Brain Phospholipids	407
5.1	Model of Fatty Acid Recycling	407
5.2	Rates of Fatty Acid Incorporation into the <i>sn</i> -1 Position of Phospholipids	409
5.3	Rates of Fatty Acid Incorporation into the <i>sn</i> -2 Position of Phospholipids	409
5.4	ATP Consumption by Fatty Acid Recycling	409
6	ATP Consumption for Maintaining Membrane Phospholipid Asymmetries	409
6.1	Aminophospholipid Asymmetries in Membranes	409
6.2	ATP Consumption by Aminophospholipid Translocation	410
7	ATP Consumption by the Phosphatidylinositol Cycle	411
7.1	ATP Consumption for Phosphorylation of Inositol-Containing Phospholipids from Studies in Platelets	412
7.2	ATP Consumption for the De Novo Biosynthesis of Inositol-Containing Phospholipids from Studies in Cultured Neurons	413
8	ATP Consumption by Synthesis of Brain Ether Phospholipids	414
8.1	Energy Requirement for Ether Phospholipid Synthesis	416
9	Disruption of Phospholipid Metabolism Requires Augmented ATP Consumption to Reestablish Membrane Homeostasis	417
9.1	Cerebral Ischemia	417
9.2	Possible Therapies for Ischemia Related to ATP Debt	418
10	Discussion	419

Abstract: Until recently, phospholipid metabolism was considered to consume less than 2% of net brain ATP consumption. We now estimate that the consumption rate by phospholipids is much higher, as much as 26% of net brain ATP consumption. A high rate is consistent with evidence that phospholipids participate in dynamic brain signaling and membrane-recycling processes. We calculate that 1.4% of net brain ATP consumption is used for de novo synthesis of ether phospholipids, 5% for recycling of fatty acids within phospholipids, 7.7% for maintaining membrane asymmetries of charged aminophospholipids, and about 12% for maintaining the phosphorylation state and de novo biosynthesis of inositol-containing phospholipids involved in phosphatidylinositol signaling. Some of these estimates should be confirmed by direct measurements in the brain. In pathological conditions such as cerebral ischemia, in which ATP production becomes limited, phospholipid breakdown is accelerated and cell death can ensue. Satisfying ATP demands to restore phospholipid integrity should be a consideration in treating such conditions.

List of Abbreviations: CDP, cytosine diphosphate; CMP, cytosine monophosphate; CTP, cytosine triphosphate; COX, cyclooxygenase; DAG, 1,2-diacyl-*sn*-glycerol; Ins, myo-inositol; DHAP, dihydroxyacetonephosphate; g brain, gram wet weight of brain; GAP, glyceraldehyde phosphate; Ins, *myo*-inositol; 1,4,5-InsP₃, inositol 1,4,5-trisphosphate; NADH, nicotinamide adenine dinucleotide reduced form; PAF, platelet activating factor; NSAID, non-steroidal anti-inflammatory drug; PakCho, 1-*O*-alkyl-2-acyl-*sn*-glycero-3-phosphocholine; PakEtn, 1-*O*-alkyl-2-acyl-*sn*-glycero-3-phosphoethanolamine; PakOH, 1-*O*-alkyl-2-acyl-*sn*-glycero-3-phosphate; PGE₂, prostaglandin E₂; PlsCho, 1-*O*-alk-1'-enyl-2-acyl-*sn*-glycero-3-phosphocholine; PlsEtn, 1-*O*-alk-1'-enyl-2-acyl-*sn*-glycero-3-phosphoethanolamine; PLA₂, phospholipase A₂; cPLA₂, cytosolic PLA₂; sPLA₂, secretory PLA₂; PLC, phospholipase C; PtdEtn, phosphatidylethanolamine; PtdSer, phosphatidylserine; PtdIns, phosphatidylinositol; PtdIns4-P, phosphatidylinositol-4-phosphate; PtdIns4,5-P₂, phosphatidylinositol-4,5-bisphosphate; PtdOH, 1,2-diacyl-*sn*-glycero-3-phosphate; PUFAs, polyunsaturated fatty acids; *sn*, stereospecifically numbered

1 Introduction

The adult human brain constitutes 2% of body weight, yet consumes about 20% of the body's oxygen and glucose for the production of energy in the form of ATP (Clarke and Sokoloff, 1994). A considerable portion of the ATP produced is required by the ouabain-sensitive Na⁺/K⁺-ATPase exchange pump, which redistributes K⁺ as well as 4–5 μmol Na⁺/g wet weight brain/min (Lowry, 1975) to maintain cell membrane potential (Rapoport, 1970, 1971; Albers et al., 1994).

The estimated rate of ATP use by the Na⁺/K⁺-ATPase pump is based on an observed 50% decrease in resting oxygen consumption following addition of ouabain to rat brain slices (Whittam, 1962; Whittam and Blond, 1964; Vierbuchen et al., 1979). More recent analyses, including further scrutiny of "ouabain-sensitive O₂ consumption," however, have lowered the cation pump requirement to 25–40% of the net brain ATP utilization (Albers et al., 1994). ATP is also required to maintain a low cytosolic free calcium concentration by the action of the sarcoplasmic/endoplasmic reticulum calcium ATPase (Pottorf et al., 2001), and an additional 10% of the brain's ATP is used for synthetic purposes (Lowry, 1975; Vierbuchen et al., 1979). These calculations leave about 50% in an unknown "black box."

One possibility is that the black box includes ATP utilized by phospholipid metabolism. Phospholipids constitute 45% of total brain dry weight and are intimately involved in active membrane remodeling and signaling processes (Ansell, 1973; Miller et al., 1977; Dawson, 1985; Fisher and Agranoff, 1985; Horrocks, 1985; Berridge and Irvine, 1989; Bazán, 1990; Hokin and Dixon, 1993; Glaser and Gross, 1994; Cooper et al., 2003). Some signaling processes, particularly those concerned with neurotransmission, involve the activation of phospholipase C (PLC) to initiate the phosphatidylinositol (PtdIns) cycle, or the activation of phospholipase A₂ (PLA₂) to release the second messenger, arachidonic acid (20:4 n-6), from brain phospholipids (Fisher and Agranoff, 1985; Shimizu and Wolfe, 1990; Cooper et al., 2003). These processes must be very rapid, as neurotransmission occurs on a timescale of milliseconds (Shepherd, 1979). However, despite evidence for active brain phospholipid metabolism, until recently (Purdon and Rapoport, 1998;

Purdon et al., 2002) phospholipid metabolism was considered to consume less than 2% of net ATP produced by brain oxidative metabolism (Clarke and Sokoloff, 1994).

There are several reasons for the prior low estimate of ATP consumption by brain phospholipid metabolism. One is that it was widely held that turnover rates of brain phospholipid components, as well as brain phospholipid synthesis rates, were slow and thus consumed ATP slowly (Sun, 1977; Sun and Su, 1979; Porcellati et al., 1983; Horrocks, 1990). This notion was supported by studies in which slopes of decline of radioactivity in individual brains or retinal phospholipids were measured after the intracerebral or intraretinal injection of a radiolabeled phospholipid precursor (Freysz et al., 1969; Horrocks et al., 1975; Miller et al., 1977; Porcellati et al., 1983; Stinson et al., 1991; DeMar et al., 2004). These slopes suggested that half-lives of phospholipid components were weeks to months, and appeared to agree with the long half-lives for the recovery of brain lipid composition in rats following dietary deprivation of nutritionally essential n-3 polyunsaturated fatty acids (PUFAs) (▶ [Table 4.6-1](#)).

■ **Table 4.6-1**

PUFA half-lives in nervous system phospholipids from intratissue injection or feeding studies

Method	Fatty acid	Species	Half-life (days)
Deprivation-supplementation (brain)	Docosahexaenoic	Rat	11 ^a
Deprivation-supplementation (brain)	Docosahexaenoic	Macaque	17–21 ^b
Intracerebral injection (brain)	Arachidonic	Mouse	11–14 ^c
Intraretinal injection (retina)	Docosahexaenoic	Rat	33 ^d
	Docosahexaenoic	Rat	19 ^e

^aMoriguchi et al. (2001)

^bConnor et al. (1990)

^cSun and Su (1979)

^dDeMar et al. (2004)

^eStinson et al. (1991)

The half-lives calculated from the slopes or following dietary n-3 PUFA deprivation ignored recycling of phospholipid components, which often characterizes phospholipid metabolism (Lands and Crawford, 1976; Sun and MacQuarrie, 1989; Robinson et al., 1992; Rapoport, 2003; DeMar et al., 2004). When recycling was taken into account using *in vivo* methods that measure rates of incorporation of a tracer from the brain precursor pool (see below), half-lives of phospholipid components were found to be much shorter (minutes to hours), consistent with rapid acylation–deacylation (Shetty et al., 1996; Rapoport, 2001; Rapoport et al., 2001; Rosenberger et al., 2002).

Some prior studies suggesting long half-lives also ignored metabolic compartmentation. If metabolism largely occurs in a small, rapidly turning-over brain compartment, analyzing only whole brains can give unrealistic long half-lives (Paltauf, 1994; Lee, 1998; Rosenberger et al., 2002, 2004). Quantitative autoradiography and subcellular fractionation have been used to distinguish active from less active brain metabolic compartments in order to calculate appropriate half-lives and turnover rates (DeGeorge et al., 1991; Jones et al., 1996, 1997; Rosenberger et al., 2002; Rapoport, 2003).

2 General Compartmental Model for Calculating Half-Lives and Turnover Rates of Brain Lipids and Their Components

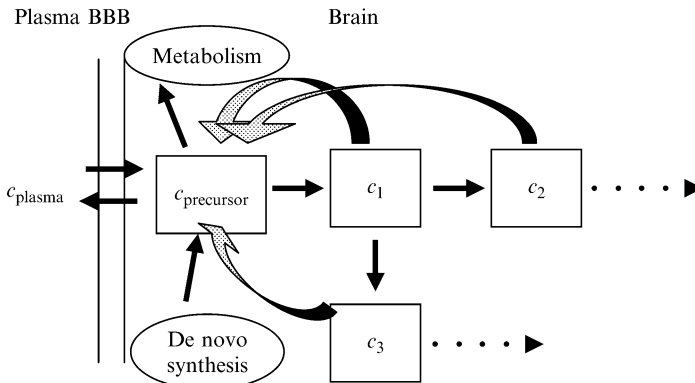
Our laboratory has developed methods that take into account recycling and compartmentation, to calculate half-lives and turnover rates of brain phospholipids and their components in unanesthetized rodents (Robinson et al., 1992; Rapoport, 2001). A labeled compound (radiotracer or heavy isotope) that can be incorporated into a brain phospholipid is administered by programmed intravenous infusion (Patlak and

Pettigrew, 1976). The arterial plasma input function to the brain (integrated arterial plasma-specific activity) is measured until the animal is killed, and the brain is subjected to high-energy microwaving to stop enzyme activity. Analytical techniques are used to measure labeled and cold concentrations of lipids of interest, and brain fractionation and quantitative autoradiography are performed as necessary (Jones et al., 1996, 1997; Rabin et al., 1998b; Rosenberger et al., 2002; Lee et al., 2004a).

Figure 4.6-1 illustrates a “general” compartmental model (Rapoport, 2001, 2005) in which a substance (potential lipid precursor) passes from the plasma into a brain precursor pool across the blood–brain barrier (compartments prior to the precursor pool are not shown), from which it can be incorporated into “stable” lipid compartments, $i = 1, 2, 3 \dots$, arranged in parallel and/or in series. Right-to-left arrows indicate that the substance can be recycled back from the stable lipid to the precursor pool. An additional contribution to the precursor pool can be de novo synthesis, whereas additional loss may be due to β -oxidation or other degradative processes.

Figure 4.6-1

Generic model for determining fluxes, turnover rates, and half-lives in brain lipid compartments. A substance in plasma at concentration c_{plasma} crosses the blood–brain barrier to enter the brain precursor pool at concentration $c_{\text{precursor}}$, from which it can be distributed by serial or parallel steps into stable brain lipid compartments at concentrations c_i ($i = 1, 2, 3 \dots$). Reverse arrows indicate back fluxes of the tracer from the compartments to the precursor pool. De novo synthesis can contribute to the precursor pool, whereas the substance can be lost from the precursor pool by metabolism. Modified from Rapoport (2005)



To quantify incorporation of the unlabeled substance from the brain precursor pool into lipid $i = 1$ during infusion of label at constant (steady state) brain and plasma lipid concentrations, it is necessary to measure the ratio between its specific activity in the brain precursor pool and its specific activity in plasma as a function of time. This ratio is termed the “dilution factor” λ

$$\lambda = \frac{\left[\frac{c_{\text{precursor}}^*}{c_{\text{precursor}}} \right]}{\left[\frac{c_{\text{plasma}}^*}{c_{\text{plasma}}} \right]}, \quad (1)$$

where c_{plasma}^* and c_{plasma} are the respective labeled and unlabeled plasma concentrations of the substance, and $c_{\text{precursor}}^*$ and $c_{\text{precursor}}$ are the respective labeled and unlabeled precursor pool concentrations. At steady-state radioactivity in the plasma and precursor pool, λ exactly equals the flux of the substance from plasma into the precursor pool divided by the sum of fluxes from all sources into that pool (Robinson et al., 1992; Purdon et al., 1997; Chikhale et al., 2001). Thus, λ represents the extent to which the plasma-derived substance (which can be labeled) is “diluted” by the substance derived from other sources (e.g., from de novo synthesis, release from stable lipids).

An incorporation coefficient, k_i^* , is calculated as radioactivity in a “stable” lipid compartment i at time of death T , $c_{\text{brain},i}^*(T)$, divided by integrated plasma radioactivity to T , where t is time after beginning infusion

$$k_i^* = \frac{c_{\text{brain},i}^*(T)}{\int_0^T c_{\text{plasma}}^* dt}. \quad (2)$$

Then, the rate of incorporation $J_{\text{FA},i}$ of the unlabeled substance (for convenience designated as FA) from the brain precursor pool into lipid $i=1$ equals

$$J_{\text{FA},i} = \frac{k_i^* c_{\text{plasma}}}{\lambda}, \quad (3)$$

and the substance’s turnover rate $F_{\text{FA},i}$ and half-life $t_{1/2,i}$ in i equals

$$F_{\text{FA},i} = \frac{J_{\text{FA},i}}{c_{\text{brain},i}} \quad (4a)$$

and

$$t_{1/2,i} = 0.693/F_{\text{FA},i}. \quad (4b)$$

Transfer from compartment $i = 1$ to compartments $i = 2, 3, 4 \dots$ over time can be represented in the form of [Eq. 16a–c](#).

Evidence indicates that the brain unesterified fatty acid pool is metabolically active and not isolated from rapid equilibration events, and that acyl-CoA represents the final precursor pool before the incorporation of the fatty acid into membrane lipids. For example, intravenous infusion of labeled arachidonic acid in rats rapidly labels the brain unesterified fatty acid and arachidonoyl-CoA pools, and within 1 min most of the label is found as esterified arachidonic acid in brain phospholipids (Washizaki et al., 1994). Similarly, changes in brain unesterified arachidonic acid and arachidonoyl-CoA proceed in parallel during and following ischemia (Rabin et al., 1998a).

The rate of ATP consumption due to incorporation of the substance into lipid $i = 1$ equals the product of $J_{\text{FA},i}$ and ATP stoichiometry, S ,

$$\text{Rate of consumption} = S \times J_{\text{FA},i}. \quad (5)$$

[Eq. 5](#) can be generalized to any metabolic process whose stoichiometry and rate are known.

3 Net Rate of ATP Consumption by Mammalian Brain

It would be worthwhile reviewing estimates of net brain ATP production before considering what fraction of net production is used by phospholipid metabolism (Purdon and Rapoport, 1998; Purdon et al., 2002). One estimate was derived from the measured rate of oxygen consumption by a 1,400 g human brain: 49 ml O_2/min (Clarke and Sokoloff, 1994). Assuming that almost all brain oxygen is used for carbohydrate oxidation (the value actually is about 90% (Siesjö, 1978)) and a 20% efficiency of energy conversion for synthesizing the high-energy phosphate bonds of ATP (which has an energy of hydrolysis of 7 kcal/1,000 mmol), the energy equivalent of this rate of ATP synthesis is 0.25 kcal/min. Accordingly, the rate of ATP production by a 1400 g human brain is 7.1 mmol/min (Clarke and Sokoloff, 1994),

$$(0.25 \text{ kcal/min}) \times 0.20(1,000 \text{ mmol/7 kcal}) = 7.1 \text{ mmol of ATP/min}. \quad (6)$$

Another estimate for net brain ATP production was derived by recognizing that glucose is the preferred substrate for the oxygen used to reoxidize nicotinamide adenine dinucleotide (NADH), and in principle will yield 2.5 ATP per oxygen atom consumed. A value of 2.5 is considered to represent the best estimate of a “mechanistic” P/O ratio (Hinkle et al., 1991). Taking oxygen consumption by the human brain as 49 ml/min/1400 g (see above) or 2.18 mol/min/g and assuming that glucose being the substrate, most

oxygen is used to reoxidize NADH and ATP production equals 10.9 mmol of ATP/min/g. The mechanistic P/O ratio can be used to estimate an actual or “effective” P/O ratio by taking into account the fraction of tissue oxygen consumption that is involved with nonmitochondrial oxygen consumption (10%) and also coupled to the proton leak (20%) (Rolfe and Brown, 1997). With these approximations, the “effective” tissue P/O ratio equals $0.7 \times 2.5 = 1.75$ for mitochondrial oxidative phosphorylation (Zachowski and Gaudry-Talarmin, 1990; Hinkle et al., 1991; Williamson and Schlegel, 1994; Rolfe and Brown, 1997; Purdon and Rapoport, 1998), which gives a production rate of 7.7 mmol ATP/min by the 1400 g brain (Purdon and Rapoport, 1998),

$$(49 \text{ ml of O}_2)/(22.4 \text{ ml/mmol}) \times (2 \text{ mol of O/mol of O}_2) \times (1.75 \text{ mol of P/mol of O}_2) \\ = 7.7 \text{ mol of ATP/min.} \quad (7)$$

This rate is virtually identical to Clarke and Sokoloff’s estimate of 7.1 mmol of ATP/min/1400 g for the human brain (Clarke and Sokoloff, 1994), which is equal to 83 nmol of ATP/s/g. Because energy metabolism is 2.5 times higher in rats than in human brain (Sokoloff, 1977), ATP production (equal to consumption) by rat brain will be taken as 208 nmol/s/g for subsequent analyses

$$(83 \text{ nmol/s/g human brain}) \times 2.5 = 208 \text{ nmol/s/g rat brain.} \quad (8)$$

In the above calculations, we ignored any contribution of long-chain fatty acids to brain oxygen consumption or ATP production. After entering the brain from the plasma, these fatty acids are partly subjected to β -oxidation within mitochondria (Lehninger et al., 1993). The fraction subjected to β -oxidation is high for saturated fatty acids like palmitic acid and for polyunsaturated α -linolenic (18:3 n-3) and linoleic (18:2 n-6) acids, but low (<10%) for polyunsaturated docosahexaenoic acid (22:6 n-3) and arachidonic acid (Miller et al., 1987; Washizaki et al., 1994; Rapoport, 2001; DeMar et al., 2005). These differences likely reflect differences in fatty acid selectivity of the mitochondrial carnitine *O*-palmitoyl transferase process (Gavino and Gavino, 1991; DeMar et al., 2005). β -Oxidation first converts long-chain fatty acids within mitochondria to acetyl-CoA moieties with the production of ATP, and these moieties are largely used for the de novo synthesis of glutamate and other amino acids, glutamine, saturated fatty acids, cholesterol, and other carbon compounds (Miller et al., 1987; DeMar et al., 2005). Very little is used for the Krebs’s cycle formation of CO₂ and H₂O. Thus, the rate of CO₂ formation from long-chain fatty acids represents less than 3% of the brain’s net CO₂ formation rate (Allweis et al., 1966; Carey, 1975; Horrocks and Harder, 1983), and conversion of palmitate to two carbon fragments is 30–40 times its rate of conversion to CO₂ and H₂O in cultured astrocytes (Murphy et al., 1992a; Blazquez et al., 1998). We therefore ignore (see above) the contribution of fatty acid oxidation to net ATP production, and assume like other investigators (Siesjö, 1978; Clarke and Sokoloff, 1994) that ATP in the brain is formed entirely by the oxidation of glucose.

4 Estimated Rates of ATP Consumption by Different Metabolic Processes Involving Phospholipids

Table 4.6-2 presents estimates of ATP consumption by each of the five brain phospholipid metabolic processes. These estimates will be discussed in detail in the following sections. The estimated metabolic rates of these processes (first data column) when multiplied by the respective ATP stoichiometry *S* (Eq. 5) (second data column) provide respective rates of ATP consumption in nmol/s/g in the rat brain and as a percent of the net brain ATP consumption, i.e., 208 nmol/s/g (Eq. 8). The metabolic rates of recycling (acylation–deacylation) of long-chain fatty acids in different phospholipids and of synthesis of ether phospholipids were obtained from direct measurements in unanesthetized rats (Table 4.6-2). The rates of turnover and phosphorylation of the PtdIns cycle and of maintaining aminophospholipid asymmetries were extrapolated from other data. The five processes are estimated to consume ATP at a rate of 26% of the net brain rate.

Knowing that the brain phospholipid metabolism consumes ATP at a high rate has more than a heuristic value. A high rate confirmed the importance of phospholipid metabolism in brain function and structure, and also suggests that phospholipids influenced brain evolution processes that depended

■ Table 4.6-2

Estimated ATP consumption by phospholipid metabolism in rat brain

Metabolic process	Rate (nmol/s/g)	ATP stoichiometry (S)	ATP consumption (nmol/s/g)	Percent net ATP consumption ^a
Fatty acid turnover in <i>sn</i> -1 and <i>sn</i> -2 positions of phospholipids	5.2	2	10.4	5
De novo PtdIns synthesis ^b	0.063	9	0.57	0.27
Maintenance of PtdIns phosphorylation state ^c		5	24.8	12
De novo synthesis of ether phospholipids ^d		10–13	2.9	1.4
Maintenance of aminophospholipid asymmetries ^e		1:1 (ATP/phospholipid)	16	7.7
Sum			54.7	26.4

^aSee ▶ Sect. 4. 208 nmol/s/g

^bExtrapolated from cultured mouse neurons (Chikhale et al., 2001)

^cExtrapolated from phosphorylation rates of unstimulated human platelets (▶ Table 4.6-4) (Verhoeven et al., 1987)

^d▶ Table 4.6-5

^eExtrapolated from human erythrocytes (Bitbol and Devaux, 1988). Rate of consumption in humans multiplied by 2.5 to obtain the respective rate in rats. Modified from Purdon and Rapoport (1998) and Purdon et al. (2002)

on energy constraints (Leonard, 2001; Peters et al., 2004). Additionally, in neuropathological conditions in which phospholipids are broken down and their components released, recovery of tissue integrity will require ATP consumption above normal. If the initial insult (e.g., ischemia, hypoglycemia, hypoxia) is accompanied by reduced ATP synthesis, the ATP debt may be difficult to meet, and cell dysfunction and death will be promoted (see ▶ Sect. 10).

5 ATP Consumption by Fatty Acid Recycling (Acylation–Deacylation) in Brain Phospholipids

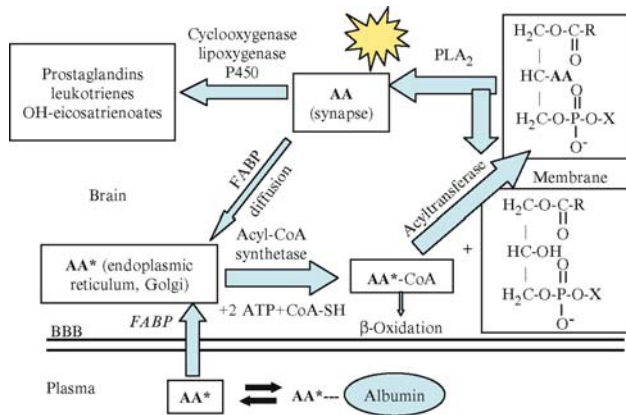
5.1 Model of Fatty Acid Recycling

▶ Figure 4.6-2 presents a model (extension of ▶ Figure 4.6-1) that we have used to quantify half-lives and turnover rates of long-chain fatty acids in rat brain phospholipids (Robinson et al., 1992; Rapoport, 2003). It illustrates the “arachidonic acid cascade” (Shimizu and Wolfe, 1990; Fitzpatrick and Soberman, 2001). Arachidonic acid is released (in compartment designated as the synapse) from the stereospecifically numbered (*sn*)-2 position of phospholipids by PLA₂ activation (*star*), where it can be converted to bioactive eicosanoids by enzymes such as cyclooxygenase (COX)-2. The remainder is transported via a fatty acid-binding protein (FABP) to the endoplasmic reticulum, where it can freely exchange with labeled and unlabeled arachidonic acid in the plasma and be converted to arachidonoyl-CoA by an acyl-CoA synthetase with the consumption of two ATPs (Waku, 1992). From the acyl-CoA pool, arachidonic acid can be esterified into a lysophospholipid by an acyltransferase or transferred to mitochondria or peroxisomes to undergo β-oxidation.

When infusing a radiolabeled long-chain fatty acid intravenously into an unanesthetized rat to produce a step elevation in plasma radioactivity, the specific activity of the brain acyl-CoA pool will equilibrate with the plasma specific activity in less than 2 min, at which point λ for acyl-CoA (▶ Eq. 1) becomes constant (Washizaki et al., 1994; Grange et al., 1995). This and the fact that about 90% of the brain label is esterified in phospholipids within 1–2 min after entering brain confirm very rapid recycling of fatty acids in brain phospholipids (▶ Figure 4.6-2).

Figure 4.6-2

Model of brain arachidonic acid cascade. Arachidonic acid (AA), esterified at the *sn*-2 position of a phospholipid, is liberated by the activation (*star*) of phospholipase A₂ (PLA₂) at the synapse. A lysophospholipid also is formed. A fraction of the unesterified AA is converted to eicosanoids by cyclooxygenase, lipoxygenase, or P-450 enzymes, whereas the remainder is transported by a fatty acid-binding protein (FABP) to the endoplasmic reticulum. From there, AA is converted to arachidonoyl-CoA by an acyl-CoA synthetase with the consumption of two ATPs per molecule, then reesterified into an available lysophospholipid by an acyltransferase. It also can be lost by β -oxidation in mitochondria or peroxisomes, or by other pathways (not shown). The endoplasmic reticulum compartment is in very rapid equilibrium with the unesterified unlabeled AA or labeled AA* in plasma, whereas the synaptic compartment does not exchange with plasma (Rosenberger et al., 2004). From Rapoport (2001)



Published values for the dilution coefficient λ of different acyl-CoAs range from 0.01 to 0.04 (0.02–0.03 in Table 4.6-3), also supporting marked fatty acid recycling within brain phospholipids (Robinson et al., 1992; Shetty et al., 1996; Rapoport et al., 1997). Fatty acid half-lives derived with these values, $t_{1/2,i}(\text{recycling})$ (Eq. 4b) may be only a few hours (Table 4.6-3) (only 10 min in the case of some polyunsaturated molecular species of arachidonoyl-containing phosphatidylcholine) (Shetty et al., 1996) compared with much longer half-lives calculated by the slope method, $t_{1/2,i}(\text{slope})$, which ignore recycling (Table 4.6-1). The two half-lives are related via λ as follows (Rapoport, 2001; DeMar et al., 2004):

$$t_{1/2,i}(\text{slope}) = t_{1/2,i}(\text{recycling})/\lambda. \quad (9)$$

Table 4.6-3

Half-lives of fatty acid recycling in rat brain phospholipids

Fatty acid	Dilution factor ($\lambda_{\text{acyl-CoA}}$) ^a	Half-life (h)		
		Phosphatidylcholine	Phosphatidylinositol	Phosphatidylethanolamine
Arachidonic acid (20:4 n-6)	0.03	3.4	2.9	47
Docosahexaenoic acid (22:6 n-3)	0.03	3.9	22	58
Palmitic acid (16:0)	0.02	2.4	9.9	17

$$^a \lambda_{\text{acyl-CoA}} = \frac{c_{\text{acyl-CoA}}^{\text{ER}}/c_{\text{acyl-CoA}}^{\text{plasma}}}{c_{\text{plasma}}/c_{\text{plasma}}}$$

From Chang et al. (1999), Grange et al. (1995), and Washizaki et al. (1994)

5.2 Rates of Fatty Acid Incorporation into the *sn*-1 Position of Phospholipids

Intravenously injected palmitic acid (16:0), a saturated fatty acid, preferentially enters the *sn*-1 position of brain phospholipids (Nariai et al., 1994). The sum of $J_{FA,i}$ (Eq. 3) for incorporation of palmitic acid into rat brain phospholipids plus neutral lipid equals 0.78 nmol/s/g brain (Grange et al., 1995). The brain concentration of esterified palmitic acid is 28 $\mu\text{mol/g}$ (Rehncrona et al., 1982), whereas total esterified fatty acid is 111.9 $\mu\text{mol/g}$, with half (56 $\mu\text{mol/g}$) in the *sn*-1 position (Rehncrona et al., 1982). Assuming that palmitate is only at the *sn*-1 position of phospholipids (small amounts may be found in triacylglycerol and cholesterol ester), palmitate must then represent half of the fatty acid at the *sn*-1 position (i.e., 28 $\mu\text{mol/g}$). If rates of incorporation of the remaining fatty acids into the *sn*-1 position approximate that of palmitate, the sum of their $J_{FA,i}$ equals 2×0.78 nmol/s/g or 1.56 nmol/s/g (Purdon and Rapoport, 1998).

5.3 Rates of Fatty Acid Incorporation into the *sn*-2 Position of Phospholipids

Intravenously injected radiotracers of polyunsaturated arachidonic and docosahexaenoic (22:6 n-3) acids almost exclusively enter the *sn*-2 position of rat brain phospholipids (DeGeorge et al., 1991; Nariai et al., 1994). The sum of $J_{FA,i}$ (Eq. 3) for arachidonic acid into total phospholipids + neutral lipids equals 0.72 nmol/s/g (Washizaki et al., 1994). The brain concentration of esterified arachidonic acid is 11.3 $\mu\text{mol/g}$, 20% of the 56 μmol of fatty acids in the *sn*-2 position (Rehncrona et al., 1982). If the remaining fatty acids enter the *sn*-2 position at the same rate as arachidonic acid, the net rate of incorporation is $0.72 \text{ nmol/s/g} \times 5 = 3.60$ nmol/s/g.

5.4 ATP Consumption by Fatty Acid Recycling

The above calculations indicate that the net rate of incorporation of long-chain fatty acids into the *sn*-1 and *sn*-2 positions of rat brain phospholipids equals

$$1.56(\textit{sn-1}) \text{ nmol/s/g} + 3.6(\textit{sn-2}) \text{ nmol/s/g} = 5.2 \text{ nmol/s/g.} \quad (10)$$

The generation of acyl-CoA from unesterified fatty acids and ATP by acyl-CoA synthetase occurs in two steps that include formation of a fatty acid-AMP intermediate and conversion of ATP to AMP and PP_i (Waku, 1992; Hisanaga et al., 2004). Adenylate kinase catalyzes the reversible phosphotransfer between ADP, ATP, and AMP that can yield two ADP molecules from AMP with the consumption of one ATP; the process is a component in an integrated phosphotransfer system between sites of ATP consumption and production (Dzeja et al., 2004). Adenylate kinase is found in the brain (Janssen et al., 2004) and its conversion of AMP to ADP, followed by the generation of ATP from ADP by oxidative phosphorylation, indicates that overall two ATPs are required for acyl-CoA formation. Thus, ATP consumption to support fatty acid incorporation into rat brain phospholipids equals (from Eq. 5)

$$5.2 \text{ nmol/s/g} \times 2 = 10.4 \text{ nmol of ATP/s/g.} \quad (11)$$

This rate represents 5% of the 208 nmol/s/g of ATP consumed by rat brain (Table 4.6-2) (Purdon and Rapoport, 1998).

6 ATP Consumption for Maintaining Membrane Phospholipid Asymmetries

6.1 Aminophospholipid Asymmetries in Membranes

Studies of different cell types indicate that phospholipids in membranes of the endoplasmic reticulum, Golgi apparatus, and mitochondria are symmetrically disposed, due to randomization by an ATP-independent protein that acts on phospholipids synthesized de novo on the membrane surfaces (Herrmann et al., 1990;

Zachowski and Gaudry-Talarmain, 1990; Williamson and Schlegel, 1994). In contrast, plasma membrane phospholipids are distributed asymmetrically, with the charged aminophospholipids, phosphatidylserine (PtdSer) and phosphatidylethanolamine (PtdEtn), largely located on the inside (cytosolic) surface. This asymmetry is produced by an ATP-linked aminophospholipid translocase that can transfer an aminophospholipid in either direction with the consumption of one ATP (Bitbol and Devaux, 1988; Zachowski and Gaudry-Talarmain, 1990; Belezny et al., 1993; Williamson and Schlegel, 1994; Diaz and Schroit, 1996).

There is considerable evidence for charged aminophospholipid asymmetry at brain cell membranes. Ischemia results in exteriorization of PtdSer in neurons (Walton et al., 1997), as does apoptosis. The putative aminophospholipid translocase has been identified in the bovine brain (Ding et al., 2000). However, direct data are unavailable for the rates of formation of phospholipid membrane asymmetry in brain. We therefore will calculate these rates and their ATP consumption using data from the human erythrocyte.

With a total PtdSer concentration of 9 $\mu\text{mol/g}$ in rat brain (Wells and Dittmer, 1967), PtdSer at the inner leaflet of brain plasma membranes can be taken to be 7 $\mu\text{mol/g}$ (Purdon and Rapoport, 1998). The brain PtdEtn concentration is 25.7 $\mu\text{mol/g}$ (Wells and Dittmer, 1967), and studies in different tissues suggest that 45% of this PtdEtn is distributed symmetrically in nuclear (5%), Golgi (10%), lysosomal (10%), and mitochondrial (25%) membranes (Williamson and Schlegel, 1994; Allan, 1996). The remaining 55% (14.1 mmol/g) can be taken as asymmetrically disposed in the plasma membrane due to the action of an aminophospholipid translocase. On the basis of its distribution in human erythrocyte membranes, 85% of plasma membrane PtdEtn should be on the inner surface and 15% on the outer surface, at a ratio of 5.71. This gives $(25.7 \mu\text{mol/g} \times 0.55) \times 0.85 = 12.0 \mu\text{mol/g}$ on the cytoplasmic side and $(25.7 \mu\text{mol/g} \times 0.55) \times 0.15 = 2.1 \mu\text{mol/g}$ on the cell surface (Zachowski and Gaudry-Talarmain, 1990; Williamson and Schlegel, 1994; Diaz and Schroit, 1996; Purdon and Rapoport, 1998).

6.2 ATP Consumption by Aminophospholipid Translocation

Figure 4.6-3 illustrates the asymmetric distribution of aminophospholipids across a membrane bilayer, where $k_{\text{out} \rightarrow \text{in}}$ and $k_{\text{in} \rightarrow \text{out}}$ are rate constants (s^{-1}) for inward (outside to inside) and outward fluxes, respectively, and $k_{\text{in} \rightarrow \text{out}} < k_{\text{out} \rightarrow \text{in}}$. We define flux from outside to inside as

$$J_{\text{in}} = k_{\text{out} \rightarrow \text{in}} c_{\text{out}} \quad (12a)$$

and efflux as

$$J_{\text{out}} = k_{\text{in} \rightarrow \text{out}} c_{\text{in}}, \quad (12b)$$

where c_{in} and c_{out} are the aminophospholipid concentrations on the inside and outside of the membrane, respectively. At steady state,

$$J_{\text{in}} = J_{\text{out}}. \quad (12c)$$

For PtdEtn, c_{in} and c_{out} are 12.0 $\mu\text{mol/g}$ and 2.1 $\mu\text{mol/g}$, respectively (see above), and thus

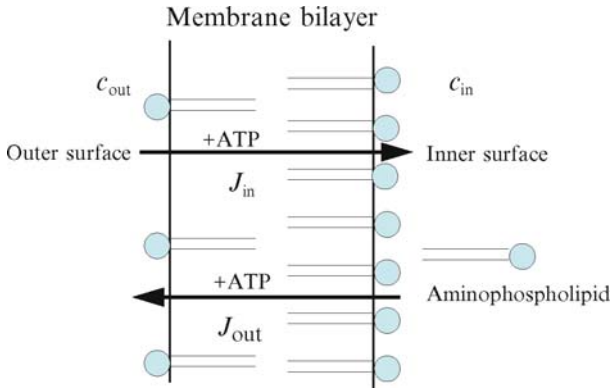
$$\frac{k_{\text{out} \rightarrow \text{in}}}{k_{\text{in} \rightarrow \text{out}}} = \frac{c_{\text{in}}}{c_{\text{out}}} = 5.71. \quad (13)$$

In human erythrocyte membranes, $k_{\text{in} \rightarrow \text{out}} = 1.50 \times 10^{-4} \text{ s}^{-1}$ for PtdEtn (Bitbol and Devaux, 1988), and by Eq. 13 $k_{\text{out} \rightarrow \text{in}} = 8.57 \times 10^{-4} \text{ s}^{-1}$. J_{in} and J_{out} for PtdEtn both equal 1.8 nmol/s/g . Additionally, using $k_{\text{in} \rightarrow \text{out}} = 2 \times 10^{-4} \text{ s}^{-1}$ for PtdSer in human erythrocytes (Bitbol and Devaux, 1988) and $c_{\text{in}} = 7 \mu\text{mol/g}$ (see above), J_{out} and J_{in} for PtdSer both equal 1.4 nmol/s/g .

Given the 1:1 stoichiometry between transmembrane aminophospholipid flux and ATP consumption (Bitbol and Devaux, 1988; Belezny et al., 1993; Diaz and Schroit, 1996), ATP consumption for the

■ **Figure 4.6-3**

Model of plasma membrane bilayer. The aminophospholipids, phosphatidylserine and phosphatidylethanolamine, are concentrated on the inner (cytoplasmic) surface. $J_{in \rightarrow out}$ represents inward-to-outward flux, whereas $J_{out \rightarrow in}$ represents outward-to-inward flux of aminophospholipids. ATP is required for both fluxes at a stoichiometry of 1:1. From Purdon and Rapoport (1998)



bidirectional transfer of PtdEtn and PtdSer equals 3.6 nmol/s/g and 2.8 nmol/s/g, respectively (Purdon and Rapoport, 1998), a total of 6.4 nmol/s/g. Extrapolating to the human brain, and then to the rat brain by multiplying the rate in humans by 2.5, gives a rate of 16 nmol/s/g, or 7.7% of the net brain rate (▶ [Table 4.6-2](#)).

7 ATP Consumption by the Phosphatidylinositol Cycle

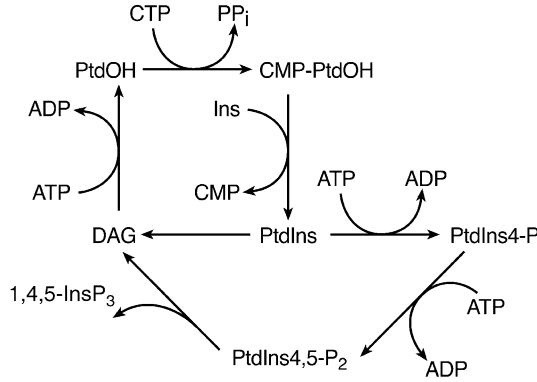
The de novo synthesis of inositol-containing phospholipids involves the formation of 1,2-diacyl-*sn*-glycero-3-phosphate (PtdOH) from glyceraldehyde phosphate (GAP), followed by incorporation of *myo*-inositol and later by phosphorylation to produce phosphatidylinositol-4-phosphate (PtdIns4-P) and phosphatidylinositol-4,5-bisphosphate (PtdIns4,5-P₂). Nine moles of ATP are consumed by this de novo pathway (Verhoeven et al., 1987; Fisher et al., 1992).

The terminal portion of this de novo pathway is modulated by neuroreceptor-initiated activation of PLC via a GTP-linked protein (Fisher et al., 1992; Hokin and Dixon, 1993; Agranoff and Fisher, 1994; Hajra, 1995; Cooper et al., 2003). The resultant hydrolysis of PtdIns4,5-P₂ produces two second messengers, inositol-1,4,5-trisphosphate (1,4,5-InsP₃) and 1,2-diacyl-*sn*-glycerol (DAG). 1,4,5-InsP₃ can promote the release of intracellular Ca²⁺, whereas DAG can activate protein kinase C. To complete the PtdIns signaling cycle (▶ [Figure 4.6-4](#)), DAG is phosphorylated by a receptor-linked diglyceride kinase and subsequently converted to the cytosine monophosphate (CMP) derivative of phosphatidic acid. PtdIns, which then is formed by an exchange of *myo*-inositol for CMP, undergoes phosphorylation to PtdIns4-P and PtdIns4,5-P₂ by selective kinases.

This recycling of diglyceride through the PtdIns cycle consumes 5 moles of ATP—one for converting PtdIns to PtdIns4-P, one for converting PtdIns4-P to PtdIns4,5-P₂, one for converting DAG to PtdOH, and two for converting PtdOH to CMP-PtdOH (Pediconi and Barrantes, 1990; Fisher et al., 1992; Tong and Sun, 1996). It is not possible from available data to determine the relative contributions of de novo synthesis and of the PtdIns cycle (▶ [Figure 4.6-4](#)) to ATP consumption for the reformation of PtdIns4,5-P₂ following its hydrolysis by PLC. We therefore consider that recovery requires between 5 and 9 moles of ATP per turn of the PtdIns cycle (Purdon et al., 2002) (see ▶ [Table 4.6-2](#)).

■ **Figure 4.6-4**

Pathways of the phosphatidylinositol (PtdIns) cycle. PtdOH, 1,2-diacyl-*sn*-glycero-3-phosphate; PtdIns, phosphatidylinositol; PtdIns4-P, phosphatidylinositol-4-phosphate; PtdIns4,5-P₂, phosphatidylinositol-4,5-bisphosphate; 1,4,5-InsP₃, inositol 1,4,5-trisphosphate; CMP, cytosine monophosphate; CDP, cytosine diphosphate; DAG, diacylglycerol, Ins, *myo*-inositol. From Purdon et al. (2002)



7.1 ATP Consumption for Phosphorylation of Inositol-Containing Phospholipids from Studies in Platelets

Maintenance of a suitable concentration of receptor-associated PtdIns4,5-P₂ is crucial for the PLC generation of second messengers, 1,4,5-InsP₃ and DAG. The action of the PtdIns cycle reclaims PLC-generated diglyceride that would otherwise be lost by the action of mono/diglyceride lipases. In addition, PtdIns4-P/PtdIns4,5-P kinases/phosphatases maintain a high turnover of phosphates at the 4/5 positions of the inositol ring, which in turn ensures rapid replacement of depleted PtdIns4-P and PtdIns4,5-P from PtdIns in stimulated cells. This high turnover rate was demonstrated in the brain *in vivo*, where the intracerebral injection of [³²P]P_i-radiolabeled ATP resulted in high radioactivity in brain PtdIns4-P and PtdIns4,5-P (Sun and Lin, 1989).

To estimate the rate of ATP consumption required for maintaining the high turnover of PtdIns4-P and PtdIns4,5-P₂, the kinetics of phosphate turnover in inositol-containing phospholipids of the PtdIns cycle were studied in isolated unstimulated human platelets that were exposed to [³²P]P_i in platelet-rich plasma (Verhoeven et al., 1987). In these platelets, the species PtdIns, PtdIns4-P, and PtdIns4,5-P₂ were rapidly labeled, and their specific activities increased linearly and equally with the β and γ phosphates of the metabolic ATP. At the steady state, radioactivity in PtdIns, PtdIns4-P, and PtdIns4,5-P₂ was 0.7%, 1.9%, and 3.6 % of ATP radioactivity, respectively (Verhoeven et al., 1987).

The first row of Table 4.6-4 gives radioactivity in the three PtdIns species in platelets exposed to [³²P]P_i, as a percent of ATP radioactivity. In the second row are rates of ATP consumption by the three species in 10¹¹ platelets. In the third are the platelet phospholipid concentrations, and in the fourth are rates of ATP consumption per nmol platelet phospholipid. Knowing the concentration of the respective phospholipid in microwaved rat brain (fifth row) (Soukup et al., 1978; Nishihara and Keenan, 1985; Reddy and Bazan, 1987) gives the rate of ATP consumption for that phospholipid in both human and rat brain (sixth row). The sum of these rates in the human brain, when multiplied by 2.5, gives a rate of 24.8 nmol ATP/s/g for the rat brain, or 12% of the net brain ATP consumption (last column and Table 4.6-2). This rate is estimated to maintain phosphate turnover in all three of the inositol-containing phospholipids in the unstimulated brain.

■ **Table 4.6-4**

Brain ATP consumption by the phosphatidylinositol cycle obtained from the consumption rates of three inositol-containing phospholipids in human platelets

Measurement	PtdIns	PtdIns4-P	PtdIns4,5-P ₂
Platelet phospholipid radioactivity as percent ATP radioactivity ^a	0.7	1.9	3.6
Nanomoles of ATP consumed per second per nanomole phospholipid in 10 ¹¹ platelets	0.47	1.27	2.4
Phospholipid in 10 ¹¹ platelets ^a (nmol)	1600	170	160
Picamoles of ATP consumed per second per nanomole phospholipid in 10 ¹¹ platelets	0.29	7.47	15
Phospholipid (nmol)/g of rat brain ^b	2004	204	524
ATP (nmol)/s/g human (rat) brain ^c	0.6 (1.5)	1.5 (3.75)	7.8 (19.5)
Percent net brain ATP consumption ^d	0.7	1.8	9.5

PtdIns phosphatidylinositol, *PtdIns4-P* phosphatidylinositol-4-phosphate, *PtdIns4,5-P₂* phosphatidylinositol-4,5-bisphosphate

Adapted from Purdon et al. (2002)

^aVerhoeven et al. (1987)

^bNishihara and Keenan (1985), Reddy and Bazan (1987) and Soukup et al. (1978)

^cRate in rats is 2.5 times the human rate

^d208 nmol/s/g for rat brain and 83 nmol/s/g for human brain (cf [▶ Sect. 5](#))

7.2 ATP Consumption for the De Novo Biosynthesis of Inositol-Containing Phospholipids from Studies in Cultured Neurons

Myo-inositol incorporation into PtdIns has been quantified in cultured cortical neurons from the fetal mouse using a three-compartmental model consisting of *myo*-inositol in the extracellular bath, intracellular precursor *myo*-inositol, and intracellular PtdIns (PtdIns, PtdIns4-P, and PtdIns4,5-P₂) (Chikhale et al., 2001). The cells were exposed to deuterium-labeled *myo*-inositol (*myo*-[²H₆]inositol) at a specific activity of 1 at $t = 0$, after which time-dependent changes in specific activities of intracellular *myo*-inositol and PtdIns were measured using mass spectrometry. The rate of *myo*-inositol incorporation into PtdIns, J_{PtdIns} , is given as a form of [▶ Eq. 3](#)

$$J_{\text{PI}} = \left[\frac{c_{\text{cell,PI}}^*(T)}{\int_0^T \lambda(t) c_{\text{bath,myo-inositol}}^* dt} \right] c_{\text{bath,myo-inositol}} = \frac{c_{\text{cell,PI}}^*(T)}{\int_0^T \lambda(t) dt}, \quad (14)$$

where $c_{\text{bath,myo-inositol}}^* = c_{\text{bath,myo-inositol}}$ are constant and equal (bath specific activity = 1), and (cf [▶ Eq. 1](#))

$$\lambda(t) = c_{\text{cell,myo-inositol}}^*(t) / c_{\text{cell,myo-inositol}}. \quad (15)$$

$c_{\text{cell,myo-inositol}}^*(t)$ and $c_{\text{cell,myo-inositol}}$ are time-dependent labeled and time-independent unlabeled cell *myo*-inositol concentrations, respectively; $\lambda(t)$ is a time-dependent dilution factor ([▶ Eq. 1](#)), since cell *myo*-inositol-specific activity approaches equilibrium very slowly with bath specific activity (Chikhale et al., 2001); $c_{\text{cell,PI}}^*(T)$ is the labeled concentration of PtdIns in the cell at time T of sampling. Using *Eqs. 14* and *15*, J_{PtdIns} , the initial rate of entry of *myo*-[²H₆]inositol from the bath into PtdIns, was calculated as 315 nmol/h/g protein. This rate gave PtdIns turnover ([▶ Eq. 4a](#)) as 10.3% per hour, equivalent to a half-life ([▶ Eq. 4b](#)) of 6.8 h. (Preliminary results obtained by infused *myo*-[²H₆]inositol i.p. in vivo in rats suggest that the in vivo half-life is $\ll 6.8$ h (Ma et al., 2006).

The PtdIns concentration in the rat brain is 2.2 mmol/g (Ansell, 1973). Assuming a turnover rate of 10.3% per hour from the cultured neuron data, the rate of PtdIns formation equals 227 nmol/h/g or

0.063 nmol/s/g (Purdon et al., 2002). As the cultured neuron experiments were performed in the absence of an agonist, we assume that there was no neuroreceptor mediated activation of the PtdIns cycle and no recycling of diglycerides because the action of “PtdIns cycle” diglyceride kinase is linked to receptor occupancy (Holmsen et al., 1992). We also assume that the diglyceride produced by low PLC activity in unstimulated neurons was completely hydrolyzed by diglyceride and monoglyceride lipases. Therefore, as 9 moles of ATP are required for each mole of *myo*-inositol turning over in the PtdIns cycle (the higher number is for de novo synthesis, see above), the estimated rate of ATP consumption for de novo synthesis is 0.57 nmol/s/g or 0.27 % of the 208 nmol/s/g of ATP consumed by rat brain (▶ [Table 4.6-2](#)). The lower value of five ATPs per turn of the PtdIns cycle would be required for calculating ATP consumption in the presence of an agonist.

In summary, the human platelet and mouse neuronal culture data suggest that the de novo synthesis pathway involving inositol-containing phospholipids consumes 0.27% of net brain ATP consumption and that maintenance of their phosphorylation state may require 12% of net brain ATP consumption.

8 ATP Consumption by Synthesis of Brain Ether Phospholipids

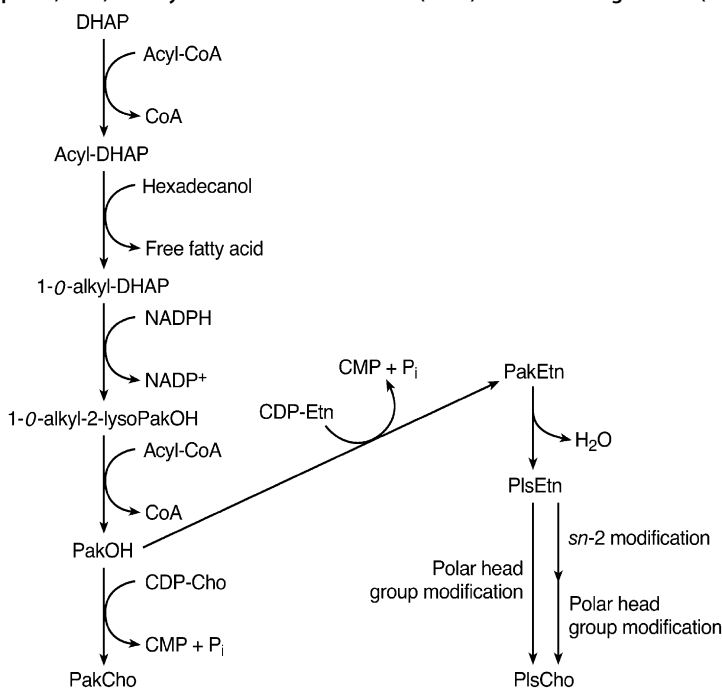
Ether phospholipids have a 1-*O*-alkyl (plasmanyl) or a 1-*O*-alk-1'-enyl (plasmenyl) linkage at the *sn*-1 position of the glycerol backbone, and in mammals belong almost exclusively to the choline and ethanolamine glycerophospholipid classes (Ansell, 1973). In human brain, plasmenyl-type ether phospholipids (plasmalogens) comprise approximately 23% of total phospholipids (Panganamala et al., 1971), while in rat brain and monkey spinal cord 33–35% of myelin phospholipids are plasmalogens (Horrocks, 1967; Eng and Noble, 1968). Evidence suggests a primary structural role for them in myelin, but a primary dynamic role in the gray matter, involving signal transduction, membrane fusion, vesicle formation, antioxidant function, and synaptic plasticity (Rosenberger et al., 2002). Nevertheless, measurements of radioactive decay, following ether phospholipid labeling by intracerebrally injected [¹⁴C]ethanolamine, [³H]glycerol, [¹⁴C]choline, or [³²P]phosphate, have suggested long half-lives: 11–58 days in myelin and microsomes, 30 days in whole brain, and 6–9.5 days in neurons and glia (Freysz et al., 1969; Horrocks et al., 1975; Miller et al., 1977).

▶ [Figure 4.6-5](#) illustrates steps in the de novo synthesis of brain ether phospholipids (Rosenberger et al., 2002), and ▶ [Table 4.6-5](#) shows the stepwise ATP consumption rates. Glucose is converted through a series of reactions to dihydroxyacetonephosphate (DHAP) and GAP (Bell and Coleman, 1980). DHAP is the precursor for the de novo synthesis of ether phospholipids (Pollock et al., 1976; Hajra, 1995; Lee, 1998), whereas GAP is the precursor for the de novo synthesis of diacyl-type phospholipids (Pollock et al., 1976; Bell and Coleman, 1980; Hajra, 1995). At the onset, 1 mole of ATP is consumed per molecule of DHAP derived from glucose. The *sn*-1 position of DHAP is esterified in peroxisomes with a fatty acid. Additionally, the fatty acid component (e.g., hexadecanoic acid) of acyl-CoA is reduced and released as alcohol (Pollock et al., 1976; Hajra, 1995; Lee, 1998; Rosenberger et al., 2002). Formation of acyl-CoA from a fatty acid molecule requires cytosine triphosphate (CTP) and releases PP_i and CMP. Two moles of ATP are required to regenerate CTP (Purdon and Rapoport, 1998). Alkyl-DHAP synthase generates an alkyl or ether linkage at the *sn*-1 position by exchanging a long-chain fatty alcohol for the fatty acid. Therefore, generating the ether linkage at the *sn*-1 position of ether phospholipids requires 4 moles of ATP per mole of DHAP. Following its migration to the endoplasmic reticulum, the 1-*O*-alkyl-2-lyso-*sn*-glycero-3-phosphate is acylated at the *sn*-2 position to form 1-*O*-alkyl-2-acyl-*sn*-glycero-3-phosphate (PakOH) (Pollock et al., 1976; Hajra, 1995; Lee, 1998). Thus, 7 moles of ATP are required to produce 1 mole of PakOH, of which 6 moles are consumed for the production of 3 moles of acyl-CoA and another for the phosphorylation at the *sn*-3 carbon (▶ [Table 4.6-5](#)).

PakOH is converted to 1-*O*-alkyl-2-acylglycerol by a phosphohydrolase within the endoplasmic reticulum (Pollock et al., 1976; Hajra, 1995; Lee, 1998). The resulting ether-containing diglyceride is converted to 1-*O*-alkyl-2-acyl-*sn*-glycero-3-phosphocholine (PakCho) or 1-*O*-alkyl-2-acyl-*sn*-glycero-3-phosphoethanolamine (PakEtn) by the respective choline/ethanolamine phosphotransferases. Activation of choline or ethanolamine to form the CMP derivative prior to incorporation into PakCho or PakEtn requires 3 moles

■ Figure 4.6-5

Biosynthetic pathways in the de novo synthesis of ether phospholipids. PakOH, 1-*O*-alkyl-2-acyl-*sn*-glycerol-3-phosphate; PakEtn, 1-*O*-alkyl-2-acyl-*sn*-glycerol-3-phosphoethanolamine; PakCho, 1-*O*-alkyl-2-acyl-*sn*-glycerol-3-phosphocholine; PlsEtn, 1-*O*-alk-1'-enyl-2-acyl-*sn*-glycerol-3-phosphoethanolamine; PlsCho, 1-*O*-alk-1'-enyl-2-acyl-*sn*-glycerol-3-phosphocholine; DHAP, dihydroxyacetonephosphate; CMP, cytosine monophosphate; CDP, cytosine diphosphate; CoA, coenzyme A. From Purdon et al. (2002) and Rosenberger et al. (2002)



■ Table 4.6-5

ATP consumption by ether phospholipid biosynthesis in gray matter microsomes of rat brain

Ether phospholipid	Synthesis rate ^a (nmol/s/g)	ATP stoichiometry	ATP consumption ^b (nmol/s/g)
PakOH	0.18	7	1.26
PakCho	0.02	3	0.06
PakEtn	0.16	3	0.48
PlsEtn	0.46	0	0
PlsCho	0.36	3	1.08
Total			2.88

PakCho 1-*O*-alkyl-2-acyl-*sn*-glycerol-3-phosphocholine, PakEtn 1-*O*-alkyl-2-acyl-*sn*-glycerol-3-phosphoethanolamine, PakOH 1-*O*-alkyl-2-acyl-*sn*-glycerol-3-phosphate, PlsCho 1-*O*-alk-1'-enyl-2-acyl-*sn*-glycerol-3-phosphocholine, PlsEtn 1-*O*-alk-1'-enyl-2-acyl-*sn*-glycerol-3-phosphoethanolamine

^aRosenberger et al. (2002)

^bPurdon et al. (2002)

of ATP. Thus, the synthesis of 1 mole of PakCho or PakEtn requires 10 moles of ATP, 7 moles to make PakOH and 3 moles to introduce the polar-head group.

The *sn*-1 ether linkage of PakEtn is desaturated at the 1'-position to form the vinyl ether linkage of 1-O-alk-1'-enyl-2-acyl-*sn*-glycero-3-phosphoethanolamine (PlsEtn) by a combination of a cytochrome *b*₅/NADH/cytochrome *b*₅ reductase and a cyanide-sensitive δ -1 alkyl desaturase. ATP is not involved in this process. The δ -1 alkyl desaturase system does not convert PakCho to 1-O-alk-1'-enyl-2-acyl-*sn*-glycero-3-phosphocholine (PlsCho). Instead, PlsCho is derived from PlsEtn by an alternate pathway (Lee, 1998). ATP requirements for these steps are dictated by the formation of choline phosphate and its exchange with the phosphoethanolamine found in PlsEtn by choline phosphotransferase (Ford and Gross, 1994; Lee, 1998). Therefore, synthesis of PlsCho from PlsEtn consumes an additional 3 moles of ATP, requiring a total of 13 moles of ATP per mole PlsCho formed by de novo biosynthesis.

8.1 Energy Requirement for Ether Phospholipid Synthesis

Ether phospholipid synthesis occurs in peroxisomes and microsomes, which contain 8% of brain ether phospholipids (Paltauf, 1994; Snyder, 1996; Lee, 1998). A kinetic model, based on known pathways and compartments of brain ether phospholipid synthesis (Figure 4.6-5), was applied to the data generated by measuring the incorporation of intravenously infused [1,1-³H]hexadecanol into brain ether phospholipids of unanesthetized rats (Rosenberger et al., 2002). Labeled and unlabeled concentrations were determined in plasma and in different fractions of the rat brain up to 120 min following a 5-min intravenous infusion of [1,1-³H]hexadecanol.

Radioactivities of plasma hexadecanol ($c_{\text{plasma,hex}}^*$), brain hexadecanol, and ether phospholipids were measured from the start of [1,1-³H]hexadecanol infusion at time 0 (Rosenberger et al., 2002). A coefficient ($k_{i-1 \rightarrow i}^*$) for the unilateral transfer of labeled hexadecanol from compartment $i-1$ to product compartment i was calculated as the ratio of brain radioactivity $c_{\text{brain},i}^*(T_2)$ in i at time T_2 and integrated radioactivity of the precursor $i-1$ between T_1 and T_2 (input function), where T_1 and T_2 were chosen to cover the initial linear increase of radioactivity in compartment i

$$dc_{\text{brain},i}^*/dt = k_{i-1 \rightarrow i}^* c_{\text{brain},i-1}^* \quad (16a)$$

and

$$k_{i-1 \rightarrow i}^* = \frac{c_{\text{brain},i}^*(T_2)}{\int_{T_1}^{T_2} c_{\text{brain},i-1}^* dt} \quad (16b)$$

To calculate unlabeled mass flux of ether phospholipid from $i-1$ to i (the synthesis rate of i) in units of nmol/min/g brain, we multiply $k_{i-1 \rightarrow i}^*$ by the unlabeled concentration of $i-1$ (nmol/g) in the brain fraction in which the synthesis of i takes place, namely the peroxisome-microsomal fraction (Paltauf, 1994; Snyder, 1996; Lee, 1998). Where $c_{\text{brain},i}$ nmol/g is the unlabeled concentration of i in the microsomal-peroxisomal fraction, the flux of $i-1$ into i ($J_{i-1 \rightarrow i}$) or the rate of synthesis of i equals

$$J_{i-1 \rightarrow i} = k_{i-1 \rightarrow i}^* c_{\text{brain},i-1} \quad (16c)$$

Products of individual ether phospholipids, their synthesis rates, and their respective ATP stoichiometries S (Eq. 5) are presented in Table 4.6-5. With regard to the rate of PlsEtn synthesis, the estimate of 0.46 nmol/min/g by the [1,1-³H]hexadecanol infusion method is comparable to the 0.53 nmol/min/g obtained when measuring [³H]glycerol incorporation into PlsEtn (Masuzawa et al., 1984), supporting the [1,1-³H]hexadecanol method. Seven and 10 moles of ATP are required for the biosynthesis of PakOH, and PakCho plus PakEtn, respectively, whereas 13 moles are required for the biosynthesis of PlsCho. Thus, net ATP consumption by de novo synthesis of ether phospholipids is approximately 2.88 nmol/s/g, which is 1.4% of the total ATP consumed by the rat brain (Table 4.6-2).

9 Disruption of Phospholipid Metabolism Requires Augmented ATP Consumption to Reestablish Membrane Homeostasis

In view of the dependence of brain phospholipid metabolism on a high rate of ATP synthesis (● [Table 4.6-2](#)), pathological conditions that interfere with the synthesis of ATP or that consume excessive amounts of ATP will disrupt phospholipid metabolism. Examples of the former conditions are cerebral ischemia (Bazán and Rodríguez de Turco, 1980; Edgar et al., 1982; Rehncrona et al., 1982; Ikeda et al., 1986; Rabin et al., 1998b), anoxia–hypoxia (Gardiner et al., 1981), inhibition of mitochondrial oxidative phosphorylation by carbon monoxide or cyanide (Li et al., 2002), and hypoglycemia (Ikeda et al., 1987). Conditions that augment ATP consumption include prolonged convulsions, electroshock, and glutamate-mediated excitotoxicity (Dunn, 1973; Folbergrova et al., 1981; McCandless et al., 1982; Reddy and Bazan, 1987; Kosenko et al., 1994).

In general, ATP is required for anabolic reactions, while catabolic reactions can occur in the absence of ATP. In the absence of ATP, there will be a depletion of various phospholipids through different pathways and a buildup of phospholipid breakdown products. Brain ATP depletion will lead to loss of the PtdIns cycle phospholipids with increased 1,4,5-InsP₃ and DAG and their degradation products. Aminophospholipid asymmetries across cell membranes will dissipate with PtdSer being increasingly exteriorized (Walton et al., 1997), disturbances in ether phospholipid synthesis will yield increasing amounts of lysophospholipids, and unesterified long-chain fatty acids will accumulate from all phospholipids (Williamson and Schlegel, 1994; Rabin et al., 1998a; Farooqui and Horrocks, 2001; Furuta et al., 2003).

Brain ATP depletion also will cause rapid membrane depolarization because of failure of the Na⁺/K⁺-ATPase and other ATP-dependent ion pumps, leading to excitotoxicity with the release of glutamate and aspartate from intracellular stores (Choi and Rothman, 1990; Lees, 1991; Siesjo et al., 1991). Furthermore, ATP-dependent glutamate reuptake will be interrupted and may even run backward (Rossi et al., 2000). Ca²⁺ entry into cells via ionotropic glutamatergic receptors (Frandsen and Schousboe, 1993; Weichel et al., 1999) will activate Ca²⁺-dependent enzymes including calmodulin-dependent protein kinase II (Colbran, 2004), calpain (Hewitt et al., 1998), PLC γ (Gurd and Bissoon, 1997), cytosolic PLA₂ (cPLA₂), and secretory PLA₂ (sPLA₂) (Weichel et al., 1999; Kolko et al., 2002; Rodríguez De Turco et al., 2002). Activation of the phospholipases in turn will catabolize membrane phospholipids to unesterified fatty acids, lysophospholipids, platelet activating factor (PAF), and other products that, at high concentrations, can be neurotoxic by any of a number of mechanisms beyond the scope of this chapter (Sun and Gilboe, 1994; Katsuki and Okuda, 1995; Atsumi et al., 1997; Bazan, 1998; Brash, 2001; Pompeia et al., 2003; Penzo et al., 2004). If phospholipid homeostasis is to recover from such events, not only must mitochondrial oxidative phosphorylation be reestablished to supply ATP at a normal rate, but extra ATP must be synthesized to reincorporate the high concentration of various phospholipid components (e.g., lysophospholipids, fatty acids, free choline) (Narita et al., 2000; Farooqui and Horrocks, 2001; Rami et al., 2003).

9.1 Cerebral Ischemia

Cerebral ischemia is an example in which phospholipid changes occur because of reduced ATP availability. ● [Table 4.6-6](#) illustrates that 5 min of total cerebral ischemia in the gerbil increased the net brain unesterified fatty acid concentration 4.5-fold, with a maximum fractional increase (10-fold) in the arachidonic acid concentration (Rabin et al., 1998a). For recovery to occur if perfusion were reestablished, reacylation of excess unesterified fatty acid integrated over time would have to occur at a 4.5-fold normal rate, as would ATP consumption by reacylation. ● [Table 4.6-7](#) shows, furthermore, that initial reacylation was accelerated for arachidonic acid compared with palmitic acid during reperfusion after 5 min of ischemia in the gerbil brain (Rabin et al., 1998a). This selectively may have reflected selectivity of acyl-CoA synthetases for arachidonic acid over palmitic acid (Kang et al., 1997).

■ Table 4.6-6

Unesterified fatty acid and Acyl-CoA concentrations in Gerbil brain after 5 min of ischemia followed by 5 min of reperfusion

Fatty acid	Fatty acid concentration (nmol/g wet wt.)		Acyl-CoA concentration (nmol/g wet wt.)	
	Control	Ischemia–reperfusion	Control	Ischemia–reperfusion
16:0 (palmitic)	34.3 ± 2.1	81.2 ± 10.0**	11.7 ± 0.8	8.8 ± 1.0*
16:1 (palmitoleic)	1.9 ± 0.4	1.2 ± 0.4		
18:0 (stearic)	35.9 ± 4.1	199.0 ± 26.0***	3.5 ± 0.3	5.0 ± 0.5
18:1 (oleic)	15.0 ± 2.2	49.3 ± 8.7**	10.8 ± 0.9	10.0 ± 1.1
18:2 n-6 (linoleic)	3.8 ± 0.8	8.6 ± 1.5*	1.3 ± 0.2	0.6 ± 0.2**
18:3 n-3 (α-linolenic)	1.1 ± 0.4	1.7 ± 0.4		
20:4 n-6 (arachidonic)	3.4 ± 1.2	94.8 ± 20.4**	1.4 ± 0.2	7.6 ± 0.7***
22:6 n-3 (docosahexaenoic)	1.2 ± 0.4	16.3 ± 4.0**	1.3 ± 0.2	0.3 ± 0.1***
Sum	96.6	452.1	30	32.3

Mean ± SEM ($n = 8-10$). Differs from control mean: * $p < 0.05$, ** $p < 0.01$, *** $p < 0.01$

From Rabin et al.

■ Table 4.6-7

Incorporation rates J_{FA} of arachidonic and palmitic acids into gerbil brain phospholipids after 5 min of ischemia followed by 5 min of reperfusion: effect of EGb 761

Fatty acid	Control	Ischemia–reperfusion	
		J_{FA}^a (No EGb 761)	J_{FA}^a (EGb 761)
Arachidonic acid	10.5 ± 1.4	25.4 ± 3.9**	37.8 ± 3.4***,°
Palmitic acid	70.9 ± 9.0	75.0 ± 9.8	73.6 ± 10.9

^aSee Rabin et al. (1998b) for units

Mean ± SEM ($n = 8-10$)

Differs from control mean: * $p < 0.05$, ** $p < 0.01$, *** $p < 0.01$

^oDiffers from ischemia–reperfusion mean without EGb 761, $p < 0.05$

9.2 Possible Therapies for Ischemia Related to ATP Debt

In view of a high rate of ATP consumption by phospholipid metabolism, anti-ischemia therapy might profitably focus on reducing ATP demand by phospholipid metabolism and on ameliorating the toxic effects of phospholipid breakdown products. Two regions need be considered, infarcted areas where neurons die within 5 min of total ischemia (Symon, 1993) (thus therapy must be immediate) and the surrounding area (penumbra) where blood flow may be compromised without causing immediate neuronal death (Hossmann, 1994; Narita et al., 2000; Baron, 2001; Heiss et al., 2004).

ATP consumption might be reduced in ischemia by blocking ionotropic glutamatergic receptors that allow Ca^{2+} into cells to activate phospholipases (Gorgulu et al., 2000; Willard et al., 2000; Mattson, 2003; Aarts and Tymianski, 2004), whereas inhibitors could be used to block PLA₂ enzymes directly. A number of inhibitors of cPLA₂, which is arachidonic acid-selective and Ca^{2+} -dependent (Dennis, 1994), have been proposed in this regard. These include 2-oxoamines (Kokotos et al., 2002), 1,3-disubstituted propane-2 skeleton drugs (Connolly et al., 2002), arachidonoyl-trifluoromethylketone (Riendeau et al., 1994), and bilobalide, a sesquiterpene trilactone ingredient of ginkgo biloba (Weichel et al., 1999; Defeudis, 2002).

Additionally, chronic administration of lithium and carbamazepine to rats has been reported to downregulate parts of the brain arachidonic acid cascade—cPLA₂ transcription, cyclooxygenase (COX)-2 activity, and the production of prostaglandin E₂ (PGE₂) (Chang and Jones, 1998; Rintala et al., 1999; Bosetti et al., 2002; Ghelardoni et al., 2004; Weerasinghe et al., 2004), while slowing arachidonic acid recycling in brain phospholipids (Chang et al., 1996, 1999, 2001; Lee et al., 2004b). Consistent with these effects, these drugs can reduce brain damage in animal models of ischemia (Murakami and Furui, 1994; Nonaka and Chuang, 1998). To the degree that generation of phospholipid components such as unesterified fatty acids and lysophospholipids is inhibited, the ATP requirements for their reincorporation will be reduced.

Nonsteroidal anti-inflammatory drugs (NSAIDs) that inhibit COX-2 and thus oxidation of arachidonic acid to PGE₂ (Figure 4.6-2) also can be neuroprotective in experimental cerebral ischemia (Iadecola and Ross, 1997). Antagonists to receptors of PAF (Liu et al., 2001), lysophospholipid (Lynch and Macdonald, 2002), PGE₂ (McCullough et al., 2004), and to nonenzymatic oxidation products of PUFAs (Gottlieb, 2003) may prove useful. Reduction of reactive oxygen species acting on brain lipids has been widely considered (Adibhatla et al., 2003). Once high levels of lysophospholipids and unesterified arachidonic acid are produced, it is important to remove the membrane perturbation and toxic effects by reacylation. Pharmacological inhibition of arachidonate derivitization will leave suitable levels of arachidonic acid for rapid reacylation of lysophospholipid; otherwise, the lysophospholipid will remain as a membrane perturbant ultimately to be broken down by lysophospholipase, which will necessitate replacement of phospholipid by the slower *de novo* pathway.

If brain ATP synthesis can be restored during reperfusion, fatty acid reincorporation into available lysophospholipid might be enhanced by drugs like ciprofibrate, which activate peroxisomal proliferator-activated receptor α (PPAR α) and upregulate brain acyl-CoA synthetase activity (Cullingford et al., 2002). In this regard, EGb 761, a component of ginkgo biloba that is neuroprotective in experimental cerebral ischemia (Spinnewyn, 1992; Chandrasekaran et al., 2001), accelerates arachidonic acid reincorporation into brain phospholipid after transient ischemia (Table 4.6-7) (Rabin et al., 1998b).

10 Discussion

In contrast to the assertion that brain phospholipid metabolism consumes less than 2% of net brain ATP consumption (Clarke and Sokoloff, 1994), our calculations (Table 4.6-2) indicate that the percentage approximates 26% (Purdon and Rapoport, 1998; Purdon et al., 2002). Even this range may be a lower bound, as a lack of knowledge of their metabolic rates does not allow us at this time to estimate brain ATP consumption by anandamide synthesis from arachidonic acid (Pestonjamas and Burstein, 1998), protein acylation (DeMar et al., 1996), *de novo* synthesis and turnover of 1,2-diacyl phospholipids, triglycerides, diglycerides, cholesterol, steroids, and isoprenoids (Lehninger et al., 1993; Cunnane et al., 1998), recycling of choline and other bases within phospholipids (Ford and Gross, 1994), and other lipid metabolic processes.

A high rate of ATP consumption by brain phospholipid metabolism is consistent with evidence that phospholipids participate in multiple active processes, including synaptic neurotransmission and membrane remodeling (see Sect. 1). A high rate was derived from evidence for high rates of a number of brain phospholipid metabolic processes with half-lives of minutes to hours, which were estimated in part using appropriate kinetic models (Figure 4.6-1). The prior slope and feeding studies that suggested half-lives of days to months (Table 4.6-1) had ignored recycling and compartmentation in brain phospholipid metabolism.

In unanesthetized rats, we calculated that recycling of long-chain fatty acids in rat brain phospholipids consumes about 5% of net brain ATP consumed, when measuring rates of incorporation of their radiolabels via the precursor acyl-CoA pool, and when taking into account the dilution factor λ (equation 1). We also estimated that *de novo* synthesis of brain ether phospholipids consumes approximately 1.4% of the net brain ATP consumption, when using data obtained by injecting [1,1-³H]hexadecanol intravenously in unanesthetized rats and by measuring tracer distribution over time in individual brain ether phospholipids (Rosenberger et al., 2002). Additionally, we extrapolated ATP consumption for

maintaining brain membrane asymmetries of aminophospholipids as 7.7 % of the net brain ATP consumption, using data from human erythrocyte membranes. Extrapolation from measurements on nonstimulated human platelets exposed to [^{32}P]P_i suggested that maintaining the state of phosphorylation of inositol-containing phospholipids to support the PtdIns cycle consumes an additional 12% of the net brain ATP consumption, whereas an ATP consumption rate of 0.27 % by de novo synthesis was obtained from studies on isolated fetal mouse neurons exposed to deuterated *myo*-inositol. However, it is likely that the latter value is a marked underestimate, as cultured neurons lack normal synaptic connections and critical growth factors and have a slowed PtdIns cycle compared with neurons in situ since they are not activated (Brusa et al., 1992; Hertz and Peng, 1992; Holmsen et al., 1992; Murphy et al., 1992b; Rowlands et al., 2001). Indeed, stimulation of cultured neurons by appropriate agonists can accelerate the PtdIns cycle tenfold (Gammon et al., 1989; del Rio et al., 1999), and studies suggest shorter half-lives of inositol-containing phospholipids in the brain in vivo than in cultured neurons (Ma et al., 2006).

In pathological conditions accompanied by ATP insufficiency, brain lipid metabolism is markedly disturbed and large amounts of unesterified fatty acids and other products are released from phospholipids. For the brain to recover without permanent sequelae, phospholipids that have been degraded have to be resynthesized de novo, fatty acids that have been released have to be reincorporated, and membrane asymmetries of aminophospholipids have to be reestablished. Thus, enhancing ATP production, reducing ATP demand, interfering with the toxic effects of high concentrations of phospholipid products, and decreasing the release while stimulating reincorporation of phospholipid components should be considered as potential therapeutic strategies.

A limitation of the results in [Table 4.6-2](#) is that ATP consumption rates by only two brain lipid metabolic processes, fatty acid recycling within phospholipids and synthesis of ether phospholipids, were calculated directly from data obtained unanesthetized rats. Consumption rates for the phosphorylation of inositol-containing phospholipids and for maintaining aminophospholipid asymmetries were extrapolated from other tissue preparations in rodents or humans, whereas consumption by additional lipid metabolic processes could not be evaluated because the relevant data are unavailable (Lehninger et al., 1993). This makes our estimated consumption rate of 26% of the net brain ATP consumption tentative. However, by identifying approaches to calculate these rates in vivo and by emphasizing their importance, we hope that this review will stimulate efforts to obtain more precise estimates of the energy consumption by brain phospholipid metabolism in health and disease.

References

- Aarts MM, Tymianski M. 2004. Molecular mechanisms underlying specificity of excitotoxic signaling in neurons. *Curr Mol Med* 4: 137-147.
- Adibhatla RM, Hatcher JF, Dempsey RJ. 2003. Phospholipase A₂, hydroxyl radicals, and lipid peroxidation in transient cerebral ischemia. *Antioxid Redox Signal* 5: 647-654.
- Agranoff BW, Fisher SK. 1994. Phosphoinositides. *Basic neurochemistry*, 5th edition. Siegel GJ, Agranoff BW, Albers RW, Molinoff PB, editors. New York: Raven Press; pp. 417-448.
- Albers RW, Siegel GJ, Stahl WL. 1994. Membrane transport. *Basic neurochemistry*. Siegel GJ, Agranoff BW, Albers RW, Molinoff PB, editors. New York: Raven Press; pp. 49-74.
- Allan D. 1996. Mapping the lipid distribution in the membranes of BHK cells (mini-review). *Mol Membr Biol* 13: 81-84.
- Allweis C, Landau T, Abeles M, Magnes J. 1966. The oxidation of uniformly labelled albumin-bound palmitic acid to CO₂ by the perfused cat brain. *J Neurochem* 13: 795-804.
- Ansell GB. 1973. Phospholipids and the nervous system. Form and function of phospholipids. Ansell GB, Hawthorne JN, Dawson RMC, editors. New York: Elsevier; pp. 377-422.
- Atsumi G, Murakami M, Tajima M, Shimbara S, Hara N, et al. 1997. The perturbed membrane of cells undergoing apoptosis is susceptible to type II secretory phospholipase A₂ to liberate arachidonic acid. *Biochim Biophys Acta* 1349: 43-54.
- Baron JC. 2001. Perfusion thresholds in human cerebral ischemia: Historical perspective and therapeutic implications. *Cerebrovasc Dis* 11(Suppl 1): 2-8.
- Bazán NG. 1990. Supply of n-3 polyunsaturated fatty acids and their significance in the central nervous system.

- Nutrition and the brain. Wurtman RJ, Wurtman JJ, editors. New York: Raven Press; pp. 1-24.
- Bazan NG. 1998. The neuromessenger platelet-activating factor in plasticity and neurodegeneration. *Prog Brain Res* 118: 281-291.
- Bazán NG, Rodríguez de Turco EB. 1980. Membrane lipids in the pathogenesis of brain edema: Phospholipids and arachidonic acid, the earliest membrane components changed at the onset of ischemia. *Adv Neurol* 28: 197-205.
- Beleznyay Z, Zachowski A, Devaux PF, Navazo MP, Ott P. 1993. ATP-dependent aminophospholipid translocation in erythrocyte vesicles: Stoichiometry of transport. *Biochemistry* 32: 3146-3152.
- Bell RM, Coleman RA. 1980. Enzymes of glycerolipid synthesis in eukaryotes. *Annu Rev Biochem* 49: 459-487.
- Berridge MJ, Irvine RF. 1989. Inositol phosphates and cell signalling. *Nature* 341: 197-205.
- Bitbol M, Devaux PF. 1988. Measurement of outward translocation of phospholipids across human erythrocyte membrane. *Proc Natl Acad Sci USA* 85: 6783-6787.
- Blazquez C, Sanchez C, Velasco G, Guzman M. 1998. Role of carnitine palmitoyltransferase I in the control of ketogenesis in primary cultures of rat astrocytes. *J Neurochem* 71: 1597-1606.
- Bosetti F, Rintala J, Seemann R, Rosenberger TA, Contreras MA, et al. 2002. Chronic lithium downregulates cyclooxygenase-2 activity and prostaglandin E(2) concentration in rat brain. *Mol Psychiatry* 7: 845-850.
- Brash AR. 2001. Arachidonic acid as a bioactive molecule. *J Clin Invest* 107: 1339-1345.
- Brusa R, Eva C, Oberto A, Peila R, Ricci Galamero S, et al. 1992. Downregulation of muscarinic receptor subtypes messenger RNA in rat primary culture of corticostriatal neurons. *Pharmacol Res* 25(Suppl 1): 121-122.
- Carey EM. 1975. A comparative study of the metabolism of de novo synthesized fatty acids from acetate and glucose, and exogenous fatty acids, in slices of rabbit cerebral cortex during development. *J Neurochem* 24: 237-244.
- Chandrasekaran K, Mehrabian Z, Spinnewyn B, Drieu K, Fiskum G. 2001. Neuroprotective effects of bilobalide, a component of the *Ginkgo biloba* extract (EGb 761), in gerbil global brain ischemia. *Brain Res* 922: 282-292.
- Chang MC, Bell JM, Purdon AD, Chikhale EG, Grange E. 1999. Dynamics of docosahexaenoic acid metabolism in the central nervous system: Lack of effect of chronic lithium treatment. *Neurochem Res* 24: 399-406.
- Chang MC, Contreras MA, Rosenberger TA, Rintala JJ, Bell JM, et al. 2001. Chronic valproate treatment decreases the in vivo turnover of arachidonic acid in brain phospholipids: A possible common effect of mood stabilizers. *J Neurochem* 77: 796-803.
- Chang MC, Jones CR. 1998. Chronic lithium treatment decreases brain phospholipase A2 activity. *Neurochem Res* 23: 887-892.
- Chang MCJ, Grange E, Rabin O, Bell JM, Allen DD, et al. 1996. Lithium decreases turnover of arachidonate in several brain phospholipids. *Neurosci Lett* 220: 171-174.
- Chikhale EG, Balbo A, Galdzicki Z, Rapoport SI, Shetty HU. 2001. Measurement of *myo*-inositol turnover in phosphatidylinositol: Description of a model and mass spectrometric method for cultured cortical neurons. *Biochemistry* 40: 11114-11120.
- Choi DW, Rothman SM. 1990. The role of glutamate neurotoxicity in hypoxic-ischemic neuronal death. *Annu Rev Neurosci* 13: 171-182.
- Clarke DD, Sokoloff L. 1994. Circulation and energy metabolism of the brain. *Basic neurochemistry: Molecular, cellular, and medical aspects*. Siegel GJ, Agranoff BW, Albers RW, Molinoff MD, editors. New York: Raven Press; pp. 645-680.
- Colbran RJ. 2004. Protein phosphatases and calcium/calmodulin-dependent protein kinase II-dependent synaptic plasticity. *J Neurosci* 24: 8404-8409.
- Connolly S, Bennion C, Botterell S, Croshaw PJ, Hallam C, et al. 2002. Design and synthesis of a novel and potent series of inhibitors of cytosolic phospholipase A(2) based on a 1,3-disubstituted propan-2-one skeleton. *J Med Chem* 45: 1348-1362.
- Connor WE, Neuringer M, Lin DS. 1990. Dietary effects on brain fatty acid composition: The reversibility of n-3 fatty acid deficiency and turnover of docosahexaenoic acid in the brain, erythrocytes, and plasma of rhesus monkeys. *J Lipid Res* 31: 237-247.
- Cooper J, Bloom FE, Roth RH. 2003. *The biochemical basis of neuropharmacology*. Oxford University Press; Oxford: p. 404.
- Cullingford TE, Dolphin CT, Sato H. 2002. The peroxisome proliferator-activated receptor alpha-selective activator ciprofibrate upregulates expression of genes encoding fatty acid oxidation and ketogenesis enzymes in rat brain. *Neuropharmacology* 42: 724-730.
- Cunnane SC, Belza K, Anderson MJ, Ryan MA. 1998. Substantial carbon recycling from linoleate into products of de novo lipogenesis occurs in rat liver even under conditions of extreme dietary linoleate deficiency. *J Lipid Res* 39: 2271-2276.
- Dawson RMC. 1985. *Enzymic pathways of phospholipid metabolism in the nervous system*. Phospholipids in nervous tissues. Eichberg J, editor. New York: John Wiley & Sons; pp. 45-78.
- Defeudis FV. 2002. Bilobalide and neuroprotection. *Pharmacol Res* 46: 565-568.
- DeGeorge JJ, Nariai T, Yamazaki S, Williams WM, Rapoport SI. 1991. Arecoline-stimulated brain incorporation of

- intravenously administered fatty acids in unanesthetized rats. *J Neurochem* 56: 352-355.
- Del Rio E, Bevilacqua JA, Marsh SJ, Halley P, Caulfield MP. 1999. Muscarinic M1 receptors activate phosphoinositide turnover and Ca^{2+} mobilization in rat sympathetic neurons, but this signalling pathway does not mediate M-current inhibition. *J Physiol* 520: 101-111.
- DeMar JC Jr, Ma K, Bell JM, Rapoport SI. 2004. Half-lives of docosahexaenoic acid in rat brain phospholipids are prolonged by 15 weeks of nutritional deprivation of n-3 polyunsaturated fatty acids. *J Neurochem* 91: 1125-1137.
- DeMar JC Jr, Ma K, Chang L, Bell JM, Rapoport SI. 2005. α -Linolenic acid does not contribute appreciably to docosahexaenoic acid within brain phospholipids of adult rats fed a diet enriched in docosahexaenoic acid. *J Neurochem* 94: 1063-1076.
- DeMar JC Jr, Wensel TG, Anderson RE. 1996. Biosynthesis of the unsaturated 14-carbon fatty acids found on the N termini of photoreceptor-specific proteins. *J Biol Chem* 271: 5007-5016.
- Dennis EA. 1994. Diversity of group types, regulation, and function of phospholipase A2. *J Biol Chem* 269: 13057-13060.
- Diaz C, Schroit AJ. 1996. Role of translocases in the generation of phosphatidylserine asymmetry. *J Membr Biol* 151: 1-9.
- Ding J, Wu Z, Crider BP, Ma Y, Li X, et al. 2000. Identification and functional expression of four isoforms of ATPase II, the putative aminophospholipid translocase. Effect of isoform variation on the ATPase activity and phospholipid specificity. *J Biol Chem* 275: 23378-23386.
- Dunn A. 1973. The dependence of brain ATP content on cerebral electroshock current. *Brain Res* 61: 442-445.
- Dzeja PP, Terzic A, Wieringa B. 2004. Phosphotransfer dynamics in skeletal muscle from creatine kinase gene-deleted mice. *Mol Cell Biochem* 256-257: 13-27.
- Edgar AD, Strosznajder J, Horrocks LA. 1982. Activation of ethanolamine phospholipase A₂ in brain during ischemia. *J Neurochem* 39: 1111-1116.
- Eng LF, Noble EP. 1968. The maturation of rat brain myelin. *Lipids* 3: 157-162.
- Farooqui AA, Horrocks LA. 2001. Plasmalogens: Workhorse lipids of membranes in normal and injured neurons and glia. *Neuroscientist* 7: 232-245.
- Fisher SK, Agranoff BW. 1985. The biochemical basis and functional significance of enhanced phosphatidate and phosphoinositide turnover. Phospholipids in nervous tissues. Eichberg J, editor. New York: John Wiley & Sons; pp. 241-295.
- Fisher SK, Heacock AM, Agranoff BW. 1992. Inositol lipids and signal transduction in the nervous system: An update. *J Neurochem* 58: 18-38.
- Fitzpatrick FA, Soberman R. 2001. Regulated formation of eicosanoids. *J Clin Invest* 107: 1347-1351.
- Folbergrova J, Ingvar M, Siesjo BK. 1981. Metabolic changes in cerebral cortex, hippocampus, and cerebellum during sustained bicuculline-induced seizures. *J Neurochem* 37: 1228-1238.
- Ford DA, Gross RW. 1994. The discordant rates of sn-1 aliphatic chain and polar head group incorporation into plasmalogen molecular species demonstrate the fundamental importance of polar head group remodeling in plasmalogen metabolism in rabbit myocardium. *Biochemistry* 33: 1216-1222.
- Frandsen A, Schousboe A. 1993. Excitatory amino acid-mediated cytotoxicity and calcium homeostasis in cultured neurons. *J Neurochem* 60: 1202-1211.
- Freysz L, Bieth R, Mandel P. 1969. Kinetics of the biosynthesis of phospholipids in neurons and glial cells isolated from rat brain cortex. *J Neurochem* 16: 1417-1424.
- Furuta Y, Uehara T, Nomura Y. 2003. Correlation between delayed neuronal cell death and selective decrease in phosphatidylinositol 4-kinase expression in the CA1 subfield of the hippocampus after transient forebrain ischemia. *J Cereb Blood Flow Metab* 23: 962-971.
- Gammon CM, Allen AC, Morell P. 1989. Bradykinin stimulates phosphoinositide hydrolysis and mobilization of arachidonic acid in dorsal root ganglion neurons. *J Neurochem* 53: 95-101.
- Gardiner M, Nilsson B, Rehncrona S, Siesjo BK. 1981. Free fatty acids in the rat brain in moderate and severe hypoxia. *J Neurochem* 36: 1500-1505.
- Gavino GR, Gavino VC. 1991. Rat liver outer mitochondrial carnitine palmitoyltransferase activity towards long-chain polyunsaturated fatty acids and their CoA esters. *Lipids* 26: 266-270.
- Ghelardoni S, Tomita YA, Bell JM, Rapoport SI, Bosetti F. 2004. Chronic carbamazepine selectively downregulates cytosolic phospholipase A2 expression and cyclooxygenase activity in rat brain. *Biol Psychiatry* 56: 248-254.
- Glaser PE, Gross RW. 1994. Plasmenylethanolamine facilitates rapid membrane fusion: A stopped-flow kinetic investigation correlating the propensity of a major plasma membrane constituent to adopt an HII phase with its ability to promote membrane fusion. *Biochemistry* 33: 5805-5812.
- Gorgulu A, Kins T, Cobanoglu S, Unal F, Izgi NI, et al. 2000. Reduction of edema and infarction by memantine and MK-801 after focal cerebral ischaemia and reperfusion in rat. *Acta Neurochir (Wien)* 142: 1287-1292.

- Gottlieb RA. 2003. Cytochrome P450: Major player in reperfusion injury. *Arch Biochem Biophys* 420: 262-267.
- Grange E, Deutsch J, Smith QR, Chang M, Rapoport SI, et al. 1995. Specific activity of brain palmitoyl-CoA pool provides rates of incorporation of palmitate in brain phospholipids in awake rats. *J Neurochem* 65: 2290-2298.
- Gurd JW, Bissoon N. 1997. The N-methyl-D-aspartate receptor subunits NR2A and NR2B bind to the SH2 domains of phospholipase C-gamma. *J Neurochem* 69: 623-630.
- Hajra AK. 1995. Glycerolipid biosynthesis in peroxisomes (microbodies). *Prog Lipid Res* 34: 343-364.
- Heiss WD, Sobesky J, Hesselmann V. 2004. Identifying thresholds for penumbra and irreversible tissue damage. *Stroke* 35: 2671-2674.
- Herrmann A, Zachowski A, Devaux PF. 1990. Protein-mediated phospholipid translocation in the endoplasmic reticulum with a low lipid specificity. *Biochemistry* 29: 2023-2027.
- Hertz L, Peng L. 1992. Energy metabolism at the cellular level of the CNS. *Can J Physiol Pharmacol* 70(Suppl): S145-S157.
- Hewitt KE, Lesiuk HJ, Tauskela JS, Morley P, Durkin JP. 1998. Selective coupling of mu-calpain activation with the NMDA receptor is independent of translocation and autolysis in primary cortical neurons. *J Neurosci Res* 54: 223-232.
- Hinkle PC, Kumar MA, Resetar A, Harris DL. 1991. Mechanistic stoichiometry of mitochondrial oxidative phosphorylation. *Biochemistry* 30: 3576-3582.
- Hisanaga Y, Ago H, Nakagawa N, Hamada K, Ida K, et al. 2004. Structural basis of the substrate-specific two-step catalysis of long chain fatty acyl-CoA synthetase dimer. *J Biol Chem* 279: 31717-31726.
- Hokin LE, Dixon JF. 1993. The phosphoinositide signalling system. I. Historical background. II. Effects of lithium on the accumulation of second messenger inositol 1,4,5-trisphosphate in brain cortex slices. *Prog Brain Res* 98: 309-315.
- Holmsen H, Hindenes JO, Fukami M. 1992. Glycerophospholipid metabolism: Back to the future. *Thromb Res* 67: 313-323.
- Horrocks L. 1985. Metabolism and function of fatty acids in brain. Phospholipids in nervous tissues. Eichberg J, editor. New York: John Wiley & Sons; pp. 173-199.
- Horrocks LA. 1967. Composition of myelin from peripheral and central nervous systems of the squirrel monkey. *J Lipid Res* 8: 569-576.
- Horrocks LA. 1990. Metabolism of adrenergic and arachidonic acids in nervous system phospholipids. Phospholipids. Hanin I, Pepeu G, editors. New York: Plenum; pp. 51-58.
- Horrocks LA, Harder HW. 1983. Fatty acids and cholesterol. Handbook of neurochemistry. Lajtha A, editor. New York: Plenum; pp. 1-16.
- Horrocks LA, Toews AD, Tompson DK, Chin JY. 1975. Synthesis and turnover of brain phosphoglycerides—results, methods of calculation and interpretation. Function and metabolism of phospholipids in the central and peripheral nervous systems. Porcellati G, Amaducci L, Galli C, editors. New York: Plenum Press.
- Hossmann KA. 1994. Viability thresholds and the penumbra of focal ischemia. *Ann Neurol* 36: 557-565.
- Iadecola C, Ross ME. 1997. Molecular pathology of cerebral ischemia: Delayed gene expression and strategies for neuroprotection. *Ann N Y Acad Sci* 835: 203-217.
- Ikeda M, Yoshida S, Busto R, Santiso M, Ginsberg MD. 1986. Polyphosphoinositides as a probable source of brain free fatty acids accumulated at the onset of ischemia. *J Neurochem* 47: 123-132.
- Ikeda M, Yoshida S, Busto R, Santiso M, Martinez E, et al. 1987. Cerebral phosphoinositide and energy metabolism during and after insulin-induced hypoglycemia. *J Neurochem* 49: 100-106.
- Janssen E, Kuiper J, Hodgson D, Zingman LV, Alekseev AE, et al. 2004. Two structurally distinct and spatially compartmentalized adenylate kinases are expressed from the AK1 gene in mouse brain. *Mol Cell Biochem* 256-257: 59-72.
- Jones CR, Arai T, Bell JM, Rapoport SI. 1996. Preferential in vivo incorporation of [³H]arachidonic acid from blood into rat brain synaptosomal fractions before and after cholinergic stimulation. *J Neurochem* 67: 822-829.
- Jones CR, Arai T, Rapoport SI. 1997. Evidence for the involvement of docosahexaenoic acid in cholinergic stimulated signal transduction at the synapse. *Neurochem Res* 22: 663-670.
- Kang MJ, Fujino T, Sasano H, Minekura H, Yabuki N, et al. 1997. A novel arachidonate-preferring acyl-CoA synthetase is present in steroidogenic cells of the rat adrenal, ovary, and testis. *Proc Natl Acad Sci USA* 94: 2880-2884.
- Katsuki H, Okuda S. 1995. Arachidonic acid as a neurotoxic and neurotrophic substance. *Prog Neurobiol* 46: 607-636.
- Kokotos G, Kotsovolou S, Six DA, Constantinou-Kokotou V, Beltzner CC, et al. 2002. Novel 2-oxoamide inhibitors of human group IVA phospholipase A(2). *J Med Chem* 45: 2891-2893.
- Kolko M, de Turco EB, Diemer NH, Bazan NG. 2002. Secretory phospholipase A2-mediated neuronal cell death involves glutamate ionotropic receptors. *Neuroreport* 13: 1963-1966.
- Kosenko E, Kaminsky Y, Grau E, Minana MD, Marcaida G, et al. 1994. Brain ATP depletion induced by acute ammonia intoxication in rats is mediated by activation of the

- NMDA receptor and Na⁺,K⁺-ATPase. *J Neurochem* 63: 2172-2178.
- Lands WEM, Crawford CG. 1976. Enzymes of membrane phospholipid metabolism. The enzymes of biological membranes. Martonosi A, editor. New York: Plenum; pp. 3-85.
- Lee H, Villacreses NE, Rapoport SI, Rosenberger TA. 2004a. In vivo imaging detects a transient increase in brain arachidonic acid metabolism: A potential marker of neuroinflammation. *J Neurochem* 91: 936-945.
- Lee HJ, Bazinet RP, Chang L, Rapoport SI. 2004b. Effects of carbamazepine, an antiepileptic drug, on the turnover of arachidonic and docosahexaenoic acids in brain phospholipids of the awake rat. *Abstr Soc Neurosci*: 906.9.
- Lee TC. 1998. Biosynthesis and possible biological functions of plasmalogens. *Biochim Biophys Acta* 1394: 129-145.
- Lees GJ. 1991. Inhibition of sodium-potassium-ATPase: A potentially ubiquitous mechanism contributing to central nervous system neuropathology. *Brain Res Brain Res Rev* 16: 283-300.
- Lehninger AL, Nelson DL, Cox MM. 1993. Principles of biochemistry. New York: Worth Press; pp. 1090.
- Leonard BE. 2001. Stress, norepinephrine and depression. *J Psychiatry Neurosci* 26(Suppl): S11-S16.
- Li L, Prabhakaran K, Shou Y, Borowitz JL, Isom GE. 2002. Oxidative stress and cyclooxygenase-2 induction mediate cyanide-induced apoptosis of cortical cells. *Toxicol Appl Pharmacol* 185: 55-63.
- Liu XH, Eun BL, Barks JD. 2001. Platelet-activating factor antagonist BN 50730 attenuates hypoxic-ischemic brain injury in neonatal rats. *Pediatr Res* 49: 804-811.
- Lowry OH. 1975. Energy metabolism in brain and its control. *Brain Work, Alfred Benzon Symposium VIII*. Ingvar DH, Lassen NA, editors. New York: Academic Press; pp. 48-64.
- Lynch KR, Macdonald TL. 2002. Structure-activity relationships of lysophosphatidic acid analogs. *Biochim Biophys Acta* 1582: 289-294.
- Ma K, Deutsch J, Villacreses N, Rosenberger TA, Rapoport SI, Shetty HU. 2006. Measuring brain uptake and incorporation into brain phosphatidylinositol of plasma myo-[²H₆] inositol in unanesthetized rats: A new approach to estimate the in vivo brain phosphatidylinositol turnover rate. *Neurochem Lett* June 22 (Epub).
- Masuzawa Y, Sugiura T, Ishima Y, Waku K. 1984. Turnover rates of the molecular species of ethanolamine plasmalogen of rat brain. *J Neurochem* 42: 961-968.
- Mattson MP. 2003. Excitotoxic and excitoprotective mechanisms: Abundant targets for the prevention and treatment of neurodegenerative disorders. *Neuromolecular Med* 3: 65-94.
- McCandless DW, Abel MS, Schwartzenburg FC Jr. 1982. Iso-niazid induced seizures and cerebral cortical and cerebellar energy metabolism. *J Neurosci Res* 7: 419-430.
- McCullough L, Wu L, Haughey N, Liang X, Hand T, et al. 2004. Neuroprotective function of the PGE2 EP2 receptor in cerebral ischemia. *J Neurosci* 24: 257-268.
- Miller JC, Gnaedinger JM, Rapoport SI. 1987. Utilization of plasma fatty acid in rat brain: Distribution of [14-C]palmitate between oxidative and synthetic pathways. *J Neurochem* 49: 1507-1514.
- Miller SL, Benjamins JA, Morell P. 1977. Metabolism of glycerophospholipids of myelin and microsomes in rat brain. Reutilization of precursors. *J Biol Chem* 252: 4025-4037.
- Moriguchi T, Loewke J, Garrison M, Catalan JN, Salem N Jr. 2001. Reversal of docosahexaenoic acid deficiency in the rat brain, retina, liver, and serum. *J Lipid Res* 42: 419-427.
- Murakami A, Furui T. 1994. Effects of the conventional anticonvulsants, phenytoin, carbamazepine, and valproic acid, on sodium-potassium-adenosine triphosphatase in acute ischemic brain. *Neurosurgery* 34:1047-1051; discussion 1051.
- Murphy MG, Jollimore C, Crocker JF, Her H. 1992a. Beta-oxidation of [1-14C]palmitic acid by mouse astrocytes in primary culture: Effects of agents implicated in the encephalopathy of Reye's syndrome. *J Neurosci Res* 33: 445-454.
- Murphy TH, Wright DD, Baraban JM. 1992b. Phosphoinositide turnover associated with synaptic transmission. *J Neurochem* 59: 2336-2339.
- Nariai T, DeGeorge JJ, Greig NH, Genka S, Rapoport SI, et al. 1994. Differences in rates of incorporation of intravenously injected radiolabeled fatty acids into phospholipids of intracerebrally implanted tumor and brain in awake rats. *Clin Exp Metastasis* 12: 213-225.
- Narita K, Kubota M, Nakane M, Kitahara S, Nakagomi T, et al. 2000. Therapeutic time window in the penumbra during permanent focal ischemia in rats: Changes of free fatty acids and glycerophospholipids. *Neurol Res* 22: 393-400.
- Nishihara M, Keenan RW. 1985. Inositol phospholipid levels of rat forebrain obtained by freeze-blowing method. *Biochim Biophys Acta* 835: 415-418.
- Nonaka S, Chuang DM. 1998. Neuroprotective effects of chronic lithium on focal cerebral ischemia in rats. *Neuroreport* 9: 2081-2084.
- Paltauf F. 1994. Ether lipids in biomembranes. *Chem Phys Lipids* 74: 101-139.
- Panganamala RV, Horrocks LA, Geer JC, Cornwell DG. 1971. Positions of double bonds in the monounsaturated alk-1-enyl groups from the plasmalogens of human heart and brain. *Chem Phys Lipids* 6: 97-102.

- Patlak CS, Pettigrew KD. 1976. A method to obtain infusion schedules for prescribed blood concentration time courses. *J Appl Physiol* 40: 458-463.
- Pediconi MF, Barrantes FJ. 1990. Brain asymmetry in phospholipid polar head group metabolism: Parallel *in vivo* and *in vitro* studies. *Neurochem Res* 15: 25-32.
- Penzo D, Petronilli V, Angelin A, Cusan C, Colonna R, et al. 2004. Arachidonic acid released by phospholipase A(2) activation triggers Ca(2+)-dependent apoptosis through the mitochondrial pathway. *J Biol Chem* 279: 25219-25225.
- Pestonjamas VK, Burstein SH. 1998. Anandamide synthesis is induced by arachidonate mobilizing agonists in cells of the immune system. *Biochim Biophys Acta* 1394: 249-260.
- Peters A, Schweiger U, Pellerin L, Hubold C, Oltmanns KM, et al. 2004. The selfish brain: Competition for energy resources. *Neurosci Biobehav Rev* 28: 143-180.
- Pollock RJ, Hajra AK, Agranoff BW. 1976. Incorporation of D-[3-³H, U-¹⁴C] glucose into glycerolipid via acyl dihydroxyacetone phosphate untransformed and viral-transformed BHK-21-c13 fibroblasts. *J Biol Chem* 251: 5149-5154.
- Pompeia C, Lima T, Curi R. 2003. Arachidonic acid cytotoxicity: Can arachidonic acid be a physiological mediator of cell death? *Cell Biochem Funct* 21: 97-104.
- Porcellati G, Goracci G, Arienti G. 1983. Lipid turnover. *Handbook of neurochemistry*, Vol. 5. Lajtha A, editor. New York: Plenum; pp. 277-294.
- Pottorf WJ, De Leon DD, Hessinger DA, Buchholz JN. 2001. Function of SERCA mediated calcium uptake and expression of SERCA3 in cerebral cortex from young and old rats. *Brain Res* 914: 57-65.
- Purdon AD, Rapoport SI. 1998. Energy requirements for two aspects of phospholipid metabolism in mammalian brain. *Biochem J* 335: 313-318.
- Purdon AD, Rosenberger TA, Shetty HU, Rapoport SI. 2002. Energy consumption by phospholipid metabolism in mammalian brain. *Neurochem Res* 27: 1641-1647.
- Purdon D, Arai T, Rapoport SI. 1997. No evidence for direct incorporation of esterified palmitic acid from plasma into brain lipids of awake adult rat. *J Lipid Res* 38: 526-530.
- Rabin O, Chang MC, Grange E, Bell J, Rapoport SI, et al. 1998a. Selective acceleration of arachidonic acid reincorporation into brain membrane phospholipids following transient ischemia in awake gerbil. *J Neurochem* 70: 325-334.
- Rabin O, Drieu K, Grange E, Chang MC, Rapoport SI, et al. 1998b. Effects of EGb 761 on fatty acid reincorporation during reperfusion following ischemia in the brain of the awake gerbil. *Mol Chem Neuropathol* 34: 79-101.
- Rami A, Sims J, Botez G, Winckler J. 2003. Spatial resolution of phospholipid scramblase 1 (PLSCR1), caspase-3 activation and DNA-fragmentation in the human hippocampus after cerebral ischemia. *Neurochem Int* 43: 79-87.
- Rapoport SI. 1970. The sodium-potassium exchange pump: Relation of metabolism to electrical properties of the cell. I. *Theory Biophys. J* 10: 246-259.
- Rapoport SI. 1971. The sodium-potassium exchange pump. II. Analysis of Na⁺-loaded frog sartorius muscle. *Biophys J* 11: 631-647.
- Rapoport SI. 2001. *In vivo* fatty acid incorporation into brain phospholipids in relation to plasma availability, signal transduction and membrane remodeling. *J Mol Neurosci* 16: 243-261.
- Rapoport SI. 2003. *In vivo* approaches to quantifying and imaging brain arachidonic and docosahexaenoic acid metabolism. *J Pediatr* 143: S26-S34.
- Rapoport SI. 2005. *In vivo* approaches and rationale for quantifying kinetics and imaging of brain lipid metabolic pathways. *Prostaglandins Other Lipid Mediators*. 77: 185-186.
- Rapoport SI, Chang MCJ, Spector AA. 2001. Delivery and turnover of plasma-derived essential PUFAs in mammalian brain. *J Lipid Res* 42: 678-685.
- Rapoport SI, Purdon D, Shetty HU, Grange E, Smith Q, et al. 1997. *In vivo* imaging of fatty acid incorporation into brain to examine signal transduction and neuroplasticity involving phospholipids. *Ann N Y Acad Sci* 820: 56-74.
- Reddy TS, Bazan NG. 1987. Arachidonic acid, stearic acid, and diacylglycerol accumulation correlates with the loss of phosphatidylinositol 4,5-bisphosphate in cerebrum 2 seconds after electroconvulsive shock: Complete reversal of changes 5 minutes after stimulation. *J Neurosci Res* 18: 449-455.
- Rehncrona S, Westerberg E, Åkesson B, Siesjö BK. 1982. Brain cortical fatty acids and phospholipids during and following complete and severe incomplete ischemia. *J Neurochem* 38: 84-93.
- Riendeau D, Guay J, Weech PK, Laliberte F, Yergey J, et al. 1994. Arachidonyl trifluoromethyl ketone, a potent inhibitor of 85-kDa phospholipase A2, blocks production of arachidonate and 12-hydroxyeicosatetraenoic acid by calcium ionophore-challenged platelets. *J Biol Chem* 269: 15619-15624.
- Rintala J, Seemann R, Chandrasekaran K, Rosenberger TA, Chang L, et al. 1999. 85 kDa cytosolic phospholipase A2 is a target for chronic lithium in rat brain. *Neuroreport* 10: 3887-3890.
- Robinson PJ, Noronha J, DeGeorge JJ, Freed LM, Nariai T, et al. 1992. A quantitative method for measuring regional *in vivo* fatty-acid incorporation into and turnover within brain phospholipids: Review and critical analysis. *Brain Res Rev* 17: 187-214.

- Rodriguez De Turco EB, Jackson FR, DeCoster MA, Kolko M, Bazan NG. 2002. Glutamate signalling and secretory phospholipase A2 modulate the release of arachidonic acid from neuronal membranes. *J Neurosci Res* 68: 558-567.
- Rolfé DFS, Brown GC. 1997. Cellular energy utilization and molecular origin of standard metabolic rate in mammals. *Physiol Rev* 77: 731-758.
- Rosenberger TA, Oki J, Purdon AD, Rapoport SI, Murphy EJ. 2002. Rapid synthesis and turnover of brain microsomal ether phospholipids in the adult rat. *J Lipid Res* 43: 59-68.
- Rosenberger TA, Villacreses NE, Hovda JT, Bosetti F, Weerasinghe G, et al. 2004. Rat brain arachidonic acid metabolism is increased by a 6-day intracerebral ventricular infusion of bacterial lipopolysaccharide. *J Neurochem* 88: 1168-1178.
- Rossi DJ, Oshima T, Attwell D. 2000. Glutamate release in severe brain ischaemia is mainly by reversed uptake. *Nature* 403: 316-321.
- Rowlands DK, Kao C, Wise H. 2001. Regulation of prostacyclin and prostaglandin E(2) receptor mediated responses in adult rat dorsal root ganglion cells in vitro. *Br J Pharmacol* 133: 13-22.
- Shepherd GM. 1979. *The synaptic organization of the brain*. New York: Oxford University Press; pp. 436.
- Shetty HU, Smith QR, Washizaki K, Rapoport SI, Purdon AD. 1996. Identification of two molecular species of rat brain phosphatidylcholine that rapidly incorporate and turn over arachidonic acid in vivo. *J Neurochem* 67: 1702-1710.
- Shimizu T, Wolfe LS. 1990. Arachidonic acid cascade and signal transduction. *J Neurochem* 55: 1-15.
- Siesjö BK. 1978. *Brain energy metabolism*. Chichester: John Wiley & Sons; pp. 1-607.
- Siesjö BK, Memezawa H, Smith ML. 1991. Neurocytotoxicity: Pharmacological implications. *Fundam Clin Pharmacol* 5: 755-767.
- Snyder F. 1996. Ether-linked lipids and their bioactive species: Occurrence, chemistry, metabolism, regulation, and function. *Biochemistry of lipids, lipoproteins, and membranes*. Vance DE, Vance JE, editors. New York: Elsevier; pp. 183-210.
- Sokoloff L. 1977. Relation between physiological function and energy metabolism in the central nervous system. *J Neurochem* 29: 13-26.
- Soukup JF, Friedel RO, Shanberg SM. 1978. Microwave irradiation fixation for studies of polyphosphoinositide metabolism in brain. *J Neurochem* 30: 635-637.
- Spinnewyn B. 1992. Ginkgo biloba extract (EGb 761) protects against delayed neuronal death in gerbils. *Advances in ginkgo biloba extract research. Effects of Ginkgo biloba extract (EGb 761) on the central nervous system*. Christen Y, Constantin J, Lacour M, editors. Paris: Elsevier; pp. 113-118.
- Stinson AM, Wiegand RD, Anderson RE. 1991. Recycling of docosahexaenoic acid in rat retinas during n-3 fatty acid deficiency. *J Lipid Res* 32: 2009-2017.
- Sun D, Gilboe DD. 1994. Ischemia-induced changes in cerebral mitochondrial free fatty acids, phospholipids, and respiration in the rat. *J Neurochem* 62: 1921-1928.
- Sun GY. 1977. Metabolism of arachidonate and stearate injected simultaneously into the mouse brain. *Lipids* 12: 661-665.
- Sun GY, Lin TN. 1989. Time course for labeling of brain membrane phosphoinositides and other phospholipids after intracerebral injection of [³²P]-ATP. Evaluation by an improved HPTLC procedure. *Life Sci* 44: 689-696.
- Sun GY, MacQuarrie RA. 1989. Deacylation-reacylation of arachidonoyl groups in cerebral phospholipids. *Ann N Y Acad Sci* 559: 37-55.
- Sun GY, Su KL. 1979. Metabolism of arachidonoyl phosphoglycerides in mouse brain subcellular fractions. *J Neurochem* 32: 1053-1059.
- Symon L. 1993. Recovery of brain function following ischemia. *Acta Neurochir Suppl (Wien)* 57: 102-109.
- Tong W, Sun GY. 1996. Effects of ethanol on phosphorylation of lipids in rat synaptic plasma membranes. *Alcohol Clin Exp Res* 20: 1335-1339.
- Verhoeven AJ, Tysnes OB, Aarbakke GM, Cook CA, Holmsen H. 1987. Turnover of the phosphomonoester groups of polyphosphoinositol lipids in unstimulated human platelets. *Eur J Biochem* 166: 3-9.
- Vierbuchen M, Gunawan J, Debuch H. 1979. Studies on the hydrolysis of 1-alkyl-*sn*-glycero-3-phosphoethanolamine in subcellular fractions of rat brain. *Hoppe Seyler's Z. Physiol Chem* 360: 1091-1097.
- Waku K. 1992. Origins and fates of fatty acyl-CoA esters. *Biochim Biophys Acta* 1124: 101-111.
- Walton M, Sirimanne E, Reutelingsperger C, Williams C, Gluckman P, et al. 1997. Annexin V labels apoptotic neurons following hypoxia-ischemia. *Neuroreport* 8: 3871-3875.
- Washizaki K, Smith QR, Rapoport SI, Purdon AD. 1994. Brain arachidonic acid incorporation and precursor pool specific activity during intravenous infusion of unesterified [³H]arachidonate in the anesthetized rat. *J Neurochem* 63: 727-736.
- Weerasinghe GR, Rapoport SI, Bosetti F. 2004. The effect of chronic lithium on arachidonic acid release and metabolism in rat brain does not involve secretory phospholipase A2 or lipoxygenase/cytochrome P450 pathways. *Brain Res Bull* 63: 485-489.
- Weichel O, Hilgert M, Chatterjee SS, Lehr M, Klein J. 1999. Bilobalide, a constituent of *Ginkgo biloba*, inhibits NMDA-induced phospholipase A2 activation and phospholipid breakdown in rat hippocampus. *Naunyn Schmiedeberg's Arch Pharmacol* 360: 609-615.

- Wells MA, Dittmer JC. 1967. A comprehensive study of the postnatal changes in the concentration of the lipids of developing rat brain. *Biochemistry* 6: 3169-3175.
- Whittam R. 1962. The dependence of the respiration of brain cortex on active cation transport. *Biochem J* 82: 205-212.
- Whittam R, Blond DM. 1964. Respiratory control by an adenosine triphosphatase involved in active transport in brain cortex. *Biochem J* 92: 147-158.
- Willard LB, Hauss-Wegrzyniak B, Danysz W, Wenk GL. 2000. The cytotoxicity of chronic neuroinflammation upon basal forebrain cholinergic neurons of rats can be attenuated by glutamatergic antagonism or cyclooxygenase-2 inhibition. *Exp Brain Res* 134: 58-65.
- Williamson P, Schlegel RA. 1994. Back and forth: The regulation and function of transbilayer phospholipid movement in eukaryotic cells. *Mol Membr Biol* 11: 199-216.
- Zachowski A, Gaudry-Talarmin YM. 1990. Phospholipid transverse diffusion in synaptosomes: Evidence for the involvement of the aminophospholipid translocase. *J Neurochem* 55: 1352-1356.

4.7 Ion Transport and Energy Metabolism

O. Vergun · K. E. Dineley · I. J. Reynolds

1	Introduction	430
2	The Main Energy-Consuming Ion Transport Systems in the Brain	431
2.1	Sodium and Potassium Transport	431
2.1.1	Na ⁺ /K ⁺ -ATPase	432
2.1.2	Secondary Active Na ⁺ -Coupled Transport Systems	434
2.2	Calcium Transport	436
2.2.1	Plasma Membrane Ca ²⁺ Pump	437
2.2.2	Plasmalemmal Na ⁺ /Ca ²⁺ Exchange	439
2.2.3	Endoplasmic Reticulum Ca ²⁺ Pump	440
2.2.4	Mitochondrial Ca ²⁺ Uptake	442
2.3	Zinc Transport	442
3	Spatial and Functional Interdependence of Energy Consumption and Energy Production in the Brain	444
3.1	Mechanisms Controlling Energy Production	444
3.2	Energy Production Is Spatially Dynamic and Regulated by Mitochondrial Trafficking	446
4	Interactions Between Ion Transport and Energy Metabolism in Pathology	448
4.1	In Vivo and In Vitro Perspectives on Ion Transport and Brain Injury	448
4.2	Failure of Ion Homeostasis and Energy Metabolism During Excitotoxic Insult	449
4.2.1	Interactions Between Energy Supply, Ion Transport, and Glutamate	450
4.2.2	NMDA Receptor-Mediated Ca ²⁺ Overload and Energy Production	452
4.2.3	Mitochondrial Ca ²⁺ Uptake and Neuronal Injury	454
4.3	Effects of Zn ²⁺ on Energy Metabolism	456
5	Conclusions	457

Abstract: There is an intimate relationship between ion transport and energy metabolism in the brain. All ion transport is driven directly or indirectly by ATP, and the support of ion homeostasis represents the largest demand on energy production in the brain. Failure of ion homeostasis because of the interruption of energy generation has devastating consequences. This chapter reviews the principal mechanisms responsible for maintaining homeostasis of Na^+ , K^+ , and Ca^{2+} , and the mechanisms controlling Zn^{2+} as an example of trace metal transport. The chapter also discusses the interplay between ion loads and energy production. Finally, we present a description of some of the mechanisms that link pathophysiological states with alterations in ion transport and energy metabolism.

List of Abbreviations: $[\text{Ca}^{2+}]_e$, $[\text{Na}^+]_e$, $[\text{K}^+]_e$, $[\text{Clu}]_e$, extracellular concentrations of Ca^{2+} , Na^+ , K^+ and glutamate; $[\text{Ca}^{2+}]_c$, $[\text{Na}^+]_c$, $[\text{Zn}^{2+}]_c$, cytosolic concentrations of Ca^{2+} , Na^+ , Zn^{2+} ; pH_i , intracellular pH; $[\text{ATP}]_i$, intracellular ATP concentration; Na^+/K^+ -ATPase, sodium/potassium ATPase; $\text{Na}^+/\text{Ca}^{2+}$, sodium/potassium exchanger; Na^+/H^+ , sodium/proton exchanger; ER, endoplasmic reticulum; PMCA, plasma membrane Ca^{2+} ATPase; SERCA, sarco(endo)plasmic reticulum Ca^{2+} ATPase; RyR, ryanodine receptor; IP_3 , 1,4,5-inositol trisphosphate; IP_3R , 1,4,5-inositol trisphosphate receptor; CCE, capacitative Ca^{2+} entry; $\Delta\Psi_m$, mitochondrial membrane potential; ROS, reactive oxygen species; NMDA, *N*-methyl-D-aspartate; FCCP, carbonyl cyanide *p*-trifluoromethoxyphenyl hydrazone; MK801, (+)5-methyl-10-11-dihydro-5*N*-dibenzocyclohepten-5,10-imine; CNQX, 6-cyano-7-nitroquinoxaline-2,3-dione; CDF, cation diffusion facilitator; GAPDH, glyceraldehyde-3-phosphate dehydrogenase; KGDHC, alpha-ketoglutarate dehydrogenase complex; LAPD, lipoamide dehydrogenase; MT, metallothionein; ROS, reactive oxygen species; ZIP, zinc-responsive transporter-, iron-responsive transporter-like protein; ZnT, zinc transporter; VCaCh, voltage-gated Ca^{2+} channel; VNaCh, voltage-gated sodium channel; LGCh, ligand-gated channel; KCh, potassium channel; MCaU, mitochondrial calcium uniporter

1 Introduction

All cellular functions are directly or indirectly dependent on energy supply. The fundamental function of neurons can be described as a receiving, processing, and transferring of information, which occur in the form of electrical and chemical signals mediated by ion transport and ionic gradients. Therefore, the majority of energy in the brain (about 60% of total energy) is used to support ion movement (Erecinska and Silver, 1994). Most of this expense is attributed to the maintenance of three ions: Na^+ , K^+ , and Ca^{2+} . This is because the cell must generate a large gradient for these ions across the cellular membranes to accomplish their functions, and movement of ions against their concentration and electrical gradient requires energy expenditure. In this chapter, we review the main mechanisms for the regulation of Na^+ , K^+ , and Ca^{2+} homeostasis. There are numerous other ionic species transported across cell membranes in the brain. These include ions like protons, chloride, and phosphate, trace metals including Zn^{2+} , Cu^{2+} , and Fe^{3+} , and a multitude of organic acids. We will not attempt to review transport mechanisms and energy demands for all of these species. In some cases, these mechanisms are covered elsewhere in this volume, while in others relatively little is known about the transport mechanisms. For example, while Mg^{2+} is an abundant metal in the brain, we do not consider it here. Although some evidence (Stout et al., 1996) supports the presence of Mg^{2+} transporters in the brain, very little is known about the mechanisms of Mg^{2+} transport in neurons or glia. We have elected to provide an example of trace metal handling, and we use Zn^{2+} as the prototype. Zn^{2+} is a relatively abundant trace metal, is clearly subject to active transport, and under circumstances of homeostatic deregulation can interact with energy metabolism to impair cell viability. In this regard, Zn^{2+} is much like Ca^{2+} in its utility and liability, and these general properties resemble those of Fe^{3+} and Cu^{2+} .

Unlike other tissues, the brain energy supply is critically dependent on oxidative metabolism, and 95% of total ATP in the brain is estimated to be generated in mitochondria. Thus, while constituting only 2% of the total body weight, the brain consumes about 20% of total oxygen (Silver and Erecinska, 1998). Another peculiarity of the brain is very small energy reserves. These two factors make the brain extremely sensitive to oxygen supply: within 90 seconds of ischemia, rat cerebrocortical $[\text{ATP}]/[\text{ADP}]$ ratio falls from 10 to 0.4

(Katsura et al., 1993). However, under physiological conditions the ATP level remains nearly constant. This is accomplished by tight spatial and functional coupling between energy demand and production. The majority of metabolic energy used in the brain is devoted to ion transport; this implies that the transport of ions and energy production must also be coupled. We describe some of these interactions. The unique architecture of neurons introduces another key parameter, namely the spatial relationships between energy demand and production; so we also consider the temporal and spatial aspects of energy production in relation to the demands placed by ion transport.

Finally, we consider interactions between ion transport and energy production from a pathophysiological standpoint. It has long been appreciated that loss of substrates for energy production in the brain results in a rapid alteration in ion homeostasis, and that these alterations are likely to contribute to the key pathogenic mechanisms associated with cerebral ischemia, seizures, and traumatic injury. While earlier reviews focused on studies that described the nature of the ionic changes in intact but injured brains, more recently the mechanisms that potentially underlie these changes have been elucidated. Our discussion here focuses on mechanisms that link excessive ionic burdens to altered energy metabolism, with specific attention to Ca^{2+} , Na^+ , and Zn^{2+} .

2 The Main Energy-Consuming Ion Transport Systems in the Brain

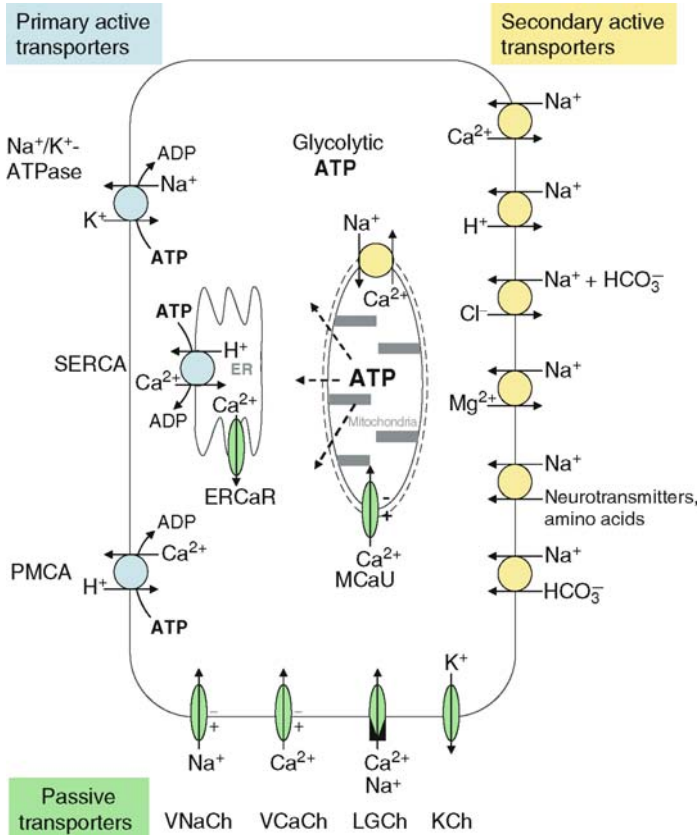
In this section, we discuss several energy-dependent ion transporters that are the main mediators of brain ion homeostasis. Some ion transporters require ATP as a direct source of energy, while many others use energy stored in the form of ion gradients. In terms of energy usage, ion transporters can be either active or passive. Active transport creates an ionic gradient across the plasma membrane or across the boundary of an intracellular compartment, whereas passive transport allows a species to simply move down a previously established electrochemical gradient. Active transport includes primary and secondary active transport. Primary active transporters, like ion pumps, require immediate hydrolysis of ATP to move a given species against its electrochemical gradient, whereas the movement of ions by secondary active transporters is coupled to the movement of another species down its preexisting ion gradient. Passive transporters, such as ion channels, allow ions to pass the membrane down their electrochemical gradients without an immediate cost of energy. Ion movement by passive transport can continue only as long as an electrochemical gradient persists. In the case of passive transport, it is thus necessary to consider the energy required to establish the gradient in the first place. Examples of different types of ion transporters discussed in this section are schematically presented in [Figure 4.7-1](#).

2.1 Sodium and Potassium Transport

An abundance of energy is used to maintain Na^+ and K^+ gradients. Maintenance of Na^+ and K^+ gradients across the plasma membrane is the most energy-intensive process for the neuron, and is estimated to account for 50% of total brain expenditure (Hansen, 1985). The extracellular concentration of Na^+ in the brain is high (130–150 mM) whereas the intracellular is low (20–25 mM). K^+ is distributed conversely, with external K^+ at about 3 mM and the intracellular much higher (85 mM in neurons and 135 mM in glia) (Erecinska and Silver, 1994). The differences in ion distribution between extra- and intracellular compartments control osmotic balance and cellular volume. Moreover, the distribution of Na^+ and K^+ creates an electrochemical gradient across the plasma membrane, which is critical for maintenance of the resting membrane potential and propagation of action potentials. Movement of Na^+ and K^+ down their respective electrochemical gradients during a single action potential does not significantly alter the concentrations of these cations, but repetitive spike activity can have a substantial impact. An additional intracellular Na^+ burden is imposed by various transporters and channels. These include Na^+ -permeable receptor-activated ion channels and a number of Na^+ -dependent transporters, for example, Na^+ cotransport with amino acids and $\text{Na}^+/\text{Ca}^{2+}$, Na^+/H^+ , and $\text{Na}^+/\text{HCO}_3^-/\text{Cl}^-$ antiporters. In spite of the extensive use of the Na^+ gradient as a driving force for numerous homeostatic mechanisms, intracellular and extracellular concentrations of Na^+ and K^+ do not meaningfully change during physiological activity as long as energy homeostasis is

■ Figure 4.7-1

A wide variety of transporters is important for maintaining ion homeostasis. Primary active transporters include plasma membrane Na^+/K^+ -ATPase, PMCA, and the SERCA. Each hydrolyzes ATP in order to move an ionic species against its concentration gradient. The movement of various species against their concentration gradient by secondary active transporters is often coupled to Na^+ transport. Plasma membrane secondary active transporters include transporters that use the large inward Na^+ gradient to export Ca^{2+} , H^+ , Cl^- and Mg^{2+} , in antiport fashion, as well as to drive the influx of neurotransmitters, amino acids, and HCO_3^- in symport fashion. Plasma membrane passive transporters are ion channels such as voltage- and ligand-gated channels for Ca^{2+} (VCaCh, LGCh), Na^+ (VNaCh, LGCh), and K^+ channels (KCh). The mitochondrial uniporter (MCAU) is a high capacity Ca^{2+} uptake mechanism driven by the mitochondrial membrane potential



sufficient to support a restoration of ionic gradients. The only mechanism for active transport of Na^+ against its concentration gradient is the plasma membrane Na^+/K^+ -ATPase.

2.1.1 Na^+/K^+ -ATPase

A mechanism for the pumping of Na^+ from mammalian cells was first suggested by Dean (1941). In the early 1950s, an energy-dependent outward transport of Na^+ against its electrochemical gradient was established in experiments with squid giant axons. Skou later discovered that crab nerves contain an ATPase activated by both Na^+ and K^+ (Skou, 1957). Found so far in every mammalian cell studied, the

Na^+/K^+ -ATPase is an ion-stimulated, membrane-bound enzyme responsible for the extrusion of Na^+ from the cell for exchange to K^+ .

The Na^+/K^+ -ATPase is composed of α and β subunits. It is now well established that the Na^+/K^+ -ATPase is a multigene product comprised of α and β subunits. The purified enzyme contains α and β chains in a 1:1 ratio and has a strong tendency to form $(\alpha\beta)_2$ or higher complexes. However, $(\alpha\beta)_2$ formation is not necessary for enzymatic activity (Lauger, 1991). There is evidence that, in native membranes, the enzyme is an oligomer with quaternary structure (Ivanov et al., 2004). A γ subunit was also identified; however, little is known about its structure, specificity, and function. Enzymatic function of the protein occurs through the catalytic α -subunit, which contains Na^+ - and K^+ -binding sites and the phosphorylation site, whereas β is a glycoprotein subunit, whose complete role is not fully understood. Four α isoforms (ATP1A1, ATP1A2, ATP1A3, and ATP1A4) and three β isoforms (ATP1B1, ATP1B2, and ATP1B3), coded by different genes, have been described (see Vague et al. (2004) for review). In the nervous system ATP1A1, ATP1A2, ATP1A3 and ATP1B1 and ATP1B2 are expressed (Hieber et al., 1991), and the specific isoform distribution depends on cell type. For example, different types of neurons were shown to possess high levels of mRNA for ATP1A1, ATP1A2, ATP1A3, and ATP1B2, whereas in glia the expression of the catalytic subunit was low, corresponding with less functional sodium pump activity (Brines et al., 1991; Hieber et al., 1991). It was shown that different isoforms have a specific localization within cellular compartments and also have different affinities for Na^+ (Shyjan et al., 1990; Brines and Robbins, 1993).

Kinetics and stoichiometry of the Na^+/K^+ -ATPase. The binding sites for Na^+ and ATP are located on the cytosolic side of α -subunit, whereas K^+ binds at the extracellular side. For each molecule of ATP, three molecules of Na^+ and two molecules of K^+ are pumped. Only in extreme conditions uncommon to live cells is this stoichiometry changed, such as in the complete absence of extracellular K^+ , or Na^+ being less than 1mM. As each cycle of the pump transports three positive charges out of and two positive charges into the cell, the Na^+/K^+ pump creates an electrical current that favors hyperpolarization of the plasma membrane. Two principal conformations of the pump were proposed: E_1 , in which the Na^+ - and ATP-binding sites face inward, and E_2 , which has the K^+ - and P_i -binding sites outward (Lauger, 1991). When Na^+ is bound at the intracellular site, phosphorylation by ATP promotes trapping of Na^+ inside of the protein (E_1 conformation). At this stage, the enzyme is ready to switch to E_2 . In E_2 , the protein releases Na^+ to the extracellular side and binds K^+ , which is trapped by dephosphorylation, after which the enzyme changes back to E_1 . Since Na^+ translocation is associated with a movement of charge, transition from E_1 to E_2 is the most energy-consuming process.

The Na^+/K^+ -ATPase is controlled predominantly by intracellular Na^+ . The Na^+/K^+ -ATPase is highly specific to Na^+ . Li^+ is the only metal that can substitute for Na^+ , but is 20 times less powerful in activating the enzyme (Beauge, 1978). The pump has comparatively low specificity for K^+ , and a variety of other monovalent cations such as Rb^+ , Cs^+ , and Tl^+ are transported about as well as K^+ (Karlsh et al., 1978). Indeed, $^{86}\text{Rb}^+$ has been widely used to characterize pump properties. Affinities of the pump for different substrates have been reviewed by Lauger (1991). The affinity for Na^+ and K^+ may vary, depending on the specific state of the pump, membrane potential, or concentrations of other ligands. Moreover, the affinity of the isolated enzyme may vary depending on the method of isolation. Because of these complications, the binding sites are usually characterized by apparent affinities (K_m). The K_m of brain ATPase for Na^+ was estimated as 15–20 mM at the cytoplasmic side, and <2 mM for K^+ at the extracellular side (Kimelberg et al., 1978). As the extracellular K^+ concentration in the brain is about 3 mM, the external K^+ site is nearly saturated. Data obtained from different models suggest a K_m for Na^+ at the cytoplasmic (uptake) side that is as much as 1000-times that of the extracellular (release) side. For K^+ , the external (uptake) K_m is only about 50-times higher than the K_m for the cytoplasmic (release) side (see Lauger (1991) for review). Thus, under physiological conditions, the activity of the neuronal enzyme, and consequently the rate of energy consumption, is controlled predominantly by the concentration of intracellular Na^+ .

The cardiac glycoside ouabain specifically inhibits Na^+/K^+ -ATPase. Pharmacological inhibition of Na^+/K^+ -ATPase activity is one of the most often used techniques for defining enzyme activity. Among known inhibitors of Na^+/K^+ -ATPase, cardiac glycosides are the most specific. Ouabain (or G-strophanthin) is a cardiac glycoside that displays nearly absolute specificity for Na^+/K^+ -ATPase (Glynn, 1985), and therefore has been useful in identifying the presence and function of this ATPase in a variety of tissues. Ouabain binds to the

extracellular side of the enzyme, blocking its transition from E_2 to E_1 . The apparent affinity may vary depending on the enzyme's current conformation state. Thus, changes in Na^+ , K^+ , or ATP concentrations and membrane potential can influence the affinity of the pump for ouabain. Sensitivity to ouabain is determined by the α subunit, and different isoforms vary in their affinity for the inhibitor (Horisberger et al., 1991).

ATP: A primary substrate for Na^+/K^+ -ATPase. ATP, a primary substrate for Na^+/K^+ -ATPase, binds to the pump as a MgATP complex. Two apparent affinities for ATP were shown for the isolated enzyme: in the E_1 conformation, K_m for ATP is $<1 \mu\text{M}$; in E_2 , the K_m is 0.3–0.5 mM (Glynn and Karlish, 1975). Binding of ATP to the high-affinity site activates a phosphorylation reaction, whereas ATP bound to the low-affinity site promotes transition from E_2 to E_1 (Lauger, 1991). Thus, ATP has a dual role in the enzyme activation: it acts as a phosphorylating agent as well as an allosteric activator. Other nucleotides can be hydrolyzed by the ATPase, but with rates of only 15%–0.5% of the ATP activity, in the following decreasing order: CTP $>$ ITP $>$ GTP $>$ UTP $>$ TTP (Schuermans Stekhoven and Bonting, 1981).

Mg^{2+} is also involved in the regulation of Na^+/K^+ -ATPase activity. Together with ATP, it forms a complex which is a substrate for the ATPase and serves as a cosubstrate binding to the regulatory site of the enzyme (Richards, 1988). At high concentration, Mg^{2+} inhibits the pump (Sachs, 1988).

Na^+/K^+ -ATPase is a main energy consumer and is fueled predominantly by oxidative phosphorylation. In many studies the energy-linked functions of Na^+/K^+ -ATPase were analyzed by the ouabain-sensitive redistribution of Na^+ and K^+ , changes in oxygen and glucose uptake, and production of lactate. During enhanced neuronal activity extracellular K^+ rises to 12 mM, and can rise even higher under pathological conditions such as spreading depression or hypoxia. A redistribution of Na^+ and K^+ considerably increases energy metabolism. In numerous models for instance, glucose utilization increased almost linearly with the frequency of action potentials during electrical stimulation (see Sokoloff (1993) for review). Moreover, ouabain prevented the enhancement of glucose uptake, indicating that Na^+/K^+ -ATPase activity is closely linked to energy utilization.

As demonstrated in experiments on isolated brain synaptosomes, oxidative phosphorylation plays a predominant role in neuronal energy production. It was found that glycolysis is not sufficient to support Na^+/K^+ -ATPase activity and that $>90\%$ of energy used for the enzyme activity is derived from oxidative phosphorylation (Erecinska and Dagoni, 1990). Numerous studies have demonstrated a proportional increase in oxygen consumption and extracellular K^+ accumulation in response to increased central nervous system (CNS) activity which can be inhibited by ouabain. This demonstrates that oxidative metabolism of glucose almost exclusively supports Na^+ -pump activity in nervous tissue. In numerous other models it was calculated that about 40%–50% of O_2 in the resting brain is utilized by Na^+/K^+ transport (see Clausen et al. (1991) for review). This strong oxygen dependence of Na^+ and K^+ homeostasis is a specific property of neuronal tissue. In contrast, liver Na^+/K^+ transport uses only about 5% of the O_2 consumption (Folke and Sestoft, 1977).

2.1.2 Secondary Active Na^+ -Coupled Transport Systems

Numerous secondary active transporters are powered by the Na^+ gradient. The large inward Na^+ gradient drives a variety of secondary active transporters. With these transporters, the electrochemical gradient, and not ATP, provides the driving force. Many of those proteins were identified in the CNS and most of them are well characterized. Na^+ gradient-dependent transporters found in the CNS are members of the 13 families of proteins encoded by solute carrier (SLC) gene series (Hediger et al., 2004). For more detailed information about these proteins, we refer to the series of recent minireviews:

- The high-affinity glutamate and neuronal amino acid transporter family, SLC1 (Kanai and Hediger, 2003, 2004);
- The bicarbonate transporter family, SLC4 (Romero et al., 2004);
- The sodium–glucose cotransporter family, SLC5 (Wright and Turk, 2004);
- The sodium- and chloride-dependent neurotransmitter transporter family, SLC6 (Chen et al., 2004);
- The cationic amino acid transporter/glycoprotein-associated family, SLC7 (Verrey et al., 2004);
- The $\text{Na}^+/\text{Ca}^{2+}$ exchanger family, SLC8 (Quednau et al., 2004);

- The Na^+/H^+ exchanger family, SLC9 (Orlowski and Grinstein, 2004);
- The sodium bile salt cotransport family, SLC10 (Hagenbuch and Dawson, 2004);
- The human Na^+ -sulfate/carboxylate cotransporter family, SLC13 (Markovich and Murer, 2004);
- The Na^+ -dependent ascorbic acid transporter family, SLC23 (Takanaga et al., 2004);
- The $\text{Na}^+/\text{Ca}^{2+}$ - K^+ exchanger family, SLC24 (Schnetkamp, 2004);
- The Na^+ -coupled nucleoside transport family, SLC28 (Gray et al., 2004);
- The type II Na^+ -phosphate cotransporter family, SLC34 (Murer et al., 2004);
- The System A & N, sodium-coupled neutral amino acid transporter family, SLC38 (Mackenzie and Erickson, 2004).

A complete list of these protein families and their members encoded by the SLC gene series is published on <http://www.pharmaconference.org/>

Because functions of these transporters are not directly coupled to ATP hydrolysis, but rather depend on the Na^+ gradient (and therefore on the activity of Na^+/K^+ -ATPase), we provide a limited description of three of these ion transport systems to give a perspective on the properties of Na^+ -linked transporters, when considered as a class. The examples chosen include transporters that may also have an important impact under conditions of neuronal injury. The $\text{Na}^+/\text{Ca}^{2+}$ exchanger, which plays an important role in the regulation of cellular Ca^{2+} homeostasis, is discussed in the next section.

Na^+ -dependent glutamate transporters. Na^+ -dependent glutamate transporters encoded by five genes are found in neuronal (SLC1A1, SLC1A6, and SLC1A7) and glial (SLC1A2 and SLC1A3) cells. These and other neurotransmitter transporters play a key role in the CNS function by regulating synaptic activity by clearing neurotransmitters from the extracellular space. It was calculated by Attwell and Laughlin (2001) that 2.67 ATP molecules are used to recycle each glutamate molecule. Glutamate is sequestered across the plasma membrane in a large gradient: cytosolic glutamate is in the millimolar range, whereas extracellular glutamate is low micromolar. Therefore, pumping glutamate into the cell against its electrochemical gradient is an energy-demanding process. Reuptake of glutamate from the synaptic cleft consumes 3%–4% of total energy in the brain (Ames, 2000). It is important to note that glutamate transport is also electrogenic; for each imported Glu^- , three molecules of Na^+ and one molecule of H^+ are also imported, while one molecule of K^+ is exported. The glutamate transporter plays a crucial role in limiting extracellular glutamate concentrations, and thus the activation of ionotropic and metabotropic glutamate receptors. When energy supply is limited, for example during brain ischemia or hypoxia, Na^+ and K^+ gradients collapse, the plasma membrane depolarizes, and glutamate transport can reverse so that glutamate is pumped out of neurons and glia into the extracellular space. As discussed below, accumulation of extracellular glutamate overactivates glutamate receptors, inducing a massive Ca^{2+} influx, which in turn triggers excitotoxic processes that lead to cell death. (See *Chapter 4.2* for a more detailed discussion about the interaction of metabolism and neurotransmitters.)

Na^+/H^+ exchange. Na^+/H^+ exchange operates in all cell types. All of eight mammalian isoforms (SLC9A1–8) of the Na^+/H^+ exchanger are expressed in the brain. They show considerable heterogeneity in cell-type expression and membrane localization (Orlowski and Grinstein, 2004). In mammalian cells, Na^+/H^+ antiport is electroneutral with a stoichiometry of $1\text{Na}^+:1\text{H}^+$. Since the plasmalemmal electrochemical gradient for Na^+ at normal conditions is dominant over H^+ , there is a significant driving force for Na^+ influx and H^+ efflux. Thus, one of the physiological roles of this transport system is the extrusion of excess acid accumulated by cellular metabolism and the fine control of intracellular pH. A second function involves regulation of cell volume, because Na^+ influx is coupled to Cl^- and H_2O uptake. The plasmalemmal Na^+/H^+ exchanger has a single binding site for Na^+ with K_{Na} in the range 5–50 mM, depending on the isoform (Szabo et al., 2000). The activity of the exchanger is stimulated by low intracellular pH. Although it does not require hydrolysis of ATP for ion translocation, intracellular ATP was shown to optimize its operation (Orlowski and Grinstein, 2004). Low ATP reduced affinity for intracellular H^+ ; however, the mechanism for this is unclear. Alteration of Na^+/H^+ exchange is associated with many pathological conditions including essential hypertension, diabetes, and ischemia/reperfusion.


$\text{Na}^+/\text{HCO}_3^-$ transport. $\text{Na}^+/\text{HCO}_3^-$ transport is another Na^+ -coupled system involved in the regulation of intracellular pH buffering and cell volume. At least three Na^+ -coupled HCO_3^- transporter isoforms are

found in the brain (Romero et al., 2004). They include two $\text{Na}^+/\text{HCO}_3^-$ cotransporters (SLC4A4 and SLC4A7) which import both Na^+ and HCO_3^- ions, and $\text{Na}^+/\text{HCO}_3^-/\text{Cl}^-$ exchanger (SLC4A8) which imports Na^+ and HCO_3^- in exchange for export of Cl^- . Depending on the isoform, $\text{Na}^+/\text{HCO}_3^-$ cotransport can be electroneutral, with a stoichiometry of 1:1, or electrogenic, carrying $1\text{Na}^+:2\text{HCO}_3^-$. The $\text{Na}^+/\text{HCO}_3^-/\text{Cl}^-$ exchanger transports $1\text{Na}^+:2\text{HCO}_3^-:1\text{Cl}^-$, thus it is electroneutral. In the squid axon, $\text{Na}^+/\text{HCO}_3^-/\text{Cl}^-$ transport required intracellular ATP, but was independent of ATP hydrolysis (Boron et al., 1988).

2.2 Calcium Transport

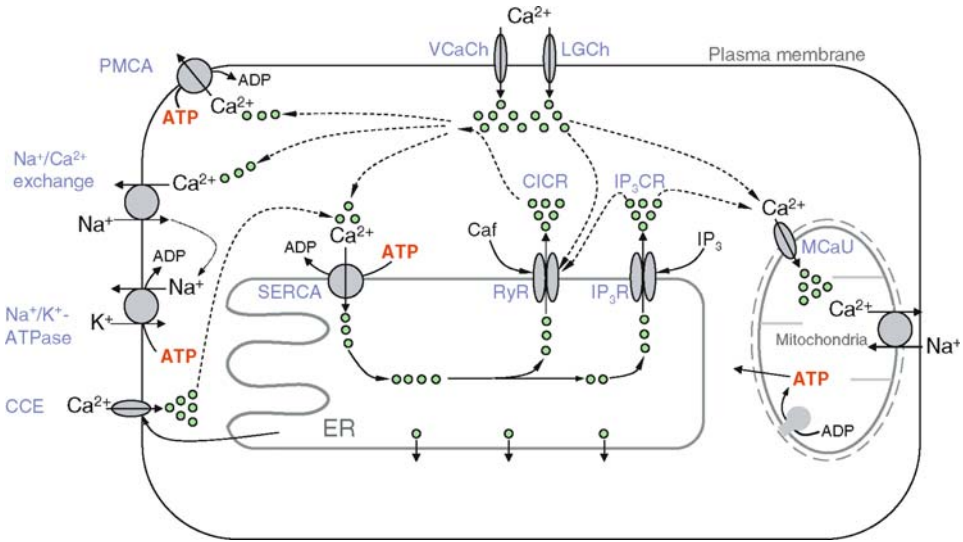
Calcium as a main “signaling” cation in the cell. As described by Carafoli (2002) in his brief “calcium signaling saga,” the calcium era began more than 120 years ago in London, where in 1883 Sidney Ringer discovered that isolated hearts contracted beautifully in saline made with “hard” London tap water, but stopped when buffer was instead made with distilled water. Thus a novel function for Ca^{2+} , apart from being a structural element for bone and teeth, was discovered: “It carried the signal that initiated heart contraction.” Fragmented experimental evidence for a role of Ca^{2+} in the cell was accumulated over ensuing decades, and only in the late 1950s were the first pioneers able to fully appreciate the importance of these observations: in 1959 Otto Loewy proclaimed “*Ja Kalzium, das ist alles!*”. It is now indisputable that calcium is a critical signaling cation in the cell. Ca^{2+} is an important second messenger that activates many cellular pathways and is involved in a plethora of cellular processes including neurotransmitter release, synaptic plasticity, growth of neuronal processes, and gene transcription. Most germane to this discussion, Ca^{2+} is required for the activation of many enzymes, including those of the respiratory chain, and is therefore important in regulating mitochondrial energy production.

A large gradient for Ca^{2+} allows fast changes in cytosolic Ca^{2+} concentration. The concentration of free Ca^{2+} in the cytosol ($[\text{Ca}^{2+}]_c$) in resting cells is very low, about 0.1 μM , whereas extracellular Ca^{2+} is about 1.2–1.9 mM. This gradient of roughly four orders of magnitude drives Ca^{2+} ions into the cytosol from the extracellular space, providing a rapid response mechanism for various stimuli. On the other hand, maintaining resting cytosolic Ca^{2+} at a low concentration is a process of high energy demand. The plasma membrane has very restricted and tightly controlled Ca^{2+} influx pathways. However, as a result of the large transmembrane gradient, even a minor increase in plasma membrane Ca^{2+} permeability can result in significant elevations in $[\text{Ca}^{2+}]_c$ and, consequently, activation of Ca^{2+} -dependent cellular pathways. Rapid increases in cytosolic Ca^{2+} can result from Ca^{2+} influx through plasmalemmal voltage- and receptor-operated channels, as well as release of Ca^{2+} from intracellular stores. Ca^{2+} can fulfill its regulatory functions only if changes in its cytosolic levels are carefully buffered.

Calcium clearance mechanisms specifically regulate the shape of Ca^{2+} transients. The mechanisms for the recovery of elevated $[\text{Ca}^{2+}]_c$ include Ca^{2+} extrusion by the plasma membrane Ca^{2+} ATPase (PMCA) and the $\text{Na}^+/\text{Ca}^{2+}$ exchanger, Ca^{2+} sequestration by the endoplasmic reticulum Ca^{2+} pump (SERCA), and by mitochondrial Ca^{2+} uptake. Each of these mechanisms has a specific role in the regulation of the shape of Ca^{2+} transients, which is based on its localization, capacity, and affinity for Ca^{2+} , and this in turn modifies the characteristics of Ca^{2+} signals. Evidences suggest that mitochondria and endoplasmic reticulum (ER) are responsible for fast control of Ca^{2+} signals, whereas PMCA and $\text{Na}^+/\text{Ca}^{2+}$ exchange are important for long-term maintenance. The PMCA is a very high-affinity transport system sensitive to small $[\text{Ca}^{2+}]_c$ changes and could contribute to the maintenance of basal $[\text{Ca}^{2+}]_c$ in resting cells, while the $\text{Na}^+/\text{Ca}^{2+}$ exchanger is a low-affinity but higher capacity transporter that is more important in correcting larger amplitude changes. All of these Ca^{2+} clearance mechanisms depend directly or indirectly on energy. With the exception of mitochondrial Ca^{2+} uptake, Ca^{2+} ions must be pumped against their concentration gradient, which makes this process highly energy intensive. Indeed, after Na^+ and K^+ , Ca^{2+} is the third most expensive cation in terms of brain energy utilization. Although estimates of the energy required for Ca^{2+} transporters are uncertain owing to the complexity of the regulation of cellular Ca^{2+} , transport of Ca^{2+} consumes an estimated 3%–7% of total brain energy (Ames, 2000). The main transport Ca^{2+} systems are schematically shown in  Figure 4.7-2. Because many vital cellular processes are affected by Ca^{2+} , impaired evacuation of cytosolic Ca^{2+} leads to dangerous pathologies which will be discussed in the next section.

■ Figure 4.7-2

The main energy-consuming pathways for the maintenance of $[Ca^{2+}]_i$. Under normal circumstances, extracellular Ca^{2+} enters the cells largely via voltage- and ligand-gated ion channels (VCaCh, LGCh). The major mechanisms for Ca^{2+} clearance include (1) the plasma membrane Na^+/Ca^{2+} exchanger; (2) the mitochondrial Ca^{2+} uniporter (MCuU); (3) the plasma membrane Ca^{2+} ATPase (PMCA) and (4) sarco(endoplasmic) reticulum Ca^{2+} ATPase (SERCA). Inositol-1,4,5-triphosphate (IP_3R) and ryanodine receptors (RyR) associated with the endoplasmic reticulum (ER) amplify VCaCh- and LGCh-induced $[Ca^{2+}]_i$ increases by Ca^{2+} -induced Ca^{2+} release and caffeine (CICR and caf) and IP_3 - Ca^{2+} release (IP_3CR). ER Ca^{2+} release plays a major role in Ca^{2+} signaling in nonneuronal cells. Depletion of the ER activates store-operated channels and initiates capacitative Ca^{2+} enter (CCE), which is responsible for the refilling of ER with Ca^{2+} . All Ca^{2+} transport systems are energy dependent and use ATP hydrolysis or previously established ion gradients as a driving force for Ca^{2+} movement



2.2.1 Plasma Membrane Ca^{2+} Pump

The Ca^{2+} -dependent ATPase (PMCA) was first identified in human red cells by Dunham and Glynn (1961). Later Schatzmann (1966) showed that it is responsible for exporting Ca^{2+} from the cell. For many years its biochemical properties were studied in erythrocytes, and only in the mid and late 1970s was an ATP-dependent and Na^+ -independent Ca^{2+} extrusion revealed in neuronal cells (Robinson, 1976; DiPolo, 1978). It is now generally accepted that PMCA protein is ubiquitously expressed. The amount of PMCA in different tissues usually does not exceed 0.1%–0.3% of total membrane protein, however neuronal tissues contain up to ten times more PMCA than nonexcitable cells (Guerini, 1998b), indicating the importance of PMCA in neuronal Ca^{2+} homeostasis. Because the pump is a high-affinity, low-capacity system, the PMCA is most important in restoring resting $[Ca^{2+}]_i$ after modest Ca^{2+} loads, and for maintaining $[Ca^{2+}]_i$ under resting conditions. The plasmalemmal Ca^{2+} ATPase is the only primary active transporter that pumps Ca^{2+} out of the cell. Erecinska and Silver (1989) used the calculations of Sanchez-Armass and Blaustein (1987) to estimate that the PMCA uses about 0.3%–0.5% of total ATP in the brain.

Kinetics and stoichiometry of the PMCA. The PMCA belongs to the P-type family of ion-motive ATPases. The enzyme oscillates between a high-affinity E_1 conformation with a catalytic site for ATP ($K_m \approx 1 \mu M$) and a low-affinity E_2 conformation with a noncatalytic site for ATP ($K_m \approx 100\text{--}300 \mu M$) (Lauger, 1991). Ca^{2+} binds to the E_1 conformation at the cytoplasmic side of the membrane ($K_m \approx 0.1\text{--}1 \mu M$ in the presence of calmodulin). Phosphorylation by ATP catalyzes the transformation of E_1 to E_2 and translocation of Ca^{2+} to the extracellular side where the enzyme has low Ca^{2+} affinity ($K_m > 10 \mu M$). Phosphorylation of the enzyme

at the low-affinity site (E_2) accelerates a returning of the pump to the E_1 conformation. Only ATP can catalyze the reaction; other triphosphates are ineffective. PMCA transports one molecule of Ca^{2+} per hydrolyzed ATP (Garrahan and Rega, 1990). It is well established that the PMCA functions as an obligatory $\text{Ca}^{2+}/\text{H}^+$ exchanger with a probable stoichiometry of 1:1, though it can be 1:2 depending on the method of enzyme isolation (Carafoli, 1994).

An important difference between the PMCA and other P-type pumps is that the PMCA is regulated by multiple cellular mechanisms. The most potent activator of the PMCA is calmodulin. Although not essential for Ca^{2+} pump activity, calmodulin binding increases the maximal turnover rate of the pump owing to an increase of apparent affinity for Ca^{2+} : $K_m(\text{Ca})$ decreases in the presence of calmodulin from about 10–20 μM to about 0.5 μM (Carafoli, 1994). Calmodulin accelerates the reaction either by binding directly to the enzyme or through the activation of a calmodulin-dependent protein kinase. The affinity of the pump for calmodulin is very high, with a K_D of 5–50 nM, depending on the PMCA isoform. Other activators include acidic phospholipids, long-chain polyunsaturated fatty acids, protein kinase A, and protein kinase C. Mg^{2+} ions also significantly increase PMCA activity, and activity drops to less than 5% of maximum in the absence of Mg^{2+} . In contrast to Na^+/K^+ -ATPase, Mg^{2+} is not absolutely required for Ca^{2+} translocation (Garrahan and Rega, 1990). Mg^{2+} promotes both the rate of the phosphorylation (with a half-maximal effect at about 100 μM) and the conversion of E_2 into E_1 . High intracellular Mg^{2+} (>2 mM) is inhibitory. Among other divalent cations Sr^{2+} , but not Ba^{2+} or Mn^{2+} , can be effectively transported by the pump (Schatzmann and Vincenzi, 1969; Graf et al., 1982).

PMCA isoforms have different sensitivities to calmodulin and their expression is age dependent. The regulation of the PMCA-evoked Ca^{2+} extrusion from the cell depends on the expression of the enzyme isoforms. PMCA is encoded by four different genes found in humans and the rat: ATP2B1, ATP2B2, ATP2B3, and ATP2B4. Because of alternative mRNA splicing, more than 20 variants exist (Guerini, 1998b). Whereas ATP2B1 and 4 are expressed in all tissues, ATP2B2 and 3 are specific to brain and heart. Their most significant difference is their affinity for calmodulin, which is 3–4 times higher in ATP2B2 than in other isoforms (Guerini, 1998b). The physiological impact of this difference remains unclear. It has been demonstrated that PMCA mRNA and proteins are distributed heterogeneously in different CNS regions (Carafoli, 1994; Stahl et al., 1994; Stauffer et al., 1995; Burette et al., 2003). It is also interesting that the expression of the different isoforms changes during development and depends on neuronal Ca^{2+} loading. Thus, isoforms 2, 3, and 1CII, which are expressed copiously in the cerebellum of adult but not neonatal rats, were highly upregulated in cerebellar granule cells after 7–9 days in culture under membrane-depolarizing conditions. Conversely, expression of isoform 4 in the adult cerebellum was downregulated by membrane depolarization. These changes required L-type Ca^{2+} channel activation (Guerini et al., 1999). In whole animal hippocampus, as well as in cultured hippocampal neurons, all the PMCA isoforms are upregulated with maturity (Jensen et al., 2004; Kip et al., 2006).

Functional impact of brain PMCA. Owing to a lack of specific modulators of the PMCA, the study of its physiological function in living cells has proven challenging. The pump can be inhibited by vanadate, La^{3+} , N-ethylmaleimide (NEM, an inhibitor of calmodulin) calmidazolium, and carboxyeosin. Steroid hormones also modulate the pump activity (Deliconstantinos, 1988; Zylinska et al., 1999). However, all of these compounds have other effects on cellular functions at concentrations similar to those used to inhibit the PMCA. A novel and apparently selective peptide inhibitor of PMCA, caloxin 1A1, was found by screening a peptide library (Chaudhary et al., 2001); however, it has not yet been used extensively in neuronal cells. There is comparatively more information regarding the biochemical properties of the isolated enzyme, but the limited pharmacopoeia means that data is lacking regarding the role of the pump in $[\text{Ca}^{2+}]_c$ recovery after physiological or pathological calcium loads. Because of its high Ca^{2+} affinity, the pump has long been considered as mainly important for maintaining basal $[\text{Ca}^{2+}]_c$. However, there is increasing evidence for a more active role in $[\text{Ca}^{2+}]_c$ recovery after small-amplitude Ca^{2+} transients (Benham et al., 1992; Pottorf and Thayer, 2002; Wanaverbecq et al., 2003). A dominant role for the PMCA was proposed in Ca^{2+} recovery after short-duration stimulation of NMDA receptors in cultured cerebellar neurons (Khodorov et al., 1995). Recent data further show that the enzyme is not uniformly distributed within the cell, instead its density is increased in high metabolic subdomains, such as (1) dendritic spines of cerebellar Purkinje cells (Hillman et al., 1996), (2) transmitter release sites (Juhaszova et al., 2000), (3) growth cones of developing neurons

and dendritic spines in mature neurons (Kip et al., 2006), and (4) active zones of nerve terminals (Blaustein et al., 2002; Kip et al., 2006). Heterogeneous expression of PMCA isoforms in different cell types and specific localization in subcellular microdomains with larger Ca^{2+} traffic suggest that the PMCA is a more dynamic, but local, regulator of $[\text{Ca}^{2+}]_c$ than previously has been appreciated.

2.2.2 Plasmalemmal $\text{Na}^+/\text{Ca}^{2+}$ Exchange

Evidence for Na^+ -dependent Ca^{2+} transport has been accumulating since the end of nineteenth century. In late 1960s, three different groups independently concluded that Na^+ and Ca^{2+} were antiported through the plasma membrane of cardiac muscle, intestine, and giant squid axon (Reuter and Seitz, 1968; Baker et al., 1969; Martin and DeLuca, 1969). Since then, the $\text{Na}^+/\text{Ca}^{2+}$ exchanger was identified in most cell types of both vertebrates and invertebrates. The plasma membrane $\text{Na}^+/\text{Ca}^{2+}$ exchanger is a secondary active transporter, thus ATP hydrolysis is not a direct energy source for ion movement. Its affinity for Ca^{2+} is about 10-fold lower and its capacity 10- to 50-fold higher than the PMCA (Blaustein and Lederer, 1999). As the largest capacity Ca^{2+} extrusion system, the $\text{Na}^+/\text{Ca}^{2+}$ exchanger is critical for $[\text{Ca}^{2+}]_c$ recovery after loads, as well as in maintaining low intracellular Ca^{2+} . The Na^+ gradient across the plasma membrane is the driving force for Ca^{2+} extrusion. Therefore, energy utilized by $\text{Na}^+/\text{Ca}^{2+}$ transport is coupled to the Na^+/K^+ -ATPase. Erecinska and Silver (1989) estimated that the $\text{Na}^+/\text{Ca}^{2+}$ exchanger utilizes about 2%–3% of total ATP consumption in the brain. It is important to note that this assumes perfect coupling between $\text{Na}^+/\text{Ca}^{2+}$ exchange and Na^+/K^+ -ATPase (i.e., no energy losses during the reaction).

Cardiac/neuronal type of the $\text{Na}^+/\text{Ca}^{2+}$ exchanger is dominant in the brain. Six genes encoding the $\text{Na}^+/\text{Ca}^{2+}$ exchanger have been identified in mammals: three for $\text{Na}^+/\text{Ca}^{2+}$ exchange (SLC8A1, SLC8A2 and SLC8A3) and three for $\text{Na}^+/\text{Ca}^{2+} + \text{K}^+$ exchange (SLC24A1, SLC24A2, and SLC24A3) (Blaustein and Lederer, 1999). The dominant type of the exchanger in the brain is SLC8A1, a “cardiac/neuronal type” with a stoichiometry of $3\text{Na}^+ : 1\text{Ca}^{2+}$ (Blaustein and Lederer, 1999), although SLC8A2 and SLC8A3 are also expressed in the CNS. All three K^+ -dependent isoforms ($4\text{Na}^+ / 1\text{Ca}^{2+} + 1\text{K}^+$) were also identified in the brain. However, relatively little is known about their role in regulating neuronal Ca^{2+} homeostasis (Tsoi et al., 1998; Kraev et al., 2001; Kiedrowski et al., 2004).

Kinetics and stoichiometry of $\text{Na}^+/\text{Ca}^{2+}$ exchange. The biochemical properties of the $\text{Na}^+/\text{Ca}^{2+}$ exchanger have been studied most intensively on the squid giant axon and the mammalian cardiac myocyte. Depending on ion composition and the regulatory factors present, the exchanger can operate in four modes: $\text{Na}^+_o/\text{Ca}^{2+}_i$ (forward mode), $\text{Na}^+_i/\text{Ca}^{2+}_o$ (reverse mode), and $\text{Na}^+_o/\text{Na}^+_i$ and $\text{Ca}^{2+}_o/\text{Ca}^{2+}_i$ (homologous modes). SLC8A1 stoichiometry is the same in forward and reverse modes i.e., $3\text{Na}^+ : 1\text{Ca}^{2+}$. The mode of the exchange operation is determined by the electrochemical gradient across the plasma membrane.

As the $\text{Na}^+/\text{Ca}^{2+}$ exchanger is highly regulated, many factors including monovalent and divalent cation concentrations and metabolites will affect the exchanger’s kinetics and velocity. The molecular and kinetic properties of the $\text{Na}^+/\text{Ca}^{2+}$ exchanger are described in detail in numerous original reports and reviews. Recent comprehensive reviews include those by Reeves and coworkers (1994), Guerini (1998a), Blaustein and Lederer (1999), and DiPolo and Beauge (2006). Briefly, because three molecules of Na^+ are transported in exchange for one molecule of Ca^{2+} , the exchanger is electrogenic and, consequently, its operation is voltage sensitive. The exchanger has both transport and nontransport (regulatory) sites for Na^+ and Ca^{2+} . Na^+ and Ca^{2+} can bind to sites on the external and internal sides of the membrane in competitive fashion. K_m values for Na^+ vary from 15 to 70 mM depending on the cell type and preparation. In vertebrates, affinity at the intracellular side is about ~8-fold lower than at the extracellular side, while in squid axons there is no such difference (DiPolo and Beauge, 2006). Measurement of the apparent affinities for Ca^{2+} is complicated because of many regulatory factors. In different preparations, K_m for Ca^{2+} at the intracellular side is 10–100 times lower than at the extracellular side (DiPolo and Beauge, 2006). In different reports, K_m at the cytoplasmic side in the presence of ATP varies from 0.6 to 2.5 μM (Reeves, 1990).

Nontransported Na^+ , Ca^{2+} , and H^+ regulate activity of the $\text{Na}^+/\text{Ca}^{2+}$ exchange. Intracellular Ca^{2+} and Na^+ can regulate the activity of the transporter by binding to the nontransport sites. Binding of Ca^{2+} to a

regulatory site on the intracellular side is absolutely required for both forward and reverse mode transport. In contrast, Na^+ binding to the regulatory site inhibits the exchanger. Enhanced Ca^{2+} binding can thus reduce the inhibitory action of Na^+ . Exchanger activity depends on intracellular pH, so that internal acidification strongly inhibits whereas internal alkalization activates the transporter. External pH changes have no effect. According to the model proposed by DiPolo and Beauge (2006), H^+ interacts with Ca^{2+}_i and Na^+_i at their regulatory sites but not at the sites responsible for transporting the ions; H^+ competes with Ca^{2+} , enhancing the inhibitory action of Na^+_i . The actual value of pH at which the exchanger is inhibited depends on Ca^{2+} and Na^+ concentrations. At constant cytoplasmic Na^+ (100 mM) and Ca^{2+} (4 μM) concentrations, and absence of ATP, a decrease in pH from 7.8 to 6.8 reduced the exchange current by several times in voltage-clamped myocytes of guinea pig (Hilgemann et al., 1992).

Although the $\text{Na}^+/\text{Ca}^{2+}$ exchanger uses the electrochemical ion gradients as a driving force and ATP hydrolysis is not required for its catalytic activity, ATP significantly facilitates ion transport. The K_m for ATP varies in different cell types, and for mammalian nerve vesicles it was calculated at about 300 μM (Berberian et al., 2002). The activation of the exchanger by ATP is due to an increase in the affinity for internal Ca^{2+} and external Na^+ at their transport sites (Blaustein and Santiago, 1977) and a decrease of the Na^+_i -dependent inhibition (DiPolo and Beauge, 2006). In squid axons, the affinity for external Na^+ at the transport site is increased by ATP by about threefold, and for internal Ca^{2+} by about 10-fold (DiPolo and Beauge, 2006).

There are no potent or selective drugs for the inhibition of the $\text{Na}^+/\text{Ca}^{2+}$ exchanger. Nonselective inhibitors include amiloride analogs N^5 -(2,4-dimethylbenzyl)amiloride and 3,4-dichlorobenzamil (the most effective inhibitor), antiarrhythmic agents quinacrine and bepridil, various local and general anesthetics, some synthetic peptides, and various inorganic cations including La^{3+} , Mg^{2+} , Cd^{2+} , Co^{2+} , Mn^{2+} , Zn^{2+} , and Ni^{2+} .

Investigation of the physiological role of the $\text{Na}^+/\text{Ca}^{2+}$ exchanger in nerve cells. At resting Na^+ concentrations and resting membrane potential, and with an abundance of intracellular ATP, increased $[\text{Ca}^{2+}]_c$ will activate forward mode exchange, facilitating the extrusion of Ca^{2+} and $[\text{Ca}^{2+}]_c$ recovery. However, under conditions typical for hypoxia such as increased $[\text{Na}^+]_o$, ATP depletion, and intracellular acidification, the extrusion of Ca^{2+} can be reduced or even reversed, providing an additional route for Ca^{2+} influx (Hoyt et al., 1998).

Despite a lack of specific inhibitors, the role of $\text{Na}^+/\text{Ca}^{2+}$ exchanger in transporting neuronal Ca^{2+} has been investigated. The $\text{Na}^+/\text{Ca}^{2+}$ exchanger proteins are highly expressed in neurons, especially in the synapses and growth cones (Luther et al., 1992) where the concentration of Ca^{2+} channels is higher and larger amounts of Ca^{2+} must be exported from the cell to maintain normal $[\text{Ca}^{2+}]_c$. Elevated $[\text{Ca}^{2+}]_c$ in the presynaptic terminals triggers neurotransmitter release. In a number of models, blockade of $\text{Na}^+/\text{Ca}^{2+}$ exchange following elevation of $[\text{Ca}^{2+}]_c$ enhances neurotransmitter release, which is consistent with a role for $\text{Na}^+/\text{Ca}^{2+}$ exchange in clearing Ca^{2+} from active secretory zones (Thayer et al., 2002).

Because Na^+ -dependent Ca^{2+} efflux is the highest capacity Ca^{2+} extrusion system in the cell, the exchanger must mediate long-term recovery after increased neuronal activity. Its role in acute recovery after the stimulation of NMDA receptors was also investigated. Substitution of *N*-methyl-D-glucamine (NMDG⁺) for Na^+ dramatically delayed $[\text{Ca}^{2+}]_c$ recovery after NMDA stimulation in cultured cortical neurons, suggesting that $\text{Na}^+/\text{Ca}^{2+}$ exchange is an important factor in the Ca^{2+} recovery after glutamate-induced Ca^{2+} loads (White and Reynolds, 1995). However, in cerebellar granule cells NMDG⁺ substitution caused release of endogenous glutamate, and delayed $[\text{Ca}^{2+}]_c$ recovery after glutamate was abolished by NMDA receptor inhibition, arguing against the role of $\text{Na}^+/\text{Ca}^{2+}$ exchange in Ca^{2+} recovery after glutamate stimulus (Storozhevkyh et al., 1998).

2.2.3 Endoplasmic Reticulum Ca^{2+} Pump

Discovered in 1961 in muscle sarcoplasmic reticulum, the sarco(endo)plasmic reticulum Ca^{2+} ATPase (SERCA) is an intracellular primary active transporter which uses the energy of ATP hydrolysis for the movement of Ca^{2+} (Hasselbach and Makinose, 1961).

The function of SERCA is to pump Ca^{2+} from the cytosol into the ER lumen where the concentration of free Ca^{2+} exceeds that of the cytosol by a factor of about 10,000. Ca^{2+} cations continuously leak across the

ER membrane, and SERCA counteracts this by pumping Ca^{2+} back in. Thus, inhibition of SERCA leads to depletion of Ca^{2+} stores.

ER Ca^{2+} represents a dynamic pool with potential for a dual role in regulating cytosolic Ca^{2+} : it may contribute to Ca^{2+} buffering by activation of SERCA, or it may be a source of Ca^{2+} by activation of ER Ca^{2+} release channels. ER Ca^{2+} is released by the activation of ryanodine receptor (RyR) channels and 1,4,5-inositol trisphosphate receptor (IP_3R) channels and is critical for fast $[\text{Ca}^{2+}]_c$ elevations in nonneuronal cells. In astrocytes, for example, ER Ca^{2+} release is a main mechanism for the propagation of Ca^{2+} waves (Duchen, 2004). Ca^{2+} entering the cytoplasm via voltage- or ligand-gated channels acts as a second messenger and activates RyR. This, in turn, initiates Ca^{2+} release from the ER and thereby depletion of stores. In case of IP_3R -mediated Ca^{2+} release, IP_3 acts as a second messenger to stimulate the receptors. Depletion of calcium stores in the ER activates store-operated Ca^{2+} channels in the plasma membrane, and Ca^{2+} entering the cytoplasm promotes store refilling, a process called “capacitative Ca^{2+} entry” (CCE). Because ER is able to amplify $[\text{Ca}^{2+}]_c$ increases only under conditions when stores are replete of Ca^{2+} , this function of ER is dependent on the proper operation of SERCA and consequently on the metabolic state of the cell. There is also a close physical and functional interrelation between ER and mitochondria that is important in shaping cytoplasmic Ca^{2+} signals. (For more details about ER-mediated Ca^{2+} signaling see Chapter 6.2). The ER and associated IP_3R and RyR receptors are widely distributed in neurons, and there is evidence of ER-associated Ca^{2+} elevations in response to physiological stimulus (Simpson et al., 1995; Verkhratsky and Petersen, 2002).

The second role of the ER, which is also related to its Ca^{2+} capacity, involves posttranslational modification of proteins, or “protein folding.” The accumulation of unfolded proteins in the ER and Ca^{2+} -depletion of the ER by the inhibition of SERCA results in ER stress response. The ER stress response includes initiation of cellular adaptive mechanisms for the regulation of protein synthesis, but also may upregulate the synthesis of proapoptotic proteins leading to cell death (Pahl and Baeuerle, 1995). Thus, inhibition of SERCA triggers apoptotic cell death (Verkhratsky and Petersen, 2002; Verkhratsky, 2005).

A third intriguing possibility is that the ER serves as a tunnel for transporting Ca^{2+} throughout the cell (Mogami et al., 1997; Verkhratsky and Petersen, 2002). Since the cell has very large capacity Ca^{2+} buffering systems, only 0.05%–1% of Ca^{2+} in the cytosol remains free, and the diffusion of Ca^{2+} in the cytosol is slow and limited in distance (Meyer et al., 1988), which restricts the diffusibility of the cation. It would take a long time for Ca^{2+} to diffuse, for example, from the plasma membrane to the nucleus. Because ER buffering capacity is lower than the cytosol’s, free Ca^{2+} in the ER varies between 100–600 μM (Verkhratsky and Petersen, 2002); this would allow faster Ca^{2+} diffusion to other cellular domains, and would enable the “tunneling” effect.

Kinetics and stoichiometry of SERCA. The reaction cycle of SERCA is similar to that of the Na^+/K^+ -ATPase (Lauger, 1991). The enzyme adopts two conformations: E_1 and E_2 . In E_1 it binds with high affinity two molecules of Ca^{2+} and one of ATP at a cytosolic site ($K_m \approx 1 \mu\text{M}$ and 2 μM , respectively). When phosphorylated, the Ca^{2+} ions become occluded. E_1 then transitions to E_2 , which is a low-affinity Ca^{2+} conformation ($K_m \approx 1 \text{ mM}$) facing the ER lumen, allowing Ca^{2+} release into the ER lumen. After Ca^{2+} release, the enzyme returns to E_1 . As with the Na^+/K^+ -ATPase, $E_2 \rightarrow E_1$ transition is accelerated by ATP binding to a low-affinity cytosolic site ($K_m \approx 20\text{--}50 \mu\text{M}$). Like the PMCA, SERCA is an obligatory H^+ exchanger, pumping cytosolic Ca^{2+} in exchange for luminal H^+ , shifting the luminal pH toward the alkaline. The exchange is thought to be electrogenic, with proposed stoichiometries of $2\text{Ca}^{2+}:\text{2H}^+$ (Yu et al., 1993) or $1\text{Ca}^{2+}:\text{1H}^+$ (Hao et al., 1994). SERCA is regulated by ER Ca^{2+} , and a reduction of luminal Ca^{2+} activates the pump. Two ER proteins were shown to modulate SERCA activity. The Ca^{2+} -sensitive protein calreticulin activates the enzyme directly when luminal Ca^{2+} is low (John et al., 1998). Another protein, ERp57, modulates the redox state of SERCA, which is also Ca^{2+} dependent (Li and Camacho, 2004).

Three isoforms of SERCA are expressed in the brain. SERCA is encoded by three genes SERCA1, SERCA2, and SERCA3 (so-called ATP2A1-3), two of which—SERCA2 (of which there are two isoforms, SERCA2a and SERCA2b) and SERCA3—are expressed in the brain (Meldolesi, 2001). SERCA2b is ubiquitously expressed in the brain, whereas SERCA2a and SERCA3 are found only in the cerebellar Purkinje neurons. The physiological role of SERCA3 remains unclear since a genetic deletion of this protein did not result in phenotypic change (Baba-Aissa et al., 1996; Verkhratsky, 2005).

Specific inhibitors of SERCA. As is the case with all P-type pumps, the SERCA is blocked by La^{3+} and orthovanadate (Szasz et al., 1978). In contrast to PMCA, specific membrane-permeable inhibitors are available, which obviously presents a huge advantage for elucidating SERCA's physiological role. These are the irreversible inhibitor thapsigargin and the reversible inhibitor cyclopiazonic acid. The most specific inhibitor is thapsigargin with a $K_D \approx 20$ nM. Cyclopiazonic acid blocks the pump in the concentrations of about 20–50 μM (Verkhatsky, 2005).

2.2.4 Mitochondrial Ca^{2+} Uptake

Mitochondria have a dual role in the regulation of cellular ion transport. First, mitochondria are the main energy source for other ion transport systems, as discussed above. Second, mitochondria directly regulate intracellular Ca^{2+} through uptake and release. Ca^{2+} moves into the mitochondria passively by virtue of the large mitochondrial transmembrane potential, and therefore import of Ca^{2+} does not require ATP hydrolysis. However, mitochondrial Ca^{2+} uptake influences cellular energy metabolism via regulation of matrix dehydrogenases of the citric acid cycle (McCormack and Denton, 1980) essential to ATP production. In addition, mitochondrial Ca^{2+} accumulation occurs at the expense of the mitochondrial proton gradient, which limits ATP synthesis (Nicholls and Budd, 2000). Since mitochondrial ion transport systems are only indirectly coupled to ATP consumption, and because mechanisms of mitochondrial Ca^{2+} uptake and for the regulation of mitochondrial ATP production are described in detail in the previous chapters, we only briefly discuss this issue.

Mitochondrial Ca^{2+} uniporter is a high-affinity selective ion channel. Mitochondria Ca^{2+} uptake occurs through the Ca^{2+} uniporter, located on the inner mitochondrial membrane, and is driven by the electrochemical gradient. From the mid-1970s until recently, the Ca^{2+} uniporter was assumed to be a low-affinity ion transport system, and therefore most responsible for clearance of large Ca^{2+} loads. However, recent data suggest it is a Ca^{2+} -selective channel with extremely high affinity for Ca^{2+} (≤ 2 nM) (Kirichok et al., 2004), and this is consistent with studies showing mitochondrial calcium accumulation following physiological Ca^{2+} loads (Werth and Thayer, 1994). We have also shown that the mitochondrial membrane potential ($\Delta\Psi_m$) of isolated brain mitochondria is extremely sensitive to low concentrations of external calcium. Addition of 30–70 nM Ca^{2+} induced transient mitochondrial depolarizations (Vergun and Reynolds, 2004, 2005b). These data favor a role for mitochondria in regulating basal $[\text{Ca}^{2+}]_i$ in brain cells.

Mitochondria provide a rapid Ca^{2+} clearance system in neurons. It is now obvious that mitochondrial Ca^{2+} sequestration is important for rapid clearance after large Ca^{2+} loads imposed by voltage-gated and ligand-gated channels, and in shaping amplitude and duration of Ca^{2+} transients after physiological stimuli (Werth and Thayer, 1994; Jouaville et al., 1995; Budd and Nicholls, 1996a; Khodorov et al., 1996a, b; Wang and Thayer, 1996; Babcock et al., 1997; Boitier et al., 1999). Because Ca^{2+} sequestration by mitochondria is the fastest Ca^{2+} clearance system, it is therefore best suited for rapid removal of Ca^{2+} from the cytosol. Excessive mitochondrial Ca^{2+} accumulation during prolonged stimulation of glutamate receptors results in the acute dissipation of the $\Delta\Psi_m$ and eventually leads to neuronal death. Possible mechanisms underlying neuronal injury, and the role of mitochondria in the perturbation of neuronal Ca^{2+} homeostasis is discussed in the next section.

Mitochondria are unique organelles because they can adjust energy production to cellular needs not only by the regulation of intensity of ATP synthesis but also by moving to the specific locations where energy demand is intense. This is especially important for neuronal cells because of their morphology and continuously changing energy requirements associated with neuronal plasticity. This is discussed in more detail below.

2.3 Zinc Transport

Zn^{2+} has emerged as an important cation in the brain for signaling and neurotoxicity (Choi and Koh, 1998) and is suitable as an exemplar cation for the consideration of the interaction between trace metals and energy homeostasis. Heterogeneously distributed in the brain, Zn^{2+} is especially abundant in neurons

where it is stored with glutamate in presynaptic vesicles. Zn^{2+} is a relatively potent neurotoxin, and there is no doubt that Zn^{2+} deregulation occurs during neuronal death associated with various CNS pathologies, including stroke, epilepsy, trauma, and possibly Alzheimer's disease. In the context of the excitotoxic sequelae, however, it is yet uncertain whether zinc deregulation is an early, causative event as opposed to a later secondary event. Zn^{2+} can accumulate in neurons because it can mimic calcium and thus enter through various calcium pathways, including voltage-gated channels, ionotropic glutamate receptors, and the Na^+/Ca^{2+} exchanger, or as a result of oxidant-induced alteration of Zn^{2+} -binding proteins (Sensi et al., 1997; Cheng and Reynolds, 1998; Aizenman et al., 2000). It is also clear that there are many Zn^{2+} transporters distinct from these Zn^{2+} transporting pathways, and these are described below.

The effective study of Zn^{2+} neurobiology is limited by the ability to monitor zinc in its native environment. Many approaches such as atomic absorption or plasma emission spectroscopies allow sensitive detection of total Zn^{2+} in tissues and cells; however, they are not useful for discerning the relatively small fraction of Zn^{2+} that is free compared with the much larger quantity of zinc that is bound to intracellular proteins. ^{65}Zn is similarly useful for whole-cell measurements, as well as turnover studies. Commercially available live-cell fluorescent indicators sensitive to Zn^{2+} have been particularly useful, but it is important to note that such techniques are probably semiquantitative at best (Dineley et al., 2002). Indeed, though many reports use standard calibration techniques (Gryniewicz et al., 1985) to make precise quantitative statements regarding intracellular Zn^{2+} concentrations, such numbers are probably crude estimates at best.

Most tissue zinc is bound to intracellular proteins, and thus is comparatively immobile. The vesicular pool can be mobilized during neuronal activity, and some estimates indicate that such activity can lead to high localized concentrations in the extracellular space (Frederickson et al., 2005). Because Zn^{2+} modulates the activity of various channels and transporters, and because Zn^{2+} in the synapse may contribute to the death of postsynaptic targets, vesicular zinc has held special interest. However, it must be stated clearly that no definitive function can yet be ascribed to vesicular zinc or its release, and here it is important to note that genetically engineered mice lacking nearly all detectable vesicular brain zinc are strikingly normal (Cole et al., 1999; Cole et al., 2000; Cole et al., 2001).

Total zinc inside a mammalian cell is on the order of 200 μM , but determining the small fraction that is free in ionic form is an area of intense investigation. Historically, estimates range in the high pico- to low nanomolar range. Bozym and colleagues recently used a carbonic anhydrase-like fluorescent biosensor to estimate $[Zn^{2+}]_c$ at ~ 5 pM in PC12 and Chinese hamster ovary cells (Bozym et al., 2006). Whatever its precise value, free Zn^{2+} is exceedingly low and kept so in part by a variety of Zn^{2+} -binding proteins. Any increase must be ephemeral, because prolonged elevation of Zn^{2+} is patently lethal to neurons and glia (Yokoyama et al., 1986; Dineley et al., 2000).

In addition to metal-binding proteins, it is now beyond doubt that cells possess a variety of metal transporters that move Zn^{2+} with relative specificity. The first mammalian zinc transporter, ZnT1, was cloned and characterized in 1995 by Palmiter and Findley (Palmiter and Findley, 1995), and candidate human zinc transporters now number over 20. Zn^{2+} transporters have been classified into two categories: cation diffusion facilitators (CDFs or SLC30 family) and Zrt (zinc responsive transporter) Irt (iron responsive transporter)-like proteins (ZIPs). A comprehensive review is provided by Gaither and Eide, (2001) and more recently by Kambe and colleagues (Kambe et al., 2004). Here, we briefly summarize some fundamental properties.

Eukaryotic metal transporters include CDFs and ZIPs. CDFs are metal transporters that remove zinc from the cytoplasm. The CDF family includes zinc transporters (ZnT) 1–8. Though still poorly characterized in terms of function, all members of this family are believed to remove Zn^{2+} from the cytoplasm either by efflux through the plasma membrane or by transport into intracellular compartments or by both mechanisms. Each zinc transporter is between 300 and 550 amino acids in length, and hydrophobicity plots predict that all members have six transmembrane domains. Both the N and C termini are cytoplasmic, and a histidine-rich loop between transmembrane domains four and five may function in zinc binding. Another potential metal-binding motif is found in the histidine rich C terminus. The amphipathic transmembrane domains I, II, and V are conserved between CDFs and are speculated to mediate substrate transport. Some members of the CDF family are transcriptionally regulated by metals, and there is evidence that intracellular zinc may directly control CDF protein levels. Zinc administered by gavage in mice, for example, increased

the levels of ZnT1 and ZnT2 mRNA in the small intestine and kidneys (McMahon and Cousins, 1998a,b; Liuzzi et al., 2001). There is very little data regarding the precise mechanism by which CDFs transport Zn^{2+} , though they are not believed to require ATP, as none possesses any known ATP-binding motif. Functional CDFs are assumed to be composed of multimers, because six domains are probably insufficient to form a channel, and dominant-negative interactions have been described (Palmiter and Findley, 1995).

The ZIP family of transporters import Zn^{2+} from across the plasma membrane. Zrt-Irt-like proteins, or ZIPs, comprise a second family of metal transporters found in mammals. ZIPs are believed to mediate zinc import across the plasma membrane but, as with CDFs, definitive function for most of these proteins is not yet at hand. ZIP proteins usually possess eight transmembrane domains, with extracellular amino and carboxy termini. The cytoplasmic loop between domains III and IV varies in length and sequence between different ZIPs, but it is generally histidine rich and is therefore a candidate Zn^{2+} -binding site. Domains V and VI are predicted to participate in pore formation, as they contain histidine residues highly conserved between different ZIPs. As with CDFs, there is evidence that zinc can modulate the expression of some ZIP members. However, while Zn^{2+} regulation of CDFs presumably results from the direct interaction of Zn^{2+} with transcriptional promoter elements, zinc regulation of ZIPs appears more indirect in that Zn^{2+} may bind to the transporter, inducing a conformation change that renders the protein more susceptible to proteolytic degradation through endosomal pathways.

Energy requirements for CDF and ZIP remain unclear. Little is known regarding the source of energy for any mammalian CDFs or ZIPs. One of the more extensively studied transporters, ZnT1, is thought to export Zn^{2+} from BHK cells via a secondary active mechanism, because inhibition of energy production had no effect. However, various standard manipulations of extracellular buffer (e.g., removal of Na^+ , Cl^- , excess K^+ , etc) also did not change the rate of transport (Palmiter and Findley, 1995). Similarly, HCO_3^- transport might account Zn^{2+} influx via hZip2 (Gaither and Eide, 2000).

The mystery is deepened by a fundamental lack of knowledge regarding the Zn^{2+} transmembrane gradient, which stems from the great difficulty of determining free Zn^{2+} concentrations on either side of it. In their recent work, Bozym and colleagues (Bozym et al., 2006) estimated extracellular Zn^{2+} in the medium at 10 nM. If both intra- and extracellular calculations are correct, then ZnT1, for example (which is present in PC12 cells and neurons), is exporting Zn^{2+} against a gradient approaching 10,000. Extrapolating these figures to a Nernstian consideration of a resting neuron at -70 mV, it is evident that passive Zn^{2+} efflux would not occur below a Zn^{2+} reversal potential of $+120$ mV. Thus, according to these calculations, removing Zn^{2+} from the cytoplasm certainly requires some form of energy expenditure, while Zn^{2+} import ought to be passive. Naturally, any burden associated with import and export could be minimized if zinc movement coincided with voltage changes. And while a comprehensive treatment is outside the scope of this review, it should be noted that the total cost of maintaining Zn^{2+} homeostasis must consider the expense of synthesizing Zn^{2+} -binding proteins such as metallothionein. Clearly, it is challenging to determine the energetic burden of maintaining $[\text{Zn}^{2+}]_c$ homeostasis.

3 Spatial and Functional Interdependence of Energy Consumption and Energy Production in the Brain

In the brain, where energy reserves are extremely limited, there is a very tight interdependence of the activity of energy-producing and energy-consuming enzymes. An increase in the rate of ATP utilization during neuronal activity results in activation of glycolysis and oxidative phosphorylation. This is accomplished by both ionic regulation and close spatial localization of the enzymes. In this section, we will discuss the properties of functional and spatial regulation of ATP synthesis.

3.1 Mechanisms Controlling Energy Production

At physiological conditions, the total content of adenine nucleotides (ATP, ADP, and AMP) in the brain is about $3 \mu\text{mol/g}$ wet weight with ATP exceeding ADP and AMP by about 10 and 100 times, respectively.

Thus, the total content of ATP is about 2.7–2.9 $\mu\text{mol/g}$ wet weight and ADP is about 0.19–0.38 $\mu\text{mol/g}$ wet weight (Erecinska and Silver, 1994). Cytosolic ATP is about 3 mM (Erecinska and Silver, 1989), though of course there are variations between different cell types and between intracellular microdomains of the same cell. Free nucleotide concentrations are not however a useful indicator of energy turnover in a cell, because ATP-utilizing reactions depend on the ATP/ADP ratio as the major driving force.

Methods for the estimation of the rate of energy consumption in tissues are based on the calculation of glucose and oxygen utilization and include: the measurement of glucose consumption with retention of 2-deoxyglucose; measurement of labeled phosphates in H_2^{18}O -exposed tissue (Dawis et al., 1989); detection of ^{13}C label on $[1-^{13}\text{C}]$ glucose using nuclear magnetic resonance spectroscopy (MRS) (Mason et al., 1995); and measurement of ^{18}F fluoro-2-deoxyglucose, ^{11}C glucose, or $^{15}\text{O}_2$ by using positron emission tomography (Phelps et al., 1982). The rate of oxidative phosphorylation was studied by measurements of changes in capillary $p\text{O}_2$ (Vanzetta and Grinvald, 1999), level of cytochrome oxidase activity (Wong-Riley, 1989) and heat production, oxyhemoglobin and deoxyhemoglobin levels, and NADH fluorescence. Clark-type oxygen electrode is widely used for the measurement of oxygen consumption in cell suspension, synaptosomes, or isolated mitochondria. Generally, these techniques do not allow assessment of function at the single living cell or subcellular levels. However, in recent studies Jakobsons and Nicholls (2004) measured the rate of oxygen consumption in living cultured cells using an oxygen electrode in combination with fluorescence imaging techniques for the simultaneous monitoring of other cellular parameters.

The level of energy turnover correlates with neuronal activity. In combination, these techniques reveal two key mechanisms for regulating ATP synthesis. The first is the established mechanism by which ATP production is increased in response to elevated ATP demand. There are several steps in glycolysis where enzyme activity is regulated by ATP or ADP such that changes in nucleotide levels regulate activity of the key synthesis pathways. This has been demonstrated clearly in neurons in the experiments discussed above where inhibition of Na^+/K^+ -ATPase decreases glucose utilization, presumably by decreasing the demand for ATP (McCormack and Denton, 1993; Sokoloff, 1993). Many studies have shown that increased neuronal activity proportionally increases the rate of glucose utilization and oxidative metabolism (Sokoloff, 1996, 1999; Sokoloff et al., 1996).

The second key process is the regulation by calcium of glycolysis, oxidative phosphorylation, and ATP synthesis. As discussed by McCormack and Denton (1993), elevated cellular activity results in increased cytosolic calcium, which can be accumulated by mitochondria. Elevated matrix calcium then alters the activity of several matrix dehydrogenases and also the F_1F_0 ATP synthase, with the resulting enhancement of ATP synthesis. Under physiological conditions, then, both ATP demand and mitochondrial calcium accumulation help to match ATP synthesis to ionic homeostasis.

Spatial distribution of enzymes and cellular compartmentalization enhances efficiency of energy use and increases rate of the reactions. Because diffusion of respiratory substrates and ATP within the cell is relatively slow (Ovadi and Saks, 2004), there must exist special cellular mechanisms to facilitate the transport of substrates to enzymes. This is particularly important for neurons, where metabolic demand is often high in compartments situated far from the cell soma, such as axons and nerve terminals. Ideally, the mechanism should include a close spatial localization of the enzyme in the catabolic pathway that facilitates the passing of metabolic substrates from one enzyme to the next, which should increase the rate of the reaction. A spatial organization of glycolytic enzymes in the different cell types was well characterized over the last few decades. A significant fraction of glycolytic enzymes associate with mitochondrial membranes, which enhances supply of mitochondria with respiratory substrates (Crane and Sols, 1953). There is also close localization of energy-producing and energy-consuming enzymes. For example, Hevner and colleagues (1992) showed a similar distribution of cytochrome oxidase and Na^+/K^+ -ATPase in monkey hippocampus and striate cortex and that the activity of both enzymes can be altered by tetrodotoxin.

The heterogeneous distribution of energy-producing enzymes has been shown in different brain regions, cell types, and even in different subcellular locations in studies that concluded that the density of these enzymes are higher in the regions with higher energy demands. Particularly important was the work of Wong-Riley (1989), who used the amount of mitochondrial enzyme cytochrome oxidase as a marker of metabolic activity. The histochemical localization of cytochrome oxidase has shown that a number of anatomical nuclei in the brain that exhibit high levels of spontaneous and synaptic activities, such as the

brain stem auditory relay nuclei and CA3 of the hippocampus, have higher levels of cytochrome oxidase (Wong-Riley et al., 1978; Wong-Riley, 1989). The high level of metabolism shown by the cytochrome oxidase activity was also found in physiologically highly active nuclei of the basal ganglia, thalamus, brain stem, and spinal cord (Wong-Riley, 1989).

The detailed analysis of the histochemical localization of cytochrome oxidase revealed the differences in the distribution of this enzyme in different cell types. Thus, the density of mitochondria reactive for cytochrome oxidase in glutamatergically (excitatory) innervated GABAergic neurons was three times higher than that in glutamatergic neurons that received GABAergic inhibitory innervation (Nie and Wong-Riley, 1995, 1996). This supports the hypothesis that energy metabolism in postsynaptic neurons correlates with the proportion of excitatory synapses they receive.

Additional evidence showing that energy-producing enzymes are positioned near sites of high demand was obtained from studies of mitochondrial and glycolytic enzyme localization and activity. In the visual cortex neuropil, the highest density of mitochondria was found in dendrites (62%), while in axons and in glia, it was only 36% and 2%, respectively (Wong-Riley, 1989). Mitochondrial density correlated well with predictions of energy consumption in different cell compartments as calculated by Attwell and Laughlin. Their model analyzed energy expenditure in gray matter based on published data from rodents (Attwell and Laughlin, 2001). The correlation between the mitochondrial distribution and predicted energy usage indicates that the greatest fraction of mitochondria is localized in the dendrites, which are the neuronal compartments with the highest density of ion transporters and the highest level of energy metabolism. Other subcellular regions with high energy demand and very small energy reserves such as synaptic nerve endings have high hexokinase activity, high rate of glucose glycolysis, and oxidative metabolism (Kauppinen and Nicholls, 1986).

The model by Attwell and Laughlin predicted that the largest fraction of energy in gray matter is consumed by action potentials. At a frequency of 4 Hz, action potentials consume 47% of the energy, postsynaptic effects of glutamate consume 34%, and the resting potential in glia and neurons consumes 13% (Attwell and Laughlin, 2001). While most energy consumed for signaling-related processes is used by neurons, glial cells contribute significantly to energy turnover. Among the glia, astrocytes have the highest metabolism (Hertz and Dienel, 2002). High activity of cytochrome oxidase was shown in astrocytes from glutamatergic regions (Aoki et al., 1987) indicating that astrocyte energy metabolism is influenced by neuronal activity. Since astrocytes are responsible for the major part of glutamate uptake, which requires Na^+ cotransport, the main energy-consuming process in astrocytes is Na^+/K^+ pumping, although clearly other processes also contribute to the total energy consumption. Although it was initially thought that the astrocytes depend more on the glycolytic source of energy, new data obtained from in vivo nuclear magnetic resonance (NMR) studies suggest that about one-third of glucose metabolism in cerebral cortex under resting conditions occurs in astrocytes (Hertz and Dienel, 2002; Hyder et al., 2006). Since astrocytes contribute about 30% of cortical volume, it can be concluded that astrocytes and neurons have similar oxidative rates; the latter was also confirmed in in vitro studies of oxidative metabolism in neuronal and astrocyte cultures (Hertz and Dienel, 2002; Hertz et al., 2006). Only very tiny astrocytic processes such as filopodia and lamellipodia, which are too thin to accommodate mitochondria, are dependent on ATP derived from glycolysis and glycogenolysis (Hertz et al., 2006). For a more detailed analysis of glial-neuronal metabolic interaction, see *Chapter 3* of this volume.

3.2 Energy Production Is Spatially Dynamic and Regulated by Mitochondrial Trafficking

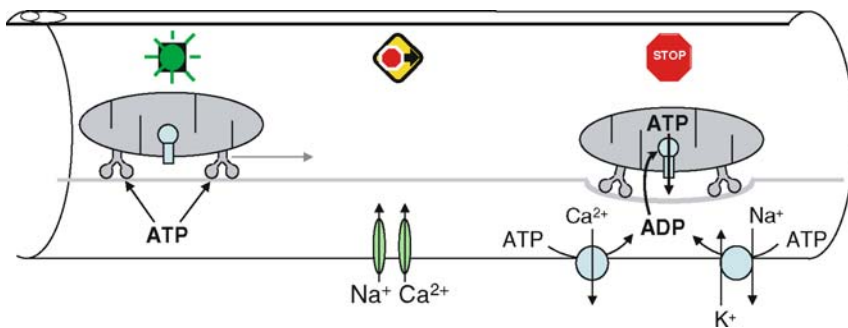
It is well known that mitochondria are mobile organelles that can travel long distances along neurites. It was suggested that axonal mitochondria move along microtubules and that mitochondrial transport implicates motor protein kinesin for movement in an anterograde direction and dynein in a retrograde direction. For short-range movement, mitochondria can be transported by myosin motors along actin filaments (Hollenbeck and Saxton, 2005). However, the mechanisms responsible for the regulation of mitochondrial trafficking are not completely understood. One principle that has emerged recently with

the advent of high-resolution time-lapse imaging is that mitochondrial trafficking in neurons depends on effective ATP production. Results from our laboratory showed that mitochondrial movement in cultured central neurons was inhibited by the uncoupler FCCP as well as the ATPase inhibitor oligomycin (Rintoul et al., 2003), suggesting that mitochondria may generate their own fuel for movement. Consistent with this observation, mitochondrial calcium overloading and NO exposure, both of which depolarize mitochondria, inhibit movement (Rintoul et al., 2003; Rintoul et al., 2006). Whereas an abundance of mitochondria at cellular compartments of high energy demand, such as synapses, was well known, recent data suggest that synapses are recruitment sites for mitochondria. For example, as mitochondria move through processes they make transient stops at synaptic sites (Chang et al., 2006). In this study, cultured cortical neurons exhibited spontaneous synaptic activity, which was abolished by the Na^+ channel blocker, tetrodotoxin, and enhanced by veratridine, an inhibitor of Na^+ channel inactivation. Blocking Na^+ channels significantly decreased mitochondrial recruitment, whereas an increase in Na^+ influx caused by veratridine attracted mitochondria to postsynaptic sites. This is consistent with the work of Mironov (2006) who also showed a slowing of mitochondria at active synapses and acceleration after inhibition with tetrodotoxin and ω -conotoxin GVIA. Furthermore, alteration of mitochondrial velocity after KCl-induced membrane depolarization did not depend on Ca^{2+} , favoring the hypothesis that decreased ATP rather than changing Ca^{2+} concentration alters mitochondrial velocity.

Though much remains unclear regarding the mechanisms which regulate mitochondrial movement, based on the data discussed above we might speculate that intense energy consumption during synaptic activity decreases local ATP content, which prevents further mitochondrial movement. Likewise, a decreased ATP/ADP ratio as well as increased mitochondrial Ca^{2+} uptake activates glycolysis and oxidative phosphorylation. If the local ATP level rises sufficiently to support mitochondrial movement, the mitochondrion moves on until ATP synthesis is reengaged at the next low-energy site (▶ [Figure 4.7-3](#)). Direct examination of this hypothesis would require simultaneous measurement of mitochondrial movement and

■ **Figure 4.7-3**

Energy demand regulates mitochondrial trafficking. Mitochondrial trafficking in neuronal processes requires ATP generation by the mitochondria themselves. Although the processes governing the distribution and movement of mitochondria are not fully understood, it is becoming clear that alterations in ion flux represent one key regulatory mechanism. Thus, mitochondrial movement may change in response to Ca^{2+} accumulation in the matrix, which impairs mitochondrial ATP synthesis. Alternatively, changing the local concentration of ATP by increasing its utilization by ion pumps might represent another key mechanism for regulating trafficking, with the net result that mitochondria reside at subcellular locations of highest energy demand



local concentrations of ATP. Unfortunately, tools for measuring ATP in the different intracellular compartments are limited. Rizzuto's group first attempted to measure ATP in cellular microdomains using luciferase-transfected MIN6 cells. They demonstrated that ATP changes in response to elevated extracellular glucose are different for different cellular subdomains (i.e., the cytosol, mitochondrial matrix, and under

the plasma membrane) (Kennedy et al., 1999). Measurements of ATP in the subdomains of neurons have not yet been performed.

If the local ATP concentration is involved in the regulation of mitochondrial trafficking, it is unlikely that this is the only mechanism. For example, it was shown that Zn^{2+} stopped mitochondrial movement in dendrites and axons within minutes (Malaiyandi et al., 2005b). The precise mechanisms behind the phenomenon are unclear; however, inhibition of PI3 kinase ameliorated the movement effects and toxicity. This raises the possibility that there may be modulation of mitochondrial transport on microtubules or actin, or alterations in docking mechanisms, in addition to the regulation of availability of ATP.

The production of ATP at a site of high energy demand is a very economic way to fuel cellular functions. Thus, viewing it from the standpoint of evolution, it is quite possible that mitochondria have become the main source of energy in the brain not only because they oxidize glucose more profitably than glycolysis, but also because mitochondria can serve as “mobile fuel stations” capable of delivering large quantities of ATP directly to hot spots. Such a mechanism is especially useful to neurons, in which ATP requirements vary considerably depending on the level of activity.

4 Interactions Between Ion Transport and Energy Metabolism in Pathology

It has been clear for many years that many pathological states in the brain are associated with altered ion transport and/or energy metabolism. The mechanisms that link altered energy metabolism, loss of ion homeostasis, and neuronal dysfunction or death are becoming more clear, especially as the result of more recent *in vitro* studies. However, much of the understanding of the fundamental principles of altered neuronal metabolism in pathological states originated from *in vivo* studies, which have the obvious advantage of more accurately recapitulating the pathological state. In this section, we focus on the more recently developed mechanistic understanding of cellular and biochemical events in brain injury. These studies complement and extend the previous *in vivo* findings. However, as revealed by studies with trace metals like Zn^{2+} , a number of additional pathogenic interactions between ion transport and energy metabolism may be revealed with the additional resolution provided by the *in vitro* approach. Notwithstanding, we will begin this section with an overview of the comparison of *in vivo* and *in vitro* approaches.

4.1 In Vivo and In Vitro Perspectives on Ion Transport and Brain Injury

The topic of ion distribution and energetics in the intact mammalian brain has been the subject of several detailed reviews (Hansen, 1985; Erecinska and Silver, 1994). These reviews provide a detailed description of ion distribution between the intra- and extracellular compartments and the impact of injury. There is little value in recapitulating these conclusions in detail. Nevertheless, it is helpful to describe some of the key conclusions, to provide the appropriate context for the discussion of findings, using *in vitro* methods, that will follow.

Extracellular ion concentrations in the “resting” brain are reported to be 2.2–4.6 mM for K^+ , 133–154 mM for Na^+ , 1.2–1.5 mM for Ca^{2+} , and 129–149 mM for Cl^- (as reviewed by Erecinska and Silver (1994)). Increased or altered brain activity in the form of seizures, spreading depression, or anoxia results in an ionic redistribution such that extracellular K^+ increases into the 10–80 mM range, while Na^+ and Ca^{2+} both drop. Notably, extracellular Ca^{2+} can decrease by a factor of ten or more. These changes reflect a combination of the activation of ion transport pathways (e.g., voltage- and ligand-gated ion channels) and, in pathological conditions, the failure of homeostatic mechanisms due to the decrease in ATP production. The injury-associated changes in extracellular ion concentrations are temporally and spatially heterogeneous. For example, extracellular changes in ion concentrations in white matter typically occur more slowly than in gray matter, and several studies have reported a transient increase in extracellular Ca^{2+} at the onset of anoxia (Brown et al., 1998; Kumura et al., 1999). This increase is likely to reflect a decrease in the volume of the extracellular space in white matter, rather than an efflux of the ion. However, a key feature

reflected in these models is the restricted volume of the extracellular compartment, and as a consequence, the net flux of ions like Ca^{2+} into cells is effectively limited. Without question, studies using *in vivo* models offer the greatest insight into the most relevant parameters to understand human brain injury. However, it remains challenging to measure certain parameters, such as intracellular ion concentrations, in intact animal models, and it is also challenging to study molecular mechanisms of injury because of the difficulties in effectively controlling the cellular environment.

Many of the advances in the understanding of mechanisms and ion transport pathways involved in cellular injury have come from *in vitro* studies of neurons and glia. However, there are obvious compromises with this approach. Typically, brain tissues are removed from their normal environment, damaged or deafferented during the extraction process, maintained in artificial solutions, and exposed to supraphysiological oxygen concentrations. When cultured tissues are used, it is typical to see an adaptation in cellular metabolism such that glycolysis is enhanced while oxidative phosphorylation is depressed (Vergun et al., 2003). Nevertheless, these simplified preparations do allow certain techniques to be more readily applied, including measurements of intracellular ion concentrations, and the study of ion transport pathways by ionic substitution is much more readily accomplished.

It is reasonable to ask whether the extent of the compromises associated with *in vitro* experimentation is such that the subsequent results lack physiological or pathophysiological relevance. For example, as discussed below, it is widely believed that NMDA receptor-mediated Ca^{2+} entry is a critical contributor to excitotoxic injury to neurons, based on a number of *in vitro* studies (Choi, 1987). This provides an attractive mechanism to link the observation of ischemia-induced elevations in extracellular glutamate (Benveniste et al., 1984) to delayed cell death. Subsequent observations that NMDA antagonists can prevent ischemia-induced neuronal injury would appear to confirm the relevance of the *in vitro* model (Simon et al., 1984). However, there can be no argument that *in vitro* experiments misrepresent the nature of the Ca^{2+} signal associated with cell injury, because these experiments almost inevitably are performed with high Ca^{2+} in the extracellular solution, and the extracellular solution essentially represents an infinite volume. This is quite unlike the situation in the intact brain where the extracellular volume is quite limited and the Ca^{2+} concentration drops quickly to relatively low levels at the onset of injury. At this time, the prevailing view appears to be that the advantages of *in vitro* models outweigh their limitations, although continued efforts to reconcile findings between both approaches are clearly warranted. Given that previous reviews have covered findings on *in vivo* models in some depth, we will focus on *in vitro* models of neuronal injury in this chapter.

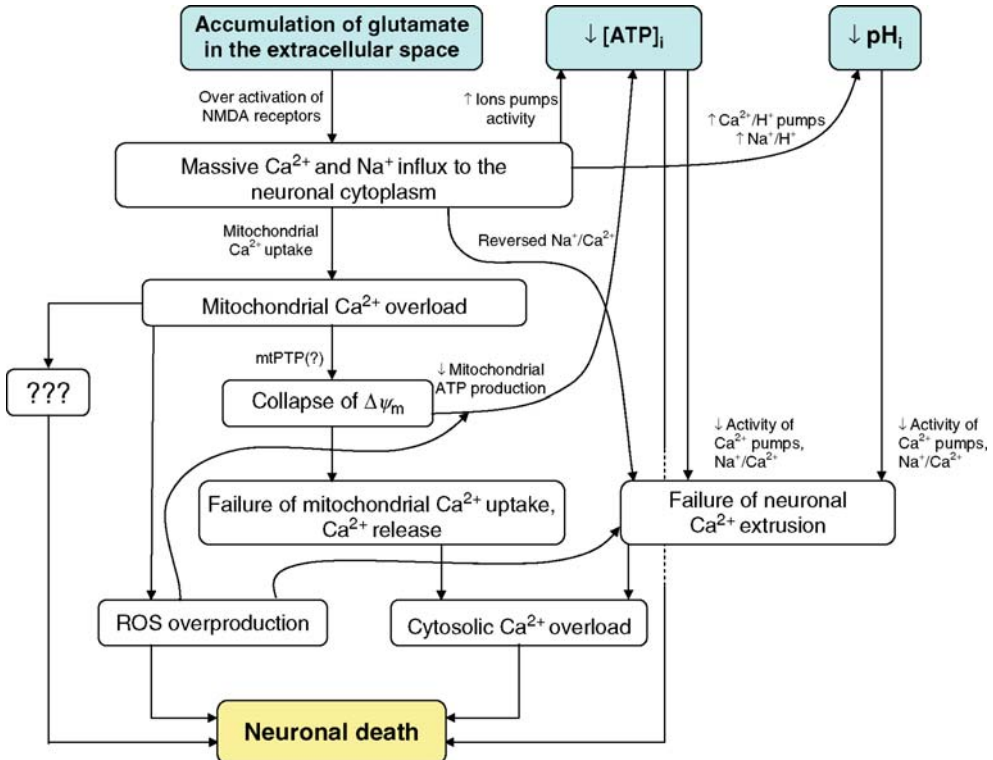
4.2 Failure of Ion Homeostasis and Energy Metabolism During Excitotoxic Insult

One of the pathological conditions which entails fast and severe ATP depletion is brain hypoxia/ischemia. Though mechanisms leading to hypoxia-induced neurodegeneration are incompletely understood, it is now clear that the overstimulation of glutamate receptors by excess extracellular glutamate and massive Ca^{2+} influx through NMDA channels play a central role. In this section, we use the excitotoxic neuronal injury model as an example of neuronal pathology that involves faulty energy metabolism and deregulation of numerous ion transporters. The present review does not attempt to discuss all of the pathological events leading to CNS damage during brain hypoxia or ischemia. For a comprehensive review on this topic, see Lipton (1999).

For heuristic considerations, we will divide the hypoxia-induced sequence of pathological events resulting in the collapse of ion homeostasis into two phases: first, the processes triggered by deficient oxygen supply leading to accumulation of lethal concentrations of glutamate in the extracellular space (▶ [Figure 4.7-4](#)); second, the processes triggered by the overstimulation of glutamate receptors leading to the deregulation of ion homeostasis and neuronal death (▶ [Figure 4.7-5](#)). It must be emphasized however that this separation of excitotoxic processes is somewhat artificial, because events “upstream” or “downstream” of glutamate receptor activation often directly affect each other.

■ Figure 4.7-5

Excitotoxicity triggered by failed energy metabolism is a complex pathological regenerative process. Figure 4.7-5 considers intracellular excitotoxic events in detail. High extracellular glutamate causes cytosolic Ca^{2+} and Na^+ overload via opening of NMDA receptors/channels. Mitochondrial Ca^{2+} uptake overloads the matrix, resulting in mitochondrial depolarization and further decline in ATP production. Mitochondrial failure might also be marked by large changes in mitochondrial permeability (i.e., mitochondrial permeability transition) that promote the release of apoptogens and other species into the cytosol. These events, together with falling ATP levels and intracellular acidosis, cause further loss of cytoplasmic Ca^{2+} homeostasis, increase ROS accumulation, and eventually kill the neuron



In this reversed mode of operation of the ATP-synthase, protons are pumped out of the matrix via the ATP synthase while ATP is hydrolyzed to ADP and phosphate (Nicholls and Ferguson, 2002).

Because $\Delta\Psi_m$ is an important driving force for mitochondrial Ca^{2+} uptake, low $\Delta\Psi_m$ reduces mitochondrial Ca^{2+} sequestration and impairs cytosolic Ca^{2+} regulation. Consequently, the work of correcting any $[\text{Ca}^{2+}]_c$ elevations falls disproportionately on ATP-driven Ca^{2+} pumps, which presents an additional ATP burden in a neuron that has already been energetically compromised.


As was discussed earlier, the main neuronal ATP consumer is the Na^+/K^+ -ATPase. Under conditions when ATP supply is limited, the Na^+/K^+ -ATPase is unable to maintain Na^+ and K^+ gradients. This results in increased $[\text{K}^+]_e$ and plasma membrane depolarization. In rat brain cortex, increased $[\text{K}^+]_e$ during anoxia was shown to be biphasic: a small transient increase in $[\text{K}^+]_e$ up to about 10 mM with concurrent increase of electroencephalogram activity lasting for about 2 min, followed by a fast secondary rise in $[\text{K}^+]_e$ reaching about 60 mM within a few seconds of cessation of neuronal activity. During the next few minutes $[\text{K}^+]_e$ gradually rose to 80 mM (Hansen, 1985). The first phase can be prolonged by increasing glucose stores (Hansen, 1985) indicating that energy limitations can play a critical role in the onset of the second phase.

Increased neuronal activity during the first phase activates ion pumps, leading to a further reduction of [ATP].

Collapse of Na^+ and K^+ gradients and plasma membrane depolarization promote accumulation of high doses of glutamate in the extracellular space. The calculations of changes in extracellular glutamate concentrations has shown that $[\text{Glu}]_e$ rises during ischemia up to about $60 \mu\text{mol/L}$ (Rossi et al., 2000). As a result the neuronal glutamate receptors (NMDA receptors seems to play a dominant role) become activated for prolonged periods, initiating Ca^{2+} -dependent pathological processes that eventually result in cell death. This turns glutamate from an excitatory neurotransmitter to a powerful neurotoxin (Olney, 1978). It appears that the main mechanism for the glutamate release is a reversed operation of the glutamate transporters (Seki et al., 1999; Rossi et al., 2000). As discussed previously, the major driving force for glutamate transport is the Na^+ gradient, but K^+ and H^+ gradients are also involved. At physiological conditions, each cycle of the transporter pumps 1Glu^- , 3Na^+ , and 1H^+ into the cytoplasm while moving 1K^+ out of the cell. Since all these ions become deregulated when cellular energy is limited, the transporter is unable to operate in the normal mode, and instead of returning glutamate back into the cytosol, it releases glutamate from neurons and glia into the extracellular space. The pump is also electrogenic therefore membrane depolarization also promotes reverse mode operation. It was shown that during ischemia reversal of the astrocytic glutamate transporter GLT-1 and swelling-induced release of glutamate from astrocytes were the main contributors to the glutamate accumulated in the striatum, where about 50% of glutamate released was due to the reversed glutamate transporter (Seki et al., 1999).

4.2.2 NMDA Receptor-Mediated Ca^{2+} Overload and Energy Production

There is now a large body of data describing the complex interactions between NMDA receptor activation, calcium entry, and altered energy metabolism. Much of this work has been done in cultured neurons, and prior to discussing these findings it is appropriate to consider the nature of the experimental system most commonly used. Advantages of primary neuronal cultures include: (1) the accessibility of a simpler experimental system; (2) the ability to exercise greater control over potentially confounding variables; (3) the convenience of using ion-sensitive and potentiometric fluorescence probes in individual cells; (4) the easy and fast delivery of drugs to cells without having to penetrate a blood–brain barrier and (5) the ability to resolve the distribution of ions and cellular organelles at the subcellular level. Some potential disadvantages of cell culture compared with *in vivo* models include: (1) cultured neurons are more glycolytic compared with the brain neurons (Nicholls and Budd, 2000) and may thus not accurately represent the bioenergetic state of neurons *in situ*; (2) cultured neurons do not develop as many synaptic connections as they would in the brain; (3) cultured neurons are usually prepared from embryonic or early postnatal brains and generally survive for only 2–3 weeks in culture, therefore cultured neurons must necessarily be regarded as much younger than those from adult animals. This last consideration may be very important in the comparison of *in vivo* and *in vitro* data, because an aged brain is much more sensitive to hypoxia than a young one. Thus, some caution is necessary when results from cultured neurons are used to reflect physiological and pathological processes thought to take place in the living brain.

Although the hypoxia-induced neuronal pathology complex involves deregulation of homeostasis of many ions, excessive intracellular Ca^{2+} is thought to be a key event causing cell death. The usual view is that high $[\text{Ca}^{2+}]_e$ for prolonged periods alters cellular signaling, overactivates proteases, phospholipases, and possibly endonucleases, and alters phosphorylation of proteins, which secondarily affects protein synthesis and gene expression (Nicotera et al., 1992). Mitochondrial Ca^{2+} overload produces additional toxic effects on neurons.  *Figure 4.7-5* shows the accrual of pathological events in a neuron subjected to prolonged glutamate receptor activation under conditions of decreased [ATP] and pH_i . This simplified scheme does not represent all pathological pathways taking place in the ischemic brain; nevertheless it readily conveys the complexities associated with toxic ion deregulation. Experiments using cultured primary neurons have identified certain events in the hypoxia-triggered pathological sequel, and glutamate accumulation in the hypoxic brain can be mimicked by exposing cultured cells to high levels of glutamate. From such experiments, it is now well established that activation of NMDA receptors triggers Ca^{2+} -dependent excitotoxicity and neuronal

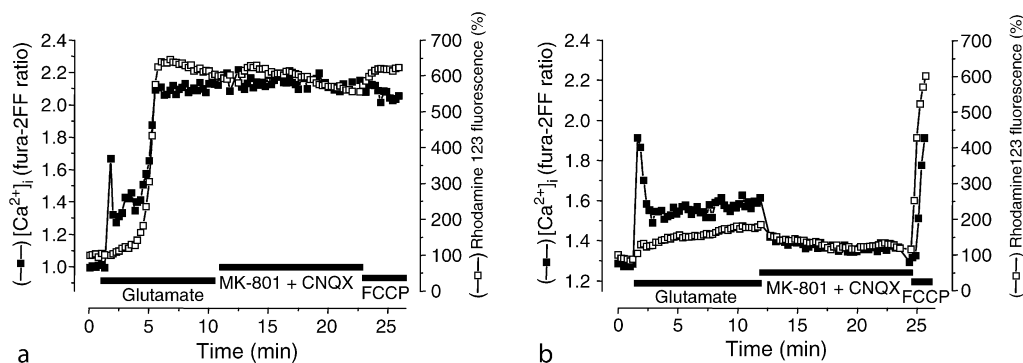
death (Choi, 1987; Choi et al., 1988; Manev et al., 1989; de Erausquin et al., 1990; Michaels and Rothman, 1990; Dubinsky and Rothman, 1991). This conclusion is supported by three fundamental observations: (1) glutamate exposure induces delayed (~ 24 h after glutamate insult) neuronal death; (2) toxicity can be prevented by the selective inhibition of NMDA receptor channels or removal of Ca^{2+} from the extracellular medium; and (3) specific agonists of non-NMDA glutamate receptors are only mildly toxic following short-term exposure compared with acute NMDA treatment. In primary neuronal cultures, relatively short (5–20 min) exposure to 10–500 μM glutamate is sufficient to trigger widespread delayed excitotoxicity.

Increased $[\text{Ca}^{2+}]_c$ by stimulation of NMDA receptors correlates with neuronal toxicity. Recently, Khodorov (2004) extensively reviewed the mechanisms of the glutamate-induced, sustained elevations of $[\text{Ca}^{2+}]_c$ in cultured neurons, and provided a comprehensive body of references on this topic. Accordingly, we here discuss only briefly the main pathologies of ion transport systems that lead to neuronal Ca^{2+} deregulation and cell death.

Work using fluorescence Ca^{2+} indicators revealed that glutamate induces a biphasic increase in $[\text{Ca}^{2+}]_c$ in cultured neurons (Castilho et al., 1998; Keelan et al., 1999; Vergun et al., 1999; Nicholls and Budd, 2000; Chinopoulos et al., 2004; Bano et al., 2005). The example of the glutamate-induced neuronal Ca^{2+} response is shown in [Figure 4.7-6](#). While the neurons are able to recover after small Ca^{2+} loads ([Figure 4.7-6b](#)), a secondary profound phase is irreversible ([Figure 4.7-6a](#)). In cerebellar granule cells, the secondary

■ Figure 4.7-6

Glutamate-induced changes in neuronal $[\text{Ca}^{2+}]_c$ and mitochondrial membrane potential. (a) Intense glutamate stimulation (100 μM) causes a biphasic $[\text{Ca}^{2+}]_c$ rise (fura-2FF, left axis) accompanied by a collapse of mitochondrial potential (increase in rhodamine 123 fluorescence, right axis), which are irreversible. These traces were obtained from hippocampal neurons maintained in culture for 16 days (16DIV). (b) Moderate glutamate-induced $[\text{Ca}^{2+}]_c$ loads are associated with a small mitochondrial depolarization, which is completely reversible. These traces were obtained from 8DIV hippocampal neurons. (Reprinted from Journal of Physiology; Vergun et al. (1999) copyright 1999 the physiological society)



$[\text{Ca}^{2+}]_c$ increase (“delayed calcium deregulation”) appeared with a longer, 30–60 min, delay (Castilho et al., 1999; Nicholls and Budd, 2000). Many reports demonstrated that the postglutamate Ca^{2+} disturbance correlates with delayed neuronal death (Ogura et al., 1988; Manev et al., 1989; de Erausquin et al., 1990; Tymianski et al., 1993; Rajdev and Reynolds, 1994; Vergun et al., 2001).

It was initially thought that the failure of neurons to restore Ca^{2+} after toxic glutamate treatments is associated with an increased Ca^{2+} permeability of the plasma membrane. However, measurements of Mn^{2+} quenching of fura-2 fluorescence, which is an indicator of Ca^{2+} permeability, have demonstrated that Ca^{2+} permeability in the postglutamate period is even lower than during glutamate exposure (Khodorov et al., 1996c). Accordingly, an inhibition of glutamate receptors (for example by MK801+CNQX, [Figure 4.7-6](#)) or even a removal of Ca^{2+} from the external buffer does not improve $[\text{Ca}^{2+}]_c$ recovery (Carafoli et al., 1996;

Castilho et al., 1998; Vergun et al., 1999). Thus it appears that perturbation of cytosolic Ca^{2+} homeostasis induced by high glutamate is due rather to failure of neuronal Ca^{2+} clearance systems than to enhanced Ca^{2+} influx.

The first and simplest explanation for failed Ca^{2+} extrusion would be a decrease in cytosolic ATP level. The role of ATP depletion in the glutamate-induced Ca^{2+} deregulation was first confirmed in experiments on cerebellar granule cells by Nicholls and colleagues (Budd and Nicholls, 1996a, b; Castilho et al., 1998). They demonstrated that when mitochondrial respiration was inhibited by rotenone, blockade of NMDA receptors was not sufficient to restore glutamate-evoked $[\text{Ca}^{2+}]_c$ increase. However, if the hydrolysis of glycolytic ATP by a reversed mode of ATP-synthase was prevented by oligomycin, the cells were able to restore the resting $[\text{Ca}^{2+}]_c$. This suggests that prevention of consumption of ATP by the ATP-synthase was sufficient to restore calcium homeostasis by maintaining glycolysis-driven cellular ATP production. However, if mitochondrial respiration was not inhibited prior to the glutamate application, oligomycin was not able to protect hippocampal neurons against Ca^{2+} deregulation, suggesting that not only ATP depletion but also other factors are implicated in glutamate-induced ionic deregulations (Khodorov, 2004). Other studies show that even small doses of glutamate, which did not disturb Ca^{2+} homeostasis in control cultured cortical neurons, caused irreversible $[\text{Ca}^{2+}]_c$ deterioration when both glycolytic and mitochondrial ATP production were suppressed by 2-deoxy-D-glucose. Rescue of mitochondrial ATP synthesis by pyruvate completely reversed the toxic effect of 2-deoxy-D-glucose (Vergun et al., 2003). Collectively, these data indicate that depletion of ATP is one of the major pathological events leading to the glutamate-induced deterioration of Ca^{2+} homeostatic systems.

Neuronal Na^+ overload further deteriorates Ca^{2+} homeostasis. In addition to the failure of Na^+ extrusion from the cell due to deterioration of Na^+/K^+ -ATPase, Na^+ loading occurs via activated AMPA and NMDA receptor channels. In experiments on cultured hippocampal neurons, it was estimated that glutamate increases $[\text{Na}^+]_c$ from 6–8 mM to 30–45 mM (Pinelis et al., 1994). Concurrent recordings of $[\text{Na}^+]_c$ and $[\text{Ca}^{2+}]_c$ have shown a correlation between $[\text{Na}^+]_c$ and $[\text{Ca}^{2+}]_c$ recovery in the postglutamate period, and neurons which failed to recover $[\text{Na}^+]_c$ were also unable to restore basal $[\text{Ca}^{2+}]_c$ (Kiedrowski and Costa, 1995). Sustained elevations of $[\text{Na}^+]_c$ during and after glutamate exposure, especially under conditions of depleted [ATP], can inhibit Ca^{2+} extrusion by $\text{Na}^+/\text{Ca}^{2+}$ exchange and even reverse its operation, providing a route for additional Ca^{2+} entry. However, some evidence suggests that ATP depletion, intracellular acidification, and ROS suppress both modes of $\text{Na}^+/\text{Ca}^{2+}$ exchange during hypoxic conditions (Khodorov, 2004).

Role of intracellular acidification in the ion transport failure. In cultured neurons, intracellular pH was measured using pH-sensitive fluorescence indicators. Glutamate decreased pH_i from 7.0–7.2 to 6.5–6.8 in a Ca^{2+} -dependent manner (Hartley and Dubinsky, 1993; Irwin et al., 1994; Wang et al., 1994; Khodorov, 2004). While glutamate-induced acidification is incompletely understood, important mechanisms might include (1) inhibition of Na^+/H^+ exchange when Na^+ influx is greatly increased (Valkina et al., 1993; Khodorov et al., 1994) and (2) activation of PMCA which extrudes Ca^{2+} in exchange for H^+ (Trapp et al., 1996; Wu et al., 1999). Glutamate-induced acidification is also reproduced in animal models: ischemia dropped extracellular pH in the brain of animals under hyperglycemic conditions to 5.95, while in normoglycemic animals, only to 6.6 (Smith et al., 1986; Siesjo, 1992; Kristian, 2004). Intracellular acidification might have opposite consequences. On one hand it may be protective because low pH inhibits ion fluxes through plasma membrane channels, and therefore would preserve ATP. Conversely, acidification might contribute to ion deregulation because operation of Ca^{2+} pumps, $\text{Na}^+/\text{Ca}^{2+}$ exchanger, and Na^+/H^+ exchanger are all inhibited by acidosis. Obviously, any impairment of these transporters would exacerbate Ca^{2+} deregulation.

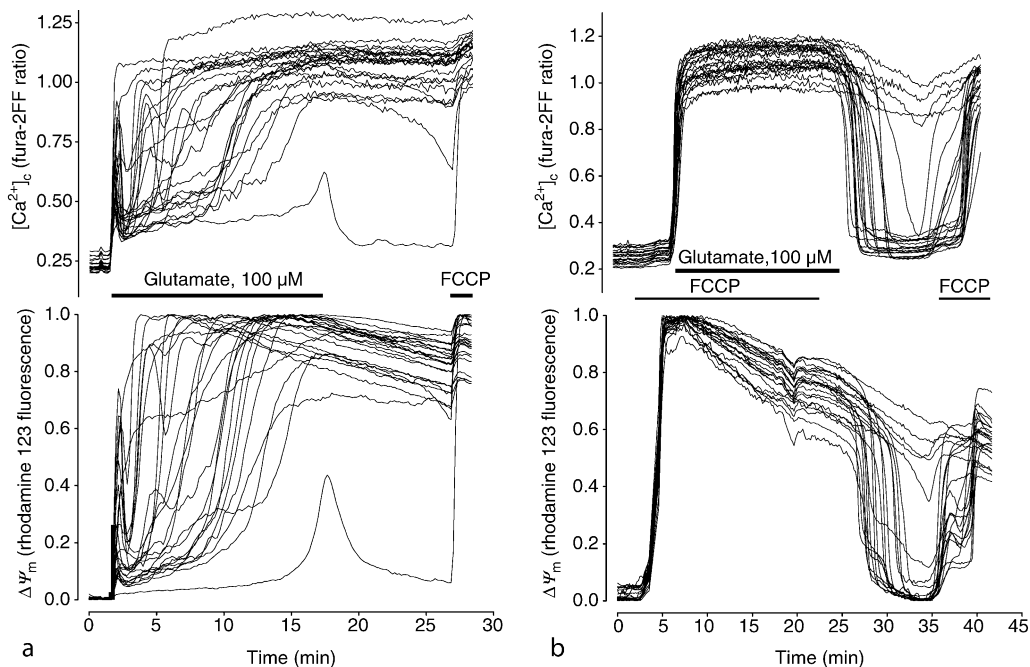
4.2.3 Mitochondrial Ca^{2+} Uptake and Neuronal Injury

Several groups showed mitochondrial depolarization follows NMDA receptor activation (Isaev et al., 1996; Nieminen et al., 1996; Schinder et al., 1996; White and Reynolds, 1996). Subsequently, a large body of work has clarified the role of mitochondrial depolarization during excitotoxic stimulus. Several mechanisms

for this depolarization are possible, including dissipation of the mitochondrial membrane potential by calcium cycling across the inner membrane, some form of inhibition of electron transport by calcium overload, or due to the activation of the mitochondrial permeability transition pore (PTP). **Figure 4.7-6** shows that mitochondria depolarize in parallel with $[Ca^{2+}]_c$ rises. A striking correlation was found between glutamate-induced collapse of $\Delta\Psi_m$ and deterioration of Ca^{2+} homeostasis in the experiments with simultaneous measurements of $[Ca^{2+}]_c$ and mitochondrial potential (Khodorov et al., 1996b; Vergun et al., 1999). However, it has become clear that mitochondrial depolarization alone is insufficient to cause irreversible Ca^{2+} loading and toxicity. In fact, depolarization of mitochondria by the protonophore FCCP protected against glutamate toxicity (Stout et al., 1998). This work demonstrated that decreased mitochondrial Ca^{2+} uptake in glutamate-treated neurons resulted in very large but relatively nontoxic cytosolic Ca^{2+} loads. These and earlier results (Budd and Nicholls, 1996a) led to the conclusion that glutamate-induced neuronal death requires mitochondrial Ca^{2+} uptake. **Figure 4.7-7** clearly demonstrates that depolarization of mitochondria by FCCP prior to glutamate treatment completely reversed the sustained postglutamate $[Ca^{2+}]_c$ plateau. Thus, it is important to distinguish between Ca^{2+} -induced mitochondrial depolarization, which in most cases is irreversible and correlates with neuronal death, and mitochondrial depolarization that precludes Ca^{2+} uptake during glutamate exposure, which is protective. Nevertheless, the two mechanisms are clearly not mutually exclusive. This leaves open the question of how mitochondrial depolarization is linked to neuronal death. Candidate mechanisms include ROS accumulation and activation of PTP.

Figure 4.7-7

Acute inhibition of mitochondrial Ca^{2+} uptake spares neurons from glutamate-induced $[Ca^{2+}]_c$ deregulation. (a). $[Ca^{2+}]_c$ is deregulated and mitochondrial membrane potential ($\Delta\Psi_m$) is lost in neurons exposed to excess glutamate. (b). Prevention of mitochondrial Ca^{2+} uptake by mitochondria depolarization (with a protonophore FCCP, 750 nM) before glutamate treatment results in large cytosolic Ca^{2+} loads, but neurons are later able to restore both $[Ca^{2+}]_c$ and $\Delta\Psi_m$. Each trace represents a single cortical cultured neuron from a group on a coverslip; $[Ca^{2+}]_c$ and $\Delta\Psi_m$ were simultaneously monitored with fura-2FF and rhodamine 123, respectively



Contribution of ROS to the delay neuronal death during excitotoxicity. Glutamate was found to increase ROS production in cultured neurons (Lafon-Cazal et al., 1993; Reynolds and Hastings, 1995; Castilho et al., 1999), and data suggest that under these circumstances ROS arise mainly from mitochondria. (For detailed mechanisms of mitochondrial ROS generation, see *Chapter 5.3* (Brookes and Sheu)). The generation of ROS can damage many ion transport systems (Kourie, 1998). Indeed, a large amount of data show that antioxidants protect against excitotoxicity, favoring a role for ROS in the hypoxia-induced ion deregulation (Monyer and Choi, 1990; Dykens, 1994; Carriedo et al., 1998). A role for ROS in triggering PTP during excitotoxic insult is suggested in many reviews and original reports. However, no evidence of ROS overproduction during a 10 min glutamate treatment was found in hippocampal cultured neurons, even though antioxidants partially protected neurons from delayed death (Vergun et al., 2001). This supports the notion that ROS damage occurs downstream of the acute mitochondrial depolarization and Ca^{2+} deregulation. However, increased ROS accumulation during glutamate treatment and a delay in the secondary Ca^{2+} deregulation in the presence of antioxidant was observed in cerebellar granule cells (Castilho et al., 1999). Taking into account that Ca^{2+} regulation of ROS production depends on the metabolic state of mitochondria (Votyakova and Reynolds, 2001), it is possible that mitochondria in these two culture preparations responded differently to pathological Ca^{2+} loads.

The role of mitochondrial permeability transition pore in glutamate toxicity is controversial. Increased Ca^{2+} in the mitochondrial matrix, ROS accumulation, and intracellular acidification are conditions that promote activation of PTP. The structure, function, regulation, molecular basis, and controversy regarding the PTP in the CNS are discussed in *Chapter 6.4* by Wieloch. Here, we will only briefly note that there is much disagreement over the role and even the existence of PTP in neurons. Overall, the majority of data supporting a role for PTP in glutamate excitotoxicity come from experiments using isolated mitochondria, whereas the phenomenon is much more difficult to observe in intact cells. A variety of reasons might account for such discrepancies. First, the most potent inhibitor of PTP, cyclosporin A, is not a specific blocker of PTP in situ. Second, it is not possible to isolate pure neuronal mitochondria, and preparations from neural tissue will inevitably contain a mix of glial and neuronal mitochondria. Third, mitochondria are usually isolated from adult tissue whereas the cultured neurons are prepared from immature animals. Variations resulting from this last consideration were recently tested in mitochondria isolated from young (2–4-days old) or mature (4-weeks old) rat brains. In experiments monitoring $\Delta\Psi_m$, we found that mitochondria from older brains were much more sensitive to Ca^{2+} and PTP modulators than those from younger brains (Vergun and Reynolds, 2005a).

Excitotoxicity triggered by failed energy metabolism involves many interdependent factors. Hypoxia-induced pathological processes are very complex and include depression of many ion transport systems (see [Figures 4.7-4](#) and [4.7-5](#)). Because downstream pathologies exacerbate earlier deregulations, the entire hypoxic sequel becomes a pathological regenerative process. In many cases, neuronal death cannot be prevented by simply blocking a single step in the whole spectrum of events. Yet not all of the players in the hypoxia-induced brain pathology are known, and a vast body of work supports the theory that mitochondrial dysfunction, mitochondrial Ca^{2+} overload, and collapse of neuronal Ca^{2+} homeostasis are key events leading to the neuronal death.

4.3 Effects of Zn^{2+} on Energy Metabolism

The preceding section illustrates a key series of events that may link ion flux to neuronal injury. These events are largely the consequence of excessive ion loading of mitochondria. One can reasonably claim that excessive zinc is toxic, but the mechanisms of injury are distinct in that the injury does not appear to be the direct consequence of exceeding the ion transport capacity of mitochondria or of any other key organelle. There is little doubt that excess Zn^{2+} results in accumulation of ROS in cultured neurons, however, the mechanism by which this occurs remains unclear. Zinc causes lipid peroxidation, and antioxidants ameliorate Zn^{2+} -induced injury (Kim et al., 1999a, b; Noh et al., 1999). Data from Weiss and colleagues show that zinc causes ROS accumulation that appears to originate from mitochondria (Sensi et al., 1999, 2000). Other evidence indicates that excess Zn^{2+} triggers superoxide production from NADPH

oxidase (Noh and Koh, 2000). Recent data from our laboratory suggests that ROS accumulation, secondary to neuronal Ca^{2+} overload, causes rapid mobilization of Zn^{2+} (Devinney et al., 2005).

As it is evident that ROS can result from excess Zn^{2+} , it is equally clear that excess ROS can liberate zinc from protein-bound stores, and numerous groups using different models have shown that various oxidants elevate Zn^{2+} (Fliss and Menard, 1992; Aizenman et al., 2000; St Croix et al., 2002). Thus it appears that ROS and Zn^{2+} homeostasis are interdependent, and deregulation of one leads to deregulation of the other. Furthermore, Aizenman's group has elucidated a pathway that links the Zn^{2+} -ROS axis to apoptosis triggered by K^+ efflux. In their scheme, oxidant burden leads to increased Zn^{2+} , activating p38 kinase. p38 then enhances K^+ efflux via kv2.1-encoded channels (McLaughlin et al., 2001; Pal et al., 2003).

Additional effects of zinc on energy metabolism. Beyond the mechanisms described above, there are several additional ways in which changes in intracellular Zn^{2+} regulates cellular energy metabolism. A role in energy metabolism has been suggested for the metallothioneins (MTs), a family of small (6–7 kDa) zinc-binding proteins, ubiquitously expressed, and of unknown function. Vallee's group demonstrated that (1) MTs may be imported into isolated liver mitochondria, (2) MT-derived Zn^{2+} inhibits mitochondrial O_2 utilization, and (3) MT binds ATP in a 1:1 stoichiometry ((Jiang et al. (1998); Ye et al. (2001); but see Zangger et al. (2000)). Others claimed that disruption of certain MT genes results in obesity in mice (Beattie et al., 1998), but it is not clear if the results of this study are confounded by genetic background effects (Palmiter, 1998). Given that most null mice and cells grow relatively normally, MT is either a redundant or unimportant regulator of cellular energy status.

Two glycolytic enzymes that might be inhibited during Zn^{2+} overload are glyceraldehyde-3-phosphate dehydrogenase (GAPDH; $\text{IC}_{50} \sim 400$ nM) and phosphofructokinase ($\text{IC}_{50} \sim 1.5$ μM). In cultured neurons, Choi's group showed that elevated Zn^{2+} reduced ATP levels in a manner consistent with blocked glycolysis, i.e., accumulation of upstream metabolites dihydroxyacetone phosphate and fructose-1,6-bisphosphate and depletion of downstream metabolites 1,3-bisphosphoglycerate and pyruvate (Sheline et al., 2000). Furthermore, Zn^{2+} -induced neurotoxicity could be prevented by addition of pyruvate. Taken together, these results suggest that inhibition of glycolysis could be an important mechanism of Zn^{2+} -induced neurotoxicity.

There is some evidence that Zn^{2+} can inhibit enzymes of the tricarboxylic acid cycle. In preparations from isolated rat liver mitochondria, Zn^{2+} inhibited the α -ketoglutarate dehydrogenase complex (KGDHC) with an apparent K_i of ~ 1 μM , although the authors figured the true K_i to be nearer 100 nM (Brown et al., 2000). Inhibition probably occurs at a catalytic disulfide of the lipoamide dehydrogenase (LADH) subunit. Notably, zinc inhibition of LADH is also associated with increased production of H_2O_2 and superoxide (Gazaryan et al., 2002).

Numerous reports suggest that $[\text{Zn}^{2+}]_i$ accumulation causes mitochondrial depolarization in cultured neurons (Sensi et al., 1997; Sensi et al., 2000). In our hands, Zn^{2+} is not a particularly effective agent for inducing mitochondrial depolarization in cells, whether delivered by depolarization or by use of the Zn^{2+} -selective ionophore pyrithone (Dineley et al., 2000; Malaiyandi et al., 2005b). Any in situ mitochondrial depolarization we observed occurred in response to high and sustained Zn^{2+} loads. Isolated brain mitochondria are by comparison more sensitive and depolarize relatively quickly in response to submicromolar Zn^{2+} (Dineley et al., 2005). Discrepancies between mitochondria in isolated preparations and whole cells might be explained by the abundance of Zn^{2+} -binding proteins in the cell, which of course are lost or diluted during organelle isolation. While Zn^{2+} can enter the matrix through a pathway consistent with the uniporter, matrix zinc does not appear necessary to cause depolarization, and moreover Zn^{2+} depolarization can be rapidly reversed with an impermeant chelator (Dineley et al., 2005; Malaiyandi et al., 2005a). Taken together, these results suggest that inhibition is probably occurring at an externally accessible site.

5 Conclusions

The work discussed in this chapter clearly describes the intricate link between ion homeostasis and energy metabolism in cells. The large proportion of energy production devoted to ion homeostasis appropriately reflects the importance of this series of mechanisms to the normal functioning of the CNS. The abundance

of ways in which disordered ion homeostasis leads to cell pathology provides an additional confirmation of the central importance of these mechanisms.

References

- Aizenman E, Stout AK, Hartnett KA, Dineley KE, McLaughlin B, et al. 2000. Induction of neuronal apoptosis by thiol oxidation: Putative role of intracellular zinc release. *J Neurochem* 75: 1878-1888.
- Ames A 3rd. 2000. CNS energy metabolism as related to function. *Brain Res Rev* 34: 42-68.
- Aoki C, Milner TA, Sheu KF, Blass JB, Pickel VM. 1987. Regional distribution of astrocytes with intense immunoreactivity for glutamate dehydrogenase in rat brain: Implications for neuron-glia interactions in glutamate transmission. *J Neurosci* 7: 2214-2231.
- Attwell D, Laughlin SB. 2001. An energy budget for signaling in the grey matter of the brain. *J Cereb Blood Flow Metab* 21: 1133-1145.
- Baba-Aissa F, Raeymaekers L, Wuytack F, De Greef C, Missiaen L, et al. 1996. Distribution of the organellar Ca^{2+} transport ATPase SERCA2 isoforms in the cat brain. *Brain Res* 743: 141-153.
- Babcock DF, Herrington J, Goodwin PC, Park YB, Hille B. 1997. Mitochondrial participation in the intracellular Ca^{2+} network. *J Cell Biol* 136: 833-844.
- Baker PF, Blaustein MP, Hodgkin AL, Steinhardt RA. 1969. The influence of calcium on sodium efflux in squid axons. *J Physiol* 200: 431-458.
- Bano D, Young KW, Guerin CJ, Lefevre R, Rothwell NJ, et al. 2005. Cleavage of the plasma membrane $\text{Na}^+/\text{Ca}^{2+}$ exchanger in excitotoxicity. *Cell* 120: 275-285.
- Beattie JH, Wood AM, Newman AM, Bremner I, Choo KH, et al. 1998. Obesity and hyperleptinemia in metallothionein (-I and -II) null mice. *Proc Natl Acad Sci USA* 95: 358-363.
- Beauge L. 1978. Activation by lithium ions of the inside sodium sites in Na^+/K^+ -ATPase. *Biochim Biophys Acta* 527: 472-484.
- Benham CD, Evans ML, McBain CJ. 1992. Ca^{2+} efflux mechanisms following depolarization evoked calcium transients in cultured rat sensory neurons. *J Physiol* 455: 567-583.
- Benveniste H, Drejer J, Schousboe A, Diemer NH. 1984. Elevation of the extracellular concentrations of glutamate and aspartate in rat hippocampus during transient cerebral ischemia monitored by intracerebral microdialysis. *J Neurochem* 43: 1369-1374.
- Berberian G, Asteggiano C, Pham C, Roberts S, Beauge L. 2002. MgATP and phosphoinositides activate $\text{Na}^+/\text{Ca}^{2+}$ exchange in bovine brain vesicles. Comparison with other $\text{Na}^+/\text{Ca}^{2+}$ exchangers. *Pflugers Arch* 444: 677-684.
- Blaustein MP, Lederer WJ. 1999. Sodium/calcium exchange: Its physiological implications. *Physiol Rev* 79: 763-854.
- Blaustein MP, Santiago EM. 1977. Effects of internal and external cations and of ATP on sodium-calcium and calcium-calcium exchange in squid axons. *Biophys J* 20: 79-111.
- Blaustein MP, Juhaszova M, Golovina VA, Church PJ, Stanley EF. 2002. Na/Ca exchanger and PMCA localization in neurons and astrocytes: Functional implications. *Ann N Y Acad Sci* 976: 356-366.
- Boitier E, Rea R, Duchen MR. 1999. Mitochondria exert a negative feedback on the propagation of intracellular Ca^{2+} waves in rat cortical astrocytes. *J Cell Biol* 145: 795-808.
- Boron WF, Hogan E, Russell JM. 1988. pH-sensitive activation of the intracellular pH regulation system in squid axons by ATP- γ -S. *Nature* 332: 262-265.
- Bozym RA, Thompson RB, Stoddard AK, Fierke C. 2006. Measuring picomolar intracellular exchangeable zinc in PC-12 cells using a ratiometric fluorescence biosensor. *ACS Chem Biol* 1: 103-111.
- Brines ML, Robbins RJ. 1993. Cell-type specific expression of Na^+/K^+ -ATPase catalytic subunits in cultured neurons and glia: Evidence for polarized distribution in neurons. *Brain Res* 631: 1-11.
- Brines ML, Gulanski BI, Gilmore-Hebert M, Greene AL, Benz EJ Jr, et al. 1991. Cytoarchitectural relationships between [^3H]ouabain binding and mRNA for isoforms of the sodium pump catalytic subunit in rat brain. *Brain Res Mol Brain Res* 10: 139-150.
- Brown AM, Fern R, Jarvinen JP, Kaila K, Ransom BR. 1998. Changes in $[\text{Ca}^{2+}]_0$ during anoxia in CNS white matter. *Neuroreport* 9: 1997-2000.
- Brown AM, Kristal BS, Effron MS, Shestopalov AI, Ullucci PA, et al. 2000. Zn^{2+} inhibits α -ketoglutarate-stimulated mitochondrial respiration and the isolated α -ketoglutarate dehydrogenase complex. *J Biol Chem* 275: 13441-13447.
- Budd SL, Nicholls DG. 1996a. A reevaluation of the role of mitochondria in neuronal Ca^{2+} homeostasis. *J Neurochem* 66: 403-411.
- Budd SL, Nicholls DG. 1996b. Mitochondria, calcium regulation, and acute glutamate excitotoxicity in cultured cerebellar granule cells. *J Neurochem* 67: 2282-2291.
- Burette A, et al. 2003. Isoform-specific distribution of the plasma membrane Ca^{2+} ATPase in the rat brain. *J Comp Neurol* 467(4): 464-476.

- Carafoli E. 1994. Biogenesis: Plasma membrane calcium ATPase: 15 years of work on the purified enzyme. *FASEB J* 8: 993-1002.
- Carafoli E. 2002. Calcium signaling: A tale for all seasons. *Proc Natl Acad Sci USA* 99: 1115-1122.
- Carafoli E, Garcia-Martin E, Guerini D. 1996. The plasma membrane calcium pump: Recent developments and future perspectives. *Experientia* 52: 1091-1100.
- Carriedo SG, Yin HZ, Sensi SL, Weiss JH. 1998. Rapid Ca^{2+} entry through Ca^{2+} -permeable AMPA/kainate channels triggers marked intracellular Ca^{2+} rises and consequent oxygen radical production. *J Neurosci* 18: 7727-7738.
- Castilho RF, Hansson O, Ward MW, Budd SL, Nicholls DG. 1998. Mitochondrial control of acute glutamate excitotoxicity in cultured cerebellar granule cells. *J Neurosci* 18: 10277-10286.
- Castilho RF, Ward MW, Nicholls DG. 1999. Oxidative stress, mitochondrial function, and acute glutamate excitotoxicity in cultured cerebellar granule cells. *J Neurochem* 72: 1394-1401.
- Chang DT, Honick AS, Reynolds IJ. 2006. Mitochondrial trafficking to synapses in cultured primary cortical neurons. *J Neurosci* 26: 7035-7045.
- Chaudhary J, Walia M, Matharu J, Escher E, Grover AK. 2001. Caloxin: A novel plasma membrane Ca^{2+} pump inhibitor. *Am J Physiol Cell Physiol* 280: C1027-C1030.
- Chen NH, Reith ME, Quick MW. 2004. Synaptic uptake and beyond: The sodium- and chloride-dependent neurotransmitter transporter family SLC6. *Pflugers Arch* 447: 519-531.
- Cheng C, Reynolds IJ. 1998. Calcium-sensitive fluorescent dyes can report increases in intracellular free zinc concentration in cultured forebrain neurons. *J Neurochem* 71: 2401-2410.
- Chinopoulos C, Gerencser AA, Doczi J, Fiskum G, Adam-Vizi V. 2004. Inhibition of glutamate-induced delayed calcium deregulation by 2-APB and La^{3+} in cultured cortical neurons. *J Neurochem* 91: 471-483.
- Choi DW. 1987. Ionic dependence of glutamate neurotoxicity. *J Neurosci* 7: 369-379.
- Choi DW, Koh JY. 1998. Zinc and brain injury. *Annu Rev Neurosci* 21: 347-375.
- Choi DW, Koh JY, Peters S. 1988. Pharmacology of glutamate neurotoxicity in cortical cell culture: Attenuation by NMDA antagonists. *J Neurosci* 8: 185-196.
- Clausen T, Van Hardevelde C, Everts ME. 1991. Significance of cation transport in control of energy metabolism and thermogenesis. *Physiol Rev* 71: 733-774.
- Cole TB, Martyanova A, Palmiter RD. 2001. Removing zinc from synaptic vesicles does not impair spatial learning, memory, or sensorimotor functions in the mouse. *Brain Res* 891: 253-265.
- Cole TB, Robbins CA, Wenzel HJ, Schwartzkroin PA, Palmiter RD. 2000. Seizures and neuronal damage in mice lacking vesicular zinc. *Epilepsy Res* 39: 153-169.
- Cole TB, Wenzel HJ, Kafer KE, Schwartzkroin PA, Palmiter RD. 1999. Elimination of zinc from synaptic vesicles in the intact mouse brain by disruption of the ZnT3 gene. *Proc Natl Acad Sci USA* 96: 1716-1721.
- Crane RK, Sols A. 1953. The association of hexokinase with particulate fractions of brain and other tissue homogenates. *J Biol Chem* 203: 273-292.
- Dawis SM, Walseth TF, Deeg MA, Heyman RA, Graeff RM, et al. 1989. Adenosine triphosphate utilization rates and metabolic pool sizes in intact cells measured by transfer of ^{18}O from water. *Biophys J* 55: 79-99.
- de Erausquin GA, Manev H, Guidotti A, Costa E, Brooker G. 1990. Gangliosides normalize distorted single-cell intracellular free Ca^{2+} dynamics after toxic doses of glutamate in cerebellar granule cells. *Proc Natl Acad Sci USA* 87: 8017-8021.
- Dean RD. 1941. Theories of electrolyte equilibrium in muscle. *Biol Symp* 3: 331-348.
- Deliconstantinos G. 1988. Structure-activity relationship of cholesterol and steroid hormones with respect to their effects on the Ca^{2+} -stimulated ATPase and lipid fluidity of synaptosomal plasma membranes from dog and rabbit brain. *Comp Biochem Physiol B* 89: 585-594.
- Devinney MJ 2nd, Reynolds IJ, Dineley KE. 2005. Simultaneous detection of intracellular free calcium and zinc using fura-2FF and FluoZin-3. *Cell Calcium* 37: 225-232.
- Dineley KE, Malaiyandi LM, Reynolds IJ. 2002. A reevaluation of neuronal zinc measurements: Artifacts associated with high intracellular dye concentration. *Mol Pharmacol* 62: 618-627.
- Dineley KE, Richards LL, Votyakova TV, Reynolds IJ. 2005. Zinc causes loss of membrane potential and elevates reactive oxygen species in rat brain mitochondria. *Mitochondrion* 5: 55-65.
- Dineley KE, Scanlon JM, Kress GJ, Stout AK, Reynolds IJ. 2000. Astrocytes are more resistant than neurons to the cytotoxic effects of increased $[\text{Zn}^{2+}]_i$. *Neurobiol Dis* 7: 310-320.
- DiPolo R. 1978. Ca-pump driven by ATP in squid axons. *Nature* 274: 390-392.
- DiPolo R, Beauge L. 2006. Sodium/calcium exchanger: Influence of metabolic regulation on ion carrier interactions. *Physiol Rev* 86: 155-203.
- Dubinsky JM, Rothman SM. 1991. Intracellular calcium concentrations during "chemical hypoxia" and excitotoxic neuronal injury. *J Neurosci* 11: 2545-2551.
- Duchen MR. 2004. Mitochondria in health and disease: Perspectives on a new mitochondrial biology. *Mol Aspects Med* 25: 365-451.
- Dunham ET, Glynn IM. 1961. Adenosinetriphosphatase activity and the active movements of alkali metal ions. *J Physiol* 156: 274-293.

- Dykens JA. 1994. Isolated cerebral and cerebellar mitochondria produce free radicals when exposed to elevated Ca^{2+} and Na^+ : Implications for neurodegeneration. *J Neurochem* 63: 584-591.
- Erecinska M, Dagani F. 1990. Relationships between the neuronal sodium/potassium pump and energy metabolism. Effects of K^+ , Na^+ , and adenosine triphosphate in isolated brain synaptosomes. *J Gen Physiol* 95: 591-616.
- Erecinska M, Silver IA. 1989. ATP and brain function. *J Cereb Blood Flow Metab* 9: 2-19.
- Erecinska M, Silver IA. 1994. Ions and energy in mammalian brain. *Prog Neurobiol* 43: 37-71.
- Fliss H, Menard M. 1992. Oxidant-induced mobilization of zinc from metallothionein. *Arch Biochem Biophys* 293: 195-199.
- Folke M, Sestoft L. 1977. Thyroid calorigenesis in isolated, perfused rat liver: Minor role of active sodium-potassium transport. *J Physiol* 269: 407-419.
- Frederickson CJ, Koh JY, Bush AI. 2005. The neurobiology of zinc in health and disease. *Nat Rev Neurosci* 6: 449-462.
- Gaither LA, Eide DJ. 2000. Functional expression of the human hZIP2 zinc transporter. *J Biol Chem* 275: 5560-5564.
- Gaither LA, Eide DJ. 2001. Eukaryotic zinc transporters and their regulation. *Biometals* 14: 251-270.
- Garrahan P, Rega A. 1990. Plasma Membrane Calcium Pump In: Intracellular calcium regulation. Felix Bronner, editor. New York: Wiley-Liss, pp. 271-303.
- Gazaryan IG, Krasnikov BF, Ashby GA, Thorneley RN, Kristal BS, et al. 2002. Zinc is a potent inhibitor of thiol oxidoreductase activity and stimulates reactive oxygen species production by lipoamide dehydrogenase. *J Biol Chem* 277: 10064-10072.
- Glynn IM. 1985. The Na^+/K^+ -transporting adenosine triphosphatase. *The Enzymes of Biological Membranes*. 2nd edition. Martonosi AN, editor. Plenum Press, New York, 3: 35-114.
- Glynn IM, Karlsh SJ. 1975. The sodium pump. *Annu Rev Physiol* 37: 13-55.
- Graf E, Verma AK, Gorski JP, Lopaschuk G, Niggli V, et al. 1982. Molecular properties of calcium-pumping ATPase from human erythrocytes. *Biochemistry* 21: 4511-4516.
- Gray JH, Owen RP, Giacomini KM. 2004. The concentrative nucleoside transporter family, SLC28. *Pflügers Arch* 447: 728-734.
- Grynkiwicz G, Poenie M, Tsien RY. 1985. A new generation of Ca^{2+} indicators with greatly improved fluorescence properties. *J Biol Chem* 260: 3440-3450.
- Guerini D. 1998a. The Ca^{2+} pumps and the $\text{Na}^+/\text{Ca}^{2+}$ exchangers. *Biometals* 11: 319-330.
- Guerini D. 1998b. The significance of the isoforms of plasma membrane calcium ATPase. *Cell Tissue Res* 292: 191-197.
- Guerini D, Garcia-Martin E, Gerber A, Volbracht C, Leist M, et al. 1999. The expression of plasma membrane Ca^{2+} pump isoforms in cerebellar granule neurons is modulated by Ca^{2+} . *J Biol Chem* 274: 1667-1676.
- Hagenbuch B, Dawson P. 2004. The sodium bile salt cotransport family SLC10. *Pflügers Arch* 447: 566-570.
- Hansen AJ. 1985. Effect of anoxia on ion distribution in the brain. *Physiol Rev* 65: 101-148.
- Hao L, Rigaud JL, Inesi G. 1994. $\text{Ca}^{2+}/\text{H}^+$ countertransport and electrogenicity in proteoliposomes containing erythrocyte plasma membrane Ca-ATPase and exogenous lipids. *J Biol Chem* 269: 14268-14275.
- Hartley Z, Dubinsky JM. 1993. Changes in intracellular pH associated with glutamate excitotoxicity. *J Neurosci* 13: 4690-4699.
- Hasselbach W, Makinose M. 1961. The calcium pump of the "relaxing granules" of muscle and its dependence on ATP-splitting. *Biochem Z* 333: 518-528.
- Hediger MA, Romero MF, Peng JB, Rolfs A, Takanao H, et al. 2004. The ABCs of solute carriers: Physiological, pathological, and therapeutic implications of human membrane transport proteins. Introduction. *Pflügers Arch* 447: 465-468.
- Hertz L, Diemel GA. 2002. Energy metabolism in the brain. *Int Rev Neurobiol* 51: 1-102.
- Hertz L, Peng L, Diemel GA. 2006. Energy metabolism in astrocytes: High rate of oxidative metabolism and spatiotemporal dependence on glycolysis/glycogenolysis. *J Cereb Blood Flow Metab*.
- Hevner RF, Duff RS, Wong-Riley MT. 1992. Coordination of ATP production and consumption in brain: Parallel regulation of cytochrome oxidase and Na^+/K^+ -ATPase. *Neurosci Lett* 138: 188-192.
- Hieber V, Siegel GJ, Fink DJ, Beaty MW, Mata M. 1991. Differential distribution of Na/K-ATPase α isoforms in the central nervous system. *Cell Mol Neurobiol* 11: 253-262.
- Hilgemann DW, Matsuoka S, Nagel GA, Collins A. 1992. Steady-state and dynamic properties of cardiac sodium-calcium exchange. Sodium-dependent inactivation. *J Gen Physiol* 100: 905-932.
- Hillman DE, Chen S, Bing R, Penniston JT, Llinas R. 1996. Ultrastructural localization of the plasmalemmal calcium pump in cerebellar neurons. *Neuroscience* 72: 315-324.
- Hollenbeck PJ, Saxton WM. 2005. The axonal transport of mitochondria. *J Cell Sci* 118: 5411-5419.
- Horisberger JD, Lemas V, Kraehenbuhl JP, Rossier BC. 1991. Structure-function relationship of Na/K-ATPase. *Annu Rev Physiol* 53: 565-584.
- Hoyt KR, Arden SR, Aizenman E, Reynolds IJ. 1998. Reverse $\text{Na}^+/\text{Ca}^{2+}$ exchange contributes to glutamate-induced intracellular Ca^{2+} concentration increases in cultured rat forebrain neurons. *Mol Pharmacol* 53: 742-749.
- Hyder F, Patel AB, Gjedde A, Rothman DL, Behar KL, et al. 2006. Neuronal-glial glucose oxidation and glutamatergic-GABAergic function. *J Cereb Blood Flow Metab* 26: 865-877.

- Irwin RP, Lin SZ, Long RT, Paul SM. 1994. *N*-methyl-D-aspartate induces a rapid, reversible, and calcium-dependent intracellular acidosis in cultured fetal rat hippocampal neurons. *J Neurosci* 14: 1352-1357.
- Isaev NK, Zorov DB, Stelmashook EV, Uzbekov RE, Kozhemyakin MB, et al. 1996. Neurotoxic glutamate treatment of cultured cerebellar granule cells induces Ca^{2+} -dependent collapse of mitochondrial membrane potential and ultrastructural alterations of mitochondria. *FEBS Lett* 392: 143-147.
- Ivanov AV, Gable ME, Askari A. 2004. Interaction of SDS with Na^+/K^+ -ATPase: SDS-solubilized enzyme retains partial structure and function. *J Biol Chem* 279: 29832-29840.
- Jekabsons MB, Nicholls DG. 2004. In situ respiration and bioenergetic status of mitochondria in primary cerebellar granule neuronal cultures exposed continuously to glutamate. *J Biol Chem* 279: 32989-33000.
- Jensen TP, Buckby LE, Empson RM. 2004. Expression of plasma membrane Ca^{2+} ATPase family members and associated synaptic proteins in acute and cultured organotypic hippocampal slices from rat. *Brain Res Dev Brain Res* 152: 129-136.
- Jiang LJ, Maret W, Vallee BL. 1998. The ATP-metallothionein complex. *Proc Natl Acad Sci USA* 95: 9146-9149.
- John LM, Lechleiter JD, Camacho P. 1998. Differential modulation of SERCA2 isoforms by calreticulin. *J Cell Biol* 142: 963-973.
- Jouaville LS, Ichas F, Holmuhamedov EL, Camacho P, Lechleiter JD. 1995. Synchronization of calcium waves by mitochondrial substrates in *Xenopus laevis* oocytes. *Nature* 377: 438-441.
- Juhászová M, Church P, Blaustein MP, Stanley EF. 2000. Location of calcium transporters at presynaptic terminals. *Eur J Neurosci* 12: 839-846.
- Kambe T, Yamaguchi-Iwai Y, Sasaki R, Nagao M. 2004. Overview of mammalian zinc transporters. *Cell Mol Life Sci* 61: 49-68.
- Kanai Y, Hediger MA. 2003. The glutamate and neutral amino acid transporter family: Physiological and pharmacological implications. *Eur J Pharmacol* 479: 237-247.
- Kanai Y, Hediger MA. 2004. The glutamate/neutral amino acid transporter family SLC1: Molecular, physiological, and pharmacological aspects. *Pflugers Arch* 447: 469-479.
- Karlish SJ, Yates DW, Glynn IM. 1978. Conformational transitions between Na^+ -bound and K^+ -bound forms of Na^+/K^+ -ATPase, studied with formycin nucleotides. *Biochim Biophys Acta* 525: 252-264.
- Katsura K, Rodriguez de Turco EB, Folbergrova J, Bazan NG, Siesjö BK. 1993. Coupling among energy failure, loss of ion homeostasis, and phospholipase A2 and C activation during ischemia. *J Neurochem* 61: 1677-1684.
- Kauppinen RA, Nicholls DG. 1986. Synaptosomal bioenergetics. The role of glycolysis, pyruvate oxidation, and responses to hypoglycemia. *Eur J Biochem* 158: 159-165.
- Keelan J, Vergun O, Duchen MR. 1999. Excitotoxic mitochondrial depolarization requires both calcium and nitric oxide in rat hippocampal neurons. *J Physiol* 520 Pt 3: 797-813.
- Kennedy HJ, Pouli AE, Ainscow EK, Jouaville LS, Rizzuto R, et al. 1999. Glucose generates sub-plasma membrane ATP microdomains in single islet β -cells. Potential role for strategically located mitochondria. *J Biol Chem* 274: 13281-13291.
- Khodorov B. 2004. Glutamate-induced deregulation of calcium homeostasis and mitochondrial dysfunction in mammalian central neurons. *Prog Biophys Mol Biol* 86: 279-351.
- Khodorov B, Pinelis V, Storozhevych T, Vergun O, Vinskaya N. 1996a. Dominant role of mitochondria in protection against a delayed neuronal Ca^{2+} overload induced by endogenous excitatory amino acids following a glutamate pulse. *FEBS Lett* 393: 135-138.
- Khodorov B, Pinelis V, Vergun O, Storozhevych T, Vinskaya N. 1996b. Mitochondrial deenergization underlies neuronal calcium overload following a prolonged glutamate challenge. *FEBS Lett* 397: 230-234.
- Khodorov BI, Fayuk DA, Koshelev SG, Vergun OV, Pinelis VG, et al. 1996c. Effect of a prolonged glutamate challenge on plasmalemmal calcium permeability in mammalian central neurons. Mn^{2+} as a tool to study calcium influx pathways. *Int J Neurosci* 88: 215-241.
- Khodorov B, Pinelis V, Vergun O, Storozhevych T, Fajuk D, et al. 1995. Dramatic effects of external alkalinity on neuronal calcium recovery following a short-duration glutamate challenge: The role of the plasma membrane $\text{Ca}^{2+}/\text{H}^+$ pump. *FEBS Lett* 371: 249-252.
- Khodorov B, Valkina O, Turovetsky V. 1994. Mechanisms of stimulus-evoked intracellular acidification in frog nerve fibers. *FEBS Lett* 341: 125-127.
- Kiedrowski L, Costa E. 1995. Glutamate-induced destabilization of intracellular calcium concentration homeostasis in cultured cerebellar granule cells: Role of mitochondria in calcium buffering. *Mol Pharmacol* 47: 140-147.
- Kiedrowski L, Czyz A, Baranauskas G, Li XF, Lytton J. 2004. Differential contribution of plasmalemmal Na/Ca exchange isoforms to sodium-dependent calcium influx and NMDA excitotoxicity in depolarized neurons. *J Neurochem* 90: 117-128.
- Kim EY, Koh JY, Kim YH, Sohn S, Joe E, et al. 1999a. Zn^{2+} entry produces oxidative neuronal necrosis in cortical cell cultures. *Eur J Neurosci* 11: 327-334.
- Kim YH, Kim EY, Gwag BJ, Sohn S, Koh JY. 1999b. Zinc-induced cortical neuronal death with features of apoptosis and necrosis: Mediation by free radicals. *Neuroscience* 89: 175-182.
- Kimelberg HK, Biddelcome S, Narumi S, Bourke RS. 1978. ATPase and carbonic anhydrase activities of bulk-isolated

- neuron, glia, and synaptosome fractions from rat brain. *Brain Res* 141: 305-323.
- Kip SN, Gray NW, Burette A, Canbay A, Weinberg RJ, et al. 2006. Changes in the expression of plasma membrane calcium extrusion systems during the maturation of hippocampal neurons. *Hippocampus* 16: 20-34.
- Kirichok Y, Krapivinsky G, Clapham DE. 2004. The mitochondrial calcium uniporter is a highly selective ion channel. *Nature* 427: 360-364.
- Kourie JJ. 1998. Interaction of reactive oxygen species with ion transport mechanisms. *Am J Physiol* 275: C1-C24.
- Kraev A, Quednau BD, Leach S, Li XF, Dong H, et al. 2001. Molecular cloning of a third member of the potassium-dependent sodium-calcium exchanger gene family, NCKX3. *J Biol Chem* 276: 23161-23172.
- Kristian T. 2004. Metabolic stages, mitochondria, and calcium in hypoxic/ischemic brain damage. *Cell Calcium* 36: 221-233.
- Kumura E, Graf R, Dohmen C, Rosner G, Heiss WD. 1999. Breakdown of calcium homeostasis in relation to tissue depolarization: Comparison between gray and white matter ischemia. *J Cereb Blood Flow Metab* 19: 788-793.
- Lafon-Cazal M, Pietri S, Culcasi M, Bockaert J. 1993. NMDA-dependent superoxide production and neurotoxicity. *Nature* 364: 535-537.
- Lauger P. 1991. *Electrogenic Ion Pumps*. Sunderland, MA: Sinauer Associates.
- Li Y, Camacho P. 2004. Ca^{2+} -dependent redox modulation of SERCA 2b by ERp57. *J Cell Biol* 164: 35-46.
- Lipton P. 1999. Ischemic cell death in brain neurons. *Physiol Rev* 79: 1431-1568.
- Liuzzi JP, Blanchard RK, Cousins RJ. 2001. Differential regulation of zinc transporter 1, 2, and 4 mRNA expression by dietary zinc in rats. *J Nutr* 131: 46-52.
- Luther PW, Yip RK, Bloch RJ, Ambesi A, Lindenmayer GE, et al. 1992. Presynaptic localization of sodium/calcium exchangers in neuromuscular preparations. *J Neurosci* 12: 4898-4904.
- Mackenzie B, Erickson JD. 2004. Sodium-coupled neutral amino acid (System N/A) transporters of the SLC38 gene family. *Pflugers Arch* 447: 784-795.
- Malaiyandi LM, Vergun O, Dineley KE, Reynolds JJ. 2005a. Direct visualization of mitochondrial zinc accumulation reveals uniporter-dependent and -independent transport mechanisms. *J Neurochem* 93: 1242-1250.
- Malaiyandi LM, Honick AS, Rintoul GL, Wang QJ, Reynolds JJ. 2005b. Zn^{2+} inhibits mitochondrial movement in neurons by phosphatidylinositol-3-kinase activation. *J Neurosci* 25: 9507-9514.
- Manev H, Favaron M, Guidotti A, Costa E. 1989. Delayed increase of Ca^{2+} influx elicited by glutamate: Role in neuronal death. *Mol Pharmacol* 36: 106-112.
- Markovich D, Murer H. 2004. The SLC13 gene family of sodium sulphate/carboxylate cotransporters. *Pflugers Arch* 447: 594-602.
- Martin DL, DeLuca HF. 1969. Influence of sodium on calcium transport by the rat small intestine. *Am J Physiol* 216: 1351-1359.
- Mason GF, Gruetter R, Rothman DL, Behar KL, Shulman RG, et al. 1995. Simultaneous determination of the rates of the TCA cycle, glucose utilization, α -ketoglutarate/glutamate exchange, and glutamine synthesis in human brain by NMR. *J Cereb Blood Flow Metab* 15: 12-25.
- McCormack JG, Denton RM. 1980. Role of calcium ions in the regulation of intramitochondrial metabolism. Properties of the Ca^{2+} -sensitive dehydrogenases within intact uncoupled mitochondria from the white and brown adipose tissue of the rat. *Biochem J* 190: 95-105.
- McCormack JG, Denton RM. 1993. Mitochondrial Ca^{2+} transport and the role of intramitochondrial Ca^{2+} in the regulation of energy metabolism. *Dev Neurosci* 15: 165-173.
- McLaughlin B, Pal S, Tran MP, Parsons AA, Barone FC, et al. 2001. p38 activation is required upstream of potassium current enhancement and caspase cleavage in thiol oxidant-induced neuronal apoptosis. *J Neurosci* 21: 3303-3311.
- McMahon RJ, Cousins RJ. 1998a. Mammalian zinc transporters. *J Nutr* 128: 667-670.
- McMahon RJ, Cousins RJ. 1998b. Regulation of the zinc transporter ZnT-1 by dietary zinc. *Proc Natl Acad Sci USA* 95: 4841-4846.
- Meldolesi J. 2001. Rapidly exchanging Ca^{2+} stores in neurons: Molecular, structural, and functional properties. *Prog Neurobiol* 65: 309-338.
- Meyer T, Holowka D, Stryer L. 1988. Highly cooperative opening of calcium channels by inositol-1,4,5-trisphosphate. *Science* 240: 653-656.
- Michaels RL, Rothman SM. 1990. Glutamate neurotoxicity in vitro: Antagonist pharmacology and intracellular calcium concentrations. *J Neurosci* 10: 283-292.
- Mironov SL. 2006. Spontaneous and evoked neuronal activities regulate movements of single neuronal mitochondria. *Synapse* 59: 403-411.
- Mogami H, Nakano K, Tepikin AV, Petersen OH. 1997. Ca^{2+} flow via tunnels in polarized cells: Recharging of apical Ca^{2+} stores by focal Ca^{2+} entry through basal membrane patch. *Cell* 88: 49-55.
- Monyer H, Choi DW. 1990. Glucose deprivation neuronal injury in vitro is modified by withdrawal of extracellular glutamine. *J Cereb Blood Flow Metab* 10: 337-342.
- Murer H, Forster I, Biber J. 2004. The sodium phosphate cotransporter family SLC34. *Pflugers Arch* 447: 763-767.
- Nicholls DG, Budd SL. 2000. Mitochondria and neuronal survival. *Physiol Rev* 80: 315-360.

- Nicholls DG, Ferguson SJ. 2002. *Bioenergetics*, 3rd Edition: San Diego, Academic Press.
- Nicotera P, Bellomo G, Orrenius S. 1992. Calcium-mediated mechanisms in chemically induced cell death. *Annu Rev Pharmacol Toxicol* 32: 449-470.
- Nie F, Wong-Riley MT. 1995. Double labeling of GABA and cytochrome oxidase in the macaque visual cortex: Quantitative EM analysis. *J Comp Neurol* 356: 115-131.
- Nie F, Wong-Riley MT. 1996. Differential glutamatergic innervation in cytochrome oxidase-rich and -poor regions of the macaque striate cortex: Quantitative EM analysis of neurons and neuropil. *J Comp Neurol* 369: 571-590.
- Nieminen AL, Petrie TG, Lemasters JJ, Selman WR. 1996. Cyclosporin A delays mitochondrial depolarization induced by *N*-methyl-D-aspartate in cortical neurons: Evidence of the mitochondrial permeability transition. *Neuroscience* 75: 993-997.
- Noh KM, Koh JY. 2000. Induction and activation by zinc of NADPH oxidase in cultured cortical neurons and astrocytes. *J Neurosci* 20: RC111.
- Noh KM, Kim YH, Koh JY. 1999. Mediation by membrane protein kinase C of zinc-induced oxidative neuronal injury in mouse cortical cultures. *J Neurochem* 72: 1609-1616.
- Ogura A, Miyamoto M, Kudo Y. 1988. Neuronal death in vitro: Parallelism between survivability of hippocampal neurones and sustained elevation of cytosolic Ca^{2+} after exposure to glutamate receptor agonist. *Exp Brain Res* 73: 447-458.
- Olney JW. 1978. *Neurotoxicity of excitatory amino acids*. New York: Raven.
- Orlowski J, Grinstein S. 2004. Diversity of the mammalian sodium/proton exchanger SLC9 gene family. *Pflugers Arch* 447: 549-565.
- Ovadi J, Saks V. 2004. On the origin of intracellular compartmentation and organized metabolic systems. *Mol Cell Biochem* 256-257: 5-12.
- Pahl HL, Baeuerle PA. 1995. A novel signal transduction pathway from the endoplasmic reticulum to the nucleus is mediated by transcription factor NF- κ B. *Embo J* 14: 2580-2588.
- Pal S, Hartnett KA, Nerbonne JM, Levitan ES, Aizenman E. 2003. Mediation of neuronal apoptosis by Kv2.1-encoded potassium channels. *J Neurosci* 23: 4798-4802.
- Palmiter RD. 1998. The elusive function of metallothioneins. *Proc Natl Acad Sci USA* 95: 8428-8430.
- Palmiter RD, Findley SD. 1995. Cloning and functional characterization of a mammalian zinc transporter that confers resistance to zinc. *Embo J* 14: 639-649.
- Phelps ME, Mazziotta JC, Huang SC. 1982. Study of cerebral function with positron computed tomography. *J Cereb Blood Flow Metab* 2: 113-162.
- Pinelis VG, Segal M, Greenberger V, Khodorov BI. 1994. Changes in cytosolic sodium caused by a toxic glutamate treatment of cultured hippocampal neurons. *Biochem Mol Biol Int* 32: 475-482.
- Pottorf WJ, Thayer SA. 2002. Transient rise in intracellular calcium produces a long-lasting increase in plasma membrane calcium pump activity in rat sensory neurons. *J Neurochem* 83: 1002-1008.
- Quednau BD, Nicoll DA, Philipson KD. 2004. The sodium/calcium exchanger family-SLC8. *Pflugers Arch* 447: 543-548.
- Rajdev S, Reynolds IJ. 1994. Glutamate-induced intracellular calcium changes and neurotoxicity in cortical neurons in vitro: Effect of chemical ischemia. *Neuroscience* 62: 667-679.
- Reeves JP. 1990. *Sodium-Calcium Exchange*: Alan R. Liss, Inc. New York.
- Reeves JP, Condrescu M, Chernaya G, Gardner JP. 1994. Na^{+}/Ca^{2+} antiport in the mammalian heart. *J Exp Biol New York*: 196: 375-388.
- Reuter H, Seitz N. 1968. The dependence of calcium efflux from cardiac muscle on temperature and external ion composition. *J Physiol* 195: 451-470.
- Reynolds IJ, Hastings TG. 1995. Glutamate induces the production of reactive oxygen species in cultured forebrain neurons following NMDA receptor activation. *J Neurosci* 15: 3318-3327.
- Richards DE. 1988. Occlusion of cobalt ions within the phosphorylated forms of the $Na^{+}-K^{+}$ pump isolated from dog kidney. *J Physiol* 404: 497-514.
- Rintoul GL, Bennett VJ, Papaconstantinou NA, Reynolds IJ. 2006. Nitric oxide inhibits mitochondrial movement in forebrain neurons associated with disruption of mitochondrial membrane potential. *J Neurochem* 97: 800-806.
- Rintoul GL, Filiano AJ, Brocard JB, Kress GJ, Reynolds IJ. 2003. Glutamate decreases mitochondrial size and movement in primary forebrain neurons. *J Neurosci* 23: 7881-7888.
- Robinson JD. 1976. (Ca + Mg)-stimulated ATPase activity of a rat brain microsomal preparation. *Arch Biochem Biophys* 176: 366-374.
- Romero MF, Fulton CM, Boron WF. 2004. The SLC4 family of HCO_3^{-} transporters. *Pflugers Arch* 447: 495-509.
- Rossi DJ, Oshima T, Attwell D. 2000. Glutamate release in severe brain ischemia is mainly by reversed uptake. *Nature* 403: 316-321.
- Sachs J. 1988. Interaction of magnesium with the sodium pump of the human red cell. *J Physiol (Lond)* 400: 575-591.
- Sanchez-Armass S, Blaustein MP. 1987. Role of sodium-calcium exchange in regulation of intracellular calcium in nerve terminals. *Am J Physiol* 252: C595-C603.
- Schatzmann HJ. 1966. ATP-dependent Ca^{2+} extrusion from human red cells. *Experientia* 22: 364-365.
- Schatzmann HJ, Vincenzi FF. 1969. Calcium movements across the membrane of human red cells. *J Physiol* 201: 369-395.
- Schinder AF, Olson EC, Spitzer NC, Montal M. 1996. Mitochondrial dysfunction is a primary event in glutamate neurotoxicity. *J Neurosci* 16: 6125-6133.

- Schnetkamp PP. 2004. The SLC24 $\text{Na}^+/\text{Ca}^{2+}\text{-K}^+$ exchanger family: Vision and beyond. *Pflugers Arch* 447: 683-688.
- Schuurmans Stekhoven F, Bonting SL. 1981. Transport adenosine triphosphatases: -Properties and functions. *Physiol Rev* 61: 1-76.
- Seki Y, Feustel PJ, Keller RW Jr, Tranmer BI, Kimelberg HK. 1999. Inhibition of ischemia-induced glutamate release in rat striatum by dihydrokinate and an anion channel blocker. *Stroke* 30: 433-440.
- Sensi SL, Canzoniero LM, Yu SP, Ying HS, Koh JY, et al. 1997. Measurement of intracellular free zinc in living cortical neurons: Routes of entry. *J Neurosci* 17: 9554-9564.
- Sensi SL, Yin HZ, Weiss JH. 1999. Glutamate triggers preferential Zn^{2+} flux through Ca^{2+} -permeable AMPA channels and consequent ROS production. *Neuroreport* 10: 1723-1727.
- Sensi SL, Yin HZ, Weiss JH. 2000. AMPA/kainate receptor-triggered Zn^{2+} entry into cortical neurons induces mitochondrial Zn^{2+} uptake and persistent mitochondrial dysfunction. *Eur J Neurosci* 12: 3813-3818.
- Sheline CT, Behrens MM, Choi DW. 2000. Zinc-induced cortical neuronal death: Contribution of energy failure attributable to loss of NAD^+ and inhibition of glycolysis. *J Neurosci* 20: 3139-3146.
- Shyjan AW, Cena V, Klein DC, Levenson R. 1990. Differential expression and enzymatic properties of the Na^+/K^+ -ATPase α 3 isoenzyme in rat pineal glands. *Proc Natl Acad Sci USA* 87: 1178-1182.
- Siesjo BK. 1992. Pathophysiology and treatment of focal cerebral ischemia. Part II: Mechanisms of damage and treatment. *J Neurosurg* 77: 337-354.
- Silver IA, Erecinska M. 1998. Oxygen and ion concentrations in normoxic and hypoxic brain cells. New York: Plenum Press.
- Simon RP, Swan JH, Griffiths T, Meldrum BS. 1984. Blockade of *N*-methyl-D-aspartate receptors may protect against ischemic damage in the brain. *Science* 226: 850-852.
- Simpson PB, Challiss RA, Nahorski SR. 1995. Neuronal Ca^{2+} stores: Activation and function. *Trends Neurosci* 18: 299-306.
- Skou JC. 1957. The influence of some cations on an adenosine triphosphatase from peripheral nerves. *Biochim Biophys Acta* 23: 394-401.
- Smith ML, von Hanwehr R, Siesjo BK. 1986. Changes in extra- and intracellular pH in the brain during and following ischemia in hyperglycemic and in moderately hypoglycemic rats. *J Cereb Blood Flow Metab* 6: 574-583.
- Sokoloff L. 1993. Sites and mechanisms of function-related changes in energy metabolism in the nervous system. *Dev Neurosci* 15: 194-206.
- Sokoloff L. 1996. Cerebral metabolism and visualization of cerebral activity. *Comprehensive Human Physiology*. Greger G, Windhorst U, editors. Heidelberg: Springer-Verlag; pp. 579-602.
- Sokoloff L. 1999. Energetics of functional activation in neural tissues. *Neurochem Res* 24: 321-329.
- Sokoloff L, Takahashi S, Gotoh J, Driscoll BF, Law MJ. 1996. Contribution of astroglia to functionally activated energy metabolism. *Dev Neurosci* 18: 344-352.
- Stahl WL, Keeton TP, Eakin TJ. 1994. The plasma membrane Ca^{2+} -ATPase mRNA isoform PMCA 4 is expressed at high levels in neurons of rat piriform cortex and neocortex. *Neurosci Lett* 178(2): 267-270.
- Stauffer TP, Guerini D, Carafoli E. 1995. Tissue distribution of the four gene products of the plasma membrane Ca^{2+} pump. A study using specific antibodies. *J Biol Chem* 270(20): 12184-12190.
- St Croix CM, Wasserloos KJ, Dineley KE, Reynolds IJ, Levitan ES, et al. 2002. Nitric oxide-induced changes in intracellular zinc homeostasis are mediated by metallothionein/thionein. *Am J Physiol Lung Cell Mol Physiol* 282: L185-L192.
- Storozhevych T, Grigortsevich N, Sorokina E, Vinskaya N, Vergun O, et al. 1998. Role of $\text{Na}^+/\text{Ca}^{2+}$ exchange in regulation of neuronal Ca^{2+} homeostasis requires re-evaluation. *FEBS Lett* 431: 215-218.
- Stout AK, Li-Smerin Y, Johnson JW, Reynolds IJ. 1996. Mechanisms of glutamate-stimulated Mg^{2+} influx and subsequent Mg^{2+} efflux in rat forebrain neurons in culture. *J Physiol* 492 (Pt 3): 641-657.
- Stout AK, Raphael HM, Kanterewicz BI, Klann E, Reynolds IJ. 1998. Glutamate-induced neuron death requires mitochondrial calcium uptake. *Nat Neurosci* 1: 366-373.
- Szabo EZ, Numata M, Shull GE, Orłowski J. 2000. Kinetic and pharmacological properties of human brain Na^+/H^+ exchanger isoform 5 stably expressed in Chinese hamster ovary cells. *J Biol Chem* 275: 6302-6307.
- Szasz I, Sarkadi B, Schubert A, Gardos G. 1978. Effects of lanthanum on calcium-dependent phenomena in human red cells. *Biochim Biophys Acta* 512: 331-340.
- Takanaga H, Mackenzie B, Hediger MA. 2004. Sodium-dependent ascorbic acid transporter family SLC23. *Pflugers Arch* 447: 677-682.
- Thayer SA, Usachev YM, Pottorf WJ. 2002. Modulating Ca^{2+} clearance from neurons. *Front Biosci* 7: d1255-d1279.
- Trapp S, Luckermann M, Kaila K, Ballanyi K. 1996. Acidosis of hippocampal neurons mediated by a plasmalemmal $\text{Ca}^{2+}/\text{H}^+$ pump. *Neuroreport* 7: 2000-2004.
- Tsoi M, Rhee KH, Bungard D, Li XF, Lee SL, et al. 1998. Molecular cloning of a novel potassium-dependent sodium-calcium exchanger from rat brain. *J Biol Chem* 273: 4155-4162.
- Tymianski M, Charlton MP, Carlen PL, Tator CH. 1993. Secondary Ca^{2+} overload indicates early neuronal injury which precedes staining with viability indicators. *Brain Res* 607: 319-323.

- Vague P, Coste TC, Jannot MF, Raccach D, Tsimaratos M. 2004. C-peptide, Na⁺, K⁺-ATPase, and diabetes. *Exp Diabetes Res* 5: 37-50.
- Valkina ON, Vergun OV, Turovetsky VB, Khodorov BI. 1993. Effects of repetitive stimulation, veratridine, and ouabain on cytoplasmic pH in frog nerve fibers: Role of internal Na⁺. *FEBS Lett* 334: 83-85.
- Vanzetta I, Grinvald A. 1999. Increased cortical oxidative metabolism due to sensory stimulation: Implications for functional brain imaging. *Science* 286: 1555-1558.
- Vergun O, Reynolds IJ. 2004. Fluctuations in mitochondrial membrane potential in single isolated brain mitochondria: Modulation by adenine nucleotides and Ca²⁺. *Biophys J* 87: 3585-3593.
- Vergun O, Reynolds IJ. 2005a. Developmental changes in the properties of Ca²⁺-induced depolarization in brain mitochondria. *Soc Neurosci Abstr* 550.6.
- Vergun O, Reynolds IJ. 2005b. Distinct characteristics of Ca²⁺-induced depolarization of isolated brain and liver mitochondria. *Biochim Biophys Acta* 1709: 127-137.
- Vergun O, Han YY, Reynolds IJ. 2003. Glucose deprivation produces a prolonged increase in sensitivity to glutamate in cultured rat cortical neurons. *Exp Neurol* 183: 682-694.
- Vergun O, Keelan J, Khodorov BI, Duchon MR. 1999. Glutamate-induced mitochondrial depolarization and perturbation of calcium homeostasis in cultured rat hippocampal neurons. *J Physiol* 519 (Pt 2): 451-466.
- Vergun O, Sobolevsky AI, Yelshansky MV, Keelan J, Khodorov BI, et al. 2001. Exploration of the role of reactive oxygen species in glutamate neurotoxicity in rat hippocampal neurons in culture. *J Physiol* 531: 147-163.
- Verkhratsky A. 2005. Physiology and pathophysiology of the calcium store in the endoplasmic reticulum of neurons. *Physiol Rev* 85: 201-279.
- Verkhratsky A, Petersen OH. 2002. The endoplasmic reticulum as an integrating signalling organelle: From neuronal signalling to neuronal death. *Eur J Pharmacol* 447: 141-154.
- Verrey F, Closs EI, Wagner CA, Palacin M, Endou H, et al. 2004. CATs and HATs: The SLC7 family of amino acid transporters. *Pflugers Arch* 447: 532-542.
- Votyakova TV, Reynolds IJ. 2001. $\Delta\Psi_m$ -Dependent and -independent production of reactive oxygen species by rat brain mitochondria. *J Neurochem* 79: 266-277.
- Wanaverbecq N, Marsh SJ, Al-Qatari M, Brown DA. 2003. The plasma membrane calcium-ATPase as a major mechanism for intracellular calcium regulation in neurons from the rat superior cervical ganglion. *J Physiol* 550: 83-101.
- Wang GJ, Thayer SA. 1996. Sequestration of glutamate-induced Ca²⁺ loads by mitochondria in cultured rat hippocampal neurons. *J Neurophysiol* 76: 1611-1621.
- Wang GJ, Randall RD, Thayer SA. 1994. Glutamate-induced intracellular acidification of cultured hippocampal neurons demonstrates altered energy metabolism resulting from Ca²⁺ loads. *J Neurophysiol* 72: 2563-2569.
- Werth JL, Thayer SA. 1994. Mitochondria buffer physiological calcium loads in cultured rat dorsal root ganglion neurons. *J Neurosci* 14: 348-356.
- White RJ, Reynolds IJ. 1995. Mitochondria and Na⁺/Ca²⁺ exchange buffer glutamate-induced calcium loads in cultured cortical neurons. *J Neurosci* 15: 1318-1328.
- White RJ, Reynolds IJ. 1996. Mitochondrial depolarization in glutamate-stimulated neurons: An early signal specific to excitotoxin exposure. *J Neurosci* 16: 5688-5697.
- Wong-Riley MT. 1989. Cytochrome oxidase: An endogenous metabolic marker for neuronal activity. *Trends Neurosci* 12: 94-101.
- Wong-Riley MT, Merzenich MM, Leake PA. 1978. Changes in endogenous enzymatic reactivity to DAB induced by neuronal inactivity. *Brain Res* 141: 185-192.
- Wright EM, Turk E. 2004. The sodium/glucose cotransport family SLC5. *Pflugers Arch* 447: 510-518.
- Wu ML, Chen JH, Chen WH, Chen YJ, Chu KC. 1999. Novel role of the Ca²⁺-ATPase in NMDA-induced intracellular acidification. *Am J Physiol* 277: C717-C727.
- Ye B, Maret W, Vallee BL. 2001. Zinc metallothionein imported into liver mitochondria modulates respiration. *Proc Natl Acad Sci USA* 98: 2317-2322.
- Yokoyama M, Koh J, Choi DW. 1986. Brief exposure to zinc is toxic to cortical neurons. *Neurosci Lett* 71: 351-355.
- Yu X, Carroll S, Rigaud JL, Inesi G. 1993. H⁺ countertransport and electrogenicity of the sarcoplasmic reticulum Ca²⁺ pump in reconstituted proteoliposomes. *Biophys J* 64: 1232-1242.
- Zangger K, Oz G, Armitage IM. 2000. Re-evaluation of the binding of ATP to metallothionein. *J Biol Chem* 275: 7534-7538.
- Zylinska L, Gromadzinska E, Lachowicz L. 1999. Short-time effects of neuroactive steroids on rat cortical Ca²⁺-ATPase activity. *Biochim Biophys Acta* 1437: 257-264.

Regulation of Metabolic Fluxes and Metabolic Shuttling by Neural Environment

5.1 Acid–Base Transport and pH Regulation

J. W. Deitmer

1	<i>Introduction</i>	470
2	<i>The Distribution of Acid and Base in the Brain</i>	471
3	<i>H⁺ Buffering and Muffling</i>	472
4	<i>pH Changes Following Neuronal Activity</i>	473
5	<i>pH Regulation in the Brain</i>	474
5.1	Neuronal pH Regulation and pH Sensitivity	474
5.2	The Role of Glial Cells for Acid/Base Regulation	476
6	<i>Acid/Base-Coupled Metabolite Transporters</i>	477
6.1	MCT1 and Energy Transfer Between Glial Cells and Neurons	477
6.2	Neurotransmitter Uptake Carriers	480
7	<i>Pathological Events Related to Acid–Base Regulation</i>	480
8	<i>Conclusions</i>	481

Abstract: In the brain, neurons and glial cells are equipped with a number of acid–base-coupled ion and metabolite transporters, which affect intra- and extracellular pH. The pH changes can be fast and multiphasic, which can be considered as “H⁺ signaling” in cells and tissues. Since many biological processes, such as metabolic activity, synaptic transmission, and electrical excitability, as well as most enzymatic processes in the cells, are dependent on and/or modulated by H⁺, changes in pH may be involved in shaping intra- and intercellular signaling patterns. The ubiquitous enzyme carbonic anhydrase (CA), which helps to modify the kinetics of pH changes, may increase the buffering capacity in cells or cellular compartments, and can enhance the activity of some acid–base transporters by binding and forming “transport metabolons” with these proteins. Some acid–base transporters, such as the Na⁺/H⁺ exchanger (NHE), the Cl[−]/HCO₃[−] exchanger (anion exchanger, AE), or the Na⁺/HCO₃[−] cotransporter (NBC), are more directly involved in the regulation of intra- and extracellular pH, while other transporters, which primarily transport, e.g., neurotransmitters (glutamate), neurotransmitter precursors (glutamine), or energetic compounds (lactate), co- or countertransport H⁺ as cosubstrate across the cell membrane, and are therefore affected by the H⁺ gradient. Protons gate acid-sensing ion channels (ASICs) involved in the perception of pain, touch, and heat. Pathological pH changes are associated with hypoxia and ischemia and subsequent lactic acidosis. Hence, changes of pH in the nervous system, as affected by intra- and extracellular H⁺ buffering capacity, metabolically released acids, and the activity of acid–base transporters in cell membranes, modulate neuronal activity and glial functions.

1 Introduction

In nerve and glial cells, and in the extracellular spaces (ECS) of nervous systems, pH changes can be evoked by neuronal activity, by neurotransmitters and neuromodulators, by active cellular pH regulation, by secondary transporters carrying acid/base equivalents, and by metabolic processes. In particular, neurotransmission mediated by glutamate, γ -aminobutyric acid (GABA), or glycine as the transmitters is associated with intra- and extracellular pH changes, which can be large and rapid, with kinetics not unlike intracellular calcium transients. However, *unlike* intracellular calcium changes that rise and then recover, pH shifts can occur in two directions, namely in acid and alkaline directions. Indeed, since acid/base fluxes with different time courses may be elicited by a stimulus, for example, by a brief train of action potentials, the pH changes, particularly in the ECS, may be multiphasic. These multiphasic changes in extracellular pH (pH_o) may in turn affect the electrical and synaptic activity of neurons, and could modulate extracellular enzyme activity.

Rapid pH transients may actually be signals rather than only a result of inadequate homeostatic acid–base regulation. Analogous to the signaling pattern of other ions, such as calcium and potassium, transient shifts of protons and bicarbonate, together with carbon dioxide and carbonic anhydrase (CA) activity, may influence or initiate functional processes in the nervous system. These include pH-induced changes of neuronal excitability, synaptic activity, the modulation of gap junctions (connexins) and thus of electrical synapses and the glial syncytium, transport processes in which acid or base is involved, and regulation of enzyme activities. Proton signaling in cells and in local extracellular domains, particularly in the micro-environment of synapses, could well contribute to information processing in nervous systems (Chesler and Kaila, 1992; Deitmer and Rose, 1996).

Functionally, pH_o changes will modify processes at the extracellular surface of cells, resulting in the modulation of neuronal excitability and synaptic transmission, as well as of a variety of membrane carriers. For instance, ionotropic glutamate receptors of the *N*-methyl-D-aspartate (NMDA) type are highly sensitive to pH_o, and synaptic transmission via these receptors is suppressed if pH_o falls below 7.0 (Traynelis and Cull-Candy, 1990). Furthermore, since synaptic vesicles are acidic (pH 5.6, Miesenbock et al., 1998), a transient, local fall of extracellular pH is associated with their exocytosis during synaptic transmission, suggesting that pH changes at the synapse may be significant and can hence influence synaptic transmission. Indeed, transient inhibition of the presynaptic Ca²⁺ current, presumably due to an acidification in the

synaptic cleft, has been reported in mammalian photoreceptors (DeVries, 2001). Many of these aspects related to pH regulation and H^+ signaling properties in the brain have been reviewed recently in more detail (Putnam, 2001; Chesler, 2003; Deitmer, 2004; Coles and Deitmer, 2005).

2 The Distribution of Acid and Base in the Brain

The intracellular, cytosolic pH (pH_i) of neurons and glial cells is actively maintained at a value usually between 7.0 and 7.4, which is similar to the extracellular pH value (pH_o) in nervous tissue (7.1–7.3). Thus, “resting” intra- and extracellular pH ranges between 40 and 100 nM free H^+ concentration. This means that there is often only a small chemical gradient of H^+ concentration, if any, across the cell membranes of “resting” neurons and glial cells. The main driving force of H^+ from outside to inside of a cell is the negative membrane potential. Any conductance of the cell membrane for H^+ and/or HCO_3^- at cell membrane potentials negative to -30 mV would result in a gain of acid or loss of base, and would hence lead to an intracellular acidification.

In isolated cells and tissues, pH_i depends on whether the preparation is bathed in a solution buffered with a standard buffer, such as HEPES, or with CO_2 and HCO_3^- . In general, the steady-state pH_i is lower in CO_2/HCO_3^- -buffered saline by 0.1–0.4 pH units. Neurons are the main consumers of ATP, and therefore the main producers of CO_2 (Attwell and Laughlin, 2001). The link between CO_2 production and pH is the CO_2/HCO_3^- buffer system, which plays a major role for the maintenance of pH both intra- and extracellularly (see below).

The proton equilibrium potential hence ranges between 0 and -30 mV in most animal cells. At a negative cell membrane potential of brain cells between -40 and -90 mV, the total H^+ gradient therefore amounts to 10–90 mV. Acid must be actively extruded by the cells against this electrochemical gradient, which requires energy. In most cells, this energy is provided by the Na^+ gradient, which drives the Na^+/H^+ exchanger (NHE) and other acid/base transport systems. The different isoforms of the NHE are the most prominent and ubiquitous transport proteins for acid extrusion in animal cells, and their malfunction is associated with a variety of diseases (Harris and Fliegel, 1999; Putney et al., 2002; Bobulescu et al., 2005). The NHE helps the cytoplasm to maintain a more alkaline pH than the acid/base electrochemical equilibrium across the plasma membrane, which can be calculated to be around 6.4–6.8 in most animal cells. When cells become alkaline beyond their steady-state pH_i , base equivalents are extruded mainly by the anion exchanger (AE), i.e., the Cl^-/HCO_3^- exchanger.

The biological need for active maintenance of cytosolic pH is usually explained by the steep pH dependence of many enzymatic processes in cells, which have their optimum at a pH of around 7.0 or higher. Although the proton gradient across animal plasma membranes is not very large, and amounts to only about half the size of the Na^+ gradient, it is also a significant source of energy, which can be used to fuel secondary transport (see below). Thus, membrane transporters can be fueled by the H^+ gradient, and they may, in addition, be modulated on the protein level by intra- and/or extracellular pH. In order to understand the mechanisms of the acid and alkaline transients, it is often necessary to monitor pH in all three compartments of the tissue: in neurons, in glial cells, and in the ECS. The pH shifts in the ECS are often, for example, during membrane fluxes of acid or base, approximate mirror images of intracellular pH changes. However, it is usually difficult to make an accurate quantitative inverse match, partly because the volumes and spatial distributions of the cells involved are uncertain, and because H^+ ions effectively diffuse very rapidly through extracellular clefts. In addition, we still know little about intracellular handling of H^+ , particularly the capacity and time courses of sequestration of H^+ by intracellular organelles.

Our interpretation of acid/base fluxes in tissues is restricted by the method employed to measure intra- and extracellular pH. pH-sensitive, neutral carrier microelectrodes, which are impaled into larger cells and into ECS of a tissue and provide an “online” recording of pH, and fluorescent probes (e.g., 2',7'-(bis carboxyethyl)-5,6-carboxyfluorescein, BCECF), which can be loaded into cells or distributed in tissues, and measured by fluorescence microscopy, can be used for measuring pH in cells and tissues. The pH-sensitive microelectrodes are very reliable, but relatively slow, and they may cause some damage to the tissue, while pH-sensitive dyes are basically noninvasive and fast, but more difficult to calibrate, and they bleach, which

can produce radicals harmful to cells and tissue. A more detailed account of the different methods to determine cell and tissue pH are given in methodological books and reviews (Tsien and Waggoner, 1995; Deitmer and Rose, 1996; Deitmer and Schild, 2000).

3 H⁺ Buffering and Muffling

The free H⁺ concentration in cells is in the nanomolar range, and the high buffer capacity of cells provides a reservoir of acid equivalents in the millimolar range. In other words, there is a pool of protons in rapid exchange between buffer sites and free solution, some 10⁵ protons being buffered for each one in solution. The buffer capacity β is measured in mM acid or base needed to shift the pH by one unit. The value β in cells is itself dependent on pH and on the buffer, for example, on whether CO₂/HCO₃⁻ is present or not. In experiments on isolated tissues or cells, β is usually measured either in the nominal absence of CO₂/HCO₃⁻ (the “intrinsic buffer capacity” β_i) or in the presence of CO₂/HCO₃⁻, providing the “total buffer capacity” β_t . The difference between β_t and β_i gives the bicarbonate-dependent buffer capacity β_{CO_2} .

For neurons and glial cells, β_i has been measured to be 10–40 mM, and β_{CO_2} , which is approximately 2.3 times the HCO₃⁻ concentration (Roos and Boron, 1981), is between 14 mM (corresponding to 6 mM HCO₃⁻ at a pHi of 6.8) and 40 mM (corresponding to 17 mM HCO₃⁻ at a pHi of 7.2) in the presence of 5% CO₂. Hence, β_t is usually between 24 and 80 mM in nerve and glial cells. The CO₂/HCO₃⁻ system contributes a large part of the pH buffering in cells and tissues. Its effectiveness, and in particular its kinetics, depends on the activity of CA, which catalyzes the reaction CO₂ + H₂O \longleftrightarrow HCO₃⁻ + H⁺, and hence speeds up equilibration between CO₂ and H⁺/HCO₃⁻. In the absence of this enzyme, the reaction is slow, and CA can accelerate the reversible conversion of CO₂ by many hundredfold, depending on the isoform and concentration of the enzyme (Maren, 1967, 1988). Within the vertebrate nervous system, CA is primarily present in oligodendrocytes (Cammer, 1984; Tong et al., 2000) and astrocytes (Giacobini, 1962; Sapirstein et al., 1984). Because of the rapid conversion of CO₂ to H⁺ and HCO₃⁻ by CA, glial cells may act as sinks for CO₂ (Newman, 1994; Deitmer and Rose, 1996), resulting in a rise of H⁺ and HCO₃⁻ and subsequent activation of H⁺ and HCO₃⁻-coupled transporters.

Little is known about the intrinsic (i.e., non-CO₂/HCO₃⁻) buffer capacity of the extracellular fluid. Nonbicarbonate buffering is believed to take place due to the collective contributions of inorganic phosphate and various proteins and amino acids. There is no quantitative measurement for the extracellular intrinsic buffer capacity in mammalian brain; however, in the leech central nervous system, extracellular intrinsic buffer capacity was estimated to be up to about 5 mM (Deitmer and Rose, 1996), presumably a minor component of the total extracellular buffer capacity. Given the small volume fraction of the extracellular compartment (Nicholson and Sykova, 1998; Nicholson, 2005), the interstitial buffer reservoir per unit volume is low compared with that of the intracellular space. These two factors render much larger pH changes in the ECS than in the cytosol of the cells. Changes of pH_o following the addition of a weak acid or ammonium have been used to estimate the relative buffer capacity in the ECS in different buffer solutions. In the presence of the CA inhibitors ethoxzolamide or benzolamide, the increase in buffer capacity due to CO₂/HCO₃⁻ can be reversed, suggesting that the CA activity not only enhances intracellular but also extracellular buffer capacity, and that the buffer capacity contributed by the CO₂/HCO₃⁻ buffer system largely depends on CA activity (Thomas et al., 1991; Chen and Chesler, 1992; Deitmer, 1992; Chesler et al., 1994). There is recent evidence regarding the presence of CA IV and CA XIV isoforms and their contribution to extracellular buffering in the central nervous system (Shah et al., 2005; Svichar et al., 2005). Major CA activity is also associated with the cerebrospinal fluid, where the enzyme is involved in HCO₃⁻ formation (Maren, 1979).

The *recovery* from pH_o changes in the tissue depends mainly on acid/base transport across the cell membranes, and therefore often reflects intracellular pH changes. Thus, the cells may sense pH_i changes in neighboring cells by the pH changes in the ECS. When trying to measure buffering power, it is often assumed that the pH changes truly reflect the H⁺ binding capacity (chemical buffering) of a cellular or extracellular compartment. However, this may not be so, because the time course of monitoring pH is presumably slow not only in relation to chemical buffering (which can be fast), but also with respect to the

transport of acid/base equivalents via the plasma membrane and across organellar membranes in the cells (sequestration). Hence, it must be expected that “immediate” pH changes, as are used to determine buffer capacity, are not only affected by chemical buffering, but also by transport and sequestration of acid/base equivalents. Therefore, the term “H muffling” has been introduced, which includes all fast processes, and contributes to the damping of measured pH changes; H^+ muffling is also denoted as “physiological buffering” or “apparent buffer capacity,” to be distinguished from pure chemical buffering, which probably cannot be measured accurately in living cells and tissues (Thomas et al., 1991).

The activity of an electrogenic sodium bicarbonate cotransporter (NBCe1), which is present predominantly in glial cells in nervous tissue (Deitmer and Rose, 1996; Chesler, 2003), has recently been shown to affect cellular buffering (Becker and Deitmer, 2004). Heterologously expressed in *Xenopus* oocytes, NBCe1 not only increased the buffer capacity of the cells, but also rendered the intracellular buffer capacity dependent on the cell membrane potential. This suggests that depolarized glial cells, after activation of ionotropic glutamate receptor channels (Verkhatsky and Steinhäuser, 2000), acquire a larger cytosolic buffer capacity due to inward transport of bicarbonate via NBCe1. This increased buffer capacity may help to muffle pH_i changes as induced by neurotransmitter carriers, such as the excitatory amino acid transporters (EAATs), or metabolite-coupled acid/base transporters (see below).

4 pH Changes Following Neuronal Activity

Neuronal activity leads to defined changes of intra- and extracellular pH in central nervous systems of both vertebrates and invertebrates (Deitmer and Rose, 1996; Chesler, 2003). These consist of mono- or multiphasic pH shifts, indicating that they might originate from multiple sources and/or via multiple processes. Because of the increase in $[K^+]_o$ and because of excitatory neurotransmitters during neuronal activity, glial cells may respond to the activity of neighboring neurons with a substantial depolarization of their cell membrane, accompanied by an intracellular alkalization. In the rat cortex, the stimulus-evoked glial depolarization is accompanied by an intracellular alkalization of astrocytes, the amplitude of which is dependent on the extent of the depolarization (Chesler and Kraig, 1989). In the ECS, the nerve stimulation that elicits an intragial alkalization also evokes an acid transient in the ECS. Interestingly, while the intragial pH shift was unaffected by the CA inhibitor ethoxyzolamide, the extracellular pH transient was converted or enhanced to a large alkaline transient following inhibition of CA activity (Chen and Chesler, 1992; Rose and Deitmer, 1995b). This suggests that these pH_o changes are greatly affected by the activity of extracellular and/or intracellular CA.

Several lines of evidence suggest that the depolarization-induced alkalization of glial cells in both vertebrate and invertebrate preparations is due to inward transport of bicarbonate via the electrogenic Na^+/HCO_3^- cotransporter (NBC), activated by the K^+ -induced membrane depolarization (Deitmer and Szatkowski, 1990; Grichtchenko and Chesler, 1994; Pappas and Ransom, 1994; Bevensee et al., 1997). In the cortex, the glial alkaline shift was partly inhibited in Na^+ -free saline and turned into a small acidification when the K^+ -induced depolarization was reduced by the application of Ba^{2+} (Chesler and Kraig, 1989; Grichtchenko and Chesler, 1994). The stimulus-induced alkalization of the leech giant glial cell was turned into an acidification by all experimental protocols suppressing the activation of the NBC: (1) by voltage-clamping the glial cell (Rose and Deitmer, 1994), (2) in the presence of the stilbene, DIDS (4,4'-diisothiocyano-2,2'-stilbene-disulfide), and (3) in CO_2 , HCO_3^- -free saline (Rose and Deitmer, 1995a, b). Suppressing glial depolarization during nerve root stimulation not only reversed intragial pH change, but also uncovered an alkaline pH_o transient, which preceded the extracellular acidification (Rose and Deitmer, 1994).

Neurons and glial cells have a variety of transmitter receptors coupled to ion channels. The activation of these ionotropic receptors can induce pH transients in nervous systems, which are either due to the action of neurotransmitters themselves by both HCO_3^- -dependent and -independent mechanisms, or are secondary to membrane potential changes (Chesler and Kaila, 1992; Munsch and Deitmer, 1994). The majority of available data relates to pH changes induced by GABA and glutamate, while the effects of other transmitters on pH_o or pH_i in the nervous system have been investigated in only a few systems. It has become clear,

however, that there may be complex interactions between transmitter effects on both glial cells and neurons and pH_o or pH_i changes, including not only the activation of ionotropic receptor-operated channels, but also transmitter and metabolite carriers, which may contribute to acid/base fluxes (see below).

Perturbations of pH can induce a variety of changes in cellular functions in nervous systems, from the activation or inhibition of ionic currents, to alterations in overall neuronal excitability, and to modulation of enzyme activities (Chesler, 1990, 2003; Deitmer and Rose, 1996). Such pH shifts may be associated with acid/base secretion, lactate transport, cell volume changes, glutamate uptake and glutamine efflux, alteration in gap junctional communication, and metabolic processes (some of which will be discussed below and in related chapters of this volume). Often, these pH-dependent processes are linked to, or might induce, a cascade of H^+ -induced signals in nervous systems. For example, pH modulation of gap junctions might result in a change in synchronous activity in neurons. In glial cells, transmitter release through hemichannels in the glial cell membrane, as suggested for ATP and glutamate (Cotrina et al., 2000; Ye et al., 2003), may be pH-dependent. In addition, pH-dependent Cl^- regulation (via AE) in neurons and glial cells, and HCO_3^- -permeable receptor channels activated by GABA or glycine, affects synaptic inhibition in nervous systems (Kaila, 1994). In addition, pH changes are often accompanied by changes in calcium, sodium, and other ions, by coupling with one of these ions on carriers, which can result in rather complex changes with respect to the performance of glial cells and neurons.

5 pH Regulation in the Brain

The plasma membranes of neurons and glial cells contain a variety of acid/base-transporting proteins, most of them being counter- or cotransporters with sodium and/or chloride as the co- or counterion for protons and bicarbonate. In general, influx or extrusion of protons or bicarbonate into or out of the cells to regulate pH_i always changes pH_o also. The magnitudes of the changes depend on four main variables: (1) the amount of acid/base flux across the cell membranes, (2) the volume of the ECS, (3) the buffering power of the ECS fluid, and (4) the removal of acid/base equivalents from the ECS.

All four variables may affect neuronal functioning, in particular electrical and synaptic activity, and hence information processing, by modulating the magnitude and kinetics of the pH_o transients. For a given initial acid/base flux, the magnitude of the pH_o change is greater if the extracellular domain is small and has weak buffering capacity, and attenuated if the effective extracellular volume is large and the buffering capacity larger. The effectiveness of pH_o regulation, i.e., acid/base fluxes that counteract shifts in pH_o , depends on, among other factors, the density and activity of acid/base transporters in adjacent cell membranes. pH_o shifts can be rapid and brief, lasting only seconds, and may be signals rather than only a result of inadequate homeostatic acid/base regulation (see also Deitmer and Rose, 1996; Deitmer, 2004).

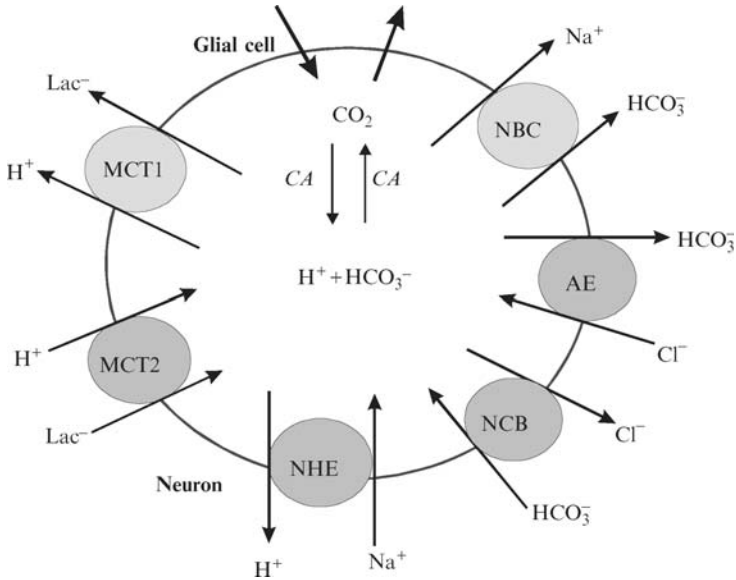
Like many other cell types, neurons and glial cells use a variety of acid/base transport systems for their intracellular pH (pH_i) regulation (▶ [Figure 5.1-1](#)). As with most cells, they use various isoforms of NHE and AE. So far, five isoforms of NHE have been detected in the brain, some of which seem to be restricted to certain brain areas (Ma and Haddad, 1997). Like most *epithelial* cells, glial cells use, in addition to the NHE and the AE, an electrogenic $\text{Na}^+/\text{HCO}_3^-$ cotransporter (NBCe), which is apparently not active in neurons, despite evidence for transporter messenger RNA (mRNA) and protein also in neurons (Schmitt et al., 2000). In situ hybridization revealed NBC mRNA expression throughout the rat central nervous system, with particularly high levels in the olfactory bulb, the hippocampus dentate gyrus, and the cerebellum (Schmitt et al., 2000).

5.1 Neuronal pH Regulation and pH Sensitivity

The predominant pH-regulating transporters in neurons are the NHE, a sodium-dependent chloride/bicarbonate exchanger (NCB) and the AE; recently, an electroneutral NBC has been reported for hippocampal neurons (Cooper et al., 2005). The Na^+ -coupled exchangers extrude acid, AE usually extrudes base, helping to maintain or return the intracellular pH in “resting” neurons between 7.0 and 7.4 (▶ [Figure 5.1-1](#)). In neurons, the uptake of H^+ and lactate via the monocarboxylate transporter 2 (MCT2) would stimulate

■ Figure 5.1-1

The main acid/base-regulating transport systems and monocarboxylate transporter (MCT) across the neuronal and glial cell membrane: Na^+/H^+ exchanger (NHE), $\text{Cl}^-/\text{HCO}_3^-$ exchanger (or anion exchanger, AE), Na^+ -dependent $\text{Cl}^-/\text{HCO}_3^-$ exchanger (NCB), $\text{Na}^+/\text{HCO}_3^-$ cotransporter (NBC), glial MCT1 and neuronal MCT2. Carbonic anhydrase (CA) catalyzes CO_2 , diffusing into the cell, to H^+ and HCO_3^-



NHE to extrude H^+ , resulting in a net uptake of Na^+ and lactate (Figure 5.1-1). As expected, recovery from cytosolic acid load in hippocampal neurons is impaired in mice lacking NHE1 (Yao et al., 1999).

Electrical activity or membrane depolarization results in intracellular acidification (Rose and Deitmer, 1995a, b). In cerebellar Purkinje neurons, these acid shifts were significantly larger in dendrites than in the soma (Schwiening and Willoughby, 2002; Willoughby and Schwiening, 2002). The depolarization-induced acidifications were, at least in part, related to Ca^{2+} entry and Ca^{2+} release from intracellular stores (endoplasmic reticulum (ER), mitochondria) in neurons (Willoughby et al., 2001; Yao and Haddad, 2004). In snail neurons, strong depolarization activated H^+ channels; this led to H^+ efflux and an acidification at the outer face of the cell membrane (Thomas, 1988; Byerly and Suen, 1989).

Intracellular pH regulation in neurons, as in most other cells, is directly related to the intracellular Na^+ level via the potent NHE, and hence to other Na^+ -dependent membrane transporters, in particular the Na/K-ATPase. A rise in intracellular Na^+ , as the result of enhanced Na^+ influx and/or inadequate regulation by the Na/K-ATPase, may lead to an increase in both H^+ and Ca^{2+} in the cytosol due to decreased NHE and $\text{Na}^+/\text{Ca}^{2+}$ exchange at a reduced transmembrane Na^+ gradient. Through these and other mechanisms, the levels of the intracellular H^+ , Ca^{2+} , and Na^+ are linked to each other and to various ion channels, and Na^+ - and acid/base-coupled membrane transporters. In addition, electrogenic transporter activity is linked to membrane potential changes, and is thus modulated by neuronal activity. Functional interaction was indeed reported between NHE1 and voltage-sensitive Na^+ channels, and an increased excitability of hippocampal neurons in NHE knockout mice (Gu et al., 2001). Direct binding between CA and NHE1 was shown to double H^+ flux (Li et al., 2002), although it remains to be shown that CA is involved in neuronal acid regulation via NHE.

Regulation of pH is particularly important for neurons in chemosensitive areas of the brain (reviewed by Putnam, 2001; Putnam et al., 2004; Shimokawa et al., 2005). Changes of intracellular pH in response of central chemosensitive neurons to increased CO_2 and/or H^+ levels may affect the electrical activity of these neurons. Many neurons of the retrotrapezoid nucleus are highly responsive to hypercapnic acidosis, which

may reflect synaptically driven and intrinsic mechanisms of CO₂ sensitivity (Ritucci et al., 2005). Neuronal excitability may be affected by modulation of pH-sensitive K⁺ channels; a rise in the extra- and/or intracellular H⁺ level decreasing the open probability of K⁺ channels would enhance neuronal excitability, thus mediating the CO₂ sensitivity of chemosensitive neurons.

Additional links between neuronal pH shifts and pH regulation and neuronal functions are associated with H⁺-gated or H⁺-permeable ion channels, in particular the acid-sensing ion channels (ASICs; Akaike and Ueno, 1994; Waldmann and Lazdunski, 1998; Bianchi and Driscoll, 2002). Extracellular acidification itself may gate ASICs, a family of amiloride-sensitive, ligand-gated and Ca²⁺-permeable Na⁺ channels, which are expressed in neurons (Waldmann et al., 1997a, b). A local rise of protons activating ASICs may also contribute to synaptic plasticity in the central nervous system (Wemmie et al., 2002). ASIC-null mice had reduced excitatory postsynaptic potentials and NMDA receptor activation during high-frequency stimulation of hippocampal neurons. Moreover, loss of ASICs impaired hippocampal long-term potentiation, and ASIC-null mice displayed defective spatial learning and eye blink conditioning. ASICs also affect a variety of sensory functions that includes perception of gentle touch, harsh touch, heat, sour taste, and pain (McCleskey and Gold, 1999; Bianchi and Driscoll, 2002).

5.2 The Role of Glial Cells for Acid/Base Regulation

Glial cells have been ascribed a special role for acid/base regulation in the brain, in particular ECS (Chelser and Kaila, 1992; Deitmer and Rose, 1996; Chesler, 2003; Deitmer, 2004). However, pH regulation is linked to functional “signaling” of acid and base shifts in the brain. This is to say that the extracellular pH is subject to the acid/base-coupled transport processes, which are regulated not only by pH but also by concentration gradients of other ions involved (often sodium), and by metabolites associated with these carrier systems. On the other hand, extracellular pH shifts must not necessarily be suppressed by active pH regulation, but may be part of H⁺ signaling (Deitmer and Rose, 1996; Deitmer, 2000, 2002). Thus, acid/base-coupled transporters modulate each other (Becker et al., 2004), when activated together. The export of H⁺ and lactate from glial cells via the monocarboxylate transporter 1 (MCT1) activates NBC, resulting in a net loss of Na⁺ and lactate from the glial cell (▶ *Figure 5.1-1*).

A prominent role must also be assigned to CA, which not only accelerates the reversible conversion of CO₂ and H⁺/HCO₃⁻ but also enhances acid/base transport. Some CA isoforms directly bind to a variety of acid/base-coupled transporters, such as AE, NBC, NHE, and MCT1 (Vince and Reithmeier, 1998, 2000; Li et al., 2002; Alvarez et al., 2003; Becker et al., 2005). The interactions between acid/base-coupled transporters, among each other and with the CA, and the role of protein–protein interactions in general, appear to open new insights into the network of membrane transporters.

The major pH regulating system in glial cells is the electrogenic NBC, which has not been observed to be functional in neurons so far. The NBC has been described in nearly all types of macroglial cells, including astrocytes, oligodendrocytes, Schwann cells, and retinal Müller glial cells (*cf* Deitmer and Rose, 1996). A stoichiometry of 1 Na⁺:2 HCO₃⁻ has also been reported for the mammalian renal NBC expressed in frog oocytes (Romero et al., 1997; Heyer et al., 1999). In contrast to NHE, NBC is reversible and can shuttle base equivalents in both directions across the glial cell membrane, and it can be regarded as a regulator of pH_o also. Reduction of the pH_o by reducing the HCO₃⁻ concentration evoked an inward current in leech glial cells (Deitmer, 1991; Munsch and Deitmer, 1994) and rat astrocytes (Brune et al., 1994) mediated by the NBC. The glial NBC is electrogenic and cotransports one Na⁺ with two HCO₃⁻ (Deitmer and Schlue, 1989; Deitmer and Schneider, 1995; Bevensee et al., 2000). This is consistent with activation of an outward-going electrogenic Na⁺/HCO₃⁻ cotransport. When CO₂/HCO₃⁻ is introduced, for example, when changing from a nonbicarbonate, HEPES-buffered saline to a CO₂/HCO₃⁻-buffered saline, NBC is activated in the inward direction, leading to a membrane hyperpolarization, an intracellular alkalization, and a rise in Na_i⁺.

In most studies, NBC was detected during addition or removal of CO₂/HCO₃⁻. Addition of CO₂/HCO₃⁻ resulted in an intracellular alkaline shift and a rise in intracellular Na⁺ (Na_i⁺), while removal of CO₂/HCO₃⁻ reversed these pH_i and Na_i⁺ changes. Simultaneously, the glial membrane hyperpolarized and depolarized, respectively, during these buffer changes due to reversibility of this electrogenic cotransporter (Deitmer,

1991). There was a reversible rise in Na_i^+ during the exposure to $\text{CO}_2/\text{HCO}_3^-$ in leech glial cells (Deitmer, 1992) and in cultured rat hippocampal astrocytes (Rose and Ransom, 1996). Reduction of the pH_o by reducing the HCO_3^- concentration evoked an inward current in leech glial cells (Deitmer, 1991; Munsch and Deitmer, 1994) and rat astrocytes (Brune et al., 1994).

The direction in which the NBC operates depends on the pH_i and pH_o (and HCO_3^-), the $[\text{Na}_i^+]$, and the membrane potential (Deitmer, 1991; Deitmer and Schneider, 1995). The cotransporter could also be reversed in retinal Müller glial cells (Newman, 1991), i.e., operating inwardly *and* outwardly, depending on the thermodynamic conditions. This is also reflected by the pH_i changes induced by slow voltage steps in voltage-clamped leech giant neuropil glial cells. De- and hyperpolarizing voltage steps resulted in an intragial alkalization and acidification, respectively, providing an extrapolated change of one pH unit/110 mV membrane potential change, supporting a stoichiometry of 2 $\text{HCO}_3^-:1 \text{Na}^+$ (Deitmer and Schneider, 1995). The cotransporter appears to have a remarkably high affinity for HCO_3^- , since it was found to be active even in the nominal absence of $\text{CO}_2/\text{HCO}_3^-$, when the extracellular bicarbonate concentration is usually less than 0.3 mM due to CO_2 (Deitmer and Schneider, 1998). Expressed in frog oocytes, the NBC significantly contributes to the apparent cytosolic buffer capacity (Becker et al., 2004), and may thus enhance the efficacy of other acid/base transport systems. This is supported by the binding of CA to the NBC, rendering the transport activity of the NBC significantly more efficient by forming a “transport metabolon” with CA (Alvarez et al., 2003). The NBC from rat brain has recently been cloned, and expressed in frog oocytes (Giffard et al., 2000). *In situ* hybridization revealed NBC mRNA expression throughout the rat central nervous system, with particularly high levels in the olfactory bulb, the hippocampus dentate gyrus, and the cerebellum (Bevensee et al., 2000; Schmitt et al., 2000).

6 Acid/Base-Coupled Metabolite Transporters

Protons and bicarbonate are coupled to a variety of metabolite carrier systems in glial cells and neurons. They are either inorganic ion transporters, such as NHE, AE, or NBC, which are related to intra- and extracellular pH regulation (see above), or might be employed to drive acid/base-coupled metabolite transporters, such as the monocarboxylate transporter (MCT) or some amino acid transporters. Even if protons and bicarbonate do not essentially contribute to the driving force, the coupling of either of these ions renders the pH a regulator of these membrane transporters (Becker and Deitmer, 2004). Indeed, though the Na^+ gradient plays the dominant role for many carrier systems in animal cells, some transporters are driven by, or coupled to, the $\text{H}^+/\text{HCO}_3^-$ gradient. Here, only few examples are discussed for such transporters; other examples are discussed in other chapters of this volume.

6.1 MCT1 and Energy Transfer Between Glial Cells and Neurons

The MCT proteins belong to a family of transporters including multiple isoforms, which carry monocarboxylate anions, such as lactate, pyruvate, acetoacetate, and ketone bodies, in cotransport with a proton in an electroneutral manner across the cell membrane (▶ [Figure 5.1-1](#)). Their activity can result in the release of lactate or other monocarboxylates from astroglial cells into the ECS. According to the lactate shuttle hypothesis, the monocarboxylic acids are then taken up by neurons via the neuronal MCT isoforms and are consumed to generate ATP (Magistretti et al., 1999; Aubert et al., 2005). The characteristics of MCTs in general (Halestrap and Price, 1999), and their distribution and function in the central nervous system in particular, have been discussed elsewhere (Dienel and Cruz, 2004; Hertz and Dienel, 2005; Pierre and Pellerin, 2005).

The lactate in astroglial cells is produced from glycolysis, whereby pyruvate, instead of being channeled into the tricarboxylic acid (TCA) cycle, is converted into lactate by lactate dehydrogenase (LDH) isoform 5 (Dringen et al., 1993; Bittar et al., 1996; Magistretti et al., 1999). From the 36 ATP derived from one glucose, two are retained by the glial cells during glycolysis, while 34 ATP can be transferred to neurons in the form of lactate. The release of lactate from glial cells and the uptake of lactate into neurons, a process that is

suggested by a number of studies (Walz and Mukieri, 1988; Dringen et al., 1993; Poitry-Yamate et al., 1995; Fray et al., 1996; Hu and Wilson, 1997; Schurr et al., 1997; Bouzier et al., 2000; Vega et al., 2003), but is also disputed (Chih et al., 2001; Diemel and Cruz, 2004), may enable a major transfer of energy from glial cells to neurons. The direction of this transfer is also favored by the different substrate affinities of the glial MCT1 and the neuronal MCT2, which are almost one order of magnitude apart (Bröer et al., 1997, 1998; Halestrap and Price, 1999); glial MCT1 has a K_m value for lactate of 3–5 mM, and neuronal MCT2 has a K_m value for lactate of around 0.5 mM. However, the condition under which this lactate shuttle is employed for transferring energy from glial cells to neurons remains to be clarified (Hertz and Diemel, 2005).

According to the lactate shuttle hypothesis, the lactate released from glial cells is taken up by neurons and converted to pyruvate, catalyzed by LDH-1. Pyruvate is then channeled into the TCA cycle and ultimately generates ATP and CO_2 by oxidative metabolism. Neurons need a sufficient level of ATP (Attwell and Laughlin, 2001), which they can derive from glucose as well as from lactate, to maintain their electrical and synaptic activity (Schurr et al., 1988, 1999; Izumi et al., 1997). During energy deprivation, added monocarboxylates have been shown to restore synaptic function and are neuroprotective in acute brain slices, isolated optic nerve, and neuronal cultures (Izumi et al., 1997; Schurr et al., 1997, 2001; Maus et al., 1999; Wender et al., 2000; Cater et al., 2001; Brown et al., 2004).

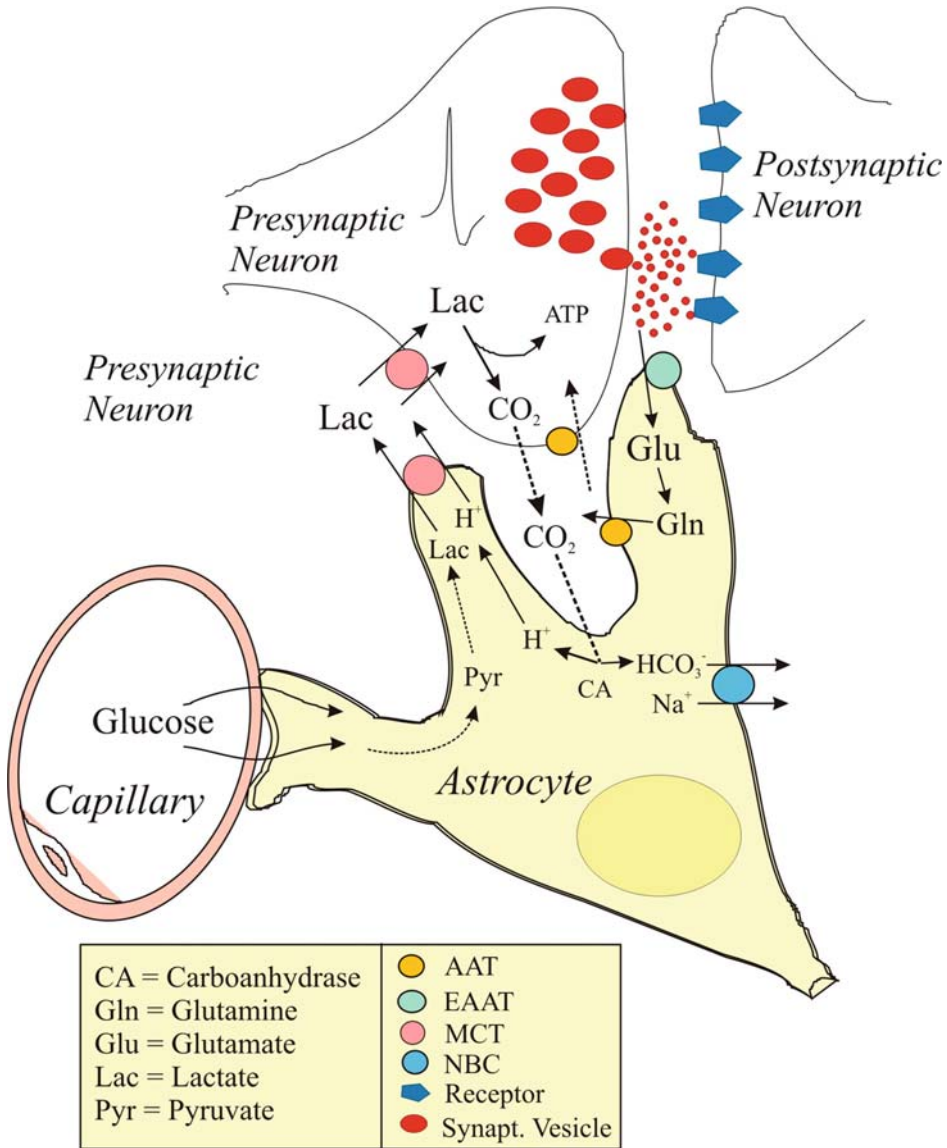
In a hypothetical scenario, some metabolic interactions between glial cells and neurons, here pre- and postsynaptic domains, are shown (🔗 [Figure 5.1-2](#)). When neurons are active, CO_2 leaves the neurons by diffusing through the cell membrane into the ECS, and from there into glial cells. Because of high CA activity in astroglial cells, CO_2 is converted to protons and bicarbonate, and hence creates a persisting gradient of CO_2 into the glial cells. Subsequently, protons and bicarbonate are extruded from the glial cytoplasm, or are metabolically consumed. A high glial CA activity works toward establishing an equilibrium between CO_2 , H^+ , and HCO_3^- , thus enabling continuous diffusion of CO_2 into the glial cells. Intracellular HCO_3^- would activate the NBC in the glial membrane in the outward direction, sustained by the production of HCO_3^- . Together with HCO_3^- , Na^+ is extruded by the NBC against a steep gradient, and the intracellular acidification then activates NHE, which would counteract the extrusion of Na^+ and HCO_3^- by the NBC. Intragial pH, however, in contrast to neuronal pH, is presumably less dominated by NHE (Brune et al., 1994; Bevensee et al., 1997; Deitmer and Schneider, 1998), due to the presence of NBC. In addition, in most cell types, activation of NHE requires a pH_i value lower than 7.2 and is significantly reduced at low pH_o , as can be induced by neuronal activity (Deitmer and Rose, 1996; Putney et al., 2002).

The extrusion of HCO_3^- may counteract extracellular acidosis (as induced by lactate secretion or NHE activity), and enhances the extracellular buffering capacity (Thomas et al., 1991). The HCO_3^- may also be converted during the consumption of protons to CO_2 by *extracellular CA* activity, thus recycling CO_2 , which could then again diffuse into the glial cells (Deitmer, 2002). There is also evidence for extracellular (interstitial) location of CA activity (Chen and Chesler, 1992; Deitmer, 1992; Tong et al., 2000), which could enhance lactate transport across cell membranes in general (Becker et al., 2005), and of glial cells and neurons in particular (Svichar and Chesler, 2003). The Na^+ extrusion via the NBC, which can be stimulated by lowering pH_o and membrane hyperpolarization (Deitmer, 1991; Deitmer and Schneider, 1995), would relieve some of the load resting on the glial Na/K-ATPase, which has to cope with a potentially large Na^+ influx associated with various sodium-driven processes in glial cells, particularly the high-affinity glutamate uptake. However, a direct link between the NBC and the Na/K-ATPase in the manner suggested here has not yet been shown. The bicarbonate-driven sodium efflux might save energy, which glial cells can either deliver to neurons or use themselves to prevent the dissipation of the sodium gradient, which in turn may lead to a calcium overload (Attwell and Laughlin, 2001), and, possibly, to apoptosis (Choi, 1992). On the other hand, glial membrane depolarization, extracellular alkalinization, and/or intragial acidification favor the transport of Na^+ and HCO_3^- via the electrogenic NBC into glial cells.

Interestingly, in glial cells, where MCT1 and NBC operate together, the shuttling of bicarbonate by NBC can support lactate transport by increasing the effective H^+ buffering capacity. Heterologously expressed in *Xenopus* oocytes, it was shown that the presence of NBCe1 can double the lactate transport capacity

Figure 5.1-2

Some possible interactions between glial cells and neurons, here represented by pre- and postsynaptic sites, with respect to energy transfer, glutamate/glutamine shuttle, and acid/base movements. Glucose is taken up by an astrocytic endfoot at the blood capillary, in part converted to pyruvate (Pyr) and lactate (Lac), which is transferred to neurons via monocarboxylate transporters (MCTs). Neuronal release of glutamate (Glu) by the presynaptic terminal acts at postsynaptic glutamate receptors, and is cleared from the synaptic cleft in part by glial glutamate uptake carriers (EAATs), where it is converted to glutamine (Gln) and shuttled back to neurons via neutral amino acid transporters (AATs). Active neurons release CO₂ produced by oxidative phosphorylation, which diffuses across the cell membranes of neurons and glial cells, where it is converted to H⁺ and HCO₃⁻ by the activity of carbonic anhydrase (CA). Intraglial H⁺ can be used to drive the efflux of lactate via MCT, and HCO₃⁻ stimulates outwardly directed Na⁺/HCO₃⁻ cotransporter (NBC), which would help to buffer the extracellular (synaptic) space. For further details see text



of MCT1 (Becker et al., 2004). Furthermore, CA appears to bind also to MCT1 and enhance lactate transport, a process that does not depend on the catalytic activity of the enzyme (Becker et al., 2005). Hence, by means of protein–protein interaction, acid/base-coupled transport appears to be subject to regulation or modulation by associated and/or functionally related proteins, which may directly bind to the carriers.

6.2 Neurotransmitter Uptake Carriers

The uptake of synaptically released neurotransmitters into neurons and glial cells is often coupled to the transport of acid/base equivalents. Glutamate uptake via EAATs, which is mainly fuelled by the inwardly directed Na^+ gradient, also transports H^+ into the cell (Anderson and Swanson, 2000; Danbolt, 2001). Thus, during increased activity of excitatory neurons releasing glutamate, glial EAAT1-2 and neuronal EAAT3–5 are activated and acidify the cytosol during the uptake of this neurotransmitter (Amato et al., 1994; Deitmer and Schneider, 1998). The glutamate is either metabolized or, more commonly, converted to glutamine by the ATP-consuming and pH-sensitive glutamine synthetase in glial cells, and as such recycled via the glutamate–glutamine shuttle to neurons (Hertz et al., 1999). Since three Na^+ ions are transported during one cycle with the EAAT, it is not clear what functional significance can be ascribed to the cotransport of one acid equivalent, since the contribution of one H^+ to the force driving glutamate into the cells is only about one-sixth of that provided by the three Na^+ ions. Certainly, acidosis or alkalosis may stimulate or reduce glutamate transport to some extent due to the cotransport of one proton.

Glutamine, which is not a neurotransmitter, can be transported out of the glial cells and taken up by neurons, where it is converted back to glutamate by transaminase activity. Both astrocytes and neurons exhibit a variety of neutral amino acid transporters that transport glutamine and other amino acids (Bröer and Brookes, 2001). One of the systems related to glutamine transport in astrocytes is the system N (SN1, now SNAT3, and SNAT5, *SLC38A3/5*), which cotransports one glutamine with one Na^+ in exchange for one H^+ in an electroneutral transfer (Chaudhry et al., 1999; Fei et al., 2000). In addition, a conductance for H^+ and/or Na^+ has been suggested for the SNAT3-mediated glutamine transport, which is not stoichiometrically coupled to the amino acid transport (Chaudhry et al., 2001; Bröer et al., 2002). Because of the steep gradient of glutamine, this transport system can mediate both influx and efflux of glutamine. The SNAT3/5 system is one of the major pathways for glutamine efflux from cultured rat astrocytes (Deitmer et al., 2003; Cubelos et al., 2005). Intra- and extracellular pH changes can modulate the release and uptake of glutamine via SNAT3/5 according to the H^+ gradient. The other glutamine transporters used by glial cells and neurons, such as system L (a Na^+ -independent pathway preferring bulky and branched-chain substrates typified by leucine, hence “L”) and system A (a Na^+ -dependent pathway preferring short-chain substrates typified by alanine) transport systems, however, are not associated with the transport of acid or base, although they may exhibit some pH sensitivity (Bröer and Brookes, 2001).

7 Pathological Events Related to Acid–Base Regulation

There is a number of pathological processes related to the impairment or the failure of acid–base regulation in the brain; in particular, hypoxia, anoxia, glucose deprivation, and conditions associated with ischemia can severely interfere with the normal acid–base homeostasis in the brain as in other tissues. Oxidative stress decreases the activity of NHE and hence the intracellular pH as shown in rat solitary complex neurons (Mulkey et al., 2004). Hyperosmotic changes in the brain, which cause shrinkage of cells, can lead to intracellular alkalinization due to activation of NHE (Shrode et al., 1995; Ritter et al., 2001). Changes in cellular and tissue pH are associated with hyperammonemia, which results from liver failure or urea cycle enzyme deficiencies, leading to brain edema and hepatic encephalopathy (Felipo and Butterworth, 2002; Suarez et al., 2002).

Since the brain is a major energy consumer, normal brain function requires complete oxidation of glucose. During hypoxia or ischemia, oxygen deficiency leads to a switch from aerobic to anaerobic glycolysis. This, in turn, has a number of consequences, some of which mitigate the deleterious effects of hypoxia/ischemia, while others appear to aggravate the damage to neurons and glial cells. The role of glial cells and glial pH regulation in acute hypoxia/ischemia for brain injury has recently been reviewed (Yao and Haddad, 2004; Chesler, 2005; Nedergaard and Dirnagl, 2005). In astrocytes, lactate production by glycolysis is increased during ischemia to meet the energy requirements, and lactate release from astrocytes is greatly enhanced (Dienel and Hertz, 2005). The release of lactate and increased ATP hydrolysis are the major sources of the extracellular acidosis observed during hypoxia/ischemia (Nedergaard et al., 1991; Siesjö et al., 1996). Although electrical excitability of the majority of neurons is decreased during acidosis due to suppression of voltage-activated ion channels (DeVries, 2001) and synaptic NMDA–glutamate receptor channels (Traynelis and Cull-Candy, 1990), the overall effect of tissue acidosis appears to be deleterious. This may be due to a number of processes, some of which are related to increased Na^+ and Ca^{2+} levels in the cells, which can be due to increased influx or reduced efflux of these ions. Cytotoxic elevation of intracellular Ca^{2+} can occur during reperfusion due to activated NHE, cytosolic Na^+ loading, and resultant reversal of $\text{Na}^+/\text{Ca}^{2+}$ exchange (Chesler, 2005). Impaired regulation of cytosolic Na^+ and Ca^{2+} subsequently leads to Ca^{2+} overload and eventually cell death (Choi, 1995). The main pathways for acid-linked Ca^{2+} influx are reversed $\text{Na}^+/\text{Ca}^{2+}$ exchange following increased intracellular Na^+ levels (see Chesler, 2005), and Ca^{2+} -permeable ASICs (Waldmann et al., 1997a, b). Indeed, blocking these ASICs or knocking the ASIC1a gene out protects the brain from ischemic injury, suggesting that ASICs are responsible for glutamate-independent, acidosis-mediated brain injury during ischemia. Thus, acidosis can injure the brain via membrane receptor-mediated mechanisms with subsequent Ca^{2+} overload (Xiong et al., 2004). This appears to be a major, glutamate-independent pathological process underlying ischemic brain damage, directly mediated by extracellular acid shifts.

8 Conclusions

For nearly all events related to pH changes in nervous tissue, the presence of CO_2 and HCO_3^- has a great impact on neuronal functions. HCO_3^- determines the buffering capacity to a large extent; the presence of $\text{CO}_2/\text{HCO}_3^-$ enables HCO_3^- flux through GABA_A receptor channels and thereby modifies the inhibitory synaptic potentials, and stimulates the powerful glial electrogenic $\text{Na}^+/\text{HCO}_3^-$ cotransporter and other carriers such as Na^+ -dependent and Na^+ -independent $\text{Cl}^-/\text{HCO}_3^-$ exchange. CO_2 , as a gas that easily permeates membranes, rapidly dissipates from any location where it is formed through cells and tissues, and together with a high enzyme activity of CA provides an effective and high buffer capacity even at relatively low concentrations. Intra- and extracellular pH shifts can gate, drive, and modulate ion channels and transporters, and can hence help to shape the performance of neurons and glial cells. The fast production of H^+ and HCO_3^- , wherever CO_2 meets CA, may shape the pH transients in brain tissue. This also supports the idea that these acid/base equivalents and CO_2 have signaling properties in the brain, with CA as an essential element determining the shape of the acid/base shifts in time and space within nervous systems. Hence, acid/base regulation is not just a homeostatic process necessary to provide a physiological platform for enzymatic processes, but the rise and fall of H^+ may have similar significance for intra- and intercellular signaling as Ca^{2+} transients. H^+ and Ca^{2+} are both maintained at submicromolar concentration as their basic level due to tight regulation, and they are both highly buffered. The mechanisms of H^+ signaling during normal and pathophysiological processes in the brain need to be further elucidated to appreciate their significance for the performance of neurons and glial cells.

Acknowledgments

The studies conducted by us have been supported by grants from the Deutsche Forschungsgemeinschaft (De 231).

References

- Akaike N, Ueno S. 1994. Proton-induced current in neuronal cells. *Prog Neurobiol* 43: 73–83.
- Alvarez BV, Loiselle FB, Supuran CT, Schwartz GJ, Casey JR. 2003. Direct extracellular interaction between carbonic anhydrase IV and the human NBC1 sodium/bicarbonate co-transporter. *Biochemistry* 42: 12321–12329.
- Amato A, Ballerini L, Attwell D. 1994. Intracellular pH changes produced by glutamate uptake in rat hippocampal slices. *J Neurophysiol* 72: 1686–1696.
- Anderson CM, Swanson RA. 2000. Astrocyte glutamate transport: Review of properties, regulation, and physiological functions. *Glia* 32: 1–14.
- Attwell D, Laughlin SB. 2001. An energy budget for signaling in the grey matter of the brain. *J Cereb Blood Flow Metab* 21: 11–33.
- Aubert A, Costalat R, Magistretti PJ, Pellerin L. 2005. Brain lactate kinetics: Modeling evidence for neuronal lactate uptake upon activation. *Proc Natl Acad Sci USA* 102: 16448–16453.
- Becker HM, Bröer S, Deitmer JW. 2004. Facilitated lactate transport by MCT1 when coexpressed with the sodium bicarbonate cotransporter (NBC) in *Xenopus* oocytes. *Biophys J* 86: 235–247.
- Becker HM, Deitmer JW. 2004. Voltage dependence of H⁺ buffering mediated by sodium-bicarbonate cotransport expressed in *Xenopus* oocytes. *J Biol Chem* 279: 28057–28062.
- Becker HM, Hirnet D, Fecher-Trost C, Sültemeyer D, Deitmer JW. 2005. Transport activity of MCT1 expressed in *Xenopus* oocytes is increased by interactions with carbonic anhydrase. *J Biol Chem* 280: 39882–39889.
- Bevensee MO, Apkon M, Boron WF. 1997. Intracellular pH regulation in cultured astrocytes from rat hippocampus. II. Electrogenic Na/HCO₃ cotransport. *J Gen Physiol* 110: 467–483.
- Bevensee MO, Schmitt BM, Choi I, Romero MF, Boron WF. 2000. An electrogenic Na⁺-HCO₃⁻ cotransporter (NBC) with a novel COOH-terminus cloned from rat brain. *Am J Physiol Cell Physiol* 278: C1200–C1211.
- Bianchi L, Driscoll M. 2002. Protons at the gate: DEG/EnaC ion channels help us feel and remember. *Neuron* 34: 337–340.
- Bittar PG, Charnay Y, Pellerin L, Bouras C, Magistretti PJ. 1996. Selective distribution of lactate dehydrogenase isoenzymes in neurons and astrocytes of human brain. *J Cereb Blood Flow Metab* 16: 1079–1089.
- Bobulescu IA, Di Sole F, Moe OW. 2005. Na⁺/H⁺ exchangers: Physiology and link to hypertension and organ ischemia. *Curr Opin Nephrol Hypertens* 14: 485–494.
- Bouzier A, Thiaudiere E, Biran M, Rouland R, Canioni P, et al. 2000. The metabolism of [3-(13)C]lactate in the rat brain is specific of a pyruvate carboxylase-deprived compartment. *J Neurochem* 75: 480–486.
- Bröer A, Albers A, Setiawan I, Edwards RH, Chaudhry FA, et al. 2002. Regulation of the glutamine transporter SN1 by extracellular pH and intracellular sodium ions. *J Physiol* 539: 3–14.
- Bröer S, Brookes N. 2001. Transfer of glutamine between astrocytes and neurons. *J Neurochem* 77: 705–719.
- Bröer S, Rahman B, Pellegrini G, Pellerin L, Martin JL, et al. 1997. Comparison of lactate transport in astroglial cells and monocarboxylate transporter 1 (MCT 1) expressing *Xenopus laevis* oocytes. Expression of two different monocarboxylate transporters in astroglial cell and neurons. *J Biol Chem* 272: 30096–30102.
- Bröer S, Schneider HP, Bröer A, Rahman B, Hamprecht B, et al. 1998. Characterization of the monocarboxylate transporter 1 expressed in *Xenopus laevis* oocytes by changes in cytosolic pH. *Biochem J* 333: 167–174.
- Brown AM, Tekkök SB, Ransom BR. 2004. Energy transfer from astrocytes to axons: The role of CNS glycogen. *Neurochem Int* 45: 529–536.
- Brune T, Fetzer S, Backus K, Deitmer JW. 1994. Evidence for electrogenic sodium-bicarbonate cotransport in cultured rat cerebellar astrocytes. *Pflügers Arch* 429: 64–71.
- Byerly L, Suen Y. 1989. Characterization of proton currents in neurones of the snail, *Lymnaea stagnalis*. *J Physiol* 413: 75–89.
- Cammer W. 1984. Carbonic anhydrase in oligodendrocytes and myelin in the central nervous system. *Ann N Y Acad Sci* 429: 494–497.
- Cater H L, Benham CD, Sundstrom LE. 2001. Neuroprotective role of monocarboxylate transport during glucose deprivation in slice cultures of rat hippocampus. *J Physiol* 531.2: 459–466.
- Chaudhry FA, Krizaj D, Larsson P, Reimer RJ, Wreden C, et al. 2001. Coupled and uncoupled proton movement by amino acid transport system N. *EMBO J* 20: 7041–7051.
- Chaudhry FA, Reimer RJ, Krizaj D, Barber D, Storm-Mathiesen J, et al. 1999. Molecular analysis of system N suggests novel physiological roles in nitrogen metabolism and synaptic transmission. *Cell* 99: 769–780.
- Chen JC, Chesler M. 1992. pH transients evoked by excitatory synaptic transmission are increased by inhibition of extracellular carbonic anhydrase. *Proc Natl Acad Sci USA* 89: 7786–7790.
- Chesler M. 1990. The regulation and modulation of pH in the nervous system. *Prog Neurobiol* 34: 401–427.

- Chesler M. 2003. Regulation and modulation of pH in the brain. *Physiol Rev* 83: 1183-1221.
- Chesler M. 2005. Failure and function of intracellular pH regulation in acute hypoxic–ischemic injury of astrocytes. *Glia* 50: 398-406.
- Chesler M, Chen JC, Kraig RP. 1994. Determination of extracellular bicarbonate and carbon dioxide concentrations in brain slices using carbonate and pH-selective microelectrodes. *J Neurosci Methods* 53: 129-136.
- Chesler M, Kaila K. 1992. Modulation of pH neuronal activity. *Trends Neurosci* 15: 396-402.
- Chesler M, Kraig RP. 1989. Intracellular pH transients of mammalian astrocytes. *J Neurosci* 9: 2011-2019.
- Chih CP, Lipton P, Roberts Jr. EL. 2001. Do active cerebral neurons really use lactate rather than glucose? *Trends Neurosci* 24: 573-578.
- Choi DW. 1992. Excitotoxic cell death. *J Neurobiol* 23: 1261-1276.
- Choi DW. 1995. Calcium: Still center-stage in hypoxic–ischemic neuronal death. *Trends Neurosci* 18: 58-60.
- Coles JA, Deitmer JW. 2005. Extracellular potassium and pH: Homeostasis and signaling. *Neuroglia*, 2nd ed. Kettenmann H, Ransom BR, editors. Oxford University Press; pp. 334-345.
- Cooper DS, Saxena NC, Yang HS, Lee HJ, Moring AG, Lee A, Choi I. 2005. Molecular and functional characterization of the electroneutral Na/HCO₃ cotransporter NBCn1 in rat hippocampal neurons. *J Biol Chem* 280: 17823-17830.
- Cotrina ML, Lin JH, Lopez-Garcia JC, Naus CC, Nedergaard M. 2000. ATP-mediated glia signaling. *J Neurosci* 20: 2835-2844.
- Cubelos B, Gonzales-Gonzales IM, Gimenez C, Zafra F. 2005. Amino acid transporter SNAT5 localizes to glial cells in the rat brain. *Glia* 49: 230-244.
- Danbolt NC. 2001. Glutamate uptake. *Prog Neurobiol* 65: 1-105.
- Deitmer JW. 1991. Electrogenic sodium-dependent bicarbonate secretion by glial cells of the leech central nervous system. *J Gen Physiol* 98: 637-655.
- Deitmer JW. 1992. Evidence for glial control of extracellular pH in the leech central nervous system. *Glia* 5: 43-47.
- Deitmer JW. 2000. Glial strategy for metabolic shuttling and neuronal function. *Bioessays* 22: 747-752.
- Deitmer JW. 2002. A role for CO₂ and bicarbonate transporters in metabolic exchanges in the brain. *J Neurochem* 80: 721-726.
- Deitmer JW. 2004. pH regulation and acid/base-mediated transport in glial cells. *Glial neuronal signaling*. Hatton GI, Parpura V, editors. Boston, London: Kluwer Academic Publishers; pp. 263-277.
- Deitmer JW, Bröer A, Bröer S. 2003. Glutamine efflux from astrocytes is mediated by multiple pathways. *J Neurochem* 87: 127-135.
- Deitmer JW, Rose CR. 1996. pH regulation and proton signalling by glial cells. *Prog Neurobiol* 48: 73-103.
- Deitmer JW, Schild D. 2000. Ca²⁺ und pH. Ionenmessungen in Zellen und Geweben. *Labor in focus*. Heidelberg, Berlin: Spektrum Akademischer Verlag GmbH; pp. 1-164.
- Deitmer JW, Schlue WR. 1989. An inwardly directed electrogenic sodium-bicarbonate cotransport in leech glial cells. *J Physiol (Lond)* 411: 179-194.
- Deitmer JW, H-P. Schneider 1995. Voltage-dependent clamp of intracellular pH of identified leech glial cells. *J Physiol (Lond)* 485: 157-166.
- Deitmer JW, H-P. Schneider 1998. Acid–base transport across the leech giant glial cell membrane at low external bicarbonate concentrations. *J Physiol* 512.2: 459-469.
- Deitmer JW, Szatkowski M. 1990. Membrane potential dependence of intracellular pH regulation by identified glial cells in the leech central nervous system. *J Physiol* 421: 617-631.
- De Vries SH. 2001. Exocytosed protons feedback to suppress the Ca²⁺ current in mammalian cone photoreceptors. *Neuron* 32: 1107-1117.
- Dienel GA, Cruz NF. 2004. Nutrition during brain activation: Does cell-to-cell lactate shuttling contribute significantly to sweet and sour food for thought? *Neurochem Int* 45: 321-351.
- Dienel GA, Hertz L. 2005. Astrocytic contributions to bioenergetics of cerebral ischemia. *Glia* 50: 362-388.
- Dringen R, Gebhardt R, Hamprecht B. 1993. Glycogen in astrocytes: Possible function as lactate supply for neighboring cells. *Brain Res* 623: 208-214.
- Fei YJ, Romero MF, Krause M, Liu JC, Huang W, et al. 2000. A novel H(+)-coupled oligopeptide transporter (OPT3) from *Caenorhabditis elegans* with a predominant function as a H(+) channel and an exclusive expression in neurons. *J Biol Chem* 275: 9563-9571.
- Felipo V, Butterworth RF. 2002. Neurobiology of ammonia. *Prog Neurobiol* 67: 259-279.
- Fray AE, Boutelle M, Fillenz M. 1996. The mechanisms controlling physiologically stimulated changes in rat brain glucose and lactate: A microdialysis study. *J Physiol (Lond)* 496: 49-57.
- Giacobini E. 1962. A cytochemical study of the localization of carbonic anhydrase in the nervous system. *J Neurochem* 9: 169-177.
- Giffard RG, Papadopoulos MC, van Hooft AC, Xu L, Giuffrida R, et al. 2000. The electrogenic sodium bicarbonate cotransporter: Developmental expression in rat brain and possible role in acid vulnerability. *J Neurosci* 20: 1001-1008.

- Grichtenko JJ, Chesler M. 1994. Depolarization-induced alkalinization of astrocytes in gliotic hippocampal slices. *Neuroscience* 62: 1071-1078.
- Gu XQ, Yao H, Haddad GG. 2001. Increased neuronal excitability and seizures in the Na^+/H^+ exchanger null mutant mouse. *Am J Physiol Cell Physiol* 281: C496-C503.
- Halestrap AP, Price NT. 1999. The proton-linked monocarboxylate transporter (MCT) family: Structure, function and regulation. *Biochem J* 343: 281-299.
- Harris C, Fliegel L. 1999. Amiloride and the Na^+/H^+ exchanger protein: Mechanism and significance of inhibition of the Na^+/H^+ exchanger. *Int J Mol Med* 3: 315-321.
- Hertz L, Dienel GA. 2005. Lactate transport and transporters: General principles and functional roles in brain cells. *J Neurosci Res* 79: 11-18.
- Hertz L, Dringen R, Schousboe A, Robinson SR. 1999. Astrocytes: Glutamate producers for neurons. *J Neurosci Res* 57: 417-428.
- Heyer M, Müller-Berger S, Romero MF, Boron WF, Frömter E. 1999. Stoichiometry of the rat kidney $\text{Na}^+-\text{HCO}_3^-$ cotransporter expressed in *Xenopus laevis* oocytes. *Eur J Physiol* 438: 322-329.
- Hu Y, Wilson GS. 1997. A temporary local energy pool coupled to neuronal activity: Fluctuations of extracellular lactate levels in rat brain monitored with rapid-response enzyme-based sensor. *J Neurochem* 69: 1484-1490.
- Izumi Y, Benz AM, Katsuki H, Zorumski CF. 1997. Endogenous monocarboxylates sustain hippocampal synaptic function and morphological integrity during energy deprivation. *J Neurosci* 17: 9448-9457.
- Kaila K. 1994. Ionic basis of GABAA receptor channel function in the nervous system. *Prog Neurobiol* 42: 489-537.
- Li X, Alvarez B, Casey JR, Reithmeier RA, Fliegel L. 2002. *J Biol Chem* 277: 36085-36091.
- Ma E, Haddad GG. 1997. Expression and localization Na^+/H^+ exchanges in rat central nervous system. *Neuroscience* 79: 591-603.
- Magistretti PJ, Pellerin L, Rothman DL, Shulman RG. 1999. Energy on demand. *Science* 283: 496-497.
- Maren TH. 1967. Carbonic anhydrase: Chemistry, physiology, and inhibition. *Physiol Rev* 47: 595-781.
- Maren TH. 1979. Effect of varying CO_2 equilibria on rates of HCO_3^- formation in cerebrospinal fluid. *J Appl Physiol* 47: 471-477.
- Maren TH. 1988. The kinetics of HCO_3^- synthesis related to fluid secretion, pH control, and CO_2 elimination. *Annu Rev Physiol* 50: 695-717.
- Maus M, Marin P, Israel M, Glowinski J, Premont J. 1999. Pyruvate and lactate protect striatal neurons against *N*-methyl-D-aspartate-induced neurotoxicity. *Eur J Neurosci* 11: 3215-3224.
- McCleskey EW, Gold MS. 1999. Ion channels of nociception. *Annu Rev Physiol* 61: 835-856.
- Miesenböck G, De Angelis DA, Rothman JE. 1998. Visualizing secretion and synaptic transmission with pH-sensitive green fluorescent proteins. *Nature* 394: 192-195.
- Mulkey DK, Henderson 3rd, RA Ritucci NA, Putnam RW, Dean JB. 2004. Oxidative stress decreases pHi and Na^+/H^+ exchange and increases excitability of solitary complex neurons from rat brain slices. *Am J Physiol Cell Physiol* 286: C940-C951.
- Munsch T, Deitmer JW. 1994. Sodium-bicarbonate cotransport current in identified leech glial cells. *J Physiol* 474: 43-55.
- Nedergaard M, Dirnagl U. 2005. Role of glial cells in cerebral ischemia. *Glia* 50: 281-286.
- Nedergaard M, Goldman SA, Desai S, Pulsinelli WA. 1991. Acid-induced death in neurons and glia. *J Neurosci* 11: 2489-2497.
- Newman EA. 1991. Sodium-bicarbonate cotransport in retinal Müller (glial) cells of the salamander. *J Neurosci* 11: 3972-3983.
- Newman EA. 1994. A physiological measure of carbonic anhydrase in Muller cells. *Glia* 11: 291-299.
- Nicholson C. 2005. Factors governing diffusing molecular signals in brain extracellular space. *J Neural Transm* 112: 29-44.
- Nicholson C, Sykova E. 1998. Extracellular space structure revealed by diffusion analysis. *Trends Neurosci* 21: 207-215.
- Pappas CA, Ransom B. 1994. Depolarization-induced alkalinization (DIA) in rat hippocampal astrocytes. *J Neurophysiol* 72: 2816-2826.
- Pierre K, Pellerin L. 2005. Monocarboxylate transporters in the central nervous system: Distribution, regulation and function. *J Neurochem* 94: 1-14.
- Poitry-Yamate CL, Poitry S, Tscapopoulos M. 1995. Lactate released by Müller glial cells is metabolized by photoreceptors from mammalia retina. *J Neurosci* 15: 51795191.
- Putnam RW. 2001. Intracellular pH regulation of neurons in chemosensitive and nonchemosensitive areas of brain slices. *Respir Physiol* 129: 37-56.
- Putnam RW, Filosa JA, Ritucci NA. 2004. Cellular mechanisms involved in CO_2 and acid signaling in chemosensitive neurons. *Am J Physiol Cell Physiol* 287: C1493-C1526.
- Putney LK, Denker SP, Barber DL. 2002. The changing face of the Na^+/H^+ exchanger, NHE1: Structure, regulation, and cellular actions. *Annu Rev Pharmacol Toxicol* 42: 527-552. Review.
- Ritter M, Fuerst J, Woll E, Chwatal S, Gschwentner M, et al. 2001. Na^+/H^+ exchangers: Linking osmotic dysequilibrium to modified cell function. *Cell Physiol Biochem* 11: 1-18.
- Ritucci NA, Erlichman JS, Leiter JC, Putnam RW. 2005. Response of membrane potential and intracellular pH to

- hypercapnia in neurons and astrocytes from rat retrotrapezoid nucleus. *Am J Physiol Regul Integr Comp Physiol* 289: R851–R861.
- Romero MF, Hediger MA, Boulpaep EL, Boron WF. 1997. Expression cloning and characterization of a renal electrogenic $\text{Na}^+/\text{HCO}_3^-$ cotransporter. *Nature* 387: 409–413.
- Romero MF, Hediger MA, Boulpaep EL, Boron WF. 1997. Expression cloning and characterization of a renal electrogenic $\text{Na}^+/\text{HCO}_3^-$ cotransporter. *Nature* 387: 409–413.
- Roos A, Boron WF. 1981. Intracellular pH. *Physiol Rev* 61: 296–434.
- Rose CR, Deitmer JW. 1994. Evidence that glial cells modulate extracellular pH transients induced by neuronal activity in the leech central nervous system. *J Physiol* 481(Pt 1): 1–5.
- Rose CR, Deitmer JW. 1995a. Stimulus-evoked changes of extra- and intracellular pH in the leech central nervous system. I. Bicarbonate dependence. *J Neurophysiol* 73: 125–131.
- Rose CR, Deitmer JW. 1995b. Stimulus-evoked changes of extra- and intracellular pH in the leech central nervous system. II. Mechanisms and maintenance of pH homeostasis. *J Neurophysiol* 73: 132–140.
- Rose CR, Ransom BR. 1996. Mechanisms of H^+ and Na^+ changes induced by glutamate, kainate, and D -aspartate in rat hippocampal astrocytes. *J Neurosci* 16: 5393–5404.
- Sapirstein VS, Stocchi P, Gilbert JM. 1984. Properties and function of brain carbonic anhydrase. *Ann N Y Acad Sci* 429: 481–493.
- Schmitt BM, Berger UV, Douglas RM, Bevenssee MO, Hediger MA, et al. 2000. Na/HCO_3 cotransporters in rat brain: Expression in glia, neurons and choroid plexus. *J Neurosci* 20: 6839–6848.
- Schurr A, Miller JJ, Payn RS, Rigor BM. 1999. An increase in lactate output by brain tissue serves to meet the energy needs of glutamate-activated neurons. *J Neurosci* 19: 34–39.
- Schurr A, Payne RS, Miller JJ, Rigor BM. 1997. Brain lactate is an obligatory aerobic energy substrate for functional recovery after hypoxia: Further in vitro validation. *J Neurochem* 69: 423–426.
- Schurr A, Payne RS, Miller JJ, Tseng MT, Rigor BM. 2001. Blockade of lactate transport exacerbated delayed neuronal damage in a rat model of cerebral ischemia. *Brain Res* 895: 268–272.
- Schurr A, West CA, Rigor BM. 1988. Lactate-supported synaptic function in the rat hippocampal slice preparation. *Science* 240: 1326–1328.
- Schwiening CJ, Willoughby D. 2002. Depolarization-induced pH microdomains and their relationship to calcium transients in isolated snail neurons. *J Physiol* 538: 371–382.
- Shah GN, Ulmasov B, Waheed A, Becker T, Makani S, et al. 2005. Carbonic anhydrase IV and XIV knockout mice: Roles of the respective carbonic anhydases in buffering the extracellular space in brain. *Proc Natl Acad Sci USA* 102: 16771–16776.
- Shimokawa N, Dikic I, Sugama S, Koibuchi N. 2005. Molecular responses to acidosis of central chemosensitive neurons in brain. *Cell Signal* 17: 799–808.
- Shrode LD, Klein JD, O'Neill WC, Putnam RW. 1995. Shrinkage-induced activation of Na^+/H^+ exchange in primary rat astrocytes: Role of myosin light-chain kinase. *Am J Physiol* 269: C257–C266.
- Siesjö BK, Katsura K, Kristian T. 1996. Acidosis-related damage. *Adv Neurol* 71: 209–233.
- Suarez I, Bodega G, Fernandez B. 2002. Glutamine synthetase in brain: Effect of ammonia. *Neurochem Int* 41: 123–142.
- Svichar N, Chesler M. 2003. Surface carbonic anhydrase activity on astrocytes and neurons facilitate lactate transport. *Glia* 41: 415–419.
- Svichar N, Esquenazi S, Waheed A, Sly WS, Chesler M. 2006. Functional demonstration of surface carbonic anhydrase IV on rat astrocytes. *Glia* 53: 241–247.
- Thomas RC. 1988. Changes in the surface pH of voltage-clamped snail neurones apparently caused by H^+ fluxes through a channel. *J Physiol* 398: 313–327.
- Thomas RC, Coles JA, Deitmer JW. 1991. Homeostatic muffling. *Nature* 350: 564.
- Tong CK, Brion LP, Suarez C, Chesler M. 2000. Interstitial carbonic anhydrase (CA) activity in brain is attributable to membrane-bound CA type IV. *J Neurosci* 20: 8247–8253.
- Traynelis SF, Cull-Candy SG. 1990. Proton inhibition of N -methyl- D -aspartate receptors in cerebellar neurons. *Nature* 345: 347–350.
- Tsacopoulos M, Magistretti PJ. 1996. Metabolic coupling between glia and neurons. *J Neurosci* 16: 877–885.
- Tsien RY, Waggoner A. 1995. Fluorophores for confocal microscopy. *Photophysics and photochemistry. Handbook of biological confocal microscopy*, 2nd ed. editor. Pawley JB, New York: Plenum Press; pp. 267–279.
- Vega C, Martiel JL, Drouhault D, Burckhart MF, Coles JA. 2003. Uptake of locally applied deoxyglucose, glucose and lactate by axons and Schwann cells of rat vagus nerve. *J Physiol* 546: 551–564.
- Verkhatsky A, Steinhäuser C. 2000. Ion channels in glial cells. *Brain Res Brain Res Rev* 32: 380–412.
- Vince JW, Reithmeier RA. 1998. Carbonic anhydrase II binds to the carboxyl terminus of human band 3, the erythrocyte $\text{Cl}^-/\text{HCO}_3^-$ exchanger. *J Biol Chem* 273: 28430–28437.
- Vince JW, Reithmeier RA. 2000. Identification of the carbonic anhydrase II binding site in the $\text{Cl}^-/\text{HCO}_3^-$ anion exchanger AE1. *Biochemistry* 39: 5527–5533.
- Waldmann R, Bassilana F, de Weille J, Champigny G, Heurteaux C. 1997a. Molecular cloning of a non-inactivating

- proton-gated Na^+ channel specific for sensory neurons. *J Biol Chem* 272: 20975-20978.
- Waldmann R, Champigny G, Bassilana F, Heurteaux C, Lazdunski M. 1997b. A proton-gated cation channel involved in acid-sensing. *Nature* 386: 173-177.
- Waldmann R, Lazunski M. 1998. H^+ -gated cation channels: Neuronal acid sensors in the NaC/DEG family of ion channels. *Curr Opin Neurobiol* 8: 418-424.
- Walz W, Mukerji S. 1988 Lactate production and release in cultured astrocytes. *Neurosci Lett* 86: 296-300.
- Wemmie JA, Chen J, Askwith CC, Hruska-Hagermann AM, Price MP, et al. 2002. The acid-activated ion channel ASIC contributes to synaptic plasticity, learning and memory. *Neuron* 34: 463-477.
- Wender R, Brown AM, Fern R, Swanson RA, Farrell K, et al. 2000. Astrocytic glycogen influences axon function and survival during glucose deprivation in central white matter. *J Neurosci* 15: 6804-6810.
- Willoughby D, Schwenning CJ. 2002. Electrically evoked dendritic pH transients in rat cerebellar Purkinje cells. *J Physiol* 544: 487-499.
- Willoughby D, Thomas RC, Schwenning CJ. 2001. The effects of intracellular pH changes on resting cytosolic calcium in voltage-clamped snail neurons. *J Physiol* 530: 405-416.
- Xiong ZG, Zhu XM, Chu XP, Minami M, Hey J, et al. 2004. Neuroprotection in ischemia: Blocking calcium-permeable acid-sensing ion channels. *Cell* 118: 687-698.
- Yao H, Haddad GG. 2004. Calcium and pH homeostasis in neurons during hypoxia and ischemia. *Cell Calcium* 36: 247-255.
- Yao H, Ma E, Gu XQ, Haddad GG. 1999. Intracellular pH regulation of CA1 neurons in $\text{Na}^+(\text{+})\text{H}^+(\text{+})$ isoform 1 mutant mice. *J Clin Invest* 104: 637-645.
- Ye ZC, Wyeth MS, Baltan-Tekkok S, Ransom BR. 2003. Functional hemichannels in astrocytes: A novel mechanism of glutamate release. *J Neurosci* 23: 3588-3596.

5.2 Nitric Oxide in Regulation of Mitochondrial Function, Respiration, and Glycolysis

J. P. Bolaños · A. Almeida

1	Introduction	488
2	Biosynthesis and Metabolism of NO in the Brain	488
2.1	Formation of Peroxynitrite	488
2.2	Interactions of NO and Peroxynitrite with Sulfhydryl Groups	489
2.3	Peroxynitrite Targets Tyrosine	490
3	NO Ubiquitously Targets Mitochondrial Function	490
3.1	NO Regulates Mitochondrial Function in the Brain	492
3.2	Molecular Mechanisms Through Which NO Inhibits Mitochondrial Function	493
3.2.1	Reversible Inhibition of Cytochrome c Oxidase by NO	493
3.2.2	Inhibition of Mitochondrial Complex I by Peroxynitrite	493
3.2.3	Persistent Inhibition of Cytochrome c Oxidase by Peroxynitrite	494
3.2.4	Effects of NO and Peroxynitrite on the Krebs Cycle	495
3.3	NO-Mediated Inhibition of Cytochrome c Oxidase and Cell Signaling	495
3.4	NO, the Mitochondrial Permeability Pore and Mitochondrial Membrane Potential	496
3.5	NO Regulates Brain Cytochrome c Oxidase Activity In Vivo	497
3.6	Neurotoxic Versus Neuroprotective Roles for NO and Peroxynitrite	499
3.7	Role of Glial-Derived NO in Hypoxia/Ischemia	499
4	The Role of Astrocytes in Neuronal Function and Energy Metabolism	500
4.1	Role of Astrocytes in Glucose Homeostasis in the Brain	500
4.2	Main Glucose Carriers in Neural Cells	501
4.3	NO Upregulates Glucose Uptake in Astrocytes	502
4.4	Direct Stimulation of Glucose Uptake by NO	502
4.5	Regulation of the Pentosephosphate Pathway by NO and Peroxynitrite	504
4.5.1	Peroxynitrite Activates the Pentosephosphate Pathway in Astrocytes	504
4.5.2	Neuroprotection by Low Doses of Peroxynitrite	504
4.5.3	Glucose Protects Neurons Against Glutamate-Induced Neurotoxicity	505
4.6	NO and Glyceraldehyde-3-Phosphate Dehydrogenase	506
4.7	Activation of Glycolysis by NO Protects Astrocytes from Cell Death	506
4.7.1	NO Activates Glycolysis at the Level of 6-Phosphofructo-1-Kinase	508
4.7.2	Role of AMP-Activated Protein Kinase in NO-Mediated Glycolytic Activation	508
5	Concluding Remarks	508

1 Introduction

After the discovery of its biological activity, nitric oxide (NO) has been shown to play essential functions in the modulation of vascular tone (Ignarro et al., 1987; Palmer et al., 1987), neurotransmission (Garthwaite et al., 1988), and the immune system (Hibbs et al., 1988; Stuehr and Nathan, 1989). Formed by a family of NO synthases (NOS), NO mainly binds to soluble guanylyl cyclase and mitochondrial cytochrome *c* oxidase and thus mediates cellular signaling cascades. The binding of NO with soluble guanylyl cyclase allosterically activates the enzyme, which strongly increases cyclic GMP concentrations. In smooth muscle cells, endothelial-derived NO thus switches on cyclic GMP-activated protein kinase, which mediates the relaxation that leads to vasodilatation. The binding of NO with the α - α_3 binuclear center of cytochrome *c* oxidase rapidly decreases the affinity of the enzyme complex for O₂, hence inhibiting the mitochondrial electron flux and ATP synthesis.

The interactions with these targets suggest that NO plays critical pathophysiological roles that only recently are beginning to be understood. Here, we shall describe the biosynthesis and regulation of NO in the brain, as well as the cellular consequences derived from the interaction of NO with cytochrome *c* oxidase and other mitochondrial constituents. Finally, we shall study how these interactions modulate brain energy metabolism under normal and pathological situations.

2 Biosynthesis and Metabolism of NO in the Brain

NO is synthesized by the NO synthase (NOS)-catalyzed reaction from L-arginine, which is converted to L-citrulline (Palmer et al., 1988; Bredt and Snyder, 1990; Knowles and Moncada, 1994) (▶ [Figure 5.2-1](#)). Although it is most actively formed in the cerebellum (Bredt et al., 1990), all brain cells are able to synthesize NO (Murphy et al., 1993; Murphy and Grzybicki, 1996). In postsynaptic neurons, NO is formed after glutamate-mediated activation of its receptors, mainly the *N*-methyl-D-aspartate (NMDA) subtype. After this activation, Ca²⁺ is transiently increased in the cytosol and forms a complex with calmodulin that binds to and activates constitutive neuronal NOS (nNOS or NOS1) (Knowles and Moncada, 1994).

Glial cells (astrocytes, microglia, and oligodendrocytes) synthesize NO after the transcriptional expression of a calcium-independent inducible NOS isoform (iNOS or NOS2). In vivo factors that promote iNOS induction include sepsis and ischemia (▶ [Figure 5.2-1](#)). Experimentally, iNOS induction in glial cells can be promoted by incubation with the endotoxin lipopolysaccharide (LPS) or with certain cytokines, such as interferon- γ , tumor necrosis factor- α or interleukin-1 β , which act through their specific plasma membrane receptors (Murphy et al., 1993; Nomura and Kitamura, 1993; Murphy and Grzybicki, 1996; Merrill et al., 1997). nNOS activation synthesizes NO in pulses, whereas iNOS activity allows NO to be accumulated in a steady-state manner.

Endothelial cells from brain microvessels release NO after the interaction of an agonist (e.g., acetylcholine) with the plasma membrane receptor, which promotes Ca²⁺ entry and activation of the constitutive Ca²⁺-dependent endothelial NOS isoform (eNOS or NOS3) (Knowles and Moncada, 1994) (▶ [Figure 5.2-1](#)). The NO formed by eNOS activation diffuses to the neighboring smooth muscle cells and activates soluble guanylyl cyclase, thereby triggering the cyclic GMP-dependent muscle relaxation that leads to vasodilatation (Rees et al., 1989).

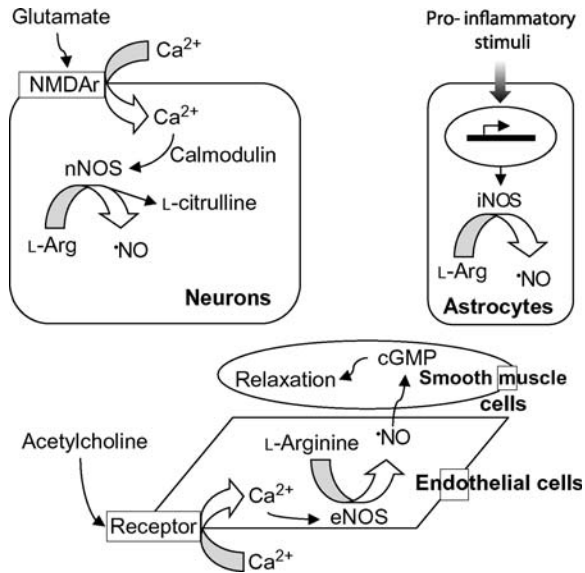
At least under experimental conditions, all brain cell types have been shown to be able to express all NOS isoforms. In fact, astrocytes were first reported to produce NO via constitutive nNOS activity (Agulló and García, 1992a, b; Galea et al., 1992; Simmons and Murphy, 1992). In addition, endothelial cells (Kilbourn and Belloni, 1990) and neurons (Minc-Golomb et al., 1996) can express iNOS after treatment with LPS plus cytokine.

2.1 Formation of Peroxynitrite

It is now well accepted that NO biosynthesis may be followed by a concomitant formation of peroxynitrite anion (ONOO⁻), which is formed by the rapid and spontaneous reaction of NO with superoxide (O₂⁻)

■ Figure 5.2-1

Nitric oxide (NO) synthesis in brain cells. In neurons, glutamate-mediated *N*-methyl-D-aspartate receptor (NMDAr) stimulation triggers intracellular Ca^{2+} accumulation. Ca^{2+} binds to calmodulin and activates neuronal nitric oxide synthase (nNOS) isoform, which forms NO and citrulline from arginine. In astrocytes, certain proinflammatory stimuli promote the transcriptional induction of iNOS (inducible isoform), which forms large amounts of NO in a Ca^{2+} -independent manner. A similar mechanism operates in microglial cells (not shown). In blood vessels, acetylcholine stimulates its receptor placed in the membrane of the endothelial cells, promoting intracellular Ca^{2+} accumulation and activation of endothelial NOS isoform (eNOS). eNOS-mediated NO is released to the neighboring smooth muscle cells, herein inducing cyclin GMP-mediated relaxation



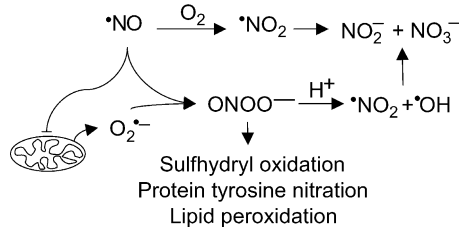
(Blough and Zafiriou, 1985) (▶ Figure 5.2-2). It is difficult to predict the precise intracellular conditions leading to peroxynitrite formation, although it appears clear that it is most favored under situations in which NO biosynthesis is associated with enhanced $\text{O}_2^{\bullet -}$ formation and/or impaired $\text{O}_2^{\bullet -}$ dismutation. Although peroxynitrite is only stable in alkaline solutions, it has a pK_a of ~ 6.8 and is thus rapidly protonated at physiological pH values to form peroxynitrous acid (ONOOH) (Beckman et al., 1990). The half-life of ONOOH is ~ 1 s, giving rise to chemical species with hydroxyl radical ($\bullet\text{OH}$)-like reactivity and nitrogen dioxide ($\bullet\text{NO}_2$). The latter two free radicals spontaneously form the more stable nitric acid at physiological pH (Beckman et al., 1990). The occurrence of such radical-mediated reactions confers peroxynitrite pro-oxidant properties that are thought to be responsible for the execution of the neurotoxic NO-mediated responses (Beckman et al., 1990; Lipton et al., 1993; Bonfoco et al., 1995; Bolaños et al., 1997). However, this is a controversial issue that has been recently revisited (Bolaños et al., 2004) (see ▶ Sect. 4.5.2).

2.2 Interactions of NO and Peroxynitrite with Sulfhydryl Groups

Sulfhydryl groups are crucial for many active sites and the native conformation of many enzymes. Accordingly, the oxidation of these groups has long been known to change protein function. Radi et al. (1991) were the first to report that peroxynitrite, but not peroxynitrous acid, targets sulfhydryl (cysteine and the thiol group of albumin) oxidation, yielding the corresponding disulfide products (▶ Figure 5.2-2). A number of subsequent studies confirmed that the redox status of intracellular reduced glutathione

■ **Figure 5.2-2**

Main pathways for nitric oxide (NO) degradation. After inhibition of cytochrome *c* oxidase, NO enhances superoxide ($O_2^{\bullet -}$) generation from mitochondria. Superoxide reacts with NO and forms peroxynitrite anion ($ONOO^-$). NO also reacts with O_2 forming nitrogen dioxide radical ($\bullet NO_2$), which rapidly decomposes to stable products nitrite (NO_2^-) and nitrate (NO_3^-). Peroxynitrite oxidizes sulfhydryls, nitrates tyrosine residues in proteins, and causes lipid peroxidation, but at physiological pH rapidly protonates and forms nitrogen dioxide radical and hydroxyl radical before decomposing to nitrite and nitrate



(GSH)—the major antioxidant thiol in mammalian cells—would be a critical factor in dictating cellular susceptibility to the actions of peroxynitrite (Bolaños et al., 1995, 1996).

Peroxynitrite also reacts with GSH to form S-nitrosoglutathione (GSNO) (Moro et al., 1994), and GSNO may act as a storage or transport form of NO possibly exerting physiological functions (Stamler et al., 1992; Moro et al., 1994, 1995; Jia et al., 1996) or cytoprotection (Clancy et al., 1994; Rauhala et al., 1998). However, the major source for GSNO is the reaction of GSH with NO (Stamler et al., 1992; Clancy et al., 1994; Schrammel et al., 2003). It appears that the relatively high carbon dioxide (CO_2) concentration occurring environmentally ($\sim 0.5\%$) and experimentally (5–10%) slows down GSNO formation from peroxynitrite (Mayer et al., 1998).

2.3 Peroxynitrite Targets Tyrosine

Tyrosine, an amino acid with regulatory functions in most proteins, can be nitrated by peroxynitrite to form 3-nitrotyrosine (Ischiropoulos et al., 1992) (🔗 [Figure 5.2-2](#)), a phenomenon that may regulate cellular functions. Low-molecular-weight metal complex-containing proteins, such as superoxide dismutase (SOD), favor such reactions (Beckman et al., 1992). In addition, peroxynitrite promotes the dimerization of tyrosine residues in proteins, forming 3,3'-dityrosine complexes (van der Vliet et al., 1996), whose pathophysiological role still requires clarification. Strikingly, CO_2 , which inhibits sulfhydryl nitrosation, favors 3-nitrotyrosination through the formation of a CO_2 -peroxynitrite adduct (Lymer et al., 1996; Uppu et al., 1996). Therefore, under most experimental and physiological conditions, where CO_2 is present at considerable concentrations, peroxynitrite would mainly oxidize sulfhydryls (to disulfides) and nitrate tyrosines (to 3-nitrotyrosines).

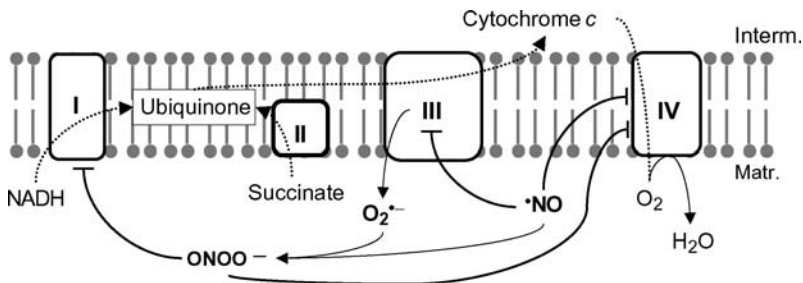
3 NO Ubiquitously Targets Mitochondrial Function

Just after the discovery of the biological activity of NO, intense efforts were made to identify the molecular targets of the free radical. Regardless of the well-known interaction of NO with soluble guanylyl cyclase, Hibbs' group demonstrated that NO interacted with mitochondrial function. Thus, Drapier and Hibbs (1988) reported that activated (LPS- and interferon- γ -treated) macrophages showed NO-mediated inhibition of malate- and succinate-dependent cellular O_2 consumption, suggesting inhibition at the level of the NADH-ubiquinone reductase (complex I) and succinate-ubiquinone reductase (complex II) of the

mitochondrial respiratory chain (Hibbs et al., 1988; Sung and Dietert, 1994). Similar mechanisms were found to be responsible for the NO-mediated macrophage killing of neighboring tumor cells (Stuehr and Nathan, 1989; Amber et al., 1991). Other groups later identified different mitochondrial targets of NO and peroxynitrite in a wide range of biological systems, including isolated heart mitochondria (Radi et al., 1994), intact astrocytes and neurons (Bolaños et al., 1994, 1995), and macrophages (Szabó and Salzman, 1995; Szabó et al., 1996) (🔗 [Figure 5.2-3](#)).

■ Figure 5.2-3

Major targets of the mitochondrial respiratory chain by nitric oxide (NO) and peroxynitrite. NO rapidly and reversibly inhibits cytochrome *c* oxidase (complex IV) by competing with O₂. This causes an increase in the reduced state of upstream cytochromes of the mitochondrial respiratory chain. In addition, when persistently present, NO interferes with ubiquinone–cytochrome *c* reductase (complex III) activity and increases the rate of O₂^{•−} generation by the mitochondrial respiratory chain. By reaction of O₂^{•−} with NO, the mitochondria can thus form peroxynitrite, which can persistently inhibit both NADH–ubiquinone reductase (complex I) and cytochrome *c* oxidase activities



In hepatocytes, the rate of O₂ consumption from citrate, malate, and succinate (Stadler et al., 1991; Phillips et al., 1996) and, in isolated liver mitochondria, from ascorbate plus tetramethylphenylenediamine (TMPD, an artificial substrate of cytochrome *c* oxidase) (Schweizer and Richter, 1994) is inhibited through an NO-dependent mechanism. In addition, endogenous NO production also inhibits mitochondrial (but not cytosolic) aconitase activity in hepatocytes (Stadler et al., 1991; Phillips et al., 1996) and decreases cellular ATP content (Kitade et al., 1996). Furthermore, hepatoma cell cytotoxicity by activated Kupffer cells is NO-mediated, as revealed by rhodamine 123 fluorescence studies (Kurose et al., 1995; Fukumura et al., 1996).

In fibroblasts, LPS/interferon- γ treatment inhibits malate- and succinate-driven cellular respiration in an L-arginine-dependent manner (Dijkmans and Billiau, 1991). In vascular smooth muscle cells, endogenously generated NO inhibits pyruvate-, succinate-, and ascorbate/TMPD-dependent rate of cellular respiration (Geng et al., 1992). Overall cell respiration rates are also inhibited by an NO-mediated mechanism in isolated perfused lung (Sakai et al., 1996), isolated alveolar type II cells (Miles et al., 1996), and Ehrlich ascites tumor cells (Inai, 1996).

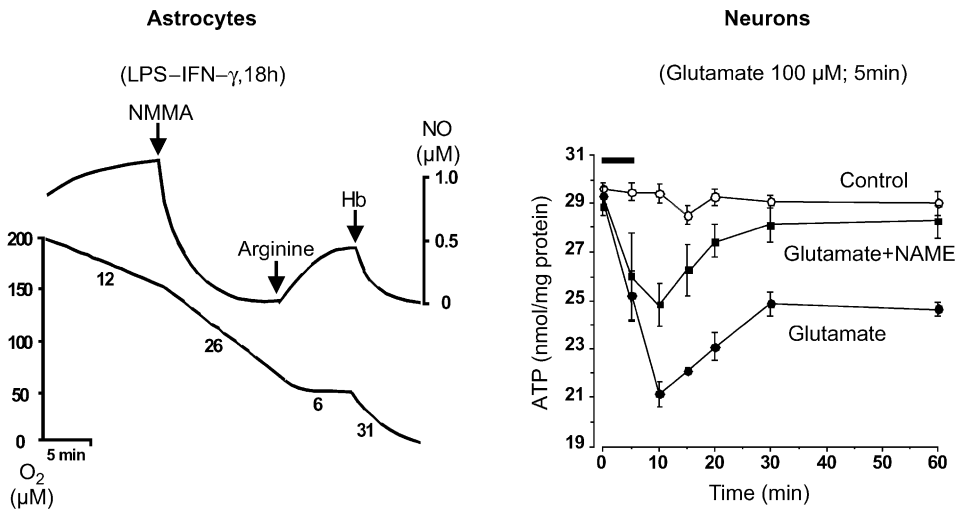
In skeletal muscle mitochondria, O₂ consumption is inhibited by an NO-mediated mechanism (Cleeter et al., 1994; Kobzik et al., 1995) through reversible inhibition of cytochrome *c* oxidase activity (Cleeter et al., 1994). In heart mitochondria, peroxynitrite inhibits glutamate- and succinate-dependent O₂ consumption (Radi et al., 1994), and succinate dehydrogenase, ATPase, and cytochrome *c* oxidase activities in intact mitochondria; NADH–ubiquinone reductase activity is only inhibited in sonicated mitochondria. Other studies performed with heart mitochondria also revealed that NO inhibits O₂ consumption (Borutaité and Brown, 1996) and reversibly inhibits cytochrome *c* oxidase and succinate dehydrogenase activities, whereas peroxynitrite inhibits succinate dehydrogenase and ATPase activities (Cassina and Radi, 1996).

3.1 NO Regulates Mitochondrial Function in the Brain

Most initial studies regarding the interaction of NO with mitochondria were performed in macrophages, hepatocytes, and heart and muscle mitochondria. However, the first demonstration that endogenous NO interacts with brain mitochondrial function was performed in cultured astrocytes (Bolaños et al., 1994). This work reported that iNOS-derived NO from activated astrocytes (by incubating these cells with LPS and interferon- γ for 18 h) inhibits (by $\sim 25\%$) cytochrome *c* oxidase activity. The remaining complexes of the mitochondrial respiratory chain are unaffected, unless the incubation period is extended to nearly 2 days, when succinate-cytochrome *c* reductase activity (i.e., transfer of electrons from succinate through cytochrome *c* by complexes II and III) is also inhibited (Bolaños et al., 1994). Since such effects were completely prevented by blocking iNOS activity with *N*-monomethyl-L-arginine methyl ester (L-NAME), it was concluded that the inhibition of cytochrome *c* oxidase activity was due to the endogenous formation of NO (► Figure 5.2-4).

■ Figure 5.2-4

Evidence for nitric oxide (NO)-mediated reversible inhibition of respiration and ATP synthesis in intact brain cells. Astrocytes (*left panel*) were activated to generate endogenous NO from iNOS-dependent activity, after incubation of cells with lipopolysaccharide (LPS) and interferon- γ (IFN- γ) for 18 h. NO traces reveal steady state NO formation that can be blocked by *N*-monomethyl-L-arginine (NMMA), reversed by excess arginine and blocked again by hemoglobin (Hb). Estimation of O₂ concentrations in the chamber shows inverse and reversible relationship between oxygen consumption rates (given in numbers under traces) and NO concentrations. Neurons (*right panel*) were activated by incubation with glutamate (100 μ M for 5 min; shown by the bar). After washout, neurons were further incubated in the absence of glutamate and ATP concentrations were measured. Coincubation of glutamate with *N*-monomethyl-L-arginine methyl ester (NAME) prevented by $\sim 50\%$ the transient decrease in ATP concentrations, and fully the long-term decrease in ATP concentrations. Reproduced with amendments and permission from Brown et al. (1995) and Almeida and Bolaños (2001)



The inhibition of mitochondrial function by NO in brain tissue was confirmed by the study of Mitrovic et al. (1994), who observed that succinate dehydrogenase activity is inhibited in oligodendrocytes incubated with an NO donor. The rate of O₂ consumption can also be decreased in synaptosomes following exposure to NO donors (Erecinska et al., 1995) or to authentic NO gas (Brown and Cooper, 1994; Schweizer and Richter, 1994), and in brain submitochondrial particles incubated with an NO donor or peroxynitrite (Lizasoain et al., 1996). Exogenous NO application to hippocampal cells rapidly and reversibly inhibits

neuronal energy production (Brorson et al., 1999). Taken together, these works strongly suggest that the mitochondria from neural cells represent an important physiological or pathophysiological target of NO.

3.2 Molecular Mechanisms Through Which NO Inhibits Mitochondrial Function

In intact astrocytes, endogenous NO reversibly modulates mitochondrial respiration (Brown, 1995) in a manner resembling the reversible inhibition of cytochrome *c* oxidase by exogenous NO in isolated muscle mitochondria (Cleeter et al., 1994) or in synaptosomes (Brown and Cooper, 1994). Thus, endogenous NO formation from iNOS activity in astrocytes inhibits cytochrome *c* oxidase activity both persistently (Bolaños et al., 1994) and reversibly (Brown, 1995). While the former effect would have neurotoxic effects (Bolaños et al., 1994, 1997), the latter would be responsible for the rapid regulation of cellular functions (Brown, 1995; Brown et al., 1995).

3.2.1 Reversible Inhibition of Cytochrome *c* Oxidase by NO

Not only does NO closely resemble O₂, but it also has one unpaired electron, which has enabled the observation, by electron paramagnetic resonance, that it forms adducts with cytochrome *c* oxidase. Consequently, for many years, NO has been used as a biochemical probe for the study of O₂-binding proteins, such as cytochrome *c* oxidase. Most such studies were performed on purified proteins from isolated heart mitochondria or heart submitochondrial particles (Keilin and Hartree, 1939; Wainio, 1955; Beinert et al., 1962; Kon, 1968, 1969; Kon and Kataoka, 1969; Blokzijl-Homan and Van Gelder, 1971; Wilson et al., 1976; Stevens et al., 1979a, b; Brudvig et al., 1980; Boelens et al., 1982, 1983, 1984; Lobrutto et al., 1984). These studies contributed valuably to clarifying the structure and catalytic activity of cytochrome *c* oxidase (Malmström, 1979) and also confirmed that NO reversibly binds to the Fe²⁺ center of cytochrome *a*₃ and to the Cu_B²⁺ center of cytochrome *c* oxidase (Stevens et al., 1979a, b; Brudvig et al., 1980). However, since the importance of NO in biology did not become apparent until 1987 (Palmer et al., 1987), the above studies never stressed the pathophysiological relevance of NO binding to cytochrome *c* oxidase. Brudvig et al. (1980) also reported that purified cytochrome *c* oxidase is able to catalyze both the oxidation and the reduction of NO, thus leading to NO breakdown, as later confirmed in isolated heart mitochondria (Borutaitė and Brown, 1996). Subsequent studies performed in several biological systems revealed that the interaction of NO with cytochrome *c* oxidase leads to reversible inhibition of O₂ consumption, as indicated above (Brown and Cooper, 1994; Cleeter et al., 1994; Brown et al., 1995; Cassina and Radi, 1996; Poderoso et al., 1996). The underlying mechanism involves the binding of NO with reduced (Fe²⁺) cytochrome *a*₃ (Stevens et al., 1979a, b; Brudvig et al., 1980; Cleeter et al., 1994; Cassina and Radi, 1996; Poderoso et al., 1996) to form a nitrosyl-heme complex through the donation of one electron to ferric (Fe³⁺) cytochrome *a*₃ (Radi, 1996), then apparently interacting with the Cu_B²⁺ center (Stevens et al., 1979a, b; Brudvig et al., 1980; Cleeter et al., 1994). These mechanisms explain the competition of NO with O₂ that results in the reversible inhibition of cytochrome *c* oxidase activity (Brown and Cooper, 1994; Cleeter et al., 1994; Brown et al., 1995) (► [Figure 5.2-4](#)). Such rapid and reversible modulation of cytochrome *c* oxidase activity suggests a physiological route through which NO can control cellular functions (Brown, 1995; Darley-Usmar et al., 1995; Takehara et al., 1995; Torres et al., 1995).

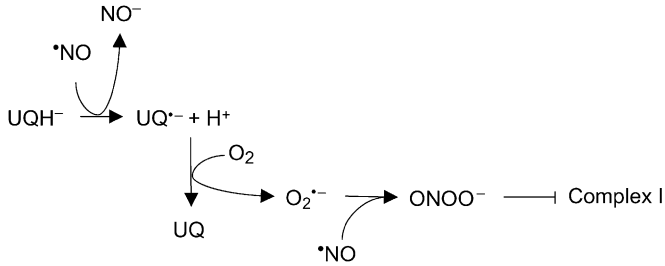
3.2.2 Inhibition of Mitochondrial Complex I by Peroxynitrite

Poderoso et al. (1996) reported that in heart mitochondria NO promotes the single-electron oxidation of ubiquinol to semiquinone, hence interfering with the transfer of the electron to cytochrome *b*. Since semiquinone is an effective source of O₂^{•-} in mitochondria, the presence of NO can enhance O₂^{•-}, with

which it reacts to form peroxynitrite. Consequently, persistent exposure of mitochondria to NO could produce peroxynitrite, which in turn might be responsible for the damage to complex I previously reported in macrophages and heart mitochondria (Clementi et al., 1998; Riobó et al., 2001) (🔗 [Figure 5.2-5](#)). In fact,

■ **Figure 5.2-5**

Persistent incubation of mitochondria with nitric oxide (NO) generates superoxide and peroxynitrite. NO promotes the one electron oxidation of ubiquinol (UQH⁻) to form semiquinone (UQ^{•-}). Semiquinone transfers one electron to O₂ and forms O₂^{•-} and ubiquinone (UQ). By the spontaneous reaction of NO with O₂^{•-}, mitochondria can thus form peroxynitrite, which can inhibit the activity of complex I



the early studies by Hibbs' group suggested that NO (or a related species) would attack the iron–sulfur clusters present in complexes I and II, and thus explained the inactivation of their activities (Drapier and Hibbs, 1988). However, the precise mechanism of complex I inactivation by NO or by peroxynitrite is not yet fully understood. In this sense, in isolated synaptosomes Cooper and Brown (1995) reported no correlation between electron paramagnetic resonance-detectable iron–sulfur–dinitrosyl complexes and O₂ consumption due to NO treatment, ruling out this mechanism, at least in these brain-derived preparations. However, it has also been suggested that peroxynitrite (either added directly or formed in situ from NO) could nitrate (and inactivate) tyrosine residues of the essential domains of complex I (Riobó et al., 2001). There is also evidence for the inactivation of complex I by NO-mediated S-nitrosylation of essential sulfhydryl groups of the protein (Clementi et al., 1998; Brown and Borutaite, 2004). Thus, Clementi et al. (1998) showed that NO-mediated inhibition of complex I could be reversed by GSH, suggesting an S-nitrosylation mechanism. Indeed, previous data obtained in isolated (heart and brain) mitochondria and intact neurons and astrocytes had shown that complex I activity was unaffected by peroxynitrite (Bolaños et al., 1994, 1995; Radi et al., 1994; Cassina and Radi, 1996) unless the intact nature of the mitochondria had previously been disrupted by sonication (Radi et al., 1994) or the cellular GSH status had previously been severely compromised (Barker et al., 1996). Together, these studies strongly support the notion that GSH protects mitochondria from NO and/or peroxynitrite-mediated complex I inhibition. Interestingly, in the substantia nigra of the brain of Parkinson's disease presymptomatic patients, GSH is severely depleted (Jenner et al., 1992). Moreover, complex I activity is compromised in the same brain region (Schapira et al., 1990a, b). Accordingly, it could be speculated that excessive NO production in the brain might contribute to the neuronal energy deficiency observed in this neurodegenerative disease (Hunot et al., 1996).

3.2.3 Persistent Inhibition of Cytochrome *c* Oxidase by Peroxynitrite

In neurons and in isolated heart mitochondria, exogenous peroxynitrite causes persistent inhibition of cytochrome *c* oxidase activity (Radi et al., 1994; Bolaños et al., 1995). Interestingly, the persistent inhibition of cytochrome *c* oxidase observed in astrocytes after iNOS induction can be prevented by SOD (Bolaños et al., 1994), suggesting the involvement of peroxynitrite in the effect. In fact, at the level of complex III activity peroxynitrite is formed by mitochondria only after prolonged NO exposure, as indicated in the (🔗 [Sect. 3.2.2](#)) (Riobó et al., 2001).

The mechanism responsible for such inhibition appears to involve direct disruption of Cu_A²⁺ (Sharpe and Cooper, 1998), and it is sensitive to the GSH redox status of the biological system used. Thus,

peroxynitrite peroxidates lipids (Radi et al., 1991), including cardiolipin, an inner mitochondrial membrane lipid susceptible to free radical peroxidation that is specifically required for maximal cytochrome *c* oxidase catalytic activity (Soussi et al., 1990). In support of this, Trolox, a vitamin E analog and an inhibitor of lipid peroxidation, protects cytochrome *c* oxidase from endogenous NO-mediated damage in astrocytes (Heales et al., 1994). Furthermore, cytochrome *c* oxidase activity in the heart is in the mitochondrial complex, which is least vulnerable to peroxynitrite (Radi et al., 1994; Cassina and Radi, 1996). Since the mitochondrial membrane cardiolipin concentration in heart is very high (White, 1973), it is conceivable that cardiolipin could be a primary target of peroxynitrite-mediated cytochrome *c* oxidase damage in the brain. Regardless of whether it is direct or indirect, the persistent inhibition of cytochrome *c* oxidase by peroxynitrite in the brain might have important pathophysiological consequences.

In mitochondria isolated from brain or heart, peroxynitrite rapidly triggers a loss of succinate–cytochrome *c* reductase (complex II–III)-specific activity (Radi et al., 1994; Bolaños et al., 1995). Intriguingly, the respiratory control ratio, using succinate as substrate, is unaffected by peroxynitrite treatment to isolated brain mitochondria under similar circumstances (Riobó et al., 2001). No explanation is available for this discrepancy, but it is possible that the extent of complex II–III inhibition by peroxynitrite would be below the threshold of mitochondrial electron transport impairment.

3.2.4 Effects of NO and Peroxynitrite on the Krebs Cycle

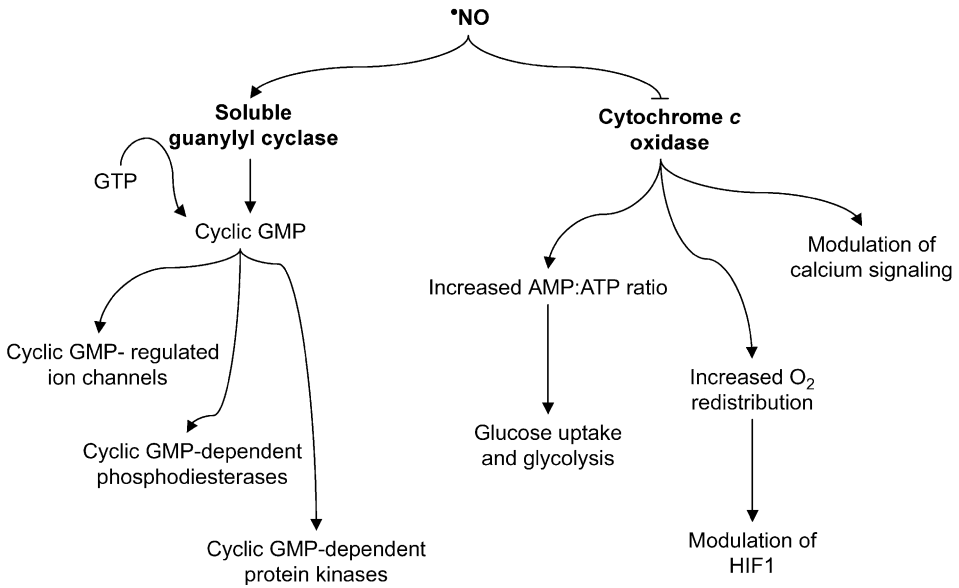
In purified preparations, peroxynitrite, but not NO itself, inhibits aconitase activity, apparently through inactivation of the iron–sulfur cluster prosthetic group (Castro et al., 1994; Hausladen and Fridovich, 1994). In intact microglial cells, α -ketoglutarate dehydrogenase activity is impaired by NO formed endogenously from iNOS activity (Park et al., 1999). It remains to be established whether the inhibition of aconitase and α -ketoglutarate dehydrogenase activities reaches the threshold of Krebs cycle impairment. If so, these observations add support to the notion that NO metabolism may be an important target to combat the brain energy deficiency associated with neurodegenerative diseases.

3.3 NO-Mediated Inhibition of Cytochrome *c* Oxidase and Cell Signaling

At the cellular level, the interaction of NO with cytochrome *c* oxidase has important consequences for the regulation of cell signaling pathways (Figure 5.2-6). For instance, the transient decrease in ATP biosynthesis that follows inhibition of cytochrome *c* oxidase by NO is accompanied by a concomitant increase in AMP concentrations (Cidad et al., 2004), which has been shown to trigger the activation of AMP-activated protein kinase (AMPK) (Almeida et al., 2004). In view of the relevance of these findings for glucose metabolism, this issue will be discussed later (see Sect. 4.7). In addition, in intact cells endogenous NO promotes the reduction of cytochrome a_3 of cytochrome *c* oxidase at O_2 concentrations compatible with those found physiologically in body tissues (Palacios-Callender et al., 2004). Moreover, the NO-dependent reduction of cytochrome a_3 occurs at O_2 concentrations that are higher than those impairing the rate of O_2 consumption. These observations suggest that endogenous NO allows cells to continue consuming oxygen even at very low O_2 concentrations. Furthermore, the increased degree of the reduction status of mitochondrial electron transport chain cytochromes favors the single-electron donation to molecular oxygen, hence releasing $O_2^{\bullet -}$, which can subsequently trigger the activation of transcription factors such as nuclear factor κB (Palacios-Callender et al., 2004). During hypoxia, cytochrome *c* oxidase inhibition by NO is stronger, and hence O_2 can be redistributed to other nonrespiratory oxygen-dependent targets (Trimmer et al., 2001), such as prolyl hydroxylases (Hagen et al., 2003). In the presence of O_2 , prolyl hydroxylases are needed to destabilize hypoxia-inducible factor (HIF) 1 alpha (HIF1- α), a transcription factor that, when stabilized, upregulates genes associated with glycolysis. Thus, during the NO-mediated inhibition of cytochrome *c* oxidase in hypoxia, prolyl hydroxylases do not register hypoxia, and hence HIF1- α continues to be destabilized (Hagen et al., 2003). Accordingly, NO downregulates hypoxia-dependent HIF1- α transcription factor activation in response to hypoxia. Finally, NO-mediated interference with the

■ Figure 5.2-6

Nitric oxide (NO) signaling pathways. NO activates soluble guanylyl cyclase to form cyclic GMP. Cyclic GMP thus mediates a number of cell signaling cascades, such as regulation of ion channels, cyclic GMP-dependent phosphodiesterases, or cyclic GMP-dependent protein kinases. On the other hand, NO reversibly inhibits cytochrome *c* oxidase in a competitive way with O₂. This interaction can be amplified by, at least, three ways. Thus, the inhibition of ATP synthesis transiently increases the AMP:ATP ratio, which is the trigger of AMP-activated protein kinase (AMPK) stimulation, leading to several effects, including activation of glucose uptake and glycolysis. At low O₂ concentrations, endogenous NO allows O₂ redistribution to other O₂ nonrespiratory targets, such as prolyl hydroxylases. These do not register hypoxia and hence continue degrading hypoxia inducible factor 1- α (HIF1). Finally, mitochondrial calcium signaling is modulated by the energetic effect of NO-mediated inhibition of respiration



mitochondrial respiratory chain induces changes in mitochondrial Ca²⁺ flux (Brorson and Zhang, 1997; Brorson et al., 1997), which induces the activation of endoplasmic reticulum stress-regulated transcription factor (Xu et al., 2004). Together, these observations strongly support the notion that the interaction of NO with cytochrome *c* oxidase is a molecular switch involved in the regulation of cell signaling pathways (▶ Figure 5.2-6).

Recently, a novel biogenic function for NO in mitochondria has been shown (Nisoli et al., 2003). In this sense, endogenous NO triggers the biogenesis of mitochondria from a variety of cell types through a mechanism that involves cyclic GMP and peroxisome proliferator-activated receptor- γ coactivator (Nisoli et al., 2003). Such an increase in mitochondrial proliferation affords functional mitochondria (Nisoli et al., 2004), and confirms and expands previous observations indicating the effect of endogenous NO on mitochondrial maturation (Almeida et al., 1999). These results provide novel insight into the interaction of NO with mitochondria (Brown, 2003).

3.4 NO, the Mitochondrial Permeability Pore and Mitochondrial Membrane Potential

NO and peroxynitrite promote permeability transition pore (PTP) activity (Packer and Murphy, 1994, 1995; Schweizer and Richter, 1996). Among other factors, a loss of mitochondrial membrane potential

($\Delta\psi_m$) triggers PTP opening (Tatton and Olanow, 1999). It can thus be speculated that the inhibition of the mitochondrial respiratory chain by NO or the reported increased proton leak due to peroxynitrite (Brookes et al., 1998) may contribute to PTP opening. In agreement with this, endogenous (Almeida and Bolaños, 2001) NO causes a loss in $\Delta\psi_m$ in intact neurons exposed to glutamate. The enhancements in mitochondrial Ca^{2+} that follow glutamate receptor activation (Wang et al., 1994; White and Reynolds, 1996; Keelan et al., 1999) reinforce $\Delta\psi_m$ loss and PTP opening. PTP opening promotes the exchange of solutes and small proteins between the mitochondrial matrix and the cytosol (Tatton and Olanow, 1999) and these phenomena lead to mitochondrial swelling, rupture of the outer mitochondrial membrane, and release of proapoptotic factors such as cytochrome *c* (Tatton and Olanow, 1999).

Mitochondria from different cell types and tissues (e.g., brain versus liver) respond differentially to Ca^{2+} in modulating PTP (Kristian et al., 2000). Interestingly, identical concentrations of NO can trigger opposite effects on $\Delta\psi_m$, depending on the cell type. Thus, $\Delta\psi_m$ increases in astrocytes (Almeida et al., 2001) and macrophages (Beltrán et al., 2000) after NO treatment. In contrast, $\Delta\psi_m$ decreases in neurons incubated with identical amounts of NO (Almeida et al., 2001) (🔗 [Figure 5.2-7](#)).

The molecular mechanism responsible for the maintenance (Takuma et al., 2001) of or increase (Beltrán et al., 2000; Almeida et al., 2001) in $\Delta\psi_m$ observed in certain cell types is controversial. NO could exert its antiapoptotic effect in astrocytes by blocking permeability transition through a cyclic GMP-dependent mechanism (Takuma et al., 2001). However, other authors have suggested that this would be a cyclic GMP-independent phenomenon and an indirect consequence of the inhibition of the mitochondrial respiratory chain (Beltrán et al., 2000; Almeida et al., 2001). Thus, the hyperpolarizing and antiapoptotic effects of NO are abolished by inhibiting glycolysis in astrocytes. Accordingly, it was suggested that glycolytically generated ATP would compensate for the loss of $\Delta\psi_m$ by driving ATPase activity in the reverse direction (Almeida et al., 2001), as previously reported (Dimroth et al., 2000). Other cell types such as eosinophils, which contain small numbers of mitochondria, generate their $\Delta\psi_m$ through the hydrolysis of ATP by F_1F_0 -ATPase (Peachman et al., 2001).

Whatever the mechanism responsible for increased $\Delta\psi_m$, NO triggers dual effects on cell viability. Cells lacking the ability to switch on glycolysis (such as neurons) undergo $\Delta\psi_m$ loss and apoptotic cell death soon after mitochondrial respiratory chain inhibition by NO. In contrast, cells having the ability to switch on glycolysis upon NO-mediated mitochondrial inhibition (astrocytes or macrophages) maintain sufficient ATP to generate $\Delta\psi_m$ and survive (Almeida et al., 2001) (🔗 [Figure 5.2-7](#)).

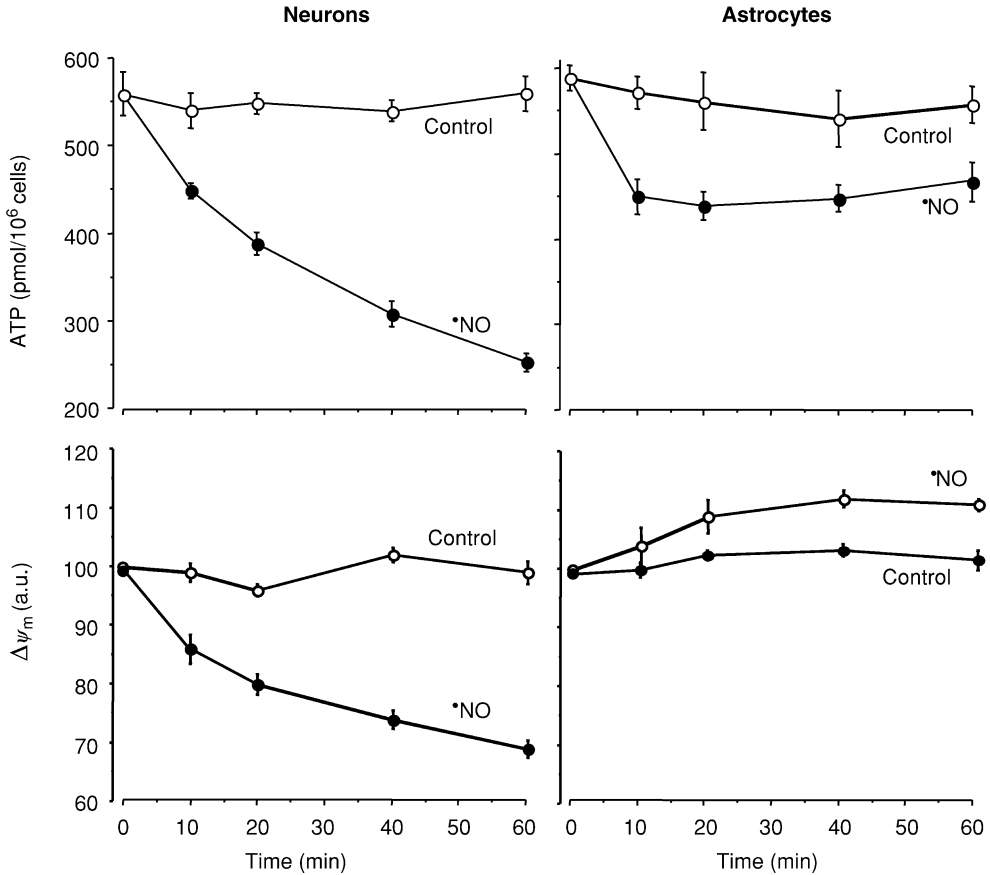
3.5 NO Regulates Brain Cytochrome *c* Oxidase Activity In Vivo

Cytochrome *c* oxidase activity is considered to be an endogenous metabolic marker for neuronal activity (Wong-Riley, 1989). In the central nervous system, cytochrome *c* oxidase colocalizes with nNOS and the NMDA receptor (Zhang and Wong-Riley, 1996), suggesting that the endogenous formation of NO could regulate this mitochondrial complex. To demonstrate this, cortical neurons were incubated with 100 μM glutamate, compatible with the estimated amino acid levels within the synaptic cleft, which range from 2 to 1,000 μM (Meldrum, 2000), for a 5-min pulse. This protocol allowed a rapid and transient triggering of the NMDA receptor that was accompanied by a rapid and reversible inhibition of mitochondrial ATP synthesis (Almeida and Bolaños, 2001). A large proportion of this inhibition was prevented by NOS inhibitors, suggesting the involvement of endogenous NO from nNOS activity. Despite this, no direct evidence demonstrating that endogenous NO reversibly inhibits cytochrome *c* oxidase activity in intact neurons has been reported so far, even though the above experiments (Almeida and Bolaños, 2001) strongly support this notion.

Cytochrome *c* oxidase inhibition in vivo can be estimated by assessing the reduction status of mitochondrial cytochromes. Using this approach, it has recently been reported that the reduced state of cytochrome *c* oxidase in the brain tissue of adult rats subjected to transient ischemia is not prevented by exogenous administration of NOS inhibitors (De Visscher et al., 2002). Although this argues against a possible role for reversible cytochrome *c* oxidase inhibition by NO in vivo, these results have been questioned on the basis that it is not clear whether, in the adult brain, the NOS inhibitors used crossed

■ Figure 5.2-7

Nitric oxide (NO) maintains mitochondrial membrane potential in astrocytes, but depolarizes neuronal mitochondria. NO was persistently added to either neurons or astrocytes at concentrations causing full blockade of mitochondrial respiration (not shown). ATP concentrations progressively decreased in neurons (*left upper panel*) and only transiently in astrocytes (*right upper panel*). In neurons, mitochondrial membrane potential ($\Delta\psi_m$) was decreased (*left bottom panel*), whereas $\Delta\psi_m$ in astrocytes was maintained or slightly increased (*right bottom panel*). The increased glycolytic rate observed in astrocytes treated with NO (not shown) suggested that glycolytically generated ATP contributed to maintain ATP concentrations and $\Delta\psi_m$. Reproduced with amendments and permission from Almeida et al. (2001)



the blood–brain barrier (Cooper, 2003). Accordingly, the role for NO in reversibly modulating brain cytochrome *c* oxidase activity *in vivo* remains to be fully elucidated.

As mentioned above, NO-mediated modulation of cytochrome *c* oxidase occurs in competition with O₂. Under most experimental conditions, cell and tissue preparations are exposed to atmospheric O₂ concentrations (~175–200 μ M), whereas *in vivo* they are subjected to O₂ concentrations that are one order of magnitude lower (~10–30 μ M). This implies that the NO concentrations needed to block cytochrome *c* oxidase activity *in vivo* are much lower than those needed to affect the activity of the enzyme in the test tube. In this context, recent experiments have reported that NO (added to brain slices at concentrations similar to those produced by nNOS activity) activates soluble guanylyl cyclase but does not inhibit cytochrome *c* oxidase when O₂ concentrations are ~30 μ M (Bellamy et al., 2002). However, lowering O₂

concentrations to $\sim 5 \mu\text{M}$ increased the sensitivity of cytochrome *c* oxidase to NO (Bellamy et al., 2002). These results suggest that neuronal energy metabolism is compromised under pathological conditions associated with reduced blood supply to the brain, such as stroke.

3.6 Neurotoxic Versus Neuroprotective Roles for NO and Peroxynitrite

Soon after the observation that NO plays a role in neurotransmission (Garthwaite et al., 1988; Knowles et al., 1989) it was reported that NO accounts for the neurotoxicity of excess NMDA receptor activation (Dawson et al., 1991, 1993; Dawson and Dawson, 1996). However, other authors failed to reproduce such an effect (Keynes et al., 2004), although the considerable differences in the systems and protocols used might explain such discrepancies. For instance, Dawson et al. (1993) pointed out that the age of the neuronal cultures used is an essential issue, since only old cultures (i.e., 14–21 days *in vitro*) showing prominent NMDA receptor expression are vulnerable to NO-dependent neurotoxicity. Keynes et al. (2004) recently reported that the neurons of hippocampal organotypic slices fully expressing NMDA receptors are resistant to NMDA receptor-mediated nNOS activation. Furthermore, these authors found that exogenous NO is nontoxic to neurons in this experimental system, at least up to concentrations of $4.5 \mu\text{M}$. It should be mentioned that organotypic cultures of brain sections conserve intact glial cells, such as astrocytes. Since astrocytes have a robust antioxidant system (Dringen, 2000), it is possible that these cells could help neurons to scavenge part of the added NO. This would lead to an overestimation of the concentration of NO that is neurotoxic. In fact, similar concentration values of exogenous NO ($5 \mu\text{M}$) strongly inhibit mitochondrial ATP synthesis in hippocampal neurons in cultures without astrocytes (Brorson et al., 1999). These results suggest that the discrepancy among the results of the different groups regarding the susceptibility of neurons to NO could be due to the experimental protocol used.

Different cell types respond differentially to NO. Glial cells are more resistant than neurons to excess NO (Mitrovic et al., 1994; Bolaños et al., 1995). Possible factors dictating this differential susceptibility are GSH concentrations and the specific activity of antioxidant enzymes such as SOD, catalase, or glutathione peroxidase (Sagara et al., 1993; Makar et al., 1994; Bolaños et al., 1995; Dringen, 2000). GSH decreases in neurons, but not in astrocytes, when these cells are incubated with peroxynitrite (Bolaños et al., 1995) or with H_2O_2 (Dringen et al., 1999). Toxicity in astrocytes is only found when these cells are depleted of GSH before incubation with peroxynitrite (Barker et al., 1996). Together, these results strongly suggest that the cellular GSH status is a contributing factor that dictates the differential responses of neural cells to NO-mediated toxicity (Bolaños et al., 1996).

3.7 Role of Glial-Derived NO in Hypoxia/Ischemia

Since the synthesis of NO by glial cells requires the transcriptional induction of iNOS, these cells can only form NO after a lag ($\sim 2\text{--}4$ h) period, and not instantaneously, as in the case of neurons. In addition, to activate the transcriptional machinery that leads to new iNOS protein synthesis, the activating factors must reach the extracellular space. In fact, proinflammatory situations associated with the loss of an intact blood–brain barrier, such as multiple sclerosis or brain sepsis, stimulate glial cells to produce NO in an iNOS-dependent manner (Murphy and Grzybicki, 1996). Other neurological disorders, such as Alzheimer's disease, are also associated with glial NO production (Yankner, 1996).

Brain ischemia is one of the most generally accepted pathogenic conditions associated with iNOS-dependent glial NO formation. Thus, episodes of ischemia followed by reoxygenation promote the transcriptional induction of iNOS in astrocytes by interleukin-1 (Maeda et al., 1994). There is considerable evidence suggesting that such astrocyte-derived NO plays a neurotoxic role in ischemia/reoxygenation *in vivo* (Faraci and Brian, 1994; Gehrmann et al., 1995; Wood, 1995; Iadecola, 1997; Bidmon et al., 1998; Bolaños and Almeida, 1999). The intracellular constituents of necrotic neurons, which are released after an ischemic episode, can also promote glial activation and NO production. Such glial-derived NO may in turn be deleterious to still alive neighboring neurons. The mechanism of this neurotoxicity possibly involves

mitochondrial respiratory chain inhibition (Bolaños et al., 1996; Stewart et al., 1998). It should be noticed that in addition to excess NO, cytoprotective factors can also be transferred from glia to neurons (Bolaños et al., 1996; Dringen, 2000). Accordingly, neuronal damage is apparent only when the defense mechanisms of the brain are seriously compromised.

Increasing evidence strongly suggests that endothelial-derived NO (from eNOS activity), in contrast to glial-derived NO, plays an important neuroprotective role during ischemia (Gajkowska and Mossakowski, 1997; Stagliano et al., 1997). Thus, when there is a lack of oxygen that is associated with transient interruptions of the blood supply to the brain, cytosolic Ca^{2+} is accumulated and this activates eNOS in endothelial cells (reviewed in Bolaños and Almeida, 1999). Consequently, eNOS-derived NO would produce vasorelaxation, which improves the blood supply to the infarcted area, hence contributing to preventing neuronal damage.

4 The Role of Astrocytes in Neuronal Function and Energy Metabolism

The brain is a vulnerable organ that depends on an efficient and continuous supply of oxygen and energy substrates from the blood. A single transient lapse in that supply rapidly leads to unconsciousness and, after only a few minutes, to irreversible alterations that may cause neuronal death (Clarke and Sokoloff, 1994). Neurotransmission is one of highest energy-demanding processes in mammals, and hence a continuous supply of substrates is necessary to keep the axonal membrane potential active (Hawkins, 1985). Astrocytes help neurons in this function. In fact, these glial cells surround capillary blood vessels (Morgello et al., 1995; Kacem et al., 1998) and synaptic spaces (Blumcke et al., 1995; Grosche et al., 1999). This strategic localization allows astrocytes to remove synaptic neurotransmitters (Mennerick and Zorumski, 1994) and to shuttle metabolic substrates between intracerebral vessels and neurons (Magistretti et al., 1986; Tsacopoulos and Magistretti, 1996).

The blood–brain barrier restricts the range of available ready-to-use metabolic substrates by neural cells to those having an efficient carrier system. In the mammalian brain, glucose is the most important metabolic substrate (Clarke and Sokoloff, 1994). Indeed, the endothelial cells that form the blood–brain barrier express a suitable glucose transport system, i.e., the energy-independent glucose transporter Glut1. Glut1 has a K_m for glucose that is sufficiently high to prevent any failure in the brain supply of this substrate, at least under normoglycemic conditions (Partridge et al., 1990; Maher et al., 1993). However, several pathological situations, such as stroke, are associated with reductions in the blood supply to the brain. In these cases, activation of glucose transport systems having lower K_m values for glucose, such as Glut3, becomes necessary to prevent brain energy deficiency. In either case, astrocytes are the first neural cell type having the ability to take up glucose from the blood for transfer to neurons. The regulation of glucose transport by NO in astrocytes is therefore very relevant and will receive further attention in this chapter.

4.1 Role of Astrocytes in Glucose Homeostasis in the Brain

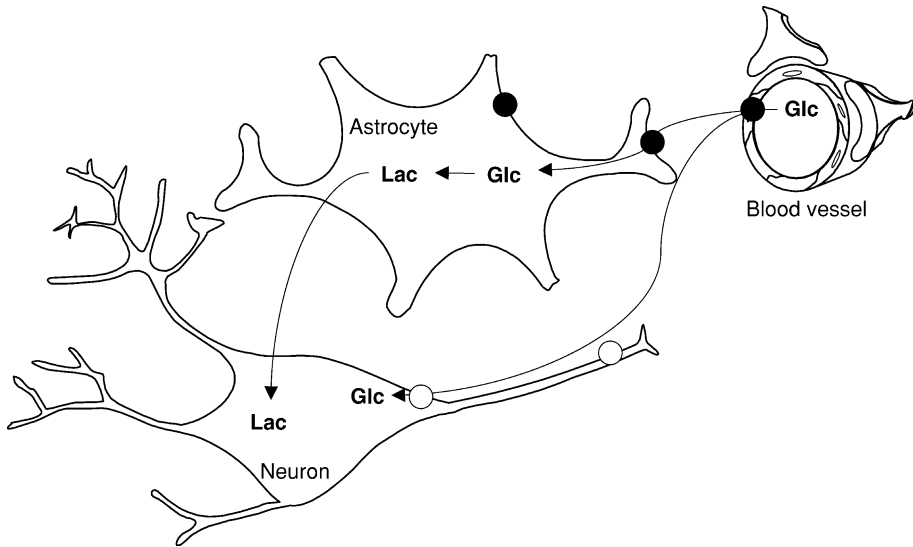
Regardless of its energetic potential, glucose is the main precursor for fatty acids, cholesterol, neurotransmitters, amino acids, glycerol-3-phosphate and, of glycogen biosyntheses in astrocytes within the brain (Cataldo and Broadwell, 1986). An important fraction of glucose entering the brain is oxidized through the pentosephosphate pathway, which is the main cellular source of NADPH and ribose-5-phosphate. During long-term starvation, such as that occurring during the suckling period, the brain can adapt itself to using alternative substrates such as lactate or ketone bodies (Medina et al., 1980, 1990; Vicario et al., 1991; Almeida et al., 1992; Taberner et al., 1993; Pellerin, 2003).

Astrocytes play critical roles in brain energy homeostasis, in part because they are strategically localized in the brain network (Andriezen, 1893). They channel metabolic substrates between the blood and neurons; through their end-feet processes, astrocytes surround blood vessels (Morgello et al., 1995; Kacem et al., 1998), and can readily take up the glucose arriving from the blood through endothelial cells. Moreover, the astrocytic processes that surround synapses (Blumcke et al., 1995; Grosche et al., 1999) contribute to

modulating energy metabolism as a function of neuronal synaptic activity. After being taken up by astrocytes, glucose is rapidly and efficiently distributed, in the form of glucose-6-phosphate, to the most inaccessible zones of the brain through gap junctions (Taberero et al., 1996; Giaume et al., 1997) (▶ [Figure 5.2-8](#)).

■ **Figure 5.2-8**

Main glucose carriers in brain cells. *Glut1* glucose (gluc) carriers are mainly expressed in endothelial cells and astrocytes (filled circles), whereas *Glut3* glucose carriers (empty circles) are expressed in neurons. Astrocytes take up glucose from the blood and can convert it into lactate, which can be released and taken up (lactate transporters are not shown) by neighboring neurons. Expression of a high-affinity-like *Glut3* transporter in neurons permits utilization of extracellular glucose under situations in which blood glucose supply is low (i.e., stroke)



Astrocytes are the only neural cell type having a reservoir of glycogen (Wiesinger et al., 1997). This allows a transient supply of energy substrate during ischemia and during physiologic neurotransmission. In fact, the conversion of glycogen to glucose-6-phosphate is stimulated by synaptic activity (Pellerin and Magistretti, 1994). Glucose-6-phosphate can be converted to lactate (Dringen and Hamprecht, 1992; Dringen et al., 1993) and further released to the interstitial space to be taken up by surrounding neurons, which use lactate as an alternative energy substrate (Medina et al., 1990). In fact, lactate preserves neuronal activity during hypoglycemic episodes and is neuroprotective under certain pathophysiological conditions (Schurr et al., 1988, 1997) (reviewed in Pellerin, 2003). However, neuroprotection can only be maintained transiently because the ability of astrocytes to store glycogen is very limited (Dringen and Hamprecht, 1992; Dringen et al., 1993). Thus, astrocytes must express suitable systems for taking up glucose efficiently enough to support neuronal energy metabolism during such stressful conditions (▶ [Figure 5.2-8](#)).

4.2 Main Glucose Carriers in Neural Cells

In mammals, glucose is taken up through the sodium-dependent (SGLT) and the sodium-independent (Glut) families of glucose transporters. The former group comprises at least six members (SGLT1–6) that are expressed at the apical membrane of kidney and intestinal epithelial cells, but not in brain cells. The

SGLT system takes up glucose as a function of the glucose concentration gradient and therefore indirectly requires energy in the form of ATP (Wood and Trayhurn, 2003). The second family (Glut) is expressed in all cells, including neural cells, which take up glucose through a facilitative, energy-independent process enabled by the glucose concentration gradient (Gorovits and Charron, 2003). Up to 14 Glut members have been identified in humans (Mueckler et al., 1985; Birnbaum et al., 1986; Joost and Thorens, 2001; Wu and Freeze, 2002), but in the brain the major glucose transporters expressed are Glut1 and Glut3, although Glut4, Glut5, Glut2, and Glut8 are also expressed to a lesser extent. All brain cell types appear to express Glut1 (Maher, 1995), although the expression of Glut1 in cultured neurons is believed to be an adaptive consequence to in vitro conditions (Maher et al., 1994) (🔗 [Figure 5.2-8](#)). The expression of Glut3 is confined to neurons (Nagamatsu et al., 1993; Choeiri et al., 2002) and, in light of the kinetic parameters, it appears that Glut3 transporter activity is responsible for the high affinity for glucose shown by cerebellar neurons (Gould et al., 1991; Pessin and Bell, 1992; Maher et al., 1994). This observation has led to the notion that Glut3 activity in neurons would confer protection to these cells against hypoglycemic episodes (Maher et al., 1994). Furthermore, brain Glut4 immunostaining colocalizes with Glut3 in neurons, suggesting that these transporters might cooperate during a deficiency in the supply of glucose (Apelt et al., 1999).

4.3 NO Upregulates Glucose Uptake in Astrocytes

Cell activation in vitro by incubation with LPS and or cytokines stimulates NO-dependent glucose utilization in a broad range of cell types, including macrophages, epithelial cells, smooth muscle cells, endothelial cells, fibroblasts, and pancreatic islets (Dijkmans and Billiau, 1991; Geng et al., 1992; Welsh and Sandler, 1992; Albina and Mastrofrancesco, 1993; Spolarics and Spitzer, 1993; Bolaños et al., 1994; Le Goffe et al., 2002). Thus, astrocytes (García-Nogales et al., 1999), macrophages (Albina and Mastrofrancesco, 1993), and epithelial cells (Le Goffe et al., 2002) respond to LPS and cytokine-mediated activation by increasing glucose consumption. Further metabolism of glucose through glycolysis and the pentosephosphate pathway probably serve to compensate for the loss of ATP and GSH oxidation induced by NO and peroxynitrite (García-Nogales et al., 1999, 2003).

The mechanism through which NO increases the rate of glucose uptake has been studied in astrocytes. Using 2-deoxy-D-[U-¹⁴C]glucose, it was reported that the activation of astrocytes with LPS results in an increase in the uptake process (Cidad et al., 2001). 2-Deoxy-D-glucose is a glucose analog that is taken up and is phosphorylated by hexokinase(s), but the product (2-deoxy-D-glucose-6-phosphate) is not metabolized further, remaining entrapped within the cells. The measurement of radioactive cells thus represents a good index of the uptake process, at least when this process is measured at relatively low extracellular glucose concentrations. Owing to the relatively low K_m values of hexokinase(s) (~100 μ M), the overall glucose uptake process may be limited. In fact, the uptake of glucose by activated astrocytes is most efficient when extracellular glucose concentrations are below 250 μ M (Cidad et al., 2001), strongly suggesting an increase in the affinity for glucose (🔗 [Figure 5.2-9](#)).

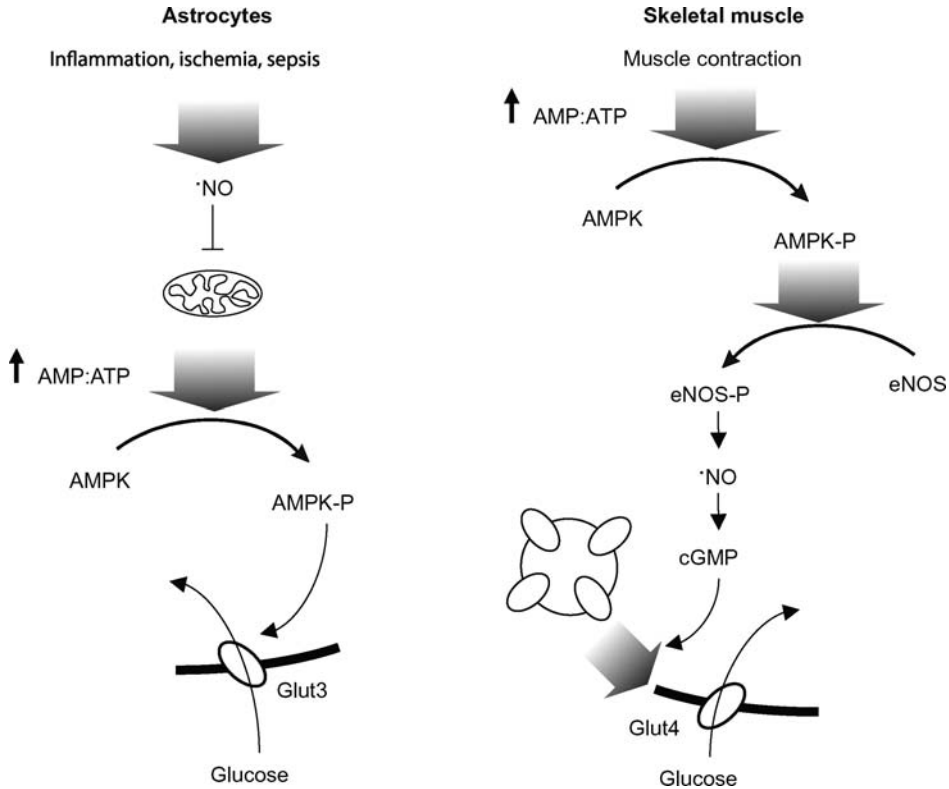
Both transcriptional and posttranslational mechanisms appear to be responsible for the increased affinity of astrocytes for glucose. The high-affinity Glut3 glucose transporter is not normally expressed in astrocytes, but is constitutively expressed in neurons (Bell et al., 1993; Maher et al., 1994; Cidad et al., 2001). Shortly (as from ~4 h) after incubation of astrocytes with LPS (1 μ g/ml), with a low-oxygen atmosphere (~3% O₂) or with a low-glucose medium, Glut3 mRNA and protein levels increase dramatically (Cidad et al., 2001). The increased abundance of Glut3 mRNA can be abolished with an inhibitor of nuclear factor κ B (NF- κ B) (Cidad et al., 2001). Since NF- κ B transcriptionally promotes iNOS expression by LPS (Xie et al., 1994), it has been suggested that the acquired increase in affinity of astrocytes for glucose may serve to protect the brain against stressful conditions.

4.4 Direct Stimulation of Glucose Uptake by NO

Besides the transcriptional induction of glucose transporter in astrocytes by LPS, endogenous NO also stimulates glucose uptake (Cidad et al., 2001) (🔗 [Figure 5.2-9](#)). This NO-dependent increase in glucose

■ Figure 5.2-9

Different mechanisms for glucose transport activation by nitric oxide (NO). In astrocytes (*left panel*), NO-dependent inhibition of mitochondrial respiration increases the AMP:ATP ratio, which is the trigger for AMPK phosphorylation (AMPK-P) and activation. As a result of this, Glut3-mediated glucose uptake is rapidly increased. In skeletal muscle cells (*right panel*), the trigger of increased AMP:ATP ratio is muscle contraction. AMPK is then activated to promote phosphorylation and activation of endothelial NOS isoform (eNOS-P). NO so formed facilitates Glut4 glucose transporter translocation to the plasma membrane in a cyclic GMP-dependent manner



uptake seems to be a compensatory energetic effect that is initially triggered by inhibition of the mitochondrial respiratory chain. Moreover, AMPK, a cell energy sensor that is activated (by phosphorylation of its α_1 -subunit at Thr-172) in response to high AMP:ATP ratios (Hardie et al., 1989), appears to be involved. AMPK triggers the phosphorylation of metabolic substrates to maintain the energy balance (Carling, 2004), and recent evidence has shown that treatment of astrocytes with either exogenous or endogenous NO promotes the phosphorylation of Thr-172 of α_1 -AMPK (Almeida et al., 2004). This activation of AMPK occurs secondary to the inhibition of cytochrome *c* oxidase by NO, which increases the AMP:ATP ratio by \sim fivefold (Cidad et al., 2004). NO-dependent AMPK stimulation was followed by an increase in Glut3 (and Glut1)-mediated glucose uptake (Cidad et al., 2004). The precise mechanism by which AMPK stimulates glucose transporters is unknown, but it does not involve carrier translocation from intracellular stores or a cyclic GMP-dependent pathway (Cidad et al., 2004). This mechanism contrasts with the observed stimulation of glucose uptake in skeletal muscle cells, which mainly express Glut4 (but not the Glut1 or Glut3 glucose transporter isoforms). In these cells, NO activates glucose uptake in a cyclic GMP-dependent fashion (Etgen et al., 1997; Roberts et al., 1997) by promoting Glut4 translocation to the plasma membrane

(Fryer et al., 2000) (▶ *Figure 5.2-9*). More intriguingly, this cascade is initiated by AMPK, which is stimulated after the increase in the AMP:ATP ratio that follows muscle contraction. The endothelial NOS isoform (eNOS) is phosphorylated and activated by AMPK during the energy loss associated with ischemia in the rat heart (Chen et al., 1999). Thus, the activation of AMPK by the addition of exogenous AMP analog triggers eNOS-mediated NO production, which is responsible for the cGMP-dependent glucose uptake observed in skeletal muscle cells (Fryer et al., 2000). AMPK can also stimulate glucose uptake in cells that mainly express Glut1, but not Glut4, Glut2, or Glut3, such as rat liver epithelial clone 9 cells (Shi et al., 1995), 3T3-L1 pre-adipocytes, or myoblasts (Abbud et al., 2000), although the mechanism involves cyclic GMP-independent direct activation of the transporter at the plasma membrane (Abbud et al., 2000; Barnes et al., 2002). Accordingly, the mechanism through which NO and AMPK stimulate glucose uptake appears to depend on the cell type and on the major glucose carrier expressed in that cell type. In astrocytes, the modulation of mitochondrial function by NO may thus represent an indirect mechanism for the regulation of glucose metabolism.

4.5 Regulation of the Pentosephosphate Pathway by NO and Peroxynitrite

Since both NO and peroxynitrite oxidize sulfhydryls, including GSH (Radi et al., 1991; Clancy et al., 1994), it has been suggested that the intracellular concentration of GSH would dictate the susceptibility of neurons to these nitrogen-derived species (Bolaños et al., 1996; Clementi et al., 1998; Bal-Price and Brown, 2000). Unlike neurons, astrocytes can efficiently maintain GSH status in its reduced form (Bolaños et al., 1994, 1995). Glucose oxidation through the pentosephosphate pathway appears to play a key role in this maintenance. This metabolic route is considered to be essential for the regeneration of GSH from GSSG. For instance, hepatocytes are prone to H₂O₂-mediated activation of glucose-6-phosphate dehydrogenase (G6PD), the enzyme that catalyzes the first rate-limiting step in the oxidative branch of the pentosephosphate pathway (Spolarics et al., 1996; Ursini et al., 1997). Furthermore, the stimulation of this pathway in neurons (Ben-Yoseph et al., 1996) and astrocytes (Kussmaul et al., 1999) has been proposed to elicit a protective action against H₂O₂ toxicity through the regeneration of NADPH, a cofactor necessary for GSH recovery from GSSG (Kletzien et al., 1994; Salvemini et al., 1999) (▶ *Figure 5.2-10*).

4.5.1 Peroxynitrite Activates the Pentosephosphate Pathway in Astrocytes

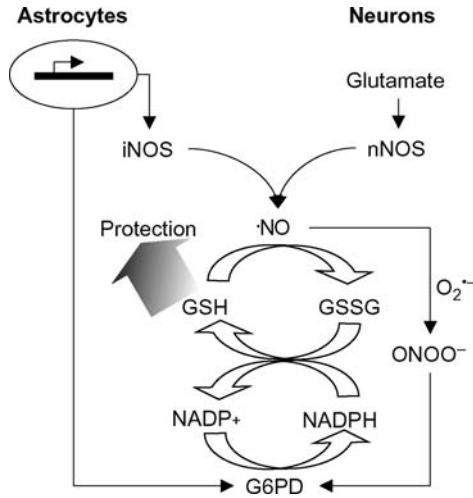
Glucose utilization through the pentosephosphate pathway is stimulated by incubation of astrocytes with LPS (1 μg/ml, 18 h). This may be responsible for the protection of astrocytes against endogenous NO-mediated GSH oxidation (García-Nogales et al., 1999). Since LPS-stimulated astrocytes synthesize O₂^{•-} by iNOS-dependent activity (Xia et al., 1998), it has been suggested that peroxynitrite could be involved in the effect. Thus, direct incubation of astrocytes with peroxynitrite (10 boli of 50 μM during 5 min) triggers rapid pentosephosphate pathway activation and NADPH accumulation (García-Nogales et al., 2003). Investigation of the mechanism responsible revealed a stimulation of G6PD activity, as demonstrated by an increased ratio of 6-phosphogluconate to glucose-6-phosphate, i.e., the product and substrate of G6PD, respectively (García-Nogales et al., 2003) (see *Chapter 1.3*). Together, these results suggest that glucose oxidation through the pentosephosphate pathway is cytoprotective against excess NO (▶ *Figure 5.2-10*).

4.5.2 Neuroprotection by Low Doses of Peroxynitrite

Neurons rapidly (within 1 h) undergo apoptotic death upon exposure to either endogenous (Dawson et al., 1991; Bonfoco et al., 1995; Almeida and Bolaños, 2001) or exogenous (Almeida et al., 2001) excess NO. Strikingly, pretreatment of neurons with peroxynitrite (either 10 boli of 50 μM for 5 min or continuous from 1 mM of the peroxynitrite donor, SIN-1) prevents neuronal death shortly (1 h) after NO treatment. However, the degree of protection is lost thereafter (to ~60% of protection after 4 h, and to ~25% after 8 h)

■ Figure 5.2-10

Activation of the pentosephosphate pathway in astrocytes and in neurons by peroxynitrite. In astrocytes, proinflammatory situations promote the transcriptional induction of iNOS and glucose-6-phosphate dehydrogenase (G6PD), the rate-limiting enzyme of the pentosephosphate pathway. iNOS-dependent NO formation oxidizes glutathione (GSH), but the induction of G6PD forms sufficient NADPH to regenerate GSH from oxidized glutathione (GSSG) and thus prevent further GSH depletion. In addition, peroxynitrite (formed from NO and $O_2^{\bullet-}$ in neurons by glutamate receptor-mediated activation) can rapidly activate G6PD activity, which transiently contributes to prevent neuronal GSH oxidation and cell death



and parallels the redox GSH status (García-Nogales et al., 2003). Since GSH oxidation plays a role in NO-mediated neuronal apoptotic death (Bolaños et al., 1996; Eu et al., 2000; Sastry and Rao, 2000; Almeida and Bolaños, 2001), it is tempting to speculate that peroxynitrite-mediated cytoprotection would be associated with the ability of peroxynitrite to reactivate the pentosephosphate pathway and NADPH. Maintenance of the reduced status of GSH after peroxynitrite treatment would hence occur at the expense of increased availability of NADPH, which serves as a cofactor for GSH reductase activity.

The transient neuroprotective role for peroxynitrite (García-Nogales et al., 2003) is in apparent contradiction with the widely held assumption that peroxynitrite would be the NO-derived neurotoxic effector molecule (Beckman et al., 1990; Lipton et al., 1993; Bolaños et al., 1995; Bonfoco et al., 1995). In light of these results, a major conclusion is that the interference of peroxynitrite with energy metabolism and neurotoxicity is an issue that should be revisited. NO affords protection against $O_2^{\bullet-}$ (Oury et al., 1992; Lafon-Cazal et al., 1993; Rauhala et al., 1998; Mohanakumar et al., 2002) and H_2O_2 -mediated cytotoxicity (Chang et al., 1996; Wink et al., 1996). Since peroxynitrite is formed spontaneously from NO and $O_2^{\bullet-}$ (Beckman et al., 1990), it could be surmised that peroxynitrite would be the factor that mediates such NO-derived protective responses. Taken together, the results of García-Nogales et al. (2003) may provide a clue for understanding the existing controversy concerning the role of NO formation in cell death/survival decisions.

4.5.3 Glucose Protects Neurons Against Glutamate-Induced Neurotoxicity

Glucose has been found to prevent glutamate (100 μ M for 5 min)-mediated energy depletion and neuronal death (Delgado-Esteban et al., 2000). This phenomenon cannot be due to a nonspecific effect, since the inactive enantiomer L-glucose, not recognized by hexose transporters, is not effective. These results suggest

that the neuroprotective effects of glucose would be due to its uptake and further intracellular metabolism. Lactate release is unchanged following exposure to glutamate, ruling out the possibility that the neuroprotective effect of glucose might be due to compensated glycolysis (Delgado-Esteban et al., 2000). In contrast, D- but not L-glucose abolishes the glutamate-mediated GSH oxidation and NADPH loss caused by glutamate-receptor stimulation (Delgado-Esteban et al., 2000). These results are consistent with the notion that the neuroprotective effect of glucose would be due to its metabolism through the pentosephosphate pathway. Whether glucose utilization exerts neuroprotection *in vivo* is unknown, but it is interesting to note that postmortem brain samples from Alzheimer's disease patients show decreased Glut1 and Glut3 levels (Maher et al., 1994), pointing to brain energy dysfunction as a contributing factor in degenerating neurons.

4.6 NO and Glyceraldehyde-3-Phosphate Dehydrogenase

Glyceraldehyde-3-phosphate dehydrogenase (G3PD) is a NAD^+ -requiring glycolytic enzyme. Together with phosphoglycerate kinase, G3PD is an enzyme responsible for the substrate-level phosphorylation of ADP in the glycolysis pathway (Lehninger et al., 1995). The specific activity of G3PD is inhibited by both endogenous and exogenous NO in cellular extracts obtained from a range of cellular systems (Molina y Vedia et al., 1992; Zhang and Snyder, 1992). These observations are intriguing (Mateo et al., 1995) since, under identical conditions, NO also stimulates the flux of glucose consumption through glycolysis, as measured by the rate of lactate formation (Messmer and Brune, 1996). A possible explanation for this apparent paradox would be that the degree of G3PD inhibition does not reach the threshold to limit glycolytic flux (Erecinska et al., 1995). Nevertheless, such an explanation does not justify the enhancement in the glycolytic flux caused by NO. Indeed, NO-releasing donors given to intact red cells promote the release of G3PD to the cytosol from a membrane protein band 3, leading to increased enzyme activity (Galli et al., 2002).

NO and peroxynitrite can interfere with G3PD in different ways that might provide a novel insight into the relationship between G3PD activity and the glycolytic pathway. Initially, it was reported that S-nitrosylates a critical Cys-149 residue of G3PD (Molina y Vedia et al., 1992; Zhang and Snyder, 1992). Such protein modification reversibly inhibits G3PD *in vitro* activity. Later studies revealed that this modification favors the subsequent linking of NADH to G3PD (Mohr et al., 1996), leading to irreversible inhibition of the enzyme. Whether NADH or NAD^+ is the cofactor that actually binds to G3PD is controversial (Mohr et al., 1996). In this context, Wu et al. (1997) suggested that NAD^+ would be the interacting cofactor, and the resulting NAD-G3PD complex would be kept inactive by binding to actin. These authors further reported that the increased glycolytic flux to lactate observed in cells treated with NO might provide the necessary NAD^+ to facilitate the binding of this cofactor to G3PD, further stimulating its inactivation (Wu et al., 1997).

NO depletes ATP stores in most cells, possibly by inhibiting mitochondrial ATP synthesis. However, certain cell types do not suffer from inhibition of mitochondrial ATP synthesis but decrease their ATP levels in close correlation with G3PD inhibition. Thus, the NO-mediated inhibition of G3PD dehydrogenase activity occurs in parallel with increased G3PD acyl phosphatase activity (Mallozzi et al., 1997). This observation suggests that NO uncouples the glycolytic flux from the substrate-level phosphorylation, leading to ATP depletion. The theoretical implication is that despite promoting increased flux through glycolysis NO abolishes ATP generation by this pathway. The facts, however, show that NO stimulates the glycolytic pathway to maintain ATP concentrations (Almeida et al., 2001).

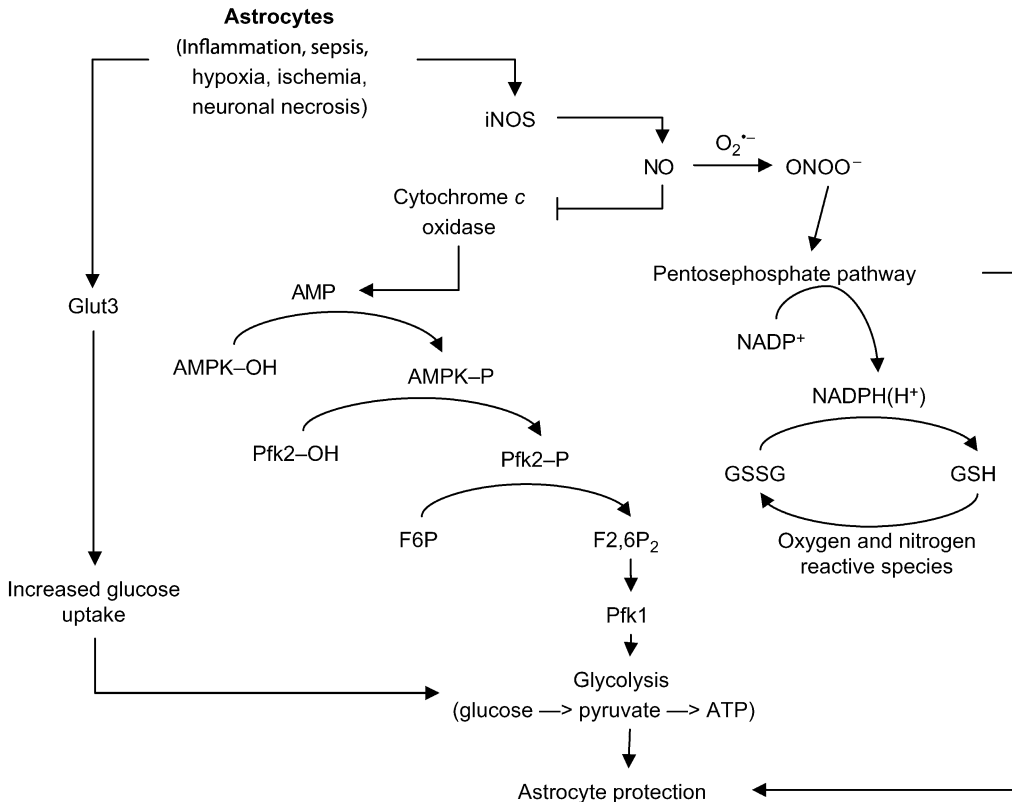
4.7 Activation of Glycolysis by NO Protects Astrocytes from Cell Death

Astrocytes have long been considered as glycolytic cells, since mitochondrial toxins such as antimycin stimulate glucose metabolism through this pathway. In contrast, neurons do not easily elicit glycolysis

under similar circumstances (Pauwels et al., 1985; Walz and Mukerji, 1988). In keeping with this, incubation of astrocytes and neurons with NO inhibits the rate of O_2 consumption by $\sim 85\%$, whereas glycolysis is only enhanced in the former cells (Almeida et al., 2001). Increased glycolysis allows astrocytes to maintain ATP concentrations and cell death, unless glucose is removed from the medium (Almeida et al., 2001). In contrast, neuronal ATP concentrations progressively decrease due to NO, leading to cell death. These correlations suggest that the inhibition of mitochondrial respiration by NO would be associated with an upregulation of the glycolytic flux in astrocytes to prevent the depletion of ATP (Almeida et al., 2001) (see [Figure 5.2-11](#)).

Figure 5.2-11

Coordinated upregulation of glucose utilization contributes to prevent cellular death upon excess nitric oxide (NO) formation. Astrocytes generate large amounts of NO that inhibits cytochrome c oxidase, increases the AMP:ATP ratio, and promotes AMPK phosphorylation and activation. Active AMPK thus activates 6-phosphofructo-2-kinase (Pfk2), which forms fructose-2,6-bisphosphate (F2,6P₂), i.e., the most potent positive effector of 6-phosphofructo-1-kinase (Pfk1). The glycolytic pathway is thus rapidly activated and ATP can be generated to maintain $\Delta\psi_m$ and prevent from apoptotic cell death. On the other hand, transcriptionally induced Glut3, and AMPK-mediated activation of Glut3 (see [Figure 5.2-9](#)) contributes to this sequence of events by supplying intracellular glucose for glycolysis. Under these circumstances, G6PD is induced, and activated by peroxynitrite (see [Figure 5.2-10](#)). This allows for sufficient NADPH generation to keep glutathione reduced and hence contributes to prevention from oxidative stress and cell death



4.7.1 NO Activates Glycolysis at the Level of 6-Phosphofructo-1-Kinase

Besides hexokinase and pyruvate kinase, 6-phosphofructo-1-kinase (Pfk1) is the key rate-limiting step in the glycolytic pathway (Lehninger et al., 1995). Treatment of astrocytes with inhibitors of mitochondrial ATP synthesis such as potassium cyanide, oligomycin, or NO promotes a rapid activation of Pfk1 activity in intact cells (Almeida et al., 2004), as measured with the fructose-6-phosphate (F6P)/fructose-1,6-bisphosphate (F1,6P₂) ratio. No effect of NO on purified enzyme activity is observed, suggesting that the activation of Pfk1 in intact cells would be indirect. Intracellular levels of fructose-2,6-bisphosphate (F2,6P₂), the most powerful Pfk1 allosteric activator (Hers and Van Schaftingen, 1982), rapidly (~5 min) and time-dependently (up to 60 min) accumulate in astrocytes, but not in neurons, after NO incubation (Almeida et al., 2004). These results suggest that NO would activate Pfk1 after 6-phosphofructo-2-kinase (Pfk2), the F2,6P₂-forming enzyme, has been activated (🔗 [Figure 5.2-11](#)).

Reverse transcriptase polymerase chain reaction (RT-PCR) analysis for Pfk2 reveals that astrocytes mainly express isoform Pfk2.3, which has the highest kinase/bisphosphatase activity ratio (Manzano et al., 1998). Western blot analysis of that isoenzyme revealed higher Pfk2.3 contents in astrocytes than in neurons (Almeida et al., 2004). Furthermore, RNA interference against Pfk2.3 renders astrocytes unable to increase F2,6P₂, Pfk1 activity, and glycolysis upon NO treatment. These results strongly suggest that Pfk2.3 would be essential for NO-mediated Pfk1 activation and glycolytic stimulation (Almeida et al., 2004). Furthermore, the NO-dependent activation of Pfk2 is a cyclic GMP-independent phenomenon and requires prior inhibition of mitochondrial respiration (Almeida et al., 2004).

4.7.2 Role of AMP-Activated Protein Kinase in NO-Mediated Glycolytic Activation

In response to *in vivo* ischemia, Pfk2 (isoform Pfk2.2) is phosphorylated (and activated) by AMPK in the heart (Marsin et al., 2000). In response to NO, astrocytes show AMPK activation, as judged by AMPK- α_1 subunit Thr¹⁷² phosphorylation (Almeida et al., 2004). Depletion of AMPK- α_1 by RNA interference renders astrocytes unable to form F2,6P₂, thereby preventing Pfk1 and glycolysis activation in response to NO (Almeida et al., 2004). Together, these observations are compatible with the notion that the mechanism through which NO activates glycolysis first involves the inhibition of mitochondrial respiration, leading to enhancement of AMP:ATP ratio. When transiently increased, the AMP:ATP ratio would activate AMPK, which phosphorylates and activates Pfk2 to form F2,6P₂. Hence, elevations in F2,6P₂ would stimulate Pfk1 activity allosterically, leading to the observed rapid increase in the glycolytic flux (Almeida et al., 2004) (🔗 [Figure 5.2-11](#)).

Western blot and biochemical analyses have revealed that neurons virtually lack Pfk2 protein and activity (Almeida et al., 2004). Moreover, incubation with NO at concentrations that do not affect astrocytic survival kills neurons, and disruption of either AMPK or Pfk2.3 affords astrocytes that are vulnerable to NO. These data indicate that the ability of NO to activate glycolysis promotes protection only in those cells that have the appropriate biochemical glycolytic machinery, such as Pfk2. Thus, the synthesis of ATP by the glycolytic pathway is a transient response of certain cell types to compensate for the energy failure that would otherwise lead to cell death.

5 Concluding Remarks

The brain actively synthesizes NO and peroxynitrite. These nitrogen-derived species trigger a cascade of biochemical effects, including inhibition of cytochrome *c* oxidase and oxidation of GSH in both astrocytes and neurons. Despite promoting a profound degree of mitochondrial inhibition, astrocytes show remarkable resistance to NO and peroxynitrite; in contrast, neurons are highly vulnerable. Recent evidence suggests that these nitrogen-derived reactive species would modulate the key regulatory steps of glucose metabolism that would dictate cellular survival. Upregulation of the high-affinity glucose transporter, the stimulation of glycolysis at Pfk1, and activation of pentosephosphate pathway at G6PD may be important sites of action.

The orchestrated stimulation of these glucose-metabolizing pathways by NO would represent a transient attempt by the brain to compensate for energy impairment and oxidative stress, and thus to emerge from an otherwise pathological outcome.

Acknowledgments

J.P.B. is funded by the Spanish Ministry of Science and Education (grant SAF2004-2038) and the Junta de Castilla-León (grant SA081/04). A.A.P. is funded by the Fondo de Investigación Sanitaria (grant FIS03/1055) and the Junta de Castilla-León (grant SA020/02). The authors wish to thank Dr. María Delgado-Esteban, Dr. Paula García-Nogales, Dr. Victoria Vega-Agapito, Dr. Pilar Ciudad, Dr. Emilio Fernández, Prof. Jose M. Medina, Dr. Simon J. Heales, Prof. John B. Clark, Dr. Guy C. Brown, and Prof. Salvador Moncada for exciting collaborative efforts that led to part of the results discussed in this chapter.

References

- Abbud W, Habinowski S, Zhang JZ, Kendrew J, Elkairi FS, et al. 2000. Stimulation of AMP-activated protein kinase (AMPK) is associated with enhancement of Glut1-mediated glucose transport. *Arch Biochem Biophys* 380: 347-352.
- Agulló L, García A. 1992a. Characterization of noradrenaline-stimulated cyclic GMP formation in brain astrocytes in culture. *Biochem J* 288: 619-624.
- Agulló L, García A. 1992b. Different receptors mediate stimulation of nitric oxide-dependent cyclic GMP formation in neurons and astrocytes in culture. *Biochem Biophys Res Commun* 182: 1362-1368.
- Albina JE, Mastrofrancesco B. 1993. Modulation of glucose metabolism in macrophages by products of nitric oxide synthase. *Am J Physiol* 264: C1594-C1599.
- Almeida A, Almeida J, Bolaños JP, Moncada S. 2001. Different responses of astrocytes and neurons to nitric oxide: The role of glycolytically-generated ATP in astrocyte protection. *Proc Natl Acad Sci USA* 98: 15294-15299.
- Almeida A, Bolaños JP. 2001. A transient inhibition of mitochondrial ATP synthesis by nitric oxide synthase activation triggered apoptosis in primary cortical neurons. *J Neurochem* 77: 676-690.
- Almeida A, Bolaños JP, Medina JM. 1992. Ketogenesis from lactate in rat liver during the perinatal period. *Pediatr Res* 31: 415-418.
- Almeida A, Bolaños JP, Medina JM. 1999. Nitric oxide mediates brain mitochondrial maturation immediately after birth. *FEBS Lett* 452: 290-294.
- Almeida A, Moncada S, Bolaños JP. 2004. Nitric oxide switches on glycolysis through the AMP protein kinase and 6-phosphofructo-2-kinase pathway. *Nat Cell Biol* 6: 45-51.
- Amber IJ, Hibbs JB Jr, Parker CJ, Johnson BB, Taintor RR, et al. 1991. Activated macrophage conditioned medium: Identification of the soluble factors inducing cytotoxicity and the L-arginine dependent effector molecule. *J Leukoc Biol* 49: 610-620.
- Andriezen WL. 1893. On a system of fibre-like cells surrounding the blood vessels of the brain of man and mammals, and its physiological significance. *Int Monatsschr Anat Physiol* 10: 532-540.
- Apelt J, Mehlhorn G, Schliebs R. 1999. Insulin-sensitive GLUT4 glucose transporters are colocalized with GLUT3-expressing cells and demonstrate a chemically distinct neuron-specific localization in rat brain. *J Neurosci Res* 57: 693-705.
- Bal-Price A, Brown GC. 2000. Nitric-oxide-induced necrosis and apoptosis in PC12 cells mediated by mitochondria. *J Neurochem* 75: 1455-1464.
- Barker JE, Bolaños JP, Land JM, Clark JB, Heales SJR. 1996. Glutathione protects astrocytes from peroxynitrite-mediated mitochondrial damage: Implications for neuronal/astrocytic trafficking and neurodegeneration. *Dev Neurosci* 18: 391-396.
- Barnes K, Ingram JC, Porras OH, Barros LF, Hudson ER, et al. 2002. Activation of GLUT1 by metabolic and osmotic stress: Potential involvement of AMP-activated protein kinase (AMPK). *J Cell Sci* 115: 2433-2442.
- Beckman JS, Beckman TW, Chen J, Marshall PA, Freeman BA. 1990. Apparent hydroxyl radical production by peroxynitrite: Implications for endothelial injury from nitric oxide and superoxide. *Proc Natl Acad Sci USA* 87: 1620-1624.
- Beckman JS, Ischiropoulos H, Zhu J, van der Woerd M, Smith C, et al. 1992. Kinetics of superoxide dismutase- and iron-catalyzed nitration of phenolics by peroxynitrite. *Arch Biochem Biophys* 298: 438-445.
- Beinert H, Griffith DE, Wharton DC, Sands RH. 1962. Properties of the copper associated with cytochrome oxidase as

- studied by paramagnetic resonance spectroscopy. *J Biol Chem* 237: 2337-2346.
- Bell GI, Burant CF, Takeda J, Gould GW. 1993. Structure and function of mammalian facilitative sugar transporters. *J Biol Chem* 268: 19161-19164.
- Bellamy TC, Griffiths C, Garthwaite J. 2002. Differential sensitivity of guanylyl cyclase and mitochondrial respiration to nitric oxide measured using clamped concentrations. *J Biol Chem* 277: 31801-31807.
- Beltrán B, Mathur A, Duchon MR, Erusalimsky JD, Moncada S. 2000. The effect of nitric oxide on cell respiration: A key to understanding its role in cell survival or death. *Proc Natl Acad Sci USA* 97: 14602-14607.
- Ben-Yoseph O, Boxer PA, Ross BD. 1996. Assessment of the role of the glutathione and pentose phosphate pathways in the protection of primary cerebrocortical cultures from oxidative stress. *J Neurochem* 66: 2329-2337.
- Bidmon HJ, Wu J, Buchkremer-Ratzmann I, Mayer B, Witte OW, et al. 1998. Transient changes in the presence of nitric oxide synthases and nitrotyrosine immunoreactivity after focal cortical lesions. *Neuroscience* 82: 377-395.
- Birnbaum MJ, Haspel HC, Rosen OM. 1986. Cloning and characterization of a cDNA encoding the rat brain glucose-transporter protein. *Proc Natl Acad Sci USA* 83: 5784-5788.
- Blokzijl-Homan MFJ, Van Gelder BF. 1971. Biochemical and biophysical studies on cytochrome *aa₃* III. The EPR spectrum of NO-ferrocycytochrome *a₃*. *Biochim Biophys Acta* 234: 493-498.
- Blough NV, Zafiriou OC. 1985. Reactions of superoxide with nitric oxide to form peroxynitrite in alkaline aqueous solution. *Inorg Chem* 24: 3502-3504.
- Blumcke I, Eggl P, Celio MR. 1995. Relationship between astrocytic processes and "perineuronal nets" in rat neocortex. *Glia* 15: 131-140.
- Boelens R, Rademaker H, Pel R, Wever R. 1982. Electron paramagnetic-RES studies of the photo-dissociation reactions of cytochrome *c* oxidase nitric oxide complexes. *Biochim Biophys Acta* 679: 84-94.
- Boelens R, Rademaker H, Wever R, Vangelder BF. 1984. The cytochrome *c* oxidase azide nitric oxide complex as a model for the oxygen binding site. *Biochim Biophys Acta* 765: 196-209.
- Boelens R, Wever R, Vangelder BF, Rademaker H. 1983. An electron paramagnetic-RES study of the photo-dissociation reactions of oxidized cytochrome *c* oxidase nitric oxide complexes. *Biochim Biophys Acta* 724: 176-183.
- Bolaños JP, Almeida A. 1999. Roles of nitric oxide in brain hypoxia-ischemia. *Biochim Biophys Acta* 1411: 415-436.
- Bolaños JP, Almeida A, Stewart V, Peuchen S, Land JM, et al. 1997. Nitric oxide-mediated mitochondrial damage in the brain: Mechanisms and implications for neurodegenerative diseases. *J Neurochem* 68: 2227-2240.
- Bolaños JP, García-Nogales P, Almeida A. 2004. Provoking neuroprotection by peroxynitrite. *Curr Pharm Des* 10: 867-877.
- Bolaños JP, Heales SJR, Land JM, Clark JB. 1995. Effect of peroxynitrite on the mitochondrial respiratory chain: Differential susceptibility of neurones and astrocytes in primary cultures. *J Neurochem* 64: 1965-1972.
- Bolaños JP, Heales SJR, Peuchen S, Barker JE, Land JM, et al. 1996. Nitric oxide-mediated mitochondrial damage: A potential neuroprotective role for glutathione. *Free Radic Biol Med* 21: 995-1001.
- Bolaños JP, Peuchen S, Heales SJR, Land JM, Clark JB. 1994. Nitric oxide-mediated inhibition of the mitochondrial respiratory chain in cultured astrocytes. *J Neurochem* 63: 910-916.
- Bonfoco E, Krainc C, Ankarcrona M, Nicotera P, Lipton SA. 1995. Apoptosis and necrosis: Two distinct events induced, respectively, by mild and intense insults with *N*-methyl-D-aspartate or nitric oxide/superoxide in cortical cell cultures. *Proc Natl Acad Sci USA* 92: 7162-7166.
- Borutaité V, Brown GC. 1996. Rapid reduction of nitric oxide by mitochondria, and reversible inhibition of mitochondrial respiration by nitric oxide. *Biochem J* 315: 295-299.
- Bredt DS, Hwang PM, Snyder SH. 1990. Localization of nitric oxide synthase indicating a neural role for nitric oxide. *Nature* 347: 768-770.
- Bredt DS, Snyder SH. 1990. Isolation of nitric oxide synthetase, a calmodulin-requiring enzyme. *Proc Natl Acad Sci USA* 87: 682-685.
- Brookes PS, Land JM, Clark JB, Heales SJR. 1998. Peroxynitrite and brain mitochondria: Evidence for increased proton leak. *J Neurochem* 70: 2195-2202.
- Brorson JR, Schumacker PT, Zhang H. 1999. Nitric oxide acutely inhibits neuronal energy metabolism. *J Neurosci* 19: 147-158.
- Brorson JR, Sulit RA, Zhang H. 1997. Nitric oxide disrupts Ca^{2+} homeostasis in hippocampal neurons. *J Neurochem* 68: 95-105.
- Brorson JR, Zhang H. 1997. Disrupted $[Ca^{2+}]_i$ homeostasis contributes to the toxicity of nitric oxide in cultured hippocampal neurons. *J Neurochem* 69: 1882-1889.
- Brown GC. 1995. Nitric oxide regulates mitochondrial respiration and cell functions by inhibiting cytochrome oxidase. *FEBS Lett* 369: 136-139.
- Brown GC. 2003. NO says yes to mitochondria. *Science* 299: 838-839.
- Brown GC, Bolaños JP, Heales SJR, Clark JB. 1995. Nitric oxide produced by activated astrocytes rapidly and reversibly inhibits cellular respiration. *Neurosci Lett* 193: 201-204.

- Brown GC, Borutaite V. 2004. Inhibition of mitochondrial respiratory complex I by nitric oxide, peroxynitrite and S-nitrosothiols. *Biochim Biophys Acta* 1658: 44-49.
- Brown GC, Cooper CE. 1994. Nanomolar concentrations of nitric oxide reversibly inhibit synaptosomal respiration by competing with oxygen at cytochrome oxidase. *FEBS Lett* 356: 295-298.
- Brudvig GW, Stevens TH, Chan SI. 1980. Reactions of nitric oxide with cytochrome *c* oxidase. *Biochemistry* 19: 5275-5285.
- Carling D. 2004. The AMP-activated protein kinase cascade—a unifying system for energy control. *Trends Biochem Sci* 29: 18-24.
- Cassina A, Radi R. 1996. Differential inhibitory action of nitric oxide and peroxynitrite on mitochondrial electron transport. *Arch Biochem Biophys* 328: 309-316.
- Castro L, Rodríguez M, Radi R. 1994. Aconitase is readily inactivated by peroxynitrite, but not by its precursor, nitric oxide. *J Biol Chem* 269: 29409-29415.
- Cataldo AM, Broadwell RD. 1986. Cytochemical identification of cerebral glycogen and glucose-6-phosphatase activity under normal and experimental conditions. I. Neurons and glia. *J Electron Microscop Tech* 3: 413-437.
- Chang J, Rao NV, Markewitz BA, Hoidal JR, Michael JR. 1996. Nitric oxide donor prevents hydrogen peroxide-mediated endothelial cell injury. *Am J Physiol* 270: L931-L949.
- Chen ZP, Mitchelhill KI, Michell BJ, Stapleton D, Rodriguez-Crespo I, et al. 1999. AMP-activated protein kinase phosphorylation of endothelial NO synthase. *FEBS Lett* 443: 285-289.
- Choeiri C, Staines W, Messier C. 2002. Immunohistochemical localization and quantification of glucose transporters in the mouse brain. *Neuroscience* 111: 19-34.
- Cidad P, Almeida A, Bolaños JP. 2004. Inhibition of mitochondrial respiration by nitric oxide rapidly stimulates cytoprotective GLUT3-mediated glucose uptake through 5'-AMP-activated protein kinase. *Biochem J* 384: 629-636.
- Cidad P, García-Nogales P, Almeida A, Bolaños JP. 2001. Expression of glucose transporter GLUT3 by endotoxin in cultured rat astrocytes: The role of nitric oxide. *J Neurochem* 79: 17-24.
- Clancy RM, Levartovsky D, Leszczynska-Piziak J, Yegudin J, Abramson S. 1994. Nitric oxide reacts with intracellular glutathione and activates the hexose monophosphate shunt in human neutrophils: Evidence for S-nitrosoglutathione as a bioactive intermediary. *Proc Natl Acad Sci USA* 91: 3680-3684.
- Clarke DD, Sokoloff L. 1994. Circulation and energy metabolism of the brain. *Basic neurochemistry*. Siegel GJ, Agranoff BW, Albers RW, Molinoff PB, editors. New York: Raven Press; pp. 645-680.
- Cleeter MWJ, Cooper JM, Darley-USmar VM, Moncada S, Schapira AH. 1994. Reversible inhibition of cytochrome *c* oxidase, the terminal enzyme of the mitochondrial respiratory chain, by nitric oxide. Implications for neurodegenerative diseases. *FEBS Lett* 345: 50-54.
- Clementi E, Brown GC, Feelisch M, Moncada S. 1998. Persistent inhibition of cell respiration by nitric oxide: Crucial role of S-nitrosylation of mitochondrial complex I and protective action of glutathione. *Proc Natl Acad Sci USA* 95: 7631-7636.
- Cooper CE. 2003. Competitive, reversible, physiological? inhibition of mitochondrial cytochrome oxidase by nitric oxide. *IUBMB Life* 55: 591-597.
- Cooper CE, Brown GC. 1995. The interactions between nitric oxide and brain nerve terminals as studied by electron paramagnetic resonance. *Biochem Biophys Res Commun* 212: 404-412.
- Darley-USmar V, Wiseman H, Halliwell B. 1995. Nitric oxide and oxygen radicals: A question of balance. *FEBS Lett* 369: 131-135.
- Dawson VL, Dawson TM. 1996. Nitric oxide neurotoxicity. *J Chem Neuroanat* 10: 179-190.
- Dawson VL, Dawson TM, Bartley DA, Uhl GR, Snyder SH. 1993. Mechanisms of nitric oxide-mediated neurotoxicity in primary brain cultures. *J Neurosci* 13: 2651-2661.
- Dawson VL, Dawson TM, London ED, Bredt DS, Snyder SH. 1991. Nitric oxide mediates glutamate neurotoxicity in primary cortical cultures. *Proc Natl Acad Sci USA* 88: 6368-6371.
- Delgado-Esteban M, Almeida A, Bolaños JP. 2000. D-glucose prevents glutathione oxidation and mitochondrial damage after glutamate receptor stimulation in rat cortical primary neurons. *J Neurochem* 75: 1618-1624.
- De Visscher G, Springett R, Delpy DT, Van Reempts J, Borgers M, et al. 2002. Nitric oxide does not inhibit cerebral cytochrome oxidase in vivo or in the reactive hyperemic phase after brief anoxia in the adult rat. *J Cereb Blood Flow Metab* 22: 515-519.
- Dijkmans R, Billiau A. 1991. Interferon-g/lipopolysaccharide-treated mouse embryonic fibroblasts are killed by a glycolysis/L-arginine-dependent process accompanied by depression of mitochondrial respiration. *Eur J Biochem* 202: 151-159.
- Dimroth P, Kaim G, Matthey U. 2000. Crucial role of the membrane potential for ATP synthesis by F(1)F(0) ATP synthases. *J Exp Biol* 203: 51-59.
- Drapier J-C, Hibbs JB Jr. 1988. Differentiation of murine macrophages to express nonspecific cytotoxicity for tumor cells results in L-arginine-dependent inhibition of mitochondrial iron-sulfur enzymes in the macrophage effector cells. *J Immunol* 140: 2829-2838.

- Dringen R. 2000. Metabolism and functions of glutathione in brain. *Prog Neurobiol* 62: 649-671.
- Dringen R, Gebhardt R, Hamprecht B. 1993. Glycogen in astrocytes: Possible function as lactate supply for neighboring cells. *Brain Res* 623: 208-214.
- Dringen R, Hamprecht B. 1992. Glucose, insulin, and insulin-like growth factor I regulate the glycogen content of astroglia-rich primary cultures. *J Neurochem* 58: 511-517.
- Dringen R, Kussmaul L, Gutterer JM, Hirrlinger J, Hamprecht B. 1999. The glutathione system of peroxide detoxification is less efficient in neurons than in astrocytes. *J Neurochem* 72: 2523-2530.
- Erecinska M, Nelson D, Vanderkooi JM. 1995. Effects of NO-generating compounds on synaptosomal energy metabolism. *J Neurochem* 65: 2699-2705.
- Etgen GJ Jr, Fryburg DA, Gibbs EM. 1997. Nitric oxide stimulates skeletal muscle glucose transport through a calcium/contraction- and phosphatidylinositol-3-kinase-independent pathway. *Diabetes* 46: 1915-1919.
- Eu JP, Liu L, Zeng M, Stamler JS. 2000. An apoptotic model for nitrosative stress. *Biochemistry* 39: 1040-1047.
- Faraci FM, Brian JE. 1994. Nitric oxide and the cerebral circulation. *Stroke* 25: 692-703.
- Fryer LG, Hajdich E, Rencurel F, Salt IP, Hundal HS, et al. 2000. Activation of glucose transport by AMP-activated protein kinase via stimulation of nitric oxide synthase. *Diabetes* 49: 1978-1985.
- Fukumura D, Yonei Y, Kurose I, Saito H, Ohishi T, et al. 1996. Role of nitric oxide in Kupffer cell-mediated hepatoma cell cytotoxicity. *Hepatology* 24: 141-149.
- Gajkowska B, Mossakowski MJ. 1997. Endothelial nitric oxide synthase in vascular endothelium of rat hippocampus after ischemia: Evidence and significance. *Folia Neuropathol* 35: 171-180.
- Galea E, Feinstein DL, Reis DJ. 1992. Induction of calcium-independent nitric oxide synthase activity in primary rat glial cultures. *Proc Natl Acad Sci USA* 89: 10945-10949.
- Galli F, Rossi R, Di Simplicio P, Floridi A, Canestrari F. 2002. Protein thiols and glutathione influence the nitric oxide-dependent regulation of the red blood cell metabolism. *Nitric Oxide* 6: 186-199.
- García-Nogales P, Almeida A, Bolaños JP. 2003. Peroxynitrite protects neurons against nitric oxide-mediated apoptosis. A key role for glucose-6-phosphate dehydrogenase activity in neuroprotection. *J Biol Chem* 278: 864-874.
- García-Nogales P, Almeida A, Fernández E, Medina JM, Bolaños JP. 1999. Induction of glucose-6-phosphate dehydrogenase by lipopolysaccharide contributes to preventing nitric oxide-mediated glutathione depletion in cultured rat astrocytes. *J Neurochem* 72: 1750-1758.
- Garthwaite J, Charles SL, Chess-Williams R. 1988. Endothelium-derived relaxing factor release on activation of NMDA receptors suggests a role as intercellular messenger in the brain. *Nature* 336: 385-387.
- Gehrmann J, Banati RB, Wiessner C, Hossmann KA, Kreutzberg GW. 1995. Reactive microglia in cerebral ischemia. An early mediator of tissue damage. *Neuropathol Appl Neurobiol* 21: 277-289.
- Geng Y-J, Hansson GK, Holme E. 1992. Interferon-gamma and tumor necrosis factor synergize to induce nitric oxide production and inhibit mitochondrial respiration in vascular smooth muscle cells. *Circ Res* 71: 1268-1276.
- Giaume C, Taberner A, Medina JM. 1997. Metabolic trafficking through astrocytic gap junctions. *Glia* 21: 114-123.
- Gorovits N, Charron MJ. 2003. What we know about facilitative glucose transporters. Lessons from cultured cells, animal models and human studies. *Biochem Mol Biol Educ* 13: 163-172.
- Gould GW, Thomas HM, Jess TJ, Bell GI. 1991. Expression of human glucose transporters in *Xenopus* oocytes: Kinetic characterization and substrate specificities of the erythrocyte, liver, and brain isoforms. *Biochemistry* 30: 5139-5145.
- Grosche J, Matyash V, Moller T, Verkhatsky A, Reichenbach A, et al. 1999. Microdomains for neuron-glia interaction: Parallel fiber signaling to Bergmann glial cells. *Nat Neurosci* 2: 139-143.
- Hagen T, Taylor CT, Lam F, Moncada S. 2003. Redistribution of intracellular oxygen in hypoxia by nitric oxide: Effect on HIF1alpha. *Science* 302: 1975-1978.
- Hardie DG, Carling D, Sim ATR. 1989. The AMP-activated protein kinase: A multisubstrate regulator of lipid metabolism. *Trends Biochem Sci* 14: 20-23.
- Hausladen A, Fridovich I. 1994. Superoxide and peroxynitrite inactivate aconitases, but nitric oxide does not. *J Biol Chem* 269: 29405-29408.
- Hawkins R. 1985. Cerebral energy metabolism. Cerebral energy metabolism and metabolic encephalopathy. McCandless DW, editor. Plenum Press; New York: pp 3-17.
- Heales SJR, Bolaños JP, Land JM, Clark JB. 1994. Trolox protects mitochondrial complex IV from nitric oxide-mediated damage in astrocytes. *Brain Res* 668: 243-245.
- Hers HG, Van Schaftingen E. 1982. Fructose 2,6-bisphosphate 2 years after its discovery. *Biochem J* 206: 1-12.
- Hibbs JB Jr, Taintor RR, Vavrin Z, Rachlin EM. 1988. Nitric oxide: A cytotoxic activated macrophage effector molecule. *Biochem Biophys Res Commun* 157: 87-94.
- Hunot S, Boissiere F, Faucheux B, Brugg B, Mouattprigent A, et al. 1996. Nitric oxide synthase and neuronal vulnerability in Parkinson's disease. *Neuroscience* 72: 355-363.
- Iadecola C. 1997. Bright and dark sides of nitric oxide in ischemic brain injury. *Trends Neurosci* 20: 132-139.
- Ignarro LJ, Buga GM, Wood KS, Byrns RE, Chaudhuri G. 1987. Endothelium-derived relaxing factor produced and

- released from artery and vein is nitric oxide. *Proc Natl Acad Sci USA* 84: 9265-9269.
- Inai Y, Takehara Y, Yabuki M, Sato EF, Akiyama J, Yasuda T, Inoue M, Horton AA, Utsumi K. 1996. Oxygen-dependent-regulation of Ehrlich ascites tumor cell respiration by nitric oxide. *Cell Struct Funct* 21: 151-157.
- Ischiropoulos H, Zhu LC, Chen J, Tsai M, Martin JC, et al. 1992. Peroxynitrite-mediated tyrosine nitration catalyzed by superoxide dismutase. *Arch Biochem Biophys* 298: 431-437.
- Jenner P, Dexter DT, Sian J, Schapira AHV, Marsden CD. 1992. Oxidative stress as a cause of nigral cell death in Parkinson's disease and incidental Lewy body disease. *Ann Neurol* 32: S82-S87.
- Jia L, Bonaventura C, Bonaventura J, Stamler JS. 1996. S-nitrosohaemoglobin: A dynamic activity of blood involved in vascular control. *Nature* 380: 221-226.
- Joost HG, Thorens B. 2001. The extended GLUT-family of sugar/polyol transport facilitators: Nomenclature, sequence characteristics, and potential function of its novel members (review). *Mol Membr Biol* 18: 247-256.
- Kacem K, Lacombe P, Seylaz J, Bonvento G. 1998. Structural organization of the perivascular astrocyte endfeet and their relationship with the endothelial glucose transporter: A confocal microscopy study. *Glia* 23: 1-10.
- Keelan J, Vergun O, Duchon MR. 1999. Excitotoxic mitochondrial depolarisation requires both calcium and nitric oxide in rat hippocampal neurons. *J Physiol* 520: 797-813.
- Keilin D, Hartree EF. 1939. Cytochrome and cytochrome oxidase. *Proc Roy Soc London Ser B* 127: 167-191.
- Keynes RG, Dupont S, Garthwaite J. 2004. Hippocampal neurons in organotypic slice culture are highly resistant to damage by endogenous and exogenous nitric oxide. *Eur J Neurosci* 19: 1163-1173.
- Kilbourn RG, Belloni P. 1990. Endothelial cell production of nitrogen oxides in response to interferon in combination with tumor necrosis factor, interleukin-1, or endotoxin. *J Natl Cancer Inst* 82: 772-776.
- Kitade H, Kanemaki T, Sakitani K, Inoue K, Matsui Y, et al. 1996. Regulation of energy metabolism by interleukin-1-beta, but not by interleukin-6, is mediated by nitric oxide in primary cultured rat hepatocytes. *Biochim Biophys Acta* 1311: 20-26.
- Kletzien RF, Harris PKW, Foellmi LA. 1994. Glucose-6-phosphate dehydrogenase: A housekeeping enzyme subject to tissue-specific regulation by hormones, nutrients, and oxidant stress. *FASEB J* 8: 174-181.
- Knowles RG, Moncada S. 1994. Nitric oxide synthases in mammals. *Biochem J* 298: 249-258.
- Knowles RG, Palacios M, Palmer RMJ, Moncada S. 1989. Formation of nitric oxide from L-arginine in the central nervous system: A transduction mechanism for stimulation of the soluble guanylate cyclase. *Proc Natl Acad Sci USA* 86: 5159-5162.
- Kobzik L, Stringer B, Balligand J-L, Reid MB, Stamler JS. 1995. Endothelial type nitric oxide synthase in skeletal muscle fibers: Mitochondrial relationships. *Biochem Biophys Res Commun* 211: 375-381.
- Kon H. 1968. Paramagnetic resonance study of nitric oxide haemoglobin. *J Biol Chem* 243: 4350-4357.
- Kon H. 1969. Electron paramagnetic resonance of nitric oxide cytochrome c. *Biochem Biophys Res Commun* 35: 423-427.
- Kon H, Kataoka N, 1969. Electron paramagnetic resonance of nitric oxide-protoheme complexes with some nitrogenous base. Model systems of nitric oxide hemoproteins. *Biochemistry* 8: 4757-4762.
- Kristian T, Gertsch J, Bates TE, Siesjö BK. 2000. Characteristics of the calcium-triggered mitochondrial permeability transition in non-synaptic brain mitochondria: Effect of cyclosporin A and ubiquinone 0. *J Neurochem* 74: 1999-2009.
- Kurose I, Ebinuma H, Higuchi H, Yonei Y, Saito H, et al. 1995. Nitric oxide mediates mitochondrial dysfunction in hepatoma cells induced by nonactivated Kupffer cells: Evidence implicating ICAM-1-dependent process. *J Gastroenterol Hepatol* 10: S68-S71.
- Kussmaul L, Hamprecht B, Dringen R. 1999. The detoxification of cumene hydroperoxide by the glutathione system of cultured astroglial cells hinges on hexose availability for the regeneration of NADPH. *J Neurochem* 73: 1246-1253.
- Lafon-Cazal M, Pietri S, Culcasi M, Bockaert J. 1993. NMDA-dependent superoxide production and neurotoxicity. *Nature* 364: 535-537.
- Le Goffe C, Vallette G, Charrier L, Candelon T, Bou-Hanna C, et al. 2002. Metabolic control of resistance of human epithelial cells to H₂O₂ and NO stresses. *Biochem J* 364: 349-359.
- Lehninger AL, Nelson DL, Cox MM. 1995. Principles of biochemistry. New York: Worth Publishers.
- Lipton SA, Choi YB, Pan ZH, Lei SZ, Chen HSV, et al. 1993. A redox-based mechanism for the neuroprotective and neurodestructive effects of nitric oxide and related nitroso-compounds. *Nature* 364: 626-632.
- Lizasoain I, Moro MA, Knowles RG, Darley-Usmar V, Moncada S. 1996. Nitric oxide and peroxynitrite exert distinct effects on mitochondrial respiration which are differentially blocked by glutathione or glucose. *Biochem J* 314: 877-880.
- Lobrutto R, Wei YH, Yoshida S, Vancamp HL, Scholes CP, et al. 1984. Electron paramagnetic resonance resolved (EPR-resolved) kinetics of cryogenic nitric oxide recombination to cytochrome c oxidase and myoglobin. *Biophys J* 45: 473-479.

- Lymar SV, Jiang Q, Hurst JK. 1996. Mechanism of carbon dioxide-catalyzed oxidation of tyrosine by peroxynitrite. *Biochemistry* 35: 7855-7861.
- Maeda Y, Matsumoto M, Hori O, Kuwabara K, Ogawa S, et al. 1994. Hypoxia/reoxygenation-mediated induction of astrocyte interleukin-6. A paracrine mechanism potentially enhancing neuron survival. *J Exp Med* 180: 2297-2308.
- Magistretti PJ, Hof PR, Martin JL. 1986. Adenosine stimulates glycogenolysis in mouse cerebral cortex: A possible coupling mechanism between neuronal activity and energy metabolism. *J Neurosci* 6: 2558-2562.
- Maher F. 1995. Immunolocalization of GLUT1 and GLUT3 glucose transporters in primary cultured neurons and glia. *J Neurosci Res* 42: 459-469.
- Maher F, Vannucci SJ, Simpson IA. 1993. Glucose transporter isoforms in brain: Absence of GLUT3 from the blood-brain barrier. *J Cereb Blood Flow Metab* 13: 342-345.
- Maher F, Vannucci SJ, Simpson IA. 1994. Glucose transporter proteins in brain. *FASEB J* 8: 1003-1011.
- Makar TK, Nedergaard M, Preuss A, Gelbard AS, Perumal AS, et al. 1994. Vitamin E, ascorbate, glutathione, glutathione disulfide, and enzymes of glutathione metabolism in cultures of chick astrocytes and neurones: Evidence that astrocytes play an important role in antioxidative processes in the brain. *J Neurochem* 62: 45-53.
- Mallozzi C, Di Stasi AMM, Minetti M. 1997. Peroxynitrite modulates tyrosine-dependent signal transduction pathway of human erythrocyte band 3. *FASEB J* 11: 1281-1290.
- Malmström BG. 1979. Cytochrome *c* oxidase. Structure and catalytic activity. *Biochim Biophys Acta* 549: 281-303.
- Manzano A, Rosa JL, Ventura F, Perez JX, Nadal M, et al. 1998. Molecular cloning, expression, and chromosomal localization of a ubiquitously expressed human 6-phosphofructo-2-kinase/ fructose-2, 6-bisphosphatase gene (PFKFB3). *Cytogenet Cell Genet* 83: 214-217.
- Marsin AS, Bertrand L, Rider MH, Deprez J, Beauloye C, et al. 2000. Phosphorylation and activation of heart PFK-2 by AMPK has a role in the stimulation of glycolysis during ischaemia. *Curr Biol* 10: 1247-1255.
- Mateo RB, Reichner JS, Mastrofrancesco B, Kraft-Stolar D, Albina JE. 1995. Impact of nitric oxide on macrophage glucose metabolism and glyceraldehyde-3-phosphate dehydrogenase activity. *Am J Physiol* 268: C669-C675.
- Mayer B, Pfeiffer S, Schrammel A, Koelsing D, Schmidt K, et al. 1998. A new pathway of nitric oxide/cyclic GMP signalling involving S-nitrosoglutathione. *J Biol Chem* 273: 3264-3270.
- Medina JM, Cuezva JM, Mayor F. 1980. Non-gluconeogenic fate of lactate during the early neonatal period in the rat. *FEBS Lett* 114: 132-134.
- Medina JM, Fernández E, Bolaños JP, Vicario C, Arizmendi C. 1990. Fuel supply to the brain during the early postnatal period. Endocrine and biochemical development of the fetus and neonate. Cuezva JM, Pascual-Leone AM, Patel MS, editors. Plenum Press; New York: pp. 175-194.
- Meldrum BS. 2000. Glutamate as a neurotransmitter in the brain: Review of physiology and pathology. *J Nutr* 130: 1007S-1015S.
- Mennerick S, Zorumski CF. 1994. Glial contributions to excitatory neurotransmission in cultured hippocampal cells. *Nature* 368: 59-62.
- Merrill JE, Murphy SP, Mitrovic B, Mackenzie-Graham A, Dopp JC, et al. 1997. Inducible nitric oxide synthase and nitric oxide production by oligodendrocytes. *J Neurosci Res* 48: 372-384.
- Messmer UK, Brune B. 1996. Modification of macrophage glyceraldehyde-3-phosphate dehydrogenase in response to nitric oxide. *Eur J Pharmacol* 302: 171-182.
- Miles PR, Bowman L, Huffman L. 1996. Nitric oxide alters metabolism in isolated alveolar type-II cells. *Am J Physiol* 15: L23-L30.
- Minc-Golomb D, Yadid G, Tsarfaty I, Resau JH, Schwartz JP. 1996. In vivo expression of inducible nitric oxide synthase in cerebellar neurons. *J Neurochem* 66: 1504-1509.
- Mitrovic B, Ignarro LJ, Montestruque S, Smoll A, Merrill JE. 1994. Nitric oxide as a potential pathological mechanism in demyelination: Its differential effects on primary glial cells in vitro. *Neuroscience* 61: 575-585.
- Mohanakumar KP, Thomas B, Sharma SM, Muralikrishnan D, Chowdhury R, et al. 2002. Nitric oxide: An antioxidant and neuroprotector. *Ann N Y Acad Sci* 962: 389-401.
- Mohr S, Stamler JS, Brune B. 1996. Posttranslational modification of glyceraldehyde-3-phosphate dehydrogenase by S-nitrosylation and subsequent NADH attachment. *J Biol Chem* 271: 4209-4214.
- Molina y Vedia L, McDonald B, Reep B, Brüne B, Di Silvio M, et al. 1992. Nitric oxide-induced S-nitrosylation of glyceraldehyde-3-phosphate dehydrogenase inhibits enzymatic activity and increases endogenous ADP-ribosylation. *J Biol Chem* 267: 24929-24932.
- Morgello S, Uson RR, Schwartz EJ, Haber RS. 1995. The human blood-brain barrier glucose transporter (GLUT1) is a glucose transporter of gray matter astrocytes. *Glia* 14: 43-54.
- Moro MA, Darley-Usmar VM, Goodwin DA, Read NG, Zamora-Pino R, et al. 1994. Paradoxical fate and biological action of peroxynitrite on human platelets. *Proc Natl Acad Sci USA* 91: 6702-6706.
- Moro MA, Darley-Usmar VM, Lizasoain YS, Knowles RG, Radomski MW, Moncada S. 1995. The formation of nitric oxide donors from peroxynitrite. *Br J Pharmacol* 116: 1999-2004.
- Mueckler M, Caruso C, Baldwin SA, Panico M, Blench I, et al. 1985. Sequence and structure of a human glucose transporter. *Science* 229: 941-945.

- Murphy S, Grzybicki D. 1996. Glial NO. Normal and pathological roles. *Neuroscientist* 2: 90-99.
- Murphy S, Simmons ML, Agulló L, García A, Feinstein DL, et al. 1993. Synthesis of nitric oxide in CNS glial cells. *Trends Neurosci* 16: 323-328.
- Nagamatsu S, Sawa H, Kamada K, Nakamichi Y, Yoshimoto K, et al. 1993. Neuron-specific glucose transporter (NSGT): CNS distribution of GLUT3 rat glucose transporter (RGT3) in rat central neurons. *FEBS Lett* 334: 289-295.
- Nisoli E, Clementi E, Paolucci C, Cozzi V, Tonello C, et al. 2003. Mitochondrial biogenesis in mammals: The role of endogenous nitric oxide. *Science* 299: 896-899.
- Nisoli E, Falcone S, Tonello C, Cozzi V, Palomba L, et al. 2004. Mitochondrial biogenesis by NO yields functionally active mitochondria in mammals. *Proc Natl Acad Sci USA* 101: 16507-16512.
- Nomura Y, Kitamura Y. 1993. Inducible nitric oxide synthase in glial cells. *Neurosci Res* 18: 103-107.
- Oury TD, Ho YS, Piantadosi CA, Crapo JD. 1992. Extracellular superoxide dismutase, nitric oxide, and central nervous system O₂ toxicity. *Proc Natl Acad Sci USA* 89: 9715-9719.
- Packer MA, Murphy MP. 1994. Peroxynitrite causes calcium efflux from mitochondria which is prevented by cyclosporin A. *FEBS Lett* 345: 237-240.
- Packer MA, Murphy MP. 1995. Peroxynitrite formed by simultaneous nitric oxide and superoxide generation causes cyclosporine A-sensitive mitochondrial calcium efflux and depolarization. *Eur J Biochem* 234: 231-239.
- Palacios-Callender M, Quintero M, Hollis VS, Springett RJ, Moncada S. 2004. Endogenous NO regulates superoxide production at low oxygen concentrations by modifying the redox state of cytochrome c oxidase. *Proc Natl Acad Sci USA* 101: 7630-7635.
- Palmer RM, Ashton DS, Moncada S. 1988. Vascular endothelial cells synthesize nitric oxide from L-arginine. *Nature* 333: 664-666.
- Palmer RMJ, Ferrige AG, Moncada S. 1987. Nitric oxide release accounts for the biological activity of endothelium-derived relaxing factor. *Nature* 327: 524-526.
- Pardridge WM, Boado RJ, Farrell CR. 1990. Brain-type glucose transporter (GLUT-1) is selectively localized to the blood-brain barrier. Studies with quantitative Western blotting and in situ hybridization. *J Biol Chem* 265: 18035-18040.
- Park LCH, Zhang H, Sheu KFR, Calingasan NY, Kristal BS, et al. 1999. Metabolic impairment induces oxidative stress, compromises inflammatory responses, and inactivates a key mitochondrial enzyme in microglia. *J Neurochem* 72: 1948-1958.
- Pauwels PJ, Opperdoes FR, Trouet A. 1985. Effects of antimycin, glucose deprivation, and serum on cultures of neurons, astrocytes, and neuroblastoma cells. *J Neurochem* 44: 143-148.
- Peachman KK, Lyles DS, Bass DA. 2001. Mitochondria in eosinophils: Functional role in apoptosis but not respiration. *Proc Natl Acad Sci USA* 98: 1717-1722.
- Pellerin L. 2003. Lactate as a pivotal element in neuron-glia metabolic cooperation. *Neurochem Int* 43: 331-338.
- Pellerin L, Magistretti PJ. 1994. Glutamate uptake into astrocytes stimulates aerobic glycolysis: A mechanism coupling neuronal activity to glucose utilization. *Proc Natl Acad Sci USA* 91: 10625-10629.
- Pessin JE, Bell GI. 1992. Mammalian facilitative glucose transporter family: Structure and molecular regulation. *Annu Rev Physiol* 54: 911-930.
- Phillips JD, Kinikini DV, Yu Y, Guo B, Leibold EA. 1996. Differential regulation of IRP1 and IRP2 by nitric oxide in rat hepatoma cells. *Blood* 87: 2983-2992.
- Poderoso JJ, Carreras MC, Lisdero C, Riobó N, Schöper F, et al. 1996. Nitric oxide inhibits electron transfer and increases superoxide radical production in rat heart mitochondria and submitochondrial particles. *Arch Biochem Biophys* 328: 85-92.
- Radi R. 1996. Reactions of nitric oxide with metalloproteins. *Chem Res Toxicol* 9: 828-835.
- Radi R, Beckman JS, Bush KM, Freeman BA. 1991. Peroxynitrite oxidation of sulfhydryls. The cytotoxic potential of superoxide and nitric oxide. *J Biol Chem* 266: 4244-4250.
- Radi R, Rodríguez M, Castro L, Telleri R. 1994. Inhibition of mitochondrial electron transport by peroxynitrite. *Arch Biochem Biophys* 308: 89-95.
- Rauhala P, Lin AM, Chiueh CC. 1998. Neuroprotection by S-nitrosoglutathione of brain dopamine neurons from oxidative stress. *FASEB J* 12: 165-173.
- Rees DD, Palmer RJM, Moncada S. 1989. Role of endothelium-derived nitric oxide in the regulation of blood pressure. *Proc Natl Acad Sci USA* 86: 3375-3378.
- Riobó NA, Clementi E, Melani M, Boveris A, Cadenas E, Moncada S, Poderoso JJ. 2001. Nitric oxide inhibits mitochondrial NADH: Ubiquinone reductase activity through peroxynitrite formation. *Biochem J* 359: 139-145.
- Roberts CK, Barnard RJ, Scheck SH, Balon TW. 1997. Exercise-stimulated glucose transport in skeletal muscle is nitric oxide dependent. *Am J Physiol* 273: E220-225.
- Sagara J, Miura K, Bannai S. 1993. Maintenance of neuronal glutathione by glial cells. *J Neurochem* 61: 1672-1676.
- Sakai T, Ishizaki T, Nakai T, Miyabo S, Matsukawa S, et al. 1996. Role of nitric oxide and superoxide anion in leukotoxin-induced, 9,10-epoxy-12-octadecenoate-induced mitochondrial dysfunction. *Free Radic Biol Med* 20: 607-612.

- Salvemini F, Franzé A, Iervolino A, Filosa S, Salzano S, et al. 1999. Enhanced glutathione levels and oxidoresistance mediated by increased glucose-6-phosphate dehydrogenase expression. *J Biol Chem* 274: 2750-2757.
- Sastry PS, Rao KS. 2000. Apoptosis and the nervous system. *J Neurochem* 74: 1-20.
- Schapira AHV, Cooper JM, Dexter D, Clark JB, Jenner P, et al. 1990a. Mitochondrial complex I deficiency in Parkinson's disease. *J Neurochem* 54: 823-827.
- Schapira AHV, Mann VM, Cooper JM, Dexter D, Daniel SE, et al. 1990b. Anatomic and disease specificity of NADH CoQ₁ reductase (complex I) deficiency in Parkinson's disease. *J Neurochem* 55: 2142-2145.
- Schrammel A, Gorren ACF, Schmidt K, Pfeiffer S, Mayer B. 2003. S-nitrosation of glutathione by nitric oxide, peroxy-nitrite, and *NO/O₂•. *Free Radic Biol Med* 34: 1078-1088.
- Schurr A, Payne RS, Miller JJ, Rigor BM. 1997. Brain lactate is an obligatory aerobic energy substrate for functional recovery after hypoxia: Further in vitro validation. *J Neurochem* 69: 423-426.
- Schurr A, West CA, Rigor BM. 1988. Lactate-supported synaptic function in the rat hippocampal slice preparation. *Science* 240: 1326-1328.
- Schweizer M, Richter C. 1994. Nitric oxide potently and reversibly deenergizes mitochondria at low oxygen tension. *Biochem Biophys Res Commun* 204: 169-175.
- Schweizer M, Richter C. 1996. Peroxynitrite stimulates the pyridine nucleotide-linked Ca²⁺ release from intact rat liver mitochondria. *Biochemistry* 35: 4524-4528.
- Sharpe MA, Cooper CE. 1998. Interaction of peroxynitrite with mitochondrial cytochrome oxidase. *J Biol Chem* 273: 30961-30972.
- Shi Y, Liu H, Vanderburg G, Samuel SJ, Ismail-Beigi F, et al. 1995. Modulation of GLUT1 intrinsic activity in clone 9 cells by inhibition of oxidative phosphorylation. *J Biol Chem* 270: 21772-21778.
- Simmons ML, Murphy S. 1992. Induction of nitric oxide synthase in glial cells. *J Neurochem* 59: 897-905.
- Soussi B, Idstrom J-P, Schersten T, Bylund-Fellenius A-C. 1990. Cytochrome c oxidase and cardiolipin alterations in response to skeletal muscle ischaemia and reperfusion. *Acta Physiol Scand* 138: 107-114.
- Spolarics Z, Spitzer JJ. 1993. Augmented glucose use and pentose cycle activity in hepatic endothelial cells after in vivo endotoxemia. *Hepatology* 17: 615-620.
- Spolarics Z, Stein DS, García ZC. 1996. Endotoxin stimulates hydrogen peroxide detoxifying activity in rat hepatic endothelial cells. *Hepatology* 24: 691-696.
- Stadler J, Billiar TR, Curran RD, Stuehr DJ, Ochoa JB, et al. 1991. Effect of exogenous and endogenous nitric oxide on mitochondrial respiration of rat hepatocytes. *Am J Physiol* 260: C910-C916.
- Stagliano NE, Dietrich WD, Prado R, Green EJ, et al. 1997. The role of nitric oxide in the pathophysiology of thromboembolic stroke in the rat. *Brain Res* 759: 32-40.
- Stamler JS, Simon DI, Jaraki O, Osborne JA, Francis S, et al. 1992. S-nitrosylation of tissue-type plasminogen activator confers vasodilatory and antiplatelet properties on the enzyme. *Proc Natl Acad Sci USA* 89: 87-91.
- Stevens TH, Bocian DF, Chan SI. 1979a. EPR studies of ¹⁵NO-ferrocyclochrome a₃ in cytochrome c oxidase. *FEBS Lett* 97: 314-316.
- Stevens TH, Brudvig GW, Bocian DF, Chan SI. 1979b. Structure of cytochrome a₃-Cu_{a3} couple in cytochrome c oxidase as revealed by nitric oxide binding studies. *Proc Natl Acad Sci USA* 76: 3320-3324.
- Stewart VC, Land JM, Clark JB, Heales SJR. 1998. Pretreatment of astrocytes with interferon- α/β prevents neuronal mitochondrial respiratory chain damage. *J Neurochem* 70: 432-434.
- Stuehr DJ, Nathan CF. 1989. Nitric oxide. A macrophage product responsible for cytostasis and respiratory inhibition in tumour target cells. *J Exp Med* 169: 1543-1555.
- Sung Y-J, Dietert RR. 1994. Nitric oxide (*NO)-induced mitochondrial injury among chicken *NO-generating and target leukocytes. *J Leukoc Biol* 56: 52-58.
- Szabó C, Day BJ, Salzman AL. 1996. Evaluation of the relative contribution of nitric oxide and peroxynitrite to the suppression of mitochondrial respiration in immunostimulated macrophages using a manganese mesoporphyrin superoxide dismutase mimetic and peroxynitrite scavenger. *FEBS Lett* 381: 82-86.
- Szabó C, Salzman AL. 1995. Endogenous peroxynitrite is involved in the inhibition of mitochondrial respiration in immuno-stimulated J774.2 macrophages. *Biochem Biophys Res Commun* 209: 739-743.
- Tabernerero A, Bolaños JP, Medina JM. 1993. Lipogenesis from lactate in rat neurons and astrocytes in primary culture. *Biochem J* 294: 635-638.
- Tabernerero A, Giaume C, Medina JM. 1996. Endothelin-1 regulates glucose utilization in cultured astrocytes by controlling intercellular communication through gap junctions. *Glia* 16: 187-195.
- Takehara Y, Kanno T, Yoshioka T, Inoue M, Utsumi K. 1995. Oxygen-dependent regulation of mitochondrial energy metabolism by nitric oxide. *Arch Biochem Biophys* 323: 27-32.
- Takuma K, Phuagphong P, Lee E, Mori K, Baba A, et al. 2001. Anti-apoptotic effect of cGMP in cultured astrocytes. Inhibition by cGMP-dependent protein kinase of mitochondrial permeable transition pore. *J Biol Chem* 276: 48093-48099.
- Tatton WH, Olanow CW. 1999. Apoptosis in neurodegenerative diseases: The role of mitochondria. *Biochim Biophys Acta* 1410: 195-213.

- Torres J, Darley-Usmar VM, Wilson MT. 1995. Inhibition of cytochrome *c* oxidase in turnover by nitric oxide: Mechanism and implications for control of respiration. *Biochem J* 312: 169-173.
- Trimmer BA, Aprille JR, Dudzinski DM, Lagace CJ, Lewis SM, et al. 2001. Nitric oxide and the control of firefly flashing. *Science* 292: 2486-2488.
- Tsacopoulos M, Magistretti PJ. 1996. Metabolic coupling between glia and neurons. *J Neurosci* 16: 877-885.
- Uppu RM, Squadrito GL, Pryor WA. 1996. Acceleration of peroxynitrite oxidations by carbon dioxide. *Arch Biochem Biophys* 327: 335-343.
- Ursini MV, Parrella A, Rosa G, Salzano S, Martini G. 1997. Enhanced expression of glucose-6-phosphate dehydrogenase in human cells sustaining oxidative stress. *Biochem J* 323: 801-806.
- Van der Vliet A, Eiserich JP, Kaur H, Cross CE, Halliwell B. 1996. Nitrotyrosine as biomarker for reactive nitrogen species. *Methods Enzymol* 269: 175-184.
- Vicario C, Arizmendi C, Malloch G, Clark JB, Medina JM. 1991. Lactate utilization by isolated cells from early neonatal rat brain. *J Neurochem* 57: 1700-1707.
- Wainio WW. 1955. Reactions of cytochrome oxidase. *J Biol Chem* 212: 723-733.
- Walz W, Mukerji S. 1988. Lactate release from cultured astrocytes and neurons: A comparison. *Glia* 1: 366-370.
- Wang GJ, Randall RD, Thayer SA. 1994. Glutamate-induced intracellular acidification of cultured hippocampal neurons demonstrates altered energy metabolism resulting from Ca^{2+} loads. *J Neurophysiol* 72: 2563-2569.
- Welsh N, Sandler S. 1992. Interleukin-1 beta induces nitric oxide production and inhibits the activity of aconitase without decreasing glucose oxidation rates in isolated mouse pancreatic islets. *Biochem Biophys Res Commun* 182: 333-340.
- White DA. 1973. The phospholipid composition of mammalian tissues. Form and function of phospholipids. Ansell GB, Hawthorne JN, Dawson RMC, editors. Amsterdam: Elsevier Science; pp 441-482.
- White RJ, Reynolds IJ. 1996. Mitochondrial depolarization in glutamate-stimulated neurons: An early signal specific to excitotoxic exposure. *J Neurosci* 16: 5688-5697.
- Wiesinger H, Hamprecht B, Dringen R. 1997. Metabolic pathways for glucose in astrocytes. *Glia* 21: 22-34.
- Wilson DF, Erecinska M, Owen CS. 1976. Some properties of the redox components of cytochrome *c* oxidase and their reactions. *Arch Biochem Biophys* 175: 160-172.
- Wink DA, Cook JA, Pacelli R, DeGraff W, Gamson J, et al. 1996. The effect of various nitric oxide-donor agents on hydrogen peroxide-mediated toxicity: A direct correlation between nitric oxide formation and protection. *Arch Biochem Biophys* 331: 241-248.
- Wong-Riley MTT. 1989. Cytochrome oxidase: An endogenous metabolic marker for neuronal activity. *Trends Neurosci* 12: 94-101.
- Wood IS, Trayhurn P. 2003. Glucose transporters (GLUT and SGLT): Expanded families of sugar transport proteins. *Br J Nutr* 89: 3-9.
- Wood PL. 1995. Microglia as a unique cellular target in the treatment of stroke. Potential neurotoxic mediators produced by activated microglia. *Neurol Res* 17: 242-248.
- Wu K, Aoki C, Elste A, Rogalski-Wilk AA, Siekevitz P. 1997. The synthesis of ATP by glycolytic enzymes in the postsynaptic density and the effect of endogenous generated nitric oxide. *Proc Natl Acad Sci USA* 94: 13273-13278.
- Wu X, Freeze HH. 2002. GLUT14, a duplicon of GLUT3, is specifically expressed in testis as alternative splice forms. *Genomics* 80: 553-557.
- Xia Y, Roman JJ, Masters BS, Zweier JL. 1998. Inducible nitric oxide synthase generates superoxide from the reductase domain. *J Biol Chem* 273: 22635-22639.
- Xie Q-W, Kashiwabara Y, Nathan C. 1994. Role of transcription factor NF- κ B/rel in induction of nitric oxide synthase. *J Biol Chem* 269: 4705-4708.
- Xu W, Liu L, Charles IG, Moncada S. 2004. Nitric oxide induces coupling of mitochondrial signalling with the endoplasmic reticulum stress response. *Nat Cell Biol* 6: 1129-1134.
- Yankner BA. 1996. Mechanisms of neuronal degeneration in Alzheimer's disease. *Neuron* 16: 921-932.
- Zhang J, Snyder SH. 1992. Nitric oxide stimulates auto-ADP-ribosylation of glyceraldehyde-3-phosphate dehydrogenase. *Proc Natl Acad Sci USA* 89: 9382-9385.
- Zhang C, Wong-Riley MTT. 1996. Do nitric oxide synthase, NMDA receptor subunit R1 and cytochrome oxidase colocalize in the rat central nervous system? *Brain Res* 729: 205-215.

5.3 Mitochondrial Production of Oxidants and Their Role in the Regulation of Cellular Processes

P. S. Brookes

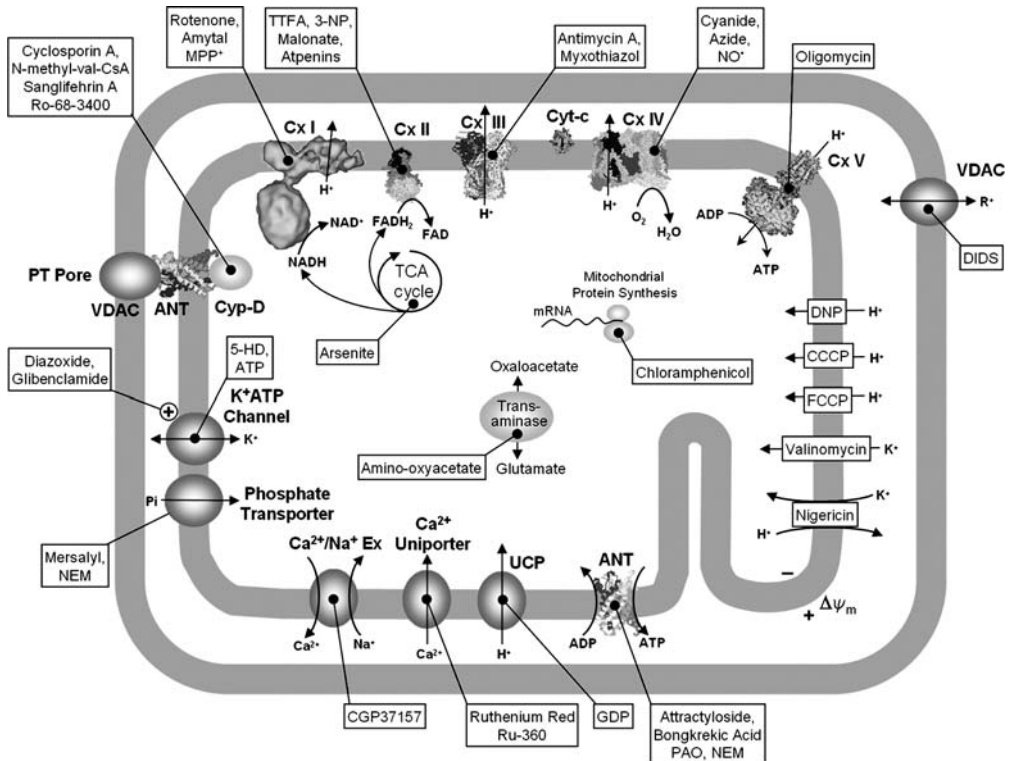
1	General Concepts on Reactive Oxygen Species	521
1.1	Nomenclature	521
1.2	O ₂ as Substrate	522
1.3	Local Conditions	522
1.4	Nitric Oxide	523
2	ROS “Weights and Measures”	523
2.1	Quantifying ROS—Fluorescent Probes	523
2.2	Use of Inhibitors and Antioxidants	525
2.3	So, How Much ROS?	525
2.4	End Points Versus Kinetic Rates	526
3	Mitochondria as a Source of ROS	526
3.1	The Energy “Plumbing” of Mitochondria and ROS Leakage	526
3.2	ROS from the Respiratory Chain	526
3.3	ROS from the Tricarboxylic Cycle	528
3.4	ROS from Other Mitochondrial Sources	529
3.5	Regulation of Mitochondrial ROS Generation	529
3.6	Mitochondrial Generation of RNS	530
4	Neuron-Specific Aspects of Mitochondrial ROS Generation	531
4.1	Neuronal Mitochondria Versus Glial/Astrocytic Mitochondria	531
4.2	Neuronal Excitotoxicity, Ca ²⁺ Overload, and ROS	531
5	Cell Signaling by ROS	533
5.1	ROS Are Cell Signaling Molecules	533
5.2	Specific Examples of ROS Cell Signaling	533
5.3	Mitochondrial ROS and NO• in Cell Signaling	534
5.4	Redox-Sensitive Transcription Factors	535
5.5	ROS-Sensitive Ion Channels	535
5.6	Mitochondria in Apoptotic Signaling—Role of ROS	536
5.7	Hypoxic Signaling and Mitochondrial ROS	536
6	Pathological Effects of Mitochondrial ROS	537
6.1	Stroke	537
6.2	Ischemic Preconditioning in the Brain; the Role of ROS and Mitochondria	537
6.3	Neurodegeneration	538
6.4	Therapeutic Strategies	538
7	Closing Remarks	539

Abstract: The other chapters in this volume provide an introduction to the general topic of mitochondrial energy metabolism. In this chapter, the mitochondrial generation of reactive oxygen species (ROS) is covered in more detail, addressing both established and novel concepts in this field. By way of introduction, [▶ Figure 5.3-1](#) shows a schematic of the mitochondrion indicating the inhibitory positions of several pharmacologic tools that have been used in the study of mitochondria over the past few decades. Much of the literature describing mitochondrial function relies heavily on the use of these inhibitors, and it is therefore hoped that this diagram may aid not only in the subsequent understanding of mitochondrial ROS generation, but in the wider understanding of mitochondrial function outlined in this volume.

A single caveat surrounds the use of this diagram as a reference for determining which inhibitors to use in a given set of experiments: virtually all of the compounds listed were discovered and initially tested in

■ **Figure 5.3-1**

Pharmacologic tools used in mitochondrial research. Names of mitochondrial enzymes and carriers are in bold and pharmacologic agents are in boxes. Inhibitors are denoted by a filled circle (●), activators by a plus sign. The mitochondrial membrane potential (positive outside, negative inside) is denoted by $\Delta\psi_m$. *ANT* adenine nucleotide translocase, *CCCP* carbonyl cyanide m-chloro phenylhydrazone, *Cyp-D* cyclophilin D, *Cyt-c* cytochrome c, *Cx I* complex I (NADH dehydrogenase), *Cx II* complex II (succinate dehydrogenase), *Cx III* complex III (ubiquinol/cytochrome c oxidoreductase), *Cx IV* complex IV (cytochrome c oxidase), *Cx V* complex V (ATP synthase), *DIDS* 4,4-diisothiocyanato-stilbene-2,2'-disulphonate, *DNP* dinitrophenol, *FCCP* carbonyl cyanide p-[trifluoromethoxy]-phenylhydrazone, *GDP* guanosine diphosphate, *5-HD* 5-hydroxydecanoate, *MPP⁺* 1-methyl-4-phenylpyridinium, *NEM* N-ethyl maleimide, *3-NP* 3-nitropropionate, *NO^{*}* nitric oxide, *PAO* phenylarsine oxide, *RNS* reactive nitrogen species, *ROS* reactive oxygen species, *TFA* thenoyl-trifluoroacetic acid, *UCP* uncoupling protein, *VDAC* voltage-dependent anion channel



isolated mitochondrial systems, but their specificity in cellular systems and in whole organs and organisms is less certain.

1 General Concepts on Reactive Oxygen Species

1.1 Nomenclature

An introduction to the nomenclature and terminology used to describe ROS biochemistry is necessary, since there are several confusing and conflicting terms in use. “Reactive oxygen species” (ROS) is a term applied to molecules that are derived from oxygen, and have a high reactivity toward other molecules. The term “free radical” is generally used to describe a radical, i.e., a molecule with a free unpaired electron. The “free” notation strictly refers to the radical being capable of independent existence, and able to react with other molecules, although often the terms “radical” and “free radical” are used interchangeably. Radicals are denoted by the dot superscript sign (\bullet). The term “ROS” is used almost interchangeably with “free radical” in the literature, although it should be noted that not all free radicals are ROS; there are several non-oxygen-based radicals such as the tyrosyl and ascorbyl radicals (Tyr^\bullet and Asc^\bullet , respectively). Similarly not all ROS are free radicals; for example hydrogen peroxide (H_2O_2) and peroxyntirite (ONOO^-) are not radicals. In addition the term “reactive nitrogen species” (RNS) has recently come into use, to describe a subset of ROS derived from nitric oxide (NO^\bullet). Again, confusion can arise since not all RNS can be strictly classified ROS and vice versa. An example is ONOO^- , which is both an ROS and an RNS.

For most purposes, use of the terms “ROS” or “RONS” (reactive oxygen and nitrogen species) is preferred, since it encompasses a large number of species, and is especially applicable to situations in which the exact molecular species is unknown. For example “mitochondrial ROS generation” covers the concept that mitochondria can make O_2^\bullet , H_2O_2 , ONOO^- , LOOH , or a variety of other species. [Table 5.3-1](#) shows a listing of some common free radicals, ROS, RNS, and antioxidants encountered in biological systems, with their varying nomenclature. For further reading, the Society for Free Radical Biology and Medicine

Table 5.3-1

Reactive oxygen species, reactive nitrogen species, free radicals, and antioxidants commonly encountered in biological systems. Names listed are the formal ones, with other (often more commonly used) names listed on the right

Symbol/abbreviations	Name	Other names
$\text{O}_2^{\bullet-}$	Superoxide anion radical	Superoxide
HO_2^\bullet	Hydroperoxyl radical	Protonated superoxide
OH^\bullet	Hydroxyl radical	
H_2O_2	Hydrogen peroxide	
LOO^\bullet	Lipid hydroperoxyl radical	
LOOH	Lipid hydroperoxide	Lipid peroxide
NO^\bullet	Nitric oxide	
ONOO^-	Peroxyntirite anion	Peroxyntirite
ONOOH	Peroxyntirous acid	
Asc	Ascorbate	Vitamin C
GSH	Reduced glutathione	Glutathione
GSSG	Oxidized glutathione	Glutathione disulfide
α -Toc	α -Tocopherol	Vitamin E
SOD	Superoxide dismutase	Cu/Zn SOD or Mn SOD
CAT	Catalase	

(SFRBM) website has an excellent “virtual free radical school,” with several articles and slide shows on basic concepts in free radical research (<http://www.medicine.uiowa.edu/FRRB/VirtualSchool/Virtual.html>).

1.2 O₂ as Substrate

The ultimate substrate for generation of all ROS is molecular oxygen (O₂), with the sequential one electron reduction of O₂ yielding O₂^{•-} → H₂O₂ → OH[•] → H₂O. It is remarkable that the mitochondrial enzyme cytochrome *c* oxidase is able to convert O₂ to H₂O without releasing any of these intermediates, by keeping them bound during its enzymatic cycle. However, as discussed in more detail below, this is not the case for some of the other mitochondrial respiratory complexes, which can leak electrons to O₂, making the superoxide anion radical, O₂^{•-}.

The absolute requirement for O₂ in ROS generation brings up a serious issue in much of the literature on the topic of mitochondrial ROS generation, including much of that cited in this review; nearly all mitochondrial experiments are performed at saturating O₂ tensions (air-saturated buffers, ~200 μM), while cells typically exist at much lower O₂ tensions (5–20 μM) (Wilson et al., 1979; Gnaiger et al., 1995). In fact, it is arguable that at the O₂ tensions experienced by mitochondria inside cells (2–20 μM), ROS generation may be severely oxygen-limited. Despite this shortcoming, much work continues to be performed at relatively high O₂ tensions owing to the difficulties in maintaining low steady-state O₂ tensions in experimental systems. It is therefore useful to remember that the absolute quantities of ROS measured at saturating O₂ in isolated cell and mitochondrial systems may not be applicable to mitochondria in situ.

1.3 Local Conditions

Another important consideration in ROS biochemistry is the impact of microenvironment on the precise chemical reactions. This is especially true for the mitochondrion, which offers not only an extremely hydrophobic membrane environment but also an alkaline matrix pH, the presence of a large concentration of reducing equivalents such as GSH, and the presence of several metal ions.

One example of the impact of a variable such as pH is the behavior of superoxide (O₂^{•-}) in mitochondria (DeGrey, 2002). The pK_a of the O₂^{•-} ↔ HO₂[•] pair is ~4.8, meaning that the superoxide made in the acidic environment of the intermembrane space will be more protonated (HO₂[•]), while superoxide made in the alkaline matrix will be anionic (O₂^{•-}). Since HO₂[•] is uncharged, it can move across membranes quicker than O₂^{•-}, giving HO₂[•] an entirely different biochemical reactivity than its unprotonated congener. An excellent review of the biochemical importance of HO₂[•] (DeGrey, 2002) highlights the differential rates of dismutation (to H₂O₂) of these species.

Another example of the importance of mitochondrial microenvironment is the biochemistry of peroxynitrite (ONOO⁻). The pK_a of the ONOO⁻ ↔ ONOOH couple is ~7, and the chemical reactivities of ONOO⁻ and ONOOH are very different, yielding differential amounts of oxidation, tyrosine nitration, and S-nitrosation (Pryor and Squadrito, 1995; Uppu et al., 1998).

A third example of the way in which microenvironment can impact ROS biochemistry is the hydrophobic nature of NO[•]. Nitric oxide partitions preferentially into biological membranes (around eightfold), while O₂ partitions around threefold. Since the reaction between NO[•] and O₂ is second order with respect to NO[•], this has the effect of an approximate 300-fold increase in the rate of reaction in membranes versus in the aqueous phase (Liu et al., 1998; Shiva et al., 2001). Thus, when membranes are present the reaction between NO[•] and O₂ is faster and NO[•] bioavailability is decreased. Since the mitochondrion represents one of the most membranous environments in the cell, the mitochondrial membrane is a very effective regulator of NO[•] availability (Shiva et al., 2001).

A final example is the presence of manganese superoxide dismutase (Mn SOD, SOD2) in the mitochondrial matrix. Thus, O₂^{•-} made facing the matrix will be dismuted to H₂O₂, for release into the cytosol by permeation across the inner and outer membranes (St-Pierre et al., 2002; Muller et al., 2004),

while $O_2^{\bullet-}$ made facing the intermembrane space will be released into the cytosol as $O_2^{\bullet-}$, through the voltage-dependent anion channel (VDAC) (Han et al., 2003a, b). In addition, the presence of a subpopulation of SOD1 (Cu/Zn SOD) in the intermembrane space continues to be a subject of debate (Weisiger and Fridovich, 1973; Okado-Matsumoto and Fridovich, 2001).

1.4 Nitric Oxide

The chapter by Bolaños et al. in this volume details several of the neuron-specific aspects of NO^{\bullet} interactions with mitochondria. As alluded to in the above paragraph, NO^{\bullet} has an overbearing impact on mitochondrial ROS biochemistry. The most notable effect is the diffusion-limited reaction between NO^{\bullet} and $O_2^{\bullet-}$, yielding $ONOO^-$ (Packer et al., 1996; Pryor and Squadrito, 1998; Uppu et al., 1998). This radical-radical reaction can occur so quickly that NO^{\bullet} competes with SOD for $O_2^{\bullet-}$ (Beckman et al., 1990), essentially meaning that whenever there is NO^{\bullet} around, any $O_2^{\bullet-}$ made will be converted to $ONOO^-$.

The other main impact of NO^{\bullet} on mitochondrial ROS is the ability of NO^{\bullet} to modulate ROS generation via its effects on respiration. NO^{\bullet} is a potent reversible inhibitor of cytochrome *c* oxidase (Cleeter et al., 1994; Brown, 2000; Shiva et al., 2001), and the resultant blockage of the respiratory chain has been proposed to result in enhanced ROS generation from the upstream complexes (Poderoso et al., 1996; Brookes and Darley-Usmar, 2002). In this manner, mitochondria may be considered as “redox signaling boxes,” since they may take an NO^{\bullet} cell signal and turn it into an oxidative cell signal. Evidence for such a pathway in endothelial cells has recently been shown (Palacios-Callender et al., 2004).

Combining the phenomena of $NO^{\bullet}/O_2^{\bullet-}$ reactivity, and NO^{\bullet} 's proposed ability to stimulate mitochondrial $O_2^{\bullet-}$ generation, one might guess that NO^{\bullet} addition to mitochondria would cause generation of $ONOO^-$, and in fact this has been directly demonstrated at high concentrations of NO^{\bullet} (Packer et al., 1996). Such an observation raises a critical issue when considering NO^{\bullet} effects on mitochondria: that of concentration. While a full discussion of NO^{\bullet} effects is given in the chapter by Bolaños et al., these effects can be briefly summarized by saying that low “physiological” levels of NO^{\bullet} are beneficial to mitochondria and cell functionality, whereas high “pathological” levels of NO^{\bullet} are detrimental. While this is a gross oversimplification of a constantly growing field, a key example is the induction of the mitochondrial permeability transition (PT) pore, which is inhibited by low $[NO^{\bullet}]$, but stimulated at high $[NO^{\bullet}]$ (Brookes et al., 2000). While beneficial effects of exogenously added $ONOO^-$ have been shown in some systems (Ronson et al., 1999; Garcia-Nogales et al., 2003), the mechanism is unknown and may involve conversion of $ONOO^-$ back to NO^{\bullet} by buffer components such as HEPES, or the secondary generation of *s*-nitrosothiols (Nossuli et al., 1998).

2 ROS “Weights and Measures”

2.1 Quantifying ROS—Fluorescent Probes

One of the key issues facing ROS quantitation today is defining which exact molecular species is involved, and there are very few methods that can achieve this unequivocally. Electron paramagnetic resonance (EPR) is one such method (Valgimigli et al., 2001; Davies and Hawkins, 2004; Villamena and Zweier, 2004), in which the spin traps (probes) used can show high specificity for individual radical species, although this method is usually beyond the financial or accessibility level of most laboratories, and technical limitations (such as temperature requirements) can limit its application to intricate biological systems. Interestingly, a recent innovation is immuno-spin trapping, in which protein-bound radicals can be visualized using antibodies to the spin trap/probe molecule (Mason, 2004).

The most commonly used technique for the quantitation of ROS is fluorescence, with a wide variety of probes available for use in both microscopic and bulk fluorimetric systems (Brandes and Janiszewski, 2005). A list of some of the most commonly used probes and their specificities and pitfalls is shown in [Table 5.3-2](#). ROS probes can also be further divided into those that react directly with ROS and those that

■ **Table 5.3-2**
Commonly used ROS probes

Abbreviations	Uses	Detects	Pitfalls
DCF-DA	C, F	Superoxide, H ₂ O ₂ , ONOO ⁻	Reacts with cyt-c
DHE	C	O ₂ ^{•-} no kinetic rates	
DHR 123		ONOO ⁻	
CMX-ROS			
Amplex Red	M	H ₂ O ₂ , LOOH	NADH artifacts
Homovallinic acid	M	H ₂ O ₂	Reacts with ONOO ⁻
Mito-sox-red	M, F	O ₂ ^{•-} no kinetic rates	
DAF	C, M	NO [•] , NO ₂ ⁻ , N ₂ O ₃	Reacts with ascorbate
Lucigenin	C, M	O ₂ ^{•-} , H ₂ O ₂ , ONOO ⁻	Redox cycles
Coelenterazine	C, M	O ₂ ^{•-}	

Uses: C cell microscopy, M isolated mitochondria, F FACS or bulk fluorescence

require an enzymatic activity to give a signal. For example many assays of ROS use peroxidase (usually from horseradish) as an auxiliary enzyme, relying on the generation of the enzyme compound-I from H₂O₂, and it is compound-I that then reacts with the probe to give a fluorescent product. Another common practice when studying mitochondria is to include SOD in the incubations, to convert any O₂^{•-} to H₂O₂, thereby ensuring that all ROS released from the mitochondria end up as H₂O₂, to be detected by the fluorescent system.

It should be noted that the field of fluorescent ROS detection is a rapidly evolving one, with new compounds being introduced to the market on an almost monthly basis. It is beyond the scope of this chapter to discuss the merits of each individual compound, but typically a “grace” period of around 1 year follows the release of a new compound, before an artifact is discovered, such as reaction of the probe with other cellular components. For example the probe DCF is now known to react with cytochrome *c* (Burkitt and Wardman, 2001), DAF is known to react with ascorbate (Zhang et al., 2002), and Amplex red may suffer artifacts from reaction with NADH (Votyakova and Reynolds, 2004), thereby limiting the broad application of conclusions drawn from early experiments using these compounds. Nowadays, the most valid approach to the determination of ROS is one that encompasses multiple different probes and experimental systems. For example a combined approach using DCF-DA, DHE, and mito-sox-red would be considered adequate, since each of these probes has different chemical bases for its reactivity with the ROS being studied, and therefore it is hoped they would not all be subject to the same artifacts.

Several chemiluminescent probes also exist for ROS determination, although these probes have fallen out of fashion in recent years, in favor of fluorescent probes. This was mostly due to the discovery that the probe lucigenin can redox-cycle, and actually generates ROS during this cycling (Tarpey et al., 1999). These problems have been solved more recently by the use of modern probes such as coelenterazine. Another disadvantage of chemiluminescent probes is their complex kinetics. Fluorescent probes, once they have reacted with an ROS, will yield a product that continues to fluoresce. Thus, the fluorescent signal can easily be measured and the kinetics (rate of ROS generation) quantified, since the signal always increases. In contrast, the product of an ROS and a chemiluminescent probe is a short-lived luminescent species that ceases to give off light once it has returned to the ground state. Thus, the traces obtained from chemiluminescent experiments exhibit complex shapes, and it is often difficult to obtain data on rates of ROS generation, since one is essentially measuring the steady-state level of a species that is being both made and degraded simultaneously.

A final note on kinetics should be added with respect to dyes such as DHE and its derivative mito-sox-red. These dyes work by intercalation of the oxidized product into DNA to give a fluorescent signal. Under certain circumstances the rate-limiting step for the fluorescence increase may be the DNA intercalation and not the ROS generation, and therefore these dyes cannot be used quantitatively to determine rates of ROS generation, and are best suited to end-point assays.

2.2 Use of Inhibitors and Antioxidants

Much of the current literature assigning an ROS signal to mitochondria comes from the use of two classes of inhibitors: (1) mitochondrial pharmacologic agents and (2) antioxidants (reviewed in Levenon et al., 2001; Brookes et al., 2002b; Waypa and Schumacker, 2005). The former (see [Figure 5.3-1](#)) have been developed over several decades of research on isolated mitochondria, and their application to cells and tissues should always be with caution, since these compounds may react with nonmitochondrial cellular components, which they were never designed to encounter. For example rotenone is an excellent dissociator of microtubules (Brinkley et al., 1974), antimycin A mimics the BH₃ domain of proapoptotic Bcl family proteins (Tzung et al., 2001), and uncouplers such as FCCP will uncouple the proton gradients across all membranes in a cell, not just the mitochondrial inner membrane. Thus, in a manner similar to fluorescent probes, the most reliable approach is to pool results from several different inhibitors with different mechanisms of action. Furthermore, with the advent of novel genetic tools such as siRNA, reliance on a purely pharmacologic approach to the manipulation of mitochondrial enzyme activity is no longer necessary (Brunelle et al., 2005).

In the case of antioxidants, one of the most reliable ways to assign a biological activity to an ROS is to see if the effect can be reversed by an antioxidant or radical scavenger. Examples include the use of oxyhemoglobin (Feelisch et al., 1996) or carboxy-PTIO (Maeda et al., 1994) to scavenge NO[•], the use of N-acetyl cysteine as a general thiol antioxidant and precursor for GSH synthesis, uric acid to scavenge ONOO⁻, or superoxide dismutase to scavenge O₂^{•-}. In certain cases, the specificity of such scavengers should be viewed with caution, and this is all the more applicable to the hydroxyl radical (OH[•]). The extreme reactivity of OH[•] with just about any biomolecule, including water (at a concentration of 55 molar), means there is essentially no such thing as a specific OH[•] scavenger, and it is difficult to assign a biological effect to OH[•] over another reactive species.

The development of novel targeted antioxidants, especially mitochondria-targeted compounds, is proceeding rapidly. Key examples include mitochondria-targeted forms of α -tocopherol and ubiquinone (Smith et al., 1999; Coulter et al., 2000). Such compounds will be of great use in deciphering the spatial distribution of ROS within the cell, and as therapeutics in the prevention of oxidative stress diseases (see [Sect. 7](#)).

2.3 So, How Much ROS?

The most widely heard phrase when referring to mitochondrial ROS generation is “mitochondria are the most significant source of ROS in the cell.” While this may indeed be the case under certain pathologic conditions, it is not generally applicable to all cell types and conditions. In the case of isolated mitochondria, ROS generation (mostly H₂O₂ measurements) is in the range of tens of nanomoles/min/mg protein (Boveris et al., 1972; Boveris and Chance, 1973; Cadenas and Boveris, 1977; Poderoso et al., 1996; St-Pierre et al., 2002; Han et al., 2003a, b; Turrens, 2003; Muller et al., 2004; Palacios-Callender et al., 2004)). This varies greatly depending on two major factors: (1) the respiratory substrate that the mitochondria are supplied with, and (2) the state of the mitochondria, i.e., state 3 or 4 respiration, uncoupled, or inhibited by compounds such as antimycin A or rotenone. In addition, tissue-specific differences are present, such that heart, muscle, and brain mitochondria typically make two- to threefold more ROS than those from liver and kidney. However, since ROS generation rates are usually normalized per milligram of mitochondrial protein, and mitochondria from heart/muscle/brain contain a greater complement of cytochromes (Rossignol et al., 2000), such differences may not represent different properties at the molecular level in the individual respiratory complexes.

Interestingly, ROS generation appears to show a general correlation with metabolic rate (see Brookes, 2005, for review); thus mitochondria from smaller animals such as mice exhibit greater rates of ROS generation than larger animals such as humans. This relationship is believed to underlie the mitochondrial free radical theory of aging, whereby animals with a higher metabolic rate have shorter lifespan (Sohal and Weindruch, 1996; Barja, 2002; Harper et al., 2004). From an experimental perspective however, this means that results obtained in one experimental tissue/organ/organism system may not be generally applicable to other systems.

2.4 End Points Versus Kinetic Rates

Another issue in mitochondrial ROS quantitation is the lifetime of the ROS in question, and (as discussed above) the fluorescent or luminescent product to be quantified. In the case of luminescent probes, the lifetime of the luminescent species can impact the measurement, such that it is often difficult to know whether to quantify the absolute luminescence, the rate of increase in luminescence, or the area under the curve. Similarly, several probes such as DCF undergo spontaneous auto-oxidation under standard experimental systems, such that there is an increased fluorescence even in the absence of a biological stimulus. In these cases, careful baseline correction and subtraction is required if quantitation of the absolute rate of ROS generation is needed.

One extreme solution that has been proposed to overcome these quantitation difficulties is the physical separation of mitochondria from the measurement system (Staniek and Nohl, 1999). In this method, mitochondria are pelleted by centrifugation and ROS quantified in the supernatant. However, such a method relies on the long-term stability of the ROS being quantified, inevitably leading to underestimation of ROS amounts. Indeed, the conclusion that can be drawn from such studies is that mitochondria do not make ROS at all (Nohl et al., 2003a, b). Clearly, given the opening statement of this section that mitochondria are the most significant source of ROS in the cell, the answer lies somewhere in between these extreme viewpoints.

Overall, the methodology by which mitochondrial ROS are quantified can be fraught with artifacts and caveats. However, careful choice of reagents and experimental systems, coupled with a multipronged approach, can yield reliable, reproducible data.

3 Mitochondria as a Source of ROS

Mitochondria are a significant cellular source of ROS, and under certain conditions may indeed be the dominant cellular source of ROS (Boveris et al., 1972; Boveris and Chance, 1973; Cadenas et al., 1977; Turrens, 2003). The primary ROS generated in the organelle is superoxide ($O_2^{\bullet-}$), which is then converted to H_2O_2 by spontaneous dismutation or by SOD. H_2O_2 can also be further transformed to OH^{\bullet} in the presence of metal ions by Fenton chemistry, although metal chaperone proteins in the mitochondrial matrix likely prevent this from occurring in the organelle. [Figure 5.3-2](#) shows a schematic of the mitochondrion, highlighting the major sources of ROS, each of which are discussed in detail later.

3.1 The Energy “Plumbing” of Mitochondria and ROS Leakage

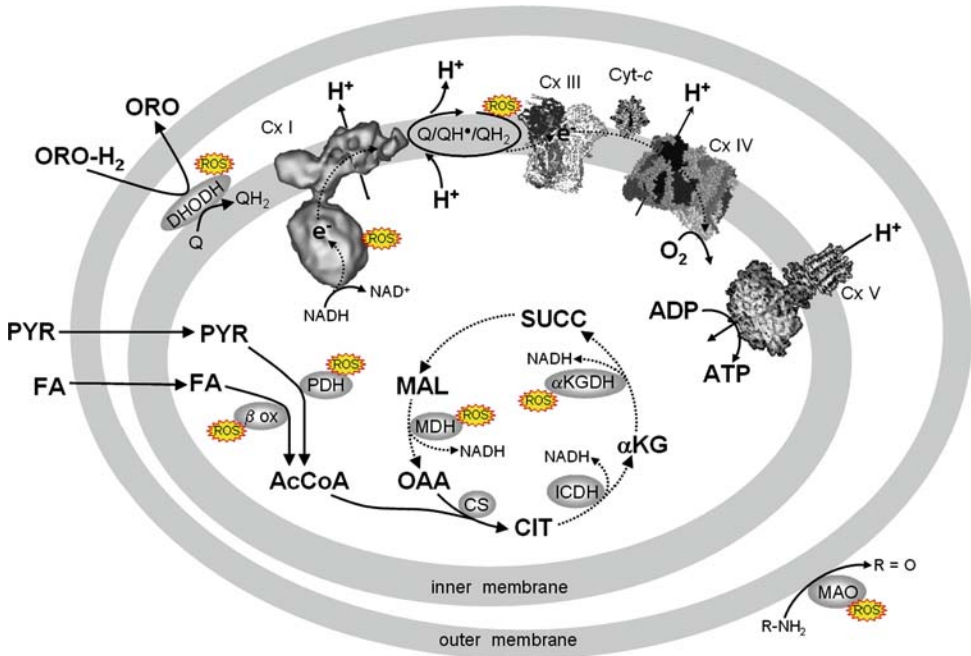
In considering mitochondrial ROS generation, a helpful analogy is to think of energy and electron flow through mitochondria as a series of water pipes. When one of the pipes becomes blocked, electrons leak out and react with O_2 to form ROS. [Figure 5.3-3](#) outlines the network of energy/electron flow in mitochondrial oxidative phosphorylation, highlighting the important sites for ROS generation, and the fact that inhibition downstream of these sites results in a buildup of electrons, and greater ROS formation. All of the known regulators of mitochondrial ROS generation act at one or more of these sites, including compounds such as rotenone (complex I), antimycin (complex III), NO^{\bullet} (complex IV), uncouplers (H^+ leak), and ADP.

3.2 ROS from the Respiratory Chain

The main mitochondrial $O_2^{\bullet-}$ source is believed to be the ubisemiquinone radical (QH^{\bullet}), formed at the complex III Q_O site, facing the intermembrane space (Cadenas et al., 1977; St-Pierre et al., 2002; Han et al., 2003a, b), although some $O_2^{\bullet-}$ may also be released to the matrix from this site (Muller et al., 2004). Inhibitors of complex III including antimycin A and myxothiazol are typically used to demonstrate increased ROS from complex III ([Figure 5.3-1](#)). Two related parameters that regulate ROS generation

■ Figure 5.3-2

Schematic of mitochondrial oxidative phosphorylation, showing major sites of reactive oxygen species (ROS) generation. Complex II and several intermediates of the tricarboxylic (TCA) cycle are omitted for clarity. Pathways of electron flux are denoted by the dotted arrows. The intermediates of the Q cycle are abbreviated Q (ubiquinone), QH[•] (ubisemiquinone radical), and QH₂ (ubiquinol). Other abbreviations as per [Figure 5.3-1](#), except for the following: *AcCoA* acetyl coenzyme A, *αKG* α-ketoglutarate, *αKGDH* α-ketoglutarate dehydrogenase, *β-ox* fatty acid β oxidation, *CIT* citrate, *CS* citrate synthase, *DHODH* dihydroorotate dehydrogenase, *FA* fatty acids, *MAL* malate, *MAO* monoamine oxidase, *OAA* oxaloacetate, *ORO* orotate, *ORO-H₂* dihydroorotate, *PYR* pyruvate, *SUCC* succinate. The main sites of ROS generation are complex I (facing the matrix side), complex III Q cycle (facing the intermembrane space), PDH, MDH, and α-KGDH (in the TCA cycle), DHODH, the electron transfer flavoprotein of fatty acid β-oxidation, and at monoamine oxidase during the deamination of monoamines (R-NH₂) to aldehydes (R = O)

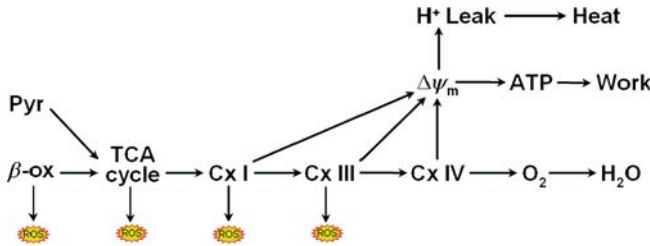


at complex III are the effective concentration of QH[•], which is increased when the distal respiratory chain is inhibited and the frequency of QH[•] occurrence, which is increased when the respiratory chain turns over more quickly. Thus, both stimulation and inhibition of mitochondrial oxidative phosphorylation can result in enhanced ROS generation.

In addition to complex III, more recent evidence favors complex I as a significant source of O₂^{•-} generation, facing the matrix (St-Pierre et al., 2002), although the exact site within the complex is unclear, with the FMN cofactor, the various Fe-S clusters, and the Q binding sites all being proposed as sources of ROS. Rotenone and other distal complex I inhibitors can cause O₂^{•-} generation facing the matrix side of the inner membrane, and recent reports suggest that glutathionylation (Taylor et al., 2003) of complex I or phosphorylation by PKA (Raha et al., 2002) can elevate ROS generation, but the physiologic or pathologic significance of this is unclear. In addition, *in vitro* experiments show that electrons entering at complex II (succinate dehydrogenase) can flow backward through complex I to make ROS (St-Pierre et al., 2002), although *in vivo* this would be prevented by forward electron flow through complex I from NADH, except under pathologic conditions in which NADH is depleted (see [Figure 5.3-2](#)). Notably, it has been shown that complex I can be S-nitrosated (covalent attachment of NO[•] to a cysteine residue) following exposure of mitochondria to NO[•] donors (Clementi et al., 1998; Burwell et al., 2005).

■ **Figure 5.3-3**

The electron and energy flux “plumbing” of mitochondrial oxidative phosphorylation. Using water pipes as an analogy for electron and energy flow through mitochondria, each of the steps in bold may be thought of as a branch point or a control valve. Examples of this system in action include the following: (1) Elevated H^+ dissipates $\Delta\psi_m$ as heat, preventing feedback inhibition of the respiratory chain and therefore decreasing reactive oxygen species (ROS) generation. (2) Inhibition of complex IV by lack of O_2 , or by inhibitors such as NO^* , feedback inhibits the respiratory chain, shifting the flow of electrons toward ROS generation



The primary factor governing mitochondrial ROS generation by respiratory complexes I or III is the redox state of the respiratory chain. Since the respiratory chain complexes are proton pumps, this property is inherently governed by the transmembrane potential ($\Delta\psi_m$), which can feedback inhibit the pumps when sufficiently high. This is highlighted in [Figure 5.3-3](#), in which $\Delta\psi_m$ is shown as a central factor in the flow diagram of mitochondrial energy metabolism. Things that cause a buildup of $\Delta\psi_m$ can increase ROS, while things that dissipate $\Delta\psi_m$ can decrease ROS. This concept has recently been demonstrated experimentally (Korshunov et al., 1997; Starkov and Fiskum, 2003). Indeed, the activation of “mild” uncoupling or proton leak pathways across the mitochondrial inner membrane (possibly mediated by uncoupling proteins, UCPs) is emerging as a significant protective strategy in pathological conditions where overproduction of ROS is implicated, such as cardiac ischemia–reperfusion (I–R) injury (Minners et al., 2000, 2001; Ganote and Armstrong, 2003; Teshima et al., 2003; Hoerter et al., 2004; McLeod et al., 2004). This phenomenon is discussed in more detail in the chapter by Dugan *et al.* on mitochondrial uncoupling.

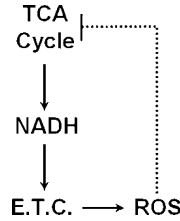
3.3 ROS from the Tricarboxylic Cycle

An exciting recent development in the field of mitochondrial ROS research is the realization that several dehydrogenases in the tricarboxylic cycle (TCA) cycle can generate ROS. Most notably, α -ketoglutarate dehydrogenase (α -KGDH) and pyruvate dehydrogenase (PDH) have been identified as sources of ROS (Starkov et al., 2004; Tretter and Adam-Vizi, 2004). Both these enzymes contain miniature electron transport chains, including α -lipoic acid, NADH, and flavin binding sites. The precise site within these chains where electrons may interact with O_2 to generate ROS is not yet known.

Additionally, several of the TCA cycle enzymes are sensitive to inhibition by oxidants. The most widely studied example is aconitase, whose Fe–S center has been shown to be damaged by several different types of ROS and RNS (Castro et al., 1994). Indeed, inhibition of mitochondrial aconitase is often used as an indicator of intramitochondrial ROS generation (Muller et al., 2004). Similarly, α -KGDH has been shown by several authors to be inhibited under conditions of oxidative stress (Humphries and Szveda, 1998; Tretter and Adam-Vizi, 2000). Interestingly, such inhibition of the TCA cycle dehydrogenases would slow down the entry of electrons into the respiratory chain, by decreasing the generation of NADH, and this in turn would slow down ROS generation by complexes I and III. This has led to the proposal that redox-sensitive TCA cycle enzymes and the respiratory chain may be involved in a feedback loop type of regulation mechanism, as depicted in [Figure 5.3-4](#). Such a feedback loop would function as a safety valve, to prevent overproduction of ROS by the respiratory chain (Armstrong et al., 2004).

■ Figure 5.3-4

Feedback regulation of the tricarboxylic (TCA) cycle by reactive oxygen species (ROS) generation. Several enzymes in the TCA cycle are inhibited by ROS, and this in turn would limit the flow of electrons in the respiratory chain (via NADH), thereby inhibiting further ROS generation. Such a system may help to limit overproduction of ROS in pathologic situations



3.4 ROS from Other Mitochondrial Sources

Three other notable sources of ROS are present in the mitochondrion (▶ Figure 5.3-2). The first is the electron transfer flavoprotein of fatty acid β -oxidation, which has been shown to be a significant source of ROS under conditions where mitochondria are oxidizing palmitoylcarnitine as a respiratory substrate (Boveris et al., 1972; Boveris and Chance, 1973; St-Pierre et al., 2002). The second is monoamine oxidase (MAO), which is located on the mitochondrial outer membrane and participates in the degradation of neurotransmitters, generating H_2O_2 in the process (Werner and Cohen, 1991). The upregulation of MAO, and a consequent increase in H_2O_2 generation, has been implicated in several pathological conditions including Parkinson's disease (Cohen, 2000) and cardiac hypertrophy (de Chaplain et al., 1968). The third is the enzyme dihydroorotate dehydrogenase (DHOD), an important mediator of pyrimidine biosynthesis, which is an additional mitochondrial source of ROS (Forman and Kennedy, 1976).

3.5 Regulation of Mitochondrial ROS Generation

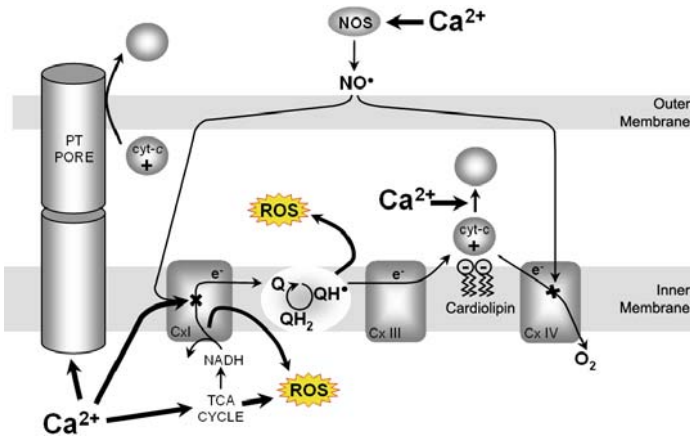
Mitochondrial ROS generation appears to be a tightly regulated process, and as discussed in the preceding sections, there are several physiological effectors that can impact ROS generation from the organelle. Among the most widely studied are Ca^{2+} and NO^\bullet .

There have been several studies on the regulation of mitochondrial ROS generation by Ca^{2+} . In a recent review (Brookes et al., 2004), we highlighted the potential mechanisms by which Ca^{2+} can impact ROS generation, as summarized in ▶ Figure 5.3-5 (the legend to this figure gives a stepwise explanation of each of these mechanisms, and overall it appears that the situation is a lot more complicated than merely a simple acceleration of oxidative phosphorylation by Ca^{2+}). It is also worth noting that many of these mechanisms are based on experiments in isolated enzymes or organelles, and it is not clear which (if any) will be prevalent at the whole-cell level. For example, the micromolar level of Ca^{2+} required to stimulate the dehydrogenases of the TCA cycle (McCormack and Denton, 1993) means that in typical isolated mitochondrial preparations these enzymes are already supersaturated with Ca^{2+} .

The effects of Ca^{2+} are also tissue-specific (reviewed in Gunter et al., 2004), especially with respect to transport mechanisms, and depend on various other parameters such as the respiratory state of the mitochondria. For example, Ca^{2+} diminishes ROS from both complexes I and III under normal conditions, and enhances ROS when these complexes are inhibited (Cadenas and Boveris, 1980; Kowaltowski et al., 1998; Starkov et al., 2002; Sousa et al., 2003). The exact mechanism of Ca^{2+} -induced ROS generation by direct action on the respiratory complexes is unclear, although it may involve changes in their 3D conformation or structure. Indeed, Ca^{2+} is reported to alter the spectrum of cytochromes a/a_3 in isolated complex IV (Wikstrom and Saari, 1975), and we have shown that Ca^{2+} exposes novel mitochondrial targets for nitration by $ONOO^-$ (Brookes and Darley-Usmar, 2004), consistent with protein conformational

■ Figure 5.3-5

Mechanisms for Ca^{2+} stimulation of mitochondrial reactive oxygen species (ROS) generation. Thick arrows represent effects of Ca^{2+} . Complex II is omitted for clarity. Direct stimulation of the tricarboxylic (TCA) cycle by Ca^{2+} can enhance electron flow into the respiratory chain, while Ca^{2+} stimulation of NOS and subsequent NO^\bullet generation would inhibit respiration at complex IV. These events (alone or in combination) would enhance ROS generation from the Q cycle. In addition NO^\bullet and Ca^{2+} together can inhibit complex I, possibly enhancing ROS generation from this complex. Ca^{2+} also dissociates cytochrome *c* from its binding site on the inner membrane, at cardiolipin, and at high concentrations triggers permeability transition (PT) pore opening and cytochrome *c* release across the outer membrane. Both these events would lead to a blockade of electron flux at complex III, thereby also enhancing ROS generation at the Q cycle



changes. Ultimately, differences in the subunit composition of the respiratory complexes between tissues may underlie the tissue specificity of Ca^{2+} effects on ROS generation.

Another important aspect of the effects of Ca^{2+} on ROS generation is the role of the mitochondrial PT pore (Crompton, 1999; Brookes et al., 2000, 2004; Halestrap et al., 2002; DiLisa et al., 2003). The PT pore is a large assembly of inner- and outer-membrane proteins that is triggered by excess Ca^{2+} and a variety of oxidants such as ONOO^- . The interactions between ROS, Ca^{2+} , and the PT pore can be summarized by saying that ROS generation appears to increase following PT pore opening, but may also be involved, in an autocatalytic manner, in the actual opening mechanism of the PT pore itself. An extensive review of the PT pore is given in the chapter by Wieloch et al. in this volume.

3.6 Mitochondrial Generation of RNS

No discussion of mitochondrial ROS generation would be complete without mentioning the putative mitochondrial NO^\bullet synthase (mtNOS). While initial reports of mtNOS were intriguing (Bates et al., 1995; Ghafourifar and Richter, 1997; Giulivi et al., 1998), the experimental evidence is somewhat equivocal, and several recent papers have questioned the existence of this enzyme (Lacza et al., 2003b, 2005; Brookes, 2004; Gao et al., 2004; Tay et al., 2004). Controversy still surrounds the amount of NO^\bullet made by the putative mtNOS (reported rates vary by 150,000-fold), the purity/contamination of mitochondrial preparations, and the specificity of NOS assays used. This is not to say that NO^\bullet is not an important regulator of mitochondrial function, which it clearly is, but merely to highlight that making NO^\bullet inside the mitochondrion is not necessary to explain the effects of this radical on mitochondrial function.

A very exciting recent development is the discovery that the plant *Arabidopsis thaliana* possesses a unique isoform of NOS (termed “atNOS”), which is structurally unrelated to the other classical NOS isoforms, and contains a mitochondrial targeting sequence (Guo and Crawford, 2005). The discovery of a mammalian homolog of this protein would represent a significant advance for the field, but would also render obsolete much of the work to date on classical NOS isoforms in mitochondria.

4 Neuron-Specific Aspects of Mitochondrial ROS Generation

Much of the work on mitochondrial ROS generation has been performed using common isolated mitochondrial preparations such as those from rat heart and liver. As discussed above, there are tissue differences between mitochondria (Rossignol et al., 2000), such as the content of respiratory complexes and preferences for respiratory substrates (see chapter by Perkins et al.). In this section, the aspects of neuronal function that impact neuronal mitochondrial ROS generation are discussed.

4.1 Neuronal Mitochondria Versus Glial/Astrocytic Mitochondria

As mentioned earlier, the ability of MAO to make H_2O_2 has unique import for brain mitochondria, since the metabolism of neurotransmitters is a critical function in neurons and astrocytes. In particular, it has been proposed that selective neurotoxicity caused by complex I inhibition in Parkinson's disease (Schapira et al., 1989) may be due to MAO-derived ROS (Cohen, 2000).

As emphasized elsewhere in this book, metabolic function in different types of brain cells is highly differentiated. For example, it has now been demonstrated with two-photon microscopic evidence that astrocytes primarily perform glycolysis, and shuttle lactate to neurons, which then further metabolize lactate via oxidative phosphorylation to yield ATP (Kasischke et al., 2004).

Whether the ROS generation varies between neuronal and astrocytic mitochondria remains largely understudied. The main reason for this is the lack of reliable methods for isolating distinct subpopulations of mitochondria from neuronal tissue. Although recent advances have been made in the area of mitochondrial isolation from different types of cultured cells such as neurons and astrocytes (Kristian et al., 2005), the majority of isolated mitochondrial experiments use whole-brain homogenates as the starting material for preparations, and are weighted toward nonsynaptosomal populations (Lai et al., 1977). There have been attempts to examine ROS generation in unique neuronal populations, such as those from the substantia nigra (in the context of Parkinsonism), but these studies are limited in number (Goldberg et al., 2003), and are hampered by difficulties in isolating sufficient quantities of mitochondrial material, especially when using transgenic mice as tissue source.

An interesting aspect of considering heterogeneity between mitochondrial populations is the idea that mitochondria within the same neuron may behave differently depending on their position within the cell. It has recently been demonstrated that mitochondria within dendrites have higher membrane potentials than those in the cell body (Miller and Sheetz, 2004). As discussed earlier, $\Delta\psi_m$ is a key regulator of mitochondrial ROS generation (Starkov and Fiskum, 2003), and thus it would seem logical that dendritic mitochondria may make more ROS. Notably, it has been shown that the susceptibility of mitochondria to oxidative stress is particularly high in nerve terminals (Chinopoulos and Adam-Vizi, 2001).

Another factor to consider between neurons and astrocytes is their antioxidant capacity. Extensive work has now shown that neurons are essentially "antioxidant poor," and get most of their antioxidant capacity from astrocytes (Barker et al., 1996; Peuchen et al., 1997; Heales et al., 1999; Stewart et al., 2002; Heales et al., 2004). This includes the shuttling of glutathione and its precursors from astrocytes to neurons, and the export of extracellular SOD from astrocytes (Stewart et al., 2002). Notably, mitochondria do not make their own GSH, and have to import it from the cytosol (Fernandez-Checa et al., 1998; Reed, 2004). Thus, since neuronal mitochondria get most of their GSH from astrocytes, it would appear that any disruption in the antioxidant shuttling machinery between these two types of brain cells may have a significant impact on neuronal mitochondrial redox status and ROS generation.

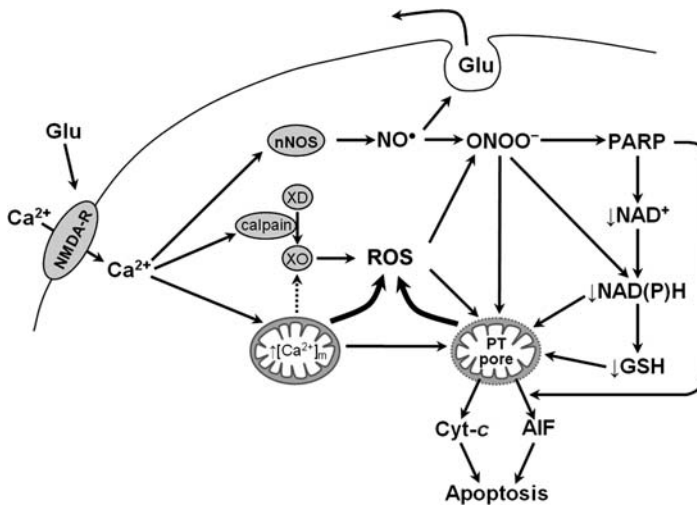
4.2 Neuronal Excitotoxicity, Ca^{2+} Overload, and ROS

Excitotoxicity is a phenomenon in which neuronal cells undergo necrosis or apoptosis in response to overexposure to excitatory amino acids such as glutamate (Sattler and Tymianski, 2001). Prolonged NMDA receptor activation leads to massive Ca^{2+} influx, resulting in Ca^{2+} overload and cell death. Presently there

are two models for the mechanism of excitotoxicity: the mitochondrial Ca^{2+} hypothesis and the nuclear PARP hypothesis, with both models emphasizing a key role for ROS. The interplay between these two models is shown in [Figure 5.3-6](#).

Figure 5.3-6

Mitochondrial reactive oxygen species (ROS) in neuronal excitotoxicity. Following NMDA-receptor (NMDA-R) activation, Ca^{2+} influx leads to stimulation of nNOS and NO^\bullet generation. In addition, both Ca^{2+} accumulation by mitochondria and activation of xanthine oxidase (XO) by calpain lead to ROS generation. ROS and NO^\bullet then combine to make peroxynitrite (ONOO^-), which activates PARP. This then leads to pyridine nucleotide depletion, which subsequently leads to energetic dysfunction and loss of antioxidant capacity (GSH). Alone or in combination, low GSH, ROS, ONOO^- , and Ca^{2+} all contribute to mitochondrial permeability transition (PT) pore opening and release of proapoptotic proteins such as cytochrome *c* and AIF, eventually leading to cell death



The mitochondrial Ca^{2+} hypothesis centers on mitochondrial Ca^{2+} overload as a central event, leading to enhanced generation of mitochondrial ROS, opening of the PT pore, and release of proapoptotic proteins such as cytochrome *c* (Stout et al., 1998; Nicholls et al., 1999; Duchen, 2000). In support of this, inhibition of mitochondrial Ca^{2+} accumulation prevents excitotoxicity. Moreover, during the progression to cell death, a secondary increase in cytosolic Ca^{2+} occurs, termed “delayed Ca^{2+} deregulation” (DCD), and it appears that the speed of DCD is strongly dependent on the magnitude of mitochondrial Ca^{2+} accumulation, suggesting that mitochondrial Ca^{2+} release (possibly via the PT pore) causes DCD.

Parallel to the mitochondrial Ca^{2+} hypothesis, a role for poly-ADP-ribose polymerase-1 (PARP-1) in excitotoxicity has been established (Szabo and Dawson, 1998; Pieper et al., 1999), in which NMDA-receptor-mediated Ca^{2+} influx leads to activation of neuronal nitric oxide synthase (nNOS), excessive production of NO^\bullet (Dawson et al., 1991), and activation of proteases that cleave and activate xanthine oxidase, leading to ROS generation. Subsequent ONOO^- generation (from NO^\bullet and $\text{O}_2^{\bullet-}$) damages DNA, and activates PARP-1, which then catalyzes NAD^+ hydrolysis and depletion, leading to cellular energy crisis and eventually cell death. Notably, PARP-1 activation leads to the release of cytochrome *c*, which would further enhance mitochondrial ROS generation. This may occur through $\text{ONOO}^-/\text{Ca}^{2+}$ -dependent PT pore opening (Brookes and Darley-Usmar, 2004).

A scheme incorporating both of these models is shown in [Figure 5.3-6](#), highlighting the central role of mitochondria and ROS generation. Further interaction between PARP-1 and ROS could occur at the level

of $\text{NAD(P)}^+/\text{NAD(P)H}$, since glutathione reductase (GR) requires NAD(P)H to reduce GSSG back to GSH, and thus NAD(P)^+ depletion would deplete the reducing substrate NAD(P)H , leading to loss of GSH, and consequently more ROS generation.

Overall, the pathways of cell injury and death in neuronal excitotoxicity highlight the central role of mitochondrial ROS generation and Ca^{2+} overload, and the complex interaction between the mitochondrion and its unique neuronal environment, to bring about cell death.

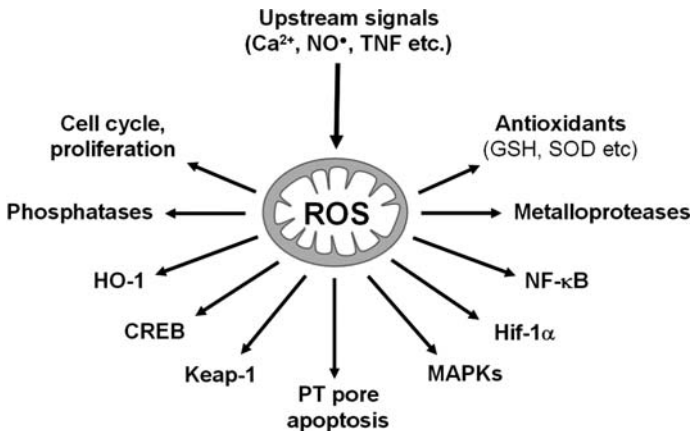
5 Cell Signaling by ROS

5.1 ROS Are Cell Signaling Molecules

When one thinks of a typical cell signaling molecule such as cAMP, a series of properties emerge that are the defining hallmarks of a cellular second messenger, including (1) made enzymatically, (2) binding to specific targets, (3) compartmentalization, (4) short half-life, (5) often degraded enzymatically, and (6) diffusible. When this set of rules is applied to free radicals, it is immediately apparent that both ROS and RNS can be defined as second messengers. The remainder of this chapter will deal with some of the cell signaling pathways that can be regulated by ROS, with an emphasis on ROS from mitochondria. [Figure 5.3-7](#) shows a variety of cell signaling pathways impacted by mitochondrial ROS generation.

Figure 5.3-7

Cell signaling pathways that are impacted by mitochondria-derived reactive oxygen species (ROS)



5.2 Specific Examples of ROS Cell Signaling

The idea that a “tonal” rate of ROS generation is essential for cell survival has been gaining popularity in recent years. This overturns the notion that mitochondrial ROS are merely damaging by-products of respiration (Harman, 2003), and instead suggests that mitochondrial ROS are important for a variety of cellular processes (Levonen et al., 2001; Brookes et al., 2002b). Illustratively, cytosolic Cu/Zn SOD^{-/-} mice are viable, while mitochondrial Mn SOD^{-/-} mice are not (Huang et al., 1997). The fact that Cu/Zn SOD cannot compensate for the loss of Mn SOD suggests a much more subtle, compartmentalized role for these enzymes than mere damage limitation and ROS detoxification. Several recent studies have shown that perturbations in mitochondrial ROS generation can affect diverse redox signaling pathways such as the cell

cycle (Sauer et al., 2001), cell proliferation (Kim et al., 2001), apoptosis (Li et al., 2003), metalloproteinase function (Ranganathan et al., 2001), oxygen sensing (Chandel et al., 2000, Brunelle et al., 2005, Waypa and Schumacker, 2005), protein kinases (Ranganathan et al., 2001, Ramachandran et al., 2002), phosphatases (Pomytkin and Kolesova, 2002), enzymes such as heme-oxygenase (Chang et al., 2003), growth factor signaling (Thannickal and Fanburg, 1995), and a multitude of transcription factors (Hongpaisan et al., 2003, Itoh et al., 2005) (see [Figure 5.3-7](#)).

Various extracellular stimuli have been shown to increase the production of ROS by the mitochondrial respiratory chain, thereby causing a shift in overall redox balance and subsequent initiation of downstream signaling cascades (Droge, 2002). Among the first such discovered was the cytotoxic and gene-regulating effects of TNF α , shown to be mediated by mitochondrial ROS formation (Schulze-Osthoff et al., 1992; Hennet et al., 1993). Although studies on specific sites in the respiratory chain rely upon the use of inhibitors, and are therefore difficult to interpret, increased production of mitochondrial ROS by TNF α and ceramide has been localized at the cytochrome *bc*₁ segment of complex III (Schulze-Osthoff et al., 1992; Garcia-Ruiz et al., 1997; Di Paola et al., 2000).

More recently, a number of other cell signaling pathways have been suggested to be relayed through mitochondria, including activation of protein kinase C (Lee et al., 2004) and nuclear factor κ B (NF- κ B) (Kiritooshi et al., 2003) by high glucose, c-Jun N-terminal kinase (JNK)-dependent activation of glycogen synthase (Nemoto et al., 2000), and activation of NF- κ B by angiotensin II (Pueyo et al., 2000). Furthermore, cell signaling pathways initiated by ROS, such as activation of extracellular signal regulated kinases (ERK1/2), actually require an intact respiratory chain to function properly (Abas et al., 2000; Bogoyevitch et al., 2000). Notably, a number of these signaling molecules have recently been shown to be present in unique isoforms within the mitochondrion, including JNK (He et al., 1999), PKC and MAPKs (Baines et al., 2002), Src (Itoh et al., 2005), and PKA (Raha et al., 2002). Identification of the mitochondrial phosphorylation targets of these kinases will greatly enhance our understanding of mitochondrial signaling pathways. Indeed, recently developed proteomics tools are already making significant advances in this area (Schulenberg et al., 2004).

In this regard, it is of particular interest that a mitochondria-targeted antioxidant (mito-ubiquinone) has been shown to inhibit apoptosis caused by external administration of H₂O₂ (Kelso et al., 2001). This suggests a role for secondary ROS production by mitochondria in H₂O₂-induced apoptosis. Inhibition of mitochondrial respiration can also trigger signaling events. For example, complex I inhibition by the Parkinsonian neurotoxin 1-methyl-4-phenylpyridium (MPP⁺) has been shown to activate JNK and NF- κ B in an ROS-dependent manner (Cassarino et al., 2000).

At this point, much of the work on ROS in cell signaling has focused on the effects of an increase in ROS. However, it should be noted that because ROS are continually being produced by mitochondria, providing a basal “ROS tone,” it is also likely that in certain scenarios, decreases in ROS generation may act as cell signals. While specific examples of this have been difficult to find, it is noteworthy that “overdosing” of antioxidants in experimental systems can produce pathological outcomes. For example in cardiac I–R injury, a condition where ROS undoubtedly play a pathologic role, administering too much SOD actually overcomes any beneficial effect seen at low concentrations, and is detrimental to recovery (Omar et al., 1990). The recent implication of ROS as important cell signals in protective pathways such as ischemic preconditioning (IPC) (Kevin et al., 2005) suggests that removing all ROS may not be a good idea.

5.3 Mitochondrial ROS and NO[•] in Cell Signaling

A concept that has increasingly received attention recently is the possible role of NO[•] in these mitochondrial ROS signaling events (see also the chapter by Bolaños et al.). Intriguingly, the protective effect of endogenously produced NO[•] against the cytotoxicity of H₂O₂ is lost when cells devoid of respiring mitochondria (ρ^0) are used, implying that NO[•] plays a critical role in defense against oxidative stress through regulation of respiration (Paxinou et al., 2001).

Two other signaling pathways that may be impacted by NO[•]–mitochondrial interactions have also not been widely considered. One is the generation of arachidonate-derived lipid signaling species

(e.g. isoprostanes, isofurans, and neuroprostanes) in mitochondria by oxidative pathways; the inhibitory effects of NO^\bullet on lipid oxidation (Rubbo et al., 1995) would impact upon this. A second is the inhibition of ATP synthesis by NO^\bullet , since many cell signaling cascades include protein kinases, which require ATP as a substrate. Recent studies showing that activation of ERK1/2 depends on cellular ATP level (Abas et al., 2000; Bogoyevitch et al., 2000) supports this notion.

5.4 Redox-Sensitive Transcription Factors

Cellular redox status, which is partially regulated by mitochondrial ROS generation, has the potential to impact a number of nuclear transcription factors. Several of these factors are themselves directly redox sensitive. For example, GABP α (a murine homolog of nuclear respiratory factor-2, or Nrf-2) is a transcription factor involved in the regulation of many nuclear-encoded mitochondrial proteins such as cytochrome *c* oxidase subunits IV and Vb, and is redox-regulated through the oxidation/reduction of one or more cysteine residues in its DNA-binding and dimerization domains (Martin et al., 1996). Another example is the peroxisome proliferator activated receptors (PPARs), a family of nuclear receptors whose natural ligands are thought to be electrophilic lipid oxidation products such as 15d-PGJ₂. Recently, PPAR- γ was found to be expressed in platelets, which have no nucleus (Akbiyik et al., 2004), suggesting possible nonnuclear functions of these receptors. Notably, many PPAR γ ligands have been shown to act directly on mitochondria (Landar et al., 2005; Martinez et al., 2005).

One of the key events that appears to be regulated by mitochondria-derived ROS is the balance between cell proliferation and differentiation. This is achieved through the regulation of several redox-sensitive transcription factors and upstream signaling molecules, such as Nrf-2, AP-1, and NF- κ B. This is particularly important for cancer cells, and indeed several genes that may impact mitochondrial ROS generation (including p53 and members of the Bcl family) are oncogenes (Hockenbery et al., 1993; Karawajew et al., 2005). In addition, important properties for cancer cells, such as tumor metastatic capacity, have been shown to be regulated by mitochondrial ROS generation (Kim et al., 2001; Nelson et al., 2003). Metastasis and cell migration are also greatly facilitated by matrix metalloproteases, which are activated by ROS (Ranganathan et al., 2001).

The recent discovery that mitochondrial biogenesis is regulated by a pathway that is sensitive to NO^\bullet (Nisoli et al., 2003) raises the possibility that mitochondria, by generating ROS, may be able to regulate their own biogenesis through a redox signaling mechanism.

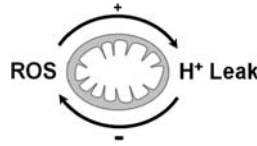
5.5 ROS-Sensitive Ion Channels

Several ion channels have now been identified as sensitive to redox regulation. This typically involves the modification of a cysteine residue, as is the case with the ryanodine receptor (RyR) (Marengo et al., 1998; Xu et al., 1998). The recent discovery of a mitochondrial RyR in certain tissues (Buetner et al., 2001) again suggests mitochondrial autoregulation via redox signaling (cf [Sect. 5.4](#)). Another example is the putative mitochondrial K_{ATP}^+ channel (see [Sect. 6.2](#)), which is sensitive to NO^\bullet and a variety of oxidants and antioxidants (Dahlem et al., 2004). In addition, the IP₃ receptor is redox sensitive (Hilly et al., 1993). Thus, mitochondrial ROS have the potential to impact ion gradients both within the organelle itself and beyond.

An interesting example of redox modulation of ion channels is the mitochondrial UCPs (see also the chapter by Dugan et al.). It has recently been shown that UCPs are activated by $\text{O}_2^{\bullet-}$ and by lipid oxidation products (Echtay et al., 2002, 2003), resulting in enhanced mitochondrial H^+ leak and thus decreased ROS generation (see [Sect. 4.2](#)). Thus, it has been proposed that H^+ leak and ROS generation may in fact reside in an autoregulatory feedback loop, as depicted in [Figure 5.3-8](#) (Brookes, 2005). The exact mechanism by which ROS can activate UCPs is unknown, although it is noted that UCPs contain several well-conserved cysteine residues on the loops in between their transmembrane helices.

■ **Figure 5.3-8**

Feedback loop between mitochondrial reactive oxygen species (ROS) generation and H⁺ leak. Several studies show that H⁺ leak is stimulated by ROS, and that ROS generation is inhibited by H⁺ leak. The molecular entities that mediate these phenomena are unknown, but may include uncoupling proteins



5.6 Mitochondria in Apoptotic Signaling—Role of ROS

As discussed earlier (and in the chapter by Fiskum et al.), ROS appear to play a key role in the triggering and autocatalytic phase of PT pore opening. In addition, PT pore opening results in enhanced mitochondrial ROS generation. The physiologic end point of the PT pore is in the regulation of apoptosis through the controlled release of cytochrome *c* into the cytosol.

Notably, in addition to the PT pore itself being a redox sensor, several other aspects of the apoptotic signaling cascade are sensitive to ROS. For example, both caspases and the release of cytochrome *c* can be inhibited by NO[•] (Brookes et al., 2000; Mannick et al., 2001). Furthermore, it has been proposed that the assembly of the apoptosome, which governs the triggering of caspase 9, is a redox-driven process (Suto et al., 2005). Indeed, it has been proposed that the redox status of cytochrome *c* can govern its participation in downstream apoptotic signaling (Hancock et al., 2001).

A further example of the importance of redox signaling in apoptosis was the recent discovery that apoptosis-inducing factor (AIF), a mitochondrial protein released during apoptosis, contains a flavin, and is a redox-active protein, although its precise function within mitochondria is not known (Miramar et al., 2001). Clearly, the mitochondrial generation of ROS during apoptosis has the potential to impact such signaling. In addition, a growing body of evidence suggests that the regulatory Bcl family of proteins, whose site of action is the mitochondrion, are able to regulate cellular redox status (Hockenbery et al., 1993), although it is not known if this effect is channeled through the mitochondrion.

5.7 Hypoxic Signaling and Mitochondrial ROS

Mitochondria-derived ROS are believed to be critical for the signaling events that occur in hypoxia (Chandel et al., 2000; Brunelle et al., 2005; Waypa and Schumacker, 2005). One proposed mechanism involves O₂ limitation at cytochrome *c* oxidase (complex IV), causing a backup of electrons in the respiratory chain, and enhanced electron leakage to O₂^{•-} from the upstream respiratory complexes I and III (see ▶ [Figures 5.3-2](#) and ▶ [5.3-3](#)). Evidence for a hypoxic increase in mitochondrial ROS comes from the use of mitochondrial pharmacologic agents such as rotenone, antimycin, and FCCP in isolated cell and tissue preparations. Since the ultimate substrate for ROS generation is O₂, inherent in this signaling paradigm is a paradoxical increase in ROS production while its substrate availability decreases. Thus, it has been alternately proposed that mitochondrial ROS generation actually decreases at low [O₂] (Archer et al., 1993; Moudgil et al., 2005).

One cellular factor with the potential to impact hypoxic signaling is NO[•], which can increase the K_m of cytochrome *c* oxidase for O₂ (Cooper et al., 2003). Thus, in the presence of NO[•], respiration would become inhibited at higher O₂ tensions than in the absence of NO[•]. Indeed, it has been proposed that NO[•] modulation of mitochondrial respiration is responsible for activation of Hif-1α under hypoxic conditions (Palacios-Callender et al., 2004).

The direction of mitochondrial ROS generation (increased or decreased) in hypoxia is further complicated when one considers the role of Δψ_m as a key regulator of ROS generation (see ▶ [Figure 5.3-3](#), Starkov and Fiskum 2003, and the chapter by Fiskum et al.). A paradox exists in the literature regarding the effects of

low $[O_2]$ on mitochondrial coupling efficiency, with claims for both increased (Kramer and Pearlstein, 1993) and decreased (Gnaiger et al., 2000) uncoupling at low $[O_2]$. In addition, since Ca^{2+} has multiple effects on mitochondria (vide supra), the recent discovery that hypoxia can impact Ca^{2+} signaling (Aley et al., 2004) further complicates this story.

A further level of complexity to the role of mitochondria in hypoxic signaling is added when it is considered that the substrates and products for the oxygen-sensitive prolyl hydroxylase (PHD) enzymes, which regulate Hif-1 α stability, are intermediates of the TCA cycle (Selak et al., 2005). A complex crosstalk is proposed to occur between the TCA cycle and PHD signaling, and overall it appears that the exact role of mitochondria and ROS in hypoxic signaling may be unique to particular cell/organ systems, and requires much further investigation.

6 Pathological Effects of Mitochondrial ROS

As discussed in [Sect. 5.2](#), mitochondria-derived ROS appear to play a unique role in neuronal excitotoxicity. In the remainder of this section, other aspects of the role of mitochondrial ROS in neuropathology will be briefly discussed.

6.1 Stroke

Neuronal I–R injury (stroke) shares many mechanistic links at the mitochondrial level with myocardial I–R (heart attack), and with excitotoxicity ([Sect. 5.2](#)). This includes mitochondrial Ca^{2+} overload, a multitude of energetic dysfunctions at the level of the organelle, enhanced ROS generation, and oxidative damage to mitochondria, PT pore opening, and cytochrome *c* release (Hayashi and Abe, 2004).

Notably, there appears to be a significant level of protection from stroke afforded by estrogens, and at least some of this protection appears to be conferred at the mitochondrial level (Simpkins et al., 2005). While gender differences in mitochondrial function overall have been very poorly studied, it is known that both estrogen alone (Stirone et al., 2005) and several estrogen-like polyphenolic compounds from red wines and soy products (Brookes et al., 2002a) can exert protective effects through the mitochondrion. This is in addition to any antioxidant activity within the compounds themselves.

6.2 Ischemic Preconditioning in the Brain; the Role of ROS and Mitochondria

IPC refers to the phenomenon whereby exposure of a tissue (usually heart or brain) to short periods of nonpathologic I–R can protect from a later prolonged pathologic I–R event (Murry et al., 1986; Perez-Pinzon et al., 2004; Ratan et al., 2004). There are two “windows” of IPC, the first taking minutes to develop and lasting 2–3 h and the second taking >6 h to develop and lasting up to 3 days.

The cell signaling pathways of IPC are intricate and poorly understood at the molecular level. Key players are believed to be PKC, mitochondrial ROS generation, MAP kinases, and NO^{\bullet} . In addition, as for ischemic injury itself (stroke versus heart attack, see [Sect. 6.1](#)), there exists significant overlap in the literature between IPC studies in the brain and the heart, and a large degree of convergence is present at the level of the mitochondrion. Among the most intriguing proposals is the existence of an ATP-sensitive potassium (K_{ATP}^+) channel in the mitochondrial inner membrane (Liu et al., 1998; Bajgar et al., 2001; Dos Santos et al., 2002). Opening of this channel is proposed to confer protection by several mechanisms:

1. a small decrease in $\Delta\psi_m$, which would decrease mitochondrial ROS generation.
2. A small decrease in $\Delta\psi_m$, which would diminish mitochondrial Ca^{2+} accumulation.
3. Regulation of mitochondrial volume, which would impact formation of PT pore complexes by altering contact sites between the inner and outer membranes.

Several cardioprotective and neuroprotective drugs, most notably diazoxide, are proposed to work via mitochondrial K_{ATP}^+ channels (Liu et al., 1998). However, the molecular identity of the mitochondrial K_{ATP}^+

channel remains unclear. While some authors claim it is composed of SUR and KIR subunits, akin to plasma membrane K_{ATP}^+ channels (Lacza et al., 2003a), others claim it is a conglomeration of existing inner-membrane proteins including complex II (succinate dehydrogenase) (Ardehali et al., 2004). Indeed, several inhibitors of complex II (e.g., 3-nitropropionate, malonate) are known to elicit protection from neuronal I–R injury (Garnier et al., 2002; Ardehali et al., 2004).

In addition to IPC, an exciting recent finding is the ability of volatile anesthetics (isoflurane, sevoflurane, etc.) to elicit preconditioning (De Hert et al., 2005; Payne et al., 2005). In a manner similar to preconditioning agents such as diazoxide, these agents are thought to work via opening of mitochondrial K_{ATP}^+ channels and subsequent ROS generation. Interestingly, the inert gas xenon has also recently been shown to elicit neuroprotection by a preconditioning type of mechanism (Ma et al., 2005). Clearly, the continued development of agents that mimic IPC is of great clinical promise in the prevention of mitochondrial dysfunction and neuronal death within the setting of stroke.

6.3 Neurodegeneration

As discussed extensively elsewhere in this volume, several neurodegenerative conditions have been linked to mitochondrial defects. However, since almost all neurodegenerative conditions involve loss of neurons via apoptosis, by default they involve mitochondria. Distinguishing those diseases in which mitochondria have a unique pathologic role above and beyond simple participation in the apoptotic cascade is difficult, but a partial list includes Parkinson's (Schapira et al., 1989; Cohen, 2000; Chinopoulos and Adam-Vizi, 2001), Alzheimer's (Blass and Gibson, 1991; Yan and Stern, 2005), and Huntington's diseases (Choo et al., 2004, Milakovic and Johnson, 2005), multiple sclerosis (Heales et al., 1999, Andrews et al., 2005), Friedrich's ataxia (Wilson and Roof, 1997), and amyotrophic lateral sclerosis (ALS, Lou Gehrig's disease) (Kruman et al., 1999; Beal, 2000; Chung et al., 2003).

Specific examples of mitochondrial functional defects in neurodegenerative diseases include reports of decreased complex I activity in Parkinson's disease, and decreased complex IV activity in Alzheimer's disease. Notably, these mitochondrial defects do not appear to be present in all cases, and very few causative links to disease progression have been established. Trials of antioxidant therapies in neurodegenerative diseases are currently in development.

Of particular interest is ALS, since the familial form of this disease has been linked to a mutation in Cu/Zn SOD (Kruman et al., 1999). While it is still being debated whether the mitochondrial intermembrane space contains a population of Cu/Zn SOD (Weisiger and Fridovich, 1973; Okado-Matsumoto and Fridovich, 2001), it has been noted that mice expressing the G93A mutated form of Cu/Zn SOD show elevated levels of Mn SOD in their mitochondria, suggesting a link between mitochondrial ROS generation and the pathogenesis of this disease (Chung et al., 2003).

Another interesting development within the context of Huntington's disease (HD) is the discovery that the neurotransmitter gas sulfide can inhibit mitochondrial function (Eghbal et al., 2004). Sulfide is made in cells by cystathionine- β -synthase (CBS), which has been shown to functionally interact with the Huntingtin protein (Boutell et al., 1998), although it is not clear at this stage if any of the pathology of HD is mediated by sulfide effects on mitochondria. Notably, H_2S /mitochondrial toxicity may also underlie some of the pathology of Down's Syndrome (DS), since CBS is carried on chromosome 21, and therefore DS individuals have more CBS than usual.

6.4 Therapeutic Strategies

Trials of nontargeted antioxidants in several disease conditions have yielded disappointing results. For example, one large study (>20,000 patients, 5-year follow-up) found no beneficial effects on any disease parameter measured, for an antioxidant vitamin cocktail (α -tocopherol, ascorbate, β -carotene) (Collins et al., 2002). Such studies have encouraged the search for antioxidants directed at the source of the ROS: mitochondria.

There are several drug design strategies for targeting antioxidants to mitochondria (see Coulter et al., 2000, Brookes et al., 2004, for reviews). These include the following:

1. Attachment to a positively charged lipophilic group, to facilitate delivery across the mitochondria inner membrane, driven by the $\Delta\psi_m$.
2. Design of a pro-drug that is cleaved to its active form by an enzyme uniquely localized in the mitochondrion.
3. Exploitation of unique mitochondrial carrier proteins.
4. Use of novel liposomal technologies to increase the concentration of a drug in the vicinity of mitochondria.

Several compounds from the laboratory of Michael Murphy have successfully utilized the first strategy to deliver drugs to the mitochondrial matrix. These compounds have been successful in animal models (Adlam et al., 2005), and may eventually find clinical use in the treatment of conditions such as Friedrich's ataxia (Jauslin et al., 2003).

Another strategy that is gaining increasing acceptance is the use of traditional mitochondrial inhibitors in animal disease models. For example as discussed above, 3-NP and malonate (complex II inhibitors) appear capable of chemically preconditioning the brain and heart to protect from I-R injury (Garnier et al., 2002). Similarly, low concentrations of the mitochondrial uncouplers such as DNP have been shown to confer protection from I-R injury (Minners et al., 2000, 2001). In addition, reversible inhibition of complex I has been shown to protect the heart from ischemic injury (Lesnfsky et al., 2004). While the use of such pharmacologic strategies may depend on the nature of the condition to be treated (chronic versus acute versus elective/perioperative/surgical), overall it is expected that in the coming years, a growing number of mitochondrially targeted drugs, both antioxidant and otherwise, will become available for the prevention and/or reversal of neurodegenerative oxidative stress conditions.

7 Closing Remarks

Our knowledge of the complex roles that mitochondrial ROS generation can play in physiology and pathology has expanded drastically in recent years. From the very naive belief that ROS are merely by-products of respiration that damage macromolecules and contribute to aging, we have evolved to the current paradigm that mitochondrial ROS generation is a tightly regulated process, with important roles in all aspects of cell signaling and survival. While there can be little doubt that enhanced mitochondrial ROS generation is involved in disease pathogenesis, the "sledgehammer" approach of antioxidant therapy has yielded disappointing results, making it clear that future therapies will have to take account of the subtle signaling roles of mitochondrial ROS. The development of spatiotemporally targeted antioxidants remains a distant therapeutic goal.

Acknowledgments

I am grateful to Sergiy Nadtochiy (Rochester) for insightful discussions during the preparation of this manuscript, and to NIH (NHLBI, RO1 HL71158) and the University of Rochester's Mitochondrial Research Interest Group for research funding.

References

- Abas L, Bogoyevitch MA, Guppy M. 2000. Mitochondrial ATP production is necessary for activation of the extracellular-signal-regulated kinases during ischaemia/reperfusion in rat myocyte-derived H9c2 cells. *Biochem J* 349: 119-126.
- Adlam VJ, Harrison JC, Porteous CM, James AM, Smith RA, et al. 2005. Targeting an antioxidant to mitochondria decreases cardiac ischemia-reperfusion injury. *FASEB J* 19: 1088-1095.

- Akbiyik F, Ray DM, Gettings KF, Blumberg N, Francis CW, et al. 2004. Human bone marrow megakaryocytes and platelets express PPAR γ , and PPAR γ agonists blunt platelet release of CD40 ligand and thromboxanes. *Blood* 104: 1361-1368.
- Aley PK, Porter KE, Boyle JP, Kemp PJ, Peers C. 2004. Hypoxic modulation of Ca²⁺ signaling in human venous endothelial cells. Multiple roles for reactive oxygen species. *J Biol Chem* 280: 13349-13354.
- Andrews HE, Nichols PP, Bates D, Turnbull DM. 2005. Mitochondrial dysfunction plays a key role in progressive axonal loss in multiple sclerosis. *Med Hypotheses* 64: 669-677.
- Archer SL, Huang J, Henry T, Peterson D, Weir EK. 1993. A redox-based O₂ sensor in rat pulmonary vasculature. *Circ Res* 73: 1100-1112.
- Ardehali H, Chen Z, Ko Y, Mejia-Alvarez R, Marban E. 2004. Multiprotein complex containing succinate dehydrogenase confers mitochondrial ATP-sensitive K⁺ channel activity. *Proc Natl Acad Sci USA* 101: 11880-11885.
- Armstrong JS, Whiteman M, Yang H, Jones DP. 2004. The redox regulation of intermediary metabolism by a superoxide-aconitase rheostat. *Bioessays* 26: 894-900.
- Baines CP, Zhang J, Wang GW, Zheng YT, Xiu JX, et al. 2002. Mitochondrial PKC ϵ and MAPK form signaling modules in the murine heart: Enhanced mitochondrial PKC ϵ -MAPK interactions and differential MAPK activation in PKC ϵ -induced cardioprotection. *Circ Res* 90: 390-397.
- Bajgar R, Seetharaman S, Kowaltowski AJ, Garlid KD, Paucek P. 2001. Identification and properties of a novel intracellular (mitochondrial) ATP-sensitive potassium channel in brain. *J Biol Chem* 276: 33369-33374.
- Barja G. 2002. Rate of generation of oxidative stress-related damage and animal longevity. *Free Radic Biol Med* 33: 1167-1172.
- Barker JE, Bolanos JP, Land JM, Clark JB, Heales SJ. 1996. Glutathione protects astrocytes from peroxynitrite-mediated mitochondrial damage: Implications for neuronal/astrocytic trafficking and neurodegeneration. *Dev Neurosci* 18: 391-396.
- Bates TE, Loesch A, Burnstock G, Clark JB. 1995. Immunocytochemical evidence for a mitochondrially located nitric oxide synthase in brain and liver. *Biochem Biophys Res Commun* 213: 896-900.
- Beal MF. 2000. Mitochondria and the pathogenesis of ALS. *Brain* 123: 1291-1292.
- Beckman JS, Beckman TW, Chen J, Marshall PA, Freeman BA. 1990. Apparent hydroxyl radical production by peroxynitrite: Implications for endothelial injury from nitric oxide and superoxide. *Proc Natl Acad Sci USA* 87: 1620-1624.
- Beutner G, Sharma VK, Giovannucci DR, Yule DJ, Sheu S-S. 2001. Identification of a ryanodine receptor in rat heart mitochondria. *J Biol Chem* 276: 21482-21488.
- Blass JP, Gibson GE. 1991. The role of oxidative abnormalities in the pathophysiology of Alzheimer's disease. *Rev Neurol (Paris)* 147: 513-525.
- Bogoyevitch MA, Ng DC, Court NW, Draper KA, Dhillion A, et al. 2000. Intact mitochondrial electron transport function is essential for signaling by hydrogen peroxide in cardiac myocytes. *J Mol Cell Cardiol* 32: 1469-1480.
- Boutell JM, Wood JD, Harper PS, Jones AL. 1998. Huntingtin interacts with cystathionine beta-synthase. *Hum Mol Genet* 7: 371-378.
- Boveris A, Chance B. 1973. The mitochondrial generation of hydrogen peroxide. General properties and effect of hyperbaric oxygen. *Biochem J* 134: 707-716.
- Boveris A, Oshino N, Chance B. 1972. The cellular production of hydrogen peroxide. *Biochem J* 128: 617-630.
- Brandes RP, Janiszewski M. 2005. Direct detection of reactive oxygen species ex-vivo. *Kidney Int* 67: 1662-1664.
- Brinkley BR, Barham SS, Barranco SC, Fuller GM. 1974. Rotenone inhibition of spindle microtubule assembly in mammalian cells. *Exp Cell Res* 85: 41-46.
- Brookes P, Darley-USmar VM. 2002. Hypothesis: The mitochondrial NO[•] signaling pathway, and the transduction of nitrosative to oxidative cell signals: An alternative function for cytochrome *c* oxidase. *Free Radic Biol Med* 32: 370-374.
- Brookes PS. 2004. Mitochondrial nitric oxide synthase. *Mitochondrion* 3: 187-204.
- Brookes PS. 2005. Mitochondrial H⁺ leak and ROS generation: An odd couple. *Free Radic Biol Med* 38: 12-23.
- Brookes PS, Darley-USmar VM. 2004. Role of calcium and superoxide dismutase in sensitizing mitochondria to peroxynitrite-induced permeability transition. *Am J Physiol* 286: H39-H46.
- Brookes PS, Digerness SB, Parks DA, Darley-USmar VM. 2002a. Mitochondrial function in response to cardiac ischemia-reperfusion after oral treatment with quercetin. *Free Radic Biol Med* 32: 1220-1228.
- Brookes PS, Levenon AL, Shiva S, Sarti P, Darley-USmar VM. 2002b. Mitochondria: Regulators of signal transduction by reactive oxygen and nitrogen species. *Free Radic Biol Med* 33: 755-764.
- Brookes PS, Salinas EP, Darley-USmar K, Eiserich JP, Freeman BA, et al. 2000. Concentration-dependent effects of nitric oxide on mitochondrial permeability transition and cytochrome *c* release. *J Biol Chem* 275: 20474-20479.
- Brookes PS, Yoon Y, Robotham JL, Anders MW, Sheu S-S. 2004. Calcium, ATP, and ROS: A mitochondrial love-hate triangle. *Am J Physiol* 287: C817-C833.
- Brown GC. 2000. Nitric oxide as a competitive inhibitor of oxygen consumption in the mitochondrial respiratory chain. *Acta Physiol Scand* 168: 667-674.

- Brunelle JK, Bell EL, Quesada NM, Vercauteren K, Tiranti V, et al. 2005. Oxygen sensing requires mitochondrial ROS but not oxidative phosphorylation. *Cell Metab* 1: 409-414.
- Burkitt MJ, Wardman P. 2001. Cytochrome *c* is a potent catalyst of dichlorofluorescein oxidation: Implications for the role of reactive oxygen species in apoptosis. *Biochem Biophys Res Commun* 282: 329-333.
- Burwell LS, Tompkins AJ, Brookes PS. 2006. Direct evidence for S-nitrosation of mitochondrial complex I. *Biochem J* 394: 627-634.
- Cadenas E, Boveris A. 1980. Enhancement of hydrogen peroxide formation by protophores and ionophores in antimycin-supplemented mitochondria. *Biochem J* 188: 31-37.
- Cadenas E, Boveris A, Ragan CI, Stoppani AO. 1977. Production of superoxide radicals and hydrogen peroxide by NADH-ubiquinone reductase and ubiquinol-cytochrome *c* reductase from beef-heart mitochondria. *Arch Biochem Biophys* 180: 248-257.
- Cassarino DS, Halvorsen EM, Swerdlow RH, Abramova NN, Parker WD Jr, et al. 2000. Interaction among mitochondria, mitogen-activated protein kinases, and nuclear factor-kappaB in cellular models of Parkinson's disease. *J Neurochem* 74: 1384-1392.
- Castro L, Rodriguez M, Radi R. 1994. Aconitase is readily inactivated by peroxynitrite, but not by its precursor, nitric oxide. *J Biol Chem* 269: 29409-29415.
- Chandel NS, McClintock DS, Feliciano CE, Wood TM, Melendez JA, et al. 2000. Reactive oxygen species generated at mitochondrial complex III stabilize hypoxia-inducible factor-1alpha during hypoxia: A mechanism of O₂ sensing. *J Biol Chem* 275: 25130-25138.
- Chang SH, Garcia J, Melendez JA, Kilberg MS, Agarwal A. 2003. Haem oxygenase 1 gene induction by glucose deprivation is mediated by reactive oxygen species via the mitochondrial electron-transport chain. *Biochem J* 371: 877-885.
- Chinopoulos C, Adam-Vizi V. 2001. Mitochondria deficient in complex I activity are depolarized by hydrogen peroxide in nerve terminals: Relevance to Parkinson's disease. *J Neurochem* 76: 302-306.
- Choo YS, Johnson GV, MacDonald M, Detloff PJ, Lesort M. 2004. Mutant huntingtin directly increases susceptibility of mitochondria to the calcium-induced permeability transition and cytochrome *c* release. *Hum Mol Genet* 13: 1407-1420.
- Chung YH, Joo KM, Lee YJ, Cha CI. 2003. Immunohistochemical study on the distribution of MnSOD in the central nervous system of the transgenic mice expressing a human Cu/Zn SOD mutation. *Brain Res* 990: 215-220.
- Cleeter MW, Cooper JM, Darley-Usmar VM, Moncada S, Schapira AH. 1994. Reversible inhibition of cytochrome *c* oxidase, the terminal enzyme of the mitochondrial respiratory chain, by nitric oxide. Implications for neurodegenerative diseases. *FEBS Lett* 345: 50-54.
- Clementi E, Brown GC, Feelisch M, Moncada S. 1998. Persistent inhibition of cell respiration by nitric oxide: Crucial role of S-nitrosylation of mitochondrial complex I and protective action of glutathione. *Proc Natl Acad Sci USA* 95: 7631-7636.
- Cohen G. 2000. Oxidative stress, mitochondrial respiration, and Parkinson's disease. *Ann N Y Acad Sci* 899: 112-120.
- Collins R, Peto R, Armitage J. 2002. The MRC/BHF Heart Protection Study: Preliminary results. *Int J Clin Pract* 56: 53-56.
- Cooper CE, Davies NA, Psychoulis M, Canevari L, Bates TE, et al. 2003. Nitric oxide and peroxynitrite cause irreversible increases in the K_M for oxygen of mitochondrial cytochrome oxidase: In vitro and in vivo studies. *Biochim Biophys Acta* 1607: 27-34.
- Coulter CV, Kelso GF, Lin TK, Smith RA, Murphy MP. 2000. Mitochondrially targeted antioxidants and thiol reagents. *Free Radic Biol Med* 28: 1547-1554.
- Crompton M. 1999. The mitochondrial permeability transition pore and its role in cell death. *Biochem J* 341: 233-249.
- Dahlem YA, Horn TF, Buntinas L, Gonoï T, Wolf G, et al. 2004. The human mitochondrial K_{ATP} channel is modulated by calcium and nitric oxide: A patch-clamp approach. *Biochim Biophys Acta* 1656: 46-56.
- Davies MJ, Hawkins CL. 2004. EPR spin trapping of protein radicals. *Free Radic Biol Med* 36: 1072-1086.
- Dawson VL, Dawson TM, London ED, Bredt DS, Snyder SH. 1991. Nitric oxide mediates glutamate neurotoxicity in primary cortical cultures. *Proc Natl Acad Sci USA* 88: 6368-6371.
- De Chaplain J, Krakoff LR, Axelrod J. 1968. Increased monomine oxidase activity during the development of cardiac hypertrophy in the rat. *Circ Res* 23: 361-369.
- De Grey AD. 2002. HO₂•: The forgotten radical. *DNA Cell Biol* 21: 251-257.
- De Hert SG, Turani F, Mathur S, Stowe DF. 2005. Cardioprotection with volatile anesthetics: Mechanisms and clinical implications. *Anesth Analg* 100: 1584-1593.
- Di Paola M, Cocco T, Lorusso M. 2000. Ceramide interaction with the respiratory chain of heart mitochondria. *Biochemistry* 39: 6660-6668.
- Dos Santos P, Kowaltowski AJ, Laclau MN, Seetharaman S, Paucek P, et al. 2002. Mechanisms by which opening the mitochondrial ATP-sensitive K⁺ channel protects the ischemic heart. *Am J Physiol* 283: H284-H295.

- Droge W. 2002. Free radicals in the physiological control of cell function. *Physiol Rev* 82: 47-95.
- Duchen MR. 2000. Mitochondria and calcium: From cell signalling to cell death. *J Physiol* 529: 57-68.
- Echtay KS, Esteves TC, Pakay JL, Jekabsons MB, Lambert AJ, et al. 2003. A signalling role for 4-hydroxy-2-nonenal in regulation of mitochondrial uncoupling. *EMBO J* 22: 4103-4110.
- Echtay KS, Murphy MP, Smith RA, Talbot DA, Brand MD. 2002. Superoxide activates mitochondrial uncoupling protein 2 from the matrix side. Studies using targeted antioxidants. *J Biol Chem* 277: 47129-47135.
- Eghbal MA, Pennefather PS, O'Brien PJ. 2004. H₂S cytotoxicity mechanism involves reactive oxygen species formation and mitochondrial depolarisation. *Toxicology* 203: 69-76.
- Feelisch M, Kubitzek D, Werringloer J. 1996. The oxyhemoglobin assay. *Methods in nitric oxide research*. Feelisch M, Stamler JS, editors. England: Wiley; pp. 455-478.
- Fernandez-Checa JC, Kaplowitz N, Garcia-Ruiz C, Colell A. 1998. Mitochondrial glutathione: Importance and transport. *Semin Liver Dis* 18: 389-401.
- Forman HJ, Kennedy J. 1976. Dihydroorotate-dependent superoxide production in rat brain and liver. A function of the primary dehydrogenase. *Arch Biochem Biophys* 173: 219-224.
- Ganote CE, Armstrong SC. 2003. Effects of CCCP-induced mitochondrial uncoupling and cyclosporin A on cell volume, cell injury and preconditioning protection of isolated rabbit cardiomyocytes. *J Mol Cell Cardiol* 35: 749-759.
- Gao S, Chen J, Brodsky SV, Huang H, Adler S, et al. 2004. Docking of endothelial nitric oxide synthase (eNOS) to the mitochondrial outer membrane: A pentabasic amino acid sequence in the autoinhibitory domain of eNOS targets a proteinase K-cleavable peptide on the cytoplasmic face of mitochondria. *J Biol Chem* 279: 15968-15974.
- Garcia-Nogales P, Almeida A, Bolanos JP. 2003. Peroxynitrite protects neurons against nitric oxide-mediated apoptosis. A key role for glucose-6-phosphate dehydrogenase activity in neuroprotection. *J Biol Chem* 278: 864-874.
- Garcia-Ruiz C, Colell A, Mari M, Morales A, Fernandez-Checa JC. 1997. Direct effect of ceramide on the mitochondrial electron transport chain leads to generation of reactive oxygen species. Role of mitochondrial glutathione. *J Biol Chem* 272: 11369-11377.
- Garnier P, Bertrand N, Demougeot C, Prigent-Tessier A, Marie C, et al. 2002. Chemical preconditioning with 3-nitropropionic acid: Lack of induction of neuronal tolerance in gerbil hippocampus subjected to transient forebrain ischemia. *Brain Res Bull* 58: 33-39.
- Ghafourifar P, Richter C. 1997. Nitric oxide synthase activity in mitochondria. *FEBS Lett* 418: 291-296.
- Giulivi C, Poderoso JJ, Boveris A. 1998. Production of nitric oxide by mitochondria. *J Biol Chem* 273: 11038-11043.
- Gnaiger E, Mendez G, Hand SC. 2000. High phosphorylation efficiency and depression of uncoupled respiration in mitochondria under hypoxia. *Proc Natl Acad Sci USA* 97: 11080-11085.
- Gnaiger E, Steinlechner-Maran R, Mendez G, Eberl T, Margreiter R. 1995. Control of mitochondrial and cellular respiration by oxygen. *J Bioenerg Biomembr* 27: 583-596.
- Goldberg MS, Fleming SM, Palacino JJ, Cepeda C, Lam HA, et al. 2003. Parkin-deficient mice exhibit nigrostriatal deficits but not loss of dopaminergic neurons. *J Biol Chem* 278: 43628-43635.
- Gunter TE, Yule DI, Gunter KK, Elisev RA, Salter JD. 2004. Calcium and mitochondria. *FEBS Lett* 567: 96-102.
- Guo FQ, Crawford NM. 2005. Arabidopsis nitric oxide synthase1 is targeted to mitochondria and protects against oxidative damage and dark-induced senescence. *Plant Cell* 17: 3436-3450.
- Halestrap AP, McStay GP, Clarke SJ. 2002. The permeability transition pore complex: Another view. *Biochimie* 84: 153-166.
- Han D, Antunes F, Canali R, Rettori D, Cadenas E. 2003a. Voltage-dependent anion channels control the release of the superoxide anion from mitochondria to cytosol. *J Biol Chem* 278: 5557-5563.
- Han D, Canali R, Rettori D, Kaplowitz N. 2003b. Effect of glutathione depletion on sites and topology of superoxide and hydrogen peroxide production in mitochondria. *Mol Pharmacol* 64: 1136-1144.
- Hancock JT, Desikan D, Neill SJ. 2001. Does the redox status of cytochrome *c* act as a fail-safe mechanism in the regulation of programmed cell death? *Free Radic Biol Med* 31: 697-703.
- Harman D. 2003. The free radical theory of aging. *Antioxid Redox Signal* 5: 557-561.
- Harper ME, Bevilacqua L, Hagopian K, Weindruch R, Ramsey JJ. 2004. Ageing, oxidative stress, and mitochondrial uncoupling. *Acta Physiol Scand* 182: 321-331.
- Hayashi T, Abe K. 2004. Ischemic neuronal cell death and organelle damage. *Neuro Res* 26: 827-834.
- He H, Li HL, Lin A, Gottlieb RA. 1999. Activation of the JNK pathway is important for cardiomyocyte death in response to simulated ischemia. *Cell Death Differ* 6: 987-991.
- Heales SJ, Bolanos JP, Stewart VC, Brookes PS, Land JM, et al. 1999. Nitric oxide, mitochondria and neurological disease. *Biochim Biophys Acta* 1410: 215-228.
- Heales SJ, Lam AA, Duncan AJ, Land JM. 2004. Neurodegeneration or neuroprotection: The pivotal role of astrocytes. *Neurochem Res* 29: 513-519.

- Hennet T, Richter C, Peterhans E. 1993. Tumour necrosis factor- α induces superoxide anion generation in mitochondria of L929 cells. *Biochem J* 289: 587-592.
- Hilly M, Pietri-Rouxel F, Coquil JF, Guy M, Mauger JP. 1993. Thiol reagents increase the affinity of the inositol 1,4,5-trisphosphate receptor. *J Biol Chem* 268: 16488-16494.
- Hockenbery DM, Oltvai ZN, Yin XM, Milliman CL, Korsmeyer SJ. 1993. Bcl-2 functions in an antioxidant pathway to prevent apoptosis. *Cell* 75: 241-251.
- Hoerter J, Gonzales-Barroso M, Couplan E, Mateo P, Gelly C, et al. 2004. Mitochondrial uncoupling protein 1 expressed in the heart of transgenic mice protects against ischemic-reperfusion damage. *Circulation* 110: 528-533.
- Hongpaisan J, Winters CA, Andrews SB. 2003. Calcium-dependent mitochondrial superoxide modulates nuclear CREB phosphorylation in hippocampal neurons. *Mol Cell Neurosci* 24: 1103-1115.
- Huang TT, Yasunami M, Carlson EJ, Gillespie AM, Reaume AG, et al. 1997. Superoxide-mediated cytotoxicity in superoxide dismutase-deficient fetal fibroblasts. *Arch Biochem Biophys* 344: 424-432.
- Humphries KM, Swzeda LI. 1998. Selective inactivation of alpha-ketoglutarate dehydrogenase and pyruvate dehydrogenase: Reaction of lipoic acid with 4-hydroxy-2-nonenal. *Biochemistry* 37: 15835-15841.
- Itoh S, Lemay S, Osawa M, Che W, Duan Y, et al. 2005. Mitochondrial Dok-4 recruits Src kinase and regulates NF- κ B activation in endothelial cells. *J Biol Chem* 280: 26383-26396.
- Jauslin ML, Meier T, Smith RA, Murphy MP. 2003. Mitochondria-targeted antioxidants protect Friedreich ataxia fibroblasts from endogenous oxidative stress more effectively than untargeted antioxidants. *FASEB J* 17: 1972-1974.
- Karawajew L, Rhein P, Czerwonny G, Ludwig WD. 2005. Stress-induced activation of the p53 tumor suppressor in leukemia cells and normal lymphocytes requires mitochondrial activity and reactive oxygen species. *Blood* 105: 4767-4775.
- Kasischke KA, Vishwasrao HD, Fisher PJ, Zipfel WR, Webb WW. 2004. Neural activity triggers neuronal oxidative metabolism followed by astrocytic glycolysis. *Science* 305: 99-103.
- Kelso GE, Porteous CM, Coulter CV, Hughes G, Porteous WK, et al. 2001. Selective targeting of a redox-active ubiquinone to mitochondria within cells: Antioxidant and antiapoptotic properties. *J Biol Chem* 276: 4588-4596.
- Kevin LG, Novalija E, Stowe DF. 2005. Reactive oxygen species as mediators of cardiac injury and protection: The relevance to anesthesia practice. *Anesth Analg* 101: 1275-1287.
- Kim KH, Rodriguez AM, Carrico PM, Melendez JA. 2001. Potential mechanisms for the inhibition of tumor cell growth by manganese superoxide dismutase. *Antioxid Redox Signal* 3: 361-373.
- Kiritoshi S, Nishikawa T, Sonoda K, Kukidome D, Senokuchi T, et al. 2003. Reactive oxygen species from mitochondria induce cyclooxygenase-2 gene expression in human mesangial cells: Potential role in diabetic nephropathy. *Diabetes* 52: 2570-2577.
- Korshunov SS, Skulachev VP, Starkov AA. 1997. High protonic potential actuates a mechanism of production of reactive oxygen species in mitochondria. *FEBS Lett* 416: 15-18.
- Kowaltowski AJ, Naia-da-Silva ES, Castilho RF, Vercesi AE. 1998. Ca^{2+} -stimulated mitochondrial reactive oxygen species generation and permeability transition are inhibited by dibucaine or Mg^{2+} . *Arch Biochem Biophys* 359: 77-81.
- Kramer RS, Pearlstein RD. 1993. Reversible uncoupling of oxidative phosphorylation at low oxygen tension. *Proc Natl Acad Sci USA* 80: 5807-5811.
- Kristian T, Hopkins IB, McKenna MC, Fiskum G. 2006. Isolation of mitochondria with high respiratory control from primary cultures of neurons and astrocytes using nitrogen cavitation. *J Neurosci Methods* 152: 136-143.
- Kruman II, Pedersen WA, Springer JE, Mattson MP. 1999. ALS-linked Cu/Zn-SOD mutation increases vulnerability of motor neurons to excitotoxicity by a mechanism involving increased oxidative stress and perturbed calcium homeostasis. *Exp Neurol* 160: 28-39.
- Lacza Z, Pankotai E, Csordas A, Gero D, Kiss L, et al. 2006. Mitochondrial NO and reactive nitrogen species production: Does mtNOS exist? *Nitric Oxide* 14(2): 162-168.
- Lacza Z, Snipes JA, Miller AW, Szabo C, Grover G, et al. 2003a. Heart mitochondria contain functional ATP-dependent K^+ channels. *J Mol Cell Cardiol* 35: 1339-1347.
- Lacza Z, Snipes JA, Zhang J, Horvath EM, Figueroa JP, et al. 2003b. Mitochondrial nitric oxide synthase is not eNOS, nNOS or iNOS. *Free Radic Biol Med* 35: 1217-1228.
- Lai JC, Walsh JM, Dennis SC, Clark JB. 1977. Synaptic and non-synaptic mitochondria from rat brain: Isolation and characterization. *J Neurochem* 28: 625-631.
- Landar A, Shiva S, Levonen AL, Oh JY, Zaragoza C, et al. 2006. Induction of the permeability transition and cytochrome *c* release by 15-deoxy prostaglandin J_2 in mitochondria. *Biochem J* 394: 185-195.
- Lee HB, Yu MR, Song JS, Ha H. 2004. Reactive oxygen species amplify protein kinase C signaling in high glucose-induced fibronectin expression by human peritoneal mesothelial cells. *Kidney Int* 65: 1170-1179.
- Lesnefsky EJ, Chen Q, Moghaddas S, Hassan MO, Tandler B, et al. 2004. Blockade of electron transport during ischemia protects cardiac mitochondria. *J Biol Chem* 279: 47961-47967.

- Levonen AL, Patel RP, Brookes P, Go YM, Jo H, et al. 2001. Mechanisms of cell signaling by nitric oxide and peroxynitrite: From mitochondria to MAP kinases. *Antioxid Redox Signal* 3: 215-229.
- Li N, Ragheb K, Lawler G, Sturgis J, Rajwa B, et al. 2003. Mitochondrial complex I inhibitor rotenone induces apoptosis through enhancing mitochondrial reactive oxygen species production. *J Biol Chem* 278: 8516-8525.
- Liu X, Miller MJ, Joshi MS, Thomas DD, Lancaster JR Jr. 1998. Accelerated reaction of nitric oxide with O₂ within the hydrophobic interior of biological membranes. *Proc Natl Acad Sci USA* 95: 2175-2179.
- Liu Y, Sato T, O'Rourke B, Marban E. 1998. Mitochondrial ATP-dependent potassium channels: Novel effectors of cardioprotection? *Circulation* 97: 2463-2469.
- Ma D, Hossain M, Pettet GK, Luo Y, Lim T, et al. 2006. Xenon preconditioning reduces brain damage from neonatal asphyxia in rats. *J Cereb Blood Flow Metab* 26: 199-208.
- Maeda H, Akaike T, Yoshida M, Suga M. 1994. Multiple functions of nitric oxide in pathophysiology and microbiology: Analysis by a new nitric oxide scavenger. *J Leukoc Biol* 56: 588-592.
- Mannick JB, Schonhoff C, Papeta N, Ghafourifar P, Szibor M, et al. 2001. S-nitrosylation of mitochondrial caspases. *J Cell Biol* 154: 1111-1116.
- Marengo JJ, Hidalgo C, Bull R. 1998. Sulfhydryl oxidation modifies the calcium dependence of ryanodine-sensitive calcium channels of excitable cells. *Biophys J* 74: 1263-1277.
- Martin ME, Chinenov Y, Yu M, Schmidt TK, Yang XY. 1996. Redox regulation of GA-binding protein- α DNA binding activity. *J Biol Chem* 271: 25617-25623.
- Martinez B, Perez-Castillo A, Santos A. 2005. The mitochondrial respiratory complex I is a target for 15-deoxy- $\Delta^{12,14}$ -prostaglandin J₂ action. *J Lipid Res* 46: 736-743.
- Mason RP. 2004. Using anti-5,5-dimethyl-1-pyrroline N-oxide (anti-DMPO) to detect protein radicals in time and space with immuno-spin trapping. *Free Radic Biol Med* 36: 1214-1223.
- McCormack JG, Denton RM. 1993. Mitochondrial Ca²⁺ transport and the role of intramitochondrial Ca²⁺ in the regulation of energy metabolism. *Dev Neurosci* 15: 165-173.
- McLeod C, Hoyt R, Sack M. 2004. UCP-2, a functional target in delayed preconditioning induced cardioprotection? *Cardiovasc J S Afr* 15: S4.
- Milakovic T, Johnson GV. 2005. Mitochondrial respiration and ATP production are significantly impaired in striatal cells expressing mutant huntingtin. *J Biol Chem* 280: 30773-30782.
- Miller KE, Sheetz MP. 2004. Axonal mitochondrial transport and potential are correlated. *J Cell Sci* 117: 2791-2804.
- Minners J, Lacerda L, McCarthy J, Meiring JJ, Yellon DM, et al. 2001. Ischemic and pharmacological preconditioning in Girardi cells and C2C12 myotubes induce mitochondrial uncoupling. *Circ Res* 89: 787-792.
- Minners J, van den Bos EJ, Yellon D, Schwalb H, Opie L, et al. 2000. Dinitrophenol, cyclosporine A, and trimetazidine modulate preconditioning in the isolated rat heart: Support for a mitochondrial role in cardioprotection. *Cardiovasc Res* 47: 68-73.
- Miramar MD, Costantini P, Ravagnan L, Saraiva LM, Haouzi D, et al. 2001. NADH oxidase activity of mitochondrial apoptosis-inducing factor. *J Biol Chem* 276: 16391-16398.
- Moudgil R, Michelakis ED, Archer SL. 2005. Hypoxic pulmonary vasoconstriction. *J Appl Physiol* 98: 390-403.
- Muller FL, Liu Y, Van Remmen H. 2004. Complex III releases superoxide to both sides of the inner mitochondrial membrane. *J Biol Chem* 279: 49064-49073.
- Murry CE, Jennings RB, Reimer KA. 1986. Preconditioning with ischemia: A delay of lethal cell injury in ischemic myocardium. *Circulation* 74: 1124-1136.
- Nelson KK, Ranganathan AC, Mansouri J, Rodriguez AM, Providence KM, et al. 2003. Elevated sod2 activity augments matrix metalloproteinase expression: Evidence for the involvement of endogenous hydrogen peroxide in regulating metastasis. *Clin Cancer Res* 9: 424-432.
- Nemoto S, Takeda K, Yu ZX, Ferrans VJ, Finkel T. 2000. Role for mitochondrial oxidants as regulators of cellular metabolism. *Mol Cell Biol* 20: 7311-7318.
- Nicholls DG, Budd SL, Ward MW, Castilho RF. 1999. Excitotoxicity and mitochondria. *Biochem Soc Symp* 66: 55-67.
- Nisoli E, Clementi E, Paolucci C, Cozzi V, Tonello C, et al. 2003. Mitochondrial biogenesis in mammals: The role of endogenous nitric oxide. *Science* 299: 896-899.
- Nohl H, Gille L, Kozlov A, Staniek K. 2003a. Are mitochondria a spontaneous and permanent source of reactive oxygen species? *Redox Rep* 8: 135-141.
- Nohl H, Kozlov AV, Gille L, Staniek K. 2003b. Cell respiration and formation of reactive oxygen species: Facts and artefacts. *Biochem Soc Trans* 6: 1308-1311.
- Nossuli TO, Hayward R, Jensen D, Scalia R, Lefer AM. 1998. Mechanisms of cardioprotection by peroxynitrite in myocardial ischemia and reperfusion injury. *Am J Physiol* 275: H509-H519.
- Okado- Matsumoto A, Fridovich I. 2001. Subcellular distribution of superoxide dismutases (SOD) in rat liver: Cu,Zn-SOD in mitochondria. *J Biol Chem* 276: 38388-38393.
- Omar BA, Gad NM, Jordan MC, Striplin SP, Russell WJ, et al. 1990. Cardioprotection by Cu,Zn-superoxide dismutase is lost at high doses in the reoxygenated heart. *Free Radic Biol Med* 9: 465-471.
- Packer MA, Porteous CM, Murphy MP. 1996. Superoxide production by mitochondria in the presence of nitric

- oxide forms peroxynitrite. *Biochem Mol Biol Int* 40: 527-534.
- Palacios-Callender M, Quintero M, Hollis VS, Springett RJ, Moncada S. 2004. Endogenous NO regulates superoxide production at low oxygen concentrations by modifying the redox state of cytochrome *c* oxidase. *Proc Natl Acad Sci USA* 101: 7630-7635.
- Paxinou E, Weisse M, Chen Q, Souza JM, Hertkorn C, et al. 2001. Dynamic regulation of metabolism and respiration by endogenously produced nitric oxide protects against oxidative stress. *Proc Natl Acad Sci USA* 98: 11575-11580.
- Payne RS, Akca O, Roewer N, Schurr A, Kehl F. 2005. Sevoflurane-induced preconditioning protects against cerebral ischemic neuronal damage in rats. *Brain Res* 1034: 147-152.
- Perez-Pinzon MA. 2004. Neuroprotective effects of ischemic preconditioning in brain mitochondria following cerebral ischemia. *J Bioenerg Biomembr* 36: 323-327.
- Peuchen S, Bolanos JP, Heales SJ, Almeida A, Duchon MR, et al. 1997. Interrelationships between astrocyte function, oxidative stress and antioxidant status within the central nervous system. *Prog Neurobiol* 52: 261-281.
- Pieper AA, Verma A, Zhang J, Snyder SH. 1999. Poly (ADP-ribose) polymerase, nitric oxide and cell death. *Trends Pharmacol Sci* 20: 171-181.
- Poderoso JJ, Carreras MC, Lisdero C, Riobo N, Schopfer F, et al. 1996. Nitric oxide inhibits electron transfer and increases superoxide radical production in rat heart mitochondria and submitochondrial particles. *Arch Biochem Biophys* 328: 85-92.
- Pomytkin IA, Kolesova OE. 2002. Key role of succinate dehydrogenase in insulin-induced inactivation of protein tyrosine phosphatases. *Bull Exp Biol Med* 133: 568-570.
- Pryor WA, Squadrito GL. 1995. The chemistry of peroxynitrite: A product from the reaction of nitric oxide with superoxide. *Am J Physiol* 268: L699-L722.
- Pueyo ME, Gonzalez W, Nicoletti A, Savoie F, Arnal JF, et al. 2000. Angiotensin II stimulates endothelial vascular cell adhesion molecule-1 via nuclear factor-kappaB activation induced by intracellular oxidative stress. *Arterioscler Thromb Vasc Biol* 20: 645-651.
- Raha S, Myint AT, Johnstone L, Robinson BH. 2002. Control of oxygen free radical formation from mitochondrial complex I: Roles for protein kinase A and pyruvate dehydrogenase kinase. *Free Radic Biol Med* 32: 421-430.
- Ramachandran A, Moellering D, Go Y-M, Shiva S, Levonen A-L, et al. 2002. Activation of c-Jun N-terminal kinase and apoptosis in endothelial cells mediated by endogenous generation of hydrogen peroxide. *Biol Chem* 383: 693-701.
- Ranganathan AC, Nelson KK, Rodriguez AM, Kim KH, Tower GB, et al. 2001. Manganese superoxide dismutase signals matrix metalloproteinase expression via H₂O₂-dependent ERK1/2 activation. *J Biol Chem* 276: 14264-14270.
- Ratan RR, Siddiq A, Aminova L, Lange PS, Langley B, et al. 2004. Translation of ischemic preconditioning to the patient: Prolyl hydroxylase inhibition and hypoxia inducible factor-1 as novel targets for stroke therapy. *Stroke* 35(S1): 2687-2689.
- Reed DJ. 2004. Mitochondrial glutathione and chemically induced stress including ethanol. *Drug Metab Rev* 36: 569-582.
- Ronson RS, Nakamura M, Vinten-Johansen J. 1999. The cardiovascular effects and implications of peroxynitrite. *Cardiovasc Res* 44: 47-59.
- Rosignol R, Letellier T, Malgat M, Rocher C, Mazat JP. 2000. Tissue variation in the control of oxidative phosphorylation: Implication for mitochondrial diseases. *Biochem J* 347: 45-53.
- Rubbo H, Parthasarathy S, Barnes S, Kirk M, Kalyanaram B, et al. 1995. Nitric oxide inhibition of lipoxygenase-dependent liposome and low-density lipoprotein oxidation: Termination of radical chain propagation reactions and formation of nitrogen-containing oxidized lipid derivatives. *Arch Biochem Biophys* 324: 15-25.
- Sattler R, Tymianski M. 2001. Molecular mechanisms of glutamate receptor-mediated excitotoxic neuronal cell death. *Mol Neurobiol* 24: 107-129.
- Sauer H, Wartenberg M, Hescheler J. 2001. Reactive oxygen species as intracellular messengers during cell growth and differentiation. *Cell Physiol Biochem* 11: 173-186.
- Schapira AH, Cooper JM, Dexter D, Jenner P, Clark JB, et al. 1989. Mitochondrial complex I deficiency in Parkinson's disease. *Lancet* 1(8649): 1269.
- Schulenberg B, Goodman TN, Aggeler R, Capaldi RA, Patton WF. 2004. Characterization of dynamic and steady-state protein phosphorylation using a fluorescent phosphoprotein gel stain and mass spectrometry. *Electrophoresis* 25: 2526-2532.
- Schulze-Osthoff K, Bakker AC, Vanhaesebroeck B, Beyaert R, Jacob WA, et al. 1992. Cytotoxic activity of tumor necrosis factor is mediated by early damage of mitochondrial functions. Evidence for the involvement of mitochondrial radical generation. *J Biol Chem* 267: 5317-5323.
- Selak MA, Armour SM, MacKenzie ED, Boulahbel H, Watson DG, et al. 2005. Succinate links TCA cycle dysfunction to oncogenesis by inhibiting HIF- α prolyl hydroxylase. *Cancer Cell* 7: 77-85.
- Shiva S, Brookes PS, Patel RP, Anderson PG, Darley-Usmar VM. 2001. Nitric oxide partitioning into mitochondrial membranes and the control of respiration at cytochrome *c* oxidase. *Proc Natl Acad Sci USA* 98: 7212-7217.
- Simpkins JW, Wang J, Wang X, Perez E, Prokai L, et al. 2005. Mitochondria play a central role in estrogen-induced neuroprotection. *Curr Drug Target CNS Neurol Disord* 4: 69-83.

- Smith RA, Porteous CM, Coulter CV, Murphy MP. 1999. Selective targeting of an antioxidant to mitochondria. *Eur J Biochem* 263: 709-716.
- Sohal RS, Weindruch R. 1996. Oxidative stress, caloric restriction, and aging. *Science* 273: 59-63.
- Sousa SC, Maciel EN, Vercesi AE, Castilho RF. 2003. Ca²⁺-induced oxidative stress in brain mitochondria treated with the respiratory chain inhibitor rotenone. *FEBS Lett* 543: 179-183.
- Staniek K, Nohl H. 1999. H₂O₂ detection from intact mitochondria as a measure for one-electron reduction of dioxygen requires a non-invasive assay system. *Biochim Biophys Acta* 1413: 70-80.
- Starkov AA, Fiskum G. 2003. Regulation of brain mitochondrial H₂O₂ production by membrane potential and NAD (P)H redox state. *J Neurochem* 86: 1101-1107.
- Starkov AA, Fiskum G, Chinopoulos C, Lorenzo BJ, Browne SE, et al. 2004. Mitochondrial alpha-ketoglutarate dehydrogenase complex generates reactive oxygen species. *J Neurosci* 24: 7779-7788.
- Starkov AA, Polster BM, Fiskum G. 2002. Regulation of hydrogen peroxide production by brain mitochondria by calcium and Bax. *J Neurochem* 83: 220-228.
- Stewart VC, Stone R, Gegg ME, Sharpe MA, Hurst RD, et al. 2002. Preservation of extracellular glutathione by an astrocyte derived factor with properties comparable to extracellular superoxide dismutase. *J Neurochem* 83: 984-991.
- Stirone C, Duckles SP, Krause DN, Procaccio V. 2005. Estrogen increases mitochondrial efficiency and reduces oxidative stress in cerebral blood vessels. *Mol Pharmacol* 68(4): 959-965.
- Stout AK, Raphael HM, Kanterewicz BI, Klann E, Reynolds IJ. 1998. Glutamate-induced neuron death requires mitochondrial calcium uptake. *Nat Neurosci* 1: 366-373.
- St-Pierre J, Buckingham JA, Roebuck SJ, Brand MD. 2002. Topology of superoxide production from different sites in the mitochondrial electron transport chain. *J Biol Chem* 277: 44784-44790.
- Suto D, Sato K, Ohba Y, Yoshimura T, Fujii J. 2005. Suppression of the pro-apoptotic function of cytochrome *c* by singlet oxygen via a heme redox state-independent mechanism. *Biochem J* 392: 399-406.
- Szabo C, Dawson VL. 1998. Role of poly(ADP-ribose) synthetase in inflammation and ischaemia-reperfusion. *Trends Pharmacol Sci* 19: 287-298.
- Tarpey MM, White CR, Suarez E, Richardson G, Radi R, et al. 1999. Chemiluminescent detection of oxidants in vascular tissue. Lucigenin but not coelenterazine enhances superoxide formation. *Circ Res* 84: 1203-1211.
- Tay YM, Lim KS, Sheu FS, Jenner A, Whiteman M, et al. 2004. Do mitochondria make nitric oxide? No. *Free Radic Res* 38: 591-599.
- Taylor ER, Hurrell F, Shannon RJ, Lin TK, Hirst J, et al. 2003. Reversible glutathionylation of complex I increases mitochondrial superoxide formation. *J Biol Chem* 278: 19603-19610.
- Teshima Y, Akao M, Jones S, Marban E. 2003. Uncoupling protein-2 overexpression inhibits mitochondrial death pathway in cardiomyocytes. *Circ Res* 93: 192-200.
- Thannickal VJ, Fanburg BL. 1995. Activation of an H₂O₂-generating NADH oxidase in human lung fibroblasts by transforming growth factor beta 1. *J Biol Chem* 270: 30334-30338.
- Tretter L, Adam-Vizi V. 2000. Inhibition of Krebs cycle enzymes by hydrogen peroxide: A key role of α -ketoglutarate dehydrogenase in limiting NADH production under oxidative stress. *J Neurosci* 20: 8972-8979.
- Tretter L, Adam-Vizi V. 2004. Generation of reactive oxygen species in the reaction catalyzed by alpha-ketoglutarate dehydrogenase. *J Neurosci* 24: 7771-7778.
- Turrens JF. 2003. Mitochondrial formation of reactive oxygen species. *J Physiol* 552: 335-344.
- Tzung SP, Kim KM, Basanez G, Giedt CD, Simon J, et al. 2001. Antimycin A mimics a cell-death-inducing Bcl-2 homology domain 3. *Nat Cell Biol* 3: 183-191.
- Uppu RM, Lemercier JN, Squadrito GL, Zhang H, Bolzan RM, et al. 1998. Nitrosation by peroxynitrite: Use of phenol as a probe. *Arch Biochem Biophys* 358: 1-16.
- Valgimigli L, Pedullì GF, Paolini M. 2001. Measurement of oxidative stress by EPR radical-probe technique. *Free Radic Biol Med* 31: 708-716.
- Villamena FA, Zweier JL. 2004. Detection of reactive oxygen and nitrogen species by EPR spin trapping. *Antioxid Redox Signal* 6: 619-629.
- Votyakova TV, Reynolds IJ. 2004. Detection of hydrogen peroxide with Amplex Red: Interference by NADH and reduced glutathione auto-oxidation. *Arch Biochem Biophys* 431: 138-144.
- Waypa GB, Schumacker PT. 2005. Hypoxic pulmonary vasoconstriction: Redox events in oxygen sensing. *J Appl Physiol* 98: 404-414.
- Weisiger RA, Fridovich I. 1973. Superoxide dismutase. Organelle specificity. *J Biol Chem* 248: 3582-3592.
- Werner P, Cohen G. 1991. Intramitochondrial formation of oxidized glutathione during the oxidation of benzylamine by monoamine oxidase. *FEBS Lett* 280: 44-46.
- Wikstrom M, Saari HA. 1975. Spectral shift in cytochrome *a* induced by calcium ions. *Biochim Biophys Acta* 408: 170-179.

- Wilson DE, Erecinska M, Drown C, Silver IA. 1979. The oxygen dependence of cellular energy metabolism. *Arch Biochem Biophys* 195: 485-493.
- Wilson RB, Roof DM. 1997. Respiratory deficiency due to loss of mitochondrial DNA in yeast lacking the frataxin homologue. *Nat Genet* 16: 352-357.
- Xu L, Eu JP, Meissner G, Stamler JS. 1998. Activation of the cardiac calcium release channel (ryanodine receptor) by poly-S-nitrosylation. *Science* 279: 234-237.
- Yan SD, Stern DM. 2005. Mitochondrial dysfunction and Alzheimer's disease: Role of amyloid-beta peptide alcohol dehydrogenase (ABAD). *Int J Exp Pathol* 86: 161-171.
- Zhang X, Kim WS, Hatcher N, Potgieter K, Moroz LL, et al. 2002. Interfering with nitric oxide measurements. 4,5-diaminofluorescein reacts with dehydroascorbic acid and ascorbic acid. *J Biol Chem* 277: 48472-48478.

5.4 Uncoupling Proteins

J. S. Kim-Han · S. S. Ali · L. L. Dugan

<i>1 Introduction to Mitochondrial Uncoupling Proteins</i>	<i>550</i>
<i>2 Regulation of Uncoupling Protein Expression</i>	<i>551</i>
<i>3 Regulation of UCP Activity</i>	<i>551</i>
<i>4 Physiological Roles of UCPs in Metabolism</i>	<i>558</i>
<i>5 Uncoupling Proteins and Regulation of Reactive Oxygen Species Generation</i>	<i>560</i>
<i>6 Overview of the Involvement of UCPs in Systemic Disease States</i>	<i>560</i>
<i>7 UCPs in Brain</i>	<i>561</i>
<i>8 Summary</i>	<i>562</i>

Abstract: Mitochondrial oxidation of fuel generates an electrochemical gradient via outward pumping of protons by the electron transport chain. ATP production via ATP synthase is then facilitated by the inward flux of protons down the gradient. However, during the 1970s, David Nicholls and colleagues found that the electrochemical gradient could be uncoupled from ATP production in brown adipose tissue (BAT) to produce heat, and that this uncoupling was due to activation of the prototypic mitochondrial uncoupling protein (UCP1) (Nicholls, 2001). Subsequently, a family of related proteins has been described and several of these putative uncoupling proteins (UCPs) are expressed in brain. This chapter describes these proteins and their proposed roles in health and disease.

List of Abbreviations: ANT, adenine nucleotide translocase; BAT, brown adipose tissue; BSA, bovine serum albumin; GPX1, glutathione peroxidase; KA, kainic acid; LPS, lipopolysaccharide; MC, mitochondrial carrier; MnSOD, mitochondrial superoxide dismutase; MPTP, 1-methyl-4-phenyl-1,2,5,6-tetrahydropyridine; ORF, open reading frame; PPARs, peroxisome proliferator-activated receptors; ROS, reactive oxygen species; SOD, superoxide dismutase; TCA, tricarboxylic acid; UCPs, uncoupling proteins

1 Introduction to Mitochondrial Uncoupling Proteins

Mitochondria are the main power plants in eukaryotic cells, producing ATP as a high-energy storage form, a process which is regulated by many factors including diet, temperature, and energy demands (see also *Chapters 1.1* and *1.6*). As first proposed by Mitchell (1961), the driving force for ATP production is the proton electrochemical gradient (Δp), established by the electron transport chain across the inner mitochondrial membrane between the mitochondrial matrix and the intermembrane space. Many proteins, including the ADP/ATP carrier, glutamate/aspartate carrier, and phosphate carrier, harness components of Δp for their functions. Dissipation of Δp without concomitant ATP synthesis has been termed uncoupling. Nicholls and colleagues first recognized that the protein-mediated uncoupling activity in brown adipose tissues (BAT), which helps maintain the body temperature of newborn infants, was due to a specific mitochondrial protein, uncoupling protein 1 (UCP1) (Nicholls and Locke, 1984). This novel protein was found to utilize Δp to generate heat instead of ATP. UCP1 is now known to be responsible for nonshivering thermogenesis in both newborns and hibernating mammals (Nicholls et al., 1984; Boyer, et al., 1998; Klingenberg, 1999), and recent studies in *ucp1* knockout mice suggest that UCP1 is, in fact, the sole effector for thermogenesis in BAT (Enerback et al., 1997; Matthias et al., 2000).

The human *UCP1* gene, located on chromosome 4, has 6 exons encoding a protein of 305 amino acids. The ~32-kDa UCP1 protein has six transmembrane domains, three mitochondrial carrier protein motifs, and a nucleotide-binding domain. Uncoupling proteins (UCPs) are members of the large family of mitochondrial carrier (MC) proteins, which are expressed in organisms ranging from single-cell forms to mammals. The solute carrier protein 25 (SLC25) genes represent the human MC family. On the basis of sequence similarity with UCP1, a number of members of the SLC25 family of MC proteins (Palmieri, 2004) have been proposed to be putative mitochondrial UCPs. To date, more than 45 genes encoding UCP-like proteins have been described in single-cell organisms, plants, and animals (Ledesma et al., 2002), and many of these putative UCP genes have been cloned, allowing their function and regulation to be studied (Bouillaud et al., 2001).

The “novel” UCPs, UCP2 and UCP3, are 56% and 57% homologous to UCP1, respectively. UCP2 message is broadly expressed, whereas UCP3 is detected principally in BAT and skeletal muscle (Bouillaud et al., 2001). The human *UCP2* and *UCP3* genes are located on chromosome 11 within a 7-kb region, and may represent a gene duplication event. UCP3 has two splice variants encoding 275- and 312-amino-acid proteins. UCP4 and UCP5 (also known as brain mitochondrial carrier protein 1, BMCP1) have recently been added to the family of UCPs. Both are expressed primarily in the central nervous system (CNS) (Sanchis et al., 1998; Mao et al., 1999), suggesting that they may have specific roles in CNS function. Like UCP1, the putative UCPs (UCP2–5) are believed to be located in the inner mitochondrial membrane. However, a mitochondrial location for all UCP family members has not been definitively shown. Another

gene, SLC25A30, from the RIKEN cDNA library, was recently reported to have a high degree of sequence homology to UCP5/BMCP1 but has not yet been studied.

2 Regulation of Uncoupling Protein Expression

As shown in [Table 5.4-1](#), expression of UCP family members can be regulated at the mRNA level by a wide range of conditions and stimuli, including temperature, diet, leptin, insulin, endotoxin, and inflammatory cytokines. In addition, changes in expression of UCP family members in response to a given stimulus differ in both a tissue-specific and UCP-specific manner ([Table 5.4-1](#)). Of note, however, even under conditions in which expression of UCP2, UCP3, and UCP5 are induced, expression of these family members is 1–2 orders of magnitude lower than that of UCP1 in BAT. The pathways that link a specific stimulus to a change in UCP expression have not been identified under all circumstances, but increased levels of fatty acids appear to be one mechanism. For example, cold exposure upregulates UCP1 mRNA and protein in BAT through β_3 -adrenergic receptors via fatty acids released from triglycerides (Cannon and Nedergaard, 2004). Fasting and high-fat diets also regulate the expression of several UCPs through changes in circulating free-fatty acids (FFAs), which may, in turn, be under the control of peroxisome proliferator-activated receptors (PPARs).

Despite extensive studies on the expression of UCP message, regulation of protein expression is rarely reported. In part, this reflects problems with currently available UCP antibodies, including both private and commercial antibodies. Many of the published antibodies for UCP2–4 detect bands in the 32–36 kDa range for their respective proteins in knockout mice (L.L. Dugan and J.S. Kim-Han, unpublished data), suggesting that they are not specific for a given UCP isoform, and indicating that well-characterized antibodies would be extremely useful tools for future studies on the UCPs. This issue is especially important because regulation of UCP mRNA has not, in many cases, been followed by changes in UCP protein expression (Sivitz et al., 1999; Jakus et al., 2002). For example, changes in UCP2 mRNA frequently fail to result in any change in protein expression (Pecqueur et al., 2001; Ealey et al., 2002). This dissociation between message and protein likely reflects the presence of an upstream AUG start codon and alternative open reading frame (ORF) in the 5'-untranslated region of the UCP2 message (Pecqueur et al., 2001). Upstream ORFs have been identified for the UCP2, UCP3, and UCP5 message, and these can result in reduced translational efficiency (Pecqueur et al., 2001). Therefore, other posttranscriptional mechanisms including changes in mRNA stability need to be studied for these proteins. Finally, in addition to posttranscriptional regulation of UCP expression, two splice variants for UCP3 (Chung et al., 1999) and more than six splice variants for UCP5 (L.L. Dugan and J.S. Kim-Han, unpublished data) have been identified, suggesting further complexity in the regulation of UCP gene expression. It is clear that regulation of the uncoupling protein family members is complex, occurring at the level of both transcription and translation. The presence of alternative initiation sites (UCP2, UCP3, and UCP5) which can affect translational efficiency, and the identification of a splice variant for UCP3 which decreases mRNA/protein stability (Chung et al., 1999) highlight the difficulty in assuming that mRNA levels predicts protein expression (and then further, uncoupling activity). Thus, it is important to be aware that interpreting mRNA expression as predictive of the presence of UCP protein or its activity should be done with a high degree of caution.

3 Regulation of UCP Activity

In addition to transcriptional and translational regulation of UCP protein expression, the uncoupling activity of UCP1, UCP2, and UCP3 is dependent on a number of cofactors. These cofactors are best characterized for UCP1 ([Figure 5.4-1](#)). UCP1 is activated by low (nM– μ M) concentrations of FFAs (Gonzalez-Barroso et al., 1996; Echtay et al., 2001). The preference of UCP1 and other UCP isoforms for specific FFA species has not been fully defined but may differ between UCP members. Activation of UCP1 by FFAs can be reversed by inclusion of bovine serum albumin (BSA), which binds and removes FFAs

Table 5.4-1
Regulation of UCP1 and other putative uncoupling proteins

Model	Stimulants	UCP	Reference
Penguin	Pectoralis muscle	avUCP mRNA↑	Talbot et al. (2004)
Chicken	SM	avUCP mRNA↑	Toyomizu et al. (2002)
Rat	BAT	BAT-UCP1 mRNA & protein ↑, UCP3 mRNA↑, protein↓,GM-UCP1 mRNA↑, UCP3 mRNA↑, protein (nc)	Jakus et al. (2002)
	Gastrocnemius muscle (GM)	UCP3 mRNA↑, UCP5(nc)	Mizuno et al. (2000)
Rat	Spinal cord (SC)	SC-UCP2↑, UCP5(nc)	
	Brain (B)	B-0UCP2(nc), UCP5(nc)	
Rat	L6 myotube	B-UCP5↓ (26M), UCP2↑ (12, 26M)	Nagase et al. (2001)
	Colon	UCP2↑, UCP3↑	Bassaganya-Riera et al. (2004)
Rat	C57Bl/6J mouse	UCP1↑, UCP3↑	Ealey et al. (2002)
Rat	Mammary gland, BAT, WAT	In rats, UCP1↓, UCP2↑, UCP3↓ (mRNA & protein)	
	C57Bl/6 mouse	In mice, UCP3 mRNA & protein↑	
Mouse	BAT	UCP1↓, UCP2↑, UCP3↓	Takahashi et al. (2002)
Rat	Liver	UCP2↑	Armstrong and Towle (2001)
	Myotube	(Aspirin blocked the increase) UCP2↑	Chevillotte et al. (2001)
Rat	Cardiomyocytes	UCP2 mRNA↑	Van der Lee (2000)
		(+Glucose or Phenylephrine –no effect, +T3-synergistic effect) UCP2 mRNA↑ UCP2 mRNA↑	

KK-Ay mouse	BAT	GH	BAT: UCP1↑, UCP2↑, UCP3(nc) UCP1(nc), UCP2(nc), UCP3(nc)	Hioki et al. (2004)
C57Bl/6J mouse	Gastrocnemius muscle (GM) Subcutaneous WAT (SW)		GM: UCP1↑, UCP2↑, UCP3↑ UCP1(nc), UCP2(nc), UCP3(nc) SW: UCP1↑, UCP2(nc), UCP3(nc)UCP1(nc), UCP2(nc), UCP3(nc) UCP1↓	
Rat	BAT (adipocytes)	EGF, NCS, FGF	UCP1 mRNA-protein↑	Garcia and Obregon (2002) Tsuchida et al. (2001)
Obese diabetic mouse	BAT	BDNF		
Rat	SM, adipose tissue In vitro-no effect	EGF, 7 days	UCP2(nc), UCP3↑	Pederson et al. (2000)
Rat	BAT	Fasting	UCP1↓, UCP2(nc), UCP3↓	Xiao XQ et al. (2004)
	SM	Lactation	UCP1↓, UCP2(nc), UCP3↓	
		Fasting	UCP2(nc), UCP3↓	
		Lactation	UCP2(nc), UCP3↑	
Rat	Muscles	Fasting 46 hr	G: UCP2↑, UCP3↑ T: UCP2↑, UCP3↑ S: UCP2(nc), UCP3(nc)	Samec et al. (2002)
	Gastrocnemius (G) Tibialis anterior (T) Soleus (S)			
Rat	BAT	Fasting	UCP1 mRNA↓, (Leptin-sensitive) UCP1 protein↓, (Leptin-insensitive) UCP3(nc) (both mRNA and protein)	Sivitz et al. (1999)
Rat	Heart	Fasting	UCP2(nc), UCP3↑	Young et al. (2001)
Mouse	SM, BAT	Fasting (F) after birth	SM-UCP3↓ (F+lipid ↑↑, F+leptin↑, F+glucose-), UCP2(nc) BAT-UCP1(nc) (F+glucose↑)	Villarroya et al. (2001)

Table 5.4-1 (continued)

Model	Stimulants	UCP	Reference
Rat	SM	UCP3 mRNA↑	Boss et al. (1998)
Rat	iBAT	UCP3 mRNA(nc)	
Rat	SM	iBAT-UCP1↑, UCP2(nc), UCP3↑	Margareto et al. (2001)
Rat	Pancreatic islets	SM-UCP2(nc), UCP3↑	Li et al. (2003)
Mouse	INS-1 cells	UCP2 mRNA↓	
Mouse	Liver, SM		
	IL-1β,	Liver-UCP2↓↑, UCP5↓(bc)	Yu et al. (2000)
	TNFα+IL-1β	SM-UCP2↓↑, UCP3↑(bc), UCP5↓↑	
	LPS	UCP2 mRNA↑(in hepatocytes, not in macrophages) (TNF-sensitive) UCP2 mRNA↑	Cortez-Pirnte et al. (1998)
Rat	Liver	UCP1 protein↑, UCP2 protein(nc), UCP3 protein(nc)	Valverde et al. (2003)
Mouse	Brown adipocytes		
	TNFα	BAT-4d: UCP1↑, UCP2(nc), UCP3↑,	
	Insulin (IRS-med.)	25d: UCP1(nc), UCP2↑, UCP3(nc)RP-	Gullicksen et al. (2002)
Mouse	Leptin, 4 days (4d) injection, 21 days (25d) recovery	4d: UCP1↑, UCP2↑, UCP3↑	
		25d: UCP1↑↑, UCP2↑, UCP3(nc)EWAT-4d: UCP1(nc), UCP2↑, UCP3↑	
		25d: UCP1(nc), UCP2↑, UCP3(nc)ING-	
		4d: UCP1(nc), UCP2↓, UCP3(nc)25d: UCP1(nc), UCP2↑, UCP3(nc)	
		Leptin↑, UCP3↓	Kotz et al. (2000)
Rat	Acromiotrapezius	UCP2 mRNA↑	Zhou et al. (1997)
ZDF +/- lean rat	Leptin	UCP2↑ (EWAT, 75%)	Scarpace et al. (1997, 1998)
Brown-Norway rat	Leptin	UCP3↑ (BAT, 70%)	
Rat	Hypoxia	UCP3↓	Essop et al. (2004)
Rat	Exercise	UCP2 mRNA↑	Zhou et al. (2000)
	Hypoxia	UCP2 mRNA↑	
	AICAR	UCP2 mRNA & protein↑	

Rat	BAT	Bezafibrate	UCP1↓, UCP2(nc), UCP3(nc)	Mori et al. (2004)
Rat	Gastrocnemius muscle	Thiazolidinediones	UCP3↑	Brunmair et al. (2004)
Rat	Cultured preadipocytes	Bezafibrate, Wy14643, Troglitazone	UCP2↑, UCP3↑↑ UCP2(nc), UCP3↑ UCP2(nc), UCP3↑↑ UCP1↓	Cabrero et al. (2000)
C57Bl/6N mouse	BAT	H1R KO	UCP2 mRNA↑	Masaki et al. (2004b)
Mouse	WAT	IRS-1 KO	UCP1 mRNA↓	Masaki et al. (2004)
	BAT	Leptin	UCP1 mRNA↑	Masaki et al. (2003)
Rat	BAT	MT II	UCP1 mRNA↑	Williams et al. (2003)
Rat	SM	CLFS	UCP3 mRNA↓, UCP3 protein↑	Putman et al. (2004)
Rat	TA muscle	AICAR	UCP3 mRNA↓, protein↑	Putman et al. (2003)
Rat	Soleus muscle, heart	High-fat diet	UCP3 mRNA↑	Stavinoha et al. (2004)
	Heart	Fasting	UCP3 mRNA↑	
		Diabetes	UCP3 mRNA↑	
		WY-14643	UCP3 mRNA↑	
		Hypertrophy	UCP3 mRNA↓	
		Hypoxia	UCP3 mRNA↓	
Rat	Lung	CR	UCP2 mRNA↑	Xiao H et al. (2004)
Rat	Heart, SM	T3	UCP3 mRNA↑	Queiroz et al. (2004)
Human	SMAdipose tissue	T3	SM-UCP2↑, UCP3↑	Barbe et al. (2001)
			AT-UCP2 (in vivo & in vitro)	
Obese mouse		C75 30 days	UCP3 mRNA↑	Cha et al. (2004)
Rat	Adipocytes	Pancreastatin	UCP2 mRNA↑	Gonzalez-Yanes and Sanchez-margalet (2003)
			UCP1	Masanés et al. (2002)
Lean rat	Muscle	Low protein diet	UCP↓	
Obese rat	BAT	High protein diet	UCP↑	
	Subcutaneous WAT		UCP(nc) UCP3↓	

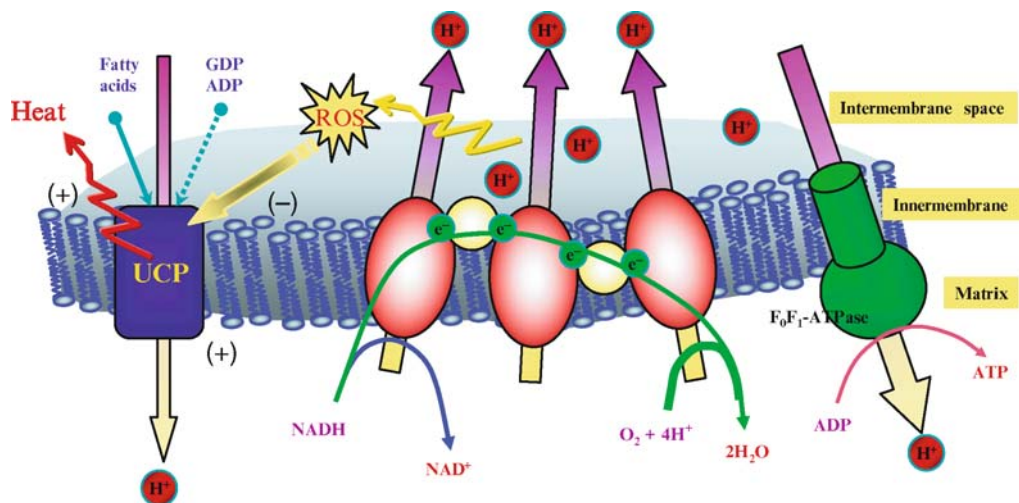
Table 5.4-1 (continued)

Model	Stimulants	UCP	Reference
Human	SM	UCP3 mRNA↑	Cameron-Smith et al. (2003)
Mice	High-fat diet High-carb diet	UCP3 mRNA-	Murase et al. (2002)
Human	Small intestine Islets	UCP2 mRNA↑ UCP2 ↑ (Leptin-sensitive)	Brown et al. (2002)

AA: arachidonic acid
 AICAR: AMPK (5'-AMP activated protein kinase) activator
 ALADG: α -linolenic acid rich diacylglycerol
 BAT: brown adipose tissue
 bc: back to the control level
 C75: fatty acid synthase inhibitor
 Ciglitazone: PPAR α ligand
 CLA: conjugated linoleic acid
 CLFS: chronic low frequency stimulation
 CR: calori-restriction
 EPA: eicosapentaenoic acid
 EWAT: epididymal WAT
 GH: growth hormone
 ING: Inguinal WAT
 L-165041: PPAR β agonist
 MT II: melanocortin $\frac{3}{4}$ receptor agonist
 nc: no change
 NCS: newborn calf serum
 Pancreastatin: a chromogranin A-derived peptide
 PUFA: polyunsaturated fatty acid
 RP: retroperitoneal
 SM: skeletal muscle
 T3: triiodothyronine
 WAT: white adipose tissue
 WY14643: PPAR gamma ligand

■ Figure 5.4-1

Regulation of uncoupling protein activity in mitochondria. The proton gradient between the mitochondrial matrix and intermembrane space is established by the mitochondrial electron transport chain (ETC), which is the driving force for ATP production by F_0F_1 -ATPase. Uncoupling proteins (UCPs) use the proton gradient to produce heat instead of ATP. UCPs are activated by fatty acids and inhibited by the purine nucleotides (GDP and ADP). Reactive oxygen species (ROS) is generated by single electron transfer from the ETC to O_2



from the UCP protein (Klingenberg, 1999). Although it is clear that UCP1 activity is highly regulated by fatty acids, a controversy has evolved about whether FFA not only are “activators” of UCP uncoupling through a specific, high-affinity binding site but also are “transported substrates” of UCPs, being cotransported with protons under selected circumstances (Garlid et al., 2000; Rousset et al., 2004). This alternative fatty acid transport activity has been most convincingly shown to date for UCP1 and UCP3. The ability of FFAs to activate UCPs is especially interesting in light of the observations that different fatty acid pools are released by varying stimuli, including ischemia and traumatic injury (Bazan Jr., 1970; Lazarewicz et al., 1972; Kuwashima et al., 1978; Agardh et al., 1982; Hillered and Chan, 1988; Stephenson et al., 1999; Phillis and O’Regan, 2004). Since both cerebral ischemia and traumatic brain injury are associated with increased ROS production, likely via glutamate receptor-mediated excitotoxicity and calcium dysregulation, one can speculate that increased fatty acid levels might activate one or more UCPs in the brain in an attempt to normalize mitochondrial ROS production.

UCP1 uncoupling activity is inhibited by purine nucleotides through binding to a specific nucleotide-binding site. ATP, ADP, GTP, and GDP all can bind to this site, although ADP is a better inhibitor of UCP1 than ATP, GTP, or GDP. The concentrations of these nucleotides reported to provide full inhibition of UCP1 activity range from $<50 \mu\text{M}$ to $100 \mu\text{M}$. The best estimates of cytosolic ADP plus ATP, however, are $>5 \text{ mM}$. Thus, the concentration required for maximal inhibition through this site is far below the physiological concentrations of purine nucleotides, raising the question of whether nucleotide-dependent inhibition of UCPs is ever released under physiologic conditions. There is an additional dilemma raised by studies that report the activation of UCPs by molecules such as ubiquinone, since in the presence of saturating physiological concentrations of purine nucleotides, it is difficult to understand how UCP activity can still be stimulated.

Another question related to the nucleotide-binding site is to what extent UCP activity through this site is regulated by the concentration of ADP (or GDP) versus the ratio of ADP/ATP (or GDP/GTP). UCP1, UCP2, UCP3, and UCP5 all appear to possess an active nucleotide-binding site based on the presence of a similar protein sequence to the site in UCP1, although regulation of uncoupling via the site has been only

shown for UCP1–3. There is a suggestion that these proteins differ in their preference for ATP/ADP versus GTP/GDP. In addition to being regulated by FFAs and purine nucleotides, UCP1 has also been reported to require ubiquinone as a necessary cofactor (Echtay et al., 2000), although the requirement for ubiquinone has not been clearly demonstrated in other model systems, such as yeast and reconstituted liposomes (Jaburek and Garlid, 2003; Esteves et al., 2004).

UCP1 has been reported to be activated by superoxide radical ($O_2^{\bullet -}$) as well (Echtay et al., 2002). Superoxide-mediated uncoupling of mitochondria is inhibited by GDP and requires fatty acids, supporting the involvement of one or more UCPs in the increased proton conductance. This uncoupling was reversible, pH dependent, and sensitive to superoxide dismutase (SOD), but not to catalase (Echtay et al., 2002), indicating that a superoxide-dependent product, but not H_2O_2 , was the reactive oxygen species (ROS) responsible for activation. Consistent with this, endogenously generated superoxide increases proton conductance through the activation of UCP3 in skeletal muscle (Talbot et al., 2004). Recently, Krauss and coworkers reported activation of UCP2 by superoxide generated by mitochondria isolated from kidney or spleen (Krauss et al., 2003). Exogenously generated superoxide also resulted in UCP2 activation in thymocytes and B cells in mice, and activation was inhibited by MnTBAP, a SOD mimetic, and by the mitochondrial superoxide dismutase (MnSOD), but not by glutathione peroxidase 1 (GPX1). Although UCP activation by superoxide is absent in UCP2 knockout mice, supporting the idea that UCP2 activity may be dependent on superoxide, another study (Couplan et al., 2002) failed to observe activation of UCP2 by superoxide. Since other UCP isoforms, specifically UCP1 (Echtay et al., 2002) and UCP3 (Echtay et al., 2002; Talbot et al., 2004), have also been reported to be activated by superoxide, changes in expression of other UCPs in UCP2(–/–) mice, as has been previously reported (de Bilbao et al., 2004), should be excluded as a possible mechanism for this result. Of note, Li and coworkers pointed out that the superoxide-generating system employed for some of these studies (xanthine oxidase metabolism of xanthine; XO/XA) consumes O_2 in the process of producing superoxide, thus reducing $[O_2]$ in the reaction mixture and thereby altering mitochondrial respiratory function (Li et al., 2002). The levels of superoxide generated by XO/XA in many of these studies are also several orders of magnitude greater than ever seen in vivo. Experiments using in vitro reconstitution systems could give more direct answers to these questions.

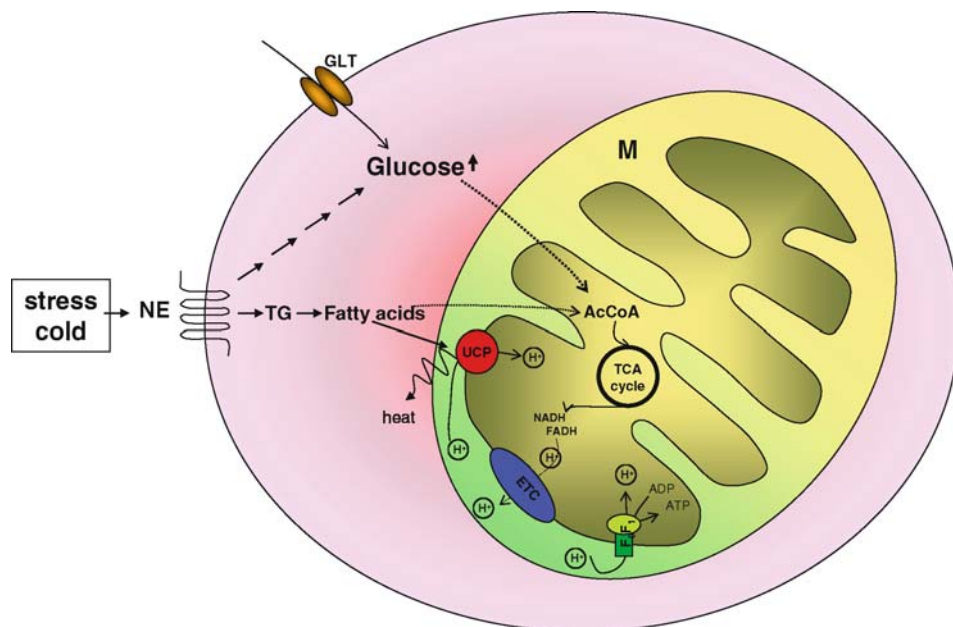
Products of lipid peroxidation such as 4-hydroxynonenal and related compounds induce proton conductance of mitochondria through UCP1, UCP2, UCP3, and the adenine nucleotide translocase (ANT) in animals (Echtay et al., 2003), and through StUCP in plants (Smith et al., 2004). Cleaved hydroperoxy-fatty acids and hydroxy-fatty acid have also been reported to activate UCP2 and promote feedback downregulation of mitochondrial ROS production (Brand et al., 2004).

4 Physiological Roles of UCPs in Metabolism

The original function of UCP1 in BAT was believed to be the control of body temperature in newborns and in rodents. Upon exposure to cold, BAT mitochondria increase their consumption of O_2 and begin to produce heat instead of ATP (▶ [Figure 5.4-2](#)). In addition, when β_3 -adrenergic receptors in BAT are activated by norepinephrine, metabolism of lipids and glucose is increased dramatically. BAT recruits triglycerides as a fuel source, releasing fatty acids that are then used as substrate for oxidative respiration via β -oxidation (Cannon and Nedergaard, 2004). Although the function of UCP1 as a thermogenic protein has been clearly established, there is now evidence that it may also be involved in the regulation of weight and body composition. Despite enlarged lipid vacuoles in the BAT of *Ucp1* (–/–) mice, these animals do not develop early obesity even on a high-fat diet (Enerback et al., 1997). Interestingly, however, *Ucp1* (–/–) mice maintained on a high-fat diet become obese as they age, suggesting biological changes associated with the aging process may interact with UCP1 to modify its effects (Kontani et al., 2005). Mitochondria isolated from *Ucp1*-deficient mice also show no decrease in their respiratory rate after addition of GDP, which would normally be expected to inhibit *Ucp1* activity through its binding to the guanine nucleotide-binding site. Finally, no changes in the mitochondrial membrane potential or O_2 consumption were apparent after application of norepinephrine or addition of GDP to *Ucp1* (–/–) mice. These data point to UCP1 as the predominant UCP in BAT (Matthias et al., 1999).

■ Figure 5.4-2

Action of uncoupling proteins in BAT. Upon exposure to stress and cold, norepinephrine activates β -adrenergic receptors, leading to lipolysis and release of free-fatty acids (FFAs). The concentration of glucose is also increased by upregulation of glucose transporters and by glycogenolysis. When BAT is active, consumption of lipids and glucose increases. Mitochondrial respiration is accelerated, resulting in thermogenesis. (M, mitochondria; NE, norepinephrine; TG, triglyceride; GLT, glucose transporters; UCPs, uncoupling proteins; ETC, electron transport chain; F_0F_1 , F_0F_1 -ATP synthase; AcCoA, acetyl-CoA)



The physiological functions of UCPs other than UCP1 have not been established, although evidence suggests that these proteins are not important for thermogenesis (Arsenijevic et al., 2000; Zhang et al., 2001). Alternatively, it might be considered that the involvement of UCPs in regulating ATP production as one aspect of their function, data to date suggest that this is generally not true. Levels of ATP and interrelated high-energy phosphates are tightly regulated and maintained by highly integrated mechanisms, with mitochondria being the main source of ATP in eukaryotes via oxidative phosphorylation. Although activation or overexpression of UCP1 decreases the proton gradient across the inner membrane, it does not appear to significantly reduce the cellular concentration of ATP, reflecting the fact that ATP levels are controlled by multiple regulatory steps (see *Chapters 1.1* and *1.6*). For example, activation of UCP in plants causes a compensatory increase in tricarboxylic acid (TCA) cycle activity (Smith et al., 2004). Chronic treatment with triiodothyronine (T3) or acute treatment with a chemical uncoupler decreases mitochondria coupling without producing a significant change in the ATP synthesis rate, but results in increased TCA cycle flux (Jucker et al., 2000). On the other hand, deletion of UCP1 has been reported to increase ATP production without detectable changes in TCA cycle flux or whole-body metabolism (Cline et al., 2001; Zhang et al., 2001). Although this seems to contradict basic bioenergetic principals, there is evidence that adenylate and creatine kinases, which are regulated by ATP, may maintain steady-state concentrations of ATP independent of alterations in ATP synthesis (Dzeja, 1998), highlighting the integrated metabolism of cellular bioenergetics.

Of interest, UCP2 is reported to mediate hypermetabolism caused by oxidative stress and glucagon in hepatocyte cultures (Lee et al., 2003), although the exact mechanism behind this action remains to be

determined. However, given the lack of evidence that the novel UCPs are involved in thermogenesis or simple regulation of cellular energy production, the question of what other, nonthermogenic, function(s) are performed is an area of active research. As discussed further below, regulation of ROS flux from mitochondria is one proposed function.

5 Uncoupling Proteins and Regulation of Reactive Oxygen Species Generation

UCP1 is one of the most highly-expressed proteins in BAT mitochondria, representing 7%–15% of total mitochondrial protein. In contrast, the other UCP family members have been estimated to represent only 0.01%–0.06% of total mitochondrial protein in various tissues (Martin et al., 1986; Garlid et al., 1995). The observation that the newer UCPs are expressed at such low levels has prompted the introduction of the concept of “mild uncoupling” (Skulachev, 1998), which suggests that physiological regulation of mitochondrial ROS production occurs through modest changes in ψ_m .

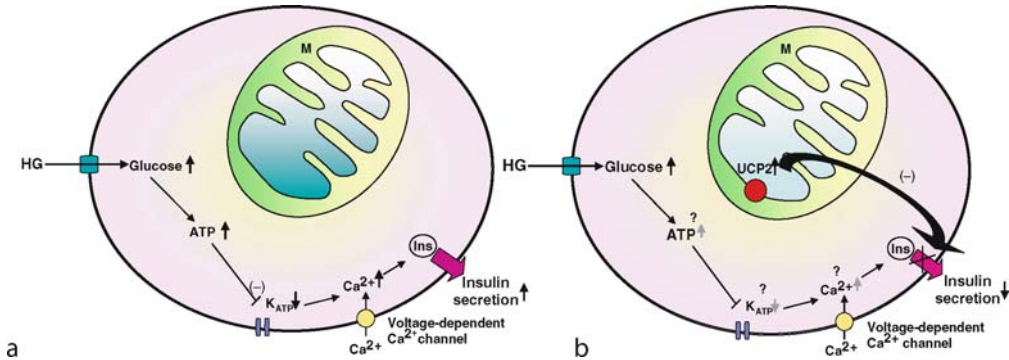
Mitochondria are one of the main sources of intracellular ROS. A single electron transfer from the electron transport chain to O_2 during normal mitochondrial respiration occurs primarily at complexes I and III (Cadenas et al., 1977; Casteilla et al., 2001; Brand et al., 2004), producing superoxide radical ($O_2^{\bullet-}$). Mitochondrial production of $O_2^{\bullet-}$ appears to be dependent on the mitochondrial membrane potential (Ψ_m) (Skulachev, 1998), with a small decrease in Ψ_m producing a dramatic reduction in ROS (Korshunov et al., 1997; Miwa and Brand, 2003). A recent report, however, indicated that mitochondrial superoxide production may be more dependent on the pH gradient (ΔpH) across the mitochondrial inner membrane than on ψ_m (Lambert and Brand, 2004). Activation of UCPs has been proposed as one means to reduce both Ψ_m and ΔpH , and thereby decrease mitochondrial generation of ROS. Mild uncoupling has, in fact, been proposed as one of the key modulators of cellular metabolism and signal transduction via regulation of mitochondrial ROS production (Brookes et al., 2002; Forman et al., 2004). This concept is supported by in vitro and in vivo findings (Skulachev, 1998). Both ψ_m and production of hydrogen peroxide was increased by GDP, presumably by inhibiting uncoupling protein activity, in mitochondria from BAT and liver (Negre-Salvayre et al., 1997). Macrophages from *Ucp2(-/-)* mice produce more ROS, resulting in enhanced resistance to toxoplasmosis infection (Arsenijevic et al., 2000). Antisense treatment to decrease UCP2 expression also increased ROS production and lipid peroxidation in murine endothelial cells (Duval et al., 2002). Furthermore, calorie restriction, which induces UCP3 expression in rat muscle, decreases mitochondrial H_2O_2 production (Bevilacqua et al., 2004). Glucose-induced ROS production, resulting from early mitochondrial hyperpolarization, was inhibited by UCP3 and UCP1 overexpression in DRG neurons (Vincent et al., 2004). In brain mitochondria, UCP2 overexpression also reduces mitochondrial ROS generation (Negre-Salvayre et al., 1997; Nishikawa et al., 2000; Mattiasson et al., 2003). The potential for UCPs to regulate mitochondrial ROS flux could have important effects on cellular metabolism and signaling, as a number of key intracellular signaling cascades have redox-sensitive components (Finkel, 2001, 2003).

6 Overview of the Involvement of UCPs in Systemic Disease States

Because of UCPs involvement in mitochondrial bioenergetics, they have been speculated to be linked to a number of conditions with altered metabolism, including diabetes. The UCP2 gene has been specifically linked to obesity and hyperinsulinemia (Fleury et al., 1997). UCP2 has been proposed to be a negative regulator for glucose-induced insulin secretion in pancreatic β -cells (Chan et al., 2001) (🔗 [Figure 5.4-3](#)). High glucose stimulates ATP production through glycolysis, resulting in an increase in the ATP/ADP ratio, followed by activation of K_{ATP} channels, increased cytosolic Ca^{2+} , and secretion of insulin. K_{ATP} channels are inhibited by intracellular ATP and activated by ADP (Ashcroft et al., 1989). Overexpression of UCP2 in isolated pancreatic islets resulted in decreased ATP content and blocked glucose-induced insulin secretion (Chan et al., 1999, 2001). ROS-mediated activation of UCP2 has been shown to be an important determinant of impaired glucose-stimulated insulin secretion (Krauss et al., 2003). *Ucp2(-/-)* mice demonstrate

■ Figure 5.4-3

Uncoupling proteins (UCPs) in insulin secretion. (a) High [glucose] increases ATP production through glycolysis, resulting in an increase in the ATP/ADP ratio, followed by inhibition of K_{ATP} channels and subsequent depolarization of the plasma membrane, increased cytosolic Ca^{2+} , and the secretion of insulin. (b) Overexpression of UCP2 in isolated pancreatic islets blocks glucose-induced insulin secretion. (M, mitochondria; HG, high glucose; Ins, insulin)



increased ATP levels, higher glucose-induced insulin secretion, and decreased hyperglycemia (Zhang et al., 2001) with no difference from WT mice in body weight when placed on a high-fat diet, and no difference in body temperature upon exposure to cold (Arsenijevic et al., 2000). Inhibition of glucose–insulin secretion by UCP2 does not appear to be caused by a decrease in the ATP/ADP ratio resulting from uncoupling, but due to some other aspect of the UCP2 protein or its activity (Hong et al., 2001). UCP2 is also involved in PPAR- γ -mediated effects of FFAs on glucose-induced insulin secretion (Patane et al., 2002). Furthermore, PPAR- γ overexpression causes induction of *Ucp2*, resulting in decreased insulin, but not glucagon, secretion (Ito et al., 2004). High-fat diets increase triglycerides in pancreatic islet cells and insulin secretion by glucose in β cells from wild-type mice, but not in *Ucp2*($-/-$) mice (Joseph et al., 2004). Finally, arachidonic acid released by cPLA₂ induces expression of UCP2, leading to enhanced glucose-induced insulin secretion (Milne et al., 2005). It is speculated that this reflects PPAR- γ -mediated glucose uptake and lactate production, although the involvement of UCP2 has not been fully established (Dello Russo et al., 2003). Links between systemic diseases and the other UCPs have not been established, although as discussed below, emerging data suggest that in the brain, UCPs may have a unique role in neurodegenerative diseases and the response to CNS injury.

7 UCPs in Brain

Message for UCP2, UCP4, and BMCP1/UCP5 has been found in the brain, but the overall amount of UCP protein in the brain, as measured by 3H -GTP binding, is substantially lower than in BAT (UCP1) or spleen (primarily UCP2), although higher than in kidney, skeletal muscle, or liver (Urbankova et al., 2003). UCP2, which shows substantial expression in multiple other organs and only modest expression in brain, is localized to a few specific brain regions under physiological conditions. UCP2 is most highly expressed in the paraventricular, supraoptic, and suprachiasmatic nuclei of the hypothalamus, the main control center for thermogenesis (Horvath et al., 1999). UCP2 is also expressed in the CA1 and CA3 of the hippocampus and the basolateral amygdaloid nucleus in the rat brain (Richard et al., 2001). Surprisingly, UCP2 was found to be expressed in the tyrosine hydroxylase-positive neurons of the substantia nigra in primates (Horvath et al., 2003). UCP2 expression is mainly neuronal and not present to any extent in astrocytes and microglia under basal conditions (Richard et al., 2001). However, UCP2 mRNA expression is upregulated in regions affected by injury in pathological conditions such as transient ischemia (Bechmann et al., 2002;

de Bilbao et al., 2004; MacManus et al., 2004), sublethal ischemia (Mattiasson et al., 2003), chemically induced seizures (Diano et al., 2003), and kainic acid (KA) lesioning (Clavel et al., 2003). Induction of UCP2 mRNA by KA was mainly observed in neurons and was greater in 129T2SvEmsJ mice, a KA-sensitive strain, than in C57BL/6J mice, which are relatively insensitive to KA-induced neurodegeneration, suggesting that UCP2 could have an important role in modifying excitotoxic neuronal injury (Clavel et al., 2003). On the basis of the findings that *Ucp2*($-/-$) mice have enhanced resistance to toxoplasmosis, Ucp2 has also been proposed as a modifier of immune cell function. Consistent with this, lipopolysaccharide (LPS) induces UCP2 mRNA, but not UCP5 mRNA, in the mouse brain (Busquets et al., 2001). This may be relevant to the neuroprotection observed in a number of studies, since leukocytes including neutrophils and microglia may contribute to tissue injury ischemia, Alzheimer's disease, and Parkinson's disease. Increased UCP2 expression in inflammatory cells could reduce ROS production, and decrease secondary tissue damage. In addition, since ROS are involved in destabilizing the blood-brain barrier, changes in inflammatory cell ROS production might be neuroprotective specifically by modifying CNS inflammation and secondary loss of blood-brain barrier integrity.

UCP4 message is found predominantly in the brain (Mao et al., 1999), whereas UCP5 is expressed not only in the brain but also in other tissues including heart and kidney (Sanchis et al., 1998; Kondou et al., 2000; Kim-Han et al., 2001). UCP5 mRNA is induced by acute hypoxia or oxidative stress (hyperoxia, 4-hydroxynonenal, or *t*-butylhydroperoxide) in SH-SY5Y neuroblastoma cells. Expression is also increased by transient global cerebral ischemia, and decreased by chronic hypoxia, in rats (Pichiule et al., 2003), but unaltered by cerebral ischemia in adult (de Bilbao et al., 2004) or neonatal (J.S. Kim-Han, S.A. Reichert, and L.L. Dugan, unpublished data) mice. The functional significance of changes in UCP5 expression has not yet been determined. However, an isoform of UCP5 mRNA in fruit flies is also found predominantly in the head of adult flies (Fridell et al., 2004), supporting an important and retained function for this putative UCP in the CNS. Recently, expression of UCP1 and UCP3 mRNAs has been reported in the brain as well (Lengacher et al., 2004; Vincent et al., 2004). Thus, although message for all UCP isoforms has been detected in brain, the functional roles of these proteins in brains have been investigated primarily for UCP2.

Recently, UCP2 was reported to modify ROS production and dopaminergic neurotoxicity in a Parkinson's disease model, using UCP2 knockout and transgenic mice mice lesioned with 1-methyl-4-phenyl-1,2,5,6-tetrahydropyridine (MPTP) (Andrews et al., 2005). In addition, short-term oral administration of ubiquinone caused nigral mitochondrial uncoupling and prevented dopamine cell loss after MPTP administration in monkeys (Horvath, 2003). The protective effect of ubiquinone may have been due to activation of UCP2.

8 Summary

UCPs are normally expressed in the brain and are regulated by CNS injury in affected brain regions, where they are postulated to cause mild uncoupling and thereby reduce ROS production by mitochondria. Mitochondrial ROS generation in pathological conditions is believed to depend on mitochondrial membrane potential, and despite a number of questions that remain to be answered, evidence suggests overexpression of UCPs can be neuroprotective. The mechanisms underlying neuroprotection may include regulation of ROS, or alternatively, changes in Ca^{2+} handling by neurons. Mitochondrial membrane potential is the main regulator of mitochondrial Ca^{2+} uptake, and many Ca^{2+} -dependent pathways are involved in neuronal cell death. Understanding the role of mild uncoupling on Ca^{2+} homeostasis and mitochondrial free radical generation in excitotoxicity will advance our understanding of a key mechanism involved in neurotoxicity (Nicholls et al., 2003). While the importance of mitochondrial UCPs to the more general process of mitochondrial metabolism and bioenergetics in brain has not been determined, recent studies showed that overexpression of UCP results in growth inhibition in yeast (Bathgate 1992; Sanchis et al., 1998), an effect that may be related not only to changes in energy metabolism such as reduced ATP production but also may reflect dysregulation of redox-sensitive pathways, including activation of MAPK

signaling. UCP expression can be proapoptotic as well as antiapoptotic, depending on transcriptional and biochemical regulation (Mills et al., 2002; Dejean et al., 2004).

The idea that UCPs regulate mitochondrial ROS production places these proteins in the intriguing position of integrating metabolic function and oxidative stress in the brain. Although it has been suggested that UCP proteins regulate many other aspects of cell biology, including expression of antioxidant defense systems and mitochondrial biogenesis, careful studies will be needed to identify the detailed mechanisms responsible for their neuroprotective effects. Elucidating the mechanisms of UCP action in the regulation of energy metabolism and ROS generation will enhance our understanding of how mitochondria respond to both physiological and pathological conditions.

References

- Agarhd CD, Chapman AG, Pelligrino D, Siesjo BK. 1982. Influence of severe hypoglycemia on mitochondrial and plasma membrane function in rat brain. *J Neurochem* 38: 662-668.
- Andrews ZB, Horvath B, Barnstable CJ, Elseworth J, Yang L, et al. 2005. Uncoupling protein-2 is critical for nigral dopamine cell survival in a mouse model of Parkinson's disease. *J Neurosci* 25: 184-191.
- Armstrong MB, Towle HC. 2001. Polyunsaturated fatty acids stimulate hepatic UCP-2 expression via a PPAR α -mediated pathway. *Am J Physiol Endocrinol Metab* 281: E1197-E1204.
- Arsenijevic D, Onuma H, Pecqueur C, Raimbault S, Manning BS, et al. 2000. Disruption of the uncoupling protein-2 gene in mice reveals a role in immunity and reactive oxygen species production. *Nat Genet* 26: 435-439.
- Ashcroft FM, Kakei M, Gibson JS, Gray DW, Sutton R. 1989. The ATP- and tolbutamide-sensitivity of the ATP-sensitive K-channel from human pancreatic β cells. *Diabetologia* 32: 591-598.
- Barbe P, Larrouy D, Boulanger C, Chevillotte E, Viguier N, et al. 2001. Triiodothyronine-mediated upregulation of UCP2 and UCP3 mRNA expression in human skeletal muscle without coordinated induction of mitochondrial respiratory chain genes. *FASEB J* 15: 13-15.
- Bassaganya-Riera J, Reynolds K, Martino-Catt S, Cui Y, Hennighausen L, et al. 2004. Activation of PPAR- γ and - δ by conjugated linoleic acid mediates protection from experimental inflammatory bowel disease. *Gastroenterology* 127: 777-791.
- Bathgate B, Freebairn EM, Greenland AJ, Reid GA. 1992. Functional expression of the rat brown adipose tissue uncoupling protein in *Saccharomyces cerevisiae*. *Mol Microbiol* 6: 363-370.
- Bazan NG Jr. 1970. Effects of ischemia and electroconvulsive shock on free fatty acid pool in the brain. *Biochim Biophys Acta* 218: 1-10.
- Bechmann I, Diano S, Warden CH, Bartfai T, Nitsch R, et al. 2002. Brain mitochondrial uncoupling protein 2 (UCP2): A protective stress signal in neuronal injury. *Biochem Pharmacol* 64: 363-367.
- Bevilacqua L, Ramsey JJ, Hagopian K, Weindruch R, Harper ME. 2004. Effects of short- and medium-term calorie restriction on muscle mitochondrial proton leak and reactive oxygen species production. *Am J Physiol Endocrinol Metab* 286: E852-E861.
- Boss O, Samec S, Kuhne F, Bijlenga P, Assimakopoulos-Jeannet F, et al. 1998. Uncoupling protein-3 expression in rodent skeletal muscle is modulated by food intake but not by changes in environmental temperature. *J Biol Chem* 273: 5-8.
- Bouillaud F, Couplan E, Pecqueur C, Ricquier D. 2001. Homologues of the uncoupling protein from brown adipose tissue (UCP1): UCP2, UCP3, BMCP1, and UCP4. *Biochim Biophys Acta* 1504: 107-119.
- Boyer BB, Barnes BM, Lowell BB, Grujic D. 1998. Differential regulation of uncoupling protein gene homologues in multiple tissues of hibernating ground squirrels. *Am J Physiol* 275: R1232-R1238.
- Brand MD, Affourtit C, Esteves TC, Green K, Lambert AJ, et al. 2004. Mitochondrial superoxide: Production, biological effects, and activation of uncoupling proteins. *Free Radic Biol Med* 37: 755-767.
- Brookes PS, Levenon AL, Shiva S, Sarti P, Darley-Usmar VM. 2002. Mitochondria: Regulators of signal transduction by reactive oxygen and nitrogen species. *Free Radic Biol Med* 33: 755-764.
- Brown JE, Thomas S, Digby JE, Dunmore SJ. 2002. Glucose induces and leptin decreases expression of uncoupling protein-2 mRNA in human islets. *FEBS Lett* 513: 189-192.
- Brunmair B, Gras F, Wagner L, Artwohl M, Zierhut B, et al. 2004. Expression of uncoupling protein-3 mRNA in rat skeletal muscle is acutely stimulated by thiazolidinediones: An exercise-like effect? *Diabetologia* 47: 1611-1614.
- Busquets S, Alvarez B, Van Royen M, Figueras MT, Lopez-Soriano FJ, et al. 2001. Increased uncoupling protein-2 gene expression in brain of lipopolysaccharide-injected mice: Role of tumour necrosis factor- α ? *Biochim Biophys Acta* 1499: 249-256.

- Cabrero A, Alegret M, Sanchez RM, Adzet T, Laguna JC, et al. 2000. Downregulation of uncoupling protein-3 and -2 by thiazolidinediones in C2C12 myotubes. *FEBS Lett* 484: 37-42.
- Cadenas E, Boveris A, Ragan CI, Stoppani AO. 1977. Production of superoxide radicals and hydrogen peroxide by NADH-ubiquinone reductase and ubiquinol-cytochrome *c* reductase from beef-heart mitochondria. *Arch Biochem Biophys* 180: 248-257.
- Cameron-Smith D, Burke LM, Angus DJ, Tunstall RJ, Cox GR, et al. 2003. A short-term, high-fat diet upregulates lipid metabolism and gene expression in human skeletal muscle. *Am J Clin Nutr* 77: 313-318.
- Cannon B, Nedergaard J. 2004. Brown adipose tissue: Function and physiological significance. *Physiol Rev* 84: 277-359.
- Casteilla L, Rigoulet M, Penicaud L. 2001. Mitochondrial ROS metabolism: Modulation by uncoupling proteins. *IUBMB Life* 52: 181-188.
- Cha SH, Hu Z, Lane MD. 2004. Long-term effects of a fatty acid synthase inhibitor on obese mice: Food intake, hypothalamic neuropeptides, and UCP3. *Biochem Biophys Res Commun* 317: 301-308.
- Chan CB, De Leo D, Joseph JW, McQuaid TS, Ha XF, et al. 2001. Increased uncoupling protein-2 levels in β -cells are associated with impaired glucose-stimulated insulin secretion: Mechanism of action. *Diabetes* 50: 1302-1310.
- Chan CB, Mac Donald PE, Saleh MC, Johns DC, Marban E, et al. 1999. Overexpression of uncoupling protein 2 inhibits glucose-stimulated insulin secretion from rat islets. *Diabetes* 48: 1482-1486.
- Chevillotte E, Rieusset J, Roques M, Desage M, Vidal H. 2001. The regulation of uncoupling protein-2 gene expression by ω -6 polyunsaturated fatty acids in human skeletal muscle cells involves multiple pathways, including the nuclear receptor peroxisome proliferator-activated receptor β . *J Biol Chem* 276: 10853-10860.
- Chung WK, Luke A, Cooper RS, Rotini C, Vidal-Puig A, et al. 1999. Genetic and physiologic analysis of the role of uncoupling protein 3 in human energy homeostasis. *Diabetes* 48: 1890-1895.
- Clavel S, Paradis E, Ricquier D, Richard D. 2003. Kainic acid upregulates uncoupling protein-2 mRNA expression in the mouse brain. *Neuroreport* 14: 2015-2017.
- Cline GW, Vidal-Puig AJ, Dufour S, Cadman KS, Lowell BB, et al. 2001. In vivo effects of uncoupling protein-3 gene disruption on mitochondrial energy metabolism. *J Biol Chem* 276: 20240-20244.
- Cortez-Pinto H, Yang SQ, Lin HZ, Costa S, Hwang CS, et al. 1998. Bacterial lipopolysaccharide induces uncoupling protein-2 expression in hepatocytes by a tumor necrosis factor- α -dependent mechanism. *Biochem Biophys Res Commun* 251: 313-319.
- Couplan E, del Mar Gonzalez-Barroso M, Alves-Guerra MC, Ricquier D, Goubern M, et al. 2002. No evidence for a basal, retinoic, or superoxide-induced uncoupling activity of the uncoupling protein 2 present in spleen or lung mitochondria. *J Biol Chem* 277: 26268-26275.
- de Bilbao F, Arsenijevic D, Vallet P, Hjelle OP, Ottersen OP, et al. 2004. Resistance to cerebral ischemic injury in UCP2 knockout mice: Evidence for a role of UCP2 as a regulator of mitochondrial glutathione levels. *J Neurochem* 89: 1283-1292.
- Dejean L, Camara Y, Sibille B, Solanes G, Villarroya F. 2004. Uncoupling protein-3 sensitizes cells to mitochondrial-dependent stimulus of apoptosis. *J Cell Physiol* 201: 294-304.
- Dello Russo C, Gavriluk V, Weinberg G, Almeida A, Bolanos JP, et al. 2003. Peroxisome proliferator-activated receptor γ thiazolidinedione agonists increase glucose metabolism in astrocytes. *J Biol Chem* 278: 5828-5836.
- Diano S, Matthews RT, Patrylo P, Yang L, Beal MF, et al. 2003. Uncoupling protein 2 prevents neuronal death including that occurring during seizures: A mechanism for preconditioning. *Endocrinology* 144: 5014-5021.
- Duval C, Negre-Salvayre A, Dogilo A, Salvayre R, Penicaud L, et al. 2002. Increased reactive oxygen species production with antisense oligonucleotides directed against uncoupling protein 2 in murine endothelial cells. *Biochem Cell Biol* 80: 757-764.
- Dzeja PP, Zeleznikar RJ, Goldberg ND. 1998. Adenylate kinase: Kinetic behavior in intact cells indicates it is integral to multiple cellular processes. *Mol Cell Biochem* 184: 169-182.
- Ealey KN, El-Sohemy A, Archer MC. 2002. Effects of dietary conjugated linoleic acid on the expression of uncoupling proteins in mice and rats. *Lipids* 37: 853-861.
- Echtay KS, Esteves TC, Pakay JL, Jekabsons MB, Lambert AJ, et al. 2003. A signaling role for 4-hydroxy-2-nonenal in regulation of mitochondrial uncoupling. *EMBO J* 22: 4103-4110.
- Echtay KS, Roussel D, St-Pierre J, Jekabsons MB, Cadenas S, et al. 2002. Superoxide activates mitochondrial uncoupling proteins. *Nature* 415: 96-99.
- Echtay KS, Winkler E, Frischmuth K, Klingenberg M. 2001. Uncoupling proteins 2 and 3 are highly active H^+ transporters and highly nucleotide sensitive when activated by coenzyme Q (ubiquinone). *Proc Natl Acad Sci USA* 98: 1416-1421.
- Echtay KS, Winkler E, Klingenberg M. 2000. Coenzyme Q is an obligatory cofactor for uncoupling protein function. *Nature* 408: 609-613.
- Enerback S, Jacobsson A, Simpson EM, Guerra C, Yamashita H, et al. 1997. Mice lacking mitochondrial uncoupling protein are cold-sensitive but not obese. *Nature* 387: 90-94.

- Essop MF, Razeghi P, McLeod C, Young ME, Taegtmeier H, et al. 2004. Hypoxia-induced decrease of UCP3 gene expression in rat heart parallels metabolic gene switching but fails to affect mitochondrial respiratory coupling. *Biochem Biophys Res Commun* 314: 561-564.
- Esteves TC, Ehtay KS, Jonassen T, Clarke CF, Brand MD. 2004. Ubiquinone is not required for proton conductance by uncoupling protein 1 in yeast mitochondria. *Biochem J* 379: 309-315.
- Finkel T. 2001. Reactive oxygen species and signal transduction. *IUBMB Life* 52: 3-6.
- Finkel T. 2003. Oxidant signals and oxidative stress. *Curr Opin Cell Biol* 15: 247-254.
- Fleury C, Neverova M, Collins S, Raimbault S, Champigny O, et al. 1997. Uncoupling protein-2: A novel gene linked to obesity and hyperinsulinemia. *Nat Genet* 15: 269-272.
- Forman HJ, Fukuto JM, Torres M. 2004. Redox signaling: Thiol chemistry defines which reactive oxygen and nitrogen species can act as second messengers. *Am J Physiol Cell Physiol* 287: C246-C256.
- Fridell YW, Sanchez-Blanco A, Silvia BA, Helfand SL. 2004. Functional characterization of a *Drosophila* mitochondrial uncoupling protein. *J Bioenerg Biomembr* 36: 219-228.
- Garcia B, Obregon MJ. 2002. Growth factor regulation of uncoupling protein-1 mRNA expression in brown adipocytes. *Am J Physiol Cell Physiol* 282: C105-112.
- Garlid KD, Jaburek M, Jezek P, Varecha M. 2000. How do uncoupling proteins uncouple? *Biochim Biophys Acta* 1459: 383-389.
- Garlid KD, Sun X, Paucek P, Woldegiorgis G. 1995. Mitochondrial cation transport systems. *Methods Enzymol* 260: 331-348.
- Gonzalez-Barroso MM, Fleury C, Arechaga I, Zaragoza P, Levi-Meyrueis C, et al. 1996. Activation of the uncoupling protein by fatty acids is modulated by mutations in the C-terminal region of the protein. *Eur J Biochem* 239: 445-450.
- Gonzalez-Yanes C, Sanchez-Margalet V. 2003. Pancreastatin, a chromogranin A-derived peptide, inhibits leptin and enhances UCP-2 expression in isolated rat adipocytes. *Cell Mol Life Sci* 60: 2749-2756.
- Gullicksen PS, Flatt WP, Dean RG, Hartzell DL, Baile CA. 2002. Energy metabolism and expression of uncoupling proteins 1, 2, and 3 after 21 days of recovery from intracerebroventricular mouse leptin in rats. *Physiol Behav* 75: 473-482.
- Hillered L, Chan PH. 1988. Role of arachidonic acid and other free fatty acids in mitochondrial dysfunction in brain ischemia. *J Neurosci Res* 20: 451-456.
- Hioki C, Yoshida T, Kogure A, Takakura Y, Umekawa T, et al. 2004. Effects of growth hormone (GH) on mRNA levels of uncoupling proteins 1, 2, and 3 in brown and white adipose tissues and skeletal muscle in obese mice. *Horm Metab Res* 36: 607-613.
- Hong Y, Fink BD, Dillon JS, Sivitz WI. 2001. Effects of adenoviral overexpression of uncoupling protein-2 and -3 on mitochondrial respiration in insulinoma cells. *Endocrinology* 142: 249-256.
- Horvath TL, Diano S, Leranth C, Garcia-Segura LM, Cowley MA, et al. 2003. Coenzyme Q induces nigral mitochondrial uncoupling and prevents dopamine cell loss in a primate model of Parkinson's disease. *Endocrinology* 144: 2757-2760.
- Horvath TL, Warden CH, Hajos M, Lombardi A, Goglia F, et al. 1999. Brain uncoupling protein 2: Uncoupled neuronal mitochondria predict thermal synapses in homeostatic centers. *J Neurosci* 19: 10417-10427.
- Ito E, Ozawa S, Takahashi K, Tanaka T, Katsuta H, et al. 2004. PPAR- γ overexpression selectively suppresses insulin secretory capacity in isolated pancreatic islets through induction of UCP-2 protein. *Biochem Biophys Res Commun* 324: 810-814.
- Jaburek M, Garlid KD. 2003. Reconstitution of recombinant uncoupling proteins: UCP1, -2, and -3 have similar affinities for ATP and are unaffected by coenzyme Q10. *J Biol Chem* 278: 25825-25831.
- Jakus PB, Sipos K, Kispal G, Sandor A. 2002. Opposite regulation of uncoupling protein 1 and uncoupling protein 3 in vivo in brown adipose tissue of cold-exposed rats. *FEBS Lett* 519: 210-214.
- Joseph JW, Koshkin V, Saleh MC, Sivitz WI, Zhang CY, et al. 2004. Free fatty acid-induced β -cell defects are dependent on uncoupling protein 2 expression. *J Biol Chem* 279: 51049-51056.
- Jucker BM, Dufour S, Ren J, Cao X, Previs SF, et al. 2000. Assessment of mitochondrial energy coupling in vivo by $^{13}\text{C}/^{31}\text{P}$ NMR. *Proc Natl Acad Sci USA* 97: 6880-6884.
- Kim-Han JS, Reichert SA, Quick KL, Dugan LL. 2001. BMCP1: A mitochondrial uncoupling protein in neurons which regulates mitochondrial function and oxidant production. *J Neurochem* 79: 658-668.
- Klingenberg M. 1999. Uncoupling protein—a useful energy dissipator. *J Bioenerg Biomembr* 31: 419-430.
- Kondou S, Hidaka S, Yoshimatsu H, Tsuruta Y, Itateyama E, et al. 2000. Molecular cloning of rat brain mitochondrial carrier protein-1 cDNA and its upregulation during postnatal development. *Biochim Biophys Acta* 1457: 182-189.
- Kontani Y, Wang Y, Kimura K, Inokuma KI, Saito M, et al. 2005. UCP1 deficiency increases susceptibility to diet-induced obesity with age. *Aging Cell* 4: 147-155.
- Korshunov SS, Skulachev VP, Starkov AA. 1997. High protonic potential actuates a mechanism of production of reactive oxygen species in mitochondria. *FEBS Lett* 416: 15-18.

- Kotz CM, Wang CF, Briggs JE, Levine AS, Billington CJ. 2000. Effect of NPY in the hypothalamic paraventricular nucleus on uncoupling proteins 1, 2, and 3 in the rat. *Am J Physiol Regul Integr Comp Physiol* 278: R494-R498.
- Krauss S, Zhang CY, Scorrano L, Dalgaard LT, St-Pierre J, et al. 2003. Superoxide-mediated activation of uncoupling protein 2 causes pancreatic β cell dysfunction. *J Clin Invest* 112: 1831-1842.
- Kuwashima J, Nakamura K, Fujitani B, Kadokawa T, Yoshida K, et al. 1978. Relationship between cerebral energy failure and free fatty acid accumulation following prolonged brain ischemia. *Jpn J Pharmacol* 28: 277-287.
- Lambert AJ, Brand MD. 2004. Superoxide production by NADH: Ubiquinone oxidoreductase (complex I) depends on the pH gradient across the mitochondrial inner membrane. *Biochem J* 382: 511-517.
- Lazarewicz JW, Strosznajder J, Gromek A. 1972. Effects of ischemia and exogenous fatty acids on the energy metabolism in brain mitochondria. *B Acad Pol Sci Biol* 20: 599-606.
- Ledesma A, de Lacoba MG, Rial E. 2002. The mitochondrial uncoupling proteins. *Genome Biol* 3: REVIEWS3015.
- Lee K, Berthiaume F, Stephanopoulos GN, Yarmush ML. 2003. Induction of a hypermetabolic state in cultured hepatocytes by glucagon and H_2O_2 . *Metab Eng* 5: 221-229.
- Lengacher S, Magistretti PJ, Pellerin L. 2004. Quantitative RT-PCR analysis of uncoupling protein isoforms in mouse brain cortex: Methodological optimization and comparison of expression with brown adipose tissue and skeletal muscle. *J Cereb Blood Flow Metab* 24: 780-788.
- Li G, Klein RL, Matheny M, King MA, Meyer EM, et al. 2002. Induction of uncoupling protein 1 by central interleukin-6 gene delivery is dependent on sympathetic innervation of brown adipose tissue and underlies one mechanism of body weight reduction in rats. *Neuroscience* 115: 879-889.
- Li LX, Yoshikawa H, Egeberg KW, Grill V. 2003. Interleukin- β swiftly downregulates UCP-2 mRNA in β -cells by mechanisms not directly coupled to toxicity. *Cytokine* 23: 101-107.
- MacManus JP, Graber T, Luebbert C, Preston E, Rasquinha I, et al. 2004. Translation-state analysis of gene expression in mouse brain after focal ischemia. *J Cereb Blood Flow Metab* 24: 657-667.
- Mao W, Yu XX, Zhong A, Li W, Brush J, et al. 1999. UCP4, a novel brain-specific mitochondrial protein that reduces membrane potential in mammalian cells. *FEBS Lett* 443: 326-330.
- Margaretto J, Marti A, Martinez JA. 2001. Changes in UCP mRNA expression levels in brown adipose tissue and skeletal muscle after feeding a high-energy diet and relationships with leptin, glucose, and PPAR γ . *J Nutr Biochem* 12: 130-137.
- Martin WH, DiResta DJ, Garlid KD. 1986. Kinetics of inhibition and binding of dicyclohexylcarbodiimide to the 82,000-dalton mitochondrial K^+/H^+ antiporter. *J Biol Chem* 261: 12300-12305.
- Masaki T, Chiba S, Noguchi H, Yasuda T, Tobe K, et al. 2004. Obesity in insulin receptor substrate-2-deficient mice: Disrupted control of arcuate nucleus neuropeptides. *Obes Res* 12: 878-885.
- Masaki T, Chiba S, Yasuda T, Noguchi H, Kakuma T, et al. 2004b. Involvement of hypothalamic histamine H_1 receptor in the regulation of feeding rhythm and obesity. *Diabetes* 53: 2250-2260.
- Masaki T, Yoshimichi G, Chiba S, Yasuda T, Noguchi H, et al. 2003. Corticotropin-releasing hormone-mediated pathway of leptin to regulate feeding, adiposity, and uncoupling protein expression in mice. *Endocrinology* 144: 3547-3554.
- Masanés RM, Yubero P, Rafecas I, Remesar X. 2002. Changes in UCP expression in tissues of Zucker rats fed diets with different protein content. *J Physiol Biochem* 58: 135-141.
- Matthias A, Jacobsson A, Cannon B, Nedergaard J. 1999. The bioenergetics of brown fat mitochondria from UCP1-ablated mice. Ucp1 is not involved in fatty acid-induced deenergization ("uncoupling"). *J Biol Chem* 274: 28150-28160.
- Matthias A, Ohlson KB, Fredriksson JM, Jacobsson A, Nedergaard J, et al. 2000. Thermogenic responses in brown fat cells are fully UCP1 dependent. UCP2 or UCP3 do not substitute for UCP1 in adrenergically or fatty acid-induced thermogenesis. *J Biol Chem* 275: 25073-25081.
- Mattiasson G, Shamloo M, Gido G, Mathi K, Tomasevic G, et al. 2003. Uncoupling protein-2 prevents neuronal death and diminishes brain dysfunction after stroke and brain trauma. *Nat Med* 9: 1062-1068.
- Mills EM, Xu D, Fergusson MM, Combs CA, Xu Y, et al. 2002. Regulation of cellular oncosis by uncoupling protein 2. *J Biol Chem* 277: 27385-27392.
- Milne HM, Burns CJ, Squires PE, Evans ND, Pickup J, et al. 2005. Uncoupling of nutrient metabolism from insulin secretion by overexpression of cytosolic phospholipase A_2 . *Diabetes* 54: 116-124.
- Mitchell P. 1961. Coupling of phosphorylation to electron and hydrogen transfer by a chemiosmotic type of mechanism. *Naturwissenschaften* 191: 144-148.
- Miwa S, Brand MD. 2003. Mitochondrial matrix reactive oxygen species production is very sensitive to mild uncoupling. *Biochem Soc Trans* 31: 1300-1301.
- Mizuno T, Miura-Suzuki T, Yamashita H, Mori, N. 2000. Distinct regulation of brain mitochondrial carrier protein-1 and uncoupling protein-2 genes in the rat brain during cold exposure and aging. *Biochem Biophys Res Commun* 278: 691-697.
- Mori Y, Tokutate Y, Oana F, Matsuzawa A, Akahane S, et al. 2004. Bezafibrate-induced changes over time in the expression of uncoupling protein (UCP) mRNA in the tissues: A

- study in spontaneously type-2 diabetic rats with visceral obesity. *J Atheroscler Thromb* 11: 224-231.
- Murase T, Nagasawa A, Suzuki J, Wakisaka T, Hase T, et al. 2002. Dietary α -linolenic acid-rich diacylglycerols reduce body weight gain accompanying the stimulation of intestinal β -oxidation and related gene expressions in C57BL/KsJ-db/db mice. *J Nutr* 132: 3018-3022.
- Nagase I, Yoshida T, Saito M. 2001. Upregulation of uncoupling proteins by β -adrenergic stimulation in L6 myotubes. *FEBS Lett* 494: 175-180.
- Negre-Salvayre A, Hirtz C, Carrera G, Cazenave R, Trolly M, et al. 1997. A role for uncoupling protein-2 as a regulator of mitochondrial hydrogen peroxide generation. *FASEB J* 11: 809-815.
- Nicholls DG. 2001. A history of UCP1. *Biochem Soc Trans* 29: 751-755.
- Nicholls DG, Locke RM. 1984. Thermogenic mechanisms in brown fat. *Physiol Rev* 64: 1-64.
- Nicholls DG, Snelling R, Rial E. 1984. Proton and calcium circuits across the mitochondrial inner membrane. *Biochem Soc Trans* 12: 388-390.
- Nicholls DG, Vesce S, Kirk L, Chalmers S. 2003. Interactions between mitochondrial bioenergetics and cytoplasmic calcium in cultured cerebellar granule cells. *Cell Calcium* 34: 407-424.
- Nishikawa T, Edelstein D, Du XL, Yamagishi S, Matsumura T, et al. 2000. Normalizing mitochondrial superoxide production blocks three pathways of hyperglycaemic damage. *Nature* 404: 787-790.
- Palmieri F. 2004. The mitochondrial transporter family (SLC25): Physiological and pathological implications. *Pflugers Arch* 447: 689-709.
- Patane G, Anello M, Piro S, Vigneri R, Purrello F, et al. 2002. Role of ATP production and uncoupling protein-2 in the insulin secretory defect induced by chronic exposure to high glucose or free fatty acids and effects of peroxisome proliferator-activated receptor- γ inhibition. *Diabetes* 51: 2749-2756.
- Pecqueur C, Alves-Guerra MC, Gelly C, Levi-Meyrueis C, Couplan E, et al. 2001. Uncoupling protein 2, in vivo distribution, induction upon oxidative stress, and evidence for translational regulation. *J Biol Chem* 276: 8705-8712.
- Pedersen SB, Kristensen K, Bruun JM, Flyvbjerg A, Vinter-Jensen L, et al. 2000. Systemic administration of epidermal growth factor increases UCP3 mRNA levels in skeletal muscle and adipose tissue in rats. *Biochem Biophys Res Commun* 279: 914-919.
- Phillis JW, O'Regan MH. 2004. A potentially critical role of phospholipases in central nervous system ischemic, traumatic, and neurodegenerative disorders. *Brain Res Brain Res Rev* 44: 13-47.
- Pichiule P, Chavez JC, LaManna JC. 2003. Oxygen and oxidative stress modulate the expression of uncoupling protein-5 in vitro and in vivo. *Adv Exp Med Biol* 540: 103-107.
- Putman CT, Dixon WT, Pearcey JA, Maclean IM, Jendral MJ, et al. 2004. Chronic low-frequency stimulation upregulates uncoupling protein-3 in transforming rat fast-twitch skeletal muscle. *Am J Physiol Regul Integr Comp Physiol* 287: R1419-R1426.
- Putman CT, Kiricsi M, Pearcey J, MacLean IM, Bamford JA, et al. 2003. AMPK activation increases uncoupling protein-3 expression and mitochondrial enzyme activities in rat muscle without fibre type transitions. *J Physiol* 551: 169-178.
- Queiroz MS, Shao Y, Ismail-Beigi F. 2004. Effect of thyroid hormone on uncoupling protein-3 mRNA expression in rat heart and skeletal muscle. *Thyroid* 14: 177-185.
- Richard D, Clavel S, Huang Q, Sanchis D, Ricquier D. 2001. Uncoupling protein 2 in the brain: Distribution and function. *Biochem Soc Trans* 29: 812-817.
- Roussel S, Alves-Guerra MC, Mozo J, Miroux B, Cassard-Doulcier AM, et al. 2004. The biology of mitochondrial uncoupling proteins. *Diabetes* 53 Suppl 1: S130-S135.
- Samec S, Seydoux J, Russell AP, Montani JB, Dulloo AG. 2002. Skeletal muscle heterogeneity in fasting-induced upregulation of genes encoding UCP2, UCP3, PPAR γ , and key enzymes of lipid oxidation. *Pflugers Arch* 445: 80-86.
- Sanchis D, Fleury C, Chomiki N, Gubern M, Huang Q, et al. 1998. BMCP1, a novel mitochondrial carrier with high expression in the central nervous system of humans and rodents, and respiration uncoupling activity in recombinant yeast. *J Biol Chem* 273: 34611-34615.
- Scarpace PJ, Matheny M, Pollock BH, Tumer N. 1997. Leptin increases uncoupling protein expression and energy expenditure. *Am J Physiol* 273: E226-E230.
- Scarpace PJ, Nicolson M, Matheny M. 1998. UCP2, UCP3, and leptin gene expression: Modulation by food restriction and leptin. *J Endocrinol* 159: 349-357.
- Sivitz WI, Fink BD, Donohoue PA. 1999. Fasting and leptin modulate adipose and muscle uncoupling protein: Divergent effects between messenger ribonucleic acid and protein expression. *Endocrinology* 140: 1511-1519.
- Skulachev VP. 1998. Uncoupling: New approaches to an old problem of bioenergetics. *Biochim Biophys Acta* 1363: 100-124.
- Smith AM, Ratcliffe RG, Sweetlove LJ. 2004. Activation and function of mitochondrial uncoupling protein in plants. *J Biol Chem* 279: 51944-51952.
- Stavinoha MA, RaySpellicy JW, Essop MF, Gravelleau C, Abel ED, et al. 2004. Evidence for mitochondrial thioesterase 1 as a peroxisome proliferator-activated receptor- α -regulated gene in cardiac and skeletal muscle. *Am J Physiol Endocrinol Metab* 287: E888-E895.

- Stephenson D, Rash K, Smalstig B, Roberts E, Johnstone E, et al. 1999. Cytosolic phospholipase A2 is induced in reactive glia following different forms of neurodegeneration. *Glia* 27: 110-128.
- Takahashi Y, Kushiro M, Shinohara K, Ide T. 2002. Dietary conjugated linoleic acid reduces body fat mass and affects gene expression of proteins regulating energy metabolism in mice. *Comp Biochem Physiol B Biochem Mol Biol* 133: 395-404.
- Talbot DA, Lambert AJ, Brand MD. 2004. Production of endogenous matrix superoxide from mitochondrial complex I leads to activation of uncoupling protein 3. *FEBS Lett* 556: 111-115.
- Toyomizu M, Ueda M, Sato S, Seki Y, Sato K, et al. 2002. Cold-induced mitochondrial uncoupling and expression of chicken UCP and ANT mRNA in chicken skeletal muscle. *FEBS Lett* 529: 313-318.
- Tsuchida A, Nonomura T, Ono-Kishino M, Nakagawa T, Taiji M, et al. 2001. Acute effects of brain-derived neurotrophic factor on energy expenditure in obese diabetic mice. *Int J Obes Relat Metab Disord* 25: 1286-1293.
- Urbankova E, Hanak P, Skobisova E, Ruzicka M, Jezek P. 2003. Substitutional mutations in the uncoupling protein-specific sequences of mitochondrial uncoupling protein UCP1 lead to the reduction of fatty acid-induced H⁺ uniport. *Int J Biochem Cell Biol* 35: 212-220.
- Valverde AM, Arribas M, Mur C, Navarro P, Pons S, Cassard-Doulcier AM, Kahn CR, Benito M. 2003. Insulin-induced up-regulated uncoupling protein-1 expression is mediated by insulin receptor substrate 1 through the phosphatidylinositol 3-kinase/Akt signaling pathway in fetal brown adipocytes. *J Biol Chem* 278: 10221-10231.
- Van Der Lee KA, Willemsen PH, Van Der Vusse GJ, Van Bilsen M. 2000. Effects of fatty acids on uncoupling protein-2 expression in the rat heart. *FASEB J* 14: 495-502.
- Villarroya F, Brun S, Giralt M, Camara Y, Solanes G, et al. 2001. Gene expression of leptin and uncoupling proteins: Molecular end-points of fetal development. *Biochem Soc Trans* 29: 76-80.
- Vincent AM, Olzmann JA, Brownlee M, Sivitz WI, Russell JW. 2004. Uncoupling proteins prevent glucose-induced neuronal oxidative stress and programmed cell death. *Diabetes* 53: 726-734.
- Williams DL, Bowers RR, Bartness TJ, Kaplan JM, Grill HJ. 2003. Brainstem melanocortin 3/4 receptor stimulation increases uncoupling protein gene expression in brown fat. *Endocrinology* 144: 4692-4697.
- Xiao H, Massaro D, Massaro GD, Clerch LB. 2004. Expression of lung uncoupling protein-2 mRNA is modulated developmentally and by caloric intake. *Exp Biol Med (Maywood)* 229: 479-485.
- Xiao XQ, Grove KL, Grayson BE, Smith MS. 2004. Inhibition of uncoupling protein expression during lactation: Role of leptin. *Endocrinology* 145: 830-838.
- Young ME, Patil S, Ying J, Depre C, Ahuja HS, et al. 2001. Uncoupling protein 3 transcription is regulated by peroxisome proliferator-activated receptor (α) in the adult rodent heart. *FASEB J* 15: 833-845.
- Yu XX, Mao W, Zhong A, Schow P, Brush J, et al. 2000. Characterization of novel UCP5/BMCP1 isoforms and differential regulation of UCP4 and UCP5 expression through dietary or temperature manipulation. *FASEB J* 14: 1611-1618.
- Zhang CY, Baffy G, Perret P, Krauss S, Peroni O, et al. 2001. Uncoupling protein-2 negatively regulates insulin secretion and is a major link between obesity, β cell dysfunction, and type-2 diabetes. *Cell* 105: 745-755.
- Zhou M, Lin BZ, Coughlin S, Vallega G, Pilch PF. 2000. UCP-3 expression in skeletal muscle: Effects of exercise, hypoxia, and AMP-activated protein kinase. *Am J Physiol Endocrinol Metab* 279: E622-E629.
- Zhou YT, Shimabukuro M, Koyama K, Lee Y, Wang MY, et al. 1997. Induction by leptin of uncoupling protein-2 and enzymes of fatty acid oxidation. *Proc Natl Acad Sci USA* 94: 6386-6390.

5.5 Actions of Toxins on Cerebral Metabolism at the Cellular Level

U. Sonnewald · T. Syversen · A. Schousboe · H. Waagepetersen · M. Aschner

1	Introduction	570
2	¹³C Nuclear Magnetic Resonance Spectroscopy to Study Brain Metabolism	570
3	Astrocyte–Neuron Interactions	570
4	Methionine Sulfoximine: A Tool to Probe Astrocyte–Neuron Interactions	573
5	3-Nitropropionic Acid	574
5.1	Effect of 3-NPA on [U- ¹³ C]Glutamate Metabolism in Neurons	575
5.2	Effect of 3-NPA on [U- ¹³ C]Glutamate Metabolism in Astrocytes	575
5.3	Energy Metabolism in the Presence of 3-NPA	577
5.4	Use of 3-NPA to Probe Pyruvate Carboxylation	577
6	Aminoxyacetic Acid: A blocker of transamination	578
6.1	Effect of AOAA on [U- ¹³ C]Glutamate Metabolism in Astrocytes	579
7	Methylmercury	579
7.1	Metabolic Effects of MeHg on Cerebral Astrocytes	580
7.2	Metabolic Effects of MeHg on Cerebellar Astrocytes	580
7.3	Effects of MeHg on GSH Precursor Transport	581

Abstract: Neurotoxins can cause disease by interfering with brain metabolism. The present chapter describes metabolic effects of methionine sulfoximine (MSO), 3-nitropropionic acid (3-NPA), aminooxyacetic acid (AOAA), and methylmercury (MeHg) on astrocytes and neurons in culture. Often toxins act in a cell-specific manner, which is the case for MSO acting mostly on astrocytes, whereas MeHg, AOAA, and 3-NPA exert their effects mostly on neurons. In the case of MeHg this effect is possibly mediated via astrocytes. The adverse cellular effects of these toxic compounds can be used for probing metabolism and creating animal models of disease, thus providing means for a better understanding of the etiology of neurological disorders, as well as for testing the effectiveness of potential treatment modalities.

1 Introduction

Environmental toxins have had devastating effects on human and animal health throughout the centuries. Toxins may be produced by plants, microorganisms, or human activity (i.e., industrial processing and waste) and they often enter organisms via food or air. Improved understanding of biological processes has led to increasing awareness of these dangers and better methods have been devised for food preservation and environmental protection and remediation. However, in spite of this, human exposure to toxic compounds in the environment persists, especially in third world and developing countries. Furthermore, the mechanisms of action of a number of toxins are still unresolved and much remains to be discovered. Despite these adverse effects of toxins, such compounds may serve as important tools to map metabolic pathways and interactions between different cell types. This chapter provides information about the effects of several toxins both on astrocytes and neurons, with special emphasis on the use of ^{13}C nuclear magnetic resonance (NMR) spectroscopy in this area.

2 ^{13}C Nuclear Magnetic Resonance Spectroscopy to Study Brain Metabolism

Even though the brain accounts for only 2% of body weight it consumes 25% of the total glucose. Thus, glucose metabolism is important for the brain and there are a number of methods available for studying this metabolism. The present chapter concentrates on cerebral metabolism of ^{13}C -labeled glucose (and other substrates). The ^{13}C labeling approach is analogous to conventional ^{14}C labeling experiments. Detection methods for ^{13}C include mass spectrometry (MS) and NMR spectroscopy. A significant advantage of NMR is the fact that it has a wide range of applicability. It can be performed on purified compounds, extracts, superfused cells or tissues, and living animals or humans. It is particularly superior to ^{14}C methods since the location of the label within a specific molecule can be obtained by ^{13}C NMR spectroscopy. MS is very useful for analysis of labeling since, in contrast to NMR, it has a superb sensitivity. Thus, the combination of NMR and MS can provide valuable information about intermediary metabolism (Sonnewald et al., 1996a). In order to understand the results obtained from studies using ^{13}C -labeled glucose or other substrates it is important to know the particular metabolic compartmentation in the brain involving astrocytes and neurons (● [Figure 5.5-1](#)).

3 Astrocyte–Neuron Interactions

During development, axons trace complex and stereotypic trajectories, and cell number is regulated to achieve correct connectivity and brain size. Axon guidance decisions are made as axons interact with astrocytes (e.g., radial glia). Neuron–glia interactions also play critical roles in neuronal differentiation and survival, and the formation, function, and maintenance of synapses. The synaptic properties of cultured retinal ganglion cells in the presence or absence of astrocytes have been investigated. The presence of astrocytes was shown to significantly increase the total number of synaptic contacts per neuron and their efficiency by promoting a number of presynaptic and postsynaptic changes, such as aggregation

and colocalization of presynaptic and postsynaptic proteins into synapses. Furthermore, reversal of these effects was noted upon the removal of astrocytes, indicating that induction, as well as maintenance of efficient synaptic contacts, is under the control of astrocyte-derived signals (Ulliam et al., 2001).

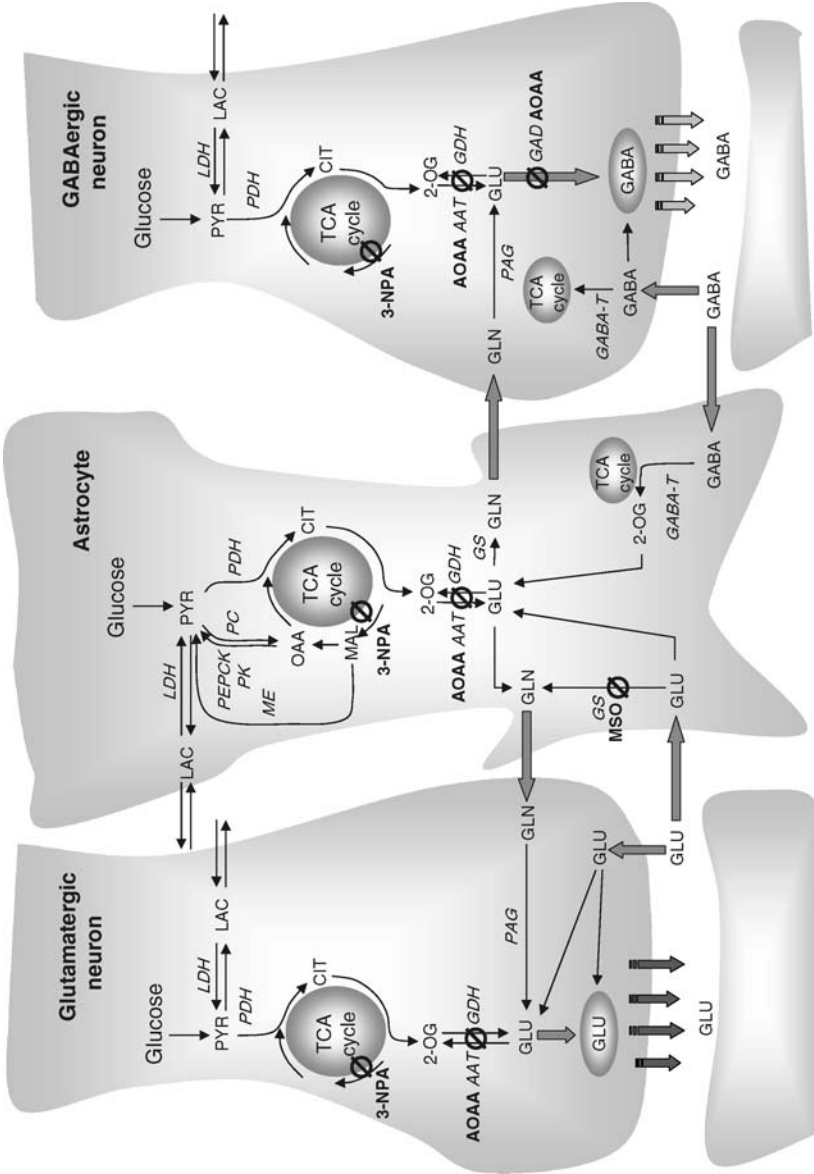
Neurotoxicity associated with interference in various developmental aspects such as cell differentiation, cell migration, and synaptogenesis is exemplified by lead exposure. Lead has been shown to be neurotoxic during neural differentiation (Petit and LeBoutillier, 1979; Alfano et al., 1983) and synaptogenesis (Bull et al., 1983; Oberto et al., 1996). However, lead seems to have its most pronounced effects during the later stages of brain development, perhaps by interfering with the trimming/pruning of synaptic connections (thus affecting the number of synaptic connections; synaptogenesis) and apoptosis (causing neuronal death) (Oberto et al., 1996). Lead can also produce significant decreases in the formation of myelin, particularly during late gestational development and during the postnatal period (Mendola et al., 2002).

Another developmental toxin is ethanol. In addition to affecting neurons, developmental exposure to ethanol has been shown to affect glial cells (Phillips, 1992). Evidence exists of abnormal glial migration in humans with fetal alcohol syndrome (FAS), as well as in primates and rats exposed to ethanol during development (Clarren, 1986; Miller and Robertson, 1993), and a reduction in glial cell number has been reported in rat models of FAS (Miller and Potempa, 1990; Perez-Torrero et al., 1997). In children affected by FAS, hypoplasia of the corpus callosum and anterior commissure, two areas originally formed by neuroglial cells, has been reported (Riley et al., 1995).

In the mature central nervous system (CNS), the metabolic interaction between neurons and astrocytes is crucial for energy metabolism in the brain, as well as for *de novo* synthesis of the most abundant neurotransmitters glutamate and γ -aminobutyrate acid (GABA). Astrocytes express enzymes that are absent in neurons and vice versa (Hertz et al., 1992). The important concept of exchange of metabolites between astrocytes and neurons was developed subsequent to basic studies of glutamate and glutamine metabolism (Lajtha et al., 1959; Berl et al., 1961) and resulted in the proposal of a glutamate–glutamine cycle linking glutamatergic neurons and astrocytes (Figure 5.5-1, van den Berg and Garfinkel, 1971). In this scheme glutamate released from neurons in glutamatergic neurotransmission is mainly taken up by astrocytes (Gegelashvili and Schousboe, 1997, 1998) and this is compensated for by a flow of glutamine from astrocytes to neurons. Another important finding is that anaplerosis, which is necessary for the operation of the tricarboxylic acid (TCA) cycle, is only present in astrocytes and is carried out by pyruvate carboxylase (PC) (Yu et al., 1983; Shank et al., 1985; Cesar and Hamprecht, 1995). This process generates a molecule of oxaloacetate by *de novo* synthesis, which may condense with acetyl-CoA to provide net synthesis of the TCA cycle intermediate α -ketoglutarate, from which glutamate can be formed by transamination (Westergaard et al., 1996). Subsequently, glutamine may be synthesized from glutamate in the reaction catalyzed by glutamine synthetase (GS), which, like PC, is exclusively expressed in glial cells (Martinez-Hernandez et al., 1977). Glial–neuronal interaction is also important for termination of glutamatergic and GABAergic activity by uptake of these neurotransmitters, especially glutamate, in astrocytes (see above).

Figure 5.5-1

Schematic representation of key metabolic processes and of release and uptake of neurotransmitters in glutamatergic and GABAergic synapses interacting with a surrounding astrocyte. The vesicular pools of glutamate and GABA are indicated by ellipses. Glucose metabolism, lactate generation or utilization, and tricarboxylic acid (TCA) cycle metabolism are indicated in all three cellular compartments. Moreover, the glutamate–glutamine cycle including the glutamine synthetase (GS) reaction is indicated in the glutamatergic neuron–astrocyte interaction. Analogously, the GABA–glutamate–glutamine cycle including the GABA transaminase (GABA-T) and glutamate decarboxylase (GAD) reactions is indicated in the GABAergic neuron–astrocyte interaction. In the astrocytic compartment pyruvate carboxylation to oxaloacetate via pyruvate carboxylase (PC) is indicated. Additionally, pyruvate recycling via phosphoenol pyruvate kinase (PEPCK) and pyruvate kinase (PK) or malic enzyme (ME) is shown. One arrow does not imply one reaction only. CIT, citrate; GAD, glutamate decarboxylase; GABA-T, GABA transaminase; GLN, glutamine; GLU, glutamate; GS, glutamine synthetase; MAL, malate; ME, malic enzyme; 2-OG, 2-oxoglutarate; PAG, phosphate-activated glutaminase; PC, pyruvate carboxylase; PDH, pyruvate dehydrogenase; PYR pyruvate; TCA, tricarboxylic acid



■ Figure 5.5-1 (continued)

Astrocytic glutamate transporters are critical components in coupling neuronal glutamatergic activity and neuronal energy utilization (Cholet et al., 2001). Communication within the astrocyte network or between neurons is carried out via electrical coupling through gap junctions (Froes et al., 1999; Alvarez-Maubecin et al., 2000; Bennett and Zukin, 2004), suggesting the possible existence of rapid regulatory crosstalk networks during synaptic transmission. Astrocytes also express a repertoire of neurotransmitter receptors mirroring that of neighboring synapses (Simard and Nedergaard, 2004). Calcium signaling occurs between astrocytes both by the gap junction-mediated pathway and by extracellularly using the P2 receptor-mediated pathway (John et al., 1999). These observations indicate that the mechanisms underlying information processing in the CNS may be substantially more complex and plastic than has previously been appreciated. Additional findings invoke the astrocyte's own form of excitability and neurotransmitter release (i.e., glutamate) via a novel process sensitive to blockers of exocytosis and involving cyclooxygenase eicosanoids (Vesce et al., 1999). Thus, the astrocyte is now viewed as an active participant in synaptic transmission, and is perhaps even involved in the processing of information in the CNS, a staggering departure from the classical dogma that the astrocytes serve only as physical support for juxtaposed neurons.

The symbiotic relationship between neurons and glia is also exemplified by the neuronal dependence on astrocyte-derived thiols for the maintenance of stable glutathione (GSH) concentrations (Dringen and Hirrlinger, 2003). GSH (γ -glutamylcysteinylglycine) is synthesized in two steps by the actions of γ -glutamylcysteine synthetase forming γ -glutamylcysteine from cysteine and glutamate, followed by the addition of glycine by GSH synthetase. It is a major antioxidant in mammalian cell systems, constituting approximately 90% of the intracellular nonprotein thiols, and it is crucial in conjugation and elimination of various toxic molecules, and the maintenance of the intracellular redox status. Recent results suggest that intracellular GSH can modulate the toxic effects of arsenic (Hirano et al., 2004). GSH deficiency is connected to a number of neurodegenerative disorders (Bains and Shaw, 1997; Dringen and Hirrlinger, 2003), enhancing the toxic effects of insults that act via generation of reactive oxygen species (ROS) such as that occurring during reperfusion after ischemia (Mizui et al., 1992), treatment with 6-hydroxydopamine (Pileblad et al., 1992) and 1-methyl-4-phenylpyridinium (Wullner et al., 1996). In vitro, GSH depletion leads to increased astrocytic swelling and excitatory amino acid (EAA) release, whereas increased GSH reduces both of these effects (Aschner et al., 1994). In general, GSH levels are lower in neurons than in astrocytes (Sagara et al., 1993), rendering the former more susceptible to increased intracellular levels of ROS. Recent studies have established that cysteine and GSH are unstable and are oxidized to their disulfide forms under aerobic conditions, and that constant release of cysteine and GSH by astrocytes is essential for the maintenance of stable levels of thiols in the CNS (Dringen et al., 1999; Shanker et al., 2001a, b; Dringen and Hirrlinger, 2003).

4 Methionine Sulfoximine: A Tool to Probe Astrocyte–Neuron Interactions

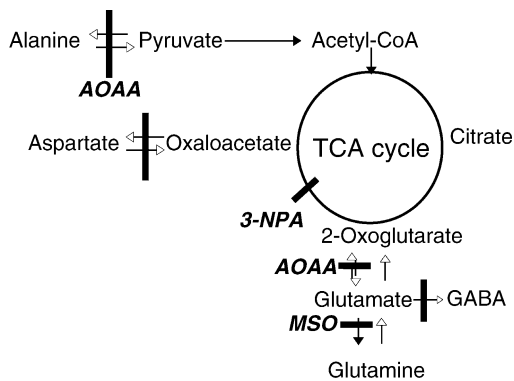
Methionine sulfoximine (MSO) is a rare amino acid and an irreversible inhibitor of the astrocyte-specific enzyme, GS (Albrecht and Norenberg, 1990). This enzyme catalyzes the conversion of glutamate to glutamine in the presence of ammonia. When administered to animals, MSO leads to rapid convulsions (Bernard-Helary et al., 2000). Although at present there appears to be no known environmental exposure to MSO, the literature is replete with examples of accidental poisonings with this compound. It occurs in nature or as a by-product of some forms of food processing. A notable example of the latter was a former method for bleaching wheat flour, using nitrogen trichloride, the “agene process,” in use for most of the first 50 years of the nineteenth century. “Agenized” flour was found to be responsible for various neurological disorders in animals. Oxidation of methionine residues during the bleaching process of wheat proteins is believed to have led to the formation of the toxic species, MSO. The agene process was subsequently discontinued in the United States and the United Kingdom circa 1950 (Shaw et al., 1999). Wheat flour that had been bleached with agene and accidentally consumed by dogs led to “running fits,” “canine hysteria,” convulsions, and anoxia (Lewey, 1950). At the morphological level, ingestion of large amounts of adulterated flour resulted in neuronal cell loss in the hippocampal fascia dentata and pyramidal cell layer, in the short-association fibers and the lower layers of the cerebral cortex, and in cerebellar Purkinje cells

(Lewey, 1950). MSO injection leads to large increases of glycogen levels (Folbergrova, 1973), primarily within astrocytic cell bodies, but not in other neuroglial cells or neurons (Phelps, 1975).

The role of glutamine as precursor for GABA was probed using ^{13}C -labeled glucose and acetate. NMR spectroscopy and MS was performed on extracts from cortical neurons, astrocytes, and cocultures of neurons on astrocytes (Sonnewald et al., 1993a). It could be shown that $[1\text{-}^{13}\text{C}]$ glucose labeled GABA both in neurons and in cocultures whereas $[2\text{-}^{13}\text{C}]$ acetate only labeled GABA in cocultures. This clearly indicated that a labeled precursor from astrocytes was transferred to the neurons for GABA synthesis. In accordance with this it was previously demonstrated by NMR spectroscopy analysis of medium from the different cell types that astrocytes released both citrate and glutamine (Sonnewald et al., 1991), which could serve as precursors for GABA. Westergaard et al. (1994) have shown that citrate is not taken up into cultured cerebellar neurons and therefore it is unlikely that it can be transported into the cortical neurons to act as precursor for GABA formation. However, glutamine could be an excellent candidate for GABA label. In order to probe this, MSO was used to block GS (Figure 5.5-2). In astrocytes no glutamine synthesis was detectable by NMR, and by using the above-mentioned cocultures and $[2\text{-}^{13}\text{C}]$ acetate in the presence of

Figure 5.5-2

Schematic presentation of the ways inhibitors can block different steps in the tricarboxylic acid (TCA) cycle. AOAA, aminooxyacetic acid; MSO, methionine sulfoximine; 3-NPA, 3-nitropropionic acid



MSO, it could be shown that GABA synthesis was strongly reduced (Sonnewald et al., 1993b). Thus glutamine released by astrocytes can, after conversion to glutamate, function as a precursor for the inhibitory neurotransmitter GABA in accordance with previous studies (Reubi et al., 1978). This extends the concept of the glutamate–glutamine cycle to a glutamate–glutamine–GABA cycle. The drain of GABA from neurons to astrocytes is relatively modest (Peng et al., 1993; Schousboe et al., 2004) and glutamine transport has been shown to be more intense in glutamatergic neurons than in cortical neurons and astrocytes (Varoqui et al., 2000). Furthermore, using MSO and inhibitors of the glial TCA cycle trifluoroacetic acid revealed that a considerable portion of the energy required to support glutamine synthesis is derived from the oxidative metabolism of glucose in the astroglia (Garcia-Espinosa et al., 2004).

5 3-Nitropropionic Acid

3-Nitropropionic acid (3-NPA) has been reported to act as an irreversible inhibitor of succinate dehydrogenase (Alston et al., 1977; Coles et al., 1979) and a reversible inhibitor of fumarase (Porter and Bright, 1980). Succinate dehydrogenase is part of both the TCA cycle (Figure 5.5-2) and complex II of the mitochondrial electron transport chain. 3-NPA is found in various species of nitro-containing *Astragalus*

(James et al., 1980). Systemic administration of 3-NPA to experimental animals results in selective striatal lesions (Brouillet et al., 1993; Wullner et al., 1994). Similar to the late age of onset for Huntington's disease and other neurodegenerative diseases, 3-NPA causes age-dependent neurotoxicity in rodents (Brouillet, 1993; Wullner et al., 1994). In agreement with its action on complex II Beal et al. (1993) have shown that 3-NPA inhibits synaptosomal respiration in a dose-dependent manner. With glutamine and 3-NPA in the medium, both glutamate and GABA increased inside the synaptosomes and the external concentration of glutamate rose, lending further evidence for an excitotoxic mechanism in neurodegeneration (Beal et al., 1993). In mice injected subcutaneously with 3-NPA an increased GABA concentration was observed, whereas glutamate was slightly decreased (Hassel and Sonnewald, 1995b). Furthermore, by using [1- ^{13}C] glucose or [2- ^{13}C]acetate in combination with NMR spectroscopy, it could be shown that 3-NPA inhibited neurons more than glial cells (Hassel and Sonnewald, 1995).

To further explore this differential vulnerability, the effect of blocking succinate dehydrogenase both in astrocytes and in neurons was studied using [U- ^{13}C]glutamate as a substrate (Sonnewald et al., 1996b; Bakken et al., 1997). 3-NPA was additionally used to determine pyruvate carboxylation and metabolism of [3- ^{13}C]malate in brain cells (Alves et al., 2000; Waagepetersen et al., 2001).

5.1 Effect of 3-NPA on [U- ^{13}C]Glutamate Metabolism in Neurons

[U- ^{13}C]Glutamate can enter the TCA cycle after conversion to 2-oxoglutarate (2-OG) (▶ [Figure 5.5-3](#)). [U- ^{13}C]Malate and [U- ^{13}C]oxaloacetate are formed after several steps, and [U- ^{13}C]lactate and [U- ^{13}C]aspartate can be synthesized thereafter (Sonnewald et al., 1993a, 1996b). In the presence of unlabeled glucose, unlabeled pyruvate is produced through glycolysis and can serve as the precursor of acetyl-CoA. The condensation of labeled oxaloacetate and unlabeled acetyl-CoA will lead to the synthesis of [1,2,3- ^{13}C]glutamate via the TCA cycle.

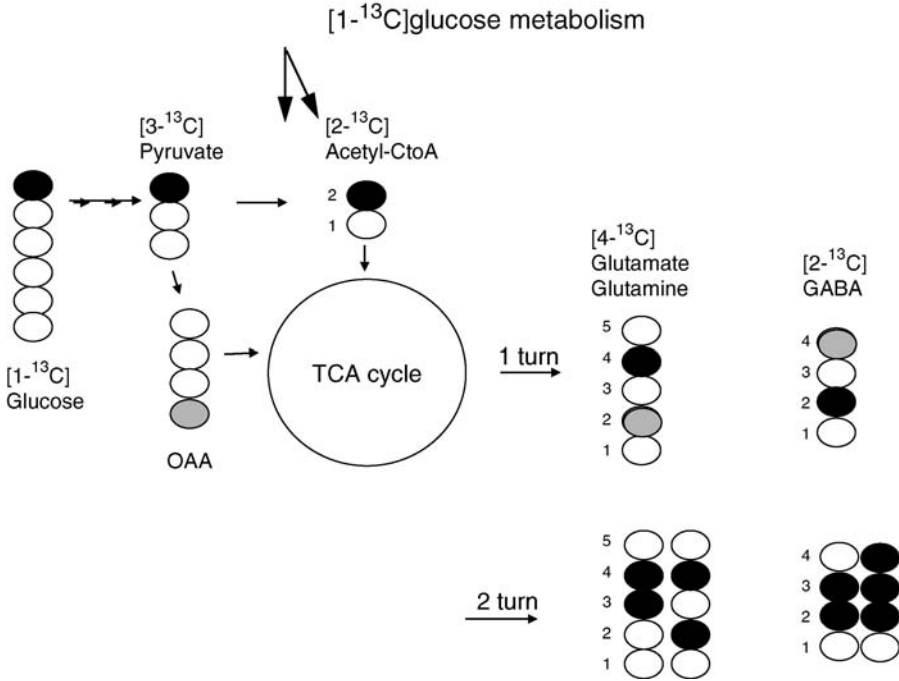
In cerebellar granule neurons, TCA cycle activity was efficiently blocked by 3 mM 3-NPA (Sonnewald et al., 1996b) and metabolism of [U- ^{13}C]glutamate was restricted to the formation of succinate. Only the uniformly labeled isotopomer of glutamate could be detected by NMR spectroscopy and the amount of labeled glutamate within the cells was decreased compared with control, which agrees well with the observations in synaptosomes (Beal et al., 1993). Lactate labeling through the TCA cycle as observed previously in vitro (Sonnewald et al., 1996b) and in mice in vivo (Hassel and Sonnewald, 1995a) was abolished by 3 mM 3-NPA in cerebellar granule neurons (Sonnewald et al., 1996b).

5.2 Effect of 3-NPA on [U- ^{13}C]Glutamate Metabolism in Astrocytes

To probe if astrocytes are indeed less sensitive than neurons to 3-NPA, cultured astrocytes were incubated in the presence of two different concentrations of 3-NPA (3 and 10 mM) using [U- ^{13}C]glutamate as the substrate (Bakken et al., 1997). For labeling patterns of [U- ^{13}C]glutamate metabolism in astrocytes, see ▶ [Figure 5.5-4](#). As in neurons, 3-NPA clearly affected glutamate metabolism in astrocytes. Succinate accumulated intra- and extracellularly and intracellular glutamate and glutamine concentrations were reduced. In the control group, the succinate concentration was too small to be detected by ^{13}C NMR spectroscopy. After 3-NPA treatment (both 3 and 10 mM) no label was detected in aspartate. However, label appeared in lactate in astrocytes receiving 3 mM 3-NPA, and intracellular [1,2,3- ^{13}C]glutamate and extracellular [1,2,3- ^{13}C]glutamine were also still present in cells receiving 3 mM 3-NPA, although both were significantly reduced. Such labeling from [U- ^{13}C]glutamate is only possible using precursors from the TCA cycle, indicating that 3 mM 3-NPA was not sufficient to achieve a complete inhibition of the TCA cycle. With 10 mM 3-NPA, TCA cycle conversion of [U- ^{13}C]glutamate to metabolites was restricted to the formation of succinate. Since, as shown above, in neurons a 3 mM concentration of 3-NPA was sufficient to block TCA cycle metabolism, it appears that astrocytes are more resistant to the effects of 3-NPA, which is in agreement with the study in mice (Hassel et al., 1995).

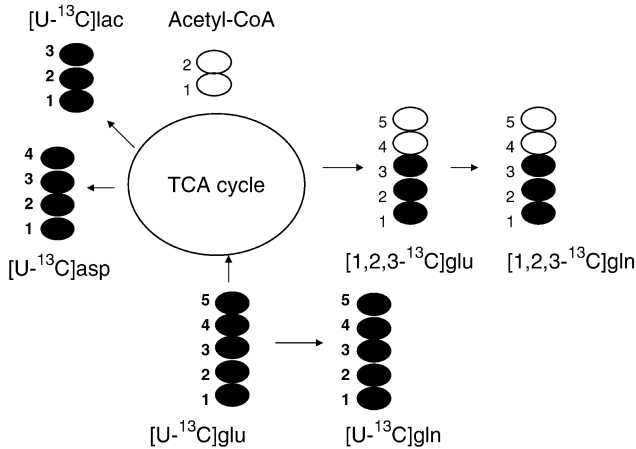
■ Figure 5.5-3

Labeling patterns of tricarboxylic acid (TCA) cycle-related amino acids originating from metabolism of $[1-^{13}\text{C}]$ glucose. Black and gray circles indicate ^{13}C -labeled atoms. Metabolism of $[3-^{13}\text{C}]$ pyruvate involving the pyruvate dehydrogenase (PDH) complex and generation of labeled intermediates in two consecutive turns of the TCA cycle (black circles). $[3-^{13}\text{C}]$ pyruvate metabolism via the pyruvate carboxylation (PC) pathway (gray circles). Note that carboxylation produces $[2-^{13}\text{C}]$ glutamate and glutamine and $[4-^{13}\text{C}]$ GABA. Full circle represents ^{13}C and empty circle ^{12}C



■ Figure 5.5-4

Schematic representation of possible isotopomers arising from $[U-^{13}\text{C}]$ glutamate in astrocytes. Full circle represents ^{13}C ; asp, aspartate; glu, glutamate; gln, glutamine



5.3 Energy Metabolism in the Presence of 3-NPA

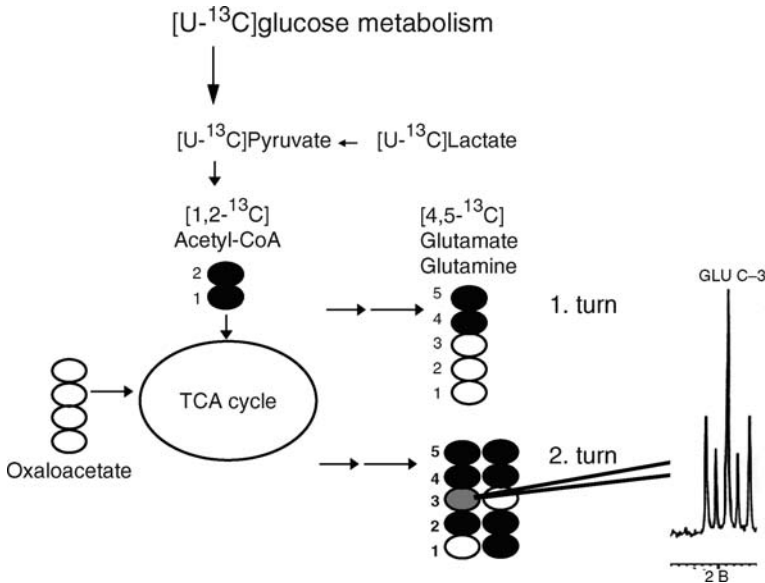
It has been shown that 3-NPA caused a significant fall in ATP both in synaptosomes (Beal et al., 1993) and in neuronal cultures of murine frontal cortex (Sonnewald et al., 1996b). Intrastriatal injection of 3-NPA has also been reported to result in a reduced ATP content within 3 h in the area close to the injection site. In cultured cortical astrocytes a decrease in ATP, although not significant, was observed after incubation with 3-NPA (Bakken et al., 1997). These results suggest that astrocytic ATP stores are less vulnerable to 3-NPA intoxication than neuronal ATP stores. A possible explanation may be the glial localization of PC, which is essential for de novo synthesis of glutamine in astrocytes and subsequently glutamate and GABA in neurons, as discussed earlier. Indeed, there are indications of an increased PC activity in 3-NPA-treated astrocytes since the glucose consumption was increased although lactate production was decreased (Bakken et al., 1997). On the contrary, in synaptosomes, where PC is unlikely to be present, lactate concentration increased after 3-NPA treatment (Beal et al., 1997).

5.4 Use of 3-NPA to Probe Pyruvate Carboxylation

As mentioned above, pyruvate carboxylation is thought to be localized in astrocytes. However, an earlier report suggests that neurons are also capable of pyruvate carboxylation, possibly via malic enzyme (Hassel and Brathe, 2000). 3-NPA can be used to probe carboxylation when combined with administration of ¹³C-labeled glucose and/or lactate. Pyruvate carboxylation will lead to labeling of the C-3 position of glutamate (● Figure 5.5-5). However, cycling of the label will also result in this labeling pattern (● Figure 5.5-6). Using 3-NPA, cycling can be abolished and under these conditions labeling of the C-3 position in glutamate will be

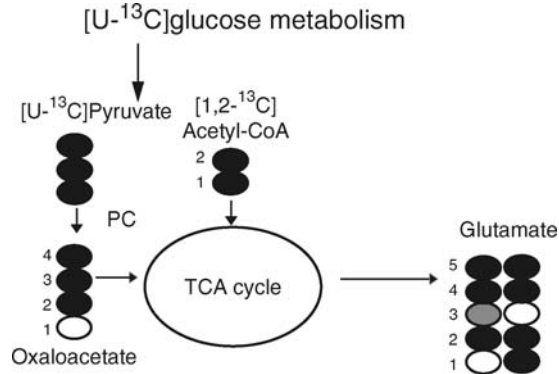
■ Figure 5.5-5

Labeling patterns of tricarboxylic acid (TCA) cycle-related amino acids originating from metabolism of [U-¹³C] glucose and [U-¹³C]lactate. Metabolism of [U-¹³C]pyruvate involving the pyruvate dehydrogenase (PDH) complex and generation of labeled intermediates in two consecutive turns of the TCA cycle. Full circle represents ¹³C and empty circle ¹²C. Inserted is part of the nuclear magnetic resonance (NMR) spectrum in the C-3 region of glutamate. The doublet represents [3,4,5-¹³C]glutamate



■ **Figure 5.5-6**

Labeling patterns of tricarboxylic acid (TCA) cycle-related amino acids originating from metabolism of $[U-^{13}C]$ glucose and $[U-^{13}C]$ lactate. Metabolism of $[U-^{13}C]$ pyruvate involving the pyruvate carboxylation (PC) pathway. Full circle represents ^{13}C and empty circle ^{12}C



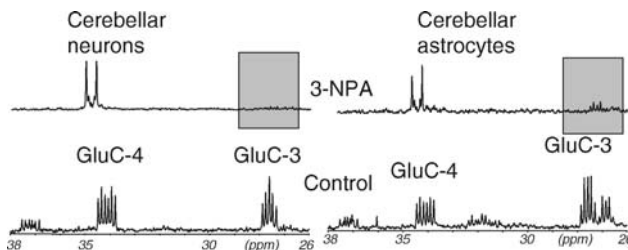
a sign of carboxylation. Using this approach, Waagepetersen et al. (2001) incubated astrocytes and neurons in medium containing $[U-^{13}C]$ glucose and $[U-^{13}C]$ lactate in the presence of 3-NPA. TCA cycle activity was clearly stopped by 3-NPA at the succinate dehydrogenase step in both culture types as evidenced by a buildup of succinate (Waagepetersen et al., 2001). Labeling of aspartate and the C-3 position of glutamate was abolished in neurons in the presence of 3-NPA (▶ [Figure 5.5-7](#)). In astrocytes, however, labeled glutamate and glutamine derived from pyruvate carboxylation were detected (▶ [Figure 5.5-7](#)). This supports the notion that only astrocytes are capable of carboxylation and thus anaplerosis in the brain.

6 Aminoxyacetic Acid: A blocker of transamination

Aminoxyacetic acid (AOAA) inhibits the major transaminases: aspartate aminotransferase (AAT) and alanine aminotransferase (ALAT), both in the cytosol and in mitochondria. AAT is an essential component of the malate–aspartate shuttle, which is also important in brain. This shuttle transports reduction equivalents of NADH from cytosol into mitochondria. An increasing number of observations suggest

■ **Figure 5.5-7**

^{13}C Nuclear magnetic resonance (NMR) spectra of cell extracts from cerebellar neurons (spectra on the left) and astrocytes (spectra on the right) incubated for 4 h in serum-free DMEM containing 2.5 mM $[U-^{13}C]$ glucose and 1 mM $[U-^{13}C]$ lactate in combination with 3-NPA (3 mM for neurons (*top*) and 10 mM for astrocytes (*top*)). It should be noted that the spectra are scaled individually and do not represent actual amounts. GluC-4, glutamate C-3; GluC-4, glutamate C-4; ppm, part per million



that neurodegenerative diseases may be associated with aberrations in energy metabolism and the handling of glutamate (Fiskum et al., 1999; Murphy et al., 1999). Glutamate metabolism is thus a central issue in several of the major brain pathologies. Animal models of neurodegenerative diseases have been created employing inhibitors of mitochondrial energy metabolism. The malate–aspartate shuttle may be regarded as part of this metabolism and AOAA has been shown to produce striatal lesions characteristic of neurodegenerative diseases (Beal et al., 1991).

6.1 Effect of AOAA on [U-¹³C]Glutamate Metabolism in Astrocytes

Different conclusions with regard to the significance and mechanism of glutamate metabolism through the TCA cycle have been reached. In one study it could be demonstrated that the extent of oxidation is coupled to the glutamate concentration (McKenna et al., 1996). A prerequisite for entry of exogenous glutamate into the TCA cycle is the conversion of glutamate to 2-OG, which can take place via transamination or deamination. In order to probe the significance of transamination for the oxidative metabolism of glutamate, AOAA has been used (Yu et al., 1982; Farinelli and Nicklas, 1992). As mentioned above, [U-¹³C]glutamate can enter the TCA cycle and this may lead to the formation of ¹³C-labeled aspartate, lactate, and in some cases also citrate (Sonnewald et al., 1993a). Aspartate formation is dependent on transamination and will thus not take place in the presence of AOAA. Formation of lactate and citrate is, however, independent of transamination and only requires [U-¹³C]glutamate entry into the TCA cycle. As can be seen in [Table 5.5-1](#) both lactate and citrate concentrations were unaffected by the presence of AOAA. Thus, as originally proposed (Yu et al., 1982) it was shown that transamination played only a minor

■ **Table 5.5-1**

Amounts of ¹³C (nmol/mg protein) in metabolites in medium from cerebral cortical astrocytes

Medium	Control (n=4)	AOAA (n=4)
Lactate total	215 ± 27	178 ± 15
[1,2,3- ¹³ C]lactate	188 ± 11	153 ± 11
Lactate % enrichment	15 ± 1.8	10 ± 1.4
Citrate C-2+4	33 ± 6	36 ± 4

Astrocytes were incubated with medium containing [U-¹³C]glutamate (0.5 mM) for 2 h. Medium was analyzed by ¹³C NMR spectroscopy. Results are presented as mean “+/-” SEM (results from Sonnewald et al., 1993a).

role in formation of 2-OG from glutamate (Westergaard et al., 1996). However, this process appeared to be the major pathway for the opposite reaction, i.e., for formation of glutamate from 2-OG. This is based on the finding that formation of [1,2,3-¹³C]glutamate and glutamine (a sign of TCA cycle activity) was strongly reduced in the presence of AOAA. An explanation for the pronounced decrease of these isotopomers is that transamination is the major pathway for glutamate formation from 2-OG, which is in accordance with the low affinity of GDH for ammonia (Cooper and Plum, 1987). A further indication that GDH may be important for glutamate degradation and normal brain function comes from the demonstration that the neurodegenerative disorder olivopontocerebellar atrophy is linked to impairment of GDH activity (Plaitakis et al., 1984).

7 Methylmercury

Methylmercury (MeHg) is an environmental contaminant that continues to pose a significant risk to human health. There has been considerable attention in the scientific and health policy fora on the question of whether MeHg intake from a diet high in fish is associated with aberrant CNS function. A recent study in the Faeroe Islands (Steuerwald et al., 2000) suggests that fetal exposure at levels attained by mothers eating

fish regularly during pregnancy is associated with neurological deficits in their offspring. Notably, this outcome has not been replicated in children in the Republic of the Seychelles (Axtell et al., 2000). However, a major confounding factor in these studies is the substantial exposure to polychlorinated biphenyls (PCBs) in the Faeroe Islands compared with the exposure in the Seychelles and the possible neurobehavioral effects of such coexposure (Newland, 2002).

The Minamata disease in Japan in the 1950s was due to excess exposure to MeHg and is still a prime source of neuropathology data on humans (Eto, 1997). The major neuropathological change after MeHg exposure is the extensive loss of cerebellar granule cells and this effect appears to involve an apoptotic process (Nagashima et al., 1996; Eto, 1997). Although not the only cell type to be adversely affected by MeHg, astrocytes appear to play a key role in MeHg-induced toxicity. After chronic *in vivo* exposure in nonhuman primates, MeHg preferentially accumulates in astrocytes (and to some degree in microglia; Charleston et al., 1994, 1996), resulting in astrocytic swelling (Aschner et al., 1990; Charleston et al., 1994, 1996). Furthermore, coapplication of nontoxic concentrations of MeHg and glutamate leads to the typical appearance of neuronal lesions associated with excitotoxic effects (Matyja and Albrecht, 1993). Furthermore, in the absence of glutamate, neurons are unaffected by acute exposure to mercury-containing compounds, suggesting that neuronal dysfunction is secondary to disturbances in astrocytes (Brookes, 1992), possibly affecting glutamate homeostasis (Schousboe et al., 2004).

7.1 Metabolic Effects of MeHg on Cerebral Astrocytes

The effect of MeHg on glutamate metabolism in rat cerebral cortical astrocytes has been studied by ^{13}C NMR spectroscopy (Allen et al., 2001). Cerebral cortical astrocytes pretreated with MeHg, 1 μM for 24 h or 10 μM for 30 min, were subsequently incubated with 0.5 mM $[\text{U}-^{13}\text{C}]$ glutamate for 2 h in growth media containing 10% serum. High-pressure liquid chromatography (HPLC) analysis of amino acids showed no changes in concentrations between groups. Furthermore, the amounts of most metabolites synthesized from $[\text{U}-^{13}\text{C}]$ glutamate were also unchanged in the presence of MeHg. However, formation of $[\text{U}-^{13}\text{C}]$ lactate was decreased in cells exposed to 10 μM MeHg for 30 min while labeled aspartate was not changed. It should be noted that both $[\text{U}-^{13}\text{C}]$ lactate and $[\text{U}-^{13}\text{C}]$ aspartate can only be derived from $[\text{U}-^{13}\text{C}]$ glutamate via mitochondrial metabolism and it is known that MeHg inhibits mitochondrial activity in both neurons and astrocytes (Sanfeliu et al., 2001). $[\text{U}-^{13}\text{C}]$ glutamate enters the TCA cycle after conversion to 2- $[\text{U}-^{13}\text{C}]$ oxoglutarate, and $[\text{U}-^{13}\text{C}]$ aspartate is formed from $[\text{U}-^{13}\text{C}]$ oxaloacetate, as is $[\text{U}-^{13}\text{C}]$ lactate via phosphoenolpyruvate. $[\text{U}-^{13}\text{C}]$ lactate can also be formed from $[\text{U}-^{13}\text{C}]$ malate. This differential effect on labeled aspartate and lactate indicated cellular compartmentation, as also shown in other studies (Qu et al., 1999, 2001; Sonnewald et al., 2004), and thus selective vulnerability of mitochondria within the astrocytes to the effects of MeHg. The decreased lactate production from glutamate might affect the metabolism of surrounding neurons since lactate has been proposed as an important substrate for these cells (Pellerin, 2003).

7.2 Metabolic Effects of MeHg on Cerebellar Astrocytes

The effect of MeHg on $[\text{U}-^{13}\text{C}]$ glutamate metabolism was also studied in cerebellar astrocytes from mice using ^{13}C NMR spectroscopy (Qu et al., 2003). The cerebellar cells were preincubated in medium containing 25 or 50 μM MeHg and 10% fetal calf serum for 4 h and subsequently in fresh medium with $[\text{U}-^{13}\text{C}]$ glutamate (0.5 mM) for 2 h. Labeled glutamate, glutamine, and aspartate were observed in both cell extracts and media. Labeled GSH was present in the cell extracts and labeled lactate and alanine in the media. The amount of labeled glutamate removed from the media (by uptake into the cells) was decreased in the 50 μM MeHg group. Furthermore, the levels of both labeled and unlabeled glutamine were decreased, possibly indicating a decreased synthesis and/or increased degradation. However, an increase was observed for GSH in the 25 μM group, which might be due to an upregulated synthesis of GSH in response to the toxic effects of MeHg as GSH has been shown to have important protective properties toward MeHg cellular toxicity (Sarafian et al., 1996). The percentage of $[\text{U}-^{13}\text{C}]$ glutamate used for the synthesis of metabolites from the

TCA cycle was increased in the presence of 50 μM MeHg. However, the percentage used for energy production was decreased in both groups, indicating selective mitochondrial vulnerability due to the inhibitory effect of MeHg. Such MeHg-induced loss of mitochondrial respiratory functions has been demonstrated in several studies both *in vivo* and *in vitro*, and has been proposed as a major mechanism of MeHg neurotoxicity. However, a wide range of toxic effects can be induced by MeHg in the CNS and the relative importance of the various mechanisms involved has yet to be determined (for a review, see Sanfeliu et al., 2003).

7.3 Effects of MeHg on GSH Precursor Transport

It has been hypothesized that oxidative damage may be the primary mechanism underlying the neurotoxicity induced by MeHg and other organometals since ROS formation was selectively increased in response to MeHg exposure in cerebellum, an area known to be specifically vulnerable to MeHg (Ali et al., 1992). It has been suggested that neurons maintain their GSH level by taking up cysteine provided by glial cells (Sagara et al., 1993). Synthesis of GSH is rate-limited by this amino acid. As recently shown (Allen et al., 2001), both cerebral astrocytes and cerebral and hippocampal neurons readily accumulate cysteine. Approximately 80–90% of cysteine uptake is sodium-dependent (with XAG system as the major contributor and ASC system, the neutral amino acids transporter system, as the minor contributor) in all these cell types. MeHg exposure is associated with a significant concentration-dependent inhibition of cysteine transport in astrocytes, but not in neurons, and this effect can be traced to the inhibition of both XAG and the ASC transport systems (Shanker et al., 2001a, b). A significant concentration-dependent inhibition of cysteine (and also of cystine) uptake in astrocytes was also observed with glutamate, suggesting that the latter may, at least in part, be mediating this MeHg response. The lack of an inhibitory effect on neurons cannot be fully explained, but some of the possible mechanisms include (1) a comparatively more efficient transport system for MeHg in astrocytes compared with in neurons, and (2) indirect inhibition of uptake in astrocytes secondary to reduced uptake and increased efflux of glutamate, with glutamate acting as a surrogate inhibitor of cysteine/cystine transport.

Acknowledgments

This work was supported by grants from the Danish Medical Research Council, the Lundbeck Foundation (to AS and HSW) and US Public Health Service Grant ES07331 to MA.

References

- Albrecht J, Norenberg MD. 1990. L-methionine-DL-sulfoximine induces massive efflux of glutamine from cortical astrocytes in primary culture. *Eur J Pharmacol* 182: 587-589.
- Alfano DP, Petit TL, Le Bouillier JC. 1983. Development and plasticity of the hippocampal-cholinergic system in normal and early lead exposed rats. *Brain Res* 312: 117-124.
- Ali SF, Le Bel CP, Bondy SC. 1992. Reactive oxygen species formation as a biomarker of methylmercury and trimethyltin neurotoxicity. *Neurotoxicology* 13: 637-648.
- Allen JW, El-Oqayli H, Aschner M, Syversen T, Sonnewald U. 2001. Methylmercury has a selective effect on mitochondria in cultured astrocytes in the presence of [^{13}C]glutamate. *Brain Res* 908: 149-154.
- Alston TA, Mela L, Bright HJ. 1977. 3-Nitropropionate, the toxic substance of indigofera, is a suicide inactivator of succinate dehydrogenase. *Proc Natl Acad Sci USA* 74: 3767-3771.
- Alvarez-Maubecin V, Garcia-Hernandez F, Williams JT, Van Bockstaele, EJ. 2000. Functional coupling between neurons and glia. *J Neurosci* 20: 4091-4098.
- Alves PM, Nunes R, Zhang C, Maycock CD, Sonnewald U, et al. 2000. Metabolism of [^{13}C]malate in primary cultures of mouse astrocytes. *Dev Neurosci* 22: 456-462.
- Aschner M, Eberle N, Miller K, Kimelberg HK. 1990. Interaction of methylmercury with rat primary astrocyte cultures: Effects on rubidium uptake and efflux and induction of swelling. *Brain Res* 530: 245-250.

- Aschner M, Mullaney KJ, Wagoner D, Lash LH, Kimelberg HK. 1994. Intracellular glutathione (GSH) levels modulate mercuric chloride (MC)- and methylmercuric chloride (MeHgCl)-induced amino acid release from neonatal rat primary astrocytes cultures. *Brain Res* 664: 133-140.
- Axtell CD, Cox C, Myers GJ, Davidson PW, Choi AL, et al. 2000. Association between methylmercury exposure from fish consumption and child development at five and a half years of age in the Seychelles Child Development Study: An evaluation of nonlinear relationships. *Environ Res* 84: 71-80.
- Bains JS, Shaw CA. 1997. Neurodegenerative disorders in humans: The role of glutathione in oxidative stress-mediated neuronal death. *Brain Res Rev* 25: 335-358.
- Bakken IJ, Johnsen SF, White LR, Unsgard G, Aasly J, et al. 1997. NMR spectroscopy study of the effect of 3-nitropropionic acid on glutamate metabolism in cultured astrocytes. *J Neurosci Res* 47: 642-649.
- Beal MF, Brouillet E, Jenkins B, Henshaw R, Rosen B, et al. 1993. Age-dependent striatal excitotoxic lesions produced by the endogenous mitochondrial inhibitor malonate. *J Neurochem* 61: 1147-1150.
- Beal MF, Swartz KJ, Hyman BT, Storey E, Finn SE, et al. 1991. Aminoxyacetic acid results in excitotoxic lesions by a novel indirect mechanism. *J Neurochem* 57: 1068-1073.
- Bennett MV, Zukin RS. 2004. Electrical coupling and neuronal synchronization in the mammalian brain. *Neuron* 41: 495-511.
- Berl S, Lajtha A, Waelsch H. 1961. Amino acid and protein metabolism of the brain-VI. Cerebral compartments of glutamic acid metabolism. *J Neurochem* 7: 322-332.
- Bernard-Helary K, Lapouble E, Ardourel M, Hevor T, Cloix JF. 2000. Correlation between brain glycogen and convulsive state in mice submitted to methionine sulfoximine. *Life Sci* 67: 1773-1781.
- Brookes N. 1992. In vitro evidence for the role of glutamate in the CNS toxicity of mercury. *Toxicology* 76: 245-256.
- Brouillet E, Jenkins BG, Hyman BT, Ferrante RJ, Kowall NW, et al. 1993. Age-dependent vulnerability of the striatum to the mitochondrial toxin 3-nitropropionic acid. *J Neurochem* 60: 356-359.
- Bull RJ, McCauley PT, Taylor DH, Crofton KM. 1983. The effects of lead on the developing central nervous system of the rat. *Neurotoxicology* 4: 1-17.
- Cesar M, Hamprecht B. 1995. Immunocytochemical examination of neural rat and mouse primary cultures using monoclonal antibodies raised against pyruvate carboxylase. *J Neurochem* 64: 2312-2318.
- Charleston JS, Body RL, Bolander RP, Mottet NK, Vahter ME, et al. 1996. Changes in the number of astrocytes and microglia in the thalamus of the monkey *Macaca fascicularis* following long-term subclinical methylmercury exposure. *Neurotoxicology* 17: 127-138.
- Charleston JS, Bolander RP, Mottet NK, Body RL, Vahter ME, et al. 1994. Increases in the number of reactive glia in the visual cortex of *Macaca fascicularis* following subclinical long-term methyl mercury exposure. *Toxicol Appl Pharmacol* 129: 196-206.
- Cholet N, Pellerin L, Welker E, Lacombe P, Seylaz J, et al. 2001. Local injection of antisense oligonucleotides targeted to the glial glutamate transporter GLAST decreases the metabolic response to somatosensory activation. *J Cereb Blood Flow Metab* 21: 404-412.
- Clarren SK. 1986. Neuropathology in fetal alcohol syndrome. Alcohol and brain development. West JR, editor. New York: Oxford University Press; pp. 158-166.
- Coles CJ, Edmondson DE, Singer TP. 1979. Inactivation of succinate dehydrogenase by 3-nitropropionate. *J Biol Chem* 254: 5161-5167.
- Cooper AJ, Plum F. 1987. Biochemistry and physiology of brain ammonia. *Physiol Rev* 67: 440-519.
- Dringen R, Hirrlinger J. 2003. Glutathione pathways in the brain. *Biol Chem* 384: 505-516.
- Dringen R, Pfeiffer B, Hamprecht B. 1999. Synthesis of the antioxidant glutathione in neurons: Supply by astrocytes of CysGly as precursor for neuronal glutathione. *J Neurosci* 19: 562-569.
- Erecinska M, Nelson D. 1994. Effects of 3-nitropropionic acid on synaptosomal energy and transmitter metabolism: Relevance to neurodegenerative brain diseases. *J Neurochem* 63: 1033-1041.
- Eto K. 1997. Pathology of Minamata disease. *Toxicol Pathol* 25: 614-623.
- Farinelli SE, Nicklas WJ. 1992. Glutamate metabolism in rat cortical astrocyte cultures. *J Neurochem* 58: 1905-1915.
- Fiskum G, Murphy AN, Beal MF. 1999. Mitochondria in neurodegeneration: Acute ischemia and chronic neurodegenerative diseases. *J Cereb Blood Flow Metab* 19: 351-369.
- Folbergrova, J. 1973. Glycogen and glycogen phosphorylase in the cerebral cortex of mice under the influence of methionine sulphoximine. *J Neurochem* 20: 547-557.
- Froes MM, Correia AH, Garcia-Abreu J, Spray DC, Campos de Carvalho AC, et al. 1999. Gap-junctional coupling between neurons and astrocytes in primary central nervous system cultures. *Proc Natl Acad Sci USA* 96: 7541-7546.
- Garcia-Espinosa MA, Rodrigues TB, Sierra A, Benito M, Fonseca C, et al. 2004. Cerebral glucose metabolism and the glutamine cycle as detected by in vivo and in vitro ¹³C NMR spectroscopy. *Neurochem Int* 45: 297-303.
- Gegelashvili G, Schousboe A. 1997. High affinity glutamate transporters: Regulation of expression and activity. *Mol Pharmacol* 52: 6-15.

- Gegelashvili G, Schousboe A. 1998. Cellular distribution and kinetic properties of high-affinity glutamate transporters. *Brain Res Bull* 45: 233-238.
- Hassel B, Brathe A. 2000. Neuronal pyruvate carboxylation supports formation of transmitter glutamate. *J Neurosci* 20: 1342-1347.
- Hassel B, Sonnewald U. 1995a. Glial formation of pyruvate and lactate from TCA cycle intermediates: Implications for the inactivation of transmitter amino acids? *J Neurochem* 65: 2227-2234.
- Hassel B, Sonnewald U. 1995b. Selective inhibition of the tricarboxylic acid cycle of GABAergic neurons with 3-nitropropionic acid in vivo. *J Neurochem* 65: 1184-1191.
- Hertz L, Peng L, Westergaard N, Yudkoff M, Schousboe A. 1992. Neuronal-astrocytic interactions in metabolism of transmitter amino acids of the glutamate family. *Alfred Benzon Symposium* 32, *Drug Research Related to Neuroactive Amino Acids*. Schousboe A, Diemer NH, Kofod H, editors. Copenhagen: Munksgaard, pp. 30-48.
- Hirano S, Kobayashi Y, Cui X, Kanno S, Hayakawa T, et al. 2004. The accumulation and toxicity of methylated arsenicals in endothelial cells: Important roles of thiol compounds. *Toxicol Appl Pharmacol* 198: 458-467.
- James LF, Hartley WJ, Williams MC, Van Kampen KR. 1980. Field and experimental studies in cattle and sheep poisoned by nitro-bearing *Astragalus* or their toxins. *Am J Vet Res* 41: 377-382.
- John GR, Scemes E, Suadicani SO, Liu JS, Charles PC, et al. 1999. IL-1 β differentially regulates calcium wave propagation between primary human fetal astrocytes via pathways involving P2 receptors and gap junction channels. *Proc Natl Acad Sci USA* 96: 11613-11618.
- Lajtha A, Berl S, Waelsch H. 1959. Amino acid and protein metabolism of the brain-IV. the metabolism of glutamic acid. *J Neurochem* 3: 322-332.
- Lewey FH. 1950. Neuropathological changes in nitrogen trichloride intoxication of dogs. *J Neuropathol Exp Neurol* 9: 397-405.
- Martinez-Hernandez A, Bell KP, Norenberg MD. 1977. Glutamine synthetase: Glial localization in brain. *Science* 195: 1356-1358.
- Matyja E, Albrecht J. 1993. Ultrastructural evidence that mercuric chloride lowers the threshold for glutamate neurotoxicity in an organotypic culture of rat cerebellum. *Neurosci Lett* 158: 155-158.
- McKenna MC, Sonnewald U, Huang X, Stevenson J, Zielke HR. 1996. Exogenous glutamate concentration regulates the metabolic fate of glutamate in astrocytes. *J Neurochem* 66: 386-393.
- Mendola P, Selevan SG, Gutter S, Rice D. 2002. Environmental factors associated with a spectrum of neurodevelopmental deficits. *Ment Retard Dev Disabil Res Rev* 8: 188-197.
- Miller MW, Potempa G. 1990. Numbers of neurons and glia in mature rat somatosensory cortex: Effects of prenatal exposure to ethanol. *J Comp Neurol* 293: 92-102.
- Miller MW, Robertson S. 1993. Prenatal exposure to ethanol alters the postnatal development and transformation of radial glia to astrocytes in the cortex. *J Comp Neurol* 337: 252-266.
- Mizui T, Kinouchi H, Chan PH. 1992. Depletion of brain glutathione by buthionine sulfoximine enhances cerebral ischemic injury in rats. *Am J Physiol* 530: 313-317.
- Murphy AN, Fiskum G, Beal MF. 1999. Mitochondria in neurodegeneration: Bioenergetic function in cell life and death. *J Cereb Blood Flow Metab* 19: 231-245.
- Nagashima K, Fujii Y, Tsukamoto T, Nukuzuma S, Satoh M, et al. 1996. Apoptotic process of cerebellar degeneration in experimental methylmercury intoxication of rats. *Acta Neuropathol* 91: 72-77.
- Newland MC. 2002. Neurobehavioral toxicity of methylmercury and PCBs—effects-profiles and sensitive populations. *Environ Toxicol Pharmacol* 12: 119-128.
- Oberto A, Marks N, Evans HL, Guidotti A. 1996. Lead (Pb+2) promotes apoptosis in newborn rat cerebellar neurons: Pathological implications. *J Pharmacol Exp Ther* 279: 435-442.
- Pellerin L. 2003. Lactate as a pivotal element in neuron–glia metabolic cooperation. *Neurochem Int* 43: 331-338.
- Peng L, Hertz L, Huang R, Sonnewald U, Petersen SB, et al. 1993. Utilization of glutamine and of TCA cycle constituents as precursors for transmitter glutamate and GABA. *Dev Neurosci* 15: 367-377.
- Perez-Torrero E, Duran P, Granados L, Gutierrez-Ospina G, Cintra L, Diaz-Cintra S. 1997. Effects of acute prenatal ethanol exposure on Bergmann glia cells early postnatal development. *Brain Res* 746: 305-308.
- Petit TL, Le Boutillier JC. 1979. Effects of lead exposure during development on neocortical dendritic and synaptic structure. *Exp Neurol* 64: 482-492.
- Phelps CH. 1975. An ultrastructural study of methionine sulphoximine-induced glycogen accumulation in astrocytes of the mouse cerebral cortex. *J Neurocytol* 4: 479-490.
- Phillips DE. 1992. Effects of alcohol on the development of glial cells and myelin. *Alcohol and neurobiology*. Brain development and hormone regulation. Watson RR, editor. Boca Raton, FL: CRC Press; pp. 83-108.
- Pileblad E, Magnusson T. 1992. Increase in rat brain glutathione following intracerebroventricular administration of gamma-glutamylcysteine. *Biochem. Pharmacol* 44: 895-903.
- Plaitakis A, Berl S, Yahr MD. 1984. Neurological disorders associated with deficiency of glutamate dehydrogenase. *Ann Neurol* 15: 144-153.
- Porter DJ, Bright HJ. 1980. 3-Carbanionic substrate analogues bind very tightly to fumarase and aspartase. *J Biol Chem* 255: 4772-4780.

- Qu H, Faero E, Jorgensen P, Dale O, Gisvold SE, et al. 1999. Decreased glutamate metabolism in cultured astrocytes in the presence of thiopental. *Biochem Pharmacol* 58: 1075-1080.
- Qu H, Syversen T, Aschner M, Sonnewald U. 2003. Effect of methylmercury on glutamate metabolism in cerebellar astrocytes in culture. *Neurochem Int* 43: 411-416.
- Qu H, der van GM, Le MT, Sonnewald U. 2001. The effect of thiopental on glutamate metabolism in mouse cerebellar astrocytes in vitro. *Neurosci Lett* 304: 141-144.
- Reubi J-C, der Berg Van C, Cuénod M. 1978. Glutamine as precursor for the GABA and glutamate transmitter pools. *Neurosci Lett* 10: 171-174.
- Riley EP, Mattson SN, Sowell ER, Jernigan TL, Sobel DF, et al. 1995. Abnormalities in the corpus callosum in children prenatally exposed to alcohol. *Alcohol Clin Exp Res* 19: 1198-1202.
- Sagara JI, Miura K, Bannai S. 1993. Maintenance of neuronal glutathione by glial cells. *J Neurochem* 61: 1672-1676.
- Sanfeliu C, Sebastia J, Cristofol R, Rodriguez-Farre E. 2003. Neurotoxicity of organomercurial compounds. *Neurotox Res* 5: 283-305.
- Sanfeliu C, Sebastia J, Kim SU. 2001. Methylmercury neurotoxicity in cultures of human neurons, astrocytes, neuroblastoma cells. *Neurotoxicology* 22: 317-327.
- Sarafian TA, Bredesen DE, Verity MA. 1996. Cellular resistance to methylmercury. *Neurotoxicology* 17: 27-36.
- Schousboe A, Sarup A, Bak LK, Waagepetersen HS, Larsson OM. 2004. Role of astrocytic transport processes in glutamatergic and GABAergic neurotransmission. *Neurochem Int* 45: 512-527.
- Shank RP, Bennett GS, Freytag SO, Campbell GL. 1985. Pyruvate carboxylase: An astrocyte-specific enzyme implicated in the replenishment of amino acid neurotransmitter pools. *Brain Res* 329: 364-367.
- Shanker G, Allen JW, Mutkus LA, Aschner M. 2001a. The uptake of cysteine in cultured primary astrocytes and neurons. *Brain Res* 902: 156-163.
- Shanker G, Allen JW, Mutkus LA, Aschner M. 2001b. Methylmercury inhibits cysteine uptake in cultured primary astrocytes, but not in neurons. *Brain Res* 914: 159-165.
- Shaw CA, Bains JS, Pasqualotto BA, Curry K. 1999. Methionine sulfoximine shows excitotoxic actions in rat cortical slices. *Can J Physiol Pharmacol* 77: 871-877.
- Simard M, Nedergaard M. 2004. The neurobiology of glia in the context of water and ion homeostasis. *Neuroscience* 129: 877-896.
- Sonnewald U, Schousboe A, Qu H, Waagepetersen HS. 2004. Intracellular metabolic compartmentation assessed by ^{13}C magnetic resonance spectroscopy. *Neurochem Int* 45: 305-310.
- Sonnewald U, Westergaard N, Jones P, Taylor A, Bachelard HS, et al. 1996a. Metabolism of $[\text{U}-^{13}\text{C}_5]$ glutamine in cultured astrocytes studied by NMR spectroscopy: First evidence of astrocytic pyruvate recycling. *J Neurochem* 67: 2566-2572.
- Sonnewald U, White LR, Odegard E, Westergaard N, Bakken JJ, et al. 1996b. MRS study of glutamate metabolism in cultured neurons/glia. *Neurochem Res* 21: 987-993.
- Sonnewald U, Westergaard N, Krane J, Unsgard G, Petersen SB, et al. 1991. First direct demonstration of preferential release of citrate from astrocytes using ^{13}C NMR spectroscopy of cultured neurons and astrocytes. *Neurosci Lett* 128: 235-239.
- Sonnewald U, Westergaard N, Petersen SB, Unsgard G, Schousboe A. 1993a. Metabolism of $[\text{U}-^{13}\text{C}]$ glutamate in astrocytes studied by ^{13}C NMR spectroscopy: Incorporation of more label into lactate than into glutamine demonstrates the importance of the tricarboxylic acid cycle. *J Neurochem* 61: 1179-1182.
- Sonnewald U, Westergaard N, Schousboe A, Svendsen JS, Unsgard G, et al. 1993b. Direct demonstration by ^{13}C NMR spectroscopy that glutamine from astrocytes is a precursor for GABA synthesis in neurons. *Neurochem Int* 22: 19-29.
- Steuerwald U, Weihe P, Jorgensen PJ, Bjerre K, Brock J, et al. 2000. Maternal seafood diet, methylmercury exposure, and neonatal neurologic function. *Pediatrics* 136: 599-605.
- den Berg Van CJ, Garfinkel D. 1971. A stimulation study of brain compartments. Metabolism of glutamate and related substances in mouse brain. *Biochem J* 123: 211-218.
- Ullian EM, Sapperstein SK, Cgristopherson KS, Barres BA. 2001. Control of synapse number by glia. *Science* 291: 657-670.
- Varoqui H, Zhu H, Yao D, Ming H, Erickson JD. 2000. Cloning and functional identification of a neuronal glutamine transporter. *J Biol Chem* 275: 4049-4054.
- Vesce S, Bezzi P, Volterra A. 1999. The highly integrated dialogue between neurons and astrocytes in brain function. *Sci Prog* 82(Pt 3): 251-270.
- Waagepetersen HS, Qu H, Schousboe A, Sonnewald U. 2001. Elucidation of the quantitative significance of pyruvate carboxylation in cultured cerebellar neurons and astrocytes. *J Neurosci Res* 66: 763-770.
- Westergaard N, Drejer J, Schousboe A, Sonnewald U. 1996. Evaluation of the importance of transamination versus deamination in astrocytic metabolism of $[\text{U}-^{13}\text{C}]$ glutamate. *Glia* 17: 160-168.
- Westergaard N, Sonnewald U, Unsgard G, Peng L, Hertz L, et al. 1994. Uptake, release, and metabolism of citrate in neurons and astrocytes in primary cultures. *J Neurochem* 62: 1727-1733.

- Wullner U, Loschmann PA, Schulz JB, Schmid A, Dringen R, et al. 1996. Glutathione depletion potentiates MPTP and MPP⁺ toxicity in nigral dopaminergic neurones. *Neuroreport* 7: 921-923.
- Wullner U, Young AB, Penney JB, Beal MF. 1994. 3-Nitropropionic acid toxicity in the striatum. *J Neurochem* 63: 1772-1781.
- Yu AC, Drejer J, Hertz L, Schousboe A. 1983. Pyruvate carboxylase activity in primary cultures of astrocytes and neurons. *J Neurochem* 41: 1484-1487.
- Yu AC, Schousboe A, Hertz L. 1982. Metabolic fate of ¹⁴C-labeled glutamate in astrocytes in primary cultures. *J Neurochem* 39: 954-960.

Interaction of Mitochondria with Cytosol and Other Organelles

6.1 Mitochondrial/Cytosolic Interactions via Metabolite Shuttles and Transporters

K. F. LaNoue · V. Carson · D. A. Berkich · S. M. Hutson

1	Introduction	590
2	Metabolite Shuttles Between and Within Cells in the Brain	591
2.1	The Glutamate/Glutamine Cycle	591
2.2	The Pyruvate/Glutamate Cycle	593
2.3	The Astrocyte/Neuron Lactate Shuttle	596
2.4	The Malate/Aspartate Shuttle	598
2.4.1	Transport of Reducing Equivalents from the Cytosol into Mitochondria	598
2.4.2	NADH and FADH ₂ Fluorescent Images and Signals from Brain Slices and Cerebellar Cortex In Vivo	599
2.5	The GABA Shunt: γ -Aminobutyrate Metabolism in the Brain	601
2.5.1	GABA: Neurotransmission	601
2.5.2	GABA Catabolism	602
3	The Role of Mitochondrial Transporters in the Brain	605
3.1	The Glutamate/Glutamine Cycle	606
3.2	The Pyruvate/Glutamate Cycle	606
3.3	The Lactate Shuttle and the Role of the Malate/Aspartate Shuttle	607
3.3.1	The Aspartate/Glutamate Carrier and the Lactate Shuttle Hypothesis	607
3.3.2	Glial Catabolism of Aspartate and the Malate/ α -Ketoglutarate Mitochondrial Exchanger (the Oxoglutarate Carrier)	609
3.4	The GABA Shunt in Astrocytes	609
4	Conclusions and Summary	611

Abstract: This chapter concerns the metabolism of glutamate, aspartate, and γ -aminobutyric acid (GABA) in the central nervous system. There appears to be a striking interplay between the metabolism of these neurotransmitters and the levels available for neurotransmission. The interplay is mediated by various inter- and intracellular metabolic cyclic shuttle systems that actively transport the transmitters into astrocytes after their release to the synaptic space and then catalyze the return of derivatives of these compounds to the neurons for transmitter regeneration.

The intercellular shuttle systems considered are the glutamate/glutamine cycle, the aspartate/glutamine cycle, the GABA/glutamine cycle, and the astrocyte/neuron lactate shuttle. Shuttle systems that operate intracellularly, within astrocytes, are also considered. These intracellular shuttles include one that converts glutamate to lactate and then via a different pathway, lactate back to glutamate. Lastly, we consider the well-known malate/aspartate cycle that acts within cells to transport reducing equivalents generated in the cytosol from the cytosol to the mitochondria. We postulate that differences in the activity of this cycle in different cell types influence metabolic traffic flow. The specific expression of the cycle within the brain, the physiological advantages of spatial specificity, and the molecular basis for the specificity are considered and discussed.

List of Abbreviations: ADP, adenosine diphosphate; AGC, aspartate/glutamate carrier; ATP, adenosine triphosphate; BCAA, branched-chain amino acid; BCAT, branched-chain aminotransferase; BCKA, branched-chain keto acid; CNQX, 6-cyano-7-nitroquinoxaline-2,3-dione, AMPA receptor antagonist; ECF, extracellular fluid; FADH, flavin adenine dinucleotide, reduced; FP, flavoproteins; GABA-T, GABA aminotransferase; GABA, gamma-aminobutyric acid; GAD, glutamate decarboxylase; GAT, GABA transporter proteins; GC1 and GC2, glutamate hydroxyl ion exchange carriers; GFAP, glial fibrillary acidic protein; GLT1, sodium linked glutamate transporter; GLUT, glucose transporters; MC, mitochondrial carriers; MDH, malate dehydrogenase; ME, malic enzyme; NADH, nicotinamide adenine dinucleotide, reduced; NADP, nicotinamide adenine dinucleotide phosphate; NADPH, nicotinamide adenine dinucleotide phosphate, reduced; NMR, nuclear magnetic resonance; OGC, oxoglutarate carrier; PC, pyruvate carboxylase; PEP, phosphoenolpyruvate; PEPCK, phosphoenolpyruvate carboxykinase; PET, positron emission tomography; RNA, ribonucleic acid; SAT1 and SAT2, glutamine transporters; SN1, glial sodium linked glutamine transporter; SSADH, succinate semialdehyde dehydrogenase; TCA, tricarboxylic acid; $\Delta\mu\text{H}^+$, electrochemical proton gradient

1 Introduction

Proteins that catalyze mitochondrial/cytosolic interactions in the brain not only provide ATP for maintenance of membrane Na^+ , K^+ , and H^+ gradients, but these proteins also support the brain's specific mission, i.e., neurotransmission. Moreover, new data about cell-specific expression of proteins that support mitochondrial/cytosolic interactions in the brain have provided insight into recent controversies about synthesis and disposal of specific neurotransmitters (del Arco et al., 2002; Ramos et al., 2003; Palmieri, 2004; Dolce et al., 2005; Molinari et al., 2005).

Many mitochondrial/cytosolic interactions are catalyzed by a single large family of proteins, mitochondrial carriers (MC), embedded in the inner membrane of the mitochondria. So far, 30 human mitochondrial carrier proteins have been identified, isolated, sequenced, cloned, and overexpressed (Agrimi et al., 2004; Fiermonte et al., 2004; Palmieri, 2004; Dolce et al., 2005). They belong to a single family of genes (SLC30) with similar structures. Their polypeptide chains consist of three tandem repeats of about 100 amino acids. Each repeat has a similar sequence. All family members that have been studied appear to function as homodimers, however some carriers, although identified using functional studies with isolated mitochondria, have not yet been molecularly characterized. Carrier proteins responsible for some essential mitochondrial transport activities, such as pyruvate transport, branched-chain α -keto acid (BCKA) transport, and glutamine transport are still not identified. An excellent review provides more details about these transporters, their structure/function relationships, and their physiology (Palmieri, 2004).

Transporters that support mitochondrial/cytosolic interactions are cell-type specific, and it appears that the expression of the mitochondrial transporters is determined by tissue function (LaNoue and Schoolwerth, 1979, 1984). The transporter for citrulline and ornithine, which is required for urea synthesis,

is expressed predominantly in liver mitochondria (McGivan et al., 1977; Indiveri et al., 1994; Fiermonte et al., 2003), while the ATP/ADP exchange transporter is almost ubiquitous (Graham et al., 1997; Fiore et al., 1998; Dolce et al., 2005). There are four ATP/ADP exchange transporter isoforms (Dolce et al., 2005) and expression of different isoforms is organ specific (Fiore et al., 1998).

Most of the common transporters are expressed in brain mitochondria and these include those for the amino acids that also serve as neurotransmitters. Examples are aspartate, glutamate, and γ -aminobutyric acid (GABA). A recent popular textbook of neuroscience (Deutch and Roth, 1999) states: "A key difference between the catecholamine transmitters and the amino acid transmitters is that the latter are derived from intermediary glucose metabolism. This dual role for the amino acid transmitters means there must be mechanisms to segregate the transmitter and general metabolic pools of the amino acid transmitters." In truth it appears there is little true segregation, but instead the mitochondrial carriers act as traffic directors. The traffic in many cases forms cyclic shuttles between cell types and within cells. The shuttles are needed to maintain brain neurotransmitter and energy homeostasis. The mitochondrial carriers provide the roads and bridges on which shuttle traffic flows. The metabolic shuttles are defined in the first part of the chapter and in the second we describe the mitochondrial carriers that characterize these shuttle pathways.

2 Metabolite Shuttles Between and Within Cells in the Brain

The cells of the brain most actively involved in glutamatergic and GABAergic neurotransmission are the pre- and postsynaptic glutamatergic and GABAergic neurons. Presynaptic neurons are defined as those that release neurotransmitter and postsynaptic neurons are those that have receptors that sense the presence of neurotransmitters released into synaptic clefts. Presynaptic neurons can be specifically glutamatergic or GABAergic. Interneurons are frequently GABAergic. Postsynaptic neurons can have one or more types of glutamatergic receptors, as well as GABAergic receptors within the same neuron but in separate synapses.

Our laboratories have studied metabolism in the central nervous system using rat brain cells in culture (Gamberino et al., 1997; Hutson et al., 1998), adult rats in vivo (Oz et al., 2004; Xu et al., 2004), and rat retinas ex vivo (Lieth et al., 2000, 2001; LaNoue et al., 2001). The retina is a useful model for many metabolic studies, because it is an easily accessible part of the brain amenable to investigation and has high glutamatergic activity. The photoreceptor cells of the retina release glutamate from synaptic vesicles. Subsequent layers of neurons are largely glutamatergic or GABAergic. Some astrocytes of the retina are called Müller cells and stretch radially through the retina. The metabolism, cell/cell interactions, and mitochondrial/cytosolic interactions are very similar in the retina and in the brain. Our recent studies have directly compared glutamate metabolism in the retina with that in the whole brain. Ratios of glutamate neurotransmission to de novo synthesis of glutamate and to glutamate oxidative disposal were found to be remarkably similar between whole in vivo brain and ex vivo retina (Lieth et al., 2001; Oz et al., 2004; Xu et al., 2004).

2.1 The Glutamate/Glutamine Cycle

The glutamate/glutamine cycle encompasses the release of glutamate from the presynaptic neuron and its metabolic fate after release into the synapse and binding to the postsynaptic neuron. Glutamate can be neurotoxic if allowed to stay in the inter membrane space, and this section explains how glutamate is detoxified by uptake into brain astrocytes. Astrocytes are not neurons but act as neuron-supporting cells and have processes that extend into the synaptic space. Astrocytes take up glutamate from the synaptic space to stop neurotransmission and then convert it to glutamine that acts as a precursor for the restoration of neuronal glutamate.

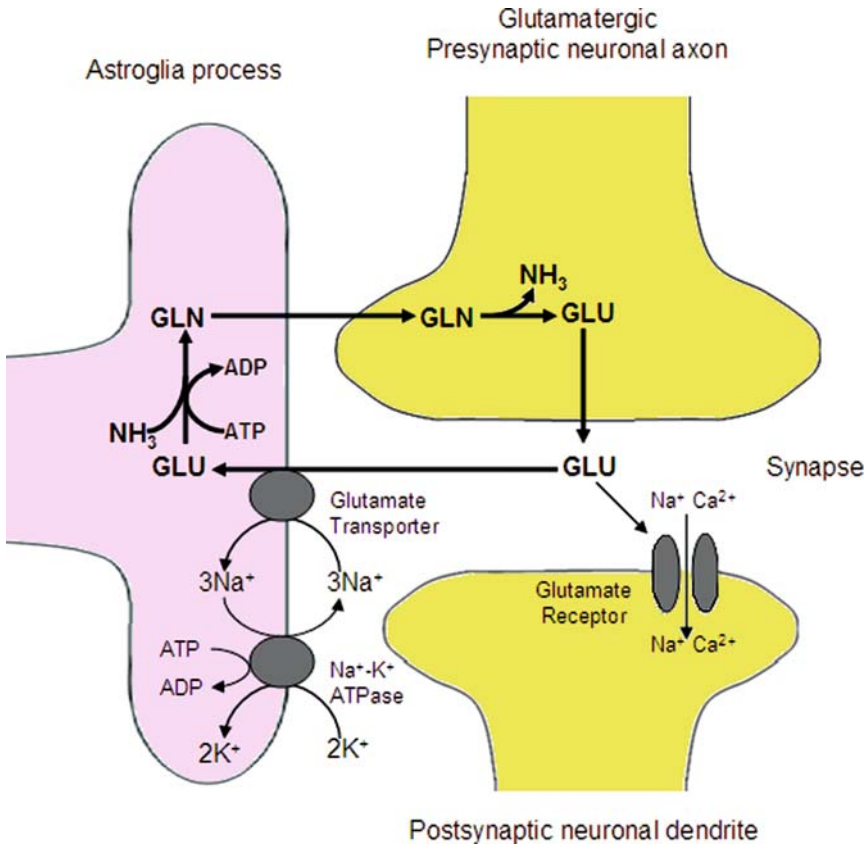
Evidence for the glutamate/glutamine cycle was first obtained over 30 years ago. Berl and his coworkers (Waelsch et al., 1964; Berl et al., 1968) observed that when ^{14}C -acetate or $^{14}\text{CO}_2$ were infused into the brain of rats, and glutamate and glutamine were subsequently isolated, the glutamine had a much higher ^{14}C -specific activity than glutamate. This was puzzling in view of the known substrate/product ratio of glutamate and glutamine but Berl et al. (Waelsch et al., 1964; Berl et al., 1968) explained this on the supposition that glutamate is synthesized from acetate or $^{14}\text{CO}_2$ in one particular cell type which maintains a very small glutamate pool. This pool provides substrate for the synthesis of glutamine, which is then

forwarded to a second cell where glutamine is converted to glutamate. They proposed that the second cell contains a large pool of glutamate, thus diluting the ^{14}C .

Later studies (Minchin and Beart, 1975; Martinez-Hernandez et al., 1977; Norenberg, 1979) demonstrated that while astrocytes are the site of glutamine synthesis, glutamatergic neurons are the cells with the large glutamate pool that is derived from glutamine. Then it became clear that a glutamate/glutamine cycle existed between the two cell types (Figure 6.1-1). The cycle was completed as the synaptic glutamate synthesized from glutamine was released as neurotransmitter and was taken up into the astrocytes by a high-affinity Na^+ -linked glutamate transporter in the astrocytic cell membrane (Rothstein et al., 1994; Sonnewald et al., 2002).

■ **Figure 6.1-1**

The glutamate/glutamine cycle. Presynaptic and postsynaptic neurons are shown *light gray*, astroglia *dark gray*, and membrane proteins *black*. The scheme is designed to illustrate means by which the glutamatergic synaptic cleft is rapidly cleared of glutamate to prevent glutamatergic neurotoxicity and at the same time maintain presynaptic glutamate homeostasis. GLN = glutamine; GLU = glutamate



This scheme coincides with the textbook suggestion (Deutch and Roth, 1999) that neurotransmission is segregated from metabolism. However, it does not explain 40-year old data showing that if one infuses $\text{H}^{14}\text{CO}_3^-$ into the brain (Waelsch et al., 1964; Berl et al., 1968), the brain glutamine subsequently isolated has a much higher specific activity than brain glutamate. Recent publications confirm these results (Xu et al., 2004) and show that glutamate carbon can enter the glutamate/glutamine cycle from the glia, synthesized anaplerotically from CO_2 and pyruvate. Metabolism is not segregated from neurotransmission, but metabolites are carefully channeled from metabolic pools to a pool packaged in synaptic vesicles. In

contrast when [$1\text{-}^{13}\text{C}$]glucose is infused, the ^{13}C enrichment of glutamine and glutamate are the same (Sibson et al., 1997, 1998), and unlabeled glucose in the infusate does not dilute the carbon 14 label in glutamine (Oz et al., 2004; Xu et al., 2004). This suggests that glucose labeling of tricarboxylic acid (TCA) cycle intermediates in the glia is limited.

2.2 The Pyruvate/Glutamate Cycle

This section of the chapter provides an outline of an alternate metabolic route branching from the glutamate/glutamine cycle after glutamate enters the astrocyte. The astrocytic glutamate is not committed to amidation and direct return to the presynaptic neuron as implied in [Figure 6.1-1](#) but instead can enter the citric acid cycle to be oxidized. We emphasize here the regulatory role that the astrocytic conversion of glutamate to pyruvate may have in maintaining homeostasis of neuronal glutamate.

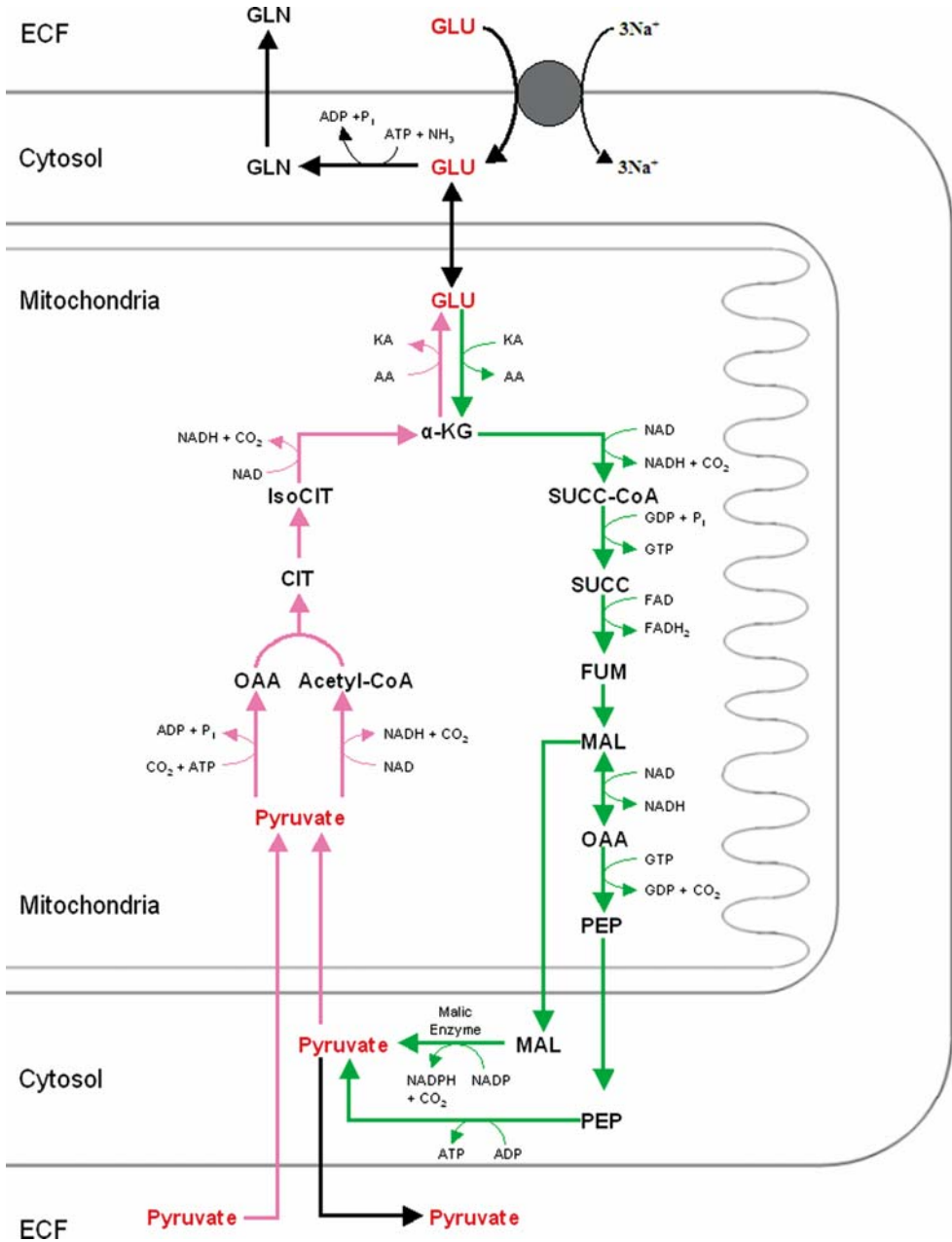
Studies of the fate of labeled glutamate incubated with cultured astrocytes (Sonnewald et al., 1993; Hassel and Sonnewald, 1995; Gamberino et al., 1997; Hutson et al., 1998) led to the suggestion that another cycle operates within the astrocytes and perhaps between astrocytes and neurons which we have called the pyruvate/glutamate cycle (Lieth et al., 2001; Xu et al., 2004) (see [Figure 6.1-2](#)). Key enzymes of the cycle, malic enzyme (ME), phosphoenolpyruvate carboxykinase (PEPCK), and pyruvate carboxylase (PC), have been identified in retinas (Lieth et al., 2001), in cultured astrocytes (Schmoll et al., 1995; Bakken et al., 1997; Cruz et al., 1998; Vogel et al., 1998; McKenna et al., 2000), in brain extracts (Sharma and Patnaik, 1983; Patel, 1989), and in adult brains (Vogel et al., 1998). As shown in [Figure 6.1-2](#), when the glutamate enters the glia, after its release as neurotransmitter, it can be amidated to glutamine or it can be transaminated to α -ketoglutarate, passing the amino group to a BCKA or to pyruvate. Proceeding around the citric acid cycle, α -ketoglutarate is converted to malate. The malate can go around the citric acid cycle again if excess pyruvate or acetyl-CoA is available. Alternatively, malate can be decarboxylated to pyruvate. Decarboxylation is achieved by cytosolic or mitochondrial ME or by PEPCK. ME decarboxylates malate directly using NADP to accept electrons, and forms CO_2 and pyruvate. Also, oxaloacetate formed from malate can be decarboxylated and phosphorylated by the mitochondrial isoform of PEPCK to form PEP, which is converted to pyruvate by cytosolic pyruvate kinase. Both lead to the generation of extra pyruvate and loss of a TCA cycle intermediate. This is the downward (dark gray arrows) arm of the cycle illustrated in [Figure 6.1-2](#).

Early data in support of this downward arm was gathered using cultured neonatal astrocytes. The data demonstrated the conversion of ^{13}C - or ^{14}C -glutamate to ^{13}C - (Sonnewald et al., 1993; Hassel and Sonnewald, 1995) or ^{14}C -lactate (Gamberino et al., 1997; Hutson et al., 1998). Firm data demonstrating that this downward arm of the cycle operates in intact neuronal tissue was generated recently using isolated excised retinas (Lieth et al., 2001). When incubated with $\text{H}^{14}\text{CO}_3^-$, large amounts of ^{14}C -lactate are produced in the ex vivo retina. This labeling of lactate by $^{14}\text{CO}_2$ had to have occurred in the same cell (the glial Müller cell) that expresses both PC and ME (or PEPCK). The reasoning is as follows: When $^{14}\text{CO}_2$ is condensed with pyruvate to form ^{14}C -oxaloacetate via PC, only the carboxyl group next to the keto group of α -ketoglutarate and the amidated carbon group next to the carboxyl group of glutamate are labeled. Both these labeled carbons are converted to $^{14}\text{CO}_2$ by isocitrate dehydrogenase and α -ketoglutarate

■ Figure 6.1-2

The pyruvate/glutamate cycle of the astrocyte. The scheme illustrates how some glutamate after entering the astrocyte (instead of being amidated to glutamine) can be converted to pyruvate. This pathway (shown in *dark gray arrows*) includes some citric acid cycle intermediates and a decarboxylating enzyme, either malic enzyme (ME1 or 2) or mitochondrial phosphoenolpyruvate carboxykinase (PEPCKm). It produces one pyruvate per glutamate. In order to maintain homeostasis of citric acid cycle intermediates and glutamate there is a pathway for de novo synthesis of glutamate. This pathway (shown in *light gray arrows*) requires two molecules of pyruvate (one more than is produced) in the downward (*dark gray arrows*) arm of the cycle. The extra pyruvate may be provided by neuronal metabolism of glutamate and lactate (see text). GLN, glutamine; GLU, glutamate; α -KG, α -ketoglutarate; SUCC-CoA, succinyl CoA; SUCC, succinate; FUM, fumarate; MAL, malic acid; OAA, oxaloacetate; PEP, phosphoenolpyruvate; CIT, citrate; IsoCIT, isocitrate

Figure 6.1-2 (continued)



dehydrogenase. The succinate formed is unlabeled. The Müller cells in the retina and the astrocytes in the brain are the major sites of PC expression. Therefore, the ^{14}C -labeled oxaloacetate can easily reach malate in the Müller cells by equilibration via malate dehydrogenase (MDH), but it would be difficult to label malate with $^{14}CO_2$ in the neurons that express very little if any PC. When $[1-^{14}C]\alpha$ -ketoglutarate and $[1-^{14}C]$ glutamate from the glia enter the neurons as glutamine, their oxidation in the citric acid cycle removes the label. Therefore, when ^{14}C from $^{14}CO_2$ was observed to produce large amounts of ^{14}C -lactate in the intact ex vivo

retina, we were able to conclude that the ^{14}C -lactate is generated in the Müller cells and not in the neurons, and that decarboxylation of malate via ME or PEPCK forms the ^{14}C -labeled lactate/pyruvate in the glia.

Flux through the pyruvate/glutamate cycle, initially called pyruvate/pyruvate cycling, was also measured in intact brains using ^{13}C -NMR spectroscopy, but the cellular location of the pathway is still contested (Cruz and Cerdan, 1999). One study suggested that pyruvate cycling was a neuronal phenomenon (Hassel and Brathe, 2000). The NADP^+ -dependent cytosolic (ME1) and mitochondrial (ME2) isozymes are both expressed in brain (Vogel et al., 1998). The neuronal vs. glial expression of these isozymes has not been determined. Kinetic properties of both indicate that they catalyze carboxylation of malate to pyruvate. Thus, the downward arm of the cycle has been demonstrated in glia and may also occur in neurons. However, the downward arm of the cycle may not depend solely on NADP -dependent ME but may instead be catalyzed by the mitochondrial isoform of PEPCK which decarboxylates oxaloacetate to form phosphoenolpyruvate and CO_2 . Abundant expression of this mitochondrial enzyme in the adult brain has been reported (Sharma and Patnaik, 1983; Patel, 1989). The relative importance of the two isoforms of ME and of PEPCK has not been resolved and may only be resolved by disrupting the respective genes or infusing specific siRNAs onto the brain ventricles.

If the cycle only operates in the direction of glutamate to pyruvate, the loss of citric acid cycle intermediates by decarboxylation would not be sustainable (i.e., the TCA cycle would shut down). As shown in [Figure 6.1-2](#), de novo synthesis (anaplerosis), catalyzed by PC, provides the needed homeostasis of citric acid cycle intermediates, and thereby the upward arm of the cycle. Separate control of the two arms of the cycle can raise or lower citric acid cycle intermediate pool sizes and regulate glutamate levels.

Another controversial issue has been the magnitude and relative importance of the anaplerotic synthesis of glutamate from CO_2 and pyruvate (the upward arm of the pyruvate/glutamate cycle) (Shank et al., 1993; Lapidot and Gopher, 1997; Sibson et al., 1997, 1998, 2001; Henry et al., 2002). Because PC is localized in glia, a complete cycle occurs in astrocytes.

Measurements of anaplerotic fluxes from pyruvate and CO_2 to glutamine have been estimated by infusing $[1-^{13}\text{C}]$ glucose in vivo into rat or human brains and by following the time course of product formation. Values for anaplerosis that depended on model assumptions varied widely from 1 to 35% of total glutamine synthesis (Shank et al., 1993; Lapidot and Gopher, 1997; Sibson et al., 1997, 1998, 2001; Gruetter et al., 2001; Henry et al., 2002). Other studies assessed glial anaplerosis by using the glial-specific tracer, ^{13}C -acetate (Bluml et al., 2002; Lebon et al., 2002). Because acetate actively labels the glial citric acid cycle, but is not metabolized in neurons it can be used to obtain an upper limit for glial anaplerosis. An estimated upper limit for glial synthesis of glutamate in the human brain was 30% (Bluml et al., 2002; Lebon et al., 2002) of the rate of neurotransmission (glutamine synthesis).

As conclusions drawn using ^{13}C -NMR techniques were model dependent, our laboratory initiated studies of de novo glutamate synthesis with ex vivo retinas using $\text{H}^{14}\text{CO}_3^-$ as substrate for anaplerosis (Lieth et al., 2000, 2001). By incubating the retinas with $\text{H}^{14}\text{CO}_3^-$ and pyruvate, it was possible to evaluate anaplerotic synthesis directly by the rate of incorporation of ^{14}C from CO_2 into glutamate as well as to calculate the rate of the glutamate/glutamine cycle. De novo synthesis accounted for the full 30% of the total synthesis of glutamine. Subsequent studies using a similar approach were carried out in collaboration with the Gruetter group in Minneapolis in which we perfused awake rats with a combination of $\text{H}^{14}\text{CO}_3^-$ and $[1-^{13}\text{C}]$ glucose infused together at a constant rate (Oz et al., 2004; Xu et al., 2004). Two different methods were then used to calculate de novo synthesis of glutamate, one in which anaplerosis was measured directly by the incorporation of ^{14}C from $\text{H}^{14}\text{CO}_3^-$ into whole brain glutamate and the other in which anaplerosis was calculated more indirectly from the distribution of ^{13}C -products of $[1-^{13}\text{C}]$ glucose. The two methods agreed and the results also indicated that the rate of anaplerosis increases with increased neurotransmission (Oz et al., 2004) and that it is glial in origin. The rate of de novo synthesis of glutamate was estimated to be at the high end of previous estimates or about 30% of the rate of neurotransmission.

Important questions remain however about the control of flux in the two halves of the cycle and the physiological role of the cycle. The high ratio of anaplerotic flux flowing through the pyruvate/glutamate cycle is difficult to comprehend in the absence of an appreciation for the other half of the pyruvate/glutamate cycle i.e., the conversion of the glutamate to pyruvate after glutamate is released into the synaptic space by neurons. Early studies (Shank et al., 1993) assumed that anaplerosis was a means to replenish the glutamate carbon skeleton lost by efflux of glutamine from the brain. However, loss of glutamate via glutamine efflux to the


circulation is slow compared with the rates of anaplerosis. Thus, these high anaplerotic rates imply active TCA cycle decarboxylation to form pyruvate, i.e., they are the other half of the proposed pyruvate/glutamate cycle. The cycle occurs primarily in astrocytes where it is tied to the glutamate/glutamine cycle.

Finally, the “forward” anaplerotic half of the pyruvate/glutamate cycle requires a source of nitrogen for the conversion of α -ketoglutarate to glutamate within the brain astrocytes. The astrocyte-specific mitochondrial isoform of branched-chain aminotransferase catalyzes a large fraction of the nitrogen transfer (Hutson, 1988; Sweatt et al., 2004). Studies using ^{15}N have shown that nitrogen is efficiently transferred from branched-chain amino acids (BCAA) to glutamate and to the α -amino group of glutamine in subcellular brain fractions, primary cell cultures in vitro, and in vivo animal models (Yudkoff et al., 1983; Matsuo et al., 1993; Kanamori et al., 1998; Sakai et al., 2004). In vivo incorporation of ^{15}N from leucine into glutamate, glutamine, and GABA has been reported in mice (Matsuo et al., 1993), and Kanamori et al. (1998) estimated that leucine provides $\sim 25\%$ of glutamate nitrogen in rat brains. During 9 h of continuous intragastric feeding in rats, Sakai et al. (2004) estimated that at least 50% of brain glutamate α -amino nitrogen was derived from leucine. As very little of the glutamate α -amino nitrogen is derived from NH_3 , it seems that glutamate dehydrogenase is not the source of the nitrogen.

There are two isoforms of the branched-chain aminotransferase enzyme (BCAT) in mammals. One form, BCATm (the mitochondrial isoform), is expressed ubiquitously in mitochondria throughout the body whereas the other, BCATc, is expressed mainly in the cytosol of the central nervous system (Hutson et al., 2005). In brain, BCATm is expressed in astrocytes, whereas the BCATc isozyme is found in neurons (Hutson et al., 2001; Sweatt et al., 2004). BCATc accounts for 60–70% of total brain BCAT activity (Goto et al., 1977; Ichihara, 1985; Hall et al., 1993; Yudkoff et al., 1996). In the rat nervous system, BCATc is expressed in selected populations of glutamatergic and GABAergic neurons (Goto et al., 1977; Sweatt et al., 2004). Our group has proposed a role for BCAAs in the direct regulation of de novo synthesis of glutamate (Jouvet et al., 2000; Hutson et al., 2001, 2005; Lieth et al., 2001). The BCAT nitrogen shuttle in which glial BCATm produces glutamate for glutamine synthesis and in which BCATc in the neurons replenishes the BCAA pool for use in the glia is part of the pyruvate/glutamate cycle and is required as a means to regulate the size of the glutamate neurotransmitter pool. It was demonstrated that the availability of BCAA and the activity of BCATs may regulate glutamate levels using isolated excised retinas (Lieth et al., 2001).

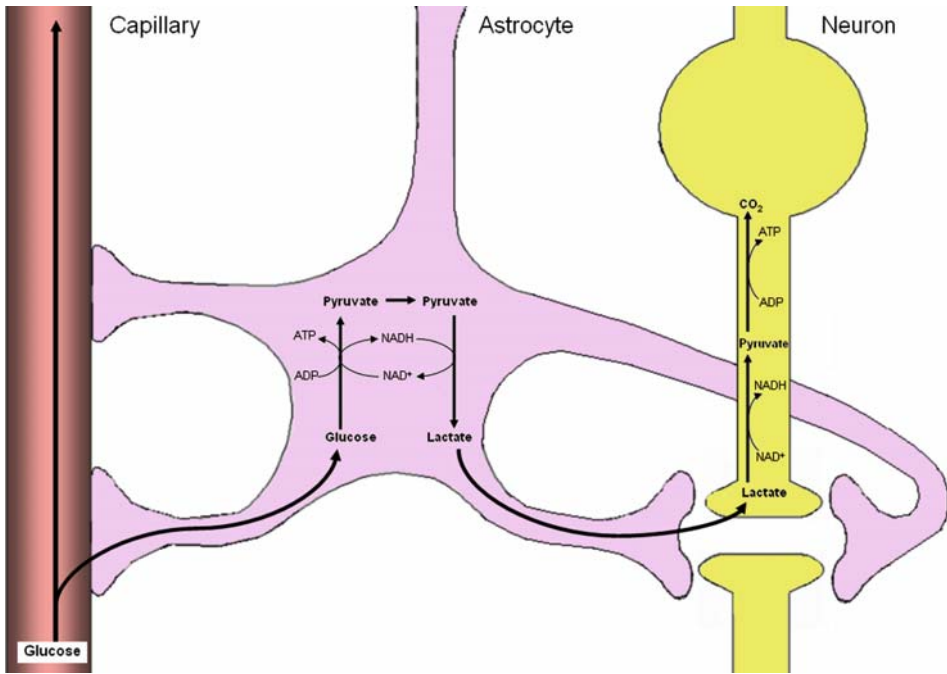
2.3 The Astrocyte/Neuron Lactate Shuttle

An astrocyte/neuron lactate shuttle has been proposed recently and has generated much controversy. The shuttle hypothesis proposes that there is little glucose oxidation in astrocytes, but that the astrocytes act as a gateway for glucose entering the brain from the vasculature. Astrocytes convert the glucose glycolytically to lactate without oxidizing it to CO_2 and H_2O and then release lactate for use by the neurons. In the hands of some investigators (Pellerin and Magistretti, 1994; Magistretti and Pellerin, 1999) but not others (Walz and Mukerji, 1988; Dienel and Hertz, 2001), this hypothesis is supported (or not) by data using cultured astrocytes. This section describes the controversy as well as data for and against the hypothesis.

When increases in glucose consumption due to increases in neuronal transmission were measured by positron emission tomography (PET) or by arteriovenous $p\text{O}_2$ differences in order to estimate rates of oxygen consumption (Mangia et al., 2003; Dienel and Cruz, 2004), much larger percent changes in glucose disappearance than in O_2 consumption have been observed in some areas of the brain such as the visual cortex (Fox et al., 1988; Ribeiro et al., 1993) and the retina (Wang et al., 1997). To understand this phenomenon, Magistretti and coworkers (Magistretti and Pellerin, 1999; Magistretti et al., 1999) measured glucose uptake in cultured astrocytes as a function of Na^+ -linked glutamate uptake (Pellerin and Magistretti, 1994; Pellerin et al., 1998). Glucose conversion to lactate increased when cultured astrocytes were exposed to glutamate. Glutamate requires Na^+ cotransport, which consumes energy and lowers ATP and should therefore stimulate O_2 consumption. Nevertheless, these workers observed that glutamate uptake stimulated glucose uptake but not oxidation. Magistretti and Pellerin (Pellerin and Magistretti, 1994; Magistretti and Pellerin, 1999) have proposed an astrocytic/neuronal lactate shuttle, illustrated in  [Figure 6.1-3](#). This shuttle could under some circumstances result in measurements of higher rates of glycolysis than glucose oxidation.

■ Figure 6.1-3

The lactate shuttle hypothesis. The hypothetical lactate shuttle illustrates a proposed pathway for glucose in astrocytes. Astrocytic processes (gray) surround blood vessels (left) in the brain and provide a partial barrier for direct access of glucose to the neurons (light gray). Glycolysis of glucose produces NADH in the cytosol at the glyceraldehyde dehydrogenase step. This NADH cannot be converted back to NAD directly by mitochondria because NAD^+ and NADH are impermeable to the mitochondria. No shuttle system for getting NADH electrons into mitochondria has been demonstrated in astrocytes, although one is present in neurons. As shown, regeneration of NAD^+ in the astrocytes can be accomplished therefore, by comparison of pyruvate to lactate and export of lactate from astrocytes to the neurons (light gray)



This scheme has not been universally accepted. Many of the criticisms concern the emphasis of the original authors (Magistretti, Pellerin, and coworkers) on the presumed preference of neurons for lactate over glucose. This preference cannot be demonstrated in neurons (Walz and Mukerji, 1988; Dienel and Hertz, 2001). Also, it is clear that neurons *in situ* have abundant low K_m glucose transporters (GLUT3) and active glycolytic enzymes (Walz and Mukerji, 1988; Maher et al., 1994; Dienel and Hertz, 2001). Moreover, astrocytes have abundant amounts of mitochondria and there seems no reason that these mitochondria do not oxidize lactate. Moreover, depending on the particular preparation of cultured astrocytes, glutamate sometimes does not stimulate glycolysis but instead increases O_2 consumption (Gramsbergen et al., 2003; Liao and Chen, 2003). For example, Eriksson et al. (1995) reported increased respiration in astrocytes in response to glutamate. Both cultured astrocytes and neurons produce and use lactate *in vitro* (Lopes-Cardozo et al., 1986; Walz and Mukerji, 1988; Medina et al., 1999; Dienel and Hertz, 2001). Moreover, it seems unlikely that the greater capacity for oxidation of lactate by neurons compared to astrocytes is due to kinetic parameters of different isoforms of lactate dehydrogenase. The difficulty in oxidizing lactate may be the result of impaired ability of astrocytes *in vivo* to transport reducing equivalents generated by the glycolytic pathway into astrocyte mitochondria. The difficulty in transporting reducing equivalents from the cytosol into the mitochondria derives from the finding that NADH is impermeable to the mammalian mitochondrial inner membrane. Specific metabolite shuttles are required for the transfer of NADH reducing equivalents into mitochondria. Perhaps, preparations of cultured astrocytes express various amounts of the enzymes and transport proteins of these shuttles while *in vivo* astrocytes produce less.

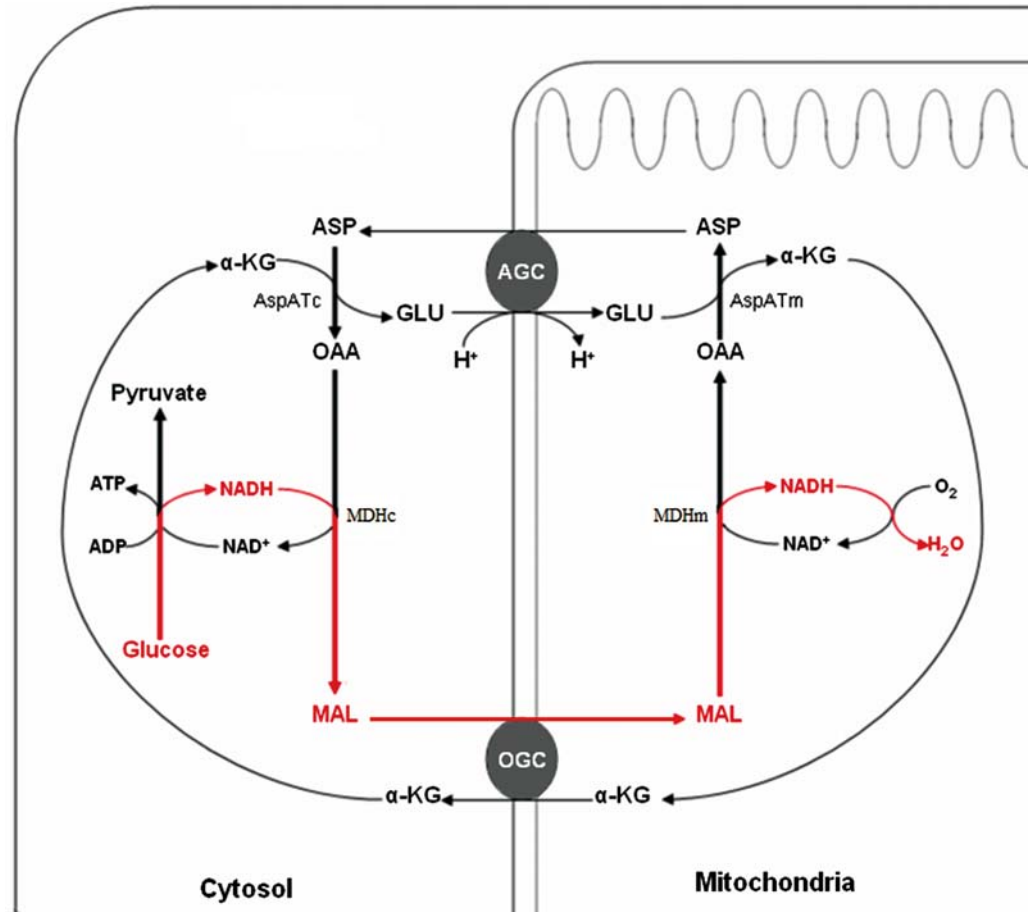
2.4 The Malate/Aspartate Shuttle

2.4.1 Transport of Reducing Equivalents from the Cytosol into Mitochondria

The malate/aspartate cycle is a metabolite shuttle present in most cells. It transports the reducing equivalents produced by glycolysis and alcohol or sorbitol oxidation into mitochondria for oxidation. As NADH and NAD⁺ are impermeable to the mitochondrial membrane, the reducing equivalents (electrons) have to get into the mitochondria carried by permeable metabolites that can be oxidized inside the mitochondria and the products carried out. [▶ Figure 6.1-4](#) illustrates the shuttle. Low malate/aspartate cycle activity in astrocytes would produce the controversial data, and thus leading to the lactate shuttle

■ Figure 6.1-4

The malate/aspartate shuttle. The scheme shown traces the path used in many cell types in order to transport reducing equivalents generated in the cytosol into the mitochondria for use by the mitochondrial electron transfer chain. A shuttle system is required since NADH is impermeable to the mitochondrial membrane. The gray arrows show the path taken by electrons into the mitochondria. MDHc, cytosolic malate dehydrogenase; MDHm, mitochondrial malate dehydrogenase; AspATc, cytosolic aspartate aminotransferase; AspATm, mitochondrial aspartate aminotransferase; ASP, aspartate; GLU, glutamate; α -KG, α -ketoglutarate; OAA, oxaloacetate; AGC, aspartate/glutamate carrier; OGC, α -ketoglutarate (oxoglutarate) carrier; MAL, malate



hypothesis. Recent data tracing localized changes in NADH and FADH₂ in brain slices and whole brain that accompany increases in neurotransmission address this issue. They support the concept that local controls of reducing equivalent transport is an important part of brain function.

For glucose to be oxidized, the reducing equivalents generated by glycolysis at the glyceraldehyde-3-phosphate dehydrogenase step (formation of NADH) must be transferred from the cytosol to the mitochondria by the malate/aspartate shuttle. Cytosolic NADH cannot be transported directly into the mitochondria because the inner mitochondrial membrane is impermeable to NADH (Purvis and Lowenstein, 1961) and because the NADH/NAD⁺ ratio is approximately 100-fold higher in the mitochondrial matrix than in the cytosol (Williamson et al., 1967).

As shown in [Figure 6.1-4](#), cytosolic NADH is oxidized to NAD⁺ in the cytosol in a reaction catalyzed by cytosolic MDHc (Castiglione-Morelli et al., 2004). Malate is then transported into the mitochondria in exchange for α -ketoglutarate by the α -ketoglutarate/malate exchange carrier (LaNoue and Schoolwerth, 1979; Runswick et al., 1990; Morozzo della Rocca et al., 2003; Castiglione-Morelli et al., 2004). The α -ketoglutarate is transaminated by mitochondrial aspartate aminotransferase to form glutamate and oxaloacetate. The oxaloacetate is now in a position to oxidize another molecule of NADH, and the glutamate is transported into mitochondria in exchange for aspartate on the aspartate/glutamate carrier (AGC) (Palmieri et al., 2001; Morozzo della Rocca et al., 2003). Gray arrows in [Figure 6.1-4](#) trace the path of the electrons from cytosolic NADH to O₂.

As the malate/aspartate cycle is necessary for the oxidation of cytosolic NADH, its activity in cells influences levels of NADH that accumulate in the presence of glucose. When glycolysis increases, activity of the shuttle becomes rate limiting. In the perfused heart, as workload increases in the presence of glucose, NADH/NAD⁺ ratios increase (Kobayashi and Neely, 1979) even though O₂ supply is adequate, suggesting that transport of reducing equivalents across the mitochondrial membrane becomes limiting for glucose and lactate oxidation. Similarly, transaminase inhibitors that block aspartate aminotransferase isozymes stop oxidation of lactate but allow pyruvate oxidation in liver (Rognstad, 1980), heart (Williamson et al., 1973), and brain (Cheeseman and Clark, 1988). As NADH increases, NAD⁺ decreases. The lactate/pyruvate ratio is in thermodynamic equilibrium (via lactate dehydrogenase) with the NADH/NAD⁺ ratio. This increases the ratio of lactate to pyruvate, and lactate efflux from astrocytes increases. Therefore, the lactate shuttle hypothesis proposed by Magistretti and coworkers could be the result of an impaired malate/aspartate shuttle in astrocytes. If so, the ratio of NADH/NAD⁺ in the astrocyte cytosol should increase with increases in neuronal activity. Neuronal mitochondrial NADH and reduced flavoprotein may decrease in response to increased respiration. As NADH and oxidized flavoproteins (FPs) emit robust fluorescent signals, these mitochondrial chromophores can and have been used to monitor energy metabolism. Recent studies of NADH and FP fluorescent signals in brain slices (Kasischke et al., 2004; Pellerin and Magistretti, 2004) address these possibilities.

2.4.2 NADH and FADH₂ Fluorescent Images and Signals from Brain Slices and Cerebellar Cortex In Vivo

The original formulation of the astrocyte/lactate shuttle hypothesis suggested that an early increase in Na⁺-linked glutamate uptake led to release of lactate from astrocytes (Magistretti and Pellerin, 1999; Magistretti et al., 1999). If so, then neurons would use lactate in preference to glucose as a fuel. The ratio of NADH/NAD⁺ in the astrocyte cytosol should increase almost immediately with increases in neuronal activity and at the same time neuronal mitochondrial NADH and reduced FP should decrease as oxygen consumption increases to meet the increased needs for ATP synthesis. Fluorescent signals from these mitochondrial chromophores can and have been used to monitor energy metabolism in heart and liver (Olson and Thurman, 1987; Blinova et al., 2004), in intact brain in vivo (Reinert et al., 2004), and in brain slices in vitro (Kasischke et al., 2004; Pellerin and Magistretti, 2004).

Studies designed using these techniques to test the astrocyte/neuron shuttle hypothesis have produced conflicting results. Mangia and coworkers (2003) used time-resolved proton magnetic resonance spectroscopy to follow rapid changes in lactate in the in vivo brain after brief visual stimulation. Lactate decreased at

5 s and recovered to baseline at 12 s. They concluded that increases in lactate did not drive its preferential use by neurons. Recent studies of fluorescent NADH signals in brain hippocampal slices by other workers showed that electrical stimulation produces a striking biphasic change in the fluorescent mitochondrial cofactors NADH and FP (Mangia et al., 2003; Kasischke et al., 2004; Reinert et al., 2004). An early phase (0–20 s) appears to represent oxidation of NADH to NAD^+ and a later, prolonged phase (20–60 s) represents reduction (NAD^+ to NADH). Efforts to understand these changes initially led to the conclusion that the early oxidative phase was due to increased flow through the electron transport chain to O_2 , due to an increase in the demand for ATP in either neurons or glia. The later phase (reduction of mitochondrial NAD^+ to NADH) was assumed to be secondary to Ca^{2+} stimulation of Ca^{2+} -sensitive citric acid cycle dehydrogenases located in postsynaptic neurons. Studies by Kann et al. (2003) provided support for this concept.

Better spatial resolution than had been available previously to monitor oxidation/reduction fluorescent signal responses to electrical stimulation was obtained by Kasischke. The multiphoton microscopy used (Denk et al., 1990; Bennett et al., 1996; Patterson et al., 2000; Kann et al., 2003) provided subcellular metabolic imaging with a resolution of 1–2 μm . This allowed identification of astrocytes expressing green fluorescent protein under the control of the glial fibrillary acidic protein (GFAP) promoter, a protein specific to brain astrocytes. Fluorescent changes could then be tracked separately in the astroglial and neuronal compartments. The two phases of the response to electrical stimulation were resolved into an early neuronal oxidation of NADH and a late astrocytic reduction of NAD^+ , possibly cytosolic, due to a stimulation of glycolysis (Pellerin and Magistretti, 2004). When postsynaptic glutamatergic receptors were blocked with CNQX (AMPA receptor antagonist), the early oxidative transient was almost completely blocked, but the slower reductive transient was reduced by only 40%. This suggests that the early phase represents NADH oxidation in postsynaptic neurons, and the late phase is due in large part to events in the glia secondary to presynaptic release of neurotransmitter, and therefore supports the lactate shuttle hypothesis.

Shuttleworth et al. (2003) have discounted the theory that the late reductive transient is the result of Ca^{2+} stimulation of citric acid cycle enzymes. They measured fluorescent responses of hippocampal slices to neuronal stimulation and reported the same biphasic NAD(P)H responses as other workers. However, the fluorescent responses were initiated in two different ways: (1) by electrical stimulation and (2) by administration of glutamate directly over the slice using a microelectrode. The response to glutamate was not influenced by Ca^{2+} in the presynaptic neuron. When Ca^{2+} was omitted from the bath medium and electrical stimulation was applied, there was of course no early oxidative NADH response. However, when glutamate infusion was used as the stimulus, there was a biphasic response and no effect of Ca^{2+} was observed on either the initial oxidative response or the late reductive phase. These authors also reported, in agreement with Kasischke et al. (2004), that the two phases do not colocalize. However, their study was at odds with the Kasischke report, because the influence of the glutamate receptor blocker CNQX (in their hands) completely blocked both phases of the response to neuronal activation. Another problem brought to light by Shuttleworth et al. (2003) involves the response of FP fluorescence to electrical stimulation. FPs are integral components of the mitochondrial electron transfer chain, and they fluoresce at excitation and emission wavelengths distinct from those of NADH. FPs are strictly mitochondrial, and fluoresce only in the oxidized state. Somewhat surprisingly, they respond to electrical stimuli in neural tissues with the same biphasic (but inverted) pattern as NADH. Therefore, Shuttleworth et al. (2003) concluded that both signals (NADH and FP) are emitted by mitochondria and that the late phase NADH cannot be cytosolic. Nevertheless, it does appear that the amplitude of the late reductive FP signal is small compared to the initial oxidative response of the NADH signals. Therefore, the late phase signal may be composed of both cytosolic NADH and mitochondrial FP responses.

A third study, conducted by Reinert et al. (2004), recorded FP signals from the cerebral cortex *in vivo* rather than from *ex vivo* hippocampal slices. Neuronal activity was induced by surface electrical stimulation. NADH signals were too weak to measure, but FP signals were robust. Reinert et al. (2004), like Shuttleworth et al. (2003), recorded effects of removal of calcium from the bath, and blockade of postsynaptic glutamate receptors by CNQX. The FPs exhibited biphasic fluorescent signals similar to the NADH fluorescent signals reported by Kasischke et al. (2004). This reemphasizes the point that at least part of the late, reductive signal must be mitochondrial. An increase in stimulus duration increased the magnitude of the later reductive phase. *In vivo* study of the surface of the cerebellar cortex (Reinert et al., 2004) indicated

that Ca^{2+} removal from the medium blocks both phases, but since the stimulus was electrical this was in agreement with the findings of Shuttleworth et al. (2003) and simply reasserts the dependence of the presynaptic neurons on Ca^{2+} for the initiation of neurotransmitter release. The influence of the postsynaptic glutamate blocker CNQX was also studied by Reinert et al. (2004). These workers obtained results compatible with the lactate shuttle hypothesis since the early oxidative phase was blocked completely, but the late phase was only blocked by 50%. This contradicts the studies of Shuttleworth et al. (2003), but are in agreement with those of Kasischke et al. (2004).

Taken together it appears that the late phase probably originates in the astrocytes but a part of the late signal response originates in the mitochondria. The reason for the delay in the appearance of the late phase is puzzling especially in view of the studies of Jahr and coworkers (Diamond and Jahr, 2000; Wadiche et al., 2006) that suggest the uptake of glutamate into the glia from the synapse is rapid. However, a recent review article by Cerdan et al (2006) may shed some light. Cerdan suggests that neither lactate nor NADH accumulates in the astrocytes initially, but lactate quickly diffuses out into the extracellular space to be taken up by neurons. Neurons have a more active malate/aspartate cycle than astrocytes and can readily consume the NADH generated when the lactate is converted to pyruvate. Not all the pyruvate generated in the neurons may enter the neuronal citric acid cycle. Some may diffuse back to the astrocyte, providing a vigorous late phase reduction in astrocyte mitochondrial NADH.

2.5 The GABA Shunt: γ -Aminobutyrate Metabolism in the Brain

2.5.1 GABA: Neurotransmission

Whereas glutamate is the major excitatory transmitter in the brain, GABA is the major inhibitory transmitter (Esclapez et al., 1997; Beleboni et al., 2004). Postsynaptic GABA receptors hyperpolarize the neuronal membrane, thus opposing the influence of depolarizing glutamate receptors. GABA catabolism following its release as neurotransmitter takes place in both the neurons and the astrocytes and is dependent on the intramitochondrial enzyme, GABA transaminase. This section focuses on events in the astrocyte where the products of GABA transaminase can follow alternate metabolic pathways. These pathways lead either to the synthesis of glutamine in the astrocyte cytosol or to the conversion of GABA carbon to pyruvate via the degradative arm of the pyruvate/glutamate cycle. The first pathway should maintain GABA at high levels; the second pathway may lower GABA levels. Factors that might alter the path chosen are discussed.

The dual roles of the two amino acid transmitters (glutamate and GABA) require the presence of mechanisms to segregate the two transmitters and their metabolic products and precursors. This is an especially critical problem because glutamate is the immediate precursor for GABA synthesis. Presynaptic neurons in this system are either GABAergic or glutamatergic (Holmes et al., 1994; Sheikh and Martin, 1998; Tian et al., 1999; Gutierrez, 2003). GABA neurons in the brain can be identified by their prominent expression of glutamate decarboxylase (GAD). GAD converts glutamate to GABA by decarboxylating the 1-C of glutamate. Thus, the 2-C of glutamate becomes the γ -carbon of GABA attached to the amino group, and the 5-C of glutamate becomes the α -carbon of GABA. There are two isoforms of GAD, GAD65 and GAD67, which are products of different genes. GAD67 is predominantly cytosolic and accounts for most GABA synthesis (Christgau et al., 1992; Condie et al., 1997). Mutation of GAD67 reduces GABA levels in the brain to only 10% of that in normal brains. Conversely, inhibition of GAD65 does not decrease GAD levels dramatically but does produce neurological symptoms. GAD65 is present in neuronal terminals, bound to the synaptic vesicle. This isozyme binds pyridoxal phosphate less tightly than the GAD67 isozyme and it also catalyzes a slower transamination reaction that produces inactive apoGAD (without bound cofactor) (Battaglioli et al., 2003). This apo-/holoenzyme cycle of inactivation and reactivation is more important in regulating the activity of GAD65 than of GAD67. A rare genetic mutation of GAD65 causes seizures and hampers isozyme activity in the absence of excess dietary pyridoxine cofactor. It is clear therefore that GAD65 plays an essential but somewhat mysterious role in the synaptic transmission of GABA in nerve terminals.

GABA is released into neuronal synapses and produces inhibitory signals via GABA receptors on postsynaptic neurons (Hill and Bowery, 1981; Beleboni et al., 2004). Some of these postsynaptic neurons

also express glutamate receptors. GABA receptors exhibit significant heterogeneity and can be divided into two general classes (Mohler et al., 2002). One class is called ionotropic and includes GABA_A and GABA_C receptors that open Cl⁻ channels, and therefore hyperpolarize postsynaptic membranes and oppose stimulatory depolarization by glutamate. GABA_B receptors on the other hand transduce signals via G-proteins and produce slow, long-lasting inhibition of depolarization. Covering the diversity and pharmacology of these receptors is beyond the scope of this chapter. Instead our focus is on GABA metabolism and the potential that the components of the GABA metabolic pathways have as pharmacological targets.

2.5.2 GABA Catabolism

After release into the synaptic space and transient binding to GABA receptors, GABA is transported via GABA transporters back into the neurons or astrocytes. At least four specific GABA transporter (GAT) proteins are expressed in the central nervous system (Dodd et al., 1989; Borden, 1996; Gadea and Lopez-Colome, 2001; Conti et al., 2004). Four genes encoding the GABA transporters of the central nervous system (GAT-1, GAT-2, GAT-3, and BGT1) have been found. GATs 1 and 3 are expressed in the cerebral cortex and their distribution and cellular localization have been determined using electron microscopic immunocytochemical techniques. They are located in synaptic sites where they mediate GABA uptake at fast inhibitory synapses and shape inhibitory postsynaptic responses. The other GATs may play roles in regulation of cortical maturation or they may regulate diffusion between synapses and regulate levels of GABA in the cerebrospinal fluid (Conti et al., 2004). GAT-1 is the most abundant and predominantly expressed in presynaptic neurons whereas GAT-3 is less abundant and predominantly expressed in astrocytes forming part of the GABAergic synapse (Borden, 1996; Conti et al., 2004). Early studies using primary cultures of neurons and astrocytes led to the assumption that uptake of GABA from GABAergic synapse is primarily due to neuronal uptake (Schousboe, 1981). All GATs are Na⁺/Cl⁻-linked and electrogenic, driving removal of GABA from the synaptic space against a gradient. Like glutamate, energy is required for GABA uptake. Depolarization or a decrease in the Na⁺ gradients can lead to a GABA “leak” from presynaptic neurons and this produces inhibitory GABA signals (Belhage et al., 1993; Borden, 1996; Wu et al., 2001; Allen et al., 2004; Schousboe et al., 2004). In recent years, specific inhibitors of one or the other of these transporters have been sought and a few identified (Schousboe, 2000). Most GABA transport blockers are nonspecific, raise GABA levels in the synaptic space, and therefore are anticonvulsant in animal models. One GABA transport inhibitor, *N*-methyl-exo-4,5,6,7-tetrahydroisoxazolo[4,5-*c*]pyridin-3-ol, preferentially inhibits astrocytic transport of GABA and is a particularly potent and effective anticonvulsant (Schousboe, 2000; Sarup et al., 2003). Microdialysis studies show that it is more effective than nipecotinic acid, a drug that strongly inhibits both neuronal and astrocytic GABA transport (Juhász et al., 1997; Schousboe, 2000). This suggests that the astrocyte GAT is especially important in increasing synaptic GABA levels by inhibiting its uptake from the synapse.

When taken up by neurons, some GABA is repackaged into synaptic vesicles in the axon terminal, but the remaining GABA enters a catabolic pathway. This catabolic pathway is more active in the astrocytes where it cannot be repackaged into synaptic vesicles. In both cell types, the catabolic pathway is initiated by transamination of GABA with α -ketoglutarate via a mitochondrial enzyme called GABA aminotransferase (GABA-T). The GABA must be transported into the mitochondria, but the mitochondrial transporter that catalyzes this process has not been identified. Inhibitors of GABA-T such as gabaculine (3-amino-2,3-dihydrobenzoic acid) and 8-vinyl GABA have been studied and have anticonvulsant activity in animal models (Sarup et al., 2003). They have a profound influence on brain glutamate, glutamine, and GABA levels. In one study (Pierard et al., 1999), gabaculine was given systemically to rats and its influence on metabolism studied using 2D-¹H NMR spectroscopy to monitor whole brain levels of GABA, glutamate, glutamine, and aspartate. Extracellular levels were monitored specifically using microdialysis. There was a large, sigmoidal increase in GABA both intracellularly and extracellularly. The increase leveled off at about 6 h when it reached 3000% intracellularly and ~800% extracellularly. Following a similar time course, glutamate and glutamine levels (intracellular and extracellular) declined 60%. These studies illustrate an important metabolic interaction between the glutamatergic and GABAergic pathways.

GABA-T is a mitochondrial enzyme that uses α -ketoglutarate as a transamination partner with GABA (Schousboe et al., 1977; Park et al., 1993). There is no requirement for mitochondrial α -ketoglutarate transport into the mitochondria since it is generated by the mitochondrial citric acid cycle. The products of GABA-T transamination are glutamate and succinic semialdehyde (Sherif and Ahmed, 1995; Tillakaratne et al., 1995). The enzyme succinate semialdehyde dehydrogenase (SSADH) oxidizes the aldehyde to a carboxyl group to produce succinate. This pathway is shown in [Figure 6.1-5a](#) and the overall equation is shown below.



■ **Figure 6.1-5**

(a) GABA conversion to pyruvate in astrocytes lining a GABAergic synapse. A hypothetical pathway is described that leads to irreversible conversion of GABA carbon to pyruvate. The pathway is similar to the glutamate to pyruvate arm of the cycle described in [Figure 6.1-2](#). The citric acid cycle pool is conserved in this scheme only by equimolar transamination of glutamate to α -ketoglutarate inside the mitochondria using pyruvate or BCKA. The GABA carbon may be restored by de novo activity of pyruvate carboxylase (PC), forming oxaloacetate (OAA), which can then be converted stepwise to α -KG rather than glutamate, and then to glutamine (not shown) (b) An alternate scheme for GABA catabolism. An alternate possibility is that GABA is transaminated inside the mitochondria, but the succinate formed is not decarboxylated and recycles with the rest of the citric acid cycle intermediates. A source of acetyl CoA is required for the cycling. Glutamate effluxes from the mitochondria and is not converted to α -ketoglutarate but instead aminated to glutamine and returns to the presynaptic GABAergic neuron for the regeneration of the synaptic vesicle GABA. This pathway maintains GABA homeostasis without the need for PC. GABA, γ -aminobutyric acid; SSA, succinic semialdehyde; SUCC, succinate; FUM, fumarate; MAL, malate; GLU, glutamate; α -KG, α -ketoglutarate; KA, keto acid; AA, amino acid; OAA, oxaloacetate; CIT, citrate; isoCit, isocitrate; Succ-CoA, succinyl CoA; GLN, glutamine

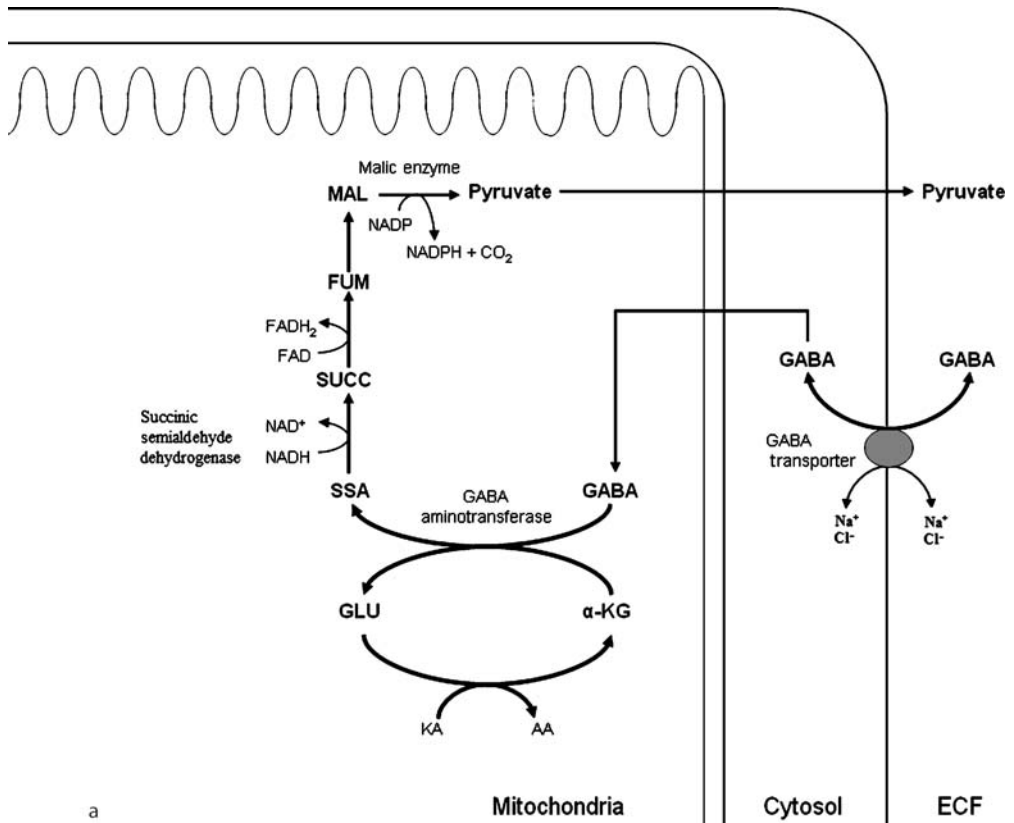
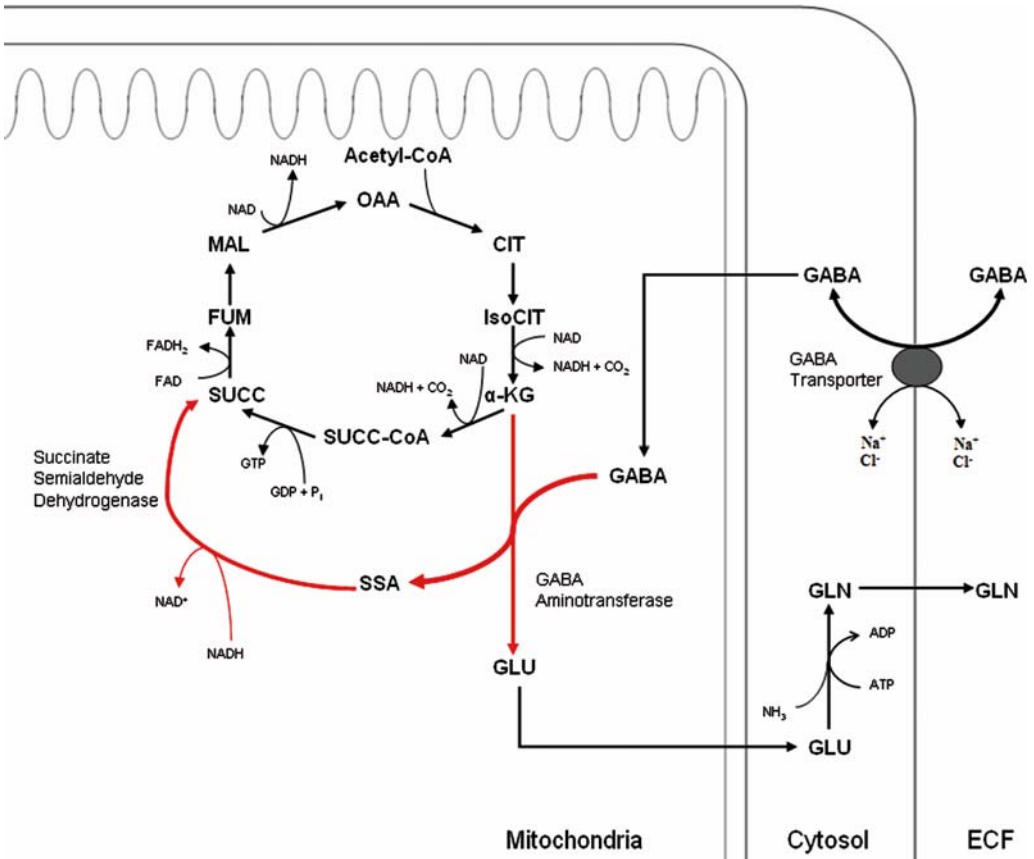


Figure 6.1-5 (continued)



The pathway is frequently referred to as the GABA shunt because it shunts the α -ketoglutarate in the mitochondria directly to succinate, bypassing succinyl CoA thiokinase without gain or loss of citric acid cycle intermediates, i.e., α -ketoglutarate is used but succinate is produced. Nevertheless, the shunt consumes energy since one NADH is used and the substrate-level phosphorylation step at succinate thiokinase is bypassed. The shunt metabolizes succinate semialdehyde very rapidly because the semialdehyde dehydrogenase has a low K_m and is bound tightly to GABA-T, forming a metabolon that can efficiently channel the product of GABA-T to SSADH (Hearl and Churchich, 1984). An alternate pathway is available if SSADH activity is low. This pathway reduces rather than oxidizes the semialdehyde group to a hydroxyl moiety, producing γ -hydroxybutyric acid (Gupta et al., 2003). Except in SSADH deficiency, only small amounts of this compound accumulate. In SSADH deficiency, which is a rare autosomal activity, γ -hydroxybutyric acid accumulates up to 1200-fold in the cerebrospinal fluid (Gupta et al., 2003). The symptoms include mental retardation and ataxia, and seizures occur in about half the affected children.

We speculated above that the glutamate produced by the GABA-T reaction in the astrocytes may take different pathways. If the glutamate remains in the mitochondria for catalysis, this may produce a decrease in total brain GABA. Alternatively, glutamate may exit the mitochondria where it can be converted to glutamine in the cytosol. Efflux of glutamate from mitochondria is catalyzed by one or both of two glutamate hydroxyl ion exchange carriers (GC₁ and GC₂) (Palmieri, 2004). Efflux via one of these carriers may not be energetically favorable because it involves cotransport of glutamate in exchange for a hydroxyl

ion against a proton gradient. The glutamate in the cytosol may be amidated to glutamine, return to the GABA neurons where the glutamine can be converted to glutamate, and then decarboxylated to GABA.

It is likely that at least some glutamate will not be released from the mitochondria but instead metabolized inside the mitochondria by transamination or deamidation by glutamate dehydrogenase. Our studies of aminotransferase expression in glia of the retina (LaNoue et al., 2001) suggest that alanine aminotransferase and BCATm, but not aspartate aminotransferase, are expressed in *in situ* astrocyte mitochondria. BCATm, discussed earlier, catalyzes transamination of glutamate with BCKAs forming α -ketoglutarate and BCAAs. Previous studies (Hutson et al., 1998; Magistretti and Pellerin, 1999; Lieth et al., 2001; Sweatt et al., 2004) have shown that this transaminase has a prominent role along with alanine aminotransferase in regulating synthesis and degradation of glial glutamate. It is likely that high levels of BCKA or high levels of pyruvate will favor the internal pathway. ^{15}N NMR studies indicate that 30–50% of the nitrogen atoms in whole brain glutamate is derived from BCAA (Kanamori et al., 1998) and only a very small percent is derived from ammonia. This suggests that glutamate dehydrogenase does not play an important role in glutamate synthesis or oxidation in astrocytes. Therefore, it probably does not play a major role in GABA metabolism. The two scenarios for GABA metabolism are illustrated in [▶ Figure 6.1-5a](#) and [▶ 5b](#). In [▶ Figure 6.1-5a](#), the possibility that GABA catabolism in the astrocytes could cause a decline in the brain GABA pool is emphasized.

Regardless of the pathway chosen, GABA-T inhibition does lower glutamine levels. The GABA-T catabolic pathway contributes significantly to whole brain glutamine levels, since inhibition of GABA-T lowers steady-state glutamine levels by 60% (Pierard et al., 1999). A major difference between the metabolic pathway of glutamate derived from glutamatergic neural activity and that derived from GABAergic neural activity is that the glutamate derived from GABA is generated inside the mitochondria whereas it initially appears in the cytosol following glutamatergic neural activity. If GABAergic glutamate remains in the mitochondria and BCKAs are high, it can be transaminated to α -ketoglutarate and oxidized in the citric acid cycle and decarboxylated to pyruvate (see [▶ Sect. 2.2](#)). This amounts to irreversible disposal of GABA. Alternatively, the glutamate may leave the mitochondria on the glutamate/hydroxyl carrier. Glutamine synthetase will convert it to glutamine, which enters glutamatergic or GABAergic presynaptic neurons. In light of the assumption that most synaptic GABA can return directly to presynaptic GABA neurons and be repackaged into synaptic vesicles, it is difficult to understand why a GABA transport inhibitor that blocks both glial and neuronal GABA uptake from the synapse raises synaptic GABA levels less than the one which is more specific for glial uptake (Juhász et al., 1997). Similarly, it is strange that inhibiting GABA-T, which is predominantly glial, has a more dramatic effect on brain GABA levels than most of the transport inhibitors (compare Juhász et al. (1997) and Pierard et al. (1999)). Measurements of brain GABA levels in currently available BCATm knockout mice may permit evaluation of the importance of the BCATm pathway in GABA catabolism.

3 The Role of Mitochondrial Transporters in the Brain

Studies of the role of mitochondrial translocases in brain function and in control of neurotransmission have recently begun to yield important information. Nevertheless, there are challenges to progress due to the variety of brain cell types (e.g., neurons, astroglia, oligodendrocytes) that are metabolically differentiated to perform their various functions. Neurons store neurotransmitters, generate ATP oxidatively, and express a variety of membrane proteins needed to appropriately generate cytosolic free Ca^{2+} pulses and fuse vesicle membranes with plasma membranes in response to Ca^{2+} pulses. Astroglia are differentiated to support the work of the neurons, helping provide substrates for neuronal use, and removing byproducts of neurotransmission. On the other hand, oligodendrocytes must synthesize phospholipids for myelin synthesis (Salvati et al., 1996). As cytosolic reducing equivalents are needed for cytosolic fatty acid synthesis, a robust malate/aspartate shuttle would be counter-productive for oligodendrocytes. Adipocytes, for example, do not express AGC (Palmieri, 2004).

The elucidation of roles of the different cell types in the brain has been facilitated by the development of techniques for culturing individual brain cell types to study their metabolic behavior in isolation.

A criticism of this approach is that the cells change in culture and become less differentiated or, in the case of embryonic or neonatal cells, do not differentiate completely. Likewise the absence or presence of other brain cells in the same culture dish can influence expression of key enzymes and transporters.

Another approach involves the separation of mitochondria from different populations of cells. There are two common methods of isolating mitochondria from brain. One excludes “synaptosomal” (neuronal?) mitochondria (Clark and Nicklas, 1970) using a Ficoll gradient system. The other method attempts to isolate a more general population of mitochondria (Rosenthal et al., 1987). As these mitochondrial preparations both contain mitochondria from a variety of cell types, they are not useful in determining cell-specific expression of mitochondrial transporters. Using immunohistochemistry for determining cell-specific expression of mitochondrial carriers may produce a clearer picture of cell/cell and cytosolic/mitochondrial interactions in the brain. Information currently available regarding the expression of mitochondrial transporters in the brain is summarized below and organized according to their participation in the various metabolic cycles, shuttles, and shunts, as previously discussed.

3.1 The Glutamate/Glutamine Cycle

Only plasma membrane transporters are involved in this metabolic pathway. The traffic between the glia and the neurons following synaptic release of glutamate from the neurons is catalyzed by plasma membrane transporters of glutamate and glutamine. Glutamate, after release into the synaptic space, is transported into the astrocytes by a high-affinity electrogenic Na^+ -linked glutamate transporter (GLT1) (Aschner, 2000). Possible inhibition of glutamate inward transport (GLT1) or outward leak as a consequence of increases in intragial glutamate has not, as far as we know, been studied. The mitochondrial transporters of glutamate, α -ketoglutarate, BCAA, and BCKA constitute determinants of glutamate metabolism in the glia and of regulators of intragial glutamate levels.

The glutamine synthesized in the glia from glutamate is transported out of the glia by a Na^+ -linked transporter (SN1) (Chaudhry et al., 1999; Boulland et al., 2002). SN1 catalyzes cotransport of glutamine with one Na^+ in exchange for H^+ (Chaudhry et al., 1999; Broer et al., 2002). Proteins in the neuronal plasma membrane then transport glutamine into the neuronal cytosol. These two are called SAT1 and SAT2. Both are Na^+ -dependent unidirectional saturable transporters (Reimer et al., 2000; Varoqui et al., 2000; Broer and Brookes, 2001; Armano et al., 2002; Kanamori and Ross, 2005). An interesting *in vivo* study of regulation of ECF glutamine suggests that the bidirectional nature of the glial glutamine transporter SN1 allows it to regulate ECF glutamine by suppressing glutamine efflux from astrocytes when ECF glutamine concentrations rise (Kanamori and Ross, 2005).

3.2 The Pyruvate/Glutamate Cycle

The pyruvate/glutamate cycle (➤ Sect. 2.2) and the pathways involved are illustrated in ➤ Figure 6.1-2. These pathways regulate glutamate disposal in the glia and therefore are able to influence intragial glutamate levels, which in turn probably determine rates of glutamine synthesis.

Mitochondrial transporters required for the pyruvate/glutamate cycle include (1) the glutamate/hydroxyl carrier; (2) the mitochondrial transporters of BCAA and alanine; and (3) the mitochondrial transporter of branched-chain keto acids (BCKAs). Citric acid cycle enzymes as well as ME, PEPCK, pyruvate kinase, and PC are likewise essential. If cytosolic ME catalyzes decarboxylation to pyruvate, then malate must be transported from the mitochondria, and this would involve participation of the dicarboxylate carrier. If PEP is part of the pathway, it must be transported out of the mitochondria.

When glutamate enters the glia from the synaptic space, it can be amidated to glutamine, transaminated to α -ketoglutarate by aspartate aminotransferase, or transported into the glial mitochondria via one of the two glutamate hydroxyl carriers (Palmieri, 2004). Thus, the glutamate/hydroxyl carrier likely plays an important

role in disposing of excess glutamate when rates of glutamatergic neurotransmission are high. Mitochondrial enzymes that convert the glutamate to α -ketoglutarate include BCATm, alanine aminotransferase, and glutamate dehydrogenase. Glutamate dehydrogenase is abundantly expressed in glia but does not appear to be very active under most physiological conditions.

The potential importance of the glutamate/hydroxyl mitochondrial transporter in regulating glial disposal of glutamate is apparent from the fact that a rare, naturally occurring mutation of this transporter causes a form of neonatal myoclonic epilepsy (Molinari et al., 2005). There are two mammalian glutamate carriers (GC1 and GC2) so far identified that catalyze mitochondrial glutamate/hydroxyl exchange (Molinari et al., 2005). Their genes, SLC25A18 and SLC25A22, were selected as possible candidates for inclusion in the SLC30 category by screening eukaryotic databases with the sequences of the known glutamate/aspartate carrier genes. The amino acid sequences of the two glutamate/hydroxyl carriers are 63% identical to each other (Fiermonte et al., 2002). Their kinetic parameters differ, however, since GC1 has a very high K_m for glutamate (4–5 mM) and GC2 has a 20-fold lower K_m (0.2 mM). The V_{max} of GC1 is higher than that for GC2 (Fiermonte et al., 2002). GC1 is more abundant than GC2 in all tissues except brain where the two are expressed equally, but perhaps in different cell types. It is likely that the role of GC1 in most tissues is to deal with excesses of metabolic glutamate. The mutation of the glutamate/hydroxyl carrier (GC1) that causes the severe neonatal epilepsy is a proline206/leucine substitution in the GC1 protein (Molinari et al., 2005). Expression studies show that during human development the gene for GC1 is specifically expressed in brain in areas that contribute to the initiation and control of myoclonic seizures (Molinari et al., 2005).

3.3 The Lactate Shuttle and the Role of the Malate/Aspartate Shuttle

3.3.1 The Aspartate/Glutamate Carrier and the Lactate Shuttle Hypothesis

As described in [Sect. 2.3](#), Magistretti and coworkers (Pellerin and Magistretti, 1994) have published studies that suggest that brain astrocytes produce lactate from glucose but astrocytes do not oxidize it to CO_2 and H_2O . Instead, they suggest that lactate may be exported into the extracellular fluid and taken up by neurons for oxidation. Our studies (LaNoue et al., 2001) of the influence of a series of different transaminase inhibitors on glutamate metabolism in the retina suggested that the anomalies of lactate metabolism in the brain might be due to low expression of a malate/aspartate shuttle in retinal Müller cells.

Relevant studies by Ramos et al. (2003) indicated that in adult mice only one of the two possible AGC isoforms is expressed in the brain. The two protein isoforms of AGC, which catalyze unidirectional exchange of cytosolic glutamate H^+ for intramitochondrial aspartate, are called aralar and citrin (Palmieri, 2004). In neonatal mice, both are expressed, but aralar is neuronal and citrin exclusively glial. Ramos et al. (2003) found that during the first two postnatal weeks, citrin expression ceases in cultured glia and is replaced by a low amount of aralar. Thus, in adult rats only aralar1 is expressed and can be detected in neurons. Aralar may be present in glia in amounts too low for detection by immunohistochemical techniques. Low expression of AGC will make it difficult for glucose or lactate to be oxidized in glia. Oligodendrocytes are an exception since in these cells reducing equivalents are consumed for fatty acid synthesis.

Aralar mRNA and protein are expressed throughout neuron-rich areas in the central nervous system. There are clear enrichments in sets of neuronal nuclei in the brain stem and in the ventral horn of the spine. These same neurons express high levels of cytochrome *c* oxidase, a specific marker for mitochondria. Strangely, there are areas where the neurons do not express AGC and it is unclear how NADH generated in the cytosol is reoxidized to NAD^+ without generating lactate, since, as discussed previously, NAD^+ and NADH are impermeable to the mitochondrial membrane.

There is another pathway, called the glycerol phosphate shuttle, expressed in some cells, which can transport reducing equivalents from NADH into mitochondria. It is not as active as the malate/aspartate shuttle and is usually present in combination with components of the malate/aspartate cycle. One might

assume that neurons that do not express either one of the AGC isoforms express the components of the glycerol phosphate shuttle. However, this does not appear to be the case.

The two enzymes needed for the glycerol phosphate shuttle are cytosolic glycerol phosphate dehydrogenase and mitochondrial glycerol phosphate dehydrogenase. Glycerol metabolism has been carefully examined in a recent report by Hassel et al. (Nguyen et al., 2003) who show that glycerol itself is actively metabolized in brain, especially in GABAergic neurons, secondary to expression of neuronal glycerol kinase. Mitochondrial glycerol phosphate dehydrogenase is expressed in these neurons but the cytosolic enzyme that could complete the reduction shuttle is absent or low in neurons but active in white matter, presumably oligodendrocytes. This suggests that the glycerol phosphate shuttle, which requires both enzymes in the same cell, is not active in the brain.

This conclusion is supported by an earlier study in which a transgenic mouse, with the gene for cytosolic glycerol phosphate dehydrogenase mutated to an inactive form, exhibited no abnormal phenotypic behavior (MacDonald and Marshall, 2001). It is not clear how glucose and lactate are oxidized in neurons that lack AGC, since they seem to lack a reducing equivalent shuttle. The two mitochondrial transporters needed for this shuttle are the AGC and the α -ketoglutarate/malate exchanger. The role of the AGCs in transporting reducing equivalents was recognized a number of years ago (LaNoue and Tischler, 1974) but the AGCs were only recently cloned, identified, and sequenced (Palmieri et al., 2001).

The two AGC isoforms are products of separate genes but have similar structures. The C terminus has a three-fold axis of symmetry with six membrane-spanning domains. The N terminus is composed of a large cytosolic domain (\sim half the protein) that includes four calcium-binding domains. These proteins are two of only three members of the MC30 family that are stimulated by calcium in the physiological range. The AGCs are widely expressed in mammalian tissues but AGC1 (aralar) is found principally in excitable tissues while AGC2 (citrin) is absent from the brain, but may be the only AGC carrier expressed in the liver. Both isoforms are present in the heart. AGC2 is called citrin because a defect in its gene causes a naturally occurring hereditary metabolic disease called citrullinemia (Kobayashi et al., 1999), a fatal adult onset disease characterized by hyperammonemia and an inability to synthesize citrulline. The slow onset of the disease suggests that factors other than the absence of the citrin gene may participate in the pathology of citrullinemia. This speculation is supported by observations that knockout mice, in which the citrin gene has been disrupted, have only a mild metabolic deficiency in citrulline synthesis (Sinasc et al., 2004).

Both AGC transporters (aralar and citrin) catalyze the exchange of protonated glutamate for anionic aspartate, and therefore the exchange only occurs in the direction of glutamate in and aspartate out. The large electrochemical potential gradient ($\Delta\mu\text{H}^+$) across the mitochondrial inner membrane prevents reversal and leak of reducing equivalents out of the mitochondria. The exchange is powered by $\Delta\mu\text{H}^+$, and this is an important aspect of its physiological function. The ratio of NADH/NAD⁺ is \sim 100-fold higher inside the mitochondria than outside (Williamson et al., 1967). Early studies showed that if the H⁺ gradient across the mitochondrial membrane is dissipated by proton ionophores, exchange of aspartate for glutamate is stopped (LaNoue et al., 1974). It is not possible to move the reducing equivalents from cytosolic NADH into the mitochondria without the power input supplied by AGC via the electrochemical proton gradient ($\Delta\mu\text{H}^+$) (LaNoue and Schoolwerth, 1979).

Thus, AGC is a necessary component of the mechanism that catalyzes transfer (into mitochondria) of reducing equivalents generated during glycolysis. When the aralar gene is disrupted, rodents live only briefly. Our group recently used immunohistochemistry to locate AGC in the retina. AGC was easily detectable in photoreceptor cells and also in the neurons of the inner retina. However, no overlap between vimentin (a Müller cell glial-specific marker) and AGC could be detected. The study has only been published in abstract form (LaNoue et al. 2005). It seems likely that the observed AGC distribution in the retina is similar to that in whole brain. Our preliminary experiments and the studies of Ramos et al. (2003) support this suggestion. Low expression of AGC in the glia and astrocytes of the retina as well as the rest of the brain may explain why lactate derived from glucose is poorly oxidized in glia of the brain and retina. Inconsistencies between whole brain estimates of the effect of neurotransmission on glucose uptake as estimated by PET versus complete oxidation of glucose (Dienel and Cruz, 2004) can also be explained in part by the compartmentalization of lactate metabolism and by the absence or low expression of AGC in astrocytes. This remains a controversial assertion however and requires confirmation by other laboratories.

3.3.2 Glial Catabolism of Aspartate and the Malate/ α -Ketoglutarate Mitochondrial Exchanger (the Oxoglutarate Carrier)

The oxoglutarate carrier (OGC) not only plays an essential role in the malate/aspartate cycle (see [▶ Figure 6.1-4](#)) but also is essential in other metabolic pathways used by the brain astrocytes. In this section, we describe the molecular characteristics of OGC. We also propose a pathway for aspartate catabolism, which requires the OGC carrier.

The OGC has been isolated, sequenced, and its activity reconstituted in proteoliposomes. Its kinetic parameters have been carefully investigated and powerful inhibition by phthalic acid has been recognized (Palmieri, 2004). There appears to be only a single gene for this carrier at least in cow, man, and rat. The reaction mechanism and kinetics of the reconstituted OGC have been investigated extensively by mutational analysis. This was made possible because the OGC carrier can be overexpressed in *Escherichia coli*. It was in fact the first mitochondrial carrier to be overexpressed and refolded into a reconstitutively active state (Fiermonte et al., 1993). A combination of cis-scanning mutagenesis, chemical modification, and spin-labeling studies identified a water-accessible face of OGC helix IV. This face probably lines part of the substrate translocation pathway. Its active form is a dimer and the translocation mechanism likely involves alternate site activation, with both monomers forming alternate translocation pathways (Stipani et al., 2001; Morozzo della Rocca et al., 2003).

The OGC carrier is required for the malate/aspartate shuttle. Both AGC and OGC are active in mitochondrial preparations isolated from whole brain. Preliminary immunohistochemical estimates of OGC distribution in the retina indicate that it is expressed in both neurons and glia. Widespread expression of OGC in retinal Müller cells may reflect the need for uptake and metabolism of aspartate. Aspartate is a neurotransmitter and it is taken up by the glia after release from nerve endings, using the same Na^+ -linked transporter that conveys glutamate into the glia (Malandro and Kilberg, 1996). A hypothetical scheme for the metabolism of aspartate in glia and the net synthesis of glutamine is shown in [▶ Figure 6.1-6](#).

Aspartate cannot enter mitochondria after it gains access to the cytosol because of the absence of the AGC in glia and the presence of $\Delta\mu\text{H}^+$ across the mitochondrial membrane. Aspartate is transaminated to oxaloacetate in the cytosol, consuming cytosolic α -ketoglutarate and forming glutamate. The glutamate formed in the cytosol from the α -ketoglutarate carbon can be converted to cytosolic glutamine, which exits astrocytes via the plasma membrane glutamine carrier (Reimer et al., 2000; Varoqui et al., 2000; Armano et al., 2002).

Cytosolic oxaloacetate formed from aspartate in this way may be reduced to malate by MDHc using the excess amounts of NADH generated by glycolysis in the retinal Müller cell cytosol. Malate generated in the cytosol can reenter the mitochondria in exchange for α -ketoglutarate via OGC.

OGC is clearly essential in this scheme, which generates glutamate, then glutamine from aspartate, and generates NAD^+ from cytosolic NADH without involving AGC. Oxidation of NADH would allow pyruvate to be generated from glucose in the cytosol. Transport of pyruvate into the mitochondria provides substrate for PC and de novo glutamate synthesis. Additional pyruvate may be generated by the malate/aspartate cycle expressed in neurons. This neuronal pyruvate may diffuse back to the glia through the extracellular space (Cerdan et al., 2006) and supply PC and pyruvate dehydrogenase with adequate substrate.

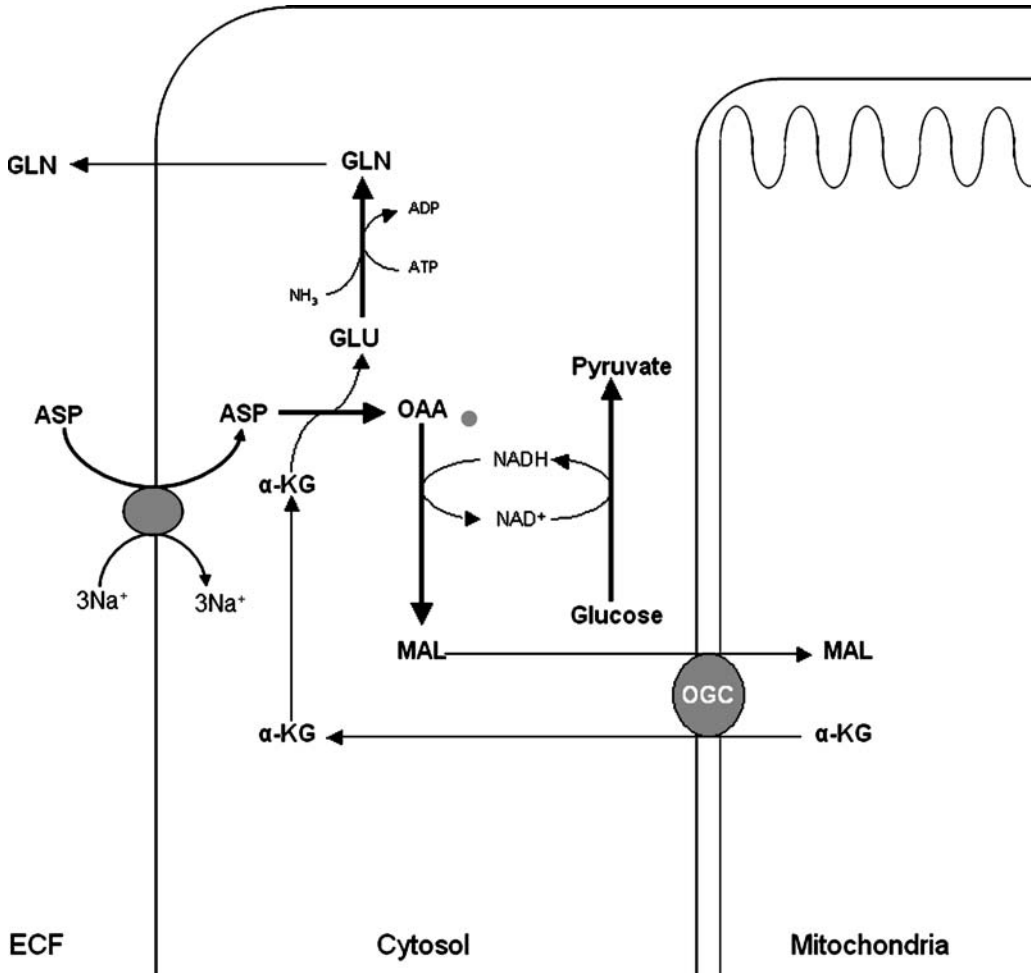
3.4 The GABA Shunt in Astrocytes

The astrocytic GABA shunt has been discussed and is illustrated in [▶ Figure 6.1-5a](#) and [▶ 5b](#). GABA recycling does not require mitochondrial transporters if GABA released as neurotransmitter is taken up from the synapse directly into presynaptic GABAergic neurons. Mitochondrial carriers do become involved when the GABA is catabolized to succinic semialdehyde by GABA-T. Another product of the GABA-T reaction is glutamate. Glutamate can leave the neuronal mitochondria on the glutamate/hydroxyl carrier and then be converted to GABA by GAD.

A fraction of the GABA in the synaptic cleft is transported into the astrocytes on Na^+/Cl^- -linked GABA transporters. This is followed by uptake into the mitochondria on a GABA transporter, which has not yet

■ Figure 6.1-6

Aspartate catabolism in astrocytes. Aspartate is an excitatory neurotransmitter that uses the same Na^+ -linked transporter to enter the astrocytic cytosol as glutamate. The scheme emphasizes the likelihood that aspartate catabolism is dependent on cytosolic aspartate aminotransferase, which generates oxaloacetate. Its catabolism, unlike that of glutamate, results in the consumption of cytosolic reducing equivalents when oxaloacetate is reduced to malate. The consumption of cytosolic NADH allows glucose to be oxidized to pyruvate without conversion to lactate. ASP, aspartate; OAA, oxaloacetate; GLN, glutamine; GLU, glutamate; α -KG, α -ketoglutarate; MAL, malate



been characterized. Inside the mitochondria, GABA is transaminated by GABA-T producing succinic semialdehyde and glutamate. Succinic semialdehyde is oxidized to succinate, which may continue around the citric acid cycle. The glutamate carbon on the other hand, in order to maintain a constant pool of citric acid cycle intermediates, must be transported out of the mitochondria possibly on the glutamate/hydroxyl carrier. Alternatively, the glutamate can be transaminated by pyruvate or BCAA. Both ketoacids can be transported in or out of the mitochondria. Although these branched-chain transporters are functionally characterized, they have not been isolated or cloned. The transporters of the amino acid products, BCAA

and alanine, have also been described and analyzed kinetically, but not yet isolated. The participation of BCKA and pyruvate in astrocytic glutamate catabolism have been demonstrated (Lieth et al., 2000, 2001), but their participation in GABA catabolism has not been reported.

4 Conclusions and Summary

Mitochondrial transporters in the central nervous system influence brain metabolism and neurotransmission. Their roles in this arena are generally under appreciated and poorly understood, largely because of the difficulty involved in isolating and studying a single type of cell in specialized areas of the brain. Pure brain mitochondrial preparations expressing a single enzymatic profile from a single cell type are not available. Original studies of brain mitochondria used a preparation termed “nonsynaptosomal,” in which mitochondrial preparations were placed on a Ficoll gradient and separated into a light fraction containing mitochondria encapsulated within plasma membranes and a heavier fraction that did not include cytosolic enzymes (Clark and Nicklas, 1970). However, encapsulated mitochondria can come from neuronal synapses or from the processes of astrocytes. Pure astrocytic or pure neuronal preparations can be obtained only from cell cultures but this is usually not done. Yields are poor from cultured cells. Data from cultured cells can also be misleading. For example, cultured astrocytes express both AGC isoforms (Ramos et al., 2003). Important progress has been made recently, attained utilizing genetic techniques, immunocytochemistry, and fluorescent microscopy using new techniques with a capacity for exceptional spatial resolution (Kasischke et al., 2004).

Acknowledgments

The authors would like to acknowledge funding from the Juvenile Diabetes Research Foundation (KFL) and the National Institutes of Health (RO1 NS38641, SMH).

References

- Agrimi G, et al. 2004. Identification of the human mitochondrial S-adenosylmethionine transporter: Bacterial expression, reconstitution, functional characterization, and tissue distribution. *Biochem J* 379(Pt 1): 183-190.
- Allen NJ, Karadottir R, Attwell D. 2004. Reversal or reduction of glutamate and GABA transport in CNS pathology and therapy. *Pflugers Arch* 449: 132-142.
- Armano S, et al. 2002. Localization and functional relevance of system A neutral amino acid transporters in cultured hippocampal neurons. *J Biol Chem* 277: 10467-10473.
- Aschner M. 2000. Neuron-astrocyte interactions: Implications for cellular energetics and antioxidant levels. *Neurotoxicology* 21: 1101-1107.
- Bakken IJ, et al. 1997. Lactate formation from [U - ^{13}C]aspartate in cultured astrocytes: Compartmentation of pyruvate metabolism. *Neurosci Lett* 237: 117-120.
- Battaglioli G, Liu H, Martin DL. 2003. Kinetic differences between the isoforms of glutamate decarboxylase: Implications for the regulation of GABA synthesis. *J Neurochem* 86: 879-887.
- Beleboni RO, et al. 2004. Pharmacological and biochemical aspects of GABAergic neurotransmission: Pathological and neuropsychobiological relationships. *Cell Mol Neurobiol* 24: 707-728.
- Belhage B, Hansen GH, Schousboe A. 1993. Depolarization by K^+ and glutamate activates different neurotransmitter release mechanisms in GABAergic neurons: Vesicular versus nonvesicular release of GABA. *Neuroscience* 54: 1019-1034.
- Bennett BD, et al. 1996. Quantitative subcellular imaging of glucose metabolism within intact pancreatic islets. *J Biol Chem* 271: 3647-3651.
- Berl S, Nicklas WJ, Clarke DD. 1968. Compartmentation of glutamic acid metabolism in brain slices. *J Neurochem* 15: 131-140.
- Blinova K, et al. 2004. Fluctuation analysis of mitochondrial NADH fluorescence signals in confocal and two-photon microscopy images of living cardiac myocytes. *J Microsc* 213(Pt 1): 70-75.
- Bluml S, et al. 2002. Tricarboxylic acid cycle of glia in the in vivo human brain. *NMR Biomed* 15: 1-5.

- Borden LA. 1996. GABA transporter heterogeneity: Pharmacology and cellular localization. *Neurochem Int* 29: 335-356.
- Boulland JL, et al. 2002. Cell-specific expression of the glutamine transporter SN1 suggests differences in dependence on the glutamine cycle. *Eur J Neurosci* 15: 1615-1631.
- Broer A, et al. 2002. Regulation of the glutamine transporter SN1 by extracellular pH and intracellular sodium ions. *J Physiol* 539(Pt 1): 3-14.
- Broer S, Brookes N. 2001. Transfer of glutamine between astrocytes and neurons. *J Neurochem* 77: 705-719.
- Castiglione-Morelli MA, et al. 2004. Solution structure of the first and second transmembrane segments of the mitochondrial oxoglutarate carrier. *Mol Membr Biol* 21: 297-305.
- Cerdan S, et al. 2006. The redox switch/redox coupling hypothesis. *Neurochem Int*. In Press. 48: 523-530.
- Chaudhry FA, et al. 1999. Molecular analysis of system N suggests novel physiological roles in nitrogen metabolism and synaptic transmission. *Cell* 99: 769-780.
- Cheeseman AJ, Clark JB. 1988. Influence of the malate-aspartate shuttle on oxidative metabolism in synaptosomes. *J Neurochem* 50: 1559-1565.
- Christgau S, et al. 1992. Membrane anchoring of the autoantigen GAD65 to microvesicles in pancreatic β -cells by palmitoylation in the NH₂-terminal domain. *J Cell Biol* 118: 309-320.
- Clark JB, Nicklas WJ. 1970. The metabolism of rat brain mitochondria. Preparation and characterization. *J Biol Chem* 245: 4724-4731.
- Condie BG, et al. 1997. Cleft palate in mice with a targeted mutation in the γ -aminobutyric acid-producing enzyme glutamic acid decarboxylase 67. *Proc Natl Acad Sci USA* 94: 11451-11455.
- Conti F, Minelli A, Melone M. 2004. GABA transporters in the mammalian cerebral cortex: Localization, development, and pathological implications. *Brain Res Brain Res Rev* 45: 196-212.
- Cruz F, Cerdan S. 1999. Quantitative ¹³C NMR studies of metabolic compartmentation in the adult mammalian brain. *NMR Biomed* 12: 451-462.
- Cruz F, et al. 1998. Ontogeny and cellular localization of the pyruvate recycling system in rat brain. *J Neurochem* 70: 2613-2619.
- del Arco A, et al. 2002. Expression of the aspartate/glutamate mitochondrial carriers, aralar1 and citrin, during development and in adult rat tissues. *Eur J Biochem* 269: 3313-3320.
- Denk W, Strickler JH, Webb WW. 1990. Two-photon laser scanning fluorescence microscopy. *Science* 248: 73-76.
- Deutch A, Roth R. 1999. Neurotransmitters. *Fundamental Neuroscience*. Zigmond MS, et al. editors. New York: Academic Press; p. 212.
- Diamond JS, Jahr CE. 2000. Synaptically released glutamate does not overwhelm transporters on hippocampal astrocytes during high-frequency stimulation. *J Neurophysiol* 83: 2835-2843.
- Dienel GA, Cruz NF. 2004. Nutrition during brain activation: Does cell-to-cell lactate shuttling contribute significantly to sweet and sour food for thought? *Neurochem Int* 45: 321-351.
- Dienel GA, Hertz L. 2001. Glucose and lactate metabolism during brain activation. *J Neurosci Res* 66: 824-838.
- Dodd PR, et al. 1989. Uptake of γ -aminobutyric acid and L-glutamic acid by synaptosomes from postmortem human cerebral cortex: Multiple sites, sodium dependence, and effect of tissue preparation. *Brain Res* 490: 320-331.
- Dolce V, et al. 2005. A fourth ADP/ATP carrier isoform in man: Identification, bacterial expression, functional characterization, and tissue distribution. *FEBS Lett* 579: 633-637.
- Eriksson G, et al. 1995. Sodium-dependent glutamate uptake as an activator of oxidative metabolism in primary astrocyte cultures from newborn rat. *Glia* 15: 152-156.
- Esclapez M, et al. 1997. Operative GABAergic inhibition in hippocampal CA1 pyramidal neurons in experimental epilepsy. *Proc Natl Acad Sci USA* 94: 12151-12156.
- Fiermonte G, et al. 2002. Identification of the mitochondrial glutamate transporter. Bacterial expression, reconstitution, functional characterization, and tissue distribution of two human isoforms. *J Biol Chem* 277: 19289-19294.
- Fiermonte G, et al. 2003. The mitochondrial ornithine transporter. Bacterial expression, reconstitution, functional characterization, and tissue distribution of two human isoforms. *J Biol Chem* 278: 32778-32783.
- Fiermonte G, et al. 2004. Identification of the mitochondrial ATP-Mg/P_i transporter. Bacterial expression, reconstitution, functional characterization, and tissue distribution. *J Biol Chem* 279: 30722-30730.
- Fiermonte G, Walker JE, Palmieri F. 1993. Abundant bacterial expression and reconstitution of an intrinsic membrane transport protein from bovine mitochondria. *Biochem J* 294(Pt 1): 293-299.
- Fiore C, et al. 1998. The mitochondrial ADP/ATP carrier: Structural, physiological, and pathological aspects. *Biochimie* 80: 137-150.
- Fox PT, et al. 1988. Nonoxidative glucose consumption during focal physiologic neural activity. *Science* 241: 462-464.
- Gadea A, Lopez-Colome AM. 2001. Glial transporters for glutamate, glycine, and GABA: II. GABA transporters. *J Neurosci Res* 63: 461-468.
- Gamberino WC, et al. 1997. Role of pyruvate carboxylase in facilitation of synthesis of glutamate and glutamine in cultured astrocytes. *J Neurochem* 69: 2312-2325.
- Goto M, Shinno H, Ichihara A. 1977. Isozyme patterns of branched-chain amino acid transaminase in human tissues and tumors. *Gann* 68: 663-667.

- Graham BH, et al. 1997. A mouse model for mitochondrial myopathy and cardiomyopathy resulting from a deficiency in the heart/muscle isoform of the adenine nucleotide translocator. *Nat Genet* 16: 226-234.
- Gramsbergen JB, et al. 2003. Quantitative on-line monitoring of hippocampus glucose and lactate metabolism in organotypic cultures using biosensor technology. *J Neurochem* 85: 399-408.
- Gruetter R, Seaquist ER, Ugurbil K. 2001. A mathematical model of compartmentalized neurotransmitter metabolism in the human brain. *Am J Physiol Endocrinol Metab* 281: E100-E112.
- Gupta M, et al. 2003. Murine succinate semialdehyde dehydrogenase deficiency. *Ann Neurol* 54 Suppl 6: S81-S90.
- Gutierrez R. 2003. The GABAergic phenotype of the glutamatergic granule cells of the dentate gyrus. *Prog Neurobiol* 71: 337-358.
- Hall TR, et al. 1993. Branched-chain aminotransferase isoenzymes. Purification and characterization of the rat brain isoenzyme. *J Biol Chem* 268: 3092-3098.
- Hassel B, Brathe A. 2000. Neuronal pyruvate carboxylation supports formation of transmitter glutamate. *J Neurosci* 20: 1342-1347.
- Hassel B, Sonnewald U. 1995. Glial formation of pyruvate and lactate from TCA cycle intermediates: Implications for the inactivation of transmitter amino acids? *J Neurochem* 65: 2227-2234.
- Hearl WG, Churchich JE. 1984. Interactions between 4-aminobutyrate aminotransferase and succinic semialdehyde dehydrogenase, two mitochondrial enzymes. *J Biol Chem* 259: 11459-11463.
- Henry PG, et al. 2002. Decreased TCA cycle rate in the rat brain after acute 3-NP treatment measured by in vivo ^1H - ^{13}C NMR spectroscopy. *J Neurochem* 82: 857-866.
- Hill DR, Bowery NG. 1981. ^3H -baclofen and ^3H -GABA bind to bicuculline-insensitive GABA B sites in rat brain. *Nature* 290: 149-152.
- Holmes CJ, Mainville LS, Jones BE. 1994. Distribution of cholinergic, GABAergic, and serotonergic neurons in the medial medullary reticular formation and their projections studied by cytotoxic lesions in the cat. *Neuroscience* 62: 1155-1178.
- Hutson SM. 1988. Subcellular distribution of branched-chain aminotransferase activity in rat tissues. *J Nutr* 118: 1475-1481.
- Hutson SM, et al. 1998. Role of branched-chain aminotransferase isoenzymes and gabapentin in neurotransmitter metabolism. *J Neurochem* 71: 863-874.
- Hutson SM, Lieth E, La Noue KF. 2001. Function of leucine in excitatory neurotransmitter metabolism in the central nervous system. *J Nutr* 131: 846S-850S.
- Hutson S, Sweatt A, La Noue K. 2005. Branched-chain amino acids in brain. *Handbook of Neurochemistry and Molecular Neurobiology*. Oja S, Schousboe A, Saransaari P, editors. New York: Springer.
- Hutson SM, Sweatt AJ, Lanoue KF. 2005. Branched-chain [corrected] amino acid metabolism: Implications for establishing safe intakes. *J Nutr* 135: 1557S-1564S.
- Ichihara A. 1985. Aminotransferases of branched-chain amino acids. *Transaminases*. Christen P, Metzler D, editors. New York: John Wiley and Sons; pp. 430-438.
- Indiveri C, Palmieri L, Palmieri F. 1994. Kinetic characterization of the reconstituted ornithine carrier from rat liver mitochondria. *Biochim Biophys Acta* 1188: 293-301.
- Jouvet P, et al. 2000. Branched-chain amino acids induce apoptosis in neural cells without mitochondrial membrane depolarization or cytochrome *c* release: Implications for neurological impairment associated with maple syrup urine disease. *Mol Biol Cell* 11: 1919-1932.
- Juhász G, et al. 1997. Differential effects of nipecotic acid and 4,5,6,7-tetrahydroisoxazolo[4,5-c]pyridin-3-ol on extracellular γ -aminobutyrate levels in rat thalamus. *Eur J Pharmacol* 331: 139-144.
- Kanamori K, Ross BD. 2005. Suppression of glial glutamine release to the extracellular fluid studied in vivo by NMR and microdialysis in hyperammonemic rat brain. *J Neurochem* 94: 74-85.
- Kanamori K, Ross BD, Kondrat RW. 1998. Rate of glutamate synthesis from leucine in rat brain measured in vivo by ^{15}N NMR. *J Neurochem* 70: 1304-1315.
- Kann O, et al. 2003. Coupling of neuronal activity and mitochondrial metabolism as revealed by NAD(P)H fluorescence signals in organotypic hippocampal slice cultures of the rat. *Neuroscience* 119: 87-100.
- Kasischke KA, et al. 2004. Neural activity triggers neuronal oxidative metabolism followed by astrocytic glycolysis. *Science* 305: 99-103.
- Kobayashi K, et al. 1999. The gene mutated in adult-onset type II citrullinemia encodes a putative mitochondrial carrier protein. *Nat Genet* 22: 159-163.
- Kobayashi K, Neely JR. 1979. Control of maximum rates of glycolysis in rat cardiac muscle. *Circ Res* 44: 166-175.
- La Noue KF, et al. 2001. Role of specific aminotransferases in de novo glutamate synthesis and redox shuttling in the retina. *J Neurosci Res* 66: 914-922.
- La Noue KF. 2005. Malate aspartate shuttle and glucose consumption in the brain. Abstract 10206 in American Society of Neurochemistry, 36th annual meeting. Madison, WI.
- La Noue KF, Bryla J, Bassett DJ. 1974. Energy-driven aspartate efflux from heart and liver mitochondria. *J Biol Chem* 249: 7514-7521.
- La Noue KF, Schoolwerth AC. 1979. Metabolite transport in mitochondria. *Annu Rev Biochem* 48: 871-922.
- La Noue KF, Schoolwerth A. 1984. Metabolite transport in mammalian mitochondria. *Bioenergetics*. Amsterdam: Elsevier; pp. 221-268.

- La Noue KF, Tischler ME. 1974. Electrogenic characteristics of the mitochondrial glutamate-aspartate antiporter. *J Biol Chem* 249: 7522-7528.
- Lapidot A, Gopher A. 1997. Quantitation of metabolic compartmentation in hyperammonemic brain by natural abundance ^{13}C -NMR detection of ^{13}C - ^{15}N coupling patterns and isotopic shifts. *Eur J Biochem* 243: 597-604.
- Lebon V, et al. 2002. Astroglial contribution to brain energy metabolism in humans revealed by ^{13}C nuclear magnetic resonance spectroscopy: Elucidation of the dominant pathway for neurotransmitter glutamate repletion and measurement of astrocytic oxidative metabolism. *J Neurosci* 22: 1523-1531.
- Liao SL, Chen CJ. 2003. L-glutamate decreases glucose utilization by rat cortical astrocytes. *Neurosci Lett* 348: 81-84.
- Lieth E, et al. 2000. Diabetes reduces glutamate oxidation and glutamine synthesis in the retina. The Penn state retina research group. *Exp Eye Res* 70: 723-730.
- Lieth E, et al. 2001. Nitrogen shuttling between neurons and glial cells during glutamate synthesis. *J Neurochem* 76: 1712-1723.
- Lopes-Cardozo M, Larsson O.M, Schousboe A. 1986. Acetoacetate and glucose as lipid precursors and energy substrates in primary cultures of astrocytes and neurons from mouse cerebral cortex. *J Neurochem* 46: 773-778.
- Mac Donald MJ, Marshall LK. 2001. Survey of normal appearing mouse strain which lacks malic enzyme and NAD^+ -linked glycerol phosphate dehydrogenase: Normal pancreatic β cell function but abnormal metabolite pattern in skeletal muscle. *Mol Cell Biochem* 220: 117-125.
- Magistretti PJ, et al. 1999. Energy on demand. *Science* 283: 496-497.
- Magistretti PJ, Pellerin L. 1999. Astrocytes couple synaptic activity to glucose utilization in the brain. *News Physiol Sci* 14: 177-182.
- Maher F, Vannucci SJ, Simpson IA. 1994. Glucose transporter proteins in brain. *FASEB J* 8: 1003-1011.
- Malandro MS, Kilberg MS. 1996. Molecular biology of mammalian amino acid transporters. *Annu Rev Biochem* 65: 305-336.
- Mangia S, et al. 2003. Issues concerning the construction of a metabolic model for neuronal activation. *J Neurosci Res* 71: 463-467.
- Mangia S, et al. 2003. The aerobic brain: Lactate decrease at the onset of neural activity. *Neuroscience* 118: 7-10.
- Martinez-Hernandez A, Bell KP, Norenberg MD. 1977. Glutamine synthetase: Glial localization in brain. *Science* 195: 1356-1358.
- Matsuo Y, Yagi M, Walser M. 1993. Arteriovenous differences and tissue concentrations of branched-chain ketoacids. *J Lab Clin Med* 121: 779-784.
- McGivan JD, Bradford NM, Beavis AD. 1977. Factors influencing the activity of ornithine aminotransferase in isolated rat liver mitochondria. *Biochem J* 162: 147-156.
- McKenna MC, et al. 2000. Mitochondrial malic enzyme activity is much higher in mitochondria from cortical synaptic terminals compared with mitochondria from primary cultures of cortical neurons or cerebellar granule cells. *Neurochem Int* 36: 451-459.
- Medina JM, Giaume C, Taberner A. 1999. Metabolic coupling and the role played by astrocytes in energy distribution and homeostasis. *Adv Exp Med Biol* 468: 361-371.
- Minchin MC, Beart PM. 1975. Compartmentation of amino acid metabolism in the rat dorsal root ganglion—a metabolic and autoradiographic study. *Brain Res* 83: 437-449.
- Mohler H, Fritschy JM, Rudolph U. 2002. A new benzodiazepine pharmacology. *J Pharmacol Exp Ther* 300: 2-8.
- Molinari F, et al. 2005. Impaired mitochondrial glutamate transport in autosomal recessive neonatal myoclonic epilepsy. *Am J Hum Genet* 76: 334-339.
- Morozzo della Rocca B, et al. 2003. The mitochondrial oxoglutarate carrier: Structural and dynamic properties of transmembrane segment IV studied by site-directed spin labeling. *Biochemistry* 42: 5493-5499.
- Nguyen NH, Brathe A, Hassel B. 2003. Neuronal uptake and metabolism of glycerol and the neuronal expression of mitochondrial glycerol-3-phosphate dehydrogenase. *J Neurochem* 85: 831-842.
- Norenberg M. 1979. Distribution of glutamine synthetase in rat central nervous system. *J Histochem Cytochem* 27: 756-762.
- Olson MJ, Thurman RG. 1987. Quantitation of ketogenesis in periportal and pericentral regions of the liver lobule. *Arch Biochem Biophys* 253: 26-37.
- Oz G, et al. 2004. Neuroglial metabolism in the awake rat brain: CO_2 fixation increases with brain activity. *J Neurosci* 24: 11273-11279.
- Palmieri F. 2004. The mitochondrial transporter family (SLC25): Physiological and pathological implications. *Pflügers Arch* 447: 689-709.
- Palmieri L, et al. 2001. Citrin and aralar1 are Ca^{2+} -stimulated aspartate/glutamate transporters in mitochondria. *EMBO J* 20: 5060-5069.
- Park J, Osei YD, Churchich JE. 1993. Isolation and characterization of recombinant mitochondrial 4-aminobutyrate aminotransferase. *J Biol Chem* 268: 7636-7639.
- Patel M. 1989. CO_2 -fixing enzymes in *Neuromethods: Carbohydrate and Energy Metabolism*. Boulton A, Baker G, editors. Clifton, NJ: The Humana Press, Inc.; pp. 309-340.
- Patterson GH, et al. 2000. Separation of the glucose-stimulated cytoplasmic and mitochondrial NAD(P)H responses in pancreatic islet β cells. *Proc Natl Acad Sci USA* 97: 5203-5207.

- Pellerin L, et al. 1998. Evidence supporting the existence of an activity-dependent astrocyte–neuron lactate shuttle. *Dev Neurosci* 20: 291-299.
- Pellerin L, Magistretti PJ. 1994. Glutamate uptake into astrocytes stimulates aerobic glycolysis: A mechanism coupling neuronal activity to glucose utilization. *Proc Natl Acad Sci USA* 91: 10625-10629.
- Pellerin L, Magistretti PJ. 2004. Neuroscience. Let there be (NADH) light. *Science* 305: 50-52.
- Pierard C, et al. 1999. Effects of GABA-transaminase inhibition on brain metabolism and amino acid compartmentation: An in vivo study by 2D ¹H-NMR spectroscopy coupled with microdialysis. *Exp Brain Res* 127: 321-327.
- Purvis JL, Lowenstein JM. 1961. The relation between intra- and extramitochondrial pyridine nucleotides. *J Biol Chem* 236: 2794-2803.
- Ramos M, et al. 2003. Developmental changes in the Ca²⁺-regulated mitochondrial aspartate–glutamate carrier aralar1 in brain and prominent expression in the spinal cord. *Brain Res Dev Brain Res* 143: 33-46.
- Reimer RJ, et al. 2000. Amino acid transport system A resembles system N in sequence but differs in mechanism. *Proc Natl Acad Sci USA* 97: 7715-7720.
- Reinert, KC, et al. 2004. Flavoprotein autofluorescence imaging of neuronal activation in the cerebellar cortex in vivo. *J Neurophysiol* 92: 199-211.
- Ribeiro L, et al. 1993. Cerebral blood flow and metabolism during nonspecific bilateral visual stimulation in normal subjects. *Quantification of Brain Function: Tracer Kinetics and Image Analysis in Brain PET*. Unemura K, et al. editors. Amsterdam: Elsevier; pp. 229-234.
- Rognstad R. 1980. Effects of ethyl hydrazinoacetate on gluconeogenesis and on ethanol oxidation in rat hepatocytes. *Biochim Biophys Acta* 628: 116-118.
- Rosenthal RE, et al. 1987. Cerebral ischemia and reperfusion: Prevention of brain mitochondrial injury by lidoflazine. *J Cereb Blood Flow Metab* 7: 752-758.
- Rothstein JD, et al. 1994. Localization of neuronal and glial glutamate transporters. *Neuron* 13: 713-25.
- Runswick MJ, et al. 1990. Sequence of the bovine 2-oxoglutarate/malate carrier protein: Structural relationship to other mitochondrial transport proteins. *Biochemistry* 29: 11033-11040.
- Sakai R, et al. 2004. Leucine-nitrogen metabolism in the brain of conscious rats: Its role as a nitrogen carrier in glutamate synthesis in glial and neuronal metabolic compartments. *J Neurochem* 88: 612-622.
- Salvati S, et al. 1996. Accelerated myelinogenesis by dietary lipids in rat brain. *J Neurochem* 67: 1744-1750.
- Sarup A, et al. 2003. Effects of 3-hydroxy-4-amino-4,5,6,7-tetrahydro-1,2-benzoxazol (exo-THPO) and its N-substituted analogs on GABA transport in cultured neurons and astrocytes and by the four cloned mouse GABA transporters. *Neurochem Int* 43: 445-451.
- Sarup A, Larsson OM, Schousboe A. 2003. GABA transporters and GABA transaminase as drug targets. *Curr Drug Targets CNS Neurol Disord* 2: 269-277.
- Schmoll D, et al. 1995. Significant amounts of glycogen are synthesized from 3-carbon compounds in astroglial primary cultures from mice with participation of the mitochondrial phosphoenolpyruvate carboxykinase isoenzyme. *Eur J Biochem* 227: 308-315.
- Schousboe A. 1981. Transport and metabolism of glutamate and GABA in neurons and glial cells. *Int Rev Neurobiol* 22: 1-45.
- Schousboe A. 2000. Pharmacological and functional characterization of astrocytic GABA transport: A short review. *Neurochem Res* 25: 1241-1244.
- Schousboe I, Bro B, Schousboe A. 1977. Intramitochondrial localization of the 4-aminobutyrate-2-oxoglutarate transaminase from ox brain. *Biochem J* 162: 303-307.
- Schousboe, A, et al. 2004. Role of astrocytic transport processes in glutamatergic and GABAergic neurotransmission. *Neurochem Int* 45: 521-527.
- Shank RP, Leo GC, Zielke HR. 1993. Cerebral metabolic compartmentation as revealed by nuclear magnetic resonance analysis of D-[1-¹³C]glucose metabolism. *J Neurochem* 61: 315-323.
- Sharma R, Patnaik SK. 1983. Induction of phosphoenolpyruvate carboxykinase by hydrocortisone in rat liver and brain as a function of age. *Biochem Int* 7: 535-540.
- Sheikh SN, Martin DL. 1998. Elevation of brain GABA levels with vigabatrin (γ -vinylGABA) differentially affects GAD65 and GAD67 expression in various regions of rat brain. *J Neurosci Res* 52: 736-741.
- Sherif FM, Ahmed SS. 1995. Basic aspects of GABA-transaminase in neuropsychiatric disorders. *Clin Biochem* 28: 145-154.
- Shuttleworth CW, Brennan AM, Connor JA. 2003. NAD(P)H fluorescence imaging of postsynaptic neuronal activation in murine hippocampal slices. *J Neurosci* 23: 3196-3208.
- Sibson NR, et al. 1997. In vivo ¹³C NMR measurements of cerebral glutamine synthesis as evidence for glutamate–glutamine cycling. *Proc Natl Acad Sci USA* 94: 2699-2704.
- Sibson NR, et al. 1998. Stoichiometric coupling of brain glucose metabolism and glutamatergic neuronal activity. *Proc Natl Acad Sci USA* 95: 316-321.
- Sibson NR, et al. 2001. In vivo ¹³C NMR measurement of neurotransmitter glutamate cycling, anaplerosis, and TCA cycle flux in rat brain during. *J Neurochem* 76: 975-989.
- Sinasac DS, et al. 2004. Slc25a13-knockout mice harbor metabolic deficits but fail to display hallmarks of adult-onset type II citrullinemia. *Mol Cell Biol* 24: 527-536.

- Sonnenwald U, et al. 1993. Metabolism of [^{13}C]glutamate in astrocytes studied by ^{13}C NMR spectroscopy: Incorporation of more label into lactate than into glutamine demonstrates the importance of the tricarboxylic acid cycle. *J Neurochem* 61: 1179-1182.
- Sonnenwald U, Qu H, Aschner M. 2002. Pharmacology and toxicology of astrocyte–neuron glutamate transport and cycling. *J Pharmacol Exp Ther* 301: 1-6.
- Stipani V, et al. 2001. The mitochondrial oxoglutarate carrier: Cysteine-scanning mutagenesis of transmembrane domain IV and sensitivity of Cys mutants to sulfhydryl reagents. *Biochemistry* 40: 15805-15810.
- Sweatt AJ, et al. 2004. Branched-chain amino acids and neurotransmitter metabolism: Expression of cytosolic branched-chain aminotransferase (BCATc) in the cerebellum and hippocampus. *J Comp Neurol* 477: 360-370.
- Tian N, et al. 1999. The role of the synthetic enzyme GAD65 in the control of neuronal γ -aminobutyric acid release. *Proc Natl Acad Sci USA* 96: 12911-12916.
- Tillakaratne NJ, Medina-Kauwe L, Gibson KM. 1995. γ -Aminobutyric acid (GABA) metabolism in mammalian neural and nonneural tissues. *Comp Biochem Physiol A Physiol* 112: 247-263.
- Varoqui H, et al. 2000. Cloning and functional identification of a neuronal glutamine transporter. *J Biol Chem* 275: 4049-4054.
- Vogel R, Hamprecht B, Wiesinger H. 1998. Malic enzyme isoforms in astrocytes: Comparative study on activities in rat brain tissue and astroglia-rich primary cultures. *Neurosci Lett* 247: 123-126.
- Wadiche JI, Tzingounis AV, Jahr CE. 2006. Intrinsic kinetics determine the time course of neuronal synaptic transporter currents. *Proc Natl Acad Sci USA* 103: 1083-1087.
- Waelisch H, et al. 1964. Quantitative aspects of CO_2 fixation in mammalian brain in vivo. *J Neurochem* 11: 717-728.
- Walz W, Mukerji S. 1988. Lactate release from cultured astrocytes and neurons: A comparison. *Glia* 1: 366-370.
- Wang L, Tornquist P, Bill A. 1997. Glucose metabolism of the inner retina in pigs in darkness and light. *Acta Physiol Scand* 160: 71-74.
- Williamson DH, Lund P, Krebs HA. 1967. The redox state of free nicotinamide adenine dinucleotide in the cytoplasm and mitochondria of rat liver. *Biochem J* 103: 514-527.
- Williamson JR, et al. 1973. Mitochondrial-cytosolic interactions in cardiac tissue: Role of the malate–aspartate cycle in the removal of glycolytic NADH from the cytosol. *Symp Soc Exp Biol* 27: 241-281.
- Wu Y, Wang W, Richerson GB. 2001. GABA transaminase inhibition induces spontaneous and enhances depolarization-evoked GABA efflux via reversal of the GABA transporter. *J Neurosci* 21: 2630-2639.
- Xu Y, et al. 2004. Whole-brain glutamate metabolism evaluated by steady-state kinetics using a double-isotope procedure: Effects of gabapentin. *J Neurochem* 90: 1104-1116.
- Yudkoff M, et al. 1983. [^{15}N] leucine as a source of [^{15}N] glutamate in organotypic cerebellar explants. *Biochem Biophys Res Commun* 115: 174-179.
- Yudkoff M, et al. 1996. Astrocyte leucine metabolism: Significance of branched-chain amino acid transamination. *J Neurochem* 66: 378-385.

6.2 Mitochondrial-Endoplasmic Reticulum Interactions

G. Szabadkai · R. Rizzuto

1	<i>Introduction</i>	618
2	<i>Structural Basis of the Interorganellar Interaction</i>	618
2.1	Structural Determinants of the Mitochondrial Network—A Snapshot and Its Evolutionary Origin	618
2.2	Parallel Evolution of Secretory Membranes, the ER, and the Endosymbiont Mitochondria	619
2.3	Spatial Colocalization and Physical Interaction Between the ER and Mitochondrial Networks—The MAM Fraction of ER	622
3	<i>Control of Metabolic Flux Between Mitochondria and ER</i>	622
3.1	The Mitochondrial Inner Membrane	622
3.2	The Mitochondrial Intermembrane Space	623
3.3	The Outer Membrane—Metabolic Channeling Through the VDAC Pore	624
3.4	VDAC in the Center of Protein Complexes Regulating Metabolic Channeling	624
3.5	The ATP Microdomain at the ER-Mitochondrial Interface	625
4	<i>Ca²⁺ Channeling Between the ER and Mitochondria</i>	626
4.1	Functional Properties of Mitochondrial Ca ²⁺ Uptake	626
4.2	Modification of Mitochondrial Ca ²⁺ Uptake by Modifying ER Ca ²⁺ Release	627
4.3	Mitochondrial Morphology Determines the Efficiency of Ca ²⁺ Channeling from the ER	628
4.4	Ca ²⁺ Signaling in Apoptosis and Mitochondrial Shape	630
5	<i>The Role of ER and Mitochondria and Their Contacts in Phospholipid Biosynthesis</i>	630
6	<i>ER–Mitochondria Contacts and Sphingolipid Metabolism</i>	632
7	<i>Protein Transport and Folding at the ER–Mitochondrial Interface</i>	632
8	<i>Summation, Challenging Problems, and Further Avenues</i>	633

List of Abbreviations: ACS, acyl-CoA synthetase; AT, acyltransferase; CL, cardiolipin; DG, diacylglycerol; FA, fatty acid; G-3-P, glycerol-3-phosphate; GPAT, glycerol-3-phosphate acyltransferase; PA, phosphatidic acid; PAB, phosphatidic acid phosphatase; PC, phosphatidylcholine; PE, phosphatidylethanolamine; PEMT, phosphatidylethanolamine *N*-methyltransferase; PG, phosphatidylglycerol; PI, phosphatidylinositol; PS, phosphatidylserine; PSD, phosphatidylserine decarboxylase; PSS, phosphatidylserine synthase

1 Introduction

More than 50 years of progress has provided structural details and functional consequences of the intercompartmental interactions between the mitochondrial and endoplasmic reticulum (ER) networks of eukaryotic cells. Biochemical approaches have characterized several membrane components clustered in interacting protein complexes, such as the protein import machinery of both organelles, components of the mitochondrial inner and outer membrane contact sites, division and fusion machineries of mitochondria, and most recently connections of the mitochondrial and ER networks. Moreover, the ER shares several metabolic pathways with the mitochondria: amino acid, lipid, carbohydrate, and even protein cycling exists between these two organelles, and their interrelated role in Ca^{2+} -, ROS-, and ATP signaling is not doubted any more. In addition to playing a crucial role in the subsistence of the organelles, it has now been recognized that these complex interactions are involved in basic cellular processes such as cell growth, metabolism, and death processes.

2 Structural Basis of the Interorganellar Interaction

Recently, a series of proteins, mainly mechanochemical enzymes (large GTPases), were shown to drive the formation of the shape of mitochondria by regulating its continuous fusion and fission events. The dynamic formation of the ER network seems to work through conceptually different processes, but recent studies revealed possible links in the parallel evolution of the two organelles, which might shed new light also on their interactions.

2.1 Structural Determinants of the Mitochondrial Network—A Snapshot and Its Evolutionary Origin

Mitochondria form a dynamic and highly variable network in eukaryotic cells, depending on the organism, the cell type, and the developmental stage (Bereiter-Hahn, 1990; Yaffe, 1999). However, this complexity might reflect a complex evolutionary path evolving from their α -proteobacterial ancestor (Gray et al., 1999). Indeed, the recent discovery of protein components driving the fusion and fission of mitochondria differ from the ones found in the genome of their prokaryotic ancestor. Division of bacteria relies on the formation of a ring underneath the inner cell membrane, of which the main component is FtsZ, a GTP-dependent mechanochemical enzyme. This FtsZ ring can be found in mitochondria of some primitive eukaryotes, but mitochondria of fungi, plants, and animals have lost this division component (Osteryoung and Nunnari, 2003). While eukaryotic tubulin seems to have close relations to FtsZ, eukaryotic cells developed a new group of proteins serving to drive the dynamics of intracellular membranes, still using GTP as source of free-energy changes. The first “large GTPase” found to be involved in the dynamic formation of the mitochondrial network was the *Drosophila* protein *fzo* (stands for fuzzy onion), which was shown to mediate the fusion of mitochondria during the meiotic stage of spermatogenesis (Hales and Fuller, 1997). Mitochondria of spermatogonia of *fzo* mutant flies showed an aberrant morphology, and importantly this change led to nonfunctional sperm formation, and thus to sterility of the affected flies. Following the discovery of the *fzo* gene product and its homologs in yeast, animals, and humans, a large family of GTPases has now been described driving both fusion and fission of mitochondria (Mozdy and Shaw, 2003; Westermann, 2003; Meeusen and Nunnari, 2005). The [table below](#) summarizes the currently

known components of the mitochondrial division and fusion apparatus (▶ [Table 6.2-1](#)), while the proposed mechanisms of fusion and fission is shown on ▶ [Figure 6.2-1](#). The figure legend also includes a short description of these processes.

■ **Table 6.2-1**
Components of the mitochondrial division and fusion machinery

Protein	Species	Function	Localization ^a
FtsZ-mt	Primitive eukaryotes	Fission, ring formation	M
CmDnm1	Red algae	Fission	Cytosolic side of OMM
Dnm-1, Drp-1	Fungi, animals	Fission	Cytosol→OMM
ADL-2b	Plants		
Fis1, hFis1	Fungi, animals	Fission	OMM integral protein
Mdv1	Budding yeast	Fission	Cytosolic surface of OMM
Erp1, endophilin-related protein	Fungi, animals	Fission	OMM
Endophilin B1	Animals	Fission	Cytosol→OMM
DAP3 (death-associated protein-3)	Mammals	Fission?	M
MPT18	Drosophila, mammals	Fission	OMM? required for Fis action
Gag3p/Mdv1p/Net2p	Yeast	Fission	OMM
Rab32 small GTPase	Mammals	OMM-associated AKAP, regulates fission	OMM
Fzo1/ Mfn1,2 (Mitofusin-1,2)	Fungi, animals	Fusion	OMM
Opa1/Mgm1	Fungi, animals	IMM fusion	IMS, tethered to IMM
Pcp1 (Mgm37) (rhomboid-type protease)	Fungi, animals	Fusion, processing of Mgm1	IMS
Mitochondrial Rho GTPase, miro-1,2 (Gem1p, yeast)	Yeast, Drosophila, human	Fusion	OMM
Ugo1	Yeast	Fusion	OMM, links Fzo1 and Mgm1

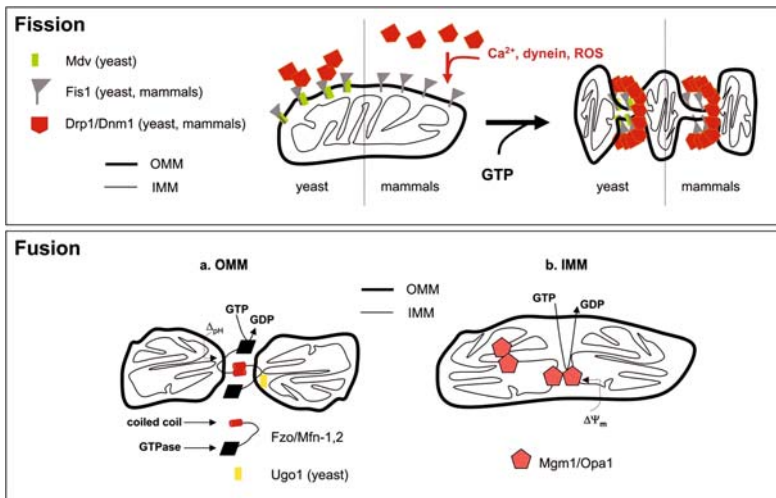
^aM: mitochondrial matrix; OMM: mitochondrial outer membrane; IMM: mitochondrial inner membrane; IMS: mitochondrial intermembrane space

2.2 Parallel Evolution of Secretory Membranes, the ER, and the Endosymbiont Mitochondria

The ER is a membrane enclosed, almost completely continuous (Federovitch et al., 2005; Levine and Rabouille, 2005) organelle that is central to numerous processes critical to the proper functioning of all eukaryotic cells (Baumann and Walz, 2001; Voeltz et al., 2002). The ER, contiguous with the nuclear envelope membrane, forms a membranous network in the cell that is the major site of lipid biosynthesis and protein folding and is the entry point into the secretory pathway. Thus, the ER can be considered the common ancestor of all membranes downstream in this pathway, including the Golgi complex, secretory vesicles, the lysosome, and the plasma membrane.

■ **Figure 6.2-1**

Mechanisms of fission (division) and fusion in the mitochondrial network. The components with known function in yeast and mammalian mitochondrial division are shown separately on the *upper panel*. Fis1 in both systems functions as an anchor for Drp-1/Dnm1. Dnm1, in yeast, is localized on the OMM surface, while in mammals Drp-1 is translocated following Ca^{2+} , ROS signals by a mechanism involving the molecular motor dynein. In the presence of GTP, Drp-1/Dnm-1 form aggregates, and by a currently unknown mechanism, induces fission through the Dnm1/Fis1/Mdv complexes in yeast or Drp1/Fis1 complexes in mammals. The *lower panel* illustrates the two phases (inner membrane and outer membrane) of fusion between mitochondrial particles. (a) For the fusion of the OMM, maintenance of the ΔpH through the IMM is necessary, and it proceeds by the interaction between mitofusin/fzo molecules, bearing coiled-coil interactory domains and GTPase domains. In yeast, fzo interacts with Ugo1, most probably transducing the fusion signal between the two membranes. (b) In contrast, the fusion of the IMM requires polarized mitochondria (maintained $\Delta\psi_m$) and a GTP-dependent process driven by the IMM protein Opa1/Mgm1. This protein has been shown to participate also in cristae remodeling



ER biogenesis is a result of coordinate activation of protein and lipid biosynthetic pathways, as deduced from experiments showing the interdependency of two known pathways, the unfolded protein response (UPR) and inositol response pathways (Federovitch et al., 2005). Accumulation of unfolded proteins leads to activation of a transcriptome including ER chaperones to ensure proper folding in the ER lumen, but concerted activation of genes involved in phospholipid synthesis can be observed in these cases, which normally respond to inositol starvation (Cox et al., 1997; Powell and Latterich, 2000). Similar mechanisms might be operating in higher animals during normal ER biogenesis and the so-called “ER stress” conditions (Szczesna-Skorupa et al., 2004), which now seem to be involved in the pathogenesis of several diseases (Rao and Bredesen, 2004; Paschen and Mengesdorf, 2005; Xu et al., 2005; see details of neurodegenerative diseases in chapter 4.6).

The questions however remain: how the normal structure of the ER is maintained, and what is the role and mechanism of membrane fusion and fission events in the dynamics of the ER network? The ATP-dependent membrane fusion in the secretory pathway is generally mediated by specific pairing between vesicle-associated SNAP receptors (v-SNAREs; the VAMP family) and target membrane-associated SNAREs (t-SNAREs; the syntaxin and SNAP-25 families) (Weber et al., 1998; Lin and Scheller, 2000; Jahn and Grubmuller, 2002). As follows, a recent working model for ER homotypic fusion involves a t-t-SNARE interaction (for review see Uchiyama and Kondo (2005)). Importantly, several interacting proteins have

been recently described to regulate this process, among which the most important ones are members of the small GTPase family of proteins, thought to determine organelle identity and their intracellular trafficking (for review see Munro (2004)). Along these lines, a tempting parallel regulation could be proposed for both the ER and mitochondrial membrane dynamics. Indeed, the growing protein family of mitochondrial fusion/fission machinery has now been shown to include specialized proteins of the Rho family GTPases (*mitochondrial Rho* GTPase, Miro-1,2). Human Miro and its orthologs in *Drosophila* and yeast (*Gem1p*) are all characterized by the presence of two GTPase domains and, intriguingly, also two Ca^{2+} -binding EF hand domains (Fransson et al., 2003; Frederick et al., 2004; Guo et al., 2005). According to these findings, Miro proteins thus may provide a direct link to Ca^{2+} regulation of mitochondrial dynamics, in analogy with other integrated GTPase and Ca^{2+} -signaling pathways (for review see Aspenstrom (2004)). Recent work unraveled an important role of the large GTPase mitochondrial fusion factor mitofusin-2 in regulating vascular hyperplasia through the regulation of Ras(p21) activity (Chen et al., 2004), showing for the first time a physical and functional interaction between these signaling pathways. In yeast, Rab family proteins were shown to be necessary for fusion competence of ER membranes (Barrowman et al., 2003), as well as in the synchronization of mitochondrial fission in mammalian cells (Alto et al., 2002). Ultimately, it was shown that movement of mitochondria is controlled by the small GTPase RhoA through regulating their association with actin via formin family proteins (Minin et al., 2006). We can just imagine that further work will explore more details on this topic, characterizing parallel events in the membrane dynamics of the ER and mitochondrial networks.

What can be the significance of these findings? The recent explosion of genomic data allowed reconstructing the extensive evolutionary view of the Ras family of small G-proteins, the main regulators of membrane dynamics, giving insight also on the formation of intracellular membrane networks (Jekely, 2003). Importantly, the superfamily of Ras GTPases, now consisting of at least seven families of proteins (Sar1, Arf, SRb, Rab, Ran, Ras, and Rho) (Leipe et al., 2002)) has no orthologs among prokaryotes and they diversified at a very early stage of eukaryotic evolution. The reconstruction of the Ras family evolutionary tree shows that the secretory tubulovesicular intracellular membrane system, the ancestor of the ER and the Golgi complex system and a primitive form of the nuclear membranes, paved the way for the origin of endo/phagocytosis. Thus, this pathway served also to establish the way for the endosymbiont mitochondria (and chloroplasts). Indeed, first the Sar1/Arf/SRb sequences split off from all other small GTPases suggesting that secretory endomembranes evolved in a very early eukaryote, and thus serving also as a basis for the connection to the plasma membrane and the cell exterior and ultimately for the reverse process of endo/phagocytosis. This event was followed by the evolution of (1) Rab proteins (Pfeffer, 2001), regulating intracellular vesicle transport and fusion; (2) Rho family proteins (Ridley, 2001), primarily involved in the regulation of the actin cytoskeleton; and together with (3) Ras, in the transduction of extracellular signals. Importantly, these three classes of proteins are essential for present-day phagocytosis (Takai et al., 2001). Along these lines, a general scheme that emerged to ensure the specificity of membrane traffic and interactions between different organelle membranes in the secretory pathway is the surface targeting of peripheral membrane proteins (for review see Munro (2002)). Several mechanisms have been proposed to underlie this process, including recruitment of specific small GTPases on the membrane surface and exposure of specific lipid domains on the organelle membrane. The former mechanism depends on specific GTP exchange factors (GEFs) that convert the members of the ADP-ribosylation factor (Arf/Sar) small GTPase protein family to the GTP bound form. The ER-resident transmembrane GEF protein, Sec12, is involved in ER–Golgi complex vesicular transport (Weissman et al., 2001), while the TRAPP GEF membrane-associated complex, leading the activation of Rab proteins (Sacher et al., 2001), participates in the retrograde Golgi complex–ER transport. Interestingly, Rab family proteins are also needed for fusion competence of ER membranes, as shown in yeast (Barrowman et al., 2003).

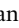
In summary, on the basis of these results which reveal a key role of the Ras family GTPases in the regulation of membrane dynamics in the secretory membrane networks, and more recently in mitochondria, we suggest that the parallel evolution of the these organelles during the genesis of the eukaryotic cells also served as a basis for their interaction.

2.3 Spatial Colocalization and Physical Interaction Between the ER and Mitochondrial Networks—The MAM Fraction of ER

Parallel to the functional characterization of the membrane dynamics of ER-mitochondrial networks, significant progress has been made in exploring the morphological characteristics of their interaction. This topic is extensively covered and illustrated in the chapter 4.6; here we just mention that the close synaptic-like apposition of the organelles was clearly demonstrated in a broad variety of cell types using light and electron microscopic studies, (Mannella et al., 1998; Rizzuto et al., 1998; Marsh et al., 2001; Frey et al., 2002).

It is now generally accepted that even if the ER forms a structurally cohesive network, it contains also functionally and structurally separate subdomains, generally specialized to a defined function (for recent review see Levine et al. (2005)). Indeed, the mitochondrial-ER interface seems to be one of these specialized domains, containing smooth ER membrane, devoid of attached ribosomes (Wang et al., 2000). This specific ER compartment involved in interactions with mitochondria is called the mitochondria-associated ER membrane (MAM). Originally it was described by its enrichment of lipid synthetic and transfer activities, but now it has an emerging role in other signaling pathways, like Ca^{2+} signaling (Filippin et al., 2003), and most probably in apoptotic signaling following ER modifications. These functions of the MAM are discussed later in detail in the sections dealing with lipid and Ca^{2+} signaling, as well as another chapters in this volume.

3 Control of Metabolic Flux Between Mitochondria and ER

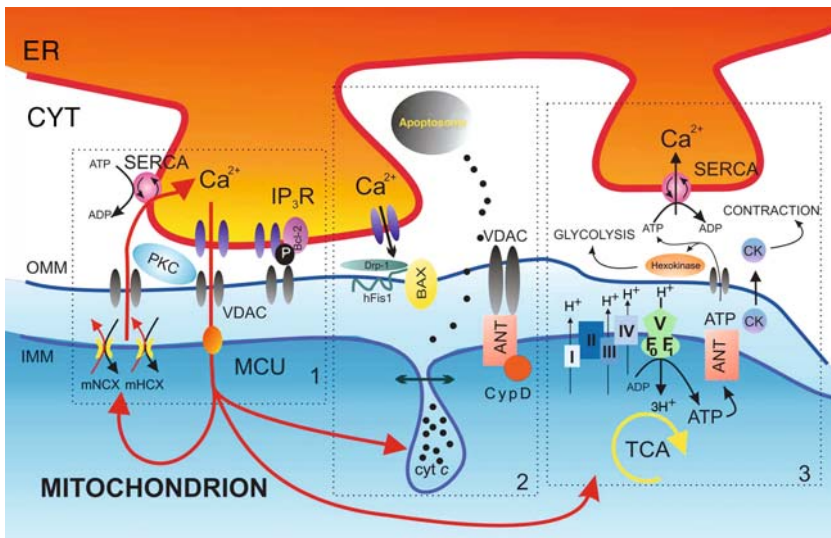
Mitochondria are in the center of a large variety of metabolic processes in eukaryotic cells such as the generation of ATP through oxidative phosphorylation, the Krebs cycle, fatty acid β -oxidation, the urea cycle, ketone body synthesis, and amino acid metabolism. All of these processes require intense transport of metabolites between mitochondria and extramitochondrial sites. Here, we summarize current knowledge regarding metabolic transport supporting energy-dependent processes specifically in the ER, which features feeding ER with ATP by exchanging it to ADP. At the molecular level, all the above processes have to be carried out by a large number of different proteins residing on the mitochondrial inner membrane (IMM), the mitochondrial intermembrane space (IMS), and the mitochondrial outer membrane (OMM).  *Figure 6.2-2* describes schematically the metabolic ER-mitochondrial interacting unit in the context of Ca^{2+} - and apoptotic signaling.

3.1 The Mitochondrial Inner Membrane

Most of the ATP, supplied by mitochondrial oxidative phosphorylation, is exported to the IMS by adenine nucleotide translocase (ANT, also called ATP/ADP translocator) in exchange for incoming ADP. The exchanger exists in two conformations depending on the nucleotide-binding either facing the matrix (*m* conformation) or the IMS space (*c* conformation). Expression of three different isoforms of ANT has been so far reported. In rat and mouse, ANT-1 is mainly present in the brain, kidneys, skeletal muscles, and the heart, whereas isotype ANT-2 is predominant in other tissues, and ANT-3 is present in small amount in all tissues (Stepien et al., 1992; Doerner et al., 1997). Thus, it is evident that ANT-1, ANT-2, and ANT-3 might coexist in a single mitochondrion. In this respect, it was shown that peripheral inner mitochondrial membrane contains all isoforms of ANT, whereas in cristae membranes ANT-2 isoform is present exclusively (Vyssokikh et al., 2001). This may suggest specific functions of particular ANT isoforms. Indeed, ANT at mitochondrial contact sites between the IMM and OMM takes part in the formation of protein complexes and regulates the permeability of mitochondrial membranes (see below). Importantly, the interactions depend on the conformational state of the ANT protein. By confirming the isoform specificity of the ANT proteins, we have shown that of the three isoforms only ANT-1 and ANT-3 were able to change mitochondrial Ca^{2+} uptake following agonist stimulation (M. Wieckowski, G. Szabadkai, and R. Rizzuto, manuscript in preparation). An alternative pathway for ATP export from the mitochondrial matrix can be

■ Figure 6.2-2

Schematic representation of interconnecting functional units of the ER and mitochondrial networks. Modified from Bianchi et al. (2004). Three different microdomains are outlined (*dotted boxes*): (1) The Ca^{2+} signaling microdomain comprises the Ca^{2+} release channel (IP_3R) of the ER, the VDAC of the OMM, and the MCU of the IMM, while Ca^{2+} recycling occurs through Ca^{2+} exchangers of the IMM and the SERCA pump of the ER. (2) Apoptotic mechanism on the mitochondrial outer membrane (OMM) and in the intermembrane space: Ca^{2+} -dependent translocation of the fission factor Drp-1 participates in the proapoptotic Bcl-2 family member-mediated outer membrane permeabilization and cytochrome *c* release, which leads to the activation of the effector caspases of the apoptosome. In addition, Ca^{2+} in concert with other factors induces the opening of mitochondrial permeability transition pore (PTP), most probably composed of the IMM component ANT-cyp-D complex and the OMM component VDAC. (3) Metabolic microdomain and the route of mitochondrially produced ATP. Continuous cycling of ATP and ADP occurs both through the IMM and OMM. The ANT is responsible for the former, while the VDAC channel mediates the transport through the OMM. The CK enzyme is an important component of the cycling machinery, supplying energy for ATP-dependent ER or sarcoplasmic reticulum processes, such as Ca^{2+} uptake through the SERCA pumps



fulfilled by another member of the mitochondrial carrier family, the deoxynucleotide carrier or the ATP-Mg/Pi exchange carrier, supplementing the role of ANT under certain conditions (Palmieri, 2004).

3.2 The Mitochondrial Intermembrane Space

In muscle and brain cells, phosphocreatine and adenylate kinase shuttles provide a link between ATP-producing and ATP-consuming sites (Bessman and Geiger, 1981; Saks et al., 1996; Dzeja and Terzic, 2003; Joubert et al., 2004). The functional coupling between mitochondrial creatine kinase (CK) and ANT has been identified, as a part of the phosphocreatine shuttle, by stimulating oxidative phosphorylation with creatine, and has been characterized by a number of studies (see references in Dzeja and Terzic, 2003; Ovadi and Saks (2004)). More recently, a model based on experimental data obtained from heart tissue has been established, efficiently describing metabolic channeling in the IMS (Vendelin et al., 2004). Further structural studies also suggest that compartmentalization in the IMS also occurs between the intracristal and external IMS space. Indeed, simulations indicate that narrow cristae junctions restrict diffusion between intracristal and external compartments, causing depletion of ADP and decreased ATP output inside the cristae (Mannella et al., 2001).

3.3 The Outer Membrane—Metabolic Channeling Through the VDAC Pore

The mitochondria of all eukaryotic organisms studied so far have at least one isoform of the voltage-dependent anion channel (VDAC), which, after reconstitution into planar phospholipid membranes, forms a voltage-regulated channel with highly conserved characteristics (Colombini, 1989). The pathway formed through the membrane by VDAC has channel properties similar to channels involved in ion transport, but they evolved to generate a large pathway because of the large size of the permeating species, i.e., the metabolic anions that must travel between the cytosol and mitochondrial spaces. The main anions transported by VDAC are ATP/ADP, NADH, and phosphate anions (Rostovtseva et al., 2002). It is assumed that the permeability pathway may be optimized for ATP flux since several cellular activities demand a high rate of flux of ATP through the OMM (i.e., through VDAC).

VDACs have different functional states that differ in their conductance of nonelectrolyte substances and both cations and anions (reviewed in Colombini (2004); Rostovtseva et al. (2005)). At a voltage smaller than 30 mV the pore has a diameter of 4 nm and is in the anion selective, high conductance “open” state (3–4 ns). Above 30 mV the diameter of the pore is reduced to 2 nm. The conductance decreases to 2 ns and ion selectivity changes to cation selectivity (“closed” state). The closure of VDAC greatly reduces the ability of anionic metabolites to diffuse between the cytosolic and the mitochondrial spaces. This selectivity, however, does not simply rely on the charge of the metabolite, but seems to involve specific-binding sites in the channel pore, as recently shown for ATP (Komarov et al., 2005). Importantly, restrictions in the flow of adenine nucleotides between the mitochondria and the cytosol has been shown to occur in the initial stages of apoptosis (see Rostovtseva et al. (2005) and chapter xx).

There are numerous reported mechanisms by which VDAC can undergo a transition from the open to the closed state. Strong evidence now exists for a potential across the outer membrane, which is sufficient to close VDAC (Colombini, 2004; Porcelli et al., 2005). Indeed, it appears that voltage changes through macromolecular charge variation (e.g., volume changes in the intermembrane space, protein phosphorylation, etc.) under different metabolic and signaling states might indirectly regulate VDAC activity. Recently, the generation of a potential across the outer membrane was also proposed to be coupled to the metabolic cycling and translocation of ATP, ADP, and P_i through the inner membrane (Elkeles et al., 1997). Moreover, as the values of the voltage-gating parameters are highly conserved among very diverse species, it was suggested to be an important regulatory parameter (Colombini, 1989).

Experiments measuring the apparent K_d of IMS enzymes (e.g., adenylate kinase or creatine kinase) for external ATP show that in permeabilized cells (mimicking *in situ* mitochondria) its value is significantly higher as compared with isolated mitochondria, demonstrating that a large fraction of the channels is closed under resting conditions (Colombini, 1980). This property of VDAC allows its modification toward both opening and closing the channel under (patho)physiological conditions. Indeed, there is a long list of other factors which regulate VDAC state: osmotic pressure (Zimmerberg and Parsegian, 1986), polyanions including charged proteins and nucleic acids (Mangan and Colombini, 1987; Colombini, 1989; Szabo et al., 1998), NADH (Lee et al., 1994), tBid (Rostovtseva et al., 2004), and phosphorylation by protein kinase A (Bera and Ghosh, 2001). Cytoskeletal and chaperone proteins were also shown to modify VDAC conductance, such as G-actin in yeast (Xu et al., 2001), the dynein light-chain component TCTEL, filamin B, and mtHSP70 ((Schwarzer et al., 2002) and G. Szabadkai, unpublished). In contrast, some factors promote VDAC opening: aluminum trihydroxide and other metal trihydroxides (Zhang and Colombini, 1989) and Bcl_{XL} (Vander Heiden et al., 2001). Phosphorylation of the channel by CamKII has been also shown in synaptosomes; however, it is not known how it affects channel conductance (Yoshimura et al., 2002).

3.4 VDAC in the Center of Protein Complexes Regulating Metabolic Channeling

The abundant OMM protein VDAC plays a crucial role in the organization of communication between mitochondria and other cellular components, particularly the ER. A key aspect of this coordination is the

reversible formation of complexes with other proteins. In this part of the chapter, we describe the currently known interactions and their possible role in bioenergetic exchange between the two organelles.

The most cited protein to be associated with VDAC from its cytosolic side is hexokinase (HK) (for reviews see Shoshan-Barmatz and Gincel (2003); Rostovtseva et al. (2005); Vyssokikh and Brdiczka (2004)). Measurement of the molecular mass of the isolated VDAC and HK complexes suggested that HK binds to VDAC in a tetrameric form (Beutner et al., 1996). Hexokinase I (HKI) converted VDAC channels reconstituted into planar membranes into a close conformation in a glucose-6-phosphate-dependent manner (Azoulay-Zohar et al., 2004). Interestingly, the glucose-6-phosphate metabolizing enzyme G-6-Pase was shown to be present in the mitochondria-associated membrane fraction of the ER, suggesting that VDAC activity might be regulated also from the ER side. This effect of HKI was also interpreted as an antiapoptotic mechanism, preventing opening of the mitochondrial permeability transition pore (PTP) (see below and chapter 4.6).

On the other hand, another more complex model was proposed by Brdiczka and coworkers to explain the role of VDAC/HK interactions (Vyssokikh and Brdzicka, 2004). According to their model, VDAC might exist in different OMM locations in different complexes. Outside of the OMM-IMM contact sites, VDAC in its open conformation forms complexes with the intermembrane space CK enzyme (see below) more readily, and through this protein it is also linked to the IMM-localized ANT. This constellation allows efficient transfer of ATP and creatine-P to the cytosol, supplying free energy also to the ER and the sarcoplasmic reticulum of muscle cells. In the contact sites, VDAC is present mostly in a closed state in direct contact with ANT from the IM and HKI on its cytosolic face. This complex is still able to transfer ATP out from the mitochondrial matrix and also through the OMM, but somehow this ATP seems to be restricted to the use of HK itself. Destabilization of the complex by detachment of HKI from VDAC (which can be induced by the proapoptotic Bcl-2 family member Bax or G-6-P) renders the VDAC-ANT complex sensitive to Ca^{2+} and ROS, which induces PTP opening.

It should be mentioned that growth factors, acting on cell survival signaling pathways (Akt/PKB), were shown to exert their effect also by increasing the binding of type II hexokinase (HKII) to the mitochondrial surface (Pastorino and Hoek, 2003), a pathway having an important role also in tumorigenesis (Pedersen et al., 2002). Mitochondrial binding of HKII to the outer mitochondrial membrane has been shown to inhibit Bax-induced cytochrome *c* release and apoptosis in HeLa cells (Pastorino et al., 2002). Moreover, the interactor of HKII was also identified as VDAC, but the exact effect of its binding to the channel has not yet been clarified (Nakashima et al., 1986).

3.5 The ATP Microdomain at the ER-Mitochondrial Interface

An intriguing prospect in interorganelle communication was disclosed by the studies of Ventura-Clapier and coworkers on creatine kinase-deficient (CK $-/-$) mice, extending the importance of ER/SR-mitochondria contacts to a possible metabolic crosstalk between these organelles. In permeabilized cardiac muscle fibers, they observed a direct channeling of adenine nucleotides from mitochondria, ensuring an efficient energy supply to the sarcoplasmic reticulum Ca^{2+} ATPases and myofilaments in which CK and the phosphoryl-creatine (PC) shuttle play a crucial role (Kaasik et al., 2001). Moreover, they observed that in CK $-/-$ mice a structural reorganization of mitochondria, myofilaments, and SR leads to a development of a more intimate contact between these organelles and functional units ensuring direct ATP supply even to a level that compensates the lack of CK, and thus even the PC shunt (Crozatier et al., 2002). This contact can even be bidirectional, as the SR-attached glycolytic enzyme complexes may supply substrates (e.g., pyruvate) to the mitochondria in a compartmentalized manner (for review see Ventura-Clapier et al. (2004)). In this respect, the central localization of glucokinase/hexokinase on the outer part of VDAC in the OMM may also provide a core for such a metabolic coupling (Azoulay-Zohar et al., 2004; Vyssokikh et al., 2004).

An evident extension of these findings is that metabolic channeling does not happen only in this microcompartment between the ER-mitochondrial surfaces, but might be a general phenomenon underlying cellular metabolic processes (Ovadi and Saks, 2004). Indeed, compartmentalization of glucose metabolism in

muscle and neuronal cells was shown to be driven by the association of metabolic enzymes (GAPDH, aldolase, and phosphofruktokinase) with the microtubular network (Ovadi et al., 2004). Moreover, in this study, mutations of components of this system (e.g., triosephosphate isomerase enzymopathy) have been shown to underlie neurodegenerative pathologies.

4 Ca²⁺ Channeling Between the ER and Mitochondria

Our current view on ER-mitochondrial interactions arose from the investigation of Ca²⁺ signal transmission between these organelles, an affirmation which might reflect its importance in cellular signaling and also the availability of technical approaches to study Ca²⁺ signals. Introduction of protein-based probes like aequorins and GFP/YFP fusion proteins with genetically engineered Ca²⁺-binding sites (Chiesa et al., 2001; Bianchi et al., 2004) targeted to virtually any desired subcellular location facilitated profoundly the development of this field.

4.1 Functional Properties of Mitochondrial Ca²⁺ Uptake

The outer mitochondrial membrane (OMM) is permeable to ions of a limited size, owing to the abundance of the large conductance channel VDAC (for the role of the channel in metabolic channeling, see above). Indeed, recent data show that the availability and selective placement of VDAC channels at ER/mitochondria contact sites facilitates mitochondrial Ca²⁺ accumulation, in line with the idea that the latter process requires the fast and efficient transfer of Ca²⁺ microdomains from the mouth of the Ca²⁺ channels located in neighboring ER to the transporters of the IMM (Gincel et al., 2001; Rapizzi et al., 2002). The IMM is an ion impermeable membrane, forming foldings into the internal space known as cristae (Frey et al., 2002). As discussed earlier, the activity of respiratory chain complexes allows the translocation of H⁺ in the IMS, with consequent generation of an electrochemical gradient ($\Delta\mu_{\text{H}}$), composed of a chemical (ΔpH) and electrical ($\Delta\psi_{\text{m}}$) component, according to the Nernst equation:

$$\Delta\mu_{\text{H}} = zF\Delta\psi_{\text{m}} + RT \ln[\text{H}^+]_{\text{in}}/[\text{H}^+]_{\text{out}}$$

In mitochondria, most of the $\Delta\mu_{\text{H}}$ established by the respiratory chain is supposed to be in the form of $\Delta\psi_{\text{m}}$ (~180 mV), thus providing a huge driving force for Ca²⁺ entry into the organelle. Indeed, collapse of the $\delta\mu_{\text{H}}$ by protonophores such as *p*-[trifluoromethoxy]phenylhydrazine (FCCP) abolishes mitochondrial Ca²⁺ uptake both in vivo and in isolated organelle preparations. As to the uptake route, its molecular identity is still unknown. Ca²⁺ transport kinetic measurements on isolated mitochondria (for review see Bernardi (1999)) and recent electrophysiological experiments on mitoplasts (Kirichok et al., 2004) suggest that it is a gated channel rather than a carrier, showing a Ca²⁺-activated second-order kinetics, with a Ca²⁺ activation and a Ca²⁺ transport site. On the basis of these properties, the rate of mitochondrial Ca²⁺ uptake through the channel was shown to be significant only above an “activatory” threshold (200–300 nM), also known as the set point. The concentration dependence fits a second order Hill equation while the membrane potential dependence allows defining its mechanism as a “uniporter” (i.e., transport across the membrane driven only by the electrochemical gradient with no immediate exchange or cotransport of other ions). The uniporter can also transport Sr²⁺, Mn²⁺, Ba²⁺, Fe²⁺, and La³⁺ in descending order of selectivity, and appears to be gated by local adenine nucleotide concentrations (ATP > ADP > AMP) at a site located at the outer surface of the inner membrane (Bernardi, 1999). Its currently known inhibitors are ruthenium red (or its subcomponent Ru360), lanthanides, and CsA at high concentrations; however, these compounds are far from being specific for this Ca²⁺ channel. Recently, this site was even proposed to be a purinergic-like receptor present in the inner mitochondrial membrane (Belous et al., 2004).

Reflecting the Ca²⁺-dependent Ca²⁺ uptake mechanism with relatively low affinity by the uniporter, efficient mitochondrial Ca²⁺ uptake in intact cells was shown to be dependent on the close apposition of mitochondria to Ca²⁺ release (ER) and entry sites (plasma membrane), where microdomains with high [Ca²⁺] are formed (Rizzuto et al., 1998; Csordas et al., 1999). Ca²⁺-dependent stimulation of NAD(P)H

and consequent ATP production, through activation of Ca^{2+} -sensitive dehydrogenases and metabolite carriers, serve to adapt energy and substrate production to increased cellular needs (McCormack et al., 1990; Lasorsa et al., 2003). In addition, mitochondria serve also as an intracellular Ca^{2+} buffer, shaping cellular Ca^{2+} signals (Tinel et al., 1999; Duchen, 2000). On the other hand, mitochondrial Ca^{2+} loading, originating from Ca^{2+} release from the ER, has been shown to play a crucial role in apoptosis induction caused by certain proapoptotic stimuli, such as C_2 -ceramide (Szalai et al., 1999; Pinton et al., 2001). C_2 -ceramide was shown to directly induce Ca^{2+} release from the ER Ca^{2+} store (Pinton et al., 2001) and also to sensitize mitochondria to Ca^{2+} impulses from InsP_3 receptor (InsP_3R)- or ryanodine receptor (RyR)-mediated Ca^{2+} release, leading to mitochondrial permeability transition (MPT) and depolarization (Szalai et al., 1999). This is followed by the release of proapoptotic factors activating the effector caspases, finally triggering apoptotic cell death (Orrenius et al., 2003). Importantly, mitochondrial depolarization in these cases is propagated as a wave throughout the cells, pointing to a fundamental role of mitochondrial network integrity in apoptotic signaling (Pacher and Hajnoczky, 2001).

Obviously, in these dynamic physiological fluctuations of $[\text{Ca}^{2+}]_m$, pathways must be operative to allow the rapid reextrusion of Ca^{2+} . Moreover, given that mitochondria utilize $\delta\psi_m$ to facilitate Ca^{2+} uptake, the extrusion of the ion is energetically uphill. In mitochondria of vertebrates, two different routes for Ca^{2+} efflux have been characterized, the $\text{Na}^+/\text{Ca}^{2+}$ (mNCC) and $\text{H}^+/\text{Ca}^{2+}$ (mHCX) exchangers. These systems (also undefined at the molecular level) utilize the driving force for Na^+ or H^+ entry into mitochondria, respectively, to extrude Ca^{2+} ions, and are commonly referred to as the Na^+ -dependent (NCE) and Na^+ -independent (NICE) pathways of Ca^{2+} efflux. In heart, brain, skeletal muscle, parotid gland, adrenal cortex, and brown fat (i.e., mostly but not exclusively excitable tissues), the Na^+ -dependent mechanism is the dominant one, while many nonexcitable tissues, such as liver, kidney, lung, and smooth muscle appear to rely mostly on the Na^+ -independent mechanism. As to the stoichiometry of the exchange, work has been carried out mostly for the NCE, indicating an exchange of $3 \text{Na}^+/2 \text{Ca}^{2+}$ (Bernardi, 1999; Gunter et al., 2000). The NCE, and with lower affinity the NICE, have been shown to be inhibited by a number of cell-permeant drugs, which include known blockers of voltage-dependent Ca^{2+} channels of the plasma membrane, e.g., verapamil and diltiazem, as well as compounds such as CGP37157, which exhibit a much larger selectivity for the NCE. Thus, in distinction to the uniporter, specific pharmacological tools are available for modulating the activity of the exchangers in intact cells.

In addition to these Ca^{2+} transport mechanisms, a channel of major pathophysiological interest has been characterized in the past years, commonly referred as the PTP (see above) (Bernardi et al., 1998). This high-conductance channel is supposed to be a multiprotein complex (the putatively essential components being VDAC, ANT, and cyclophilin D) activated by Ca^{2+} increases in the mitochondrial matrix and oxidation of critical cysteines (Crompton, 2000; Halestrap et al., 2002; He and Lemasters, 2002). The opening of PTP has been shown to be a trigger for the release of IMS components into the cytosol, and thus cellular commitment to death (Green and Kroemer, 2004). Thus, PTP can be regarded as a bonafide intramitochondrial Ca^{2+} target. As to the possibility that it can intervene in mitochondrial Ca^{2+} homeostasis, it is unlikely that it represents an alternative efflux pathway (as sometimes proposed), except in cases in which the almost complete collapse of $\Delta\psi_m$ provides a driving force for efflux, rather than accumulation, of the cation (Ichas and Mazat, 1998). It is possible, however, that when PTP opens, it transiently reduces $\Delta\psi_m$, and thus strongly affects, in some situations, Ca^{2+} transport through the uniporter. The recent availability of novel specific inhibitors of PTP (cyclosporin analogues) (Petronilli et al., 1994; Waldmeier et al., 2002), Ro 68-3400, acting on VDAC (Cesura et al., 2003)) will now allow to address these and other issues regarding PTP in the future years.

4.2 Modification of Mitochondrial Ca^{2+} Uptake by Modifying ER Ca^{2+} Release

The first observations pointing to a major role of the releasable Ca^{2+} pool of the ER on mitochondrial Ca^{2+} uptake came from the exploration of the mechanism of antiapoptotic action of Bcl-2 (Tsujimoto et al., 1985a, b; Reed et al., 1987; Korsmeyer et al., 1990; Reed, 1994). Bcl-2 has been detected in association with the outer mitochondrial membrane, with the ER, and with the nucleus, and a cytoplasmic form of Bcl-2 is

also known to exist (Tanaka et al., 1993; Lithgow et al., 1994). Moreover, an effect on cellular ion homeostasis is suggested by the observation that Bcl-2 forms ion channels of limited cation selectivity when added to lipid bilayers, thus potentially interfering with ion fluxes in organelles (Minn et al., 1997; Schendel et al., 1998). The first evidence of an effect of Bcl-2 on ER Ca^{2+} homeostasis was obtained by Distelhorst and coworkers, who showed in stably expressing clones of WEHI7.2 lymphoma cells a reduction in the thapsigargin-induced efflux of Ca^{2+} from the ER (Lam et al., 1994). In turn, its use targeted aequorins and GFP-based Ca^{2+} indicators, allowing the direct measurement of Ca^{2+} concentration in the ER of cells transiently expressing Bcl-2. It was shown that Bcl-2 overexpression in HeLa (Pinton et al., 2000) or HEK-293 cells (Foyouzi-Youssefi et al., 2000) causes a reduction of the steady state $[\text{Ca}^{2+}]_{\text{er}}$, and thus of the amount of agonist-releasable Ca^{2+} pool, due to an increase in the Ca^{2+} leak across the ER membrane (Pinton et al., 2000). Importantly, the observed reduction of steady state $[\text{Ca}^{2+}]_{\text{er}}$ was sufficient to reduce agonist-induced $[\text{Ca}^{2+}]$ increase in the cytoplasm and Ca^{2+} uptake into mitochondria. Steady state $[\text{Ca}^{2+}]_{\text{er}}$ was reduced not only by Bcl-2 overexpression, but also by a variety of experimental approaches such as incubation at lower extracellular $[\text{Ca}^{2+}]$, partial inhibition of the ER Ca^{2+} ATPase, or overexpression of the plasma membrane Ca^{2+} ATPase, and there was marked inhibition of Ca^{2+} uptake into the mitochondria (Pinton et al., 2001). Similarly, following overexpression of calreticulin (an abundant luminal ER Ca^{2+} buffer) which does not raise $[\text{Ca}^{2+}]_{\text{er}}$, but does increase the releasable Ca^{2+} pool, mitochondrial Ca^{2+} uptake was drastically reduced upon C_2 -ceramide treatment (Pinton et al., 2001). These effects can be accounted for the protective effect of Bcl-2 and reduction of $[\text{Ca}^{2+}]_{\text{er}}$ in general against Ca^{2+} -dependent apoptotic stimuli.

Scorrano and coworkers (2003) provided further evidence in favor of the hypothesis that Ca^{2+} movement from the ER to mitochondria is a key process in the activation of apoptosis by a number of stimuli. They showed that mouse embryonic fibroblasts deficient of the two proapoptotic proteins Bax and Bak (double knockout, DKO cells) are markedly resistant to a variety of apoptotic stimuli and have a much reduced Ca^{2+} concentration in the ER. If the ER Ca^{2+} levels are restored by recombinantly overexpressing the sarco-endoplasmic reticulum Ca^{2+} ATPase (SERCA), not only mitochondrial Ca^{2+} uptake in response to stimulation is reestablished, but also the cells' sensitivity to apoptotic stimuli such as arachidonic acid, C_2 -ceramide, and oxidative stress is regained. These results are in line with previous work by Ma and coworkers (1999) demonstrating that SERCA overexpression in COS cells causes ER Ca^{2+} overload and increases spontaneous apoptosis. The work of Scorrano and coworkers further demonstrated that another group of apoptotic stimuli (staurosporine and etoposide) is partially insensitive to these alterations in the levels of ER Ca^{2+} , while they require the presence of proapoptotic proteins on the mitochondrial membrane. Thus, Bax specifically targeted to the outer mitochondrial membrane did not induce any change in $[\text{Ca}^{2+}]_{\text{er}}$ but made cells sensitive to apoptosis induced by the BH3-only protein tBID.

4.3 Mitochondrial Morphology Determines the Efficiency of Ca^{2+} Channeling from the ER

The idea that mitochondrial shape may participate in local and global Ca^{2+} signaling developed from the tools that were provided by the understanding of how mitochondrial structure is dynamically regulated. The use of targeted recombinant aequorin probes showed that upon agonist stimulation an efficient mitochondrial Ca^{2+} signal, generally in the 5–100 μM range, follows a much lower cytoplasmic $[\text{Ca}^{2+}]$ elevation. Mitochondrial Ca^{2+} uptake was shown to depend on the capacity of mitochondria to sense high $[\text{Ca}^{2+}]$ microdomains generated by the opening of neighboring ER or plasma membrane Ca^{2+} channels (Rizzuto et al., 1998). The recent development of GFP-based Ca^{2+} probes (Miyawaki, 2003) allowed to obtain spatial information about organelle Ca^{2+} signaling. Moreover, as described above, a series of proteins have been described, which are involved in mitochondrial fusion and fission events. Indeed, recent observations indicate the participation of the mitochondrial fission machinery in the mitochondrial and cellular Ca^{2+} homeostasis and in different apoptotic pathways. The first indication that mitochondrial division modifies cellular Ca^{2+} signals has been reported by Demarex and coworkers, who showed, that in hFis1 overexpressing cells, having fragmented mitochondrial network, the capacitative Ca^{2+} influx (CCI)

pathway is inhibited (Frieden et al., 2004). However, hFis1 did not only induce fragmentation of mitochondria, but also an apparent decrease in the total mitochondrial volume and a striking perinuclear aggregation of remaining mitochondrial particles, a phenomenon frequently occurring during cell death (described also by others as an important step in “thread-grain” transition of the mitochondrial network) (Skulachev 2004). Owing to this rearrangement, the mitochondrial-ER contacts are increased in the perinuclear space, leading to the preservation of the efficiency of Ca^{2+} signal transmission, and thus virtually no change of net mitochondrial Ca^{2+} uptake during agonist-induced Ca^{2+} signals occurs. A similar effect on mitochondrial morphology and Ca^{2+} signaling was also described using HIV protease inhibitors (Roumier et al., 2005).

In contrast to the effect of hFis, in our laboratory we have shown the modification of mitochondrial Ca^{2+} uptake also during IP_3 -induced Ca^{2+} release from the ER in Drp-1 overexpressing cells (Szabadkai et al., 2004). Importantly, Drp-1 overexpression caused mitochondrial fragmentation without drastic rearrangement of the network, preserving its overall volume and the extent of colocalization with the ER. These experiments also shed light on the nature of Ca^{2+} uptake in a continuous mitochondrial network, showing that mitochondrial Ca^{2+} uptake takes place at preferential Ca^{2+} uptake sites (hot spots), distantly localized in the network, and lateral diffusion of Ca^{2+} along the tubular mitochondria led to the complete filling of the network during maximal stimulation of ER Ca^{2+} release. These hot spots most likely represent the high Ca^{2+} microdomains at the ER Ca^{2+} release sites, and the result implies that the fragmentation of the mitochondrial network, induced by Drp-1, leads to a more heterogeneous (and reduced in mean) $[\text{Ca}^{2+}]_m$ response, given that individual mitochondrial particles remain without direct connection to Ca^{2+} sources (Szabadkai et al., 2004).

In addition to the expansion of knowledge on the dynamic fusion and fission events maintaining the mitochondrial network, recently a genetic program that determines mitochondrial biogenesis has also been described. In this pathway, a crucial role is played by the peroxisome proliferator-activated receptor- γ (PPAR γ) coactivator 1 α (PGC-1 α), which, interacting with different nuclear receptors, activates nuclear and mitochondrial transcription factors. In turn, the modification of the gene expression profile augments mitochondrial capability to produce ATP and heat during cellular activation, differentiation, and adaptive thermogenesis (for review see Puigserver and Spiegelman (2003)). We have shown that increased mitochondrial biogenesis affects also its Ca^{2+} -handling capacity, through a change in mitochondrial volume and Ca^{2+} -buffering capacity, and probably by directly modifying the expression of components of the mitochondrial Ca^{2+} uptake pathway (Bianchi et al., 2005). Indeed, the activity of the Ca^{2+} uniporter was reduced, while the Ca^{2+} diffusion area in the mitochondrial network was significantly increased following Ca^{2+} release from the ER in PGC-1 α -overexpressing cells.

In addition to the above studies regarding the effect of mitochondrial shape on global and mitochondrial Ca^{2+} signals, the intracellular distribution of mitochondria has also been recently shown to have an important effect on the spatiotemporal distribution of the cellular Ca^{2+} signal. The pioneering work of O.H. Petersen and coworkers highlighted the importance of the strategic positioning of mitochondria at the border of the apical region of pancreatic acinar cells, delimiting Ca^{2+} signal following IP_3 -mediated Ca^{2+} release from the ER (Petersen et al., 1999; Tinel et al., 1999). Mitochondria buffer Ca^{2+} very efficiently at these sites that no Ca^{2+} elevation can be detected at the basolateral region of these polarized cells. Recent work in “less” polarized epithelial and endothelial cells worked out further this concept, as follows. First, Malli et al. have shown that in HeLa cells, during sustained stimulation with Ca^{2+} -mobilizing agents, Ca^{2+} refilling of the ER occurs through trans-mitochondrial Ca^{2+} flux, i.e., Ca^{2+} uptake by mitochondria near the near plasma membrane and subsequent Ca^{2+} release through Na/Ca^{2+} exchange. This Ca^{2+} flux appeared to be essential for the ability of mitochondria to generate subplasmalemmal microdomains of low $[\text{Ca}^{2+}]$ in order to maintain the CCI and to sustain the transfer of Ca^{2+} from the extracellular (EC) space to the ER (Malli et al., 2003). Further work by the groups of Demarex and Graier extended this observation, showing that in the absence of IP_3 , the ER is able to refill independently of mitochondria by sequestering Ca^{2+} entering from the EC space in a subplasmalemmal microdomain between the ER and the plasma membrane. However, in the presence of IP_3 , subplasmalemmal ER domains generate high $[\text{Ca}^{2+}]$, thereby preventing the CCI by negative feedback inhibition (Malli et al., 2005) and activating plasma membrane Ca^{2+} ATPases and Ca^{2+} extrusion (Frieden et al., 2005).

4.4 Ca²⁺ Signaling in Apoptosis and Mitochondrial Shape

A striking general feature of apoptotic cells is the breakdown of the mitochondrial network, and thus the elegant experiments of Youle and coworkers bridging the Bax-mediated mitochondrial apoptotic pathway to the Drp-1-mediated mitochondrial fragmentation (Frank et al., 2001) and the inhibition of mitochondrial fusion (Karbowski et al., 2004) took place almost immediately, which is common knowledge in the field of mitochondrial studies. Particularly important from the point of view of this chapter was the following demonstration, that in the BAP31-mediated apoptotic pathway, a Ca²⁺-dependent translocation of Drp-1 could be observed on the mitochondrial OM surface, following Ca²⁺ release from the ER, leading to mitochondrial fragmentation and release of proapoptotic factors from the MIMS (Breckenridge et al., 2003). According to these results one could envisage a simple model in which the concerted activation of mitochondrial fission factors and proapoptotic proteins like Bax and the death-associated protein 3 (DAP3) (Mukamel and Kimchi, 2004) promote apoptosis in a presumably Ca²⁺-dependent way (see above). However, some current observations seem to complicate this view. First, Drp-1-induced mitochondrial fragmentation per se was repeatedly shown to be innocuous to the cell (Karbowski et al., 2002; Szabadkai et al., 2004) (but see also hFis1 (Yoon et al., 2003)). Second, this “safe” fragmentation was even able to protect cells selectively against ceramide-induced ER Ca²⁺ release-dependent apoptosis (Szabadkai et al., 2004). These data, taken together with the seemingly tight regulation of the mitochondrial division pathway (dynamic connection of Drp-1 with the cytoskeleton) (Varadi et al., 2004) (Sumo-1 conjugation of Drp-1) (Harder et al., 2004), suggest that in the field of mitochondrial connectivity regulation and its relationship to Ca²⁺ homeostasis and apoptosis, much remains to be understood.

5 The Role of ER and Mitochondria and Their Contacts in Phospholipid Biosynthesis

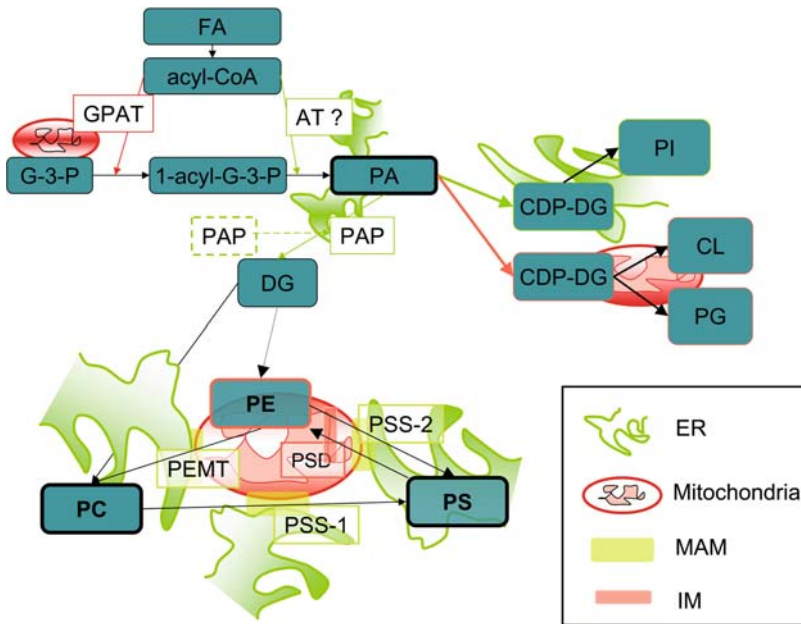
Lipid and protein components of biological membranes are synthesized and assembled into biological membranes. Apart from their evident structural role by creating the environment for proper functioning of membrane proteins, phospholipids were recently shown to be involved directly in key regulatory functions within mammalian cells. For example, phosphatidylinositol-4,5-bisphosphate is the precursor of both IP₃, a signaling molecule that promotes the release of intracellular calcium (Bootman et al., 2002), and diacylglycerol, another signaling molecule that activates several isoforms of protein kinase C (Nishizuka, 1984). Phosphatidylcholine (PC), the most abundant phospholipid in eukaryotic cell membranes, can be cleaved by phospholipases to generate diacylglycerol, lysophosphatidylcholine, phosphatidic acid (PA), and arachidonic acid, all of which have been implicated in lipid second messenger roles. Phosphatidylserine (PS), although quantitatively, a relatively minor phospholipid in mammalian cell membranes, has become a major focus of interest because externalization of PS on the outside of apoptotic cells is believed to be the recognition signal by which apoptotic cells are removed by phagocytes (Fadok et al., 2001). Here we briefly review the general metabolism of phospholipids with respect to their localization to the mitochondrial-ER interface (for an excellent review of this expanding field, which served also as a base of this description, see Vance and Vance (2004)).

PA is a key building block of all the mammalian phospholipids and is also a precursor of the triacylglycerols. The donor of the fatty acyl chains for PA synthesis is acyl-CoA. The different acyl-CoA synthetase isoforms (Kim et al., 2001) are thought to produce pools of acyl-CoA that are channeled into distinct metabolic pathways, i.e., either for phospholipid or triacylglycerol synthesis (Coleman et al., 2000).

For PA synthesis, glycerol-3-phosphate is first converted into 1-acylglycerol-3-phosphate (lysophosphatidic acid) by the action of glycerol-3-phosphate acyltransferase (see [Figure 6.2-3](#)). Two isoforms of this key enzyme have been identified that are encoded by different genes and have distinct subcellular locations (Dircks and Sul, 1997). One isoform is restricted to the OMM whereas the other is associated with the ER. Interestingly, the OMM enzyme primarily uses saturated rather than unsaturated acyl-CoAs, and thus it has been proposed that this isoform is responsible for establishing the most frequently found fatty acid distribution of phospholipids and triacylglycerols, i.e., a saturated fatty acyl chain at the *sn*-1 position.

■ **Figure 6.2-3**

Phospholipid biosynthetic pathways and their relative localization to the ER and mitochondrial network in mammalian cells



The acyltransferase catalyzing the second acylation step in PA synthesis has not been well characterized. The enzymatic activity, which preferentially utilizes unsaturated fatty acyl-CoAs, resides primarily on ER membranes, but there is also low activity in mitochondria. Thus, 1-acylglycerol-3-phosphate generated in mitochondria has been proposed to be transferred to the ER for subsequent conversion to PA (Das et al., 1992).

PA is a branch point for the synthesis of all of the phospholipids, as shown on [Figure 6.2-3](#).

It can be converted to CDP-diacylglycerol that is used for the synthesis of phosphatidylinositol (PI), phosphatidylglycerol (PG), and cardiolipin (CL). Mammalian CDP-diacylglycerol synthase, which converts PA into CDP-diacylglycerol, is present in both mitochondrial and microsomal fractions, although 90–95% of the activity resides in microsomes. The enzymes in the two different locations have distinct properties. A hypothesis for why mammalian cells express two CDP-diacylglycerol synthases is that the two isoforms are compartmentalized according to their function (Vance, 1998). Accordingly, the microsomal isoform of CDP-diacylglycerol synthase might be used for PI synthesis in the ER, while the mitochondrial isoform might be used for synthesis of the predominantly mitochondrial phospholipids, PG and CL.

The biosynthesis of PC, PE, and PS requires a source of diacylglycerol that is generated through the hydrolysis of PA. The enzyme catalyzing this reaction is phosphatidic acid phosphatase. This phosphatase translocates to the ER from the cytosol, gaining a more active conformation. Consequently, PC and PE can be formed through the CDP-choline and CDP-ethanolamine pathway, respectively. However, PC, PE, and PS are also interconverted between each other, catalyzed by enzymes mainly residing at the ER–mitochondria interface. The relative importance of different synthetic pathways is intensely investigated now using mainly knockout animal models of different enzyme components (Vance and Vance, 2005).

Mitochondria, particularly the IMM, are enriched in PE compared with other organelles, and virtually all PE in mitochondrial membranes is synthesized in situ in mitochondria from PS decarboxylase (Shiao et al., 1995). As PS decarboxylase is an IMM integral membrane protein whose active site is located in the IMS (Zborowski et al., 1983), PS should be transported from the ER/MAM fraction to this site. The transport of PS from its site of synthesis in MAM and ER to the mitochondria has also been proposed to

occur via regions of close apposition, or contact sites, between the MAM and OMM (Voelker, 1989a, b; Vance, 1990, 1991). Interestingly, in neurons, the apposition points between the ER and mitochondria appear to punctuate, suggesting a highly specific interaction (Perkins et al., 1997, 2001). Recent genetic studies in yeast and mammals have identified some components of the transport machinery (for review see Voelker (2005)); its exact mechanism still remains to be elucidated.

The enzymes responsible for the synthesis of PC via the methylation of PE (PEMT-2) also reside in the MAM fraction of ER, while the bulk ER contains another PEMT activity, presumably originating from the same gene (Walkey et al., 1997).

PS is synthesized in mammalian cells by a Ca^{2+} -dependent base-exchange reaction using both PC and PE as substrates (reviewed recently in Vance (2003)). The enzyme responsible for the reaction, PS synthase (PSS), resides almost exclusively in the MAM and has two isoforms. PSS-1 catalyzes the base exchange of serine with PC, whereas PSS-2 catalyzes serine exchange with PE. This localization of the enzymes is consistent with the proposed role of MAM in mediating the transport of newly synthesized PS into mitochondria, used in PE synthesis, (see above) and confirms the central role of the ER–mitochondria interaction in the metabolism of phospholipids regulating basic cellular functions.

6 ER–Mitochondria Contacts and Sphingolipid Metabolism

Sphingolipid metabolites are now recognized as key players in signal transduction following cellular responses to stress. Among these metabolites, ceramide has been shown to play a role in cell cycle arrest, differentiation, and apoptosis (for recent reviews see Hannun and Luberto (2000); van Blitterswijk et al. (2003)). Ceramide can be generated in cells by sphingomyelin hydrolysis or de novo synthesis. Thus, ceramide is synthesized at the cytosolic face of the ER (Merrill Jr., 2002), or formed in mitochondria (Bionda et al., 2004), or generated by sphingomyelinases (SMases) of the ER (Ardail et al., 2003). Moreover, ceramide may be directly imported from the ER via intimate membrane contact between the two organelles (Ardail et al., 1993; Marsh et al., 2001), underlying the importance of the MAM fraction also in this important biosynthetic pathway.

7 Protein Transport and Folding at the ER–Mitochondrial Interface

The conversion of genetic information into functional proteins is initiated by the ribosomes, localized in the cytoplasm and associated with ER membranes, where mRNA is translated into linear polypeptides. There are, however, two further very important steps in protein synthesis: (1) the folding of the newly translated polypeptides into their functional three-dimensional conformations and (2) the sorting of nascent proteins to their cellular destination, also to mitochondrial compartments and the ER, the latter being the first step in the secretory pathway/plasma membrane targeting. Recent awareness on these processes has shed light on the function of a large protein family called “molecular chaperones,” which fulfill both the above roles. We describe here briefly the main pathways discovered recently that sort and fold proteins destined to the ER and mitochondria.

As nascent polypeptide chains emerge from ribosomes they bind to a 70-kDa heat-shock protein member (Hsc70 in mammals), which undergoes an ATPase cycle, using the free energy of ATP hydrolysis for polypeptide binding, released by the exchange of ADP to a new ATP. The aim of the cycle is to ensure conformational change in the nascent polypeptide chain, in order to obtain its functional conformation (Bukau and Horwich, 1998; Hartl and Hayer-Hartl, 2002). Its ATPase activity is stimulated by the cofactor/co-chaperones (the 40-kDa heat-shock protein Hsp40, also known as Hdj1 or Hdj2 in mammals). Intriguingly, co-chaperones of Hsc70 and Hsp90 are not found in bacteria, but arose after the symbiotic development of eukaryotic cells, pointing to their possible (but less studied) role in organellar interactions. Nucleotide exchange factors (Bcl-2-associated athanogene-1 (BAG1) and Hsp70-binding protein (HspBp1)) stimulate ADP/ATP exchange, and thus the release of folded chaperone substrates (for review see Young et al. (2004)). In eukaryotes, cytosolic Hsc70 functions on certain polypeptides together

with the homodimeric Hsp90. From yeast to mammals, Hsp90 functions in the folding of a particular set of proteins, including transcription factors, regulatory kinases, and numerous other proteins that apparently lack common structural or functional features. The biochemical mechanisms of Hsp90 are less well understood compared with Hsc70, and it might function on more compact folding intermediates (Young et al., 2001; Pratt and Toft, 2003). Importantly, in addition to its role in polypeptide folding, the Hsc70–Hsp90 machinery can be adapted by some co-chaperone proteins to function in protein sorting either to intracellular organelles or to the proteasome for degradation (Young et al., 2003a; Soti et al., 2005).

The mitochondrial proteome consists of about 500–1500 proteins of which only a minor fraction (8 proteins in yeast and 13 in humans) is encoded by mitochondrial DNA. Thus, virtually all mitochondrial proteins must be transported from their site of synthesis in the cytosol to the various mitochondrial subcompartments. Mitochondrial proteins are mostly synthesized as precursor polypeptides in the cytosol and are imported posttranslationally into the organelle (Truscott et al., 2003). Hsc70, together with Hdj1 or Hdj2, are known to maintain the solubility of the mitochondrial proteins (Deshaies et al., 1988) and mediate their targeting to the mitochondrial import receptor 70-kDa translocase of the outer mitochondrial membrane (TOM70). Matrix proteins must traverse both the OMM and IMM, which is ensured by the coordinate action of protein translocase complexes found in both membranes (TOM and TIM22 complexes, respectively) (Neupert and Brunner, 2002; Pfanner et al., 2004). Integral IMM proteins of the solute carrier family are inserted into the IMM through the action of a specialized TIM complex called TIM22. In both mammals and yeast, TOM70 recognizes the precursor protein-binding chaperones through its co-chaperone TPR-clamp domain, and this docking step is important for the transfer of the precursors to the import receptor and the mitochondrial import machinery (Young et al., 2003b). Mitochondrial precursors with amino-terminal presequences rely on the main import receptor TOM20 and, in mammals; these precursors can be maintained in the cytosol by HSC70 and the co-chaperone XAP2/AIP, which can contact TOM20 directly (Yano et al., 2003).

In an independent pathway, Ydj1, which is the yeast homolog of HDJ2, transiently associates with membranes through its covalently attached lipid moiety, and assists the HSC70 (Ssa in yeast)-mediated posttranslational targeting of some proteins to both mitochondria and the ER (Becker et al., 1996). Indeed, other reports, analyzing alternative mitochondrial and ER targeting sequences (e.g., tail anchors), show that the two organelles may share particular proteins, including also integral membrane proteins. For these membrane proteins, posttranslational insertion into the mitochondria tends to occur if cotranslational insertion into the ER is inefficient (Colombo et al., 2005; Miyazaki et al., 2005; van Herpen et al., 2005).

As a concluding note, we believe that the emerging field of protein interaction network characterization will certainly lead to innovative new results and ideas to describe the nature of interaction of the ER and mitochondria. Moreover, even if this field in 2005 seems to be only in its infancy, we have high hopes that it will also provide insight into major pathologies like cancer, metabolic and neurodegenerative diseases, as described by our colleagues in related chapters of the handbook.

8 Summation, Challenging Problems, and Further Avenues

Different fields of recent and significant research advancements have merged to characterize the close morphological and functional interaction between the ER and mitochondria. These fields include the advanced high-resolution 3D imaging of intracellular ultrastructure; disclosure of determinants of mitochondrial shape and dynamics, common regulatory factors of ER and mitochondrial shape; characterization of Ca^{2+} and phospholipid transport between these organelles; induction of apoptosis through ER–mitochondria interactions, and last but not at least; the protein sorting machinery of which the components might participate significantly in the ER–mitochondrial interaction. Further research should concentrate on the development of these particular issues in order to respond questions of immediate interest:

1. What are the molecular components responsible for bridging physically the ER and mitochondria and underlie their functional interaction?

2. What are the components of the mitochondrial and ER fusion/fission machinery that participate also in their interaction?
3. Are there cell-type specific differences in the morphology and components of interaction?
4. Does the interaction change during pathophysiological conditions?
5. Do intracellular signaling pathways regulate the interplay between the organelles?

These questions will be resolved by applying imaging, proteomic, and genetic models in which the ER-mitochondrial interaction changes, and by applying models in which targeted changes of the interaction will be possible.

References

- Alto NM, Soderling J, Scott JD. 2002. Rab32 is an A-kinase anchoring protein and participates in mitochondrial dynamics. *J Cell Biol* 158: 659-668.
- Ardail D, Gasnier F, Lerme F, Simonot C, Louisot, P, et al. 1993. Involvement of mitochondrial contact sites in the subcellular compartmentalization of phospholipid biosynthetic enzymes. *J Biol Chem* 268: 25985-25992.
- Ardail D, Popa I, Bodennec J, Louisot P, Schmitt D, et al. 2003. The mitochondria-associated endoplasmic reticulum sub-compartment (MAM fraction) of rat liver contains highly active sphingolipid-specific glycosyltransferases. *Biochem J* 371: 1013-1019.
- Aspenstrom P. 2004. Integration of signaling pathways regulated by small GTPases and calcium. *Biochim Biophys Acta* 1742: 51-58.
- Azoulay-Zohar H, Israelson A, Abu-Hamad S, Shoshan-Barmatz V. 2004. In self-defense: Hexokinase promotes voltage-dependent anion channel closure and prevents mitochondria-mediated apoptotic cell death. *Biochem J* 377: 347-355.
- Barrowman J, Wang W, Zhang Y, Ferro-Novick S. 2003. The Yip1p.Yif1p complex is required for the fusion competence of endoplasmic reticulum-derived vesicles. *J Biol Chem* 278: 19878-19884.
- Baumann O, Walz B. 2001. Endoplasmic reticulum of animal cells and its organization into structural and functional domains. *Int Rev Cytol* 205: 149-214.
- Becker J, Walter W, Yan W, Craig, EA. 1996. Functional interaction of cytosolic Hsp70 and a DnaJ-related protein, Ydj1p, in protein translocation in vivo. *Mol Cell Biol* 16: 4378-4386.
- Belous A, Wakata A, Knox CD, Nicoud IB, Pierce J, et al. 2004. Mitochondrial P2Y-like receptors link cytosolic adenosine nucleotides to mitochondrial calcium uptake. *J Cell Biochem* 92: 1062-1073.
- Bera AK, Ghosh S. 2001. Dual mode of gating of voltage-dependent anion channel as revealed by phosphorylation. *J Struct Biol* 135: 67-72.
- Bereiter-Hahn J. 1990. Behavior of mitochondria in the living cell. *Int Rev Cytol* 122: 1-63.
- Bernardi P. 1999. Mitochondrial transport of cations: Channels, exchangers, and permeability transition. *Physiol Rev* 79: 1127-1155.
- Bernardi P, Colonna R, Costantini P, Eriksson O, Fontaine E, et al. 1998. The mitochondrial permeability transition. *Biofactors* 8: 273-281.
- Bessman SP, Geiger PJ. 1981. Transport of energy in muscle: The phosphorylcreatine shuttle. *Science* 211: 448-452.
- Beutner G, Ruck A, Riede B, Welte W, Brdiczka, D. 1996. Complexes between kinases, mitochondrial porin and adenylate translocator in rat brain resemble the permeability transition pore. *FEBS Lett* 396: 189-195.
- Bianchi K, Rimessi A, Prandini A, Szabadkai G, Rizzuto R. 2004. Calcium and mitochondria: Mechanisms and functions of a troubled relationship. *Biochim Biophys Acta* 1742: 119-131.
- Bianchi K, Vandecasteele G, Carli C, Romagnoli A, Szabadkai G, et al. 2005. Regulation of Ca²⁺ signaling and Ca²⁺-mediated cell death by the transcriptional coactivator PGC-1 α . *Cell Death Differ* 13: 586-596.
- Bionda C, Portoukalian J, Schmitt D, Rodriguez-Lafrasse C, Ardail D. 2004. Subcellular compartmentalization of ceramide metabolism: MAM (mitochondria-associated membrane) and/or mitochondria? *Biochem J* 382: 527-533.
- Bootman M, Berridge M, Roderick H. 2002. Calcium signaling: More messengers, more channels, more complexity. *Curr Biol* 12: R563-R565.
- Breckenridge DG, Stojanovic M, Marcellus RC, Shore GC. 2003. Caspase cleavage product of BAP31 induces mitochondrial fission through endoplasmic reticulum calcium signals, enhancing cytochrome *c* release to the cytosol. *J Cell Biol* 160: 1115-1127.
- Bukau B, Horwich AL. 1998. The Hsp70 and Hsp60 chaperone machines. *Cell* 92: 351-366.
- Cesura AM, Pinard E, Schubel R, Goetschy V, Friedlein A, et al. 2003. The voltage-dependent anion channel is the

- target for a new class of inhibitors of the mitochondrial permeability transition pore. *J Biol Chem* 278: 49812-49818.
- Chen KH, Guo X, Ma D, Guo Y, Li Q, et al. 2004. Dysregulation of HSG triggers vascular proliferative disorders. *Nat Cell Biol* 6: 872-883.
- Chiesa A, Rapizzi E, Tosello V, Pinton P, de Virgilio M, et al. 2001. Recombinant aequorin and green fluorescent protein as valuable tools in the study of cell signaling. *Biochem J* 355: 1-12.
- Coleman RA, Lewin TM, Muoio DM. 2000. Physiological and nutritional regulation of enzymes of triacylglycerol synthesis. *Annu Rev Nutr* 20: 77-103.
- Colombini M. 1980. Structure and mode of action of a voltage-dependent anion-selective channel (VDAC) located in the outer mitochondrial membrane. *Ann N Y Acad Sci* 341: 552-563.
- Colombini M. 1989. Voltage gating in the mitochondrial channel, VDAC. *J Membr Biol* 111: 103-111.
- Colombini M. 2004. VDAC: The channel at the interface between mitochondria and the cytosol. *Mol Cell Biochem* 256-257: 107-115.
- Colombo S, Longhi R, Alcaro S, Ortuso F, Sprocati T, et al. 2005. *N*-myristoylation determines dual targeting of mammalian NADH-cytochrome *b5* reductase to ER and mitochondrial outer membranes by a mechanism of kinetic partitioning. *J Cell Biol* 168: 735-745.
- Cox JS, Chapman RE, Walter P. 1997. The unfolded protein response coordinates the production of endoplasmic reticulum protein and endoplasmic reticulum membrane. *Mol Biol Cell* 8: 1805-1814.
- Crompton M. 2000. Mitochondrial intermembrane junctional complexes and their role in cell death. *J Physiol* 529 Pt 1: 11-21.
- Crozati B, Badoual T, Boehm E, Ennezat PV, Guenoun T, et al. R. 2002. Role of creatine kinase in cardiac excitation-contraction coupling: Studies in creatine kinase-deficient mice. *FASEB J* 16: 653-660.
- Csordas G, Thomas AP, Hajnoczky G. 1999. Quasi-synaptic calcium signal transmission between endoplasmic reticulum and mitochondria. *EMBO J* 18: 96-108.
- Das AK, Horie S, Hajra AK. 1992. Biosynthesis of glycerolipid precursors in rat liver peroxisomes and their transport and conversion to phosphatidate in the endoplasmic reticulum. *J Biol Chem* 267: 9724-9730.
- Deshaies RJ, Koch BD, Werner-Washburne M, Craig EA, Schekman R. 1988. A subfamily of stress proteins facilitates translocation of secretory and mitochondrial precursor polypeptides. *Nature* 332: 800-805.
- Dircks LK, Sul HS. 1997. Mammalian mitochondrial glycerol-3-phosphate acyltransferase. *Biochim Biophys Acta* 1348: 17-26.
- Doerner A, Pauschinger M, Badorff A, Noutsias M, Giessen S, et al. 1997. Tissue-specific transcription pattern of the adenine nucleotide translocase isoforms in humans. *FEBS Lett* 414: 258-262.
- Duchen MR. 2000. Mitochondria and calcium: From cell signaling to cell death. *J Physiol* 529 Pt 1: 57-68.
- Dzeja PP, Terzic A. 2003. Phosphotransfer networks and cellular energetics. *J Exp Biol* 206: 2039-2047.
- Elkeles A, Breiman A, Zizi M. 1997. Functional differences among wheat voltage-dependent anion channel (VDAC) isoforms expressed in yeast. Indication for the presence of a novel VDAC-modulating protein? *J Biol Chem* 272: 6252-6260.
- Fadok VA, de Cathelineau A, Daleke DL, Henson PM, Bratton DL. 2001. Loss of phospholipid asymmetry and surface exposure of phosphatidylserine is required for phagocytosis of apoptotic cells by macrophages and fibroblasts. *J Biol Chem* 276: 1071-1077.
- Federovitch CM, Ron D, Hampton RY. 2005. The dynamic ER: Experimental approaches and current questions. *Curr Opin Cell Biol* 17: 409-414.
- Filippin L, Magalhaes PJ, Di Benedetto G, Colella M, Pozzan T. 2003. Stable interactions between mitochondria and endoplasmic reticulum allow rapid accumulation of calcium in a subpopulation of mitochondria. *J Biol Chem* 278: 39224-39234.
- Foyouzi-Youssefi R, Arnaudeau S, Borner C, Kelley WL, Tschopp J, et al. 2000. Bcl-2 decreases the free Ca²⁺ concentration within the endoplasmic reticulum. *Proc Natl Acad Sci USA* 97: 5723-5728.
- Frank S, Gaume B, Bergmann-Leitner ES, Leitner WW, Robert EG, et al. 2001. The role of dynamin-related protein 1, a mediator of mitochondrial fission, in apoptosis. *Dev Cell* 1: 515-525.
- Fransson A, Ruusala A, Aspenstrom P. 2003. Atypical Rho GTPases have roles in mitochondrial homeostasis and apoptosis. *J Biol Chem* 278: 6495-6502.
- Frederick RL, McCaffery JM, Cunningham KW, Okamoto K, Shaw JM. 2004. Yeast Miro GTPase, Gem1p, regulates mitochondrial morphology via a novel pathway. *J Cell Biol* 167: 87-98.
- Frey TG, Renken CW, Perkins GA. 2002. Insight into mitochondrial structure and function from electron tomography. *Biochim Biophys Acta* 1555: 196-203.
- Frieden M, James D, Castelbou C, Danckaert A, Martinou JC, et al. 2004. Ca²⁺ homeostasis during mitochondrial fragmentation and perinuclear clustering induced by hFis1. *J Biol Chem* 279: 22704-22714.
- Frieden M, Arnaudeau S, Castelbou C, Demaurex N. 2005. Subplasmalemmal mitochondria modulate the activity of plasma membrane Ca²⁺-ATPases. *J Biol Chem* 280: 43198-43208.

- Gincel D, Zaid H, Shoshan-Barmatz V. 2001. Calcium binding and translocation by the voltage-dependent anion channel: A possible regulatory mechanism in mitochondrial function. *Biochem J* 358: 147-155.
- Gray MW, Burger G, Lang BF. 1999. Mitochondrial evolution. *Science* 283: 1476-1481.
- Green DR, Kroemer G. 2004. The pathophysiology of mitochondrial cell death. *Science* 305: 626-629.
- Gunter TE, Buntinas L, Sparagna G, Eliseev R, Gunter K. 2000. Mitochondrial calcium transport: Mechanisms and functions. *Cell Calcium* 28: 285-296.
- Guo X, Macleod GT, Wellington A, Hu F, Panchumarthi S, et al. 2005. The GTPase dMiro is required for axonal transport of mitochondria to *Drosophila* synapses. *Neuron* 47: 379-393.
- Hales KG, Fuller MT. 1997. Developmentally regulated mitochondrial fusion mediated by a conserved, novel, predicted GTPase. *Cell* 90: 121-129.
- Halestrap AP, McStay GP, Clarke SJ. 2002. The permeability transition pore complex: Another view. *Biochimie* 84: 153-166.
- Hannun YA, Luberto C. 2000. Ceramide in the eukaryotic stress response. *Trends Cell Biol* 10: 73-80.
- Harder Z, Zunino R, McBride H. 2004. Sumo1 conjugates mitochondrial substrates and participates in mitochondrial fission. *Curr Biol* 14: 340-345.
- Hartl FU, Hayer-Hartl M. 2002. Molecular chaperones in the cytosol: From nascent chain to folded protein. *Science* 295: 1852-1858.
- He L, Lemasters JJ. 2002. Regulated and unregulated mitochondrial permeability transition pores: A new paradigm of pore structure and function? *FEBS Lett* 512: 1-7.
- Ichaz F, Mazat JP. 1998. From calcium signaling to cell death: Two conformations for the mitochondrial permeability transition pore. Switching from low- to high-conductance state. *Biochim Biophys Acta* 1366: 33-50.
- Jahn R, Grubmuller H. 2002. Membrane fusion. *Curr Opin Cell Biol* 14: 488-495.
- Jekely G. 2003. Small GTPases and the evolution of the eukaryotic cell. *Bioessays* 25: 1129-1138.
- Joubert F, Mateo P, Gillet B, Beloel JC, Mazet JL, et al. 2004. CK flux or direct ATP transfer: Versatility of energy transfer pathways evidenced by NMR in the perfused heart. *Mol Cell Biochem* 256-257: 43-58.
- Kaasik A, Veksler V, Boehm E, Novotova M, Minajeva A, et al. 2001. Energetic cross talk between organelles: Architectural integration of energy production and utilization. *Circ Res* 89: 153-159.
- Karbowski M, Arnould D, Chen H, Chan DC, Smith CL, et al. 2004. Quantitation of mitochondrial dynamics by photo-labeling of individual organelles shows that mitochondrial fusion is blocked during the Bax activation phase of apoptosis. *J Cell Biol* 164: 493-499.
- Karbowski M, Lee YJ, Gaume B, Jeong SY, Frank S, et al. 2002. Spatial and temporal association of Bax with mitochondrial fission sites, Drp1, and Mfn2 during apoptosis. *J Cell Biol* 159: 931-938.
- Kim JH, Lewin TM, Coleman RA. 2001. Expression and characterization of recombinant rat Acyl-CoA synthetases 1, 4, and 5. Selective inhibition by triacsin C and thiazolidinediones. *J Biol Chem* 276: 24667-24673.
- Kirichok Y, Kravinsky G, Clapham DE. 2004. The mitochondrial calcium uniporter is a highly selective ion channel. *Nature* 427: 360-364.
- Komarov AG, Deng D, Craigen WJ, Colombini M. 2005. New insights into the mechanism of permeation through large channels. *Biophys J* 89: 3950-3959.
- Korsmeyer SJ, McDonnell TJ, Nunez G, Hockenbery D, Young R. 1990. Bcl-2: B cell life, death, and neoplasia. *Curr Top Microbiol Immunol* 166: 203-207.
- Lam M, DUBYAK G, Chen L, Nunez G, Miesfeld RL, et al. 1994. Evidence that Bcl-2 represses apoptosis by regulating endoplasmic reticulum-associated Ca^{2+} fluxes. *Proc Natl Acad Sci USA* 91: 6569-6573.
- Lasorsa FM, Pinton P, Palmieri L, Fiermonte G, Rizzuto R, et al. 2003. Recombinant expression of the Ca^{2+} -sensitive aspartate/glutamate carrier increases mitochondrial ATP production in agonist-stimulated Chinese hamster ovary cells. *J Biol Chem* 278: 38686-38692.
- Lee AC, Zizi M, Colombini M. 1994. β -NADH decreases the permeability of the mitochondrial outer membrane to ADP by a factor of 6. *J Biol Chem* 269: 30974-30980.
- Leipe DD, Wolf YI, Koonin EV, Aravind L. 2002. Classification and evolution of P-loop GTPases and related ATPases. *J Mol Biol* 317: 41-72.
- Levine T, Rabouille C. 2005. Endoplasmic reticulum: One continuous network compartmentalized by extrinsic cues. *Curr Opin Cell Biol* 17: 362-368.
- Lin RC, Scheller RH. 2000. Mechanisms of synaptic vesicle exocytosis. *Annu Rev Cell Dev Biol* 16: 19-49.
- Lithgow T, van Driel R, Bertram JF, Strasser A. 1994. The protein product of the oncogene bcl-2 is a component of the nuclear envelope, the endoplasmic reticulum, and the outer mitochondrial membrane. *Cell Growth Differ* 5: 411-417.
- Ma TS, Mann DL, Lee JH, Gallinghouse GJ. 1999. SR compartment calcium and cell apoptosis in SERCA overexpression. *Cell Calcium* 26: 25-36.
- Malli R, Frieden M, Osibow K, Zoratti C, Mayer M, et al. 2003. Sustained Ca^{2+} transfer across mitochondria is essential for mitochondrial Ca^{2+} buffering, store-operated Ca^{2+} entry, and Ca^{2+} store refilling. *J Biol Chem* 278: 44769-44779.

- Malli R, Frieden M, Trenker M, Graier WF. 2005. The role of mitochondria for Ca^{2+} refilling of the endoplasmic reticulum. *J Biol Chem* 280: 12114-12122.
- Mangan PS, Colombini M. 1987. Ultrasteep voltage dependence in a membrane channel. *Proc Natl Acad Sci USA* 84: 4896-4900.
- Mannella CA, Buttle K, Rath BK, Marko, M. 1998. Electron microscopic tomography of rat-liver mitochondria and their interaction with the endoplasmic reticulum. *Biofactors* 8: 225-228.
- Mannella CA, Pfeiffer DR, Bradshaw PC, Moraru II, Slepchenko B, et al. 2001. Topology of the mitochondrial inner membrane: Dynamics and bioenergetic implications. *IUBMB. Life* 52: 93-100.
- Marsh BJ, Mastronarde DN, Buttle KF, Howell KE, McIntosh JR. 2001. Organellar relationships in the Golgi region of the pancreatic β cell line, HIT-T15, visualized by high-resolution electron tomography. *Proc Natl Acad Sci USA* 98: 2399-2406.
- McCormack JG, Halestrap AP, Denton RM. 1990. Role of calcium ions in regulation of mammalian intramitochondrial metabolism. *Physiol Rev* 70: 391-425.
- Meeusen SL, Nunnari J. 2005. How mitochondria fuse. *Curr Opin Cell Biol* 17: 389-394.
- Merrill AH, Jr. 2002. De novo sphingolipid biosynthesis: Necessary, but dangerous, pathway. *J Biol Chem* 277: 25843-25846.
- Minin AA, Kulik AV, Gyoeva FK, Li Y, Goshima G, et al. 2006. Regulation of mitochondria distribution by RhoA and formins. *J Cell Sci* 119: 659-670.
- Minn AJ, Velez P, Schendel SL, Liang H, Muchmore SW, et al. 1997. Bcl-x(L) forms an ion channel in synthetic lipid membranes. *Nature* 385: 353-357.
- Miyawaki A. 2003. Fluorescence imaging of physiological activity in complex systems using GFP-based probes. *Curr Opin Neurobiol* 13: 591-596.
- Miyazaki E, Kida Y, Mihara K, Sakaguchi M. 2005. Switching the sorting mode of membrane proteins from cotranslational endoplasmic reticulum targeting to posttranslational mitochondrial import. *Mol Biol Cell* 16: 1788-1799.
- Mozdy AD, Shaw JM. 2003. A fuzzy mitochondrial fusion apparatus comes into focus. *Nat Rev Mol Cell Biol* 4: 468-478.
- Mukamel Z, Kimchi A. 2004. Death-associated protein 3 localizes to the mitochondria and is involved in the process of mitochondrial fragmentation during cell death. *J Biol Chem* 279: 36732-36738.
- Munro S. 2002. Organelle identity and the targeting of peripheral membrane proteins. *Curr Opin Cell Biol* 14: 506-514.
- Munro S. 2004. Organelle identity and the organization of membrane traffic. *Nat Cell Biol* 6: 469-472.
- Nakashima RA, Mangan PS, Colombini M, Pedersen PL. 1986. Hexokinase receptor complex in hepatoma mitochondria: Evidence from N,N' -dicyclohexylcarbodiimide-labeling studies for the involvement of the pore-forming protein VDAC. *Biochemistry* 25: 1015-1021.
- Neupert W, Brunner M. 2002. The protein import motor of mitochondria. *Nat Rev Mol Cell Biol* 3: 555-565.
- Nishizuka Y. 1984. Turnover of inositol phospholipids and signal transduction. *Science* 225: 1365-1370.
- Orrenius S, Zhivotovsky B, Nicotera P. 2003. Regulation of cell death: The calcium-apoptosis link. *Nat Rev Mol Cell Biol* 4: 552-565.
- Osteryoung KW, Nunnari J. 2003. The division of endosymbiotic organelles. *Science* 302: 1698-1704.
- Ovadi J, Saks V. 2004. On the origin of intracellular compartmentation and organized metabolic systems. *Mol Cell Biochem* 256-257: 5-12.
- Ovadi J, Orosz F, Hollan S. 2004. Functional aspects of cellular microcompartmentation in the development of neurodegeneration: Mutation induced aberrant protein-protein associations. *Mol Cell Biochem* 256-257: 83-93.
- Pacher P, Hajnoczky G. 2001. Propagation of the apoptotic signal by mitochondrial waves. *EMBO J* 20: 4107-4121.
- Palmieri F. 2004. The mitochondrial transporter family (SLC25): Physiological and pathological implications. *Pflügers Arch* 447: 689-709.
- Paschen W, Mengesdorf T. 2005. Endoplasmic reticulum stress response and neurodegeneration. *Cell Calcium* 38: 409-415.
- Pastorino JG, Hoek JB. 2003. Hexokinase II: The integration of energy metabolism and control of apoptosis. *Curr Med Chem* 10: 1535-1551.
- Pastorino JG, Shulga N, Hoek JB. 2002. Mitochondrial binding of hexokinase II inhibits Bax-induced cytochrome c release and apoptosis. *J Biol Chem* 277: 7610-7618.
- Pedersen PL, Mathupala S, Rempel A, Geschwind JF, Ko YH. 2002. Mitochondrial-bound type II hexokinase: A key player in the growth and survival of many cancers and an ideal prospect for therapeutic intervention. *Biochim Biophys Acta* 1555: 14-20.
- Perkins G, Renken C, Martone ME, Young SJ, Ellisman M, et al. 1997. Electron tomography of neuronal mitochondria: Three-dimensional structure and organization of cristae and membrane contacts. *J Struct Biol* 119: 260-272.
- Perkins GA, Renken CW, Frey TG, Ellisman MH. 2001. Membrane architecture of mitochondria in neurons of the central nervous system. *J Neurosci Res* 66: 857-865.
- Petersen OH, Burdakov D, Tepikin AV. 1999. Polarity in intracellular calcium signaling. *Bioessays* 21: 851-860.
- Petronilli V, Nicolli A, Costantini P, Colonna R, Bernardi P. 1994. Regulation of the permeability transition pore, a

- voltage-dependent mitochondrial channel inhibited by cyclosporin A. *Biochim Biophys Acta* 1187: 255-259.
- Pfanner N, Wiedemann N, Meisinger C, Lithgow T. 2004. Assembling the mitochondrial outer membrane. *Nat Struct Mol Biol* 11: 1044-1048.
- Pfeffer SR. 2001. Rab GTPases: Specifying and deciphering organelle identity and function. *Trends Cell Biol* 11: 487-491.
- Pinton P, Ferrari D, Magalhaes P, Schulze-Osthoff K, Di Virgilio F, et al. 2000. Reduced loading of intracellular Ca^{2+} stores and downregulation of capacitative Ca^{2+} influx in Bcl-2-overexpressing cells. *J Cell Biol* 148: 857-862.
- Pinton P, Ferrari D, Rapizzi E, Di Virgilio FD, Pozzan T, et al. 2001. The Ca^{2+} concentration of the endoplasmic reticulum is a key determinant of ceramide-induced apoptosis: Significance for the molecular mechanism of Bcl-2 action. *EMBO J* 20: 2690-2701.
- Porcelli AM, Ghelli A, Zanna C, Pinton P, Rizzuto R, et al. 2005. pH difference across the outer mitochondrial membrane measured with a green fluorescent protein mutant. *Biochem Biophys Res Commun* 326: 799-804.
- Powell KS, Latterich M. 2000. The making and breaking of the endoplasmic reticulum. *Traffic* 1: 689-694.
- Pratt WB, Toft DO. 2003. Regulation of signaling protein function and trafficking by the Hsp90/Hsp70-based chaperone machinery. *Exp Biol Med (Maywood)* 228: 111-133.
- Puigserver P, Spiegelman BM. 2003. Peroxisome proliferator-activated receptor- γ coactivator 1 α (PGC-1 α): Transcriptional coactivator and metabolic regulator. *Endocr Rev* 24: 78-90.
- Rao RV, Bredesen DE. 2004. Misfolded proteins, endoplasmic reticulum stress, and neurodegeneration. *Curr Opin Cell Biol* 16: 653-662.
- Rapizzi E, Pinton P, Szabadkai G, Wiekowski MR, Vandecasteele G, et al. 2002. Recombinant expression of the voltage-dependent anion channel enhances the transfer of Ca^{2+} microdomains to mitochondria. *J Cell Biol* 159: 613-624.
- Reed JC. 1994. Bcl-2 and the regulation of programmed cell death. *J Cell Biol* 124: 1-6.
- Reed JC, Tsujimoto Y, Alpers JD, Croce CM, Nowell PC. 1987. Regulation of Bcl-2 protooncogene expression during normal human lymphocyte proliferation. *Science* 236: 1295-1299.
- Ridley AJ. 2001. Rho family proteins: Coordinating cell responses. *Trends Cell Biol* 11: 471-477.
- Rizzuto R, Pinton P, Carrington W, Fay FS, Fogarty KE, et al. 1998. Close contacts with the endoplasmic reticulum as determinants of mitochondrial Ca^{2+} responses. *Science* 280: 1763-1766.
- Rostovtseva TK, Antonsson B, Suzuki M, Youle RJ, Colombini M, et al. 2004. Bid, but not Bax, regulates VDAC channels. *J Biol Chem* 279: 13575-13583.
- Rostovtseva TK, Komarov A, Bezrukov SM, Colombini M. 2002. VDAC channels differentiate between natural metabolites and synthetic molecules. *J Membr Biol* 187: 147-156.
- Rostovtseva TK, Tan W, Colombini M. 2005. On the role of VDAC in apoptosis: Fact and fiction. *J Bioenerg Biomembr* 37: 129-142.
- Roumier T, Szabadkai G, Simoni AM, Perfettini JL, Paulau AL, et al. 2005. HIV-1 protease inhibitors and cytomegalovirus vMIA induce mitochondrial fragmentation without triggering apoptosis. *Cell Death Differ* 13: 348-351.
- Sacher M, Barrowman J, Wang W, Horecka J, Zhang Y, et al. 2001. TRAPP I implicated in the specificity of tethering in ER-to-Golgi transport. *Mol Cell* 7: 433-442.
- Saks VA, Ventura-Clapier R, Aliev MK. 1996. Metabolic control and metabolic capacity: Two aspects of creatine kinase functioning in the cells. *Biochim Biophys Acta* 1274: 81-88.
- Schendel SL, Montal M, Reed JC. 1998. Bcl-2 family proteins as ion channels. *Cell Death Differ* 5: 372-380.
- Schwarzer C, Barnikol-Watanabe S, Thinnies FP, Hilschmann N. 2002. Voltage-dependent anion-selective channel (VDAC) interacts with the dynein light chain Tctex1 and the heat-shock protein PBP74. *Int J Biochem Cell Biol* 34: 1059-1070.
- Scorrano L, Oakes SA, Opferman JT, Cheng EH, Sorcinelli MD, et al. 2003. Bax and Bak regulation of endoplasmic reticulum Ca^{2+} : A control point for apoptosis. *Science* 300: 135-139.
- Shiao YJ, Lupo G, Vance JE. 1995. Evidence that phosphatidylserine is imported into mitochondria via a mitochondria-associated membrane and that the majority of mitochondrial phosphatidylethanolamine is derived from decarboxylation of phosphatidylserine. *J Biol Chem* 270: 11190-11198.
- Shoshan-Barmatz V, Gincel D. 2003. The voltage-dependent anion channel: Characterization, modulation, and role in mitochondrial function in cell life and death. *Cell Biochem Biophys* 39: 279-292.
- Soti C, Pal C, Papp B, Csermely P. 2005. Molecular chaperones as regulatory elements of cellular networks. *Curr Opin Cell Biol* 17: 210-215.
- Skulachev VP, Bakeeva LE, Chernyak BV, Domnina LV, Minin AA, et al. 2004. Thread-grain transition of mitochondrial reticulum as a step of mitoptosis and apoptosis. *Mol Cell Biochem* 256-257: 341-358.
- Stepien G, Torroni A, Chung AB, Hodge JA, Wallace DC. 1992. Differential expression of adenine nucleotide translocator isoforms in mammalian tissues and during muscle cell differentiation. *J Biol Chem* 267: 14592-14597.
- Szabadkai G, Simoni AM, Chami M, Wiekowski MR, Youle RJ, et al. 2004. Drp-1-dependent division of the mitochondrial network blocks intraorganellar Ca^{2+} waves and protects against Ca^{2+} -mediated apoptosis. *Mol Cell* 16: 59-68.
- Szabo I, Bathori G, Tombola F, Coppola A, Schmehl I, et al. 1998. Double-stranded DNA can be translocated across a

- planar membrane containing purified mitochondrial porin. *FASEB J* 12: 495-502.
- Szalai G, Krishnamurthy R, Hajnoczky G. 1999. Apoptosis driven by IP₃-linked mitochondrial calcium signals. *EMBO J* 18: 6349-6361.
- Szczesna-Skorupa E, Chen CD, Liu H, Kemper B. 2004. Gene expression changes associated with the endoplasmic reticulum stress response induced by microsomal cytochrome P450 overproduction. *J Biol Chem* 279: 13953-13961.
- Takai Y, Sasaki T, Matozaki T. 2001. Small GTP-binding proteins. *Physiol Rev* 81: 153-208.
- Tanaka S, Saito K, Reed JC. 1993. Structure-function analysis of the Bcl-2 oncoprotein. Addition of a heterologous transmembrane domain to portions of the Bcl-2 β protein restores function as a regulator of cell survival. *J Biol Chem* 268: 10920-10926.
- Tinel H, Cancela JM, Mogami H, Gerasimenko JV, Gerasimenko OV, et al. 1999. Active mitochondria surrounding the pancreatic acinar granule region prevent spreading of inositol trisphosphate-evoked local cytosolic Ca²⁺ signals. *EMBO J* 18: 4999-5008.
- Truscott KN, Brandner K, Pfanner N. 2003. Mechanisms of protein import into mitochondria. *Curr Biol* 13: R326-R337.
- Tsujimoto Y, Cossman J, Jaffe E, Croce CM. 1985a. Involvement of the bcl-2 gene in human follicular lymphoma. *Science* 228: 1440-1443.
- Tsujimoto Y, Jaffe E, Cossman J, Gorham J, Nowell PC, et al. 1985b. Clustering of breakpoints on chromosome 11 in human B cell neoplasms with the t(11;14) chromosome translocation. *Nature* 315: 340-343.
- Uchiyama K, Kondo H. 2005. p97/p47-mediated biogenesis of Golgi and ER. *J Biochem (Tokyo)* 137: 115-119.
- van Blitterswijk WJ, van der Luit AH, Veldman RJ, Verheij M, Borst J. 2003. Ceramide: Second messenger or modulator of membrane structure and dynamics? *Biochem J* 369: 199-211.
- van Herpen RE, Oude Ophuis RJ, Wijers M, Bennink MB, van de Loo FA, et al. 2005. Divergent mitochondrial and endoplasmic reticulum association of DMPK splice isoforms depends on unique sequence arrangements in tail anchors. *Mol Cell Biol* 25: 1402-1414.
- Vance JE. 1990. Phospholipid synthesis in a membrane fraction associated with mitochondria. *J Biol Chem* 265: 7248-7256.
- Vance JE. 1991. Newly made phosphatidylserine and phosphatidylethanolamine are preferentially translocated between rat liver mitochondria and endoplasmic reticulum. *J Biol Chem* 266: 89-97.
- Vance JE. 1998. Eukaryotic lipid-biosynthetic enzymes: The same but not the same. *Trends Biochem Sci* 23: 423-428.
- Vance JE. 2003. Molecular and cell biology of phosphatidylserine and phosphatidylethanolamine metabolism. *Prog Nucleic Acid Res Mol Biol* 75: 69-111.
- Vance JE, Vance DE. 2004. Phospholipid biosynthesis in mammalian cells. *Biochem Cell Biol* 82: 113-128.
- Vance JE, Vance DE. 2005. Metabolic insights into phospholipid function using gene-targeted mice. *J Biol Chem* 280: 10877-10880.
- Vander Heiden MG, Li XX, Gottlieb E, Hill RB, Thompson CB, et al. 2001. Bcl-xL promotes the open configuration of the voltage-dependent anion channel and metabolite passage through the outer mitochondrial membrane. *J Biol Chem* 276: 19414-19419.
- Varadi A, Johnson-Cadwell LI, Cirulli V, Yoon Y, Allan VJ, et al. 2004. Cytoplasmic dynein regulates the subcellular distribution of mitochondria by controlling the recruitment of the fission factor dynamin-related protein-1. *J Cell Sci* 117: 4389-4400.
- Vendelin M, Lemba M, Saks VA. 2004. Analysis of functional coupling: Mitochondrial creatine kinase and adenine nucleotide translocase. *Biophys J* 87: 696-713.
- Ventura-Clapier R, Kaasik A, Veksler, V. 2004. Structural and functional adaptations of striated muscles to CK deficiency. *Mol Cell Biochem* 256-257: 29-41.
- Voelker DR. 1989a. Phosphatidylserine translocation to the mitochondrion is an ATP-dependent process in permeabilized animal cells. *Proc Natl Acad Sci USA* 86: 9921-9925.
- Voelker DR. 1989b. Reconstitution of phosphatidylserine import into rat liver mitochondria. *J Biol Chem* 264: 8019-8025.
- Voelker DR. 2005. Bridging gaps in phospholipid transport. *Trends Biochem Sci* 30: 396-404.
- Voeltz GK, Rolls MM, Rapoport TA. 2002. Structural organization of the endoplasmic reticulum. *EMBO Rep* 3: 944-950.
- Vyssokikh M, Brdiczka D. 2004. VDAC and peripheral channeling complexes in health and disease. *Mol Cell Biochem* 256-257: 117-126.
- Vyssokikh MY, Katz A, Rueck A, Wuensch C, Dorner A, et al. 2001. Adenine nucleotide translocator isoforms 1 and 2 are differently distributed in the mitochondrial inner membrane and have distinct affinities to cyclophilin D. *Biochem J* 358: 349-358.
- Waldmeier PC, Feldtrauer JJ, Qian T, Lemasters JJ. 2002. Inhibition of the mitochondrial permeability transition by the nonimmunosuppressive cyclosporin derivative NIM811. *Mol Pharmacol* 62: 22-29.
- Walkey CJ, Donohue LR, Bronson R, Agellon LB, Vance DE. 1997. Disruption of the murine gene encoding phosphatidylethanolamine N-methyltransferase. *Proc Natl Acad Sci USA* 94: 12880-12885.
- Wang HJ, Guay G, Pogan L, Sauve R, Nabi, IR. 2000. Calcium regulates the association between mitochondria and a

- smooth subdomain of the endoplasmic reticulum. *J Cell Biol* 150: 1489-1498.
- Weber T, Zemelman BV, McNew JA, Westermann B, Gmachl M, et al. 1998. SNAREpins: Minimal machinery for membrane fusion. *Cell* 92: 759-772.
- Weissman JT, Plutner H, Balch WE. 2001. The mammalian guanine nucleotide exchange factor mSec12 is essential for activation of the Sar1 GTPase-directing endoplasmic reticulum export. *Traffic* 2: 465-475.
- Westermann B. 2003. Mitochondrial membrane fusion. *Biochim Biophys Acta* 1641: 195-202.
- Xu C, Bailly-Maitre B, Reed JC. 2005. Endoplasmic reticulum stress: Cell life and death decisions. *J Clin Invest* 115: 2656-2664.
- Xu X, Forbes JG, Colombini M. 2001. Actin modulates the gating of *Neurospora crassa* VDAC. *J Membr Biol* 180: 73-81.
- Yaffe MP. 1999. The machinery of mitochondrial inheritance and behavior. *Science* 283: 1493-1497.
- Yano M, Terada K, Mori M. 2003. AIP is a mitochondrial import mediator that binds to both import receptor Tom20 and preproteins. *J Cell Biol* 163: 45-56.
- Yoon Y, Krueger EW, Oswald BJ, McNiven MA. 2003. The mitochondrial protein hFis1 regulates mitochondrial fission in mammalian cells through an interaction with the dynamin-like protein DLP1. *Mol Cell Biol* 23: 5409-5420.
- Yoshimura Y, Shinkawa T, Taoka M, Kobayashi K, Isobe T, et al. 2002. Identification of protein substrates of Ca^{2+} /calmodulin-dependent protein kinase II in the postsynaptic density by protein sequencing and mass spectrometry. *Biochem Biophys Res Commun* 290: 948-954.
- Young JC, Agashe VR, Siegers K, Hartl FU. 2004. Pathways of chaperone-mediated protein folding in the cytosol. *Nat Rev Mol Cell Biol* 5: 781-791.
- Young JC, Barral JM, Ulrich HF. 2003a. More than folding: Localized functions of cytosolic chaperones. *Trends Biochem Sci* 28: 541-547.
- Young JC, Hoogenraad NJ, Hartl FU. 2003b. Molecular chaperones Hsp90 and Hsp70 deliver preproteins to the mitochondrial import receptor Tom70. *Cell* 112: 41-50.
- Young JC, Moarefi I, Hartl FU. 2001. Hsp90: A specialized but essential protein-folding tool. *J Cell Biol* 154: 267-273.
- Zborowski J, Dygas A, Wojtczak L. 1983. Phosphatidylserine decarboxylase is located on the external side of the inner mitochondrial membrane. *FEBS Lett* 157: 179-182.
- Zhang DW, Colombini M. 1989. Inhibition by aluminum hydroxide of the voltage-dependent closure of the mitochondrial channel, VDAC. *Biochim Biophys Acta* 991: 68-78.
- Zimmerberg J, Parsegian VA. 1986. Polymer inaccessible volume changes during opening and closing of a voltage-dependent ionic channel. *Nature* 323: 36-39.

6.3 Mitochondria-Nucleus Energetic Communication: Role for Phosphotransfer Networks in Processing Cellular Information

P. P. Dzeja · A. Terzic

1	<i>Introduction</i>	642
2	<i>Mechanisms of Intracellular Energetic Communication</i>	643
2.1	Simple Diffusion	645
2.2	Facilitated Diffusion	645
2.3	Metabolite Channeling	646
2.4	Reaction-Diffusion	646
2.5	Ligand Conduction	647
3	<i>Phosphotransfer Reactions in Mitochondrial-Nuclear Energetic Communication</i>	648
4	<i>Phosphotransfer-Mediated Metabolic Signaling</i>	651
5	<i>Phosphotransfer Networks in Processing and Integrating Cellular Information</i>	654
6	<i>Concluding Remarks</i>	657

Abstract: Metabolic networks composed of the creatine kinase, adenylate kinase, and glycolytic phosphotransfer reactions are integral components of the cellular energetic infrastructure. Collectively, these pathways facilitate transfer and distribution of high-energy phosphoryls produced in the mitochondria through structured cytosolic and nuclear compartments. In this way, intracellular phosphotransfer relays secure efficient energetic and metabolic signaling, and thereby determining the fidelity of a range of cellular responses, including nucleocytoplasmic, metabolic, and genomic communications. The role and contribution of individual phosphotransfer enzymes depends on the species, tissue, developmental stage, or (patho) physiological state, underscoring the plasticity of the cellular energetic system in governing metabolic homeostasis. Catalyzed phosphotransfer along with related systems such as nucleoside diphosphate kinase (NDPK) play a vital role in organs with intense and fluctuating energy and signaling demands such as the heart or brain. Deletion of phosphotransfer enzyme isoforms compromises diverse cellular functions, including metabolic signaling, information processing, and adaptation of cellular energy metabolism to stress. Adaptive genetic reprogramming in conditions of phosphotransfer enzyme deficits is required to safeguard optimal cellular energetics. Emerging data indicate that coupling of phosphotransfer enzymes with metabolic sensors and phosphoryl-transferring protein kinase cascades comprises a unified intracellular energy/signal transduction matrix capable of processing, delivering, and retrieving cellular information. Here, recent evidence demonstrating the significance of compartmentalized and dynamically superimposed interactions of adenylate kinase, creatine kinase, and glycolytic enzyme-catalyzed phosphotransfers in orchestrating cytosolic and nuclear energetics is highlighted.

List of Abbreviations: AMPK, AMP-activated protein kinase; GAPDH, glyceraldehydes-3-phosphate dehydrogenase; β -GPA, beta-guanidinopropionic acid; K_{ATP} , ATP-sensitive potassium channel; NDPK, nucleoside diphosphate kinase; PFK, phosphofructokinase

1 Introduction

Efficient coordination of energy supply and demand, secured through metabolic signaling, is central for normal cell function and stress response. Phosphotransfer networks, composed of adenylate kinase, creatine kinase, nucleoside diphosphate kinase (NDPK), and glycolytic enzymes, have emerged as prototypic intracellular energetic signaling pathways integral to the maintenance of cellular homeostasis (Wallimann et al., 1992; Saks et al., 1994; de Groof et al., 2001; Dzeja and Terzic, 2003; Ingwall, 2004). These networks facilitate communication of high-energy phosphoryls and metabolic signals between cellular compartments, adjusting cellular energy flux in response to functional load (Dzeja et al., 1998, 2004; Boehm et al., 2000; Janssen et al., 2000, 2003b; Saks et al., 2004). As such, the governance of ATP-requiring and ATP-responding cellular components and their integration with cellular energetic and signaling systems is accomplished through the dynamics of phosphotransfer-mediated intracellular nucleotide exchange (Dzeja and Terzic, 1998; Carrasco et al., 2001; Abraham et al., 2002; Neumann et al., 2003; Allen and Dunaway-Mariano, 2004). Efficient intracellular energetic communication is of particular importance in organs with sudden and fluctuating energy demands such as the heart and brain (Wallimann and Hemmer, 1994; Dzeja et al., 1999a; Ames, 2000; Kekelidze et al., 2001; Jost et al., 2002). A case in point is the energy transfer in photoreceptors and neurons, where ATP-generating and ATP-consuming processes are separated by large distances (Hemmer et al., 1993; Notari et al., 2001; Streijger et al., 2004). Similarly, the energy demands of the contracting muscle require efficient communication of energetic signals (Saks et al., 1994; Dzeja and Terzic, 2003).

The distribution of metabolic flux among individual phosphotransfer systems, under different metabolic states, could in turn regulate vital ATP-sensitive cellular processes, including ion conduction, nuclear-cytoplasmic information exchange, receptor-mediated signal transduction, cytoskeletal organization, and cell motility (Mahajan et al., 2000; Abraham et al., 2002; Dzeja et al., 2002; Hipe et al., 2003; Picher and Boucher, 2003). The interaction with adenylate kinase and creatine kinase has been directly implicated in the activity of diverse metabolic sensors, such as the AMP-activated protein kinase (AMPK) and the ATP-sensitive potassium (K_{ATP}) channel, and in the overall ability of the cell to withstand metabolic stress

(Dzeja et al., 1998; Bergeron et al., 2001; Carrasco et al., 2001; Pucar et al., 2001; Zingman et al., 2001, 2002b; Hardie, 2003; Pucar et al., 2004; Alekseev et al., 2005). Metabolic and functional alterations induced by transgenic deficiency of individual phosphotransfer isoforms precipitate a broad spectrum of genetic reprogramming with a resulting wide range of cellular adaptations, underscoring the fundamental role of energetic pathways in sustaining efficient yet vibrant cellular energetics (van Deursen et al., 1993; Saupe et al., 1998; Janssen et al., 2000, 2003a; Dzeja et al., 2004). Moreover, recent gene-knockout studies, where single or multiple phosphotransfer enzymes are disrupted, have opened new perspectives in the intimate understanding of cellular energetic and metabolic signaling networks and their integration with genetic, biosynthetic, membrane electrical, and receptor-mediated signal transduction events within the cellular environment (Steehgs et al., 1997; Boehm et al., 2000; Pucar et al., 2000, 2002; Dzeja and Terzic, 2003; Ingwall, 2004; Spindler et al., 2004). Taken together, with the emerging identification of scaffolding proteins and their support of the spatial organization of phosphotransfer networks, the efficiency and specificity of high-energy phosphoryl distribution has been recognized as necessary in securing a harmonious coordination of diverse cellular processes (Dzeja et al., 2000; Horneman et al., 2003; Neumann et al., 2003; Saks et al., 2004; Dzeja and Terzic, 2005). A case in point is the adaptor protein DRAL/FHL-2, involved in the anchoring of creatine kinase, adenylate kinase, and phosphofructokinase (PFK) to sites of high-energy consumption in the cardiac sarcomere (Lange et al., 2002). Similarly, the Oda5p protein anchors adenylate kinase in the proximity of the dynein arm ensuring that both the high-energy phosphate bonds of ATP are efficiently utilized at the major site of power production of the microtubule motors that are involved in diverse cellular movements (Wirschell et al., 2004). In this regard, overexpression of adenylate kinase isoforms contributes to the precise movements of the extraocular muscle (Andrade et al., 2003). We here summarize recent evidence regarding the importance of phosphotransfer networks in the regulation of the mitochondrial-nuclear energetic communication, metabolic signaling, and processing of cellular information.

2 Mechanisms of Intracellular Energetic Communication

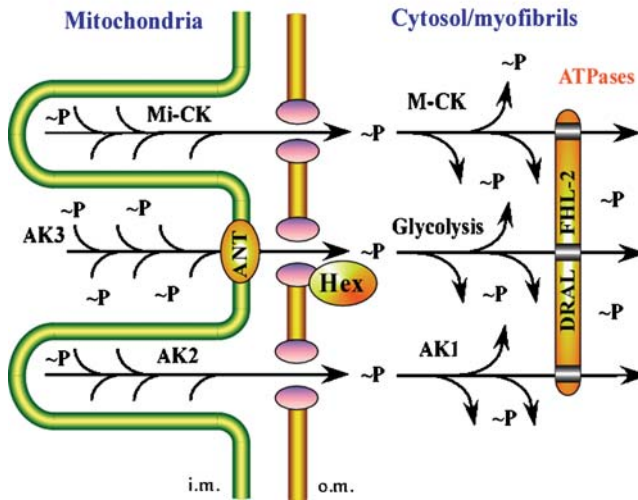
In the cell, major sites of energy transformation and ATP production are spatially separated from sites of ATP-energy utilization that support vital cellular functions. Progress has been made in elucidating the cytoarchitectural, convectional, and enzymatic mechanisms that facilitate the coupling and coordination of energy transduction processes with the metabolic, mechanical, and electrical activities of the cell (Hochachka, 1999; Janssen et al., 2000; Kaasik et al., 2001; Saks et al., 2001; Abraham et al., 2002; Selivanov et al., 2004). Cytoplasmic streaming, positioning of mitochondria and their movement in response to changes in energy utilization, along with formation of enzymatic and mitochondrial-myofibrillar complexes, have all been shown to contribute to the facilitation of intracellular energetic communication (Harold, 1991; Hollenbeck, 1996; Hochachka, 1999; Lange et al., 2002; Saks et al., 2004). However, topological arrangements apparently are not sufficient on their own to fulfill cellular energetic needs (Boehm et al., 2000; Dzeja et al., 2000; de Groof, 2001; Dzeja and Terzic, 2003). In this regard, a new role has emerged for spatially arranged intracellular enzymatic networks catalyzed by creatine kinase, adenylate kinase, and glycolytic enzymes, supporting high-energy phosphoryl transfer and signal communication between ATP-generating and ATP-consuming/ATP-sensing processes (Wallimann et al., 1992; Saks et al., 1994; Dzeja et al., 1998, 2000, 2004; Joubert et al., 2002; Ingwall, 2004) (🔵 [Figure 6.3-1](#)).

Creatine kinase is a major phosphotransfer system in cells with high-energy demand, and it acts in concert with other enzymatic systems to facilitate intracellular energetic communication (Bessman and Carpenter, 1985; Jacobus, 1985; Saks et al., 1994; Joubert et al., 2002; Dzeja and Terzic, 2003; Neumann et al., 2003). Energy transfer does not exclusively rely on creatine kinase (Zelevnikar et al., 1995; Dzeja et al., 1998, 1999b, 2004; Boehm et al., 2000; Janssen et al., 2000, 2003b). Parallel to the creatine kinase system is the adenylate kinase-catalyzed high-energy phosphoryl shuttle (🔵 [Figure 6.3-1](#)), which provides a unique capability for transfer and utilization of both β - and γ -phosphoryls of the ATP molecule, doubling its energetic potential (Dzeja et al., 1985, 1996, 1999b; Zelevnikar et al., 1990). Tissues with high-energy demands are also characterized by robust phosphoryl exchange catalyzed by glycolytic phosphotransfer enzymes (Kingsley-Hickman et al., 1987; Portman, 1994). Depending on metabolic

■ Figure 6.3-1

Integrated cellular phosphotransfer network facilitates high-energy phosphoryl export from mitochondria, with delivery and distribution to remote cellular ATPases. High-energy phosphoryls ($\sim P$), produced in mitochondria, are exported into the cytosol and delivered to remote cellular ATPases. Delivery is mediated and facilitated by three major phosphotransfer reactions comprising the intracellular phosphotransfer network. Network infrastructure is maintained by the interaction of phosphotransfer enzymes with cellular constituents mediated by specific protein domains, protein acetylation, myristoylation, and by anchor proteins (e.g., DRAL/FHL-2). MI-CK and M-CK, mitochondrial and cytosolic isoforms of CK, respectively; AK1 and AK2, cytosolic and mitochondrial isoforms of AK, respectively; AK3, mitochondrial matrix AK isoform; ANT, adenine nucleotide translocator; Hex, hexokinase; DRAL/FHL-2, phosphotransfer enzyme anchor LIM domain protein; i.m. and o.m., inner and outer membranes, respectively

Cellular bioenergetics infrastructure



needs, there is a tight regulation of glycolytic enzyme binding to the mitochondrial outer membrane and to cellular ATP-consumption sites (Gerbitz et al., 1996; Cesar and Wilson, 1998; Ikemoto et al., 2003). This facilitates high-energy phosphoryl transfer from mitochondria to sites of ATP utilization through the glycolytic network (Dzeja et al., 2004). Energy-rich phosphoryls from ATP, used to phosphorylate glucose and fructose-6-phosphate at the mitochondrial site, traverse the glycolytic pathway and can be used to phosphorylate ADP through pyruvate kinase-catalyzed reactions at remote ATP-utilization sites (Figure 6.3-1). There is a close functional interaction and potential for substitution between creatine kinase, adenylate kinase, and glycolytic phosphotransfer systems (Dzeja and Terzic, 2003). Indeed, such alternative high-energy phosphoryl routes may rescue cellular bioenergetics under conditions of compromised creatine kinase-catalyzed phosphotransfer (Dzeja et al., 2004). The glycolytic phosphotransfer system has a distinct significance in brain energetics (as discussed in Chapter 4) supporting ATP-dependent processes separated from mitochondria at much larger distances compared with nonneuronal cells (Ames, 2000; Gjedde, 2001). The function of the newly discovered adaptor protein DRAL/FHL-2, which is involved in anchoring creatine kinase, adenylate kinase, and glycolytic enzymes to sites of high-energy phosphoryl consumption (Lange et al., 2002), is apparently to maintain the structural integrity of the intracellular phosphotransfer network (Figure 6.3-1). Mutations in the FHL-2 family of proteins are associated with human heart disease (Lange et al., 2002). The expression of FHL family proteins is not detected in the brain where other principles or distinct anchoring proteins could be involved in the topological arrangement of intracellular phosphotransfer networks. As such, membrane anchoring of phosphotransfer enzymes

through protein alkylation or phosphorylation could provide organized phosphotransfer pathways to synchronize energy supply to membrane ATPases, and thus harmonizing the operation of ATP/ADP-sensitive receptors and ion channels, important components of the brain cell function (Wallimann and Hemmer, 1994; Dzeja and Terzic, 1998; Janssen et al., 2004). Indeed, membrane-bound creatine kinases and adenylate kinases are characteristic for brain cell types (Nagy et al., 1989; Wallimann and Hemmer, 1994; Inouye et al., 1999).

Energy transfer and feedback signal communication through the exchange of nucleotides and other high-energy carrying molecules between ATP-consuming and ATP-producing processes could be accomplished by several mechanisms. These are described individually in the following sections.

2.1 Simple Diffusion

Diffusion is an intrinsic feature of molecular processes determining random movement of molecules down the concentration gradient. In the cellular environment, simple diffusion of molecules is hampered by high structural organization and viscosity of the cytoplasm (Luby-Phelps, 2000; Vendelin et al., 2004). Formulations of diffusional fluxes have been developed to account for such high density, inhomogeneous, and spatially confined environments (Andreucci et al., 2003; Roussel and Roussel, 2004). The localization of mitochondria in close proximity with cellular energy-utilizing processes and their movement in response to activation of ATP-utilizing reactions (Hollenbeck, 1996) suggest that the distance of energy transfer is critical for adequate energy supply. However, energy transfer by diffusional exchange of adenine nucleotides is kinetically and thermodynamically inefficient since it requires a significant concentration gradient (Meyer et al., 1984; Jacobus, 1985; Dzeja et al., 1999b). This would result in ATPase inhibition by end products (P_i , ADP, H^+), the inability to sustain free energy of ATP hydrolysis (ΔG_{ATP}) at sites of ATP utilization at an appropriate magnitude above the threshold value, and ultimately in energy dissipation during transmission (Kammermeier, 1997; Dzeja et al., 2000; Dzeja and Terzic, 2003). A low concentration of intracellular ADP, necessary to sustain a high ATP/ADP ratio and ΔG_{ATP} , is considered the limiting factor in diffusional feedback communication from ATPases to mitochondrial oxidative phosphorylation (Jacobus, 1985; Saks et al., 2003). Also, diffusional nucleotide exchange cannot provide a uniform energy supply to all ATPases such as in the center of myofibrils, where ATP deficiency can cause formation of rigor bridges (Ventura-Clapier and Veksler, 1994). To achieve normal contraction of isolated myofibers, about ten times higher concentration of bulk ATP should be provided (Bendall, 1969). The same is true with DNA synthesis where much higher concentrations of deoxyribonucleotides are required *in vitro* compared with conditions *in vivo* (Mathews, 1985). If all energy-requiring cellular processes competed for a common pool of ATP, one low K_m /high V_{max} ATPase might effectively eliminate access of other processes to ATP (Masters, 1991). Thus, in the intracellular environment, diffusional exchange of molecules and even small ions is restricted, and concentration gradients build up (Kemp et al., 1998; Kongas and van Beek, 2002). Diffusional restrictions for water molecule movement in the brain are used for tissue microarchitecture and microdynamic imaging using diffusion tensor NMR (Le Bihan, 2003). Molecular diffusion is impaired in disease processes such as brain ischemia (Le Bihan, 2003), and a reduced diffusivity of signaling molecules within the brain's interstitial space due to amyloid deposits contributes to the cognitive impairment in Alzheimer's disease (Mueggler et al., 2004).

2.2 Facilitated Diffusion

Facilitated diffusion is a carrier-mediated process for accelerated transport of molecules across impermeable membranes or throughout the cellular cytosol and extracellular space. According to this mechanism, reversible combination of a ligand with a protein macromolecule results in enhancement of diffusion due to fluxes of both free- and carrier-bound ligand (Wittenberg, 1970). This type of mechanism has been applied to myoglobin- and hemoglobin-facilitated oxygen diffusion (Wittenberg, 1970) as well as to creatine kinase (Meyer et al., 1984) and carbonic anhydrase (Enns, 1967; Stewart et al., 1999) reactions with regard to accelerated metabolite and ion transfer. In the latter, the diffusive flux of substance X in one metabolic

pathway is effectively increased when it participates in an equilibrium reaction with another substance Y since the total flux of X in the pathway is the sum of X and Y fluxes (Meyer et al., 1984). However, this is likely more a reflection of the reaction-diffusion mechanism associated with the reaction front or disequilibrium movement and flux wave propagation (Goldbeter and Nicolis, 1976; Vandelin et al., 2000). Also, the classic example of myoglobin-facilitated oxygen diffusion has been lately questioned due to findings of relatively low mobility of myoglobin in the crowded muscle cytosol (Jurgens et al., 1994; Wittenberg and Wittenberg, 2003). Measurements of intracellular distribution of myoglobin show that this protein displays a clustered pattern of localization parallel to mitochondrial arrays (Takahashi and Asano, 2002). Even immobilized hemoglobin or carbonic anhydrase can markedly increase the rate of O₂ or CO₂ movement (Hemmingsen, 1962; Trachtenberg et al., 1999), which is consistent with the proposed ligand conduction mechanism rather than facilitated diffusion (Dzeja and Terzic, 2003).

2.3 Metabolite Channeling

In living cells, there are numerous stable enzymatic complexes where metabolites are transferred directly from one to the other consecutive component without equilibration with the common intracellular pool (Welch and Easterby, 1994; Ovadi and Saks, 2004). The occurrence of channeling or direct transfer through transient association of enzymes during metabolic activity has important kinetic as well as regulatory implications (Saks et al., 1994; Welch and Easterby, 1994). Selective channeling of intermediates increases the economy and efficiency of enzymatic processes and enables preferential routing of metabolic fluxes through branched pathways in the crowded cellular environment (Srivastava and Bernhard, 1987; Aflalo, 1991; Ovadi and Saks, 2004). In principle, metabolite channeling or the “bucket brigade” type of action could occur between associated single types of phosphotransfer enzymes forming molecular wires or clusters (Wallimann et al., 1992; Appleby et al., 1996; Dzeja and Terzic, 1998). In this regard, direct metabolite channeling has been demonstrated between complexes of phosphotransfer enzymes with the adenine nucleotide translocator in mitochondria as well as with cellular ATPases (Saks et al., 1994). It is unresolved whether substrate channeling is effective at longer distances within enzymatic clusters. In the cytosolic compartment and in the mitochondrial intermembrane space, sequential phosphotransfer reactions could operate through the mechanism of reaction-diffusion or ligand conduction (Dzeja et al., 1998; Dzeja and Terzic, 2005).

2.4 Reaction-Diffusion

In biological and chemical systems which are not well mixed, enzymatic and chemical reactions are associated with substrate and product diffusion, triggering reaction front propagations, inhomogeneous spatial concentration patterns, and chemical or metabolic waves (Goldbeter and Nicolis, 1976; Mair and Muller, 1996; Vandelin et al., 2000). Reaction-diffusion phenomena have a broad biological significance, regulating the spatiotemporal behavior of genetic, metabolic, and electrophysiological processes (Saks et al., 2000; Roussel and Roussel, 2004; Selivanov et al., 2004). In searching how cells overcome diffusional limitations for energy transfer in the highly structured intracellular milieu, it has been suggested that the displacement of equilibrium of creatine kinase or glycolytic reactions in one cellular locale could be rapidly transmitted through a near-equilibrium network in the form of a sharp concentration wavefront over macroscopic distances (Nagle, 1970; Goldbeter and Nicolis, 1976). This has led to the concept of flux transfer chains along which an incoming flux wave could be instantaneously transmitted in either direction (Reich and Sel'kov, 1981), as well as to the node of a “phosphocreatine circuit” (Wallimann et al., 1992). It is known that flux wave propagation along rapid equilibrating chemical and biological reactions can proceed much faster than diffusion of reactants (Goldbeter and Nicolis, 1976; Mair and Muller, 1996). The rate of wave front movement in these systems is equal to the square root of the reaction velocity constant and the diffusion coefficient (Mair and Muller, 1996). These calculations provide an important indication why the total activity of many enzymes catalyzing near-equilibrium reactions in the cell surpasses apparent physiological needs (Saks et al., 1994). Reaction-diffusion models have been successfully applied to describe the

organization and dynamic behavior of the complex cellular energetic system (Meyer et al., 1984; Wallimann et al., 1992; Kemp et al., 1998). Indeed, “metabolic waves” have been observed to propagate rapidly throughout the entire cell (Mair and Muller, 1996; Kindzelskii and Petty, 2002) and oscillations in energy metabolism appear to govern cellular electrical activity, biological information processing, and functional response (O’Rourke et al., 1994; Welch, 1996; Dzeja and Terzic, 2003). The phosphotransfer enzyme adenylate kinase is one of the principal components in the generation of metabolic oscillations by sustaining dynamic fluctuations of adenine nucleotide ratios (Welch, 1977; Mair and Muller, 1996). In this regard, a term, excitable “adenylate kinase medium” has been proposed (Kohen et al., 1985) to emphasize the significance of this enzyme in conveying energetic and metabolic signals (Carrasco et al., 2001; Dzeja et al., 2002).

2.5 Ligand Conduction

Ligand conduction stems from the proton conduction mechanism (Grotthuss mechanism), a much faster transfer of protons in strong acid solutions compared with simple diffusion (Pomes and Roux, 2002). This phenomenon, which was recently refined using modern computer simulation, is referred to as “walking without moving” (Tuckerman et al., 2002). According to the ligand conduction mechanism, a triggering ligand induces a series of propagations in a coupled system resulting in the almost instantaneous appearance of an equivalent ligand at the distant end. Ligand conduction occurs along spatially oriented water and protein molecules (“proton wires”) (Pomes and Roux, 2002), in transmembrane ion channels (single-file ion conduction) (Berneche and Roux, 2001), in the mitochondrial respiratory chain (electron and proton conduction) (Mitchell, 1979), in vascular plants, aquaporin channels and carbon nanotubes (water conduction) (Tournaire-Roux et al., 2003; Zhu and Schulten, 2003; Agre et al., 2004), and in the extracellular space and fluid channels of the inner ear (fluid conduction) (Mhatre et al., 2002; Pozrikidis and Farrow, 2003; Mueggler et al., 2004). Bacterial phosphorelay-type sugar transport, signal transduction through receptor–G-protein–protein kinase cascades, and propagation of conformational changes through linear chains of protein molecules apparently also occur by ligand or structural conduction mechanisms (Appleby et al., 1996; Lu et al., 1996; Bray and Duke, 2004). In addition, myoglobin- and hemoglobin-facilitated oxygen diffusion could be accomplished through the ligand conduction mechanism by “hopping” of oxygen molecules along the network of relatively immobile carrier molecules (Takahashi and Asano, 2002). This is indicated from direct measurements of oxygen diffusion using ^{18}O isotopes (Hemmingsen, 1962) and from other considerations (Wittenberg and Wittenberg, 2003). Ligand conduction mechanism is also suggested for the carbonic anhydrase-catalyzed intracellular and paracellular CO_2 , H^+ , and H_2O transfer pathways (Dzeja and Terzic, 2003). In this regard, carbonic anhydrase networks by forming planar H^+ conduction pathways along cell surface or mucosa, which could prevent direct H^+ entrance and protect cells from acid damage (Kivela et al., 2005; Marcus et al., 2005). Thus, growing evidence suggests the versatility of ligand conduction in different cellular processes.

By addressing vectorial behavior of chemiosmotic systems, the principle of vectorial ligand conduction has been formulated as a basic mechanism for operation of metabolic and transport processes within the cell (Mitchell, 1979). According to this principle, “vectorial metabolism” is represented by a network of spatiotemporal pathways along which ligands, including solutes, ions, chemical groups, electrons, and catalytic compounds and complexes, are conducted by articulated movements that occur in the direction of the thermodynamically natural escaping tendency (Mitchell, 1991). Subsequently, this principle was applied to the chains of sequential rapid equilibrating reactions catalyzed by creatine kinase and adenylate kinase (“phosphoryl wires”) as a mechanism for facilitated high-energy phosphoryl transfer between ATP-consuming and ATP-generating sites in the cell (Zeleznikar et al., 1995; Dzeja et al., 1998). In these chains, a series of rapidly equilibrating reactions catalyzed by cellular phosphotransferases provide the driving force for high-energy phosphoryl flux (Wallimann et al., 1992; Saks et al., 1994; Dzeja et al., 1998). According to this mechanism, incoming ligands at one end of the system “push” adjacent ligands, thereby triggering a propagation of disequilibrium through an entire cluster of enzymes catalyzing rapid equilibration among substrates. In this type of system, ligands do not move the entire length of the pathway, as molecules arriving at the distal sites of this sequence represent the equivalent rather than the specific molecule generated at the

origination site. This would provide directionality to the metabolic system and contribute to the efficiency and accuracy of energetic signaling (Carrasco et al., 2001; Abraham et al., 2002; Dzeja and Terzic, 2003; Hodgson et al., 2003). The occurrence of ligand conduction apparently requires more structured and organized systems (Dzeja et al., 1998; Pomes and Roux, 2002), such as enzymatic clusters or molecular wires (Wegmann et al., 1992; Wild et al., 1997), while reaction-diffusion and metabolic wave propagation can take place also in a dispersed soluble system such as cellular extracts (Mair and Muller, 1996). Thus, the ligand conduction mechanism contrasts with the traditional diffusion theory and also with the “metabolite channeling” concept by operating independently of cytosolic ligand concentrations and without the movement of a specific ligand through the entire length of the pathway (Dzeja et al., 1998).

It was determined that the effective substrate transfer (conduction), independent of bulk concentration, occurs when enzymes are spaced apart less than 10 nm (Fossel and Hoefeler, 1987). Using this data and the relationship between the total number of unidirectional phosphotransfers, determined by ^{31}P NMR (Kingsley-Hickman et al., 1987), and the net phosphoryl flux, determined by the ^{18}O -labeling technique (Pucar et al., 2001, 2002), it can be calculated that the average length of intracellular phosphoryl conduction pathways ranges from 0.5 to 1.0 μm (Dzeja et al., 1998). This length roughly corresponds to the average distance between the centers of mitochondria and myofibrils. Another feature, underscoring thermodynamic efficiency, is that enzymatic ligand conduction systems are capable of operating with minimal or no concentration gradients (Dzeja et al., 1998; Dzeja and Terzic, 2003). This could explain why changes in cellular adenine nucleotide concentrations are most often not observed even with marked increases in metabolic flux (Balaban, 1990; Saks et al., 1994).

Intracellular energetic and metabolic signal communication can employ simultaneously several different mechanisms depending on the cell type and specific compartment, structural organization, and topological arrangement of enzymatic networks (Dzeja and Terzic, 2003). While the spatial heterogeneity and directionality of enzyme-catalyzed process is not essential in well-mixed conditions *in vitro*, this becomes a vital entity in highly organized living matter (Harold, 1991), with cluster organization and the high rate of unidirectional phosphoryl exchange in phosphotransfer systems promoting ligand conduction and signal communication at cellular distances (Wallimann et al., 1992; Dzeja et al., 1998; Dzeja and Terzic, 2003).

3 Phosphotransfer Reactions in Mitochondrial-Nuclear Energetic Communication

Mitochondrial-nuclear intercommunication proceeds at the genomic, metabolic/energetic, and signaling levels (Poyton and McEwen, 1996; Cyert, 2001; Dawson and Dawson, 2004). Nuclear-coded proteins regulate mitochondrial morphology, intracellular localization, and functional activity (Bach et al., 2003). Conversely, mitochondrial proteins and generated signals affect nuclear processes leading to altered gene expression or cell death through apoptosis (Fulco et al., 2003; Dawson and Dawson, 2004; Templeton and Moorhead, 2004). With respect to energetic communication, intense nuclear functions including DNA replication, nucleosome and chromatin remodeling, gene transcription, and transport of macromolecules inside the nucleus and across the nuclear envelope require efficient energy supply, yet the nucleus is secluded from major cellular ATP generation sites such as mitochondria (Mattaj and Englmeier, 1998; Dzeja et al., 2002; Ohba et al., 2004). The nuclear ATP pool is compartmentalized (Rapaport, 1980), and the ATP level in the nucleus depends on the intensity of energy-consuming processes (Gajewski et al., 2003). Organized enzymatic complexes of nucleotide-metabolizing and phosphotransfer enzymes are involved in maintaining nuclear dNTP ratios and their channeling into the DNA replication machinery (Mathews, 1985). Although the nuclear compartment contains glycolytic enzymes, the entry point for high-energy phosphoryls into the glycolytic pathway catalyzed by hexokinase usually is localized at the mitochondrial site (Ottaway and Mowbray, 1977; Gerbitz et al., 1996; Cesar and Wilson, 1998). This suggests that glycolytic energy transfer shuttles between mitochondria and nucleus (Dzeja et al., 2004).

Beside hexokinase, the mitochondrial outer membrane and intermembrane space harbor several phosphotransfer enzymes, which participate in the energetic communication between ATP-consuming processes in the cytosol and oxidative phosphorylation in mitochondria (Wyss et al., 1992; Gerbitz et al., 1996;

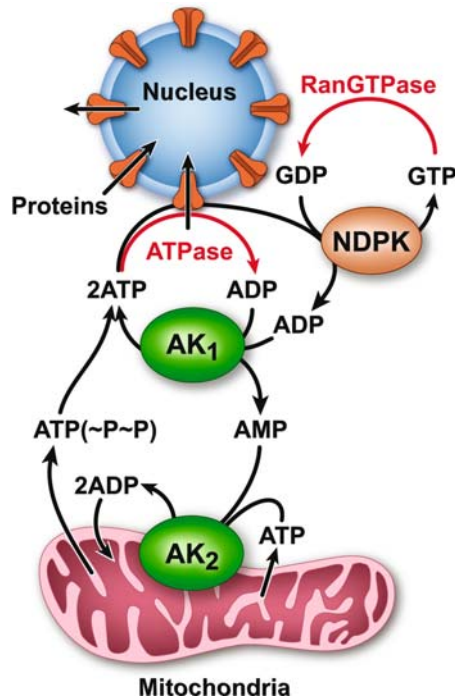
Laterveer et al., 1996; Dzeja et al., 2004). With condensed mitochondrial structures and a narrow intermembrane/intracristal space, creatine kinase and adenylate kinase appear necessary in conducting the ADP stimulatory signal through the adenine nucleotide translocator to matrix ATP-synthases (Gellerich et al., 1994; Saks et al., 1994; Laterveer et al., 1996; Dzeja and Terzic, 2003). Disruption of the adenylate kinase gene impedes ATP export and mitochondria-cytosolic communication (Bandlow et al., 1988). Inactivation of adenylate kinase by gene replacement disrupts adenine nucleotide homeostasis and reduces cell viability (Counago and Shamoo, 2005). Deletion of UbCKmit, a mitochondrial creatine kinase isoform, disrupts neural energetics during seizures, while deletion of ScCKmit has a lesser effect in the heart, merely compromising the ability to maintain normal high-energy phosphate levels (Kekelidze et al., 2001; Spindler et al., 2002). In this regard, in brain mitochondria, adenylate kinase, which could be of cytosolic origin (AK1 or AK5), is less active and the compensatory potential consequently lower than in the heart (Walker and Dow, 1982; Wustmann et al., 1987). NDPK ($\text{ATP} + \text{NDP} \leftrightarrow \text{ADP} + \text{NTP}$) present in the mitochondrial intermembrane space also facilitates the reception of cytosolic nucleoside diphosphate-based signals and provides a link between ATP generation and energy distribution to synthetic GTP-, UTP-, and CTP-requiring processes (Gerbitz et al., 1996; Dzeja et al., 2002). Similarly hexokinase, bound to the outer membrane of mitochondria, directs high-energy phosphoryls through the glycolytic phosphotransfer network in response to cellular energetic signals (Cesar and Wilson, 1998; Dzeja et al., 2004). Thus, functional interaction and complementation of creatine kinase, adenylate kinase, and NDPK phosphotransfer relays in the intermembrane/intracristal space along with porin-bound hexokinase provide a mechanism for the integrated response of mitochondrial oxidative phosphorylation to increased cellular energy demand (Saks et al., 1994; Roberts et al., 1997; Dzeja et al., 1999b; Dzeja and Terzic, 2003).

Creatine kinase and adenylate kinase isoforms, depending on the developmental or functional state, are found in the nucleus or bound to the nuclear envelope (Criss, 1970; Manos and Bryan, 1993; Chen et al., 1995). Recently, a novel nuclear adenylate kinase isoform, AK6, has been characterized (Ren et al., 2005). Also, a membrane-bound AK1 β isoform, which has been implicated in p53-dependent cell-cycle arrest (Collavin et al., 1999), has been found associated with the nuclear envelope (Janssen et al., 2004). Adenylate kinase isoforms in the brain may further contribute to neuronal maturation and regeneration (Inouye et al., 1998; Yoneda et al., 1998). Glycolytic enzymes are markedly elevated in nuclei of regenerating cells, suggesting increased nuclear energetic needs (Ottaway and Mowbray, 1977). Recently, it was demonstrated that mitochondrial ATP production is required to support energy-consuming processes at the nuclear envelope, while glycolysis alone was insufficient to perform such a function (Dzeja et al., 2002). Although mitochondrial clustering around the nucleus reduces the distance of energy transfer, oxidative phosphorylation and simple nucleotide diffusion are inefficient to meet energy requirements for nucleocytoplasmic communication. Adenylate kinase phosphotransfer was identified to direct transmission of high-energy phosphoryls from mitochondria to the nucleus, maintaining the optimal nucleotide ratios required for active nuclear transport (Dzeja et al., 2002) (🔗 [Figure 6.3-2](#)). Moreover, adenylate kinase coupled with NDPK secures phosphoryl transfer between ATP and GTP, as both nucleoside triphosphates are necessary for active nuclear transport (Perez-Terzic et al., 2001; Dzeja and Terzic, 2003). A mechanistic basis for thermodynamically efficient coupling of cell energetics with nuclear pore function lies in the unique property of adenylate kinase catalysis, which transfers both β - and γ -phosphoryls of ATP, doubling the energetic potential of ATP as an energy-carrying molecule (Dzeja et al., 1985, 1999b). Inhibition of nuclear transport by disruption of the adenylate kinase relay can be rescued through upregulation of alternative phosphotransfer pathways, such as the creatine kinase system, which regulates both adenine and guanine nucleotide ratios (Wallimann et al., 1992; Dzeja et al., 2002). Indeed, creatine kinase is bound to the nuclear membrane and present in the nucleus, providing an energy transfer shuttle capability (Manos and Bryan, 1993; Chen et al., 1995).

Variations of phosphotransfer enzyme activity in the cytosol and nucleus correlate with the intensity of nuclear processes in normal and diseased conditions, underscoring the significance of maintained phosphotransfer in directing cellular energy flow (Ottaway and Mowbray, 1977; Manos and Bryan, 1993; Dzeja and Terzic, 2003). Thus, phosphotransfer reactions are essential in providing energy for nuclear processes spatially separated from mitochondrial sites of energy transduction and regulate exchange of molecules and information between the cytosol and nucleus.

Figure 6.3-2

Adenylate kinase energy transfer shuttle facilitates energetic communication between mitochondria and nucleus. Concerted action of mitochondrial (AK2) and cytosolic (AK1) adenylate kinases provide a mechanism for transfer and utilization of two high-energy phosphoryls (i.e., β and γ) in one ATP molecule. AK1 coupled with nucleoside diphosphate kinase (NDPK) at the nuclear envelope secures phosphoryl transfer between ATP and GTP, as both nucleoside triphosphates are necessary for active nuclear transport. Depending on cell type, developmental stage and physiological conditions parallel creatine kinase, and glycolytic phosphotransfer systems (Figure 6.3-1) can also contribute to mitochondria–nucleus energetic communication



In this regard, NDPK-phosphotransfer deficient cells have highly biased nucleoside triphosphate pools, including marked elevations of CTP and dCTP, and a strong mutator phenotype (Bernard et al., 2000). Imbalance in cellular nucleotide ratios results in increased genetic error frequency (Bebenek et al., 1992), with NDPK, a product of the tumor suppressor gene *Nm23*, mutations affecting the processing of genetic information (Lacombe et al., 2000). Adenylate kinase in the nucleus is responsible for conversion of dADP to dATP, while creatine kinase can phosphorylate and convert deoxynucleotide diphosphates (dNDPs) into dNTP and facilitate DNA mismatch repair, an energy-requiring process (Mathews, 1985; Glazer et al., 1987). Thus, interactions between phosphotransfer enzymes in the nucleus secure proper nucleotide ratios and the fidelity of processing genetic information.

Glycolytic substrates, both in wild type and mtDNA mutant cells, are able to maintain adequate ATP supplies in all compartments including the nucleus (Gajewski et al., 2003). Conversely, with the mitochondrial substrate pyruvate, ATP levels collapse in all compartments of mutant cells with nonfunctional mitochondria. It is suggested that depletion of nuclear ATP plays an important role in disease pathogenesis in conditions of mitochondrial dysfunction (Gajewski et al., 2003). In wild-type cells, normal levels of ATP can be maintained with pyruvate in the cytosol and in the subplasma membrane region, but are reduced in the nucleus. The severe decrease in nuclear ATP content under conditions of compromised cytosolic glycolytic phosphotransfer implies that other phosphotransfer systems in this type of cells are not

sufficiently active to provide ATP and to sustain proper nucleotide ratios in the nuclear compartment. It also may suggest that coordinated action between several phosphotransfer relays is required to sustain efficient nuclear energetics. In this regard, the presence of glucose and basal glycolytic phosphotransfer is usually necessary for mitochondrial substrate signaling to plasma membrane metabolic sensors such as K_{ATP} channels implicated in induction of hormone secretion (Tarasov et al., 2004).

Beside ATP requirements, the nucleus possesses several metabolic sensors which are regulated by nuclear AMP/ATP and $NAD^+/NADH$ ratios (Fjeld et al., 2003; McGee et al., 2003). Nuclear translocation of the metabolic sensor AMPK mediates exercise-induced gene expression, regulates phosphorylation and acetylation of nuclear transport factors affecting their activity, and is critical for hypoxia-inducible factor-1 transcriptional activity (Lee et al., 2003; McGee et al., 2003; Wang et al., 2004). Silent information regulator Sir2 is an active NAD^+ -dependent deacetylase critical in transcription silencing and in linking chromatin function with cellular metabolic networks (Denu, 2003; Blander and Guarente, 2004). Another transcriptional corepressor CtBP has been identified as a nuclear redox sensor mediating nuclear $NAD^+/NADH$ effects on cell differentiation, development, and transformation (Fjeld et al., 2003). Thus, emerging data on the energy supply to nuclear processes and metabolic signaling have advanced our understanding of metabolic requirements and energetic costs of processing and distributing genetic information.

4 Phosphotransfer-Mediated Metabolic Signaling

Metabolic signaling cascades are essential in vital cellular processes integrating gene expression, metabolism, and response to stress, with their deficit associated with diseases under the wide umbrella of the “metabolic syndrome” (Carrasco et al., 2001; Hardie, 2003; Hodgson et al., 2003; Carling, 2004; Tokunaga et al., 2004; Wang et al., 2004). Understanding the principles governing the integration and synchronization of metabolic sensors with cellular metabolism is important for regulation of cellular energetic and ionic homeostasis as well as for hormonal balance and food intake (Dzeja and Terzic, 1998; Carling, 2004; Minami et al., 2004; Tarasov et al., 2004). Phosphotransfer reactions have emerged as principal signal generators and relays coupling cellular metabolism and metabolic sensors (Dzeja and Terzic, 1998, 2003; Hardie, 2003). In particular, adenylate kinase-generated AMP and AMPK are integral to metabolic signaling, balancing cellular ATP production and utilization priorities and increasing cell tolerance to stress (Hardie, 2003; Xing et al., 2003; Frederich et al., 2005). Moreover, the adenylate kinase–AMP–AMPK pathway integrates complex mTOR, TSC2, LKB1, 14-3-3, and K_{ATP} channel-signaling cascades, required in the regulation of vital cellular functions (Carrasco et al., 2001; Carling, 2004; Mak and Yeung, 2004; Rubio et al., 2004; Selivanov et al., 2004; Tokunaga et al., 2004).

The microenvironment of the prototypic metabolic sensor, the K_{ATP} channel, harbors several phosphotransfer enzymes, including adenylate, creatine, and pyruvate kinases, as well as other glycolytic enzymes that are able to transfer phosphoryls between ATP and ADP in the absence of major changes in cytosolic levels of adenine nucleotides (Weiss and Lamp, 1987; Dzeja and Terzic, 1998; Carrasco et al., 2001; Abraham et al., 2002; Crawford et al., 2002; Hodgson et al., 2003; Alekseev et al., 2005). These phosphotransfer reactions are governed by the metabolic status of a cell, and their phosphotransfer rates closely correlate with K_{ATP} channel activity (Zingman et al., 2001). Thus, through delivery and removal of adenine nucleotides at the channel site, phosphotransfer reactions regulate the dynamics of ATP and ADP exchange in the immediate vicinity of the channel, and thereby the probability of K_{ATP} channel opening (Zingman et al., 2001; Selivanov et al., 2004; Alekseev et al., 2005). In this way, coordinated phosphotransfer reactions could provide a transduction mechanism coupling cellular metabolic signals with K_{ATP} channel-associated functions such as hormone secretion, membrane electrical activity, brain glucose sensing, regulation of vasculature tone and cerebral circulation as well as protection against metabolic stress (Dzeja and Terzic, 1998; Zingman et al., 2002a; Gumina et al., 2003; Kane et al., 2004; Minami et al., 2004; Tarasov et al., 2004).

While regimented K_{ATP} channel activity regulates membrane electrical events and associated cellular functions (Zingman et al., 2002b; Liu et al., 2004; Minami et al., 2004), unregulated channel opening can precede loss of membrane excitability, excessive vasodilatation, and consequently cardiac and brain functional arrest (Weiss and Lamp, 1987; Englert et al., 2003). Therefore, systems regulating K_{ATP} channel

activity in response to functional and metabolic changes and preventing uncontrolled channel gating during metabolic disturbances are warranted (Dzeja and Terzic, 1998; Hodgson et al., 2003). In this regard, knockout of the creatine kinase M-CK gene shifts signal delivery to K_{ATP} channels through the glycolytic system (Dzeja et al., 2004), generating a phenotype with increased electrical vulnerability to disturbances in glucose metabolism (Abraham et al., 2002). Adenylate kinase, which phosphotransfer flux along with AMP concentration markedly increases under stress, contributes to the response of K_{ATP} channels to metabolic challenge (Carrasco et al., 2001; Pucar et al., 2004). Adenylate kinase associates with the K_{ATP} channel complex, anchoring cellular phosphotransfer network and facilitating delivery of mitochondrial stress signals to the submembrane environment. Deletion of the cytosolic adenylate kinase gene (AK1) compromises nucleotide exchange at the channel site and impedes communication between mitochondria and K_{ATP} channels, rendering cellular metabolic sensing defective (Carrasco et al., 2001). Conversely, over-expression of adenylate kinase results in excessive activation of K_{ATP} channels (Brochiero et al., 2001). Also, complementation of membrane-bound AK1 β activity in neuroblastoma cells, in the presence of appropriate levels of ATP and AMP, promotes opening of the K_{ATP} channel (Janssen et al., 2004). In neurons, opening of K_{ATP} channels reduces the frequency of action potentials, thereby serving a protective function (Yamada et al., 2001). Existence of synaptic plasma membrane-associated adenylate kinase activity has been reported earlier for rat and human brains (Nagy et al., 1989; Janssen et al., 2004). In this regard, both creatine kinase and glycolytic phosphotransfers suppress adenylate kinase-mediated nucleotide exchange (Olson et al., 1996; Dzeja et al., 1998) and maintain K_{ATP} channel in a predominantly closed state (Weiss and Lamp, 1987; Abraham et al., 2002). Thus, complementation between creatine kinase, adenylate kinase, and glycolytic systems provides a mechanistic basis for metabolic sensor function in response to alterations in intracellular phosphotransfer fluxes (Dzeja and Terzic, 1998; Carrasco et al., 2001; Abraham et al., 2002).

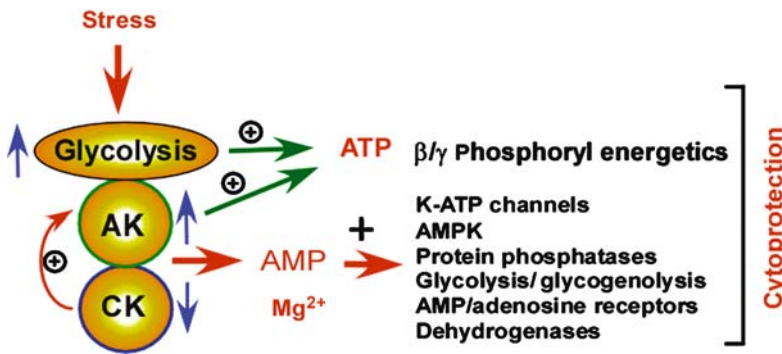
Adenylate kinase is ubiquitously present in all cell types and its activity surpasses by several folds an apparent need for adenine nucleotide synthesis *de novo*, one of the classical functions of this enzyme (Noda, 1973). Adenylate kinase family includes several isoforms (AK1–AK7) with distinct tissue distribution and subcellular localization (Tanabe et al., 1993; Ruan et al., 2002; Janssen et al., 2004). In the presence of adenylate kinase, small changes in the balance between ATP and ADP translate into relative large changes in the concentration of AMP, so that enzymes and metabolic sensors, such as AMPK, that are affected by AMP can respond with high sensitivity and fidelity to stress signals (Dzeja et al., 1998; Hardie, 2003; Pucar et al., 2004). Phosphoryl-labeling experiments indicate that in intact muscle metabolically active ADP and AMP concentrations are much higher than those obtained from enzyme equilibrium calculations, reflecting rapid exchange of nucleotides between the free and bound states (Dzeja et al., 1998; Barany and Tombe, 2004). This may involve the mechanism of “kinetic entrapment” and distribution of a large percentage of the cytosolic ADP and AMP among reversible nucleotide-binding/consuming reactions, which would continue to function as the metabolically active pool participating in enzymatic relays for metabolic signals (Dzeja et al., 1998; Dzeja and Terzic, 2003). In this regard, metabolic dynamics and the number of signaling molecules in the microenvironment (“sensing zone”) of metabolic sensor rather than static bulk AMP concentration would determine AMPK activation, similarly to the role of cAMP and cGMP fluxes in regulation of their specific targets (Dawis et al., 1988). This could explain why sometimes AMPK activation does not correlate with calculated intracellular AMP levels (Frederich et al., 2005). Future development of fluorescent reporters sensing intracellular free ADP and AMP concentrations would greatly facilitate our understanding of cellular energetic signaling.

An increase in intracellular AMP stimulates glycolysis and glycogenolysis due to activation of PFK and phosphorylase b, respectively (Ottaway and Mowbray, 1977). Through positive and negative nucleotide feedback interactions, adenylate kinase is a principal component in generating glycolytic oscillations and maintaining the dynamics of cellular nucleotide exchange (Welch, 1977; Mair and Muller, 1996; Dzeja et al., 1998). Recent evidence further implicates AMP signaling in metabolic regulation through AMPK and other AMP-sensitive cellular components (Carrasco et al., 2001; Hardie, 2003; Pucar et al., 2004). Indeed, AMP signaling affects mitochondrial biogenesis and respiration, increasing the muscle energetic capacity (Zong et al., 2002; Tokunaga et al., 2004; Dzeja and Terzic, 2005). Moreover, AMPK associates with glycogen particles and could be a target for AMP to inhibit glycogen synthesis and/or activate glycogenolysis/glycolysis by diverting glucose-6-phosphate into ATP-producing pathways (Polekhina et al., 2003). Beside

AMP, AMPK-mediated PFK activation contributes to stimulation of heart glycolysis during ischemia (Marsin et al., 2000; Xing et al., 2003). Thus, stress-induced changes in adenylate kinase and creatine kinase equilibriums trigger $\text{AMP} \rightarrow \text{AMPK}$, K_{ATP} and other signaling cascades, producing adaptive responses in the metabolic and ion channel systems (🔗 [Figure 6.3-3](#)).

■ **Figure 6.3-3**

Interaction of the adenylate kinase (AK), creatine kinase (CK), and glycolytic phosphotransfer system in stress-induced energetic and metabolic signaling triggers protective response. Metabolic or functional stress results in the fall of ATP/ADP and creatine phosphate/creatine ratios, which increase AK flux resulting in AMP production and high AMP/ATP ratio. This triggers activation of stress response energetic pathways (increase utilization of ATP β - and γ -phosphoryls) and signaling cascades such as AMP-activated protein kinase (AMPK), ATP-sensitive potassium channel (K-ATP), and glycolysis/glycogenolysis. Recently discovered AMP-receptors, along with $\text{AMP} \rightarrow$ adenosine signaling, could contribute to the increased blood flow and tissue oxygen delivery. Parallel to AMP, Mg^{2+} signaling, originating from the MgATP^{2-} complex during ATP consumption and governed by the AK equilibrium, could activate Mg^{2+} -dependent protein kinases/phosphatases and dehydrogenases, promoting signal transduction and mitochondrial substrate oxidation



Upon hypoxic stress, production of phosphocreatine in mitochondria is compromised due to unfavorable thermodynamic and kinetic conditions, leading to depletion of cytosolic energy stores (Wallimann et al., 1992; Dzeja et al., 2000; Saks et al., 2004). Accordingly, creatine kinase-catalyzed phosphotransfer, measured by ^{18}O -assisted ^{31}P NMR in the direction of creatine phosphate production, is reduced under hypoxic challenge (Pucar et al., 2004). Concomitantly, adenylate kinase-catalyzed ^{18}O -labeling of β -ADP and β -ATP is increased, resulting in doubling of adenylate kinase flux. Such activation of adenylate kinase can protect heart muscle under hypoxia by regenerating ATP, providing a transfer mechanism for ATP between production and consumption sites, and ultimately initiating AMP and adenosine signaling (🔗 [Figure 6.3-3](#)) (Dzeja et al., 1999b; Pucar et al., 2000, 2002, 2004). Indeed, adenylate kinase remains active in its ATP regenerating and transferring role as long as ADP is available and the enzyme is not inhibited by a buildup of AMP (Noda, 1973; Savabi, 1994). In addition, adenylate kinase serves a distinct metabolic signaling role by translating small alterations in the ATP and ADP balance into large changes in AMP levels (Dzeja et al., 1998; Dzeja and Terzic, 2003). In this way, adenylate kinase phosphotransfer communicates metabolic signals to K_{ATP} channels, AMPK, and adenosine receptors—metabolic sensors implicated in stress adaptation and cardioprotection (Carrasco et al., 2001; Hardie, 2003; Picher and Boucher, 2003). ^{18}O -assisted ^{31}P NMR analysis indicates that a hypoxia-induced increase in AMP phosphorylation ($\text{ATP} + \text{AMP} \leftrightarrow 2\text{ADP}$) would amplify metabolic signals by providing two molecules of ADP for each ATP removed from ATP-sensitive cellular components (Dzeja and Terzic, 1998; Pucar et al., 2004). Thus, redistribution of flux between adenylate kinase and creatine kinase phosphotransfer, observed under hypoxic challenge, contributes to a reduction in the bioenergetic deficit and initiates signaling pathways that promote cellular protection (Pucar et al., 2001, 2004).

The interrelationship between adenylate kinase and creatine kinase is mediated not only by adenine nucleotide substrates but also by AMPK. Indeed, AMPK activated by adenylate kinase-generated AMP phosphorylates and modulates the activity of creatine kinase (Ponticos et al., 1998). AMPK is an energy-sensing enzyme strongly activated during muscle contraction and metabolic stress due to acute decreases in ATP/ADP and phosphocreatine/creatine ratios (Hardie, 2003; Carling, 2004). In this regard, chronic phosphocreatine depletion during β -GPA supplementation increases brain adenylate kinase activity (Holtzman et al., 1998) and muscle adenylate kinase flux (P. P Dzeja et al., unpublished) accompanied by AMPK activation associated with increased cytochrome *c* content and muscle mitochondrial density (Bergeron et al., 2001). These data demonstrate that, by sensing the energy status of the muscle cell, the adenylate kinase, creatine kinase, and AMPK signaling triad is a critical regulator involved in the initiation of mitochondrial biogenesis, thereby increasing the energy-transducing capacity of the cell (Zong et al., 2002). In this regard, glycolytic phosphotransfer and separate glycolytic enzymes, such as GAPDH and glucokinase/hexokinase, have specific signaling roles beyond their metabolic function in regulating gene expression and protecting against oxidative stress or apoptotic stimuli-induced cell death (Tatton et al., 2000; Pastorino and Hoek, 2003).

Thus, phosphotransfer-mediated integration and synchronization of metabolic sensors with the dynamics of cellular metabolism is critical for regulation of genetic, energetic, electrical, and signal transduction processes that determine cell viability and functional activity. Moreover, more and more evidence is emerging about the direct relationship between defects in metabolic signaling and disease processes, such as heart failure, diabetes, obesity, cancer, and neurodegeneration.

5 Phosphotransfer Networks in Processing and Integrating Cellular Information

As discussed above, energetic- and metabolic-signaling roles render adenylate kinase and creatine kinase as important components of cellular physiology determining the fidelity of metabolic response and functional perfection. Yet several lines of evidence suggest that intracellular and paracellular phosphotransfer networks may have functions beyond metabolic signaling, energy supply, and distribution, such as in the integration of cellular information, computation, and memory processing.

Deletion of brain B-CK or UbCKmit isoforms indicate that creatine kinase phosphotransfer is fundamental to processes that involve exploration and habituation, spatial learning, and acoustic startle reflex (Jost et al., 2002; Streijger et al., 2004). Mice lacking both brain creatine kinase isoforms have reduced body weight, and demonstrate severely impaired spatial learning, lower nest-building activity, and diminished acoustic startle reflex response (Streijger et al., 2005). Creatine deficiency in humans is associated with movement disorders, mental retardation, severe language delay, autistic-like behavior, and electroencephalographic abnormalities (Stockler et al., 1994; Bianchi et al., 2000; Leuzzi, 2002; Schuze et al., 2003). This occurs in spite of normal brain ATP levels and other metabolic parameters (Bianchi et al., 2000). A novel X-linked mental retardation syndrome was recently identified, resulting from creatine deficiency in the brain caused by mutations in the creatine transporter gene (Rosenberg et al., 2004). The hallmarks of the disorder are mental retardation, learning disabilities, expressive speech and language delay, epilepsy, developmental delay, and autistic behavior (Salomons et al., 2003). In humans, genetic adenylate kinase deficiency or losses of adenylate kinase from the brain after surgery are associated with compromised intellectual function (Aberg et al., 1982; Toren et al., 1994). Similarly, disturbances in glycolytic phosphotransfer system are associated with deficient memory formation and retrieval (Hoyer, 2003).

Coupled near-equilibrium enzymatic networks have the ability to provide a precise control similar to a “digital” type of regulation, such that each ATP conversion to ADP, P_i , and H^+ will be signaled to an equivalent stoichiometry of ADP, P_i , and H^+ transformation to ATP (Saks et al., 1994; Dzeja et al., 2000; Neumann et al., 2003). It was suggested that information can be encoded in the dynamic behavior of a chemical oscillating system by forcing the system to follow a desired trajectory (Dolnik and Bollt, 1998). As such, conversion of 2 ADP to ATP plus AMP and vice versa by adenylate kinase reaction will output signals to ATP-, AMP-, and ADP-sensitive cellular components inducing oscillatory behavior of metabolic,

electrical, and signal-transducing systems (Welch, 1977; Mair and Muller, 1996; Dzeja and Terzic, 2003). It was noted that the adenylate kinase reaction and factors regulating it contribute significantly to the solution of the information-coding algorithm in living cells (Kremen, 1982). Also, analogies have been drawn between the computational aspects of information processing and the enzymatic events of cellular metabolism (Welch, 1996). In line with this is the notion that information processing proceeds through the tightly organized networks, that information flows freely and independently yet patterned, so that the necessary contact and transactions are made quickly and efficiently (Laughlin, 2001).

While nucleotide pool output follows laws of thermodynamics and kinetics, it is regulated primarily by informational requirements. In processes requiring information supply, such as nucleic acid and protein synthesis, error-reducing mechanisms are necessary. According to Shannon (1948), the fraction of errors introduced by noise during message transmission can be reduced only at the expense of additional information supply. Also, as noted by Welch (1996), diffusion of molecules by itself is a dissipative phenomenon. Thus, when metabolic processes take place in bulk solution, there is a considerable energy cost to the cell in the spatiotemporal conveyance of coherent biochemical information. For efficient coupling of energy and metabolic signal sources with molecular motors and metabolic sensors and, therefore, for “activity-causal” information flow, a specific spatial organization of enzymatic components is required in order to increase the kinetic efficiency and to minimize the heat-exchange during energy and signal transduction (McClare, 1971; Dzeja and Terzic, 2003). In protein synthesis, for example, very high relative amounts of ATP and GTP and coupled phosphotransfer reactions are required to enhance the translation fidelity (Kremen, 1982). The same is true for DNA synthesis and transcription, where high local pools of dNTP maintained by phosphotransfer reactions are necessary (Mathews, 1985). Imbalance in nuclear nucleotide ratios results in increased genetic error frequency (Bebenek et al., 1992; Lu et al., 1996). Thus, for efficient cellular information transfer organized enzymatic pathways are required, which provide directionality, increase fidelity, and reduce signaling errors.

Adenylate kinase equilibrium governs not only adenine nucleotide species but also free magnesium (Mg^{2+}) levels within cells (Rose, 1968; Igamberdiev and Kleczkowski, 2001). It was suggested that Mg^{2+} , released from the $MgATP^{2-}$ complex during ATP consumption, could serve as a feedback signal conveying information regarding alterations in the adenine nucleotide pool to different cellular compartments (Blair, 1970). In this regard, creatine kinase also regulates adenine nucleotide and adenylate kinase equilibria, and consequently can shape Mg^{2+} signaling (Vincent and Blair, 1970). Conversely, both creatine kinase and adenylate kinase reactions by itself are highly dependent on Mg^{2+} concentration (Noda, 1973; Saks et al., 1978), changes of which would produce feedback signals tuning the initial response. In this way, nucleotide-based information processing could be complemented with simultaneous Mg^{2+} signaling affecting critical cellular components, ranging from dehydrogenases, DNA polymerases, ion channels, and protein kinases/phosphatases (Takaya et al., 2000; Politi and Preston, 2003; Schmitz et al., 2003; Yang et al., 2004). Thus, phosphotransfer networks could serve a function of coding, processing, and transferring cellular information and, in conjunction with protein kinase/phosphatase cascades and Mg^{2+} signaling, be part of the mechanism facilitating memory storage and retrieval. Indeed, Mg^{2+} deficiency disturbs many brain functions (Galland, 1991–92), while Mg^{2+} therapy restores and improves cognitive performance (Hoane et al., 2003).

The critical role of adenylate kinase and creatine kinase in information processing stems from several physiological and pathophysiological observations. It was noted that there is a close linear relationship between impaired cerebral energy state and brain memory dysfunction (Kjekshus et al., 1980; Aberg et al., 1982). The disturbance in energy metabolism may have impacts on energy-consuming processes markedly reducing cognitive reserve (Hoyer et al., 2004). A linear relationship between cerebral phosphocreatine concentration and memory capacities has been found (Plaschke et al., 2000; Ross and Sachdev, 2004). Indeed, creatine supplementation has a significant positive effect on both working memory and intelligence (Rae et al., 2003). In this regard, photic stimulation increases the creatine kinase unidirectional rate in the visual cortex without significant changes of steady-state concentration of high-energy phosphate compounds, indicating that phosphocreatine turnover is elevated during increased neuronal activity (Chen et al., 1997). Similarly, photic stimulation increases adenylate kinase-mediated ATP β -phosphoryl turnover in photoreceptors (Dawis et al., 1988). ^{32}P -labeling studies of adenine nucleotides indicate that adenylate kinase is active in the brain and that its phosphotransfer rate is activated by drugs improving cerebral

circulation and memory dysfunction (Kanig and Hoffmann, 1979). Recently, an important discovery has been made linking hypothalamic AMPK to regulation of food intake and obesity (Minokoshi et al., 2004). This protein kinase serving as master metabolic sensor responds to adenylate kinase-generated AMP, and plays a critical role in hormonal and nutrient-derived anorexigenic and orexigenic signaling (Hardie, 2003; Minokoshi et al., 2004). Thus, the adenylate kinase/creatine kinase→AMP→AMPK-signaling cascade represents a new modality in brain functioning and body energy balance.

Glycolytic phosphotransfer network, which acts in parallel to creatine kinase and adenylate kinase systems (Dzeja et al., 2004), has also important functions in information processing and memory storage (Hoyer, 2003). Glucose has been found to improve learning and memory in humans and laboratory animals, but the underlying mechanisms are unknown (Hoyer, 2003; Messier, 2004). Among possible mechanisms by which peripheral glucose might act on memory storage is activation of glycolytic phosphotransfer, which has important roles in energetic signal communication and their spatial distribution in cells with large dimensions such as neurons (Goldbeter and Nicolis, 1976; Dzeja and Terzic, 2003; Dzeja et al., 2004). Glucose can also affect substrate cycles mediated by membrane-bound glycolytic enzymes (Chaplain, 1979; Weiss and Lamp, 1987). Associated with these cycles are slow oscillations in membrane potential, which could be brought about by the cyclic fluctuations of H^+ ions and ATP/ADP in the immediate vicinity of the membrane (O'Rourke et al., 1994). Memory facilitation and consolidation under glycolytic modifiers could also be demonstrated in avoidance- and discrimination-learning trials with honey bees and rats, which are consistent with the metabolic nature of the slow-wave rhythmicity in vertebrate microneurons (Chaplain, 1979). Another mechanism by which glucose could affect brain cognitive function is related to the ability of glycolytic phosphotransfer to regulate K_{ATP} channels (Weiss and Lamp, 1987; Dzeja and Terzic, 1998). In this regard, glucose effect on memory storage was attenuated and enhanced by pretreatment with minoxidil and glibenclamide, an opener and inhibitor of K_{ATP} channel, respectively (Rashidy-Pour, 2001). Thus, enhanced glycolytic phosphotransfer could be linked to ATP-sensitive cellular components, including membrane ATPases, ion channels, and nuclear factors regulating neuronal activity and information processing (Dzeja and Terzic, 2003; Hoyer, 2003).

In brain, another phosphotransfer enzyme NDPK and its coding gene, *Nm23*, have been implicated to modulate neuronal cell proliferation, differentiation, and neurite outgrowth as well as tumor metastasis (Kim et al., 2002). Its activity is decreased in Alzheimer's disease and Down's syndrome (Kim et al., 2002). NDPK-catalyzed GDP to GTP conversion regulates G-protein-mediated signaling, nuclear transport, dynamin-dependent synaptic vesicle recycling, and microtubule assembly–disassembly (Huitorel et al., 1984; Krishnan et al., 2001; Dzeja et al., 2002; Hippe et al., 2003). New evidence links cytoskeleton dynamics with synaptic connectivity, information processing, and cognitive function (Tuszynski et al., 1998; van Galen and Ramakers, 2005). Axons can send a message to the cell body by mechanisms that require a complex of the microtubule motor dynein and proteins that mediate nuclear-cytoplasmic transport (Hanz et al., 2003). In this regard, recent data indicate that mitochondria stall near synapses when neurons are activated (providing energy and acquiring information) and increase their movement (transferring information) when neurons are silent (Li et al., 2004). Interestingly, mitochondrial positioning in synapses is enhanced by supplementation of creatine, which facilitates creatine kinase phosphotransfer (Li et al., 2004). It is plausible that phosphotransfer-modulated microtubule networks and associated mitochondrial movements from synapses to the cell body along with nuclear transport could be involved in neurocomputational processes, information transfer, and memory engram (Hollenbeck, 1996; Tuszynski et al., 1998).

Information processing in the brain takes place not only intracellularly but also extracellularly and between different types of cells (Wang et al., 2000; Laughlin, 2001; Gjeddé, 2002). In brain, ecto-adenylate kinase is an integral part of the synaptosomal ATP-metabolizing enzyme cascade, regulating ATP, AMP, and adenosine signaling (Nagy et al., 1989; Joseph et al., 2003). In other cell types ecto-adenylate kinase provides a mechanism for propagation of nucleotide-based signals along cellular surface, thus coordinating multiple receptor-mediated signaling events (Yegutkin et al., 2002; Picher and Boucher, 2003). Both ATP and adenosine signaling, manifested in intercellular ATP waves, are critical for normal brain functioning (Wang et al., 2000; Latini and Pedata, 2001; Newman, 2003). This type of dynamic nucleotide-based signaling could be linked with extracellular glutamate waves and related signal transduction (Innocenti et al., 2000). Recently, a specific AMP-receptor has been discovered too (Inbe et al., 2004). In this regard,

extracellular AMP can regulate endocytosis and glycolytic activity in different cell types (Westmoreland et al., 1986; Mazurek et al., 1997). Adenylate kinase-catalyzed generation of AMP and its subsequent hydrolysis can produce adenosine which is a ubiquitous homeostatic substance released from most cells, including neurons and glia (Berne, 1980). Once in the extracellular space, adenosine modifies cell functioning by operating G-protein-coupled receptors that can inhibit (A1) or enhance (A2) neuronal communication. Manipulations of adenosine receptors influence sleep and arousal, cognition and memory, neuronal damage and degeneration, as well as neuronal maturation (Ribeiro et al., 2002). The popularity of caffeine as a psychoactive drug is due to its stimulant properties, which depend on its ability to reduce adenosine transmission in the brain (Fisone et al., 2004). The important consequence of adenosine antagonism by caffeine is cholinergic stimulation, which leads to improvement of higher cognitive functions, particularly memory (Riedel et al., 1995). In this regard, redistribution in cellular phosphotransfer flux and in AMP/adenosine signaling during transient cerebral ischemia, as occurring in hypoxic and “preconditioned” hearts (Pucar et al., 2000, 2004), could be a reason for the dysfunctional learning and memory behavior (Hoyer, 2003; Hoyer et al., 2004).

A new emerging modality in extracellular and intracellular nucleotide signaling and information processing is cAMP→AMP→adenosine/AMPK pathway sequentially connecting cAMP- and AMP-response elements (Jackson et al., 2003). In this pathway cAMP signaling is followed by conversion of cAMP by phosphodiesterases to AMP that activates the AMP-signaling cascade (Downs et al., 2002). The role of adenylate kinase in this system is envisioned to propagate AMP metabolic signals along the membrane surface or within the cytosolic space and nuclear compartment where AMPK resides (Dzeja et al., 1998; Turnley et al., 1999; Picher and Boucher, 2003; Wang et al., 2004). Consequently, production of adenosine from AMP by 5'-nucleotidase could stimulate adenosinergic-signaling pathways (Berne, 1980). In this regard, both the cAMP-response element binding protein (CREB), a transcription factor, and protein kinase C (PKC), are implicated in the formation of long-term memory (Alvarez-Jaimes et al., 2005). Moreover, cAMP-dependent protein kinase A (PKA)-signaling pathway maintains the cytoplasmic localization of AMPK in glucose-grown cells (Hedbacker et al., 2004). Conversely, AMPK activation is linked with the reduction in cAMP-mediated signaling (Walker et al., 2003). The association of PKC with phosphotransfer enzymes creatine kinase and glyceraldehyde-3-phosphate dehydrogenase, and the regulation of creatine kinase activity by PKC-mediated phosphorylation (Wallimann et al., 1992; Reiss et al., 1996), further emphasize the importance of the integrated cellular phosphotransfer network.

Thus, this kind of integration of cyclic nucleotide→nucleotide→nucleoside signaling provides a means for coordination of diverse signaling events and information flow from one system to another. The significance of organized receptor-mediated and metabolic-signaling networks is growing, and the current challenge is to separate the effects of cAMP from those produced by AMP (and perhaps the effects of cGMP from GMP) in the subsequent signal transduction steps (Downs et al., 2002). In this regard, both cAMP and cGMP have important functions in brain memory processing (Boess et al., 2004) and their signaling cascades are regulated by cellular energy metabolism through phosphotransfer relays (Dawis et al., 1988; Ruiz-Stewart et al., 2004).

6 Concluding Remarks

Phosphotransfer networks provide the cell with mechanisms supporting energetic communication and the integration and transmission of a vast amount of metabolic information. Interaction and complementation between creatine kinase, adenylate kinase, and glycolytic phosphotransfers have significant impact on the efficiency of energy transformation, transfer, and utilization processes, providing energy supply pathways from mitochondria to separate cellular compartments such as the nucleus. Phosphotransfer enzymes are critical in transduction of metabolic signals governing cellular electrical activity, hormone secretion, and response to stress. Coupling energetic phosphotransfer enzymes with metabolic sensors and phosphoryl-transferring protein kinase cascades comprises a unified intracellular energy signal transduction matrix capable of processing, delivering, storing, and retrieving cellular information. These integrated dynamic networks have a critical impact on brain cognitive function and memory processing. Further elucidation of molecular mechanisms controlling energetic signaling will contribute to a new understanding of metabolic disorders.

References

- Aberg T, Ronquist G, Tyden H, Ahlund P, Bergstrom K. 1982. Release of adenylate kinase into cerebrospinal fluid during open-heart surgery and its relation to postoperative intellectual function. *Lancet* 1: 1139-1142.
- Abraham MR, Selivanov VA, Hodgson DM, Pucar D, Zingman LV, et al. 2002. Coupling of cell energetics with membrane metabolic sensing. Integrative signaling through creatine kinase phosphotransfer disrupted by M-CK gene knockout. *J Biol Chem* 277: 24427-24434.
- Aflalo C. 1991. Biologically localized firefly luciferase: A tool to study cellular processes. *Int Rev Cytol* 130: 269-323.
- Agre P, Nielsen S, Ottersen OP. 2004. Towards a molecular understanding of water homeostasis in the brain. *Neuroscience* 129: 849-850.
- Alekseev AE, Hodgson DM, Karger AB, Park S, Zingman LV, et al. 2005. ATP-sensitive K^+ channel/enzyme multimer: Metabolic gating in the heart. *J Mol Cell Cardiol* 38: 895-905.
- Allen KN, Dunaway-Mariano D. 2004. Phosphoryl group transfer: Evolution of a catalytic scaffold. *Trends Biochem Sci* 29: 495-503.
- Alvarez-Jaimes L, Centeno-Gonzalez M, Feliciano-Rivera M, Maldonado-Vlaar CS. 2005. Dissociation of the effect of spatial behaviors on the phosphorylation of cAMP-response element binding protein (CREB) within the nucleus accumbens. *Neuroscience* 130: 833-842.
- Ames A. 2000. CNS energy metabolism as related to function. *Brain Res Rev* 34: 42-68.
- Andrade FH, Merriam AP, Guo W, Cheng G, McMullen CA, et al. 2003. Paradoxical absence of M lines and downregulation of creatine kinase in mouse extraocular muscle. *J Appl Physiol* 95: 692-699.
- Andreucci D, Bisegna P, Caruso G, Hamm HE, Di Benedetto E. 2003. Mathematical model of the spatiotemporal dynamics of second messengers in visual transduction. *Biophys J* 85: 1358-1376.
- Appleby JL, Parkinson JS, Bourret RB. 1996. Signal transduction via the multistep phosphorelay: Not necessarily a road less traveled. *Cell* 86: 845-848.
- Bach D, Pich S, Soriano FX, Vega, N., Baumgartner B, et al. 2003. Mitofusin-2 determines mitochondrial network architecture and mitochondrial metabolism. A novel regulatory mechanism altered in obesity. *J Biol Chem* 278: 17190-17197.
- Balaban RS. 1990. Regulation of oxidative phosphorylation in the mammalian cell. *Am J Physiol* 258: C377-C389.
- Bandlow W, Strobel G, Zoglowek C, Oechsner U, Magdolen V. 1988. Yeast adenylate kinase is active simultaneously in mitochondria and cytoplasm and is required for nonfermentative growth. *Eur J Biochem* 178: 451-457.
- Barany M, de Tombe PP. 2004. Rapid exchange of actin-bound nucleotide in perfused rat heart. *Am J Physiol* 286: H1394-H401.
- Bebenek K, Roberts JD, Kunkel TA. 1992. The effects of dNTP pool imbalances on frameshift fidelity during DNA replication. *J Biol Chem* 267: 3589-3596.
- Bendall JR. 1969. *Muscles, Molecules, and Movement*. London: Heinemann Educational Books; p. 219.
- Bergeron R, Ren JM, Cadman KS, Moore IK, Perret P, et al. 2001. Chronic activation of AMP kinase results in NRF-1 activation and mitochondrial biogenesis. *Am J Physiol* 281: E1340-E1346.
- Bernard MA, Ray NB, Olcott MC, Hendricks SP, Mathews CK. 2000. Metabolic functions of microbial nucleoside diphosphate kinases. *J Bioenerg Biomembr* 32: 259-267.
- Berne RM. 1980. The role of adenosine in the regulation of coronary blood flow. *Circ Res* 47: 807-813.
- Berneche S, Roux B. 2001. Energetics of ion conduction through the K^+ channel. *Nature* 414: 73-77.
- Bessman SP, Carpenter CL. 1985. The creatine-creatine phosphate energy shuttle. *Annu Rev Biochem* 54: 831-862.
- Bianchi MC, Tosetti M, Fornai F, Alessandri MG, Cipriani P, et al. 2000. Reversible brain creatine deficiency in two sisters with normal blood creatine level. *Ann Neurol* 47: 511-513.
- Blair JM. 1970. Magnesium, potassium, and the adenylate kinase equilibrium. Magnesium as a feedback signal from the adenine nucleotide pool. *Eur J Biochem* 13: 384-390.
- Blander G, Guarente L. 2004. The Sir2 family of protein deacetylases. *Annu Rev Biochem* 73: 417-435.
- Boehm E, Ventura-Clapier R, Mateo P, Lechene P, Veksler V. 2000. Glycolysis supports calcium uptake by the sarcoplasmic reticulum in skinned ventricular fibers of mice deficient in mitochondrial and cytosolic creatine kinase. *J Mol Cell Cardiol* 32: 891-902.
- Boess FG, Hendrix M, van der Staay FJ, Erb C, Schreiber R, et al. 2004. Inhibition of phosphodiesterase 2 increases neuronal cGMP, synaptic plasticity and memory performance. *Neuropharmacology* 47: 1080-1092.
- Bray D, Duke T. 2004. Conformational spread: The propagation of allosteric states in large multiprotein complexes. *Annu Rev Biophys Biomol Struct* 33: 53-73.
- Brochiero E, Coady MJ, Klein H, Laprade R, Lapointe JY. 2001. Activation of an ATP-dependent K^+ conductance in *Xenopus* oocytes by expression of adenylate kinase cloned from renal proximal tubules. *Biochim Biophys Acta* 1510: 29-42.
- Carling D. 2004. The AMP-activated protein kinase cascade—a unifying system for energy control. *Trends Biochem Sci* 29: 18-24.

- Carrasco AJ, Dzeja PP, Alekseev AE, Pucar D, Zingman LV, et al. 2001. Adenylate kinase phosphotransfer communicates cellular energetic signals to ATP-sensitive potassium channels. *Proc Natl Acad Sci USA* 98: 7623-7628.
- Cesar MC, Wilson JE. 1998. Further studies on the coupling of mitochondrially bound hexokinase to intramitochondrially compartmented ATP, generated by oxidative phosphorylation. *Arch Biochem Biophys* 350: 109-117.
- Chaplain RA. 1979. Metabolic control of neuronal pacemaker activity and the rhythmic organization of central nervous functions. *J Exp Biol* 81: 113-130.
- Chen L, Roberts R, Friedman DL. 1995. Expression of brain-type creatine kinase and ubiquitous mitochondrial creatine kinase in the fetal rat brain: Evidence for a nuclear energy shuttle. *J Comp Neurol* 363: 389-401.
- Chen W, Zhu XH, Adriany G, Ugurbil K. 1997. Increase of creatine kinase activity in the visual cortex of human brain during visual stimulation: A ^{31}P magnetization transfer study. *Magn Reson Med* 38: 551-557.
- Collavin L, Lazarevic D, Utrera R, Marzinotto S, Monte M, et al. 1999. wt p53 dependent expression of a membrane-associated isoform of adenylate kinase. *Oncogene* 18: 5879-5888.
- Counago R, Shamooy Y. 2005. Gene replacement of adenylate kinase in the gram-positive thermophile *Geobacillus stearothermophilus* disrupts adenine nucleotide homeostasis and reduces cell viability. *Extremophiles* 2005 Jan 13.
- Crawford RM, Ranki HJ, Botting CH, Budas GR, Jovanovic A. 2002. Creatine kinase is physically associated with the cardiac ATP-sensitive K^+ channel in vivo. *FASEB J* 16: 102-104.
- Criss WE. 1970. Rat liver adenosine triphosphate: Adenosine monophosphate phosphotransferase activity. II. Subcellular localization of adenylate kinase isozymes. *J Biol Chem* 245: 6352-6356.
- Cyert MS. 2001. Regulation of nuclear localization during signaling. *J Biol Chem* 276: 20805-20808.
- Dawis SM, Graeff RM, Heyman RA, Walseth TF, Goldberg ND. 1988. Regulation of cyclic GMP metabolism in toad photoreceptors. Definition of the metabolic events subserving photoexcited and attenuated states. *J Biol Chem* 263: 8771-8785.
- Dawson VL, Dawson TM. 2004. Deadly conversations: Nuclear-mitochondrial cross talk. *J Bioenerg Biomembr* 36: 287-294.
- de Groof AJ, Oerlemans FT, Jost CR, Wieringa B. 2001. Changes in glycolytic network and mitochondrial design in creatine kinase-deficient muscles. *Muscle Nerve* 24: 1188-1196.
- Denu JM. 2003. Linking chromatin function with metabolic networks: Sir2 family of NAD^+ -dependent deacetylases. *Trends Biochem Sci* 28: 41-48.
- Dolnik M, Bollt EM. 1998. Communication with chemical chaos in the presence of noise. *Chaos* 8: 702-710.
- Downs SM, Hudson ER, Hardie DG. 2002. A potential role for AMP-activated protein kinase in meiotic induction in mouse oocytes. *Dev Biol* 245: 200-212.
- Dzeja PP, Terzic A. 1998. Phosphotransfer reactions in the regulation of ATP-sensitive K^+ channels. *FASEB J* 12: 523-529.
- Dzeja PP, Terzic A. 2003. Phosphotransfer networks and cellular energetics. *J Exp Biol* 206: 2039-2047.
- Dzeja PP, Terzic A. 2005. Adenylate kinase and creatine kinase phosphotransfer in the regulation of mitochondrial respiration and cellular energetic efficiency. Vial C, Uversky N, Creatine Kinase Biochemistry, Physiology, Structure and Function. Nova Science Publishers. New York:editors.
- Dzeja PP, Bortolon R, Perez-Terzic C, Holmuhamedov EL, Terzic A. 2002. Energetic communication between mitochondria and nucleus directed by catalyzed phosphotransfer. *Proc Natl Acad Sci USA* 99: 10156-10161.
- Dzeja P, Kalvenas A, Toleikis A, Praskevicius A. 1985. The effect of adenylate kinase activity on the rate and efficiency of energy transport from mitochondria to hexokinase. *Biochem Int* 10: 259-265.
- Dzeja PP, Pucar D, Redfield MM, Burnett JC, Terzic A. 1999a. Reduced activity of enzymes coupling ATP-generating with ATP-consuming processes in the failing myocardium. *Mol Cell Biochem* 201: 33-40.
- Dzeja PP, Redfield MM, Burnett JC, Terzic A. 2000. Failing energetics in failing hearts. *Curr Cardiol Rep* 2: 212-217.
- Dzeja PP, Terzic A, Wieringa B. 2004. Phosphotransfer dynamics in skeletal muscle from creatine kinase gene-deleted mice. *Mol Cell Biochem* 256-257: 13-27.
- Dzeja PP, Vitkevicius KT, Redfield MM, Burnett JC, Terzic A. 1999b. Adenylate kinase-catalyzed phosphotransfer in the myocardium: Increased contribution in heart failure. *Circ Res* 84: 1137-1143.
- Dzeja PP, Zeleznikar RJ, Goldberg ND. 1996. Suppression of creatine kinase-catalyzed phosphotransfer results in increased phosphoryl transfer by adenylate kinase in intact skeletal muscle. *J Biol Chem* 271: 12847-12851.
- Dzeja PP, Zeleznikar RJ, Goldberg ND. 1998. Adenylate kinase: Kinetic behavior in intact cells indicates it is integral to multiple cellular processes. *Mol Cell Biochem* 84: 169-182.
- Englert HC, Heitsch H, Gerlach U, Knieps S. 2003. Blockers of the ATP-sensitive potassium channel SUR2A/Kir6.2: A new approach to prevent sudden cardiac death. *Curr Med Chem* 1: 253-271.
- Enns T. 1967. Facilitation by carbonic anhydrase of carbon dioxide transport. *Science* 155: 44-47.

- Fisone G, Borgkvist A, Usiello A. 2004. Caffeine as a psychomotor stimulant: Mechanism of action. *Cell Mol Life Sci* 61: 857-872.
- Fjeld CC, Birdsong WT, Goodman RH. 2003. Differential binding of NAD⁺ and NADH allows the transcriptional corepressor carboxyl-terminal binding protein to serve as a metabolic sensor. *Proc Natl Acad Sci USA* 100: 9202-9207.
- Fossel ET, Hoefeler H. 1987. A synthetic functional metabolic compartment. The role of propinquity in a linked pair of immobilized enzymes. *Eur J Biochem* 170: 165-171.
- Frederich M, Zhang L, Balschi JA. 2005. Hypoxia and AMP independently regulate AMP-activated protein kinase activity in the heart. *Am J Physiol Heart Circ Physiol* 288: H2412-H2421.
- Fulco M, Schiltz RL, Iezzi S, King MT, Zhao P, et al. 2003. Sir2 regulates skeletal muscle differentiation as a potential sensor of the redox state. *Mol Cell* 12: 51-62.
- Gajewski CD, Yang L, Schon EA, Manfredi G. 2003. New insights into the bioenergetics of mitochondrial disorders using intracellular ATP reporters. *Mol Biol Cell* 14: 3628-3635.
- Galland L. 1991-1992. Magnesium, stress, and neuropsychiatric disorders. *Magnes Trace Elem* 10: 287-301.
- Gellerich FN, Kapischke M, Kunz W, Neumann W, Kuznetsov A, et al. 1994. The influence of the cytosolic oncotic pressure on the permeability of the mitochondrial outer membrane for ADP: Implications for the kinetic properties of mitochondrial creatine kinase and for ADP channeling into the intermembrane space. *Mol Cell Biochem* 133-134: 85-104.
- Gerbitz KD, Gempel K, Brdiczka D. 1996. Mitochondria and diabetes. Genetic, biochemical, and clinical implications of the cellular energy circuit. *Diabetes* 45: 113-126.
- Gjedde A. 2001. Brain energy metabolism and the physiological basis of the hemodynamic response. *Functional MRI—An Introduction to Methods*. Jezard P, Matthews PM, Smith S, editors. Oxford: Oxford University Press; pp. 37-65.
- Glazer PM, Sarkar SN, Chisholm GE, Summers WC. 1987. DNA mismatch repair detected in human cell extracts. *Mol Cell Biol* 7: 218-224.
- Goldbeter A, Nicolis G. 1976. An allosteric enzyme model with positive feedback applied to glycolytic oscillations. *Prog Theor Biol* 4: 65-160.
- Gumina RJ, Pucar D, Bast P, Hodgson DM, Kurtz CE, et al. 2003. Knockout of Kir6.2 negates ischemic preconditioning-induced protection of myocardial energetics. *Am J Physiol* 284: H2106-H2113.
- Hanz S, Perlson E, Willis D, Zheng JQ, Massarwa R, et al. 2003. Axoplasmic importins enable retrograde injury signaling in lesioned nerve. *Neuron* 40: 1095-10104.
- Hardie DH. 2003. The AMP-activated protein kinase cascade: The key sensor of cellular energy status. *Endocrinology* 144: 5179-5183.
- Harold FM. 1991. Biochemical topology: From vectorial metabolism to morphogenesis. *Biosci Rep* 11: 347-385.
- Hedbacker K, Townley R, Carlson M. 2004. Cyclic AMP-dependent protein kinase regulates the subcellular localization of Snf1-Sip1 protein kinase. *Mol Cell Biol* 24: 1836-1843.
- Hemmer W, Riesinger I, Wallimann T, Eppenberger HM, Quest AF. 1993. Brain-type creatine kinase in photoreceptor cell outer segments: Role of a phosphocreatine circuit in outer segment energy metabolism and phototransduction. *J Cell Sci* 106: 671-683.
- Hemmingsen E. 1962. Accelerated exchange of oxygen-18 through a membrane containing oxygen-saturated hemoglobin. *Science* 135: 733-734.
- Hippe HJ, Lutz S, Cuello F, Knorr K, Vogt A, et al. 2003. Activation of heterotrimeric G proteins by a high-energy phosphate transfer via nucleoside diphosphate kinase (NDPK) B and Gβ subunits. Specific activation of Gα_s by an NDPK B Gβγ complex in H10 cells. *J Biol Chem* 278: 7227-7233.
- Hoane MR, Knotts AA, Akstulewicz SL, Aquilano M, Means LW. 2003. The behavioral effects of magnesium therapy on recovery of function following bilateral anterior medial cortex lesions in the rat. *Brain Res Bull* 60: 105-114.
- Hochachka PW. 1999. The metabolic implications of intracellular circulation. *Proc Natl Acad Sci USA* 96: 12233-12239.
- Hodgson DM, Zingman LV, Kane GC, Perez-Terzic C, Bienengraeber M, et al. 2003. Cellular remodeling in heart failure disrupts K_{ATP} channel-dependent stress tolerance. *EMBO J* 22: 1732-1742.
- Hollenbeck PJ. 1996. The pattern and mechanism of mitochondrial transport in axons. *Front Biosci* 1: D91-D102.
- Holtzman D, Brown M, O'Gorman E, Allred E, Wallimann T. 1998. Brain ATP metabolism in hypoxia-resistant mice fed guanidinopropionic acid. *Dev Neurosci* 20: 469-477.
- Hornemann T, Kempa S, Himmel M, Hayess K, Furst DO, et al. 2003. Muscle-type creatine kinase interacts with central domains of the M-band proteins myomesin and M-protein. *J Mol Biol* 332: 877-887.
- Hoyer S. 2003. Memory function and brain glucose metabolism. *Pharmacopsychiatry* 36: S62-S67.
- Hoyer S, Lannert H, Latteier E, Meisel T. 2004. Relationship between cerebral energy metabolism in parietotemporal cortex and hippocampus and mental activity during aging in rats. *J Neural Transm* 111: 575-589.
- Huitorel P, Simon C, Pantaloni D. 1984. Nucleoside diphosphate kinase from brain. Purification and effect on microtubule assembly in vitro. *Eur J Biochem* 144: 233-241.

- Igamberdiev AU, Kleczkowski LA. 2001. Implications of adenylate kinase-governed equilibrium of adenylates on contents of free magnesium in plant cells and compartments. *Biochem J* 360: 225-231.
- Ikemoto A, Bole DG, Ueda T. 2003. Glycolysis and glutamate accumulation into synaptic vesicles. Role of glyceraldehyde phosphate dehydrogenase and 3-phosphoglycerate kinase. *J Biol Chem* 278: 5929-5940.
- Inbe H, Watanabe S, Miyawaki M, Tanabe E, Encinas JA. 2004. Identification and characterization of a cell-surface receptor, P2Y15, for AMP and adenosine. *J Biol Chem* 279: 19790-19799.
- Ingwall JS. 2004. Transgenesis and cardiac energetics: New insights into cardiac metabolism. *J Mol Cell Cardiol* 37: 613-623.
- Innocenti B, Parpura V, Haydon PG. 2000. Imaging extracellular waves of glutamate during calcium signaling in cultured astrocytes. *J Neurosci* 20: 1800-1808.
- Inouye S, Seo M, Yamada Y, Nakazawa A. 1998. Increase of adenylate kinase isozyme 1 protein during neuronal differentiation in mouse embryonal carcinoma P19 cells and in rat brain primary cultured cells. *J Neurochem* 71: 125-133.
- Inouye S, Yamada Y, Miura K, Suzuki H, Kawata K, et al. 1999. Distribution and developmental changes of adenylate kinase isozymes in the rat brain: Localization of adenylate kinase 1 in the olfactory bulb. *Biochem Biophys Res Commun* 254: 618-622.
- Jackson EK, Mi Z, Zhu C, Dubey RK. 2003. Adenosine biosynthesis in the collecting duct. *J Pharmacol Exp Ther* 307: 888-896.
- Jacobus WE. 1985. Respiratory control and the integration of heart high-energy phosphate metabolism by mitochondrial creatine kinase. *Annu Rev Physiol* 47: 707-725.
- Janssen E, de Groof A, Wijers M, Fransen J, Dzeja PP, et al. 2003a. Adenylate kinase 1 deficiency induces molecular and structural adaptations to support muscle energy metabolism. *J Biol Chem* 278: 12937-12945.
- Janssen E, Dzeja PP, Oerlemans F, Simonetti AW, Heerschap A, et al. 2000. Adenylate kinase 1 gene deletion disrupts muscle energetic economy despite metabolic rearrangement. *EMBO J* 19: 6371-6381.
- Janssen E, Kuiper J, Hodgson D, Zingman LV, Alekseev AE, et al. 2004. Two structurally distinct and spatially compartmentalized adenylate kinases are expressed from the AK1 gene in mouse brain. *Mol Cell Biochem* 256-257: 59-72.
- Janssen E, Terzic A, Wieringa B, Dzeja PP. 2003b. Impaired intracellular energetic communication in muscles from creatine kinase and adenylate kinase (M-CK/AK1) double knockout mice. *J Biol Chem* 278: 30441-30449.
- Joseph SM, Buchakjian MR, Dubyak GR. 2003. Colocalization of ATP release sites and ecto-ATPase activity at the extracellular surface of human astrocytes. *J Biol Chem* 278: 23331-23342.
- Jost CR, Van Der Zee CE, Zandt HJ, Oerlemans F, Verheij M, et al. 2002. Creatine kinase B-driven energy transfer in the brain is important for habituation and spatial learning behavior, mossy fiber field size, and determination of seizure susceptibility. *Eur J Neurosci* 15: 1692-1706.
- Joubert F, Mazet JL, Mateo P, Hoerter JA. 2002. ³¹P NMR detection of subcellular creatine kinase fluxes in the perfused rat heart: Contractility modifies energy transfer pathways. *J Biol Chem* 277: 18469-18476.
- Jurgens KD, Peters T, Gros G. 1994. Diffusivity of myoglobin in intact skeletal muscle cells. *Proc Natl Acad Sci USA* 91: 3829-3833.
- Kaasik A, Veksler V, Boehm E, Novotova M, Minajeva A, et al. 2001. Energetic crosstalk between organelles: Architectural integration of energy production and utilization. *Circ Res* 89: 153-159.
- Kammermeier H. 1997. Myocardial cell energetics. *Adv Exp Biol* 430: 89-96.
- Kane GC, Behfar A, Yamada S, Perez-Terzic C, O'Coilain F, et al. 2004. ATP-sensitive K⁺ channel knockout compromises the metabolic benefit of exercise training, resulting in cardiac deficits. *Diabetes* 53: S169-S175.
- Kanig K, Hoffmann KH. 1979. ³²P incorporation in adenosine phosphates of the rat brain after oral application of vincamine for 2 weeks. *Arzneimittelforschung* 29: 33-34.
- Kekelidze T, Khait I, Togliatti A, Benzecry JM, Wieringa B, et al. 2001. Altered brain phosphocreatine and ATP regulation when mitochondrial creatine kinase is absent. *J Neurosci Res* 66: 866-872.
- Kemp GJ, Manners DN, Clark JF, Bastin ME, Radda GK. 1998. Theoretical modeling of some spatial and temporal aspects of the mitochondrion/creatine kinase/myofibril system in muscle. *Mol Cell Biochem* 184: 249-289.
- Kim SH, Fountoulakis M, Cairns NJ, Lubec G. 2002. Human brain nucleoside diphosphate kinase activity is decreased in Alzheimer's disease and Down's syndrome. *Biochem Biophys Res Commun* 296: 970-975.
- Kindzelskii AL, Petty HR. 2002. Apparent role of traveling metabolic waves in oxidant release by living neutrophils. *Proc Natl Acad Sci USA* 99: 9207-9212.
- Kingsley-Hickman PB, Sako EY, Mohanakrishnan P, Robitaille PM, From AH, et al. 1987. ³¹P NMR studies of ATP synthesis and hydrolysis kinetics in the intact myocardium. *Biochemistry* 26: 7501-7510.
- Kivela AJ, Kivela J, Saarnio J, Parkkila S. 2005. Carbonic anhydrases in normal gastrointestinal tract and gastrointestinal tumors. *World J Gastroenterol* 11: 155-163.
- Kjekshus JK, Vaagenes P, Hetland O. 1980. Assessment of cerebral injury with spinal fluid creatine kinase (CSF-CK)

- in patients after cardiac resuscitation. *Scand J Clin Lab Invest* 40: 437-444.
- Kohen E, Welch GR, Kohen C, Hirschberg JG, Bereiter-Hahn J. 1985. Experimental analysis of spatiotemporal organization of metabolism in intact cells: The enigma of "Metabolic Channeling" and "Metabolic Compartmentation." *The Organization of Cell Metabolism*, Vol. 127. Welch GR, Clegg JS, editors. New York: Plenum Press; pp. 251-275.
- Kongas O, van Beek JH. 2002. Diffusion barriers for ADP in the cardiac cell. *Mol Biol Rep* 29: 141-144.
- Kremen A. 1982. Informational aspects of Gibbs function output from nucleotide pools and of the adenylate kinase reaction. *J Theor Biol* 96: 425-441.
- Krishnan KS, Rikhy R, Rao S, Shivalkar M, Mosko M, et al. 2001. Nucleoside diphosphate kinase, a source of GTP, is required for dynamin-dependent synaptic vesicle recycling. *Neuron* 30: 197-210.
- Lacombe ML, Milon L, Munier A, Mehus JG, Lambeth DO. 2000. The human Nm23/nucleoside diphosphate kinases. *J Bioenerg Biomembr* 32: 247-258.
- Lange S, Auerbach D, McLoughlin P, Perriard E, Schafer BW, et al. 2002. Subcellular targeting of metabolic enzymes to titin in heart muscle may be mediated by DRAL/FHL-2. *J Cell Sci* 115: 4925-4936.
- Laterveer FD, Nicolay K, Gellerich FN. 1996. ADP delivery from adenylate kinase in the mitochondrial intermembrane space to oxidative phosphorylation increases in the presence of macromolecules. *FEBS Lett* 386: 255-259.
- Latini S, Pedata F. 2001. Adenosine in the central nervous system: Release mechanisms and extracellular concentrations. *J Neurochem* 79: 463-484.
- Laughlin SB. 2001. Energy as a constraint on the coding and processing of sensory information. *Curr Opin Neurobiol* 11: 475-480.
- Le Bihan D. 2003. Looking into the functional architecture of the brain with diffusion MRI. *Nat Rev Neurosci* 4: 469-480.
- Lee M, Hwang JT, Lee HJ, Jung SN, Kang I, et al. 2003. AMP-activated protein kinase activity is critical for hypoxia-inducible factor-1 transcriptional activity and its target gene expression under hypoxic conditions in DU145 cells. *J Biol Chem* 278: 39653-39661.
- Leuzzi V. 2002. Inborn errors of creatine metabolism and epilepsy: Clinical features, diagnosis, and treatment. *J Child Neurol* 17: 3589-3597.
- Li Z, Okamoto K, Hayashi Y, Sheng M. 2004. The importance of dendritic mitochondria in the morphogenesis and plasticity of spines and synapses. *Cell* 119: 873-887.
- Liu XK, Yamada S, Kane GC, Alekseev AE, Hodgson DM, et al. 2004. Genetic disruption of Kir6.2, the pore-forming subunit of ATP-sensitive K⁺ channel, predisposes to catecholamine-induced ventricular dysrhythmia. *Diabetes* 53: S165-S168.
- Lu Q, Park H, Egger LA, Inouye M. 1996. Nucleoside-diphosphate kinase-mediated signal transduction via histidyl-aspartyl phosphorelay systems in *Escherichia coli*. *J Biol Chem* 271: 32886-32893.
- Luby-Phelps K. 2000. Cytoarchitecture and physical properties of cytoplasm: Volume, viscosity, diffusion, intracellular surface area. *Int Rev Cytol* 192: 189-221.
- Mahajan VB, Pai KS, Lau A, Cunningham DD. 2000. Creatine kinase, an ATP-generating enzyme, is required for thrombin receptor signaling to the cytoskeleton. *Proc Natl Acad Sci USA* 97: 12062-12067.
- Mair T, Muller SC. 1996. Traveling NADH and proton waves during oscillatory glycolysis in vitro. *J Biol Chem* 271: 627-630.
- Manos P, Bryan GK. 1993. Cellular and subcellular compartmentation of creatine kinase in brain. *Dev Neurosci* 15: 271-279.
- Mak BC, Yeung RS. 2004. The tuberous sclerosis complex genes in tumor development. *Cancer Invest* 22: 588-603.
- Marcus EA, Moshfegh AP, Sachs G, Scott DR. 2005. The periplasmic α -carbonic anhydrase activity of *Helicobacter pylori* is essential for acid acclimation. *J Bacteriol* 187: 729-738.
- Marsin AS, Bertrand L, Rider MH, Deprez J, Beauloye C, et al. 2000. Phosphorylation and activation of heart PFK-2 by AMPK has a role in the stimulation of glycolysis during ischaemia. *Curr Biol* 10: 1247-1255.
- Masters C. 1991. Cellular differentiation and the micro-compartmentation of glycolysis. *Mech Ageing Dev* 61: 11-22.
- Mathews CK. 1985. Enzymatic channeling of DNA precursors. *Basic Life Sci* 31: 47-66.
- Mattaj JW, Englmeier L. 1998. Nucleocytoplasmic transport: The soluble phase. *Annu Rev Biochem* 67: 265-306.
- Mazurek S, Boschek CB, Eigenbrodt E. 1997. The role of phosphometabolites in cell proliferation, energy metabolism, and tumor therapy. *J Bioenerg Biomembr* 29: 315-330.
- McClare CW. 1971. Chemical machines, Maxwell's demon, and living organisms. *J Theor Biol* 30: 1-34.
- McGee SL, Howlett KF, Starkie RL, Cameron-Smith D, Kemp BE, et al. 2003. Exercise increases nuclear AMPK α 2 in human skeletal muscle. *Diabetes* 52: 926-928.
- Messier C. 2004. Glucose improvement of memory: A review. *Eur J Pharmacol* 490: 33-57.
- Meyer RA, Sweeney HL, Kushmerick MJ. 1984. A simple analysis of the "phosphocreatine shuttle." *Am J Physiol* 246: C365-C377.
- Mhatre AN, Stern RE, Li J, Lalwani AK. 2002. Aquaporin 4 expression in the mammalian inner ear and its role in hearing. *Biochem Biophys Res Commun* 297: 987-996.
- Minami K, Miki T, Kadowaki T, Seino S. 2004. Roles of ATP-sensitive K⁺ channels as metabolic sensors: Studies of Kir6.2 null mice. *Diabetes* 53: S176-S180.

- Minokoshi Y, Alquier T, Furukawa N, Kim YB, Lee A, et al. 2004. AMP-kinase regulates food intake by responding to hormonal and nutrient signals in the hypothalamus. *Nature* 428: 569-574.
- Mitchell P. 1979. Compartmentation and communication in living systems. Ligand conduction: A general catalytic principle in chemical, osmotic, and chemiosmotic reaction systems. *Eur J Biochem* 95: 1-20.
- Mitchell P. 1991. Foundations of vectorial metabolism and osmochemistry. *Biosci Rep* 11: 297-344.
- Mueggler T, Meyer-Luehmann M, Rausch M, Staufenbiel M, Jucker M, et al. 2004. Restricted diffusion in the brain of transgenic mice with cerebral amyloidosis. *Eur J Neurosci* 20: 811-817.
- Nagle S. 1970. Regulation problems in the energy metabolism of the myocardium. *Wien Klin Wochenschr* 48: 1075-1089.
- Nagy AK, Shuster TA, Delgado-Escueta AV. 1989. Rat brain synaptosomal ATP: AMP-phosphotransferase activity. *J Neurochem* 53: 1166-1172.
- Neumann D, Schlattner U, Wallimann T. 2003. A molecular approach to the concerted action of kinases involved in energy homeostasis. *Biochem Soc Trans* 31: 169-174.
- Newman EA. 2003. Glial cell inhibition of neurons by release of ATP. *J Neurosci* 23: 1659-1666.
- Noda L. 1973. Adenylate kinase. The *Enzymes*, Vol. 8. Boyer PD, editor. New York: Academic Press; pp. 279-305.
- Notari L, Pepe IM, Cugnoli C, Morelli A. 2001. Adenylate kinase activity in rod outer segments of bovine retina. *Biochim Biophys Acta* 1504: 438-443.
- Ohba T, Schirmer EC, Nishimoto T, Gerace L. 2004. Energy- and temperature-dependent transport of integral proteins to the inner nuclear membrane via the nuclear pore. *J Cell Biol* 167: 1051-1062.
- Olson LK, Schroeder W, Robertson RP, Goldberg ND, Walseth TF. 1996. Suppression of adenylate kinase-catalyzed phosphotransfer precedes and is associated with glucose-induced insulin secretion in intact HIT-T15 cells. *J Biol Chem* 271: 16544-16552.
- O'Rourke B, Ramza BM, Marban E. 1994. Oscillations of membrane current and excitability driven by metabolic oscillations in heart cells. *Science* 265: 962-966.
- Ottaway JH, Mowbray J. 1977. The role of compartmentation in the control of glycolysis. *Curr Top Cell Regul* 12: 107-208.
- Ovadi J, Saks V. 2004. On the origin of intracellular compartmentation and organized metabolic systems. *Mol Cell Biochem* 256-257: 5-12.
- Pastorino JG, Hoek JB. 2003. Hexokinase II: The integration of energy metabolism and control of apoptosis. *Curr Med Chem* 10: 1535-1551.
- Perez-Terzic C, Gacy AM, Bortolon R, Dzeja PP, Pucaat M, et al. 2001. Directed inhibition of nuclear import in cellular hypertrophy. *J Biol Chem* 276: 20566-20571.
- Picher M, Boucher RC. 2003. Human airway ecto-adenylate kinase. A mechanism to propagate ATP signaling on airway surfaces. *J Biol Chem* 278: 11256-1164.
- Plaschke K, Yun SW, Martin E, Hoyer S, Bardenheuer HJ. 2000. Linear relation between cerebral phosphocreatine concentration and memory capacities during permanent brain vessel occlusions in rats. *Ann NY Acad Sci* 903: 299-306.
- Polekhina G, Gupta A, Michell BJ, van Denderen B, Murthy S, et al. 2003. AMPK β subunit targets metabolic stress sensing to glycogen. *Curr Biol* 13: 867-871.
- Politi HC, Preston RR. 2003. Is it time to rethink the role of Mg^{2+} in membrane excitability? *Neuroreport* 14: 659-668.
- Pomes R, Roux B. 2002. Molecular mechanism of H^+ conduction in the single-file water chain of the gramicidin channel. *Biophys J* 82: 2304-2316.
- Ponticos M, Lu QL, Morgan JE, Hardie DG, Partridge TA, et al. 1998. Dual regulation of the AMP-activated protein kinase provides a novel mechanism for the control of creatine kinase in skeletal muscle. *EMBO J* 17: 1688-1699.
- Portman MA. 1994. Measurement of unidirectional $P_i \rightarrow$ ATP flux in lamb myocardium in vivo. *Biochim Biophys Acta* 1185: 221-227.
- Poyton RO, McEwen JE. 1996. Cross talk between nuclear and mitochondrial genomes. *Annu Rev Biochem* 65: 563-607.
- Pozrikidis C, Farrow DA. 2003. A model of fluid flow in solid tumors. *Ann Biomed Eng* 31: 181-194.
- Pucar D, Bast P, Gumina RJ, Lim L, Drahl C, et al. 2002. Adenylate kinase AK1 knockout heart: Energetics and functional performance under ischemia-reperfusion. *Am J Physiol* 283: H776-H782.
- Pucar D, Dzeja PP, Bast P, Gumina RJ, Drahl C, et al. 2004. Mapping hypoxia-induced bioenergetic rearrangements and metabolic signaling by ^{18}O -assisted ^{31}P NMR and 1H NMR spectroscopy. *Mol Cell Biochem* 256-257: 281-289.
- Pucar D, Dzeja PP, Bast P, Juranic N, Macura S, et al. 2001. Cellular energetics in the preconditioned state: Protective role for phosphotransfer reactions captured by ^{18}O -assisted ^{31}P NMR. *J Biol Chem* 276: 44812-44819.
- Pucar D, Janssen E, Dzeja PP, Juranic N, Macura S, et al. 2000. Compromised energetics in the adenylate kinase AK1 gene knockout heart under metabolic stress. *J Biol Chem* 275: 41424-41429.
- Rae C, Digney AL, McEwan SR, Bates TC. 2003. Oral creatine monohydrate supplementation improves brain performance: A double-blind, placebo-controlled, cross-over trial. *Proc R Soc Lond B Biol Sci* 270: 2147-2150.
- Rapaport E. 1980. Compartmentalized ATP pools produced from adenosine are nuclear pools. *J Cell Physiol* 105: 267-274.
- Rashdy-Pour A. 2001. ATP-sensitive potassium channels mediate the effects of a peripheral injection of glucose on

- memory storage in an inhibitory avoidance task. *Behav Brain Res* 126: 43-48.
- Reich JG, Sel'kov EE. 1981. *Energy Metabolism of the Cell: A Theoretical Treatise*. London: Academic Press; pp 95-107.
- Reiss N, Hermon J, Oplatka A, Naor Z. 1996. Interaction of purified protein kinase C with key proteins of energy metabolism and cellular motility. *Biochem Mol Biol Int* 38: 711-719.
- Ren H, Wang L, Bennett M, Liang Y, Zheng X, et al. 2005. The crystal structure of human adenylate kinase 6: An adenylate kinase localized to the cell nucleus. *Proc Natl Acad Sci USA* 102: 303-308.
- Ribeiro JA, Sebastiao AM, de Mendonca A. 2002. Adenosine receptors in the nervous system: Pathophysiological implications. *Prog Neurobiol* 68: 377-392.
- Riedel W, Hogervorst E, Lebourg R, Verhey F, van Praag H, et al. 1995. Caffeine attenuates scopolamine-induced memory impairment in humans. *Psychopharmacology (Berl)* 122: 158-168.
- Roberts J, Aubert S, Gout E, Bligny R, Douce R. 1997. Cooperation and competition between adenylate kinase, nucleoside diphosphokinase, electron transport, and ATP synthase in plant mitochondria studied by ^{31}P -nuclear magnetic resonance. *Plant Physiol* 113: 191-199.
- Rose IA. 1968. The state of magnesium in cells as estimated from the adenylate kinase equilibrium. *Proc Natl Acad Sci USA* 61: 1079-1086.
- Rosenberg EH, Almeida LS, Kleefstra T, deGrauw RS, Yntema HG, et al. 2004. High prevalence of SLC6A8 deficiency in X-linked mental retardation. *Am J Hum Genet* 75: 97-105.
- Ross AJ, Sachdev PS. 2004. Magnetic resonance spectroscopy in cognitive research. *Brain Res Brain Res Rev* 44: 83-102.
- Roussel CJ, Roussel MR. 2004. Reaction-diffusion models of development with state-dependent chemical diffusion coefficients. *Prog Biophys Mol Biol* 86: 113-160.
- Ruan Q, Chen Y, Gratton E, Glaser M, Mantulin WW. 2002. Cellular characterization of adenylate kinase and its isoform: Two-photon excitation fluorescence imaging and fluorescence correlation spectroscopy. *Biophys J* 83: 3177-3187.
- Rubio MP, Geraghty KM, Wong BH, Wood NT, Campbell DG, et al. 2004. 14-3-3-affinity purification of over 200 human phosphoproteins reveals new links to regulation of cellular metabolism, proliferation, and trafficking. *Biochem J* 379: 395-408.
- Ruiz-Stewart I, Tiyyagura SR, Lin JE, Kazerounian S, Pitari GM, et al. 2004. Guanylyl cyclase is an ATP sensor coupling nitric oxide signaling to cell metabolism. *Proc Natl Acad Sci USA* 101: 37-42.
- Saks VA, Kaambre T, Sikk P, Eimre M, Orlova E, et al. 2001. Intracellular energetic units in red muscle cells. *Biochem J* 356: 643-657.
- Saks VA, Khuchua ZA, Vasilyeva EV, Belikova OY, Kuznetsov AV. 1994. Metabolic compartmentation and substrate channeling in muscle cells. Role of coupled creatine kinases in *in vivo* regulation of cellular respiration—a synthesis. *Mol Cell Biochem* 133-134: 155-192.
- Saks VA, Kongas O, Vendelin M, Kay L. 2000. Role of the creatine/phosphocreatine system in the regulation of mitochondrial respiration. *Acta Physiol Scand* 168: 635-641.
- Saks V, Kuznetsov A, Andrienko T, Ussov Y, Appaix F, et al. 2003. Heterogeneity of ADP diffusion and regulation of respiration in cardiac cells. *Biophys J* 84: 3436-3456.
- Saks VA, Kuznetsov AV, Vendelin M, Guerrero K, Kay L, et al. 2004. Functional coupling as a basic mechanism of feedback regulation of cardiac energy metabolism. *Mol Cell Biochem* 256-257: 185-199.
- Saks VA, Rosenshtraukh LV, Smirnov VN, Chazov EI. 1978. Role of creatine phosphokinase in cellular function and metabolism. *Can J Physiol Pharmacol* 56: 691-706.
- Salomons GS, van Dooren SJ, Verhoeven NM, Marsden D, Schwartz C, et al. 2003. X-linked creatine transporter defect: An overview. *J Inher Metab Dis* 26: 309-318.
- Saupe KW, Spindler M, Tian R, Ingwall JS. 1998. Impaired cardiac energetics in mice lacking muscle-specific isoenzymes of creatine kinase. *Circ Res* 82: 898-907.
- Savabi F. 1994. Interaction of creatine kinase and adenylate kinase systems in muscle cells. *Mol Cell Biochem* 133-134: 145-152.
- Schmitz C, Perraud AL, Johnson CO, Inabe K, Smith MK, et al. 2003. Regulation of vertebrate cellular Mg^{2+} homeostasis by TRPM7. *Cell* 114: 191-200.
- Schulze A, Bachert P, Schlemmer H, Harting I, Polster T, et al. 2003. Lack of creatine in muscle and brain in an adult with GAMT deficiency. *Ann Neurol* 53: 248-251.
- Selivanov VA, Alekseev AE, Hodgson DM, Dzeja PP, Terzic A. 2004. Nucleotide-gated K-ATP channels integrated with creatine and adenylate kinases: Amplification, tuning, and sensing of energetic signals in the compartmentalized cellular environment. *Mol Cell Biochem* 256-257: 243-256.
- Shannon CE. 1948. A mathematical theory of communication. *Bell Sys Tech J* 27: 379-423/623-656.
- Spindler M, Meyer K, Stromer H, Leupold A, Boehm E, et al. 2004. Creatine kinase-deficient hearts exhibit increased susceptibility to ischemia-reperfusion injury and impaired calcium homeostasis. *Am J Physiol* 287: H1039-H1045.
- Spindler M, Niebler R, Remkes H, Horn M, Lanz T, et al. 2002. Mitochondrial creatine kinase is critically necessary for normal myocardial high-energy phosphate metabolism. *Am J Physiol* 283: H680-H687.
- Srivastava DK, Bernhard SA. 1987. Biophysical chemistry of metabolic reaction sequences in concentrated enzyme solution and in the cell. *Annu Rev Biophys Biophys Chem* 16: 175-204.

- Steeghs K, Benders A, Oerlemans F, de Haan A, Heerschap A, et al. 1997. Altered Ca^{2+} responses in muscles with combined mitochondrial and cytosolic creatine kinase deficiencies. *Cell* 89: 93-103.
- Stewart AK, Boyd CA, Vaughan-Jones RD. 1999. A novel role for carbonic anhydrase: Cytoplasmic pH gradient dissipation in mouse small intestinal enterocytes. *J Physiol* 516: 209-217.
- Stockler S, Holzbach U, Hanefeld F, Marquardt I, Helms G, et al. 1994. Creatine deficiency in the brain: A new, treatable inborn error of metabolism. *Pediatr Res* 36: 409-413.
- Streijger F, Jost CR, Oerlemans F, Ellenbroek BA, Cools AR, et al. 2004. Mice lacking the UbCKmit isoform of creatine kinase reveal slower spatial learning acquisition, diminished exploration and habituation, and reduced acoustic startle reflex responses. *Mol Cell Biochem* 256-257: 305-318.
- Streijger F, Oerlemans F, Ellenbroek BA, Jost CR, Wieringa B, et al. 2005. Structural and behavioral consequences of double deficiency for creatine kinases B-CK and UbCKmit. *Behav Brain Res* 157: 219-234.
- Takahashi E, Asano K. 2002. Mitochondrial respiratory control can compensate for intracellular O_2 gradients in cardiomyocytes at low PO_2 . *Am J Physiol* 283: H871-H878.
- Takaya J, Higashino H, Kobayashi Y. 2000. Can magnesium act as a second messenger? Current data on translocation induced by various biologically active substances. *Magnes Res* 13: 139-146.
- Tanabe T, Yamada M, Noma T, Kajii T, Nakazawa A. 1993. Tissue-specific and developmentally regulated expression of the genes encoding adenylate kinase isozymes. *J Biochem (Tokyo)* 113: 200-207.
- Tarasov A, Dusonchet J, Ashcroft F. 2004. Metabolic regulation of the pancreatic β -cell ATP-sensitive K^+ channel: A pas de deux. *Diabetes* 53: S113-S122.
- Tatton WG, Chalmers-Redman RM, Elstner M, Leesch W, Jagodzinski FB, et al. 2000. Glycerinaldehyde-3-phosphate dehydrogenase in neurodegeneration and apoptosis signaling. *J Neural Transm* 60: 77-100.
- Templeton GW, Moorhead GB. 2004. A renaissance of metabolite sensing and signaling: From modular domains to riboswitches. *Plant Cell* 16: 2252-2257.
- Tokunaga C, Yoshino K, Yonezawa K. 2004. mTOR integrates amino acid- and energy-sensing pathways. *Biochem Biophys Res Commun* 313: 443-446.
- Toren A, Brok-Simoni F, Ben-Bassat I, Holtzman F, Mandel M, et al. 1994. Congenital hemolytic anemia associated with adenylate kinase deficiency. *Br J Haematol* 87: 376-380.
- Tournaire-Roux C, Sutka M, Javot H, Gout E, Gerbeau P, et al. 2003. Cytosolic pH regulates root water transport during anoxic stress through gating of aquaporins. *Nature* 425: 393-397.
- Trachtenberg MC, Tu CK, Landers RA, Willson RC, McGregor ML, et al. 1999. Carbon dioxide transport by proteic and facilitated transport membranes. *Life Support Biosph Sci* 6: 293-302.
- Tuckerman ME, Marx D, Parrinello M. 2002. The nature and transport mechanism of hydrated hydroxide ions in aqueous solution. *Nature* 417: 925-929.
- Turnley AM, Stapleton D, Mann RJ, Witters LA, Kemp BE, et al. 1999. Cellular distribution and developmental expression of AMP-activated protein kinase isoforms in mouse central nervous system. *J Neurochem* 72: 1707-1716.
- Tuszynski JA, Brown JA, Hawrylak P. 1998. Dielectric polarization, electrical conduction, information processing, and quantum computation in microtubules. Are they plausible? *Philos Transact A Math Phys Eng Sci* 356: 1897-1926.
- van Deursen J, Heerschap A, Oerlemans F, Ruitenbeek W, Jap P, et al. 1993. Skeletal muscle of mice deficient in muscle creatine kinase lack burst activity. *Cell* 74: 621-631.
- van Galen EJ, Ramakers GJ. 2005. Rho proteins, mental retardation, and the neurobiological basis of intelligence. *Prog Brain Res* 147: 295-317.
- Vendelin M, Kongas O, Saks V. 2000. Regulation of mitochondrial respiration in heart cells analyzed by reaction-diffusion model of energy transfer. *Am J Physiol* 278: C747-C764.
- Vendelin M, Lemba M, Saks VA. 2004. Analysis of functional coupling: Mitochondrial creatine kinase and adenine nucleotide translocase. *Biophys J* 87: 696-713.
- Ventura-Clapier R, Veksler V. 1994. Myocardial ischemic contracture. Metabolites affect rigor tension development and stiffness. *Circ Res* 74: 920-929.
- Vincent A, Blair JM. 1970. The coupling of the adenylate kinase and creatine kinase equilibria. Calculation of substrate and feedback signal levels in muscle. *FEBS Lett* 7: 239-244.
- Walker EJ, Dow JW. 1982. Location and properties of two isoenzymes of cardiac adenylate kinase. *Biochem J* 203: 361-369.
- Walker J, Jijon HB, Churchill T, Kulka M, Madsen KL. 2003. Activation of AMP-activated protein kinase reduces cAMP-mediated epithelial chloride secretion. *Am J Physiol* 285: G850-G860.
- Wallimann T, Hemmer W. 1994. Creatine kinase in nonmuscle tissues and cells. *Mol Cell Biochem* 133-134: 193-220.
- Wallimann T, Wyss M, Brdiczka D, Nicolay K, Eppenberger HM. 1992. Intracellular compartmentation, structure, and function of creatine kinase isoenzymes in tissues with high and fluctuating energy demands: The "phosphocreatine circuit" for cellular energy homeostasis. *Biochem J* 28: 21-40.
- Wang Z, Haydon PG, Yeung ES. 2000. Direct observation of calcium-independent intercellular ATP signaling in astrocytes. *Anal Chem* 72: 2001-2007.

- Wang W, Yang X, Kawai T, Lopez de Silanes I, Mazan-Mamczarz K, et al. 2004. AMP-activated protein kinase-regulated phosphorylation and acetylation of importin α 1: Involvement in the nuclear import of RNA-binding protein HuR. *J Biol Chem* 279: 48376-4888.
- Wegmann G, Zanolla E, Eppenberger HM, Wallimann, T. 1992. In situ compartmentation of creatine kinase in intact sarcomeric muscle: The acto-myosin overlap zone as a molecular sieve. *J Muscle Res Cell Motil* 13: 420-435.
- Weiss JN, Lamp ST. 1987. Glycolysis preferentially inhibits ATP-sensitive K^+ channels in isolated guinea pig cardiac myocytes. *Science* 238: 67-69.
- Welch GR. 1977. On the role of organized multienzyme systems in cellular metabolism: A general synthesis. *Prog Biophys Mol Biol* 32: 103-191.
- Welch GR. 1996. The enzymatic basis of information processing in the living cell. *Biosystems* 38: 147-153.
- Welch GR, Easterby JS. 1994. Metabolic channeling versus free diffusion: Transition-time analysis. *Trends Biochem Sci* 19: 193-197.
- Westmoreland CA, Koke JR, Bittar N. 1986. AMP stimulation of endocytotic transport from canine coronary circulation into myocytes. *Cytobios* 46: 201-210.
- Wild K, Grafmuller R, Wagner E, Schulz GE. 1997. Structure, catalysis, and supramolecular assembly of adenylate kinase from maize. *Eur J Biochem* 250: 326-331.
- Wirschell M, Pazour G, Yoda A, Hirano M, Kamiya R, et al. 2004. Oda5p, a novel axonemal protein required for assembly of the outer dynein arm and an associated adenylate kinase. *Mol Biol Cell* 15: 2729-2741.
- Wittenberg JB. 1970. Myoglobin-facilitated oxygen diffusion and the role of myoglobin in oxygen entry into muscle. *Physiol Rev* 50: 559-636.
- Wittenberg JB, Wittenberg BA. 2003. Myoglobin function reassessed. *J Exp Biol* 206: 2011-2020.
- Wustmann C, Petzold D, Fischer HD, Kunz W. 1987. ATP-metabolizing enzymes in suspensions of isolated coupled rat brain mitochondria. *Biomed Biochim Acta* 46: 331-340.
- Wyss M, Smeitink J, Wevers RA, Wallimann T. 1992. Mitochondrial creatine kinase: a key enzyme of aerobic energy metabolism. *Biochim Biophys Acta* 1102: 119-166.
- Xing Y, Musi N, Fujii N, Zou L, Luptak I, et al. 2003. Glucose metabolism and energy homeostasis in mouse hearts over-expressing dominant negative α 2 subunit of AMP-activated protein kinase. *J Biol Chem* 278: 28372-28377.
- Yamada K, Ji JJ, Yuan H, Miki T, Sato S, et al. 2001. Protective role of ATP-sensitive potassium channels in hypoxia-induced generalized seizure. *Science* 292: 1543-1546.
- Yang L, Arora K, Beard WA, Wilson SH, Schlick T. 2004. Critical role of magnesium ions in DNA polymerase β 's closing and active site assembly. *J Am Chem Soc* 126: 8441-8453.
- Yegutkin GG, Henttinen T, Samburski SS, Spychala J, Jalkanen S. 2002. The evidence for two opposite, ATP-generating and ATP-consuming, extracellular pathways on endothelial and lymphoid cells. *Biochem J* 367: 121-128.
- Yoneda T, Sato M, Maeda M, Takagi H. 1998. Identification of a novel adenylate kinase system in the brain: Cloning of the fourth adenylate kinase. *Brain Res Mol Brain Res* 62: 187-195.
- Zhu F, Schulten K. 2003. Water and proton conduction through carbon nanotubes as models for biological channels. *Biophys J* 85: 236-244.
- Zeleznikar RJ, Dzeja PP, Goldberg ND. 1995. Adenylate kinase-catalyzed phosphoryl transfer couples ATP utilization with its generation by glycolysis in intact muscle. *J Biol Chem* 270: 7311-7319.
- Zeleznikar RJ, Heyman RA, Graeff RM, Walseth TE, Dawis SM, et al. 1990. Evidence for compartmentalized adenylate kinase catalysis serving a high-energy phosphoryl transfer function in rat skeletal muscle. *J Biol Chem* 265: 300-311.
- Zingman LV, Alekseev AE, Bienengraeber M, Hodgson D, Karger AB, et al. 2001. Signaling in channel/enzyme multimers: ATPase transitions in SUR module gate ATP-sensitive K^+ conductance. *Neuron* 31: 233-245.
- Zingman LV, Hodgson DM, Bast PH, Kane GC, Perez-Terzic C, 2002a. Kir6.2 is required for adaptation to stress. *Proc Natl Acad Sci USA* 99: 13278-13283.
- Zingman LV, Hodgson DM, Bienengraeber M, Karger AB, Kathmann EC, et al. 2002b. Tandem function of nucleotide-binding domains confers competence to sulfonylurea receptor in gating ATP-sensitive K^+ channels. *J Biol Chem* 277: 14206-14210.
- Zong H, Ren JM, Young LH, Pypaert M, Mu J, et al. 2002. AMP kinase is required for mitochondrial biogenesis in skeletal muscle in response to chronic energy deprivation. *Proc Natl Acad Sci USA* 99: 15983-15987.

6.4 Mitochondrial Permeability Transition in the CNS—Composition, Regulation, and Pathophysiological Relevance

T. Wieloch · G. Mattiasson · M. J. Hansson · E. Elmér

1	Introduction	668
2	Historical Overview	668
3	Proteomics of MPT	669
3.1	Adenine Nucleotide Translocase	671
3.2	Voltage-Dependent Anion Channel	672
3.3	Cyclophilin D	672
3.4	Mitochondrial Creatine Kinase	673
3.5	The Peripheral Benzodiazepine Receptor	674
3.6	Bcl-2 Family of Proteins	674
3.7	The Hypothetical Permeability Transition Pore	674
4	Regulation of MPT	675
4.1	Methods for MPT Analysis in Isolated Mitochondria	675
4.2	Calcium Ions	677
4.3	Adenine Nucleotides and Inorganic Phosphate	678
4.4	Extramitochondrial and Intramitochondrial pH	678
4.5	Inner Membrane Potential	679
4.6	Oxidants and the Mitochondrial Redox State	679
4.7	Free Fatty Acids	680
4.8	Pharmacological (Nonendogenous) Regulators of the MPT	681
5	Pathophysiological Importance of MPT	681
5.1	Glutamate Toxicity	685
5.2	Acute Brain Injury	685
5.3	Chronic Neurodegenerative Disease	688
5.4	Astrocytic Dysfunction	688
6	Physiological Relevance of MPT	689

Abstract: Mitochondrial permeability transition (MPT) is induced in isolated brain mitochondria by calcium and oxidants and is inhibited by adenine nucleotides. When induced, MPT is associated with equilibration of solutes of <1500 Da across the inner mitochondrial membrane. A persistent induction of MPT depolarizes the inner membrane and causes cessation of ATP synthesis, swelling of the matrix, and bursting of the mitochondrial membranes. The rupture of the membranes releases calcium stored in the mitochondrial matrix and apoptogenic factors from the intermembrane space, leading to cell death. MPT has been implicated in acute brain injury and neurodegenerative disease since inhibitors of MPT such as cyclosporin A (CsA) are brain protective. Whether MPT has a physiological role is unclear, but MPT may be important in calcium homeostasis under conditions of excessive neuronal activity.

1 Introduction

The mitochondrion is an organelle involved in multiple cellular functions in the central nervous system (CNS), including energy production, regulation of ion homeostasis, and cell death. The integrity of its inner and outer membranes is of central importance for these functions. The protonmotive force formed across the inner mitochondrial membrane during the oxidation of substrates by the electron transport chain (ETC) enzymes drives the generation of ATP and in particular the maintenance of cellular calcium homeostasis. This is not only of importance for normal cellular function but also for cell survival since loss of neuronal ATP and calcium homeostasis will lead to cellular catabolism, calcium toxicity, and eventually to cell death. Also, the integrity of the outer membrane of mitochondria, though permeable for low-molecular weight solutes, is of importance for life and death decisions, since it harbors molecules that may activate programmed cell death, apoptosis.

In this chapter, we present current views of a particular property of mitochondria, the mitochondrial permeability transition (MPT), with special reference to the CNS. The MPT is characterized by a sudden increase in mitochondrial inner membrane permeability preferentially induced by elevated intramitochondrial calcium levels and oxidative stress. This leads to the opening of a membrane pore, which allows solutes of approximately 1500 Da to be equilibrated, causing mitochondrial membrane potential to dissipate, and inhibition of ATP synthesis. It also allows water to enter the mitochondrial matrix, leading to mitochondrial swelling due to the colloidal osmotic pressure exerted by the high protein content of the mitochondrial matrix. If swelling is extensive, the outer membrane ruptures and proteins are released from the intermembrane spaces, causing cell demise (apoptosis). While the involvement of MPT in the pathological processes is evident (Crompton and Costi, 1988; Kim et al., 2003; Green and Kroemer, 2004; Dubinsky, 2005; Halestrap, 2005; Spierings et al., 2005; Bernardi et al., 2006), its physiological role is unclear (Gunter and Pfeiffer, 1990; Bernardi and Petronilli, 1996; Ichas and Mazat, 1998).

We start this chapter with a historical overview, since many fundamental discoveries that led to the characterization of the MPT were made in the late 1940s and early 1950s. Also, because the story of MPT is a beautiful example of how persistent research of a biological phenomenon, which was by many considered to be an *in vitro* artifact, has led to the discovery of an important factor involved in disease. We then describe the molecular entities of MPT and how the MPT is regulated in brain mitochondria, and finally we discuss the involvement of MPT in CNS disease and injury as well as its possible physiological role.

2 Historical Overview

Mitochondrial swelling, a hallmark of MPT induction, was earlier associated with inhibition of oxidative phosphorylation and mitochondrial calcium uptake. Calcium was found to be a potent inhibitor of mitochondrial oxidative ATP formation (Potter, 1947; Lehninger, 1949), and chelation of calcium ions with EDTA prevented mitochondrial swelling (Slater and Cleland, 1953; Hunter and Ford, 1955). The fact that the swelling was not readily reversible and was associated with loss of ATP required for critical cellular

functions indicated that there was no obvious physiological role of the calcium-induced swelling process. In fact, in order to obtain preparations of viable mitochondria for functional studies, swelling was considered an artifact induced during mitochondrial preparation that should be avoided by addition of EDTA. Still, a series of detailed studies by Haworth and Hunter established the concept of MPT. Calcium was found to trigger structural changes of the mitochondria (swelling) by increasing the permeability of the inner mitochondrial membrane (Hunter et al., 1976), concomitant with the release of solutes of approximately 1000 Da from the mitochondria (Haworth and Hunter, 1979). In the search for trigger sites of the MPT, ADP, NADH, magnesium, and hydrogen ions were identified as inhibitors of calcium-induced MPT (Hunter and Haworth, 1979a). Furthermore, while bongkrekic acid and ADP inhibited MPT, atractyloside was found to be an activator, strongly linking the adenine nucleotide translocase (ANT) to the phenomenon of MPT (Hunter and Haworth, 1979b). Since fatty acids also induced swelling of mitochondria and inhibited oxidative phosphorylation, an alternative explanation for MPT was provided, suggesting that PLA2 activated by calcium influx increased mitochondrial permeability by generating lysophospholipids and fatty acids (Pfeiffer et al., 1979). Subsequent studies increased the list of modulators of the MPT, including local anesthetics and calcium or calmodulin antagonists (for review, see Gunter and Pfeiffer (1990)).

Concurrently with the findings of the calcium dependence of MPT and the toxicity of calcium overload in heart (Leder et al., 1969), liver (Schanne et al., 1979), and brain (Siesjo, 1981), ischemia was recognized, which led to the proposal that MPT may be involved in reperfusion injury following ischemic damage to tissues (Al-Nasser and Crompton, 1986).

While investigating the toxic effect of the immunosuppressant CsA on isolated mitochondria, Fournier and coworkers found that the compound inhibited calcium efflux from mitochondria and allowed excessive uptake of calcium ions into the matrix (Fournier et al., 1987). Crompton and coworkers followed up on this finding and demonstrated that CsA is a strong inhibitor of calcium-induced MPT in heart mitochondria in the presence of inorganic phosphate (P_i) or during oxidative conditions, and suggested that MPT may have a detrimental function during the reoxygenation phase following ischemia that could be prevented by inhibitors of the MPT such as CsA (Crompton et al., 1988). Still, CsA inhibited calcium-dependent MPT without affecting PLA2 activity (Broekemeier et al., 1989) suggesting that MPT may be activated either by a CsA-sensitive or by a CsA-insensitive pathway (Broekemeier and Pfeiffer, 1989). Halestrap and coworkers demonstrated that cyclophilin D (CypD), a cyclophilin specific for the mitochondrial matrix (Connern and Halestrap, 1992), induced the MPT at high calcium concentrations by binding to ANT, and that CsA prevents calcium-induced MPT by inhibiting the binding of CypD to ANT (Halestrap and Davidson, 1990). The MPT was also studied in mitoplasts and had characteristics of a giant ion channel with conductance of 1.3 nS (Petronilli et al., 1989) and a pore size of 3 nm, which allowed solutes of <1500 Da to equilibrate, and this was inhibited by CsA (Szabo and Zoratti, 1991).

Whether MPT fulfills a physiological function is still an enigma (Gunter and Pfeiffer, 1990; Bernardi et al., 2006). The robust protection attained by CsA in *in vitro* and *in vivo* models of lethal cell stress in liver (Broekemeier et al., 1992; Imberti et al., 1992; Kass et al., 1992; Snyder et al., 1992), heart (Duchen et al., 1993; Griffiths and Halestrap, 1995), and brain (Shiga et al., 1992; Uchino et al., 1995) strongly implied the MPT in pathological processes. In 1995, Zamzami and coworkers demonstrated that mitochondrial membrane depolarization preceded apoptosis *in vivo* and *in vitro* and that MPT could be inhibited by Bcl-2 (Zamzami et al., 1995a, b). The fact that bongkrekic acid and CsA also inhibited apoptosis implied the involvement of MPT in apoptosis (Zamzami et al., 1996).

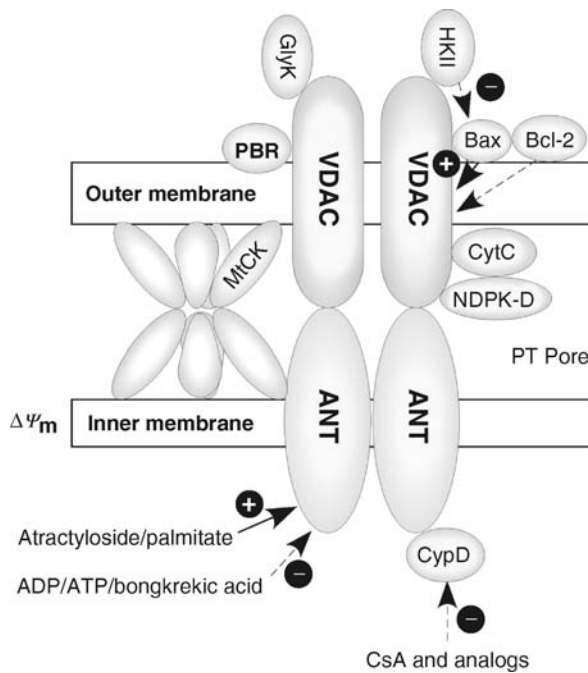
3 Proteomics of MPT

The MPT is thought to be accomplished through a dynamic multiprotein complex, a permeability transition pore (PTP), located at the contact site between the inner and outer mitochondrial membranes, a site of metabolic coordination between the mitochondrial matrix, the intermembrane space, and the cytosol (Knoll and Brdiczka, 1983; Adams et al., 1989; Halestrap et al., 2000; Halestrap and Brennerb, 2003; Palmieri, 2004; Brdiczka et al., 2006).

Despite detailed functional characterization, the exact composition of the molecular components that induce MPT is still elusive. However, the prevalent hypothesis is that the PTP involves proteins from the outer membrane (voltage-dependent anion channel (VDAC or porin), the peripheral benzodiazepine receptor (PBR)), the inner membrane (ANT), and the matrix (CypD) (Halestrap and Davidson, 1990; Zoratti and Szabo, 1995; Halestrap et al., 1997a, b; Crompton et al., 1998; Marzo et al., 1998b; Crompton, 1999; Crompton et al., 1999; Halestrap, 1999; Crompton et al., 2002; Halestrap and Brennerb, 2003; Verrier et al., 2003) (● Figure 6.4-1). In support of this hypothesis, it has been shown that pharmacological agents that target VDAC, ANT (in particular atractylate and bongkreic acid), or CypD (in particular CsA) can

■ Figure 6.4-1

The mitochondrial permeability transition pore (PTP) depicting the inner and outer mitochondrial membranes with the PTP core components: the adenine nucleotide translocase (ANT), the voltage-dependent anion channel (VDAC), and cyclophilin D (CypD). Other proteins thought to modulate mitochondrial permeability transition are octameric mitochondrial creatine kinase (MtCK), mitochondrial nucleoside diphosphate kinase D (NDPK-D), cytochrome c (CytC), hexokinase (HKII), glycerol kinase (GlyK), the peripheral benzodiazepine receptor (PBR), and pro- and antiapoptotic members of the Bcl-2 family (Bax and Bcl-2, respectively). Activators (atractyloside, palmitate) and inhibitors (ADP/ATP/ bongkreic acid) of ANT as well as inhibitors of CypD (CsA and analogs) are depicted



stimulate or inhibit MPT induction in isolated mitochondria *in vitro* (Cesura et al., 2003; Halestrap and Brennerb 2003; Waldmeier et al., 2003) as well as *in vivo* (Friberg et al., 1998). It is often assumed that outer and inner membrane pore components associate at “contact sites,” which are enriched in ANT and VDAC, forming a PTP through interaction with other proteins (Beutner et al., 1996; Beutner et al., 1998). Analysis of the protein content of such contact sites in brain mitochondria has revealed the presence of ANT, VDAC, hexokinase, and CypD (Beutner et al., 1996; Beutner et al., 1998). When reconstituted into liposomes or artificial membranes, these proteins formed channels similar to the PTP (Beutner et al., 1996; Beutner et al., 1998). However, the same investigators also found that PTP-like pores could be formed in protein fractions

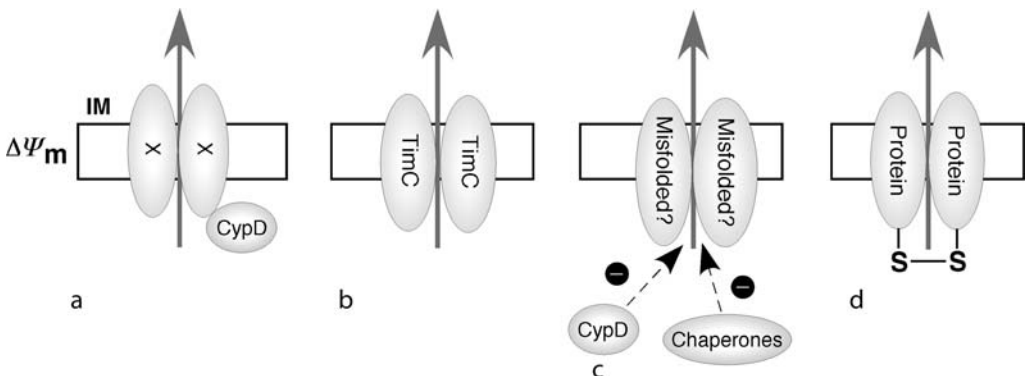
that lacked VDAC or ANT (Beutner et al., 1996), suggesting that both ANT and VDAC are possible, but not necessary components of the PTP in the brain. These findings are supported by recent findings in genetically modified mice, implicating that ANT (Kokoszka et al., 2004) and CypD (Baines et al., 2005; Basso et al., 2005; Nakagawa et al., 2005; Schinzel et al., 2005) are modulatory, rather than obligatory, for MPT. Similar studies for the VDAC isoforms are so far inconclusive (see Sect. 4.2). Still, it is likely that the core PTP components are responsible for the MPT under pathophysiological conditions (Halestrap, 2005).

3.1 Adenine Nucleotide Translocase

ANT is an antiporter that transfers adenine nucleotides (ADP/ATP) between the cytoplasm and the mitochondrial matrix. The ADP/ATP-binding site of ANT is either on the matrix (m-state) or on the cytoplasmic (c-state) side of the inner membrane. The ANT may be deformed by calcium ions into a nonselective pore when it is in the c-state, a process catalyzed by CypD. Several other ligands that modulate ANT and MPT activation also affect ANT conformation. For example, atractylate stabilizes ANT in the c-state and promotes MPT, while bongkreikic acid stabilizes it in the m-state and inhibits MPT (Schultheiss and Klingenberg, 1984). The strong regulatory role of ANT on MPT activation led to the suggestion that the PTP could be formed by ANT (Halestrap and Brennerb, 2003). This suggestion is supported by the findings that purified ANT can be induced to form calcium-sensitive high-conductance pores in artificial membranes (Brustovetsky and Klingenberg, 1996; Brenner et al., 2000; Brustovetsky et al., 2002b) and that ANT-induced pore formation may involve a specific conformational change and/or oligomerization to varying degrees in muscle, heart, liver, kidney, and brain mitochondria (Faustin et al., 2004). In addition, over-expression of some ANT isoforms (human ANT1 and 3 but not ANT2) can induce cell death in cultured cells (Bauer et al., 1999; Zamora et al., 2004) while transfection-enforced expression of CypD can inhibit cell death induced by ANT1 in cultured cells (Bauer et al., 1999; Lin and Lechleiter, 2002; Schubert and Grimm, 2004). The protective effect of CypD in this context may be due to its isomerase activity which overcomes the apoptogenic effects of misfolded ANT1 protein (🔗 Figure 6.4-2).

■ Figure 6.4-2

Hypothetical drawings of MPT-based mechanisms for permeabilization of the inner mitochondrial membrane (IM). (a) The “classical” mitochondrial permeability transition pore (PTP), comprised of protein complexes in the inner membrane, typically the ANT. Since ANT is a common but not necessary pore component, the components have been named “X” to reflect that ANT can be replaced by other proteins such as UCPCs, transporters, or transmembrane proteins. Opening of the inner membrane complex in this model is stimulated by binding of cyclophilin D (CypD). (b) Membrane permeabilization by complexes of proteins involved in mitochondrial protein import complex (TimC). (c) Membrane permeabilization by complexes of misfolded membrane proteins. (d) Membrane permeabilization by crosslinking of inner membrane proteins



The involvement of the ANT in MPT and the role of the MPT in apoptotic processes was investigated by Kokoszka and coworkers (2004), who used genetically modified mice where the genes encoding the two isoforms of the ANT (ANT1 and ANT2) were selectively eliminated in the liver. Somewhat surprisingly, ANT-deficient and control mitochondria were able to undergo a calcium-dependent, CsA-inhibitable permeability transition. This demonstrated that the ANT is not required for induction of MPT and that ANT is not the only binding partner of CypD. As expected, the absence of the ANT resulted in the selective loss of MPT regulation by ANT ligands such as atractyloside and ADP. These findings suggest that low (undetectable) levels of ANT could not explain the induction of MPT observed, but rather that other mitochondrial components induced MPT. Further, MPT was also induced by oxidative stress, demonstrating that ANT is not the (only) site of oxidative induction of PTP in mouse liver mitochondria (Armstrong, 2006). The MPT in ANT-deficient mitochondria required three-fold higher levels of calcium ions for activation when compared with control mitochondria. One interpretation of these data is that ANT, being the most abundant inner mitochondrial membrane protein, is a main modulator of MPT, yet if absent can be substituted by other components in the induction of MPT (Kokoszka et al., 2004).

3.2 Voltage-Dependent Anion Channel

It has been suggested that MPT is dependent on the interaction between the inner and outer membranes, since MPT did not occur in mitoplasts (only inner membrane) (Le-Quoc and Le-Quoc, 1985). The identity of outer membrane proteins that may associate with ANT to form a PTP was investigated using gel chromatography with immobilized ANT. The result of these studies identified VDAC as a potential partner of ANT in heart (Crompton et al., 1998; Woodfield et al., 1998) and brain mitochondria (Beutner et al., 1996; Beutner et al., 1998). Similar results have also been obtained using coimmunoprecipitation with VDAC in brain, heart, and liver mitochondria, although these experiments found several potential partners of ANT besides VDAC, including endoplasmic reticulum (ER) proteins (Verrier et al., 2004). VDAC may be incorporated into artificial membranes to form pores with electrophysiological properties similar to those of MPT (Szabo et al., 1993; Szabo and Zoratti, 1993). The activity of such channels is modulated in fashions similar to those of the MPT (Costantini et al., 1996; Fontaine et al., 1998a; Pastorino and Hoek, 2003), i.e., by NADH, calcium, and glutamate (Zizi et al., 1994; Gincel et al., 2001; Gincel and Shoshan-Barmatz, 2004), and by binding of hexokinase (Pastorino et al., 2002; Majewski et al., 2004b; Pastorino et al., 2005). The evidence for involvement of VDAC in MPT is thus mostly indirect, and definite proof using knockout studies *in vivo* is hard to obtain since VDAC is expressed in three isoforms (VDAC1–3) (Blachly-Dyson and Forte, 2001), all with channel-forming ability (Xu et al., 1999). VDAC1 or -3 knockout mice are viable (Sampson et al., 2001), while knocking out VDAC2 is lethal before birth (Cheng et al., 2003). Using VDAC1 (–/–) mice, it was recently suggested that VDAC1 is not necessary for MPT in isolated liver mitochondria (Krauskopf et al., 2006). Alternate strategies to block all VDAC activity and to obtain conclusive evidence of its role in MPT *in vivo* are needed.

3.3 Cyclophilin D

CypD has peptidylprolyl *cis-trans* isomerase activity and is thought to facilitate a calcium-triggered conformational change in the ANT, converting it to an “open” pore configuration. Furthermore, CypD appears to exert a regulatory function and is the putative target for CsA inhibition of pore activity (Halestrap and Davidson, 1990) by binding *in vitro* to complexes of the VDAC and the ANT. Although the role of the ANT remains unclear (Bernardi et al., 2001; Waldmeier et al., 2003; Halestrap, 2004; Kokoszka et al., 2004), recent work using mice lacking CypD (CypD knockout mice) defined the role of CypD beyond doubt in liver (Baines et al., 2005; Basso et al., 2005; Nakagawa et al., 2005; Schinzel et al., 2005), fibroblasts (Baines et al., 2005; Schinzel et al., 2005), heart (Baines et al., 2005; Nakagawa et al., 2005), and brain (Baines et al., 2005; Schinzel et al., 2005). These animals appear to have a normal phenotype, and

the investigators found that mitochondria from mice lacking CypD no longer responded to CsA treatment following calcium challenge. However, the MPT can still be induced in isolated liver mitochondria, though at much higher calcium concentrations, i.e., at similar calcium levels as in normal mitochondria treated with CsA (Basso et al., 2005). These results demonstrate that the role of CypD is to facilitate a conformational change that can occur in the absence of CypD, if the stimulus (calcium and oxidative stress) is strong enough, and imply CsA as a “desensitizer” rather than a blocker of the MPT.

3.4 Mitochondrial Creatine Kinase

Although speculative, a core PTP complex composed of ANT, VDAC, and CypD can be envisaged (▶ [Figure 6.4-1](#)) that interacts with optional proteins (Crompton, 2000; Crompton et al., 2002). This has been demonstrated in kidney mitochondria for kinases that preferentially use mitochondrial ATP in the intermembrane space such as mitochondrial creatine kinase (MtCK) or mitochondrial nucleoside diphosphate kinase D (Milon et al., 2000). In brain mitochondria, hexokinase and glycerol kinase can interact with the PTP at the cytosolic side of VDAC (Beutner et al., 1996). Also, CypD at the matrix side of ANT in liver mitochondria (McGuinness et al., 1990; Woodfield et al., 1998), cytochrome *c* (CytC) at the intermembrane side of VDAC in kidney mitochondria (Mannella, 1998; Vyssokikh et al., 2004), the PBR in the brain (Jorda et al., 2005), and members of the Bcl-2 family (Green and Kroemer, 2004) are additional proteins that can interact with the core proteins and regulate the MPT (McEnery et al., 1992; Zoratti and Szabo, 1995; Jorda et al., 2005).

The composition and function of the contact site complexes are controversial, but they have been suggested to participate in the transfer of metabolites and in regulation of cellular energy utilization and apoptosis. Moreover, results from several model systems suggest that these complexes may also allow cross talk between apoptotic signaling and metabolism, where apoptosis is controlled by metabolic state and vice versa (Gottlob et al., 2001; Bryson et al., 2002; Pastorino et al., 2002; Azoulay-Zohar et al., 2004; Green and Kroemer, 2004; Majewski et al., 2004a; Vyssokikh et al., 2004). An involvement of MtCK in MPT and mitochondrial ultrastructure has been demonstrated in liver mitochondria isolated either from transgenic mice that overexpress MtCK (Miller et al., 1997) or from wild-type animals that lack MtCK (O’Gorman et al., 1997; Dolder et al., 2003). These experiments clearly show that MtCK, in complexes with ANT and together with its substrates, is able to delay or even prevent calcium-induced MPT (Dolder et al., 2001). It is not the presence of MtCK per se that inhibits MPT, but more precisely its enzymatic activity and its correct localization in mitochondrial complexes. MtCK exists as dimers or octamers, and the octameric complexes are the structural basis for the functional coupling of MtCK with ATP transport, and also promote formation of “contact sites” between the outer and inner mitochondrial membranes (Speer et al., 2005). No effect on MPT is observed if the enzyme is not supplied with its appropriate substrates or if it is only added externally to mitochondria that lack endogenous MtCK (Dolder et al., 2003). This can be explained by the functional coupling of octameric MtCK to ANT (▶ [Figure 6.4-1](#)), which is stabilized when MtCK is provided with substrate (particularly creatine). However, administration of creatine had no significant effect on MPT in isolated brain mitochondria or in brain mitochondria isolated from rats fed with creatine (Brustovetsky et al., 2001). Still, creatine was neuroprotective in MtCK knockout animals (Klivenyi et al., 2004). This suggests that the protective effect of creatine is not mediated by the direct effect of MtCK complexes on MPT, but rather that MtCK maintains energy levels (PCr and ATP) within the cell, as well as a high ADP concentration in the mitochondrial matrix, which in turn is known to effectively inhibit MPT (O’Gorman et al., 1997; Dolder et al., 2001; Dolder et al., 2003). Thus, MtCK could play the role of an energy sensor, coupling cellular energy state to programmed cell death. A similar mechanism may apply for the antiapoptotic effect of hexokinase (Gottlob et al., 2001; Bryson et al., 2002; Pastorino et al., 2002; Azoulay-Zohar et al., 2004; Majewski et al., 2004a), which is located at the cytosolic side of VDAC or VDAC/ANT complexes in brain mitochondria (Beutner et al., 1996), and which also preferentially uses mitochondrial ATP. Hexokinase has also been suggested to be antiapoptotic by inhibiting binding of Bax to VDAC (Vyssokikh et al., 2004).

3.5 The Peripheral Benzodiazepine Receptor

The PBR is located in the outer mitochondrial membrane (Anholt et al., 1986). It is found at varying levels in several tissues and is highly expressed e.g., in cells producing steroid hormones where it promotes the transport of cholesterol into the mitochondrial matrix (Papadopoulos et al., 1997) as well as in cardiac myocytes. Cholesterol in the mitochondrial inner membrane has been suggested to alter membrane fluidity, thereby impairing ANT-mediated MPT in liver mitochondria (Colell et al., 2003). The PBR binds to VDAC and the ANT in kidney mitochondria (McEnery, 1992) and has been suggested to affect MPT in heart mitochondria (Kinnally et al., 1993). The effect of PBR on MPT seems to be dependent on cell- or tissue type, and both stimulation and inhibition of MPT have been reported (Bono et al., 1999; Berson et al., 2001; Chelli et al., 2001). In isolated rat forebrain mitochondria, MPT, mitochondrial swelling, and release of CytC was inhibited by ligands of the PBR (Parker et al., 2002). Thus, PBR may be part of the pore complex, but owing to the lack of PBR-specific drugs in combination with the fact that PBR knockout leads to embryonic lethality (Papadopoulos et al., 1997) it is presently difficult to establish if PBR has a critical role in MPT.

3.6 Bcl-2 Family of Proteins

The proapoptotic Bcl-2 family members, e.g., Bax, Bak, Bad, Bim, and Bid can induce release of apoptogenic factors by oligomerization in the mitochondrial membrane (Spierings et al., 2005; Garrido et al., 2006). This effect is counteracted by the antiapoptotic Bcl-2 family members. It has been suggested that Bax and Bak may associate with VDAC (for review, see Crompton, (2003)), and induce mitochondrial depolarization in a calcium-dependent, CsA-inhibitable fashion. This would indicate that Bax- and Bak-induced mitochondrial changes may be mediated through a mechanism similar to MPT in liposomes (Marzo et al., 1998a; Brenner et al., 2000), liver mitochondria (Narita et al., 1998; Pastorino et al., 1999), and cultured cells (Pastorino et al., 1998). However, since calcium-induced MPT can occur efficiently in liver cells deficient in Bax/Bak (Scorrano et al., 2002), Bax/Bak do not seem to have a critical function, but rather a modulatory function in the activation of MPT. In brain mitochondria, release of CytC can be induced by Bid in combination with Bak or Bax, possibly involving VDAC in a mechanism that is not inhibited by CsA (Brustovetsky et al., 2003b; Brustovetsky et al., 2005b). Still, it is possible that the PTP through cristae remodeling acts in concert with the proapoptotic Bcl-2 family members to release CytC (Scorrano et al., 2002). Also tBid may act independently on mitochondria through reorganization of cardiolipin in the inner mitochondrial membrane, thereby affecting the activity of the ANT (Gonzalez et al., 2005). The literature on the role of the proapoptotic Bcl-2 family members in the induction of cell death is complex, and results from different model systems are often conflicting. It seems clear that proapoptotic members may induce release of apoptogenic proteins from mitochondria independently of MPT, but that they sometimes may act in concert with components of, or with the PTP complex (🔗 [Figure 6.4-1](#)), to modulate its activity. The role of Bax and Bak in MPT in the brain is thus unclear and has recently been reviewed elsewhere (Jemmerson et al., 2005).

3.7 The Hypothetical Permeability Transition Pore

The prevailing hypothesis of MPT is that it is induced by opening of a pore composed of proteins from both the inner and outer mitochondrial membranes. The emerging conclusion is that MPT should be regarded as a phenomenon that can be accomplished using the “classical core components” ANT, VDAC, and CypD, although none of these components appear to be critical for MPT to occur. Rather, several or all of the “core components” may be replaced by other, largely unidentified, components that may associate to form the PTP in a dynamic interplay (🔗 [Figure 6.4-2a](#)). Such alternative MPT-inducing pore proteins could be of the mitochondrial carrier family e.g., the uncoupling proteins (UCPs) (Gonzalez-Barroso et al., 1997) or the bimembrane spanning mitochondrial protein transport system Tom/Tim or SAM50 (🔗 [Figure 6.4-2b](#))

(Newmeyer and Ferguson-Miller, 2003; Paschen et al., 2003; Pfanner et al., 2004; Wiedemann et al., 2004; Zoratti et al., 2005). Also, it is conceivable that permeability pores can be formed by aggregation of misfolded (🔗 [Figure 6.4-2c](#)) or crosslinked integral membrane proteins, (🔗 [Figure 6.4-2d](#)), and that chaperone-like proteins (such as CypD) initially block conductance through these misfolded protein clusters (Kowaltowski et al., 2001; He and Lemasters, 2002; Armstrong, 2006). The presence of recruited proteins in the PTP may be optional and depends on tissue and cell type as well as the circumstances under which the mitochondrial PTP is formed. Hence, variation in the features of MPT are obvious, and the underlying molecular entity for MPT still elusive.

4 Regulation of MPT

4.1 Methods for MPT Analysis in Isolated Mitochondria

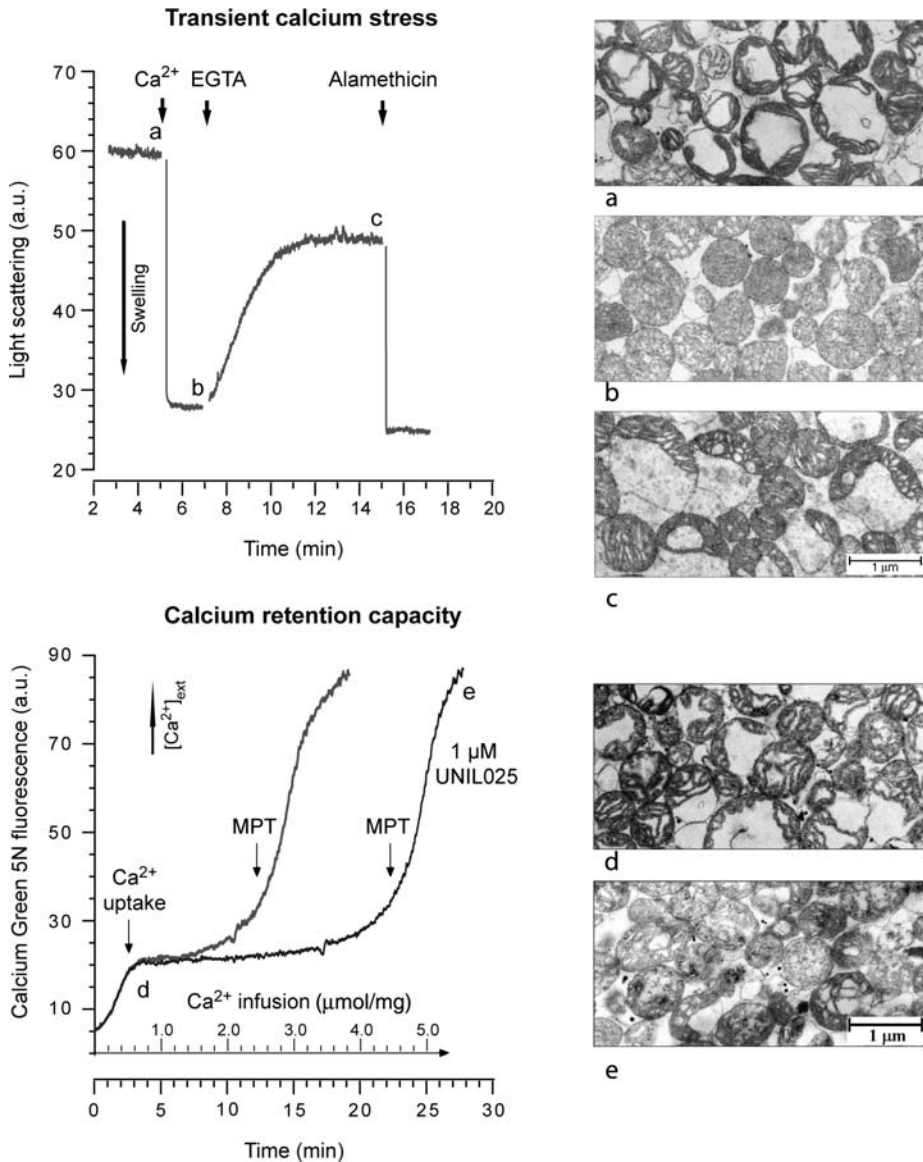
MPT is an all-or-none phenomenon at the single mitochondrial level (Haworth and Hunter, 1979), but a population of mitochondria *in vitro* will undergo MPT at a rate and extent depending on the prevailing experimental conditions. The process of MPT in a studied population is therefore not always instantaneous since there are subtle differences in resistance to MPT induction among mitochondria. Notably, a slow rate of MPT will reflect a change in the distribution of permeabilized to nonpermeabilized mitochondria, rather than gradual MPT in the entire mitochondrial population (Gunter and Pfeiffer, 1990).

Numerous studies on the regulation of MPT in isolated mitochondria have been conducted over the last 50 years (for extensive review see Gunter and Pfeiffer (1990); Zoratti and Szabo (1995); Bernardi (1999); Crompton (1999)) using experimental conditions where mitochondria are either energized (with mitochondrial substrates present in the reaction mixture) or de-energized, two experimental paradigms that provide complementary information. For studies of extra- and intramitochondrial regulators of the MPT as well as pharmacological modulators of MPT, nonrespiring (de-energized) mitochondria are often employed in which a defined free matrix calcium concentration can be set. The absence of mitochondrial substrates and inhibition of the respiratory chain prevent the formation of a membrane potential and hence prevents calcium uptake into the matrix, and by addition of a calcium ionophore, equilibration of calcium ions across the inner mitochondrial membrane is facilitated (Hunter and Haworth, 1979b; Halestrap and Davidson, 1990; Bernardi, 1992). Energized, respiring mitochondria are preferentially used for studying the dynamics of MPT induction, for example, the conductance states of MPT or MPT induction in relation to changes in membrane potential, calcium movements, or generation of free radicals (Zoratti and Szabo, 1995; Ichas et al., 1997).

The MPT can readily be studied by different physicochemical methods. In energized mitochondria, the free permeability to protons during MPT will result in uncoupling of oxidative phosphorylation, which can be monitored using oxygen-sensitive electrodes in airtight chambers. Also, positively charged fluorescent probes or ions such as TPP⁺ accumulate electrophoretically into the matrix according to the magnitude of the inner membrane potential and can be utilized to monitor changes in the membrane potential. The increased permeability causes a structural change and swelling, which can be detected in both de-energized and energized mitochondria by light absorbance/transmission or 90° light scattering, reflecting the turbidity of mitochondria in suspension. The decrease in light scattering has been tightly correlated to the proportion of mitochondria undergoing a structural change (Hunter and Haworth, 1979b). Electrophysiological examination of mitoplasts with patch-clamp can also be employed to study permeability of the inner mitochondrial membrane, and the MPT has been closely correlated to high conductance states around 1 nS (Kinnally et al., 1989; Petronilli et al., 1989). Further, the redox status of pyridine nucleotides is rapidly changed upon permeabilization and can be monitored by the autofluorescence of NADH. Finally, the capacity of mitochondria to take up and buffer extramitochondrial loads of calcium can be followed by nonpermeable calcium-sensitive fluorescent probes. Examples of MPT assays are illustrated in 🔗 [Figure 6.4-3](#). Importantly, changes in oxygen consumption, membrane potential, morphology (swelling), and alterations in the mitochondrial redox state can occur independently of MPT. Therefore, a single parameter or assay may not be sufficient evidence of permeability transition.

■ Figure 6.4-3

Induction of permeability transition in isolated brain mitochondria by calcium. Mitochondria are suspended in KCl-based buffer at 37°C (125 mM KCl, 20 mM Trizma base, 2 mM P_i , 1 mM $MgCl_2$, pH 7.2) oxidizing NADH-linked substrates. *Top graph displays changes in light scattering, reflecting mitochondrial morphology. Calcium administration induces a rapid decrease in light scattering indicative of mitochondrial swelling. Chelation of calcium by EGTA reverses the mitochondrial swelling to a large extent. Lower graph depicts changes in fluorescence of the extramitochondrial Ca^{2+} -sensitive probe Calcium Green 5N upon a continuous infusion of calcium to the media. In the presence of 200 μM ADP, mitochondria take up and retain calcium to a threshold at which permeability transition (MPT) is induced. The calcium retention capacity (CRC) is increased by the cyclophilin D inhibitor *N*-methyl-D-alanine³-*N*-ethyl-valine⁴-cyclosporin-A (UNIL025). (a–e) The electron micrographs display the ultrastructural appearances of mitochondria at the respective experimental conditions*



Brain mitochondria have been suggested to exhibit unique MPT characteristics. Their relative ability to undergo MPT is currently debated, and the regulation and pharmacological modulation of brain MPT have been shown to differ from that of other commonly studied mitochondria. In the following sections, MPT regulation in isolated mitochondria in general and in brain mitochondria in particular is reviewed.

4.2 Calcium Ions

Mitochondrial calcium overload is the prime trigger for MPT. Calcium ions move electrophoretically into the mitochondrial matrix through the calcium uniporter and the efflux (in liver and brain mitochondria) occurs by the $\text{Na}^+/\text{Ca}^{2+}$ and Na^+/H^+ antiporters in the inner membrane (Crompton et al., 1977; Crompton and Heid, 1978). The calcium uptake is driven by the proton electrochemical gradient (protonmotive force) (≈ 180 mV) (Δp), which consists of an inner membrane potential ($\Delta\Psi_m$) (≈ 150 mV) and a pH gradient of -0.5 units (matrix alkaline). The protonmotive force drives the ATP synthesis of mitochondria, while the $\Delta\Psi_m$ determines the rate of calcium uptake (Nicholls and Ward, 2000). At physiological levels of phosphate, mitochondria accumulate calcium and extrude one proton per calcium ion, leading to matrix alkalinization and formation of calcium complexes, supposedly $\text{Ca}_3(\text{PO}_4)_2$ (Lehninger et al., 1967; Chalmers and Nicholls, 2003), thereby strictly regulating intramitochondrial free calcium. Hence, the intramitochondrial pH will determine the total amount of calcium that can be sequestered prior to MPT (Chalmers and Nicholls, 2003; Nicholls and Chalmers, 2004). It is currently unknown what determines the calcium set point for triggering MPT, but it is likely determined by the amount of accumulated intramitochondrial calcium and available MPT regulators.

The mechanism for calcium-activated MPT is largely unknown, but two alternative mechanisms have been suggested. Calcium ions bind to ANT at a site on the matrix side of the protein, inducing a conformational change and pore formation (Halestrap, 2006), or bind to negatively charged cardiolipin at the inner leaflet of the inner membrane, which destabilizes the ANT–cardiolipin interactions, which are essential for normal ANT function and gating (Hoffmann et al., 1994; Crompton, 2003). The effect of calcium is competitively counteracted by several divalent cations such as Mg^{2+} , Sr^{2+} , and Mn^{2+} (Haworth and Hunter, 1979; Bernardi et al., 1992).

Regulation of calcium-induced MPT in brain mitochondria under de-energized conditions is similar to that of heart and liver mitochondria (Friberg et al., 1999; Hansson et al., 2003), while under energized conditions, differences have been reported. Brain mitochondrial MPT has been shown to exhibit dual responses to calcium challenge, exhibiting membrane depolarization with or without appreciable mitochondrial swelling (Brustovetsky and Dubinsky, 2000). Several reports demonstrate that, in contrast to liver mitochondria, only a subpopulation of energized brain mitochondria undergo calcium-induced MPT (Andreyev et al., 1998; Berman et al., 2000; Kristian et al., 2002; Kobayashi et al., 2003). This suggests the presence of distinct subpopulations of brain mitochondria, and that some of the mitochondrial populations originate from different cell types or brain regions and are resistant to MPT (Kristian et al., 2002). Other reports have not found evidence for subpopulations of energized mitochondria resistant to calcium-induced MPT (Hansson et al., 2004a), similar to what is seen in liver mitochondria. Several factors could contribute to these discrepancies. Mitochondria isolated from brain tissue are derived from a heterogeneous mixture of glial and neuronal origins, and differences in MPT sensitivity have been demonstrated between nonsynaptic and synaptic mitochondria (Brown et al., 2006), astrocytic and neuronal mitochondria (Bambrick et al., 2006), and between mitochondria derived from different regions within the CNS (Friberg et al., 1999; Mattiasson et al., 2003; Brustovetsky et al., 2003a). Isolation protocols for brain mitochondria are not uniform and usually differ from those historically used in studies of liver and heart mitochondria. Methodological aspects of MPT detection may also influence the experimental outcome. For example, monitoring structural changes and swelling with the light absorbance assay generally results in a lower response following calcium-induced MPT in brain mitochondria (Berman et al., 2000; Brustovetsky et al., 2002a) compared with detection by 90° light scattering (Hansson et al., 2004a). A lower maximal swelling response in brain mitochondria compared with liver mitochondria, which is often interpreted as an apparent relative inability to swell, could be explained by different

physical properties (e.g., size, density). On the other hand, liver and brain mitochondria respond similarly with respect to changes in membrane potential, NAD(P)H redox status and calcium retention capacity (CRC), detected using functional MPT assays (Chalmers and Nicholls, 2003; Panov et al., 2004). However, brain mitochondria have been proposed to sequester more insoluble forms of calcium phosphates than liver mitochondria, possibly explaining the reduced sensitivity to calcium under certain conditions (Panov et al., 2004). In brain mitochondria as well as in mitochondria from other tissues, calcium-induced MPT is rapidly reversible upon calcium chelation by EGTA (Hunter et al., 1976; Petronilli et al., 1994b; Hansson et al., 2004a). The reversal of MPT is also followed by a morphological recovery provided that the duration of MPT is not extensive (● [Figure 6.4-3](#)).

4.3 Adenine Nucleotides and Inorganic Phosphate

The adenine nucleotides ADP and ATP are potent inhibitors of MPT induction, whereas nucleotides not transported by ANT have no effect on MPT (Hunter and Haworth, 1979b; Zoratti and Szabo, 1995; Halestrap et al., 1998; Bernardi, 1999; Crompton, 1999). Also, in isolated brain mitochondria and in a system reconstituting MPT, both ADP and ATP are potent inhibitors of MPT (Nicholls and Scott, 1980; Beutner et al., 1998; Kristian et al., 2002; Chinopoulos et al., 2003; Robertson et al., 2004). Likewise, ATP and in particular ADP, but not AMP, cAMP, GTP, GDP, cGDP, GMP, cGMP, ITP, IDP and adenosine, increased brain mitochondrial CRC (Rottenberg and Marbach, 1990).

ADP is considered the most potent adenine nucleotide inhibitor of MPT with two ANT-binding sites, one of which is located on the matrix side (Hunter and Haworth, 1979b; Halestrap et al., 1998). The physiological concentration of free ADP in the neuronal cytoplasm is 10–100 μM (Veech et al., 1979; Erecinska and Silver, 1989), the concentration range within which ADP inhibition of brain MPT is most dynamic (Rottenberg and Marbach, 1990). Brain mitochondria, in contrast to liver mitochondria, are also resistant to MPT induction by calcium in the presence of physiological concentrations of ATP (Andreyev et al., 1998).

P_i is an inducer of MPT that acts in concert with calcium ions. High levels of P_i potentiate calcium-induced swelling in de-energized and energized mitochondria from various tissues, including the brain (Azzi and Azzone, 1965; Crompton and Costi, 1988; Zoratti and Szabo, 1995; Kristal and Dubinsky, 1997; Sims and Anderson, 2002). The mechanisms for the sensitization of MPT by P_i are largely unknown. High concentrations of P_i may influence matrix pH, hydrogen peroxide production, and free magnesium ion levels (Jung et al., 1990; Zoratti and Szabo, 1995; Kowaltowski et al., 1996) and may reduce matrix ATP/ADP content, thereby promoting MPT (Lapidus and Sokolove, 1994). The capacity of isolated brain mitochondria to accumulate calcium before the induction of MPT decreases by about 50% when extramitochondrial P_i increases from 2 mM (the levels of P_i in brain tissue) to 5 mM (concentrations readily attained during ischemia) (Chalmers and Nicholls, 2003). However, P_i is obligatory for maintaining free low calcium levels in the mitochondrial matrix by forming calcium phosphate complexes (Lehninger et al., 1967; Chalmers and Nicholls, 2003).

4.4 Extramitochondrial and Intramitochondrial pH

Low external pH protects against spontaneous swelling of mitochondria in vitro (Raaflaub, 1953) and lowering pH under controlled de-energized conditions decreases the probability of MPT induction (Haworth and Hunter, 1979, 1980). In liver and heart mitochondria, the rate of MPT induction (in de-energized conditions) at pH 6.0 is less than 10% of that at pH 7.4 (Halestrap, 1991). In addition, MPT induced by the thiol-oxidizing agent phenylarsine oxide in de-energized liver mitochondria is prevented below pH 7.0 (Bernardi, 1992). The pH sensitivity of MPT induction appears to be due to reversible protonation of histidyl residues on protein components on the matrix side of the inner membrane (Nicolli et al., 1993). Alternatively, protons act on calcium-binding sites on the inner membrane, similarly as seen for divalent cations (Haworth and Hunter, 1979; Haworth and Hunter, 1980; Halestrap, 1991).

In de-energized brain mitochondria, the influence of pH on calcium-activated MPT is similar to that observed in liver and heart mitochondria. MPT is inhibited at $\text{pH} < 7.0$ and facilitated during alkalosis ($\text{pH} 7.5$)

(Friberg et al., 1999). In isolated energized mitochondria from brain, liver, and heart energized by either complex I- or complex II-linked substrates, acidic pH promotes rather than inhibits calcium-induced MPT activation (Kristian et al., 2001). This effect has been attributed to an increased rate of phosphate transport, overriding the preventive effect of protons on MPT seen under de-energized conditions (Kristian et al., 2001). Importantly, acidification of the matrix compartment will decrease the solubility of stored calcium phosphates (Nicholls and Chalmers, 2004). For $\text{Ca}_3(\text{PO}_4)_2$, a change in 0.5 pH units would destabilize the complex and increase the level of free calcium from about 2 μM to 100 μM (Nicholls and Chalmers, 2004), increasing the probability of MPT.

4.5 Inner Membrane Potential

The driving force for mitochondrial uptake of calcium through the uniporter is mainly determined by the inner membrane potential ($\Delta\Psi_m$), produced by the ETC or by reversal of the ATP synthase at the expense of ATP. It has been suggested that a high membrane potential tends to stabilize the components of MPT in the closed conformation (Bernardi, 1992), mediated through a putative voltage-sensor translating both the transmembrane potential and the mitochondrial surface potential into MPT induction (Petronilli et al., 1993b). Also, it has been proposed that proteins involved in MPT contain a potential-sensitive component, e.g., critical arginine residues (Johans et al., 2005). The fraction of mitochondria undergoing MPT increases with increasing depolarization, attained by uncoupling agents, but varies depending on the presence of inducers or inhibitors of the MPT (Petronilli et al., 1993a). Isolated mitochondria not preloaded with calcium and mitochondria studied *in situ* in cell cultures do not respond with immediate MPT activation when exposed to uncouplers (Nieminen et al., 1995), whereas other studies have suggested a calcium-independent MPT induced by depolarization (Scorrano et al., 1997; Minamikawa et al., 1999).

The sensitivity of MPT to uncoupling agents could be related to alteration in the balance of endogenous inhibitors and inducers of the MPT or to the intramitochondrial acidification resulting from an increased proton conductance (Nicholls and Chalmers, 2004). Depolarization can lower NADPH/NADP and GSH/GSSG ratios making the mitochondria vulnerable to oxidative stress, particularly thiol oxidation, which could influence the threshold for MPT induction. It is also possible that ANT has a membrane potential sensor (Halestrap et al., 1998).

Many of the compounds stimulating calcium-induced MPT such as heavy metals, arsenate, fatty acids, pesticides, quinones, and sulfhydryl reagents are likely to affect MPT indirectly by acting on one or several PTP regulators, such as the membrane potential, the intramitochondrial pH, or the level of oxidative stress, thus changing the threshold of MPT induction (Petronilli et al., 1993a).

4.6 Oxidants and the Mitochondrial Redox State

Besides calcium, oxidative stress is considered to be an important trigger of MPT *in vitro* and *in vivo* (Zoratti and Szabo, 1995; Bernardi, 1999; Crompton, 1999). Peroxides are effective inducers of MPT in combination with calcium in isolated liver and heart mitochondria (Beatrice et al., 1982; Crompton and Costi, 1988; Novgorodov et al., 1992; Kushnareva and Sokolove, 2000). Peroxides oxidize the GSH pool, and subsequently the pyridine nucleotide pool (Crompton, 1999). The redox state of the pyridine nucleotides NADH/NAD or NADPH/NADP greatly influences the probability of MPT (Hunter and Haworth, 1979b), by their equilibration with protein thiol groups of the inner mitochondrial membrane. Under normal conditions, the highly reduced state of intramitochondrial glutathione maintains the dithiols of proteins in a reduced state. Oxidative stress may facilitate MPT by inducing oxidation of vicinal thiols, cross-linking dithiols to disulfides on components of the MPT pore (Fagian et al., 1990; Petronilli et al., 1994a; Armstrong, 2006). The sulfhydryl group reagents arsenite, phenylarsine oxide, and diamide mimic the effect of peroxides in inducing MPT in liver and heart mitochondria (Hunter et al., 1976; Novgorodov et al., 1990; Petronilli et al., 1994a). The modulation of MPT by oxidation of dithiols is likely in equilibrium with the glutathione redox state but is separate from the direct effect of pyridine nucleotide redox state on MPT

probability (Chernyak and Bernardi, 1996; Costantini et al., 1996). Protein thiol cross-linking may also induce MPT in the absence of calcium ions (Bernardi, 1992; Gadelha et al., 1997). In addition, the antioxidants catalase and dithiothreitol can reduce calcium and P_i -induced MPT (Kowaltowski et al., 1996).

The ANT contains thiol groups at cysteine residues, which are sensitive to oxidation by sulfhydryl reagents. These cysteine residues are within the ADP-binding site on ANT, and thiol oxidation decreases the ability of ADP to prevent MPT suggesting that oxidative stress may promote MPT by affecting nucleotide binding to ANT (Halestrap et al., 1997b; McStay et al., 2002). Studies of isolated ANT has demonstrated that its activity is dependent on closely associated cardiolipin (Hoffmann et al., 1994). Cardiolipin contains a relatively high proportion of polyunsaturated fatty acids, which makes it sensitive to damage by reactive oxygen species. Oxidative stress with lipid peroxidation may therefore sensitize ANT to pore formation by destabilizing its interaction with cardiolipin (Brustovetsky and Klingenberg, 1996; Grijalba et al., 1999; Crompton, 2003). However, mitochondria from ANT knockout mice are still sensitized to calcium-induced MPT by oxidative stress (Kokoszka et al., 2004).

Evidence of oxidative stress-induced MPT in brain mitochondria is limited and the results differ somewhat from those obtained in other tissues. While 30 μ M phenylarsine oxide increased the rate of swelling in de-energized brain mitochondria (Friberg et al., 1999), and can induce swelling independent of calcium in energized brain mitochondria (Kristian et al., 2001), 25 μ M had only minor effects on swelling in another study (Kristal and Dubinsky, 1997). *tert*-butyl hydroperoxide (up to 750 μ M) had no effect on calcium-induced swelling (Kristal and Dubinsky, 1997). As demonstrated in liver mitochondria, catalase reduces calcium-induced MPT also in brain mitochondria (Maciel et al., 2001). Oxidative stress induced by inhibitors of the respiratory complexes sensitize brain mitochondria to MPT induction (Maciel et al., 2004). Interestingly, brain mitochondria from rotenone-treated animals display an increased sensitivity to calcium-induced MPT even in the absence of the complex I inhibitor itself, implicating oxidative damage to the ETC (Panov et al., 2005).

4.7 Free Fatty Acids

Calcium-induced MPT is modulated by fatty acids and lysophospholipids, generated from phospholipids degraded by the mitochondrial calcium-activated PLA2 (Pfeiffer et al., 1979; Gadd et al., 2006). Indeed, fatty acids generated endogenously in isolated mitochondria or externally added induce large amplitude swelling in mitochondria (Lehninger and Remmert, 1959; Wojtczak and Lehninger, 1961; Lehninger, 1962). The swelling-inducing potency of fatty acids is dependent on the carbon chain length (e.g., saturated fatty acids of 12–16 carbon atoms length are particularly active) as well as the level of unsaturation, and correlates to their ability to disrupt energy coupling processes (Lardy and Pressman, 1956; Zborowski and Wojtczak, 1963). Fatty acids induce MPT (Petronilli et al., 1993b; Broekemeier and Pfeiffer, 1995; Scorrano et al., 2001), which is partially reversed by CsA (Brustovetsky et al., 1993; Starkov et al., 1994; Amerkhanov et al., 1996; Wojtczak et al., 1998; Scorrano et al., 2001). The induction of MPT is accomplished by the flipping of protonated fatty acids across the inner mitochondrial membrane bilayer, causing acidification of the mitochondrial matrix by proton release from protonated fatty acids to the alkaline matrix (uncoupling). Fatty acids that promote mitochondrial swelling also inhibit ANT and cause matrix acidification (Wojtczak et al., 1998). The swelling induced by these fatty acids, with the exception of phytanic acid, is largely inhibited by CsA (Wojtczak et al., 1998).

The relative potency of a wide range of fatty acids has been screened and compared with respect to MPT induction and uncoupling (Scorrano et al., 2001; Penzo et al., 2002). In contrast to previous studies (Zborowski and Wojtczak, 1963; Wojtczak et al., 1998), MPT induction was not strongly influenced by chain length or unsaturation, with the exception of C20 fatty acids, e.g., arachidonic acid, that induced MPT.

The MPT-inducing effect of fatty acids has been explained by their protonophoric activity with acidification of the mitochondrial matrix and dissipation of the membrane potential. Alternatively, long-chain fatty acids bind to ANT with high affinity (Schonfeld and Bohnensack, 1997) and mimic the effect of ANT activators such as carboxyatractyloside (Halestrap and Davidson, 1990; Novgorodov et al., 1994). In favor of the latter mechanism is the finding that fatty acids promote induction of MPT in an

ANT-reconstituted system, where transmembrane potential is absent (Wieckowski et al., 2000). Furthermore, synthetic protonophores, used in concentrations with a comparable uncoupling effect to that of fatty acids do not open the PTP (Wieckowski and Wojtczak, 1998; Di Paola et al., 2006).

4.8 Pharmacological (Nonendogenous) Regulators of the MPT

What defines and what are the minimal requirements of an MPT inhibitor? Compounds that interfere with respiration and membrane potential can prevent the mitochondrial uptake of calcium by reducing the electrophoretic driving force for calcium uptake. If an uncoupling agent is administered to calcium-loaded energized mitochondria, MPT is rapidly triggered. However, if an uncoupler is added before calcium is added, MPT is prevented by the reduced mitochondrial uptake of calcium. Uncouplers and ruthenium red (an inhibitor of the calcium uniporter), which prevent calcium uptake and thereby MPT, are not generally regarded as MPT inhibitors.

The swelling assays used to monitor MPT *in vitro* will not differentiate between prevention of calcium uptake (by an uncoupler) and inhibition of MPT related to intramitochondrial overload of calcium (by CypD inhibitors). Therefore, the minimal requirements for an MPT-inhibitor should include effects in additional functional assays like increased mitochondrial CRC and protection against depolarization.

With such a definition, minocycline would not be classified as an inhibitor of MPT in isolated mitochondria. Minocycline inhibits calcium-induced mitochondrial swelling (Zhu et al., 2002), but at the same time induces mitochondrial membrane depolarization and inhibits respiration, which obviously results in a decreased calcium uptake and prevention of MPT induction (Zhu et al., 2002; Cornet et al., 2004; Fernandez-Gomez et al., 2005).

Putative MPT inhibitors with relevance to brain disease are listed in [Table 6.4-1](#). The selection of compounds was based on two criteria: (1) the compounds have been evaluated as MPT blockers in assays with brain-derived mitochondria and (2) the compounds have been studied *in vivo* in acute or chronic models of brain disease, and confirmed to be inhibitors of MPT in mitochondria from other tissues than the brain.

5 Pathophysiological Importance of MPT

From experiments essentially performed during the last 10 years, a general scheme of two main mitochondria-induced cell death pathways can be outlined. One cascade encompasses apoptosis or programmed cell death activated by intricate cell-signaling cascades normally present but depressed in the cell, or initiated by particular gene programs. Apoptosis is dependent on selective mitochondrial outer membrane permeabilization caused by translocation and oligomerization of proapoptotic members of the Bcl-2 family of proteins such as Bax, on the outer leaflet of the outer mitochondrial membrane (Polster and Fiskum, 2004; Spierings et al., 2005; Garrido et al., 2006). The outer membrane permeabilization is also regulated by the antiapoptotic Bcl-2 family of proteins, including Bcl-2 and upstream cell-signaling events. Bax oligomerization is thought to form a pore or to cause irregularities in the outer mitochondrial membrane that allows release of proteins residing in the intermitochondrial space, including the regulators of apoptosis execution, e.g., CytC, Omi, and Smac. CytC activates downstream processes that ultimately result in the irreversible degradation of key cell structural and regulatory proteins, DNA fragmentation, and cell demise.

Alternatively, cell death involves activation of MPT by the factors outlined above, including elevated intracellular levels of calcium ions and oxidative stress, causing mitochondrial inner membrane permeability, swelling, and expansion of the matrix, thus leading to outer membrane permeabilization by bursting of the outer mitochondrial membrane. If MPT is persistently induced, the accompanying membrane depolarization will lead to loss of ATP formation. The subsequent inhibition of plasma membrane function will cause elevated cytosolic calcium levels. Mitochondrial calcium and glutathione are released upon MPT, thus decreasing the defense against oxidative stress. Cytosolic calcium overload will activate degradative enzymes that together with oxidative damage to proteins, lipids, and DNA will lead to cellular swelling and

Table 6.4-1
Putative inhibitors of permeability transition in brain mitochondria

Compound	Mitochondrial target	Ca ²⁺ retention capacity	Uncoupling or respiratory inhibition	Inhibition of swelling	Inhibition of depolarization	Protective in vivo	References
2-APB		+	Yes	Yes	Yes		Chinopoulos et al. (2003)
BBMP			(No)	(Yes)	(Yes)		Fuks et al. (2005)
Bongkrekic acid	ANT	+		Yes			Chinopoulos et al. (2003); Kristian (2004)
Chlorpromazine				(Yes)		Spinal cord ischemia	Zivin et al. (1989); Stavrovskaya et al. (2004)
Clomipramine			(No)	(Yes)	(Yes)	Global ischemia	Nakata et al. (1992); Stavrovskaya et al. (2004)
Clozapine				(Yes)		Excitotoxicity	Stavrovskaya et al. (2004)
CsA	CypD	+	No	Yes	Yes	Global ischemia, MCAO, trauma, ALS	Uchino et al. (1995); Butcher et al. (1997); Uchino et al. (1998); Yoshimoto and Siesjo (1999); Sullivan et al. (2000); Bai et al. (2001); Keep et al. (2001); Hansson et al. (2003); Okonkwo et al. (2003); Hansson et al. (2004a)
Deprenyl	Antioxidant		No	Yes			Czerniczyniec et al. (2006)
Desipramine				(Yes)			Stavrovskaya et al. (2004); Palmer et al. (1992)
Dibucaine	Lipids (?), PLA2	+			Yes		Hoyt et al. (1997); Panov et al. (2004)
Doxepin				(Yes)			Stavrovskaya et al. (2004)
MeAla ³ EtVal ⁴ -CsA (UNIL025)	CypD	+		Yes			Hansson et al. (2004b)
Melle ⁴ -CsA (NIM811)	CypD			Yes			Hansson et al. (2004b); Rytter et al. (2005)
Melatonin	Antioxidant		No		Yes	MCAO	Andrabi et al. (2004); Sousa and Castilho (2005)
MeVal ⁴ -CyA	CypD			Yes		MCAO	Khaspekov et al. (1999); Matsumoto et al. (1999)

Mianserin			(Yes)			Global ischemia	Karasawa et al. (1992); Stavrovskaya et al. (2004)
Minocycline	—	Yes	Yes	No		Global ischemia, MCAO, trauma, ALS, HD, PD	Yrijanheikki et al. (1998, 1999); Chen et al. (2000); Bai et al. (2001); Sanchez Mejia et al. (2001); Arvin et al. (2002); Zhu et al. (2002); Cornet et al. (2004); Teng et al. (2004); Fernandez-Gomez et al. (2005)
Monobromobimane		(No)	Yes	(Yes)		Global ischemia	Costantini et al. (1995); Abe et al. (2004)
Phosphocreatine/creatine	Thiol groups		Yes	Yes		HD, ALS, PD	Matthews et al. (1998); Klivenyi et al. (1999); Chen et al. (2000); Brustovetsky et al. (2001); Klivenyi et al. (2004)
Polyamines	Creatine kinase (?), high-energy phosphates Ca ²⁺ transport (?)	(No)	(Yes)			MCAO	Lapidus and Sokolove (1994); Coert et al. (2000); Clarkson et al. (2004); Salvi and Toninello (2004)
Promethazine	Complex 1 (?)	No	Yes	Yes		MCAO, PD	Stavrovskaya et al. (2004); Cleren et al. (2005)
Propofol			Yes			MCAO	Adembri et al. (2006)
Quinacrine	PLA2		(Yes)			MCAO	Estevez and Phillis (1997); Stavrovskaya et al. (2004)
Ro 68-3400	+	No	Yes	Yes			Cesura et al. (2003); Krauskopf et al. (2006)
Tamoxifen/hydroxytamoxifen	Antioxidant	Yes	Yes	Yes		MCAO	Kimelberg et al. (2000); Moreira et al. (2004); Moreira et al. (2005)
Trifluoperazine	PLA2	(No)	(Yes)	Yes		MCAO, spinal cord ischemia	Zivin et al. (1989); Hoyt et al. (1997); Kuroda et al. (2004); Fuks et al. (2005)
Ubiquinone O	ETC (?)	(Yes)	Yes	Yes			Fontaine et al. (1998b); Kristian et al. (2000); Fuks et al. (2005)

(Yes)/(No)—Evaluated in liver mitochondria

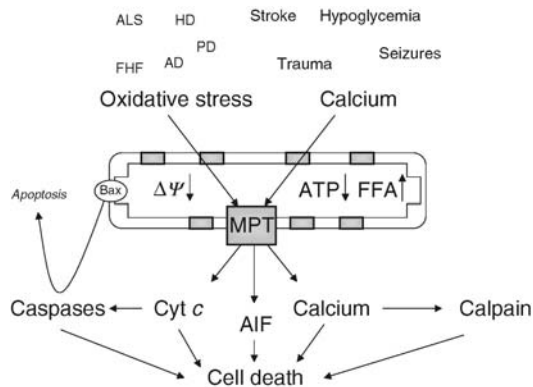
ALS, amyotrophic lateral sclerosis; 2-APB, 2-aminoethoxydiphenyl borate; BBMP, 5-(benzylsulfonyl)-4-bromo-2-methyl-3(2H)-pyridazinone; CypD, Cyclophilin D; CsA, Cyclosporin-A; ETC, electron transport chain; HD, Huntington's disease; MCAO, middle cerebral artery occlusion; PD, Parkinson's disease; PLA2, phospholipase A2; VDAC, voltage-dependent anion channel

dissolution, a process denoted as necrosis. Concomitant with outer membrane permeabilization, proteins such as apoptosis-inducing factor (AIF) are released from the intermembrane space of the mitochondria. AIF is a large protein bound to the outer membrane leaflet of the inner mitochondrial membrane that can be released by limited proteolysis by calpain I, either by a calpain present in the intermembrane space or by cytosolic calpain entering an outer mitochondrial membrane permeabilized by tBid (Polster and Fiskum, 2004). Calcium-activated calpain I will cleave and release AIF from the outer leaflet of the inner mitochondrial membrane, and subsequently AIF translocates to the nucleus and degrades DNA. The opening of the outer membrane will also release CytC, and provided that some ATP formation remains in the cell, the downstream caspase cascade can be activated. Hence, MPT activation leading to obvious necrotic cell morphology will have components of the apoptosis cascade activated. Therefore, depending on the detrimental agents involved, the severity of the insults or disease, and the cell types affected, the resulting morphological features of cell demise in the CNS may be unique (Martin et al., 1998). It appears more purposeful to define cell death by the particular underlying biochemical events leading to cell demise, rather than by semantic/morphological events (apoptosis and necrosis) (Deshpande et al., 1992; Colbourne et al., 1999). Hence, we will refrain from classifying particular disease states as caused either due to apoptosis or due to necrosis.

From a vast literature reviewed below, it is evident that MPT is involved in cell death in the brain following acute brain damage and intoxications (stroke, brain, trauma, hypoglycemic and hepatic encephalopathy) and during neurodegenerative disease such as amyotrophic lateral sclerosis, Alzheimer's disease, Huntington's disease, and Parkinson's disease (Figure 6.4-4). It has to be stressed though that cell death

Figure 6.4-4

During acute brain injury (stroke, hypoglycemia, trauma, and epilepsy) and neurodegenerative diseases such as amyotrophic lateral sclerosis (ALS), Alzheimer's disease (AD), Huntington's disease (HD), Parkinson's disease (PD), and fulminant hepatic failure the mitochondrial permeability transition (MPT) may be induced. This could lead to cell death due to ATP depletion, release of stored mitochondrial calcium ions, and release of proteins that activate factors involved in apoptosis. The induction of MPT is enhanced by elevated cytosolic calcium ions, secondary to enhanced receptor/calcium channel activation, decreased transport of calcium ions out of cells or to leaky cell membranes due to unfolded proteins (synuclein, amyloid), or aberrant covalent modifications of membrane components (oxidation, phosphorylation, hydrolysis). MPT may also be induced by oxidative stress due to an uncoupled electron transport chain (hypoxia, free fatty acids (FFA)), formation of reactive nitrogen species, or loss of antioxidants such as glutathione



following acute brain injury and neurodegenerative disease is complex and involves multiple factors that act in series or in parallel. A particular factor, such as MPT, is therefore essential in the cell death process within a distinct defined time window and a particular density (intensity) of an insult.

5.1 Glutamate Toxicity

Glutamate toxicity is one of several mechanisms implicated in acute and chronic neurodegeneration (Choi, 1988; Dirnagl et al., 1999), and involves activation of AMPA and NMDA receptors, sometimes with subsequent activation of voltage-dependent calcium channels. This leads to elevated intracellular calcium levels that, if persistent, will cause mitochondrial calcium overload, oxidative stress, and cell death (Starkov et al., 2004). In isolated cortical and hippocampal neurons, overactivation of NMDA receptors leads to a biphasic cellular calcium response. An initial rapid rise in intracellular calcium concentration to a new steady-state level is followed by a delayed (30 min–2 h) calcium deregulation with another steep rise in calcium levels (Nicholls and Budd, 1998). This late deregulation occurs concomitantly with mitochondrial membrane depolarization (Isaev et al., 1996; Schinder et al., 1996; White and Reynolds, 1996; Alano et al., 2002). In some studies, CsA progressively delays mitochondrial depolarization in a concentration-dependent manner (Nieminen et al., 1996; White and Reynolds, 1996; Alano et al., 2002) and is neuroprotective (Schinder et al., 1996). Neuronal calcium overload causes mitochondrial swelling mitigated by CsA (Dubinsky and Levi, 1998). Glutamate toxicity is accompanied by CytC release and caspase-3 activation that is inhibited by CsA and the NMDA receptor blocker MK801 (Brustovetsky et al., 2002a) and by release of AIF (Cregan et al., 2002; Wang et al., 2004), which can partially be a consequence of calcium-induced MPT induction as outlined above. Using CsA solely to inhibit MPT and cell death in cell cultures or brain tissue is insufficient to unequivocally imply the MPT in the cell death process, since CsA also inhibits calcineurin-regulated pathways. For example, under certain conditions, both CsA and FK506 protect against NMDA toxicity in primary cortical cultures, implying calcineurin in the cell death process since both FK506 and CsA inhibit calcineurin (Dawson et al., 1993). On the other hand, if CsA but not FK506 is cell protective it is more likely that the protective action of CsA is through inhibition of the MPT (Friberg et al., 1998). Hence, in seizure-prone FVB/N mice, kainate-induced damage in the hippocampus was ameliorated by treatment with CsA but not with FK506, implying MPT in seizure-induced damage (Santos and Schauwecker, 2003). A better option is to use a more selective MPT inhibitor that does not suppress calcineurin activity, such as a wide range of CsA derivatives (Bernardi et al., 1994; Waldmeier et al., 2003; Hansson et al., 2004b) or compounds unrelated to CsA (Clarke et al., 2002). For example, Alano and coworkers found that neurons treated with the cyclosporin derivative *N*-methyl-4-valine-cyclosporin (MeVal⁴-CsA) delayed cellular calcium deregulation induced by NMDA (Alano et al., 2002). Also, if MPT is transiently induced (Ichas and Mazat, 1998; Halestrap, 2005), deoxyglucose may enter the mitochondria and become trapped upon pore closure (Griffiths and Halestrap, 1995). In a model of excitotoxicity *in vivo*, NMDA was injected into the striatum and deoxyglucose was administered intravenously, and trapped in mitochondria isolated 12 h but not 8 h after the injection, a clear demonstration that MPT is induced following NMDA receptor activation (Zaidan et al., 2004). However, CsA did not protect against damage due to quinolinate injections into the striatum (Sousa et al., 2003). Suffice to say, activation of MPT during glutamate toxicity (or other neurodegenerative conditions) is one out of several mechanisms that act in concert. For example, nitric oxide-induced death of cortical neurons is accompanied by mitochondrial depolarization, and while CsA prevented the depolarization, it was not protective (Solenski et al., 2003).

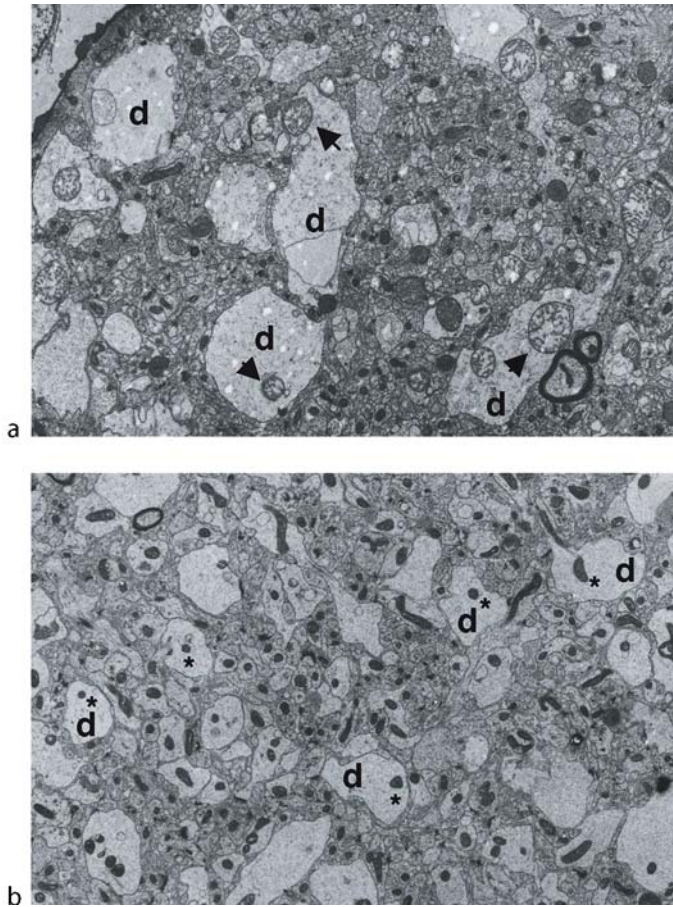
5.2 Acute Brain Injury

During severe ischemia and hypoglycemia that causes brain damage, oxygen and glucose levels decrease to an extent that oxidative phosphorylation cannot be maintained and ATP is hydrolyzed, causing P_i to accumulate. The lack of ATP will inhibit plasma membrane ion pumps, cellular calcium homeostasis will collapse, and calcium will be taken up by mitochondria, promoting MPT. Also, free fatty acid levels increase and this could enhance induction of MPT. The dentate gyrus of the hippocampus is particularly vulnerable in models of insulin-induced hypoglycemia, and the damage is partially excitotoxic (Auer et al., 1984; Wieloch, 1985). Following hypoglycemic coma, cell death develops during a period of 3–6 h, in cortex, hippocampus, and striatum. Damage in the dentate gyrus is prevented by CsA, but not by FK506 (Friberg et al.,

1998). On the ultrastructural level, mitochondria in granule cell dendrites swell markedly during hypoglycemic coma, concomitant with mitochondrial swelling, indicative of excitotoxic damage (Figure 6.4-5). In these animals, calpain and caspase-3 are activated, AIF translocated to the nucleus, and DNA is fragmented

■ **Figure 6.4-5**

Electron micrographs of the outer dendritic layer of dentate gyrus of anesthetized and artificially ventilated rats subjected to insulin-induced hypoglycemic coma for 30 min (Friberg et al., 1998) and treated with (a) vehicle and (b) CsA. Swollen dendrites are denoted (d) and arrows depict swollen mitochondria, while stars denote compact mitochondria. Note the swollen mitochondria and dendrites in vehicle-treated animals and the compact mitochondria and swollen dendrites in CsA-treated animals



(Ferrand-Drake et al., 2003). In contrast, in CsA-treated animals, condensed mitochondria are found within swollen dendrites, suggestive of membrane depolarization that allows calcium ions to enter the dendrite without causing cell death. Also, calpain activation and AIF translocation is not evident in CsA-treated animals. Hence, hypoglycemic damage in the granule cells displays all characteristics of MPT-mediated cell death. This includes mitochondrial calcium overload with mitochondrial swelling and rupture of the outer mitochondrial membrane. The elevated cellular calcium activates calpain that cleaves AIF bound to the inner mitochondrial membrane and translocates AIF to the nucleus, inducing DNA fragmentation and cell degeneration. CsA prevents all these events, strongly implying MPT in cell death.

In experimental models of brain ischemia, the detrimental processes involved are complicated, multiple, and differentially activated in time and space (Dirnagl et al., 1999). Similarly to hypoglycemia, excitotoxicity, cellular calcium overload, and oxidative stress are prime initiators of ischemic brain damage. During focal ischemia in rodents, ischemia is graded with a core of dense ischemic tissue around the occluded vessel and with decreasing ischemia around the ischemic core—the penumbra. Likewise, ATP levels are severely compromised in the core and less so in the penumbra. Also, phospholipids are degraded and the free fatty acid levels increased. Hence, cellular conditions are such that MPT may be induced. During reperfusion following stroke, mitochondria are re-energized, more calcium and P_i are taken up, aggravating mitochondrial overload and oxidative stress. Hence, during and immediately following focal ischemia, MPT may be induced. Indeed, both CsA (Shiga et al., 1992; Yoshimoto and Siesjo, 1999; Uchino et al., 2002) and FK506 (Butcher et al., 1997; Uchino et al., 2002) diminish infarct size when given during the first 3 h of reperfusion following transient middle cerebral artery occlusion (MCAO), indicative of a contribution of both MPT and calcineurin in the cell death process. More important, treatment with MeVal⁴-CsA is equally effective as CsA, demonstrating the induction and importance of MPT in experimental stroke and its potential as a future neuroprotective agent (Matsumoto et al., 1999). Also, in brain slices exposed to oxygen glucose deprivation, cell death is readily prevented by CsA and the nonimmunosuppressive CsA analog MeIle⁴-CsA, while FK506 is ineffective (Rytter et al., 2005). Likewise, in neuronal cultures CsA and MeVal⁴-CsA protected against OGD (Khaspekov et al., 1999). Subjecting CypD knockout mice (Basso et al., 2005; Nakagawa et al., 2005; Schinzel et al., 2005) to experimental stroke unequivocally demonstrated the involvement of the MPT in stroke. Hence, these mice had smaller infarct volume following transient MCAO, corroborating findings in heart and liver ischemia (Schinzel et al., 2005). Interestingly, Bax-dependent apoptosis was not affected by deletion of CypD (Nakagawa et al., 2005). This suggests that the observed TUNEL staining and the activation of the apoptosome and caspase-3 in the penumbra (Endres et al., 1998; Fink et al., 1998; Schmidt-Kastner et al., 2000) most probably is not due to classical apoptosis mediated by proapoptotic Bcl-2 proteins (Deshpande et al., 1992; Van Lookeren Campagne and Gill, 1996; Colbourne et al., 1999; Wei et al., 2004) but due to outer membrane rupture as a consequence of MPT and subsequent release of CytC and AIF. Since there is some ATP production ongoing in the penumbra, the apoptosome and the caspase-9/3 cascade can be activated.

In models simulating cardiac arrest ischemia, delayed cell death in the CA1 region of the hippocampus is dramatically reduced by CsA treatment initiated before or immediately upon reperfusion (Uchino et al., 1998). The involvement of MPT in delayed cell death is enigmatic since morphological signs of cell death do not appear until 24–72 h of reperfusion (Uchino et al., 1998). Still, CytC is released and AIF is translocated to the nucleus 24–48 h into the reperfusion phase (Cao et al., 2003). Also, no swelling of mitochondria is seen until frank neuronal necrosis appears, i.e., at 24–78 h of reperfusion (Ouyang et al., 1999). It is not clear what factors are activated or released by transient induction of MPT during ischemia and immediately following reperfusion and what factors cause cell death 24–48 h later.

In neonatal hypoxia/ischemia, the mechanisms of cell death differ from adult rodents because of the ongoing development of the nervous system, retaining inducible and constitutive apoptotic cell death programs (Hu et al., 2000; Blomgren and Hagberg, 2006). Hence, in 7-day-old rat pups exposed to transient hypoxia in combination with unilateral occlusion of the common carotid artery for 1 h, CsA did not prevent cell death or mitochondrial swelling (Puka-Sundvall et al., 2001) indicating that CypD-dependent MPT is not a prime inducer of cell death in this setting (Blomgren and Hagberg, 2006).

During brain trauma and spinal cord damage, the physical impact to the CNS tissue will, in addition to the primary injury, cause shear forces that disrupt cell structure and cell–cell interaction in areas remote from the primary lesion. This secondary injury will lead to glutamate toxicity, calcium toxicity, free radical generation, inflammation, loss of trophic support, and delayed cell death (Thompson et al., 2005). The secondary injuries may lead to progression of cell death and tissue damage for up to 1 year after the traumatic event (Smith et al., 1997). Similarly as in ischemia and hypoglycemia, cellular conditions following brain trauma are such that MPT is likely to be induced. Indeed, CsA treatment reduces traumatic brain injury (Buki et al., 1999; Okonkwo and Povlishock, 1999; Singleton et al., 2001; Sullivan et al., 2005) and also reduces cognitive and motor deficits incurred (Alessandri et al., 2002). Treating brain trauma patients with CsA has provided promising results in preliminary clinical trials (Empey et al., 2006; Merenda and Bullock, 2006).

5.3 Chronic Neurodegenerative Disease

Mitochondrial dysfunction has been implicated in hereditary neurodegenerative disease including amyotrophic lateral sclerosis, Huntington's disease, Parkinson's disease, Alzheimer's disease, Friedreich's ataxia, and others. Although the mechanisms of cell death in these conditions are unknown, they are most certainly complex, multiple, and dynamic in nature, and active over a long period. Still, the diseases have in common a defect in mitochondrial enzymes involved in oxidative phosphorylation and in handling free radicals generated by mitochondria (Beal, 1998; Schon and Manfredi, 2003). This could set the stage for MPT induction at some period during the disease process (Dubinsky, 2005) although the evidence is less compelling than what has been demonstrated in models of acute brain damage. For example, the activity of the mitochondrial α -ketoglutarate dehydrogenase complex (KGDHC), a rate-limiting enzyme of the Krebs cycle, is markedly decreased in neurodegenerative conditions. Inhibition of KGDHC with α -keto- β -methyl-n-valeric acid induces CytC release, activates caspase-3, and results in the death of PC12 cells, which is inhibited by CsA (Huang et al., 2003).

Mitochondria from patients with Huntington's disease are defective in complex II/III (Browne et al., 1997). Striatal mitochondria show increased sensitivity to MPT induction compared with cortical mitochondria, which was associated with higher CypD levels and lower sensitivity of MPT to CsA inhibition (Brustovetsky et al., 2003a). The supersensitivity of MPT to calcium in rat striatal mitochondria was seen up to 33 months of age, which implied the MPT as an important factor in Huntington's disease (LaFrance et al., 2005). However, in models of Huntington's disease using genetically modified mice (knockin of polyQ expansions or R2/6 transgenic mice), striatal mitochondria are less sensitive to calcium and MPT induction, probably owing to activation of compensatory mechanisms (Brustovetsky et al., 2005a). Still, in a model of Huntington's disease wherein 3-nitropropionic acid was injected into the striatum of Lewis rats, protection was attained by using CsA (Leventhal et al., 2000).

Mitochondria from the substantia nigra of postmortem brains from patients with Parkinson's disease are deficient in complex I. In a rat model of Parkinson's disease, electron transport was inhibited at complex I in brain mitochondria by long-term systemic infusion of rotenone, which causes increased generation of superoxide anions and hydrogen peroxide by mitochondria (Panov et al., 2005). These mitochondria required 50% less calcium to induce MPT, which could be inhibited by CsA, implying MPT in the pathogenesis of Parkinson's disease.

In a cybrid model of Alzheimer's disease, mitochondria are deficient in complex IV (cytochrome oxidase) and display increased ROS production, as is also seen in mitochondria from tissue from patients with sporadic Alzheimer's disease. The membrane potential of mitochondria from Alzheimer's disease cybrids is reduced, but increases to control levels following CsA treatment (Cassarino et al., 1998, Thiffault and Bennett, 2005). This implies the involvement of MPT in mitochondrial dysfunction and possibly in neurodegeneration in Alzheimer's disease.

In the familiar forms of amyotrophic lateral sclerosis, there is a mutation in the superoxide dismutase 1 (SOD1) gene. In the rat G93A model of ALS, overexpression of the human mutant SOD1 gene affects mitochondrial function in brain and spinal cord very early on in the course of the disease, and also causes major changes in mitochondrial morphology. Treatment of SOD1 mutant mice with CsA increases the survival rate suggesting that MPT may play a role in the pathogenesis of ALS (Keep et al., 2001; Karlsson et al., 2004).

5.4 Astrocytic Dysfunction

Astrocytes play a pivotal role in brain nutrition, development, synaptic plasticity, glutamate homeostasis, blood flow regulation, and as suppliers of trophic factors and antioxidants to CNS cells, thereby promoting neuronal survival (Nedergaard et al., 2003; Bambrick et al., 2004). Hence, dysfunctional or damaged astrocytes may contribute to brain damage by limiting fuel supply to neurons, aggravating glutamate toxicity or decreasing trophic and antioxidant support (Swanson et al., 2004). Astrocytes are sensitive to oxidative stress but less so to calcium toxicity (Robb et al., 1999). As a matter of fact, astrocytes will succumb when depleted of mitochondrial glutathione or when exposed to peroxynitrite (Anderson and

Sims, 2002), cell death likely mediated by MPT since CsA provides protection. Likewise, astrocytic death caused by OGD is prevented by CsA (Reichert et al., 2001; Dugan and Kim-Han, 2004). Astrocytic swelling is responsible for fatal brain edema seen following fulminant hepatic failure and rising serum levels of ammonia, which may partly be attributed to mitochondrial failure due to MPT (Norenberg et al., 2005). In astrocytes in culture, ammonia enhances the formation of ROS and induces MPT, which is completely inhibited by CsA but not by FK506 (Bai et al., 2001; Rama Rao et al., 2003, 2005). Also, CsA enhances mitochondrial calcium uptake capacity in astrocytes (Bambrick et al., 2006).

6 Physiological Relevance of MPT

Mitochondria are important regulators of intracellular calcium homeostasis, and it is therefore reasonable to assume that the opening of PTP under physiological conditions could constitute a cellular calcium homeostatic mechanism. During high neuronal activity, calcium will accumulate in the cytosol and subsequently in mitochondria, and there will be a need for a rapid and efficient release of stored calcium. Transient induction of MPT has been proposed to serve as a mechanism for such fast calcium release (Gunter and Pfeiffer, 1990; Bernardi and Petronilli, 1996; Ichas and Mazat, 1998). Rapid and transient MPT opening, so-called pore flickering, has been demonstrated in isolated mitochondria (Huser and Blatter, 1999) as well as in intact liver cells (Petronilli et al., 1999) and neurons (Gillesen et al., 2002). The rapid calcium release could occur through a low permeability state of the MPT (Ichas and Mazat, 1998), and it has been argued that brief induction of MPT could serve predominantly as a Ca^{2+} release channel despite its apparent lack of specificity (Bernardi and Petronilli, 1996). During release of calcium through transient MPT, a close positioning in the space of the mitochondria to the ER will allow the ER to rapidly sequester the released calcium. The MPT may thus be involved in the mitochondrial shaping and propagation of the intracellular Ca^{2+} signaling (Rutter and Rizzuto, 2000). Still, the fact that CypD knockout mice do not show any phenotype under normal laboratory conditions suggests that MPT may be preferentially activated during conditions of excessive neuronal activity.

Acknowledgments

In this chapter, we have only cited a selection of articles and apologize for any unintentional omissions. The work was supported by the Swedish Research Council (grant nr 8644) and the Swedish Brain Foundation.

References

- Abe T, Takagi N, Nakano M, Takeo S. 2004. The effects of monobromobimane on neuronal cell death in the hippocampus after transient global cerebral ischemia in rats. *Neurosci Lett* 357: 227-231.
- Adams V, Bosch W, Schlegel J, Wallimann T, Brdiczka D. 1989. Further characterization of contact sites from mitochondria of different tissues: Topology of peripheral kinases. *Biochim Biophys Acta* 981: 213-225.
- Adembri C, Venturi L, Tani A, Chiarugi A, Gramigni E, et al. 2006. Neuroprotective effects of propofol in models of cerebral ischemia: Inhibition of mitochondrial swelling as a possible mechanism. *Anesthesiology* 104: 80-89.
- Al-Nasser I, Crompton M. 1986. The reversible Ca^{2+} -induced permeabilization of rat liver mitochondria. *Biochem J* 239: 19-29.
- Alano CC, Beutner G, Dirksen RT, Gross RA, Sheu SS. 2002. Mitochondrial permeability transition and calcium dynamics in striatal neurons upon intense NMDA receptor activation. *J Neurochem* 80: 531-538.
- Alessandri B, Rice AC, Levasseur J, DeFord M, Hamm RJ, et al. 2002. Cyclosporin A improves brain tissue oxygen consumption and learning/memory performance after lateral fluid percussion injury in rats. *J Neurotrauma* 19: 829-841.
- Amerkhanov ZG, Yegorova MV, Markova OV, Mokhova EN. 1996. Carboxyatractylate- and cyclosporin A-sensitive uncoupling in liver mitochondria of ground squirrels during hibernation and arousal. *Biochem Mol Biol Int* 38: 863-870.
- Anderson MF, Sims NR. 2002. The effects of focal ischemia and reperfusion on the glutathione content of

- mitochondria from rat brain subregions. *J Neurochem* 81: 541-549.
- Andrabi SA, Sayeed I, Siemen D, Wolf G, Horn TF. 2004. Direct inhibition of the mitochondrial permeability transition pore: A possible mechanism responsible for antiapoptotic effects of melatonin. *FASEB J* 18: 869-871.
- Andreyev AY, Fahy B, Fiskum G. 1998. Cytochrome *c* release from brain mitochondria is independent of the mitochondrial permeability transition. *FEBS Lett* 439: 373-376.
- Anholt RR, Pedersen PL, De Souza EB, Snyder SH. 1986. The peripheral-type benzodiazepine receptor. Localization to the mitochondrial outer membrane. *J Biol Chem* 261: 576-583.
- Armstrong JS. 2006. Mitochondrial membrane permeabilization: The sine qua non for cell death. *Bioessays* 28: 253-260.
- Arvin KL, Han BH, Du Y, Lin SZ, Paul SM, et al. 2002. Minocycline markedly protects the neonatal brain against hypoxic-ischemic injury. *Ann Neurol* 52: 54-61.
- Auer RN, Wieloch T, Olsson Y, Siesjö BK. 1984. The distribution of hypoglycemic brain damage. *Acta Neuropathol (Berl)* 64: 177-191.
- Azoulay-Zohar H, Israelson A, Abu-Hamad S, Shoshan-Barmatz V. 2004. In self-defence: Hexokinase promotes voltage-dependent anion channel closure and prevents mitochondria-mediated apoptotic cell death. *Biochem J* 377: 347-355.
- Azzi A, Azzone GF. 1965. Swelling and shrinkage phenomena in liver mitochondria. I. Large amplitude swelling induced by inorganic phosphate and by ATP. *Biochim Biophys Acta* 105: 253-264.
- Bai G, Rama Rao KV, Murthy CR, Panickar KS, Jayakumar AR, et al. 2001. Ammonia induces the mitochondrial permeability transition in primary cultures of rat astrocytes. *J Neurosci Res* 66: 981-991.
- Baines CP, Kaiser RA, Purcell NH, Blair NS, Osinska H, et al. 2005. Loss of cyclophilin D reveals a critical role for mitochondrial permeability transition in cell death. *Nature* 434: 658-662.
- Bambrick L, Kristian T, Fiskum G. 2004. Astrocyte mitochondrial mechanisms of ischemic brain injury and neuroprotection. *Neurochem Res* 29: 601-608.
- Bambrick LL, Chandrasekaran K, Mehrabian Z, Wright C, Krueger BK, et al. 2006. Cyclosporin A increases mitochondrial calcium uptake capacity in cortical astrocytes but not cerebellar granule neurons. *J Bioenerg Biomembr* 38: 43-47.
- Basso E, Fante L, Fowlkes J, Petronilli V, Forte MA, et al. 2005. Properties of the permeability transition pore in mitochondria devoid of Cyclophilin D. *J Biol Chem* 280: 18558-18561.
- Bauer MK, Schubert A, Rocks O, Grimm S. 1999. Adenine nucleotide translocase-1, a component of the permeability transition pore, can dominantly induce apoptosis. *J Cell Biol* 147: 1493-1502.
- Beal MF. 1998. Mitochondrial dysfunction in neurodegenerative diseases. *Biochim Biophys Acta* 1366: 211-223.
- Beatrice MC, Stiers DL, Pfeiffer DR. 1982. Increased permeability of mitochondria during Ca^{2+} release induced by *t*-butyl hydroperoxide or oxalacetate. The effect of ruthenium red. *J Biol Chem* 257: 7161-7171.
- Berman SB, Watkins SC, Hastings TG. 2000. Quantitative biochemical and ultrastructural comparison of mitochondrial permeability transition in isolated brain and liver mitochondria: Evidence for reduced sensitivity of brain mitochondria. *Exp Neurol* 164: 415-425.
- Bernardi P. 1992. Modulation of the mitochondrial cyclosporin A-sensitive permeability transition pore by the proton electrochemical gradient. Evidence that the pore can be opened by membrane depolarization. *J Biol Chem* 267: 8834-8839.
- Bernardi P. 1999. Mitochondrial transport of cations: Channels, exchangers, and permeability transition. *Physiol Rev* 79: 1127-1155.
- Bernardi P, Petronilli V. 1996. The permeability transition pore as a mitochondrial calcium release channel: A critical appraisal. *J Bioenerg Biomembr* 28: 131-138.
- Bernardi P, Broekemeier KM, Pfeiffer DR. 1994. Recent progress on regulation of the mitochondrial permeability transition pore, a cyclosporin-sensitive pore in the inner mitochondrial membrane. *J Bioenerg Biomembr* 26: 509-517.
- Bernardi P, Krauskopf A, Basso E, Petronilli V, Blalchy-Dyson E, et al. 2006. The mitochondrial permeability transition from in vitro artifact to disease target. *FEBS J* 273: 2077-2099.
- Bernardi P, Petronilli V, Di Lisa F, Forte M. 2001. A mitochondrial perspective on cell death. *Trends Biochem Sci* 26: 112-117.
- Bernardi P, Vassanelli S, Veronese P, Colonna R, Szabo I, et al. 1992. Modulation of the mitochondrial permeability transition pore. Effect of protons and divalent cations. *J Biol Chem* 267: 2934-2939.
- Berson A, Descatoire V, Sutton A, Fau D, Maulny B, et al. 2001. Toxicity of alpidem, a peripheral benzodiazepine receptor ligand, but not zolpidem, in rat hepatocytes: Role of mitochondrial permeability transition and metabolic activation. *J Pharmacol Exp Ther* 299: 793-800.
- Beutner G, Ruck A, Riede B, Brdiczka D. 1998. Complexes between porin, hexokinase, mitochondrial creatine kinase, and adenylate translocator display properties of the permeability transition pore. Implication for regulation of permeability transition by the kinases. *Biochim Biophys Acta* 1368: 7-18.
- Beutner G, Ruck A, Riede B, Welte W, Brdiczka D. 1996. Complexes between kinases, mitochondrial porin, and

- adenylate translocator in rat brain resemble the permeability transition pore. *FEBS Lett* 396: 189-195.
- Blachly-Dyson E, Forte M. 2001. VDAC channels. *IUBMB Life* 52: 113-118.
- Blomgren K, Hagberg H. 2006. Free radicals, mitochondria, and hypoxia-ischemia in the developing brain. *Free Radic Biol Med* 40: 388-397.
- Bono F, Lamarche I, Prabonnaud V, Le Fur G, Herbert JM. 1999. Peripheral benzodiazepine receptor agonists exhibit potent antiapoptotic activities. *Biochem Biophys Res Commun* 265: 457-461.
- Brdiczka DG, Zorov DB, Sheu SS. 2006. Mitochondrial contact sites: Their role in energy metabolism and apoptosis. *Biochim Biophys Acta* 1762: 148-163.
- Brenner C, Cadiou H, Vieira HL, Zamzami N, Marzo I, et al. 2000. Bcl-2 and Bax regulate the channel activity of the mitochondrial adenine nucleotide translocator. *Oncogene* 19: 329-336.
- Broekemeier KM, Pfeiffer DR. 1989. Cyclosporin A-sensitive and insensitive mechanisms produce the permeability transition in mitochondria. *Biochem Biophys Res Commun* 163: 561-566.
- Broekemeier KM, Pfeiffer DR. 1995. Inhibition of the mitochondrial permeability transition by cyclosporin A during long time frame experiments: Relationship between pore opening and the activity of mitochondrial phospholipases. *Biochemistry* 34: 16440-16449.
- Broekemeier KM, Carpenter-Deyo L, Reed DJ, Pfeiffer DR. 1992. Cyclosporin A protects hepatocytes subjected to high Ca^{2+} and oxidative stress. *FEBS Lett* 304: 192-194.
- Broekemeier KM, Dempsey ME, Pfeiffer DR. 1989. Cyclosporin A is a potent inhibitor of the inner membrane permeability transition in liver mitochondria. *J Biol Chem* 264: 7826-7830.
- Brown MR, Sullivan PG, Geddes JW. 2006. Synaptic mitochondria are more susceptible to Ca^{2+} overload than non-synaptic mitochondria. *J Biol Chem* 281: 11658-11668.
- Browne SE, Bowling AC, MacGarvey U, Baik MJ, Berger SC, et al. 1997. Oxidative damage and metabolic dysfunction in Huntington's disease: Selective vulnerability of the basal ganglia. *Ann Neurol* 41: 646-653.
- Brustovetsky N, Dubinsky JM. 2000. Dual responses of CNS mitochondria to elevated calcium. *J Neurosci* 20: 103-113.
- Brustovetsky N, Klingenberg M. 1996. Mitochondrial ADP/ATP carrier can be reversibly converted into a large channel by Ca^{2+} . *Biochemistry* 35: 8483-8488.
- Brustovetsky N, Brustovetsky T, Dubinsky JM. 2001. On the mechanisms of neuroprotection by creatine and phosphocreatine. *J Neurochem* 76: 425-434.
- Brustovetsky N, Brustovetsky T, Jemmerson R, Dubinsky JM. 2002a. Calcium-induced cytochrome *c* release from CNS mitochondria is associated with the permeability transition and rupture of the outer membrane. *J Neurochem* 80: 207-218.
- Brustovetsky N, Tropschug M, Heimpele S, Heidkamper D, Klingenberg M. 2002b. A large Ca^{2+} -dependent channel formed by recombinant ADP/ATP carrier from *Neurospora crassa* resembles the mitochondrial permeability transition pore. *Biochemistry* 41: 11804-11811.
- Brustovetsky N, Brustovetsky T, Purl KJ, Capano M, Crompton M, et al. 2003a. Increased susceptibility of striatal mitochondria to calcium-induced permeability transition. *J Neurosci* 23: 4858-4867.
- Brustovetsky N, Dubinsky JM, Antonsson B, Jemmerson R. 2003b. Two pathways for tBID-induced cytochrome *c* release from rat brain mitochondria: BAK versus BAX-dependence. *J Neurochem* 84: 196-207.
- Brustovetsky N, LaFrance R, Purl KJ, Brustovetsky T, Keene CD, et al. 2005a. Age-dependent changes in the calcium sensitivity of striatal mitochondria in mouse models of Huntington's disease. *J Neurochem* 93: 1361-1370.
- Brustovetsky T, Antonsson B, Jemmerson R, Dubinsky JM, Brustovetsky N. 2005b. Activation of calcium-independent phospholipase A (iPLA) in brain mitochondria and release of apoptogenic factors by BAX and truncated BID. *J Neurochem* 94: 980-994.
- Brustovetsky NN, Egorova MV, Gnutov D, Mokhova EN, Skulachev VP. 1993. Cyclosporin A suppression of uncoupling in liver mitochondria of ground squirrel during arousal from hibernation. *FEBS Lett* 315: 233-236.
- Bryson JM, Coy PE, Gottlob K, Hay N, Robey RB. 2002. Increased hexokinase activity, of either ectopic or endogenous origin, protects renal epithelial cells against acute oxidant-induced cell death. *J Biol Chem* 277: 11392-11400.
- Buki A, Okonkwo DO, Povlishock JT. 1999. Postinjury cyclosporin A administration limits axonal damage and disconnection in traumatic brain injury. *J Neurotrauma* 16: 511-521.
- Butcher SP, Henshall DC, Teramura Y, Iwasaki K, Sharkey J. 1997. Neuroprotective actions of FK506 in experimental stroke: In vivo evidence against an antiexcitotoxic mechanism. *J Neurosci* 17: 6939-6946.
- Cao G, Clark RS, Pei W, Yin W, Zhang F, et al. 2003. Translocation of apoptosis-inducing factor in vulnerable neurons after transient cerebral ischemia and in neuronal cultures after oxygen-glucose deprivation. *J Cereb Blood Flow Metab* 23: 1137-1150.
- Cassarino DS, Swerdlow RH, Parks JK, Parker WD Jr., Bennett JP Jr. 1998. Cyclosporin A increases resting mitochondrial membrane potential in SY5Y cells and reverses the depressed mitochondrial membrane potential of Alzheimer's disease cybrids. *Biochem Biophys Res Commun* 248: 168-173.
- Cesura AM, Pinard E, Schubel R, Goetschy V, Friedlein A, et al. 2003. The voltage-dependent anion channel is the target

- for a new class of inhibitors of the mitochondrial permeability transition pore. *J Biol Chem* 278: 49812-49818.
- Chalmers S, Nicholls DG. 2003. The relationship between free and total calcium concentrations in the matrix of liver and brain mitochondria. *J Biol Chem* 278: 19062-19070.
- Chelli B, Falleni A, Salvetti F, Gremigni V, Lucacchini A, et al. 2001. Peripheral-type benzodiazepine receptor ligands: Mitochondrial permeability transition induction in rat cardiac tissue. *Biochem Pharmacol* 61: 695-705.
- Chen M, Ona VO, Li M, Ferrante RJ, Fink KB, et al. 2000. Minocycline inhibits caspase-1 and caspase-3 expression and delays mortality in a transgenic mouse model of Huntington disease. *Nat Med* 6: 797-801.
- Cheng EH, Sheiko TV, Fisher JK, Craigen WJ, Korsmeyer SJ. 2003. VDAC2 inhibits BAK activation and mitochondrial apoptosis. *Science* 301: 513-517.
- Chernyak BV, Bernardi P. 1996. The mitochondrial permeability transition pore is modulated by oxidative agents through both pyridine nucleotides and glutathione at two separate sites. *Eur J Biochem* 238: 623-630.
- Chinopoulos C, Starkov AA, Fiskum G. 2003. Cyclosporin A-insensitive permeability transition in brain mitochondria: Inhibition by 2-aminoethoxydiphenyl borate. *J Biol Chem* 278: 27382-27389.
- Choi DW. 1988. Glutamate neurotoxicity and diseases of the nervous system. *Neuron* 1: 623-634.
- Clarke SJ, McStay GP, Halestrap AP. 2002. Sanglifehrin A acts as a potent inhibitor of the mitochondrial permeability transition and reperfusion injury of the heart by binding to cyclophilin D at a different site from cyclosporin A. *J Biol Chem* 277: 34793-34799.
- Clarkson AN, Liu H, Pearson L, Kapoor M, Harrison JC, et al. 2004. Neuroprotective effects of spermine following hypoxic-ischemic-induced brain damage: A mechanistic study. *FASEB J* 18: 1114-1116.
- Cleren C, Starkov AA, Calingasan NY, Lorenzo BJ, Chen J, et al. 2005. Promethazine protects against 1-methyl-4-phenyl-1,2,3,6-tetrahydropyridine neurotoxicity. *Neurobiol Dis* 20: 701-708.
- Coert BA, Anderson RE, Meyer FB. 2000. Exogenous spermine reduces ischemic damage in a model of focal cerebral ischemia in the rat. *Neurosci Lett* 282: 5-8.
- Colbourne F, Sutherland GR, Auer RN. 1999. Electron microscopic evidence against apoptosis as the mechanism of neuronal death in global ischemia. *J Neurosci* 19: 4200-4210.
- Colell A, Garcia-Ruiz C, Lluís JM, Coll O, Mari M, et al. 2003. Cholesterol impairs the adenine nucleotide translocator-mediated mitochondrial permeability transition through altered membrane fluidity. *J Biol Chem* 278: 33928-33935.
- Connern CP, Halestrap AP. 1992. Purification and N-terminal sequencing of peptidyl-prolyl cis-trans-isomerase from rat liver mitochondrial matrix reveals the existence of a distinct mitochondrial cyclophilin. *Biochem J* 284 (Pt 2): 381-385.
- Cornet S, Spinnewyn B, Delafloffe S, Charnet C, Roubert V, et al. 2004. Lack of evidence of direct mitochondrial involvement in the neuroprotective effect of minocycline. *Eur J Pharmacol* 505: 111-119.
- Costantini P, Chernyak BV, Petronilli V, Bernardi P. 1995. Selective inhibition of the mitochondrial permeability transition pore at the oxidation-reduction sensitive dithiol by monobromobimane. *FEBS Lett* 362: 239-242.
- Costantini P, Chernyak BV, Petronilli V, Bernardi P. 1996. Modulation of the mitochondrial permeability transition pore by pyridine nucleotides and dithiol oxidation at two separate sites. *J Biol Chem* 271: 6746-6751.
- Cregan SP, Fortin A, MacLaurin JG, Callaghan SM, Cecconi F, et al. 2002. Apoptosis-inducing factor is involved in the regulation of caspase-independent neuronal cell death. *J Cell Biol* 158: 507-517.
- Crompton M. 1999. The mitochondrial permeability transition pore and its role in cell death. *Biochem J* 341 (Pt 2): 233-249.
- Crompton M. 2000. Mitochondrial intermembrane junctional complexes and their role in cell death. *J Physiol* 529 Pt (1): 11-21.
- Crompton M. 2003. On the involvement of mitochondrial intermembrane junctional complexes in apoptosis. *Curr Med Chem* 10: 1473-1484.
- Crompton M, Costi A. 1988. Kinetic evidence for a heart mitochondrial pore activated by Ca^{2+} , inorganic phosphate, and oxidative stress. A potential mechanism for mitochondrial dysfunction during cellular Ca^{2+} overload. *Eur J Biochem* 178: 489-501.
- Crompton M, Heid I. 1978. The cycling of calcium, sodium, and protons across the inner membrane of cardiac mitochondria. *Eur J Biochem* 91: 599-608.
- Crompton M, Barksby E, Johnson N, Capano M. 2002. Mitochondrial intermembrane junctional complexes and their involvement in cell death. *Biochimie* 84: 143-152.
- Crompton M, Ellinger H, Costi A. 1988. Inhibition by cyclosporin A of a Ca^{2+} -dependent pore in heart mitochondria activated by inorganic phosphate and oxidative stress. *Biochem J* 255: 357-360.
- Crompton M, Kunzi M, Carafoli E. 1977. The calcium-induced and sodium-induced effluxes of calcium from heart mitochondria. Evidence for a sodium-calcium carrier. *Eur J Biochem* 79: 549-558.
- Crompton M, Virji S, Doyle V, Johnson N, Ward JM. 1999. The mitochondrial permeability transition pore. *Biochem Soc Symp* 66: 167-179.
- Crompton M, Virji S, Ward JM. 1998. Cyclophilin-D binds strongly to complexes of the voltage-dependent anion channel and the adenine nucleotide translocase to form the permeability transition pore. *Eur J Biochem* 258: 729-735.

- Czerniczyniec A, Bustamante J, Lores-Arnaiz S. 2006. Modulation of brain mitochondrial function by deprenyl. *Neurochem Int* 48: 235-241.
- Dawson TM, Steiner JP, Dawson VL, Dinerman JL, Uhl GR, et al. 1993. Immunosuppressant FK506 enhances phosphorylation of nitric oxide synthase and protects against glutamate neurotoxicity. *Proc Natl Acad Sci USA* 90: 9808-9812.
- Deshpande J, Bergstedt K, Linden T, Kalimo H, Wieloch T. 1992. Ultrastructural changes in the hippocampal CA1 region following transient cerebral ischemia: Evidence against programmed cell death. *Exp Brain Res* 88: 91-105.
- Di Paola M, Zaccagnino P, Oliveros-Celis C, Lorusso M. 2006. Arachidonic acid induces specific membrane permeability increase in heart mitochondria. *FEBS Lett* 580: 775-781.
- Dirnagl U, Iadecola C, Moskowitz MA. 1999. Pathobiology of ischemic stroke: An integrated view. *Trends Neurosci* 22: 391-397.
- Dolder M, Walzel B, Speer O, Schlattner U, Wallimann T. 2003. Inhibition of the mitochondrial permeability transition by creatine kinase substrates. Requirement for micro-compartmentation. *J Biol Chem* 278: 17760-17766.
- Dolder M, Wendt S, Wallimann T. 2001. Mitochondrial creatine kinase in contact sites: Interaction with porin and adenine nucleotide translocase, role in permeability transition, and sensitivity to oxidative damage. *Biol Signal Recept* 10: 93-111.
- Dubinsky JM. 2005. CNS mitochondria in neurodegenerative disorders. *Antioxid Redox Signal* 7: 1089-1091.
- Dubinsky JM, Levi Y. 1998. Calcium-induced activation of the mitochondrial permeability transition in hippocampal neurons. *J Neurosci Res* 53: 728-741.
- Duchen MR, McGuinness O, Brown LA, Crompton M. 1993. On the involvement of a cyclosporin A-sensitive mitochondrial pore in myocardial reperfusion injury. *Cardiovasc Res* 27: 1790-1794.
- Dugan LL, Kim-Han JS. 2004. Astrocyte mitochondria in vitro models of ischemia. *J Bioenerg Biomembr* 36: 317-321.
- Empey PE, McNamara PJ, Young B, Rosbalt MB, Hatton J. 2006. Cyclosporin A disposition following acute traumatic brain injury. *J Neurotrauma* 23: 109-116.
- Endres M, Namura S, Shimizu-Sasamata M, Waeber C, Zhang L, et al. 1998. Attenuation of delayed neuronal death after mild focal ischemia in mice by inhibition of the caspase family. *J Cereb Blood Flow Metab* 18: 238-247.
- Erecinska M, Silver IA. 1989. ATP and brain function. *J Cereb Blood Flow Metab* 9: 2-19.
- Estevez AY, Phillis JW. 1997. The phospholipase A2 inhibitor, quinacrine, reduces infarct size in rats after transient middle cerebral artery occlusion. *Brain Res* 752: 203-208.
- Fagian MM, Pereira-da-Silva L, Martins IS, Vercesi AE. 1990. Membrane protein thiol cross-linking associated with the permeabilization of the inner mitochondrial membrane by Ca^{2+} plus prooxidants. *J Biol Chem* 265: 19955-19960.
- Faustin B, Rossignol R, Rocher C, Benard G, Malgat M, et al. 2004. Mobilization of adenine nucleotide translocators as molecular bases of the biochemical threshold effect observed in mitochondrial diseases. *J Biol Chem* 279: 20411-20421.
- Fernandez-Gomez FJ, Galindo MF, Gomez-Lazaro M, Gonzalez-Garcia C, Cena V, et al. 2005. Involvement of mitochondrial potential and calcium buffering capacity in minocycline cytoprotective actions. *Neuroscience* 133: 959-967.
- Ferrand-Drake M, Zhu C, Gido G, Hansen AJ, Karlsson JO, et al. 2003. Cyclosporin A prevents calpain activation despite increased intracellular calcium concentrations, as well as translocation of apoptosis-inducing factor, cytochrome c, and caspase-3 activation in neurons exposed to transient hypoglycemia. *J Neurochem* 85: 1431-1442.
- Fink K, Zhu J, Namura S, Shimizu-Sasamata M, Endres M, et al. 1998. Prolonged therapeutic window for ischemic brain damage caused by delayed caspase activation. *J Cereb Blood Flow Metab* 18: 1071-1076.
- Fontaine E, Eriksson O, Ichas F, Bernardi P. 1998a. Regulation of the permeability transition pore in skeletal muscle mitochondria. Modulation by electron flow through the respiratory chain complex I. *J Biol Chem* 273: 12662-12668.
- Fontaine E, Ichas F, Bernardi P. 1998b. A ubiquinone-binding site regulates the mitochondrial permeability transition pore. *J Biol Chem* 273: 25734-25740.
- Fournier N, Ducet G, Crevat A. 1987. Action of cyclosporin on mitochondrial calcium fluxes. *J Bioenerg Biomembr* 19: 297-303.
- Friberg H, Connern C, Halestrap AP, Wieloch T. 1999. Differences in the activation of the mitochondrial permeability transition among brain regions in the rat correlate with selective vulnerability. *J Neurochem* 72: 2488-2497.
- Friberg H, Ferrand-Drake M, Bengtsson F, Halestrap AP, Wieloch T. 1998. Cyclosporin A, but not FK 506, protects mitochondria and neurons against hypoglycemic damage and implicates the mitochondrial permeability transition in cell death. *J Neurosci* 18: 5151-5159.
- Fuks B, Talaga P, Huart C, Henichart JP, Bertrand K, et al. 2005. In vitro properties of 5-(benzylsulfonyl)-4-bromo-2-methyl-3(2H)-pyridazinone: A novel permeability transition pore inhibitor. *Eur J Pharmacol* 519: 24-30.
- Gadd ME, Broekemeier KM, Crouser ED, Kumar J, Graff G, et al. 2006. Mitochondrial iPLA2 activity modulates the release of cytochrome c from mitochondria and influences the permeability transition. *J Biol Chem* 281: 6931-6939.
- Gadella FR, Thomson L, Fagian MM, Costa AD, Radi R, et al. 1997. Ca^{2+} -independent permeabilization of the inner

- mitochondrial membrane by peroxynitrite is mediated by membrane protein thiol cross-linking and lipid peroxidation. *Arch Biochem Biophys* 345: 243-250.
- Garrido C, Galluzzi L, Brunet M, Puig PE, Didelot C, et al. 2006. Mechanisms of cytochrome *c* release from mitochondria. *Cell Death Differ* 13: 1423-1433.
- Gillessen T, Grasshoff C, Szinicz L. 2002. Mitochondrial permeability transition can be directly monitored in living neurons. *Biomed Pharmacother* 56: 186-193.
- Gincel D, Shoshan-Barmatz V. 2004. Glutamate interacts with VDAC and modulates opening of the mitochondrial permeability transition pore. *J Bioenerg Biomembr* 36: 179-186.
- Gincel D, Zaid H, Shoshan-Barmatz V. 2001. Calcium binding and translocation by the voltage-dependent anion channel: A possible regulatory mechanism in mitochondrial function. *Biochem J* 358: 147-155.
- Gonzalez-Barroso MM, Fleury C, Levi-Meyrueis C, Zaragoza P, Bouillaud F, et al. 1997. Deletion of amino acids 261–269 in the brown fat uncoupling protein converts the carrier into a pore. *Biochemistry* 36: 10930-10935.
- Gonzalez F, Pariselli F, Dupaigne P, Budihardjo I, Lutter M., et al. 2005. tBid interaction with cardiolipin primarily orchestrates mitochondrial dysfunctions and subsequently activates Bax and Bak. *Cell Death Differ* 12: 614-626.
- Gottlob K, Majewski N, Kennedy S, Kandel E, Robey RB, et al. 2001. Inhibition of early apoptotic events by Akt/PKB is dependent on the first committed step of glycolysis and mitochondrial hexokinase. *Genes Dev* 15: 1406-1418.
- Green DR, Kroemer G. 2004. The pathophysiology of mitochondrial cell death. *Science* 305: 626-629.
- Griffiths EJ, Halestrap AP. 1995. Mitochondrial nonspecific pores remain closed during cardiac ischemia, but open upon reperfusion. *Biochem J* 307 (Pt 1): 93-98.
- Grijalba MT, Vercesi AE, Schreier S. 1999. Ca²⁺-induced increased lipid packing and domain formation in submitochondrial particles. A possible early step in the mechanism of Ca²⁺-stimulated generation of reactive oxygen species by the respiratory chain. *Biochemistry* 38: 13279-13287.
- Gunter TE, Pfeiffer DR. 1990. Mechanisms by which mitochondria transport calcium. *Am J Physiol* 258: C755-C786.
- Halestrap A. 2005. Biochemistry: A pore way to die. *Nature* 434: 578-579.
- Halestrap AP. 1991. Calcium-dependent opening of a nonspecific pore in the mitochondrial inner membrane is inhibited at pH values below 7. Implications for the protective effect of low pH against chemical and hypoxic cell damage. *Biochem J* 278 (Pt 3): 715-719.
- Halestrap AP. 1999. The mitochondrial permeability transition: Its molecular mechanism and role in reperfusion injury. *Biochem Soc Symp* 66: 181-203.
- Halestrap AP. 2004. Mitochondrial permeability: Dual role for the ADP/ATP translocator? *Nature* 430. Brief communication.
- Halestrap AP. 2006. Calcium, mitochondria, and reperfusion injury: A pore way to die. *Biochem Soc Trans* 34: 232-237.
- Halestrap AP, Brenner C. 2003. The adenine nucleotide translocase: A central component of the mitochondrial permeability transition pore and key player in cell death. *Curr Med Chem* 10: 1507-1525.
- Halestrap AP, Davidson AM. 1990. Inhibition of Ca²⁺-induced large-amplitude swelling of liver and heart mitochondria by cyclosporin is probably caused by the inhibitor binding to mitochondrial-matrix peptidyl-prolyl *cis-trans* isomerase and preventing it interacting with the adenine nucleotide translocase. *Biochem J* 268: 153-160.
- Halestrap AP, Connern CP, Griffiths EJ, Kerr PM. 1997a. Cyclosporin A binding to mitochondrial cyclophilin inhibits the permeability transition pore and protects hearts from ischemia/reperfusion injury. *Mol Cell Biochem* 174: 167-172.
- Halestrap AP, Woodfield KY, Connern CP. 1997b. Oxidative stress, thiol reagents, and membrane potential modulate the mitochondrial permeability transition by affecting nucleotide binding to the adenine nucleotide translocase. *J Biol Chem* 272: 3346-3354.
- Halestrap AP, Gillespie JP, O'Toole A, Doran E. 2000. Mitochondria and cell death: A pore way to die? *Symp Soc Exp Biol* 52: 65-80.
- Halestrap AP, Kerr PM, Javadov S, Woodfield KY. 1998. Elucidating the molecular mechanism of the permeability transition pore and its role in reperfusion injury of the heart. *Biochim Biophys Acta* 1366: 79-94.
- Hansson MJ, Mansson R, Mattiasson G, Ohlsson J, Karlsson J, et al. 2004a. Brain-derived respiring mitochondria exhibit homogeneous, complete, and cyclosporin-sensitive permeability transition. *J Neurochem* 89: 715-729.
- Hansson MJ, Mattiasson G, Mansson R, Karlsson J, Keep MF, et al. 2004b. The nonimmunosuppressive cyclosporin analogs NIM811 and UNIL025 display nanomolar potencies on permeability transition in brain-derived mitochondria. *J Bioenerg Biomembr* 36: 407-413.
- Hansson MJ, Persson T, Friberg H, Keep MF, Rees A, et al. 2003. Powerful cyclosporin inhibition of calcium-induced permeability transition in brain mitochondria. *Brain Res* 960: 99-111.
- Haworth RA, Hunter DR. 1979. The Ca²⁺-induced membrane transition in mitochondria. II. Nature of the Ca²⁺ trigger site. *Arch Biochem Biophys* 195: 460-467.
- Haworth RA, Hunter DR. 1980. Allosteric inhibition of the Ca²⁺-activated hydrophilic channel of the mitochondrial inner membrane by nucleotides. *J Membr Biol* 54: 231-236.
- He L, Lemasters JJ. 2002. Regulated and unregulated mitochondrial permeability transition pores: A new paradigm of pore structure and function? *FEBS Lett* 512: 1-7.

- Hoffmann B, Stockl A, Schlame M, Beyer K, Klingenberg M. 1994. The reconstituted ADP/ATP carrier activity has an absolute requirement for cardiolipin as shown in cysteine mutants. *J Biol Chem* 269: 1940-1944.
- Hoyt KR, Sharma TA, Reynolds JJ. 1997. Trifluoperazine- and dibucaine-induced inhibition of glutamate-induced mitochondrial depolarization in rat cultured forebrain neurons. *Br J Pharmacol* 122: 803-808.
- Hu BR, Liu CL, Ouyang Y, Blomgren K, Siesjo BK. 2000. Involvement of caspase-3 in cell death after hypoxia-ischemia declines during brain maturation. *J Cereb Blood Flow Metab* 20: 1294-1300.
- Huang HM, Ou HC, Xu H, Chen HL, Fowler C, et al. 2003. Inhibition of α -ketoglutarate dehydrogenase complex promotes cytochrome *c* release from mitochondria, caspase-3 activation, and necrotic cell death. *J Neurosci Res* 74: 309-317.
- Hunter DR, Haworth RA, Southard JH. 1976. Relationship between configuration, function, and permeability in calcium-treated mitochondria. *J Biol Chem* 251: 5069-5077.
- Hunter DR, Haworth RA. 1979a. The Ca^{2+} -induced membrane transition in mitochondria. III. Transitional Ca^{2+} release. *Arch Biochem Biophys* 195: 468-477.
- Hunter DR, Haworth RA. 1979b. The Ca^{2+} -induced membrane transition in mitochondria. I. The protective mechanisms. *Arch Biochem Biophys* 195: 453-459.
- Hunter FE Jr, Ford L. 1955. Inactivation of oxidative and phosphorylative systems in mitochondria by preincubation with phosphate and other ions. *J Biol Chem* 216: 357-369.
- Huser J, Blatter LA. 1999. Fluctuations in mitochondrial membrane potential caused by repetitive gating of the permeability transition pore. *Biochem J* 343 Pt (2): 311-317.
- Ichas F, Mazat JP. 1998. From calcium signaling to cell death: Two conformations for the mitochondrial permeability transition pore. Switching from low- to high-conductance state. *Biochim Biophys Acta* 1366: 33-50.
- Ichas F, Jouaville LS, Mazat JP. 1997. Mitochondria are excitable organelles capable of generating and conveying electrical and calcium signals. *Cell* 89: 1145-1153.
- Imberti R, Nieminen AL, Herman B, Lemasters JJ. 1992. Synergism of cyclosporin A and phospholipase inhibitors in protection against lethal injury to rat hepatocytes from oxidant chemicals. *Res Commun Chem Path* 78: 27-38.
- Isaev NK, Zorov DB, Stelmashook EV, Uzbekov RE, Kozhemyakin MB, et al. 1996. Neurotoxic glutamate treatment of cultured cerebellar granule cells induces Ca^{2+} -dependent collapse of mitochondrial membrane potential and ultrastructural alterations of mitochondria. *FEBS Lett* 392: 143-147.
- Jemmerson R, Dubinsky JM, Brustovetsky N. 2005. Cytochrome *c* release from CNS mitochondria and potential for clinical intervention in apoptosis-mediated CNS diseases. *Antioxid Redox Signal* 7: 1158-1172.
- Johans M, Milanesi E, Franck M, Johans C, Liobikas J, et al. 2005. Modification of permeability transition pore arginine (s) by phenylglyoxal derivatives in isolated mitochondria and mammalian cells. Structure-function relationship of arginine ligands. *J Biol Chem* 280: 12130-12136.
- Jorda EG, Jimenez A, Verdaguer E, Canudas AM, Folch J, et al. 2005. Evidence in favour of a role for peripheral-type benzodiazepine receptor ligands in amplification of neuronal apoptosis. *Apoptosis* 10: 91-104.
- Jung DW, Apel L, Brierley GP. 1990. Matrix free Mg^{2+} changes with metabolic state in isolated heart mitochondria. *Biochemistry* 29: 4121-4128.
- Karasawa Y, Araki H, Otomo S. 1992. Effects of ketanserin and mianserin on delayed neuronal death induced by cerebral ischemia in Mongolian gerbils. *Psychopharmacology (Berl)* 109: 264-270.
- Karlsson J, Fong KS, Hansson MJ, Elmer E, Csiszar K, et al. 2004. Life span extension and reduced neuronal death after weekly intraventricular cyclosporin injections in the G93A transgenic mouse model of amyotrophic lateral sclerosis. *J Neurosurg* 101: 128-137.
- Kass GE, Juedes MJ, Orrenius S. 1992. Cyclosporin A protects hepatocytes against prooxidant-induced cell killing. A study on the role of mitochondrial Ca^{2+} cycling in cytotoxicity. *Biochem Pharmacol* 44: 1995-2003.
- Keep M, Elmer E, Fong KS, Csiszar K. 2001. Intrathecal cyclosporin prolongs survival of late-stage ALS mice. *Brain Res* 894: 327-331.
- Khaspekov L, Friberg H, Halestrap A, Viktorov I, Wieloch T. 1999. Cyclosporin A and its nonimmunosuppressive analog *N*-Me-Val-4-cyclosporin A mitigate glucose/oxygen deprivation-induced damage to rat cultured hippocampal neurons. *Eur J Neurosci* 11: 3194-3198.
- Kim JS, He L, Lemasters JJ. 2003. Mitochondrial permeability transition: A common pathway to necrosis and apoptosis. *Biochem Biophys Res Commun* 304: 463-470.
- Kimelberg HK, Feustel PJ, Jin Y, Paquette J, Boulos A, et al. 2000. Acute treatment with tamoxifen reduces ischemic damage following middle cerebral artery occlusion. *Neuroreport* 11: 2675-2679.
- Kinnally KW, Campo ML, Tedeschi H. 1989. Mitochondrial channel activity studied by patch-clamping mitoplasts. *J Bioenerg Biomembr* 21: 497-506.
- Kinnally KW, Zorov DB, Antonenko YN, Snyder SH, McEnery MW, et al. 1993. Mitochondrial benzodiazepine receptor linked to inner membrane ion channels by nanomolar actions of ligands. *Proc Natl Acad Sci USA* 90: 1374-1378.
- Klivenyi P, Calingasan NY, Starkov A, Stavrovskaya IG, Kristal BS, et al. 2004. Neuroprotective mechanisms of creatine

- occur in the absence of mitochondrial creatine kinase. *Neurobiol Dis* 15: 610-617.
- Klivenyi P, Ferrante RJ, Matthews RT, Bogdanov MB, Klein AM, et al. 1999. Neuroprotective effects of creatine in a transgenic animal model of amyotrophic lateral sclerosis. *Nat Med* 5: 347-350.
- Knoll G, Brdiczka D. 1983. Changes in freeze-fractured mitochondrial membranes correlated to their energetic state. Dynamic interactions of the boundary membranes. *Biochim Biophys Acta* 733: 102-110.
- Kobayashi T, Kuroda S, Tada M, Houkin K, Iwasaki Y, et al. 2003. Calcium-induced mitochondrial swelling and cytochrome *c* release in the brain: Its biochemical characteristics and implication in ischemic neuronal injury. *Brain Res* 960: 62-70.
- Kokoszka JE, Waymire KG, Levy SE, Slish JE, Cai J, et al. 2004. The ADP/ATP translocator is not essential for the mitochondrial permeability transition pore. *Nature* 427: 461-465.
- Kowaltowski AJ, Castilho RF, Vercesi AE. 1996. Opening of the mitochondrial permeability transition pore by uncoupling or inorganic phosphate in the presence of Ca^{2+} is dependent on mitochondrial-generated reactive oxygen species. *FEBS Lett* 378: 150-152.
- Kowaltowski AJ, Castilho RF, Vercesi AE. 2001. Mitochondrial permeability transition and oxidative stress. *FEBS Lett* 495: 12-15.
- Krauskopf A, Eriksson O, Craigen WJ, Forte MA, Bernardi P. 2006. Properties of the permeability transition in VDAC1 (–/–) mitochondria. *Biochim Biophys Acta* 1757: 590-595.
- Kristal BS, Dubinsky JM. 1997. Mitochondrial permeability transition in the central nervous system: Induction by calcium cycling-dependent and -independent pathways. *J Neurochem* 69: 524-538.
- Kristian T. 2004. Metabolic stages, mitochondria, and calcium in hypoxic/ischemic brain damage. *Cell Calcium* 36: 221-233.
- Kristian T, Bernardi P, Siesjo BK. 2001. Acidosis promotes the permeability transition in energized mitochondria: Implications for reperfusion injury. *J Neurotrauma* 18: 1059-1074.
- Kristian T, Gertsch J, Bates TE, Siesjo BK. 2000. Characteristics of the calcium-triggered mitochondrial permeability transition in nonsynaptic brain mitochondria: Effect of cyclosporin A and ubiquinone O. *J Neurochem* 74: 1999-2009.
- Kristian T, Weatherby TM, Bates TE, Fiskum G. 2002. Heterogeneity of the calcium-induced permeability transition in isolated nonsynaptic brain mitochondria. *J Neurochem* 83: 1297-1308.
- Kuroda S, Nakai A, Kristian T, Siesjo BK. 1997. The calmodulin antagonist trifluoperazine in transient focal brain ischemia in rats. Antischematic effect and therapeutic window. *Stroke* 28: 2539-2544.
- Kushnareva YE, Sokolove PM. 2000. Prooxidants open both the mitochondrial permeability transition pore and a low-conductance channel in the inner mitochondrial membrane. *Arch Biochem Biophys* 376: 377-388.
- LaFrance R, Brustovetsky N, Sherburne C, Delong D, Dubinsky JM. 2005. Age-related changes in regional brain mitochondria from Fischer 344 rats. *Aging Cell* 4: 139-145.
- Lapidus RG, Sokolove PM. 1994. The mitochondrial permeability transition. Interactions of spermine, ADP, and inorganic phosphate. *J Biol Chem* 269: 18931-18936.
- Lardy HA, Pressman BC. 1956. Effect of surface active agents on the latent ATPase of mitochondria. *Biochim Biophys Acta* 21: 458-466.
- Le-Quoc K, Le-Quoc D. 1985. Crucial role of sulfhydryl groups in the mitochondrial inner membrane structure. *J Biol Chem* 260: 7422-7428.
- Leder O, Doring HJ, Reindell A, Fleckenstein A. 1969. Protective effect of organic Ca antagonists (iproveratril, D 600, prenylamine) against isoproterenol-induced myocardial necrosis. *Pflugers Arch* 312: R9-10.
- Lehninger AL. 1949. Esterification of inorganic phosphate coupled to electron transport between dihydrodiphosphopyridine nucleotide and oxygen. *J Biol Chem* 178: 625-644.
- Lehninger AL. 1962. Water uptake and extrusion by mitochondria in relation to oxidative phosphorylation. *Physiol Rev* 42: 467-517.
- Lehninger AL, Remmert LF. 1959. An endogenous uncoupling and swelling agent in liver mitochondria and its enzymic formation. *J Biol Chem* 234: 2459-2464.
- Lehninger AL, Carafoli E, Rossi CS. 1967. Energy-linked ion movements in mitochondrial systems. *Adv Enzymol Relat Areas Mol Biol* 29: 259-320.
- Leventhal L, Sortwell CE, Hanbury R, Collier TJ, Kordower JH, et al. 2000. Cyclosporin A protects striatal neurons in vitro and in vivo from 3-nitropropionic acid toxicity. *J Comp Neurol* 425: 471-478.
- Lin DT, Lechleiter JD. 2002. Mitochondrial targeted cyclophilin D protects cells from cell death by peptidyl prolyl isomerization. *J Biol Chem* 277: 31134-31141.
- Maciel EN, Vercesi AE, Castilho RF. 2001. Oxidative stress in Ca^{2+} -induced membrane permeability transition in brain mitochondria. *J Neurochem* 79: 1237-1245.
- Maciel EN, Kowaltowski AJ, Schwalm FD, Rodrigues JM, Souza DO, et al. 2004. Mitochondrial permeability transition in neuronal damage promoted by Ca^{2+} and respiratory chain complex II inhibition. *J Neurochem* 90: 1025-1035.
- Majewski N, Nogueira V, Bhaskar P, Coy PE, Skeen JE, et al. 2004a. Hexokinase-mitochondria interaction mediated by Akt is required to inhibit apoptosis in the presence or absence of Bax and Bak. *Mol Cell* 16: 819-830.
- Majewski N, Nogueira V, Robey RB, Hay N. 2004b. Akt inhibits apoptosis downstream of BID cleavage via a

- glucose-dependent mechanism involving mitochondrial hexokinases. *Mol Cell Biol* 24: 730-740.
- Mannella CA. 1998. Conformational changes in the mitochondrial channel protein, VDAC, and their functional implications. *J Struct Biol* 121: 207-218.
- Martin LJ, Al-Abdulla NA, Brambrink AM, Kirsch JR, Sieber FE, et al. 1998. Neurodegeneration in excitotoxicity, global cerebral ischemia, and target deprivation: A perspective on the contributions of apoptosis and necrosis. *Brain Res Bull* 46: 281-309.
- Marzo I, Brenner C, Zamzami N, Jurgensmeier JM, Susin SA, et al. 1998a. Bax and adenine nucleotide translocator cooperate in the mitochondrial control of apoptosis. *Science* 281: 2027-2031.
- Marzo I, Brenner C, Zamzami N, Susin SA, Beutner G, et al. 1998b. The permeability transition pore complex: A target for apoptosis regulation by caspases and bcl-2-related proteins. *J Exp Med* 187: 1261-1271.
- Matsumoto S, Friberg H, Ferrand-Drake M, Wieloch T. 1999. Blockade of the mitochondrial permeability transition pore diminishes infarct size in the rat after transient middle cerebral artery occlusion. *J Cereb Blood Flow Metab* 19: 736-741.
- Matthews RT, Yang L, Jenkins BG, Ferrante RJ, Rosen BR, et al. 1998. Neuroprotective effects of creatine and cyclocreatine in animal models of Huntington's disease. *J Neurosci* 18: 156-163.
- Mattiasson G, Friberg H, Hansson M, Elmer E, Wieloch T. 2003. Flow cytometric analysis of mitochondria from CA1 and CA3 regions of rat hippocampus reveals differences in permeability transition pore activation. *J Neurochem* 87: 532-544.
- McEnery MW. 1992. The mitochondrial benzodiazepine receptor: Evidence for association with the voltage-dependent anion channel (VDAC). *J Bioenerg Biomembr* 24: 63-69.
- McEnery MW, Snowman AM, Trifiletti RR, Snyder SH. 1992. Isolation of the mitochondrial benzodiazepine receptor: Association with the voltage-dependent anion channel and the adenine nucleotide carrier. *Proc Natl Acad Sci USA* 89: 3170-3174.
- McGuinness O, Yafei N, Costi A, Crompton M. 1990. The presence of two classes of high-affinity cyclosporin A binding sites in mitochondria. Evidence that the minor component is involved in the opening of an inner-membrane Ca^{2+} -dependent pore. *Eur J Biochem* 194: 671-679.
- McStay GP, Clarke SJ, Halestrap AP. 2002. Role of critical thiol groups on the matrix surface of the adenine nucleotide translocase in the mechanism of the mitochondrial permeability transition pore. *Biochem J* 367: 541-548.
- Merenda A, Bullock R. 2006. Clinical treatments for mitochondrial dysfunctions after brain injury. *Curr Opin Crit Care* 12: 90-96.
- Miller K, Sharer K, Suhan J, Koretsky AP. 1997. Expression of functional mitochondrial creatine kinase in liver of transgenic mice. *Am J Physiol* 272: C1193-C1202.
- Milon L, Meyer P, Chiadmi M, Munier A, Johansson M, et al. 2000. The human nm23-H4 gene product is a mitochondrial nucleoside diphosphate kinase. *J Biol Chem* 275: 14264-14272.
- Minamikawa T, Williams DA, Bowser DN, Nagley P. 1999. Mitochondrial permeability transition and swelling can occur reversibly without inducing cell death in intact human cells. *Exp Cell Res* 246: 26-37.
- Moreira PI, Custodio JB, Oliveira CR, Santos MS. 2004. Hydroxytamoxifen protects against oxidative stress in brain mitochondria. *Biochem Pharmacol* 68: 195-204.
- Moreira PI, Custodio JB, Oliveira CR, Santos MS. 2005. Brain mitochondrial injury induced by oxidative stress-related events is prevented by tamoxifen. *Neuropharmacology* 48: 435-447.
- Nakagawa T, Shimizu S, Watanabe T, Yamaguchi O, Otsu K, et al. 2005. Cyclophilin D-dependent mitochondrial permeability transition regulates some necrotic but not apoptotic cell death. *Nature* 434: 652-658.
- Nakata N, Kato H, Kogure K. 1992. Protective effects of serotonin reuptake inhibitors, citalopram and clomipramine, against hippocampal CA1 neuronal damage following transient ischemia in the gerbil. *Brain Res* 590: 48-52.
- Narita M, Shimizu S, Ito T, Chittenden T, Lutz RJ, et al. 1998. Bax interacts with the permeability transition pore to induce permeability transition and cytochrome *c* release in isolated mitochondria. *Proc Natl Acad Sci USA* 95: 14681-14686.
- Nedergaard M, Ransom B, Goldman SA. 2003. New roles for astrocytes: Redefining the functional architecture of the brain. *Trends Neurosci* 26: 523-530.
- Newmeyer DD, Ferguson-Miller S. 2003. Mitochondria: Releasing power for life and unleashing the machineries of death. *Cell* 112: 481-490.
- Nicholls DG, Budd SL. 1998. Mitochondria and neuronal glutamate excitotoxicity. *Biochim Biophys Acta* 1366: 97-112.
- Nicholls DG, Chalmers S. 2004. The integration of mitochondrial calcium transport and storage. *J Bioenerg Biomembr* 36: 277-281.
- Nicholls DG, Scott ID. 1980. The regulation of brain mitochondrial calcium ion transport. The role of ATP in the discrimination between kinetic and membrane potential-dependent calcium ion efflux mechanisms. *Biochem J* 186: 833-839.
- Nicholls DG, Ward MW. 2000. Mitochondrial membrane potential and neuronal glutamate excitotoxicity: Mortality and millivolts. *Trends Neurosci* 23: 166-174.

- Niccoli A, Petronilli V, Bernardi P. 1993. Modulation of the mitochondrial cyclosporin A-sensitive permeability transition pore by matrix pH. Evidence that the pore open-closed probability is regulated by reversible histidine protonation. *Biochemistry* 32: 4461-4465.
- Nieminen AL, Petrie TG, Lemasters JJ, Selman WR. 1996. Cyclosporin A delays mitochondrial depolarization induced by *N*-methyl-D-aspartate in cortical neurons: Evidence of the mitochondrial permeability transition. *Neuroscience* 75: 993-997.
- Nieminen AL, Saylor AK, Tesfai SA, Herman B, Lemasters JJ. 1995. Contribution of the mitochondrial permeability transition to lethal injury after exposure of hepatocytes to *t*-butylhydroperoxide. *Biochem J* 307 (Pt 1): 99-106.
- Norenberg MD, Rao KV, Jayakumar AR. 2005. Mechanisms of ammonia-induced astrocyte swelling. *Metab Brain Dis* 20: 303-318.
- Novgorodov SA, Guduz TI, Brierley GP, Pfeiffer DR. 1994. Magnesium ion modulates the sensitivity of the mitochondrial permeability transition pore to cyclosporin A and ADP. *Arch Biochem Biophys* 311: 219-228.
- Novgorodov SA, Guduz TI, Kushnareva YE, Zorov DB, Kudrjashov YB. 1990. Effect of ADP/ATP antiporter conformational state on the suppression of the nonspecific permeability of the inner mitochondrial membrane by cyclosporin A. *FEBS Lett* 277: 123-126.
- Novgorodov SA, Guduz TI, Milgrom YM, Brierley GP. 1992. The permeability transition in heart mitochondria is regulated synergistically by ADP and cyclosporin A. *J Biol Chem* 267: 16274-16282.
- O'Gorman E, Beutner G, Dolder M, Koretsky AP, Brdiczka D, et al. 1997. The role of creatine kinase in inhibition of mitochondrial permeability transition. *FEBS Lett* 414: 253-257.
- Okonkwo DO, Povlishock JT. 1999. An intrathecal bolus of cyclosporin A before injury preserves mitochondrial integrity and attenuates axonal disruption in traumatic brain injury. *J Cereb Blood Flow Metab* 19: 443-451.
- Okonkwo DO, Melon DE, Pellicane AJ, Mutlu LK, Rubin DG, et al. 2003. Dose-response of cyclosporin A in attenuating traumatic axonal injury in rat. *Neuroreport* 14: 463-466.
- Ouyang YB, Tan Y, Comb M, Liu CL, Martone ME, et al. 1999. Survival- and death-promoting events after transient cerebral ischemia: Phosphorylation of Akt, release of cytochrome *c*, and activation of caspase-like proteases. *J Cereb Blood Flow Metab* 19: 1126-1135.
- Palmer GC, Harris EW, Ray R, Stagnitto ML, Schmiesing RJ. 1992. Classification of compounds for prevention of NMDA-induced seizures/mortality, or maximal electroshock and pentylenetetrazol seizures in mice and antagonism of MK801 binding in vitro. *Arch Int Pharmacodyn Ther* 317: 16-34.
- Palmieri F. 2004. The mitochondrial transporter family (SLC25): Physiological and pathological implications. *Pflügers Arch* 447: 689-709.
- Panov A, Dikalov S, Shalbuyeva N, Taylor G, Sherer T, et al. 2005. Rotenone model of Parkinson disease: Multiple brain mitochondria dysfunctions after short-term systemic rotenone intoxication. *J Biol Chem* 280: 42026-42035.
- Panov AV, Andreeva L, Greenamyre JT. 2004. Quantitative evaluation of the effects of mitochondrial permeability transition pore modifiers on accumulation of calcium phosphate: Comparison of rat liver and brain mitochondria. *Arch Biochem Biophys* 424: 44-52.
- Papadopoulos V, Amri H, Boujrad N, Cascio C, Culty M, et al. 1997. Peripheral benzodiazepine receptor in cholesterol transport and steroidogenesis. *Steroids* 62: 21-28.
- Parker MA, Bazan HE, Marcheselli V, Rodriguez de Turco EB, Bazan NG. 2002. Platelet-activating factor induces permeability transition and cytochrome *c* release in isolated brain mitochondria. *J Neurosci Res* 69: 39-50.
- Paschen SA, Waizenegger T, Stan T, Preuss M, Cyrklaff M, et al. 2003. Evolutionary conservation of biogenesis of β -barrel membrane proteins. *Nature* 426: 862-866.
- Pastorino JG, Hoek JB. 2003. Hexokinase II: The integration of energy metabolism and control of apoptosis. *Curr Med Chem* 10: 1535-1551.
- Pastorino JG, Chen ST, Tafani M, Snyder JW, Farber JL. 1998. The overexpression of Bax produces cell death upon induction of the mitochondrial permeability transition. *J Biol Chem* 273: 7770-7775.
- Pastorino JG, Hoek JB, Shulga N. 2005. Activation of glycogen synthase kinase β disrupts the binding of hexokinase II to mitochondria by phosphorylating voltage-dependent anion channel and potentiates chemotherapy-induced cytotoxicity. *Cancer Res* 65: 10545-10554.
- Pastorino JG, Shulga N, Hoek JB. 2002. Mitochondrial binding of hexokinase II inhibits Bax-induced cytochrome *c* release and apoptosis. *J Biol Chem* 277: 7610-7618.
- Pastorino JG, Tafani M, Rothman RJ, Marcineviciute A, Hoek JB, et al. 1999. Functional consequences of the sustained or transient activation by Bax of the mitochondrial permeability transition pore. *J Biol Chem* 274: 31734-31739.
- Penzo D, Tagliapietra C, Colonna R, Petronilli V, Bernardi P. 2002. Effects of fatty acids on mitochondria: Implications for cell death. *Biochim Biophys Acta* 1555: 160-165.
- Petronilli V, Cola C, Bernardi P. 1993a. Modulation of the mitochondrial cyclosporin A-sensitive permeability transition pore. II. The minimal requirements for pore induction underscore a key role for transmembrane electrical potential, matrix pH, and matrix Ca^{2+} . *J Biol Chem* 268: 1011-1016.
- Petronilli V, Cola C, Massari S, Colonna R, Bernardi P. 1993b. Physiological effectors modify voltage sensing by

- the cyclosporin A-sensitive permeability transition pore of mitochondria. *J Biol Chem* 268: 21939-21945.
- Petronilli V, Costantini P, Scorrano L, Colonna R, Passamonti S, et al. 1994a. The voltage sensor of the mitochondrial permeability transition pore is tuned by the oxidation–reduction state of vicinal thiols. Increase of the gating potential by oxidants and its reversal by reducing agents. *J Biol Chem* 269: 16638-16642.
- Petronilli V, Nicolli A, Costantini P, Colonna R, Bernardi P. 1994b. Regulation of the permeability transition pore, a voltage-dependent mitochondrial channel inhibited by cyclosporin A. *Biochim Biophys Acta* 1187: 255-259.
- Petronilli V, Miotto G, Canton M, Brini M, Colonna R, et al. 1999. Transient and long-lasting openings of the mitochondrial permeability transition pore can be monitored directly in intact cells by changes in mitochondrial calcein fluorescence. *Biophys J* 76: 725-734.
- Petronilli V, Szabo I, Zoratti M. 1989. The inner mitochondrial membrane contains ion-conducting channels similar to those found in bacteria. *FEBS Lett* 259: 137-143.
- Pfanner N, Wiedemann N, Meisinger C, Lithgow T. 2004. Assembling the mitochondrial outer membrane. *Nat Struct Mol Biol* 11: 1044-1048.
- Pfeiffer DR, Schmid PC, Beatrice MC, Schmid HH. 1979. Intramitochondrial phospholipase activity and the effects of Ca^{2+} plus *N*-ethylmaleimide on mitochondrial function. *J Biol Chem* 254: 11485-11494.
- Polster BM, Fiskum G. 2004. Mitochondrial mechanisms of neural cell apoptosis. *J Neurochem* 90: 1281-1289.
- Potter VR. 1947. The assay of animal tissues for respiratory enzymes. VI. Further studies on oxidative phosphorylation. *J Biol Chem* 169: 17-37.
- Puka-Sundvall M, Gilland E, Hagberg H. 2001. Cerebral hypoxia–ischemia in immature rats: Involvement of mitochondrial permeability transition? *Dev Neurosci* 23: 192-197.
- Raaflaub J. 1953. Swelling of isolated mitochondria of the liver and their susceptibility to physicochemical influences. *Helv Physiol Pharmacol Acta* 11: 142-156.
- Rama Rao KV, Jayakumar AR, Norenberg DM. 2003. Ammonia neurotoxicity: Role of the mitochondrial permeability transition. *Metab Brain Dis* 18: 113-127.
- Rama Rao KV, Jayakumar AR, Norenberg MD. 2005. Role of oxidative stress in the ammonia-induced mitochondrial permeability transition in cultured astrocytes. *Neurochem Int* 47: 31-38.
- Reichert SA, Kim-Han JS, Dugan LL. 2001. The mitochondrial permeability transition pore and nitric oxide synthase mediate early mitochondrial depolarization in astrocytes during oxygen–glucose deprivation. *J Neurosci* 21: 6608-6616.
- Robb SJ, Robb-Gaspers LD, Scaduto RC, Jr., Thomas AP, Connor JR. 1999. Influence of calcium and iron on cell death and mitochondrial function in oxidatively stressed astrocytes. *J Neurosci Res* 55: 674-686.
- Robertson CL, Bucci CJ, Fiskum G. 2004. Mitochondrial response to calcium in the developing brain. *Brain Res Dev Brain Res* 151: 141-148.
- Rottenberg H, Marbach M. 1990. Regulation of Ca^{2+} transport in brain mitochondria. II. The mechanism of the adenine nucleotides enhancement of Ca^{2+} uptake and retention. *Biochim Biophys Acta* 1016: 87-98.
- Rutter GA, Rizzuto R. 2000. Regulation of mitochondrial metabolism by ER Ca^{2+} release: An intimate connection. *Trends Biochem Sci* 25: 215-221.
- Rytter A, Cardoso CM, Johansson P, Cronberg T, Hansson MJ, et al. 2005. The temperature dependence and involvement of mitochondria permeability transition and caspase activation in damage to organotypic hippocampal slices following in vitro ischemia. *J Neurochem* 95: 1108-1117.
- Salvi M, Toninello A. 2004. Effects of polyamines on mitochondrial Ca^{2+} transport. *Biochim Biophys Acta* 1661: 113-124.
- Sampson MJ, Decker WK, Beaudet AL, Ruitenbeek W, Armstrong D, et al. 2001. Immotile sperm and infertility in mice lacking mitochondrial voltage-dependent anion channel type 3. *J Biol Chem* 276: 39206-39212.
- Sanchez Mejia RO, Ona VO, Li M, Friedlander RM. 2001. Minocycline reduces traumatic brain injury-mediated caspase-1 activation, tissue damage, and neurological dysfunction. *Neurosurgery* 48:1393-1399; discussion 1399–1401.
- Santos JB, Schauwecker PE. 2003. Protection provided by cyclosporin A against excitotoxic neuronal death is genotype dependent. *Epilepsia* 44: 995-1002.
- Schanne FA, Kane AB, Young EE, Farber JL. 1979. Calcium dependence of toxic cell death: A final common pathway. *Science* 206: 700-702.
- Schinder AF, Olson EC, Spitzer NC, Montal M. 1996. Mitochondrial dysfunction is a primary event in glutamate neurotoxicity. *J Neurosci* 16: 6125-6133.
- Schinzel AC, Takeuchi O, Huang Z, Fisher JK, Zhou Z, et al. 2005. Cyclophilin D is a component of mitochondrial permeability transition and mediates neuronal cell death after focal cerebral ischemia. *Proc Natl Acad Sci USA* 102: 12005-12010.
- Schmidt-Kastner R, Truettner J, Zhao W, Belayev L, Krieger C, et al. 2000. Differential changes of bax, caspase-3, and p21 mRNA expression after transient focal brain ischemia in the rat. *Brain Res Mol Brain Res* 79: 88-101.
- Schon EA, Manfredi G. 2003. Neuronal degeneration and mitochondrial dysfunction. *J Clin Invest* 111: 303-312.
- Schonfeld P, Bohnensack R. 1997. Fatty acid-promoted mitochondrial permeability transition by membrane

- depolarization and binding to the ADP/ATP carrier. *FEBS Lett* 420: 167-170.
- Schubert A, Grimm S. 2004. Cyclophilin D, a component of the permeability transition-pore, is an apoptosis repressor. *Cancer Res* 64: 85-93.
- Schultheiss HP, Klingenberg M. 1984. Immunochemical characterization of the adenine nucleotide translocator. Organ specificity and conformation specificity. *Eur J Biochem* 143: 599-605.
- Scorrano L, Ashiya M, Buttle K, Weiler S, Oakes SA, et al. 2002. A distinct pathway remodels mitochondrial cristae and mobilizes cytochrome *c* during apoptosis. *Dev Cell* 2: 55-67.
- Scorrano L, Nicolli A, Basso E, Petronilli V, Bernardi P. 1997. Two modes of activation of the permeability transition pore: The role of mitochondrial cyclophilin. *Mol Cell Biochem* 174: 181-184.
- Scorrano L, Penzo D, Petronilli V, Pagano F, Bernardi P. 2001. Arachidonic acid causes cell death through the mitochondrial permeability transition. Implications for tumor necrosis factor- α apoptotic signaling. *J Biol Chem* 276: 12035-12040.
- Shiga Y, Onodera H, Matsuo Y, Kogure K. 1992. Cyclosporin A protects against ischemia-reperfusion injury in the brain. *Brain Res* 595: 145-148.
- Siesjo BK. 1981. Cell damage in the brain: A speculative synthesis. *J Cereb Blood Flow Metab* 1: 155-185.
- Sims NR, Anderson MF. 2002. Mitochondrial contributions to tissue damage in stroke. *Neurochem Int* 40: 511-526.
- Singleton RH, Stone JR, Okonkwo DO, Pellicane AJ, Povlishock JT. 2001. The immunophilin ligand FK506 attenuates axonal injury in an impact-acceleration model of traumatic brain injury. *J Neurotrauma* 18: 607-614.
- Slater EC, Cleland KW. 1953. The effect of calcium on the respiratory and phosphorylative activities of heart-muscle sarcosomes. *Biochem J* 55: 566-590.
- Smith DH, Chen XH, Pierce JE, Wolf JA, Trojanowski JQ, et al. 1997. Progressive atrophy and neuron death for one year following brain trauma in the rat. *J Neurotrauma* 14: 715-727.
- Snyder JW, Pastorino JG, Attie AM, Farber JL. 1992. Protection by cyclosporin A of cultured hepatocytes from the toxic consequences of the loss of mitochondrial energization produced by 1-methyl-4-phenylpyridinium. *Biochem Pharmacol* 44: 833-835.
- Solenski NJ, Kostecki VK, Dovey S, Periasamy A. 2003. Nitric oxide-induced depolarization of neuronal mitochondria: Implications for neuronal cell death. *Mol Cell Neurosci* 24: 1151-1169.
- Sousa SC, Castilho RF. 2005. Protective effect of melatonin on rotenone plus Ca^{2+} -induced mitochondrial oxidative stress and PC12 cell death. *Signal* 7: 1110-1116.
- Sousa SC, Maciel EN, Vercesi AE, Castilho RF. 2003. Ca^{2+} -induced oxidative stress in brain mitochondria treated with the respiratory chain inhibitor rotenone. *FEBS Lett* 543: 179-183.
- Speer O, Back N, Buerklen T, Brdiczka D, Koretsky A, et al. 2005. Octameric mitochondrial creatine kinase induces and stabilizes contact sites between the inner and outer membrane. *Biochem J* 385: 445-450.
- Spierings D, McStay G, Saleh M, Bender C, Chipuk J, et al. 2005. Connected to death: The (unexpurgated) mitochondrial pathway of apoptosis. *Science* 310: 66-67.
- Starkov AA, Chinopoulos C, Fiskum G. 2004. Mitochondrial calcium and oxidative stress as mediators of ischemic brain injury. *Cell Calcium* 36: 257-264.
- Starkov AA, Markova OV, Mokhova EN, Arrigoni-Martelli E, Bobyleva VA. 1994. Fatty acid-induced Ca^{2+} -dependent uncoupling and activation of external pathway of NADH oxidation are coupled to cyclosporin A-sensitive mitochondrial permeability transition. *Biochem Mol Biol Int* 32: 1147-1155.
- Stavrovskaya IG, Narayanan MV, Zhang W, Krasnikov BF, Heemskerk J, et al. 2004. Clinically approved heterocyclics act on a mitochondrial target and reduce stroke-induced pathology. *J Exp Med* 200: 211-222.
- Sullivan PG, Rabchevsky AG, Hicks RR, Gibson TR, Fletcher-Turner A, et al. 2000. Dose-response curve and optimal dosing regimen of cyclosporin A after traumatic brain injury in rats. *Neuroscience* 101: 289-295.
- Sullivan PG, Rabchevsky AG, Waldmeier PC, Springer JE. 2005. Mitochondrial permeability transition in CNS trauma: Cause or effect of neuronal cell death? *J Neurosci Res* 79: 231-239.
- Swanson RA, Ying W, Kauppinen TM. 2004. Astrocyte influences on ischemic neuronal death. *Curr Mol Med* 4: 193-205.
- Szabo I, Zoratti M. 1991. The giant channel of the inner mitochondrial membrane is inhibited by cyclosporin A. *J Biol Chem* 266: 3376-3379.
- Szabo I, Zoratti M. 1993. The mitochondrial permeability transition pore may comprise VDAC molecules. I. Binary structure and voltage dependence of the pore. *FEBS Lett* 330: 201-205.
- Szabo I, De Pinto V, Zoratti M. 1993. The mitochondrial permeability transition pore may comprise VDAC molecules. II. The electrophysiological properties of VDAC are compatible with those of the mitochondrial megachannel. *FEBS Lett* 330: 206-210.
- Teng YD, Choi H, Onario RC, Zhu S, Desilets FC, et al. 2004. Minocycline inhibits contusion-triggered mitochondrial cytochrome *c* release and mitigates functional deficits after spinal cord injury. *Proc Natl Acad Sci USA* 101: 3071-3076.

- Thiffault C, Bennett JR, Jr. 2005. Cyclical mitochondrial $\Delta\Psi_M$ fluctuations linked to electron transport, F_0F_1 ATP-synthase and mitochondrial Na^+/Ca^{2+} exchange are reduced in Alzheimer's disease cybrids. *Mitochondrion* 5: 109-119.
- Thompson HJ, Lifshitz J, Marklund N, Grady MS, Graham DI, et al. 2005. Lateral fluid percussion brain injury: A 15-year review and evaluation. *J Neurotrauma* 22: 42-75.
- Uchino H, Elmer E, Uchino K, Li PA, He QP, et al. 1998. Amelioration by cyclosporin A of brain damage in transient forebrain ischemia in the rat. *Brain Res* 812: 216-226.
- Uchino H, Elmer E, Uchino K, Lindvall O, Siesjo BK. 1995. Cyclosporin A dramatically ameliorates CA1 hippocampal damage following transient forebrain ischaemia in the rat. *Acta Physiol Scand* 155: 469-471.
- Uchino H, Minamikawa-Tachino R, Kristian T, Perkins G, Narazaki M, et al. 2002. Differential neuroprotection by cyclosporin A and FK506 following ischemia corresponds with differing abilities to inhibit calcineurin and the mitochondrial permeability transition. *Neurobiol Dis* 10: 219-233.
- Van Lookeren Campagne M, Gill R. 1996. Ultrastructural morphological changes are not characteristic of apoptotic cell death following focal cerebral ischaemia in the rat. *Neurosci Lett* 21: 111-114.
- Veech RL, Lawson JW, Cornell NW, Krebs HA. 1979. Cytosolic phosphorylation potential. *J Biol Chem* 254: 6538-6547.
- Verrier F, Mignotte B, Jan G, Brenner C. 2003. Study of PTPC composition during apoptosis for identification of viral protein target. *Ann N Y Acad Sci* 1010: 126-142.
- Vysokikh M, Zorova L, Zorov D, Heimlich G, Jurgensmeier J, et al. 2004. The intramitochondrial cytochrome *c* distribution varies correlated to the formation of a complex between VDAC and the adenine nucleotide translocase: This affects Bax-dependent cytochrome *c* release. *Biochim Biophys Acta* 1644: 27-36.
- Waldmeier PC, Zimmermann K, Qian T, Tintelen-Blomley M, Lemasters JJ. 2003. Cyclophilin D as a drug target. *Curr Med Chem* 10: 1485-1506.
- Wang H, Yu SW, Koh DW, Lew J, Coombs C, et al. 2004. Apoptosis-inducing factor substitutes for caspase executors in NMDA-triggered excitotoxic neuronal death. *J Neurosci* 24: 10963-10973.
- Wei L, Ying DJ, Cui L, Langsdorf J, Yu SP. 2004. Necrosis, apoptosis, and hybrid death in the cortex and thalamus after barrel cortex ischemia in rats. *Brain Res* 1022: 54-61.
- White RJ, Reynolds IJ. 1996. Mitochondrial depolarization in glutamate-stimulated neurons: An early signal specific to excitotoxin exposure. *J Neurosci* 16: 5688-5697.
- Wieckowski MR, Wojtczak L. 1998. Fatty acid-induced uncoupling of oxidative phosphorylation is partly due to opening of the mitochondrial permeability transition pore. *FEBS Lett* 423: 339-342.
- Wieckowski MR, Brdiczka D, Wojtczak L. 2000. Long-chain fatty acids promote opening of the reconstituted mitochondrial permeability transition pore. *FEBS Lett* 484: 61-64.
- Wiedemann N, Frazier AE, Pfanner N. 2004. The protein import machinery of mitochondria. *J Biol Chem* 279: 14473-14476.
- Wieloch T. 1985. Hypoglycemia-induced neuronal damage prevented by an *N*-methyl-D-aspartate antagonist. *Science* 230: 681-683.
- Wojtczak L, Lehninger AL. 1961. Formation and disappearance of an endogenous uncoupling factor during swelling and contraction of mitochondria. *Biochim Biophys Acta* 51: 442-456.
- Wojtczak L, Wieckowski MR, Schonfeld P. 1998. Protonophoric activity of fatty acid analogs and derivatives in the inner mitochondrial membrane: A further argument for the fatty acid cycling model. *Arch Biochem Biophys* 357: 76-84.
- Woodfield K, Ruck A, Brdiczka D, Halestrap AP. 1998. Direct demonstration of a specific interaction between cyclophilin D and the adenine nucleotide translocase confirms their role in the mitochondrial permeability transition. *Biochem J* 336 (Pt 2): 287-290.
- Xu X, Decker W, Sampson MJ, Craigen WJ, Colombini M. 1999. Mouse VDAC isoforms expressed in yeast: Channel properties and their roles in mitochondrial outer membrane permeability. *J Membr Biol* 170: 89-102.
- Yoshimoto T, Siesjo BK. 1999. Posttreatment with the immunosuppressant cyclosporin A in transient focal ischemia. *Brain Res* 839: 283-291.
- Yrjanheikki J, Keinanen R, Pellikka M, Hokfelt T, Koistinaho J. 1998. Tetracyclines inhibit microglial activation and are neuroprotective in global brain ischemia. *Proc Natl Acad Sci USA* 95: 15769-15774.
- Yrjanheikki J, Tikka T, Keinanen R, Goldsteins G, Chan PH, et al. 1999. A tetracycline derivative, minocycline, reduces inflammation and protects against focal cerebral ischemia with a wide therapeutic window. *Proc Natl Acad Sci USA* 96: 13496-13500.
- Zaidan E, Nilsson M, Sims NR. 2004. Increased mitochondrial permeability in response to intrastriatal *N*-methyl-D-aspartate: Detection based on accumulation of radiolabel from [3 H]deoxyglucose. *Neurochem Res* 29: 609-616.
- Zamora M, Granel M, Mampel T, Vinas O. 2004. Adenine nucleotide translocase 3 (ANT3) overexpression induces apoptosis in cultured cells. *FEBS Lett* 563: 155-160.
- Zamzami N, Marchetti P, Castedo M, Decaudin D, Macho A, et al. 1995a. Sequential reduction of mitochondrial transmembrane potential and generation of reactive oxygen species in early programmed cell death. *J Exp Med* 182: 367-377.

- Zamzami N, Marchetti P, Castedo M, Zanin C, Vayssiere JL, et al. 1995b. Reduction in mitochondrial potential constitutes an early irreversible step of programmed lymphocyte death in vivo. *J Exp Med* 181: 1661-1672.
- Zamzami N, Marchetti P, Castedo M, Hirsch T, Susin SA, et al. 1996. Inhibitors of permeability transition interfere with the disruption of the mitochondrial transmembrane potential during apoptosis. *FEBS Lett* 384: 53-57.
- Zborowski J, Wojtczak L. 1963. Induction of swelling of liver mitochondria by fatty acids of various chain lengths. *Biochim Biophys Acta* 70: 596-598.
- Zhu S, Stavrovskaya IG, Drozda M, Kim BY, Ona V, et al. 2002. Minocycline inhibits cytochrome *c* release and delays progression of amyotrophic lateral sclerosis in mice. *Nature* 417: 74-78.
- Zivin JA, Kochhar A, Saitoh T. 1989. Phenothiazines reduce ischemic damage to the central nervous system. *Brain Res* 482: 189-193.
- Zizi M, Forte M, Blachly-Dyson E, Colombini M. 1994. NADH regulates the gating of VDAC, the mitochondrial outer membrane channel. *J Biol Chem* 269: 1614-1616.
- Zoratti M, Szabo I. 1995. The mitochondrial permeability transition. *Biochim Biophys Acta* 1241: 139-176.
- Zoratti M, Szabo I, De Marchi U. 2005. Mitochondrial permeability transitions: How many doors to the house? *Biochim Biophys Acta* 1706: 40-52.

6.5 Mitochondrial Mechanisms of Oxidative Stress and Apoptosis

L. Soane · N. Solenski · G. Fiskum

1	Introduction	704
2	Oxidative Stress	705
2.1	Contribution of Oxidative Stress to Neurodegeneration	705
2.2	Mitochondria as Sources of Reactive Oxygen Species	706
2.3	Mitochondrial Antioxidant Systems	709
2.4	Formation of Nitric Oxide in the Brain	710
2.5	NMDA Receptor and nNOS Activation Coupling	711
2.6	Mitochondrial Formation of NO	711
2.7	Mitochondria as Targets of Reactive Oxygen and Nitrogen Species	713
3	Apoptosis	715
3.1	Intrinsic and Extrinsic Apoptotic Pathways	715
3.2	Proapoptotic Bcl-2 Family Proteins	717
3.3	Antiapoptotic Bcl-2 Family Proteins	720
3.4	Antiapoptotic Drugs and Proteins	721
4	Future Directions	723

Abstract: While it has long been appreciated that mitochondrial dysfunction can lead to metabolic failure and necrotic cell death, more recent work has highlighted the central role that mitochondria play in oxidative stress and apoptosis, including their involvement in neurodegeneration. Factors that promote mitochondrial production of reactive oxygen species are not well understood but include abnormally high levels of oxygen, excessive mitochondrial accumulation of Ca^{2+} , inhibition of electron transport by nitric oxide and various toxins (including several pesticides), genetic alterations in electron transport chain proteins, and impaired detoxification by enzymes like superoxide dismutase. Mitochondrial proteins, lipids, and DNA are also highly sensitive targets of reactive oxygen and nitrogen species, due at least in part to their proximity. Oxidative stress is also one of many conditions that can trigger the release of pro-apoptotic mitochondrial proteins into the cytosol. Several release mechanisms exist and are modulated by a host of interactions between mitochondrial and extramitochondrial proteins that are susceptible to inhibition by both small chemicals and proteins. This review focuses on mitochondria as generators and targets of oxidative stress and on mitochondrial mechanisms of apoptosis in the nervous system. Attention is also focused on future research directions that may translate this knowledge into neuroprotection.

List of Abbreviations: 3-AB, 3-aminobenzamide; 6-OHDA, 6-hydroxydopamine; AD, Alzheimer's disease; AIF, apoptosis-inducing factor; ALS, amyotrophic lateral sclerosis; Apaf-1, apoptotic protease-activating factor-1; Bcl, B cell lymphoma; BH, Bcl-2 homology; ced, cell death abnormal; CAD, caspase-activated DNase; cGMP, cyclic 3',5'-guanosine monophosphate; CL, cardiolipin; CNS, central nervous system; COX, cytochrome oxidase; CytC, cytochrome c; DLC, dynein light chain; DR, death receptor; EndoG, endonuclease G; ER, endoplasmic reticulum; ETC, electron transport chain; FCCP, carbonyl cyanide 4-trifluoromethoxy-phenylhydrazone; G6PD, glucose-6-phosphate dehydrogenase; GPx, glutathione peroxidase; GSH, reduced glutathione; HIV, human immunodeficiency virus; Htra2/Omi, high temperature requirement protein A2/Omi stress-regulated endoprotease; IAP, inhibitor of apoptosis protein; IMS, intermembrane space; MPT, membrane permeability transition; MPTP, 1-methyl-4-phenyl-1,2,3,6-tetrahydropyridine; NMDA, *N*-methyl-D-aspartate; NOS, nitric oxide synthase; NPC, neural precursor cells; OMM, outer mitochondrial membrane; PARP, poly(ADP-ribose) polymerase; PCD, programmed cell death; PSD-95, postsynaptic density-95 kDa; PTD, protein transduction domain; RNS, reactive nitrogen species; ROS, reactive oxygen species; Smac/DIABLO, second mitochondria-derived activator of caspase/direct IAP-associated binding protein with low PI; SOD, superoxide dismutase; TAT, transactivator of transcription; TNF, tumor necrosis factor; Trp, transient receptor potential; TUDCA, tauroursodeoxycholic acid; UCP, Uncoupling protein; VDAC, voltage-dependent anion channel

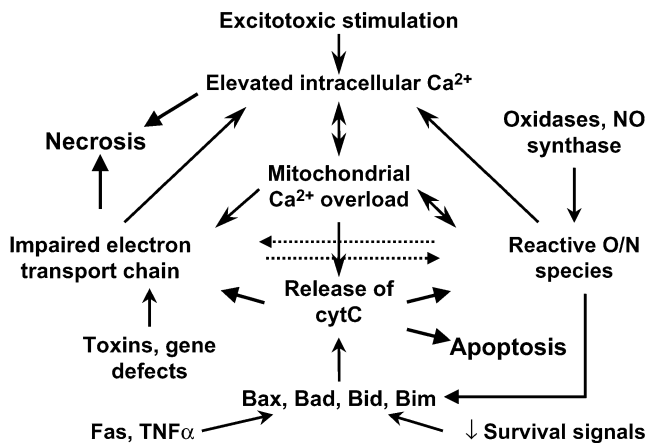
1 Introduction

Mitochondria are important mediators of cell death that occurs during both acute brain injury and chronic neurodegenerative disorders (Calabrese et al., 2001; Castellani et al., 2002; Jordan et al., 2003; Ames, 2004; Chan, 2004; Hagberg, 2004; Beal, 2005). Mitochondrial participation in cell death can be due to dysfunction caused by exogenous or endogenous toxicants (Wallace and Starkov, 2000), or to genetic alterations in the expression or activity of mitochondrial proteins and nonmitochondrial proteins that interact with mitochondria in response to stressful stimuli (Wallace, 2005). The significance of mitochondrial dysfunction was previously thought to be limited to effects on mitochondrial ATP production, and therefore to necrotic cell death. We now understand that mitochondrial mechanisms of neural cell death include oxidative stress and apoptosis, in addition to metabolic failure (🔗 [Figure 6.5-1](#)). Mild mitochondrial injury, with maintenance of near-normal cellular ATP, results in mainly apoptotic cell death. More extensive injury that causes ATP depletion shifts the form of cell death toward necrosis (Ankarcrona et al., 1995; Nicotera, 2002, 2003; Orrenius et al., 2003; Nicotera and Melino, 2004; Chiarugi, 2005).

Several fundamentally different, albeit interactive, mechanisms contribute to mitochondrial dysfunction (🔗 [Figure 6.5-1](#)). In neurons exposed to excitotoxic levels of the neurotransmitter glutamate, excessive mitochondrial accumulation of Ca^{2+} and possibly Zn^{2+} triggers several forms of mitochondrial injury

■ Figure 6.5-1

Mitochondrial mechanisms of neuronal cell death. Depending on the form of neuropathology (i.e., stroke, inflammation, Parkinson's disease, etc.), mitochondrial dysfunction is caused by various combinations of stressors, including excitotoxic elevation of intracellular Ca^{2+} , reactive O_2 and nitrogen species, toxins, gene defects, cell-death ligands (e.g., Fas and $\text{TNF}\alpha$), and altered cell survival signal transduction. Substantial inhibition of oxidative phosphorylation in cells like neurons with a high energy demand leads to cellular deenergization and necrotic cell death. Mitochondrial production of reactive oxygen and nitrogen species promotes excitotoxic neuronal Ca^{2+} dysregulation through activation of plasmalemmal transient receptor potential (Trp) channels. Mitochondrial oxidative stress also promotes apoptosis through induction of proapoptotic gene expression and other more direct mechanisms. Release of cytochrome c (CytC) into the cytosol in response to outer membrane pore formation, for example by Bax, in response to the binding of BH3-only proteins, e.g., truncated Bid, is a critical step in triggering the caspase cascade of apoptosis and can also promote formation of superoxide and impair oxidative phosphorylation



(Atlante et al., 2001; Dineley et al., 2003; Kristian, 2004; Nicholls, 2004; Sensi and Jeng, 2004; Kushnareva et al., 2005). Mitochondria are also highly sensitive targets of toxic reactive oxygen and reactive nitrogen species (ROS and RNS, respectively), generated by both mitochondrial and extramitochondrial enzymes and nonenzymatic reactions (Fiskum et al., 2004; Gibson and Huang, 2004; Patel, 2004; Sims et al., 2004; Tretter et al., 2004; Zhu et al., 2005). The currently most widely investigated mitochondrial cell death mechanism is the release of mitochondrial proapoptotic proteins into the cytosol mediated by a host of interactions between mitochondrial and extramitochondrial proteins (Kirkland and Franklin, 2003; Scorrano and Korsmeyer, 2003; Hong et al., 2004; Khosravi-Far and Esposti, 2004; Orrenius, 2004; Ouyang and Giffard, 2004; Polster and Fiskum, 2004; Reed, 2004; Culmsee and Mattson, 2005; Green, 2005; Lucken-Ardjomande and Martinou, 2005). This chapter focuses on mitochondria as mediators and targets of oxidative stress and on mitochondrial mechanisms of apoptosis in the central nervous system (CNS).

2 Oxidative Stress

2.1 Contribution of Oxidative Stress to Neurodegeneration

Several lines of evidence indicate that oxidative stress is a primary mechanism of neuronal cell death associated with a wide range of neurologic disorders. The extent of delayed neuronal death correlates well with prelethal markers of oxidative molecular alterations to lipids, proteins, and nucleic acids in both

animal models and patients (Hall, 1997; Markesbery and Carney, 1999; Bayir et al., 2002; Butterfield, 2004; Cristofori et al., 2005; Musiek et al., 2005). Moreover, these oxidative modifications are also observed at the mitochondrial level (Liu et al., 2002; Sullivan et al., 2004a; Hsu et al., 2005; Naoi et al., 2005). Neuroprotection occurs following the use of antioxidants and inhibitors of free radical-producing enzymes, some of which target mitochondria (Coulter et al., 2000; Ginsberg, 2001; Ahlemeyer and Kriegelstein, 2003; Sugimoto and Iadecola, 2003; Beal, 2004; Park et al., 2006; Simpkins et al., 2005). In addition, genetic animal models where antioxidant enzymes, including the mitochondrial enzymes manganese superoxide dismutase (SOD2) and glutathione peroxidase (GPx), are either over- or underexpressed display decreased and increased resistance, respectively, to acute and chronic neurodegeneration (Lewen et al., 2000; Van Remmen et al., 2004; McLean et al., 2005; Moskovitz, 2005).

2.2 Mitochondria as Sources of Reactive Oxygen Species

Superoxide is a normal byproduct of mitochondrial electron transport respiration and is responsible for 0.2–2.0% of mitochondrial and therefore cellular O_2 consumption (Barja, 1999; St Pierre et al., 2002). Due to its extremely short half-life, superoxide normally reacts with itself (dismutates) to form H_2O_2 , aided by SOD1 and SOD2 in the cytosol and mitochondria, respectively. The metabolism of H_2O_2 to H_2O via GPx and other peroxidases can result in oxidative stress if this causes a net oxidized shift in the redox state of glutathione and pyridine nucleotides (NAD(H) and NADP(H)). As NADPH is the direct reductant responsible for maintaining reduced glutathione (GSH) via glutathione reductase, the reduction of $NADP^+$ by mitochondrial isocitrate dehydrogenase, malic enzyme, and nicotinamide nucleotide transhydrogenase reactions is critical for detoxification of intramitochondrial peroxides (Vogel et al., 1999). GSH can also be irreversibly lost without an increase in GSSG in brain mitochondria due to formation of protein-SS-glutathione mixed disulfides (Ravindranath and Reed, 1990).

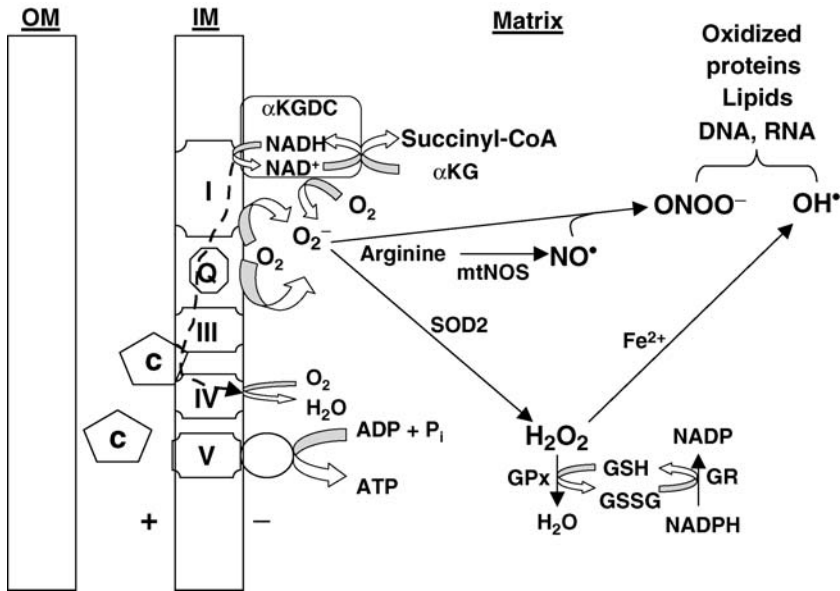
The toxicity of mitochondrially produced superoxide and H_2O_2 is also exerted by their metabolites, including the hydroxyl radical generated by metal-catalyzed reduction of H_2O_2 , and peroxynitrite ($ONOO^-$) generated by the reaction of superoxide with nitric oxide ($NO\cdot$) (Figure 6.5-2). Both of these highly reactive agents are capable of oxidatively modifying proteins, lipids, RNA, and DNA, including those found within mitochondria (Beckman and Koppenol, 1996; Heck et al., 2005).

The chemical mechanisms responsible for mitochondrial superoxide formation are not well understood. While much evidence points to the single electron reduction of O_2 by semiubiquinone during its two-step oxidation at complex III and to reactions at one or more redox sites within complex I (Turrens, 2003; Lambert and Brand, 2004; Andreyev et al., 2005), recent evidence also strongly suggests that mitochondrial matrix dehydrogenases, particularly 2-oxoglutarate dehydrogenase, contribute significantly to mitochondrial superoxide production (Starkov et al., 2004; Tretter and Adam-Vizi, 2004).

The physiological and pathological factors that regulate mitochondrial superoxide production are those that influence mitochondrial bioenergetics, and therefore the thermodynamic driving force behind superoxide production. In general, conditions that cause a net reduced shift in the redox state of the sites of superoxide formation result in increased production, and those that produce an oxidized shift in redox state, result in decreased production. The redox state is very sensitive to the rate of respiration; therefore, the rate of ROS production during maximal oxidative phosphorylation conditions (state 3 respiration) in the presence of NADH-linked oxidizable substrates, e.g., pyruvate or glutamate, is only 30% as fast as the rate observed at rest (state 4 respiration). At rest the redox state of all electron transport chain (ETC) and of matrix dehydrogenase redox centers is relatively reduced (Starkov and Fiskum, 2003). The link between oxidative phosphorylation and redox state is the generation of an electrochemical gradient of protons ($\Delta\mu_{H^+}$) across the mitochondrial inner membrane by respiration-dependent proton efflux. Therefore, conditions, in addition to ATP synthase activation, that reduce $\Delta\mu_{H^+}$ also lower the rate of superoxide generation. As the vast majority of the energy present in $\Delta\mu_{H^+}$ is in the form of the membrane potential ($\Delta\Psi$), compared to the small pH gradient, activities or chemicals that drop $\Delta\Psi$ without impairing the flow of electrons through the ETC also lower the rate of superoxide generation. For example, when isolated brain mitochondria are exposed to nanomolar concentrations of the proton ionophore FCCP (carbonyl cyanide

■ Figure 6.5-2

Mitochondrial generation and metabolism of reactive oxygen species (ROS). Normally, around 99% of the O_2 consumed by mitochondria occurs at the ETC complex IV (cytochrome oxidase), driven by electrons ultimately donated to the ETC by dehydrogenases, e.g., α -ketoglutarate dehydrogenase complex (α KGDH) and succinate dehydrogenase (complex II, not shown). Some O_2 is also reduced by a single electron reaction, forming superoxide (O_2^-), catalyzed by reactions at ETC complexes I–III and by one or more dehydrogenases, e.g., α KGDH. Superoxide is dismutated to H_2O_2 both spontaneously and enzymatically via the mitochondrial manganese superoxide dismutase (SOD2). H_2O_2 and other peroxides are further metabolized to H_2O or alcohol derivatives by one or more glutathione peroxidases (GPx). The electrons necessary for this reduction reaction come from reduced glutathione (GSH), which in turn is kept in its reduced state by glutathione reductase (GR). Excessive superoxide production occurs when the flow of electrons through the ETC is impaired by altered activities of any of the complexes due to genetic alterations, ETC inhibitory toxins (e.g., rotenone), or protein modifications (e.g., due to oxidative stress). Release of cytochrome *c* through the outer membrane also inhibits the ETC and promotes superoxide formation. Consequently, excessive H_2O_2 production can deplete mitochondria of reduced glutathione (GSH), resulting in the accumulation of lipid peroxides and oxidized proteins. In the presence of reduced iron (Fe^{2+}), the reduction of H_2O_2 leads to the formation of the highly reactive hydroxyl radical (OH^\bullet). Nitric oxide (NO), generated either extramitochondrially or via the mitochondrial nitric oxide synthase (mtNOS), can react with superoxide, forming peroxynitrite ($ONOO^-$). Peroxynitrite and hydroxyl radical are capable of oxidizing virtually all cellular molecules, including many present at the mitochondrion that are essential for cell viability



4-trifluoromethoxy-phenylhydrazine), they exhibit less than 10% drop in $\Delta\Psi$, with 50% reduction in the rate of ROS formation (Starkov and Fiskum, 2003). The concept of reducing mitochondrial ROS production by mild respiratory uncoupling has been used to explain the neuroprotection afforded *in vitro* and *in vivo* by the administration of uncoupling agents (lipid soluble weak acids like FCCP) (Ferranti et al., 2003; Maragos et al., 2003; Jin et al., 2004).

The same rationale has been applied to the finding that increased expression of mitochondrial uncoupling proteins (UCPs) provides neuroprotection (Kim-Han et al., 2001; Sullivan et al., 2004b; Andrews et al., 2005; Conti et al., 2005). While the activation of these UCPs by markers of cellular stress, including free fatty acids and ROS, is well documented (Echtay et al., 2002), the actual participation of

UCPs, other than UCP1 found in brown fat, in mitochondrial uncoupling and decreased ROS production in cells or tissues is still controversial (Nicholls, 2001).

Another potential mechanism for decreasing $\Delta\Psi$ is activation of the mitochondrial ATP-sensitive potassium channel, which has been reported to be highly expressed in brain mitochondria (Bajgar et al., 2001). Activation does cause a significant increase in mitochondrial volume (Beavis et al., 1993) but only decreases $\Delta\Psi$ by 1–2 mV (Kowaltowski et al., 2001). Nevertheless, neuroprotection is afforded by pretreatment of neurons or animals with pharmacologic activators of the mitochondrial $[K^+]$ ATP-sensitive channel blocker, diazoxide (Rajapakse et al., 2002; Mattson and Kroemer, 2003; Teshima et al., 2003). Despite the fact that mild uncoupling (i.e., reduction in $\Delta\Psi$) normally reduces mitochondrial ROS formation, numerous reports suggest that the opening of this channel somehow increases mitochondrial ROS production (Krenz et al., 2002; Busija et al., 2005; Liang et al., 2005). Activation of mitochondrial $[K^+]$ ATP channels may represent one of the primary mechanisms for ischemic preconditioning stress involving the generation of ROS as a downstream effect (Oldenburg et al., 2003).

While mitochondrial $\Delta\Psi$ and redox state are normally controlled by metabolic demand, i.e., ATP synthase activity (Dimroth et al., 2003), a number of pathological conditions can override this control. For instance, inhibition of electron flow at any redox site distal to sites of superoxide formation will cause a reduced shift in the redox state of those sites, thereby promoting superoxide formation. Examples of ETC inhibitors that produce these effects are those that target either complex IV (cyanide, sodium azide, and NO), complex III (antimycin A), complex II (methylmalonate and 3-nitropropionate), or complex I (rotenone and paraquat).

A controversial topic in this field is the involvement of mitochondrial Ca^{2+} in ROS production. Respiration-dependent mitochondrial Ca^{2+} uptake occurs via electrophoretic uniporter, and Ca^{2+} release is mediated by both $Ca^{2+}/2H^+$ and $Ca^{2+}/2Na^+$ antiports (Gunter et al., 2004). The activity of Ca^{2+} uniporter and exchangers are, under normal conditions, limited kinetically and utilize only a small fraction of the $\Delta\mu_{H^+}$. Nevertheless, they importantly regulate intramitochondrial $[Ca^{2+}]$ in a range that mediates key metabolic enzymes, e.g., pyruvate and 2-oxoglutarate dehydrogenases, thereby modulating oxidative phosphorylation. The fact that Ca^{2+} activates these dehydrogenases, resulting in a net reduced shift in mitochondrial redox state, may suggest that a physiological increase in Ca^{2+} could also increase mitochondrial superoxide formation, although this has yet to be demonstrated.

A supraphysiologic increase in intramitochondrial Ca^{2+} has been proposed to account for elevated mitochondrial ROS production in a number of cell death paradigms, including neuronal excitotoxicity (Castilho et al., 1999) and neuronal apoptosis (Mattson, 1998). One possible mechanism responsible for Ca^{2+} -induced mitochondrial ROS production is the membrane permeability transition (MPT). The MPT is induced specifically at the inner membrane by excessive mitochondrial Ca^{2+} accumulation and is promoted by an oxidized mitochondrial redox state. When MPT is fully activated, solutes up to approximately 1.5 kDa equilibrate across the membrane resulting in loss of mitochondrial metabolites (e.g., NAD(P)H, glutathione), and net uptake of osmolytes like K^+ , resulting in swelling of the matrix, and typically, rupture of the outer membrane. Outer membrane disruption results in release of soluble intermembrane proteins, e.g., adenylate kinase, cytochrome C (CytC) (Crouser et al., 2003). Treatment with calcium chelators such as BAPTA can reduce mitochondrial ROS production and promote neuroprotection (Keller et al., 1998a).

Loss of CytC can certainly stimulate mitochondrial generation of ROS by causing a reduced shift in mitochondrial redox sites associated with superoxide production (Kushnareva et al., 2002; Starkov et al., 2002). However, the MPT also causes a drop in $\Delta\Psi$ and a loss of mitochondrial pyridine nucleotides, both of which depress mitochondrial generation of ROS (Costantini et al., 1996). However, recent work from Batandier et al. suggests that even if mitochondrial NAD(H) were released into the cytosol in response to the MPT, their residual concentration in the mitochondrial matrix in equilibrium with the cytosolic pool could be sufficient to support substantial ROS production (Batandier et al., 2004). As the MPT also results in the release of mitochondrial matrix glutathione, this loss and impairment of the GPx/reductase system could explain a net increase in ROS and associated markers of oxidative stress during excitotoxicity and acute brain injury (Anderson and Sims, 2002). An attractive alternative explanation for Ca^{2+} -induced net ROS production is its potent direct inhibition of both mitochondrial GPx and reductase enzyme activities (Zoccarato et al., 2004).

The finding that MPT inhibitors, cyclosporin A and bongkreic acid, are neuroprotective both *in vitro* and *in vivo*, is supportive evidence of the role of MPT in neuronal cell death and in oxidative stress (Friberg and Wieloch, 2002). However, the use of MPT inhibitors as neuroprotectants has met with variable degrees of success (Dubinsky and Levi, 1998; Scheff and Sullivan, 1999; Kaminska et al., 2001; Uchino et al., 2002; Maciel et al., 2003; Domanska-Janik et al., 2004). This variability could be due to the fact that cyclosporin A is relatively ineffective at blocking the MPT in different cell types, including neurons, and under specific conditions, e.g., at high [ATP], or very high $[Ca^{2+}]$ (Andreyev and Fiskum, 1999; Brustovetsky and Dubinsky, 2000; Fiskum et al., 2003). Therefore, the development of more broadly effective MPT inhibitors is needed. One agent that exhibits superior inhibition of the MPT in brain mitochondria is 2-aminoethoxydiphenylborate (2-APB) (Chinopoulos et al., 2003). This drug also inhibits capacitative Ca^{2+} entry associated with Trp channels, including those activated by oxidative stress. This compound may therefore provide a multipotent approach to neuroprotection (Iwasaki et al., 2001).

Another factor that likely regulates mitochondrial superoxide production is the tissue O_2 tension. The normal cerebral cortex pO_2 is 20–40 mm Hg (30–60 $\mu M [O_2]$). The K_m for O_2 of mitochondrial complex IV (cytochrome oxidase) is approximately 1 μM . The fact that cerebral O_2 consumption is limited by tissue pO_2 at approximately 10 mm Hg (15 $\mu M [O_2]$) indicates that a large O_2 gradient exists between the interstitium and the mitochondria within the intracellular milieu (Erecinska and Silver, 2001). Several studies performed with isolated mitochondria indicate that there is a first-order relationship between $[O_2]$ and mitochondrial superoxide formation, with no evidence for saturation at up to 100% O_2 -saturated medium (Boveris and Chance, 1973). It is therefore highly likely that as tissue pO_2 rises from normoxic to hyperoxic levels, mitochondrial ROS production rises accordingly. This relationship may explain why hyperoxic resuscitation following global cerebral ischemia results in elevated markers of oxidative stress, increased neuronal death, and worse neurologic outcome than when animals are reperfused under normoxic conditions (Liu et al., 1998; Rosenthal and Fiskum, 2005; Vereczki et al., 2006). On the other hand, evidence suggests that severe hypoxia can also trigger mitochondrial ROS formation (Chandel and Schumacker, 2000). Although the mechanism for hypoxic mitochondrial ROS formation is not established, it is theoretically possible that at O_2 concentrations that limit respiration, the subsequent reduced shift in the redox state of superoxide-generating redox sites could be responsible.

2.3 Mitochondrial Antioxidant Systems

The pathologically important net production of ROS and RNS is the difference between their generation and detoxification. Mitochondria possess many nonenzymatic and enzymatic antioxidant defenses and other enzyme activities that are protective against a variety of ROS and RNS and the products of their reactions with proteins, lipids, and nucleic acids.

Mitochondria possess a very active and highly inducible manganese SOD, also known as SOD2 (Macmillan-Crow and Cruthirds, 2001). This enzyme is found exclusively in the mitochondrial matrix (▶ [Figure 6.5-2](#)) and is critical for cell viability. Supportive evidence includes data that homozygous SOD^{-/-} animals die within 10 days after birth (Li et al., 1995) and that primary neuronal cultures from the fetuses of these knockouts are extremely vulnerable to oxidative stress to the extent that they spontaneously die at normal oxygen conditions (20% of O_2) (Li et al., 1998). Heterozygote knockouts are viable, but are much more vulnerable to many forms of stress, including excitotoxicity and cerebral ischemia (Li et al., 1998; Kim et al., 2002). Similarly, overexpression of SOD2 leads to neuroprotection from excitotoxic- and NO-mediated damage (Gonzalez-Zulueta et al., 1998). In neural cell lines, overexpression of SOD2 reduces ONOO⁻ generated by NO-generating agents and protects against protein nitration, mitochondrial membrane depolarization, and apoptosis (Keller et al., 1998b). Studies indicate that CuZnSOD (SOD1), which is primarily located in the cytosol, is at least partially localized to mitochondria, although the functional significance of SOD1 in mammalian mitochondria is not known (Sturtz et al., 2001; Takeuchi et al., 2002).

A number of nonenzymatic superoxide scavenging molecules are present in mitochondria, although the degree to which they contribute to superoxide scavenging is unknown. These molecules include dihydrolipoic acid, ubiquinone, α -tocopherol, pyruvate, ascorbate, CytC, and glutathione.

Removal of H_2O_2 is important to avoid production of the hydroxyl radicals by Fenton reaction. The primary intramitochondrial system, the activities of which are responsible for the reduction of H_2O_2 and lipid peroxides (to water and alcohols accordingly), constitutes GPx and glutathione reductase (GR) (▶ *Figure 6.5-2*). The normal concentration of intramitochondrial glutathione is high (~ 10 mM), suggesting it may also act as a direct antioxidant. Depletion of either the cytoplasmic or the mitochondrial glutathione pools can have significant impact on neuronal viability (Heales and Bolanos, 2002; Gegg et al., 2003). For example, mitochondrial glutathione pool depletion in astrocytes (that are exposed to ONOO⁻ donors) results in increased cell death compared with astrocytes with an intact pool of mitochondrial glutathione (Muyderman et al., 2004; Sims et al., 2004). GPx1 is the primary GPx isoform present in mitochondria (Esworthy et al., 1997). The importance of the activity of this enzyme under even normal conditions is illustrated by the finding that mitochondria from mice lacking GPx1 produce excessive H_2O_2 and exhibit impaired respiration (Esposito et al., 2000). Overexpression of GPx1 inhibits CytC release, caspase activation, and neuronal death in experimental stroke (Hoehn et al., 2003). In addition to GPx1, mitochondria possess activity of hydroperoxide GPx (GPx4). Overexpression of this enzyme protects against cell death caused by the mitochondrial poisons cyanide and rotenone (Arai et al., 1999), and against apoptosis induced by the glycolytic inhibitor 2-deoxyglucose (Nakagawa, 2004). The activity of NADPH-dependent mitochondrial GR is necessary for reducing the oxidized glutathione generated by GPx reactions (▶ *Figure 6.5-2*). This enzyme, as noted earlier, is highly sensitive to inhibition by elevated intramitochondrial Ca^{2+} (Zoccarato et al., 2004). Exposure of neural cells to an inhibitor of GR greatly increases their sensitivity to death caused by the stimulation of endogenous H_2O_2 production (Buckman et al., 1993). Another enzyme present in mitochondria that utilizes glutathione is glutathione-S-transferase. This enzyme is thought to detoxify 4-hydroxynonenal, a highly reactive lipid peroxidation product that is toxic to mitochondria (Chen et al., 1997; Keller et al., 1997; Raza et al., 2002).

Although not as well characterized as the GPx/reductase system, the mitochondrial thioredoxin/thioredoxin reductase and glutaredoxin/glutaredoxin reductase systems are also likely important for neuroprotection (Tanaka et al., 2000). These enzyme systems reduce protein disulfides and mixed disulfides, respectively. Finally, other important antioxidant-related mitochondrial enzyme systems include NADP-dependent isocitrate dehydrogenase, malic enzyme, and the $\Delta\mu_{\text{H}^+}$ -dependent transhydrogenase. These enzymes are all important in producing the NADPH used by the GR and transferase enzymes and in the thioredoxin and glutaredoxin reductase reactions.

2.4 Formation of Nitric Oxide in the Brain

NO is a unique signaling gas molecule that binds to the heme moiety of guanylyl cyclase, causing a conformational change, activating enzyme activity, and forming guanosine 3',5'-cyclic monophosphate (cGMP). As a small gas molecule, it diffuses rapidly through cell lipid membranes, and therefore can be released from neuronal axons into the extracellular space as a potent nonreceptor-mediated signaling molecule among neurons.

NO is formed following activation of the enzyme nitric oxide synthase (NOS), which exists in three established isoforms in brain tissue, best classified by their dependency on Ca^{2+} for activation. The constitutive Ca^{2+} -dependent forms are endothelial NOS (eNOS) and neuronal NOS (nNOS), while the inducible Ca^{2+} -independent form is known as "iNOS." Although named by the tissue in which they were originally discovered, these isoforms of NOS are not tissue specific. The exact contribution of each isoform to neurotoxicity and neuroprotection during brain injury is unknown. In general, results obtained both *in vitro* and *in vivo* suggest that eNOS activation with NO acting as a vasodilator is neuroprotective, while nNOS and iNOS are thought to be neurotoxic (reviewed in Dalkara et al. (1998); Dirnagl et al. (1999)). For example, during the initial stages of brain ischemia, activation of nNOS is associated with *N*-methyl-D-aspartate (NMDA) receptor activation while activation of iNOS occurs as a consequence of stimulated macrophages or astrocytes (including microglia), mainly during the reperfusion stage. This concept of neurotoxicity vs. neuroprotection, based on isoform activation, is probably too simplistic. Important parameters are being clarified by defining the role of NO concentration as well as spatial, temporal, and

cell-type considerations. For example, evidence from rodent stroke models support the concept that nNOS is “inducible,” with a large population of neurons being activated during ischemia, particularly in the perifocal ischemic region (Eliasson et al., 1999). Similarly, the concept that upregulation of eNOS is simply neuroprotective is not accurate since eNOS, in the absence of the crucial cofactor tetrahydrobiopterin (BH4) or its substrate L-arginine, can produce large amounts of ROS. Electron flow through the eNOS enzyme becomes subsequently diverted to molecular O₂ rather than to L-arginine, leading to a condition called “eNOS uncoupling.” During this state, potentially damaging superoxide is formed rather than the expected neuroprotective vasodilatory effects of NO (Landmesser et al., 2003; Endres et al., 2004). In addition, there is a greater appreciation that nonneuronal cells, e.g., glia, contribute significantly to NO levels during ischemia, suggesting a similar critical role in mediating brain injury (Murphy, 2000).

NO has also important effects on astrocytes. In contrast to neurons, astrocytes are glycolytic cells and can metabolize glucose through the glycolytic pathways. In vitro, astrocytes exposed to exogenous NO upregulate baseline glycolysis while preserving ATP levels (Almeida et al., 2001). When neurons are exposed to supraphysiologic concentrations of NO, mitochondrial membrane collapse occurs (Solenski et al., 2003). In contrast, exposure of astrocytes to NO causes mitochondrial membrane hyperpolarization. Although speculative, this may represent a mechanism of protecting astrocytes during conditions of high NO release (such as during cerebral ischemia or hypoxia).

ONOO⁻ upregulates specific steps involved in glucose utilization by neurons. For example, ONOO⁻ rapidly activates the pentose phosphate pathway by potently stimulating the activity of glucose-6-phosphate dehydrogenase (G6PD), the rate-limiting step in this pathway. Under pathological conditions, ONOO⁻ could be formed from astrocytes upon iNOS induction, or from neurons following glutamate receptor stimulation. There is no similar NO-mediated stimulation of G6P activation in neurons, illustrating the cell-specific effects of NO within brain tissue (as reviewed in Bolanos et al. (2001); Bolanos et al. (2004a)).

2.5 NMDA Receptor and nNOS Activation Coupling

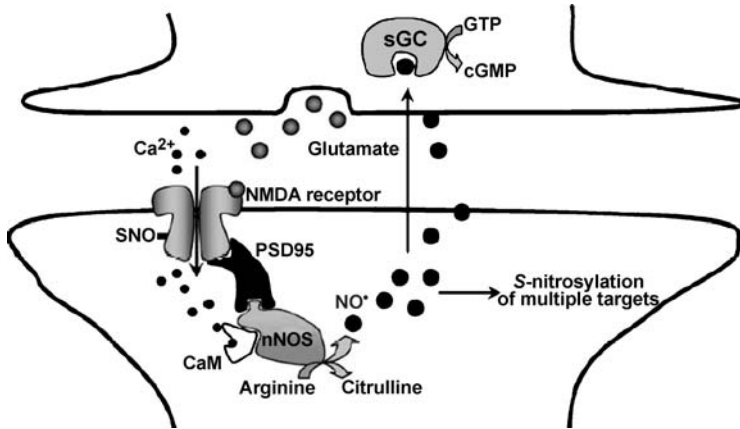
In the neuron, NO-mediated injury is coupled to NMDA receptor activation. The NMDA receptor is associated with nNOS through an important scaffolding protein known as PSD-95 (postsynaptic density-95 kDa) (Alderton et al., 2001). The binding of Ca²⁺-dependent nNOS to PSD-95 may serve to concentrate nNOS near the NMDA receptor, thus enhancing its response to Ca²⁺ during receptor activation (▶ [Figure 6.5-3](#)). The importance of this binding is illustrated by the fact that inhibited expression of PSD-95 reduces NMDA receptor-mediated activation of NOS and neuronal excitotoxic damage during focal cerebral ischemia (Sattler et al., 1999; Aarts et al., 2002). Therefore, it appears that PSD-95 is required for coupling of NMDA receptor activity to NO toxicity and imparts specificity to excitotoxic Ca²⁺ signaling (Sattler et al., 1999). Additional studies indicate that, for example, in hippocampal neurons both Ca²⁺ and NO are required for excitotoxic-related mitochondrial depolarization (Keelan et al., 1999). Thus, NO is emerging as a link between NMDA receptor activation, Ca²⁺ dysregulation, and neurotoxicity through a central mitochondrial-mediated mechanism (Almeida et al., 1999).

2.6 Mitochondrial Formation of NO

A number of investigators have reported that neuronal mitochondria produce NO in situ, catalyzed by NOS (Bates et al., 1995; Giulivi et al., 1998; Ghafourifar and Richter, 1999; Lacza et al., 2001). Prior to this discovery, it was believed that postsynaptic locations of nNOS, held by scaffolding proteins in close association with the NMDA receptor, represented the main sources for neuronal NO-related toxicity (Duchen, 2000). Much less is known, however, if mitochondrial formation of NO and/or ONOO⁻ formation in situ plays a direct role in mediating the observed NO-related mitochondrial membrane changes or if it acts as an essential cell signal to mediate cell death or survival mechanisms (Radi et al., 2002a, b). Mitochondria produce NO through a Ca²⁺-sensitive NOS identified in mitochondria isolated from liver, heart, kidney, and brain (Bates et al., 1995; Ghafourifar and Richter, 1999; Lacza et al., 2001;

■ **Figure 6.5-3**

Regulation of nitric oxide signaling by adaptor proteins. Neuronal nitric oxide synthase (nNOS) is localized to NMDA receptors by the PDZ-domain adaptor protein PSD95. Calcium entry through NMDA receptors activates nNOS by a calcium/calmodulin-dependent mechanism. NO produced by nNOS can diffuse to neighboring cells to activate soluble guanylyl cyclase or to covalently modify cysteine residues of target proteins (S-nitrosylation). Nitrosylation of NMDA receptors inhibits their activity, thereby providing a negative feedback loop to NMDA receptor signaling. (Adapted from: Boehning D, Snyder SH. Novel neural modulators. *Annu Rev Neurosci* 2003; 26:105–31. [▶ Figure 6.5-1](#)). Reprinted, with permission, from the Annual Review of Neuroscience, Volume 26(c) 2003 by Annual Reviews www.annualreviews.org.



Aguilera-Aguirre et al., 2002). However, some investigators have challenged the existence of mitochondrial NOS (Tay et al., 2004; Lacza et al., 2005).

One hypothesis under investigation is that NOS located within neuronal mitochondria is activated during pathological conditions, e.g., as hypoxia/ischemia, in a Ca^{2+} -dependent manner. The proximity of the NO formed by mtNOS to mitochondrially generated superoxide would, in turn, result in ONOO^- formation. Endogenous mitochondrial production of NO and its metabolites may therefore contribute to the oxidative modification of mitochondrial proteins. Evidence of intramitochondrial NO-mediated pathology includes the observation of parallel translocation of the mitochondrial-located proapoptotic factor CytC with nitrated proteins following brain oxygen–glucose deprivation (Alonso et al., 2002).

The physiological role of mtNOS in the cell is unknown. It has been demonstrated that mtNOS activity is functionally upregulated during hypoxia (Lacza et al., 2001). Dedkova and coworkers (2004) report that in vascular epithelial cells mitochondrial Ca^{2+} uptake rapidly activates mtNOS via phosphorylation. These investigators suggest that Ca^{2+} -activated mitochondrial NO formation may inhibit mitochondrial respiration, thereby protecting against respiration-dependent mitochondrial Ca^{2+} overload. These observations have led to the hypothesis that mitochondrial production of NO helps normalize O_2 utilization between cells at different distances from capillaries. The basic concept is that NO inhibits O_2 consumption by cells closest to the capillaries, allowing O_2 to penetrate to cells further away that would be severely hypoxic without buffering of the O_2 gradient. In this regard, mitochondrial NO together with other sources aids in dilation of blood vessels, thereby increasing cerebral blood flow and oxygenation of brain tissue at risk of becoming hypoxic (Haynes et al., 2003).

Another effect of NO is the triggering of mitochondrial biogenesis via the generation of cGMP (Nisoli et al., 2003). This process involves increased expression of transcription factors, including peroxisome proliferator-activated receptor coactivator 1 α (PGC-1 α), nuclear respiratory factor 1 (NRF-1), and mitochondrial transcription factor A (Tfam) (Gleyzer et al., 2005). eNOS is currently implicated in mitochondrial biogenesis and it is unknown if mtNOS or iNOS can also trigger new mitochondrial formation through a similar mechanism. While NO triggers transcription of these factors and increases

mitochondrial content through the cGMP pathway in PC12 neural cells (Nisoli et al., 2004), it is currently unknown whether similar effects occur in primary cultures of neurons or astrocytes or whether mitochondrial NO specifically contributes to this process.

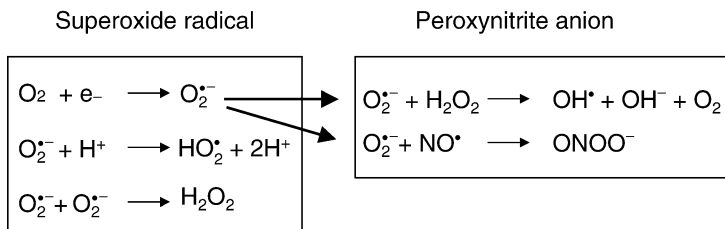
There is a paucity of data on whether intramitochondrial formation of NO and ONOO⁻ is affected by the redox state, electrochemical properties of the mitochondria, its pH, or the ionic or enzymatic milieu. There is a need to more comprehensively understand the role of NO in mitochondrial damage and function during oxidative stress. The relationship of NO reactants formed within neuronal mitochondria to Ca²⁺ homeostasis and to mitochondrial respiration is currently not well defined. For further reviews see Elfering et al. (2004); Haynes et al. (2004); and Ghafourifar and Cadenas (2005).

2.7 Mitochondria as Targets of Reactive Oxygen and Nitrogen Species

It is well established that during chronic neurodegenerative diseases and following acute brain ischemia/injury, ROS and RNS contribute to mitochondrial damage (Cao et al., 1988; Globus et al., 1995; Kil et al., 1996; Solenski et al., 1997; Brorson et al., 1999; Stewart and Heales, 2003). The origin of the ROS is multifactorial but includes mitochondria-generated superoxide (O₂⁻), hydrogen peroxide (H₂O₂), NO•, and its reactant anion, ONOO⁻ (▶ *Figure 6.5-4*). The ability of ONOO⁻ to act as a neurotoxicant when

■ **Figure 6.5-4**

Reactions forming reactive oxygen and nitrogen species



generated at relatively high concentrations is well defined (Estevez et al., 1998). However, at lower, nanomolar concentrations, ONOO⁻ is critical for triggering neuroprotective signaling, including activation of antiapoptotic pathways (Garcia-Nogales et al., 2003; Bolanos et al., 2004a, b).

NO, being a gas, can easily diffuse across biological membranes and enter mitochondria without requiring any receptor binding processes or transporting systems. In the presence of O₂⁻, ONOO⁻ anion is formed. As an uncharged lipophilic molecule, NO contains a single unpaired electron (NO•). NO can function either an electron donor (oxidant) or an electron acceptor (antioxidant). This property allows it to react with many types of molecules, including O₂, glutathione, and superoxide.

There is convincing evidence that ROS, NO, and its metabolites are toxic to mitochondria by damaging the ETC and the inner mitochondrial membrane in which the ETC resides (Brown, 1999; Kowaltowski and Vercesi, 1999; Lipton, 1999; Moncada and Erusalimsky, 2002; Carreras et al., 2004). NO inhibits ETC activity by reversibly inhibiting complex IV (cytochrome oxidase, COX). NO binds reversibly to the O₂-binding site of COX, which is an iron–copper binuclear center. At high concentrations, NO binds to the iron side, while at low concentrations, it binds to the copper side of the COX active center (reviewed in Cooper (2002)). During normal physiological conditions, the affinity of COX for O₂ is high (<1 mm Hg). During normal physiologic conditions, brain O₂ tensions are estimated to range between 20 and 40 mm Hg, i.e., significantly higher than the K_m for COX. In contrast, during cerebral ischemia and hypoxia, the combination of reduced O₂ tension and elevated NO production might result in effective competitive

inhibition of COX by NO, leading to impaired respiration and oxidative phosphorylation. Moreover, respiratory inhibition produces a reduced shift in the redox state of ETC components that, in turn, promotes the single electron reduction of O₂, forming superoxide. Elevated superoxide in the presence of elevated NO generates ONOO⁻.

ONOO⁻ can irreversibly inhibit many components of the ETC necessary for oxidative phosphorylation, including complexes I, II, and IV, and the ATP synthase (reviewed in Stewart and Heales (2003); Brown and Borutaite (2004); Carreras et al. (2004)). A variety of RNS-mediated inhibitory mechanisms have been suggested. RNS can inhibit complex I through the release of iron from the complex, modifying iron-sulfur centers, and leading to the S-nitrosylation of cysteine residues, oxidation of amines, modification of coenzymes (e.g., NADH), or nitration of tyrosine residues (Brown and Borutaite, 2004). ONOO⁻ and/or ROS (e.g., the hydroxyl radical) can inhibit important enzymes of energy metabolism (e.g., aconitase, pyruvate dehydrogenase, creatine kinase) and other mitochondrial-associated proteins including manganese superoxide dismutase (MnSOD) (MacMillan-Crow and Thompson, 1999; Han et al., 2005; Martin et al., 2005). Other functionally important nitrated mitochondrial proteins are likely to be identified, since current proteomic analysis demonstrates close to 40 different nitrated mitochondrial proteins (Elfering et al., 2004). There is evidence that NO and ONOO⁻ can both directly and indirectly activate the MPT in mitochondria (Brookes et al., 2000; Vieira et al., 2001). In neurons, ONOO⁻ formation also leads to release of intracellular zinc stores, which can induce the MPT and cause further respiratory inhibition (Dineley et al., 2003; Sensi et al., 2003; Bossy-Wetzel et al., 2004).

NO, via its effects on mitochondria, can induce necrosis or apoptosis, depending on the degree to which ATP levels are compromised (Bal-Price and Brown, 2000). The effect of NO on glycolysis in astrocytes and neurons is different. Inhibition of respiration by NO in astrocytes results in glycolytic activation, whereas stimulation of glycolysis does not occur in neurons due to cell-type specific signal transduction mechanisms (Almeida et al., 2001). In addition, both NO and ONOO⁻ are capable of upregulating specific steps in glucose metabolism through their effects on gene expression. For example, NO induces the expression of glucose transporter proteins in astrocytes as a consequence of NO-mediated inhibition of mitochondrial respiration in neurons (Cidad et al., 2004).

NO reactants can generate potent nitrating species leading to the formation of 3-nitrotyrosine in proteins. Two of the more commonly accepted *in vivo* mechanisms include the formation of either ONOO⁻ or nitrogen dioxide. Both reactants are potent unstable species capable of interacting with proteins near the site of their generation. As illustrated in [Figure 6.5-4](#), ONOO⁻ is formed by the interaction of superoxide radical, [O₂⁻], with NO and is responsible for the oxidation, nitration, and nitrosylation of a variety of proteins (reviewed in Jaffrey et al. (2001); Ischiropoulos and Gow (2005)). Nitration refers to the binding of a NO₂ group to a tyrosine or tryptophan residue, whereas nitrosylation refers to the binding of a NO group to a transition metal or cysteine residue (or other thiols). Initially it was thought that tyrosine nitration was irreversible. However, recent results indicate that tyrosine nitration can be reversible, with the existence of a repair mechanism for nitrated proteins (Ischiropoulos, 2003; Gow et al., 2004). Nitration of tyrosine residues can have important activating and inhibitory effects on regulatory proteins since it prevents tyrosine phosphorylation. Nitrosylation of cysteines is also reversible and, in general, plays a more important role in NO-mediated signal transduction. S-nitrosylation also inhibits the catalytic site of a variety of enzymes including some caspases, preventing inappropriate initiation of apoptosis (Kang et al., 2004). In contrast, nitrosylation of CytC promotes caspase activation (Cassina et al., 2000). As mentioned earlier, there are many mitochondrial proteins that undergo tyrosine nitration even under nonpathological conditions (Radi et al., 2002a, b). Therefore, although protein nitration can interfere with mechanisms of cellular regulation and play a large role in mediating mitochondrial and neuronal toxicity, it may also play an important role in normal cell physiology (reviewed in Beckman (2002); Aulak et al. (2004); Elfering et al. (2004); Radi et al. (2002a, b); Ischiropoulos and Gow (2005)).

In addition to the direct effects of ROS and RNS on critical enzymes involved in cerebral energy metabolism, indirect effects are also observed. Indirect effects include depletion of pyridine nucleotides through activation of poly(ADP-ribose) polymerase (PARP) in response to DNA oxidation (Wang et al., 2002), and release of mitochondrial NAD(H) and NADP(H) from the mitochondrial matrix into the

cytosol following activation of the MPT (Chinopoulos et al., 2003). ROS and RNS are extremely potent activators of both PARP and the MPT (Kowaltowski et al., 2000). Moreover, the metabolism of H_2O_2 and other peroxides via the GPx/reductase system can contribute to the oxidative shift in pyridine nucleotide redox state (🔗 [Figure 6.5-2](#)). Irrespective of the mechanism by which ROS and RNS cause this shift in redox state, the associated decrease in reducing power could limit detoxification of peroxides and maintenance of reduced protein sulfhydryl groups. This may have pathologic implications by contributing to the prolonged oxidative stress of acute and chronic neurodegenerative disorders.

Importantly, although the majority of effects of $ONOO^-$ on brain tissue are deleterious, at low concentrations, there is evidence that $ONOO^-$ is neuroprotective (Garcia-Nogales et al., 2003). In neural cell culture studies it appears that $ONOO^-$ upregulates G6PD activity that in turns increases NADPH, necessary for maintaining glutathione in its reduced redox state.

3 Apoptosis

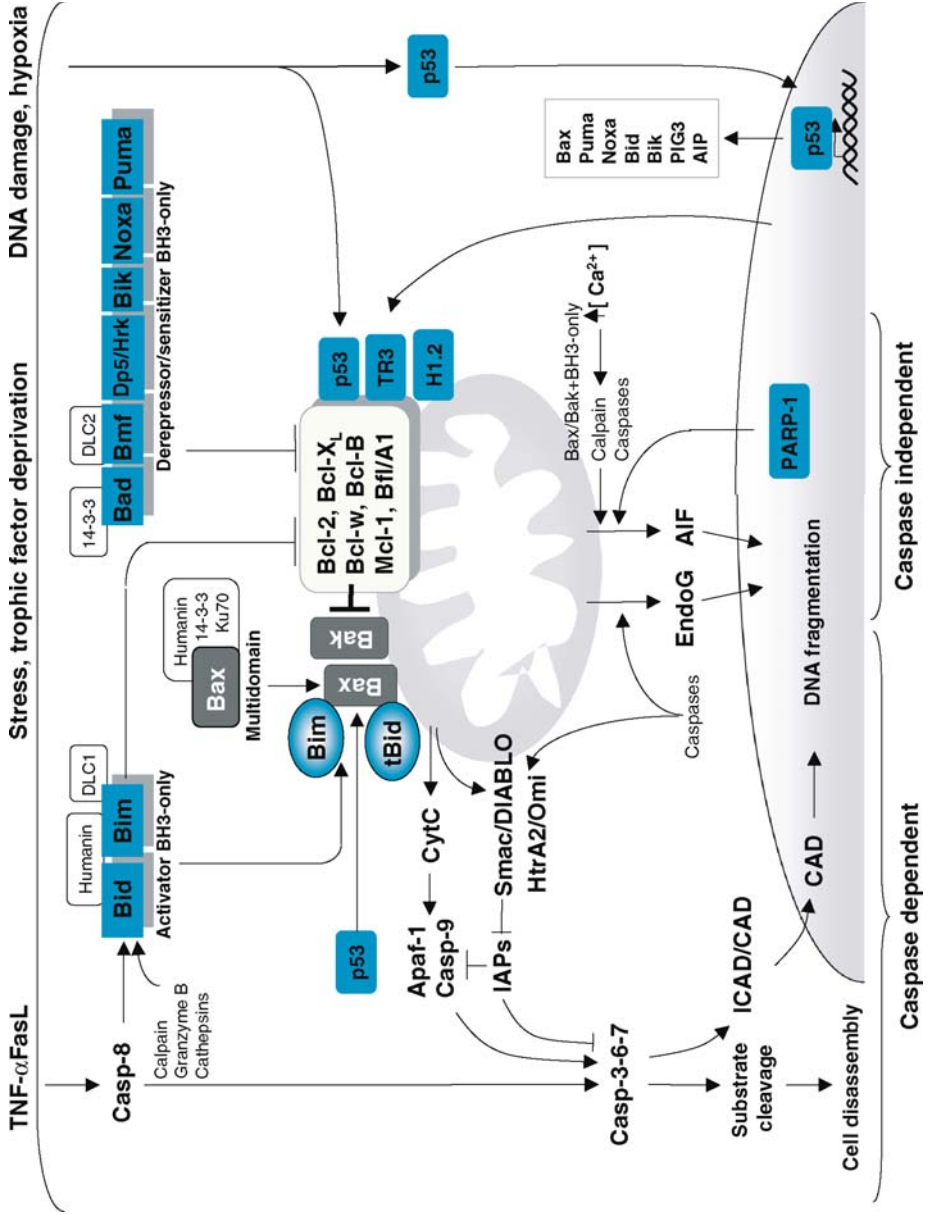
3.1 Intrinsic and Extrinsic Apoptotic Pathways

In multicellular organisms, elimination of excess and damaged cells is highly regulated and occurs through a genetically controlled pathway known as programmed cell death (PCD) or apoptosis. The genetic basis of PCD was uncovered by studies in *Caenorhabditis elegans*, where *ced-3*, *ced-9*, and *ced-4* control the initiation and execution of PCD (Horvitz, 2003). PCD is evolutionary conserved, and from *C. elegans* to mammals, its execution relies on activation of caspases, a family of aspartyl-directed cysteine proteases homologous to *ced-3*. Activation of executioner caspases (caspase-3, -7, and -6) is strictly regulated and initiated through cleavage by upstream initiator caspases (caspase -8, -9, -10, and -12) (Adams, 2003; Reed, 2004). Two major pathways of caspase activation have been discovered in mammalian cells: the intrinsic or mitochondrial pathway, and the extrinsic or death receptor pathway.

The discovery that CytC release from mitochondria is required for apoptosis (Liu et al., 1996) revealed a new and unexpected function of mitochondria. In addition to its bioenergetic function, mitochondria are also the source of potent apoptotic proteins. The key event that links mitochondria to the activation of caspases is the permeabilization of the outer mitochondrial membrane (OMM) resulting in the release of CytC and other apoptogenic proteins (apoptosis-inducing factor (AIF), Smac/DIABLO, endonuclease G (EndoG), and HtrA2/Omi) into the cytosol (reviewed in Lindholm et al. (2004)). In the presence of dATP, CytC binds to Apaf-1 (apoptotic protease-activating factor-1), the mammalian homologue of *C. elegans ced-4* and triggers activation of the initiator procaspase-9 within the apoptosome (Zou et al., 1997). Active caspase-9 then activates effector caspase-3 and -7 that in turn cleave numerous substrates responsible for DNA fragmentation and cell disassembly (🔗 [Figure 6.5-5](#)). Activation of caspase-3 and -9 is endogenously controlled by the inhibitor of apoptosis (IAP) family proteins, including XIAP, which when overexpressed, promotes neuronal survival after cerebral ischemia (Trapp et al., 2003). The IAP inhibitory step is mitigated through the release of the serine protease HtrA2/Omi and Smac/DIABLO. AIF and EndoG are also released from mitochondria, and can mediate a caspase-independent mitochondrial death pathway by promoting DNA fragmentation (Lindholm et al., 2004). The complex role of mitochondria in apoptosis is highlighted by the dual role, pro-death and -survival, of some apoptogenic proteins, e.g., AIF and HtrA2/Omi, that induce cell death when released from mitochondria, but promote neuronal survival and resistance to oxidative stress at their mitochondrial location (reviewed in Lindholm et al. (2004)).

PCD occurs as a natural process in the nervous system during development (Openheim, 1991; Lossi and Merighi, 2003) and a role for PCD in physiological aging is also suggested (Tagliatela et al., 1996). Developmental death in various regions of the brain (e.g., cerebellum, retina) occurs at early developmental stages for neural precursor cells (NPC), and later during the period of synaptogenesis, in postmitotic neurons establishing proper connections. Much of this developmental death appears to be apoptotic (Lossi and Merighi, 2003). Involvement of the intrinsic pathway is indicated by severe defects in brain development in caspase-3^{-/-} and -9^{-/-} deficient mice that exhibit supranumerary neurons and ectopic masses in the cerebral cortex,

Figure 6.5-5 Schematic representation of the intrinsic (mitochondrial) and extrinsic (death receptor) pathways of apoptosis and their regulation by the Bcl-2 family proteins. See text for details



hippocampus, and striatum. These mice are phenotypically similar to that of *apaf-1*^{-/-} mice (reviewed in Lossi and Merighi (2003)). Evidence of apoptotic death through the intrinsic pathway is found in acute (e.g., trauma, stroke) and chronic neurodegenerative disorders (e.g., Alzheimer's disease (AD), Parkinson's disease, amyotrophic lateral sclerosis (ALS)) (reviewed in Waldmeier (2003); Akhtar et al. (2004)).

Apoptotic neuronal death can also proceed through the extrinsic pathway or death receptor pathway, initiated by the binding of structurally related extracellular death ligands (e.g., tumor necrosis factor (TNF)- α , FasL/CD95L, p75^{NTR}) to the TNF receptor/death receptor (DR) family (Schulze-Osthoff et al., 1998; Khosravi-Far and Esposti, 2004). Ligation of DR results in activation of initiator caspase-8 that can efficiently activate caspase-3 in some cells types (type I). In other cell types (type II), the mitochondrial pathway is recruited through caspase-8-mediated cleavage of proapoptotic Bid that translocates to mitochondria and activates Bax and Bak. This pathway can be induced in some neurons in response to trophic factor deprivation (Raoul et al., 1999). In many acute (e.g., ischemia, trauma) and chronic CNS disorders (e.g., AD, Parkinson's disease, ALS), an inflammatory response occurs. The latter activates glia and secretion of cytokines like interleukin-1 and TNF- α (Allan and Rothwell, 2003). The importance of the extrinsic pathway is demonstrated by upregulation of Fas/FasL in the ischemic brain and the finding that apoptotic neuronal death and stroke infarct size are reduced in *fas*^{-/-} mice (Rosenbaum et al., 2000). An endoplasmic reticulum (ER)-dependent pathway is also described and relies on the initiator caspase-12 activated in response to ER-stress. This pathway is implicated in β -amyloid-induced neuronal death and in chronic neurodegeneration (Rao et al., 2004).

3.2 Proapoptotic Bcl-2 Family Proteins

Bcl-2 (B cell lymphoma) family proteins, the most important regulators of the intrinsic pathway, are expressed in both the embryonic and adult CNS, and control neuronal death during development and in pathologic conditions (see [Table 6.5-1](#)). Bcl-2 family consists of pro- and antiapoptotic proteins homologous to *C. elegans* CED-9, characterized by the presence of at least one of the four Bcl-2 homology (BH) domains. Proapoptotic Bcl-2 proteins are subdivided into multidomain (BH1–3) proteins (Bax, Bak, and Bok/Mtd) and BH3-only proteins (Bid, Bim, Bad, Bmf, Dp5/Hrk, Puma, Noxa, Bik, Bnip3). The BH3-only proteins consist of a large and structurally diverse group sharing only the amphipathic α -helical BH3 region (Adams and Cory, 1998; Gross et al., 1999).

Bcl-2 family proteins regulate cell death pathways by controlling release of proapoptotic proteins from mitochondrial intermembrane space (IMS) through regulation of the OMM permeability. Bcl-2 proteins can also function at the ER (Scorrano and Korsmeyer, 2003; Scorrano et al., 2003). A rise in OMM permeability is triggered by multidomain Bax/Bak in cooperation with BH3-only proteins. In contrast, OMM permeabilization is inhibited by antiapoptotic members (e.g., Bcl-2, Bcl-X_L). While the exact biochemical activities are not completely elucidated, the BH3-domain-dependent heterodimerization is critical for proapoptotic activity. Studies also indicate that antiapoptotic (Bcl-2, Bcl-X_L), multidomain proapoptotic (Bax, Bak), and the Bid member of the BH3-only proteins are structurally related to the membrane insertion domain of diphtheria toxin (Petros et al., 2004). Proteins sharing this structural fold can insert into lipid membranes through the central hydrophobic α 5– α 6 helical regions and form ion channels (Schendel et al., 1998). While the role of ion channel formation is unclear, Bax/Bak can also form large oligomers, which facilitate the release of CytC through the OMM (Antonsson et al., 2000).

Prior to a death stimulus, monomeric Bax can reside in the cytosol in an inactive conformation, bound to Ku70 (70-kDa polypeptide subunit of the DNA-dependent protein kinase) (Sawada et al., 2003), 14-3-3 θ protein (Nomura et al., 2003), or the short peptide humanin (Guo et al., 2003), or it can be loosely attached to mitochondria (Polster et al., 2001). Bak normally resides in mitochondria, where at least in some cells it is kept inactive by binding to OMM protein voltage-dependent anion channel (VDAC)-2 (Cheng et al., 2003). Allosteric activation of Bax results from a conformational change that exposes its N terminus. This promotes translocation to mitochondria, stable OMM insertion, oligomerization, and subsequent release of apoptogenic proteins from the IMS (Desagher et al., 1999; Nechushtan et al., 1999). The exact mechanism of Bax/Bak-mediated OMM permeabilization is still a matter of debate. Proposed mechanisms

■ Table 6.5-1

Bcl-2 family proteins in models of nervous system disorders

	Protein	Effect	Model/cells	Reference
Trophic factor deprivation	Bak ^{-/-} , Bid ^{-/-} Bad ^{-/-} Bax ^{-/-}	No protection	Cerebellar granule neurons	Putcha et al. (2002)
	Bax/Bak ^{-/-}	Protective	Cerebellar granule neurons	Putcha et al. (2002)
		Protective	Cerebellar granule neurons	Lindsten et al. (2005)
Hypoxia–ischemia	Bcl-2	Decreased infarct size	MCAO	Martinou et al. (1994)
	Bcl-X _L	Decreased infarct size	MCAO	Wiessner et al. (1999)
	TAT-Bcl-X _L	Decreased infarct size	MCAO	Cao et al. (2002); Kilic et al. (2002)
	TAT-FNK	Decreased infarct size	MCAO	Asoh et al. (2002)
	Bcl-w Bax ^{-/-}	Decreased infarct size Decreased infarct size	MCAO Neonatal hypoxia– ischemia	Sun et al. (2003) Gibson et al. (2001)
	Bid ^{-/-}	Decreased infarct size	MCAO	Plesnila et al. (2001)
Traumatic brain injury	Bcl-2	Decreased cortical and hippocampal tissue loss	Cortical impact injury	Raghupathi et al. (1998)
Excitotoxicity/Seizure- induced neurodegeneration	Bcl-2	Protective	AMPA-mediated apoptosis	McLaughlin et al. (2000)
	Bax/Bak ^{-/-}	Sensitive to NMDA	Cerebellar granule neurons	Lindsten et al. (2005)
	Mcl-1 ^{-/-}	Increased neuronal death	Pilocarpine- induced seizure	Mori et al. (2004)
Neurodegenerative disease models	Bcl-2	Protective	ALS mouse models	Kostic et al. (1997)
	Bcl-2	Protective	MPTP and 6- OHDA	Offen et al. (1998)
	Bcl-2	Protective	β-Amyloid- induced toxicity	Saille et al. (1999)
	Bcl-w	Protective	β-Amyloid- induced toxicity	Yao et al. (2005)
	Bax ^{-/-}	Protective	Parkinson's disease model; MPTP	Vila et al. (2001)
Nerve injury	Bcl-2	Protective	Optic nerve transection	Bonfanti et al. (1996)
	TAT-Bcl-X _L	Protective	Optic nerve transection	Dietz et al. (2002)
	Bax ^{-/-}	Protective	Facial nerve axotomy	Deckwerth et al. (1996)
	Dp5/Hrk ^{-/-}	Protective	Transection of hypoglossal nerve	Imaizumi et al. (2004)

include the involvement of MPT with nonselective OMM rupture following osmotic swelling (Zamzami and Kroemer, 2001), formation of a discrete protein pore by Bax/Bak or activation of an OMM existent pore, and cooperation with mitochondrial lipids to form lipidic pores (reviewed in (Polster and Fiskum, 2004)).

Reconstitution experiments demonstrate that Bax and a BH3-only protein (e.g., tBid) are the minimal components required for CytC release (Kuwana et al., 2002). While the involvement of OMM proteins (e.g., VDAC) is still debated (Shimizu et al., 1999; Rostovtseva et al., 2005), activated tetrameric Bax can form pores sufficiently large to allow passage of CytC (Saito et al., 2000). tBid-induced oligomerization of Bax is required for the release of liposome-entrapped molecules, and Bax oligomers are detected in apoptotic cells (Antonsson et al., 2000). Cooperation with mitochondrial membrane lipids, particularly cardiolipin (CL), appears to play a role in this process (Kuwana et al., 2002), and membrane lipid curvature is also important (Terrones et al., 2004). CL, an anionic phospholipid exclusively present in mitochondria in eukaryotic cells, might confer specificity for targeting of mitochondria by tBid, and is required for Bax-mediated pore formation (Kuwana et al., 2002; Iverson and Orrenius, 2004). CL is localized primarily in the inner membrane and is required for CytC binding. Therefore, its role might be to regulate the extent of CytC release after OMM permeabilization (Iverson and Orrenius, 2004; Orrenius, 2004).

Bax/BH3 domain peptide-mediated CytC release involves a selective permeabilization of the OMM without loss of the inner mitochondrial membrane integrity loss (Polster et al., 2001). Indeed, while Bax and Bak might indirectly affect MPT through regulation of ER calcium release (Scorrano et al., 2003), studies using cyclophilin D-deficient animals demonstrated that MPT is important in necrotic death but is not required for apoptotic death (Baines et al., 2005; Basso et al., 2005; Nakagawa et al., 2005). In addition to OMM permeabilization, a distinct pathway triggered by tBid results in remodeling of the inner mitochondrial membrane and cristae, and maximal release of IMS proteins (Scorrano and Korsmeyer, 2003). This additional mechanism appears to involve the BH3-independent interaction of tBid with CL (Kim et al., 2004). These structural alterations together with the mitochondrial oxidative stress induced by CytC-mediated respiratory inhibition, could, however, promote a secondary MPT and bioenergetic failure.

Unlike CytC, caspase activation is required for the release of Smac/DIABLO, EndoG, and AIF (reviewed in Lindholm et al., (2004)). AIF release also appears to involve additional mechanisms and can be induced by PARP-1 activation in a caspase-independent excitotoxic death (Dawson and Dawson, 2004; Hong et al., 2004). Recently, it was shown that its release from isolated mitochondria is promoted through cleavage by calpain (Polster et al., 2005).

BH3-only Bcl-2 family proteins act upstream of multidomain proteins as sensors of apoptotic stimuli and triggers of Bax/Bak activation. In healthy cells, they are sequestered away from mitochondria and mediate death signals in a stimulus-specific manner (Huang and Strasser, 2000). Under normal conditions, phosphorylated Bad is bound to cytosolic 14-3-3 proteins, and can be activated through dephosphorylation in response to trophic factor deprivation. The dephosphorylation of Bad by the Ca^{2+} -dependent phosphatase, calcineurin, in neurons results in binding to Bcl-X_L and cell death (Wang et al., 1999). Bim and Bmf are sequestered by binding to the cytoskeleton-associated dynein light chain 1 (DLC1) and DLC2, respectively, and can initiate death following cytoskeletal damage (Huang and Strasser, 2000). Bid has a unique role in conveying proteolytic signals to mitochondria, including those initiated by DRs. Bid activation requires exposure of the BH3 domain and occurs through proteolytic cleavage by multiple proteases (caspase-8 and -3, calpains, granzyme B, and cathepsins) (Gross et al., 1999; Cirman et al., 2004; Krajewska et al., 2004). In addition to posttranslational mechanisms, transcriptional regulation is also implicated in controlling the activity of some BH3-only proteins and is mediated by p53 following genotoxic stress (e.g., Noxa, Puma, Bid) (Culmsee and Mattson, 2005), or in the case of Dp5/Hrk and Bim, in neurons, by JNK (Harris and Johnson, Jr., 2001; Ham et al., 2005).

Mutational studies demonstrate the essential requirement of the BH3 domain for the proapoptotic activity and dimerization of BH3-only proteins. BH3 domain peptides function as specific death ligands and mimic the activity of the full-length proteins, inducing cell death in cells and CytC release from isolated mitochondria (Polster et al., 2001; Letai et al., 2002). Studies using double-deficient *bax/bak*^{-/-} mice indicate that the activity of BH3-only proteins is exclusively mediated through the Bax/Bak “gateway” (Wei et al., 2001; Zong et al., 2001). Evidence supports the existence of two functional classes of BH3

domains similar to the model proposed initially by Letai et al. (2002). Activator BH3 domains (Bid and Bim) can directly trigger a conformational activation of Bax/Bak and their oligomerization, while sensitizer/derepressor BH3 domains (Bad, Bik, Puma, Noxa, and others) bind and inactivate antiapoptotic proteins. Sensitizer/derepressor BH3 domains are unable to directly activate Bax/Bak (Letai et al., 2002; Kuwana et al., 2005).

The array of upstream apoptotic initiators is not restricted, however, to known BH3-only proteins, as non-Bcl-2 proteins that contain functional BH3-like regions, e.g., transglutaminase, translocate to mitochondria and initiate CytC release through a similar mechanism (Rodolfo et al., 2004). Other non-Bcl-2 family proteins translocate to mitochondria and induce the release of proapoptotic proteins without having a recognizable BH3 region, e.g., transcription factors (TR3 and p53), histone H1.2 (Li et al., 2000; Konishi et al., 2003; Mihara et al., 2003). In addition to its transactivation-dependent role, p53 also promotes apoptosis more directly at the mitochondria by binding to Bcl-X_L (Mihara et al., 2003). p53 can also induce CytC release from isolated mitochondria through a Bid-like mechanism by binding to and promoting Bax oligomerization (Chipuk et al., 2004). As oxidative stress is an important signal for transcriptional activation of proapoptotic genes by p53, it is possible that oxidative modification of p53 also promotes the direct interaction of this protein with Bcl-X_L. In summary, proteins other than the BH3-only subgroup might function in a similar manner, either as sensitizers or direct activators of Bax/Bak.

Studies using genetically modified animals have uncovered essential roles for proapoptotic Bcl-2 family proteins in naturally occurring developmental death and neuronal death associated with neurodegeneration (Akhtar et al., 2004; Lindsten et al., 2005) (🔗 [Table 6.5-1](#)). Targeted deletion of Bax or Bak does not result in major developmental defects. However, a reduction in apoptosis of neurons in the brainstem, hippocampus, cerebellum, dorsal root ganglia, and spinal cord is observed in Bax-deficient mice. Bax/Bak double-deficient mice do exhibit a CNS phenotype characterized by profound alterations in apoptotic death with expansion of neural progenitors cells indicating that Bax and Bak overlap functionally. Unlike single-gene deficient cells, neural progenitors cells and mature neurons derived from *bax/bak*^{-/-} mice are resistant to multiple apoptotic stimuli. The Bax/Bak checkpoint is not universally required for all forms of neuronal death, as postmitotic *bax/bak*^{-/-} neurons are still sensitive to excitotoxicity (reviewed in Lindsten et al. (2005)). A functional overlap also exists between some BH3-only proteins (Putcha et al., 2002). Major defects in apoptotic death within the brain are not observed during development in mice lacking the expression of several BH3-only proteins (Bid, Bad, Bim, Noxa, Puma) (reviewed in Akhtar et al. (2004)). Bid deficiency, however, protects neurons following ischemic injury (Plesnila et al., 2001), and Dp5/Hrk deficiency protects against axotomy-induced neuronal death (Imaizumi et al., 2004). In addition, there is evidence for the involvement of Bim and Bad in seizure-induced death (Niquet and Wasterlain, 2004). Therefore, certain BH3-only proteins are apparently involved more in pathologic apoptosis, than in developmental PCD.

3.3 Antiapoptotic Bcl-2 Family Proteins

The six Bcl-2-like antideath proteins identified in mammals (Bcl-2, Bcl-X_L, Bcl-w, Bfl/A1, Bcl-B, and Mcl-1) are characterized by the presence of all four BH domains (BH1–4). Most of these proteins have a C-terminal hydrophobic domain that anchors them to multiple intracellular membranes (nuclear, ER, and OMM), while some (e.g., Bcl-X_L) can also reside in the cytosol (Adams and Cory, 1998; Borner, 2003). Bcl-2-like proteins protect neurons and other cell types against a wide variety of apoptotic insults. Some of them, e.g., Bcl-2 and Bcl-X_L, are also protective against necrotic cell death (Myers et al., 1995; Kowaltowski et al., 2004). A role of Bcl-2 in the regulation of autophagic death is also suggested by its interaction with the autophagy-related protein, beclin (Liang et al., 1998). These multiple pro-survival activities might relate to the neuroprotective ability of Bcl-2 in pathologic conditions, where multiple neuronal death types (apoptotic, necrotic, and autophagic) are frequently observed in the brain (Yuan et al., 2003). Bcl-2 and Bcl-X_L control the developmental death of several neuronal populations and are critical for the survival of adult postmitotic, long-lived neurons (Lindsten et al., 2005). Numerous studies document the role of Bcl-2 and close

protein family members in neuronal survival in pathologic conditions such as ischemia (Martinou et al., 1994) and traumatic brain injury (Raghupathi et al., 1998). Bcl-2 is also protective in animal models of ALS (Kostic et al., 1997), Parkinson's disease models (e.g., 1-methyl-4-phenyl-1,2,3,6-tetrahydropyridine (MPTP) toxicity and 6-hydroxydopamine (6-OHDA)) (Offen et al., 1998), and against β -amyloid-induced toxicity (Saille et al., 1999). Mcl-1 protects against hippocampal neuronal cell death after seizures, as decrease of Mcl-1 level is associated with extensive apoptosis (Mori et al., 2004).

While not completely understood, the neuroprotective activity of Bcl-2 and its antiapoptotic relatives is in part due to their ability to heterodimerize and inhibit Bax/Bak-type proapoptotic proteins, and to sequester BH3-only proteins. Structural studies indicate that the molecular basis of heterodimerization is the presence of a hydrophobic groove formed by the BH3, BH2, and BH1 domains of these proteins that can fit the amphipathic α -helical BH3 domain of pro-apoptotic Bcl-2 family proteins (reviewed in Petros et al. (2004)). According to the "rheostat" model proposed by Korsmeyer, antiapoptotic proteins bind and neutralize proapoptotic proteins, and their relative balance determines cell death or survival (Korsmeyer et al., 1993). Some Bcl-2 proteins show distinct patterns of heterodimerization, e.g., Bcl-X_L binding to Bak is preferred over Bax (Sattler et al., 1997), and Bok selectively binds Mcl-1. Such specific interactions are critical for protection, as Bcl-2 is unable to protect against Bok-induced death (Hsu et al., 1997). The initial heterodimerization model is further refined by recent studies indicating that BH3-only proteins also display distinct binding affinities for antiapoptotic proteins (Chen et al., 2005). While some BH3-only proteins (Bim, Puma) can target all Bcl-2 like proteins, others bind preferentially to Bcl-2, Bcl-X_L, and Bcl-w (Bad), and Noxa binds only to Mcl-1 and A1. The increased killing efficiency of some BH3-only proteins (e.g., Bim, Puma) correlates with their ability to target and inactivate all pro-survival proteins (Chen et al., 2005). Bcl-X_L can also protect against Bim-induced CytC release independent of interaction with both Bax and Bim (Yamaguchi and Wang, 2002), indicating the existence of heterodimerization-independent mechanisms of protection.

In addition to the Bax/Bak neutralizing activity, the antiapoptotic and antinecrotic activity of Bcl-2-like proteins involves other mitochondrial processes, including mitochondrial calcium uptake capacity, MPT, and redox state (Kowaltowski et al., 2004; Kowaltowski and Fiskum, 2005). Early studies on Bcl-2, and more recently on Bcl-X_L and Mcl-1, indicated that their cytoprotective activities are in part due to increased protection against oxidative stress via elevating expression of the enzymes actively involved in the defense against ROS (Hockenbery et al., 1993; Ellerby et al., 1996; Murphy et al., 1996). This effect may involve an increased expression of intracellular defenses against ROS, e.g., through modulation of transcription factor activity and subsequent expression of antioxidant enzymes. It now appears that the increased expression of antioxidant defense systems is a "preconditioning" response to the elevation of mitochondrial ROS production by increased Bcl-2 expression (Kowaltowski and Fiskum, 2005). This response may explain Bcl-2 protection against death caused by oxidative stress throughout the cell, including at the mitochondrial level where Bcl-2 protects against Ca²⁺- and peroxide-induced MPT activation (Kowaltowski et al., 2000). The "antioxidant" mechanism of action of antideath Bcl-2 family proteins may be particularly important in acute ischemic and traumatic brain injury where excitotoxicity and oxidative stress play major roles in neuronal cell death.

3.4 Antiapoptotic Drugs and Proteins

Strategies to inhibit apoptotic neuronal death in pathologic conditions are aimed at enhancing endogenous neuroprotective response (e.g., using neurotrophic factors) or interfere with apoptosis regulators (e.g., Bcl-2 family proteins) and effectors (e.g., caspases). Recent progress in understanding the mechanisms of mitochondrial apoptotic pathway provides several therapeutic targets for neuroprotection (🔗 [Table 6.5-2](#)).

While caspase inhibitors were proven useful at protecting neurons in some experimental models (Fink et al., 1999), caspase inhibition might only delay cell death. A switch of cell death to necrosis occurs in the presence of caspase inhibitors in neurons, associated with increased PARP-1 activity (Prabhakaran et al., 2004). Potential release of caspase-independent death effectors (e.g., AIF) from mitochondria also suggests that interfering with upstream steps in the death cascade should be more effective.

■ **Table 6.5-2**
Antiapoptotic drugs and proteins

Mitochondria related antiapoptotic drugs and proteins			Reference	
Small molecular inhibitors	Bax inhibition	Dibucaine, propranolol	Polster et al. (2003)	
		TUDCA	Rodrigues et al. (2003)	
		Humanin	Luciano et al. (2005); Zhai et al. (2005)	
		BIP	Sawada et al. (2003)	
		Bci1, Bci2	Hetz et al. (2005)	
	Caspase inhibition	zVAD	Fink et al. (1999)	
		PARP inhibition	3-aminobenzamide (3-AB)	Endres et al. (1997)
	Protein transduction	p53 inhibition	PFT- α	Culmsee et al. (2001)
		Peptides	Bcl-2 BH4 peptide	Cantara et al. (2004)
			Bcl-X _L BH4 peptide	Shimizu et al. (2000)
Proteins		Bcl-X _L	Kilic et al. (2002); Cao et al. (2002); Asoh et al. (2002)	

Cells deficient in both Bax and Bak display long-term protection against multiple apoptotic stimuli (Wei et al., 2001). The discovery of several proteins that bind Bax in the cytosol and maintain its inactive conformation (humanin, Ku70, and 14-3-3) suggests a means of Bax inhibition that could translate into therapy. A cell-permeable Bax-inhibiting peptide (BIP) derived from the Bax-binding region of Ku70 protects against cell death (Sawada et al., 2003). In addition to Bax, humanin can also bind and inhibit Bid and Bim_{EL} and is effective at protecting cells when delivered through protein transduction (Luciano et al., 2005; Zhai et al., 2005). Tauroursodeoxycholic acid (TUDCA) also inhibits Bax translocation to mitochondria and is neuroprotective in a rat stroke model (Rodrigues et al., 2003). In addition to preventing Bax translocation, Bax inhibition can also be achieved at steps downstream of its insertion into OMM by two other agents, dibucaine and propranolol, that effectively inhibit Bax-induced OMM permeabilization and CytC release (Polster et al., 2003). Two inhibitors of Bax channel activity (Bci1 and Bci2) have been discovered recently, which inhibit CytC release from mitochondria without affecting Bax conformational activation, translocation, or its insertion into mitochondria. Inhibition of Bax channel activity protects against apoptosis and was neuroprotective in an animal model of global ischemia (Hetz et al., 2005). In addition to targeting core apoptotic regulators such as Bax, pharmacologic inhibition of p53 using pifithrin- α (Culmsee et al., 2001) or PARP-1 inhibitors also confer protection against ischemic injury and have therapeutic potential (Endres et al., 1997).

Recent development of protein transduction technology provides a new approach for neuroprotection by facilitating the delivery of proteins and peptides into cells and tissues including the brain (Denicourt and Dowdy, 2003). Although its mechanism remains debated, the neuroprotective potential of this strategy has been demonstrated in principle, by several studies in cells and models of brain injury in mice (Asoh et al., 2002; Cao et al., 2002; Kilic et al., 2002). Such an approach was used to deliver peptides with antiapoptotic activity, corresponding to the short BH4 domain of Bcl-2 and Bcl-X_L (Shimizu et al., 2000; Cantara et al., 2004). Delivery of the antiapoptotic Bcl-X_L as a fusion protein with the HIV-1 TAT (transactivator of transcription) protein transduction domain (PTD) has been reported to reduce the severity of ischemic injury in mice models (Asoh et al., 2002; Cao et al., 2002; Kilic et al., 2002). A TAT-Bcl-2 construct with the loop domain deleted was shown to increase the survival of primary cortical neurons following trophic factor withdrawal (Soane and Fiskum, 2005). As growing evidence indicates that protein transduction generally occurs via endocytosis, the effectiveness of this approach may be limited by the ability of transduced proteins to escape from endosomes.

4 Future Directions

The traditional view that mitochondrial participation in neurodegeneration is due primarily to impairment of ATP production has given way to an appreciation of the central roles that mitochondria play in oxidative stress and apoptosis. One current challenge is to develop an integrative view of how each of these mitochondrial cell death mechanisms interacts and to identify the specific molecules responsible for these connections. A bigger challenge is to also understand how mitochondrial cell death pathways network with a host of extramitochondrial cell stressors and effectors, e.g., loss of Ca^{2+} homeostasis, degradative enzyme activities, proteasomal dysfunction, ER stress responses, cell death and survival signal transduction pathways, and abnormal gene expression.

Considerable information can still be obtained from measurements of levels and chemical modifications of proteins, lipids, and nucleic acids present in mitochondria isolated from diseased regions of the CNS. This information will, however, be far more useful once discrete mitochondrial subfractions can be obtained, e.g., those from astrocytes and neurons, and from neuronal subregions, including presynaptic nerve endings, dendrites, axons, and soma. These new findings can then be compared to measures of mitochondrial activities using *in vitro* models of CNS injury utilizing primary cultures of neurons, astrocytes and other brain cells, and organotypic brain slice cultures. While these *in vitro* systems probably do not accurately reflect the relative contribution of different cell death mechanisms that participate in the CNS, they provide insight into mitochondrial dynamics and cell biology that are currently very limited, obtained using animal models. In particular, the influence of cellular energy demand, oxidative stress, intracellular Ca^{2+} , and apoptotic signals on mitochondrial movement, fission, and fusion and how mitochondrial structural dynamics influence mitochondrial mechanisms of death is a topic of recent interest that warrants more investigation (Bossy-Wetzell et al., 2003; Reynolds et al., 2004).

The ultimate goal shared by many neuroscientists who study mitochondria is to translate knowledge of mitochondrial cell death mechanisms into safe and effective therapy for both acute and chronic neurodegenerative disorders. Examples of mitochondrially targeted neuroprotective strategies that are at different stages of either preclinical or clinical development include MPT inhibitors (Clausen and Bullock, 2001), membrane potential sensitive antioxidants (Beal, 2004), uncouplers of oxidative phosphorylation (Jin et al., 2004), K^+ channel openers (Ferranti et al., 2003; Maragos et al., 2003; Mattson and Kroemer, 2003), alternative sources of oxidative fuel (e.g., ketone bodies and acetyl-L-carnitine) (Rosenthal et al., 1992; Veech, 2004; Prins et al., 2005), and antiapoptotic drugs (e.g., antiapoptotic Bcl-2 family mimetics) and chemical inhibitors of proapoptotic protein interactions (Cao et al., 2002; Hetz et al., 2005). This list will continue to expand and hopefully include a clinically successful approach in the near future.

References

- Aarts M, Liu Y, Liu L, Besshoh S, Arundine M, et al. 2002. Treatment of ischemic brain damage by perturbing NMDA receptor-PSD-95 protein interactions. *Science* 298: 846-850.
- Adams JM. 2003. Ways of dying: Multiple pathways to apoptosis. *Genes Dev* 17: 2481-2495.
- Adams JM, Cory S. 1998. The Bcl-2 protein family: Arbiters of cell survival. *Science* 281: 1322-1326.
- Aguilera-Aguirre L, Gonzalez-Hernandez JC, Perez-Vazquez V, Ramirez J, Clemente-Guerrero M, et al. 2002. Role of intramitochondrial nitric oxide in rat heart and kidney during hypertension. *Mitochondrion* 1: 413-423.
- Ahlemeyer B, Kriegstein J. 2003. Neuroprotective effects of *Ginkgo biloba* extract. *Cell Mol Life Sci* 60: 1779-1792.
- Akhtar RS, Ness JM, Roth KA. 2004. Bcl-2 family regulation of neuronal development and neurodegeneration. *Biochim Biophys Acta* 1644: 189-203.
- Alderton WK, Cooper CE, Knowles RG. 2001. Nitric oxide synthases: Structure, function, and inhibition. *Biochem J* 357: 593-615.
- Allan SM, Rothwell NJ. 2003. Inflammation in central nervous system injury. *Philos Trans R Soc Lond B Biol Sci* 358: 1669-1677.
- Almeida A, Almeida J, Bolanos JP, Moncada S. 2001. Different responses of astrocytes and neurons to nitric oxide: The role of glycolytically generated ATP in astrocyte protection. *Proc Natl Acad Sci USA* 98: 15294-15299.

- Almeida A, Bolanos JP, Medina JM. 1999. Nitric oxide mediates glutamate-induced mitochondrial depolarization in rat cortical neurons. *Brain Res* 816: 580-586.
- Alonso D, Encinas JM, Uttenthal LO, Bosca L, Serrano J, et al. 2002. Coexistence of translocated cytochrome *c* and nitrated protein in neurons of the rat cerebral cortex after oxygen and glucose deprivation. *Neuroscience* 111: 47-56.
- Ames BN. 2004. Delaying the mitochondrial decay of aging. *Ann N Y Acad Sci* 1019: 406-411.
- Anderson MF, Sims NR. 2002. The effects of focal ischemia and reperfusion on the glutathione content of mitochondria from rat brain subregions. *J Neurochem* 81: 541-549.
- Andrews ZB, Diano S, Horvath TL. 2005. Mitochondrial uncoupling proteins in the CNS: In support of function and survival. *Nat Rev Neurosci* 6: 829-840.
- Andreyev A, Fiskum G. 1999. Calcium-induced release of mitochondrial cytochrome *c* by different mechanisms selective for brain versus liver. *Cell Death Differ* 6: 825-832.
- Andreyev AY, Kushnareva YE, Starkov AA. 2005. Mitochondrial metabolism of reactive oxygen species. *Biochemistry (Mosc)* 70: 200-214.
- Ankarcrona M, Dypbukt JM, Bonfoco E, Zhivotovsky B, Orrenius S, et al. 1995. Glutamate-induced neuronal death: A succession of necrosis or apoptosis depending on mitochondrial function. *Neuron* 15: 961-973.
- Antonsson B, Montessuit S, Lauper S, Eskes R, Martinou JC. 2000. Bax oligomerization is required for channel-forming activity in liposomes and to trigger cytochrome *c* release from mitochondria. *Biochem J* 345: 271-278.
- Arai M, Imai H, Koumura T, Yoshida M, Emoto K, et al. 1999. Mitochondrial phospholipid hydroperoxide glutathione peroxidase plays a major role in preventing oxidative injury to cells. *J Biol Chem* 274: 4924-4933.
- Asoh S, Ohsawa I, Mori T, Katsura K, Hiraide T, et al. 2002. Protection against ischemic brain injury by protein therapeutics. *Proc Natl Acad Sci USA* 99: 17107-17112.
- Atlante A, Calissano P, Bobba A, Giannattasio S, Marra E, et al. 2001. Glutamate neurotoxicity, oxidative stress, and mitochondria. *FEBS Lett* 497: 1-5.
- Aulak KS, Koeck T, Crabb JW, Stuehr DJ. 2004. Dynamics of protein nitration in cells and mitochondria. *Am J Physiol Heart Circ Physiol* 286: H30-H38.
- Baines CP, Kaiser RA, Purcell NH, Blair NS, Osinska H, et al. 2005. Loss of cyclophilin D reveals a critical role for mitochondrial permeability transition in cell death. *Nature* 434: 658-662.
- Bajgar R, Seetharaman S, Kowaltowski AJ, Garlid KD, Paucek P. 2001. Identification and properties of a novel intracellular (mitochondrial) ATP-sensitive potassium channel in brain. *J Biol Chem* 276: 33369-33374.
- Bal-Price A, Brown GC. 2000. Nitric oxide-induced necrosis and apoptosis in PC12 cells mediated by mitochondria. *J Neurochem* 75: 1455-1464.
- Barja G. 1999. Mitochondrial oxygen radical generation and leak: Sites of production in states 4 and 3, organ specificity, and relation to aging, and longevity. *J Bioenerg Biomembr* 31: 347-366.
- Basso E, Fante L, Fowlkes J, Petronilli V, Forte MA, et al. 2005. Properties of the permeability transition pore in mitochondria devoid of cyclophilin D. *J Biol Chem* 280: 18558-18561.
- Batandier C, Leverve X, Fontaine E. 2004. Opening of the mitochondrial permeability transition pore induces reactive oxygen species production at the level of the respiratory chain complex I. *J Biol Chem* 279: 17197-17204.
- Bates TE, Loesch A, Burnstock G, Clark JB. 1995. Immunocytochemical evidence for a mitochondrially located nitric oxide synthase in brain and liver. *Biochem Biophys Res Commun* 213: 896-900.
- Bayir H, Kagan VE, Tyurina YY, Tyurin V, Ruppel RA, et al. 2002. Assessment of antioxidant reserves and oxidative stress in cerebrospinal fluid after severe traumatic brain injury in infants and children. *Pediatr Res* 51: 571-578.
- Beal MF. 2004. Mitochondrial dysfunction and oxidative damage in Alzheimer's and Parkinson's diseases and coenzyme Q10 as a potential treatment. *J Bioenerg Biomembr* 36: 381-386.
- Beal MF. 2005. Mitochondria take center stage in aging and neurodegeneration. *Ann Neurol* 58: 495-505.
- Beavis AD, Lu Y, Garlid KD. 1993. On the regulation of K⁺ uniport in intact mitochondria by adenine nucleotides and nucleotide analogs. *J Biol Chem* 268: 997-1004.
- Beckman JS. 2002. Protein tyrosine nitration and peroxynitrite. *FASEB J* 16: 1144.
- Beckman JS, Koppenol WH. 1996. Nitric oxide, superoxide, and peroxynitrite: The good, the bad, and ugly. *Am J Physiol* 271: C1424-C1437.
- Bolanos JP, Ciudad P, Garcia-Nogales P, Delgado-Esteban M, Fernandez E, et al. 2004a. Regulation of glucose metabolism by nitrosative stress in neural cells. *Mol Aspects Med* 25: 61-73.
- Bolanos JP, Garcia-Nogales P, Almeida A. 2004b. Provoking neuroprotection by peroxynitrite. *Curr Pharm Des* 10: 867-877.
- Bolanos JP, Garcia-Nogales P, Vega-Agapito V, Delgado-Esteban M, Ciudad P, et al. 2001. Nitric oxide-mediated mitochondrial impairment in neural cells: A role for glucose metabolism in neuroprotection. *Prog Brain Res* 132: 441-454.
- Bonfanti L, Strettoi E, Chierzi S, Cenni MC, Liu XH, et al. 1996. Protection of retinal ganglion cells from natural and

- axotomy-induced cell death in neonatal transgenic mice overexpressing Bcl-2. *J Neurosci* 16: 4186-4194.
- Borner C. 2003. The Bcl-2 protein family: Sensors and checkpoints for life-or-death decisions. *Mol Immunol* 39: 615-647.
- Bossy-Wetzel E, Barsoum MJ, Godzik A, Schwarzenbacher R, Lipton SA. 2003. Mitochondrial fission in apoptosis, neurodegeneration, and aging. *Curr Opin Cell Biol* 15: 706-716.
- Bossy-Wetzel E, Talantova MV, Lee WD, Scholzke MN, Harrop A, et al. 2004. Cross talk between nitric oxide and zinc pathways to neuronal cell death involving mitochondrial dysfunction and p38-activated K⁺ channels. *Neuron* 41: 351-365.
- Boveris A, Chance B. 1973. The mitochondrial generation of hydrogen peroxide. General properties and effect of hyperbaric oxygen. *Biochem J* 134: 707-716.
- Brookes PS, Salinas EP, Darley-USmar K, Eiserich JP, Freeman BA, et al. 2000. Concentration-dependent effects of nitric oxide on mitochondrial permeability transition and cytochrome *c* release. *J Biol Chem* 275: 20474-20479.
- Bronson JR, Schumacker PT, Zhang H. 1999. Nitric oxide acutely inhibits neuronal energy production. The committees on neurobiology and cell physiology. *J Neurosci* 19: 147-158.
- Brown GC. 1999. Nitric oxide and mitochondrial respiration. *Biochim Biophys Acta* 1411: 351-369.
- Brown GC, Borutaite V. 2004. Inhibition of mitochondrial respiratory complex I by nitric oxide, peroxynitrite, and S-nitrosothiols. *Biochim Biophys Acta* 1658: 44-49.
- Brustovetsky N, Dubinsky JM. 2000. Limitations of cyclosporin A inhibition of the permeability transition in CNS mitochondria. *J Neurosci* 20: 8229-8237.
- Buckman TD, Sutphin MS, Mitrovic B. 1993. Oxidative stress in a clonal cell line of neuronal origin: Effects of antioxidant enzyme modulation. *J Neurochem* 60: 2046-2058.
- Busija DW, Katakam P, Rajapakse NC, Kis B, Grover G, et al. 2005. Effects of ATP-sensitive potassium channel activators diazoxide and BMS-191095 on membrane potential and reactive oxygen species production in isolated piglet mitochondria. *Brain Res Bull* 66: 85-90.
- Butterfield DA. 2004. Proteomics: A new approach to investigate oxidative stress in Alzheimer's disease brain. *Brain Res* 1000: 1-7.
- Calabrese V, Scapagnini G, Giuffrida Stella AM, Bates TE, Clark JB. 2001. Mitochondrial involvement in brain function and dysfunction: Relevance to aging, neurodegenerative disorders, and longevity. *Neurochem Res* 26: 739-764.
- Cantara S, Donnini S, Giachetti A, Thorpe PE, Ziche M. 2004. Exogenous BH4/Bcl-2 peptide reverts coronary endothelial cell apoptosis induced by oxidative stress. *J Vasc Res* 41: 202-207.
- Cao G, Pei W, Ge H, Liang Q, Luo Y, et al. 2002. In vivo delivery of a Bcl-xL fusion protein containing the TAT protein transduction domain protects against ischemic brain injury and neuronal apoptosis. *J Neurosci* 22: 5423-5431.
- Cao W, Carney JM, Duchon A, Floyd RA, Chevion M. 1988. Oxygen free radical involvement in ischemia and reperfusion injury to brain. *Neurosci Lett* 88: 233-238.
- Carreras MC, Franco MC, Peralta JG, Poderoso JJ. 2004. Nitric oxide, complex I, and the modulation of mitochondrial reactive species in biology and disease. *Mol Aspects Med* 25: 125-139.
- Cassina AM, Hodara R, Souza JM, Thomson L, Castro L, et al. 2000. Cytochrome *c* nitration by peroxynitrite. *J Biol Chem* 275: 21409-21415.
- Castellani R, Hirai K, Aliev G, Drew KL, Nunomura A, et al. 2002. Role of mitochondrial dysfunction in Alzheimer's disease. *J Neurosci Res* 70: 357-360.
- Castilho RF, Ward MW, Nicholls DG. 1999. Oxidative stress, mitochondrial function, and acute glutamate excitotoxicity in cultured cerebellar granule cells. *J Neurochem* 72: 1394-1401.
- Chan PH. 2004. Mitochondria and neuronal death/survival signaling pathways in cerebral ischemia. *Neurochem Res* 29: 1943-1949.
- Chandel NS, Schumacker PT. 2000. Cellular oxygen sensing by mitochondria: Old questions, new insight. *J Appl Physiol* 88: 1880-1889.
- Chen JJ, Schenker S, Henderson GI. 1997. 4-hydroxynonenal levels are enhanced in fetal liver mitochondria by in utero ethanol exposure. *Hepatology* 25: 142-147.
- Chen L, Willis SN, Wei A, Smith BJ, Fletcher JI, et al. 2005. Differential targeting of prosurvival Bcl-2 proteins by their BH3-only ligands allows complementary apoptotic function. *Mol Cell* 17: 393-403.
- Cheng EH, Sheiko TV, Fisher JK, Craigen WJ, Korsmeyer SJ. 2003. VDAC2 inhibits BAK activation and mitochondrial apoptosis. *Science* 301: 513-517.
- Chiarugi A. 2005. Simple but not simpler: Toward a unified picture of energy requirements in cell death. *FASEB J* 19: 1783-1788.
- Chinopoulos C, Starkov AA, Fiskum G. 2003. Cyclosporin A-insensitive permeability transition in brain mitochondria: Inhibition by 2-aminoethoxydiphenyl borate. *J Biol Chem* 278: 27382-27389.
- Chipuk JE, Kuwana T, Bouchier-Hayes L, Droin NM, Newmeyer DD, et al. 2004. Direct activation of Bax by p53 mediates mitochondrial membrane permeabilization and apoptosis. *Science* 303: 1010-1014.

- Cidad P, Almeida A, Bolanos JP. 2004. Inhibition of mitochondrial respiration by nitric oxide rapidly stimulates cytoprotective GLUT3-mediated glucose uptake through 5'-AMP-activated protein kinase. *Biochem J* 384: 629-636.
- Cirman T, Oresic K, Mazovec GD, Turk V, Reed JC, et al. 2004. Selective disruption of lysosomes in HeLa cells triggers apoptosis mediated by cleavage of Bid by multiple papain-like lysosomal cathepsins. *J Biol Chem* 279: 3578-3587.
- Clausen T, Bullock R. 2001. Medical treatment and neuroprotection in traumatic brain injury. *Curr Pharm Des* 7: 1517-1532.
- Conti B, Sugama S, Lucero J, Winsky-Sommerer R, Wirz SA, et al. 2005. Uncoupling protein 2 protects dopaminergic neurons from acute 1,2,3,6-methyl-phenyl-tetrahydropyridine toxicity. *J Neurochem* 93: 493-501.
- Cooper CE. 2002. Nitric oxide and cytochrome oxidase: Substrate, inhibitor, or effector? *Trends Biochem Sci* 27: 33-39.
- Costantini P, Chernyak BV, Petronilli V, Bernardi P. 1996. Modulation of the mitochondrial permeability transition pore by pyridine nucleotides and dithiol oxidation at two separate sites. *J Biol Chem* 271: 6746-6751.
- Coulter CV, Kelso GF, Lin TK, Smith RA, Murphy MP. 2000. Mitochondrially targeted antioxidants and thiol reagents. *Free Radic Biol Med* 28: 1547-1554.
- Cristofori L, Tavazzi B, Gambin R, Vagnozzi R, Signoretto S, et al. 2005. Biochemical analysis of the cerebrospinal fluid: Evidence for catastrophic energy failure and oxidative damage preceding brain death in severe head injury: A case report. *Clin Biochem* 38: 97-100.
- Crouser ED, Gadd ME, Julian MW, Huff JE, Broekemeier KM, et al. 2003. Quantitation of cytochrome *c* release from rat liver mitochondria. *Anal Biochem* 317: 67-75.
- Culmsee C, Mattson MP. 2005. p53 in neuronal apoptosis. *Biochem Biophys Res Commun* 331: 761-777.
- Culmsee C, Zhu X, Yu QS, Chan SL, Camandola S, et al. 2001. A synthetic inhibitor of p53 protects neurons against death induced by ischemic and excitotoxic insults and amyloid β -peptide. *J Neurochem* 77: 220-228.
- Dalkara T, Endres M, Moskowitz MA. 1998. Mechanisms of NO neurotoxicity. *Prog Brain Res* 118: 231-239.
- Dawson VL, Dawson TM. 2004. Deadly conversations: Nuclear-mitochondrial cross talk. *J Bioenerg Biomembr* 36: 287-294.
- Deckwerth TL, Elliott JL, Knudson CM, Johnson EM Jr, Snider WD, et al. 1996. BAX is required for neuronal death after trophic factor deprivation and during development. *Neuron* 17: 401-411.
- Dedkova EN, Ji X, Lipsius SL, Blatter LA. 2004. Mitochondrial calcium uptake stimulates nitric oxide production in mitochondria of bovine vascular endothelial cells. *Am J Physiol Cell Physiol* 286: C406-C415.
- Denicourt C, Dowdy SF. 2003. Protein transduction technology offers novel therapeutic approach for brain ischemia. *Trends Pharmacol Sci* 24: 216-218.
- Desagher S, Osen-Sand A, Nichols A, Eskes R, Montessuit S, et al. 1999. Bid-induced conformational change of Bax is responsible for mitochondrial cytochrome *c* release during apoptosis. *J Cell Biol* 144: 891-901.
- Dietz GP, Kilic E, Bahr M. 2002. Inhibition of neuronal apoptosis in vitro and in vivo using TAT-mediated protein transduction. *Mol Cell Neurosci* 21: 29-37.
- Dimroth P, von Ballmoos C, Meier T, Kaim G. 2003. Electrical power fuels rotary ATP synthase. *Structure* 11: 1469-1473.
- Dineley KE, Votyakova TV, Reynolds IJ. 2003. Zinc inhibition of cellular energy production: Implications for mitochondria and neurodegeneration. *J Neurochem* 85: 563-570.
- Dirnagl U, Iadecola C, Moskowitz MA. 1999. Pathobiology of ischemic stroke: An integrated view. *Trends Neurosci* 22: 391-397.
- Domanska-Janik K, Buzanska L, Dluzniewska J, Kozłowska H, Sarnowska A, et al. 2004. Neuroprotection by cyclosporin A following transient brain ischemia correlates with the inhibition of the early efflux of cytochrome *c* to cytoplasm. *Brain Res Mol Brain Res* 121: 50-59.
- Dubinsky JM, Levi Y. 1998. Calcium-induced activation of the mitochondrial permeability transition in hippocampal neurons. *J Neurosci Res* 53: 728-741.
- Duchen MR. 2000. Mitochondria and calcium: From cell signaling to cell death. *J Physiol* 529 Pt 1: 57-68.
- Echtay KS, Murphy MP, Smith RA, Talbot DA, Brand MD. 2002. Superoxide activates mitochondrial uncoupling protein 2 from the matrix side. Studies using targeted antioxidants. *J Biol Chem* 277: 47129-47135.
- Elfering SL, Haynes VL, Traaseth NJ, Ettl A, Giulivi C. 2004. Aspects, mechanism, and biological relevance of mitochondrial protein nitration sustained by mitochondrial nitric oxide synthase. *Am J Physiol Heart Circ Physiol* 286: H22-H29.
- Eliasson MJ, Huang Z, Ferrante RJ, Sasamata M, Molliver ME, et al. 1999. Neuronal nitric oxide synthase activation and peroxynitrite formation in ischemic stroke linked to neural damage. *J Neurosci* 19: 5910-5918.
- Ellerby LM, Ellerby HM, Park SM, Holleran AL, Murphy AN, et al. 1996. Shift of the cellular oxidation-reduction potential in neural cells expressing Bcl-2. *J Neurochem* 67: 1259-1267.
- Endres M, Laufs U, Liao JK, Moskowitz MA. 2004. Targeting eNOS for stroke protection. *Trends Neurosci* 27: 283-289.
- Endres M, Wang ZQ, Namura S, Waeber C, Moskowitz MA. 1997. Ischemic brain injury is mediated by the activation of poly(ADP-ribose) polymerase. *J Cereb Blood Flow Metab* 17: 1143-1151.
- Erecinska M, Silver IA. 2001. Tissue oxygen tension and brain sensitivity to hypoxia. *Respir Physiol* 128: 263-276.

- Esposito LA, Kokoszka JE, Waymire KG, Cottrell B, Mac Gregor GR, et al. 2000. Mitochondrial oxidative stress in mice lacking the glutathione peroxidase-1 gene. *Free Radic Biol Med* 28: 754-766.
- Estevez AG, Spear N, Manuel SM, Barbeito L, Radi R, et al. 1998. Role of endogenous nitric oxide and peroxynitrite formation in the survival and death of motor neurons in culture. *Prog Brain Res* 118: 269-280.
- Esworthy RS, Ho YS, Chu FF. 1997. The Gpx1 gene encodes mitochondrial glutathione peroxidase in the mouse liver. *Arch Biochem Biophys* 340: 59-63.
- Ferranti R, da Silva MM, Kowaltowski AJ. 2003. Mitochondrial ATP-sensitive K⁺ channel opening decreases reactive oxygen species generation. *FEBS Lett* 536: 51-55.
- Fink KB, Andrews LJ, Butler WE, Ona VO, Li M, et al. 1999. Reduction of posttraumatic brain injury and free radical production by inhibition of the caspase-1 cascade. *Neuroscience* 94: 1213-1218.
- Fiskum G, Bambrick L, Kristian T, Chandrasekaran K, Chinopoulos C. 2003. Calcium-induced damage to neuron, astrocyte, and brain mitochondria. *J Neurochem* 85 (Suppl. 1), 56.
- Fiskum G, Rosenthal RE, Vereczki V, Martin E, Hoffman GE, et al. 2004. Protection against ischemic brain injury by inhibition of mitochondrial oxidative stress. *J Bioenerg Biomembr* 36: 347-352.
- Friberg H, Wieloch T. 2002. Mitochondrial permeability transition in acute neurodegeneration. *Biochimie* 84: 241-250.
- Garcia-Nogales P, Almeida A, Bolanos JP. 2003. Peroxynitrite protects neurons against nitric oxide-mediated apoptosis. A key role for glucose-6-phosphate dehydrogenase activity in neuroprotection. *J Biol Chem* 278: 864-874.
- Gegg ME, Beltran B, Salas-Pino S, Bolanos JP, Clark JB, et al. 2003. Differential effect of nitric oxide on glutathione metabolism and mitochondrial function in astrocytes and neurons: Implications for neuroprotection/neurodegeneration? *J Neurochem* 86: 228-237.
- Ghafourifar P, Cadenas E. 2005. Mitochondrial nitric oxide synthase. *Trends Pharmacol Sci* 26: 190-195.
- Ghafourifar P, Richter C. 1999. Mitochondrial nitric oxide synthase regulates mitochondrial matrix pH. *Biol Chem* 380: 1025-1028.
- Gibson GE, Huang HM. 2004. Mitochondrial enzymes and endoplasmic reticulum calcium stores as targets of oxidative stress in neurodegenerative diseases. *J Bioenerg Biomembr* 36: 335-340.
- Gibson ME, Han BH, Choi J, Knudson CM, Korsmeyer SJ, et al. 2001. BAX contributes to apoptotic-like death following neonatal hypoxia-ischemia: Evidence for distinct apoptosis pathways. *Mol Med* 7: 644-655.
- Ginsberg MD. 2001. Role of free radical reactions in ischemic brain injury. *Drug News Perspect* 14: 81-88.
- Giulivi C, Poderoso JJ, Boveris A. 1998. Production of nitric oxide by mitochondria. *J Biol Chem* 273: 11038-11043.
- Gleyzer N, Vercauteren K, Scarpulla RC. 2005. Control of mitochondrial transcription specificity factors (TFB1M and TFB2M) by nuclear respiratory factors (NRF-1 and NRF-2) and PGC-1 family coactivators. *Mol Cell Biol* 25: 1354-1366.
- Globus MY, Busto R, Lin B, Schnippering H, Ginsberg MD. 1995. Detection of free radical activity during transient global ischemia and recirculation: Effects of intraschemic brain temperature modulation. *J Neurochem* 65: 1250-1256.
- Gonzalez-Zulueta M, Ensz LM, Mukhina G, Lebovitz RM, Zwacka RM, et al. 1998. Manganese superoxide dismutase protects nNOS neurons from NMDA and nitric oxide-mediated neurotoxicity. *J Neurosci* 18: 2040-2055.
- Gow AJ, Farkouh CR, Munson DA, Posencheg MA, Ischiropoulos H. 2004. Biological significance of nitric oxide-mediated protein modifications. *Am J Physiol Lung Cell Mol Physiol* 287: L262-L268.
- Green DR. 2005. Apoptotic pathways: Ten minutes to dead. *Cell* 121: 671-674.
- Gross A, McDonnell JM, Korsmeyer SJ. 1999. Bcl-2 family members and the mitochondria in apoptosis. *Genes Dev* 13: 1899-1911.
- Gunter TE, Yule DI, Gunter KK, Eliseev RA, Salter JD. 2004. Calcium and mitochondria. *FEBS Lett* 567: 96-102.
- Guo B, Zhai D, Cabezas E, Welsh K, Nouraini S, et al. 2003. Humanin peptide suppresses apoptosis by interfering with Bax activation. *Nature* 423: 456-461.
- Hagberg H. 2004. Mitochondrial impairment in the developing brain after hypoxia-ischemia. *J Bioenerg Biomembr* 36: 369-373.
- Hall ED. 1997. Brain attack. Acute therapeutic interventions. Free radical scavengers and antioxidants. *Neurosurg Clin N Am* 8: 195-206.
- Ham J, Towers E, Gilley J, Terzano S, Randall R. 2005. BH3-only proteins: Key regulators of neuronal apoptosis. *Cell Death Differ* 12: 1015-1020.
- Han D, Canali R, Garcia J, Aguilera R, Gallaher TK, et al. 2005. Sites and mechanisms of aconitase inactivation by peroxynitrite: Modulation by citrate and glutathione. *Biochemistry* 44: 11986-11996.
- Harris CA, Johnson EM Jr. 2001. BH3-only Bcl-2 family members are coordinately regulated by the JNK pathway and require Bax to induce apoptosis in neurons. *J Biol Chem* 276: 37754-37760.
- Haynes V, Elfering S, Traaseth N, Giulivi C. 2004. Mitochondrial nitric oxide synthase: Enzyme expression, characterization, and regulation. *J Bioenerg Biomembr* 36: 341-346.
- Haynes V, Elfering SL, Squires RJ, Traaseth N, Solien J, et al. 2003. Mitochondrial nitric oxide synthase: Role in pathophysiology. *IUBMB Life* 55: 599-603.

- Heales SJ, Bolanos JP. 2002. Impairment of brain mitochondrial function by reactive nitrogen species: The role of glutathione in dictating susceptibility. *Neurochem Int* 40: 469-474.
- Heck DE, Kagan VE, Shvedova AA, Laskin JD. 2005. An epigrammatic (abridged) recounting of the myriad tales of astonishing deeds and dire consequences pertaining to nitric oxide and reactive oxygen species in mitochondria with an ancillary missive concerning the origins of apoptosis. *Toxicology* 208: 259-271.
- Hetz C, Vitte PA, Bombrun A, Rostovtseva TK, Montessuit S, et al. 2005. Bax channel inhibitors prevent mitochondrial-mediated apoptosis and protect neurons in a model of global brain ischemia. *J Biol Chem* 280, 42960-42970.
- Hockenbery DM, Oltvai ZN, Yin XM, Milliman CL, Korsmeyer SJ. 1993. Bcl-2 functions in an antioxidant pathway to prevent apoptosis. *Cell* 75: 241-251.
- Hoehn B, Yenari MA, Sapolsky RM, Steinberg GK. 2003. Glutathione peroxidase overexpression inhibits cytochrome *c* release and proapoptotic mediators to protect neurons from experimental stroke. *Stroke* 34: 2489-2494.
- Hong SJ, Dawson TM, Dawson VL. 2004. Nuclear and mitochondrial conversations in cell death: PARP-1 and AIF signaling. *Trends Pharmacol Sci* 25: 259-264.
- Horvitz HR. 2003. Worms, life, and death (Nobel lecture). *ChemBiochem* 4: 697-711.
- Hsu M, Srinivas B, Kumar J, Subramanian R, Andersen J. 2005. Glutathione depletion resulting in selective mitochondrial complex I inhibition in dopaminergic cells is via a NO-mediated pathway not involving peroxynitrite: Implications for Parkinson's disease. *J Neurochem* 92: 1091-1103.
- Hsu SY, Kaipia A, McGee E, Lomeli M, Hsueh AJ. 1997. Bok is a proapoptotic Bcl-2 protein with restricted expression in reproductive tissues and heterodimerizes with selective antiapoptotic Bcl-2 family members. *Proc Natl Acad Sci USA* 94: 12401-12406.
- Huang DC, Strasser A. 2000. BH3-only proteins—essential initiators of apoptotic cell death. *Cell* 103: 839-842.
- Imaizumi K, Benito A, Kiryu-Seo S, Gonzalez V, Inohara N, et al. 2004. Critical role for DP5/Harakiri, a Bcl-2 homology domain 3-only Bcl-2 family member in axotomy-induced neuronal cell death. *J Neurosci* 24: 3721-3725.
- Ischiropoulos H. 2003. Biological selectivity and functional aspects of protein tyrosine nitration. *Biochem Biophys Res Commun* 305: 776-783.
- Ischiropoulos H, Gow A. 2005. Pathophysiological functions of nitric oxide-mediated protein modifications. *Toxicology* 208: 299-303.
- Iverson SL, Orrenius S. 2004. The cardiolipin–cytochrome *c* interaction and the mitochondrial regulation of apoptosis. *Arch Biochem Biophys* 423: 37-46.
- Iwasaki H, Mori Y, Hara Y, Uchida K, Zhou H, et al. 2001. 2-Aminoethoxydiphenyl borate (2-APB) inhibits capacitative calcium entry independently of the function of inositol-1,4,5-trisphosphate receptors. *Receptors Channels* 7: 429-439.
- Jaffrey SR, Erdjument-Bromage H, Ferris CD, Tempst P, Snyder SH. 2001. Protein S-nitrosylation: A physiological signal for neuronal nitric oxide. *Nat Cell Biol* 3: 193-197.
- Jin Y, McEwen ML, Nottingham SA, Maragos WF, Dragicevic NB, et al. 2004. The mitochondrial uncoupling agent 2,4-dinitrophenol improves mitochondrial function, attenuates oxidative damage, and increases white matter sparing in the contused spinal cord. *J Neurotrauma* 21: 1396-1404.
- Jordan J, Cena V, Prehn JH. 2003. Mitochondrial control of neuron death and its role in neurodegenerative disorders. *J Physiol Biochem* 59: 129-141.
- Kaminska B, Figiel I, Pyszynska B, Czajkowski R, Mosieniak G. 2001. Treatment of hippocampal neurons with cyclosporin A results in calcium overload and apoptosis, which are independent on NMDA receptor activation. *Br J Pharmacol* 133: 997-1004.
- Kang YC, Kim PK, Choi BM, Chung HT, Ha KS, et al. 2004. Regulation of programmed cell death in neuronal cells by nitric oxide. *In Vivo* 18: 367-376.
- Keelan J, Vergun O, Duchon MR. 1999. Excitotoxic mitochondrial depolarization requires both calcium and nitric oxide in rat hippocampal neurons. *J Physiol* 520 Pt 3: 797-813.
- Keller JN, Guo Q, Holtsberg FW, Bruce-Keller AJ, Mattson MP. 1998a. Increased sensitivity to mitochondrial toxin-induced apoptosis in neural cells expressing mutant presenilin-1 is linked to perturbed calcium homeostasis and enhanced oxyradical production. *J Neurosci* 18: 4439-4450.
- Keller JN, Kindy MS, Holtsberg FW, St Clair DK, Yen HC, et al. 1998b. Mitochondrial manganese superoxide dismutase prevents neural apoptosis and reduces ischemic brain injury: Suppression of peroxynitrite production, lipid peroxidation, and mitochondrial dysfunction. *J Neurosci* 18: 687-697.
- Keller JN, Mark RJ, Bruce AJ, Blanc E, Rothstein JD, et al. 1997. 4-Hydroxynonenal, an aldehydic product of membrane lipid peroxidation, impairs glutamate transport, and mitochondrial function in synaptosomes. *Neuroscience* 80: 685-696.
- Khosravi-Far R, Esposti MD. 2004. Death receptor signals to mitochondria. *Cancer Biol Ther* 3: 1051-1057.
- Kil HY, Zhang J, Piantadosi CA. 1996. Brain temperature alters hydroxyl radical production during cerebral ischemia/reperfusion in rats. *J Cereb Blood Flow Metab* 16: 100-106.

- Kilic E, Dietz GP, Hermann DM, Bahr M. 2002. Intravenous TAT-Bcl-Xl is protective after middle cerebral artery occlusion in mice. *Ann Neurol* 52: 617-622.
- Kim-Han JS, Reichert SA, Quick KL, Dugan LL. 2001. BMCPI: A mitochondrial uncoupling protein in neurons that regulates mitochondrial function and oxidant production. *J Neurochem* 79: 658-668.
- Kim GW, Kondo T, Noshita N, Chan PH. 2002. Manganese superoxide dismutase deficiency exacerbates cerebral infarction after focal cerebral ischemia/reperfusion in mice: Implications for the production and role of superoxide radicals. *Stroke* 33: 809-815.
- Kim TH, Zhao Y, Ding WX, Shin JN, He X, et al. 2004. Bid-cardiolipin interaction at mitochondrial contact site contributes to mitochondrial cristae reorganization and cytochrome *c* release. *Mol Biol Cell* 7: 3061-3072.
- Kirkland RA, Franklin JL. 2003. Bax, reactive oxygen, and cytochrome *c* release in neuronal apoptosis. *Antioxid Redox Signal* 5: 589-596.
- Konishi A, Shimizu S, Hirota J, Takao T, Fan Y, et al. 2003. Involvement of histone H1.2 in apoptosis induced by DNA double-strand breaks. *Cell* 114: 673-688.
- Korsmeyer SJ, Shutter JR, Veis DJ, Merry DE, Oltvai ZN. 1993. Bcl-2/Bax: A rheostat that regulates an antioxidant pathway and cell death. *Semin Cancer Biol* 4: 327-332.
- Kostic V, Jackson-Lewis V, De Bilbao F, Dubois-Dauphin M, Przedborski S. 1997. Bcl-2: Prolonging life in a transgenic mouse model of familial amyotrophic lateral sclerosis. *Science* 277: 559-562.
- Kowaltowski AJ, Fenton RG, Fiskum G. 2004. Bcl-2 family proteins regulate mitochondrial reactive oxygen production and protect against oxidative stress. *Free Radic Biol Med* 37: 1845-1853.
- Kowaltowski AJ, Fiskum G. 2005. Redox mechanisms of cyto-protection by Bcl-2. *Antioxid Redox Signal* 7: 508-514.
- Kowaltowski AJ, Seetharaman S, Paucek P, Garlid KD. 2001. Bioenergetic consequences of opening the ATP-sensitive K⁺ channel of heart mitochondria. *Am J Physiol Heart Circ Physiol* 280: H649-H657.
- Kowaltowski AJ, Vercesi AE. 1999. Mitochondrial damage induced by conditions of oxidative stress. *Free Radic Biol Med* 26: 463-471.
- Kowaltowski AJ, Vercesi AE, Fiskum G. 2000. Bcl-2 prevents mitochondrial permeability transition and cytochrome *c* release via maintenance of reduced pyridine nucleotides. *Cell Death Differ* 7: 903-910.
- Krajewska M, Rosenthal RE, Mikolajczyk J, Stennicke HR, Wiesenthal T, et al. 2004. Early processing of Bid and caspase-6, -8, -10, -14 in the canine brain during cardiac arrest and resuscitation. *Exp Neurol* 189: 261-279.
- Krenz M, Oldenburg O, Wimpee H, Cohen MV, Garlid KD, et al. 2002. Opening of ATP-sensitive potassium channels causes generation of free radicals in vascular smooth muscle cells. *Basic Res Cardiol* 97: 365-373.
- Kristian T. 2004. Metabolic stages, mitochondria, and calcium in hypoxic/ischemic brain damage. *Cell Calcium* 36: 221-233.
- Kushnareva YE, Murphy AN, Andreyev AY. 2002. Complex I-mediated reactive oxygen species generation: Modulation by Cytochrome *c* and NAD(P)⁺ oxidation-reduction state. *Biochem J* 368: 545-553.
- Kushnareva YE, Wiley SE, Ward MW, Andreyev AY, Murphy AN. 2005. Excitotoxic injury to mitochondria isolated from cultured neurons. *J Biol Chem* 280: 28894-28902.
- Kuwana T, Bouchier-Hayes L, Chipuk JE, Bonzon C, Sullivan BA, et al. 2005. BH3 domains of BH3-only proteins differentially regulate Bax-mediated mitochondrial membrane permeabilization both directly and indirectly. *Mol Cell* 17: 525-535.
- Kuwana T, Mackey MR, Perkins G, Ellisman MH, Latterich M, et al. 2002. Bid, Bax, and lipids cooperate to form supramolecular openings in the outer mitochondrial membrane. *Cell* 111: 331-342.
- Lacza Z, Pankotai E, Csordas A, Gero D, Kiss L, et al. 2005. Mitochondrial NO and reactive nitrogen species production: Does mtNOS exist? *Nitric Oxide* 14: 162-168.
- Lacza Z, Puskar M, Figueroa JP, Zhang J, Rajapakse N, et al. 2001. Mitochondrial nitric oxide synthase is constitutively active and is functionally upregulated in hypoxia. *Free Radic Biol Med* 31: 1609-1615.
- Lambert AJ, Brand MD. 2004. Inhibitors of the quinone-binding site allow rapid superoxide production from mitochondrial NADH: Ubiquinone oxidoreductase (complex I). *J Biol Chem* 279: 39414-39420.
- Landmesser U, Dikalov S, Price SR, McCann L, Fukai T, et al. 2003. Oxidation of tetrahydrobiopterin leads to uncoupling of endothelial cell nitric oxide synthase in hypertension. *J Clin Invest* 111: 1201-1209.
- Letai A, Bassik MC, Walensky LD, Sorcinelli MD, Weiler S, et al. 2002. Distinct BH3 domains either sensitize or activate mitochondrial apoptosis, serving as prototype cancer therapeutics. *Cancer Cell* 2: 183-192.
- Lewen A, Matz P, Chan PH. 2000. Free radical pathways in CNS injury. *J Neurotrauma* 17: 871-890.
- Li H, Kolluri SK, Gu J, Dawson MI, Cao X, et al. 2000. Cytochrome *c* release and apoptosis induced by mitochondrial targeting of nuclear orphan receptor TR3. *Science* 289: 1159-1164.
- Li Y, Copin JC, Reola LF, Calagui B, Gobbel GT, et al. 1998. Reduced mitochondrial manganese superoxide dismutase activity exacerbates glutamate toxicity in cultured mouse cortical neurons. *Brain Res* 814: 164-170.
- Li Y, Huang TT, Carlson EJ, Melov S, Ursell PC, et al. 1995. Dilated cardiomyopathy and neonatal lethality in mutant

- mice lacking manganese superoxide dismutase. *Nat Genet* 11: 376-381.
- Liang HW, Xia Q, Bruce IC. 2005. Reactive oxygen species mediate the neuroprotection conferred by a mitochondrial ATP-sensitive potassium channel opener during ischemia in the rat hippocampal slice. *Brain Res* 1042: 169-175.
- Liang XH, Kleeman LK, Jiang HH, Gordon G, Goldman JE, et al. 1998. Protection against fatal Sindbis virus encephalitis by beclin, a novel Bcl-2-interacting protein. *J Virol* 72: 8586-8596.
- Lindholm D, Eriksson O, Korhonen L. 2004. Mitochondrial proteins in neuronal degeneration. *Biochem Biophys Res Commun* 321: 753-758.
- Lindsten T, Zong WX, Thompson CB. 2005. Defining the role of the Bcl-2 family of proteins in the nervous system. *Neuroscientist* 11: 10-15.
- Lipton SA. 1999. Neuronal protection and destruction by NO. *Cell Death Differ* 6: 943-951.
- Liu J, Head E, Gharib AM, Yuan W, Ingersoll RT, et al. 2002. Memory loss in old rats is associated with brain mitochondrial decay and RNA/DNA oxidation: Partial reversal by feeding acetyl-L-carnitine and/or R- α -lipoic acid. *Proc Natl Acad Sci USA* 99: 2356-2361.
- Liu X, Kim CN, Yang J, Jemmerson R, Wang X. 1996. Induction of apoptotic program in cell-free extracts: Requirement for dATP and cytochrome *c*. *Cell* 86: 147-157.
- Liu Y, Rosenthal RE, Haywood Y, Miljkovic-Lolic M, Vanderhoek JY, et al. 1998. Normoxic ventilation after cardiac arrest reduces oxidation of brain lipids and improves neurological outcome. *Stroke* 29: 1679-1686.
- Lossi L, Merighi A. 2003. In vivo cellular and molecular mechanisms of neuronal apoptosis in the mammalian CNS. *Prog Neurobiol* 69: 287-312.
- Luciano F, Zhai D, Zhu X, Bailly-Maitre B, Ricci JE, et al. 2005. Cytoprotective peptide humanin binds and inhibits proapoptotic Bcl-2/Bax family protein BimEL. *J Biol Chem* 280: 15825-15835.
- Lucken-Ardjomande S, Martinou JC. 2005. Regulation of Bcl-2 proteins and of the permeability of the outer mitochondrial membrane. *C R Biol* 328: 616-631.
- Maciel EN, Kaminski Schierle GS, Hansson O, Brundin P, Castilho RF. 2003. Cyclosporin A and Bcl-2 do not inhibit quinolinic acid-induced striatal excitotoxicity in rodents. *Exp Neurol* 183: 430-437.
- Macmillan-Crow LA, Cruthirds DL. 2001. Invited review: Manganese superoxide dismutase in disease. *Free Radic Res* 34: 325-336.
- MacMillan-Crow LA, Thompson JA. 1999. Tyrosine modifications and inactivation of active site manganese superoxide dismutase mutant (Y34F) by peroxynitrite. *Arch Biochem Biophys* 366: 82-88.
- Maragos WF, Rockich KT, Dean JJ, Young KL. 2003. Pre- or posttreatment with the mitochondrial uncoupler 2,4-dinitrophenol attenuates striatal quinolinic lesions. *Brain Res* 966: 312-316.
- Markesbery WR, Carney JM. 1999. Oxidative alterations in Alzheimer's disease. *Brain Pathol* 9: 133-146.
- Martin E, Rosenthal RE, Fiskum G. 2005. Pyruvate dehydrogenase complex: Metabolic link to ischemic brain injury and target of oxidative stress. *J Neurosci Res* 79: 240-247.
- Martinou JC, Dubois-Dauphin M, Staple JK, Rodriguez I, Frankowski H, et al. 1994. Overexpression of BCL-2 in transgenic mice protects neurons from naturally occurring cell death and experimental ischemia. *Neuron* 13: 1017-1030.
- Mattson MP. 1998. Free radicals, calcium, and the synaptic plasticity-cell death continuum: Emerging roles of the transcription factor NF- κ B. *Int Rev Neurobiol* 42: 103-168.
- Mattson MP, Kroemer G. 2003. Mitochondria in cell death: Novel targets for neuroprotection and cardioprotection. *Trends Mol Med* 9: 196-205.
- McLaughlin J, Roozendaal B, Dumas T, Gupta A, Ajilore O, et al. 2000. Sparing of neuronal function postseizure with gene therapy. *Proc Natl Acad Sci USA* 97: 12804-12809.
- McLean CW, Mirochnitchenko O, Claus CP, Noble-Haesslein LJ, Ferriero DM. 2005. Overexpression of glutathione peroxidase protects immature murine neurons from oxidative stress. *Dev Neurosci* 27: 169-175.
- Mihara M, Erster S, Zaika A, Petrenko O, Chittenden T, et al. 2003. p53 has a direct apoptogenic role at the mitochondria. *Mol Cell* 11: 577-590.
- Moncada S, Erusalimsky JD. 2002. Does nitric oxide modulate mitochondrial energy generation and apoptosis? *Nat Rev Mol Cell Biol* 3: 214-220.
- Mori M, Burgess DL, Geffrides LA, Foreman PJ, Opferman JT, et al. 2004. Expression of apoptosis inhibitor protein Mcl1 linked to neuroprotection in CNS neurons. *Cell Death Differ* 11: 1223-1233.
- Moskovitz J. 2005. Methionine sulfoxide reductases: Ubiquitous enzymes involved in antioxidant defense, protein regulation, and prevention of aging-associated diseases. *Biochim Biophys Acta* 1703: 213-219.
- Murphy AN, Bredesen DE, Cortopassi G, Wang E, Fiskum G. 1996. Bcl-2 potentiates the maximal calcium uptake capacity of neural cell mitochondria. *Proc Natl Acad Sci USA* 93: 9893-9898.
- Murphy S. 2000. Production of nitric oxide by glial cells: Regulation and potential roles in the CNS. *Glia* 29: 1-13.
- Musiek ES, Milne GL, McLaughlin B, Morrow JD. 2005. Cyclopentenone eicosanoids as mediators of neurodegeneration: A pathogenic mechanism of oxidative stress-mediated

- and cyclooxygenase-mediated neurotoxicity. *Brain Pathol* 15: 149-158.
- Muyderman H, Nilsson M, Sims NR. 2004. Highly selective and prolonged depletion of mitochondrial glutathione in astrocytes markedly increases sensitivity to peroxynitrite. *J Neurosci* 24: 8019-8028.
- Myers KM, Fiskum G, Liu Y, Simmens SJ, Bredesen DE, et al. 1995. Bcl-2 protects neural cells from cyanide/aglycemia-induced lipid oxidation, mitochondrial injury, and loss of viability. *J Neurochem* 65: 2432-2440.
- Nakagawa T, Shimizu S, Watanabe T, Yamaguchi O, Otsu K, et al. 2005. Cyclophilin D-dependent mitochondrial permeability transition regulates some necrotic but not apoptotic cell death. *Nature* 434: 652-658.
- Nakagawa Y. 2004. Role of mitochondrial phospholipid hydroperoxide glutathione peroxidase (PHGPx) as an anti-apoptotic factor. *Biol Pharm Bull* 27: 956-960.
- Naoi M, Maruyama W, Shamoto-Nagai M, Yi H, Akao Y, et al. 2005. Oxidative stress in mitochondria: Decision to survival and death of neurons in neurodegenerative disorders. *Mol Neurobiol* 31: 81-93.
- Nechushtan A, Smith CL, Hsu YT, Youle RJ. 1999. Conformation of the Bax C terminus regulates subcellular location and cell death. *EMBO J* 18: 2330-2341.
- Nicholls DG. 2001. A history of UCP1. *Biochem Soc Trans* 29: 751-755.
- Nicholls DG. 2004. Mitochondrial dysfunction and glutamate excitotoxicity studied in primary neuronal cultures. *Curr Mol Med* 4: 149-177.
- Nicotera P. 2002. Apoptosis and age-related disorders: Role of caspase-dependent and caspase-independent pathways. *Toxicol Lett* 127: 189-195.
- Nicotera P. 2003. Molecular switches deciding the death of injured neurons. *Toxicol Sci* 74: 4-9.
- Nicotera P, Melino G. 2004. Regulation of the apoptosis-necrosis switch. *Oncogene* 23: 2757-2765.
- Niquet J, Wasterlain CG. 2004. Bim, Bad, and Bax: A deadly combination in epileptic seizures. *J Clin Invest* 113: 960-962.
- Nisoli E, Clementi E, Paolucci C, Cozzi V, Tonello C, et al. 2003. Mitochondrial biogenesis in mammals: The role of endogenous nitric oxide. *Science* 299: 896-899.
- Nisoli E, Falcone S, Tonello C, Cozzi V, Palomba L, et al. 2004. Mitochondrial biogenesis by NO yields functionally active mitochondria in mammals. *Proc Natl Acad Sci USA* 101: 16507-16512.
- Nomura M, Shimizu S, Sugiyama T, Narita M, Ito T, et al. 2003. 14-3-3 interacts directly with and negatively regulates proapoptotic Bax. *J Biol Chem* 278: 2058-2065.
- Offen D, Beart PM, Cheung NS, Pascoe CJ, Hochman A, et al. 1998. Transgenic mice expressing human Bcl-2 in their neurons are resistant to 6-hydroxydopamine and 1-methyl-4-phenyl-1,2,3,6-tetrahydropyridine neurotoxicity. *Proc Natl Acad Sci USA* 95: 5789-5794.
- Oldenburg O, Cohen MV, Downey JM. 2003. Mitochondrial K_{ATP} channels in preconditioning. *J Mol Cell Cardiol* 35: 569-575.
- Oppenheim RW. 1991. Cell death during development of the nervous system. *Annu Rev Neurosci* 14: 453-501.
- Orrenius S. 2004. Mitochondrial regulation of apoptotic cell death. *Toxicol Lett* 149: 19-23.
- Orrenius S, Zhivotovsky B, Nicotera P. 2003. Regulation of cell death: The calcium-apoptosis link. *Nat Rev Mol Cell Biol* 4: 552-565.
- Ouyang YB, Giffard RG. 2004. Cellular neuroprotective mechanisms in cerebral ischemia: Bcl-2 family proteins and protection of mitochondrial function. *Cell Calcium* 36: 303-311.
- Park EM, Cho S, Frys KA, Glickstein SB, Zhou P, et al. 2006. Inducible nitric oxide synthase contributes to gender differences in ischemic brain injury. *J Cereb Blood Flow Metab* 26: 392-401.
- Patel M. 2004. Mitochondrial dysfunction and oxidative stress: Cause and consequence of epileptic seizures. *Free Radic Biol Med* 37: 1951-1962.
- Petros AM, Olejniczak ET, Fesik SW. 2004. Structural biology of the Bcl-2 family of proteins. *Biochim Biophys Acta* 1644: 83-94.
- Plesnila N, Zinkel S, Le DA, Amin-Hanjani S, Wu Y, et al. 2001. BID mediates neuronal cell death after oxygen/glucose deprivation and focal cerebral ischemia. *Proc Natl Acad Sci USA* 98: 15318-15323.
- Polster BM, Basanez G, Etxebarria A, Hardwick JM, Nicholls DG. 2005. Calpain I induces cleavage and release of apoptosis-inducing factor from isolated mitochondria. *J Biol Chem* 280: 6447-6454.
- Polster BM, Basanez G, Young M, Suzuki M, Fiskum G. 2003. Inhibition of Bax-induced cytochrome *c* release from neural cell and brain mitochondria by dibucaine and propranolol. *J Neurosci* 23: 2735-2743.
- Polster BM, Fiskum G. 2004. Mitochondrial mechanisms of neural cell apoptosis. *J Neurochem* 90: 1281-1289.
- Polster BM, Kinnally KW, Fiskum G. 2001. BH3 death domain peptide induces cell type-selective mitochondrial outer membrane permeability. *J Biol Chem* 276: 37887-37894.
- Prabhakaran K, Li L, Borowitz JL, Isom GE. 2004. Caspase inhibition switches the mode of cell death induced by cyanide by enhancing reactive oxygen species generation and PARP-1 activation. *Toxicol Appl Pharmacol* 195: 194-202.
- Prins ML, Fujima LS, Hovda DA. 2005. Age-dependent reduction of cortical contusion volume by ketones after traumatic brain injury. *J Neurosci Res* 82: 413-420.

- Putcha GV, Harris CA, Moulder KL, Easton RM, Thompson CB, et al. 2002. Intrinsic and extrinsic pathway signaling during neuronal apoptosis: Lessons from the analysis of mutant mice. *J Cell Biol* 157: 441-453.
- Radi R, Cassina A, Hodara R. 2002a. Nitric oxide and peroxynitrite interactions with mitochondria. *Biol Chem* 383: 401-409.
- Radi R, Cassina A, Hodara R, Quijano C, Castro L. 2002b. Peroxynitrite reactions and formation in mitochondria. *Free Radic Biol Med* 33: 1451-1464.
- Raghupathi R, Fernandez SC, Murai H, Trusko SP, Scott RW, et al. 1998. BCL-2 overexpression attenuates cortical cell loss after traumatic brain injury in transgenic mice. *J Cereb Blood Flow Metab* 18: 1259-1269.
- Rajapakse N, Shimizu K, Kis B, Snipes J, Lacza Z, et al. 2002. Activation of mitochondrial ATP-sensitive potassium channels prevents neuronal cell death after ischemia in neonatal rats. *Neurosci Lett* 327: 208-212.
- Rao RV, Ellerby HM, Bredesen DE. 2004. Coupling endoplasmic reticulum stress to the cell death program. *Cell Death Differ* 11: 372-380.
- Raoul C, Henderson CE, Pettmann B. 1999. Programmed cell death of embryonic motoneurons triggered through the Fas death receptor. *J Cell Biol* 147: 1049-1062.
- Ravindranath V, Reed DJ. 1990. Glutathione depletion and formation of glutathione protein-mixed disulfide following exposure of brain mitochondria to oxidative stress. *Biochem Biophys Res Commun* 169: 1075-1079.
- Raza H, Robin MA, Fang JK, Avadhani NG. 2002. Multiple isoforms of mitochondrial glutathione S-transferases and their differential induction under oxidative stress. *Biochem J* 366: 45-55.
- Reed JC. 2004. Apoptosis mechanisms: Implications for cancer drug discovery. *Oncology (Williston Park)* 18: 11-20.
- Reynolds IJ, Malaiyandi LM, Coash M, Rintoul GL. 2004. Mitochondrial trafficking in neurons: A key variable in neurodegeneration? *J Bioenerg Biomembr* 36: 283-286.
- Rodolfo C, Mormone E, Matarrese P, Ciccossanti F, Farrace MG, et al. 2004. Tissue transglutaminase is a multifunctional BH3-only protein. *J Biol Chem* 279: 54783-54792.
- Rodrigues CM, Sola S, Sharpe JC, Moura JJ, Steer CJ. 2003. Tauroursodeoxycholic acid prevents Bax-induced membrane perturbation and cytochrome *c* release in isolated mitochondria. *Biochemistry* 42: 3070-3080.
- Rosenbaum DM, Gupta G, D'Amore J, Singh M, Weidenheim K, et al. 2000. Fas (CD95/APO-1) plays a role in the pathophysiology of focal cerebral ischemia. *J Neurosci Res* 61: 686-692.
- Rosenthal RE, Fiskum G. 2005. Oxygen: Could there be too much of a good thing? *Hosp Med* 66: 76-77.
- Rosenthal RE, Williams R, Bogaert YE, Getson PR, Fiskum G. 1992. Prevention of posts ischemic canine neurological injury through potentiation of brain energy metabolism by acetyl-L-carnitine. *Stroke* 23: 1312-1317.
- Rostovtseva TK, Tan W, Colombini M. 2005. On the role of VDAC in apoptosis: Fact and Fiction. *J Bioenerg Biomembr* 37: 129-142.
- Saille C, Marin P, Martinou JC, Nicole A, London J, et al. 1999. Transgenic murine cortical neurons expressing human Bcl-2 exhibit increased resistance to amyloid β -peptide neurotoxicity. *Neuroscience* 92: 1455-1463.
- Saito M, Korsmeyer SJ, Schlesinger PH. 2000. BAX-dependent transport of cytochrome *c* reconstituted in pure liposomes. *Nat Cell Biol* 2: 553-555.
- Sattler M, Liang H, Nettesheim D, Meadows RP, Harlan JE, et al. 1997. Structure of Bcl-xL-Bak peptide complex: Recognition between regulators of apoptosis. *Science* 275: 983-986.
- Sattler R, Xiong Z, Lu WY, Hafner M, MacDonald JF, et al. 1999. Specific coupling of NMDA receptor activation to nitric oxide neurotoxicity by PSD-95 protein. *Science* 284: 1845-1848.
- Sawada M, Hayes P, Matsuyama S. 2003. Cytoprotective membrane-permeable peptides designed from the Bax-binding domain of Ku70. *Nat Cell Biol* 5: 352-357.
- Scheff SW, Sullivan PG. 1999. Cyclosporin A significantly ameliorates cortical damage following experimental traumatic brain injury in rodents. *J Neurotrauma* 16: 783-792.
- Schendel SL, Montal M, Reed JC. 1998. Bcl-2 family proteins as ion-channels. *Cell Death Differ* 5: 372-380.
- Schulze-Osthoff K, Ferrari D, Los M, Wesselborg S, Peter ME. 1998. Apoptosis signaling by death receptors. *Eur J Biochem* 254: 439-459.
- Scorrano L, Korsmeyer SJ. 2003. Mechanisms of cytochrome *c* release by proapoptotic BCL-2 family members. *Biochem Biophys Res Commun* 304: 437-444.
- Scorrano L, Oakes SA, Opferman JT, Cheng EH, Sorcinelli MD, et al. 2003. BAX and BAK regulation of endoplasmic reticulum Ca^{2+} : A control point for apoptosis. *Science* 300: 135-139.
- Sensi SL, Jeng JM. 2004. Rethinking the excitotoxic ionic milieu: The emerging role of Zn^{2+} in ischemic neuronal injury. *Curr Mol Med* 4: 87-111.
- Sensi SL, Ton-That D, Sullivan PG, Jonas EA, Gee KR, et al. 2003. Modulation of mitochondrial function by endogenous Zn^{2+} pools. *Proc Natl Acad Sci USA* 100: 6157-6162.
- Shimizu S, Konishi A, Kodama T, Tsujimoto Y. 2000. BH4 domain of antiapoptotic Bcl-2 family members closes voltage-dependent anion channel and inhibits apoptotic mitochondrial changes and cell death. *Proc Natl Acad Sci USA* 97: 3100-3105.

- Shimizu S, Narita M, Tsujimoto Y. 1999. Bcl-2 family proteins regulate the release of apoptogenic cytochrome *c* by the mitochondrial channel VDAC. *Nature* 399: 483-487.
- Simpkins JW, Wang J, Wang X, Perez E, Prokai L, et al. 2005. Mitochondria play a central role in estrogen-induced neuroprotection. *Curr Drug Targets CNS Neurol Disord* 4: 69-83.
- Sims NR, Nilsson M, Muyderman H. 2004. Mitochondrial glutathione: A modulator of brain cell death. *J Bioenerg Biomembr* 36: 329-333.
- Soane L, Fiskum G. 2005. TAT-mediated endocytotic delivery of the loop deletion Bcl-2 protein protects neurons against cell death. *J Neurochem* 95: 230-243.
- Solenski NJ, Kostecki VK, Dovey S, Periasamy A. 2003. Nitric oxide-induced depolarization of neuronal mitochondria: Implications for neuronal cell death. *Mol Cell Neurosci* 24: 1151-1169.
- Solenski NJ, Kwan AL, Yanamoto H, Bennett JP, Kassell NF, Lee KS. 1997. Differential hydroxylation of salicylate in core and penumbra regions during focal reversible cerebral ischemia. *Stroke* 28: 2545-2551.
- Starkov AA, Fiskum G. 2003. Regulation of brain mitochondrial H₂O₂ production by membrane potential and NAD (P)H redox state. *J Neurochem* 86: 1101-1107.
- Starkov AA, Fiskum G, Chinopoulos C, Lorenzo BJ, Browne SE, et al. 2004. Mitochondrial α -ketoglutarate dehydrogenase complex generates reactive oxygen species. *J Neurosci* 24: 7779-7788.
- Starkov AA, Polster BM, Fiskum G. 2002. Regulation of hydrogen peroxide production by brain mitochondria by calcium and Bax. *J Neurochem* 83: 220-228.
- Stewart VC, Heales SJ. 2003. Nitric oxide-induced mitochondrial dysfunction: Implications for neurodegeneration. *Free Radic Biol Med* 34: 287-303.
- St Pierre J, Buckingham JA, Roebuck SJ, Brand MD. 2002. Topology of superoxide production from different sites in the mitochondrial electron transport chain. *J Biol Chem* 277: 44784-44790.
- Sturtz LA, Diekert K, Jensen LT, Lill R, Culotta VC. 2001. A fraction of yeast Cu,Zn-superoxide dismutase and its metallochaperone, CCS, localize to the intermembrane space of mitochondria. A physiological role for SOD1 in guarding against mitochondrial oxidative damage. *J Biol Chem* 276: 38084-38089.
- Sugimoto K, Iadecola C. 2003. Delayed effect of administration of COX-2 inhibitor in mice with acute cerebral ischemia. *Brain Res* 960: 273-276.
- Sullivan PG, Rabchevsky AG, Keller JN, Lovell M, Sodhi A, et al. 2004a. Intrinsic differences in brain and spinal cord mitochondria: Implication for therapeutic interventions. *J Comp Neurol* 474: 524-534.
- Sullivan PG, Springer JE, Hall ED, Scheff SW. 2004b. Mitochondrial uncoupling as a therapeutic target following neuronal injury. *J Bioenerg Biomembr* 36: 353-356.
- Sun Y, Jin K, Clark KR, Peel A, Mao XO, et al. 2003. Adeno-associated virus-mediated delivery of BCL-w gene improves outcome after transient focal cerebral ischemia. *Gene Ther* 10: 115-122.
- Tagliatalata G, Gegg M, Perez-Polo JR, Williams LR, Rose GM. 1996. Evidence for DNA fragmentation in the CNS of aged Fischer-344 rats. *Neuroreport* 7: 977-980.
- Takeuchi H, Kobayashi Y, Ishigaki S, Doyu M, Sobue G. 2002. Mitochondrial localization of mutant superoxide dismutase 1 triggers caspase-dependent cell death in a cellular model of familial amyotrophic lateral sclerosis. *J Biol Chem* 277: 50966-50972.
- Tanaka T, Nakamura H, Nishiyama A, Hosoi F, Masutani H, et al. 2000. Redox regulation by thioredoxin superfamily; protection against oxidative stress and aging. *Free Radic Res* 33: 851-855.
- Tay YM, Lim KS, Sheu FS, Jenner A, Whiteman M, et al. 2004. Do mitochondria make nitric oxide? No? *Free Radic Res* 38: 591-599.
- Terrones O, Antonsson B, Yamaguchi H, Wang HG, Liu Y, et al. 2004. Lipidic pore formation by the concerted action of proapoptotic BAX and tBID. *J Biol Chem* 279: 30081-30091.
- Teshima Y, Akao M, Li RA, Chong TH, Baumgartner WA, et al. 2003. Mitochondrial ATP-sensitive potassium channel activation protects cerebellar granule neurons from apoptosis induced by oxidative stress. *Stroke* 34: 1796-1802.
- Trapp T, Korhonen L, Besselmann M, Martinez R, Mercer EA, et al. 2003. Transgenic mice overexpressing XIAP in neurons show better outcome after transient cerebral ischemia. *Mol Cell Neurosci* 23: 302-313.
- Tretter L, Adam-Vizi V. 2004. Generation of reactive oxygen species in the reaction catalyzed by α -ketoglutarate dehydrogenase. *J Neurosci* 24: 7771-7778.
- Tretter L, Sipos I, Adam-Vizi V. 2004. Initiation of neuronal damage by complex I deficiency and oxidative stress in Parkinson's disease. *Neurochem Res* 29: 569-577.
- Turrens JF. 2003. Mitochondrial formation of reactive oxygen species. *J Physiol* 552: 335-344.
- Uchino H, Minamikawa-Tachino R, Kristian T, Perkins G, Narazaki M, et al. 2002. Differential neuroprotection by cyclosporin A and FK506 following ischemia corresponds with differing abilities to inhibit calcineurin and the mitochondrial permeability transition. *Neurobiol Dis* 10: 219-233.
- Van Remmen H, Qi W, Sabia M, Freeman G, Estlack L, et al. 2004. Multiple deficiencies in antioxidant enzymes in mice

- result in a compound increase in sensitivity to oxidative stress. *Free Radic Biol Med* 36: 1625-1634.
- Veech RL. 2004. The therapeutic implications of ketone bodies: The effects of ketone bodies in pathological conditions: Ketosis, ketogenic diet, redox states, insulin resistance, and mitochondrial metabolism. *Prostaglandins Leukot Essent Fatty Acids* 70: 309-319.
- Vereczki V, Martin E, Rosenthal RE, Hof PR, Hoffman GE, et al. 2006. Normoxic resuscitation after cardiac arrest protects against hippocampal oxidative stress, metabolic dysfunction, and neuronal death. *J Cereb Blood Flow Metab* 26: 821-835.
- Vieira HL, Belzacq AS, Haouzi D, Bernassola F, Cohen I, et al. 2001. The adenine nucleotide translocator: A target of nitric oxide, peroxynitrite, and 4-hydroxynonenal. *Oncogene* 20: 4305-4316.
- Vila M, Jackson-Lewis V, Vukosavic S, Djaldetti R, Liberatore G, et al. 2001. Bax ablation prevents dopaminergic neurodegeneration in the 1-methyl-4-phenyl-1,2,3,6-tetrahydropyridine mouse model of Parkinson's disease. *Proc Natl Acad Sci USA* 98: 2837-2842.
- Vogel R, Wiesinger H, Hamprecht B, Dringen R. 1999. The regeneration of reduced glutathione in rat forebrain mitochondria identifies metabolic pathways providing the NADPH required. *Neurosci Lett* 275: 97-100.
- Waldmeier PC. 2003. Prospects for antiapoptotic drug therapy of neurodegenerative diseases. *Prog Neuropsychopharmacol Biol Psychiatry* 27: 303-321.
- Wallace DC. 2005. A mitochondrial paradigm of metabolic and degenerative diseases, aging, and cancer: A dawn for evolutionary medicine. *Annu Rev Genet* 39: 359-407.
- Wallace KB, Starkov AA. 2000. Mitochondrial targets of drug toxicity. *Annu Rev Pharmacol Toxicol* 40: 353-388.
- Wang HG, Pathan N, Ethell IM, Krajewski S, Yamaguchi Y, et al. 1999. Ca^{2+} -induced apoptosis through calcineurin dephosphorylation of BAD. *Science* 284: 339-343.
- Wang JY, Shum AY, Wang JY. 2002. Hypoxia/reoxygenation induces cell injury via different mechanisms in cultured rat cortical neurons and glial cells. *Neurosci Lett* 322: 187-191.
- Wei MC, Zong WX, Cheng EH, Lindsten T, Panoutsakopoulou V, et al. 2001. Proapoptotic BAX and BAK: A requisite gateway to mitochondrial dysfunction and death. *Science* 292: 727-730.
- Wiessner C, Allegrini PR, Rupalla K, Sauer D, Oltersdorf T, et al. 1999. Neuron-specific transgene expression of Bcl-XL but not Bcl-2 genes reduced lesion size after permanent middle cerebral artery occlusion in mice. *Neurosci Lett* 268: 119-122.
- Yamaguchi H, Wang HG. 2002. Bcl-XL protects BimEL-induced Bax conformational change and cytochrome *c* release independent of interacting with Bax or BimEL. *J Biol Chem* 277: 41604-41612.
- Yao M, Nguyen TV, Pike CJ. 2005. β -Amyloid-induced neuronal apoptosis involves c-Jun N-terminal kinase-dependent downregulation of Bcl-w. *J Neurosci* 25: 1149-1158.
- Yuan J, Lipinski M, Degterev A. 2003. Diversity in the mechanisms of neuronal cell death. *Neuron* 40: 401-413.
- Zamzami N, Kroemer G. 2001. The mitochondrion in apoptosis: How Pandora's box opens. *Nat Rev Mol Cell Biol* 2: 67-71.
- Zanelli S, Renik A, Trimmer P, Solenski N. 2006. Nitric oxide impairs mitochondrial movement in cortical neurons during hypoxia. *J Neurochem* 97(3): 724-36.
- Zhai D, Luciano F, Zhu X, Guo B, Satterthwait AC, et al. 2005. Humanin binds and nullifies Bid activity by blocking its activation of Bax and Bak. *J Biol Chem* 280: 15815-15824.
- Zhu X, Lee HG, Casadesus G, Avila J, Drew K, et al. 2005. Oxidative imbalance in Alzheimer's disease. *Mol Neurobiol* 31: 205-217.
- Zoccarato F, Cavallini L, Alexandre A. 2004. Respiration-dependent removal of exogenous H_2O_2 in brain mitochondria: Inhibition by Ca^{2+} . *J Biol Chem* 279: 4166-4174.
- Zong WX, Lindsten T, Ross AJ, MacGregor GR, Thompson CB. 2001. BH3-only proteins that bind prosurvival Bcl-2 family members fail to induce apoptosis in the absence of Bax and Bak. *Genes Dev* 15: 1481-1486.
- Zou H, Henzel WJ, Liu X, Lutschg A, Wang X. 1997. Apaf-1, a human protein homologous to *C. elegans* CED-4, participates in cytochrome *c*-dependent activation of caspase-3. *Cell* 90: 405-413.

Genes of Metabolism: Generating, Sustaining, and Modifying the Machinery of Energy Metabolism. Regulation of Gene Expression for Metabolic Enzymes

7.1 Proteomics

M. H. Maurer · W. Kuschinsky

1	<i>A Profile of Proteomics</i>	738
1.1	Proteomics: Complement to Genomic Approaches	738
1.2	Proteomics as a Screening Tool in the Neurosciences	739
2	<i>Techniques</i>	739
2.1	Two-Dimensional Gel Electrophoresis	739
2.1.1	Sample Preparation	740
2.1.2	First Dimension: Isoelectric Focusing	741
2.1.3	Second Dimension: Polyacrylamide Gel Electrophoresis	742
2.1.4	Staining Proteins in 2D Gels	743
2.1.5	Image Analysis and 2D Gel Electrophoresis Software	743
2.2	Protein Identification	746
2.2.1	Mass Spectrometry	746
2.2.2	Imaging MS	748
2.2.3	Isotope Coding for Quantification Purposes	748
2.2.4	Protein Array Technology	749
2.3	Bioinformatics	751
2.3.1	Web Databases	751
2.3.2	Online Tools	751
2.3.3	Statistical Data Analysis	754
3	<i>Proteomics and the Analysis of Cerebral Energy Metabolism</i>	754
3.1	Enzyme Function and 2D Gel Electrophoresis	754
3.2	Glucose Metabolism and Cellular Respiration	754
3.3	Mitochondrial Proteomics	759
3.4	Proteomic Studies Investigating Brain Metabolism in Brain Disease or Disease Models	759
3.4.1	Inborn Errors of Metabolism	759
3.4.2	Down's Syndrome (Trisomy 21)	759
3.4.3	Alzheimer's Disease	760
4	<i>Perspectives</i>	761
4.1	Outlook: Challenges and Issues To Be Resolved	761
4.1.1	General Considerations	761
4.1.2	Membrane Proteins	761
4.1.3	Dynamics of Protein Turnover	762
4.1.4	Quantitation	762
4.1.5	Bioinformatics	763
5	<i>Conclusion</i>	763

Abstract: Proteomics is the study of the proteome defined as the set of all proteins of a cell, an organ, or the whole organism. Currently, the proteomic approach usually combines two-dimensional (2D) gel electrophoresis and mass spectrometry (MS) as a common and powerful approach. The specific feature of proteomics is the simultaneous detection of many proteins involved in different biochemical pathways. With regard to the brain, this approach has proven to be particularly beneficial for the analysis of energy metabolism and cellular respiration. To gather proteomic information, techniques were developed to handle the large amount of data yielding a comprehensive pattern of protein alignment within brain biochemical pathways. It is expected that in future proteomics will become a routine tool in all aspects of brain cell biology and beyond those of bioenergetics, including cell development, differentiation, and cell death. Proteomics then will complement other approaches to analyze cerebral function and biochemistry under normal and disease conditions.

1 A Profile of Proteomics

1.1 Proteomics: Complement to Genomic Approaches

The term “genome” describes the whole set of genes, whereas the term “proteome” encompasses the protein complement of the genome (Wasinger et al., 1995). It subsumes the whole set of proteins of a cell, an organ, or the whole organism. The study of the proteome, called proteomics, is even more comprehensive and subsumes not only all proteins in a given compartment, but also the respective protein isoforms and modifications, as well as the information on their structure and interaction (Tyers and Mann, 2003). The genome remains relatively constant during the lifetime of an individual, but the proteome undergoes constant changes as a reaction to environmental influences on protein synthesis. Specifically, proteins are modified posttranslationally by phosphorylation, glycosylation, the addition of carbohydrate chains (methylation, acetylation), proteolytic cleavage, sulfation, and by many other biochemical reactions resulting in various isoforms of a specific protein (Mann et al., 2001; Mann and Jensen, 2003). In addition, the rate of synthesis and degradation of a specific protein can vary, resulting in different concentrations of the same protein under different conditions. Thus, the proteomic analysis represents only a “snapshot” of the pattern of protein expression at a given point of time in a specific environment.

In the context of functional genomic approaches, the proteomic analysis complements the set of diverse approaches, which include gene expression profiling using microarray technology; systematic phenotypic analysis of cells and organisms (phenomics) based on structural, ultrastructural, and functional aspects; and systematic genetics using mutational analysis and RNA interference (Tyers and Mann, 2003). Additionally, one gene and its transcript mRNA may encode for more than one protein. For example, in humans, one gene encodes for more than ten protein isoforms on an average (Gunning et al., 1998; Kim et al., 2004). Additionally, posttranslational modifications contribute to the diversity of protein isoforms (Mann and Jensen, 2003). Although there is no doubt that the levels of DNA, RNA, and protein are highly related and interconnected, several studies have found only limited correlation between transcriptomic and proteomic data (Anderson and Seilhamer, 1997; Link et al., 1997; Gygi et al., 1999b; Lee et al., 2003). Besides technical variability of the molecular screening methods applied, biological divergences contribute to the explanation of these findings: molecular half-life, synthesis and decay rates, mutations, reaction kinetics, environmental stress, cell cycle, disease, and multigenic and epigenetic influences are all factors influencing the concentrations of cellular RNA and of protein species (Humphery-Smith et al., 1997). Therefore, proteomics can be seen as an additional and complementary tool besides other exploratory data analysis approaches such as differential display, high-density nucleic acid arrays, expressed sequence tags, hybridization techniques, chromosomal linkage studies, and nucleic acid sequencing.

In principle, two main areas in the field of proteomics have been developed, each of them having its pros and cons. These fields are “profiling” and “functional” proteomics (Choudhary and Grant, 2004). The aim of proteomic profiling is to describe and index the whole set of proteins of a biological sample, which could be an organism, an organ, or a cell, or parts thereof like individual tissues or organelles. Profiling also

includes differential protein expression levels under specific experimental conditions or the comparison of different types or origins of sample material. Thus, proteomic profiling describes the inventory of proteins at a particular point of time. In contrast to the more static approach of proteomic profiling, the term functional proteomics encompasses direct functional aspects, like enzyme activity, protein interactions, and posttranslational modifications (PTMs). Although these two experimental approaches cannot be seen completely separate, profiling has been regarded to be of minor biological relevance due to its descriptive nature. However, such an opinion does not seem justified, since the cataloging of existing proteins is a basis to generate new hypotheses, which trigger further biological investigations. On the other hand, functional proteomics is based on protein profiling, since one needs to know which proteins to search for when it is intended to focus on a subset of proteins that are functionally coupled. In our understanding, both types of proteomics are valuable tools complementing other biological methodologies that help to describe the complexity of nature, and, specifically, brain function.

1.2 Proteomics as a Screening Tool in the Neurosciences

In general, proteomics can be used for a wide variety of applications, including (1) validation of genome sequences, (2) identification of novel proteins, (3) characterization of regulating (stimulating and inhibiting) proteins, (4) detection of posttranslational modifications, (5) monitoring expression patterns of large sets of proteins, (6) high-resolution protein purification, (7), detection of immunogenic proteins, e.g., in vaccine studies, (8) analysis of mechanisms of action of therapeutic agents and their toxicological relevance, and (9) identification of novel drug targets (O'Connor et al., 2000).

With regard to neurological disorders, we have to take into account the complexity of these diseases. The etiology and pathogenesis of many neurological diseases are not well defined at a molecular level. When investigating potential changes in protein expression as a basis of brain disease, several limitations have to be taken into account. The amount of deviating proteins may be less, thus obviating the detection of relevant proteins. Many details of protein interactions as well as of signaling and metabolic pathways are still not understood. In addition, the diseases themselves may not show well-defined protein targets. For example, the players in Alzheimer's disease appear to be known, but the debate of what is cause and what is epiphenomenon is still not solved. For schizophrenia, several candidate markers are discussed, but their interrelation is unknown. Proteomic technology may open new doors in the search for biomarkers and their pathophysiological interactions.

Proteomic applications in the neurosciences have been proposed for a variety of fields, including learning and memory, brain injury, ischemia, addiction, neurodegenerative diseases, polyglutamine repeat disorders, depression, anxiety, bipolar disorders, epilepsy, and brain tumors (Rohlf, 2000; Morrison et al., 2002; Kim et al., 2004). In the near future, the techniques of proteomics will be increasingly used for the development of novel pathophysiological concepts, novel diagnostic and prognostic markers, and novel therapeutic strategies.

2 Techniques

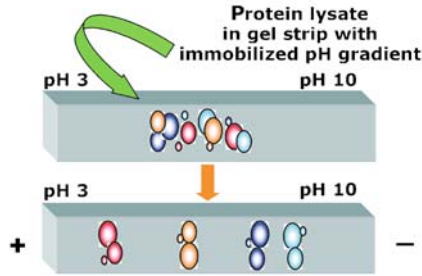
2.1 Two-Dimensional Gel Electrophoresis

The majority of proteomic results was obtained using a system of two-dimensional (2D) gel electrophoresis to separate proteins according to their isoelectric points in the first dimension and according to their molecular weight in the second dimension (▶ [Figure 7.1-1](#)). This approach allows a high-resolution separation and quantitation of at least several hundred or even thousands of proteins or polypeptides. The method is limited by the fact that only the most abundant proteins can be detected and the proteins have to be present within the given pH and molecular mass range (Görg et al., 2000; Rabilloud, 2002). The rapid development of new applications in the field of mass spectrometry (MS) has favored direct mass spectrometric approaches (Tyers and Mann, 2003), but a complete substitution of 2D gel electrophoresis by

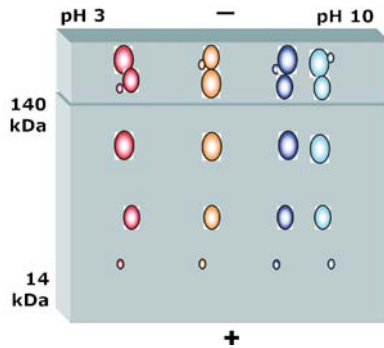
■ Figure 7.1-1

Principles of two-dimensional (2D) gel electrophoresis. In the first dimension, solubilized proteins are separated by isoelectric focusing (IEF) in a gel containing an immobilized pH gradient. After high voltage is applied, the proteins migrate to their respective isoelectric points. The gel strip of the first dimension is then attached to a polyacrylamide gel. In the second dimension, the polyacrylamide gel sieve separates the proteins according to their respective molecular weights

1st dimension: isoelectric focusing (IEF)



Second dimension: polyacrylamide gel electrophoresis (PAGE)



MS is still not possible (Dutt and Lee, 2000; Herbert et al., 2001; Ong and Pandey, 2001; Rabilloud, 2002; Patterson and Aebersold, 2003).

A typical 2D gel electrophoresis experiment consists of several subsequent steps (Freeman and Hemby, 2004):

1. sample preparation,
2. first dimension: isoelectric focusing,
3. second dimension: polyacrylamide gel electrophoresis,
4. in-gel staining of proteins,
5. digitizing of gel images and image analysis, and
6. protein identification.

In the following sections, we will describe some of the most common principles and protocols of these steps.

2.1.1 Sample Preparation

Principles of sample preparation. Sample preparation is considered the most delicate and essential step to obtain reliable 2D gel electrophoresis results (for discussion of procedures and components, as well as

additional references, see Link, 1999; Berkelman and Stenstedt, 2001; Westermeier, 2001). The aim of sample preparation is to solubilize, disaggregate, denature, and reduce the proteins in a given biological sample in order to resolve any kind of binding to other proteins or compounds of cell membranes and organelles. Ideally, the proteins should then be freely dissolved in the sample buffer.

To obtain single molecule components out of a complex mixture of proteins, it is necessary to remove all possible interacting components such as protein complexes formed with membranes, nucleic acids, or other proteins. Moreover, although unspecific aggregates must be disrupted, the precipitation of proteins under these nonphysiological conditions must be avoided. The effectiveness of solubilization depends mainly on the cell disruption method, protein concentration, choice of detergent, and composition of the sample buffer. Detergents in the sample buffer are necessary for solubilization, disaggregation, and denaturation, whereas reducing agents prevent postextraction modifications of the proteins.

Different methods of pretreatment of the samples may be employed, according to the specific application desired (Patton, 1999). For the detection of intracellular proteins, cells must be completely disrupted. Proteases should be inhibited effectively, as they are released during this process. Reagents interfering with the subsequent electrophoresis steps such as salts, small ionic molecules, ionic detergents, nucleic acids, polysaccharides, lipids, and phenolic compounds must be removed by using, for example, ultrafiltration, microdialysis, gel filtration, or precipitation/resuspension. For the analysis of subcellular compartments and organelles, differential fractioning methods like ultracentrifugation have to be applied. A special challenge is the preparation of membrane proteins. Although membrane proteins are of great interest in cell signaling research, they remain the stepchild of proteomic analysis, because sample preparation of membrane proteins is poorly compatible with current isoelectric focusing (IEF) techniques.

Cell disruption methods. Mechanical and chemical approaches can be applied to achieve cell disruption. The method of disruption should depend on the cell type of interest. For cultured cells and microorganisms, a gentle lysis method like osmotic lysis, freeze–thaw lysis, detergent lysis, or enzymatic lysis may be chosen. For cells in solid tissues and plant cells containing cell walls, more vigorous methods like sonication, French pressure cells, grinding, mechanical homogenization, and glass bead homogenization may be helpful. Differential centrifugation steps may follow in order to isolate the cell organelles of interest.

Practical application. The typical sample buffer is composed of urea (and desirably, thiourea), zwitterionic detergents like 3-[(3-cholamidopropyl)dimethylammonio]-1-propanesulfonate (CHAPS), reducing agents like dithiothreitol (DTT), and carrier ampholyte buffer. For the preparation of proteins, extracts from brain cell cultures including neurons, astrocytes, and neural stem cells are obtained. These cells are dissolved in a detergent lysis buffer containing 7 M urea, 2 M thiourea, 4% (w/v) CHAPS, 0.5% (v/v) Triton X-100, 0.5% (v/v) IPG buffer pH 3–10 (Amersham Biosciences, Uppsala, Sweden), 100 mM DTT, and 1.5 mg/ml complete protease inhibitor (Roche, Mannheim, Germany) for 1 h at room temperature in an orbital shaker (Maurer et al., 2003b, 2004). Twice the volume of lysis buffer is added to the cell pellet. For whole brains from mice (0.5 g) or rats (2 g), 2 ml of lysis buffer is recommended. The lysate should be centrifuged at 21,000g for 30 min. Protein content of the supernatant can be measured by the Bradford assay (Bradford, 1976), as this protocol is compatible with the major components of the lysis buffer (Ramagli, 1999). The supernatant should be stored at -80°C until further processing, and repeated freeze–thaw cycles should be avoided.

2.1.2 First Dimension: Isoelectric Focusing

Proteins carry either positive, negative, or zero net charge, depending on the pH of their surroundings. The pH value at which the net charge equals zero is called the isoelectric point (pI). IEF allows separating proteins according to their isoelectric points. The presence of a pH gradient in the electrophoresis gel is essential to achieve the separation of proteins in the sample, which causes proteins to move in the electric field through the pH gradient until they reach their isoelectric point. If a protein diffuses away from the isoelectric point, it will gain charge and immediately be driven back. This is the essence of the focusing

effect. A milestone in IEF technology was the introduction of immobilized pH gradient gels (Görg et al., 1988, 1998), which allowed to establish comparable and reproducible pH gradients.

The resolution depends on the slope of the pH gradient and the electric field strength. Typically, IEF is performed at high voltages (more than 1,000 V). Once the proteins have reached their final position in the pH gradient gel, there is only little ionic movement, resulting in low currents (<1 mA). Normally, a constant number of volt-hours is applied for reasons of comparison within a series of experiments, defined by the integral of the volts applied over the time.

For initial screening experiments, one may choose a pH range of 3–10 to get an overview of the total protein distribution. To study the protein pattern in greater detail, or if only a certain pH range is of interest, “zoom” gels with a narrow pH range of 1 pH unit or even less are available.

For analytical brain and cell culture experiments, a typical IEF protocol includes running 250–500 µg of the protein extract in 6 M urea, 2 M thiourea, 1 M DTT, 2% (w/v) CHAPS, and 0.5% (v/v) IPG buffer on 18 cm immobilized nonlinear pH 3–10 gradient IPG strips (Immobiline DryStrip pH 3–10 NL, Amersham Biosciences, Uppsala, Sweden), using the IPGphor apparatus (Amersham Biosciences, Uppsala, Sweden). Other pH ranges may be used, for example, “zoom gels” may resolve a single pH step. Nowadays, pH gradient gels are distributed on plastic supports to ensure easier handling and protection of the gels, which are 3 mm thick when rehydrated. After 12 h of reswelling time at 30 V to remove disturbing salts, voltages of 200, 500, and 1,000 V are applied for 1 h each. Then voltage is increased to 8,000 V within 30 min and kept constant at 8,000 V for 12 h, resulting in a total of 100,300 Vh (Maurer et al., 2003b, 2004). After an IEF protocol, the gels may be stored at –80°C until further use.

2.1.3 Second Dimension: Polyacrylamide Gel Electrophoresis

In the second dimension, a polyacrylamide gel electrophoresis (PAGE) is performed under denaturing conditions in the presence of sodium dodecylsulfate (SDS) to separate proteins according to their molecular weight. The cross-linked acrylamide polymers act as molecular sieve; thus smaller proteins migrate faster than larger ones. The intrinsic charge of the proteins does not influence electrophoresis, as the anionic detergent SDS will provide negative charges for all proteins, thus the separation is based primarily on the molecular size. The most common buffer system used for the second dimension was described by Laemmli (1970), which resolves proteins at high pH and allows the detection of relatively heavy proteins up to a molecular weight of about 250 kDa. The Tris-tricine system of Schägger and von Jagow (1987) may also be used for resolution of smaller proteins and peptides below 10 kDa.

Before running the second-dimension gels, the pH gradient gels must be equilibrated for the new running conditions. Typically, the equilibration solution contains 2% (w/v) SDS, 50 mM Tris-HCl pH 8.8, 6 M urea, 30% (v/v) glycerol, a trace of bromophenol blue, and 100 mg/10 ml DTT to preserve the reduced state of the proteins, preventing postextraction modifications of the proteins. The reducing agents improve protein solubility during IEF, which results in shorter run times and increased resolution as well as decreased horizontal streaking on the subsequent second-dimension gel. A recent study replaced DTT by tributyl phosphine for even better solubilization (Herbert et al., 1998). The first-dimension gels are incubated for 20 min. In a second equilibration step, the gels are incubated for another 20 min in a buffer where DTT is replaced by 250 mg/10 ml of the alkylating agent iodoacetamide (IAA) to prevent reoxidation, which is necessary for maintaining solubility in the second-dimension gel electrophoresis.

For the second dimension, large gels should be used to resolve several hundreds or even thousands of protein spots. Good results can be achieved using $20 \times 20 \times 0.3 \text{ cm}^3$ gel volumes. Klose and coworkers have developed the large-gel 2D electrophoresis (2DE) (Gauss et al., 1999; Klose et al., 2002), where the gel running length is 40 cm or more, but the gels are more difficult to handle than smaller ones. The final polyacrylamide concentration may vary between 5% and 20%, or gradient gels may be used, depending on the molecular size range that is to be resolved. Excellent step-by-step protocols have been described by Berkelman and Stenstedt (2001) and can be downloaded free of charge from the support section of <http://www.amershambiosciences.com>.

2.1.4 Staining Proteins in 2D Gels

After second-dimension SDS-PAGE, the separated protein spots are visualized in the gels. Most staining protocols originally developed for SDS gels can also be applied to second-dimension gels (Rabilloud, 2000). The optimal staining procedure should have (1) a high sensitivity, (2) a wide linear range for quantification, (3) an intrinsic compatibility with MS, and (4) low toxicity of the dye. Unfortunately, none of the existing staining procedures fulfill all of these requirements. On the other hand, a myriad of different staining methods and protocols has been developed based on the following:

1. Organic dyes like Coomassie Brilliant Blue R-250, Xylene Cyanine Brilliant G (better known as Coomassie Brilliant Blue G-250), Amido Black 10S, Procion Blue RS, Ponceau S, Alcian Blue, and Fast Green FCF (Wirth and Romano, 1995). The stains are mostly compatible with MS, although the methods described below are more sensitive.
2. Metal ions like silver (Blum et al., 1987; Rabilloud, 1999), zinc, and copper. Only some staining protocols allow full compatibility with MS (Shevchenko et al., 1996), although modified staining protocols show an excellent sensitivity.
3. Fluorescent dyes like SYPRO Ruby, SYPRO Orange, Cy3, and Cy5 (Patton, 2000a, b), which are compatible with MS and exhibit a sensitivity comparable with silver staining. Different excitation and emission wavelengths make these dyes well suited for differential proteome analysis of two samples in the same gel (DIGE; Ünlü et al., 1997; Ünlü, 1999).
4. Radiolabeling using the isotopes ^{14}C , ^{35}S , ^{32}P , ^3H , and ^{125}I (Wirth and Romano, 1995). Radioactive isotopes are mostly used for metabolic labeling during protein synthesis and still permit the most sensitive staining procedure. These methods require the incorporation of the isotope into living cells and therefore cannot be applied to body fluids, biopsy material, and other clinically available material from patients. Although radiolabeling can be applied to brain cell cultures and living animals, its use with regard to the human brain is limited and has not been described.

▶ [Table 7.1-1](#) compares the most common stains with regard to their detection limit and compatibility with MS.

■ **Table 7.1-1**

Comparison of the most common protein staining methods in 2D gels

Dye	Detection limit (ng)	Compatible to MALDI-MS
Coomassie Brilliant Blue R-250	>100	Yes
Blum's zinc/imidazole	>100	Yes
SYPRO Orange	>30	Yes
Coomassie Brilliant Blue G-250	>30	Yes
SYPRO Ruby	>10	Yes
Silver	>10	No
Silver + glutaraldehyde	>1	Some protocols

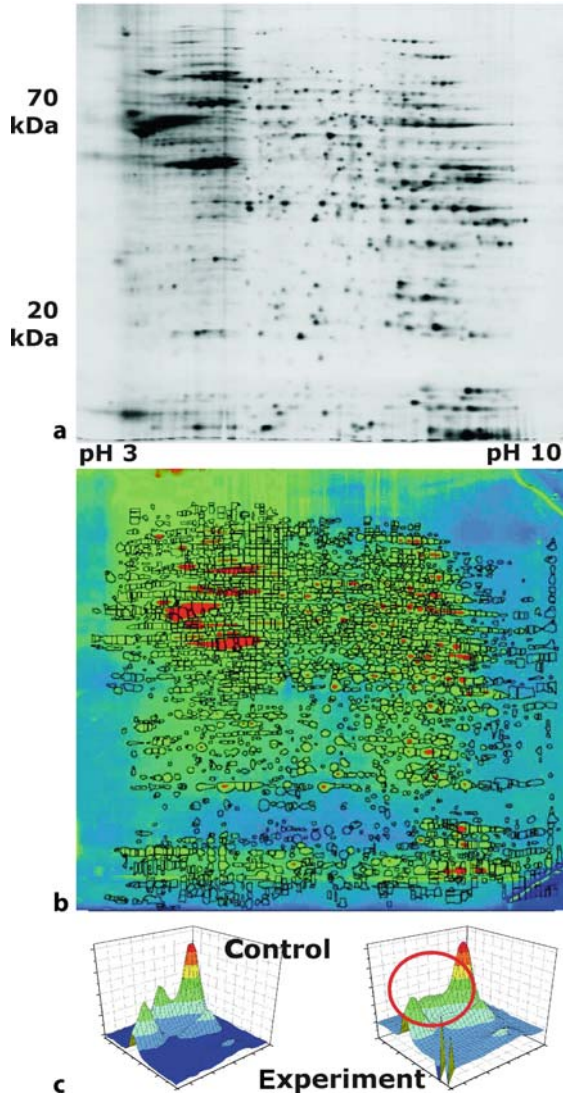
2.1.5 Image Analysis and 2D Gel Electrophoresis Software

In a typical 2D experiment, the gel image analysis steps after staining include (1) digitizing the gels, (2) spot detection and quantitation of spot parameters such as the optical density or the volumes for each protein spot, (3) comparison of different gels, and (4) data analysis (▶ [Figure 7.1-2](#)).

To this end, the stained 2DE gels are scanned and the digitized gel images subjected to image analysis. For digitizing, densitometers, CCD cameras, or laser imaging devices can be used. For proteomic experiments, specialized software is necessary to store and structure the huge amount of data. Sophisticated algorithms provide the basis for spot detection and quantitation of protein spots and intergel comparison (Garrels, 1989; Appel et al., 1997; Seillier-Moisewitsch et al., 2002; Maurer, 2004b).

■ Figure 7.1-2

Principle of two-dimensional (2D) gel analysis. (a) After protein separation, the proteins are visualized by a highly sensitive staining procedure such as silver staining. (b) Gel images are digitized and protein spots are detected by a special 2D analysis software. (c) For quantitative analysis, protein spot volumes, defined as the integral optical density of the spot area, are compared by statistical methods



In principle, spot detection relies on the accurate discrimination of the spot boundaries. A common problem is a low signal-to-noise ratio, mainly because of high gel background. Then, the gel background is subtracted and all gels in an experiment are normalized, either by external standards or by the total protein load. In the next step, gel matching is applied to geometrically align spots from different gels by mathematical algorithms (Garrels, 1989; Appel et al., 1997; Maurer et al., 2004), based on a procedure called polynomial image warping. First, an initial reference gel is chosen and several landmarks are selected on this reference image. Then corresponding spots in the experimental gel images are aligned to the reference.

Some of the software specified in [Table 7.1-2](#) requires time-consuming manual matching, whereas others provide fully automated spot detection and matching. A helpful tool integrated in some of the 2D software is the three-dimensional representation of gel spots, which allows easier detection of the spot limits and simplified spot matching (Maurer, 2004b).

Table 7.1-2
Commercially available 2D analysis software (as of September 2004)

Name	Distributor	Internet URL
DeCyder Differential Analysis Software	Amersham Biosciences, Uppsala, Sweden	www.amershambiosciences.com
Delta2D	DECODON, Greifswald, Germany	www.decodon.com
Expressionist Pro	GeneData, Martinsried, Germany	www.genedata.com
Gellab II+	Scanalytics, Fairfax, VA, USA	www.scanalytics.com
ImageMaster 2D Platinum 5.0 ^a	Amersham Biosciences, Uppsala, Sweden	www.amershambiosciences.com
ImagePlQ	Proteome Systems, Sydney, Australia	www.proteomesystems.com
Investigator HT Analyzer	Genomic Solutions, Ann Arbor, MI, USA	www.genomicsolutions.com
PDQuest 2D	BioRad, Hercules, CA, USA	www.proteomeworks.bio-rad.com
Phoretix 2D	Nonlinear Dynamics, Newcastle-upon-Tyne, UK	www.nonlinear.com
ProteinMine	Scimagix, San Mateo, CA, USA	www.scimagix.com
ProteomWeaver	Definiens Imaging, München, Germany	www.proteomweaver.com
Z3	Compugen, Tel-Aviv, Israel	www.2dgels.com

^aThe program Melanie has been incorporated into the ImageMaster 2D Platinum series only recently. Melanie has been one of the leading two-dimensional (2D) gel electrophoresis software for many years and was developed by the Swiss Institute of Bioinformatics (SIB, <http://www.isb-sib.ch>)

Of note, online tools are available for comparison of 2D images over the Internet like Flicker (<http://www.lecb.ncifcrf.gov/flicker>) (Lemkin, 1999) and GelScape (<http://www.gelscape.ualberta.ca>) (Young et al., 2004), although these programs lack automated spot detection.

A typical 2D analysis software package should include algorithms for:

1. automated spot detection with numbering, annotation, and spot filtering,
2. background subtraction,
3. calculation of geometric spot characteristics such as area, optical density, or spot volume,
4. 2D calibration for isoelectric points and molecular weight,
5. averaging multiple sample gels,
6. choosing a reference gel and modifying the reference gel by adding spots,
7. matching spots in different sample gels,
8. normalization of spots for intergel comparison,
9. statistical analysis of the results,
10. directing spot picking devices,
11. including additional data such as mass spectrograms, and
12. creating a Web-based federated database to publish the data on the Internet.

Currently available programs are given in [Table 7.1-2](#). Special care should be taken to guarantee the reproducibility of the gel analysis (Mahon and Dupree, 2001; Choe and Lee, 2003) as multiple software parameters can influence the quality of the analysis.

Several studies have compared commercially available 2D gel electrophoresis programs (Raman et al., 2002; Rosengren et al., 2003) by a standard set of gel images for parameters like spot detection, gel matching, and spot quantitation. These gel images can be downloaded from the URL <http://www.umbc.edu/proteome> and may be used for benchmarking the 2D software in the user's own lab.

2.2 Protein Identification

For protein identification, the protein spots stained and mapped on the 2D gels are excised. Manual spot cutting was used in the beginning. Later, the advantages of automated spot cutting became obvious: There is only a minimal risk of contamination of the samples, the access to the individual protein spots is highly precise, data may be automatically tracked, and these systems are well suited for high throughput applications. Therefore, manual spot picking should be avoided.

Several methods for protein identification have been developed including MS as the gold standard, amino acid sequencing, immunoaffinity identification, and protein arrays. In this chapter, we describe the most widely applied techniques for the identification of 2D gel electrophoresis spots.

2.2.1 Mass Spectrometry

Recent years have shown tremendous advances in mass spectrometric methodology and instrumentation. For the identification of proteins by MS, sensitivity, resolution, and mass accuracy, as well as the availability of sequence databases, are the most important requirements. New technologies in MS meet these prerequisites and have been successfully applied for primary sequence analysis and proteome profiling, posttranslational modifications, and protein–protein interaction analysis (Aebersold and Mann, 2003). Mass spectrometric identification of proteins is based on two independent approaches. The first is a combination of 2D gel electrophoresis and MS, whereas the second is a combination of protein purification steps, automated peptide MS/MS, and stable-isotope tagging of proteins and peptides for quantitation purposes. Three main approaches involving MS are currently used in proteomics: (1) peptide mass fingerprinting for protein identification, (2) sequence tags and postsource decay (PSD) analysis for protein or peptide sequencing, and (3) isotope coding for protein quantification.

For the typical mass spectrometric peptide mass fingerprinting, 2D gel electrophoresis is combined with MS. Therefore, the protein spots excised from the 2D gels are destained when necessary to ensure compatibility with the mass spectrometric application used. Then the spots are enzymatically digested to obtain smaller peptide fragments (Shevchenko et al., 1996). Most commonly, trypsin is the enzyme of choice, but chymotrypsin, formic acid, pepsin, inorganic cleaving agents, or combinations of these may also be used. A mass spectrometer consists of an ion source, by which the peptides are ionized, a mass analyzer, where ions are transmitted in an electromagnetic field, and an ion detector (Bakhtiar and Nelson, 2001; Aebersold and Mann, 2003). It is important to keep in mind that MS can only measure masses of molecules that can be ionized. For ionization, several methods can be used, including electron jet ionization (EI), chemical ionization (CI), fast atom bombardment (FAB), electrospray ionization (ESI), and matrix-associated laser desorption/ionization (MALDI). The mass analyzer measures the mass-to-charge ratios (m/z) of the ionized peptides. The greater the accuracy of the measurement, the easier it is to identify the protein. Most common applications for mass analyzers include quadrupole, magnetic sector field, electric sector field, time-of-flight (TOF), electric ion trap, and electromagnetic ion trap (= electron cyclotron). The detector, which may be a Faraday's cup, a conversion dynode with secondary electron multiplier, a scintillation counter, or a multichannel plate, records the arrival of ions after they have passed through the mass analyzer.

In order to identify peptides and proteins, the resulting fragment mass spectra are submitted to online sequence databases, such as the National Center for Biotechnology Information (NCBI) (<http://www.ncbi.nlm.nih.gov/>) or the SwissProt and TrEMBL databases at the ExPASy server (<http://www.expasy.org>) (▶ [Figure 7.1-3](#)).

▶ [Table 7.1-3](#) lists several online tools available for the identification of specific mass spectra. These programs compare experimental spectra with theoretical spectra of the database entries by using distinct search algorithms (Sadygov et al., 2004).

Besides this peptide mapping or “fingerprinting” approach, MS can be used for protein or peptide sequencing in a PSD analysis (Jensen et al., 1999). PSD is based on ions that are generated in the ion source but are not stable (metastable ions). To obtain amino acid sequences, peptides are selected using electronic

Figure 7.1-3

Identification of proteins by MALDI-TOF MS and database search. Digested peptide ions are embedded in a matrix and immobilized on a metal surface. Peptides are ionized by a laser beam and accelerated in an electromagnetic field. The peptides reach the detector relative to their molecular mass and their charge. The experimental spectra are compared with theoretical spectra in sequence databases to find a matching amino acid sequence

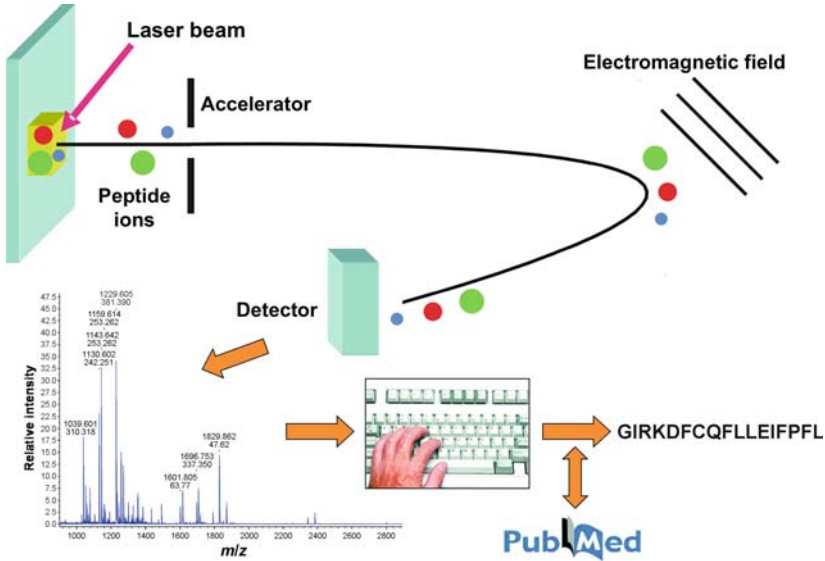


Table 7.1-3

Web-based analysis tools for data mining of peptide mass spectrograms. The measured fragment pattern is submitted to the Web search engine, which compares the fragments with in silico digested database entries

Application name	URL
Mascot	http://www.matrixscience.com
Masslynx	http://www.waters.com
MOWSE	http://www.hgmp.mrc.ac.uk/Bioinformatics/Webapp/mowse/
Peptident	http://www.expasy.org
PeptideSearch	http://www.narrador.embl-heidelberg.de/GroupPages/Homepage.html
Probid	http://projects.systemsbiology.net/probid
ProFound v4.10.5	http://129.85.19.192/profound_bin/WebProFound.exe
ProteinProspector v4.0.5	http://prospector.ucsf.edu
PROWL	http://prowl.rockefeller.edu
SEQUEST	http://fields.scripps.edu , http://www.thermo.com
SpectrumMill	http://www.chem.agilent.com/
The Global Proteome Machine, X! Tandem	http://www.thegpm.org

pulses and their decay products are focused in a differential reflector field. More commonly, ESI is combined with triple-quadrupole or quadrupole/TOF hybrid analyzers. Therefore, the ions are selected in the first quadrupole and collide in the second one. Then their spectra are registered in the third one, or in

a reflector tube. The collision of peptides with gas molecules favors the fragmentation at the bound peptide, which allows easier identification of the spectra. In both cases, suitable software tools are necessary for database screening of the mass spectra.

The two “sequence tag” methods described can also be used in combination with other one- or multidimensional separation procedures such as chromatography (Mann et al., 2001). With this approach, proteins are not separated using 2D gel electrophoresis but are digested directly in the sample. The peptide solution is then separated by one of the various liquid chromatography (LC) methods available, and the eluted peptides are directly sequenced by mass spectroscopy. Using this approach, only a small amount of peptide (down to 1–2 molecules) is necessary for identification of the protein in the database. A different approach called “accurate mass and time (AMT) tag” combines the high resolution and mass measurement accuracy of Fourier transform ion cyclotron resonance (FITRC), the high efficiency of capillary LC separation, and the peptide identification capabilities of MS/MS (Pasa-Tolic et al., 2004).

2.2.2 Imaging MS

Although the described proteomic approaches allow the analysis of the protein components of a given sample, the regional distribution of individual “proteomes” cannot be determined easily. Imaging MS, developed by Stoeckli and Caprioli, allows a regional resolution of proteins present on a cryosection (Stoeckli et al., 2001). Brain samples are cut in a cryomicrotome and embedded on a gold surface. Then small pieces of the tissue are cut by laser beam of nearly half the size of a cell. The proteins and peptides present in the cut sample are then subjected to mass spectrometric identification. Then the laser beam moves on to the next point on the grid. Technical limitations allow an average distance of cutting points of about 100 μm , but technical improvement will decrease the grid size in the future to improve spatial resolution. The whole brain section can be scanned, producing several hundreds of data points, each of them consisting of several hundreds or thousands of mass spectra. Computer-aided reconstitution of the brain section can then show the regional distribution of a given protein in the whole section. Still the number of proteins isolated by laser dissection is small (about 100 per scan) and represents only a small range of proteins of the cell (some 10,000 per cell). Moreover, this method favors cytosolic proteins, and combination with other separation and identification techniques is difficult. On the other hand, it is intriguing to have a spatial resolution of proteins on a brain section.

2.2.3 Isotope Coding for Quantification Purposes

Stable isotope tagging has been used for quantitation and sequence identification of individual proteins within complex protein mixtures (Gygi et al., 1999a). The method is based on a new class of chemical reagents called isotope-coded affinity tags (ICAT) and tandem MS. In principle, two different biological samples are tagged with a “heavy” and a “light” isotope (e.g., deuterium and hydrogen), resulting in two protein samples with “light” or “heavy” isotope labels. The samples can be mixed and separated by LC. The corresponding heavy and light peptides will coelute from the chromatography column, and relative protein expression ratios can be measured in the subsequent MS by comparing the two peak intensities for the two isotopes. Furthermore, sequence information can be acquired for these peptides by fragment analysis in the product ion mass spectrum, as described above. ICAT requires the three functional elements of a specific chemical reactivity, an isotope-coded linker, and an affinity tag.

On the basis of this method, stable isotope labeling with amino acids in cell culture (SILAC) has been introduced for special application in cell culture (Ong et al., 2003). Cells of two biological conditions are cultured in amino acid-deficient growth media supplemented with radioactive amino acids labeled with two different isotopes (e.g., ^{12}C and ^{13}C). Differentially expressed proteins can be identified in the same way as in the ICAT method. SILAC uses global protein coding and does not require the functional chemical elements of ICAT.

Isotope coding and quantification of proteins requires that (1) all proteins/peptides in the sample are coded, (2) there is only a minimal spectral overlap between the isotopes used, (3) labeling is quantitative and the isotopic isoforms are enriched, (4) postcoding sample treatment does not influence mass spectrometric identification, (5) the resulting mass spectra are not influenced by the isotope coding, and (6) coding allows multiplexing two or more samples (Julka and Regnier, 2004). Several applications for isotope coding have been developed for expression analysis, posttranslational modifications, protein–protein interactions, single amino acid polymorphism, and absolute quantitation.

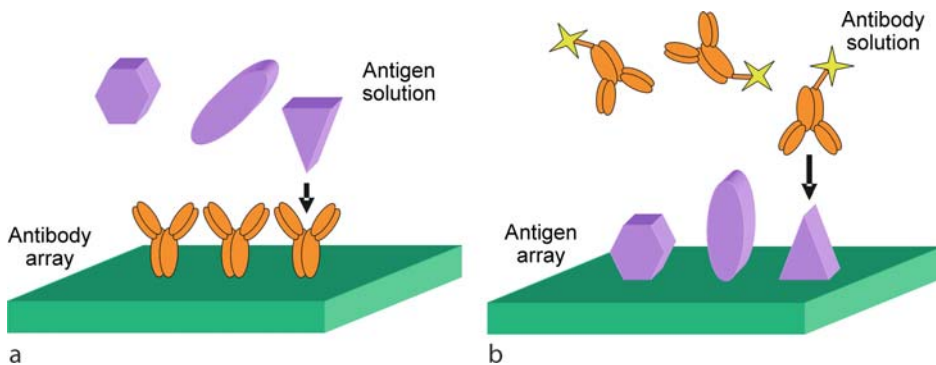
With regard to expression analysis, two different strategies are used (for review see Julka and Regnier, 2004). One is to label all peptides in a proteolytic digest of a proteome and then select specific peptides by chromatography in a second step. The other introduces isotope labels into peptides in a single-step reaction. General approaches include metabolic coding in isotopically enriched and depleted media, derivatization of primary amines, ^{18}O labeling, tagging amino and carboxyl groups at peptide termini (TACT), and esterification. Also, specific amino acids can be targeted by metabolic incorporation of amino acid-containing stable isotopes. Other ICAT reagents target cysteine, lysine, N-terminal threonine and serine, tryptophan, or methionine.

2.2.4 Protein Array Technology

As with gene chip microarrays, efforts have been undertaken to create protein-based microchips to analyze protein expression levels (James, 2002; Phizicky et al., 2003). The general principle is to immobilize protein molecules (e.g., antibodies) on a surface and to incubate with a protein sample solution (i.e., the antigens) for studying protein–protein interactions (● Figure 7.1-4).

■ Figure 7.1-4

Protein array technology. In principle, two main approaches are used. (a) In the antigen capture array, different sets of antibodies are immobilized on a solid surface. For detection of the bound protein antigens, a secondary antibody system, or prelabeling of the proteins, is necessary. (b) In the direct assay, the protein antigens are immobilized and detected by labeled antibody probes (modified from MacBeath, 2002)



Three assay systems have been developed for protein microarrays (MacBeath, 2002):

1. Sandwich immunoassays—antibodies that bind to specific proteins in the sample are arrayed on a surface. If an antigen–antibody complex is formed, the complex is detected by a labeled secondary antibody.
2. Antigen capture immunoassays—proteins in the sample are labeled by specific molecular markers. These labeled proteins are bound by antibodies arrayed on a surface.
3. Direct immunoassays—antigens of the sample are attached to the chip surface and detected by labeled antibodies.

Because of new techniques in antibody engineering (Gavilondo and Larrick, 2000), the supply of antibodies as the limiting step in these approaches can be overcome. Other techniques using different protein recognition molecules such as phage-displayed antibodies, aptamers (short oligonucleotides with high protein affinity), or molecularly imprinted polymers (MIPs) still are in methodological development and are not ready for routine use (Jenkins and Pennington, 2001; Hanash, 2003).

Similar to other genomic and proteomic approaches, two main applications for protein arrays have emerged (MacBeath, 2002). First, the so-called unbiased, or discovery-orientated approach is used to separate, quantify, and identify as many proteins in a sample as possible. Often, two samples are compared to find differentially expressed proteins. This approach is similar to the 2D gel electrophoresis experiments. The second approach, the “focused”, or “system-oriented” approach, gives a fast and less expensive way to analyze the characteristics of a large number of specified proteins. Only a subset of proteins is chosen by structural similarities due to their sequence or functional relationship, and analyzed. Microarray technology is particularly well suited for the second approach, although the proteins to be studied have to be known and well characterized.

Although gene chip and protein chip experiments share some common principles, several limitations have to be taken into account. The complexity of the proteome exceeds the complexity of the genome by decimal power. For example, the known 30,000–40,000 human genes will be translated approximately into more than 100,000–150,000 proteins. This makes it difficult to construct miniature “whole proteome” chips. Moreover, no function is known for about 75% of the proteins, which limits their diagnostic use in clinical application. It also has to be taken into account that the dynamic range of protein expression can exceed 10^7 (Kusnezow and Hoheisel, 2002), making it difficult to construct detection systems that can be applied for the whole range of expression and still show sufficient information to find differential expression (Gygi et al., 2000a).

Besides these general considerations, protein array technology has also several technical limitations compared with gene chip arrays. First, nucleic acids can be amplified by generally established techniques such as polymerase chain reaction (PCR), whereas such methods for amplification of proteins do not exist, making it difficult to provide a sufficient number of molecules for large-scale applications; second, proteins are more complex and heterogeneous than nucleic acids with regard to structure and function, which prevents a more detailed analysis of their characteristics rather than their presence in most cases; third, proteins easily lose their biological activity due to chemical modification or denaturation and therefore proteins cannot be as easily attached to chip surfaces as nucleic acids and stored for some time without losing biological activity; fourth, antibody–antigen interactions are varying in their specificity and affinity, resulting in diversities of protein binding (Jenkins and Pennington, 2001; Kusnezow and Hoheisel, 2002; Valle and Jendoubi, 2003).

One of the inherent problems of proteomics based on 2D gels is the poor resolution of membrane-bound proteins. Therefore, most of the proteins located on the cell surface are not included in 2D gels. Iwato and coworkers have recently demonstrated an elegant method for screening cell surface markers using an antibody array (Ko et al., 2005a, b). The arrays consisted of antibodies bound to cellulose membranes or glass plates. This approach made it possible to expose whole cells to the microarrays and to detect cell surface proteins by immunocytochemistry. In the future, further miniaturization and the use of additional antibodies will allow refining this attractive method in cell biology.

SELDI-TOF. Another application utilizing affinity surfaces to retain proteins based on their physical and chemical characteristics combined with direct TOF-MS is surface-enhanced laser desorption/ionization time-of-flight mass spectrometry (SELDI-TOF-MS) (Merchant and Weinberger, 2000). Protein retention is performed by chromatography with varying properties such as anion exchange, cation exchange, metal affinity, and reverse phase. By applying differing chip conditions in parallel or in series, complex biological protein mixtures can be resolved into subsets of proteins with common properties (Fung and Enderwick, 2002). The main advantage of SELDI-TOF-MS technology is in its rapid screening capabilities, which are useful for fast clinical detection of differential protein expression, e.g., in cancer and infectious disease medicine.

2.3 Bioinformatics

Though the whole field of proteomics emerged only after major technological advances, the biggest steps have been undertaken in computer technology (Chakravarti et al., 2002). Proteome informatics involves not only collection, storage, search, analysis, and classification of experimental results, but also integration, management, and retrieval of data from large-scale databases. Thus, whole proteomic technology is mainly based on computer analysis. Two-dimensional gel electrophoresis software, automated spot picking, sequence database search, proteome databases, and protein interaction maps are all dependent on powerful bioinformatic tools to translate experimental results into meaningful biological answers (Dowsey et al., 2003).

2.3.1 Web Databases

Internet databases are a common application to share proteomic data with a large number of other scientists. Because of the large size of data and a dynamic turnover of protein information including functional annotation, it is not possible in print publications any more. Numerous publications describing proteomic profiles of a large number of tissues or organisms made it necessary to develop rules for federated 2D databases (Appel et al., 1996, 1999). These rules comprehend:

1. Keyword search—Individual entries in the database must be searchable and accessible by remote keyword search.
2. Hypertext links—The database must be linked to other databases through active hypertext cross-referencing.
3. Main index—All databases of a site must have a single entry point.

An incomplete list of currently existing Internet databases can be found in [▶ Table 7.1-4](#). We have checked the hyperlinks carefully, but these databases are in current flow, as they are constantly growing and modified.

2.3.2 Online Tools

Indexing proteomes on the Web is only a part of proteomic data management. It is necessary to apply computer-aided analysis to retrieve useful information from the proteome data and to compare results from different experimental approaches.

The largest set of tools collected from the Swiss Institute of Bioinformatics can be found at the ExPASy (Expert Protein Analysis System) proteomics server at the URL <http://www.expasy.org>, including software that can be used to identify mass spectrometric data, to translate DNA into protein sequences, to search for sequence similarities, to search for protein sequence patterns, to predict posttranslational modifications and topology, to analyze the protein primary, secondary, or tertiary structure, and to align sequences (Hoogland et al., 1999; Wilkins et al., 1999).

Other resources are available:

- Gelscape (<http://www.gelscape.ualberta.ca>), an automated system for comparison of gel images (Young et al., 2004);
- Matchminer (<http://discover.nci.nih.gov/matchminer>), a tool to navigate among gene and gene product identifiers (Bussey et al., 2003);
- GoMiner (<http://discover.nci.nih.gov/gominer>), a tool for biological interpretation of genomic and proteomic data (Zeeberg et al., 2003);
- Cluster and Treeview (<http://rana.lbl.gov>), for cluster analysis of genomic and proteomic data (Eisen et al., 1998);
- Expression Profiler (<http://ep.ebi.ac.uk/EP>), a set of programs for the analysis of genomic and proteomic data sets (Vilo et al., 2003);

■ Table 7.1-4

Two-dimensional databases available on the Internet. Some of the databases are specialized in one specific tissue or cell line, whereas others comprehend a global list with links to other databases. Most databases contain proteins that have been isolated from the brain or cerebrospinal fluid and are therefore useful in brain research. (Enlarged and updated table modified from Lopez, 1999)

Name	URL	Description
2-D PAGE Aberdeen	http://www.abdn.ac.uk/~mmb023/2dhome.htm	<i>Haemophilus influenzae</i> and <i>Neisseria meningitidis</i>
Argonne Protein Mapping Group	http://www.anl.gov/BIO/PMG/	Mouse liver, human breast cell lines, pyrococcus
BALF 2D_AGE	http://www.umh.ac.be/~biochim/BALF2D.html	Mouse, human bronchoalveolar lavage fluid
Danish Centre for Human Genome Research	http://biobase.dk/cgi-bin/celis/	Human: primary keratinocytes, epithelial, hematopoietic, mesenchymal, tumors, urothelium, amnion fluid, serum, urine, proteasomes, ribosomes, phosphorylations. Mouse: epithelial, new born (ear, heart, liver, lung)
ECO2DBASE (in NCBI repository)	ftp://ncbi.nlm.nih.gov/repository/ECO2DBASE/	<i>Escherichia coli</i>
ExpASY SWISS-2DPAGE	http://www.expasy.ch/	Liver, plasma, HepG2, HepG2SP, RBC, lymphoma, CSF, macrophage-CL, erythroleukemia-CL, platelet, yeast, <i>E. coli</i> , colorectal, kidney, muscle, macrophage-like-CL, pancreatic islets, epididymus, dictyostelium
GelBank-Argonne National Lab	http://gelbank.anl.gov/overview/	42 bacterial genomes
Heart High-Performance 2-DE Database	http://www.mdc-berlin.de/~emu/heart/heart.html	Human heart
Heart-2D PAGE, The Human Myocardial Two-Dimensional (2D) Electrophoresis Protein Database	http://www.chemie.fu-berlin.de/user/pleiss/	Human heart
HSC-2D PAGE, Heart Science Centre, Harefield Hospital	http://www.harefield.nthames.nhs.uk/	Human, rat and mouse heart
Immunobiology, University of Edinburgh	http://www.ed.ac.uk/~nh/2DPAGE.html	Embryonal stem cells
INRA Maize Genome Database	http://moulon.moulon.inra.fr/imgd	Maize
IPS/LECB, NCI/FCRDC	http://www.lecb.ncifcrf.gov/ips-databases.html	Phosphoprotein, prostate, breast cancer drug screen, FAS (plasma), Cd toxicity (urine), leukemia
Joint Protein Structure Lab	http://www.ludwig.edu.au/jpsl/jpslhome.html	Human colorectal-CL, placental lysosomes
Lab. de Biochimie et Tech. des Proteines, Bobigny	http://www.smbh.univ-paris13.fr/lbtp/biochemistry/biochimie/bque.htm	Human leukemia cell lines
Large Scale Biology Corp	http://www.lsbcc.com/	Rat, mouse, human liver, corn, wheat
Max-Planck-Institut f. Infektionsbiologie	http://www.mpiib-berlin.mpg.de/2D-PAGE	<i>Mycobacterium tuberculosis</i> , vaccine strain <i>Mycobacterium bovis</i> BCG

■ Table 7.1-4 (Continued)

Name	URL	Description
Meta-Database Catalog of 2D gel images found in Web databases – 2DWG	http://www-lmmb.ncifcrf.gov/2dwgDB/2DWG.html	Set of links to www sites
Mito-pick	http://www-dsv.cea.fr/thema/MitoPick/Mito2D.html	Human mitochondria
Molecular Anatomy Laboratory	http://iupucbio1.iupui.edu/Frankw/molan.htm	Rat
Mouse Proteome Database	http://www.ukrv.de/humangenetik	Mouse brain
Partial List of Web 2D Electrophoretic Gel Databases	http://www-lecb.ncifcrf.gov/EP/table2Ddatabases.html	Set of links to 2D gel Web databases
PDD (Protein Disease Database)	http://www-lecb.ncifcrf.gov/PDD	Plasma, cerebrospinal spinal fluid, urine
PHCI-2DPAGE	http://www.gram.au.dk/	Parasite–host cell interaction, IFN- γ -induced HeLa cells
PMMA-2DPAGE	http://www.pmma.pmfhk.cz/	Human colorectal carcinoma
PPDB (Phosphoprotein Database)	http://www-lecb.ncifcrf.gov/phosphoDB/	Phosphoproteins: murine B lymphoma cells (WEHI-231)
Protein Project of Cyanobacteria	http://www.kazusa.or.jp/cyano/cyano2D/	Cyano2Dbase- <i>Synechocystis</i> sp. PCC6803
PROTEOME Inc (YPD-Yeast Protein DB)	http://www.proteome.com/	Yeast
Siena2D-PAGE	http://www.bio-mol.unisi.it/2d/2d.html	<i>Chlamydia trachomatis</i> L2, <i>Caenorhabditis elegans</i> , Human breast ductal carcinoma and histologically normal tissue, human amniotic fluid
ToothPrint DB	http://bioc111.otago.ac.nz:8001/tooth/home.htm	Dental tissue in rat
UCSF 2D PAGE	http://rafael.ucsf.edu/2DPAGEhome.html	A375 melanoma cell line
University of Greifswald, Germany	http://pc13mi.biologie.uni-greifswald.de/	<i>Bacillus subtilis</i>
Washington University Inner Ear Protein Database	http://oto.wustl.edu/thc/innerear2d.htm	Humans: inner ear
Yeast 2D gel DB, Bordeaux	http://www.ibgc.u-bordeaux2.fr/YPM	Yeast
YPD (Yeast Protein Database)	http://www.proteome.com/YPDhome.html	Yeast

- JVirGel (<http://prodoric.tu-bs.de/proteomics.php>), a tool for the construction of virtual gel images, which allows the identification of unknown proteins and the localization of known proteins on gel images (Hiller et al., 2003); and
- GenMAPP (<http://www.genemapp.org>), which allows one to display and modify own results from gene expression experiments in pathway diagrams (Dahlquist et al., 2002; Doniger et al., 2003).

We have collected a list of gene and protein expression analysis tools (Maurer, 2004a) including databases, structure prediction websites, and other data interpretation Internet pages and programs, with the emphasis on programs and sites freely available to the research community.

2.3.3 Statistical Data Analysis

One important aspect to consider is that the statistical approach used for the analysis of 2DE experiments has a major impact on the outcome of the experiment. Therefore, care must be taken to choose the appropriate statistical method.

Recently, we have compared three different statistical approaches applied to the same data set (Maurer et al., 2005). We found major differences in the results calculated by *t*-test statistics and the statistical algorithms included in the 2D software package used. Additionally, applying software for cDNA/oligonucleotide microarray experiment analysis and comparing the results to the 2D statistics showed that care should also be taken when transferring the microarray statistical algorithms to proteome data sets. Microarrays normally consist of several thousands of sequences, whereas 2D proteomic experiments identify some hundred proteins at their best, meaning that there is at least one order of magnitude between genomic and proteomic items that needs to be compared statistically. It seems that microarray software does not produce very stringent results in proteomic experiments due to the relatively small data sets in 2D analysis.

In a recent review (Boguski and McIntosh, 2003), the authors discuss statistical methods used for the identification of peptides in proteomic experiments based on MS. They compare the bioinformatics scoring systems for detecting false-positive or false-negative sequences in MS to the false detection rate (FDR) of microarray experiments. To summarize their considerations, it is important to keep in mind that for large-scale experiments such as genomics and proteomics large number of genes or proteins are misidentified just by chance. In consequence, the statistical analysis had to be more stringent or a new statistical methodology needs to be developed to address these questions. Unfortunately, there is no reliable way to deal with these issues currently.

3 Proteomics and the Analysis of Cerebral Energy Metabolism

Proteomic technology can be useful for the analysis of proteins with known enzymatic functions in cerebral cellular metabolism. Since the components of the basic metabolic pathways are well described on both the structural and the functional level, it is possible to identify the proteins involved. Using proteomic technology, the advantage to analyze a large number of these proteins at once is obvious.

3.1 Enzyme Function and 2D Gel Electrophoresis

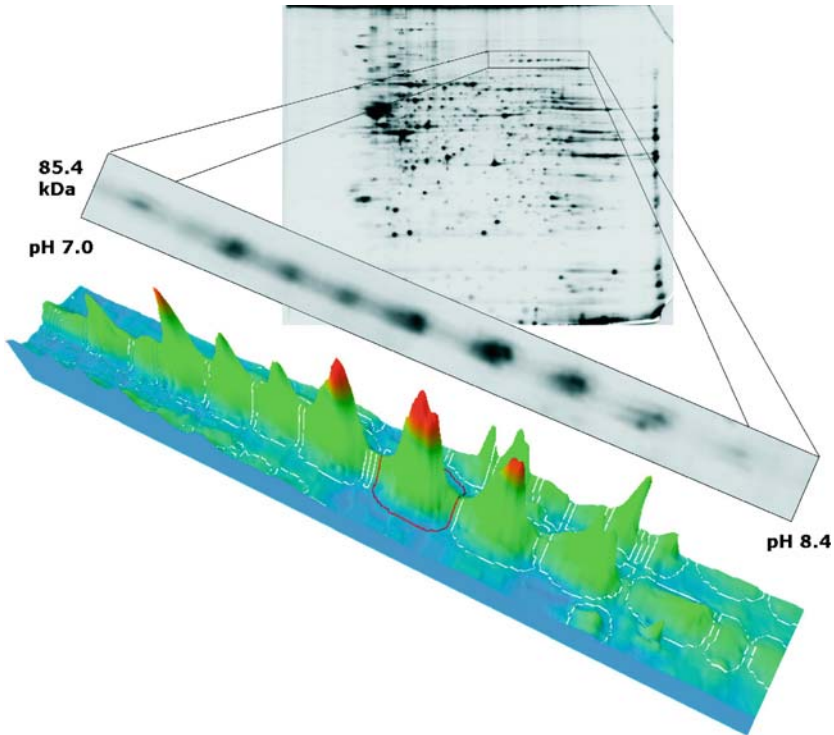
A question that needs to be addressed is whether the protein content represented by the spot volumes on 2D gels correlates with the enzymatic function of the respective protein. In an early study, Merrill and Goldman found that the amount of protein in a protein spot on 2D gels correlates well with the enzymatic function of the protein investigated (Merrill and Goldman, 1982). Since such findings may not hold for every experimental condition, care should be taken correlating protein concentration with protein function. Thus, proteins may be inactive, or they may become inactivated. In addition, 2D gel electrophoresis may result in separate isoforms, which may exert different functional effects such as different catalytic capacities that are not related to the spot volumes (▶ [Figure 7.1-5](#)). In contrast, most enzymatic tests do not separate different enzyme subtypes or isotypes, but they determine an overall enzymatic function.

3.2 Glucose Metabolism and Cellular Respiration

Proteomics based on 2D gel electrophoresis is an extremely useful tool for investigating metabolic pathways, because the majority of proteins in these pathways is located in the cytoplasm and 2DE is very well suited to separate predominantly cytoplasmic proteins due to their mostly hydrophilic properties, isoelectric points around pH 6–7, and a molecular mass up to 200 kDa.

Figure 7.1-5

Proteomics used for the identification of protein isoforms. In a two-dimensional (2D) gel experiment (Maurer et al., 2003b), we identified about 12 protein isoforms of the mitochondrial aconitase (ACO2). These isoforms are mainly generated by posttranslational modifications such as phosphorylation. A theoretical search for serine, threonine, and tyrosine phosphorylation sites at <http://www.cbs.dtu.dk> revealed a total of 30 possible sites. This means that, theoretically, the same number of protein isoform spots can be present on a 2D gel. The ACO2 enzyme plays a role in energy metabolism and iron homeostasis and is related to Friedreich's ataxia



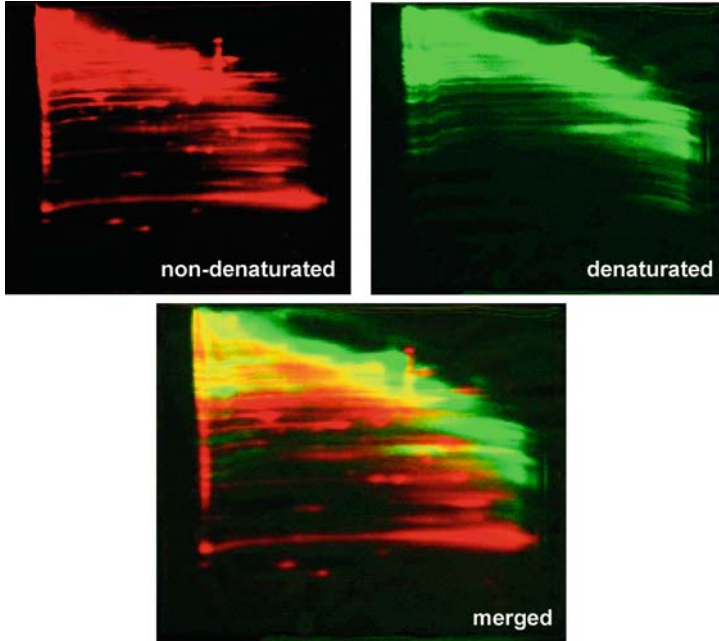
It is possible to evaluate the composition of individual components of the glycolytic pathway simultaneously. For example, different isoforms (including posttranslationally modified proteins) can be observed and their enzymatic function visualized by specific staining procedures. Of note, standard 2DE is a denaturing gel electrophoresis. This means that the protein content can be measured easily; however, for a functional analysis, other types of extraction protocols and nondenaturing gel electrophoresis have to be applied to maintain proteins in their functional state. For in-gel staining of enzymatic function, Rothe (1994) has compiled a huge collection of protocols that are an invaluable tool for subsequent functional analysis.

As a method of nondenaturing gel electrophoresis, blue-native 2D gel electrophoresis has been developed, which allows to separate intact proteins or protein complexes (Schägger and von Jagow, 1991; Schägger et al., 1994; Camacho-Carvajal et al., 2004). In contrast to standard 2DE, the first dimension is not a protein separation according to the protein isoelectric point, but rather a molecular mass separation. Therefore, the protein patterns occurring on the 2D gels are different to the gel images seen using denaturing 2DE. The blue-native 2DE is extremely useful for finding protein–protein interactions or to identify multiprotein complexes (▶ [Figure 7.1-6](#)).

Metabolic pathway analysis allows the monitoring of a large number of proteins simultaneously. Ideally, all proteins of an enzymatic pathway can be identified on the 2D gels, although only few studies aimed at

■ **Figure 7.1-6**

Identification of multiprotein complexes using blue-native two-dimensional (2D) gel electrophoresis. We separated proteins isolated from whole-cell lysates of hippocampal neural stem cells. *Upper panel:* In the first dimension, proteins were separated under nondenaturing (*left*) or denaturing (*right*) conditions, followed by a denaturing separation in the second dimension. *Lower panel:* The merged image shows monomeric proteins, multimeric proteins (*dark gray*), and the monomers of which the multimeric proteins are consisting of (*light gray*) (Maurer et al., unpublished data)



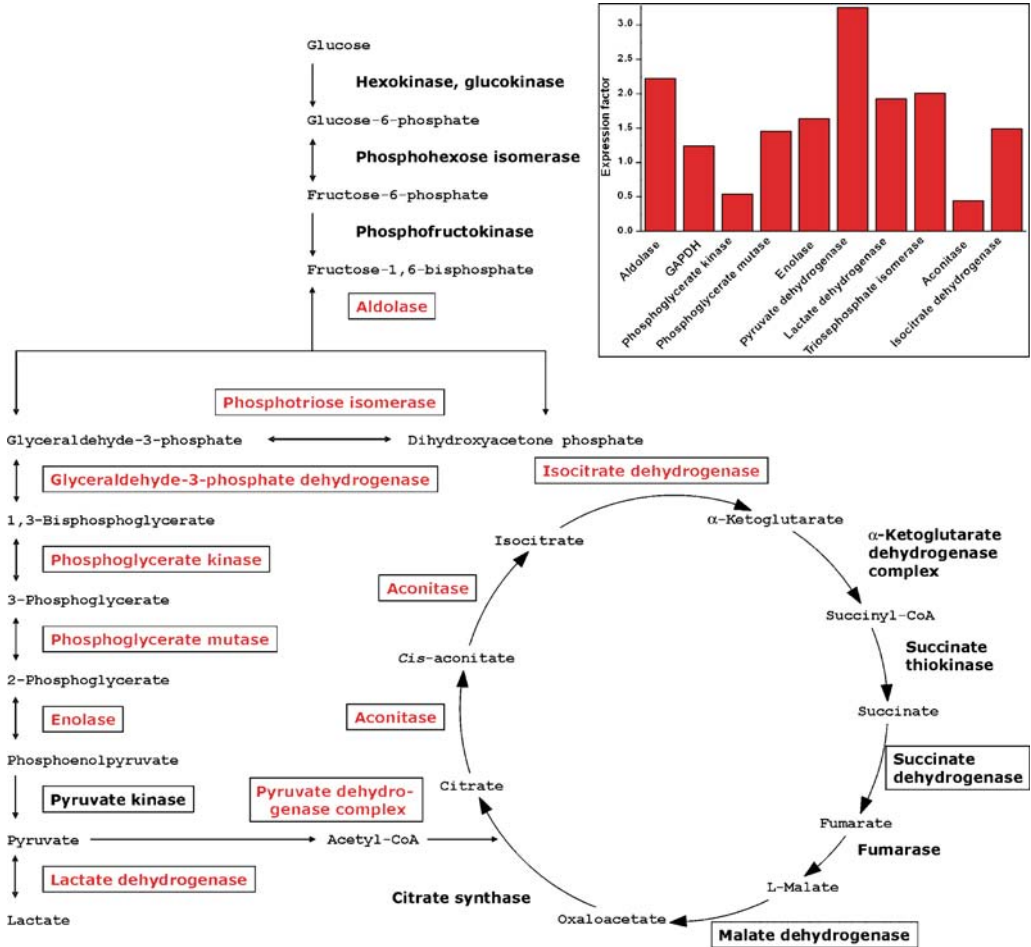
creating pathway maps for metabolic pathways. One explanation for this remarkable neglect is that the pathways are well defined, such as those of glycolysis or of the Krebs cycle. Their description in the biochemistry textbooks may leave one with the impression that these proteins are uninteresting targets for screening studies, which are always aimed at searching for new and unknown protein targets. For example, the metabolically well-known glyceraldehyde-3-phosphate dehydrogenase (GAPDH, EC 1.2.1.12), termed the “housekeeping protein” with all its connotation, reemerged as a protein with a vast variety of other functions, including the control of transcription and translation, apoptosis, and membrane fusion (Sirover, 1999).

To set a paradigm for metabolic pathway analysis, we reevaluated a proteomic study of our own to analyze proteins in metabolic pathways. We separated proteins from undifferentiated hippocampal neural stem cells by 2DE and compared the results to the protein pattern of *in vitro* differentiated cells (Maurer et al., 2004). With regard to enzymes involved in glucose metabolism, we identified nearly all of the proteins involved in glycolysis and the Krebs cycle (▶ [Figure 7.1-7](#)). Most of the identified proteins were differentially expressed under *in vitro* differentiating conditions, indicating that the cellular metabolism undergoes major changes and adapts to the new needs of the differentiated cell.

Metabolic pathway analysis in cell culture models can also be used for monitoring the effects of nutrient supply and demand. Several studies investigated the influence of different feeding conditions on cell growth and proliferation, e.g., by varying the concentration of glucose. It was possible to correlate the intracellular metabolic changes with the physiological metabolic shift in lactate and ammonia metabolism (Seow et al., 2001; Korke et al., 2004).

Figure 7.1-7

Proteomics used for metabolic pathway analysis. Proteomic technology allows monitoring a large number of proteins simultaneously. In this example, we compared changes in the proteomes of undifferentiated neural stem cells with in vitro differentiated cells (Maurer et al., 2004). We could identify a large number of enzymes involved in glycolysis and the Krebs cycle (*black boxes*), most of them showing differential protein expression upon differentiation (*italics*). *Inset*: Quantitative changes between undifferentiated and in vitro differentiated neural stem cells. The columns show the expression factor, defined as the differentiated/undifferentiated ratio



In nearly all studies involved in creating brain proteome databases (for a list of selected studies, see Table 7.1-5), the group of enzyme proteins involved in intermediary metabolism is represented most dominantly not only by number, but also as highly abundant proteins (Lubec et al., 2003). This allows pathway analysis of enzyme activity and can be used for monitoring the inborn errors of metabolism in the brain.

Proteomic methodology can also be used for chemotyping of enzyme classes. Enzymes have common structural properties defining their function. In a recent study, the authors used a combinatorial strategy to identify at least six mechanistically distinct enzyme classes of sulfonate ester-containing proteins (Adam et al., 2002).

■ **Table 7.1-5**

Brain proteome studies^a

Brain proteome databases	
Mouse brain	Eckerskorn et al. (1988), Jungblut et al. (1992), Gauss et al. (1999), Klose (1999), Tsugita et al. (2000), Klose et al. (2002)
Rat brain	Fountoulakis et al. (1999, 2000)
Human brain	Karlsson et al. (1999), Langen et al. (1999)
Human frontal cortex	Lubec et al. (2003)
Human hippocampus	Yang et al. (2004)
Human brain (HUPO, planned)	Marcus et al. (2004)
Experimental disease models	
Focal cerebral ischemia	Jacewicz et al. (1986), Kiessling et al. (1986)
Excitotoxicity	Krapfenbauer et al. (2001)
p53 knockout mouse brain (tumor suppressor gene involved in neuronal apoptosis)	Araki et al. (2000)
E1 mouse brain (epileptic seizures)	Ohmori et al. (1999)
GSK3 β transgenic mouse (Alzheimer's disease)	Tilleman et al. (2002)
Cell culture	
Neuronal hypoxia	Jin et al. (2004)
Adult rat hippocampal neuronal stem cells	Maurer et al. (2003b, 2004)
Human fetal brain stem cells	Pearce and Svendsen (1999)
Murine embryonic stem cells	Guo et al. (2001)
Postnatal rat cerebellum	Taoka et al. (2000)
Human pluripotent stem cells	Hayman and Przyborski (2004)
Human CSF and disease models	
CSF in schizophrenia, affective disorders, multiple sclerosis, neurosyphilis, AIDS, Alzheimer's disease, Parkinson's disease, infectious diseases of the brain, epilepsy, amyotrophic lateral sclerosis, polyneuropathy, and many others	Goldman et al. (1980), Harrington and Merrill (1984, 1988), Harrington et al. (1984), Walsh et al. (1984), Bracco et al. (1985), Wiederkehr et al. (1985), Pirttila et al. (1991), Wildenauer et al. (1991)
Human CSF reference map	Sanchez et al. (1995), Sickmann et al. (2000, 2002)
CSF in Alzheimer's disease	Davidsson et al. (2001, 2002), Puchades et al. (2003)
CSF in traumatic brain injury	Conti et al. (2004)
CSF in neurologically normal, elderly patients	Wenner et al. (2004)
CSF in lower back pain patients	Yuan et al. (2002)
Human brain disease	
Alzheimer's disease	Lubec et al. (1999), Castegna et al. (2002a, b, 2003), Kim et al. (2002, 2004), Tsuji et al. (2002), Butterfield et al. (2003)
Down's syndrome (trisomy 21)	Bajo et al. (2002), Jae-Kyung et al. (2003), Shin et al. (2004a)
Human brain microdialysate, stroke	Maurer et al. (2003a)

^aThis table includes a representative collection of brain proteome studies. A huge number of other brain proteomic studies could not be included due to space constraints

Rabilloud et al. (2002) investigated changes in the cellular proteome after oxidative stress. They focused on the cellular reaction to peroxiredoxins, enzymes destructing reactive oxygen species (ROS) such as peroxides. Oxidative stress also seems to play a major role in neurodegenerative diseases such as Alzheimer's disease (Castegna et al., 2002a, b; Butterfield, 2004) (see below).

3.3 Mitochondrial Proteomics

The analysis of mitochondrial proteins under normal and disease conditions has assumed importance. Mitochondria play an essential role in cellular metabolism by providing cellular energy through ATP synthesis. The enzymes for oxidative phosphorylation are located in mitochondria, as well as some of the enzymes necessary for free fatty acid metabolism and the Krebs cycle. Other biochemical pathways in mitochondria involve heme biosynthesis, ketone body generation, and hormone synthesis. Mitochondria also play a major role in the generation and degradation of ROS. Moreover, they are involved in key pathways in cellular signaling such as calcium signaling and apoptosis.

Subcellular isolation techniques enable the separation of the mitochondrial compartment of the cell, which can be analyzed in proteomic studies. Prerequisite for a functional proteomic analysis of mitochondria in disease models is the knowledge of the proteins that are normally present in mitochondria (Westermann and Neupert, 2003). A study based on liquid chromatography tandem mass spectrometry (LC-MS/MS) provided a comprehensive proteomic database of 591 proteins found in mitochondria isolated from mouse brain, heart, kidney, and liver (Mootha et al., 2003), whereas a study based on minispin affinity columns generated profiles of calcium-binding proteins, glycoproteins, and membrane proteins in the mitochondrial fraction (Lopez et al., 2000). A study using 2D gel electrophoresis provided a reference map for mitochondrial proteins (Krapfenbauer et al., 2003).

Even though mitochondria perform a multitude of different functions in cellular physiology, it is of interest to know the contribution of altered mitochondrial function to disease processes like neurodegeneration, obesity, cancer, diabetes, aging, and cardiomyopathy (Wallace, 1999). Mitochondrial proteomics may play a role in diseases where mitochondrial dysfunction has been implicated, such as in neoplastic growth (cancer), neurodegeneration (Alzheimer's disease), or metabolic disorders (diabetes). The knowledge of the mitochondrial proteome and the changes therein due to pathophysiological events will be useful for drug testing and diagnostic improvements.

3.4 Proteomic Studies Investigating Brain Metabolism in Brain Disease or Disease Models

3.4.1 Inborn Errors of Metabolism

Early studies investigated inborn errors of metabolism by means of 2D gel electrophoresis (Merrill and Goldman, 1982). The authors found alterations of proteins in lymphocytes of patients with Lesch-Nyhan syndrome, a neuropsychiatric disease that is associated with self-mutilation, spasticity, and hyperuricemia. The patients have decreased or absent levels of the purine-modifying enzyme hypoxanthine phosphoribosyltransferase (EC 2.4.2.8). Although the disease is extremely uncommon, it was one of the first neuropsychiatric diseases of which the molecular mechanisms were elucidated. The authors found 17 protein spots with differential expression; unfortunately, none of them could be identified, since MS was not developed for proteomic analysis at that time.

3.4.2 Down's Syndrome (Trisomy 21)

Down's syndrome (trisomy 21) is a common genetic cause of human mental retardation. In patients suffering from Down's syndrome, deteriorated glucose, lipid, purine, folate, and methionine/homocysteine metabolism have been reported. Lubec and Fountoulakis and coworkers have investigated proteomic changes in fetal brain tissue from patients with Down's syndrome. They found a derangement of intermediary metabolism during prenatal development, with increased protein levels of mitochondrial aconitase, NADP-linked isocitrate dehydrogenase, and pyruvate kinase as well as decreased protein expression of citrate synthase, cytosolic aspartate aminotransferase, and hypothetical proteins 4833418L03Rik protein Q9D614, mitochondrial inner-membrane protein Q16891, Nit protein 2 Q8WUF0, KIAA1185,

hypothetical protein 55.2 kDa, hypothetical protein 58.8 kDa, actin-related protein 3 β (ARP3 β), and putative GTP-binding protein PTD004 (Bajo et al., 2002; Jae-Kyung et al., 2003; Shin et al., 2004a). Also in animal models of Down's syndrome, like a transgenic mouse overexpressing human Cu/Zn superoxide dismutase I (SOD1), hypothetical hippocampal proteins of 2610008O03Rik protein Q9D0K2 and 4632432E04Rik protein Q9D358 were decreased and hypothetical protein Q99KP6 was increased, indicating an impairment of metabolism, signaling, and transcription machinery in the SOD1 transgenic brain (Shin et al., 2004b). Other studies investigating brain proteomes of transgenic mice can be found in [Table 7.1-5](#).

3.4.3 Alzheimer's Disease

Neurodegenerative disorders have been in the focus of proteomic analysis, mostly as their pathobiological events can be seen at the protein level. Neurodegenerative diseases are characterized by the loss of neurons and the intracerebral accumulation of fibrillary material. Some of the pathophysiological mechanisms have been elucidated and include (1) alterations in calcium homeostasis in the endoplasmic reticulum resulting in excitotoxicity, proteolysis, and neuronal apoptosis, (2) mitochondrial dysfunction resulting in free radical generation and impaired calcium buffering, and (3) disorganization of the cytoskeleton resulting in neurodegeneration (Tsuji et al., 2002).

Alzheimer's disease is one of the most common causes of dementia in the elderly, affecting more than 10% of the population over 65 years of age. The neuropathology of Alzheimer's disease involves irreversible progression of dementia, neuronal cell death, and accumulated protein aggregates consisting of amyloid and tau protein. Mutations that are responsible for familial Alzheimer's disease in the amyloid β precursor protein (APP) and presenilin-1 and -2 have been identified. Also, the microtubule-associated protein tau is abnormally phosphorylated, which prevents its degradation by the ubiquitin-proteasome system, resulting in an aggregation to protein complexes, the so-called tangles (Kim et al., 2004).

Studies investigating Alzheimer's disease focused mainly on two biochemical processes: (1) the formation of the neurotoxic A β peptide in senile plaques by a sequence of posttranslational modifications of the amyloid β precursor protein, and (2) the hyperphosphorylation of tau protein as the major component of tangles (Kim et al., 2004). As both pathways are not reflected by genomic alterations, several studies have applied proteomics for detecting changes in protein expression in the brains of patients with Alzheimer's disease. The main proteome alterations detected in such brains involve synaptic loss, oxidative stress, decreased glucose metabolism and protein turnover, mitochondrial dysfunction, and deficits in protein folding (Lubec et al., 1999; Castegna et al., 2002a, b, 2003; Kim et al., 2002, 2004; Tsuji et al., 2002; Butterfield et al., 2003).

Several glycolytic enzymes including α - and γ -enolase (phosphopyruvate hydratase) and glyceraldehyde-3-phosphate dehydrogenase show decreased expression in the brains of patients with Alzheimer's disease. Moreover, the expression of voltage-dependent anion channel-1 (VDAC-1) is decreased. This protein regulates the mitochondrial metabolism by controlling the ATP flux. The expression of the complex I of the mitochondrial electron transport chain (synonymously NADH:ubiquinone oxidoreductase) was also reported to be decreased, indicating that ATP production might be impaired (Butterfield, 2004). Other findings involve a decreased expression of creatine kinase (BB isoform) and triosephosphate isomerase, which are also involved in ATP production. The dysregulated energy supply may affect chemical gradients, ion channels, and finally the cell potential, resulting in neurodegeneration (Butterfield et al., 2003).

Contrary to the findings in other studies investigating the cerebrospinal fluid proteome from patients with Alzheimer's disease, the metabolic proteins could not be detected in the cerebrospinal fluid in this study, indicating that the pathological processes remain located intracellularly. The observed alterations in apolipoprotein E (ApoE) and its precursor proapolipoprotein, as well as in transthyretin, β -2 microglobulin, retinol-binding protein, and Zn- α -2 glycoprotein, may be explained by the involvement of β APP in other mechanisms like cholesterol metabolism (Davidsson et al., 2002, 2003).

A mouse model for Alzheimer's disease is the GSK3 β transgenic mouse, which overexpresses the multifunctional enzyme glycogen synthase kinase-3 β (GSK3 β). GSK3 β phosphorylates the tau protein, which then aggregates. These aggregates seem to play a pathogenetic role in Alzheimer's disease, as in the transgenic mouse, hyperphosphorylation of the tau protein is followed by increased formation of neurofibrillary tangles. Tilleman et al. (2002) used 2D gel electrophoresis to find 51 differentially expressed protein spots in the transgenic mice as compared with wild-type littermates. They identified downstream targets of the GSK3 β signaling pathways in the functional groups relating to cytoskeleton, energy metabolism, folding, signal transduction, detoxification, and oxygen scavenging.

In summary, the numerous studies investigating the proteome of diseased brain tissue or cerebrospinal fluid could not discriminate distinctively and unanimously between cause and effect of their observations. Although the metabolic changes of brain metabolism after a noxious event can be monitored, the meaning of "marker" proteins found for various diseases cannot be determined easily. Similar to the results observed in genetic testing, the observation of a specific protein in a specific condition is not necessarily related in a pathophysiological sequence of events, and its clinical relevance remains unclear. Thus, all candidate markers have to be carefully evaluated further, both in other experimental approaches in vitro and in vivo as well as in clinical trials.

4 Perspectives

4.1 Outlook: Challenges and Issues To Be Resolved

4.1.1 General Considerations

Application of proteomic techniques has inherent problems of biological and technical nature. Biological limitations concern interindividual diversity of biological samples, resulting in a large scatter of data. In addition, protein concentrations may be altered by degradation after sampling. Furthermore, results may be altered by posttranslational modifications or the influence of drugs. Finally, protein expression changes over time due to different environmental cues in development and aging, making it necessary to investigate different time points.

Technical limitations result from the fact that only a finite number of the most abundant proteins can be resolved and stained on the 2D gels, but the dynamic range of protein expression exceeds a factor of 10^7 (Tyers and Mann, 2003). The process of gel analysis is time-consuming and labor-intensive. Finally, MS requires expensive equipment as well as specially trained personnel. Future developments will be based on technological advances like miniaturization and increased automatization of instrumentation as well as further acceleration in high-throughput screening.

4.1.2 Membrane Proteins

Biological membranes are important in the processing of information, which is of special relevance for the brain. Integrated membrane proteins such as ion channels, receptors, and transporters together with cytoskeletal elements contribute to neural and astrocytic signaling. Both neurogenesis and gliogenesis require a constant flow of membranes as the basis of morphological changes. Finally, cellular metabolism in the brain is dependent on intact membranes and on integral membrane proteins that mediate the flux of metabolites.

Although it is desirable to detect membrane proteins by proteomics, membrane proteins are under-represented in 2D gels. This is due to the following: (1) They are less abundant proteins, which makes them "invisible" in the pool of cytoplasmic proteins on standard 2D gels; (2) they have mostly alkaline isoelectric points ($pI > 8$), which would require technically more difficult alkaline pH gradient gels; and (3) most of their domains are composed of hydrophobic amino acids, meaning that these proteins are rarely soluble in

the standard aqueous buffer systems used for first-dimensional IEF in 2D gel electrophoresis. Membrane proteins tend to precipitate during this step (Santoni et al., 2000). Although promising improvements including differential solubilization techniques and new surfactants and detergents for membrane protein extraction have been described (Santoni et al., 2000), electrophoresis-free methods such as direct MS have been developed (Aebersold and Mann, 2003), or alternatively, electrophoresis under nondenaturing conditions such as the blue-native 2D electrophoresis has been applied for resolution of membrane proteins (Schägger et al., 1994; Brookes et al., 2002; Camacho-Carvajal et al., 2004). Future research may also concentrate on the development of detergents to solubilize integral membrane proteins compatible with IEF, which would then allow 2D gel electrophoresis for membrane proteins.

A different approach for the analysis of membrane proteins is called multidimensional protein identification technology (MudPIT) (Washburn et al., 2001). It combines a series of prefractionation steps including membrane solubilization, enzymatic digestion of the proteins, strong cationic exchange columns (SCX technology), and reverse-phase high-pressure liquid chromatography (RP-HPLC), with the advantages of electrospray MS (ESI-MS/MS). This technique allows the rapid identification of integral membrane proteins, but it is not quantitative.

4.1.3 Dynamics of Protein Turnover

The cellular protein concentration is balanced in a constant flow from synthesis to degradation (steady state). As the current proteomic technology can only display a small section of the protein content at a given time point, rates of protein turnover need to be determined separately to get an impression of the cellular protein turnover. Pratt et al. (2002) used stable isotope-labeled amino acids to monitor mass shifts in tryptic protein fragments. This approach allows determining rates of protein turnover and protein half-lives by MS. Such an approach is easier and more comprehensive than traditional methods such as liquid scintillation or autoradiography.

4.1.4 Quantitation

In most proteomic studies, two or more groups are compared on a qualitative basis: The presence or absence of a spot is detected in one of the experimental groups. It is more difficult to obtain quantitative data, since the technique of analysis is limited: protein isolation protocols may result in enrichment or suppression of a certain protein species. The dynamic range of staining procedures must be considered, since the linear range of most stains and labels does not exceed a factor of 10^3 , but protein abundance is far beyond a factor of 10^7 . Some of these problems are circumvented by novel approaches. Gerner et al. (2002) developed a method of simultaneous fluorescent staining and radiolabeling of proteins, which allows to compare protein amounts quantitatively and to determine protein half-lives.

Two-dimensional gel electrophoresis offers the possibility of visualizing quantitative results, but the price must be paid that only a limited range of concentrations of the expressed proteins can be stained when compared with direct mass spectrometric approaches (Gygi et al., 2000b; Righetti et al., 2004). Therefore, both approaches will exist most likely side by side for the coming years.

In the future, new methods are envisioned to increase the amount of less abundant proteins in a sample. Such protein amplification machinery should amplify proteins in a way similar to PCR for nucleic acids. If the amplification step can be linearized, a direct quantitation of the protein concentration can be achieved and the protein concentration in the original sample can be calculated.

The enormous dynamic range of protein concentrations that normally exists within the cells makes it obvious that staining methods need to be improved. Such new methods should allow staining proteins in a linear range of at least 10^6 , which may come close to the actual protein concentrations. This may help to standardize experimental conditions, as prefractionation and enrichment of some protein species would become obsolete.

4.1.5 Bioinformatics

With the technical improvement of the “hardware” such as mass spectrometers, the gigantic amount of data produced by high-throughput screening methods has to be organized and evaluated. Future developments will not only be based on faster computers with larger memory and storage options, but also on new software tools to interpret proteomic data. One of the most important aims will be to calculate and model tertiary protein structures on the basis of the primary amino acid sequence. This might improve the functional classification of proteins and the search for interacting partners.

5 Conclusion

Proteomics is a screening technology for high-throughput protein analysis. In principle, it permits the description of whole sets of proteins and their functional interaction. Proteomic technology applied to the brain is mainly based on 2D gel electrophoresis for protein separation in combination with MS for protein identification. Although the technological basis of this approach is constantly improving, the application of proteomics for diagnosis and therapy is only starting and remains in the experimental stage. With regard to brain function and biochemistry, proteomics is a useful technology for monitoring the expression and function of a large number of proteins simultaneously, which will further stimulate investigations of the brain and its diseases by the use of proteomics.

Acknowledgments

This work was supported by the German Ministry of Education and Research (BMBF) in the research programs Competence Network Stroke (B2, to WK) and the National Genome Research Network NGFN-2 (N3NV-S19T05, to MHM and WK), as well as by the German Research Foundation DFG (MA 2492/2-2, to MHM and WK).

References

- Adam GC, Sorensen EJ, Cravatt BF. 2002. Proteomic profiling of mechanistically distinct enzyme classes using a common chemotype. *Nat Biotechnol* 20: 805-809.
- Aebersold R, Mann M. 2003. Mass spectrometry-based proteomics. *Nature* 422: 198-207.
- Anderson L, Seilhamer J. 1997. A comparison of selected mRNA and protein abundances in human liver. *Electrophoresis* 18: 533-537.
- Appel RD, Bairoch A, Hochstrasser DF. 1999. 2-D databases on the World Wide Web. *Methods Mol Biol* 112: 383-391.
- Appel RD, Bairoch A, Sanchez JC, Vargas JR, Golaz O, et al. 1996. Federated two-dimensional electrophoresis database: A simple means of publishing two-dimensional electrophoresis data. *Electrophoresis* 17: 540-546.
- Appel RD, Vargas JR, Palagi PM, Walther D, Hochstrasser DF. 1997. Melanie II—a third-generation software package for analysis of two-dimensional electrophoresis images: II. Algorithms. *Electrophoresis* 18: 2735-2748.
- Araki N, Morimasa T, Sakai T, Tokuoh H, Yunoue S, et al. 2000. Comparative analysis of brain proteins from p53-deficient mice by two-dimensional electrophoresis. *Electrophoresis* 21: 1880-1889.
- Bajo M, Fruehauf J, Kim SH, Fountoulakis M, Lubec G. 2002. Proteomic evaluation of intermediary metabolism enzyme proteins in fetal Down's syndrome cerebral cortex. *Proteomics* 2: 1539-1546.
- Bakhtiar R, Nelson RW. 2001. Mass spectrometry of the proteome. *Mol Pharmacol* 60: 405-415.
- Berkelman T, Stenstedt T. 2001. 2-D electrophoresis. Principles and methods. Uppsala: Amersham Biosciences.
- Blum H, Beier H, Gross HJ. 1987. Improved silver staining of plant proteins, RNA and DNA in polyacrylamide gels. *Electrophoresis* 8: 93-99.
- Boguski MS, McIntosh MW. 2003. Biomedical informatics for proteomics. *Nature* 422: 233-237.
- Bracco F, Gallo P, Tavolato B, Battistin L. 1985. Two-dimensional electrophoresis of cerebrospinal fluid proteins

- in normal and pathological conditions. *Neurochem Res* 10: 1203-1219.
- Bradford MM. 1976. A rapid and sensitive method for the quantitation of microgram quantities of protein utilizing the principle of protein-dye binding. *Anal Biochem* 72: 248-254.
- Brookes PS, Pinner A, Ramachandran A, Coward L, Barnes S, et al. 2002. High throughput two-dimensional blue-native electrophoresis: A tool for functional proteomics of mitochondria and signaling complexes. *Proteomics* 2: 969-977.
- Bussey KJ, Kane D, Sunshine M, Narasimhan S, Nishizuka S, et al. 2003. MatchMiner: A tool for batch navigation among gene and gene product identifiers. *Genome Biol* 4.
- Butterfield DA. 2004. Proteomics: A new approach to investigate oxidative stress in Alzheimer's disease brain. *Brain Res* 1000: 1-7.
- Butterfield DA, Boyd-Kimball D, Castegna A. 2003. Proteomics in Alzheimer's disease: Insights into potential mechanisms of neurodegeneration. *J Neurochem* 86: 1313-1327.
- Camacho-Carvajal MM, Wollscheid B, Aebersold R, Steimle V, Schamel WW. 2004. Two-dimensional Blue native/SDS gel electrophoresis of multi-protein complexes from whole cellular lysates: A proteomics approach. *Mol Cell Proteomics* 3: 176-182.
- Castegna A, Aksenov M, Aksenova M, Thongboonkerd V, Klein JB, Pierce WM, et al. 2002a. Proteomic identification of oxidatively modified proteins in Alzheimer's disease brain. Part I: Creatine kinase BB, glutamine synthase, and ubiquitin carboxy-terminal hydrolase L-1. *Free Radic Biol Med* 33: 562-571.
- Castegna A, Aksenov M, Thongboonkerd V, Klein JB, Pierce WM, et al. 2002b. Proteomic identification of oxidatively modified proteins in Alzheimer's disease brain. Part II: Dihydropyrimidinase-related protein 2, alpha-enolase and heat shock cognate 71. *J Neurochem* 82: 1524-1532.
- Castegna A, Thongboonkerd V, Klein JB, Lynn B, Markesbery WR, et al. 2003. Proteomic identification of nitrated proteins in Alzheimer's disease brain. *J Neurochem* 85: 1394-1401.
- Chakravarti DN, Chakravarti B, Moutsatsos I. 2002. Informatic tools for proteome profiling. *Biotechniques Suppl* 4-10, 12-15.
- Choe LH, Lee KH. 2003. Quantitative and qualitative measure of intralaboratory two-dimensional protein gel reproducibility and the effects of sample preparation, sample load, and image analysis. *Electrophoresis* 24: 3500-3507.
- Choudhary J, Grant SG. 2004. Proteomics in postgenomic neuroscience: The end of the beginning. *Nat Neurosci* 7: 440-445.
- Conti A, Sanchez-Ruiz Y, Bachi A, Beretta L, Grandi E, et al. 2004. Proteome study of human cerebrospinal fluid following traumatic brain injury indicates fibrin(ogen) degradation products as trauma-associated markers. *J Neurotrauma* 21: 854-863.
- Dahlquist KD, Salomonis N, Vranizan K, Lawlor SC, Conklin BR. 2002. GenMAPP, a new tool for viewing and analyzing microarray data on biological pathways. *Nat Genet* 31: 19-20.
- Davidsson P, Brinkmalm A, Karlsson G, Persson R, Lindbjör M, et al. 2003. Clinical mass spectrometry in neuroscience. *Proteomics and peptidomics. Cell Mol Biol (Noisy-le-grand)* 49: 681-688.
- Davidsson P, Paulson L, Hesse C, Blennow K, Nilsson CL. 2001. Proteome studies of human cerebrospinal fluid and brain tissue using a preparative two-dimensional electrophoresis approach prior to mass spectrometry. *Proteomics* 1: 444-452.
- Davidsson P, Westman-Brinkmalm A, Nilsson CL, Lindbjör M, Paulson L, et al. 2002. Proteome analysis of cerebrospinal fluid proteins in Alzheimer patients. *Neuroreport* 13: 611-615.
- Doniger SW, Salomonis N, Dahlquist KD, Vranizan K, Lawlor SC, et al. 2003. MAPPFinder: Using Gene Ontology and GenMAPP to create a global gene-expression profile from microarray data. *Genome Biol* 4: R7.
- Dowsey AW, Dunn MJ, Yang GZ. 2003. The role of bioinformatics in two-dimensional gel electrophoresis. *Proteomics* 3: 1567-1596.
- Dutt MJ, Lee KH. 2000. Proteomic analysis. *Curr Opin Biotechnol* 11: 176-179.
- Eckerskorn C, Jungblut P, Mewes W, Klose J, Lottspeich F. 1988. Identification of mouse brain proteins after two-dimensional electrophoresis and electroblotting by microsequence analysis and amino acid composition analysis. *Electrophoresis* 9: 830-838.
- Eisen MB, Spellman PT, Brown PO, Botstein D. 1998. Cluster analysis and display of genome-wide expression patterns. *Proc Natl Acad Sci USA* 95: 14863-14868.
- Fountoulakis M, Hardmaier R, Schuller E, Lubec G. 2000. Differences in protein level between neonatal and adult brain. *Electrophoresis* 21: 673-678.
- Fountoulakis M, Schuller E, Hardmeier R, Berndt P, Lubec G. 1999. Rat brain proteins: Two-dimensional protein database and variations in the expression level. *Electrophoresis* 20: 3572-3579.
- Freeman WM, Hemby SE. 2004. Proteomics for protein expression profiling in neuroscience. *Neurochem Res* 29: 1065-1081.
- Fung ET, Enderwick C. 2002. ProteinChip clinical proteomics: Computational challenges and solutions. *Biotechniques Suppl*: 34-38, 40-31.

- Garrels JI. 1989. The QUEST system for quantitative analysis of two-dimensional gels. *J Biol Chem* 264: 5269-5282.
- Gauss C, Kalkum M, Löwe M, Lehrach H, Klose J. 1999. Analysis of the mouse proteome. (I) Brain proteins: Separation by two-dimensional electrophoresis and identification by mass spectrometry and genetic variation. *Electrophoresis* 20: 575-600.
- Gavilondo JV, Larrick JW. 2000. Antibody engineering at the millennium. *Biotechniques* 29: 128-132, 134-136, 138 passim.
- Gerner C, Vejda S, Gelbmann D, Bayer E, Gotzmann J, et al. 2002. Concomitant determination of absolute values of cellular protein amounts, synthesis rates, and turnover rates by quantitative proteome profiling. *Mol Cell Proteomics* 1: 528-537.
- Goldman D, Merrill CR, Ebert MH. 1980. Two-dimensional gel electrophoresis of cerebrospinal fluid proteins. *Clin Chem* 26: 1317-1322.
- Görg A, Boguth G, Obermaier C, Harder A, Weiss W. 1998. 2-D electrophoresis with immobilized pH gradients using IPGphor isoelectric focussing system. *Life Science News* 1: 4-6.
- Görg A, Obermaier C, Boguth G, Harder A, Scheibe B, et al. 2000. The current state of two-dimensional electrophoresis with immobilized pH gradients. *Electrophoresis* 21: 1037-1053.
- Görg A, Postel W, Gunther S. 1988. The current state of two-dimensional electrophoresis with immobilized pH gradients. *Electrophoresis* 9: 531-546.
- Gunning P, Weinberger R, Jeffrey P, Hardeman E. 1998. Isoform sorting and the creation of intracellular compartments. *Annu Rev Cell Dev Biol* 14: 339-372.
- Guo X, Ying W, Wan J, Hu Z, Qian X, et al. 2001. Proteomic characterization of early-stage differentiation of mouse embryonic stem cells into neural cells induced by all-trans retinoic acid in vitro. *Electrophoresis* 22: 3067-3075.
- Gygi SP, Corthals GL, Zhang Y, Rochon Y, Aebersold R. 2000a. Evaluation of two-dimensional gel electrophoresis-based proteome analysis technology. *Proc Natl Acad Sci USA* 97: 9390-9395.
- Gygi SP, Rist B, Aebersold R. 2000b. Measuring gene expression by quantitative proteome analysis. *Curr Opin Biotechnol* 11: 396-401.
- Gygi SP, Rist B, Gerber SA, Turecek F, et al. 1999a. Quantitative analysis of complex protein mixtures using isotope-coded affinity tags. *Nat Biotechnol* 17: 994-999.
- Gygi SP, Rochon Y, Franz A, Aebersold R. 1999b. Correlation between protein and mRNA abundance in yeast. *Mol Cell Biol* 19: 1720-1730.
- Hanash S. 2003. Disease proteomics. *Nature* 422: 226-232.
- Harrington MG, Merrill CR. 1984. Two-dimensional electrophoresis and "ultrasensitive" silver staining of cerebrospinal fluid proteins in neurological diseases. *Clin Chem* 30: 1933-1937.
- Harrington MG, Merrill CR. 1988. Cerebrospinal fluid protein analysis in diseases of the nervous system. *J Chromatogr* 429: 345-358.
- Harrington MG, Merrill CR, Goldman D, Xu X, McFarlin DE. 1984. Two-dimensional electrophoresis of cerebrospinal fluid proteins in multiple sclerosis and various neurological diseases. *Electrophoresis* 5: 236-245.
- Hayman MW, Przyborski SA. 2004. Proteomic identification of biomarkers expressed by human pluripotent stem cells. *Biochem Biophys Res Commun* 316: 918-923.
- Herbert BR, Harry JL, Packer NH, Gooley AA, Pedersen SK, et al. 2001. What place for polyacrylamide in proteomics? *Trends Biotechnol* 19: S3-9.
- Herbert BR, Molloy MP, Gooley AA, Walsh BJ, Bryson WG, et al. 1998. Improved protein solubility in two-dimensional electrophoresis using tributyl phosphine as reducing agent. *Electrophoresis* 19: 845-851.
- Hiller K, Schobert M, Hundertmark C, Jahn D, Munch R. 2003. JVirGel: Calculation of virtual two-dimensional protein gels. *Nucleic Acids Res* 31: 3862-3865.
- Hoogland C, Sanchez JC, Walther D, Baujard V, Baujard O, et al. 1999. Two-dimensional electrophoresis resources available from ExPASy. *Electrophoresis* 20: 3568-3571.
- Humphery-Smith I, Cordwell SJ, Blackstock WP. 1997. Proteome research: Complementarity and limitations with respect to the RNA and DNA worlds. *Electrophoresis* 18: 1217-1242.
- Jacewicz M, Kiessling M, Pulsinelli WA. 1986. Selective gene expression in focal cerebral ischemia. *J Cereb Blood Flow Metab* 6: 263-272.
- Jae-Kyung M, Gulesserian T, Fountoulakis M, Lubec G. 2003. Deranged hypothetical proteins Rik protein, Nit protein 2 and mitochondrial inner membrane protein, Mitofilin, in fetal Down syndrome brain. *Cell Mol Biol (Noisy-le-grand)* 49: 739-746.
- James P. 2002. Chips for proteomics: A new tool or just hype? *Biotechniques Suppl*: 4-10, 12-13.
- Jenkins RE, Pennington SR. 2001. Arrays for protein expression profiling: Towards a viable alternative to two-dimensional gel electrophoresis? *Proteomics* 1: 13-29.
- Jensen ON, Wilm M, Shevchenko A, Mann M. 1999. Peptide sequencing of 2-DE gel-isolated proteins by nanoelectrospray tandem mass spectrometry. *Methods Mol Biol* 112: 571-588.
- Jin K, Mao XO, Greenberg DA. 2004. Proteomic analysis of neuronal hypoxia in vitro. *Neurochem Res* 29: 1123-1128.
- Julka S, Regnier F. 2004. Quantification in proteomics through stable isotope coding: A review. *J Proteome Res* 3: 350-363.
- Jungblut P, Dzionara M, Klose J, Wittmann-Liebold B. 1992. Identification of tissue proteins by amino acid analysis after

- purification by two-dimensional electrophoresis. *J Protein Chem* 11: 603-612.
- Karlsson K, Cairns N, Lubec G, Fountoulakis M. 1999. Enrichment of human brain proteins by heparin chromatography. *Electrophoresis* 20: 2970-2976.
- Kiessling M, Diemel GA, Jacewicz M, Pulsinelli WA. 1986. Protein synthesis in postischemic rat brain: A two-dimensional electrophoretic analysis. *J Cereb Blood Flow Metab* 6: 642-649.
- Kim SH, Fountoulakis M, Cairns NJ, Lubec G. 2002. Human brain nucleoside diphosphate kinase activity is decreased in Alzheimer's disease and Down syndrome. *Biochem Biophys Res Commun* 296: 970-975.
- Kim SI, Voshol H, van Oostrum J, Hastings TG, Cascio M, et al. 2004. Neuroproteomics: Expression profiling of the brain's proteomes in health and disease. *Neurochem Res* 29: 1317-1331.
- Klose J. 1999. Genotypes and phenotypes. *Electrophoresis* 20: 643-652.
- Klose J, Nock C, Herrmann M, Stuhler K, Marcus K, et al. 2002. Genetic analysis of the mouse brain proteome. *Nat Genet* 30: 385-393.
- Ko IK, Kato K, Iwata H. 2005a. Antibody microarray for correlating cell phenotype with surface marker. *Biomaterials* 26: 687-696.
- Ko IK, Kato K, Iwata H. 2005b. Parallel analysis of multiple surface markers expressed on rat neural stem cells using antibody microarrays. *Biomaterials* 26: 4882-4891.
- Korke R, Gatti Mde L, Lau AL, Lim JW, Seow TK, et al. 2004. Large scale gene expression profiling of metabolic shift of mammalian cells in culture. *J Biotechnol* 107: 1-17.
- Krapfenbauer K, Berger M, Friedlein A, Lubec G, Fountoulakis M. 2001. Changes in the levels of low-abundance brain proteins induced by kainic acid. *Eur J Biochem* 268: 3532-3537.
- Krapfenbauer K, Fountoulakis M, Lubec G. 2003. A rat brain protein expression map including cytosolic and enriched mitochondrial and microsomal fractions. *Electrophoresis* 24: 1847-1870.
- Kusnezow W, Hoheisel JD. 2002. Antibody microarrays: Promises and problems. *Biotechniques Suppl*: 14-23.
- Laemmli UK. 1970. Cleavage of structural proteins during the assembly of the head of bacteriophage T4. *Nature* 227: 680-685.
- Langen H, Berndt P, Roder D, Cairns N, Lubec G, et al. 1999. Two-dimensional map of human brain proteins. *Electrophoresis* 20: 907-916.
- Lee PS, Shaw LB, Choe LH, Mehra A, Hatzimanikatis V, et al. 2003. Insights into the relation between mRNA and protein expression patterns: II. Experimental observations in *Escherichia coli*. *Biotechnol Bioeng* 84: 834-841.
- Lemkin PF. 1999. Comparing 2-D electrophoretic gels across Internet databases. *Methods Mol Biol* 112: 393-410.
- Link AJ. 1999. 2-D Proteome Analysis Protocols. Humana Press, Totowa, NJ.
- Link AJ, Robison K, Church GM. 1997. Comparing the predicted and observed properties of proteins encoded in the genome of *Escherichia coli* K-12. *Electrophoresis* 18: 1259-1313.
- Lopez MF. 1999. Proteome analysis. I. Gene products are where the biological action is. *J Chromatogr B Biomed Sci Appl* 722: 191-202.
- Lopez MF, Kristal BS, Chernokalskaya E, Lazarev A, Shestopalov AI, et al. 2000. High-throughput profiling of the mitochondrial proteome using affinity fractionation and automation. *Electrophoresis* 21: 3427-3440.
- Lubec G, Krapfenbauer K, Fountoulakis M. 2003. Proteomics in brain research: Potentials and limitations. *Prog Neurobiol* 69: 193-211.
- Lubec G, Nonaka M, Krapfenbauer K, Gratzer M, Cairns N, et al. 1999. Expression of the dihydropyrimidinase related protein 2 (DRP-2) in Down syndrome and Alzheimer's disease brain is downregulated at the mRNA and dysregulated at the protein level. *J Neural Transm Suppl* 57: 161-177.
- Mac Beath G. 2002. Protein microarrays and proteomics. *Nat Genet* 32(Suppl): 526-532.
- Mahon P, Dupree P. 2001. Quantitative and reproducible two-dimensional gel analysis using Phoretix 2D Full. *Electrophoresis* 22: 2075-2085.
- Mann M, Hendrickson RC, Pandey A. 2001. Analysis of proteins and proteomes by mass spectrometry. *Annu Rev Biochem* 70: 437-473.
- Mann M, Jensen ON. 2003. Proteomic analysis of post-translational modifications. *Nat Biotechnol* 21: 255-261.
- Marcus K, Schmidt O, Schaefer H, Hamacher M, van Hall A, et al. 2004. Proteomics—application to the brain. *Int Rev Neurobiol* 61: 285-311.
- Maurer MH. 2004a. The path to enlightenment: Making sense of genomic and proteomic information. *Genomics Proteomics Bioinformatics* 2: 123-131.
- Maurer MH. 2004b. Simple method for three-dimensional representation of 2-DE spots using a spreadsheet program. *J Proteome Res* 3: 665-666.
- Maurer MH, Berger C, Wolf M, Fütterer CD, Feldmann RE Jr, et al. 2003a. The proteome of human brain microdialysate. *Proteome Sci* 1: 7.
- Maurer MH, Feldmann RE, Fütterer CD, Butlin J, Kuschinsky W. 2004. Comprehensive proteome expression profiling of undifferentiated vs. differentiated neural stem cells from adult rat hippocampus. *Neurochem Res* 29: 1129-1144.

- Maurer MH, Feldmann RE Jr, Brömme JO, Kalenka A. 2005. Comparison of statistical approaches for the analysis of proteome expression data of differentiating neural stem cells. *J Proteome Res* 4: 96-100.
- Maurer MH, Feldmann RE Jr, Fütterer CD, Kuschinsky W. 2003b. The proteome of neural stem cells from adult rat hippocampus. *Proteome Sci* 1: 4.
- Merchant M, Weinberger SR. 2000. Recent advancements in surface-enhanced laser desorption/ionization-time of flight mass spectrometry. *Electrophoresis* 21: 1164-1177.
- Merrill CR, Goldman D. 1982. Quantitative two-dimensional protein electrophoresis for studies of inborn errors of metabolism. *Clin Chem* 28: 1015-1020.
- Mootha VK, Bunkenborg J, Olsen JV, Hjerrild M, Wisniewski JR, et al. 2003. Integrated analysis of protein composition, tissue diversity, and gene regulation in mouse mitochondria. *Cell* 115: 629-640.
- Morrison RS, Kinoshita Y, Johnson MD, Uo T, Ho JT, et al. 2002. Proteomic analysis in the neurosciences. *Mol Cell Proteomics* 1: 553-560.
- O'Connor CD, Adams P, Alefounder P, Farris M, Kinsella N, et al. 2000. The analysis of microbial proteomes: Strategies and data exploitation. *Electrophoresis* 21: 1178-1186.
- Ohmori O, Hirano H, Mita T. 1999. Shifted cytosolic NADP⁺-dependent isocitrate dehydrogenase on 2-D gel in the brain of genetically epileptic E1 mice. *Neurochem Res* 24: 365-369.
- Ong SE, Foster LJ, Mann M. 2003. Mass spectrometric-based approaches in quantitative proteomics. *Methods* 29: 124-130.
- Ong SE, Pandey A. 2001. An evaluation of the use of two-dimensional gel electrophoresis in proteomics. *Biomol Eng* 18: 195-205.
- Pasa-Tolic L, Masselon C, Barry RC, Shen Y, Smith RD. 2004. Proteomic analyses using an accurate mass and time tag strategy. *Biotechniques* 37: 621-624, 626-633, 636 passim.
- Patterson SD, Aebersold RH. 2003. Proteomics: The first decade and beyond. *Nat Genet* 33(Suppl): 311-323.
- Patton WF. 1999. Proteome analysis. II. Protein subcellular redistribution: Linking physiology to genomics via the proteome and separation technologies involved. *J Chromatogr B Biomed Sci Appl* 722: 203-223.
- Patton WF. 2000a. Making blind robots see: The synergy between fluorescent dyes and imaging devices in automated proteomics. *Biotechniques* 28: 944-948, 950-947.
- Patton WF. 2000b. A thousand points of light: The application of fluorescence detection technologies to two-dimensional gel electrophoresis and proteomics. *Electrophoresis* 21: 1123-1144.
- Pearce A, Svendsen CN. 1999. Characterisation of stem cell expression using two-dimensional electrophoresis. *Electrophoresis* 20: 969-970.
- Phizicky E, Bastiaens PI, Zhu H, Snyder M, Fields S. 2003. Protein analysis on a proteomic scale. *Nature* 422: 208-215.
- Pirttila T, Mattila K, Frey H. 1991. CSF proteins in neurological disorders analyzed by immobilized PH gradient isoelectric focusing using narrow PH gradients. *Acta Neurol Scand* 83: 34-40.
- Pratt JM, Petty J, Riba-Garcia I, Robertson DH, Gaskell SJ, et al. 2002. Dynamics of protein turnover, a missing dimension in proteomics. *Mol Cell Proteomics* 1: 579-591.
- Puchades M, Hansson SE, Nilsson CL, Andreassen N, Blennow K, et al. 2003. Proteomic studies of potential cerebrospinal fluid protein markers for Alzheimer's disease. *Brain Res Mol Brain Res* 118: 140-146.
- Rabilloud T. 1999. Silver staining of 2-D electrophoresis gels. *Methods Mol Biol* 112: 297-305.
- Rabilloud T. 2000. Detecting proteins separated by 2-D gel electrophoresis. *Anal Chem* 72: 48A-55A.
- Rabilloud T. 2002. Two-dimensional gel electrophoresis in proteomics: Old, old fashioned, but it still climbs up the mountains. *Proteomics* 2: 3-10.
- Rabilloud T, Heller M, Gasnier F, Luche S, Rey C, et al. 2002. Proteomics analysis of cellular response to oxidative stress. Evidence for in vivo overoxidation of peroxiredoxins at their active site. *J Biol Chem* 277: 19396-19401.
- Ramagli LS. 1999. Quantifying protein in 2-D PAGE solubilization buffers. *Methods Mol Biol* 112: 99-103.
- Raman B, Cheung A, Marten MR. 2002. Quantitative comparison and evaluation of two commercially available, two-dimensional electrophoresis image analysis software packages, Z3 and Melanie. *Electrophoresis* 23: 2194-2202.
- Righetti PG, Camprostrini N, Pascali J, Hamdan M, Astner H. 2004. Quantitative proteomics: A review of different methodologies. *Eur J Mass Spectrom (Chichester, Eng)* 10: 335-348.
- Rohlf C. 2000. Proteomics in molecular medicine: Applications in central nervous systems disorders. *Electrophoresis* 21: 1227-1234.
- Rosengren AT, Salmi JM, Aittokallio T, Westerholm J, Lahesmaa R, et al. 2003. Comparison of PDQuest and Progenesis software packages in the analysis of two-dimensional electrophoresis gels. *Proteomics* 3: 1936-1946.
- Rothe GM. 1994. *Electrophoresis of enzymes—laboratory methods*. Berlin: Springer.
- Sadygov RG, Cociorva D, Yates JR III. 2004. Large-scale database searching using tandem mass spectra: Looking up the answer in the back of the book. *Nat Methods* 1: 195-201.
- Sanchez JC, Appel RD, Golaz O, Pasquali C, Ravier F, et al. 1995. Inside SWISS-2DPAGE database. *Electrophoresis* 16: 1131-1151.
- Santoni V, Molloy M, Rabilloud T. 2000. Membrane proteins and proteomics: Un amour impossible? *Electrophoresis* 21: 1054-1070.

- Schägger H, Cramer WA, von Jagow G. 1994. Analysis of molecular masses and oligomeric states of protein complexes by blue native electrophoresis and isolation of membrane protein complexes by two-dimensional native electrophoresis. *Anal Biochem* 217: 220-230.
- Schägger H, von Jagow G. 1987. Tricine-sodium dodecyl sulfate-polyacrylamide gel electrophoresis for the separation of proteins in the range from 1 to 100 kDa. *Anal Biochem* 166: 368-379.
- Schägger H, von Jagow G. 1991. Blue native electrophoresis for isolation of membrane protein complexes in enzymatically active form. *Anal Biochem* 199: 223-231.
- Seillier-Moiseiwitsch F, Trost DC, Moiseiwitsch J. 2002. Statistical methods for proteomics. *Methods Mol Biol* 184: 51-80.
- Seow TK, Korke R, Liang RC, Ong SE, Ou K, et al. 2001. Proteomic investigation of metabolic shift in mammalian cell culture. *Biotechnol Prog* 17: 1137-1144.
- Shevchenko A, Wilm M, Vorm O, Mann M. 1996. Mass spectrometric sequencing of proteins silver-stained polyacrylamide gels. *Anal Chem* 68: 850-858.
- Shin JH, Gulesserian T, Weitzdoerfer R, Fountoulakis M, Lubec G. 2004a. Derangement of hypothetical proteins in fetal Down's syndrome brain. *Neurochem Res* 29: 1307-1316.
- Shin JH, Yang JW, Le Pecheur M, London J, Hoeger H, et al. Altered expression of hypothetical proteins in hippocampus of transgenic mice overexpressing human Cu/Zn-superoxide dismutase 1. *Proteome Sci* 2: 2.
- Sickmann A, Dormeyer W, Wortelkamp S, Woitalla D, Kuhn W, et al. 2000. Identification of proteins from human cerebrospinal fluid, separated by two-dimensional polyacrylamide gel electrophoresis. *Electrophoresis* 21: 2721-2728.
- Sickmann A, Dormeyer W, Wortelkamp S, Woitalla D, Kuhn W, et al. 2002. Towards a high resolution separation of human cerebrospinal fluid. *J Chromatogr B Analyt Technol Biomed Life Sci* 771: 167-196.
- Sirover MA. 1999. New insights into an old protein: The functional diversity of mammalian glyceraldehyde-3-phosphate dehydrogenase. *Biochim Biophys Acta* 1432: 159-184.
- Stoeckli M, Chaurand P, Hallahan DE, Caprioli RM. 2001. Imaging mass spectrometry: A new technology for the analysis of protein expression in mammalian tissues. *Nat Med* 7: 493-496.
- Taoka M, Wakamiya A, Nakayama H, Isobe T. 2000. Protein profiling of rat cerebella during development. *Electrophoresis* 21: 1872-1879.
- Tilleman K, Stevens I, Spittaels K, Haute CV, Clerens S, et al. 2002. Differential expression of brain proteins in glycogen synthase kinase-3 transgenic mice: A proteomics point of view. *Proteomics* 2: 94-104.
- Tsugita A, Kawakami T, Uchida T, Sakai T, Kamo M, et al. 2000. Proteome analysis of mouse brain: Two-dimensional electrophoresis profiles of tissue proteins during the course of aging. *Electrophoresis* 21: 1853-1871.
- Tsuji T, Shiozaki A, Kohno R, Yoshizato K, Shimohama S. 2002. Proteomic profiling and neurodegeneration in Alzheimer's disease. *Neurochem Res* 27: 1245-1253.
- Tyers M, Mann M. 2003. From genomics to proteomics. *Nature* 422: 193-197.
- Ünlü M. 1999. Difference gel electrophoresis. *Biochem Soc Trans* 27: 547-549.
- Ünlü M, Morgan ME, Minden JS. 1997. Difference gel electrophoresis: A single gel method for detecting changes in protein extracts. *Electrophoresis* 18: 2071-2077.
- Valle RP, Jendoubi M. 2003. Antibody-based technologies for target discovery. *Curr Opin Drug Discov Devel* 6: 197-203.
- Vilo J, Kapushesky M, Kemmeren P, Sarkans U, Brazma A. 2003. Expression profiler. The analysis of gene expression data: Methods and software. Parmigiani G, Garrett ES, Irizarry R, Zeger SL, editors. New York: Springer Verlag.
- Wallace DC. 1999. Mitochondrial diseases in man and mouse. *Science* 283: 1482-1488.
- Walsh MJ, Limos L, Tourtellotte WW. 1984. Two-dimensional electrophoresis of cerebrospinal fluid and ventricular fluid proteins, identification of enriched and unique proteins, and comparison with serum. *J Neurochem* 43: 1277-1285.
- Washburn MP, Wolters D, Yates JR III. 2001. Large-scale analysis of the yeast proteome by multidimensional protein identification technology. *Nat Biotechnol* 19: 242-247.
- Wasinger VC, Cordwell SJ, Cerpa-Poljak A, Yan JX, Gooley AA, et al. 1995. Progress with gene-product mapping of the Mollicutes: *Mycoplasma genitalium*. *Electrophoresis* 16: 1090-1094.
- Wenner BR, Lovell MA, Lynn BC. 2004. Proteomic analysis of human ventricular cerebrospinal fluid from neurologically normal, elderly subjects using two-dimensional LC-MS/MS. *J Proteome Res* 3: 97-103.
- Westermann B, Neupert W. 2003. 'Omics' of the mitochondrion. *Nat Biotechnol* 21: 239-240.
- Westermeier R. 2001. *Electrophoresis in practice. A guide to methods and applications of DNA and protein separations*, 3rd ed. Weinheim: Wiley-VCH.
- Wiederkehr F, Ogilvie A, Vonderschmitt DJ. 1985. Two-dimensional gel electrophoresis of cerebrospinal fluid proteins from patients with various neurological diseases. *Clin Chem* 31: 1537-1542.

- Wildenauer DB, Korschenhausen D, Hoechtlen W, Ackenheil M, Kehl M, et al. 1991. Analysis of cerebrospinal fluid from patients with psychiatric and neurological disorders by two-dimensional electrophoresis: Identification of disease-associated polypeptides as fibrin fragments. *Electrophoresis* 12: 487-492.
- Wilkins MR, Gasteiger E, Bairoch A, Sanchez JC, Williams KL, et al. 1999. Protein identification and analysis tools in the ExPASy server. *Methods Mol Biol* 112: 531-552.
- Wirth PJ, Romano A. 1995. Staining methods in gel electrophoresis, including the use of multiple detection methods. *J Chromatogr A* 698: 123-143.
- Yang JW, Czech T, Lubec G. 2004. Proteomic profiling of human hippocampus. *Electrophoresis* 25: 1169-1174.
- Young N, Chang Z, Wishart DS. 2004. GelScape: A Web-based server for interactively annotating, manipulating, comparing and archiving 1D and 2D gel images. *Bioinformatics* 20: 976-978.
- Yuan X, Russell T, Wood G, Desiderio DM. 2002. Analysis of the human lumbar cerebrospinal fluid proteome. *Electrophoresis* 23: 1185-1196.
- Zeeberg BR, Feng W, Wang G, Wang MD, Fojo AT, et al. 2003. GoMiner: A resource for biological interpretation of genomic and proteomic data. *Genome Biol* 4: R28.

7.2 Genetics and Gene Expression of Glycolysis

J. C. LaManna · P. Pichiule · J. C. Chavez

1	<i>Glycolysis</i>	772
1.1	Introduction	772
1.2	The Glycolytic Gene Set	773
1.3	Cellular Heterogeneity	774
1.3.1	Cell Types	774
1.3.2	The Lactate Shuttle Hypothesis	774
1.4	Brain Regional Heterogeneity	775
2	<i>Hypoxia</i>	775
2.1	Hypoxic Control of Glycolysis	775
2.2	Hypoxia-Inducible Factor	775
2.2.1	Molecular Mechanism of HIF-1 Activation During Hypoxia: Oxygen Sensing Mechanism ...	776
2.2.2	Regulation of Expression of Prolyl Hydroxylases	778
2.3	Physiologic Role of HIF-1 in the CNS	778
2.4	CNS Cell Types that Accumulate HIF-1	779
2.5	Alternative Mechanisms Stabilizing HIF-1 α Under Normoxic Conditions	779
2.5.1	DFO and CoCl ₂	780
2.5.2	Growth Factors and Cytokines	780
2.5.3	Pyruvate and Succinate	780
2.5.4	Nickel	780
2.5.5	The Role of Nitric Oxide	781
2.6	Coordinate Regulation of Glycolysis-Associated Genes	781
2.6.1	Glucose Transporters	781
2.6.2	Intracellular Acid-Base Balance	781
3	<i>Ischemia</i>	781
4	<i>Aging</i>	782
5	<i>Cancer</i>	782
6	<i>Summary and Conclusions</i>	783

Abstract: Control of the glycolytic pathway is crucial for the adaptation of the cellular and organismal energy-producing systems in development, plasticity, and environmental challenges. Lack of proper regulation of glycolysis may underlie the pathology of carcinogenesis and tumorigenesis as well as the decreased adaptability and plasticity in aging. Hypoxia-inducible factor-1 (HIF-1) is a ubiquitous transcription factor that responds to hypoxia and a variety of other energy-related molecules to coordinate the upregulation of the glycolytic enzymes and glucose transporters, thus specifying the glycolytic capacity of the cell.

1 Glycolysis

1.1 Introduction

Glycolysis is an ancient metabolic pathway, present in prokaryotes and arising initially in the absence of oxygen more than 3.5 billion years ago, which provides energy in the form of ATP by substrate-level phosphorylation. This term refers to the fact that some of the intermediates in the pathway are themselves phosphorylated. The reactions in this pathway can occur in solution, i.e., there is no requirement for compartmentation, and do not need extrinsic energy supplied by light or free oxygen, deriving the needed energy from redox reactions. Glycolysis (historically called the Embden–Meyerhof pathway), a simple kind of fermentation, specifically refers to the pathway from glucose to lactate. Some go so far as to include the step of glycogen breakdown, more properly “glycogenolysis” as part of glycolysis.

Glycolysis per se is not an oxygen-dependent metabolic pathway, and in that sense, “anaerobic glycolysis” is redundant and “aerobic glycolysis” a misnomer. However, because glycolysis is regulated basically by product inhibition, when pyruvate is consumed by respiration the glycolytic rate increases rapidly. Glycolysis produces energy in the absence of oxygen, but in the presence of oxygen provides substrate to mitochondria for the far more energy-efficient (by almost 20 times) oxidative phosphorylation. Since energy is the fundamental basis of life, it is not hard to understand that oxygen availability plays a major role in controlling glycolysis. In most cells, the rate of glycolytic flux is inversely proportional to the oxygen partial pressure and in the presence of oxygen glycolysis is slowed (the so-called Pasteur effect).

The transition to an oxidizing environment from a reducing environment, beginning about 2 million years ago, produced the evolution of mechanisms that allowed for rapid upregulation and downregulation of genes to maximize energy production. In the absence of oxygen, an upregulation of glycolytic enzymes is favorable to survival, and since this is a sequential pathway, there should be a signal that upregulates the appropriate genes together. Anaerobic to aerobic evolution required development of a system for coordinately and simultaneously regulating multiple unlinked genes.

Flux through glycolysis has been traditionally considered to be controlled by three regulatory components: hexokinase (HK), phosphofructokinase (PFK), and pyruvate kinase (PKM). The remaining enzymes are considered to be operating near equilibrium and limited by substrate availability. Nevertheless, this view must be overly simplistic because it has been shown that all of the genes for the glycolytic enzymes are upregulated by hypoxia, not just the key regulatory components. This “coordinate response” (Robin et al., 1984; Webster and Murphy, 1988; Webster, 2003) indicates that glycolytic regulation is not driven purely in response to substrate flux, but suggests that the glycolytic reactions participate in multiple cell functions. The nontranscriptional control of glycolysis is covered by Bolanos in *Chapter 34* of this volume, where the rapid and allosteric nontranscriptional control of glycolysis by nitric oxide (NO) through AMP-activated protein kinase (AMPK) is discussed (Almeida et al., 2004).

The genes that code the glycolytic enzymes are distributed without a discernible pattern among the different chromosomes but have a common promoter site called the hypoxic response element (HRE), which is activated by the transcription factor HIF-1. HIF-1 is found universally, responds rapidly, and activates many other genes besides the glycolytic enzymes. Although the enzymes work sequentially in concert, and so are regulated in concert, there are specific enzymes (like glyceraldehyde-3-phosphate dehydrogenase (GAPDH)) that have other functions, and so the expression of these genes may be finetuned by alternate signals. This system is characterized by rapid switching, suggesting that the speed of response must have conferred an evolutionary advantage.

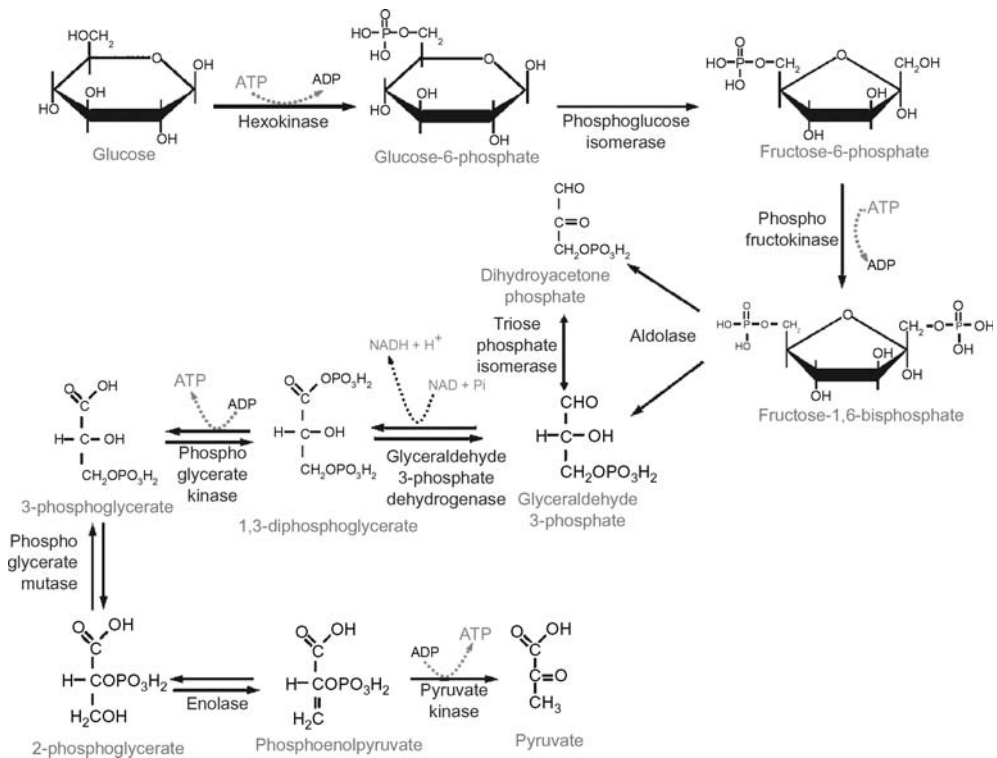
The glycolytic metabolic pathway is both ancient and pervasive, and thus it is not surprising that the component enzymes and control mechanisms are highly conserved across phyla and kingdoms. The cells of all higher organisms maintain the basic metabolic machinery for glycolysis as the substrate supply pathway for respiration.

1.2 The Glycolytic Gene Set

The glycolytic gene (Figure 7.2-1) set is defined as including 10 enzymes, or 12 when glycogen phosphorylase and lactate dehydrogenase (LDH) are included, that metabolize glucose (glycogen) to pyruvate (lactate): hexokinase (HK), phosphoglucose isomerase (PGI), phosphofructokinase (PFK), aldolase (ALD), triose phosphate isomerase (TPI), glyceraldehyde-3-phosphate dehydrogenase (GAPDH), phosphoglycerate kinase (PGK), phosphoglycerate mutase (PGM), enolase (ENO), and pyruvate kinase (PKM).

Figure 7.2-1

The glycolytic metabolic pathway from glucose to pyruvate including the enzymes at each step. The steps that use (hexokinase (HK) and phosphofructokinase (PFK)) or produce (phosphoglycerate kinase (PGK) and pyruvate kinase (PKM)) energy in the form of adenosine triphosphate (ATP) are indicated, as is the step that reduces NAD^+ (glyceraldehyde-3-phosphate dehydrogenase)



Two ATPs are used to reach fructose-1,6-bisphosphate from glucose; one at HK and the other at PFK. The action of ALD and TPI produces two molecules of glyceraldehyde-3-phosphate for each starting molecule of glucose. From there, four ATPs are produced from PGK and PK, for a net gain of two ATPs per glucose molecule along with two NADHs (from GAPDH).

1.3 Cellular Heterogeneity

1.3.1 Cell Types

The basic cell types of the brain can be roughly divided among neuronal, glial, and endothelial types. The cell types have radically different arrangements of their metabolic components, energy demands, and responses to natural and pathological challenges. Our understanding of these differences is rudimentary at best, and we have barely begun to scratch the surface regarding the differences among the various subtypes. The cellular heterogeneity makes studies of the glycolytic enzymes more difficult because most available quantitative techniques use homogeneous samples. Cellular studies of the glycolytic pathway *in vivo* require preservation of tissue structure, e.g., immunohistochemistry or *in situ* hybridization.

A simplified differential description of the basic metabolic property distinctions among neurons, glia, and endothelial cells can be ventured. Neurons may have most of the mitochondria, by a wide margin (Wong-Riley, 1989), and are, thus, thought to be highly oxidative and the site of oxygen consumption. Astroglia are known to be glycogen-laden (Phelps, 1972) and are presumed to be mostly glycolytic and the main site of glucose consumption. Endothelial cells have lower metabolic rates, but do contain mitochondria, and are presumed to generate energy primarily using the fatty acid metabolic substrate pathway (Betz and Goldstein, 1981). The picture that emerges is one of metabolic compartmentation. Endothelial cells make up a small fraction of the mass of the organ, but all substrates and oxygen must pass through them to reach the neuropil. The endothelial cell energy needs are provided by a fuel that is not used by the other cells, and thus, cannot interfere with their metabolism. Similarly, because of the structural plan of the neuropil, most of the glucose has to pass through the glial cells to reach the neurons. If the glial cell metabolic needs are met by glycogenolysis, then little or no oxygen is used, preserving the oxygen gradient to aid the supply of the oxidatively working neurons.

1.3.2 The Lactate Shuttle Hypothesis

Glycolysis has recently become the focus of intense interest because of the debate surrounding the lactate shuttle hypothesis (Magistretti et al., 1999). The implications of this hypothesis for glycolysis is that it defines specific energy metabolism patterns for neurons and glia. Glucose is purported to be taken up preferentially by astrocytes and metabolized to lactate, which then enters neurons where it is metabolized oxidatively to provide energy for neuronal activity. Transport of glucose and lactate occurs through carrier-mediated, facilitated diffusion. The necessary transporters, primarily the glucose transporter 1 (GLUT-1) and the monocarboxylate transporter 1 (MCT1), are apparently present at the appropriate membranes.

The experimental direction for examining this hypothesis has concentrated almost completely on the glutamate–glutamine mechanisms, but the glycolytic mechanisms that are involved also have significant experimental support (LaManna, 1996). For example, during neuronal activation, the fluxes of Na^+ and K^+ are also accompanied by an influx of H^+ ions into neurons, acidifying the neuronal intracellular compartment, and alkalinizing the extracellular space (Urbanics et al., 1978). This initial extracellular alkalinization is neutralized by proton efflux from astrocytes, which effectively alkalinizes the astrocyte intracellular compartment (Kraig et al., 1983; Chesler, 1990). The alkalinization of the astrocyte pH can activate PFK and, therefore, glycolysis (Hochachka and Mommsen, 1983), with the substrate primarily derived from glycogen breakdown (Swanson, 1992; Swanson et al., 1992). The astrocyte would then produce more pyruvate and lactate than needed for its own metabolic demands and the excess can be taken up by neurons through monocarboxylic acid transporter mechanisms (Assaf et al., 1990) and made available for the neuronal mitochondria (Dringen et al., 1993). Significantly, however, this hypothesis does not fully explain all the pertinent data and more developmental work needs to be done (Dienel and Cruz, 2003, 2004).

The compartmental separation of glycolysis and oxidative phosphorylation suggests that the *in vivo* responses to oxidative stress and environmental challenges may be very different in the different cell types; indeed, gene regulation may be in opposite directions in glia compared with that in neurons.

1.4 Brain Regional Heterogeneity

The brain is a metabolically heterogeneous organ. In addition to the cell type metabolic differences, there are regional differences in enzyme patterns and metabolism (Borowsky and Collins, 1989), perhaps most easily delineated in the differences in regional capillary density. These differences derive from the differences in neuronal firing patterns and structural organization of the region. In general, the capillary densities and metabolic rates are dependent on the patterns of neuronal activity, and there are signaling molecules to regulate the genes responsible for maintaining these dependencies.

2 Hypoxia

2.1 Hypoxic Control of Glycolysis

Glycolysis is positively regulated by hypoxia, and a full discussion of the acute and chronic mechanisms and consequences has recently appeared (Hochachka and Lutz, 2001). In vivo experiments in rats have shown that chronic exposure to mild hypoxia for 3 weeks was associated with an increase of 10–40% in cerebral metabolic rates for glucose (Harik et al., 1995). An overall increase in glycolysis was indicated based on a 50% increase in tissue glucose content, a 150% increase in tissue lactate, and a 25% decrease in tissue glycogen, reported in the same study, and consistent with previous reports (Musch et al., 1983). The increased glycolysis occurred in association with decreased oxidative metabolic capacity as indicated by decreased cytochrome oxidase activity (Chávez et al., 1995; LaManna et al., 1996) and decreased neuronal mitochondrial density (Stewart et al., 1997). Indeed, there is known to be a hypoxia-induced coordinate decrease in oxidative enzymes (Murphy et al., 1984).

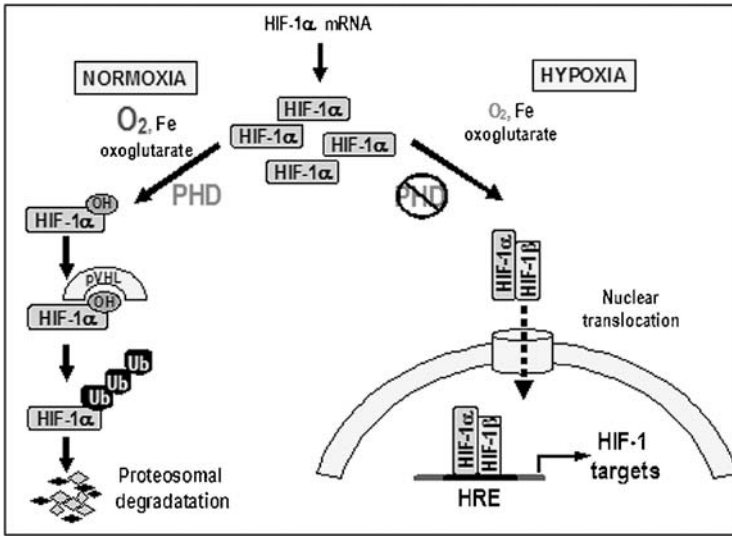
Under these hypoxic conditions, brain oxygen delivery is maintained through systemic and central adaptations. Systemically, the primary adaptations are increased ventilatory rate and packed red cell volume, while the main central adaptations are decreased consumption and increased capillary density (LaManna et al., 1992; Dunn et al., 2000). The coordination of these events implies the existence of a hypoxia-driven signaling system for upregulating the appropriate genes.

2.2 Hypoxia-Inducible Factor

The signal molecule responsible for gene upregulation in the brain in response to continued hypoxia is the hypoxia-inducible factor (HIF) (LaManna et al., 2004; Sharp and Bernaudin, 2004), as has been described for most cells in general (Bunn and Poyton, 1996). HIF (Figure 7.2-2) is a heterodimer formed by two subunits that belong to the PAS (Per, Arnt, Sim) family of basic helix–loop–helix (bHLH) transcription factors; these subunits are designated HIF- α and HIF- β (Wang and Semenza, 1995). The expression of the HIF-1 α subunits is regulated by oxygen levels (Wang et al., 1995), whereas the HIF-1 β subunits, also known as arylhydrocarbon receptor nuclear translocator (ARNT), are constitutive nuclear proteins that dimerize with other bHLH-PAS transcription factors (Wang and Semenza, 1995; Wang et al., 1995; Semenza et al., 1997; Semenza, 1998). Currently, three HIF- α subunits (HIF-1 α , HIF-2 α /EPAS1, and HIF-3 α) as well as three HIF- β subunits (HIF-1 β /ARNT1, ARNT2, and ARNT3) are known (Semenza, 1999; Talks et al., 2000). The most widely expressed α subunit in mammalian tissues is HIF-1 α ; indeed, most of our knowledge about HIF comes from studies of the mechanism regulating the expression of HIF-1 α protein and the transcriptional activity of the HIF-1 complex (HIF-1 α /HIF-1 β heterodimer). The other HIF- α subunits are regulated by a similar mechanism although they appear to have more specialized and tissue-specific functions (Semenza, 1999; Hu et al., 2003). During normoxia, the HIF-1 α protein is constitutively expressed, but it is rapidly destroyed by the ubiquitin-proteasome system, such that almost no HIF-1 α protein accumulates (Salceda and Caro, 1997; Huang et al., 1998). Under hypoxic conditions, degradation of the HIF-1 α subunit is prevented, allowing HIF-1 α to accumulate within the nucleus where it dimerizes with HIF-1 β , forming the HIF-1 transcriptional complex (Salceda and Caro, 1997; Jewell et al., 2001). HIF-1 binds to a consensus DNA sequence A/(G)CGTG within the HREs of numerous hypoxic responsive target

Figure 7.2-2

This scheme illustrates the normoxic and hypoxic HIF-1 signaling pathways leading either to proteosomal degradation or to nuclear translocation of the dimeric transcription factor



genes that include EPO, glycolytic enzymes, angiogenic factors, and glucose transporters, among others (Wang and Semenza, 1993, 1995; Wang et al., 1995; Semenza, 1999).

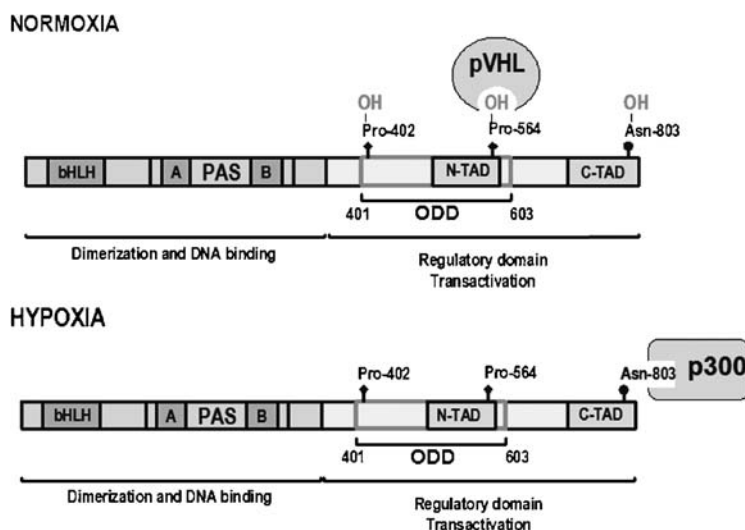
At least nine of the glycolytic enzyme genes induced by hypoxia in mammalian cells have HREs and are upregulated by HIF-1 (Webster, 2003): ALDA (Semenza et al., 1994), TPI (Seagroves et al., 2001; Gess et al., 2004), GAPDH (Graven et al., 1999; Salnikow et al., 2000; Seagroves et al., 2001), PGK1 (Firth et al., 1994; Seagroves et al., 2001), PKM (Semenza et al., 1994), PGI (Yoon et al., 2001), HK (Iyer et al., 1998), PFK (Minchenko et al., 2002), and LDHA (Firth et al., 1994, 1995; Semenza et al., 1994). The glycolytic enzymes, in contrast, are apparently not sensitive to HIF-2 α (Hu et al., 2003).

2.2.1 Molecular Mechanism of HIF-1 Activation During Hypoxia: Oxygen Sensing Mechanism

Regulation of HIF by O₂ is mediated by two distinct pathways that involve enzymatic *trans*-4-hydroxylation of two proline residues and the β -hydroxylation of an asparagine residue in the HIF- α subunits. Prolyl hydroxylation of the HIF- α subunit is carried out by an enzyme encoded by the egg-laying abnormal-9 (*Egl-9*) gene in *Caenorhabditis elegans* and *Drosophila melanogaster*. The mammalian homologs are named egg-laying nine-1 (EGLN1), EGLN2, and EGLN3 (Taylor, 2001), also called prolyl hydroxylase domain-containing proteins PHD2, PHD1, and PHD3, respectively (Epstein et al., 2001); or HIF prolyl hydroxylase HPH2, HPH3, and HPH1, respectively (Bruick and McKnight, 2001). A full exegesis of the terminology and the linkage to SM-20 has been provided by Freeman et al. (2003). Degradation of HIF- α under normoxic conditions is triggered by the posttranslational hydroxylation of the conserved proline residues, Pro-402 and Pro-564, within a region of the HIF- α protein known as the oxygen-dependent degradation (ODD) domain (Figure 7.2-3). The hydroxylated proline residues in this domain are recognized by the product of the von Hippel-Lindau tumor suppressor gene (pVHL), which acts as the recognition component of a multiprotein ubiquitin E3 ligase complex, thus targeting HIF- α to ubiquitin-mediated proteolysis in the proteasome (Maxwell et al., 1999; Ohh et al., 2000; Ivan et al., 2001; Jaakkola et al., 2001; Masson et al., 2001). This regulatory posttranslational modification is inherently oxygen-dependent, since the hydroxyl

■ Figure 7.2-3

This schematic showing the domains of the HIF-1 α transcription shows the effect of hydroxylation under normoxic conditions to provide binding sites for the von Hippel-Lindau protein (pVHL) in the oxygen-dependent degradation domain (ODD) and to block binding of p300



group is derived from molecular oxygen (Bruick and McKnight, 2001; Epstein et al., 2001; Ivan et al., 2001). The prolyl hydroxylation also requires the cofactors 2-oxoglutarate, vitamin C, and iron (II). The requirement of iron explains the hypoxic-mimetic effects of iron chelators (such as deferoxamine mesylate (DFO)) and iron antagonists (such as cobalt chloride (CoCl₂)). Under low O₂ conditions, or in the presence of iron chelators, HIF- α is not hydroxylated by PHDs and therefore HIF- α is neither recognized by pVHL nor targeted for degradation by the proteasome (Figure 7.2-2). As a result, HIF- α accumulates in the nucleus and is available to dimerize with HIF- β subunits to form the active HIF complex that activates transcription of target genes including EPO.

Hypoxia affects not only HIF- α protein stability but also the transcriptional activity of the HIF complex (Jiang et al., 1997; Pugh et al., 1997; Bruick and McKnight, 2001). The three α subunits contain two transactivation domains (TAD) that interact with transcriptional coactivators essential for gene expression (Figure 7.2-3). The amino-terminal TAD (N-TAD, aa 531–575) overlaps with the ODD domain (aa 401–603). The carboxy-terminal TAD (C-TAD, aa 786–826) is independent of the ODD domain and is able to recruit coactivators such as p300/CBP under hypoxic conditions only (Ema et al., 1999; Gu et al., 2001; Semenza, 2002). The regulation of this C-TAD involves an oxygen-dependent hydroxylation of a conserved asparagine residue (Asn-803 in HIF-1 α and Asn-851 in HIF-2 α). This hydroxylation is catalyzed by a novel asparaginyl hydroxylase that was described previously as a factor inhibiting HIF-1 (FIH-1). This asparaginyl hydroxylase is also a member of the 2-oxoglutarate- and iron-dependent dioxygenase superfamily; hence it is inhibited by hypoxia (Mahon et al., 2001; Lando et al., 2002). When the asparagine residue is hydroxylated, the C-TAD cannot interact with the transcriptional coactivator p300/CBP and the HIF-1 transcriptional activity is reduced.

Histone acetylation state is also a factor that affects HIF-1 transcriptional activity. In addition to promoting ubiquitination and degradation of HIF-1 α , VHL forms a ternary complex with HIF-1 α and the corepressor FIH-1. Both VHL and FIH-1 recruit histone deacetylases that may contribute to the loss of HIF-1 transcriptional activity under nonhypoxic conditions (Mahon et al., 2001).

In addition to hydroxylation, a new posttranslational modification of the HIF-1 α subunit has been described, where a novel HIF-1 α protein acetyl transferase called ARD1 was shown to acetylate the lysine 532 residue of HIF-1 α . This acetylation enhances the interaction of HIF-1 α with VHL, thereby augmenting

the subsequent HIF-1 α ubiquitination and proteosomal degradation. Moreover, this study showed that the expression of ARD1 is reduced by hypoxia, consistent with the accumulation of HIF-1 α during low oxygen conditions (Jeong et al., 2002). Collectively, these findings demonstrate that during hypoxia, HIF-1 is regulated by a carefully controlled signal transduction pathway in which a group of hydroxylases act as putative oxygen sensors by way of their requirement of oxygen for activity. These hydroxylases catalyze unique oxygen-dependent posttranslational modifications of the HIF-1 α subunit that control its degradation and regulate HIF transcriptional activity.

The brain expresses PHD1 at about the same levels as other major organs such as heart, liver, kidney, and skeletal muscle (Freeman et al., 2003). There is also significant expression of PHD3, which exhibits some regional specificity in that cerebral cortical structures appear to express the gene more strongly than spinal cord, cerebellum, or white matter (Freeman et al., 2003).

2.2.2 Regulation of Expression of Prolyl Hydroxylases

Little is known about the expression and functions of HIF-1 prolyl hydroxylases in the CNS. However, the regulation of HIF by the PHDs known to date, PHD1, PHD2, and PHD3, has been studied *in vitro* (in chemical assays) and in the context of a variety of nonneural cell types (Freeman et al., 2003). All three of the PHD isoforms hydroxylate HIF- α peptides *in vitro* (Bruick and McKnight, 2001; Epstein et al., 2001) and contribute to the regulation of HIF in a variety of cell contexts (Hirsila et al., 2003; Appelhoff et al., 2004). Furthermore, when overexpressed in cells, all three PHDs can suppress HRE-mediated reporter gene activity (Huang et al., 2002; Metzen et al., 2003). Despite the distinct intracellular localization patterns of exogenous PHDs, PHD1 is exclusively nuclear, PHD2, mainly cytoplasmic, and PHD3, both cytoplasmic and nuclear, and each of the PHDs can regulate nuclear HIF-1 α during hypoxia (Metzen et al., 2003). Metzen et al. also showed that endogenous PHD2 mRNA and PHD3 mRNA are hypoxia-induced. However, during normoxia, a dominant role for endogenous PHD2 has been demonstrated in a variety of nonneural cell lines (Berra et al., 2003). Furthermore, PHD2 has a greater influence on HIF-1 α than on HIF-2 α ; whereas for PHD3, the opposite pattern emerges (Appelhoff et al., 2004). Admittedly, variations in expression levels of endogenous PHD isoforms appear to be cell type- and culture condition-dependent, warranting investigation of PHDs in neural cell types. To further understand HIF regulation of EPO in the brain, study of these critical HIF regulators, i.e., the PHDs, in a neural cell context is essential. These observations suggest that a novel feedback mechanism for adjusting hypoxia-induced gene expression exist that involves regulation of PHD expression.

In a recent study, Nakayama et al. (2004) had identified a novel mechanism that regulates the availability of PHD1 and PHD3 and consequently affects the abundance of HIF-1 α . This study showed that PHD1 and PHD3 protein levels are regulated by members of the E3 ubiquitin ligase family, Siah2 and Siah1a. These E3 ligases mediate the ubiquitination and the proteasome-dependent degradation of PHD1/3 during hypoxia. Generally, PHD activity is diminished during hypoxia, although even at low oxygen concentrations residual PHD activity may persist. To overcome this residual activity, an additional mechanism of PHD regulation at the protein level is required during hypoxia to facilitate HIF-1 activation and upregulation of hypoxia-responsive genes including EPO (Simon, 2004). Regulation of PHD availability is therefore another step in the complex pathway that regulates HIF activation.

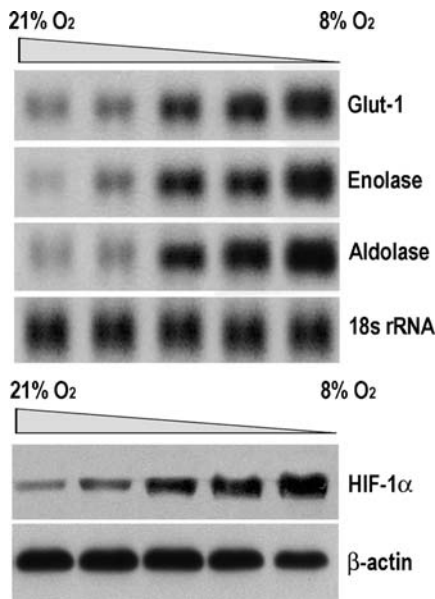
2.3 Physiologic Role of HIF-1 in the CNS

HIF-1 has a critical physiological role in the CNS. HIF-1 is absolutely required for normal development. Mouse embryos that lack HIF-1 α die at midgestation, with multiple cardiovascular defects and mesenchymal cell death (Yu et al., 1999). Also, HIF-1 α is necessary for the normal development of the brain. In a mouse model of neural cell-specific HIF-1 α deficiency, animals were viable and reached adulthood; however, they developed hydrocephalus and showed a marked reduction in brain mass (Tomita et al., 2003). In the adult brain, HIF-1 α is expressed constitutively (Stroka et al., 2001) and is further induced by hypoxia in neurons, astrocytes, ependymal cells, and possibly endothelial cells (Chávez et al., 2000). Whether HIF-1 is activated in microglia and oligodendrocytes is not known. In contrast, HIF-2 α seems

to be induced preferentially in glia and endothelial cells, but not in neurons (Wiesener et al., 2003). A recent study suggests that expression of HIF-1 α and HIF-2 α results in the induction of different HIF target genes. In particular, the expression of EPO seems to depend primarily on HIF-2 α activation (Ralph et al., 2004). In the brains of rodents exposed to hypoxia, HIF-1 α accumulation correlates with the upregulation of HIF-regulated genes that include glucose transporters (GLUT-1), glycolytic enzymes, proangiogenic factors (VEGF and Flt-1), and EPO (Bergeron et al., 1999; Chávez et al., 2000) (Figure 7.2-4). Similarly, in a

Figure 7.2-4

The upper portion demonstrates the hypoxic upregulation of the genes for the glucose transporter (GLUT-1) and the glycolytic enzymes enolase (ENO) and aldolase (ALD). The lower portion shows the accumulation of HIF-1 α protein as a function of decreasing inspired oxygen



variety of cerebral ischemia models, EPO is upregulated at the mRNA level (Bergeron et al., 1999, 2000; Sharp et al., 2001; Sharp and Bernaudin, 2004). Taken together, the in vivo and in vitro data implicate HIF as a critical mediator of EPO expression in the CNS.

2.4 CNS Cell Types that Accumulate HIF-1

In response to hypoxia, all nonaltered cells and tissues respond with an increased accumulation of HIF-1. The CNS is no different. In response to hypoxic exposure in vivo, neurons, glia, capillary endothelial cells, and ependymal cells of the choroid plexus respond with an accumulation of HIF-1 (Chávez et al., 2000). This response can be detected with an FiO₂ of 0.14 or lower (Chavez and LaManna, 2002). During postischemic reperfusion, however, the response is limited to neurons and endothelial cells (Chavez and LaManna, 2002).

2.5 Alternative Mechanisms Stabilizing HIF-1 α Under Normoxic Conditions

Although hypoxia could be considered the primary stimulator of HIF-1 accumulation, it is not the only one. Other causes of HIF-1 accumulation include growth factors, multivalent metals, NO, oxygen radicals, and cytokines.

2.5.1 DFO and CoCl₂

As noted above, DFO and CoCl₂ are classic pharmacological agents that mimic some cellular hypoxic responses, including activation of HIF-1. Numerous studies have shown that a variety of iron chelators including mimosine and DFO are potent activators of HIF, since PHD activity requires iron (Ivan et al., 2002; Warnecke et al., 2003). In addition, the divalent transition metal Cobalt (Co²⁺) has been shown to induce HIF-1 α protein accumulation under normoxic conditions. Although it was initially proposed that Co²⁺ acts by displacing iron, a recent report demonstrated that Co²⁺ induces HIF-1 α protein accumulation by disrupting the interaction between hydroxylated HIF-1 α and VHL, consequently preventing HIF-1 α ubiquitination and proteosomal degradation (Yuan et al., 2003). Both DFO and CoCl₂ have been used successfully to activate HIF and the expression of HIF target genes in neonatal rat brains and adult mouse and rat brains (Bergeron et al., 2000) and were effective in reducing brain injury associated with ischemia in different animal models (Bergeron et al., 2000).

2.5.2 Growth Factors and Cytokines

HIF-1 α protein expression, HIF-1 DNA-binding activity, and HIF-1 target gene expression under non-hypoxic conditions are induced also by a variety of growth factors and cytokines, including epidermal growth factor (EGF), fibroblast growth factor-2 (FGF-2), insulin, insulin-like growth factor-1 and -2 (IGF-1, IGF-2), tumor necrosis factor- α (TNF α), interleukin-1 β , and angiotensin II (Zelzer et al., 1998; Richard et al., 2000; Semenza, 2000a, b; Semenza et al., 2000; Zhong et al., 2000; Fukuda et al., 2002; Treins et al., 2002). These growth factors and cytokines bind their cognate receptor tyrosine kinases and activate a variety of signaling pathways, including the phosphatidylinositol-3-kinase (PI3K), the serine–threonine protein kinase Akt (protein kinase B), the mammalian target of rapamycin (mTOR, also known as FRAP), and the ERK/MAPK pathways (Semenza, 2000b, 2003). Many of these pathways have been implicated in the growth factor-mediated activation of HIF-1 in a variety of cell lines.

In the CNS, IGF-1 is so far the only growth factor that has been shown to activate the HIF pathway. Interestingly, IGF-1, IGF-2, and insulin can stimulate erythropoietin production in primary cultured astrocytes (Masuda et al., 1997). In a model of global cerebral ischemia in rats, IGF-1 mediates, in part, the activation of HIF-1 independently of hypoxia. Moreover, exogenous systemic or intracerebroventricular infusion of IGF causes HIF-1 α accumulation and expression of HIF-1 target genes, including EPO (Chavez and LaManna, 2002). In a recent study, Lopez-Lopez et al. showed that IGF-1 induces the growth of cultured brain endothelial cells through activation of HIF and its target gene, VEGF. This study also showed that systemic injection of IGF-1 in adult mice increases brain vessel density (Lopez-Lopez et al., 2004). Taken together, these data support the role of IGF-1 as an important regulator of HIF activation in the adult CNS.

2.5.3 Pyruvate and Succinate

Both pyruvate and oxaloacetate (Lu et al., 2002; Dalgard et al., 2004) cause accumulation of HIF-1 under normoxic conditions. This suggests that glycolytic and tricarboxylic intermediates can feed back on the HIF-1 metabolic pathway. Succinate can also do so directly (Selak et al., 2005) through inhibition of PHD and indirectly through the electron transport chain (Agani et al., 2000).

2.5.4 Nickel

Nickel ion and carcinogenic nickel compounds cause accumulation of HIF-1 even in the presence of oxygen (Salnikow et al., 1999, 2000). Nickel-stimulated gene expression was similar to hypoxia-induced gene expression and suggests that the carcinogenic nature of the nickel compounds is closely related to activating the oxygen stress pathway.

2.5.5 The Role of Nitric Oxide

The role of NO is still somewhat controversial. Nevertheless, there appears to be a concentration-dependent effect of NO on HIF-1 accumulation. NO prevented hypoxic accumulation of HIF-1, but this inhibition could be blocked with antioxidants or succinate (Agani et al., 2002). Higher concentrations of NO lead directly to HIF-1 stabilization, independent of oxygen levels or mitochondrial state (Mateo et al., 2003). The inhibition of HIF-1 stabilization by NO at low O₂ levels was suggested to be due to the inhibition of mitochondrial metabolism by NO binding to cytochrome *c* oxidase (Brown and Cooper, 1994; Brown, 1999) and with the subsequent decrease in oxygen consumption being responsible for a rise in intracellular oxygen that supported PHD activity and destabilized HIF-1 (Hagen et al., 2003).

2.6 Coordinate Regulation of Glycolysis-Associated Genes

2.6.1 Glucose Transporters

The hypoxia-driven upregulation of glycolysis appears to be associated with upregulation of the glucose transporter (GLUT-1) at the blood–brain barrier (BBB) (Harik et al., 1994, 1996). The increase in GLUT-1 at the BBB had two components: an increase in the density of transporters per unit capillary and an increase in the capillary density. The combination resulted in a doubling of the glucose influx in hypoxic brain tissue. The *in vivo* results were prefigured by *in vitro* data demonstrating that GLUT-1 mRNA and protein was induced by hypoxia in endothelial cells (Loike et al., 1992). The GLUT-1 transporter gene has an HRE and is responsive to HIF-1 (Ebert et al., 1995; Semenza, 2000a).

A similar effect can be seen for the major cellular glucose transporter in the brain, GLUT-3, which is also HIF-1 sensitive (Semenza, 2000a). The regulation of GLUT-3 by NO (Cidad et al., 2004) is covered in the *Chapter* by Bolanos in this volume. Here also, it appears that increased capacity for glucose flux into and out of the tissue is coordinately regulated by HIF-1.

2.6.2 Intracellular Acid–Base Balance

At first glance, the increased glycolysis in chronic hypoxia is puzzling. The rather small increases in flux cannot be efficiently replacing ATP production from oxidative metabolism, even when tissue oxygen levels are reduced (which they are not, due to angiogenesis and increased hematocrit). Therefore, there must be some other function driving the response. One possibility is that these adaptations represent a small, but important, shift in the ratio of ATP produced by glycolysis to that produced by oxidative phosphorylation. Under steady-state conditions, the proton consumed during ATP production from oxidative phosphorylation is balanced when that ATP is hydrolyzed by an ATPase. On the other hand, ATP produced in glycolysis is proton neutral until hydrolysis, which then produces net protons. Thus, an increase in the proportion of glycolytically produced ATP will acidify the tissue (Gevers, 1977; Dennis et al., 1991). During the adaptation to hypoxic exposure *in vivo*, the hypoxic ventilatory response results in decreased CO₂. This respiratory alkalosis is compensated for systemically by the excretion of plasma bicarbonate. In the CNS, the increased proton production balances the decrease in tissue CO₂ (Musch et al., 1983; Lauro and LaManna, 1997).

3 Ischemia

The primary initial effect of the loss of circulation is lack of oxygen, but ischemia, whether focal or global, reversible or irreversible, also presents a strong challenge for the cellular glycolytic system. The most obvious challenge comes from the cessation of glucose influx, but also significantly, from the accumulation of end products lactate and CO₂. In addition, ischemia results in changes in the intracellular and extracellular milieu, especially ion gradients and proton concentrations, and also includes changes in the activity

of numerous signaling molecules. Despite the fact that much of the changes that occur in glycolysis during and after ischemia have been documented, there is little insight in how to use this information to manipulate glycolytic pathways in order to ameliorate the effects of stroke and cardiac arrest and to determine the best conditions for neuroprotection and preconditioning. Most of the attention has been focused on PDH, the activity of which is clearly decreased following reperfusion after global ischemia (Martin et al., 2005).

HIF-1 accumulates during reversible focal (Bergeron et al., 1999) and reversible global ischemia (Chavez and LaManna, 2002). After resuscitation from cardiac arrest, HIF-1 remains elevated for about 1 week due to IGF-1 acting through its receptor (Chavez and LaManna, 2002). For the most part, the increase in HIF-1 is thought to be neuroprotective and elevations of HIF-1 are thought to be involved in the mechanism of preconditioning (Bergeron et al., 2000; Aminova et al., 2005), but this has not been universally supported (Helton et al., 2005).

4 Aging

Glycolysis and glycolytic flux appear to be stable during aging (Meier-Ruge et al., 1980; El-Hassan et al., 1981), but no one has yet studied whether the ability of the tissue to change enzyme levels in response to external challenges has been compromised in aging. Plasticity is impaired in aging (Riddle et al., 2003), and this may be partially related to deficiencies in the HIF-1 signaling system. Reduced HIF-1 activity has been shown to be responsible for the age-dependent defect in VEGF expression in vascular smooth muscle cells (Rivard et al., 2000).

The HIF-1 response to hypoxia, but not the response to DFO or CoCl₂, is severely attenuated in 24-month-old Fischer 344 rats (Chavez and LaManna, 2003). There also appears to be an attenuation in the capacity to form HIF-1/HRE complexes in old mice (Frenkel-Denkberg et al., 1999). It is currently unknown whether or not these are effects with a gradual or precipitous onset. The attenuated hypoxic response may be a major contributor to the increasing sensitivity to hypoxia and ischemia with age (LaManna et al., 2004).

Decreased HIF-1 function could result in decreased glycolytic enzyme levels in stressed tissue regions. Decreased glucose metabolism might lead to Tau hyperphosphorylation due to hypothermia, with significant implications for Alzheimer's disease (Planel et al., 2004). In addition, it has been shown that upregulation of glycolytic flux through HIF-1 activation is responsible for resistance to A β toxicity in primary cultures of cortical neurons (Soucek et al., 2003).

5 Cancer

A number of intriguing observations have implicated hypoxic activation of HIF-1 and accelerated glycolysis to carcinogenesis (Lu et al., 2002). Increased glycolytic activity is commonly a hallmark of primary and metastatic cancers (Gatenby and Gillies, 2004); although the molecular basis of this phenomenon and its role in carcinogenesis is controversial (Elstrom et al., 2004; Gatenby and Gillies, 2004; Thompson and Thompson, 2004). In the 1950s, Warburg reported that some cancer cells exhibit increased glycolysis despite the presence of oxygen and depend largely on this pathway for generation of ATP (Warburg, 1956); this phenomenon, i.e., the presence of aerobic glycolysis in tumors, has been dubbed the "Warburg effect" (Racker, 1972; Racker and Spector, 1981). In recent years, the imaging technique, positron emission tomography, using the glucose analog [18]fluorodeoxyglucose has consistently shown that most human cancers have significantly increased glucose uptake, which may be related to increased glycolytic flux (Czernin and Phelps, 2002). Accordingly, genes of the glycolysis pathway have been found to be overexpressed in a variety of cancers (Osthus et al., 2000). In fact, most tumor-derived cell lines also display increased glycolytic flux.

The molecular mechanism leading to upregulation of glycolysis in cancer is not well defined, and some investigators have even suggested that there is no reason to suspect that cancer cells have an abnormal glycolytic control system, but more likely are acting in response to their external milieu (Zu and Guppy,

2004). It has been proposed that the glycolytic phenotype initially arises as a response to the local hypoxic environment in premalignant lesions; in this scenario, increased expression of glycolytic enzymes is likely regulated by HIF-1 (Gatenby and Gillies, 2004). Whichever of these contrasting viewpoints is more descriptive of the actual situation, there still remains the observation that HIF-1 α is overexpressed in a wide variety of cancers (Zhong et al., 1999). That HIF-1 may play a major role in tumorigenesis is further supported by the hemangioblastomas in the CNS and retina found in von Hippel–Lindau disease, where a defect in pVHL leads to the accumulation of HIF-1 (Kaelin, 2002). Increased glycolysis leads to proton production that will require further adaptation to overcome acid-related toxicity. In this context, as carcinogenesis proceeds, selection pressures lead to proliferation of cell populations that have constitutive upregulation of glycolysis and tolerance to an acidic environment, features that presumably facilitate proliferation and invasion (Gatenby and Gillies, 2004; Brahimi-Horn and Pouyssegur, 2005).

Enhancement of glycolytic capacity confers an advantage beyond just that of anaerobic energy production. Glycolytic intermediates are involved in numerous side reactions important to cell homeostasis. For example, it has been proposed that one outcome of HIF-1-induced upregulation of glycolysis is to restore the adenosine pool, which has been found to be depleted in tumors deficient in HIF-1 β (Griffiths et al., 2002; Griffiths and Stubbs, 2003; Stubbs et al., 2003).

Tumor-associated increases in glycolysis are not exclusively regulated by HIF-1. In this regard, it has been reported that activation of Akt can stimulate glycolysis in transformed cultured cells (Xu et al., 2005). Similarly, the transcription factor c-Myc can regulate the expression of GLUT-1 and several glycolytic genes in several cancer cell lines (Osthus et al., 2000; Altenberg and Greulich, 2004). Although both HIF-1 and c-Myc upregulate GLUT-1 and glycolytic enzyme genes, the groups of upregulated genes are not identical.

6 Summary and Conclusions

HIF-1 controls the switch to glycolysis in the Pasteur effect (Seagroves et al., 2001). Oxidative stress and other stimuli that lead to increased glycolytic rates will lead to a unifying signal, coordinated through HIF-1, to upregulate glycolytic enzymes and a host of other molecules that contribute to the generation of increased glycolytic capacity in the brain.

Genetic control of glycolysis is an ancient pathway of adaptation to environmental stress. The primary control mechanism appears to be through HIF-1, thus the primary triggering variable is hypoxia, and HIF-1 is part of a tissue oxygen-sensing system. HIF-1 response allows normal development and adaptation to physiological stresses such as the chronic mild hypoxia of altitude adaptation, where the other major physiological process, HIF-1-dependent angiogenesis, also participates.

Certain pathological stimuli including ischemia also activate the HIF-1 system, presumably as an ameliorating process, but not always successfully. When there is an attenuation of the response or a more complete failure of the system, there is a significantly decreased chance for survival.

In the future, it may be possible to exploit the HIF-1 signaling system to prevent the fallout of physiological adaptation and to precondition or neuroprotect the brain from ischemic insults.

References

- Agani FH, Pichiule P, Chávez JC, La Manna J. 2000. The role of mitochondria in the regulation of hypoxia-inducible factor 1 expression during hypoxia. *J Biol Chem* 275: 35863-35867.
- Agani FH, Puchowicz MA, Chavez JC, Pichiule P, La Manna J. 2002. Role of nitric oxide in the regulation of HIF-1 α expression during hypoxia. *Am J Physiol* 283: C178-C186.
- Almeida A, Moncada S, Bolanos JP. 2004. Nitric oxide switches on glycolysis through the AMP protein kinase and 6-phosphofructo-2-kinase pathway. *Nat Cell Biol* 6: 45-51.
- Altenberg B, Greulich KO. 2004. Genes of glycolysis are ubiquitously overexpressed in 24 cancer classes. *Genomics* 84: 1014-1020.
- Aminova LR, Chavez JC, Lee J, Ryu H, Kung A, et al. 2005. Prosurvival and prodeath effects of hypoxia-inducible factor-1 α stabilization in a murine hippocampal cell line. *J Biol Chem* 280: 3996-4003.

- Appelhoff RJ, Tian YM, Raval RR, Turley H, Harris AL, et al. 2004. Differential function of the prolyl hydroxylases PHD1, PHD2, and PHD3 in the regulation of hypoxia-inducible factor. *J Biol Chem* 279: 38458-38465.
- Assaf HM, Ricci AJ, Whittingham TS, La Manna JC, Ratcheson RA, et al. 1990. Lactate compartmentation in hippocampal slices: Evidence for a transporter. *Metab Brain Dis* 5: 143-154.
- Bergeron M, Gidday JM, Yu AY, Semenza GL, Ferriero DM, et al. 2000. Role of hypoxia-inducible factor-1 in hypoxia-induced ischemic tolerance in neonatal rat brain. *Ann Neurol* 48: 285-296.
- Bergeron M, Yu AY, Solway KE, Semenza GL, Sharp FR. 1999. Induction of hypoxia-inducible factor-1 (HIF-1) and its target genes following focal ischaemia in rat brain. *Eur J Neurosci* 11: 4159-4170.
- Berra E, Benizri E, Ginouves A, Volmat V, Roux D, et al. 2003. HIF prolyl-hydroxylase 2 is the key oxygen sensor setting low steady-state levels of HIF-1 α in normoxia. *EMBO J* 22: 4082-4090.
- Betz AL, Goldstein GW. 1981. Developmental changes in metabolism and transport properties of capillaries isolated from rat brain. *J Physiol* 312: 365-376.
- Borowsky IW, Collins RC. 1989. Metabolic anatomy of brain: A comparison of regional capillary density, glucose metabolism, and enzyme activities. *J Comp Neurol* 288: 401-413.
- Brahimi-Horn MC, Pouyssegur J. 2005. The hypoxia-inducible factor and tumor progression along the angiogenic pathway. *Int Rev Cytol* 242: 157-213.
- Brown GC. 1999. Nitric oxide and mitochondrial respiration. *Biochim Biophys Acta* 1411: 351-369.
- Brown GC, Cooper CE. 1994. Nanomolar concentrations of nitric oxide reversibly inhibit synaptosomal respiration by competing with oxygen at cytochrome oxidase. *FEBS Lett* 356: 295-298.
- Bruick RK, McKnight SL. 2001. A conserved family of prolyl-4-hydroxylases that modify HIF. *Science* 294: 1337-1340.
- Bunn HF, Poyton RO. 1996. Oxygen sensing and molecular adaptation to hypoxia. *Physiol Rev* 76: 839-885.
- Chávez JC, Agani F, Pichiule P, La Manna JC. 2000. Expression of hypoxic inducible factor 1 α in the brain of rats during chronic hypoxia. *J Appl Physiol* 89: 1937-1942.
- Chavez JC, LaManna JC. 2002. Activation of hypoxia inducible factor-1 in the rat cerebral cortex after transient global ischemia: Potential role of insulin-like growth factor-1. *J Neurosci* 22: 8922-8931.
- Chavez JC, LaManna JC. 2003. Hypoxia-inducible factor-1 α accumulation in the rat brain in response to hypoxia and ischemia is attenuated during aging. *Adv Exp Med Biol* 510: 337-341.
- Chávez JC, Pichiule P, Boero J, Arregui A. 1995. Reduced mitochondrial respiration in mouse cerebral cortex during chronic hypoxia. *Neurosci Lett* 193: 169-172.
- Chesler M. 1990. The regulation and modulation of pH in the nervous system. *Prog Neurobiol* 34: 401-427.
- Cidad P, Almeida A, Bolanos JP. 2004. Inhibition of mitochondrial respiration by nitric oxide rapidly stimulates cytoprotective GLUT3-mediated glucose uptake through 5'-AMP-activated protein kinase. *Biochem J* 384: 629-636.
- Czernin J, Phelps ME. 2002. Positron emission tomography scanning: Current and future applications. *Annu Rev Med* 53: 89-112.
- Dalgard CL, Lu H, Mohyeldin A, Verma A. 2004. Endogenous 2-oxoacids differentially regulate expression of oxygen sensors. *Biochem J* 380: 419-424.
- Dennis SC, Gevers W, Opie LH. 1991. Protons in ischemia: Where do they come from; where do they go to? *J Mol Cell Cardiol* 23: 1077-1086.
- Dienel GA, Cruz NF. 2003. Neighborly interactions of metabolically-activated astrocytes in vivo. *Neurochem Int* 43: 339-354.
- Dienel GA, Cruz NF. 2004. Nutrition during brain activation: Does cell-to-cell lactate shuttling contribute significantly to sweet and sour food for thought? *Neurochem Int* 45: 321-351.
- Dringen R, Gebhardt R, Hamprecht B. 1993. Glycogen in astrocytes: Possible function as lactate supply for neighboring cells. *Brain Res* 623: 208-214.
- Dunn JF, Grinberg O, Roche M, Nwaigwe CI, Hou HG, et al. 2000. Noninvasive assessment of cerebral oxygenation during acclimation to hypobaric hypoxia. *J Cereb Blood Flow Metab* 20: 1632-1635.
- Ebert BL, Firth JD, Ratcliffe PJ. 1995. Hypoxia and mitochondrial inhibitors regulate expression of glucose transporter-1 via distinct *cis*-acting sequences. *J Biol Chem* 270: 29083-29089.
- El-Hassan A, Zubairu S, Hothersall JS, Greenbaum AL. 1981. Age-related changes in enzymes of rat brain. 1. Enzymes of glycolysis, the pentose phosphate pathway and lipogenesis. *Enzyme* 26: 107-112.
- Elstrom RL, Bauer DE, Buzzai M, Karnauskas R, Harris MH, et al. 2004. Akt stimulates aerobic glycolysis in cancer cells. *Cancer Res* 64: 3892-3899.
- Ema M, Hirota K, Mimura J, Abe H, Yodoi J, et al. 1999. Molecular mechanisms of transcription activation by HLF and HIF1 α in response to hypoxia: Their stabilization and redox signal-induced interaction with CBP/p300. *EMBO J* 18: 1905-1914.
- Epstein AC, Gleadle JM, McNeill LA, Hewitson KS, O'Rourke J, et al. 2001. *C. elegans* EGL-9 and mammalian homologs

- define a family of dioxygenases that regulate HIF by prolyl hydroxylation. *Cell* 107: 43-54.
- Firth JD, Ebert BL, Pugh CW, Ratcliffe PJ. 1994. Oxygen-related control elements in the phosphoglycerate kinase 1 and lactate dehydrogenase A genes: Similarities with the erythropoietin 3' enhancer. *Proc Natl Acad Sci USA* 91: 6496-6500.
- Firth JD, Ebert BL, Ratcliffe PJ. 1995. Hypoxic regulation of lactate dehydrogenase A. *J Biol Chem* 270: 21021-21027.
- Freeman RS, Hasbani DM, Lipscomb EA, Straub JA, Xie L. 2003. SM-20, EGL-9, and the EGLN family of hypoxia-inducible factor prolyl hydroxylases. *Mol Cells* 16: 1-12.
- Frenkel-Denkberg G, Gershon D, Levy AP. 1999. The function of hypoxia-inducible factor 1 (HIF-1) is impaired in senescent mice. *FEBS Lett* 462: 341-344.
- Fukuda R, Hirota K, Fan F, Jung YD, Ellis LM, et al. 2002. Insulin-like growth factor 1 induces hypoxia-inducible factor 1-mediated vascular endothelial growth factor expression, which is dependent on MAP kinase and phosphatidylinositol 3-kinase signaling in colon cancer cells. *J Biol Chem* 277: 38205-38211.
- Gatenby RA, Gillies RJ. 2004. Why do cancers have high aerobic glycolysis? *Nat Rev Cancer* 4: 891-899.
- Gess B, Hofbauer KH, Deutzmann R, Kurtz A. 2004. Hypoxia up-regulates triosephosphate isomerase expression via a HIF-dependent pathway. *Pflugers Arch* 448: 175-180.
- Gevers W. 1977. Generation of protons by metabolic processes in heart cells. *J Mol Cell Cardiol* 9: 867-874.
- Graven KK, Yu Q, Pan D, Roncarati JS, Farber HW. 1999. Identification of an oxygen responsive enhancer element in the glyceraldehyde-3-phosphate dehydrogenase gene. *Biochim Biophys Acta* 1447: 208-218.
- Griffiths JR, McSheehy PM, Robinson SP, Troy H, Chung YL, et al. 2002. Metabolic changes detected by in vivo magnetic resonance studies of HEPA-1 wild-type tumors and tumors deficient in hypoxia-inducible factor-1beta (HIF-1beta): Evidence of an anabolic role for the HIF-1 pathway. *Cancer Res* 62: 688-695.
- Griffiths JR, Stubbs M. 2003. Opportunities for studying cancer by metabolomics: Preliminary observations on tumors deficient in hypoxia-inducible factor 1. *Adv Enzyme Regul* 43: 67-76.
- Gu J, Milligan J, Huang LE. 2001. Molecular mechanism of hypoxia-inducible factor 1alpha-p300 interaction. A leucine-rich interface regulated by a single cysteine. *J Biol Chem* 276: 3550-3554.
- Hagen T, Taylor CT, Lam F, Moncada S. 2003. Redistribution of intracellular oxygen in hypoxia by nitric oxide: Effect on HIF1alpha. *Science* 302: 1975-1978.
- Harik N, Harik SI, Kuo N-T, Sakai K, Przybylski RJ, et al. 1996. Time course and reversibility of the hypoxia-induced alterations in cerebral vascularity and cerebral capillary glucose transporter density. *Brain Res* 737: 335-338.
- Harik SI, Behmand RA, LaManna JC. 1994. Hypoxia increases glucose transport at blood-brain barrier in rats. *J Appl Physiol* 77: 896-901.
- Harik SI, Lust WD, Jones SC, Lauro KL, Pundik S, et al. 1995. Brain glucose metabolism in hypobaric hypoxia. *J Appl Physiol* 79: 136-140.
- Helton R, Cui J, Scheel JR, Ellison JA, Ames C, et al. 2005. Brain-specific knock-out of hypoxia-inducible factor-1alpha reduces rather than increases hypoxic-ischemic damage. *J Neurosci* 25: 4099-4107.
- Hirsila M, Koivunen P, Gunzler V, Kivirikko KI, Myllyharju J. 2003. Characterization of the human prolyl 4-hydroxylases that modify the hypoxia-inducible factor. *J Biol Chem* 278: 30772-30780.
- Hochachka PW, Lutz PL. 2001. Mechanism, origin, and evolution of anoxia tolerance in animals. *Comp Biochem Physiol B Biochem Mol Biol* 130: 435-459.
- Hochachka PW, Mommsen TP. 1983. Protons and anaerobiosis. *Science* 219: 1391-1397.
- Hu CJ, Wang LY, Chodosh LA, Keith B, Simon MC. 2003. Differential roles of hypoxia-inducible factor 1alpha (HIF-1alpha) and HIF-2alpha in hypoxic gene regulation. *Mol Cell Biol* 23: 9361-9374.
- Huang J, Zhao Q, Mooney SM, Lee FS. 2002. Sequence determinants in hypoxia-inducible factor-1alpha for hydroxylation by the prolyl hydroxylases PHD1, PHD2, and PHD3. *J Biol Chem* 277: 39792-39800.
- Huang LE, Gu J, Schau M, Bunn HF. 1998. Regulation of hypoxia-inducible factor 1 alpha is mediated by an O₂-dependent degradation domain via the ubiquitin-proteasome pathway. *Proc Natl Acad Sci USA* 95: 7987-7992.
- Ivan M, Haberberger T, Gervasi DC, Michelson KS, Gunzler V, et al. 2002. Biochemical purification and pharmacological inhibition of a mammalian prolyl hydroxylase acting on hypoxia-inducible factor. *Proc Natl Acad Sci USA* 99: 13459-13464.
- Ivan M, Kondo K, Yang H, Kim W, Valiando J, et al. 2001. HIFalpha targeted for VHL-mediated destruction by proline hydroxylation: Implications for O₂ sensing. *Science* 292: 464-468.
- Iyer NV, Kotch LE, Agani F, Leung SW, Laughner E, et al. 1998. Cellular and developmental control of O₂ homeostasis by hypoxia-inducible factor 1alpha. *Gene Develop* 12: 149-162.
- Jaakkola P, Mole DR, Tian YM, Wilson MI, Gielbert J, et al. 2001. Targeting of HIF-alpha to the von Hippel-Lindau ubiquitylation complex by O₂-regulated prolyl hydroxylation. *Science* 292: 468-472.

- Jeong JW, Bae MK, Ahn MY, Kim SH, Sohn TK, et al. 2002. Regulation and destabilization of HIF-1 α by ARD1-mediated acetylation. *Cell* 111: 709-720.
- Jewell UR, Kvietikova I, Scheid A, Bauer C, Wenger RH, et al. 2001. Induction of HIF-1 α in response to hypoxia is instantaneous. *FASEB J* 15: 1312-1314.
- Jiang B-H, Zheng JZ, Leung SW, Roe R, Semenza GL. 1997. Transactivation and inhibitory domains of hypoxia-inducible factor 1 α —modulation of transcriptional activity by oxygen tension. *J Biol Chem* 272: 19253-19260.
- Kaelin WG Jr. 2002. Molecular basis of the VHL hereditary cancer syndrome. *Nat Rev Cancer* 2: 673-682.
- Kraig RP, Ferreira-Filho CS, Nicholson C. 1983. Alkaline and acid transients in cerebellar microenvironment. *J Neurophysiol* 49: 831-850.
- LaManna JC. 1996. Hypoxia/ischemia and the pH paradox. *Adv Exp Med Biol* 388: 283-292.
- LaManna JC, Chavez JC, Pichiule P. 2004. Structural and functional adaptation to hypoxia in the rat brain. *J Exp Biol* 207: 3163-3169.
- LaManna JC, Kutina-Nelson KL, Hritz MA, Huang Z, Wong-Riley MTT. 1996. Decreased rat brain cytochrome oxidase activity after prolonged hypoxia. *Brain Res* 720: 1-6.
- LaManna JC, Vendel LM, Farrell RM. 1992. Brain adaptation to chronic hypobaric hypoxia in rats. *J Appl Physiol* 72: 2238-2243.
- Lando D, Peet DJ, Gorman JJ, Whelan DA, Whitelaw ML, et al. 2002. FIH-1 is an asparaginyl hydroxylase enzyme that regulates the transcriptional activity of hypoxia-inducible factor. *Genes Dev* 16: 1466-1471.
- Lauro KL, LaManna JC. 1997. Adequacy of cerebral vascular remodeling following three weeks of hypobaric hypoxia. Examined by an integrated composite analytical model. *Adv Exp Med Biol* 411: 369-376.
- Loike JD, Cao L, Brett J, Ogawa S, Silverstein SC, et al. 1992. Hypoxia induces glucose transporter expression in endothelial cells. *Am J Physiol* 263: C326-C333.
- Lopez-Lopez C, LeRoith D, Torres-Aleman I. 2004. Insulin-like growth factor I is required for vessel remodeling in the adult brain. *Proc Natl Acad Sci USA* 101: 9833-9838.
- Lu H, Forbes RA, Verma A. 2002. Hypoxia-inducible factor 1 activation by aerobic glycolysis implicates the Warburg effect in carcinogenesis. *J Biol Chem* 277: 23111-23115.
- Magistretti PJ, Pellerin L, Rothman DL, Shulman RG. 1999. Energy on demand. *Science* 283: 496-497.
- Mahon PC, Hirota K, Semenza GL. 2001. FIH-1: A novel protein that interacts with HIF-1 α and VHL to mediate repression of HIF-1 transcriptional activity. *Genes Dev* 15: 2675-2686.
- Martin E, Rosenthal RE, Fiskum G. 2005. Pyruvate dehydrogenase complex: Metabolic link to ischemic brain injury and target of oxidative stress. *J Neurosci Res* 79: 240-247.
- Masson N, Willam C, Maxwell PH, Pugh CW, Ratcliffe PJ. 2001. Independent function of two destruction domains in hypoxia-inducible factor-1 α chains activated by prolyl hydroxylation. *EMBO J* 20: 5197-5206.
- Masuda S, Chikuma M, Sasaki R. 1997. Insulin-like growth factors and insulin stimulate erythropoietin production in primary cultured astrocytes. *Brain Res* 746: 63-70.
- Mateo J, Garcia-Lecce M, Cadenas S, Hernandez C, Moncada S. 2003. Regulation of hypoxia-inducible factor-1 α by nitric oxide through mitochondria-dependent and -independent pathways. *Biochem J* 376: 537-544.
- Maxwell PH, Wiesener MS, Chang GW, Clifford SC, Vaux EC, et al. 1999. The tumour suppressor protein VHL targets hypoxia-inducible factors for oxygen-dependent proteolysis. *Nature* 399: 271-275.
- Meier-Ruge W, Iwagoff P, Reichlmeier K, Sandoz P. 1980. Neurochemical findings in the aging brain. *Adv Biochem Psychopharmacol* 23: 323-338.
- Metzen E, Berchner-Pfannschmidt U, Stengel P, Marxsen JH, Stolze I, et al. 2003. Intracellular localisation of human HIF-1 α hydroxylases: Implications for oxygen sensing. *J Cell Sci* 116: 1319-1326.
- Minchenko A, Leshchinsky I, Opentanova I, Sang N, Srinivas V, et al. 2002. Hypoxia-inducible factor-1-mediated expression of the 6-phosphofructo-2-kinase/fructose-2,6-bisphosphatase-3 (PFKFB3) gene. Its possible role in the Warburg effect. *J Biol Chem* 277: 6183-6187.
- Murphy BJ, Robin ED, Tapper DP, Wong RJ, Clayton DA. 1984. Hypoxic coordinate regulation of mitochondrial enzymes in mammalian cells. *Science* 223: 707-709.
- Musch TI, Dempsey JA, Smith CA, Mitchell GS, Bateman NT. 1983. Metabolic acids and [H⁺] regulation in brain tissue during acclimatization to chronic hypoxia. *J Appl Physiol* 55: 1486-1495.
- Nakayama K, Frew IJ, Hagensen M, Skals M, Habelhah H, et al. 2004. Siah2 regulates stability of prolyl-hydroxylases, controls HIF1 α abundance, and modulates physiological responses to hypoxia. *Cell* 117: 941-952.
- Ohh M, Park CW, Ivan M, Hoffman MA, Kim TY, et al. 2000. Ubiquitination of hypoxia-inducible factor requires direct binding to the beta-domain of the von Hippel-Lindau protein. *Nat Cell Biol* 2: 423-427.
- Osthus RC, Shim H, Kim S, Li Q, Reddy R, et al. 2000. Deregulation of glucose transporter 1 and glycolytic gene expression by c-Myc. *J Biol Chem* 275: 21797-21800.
- Phelps CH. 1972. Barbiturate-induced glycogen accumulation in brain. An electron microscopic study. *Brain Res* 39: 225-234.
- Panel E, Miyasaka T, Launey T, Chui DH, Tanemura K, et al. 2004. Alterations in glucose metabolism induce hypothermia leading to tau hyperphosphorylation through differential inhibition of kinase and phosphatase activities:

- Implications for Alzheimer's disease. *J Neurosci* 24: 2401-2411.
- Pugh CW, O'Rourke JF, Nagao M, Gleadle JM, Ratcliffe PJ. 1997. Activation of hypoxia-inducible factor-1; definition of regulatory domains within the alpha subunit. *J Biol Chem* 272: 11205-11214.
- Racker E. 1972. Bioenergetics and the problem of tumor growth. *Am Sci* 60: 56-63.
- Racker E, Spector M. 1981. Warburg effect revisited: Merger of biochemistry and molecular biology. *Science* 213: 303-307.
- Ralph GS, Parham S, Lee SR, Beard GL, Craighan MH, et al. 2004. Identification of potential stroke targets by lentiviral vector mediated overexpression of HIF-1 alpha and HIF-2 alpha in a primary neuronal model of hypoxia. *J Cereb Blood Flow Metab* 24: 245-258.
- Richard DE, Berra E, Pouyssegur J. 2000. Nonhypoxic pathway mediates the induction of hypoxia-inducible factor 1alpha in vascular smooth muscle cells. *J Biol Chem* 275: 26765-26771.
- Riddle DR, Sonntag WE, Lichtenwalner RJ. 2003. Microvascular plasticity in aging. *Ageing Res Rev* 2: 149-168.
- Rivard A, Berthou-Soulie L, Principe N, Kearney M, Curry C, et al. 2000. Age-dependent defect in vascular endothelial growth factor expression is associated with reduced hypoxia-inducible factor 1 activity. *J Biol Chem* 275: 29643-29647.
- Robin ED, Murphy BJ, Theodore J. 1984. Coordinate regulation of glycolysis by hypoxia in mammalian cells. *J Cell Physiol* 118: 287-290.
- Salceda S, Caro J. 1997. Hypoxia-inducible factor 1 alpha (HIF-1 alpha) protein is rapidly degraded by the ubiquitin-proteasome system under normoxic conditions—its stabilization by hypoxia depends on redox-induced changes. *J Biol Chem* 272: 22642-22647.
- Salnikow K, An WG, Melillo G, Blagosklonny MV, Costa M. 1999. Nickel-induced transformation shifts the balance between HIF-1 and p53 transcription factors. *Carcinogenesis* 20: 1819-1823.
- Salnikow K, Blagosklonny MV, Ryan H, Johnson R, Costa M. 2000. Carcinogenic nickel induces genes involved with hypoxic stress. *Cancer Res* 60: 38-41.
- Seagroves TN, Ryan HE, Lu H, Wouters BG, Knapp M, et al. 2001. Transcription Factor HIF-1 is a necessary mediator of the Pasteur effect in mammalian cells. *Mol Cell Biol* 21: 3436-3444.
- Selak MA, Armour SM, Mackenzie ED, Boulahbel H, Watson DG, et al. 2005. Succinate links TCA cycle dysfunction to oncogenesis by inhibiting HIF-alpha prolyl hydroxylase. *Cancer Cell* 7: 77-85.
- Semenza GL. 1998. Hypoxia-inducible factor 1: Master regulator of O₂ homeostasis. *Curr Opin Genet Dev* 8: 588-594.
- Semenza GL. 1999. Regulation of mammalian O₂ homeostasis by hypoxia-inducible factor 1. *Annu Rev Cell Dev Biol* 15: 551-578.
- Semenza GL. 2000a. HIF-1: Mediator of physiological and pathophysiological responses to hypoxia. *J Appl Physiol* 88: 1474-1480.
- Semenza GL. 2000b. Hypoxia, clonal selection, and the role of HIF-1 in tumor progression. *Crit Rev Biochem Mol Biol* 35: 71-103.
- Semenza GL. 2002. Physiology meets biophysics: Visualizing the interaction of hypoxia-inducible factor 1 alpha with p300 and CBP. *Proc Natl Acad Sci USA* 99: 11570-11572.
- Semenza GL. 2003. Targeting HIF-1 for cancer therapy. *Nat Rev Cancer* 3: 721-732.
- Semenza GL, Agani F, Booth G, Forsythe J, Iyer N, et al. 1997. Structural and functional analysis of hypoxia-inducible factor 1. *Kidney Int* 51: 553-555.
- Semenza GL, Agani F, Feldser D, Iyer N, Kotch L, et al. 2000. Hypoxia, HIF-1, and the pathophysiology of common human diseases. *Adv Exp Med Biol* 475: 123-130.
- Semenza GL, Roth PH, Fang H-M, Wang GL. 1994. Transcriptional regulation of genes encoding glycolytic enzymes by hypoxia-inducible factor 1. *J Biol Chem* 269: 23757-23763.
- Sharp FR, Bergeron M, Bernaudin M. 2001. Hypoxia-inducible factor in brain. *Adv Exp Med Biol* 502: 273-291.
- Sharp FR, Bernaudin M. 2004. HIF1 and oxygen sensing in the brain. *Nat Rev Neurosci* 5: 437-448.
- Simon MC. 2004. Siah proteins, HIF prolyl hydroxylases, and the physiological response to hypoxia. *Cell* 117: 851-853.
- Soucek T, Cumming R, Dargusch R, Maher P, Schubert D. 2003. The regulation of glucose metabolism by HIF-1 mediates a neuroprotective response to amyloid beta peptide. *Neuron* 39: 43-56.
- Stewart PA, Isaacs H, La Manna JC, Harik SI. 1997. Ultrastructural concomitants of hypoxia-induced angiogenesis. *Acta Neuropathol* 93: 579-584.
- Stroka DM, Burkhardt T, Desbaillets I, Wenger RH, Neil DA, et al. 2001. HIF-1 is expressed in normoxic tissue and displays an organ-specific regulation under systemic hypoxia. *FASEB J* 15: 2445-2453.
- Stubbs M, Bashford CL, Griffiths JR. 2003. Understanding the tumor metabolic phenotype in the genomic era. *Curr Mol Med* 3: 49-59.
- Swanson RA. 1992. Physiologic coupling of glial glycogen metabolism to neuronal activity in brain. *Can J Physiol Pharmacol* 70: S138-S144.
- Swanson RA, Morton MM, Sagar SM, Sharp FR. 1992. Sensory stimulation induces local cerebral glycogenolysis: Demonstration by autoradiography. *Neuroscience* 51: 451-461.
- Talks KL, Turley H, Gatter KC, Maxwell PH, Pugh CW, et al. 2000. The expression and distribution of the hypoxia-inducible factors HIF-1alpha and HIF-2alpha in normal

- human tissues, cancers, and tumor-associated macrophages. *Am J Pathol* 157: 411-421.
- Taylor MS. 2001. Characterization and comparative analysis of the EGLN gene family. *Gene* 275: 125-132.
- Thompson JE, Thompson CB. 2004. Putting the rap on Akt. *J Clin Oncol* 22: 4217-4226.
- Tomita S, Ueno M, Sakamoto M, Kitahama Y, Ueki M, et al. 2003. Defective brain development in mice lacking the Hif-1alpha gene in neural cells. *Mol Cell Biol* 23: 6739-6749.
- Treins C, Giorgetti-Peraldi S, Murdaca J, Semenza GL, Van OE. 2002. Insulin stimulates hypoxia-inducible factor 1 through a phosphatidylinositol 3-kinase/target of rapamycin-dependent signaling pathway. *J Biol Chem* 277: 27975-27981.
- Urbanics R, Leniger-Follert E, Lübbers DW. 1978. Time course of changes of extracellular H⁺ and K⁺ activities during and after direct electrical stimulation of the brain cortex. *Pflüg Arch* 378: 47-53.
- Wang GL, Jiang BH, Rue EA, Semenza GL. 1995. Hypoxia-inducible factor 1 is a basic-helix-loop-helix-PAS heterodimer regulated by cellular O₂ tension. *Proc Natl Acad Sci USA* 92: 5510-5514.
- Wang GL, Semenza GL. 1993. General involvement of hypoxia-inducible factor 1 in transcriptional response to hypoxia. *Proc Natl Acad Sci USA* 90: 4304-4308.
- Wang GL, Semenza GL. 1995. Purification and characterization of hypoxia-inducible factor 1. *J Biol Chem* 270: 1230-1237.
- Warburg O. 1956. On the origin of cancer cells. *Science* 123: 309-314.
- Warnecke C, Griethe W, Weidemann A, Jurgensen JS, Willam C, et al. 2003. Activation of the hypoxia-inducible factor-pathway and stimulation of angiogenesis by application of prolyl hydroxylase inhibitors. *FASEB J* 17: 1186-1188.
- Webster KA. 2003. Evolution of the coordinate regulation of glycolytic enzyme genes by hypoxia. *J Exp Biol* 206: 2911-2922.
- Webster KA, Murphy BJ. 1988. Regulation of tissue-specific glycolytic isozyme genes: Coordinate regulation by oxygen availability in skeletal muscle cells. *Can J Zool* 66: 1046-4058.
- Wiesener MS, Jurgensen JS, Rosenberger C, Scholze CK, Horstrup JH, et al. 2003. Widespread hypoxia-inducible expression of HIF-2alpha in distinct cell populations of different organs. *FASEB J* 17: 271-273.
- Wong-Riley MTT. 1989. Cytochrome oxidase: An endogenous metabolic marker for neuronal activity. *Trends Neurosci* 12: 94-101.
- Xu RH, Pelicano H, Zhou Y, Carew JS, Feng L, et al. 2005. Inhibition of glycolysis in cancer cells: A novel strategy to overcome drug resistance associated with mitochondrial respiratory defect and hypoxia. *Cancer Res* 65: 613-621.
- Yoon DY, Buchler P, Saarikoski ST, Hines OJ, Reber HA, et al. 2001. Identification of genes differentially induced by hypoxia in pancreatic cancer cells. *Biochem Biophys Res Commun* 288: 882-886.
- Yu AY, Shimoda LA, Iyer NV, Huso DL, Sun X, et al. 1999. Impaired physiological responses to chronic hypoxia in mice partially deficient for hypoxia-inducible factor 1 α . *J Clin Invest* 103: 691-696.
- Yuan Y, Hilliard G, Ferguson T, Millhorn DE. 2003. Cobalt inhibits the interaction between hypoxia-inducible factor-alpha and von Hippel-Lindau protein by direct binding to hypoxia-inducible factor-alpha. *J Biol Chem* 278: 15911-15916.
- Zelzer E, Levy Y, Kahana C, Shilo BZ, Rubinstein M, et al. 1998. Insulin induces transcription of target genes through the hypoxia-inducible factor HIF-1 alpha/ARNT. *EMBO J* 17: 5085-5094.
- Zhong H, Chiles K, Feldser D, Laughner E, Hanrahan C, et al. 2000. Modulation of hypoxia-inducible factor 1alpha expression by the epidermal growth factor/phosphatidylinositol 3-kinase/PTEN/AKT/FRAP pathway in human prostate cancer cells: Implications for tumor angiogenesis and therapeutics. *Cancer Res* 60: 1541-1545.
- Zhong H, De Marzo AM, Laughner E, Lim M, Hilton DA, et al. 1999. Overexpression of hypoxia-inducible factor 1alpha in common human cancers and their metastases. *Cancer Res* 59: 5830-5835.
- Zu XL, Guppy M. 2004. Cancer metabolism: Facts, fantasy, and fiction. *Biochem Biophys Res Commun* 313: 459-465.

7.3 Transcriptional Integration of Mitochondrial Biogenesis

R. C. Scarpulla

1	<i>The Mitochondrial Genetic System</i>	790
1.1	Mitochondrial DNA Structure	790
1.2	mtDNA Inheritance	790
2	<i>Transcription and Replication of mtDNA</i>	792
2.1	mtDNA Replication	792
2.2	mtDNA Transcription	793
3	<i>Nuclear Regulators of Mitochondrial Biogenesis</i>	794
3.1	Transcription Factors	794
3.1.1	HAP Factors in Yeast	794
3.1.2	Nuclear Respiratory Factors	795
3.1.3	Other Nuclear Factors	799
4	<i>Transcriptional Coactivators</i>	799
4.1	PGC-1 α	799
4.1.1	PGC-1 α in Gluconeogenesis	801
4.1.2	PGC-1 α Mechanisms	802
4.2	PGC-1 α -Related Coactivators	802
4.2.1	PRC	802
4.2.2	PGC-1 β	803
5	<i>Transcriptional Links Between Mitochondrial Biogenesis and Neurological Function</i>	803

1 The Mitochondrial Genetic System

1.1 Mitochondrial DNA Structure

Major inroads have been made in understanding the molecular biology of mitochondria and in elucidating nucleo-mitochondrial interactions (Garesse and Vallejo, 2001; Scarpulla, 2002a). Early work pointed to the existence of a mitochondrial genetic system that was separate from that of the nucleus (Clayton, 2000). Subsequently, isolated mitochondria were found to have their own ribosomes, rRNA, and tRNA and could synthesize a small number of proteins. The mitochondrial translation system displayed antibiotic sensitivities that differed from those of eukaryotic cytosolic translation and more closely resembled those of prokaryotes. Genetic studies in yeast led to the observation that certain respiratory mutations displayed a cytoplasmic inheritance pattern that resulted from the random segregation of mitochondrial DNA (mtDNA) molecules during mitosis. This provided genetic evidence that mitochondria had their own DNA before its existence was demonstrated physically. This conclusion was supported by physical evidence of the existence of mtDNA in yeast and in other organisms (Nass et al., 1965). Since these early discoveries, much has been done to define the structure and gene organization of mtDNA. A complete mtDNA sequence was first obtained from humans, and sequences of mitochondrial genomes from many organisms have now been reported (<http://megasun.bch.umontreal.ca/>). A comparison of these genomic structures has established that a similar complement of genes is conserved in mtDNAs from all multicellular organisms. In vertebrates, these include genes for 13 protein subunits of respiratory complexes I, III, IV and V, 2 rRNAs, and 22 tRNAs (▶ [Figure 7.3-1](#)).

Unlike the nuclear genome where the vast majority of the DNA is devoted to repetitive sequence families, introns, and vast intergenic regions, the mtDNA of mammals and other vertebrates exhibits striking economy of sequence organization. Human mtDNA is a closed circular molecule of about 16.6 kb. Its genes are completely devoid of introns and are arranged head to tail with little or no intergenic regions. Some respiratory protein genes overlap, and the adenine nucleotides of UAA termination codons are not encoded in the mtDNA but rather are supplied by polyadenylation following RNA processing (Ojala et al., 1981). Protein-coding and rRNA genes are interspersed with tRNA genes, which demarcate the cleavage sites of RNA processing (▶ [Figure 7.3-1](#)). The only substantial noncoding region is the D-loop, which gets its name from the triple-stranded structure or displacement loop that is formed by association of the nascent H-strand in this region. The D-loop is the site of transcription initiation from bidirectional promoters and also contains the origin of H-strand DNA replication (Clayton, 2000). Notably, the structural economy found in vertebrate mtDNA is not found in plants and fungi, where the mitochondrial genomes are much larger and contain intergenic regions, introns, and multiple promoters and transcriptional units (Costanzo and Fox, 1990; Poyton and McEwen, 1996). An additional unusual characteristic is that mitochondrial genetic systems utilize genetic codes that differ slightly from the universal nuclear code and that these differences are species specific (Taanman, 1999).

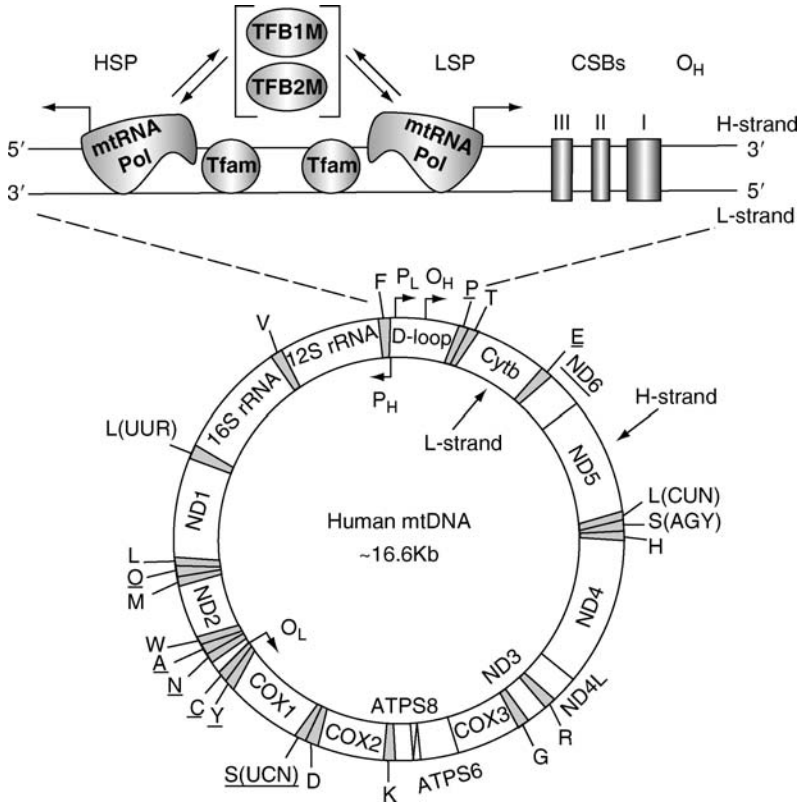
1.2 mtDNA Inheritance

The fact that mtDNA is a compartmentalized extrachromosomal element contributes to a mode of inheritance that differs from that of nuclear genes. Somatic mammalian cells generally have 10^3 – 10^4 copies of mtDNA with approximately 2–10 genomes per organelle (Satoh and Kuroiwa, 1991). The replication of these genomes is independent of the cell cycle, which is defined by nuclear DNA replication (Taanman, 1999; Clayton, 2000; Garesse and Vallejo, 2001). Some mtDNA molecules undergo multiple rounds of replication while others do not replicate. This, along with the random distribution of mtDNA during cell division, results in the segregation of sequence variants during mitosis (Shoubridge, 2000).

In mammals, the paternal mtDNA is lost during the first few embryonic cell divisions, resulting in the maternal inheritance of mtDNA (Kaneda et al., 1995; Shoubridge, 2000). In general, the paternal lineage

■ Figure 7.3-1

Schematic representation of human mitochondrial (mtDNA). The circular genetic map shows protein-coding and rRNA genes interspersed with 22 tRNA genes labeled using the single-letter amino acid designations. Protein-coding genes include cytochrome oxidase (COX) subunits 1, 2, and 3; NADH dehydrogenase (ND) subunits 1, 2, 3, 4, 4L, 5, and 6; ATP synthase (ATPS) subunits 6 and 8; cytochrome *b* (*Cytb*). ND6; and the 8 tRNA genes encoded on the L-strand are in bold type and underlined. All other genes are encoded on the H-strand. The D-loop regulatory region is expanded above showing the approximate locations for light- and heavy-strand promoters (HSP and LSP), conserved sequence blocks (CSBs), the origin of heavy-strand replication (O_H), and mitochondrial transcription complexes containing mitochondrial RNA polymerase (mtRNA Pol), Tfam, and TFB1M and TFB2M



does not contribute mtDNA to the offspring although there are individuals where the paternal lineage is represented in somatic tissues (Schwartz and Vissing, 2002). In one case, recombination between maternal and paternal genomes has been documented (Kraytsberg et al., 2004). Because mtDNA is a multicopy genome, individuals may harbor more than a single sequence, a condition known as heteroplasmy. A sequence variant that is detrimental may be tolerated in low copy, because the defective gene product(s) it encodes do not reach the threshold for disrupting respiratory function. However, sequence variants can segregate rapidly in passing from one generation to the next (Ashley et al., 1989). This can result in a defective mitochondrial phenotype in which the detrimental variant predominates in the offspring. This rapid meiotic segregation has been ascribed to a bottleneck or sampling error in the female germ line.

During oogenesis, a massive amplification of mtDNA occurs from about 10^3 copies in the primary oocyte to approximately 10^5 copies in the mature oocyte (Shoubridge, 2000). Replication of mtDNA is halted in the mature oocyte, and the population of mtDNA molecules is partitioned to the daughter cells

during early cell divisions until the copy number is diluted to approximately that found in somatic cells. Embryonic replication does not resume until the blastocyst stage of development (Piko and Taylor, 1987). The mitochondrial number is reduced to about 50 in primordial germ cells and increases to about 200 in the oogonia. Assuming the normal somatic cell number of genomes per organelle, the mtDNA copy number in germ cell progenitors is extremely small, approximately 50–100 copies. This small number results in a genetic bottleneck. Heteroplasmic mice constructed from two domestic strains were used to establish that nearly all of the mtDNA segregation occurs between the primary germ cells and the oogonia. Thus, the genetic bottleneck occurs early in the pathway of oogenesis, and segregation of sequence variants is complete before the formation of primary oocytes. Defective variants are not selectively eliminated or reduced during oogenesis or early embryonic development, indicating that optimal mitochondrial respiratory function is not required for these processes (Shoubridge, 2000).

2 Transcription and Replication of mtDNA

2.1 mtDNA Replication

New controversy has arisen over the mechanism of mtDNA replication in mammalian cells. The majority of evidence points to a classical mechanism of bidirectional replication where the replication origins for the two strands, termed heavy (H) and light (L) based on their buoyant densities, are displaced by about two-thirds of the genome (Shadel and Clayton, 1997; Clayton, 2003). This results in temporal as well as spatial separation of initiation events. Bidirectional promoters, heavy-strand promoter (HSP) and light-strand promoter (LSP), are contained within the D-loop regulatory region along with the H-strand replication origin (O_H) (▶ [Figure 7.3-1](#)). RNA transcripts initiating at LSP are cleaved at sites coinciding with three evolutionarily conserved sequence blocks (CSB I, II, and III), and H-strand replication is initiated at the sites of these cleavages (Chang et al., 1985). Thus, in this model, transcription is coupled to replication and the RNA cleavage sites mark the transition between RNA and DNA synthesis. Although nothing is known of how this transition is regulated, a stable RNA–DNA hybrid has been demonstrated (Xu and Clayton, 1995). Even after DNA synthesis begins, the nascent strand often terminates downstream from a conserved element referred to as a termination-associated sequence (TAS) (Madsen et al., 1993). This event may be important in controlling mtDNA levels and accounts for the triple-stranded D-loop structure.

Once the nascent H-strand traverses two-thirds of the genome, L-strand replication is initiated at O_L , a short noncoding region within a cluster of tRNA genes (Tapper and Clayton, 1981; Shadel and Clayton, 1997; Clayton, 2003). Upon displacement of the parental H-strand, a stem–loop structure forms at O_L (Hixson et al., 1986). This serves as the recognition site for a mitochondrial primase that produces a short RNA primer for the initiation of L-strand replication. Initiation of DNA synthesis occurs near a G+C-rich region at the base of the stem. The primase has been only partially purified and is thought to require RNA for catalytic activity (Wong and Clayton, 1986).

In marked contrast to this classical model, replication intermediates that are consistent with coupled leading- and lagging-strand replication from a single origin have also been detected (Holt et al., 2000). This mode of replication was initially observed under conditions where cells were recovering from transient mtDNA depletion (Holt et al., 2000) but is now thought to represent the predominant mechanism of replication in dividing cells (Yang et al., 2002). This conclusion has been challenged by the proponents of the classical strand displacement model on the basis that the new model is supported mainly by the detection of replication intermediates using two-dimensional gel electrophoresis (Bogenhagen and Clayton, 2003). Partially single-stranded molecules may escape detection by two-dimensional gels because of branch migration, and transcriptional intermediates might contribute to the observed pattern. In contrast, multiple lines of experimental evidence, including the precise mapping of replication origins and the detection of the predicted replication intermediates by electron microscopy, support the strand displacement model (Bogenhagen and Clayton, 2003; Clayton, 2003).

Many of the molecular constituents required for mtDNA transcription and replication have been characterized and, as expected, all are nuclear gene products. The only known mtDNA polymerase, DNA

polymerase γ , is a heterodimer of large (125–140 kDa) and small (35–54 kDa) subunits and is highly conserved from yeast to man (Lecrenier et al., 1997). A mutation of the large subunit in yeast that eliminates catalytic activity results in a loss of mtDNA without affecting cell viability (Foury, 1989). The large subunit of polymerase γ has both a 5' \rightarrow 3' polymerase as well as a 3' \rightarrow 5' exonuclease that eliminates misincorporated bases and facilitates the fidelity of mtDNA replication (Wang, 1991). The small subunit is thought to contribute to primer recognition and processivity (Insdorf and Bogenhagen, 1989; Lewis et al., 1996). The RNA primer for H-strand replication is generated by cleavage of the L-strand transcript by mitochondrial RNA-processing (MRP) endonuclease. This ribonucleoprotein contains a nucleus-encoded RNA that is essential for catalysis (MRP-RNA) and is most abundant in the nucleolus where it participates in the processing of 5.8S rRNA precursors (Shadel and Clayton, 1997). Although its association with mitochondria has been questioned (Kiss and Filipowicz, 1992), both its cleavage specificity and in situ hybridization profile argue strongly for its function in mtDNA replication (Topper et al., 1992; Li et al., 1994; Lee and Clayton, 1997). MRP RNase cleaves an R-loop containing the H-strand origin of replication at specific sites that match the in vivo priming sites.

A mitochondrial single-stranded DNA-binding protein (mtSSB) binds exposed single-stranded regions during replication. Yeast mtSSB is required for mtDNA maintenance, consistent with its role in mtDNA replication (Van Dyck et al., 1992). Genes for mammalian homologs have been characterized (Gupta and Van Tuyle, 1998), and the crystal structure of human mtSSB has been solved. MtSSB is structurally distinct from nuclear SSB but bears a strong structural similarity to the *Escherichia coli* protein (Webster et al., 1997). Topoisomerases and helicases are also associated with mitochondria. A mitochondrial protein designated as “twinkle” because of its punctate cytoplasmic staining pattern (Spelbrink et al., 2001) has a helicase domain resembling that of the bacteriophage T7 gene 4. Mutations in twinkle are associated with the autosomal dominant form of progressive external ophthalmoplegia. The inherited form of this disease is characterized by multiple deletions in mtDNA, suggesting that twinkle function is essential for maintaining the integrity of the mitochondrial genome.

2.2 mtDNA Transcription

In contrast to yeast, where transcription is initiated at approximately 20 transcriptional units (for references see Poyton and McEwen, 1996), vertebrate transcription is initiated at 2 promoters, HSP and LSP, spaced 150 nucleotides apart within the D-loop regulatory region (Montoya et al., 1983; Yoza and Bogenhagen, 1984). The H- and L-strand transcriptional units are polygenic, specifying more than one RNA gene or mRNA. In addition to the RNA primer for H-strand replication, LSP also directs the synthesis of a transcript that is processed to one mRNA and eight of the 22 tRNAs (🔗 [Figure 7.3-1](#)). The polygenic transcript directed by HSP is processed to 14 tRNAs, 12 mRNAs, and the 2 rRNAs. In both LSP and HSP, a 15-nucleotide-conserved sequence motif defines the core promoter.

LSP and HSP share an upstream enhancer that serves as the recognition site for Tfam (previously mtTF-1 and mtTFA), an HMG box protein that stimulates transcription through specific binding to the upstream enhancers (Fisher and Clayton, 1985; Shadel and Clayton, 1993; Shadel and Clayton, 1997). Like other HMG proteins, Tfam can bend and unwind DNA, properties potentially linked to its ability to stimulate transcription upon binding DNA immediately upstream from the sites of transcription initiation (Parisi and Clayton, 1991; Fisher et al., 1992). In addition, Tfam binds nonspecific DNA with high affinity and this property, along with its abundance in mitochondria, suggests that it plays a role in the stabilization and maintenance of the mitochondrial chromosome through its phased binding to nonpromoter sites (Fisher et al., 1989). A related HMG box factor from yeast, ABF2, resembles Tfam and is required for mtDNA maintenance and respiratory competence (Diffley and Stillman, 1991). Expression of Tfam in ABF2-deficient yeast cells can rescue both phenotypes, suggesting that the two proteins are functionally homologous. Despite this functional complementation, ABF2 lacks an activation domain present in Tfam and does not stimulate transcription. Tfam knockout mice exhibit embryonic lethality and depletion of mtDNA, confirming an essential role for the protein in mtDNA maintenance in mammals (Larsson et al., 1998). In addition, Tfam levels correlate well with increased mtDNA in ragged red muscle fibers and decreased

mtDNA levels in mtDNA-depleted cells (Poulton et al., 1994). The correlation with mtDNA content is also observed for mtSSB in contrast to polymerase γ , which is expressed constitutively (Schultz et al., 1998). Despite these intriguing correlations, it is unclear which, if any of these, is the key limiting factor whose expression regulates mtDNA copy number (Moraes, 2001).

In yeast, transcription is directed by a 145-kDa core polymerase encoded by *RPO41* and a 43-kDa specificity factor, also known as sc-mtTFB, encoded by *MTF1* (for references see Poyton and McEwen, 1996; Clayton, 2000; Garesse and Vallejo, 2001). The polymerase shares sequence similarities with the T7 and T3 bacteriophage polymerases, which also consist of a single subunit. The primary structure of the sc-mtTFB specificity factor bears some resemblance to the prokaryotic sigma factors (Shadel and Clayton, 1995), but a recent crystal structure reveals significant homology to rRNA methyltransferase (Schubot et al., 2001). The polymerase and specificity factor transiently interact and both are required for specific transcription initiation in vitro (Shadel and Clayton, 1993). Genetic evidence supports a functional interaction between the two factors in vivo as well.

A polymerase and a specificity factor that is required for specific initiation has been partially purified from *Xenopus laevis* (Bogenhagen, 1996). Although purification of the human polymerase has been elusive, a human cDNA that encodes a mitochondrially localized protein with sequence similarity to yeast mitochondrial and phage polymerases has been identified (Tiranti et al., 1997). A human mtTFB cDNA has also been isolated and the encoded protein has properties consistent with it being a functional homolog of sc-mtTFB (McCulloch et al., 2002). The h-mtTFB is localized to mitochondria, can bind DNA, and stimulates transcription from an L-strand promoter in vitro. More recently, two isoforms of h-mtTFB, termed TFB1M and TFB2M, have been identified (Falkenberg et al., 2002). TFB1M is identical to the original h-mtTFB isolate and has about one-tenth the transcriptional activity of TFB2M. Both proteins work together with Tfam and mtRNA polymerase to direct proper initiation from HSP and LSP (▶ [Figure 7.3-1](#)) and, like the yeast factor, both are related to rRNA methyltransferases. It is yet to be determined whether the proteins are bifunctional or whether they evolved a single function from an ancestral methyltransferase.

3 Nuclear Regulators of Mitochondrial Biogenesis

3.1 Transcription Factors

3.1.1 HAP Factors in Yeast

The cytochrome *c* and cytochrome oxidase genes have served as the prototypes for identifying regulatory factors that act on nuclear respiratory genes from both yeast and mammalian cells. In yeast, the transcriptional regulation of the major cytochrome *c* isoform, *CYC1*, is mediated by oxygen and carbon sources such as glucose and lactate through the upstream activation sites, UAS1 and UAS2 (for references see Zitomer and Lowry, 1992; Poyton and McEwen, 1996). UAS1 directs the majority of transcription under conditions of glucose repression and is dependent on a *trans*-acting factor designated as HAP1p. Heme is required for the binding of the HAP1p to the *CYC1* UAS1 in vitro suggesting that the heme dependence of UAS1 in vivo is mediated by a heme–HAP1p interaction.

UAS2 differs from UAS1 by its sensitivity to the availability of nonfermentable carbon sources and its inability to be derepressed by heme analogs (Zitomer and Lowry, 1992; Poyton and McEwen, 1996). A heterotrimeric complex consisting of HAP2p, 3p, and 4p, all of which are required for transcriptional activation, mediates regulation through UAS2 (Hahn and Guarente, 1988; Forsburg and Guarente, 1989). The HAP2p–HAP3p complex binds a CCAAT-box-like sequence motif in UAS2. HAP4p expression is subject to catabolite repression and is induced by growth in lactate. It provides an acidic transcriptional activation domain to the complex but does not bind DNA by itself (Olesen and Guarente, 1990). A fourth subunit of the complex, HAP5p, was isolated by two-hybrid screening and is required for sequence-specific DNA binding (McNabb et al., 1995).

Transcription of the *CYC7* gene is under both positive and negative control mediated by distinct *cis*-acting elements. A negative regulator, ROX1p, acts on *CYC7* and other oxygen-regulated genes (Lowry and Zitomer, 1988; Zitomer et al., 1997). A null mutation in ROX1p enhances expression of *CYC7* suggesting that ROX1p is a repressor of *CYC7* expression. ROX1p is also induced by heme and inhibits the expression of heme-repressed genes under aerobic growth conditions. Maximal heme induction of ROX1p is thought to require HAP1p. ROX1p is an HMG-box protein that is capable of binding a hypoxic consensus sequence present in *ANB1*, *CYC7*, and *COX5b* genes, among others. Like other HMG proteins, ROX1p can bend DNA. A transcriptional repression domain is located toward the carboxy-terminal end of the molecule. Thus, the regulated expression of cytochrome *c* in yeast results from the action of transcriptional activators and repressors that communicate the availability of metabolites to the transcriptional machinery.

3.1.2 Nuclear Respiratory Factors

Characterization of cytochrome *c* and cytochrome oxidase genes also led to the identification of nucleus-encoded transcription factors required for the expression of the respiratory apparatus in mammalian cells (for references see Scarpulla, 1997, 1999). Although cytochromes *c* are highly conserved at the functional level between yeast and mammals (Scarpulla and Nye, 1986), the mammalian cytochrome *c* promoter contains recognition sites for transcription factors that bear no obvious relationship to those identified in yeast (Evans and Scarpulla, 1988). Tandem Sp1 recognition sites are localized to the first intron and function synergistically to maximize promoter activity. *Cis*-elements that recognize transcription factors of the ATF/CREB family also exist in the cytochrome *c* promoter (Evans and Scarpulla, 1989; Gopalakrishnan and Scarpulla, 1994). Although CREB sites are common to cAMP- and growth-activated genes, these elements are not found in the promoters of other nuclear respiratory genes. Cytochrome *c* appears to be limiting in quiescent cells, and its transcriptional induction by serum mediates an increase in cellular respiration in preparation for cell division. CREB activation of the cytochrome *c* promoter is associated with the rapid induction of cytochrome *c* in response to serum growth factors (Herzig et al., 2000).

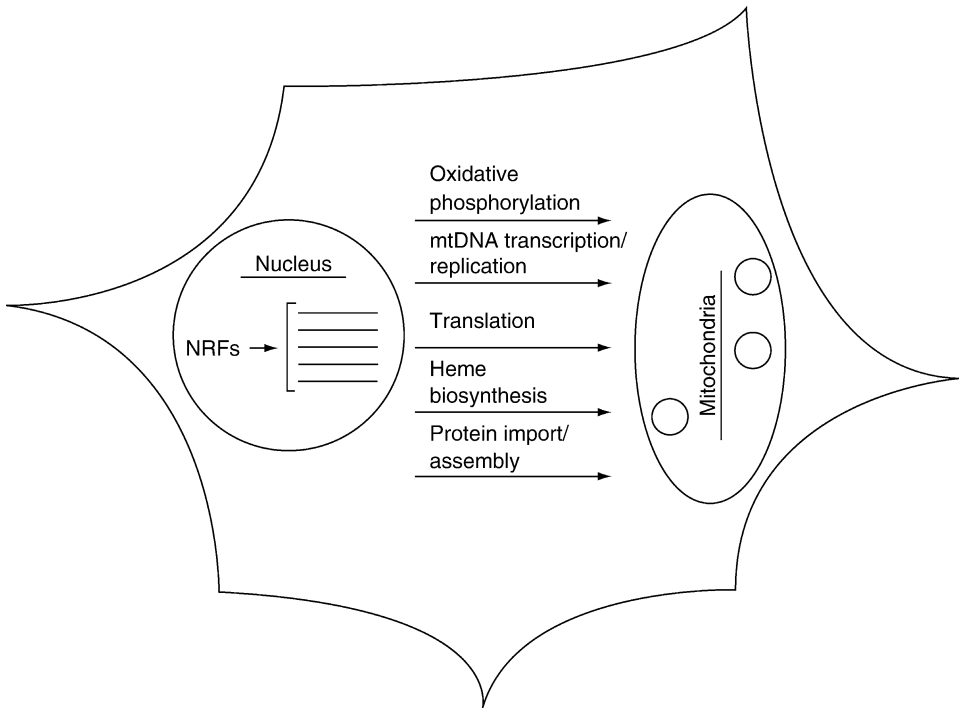
A palindromic recognition site for a transcription factor designated as NRF-1 (nuclear respiratory factor-1) also resides in the cytochrome *c* promoter (Evans and Scarpulla, 1989). The 68-kDa protein responsible for binding to this site was purified approximately 33,000-fold to near homogeneity (Chau et al., 1992). The endogenous NRF-1 present in nuclear extracts and the recombinant NRF-1 make guanine nucleotide contacts over a single turn of the DNA helix (Virbasius et al., 1993a). NRF-1 behaves as a positive regulator of transcription in *in vitro* transcription and *trans*-activation assays (Virbasius et al., 1993a). This is consistent with the presence of a carboxy-terminal transcriptional activation domain consisting of glutamine-containing clusters of hydrophobic amino acid residues (Gugneja et al., 1996). NRF-1 exists as a phosphoprotein in proliferating mammalian cells and is serine phosphorylated, within a concise amino-terminal domain, enhancing both its DNA binding (Gugneja and Scarpulla, 1997) and *trans*-activation functions (Herzig et al., 2000). NRF-1 binds its recognition site as a homodimer but phosphorylation does not appear to affect the monomer–dimer equilibrium. A glycosylated derivative of chicken NRF-1 can act as a transcriptional repressor supporting the idea that posttranslational modifications may be important regulators of NRF-1 function (Gomez-Cuadrado et al., 1995).

NRF-1 has now been linked to the expression of many genes required for mitochondrial respiration (for references see Scarpulla, 2002a, b; Kelly and Scarpulla, 2004). Although many of these genes encode subunits of the five respiratory complexes, others are involved in the expression, assembly, and function of the respiratory apparatus (Virbasius et al., 1993a). Among these are constituents of the mtDNA transcription and replication machinery, mitochondrial and cytosolic enzymes of the heme biosynthetic pathway, and components of the protein import and assembly apparatus (▶ [Figure 7.3-2](#)). These associations are consistent with the hypothesis that NRF-1 plays an integrative role in nucleo-mitochondrial interactions.

A number of recent studies that associate increases in NRF-1 mRNA or DNA-binding activity with mitochondrial biogenesis reinforce the hypothesis. Both NRF-1 and its coactivator PGC-1 α (see below) are upregulated during the adaptive response of skeletal muscle to exercise training (Murakami et al., 1998;

■ **Figure 7.3-2**

Main categories of NRF target genes involved in the expression and assembly of the mitochondrial respiratory apparatus



Baar et al., 2002). A similar response also occurs in cultured myotubules upon elevation of calcium levels, which mimics exercise-induced mitochondrial biogenesis (Ojuka et al., 2003). Treatment of rats with a creatine analog that induces muscle adaptations analogous to those observed during exercise leads to the activation of AMP-activated protein kinase. This coincides with increased NRF-1 DNA-binding activity, cytochrome *c* content, and mitochondrial density (Bergeron et al., 2001). Both NRF-1 and Tfam mRNAs are elevated in cells depleted of mtDNA, presumably as a response to increased oxidative stress (Miranda et al., 1999). NRF-1 and NRF-2 (see below) along with Tfam are also upregulated in response to lipopolysaccharide-induced oxidative damage to mitochondria, presumably to enhance mtDNA levels and OXPHOS activity (Suliman et al., 2003). Exogenous oxidants (tertiary butyl hydroperoxide) could restore NRF-1 and normal cell growth to mtDNA-depleted hepatoma cells, where reduced oxidant levels are associated with loss of NRF-1 and growth delay. However, contrary to these results, NRF-1 expression was inversely correlated with increased cytochrome *c* and cytochrome oxidase subunit V expression that occurs during postnatal myocardial development (Nau et al., 2002).

A targeted disruption of NRF-1 in mice provides *in vivo* support for the link between NRF-1 and the control of mitochondrial function (Huo and Scarpulla, 2001). The homozygous knockout results in lethality between embryonic days 3.5 and 6.5 (Table 7.3-1), and the null blastocysts fail to grow in culture despite having a normal morphology. Embryonic expression does not result from maternal carryover since the NRF-1 gene is expressed during oogenesis and in 2.5- and 3.5-day embryos. The fact that homozygous null blastocysts appear deficient in maintaining a mitochondrial membrane potential and have severely reduced mtDNA levels supports an essential role for NRF-1 in maintaining mitochondrial function. The reduction in mtDNA is not accompanied by increased apoptosis, making it unlikely that it is a by-product of a generalized increase in DNA fragmentation. There is also no apparent defect in mtDNA amplification

■ Table 7.3-1

Mouse knockouts of nucleus-encoded regulatory factors implicated in mitochondrial biogenesis

Gene knockout ^a	Viability	Mitochondrial phenotype
Tfam (germ line)	Embryonic lethal between E8.5 and E11.5	mtDNA depletion Respiratory chain deficiency
NRF-1	Embryonic lethal between E3.5 and E6.5	mtDNA depletion Loss of mitochondrial membrane potential
NRF-2 (GABP)	Preimplantation lethal	not determined
YY1	Embryonic lethal between E3.5 and E8.5	not determined
ERR α	Viable and fertile	Normal food consumption and energy expenditure Reduced lipogenesis
PGC-1 α	Viable and fertile Increased postnatal mortality	Normal mitochondrial morphology Reduced O ₂ consumption in hepatocytes Fasting hypoglycemia

^aCitations in text

during oogenesis since the mature oocytes of heterozygous mothers have a normal complement of mtDNA. This argues that the mtDNA depletion occurs between fertilization and the blastocyst stage, and most likely results from the loss of an NRF-1-dependent pathway of mtDNA maintenance. However, the loss of mtDNA does not explain the early embryonic lethality of the homozygous NRF-1 nulls. Embryos from a Tfam knockout are also depleted of mtDNA but survive to between embryonic days 8.5 and 10.5 (Larsson et al., 1998). It is likely that the loss of NRF-1 affects the expression of NRF-1 target genes, which are independent of mtDNA but required for cell growth and development.

The initial search for NRF-1 binding sites in mammalian promoters implicated the factor in a large number of primate and rodent genes whose functions are not linked directly to mitochondrial biogenesis (Virbasius et al., 1993a). These included genes encoding metabolic enzymes, components of signaling pathways, and gene products necessary for chromosome maintenance and nucleic acid metabolism, among others. Moreover, NRF-1 is among seven identified transcription factors whose recognition sites are associated at high frequency with the proximal promoters of ubiquitously expressed genes (FitzGerald et al., 2004). Chromatin immunoprecipitations (ChIP) coupled with microarray assay (ChIP-on-chip) was used to identify human promoters that are bound by NRF-1 in vivo (Cam et al., 2004). A survey of approximately 13,000 human promoters by ChIP-on-chip analysis (Ren and Dynlacht, 2004) identified 691 genes whose promoters are occupied by NRF-1 in living cells (Cam et al., 2004). As expected, a majority of these genes are involved in mitochondrial biogenesis and metabolism, including many that had not been previously identified. In addition, a large proportion function in DNA replication, mitosis, and cytokinesis. Notably, a significant subset of the NRF-1 target genes was also bound by the growth regulatory transcription factor E2F, suggesting that NRF-1 participates in the regulation of a subset of E2F-responsive genes. An NRF-1 siRNA reduced expression of several E2F target genes along with Tfam and cytochrome *c*. NRF-1 has also been implicated in the transcriptional repression of E2F1 (Efiok and Safer, 2000) and the activation of E2F6 (Kherrouche et al., 2004). These results are consistent with a role for NRF-1 in regulating cell cycle progression and developmental patterning. Although other mammalian isoforms of NRF-1 have not been found, NRF-1 is related, through its DNA-binding domain, to developmental regulatory proteins in sea urchins (Calzone et al., 1991) and *Drosophila* (Desimone and White, 1993). In addition, chicken (Gomez-Cuadrado et al., 1995), zebra fish (Becker et al., 1998), and mouse (Schaefer et al., 2000) homologs of NRF-1 have been characterized.

A second nuclear factor, NRF-2, was identified as a transcriptional activator required for the expression of cytochrome oxidase genes (for references see Scarpulla, 1997, 1999). Directly repeated NRF-2 sites

consisting of the GGAA motifs, which are characteristic of the ETS-domain family of transcription factors, are interspersed with multiple transcription initiation sites within the mouse *COXIV* promoter (Virbasius and Scarpulla, 1991; Carter et al., 1992). Human NRF-2 was purified to homogeneity from HeLa cell nuclear extracts and comprises five subunits. These include a DNA-binding α subunit and four others (β_1 , β_2 , γ_1 , and γ_2) that complex with α , but alone do not bind DNA. The NRF-2 complexes activate transcription through four directly repeated ETS-domain-binding sites in the *COXVb* promoter, suggesting that NRF-2 may also act on multiple respiratory promoters (Virbasius et al., 1993b).

Purification and molecular cloning of the five NRF-2 subunits revealed that NRF-2 is the human homolog of mouse GABP (LaMarco and McKnight, 1989). The two additional human subunits, β_1 and γ_1 , are minor splice variants of GABP subunits β_1 and β_2 (Gugneja et al., 1995). The GABP β_1 subunit, corresponding to NRF-2 β_1 and β_2 (Gugneja et al., 1995), has a dimerization domain that facilitates cooperative binding of a heterotetrameric complex to tandem binding sites (Thompson et al., 1991). In solution, GABP exists as a $\alpha\beta$ heterodimer but is induced to form the heterotetramer $\alpha_2\beta_2$ by DNA containing two or more binding sites (Chinenov et al., 2000). The crystal structure of the heterotetramer bound to DNA has been determined (Batchelor et al., 1998). All of the non-DNA-binding subunits contain a transcriptional activation domain. This domain resembles that found in NRF-1 and has been localized to a region upstream from the homodimerization domain (Gugneja et al., 1996).

In addition to the *COX* promoters, functional NRF-2 sites have been identified in a number of other genes related to respiratory chain expression (for references see Scarpulla, 2002a). These include genes for Tfam (Larsson et al., 1998; Rantanen et al., 2001) and the newly discovered mitochondrial transcription specificity factors, TFB1M and TFB2M (Falkenberg et al., 2002; McCulloch et al., 2002), involved in mitochondrial transcription and DNA replication (Rantanen et al., 2001). Three of the four human succinate dehydrogenase (complex II) subunit genes also have both NRF-1 and NRF-2 sites in their promoters (Au and Scheffler, 1998; Elbehti-Green et al., 1998; Hirawake et al., 1999). In many cases, NRF-1 sites are also present in NRF-2-dependent promoters, but this is not a general rule. For example, several *COX* promoters and the rodent Tfam (Choi et al., 2002) and TFB (Rantanen et al., 2003) promoters do not have obvious NRF-1 consensus sites. This contrasts with the human Tfam (Virbasius and Scarpulla, 1994) and TFB (Gleyzer et al., 2005) promoters, which rely upon functional NRF-1 and NRF-2 recognition sites for their activities.

The absence of NRF-1 sites in rodent Tfam and TFB promoters may mean that NRF-1 is not involved in the expression of these mitochondrial transcription factors in rodents. Alternatively, NRF-1 may bind sequences that deviate significantly from the known consensus. For example, HAP1p can bind sites with different sequences in *CYC1* and *CYC7* (Pfeifer et al., 1987). In one report, NRF-1 binding to and *trans*-activation of the rat Tfam promoter has been observed (Choi et al., 2002), whereas in another, no detectable binding was found (Dong et al., 2002). The absence of one or the other NRF site may not alter the expression of these genes if regulation is conferred by the differential expression of PGC-1 α family coactivators (see below). In a given promoter context, one or both NRF factors bound to the promoter may serve to recruit these coactivators either directly or through interactions with other proteins of the transcription complex. NRF-1 has recently been shown to interact with p300/CBP-associated factor, a coactivator with histone acetyltransferase activity (Izumi et al., 2003). It is also conceivable that in certain contexts NRFs can recruit PGC-1 α family coactivators without making direct contact with DNA. In either case, NRF-1 and/or NRF-2 may be necessary for expression of their target genes, but not sufficient to confer regulated expression.

Recently, the *in vivo* function of GABP α (NRF-2 α) was investigated by making a targeted disruption of the gene encoding this subunit in mice (Ristevski et al., 2004). As observed for the NRF-1 knockout, the GABP α homozygous null mice exhibited a periimplantation lethal phenotype (🔗 [Table 7.3-1](#)). The heterozygous nulls had wild-type levels of the protein and appeared normal. No assessment of the state of mtDNA or mitochondrial function was made in the mutant embryos, but it is likely that the early defect results from a combination of mitochondrial and nonmitochondrial deficiencies. It is notable that homozygous nulls of other Ets (E26 transformation-specific) family transcription factors also exhibit early embryonic lethality suggesting that members of this family of related transcription factors are unable to compensate for one another during embryonic development.

3.1.3 Other Nuclear Factors

Several other well-characterized regulatory factors have been implicated in the expression of respiratory genes, in particular a small subset of genes that do not appear to be dependent on NRF-1 or NRF-2. The transcription factor Sp1 is involved in the activation and repression of cytochrome c_1 (Li et al., 1996b) and adenine nucleotide translocase 2 genes (Li et al., 1996a), both of which lack NRF sites (Zaid et al., 1999). Sp1 sites are present in many GC-rich promoters including those that are NRF-dependent. NRF sites are not found in muscle-specific COX subunit genes, COXVIaH and COXVIII, which depend upon MEF-2 and/or E-box consensus elements for their expression (Wan and Moreadith, 1995). It is not surprising that the same or similar factors required for the expression of other muscle-specific genes are linked to the regulation of these tissue-specific COX subunits. In contrast, the promoter of the ubiquitously expressed liver isoform, COXVIaL, depends upon NRF-1 and NRF-2 as well as Sp1 for full activity (Seelan et al., 1996). It was noted previously that in gene pairs encoding ubiquitous and tissue-specific isoforms of a given protein, the NRF-1 site, when present, is associated with the ubiquitously expressed gene (Virbasius et al., 1993a). Finally, binding sites for the initiator element transcription factor YY1 have been detected in the promoters of genes encoding COXVb (Basu et al., 1997) and COXVIIc (Seelan and Grossman, 1997). Multiple YY1 sites in the COXVb promoter bind YY1 and possibly other factors and at least one of these sites help confer a negative regulatory effect on COXVb promoter activity (Basu et al., 1997). Two YY1 sites in the COXVIIc promoter, in conjunction with an NRF-2 site, act as positive regulators of promoter activity (Seelan and Grossman, 1997). Interestingly, YY1 knockout mice resemble the NRF-1 and NRF-2 α knockouts in that they exhibit periimplantation lethality (Donohoe et al., 1999). Thus, NRF-independent transcription of some respiratory genes needs to be accounted for in unifying transcriptional models of mitochondrial biogenesis.

4 Transcriptional Coactivators

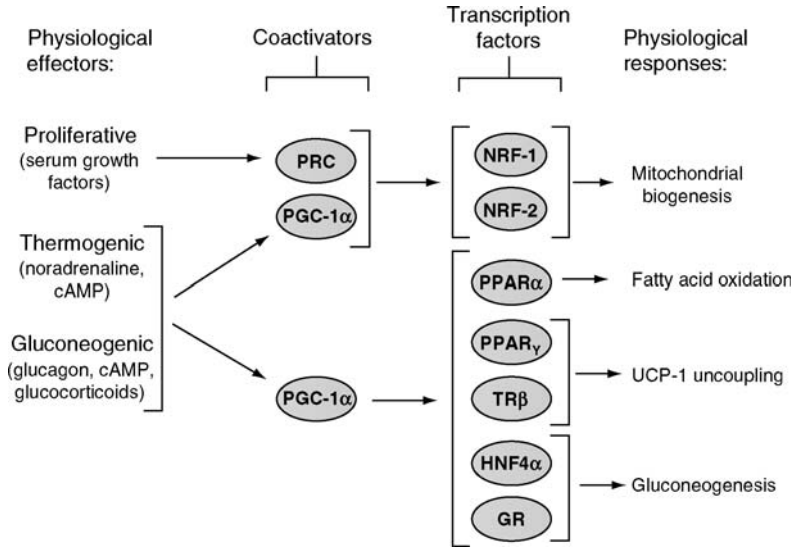
The control of respiratory chain expression by NRFs and other factors can only partly account for the complexity of mitochondrial biogenesis. For example, PPAR α controls genes of the fatty acid oxidation pathway (Gulick et al., 1994), whereas this protein has not been associated with the genes for respiratory subunits. In addition, in brown adipose tissue, cold exposure triggers a cascade of events leading to the biogenesis of mitochondria and the induction and activation of UCP-1, both of which are essential to the thermogenic response (for references see Lowell and Spiegelman, 2000; Ricquier and Bouillaud, 2000). The brown fat-specific enhancer of the UCP-1 promoter requires several ubiquitous transcription factors including thyroid and retinoic acid receptors and PPAR γ (▶ [Figure 7.3-3](#)) (for references see Silva and Rabelo, 1997). PPAR γ has a regulatory role in adipose differentiation but has not been associated with respiratory gene expression. Thus, it is important to understand how the cell integrates ubiquitous DNA-binding transcription factors into a program of mitochondrial biogenesis. At least part of the answer lies in a class of transcriptional coactivators that do not bind DNA but rather can interact with multiple transcription factors to activate or repress transcription.

4.1 PGC-1 α

PGC-1 α is a transcriptional coactivator cloned by yeast two-hybrid screening of a cDNA library derived from a differentiated brown fat cell line using PPAR γ as bait (Puigserver et al., 1998). The protein interacts with several nuclear hormone receptors including PPAR γ and can *trans*-activate the PPAR γ - and thyroid receptor β -dependent expression of the UCP-1 promoter (▶ [Figure 7.3-3](#)). PGC-1 α mRNA is markedly upregulated in brown fat upon cold exposure, supporting its involvement in thermogenic regulation. Perhaps the most striking property of PGC-1 α is that its ectopic overexpression in cultured myoblasts induces mitochondrial biogenesis (Wu et al., 1999). In addition to inducing respiratory subunit mRNAs, PGC-1 α increases COXIV and cytochrome *c* protein levels as well as the steady-state level of mtDNA. These changes coincide with increased oxygen uptake in differentiated myotubes and a visible increase in

■ Figure 7.3-3

Physiological control pathways mediated by the regulated expression of PGC-1 family coactivators. The left half of the diagram depicts physiological effectors linked to either PGC-1 α or PRC. The right half summarizes the effects of the coactivators on various transcription factors and the physiological responses



mitochondrial number. A number of observations support a major role for NRF-1 in mediating the effects of PGC-1 α on mitochondrial biogenesis. PGC-1 α and NRF-1 interact through the NRF-1 DNA-binding domain and a region of PGC-1 α that also binds PPAR γ . PGC-1 α can *trans*-activate NRF-1 target genes involved in mitochondrial respiration (▶ Figure 7.3-3). Finally, a dominant negative allele of NRF-1 blocks the effects of PGC-1 α on mitochondrial biogenesis, providing further *in vivo* evidence for an NRF-1-dependent pathway. Both NRF-1 and PGC-1 α are among a small number of genes induced in the hyperthyroid rat liver suggesting that thyroid hormone effects on mitochondria may be mediated through these factors (Weitzel et al., 2001). The functional interplay between NRF-1 and PGC-1 α appears to define a fundamental regulatory pathway for the biogenesis of mitochondria.

PGC-1 α can also upregulate genes of the mitochondrial fatty acid oxidation pathway, in keeping with a potential integrative role in mitochondrial biogenesis (Vega et al., 2000). PPAR α is an activator of this pathway and is enriched in brown fat and other tissues with high oxidative energy demands such as heart and liver. PGC-1 α expression from a retrovirus vector induces mRNAs for the enzymes of fatty acid oxidation and increases the rate of palmitate oxidation. Moreover, the coactivator can bind PPAR α and *trans*-activate PPAR α -dependent promoters, which is consistent with the idea that PGC-1 α is a regulator of mitochondrial oxidative function and biogenesis (● Figure 7.3-3). In contrast to PPAR γ , binding of PPAR α to PGC-1 α requires the LXXLL motif and is stimulated by ligand.

The effects of PGC-1 α on mitochondrial biogenesis have also been observed in cardiac cells and tissues (Lehman et al., 2000). PGC-1 α expression is induced in the postnatal mouse heart and in response to fasting. Both of these conditions increase mitochondrial energy production in the heart. Overproduction of PGC-1 α in cardiac myocytes had similar effects on the induction of respiratory subunits, oxidative enzymes, oxygen uptake, and mitochondrial biogenesis as observed for other cell types. These studies were extended to the mouse where expression of PGC-1 α from a cardiac-specific promoter resulted in massive proliferation of enlarged mitochondria in the heart (Lehman et al., 2000). This was associated with edema and dilated cardiomyopathy. Loss of PGC-1 α function was examined *in vivo* by engineering mice with a targeted disruption of the PGC-1 α gene (Lin et al., 2004). The mice were viable and showed no changes in mitochondrial abundance or morphology in liver or

brown fat. They did show modest reductions in oxygen consumption in isolated hepatocytes and in the expression of several mRNAs linked to mitochondrial function. Interestingly, brain and brown adipose were morphologically abnormal, and the mice displayed a gross neurological defect. This is intriguing in light of the long-standing link between mitochondrial function and neurodegenerative disease. It should be noted that a recently reported PGC-1 α knockout mouse differs from the original in several respects (Leone et al., 2005). It does not display postnatal mortality, defective gluconeogenesis or hyperactivity but does show increased body fat with age and hepatic steatosis upon fasting. These discrepancies may result from differences in gene targeting strategies.

Recent studies have implicated estrogen-related receptor α (ERR α) in PGC-1 α -induced mitochondrial biogenesis (Mootha et al., 2004; Schreiber et al., 2004). ERR α is an orphan nuclear receptor whose expression is elevated in tissues exhibiting a high capacity for fatty acid oxidation. It acts as a regulator of β -oxidation via its control of the medium-chain acyl-coenzyme A dehydrogenase (MCAD) promoter (Sladek et al., 1997; Vega and Kelly, 2004). PGC-1 α can interact with ERR α and induce its expression, resulting in the potent activation of MCAD gene expression (Huss et al., 2002; Schreiber et al., 2003), particularly during brown adipocyte differentiation (Vega and Kelly, 2004). Analysis of sequence motifs related to transcriptional activation by PGC-1 α revealed strong associations with ERR α and GABP α (NRF-2 α) recognition sites (Mootha et al., 2004). These motifs are conserved in the promoters of some oxidative phosphorylation genes, and PGC-1 α can drive the expression of promoters containing such sites. NRF-1 was also identified as a key contributor but was thought to be downstream of ERR α and GABP α . ERR α -binding sites are present in both cytochrome *c* and β -ATP synthase promoters, and these sites contributed to *trans*-activation by PGC-1 α but had no effect on these promoters in the absence of PGC-1 α (Schreiber et al., 2004).

The conclusion of these studies is that ERR α is an important mediator of PGC-1 α -regulated mitochondrial biogenesis. However, mice that are homozygous null for ERR α are viable and fertile and display no defects in food intake or energy expenditure, although they do have reduced fat mass and are resistant to high-fat diet-induced obesity (Luo et al., 2003). The ERR α knockouts show a modest 1.4-fold reduction in cytochrome *c* mRNA, but no changes in the expression of other respiratory subunit genes have been noted. This contrasts sharply with homozygous knockouts of other genes that are essential to mitochondrial biogenesis. For example, both Tfam (Larsson et al., 1998) and NRF-1 (Huo and Scarpulla, 2001) knockout mice die during embryonic development, and embryos are severely depleted of mtDNA (🔗 [Table 7.3-1](#)).

4.1.1 PGC-1 α in Gluconeogenesis

In addition to its role in mitochondrial biogenesis and thermogenesis, PGC-1 α has been implicated in the regulation of blood glucose levels by controlling the expression of gluconeogenic enzymes during fasting (Yoon et al., 2001). PGC-1 α levels are elevated in the livers of fasting mice and in mouse models that mimic a deficiency in insulin action. Glucocorticoids and cAMP act synergistically to induce PGC-1 α in primary liver cultures, and overexpression of PGC-1 α upregulates important gluconeogenic enzymes, resulting in increased glucose production. Phosphoenolpyruvate carboxy kinase (PEPCK) is the rate-limiting enzyme in gluconeogenesis, and PGC-1 α *trans*-activates the PEPCK promoter through glucocorticoid receptor and hepatic nuclear factor α . The transcription factor CREB is important in controlling PGC-1 α expression. Expression of the gluconeogenic pathway is reduced during fasting in CREB knockout mice because of a deficiency in ser133-phosphorylated CREB and the loss of a direct CRE-mediated CREB induction of PGC-1 α expression (Herzig et al., 2001). Glucose levels and the expression of the gluconeogenic pathway can be restored by overexpression of PGC-1 α in CREB-deficient mice. These results suggest that PGC-1 α can regulate gluconeogenesis in liver through an insulin- and cAMP-dependent mechanism (🔗 [Figure 7.3-3](#)). Surprisingly, however, the PGC-1 α -null mice constitutively activate the expression of gluconeogenic genes even in the fed state, probably through elevated CEBP β (Lin et al., 2004). Also, since reduced oxidative phosphorylation has been linked to insulin resistance one might expect that the PGC-1 α -null mice exhibit insulin resistance and obesity. Contrary to this expectation the mice were lean and insulin sensitive. This was attributed to an increased energy expenditure related to hyperactivity.

4.1.2 PGC-1 α Mechanisms

PGC-1 α has a potent transcriptional activation domain but appears devoid of histone-modifying activities. Transcriptional activation by PGC-1 α appears to be mediated by the ability of PGC-1 α to recruit other coactivators such as SRC-1 and CBP/p300 that have intrinsic histone acetyltransferase activity (Puigserver et al., 1999). Docking of PGC-1 α to a DNA-bound transcription factor is thought to induce a conformational change in PGC-1 α , which facilitates recruitment of histone-modifying coactivators. These coactivators bind the amino-terminal activation domain. PGC-1 α is also one of the few nuclear factors identified that can couple transcription and mRNA processing. The carboxy-terminal domain of PGC-1 α has an RNA recognition motif and an RS arginine and serine rich domain that are common to proteins involved in both constitutive and tissue-specific RNA splicing. This domain is required for its association with splicing factors. When these domains are intact, PGC-1 α can facilitate mRNA splicing of a target gene only when bound to a cognate promoter (Monsalve et al., 2000).

Indirect evidence suggested that a repressor, regulated by the mitogen-activated protein kinase pathway, may inhibit the PGC-1 α coactivation of steroid hormone responses (Knutti et al., 2001). Phosphorylation of PGC-1 α by this pathway presumably results in the dissociation of the PGC-1 α -receptor complex and the consequent coactivation through the steroid receptor. A good candidate for this repressor is p160 myb-binding protein, which interacts with the negative regulatory domain of PGC-1 α (Fan et al., 2004). Phosphorylation of PGC-1 α by p38 MAP kinase disrupts the binding of p160 myb-binding protein, leading to derepression of coactivator function. The activation of PGC-1 α by p38 MAP kinase can mediate the effects of cytokines on energy expenditure, possibly accounting for the negative energy balance associated with chronic disease states (Puigserver et al., 2001). In particular, cytokines could stimulate the transcriptional activity of NRF-1 only in the presence of PGC-1 α . This may lead to a cytokine-dependent increase in respiration and the induction of respiratory gene expression in muscle cells. In addition to these interactions, PGC-1 α may engage in multiple independent interactions with factors necessary for chromatin remodeling as well as those of the TRAP/mediator complex, which communicates with the general transcriptional machinery (Wallberg et al., 2003).

4.2 PGC-1 α -Related Coactivators

4.2.1 PRC

PGC-1 α is not detected in cultured fibroblasts and myoblasts that nevertheless maintain mitochondria and respiratory function. This, along with the tissue-restricted pattern of PGC-1 α expression, raised the question of whether there are relatives of PGC-1 α that differ in their mode of regulation or transcription factor specificity. A database search identified the partial sequence of a large cDNA (Nagase et al., 1998) with sequence similarity to PGC-1 α in the carboxy-terminal domain comprising the RNA recognition motif and the RS domain. A full-length cDNA was cloned and revealed additional sequence similarities with PGC-1 α , including an acidic amino-terminal region, an LXXLL signature for nuclear receptor coactivators, and a proline-rich region. The spatial conservation of these features was highly suggestive of related function, and the protein encoded by this cDNA was designated as PGC-1 α -related coactivator (PRC) (Andersson and Scarpulla, 2001).

PRC is identical to PGC-1 α in its interaction with NRF-1 and its ability to utilize NRF-1 for the *trans*-activation of NRF-1 target genes (Andersson and Scarpulla, 2001). PRC and NRF-1 colocalize to the nucleoplasm and interact both *in vitro* and *in vivo*. PGC-1 α and PRC binding to NRF-1 occurs through the NRF-1 DNA-binding domain, and NRF-1-dependent *trans*-activation by both coactivators requires the conserved amino-terminal activation domain. Interestingly, both NRF-1 and CREB sites were targets for *trans*-activation of the cytochrome *c* promoter by PRC, and recent experiments show that PRC and PGC-1 α can interact with CREB *in vitro* (unpublished). This may reflect the importance of PRC in CREB-dependent functions.

Despite the structural and functional similarities between PRC and PGC-1 α , the expression pattern of PRC was substantially different (Andersson and Scarpulla, 2001). PRC mRNA did not exhibit large tissue differences in steady-state levels except for somewhat higher levels in human skeletal muscle. In contrast to

PGC-1 α , PRC mRNA was not enriched in brown versus white fat and was only slightly elevated in brown fat upon cold exposure. This argues against a major role for PRC in adaptive thermogenesis. In contrast, PRC was expressed more abundantly in proliferating cells compared with growth-arrested cells and was rapidly and markedly induced upon serum treatment of quiescent fibroblasts (▶ [Figure 7.3-3](#)). These cell cycle changes in PRC expression were observed in the absence of detectable PGC-1 α , suggesting that PRC responds to proliferative signals rather than to thermogenic signals that govern PGC-1 α expression. Thus, it appears that PRC is a growth-regulated coactivator that may coordinate the activities of multiple transcription factors required for cell growth.

An unresolved issue is whether the constituents of the mitochondrial transcriptional machinery are coordinately induced or whether there is a single factor that is rate limiting. It was of interest to determine whether NRFs and the PGC-1 family coactivators control expression of the mitochondrial transcription specificity factors, TFB1M and TFB2M. A series of promoter mutations combined with DNA-binding assays recently established that human TFB expression depends upon both NRF-1 and NRF-2 as major determinants of promoter function (Gleyzer et al., 2005). The NRF-binding sites within the proximal promoters serve as targets for *trans*-activation by the PGC-1 family coactivators, PGC-1 α and PRC. Moreover, the expression of both TFBs is upregulated in response to serum growth factors and during L1 adipocyte differentiation where mitochondrial biogenesis is evident (Wilson-Fritch et al., 2003). Cytochrome *c* is markedly induced in both systems, as a marker of mitochondrial biogenesis. Enhanced TFB expression accompanies the induction of either PRC in response to serum growth factors or PGC-1 α during adipocyte differentiation. Ectopic expression of PGC-1 α in myoblasts results in the coordinate induction of Tfam and TFB mRNAs, as part of a pattern of gene expression similar to that observed during adipocyte differentiation. These results suggest that the coactivator can function as a limiting factor in the coordinate expression of mitochondrial transcription factors.

4.2.2 PGC-1 β

Another addition to the PGC-1 α family of coactivators was designated as PGC-1 β (Lin et al., 2002) or PERC (Kressler et al., 2002). In contrast to PRC, where the sequence similarity with PGC-1 α is confined to distinct functional domains, the sequence similarity between PGC-1 α and PGC-1 β is distributed along their entire lengths, with greater sequence conservation in the amino-terminal activation domain and the carboxy-terminal RNA-binding domain. Steady-state tissue levels of PGC-1 β mRNA parallel that of PGC-1 α , with the highest levels in brown fat, and in heart and skeletal muscle. However, PGC-1 β differs from PGC-1 α in that it is not induced in brown fat upon cold exposure (Lin et al., 2002) and it is a poor inducer of gluconeogenic gene expression in hepatocytes and liver (Lin et al., 2003; Meirhaeghe et al., 2003). This most likely results from the absence of an interaction between hepatic nuclear receptor 4 α and forkhead transcription factor 01, which mediate the expression of gluconeogenic genes. However, despite these differences, PGC-1 β binds NRF-1 and is a potent coactivator of NRF-1 target genes, leading to increased mitochondrial gene expression (Lin et al., 2002, 2003). Moreover, ectopic expression of PGC-1 β results in increased mitochondrial biogenesis and oxygen consumption (Meirhaeghe et al., 2003), although PGC-1 α has been associated with higher proton leak rates than PGC-1 β (St Pierre et al., 2003). These results demonstrate that although PGC-1 α and β are functionally divergent, they retain the ability to activate the biogenesis of mitochondria through their interaction with NRF-1 and possibly other transcription factors. Since the tissue-specific expression pattern of the two coactivators is very similar, PGC-1 β may compensate for the absence of PGC-1 α in PGC-1 α -null mice in maintaining mitochondrial function.

5 Transcriptional Links Between Mitochondrial Biogenesis and Neurological Function

Fragile X syndrome, a leading cause of heritable mental retardation, results from aberrant expression of the *FMRI* gene (Oberle et al., 1991). The failure to express *FMRI* is associated with an expansion of CGG

repeats within the 5'-untranslated region leading to abnormal methylation of the CpG islands within the promoter and transcriptional silencing (Verkerk et al., 1991). *FMR1* encodes an RNA-binding protein that may function in RNA transport between the cytoplasm and the nucleus (Feng et al., 1997). FMRP associates with translating polyribosomes and has structural features in common with hnRNPs (Corbin et al., 1997). *FMR1* knockout mice display difficulties in learning and macroorchidism, resembling those symptoms present in fragile X patients (The Dutch–Belgian Fragile X Consortium, 1994). In vivo footprinting has identified NRF-1 as one of several transcription factors interacting with the *FMR1* promoter region (Schwemmle et al., 1997; Drouin et al., 1997). NRF-1 is a major determinant of *FMR1* promoter function, and NRF-1 binding was detected in normal cells but not in those with fragile X mutations. Methylation abolishes NRF-1 binding to the promoter region and inhibits *FMR1* transcription (Kumari and Usdin, 2001). These results indicate that a failure to bind NRF-1 contributes to the loss of *FMR1* transcription in cells harboring the fragile X mutation.

NRF-1 may also be involved in the expression of several other genes required for normal neurological function. Both NRF-1 and Ets sites are present in the human gene encoding neuronal nitric oxide synthase (Hall et al., 1994). This isoform has been implicated in the regulation of neuronal functions including neuronal transmission. This may be significant since nitric oxide appears to induce mitochondrial biogenesis through its stimulatory effects on PGC-1 α expression (Nisoli et al., 2003). The increased mitochondrial content in response to nitric oxide is accompanied by increased oxygen consumption and food intake and is not restricted to brown fat but occurs in a variety of cell types. Endothelial nitric oxide synthase-null mice exhibit reductions in mitochondrial content and size along with lower oxygen consumption and ATP production (Nisoli et al., 2004). Thus, it is possible that stimulation of nitric oxide production in neuronal cells may enhance the maintenance and function of mitochondria through PGC-1 α and NRF-1.

Another NRF-1 target is the GluR2 subunit of the alpha-amino-3-hydroxy-4-isoxazole propionic acid (AMPA) subtype of glutamate receptor (Myers et al., 1998). Glutamate is the major excitatory neurotransmitter in the central nervous system and AMPA, one of several glutamate receptor subtypes, consists of combinations of multiple GluR subunits. The GluR2 subunit is particularly important in controlling permeability to calcium ions, and expression levels have been correlated with neuronal activity in visual cortical neurons (Bai and Wong-Riley, 2003). NRF-1 was identified as a major positive regulator, along with Sp1, of the GluR2 promoter by both mutational analysis and by *trans*-activation experiments (Myers et al., 1998). Although the minimal promoter showed a strong preference for neuronal cell expression, neither NRF-1 nor Sp1 showed cell-type selectivity in transient transfection experiments. The human gene encoding integrin-associated protein (IAP), also called CD47, is also regulated by NRF-1 (Chang and Huang, 2004). This protein is widely expressed in the nervous and immune systems and has been associated with learning and memory in rodents (Chang et al., 1999, 2001). An NRF-1 recognition site is conserved in mouse, rat, and human IAP gene promoters and is demonstrated to be a major determinant of human promoter function by mutational analysis, DNA-binding assays, and *trans*-activation experiments (Chang and Huang, 2004). Moreover, expression of a dominant-negative allele of NRF-1 inhibited promoter activity in transfected cells.

The association of NRF-1 with neurological function is supported by studies of NRF-1 relatives in *Drosophila* and zebra fish. Partial loss-of-function mutations in EWG, an NRF-1 relative in *Drosophila*, resulted in aberrant intersegmental axonal projection pathways in the embryo (Desimone and White, 1993). Total loss-of-function mutations in EWG are lethal to the embryo. The NRF-1 gene in zebra fish is expressed in the eye and central nervous system of developing embryos. Its disruption gives a larval–lethal phenotype accompanied by defects in the development of the central nervous system (Becker et al., 1998).

The connection between transcription factors involved in mitochondrial biogenesis and neurological function extends to NRF-2 as well. A strong correlation has been observed between NRF-2 α and cytochrome oxidase expression in the visual cortex (Nie and Wong-Riley, 1999). In this case, NRF-2 α and cytochrome oxidase were associated with metabolic state and neuronal activity in mature neurons, suggesting that NRF-2 α is important in maintaining neuronal function. Moreover, the correlation was extended to NRF-2 α mRNA, indicating that NRF-2 α may be regulated at the transcriptional level by neuronal activity (Guo et al., 2000). There is also evidence that both NRF-2 (GABP) α and β subunits

are enriched in the nucleus in response to neuronal stimulation (Zhang and Wong-Riley, 2000), and both subunits are specifically translocated to the nucleus in response to neuronal depolarization (Yang et al., 2004). These findings suggest that the nuclear translocation of NRF-2 (GABP) may serve a sensory function for the purpose of increasing metabolic gene expression, in response to changes in neuronal activity. The mechanisms by which these changes occur will be of considerable interest.

Acknowledgment

Work in the author's laboratory is supported by United States Public Health Service Grant GM32525-23 from the National Institutes of Health.

References

- Andersson U, Scarpulla RC. 2001. PGC-1-related coactivator, a novel, serum-inducible coactivator of nuclear respiratory factor 1-dependent transcription in mammalian cells. *Mol Cell Biol* 21: 3738-3749.
- Ashley MV, Laipis PJ, Hauswirth, WW. 1989. Rapid segregation of heteroplasmic bovine mitochondria. *Nucleic Acids Res* 17: 7325-7331.
- Au HC, Scheffler IE. 1998. Promoter analysis of the human succinate dehydrogenase iron-protein gene. Both nuclear respiratory factors NRF-1 and NRF-2 are required. *Eur J Biochem* 251: 164-174.
- Baar K, Wende AR, Jones TE, Marison M, Nolte LA, et al. 2002. Adaptations of skeletal muscle to exercise: Rapid increase in the transcriptional coactivator PGC-1. *FASEB J* 16: 1879-1886.
- Bai X, Wong-Riley MTT. 2003. Neuronal activity regulates protein and gene expressions of GluR2 in postnatal rat visual cortical neurons in culture. *J Neurocytol* 32: 71-78.
- Basu A, Lenka N, Mullick J, Avadhani NG. 1997. Regulation of murine cytochrome oxidase Vb gene expression in different tissues and during myogenesis—role of a YY-1 factor-binding negative enhancer. *J Biol Chem* 272: 5899-5908.
- Batchelor AH, Piper DE, De la Brousse FC, McKnight SL, Wolberger C. 1998. The structure of GABP α/β : An ETS domain ankyrin repeat heterodimer bound to DNA. *Science* 279: 1037-1041.
- Becker TS, Burgess SM, Amsterdam AH, Allende ML, Hopkins N. 1998. Not really finished is crucial for development of the zebrafish outer retina and encodes a transcription factor highly homologous to human nuclear respiratory factor 1 and avian initiation binding repressor. *Development* 124: 4369-4378.
- Bergeron R, Ren JM, Cadman KS, Moore IK, Perret P, et al. 2001. Chronic activation of AMP kinase results in NRF-1 activation and mitochondrial biogenesis. *Am J Physiol Endocrinol Metab* 281: E1340-E1346.
- Bogenhagen DF. 1996. Interaction of mtTFB and mtRNA polymerase at core promoters for transcription of *Xenopus laevis* mtDNA. *J Biol Chem* 271: 12036-12041.
- Bogenhagen DF, Clayton DA. 2003. The mitochondrial DNA replication bubble has not burst. *Trends Biochem Sci* 28: 357-360.
- Calzone FJ, Hoog C, Teplow DB, Cutting AE, Zeller RW, et al. 1991. Gene regulatory factors of the sea urchin embryo. I. Purification by affinity chromatography and cloning of P3A2, a novel DNA binding protein. *Development* 112: 335-350.
- Cam H, Balciunaite E, Blias A, Spektor A, Scarpulla RC, et al. 2004. A common set of gene regulatory networks links metabolism and growth inhibition. *Mol Cell* 16: 399-411.
- Carter RS, Bhat NK, Basu A, Avadhani NG. 1992. The basal promoter elements of murine cytochrome *c* oxidase subunit IV gene consist of tandemly duplicated ets motifs that bind to GABP-related transcription factors. *J Biol Chem* 267: 23418-23426.
- Chang DD, Hauswirth WW, Clayton DA. 1985. Replication priming and transcription initiate from precisely the same site in mouse mitochondrial DNA. *EMBO J* 4: 1559-1567.
- Chang HP, Lindberg FP, Wang HL, Huang AM, Lee EH. 1999. Impaired memory retention and decreased long-term potentiation in integrin-associated protein-deficient mice. *Learn Mem* 6: 448-457.
- Chang HP, Ma YL, Wan FJ, Tsai LY, Lindberg FP, et al. 2001. Functional blocking of integrin-associated protein impairs memory retention and decreases glutamate release from the hippocampus. *Neuroscience* 102: 289-296.
- Chang WT, Huang AM. 2004. α -Pal/NRF-1 regulates the promoter of the human integrin-associated protein/CD47 gene. *J Biol Chem* 279: 14542-14550.
- Chau CA, Evans MJ, Scarpulla RC. 1992. Nuclear respiratory factor 1 activation sites in genes encoding the gamma-subunit of ATP synthase, eukaryotic initiation factor 2 α ,

- and tyrosine aminotransferase. Specific interaction of purified NRF-1 with multiple target genes. *J Biol Chem* 267: 6999-7006.
- Chinenov Y, Henzl M, Martin ME. 2000. The α and β subunits of the GA-binding protein form a stable heterodimer in solution. *J Biol Chem* 275: 7749-7756.
- Choi YS, Lee HK, Pak YK. 2002. Characterization of the 5'-flanking region of the rat gene for mitochondrial transcription factor A (Tfam). *Biochim Biophys Acta Gene Struct Expr* 1574: 200-204.
- Clayton DA. 2000. Vertebrate mitochondrial DNA—a circle of surprises. *Exp Cell Res* 255: 4-9.
- Clayton DA. 2003. Mitochondrial DNA replication: What we know. *IUBMB Life* 55: 213-217.
- Corbin F, Bouillon M, Fortin A, Morin S, Rousseau F, et al. 1997. The fragile X mental retardation protein is associated with poly(A)+ mRNA in actively translating polyribosomes. *Hum Mol Genet* 6: 1465-1472.
- Costanzo MC, Fox TD. 1990. Control of mitochondrial gene expression in *Saccharomyces cerevisiae*. *Annu Rev Genet* 24: 91-113.
- Desimone SM, White K. 1993. The *Drosophila* erect wing gene, which is important for both neuronal and muscle development, encodes a protein which is similar to the sea urchin P3A2 DNA binding protein. *Mol Cell Biol* 13(6): 3641-3949.
- Diffley JF, Stillman B. 1991. A close relative of the nuclear, chromosomal high-mobility group protein HMG1 in yeast mitochondria. *Proc Natl Acad Sci USA* 88: 7864-7868.
- Dong XC, Ghoshal K, Majumder S, Yadav SP, Jacob ST. 2002. Mitochondrial transcription factor A and its downstream targets are up-regulated in a rat hepatoma. *J Biol Chem* 277: 43309-43318.
- Donohoe ME, Zhang X, McGinnis L, Biggers J, Li E, et al. 1999. Targeted disruption of mouse yin yang 1 transcription factor results in peri-implantation lethality. *Mol Cell Biol* 19: 7237-7244.
- Drouin R, Angers M, Dallaire N, Rose TM, Khandjian EW, et al. 1997. Structural and functional characterization of the human FMR1 promoter reveals similarities with the hnRNP-A2 promoter region. *Hum Mol Genet* 6: 2051-2060.
- Efiok BJS, Safer B. 2000. Transcriptional regulation of E2F-1 and eIF-2 genes by α -Pal: A potential mechanism for coordinated regulation of protein synthesis, growth, and the cell cycle. *Biochim Biophys Acta Mol Cell Res* 1495: 51-68.
- Elbehti-Green A, Au HC, Mascarello JT, Ream-Robinson D, Scheffler IE. 1998. Characterization of the human *SDHC* gene encoding one of the integral membrane proteins of succinate-quinone oxidoreductase in mitochondria. *Gene* 213: 133-140.
- Evans MJ, Scarpulla RC. 1988. Both upstream and intron sequence elements are required for elevated expression of the rat somatic cytochrome *c* gene in COS-1 cells. *Mol Cell Biol* 8: 35-41.
- Evans MJ, Scarpulla RC. 1989. Interaction of nuclear factors with multiple sites in the somatic cytochrome *c* promoter. Characterization of upstream NRF-1, ATF and intron Sp1 recognition sites. *J Biol Chem* 264: 14361-14368.
- Falkenberg M, Gaspari M, Rantanen A, Trifunovic A, Larsson N-G, et al. 2002. Mitochondrial transcription factors B1 and B2 activate transcription of human mtDNA. *Nat Genet* 31: 289-294.
- Fan M, Rhee J, St Pierre J, Handschin C, Puigserver P, et al. 2004. Suppression of mitochondrial respiration through recruitment of p160 myb binding protein to PGC-1 α : Modulation by p38 MAPK. *Genes Dev* 18: 278-289.
- Feng Y, Gutekunst CA, Eberhart DE, Yi H, Warren ST, et al. 1997. Fragile X mental retardation protein: Nucleocytoplasmic shuttling and association with somatodendritic ribosomes. *J Neurosci* 17: 1539-1547.
- Fisher RP, Clayton DA. 1985. A transcription factor required for promoter recognition by human mitochondrial RNA polymerase. Accurate initiation at the heavy- and light-strand promoters dissected and reconstituted in vitro. *J Biol Chem* 260: 11330-11338.
- Fisher RP, Lisowsky T, Parisi MA, Clayton DA. 1992. DNA wrapping and bending by a mitochondrial high mobility group-like transcriptional activator protein. *J Biol Chem* 267: 3358-3367.
- Fisher RP, Parisi MA, Clayton DA. 1989. Flexible recognition of rapidly evolving promoter sequences by mitochondrial transcription factor 1. *Genes Dev* 3: 2202-2217.
- FitzGerald PC, Shlyakhtenko A, Mir AA, Vinson C. 2004. Clustering of DNA sequences in human promoters. *Genome Res* 14: 1562-1574.
- Forsburg SL, Guarente L. 1989. Identification and characterization of HAP4: A third component of the CCAAT-bound HAP2/HAP3 heteromer. *Genes Dev* 3: 1166-1178.
- Foury F. 1989. Cloning and sequencing of the nuclear gene MIP1 encoding the catalytic subunit of the yeast mitochondrial DNA polymerase. *J Biol Chem* 264: 20552-20560.
- Garesse R, Vallejo CG. 2001. Animal mitochondrial biogenesis and function: A regulatory cross-talk between two genomes. *Gene* 263: 1-16.
- Gleyzer N, Vercauteren K, Scarpulla RC. 2005. Control of mitochondrial transcription specificity factors (TFB1M and TFB2M) by nuclear respiratory factors (NRF-1 and NRF-2) and PGC-1 family coactivators. *Mol Cell Biol* 25 (4): 1351-1366.
- Gomez-Cuadrado A, Martin M, Noel M, Ruiz-Carrillo A. 1995. Initiation binding receptor, a factor that binds to the transcription initiation site of the histone *h5* gene, is a glycosylated member of a family of cell growth regulators. *Mol Cell Biol* 15: 6670-6685.

- Gopalakrishnan L, Scarpulla RC. 1994. Differential regulation of respiratory chain subunits by a CREB-dependent signal transduction pathway. Role of cyclic AMP in cytochrome *c* and COXIV gene expression. *J Biol Chem* 269: 105-113.
- Gugneja S, Scarpulla RC. 1997. Serine phosphorylation within a concise amino-terminal domain in nuclear respiratory factor 1 enhances DNA binding. *J Biol Chem* 272: 18732-18739.
- Gugneja S, Virbasius CA, Scarpulla RC. 1996. Nuclear respiratory factors 1 and 2 utilize similar glutamine-containing clusters of hydrophobic residues to activate transcription. *Mol Cell Biol* 16: 5708-5716.
- Gugneja S, Virbasius JV, Scarpulla RC. 1995. Four structurally distinct, non-DNA-binding subunits of human nuclear respiratory factor 2 share a conserved transcriptional activation domain. *Mol Cell Biol* 15: 102-111.
- Gulick T, Cresci S, Caira T, Moore DD, Kelly, DP. 1994. The peroxisome proliferator-activated receptor regulates mitochondrial fatty acid oxidative enzyme gene expression. *Proc Natl Acad Sci USA* 91: 11012-11016.
- Guo, AL, Nie, F, Wong-Riley, M. 2000. Human nuclear respiratory factor 2 α subunit cDNA: Isolation, subcloning, sequencing, and in situ hybridization of transcripts in normal and monocularly deprived macaque visual system. *J Comp Neurol* 417: 221-232.
- Gupta S, Van Tuyle GC. 1998. The gene and processed pseudogenes of the rat mitochondrial single-strand DNA-binding protein: Structure and promoter strength analyses. *Gene* 212: 269-278.
- Hahn S, Guarente L. 1988. Yeast HAP2 and HAP3: Transcriptional activators in a heteromeric complex. *Science* 240: 317-321.
- Hall AV, Antoniou H, Wang Y, Cheung AH, Arbus AM, et al. 1994. Structural organization of the human neuronal nitric oxide synthase gene (*NOS1*). *J Biol Chem* 269: 33082-33090.
- Herzig RP, Scacco S, Scarpulla RC. 2000. Sequential serum-dependent activation of CREB and NRF-1 leads to enhanced mitochondrial respiration through the induction of cytochrome *c*. *J Biol Chem* 275: 13134-13141.
- Herzig S, Long FX, Jhala US, Hedrick S, Quinn R, et al. 2001. CREB regulates hepatic gluconeogenesis through the coactivator PGC-1. *Nature* 413: 179-183.
- Hirawake H, Taniwaki M, Tamura A, Amino H, Tomitsuka E, et al. 1999. Characterization of the human SDHD gene encoding the small subunit of cytochrome *b* (*cybS*) in mitochondrial succinate-ubiquinone oxidoreductase. *Biochim Biophys Acta* 1412: 295-300.
- Hixson JE, Wong TW, Clayton DA. 1986. Both the conserved stem-loop and divergent 5'-flanking sequences are required for initiation at the human mitochondrial origin of light-strand DNA replication. *J Biol Chem* 261: 2384-2390.
- Holt IJ, Lorimer HE, Jacobs, HT. 2000. Coupled leading- and lagging-strand synthesis of mammalian mitochondrial DNA. *Cell* 100: 515-524.
- Huo, L, Scarpulla, RC. 2001. Mitochondrial DNA instability and peri-implantation lethality associated with targeted disruption of nuclear respiratory factor 1 in mice. *Mol Cell Biol* 21: 644-654.
- Huss JM, Kopp RP, Kelly DP. 2002. Peroxisome proliferator-activated receptor coactivator-1 α (PGC-1 α) coactivates the cardiac-enriched nuclear receptors estrogen-related receptor- α and - γ —identification of novel leucine-rich interaction motif within PGC-1 α . *J Biol Chem* 277: 40265-40274.
- Insdorf NE, Bogenhagen DF. 1989. DNA polymerase gamma from *Xenopus laevis*. II. A 3'→5' exonuclease is tightly associated with the DNA polymerase activity. *J Biol Chem* 264: 21498-21503.
- Izumi H, Ohta R, Nagatani G, Ise T, Nakayama Y, et al. 2003. p300/CBP-associated factor (P/CAF) interacts with nuclear respiratory factor-1 to regulate the UDP-N-acetyl- α -D-galactosamine: Polypeptide N-acetylgalactosaminyltransferase-3 gene. *Biochem J* 373: 713-722.
- Kaneda H, Hayashi J, Takahama S, Taya C, Lindahl KE, et al. 1995. Elimination of paternal mitochondrial DNA in intraspecific crosses during early mouse embryogenesis. *Proc Natl Acad Sci USA* 92: 4542-4546.
- Kelly DP, Scarpulla RC. 2004. Transcriptional regulatory circuits controlling mitochondrial biogenesis and function. *Genes Dev* 18: 357-368.
- Kherrouche Z, De Launoit Y, Monte D. 2004. The NRF-1/ α PAL transcription factor regulates human E2F6 promoter activity. *Biochem J* 383: 529-536.
- Kiss T, Filipowicz W. 1992. Evidence against a mitochondrial location of the 7-2/MRP RNA in mammalian cells. *Cell* 70: 11-16.
- Knutti D, Kressler D, Kralli A. 2001. Regulation of the transcriptional coactivator PGC-1 via MAPK-sensitive interaction with a repressor. *Proc Natl Acad Sci USA* 98: 9713-9718.
- Kraytsberg Y, Schwartz M, Brown TA, Ebralidse K, Kunz WS, et al. 2004. Recombination of human mitochondrial DNA. *Science* 304: 981
- Kressler D, Schreiber SN, Knutti D, Kralli A. 2002. The PGC-1-related protein PERC is a selective coactivator of estrogen receptor α . *J Biol Chem* 277: 13918-13925.
- Kumari D, Usdin K. 2001. Interaction of the transcription factors USF1, USF2, and α -Pal/NRF-1 with the FMR1 promoter. *J Biol Chem* 276: 4357-4364.
- LaMarco KL, McKnight SL. 1989. Purification of a set of cellular polypeptides that bind to the purine-rich *cis*-regulatory element of herpes simplex virus immediate early genes. *Genes Dev* 3: 1372-1383.

- Larsson NG, Wang JM, Wilhelmsson H, Oldfors A, Rustin P, et al. 1998. Mitochondrial transcription factor A is necessary for mtDNA maintenance and embryogenesis in mice. *Nature Genetics* 18: 231-236.
- Leclercq N, Van Der Bruggen P, Foury F. 1997. Mitochondrial DNA polymerases from yeast to man: A new family of polymerases. *Gene* 185: 147-152.
- Lee DY, Clayton DA. 1997. RNase mitochondrial RNA processing correctly cleaves a novel R loop at the mitochondrial DNA leading-strand origin of replication. *Genes Dev* 11: 582-592.
- Lehman JJ, Barger PM, Kovacs A, Saffitz JE, Medeiros DM, et al. 2000. Peroxisome proliferator-activated receptor γ coactivator-1 promotes cardiac mitochondrial biogenesis. *J Clin Invest* 106: 847-856.
- Leone TC, Lehman JJ, Finck BN, Schaeffer PJ, Wende AR, Boudina S, Courtois M, Wozniak DF, Sambandam N, Bernal-Mizrachi C, Chen Z, Holloszy JO, Medeiros DM, Schmidt RE, Saffitz JE, Abel ED, Semenkovich CF, Kelly DP. 2005. PGC-1 α deficiency causes multi-system energy metabolic derangements: Muscle dysfunction, abnormal weight control and hepatic steatosis. *PLoS Biol.* 3: e101.
- Lewis DL, Farr CL, Wang YX, Lagina AT III, Kaguni LS. 1996. Catalytic subunit of mitochondrial DNA polymerase from *Drosophila* embryos—cloning, bacterial overexpression, and biochemical characterization. *J Biol Chem* 271: 23389-23394.
- Li K, Smagula CS, Parsons WJ, Richardson JA, Gonzalez M, et al. 1994. Subcellular partitioning of MRP RNA assessed by ultrastructural and biochemical analysis. *J Cell Biol* 124: 871-882.
- Li R, Hodny Z, Luciakova K, Barath P, Nelson BD. 1996a. Sp1 activates and inhibits transcription from separate elements in the proximal promoter of the human adenine nucleotide translocase 2 (*ANT2*) gene. *J Biol Chem* 271: 18925-18930.
- Li R, Luciakova K, Nelson BD. 1996b. Expression of the human cytochrome c_1 gene is controlled through multiple Sp1-binding sites and an initiator region. *Eur J Biochem* 241: 649-656.
- Lin J, Puigserver P, Donovan J, Tarr P, Spiegelman BM. 2002. PGC-1 β : A novel PGC-1-related transcription coactivator associated with host cell factor. *J Biol Chem* 277: 1645-1648.
- Lin J, Wu P, Tarr PT, Lindenberg KS, St-Pierre J, et al. 2004. Defects in adaptive energy metabolism with CNS-linked hyperactivity in PGC-1 α null mice. *Cell* 119: 121-135.
- Lin JD, Tarr PT, Yang RJ, Rhee J, Puigserver P, et al. 2003. PGC-1 β in the regulation of hepatic glucose and energy metabolism. *J Biol Chem* 278: 30843-30848.
- Lowell BB, Spiegelman BM. 2000. Towards a molecular understanding of adaptive thermogenesis. *Nature* 404: 652-660.
- Lowry CV, Zitomer RS. 1988. *ROX1* encodes a heme-induced repression factor regulating *ANBI* and *CYC7* of *Saccharomyces cerevisiae*. *Mol Cell Biol* 8: 4651-4658.
- Luo J, Sladek R, Carrier J, Bader J, Richard D, et al. 2003. Reduced fat mass in mice lacking orphan nuclear receptor estrogen-related receptor α . *Mol Bio Cell* 23: 7947-7956.
- Madsen CS, Ghivizzani SC, Hauswirth WW. 1993. Protein binding to a single termination-associated sequence in the mitochondrial DNA D-loop region. *Mol Cell Biol* 13: 2162-2171.
- McCulloch V, Seidel-Rogol BL, Shadel GS. 2002. A human mitochondrial transcription factor is related to RNA adenine methyltransferases and binds S-adenosylmethionine. *Mol Cell Biol* 22: 1116-1125.
- McNabb DS, Xing Y, Guarente L. 1995. Cloning of yeast *HAP5*: A novel subunit of a heterotrimeric complex required for CCAAT binding. *Genes Dev* 9: 47-58.
- Meirhaeghe A, Crowley V, Lenaghan C, Lelliott C, Green K, et al. 2003. Characterization of the human, mouse and rat PGC1 β (peroxisome-proliferator-activated receptor-gamma co-activator 1 β) gene in vitro and in vivo. *Biochem J* 373: 155-165.
- Miranda S, Foncea R, Guerreo J, Leighton F. 1999. Oxidative stress and upregulation of mitochondrial biogenesis genes in mitochondrial DNA-depleted HeLa cells. *Biochem Biophys Res Commun* 258: 44-49.
- Monsalve M, Wu Z, Adelman G, Puigserver P, Fan M, et al. 2000. Direct coupling of transcription and mRNA processing through the thermogenic coactivator PGC-1. *Mol Cell* 6: 307-316.
- Montoya J, Gaines GL, Attardi G. 1983. The pattern of transcription of the human mitochondrial rRNA genes reveals two overlapping transcription units. *Cell* 34: 151-159.
- Mootha VK, Handschin C, Arlow D, Xie XH, St Pierre J, et al. 2004. *Err α* and *Gabpa/b* specify PGC-1 α -dependent oxidative phosphorylation gene expression that is altered in diabetic muscle. *Proc Natl Acad Sci USA* 101: 6570-6575.
- Moraes CT. 2001. What regulates mitochondrial DNA copy number in animal cells? *Trends Genet* 17: 199-205.
- Murakami T, Shimomura Y, Yosimura A, Sokabe M, Fujitsuka N. 1998. Induction of nuclear respiratory factor-1 expression by an acute bout of exercise in rat muscle. *Biochem Biophys Acta* 1381: 113-122.
- Myers SJ, Peters J, Huang Y, Comer MB, Barthel F, et al. 1998. Transcriptional regulation of the *Glur2* gene: Neural-specific expression, multiple promoters, and regulatory elements. *J Neurosci* 18: 6723-6739.
- Nagase T, Ishikawa K, Miyajima N, Tanaka A, Kotani H, et al. 1998. Prediction of the coding region sequences of unidentified human genes. IX. The complete sequences of 100 new cDNA clones from brain which can code for large proteins in vitro. *DNA Res* 5: 31-39.

- Nass MMK, Nass S, Afzelius BA. 1965. The general occurrence of mitochondrial DNA. *Exp Cell Res* 37: 190-200.
- Nau PT, Van Natta T, Ralphe JC, Teneyck CJ, Bedell KA, et al. 2002. Metabolic adaptation of the fetal and postnatal ovine heart: Regulatory role of hypoxia-inducible factors and nuclear respiratory factor-1. *Pediatr Res* 52: 269-278.
- Nie F, Wong-Riley M. 1999. Nuclear respiratory factor-2 subunit protein: Correlation with cytochrome oxidase and regulation by functional activity in the monkey primary visual cortex. *J Comp Neurol* 404: 310-320.
- Nisoli E, Clementi E, Paolucci C, Cozzi V, Tonello C, et al. 2003. Mitochondrial biogenesis in mammals: The role of endogenous nitric oxide. *Science* 299: 896-899.
- Nisoli E, Falcone S, Tonello C, Cozzi V, Palomba L, et al. 2004. Mitochondrial biogenesis by NO yields functionally active mitochondria in mammals. *Proc Natl Acad Sci USA* 101: 16507-16512.
- Oberle I, Rousseau F, Heitz D, Kretz C, Devys D, et al. 1991. Instability of a 550-base pair DNA segment and abnormal methylation in fragile X syndrome. *Science* 252: 1097-1102.
- Ojala D, Montoya J, Attardi G. 1981. tRNA punctuation model of RNA processing in human mitochondria. *Nature* 290: 470-474.
- Ojuka EO, Jones TE, Han DH, Chen M, Holloszy JO. 2003. Raising Ca^{2+} in L6 myotubes mimics effects of exercise on mitochondrial biogenesis in muscle. *FASEB J* 17: 675-681.
- Olesen JT, Guarente L. 1990. The HAP2 subunit of yeast CCAAT transcriptional activator contains adjacent domains for subunit association and DNA recognition: Model for the HAP2/3/4 complex. *Genes Dev* 4: 1714-1729.
- Parisi MA, Clayton DA. 1991. Similarity of human mitochondrial transcription factor 1 to high mobility group proteins. *Science* 252: 965-969.
- Pfeifer K, Prezant T, Guarente L. 1987. Yeast HAP1 activator binds to two upstream activation sites of different sequence. *Cell* 49: 19-27.
- Piko L, Taylor KD. 1987. Amounts of mitochondrial DNA and abundance of some mitochondrial gene transcripts in early mouse embryos. *Dev Biol* 123: 364-374.
- Poulton J, Morten K, Freeman-Emmerson C, Potter C, Sewry C, et al. 1994. Deficiency of the human mitochondrial transcription factor h-mTFA in infantile mitochondrial myopathy is associated with mtDNA depletion. *Hum Mol Genet* 3: 1763-1769.
- Poyton RO, McEwen JE. 1996. Crosstalk between nuclear and mitochondrial genomes. *Annu Rev Biochem* 65: 563-607.
- Puigserver P, Adelmant C, Wu ZD, Fan M, Xu JM, et al. 1999. Activation of PPAR γ coactivator-1 through transcription factor docking. *Science* 286: 1368-1371.
- Puigserver P, Rhee J, Lin J, Wu Z, Yoon JC, et al. 2001. Cytokine stimulation of energy expenditure through p38 MAP kinase activation of PPAR γ coactivator-1. *Mol Cell* 8: 971-982.
- Puigserver P, Wu Z, Park CW, Graves R, Wright M, et al. 1998. A cold-inducible coactivator of nuclear receptors linked to adaptive thermogenesis. *Cell* 92: 829-839.
- Rantanen A, Gaspari M, Falkenberg M, Gustafsson CM, Larsson N-G. 2003. Characterization of the mouse genes for mitochondrial transcription factors B1 and B2. *Mamm Genome* 14: 1-6.
- Rantanen A, Jansson M, Oldfors A, Larsson N-G. 2001. Downregulation of Tfam and mtDNA copy number during mammalian spermatogenesis. *Mamm Genome* 12: 787-792.
- Ren B, Dynlacht BD. 2004. Use of chromatin immunoprecipitation assays in genome-wide location analysis of mammalian transcription factors. *Methods Enzymol* 376: 304-315.
- Ricquier D, Bouillaud F. 2000. Mitochondrial uncoupling proteins: From mitochondria to the regulation of energy balance. *J Physiol* 529: 3-10.
- Risteovski S, O'Leary DA, Thornell AP, Owen MJ, Kola I, et al. 2004. The ETS transcription factor GABP α is essential for early embryogenesis. *Mol Cell Biol* 24: 5844-5849.
- Satoh M, Kuroiwa T. 1991. Organization of multiple nucleoids and DNA molecules in mitochondria of a human cell. *Exp Cell Res* 196: 137-140.
- Scarpulla RC. 1997. Nuclear control of respiratory chain expression in mammalian cells. *J Bioenerg Biomembr* 29: 109-119.
- Scarpulla RC. 1999. Nuclear transcription factors in cytochrome *c* and cytochrome oxidase expression. *Frontiers of cellular bioenergetics: Molecular biology, biochemistry, and physiopathology*. Papa S, Guerrieri F, Tager JM, editors. London: Plenum Publishing.
- Scarpulla RC. 2002a. Nuclear activators and coactivators in mammalian mitochondrial biogenesis. *Biochem Biophys Acta* 1576: 1-14.
- Scarpulla RC. 2002b. Transcriptional activators and coactivators in the nuclear control of mitochondrial function in mammalian cells. *Gene* 286: 81-89.
- Scarpulla RC, Nye SH. 1986. Functional expression of rat cytochrome *c* in *Saccharomyces cerevisiae*. *Proc Natl Acad Sci USA* 83: 6352-6356.
- Schaefer L, Engman H, Miller JB. 2000. Coding sequence, chromosomal localization, and expression pattern of *Nrf-1*: The mouse homolog of *Drosophila* erect wing. *Genome* 11: 104-110.
- Schreiber SN, Emter R, Hock MB, Knutti D, Cardenas J, et al. 2004. The estrogen-related receptor α (ERR α) functions in PPAR γ coactivator 1 α (PGC-1 α)-induced mitochondrial biogenesis. *Proc Natl Acad Sci USA* 101: 6472-6477.

- Schreiber SN, Knutti D, Brogli K, Uhlmann T, Kralli A. 2003. The transcriptional coactivator PGC-1 regulates the expression and activity of the orphan nuclear receptor estrogen-related receptor α (ERR α). *J Biol Chem* 278: 9013-9018.
- Schubot FD, Chen CJ, Rose JP, Dailey TA, Dailey HA, et al. 2001. Crystal structure of the transcription factor sc-mtTFB offers insights into mitochondrial transcription. *Protein Sci* 10: 1980-1988.
- Schultz RA, Swoap SJ, McDaniel LD, Zhang BQ, Koon EC, et al. 1998. Differential expression of mitochondrial DNA replication factors in mammalian tissues. *J Biol Chem* 273: 3447-3451.
- Schwartz M, Vissing J. 2002. Paternal inheritance of mitochondrial DNA. *N Engl J Med* 347: 576-580.
- Schwemmle S, de Graaff E, Deissler H, Gläser D, Wöhrle D, et al. 1997. Characterization of FMR1 promoter elements by in vivo footprinting analysis. *Am J Hum Genet* 60: 1354-1362.
- Seelan RS, Gopalakrishnan L, Scarpulla RC, Grossman LI. 1996. Cytochrome *c* oxidase subunit VIIa liver isoform: Characterization and identification of promoter elements in the bovine gene. *J Biol Chem* 271: 2112-2120.
- Seelan RS, Grossman LI. 1997. Structural organization and promoter analysis of the bovine cytochrome *c* oxidase subunit VIc gene—a functional role for YY1. *J Biol Chem* 272: 10175-10181.
- Shadel GS, Clayton DA. 1993. Mitochondrial transcription initiation. Variation and conservation. *J Biol Chem* 268: 16083-16086.
- Shadel GS, Clayton DA. 1995. A *Saccharomyces cerevisiae* mitochondrial transcription factor, sc-mtTFB, shares features with sigma factors but is functionally distinct. *Mol Cell Biol* 15: 2101-2108.
- Shadel GS, Clayton DA. 1997. Mitochondrial DNA maintenance in vertebrates. *Annu Rev Biochem* 66: 409-435.
- Shoubridge EA. 2000. Mitochondrial DNA segregation in the developing embryo. *Hum Reprod* 15: 229-234.
- Silva JE, Rabelo R. 1997. Regulation of uncoupling protein gene expression. *Eur J Endocrinol* 136: 251-264.
- Sladek R, Bader J, Giguere V. 1997. The orphan nuclear receptor estrogen-related receptor α is a transcriptional regulator of the human medium-chain acyl coenzyme A dehydrogenase gene. *Mol Cell Biol* 17: 5400-5409.
- Spelbrink JN, Li FY, Tiranti V, Nikali K, Yuan QP, et al. 2001. Human mitochondrial DNA deletions associated with mutations in the gene encoding Twinkle, a phage T7 gene 4-like protein localized in mitochondria. *Nat Genet* 28: 223-231.
- St Pierre J, Lin J, Krauss S, Tarr PT, Yang RJ, et al. 2003. Bioenergetic analysis of peroxisome proliferator-activated receptor gamma coactivators 1 α and 1 β (PGC-1 α and PGC-1 β) in muscle cells. *J Biol Chem* 278: 26597-26603.
- Suliman HB, Carraway MS, Welty-Wolf KE, Whorton AR, Piantadosi CA. 2003. Lipopolysaccharide stimulates mitochondrial biogenesis via activation of nuclear respiratory factor-1. *J Biol Chem* 278: 41510-41518.
- Taanman JW. 1999. The mitochondrial genome: Structure, transcription, translation and replication. *Biochim Biophys Acta* 1410: 103-123.
- Tapper DP, Clayton DA. 1981. Mechanism of replication of human mitochondrial DNA. Localization of the 5' ends of nascent daughter strands. *J Biol Chem* 256: 5109-5115.
- The Dutch-Belgian Fragile X Consortium. 1994. Fmr1 knockout mice: A model to study fragile X mental retardation. *Cell* 78: 23-33.
- Thompson CC, Brown TA, McKnight SL. 1991. Convergence of Ets- and notch-related structural motifs in a heteromeric DNA binding complex. *Science* 253: 762-768.
- Tiranti V, Savoia A, Forti F, D'Apolito MF, Centra M, et al. 1997. Identification of the gene encoding the human mitochondrial RNA polymerase (h-mtRPOL) by cyberscreening of the expressed sequence tags database. *Hum Mol Genet* 6: 615-625.
- Topper JN, Bennett JL, Clayton DA. 1992. A role for RNAase MRP in mitochondrial RNA processing. *Cell* 70: 16-20.
- Van Dyck E, Foury F, Stillman B, Brill SJ. 1992. A single-stranded DNA binding protein required for mitochondrial DNA replication in *S. cerevisiae* is homologous to *E. coli* SSB. *EMBO J* 11: 3421-3430.
- Vega RB, Huss JM, Kelly DP. 2000. The coactivator PGC-1 cooperates with peroxisome proliferator-activated receptor α in transcriptional control of nuclear genes encoding mitochondrial fatty acid oxidation enzymes. *Mol Cell Biol* 20: 1868-1876.
- Vega RB, Kelly DP. 2004. A role for estrogen-related receptor α in the control of mitochondrial fatty acid β -oxidation during brown adipocyte differentiation. *J Biol Chem* 279: 31693-31699.
- Verkerk AJ, Pieretti M, Sutcliffe JS, Fu YH, Kuhl DP, et al. 1991. Identification of a gene (FMR-1) containing a CGG repeat coincident with a breakpoint cluster region exhibiting length variation in fragile X syndrome. *Cell* 65: 905-914.
- Virbasius CA, Virbasius JV, Scarpulla RC. 1993a. NRF-1, an activator involved in nuclear-mitochondrial interactions, utilizes a new DNA-binding domain conserved in a family of developmental regulators. *Genes Dev* 7: 2431-2445.
- Virbasius JV, Scarpulla RC. 1991. Transcriptional activation through ETS domain binding sites in the cytochrome *c* oxidase subunit IV gene. *Mol Cell Biol* 11: 5631-5638.
- Virbasius JV, Scarpulla RC. 1994. Activation of the human mitochondrial transcription factor A gene by nuclear respiratory factors: A potential regulatory link between

- nuclear and mitochondrial gene expression in organelle biogenesis. *Proc Natl Acad Sci USA* 91: 1309-1313.
- Virbasius JV, Virbasius CA, Scarpulla RC. 1993b. Identity of GABP with NRF-2, a multisubunit activator of cytochrome oxidase expression, reveals a cellular role for an ETS domain activator of viral promoters. *Genes Dev* 7: 380-392.
- Wallberg AE, Yamamura S, Malik S, Spiegelman BM, Roeder RG. 2003. Coordination of p300-mediated chromatin remodeling and TRAP/mediator function through coactivator PGC-1 α . *Mol Cell* 12: 1137-1149.
- Wan B, Moreadith RW. 1995. Structural characterization and regulatory element analysis of the heart isoform of cytochrome *c* oxidase VIa. *J Biol Chem* 270: 26433-26440.
- Wang TSF. 1991. Eukaryotic DNA polymerases. *Annu Rev Biochem* 60: 513-552.
- Webster G, Genschel J, Curth U, Urbanke C, Kang C, et al. 1997. A common core for binding single-stranded DNA: Structural comparison of the single-stranded DNA-binding proteins (SSB) from *E. coli* and human mitochondria. *FEBS Lett* 411: 313-316.
- Weitzel JM, Radtke C, Seitz HJ. 2001. Two thyroid hormone-mediated gene expression patterns in vivo identified by cDNA expression arrays in rat. *Nucleic Acids Res* 29: 5148-5155.
- Wilson-Fritch L, Burkart A, Bell G, Mendelson K, Leszyk J, et al. 2003. Mitochondrial biogenesis and remodeling during adipogenesis and in response to the insulin sensitizer rosiglitazone. *Mol Cell Biol* 23: 1085-1094.
- Wong TW, Clayton DA. 1986. DNA primase of human mitochondria is associated with structural RNA that is essential for enzymatic activity. *Cell* 45: 817-825.
- Wu Z, Puigserver P, Andersson U, Zhang C, Adelmant G, et al. 1999. Mechanisms controlling mitochondrial biogenesis and function through the thermogenic coactivator PGC-1. *Cell* 98: 115-124.
- Xu B, Clayton DA. 1995. A persistent RNA-DNA hybrid is formed during transcription at a phylogenetically conserved mitochondrial DNA sequence. *Mol Cell Biol* 15: 580-589.
- Yang MY, Bowmaker M, Reyes A, Vergani L, Angeli P, et al. 2002. Biased incorporation of ribonucleotides on the mitochondrial L-strand accounts for apparent strand-asymmetric DNA replication. *Cell* 111: 495-505.
- Yang SJ, Liang HL, Ning G, Wong-Riley MTT. 2004. Ultrastructural study of depolarization-induced translocation of NRF-2 transcription factor in cultured rat visual cortical neurons. *Eur J Neurosci* 19: 1153-1162.
- Yoon JC, Puigserver P, Chen GX, Donovan J, Wu ZD, et al. 2001. Control of hepatic gluconeogenesis through the transcriptional coactivator PGC-1. *Nature* 413: 131-138.
- Yoza BK, Bogenhagen DF. 1984. Identification and in vitro capping of a primary transcript of human mitochondrial DNA. *J Biol Chem* 259: 3909-3915.
- Zaid A, Li R, Luciakova K, Barath P, Nery S, et al. 1999. On the role of the general transcription factor Sp1 in the activation and repression of diverse mammalian oxidative phosphorylation genes. *J Bioenerg Biomembr* 31: 129-135.
- Zhang C, Wong-Riley MT. 2000. Depolarizing stimulation upregulates GA-binding protein in neurons: A transcription factor involved in the bigenomic expression of cytochrome oxidase subunits. *Eur J Neurosci* 12: 1013-1023.
- Zitomer RS, Carrico P, Deckert J. 1997. Regulation of hypoxic gene expression in yeast. *Kidney Int* 51: 507-513.
- Zitomer RS, Lowry CV. 1992. Regulation of gene expression by oxygen in *Saccharomyces cerevisiae*. *Microbiol Rev* 56: 1-11.

Metabolic Control Analysis: Modeling Local Pathway Fluxes, Control Points, System Interactions, Network Interactions

8.1 Mechanisms and Modeling of Energy Transfer Between Intracellular Compartments

V. A. Saks · M. Vendelin · M. K. Aliev · T. Kekelidze · J. Engelbrecht

1	<i>Introduction</i>	816
2	<i>Compartmentalized Energy Transfer</i>	817
3	<i>Cardiac Energy Metabolism: Experimental Basis for Modeling</i>	818
3.1	Basic Laws of Cardiac Physiology and Energetics	818
3.2	Regulation of Cellular Respiration In Vivo	819
3.3	The Phenomenon of Functional Coupling in the CK System	820
3.4	Intracellular Energetic Units	822
4	<i>Mathematical Modeling</i>	823
4.1	Basic Principles	823
4.2	Modeling Intracellular Medium: the Problems of Macromolecular Crowding and Metabolic Channeling	826
5	<i>Modeling of the Functional Coupling Mechanisms in Mitochondria</i>	826
5.1	Dynamic Compartmentation	826
5.2	Direct Transfer Mechanism	828
5.3	Probability Model of MtCK to ANT Coupling	830
5.4	The Main Results of the Probability Model	831
5.5	Thermodynamically Consistent Model of MtCK–ANT Coupling	832
5.6	Phenomenological Models	834
6	<i>Heterogeneity of ATP and ADP Diffusion and Compartmentation of Adenine Nucleotides</i>	835
7	<i>The Modeling of Compartmentalized Energy Transfer in the Cells</i>	837
7.1	Description of a Model	838
7.2	Main Results: Nonequilibrium State of the CK System	839
8	<i>Modeling the Mitochondrial Respiration Controlled by Frank–Starling Mechanism under Conditions of Metabolic Stability. Metabolic Control Analysis of the Factors of Regulation</i>	842
9	<i>CK and Brain Energy Metabolism</i>	846
9.1	The CK System and ATP Metabolism of Adult Brain	847
9.2	The CK System and ATP Metabolism in the Developing Brain	848
10	<i>Appendix: Probability Approach in Description of Enzymes and Transporters</i>	849
10.1	Mathematical Model of Free Activation of CK by Metabolites from the Medium	849
10.2	Mathematical Model of Free Activation of ANT by Metabolites from the Medium	851

Abstract: Mitochondria are the primary sources of ATP production, but the sites and processes that consume ATP are often located at considerable distances from the source of regeneration of ATP from ADP and P_i . The transfer of energy occurs in the highly organized and compartmentalized intracellular medium. The coupling of energy-producing and energy-consuming processes is important and involves metabolic channeling and functional coupling mechanisms between different enzymes, multienzyme systems, and transporters. In muscle, coupling of creatine kinase (CK) and adenylate kinase (AK) reactions is essential for minimizing energy gradients, reducing energy dissipation, and directing energy to sites and pathways for specific processes. Such processes include transfer of ATP from mitochondria to cell membrane, to myofibrils, to nucleus, or to sarcoplasmic reticulum (SR). Energy transfer via the kinase systems or localized glycolytic enzymes to membranes in order to support transport processes (e.g., glutamate loading of synaptic vesicles or Na^+/K^+ -ATPase activity) is critical for brain function, but little is known of these processes in brain cells. Therefore, this chapter provides a framework for approaching this issue in brain cells using the cardiac system as a model with description of main mechanisms involved and methods of their quantitative description. First, we analyze the experimental data showing compartmentation of the energy metabolism due to the high degree of structural organization of the cell. Then we describe the principles of mathematical modeling of biological systems, followed by mathematical and thermodynamic analysis of interaction between proteins. Finally, we use the mathematical model of the compartmentalized energy transfer to find a solution to the long-discussed problem of regulation of cardiac respiration under physiological conditions, where cardiac muscle energetics is regulated by the Frank–Starling law. Similarities and differences between compartmentalized energy transfer in cardiac and brain cells are analyzed briefly.

1 Introduction

The concept of metabolism as the sum of reactions catalyzed by enzymes in the homogenous intracellular medium, which are often in the quasi-equilibrium state (Meyer et al., 1984; Wiseman and Kushmerick, 1995; see Ingwall, 2002 for review) and can be described by a system of simple kinetic equations for diluted solutions, seems now to belong to the far and naive past. Indeed, rapid progress in experimental studies of cell structure and theoretical analysis of reactions in structurally organized medium with macromolecular crowding and multienzyme complexes has completely changed our views on cellular metabolism and its regulation. Now the basic paradigm of cellular metabolism is the compartmentation of enzymes and the compartmentation, microcompartmentation, and metabolic channeling of metabolites, including important regulators of cell life like calcium (Clegg, 1984; Ovàdi, 1995; Agius and Sherratt, 1997; Sreere, 2000; Huang et al., 2001b; Minton, 2001; Weiss and Korge, 2001; Schliwa, 2002; Hall and Minton, 2003; Ovàdi and Saks, 2004; Saks et al., 2004a; Schnell and Turner, 2004; Wang et al., 2004). This means that we now take into account the complex structural and functional organization of the cell interior and its importance for metabolic regulation. By definition, the term compartmentation is usually related to the existence of intracellular “macrocompartments”—subcellular regions that are large relative to the molecular dimension and “microcompartments” that are multiple compartments of the order of the size of metabolites. Microcompartmentation is sometimes taken to be close or synonymous to metabolic channeling, which means movement of a metabolite from enzyme to enzyme without mixing with the total pool in the same macrocompartment (Schoolwerth and LaNoue, 1980; Saks et al., 1994a; Ovàdi, 1995). However, metabolic channeling of the reaction intermediate between two enzymes (or a transporter and an enzyme) may occur by microcompartmentation or by direct transfer, but in both cases it results in a functional coupling phenomenon (see below). An important understanding is that the microcompartmentation may be of dynamic nature (Friedrich, 1985), and this may finally result in coexistence of whole sets of metabolically organized networks. The important task of highest complexity is to describe these processes quantitatively, with the aim of better understanding their mechanisms and regulation. Mathematical models have been useful tools for analysis of experimental data and for revealing regulatory mechanisms of processes of cellular energy metabolism.

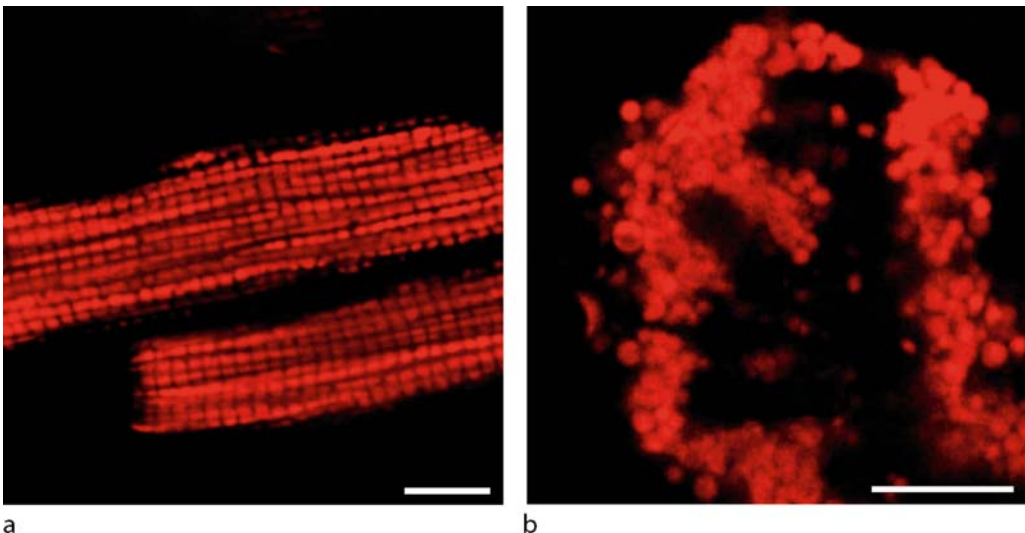
2 Compartmentalized Energy Transfer

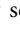
Because of their highly organized intracellular structure and unique function, which is relatively easy to measure and requires high and variable energy fluxes, cardiomyocytes are the best-studied systems with compartmentalized energy transfer and regulatory networks. High requirements for energy supply in these cells are met by aerobic oxidation of fatty acids and/or glucose coupled to ATP production in mitochondria. These processes are not considered here in detail and are described in several chapters of this volume. In all types of muscle cells, during contractions the ATP is split into ADP and inorganic phosphate in the actomyosin ATPase reaction (Goldman, 1987, 1998; Rayment et al., 1993; Cooke, 1997; Gordon et al., 2000). In brain cells, the aerobically produced ATP is used mostly to support ion gradients by Na^+/K^+ -ATPase and for processing of neurotransmitters (Ames, 2000). In cardiac cells, the specific contractile function is controlled and regulated by processes of excitation–contraction coupling, which include calcium entry across the sarcolemma via calcium channel, calcium-induced calcium release (CICR) from sarcoplasmic reticulum (SR), activation of contraction, ATP-dependent calcium uptake by SR, and its extrusion from the cells through sarcolemma by Na/Ca exchange mechanism and relaxation of sarcomeres (Opie, 1998; Bers, 2001; Carafoli, 2002; Berridge et al., 2003). The mitochondrial calcium cycle plays an active role in the regulation of cytoplasmic calcium (Rizzuto et al., 2000; Bianchi et al., 2004; Jacobson and Duchon, 2004). These events have been found to be localized in the form of calcium sparks as visualized by confocal microscopy (Bianchi et al., 2004; Wang et al., 2004). Normal muscle function depends on the fine interplay, or interaction, of energy metabolism and calcium metabolism inside the cells.

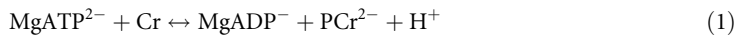
Cardiac cells have a very highly organized structure where mitochondria are localized at the A-band level within the limits of the sarcomere (Fawcett and McNutt, 1969; Sommers and Jennings, 1986; Aon et al., 2004; Vendelin et al., 2004c). [▶ Figure 8.1-1a](#) shows the typical confocal image of mitochondria in nonfixed isolated cardiomyocytes. Intermyo-fibrillar mitochondria are arranged in a highly ordered crystal-like pattern in a muscle-specific manner, with relatively small deviation in the distances between

■ Figure 8.1-1

Regular arrangement of mitochondria in cardiac cells and its alteration after treatment of permeabilized cardiomyocytes by trypsin. Confocal imaging of mitochondria using Mitotracker Red FM fluorescence. Permeabilized cells were preloaded with Mitotracker Red FM as described in Vendelin et al. (2004c). (a) Control cardiomyocytes; (b) after incubation of permeabilized cardiomyocytes with 1 μM of trypsin for 5 min at 4°C. Bar shows 10 μm . From Vendelin et al. (2004c) with permission



neighboring mitochondria (Aon et al., 2004; Vendelin et al., 2004c). Dynamic changes in mitochondrial position (Bereiter-Hahn et al., 1994; Yi et al., 2004) due to fission and fusion (Rube and van der Blik, 2004) are not characteristic of adult and healthy cardiac and skeletal muscle cells (as opposed to many other cells with less developed intracellular structure) because of their rigid intracellular structural organization, and mitochondria in these cells are morphologically unconnected (Collins and Bootman, 2003; Aon et al., 2004; Brady et al., 2004; Vendelin et al., 2004c). This regular arrangement of mitochondria is related to the highly organized cytoskeletal network in the cardiac cells (Capetanaki, 2002; Appaix et al., 2003), some components of which are very sensitive to proteolysis by proteases.  *Figure 8.1-1b* shows that after treating permeabilized cardiomyocytes with trypsin in low concentration, the arrangement of mitochondria is drastically changed and the regularity of their arrangement lost. Changes in the regular arrangement of mitochondria result in significant alterations in the regulation of respiration in permeabilized cells by ADP (Kuznetsov et al., 1996; Saks et al., 2003, 2004b) showing that the regulation of mitochondrial function and energy fluxes is closely related to the structural organization of cardiac cells (Saks et al., 2004a, b). In this structurally organized medium, the processes of energy transfer between different subcellular micro- and macrocompartments (called compartmentalized energy transfer) are of central importance. ATP is not only delivered by diffusion, but intracellular energy transfer is also facilitated via networks consisting of phosphoryl-group-transferring enzymes such as creatine kinase (CK), adenylate kinase (AK), and glycolytic phosphoryl-transferring enzymes (Bessman and Geiger, 1981; Wallimann et al., 1992; Saks et al., 1994a, b, 1995, 1998, 2004a, b; Ventura-Clapier et al., 1994; Veksler et al., 1995; Wyss and Kaddurah-Daouk, 2000; Dzeja and Terzic, 2003; Schlattner and Wallimann, 2004). CK catalyzes a reversible reaction of adenine nucleotide transphosphorylation, the forward reaction of phosphocreatine (PCr) and MgADP synthesis, and the reverse reaction of creatine (Cr) and MgATP production:



Four CK isoforms, each with compartmentalized cellular localization, exist in mammals. Specific mitochondrial CK isoenzymes (MtCK), called ubiquitous (uMtCK) and sarcomeric (sMtCK), are functionally coupled to oxidative phosphorylation (OP), producing PCr using mitochondrial ATP. PCr in turn is used for local regeneration of ATP by the muscle cytoplasmic isoform of CK (M-CK), driving myosin-ATPases or ion pump-ATPases (Schlegel et al., 1988a, b; Wallimann et al., 1992; Saks et al., 1994b, 1998, 2004b). Recent studies in CK-deficient transgenic animals indicate that energy transfer and communication between ATP-generating and ATP-utilizing sites within a muscle cell do not exclusively rely upon the activity of CK, but may rather include a number of additional intracellular phosphotransfer systems such as AK and glycolysis (Steeghs et al., 1997; Dzeja et al., 1998; de Groof et al., 2001; Dzeja and Terzic, 2003; Janssen et al., 2003). AK-catalyzed reversible phosphotransfer between ADP, ATP, and AMP molecules may process cellular signals associated with ATP production and utilization (Bessman and Geiger, 1981; Dzeja and Terzic, 2003, see also Dzeja et al. in this volume).

The existence of these complicated networks of energy transfer and signaling is related to the compartmentalization of adenine nucleotides in the cells (their distribution between different macro- and microcompartments) (McLellan et al., 1983; Geisbuhler et al., 1984; Neely and Grotyohann, 1984; Weiss and Lamp, 1987; Hoerter et al., 1988; Kennedy et al., 1999; Abraham et al., 2002), due to significant heterogeneity and local restrictions of the diffusion of adenine nucleotides in the cells. Inhibition or knockout of the CK system by genetic manipulations results in very significant loss of work capacity (Kinding et al., 2005; Momken et al., 2005).

3 Cardiac Energy Metabolism: Experimental Basis for Modeling

3.1 Basic Laws of Cardiac Physiology and Energetics

Under physiological conditions, heart function and energy metabolism are governed by the Frank–Starling law. This law states that within physiological limits, the larger the volume of the heart, the greater the energy of its contraction and the amount of chemical change at each contraction, including oxygen consumption

(Starling and Visscher, 1926; Williamson et al., 1976; Lakatta et al., 1991; Opie, 1998). This physiological mechanism of regulation of mitochondrial oxygen consumption in heart *in vivo* is related to the changes in the sarcomere length due to alterations of the left ventricle end-diastolic volume (Suga, 1990; Gordon et al., 2000).

In addition, in 1972 Neely et al. discovered the phenomenon of “metabolic stability,” showing that the intracellular levels of high-energy phosphates, ATP and PCr, are constant in aerobic heart cells and practically independent of workload and oxygen consumption (Neely et al., 1972; Balaban et al., 1986, 2002; Wan et al., 1993). Williamson et al. established quantitatively the interval of the rates of respiration dependent on the workload, regulated by the changes in the rate of left ventricular filling in accordance with the Frank–Starling mechanism: the rate of oxygen consumption by cardiac tissue changes about 15–20 times, from 6 to 12 $\mu\text{mol/g dw/min}$ during rest up to 170 $\mu\text{mol/g dw/min}$ at maximal workload under conditions of metabolic stability (Williamson et al., 1976). Under these conditions, the ATP content was not changed and the PCr content changed not more than 30%.

3.2 Regulation of Cellular Respiration In Vivo

In isolated mitochondria, respiration is intimately regulated by the availability of ADP to adenine nucleotide translocase (ANT) (Lardy and Wellman, 1952; Chance and Williams, 1956; Vignais, 1976; Brown et al., 1990; Nicholls and Ferguson, 2002; see the chapter by Nicholls in this volume). The simplest theory of respiration regulation *in vivo* is the equilibrium CK theory, according to which the ADP available to mitochondrial ANT is the cytoplasmic ADP in equilibrium with the CK reaction (Meyer et al., 1984; Kushmerick, 1995; Wiseman and Kushmerick, 1995; Ingwall, 2002). However, this theory is only of some historical interest since it does not explain the classical experimental observations of Starling, Neely, and Williamson. According to this theory, metabolic stability also means stable and relatively high cytoplasmic levels of ADP (about 50–100 μM) (Gard et al., 1985; Unitt et al., 1991, Ingwall, 2002), in comparison with the affinity of mitochondrial ANT for this substrate (10–20 μM) (Vignais, 1976; Jacobus et al., 1982a). Therefore, respiration should be activated almost maximally at rest, but this contradicts all experimental observations (Starling and Visscher, 1926; Williamson et al., 1976). The basic assumption of this theory—the CK equilibrium—is not justified (Saks and Aliev, 1996b), and the reason is that it ignores the complex structure of intracellular medium and the very well studied and described compartmentation of the CK isoenzymes in the muscle cells. Paradoxically, it is the opposite theory—that of the nonequilibrium steady-state mode of functioning of the CK isoenzymes in different directions in the distinct cellular compartments—that explains the experimental observations, as described in this chapter.

Another theory that was proposed to explain regulation of respiration under these conditions is “parallel activation” of simultaneous regulation of contraction and mitochondrial OP by calcium ions (Denton et al., 1972, 1978; Hansford, 1985; McCormack et al., 1990; Korzeniewski, 1998, 2003; Territo et al., 2001; Balaban, 2002). Rapid uptake of calcium by mitochondria (Rizzuto, 2000; Bianchi et al., 2004; Gunter et al., 2004; Jacobson and Duchon, 2004) is necessary for the activation of key dehydrogenases of the Krebs cycle and others, usually by the mechanism of increasing the affinity of these enzymes for their substrates (Hansford, 1985; McCormack et al., 1990). Elevation of $[\text{Ca}^{2+}]_i$ in cardiac cells can be easily achieved by adrenergic activation of β -receptors by activating CICR by increasing calcium influx through the slow calcium channels in the plasma membrane of cardiac cells (Bers, 2001; Berridge et al., 2003; Saucerman et al., 2003). However, both experimental and theoretical studies have shown that changes in mitochondrial calcium in response to increased calcium cycling in cytoplasm can increase the respiration rate only by a factor of 2 (Territo et al., 2001; Cortassa et al., 2003), but not by a factor of 20 as seen in experiments (Williamson et al., 1976). In addition, the Frank–Starling law, which governs cardiac work and respiration, is based on the sarcomere length-dependent increase of sensitivity of thin filaments to calcium, resulting in an increase in the number of active crossbridges involved in the contraction cycle at stable calcium concentrations in the cytoplasm (Kentish and Wrzosek, 1998; Landesber and Sideman, 1999; Shimizu et al., 2002; Kobayashi and Solaro, 2005).

The answer to the main question of regulation of cardiac cell metabolism—how spatially separated intracellular ATP consumption and ATP production (mitochondrial OP) processes are precisely matched and coordinated over a broad range of cellular functional activities and under conditions of metabolic stability—is given quantitatively only by the theory of compartmentalized energy transfer.

In this chapter, we focus on the compartmentalized energy transfer by the CK system. This is the main energy transfer pathway in normoxic adult heart cells (Dzeja and Terzic, 2003). The basic mechanism of functioning of these systems is functional coupling, which is described in the next section.

3.3 The Phenomenon of Functional Coupling in the CK System

Functional coupling means that due to the close structural proximity of enzymes, which are fixed at the membranes or in multienzyme complexes, the metabolite or metabolites are channeled from one enzyme to another instead of their free diffusion in the medium, and therefore the function of one enzyme is directly dependent on the function of another enzyme (or transporter). By this mechanism, much higher efficiency is achieved for the regulation of enzymatic reactions (Ovádi, 1995; Saks et al., 1996a; Agius and Sheratt, 1997; Saks et al., 2004a). Also, by this mechanism, excessive entropy production is avoided, in comparison with that in the disorganized metabolic system (see Schroedinger, 2000). This effective mechanism can be taken to illustrate the philosophical principle of Maxwell's demon (Saks et al., 2005) in cellular biochemistry and metabolic regulation.

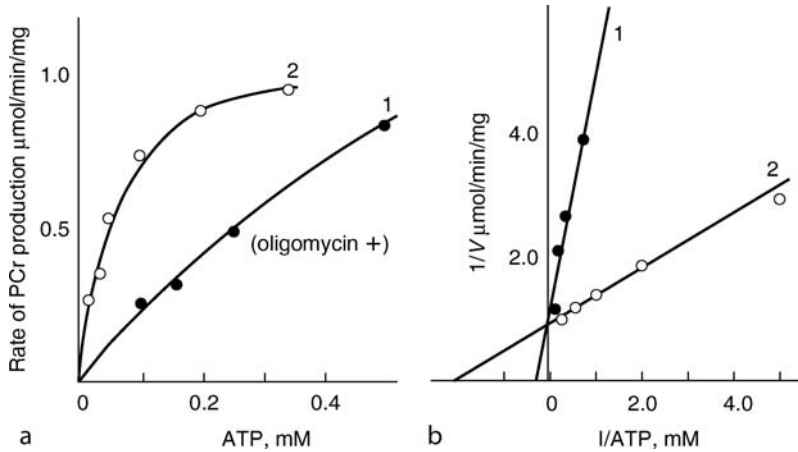
Mitochondrial CK. The most important mechanism in compartmentalized energy transfer is the functional coupling between the mitochondrial ANT and the mitochondrial isoform of CK, MtCK.

MtCK was discovered by Klingenberg's group in 1964 (Jacobs et al., 1964). This isoenzyme of CK is localized on the outer surface of the mitochondrial outer membrane, in the close vicinity of ANT (Scholte et al., 1973; Schlattner et al., 2004). When OP is not activated, the MtCK reaction does not differ kinetically and thermodynamically from that of other CK isoenzymes: the reaction favors ATP production and according to the Haldane relationship, ADP and PCr binding is more effective due to higher affinities than that of ATP and Cr, respectively (Saks et al., 1975, 1980; Jacobus and Saks, 1982b; Kenyon and Reed, 1983). Under conditions of OP, the MtCK reaction is strongly shifted in the direction of PCr synthesis and may use all ATP produced in mitochondria for PCr production (Jacobus and Lehninger, 1973; Saks et al., 1975, 1980; Jacobus and Saks, 1982b). While the kinetic constants for Cr and PCr were not changed and were the same in both conditions, OP had a specific effect on the kinetic parameters for adenine nucleotides (Jacobus and Saks, 1982b). These changes in the MtCK kinetics induced by OP are illustrated in [Figure 8.1-2](#). The figure shows the PCr production rates in rat heart mitochondria in the media with [Figure 8.1-2](#), curve 1) and without [Figure 8.1-2](#), curve 2) inhibition of OP by oligomycin. Comparison of the two curves in [Figure 8.1-2](#) clearly shows that under conditions of OP (in the system without oligomycin) MtCK is subjected to activation, which is in addition to its existing activation by substrates from the medium. Kinetic analysis of the MtCK reaction under conditions of OP revealed that the two constants for MgATP dissociation, K_{ia} and K_a , from the complexes MtCK.MgATP and MtCK.Cr.MgATP, respectively (see the *Appendix* for CK kinetic scheme) were apparently decreased (Jacobus and Saks, 1982b). The explanation proposed was the direct transfer of ATP from ANT to MtCK due to their spatial proximity, which results also in increased uptake of ATP by ANT from MtCK (reversed direct transfer), and as a result, the turnover of adenine nucleotides is increased manifold at low external concentrations of MgATP, thus maintaining high rates of OP and coupled PCr production in the presence of enough Cr. These kinetic effects are analyzed by the mathematical models given later.

The fact that mitochondrial ATP has privileged access to MtCK and increased mitochondrial turnover of adenine nucleotides in the presence of Cr was directly confirmed by the isotopic method (Barbour et al., 1984) and by the thermodynamic approach (DeFuria et al., 1980; Saks et al., 1985; Soboll et al., 1994), and by showing that inhibition of MtCK by monoclonal antibodies inhibited also the ATP/ADP exchange due to the proximity of MtCK to ANT (Saks et al., 1987). Finally, an effective competitive enzyme method for studying the functional coupling phenomenon, namely the pathway of ADP movement from MtCK back to ANT (Moreadith and Jacobus, 1982) is to use the phosphoenolpyruvate (PEP)–pyruvate kinase (PK) to

■ Figure 8.1-2

The MgATP-dependencies of the rate of PCr production in the MtCK reaction in the absence (1) and in the presence (2) of OP. Media contained 25 mM Cr. (1): OP in rat heart mitochondria was inhibited by oligomycin (5 $\mu\text{g}/\text{mg}$ of protein), and ATP concentrations were maintained by the added PK and PEP; (2): the CK reaction was coupled to OP (oligomycin and the PK system were omitted). (a) primary plots; (b) linearization of data from a, showing about tenfold decrease in apparent K_m for ATP in the coupled state and unchanged apparent maximal rate of PCr production. From Saks et al. 1980 (Fig. 10.5) with permission



trap ADP and thus to compete with ANT for this substrate (Gellerich and Saks, 1982; Gellerich et al., 1994). The functional coupling mechanism is supported by structural studies of the MtCK and its functioning performed by the Wallimann group (Wallimann et al., 1992; Fritz-Folf et al., 1996; Schlattner et al., 1998; Schlattner and Wallimann, 2004). ANT in the inner-mitochondrial membrane forms tight complexes with negatively charged cardiolipin in the ratio of 1:6 (Beyer and Klingenberg, 1985). It has been shown that positively charged MtCK is fixed to this cluster by electrostatic forces due to three C-terminal lysines that strongly interact with the negatively charged cardiolipin in complex with ANT (Muller et al., 1985; Schlattner et al., 2004). The peculiarity of MtCK, in contrast with other dimeric CK isoenzymes (MM and BB), is that it forms octamers (Schlegel et al., 1988a, b; Wallimann et al., 1992; Schlattner and Wallimann, 2004).

The structure of ANT was recently resolved at 2.2 Å (Pebay-Peyroula et al., 2003). The translocation of both ATP and ADP in the Mg-free forms is related to the conformation changes of pore-forming monomers (Pebay-Peyroula et al., 2003). This conformation change (gated pore) mechanism leads, in its simplest version, to the Ping-Pong reaction mechanism of transport (Gropp et al., 1999; Huber et al., 1999; Huang et al., 2001b). On the other hand, the kinetics of ATP–ADP exchange conforms to the sequential mechanism of the simultaneous binding of nucleotides on both sides (Duyckaerts et al., 1980). The structural data and the kinetics of ATP–ADP exchange by ANT are well fitted with each other by the hypothesis that the dimers with alternatively activated monomers function in a coordinated manner in the tetramers, where the export of ATP from mitochondria by one monomer in a dimer occurs simultaneously with the import of ADP by another monomer in another dimer (Kramer and Palmieri, 1992; Aliev and Saks, 2003).

In vivo, the functional coupling between MtCK and ANT was verified recently in studies of the energy metabolism of the heart by ^{31}P NMR inversion transfer, showing that in the intact heart cells MtCK is strongly shifted in the direction of PCr production under aerobic conditions (Joubert et al., 2002, 2004). It was also shown in MtCK-knockout mice that, as predicted by the theory described above, their hearts had lower levels of PCr and reduced postischemic recovery (Spindler et al., 2002, 2004). A new important role for MtCK is its control over ANT by preventing the opening of the mitochondrial permeability transition pore (Dolder et al., 2003), thus preventing cell death by inhibiting apoptosis and necrosis.

Myofibrillar CKs. The myofibrillar end of the Cr-PCr cycle is represented by MM isozyme of CK localized in different parts of sarcomere and functionally coupled to the actomyosin MgATPase (Wallimann et al., 1984, 1992; Wegmann et al., 1992; Ventura-Clapier and Veksler, 1994; Ventura-Clapier et al., 1994; Hornemann et al., 2003). Within the contraction cycle, ADP release is a necessary step for new binding of MgATP, for dissociation of actomyosin crossbridges, and for muscle relaxation, to start the new cycle of contraction (Goldman, 1987, 1998; Rayment et al., 1993; Gordon et al., 2000). This step is often found to be the slowest one in the contraction cycle and therefore the rate-limiting one, since MgADP may compete with MgATP for the substrate site on myosin and inhibit crossbridge detachment by MgATP, the inhibition constant K_i being in the range of 200 μM both in the MgATPase reaction and in the sliding of fluorescent actin on myosin (Cook and Pate, 1985; Yamashita et al., 1994; Sata et al., 1996; Fukuda et al., 2000; Karatzaferi et al., 2003). Thus, MgADP should be rapidly removed from actomyosin and the high local value of the MgATP/MgADP ratio and thus the local phosphorylation potential maintained. MM-CK is bound specifically to the M-line, and significant part of this isozyme is found in the space of the I-band of sarcomeres (Wegmann et al., 1992; Hornemann et al., 2003). There is increasing evidence that MM-CK is intimately involved in the contraction cycle at the level of the ADP release and ATP rebinding steps by the mechanism of functional coupling, including probably myofibrillar microcompartments of adenine nucleotides (Krause and Jacobus, 1992; Ventura-Clapier et al., 1994, 1998; Sata et al., 1996; Ogut and Brozovich, 2003).

Membrane-bound CKs. Other ATP-consuming systems are present both in the membranes of SR and in the plasmalemma (sarcolemma). Their function is to maintain ionic homeostasis and particularly, the regulation of the calcium cycle. The role of MM-CK connected to the membrane of the SR and functionally coupled to the Ca/MgATP-dependent ATPase (SERCA) is to rapidly rephosphorylate local MgADP produced in the Ca/MgATPase reaction and thus to maintain the high local value of phosphorylation potential (available free-energy level) to maintain high efficiency of calcium pumping and avoid its reversal or inhibition due to accumulation of ADP (Rossi et al., 1990; Korge et al., 1993, 1994; Minajeva et al., 1996; Steeghs et al., 1997).

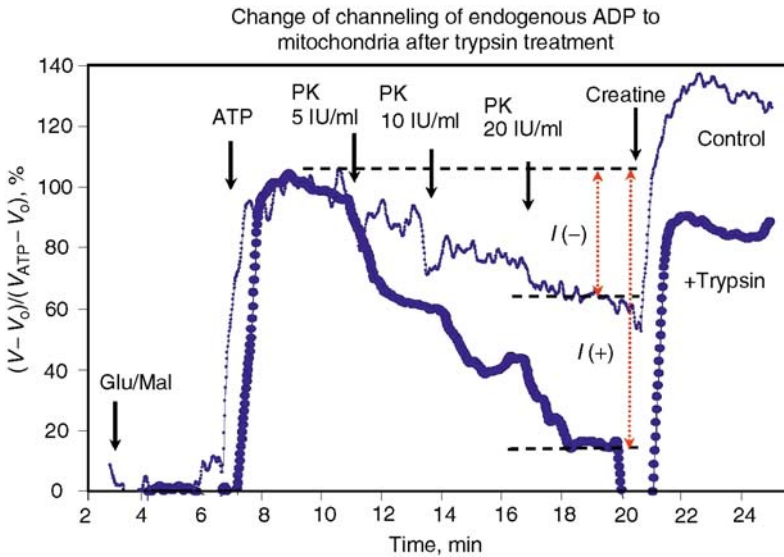
In the control of the excitation–contraction coupling in the heart an important component is the sarcolemmal membrane metabolic sensor complex (Abraham et al., 2002). Its main part is the sarcolemmal ATP-sensitive K^+ (K_{ATP}) channel acting as an alarm system to adjust cell electrical activity to the metabolic state of the cell (Lederer and Nichols, 1989; Lorenz and Terzic, 1999; Abraham et al., 2002; Crawford et al., 2002). It is the function of the sarcolemmal MM-CK to rephosphorylate the local ADP and maintain the high ATP/ADP level in these microcompartments for coordination of membrane electrical activity with cellular metabolic status, notably with the PCr level. Energy transfer and control functions are shared by whole hierarchical systems, including the AK and glycolytic systems, besides the CK system, as seen from experiments with gene manipulation (Carrasco et al., 2001; Selivanov et al., 2004). Similar metabolic sensors of cell membranes may also be of high importance in brain cells.

3.4 Intracellular Energetic Units

The intracellular energy transfer networks are structurally organized in the intracellular medium where macromolecules and organelles, including mitochondria, are involved in multiple structural and functional interactions (Kaasik et al., 2001; Saks et al., 2001, 1998, 2004a; Seppet et al., 2001; Capetanaki, 2002). [Figure 8.1-3](#) shows that in permeabilized cardiac fibers endogenous ADP is mostly channeled from MgATPases to mitochondria in cardiac cells, and demonstrates the importance of CK in respiration regulation. Respiration in permeabilized cells activated by addition of 2 mM exogenous MgATP is only slightly (not more than 40%), inhibited by the powerful added extracellular ADP-consuming system (PK + PEP), and activation of the CK system maximally activates respiration ([Figure 8.1-3](#)). This means that endogenous ADP is used by mitochondria before being made available for PK + PEP, and the local ADP produced by MtCK is not at all available for this competing system. Destruction of cell structure and regular arrangement of mitochondria by selective proteolysis makes endogenous ADP

■ Figure 8.1-3

Representative oxygen consumption traces showing changes of metabolic channeling of endogenous ADP from Ca/MgATPases to mitochondria after trypsin treatment of permeabilized fibers. For detection of ADP channeling, PK-PEP competitive enzyme method was used before and after treatment of permeabilized cardiac fibers with trypsin, leading to the disorganization of regular arrangement of mitochondria. (The first derivative of oxygraph recordings of oxygen consumption are shown, directly showing the values of respiration rate). ATP was added to the final concentration of 2 mM. *Thin line*—control fibers; *thick line*—fibers treated with 5 μ M of trypsin for 15 min at 4°C; *I(-)* and *I(+)* indicate inhibition of mitochondrial respiration by competing PK-PEP system without (-) and with (+) trypsin treatment. At the end of each experiment, creatine (Cr) (20 mM) was added. Note that Cr activates respiration in nontreated permeabilized fibers by 130% (to the state 3 level) in spite of the presence PK-PEP. After trypsin treatment the maximal Cr-activated respiration decreased by 50%. For explanations see the text. Reproduced from Saks et al. (2003) with permission



available for the PK + PEP system and decreases the activating effect of Cr (▶ Figure 8.1-3). This treatment decreases also the apparent K_m for exogenous ADP (Kuznetsov et al., 1996; Saks et al., 2001). These data illustrate the point of view that in oxidative muscle cells mitochondria are structurally organized into functional complexes with myofibrils and SR (Kaasik et al., 2001; Saks et al., 2001; Seppet et al., 2001). These complexes were called intracellular energetic units (ICEUs), the basic pattern of organization of muscle energy metabolism (Saks et al., 2001). The proposed structure of these units is shown in ▶ Figure 8.1-4.

The concept of the unitary nature of energy metabolism and ICEUs is a very useful basis for mathematical modeling of compartmentalized energy metabolism.

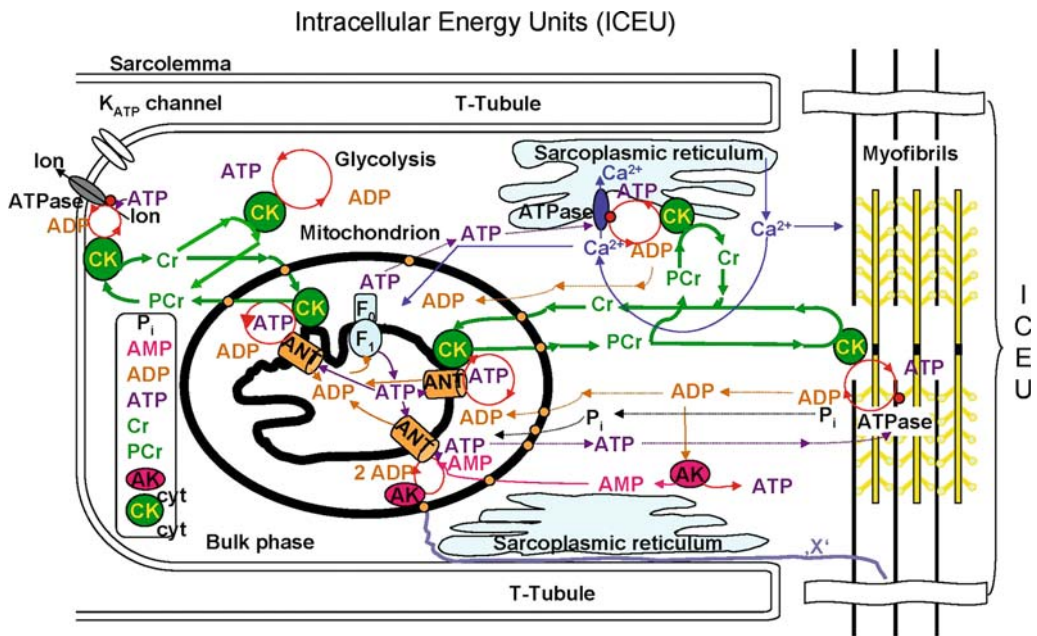
4 Mathematical Modeling

4.1 Basic Principles

There are different ways of understanding phenomena in the physical world: theories, measurements, and modeling. The latter includes mostly mathematical interpretation, i.e., casting a real-world system, process, or theory into a mathematical representation. This enhances essentially our abilities to understand and

■ Figure 8.1-4

The structural organization of the energy transfer networks of coupled CK and AK reactions within the intracellular energetic units (ICEUs). By interaction with cytoskeletal elements, the mitochondria and sarcoplasmic reticulum (SR) are precisely fixed with respect to the structure of sarcomere of myofibrils between two Z-lines and correspondingly between two T-tubules. Calcium is released from SR into the space in ICEU in the vicinity of mitochondria and sarcomeres to activate contraction and mitochondrial dehydrogenases. Adenine nucleotides within ICEU do not equilibrate rapidly with adenine nucleotides in the bulk water phase. The mitochondria, SR, and MgATPase of myofibrils and ATP-sensitive systems in sarcolemma are interconnected by metabolic channeling of reaction intermediates and energy transfer within ICEU by the CK–PCr and myokinase systems. The protein factors (still unknown and marked as X), most probably connected to the cytoskeleton, fix the position of mitochondria and probably also control the permeability of the voltage-dependent anion channel (VDAC) channels for ADP and ATP. Adenine nucleotides within ICEU and bulk water phase may be connected by some more rapidly diffusing metabolites as Cr–PCr. Synchronization of functioning of ICEUs within the cell may occur by the same metabolites (e.g., P_i or PCr) and/or by synchronized release of calcium during excitation–contraction coupling process. Reproduced from Saks et al. (2005) with permission



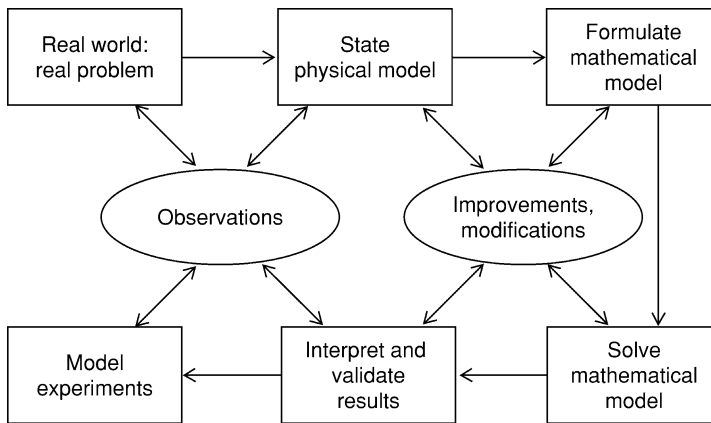
predict and possibly also control the behavior of the system being modeled. Whatever be the mathematical description, a model cannot reflect the behavior of all the systems over all the timescales and conditions, but usually can reflect either its basic (backbone) or specific (under special conditions) features. Therefore a model should always be validated and if needed improved on the basis of validation. A possible flowchart of modeling is shown in [Figure 8.1-5](#) reflecting also this important step in modeling—the validation and iterative improvement of mathematical models. Finally, modeling describes processes in the most economical ways using mathematical language and could give new insights to possible interactions or limitations of the process in general.

Mathematical modeling of biological processes means describing mathematically the physiological phenomena and structural behavior of living tissues, organs, cells, neuronal networks, and many other biological systems. It is not easy and in most cases much more difficult than, say, everyday physical processes. The reasons are as follows:

- biological systems need energy exchange with the surrounding environment and represent systems far from the thermodynamic equilibrium;
- biological systems involve many chemical reactions and transfer mechanisms where the constituents should be analyzed at the molecular level;
- the processes operate over different timescales and are spatially extended including many hierarchies;
- adaptivity should be taken into account;
- in mathematical terms the biological systems can often be described by different types of mathematical equations causing difficulties in solving them;
- in physical terms one should account for nonlinearities (additivity is lost), dissipation, activity/excitability, spatiotemporal coupling, etc.

■ **Figure 8.1-5**

Block chart of mathematical modeling (for explanation see the text)



So, in order to manage properly, the knowledge of the theory of continua, biochemistry, thermodynamics, computational methods, etc., should be interwoven into a whole on the basis of biological functions and physiology. Despite difficulties, mathematical modeling of biological systems has progressed during the last decade, supported by contemporary computing facilities and computational methods (Humphrey, 2000; Kohl et al., 2000; Hunter, 2004). This is a decisive feature and that is why *in silico* modeling (cf ● [Figure 8.1-5](#), model experiments) has assumed importance beside traditional *in vivo* and *in vitro* experimentation (cf ● [Figure 8.1-5](#), observations). Whatever the nature of processes to be modeled, besides the physical/chemical/geometrical properties, space and timescales are important, reflecting the structure of the system and its behavior. Proper modeling must use the existence of scales and this leads to certain hierarchies ordered by scales. One should distinguish two possible hierarchies: (1) structural and (2) functional. The structural hierarchy involves a strong dependence on length scales within a system in relation to the scale of excitation. Hierarchical modeling starts from the description of the whole system; later by the choice of scale parameters, a proper model is selected, leading to the asymptotically correct solution. In biological systems, one can distinguish two subcases: fundamental hierarchies like atom-molecule-cell-tissue-organ-human and specified hierarchies in cells like sarcomeres-myofibrils-fibres-muscles-heart. The architecture of biotissues is extremely rich.

The functional hierarchy in a system means that at various levels (of scale) various dynamical processes are of importance, all influencing macrobehavior. This is typical for biological systems. For example, in modeling cardiac contraction, the functional (process) hierarchy is oxygen consumption-energy transfer- Ca^{2+} signals-crossbridges-contraction. Functional hierarchies can be analyzed using a comparatively novel concept of continuum mechanics—the concept of internal variables. The concept of internal variables has its origin in thermodynamics with first ideas in the description of reacting chemical systems. Contemporary

understanding (Maugin and Muschik, 1994) rests upon the assumption that the thermodynamic state is determined by two types of variables: observable and internal. In brief, it means distinguishing between macroscopic and microscopic behavior. Macroscopic behavior is observable, governed by observable variables like stress or strain. Microscopic behavior is not observable by the external observer but nevertheless depends on corresponding variables called internal. There is a clear difference between those two types of variables. Observable variables are governed by balance laws with a kinetic energy, i.e., possess inertia, while the internal variables do not possess inertia and are governed by the kinetic equations (Maugin and Muschik, 1994; Engelbrecht et al., 2000; Maugin and Engelbrecht, 2000). The idea is that any observable variable depends on the first-level internal variable, which depends on the second-level internal variable, which depends on the third-order internal variable, etc. Such a structure describes step-by-step influence of internal variables characteristic to cell energetics.

The final aim of biomedical research is to improve patient-specific treatment strategies. For that *in silico* modeling is a powerful tool not only for describing biological processes and but also for performing *in silico* experiments (Kolston, 2000). “To think is to model”, say Kohl et al. (2000) in their vision-setting review on modeling of biological systems.

4.2 Modeling Intracellular Medium: the Problems of Macromolecular Crowding and Metabolic Channeling

In order to apply the principles of mathematical modeling to describe cell metabolism one needs to know the kinetic mechanisms and parameters of enzymes and transporters involved and to account for the real structure of the cell. The first phenomenon to be taken into account in all cells is macromolecular crowding: the high concentration of proteins in cells (Fulton, 1982; Clegg, 1984; Minton, 2001; Hall and Minton, 2003) decreases the volume for free diffusion of substrates and accordingly makes it difficult to apply correctly the enzyme kinetics and equations usually worked out in studies of enzymes in diluted solutions (Hall and Minton, 2003; Schnell and Turner, 2004). Clearly, the intracellular systems of energy metabolism are organized into functional units with dimensions of the order of one to several micrometers to avoid the possible chaos in communication because of macromolecular crowding. To account for the effects of macromolecular crowding on the enzyme kinetics, the thermodynamic activity coefficients' method may be used to find the nonideality factors (Hall and Minton, 2003; Schnell and Turner, 2004). We have worked out and used another approach to overcome these problems in describing the kinetics of enzymes in the real cells. This is the probability approach described in the *Appendix* for CK and ANT. In this case, the probabilities calculated from ratios of the concentrations are used in kinetic equations instead of the absolute values of the concentrations of substrates, products, and enzyme–substrate complexes. If the thermodynamic activity coefficients of these complexes and metabolites are close or comparable, this method allows us to find the description of experimental data with reasonable approximation to reality.

The second phenomenon is metabolic channeling (Ovådi, 1995; Ovådi and Saks, 2004) and functional coupling due to close and tight protein–protein interactions. To describe these phenomena, we have applied the probability approach and thermodynamic analysis to identify their precise mechanisms. Another effective approach, more simple, is to apply the phenomenological coefficients for the use of quantitative description of metabolic regulation in general, as will be described below.

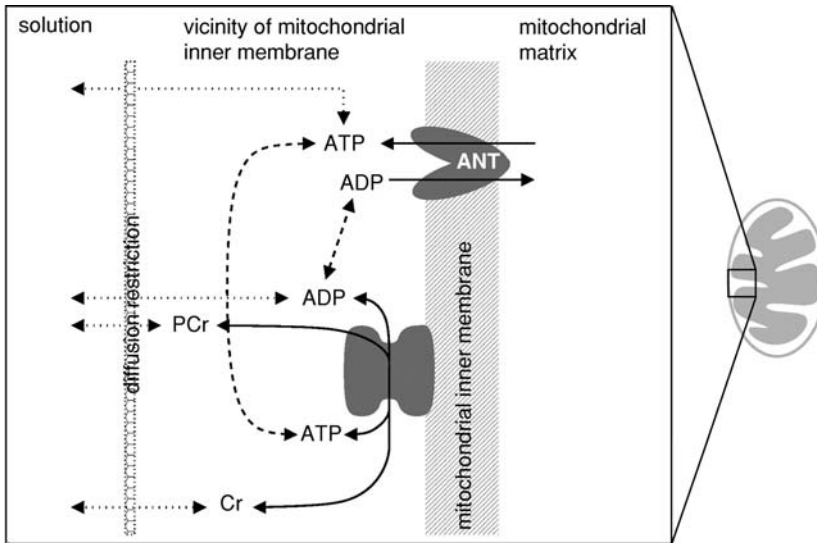
5 Modeling of the Functional Coupling Mechanisms in Mitochondria

5.1 Dynamic Compartmentation

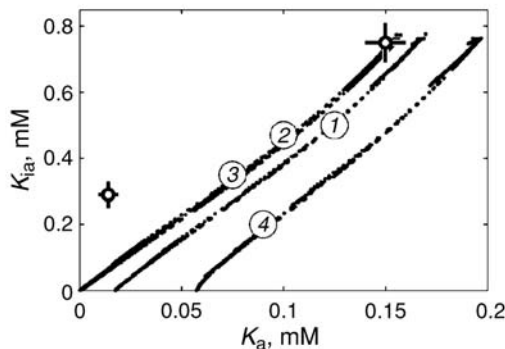
The simplest kinetic scheme that was proposed to explain the kinetic data on MtCK–ANT coupling is based on dynamic compartmentation of adenine nucleotides (Gellerich et al., 1987). According to this hypothesis, there are metabolite gradients between the solution surrounding mitochondria and the vicinity of the mitochondrial inner membrane (🔗 *Figure 8.1-6a*). Through this vicinity, ATP and ADP are exchanged

■ Figure 8.1-6

(a) Interaction between mitochondrial creatine kinase (MtCK) and adenine nucleotide translocase according to dynamic compartmentation hypothesis. Dynamic compartmentation hypothesis assumes that interaction between the proteins is the result of large ATP and ADP gradients between the vicinity of the mitochondrial inner membrane and solution surrounding mitochondria. (b) Calculated apparent dissociation constants K_a and K_i of MtCK reaction in the presence of oxidative phosphorylation (OP). Coupling between MtCK and OP was modeled according to the dynamic compartmentation hypothesis. Here, apparent dissociation constants K_a and K_i (represented by *small dots* in the figure) were computed in case of different combinations of the values of ATPase activity (v_{ATPase}) in the solution and exchange constants D_{ATP} and D_{ADP} . In the figure, the measured values are shown by *open circles* in the right upper corner (no OP) and in the left lower corner (with OP). When using the default kinetic constants of ANT transport, all combinations of computed K_a and K_i are aligned along the line with index 1 (indexes are shown within *larger empty circles*). By increasing the maximal activity of ANT by 10 or 100 times, this line can be shifted to the left (lines with indexes 2 and 3, respectively). When instead of increasing the maximal activity of ANT, the apparent dissociation constant for ATP and ADP is increased, the line shifts to the right (line with index 4). Note that regardless of the used values of ANT kinetic constants, all computed combinations of K_a and K_i were considerably adrift from the measured values of these constants in the presence of OP. Reproduced from Vendelin et al. (2004b) with permission



a



b

between MtCK and ANT. The kinetic properties of MtCK and ANT are not changed during interaction and all the changes in apparent kinetic constants measured in the experiment are due to the inability of the experimentalists to measure local ATP and ADP concentrations next to the proteins. Since the gradients of ATP and ADP between the solution and vicinity of the mitochondrial inner membrane depend on the activity of mitochondria, i.e., are not constant, this hypothesis is usually referred to as “dynamic compartmentation” hypothesis.

To check whether dynamic compartmentation hypothesis agrees with the data, one can compose a simple mathematical model based on this hypothesis and compare the model solutions with the experimental measurements (Vendelin et al., 2004b). To find out whether there exists a set of the parameter values that can reproduce both the dissociation constants for ATP altered by OP at the same time, the ATP and ADP exchange coefficients across the outer-mitochondrial membrane, ATPase activity, as well as activity of ANT were changed in the whole range of their values. Regardless of the selected parameter set, the model cannot reproduce the experimental data quantitatively (see [Figure 8.1-6b](#)). Thus, it is clear that the dynamic compartmentation hypothesis is not sufficient to reproduce the measurements and a more complex mechanism of interaction between MtCK and ANT should be used to reproduce the data (Vendelin et al., 2004b). Therefore, the alternative direct local transfer of OP-generated ATP to MtCK should be considered as a main mechanism of acceleration of aerobic PCr production in heart, skeletal muscle, and brain mitochondria.

5.2 Direct Transfer Mechanism

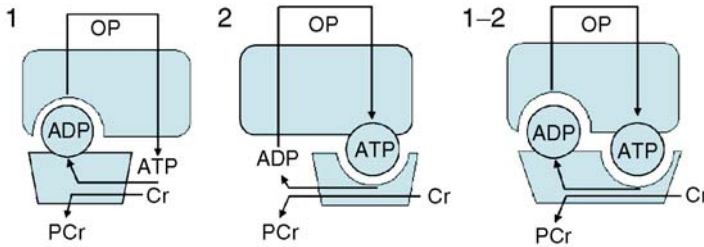
In mitochondria, ATP/ADP-translocase (ANT) transports ADP from the intermembrane (IM) space of mitochondria into their matrix space when activated by ADP from the medium. The stoichiometry of imported ADP to exported ATP is routinely 1. In mitochondria, the quantity of MtCK dimers is approximately equal to the quantity of ANT tetramers (Kuznetsov and Saks, 1986). The structural interposition of these molecular complexes, fixed by cardiolipin molecules, creates a structural basis for direct transfer (channeling) of metabolites from one complex to another without metabolite dissociation into the IM space of mitochondria. We consider the channeling between MtCK dimers (**A**) and ANT tetramers (**B**), but the results are taken to be valid also for the case of MtCK octamers (see above). In this mode of local coupling, the ANT in MtCK–ANT complexes serve as ATP donors ($\mathbf{B}_{(\text{ATP})}^{\text{D}}$) and MtCK molecules are the recipients (acceptors) of directly transferred ATP (\mathbf{A}^{R}). This coupling pathway 2, schematically shown in [Figure 8.1-7a](#), can be expressed as $\mathbf{A}^{\text{R}} \leftarrow \mathbf{B}_{(\text{ATP})}^{\text{D}}$.

In another considered mode of local OP activation, the CK dimers in CK–ANT complexes serve as ADP donors ($\mathbf{A}_{(\text{ADP})}^{\text{D}}$) and ANT tetramers are the recipients (acceptors) of directly transferred ADP (\mathbf{B}^{R}). This coupling pathway 1, schematically shown in [Figure 8.1-7a](#), can be expressed as $\mathbf{A}_{(\text{ADP})}^{\text{D}} \Rightarrow \mathbf{B}^{\text{R}}$.

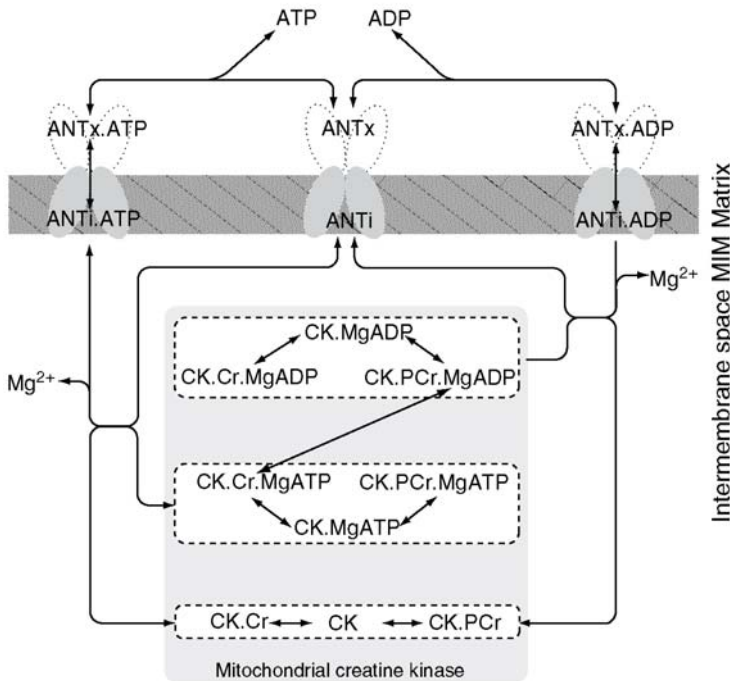
■ Figure 8.1-7

Direct transfer mechanism of coupling between mitochondrial creatine kinase (MtCK) and adenine nucleotide translocase (ANT). (a) Schematic presentation of donor–acceptor relations in local coupling between mitochondrial MtCK (*shaded trapezium*) and ANT (*shaded rectangle*). Transferred adenine nucleotide is shown by a circle associated with the donor complex, *arrows* indicate the reactions of MtCK and mitochondrial OP. Couplings in the direct reactions of MtCK and ANT: (1) local transfer of ADP from MtCK to ANT, in the sole unidirectional mode MtCK activates ANT being activated only by the substrates from medium; (2) local transfer of ATP from ANT to MtCK, in the sole unidirectional mode ANT activates MtCK being activated by ADP from medium; (1–2) bidirectional local transfer of ADP and ATP in the forward reactions of MtCK and ANT, mutual activations of MtCK and ANT without interaction with substrates in the medium in the pure mode of local coupling. This scheme is a basis for probability approach (see the text). (b) The complete kinetic scheme of interaction between MtCK and ANT according to the direct transfer hypothesis. The interaction between the proteins is considered as a sum of two interaction modes: ATP and ADP are transferred through solution (see [Figure 8.1-6a](#)) or directly channeled between the proteins. In this scheme, the direct transfer of ATP and ADP between

proteins is shown. In direct transfer mode, ATP is transferred from ANT to MtCK without leaving the two-protein complex to solution. Since MtCK has only one binding site for ATP and ADP, such transfer is possible only if this site is free, i.e., MtCK is either free (CK) or has only Cr or PCr bound (CK.Cr and CK.PCr). In the scheme, we grouped the states of MtCK according to whether ATP or ADP is bound to the enzyme or not (*white boxes* in the scheme with three states of MtCK in each group). During direct transfer of ATP from ANT to MtCK, MtCK is transferred from states CK, CK.Cr, and CK.PCr to states CK.MgATP, CK.Cr.MgATP, and CK.PCr.MgATP, respectively. In the scheme, this transfer is shown as a link between ANTi.ATP and two corresponding groups of MtCK states. Next, after MtCK reaction (link between states CK.Cr.MgATP and CK.PCr.MgADP in the scheme), ADP is transferred directly to ANT. Note, that MtCK operates with Mg-bound ATP and ADP and ANT requires Mg-free ATP and ADP forms. Thus, during direct transfer between MtCK and ANT, Mg is either bound or released, as it is shown in the scheme. This complete scheme was the basis for thermodynamically consistent analysis of coupling (see text). Reproduced from Vendelin et al. (2004b)



a



b

It is essential that pathways 1 and 2 are interrelated, pathway 1 provides local activation of OP by MtCK, and activated OP in pathway 2 provides local activation of MtCK, which is in addition to its activation by the substrates from medium (▶ [Figure 8.1-7a](#)). Therefore, coupling in the forward reactions of MtCK and ANT is bidirectional (pathways 1–2 in ▶ [Figure 8.1-7a](#)). Moreover, such bidirectional coupling simultaneously takes place in the reverse direction of the MtCK and ANT reaction (Aliev and Saks, 1994). In this respect the bidirectional coupling in MtCK–ANT complex differs from the established couplings (direct transfer of substrates) in rigid enzyme–enzyme complexes, which are mostly unidirectional (for review see Huang et al., (2001a)). ▶ [Figure 8.1-7b](#) shows the detailed kinetic scheme of these direct transfer mechanisms, which will be used for thermodynamic analysis of the coupling (see below).

It is important to emphasize that the coupling does not change the V_{\max} value of MtCK and OP, $0.99 \pm 0.07 \mu\text{mol}/\text{min}/\text{mg}$ (+) versus $1.06 \pm 0.2 \mu\text{mol}/\text{min}/\text{mg}$ (see ▶ [Figure 8.1-2](#)) (Saks, 1980; Jacobus and Saks, 1982b).

For a general analysis of the functioning of a coupled MtCK–ANT system it is important to stress that structural and functional coupling does not prevent its participants from working in completely independent modes during certain conditions. For example, it is well known that in a medium with only ADP mitochondria can carry out OP reactions without any limitations, despite the structural associations between ANT and MtCK. On the other hand, the OP inhibition does not result in inhibition of MtCK but only alters its apparent kinetic behavior (Saks et al., 1975). These facts clearly indicate that the structural associations between ANT with MtCK are rather dynamic and do not result in the formation of a completely isolated space between complexes. The metabolite molecules can leave this space, but can be trapped in it to realize the coupling.

These basic principles of direct interaction between MtCK and ANT have been accomplished mathematically in the probability model (Aliev and Saks, 1993, 1994; Aliev et al., 2003) and in the thermodynamically consistent model (Vendelin et al., 2004b) of their coupling. Both models use the basic mathematical models of free activation of MtCK and ANT by their substrates from the medium. The detailed kinetic mechanisms of these two processes—the MtCK reaction and ATP and ADP translocation by ANT—are shown in the *Appendix* with the probability model of activation of both MtCK and ANT by their substrates from the medium. Here we consider the main aspects of the probability model of CK coupling to ANT.

5.3 Probability Model of MtCK to ANT Coupling

Probability model (Aliev and Saks, 1993, 1994) realizes mathematically the following topics derived from our general analysis of coupling in MtCK–ANT system.

1. Local activations of MtCK and ANT are additional to their activations from the medium by their respective substrates.
2. The increases in MtCK and ANT rates by local coupling are achieved by the rise in a population of MtCK–ANT complexes activated by direct transfer of adenine nucleotides between counter partners in each MtCK–ANT complex in any of coupling pathways (▶ [Figure 8.1-7a](#)).
3. The sizes of populations of active local coupling complexes (P_{ActLoc}) are calculated, according to probability theory, by the product of independent probabilities of existence of a donor (P^{D}) and acceptor (P^{R}) forms of CK and ANT in each kind of coupling path:

$$P_{\text{ActLoc}} = P^{\text{D}} \times P^{\text{R}} \quad (2)$$

4. The model defines “donor” as molecular complexes of CK or ANT (▶ [Figure 8.1-7](#)), donating ADP or ATP. “Acceptor” is defined as a molecular complex, which on accepting the locally supplied ATP or ADP (▶ [Figure 8.1-7](#)) forms an effective translocation or catalytic complex. These acceptors are C.Ti and C.Di for ANT and E.Cr, E.PCr for CK (see ▶ [Figures A1a](#) and ▶ [A1b](#) in the *Appendix*). Probability model assumes that acceptance of adenine nucleotides by these acceptors leads to forming a closed conformation of complex, where the direct delivery of adenine nucleotides from donor to acceptor takes place without their diffusion out into the medium. This basic assumption of probability model, within the frameworks of the direct channeling concept, is not directly proven by respective

molecular structure analyses because of methodological problems (Pebay-Peyroula et al., 2003). Till date, we can only refer to a modern review on several enzymes where direct channeling of substrates was proven structurally (Huang et al., 2001a).

Acceptors of ATP can be classified as “immediate acceptors” (E.Cr), leading to the immediate formation of effective catalytic complexes, and “transitory acceptors,” which on binding the donated adenine nucleotide will be transformed to immediate acceptors. Transitory acceptors are E to form E.A or E.D with locally supplied ADP or ATP, respectively; E.PCr to form dead-end complex E.PCr.A with locally supplied ATP; E.Cr to form dead-end complex E.Cr.D with locally supplied ADP. Assumed peculiarity of transitory complexes with locally supplied adenine nucleotides is the noncompletely-closed configuration of formed CK-ANT substructure, allowing its exchange with the metabolites in solution. These exchanges lead, after a series of fast equilibrations with metabolites in the medium, to the formation of MtCK.A.Cr-ANT or MtCK.D.PCr-ANT complexes in a closed conformation, identical to what is formed by immediate acceptors. Transformation of MtCK.A_{loc}-ANT and CK.D_{loc}-ANT to closed conformation upon binding of Cr and PCr, respectively, is a default assumption of the probability model yet to be proven experimentally.

In the model, the effective complexes of local activation formed by immediate and transitory acceptors are summed up to obtain the pools of local activations of MtCK and ANT in different coupling pathways. Probability model describes the time course of the changes in concentrations of all acceptor and donor forms of MtCK and ANT and derived probabilities of MtCK and ANT local activations and activations by the substrates from the medium. These calculations proceed until attaining steady-state levels of all donor, acceptor, and catalytic and translocation forms of MtCK and ANT. Details of these calculations, the employed basic assumptions, parameters of modeling, and the complete set of equations can be found in Aliev and Saks (1993, 1994).

5.4 The Main Results of the Probability Model

The probability model can reproduce (Aliev and Saks, 1993, 1994) all experimental data from Jacobus and Saks’ paper (1982). The dissociation constants of coupled MtCK, obtained from kinetic analysis of these data sets, are presented in ▶ [Table 8.1-1](#). The data from ▶ [Table 8.1-1](#) indicate a close approximation of experimental data by the probability model.

■ **Table 8.1-1**

Experimental (Jacobus and Saks, 1982b) and simulated kinetic constants for rat heart mitochondrial creatine kinase as a function of oxidative phosphorylation (OP)

Dissociation constants (mM)	Without OP		With OP	
	Experimental	Used in model	Experimental	Simulated ^a
K_{ia}	0.75 ± 0.06	0.75	0.29 ± 0.04	0.16
K_a	0.15 ± 0.01	0.15	0.014 ± 0.005	0.014
K_{icr}	28.8 ± 8.45	26.0	29.4 ± 12.0	–
K_{cr}	5.20 ± 0.30	5.20	5.20 ± 2.30	5.16
K_{icp}	1.60 ± 0.20	1.6	1.40 ± 0.20	1.33
K_{cp}	20–50	24.0	20–50	7.3–20.7
V_{fw}^{maxb}	1.06 ± 0.20	1.0	0.99 ± 0.07	0.9

^aFor explanation of the constants see ▶ [Figure 8.1-A1a](#)

^b V_{fw}^{max} is the maximal rate of the direction of phosphocreatine production

The most important consequence of functional coupling of MtCK to OP is the respiration-induced shift of the MtCK reaction out of the equilibrium. As will be shown later, this phenomenon is principal for the functional role of MtCK in energy transport in heart cells.

► *Figure 8.1-8a* shows the respiration-induced shift of the MtCK reaction out of the equilibrium (Saks et al., 1985) and the reproduction of these data by the probability model (Aliev and Saks, 1994). According to this phenomenon, in the presence of OP, when the mass action ratio (Γ) of CK metabolites in the medium, i.e., ($\Gamma = ([\text{MgADP}] \cdot [\text{PCr}] / ([\text{MgATP}] \cdot [\text{Cr}]))$), favors Cr production, rat heart mitochondria (DeFuria et al., 1980) and mitoplasts (Saks et al., 1982) produce PCr at high rates. Persisting PCr production is due to the fact that MtCK coupling to ANT shifts the mass action ratio to values higher than the K_{eq} of free CK (► *Figure 8.1-8a*). The value of the shift is more than 3.8-fold according to DeFuria et al. (1980), and about 3–5 fold according to the measurements of Soboll et al. (1994) in the medium, initially containing 1 mM ATP and 10 mM Cr.

The probability model corresponds well to experimental data. At the same time, the absence of metabolite dissociation from the E.Cr.ATP_{loc} or E.PCr.ADP_{loc} complexes of CK, postulated by the probability model, precludes the reconstruction of thermodynamic profiles of coupled CK reactions.

Therefore, this model should be complemented with the thermodynamic approach to analyze the coupled reactions as described below.

5.5 Thermodynamically Consistent Model of MtCK–ANT Coupling

This analysis is based on the transition state theory that gives the rate constants of the reaction as the functions of free-energy changes during the advancement of a reaction. For the monomolecular conversion of the enzyme–substrate complex into the enzyme–product complex ($A \leftrightarrow B$), each of these states of an enzyme has a free energy associated with it: G_A and G_B for states A and B, respectively. In a generalized form, the rates of transition between two states are governed by the following equations:

$$v_+ = [A] \cdot \alpha \cdot e^{-(G_f - G_A)/RT} \quad \text{and} \quad (3)$$

$$v_- = [B] \cdot \alpha \cdot e^{-(G_f - G_B)/RT}, \quad (4)$$

where v_+ and v_- are the rates of transitions between states A and B in forward and backward directions, respectively; $[A]$ and $[B]$ are normalized concentrations; α is a factor which depends on the nature of the transition; G_f is free energy in the transition state; R is the gas constant; and T is the absolute temperature. As it is clear from the equations, the same transition state is passed during the reaction in accordance with the principle of microscopic reversibility. In equilibrium, the rates v_+ and v_- are equal, and it is easy to show that

$$[B]_{\text{eq}} / [A]_{\text{eq}} = e^{-(G_B - G_A)/RT}, \quad (5)$$

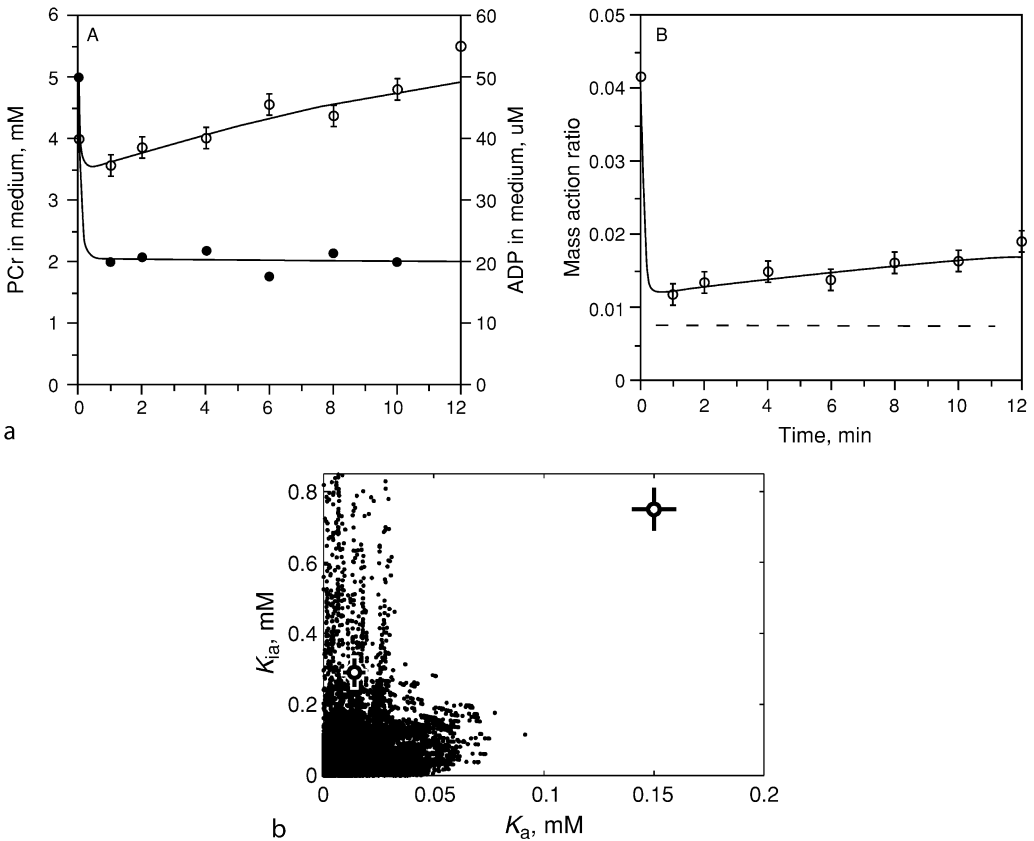
i.e., the equilibrium constant of the reaction ($K = [B]_{\text{eq}} / [A]_{\text{eq}}$) is determined by the change of the free energy of the complex ($G_B - G_A$) during the reaction and not by the free energy of the transition state. The same is true in the opposite direction, i.e., if we know the dissociation constants for substrate binding as well as the equilibrium constant for the reaction, the free energies of the enzyme states can be easily found. By depicting the free energies of all enzyme states on a graph, the free energy profile can be composed. To obtain the free energy of the MtCK states, we used the measured kinetic constants of dissociation of ATP, ADP, PCr, and Cr from MtCK as well as the measured differences in maximal rates for forward and reverse reactions.

By applying the free-energy profile during the analysis and taking into account that the transition state should be the same for each forward–backward reaction pair, the thermodynamically consistent models can be composed for CK coupled to OP (Vendelin et al., 2004b).

The interaction between MtCK and ANT was considered as a sum of two interaction modes. In the first mode, ATP and ADP are liberated into the IM space and then bound to MtCK or ANT. This mode

■ Figure 8.1-8

(a) Analysis of the experimental data on phosphocreatine (PCr) production in heart mitochondria by a probability model. Respiration-induced shift of CK reaction out the equilibrium, reported by Saks et al. (1985) (circles), and the reproduction of these data by the probability model (thin lines). A. Changes in PCr (open circles) and ADP (closed circles) concentrations. B. Changes in the mass action ratio of CK metabolites in the medium, Γ , which initially contained 0.12 mM ATP, 0.05 mM ADP, 40 mM Cr, and 4 mM PCr and substrates for respiration. Dotted line in B: apparent equilibrium constant equal to 0.0079. From Saks et al. (1985) with permission. (b) Calculated apparent dissociation constants K_a and K_{ia} of MgATP in the MtCK reaction in the presence of oxidative phosphorylation (OP). Coupling between MtCK and OP was modeled assuming direct transfer of metabolites between ANT and MtCK. Apparent dissociation constants K_a and K_{ia} (represented by small dots in the figure) are computed in case of different combinations of the free energies of MtCK-ANT complex states and free energies of transition. The measured values are shown by open circles in the right upper corner (no OP) and in the left lower corner (with OP). Note that the range of computed K_a - K_{ia} combinations covers the area near the measured values of these constants in the presence of OP. The figure is reproduced from Vendelin et al. (2004a) with permission



corresponds to the interaction between MtCK and ANT as two separate proteins without any coupling (see [Figure 8.1-6a](#)). In this case, ATP as well as all other substrates are in fast equilibrium with MtCK and the reaction follows the random Bi-Bi type mechanism (see *Appendix*). In the second mode, ATP and ADP are directly channeled between the proteins. Such channeling is possible if the acceptor protein (ANT or MtCK) has no bound ATP or ADP molecule, i.e., it can accept ATP (ADP) from the other protein

(see [Figure 8.1-7b](#)). Additionally, we assume that when MtCK accepts ATP (ADP) from ANT directly, bound ATP and ADP cannot be in fast equilibrium with the surrounding solution. Thus, the equilibration of the MtCK-binding site for ATP and ADP with the surrounding solution is prevented and the system may have different kinetics if compared to the kinetics of soluble MtCK.

By this model, one can reproduce the measured values of apparent kinetic constants of the MtCK reaction. During this test, the free energies of the states of the coupled system were varied as well as the free energies of activation. The simulation results are shown in [Figure 8.1-8b](#). Note that the region with the measured values of K_a and K_{ia} is covered by the model solution and it is possible to find such combinations of model parameters, which would lead to the measured combination of K_a and K_{ia} values. In this analysis, one can reproduce the following experiments with the same set of the model parameters: (1) changes in the apparent kinetic properties of the MtCK reaction when coupled to OP (Jacobus and Saks, 1982b; Saks et al., 1985); (2) competition between MtCK-activated mitochondrial respiration by competitive ATP-regenerating system (Gellerich and Saks, 1982); and (3) studies of radioactively labeled adenine nucleotide uptake by mitochondria in the presence of MtCK activity (Barbour et al., 1984). As a result, the free-energy profile of the coupled MtCK–ANT system was proposed (Vendelin et al., 2004b). According to our analysis, the main difference in free-energy profiles of the uncoupled and coupled MtCK reaction is the free-energy change during the reaction. In the coupled system, according to our model, due to increase of the free energy of ANT_i .ATP state the free energy decreases when ATP bound to ANT is used to synthesize PCr in the MtCK reaction. If compared with the models of direct transfer using the probability approach, the proposed mechanism does not require strong changes in the free-energy profile of the reaction of phosphate transfer itself (Vendelin et al., 2004b). The proposed detailed kinetic scheme ([Figure 8.1-7b](#)) can be used as a basis for further analysis of the kinetics of MtCK–ANT interaction. In particular, the possible mechanism of an increase of the free-energy level of the ANT_i .ATP complex when coupled to OP is intriguing and requires further experimental study.

5.6 Phenomenological Models

When we are not interested in the detailed mechanisms of functional coupling, but to describe the behavior of the whole cellular system of energy transfer, a more simple and easy method of phenomenological modeling can be used. This means that to describe the functional coupling of an enzyme with other systems (transporters or other enzymes) the kinetic equation corresponding to the mechanism of the reaction catalyzed by this enzyme in the isolated state is used also to describe its behavior in the coupled state. In the latter case, however, the parameters of equations are found by fitting it with the experimental data obtained in the coupled state. The more experimental data obtained in different conditions are used the better. Thus, instead of the real kinetic constants of the enzyme, the phenomenological constants are used to describe the changes induced by the coupled reactions. This approach was used by us to describe the behavior of compartmentalized energy transfer system and regulation of mitochondrial respiration by metabolic signaling within a whole energetic unit, ICEU (Aliev and Saks, 1997; Vendelin et al., 2000; Saks et al., 2003). By fitting the CK rate equation with multiple experimental data on its behavior in the coupled state with ANT, the phenomenological dissociation constants for adenine nucleotides were found and used in modeling the whole system (Vendelin et al., 2000; Saks et al., 2003). Another way of phenomenological modeling is to introduce into the individual enzyme equation the values of changed local concentrations of substrates, which are assumed to depend on neighboring systems. This conforms also to the model of existence of the microcompartments within the complexes (Aliev and Saks, 1997). In this way, the direct transfer mechanism between MtCK and ANT was in first approximation modeled by assuming high local ATP concentrations in the vicinity of the active center of MtCK created by ANT (Aliev and Saks, 1997, see below). These phenomenological approaches simplify the calculations, but are at the same time potential sources of the errors, if the conditions of the reaction are too far from those used for finding the values of phenomenological parameters. Therefore, the corresponding checks are required.

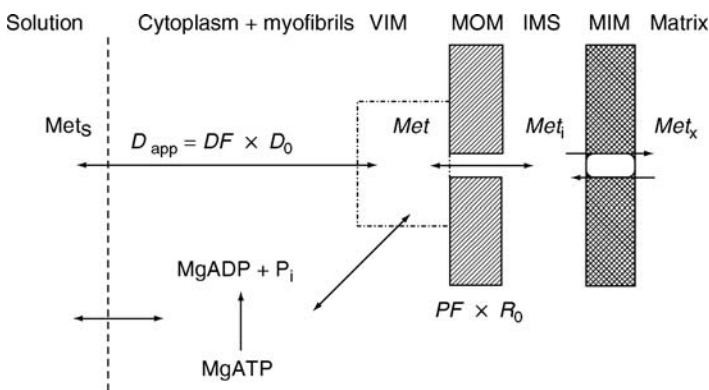
6 Heterogeneity of ATP and ADP Diffusion and Compartmentation of Adenine Nucleotides

In this section, we will use the mathematical models of intracellular diffusion and show how the latter is dependent on intracellular organization. For this, the results of experiments carried out on permeabilized cardiomyocytes and muscle fibers are used as a basis for simulation (▶ [Figures 8.1-3](#) and ▶ [8.1-4](#)). To understand the phenomenon described in ▶ [Figure 8.1-3](#) and compose the mathematical model, it is necessary to account for the diffusion of ATP and ADP molecules out of the cell before they can encounter exogenous ADP-trapping systems or into the cell before they can encounter mitochondria. Therefore, the geometry of the cell has to be taken into account to describe diffusion between the solution and the cell interior. The cardiac cell is rather elongated (about five times longer than the diameter). For simplicity, we can assume that diffusion between the cell and the solution is almost the same in all cross-sections and it is sufficient to model only one cross-section.

On the way from solution to mitochondrial inner membrane, two diffusion restrictions are encountered by ATP and ADP molecules. The first one is at the level of mitochondrial outer membrane and can be regulated by the state of voltage-dependent anion channel (VDAC) molecules (Colombini, 2001). The second one is induced by macromolecular crowding in the cell. In addition, when simulating the experiments performed on permeabilized fibers and cells, the endogenous ATPases have to be taken into account. The complete system used in the model is shown in ▶ [Figure 8.1-9](#). The aim of the model would be to find

■ Figure 8.1-9

Schematic presentation of ADP (and ATP) diffusion pathways from solution into mitochondrial matrix. Met_s , Met , Met_i , and Met_x are metabolite concentrations in the solution, in the vicinity of the mitochondria (VIM, inside ICEU), in the mitochondrial intermembrane space, and in mitochondrial matrix, correspondingly. MOM, IMS, and MIM are mitochondrial outer membrane, intermembrane space, and inner membrane, respectively. D_{app} , D_0 , and DF correspond to apparent diffusion coefficient, diffusion coefficient of metabolite in bulk water phase, and diffusion factor (see the text). R_0 is the permeability coefficient for passive diffusion of metabolite across the outer-mitochondrial membrane, and PF is the permeability factor for this metabolite. Reproduced from Saks et al. (2003) with permission



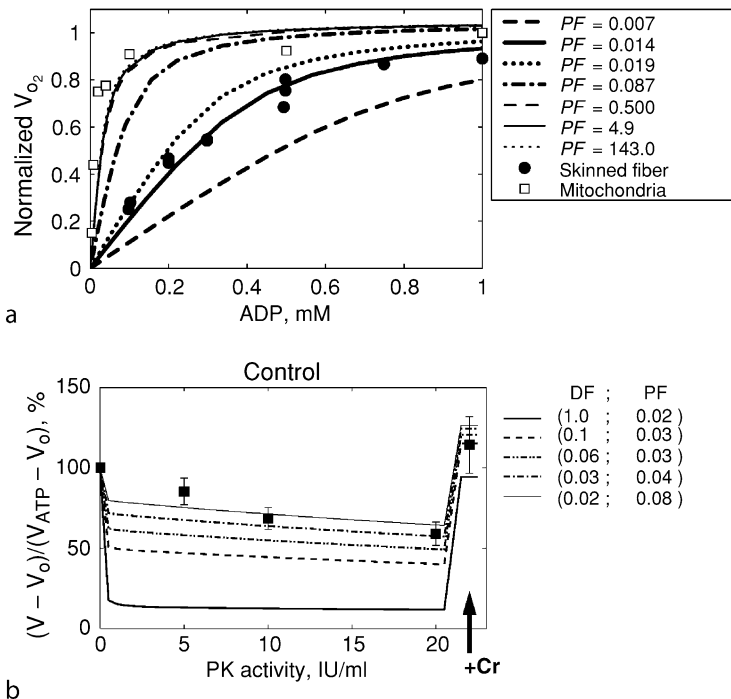
such a set of model parameters that can reproduce the following experiments: stimulation of respiration by exogenously added ADP and ATP as well as inhibition of respiration by exogenously added ADP-trapping systems (e.g., PK + PEP). For this, the model was used to determine the possible values of two factors describing the restriction of the diffusion of ADP and ATP: DF and PF . The factor DF describes the restriction of the diffusion of adenine nucleotides within the cytoplasmic (extramitochondrial) space due to macromolecular crowding and cytoskeletal structures, and the factor PF describes the decrease of the

permeability of the outer-mitochondrial membrane due to the control of VDAC by some cytoskeletal proteins (Saks et al., 1994a, 1995; Capetanaki, 2002).

The diffusion restrictions between mitochondrial inner membrane and solution influence the apparent K_m for exogenous ADP in regulating respiration by shifting it to higher values. For example, if there are no considerable diffusion restrictions encountered by molecules between solution and ANT then respiration should be stimulated by exogenous ADP, as measured for isolated mitochondria. Indeed, when we take diffusion coefficient equal to the values measured in the bulk phase and make the diffusion through mitochondrial outer membrane fast, the computed respiration rate is very close to the values measured for isolated mitochondria (open squares in [Figure 8.1-10a](#), simulations with large values of PF). However, by

Figure 8.1-10

Analysis of the experimental data on regulation of respiration in permeabilized cardiac cells and fiber by the mathematical model. (a) Dependence of the calculated mitochondrial respiration rate in permeabilized cardiac fibers on the concentration of exogenous ADP computed with different mitochondrial outer membrane permeability factors (PF). The diffusion coefficients of the metabolites within the fiber are taken to be equal to the coefficient values measured in bulk water phase of cells, i.e., there is almost no significant diffusion restriction imposed by macromolecular crowding. Simulations are compared with the measurements of respiration in isolated mitochondria (*open squares*) and in skinned fibers (*solid circles*). Note that reduction of the outer membrane permeability increases the apparent K_m (ADP) of mitochondrial respiration. Good fit with the experimental data for permeabilized fibers is obtained for $PF = 0.014$. For isolated mitochondria, good fit is obtained for $PF = 0.5$ and higher. Reproduced from Saks et al. (2003) with permission. (b) Reduction of endogenous ADP-dependent respiration rate in the presence of 2 mM MgATP by increasing PK activity in the solution. *Closed squares* are the experimental points (see [Figure 8.1-3](#)) without treatment with trypsin, *solid lines* are the calculated curves. *Arrow* indicates addition of 20 mM Cr into the solution to stimulate respiration. Note the good correlation between simulations and the measurements for DF values < 0.06 . Adapted from Saks et al. (2003) with permission



increasing diffusion restriction imposed by mitochondrial outer membrane (reduction of PF), the model can reproduce measurements on permeabilized cells and fibers (closed circles in [Figure 8.1-10a](#)). Similar results can be obtained by reducing apparent diffusion coefficient DF and keeping PF large (Saks et al., 2003). Thus, the effects of both the diffusion restrictions on the model solution are similar when the measurements of apparent K_m for exogenous ADP in permeabilized fibers or cells are simulated. Therefore, it is impossible to distinguish the contribution of each diffusion restriction using only this experiment.

Other experiments used for modeling are the experiments described in [Figure 8.1-3](#): the experiments in which respiration was activated by endogenous ADP (produced from added MgATP in the intracellular ATPase reactions) and the effects of the ADP-trapping system PK+PEP on respiration were studied. These experiments are best explained by the model in which the diffusion is mainly restricted through reduction of apparent diffusion coefficient (low values of DF), therefore the large portion of ADP does not leave the fiber and is inaccessible to PK+PEP in the solution ([Figure 8.1-10b](#)) (Saks et al., 2003). The inhibition found by the model in this case is induced partially by ADP diffusing out from the fiber as well as by PK + PEP that is diffusing into the fiber. Thus, using a combination of two experiments ([Figure 8.1-10a](#) and [b](#)) we can determine the possible values of two diffusion restrictions.

However, our modeling of the nature of the diffusion restrictions as a reduction of apparent diffusion coefficient is not clear. According to the measurements of diffusion coefficients in muscle tissue, diffusion coefficient is about two times smaller than the one measured in water (de Graaf et al., 2000). The values of apparent diffusion coefficient that we obtain from analysis of our data are smaller by an order(s) of magnitude (Saks et al., 2003). Thus, it seems that there are some diffusion restrictions which are not visible in overall diffusion coefficient measurements, but which play an important role in permeabilized fiber measurements when the mitochondrial respiration rate was used as a probe for local ADP concentration (Ovádi and Saks, 2004). Therefore, in addition to the value of the diffusion restriction, DF, we tried to estimate the distribution of this restriction in the cell. These simulations indicate that the intracellular diffusion restrictions are not distributed uniformly, but are localized in certain areas in the cell (Vendelin et al., 2004a). However, their precise localization is still unknown.

These results are consistent with the results obtained for the strong localized diffusion restrictions for ADP and ATP in cardiac cells by Abraham et al. (2002) and Selivanov et al. (2004). Earlier, Weiss and Lamp also arrived at a similar conclusion (1987). By using the microinjection technique, Bereiter-Hahn et al. showed that the average diffusion coefficient for ADP in the cells was decreased by an order of magnitude (Bereiter-Hahn et al., 1994). All these results show that the diffusion of ATP and ADP is very heterogeneous in the cell. This was recently evidenced by using the targeted recombinant luciferase technique (Kennedy H. et al., 1999).

At the present moment, however, the model with the localized diffusion restrictions should be considered as a first approximation only, and direct experiments are needed for measurement of the local diffusion rates of ATP or ADP by modern experimental techniques. Under conditions of strong local restriction of the diffusion of adenine nucleotides, the compartmentalized energy transfer by the CK-PCr and other systems becomes vitally important for the cell.

7 The Modeling of Compartmentalized Energy Transfer in the Cells

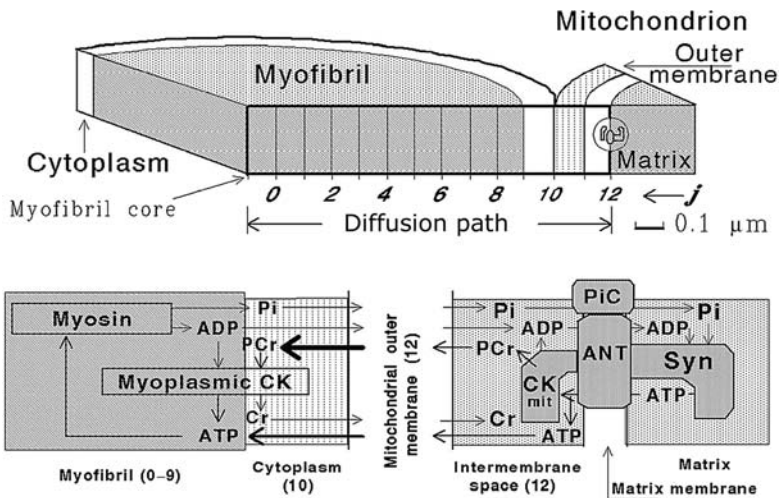
Mathematical modeling of energy exchange in working cardiac cells was performed to gain some insight on fundamental questions of cell energetics still discussed up-to-date: (1) Does cellular CK is in equilibrium state during the in vivo steady-state contractions of heart muscle, and therefore, can cellular ADP levels in the cytoplasm be predicted from measured cellular metabolite levels; (2) Do in vivo mitochondria export energy by ATP or in the form of PCr, according to the concept of the CK shuttle; (3) Do metabolite levels in the myoplasm oscillate during cardiac contractions in vivo; (4) How the cell realizes its metabolic stability, when the manifold linearly interrelated increases in cardiac work and oxygen consumption take place at the practically constant metabolite levels and at PCr/ATP ratio in the cells. Without an experimental method for the direct monitoring of cellular ADP levels, the mathematical modeling of dynamic events in cell cytoplasm remains the only choice.

7.1 Description of a Model

For these purposes, we constructed a new class of mathematical models of intracellular compartmentalized energy transport in cardiac cells, which are based mainly on the principles of chemical and enzyme kinetics (Aliev and Saks, 1997; Dos Santos et al., 2000). These models consider the dynamics of basic events of cell energetics (Figure 8.1-11): ATP hydrolysis by actomyosin ATPase during the contraction cycle, diffusional

Figure 8.1-11

The general scheme of compartmentalized energy transfer in cardiac cells (Reproduced from Dos Santos et al. (2000) with permission). In the model, the diffusional exchange of ATP, ADP, PCr, Cr, and P_i between myofibrils and mitochondria is considered along their radii and an interposed among them layer of cytoplasm. Diffusion path of $1.3 \mu\text{m}$ length includes ten $0.1 \mu\text{m}$ space units (j) in myofibril and three units in cytoplasm, mitochondrial outer membrane, and intermembrane (IM) compartments. Lower part shows compartmentation of myoplasmic CK in myofibril and cytoplasm spaces, of MtCK (CK_{mit}), adenine nucleotide translocase (ANT) and P_i Carrier (PiC) in mitochondrial IM space and of mitochondrial ATP synthase (Syn) in mitochondrial matrix space. Myofibrillar myosin provides ATP hydrolysis during myofibrillar contraction. MtCK and ANT are proposed to be coupled by high local ATP concentration arising from restricted ATP diffusion in the narrow gap (microcompartment) between coupled molecules. Arrows indicate diffusion fluxes of metabolites in compartments and between them through the mitochondrial outer membrane



exchange of metabolites between myofibril and mitochondrial compartments, VDAC-restricted diffusion of ATP and ADP across mitochondrial outer membrane, the mitochondrial synthesis of ATP by ATP synthase, ΔpH - and $\Delta\psi$ -controlled P_i and ADP transport into mitochondrial matrix, and PCr production in the coupled MtCK reaction and its utilization in the cytoplasmic CK reaction. These events are considered in a system composed of a myofibril with a radius of $1 \mu\text{m}$, a mitochondria, and a thin layer of cytoplasm interposed between them in accordance with the basic pattern of organization of muscle cell energy metabolism, the ICEUs (see Figure 8.1-4) (Aliev and Saks, 1997; Dos Santos et al., 2000; Saks et al., 2004a). The computations of diffusion and chemical events were performed for every $0.1\text{-}\mu\text{m}$ segment of a chosen diffusion path at each 0.01 ms time step (Aliev and Saks, 1997). This allows the simulation of the space-dependent changes throughout the entire cardiac cycle. The mitochondrial block of the model is based on a simple kinetic scheme of mitochondrial ATP synthase with parameters allowing the description of experimental ADP- and P_i -dependent OP in isolated mitochondria (Aliev and Saks, 1997). Mitochondrial

OP is activated by ADP and P_i produced by ATP hydrolysis in the myofibril compartment. The kinetics of ATP hydrolysis by myosin in contracting muscle was predicted from the dP/dt change in isovolumic rat heart: a linear increase in ATP hydrolysis rate up to 30 ms followed by its linear decrease to zero at the 60th ms of the contraction–relaxation cycle. The total duration of this cycle was taken to be 180 ms (Aliev and Saks, 1997). In mitochondria, the ATP/ADP translocase (ANT) and the P_i carrier (PiC) regulate the matrix concentrations of ATP, ADP, and P_i available for the ATP synthase activation. These carriers establish constant positive ADP and P_i gradients between the matrix and mitochondrial IM space. In the latest version of the model (Dos Santos et al., 2000), the ATP/ADP ratios in the matrix and activity of ATP synthase are dependent on $\Delta\psi$, the electric component of mitochondrial membrane potential. The latest version of the model employs the complete mathematical model of the PiC based on the probability approach, allowing the prediction of the dynamics of P_i accumulation in the matrix in exchange for matrix OH^- ions at the expense of mitochondrial protonmotive force, ΔpH (Dos Santos et al., 2000; Aliev et al., 2003). The model of cellular events considers CK compartmentation (🔗 [Figure 8.1-11](#)). The molecules of cytoplasmic isoenzyme of CK (MM-CK), which make up for 69% of the total activity, are taken to be distributed in the myofibrillar and cytoplasmic spaces. A remaining part of cellular CK, mitochondrial isoenzyme of CK (MtCK), is localized in the mitochondrial compartment. The resulting close proximity of MtCK and ANT allows direct channeling of adenine nucleotides between their adjacent active centers; this channeling is the actual basis for shifting the MtCK reaction toward the synthesis of PCr from translocase-supplied ATP even at high levels of ATP in the myoplasm of in vivo heart cells.

7.2 Main Results: Nonequilibrium State of the CK System

The model allows simulating several cases of cell functioning necessary for better understanding the basic mechanisms of intracellular energy transport. These cases include: system 1—the cell without CK; system 2—the cell with MM-CK and coupled MtCK; complete system 3—the cell with CK and diffusional restrictions on the mitochondrial outer membrane (🔗 [Figure 8.1-12](#)).

The main results of these simulations are shown in 🔗 [Figure 8.1-12](#), where the numbers on the curves indicate the number of the simulated system. These simulations are given for $\Delta\psi = -120$ mV, similar to that used by Aliev and Saks (1997). Metabolite contents in rat hearts when perfused with glucose at high workloads, taken from Dos Santos et al. (2000), were recalculated for free unbound water in the compartments, according to our publication (Aliev et al., 2002). The workload in these simulations was arbitrarily taken as $1.5 \text{ mmol ATP s}^{-1} \text{ kg}^{-1}$, this value is equal to half-maximal capacity of mitochondrial OP. At this workload the myoplasmic PCr/ATP ratio is in the reliable ranges of experimental data, about 1.7–1.9.

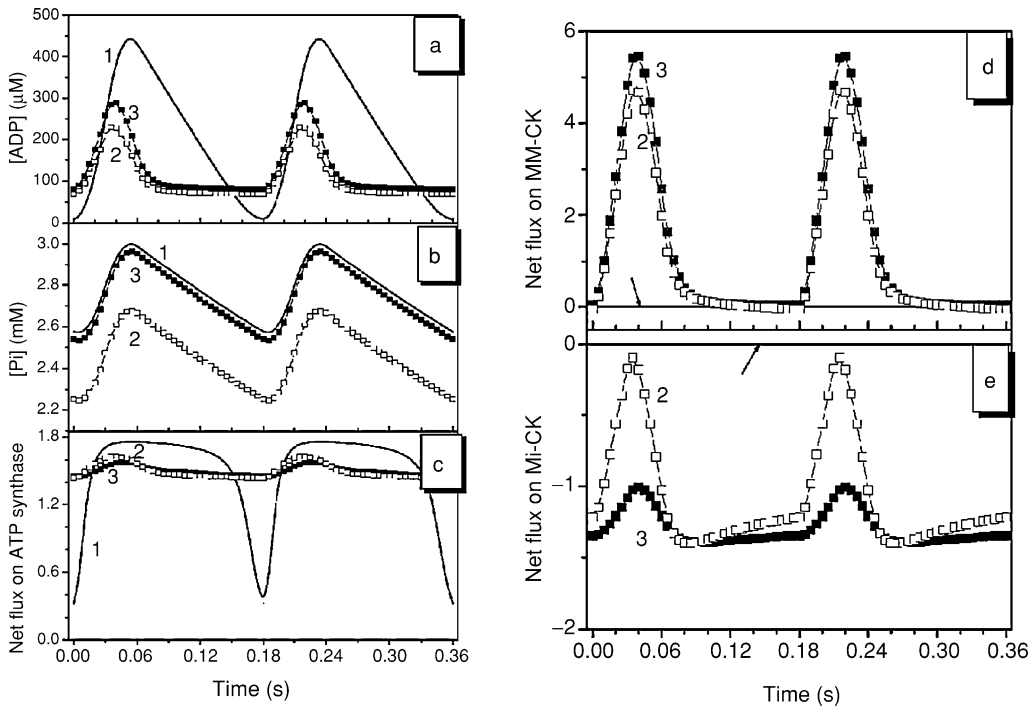
System 1: the Cell without CK. In the cell without CK (case 1), hydrolysis of cytoplasmic ATP by myofibrillar ATPase may lead to the increase in myoplasmic levels of ATP hydrolysis products, ADP and P_i , up to $753 \mu\text{M}$ in the one steady-state contraction. But the real peak values of ΔADP (🔗 [Figure 8.1-12a](#), curve 1) and ΔP_i (🔗 [Figure 8.1-12b](#), curve 1) concentrations in the myoplasm are lower, $425\text{--}437 \mu\text{M}$, due to increasing activation of mitochondrial ATP synthase (🔗 [Figure 8.1-12c](#), curve 1). Progressive decreases in myoplasmic ADP and P_i levels at the end of diastolic part of cardiac contraction cycle lead to corresponding decrease in ATP synthase activation, and the system is ready to perform the next steady-state contraction cycle.

These data clearly indicate that in case 1 the cyclic bursts of ADP and P_i levels in the myoplasm are sufficient for corresponding cyclic activation of the mitochondrial OP system, in accordance with the mechanism of simple respiratory control by ADP (Chance and Williams, 1956; Nicholls and Ferguson, 2002). Here the capacity of mitochondrial OP machine allows to attain very low end-diastolic levels of ADP ($7.7 \mu\text{M}$) and P_i (2.58 mM) in the myoplasm.

Case 1 of OP activation has several serious disadvantages. First, it supposes very high ADP levels in the myoplasm throughout the diastolic part of cardiac cycle, from 60th to 180th ms. High levels of ADP during muscle relaxation are known to decrease the rate of detachment of myosin molecules from actin filaments in the contraction cycle (Cook and Pate, 1985; Yamashita et al., 1994; Fukuda et al., 2000; Karatzaferi et al., 2003). On the other hand, high levels of ADP may activate myoplasmic AK system with consequent

Figure 8.1-12

Comparison of simulated dynamics of levels of basic oxidative phosphorylation (OP) activators (a) ADP and (b) P_i in the myofibril core with (c) activation of mitochondrial ATP synthase during steady-state contraction cycles in systems 1 (curves 1), 2 (curves), and 3 (curves 3). Net fluxes on ATP synthase are given in $\text{mmol s}^{-1} \text{kg wet mass}^{-1}$. Simulations were performed using the model with P_i -carrier kinetics (Dos Santos et al. (2000)) for workload of $1.5 \text{ mmol ATP s}^{-1} \text{kg}^{-1}$, mitochondrial $\Delta\psi = -120 \text{ mV}$. Basic metabolite contents in rat hearts for workload with 3.5 mM Ca^{2+} (Table 4, raw B in Dos Santos et al. (2000)) were recalculated for the total intracellular unbound water (529 ml kg^{-1}) and unbound water (134.6 ml kg^{-1}) in the mitochondrial matrix; the length of cardiac cycle was 0.18 s . Simulated nonequilibrium behavior of (d) myofibrillar creatine kinase and (e) mitochondrial MtCK in systems 2 and 3. Net fluxes of ATP production are given in $\text{mmol s}^{-1} \text{kg}^{-1}$, arrows indicate the position of equilibrium when net ATP production is equal to zero



degradation of cellular adenine nucleotide pool (Savabi, 1994). Increase in the workload will increase the peak value of ADP concentration further. Second, the profound cyclic activations of mitochondrial OP (Figure 8.1-12c, curve 1) may have high costs for each activation–deactivation cycle. Functioning by the direct mechanism of simple respiratory control by ADP seems to be more appropriate for cells with noncyclic activation and relatively low energy fluxes, such as hepatic cells (Bianchi et al., 2004).

System 2: the Cell with CK. The pattern of activation of cell energetics changes completely when the CK system is activated. First, in case 2, the peak value of ADP in the myofibril core decreases about twofold and the spike disappears in the beginning of the heart diastole (Figure 8.1-12a, curve 2). This event is due to activation of MM-CK (Figure 8.1-12d, curve 2) by increased levels of ADP during systole (0–60 ms).

The outstanding feature of system 2 with CK is a sustained activation of mitochondrial OP machine at maximal levels for this workload (Figure 8.1-12c, curve 2). This sustained activation arises from permanent functioning of MtCK in the direction of net ADP and PCr production (Figure 8.1-12e, curve 2). As a result, we have a complete separation of MtCK and MM-CK functions: in system 2 all reactions of ADP and PCr generation are delegated to MtCK in the mitochondrial compartment (Figure 8.1-12e, curve 2),

and restoration of the ATP pool in the myoplasm becomes delegated exclusively to MM-CK in this compartment (▶ [Figure 8.1-12d](#), curve 2).

Additional PCr production by coupled MtCK leads to a high PCr/ATP ratio close to 1.98 in the myoplasm (Dos Santos et al., 2000). This increase provides the myoplasmic diastolic values of I higher than the K_{eq} of the CK reaction thus forcing MM-CK to work only in the direction of ATP regeneration during systole (▶ [Figure 8.1-12d](#), curve 2).

The most important consequence of additional PCr production by coupled MtCK is a sharp increase in PCr export (up to 71.7% of total energy export) by mitochondria. Because in a steady state the ADP (and Cr) influx through the mitochondrial outer membrane is strictly equal to ATP (and PCr) outflux, this means that in system 2 with coupled MtCK only 28.3% of OP activation is achieved by direct activation by ADP, and a major part of activation, i.e., 71.7%, is realized through the MtCK reaction.

As a whole, the main advantages of system 2—sustained activation of OP and low ADP levels during diastolic part of cardiac contraction—are based on the cooperation of structurally and functionally separated CK isoenzymes. In this system, the early regeneration of the ATP pool in the myoplasm or directly in the myofibrillar compartment is performed by MM-CK at the expense of PCr breakdown, while all reactions of local OP activation and concomitant PCr regeneration are performed by MtCK in the mitochondrial compartment. Activation of OP by MtCK leads to $\sim 72\%$ of energy export from mitochondria by the PCr molecules.

The Complete System 3. The complete system, which is nothing but system 2 with added restrictions for ATP and ADP diffusion across the mitochondrial outer membrane, has all the advantages of system 2 (curves 3 in ▶ [Figure 8.1-12](#)), adding more sustained shift of MtCK from equilibrium in the systolic phase of cardiac cycle (▶ [Figure 8.1-12e](#), curve 3). As a result, the fraction of PCr export from mitochondria increases further up to 86.5%.

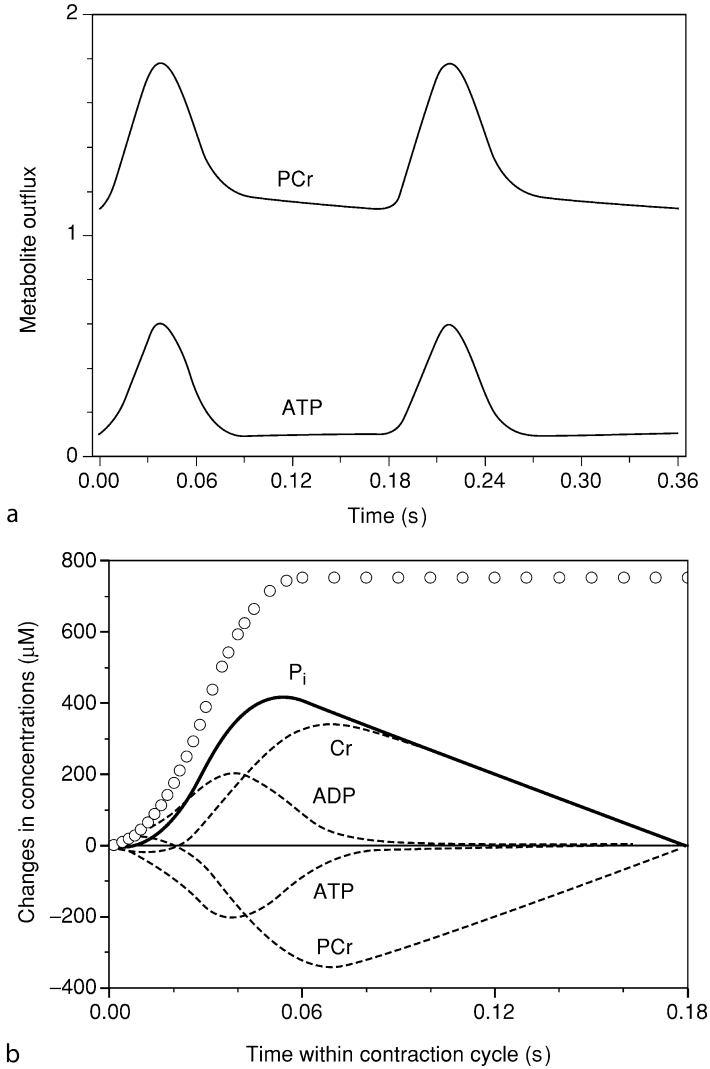
▶ [Figure 8.1-13a](#) shows the dynamics of ATP and PCr export by mitochondria in complete system 3. ATP export is substantial only in the systolic phase of cardiac cycle, coinciding with the burst in myoplasmic ADP concentration (▶ [Figure 8.1-12a](#), curve 3). The main part of OP activation comes from activation of forward MtCK reaction of PCr and local ADP production (▶ [Figure 8.1-13a](#), PCr-marked curve); it is practically exclusive in the diastole. ▶ [Figure 8.1-13a](#) also demonstrates the mechanism of OP activation, which consists of a basic persistent part (end-diastolic level of activation) and cyclic transient part (activation, additional to a basic part). The basic part of activation provides the persistent activation of ATP synthase in a whole cardiac cycle (▶ [Figure 8.1-12c](#)), while the cyclic component of activation is responsible for a considerable part of OP activation (▶ [Figure 8.1-13a](#)) during systole.

The basics of transient part of OP activation can be seen in ▶ [Figure 8.1-13b](#), showing changes of metabolite concentrations in the myofibril core. In this figure, the circles indicate the time course of ADP and P_i release into the myoplasm during one contraction cycle. While the P_i and Cr concentrations are gradually changing during the whole contraction cycle, the ADP signal persists only in the systolic phase (▶ [Figure 8.1-13b](#)). The main signals for the transient part of OP activation may come in diastole from the Cr-mediated activation of MtCK, as judged from coincidence of dynamics of P_i and Cr levels in the diastolic phase of cardiac cycle (▶ [Figure 8.1-13](#)). Note, however, that the Cr concentration changes within the range of several hundreds of μM , while its total concentration in the cell is about 10–15 mM. Thus, its relative changes are within the error range of its assay. The relative changes of ADP and P_i concentrations are, however, significant because of their low diastolic values.

The mathematical modeling of energy transfer in real working cardiac cells allows to formulate the following answers to the main questions put in the beginning of this ▶ [Section 7](#): 1) the cellular myoplasmic CK is in equilibrium state only in the diastolic part of contraction; therefore, the CK equilibrium concept can be used only for approximate estimates of diastolic levels of myoplasmic ADP; MtCK is never in the equilibrium state; 2) in real cardiac cells mitochondria export energy mostly by PCr molecules; 3) the metabolite levels in cyclically contracting cells oscillate in each cardiac contraction; the bursts of ADP levels during the systole cannot be completely damped even on an artificial 10-fold increase in the activity of MM-CK; 4) the metabolic stability in cardiac cells may be based on high background capacity of mitochondrial OP machine coupled to MtCK reaction (Aliev et al., 2003).

■ Figure 8.1-13

(a) Simulated kinetics of ATP (ATP) and PCr (PCr) diffusional export through the mitochondrial outer membrane in the complete system 3. (b) Phasic changes in metabolite concentrations in myofibril core during cardiac contraction cycle in the complete system 3. Circles indicate time course of ATP hydrolysis by myofibrils. Simulation conditions as in [Figure 8.1-12](#)



8 Modeling the Mitochondrial Respiration Controlled by Frank–Starling Mechanism under Conditions of Metabolic Stability. Metabolic Control Analysis of the Factors of Regulation

In line with the analysis described above, we investigated whether it is possible, using the model of compartmentalized energy transfer and assuming that the cytoplasmic calcium concentration is constant and ensures maximal activity of mitochondrial dehydrogenases, to reproduce the experimental data on

linear increase of the respiration rate with elevation of the workload—an important aspect of the Frank–Starling law—under conditions of metabolic stability of the heart muscle. For this, an extended model was proposed (Vendelin et al., 2000). The main addition introduced into the model described above was incorporation of OP, developed by Korzeniewski and Froncisz (1991) and Korzeniewski (1998, 2003). Such addition was made in order to calculate mitochondrial response, including changes in respiratory chain components as well as mitochondrial membrane potential to the changes in concentrations of metabolites surrounding mitochondria. The metabolites described by the model present in the myofibrils and mitochondrial IM space are ATP, ADP, AMP, PCr, Cr, and P_i . All these metabolites diffuse between the cytosolic and IM compartments, where the metabolites are involved in the CK and AK reactions. In addition, ATP is hydrolyzed in the myofibrils. The workload was changed by increasing ATPase activity, and the response of the cell in the form of increased oxygen consumption and altered metabolite concentration was computed. Thus, Frank–Starling mechanism was accounted for by increasing the rate of ADP and P_i production from MgATP in myofibrils due to increased number of crossbridges during workload elevation. In the IM space, the MtCK reaction is coupled to ANT; the coupling is moderated by a diffusional leak of the intermediates. The functional coupling between MtCK and ANT was modeled by using the phenomenological constants for the coupled MtCK reaction (Vendelin et al., 2000; Saks et al., 2003). The use of these constants instead of increased local ATP concentrations was important to calculate the supply of ADP by MtCK directly to ANT, not accounted before (Aliev and Saks, 1997). The metabolites described by the model in the matrix compartment and in the inner membrane are NADH, coenzyme Q, cytochrome C, protons, ATP, ADP, and P_i . Three coupled reactions representing the production of protonmotive force by complexes I, III, and IV are included in the model, as originally described by Korzeniewski (1998). Protonmotive force is consumed by ATP synthase and membrane leak. The ANT rate is considered to be dependent on membrane potential. P_i is transported by a phosphate carrier.

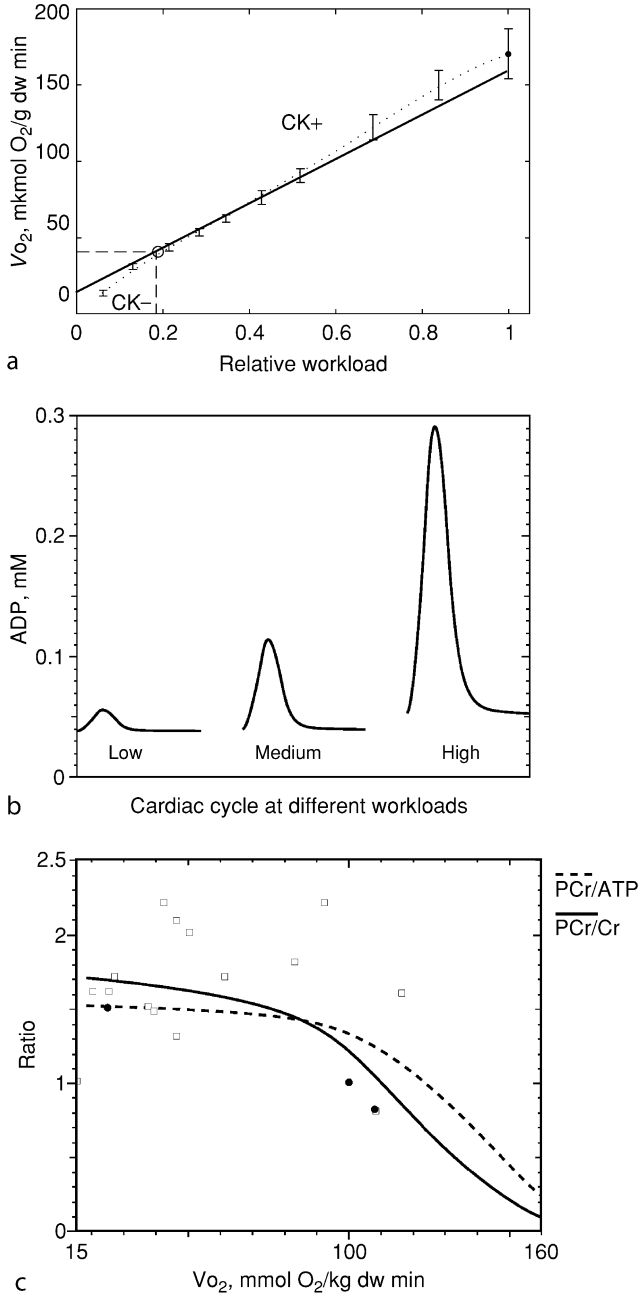
This model is available at the address: http://cens.ioc.ee/~markov/etransfer/current_model.pdf

According to simulations, the model reproduces the linear relationship between workload and oxygen consumption (● *Figure 8.1-14a*). ● *Figure 8.1-14a* shows that the feedback regulation incorporated into the model was sufficient to reproduce the experimental data in the whole physiological range of the rates of oxygen consumption, from 8–10 $\mu\text{mol min}^{-1} \text{g}^{-1}$ dry weight in resting (KCl-arrested) aerobic hearts to at least 170 $\mu\text{mol min}^{-1} \text{g}^{-1}$ dry weight in rat hearts (Williamson et al., 1976). The model describes satisfactorily the stable levels of PCr, ATP, and Cr at oxygen consumption rates up to 100 $\mu\text{mol min}^{-1} \text{g}^{-1}$ dry weight (● *Figure 8.1-14c*), in accordance with the experimental data (Williamson et al., 1976). At higher workloads the drop of PCr/Cr and PCr/ATP ratios was caused by the limitation of maximal respiration rate of 160 $\mu\text{mol min}^{-1} \text{g}^{-1}$ dry weight incorporated into the model. This maximal rate of respiration was assumed to be constant in calculations; therefore no effects of calcium on respiration were accounted for. The analysis of the model showed that the metabolic stability was observed only under conditions of functional coupling between MtCK and ANT. Analysis of the model showed that for the same total activity of the CK in the cell and for the same maximal rates of mitochondrial respiration the metabolic stability was lost when MtCK was detached from the inner-mitochondrial membrane and the functional coupling with ANT was lost (Saks et al., 2004a).

■ Figure 8.1-14

Mathematical modeling of the regulation of mitochondrial respiration in cardiac cells in vivo under physiological conditions controlled by the Frank–Starling mechanism. (a) Computed (solid line) and experimental (points with standard deviations) oxygen consumption rates. CK⁺ shows the calculations for active creatine kinase system, CK[−] shows the calculations for the cells with inactivated creatine kinases. (b) ADP profiles over cardiac cycle at different workloads. Reproduced from Vendelin et al. (2000) with permission. (c) Average phosphocreatine to ATP and phosphocreatine to creatine rates over cardiac cycles as functions of the oxygen consumption rate.

Figure 8.1-14 (continued)



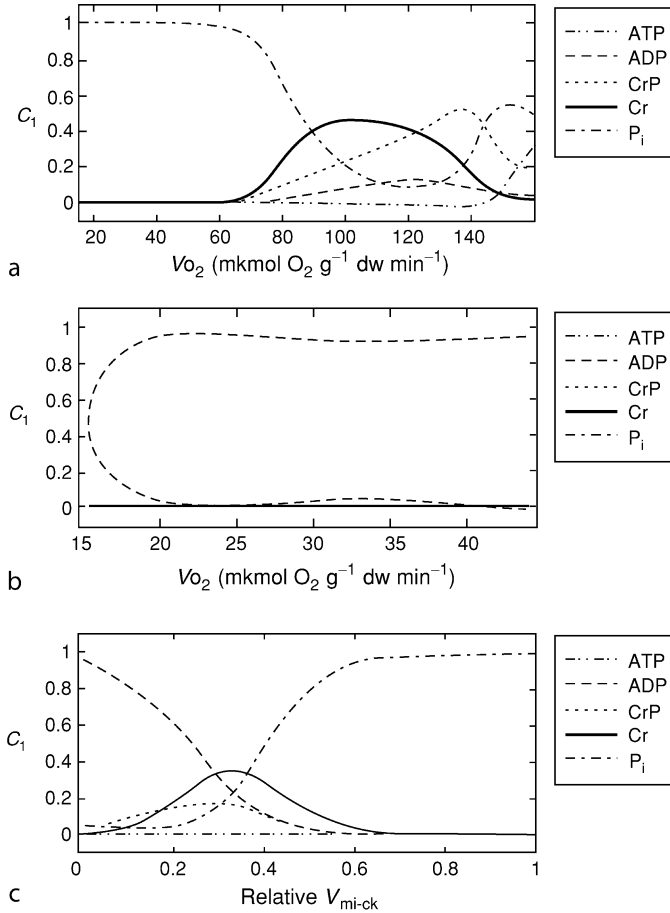
The extended model of compartmentalized energy transfer confirmed the cyclic changes in myoplasmic ADP concentrations already described above (🔗 [Figure 8.1-14b](#)). Rapid rephosphorylation of ADP released from crossbridges by myofibrillar CK produces small but opposite changes in Cr and PCr concentrations resulting in relatively significant cyclic changes in concentration of ADP in the space between MgATPases and mitochondria due to nonequilibrium steady state of the CK reaction in this space (Vendelin et al., 2000). If myoplasmic CK is structurally organized and bound to cytoskeleton, these cyclic ADP changes may move by a mechanism of vectorial conduction (Saks et al., 1994; Dzeja and Terzic, this volume). Their stimulatory effect on mitochondrial respiration is amplified by functional coupling between MtCK and ANT (Saks et al., 2004a). Accompanying changes in Cr, PCr, and ATP are within the experimental errors of their detection, thus leaving us the impression of metabolic stability (Vendelin et al., 2000). The amplitude of the ADP changes (or displacement from equilibrium in the case of vectorial ligand conduction) are remarkably altered by elevation of the workload (🔗 [Figure 8.1-14b](#)), confirming their important role in feedback metabolic regulation of respiration. The value of the model is that it allows us to use the principles of metabolic control analysis to find which of the metabolites carries the signal between ATPases and mitochondria and quantitatively evaluate its contribution into signaling (🔗 [Figure 8.1-15](#)). First, we computed the changes in metabolite concentrations induced by increase of ATPase activity. Second, we found the contribution of each of the changes of cytoplasmic metabolite concentrations to the increase of oxygen consumption. The result of the analysis is presented in the form of response coefficients indicating the relative changes in respiration rate induced by each of the metabolites (Saks et al., 2000). At low and moderate workloads, in addition to cyclic changes in ADP, OP may be regulated also by cytoplasmic P_i , providing the required feedback signal and a possibility for constant PCr/ATP ratio (Saks et al., 2000). In the coupled CK–actomyosin reactions in myofibrils, the metabolic end-products are free creatine and P_i and the feedback signal for mitochondria is represented both by parallel P_i and Cr (and by oscillating cytoplasmic ADP) fluxes (parallel regulation mechanism). Due to much lower initial concentrations of P_i , its regulatory effect on mitochondrial respiration will be stronger. After entry into mitochondria by a phosphate carrier, P_i increases the rate of ATP production coupled to oxidation on the one hand, and on the other hand increases PCr production due to functional coupling between ANT and MtCK. The final result is increased respiration and constant level of PCr—metabolic stability. This prediction of the regulatory role of P_i is in concord with the recent experimental works of Bose et al. (2003). Our simulations predict that at higher workloads the regulation is shared among the participating metabolites. If CK is inhibited or absent, OP is mainly regulated by cytoplasmic ADP levels (Saks et al., 2000). However, in this case the high workloads cannot be achieved because of product inhibition of MgATPases by high levels of cytoplasmic MgADP. This result of modeling is in good concord with many experimental data (Kapelko et al., 1988; Zweier et al., 1991; Kindig et al., 2005). In accordance with this conclusion, it was shown very recently that in CK-knockout mice the muscular work performance is decreased by factor of 10 (Monkin et al., 2005). In normal muscle cells, it is the feedback signaling of by parallel metabolic fluxes that precisely matches the energy requirements of the cell to the ATP production coupled to the mitochondrial respiration.

Thus, the regulation of cardiac cell energetics under the Frank–Starling law is quantitatively explained by metabolic feedback signaling via energy and signal transfer networks within structurally organized intracellular systems (Saks et al., 2004a; Saks et al., 2006a,b). This type of regulation results in metabolic stability (homeostasis). Revealing these important regulatory mechanisms, which are of central importance for the viability of a cardiac cell, illustrates the power of the mathematical modeling when correctly used in combination with experimental research.

Final conclusions on modeling. In modeling, it is important to determine which level is studied in the hierarchy of the cell physiology when the model is composed. As soon as this selection has been made, the models can be constructed for any of the hierarchical level. As a good starting point, several important models in energetics have been reviewed by Jafari et al. (2001). Large amount of models is collected through the Physiome project (Hunter, 2004). This and other new approaches to the modeling and analysis of biochemical reactions, pathways, and networks (Beard et al., 2004) have been recently described in *Progress of Biophysics and Molecular Biology*, (85) issues 2, 3 (2004). The number of publications in this area increases very rapidly.

■ Figure 8.1-15

Metabolic control analysis of the mathematical model of compartmentalized energy transfer. (a, b) Coefficients of responses of respiration to changes in metabolite concentrations in the cytoplasmic space as functions of the rate of oxygen consumption (workload) with (a) the active creatine kinase and (b) without it or as functions of relative MtCK activity at respiration rate equal to $41 \mu\text{mol min}^{-1} \text{g}^{-1}$ dry weight (c). Reproduced from Saks et al. (2000) with permission



9 CK and Brain Energy Metabolism

Similarities and differences between muscle and central nervous system (CNS) energy metabolism have been reviewed by Ames (2000). Brain energy (ATP) metabolism, which largely depends on aerobic glycolysis, displays marked regional differences (Clark and Sokoloff, 1999). Rates of aerobic glycolysis in cerebral gray matter (GM) are high and fluctuate rapidly with neuronal activity. In contrast, ATP metabolic rates are lower and more stable in white matter (WM). Cellular metabolic heterogeneity and intracellular differences are also present in these regions. An assessment of diffusion within cytoplasm by diffusion-weighted 1H NMR spectroscopy has indicated that the diffusion coefficients of metabolites in brain cells may be an order of magnitude lower than in extracellular fluid (Pfeuffer et al., 2000). Therefore, in the CNS cells the compartmentalized energy transfer is equally necessary (Ames, 2000).

The brain, like other tissues with high and variable rates of ATP metabolism, has high activities of the cytosolic and mitochondrial CKs and high concentrations of the guanidino reactants, PCr and Cr. The heterogeneity of brain ATP metabolism is paralleled by differences in the CK systems. GM with its rapid and variable rates of ATP synthesis has approximately equal concentrations of PCr and Cr and of the mitochondrial (MtCK) and cytosolic CK (BB-CK) isoenzymes. WM with slower and more constant rate of ATP synthesis has little Cr or MtCK.

In vivo physiological studies of the CK-catalyzed reaction have demonstrated central roles of the CK system in regulating ATP synthesis and coupling it to energy demand under stressed conditions (Ames, 2000). The latter includes animal models deficient in metabolic substrates (e.g., hypoxia) and with increased energy demand (e.g., seizures) (Howse, 1974; Holtzman, 1993a; Tsuji, 1995; Holtzman, 1998a, b). This topic has gained importance with the recently described evidence for roles of the CK system in human disease, metabolic adaptations within the CNS, and in neuroprotection. Inborn errors of Cr synthesis and transport result in marked neurological abnormalities in children. In animal models of neurodegenerative diseases, including Huntington's and amyotrophic lateral sclerosis, Cr appears to prolong life, perhaps related to recent observations that Cr and the CK system may be important in the coupling of altered cellular energetics to programmed cell death or apoptosis.

9.1 The CK System and ATP Metabolism of Adult Brain

The CK system in the adult brain, including isoenzymes, Cr transporter, reactant synthetic pathways, and enzyme activity regulation, is similar to that of heart and muscle described above (Ames, 2000). However, compared to the muscle tissues, the CK system in brain has been studied relatively little. Brain contains both cytosolic and mitochondrial CK isoenzymes (BB-CK and MtCK, respectively). The BB-CK is unique to the brain while the uMtCK is very similar to the MtCK present in the heart and smooth muscle. In line with the regional differences in ATP metabolism, BB-CK and MtCK are present in about equal concentrations in GM while in WM the BB-CK concentration is much higher compared to MtCK. Similarly, the PCr and Cr concentrations are each 5–6 mM in GM while in WM PCr is ~ 11 mM and nonphosphorylated Cr is ~ 0.5 mM (Holtzman et al., 1993a; Whittingham, 1995). The recently described Cr transporter is widely distributed in brain as in many other tissues (Loike et al., 1986; Saltarelli et al., 1996). However, unlike other tissues with high CK activities, the brain has the capacity to synthesize Cr (Defalco and Davies, 1961; Braissant et al., 2001). In brain, like in muscle, the CK activity may be regulated by AMP-activated protein kinase (AMPK), an enzyme whose activity is dependent upon concentrations of Cr and PCr (Pontikos et al., 1998).

Under normal physiologic conditions, brain ATP synthesis is almost entirely coupled to aerobic glycolysis (Siesjo et al., 1978; Erecinska et al., 1989). The cellular ATP concentration is very stable indicating close regulation of relative rates of ATP synthesis and demand. Since there is little reserve of glucose or O₂ in the brain, ATP synthesis depends upon increases in blood flow for maintaining ATP concentrations under conditions in which ATP demand can increase 50% in fractions of a second (Howse et al., 1974). In general, variability in blood flow, which directly provides glucose and O₂, appears to be the primary response to changes in ATP demand. Under conditions of metabolic activation, including seizures, the increase in local or general cerebral blood flow allows tissue and venous O₂ and glucose concentrations to exceed baseline concentrations (Kreisman, 1981; Holtzman, 1983). In contrast, hypoxia and hypoglycemia produce slowing of the electroencephalogram, which may reflect a decrease in ATP turnover (Siesjo et al., 1978).

The CK system is important in metabolic adaptations to conditions of physiological activation and seizures. The seizure is an event of widespread cerebral electrical activity and markedly increased ATP metabolism. These responses of ATP metabolism are similar in seizures and in more physiological cerebral metabolic activation, although it is not clear to what extent the seizure can be a metabolic model for cerebral activation. In addition to increased cerebral blood flow and tissue O₂ concentration, in vivo ³¹P MRS studies have shown that PCr increases up to 50% in GM but not in WM during seizures

(Holtzman et al., 1998a). The CK catalyzed reaction rate also increases in the GM. The increase in PCr concentration and the CK flux depend upon the MtCK isoenzyme since they are not present in chimeric mice in which the gene for this isoenzyme has been deleted (Kekelidze et al., 2001).

In hypoxia, cerebral PCr begins to fall only when the parenchymal cytochrome aa_3 redox state becomes more reduced, as shown with near infrared spectroscopy (Tsuji et al., 1995). In the hypoxic rat, brain PCr is depleted 50% before both PCr and ATP are lost together. This pattern of CK substrate loss during hypoxia again suggests two compartments with different coupling of the metabolism of PCr and ATP. In the posthypoxic brain, there is a change in the CK catalyzed reaction that depends upon the degree of hypoxia (Holtzman et al., 1993a; Tsuji et al., 1995). In addition, MtCK appears to regulate ATP resynthesis in the posthypoxic period (Kekelidze et al., 2001). The metabolic responses to altered ATP turnover rates mediated by the CK system are shown to be region specific in the mammalian brain (Holtzman et al., 1998). Additionally, the differential maturational changes of CK isoenzymes and CK catalyzed reaction rates in vivo were reported in WM and GM (Holtzman, 1993b; Kekelidze et al., 1999).

9.2 The CK System and ATP Metabolism in the Developing Brain

The physiology of the CK system in the developing brain is different from that of the mature brain. Studies, to date, have concentrated on effects of changes in the CK system on ATP synthesis correlated with age and with increases in brain PCr produced by systemic Cr injections. There are two developmental time courses for the CK system in the rat and mouse brain. The PCr/nucleoside triphosphate (NTP) concentration ratio increases twofold in the developmental period from days 5 to 25 or coincident with the increase in the rate of glucose and O_2 consumptions and most glycolytic and TCA cycle enzyme activities (Leong et al., 1984; Holtzman et al., 1991; Holtzman et al., 1993b). This maturational increase occurs between days 7 to 30 in the rabbit (Himwich et al., 1970; Kekelidze et al., 1999). The second developmental time course in brain ATP metabolism is that of the CK catalyzed reaction rate, which increases between days 12 to 15 in the rat and the mouse as seen in [Figure 8.1-16](#) (Holtzman et al., 1993b). This increase is coincident with the increase in glycolytic regulatory enzymes and the appearance of close coupling of ATP synthesis and demand in brain slices (Greegard et al., 1955; Holtzman et al., 1982; Leong et al., 1984). This maturational increase in CK reaction rate occurs shortly after the increase of the CK cytosolic and mitochondrial isoenzymes in the rat brain (Holtzman et al., 1993b).

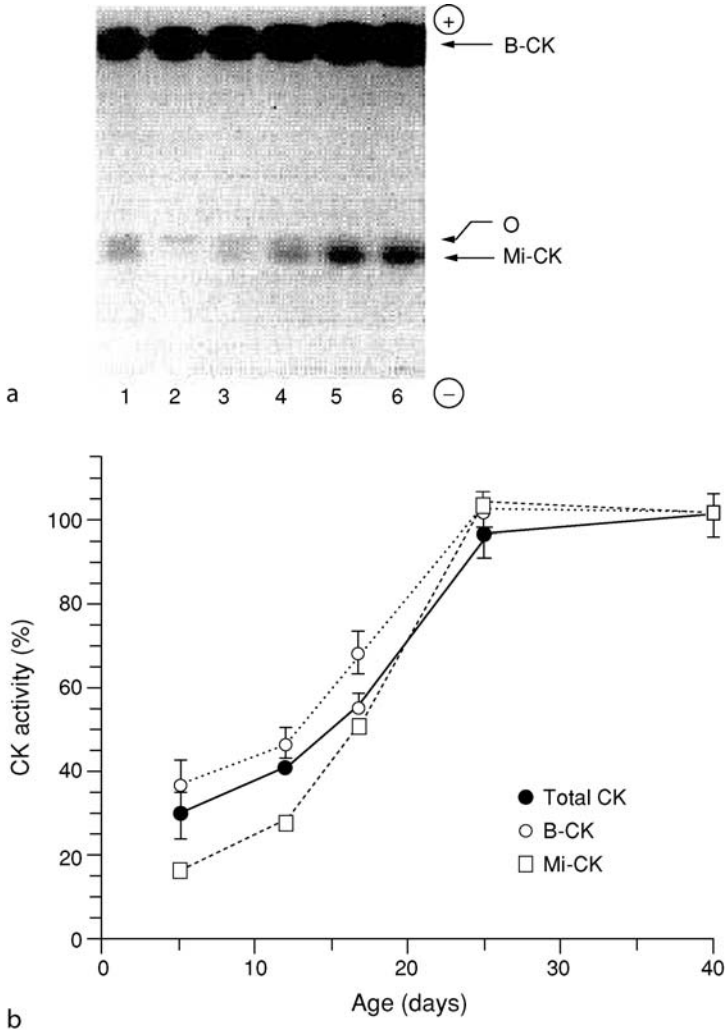
Assuming ATP levels does not change in the rabbit WM, the PCr concentration increases to the adult concentration within 3 days of starting supplemental Cr injections in 5-, 10-, 15-, 20-, and 30-day-old pups (Holtzman et al., 1998b). In GM, the PCr/NTP ratio in rabbit pups receiving supplemental Cr is 20% above controls. At each age between 5 and 30 days, the PCr level reached is the same. Thus, the ease of getting supplemental Cr into the brain decreases with maturation, which is consistent with the maturational decrease in the Cr transporter in the brain (Kekelidze et al., 2000). These observations support the proposal that Cr is predominantly synthesized in the mature brain but is transported into the immature brain.

The coupling of brain ATP and PCr losses during hypoxia changes during this developmental period (Tsuji et al., 1995b). At day 10, brain PCr is lost completely before ATP begins to decrease, while at day 20 the PCr decreases 50% before PCr and ATP decrease together. Approximately midway in the developmental period of increasing brain PCr in both rodents and rabbits, there is a period of cerebral hyperexcitability or low seizure thresholds (Schwartzkroin et al., 1984). At these ages hypoxia produces seizures in up to 80% of rat and rabbit pups (Holtzman et al., 1998b; Holtzman et al., 1999). The supplemental Cr completely blocks hypoxia-induced seizures in both the rat and the rabbit (Holtzman et al., 1998b; Holtzman et al., 1999). The mortality of the hypoxic exposures in these Cr-supplemented pups also is much less than in controls. The decreased death rates may be due to the more effective resynthesis of brain PCr and ATP after hypoxia in the Cr-supplemented rats.

At present there is no quantitative model of compartmentalized energy transfer in brain cells. The achievements in mathematical modeling of cardiac energy metabolism may give us a good example on how to approach the exciting but difficult task of quantitative description of energy metabolism in the very heterogeneous nervous system.

■ Figure 8.1-16

Zymograms (a) of the expression of the CK isoenzyme activities and (b) during postnatal rat brain development. Separation of CK isoenzymes of total brain extracts after electrophoretic separation on cellulose polyacetate strips and subsequent staining for CK activity. Lanes 2, 3, 4, 5, and 6 correspond to postnatal days 5, 12, 17, 25, and 40, respectively; lane 1 is an enriched mitochondrial fraction used as standard (adapted from Holtzman et al. (1993b))



10 Appendix: Probability Approach in Description of Enzymes and Transporters

10.1 Mathematical Model of Free Activation of CK by Metabolites from the Medium

● Figure 8.1-A1a shows the kinetic scheme of the CK reaction mechanism, which is of rapid-equilibrium random binding Bi-Bi type according to Cleland's classification (Cleland, 1967; Kenyon and Reed, 1983).

$$P(\text{E.PCr}) = [\text{E.PCr}]/[E_{\text{tot}}] = [\text{PCr}]/(K_{\text{icp}}\text{Den}) \quad (5)$$

$$P(\text{E.A.Cr}) = [\text{E.A.Cr}]/[E_{\text{tot}}] = [\text{A}][\text{Cr}]/(K_{\text{ia}}K_{\text{cr}}\text{Den}) \quad (6)$$

$$P(\text{E.PCr.A}) = [\text{E.PCr.A}]/[E_{\text{tot}}] = [\text{PCr}][\text{A}]/(K_{\text{icp}}K_{\text{ia}}\text{Den}) \quad (7)$$

$$P(\text{E.PCr.D}) = [\text{E.PCr.D}]/[E_{\text{tot}}] = [\text{PCr}][\text{D}]/(K_{\text{cp}}K_{\text{id}}\text{Den}) \quad (8)$$

$$P(\text{E.D.Cr}) = [\text{E.D.Cr}]/[E_{\text{tot}}] = [\text{D}][\text{Cr}]/(K_{\text{id}}K_{\text{icr}}\text{Den}) \quad (9)$$

In these equations the dissociation constants, K , of considered complexes are given for primary complexes with an index “i” (initial) and for ternary complexes only with the symbol for the substrate: “a” (A) for ATP, “d” (D) for ADP, “cr” (Cr) for creatine, and “cp” (PCr) for phosphocreatine. Dissociation constant of substrates from catalytically ineffective E.D.Cr and E.A.PCr dead-end complexes are given the symbol “I” (their formation is Inhibitory for the reaction); Den is an abbreviation for denominator.

With the calculated probabilities, the rates of CK reaction in the forward ($V_{\text{fw}}^{\text{CK}}$, rate constant kk_1) and reverse (V_{r}^{CK} , rate constant kk_{-1}) directions are [Figure 8.1-10a](#):

$$V_{\text{fw}}^{\text{CK}} = E_{\text{tot}}P(\text{E.A.Cr})kk_1 \quad (10)$$

$$V_{\text{r}}^{\text{CK}} = E_{\text{tot}}P(\text{E.D.PCr})kk_{-1} \quad (11)$$

The net rate ($V_{\text{net}}^{\text{CK}}$) of ADP and PCr production by CK is

$$V_{\text{net}}^{\text{CK}} = V_{\text{fw}}^{\text{CK}} - V_{\text{r}}^{\text{CK}} \quad (12)$$

At equilibrium, when $V_{\text{fw}}^{\text{CK}} = V_{\text{r}}^{\text{CK}}$, apparent equilibrium constant of CK ($K_{\text{eq}}^{\text{CK}}$) is

$$K_{\text{eq}}^{\text{CK}} = ([\text{MgADP}][\text{PCr}])/([\text{MgATP}][\text{Cr}]) \quad (13)$$

10.2 Mathematical Model of Free Activation of ANT by Metabolites from the Medium

We have used in a probability coupling model the simplest reduced version of consecutive binding scheme ([Figure 8.1-A1b](#)) with assumed fixed probabilities of $P(\text{C.T}_i) = 0.9$ and $P(\text{C.D}_i) = 0.1$ taken from experimental data (Aliev and Saks, 1993, 1994; for review see Aliev and Saks, 2003). Within the frameworks of this scheme, the carrier (C) executes the rate-limiting translocation steps only when having bound ADP (D) or ATP (T) on both its binding sites, with outer site (subscript “o”) directed to mitochondrial IM space, and inner site (subscript “i”) directed to the matrix space of mitochondria. Dissociation constants (K) for the medium with Mg^{2+} ions were taken as $K_{\text{do}} = 0.02$ mM for ADP and $K_{\text{to}} = 20$ mM for ATP (Aliev and Saks, 1993, 1994). In this reduced version, the probabilities of binding of ADP and ATP to outer site of ANT are:

$$P(\text{C.D}_o) = (D_o/K_{\text{do}})/(1 + (D_o/K_{\text{do}}) + (T_o/K_{\text{to}})) \quad (14)$$

$$P(\text{C.T}_o) = (T_o/K_{\text{to}})/(1 + (D_o/K_{\text{do}}) + (T_o/K_{\text{to}})) \quad (15)$$

By calculating the independent probabilities of adenine nucleotide binding on different surfaces of ANT, we can calculate the probability of the population of ANT complexes with simultaneous occupation of both its binding sites as the products of two independent probabilities, probabilities of adenine nucleotide binding to outer ($P(\text{C.D}_o)$, $P(\text{C.T}_o)$) and inner ($P(\text{C.D}_i)$, $P(\text{C.T}_i)$) sites of ANT. For example, $P(\text{C.D}_o, \text{T}_i) = P(\text{C.D}_o) P(\text{C.T}_i)$. With these probabilities, the ANT reaction rates in the forward ($V_{\text{D}_o\text{T}_i}$) and reverse ($V_{\text{T}_o\text{D}_i}$) directions were calculated as:

$$V_{DoTi}^C = C_{tot} P(C.D_o.T_i) k_1 \quad (16)$$

$$V_{ToDi}^C = C_{tot} P(C.T_o.D_i) k_2 \quad (17)$$

In these rate equations, subscripts indicate the kind of vectorial transport. For example, V_{DoTi} indicates 1:1 exchange of ADP in outer space (D_o) for ATP in matrix one (T_i); this exchange represents the main kind of transport in the working cell. C_{tot} designates the total amount of ANT, k_1 and k_2 are rate constants of D_oT_i and T_oD_i exchanges, respectively.

The net rate (V_{net}^C) of ATP export by ANT is:

$$V_{net}^C = V_{DoTi}^C - V_{ToDi}^C \quad (18)$$

At equilibrium, when $V_{DoTi}^C = V_{ToDi}^C$, apparent equilibrium constant of ANT (K_{eq}^C) is:

$$K_{eq}^C = ([ATP]_i[ADP]_o)/([ATP]_o[ADP]_i) \quad (19)$$

Acknowledgment

This work was supported by INSERM, France, by grants (N 5515 and 6142) from the Estonian Science Foundation, by the Marie Curie Fellowship of the European Community program "Improving Human Research Potential and the SocioEconomic Base" (M.V., contract No HPMF-CT-2002-01914), and by a grant (03-04-48891) from the Russian Foundation for Basic Researches (MKA).

References

- Abraham MR, Selivanov V, Hodgson DM, Pucar D, Zingman LV, et al. 2002. Coupling of cell energetics with membrane metabolic sensing. Integrative signaling through creatine kinase phosphotransfer disrupted by M-CK gene knockout. *J Biol Chem* 277: 24427-24427.
- Agius L, Sherratt HSA. (editors) 1997. Channelling in intermediary metabolism. London and Miami: Portland Press; pp. 1-342.
- Aliev MK, Saks VA. 1993. Quantitative analysis of the "phosphocreatine shuttle". I. A probability approach to the description of phosphocreatine production in the coupled creatine kinase-ATP/ADP-translocase-oxidative phosphorylation reaction in heart mitochondria. *Biochim Biophys Acta* 1143: 291-300.
- Aliev MK, Saks VA. 1994. Mathematical modeling of intracellular transport processes and the creatine kinase systems: A probability approach. *Mol Cell Biochem* 133/134: 333-346.
- Aliev MK, Saks VA. 1997. Compartmentalized energy transfer in cardiomyocytes: Use of mathematical modeling for analysis of in vivo regulation of respiration. *Biophys J* 73: 428-445.
- Aliev MK, Dos Santos P, Hoerter JA, Soboll S, Tikhonov AN, et al. 2002. The water content and its intracellular distribution in intact and saline perfused rat hearts revisited. *Cardiovasc Res* 53: 48-58.
- Aliev MK, Dos Santos P, Saks VA. 2003. Mathematical modeling of regulation of oxidative phosphorylation in cardiomyocytes. Creatine kinase and brain energy metabolism. Function and disease. NATO science series: Life and behavioral sciences. Vol. 342. Kekelidze T, Holtzman D, editors. Amsterdam: IOS Press; pp. 59-79.
- Aliev MK, Saks VA. 2003. Analysis of the mechanism of functioning of mitochondrial adenine nucleotide translocase using mathematical models. *Biophysics (Moscow)* 48: 1075-1085.
- Allen DG, Kentish JC. 1985. The cellular basis of the length-tension relation in cardiac muscle. *J Mol Cell Cardiol* 17: 821-840.
- Ames A. 2000. CNS energy metabolism as related to function. *Brain Res Rev* 34: 42-68.
- Aon M, Cortassa S, O'Rourke B. 2004. Percolation and criticality in a mitochondrial network. *Proc Natl Acad Sci USA* 101: 4447-4452.
- Appaix F, Kuznetsov A, Usson Y, Kay L, Andrienko T, et al. 2003. Possible role of cytoskeleton in intracellular arrangement and regulation of mitochondria. *Exp Physiol* 88: 175-190.
- Balaban RS, Kantor HL, Katz LA, Briggs RW. 1986. Relation between work and phosphate metabolite in the in vivo paced mammalian heart. *Science* 232: 1121-1123.

- Balaban RS. 2002. Cardiac energy metabolism homeostasis: Role of cytosolic calcium. *J Mol Cell Cardiol* 34: 1259-1271.
- Barbour RL, Ribauda J, Chan SH. 1984. Effect of creatine kinase activity on mitochondrial ADP/ATP transport. Evidence for a functional interaction. *J Biol Chem* 259: 8246-8251.
- Beard DA, Babson E, Curtis E, Qian H. 2004. Thermodynamic constraints for biochemical networks. *J Theor Biol* 228: 327-333.
- Bereiter-Hahn J, Voth M. 1994. Dynamics of mitochondria in living cells: Shape changes, dislocations, fusion, and fission of mitochondria. *Microsc Res Tech* 27: 198-219.
- Berridge MJ, Bootman MD, Roderick HL. 2003. Calcium signaling: Dynamics, homeostasis, and remodeling. *Nat Rev Mol Cell Biol* 4: 517-529.
- Bers D. 2001. Excitation-contraction coupling and cardiac contraction. Dordrecht: Kluwer Academic Publishers.
- Bessman SP, Geiger PJ. 1981. Transport of energy in muscle: The phosphorylcreatine shuttle. *Science* 211: 448-452.
- Beyer K, Klingenberg M. 1985. ADP/ATP carrier protein from beef heart mitochondria has high amounts of tightly bound cardiolipin, as revealed by ^{31}P nuclear magnetic resonance. *Biochemistry* 24: 3821-3826.
- Beard DA, Liang SD, Qian H. 2002. Energy balance for analysis of complex metabolic networks. *Biophys J* 83: 79-86.
- Bianchi K, Rimessi A, Prandini A, Szabadkai G, Rizzuto R. 2004. Calcium and mitochondria: Mechanisms and functions of a troubled relationship. *Biochim Biophys Acta* 1742: 119-131.
- Bose S, French S, Evans FJ, Joubert F, Balaban RS. 2003. Metabolic network control of oxidative phosphorylation: Multiple roles of inorganic phosphate. *J Biol Chem* 278: 39155-39165.
- Brady NR, Elmore SP, Van Beek J, Krab K, Courtoy PJ, et al. 2004. Coordinated behavior of mitochondria in both space and time: A reactive oxygen-species-activated wave of mitochondrial depolarization. *Biophys J* 87: 2022-2034.
- Braissant O, Henry H, Loup M, Eilers B, Bachmann C. 2001. Endogenous synthesis and transport of creatine in the rat brain: An in situ hybridization study. *Brain Res Mol Brain Res* 86: 193-201.
- Brown GC, Lakin-Thomas PL, Brand M. 1990. Control of respiration and oxidative phosphorylation in isolated rat liver cells. *Eur J Biochem* 192: 355-362.
- Capetanaki Y. 2002. Desmin cytoskeleton: A potential regulator of muscle mitochondrial behavior and function. *Trends Cardiovasc Med* 12: 339-348.
- Carafoli E. 2002. Calcium signaling: A tale for all seasons. *Proc Natl Acad Sci USA* 99: 1115-1122.
- Chance B, Williams GR. 1956. Regulatory chain and oxidative phosphorylation. *Adv Enzymol* 17: 65-134.
- Clark D, Sokoloff L. 2000. Circulation and energy metabolism. *Basic Neurochemistry*, 5th Edition. Siegal J, Agranoff B, Albers R, Fisher S, Uhler M, editors. Philadelphia: Lippincott-Raven; pp. 637-669.
- Cleland WW. 1967. Enzyme kinetics. *Annu Rev Biochem* 36: 77-112.
- Defalco A, Davies R. 1961. The synthesis of creatine by the brain of the intact rat. *J Neurochem* 7: 308-312.
- Carrasco AJ, Dzeja PP, Alekseev AE, Pucar D, Zingman LV, et al. 2001. Adenylate kinase phosphotransfer communicates cellular energetic signals to ATP-sensitive potassium channels. *Proc Natl Acad Sci USA* 98: 7623-7628.
- Clegg JS. 1984. Properties and metabolism of the aqueous cytoplasm and its boundaries. *Am J Physiol* 246: R133-R151.
- Collins TJ, Bootman MD. 2003. Mitochondria are morphologically heterogeneous within cells. *J Exp Biol* 206: 1993-2000.
- Colombini M. 2004. VDAC: The channel at the interface between mitochondria and the cytosol. *Mol Cell Biochem* 256: 107-115.
- Cook R, Pate E. 1985. The effects of ADP and phosphate on the contraction of muscle fibers. *Biophys J* 4: 789-798.
- Cooke R. 1997. Actomyosin interaction in striated muscle. *Physiol Rev* 77: 671-697.
- Cortassa S, Aon M, Marban E, Winslow RL, O'Rourke B. 2003. An integrated model of cardiac mitochondrial energy metabolism and calcium dynamics. *Biophys J* 84: 2734-2755.
- Crawford RM, Ranki HJ, Botting CH, Budas GR, Jovanovic A. 2002. Creatine kinase is physically associated with cardiac ATP-sensitive K^+ channel in vivo. *FASEB J* 16: 102-104.
- DeFuria RA, Ingwall JS, Fossel ET, Dygert MK. 1980. Microcompartmentation of the mitochondrial creatine kinase reaction. *Heart Creatine Kinase. The Integration of Enzymes for Energy Distribution*. Jacobus WE, Ingwall JS, editors. Baltimore: Williams & Wilkins; pp. 135-141.
- De Graaf RA, Van Kranenburg A, Nicolay K. 2000. In vivo ^{31}P NMR spectroscopy of ATP and phosphocreatine in rat skeletal muscle. *Biophys J* 78: 1657-1664.
- de Groof AJ, Smeets B, Groot Koerkamp MJ, Mul AN, Janssen EE, et al. 2001. Changes in mRNA expression profile underlie phenotypic adaptations in creatine kinase-deficient muscles. *FEBS Letters* 506: 73-78.
- Denton RM, Randle PJ, Martin BR. 1972. Stimulation by calcium ions of pyruvate dehydrogenase phosphate phosphatase. *Biochem J* 128: 161-163.
- Denton RM, Richards DA, Chin JG. 1978. Calcium ions and the regulation of NAD^+ -linked isocitrate dehydrogenase from the mitochondria of rat heart and other tissues. *Biochem J* 176: 899-906.

- Dolder M, Walzel B, Speer O, Schlattner U, Wallimann T. 2003. Inhibition of the mitochondrial permeability transition by creatine kinase substrates. Requirement for microcompartmentation. *J Biol Chem* 278: 17760-17766.
- Dos Santos P, Aliev MK, Diolez P, Duclos F, Bonoron-Adele S, et al. 2000. Metabolic control of contractile performance in isolated perfused rat heart. Analysis of experimental data by reaction: Diffusion mathematical model. *J Mol Cell Cardiol* 32: 1703-1734.
- Duyckaerts C, Sluse-Coffart CM, Fux JP, Sluse FE, Liebecq C. 1980. Kinetic mechanism of the exchanges catalysed by the adenine nucleotide carrier. *Eur J Biochem* 106: 1-6.
- Dzeja PP, Zeleznikar RJ, Goldberg ND. 1998. Adenylate kinase: Kinetic behaviour in intact cells indicates it is integral to multiple cellular processes. *Mol Cell Biochem* 184: 169-182.
- Dzeja P, Terzic A. 2003. Phosphotransfer networks and cellular energetics. *J Exp Biol* 206: 2039-2047.
- Engelbrecht J, Vendelin M, Maugin GA. 2000. Hierarchical internal variables reflecting microstructural properties: Application to cardiac muscle contraction. *J Non-Equilib Thermodyn* 25: 119-130.
- Erecincka M, Silver I. 1989. ATP and brain function. *J Cereb Blood Flow Metab* 9: 2-19.
- Fawcett DW, McNutt NS. 1969. The ultrastructure of the cat myocardium. I Ventricular papillary muscle. *J Cell Biol* 42: 1-45.
- Fioret C, Trezequet V, Le Saux A, Roux P, Schwimmer C, et al. 1998. The mitochondrial ADP/ATP carrier: Structural, physiological, and pathological aspects. *Biochimie* 80: 137-150.
- Friedrich P. 1985. Dynamic compartmentation in soluble multienzyme system. Organized multienzyme systems. Catalytic properties. Welch GR, editor. New York-London: Academic Press; pp. 141-176.
- Fritz-FolFK, Schnyder T, Wallimann T, Kabsch W. 1996. Structure of mitochondrial creatine kinase. *Nature* 381: 341-345.
- Fukuda N, Kajiwarra H, Ishiwata S, Kurihara S. 2000. Effects of MgATP on length dependence of tension generation in skinned rat cardiac muscle. *Circ Res* 86: e1-e6.
- Fulton AB. 1982. How crowded is the cytoplasm? *Cell* 30: 345-347.
- Gard JK, George MK, Ackerman JHJ, Eisenberg JD, Billadello JJ, et al. 1985. Quantitative ³¹P nuclear magnetic resonance analysis of metabolite concentrations in Langendorff-perfused rabbit hearts. *Biophys J* 48: 803-813.
- Geisbuhler T, Altschuld RA, Ronald W, Trewyn A, Lamka K, et al. 1984. Adenine nucleotide metabolism and compartmentation in isolated adult rat heart cells. *Circ Res* 54: 536-546.
- Gellerich F, Saks VA. 1982. Control of heart mitochondrial oxygen consumption by creatine kinase: The importance of enzyme localization. *Biochem Biophys Res Commun* 105: 1473-1481.
- Gellerich FN, Schlame M, Bohnensack R, Kunz W. 1987. Dynamic compartmentation of adenine nucleotides in the mitochondrial intermembrane space of rat heart mitochondria. *Biochim Biophys Acta* 890: 117-126.
- Gellerich FN, Kapischke M, Kunz W, Neumann W, Kuznetsov A, et al. 1994. The influence of the cytosolic oncotic pressure on the permeability of the mitochondrial outer membrane for ADP: Implications for the kinetic properties of mitochondrial creatine kinase and for ADP channeling into the intermembrane space. *Mol Cell Biochem* 133-134: 85-104.
- Goldman Y. 1987. Kinetics of the actomyosin ATPase in muscle fibers. *Annu Rev Physiol* 49: 637-654.
- Goldman Y. 1998. Wag the tail: Structural dynamics of actomyosin. *Cell* 93: 1-4.
- Gordon AM, Homsher E, Regnier M. 2000. Regulation of contraction in striated muscle. *Physiol Rev* 80: 853-924.
- Gropp T, Brustovetsky N, Klingenberg M, Müller V, Fendler K, et al. 1999. Kinetics of electrogenic transport by the ADP/ATP Carrier. *Biophys J* 77: 714-726.
- Hall D, Minton AP. 2003. Macromolecular crowding: Qualitative and semiquantitative successes, quantitative challenges. *Biochim Biophys Acta* 1649: 127-139.
- Hansford RG. 1985. Relation between mitochondrial calcium transport and control of energy metabolism. *Rev Physiol Biochem Pharmacol* 102: 1-72.
- Himwich H. 1970. Historical review. Developmental neurobiology. Himwich W, editor. Springfield: Thomas; pp. 22-44.
- Himwich H. 1951. Metabolism and cerebral disorders. Williams and Wilkins; Baltimore: p. 451.
- Hoerter JA, Lauer C, Vassort G, Gueron M. 1988. Sustained function of normoxic hearts depleted in ATP and phosphocreatine: A ³¹P NMR study. *Am J Physiol* 255: C192-C201.
- Holtzman D, Olson J, Zamvil S, Nguyen H. 1982. Maturation of potassium-stimulated respiration in rat cerebral cortical slices. *J Neurochem* 39: 274-296.
- Holtzman D, Olson J. 1983. Developmental changes in brain cellular energy metabolism in relation to seizures and their sequelae. Basic mechanisms of neuronal hyperexcitability. Jaspers H, Van Gelder N, editors. New York: Liss, Inc.; pp. 423-429.
- Holtzman D, McFarland E, Jacobs D, Offutt M, Neuringer KL. 1991. Maturation increase in mouse brain creatine kinase reaction rates shown by phosphorous magnetic resonance. *Dev Brain Res* 58: 181-188.
- Holtzman D, Tsuji M, Neuringer L, Jacobs D. 1993a. Creatine kinase reaction rates in the cyanide-poisoned mouse brain. *J Cereb Blood Flow Metab* 13: 153-161.

- Holtzman D, Tsuji M, Wallimann T, Hemmer W. 1993b. Functional maturation of creatine kinase in rat brain. *Dev Neurosci* 15: 261-270.
- Holtzman D, Mulkern RM, Cook C, Allred E, Khait I, et al. 1998. In vivo phosphocreatine and ATP in piglet cerebral gray and white matter during seizures. *Brain Res* 783: 19-27.
- Holtzman D, Togliatti A, Khait I, Jensen F. 1998b. Creatine increases survival and suppresses seizures in the hypoxic immature rat. *Pediatr Res* 44: 410-414.
- Holtzman D, Khait I, Mulkern R, Allred E, Rand R, et al. 1999. In vivo developmental changes in brain phosphocreatine and creatine kinase in normal and creatine treated rabbits. *J Neurochem* 73: 2477-2484.
- Hornemann T, Kempa S, Himmel M, Hayess K, Furst DO, et al. 2003. Muscle-type creatine kinase interacts with central domains of the M-band proteins myomesin and M-protein. *J Mol Biol* 332: 877-87.
- Howse D, Caronna D, Duffy T, Plum F. 1974. Cerebral energy metabolism, pH, and blood flow during seizures in the cat. *Am J Physiol* 227: 1444-1451.
- Huang X, Holden HM, Raushel FM. 2001a. Channeling of substrates and intermediates in enzyme-catalyzed reactions. *Annu Rev Biochem* 70: 149-180.
- Huang S-G, Oday S, Klingenberg M. 2001b. Chimers of two fused ADP/ATP carrier monomers indicate a single channel for ADP/ATP transport. *Arch Biochem Biophys* 394: 67-75.
- Huber T, Klingenberg M, Beyer K. 1999. Binding of nucleotides by mitochondrial ADP/ATP carrier as studied by ^1H Nuclear Magnetic Resonance Spectroscopy. *Biochemistry* 38: 762-769.
- Humphrey JD. 2000. Continuum biomechanics of soft biological tissues. *Proc R Soc Lond A* 459: 3-46.
- Hunter PJ. 2004. The IUPS Physiome project: A framework for computational physiology. *Prog Biophys Mol Biol* 85: 551-569.
- Ingwall JS. 2002. ATP and the heart. Dordrecht-Boston-London: Kluwer Academic Publishers; pp. 1-244.
- Jacobs H, Heldt HW, Klingenberg M. 1964. High activity of creatine kinase in mitochondria from muscle and brain and evidence for a separate mitochondrial isoenzyme of creatine kinase. *Biochem Biophys Res Commun* 16: 516-521.
- Jacobson J, Duchon MR. 2004. Interplay between mitochondria and cellular calcium signaling. *Mol Cell Biochem* 256: 209-218.
- Jacobus WE, Lehninger AL. 1973. Creatine kinase of rat mitochondria. Coupling of creatine phosphorylation to electron transport. *J Biol Chem* 248: 4803-4810.
- Jacobus WE, Moreadith RW, Vandegaer KM. 1982a. Mitochondrial respiratory control. Evidence against the regulation of respiration by extramitochondrial phosphorylation potentials or by [ATP]/[ADP] ratios. *J Biol Chem* 257: 2397-2402.
- Jacobus WE, Saks VA. 1982b. Creatine kinase of heart mitochondria: Changes in its kinetic properties induced by coupling to oxidative phosphorylation. *Arch Biochem Biophys* 219: 167-178.
- Jafri MS, Duducha SJ, O'Rourke B. 2001. Cardiac energy metabolism: Models of cellular respiration. *Annu Rev Biomed Eng* 3: 57-81.
- Janssen E, Terzic A, Wieringa B, Dzeja P. 2003. Impaired intracellular energy communication in muscles from creatine kinase and adenylate kinase (M-CK/AK1) double knockout mice. *J Biol Chem* 278: 30441-30449.
- Joubert F, Mateo P, Gillet B, Beloeil J-C, Mazet J-L, et al. 2004. CK flux or direct ATP transfer: Versatility of energy transfer pathways evidenced by NMR in the perfused heart. *Mol Cell Biochem* 256/257: 43-58.
- Joubert F, Mazet JL, Mateo P, Hoerter JA. 2002. ^{31}P NMR detection of subcellular creatine kinase fluxes in the perfused rat heart: Contractility modifies energy transfer pathways. *J Biol Chem* 277: 18469-18476.
- Kaasik A, Veksler V, Boehm E, Novotova M, Minajeva A, et al. 2001. Energetic crosstalk between organelles. Architectural integration of energy production and utilization. *Circ Res* 89: 153-159.
- Kapelko VI, Kupriyanov VV, Novikova NA, Lakomkin VL, Steinschneider A, et al. 1988. The cardiac contractile failure induced by chronic creatine and phosphocreatine deficiency. *J Mol Cell Cardiol* 20: 465-479.
- Karatzafiri C, Myburgh KH, Chinn MK, Franks-Skiba K, Cook R. 2003. Effect of an ADP analog on isometric force and ATPase activity of active muscle fibers. *Am J Physiol* 284: C816-C825.
- Kay L, Li Z, Mericskay M, Olivares J, Tranqui L, et al. 1997. Study of regulation of mitochondrial respiration in vivo. An analysis of influence of ADP diffusion and possible role of cytoskeleton. *Biochim Biophys Acta* 1322: 41-59.
- Kekelidze T, Khait I, Togliatti A, Benzycry J, Mulkern R, et al. 1999. Maturation changes in rabbit brain phosphocreatine and creatine kinase. *Ann N Y Acad Sci* 893: 309-313.
- Kekelidze T, Khait I, Togliatti A, Holtzman D. 2000. Brain creatine kinase and creatine transporter proteins in normal and creatine treated rabbit pups. *Dev Neurosci* 22: 437-443.
- Kekelidze T, Khait I, Togliatti A, Benzycry J, Wieringa B, et al. 2001. Altered brain phosphocreatine and ATP regulation when mitochondrial creatine kinase is absent. *J Neurosci Res* 66: 866-72.
- Kennedy HJ, Pouli AE, Ainscow EK, Jouaville LS, Rizzuto R, et al. 1999. Glucose generates sub-plasma membrane ATP microdomains in single islet β -cells. Potential role for strategically located mitochondria. *J Biol Chem* 274: 13281-13291.
- Kenyon GL, Reed GH. 1983. Creatine kinase: Structure-activity relationships. *Adv Enzymol* 54: 367-426.

- Kentish JC, Wrzosek A. 1998. Changes in force and cytosolic Ca^{2+} concentration after length changes in isolated rat ventricular trabeculae. *J Physiol* 506: 431-444.
- Kindig CA, Howlett RA, Sary CM, Walsh B, Hogan MC. 2005. Effects of acute creatine kinase inhibition on metabolism and tension development in isolated single myocytes. *J Appl Physiol* 98: 541-549.
- Klingenberg M. 1985. The ADP/ATP carrier in mitochondrial membranes. *The enzymes of biological membranes*, Vol. 4. Martonosi AN, editor. New York and London: Plenum Press; pp. 511-553.
- Kohl P, Noble D, Winslow RL, Hunter PT. 2000. Computational modeling of biological systems: Tools and visions. *Philos Trans R Soc Lond A* 352: 578-610.
- Korge P, Byrd SK, Campbell KB. 1993. Functional coupling between sarcoplasmic-reticulum-bound creatine kinase and Ca^{2+} ATPase. *Eur J Biochem* 213: 973-980.
- Korge P, Campbell KB. 1994. Local ATP regeneration is important for sarcoplasmic reticulum Ca^{2+} pump function. *Am J Physiol* 267: C357-C366.
- Kobayashi T, Solaro JR. 2005. Calcium, thin filaments, and the integrative biology of cardiac contractility. *Annu Rev Physiol* 67: 02.1-02.29.
- Kolston PJ. 2000. Finite-element modeling: A new tool for the biologist. *Philos Trans R Soc London A* 358: 611-631.
- Korzeniewski B. 1998. Regulation of ATP supply during muscle contraction: Theoretical studies. *Biochem J* 330: 1189-1195.
- Korzeniewski B, Zolade JA. 2001. A model of oxidative phosphorylation in mammalian skeletal muscle. *Biophys Chem* 92: 17-34.
- Korzeniewski B. 2003. Regulation of oxidative phosphorylation in different muscles and various experimental conditions. *Biochem J* 375: 799-710.
- Kramer R, Palmieri F. 1992. Metabolic carriers in mitochondria. *Molecular Mechanisms in Bioenergetics*. Ernster L, editor. Elsevier Science Publishers; Amsterdam, London, Tokyo, New York, pp. 359-384.
- Krause SM, Jacobus WE. 1992. Specific enhancement of the cardiac myofibrillar ATPase activity by bound creatine kinase. *J Biol Chem* 267: 2480-2486.
- Kreisman N, LaManna J, Rosenthal M, Sick T. 1981. Oxidative metabolic responses with recurrent seizures in rat cerebral cortex: Role of systemic factors. *Brain Res* 218: 175-188.
- Krippeit-Drews P, Backer M, Dufer M, Drews G. 2003. Phosphocreatine as a determinant of K^{+} -ATP channel activity in pancreatic β -cells. *Pflügers Arch – Eur J Physiol* 445: 556-562.
- Kushmerick MJ. 1995. Bioenergetics and muscle cell types. *Adv Exp Med Biol* 384: 175-184.
- Kuznetsov AV, Saks VA. 1986. Affinity modification of creatine kinase and ATP-ADP translocase in heart mitochondria: determination of their molar stoichiometry. *Biochem Biophys Res Comm* 134: 359-366.
- Kuznetsov AV, Tiivel T, Sikk P, Käambre T, Kay L, et al. 1996. Striking difference between slow and fast twitch muscles in the kinetics of regulation of respiration by ADP in the cells in vivo. *Eur J Biochem* 241: 909-915.
- Lakatta EG. 1991. Length modulation of muscle performance: Frank-Starling law of the heart. *The heart and cardiovascular system: Scientific foundations*. Fozzard HA, Haber E, Jennings RB, Katz AM, Morgan HE, editors. New York: Raven Press; pp. 1325-1354.
- Landesberg A. 1996. End-systolic pressure-volume relationship and intracellular control of contraction. *Am J Physiol* 270: H338-H349.
- Landesberg A, Sideman S. 1999. Regulation of energy consumption in cardiac muscle: Analysis of isometric contractions. *Am J Physiol* 276: H998-H1011.
- Lardy HA, Wellman H. 1952. Oxidative phosphorylations: Role of inorganic phosphate and acceptor systems in control metabolic rates. *J Biol Chem* 195: 215-224.
- Lederer WJ, Nichols CG. 1989. Nucleotide modulation of the activity of rat heart ATP-sensitive K^{+} channels in isolated membrane patches. *J Physiol* 419: 193-211.
- Leong S, Clark J. 1984. Regional enzyme development in rat brain: Enzymes associated with glucose utilization. *Biochem J* 218: 131-138.
- Loike J, Somes M, Silverstein S. 1986. Creatine uptake, metabolism, and efflux in human monocytes and macrophages. *Am J Physiol* 251: 128-135.
- Lorenz E, Terzic A. 1999. Physical association between recombinant cardiac ATP-sensitive K^{+} subunits Kir.6 and SUR2A. *J Mol Cell Cardiol* 31: 425-434.
- Maugin GA, Engelbrecht J. 2000. A thermodynamical viewpoint on nerve pulse dynamics. *J Non-Equilib Thermodyn* 19: 9-23.
- Maugin GA, Muschik W. 1994. Thermodynamics with internal variables, Part I: General concepts, Part II: Applications. *J Non-Equilib Thermodyn* 19: 217-249: 250-289.
- McCormack JG, Halestrap AP, Denton RM. 1990. Role of calcium ions in regulation of mammalian intramitochondrial metabolism. *Physiol Rev* 70: 391-425.
- McLellan G, Weisberg A, Winegrad S. 1983. Energy transport from mitochondria to myofibril by a creatine phosphate shuttle in cardiac cells. *Am J Physiol* 254: C423-C427.
- Meyer RA, Sweeney HL, Kushmerick MJ. 1984. A simple analysis of the “phosphocreatine shuttle”. *Am J Physiol* 246: C365-C377.
- Minajeva A, Ventura-Clapier R, Veksler V. 1996. Ca^{2+} uptake by cardiac sarcoplasmic reticulum ATPase in situ strongly depends on bound creatine kinase. *Pflügers Arch* 432: 904-912.

- Minton AP. 2001. The influence of macromolecular crowding and macromolecular confinement on biochemical reactions in biological media. *J Biol Chem* 276: 10577-10580.
- Momken I, Lechene P, Koulmann N, Fortin D, Mateo P, et al. 2005. Impaired voluntary running capacity in CK-deficient mice. *J Physiol* 565: 951-964.
- Moreadith RW, Jacobus WE. 1982. Creatine kinase of heart mitochondria. Functional coupling of ADP transfer to the adenine nucleotide translocase. *J Biol Chem* 257: 899-905.
- Muller M, Moser R, Cheneval D, Carafoli E. 1985. Cardiolipin is the membrane receptor for mitochondrial creatine phosphokinase. *J Biol Chem* 260: 3839-3843.
- Neely JR, Denton RM, England PJ, Randle PJ. 1972. The effects of increased heart work on the tricarboxylate cycle and its interactions with glycolysis in the perfused rat heart. *Biochem J* 128: 147-159.
- Neely JR, Grotyohann LW. 1984. Role of glycolytic products in damage to ischemic myocardium. Dissociation of adenosine triphosphate levels and recovery of function of reperfused ischemic hearts. *Circ Res* 55: 816-824.
- Nicholls D, Ferguson SJ. 2002. Bioenergetics. London-New York: Academic Press.
- Ogut O, Brozovich FV. 2003. Creatine phosphate consumption and the actomyosin crossbridge cycle in cardiac muscles. *Circ Res* 93: 54-60.
- Opie LH. 1998. The Heart. Physiology, from cell to circulation. Third edition. Philadelphia: Lippincott-Raven Publishers; pp. 43-63.
- Ovadi J. 1995. Cell architecture and metabolic channeling. Landes RG, editor. Austin, New York, Berlin, Heidelberg, London, Paris, Tokyo, Hong Kong, Barcelona, Budapest: Springer-Verlag.
- Ovadi J, Saks V. 2004. On the origin of intracellular compartmentation and organized metabolic systems. *Mol Cell Biochem* 256/257: 5-12.
- Pebay-Peyroula E, Dahout-Gonzalez C, Kahn R, Trezeguet V, Lauquin GJ-M, et al. 2003. Structure of mitochondrial ADP/ATP carrier in complex with carboxyatractyloside. *Nature* 426: 39-44.
- Pfeuffer J, Tkac I, Gruetter R. 2000. Extracellular-intracellular distribution of glucose and lactate in the rat brain assessed noninvasively by diffusion-weighted ^1H nuclear magnetic resonance spectroscopy in vivo. *J Cereb Blood Flow Metab* 20: 736-46.
- Ponticos M, Lu QL, Morgan JE, Hardie DG, Partridge TA, et al. 1998. Dual regulation of the AMP-activated protein kinase provides a novel mechanism for the control of creatine kinase in skeletal muscle. *EMBO J* 17(6): 1688-1699.
- Rayment I, Holden HM, Whittaker M, Yohn CB, Lorenz M, et al. 1993. Structure of the actin-myosin complex and its implications for muscle contraction. *Science* 261: 58-65.
- Rizzuto R, Bernardi P, Pozzan T. 2000. Mitochondria as all-around players of the calcium-game. *J Physiol* 529: 37-47.
- Rossi AM, Eppenberger HM, Volpe P, Cotrufo R, Wallimann T. 1990. Muscle-type MM creatine kinase is specifically bound to sarcoplasmic reticulum and can support Ca^{2+} uptake and regulate local ATP/ADP ratios. *J Biol Chem* 265: 5258-5266.
- Rube DA, van den Blik AM. 2004. Mitochondrial morphology is dynamic and varied. *Mol Cell Biochem* 256/257: 331-339.
- Saks VA, Chernousova GB, Gukovsky DE, Smirnov VN, Chazov EI. 1975. Studies of energy transport in heart cells. Mitochondrial isoenzyme of creatine phosphokinase: Kinetic properties and regulatory action of Mg^{2+} ions. *Eur J Biochem* 57: 273-290.
- Saks VA. 1980. Creatine kinase isozymes and the control of cardiac contraction. Heart creatine kinase. The integration of enzymes for energy distribution. Jacobus WE, Ingwall JS, editors. Baltimore: Williams & Wilkins; pp. 109-126.
- Saks VA, Kuznetsov AV, Kupriyanov VV, Miceli MV, Jacobus WE. 1985. Creatine kinase of rat heart mitochondria. The demonstration of functional coupling to oxidative phosphorylation in an inner membrane matrix preparation. *J Biol Chem* 260: 7757-7764.
- Saks VA, Khuchua ZA, Kuznetsov AV. 1987. Specific inhibition of ATP-ADP translocase in cardiac mitoplasts by antibodies against mitochondrial creatine kinase *Biochim Biophys Acta* 891: 138-144.
- Saks VA, Belikova YO, Kuznetsov AV. 1991. In vivo regulation of mitochondrial respiration in cardiomyocytes: Specific restrictions for intracellular diffusion of ADP. *Biochim Biophys Acta* 1074: 302-311.
- Saks VA, Vasiljeva E, Belikova Yu O, Kuznetsov AV, Lyapina S, et al. 1993. Retarded diffusion of ADP in cardiomyocytes: Possible role of mitochondrial outer membrane and creatine kinase in cellular regulation of oxidative phosphorylation. *Biochim Biophys Acta* 1144: 134-148.
- Saks VA, Khuchua ZA, Vasilyeva EV, Belikova YO, Kuznetsov A. 1994a. Metabolic compartmentation and substrate channeling in muscle cells. Role of coupled creatine kinases in in vivo regulation of cellular respiration. A synthesis. *Mol Cell Biochem* 133/134: 155-192.
- Saks VA, Ventura-Clapier R, editors. 1994b. Cellular Bioenergetics. Role of coupled creatine kinase. Dordrecht-Boston: Kluwer Academic Publishers; pp. 1-348.
- Saks VA, Ventura-Clapier R, Aliev MK. 1996a. Metabolic control and metabolic capacity: Two aspects of creatine kinase functioning in the cells. *Biochim Biophys Acta* 1274: 81-92.

- Saks VA, Aliev MK. 1996b. Is there creatine kinase equilibrium in working heart cells? *Biochem Biophys Res Commun* 227: 360-367.
- Saks VA, Tiivel T, Kay L, Novel-Chate V, Daneshrad Z, et al. 1996c. On the regulation of cellular energetics in health and disease. *Mol Cell Biochem* 160/161: 195-208.
- Saks VA, Dos Santos P, Gellerich FN, Dioloz P. 1998. Quantitative studies of enzyme-substrate compartmentation, functional coupling, and metabolic channeling in muscle cells. *Mol Cell Biochem* 184: 291-307.
- Saks VA, Kongas O, Vendelin M, Kay L. 2000. Role of the creatine/phosphocreatine system in the regulation of mitochondrial respiration. *Acta Physiol Scand* 168: 635-641.
- Saks VA, Kaambre T, Sikk P, Eimre M, Orlova E, et al. 2001. Intracellular energetic units in red muscle cells. *Biochem J* 356: 643-657.
- Saks V, Kuznetsov A, Andrienko T, Usson Y, Appaix F, et al. 2006a. Heterogeneity of ADP diffusion and regulation of respiration in cardiac cells. *Biophys J* 84: 3436-3456.
- Saks VA, Kuznetsov AV, Vendelin M, Guerro K, Seppet EK. 2004a. Functional coupling as a basic mechanism of feedback regulation of cardiac energy metabolism. *Mol Cell Biochem* 256/257: 185-199.
- Saks VA, Ventura-Clapier R, Leverve X, Rigoulet M, Rossi A, editors. 1998. *Bioenergetics of the cell: Quantitative aspects*. *Mol Cell Biol* 184:1-460.
- Saks VA, Ventura-Clapier RM, Gellerich F, Leverve X, 2004b. *Mol Cell Biochem* 256/257: 1-424.
- Saks V, Guerrero K, Vendelin M, Engelbrecht J, Seppet E. 2006a. The creatine kinase isoenzymes in organized metabolic networks and regulation of cellular respiration: A new role for Maxwell's demon. Vial C, editor. *Creatine Kinase, in series: Molecular Anatomy and Physiology of proteins* (Uversky V.N., series editor). New York: NovaScience Publisher.
- Saks VA, Dzeja P, Sehlather U, Terzic A, Nallimaun T. 2006b. *J physiol.* 576: 253-273.
- Saltarelli M, Bauman A, Moore A, Bradley C, Blakely R. 1996. Expression of the rat brain creatine transporter in situ and in transfected HeLa cells. *Dev Neurosci* 18: 524-534.
- Sata M, Sugiura S, Yamashita H, Momomura SI, Serizawa T. 1996. Coupling between myosin ATPase cycle and creatine kinase cycle facilitates cardiac actomyosin sliding in vitro: A clue to mechanical dysfunction during myocardial ischemia. *Circ* 93: 310-317.
- Saucerman JJ, Brunton LL, Michailova AP, McCulloch AD. 2003. Modeling β -adrenergic control of cardiac myocyte contractility in silico. *J Biol Chem* 278: 47997-48003.
- Savabi F. 1994. Interaction of creatine kinase and adenylate kinase systems in muscle cells. *Mol Cell Biochem* 133/134: 145-452.
- Schlattner U, Forstner M, Eder M, Stachowiak O, Fritz-Wolf K, et al. 1998. Functional aspects of the X-ray structure of mitochondrial creatine kinase: A molecular physiology approach. *Mol Cell Biochem* 184: 125-140.
- Schlattner U, Gehring F, Vernoux N, Tokarska-Schlattner M, Neumann D, et al. 2004. C-terminal lysines determine phospholipid interaction of sarcomeric mitochondrial creatine kinase. *J Biol Chem* 279: 24334-24342.
- Schlattner U, Wallimann T. 2004. Metabolite channeling: Creatine kinase microcompartments. *Encyclopedia of Biological Chemistry*, Lennorz WJ & Lake MD, Eds. Academic Press, New York, USA 2: 646-651.
- Schlegel J, Zurbriggen B, Wegmann G, Wyss M, Eppenberger HM, et al. 1988a. Native mitochondrial creatine kinase forms octameric structures. I. Isolation of two interconvertible mitochondrial creatine kinase forms, dimeric and octameric mitochondrial creatine kinase: Characterization, localization, and structure-function relationships. *J Biol Chem* 263: 16942-16953.
- Schlegel J, Wyss M, Schurch U, Schnyder T, Quest A, et al. 1988b. Mitochondrial creatine kinase from cardiac muscle and brain are two distinct isoenzymes but both form octameric molecules. *J Biol Chem* 263: 16963-16969.
- Schliwa M. 2002. The evolving complexity of cytoplasmic structure. *Nature Rev* 3: 1-6.
- Schnell S, Turner TE. 2004. Reaction kinetics in intracellular environments with macromolecular crowding: Simulations and rate laws. *Prog Biophys Mol Biol* 85: 235-260.
- Schnyder T, Rojo M, Furter R, Wallimann T. 1994. The structure of mitochondrial creatine kinase and its membrane binding properties. *Mol Cell Biochem* 133-134: 115-23.
- Scholte H. 1973. The separation and enzymatic characterization of inner and outer membranes of rat heart mitochondria. *Biochim Biophys Acta* 330: 283-293.
- Schoolweth AC, LaNoue KF. 1980. The role of microcompartmentation in the regulation of glutamate metabolism by rat kidney mitochondria. *J Biol Chem* 255: 3403-3411.
- Schroedinger E. 2000. *What is life? The physical aspect of the living cell*. London: The Folio Society; pp. 83-106.
- Schwartzkroin P. 1984. Epileptogenesis in the immature central nervous system. *Electrophysiology of epilepsy*. Schwartzkroin P, Wheal H, editors. New York: Academic Press; 389-412.
- Selivanov VA, Alekseev AE, Hodgson DM, Dzeja PP, Terzic A. 2004. Nucleotide-gated K_{ATP} channels integrated with creatine and adenylate kinases: Amplification, tuning, and sensing of energetics signals in the compartmentalized cellular environment. *Mol Cell Biol* 256/257: 243-256.
- Seppet E, Kaambre T, Sikk P, Tiivel T, Vija H, et al. 2001. Functional complexes of mitochondrial with MgATPases of myofibrils and sarcoplasmic reticulum in muscle cells. *Biochim Biophys Acta* 1504: 379-395.

- Shimizu J, Todaka K, Burkoff D. 2002. Load dependence of ventricular performance explained by model of calcium-myofibrillar interactions. *Am J Physiol* 282: H1081-H1091.
- Siesjo B. 1978. Brain energy metabolism. Chichester: John Wiley and Sons; pp. 601.
- Soboll S, Gonrad A, Hebish S. 1994. Influence of mitochondrial creatine kinase on the mitochondrial/extracellular distribution of high-energy phosphates in muscle tissue: Evidence for the leak in the creatine shuttle. *Mol Cell Biochem* 133/134: 105-115.
- Sommer JR, Jennings RB. 1986. Ultrastructure of cardiac muscle. The heart and cardiovascular system. Fozzard HA, Haber E, Jennings RB, Katz AM, Morgan HE. editors. New York: Raven Press; pp. 61-100.
- Spindler M, Niebler R, Remkes H, Horn M, Lanz T, et al. 2002. Mitochondrial creatine kinase is critically necessary for normal myocardial high-energy phosphate metabolism. *Am J Physiol* 283: H680-H687.
- Spindler M, Meyer K, Stromer H, Leupold A, Boehm E. 2004. Creatine kinase-deficient hearts exhibit increased susceptibility to ischemia/reperfusion injury and impaired calcium homeostasis. *Am J Physiol* 287: H1039-H1045.
- Srere PA. 2000. Macromolecular interactions: Tracing the roots. *Trends Biochem Sci* 25: 150-153.
- Stachowiak O, Schlattner U, Dolder M, Wallimann T. 1998. Oligomeric state and membrane binding behaviour of creatine kinase isoenzymes: Implications for cellular function and mitochondrial structure. *Mol Cell Biochem* 184: 141-151.
- Starling EH, Visscher MB. 1926. The regulation of the energy output of the heart. *J Physiol* 62: 243-261.
- Steeghs K, Benders A, Oerlemans F, de Haan A, Heerschap A, et al. 1997. Altered Ca^{2+} responses in muscles with combined mitochondrial and cytosolic creatine kinase deficiencies. *Cell* 89: 93-103.
- Suga H. 1990. Ventricular energetics. *Physiol Rev* 70: 247-277.
- Territo PR, French SA, Dunleavy MC, Evans FJ, Balaban RS. 2001. Calcium activation of heart mitochondrial oxidative phosphorylation. Rapid kinetics of mV_{O_2} , NADH, and light scattering. *J Biol Chem* 276: 2586-1599.
- Tsuji M, Naruse H, Volpe J, Holtzman D. 1995a. Cerebral oxygenation and energy state in hypoxic piglets. *Ped Research* 253-259.
- Tsuji M, Allred E, Jensen F, Holtzman D. 1995b. Sequential loss of phosphocreatine and ATP in the hypoxic immature rat brain. *Dev Brain Res* 85: 192-200.
- Veech R, Lawson JWR, Cornell NW, Krebs H. 1979. Cytosolic phosphorylation potential. *J Biol Chem* 254: 6538-6547.
- Veksler VI, Kuznetsov AV, Anfous K, Mateo P, van Deursen J, et al. 1995. Muscle creatine kinase-deficient mice. II Cardiac and skeletal muscles exhibit tissue-specific adaptation of the mitochondrial function. *J Biol Chem* 270: 19921-19929.
- Vendelin M, Kongas O, Saks V. 2000. Regulation of mitochondrial respiration in heart cells analyzed by reaction-diffusion model of energy transfer. *Am J Physiol* 278: C747-C764.
- Vendelin M, Eimre M, Seppet E, Peet N, Andrienko T, et al. 2004a. Intracellular diffusion of adenosine phosphates is locally restricted in cardiac muscle. *Mol Cell Biochem* 256/257: 229-241.
- Vendelin M, Lemba M, Saks VA. 2004b. Analysis of functional coupling: Mitochondrial creatine kinase and adenine nucleotide translocase. *Biophys J* 87: 696-713.
- Vendelin M, Beraud N, Guerrero K, Andrienko T, Kuznetsov A, et al. 2004c. Mitochondrial regular arrangement in muscle cells: A crystal-like pattern. *Am J Physiol* 288: C757-C767.
- Ventura-Clapier R, Veksler V. 1994. Myocardial ischemic contracture. Metabolites affect rigor tension development and stiffness. *Circ Res* 74: 920-929.
- Ventura-Clapier R, Veksler V, Hoerter JA. 1994. Myofibrillar creatine kinase and cardiac contraction. *Mol Cell Biochem* 133: 125-144.
- Ventura-Clapier R, Kuznetsov A, Veksler V, Boehm E, Anfous K. 1998. Functional coupling of creatine kinases in muscles: Species and tissue specificity. *Mol Cell Biochem* 184: 231-247.
- Vignais P. 1976. Molecular and physiological aspects of adenine nucleotide transport in mitochondria. *Biochim Biophys Acta* 456: 1-38.
- Wallimann T, Schlosser T, Eppenberger H. 1984. Function of M-line-bound creatine kinase as intramyofibrillar ATP regenerator at the receiving end of the phosphorylcreatine shuttle in muscle. *J Biol Chem* 259: 5238-5246.
- Wallimann T, Wyss M, Brdiczka D, Nicolay K, Eppenberger HM, et al. 1992. Intracellular compartmentation, structure, and function of creatine kinase isoenzymes in tissues with high and fluctuating energy demands: The 'phosphocreatine circuit' for cellular energy homeostasis. *Biochem J* 281: 21-40.
- Wan B, Doumen C, Duszynski J, Salama G, Vary TC, et al. 1993. Effects of cardiac work on electrical potential gradient across mitochondrial membrane in perfused rat hearts. *Am J Physiol* 265: H453-H460.
- Wang SQ, Wei C, Zhao G, Brochet D, Shen J, et al. 2004. Imaging microdomain Ca^{2+} in muscle cell. *Circ Res* 94: 1011-1022.
- Wegmann G, Zanolla E, Eppenberger HM, Wallimann T. 1992. In situ compartmentation of creatine kinase in intact sarcomeric muscle: The acto-myosin overlap zone as a molecular sieve. *J Muscle Res Cell Motil* 13: 420-435.
- Weiss JN, Lamp ST. 1987. Glycolysis preferentially inhibits ATP-sensitive K-channels in isolated guinea pig cardiac myocytes. *Science* 238: 67-69.

- Weiss JN, Korge P. 2001. The cytoplasm: No longer a well-mixed bag. *Circ Res* 89: 108-110.
- Whittingham T, Douglas A, Holtzman D. 1995. Creatine and nucleoside triphosphates in rat cerebral gray and white matter. *Metab Brain Dis* 10: 347-352.
- Williamson JR, Ford C, Illingworth J, Safer B. 1976. Coordination of cyclic acid cycle activity with electron transport flux. *Circ Res* 38, Suppl. I, 39-51.
- Wiseman RW, Kushmerick MJ. 1995. Creatine kinase equilibration follows solution thermodynamics in skeletal muscle. *J Biol Chem* 270: 12428-12438.
- Wyss M, Smeitink J, Wevers RA, Wallimann T. 1992. Mitochondrial creatine kinase: A key enzyme of aerobic energy metabolism. *Biochim Biophys Acta* 1102: 119-166.
- Wyss M, Kaddurah-Daouk R. 2000. Creatine and creatinine metabolism. *Physiological Reviews* 80: 1107-1213.
- Unitt JF, Schrader J, Brunotte F, Radda G, Seymour AM. 1991. Determination of free creatine and phosphocreatine concentrations in isolated perfused rat heart by ^1H and ^{31}P NMR. *Biochim. Biophys Acta* 1133: 115-120.
- Yamashita H, Sata M, Sugiura S, Monomura SI, Serizawa T, et al. 1994. ADP inhibits the sliding velocity of fluorescent actin filaments on cardiac and skeletal myosins. *Circ Res* 74: 1027-1033.
- Yang Z, Steele DS. 2002. Effects of phosphocreatine on SR regulation in isolated saponin-permeabilized rat cardiac myocytes. *J Physiol* 539: 767-777.
- Yi M, Weaver D, Hajnocsky G. (2004) Control of mitochondrial motility and distribution by the calcium signal: A homeostatic circuit. *J Cell Biol* 167: 661-672.
- Zweier JJ, Jacobus WE, Korecky B, Brandes-Barry Y. 1991. Bioenergetic consequences of cardiac phosphocreatine depletion induced by creatine analogue feeding. *J Biol Chem* 266: 20296-20304.

8.2 Modeling of Regulation of Glycolysis and Overall Energy Metabolism Under a Systems Biology Approach

M. Cascante · L. G. Boros · J. Boren

1	<i>Neuronal Activation and Energy Metabolism</i>	862
1.1	Metabolic Substrates	862
1.1.1	Glucose	862
1.1.2	Ketone Bodies	863
1.1.3	Fatty Acids	863
1.2	Modeling Brain Metabolic Networks	863
1.2.1	Can SIDMAP Provide New Insights to Open Questions in Brain Metabolic Regulation and Neurological Disorders?	865
2	<i>Tools to Quantitatively and Systematically Analyze Which Components Control the Metabolome and the Metabolic Flux Distribution Inside the Network</i>	867
2.1	Analysis of Metabolic Network Control Distribution in Drug Discovery and Disease	871
3	<i>Systems Biology as a Tool to Integrate Genomics, Proteomics, and Metabolomics Toward the Understanding of Brain Metabolic Regulation</i>	872

Abstract: This chapter discusses modeling of glycolysis and macromolecule synthesis in light of overall energy metabolism and glucose substrate utilization, using simpler nonbrain systems as examples. A discussion of metabolic interactions in response to dual-function neuropeptides and gut hormones, such as glucagon-like peptide-1 (GLP-1), is provided. A general introduction to metabolic network modeling includes essential concepts such as metabolic control systems, control points, and flux analysis. This chapter also discusses the ability of specific metabolic profiling tools to bring new insights to the understanding of brain metabolic regulation, to refine our grasp of neurotransmitter metabolic network interactions, and to improve the accuracy of our predictions of brain responses to drug treatments.

1 Neuronal Activation and Energy Metabolism

The nerve impulse is initiated by the depolarization of the neuronal plasma membrane. This depolarization releases potential energy earlier established through the formation of transmembrane ion gradients. The amount of energy released by depolarization is fixed, so to obtain an increase in signal intensity, an increase in the frequency sufficient to reestablish the ion gradient is necessary. For this purpose, chemical energy in the form of ATP, in an amount at least equal to the potential energy that will be consumed in the next depolarization is needed (Ockner, 2004).

The increased neuronal ATP generation creates a demand for increased availability of oxidizable substrates and increased activity of cellular mechanisms to enable its utilization. Several substrates, such as glucose, ketone bodies (β -hydroxybutyrate and acetoacetate), or free fatty acids (FFA), can be used to produce the necessary ATP for neuronal activation depending on substrate availability and the kind of cells involved.

Another important metabolic aspect of neuronal cell function is the storage and timely release of neurotransmitters upon receipt of signals, functions that require intense membrane fatty acid synthesis and turnover. Insulin production exemplifies the importance of neuropeptides in regulating *de novo* fatty acid synthesis and turnover in differentiating islet β cells as outlined later in this review. Glucagon-like peptide-1 (GLP-1) is a powerful neuropeptide regulating β cell *de novo* fatty acid synthesis and turnover with a primary target of increasing glucose carbon channeling toward fatty acid synthesis, chain elongation, and desaturation of the long chains. Further explorations of these unique metabolic effects of hormones acting in the brain, e.g., GLP-1, improve the understanding of neuronal response and neurological and psychiatric diseases and lead to the discovery of new target sites for drug interactions, with molecular mechanisms responsible for defective neurotransmitter synthesis and responses.

1.1 Metabolic Substrates

1.1.1 Glucose

Glucose uptake by the cell is mediated by members of the facilitative glucose transporters. Glucose transporter class I molecules (GLUT-1) are found in the blood–brain barrier and in astrocytes, whereas GLUT-3 is found in neurons. GLUT-3 is kinetically more efficient than GLUT-1, but this efficiency is affected *in vivo* by anatomic factors and by transporter abundance. The final end products of the complete oxidation of glucose by glycolysis and the tricarboxylic acid (TCA) cycle are CO_2 and H_2O . This oxidation yields approximately 30 ATP molecules and consumes 6 suppress ATP molecules, O_2 being the more efficient substrate. In anaerobic conditions (anaerobic glycolysis), one glucose yields two ATPs and two lactate molecules. The obtained lactate can be exported to other cells that can oxidize it, or it can be reconverted to glucose in hepatocytes by gluconeogenesis. Lactate release seems to be important to support the metabolic and energetic requirements of neurons, but a controversy about its main utilization during neuron activity exists (Chih et al., 2001).

Aerobic glycolysis is highly efficient, partly because of characteristics such as the presence of hexokinase type II, which is associated with the mitochondria. This association appears to enhance the rate and

efficiency of glucose phosphorylation and ATP synthase-mediated oxidative phosphorylation (Lemeshko, 2002).

The utilization of pyruvate produced by aerobic glycolysis in the TCA cycle is highly efficient. This results from the fact that pyruvate dehydrogenase is subject to kinase-mediated negative feedback control by high ratios of NADH/NAD, acetyl-CoA/CoA, and ATP/ADP in the mitochondrial matrix, preventing excessive oxidative decarboxylation of pyruvate to acetyl-CoA and controlling the flow of electrons into the electron transport chain. This control avoids loss of energy by disruption of the flow of electrons and prevents oxidative injury in the cell.

1.1.2 Ketone Bodies

Ketone bodies (β -hydroxybutyrate and acetoacetate) can be used by brain cells instead of glucose, and are quickly transferred to neurons and astrocytes. Moreover, utilization of ketone bodies suppresses glucose utilization. This seems to be due to the transfer of ketone bodies from plasma to brain to neuron to mitochondria, where they generate ATP. The flow from the plasma into the brain is proportional to plasma concentration as they share the same transport mechanism in the blood–brain barrier with other low-weight monocarboxylates. The ability of ketone bodies to suppress and substitute for glucose utilization in the brain can be understood via its intramitochondrial metabolism: β -hydroxybutyrate is oxidized by β -hydroxybutyrate dehydrogenase to acetoacetate, which is converted to its acyl-CoA thioester directly or by the succinyl-CoA acyltransferase entering into the oxidative pathways in the mitochondrial matrix. This metabolism will affect pyruvate dehydrogenase regulation, avoiding glucose oxidation and inhibiting pyruvate utilization, glycolysis, and glucose uptake. Because of the lack of a regulatory mechanism to prevent the increased oxidation of ketone bodies, there is an uncoupling of the oxidative phosphorylation, affecting the efficiency of this process, and an increase of the redox potential and generation of reactive oxygen species (ROS), promoting oxidative stress and cell injury.

1.1.3 Fatty Acids

Within the brain, fatty acids are utilized only in astrocytes and other glial cells, not in neurons. These long-chain fatty acids are converted to their acyl-CoA form and then an acylcarnitine derivative is obtained. The entrance of this derivative into the mitochondria is through carnitine palmitoyltransferase-I (CPT-I). Once inside the mitochondria, the fatty acid can be β -oxidized, generating acetyl-CoA, which through the TCA cycle will produce ATP. These fatty acids can also produce ketone bodies that can be exported from the astrocytes (in a manner similar to what hepatocytes do), which can then be used directly by nearby neurons in preference to glucose utilization.

Mitochondrial oxidation of fatty acids inhibits several steps of glucose uptake and glycolysis and in astrocytes it feeds gluconeogenesis. The main control point of long-chain fatty acids utilization is CPT-I, but this control is weaker than the one exerted by pyruvate dehydrogenase in glycolysis.

In summary, the metabolic behavior of brain cells depends on the cell type: neurons can oxidize glucose, lactate, ketone bodies, and TCA cycle intermediates to produce ATP, but they cannot oxidize fatty acids. On the other hand, astrocytes are more versatile, as they can also oxidize fatty acids and generate *de novo* glucose by gluconeogenesis (but they cannot export it) and export lactate and ketone bodies to the surrounding cells. In this context, it is important to model glucose metabolism when only glucose is available and also when other substrates are available, as it will indicate to us the limiting and controlling steps of the brain cells metabolism in each situation.

1.2 Modeling Brain Metabolic Networks

For a better understanding of brain metabolism it is necessary to integrate the existing data on the working of the different metabolic pathways in neurons and astrocytes, and particularly how glucose is metabolized

depending on the availability of other substrates. This integration of the data obtained in metabolic network models will be necessary to understand the relationship between the main metabolic pathways inside the cell and to comprehend the metabolic astrocyte–neuron interactions.

Metabolites are the end products of cellular regulatory processes and their levels can be regarded as the ultimate responses of biological systems to genetic and environmental changes. The metabolic phenotype is a manifestation of gene expression and it produces a metabolic fingerprint unique to its phenotype that can be related to physiological characteristics. In fact, the phenotype and function of mammalian cells greatly depend on metabolic adaptation. Thus, the metabolic profile of a given cell represents the integrated end point of many growth-modifying signaling events.

Metabolic adaptations of different cell types are not independent of their neighbors, as the excreted products of one cell type can be used as energy supplies for others, establishing a connection of the metabolic networks from one cell to another. In particular, the comprehension of brain metabolism requires a full understanding of the different metabolic characteristics of neurons and astrocytes as well as of their interactions. The highly complex and branching nature of the neuronal glucose metabolic network permits multiple metabolic end points (results) in response to changes in environmental factors for a given genomic or proteomic expression. Thus, the metabolic phenotype expression or the physiological state of neurons at a given moment cannot be simply predicted by the genome alone (or even by the proteins it encodes).

Any model of brain metabolism needs to take into account these differences in the organization of metabolic networks as well as the metabolic interactions established between these two types of brain cells.

The first question to answer before beginning to design a model is always the same: how many details on its components must we include? Must we include all the individual molecules and exhaustively compute their interactions? As Noble (2002) pointed out in a recent review on this topic, there are a lot of problems in trying to reproduce nature in a complete way, and even if we were successful in that task, the result would not be a model in the strict sense, as models are by definition partial representations. In fact, the power of a model lies in determining what is essential, allowing us to identify the controlling steps of the model system, and a complete representation of that system would leave us just as wise, or as ignorant, as before (Noble, 2002).

A second question is how to define the boundaries of a model. Traditionally, the accepted boundaries for a metabolic model have been the metabolic pathways. Models of traditional pathways (like glycolysis, the pentosephosphate pathway, the TCA cycle, and purine metabolism) have been developed for different cell lines and tissues (Sabat  et al., 1995; Curto et al., 1997). Although it is useful to analyze cell metabolism in cells in which they represent significant metabolic activities (e.g., glycolysis in yeast or the TCA cycle in anaerobic muscle), these metabolic pathway models do not provide for quantitative, systemic evaluations of full-cell metabolic reaction networks because they focus on subsets of networks without considering network-wide interactions (Papin et al., 2003).

The availability of full sets of data at the genomic level and the emerging technologies of proteomics and metabolomics show that an attempt to fully and usefully understand metabolism in any cell or tissue requires a network approach. Thus, for instance, knockouts of one or more steps in a metabolic pathway often result in a rearrangement not only of that pathway alone, but also cause a full reorganization of the network such that enzymes from other pathways are recruited to create alternative pathways that bypass the deleted step. These network rearrangements and network interactions explain failures in metabolic engineering caused by attempting to achieve significant metabolic phenotype changes solely through genetic tools, e.g., the failure to enhance ethanol production in yeast by overexpressing each enzyme in the glycolytic pathway, or the failure to increase penicillin production by overexpressing all the genes of the biosynthetic pathway in an industrial strain of the mold (Bailey, 1999).

Modeling metabolic networks in a manner that the main pathways are integrated in a single model and interactions between them are taken into account requires experimental approaches that simultaneously provide information of the different metabolic network components and the measure of metabolic fluxes through the different branches of the network.

In recent decades, an extremely large ongoing effort has continued to add to the collection of information about the characteristics of the components of metabolic networks and their interactions. This information now comprises very large databases that are updated continuously. Examples of several

such databases are those containing information on genes, proteins, small molecules, and interactions among proteins such as those housed and maintained at the US National Center for Biotechnology Information (<http://www.ncbi.nlm.nih.gov>); the Protein Data Bank (<http://www.rcb.org/pdb>); the Kyoto Encyclopedia of Genes and Genomes (<http://www.genome.jp/kegg>); and the Biomolecular Interaction Network Database (<http://bind.ca>). However, these databases depict only modular or static biochemical states and, to be more meaningful, need to be complemented with data from experiments using different substrates such as limiting substrates or pulse substrates (e.g., glucose and glycerol). The resulting plots of intracellular metabolite concentrations against time, when such measurements can be obtained, allow the useful estimation of fluxes throughout the different branches of the metabolic network.

Functional characteristics of a cellular metabolic network represent the metabolic phenotype of the cell. The characterization of metabolic functions requires the simultaneous measurement of substrate fluxes both within and among the interconnecting pathways. The simultaneous assessment of substrate flux within and among major metabolic branches inside the cellular metabolic network gives us the increasingly useful metabolic profile of a given cell.

In general, easiness or difficulty in measuring metabolic fluxes depends on the flux we want to calculate (Fell, 1997; Hellerstein, 2003). The easy part is to measure the uptake of external substrates or the output of end products fluxes, which can be calculated from the rates of disappearance or appearance of the relevant compounds. The difficult part is to determine metabolic fluxes within each internal branch of the network. The most common method used experimentally to determine fluxes is the utilization of isotope-labeled molecules. Isotope tracer studies can be carried out with stable or radioactive isotopes. Isotope labeling studies allow the introduction of the dimension of time and the quantitative measurement of specific kinetic processes occurring in any given time period. Many classical metabolic studies in recent decades have been carried out by measuring radioactivity associated with unstable isotopes such as ^3H or ^{14}C . However, relatively recent advances in mass spectrometry (MS) and nuclear magnetic resonance (NMR) technologies have resulted in a huge increase in the application of stable-isotope-based tracer methodologies to characterize the metabolic profile in different cells, tissues, and even whole organisms (van Winden et al., 2001). Currently, the utilization of stable isotopes is increasingly replacing the use of radioisotopes. Partly, this is occurring because the stable isotopes allow simultaneous quantification of multiple different specific-position and mass isotopomer molecules in one experiment, facilitating identification of the cell's use of different metabolic pathways (Boren et al., 2003). However, it has to be taken into account that tracer choice is determined by the fluxes of interest in the experiment at hand.

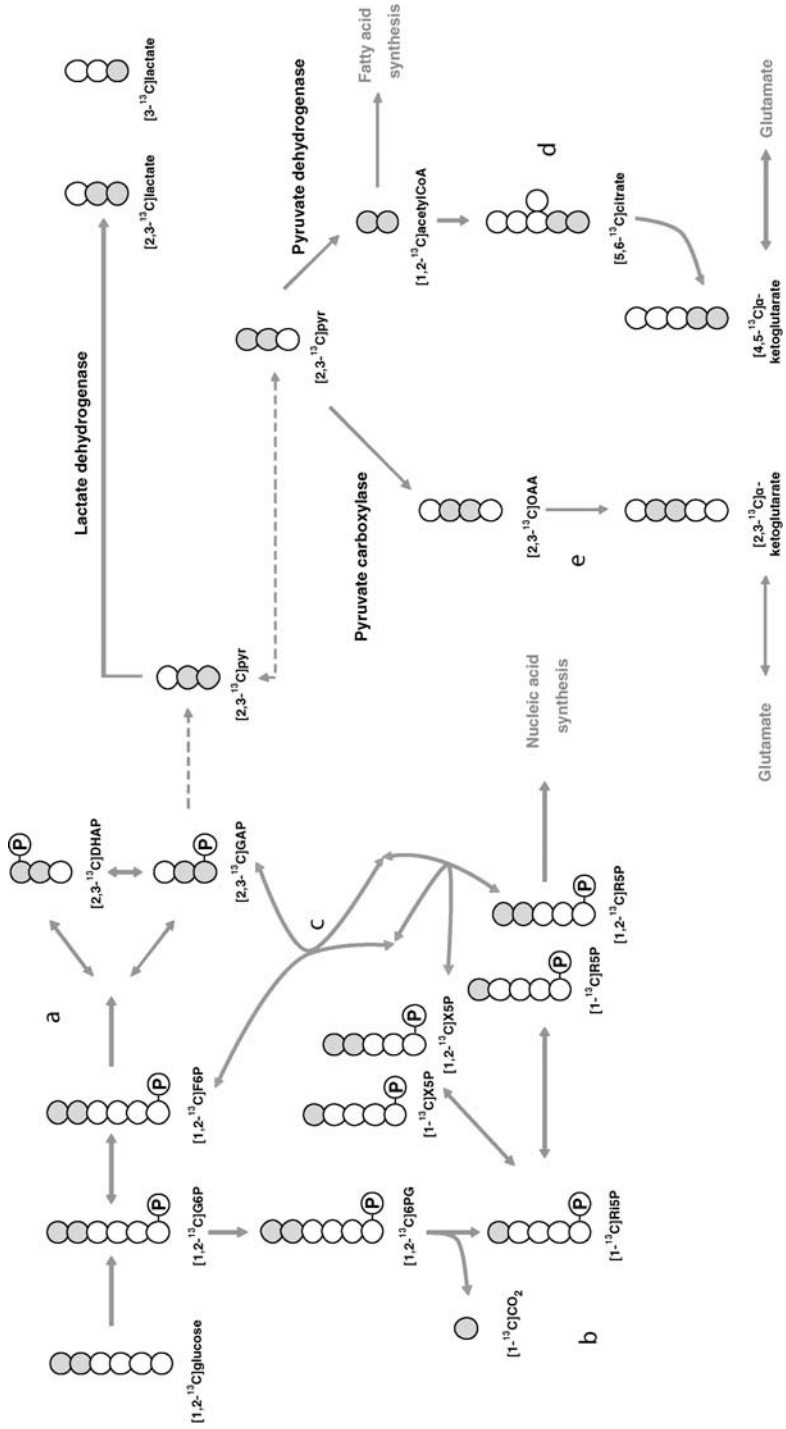
Stable-isotope-based dynamic metabolic profiling (SIDMAP) technology, combined with detailed kinetic models of the metabolic networks and appropriate software, permits quantitative characterization of the detailed routes taken by glucose carbons in the macromolecule and energy-producing metabolic reactions (Selivanov, 2004). In particular, incubation with $[1,2-^{13}\text{C}]$ glucose or uniformly labeled glucose and the use of MS enable the measurement of glucose redistribution among glycolysis and other major metabolic pathways (see [Figure 8.2-1](#)) and has been applied to various different cell types (Lee et al., 1998; Boros et al., 2002) to obtain new information on molecular-level metabolic pathway interactions in disease conditions with strong metabolic components. When applied to different types of cancer cells, the SIDMAP studies demonstrated that tumor growth is primarily determined by specific glucose metabolic reactions responsible for nucleic acid synthesis, lipid production, and TCA cycle anaplerotic flux. Significantly, these closely measured metabolic reactions showed diametrically opposite changes in response to tumor-growth-promoting or inhibiting treatments. Among these pathways, glucose intake and the nonoxidative steps of the pentose cycle, which provide the central reactions for nucleic acid ribose synthesis from glucose, are the most important pathways that directly determine tumor growth and cell transformation (Lee et al., 1998; Boren et al., 2003).

1.2.1 Can SIDMAP Provide New Insights to Open Questions in Brain Metabolic Regulation and Neurological Disorders?

Despite the fact that increasing evidence exists of the utility of SIDMAP studies in elucidating metabolic adaptations to different treatments or diseases in cells and tissues, these techniques have not been applied

Figure 8.2-1

Possible ^{13}C isotopomers formed after incubation with $[1,2-^{13}\text{C}]$ glucose as a single tracer. Labeled glucose can enter the cell and can be metabolized through glycolysis to form lactate with two labeled carbons (a). Glucose can also enter the oxidative pentosephosphate pathway (b) and be recycled back to glycolysis through the nonoxidative pentosephosphate pathway (c), forming lactate with a single carbon label. Analysis of carbon label in ribose from nucleic acids will indicate if the ribose is produced through the oxidative pathway, in which case ribose with one carbon label will be obtained, or through the nonoxidative pathway, in which case ribose with two carbon labels will be obtained. Analysis of the isotopomers from fatty acids can indicate if glucose is utilized to synthesize them. Glutamate isotopomer analysis will indicate if glucose enters the TCA cycle through the pyruvate dehydrogenase (d), or through the pyruvate carboxylase (e) enzymes, demonstrated by the position of the label in glutamate carbons



systematically to achieve a better understanding of multifactorial brain diseases and drug discovery strategies.

However, some studies of metabolic profiling using stable isotope tracer technology have been performed using labeled acetate to determine glutamine synthesis and oxidation in astrocytes, looking at the different mass and positional isotopomers of glutamate (Lee et al., 1996). This study determined that glutamine was not the main energetic substrate in astrocytes *in vivo* or *in vitro*, and that the anaplerotic flux responsible for glutamine synthesis was about 1.5 times that of the TCA cycle flux when glutamine or glucose was supplied in the medium.

A similar approach using stable isotope tracer technology and NMR instead of MS has been used to characterize the TCA cycle in cerebellar astrocytes. In this case, a mathematical model was developed to determine the relative flux of molecules through the anaplerotic versus oxidative pathways to analyze the experimental data. The model was also applied to data from granule cells and permitted identification of important differences in carbon metabolism between cerebellar astrocytes and granule cells (Merle et al., 1996).

An open question in which SIDMAP can provide new insights is in the understanding of the effect of GLP-1 in brain. GLP-1 is produced in the brain and transported along axonal networks to diverse central nervous system regions (Turton et al., 1996). It has been suggested that GLP-1 could be downstream of leptin action in the brain whereas it is still an open question whether GLP-1 needs to enter the brain to affect gut motility and food intake (Elias et al., 2000). Taking into account that increased evidence has been provided recently on the relationship between enhanced glucose metabolism and resistance to apoptosis (Danial et al., 2003), and that fatty acids induce apoptosis in β -cells (Shimabukuro et al., 1998), we hypothesize that SIDMAP characterization of GLP-1 effects on the neuronal metabolic network can help to illuminate the molecular basis of the described neuroprotective effect of GLP-1, which activates different antiapoptotic signaling pathways in specific neurons (Perry et al., 2002). This hypothesis is supported by the recent evidence provided on the effect of GLP-1 in the glucose metabolic network in pancreatic cells. These studies showed that cell differentiation and regulation of insulin release after GLP-1 treatment were accompanied by important metabolic adaptive changes that primarily affected the contribution of glucose to *de novo* fatty acid synthesis and chain elongation of the saturated long-chain species primarily utilized for triglyceride and membrane synthesis (Bulotta et al., 2003). These results indicate that a selective signaling mechanism was responsible for the differentiation-inducing metabolic effects of this hormone, being a peroxisome proliferator activated receptor-related (PPAR-related) nuclear signaling mechanism, which is a strong candidate for this action. This metabolic effect on glucose metabolic network induced by GLP-1 is totally different from the effect reported for an antitumor drug such as Gleevec, which acts through a mechanism involving tyrosine kinase inhibition. In this case, the effect on glucose metabolism was at the level of glycolysis whereas fatty acid metabolism was unaffected (Boren et al., 2001). In light of these results, it could be expected that SIDMAP characterization of GLP-1 on neuronal cells can aid in the identification of the signaling cascades and metabolic adaptations involved in the GLP-1 neuroprotective effect.

Determination of the metabolic profile, all available data on the metabolome, the kinetic parameters of each enzyme, and information on the structure of the relevant metabolic networks will serve as the basis for modeling metabolic networks and will permit us to construct detailed *in silico* metabolic models.

2 Tools to Quantitatively and Systematically Analyze Which Components Control the Metabolome and the Metabolic Flux Distribution Inside the Network

A classical question to answer when analyzing a metabolic network such as that of glucose metabolism in the brain is whether a rate-limiting reaction exists. If a rate-limiting step were to exist in a pathway, varying the activity of that step alone would change the flux in that pathway. However, as reviewed by Fell (1997), there are few definitive experimental observations of such a phenomenon and instead existing evidence suggests that most pathways are affected by the activities of several steps. Furthermore, the large number of

failures reported in the field of metabolic engineering, when trying to increase the rate of a pathway by overexpressing the predicted rate-limiting step, reinforces the concept that the control of the metabolic network is often shared among several steps (Bailey, 1999).

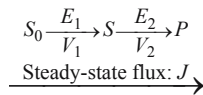
The concept that several enzymes might affect the flux in a pathway and that the effect of each enzyme on metabolite concentrations and metabolic fluxes can be quantified are the basis of two main theoretical frameworks that have been developed during the last two decades for studying the genetic, enzymatic, and substrate-level control mechanisms in metabolic networks: the biochemical systems theory (BST) developed by Savageau (Savageau, 1976; Voit, 2000) and the metabolic control analysis (MCA) (Fell, 1997; Cascante et al., 2002).

Both approaches are equivalent in essential parts as they are based on the general systems sensitivity theory (Frank, 1978). Sensitivity theory addresses the impact of changes in parameter values (or independent variables like enzyme concentrations that can be independently manipulated by genetic engineering) on responses of the integrated system. Thus, it relates properties of individual system components (local) to properties of the intact system (global).

Both theories aim to quantify how sensitive the steady-state variables (the fluxes and concentrations) are to variations in the parameters (or independent variables as, for instance, the component enzymes). These sensitivities are global or systemic properties, as they depend on all the interactions within a cellular system. Moreover, both theories seek to relate these global sensitivities to local properties of each individual metabolic reaction (enzyme reactions).

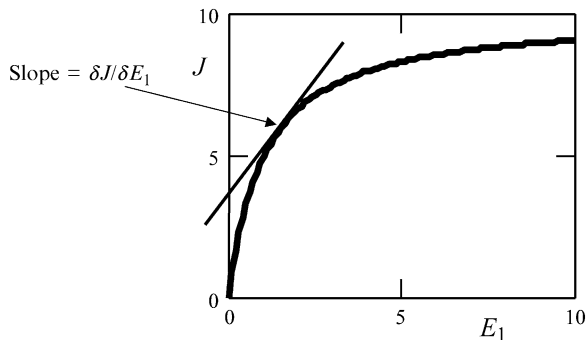
These theories have been developed almost independently of each other during the past three decades and they use different nomenclatures to describe local and global properties. In the following paragraphs, we will explain how these local and global properties are described using MCA nomenclature and we will give also the alternative of these basic concepts in BST nomenclature.

In MCA, control coefficients are defined to describe quantitatively the sensitivity of systemic variables (metabolic fluxes, intermediary metabolite concentrations, hormone secretion, brain electrical activity, etc.) to variations in enzyme activities or to any other parameters or independent variables of the system (Fell, 1997; Cascante et al., 2002). Below, we illustrate how control coefficients are defined using a simple two-step exemplary pathway:



where S_0 is the initial substrate, S the intermediary metabolite, P the final product, E_1 and E_2 are the enzymes that catalyze the two metabolic reactions, respectively; V_1 and V_2 are the corresponding local rates and J is the steady-state pathway flux.

Let us suppose first that a small change, δE_1 , is made in the amount of enzyme E_1 and that this change produces a small change, δJ , in the steady-state pathway flux, J . If the change made is small enough, then the ratio $\delta J/\delta E_1$ becomes equal to the slope of the tangent to the curve of J against E_1 .



This slope is a measure of how sensitive the flux is to variations in E_1 , but it has the disadvantage that it will depend on the units used to measure the flux and the enzyme. This slope can be made dimensionless by dividing δJ and δE_1 by the steady-state values of J and E_1 , respectively.

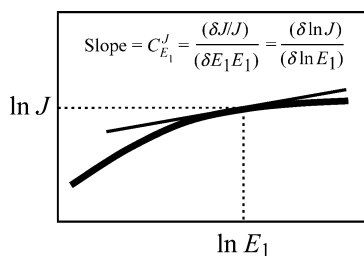
In MCA, this scaled slope is called “flux control coefficient” because it is a measure of the “control” of one enzyme on the pathway flux:

$$C_{E_1}^J = \frac{(\partial J/J)}{(\partial E_1/E_1)}.$$

Mathematically, this is equivalent to

$$C_{E_1}^J = \frac{\partial \ln J}{\partial \ln E_1},$$

and graphically it can be visualized as the slope of the tangent to the curve of $\ln J$ against $\ln E_1$:



In MCA, the meaning of “to control” is understood as “to be capable of influencing something.” In general, for metabolic fluxes or other systemic variables (Y), control coefficients of each enzyme or parameter (X) have been defined as the fractional change in the system variable (Y) over the fractional change in the enzyme activity or parameter (X):

$$C_X^Y = \frac{(\partial Y/Y)}{(\partial X/X)}$$

In BST, the same magnitude is defined as logarithmic gains:

$$L(Y, X) = \frac{\partial \ln Y}{\partial \ln X} = C_X^Y$$

Thus, logarithmic gains in BST are equal to control coefficients in MCA (see Cascante et al., 1989a, b for a more complete comparison).

Flux control coefficients are often determined by measuring these fractional changes after applying specific enzyme inhibitors. A high control coefficient indicates that the flux of the system is highly sensitive to changes in the concentration of this enzyme. For instance, control coefficients have been measured in rat hepatocytes using adenovirus-mediated enzyme overexpression. The control coefficient of glucokinase on hepatic glycogen synthesis has been reported as being close to 1 (Agius et al., 1996), indicating a true rate-limiting step. This high control coefficient can explain the abnormal hepatic glycogen synthesis in individuals with maturity-onset diabetes of the young (type II), who have just a single mutant allele (Velho et al., 1996). On the other hand, a low control coefficient indicates that the flux of the system is low in sensitivity to changes in the concentration of this enzyme. An illustrative example is the low control coefficient (lower than 0.1) reported for triose phosphate isomerase in erythrocytes (Schuster and Holzhutter, 1995). From this low control coefficient, it can be correctly predicted that individuals heterozygous for the mutated allele do not show clinical symptoms. Moreover, it has been reported that homozygous patients suffer clinical symptoms only when they present with a very low activity of this enzyme, which is in accordance with the MCA prediction for an enzyme with a very low degree of control on the pathway flux (Orosz et al., 1996; Repiso et al., 2002). The complete set of control coefficients allows us to predict the response of the system to any perturbation.

In an analogous way, control coefficients of intermediate metabolite concentrations with regard to enzymes have been defined with the same finality, which is to quantify the variation of metabolite intermediates with regard to the enzymes.

Thus, control coefficient distribution among the different steps of a pathway gives us a useful orientation from which a metabolic network can be manipulated (genetically or with drugs) to restore anomalous metabolic profiles accompanying several diseases, such as atherosclerosis or Alzheimer's disease.

Moreover, control coefficients are correlated with the kinetic properties of the pathway's enzymes. To correlate control coefficients with the kinetic properties of individual pathway enzymes, we first must define the kinetic properties of enzymes in terms of the sensitivity of the local rate to enzyme effects with variations in concentrations of its directly connected metabolites (substrates, products, effectors, etc.). In MCA, the effect of a metabolite (S) on the velocity (v_i) of the enzyme E_i is quantified by means of the elasticity coefficients, defined as the fractional change in rate of the isolated enzyme for a fractional change in substrate S , with all other effectors of the enzyme held constant at the value they have in the metabolic pathway:

$$\epsilon_S^{v_i} = \frac{(\partial v_i / v_i)}{(\partial S / S)} = \frac{\partial \ln v_i}{\partial \ln S}$$

Elasticities have positive values for substrates and metabolites (activators) that stimulate the rate of a reaction and negative values for products or inhibitors that decrease the reaction rate. They can be calculated from a rate equation using differential calculus. For example, if an enzyme obeys the Michaelis-Menten equation:

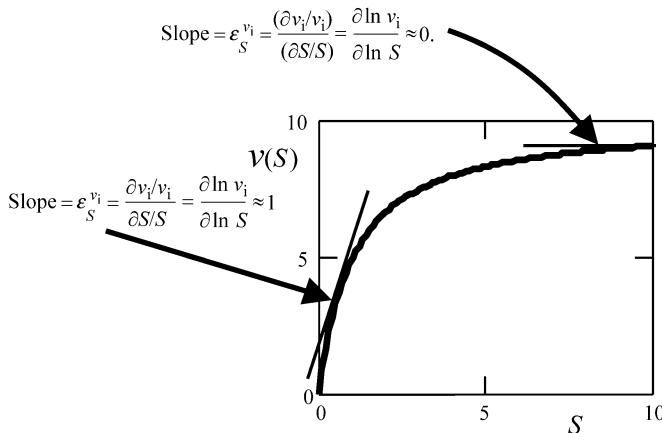
$$v = \frac{V_{\max} S}{S + K_m},$$

then the elasticity coefficients for each concentration of S can be calculated using differential calculus as:

$$\epsilon_S^v = \frac{K_m}{S + K_m}.$$

This formula facilitates observation of the link between elasticity coefficients and kinetic parameters and the typical range of values that elasticity can achieve. Elasticity coefficient values go from 1, when S is much below K_m , to 0, when S is saturated by its substrate ($S \gg K_m$). The function of elasticity in MCA is to describe quantitatively the responsiveness of an enzyme rate to a metabolite. A high-elasticity coefficient of an enzyme rate to a metabolite, S , means that the rate through the enzyme is very sensitive to a perturbation in this substrate concentration.

The elasticity coefficient of an enzyme to a metabolite can be obtained directly as the slope of the logarithm of the rate plotted against the logarithm of the metabolite concentration:



In BST, the relative derivative of rate versus metabolite concentration is named the kinetic order (g_{ij}) of the reaction, following the classical chemical kinetics nomenclature. In fact, kinetic orders are equivalent to elasticity coefficients:

$$g_{ij} = \frac{\partial v_i / v_i}{\partial S_j / S_j} = \frac{\partial \ln v_i}{\partial \ln S_j} = \varepsilon_{S_j}^{v_i}$$

Moreover, in BST individual enzyme rates, and in some cases also the net rates of synthesis or degradation of a metabolite, are described using a power-law approximation:

$$v_i = \alpha \prod_{j=1}^n X_j^{g_{ij}},$$

where X_j includes all the v_i directly connected metabolites (substrates, products, effectors, etc.).

Elasticity coefficients and control coefficients are related by the so-called connectivity theorem (Kacser and Burns, 1973, 1995). For a simple two-step metabolic pathway with a single intermediary metabolite, S, the connectivity theorem is written as:

$$C_{E_1}^J \varepsilon_s^{v_1} + C_{E_2}^J \varepsilon_s^{v_2} = 0$$

From the connectivity theorem we obtain:

$$\frac{C_{E_1}^J}{C_{E_2}^J} = \frac{\varepsilon_s^{v_2}}{\varepsilon_s^{v_1}}.$$

This ratio shows the tendency of large elasticities to be associated with small flux control coefficients and vice versa. In general, matrix equations can be written, allowing easy computation of all control coefficients in terms of the elasticity coefficients equations (Giersch, 1988; Reeder, 1988; Cascante et al., 1989a, b; Fell, 1997). Connectivity theorem allows us to easily observe that although the control coefficients are system properties of the pathway, they are explainable in terms of the kinetic properties of the constituent enzymes.

The complete set of elasticities and control coefficients allows us to predict the response of the system to any perturbation and to easily link the control properties of one enzyme with its kinetic properties.

2.1 Analysis of Metabolic Network Control Distribution in Drug Discovery and Disease

MCA has been applied in biomedicine to diagnose and understand several genetic disorders. For example, Mazat showed that control coefficient values can explain the threshold effect observed in mitochondrial diseases and used MCA to provide a possible explanation of the heterogeneous phenotypes of these pathologies (Mazat et al., 2001). Agius provided another example, which showed that the high control coefficient of glucokinase on hepatic glycogen synthesis explains the abnormalities observed in this process for patients with a single mutant allele of the glucokinase gene suffering maturity-onset diabetes of the young (type II) (Agius, 1998). Moreover, it was demonstrated that mutations of glycolytic enzymes displaying a low glycolytic flux control coefficient are recessive.

Another potentially promising area of application of MCA is the rational design of combined drug therapies, identifying particularly suitable sites for the manipulation of the metabolism with drugs. This is very useful because, as was pointed out by Salter, every enzyme in a sequence is essential for the metabolic process to work; so, the effects on metabolism are likely to be obtained with lower concentrations of the drug if an enzyme with a higher flux control coefficient is inhibited rather than one with a lower coefficient (Salter et al., 1994).

An example of the application of MCA and BST to determine the cause that led to neurological dysfunctions and mental retardation related to purine metabolism was provided by Curto et al. (1998). They modeled purine metabolism in humans utilizing different variables and looked at metabolic and flux

changes when some of these variables were altered, observing that hypoxanthine/guanine phosphoribosyl-transferase deficiency affected all the variables of the system and that the guanylate pool might be the cause of the observed neurological dysfunctions.

MCA can also provide a theoretical framework to identify key targets in disease pathways. MCA approaches the problem of drug targeting by examining the contribution of individual components within a metabolic network and quantifying it by means of control coefficients (Boros et al., 2002). For instance, a high control coefficient of a protein on an enhanced metabolite concentration associated with a pathological condition indicates that targeting this protein will result in an efficient inhibition of this metabolite accumulation. Thus, once metabolic profile differences between normal and pathological subjects are established and the steps with higher control on the relevant pathological metabolic properties are identified (steps with higher control coefficients), a rational drug design strategy can be carried out to correct the pathological situation (Cascente et al., 2002). A specific metabolic target to inhibit tumor cell growth that has been identified following such an approach is the enzyme transketolase. The control coefficient of transketolase on pentosephosphate synthesis has been reported as exceptionally high (Sabaté et al., 1995). Accordingly, it has been predicted that inhibition of transketolase will result in tumor proliferation inhibition.

3 Systems Biology as a Tool to Integrate Genomics, Proteomics, and Metabolomics Toward the Understanding of Brain Metabolic Regulation

At the threshold of the new millennium, biology faces both opportunity and challenge. The opportunity arises from the availability of complete genomic sequences and the emerging technologies of proteomics and metabolomics that inspire confidence that complex biological phenomena and systems can be understood completely (Oltvai and Barabasi, 2002; Frazier et al., 2003). This optimistic view is strengthened by the rapidly expanding technological capabilities to undertake global, whole-cell-wide analyses of gene and protein expression in mammalian cells (Phelps et al., 2002). The challenge is an increasing gap between the amount of biochemical and molecular genetic information and our understanding of the implication of these data for cell system function. In fact, life scientists have quickly realized that an encyclopedia of genes does not explain how the genome influences the phenome, nor does it provide a menu list for selecting drug targets (Huang, 2002). Moreover, the genome alone (including even the proteins it encodes) does not determine the physiological state of any cell at a given moment (Frazier et al., 2003). Thus, although genes and proteins set the stage of what “can” happen in the cell, much of the actual activity is triggered at the metabolite level: cell signaling, energy transfer, and cell-to-cell communication are regulated by metabolites (Schmidt, 2004).

To understand how the parts (genes, proteins, and metabolites) make up the whole organism, a systemic view is demanded, with genes and proteins seen more as parts of a network with the potential to affect it in certain ways, instead of as isolated entities entirely or largely determining cell function. Molecular function becomes then a function in a cellular context and not only an individual property. This change of perspective is accompanied by the recognition that bioinformatics plays an indispensable role in extracting the most relevant information from huge amounts of related data. Such a systemic view of cells demands the capacity to quantitatively predict, rather than simply qualitatively describe, cell behavior. In fact, in parallel with the data-driven research approach that focuses on speedy handling and analysis of the huge amount of data, a new approach called model-driven research (MDR) is gradually gaining influence and increased recognition.

Model-driven research takes an approach that sets up a biological model by combining the knowledge of the system with related data and simulates the behavior of the system in order to understand the biological mechanisms of the system. Typically, this is simply called systems biology (Yao, 2002) in which it is recognized that the living body is composed of numerous tissues, which include various subsystems, large and small, by which the flows of energy, material, and information are controlled. This is a hierarchical system involving subsystems such as metabolism, transcriptional control, signal transduction, the cell cycle,

and apoptosis at the cell level. All of these in turn are implemented as subsystems of interacting molecules. At a higher level, populations of cells are the subsystems of various physiological and pathological systems, organ systems, up to and including the whole body level. Systems biology aims to model and simulate the various subsystems and the interactions that are established between them, for the better understanding of life system mechanisms.

The current efforts to provide analyses of protein–protein interactions can be considered as the first steps toward the construction of interaction networks. These qualitative networks provide the basis for the quantitative spatio-temporal simulation of the evolution of a protein network at the whole-cell level. It is foreseeable that systematic data will become available in the next few years to allow the design of a virtual cell *in silico*, an accomplishment that will have an enormous impact on biomedical and pharmaceutical areas (Huang et al., 2004). With this perspective in mind, large-scale initiatives have been launched in Japan, in the USA, and to a smaller extent in Europe, aimed at the computational simulation of whole-cell functions, an example of which has been initiated at the Alliance for Cellular Signaling (Li et al., 2002). Apart from general purpose mathematical software, there are tools specifically designed to handle problems such as the modeling of metabolic and signal transduction that have been extensively used on small- and medium-sized subsystems. The next challenge is to increase the size of the systems that can be represented, by combining models of subsystems into larger wholes.

A cell is classically seen as a physical entity with a definite volume and spatial architectural substructures such as nucleus, mitochondria, Golgi bodies, ribosomes, and so on. The availability of genomic and proteomic data, as well as the growing possibility of building protein interaction maps, makes a “system view” of the cell now possible. Moreover, the use of new technologies, such as DNA and protein microarrays, two-hybrid systems, and protein-tagging techniques coupled with MS, will allow a rapid increase of the amount of information concerning protein–protein interactions (Gavin et al., 2002). From a systems biology point of view, a cell can be considered as composed of a complex network of interacting macromolecules (proteins, nucleic acids) and small molecules (lipids, carbohydrates, ions, etc.). These entities form a number of distinct, highly connected networks that make the cell a dynamic ensemble of interconnected molecular networks. If we adopt a hierarchical picture of the network, we might attribute the most relevant role to the protein networks as they trigger the fundamental activities of the cell: all the biochemical reactions are catalyzed by proteins and proteins themselves interact with each other. This fact is consistent with the view of a “central integrated” protein network, spanning the whole cellular volume (a feature particularly relevant for cells with a complex morphology, such as neurons) to which a number of functional molecular subnetworks are interconnected. For a nerve cell, an additional level of complexity is constituted by its property of electrical excitability across the cell membrane.

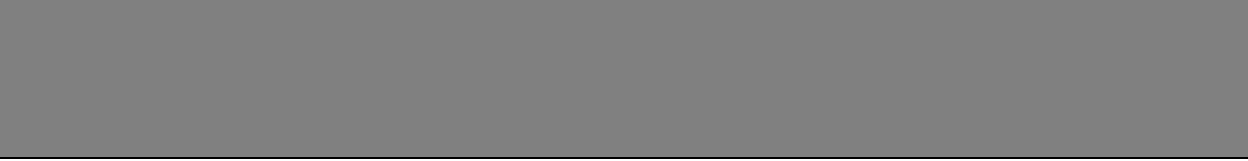
Compared with other biological systems, neuronal cells represent a greater challenge because of their structural complexity, their electrical signaling properties, and the complexity of synapses themselves, and their ability to modulate protein expression at individual synapses. Therefore, a comprehensive and quantitative understanding of neurons in the form of an *in silico* model of neuronal metabolism should contribute to the rational design of treatments for human neurodegenerative and nervous diseases.

References

- Agius L. 1998. The physiological role of glucokinase binding and translocation in hepatocytes. *Adv Enzyme Regul* 38: 303-331.
- Agius L, Peak M, Newgard CB, Gomez-Foix AM, Guinovart JJ. 1996. Evidence for a role of glucose-induced translocation of glucokinase in the control of hepatic glycogen synthesis. *J Biol Chem* 271: 30479-30486.
- Bailey JE. 1999. Lessons from metabolic engineering for functional genomics and drug discovery. *Nat Biotechnol* 17: 616-618.
- Boren J, Cascante M, Marin S, Comin-Anduix B, Centelles JJ, et al. 2001. Gleevec (STI571) influences metabolic enzyme activities and glucose carbon flow toward nucleic acid and fatty acid synthesis in myeloid tumor cells. *J Biol Chem* 276: 37747-37753.
- Boren J, Lee W-NP, Bassilian S, Centelles JJ, Lim S, et al. 2003. The stable isotope-based dynamic metabolic profile of butyrate-induced HT29 cell differentiation. *J Biol Chem* 278: 28395-28402.

- Boros LG, Cascante M, Lee WN. 2002. Metabolic profiling of cell growth and death in cancer: applications in drug discovery. *Drug Discov Today* 7: 364-372.
- Bulotta A, Perfetti R, Hui H, Boros LG. 2003. GLP-1 stimulates glucose-derived de novo fatty acid synthesis and chain elongation during cell differentiation and insulin release. *J Lipid Res* 44: 1559-1565.
- Cascante M, Boros LG, Comin-Anduix B, de Atauri P, Centelles JJ, et al. 2002. Metabolic control analysis in drug discovery and disease. *Nat Biotechnol* 20: 243-249.
- Cascante M, Franco R, Canela EI. 1989a. Use of implicit methods from general sensitivity theory to develop a systematic approach to metabolic control. I. Unbranched pathways. *Math Biosci* 94: 271-288.
- Cascante M, Franco R, Canela EI. 1989b. Use of implicit methods from general sensitivity theory to develop a systematic approach to metabolic control. II. Complex systems. *Math Biosci* 94: 289-309.
- Chih C-P, Lipton P, Roberts EL. 2001. Do active cerebral neurons really use lactate rather than glucose? *Trends Neurosci* 24: 573-578.
- Curto R, Voit EO, Cascante M. 1998. Analysis of abnormalities in purine metabolism leading to gout and to neurological dysfunctions in man. *Biochem J* 329: 477-487.
- Curto R, Voit EO, Sorribas A, Cascante M. 1997. Validation and steady-state analysis of a power-law model of purine metabolism in man. *Biochem J* 324: 761-775.
- Danial NN, Gramm CF, Scorrano L, Zhang CY, Krauss S, et al. 2003. BAD and glucokinase reside in a mitochondrial complex that integrates glycolysis and apoptosis. *Nature* 424: 952-956.
- Elias CF, Kelly JF, Lee CE, Ahima RS, Drucker DJ, et al. 2000. Chemical characterization of leptin-activated neurons in the rat brain. *J Comp Neurol* 423: 261-281.
- Fell D. 1997. *Understanding the control of metabolism*. Portland Press, Oxford.
- Frank PM. 1978. *Introduction to system sensitivity theory*. New York: Academic Press.
- Frazier ME, Johnson GM, Thomassen DG, Oliver CE, Patrinos A. 2003. Realizing the potential of the genome revolution: the genomes to life program. *Science* 300: 290-293.
- Gavin AC, Bosche M, Krause R, Grandi P, Marzioch M, et al. 2002. Functional organization of the yeast proteome by systematic analysis of protein complexes. *Nature* 415: 141-147.
- Giersch C. 1988. Control analysis of metabolic networks. 1. Homogeneous functions and the summation theorems for control coefficients. *Eur J Biochem* 174: 509-513.
- Hellerstein MK. 2003. In vivo measurement of fluxes through metabolic pathways: The missing link in functional genomics and pharmaceutical research. *Annu Rev Nutr* 23: 379-402.
- Huang S. 2002. Rational drug discovery: what can we learn from regulatory networks? *Drug Discov Today* 7: S163-S169.
- Huang TW, Tien AC, Huang WS, Lee YC, Peng CL, et al. 2004. POINT: a database for the prediction of protein-protein interactions based on the orthologous interactome. *Bioinformatics* 20: 3273-3276.
- Kacser H, Burns JA. 1973. The control of flux. *Symp Soc Exp Biol* 27: 65-104.
- Kacser H, Burns JA. 1995. The control of flux. *Biochem Soc Trans* 23: 341-366.
- Lee WN, Boros LG, Puigjaner J, Bassilian S, Lim S, et al. 1998. Mass isotopomer study of the nonoxidative pathways of the pentose cycle with [1,2-¹³C]glucose. *Am J Physiol* 274: E843-E851.
- Lee W-NP, Edmond J, Bassilian S, Morrow JW. 1996. Mass isotopomer study of glutamine oxidation and synthesis in primary culture of astrocytes. *Dev Neurosci* 18: 469-477.
- Lemeshko VV. 2002. Model of the outer membrane potential generation by the inner membrane of mitochondria. *Biophys J* 82: 684-692.
- Li J, Ning Y, Hedley W, Saunders B, Chen Y, et al. 2002. The Molecule Pages database. *Nature* 420: 716-717.
- Mazat JP, Rossignol R, Malgat M, Rocher C, Faustin B, et al. 2001. What do mitochondrial diseases teach us about normal mitochondrial functions ... that we already knew: threshold expression of mitochondrial defects. *Biochim Biophys Acta* 1504: 20-30.
- Merle M, Martin M, Villegier A, Canioni P. 1996. Mathematical modelling of the citric acid cycle for the analysis of glutamine isotopomers from cerebellar astrocytes incubated with [1-(¹³C)]glucose. *Eur J Biochem* 239: 742-751.
- Noble D. 2002. The rise of computational biology. *Nat Rev* 3: 460-463.
- Ockner RK. 2004. *Integration of metabolism, energetics, and signal transduction*. New York: Kluwer Academic/Plenum Publishers.
- Oltvai ZN, Barabasi AL. 2002. Systems biology. Life's complexity pyramid. *Science* 298: 763-764.
- Orosz F, Vertessy BG, Hollan S, Horanyi M, Ovadi J. 1996. Triosephosphate isomerase deficiency: predictions and facts. *J Theor Biol* 182: 437-447.
- Papin JA, Price ND, Wiback SJ, Fell DA, Palsson BO. 2003. Metabolic pathways in the post-genome era. *Trends Biochem Sci* 28: 250-258.
- Perry T, Haughey NJ, Mattson MP, Egan JM, Greig NH. 2002. Protection and reversal of excitotoxic neuronal damage by glucagon-like peptide-1 and exendin-4. *J Pharmacol Exp Ther* 302: 881-888.
- Phelps TJ, Palumbo AV, Beliaev AS. 2002. Metabolomics and microarrays for improved understanding of phenotypic

- characteristics controlled by both genomics and environmental constraints. *Curr Opin Biotechnol* 13: 20-24.
- Reder C. 1988. Metabolic control theory: a structural approach. *J Theor Biol* 135: 175-201.
- Repiso A, Boren J, Ortega F, Pujades A, Centelles J, et al. 2002. Triose-phosphate isomerase deficiency. Genetic, enzymatic and metabolic characterization of a new case from Spain. *Haematologica* 87: ECR12.
- Sabaté L, Franco R, Canela EI, Centelles JJ, Cascante M. 1995. A model of the pentose phosphate pathway in rat liver cells. *Mol Cell Biochem* 142: 9-17.
- Salter M, Knowles RG, Pogson CI. 1994. Metabolic control. *Essays Biochem* 28: 1-12.
- Savageau M. 1976. Biochemical system analysis. A study of function and design in molecular biology. Reading: Addison-Wesley.
- Schmidt CW. 2004. Metabolomics: what's happening downstream of DNA. *Environ Health Perspect* 112: A410-A415.
- Schuster R, Holzhutter HG. 1995. Use of mathematical models for predicting the metabolic effect of large-scale enzyme activity alterations. Application to enzyme deficiencies of red blood cells. *Eur J Biochem* 229: 403-418.
- Selivanov VA, Puigjaner J, Sillero A, Centelles JJ, Ramos-Montoya A, et al. 2004. An optimized algorithm for flux estimation from isotopomer distribution in glucose metabolites. *Bioinformatics* 20: 3387-3397.
- Shimabukuro M, Wang MY, Zhou YT, Newgard CB, Unger RH. 1998. Protection against lipoapoptosis of beta cells through leptin-dependent maintenance of Bcl-2 expression. *Proc Natl Acad Sci USA* 95: 9558-9561.
- Turton MD, O'Shea D, Gunn I, Beak SA, Edwards CM, et al. 1996. A role for glucagon-like peptide-1 in the central regulation of feeding. *Nature* 379: 69-72.
- van Winden W, Verheijen P, Heijnen S. 2001. Possible pitfalls of flux calculations based on ¹³C-labeling. *Metab Eng* 3: 151-162.
- Velho G, Petersen KF, Perseghin G, Hwang JH, Rothman DL, et al. 1996. Impaired hepatic glycogen synthesis in glucokinase-deficient (MODY-2) subjects. *J Clin Invest* 98: 1755-1761.
- Voit EO. 2000. Computational analysis of biochemical systems. Cambridge: Cambridge University Press.
- Yao T. 2002. Bioinformatics for the genomic sciences and towards systems biology. Japanese activities in the post-genome era. *Prog Biophys Mol Biol* 80: 23-42.



8.3 Modeling of Electron Transport: Implications to Mitochondrial Diseases

J.-P. Mazat · M. Beurton-Aimar · B. Faustin · T. Letellier · M. Malgat · C. Nazaret · R. Rossignol

<i>1 Introduction: Why a Model and Which Model(s)?</i>	<i>878</i>
<i>2 Metabolic Control Analysis—A Rapid Overview</i>	<i>878</i>
<i>3 Threshold in the Expression of Oxidative Phosphorylation Deficiencies</i>	<i>880</i>
<i>4 Tissue Specificity in the Expression of mtDNA Mutations</i>	<i>881</i>
<i>5 Electron Transport Models</i>	<i>882</i>
<i>6 Conclusion</i>	<i>884</i>

1 Introduction: Why a Model and Which Model(s)?

Electron transport and more generally bioenergetic metabolism in mitochondria (involving TCA cycle, β -oxidation of fatty acids, respiratory chain, and ATP-synthesis machinery) is a complex integrated system. It involves a great number of parameters and variables that the human mind has difficulty tackling simultaneously in an intuitive way. For this reason, theoretical models are useful to interpret experimental results, for instance, measured fluxes and distribution of carbon isotopes.

The analysis of the structure of metabolic networks and of their sensitivity toward perturbations is also an important point, which is the field of metabolic control analysis (MCA) described in [Sect. 2](#). This theory leads to important consequences concerning the phenotypic expression of fluxes as a function of the activity of a given step. One of these consequences is the existence of a threshold in the phenotypic expression of enzymatic deficiencies described in [Sect. 3](#). Control coefficients and threshold value measurements in different (neuronal) tissues evidence large differences, supporting the tissue specificity observed in mitochondrial bioenergetics described in [Sect. 4](#). In [Sect. 5](#), we describe the models of mitochondrial bioenergetic metabolism developed till now, and we conclude by approaching the problem of mitochondrial diseases with the help of models.

2 Metabolic Control Analysis—A Rapid Overview

It is probably in the field of oxidative phosphorylation that MCA (Kacser and Burns, 1973; Heinrich and Rapoport, 1974; Reder, 1988; see Fell (1997) for a review) showed for the first time its full possibility of prediction and explanation. At that time, researchers were arguing over the step (target) that controlled oxidative phosphorylation and energy production. It was MCA which showed that the control of oxidative phosphorylation could be shared among several steps; this was then experimentally demonstrated by Tager's group in Amsterdam (Groen et al., 1982) and at the same time by Kunz's group in Magdeburg (Bohnsack et al., 1982; Gellerich et al., 1983; Tager et al., 1983), and later by our group in yeast (Mazat et al., 1986) and rat muscle (Letellier et al., 1993).

It is beyond the scope of this chapter to detail MCA. Several reviews on the subject can be found, especially in Fell (1997) and Heinrich and Schuster (1996), and a simple presentation in Mazat and Jean-Bart (1988). Let us just say that a central parameter in MCA is the control coefficient of a step i (with the rate function v_i) on a flux F : $C_{v_i}^F$; it quantitatively expresses the effects on a flux of a perturbation of the step i . For instance, a control coefficient of 0.1 for the complex IV of oxidative phosphorylation means that a change of 10% of the activity of this complex will only entail a change of 1% in the respiratory rate; in other words one can write

$$\Delta F = C_{v_i}^F \cdot \Delta v_i \quad (1)$$

The validity of this equation is restricted to the linear neighborhood of the steady state, but as we will see later ([Figure 8.3-1](#)), this neighborhood can extend rather widely from the steady state itself.

Eq. (1) is in the same as the theoretical definition of control coefficient and an experimental way to assess the value of control coefficients, simply by measuring the variation of a flux as a result of the variations of a step, which can be experimentally performed (see [Figure 8.3-1](#)).

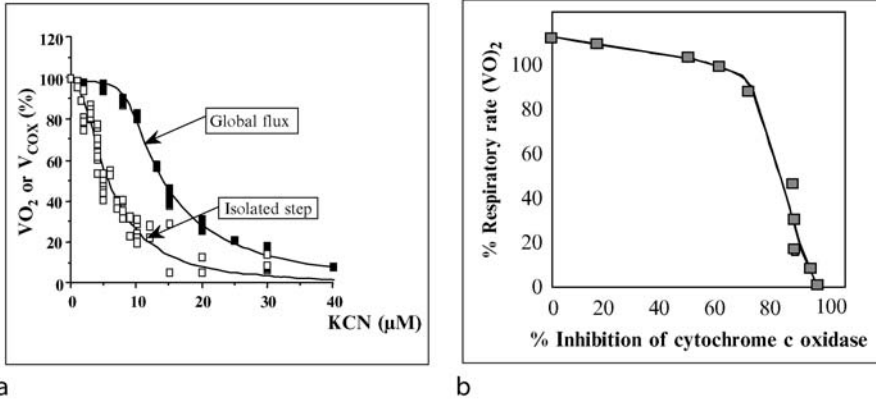
A very important consequence of the definition of control coefficient is the derivation of the summation theorem, (see Kacser and Burns (1973); Heinrich and Rapoport (1974) for the first expression in various peculiar cases; Reder (1988) for the general demonstration), which states that in a metabolic network, the sum of the flux control coefficients of every step of the network on any given flux is equal to one.

$$\sum C_{v_i}^F = 1 \quad (2)$$

This result has been largely confirmed experimentally as shown in [Table 8.3-1](#). This table also shows that the flux control is shared among different steps, definitely ending the dogma of a unique limiting step, which, being the target of regulatory signals, would direct the flux through oxidative phosphorylation.

Figure 8.3-1

(a) KCN inhibition of respiratory rate (*full square*) and of cytochrome *c* oxidase activity (*open square*) using ascorbate/TMPD as substrate (TMPD is *N,N,N',N'*-tetramethyl-*p*-phenylenediamine) and recording oxidation of reduced cytochrome *c* at 550 nm. (b) Respiratory rate as a function of cytochrome *c* oxidase inhibition. The points are the means of the data in [Figure 8.3-1a](#) corresponding to the same KCN concentrations. Adapted from Letellier T, Heinrich R, Malgat M and Mazat J-P, 1994, *Biochemical Journal*, 302, pp 171-174. (c) the Biochemical Society


Table 8.3-1

Control coefficient of oxidative phosphorylation in rat muscle and brain mitochondria (adapted from Rossignol et al. (2000))

Complexes	Cplx I	Cplx III	Cplx IV	ATP synthase	ANT	P_i carrier	Pyruvate carrier	Σ
Muscle	0.13 ± 0.03	0.22 ± 0.05	0.2 ± 0.04	0.1 ± 0.04	0.08 ± 0.03	0.08 ± 0.03	0.2 ± 0.08	1.02
Brain	0.25 ± 0.05	0.02 ± 0.02	0.02 ± 0.01	0.26 ± 0.05	0.08 ± 0.03	0.26 ± 0.05	0.26 ± 0.06	1.16

In addition, because many control coefficients are positive, Eq. (2) implies that, in these conditions, most of them must have low values, which is also largely experimentally confirmed with few exceptions (this is not a theoretical obligation); it means that the fluxes are—fortunately—not very sensitive to variations in individual enzyme activities. In other words, most of the enzymes in metabolic networks will appear as if they were in large excess, and this is an inescapable consequence of the low control coefficient values as recognized by Kacser and Burns (1980). This implies that significant changes in the oxidative phosphorylation rate have to be mediated through changes in several (if not all) of its individual steps (Fell, 1998; Korzeniewsky, 2000).

The summation theorem also implies that the distribution of flux control between the different steps of a network can vary when the steady state is changed according to a change in physiological conditions (or experimental conditions). These changes can be due to the ATP demand (rest to exercise transition for instance) or to the utilization of different respiratory substrates for example. We come back to this point in [Sect. 4](#).

Of course, the values of the flux also depend upon the rate function of the individual steps, as described in the theoretical model (see [Sect. 5](#)). In the framework of MCA, this dependence is expressed as a function of the so-called “elasticity,” which is the local expression of the rate dependence upon the

metabolites around the steady state. Control coefficients and elasticities are linked by the “connectivity theorem,” which is not described in this paper (see Mazat and Jean-Bart (1988); Heinrich and Schuster (1996); Fell (1997) for further reading on MCA).

3 Threshold in the Expression of Oxidative Phosphorylation Deficiencies

An important characteristic of mitochondrial genetics, besides maternal inheritance, is the possible heteroplasmy of mitochondrial DNA (mtDNA) in cells. The heteroplasmy of mtDNA arises from the fact that a mitochondrion contains, on average, 2–10 mtDNA molecules and that a cell may contain hundreds of mitochondria; it means that a cell may host thousands of mtDNA molecules and therefore thousands of copies of the few mtDNA genes. This is in great contrast with nuclear genes coding for mitochondrial proteins; it presumably necessitates complex regulations to assemble respiratory complexes that are built from proteins coded by both mtDNA and nuclear DNA. In addition, when an mtDNA mutation is present, not all mtDNA molecules necessarily carry the mutation so that there could exist a mixture (in the cell and maybe inside mitochondria) of mutated and normal mtDNA; the ratio of mutated mtDNA over total mtDNA is called heteroplasmy (of mtDNA in a cell). Associated with the great number of mtDNA per cell, one can understand that the heteroplasmy, which is not necessarily the same from one cell to the other, may vary continuously between 0% and 100%. The question then naturally arises: “Is the expression of a mutation proportional to the degree of heteroplasmy?”

The answer is no. In the case of null mtDNA mutations, it rapidly appeared that it is usually necessary to have a high degree of heteroplasmy (sometimes more than 90%) in order to observe the clinical signs of mitochondrial disease. In other words, when the respiration or ATP synthesis flux is recorded as a function of mtDNA heteroplasmy or as a function of the residual activity (or the inhibition as in [Figure 8.3-1b](#)) of a complex, a very slow decrease (or no decrease at all) is observed until a threshold after which the flux rapidly collapses when the mutated mtDNA amounts to 100%, in which case the activity of the complex vanishes (see [Figure 8.3-1b](#)).

Attardi’s group (Hayashi, 1991; Chomyn et al., 1992) demonstrated that in the case of the mutation MELAS (mitochondrial encephalopathy, lactic acidosis, and stroke-like episodes, mutation 3243) 10% or perhaps less of wild-type mtDNA was enough to sustain a normal respiratory rate. In 1986, Wallace had already described this phenomenon for a mutation located in the mitochondrial 16S RNA-coding gene conferring chloramphenicol resistance (Wallace, 1986, 1992). In MERRF syndrome (myoclonic epilepsy with ragged red fibers), the complete range of phenotypic and biochemical variations from normal to severely affected was found in individuals carrying between 27% and 2% wild-type mtDNA (Shoffner, 1990). In this case, a small percentage of normal mtDNA also appeared to be enough to maintain a normal phenotype. Porteous et al. (1998) built a series of cybrids (enucleated cells fused with pathological cells) containing 0–86% of a deleted mtDNA (Δ mtDNA) associated with chronic progressive external ophthalmoplegia (CPEO). In cybrids containing less than 50–55% of Δ mtDNA, the mitochondrial transmembrane potential, the rate of ATP synthesis, and the ATP/ADP ratio were the same as in the cybrids with wild-type mtDNA. However, once the proportion of Δ mtDNA exceeded this threshold, these bioenergetic parameters decreased. These observations are reviewed in Rossignol et al. (2003).

Oxidative phosphorylation deficiencies have also been experimentally simulated with specific inhibitors (Letellier et al., 1994). In the latter case, it is easy to explain the existence of a threshold (in the flux as a function of a respiratory complex inhibition), and this is well illustrated in [Figure 8.3-1](#). The ratio of the initial slopes of the two curves of [Figure 8.3-1a](#) is the control coefficient of cytochrome *c* oxidase on oxygen uptake or on ATP flux. This ratio also appears as the initial slope on the “threshold curve” ([Figure 8.3-1b](#)); the control coefficient is the variation of the flux divided by the corresponding change in the rate. In this case the value of the control coefficient is 0.2 ± 0.04 (Rossignol et al., 2000), which leads to a slow decrease of the flux as a function of cytochrome *c* oxidase inhibition; in other words, one cannot escape a plateau phase when the control coefficient is low, which is the case most of the time (see, however, exceptions in Vilani et al. (1997), (1998)). The length of the plateau is theoretically unpredictable but practically there is a rather good negative correlation between the control coefficient and the threshold

values: the lower the control coefficient, the greater the threshold value (Mazat et al., 2001). As a matter of fact, the definition of the control coefficient is local, in the linear vicinity of the steady state, while the threshold characterization is more global; the threshold value indicates the lower limit of the linear domain around the steady state. We have experimentally described several “threshold curves” and found threshold values almost always greater than 50% (Rossignol et al., 1999).

4 Tissue Specificity in the Expression of mtDNA Mutations

An important consequence of the summation theorem, widely confirmed in experimental models, is that the control coefficients can vary according to the physiological steady state of the tissue. This is the reason why we undertook a systematic study of control coefficients and their associated thresholds of the seven steps of oxidative phosphorylation in five different tissues (Rossignol et al., 1999, 2000). In these experiments, we evidenced two groups of tissues, each characterized by similar thresholds and control coefficient values: muscle and heart on the one hand, which are more controlled by the respiratory chain, and kidney and brain on the other hand, which are more controlled by the ATP synthesis machinery (ATP synthase, P_i carrier, and ATP/ADP translocator). The liver can be associated with either one of these two groups according to the complex considered.

A characteristic of brain mitochondria is their high control coefficients and low threshold values for complex I, ATP synthase, pyruvate, and the P_i carrier (Rossignol et al., 1999). If the *in vivo* values were the same as those determined on isolated mitochondria, a 50% deficiency in complex I would not have any effect in muscle or in heart but would decrease by nearly 50% ATP synthesis in brain (Fig. 2, in Rossignol et al. (1999)). Of course the situation is more complex, because these determinations have been performed on rat brain homogenate. In nonsynaptic rat brain mitochondria, Davey and Clark (1996) demonstrated a control coefficient of 0.14 for complex I, 0.15 for complex III, and 0.24 for complex IV. They found high threshold values of 72%, 70%, and 60%, respectively. In a further work (Davey et al., 1997, 1998), they compared the control of nonsynaptic and synaptic rat brain mitochondria and reported large differences in activities, controls, and thresholds in nonsynaptosomal compared with synaptosomal mitochondria. We have shown with the help of simple models that such changes in controls and thresholds could be related to the sole changes in step activities (Mazat et al., 2000). These simulations illustrate that, *in vivo*, the flux control coefficients and the shape of the threshold curves depend upon the relative activities of the complexes and the differences in the sensitivity of the complexes to intermediate metabolites (elasticities).

We also observed that the “threshold curves” can present two kinds of shape, which we called type I and type II (Rossignol et al., 1999). Type I curves are characterized by a large plateau associated with a large, well-marked threshold (as in [Figure 8.3-1b](#)). In type II curves, a plateau is no longer apparent and a threshold is hardly detectable. The plateau of type I curves is due to an excess of enzyme capacity which has to be suppressed before an effect on the flux would be appreciable. In a sense, the length of the plateau is a measure of the excess of enzyme activity. In type II curves, the enzyme reserve is small and the curve only reflects the adjustment of the metabolites inside the network, which buffer the changes in the complex activity. As a matter of fact, type II curves correspond to the last part of type I curves beginning just before the threshold point.

The two types of curves can be observed for the same complex in the same tissue but for different respiratory substrates (Rossignol et al., 1999). Thus, a difference in respiratory substrates can also be a condition changing the shape of the threshold curves. Neuronal cells principally use glucose as an energetic substrate so that the main respiratory substrate for mitochondria will be pyruvate. However, it has been proposed (Pellerin, 2003; Pellerin and Magistretti, 2004) that a high rate of glycolysis in astrocytes might lead to lactate excretion, which is used as a respiratory substrate by the neighbor neurons via pyruvate formation (Astrocyte–Neuron Lactate Shuttle Hypothesis (ANLSH)). In this context, the variations in the expression of the monocarboxylate transporters MCT1, MCT2, and MCT4 play an important role, and a clear evidence of their regulation was demonstrated by Pellerin et al. (2005). Some authors however disagree with the ANLSH hypothesis and support the conventional hypothesis, which asserts that glucose is the

primary substrate for both neurons and astrocytes during neural activity (Chih and Roberts, 2003; see also Diemel and Cruz (2004); Hertz (2004) for discussion). Alternatively, ketone bodies can also be used.

We have shown that a change in respiratory substrate can also be associated with more profound changes in the amount of functional adenine nucleotide transporter (ANT) in muscle and brain but not in liver, kidney, and heart, presumably by recruiting inactive monomers of ANT to form active dimers or tetramers (Faustin et al., 2004).

Finally, it has to be emphasized that the well-described threshold in the flux as a function of enzyme or complex activity can be augmented by nonlinear dependences in transcription of mtDNA-encoded genes and then in translation (Rossignol et al., 2003). In some cases the amount of normal transcripts decreases less than the amount of wild-type genes, just as the amount of wild-type translated proteins compared with the amount of normal transcripts. (Beziat et al., 1993; Debise et al., 1993).

5 Electron Transport Models

Oxidative phosphorylation has been modeled in order to integrate all aspects, kinetic and thermodynamic, of the chemiosmotic theory (Mitchell, 1961). One of the first models was that of Chance and Williams' (1955 and 1956), demonstrating with an analog computer the transition from state 4 to 3 following the addition of ADP. The equations representing the respiratory chain were based on the chemical hypothesis of Slater and not on Mitchell's theory. Then Rottenberg and Westerhoff and van Dam developed a Non-Equilibrium Thermodynamic Model (NET-Model) involving linear dependence of the flux as a function of the thermodynamic forces (Rottenberg, 1979; Westerhoff and van Dam, 1987). In the framework of linear nonequilibrium thermodynamics, Stucki (1980a, b) described all the states of oxidative phosphorylation dynamics (state 4, state 3, uncoupled state, etc.) in terms of energy conversion with the use of phenomenological coefficients. He looked for the optimal efficiency of the system and for the maximal net rate of ATP synthesis and calculated the degree of coupling in these conditions. Even if one can argue that oxidative phosphorylation could be out of the linear domain around equilibrium, Stucki's description is simple and points out the fundamental parameters involved: degree of coupling, thermodynamic forces, rates, optimal efficiency, phenomenological stoichiometry, etc.

Models similar to Stucki's were derived by Pietrobon et al. (1982) and Pietrobon and Caplan (1985) to describe redox-driven proton pumps and ATP synthesis in mitochondria. These models were as a matter of fact kinetic models but with the calculation of thermodynamic parameters; this evidenced the relationships between kinetics and thermodynamics. They lead to the concept of "molecular slipping" for protons (as opposed to the leak). They emphasize that the "knowledge of the distance from equilibrium of the flow-controlling ranges of the forces (i.e., the ranges of approximate linearity) turns out to be crucial for the interpretation of thermodynamic parameters determined by manipulating one of the forces while the other remains constant, as well as for the interpretation of measurements of force ratios at static head" (Pietrobon and Caplan, 1985).

Wilson et al. (1977) proposed a model essentially based on cytochrome *c* oxidase as the only rate-limiting step, quantitatively describing respiratory control (state 4 to state 3 transition); they derived a steady-state rate expression "which fits the mitochondrial respiratory rate dependence on (1) the extra-mitochondrial $[ATP]/[ADP][P_i]$ ratio; (2) the level of reduction of cytochrome *c* (or the intramitochondrial $[NAD^+]/[NADH]$) at different $[ATP]/[ADP][P_i]$ values; (3) the pH of the suspending medium". Later Wilson et al. (1979) extended their model to include the dependence on oxygen tension.

Bohnsack (1981) was probably the first to derive a quantitative model involving nearly all the components of oxidative phosphorylation linked by algebraic relationships. With the help of this model, this group was able to show that the control of oxidative phosphorylation was shared by several steps (Bohnsack et al., 1982; Gellerich et al., 1983).

Holzhtütter (1985) also took all the components of oxidative phosphorylation into consideration but did so in a dynamic model based on ordinary differential equations applied to isolated rat liver mitochondria. He was able to predict the overshoot kinetics of ΔpH , which appears when mitochondria are reoxygenated, and also that in state 3 the control is shared among the hydrogen supply, the respiratory chain, the ANT, and the proton leak to almost the same extent.

Korzeniewski and Froncisz (1991) then developed a more comprehensive model also based on ordinary differential equations, which was applied to isolated mitochondria or to intact tissues (muscle, heart, and liver). The model was used to calculate the flux control coefficient of oxidative phosphorylation (Korzeniewski and Froncisz, 1992), to fit the threshold curves in muscle (Korzeniewski and Mazat, 1996), to predict the shape of threshold curves at low oxygen pressure (Korzeniewski and Mazat, 1996), and to study the transition from rest to intensive work in muscle (Korzeniewski, 2000). It led to the concept of parallel activation. This model has also been used by Korzeniewski et al. (2001) to compare the threshold curves obtained with mitochondrial or nuclear DNA mutations.

All the previous models, based on ordinary differential equations, necessarily assumed that the mitochondrial compartments (matrix, inner membrane, and intermembrane space) were homogeneous. One of the first simulations to take into account the organization of the space for energy transduction from mitochondria to the place where ATP is used was Aliev and Saks's model (1997) on heart bioenergetics. This model, based on ordinary and partial differential equations, was carried further by Vendelin et al. (2000, 2004). It took into account the presence of creatine and adenylate kinase both in the intermembrane space and in cytosol. They ensure the conversion of ATP synthesized in mitochondria to phosphocreatine that diffuses into the cytosol where it is converted back to ATP and used; a backward diffusion of creatine closes the functional cycle. This model is described in *Chapter 8.1* with an attempt to transpose the heart model to brain energy metabolism (*Sect. 8.1.3*). The phosphocreatine/creatine kinase/creatine system is also present in brain. This is the first attempt to develop a model directed toward brain energy metabolism.

More recently, Cortassa et al. (2003) developed an "integrated model of cardiac mitochondrial energy metabolism and calcium dynamics." It includes a model of the TCA cycle, the transporters of Ca^{2+} across the mitochondrial inner membrane, and the regulation of dehydrogenases by Ca^{2+} . This model matches the supply of mitochondrial energy with the cellular demand through the variations in intracellular and intramitochondrial Ca^{2+} .

With a "systems biology" approach and in the framework of the e-cell project, Yugi and Tomita (2003) built a model of 58 reactions linking 117 metabolites. They found 286 out of 471 kinetic parameters in 45 articles. The model involves the respiratory chain, the TCA cycle, the β -oxidation of fatty acids, and the metabolite carriers of the inner mitochondrial membrane. They calculated the time course of enzyme activities and metabolite concentrations. One can criticize this model, like several others, for integrating too vast a set of parameters from different origins (human, bovine, pig, rabbit, and rat) and different tissues (heart, liver, etc.). However, one also has to recognize that it is difficult not to begin this way. We have to add that a four step scale of confidence is given which allows the user to take the results obtained from the model with care when necessary.

Palsson's group also tackles the modeling of mitochondrial energy metabolism from the structural and linear programming point of view. Ramakrishna et al. (2001) studied the constraints imposed by the stoichiometry of biochemical reactions, especially the maintenance of an NADH steady state. Flux balance analysis (FBA) was used to characterize the optimal flux distributions for maximal ATP production. The model includes glycolysis, TCA cycle, lactate production or use, and β -oxidation of fatty acids. The authors also use the representation of "phenotype phase plane" to better understand the optimal situation (for maximal ATP production) when two substrates are used simultaneously and the quantity of oxygen is limiting. Using FBA, they also characterize metabolic behavior in some genetic diseases, particularly the secretion of TCA cycle metabolites as observed in clinical studies of mitochondrial pathologies. However, this study was performed under the assumption that ATP synthesis was maximal, which is not necessarily the case. Furthermore, these authors did not take into account the rate laws of the different steps of the mitochondrial network.

In a subsequent paper from the same group, Vo et al. (2004) reconstructed mitochondrial metabolism in human cardiomyocytes based on both proteomic and biochemical data. Their metabolic network involved 189 reactions and 230 metabolites. FBA was applied to calculate optimal flux according to three separate objective functions: ATP production, heme biosynthesis, and phospholipid biosynthesis. In a more recent paper (Thiele et al., 2005), the group used linear programming and uniform random sampling to identify steady states of mitochondrial metabolism that "were consistent with the imposed physicochemical constraints and available experimental data." They applied this analysis to mitochondrial metabolism in

diabetes, ischemia, and diet. Once more, the results of these studies show the structural constraints, which have to be satisfied, but they do not take into account the reaction kinetics, which can profoundly modify the theoretical optimal production.

These last attempts show the importance of adding to models of mitochondrial metabolism the rest of energy metabolism: glycolysis, lactate metabolism, as well as amino acid metabolism, inducing new stoichiometric constraints. The main stoichiometry constraint is probably the reoxidation of NADH as shown in mitochondrial diseases. It has to be noticed that all these models, except that of Saks et al. in this handbook (*Chapter 8.1*), do not deal with brain tissue(s). Modeling the unique aspects of brain mitochondrial metabolism is a challenge; the predictions introduced by the possible interplay between astrocytes and neurons (ANLSH hypothesis) will certainly need to be taken into account in such models.

Though it is not within the scope of our study, we would like to emphasize that TCA cycle in neurological cell cultures has been modeled by Canioni's group (Portais et al., 1993; Merle et al., 1996) demonstrating the importance of pyruvate carboxylase versus pyruvate dehydrogenase activities; this model was applied to their data using NMR recording of ^{13}C -glucose metabolism.

6 Conclusion

In conclusion, we would like to focus on metabolic models in the understanding of mitochondrial diseases. Mitochondrial diseases are a group of pathologies which are characterized by the fact that several unrelated tissues can be affected leading to an unexpected association of symptoms among which neurological symptoms are always present at least some time after the onset of the disease (Di Mauro, 1985; Munnich, 1996; Wallace, 1992, 1993; Grossman and Shoubridge, 1996; Lightowers, 1997). This is presumably due to the fact that the brain and more generally neurological tissues depend closely on a constant supply of energy, a great part of which is delivered by mitochondria. This is not the only role of mitochondria in brain as in many tissues; NADH reoxidation is probably as important as ATP production. The NADH produced when neurological cells form pyruvate necessarily has to be reoxidized. This is well demonstrated by a study of stoichiometry constraints (Ramakrishna et al., 2001; Vo et al., 2004).

The study of models also points out the importance of the respiratory substrates used. Indeed the mitochondria of different tissues preferentially use different substrates and this choice confers specific characteristics on them, for instance, a different sensitivity toward some respiratory complex deficiencies (see Rossignol et al. (1999); Faustin et al. (2004)).

These properties are well described in the framework of MCA. MCA will not explain all the particular features of the expression of mutations affecting mitochondria, but it gives a framework into which these features can be logically integrated and discussed and in some cases rejected (Letellier et al., 1998). The analysis of the expression of mutations affecting mitochondrial metabolism using MCA allows one to understand several, at first sight paradoxical, properties.

First, the fact that in many cases there is not a linear correlation between the degree of the mutation (heteroplasmy in the case of mtDNA mutations) and the decrease in the fluxes. Second, MCA explains particularly well the concept of threshold, which is now well recognized in the expression of mitochondrial pathogenic mutations. It should be noticed that this concept of threshold, associated with low values of control coefficient, is general in metabolism as stressed by Kacser and Burns (1980). Third, since we know from MCA that control coefficients can be modulated by the steady state and the relative amount of mitochondrial activities in different tissues, we are not surprised that the pattern of threshold curves will be different in different tissues, and thus that the same mutation will affect different tissues in a different way.

One can imagine that the control coefficients in *in vivo* functioning cells are different from those measured in isolated mitochondria. However, if MCA applies to the *in vivo* situation, the main results of the studies on isolated mitochondria remain, i.e., the control is shared among different steps associated with different thresholds, and there are large inescapable enzymatic reserves of most of the steps in oxidative phosphorylation.

MCA demonstrates that if fluxes vary only slightly, even sometimes, for rather large changes in the step activities, it is not the case for intermediate metabolites. Their concentrations vary markedly in order to maintain steady states. In the case of oxidative phosphorylation, the accumulation of some intermediate species may generate free radicals amplifying the deleterious effects of the genetic defects.

From a more general point of view, modeling now has to integrate the huge amount of knowledge accumulated from genome sequencing and proteome analysis particularly of mitochondrial proteomes of different tissues (Taylor et al., 2003). It is also clear that a model (or models) of mitochondrial metabolism specifically devoted to neurological tissues and to their metabolic interplay has to be developed.

Acknowledgments

This work was supported by AFM and FRM and the Région Aquitaine. We thank Ms M.-N. Grangeon for correcting the English.

References

- Aliev MK, Saks VA. 1997. Compartmentalized energy transfer in cardiomyocytes: Use of mathematical modeling for analysis of in vivo regulation of respiration. *Biophys J* 73: 428-445.
- Beziat F, Morel F, Volz-Lingenhol A, Saint Paul N, Alziari S. 1993. Mitochondrial genome expression in a mutant strain of *D. subobscura*, an animal model for large-scale mtDNA deletion. *Nucleic Acids Res* 21: 387-392.
- Bohnsack R. 1981. Control of energy transformation of mitochondria. Analysis by a quantitative model. *Biochim Biophys Acta* 634: 203-218.
- Bohnsack R, Küster U, Letko G. 1982. Rate-controlling steps of oxidative phosphorylation in rat liver mitochondria. A synoptic approach of model and experiment. *Biochim Biophys Acta* 680: 271-280. The use of MCA to demonstrate for the first time that the control of oxidative phosphorylation is shared, ending in this way a long-standing riddle concerning the determination of the "controlling step"; see also Groen et al. (1982), who were very active in this field. These two articles profoundly changed the way to apprehend the regulation of oxidative phosphorylation and even the design of experiments in this field.
- Chance B, Williams GR. 1955. Respiration enzymes in oxidative phosphorylation. 1. Kinetics of oxygen utilization. *J Biol Chem* 217: 383-393.
- Chance B, Williams GR. 1956. The respiratory chain and oxidative phosphorylation. *Adv Enzymol* 17: 65-134.
- Chih C-P, Roberts EL Jr. 2003. Energy substrates for neurons during neural activity: A critical review of the astrocyte-neuron lactate shuttle hypothesis. *J Cereb Blood Flow Metab* 23: 1263-1281.
- Chomyn A, Martinuzzi A, Yoneda M, Daga A, Hurko O, et al. 1992. MELAS mutation in mtDNA-binding site for transcription termination factor causes defects in protein synthesis and in respiration but no change in levels of upstream and downstream mature transcripts. *Proc Natl Acad Sci USA* 89: 4221-4225.
- Cortassa S, Aon MA, Marban E, Winslow RL, O'Rourke B. 2003. An integrated model of cardiac mitochondrial energy metabolism and calcium dynamics. *Biophys J* 84: 2734-2755.
- Davey GP, Canevari L, Clark JB. 1997. Threshold effect in synaptosomal and nonsynaptic mitochondria from hippocampal CA1 and paramedian neocortex brain regions. *J Neurochem* 69: 2564-2570.
- Davey GP, Clark JB. 1996. Threshold effects and control of oxidative phosphorylation in nonsynaptic rat brain mitochondria. *J Neurochem* 66: 1617-1624.
- Davey GP, Penchen S, Clark JB. 1998. Energy thresholds in brain mitochondria. Potential involvement in neurodegeneration. *J Biol Chem* 273: 12753-12757.
- Debise R, Touraille S, Durand R, Alziari S. 1993. Biochemical consequences of a large deletion in the mitochondrial genome of a *Drosophila subobscura* strain. *Biochem Biophys Res Commun* 196: 355-362.
- Dienel GA, Cruz NF. 2004. Nutrition during brain activation: Does cell-to-cell lactate shuttling contribute significantly to sweet and sour food for thought? *Neurochem Int* 45: 321-351.
- Di Mauro S, Bonilla E, Zeviani M, Walton J, de Vivo DC. 1985. Mitochondrial myopathies. *Ann Neurol* 17: 521-538.
- Faustin B, Rossignol R, Rocher C, Bénard G, Malgat M, et al. 2004. Mobilization of adenine nucleotide translocators as molecular bases of the biochemical threshold effect observed in mitochondrial diseases. *J Biol Chem* 279: 20411-20421.

- Fell DA. 1997. Understanding the control of metabolism. Portland Press, Oxford. A very understandable presentation of MCA.
- Fell DA. 1998. Increasing the flux in metabolic pathways: A metabolic control analysis perspective. *Biotechnol Bioeng* 58: 121-124.
- Gellerich FN, Bohnensack R, Kunz W. 1983. Control of mitochondrial respiration. The contribution of the adenine nucleotide translocator depends on the ATP- and ADP-consuming enzymes. *Biochim Biophys Acta* 722: 381-391.
- Groen AK, Wanders RJA, Westerhoff HV, Van der Meer R, Tager JM. 1982. Quantification of the contribution of various steps to the control of mitochondrial respiration. *J Biol Chem* 257: 2754-2757. An important paper. See the comments in Bohnensack et al. (1982).
- Grossman LI, Shoubridge EA. 1996. Mitochondrial genetics and human disease. *Bioessays* 18: 983-991.
- Hayashi JI, Ohta S, Kikuchi A, Takemitsu M, Goto Y, et al. 1991. Introduction of disease-related mitochondrial DNA deletions into HeLa cells lacking mitochondrial DNA results in mitochondrial dysfunction. *Proc Natl Acad Sci USA* 88: 10614-10618.
- Heinrich R, Rapoport TA. 1974. A linear steady-state treatment of enzymatic chains. General properties, control, and effector strength. *Eur J Biochem* 42: 89-95. One of the two founding papers of MCA.
- Heinrich R, Schuster S. 1996. The regulation of cellular systems. Chapman and Hall. New-York: A very understandable presentation of MCA among other modes of modeling.
- Hertz L. 2004. The astrocyte–neuron lactate shuttle: A challenge of a challenge. *J Cereb Blood Flow Metab* 24: 1241-1248.
- Holzhütter H-G, Henke W, Dubiel W, Gerber G. 1985. A mathematical model to study short-term regulation of mitochondrial energy transduction. *Biochim Biophys Acta* 810: 252-268.
- Kacser H, Burns JA. 1973. The control of flux. *Symp Soc Exp Biol* 32: 65-104. The other founding paper of MCA.
- Kacser H, Burns JA. 1980. The molecular basis of dominance. *Genetics* 97: 639-666. A seminal paper answering the long-standing riddle concerning the equivalence of heterozygote with the normal homozygote.
- Korzeniewski B. 2000. Regulation of ATP supply in mammalian skeletal muscle during resting state→intensive work transition. *Biophys Chem* 83: 19-34.
- Korzeniewski B, Froncisz W. 1991. An extended dynamic model of oxidative phosphorylation. *Biochim Biophys Acta* 1060: 210-223.
- Korzeniewski B, Froncisz W. 1992. Theoretical studies on the control of the oxidative phosphorylation system. *Biochim Biophys Acta* 1102: 67-75.
- Korzeniewski B, Malgat M, Letellier T, Mazat J-P. 2001. Effect of binary mitochondria heteroplasmy on respiration and ATP synthesis: Implications to mitochondrial diseases. *Biochem J* 357: 835-842.
- Korzeniewski B, Mazat J-P. 1996. Theoretical studies on the control of oxidative phosphorylation in muscle mitochondria at different energy demands and oxygen concentrations. *Acta Biotheor* 44: 263-269.
- Letellier T, Heinrich R, Malgat M, Mazat J-P. 1994. The kinetic basis of the threshold effects observed in mitochondrial diseases: A systemic approach. *Biochem J* 302: 171-174.
- Letellier T, Malgat M, Mazat J-P. 1993. Control of oxidative phosphorylation in rat muscle mitochondria. Implication to mitochondrial myopathies. *Biochim Biophys Acta* 1141: 58-64.
- Letellier T, Malgat M, Rossignol R, Mazat J-P. 1998. Metabolic control analysis and mitochondrial pathologies. *Mol Cell Biochem* 184: 409-417.
- Lightowers RN, Chinnery PF, Turnbull DM, Howell N. 1997. Mammalian mitochondrial genetics: Heredity, heteroplasmy, and disease. *Trends Genet* 13: 450-455.
- Mazat J-P, Jean-Bart E. 1988. How two steps can control a flux. *Biochem Educ* 16: 28-30.
- Mazat J-P, Jean Bart E, Rigoulet M, Guerin B. 1986. Control of oxidative phosphorylation: The role of phosphate transport. *Biochim Biophys Acta* 849: 7-15.
- Mazat J-P, Rossignol R, Malgat M, Letellier T. 2000. Simple models of threshold curves in the expression of inborn errors of metabolism: Application to some experimental observations. *Dev Neurosci* 22: 399-403.
- Mazat J-P, Rossignol R, Malgat M, Rocher C, Faustin B, et al. 2001. What do mitochondrial diseases teach us about normal mitochondrial functions that we already knew: Threshold expression of mitochondrial defects. *Biochim Biophys Acta* 1504: 20-30.
- Merle M, Martin M, Villegier A, Canioni P. 1996. Mathematical modeling of the citric acid cycle for the analysis of glutamine isotopomers from cerebellar astrocytes incubated with [^{13}C]glucose. *Eur J Biochem* 239: 742-751.
- Mitchell P. 1961. Coupling of phosphorylation to electron and hydrogen transfer by a chemiosmotic type of mechanism. *Nature* 191: 144-148.
- Munnich A, Rötig A, Chrétien D, Saudubray J-M, Cormier V, et al. 1996. Clinical presentations and laboratory investigations in respiratory chain deficiency. *Eur J Pediatr* 155: 262-274.
- Pellerin L. 2003. Lactate as a pivotal element in neuron–glia metabolic cooperation. *Neurochem Int* 43: 331-338.
- Pellerin L, Halestrap AP, Pierre K. 2005. Cellular and subcellular distribution of monocarboxylate transporters in culture brain cells and in adult brain. *J Neurosci Res* 79: 55-64.

- Pellerin L, Magistretti PJ. 2004. Neuroenergetics: Calling upon astrocytes to satisfy hungry neurons. *Neuroscientist* 10: 53-62.
- Pietrobon D, Caplan SR. 1985. Flow-force relationships for a six-state proton pump model: Intrinsic uncoupling, kinetic equivalence of input and output forces, and domain of approximate linearity. *Biochemistry* 24: 5764-5776.
- Pietrobon D, Zoratti M, Azzone GF, Stucki JW, Walz D. 1982. Nonequilibrium thermodynamic assessment of redox-driven H^+ pumps in mitochondria. *Eur J Biochem* 127: 483-494.
- Portais JC, Schuster R, Merle M, Canioni P. 1993. Metabolic flux determination in C6 glioma cells using carbon-13 distribution upon $[1-^{13}C]$ glucose incubation. *Eur J Biochem* 217: 457-468.
- Porteous WK, James AM, Sheard PW, Porteous CM, Packer MA, et al. 1998. Bioenergetic consequences of accumulating the common 4977-bp mitochondrial DNA deletion. *Eur J Biochem* 257: 192-201.
- Ramakrishna R, Edwards JS, McCulloch A, Palsson BO. 2001. Flux balance analysis of mitochondrial energy metabolism: Consequences of systemic stoichiometric constraints. *Am J Physiol Regulatory Integr Comp Physiol* 280: R695-R704.
- Reder C. 1988. Metabolic control theory: A structural approach. *J Theor Biol* 135: 175-201. The general development of the theory.
- Rossignol R, Faustin B, Rocher C, Malgat M, Mazat J-P, et al. 2003. Mitochondrial threshold effects. *Biochemical J (Review)* 370: 751-762.
- Rossignol R, Letellier T, Malgat M, Rocher C, Mazat J-P. 2000. Tissue variation in the control of oxidative phosphorylation: Implication for mitochondrial diseases. *Biochem J* 347: 45-53.
- Rossignol R, Malgat M, Mazat J-P, Letellier T. 1999. Threshold effect and tissue specificity. Implication for mitochondrial cytopathies. *J Biol Chem* 274: 33426-33432.
- Rottenberg H. 1979. Nonequilibrium thermodynamics of energy conversion in bioenergetics. *Biochim Biophys Acta* 549: 225-253.
- Shoffner JM, Lott MT, Lezza AM, Seibler P, Ballinger SW, et al. 1990. Myoclonic epilepsy and ragged-red fiber disease (MERRF) is associated with a mitochondrial DNA tRNA (Lys) mutation. *Cell* 61: 931-937.
- Stucki JW. 1980a. The thermodynamic buffer enzymes. *Eur J Biochem* 109: 257-267.
- Stucki JW. 1980b. The optimal efficiency and the economic degrees of coupling of oxidative phosphorylation. *Eur J Biochem* 109: 269-283.
- Tager JM, Wanders RJA, Groen AK, Kunz W, Bohnensack R, et al. 1983. Control of mitochondrial respiration. *FEBS Lett* 151: 1-9.
- Taylor SW, Fahy E, Zhang B, Glenn GM, Warnock DE, et al. 2003. Characterization of the human heart mitochondrial proteome. *Nat Biotechnol* 21: 281-286.
- Thiele I, Price ND, Vo TD, Palsson BO. 2005. Candidate metabolic network states in human mitochondria: Impact of diabetes, ischemia, and diet. *J Biol Chem* 280: 11683-11695.
- Vendelin M, Kongas O, Saks V. 2000. Regulation of mitochondrial respiration in heart cells analyzed by reaction-diffusion model of energy transfer. *Am J Physiol* 278: C747-C764.
- Vendelin M, Lemba M, Saks VA. 2004. Analysis of functional coupling: Mitochondrial creatine kinase and adenine nucleotide translocase. *Biophys J* 87: 696-713.
- Villani G, Attardi G. 1997. In vivo control of respiration by cytochrome *c* oxidase in wild-type and mitochondrial DNA mutation-carrying human cells. *Proc Natl Acad Sci USA* 94: 1166-1171.
- Villani G, Attardi G. 1998. Low reserve of cytochrome *c* oxidase capacity in vivo in the respiratory chain of a variety of human cell types. *J Biol Chem* 273: 31829-31836.
- Vo TD, Greenberg HJ, Palsson BO. 2004. Reconstruction and functional characterization of the human mitochondrial metabolic network based on proteomic and biochemical data. *J Biol Chem* 279: 39532-39540.
- Wallace DC. 1986. Mitotic segregation of mitochondrial DNA in human cell hybrids and expression of chloramphenicol resistance. *Somat Cell Mol Genet* 12: 41-49.
- Wallace DC. 1992. Diseases of the mitochondrial DNA. *Annu Rev Biochem* 61: 1175-1212.
- Wallace, DC. 1993. Mitochondrial diseases: Genotype versus phenotype. *Trends Genet* 9: 128-133.
- Westerhoff HV, van Dam K. 1987. *Thermodynamics and Control of Free-Energy Transduction*. Amsterdam: Elsevier.
- Wilson DF, Owen CS, Erecińska M. 1979. Quantitative dependence of mitochondrial oxidative phosphorylation on oxygen concentration: A mathematical model. *Arch Biochem Biophys* 195: 494-504.
- Wilson DF, Owen CS, Holian A. 1977. Control of mitochondrial respiration: A quantitative evaluation of the roles of cytochrome *c* and oxygen. *Arch Biochem Biophys* 182: 749-762.
- Yugi K, Tomita M. 2003. A general computational model of mitochondrial metabolism in a whole organelle scale. *Bioinformatics* 1: 1-2.

8.4 Metabolomics: Concepts and Potential Neuroscience Applications

B. S. Kristal · R. Kaddurah-Daouk · M. F. Beal · W. R. Matson

1	<i>Beyond the Dogma</i>	890
2	<i>Past as Prologue</i>	891
2.1	Single Metabolites	891
2.2	Pathways I: Tracers and Flux	891
2.3	Pathways II: Simultaneous Analysis of Pathways—The HD Example	892
3	<i>Metabolomics: Promises and Current Reality</i>	892
3.1	What Is Metabolomics: Theory	892
3.2	What Is Metabolomics: Practice	893
3.2.1	Toxicology	897
3.2.2	Functional Genomics	898
3.2.3	Biomarkers/Classifiers	899
3.2.4	Flux	899
3.2.5	Insights into Neurochemistry	900
3.3	What Is Metabolomics: Current Limitations	900
4	<i>Stepping Back and Looking Forward: How Might Metabolomics Influence Research in Neuroscience?</i>	901
4.1	Problems Related to Classification	902
4.2	Problems Related to Hypothesis Generation: Novel Hypotheses Arise from a Simultaneous View of the Forest and the Trees	902
4.3	Problems Related to Fundamental Scientific Understanding of Both Physiological and Pathophysiological Processes in the CNS	903
4.4	Problems Related to Clinical Practice	904
4.5	Drug Development	905
4.6	Diagnostics and Personalized Medicine	905
4.7	A Case in Point: Initial Studies in ALS	906
4.8	A Path to the Future?	906
4.9	More Information on Metabolomics	907
5	<i>Conclusion</i>	907

Abstract: Metabolomics—the -omics face of biochemistry—may be considered as a global approach to capturing and understanding the metabolic network of a biological system. Metabolomics expands and complements the data obtained from the other three major -omics fields—genomics, transcriptomics, and proteomics. Here, we discuss the ties between metabolomics and the fields of neuroscience, neurochemistry, and neuroenergetics, and broadly outline the possible avenues in which metabolomics may facilitate studies in the nervous system.

List of Abbreviations: AD, Alzheimer’s disease; ALS, amyotrophic lateral sclerosis; CDR, clinical dementia rating; CR, caloric or dietary restriction; FANCY, functional analysis by co-responses in yeast; FTIR, Fourier transform infrared spectroscopy; FT-MS, Fourier transform mass spectrometry; GA, genetic algorithms; GABA, γ -amino butyric acid; GC-MS, gas chromatography mass spectrometry; GP, genetic programming; HD, Huntington’s disease; HPLC-EC, high-pressure (or performance) liquid chromatography separations coupled with coulometric electrode array detection; kNN, k nearest neighbor analysis; NMR, nuclear magnetic resonance; O-PLS-DA, orthogonal projection on latent structures discriminant analysis; PCA, principal components analysis; PD, Parkinson’s disease; PLS, partial least squares; PLS-DA, partial least squares projection to latent structures discriminant analysis; SIMCA, Soft Independent modeling of class analogy (note, SIMCA-P is a program that includes this algorithm); SOM, self-organizing map; STOCYSY, statistical total correlation spectroscopy

1 Beyond the Dogma

The era of molecular biology was arguably defined by what was often termed “The Central Dogma”—DNA encodes RNA encodes protein. This triad formed the basis of much of biological research over the last 50 years. It is therefore not surprising that, as the dawn of a new century led also to the dawn of a new era in biology—that of -omics and systems biology—it was these three components that led the way. Advances in genomics—the -omics field of DNA sequence analysis—has accelerated the ability to link human disease with its origins in the genome. Examples in the neurosciences include the recognition of genetic risk factors for Alzheimer’s disease (e.g., amyloid mutations, APOe4 vs APOe2 or APOe3) (Corder et al., 1993; Strittmatter et al., 1993a, b), Parkinson’s Disease (α -synuclein, Parkin, Pink1, DJ-1) (Polymeropoulos et al., 1997; Kitada et al., 1998; Klein et al., 2005; Morris, 2005), Huntington’s disease (expanded CAG repeat in the *huntingtin* gene) (Myers et al., 1993; Jenkins et al., 2005; The Huntington’s Disease Collaborative Research Groups, 1993) and amyotrophic lateral sclerosis (ALS, mutations in SOD 1) (Rosen et al., 1993). Advances in transcriptomics—the -omics field of semiquantitative mRNA analysis—has led to increased ability to generate hypotheses about patterns of gene regulation and an enhanced ability to classify certain diseases, such as leukemias (Golub et al., 1999). It is debatable whether the work in transcriptomics has, as yet, made a major impact on the neurosciences. Advances in proteomics—the -omics field of protein analysis—has led to attempts to use protein profiling to both track biochemical changes in tissues of interest and, again, to classify diseases of interest. As with transcriptomics, it is debatable whether the work in proteomics has, as yet, made a major impact on the neurosciences. While each of these technological advances is a major step forward, pieces remain missing.

Just as the missing piece of the “Central Dogma” was the field of biochemistry, one of the major missing pieces of the “-omics” revolution was the -omics field of quantitative metabolite analysis, a field whose various subfields are known by multiple names (metabolomics, metabonomics, metabolic profiling, metabolic footprinting, metanomics, etc), but now primarily termed metabolomics (Harrigan and Goodacre, 2003; Vaidyanathan et al., 2005). In contrast to classical biochemical approaches that focus tightly on single metabolites, single metabolic reactions and their kinetic properties, and defined sets of linked (i.e., precursor/product, intermediary metabolism) reactions and cycles, metabolomics collects quantitative data on a broader series of metabolites in an attempt to gain an overall picture or understanding of metabolism and metabolic shifts associated with conditions of interest. It is important to recognize here that there are at least three very different subfields within metabolomics that are potentially relevant for the neurosciences: (1) the use of metabolomics technology to address entire biochemical pathways; (2) the

use of metabolomics technologies to generate hypotheses and/or conduct general searches for affected pathways; (3) the use of metabolomics technologies for classification. These are each addressed below in several contexts. Before doing this, however, we will return briefly to consider two aspects of the intersection between biochemistry and neuroscience.

2 Past as Prologue

2.1 Single Metabolites

The ability to respond to the environment is a central function of any cell. The ability to recognize environmental cues, whether general (e.g., pain from local heating) or specific (e.g., signals from adjacent, upstream neurons), and propagate this information, is the inherent function of the nervous system. The associations of these properties with the CNS was associated with a desire to understand the signaling molecules/mechanisms involved by the early part of the twentieth century. Thus, over roughly the last half century, neurochemists have identified a series of molecules which carry out these primary messenger functions, e.g., dopamine, epinephrine, norepinephrine, serotonin, acetylcholine, GABA, substance P, bradykinin, etc. More recently, the gases NO and CO were also found to act as signaling molecules within the CNS. A second series of functions, converting the extracellular signal to one or more intracellular signals, was found to be largely the work of very few molecules, notably GTP and cAMP.

In many cases, the identification and study of these molecules required technically challenging experiments. These molecules are often present in very low levels, and they are often elevated only very transiently and/or locally. NO faced the uphill battle of showing that a gas could be involved as a signaling molecule. Thus, over years and decades, neurochemists won small, critical hard-fought victories in gradually revealing the chemistry of the brain. Once these compounds were identified, research shifted to understanding their mechanisms of regulation, synthesis and release, and the pathways that gave rise to them. Notably, however, these are molecules that are primarily thought by most, even today, as individual molecules. The next stage—the consideration of pathways—entered the picture as people asked how molecules were made, and what the limiting factors in their synthesis were. As one example, work in understanding these limitations for acetylcholine, which is limited by energy-transducing pathways, led to an understanding of hypoxia-induced loss of higher mental functions (Gibson et al., 1975, 1981). For our purposes here, however, we still note that these were studies often done one molecule at a time, even though primary consideration was on flux and attention was being paid to the concept of a pathway. Similar arguments hold when one considers studies of the defects in metabolic encephalopathies that range from primary deficits in energy-producing pathways (Blass et al., 1970) to direct inhibitory affects of toxic build up/byproducts (e.g., maple syrup urine disease) (Gibson and Blass, 1976) and to defects in chronic neurodegenerative disorders such as Alzheimer's disease (Gibson et al., 2000).

The next step arguably was the simultaneous consideration of a pathway. This step bridges the world of single molecule, mechanism-based biochemistry with the -omics world of today. We next consider two examples of this type of research.

2.2 Pathways I: Tracers and Flux

Understanding cellular function is most commonly thought of in the context of sequential reactions. Those reactions may involve energetics, gene expression, signal transduction, etc, and study of a pathway either implicitly or explicitly involves some direct or indirect consideration of the sequential changes, synthesis, and degradation that comprise pathways. As such, it is common to find that critical problems in the neurosciences are often considered in the context of pathways. For example, we consider two pathways and two approaches to the study of these, the Krebs cycle and the kynurenic acid pathway, and isotopomer (compounds whose carbon atoms are differently labeled such that the fate of specific carbons can be

followed through reactions) analysis and HPLC-EC. These have been chosen because they provide a doorway into metabolomics.

It is a useful oversimplification to consider that the Krebs tricarboxylic acid cycle, also known as the citric acid cycle, links the upstream, cytosolic pathway of glycolysis to the downstream pathways of electron transport. Determining the details of this pathway enabled us to follow the steps in which primary fuels such as glucose and fatty acids were converted into NADH and FADH₂, the primary common reducing equivalents of the cell. This left a question, however, “how was flux controlled?” The use of tracers allowed one to follow the fate of specific molecules and specific carbons. Eventually, the use of isotopomer analysis enabled us to show that the fate of certain molecules appeared to follow different paths under different conditions, to understand that neuronal and astrocytic metabolism differed, as well as to show the existence of subcompartments within these cell types (Schousboe et al., 1993; Westergaard et al., 1995a, b; Sonnewald et al., 1996; Waagepetersen et al., 2000a, b, 2002). Thus, for defined pathways of interest, tracers provide a way to study an entire pathway. From the point of view of moving closer to metabolomics, the limitation now was the movement from a technique that was limited in the scope of molecules that could be addressed, to a technology with a broader scope. The first series of studies that we are aware of this type, described below, were made in the mid-1980s, and arguably define the beginning of the critical transition in the application of -omics technology to neuroscience.

2.3 Pathways II: Simultaneous Analysis of Pathways—The HD Example

Work in the mid-1980s to early 1990s found that kynurenic acid, a broad-spectrum excitatory amino acid receptor antagonist, was reduced in the cerebral cortex of autopsy samples of patients with Huntington’s disease (HD) (Beal et al., 1990, 1992). Similar narrowly targeted, mechanistically focused studies followed in Parkinson’s and Alzheimer’s research (Matson et al., 1990; Ogawa et al., 1992). While this observation did not directly lead to an understanding of—or treatment for—HD (or Parkinson’s disease (PD) or Alzheimer’s disease (AD)), it was of particular importance for a different reason. The technology used to uncover this neurotoxin, high-pressure (or performance) liquid chromatography (HPLC) coupled with a coulometric electrode array detector system, enabled simultaneous study of not only kynurenic acid but also the majority of the two most immediately related biochemical pathways, those of tryptophan and tyrosine metabolism (Matson et al., 1984, 1987; Milbury, 1997). This approach thus became the first where researchers were able to simultaneously probe multiple biochemical pathways of interest. Related studies have been conducted in areas ranging from bear hibernation (Milbury et al., 1998) to mitochondrial changes in diabetes (Kristal et al., 1998, 1999).

The work on tracers noted above led to an ability to readily confront the changes across a single, entire pathway; the work on the coulometric array enabled one to consider multiple pathways. These two historical studies share a common theme that these were technology-driven approaches that enabled one to consider the overall context of a change or a system as well as that change itself. Of equal importance, these approaches could be done on a single system, thus removing or reducing the analytical complexity problems that would otherwise be associated with, for example, trying to tie together observations on 30 different compounds in slightly different or limited samples. These and related studies thus essentially set the stage for the metabolomics revolution.

3 Metabolomics: Promises and Current Reality

3.1 What Is Metabolomics: Theory

Metabolomics may be, and has been, both named and defined in many ways (Watkins and German, 2002; Harrigan and Goodacre, 2003; Lindon et al., 2004; Whitfield et al., 2004). For our purposes, metabolomics will be used to refer to the series of related experimental approaches to the generation and analysis of high data density data sets about small molecules that comprise a biological system. An overview of a

metabolomics experiment is shown in [▶ Figure 8.4-1](#). We believe that, over time, this approach will likely take its place alongside genomics, transcriptomics, and proteomics as the last member of the tetrad of major -omics technologies. Genomics is the blueprint, and thus a complete understanding of genomics (i.e., of the genome) would give us complete understanding of the potential of an organism. Transcriptomics gives a record of the recent usage of the genome; thus, a complete understanding of the transcriptome would give us a complete understanding of how endogenous factors (e.g., illness, physiological status such as puberty, mental state) and environmental factors (e.g., toxins, nutrients) have elicited a response from the genome. The proteome is the actualization of this response; thus, a complete understanding of the proteome would give us a “bricks and mortar” view of the organism, including its capacity to respond to certain signals (e.g., through phosphorylation events). The metabolome is comprised of the small molecules that comprise a biological system; thus, a complete understanding of the metabolome would give us insight into the second-to-second flow of signals (e.g., neurotransmitters), challenges (e.g., reactive species) and defenses (e.g., antioxidants), matter (e.g., nutrients, macromolecular building blocks, etc), and energy (e.g., ATP, NADPH) through the system. A list of some of the targets of metabolomic analysis is in [▶ Table 8.4-1](#).

Metabolomics thus gives, at least theoretically, the most temporally up-to-date view into the current status of a biological system. This is expected to be both a blessing and a curse for the field. A list of some of the other advantages and disadvantages of a metabolomics-based approach to biological problems is shown in [▶ Table 8.4-2](#). From the blessing side, this temporal ideality will mean that we can monitor a process in what amounts essentially to real time. We no longer have to be content with looking at what a system might be able to do, and we can actually begin to study what it is doing—at any resolution. For toxicity or drug studies, this means the ability to follow the metabolic consequences of a toxin through the prodromal phase, to the active phase, and through washout/recovery. For studies of mechanism, one can follow the order of events and which pathways are affected. Flux of given molecules of interest can be precisely followed, showing signaling flux through pathways and energy creation and utilization. Neurological mechanisms can be determined precisely by following neurotransmitter cascades and integrating the signaling information with information from other modalities, e.g., patch clamping. Similarly, metabolic defects are expected to give signals that are precise, for example, the build up of a metabolite such as the branched chain keto-acids in maple syrup urine disease. Furthermore, the -omics nature of the field facilitates the simultaneous study of entire pathways of interest, and makes possible discoveries heretofore unexpected.

3.2 What Is Metabolomics: Practice

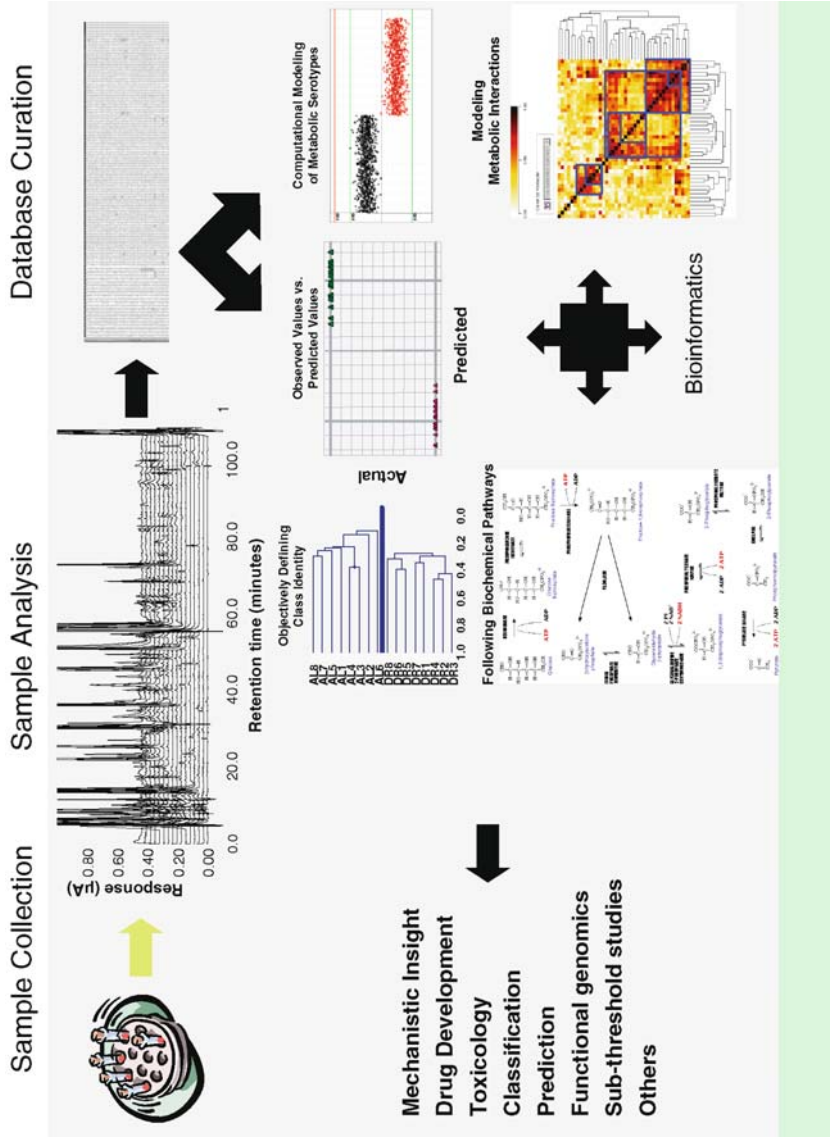
Current metabolomics practice may be considered in the context of three elements: design, data collection, and analysis.

Design of metabolomics experiments must carefully consider the unique aspects of the technology: (1) the technique can be very sensitive to picking up influences unrelated to the project, and an approach must be in place to eliminate these effects. For example, metabolomics studies readily reveal cohort identity, and initial design elements must be derived to remove this problem (Shi et al., 2002b, c, 2004b; Paolucci et al., 2004b, c). (2) Metabolomics readouts are sensitive to the moment to moment situation of the animal, and this must be accounted for, even if not the investigation target (Kristal et al., 2005). (3) The large number of variables means questions must be asked in such a way as to enable the study to be powered. (4) The technical issues and potential artifacts and sources of variation need to be addressed. This has, for example, been a slow and major aspect of our own work (Kristal et al., 1998, 2002; Bogdanov et al., 1999; Vigneau-Callahan et al., 2001; Shi et al., 2002a; Shurubor et al., 2005a, b).

Similarly, the choice of analytical platform has strong implications for the end result of the studies (Watkins and German, 2002; Harrigan and Goodacre, 2003; Lindon et al., 2004; Whitfield et al., 2004). Some of the most commonly used approaches are shown in [▶ Table 8.4-3](#). Nuclear magnetic resonance (NMR) studies are well suited for toxicological investigations. These machines have high initial costs, but yield readily automated data collection schemes, good ability to structurally identify compounds, and ultrahigh throughput and generally high quantitative accuracy. Mass spectrometry (MS) offers good

Figure 8.4-1

Schematic flowchart of a metabolomics experiment: Samples are collected and analyzed using one or more high data density analytical instruments. The chromatogram shown is from a high-pressure (or performance) liquid chromatography (HPLC)/coulometric array study, but could equally well be from nuclear magnetic resonance (NMR) or mass spectroscopy (MS), for example. This analysis generates a large database of analytes (or peaks, sometimes more than one per analyte), which is then analyzed using a series of bioinformatics approaches. Clockwise from the upper middle, the analyses shown are examples of classification on real and simulated data (in SIMCA-P, Umetrics), a correlation and clustering analysis (in Gene Linker Platinum, Improved Outcomes Software), a metabolic pathway (original diagram source unknown), and a clustering analysis in Pirouette (Infometrix). Other approaches are noted in the text. Note that many substages, such as data preprocessing and normalization, are not shown



■ **Table 8.4-1**

What can we measure in a metabolomics experiment?

What we measure	
Biochemically	Conceptually
Metabolites – small molecules	Biochemical constituents
Pathways (e.g., purine catabolites)	Excretion products
Interactive pathways (e.g., amino acid metabolism)	Precursor – product
Compound classes (e.g., lipids)	Balances (e.g., redox systems)
Conceptually linked systems (e.g., antioxidants, redox damage products)	“collection depots”
	Flux
	Snapshot view of biochemistry
	Integrated signal from genome and environment
	Short- and long-term status
	Temporal image
	Subthreshold changes (e.g., toxicology, nutrition)

■ **Table 8.4-2**

Advantages and disadvantages of metabolomic approaches

Metabolomics	
Some advantages	Some disadvantages
Sensitivity	Too Sensitive?
Allows analysis of “silent phenotypes”/ sub-threshold effects	Cohort effects, site effects, time effects
Discovery	Sample handling
Knowledge base (i.e., metabolic pathways)	Individual metabolites responsive to multiple factors genes, environment, health status, location
Limited repertoire – simplifies possibilities (2500 non-lipid endogenous metabolites?)	Experiment design must account for all factors controlled or fuzzy, multiple sources
Metabolome integrates signal	Practical
Nature and nurture – genome and environment	Setup costs
Measurement of system status/defects	Need for multiple platforms
Metabolome has the fastest response time	Early industry dominance – lots of propriety data
	Incompatible data standards

information about the elemental composition of a molecule (particularly with machines such as a Fourier transform mass spectrometry (FT-MS)) and can give further chemical identification hints when coupled with an approach that looks at ion fragments. Sensitivity is considerably better than an NMR, but quantitative accuracy is limited due to problems such as ion suppression. HPLC coupled with a coulometric array offers maximal sensitivity and quantitative precision, but at the expense of limited compound detection (only redox-active compounds are detected) and structural information. Other techniques, such as gas chromatography–mass spectrometry (GC–MS) and Fourier transform infrared (FTIR) spectroscopy have their own strengths and weaknesses. Thus, the choice of a detection platform must be carefully considered.

The informatics used to approach metabolomics data is a critical player. Informatics may be broadly broken into two classes. One class are those programs that seek to place metabolomics data into the context of systems biology and/or specific metabolic pathway representations (e.g., exPASy, <http://www.expasy.ch/>)

■ Table 8.4-3

What are the advantages and disadvantages of the different analytical tools?

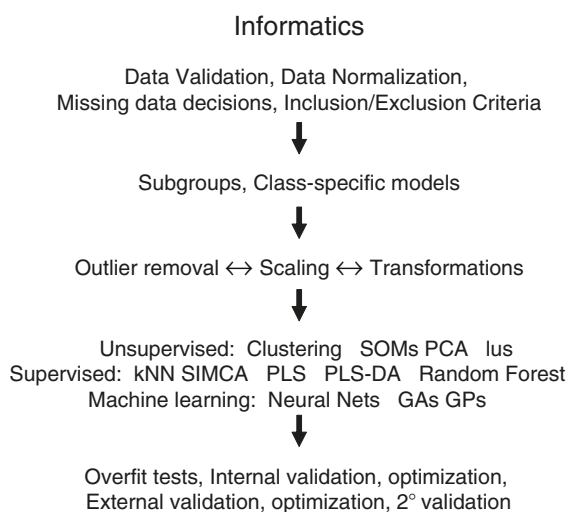
Instrument	Advantages	Disadvantages
NMR	High throughput Nondestructive Minimal or no preprocessing Broad coverage Can look at tissue Can look at living material Quantitative	Low sensitivity Split signal
CE-MS	High throughput Mass information	Low sensitivity
Triple Quad MS	Medium to high throughput Very high precision (CVs 5%)	Compounds must be known in depth
LC-MS	Medium to high throughput Mass information facilitates IDs Quantitative, but often high CVs	Some compound limitations Medium sensitivity (ion suppression and detection times)
GC-MS	High throughput Automated analysis of known compounds (libraries) Quantitative, but often high CVs Mass information	Limited to volatile compounds Medium sensitivity
HPLC-EC	High sensitivity High precision Redox specificity	No structural information Low throughput Difficult to automate Redox Specificity

Note that redox specificity can be an advantage (if the compounds you are interested in are electrochemically active, the redox specificity reduces noise) or a disadvantage (many compounds of interest are invisible)

cgi-bin/show_thumbnails.pl). These programs and approaches are similar to those used in fields such as microarray analysis, but are several years behind. Many of these efforts are based on software that is proprietary to companies in the field, or to software that has been discussed but not yet published. We therefore will not discuss this area further. Much better developed are those mathematical approaches that have focused on questions relating to classification and characterization, including the application of these approaches to problems of prediction. Standard commonly used approaches (see [Figure 8.4-2](#) for a model informatics approach) have included unsupervised approaches such as clustering (Shi et al., 2002b, c) and principal components analysis (Holmes et al., 2000; Shi et al., 2002b, c) and supervised approaches such as k-nearest neighbor analysis (kNN, supervised clustering) (Shi et al., 2004b) and soft independent modeling of class analogy (SIMCA, supervised principal components analysis), (Holmes et al., 2000; Shi et al., 2004b) and partial least squares projection to latent structures discriminant analysis (PLS-DA) (Paolucci et al., 2004b). The newer, related technique, orthogonal projection on latent structure discriminant analysis (O-PLS-DA), is also now being used to simplify interpretation of these projections. (Cloarec et al., 2005). Partial least squares is commonly used to predict and/or model continuous variables. Machine learning tools such as artificial neural nets, genetic algorithms, and genetic programs have also been used (Goodacre et al., 1998; Holmes et al., 2001; Ellis et al., 2002; Goodacre et al., 2003). Specialized approaches have included the development of geometric trajectory analysis for toxin comparison (Keun et al., 2004) and statistical total correlation spectroscopy (STOCSY) for deconvoluting NMR data (Cloarec et al., 2005). Approaches have been developed to address analytical shifts (Shurubor et al., 2005b)

■ Figure 8.4-2

Schematic flowchart of one informatics approach: The first stage in any informatics study is to generate a primary data set. This stage is followed by setting up the data set for the needed analysis, e.g., subgroup-specific and class-specific models (e.g., by incorporating dummy variables for class). The third stage begins a finer grain examination of how the experiments data will be analyzed. Once the data has been set up, analysis begins. One of many possible ways of dividing informatics approaches is shown (Abbreviations: SOM, self-organizing map; PCA, principal components analysis; kNN, k nearest neighbor; SIMCA, soft independent modeling of class analogy; PLS, partial least squares; PLS-DA, partial least squares projection to latent structures-discriminant analysis; GA, genetic algorithms; GP, genetic programming). Once apparently useful models are generated, these models must be tested, improved, and validated. Note that all stages are iterative (at least potentially), and that informatics approaches to metabolomic studies are necessarily as varied as the types of problems posed to them and the people who employ them (i.e., informatics is still arguably as much art as science). Thus, any schematic, including this one, represents only one possible approach



and to estimate the accuracy of precision measurements (Shurubor et al., 2005a). Finally, a considerable effort (Bino et al., 2004; Jenkins et al., 2004; Lindon et al., 2005) is now underway to develop standards for recording and reporting data in metabolomics studies. One goal of these efforts is to identify minimal reporting standards similar to the MIAME format used for microarray analysis.

At this point, we would like to turn to discuss some of the areas in which metabolomics is beginning to be successfully applied.

3.2.1 Toxicology

The study of the response to toxins and adverse drug reactions has been a major area of interest in the run-up that eventually became metabolomics. The instrument of choice for metabolomics-related toxicology has often been the NMR, because the severe effects of these toxins, the high levels reached by the agents and their byproducts, and the presence of metabolites of interest in urine have lent themselves well to NMR. One aspect is that these studies are beginning to give us the ability to classify target organs directly from urine or blood. In one such study, Holmes and coworkers have shown some success in classifying 13 model toxins that primarily affect liver or kidney (Holmes et al., 2001). Species specificity of toxicological responses have been studied (rat vs mouse, hydrazine), and enabled identification of different metabolic

trajectories in these species (Bollard et al., 2005a). Another issue within the toxicological applications of metabolomics is that metabolomics makes it possible to study a trajectory of response to a drug, following the course of toxicity during its acute phase and during recovery (Holmes et al., 1992; Azmi et al., 2002; Keun et al., 2004). A largely pharmaceutical consortia, Consortium for Metabonomic Toxicology (COMET), has been established to attempt to utilize metabolomic information to predict drug toxicity (Lindon et al., 2003).

3.2.2 Functional Genomics

The metabolome has shown itself to be highly responsive to changes in a system. This has led to the concept of the metabolome as the “canary in the coal mine”—the first system to give a harbinger of perturbation. It is noteworthy that this great sensitivity of metabolomics is both a major strength and a weakness. It can be a weakness because one often sees “signal” unrelated to the target perturbation; we, for example, can tell the cohort of origin of our animals (Shi et al., 2002b, c, 2004b; Paolucci et al., 2004b, c). This sensitivity has also played a role in one of the great areas of success of metabolomics—the ability to contribute to functional genomics, i.e., the attempt to ascribe functions to genes. While as yet untested in problems related to the nervous system, successes have been seen at other levels in other systems.

One area of functional genomics that has benefited from metabolomics concerns silent mutations and the related phenomena of perturbations that appear silent (e.g., knockouts, knockins, transgenics, etc). Several reviews in this area are available (Fiehn, 2002; Bino et al., 2004; Oksman-Caldentey et al., 2004).

Mutations are said to be silent when they fail to show an obvious phenotype vs cognate controls under defined conditions. In some cases, such mutations can have significant effects under different conditions (consider for example, mutations in β -amyloid, APO-E, or the presenilins in childhood vs middle-age vs elderly individuals). In other cases, flux can be rerouted through different pathways such that a defect can be “hidden.” Similar situations occur when there are multiple members (e.g., isoenzymes in a family). In still other cases, an environmental trigger is needed before an effect is seen (consider the propensity for a specific allergy, e.g., to bee stings, or the defect in phenylketonuria in the presence or absence of phenylalanine). Each of these cases makes clear the importance of determining the effects of a gene and the difficulty in determining this. The sensitivity of the metabolome to perturbation has led many to approach the problems of “silent” phenotypes. Raamsdonk et al. (2001) used metabolomics to assign functions to yeast genes involved in metabolic regulation. Their approach, called FANCY (functional analysis by coresponses in yeast), assigned metabolic pathways for unknown genes by comparing perturbations in the intracellular metabolome from these genes to those of genes whose products functioned in known pathways. Allen et al. (2003) extended this finding by showing that the metabolic footprint (compounds released into culture media) could also be used for classification. By coupling direct MS with appropriate clustering and machine learning approaches, they were able to correctly identify both different gene variants/mutants and physiological states in a system amenable to high throughput (2 min/sample). In an extreme example of the power of this approach, Weckwerth et al. (2004) used GC-MS to follow \sim 1000 metabolites in plants following suppression of sucrose synthetase isoform 2. Linear correlation analysis, in conjunction with more commonly used approaches such as clustering and statistics, allowed correct assignment of a mutation in sucrose synthetase to its role in carbohydrate and amino acid metabolism even though there were no differences in the average levels of metabolites. In an approach with a slightly different end goal, Roessner et al. (2001) started with four different genotypes known to have different modifications with pathways of sucrose metabolism. They then used these genetic variants to determine what segregated the groups. These studies lead to an understanding of metabolic groups and interrelationships within these tubers. Such studies, which give a comprehensive metabolomic view of genotype expression as phenotype, also provide a knowledge base to study future, similar variants. They directly demonstrated this point by showing that environmental perturbation could mimic the genetic variants.

Within the mammalian arena, several groups have used metabolomics approaches on transgenic and knockout animals. One collaborative group has addressed the APOE*3-Leiden mouse (Clish et al., 2004; Davidov et al., 2004). Their article provides proof of principle for using metabolomics to track the early

changes of disease. The second (Davidov et al., 2004) deals primarily with demonstrating proof of principle for linking metabolomics changes in these systems with proteomics changes. While these uses appear to differ slightly from the types of functional genomics noted above, they are conceptually similar because of the ability to walk backward on a disease path until before symptoms or observable changes occur. NMR studies on the mdx mouse (Griffin et al., 2001a, b) found disturbances in lipid, lactate, and threonine metabolism in the heart and relative concentration changes of several metabolites (taurine, creatine, glutamate, phosphatidylcholine) in heart, muscle, and, most intriguingly, brain regions (e.g., cortex). The most significant aspects of these studies likely identify the extended reach of the mdx phenotype in the transgenic animals. An NMR study of a mouse model of Batten disease found evidence of presymptomatic increases in glutamate and decreases in γ -amino butyric acid (GABA) in three brain regions as well as other variations including creatine and *N*-acetyl aspartate (Pears et al., 2005). Similar NMR analysis of a mouse model of Sandhoff disease found additional *N*-acetylhexosamine-containing oligosaccharides, consistent with the known biochemistry of the disease (Lowe et al., 2005). NMR studies of a mouse model of spinocerebellar ataxia 3 found a broadly distributed rise in glutamine levels, coupled with multiple other metabolic abnormalities in GABA, choline, phosphocholine, and lactate in the affected brain region (cerebrum) (Griffin et al., 2004).

3.2.3 Biomarkers/Classifiers

Because the metabolome is very sensitive to change and because collecting points such as serum and urine can be readily probed, searches for potential biomarkers has been a common theme in many studies. Not surprisingly, these studies, such as metabolic profiling and metabolic fingerprinting, were part of the earliest studies that presaged the coming of metabolomics itself. A key element of these studies is that they are often primarily focused on the observations and classification rather than on the variables and mechanisms.

The diversity of fields in which biomarkers have been sought is illuminating. Biomarkers have been identified for distinguishing spoiled chicken using a combination of FTIR spectroscopy and genetic algorithms (Ellis et al., 2002). The marker, which reflects onset of proteolysis, is simple to measure and could be integrated into use for determining food safety. Pyrolysis mass spectroscopy and artificial neural nets identified markers that readily distinguish methicillin-sensitive and methicillin-resistant *Staphylococcus aureus* (Goodacre et al., 1998). Again, these tools have identified a rapidly obtainable signature that could be used in a clinical setting. Other researchers have focused on the study of small metabolites to help facilitate diagnosis of pneumonia and other lung ailments (Rahman and Kelly, 2003; Hockstein et al., 2004; Hanson, III and Thaler, 2005). Brindle and coworkers have provided an NMR-based profile that may enable a noninvasive test for coronary vessel disease (Brindle et al., 2002).

Over 70 years of data have led to the recognition of caloric or dietary restriction (CR) as the most potent, robust, and reproducible known means of increasing mammalian longevity and decreasing morbidity (Weindruch and Walford, 1988; Kristal and Yu, 1994). We have previously completed proof of principle studies showing that we can identify serum metabolites that differ between ad libitum (AL) and CR rats (Shi et al., 2002c), confirmed these findings in an independent cohort (Shi et al., 2002b), and generated expert systems/trained algorithms that can objectively identify these groups (Paolucci et al., 2004b, c; Shi et al., 2004a). We have further published a series of analytical reports related to the detailed methods of these studies, assessing the analytical variability and stability of the individual components in the plasma/sera metabolome (Vigneau-Callahan et al., 2001; Shi et al., 2002a; Kristal et al., 2005; Shurubor et al., 2005a, b).

3.2.4 Flux

With the exception of the discussion of the tracer studies earlier, we have focused on the ability of metabolomics to provide a “snapshot” of metabolism—a static assessment of the system. But metabolomics can, if necessary, go further. The holistic study of flux through multiple pathways is another aspect of metabolomics. We will differentiate here and define “static studies” as those that do not study specific flux

through pathways, even if they study changes over time, and flux studies as those that attempt to ascribe values to the actual or relative number of molecules that undergo a specific reaction or set of reactions.

Before addressing flux, however, it is worth noting that addressing flux can restrict experimental options, and can make the experiments more difficult and more expensive, and thus are often not needed. For many purposes, static markers (snapshots) will be the only option. This is true, for example, when only one sample will be available (e.g., consider retrospective analysis of prospective cohort studies on samples collected 20 years ago). It is also true when it is financially unfeasible to try to collect multiple samples or to run a study under the requirements of flux analysis (e.g., consider the cost of stable isotope analysis in a routine diagnostic). Likewise, for some biochemical studies, sufficient information is gained from “static” studies that obviate the need for flux analysis (for example, the presence of certain metabolites may be diagnostic for absolute blocks in specific pathways—this is the basis of prenatal testing for some metabolic diseases). In still other cases, time-dependent studies may be assessed without demanding flux measurements. For example, multiple sequential samples are often sufficient for understanding toxicological trajectories and for clinical tests such as glucose disposal following challenges.

While these and other examples suggest the power of studies of the “static” metabolome, an understanding of flux can help us to understand complex metabolic pathways and partial inhibition of these pathways. This should not be a surprise to anyone in the neuroscience field, as flux measurements, in fact, have had a long history within neurochemistry, with one particular emphasis on the understanding of the complex intercell metabolism that occurs between neurons and astrocytes. This was noted above and is being discussed in more detail in another chapter of this book.

The metabolomics field is beginning to expand the concept of the study of flux as it has expanded the concept of the measurement of a few metabolites. Instead of focusing merely on a few metabolites, flux analysis is being expanded to follow the TCA cycle, glycolysis and gluconeogenesis, fatty acid synthesis and β oxidation, and nucleic acid synthesis in ways that enable the coordinate regulation at multiple points in the cell that need to be evaluated. The potential for these approaches has been most clearly exemplified by Boros and coworkers. These approaches have been used, for example, to study the effects of the targeted anticancer agent Gleevec (ST1571, Imatinib) (Boren et al., 2001, 2002a, b). The biggest potential for these approaches identified to date seems to be in understanding how drugs alter system level flux—a critical information for predicting and understanding drug resistance. Similar uses could readily be envisioned in studies of neurodegenerative disorders and stroke, which are associated with metabolic abnormalities (Sonnewald et al., 1994b; Haberg et al., 1998). The power of stable isotope approaches are well appreciated within the neuroscience area, as it has long been used to study cerebral metabolism, as noted above.

3.2.5 Insights into Neurochemistry

Although metabolomics studies relevant to neuroscience are in their infancy, two sets of NMR studies are worth noting. In two related studies, the downstream metabolic consequences of the activity of metabotropic (Rae et al., 2005b) and ionotropic (Rae et al., 2005a) receptor subtypes were followed and differentiated using an untargeted metabolomics approach. In another set of studies, metabolomics approaches were used to differentiate different neuroanatomic regions (Tsang et al., 2005) and cultured neuronal and glial cells (Griffin et al., 2002). The most significant aspects of these studies are the implication of the possibilities that metabolomics offers toward the investigation of neurochemical processes.

3.3 What Is Metabolomics: Current Limitations

Meeting the promise of metabolomics in these and other areas, however, will require solving a broad series of issues. Time and spatial resolution will only be as good as our ability to collect samples of interest, and may also be limited by detection technologies as smaller and smaller slices of time or space are of interest. Different detection schemes offer different advantages, but also different disadvantages. For example, NMR offers high throughput, quantitative accuracy, structural information, and high laboratory-to-laboratory

reproducibility, but is fairly insensitive. The development of cryoprobes has helped in this regard, but NMR is still considerably less sensitive than most other tools used in metabolomics. Mass spectroscopy offers high throughput, structural information, and sensitivity, but is often limited with respect to quantitative accuracy. HPLC separations coupled with coulometric array detection offer high sensitivity and quantitative accuracy, but are more limited with respect to the metabolites observed and give little or no structural information. Newer, ultrahigh-pressure HPLC systems (often termed UPLC systems) may help increase throughput in this area, but remain unproven. Hybrid technologies, such as LC-MS, can be tailored to give desired combinations of strengths and weaknesses. Two other potential concerns are costs—all of these technologies have high initial start-up costs—and technological complexity on the analytical side.

Issues of analytical complexity run through all phases of the metabolomics approach to biology. The metabolome's exquisite sensitivity to conditions means that even subtly incorrect design or conduct of experiments is generally sufficient to prevent a meaningful interpretation of the results. It is common, for example, for people in this field to be able to readily identify the labs a sample came from, a handler, or the batch origin of a sample because of inconsistent sample handling. There are at least three practical approaches to addressing this issue: (1) The minimally processed samples (e.g., whole blood) are collected and snap frozen, then handled entirely within the analytical laboratory under rigid conditions. This approach has an advantage of standardizing most phases of sample handling, and thus eliminating most aspects of analytical variability. The disadvantage is that these samples may be too complex for ideal analysis, or properties of interest may be masked by events that occur upon freeze-thawing (e.g., cell lysis). (2) Samples are collected only in a single laboratory under a rigorously defined set of conditions; this has the advantage of being the analytically cleanest solution, but can end up limiting the knowledge gained to being applicable under only very defined conditions. (3) A third possibility is to deliberately introduce a somewhat fuzzy design (Kristal et al., 2005). For example, samples can be collected in the morning (as opposed, for example, to being collected at 9:32 a.m. on Tuesday mornings), by different people, and under slightly different conditions (e.g., incubation at 4°C by placing the tube on ice for 5–30 min as opposed to 7 min and 30 s). This has the advantage of washing unstable metabolites into the noise and helping to identify robust protocols; it has the disadvantage of potentially throwing away critical information. In general, it is most critical that the investigators match the strengths and weaknesses of a given design with the critical and less critical goals of their study.

Similar complexity comes from sample design. Because the metabolome is so responsive, metabolomics signatures for factors such as drugs, illnesses, time of day, nutritive status, genetics, etc., are all reflected (Rozen et al., 2005; Bollard et al., 2005b). These signatures can be either the signal or the noise, depending on the experimental question. Controlling these factors, either strictly or through fuzzy experimental designs, can be critical to successful completion of projects of interest, particularly with respect to the robustness of the observations made.

4 Stepping Back and Looking Forward: How Might Metabolomics Influence Research in Neuroscience?

Metabolomics is sufficiently new and rapidly changing so as to make any attempt to really foresee the future naive. That said, this chapter, and ones like it (Kaddurah-Daouk et al., 2005), provide a forum where we must begin to consider such issues. It can be argued that revolutionary technical advances and conceptual changes in biomedical research over the last decade have led to a sea of change in our approaches to understanding broad areas of biology, and promise a medical revolution. Whereas the major successes of the Baconian scientific revolution of the past four centuries has been increasingly dominated by hypothesis-driven research, the -omics world may be increasingly balanced between hypothesis-driven and data-driven approaches to answer fundamental questions and address practical issues in applied biological research. Whereas the biological revolution of the previous century was a reductionist revolution, the technological advances of the -omics world will be an integrative revolution. Consistent with this, any description of metabolomics will inherently reflect issues that may also be—and indeed will be—approached with other -omics technologies as well.

With these considerations in mind, it seems safe to posit that metabolomics will have an influence on neuroscience in at least four areas, each addressed in more detail below:

1. Problems related to classification
2. Problems related to hypothesis generation
3. Problems related to fundamental scientific understanding of both physiological and pathophysiological processes in the CNS
4. Problems related to clinical practice

Consistent again with the increasingly integrative nature of the questions that we ask, there is considerable overlap between these issues. Thus, in many ways, this set of questions is more for the convenience of discussion and presentation, and increasingly less a matter of formal separation.

4.1 Problems Related to Classification

What is the underlying cause of an observed dementia? What drug is a depressed individual most likely to respond to—favorably or unfavorably? Is a given biochemical status reflective of active long-term potentiation? Which animal model best reflects disease? How are ten different animal or cellular models of a disease state related?

These questions, and many like them, are primarily biological in nature, but they also can be considered as problems of classification. Expanding on the first question, we note that dementia can have its origin in Alzheimer's, Parkinson's, stroke, and many other etiologies. Even within Alzheimer's disease, consider the evidence that there are at least two different forms. One argument in support of this statement is that changes in the relationship of changes in α -ketoglutarate dehydrogenase and clinical dementia rating (CDR) changes is different in patients who have at least one APOe4 allele as compared with those patients who do not carry the allele (Gibson et al., 2000). This strong difference is, to date, an observation at the population level. Its meaning at the individual level is unclear, as are the questions of whether someone who carries an APOe4 allele can ever get the "other" form of the disease and whether this information has any clinical relevance. The ability to recognize these forms of the disease in living patients in an objective manner could help to answer these questions, and will theoretically aid in optimal treatment. This is the type of classification problem that reflects ways in which classification problems are often nested, and metabolomics may provide a means to both ask questions like these and point to key deficits that are either similar or different between the forms of the disease(s).

Metabolomics provides another tool that can be used for classification, and, as noted above, its ability to provide current, integrated information about a situation, e.g., genotype, phenotype, history, current environment, etc., is potentially very powerful with respect to classifying and unraveling complex interrelated (or nested) problems. The potential for metabolomics to address problems of this nature is demonstrated by the growing number of studies, ranging from microbial classification studies to urine biomarkers, to our own studies of classification based on nutritive intake—each of these in their own way providing validated examples of classification studies in metabolomics. An example of using metabolomics to classify ALS patients and controls is presented below.

4.2 Problems Related to Hypothesis Generation: Novel Hypotheses Arise from a Simultaneous View of the Forest and the Trees

Metabolomics is also likely to contribute to neuroscience research through its ability to engender novel hypotheses. In general, this, along with classification, has been the great success story of the -omics era. Historically, all research begins with observation, but scientists have often focused on improving the next step, i.e., the generation of a testable hypothesis. The consequence of this is a generally negative view of what has been termed "fishing expeditions." This view is gradually changing with an appreciation that the studies being done may indeed be fishing expeditions, but they are fishing expeditions with very good nets and very

powerful ways of sorting the catch afterward! Indeed, one aspect of the power of global profiling lies in its implication that the use of -omics technologies enables one to probe scientific areas of interest poorly understood and to look for leads. This works in practice, because -omics technologies are relatively comprehensive. This enables researchers to see both “the big picture”—the forest—and, simultaneously, the individual trees as well. Thus, many nascent hypotheses can immediately be tested against other aspects of the extant data generated in the same study.

History provides a telling lesson of the importance of just how powerful seeing “the forest and the trees” can be. It was pointed out that, for decades, our view of diabetes was colored by the initial recognition of diabetes as a disease of sugar metabolism, rather than as a disease of fat metabolism (dyslipidemia) (McGarry, 1992). This has led to a focus on glucose levels, and, more importantly, a lack of focus on elements such as changes in fatty acids and their byproducts that have more recently been shown to play major roles in both the insulin resistance itself, inflammation, and the pathogenic sequelae of diabetes (Guan et al., 2002; Maeda et al., 2003; Wellen and Hotamisligil, 2003; An et al., 2004; Makowski and Hotamisligil, 2004; Maeda et al., 2005). The history of research on diabetes thus serves an example for the potential power of metabolomics, and other -omic approaches.

The historical difficulty of simultaneous analysis of multiple pathways from individual samples has often forced neuroscientists to focus their efforts on highly predefined questions. Metabolomics should open the door to a broader look at what is going on in systems ranging from basic neuronal cultures to studies within the intact brain. This broader look should open previously unconsidered vistas.

4.3 Problems Related to Fundamental Scientific Understanding of Both Physiological and Pathophysiological Processes in the CNS

Practical issues, such as cost and sample availability, are often the primary limitations in studies that seek to address the mechanisms underpinning observations associated with neuroscience processes. One aspect of this problem is that, pre-omics, it was generally possible only to ask a single question at a time, that is to say that a given investigator could only carefully follow a single line of reasoning (e.g., look at a few proteins, mRNAs, or metabolites). For studies where multiple potential mechanisms were reasonable, these limitations prevented many of these studies from even being considered. Similarly, it was very difficult to deal with midexperiment changes in design or hypotheses, as it was often impossible to go back and look at a sample in a different way. In contrast, -omics level studies inherently generate a (electronic) data set that can be “reprobed” (i.e., requeried) continually to examine fit to new hypothesis, with confirmatory testing if needed. Perhaps more importantly, as already seen in the HD example given earlier, one sees pathways and not single compounds, increasing the chance that a critical observation is not missed.

Indeed, the history of the study of neuroscience has often been writ as much by what we missed, as by what we observed. Consider the decades of work on long-term potentiation before the role for nitric oxide as a retrograde transmitter was recognized (Gally et al., 1990; Bohme et al., 1991; O’Dell et al., 1991; Schuman and Madison, 1991; Haley et al., 1992). Metabolomics has demonstrated utility in enabling new gene discoveries and mechanistic insight into plant natural product biosynthetic pathways that have been studied for decades (Broeckling et al., 2005). More specifically, these efforts have identified a novel compound involved in plant defense and multiple mechanistic responses to biotic elicitation. This work suggests that, as metabolomic approaches become more widespread in neuroscience, basic pathways now “taken for granted” as being understood will be shown to have previously unconsidered activities.

As noted earlier, studies of brain biochemistry and overall metabolism began with the studies of single metabolites of interest, such as ATP or acetylcholine. This interest then progressed to the levels of pathways with relatively few components, such as glycolysis or the Krebs tricarboxylic acid cycle, or the pathways leading to neurotransmitter synthesis. As one moved from the level of single metabolites to the levels of pathways we began to gain improved understanding of metabolism or neurotransmitter synthesis and degradation. In some cases, even the next step was taken, such as the studies linking mitochondrial energetics to neurotransmitter release. Such work has arguably dominated the last few decades. Largely missing, however, was a view of the global biology and regulation. The coming years, however, will likely

extend this integrated view. It will be possible (at least in animal models) to simultaneously monitor changes in neurotransmitter, energy metabolites, and other metabolites, such as amino acids, antioxidants, and oxidant-damage products. These types of studies will make possible the examination of disease states—or other altered states of interest—at the level of overall metabolism. Flux-based metabolomics studies give more information about subtle shifts of metabolism in neurons. An approach merging more traditional approaches to flux analysis with a conceptually more metabolomics/informatics-like approach has been used to distinguish effects at group I and II metabotropic glutamate receptors (Rae et al., 2005b). Eventually, theoretical considerations and data like these are consistent with a view that metabolomics will feed into other -omics work ongoing in systems biology.

Systems biology is, at least arguably and theoretically, the idealized combination of integrative and reductionist approaches to biology. Leaving aside quantum mechanics and nonbiological interventions (e.g., physical trauma), it is a reasonable assumption that, if one knew every critical player in every system (internal and environmental), and how each of these were related, one could essentially predict the future of an organism (or better, a population of individuals) with high levels of accuracy. In the context of the neurosciences, building *in silico* models that accurately reflect disease could enable *in silico* testing of drugs. For example, models of excitotoxicity, hypoxia, and ischemia could be used to examine the effects of stroke. Models of neurotransmitter pathways could be used to address issues in psychiatry. For these models to have utility, they will have to model the organism at the level of DNA (e.g., what is the genetic basis of interpersonal differences, how does this change response profiles), at the level of mRNA (e.g., what is the temporal pattern of response to stimuli at the genetic level), at the level of proteins (e.g., which proteins are made or degraded in response to a stimuli), at the level of metabolites (e.g., how do neurotransmitter patterns change after stimuli, how does excitotoxicity propagate), and at multiple other levels (e.g., cell, local cell–cell interactions, regional interactions, multiple cell-type interactions, blood–neuron interactions, etc). Critically, as these models become available, progress should accelerate as more and more modeling will become feasible. The future development of systems level approaches should lead to increased understanding of the integration of biological processes at the subcellular level, with eventual consequences at all levels, including the clinical.

4.4 Problems Related to Clinical Practice

The direct and indirect costs of neuropathology, neurological, and neurodegenerative illnesses likely approaches one trillion US dollars/year. Stroke-associated expenses exceed 50 billion dollars/year and those of AD exceed 100 billion/year by themselves. Stroke directly affects about 750,000 people/year, AD perhaps 30–50 percent of those in their eighties. PD incidence and prevalence rises exponentially as the population ages. Treatment of these individuals is further complicated because of the complexities inherent in geriatric medicine. Metabolomics may improve care for this population through implementing effects at the level of drug development and drug assignment (i.e., personalized medicine, pharmacometabolomics). The geriatric population is also the most difficult in which to recognize nutritional deficiencies, and the most likely to have multiple medications with detrimental interactions—even before consideration of the complications associated with altered pharmacokinetics in the geriatric population. Therefore, the geriatric population is also the population most likely to benefit from improved diagnostics and prognostic and progression markers.

Previous work on NMR studies of a limited number of metabolites primarily within energy transduction pathways suggests that more in-depth studies will give promising leads. Specifically, changes in metabolite levels have been previously associated with neurological conditions. Consideration and comparison of studies from a single lab is useful because it suggests the differences are truly disease related as opposed to, for example, platform or processing related. As such, we note a single set of examples, proton NMR studies, which focused on a small number of metabolites, were conducted by Sonnewald and several collaborations, as noted specifically below. In studies of low back pain, sciatica, and disc herniation: (1) Undifferentiated lower back pain and sciatica were both associated with evidence of increased metabolism (Zwart et al., 1997); (2) disc herniation (Garseth et al., 2002) was associated with changes in glucose, alanine, and lactate, which suggested increased aerobic metabolism in disc herniation; inositol and

creatinine were decreased; (3) spinal stenosis was associated with decreased inositol and glucose (Garseth et al., 2002). Changes between spinal stenosis and disc herniation were independent of pain level, suggesting they reflect primary disease changes and not reflections of pain. In studies of neurodegeneration: (1) Studies of HD and PD suggested that HD (Garseth et al., 2000), but not PD, was associated with general downregulations of glial energy metabolism (glycolysis and TCA cycle) (Garseth et al., 2000). (2) Studies of AD and vascular dementia found a shared common factor of unknown identity increased in CSF, but this factor was not found in ALS patients nor in PD patients (White et al., 2004). (3) Patients with multiple sclerosis were found to have lower levels of lactate and glutamine in their CSF (Aasly et al., 1997). Finally, these researchers found increased UDP-*N*-acetylhexosamines in glioblastoma extracts (Sonnewald et al., 1994a). Another group identified regions of difference within NMR spectra that appeared to partially distinguish multiple sclerosis patients from both controls and patients with other neurological problems, and that the regions of interest also differ in an experimental nonhuman primate model of the disease ('t Hart et al., 2003). Although these studies are extremely limited in the scope of molecule studies compared with modern metabolomics approaches, they still provide clear support for the concepts that detailed metabolomics profiling will find useful, differentiating details between these different diseases.

4.5 Drug Development

It can be argued that side effects limit pharmaceutical interventions in multiple ways. One aspect of the ways in which side effects can limit drugs stems from overt toxicity, often because the drug blocks a pathway that was not targeted. This toxicity can affect one or more of a number of organs, including liver, heart, or kidney. For example, some neuroactive drugs (including some antidepressants and antipsychotics) adversely affect the heart. Metabolomics, either alone or potentially in conjunction with other -omics technologies, offers the potential to address this issue rapidly, as such drugs are predicted to display aberrant metabolic signatures outside the targeted pathways. Thus, one can screen the effects of potential agents on multiple organ systems to determine whether any metabolic subset is changing significantly, and, if so, backtrack to determine the origin of the abnormality. Similarly, another problem in many medications is that they have secondary effects in the central nervous system that reduce compliance or cause secondary effects. For example, some cardiac medications leave patients feeling drowsy, often leading patients to go off the drug or place them at higher risk for accidents due to impairment. The inclusion of metabolic screens, potentially in early animal models, should enable researchers to take forward leads with less severe side effect profiles. Indeed, a major collaborative effort amongst pharmaceutical and biotech companies, called COMET, described above, is in progress to attempt to develop earlier biomarkers for specific classes of toxicity. The future development of broad-based approaches to addressing drug metabolism should facilitate the reduction in side effects.

In another application of the technology, pharmacometabolomics approaches are being developed with a view toward complementing work being done in pharmacogenomics. Aims include the ability to predict toxicity and efficacy either pretreatment or at earlier time points than currently possible, to determine subsets of patients most likely to benefit from specific therapies, and to tailor dosages.

4.6 Diagnostics and Personalized Medicine

There are at least two inherent assumptions underlying efforts to understand the risk factors for a disease. One is that early recognition of and intervention against disease can be taken to another level, i.e., accurate recognition of the propensity for disease and its prevention. The second assumption is that this would make a difference in the eventual outcome. For issues such as infectious disease, this has been demonstrated time and time again, with tremendous public health benefits (e.g., the essential elimination of smallpox and polio based on initially immunizing populations and later immunizing contacts of cases). Metabolic and neurological disorders have slightly different stories.

For specific disease, our abilities (to recognize and to intervene) are already available at the laboratory and clinical levels, with varying degrees of accuracy and utility. On one end of the spectrum, susceptibility to Huntington's disease can be predicted with 100% accuracy, but we have no intervention with clinical utility. On another side, we can recognize risk of type II diabetes with reasonable accuracy at the population level, and interventions are often effective, but individualized prediction is lower and compliance is often low. CNS disorders often lag behind other disorders with respect to both timely diagnosis and available options. For example, diagnosis of both ALS and AD is still time consuming and often by process of elimination rather than direct confirmation. Similarly, knowing which individuals are at risk for neurologically relevant effects (e.g., as side effects from drugs or from stress, such as posttraumatic stress disorder) could lead to different approaches to addressing these complications. Early recognition and diagnosis has, for example, been argued to be critical for the limited interventions available in autism. Finally, many neurological syndromes (e.g., AD, PD, autism) are defined functionally and/or morphologically/histologically, and evidence exists that these may involve subgrouping, as noted above and below. The future development of metabolic profiles for these disorders should facilitate a better scientific understanding, and consequently better interventions. By similar arguments, markers for disease progression will also aid both clinical trials and clinical practice.

When one considers the potential spectrum of possible interactions between clinical aspects of neuroscience and metabolomics, there are at least four areas in which interactions are likely. (1) Biomarkers based on metabolomics may help us to predict risk of neurological problems in an individual. (2) The identification of metabolic changes that occur as disease onset occurs would enable the use of metabolomics to assist in diagnostics. (3) Understanding both the normal and disease state may contribute to understanding of disease mechanisms, and normal physiological states can contribute to drug development. (4) Biomarkers based on metabolomics may help us both understand and follow progression. It is worth noting that the search for surrogate markers that correlate with clinical response will also be sought, although this goal has been problematic at all levels (biochemical to clinical) examined to date.

4.7 A Case in Point: Initial Studies in ALS

The four points raised above are, of course, only examples of the many potential opportunities that metabolomics offers to the neurosciences. One example of how these may be put in practice can be drawn from our own work in profiling ALS patients vs controls. We present this ALS study as an example for how the different questions that can be addressed by metabolomics can come together, not because we have solved any of these specific questions. ALS is one member of a class of motor neuron disorders, a series of diseases that lack effective treatments, and which can be difficult to diagnose. In this study (Rozen et al., 2005), we examined the metabolic profiles of two groups of ALS patients and their cognate controls. These findings are preliminary, but there appears to be a signature that distinguishes a subform of ALS associated primarily with lower motor neuron disease from the more general form of the disease. This is an example of the use of this technology for classification. This classification in turn leads to a "novel" hypothesis that there are fundamentally different mechanisms underlying these diseases, and the metabolites that are severely abnormal in lower motor neuron disease may lead us closer to identifying these mechanisms. Finally, diagnosis of ALS can be a protracted and difficult process—a signature for this disease would simplify this process, helping patients either to prepare for this devastating disease or to assure them that they have another, potential curable condition. Thus, development of a diagnostic would be a significant clinical advance.

4.8 A Path to the Future?

A comparison of the progress to date in each of the above areas with a realistic view of where we need to go as a field to make these advances clinically or scientifically meaningful would readily highlight the gap between where we are now and where we need to go to realize the potential of the metabolomics component of the -omics world (🔗 [Table 8.4-4](#)). Historically, these gaps follow from several intrinsic aspects of metabolomics:

■ **Table 8.4-4**
Challenges to progress in metabolomics

Challenges
Experimental Design
Understanding sample acquisition issues
Understanding sources of error and variation
Analytical Issues
Improving instrumentation
Analytical problem solving (eg, breakpoints)
Instrument stability and drift
Sensitivity, specificity, automation, throughput
Informatics
Developing pipelines
Multiple comparison limitations, as in microarrays
Visualization and numerical methods, fusion approaches
Language and reporting standards (MIAME Equivalent)
Integrating across genomics, transcriptomics, proteomics

1. Metabolomics reflects up-to-date information linking nature and nurture. The noise imparted by this rapidly responding sensitivity to temporal aspects of interactions between the individual and their environment can complicate analyses. This, in turn, leads to experimental design complexity, difficulty in directly reproducing experimental findings, and unique informatics problems.
2. Metabolomics has high capital expenses, which has resulted in comparatively low academic involvement.
3. Metabolomics has complex sample handling issues, which has contributed to a delay in developing multisite collaborative studies. Several such studies are, however, now working smoothly.
4. Metabolomics may be applicable in widely different areas of science, which has resulted in a fragmented effort with little interactions. One of the goals of the newly formed Metabolomics Society (<http://www.metabolomicsociety.org/>) and the journal “Metabolomics” is to help provide common ground for these diverse interests.
5. Metabolomics may require multiple platforms, leading to unique informatics problems and difficulty sharing information. This is now being addressed by proposing common standards for reporting data, as has been done in the microarray field. An international effort to address this problem is now underway, and efforts may be followed (or initiated) at <http://www.metabolomicsociety.org/mstandards.html>

4.9 More Information on Metabolomics

The combination of page limitations and the focus of this chapter on neuroscience prevent a more in-depth discussion of work ongoing in metabolomics or of the technologies and approaches that are being used in the field. Additional background may be found in the two seminal books in the field (Harrigan and Goodacre, 2003; Vaidyanathan et al., 2005), and a series of useful links may be found at <http://www.metabolomicsociety.org>. There are also several excellent reviews on the basic field (Watkins and German, 2002; Lindon et al., 2004; Whitfield et al., 2004).

5 Conclusion

The original intersection of metabolomics and medicine is lost in antiquity—the interactions between these fields likely dates to practitioners smelling and tasting the breath and urine to diagnose diseases such as diabetes as well as conditions such as inebriation. The practitioners of today have replaced the human

senses with analytical instruments that can simultaneously quantitate thousands of substances present in a biological sample of interest and with readily available software that can find the signal amongst millions or billions of pieces of data. The arrival of the -omics face of metabolism research complements the existing work in genomics, transcriptomics, and proteomics, and, like these fields, offers new approaches to understanding neuroscience and treat those afflicted with neurological diseases or neurologic injuries.

References

- Aasly J, Garseth M, Sonnewald U, Zwart JA, White LR, et al. 1997. Cerebrospinal fluid lactate and glutamine are reduced in multiple sclerosis. *Acta Neurol Scand* 95: 9-12.
- Allen J, Davey HM, Broadhurst D, Heald JK, Rowland JJ, et al. 2003. High-throughput classification of yeast mutants for functional genomics using metabolic footprinting. *Nat Biotechnol* 21: 692-696.
- An J, Muoio DM, Shiota M, Fujimoto Y, Cline GW, et al. 2004. Hepatic expression of malonyl-CoA decarboxylase reverses muscle, liver, and whole-animal insulin resistance. *Nat Med* 10: 268-274.
- Azmi J, Griffin JL, Antti H, Shore RF, Johansson E, et al. 2002. Metabolic trajectory characterization of xenobiotic-induced hepatotoxic lesions using statistical batch processing of NMR data. *Analyst* 127: 271-276.
- Beal MF, Matson WR, Storey E, Milbury PE, Ryan EA, et al. 1992. Kynurenic acid concentrations are reduced in Huntington's disease cerebral cortex. *J Neurol Sci* 108: 80-87.
- Beal MF, Matson WR, Swartz KJ, Gamache PH, Bird ED. 1990. Kynurenine pathway measurements in Huntington's disease striatum: Evidence for reduced formation of kynurenic acid. *J Neurochem* 55: 1327-1339.
- Bino RJ, Hall RD, Fiehn O, Kopka J, Saito K, et al. 2004. Potential of metabolomics as a functional genomics tool. *Trends Plant Sci* 9: 418-425.
- Blass JP, Avigan J, Uhlendorf BW. 1970. A defect in pyruvate decarboxylase in a child with an intermittent movement disorder. *J Clin. Invest* 49: 423-432.
- Bogdanov MB, Beal MF, McCabe DR, Griffin RM, Matson WR. 1999. A carbon column-based liquid chromatography electrochemical approach to routine 8-hydroxy-2'-deoxyguanosine measurements in urine and other biologic matrices: A 1-year evaluation of methods. *Free Radic Biol Med* 27: 647-666.
- Bohme GA, Bon C, Stutzmann JM, Doble A, Blanchard JC. 1991. Possible involvement of nitric oxide in long-term potentiation. *Eur J Pharmacol* 199: 379-381.
- Bollard ME, Keun HC, Beckonert O, Ebbels TM, Antti H, et al. 2005a. Comparative metabolomics of differential hydrazine toxicity in the rat and mouse. *Toxicol Appl Pharmacol* 204: 135-151.
- Bollard ME, Stanley EG, Lindon JC, Nicholson JK, Holmes E. 2005b. NMR-based metabolomic approaches for evaluating physiological influences on biofluid composition. *NMR Biomed* 18: 143-162.
- Boren J, Cascante M, Marin S, Comin-Anduix B, Centelles JJ, et al. 2001. Gleevec (STI571) influences metabolic enzyme activities and glucose carbon flow toward nucleic acid and fatty acid synthesis in myeloid tumor cells. *J Biol Chem* 276: 37747-37753.
- Boros LG, Lee WN, Cascante M. 2002a. Imatinib and chronic-phase leukemias. *N Engl J Med* 347: 67-68.
- Boros LG, Lee WN, Go VL. 2002b. A metabolic hypothesis of cell growth and death in pancreatic cancer. *Pancreas* 24: 26-33.
- Brindle JT, Antti H, Holmes E, Tranter G, Nicholson JK, et al. 2002. Rapid and noninvasive diagnosis of the presence and severity of coronary heart disease using ¹H NMR-based metabolomics. *Nat Med* 8: 1439-1444.
- Broeckling CD, Farag MA, Huhman DV, Lei Z, Naoumkina M, et al. 2005. Proceedings of the 53rd American Society for Mass Spectrometry Conference on Mass Spectrometry. Abstract.
- Clish CB, Davidov E, Oresic M, Plasterer TN, Lavine G, et al. 2004. Integrative biological analysis of the APOE*3-leiden transgenic mouse. *OMICS* 8: 3-13.
- Cloarec O, Dumas ME, Craig A, Barton RH, Trygg J, et al. 2005. Statistical total correlation spectroscopy: An exploratory approach for latent biomarker identification from metabolic ¹H NMR data sets. *Anal Chem* 77: 1282-1289.
- Corder EH, Saunders AM, Strittmatter WJ, Schmechel DE, Gaskell PC, et al. 1993. Gene dose of apolipoprotein E type 4 allele and the risk of Alzheimer's disease in late onset families. *Science* 261: 921-923.
- Davidov E, Clish CB, Oresic M, Meys M, Stochaj W, et al. 2004. Methods for the differential integrative -omic analysis of plasma from a transgenic disease animal model. *OMICS* 8: 267-288.
- Ellis DI, Broadhurst D, Kell DB, Rowland JJ, Goodacre R. 2002. Rapid and quantitative detection of the microbial spoilage of meat by Fourier transform infrared spectroscopy and machine learning. *Appl Environ Microbiol* 68: 2822-2828.

- Fiehn O. 2002. Metabolomics—the link between genotypes and phenotypes. *Plant Mol Biol* 48: 155-171.
- Gally JA, Montague PR, Reeke GN Jr, Edelman GM. 1990. The NO hypothesis: Possible effects of a short-lived, rapidly diffusible signal in the development and function of the nervous system. *Proc Natl Acad Sci USA* 87: 3547-3551.
- Garseth M, Sonnewald U, White LR, Rod M, Nygaard O, et al. 2002. Metabolic changes in the cerebrospinal fluid of patients with lumbar disc herniation or spinal stenosis. *J Neurosci Res* 69: 692-695.
- Garseth M, Sonnewald U, White LR, Rod M, Zwart JA, et al. 2000. Proton magnetic resonance spectroscopy of cerebrospinal fluid in neurodegenerative disease: Indication of glial energy impairment in Huntington chorea, but not Parkinson disease. *J Neurosci Res* 60: 779-782.
- Gibson GE, Blass JP. 1976. Inhibition of acetylcholine synthesis and of carbohydrate utilization by maple-syrup urine disease metabolites. *J Neurochem* 26: 1073-1078.
- Gibson GE, Haroutunian V, Zhang H, Park LC, Shi Q, et al. 2000. Mitochondrial damage in Alzheimer's disease varies with apolipoprotein E genotype. *Ann Neurol* 48: 297-303.
- Gibson GE, Jope R, Blass JP. 1975. Decreased synthesis of acetylcholine accompanying impaired oxidation of pyruvic acid in rat brain minces. *Biochem J* 148: 17-23.
- Gibson GE, Pulsinelli W, Blass JP, Duffy TE. 1981. Brain dysfunction in mild to moderate hypoxia. *Am J Med* 70: 1247-1254.
- Golub TR, Slonim DK, Tamayo P, Huard C, Gaasenbeek M, et al. 1999. Molecular classification of cancer: Class discovery and class prediction by gene expression monitoring. *Science* 286: 531-537.
- Goodacre R, Rooney PJ, Kell DB. 1998. Discrimination between methicillin-resistant and methicillin-susceptible *Staphylococcus aureus* using pyrolysis mass spectrometry and artificial neural networks. *J Antimicrob Chemother* 41: 27-34.
- Goodacre R, York EV, Heald JK, Scott IM. 2003. Chemometric discrimination of unfractionated plant extracts analyzed by electrospray mass spectrometry. *Phytochemistry* 62: 859-863.
- Griffin JL, Bollard M, Nicholson JK, Bhakoo K. 2002. Spectral profiles of cultured neuronal and glial cells derived from HRMAS ^1H NMR spectroscopy. *NMR Biomed* 15: 375-384.
- Griffin JL, Cemal CK, Pook MA. 2004. Defining a metabolic phenotype in the brain of a transgenic mouse model of spinocerebellar ataxia 3. *Physiol Genomics* 16: 334-340.
- Griffin JL, Williams HJ, Sang E, Clarke K, Rae C, et al. 2001a. Metabolic profiling of genetic disorders: A multitissue ^1H nuclear magnetic resonance spectroscopic and pattern recognition study into dystrophic tissue. *Anal Biochem* 293: 16-21.
- Griffin JL, Williams HJ, Sang E, Nicholson JK. 2001b. Abnormal lipid profile of dystrophic cardiac tissue as demonstrated by one- and two-dimensional magic-angle spinning ^1H NMR spectroscopy. *Magn Reson Med* 46: 249-255.
- Guan HP, Li Y, Jensen MV, Newgard CB, Steppan CM, et al. 2002. A futile metabolic cycle activated in adipocytes by antidiabetic agents. *Nat Med* 8: 1122-1128.
- Haberg A, Qu H, Haraldseth O, Unsgard G, Sonnewald U. 1998. In vivo injection of $[1-^{13}\text{C}]$ glucose and $[1,2-^{13}\text{C}]$ acetate combined with ex vivo ^{13}C nuclear magnetic resonance spectroscopy: A novel approach to the study of middle cerebral artery occlusion in the rat. *J Cereb Blood Flow Metab* 18: 1223-1232.
- Haley JE, Wilcox GL, Chapman PF. 1992. The role of nitric oxide in hippocampal long-term potentiation. *Neuron* 8: 211-216.
- Hanson CW, Thaler ER. 2005. Electronic nose prediction of a clinical pneumonia score: Biosensors and microbes. *Anesthesiology* 102: 63-68.
- Harrigan GG, Goodacre R. 2003. Metabolic profiling: Its role in biomarker discovery and gene function analysis. Kluwer Academic Publishers, Dordrecht.
- Hockstein NG, Thaler ER, Torigian D, Miller WT Jr, Deffenderfer O, et al. 2004. Diagnosis of pneumonia with an electronic nose: Correlation of vapor signature with chest computed tomography scan findings. *Laryngoscope* 114: 1701-1705.
- Holmes E, Nicholls AW, Lindon JC, Connor SC, Connelly JC, et al. 2000. Chemometric models for toxicity classification based on NMR spectra of biofluids. *Chem Res Toxicol* 13: 471-478.
- Holmes E, Nicholson JK, Bonner FW, Sweatman BC, Beddell CR, et al. 1992. Mapping the biochemical trajectory of nephrotoxicity by pattern recognition of NMR urinalysis. *NMR Biomed* 5: 368-372.
- Holmes E, Nicholson JK, Tranter G. 2001. Metabonomic characterization of genetic variations in toxicological and metabolic responses using probabilistic neural networks. *Chem Res Toxicol* 14: 182-191.
- Jenkins BG, Andreassen OA, Dedeoglu A, Leavitt B, Hayden M, et al. 2005. Effects of CAG repeat length, HTT protein length, and protein context on cerebral metabolism measured using magnetic resonance spectroscopy in transgenic mouse models of Huntington's disease. *J Neurochem* 95: 553-562.
- Jenkins H, Hardy N, Beckmann M, Draper J, Smith AR, et al. 2004. A proposed framework for the description of plant metabolomics experiments and their results. *Nat Biotechnol* 22: 1601-1606.
- Kaddurah-Daouk R, Kristal BS, Bogdanov M, Matson WR, Beal MF. 2005. Metabolomics: A new approach toward

- identifying biomarkers and therapeutic targets in CNS disorders. *Metabolome Analyses: Strategies for Systems Biology*. Vaidyanathan S, Harrigan G, Goodacre R, editors, Springer, New York.
- Keun HC, Ebbels TM, Bollard ME, Beckonert O, Antti H, et al. 2004. Geometric trajectory analysis of metabolic responses to toxicity can define treatment specific profiles. *Chem Res Toxicol* 17: 579-587.
- Kitada T, Asakawa S, Hattori N, Matsumine H, Yamamura Y, et al. 1998. Mutations in the parkin gene cause autosomal recessive juvenile parkinsonism. *Nature* 392: 605-608.
- Klein C, Djarmati A, Hedrich K, Schafer N, Scaglione C, et al. 2005. PINK1, Parkin, and DJ-1 mutations in Italian patients with early-onset parkinsonism. *Eur J Hum Genet* 13: 1086-1093.
- Kristal BS, Shurubor Y, Paolucci U, Matson WR. 2005. Methodological issues and experimental design considerations to facilitate development of robust, metabolic profile-based classification. *Metabolic Profiling: Its Role in Drug Discovery and Integration with Genomics and Proteomics*. Harrigan G, et al., editors. Dordrecht: Kluwer Academic Publishing.
- Kristal BS, Vigneau-Callahan KE, Matson WR. 1998. Simultaneous analysis of the majority of low-molecular weight, redox-active compounds from mitochondria. *Anal Biochem* 263: 18-25.
- Kristal BS, Vigneau-Callahan KE, Matson WR. 1999. Purine catabolism: Links to mitochondrial respiration and antioxidant defenses? *Arch Biochem Biophys* 370: 22-33.
- Kristal BS, Vigneau-Callahan KE, Matson WR. 2002. Simultaneous analysis of multiple redox-active metabolites from biological matrices. *Methods in Molecular Biology*, Vol. 186. Oxidative stress biomarkers and antioxidant protocols; Humana Press, Totowa, NJ; pp. 185-194.
- Kristal BS, Yu BP. 1994. Aging and its modulation by dietary restriction. *Modulation of aging processes by dietary restriction*. Yu BP, editor. Boca Raton: CRC press, Inc.; pp. 1-36.
- Lindon JC, Holmes E, Bollard ME, Stanley EG, Nicholson JK. 2004. Metabonomics technologies and their applications in physiological monitoring, drug safety assessment, and disease diagnosis. *Biomarkers* 9: 1-31.
- Lindon JC, Nicholson JK, Holmes E, Antti H, Bollard ME, et al. 2003. Contemporary issues in toxicology, the role of metabonomics in toxicology, and its evaluation by the COMET project. *Toxicol Appl Pharmacol* 187: 137-146.
- Lindon JC, Nicholson JK, Holmes E, Keun HC, Craig A, et al. 2005. Summary recommendations for standardization and reporting of metabolic analyses. *Nat Biotechnol* 23: 833-838.
- Lowe JP, Stuckey DJ, Awan FR, Jeyakumar M, Neville DC, et al. 2005. MRS reveals additional hexose N-acetyl resonances in the brain of a mouse model for Sandhoff disease. *NMR Biomed* 18: 517-526.
- Maeda K, Cao H, Kono K, Gorgun CZ, Furuhashi M, et al. 2005. Adipocyte/macrophage fatty acid-binding proteins control integrated metabolic responses in obesity and diabetes. *Cell Metab* 1: 107-119.
- Maeda K, Uysal KT, Makowski L, Gorgun CZ, Atsumi G, et al. 2003. Role of the fatty acid-binding protein mall in obesity and insulin resistance. *Diabetes* 52: 300-307.
- Makowski L, Hotamisligil GS. 2004. Fatty acid-binding proteins—the evolutionary crossroads of inflammatory and metabolic responses. *J Nutr* 134: 2464S-2468S.
- Matson WR, Bouckoms A, Svendsen C, Beal MF, Bird ED. 1990. Generating and controlling multiparameter databases for biochemical correlates of disorders. *Basic, Clinical, and Therapeutic Aspects of Alzheimer's and Parkinson's Diseases*. New York: Plenum press; pp. 513-516.
- Matson WR, Gamache PH, Beal MF, Bird ED. 1987. EC array sensor concepts and data. *Life Sci* 41: 905-908.
- Matson WR, Langials P, Volicer L, Gamache PH, Bird ED, et al. 1984. N-electrode three-dimensional liquid chromatography with electrochemical detection for determination of neurotransmitters. *Clinical Chem* 30: 1477-1488.
- McGarry JD. 1992. What if Minkowski had been agusic? An alternative angle on diabetes. *Science* 258: 766-770.
- Milbury PE. 1997. CEAS generation of large multiparameter databases for determining categorical process involvement of biomolecules. *Coulometric array detectors for HPLC*. VSP International Science Publication, Utrecht; pp. 125-141.
- Milbury PE, Vaughan MR, Farley S, Matula GJ Jr, Convertino VA, et al. 1998. A comparative bear model for immobility-induced osteopenia. *Ursus* 10: 507-520.
- Morris HR. 2005. Genetics of Parkinson's disease. *Ann Med* 37: 86-96.
- Myers RH, Mac Donald ME, Koroshetz WJ, Duyao MP, Ambrose CM, et al. 1993. De novo expansion of a (CAG) *n* repeat in sporadic Huntington's disease. *Nat Genet* 5: 168-173.
- O'Dell TJ, Hawkins RD, Kandel ER, Arancio O. 1991. Tests of the roles of two diffusible substances in long-term potentiation: Evidence for nitric oxide as a possible early retrograde messenger. *Proc Natl Acad Sci USA* 88: 11285-11289.
- Ogawa T, Matson WR, Beal MF, Myers RH, Bird ED, et al. 1992. Kynurenine pathway abnormalities in Parkinson's disease. *Neurology* 42: 1702-1706.
- Oksman-Caldentey KM, Inze D, Oresic M. 2004. Connecting genes to metabolites by a systems biology approach. *Proc Natl Acad Sci USA* 101: 9949-9950.
- Paolucci U, Vigneau-Callahan KE, Shi H, Matson WR, Kristal BS. 2004b. Development of biomarkers based on diet-dependent metabolic serotypes: Characteristics of

- component-based models of metabolic serotypes. *OMICS* 8: 221-238.
- Paolucci U, Vigneau-Callahan KE, Shi H, Matson WR, Kristal BS. 2004c. Development of biomarkers based on diet-dependent metabolic serotypes: Concerns and approaches for cohort and gender issues in serum metabolome studies. *OMICS* 8: 209-220.
- Pears MR, Cooper JD, Mitchison HM, Mortishire-Smith RJ, Pearce DA, et al. 2005. High-resolution ^1H NMR-based metabolomics indicates a neurotransmitter cycling deficit in cerebral tissue from a mouse model of Batten disease. *J Biol Chem* 280: 42508-42514.
- Polymeropoulos MH, Lavedan C, Leroy E, Ide SE, Dehejia A, et al. 1997. Mutation in the α -synuclein gene identified in families with Parkinson's disease. *Science* 276: 2045-2047.
- Raamsdonk LM, Teusink B, Broadhurst D, Zhang N, Hayes A, et al. 2001. A functional genomics strategy that uses metabolome data to reveal the phenotype of silent mutations. *Nat Biotechnol* 19: 45-50.
- Rae C, Moussa C, Griffin JL, Bubb WA, Wallis T, et al. 2005b. Group I and II metabotropic glutamate receptors alter brain cortical metabolic and glutamate/glutamine cycle activity: A ^{13}C NMR spectroscopy and metabolomic study. *J Neurochem* 92: 405-416.
- Rae C, Moussa CE, Griffin JL, Parekh SB, Bubb WA, et al. 2005a. A metabolomic approach to ionotropic glutamate receptor subtype function: A nuclear magnetic resonance in vitro investigation. *J Cereb Blood Flow Metab* 1005-1017.
- Rahman I, Kelly F. 2003. Biomarkers in breath condensate: A promising new noninvasive technique in free radical research. *Free Radic Res* 37: 1253-1266.
- Roessner U, Luedemann A, Brust D, Fiehn O, Linke T, et al. 2001. Metabolic profiling allows comprehensive phenotyping of genetically or environmentally modified plant systems. *Plant Cell* 13: 11-29.
- Rosen DR, Siddique T, Patterson D, Figlewicz DA, Sapp P, et al. 1993. Mutations in Cu/Zn superoxide dismutase gene are associated with familial amyotrophic lateral sclerosis. *Nature* 362: 59-62.
- Rozen S, Cudkovic M, Bogdanov M, Matson WR, Kristal BS, et al. 2005. Metabolomic analysis and signatures in motor neuron disease. *Metabolomics* 1: 101-108.
- Schousboe A, Westergaard N, Sonnewald U, Petersen SB, Huang R, et al. 1993. Glutamate and glutamine metabolism and compartmentation in astrocytes. *Dev Neurosci* 15: 359-366.
- Schuman EM, Madison DV. 1991. A requirement for the intercellular messenger nitric oxide in long-term potentiation. *Science* 254: 1503-1506.
- Shi H, Paolucci U, Vigneau-Callahan KE, Milbury PE, Matson WR, et al. 2004a. Development of biomarkers based on diet-dependent metabolic serotypes: Practical issues in development of expert system-based classification models in metabolomic studies. *OMICS* 8: 197-208.
- Shi H, Paolucci U, Vigneau-Callahan KE, Milbury PE, Matson WR, et al. 2004b. Development of biomarkers based on diet-dependent metabolic serotypes: Practical issues in development of expert system-based classification models in metabolomic studies. *OMICS* 8: 197-208.
- Shi H, Vigneau-Callahan KE, Matson WR, Kristal BS. 2002a. Attention to relative response across sequential electrodes improves quantitation of coulometric array. *Anal Biochem* 302: 239-245.
- Shi H, Vigneau-Callahan KE, Shestopalov AI, Milbury PE, Matson WR, et al. 2002b. Characterization of diet-dependent metabolic serotypes: Primary validation of male and female serotypes in independent cohorts of rats. *J Nutr* 132: 1039-1046.
- Shi H, Vigneau-Callahan KE, Shestopalov AI, Milbury PE, Matson WR, et al. 2002c. Characterization of diet-dependent metabolic serotypes: Proof of principle in female and male rats. *J Nutr* 132: 1031-1038.
- Shurubor Y, Matson WR, Martin RJ, Kristal BS. 2005a. Relative contribution of specific sources of systematic errors and analytical imprecision to metabolite analysis by HPLC-ECD. *Metabolomics* 1: 159-168.
- Shurubor YI, Paolucci U, Krasnikov BF, Matson WR, Kristal BS. 2005b. Analytical precision, biological variation, and mathematical normalization in high data density metabolomics. *Metabolomics* 1: 75-85.
- Sonnewald U, Isern E, Gribbestad IS, Unsgard G. 1994a. UDP-N-acetylhexosamines and hypotaurine in human glioblastoma, normal brain tissue, and cell cultures: $^1\text{H}/\text{NMR}$ spectroscopy study. *Anticancer Res* 14: 793-798.
- Sonnewald U, Muller TB, Westergaard N, Unsgard G, Petersen SB, et al. 1994b. NMR spectroscopic study of cell cultures of astrocytes and neurons exposed to hypoxia: Compartmentation of astrocyte metabolism. *Neurochem Int* 24: 473-483.
- Sonnewald U, Westergaard N, Jones P, Taylor A, Bachelard HS, et al. 1996. Metabolism of [^{13}C] glutamine in cultured astrocytes studied by NMR spectroscopy: First evidence of astrocytic pyruvate recycling. *J Neurochem* 67: 2566-2572.
- Strittmatter WJ, Saunders AM, Schmechel D, Pericak-Vance M, Enghild J, et al. 1993a. Apolipoprotein E: High-avidity binding to β -amyloid and increased frequency of type 4 allele in late-onset familial Alzheimer disease. *Proc Natl Acad Sci USA* 90: 1977-1981.
- Strittmatter WJ, Weisgraber KH, Huang DY, Dong LM, Salvesen GS, et al. 1993b. Binding of human apolipoprotein E to synthetic amyloid β peptide: Isoform-specific effects and implications for late-onset Alzheimer disease. *Proc Natl Acad Sci USA* 90: 8098-8102.

- 't Hart BA, Vogels JT, Spijksma G, Brok HP, Polman C, van der Greef J. 2003. ^1H -NMR spectroscopy combined with pattern recognition analysis reveals characteristic chemical patterns in urines of MS patients and nonhuman primates with MS-like disease. *J Neurol Sci* 212: 21-30.
- The Huntington's Disease Collaborative Research Group. 1993. A novel gene containing a trinucleotide repeat that is expanded and unstable on Huntington's disease chromosomes. *Cell* 72: 971-983.
- Tsang TM, Griffin JL, Haselden J, Fish C, Holmes E. 2005. Metabolic characterization of distinct neuroanatomical regions in rats by magic angle spinning ^1H nuclear magnetic resonance spectroscopy. *Magn Reson Med* 53: 1018-1024.
- Vaidyanathan S, Harrigan G, Goodacre R. 2005. *Metabolome analysis: Strategies for systems biology*. New York: Springer.
- Vigneau-Callahan KE, Shestopalov AI, Milbury PE, Matson WR, Kristal BS. 2001. Characterization of diet-dependent metabolic serotypes: Analytical and biological variability issues in rats. *J Nutr* 924S-932S.
- Waagepetersen HS, Qu H, Hertz L, Sonnewald U, Schousboe A. 2002. Demonstration of pyruvate recycling in primary cultures of neocortical astrocytes but not in neurons. *Neurochem Res* 27: 1431-1437.
- Waagepetersen HS, Sonnewald U, Larsson OM, Schousboe A. 2000a. A possible role of alanine for ammonia transfer between astrocytes and glutamatergic neurons. *J Neurochem* 75: 471-479.
- Waagepetersen HS, Sonnewald U, Larsson OM, Schousboe A. 2000b. Compartmentation of TCA cycle metabolism in cultured neocortical neurons revealed by ^{13}C MR spectroscopy. *Neurochem Int* 36: 349-358.
- Watkins SM, German JB. 2002. Toward the implementation of metabolomic assessments of human health and nutrition. *Curr Opin Biotechnol* 13: 512-516.
- Weckwerth W, Loureiro ME, Wenzel K, Fiehn O. 2004. Differential metabolic networks unravel the effects of silent plant phenotypes. *Proc Natl Acad Sci USA* 101: 7809-7814.
- Weindruch R, Walford R. 1988. *The retardation of aging and disease by dietary restriction*. St. Louis: Charles C. Thomas.
- Wellen KE, Hotamisligil GS. 2003. Obesity-induced inflammatory changes in adipose tissue. *J Clin Invest* 112: 1785-1788.
- Westergaard N, Sonnewald U, Petersen SB, Schousboe A. 1995a. Glutamate and glutamine metabolism in cultured GABAergic neurons studied by ^{13}C NMR spectroscopy may indicate compartmentation and mitochondrial heterogeneity. *Neurosci Lett* 185: 24-28.
- Westergaard N, Sonnewald U, Schousboe A. 1995b. Metabolic trafficking between neurons and astrocytes: The glutamate/glutamine cycle revisited. *Dev Neurosci* 17: 203-211.
- White LR, Garseth M, Aasly J, Sonnewald U. 2004. Cerebrospinal fluid from patients with dementia contains increased amounts of an unknown factor. *J Neurosci Res* 78: 297-301.
- Whitfield PD, German AJ, Noble PJ. 2004. Metabolomics: An emerging postgenomic tool for nutrition. *Br J Nutr* 92: 549-555.
- Zwart JA, Garseth M, Sonnewald U, Dale LG, White LR, et al. 1997. Nuclear magnetic resonance spectroscopy of cerebrospinal fluid from patients with low back pain and sciatica. *Spine* 22: 2112-2116.

Index

- Acetate
– in the study of pyruvate recycling, 189
- Acetoacetate, 139, 147, 154, 163, *See also* Ketone bodies
- Acetoacetyl coenzyme A (acetoacetyl-CoA), 163
- Acetoacetyl-CoA thiolase, 163, 166
- Acetyl coenzyme A (acetyl-CoA), 142, 163
- Acetylcholine, 298, 300–302, 304, 306–308
- Acid/base
– coupled transport, 476, 480
– flux, 470, 471, 474
– homeostasis, 480
– regulation, 470, 474, 476, 480
– transients, 471
– transporters, 473–477
- Acid-sensing ion channel (ASICs), 476
- Activation, *See* Brain
- Acyl-CoA
– dilution factor λ , 419
– precursor pool, *See* Compartmental model, brain
- Acyl-CoA synthetase, 407, 409, 417, 419
- Adenine Nucleotide Transporter (ANT), 879, 882
- Adenine nucleotides, 645
- Adenosine, 253
- Adenylate kinase phosphotransfers, 649, 652
- Aerobic glycolysis, 772, 782
- Aging, 298–302, 305–310, 314, 782
– antioxidants, 284, 285, 288
– free radicals, 284
– oxidative damage, 270, 281, 283
- Aglycemia, 20
- AK1 β isoform, 649
- Alanine, 140, 204, 210, 223–230
- Alcoholism, 54
- Aldolase (ALD), 242, 773
- Allose reductase, 53
- Alkyl DHAP synthase, 414
- Alpha-ketoglutarate/glutamate exchange, 64, 75
- Alzheimer's disease (AD), *See* Neurodegenerative diseases
- Amino acids
– GABA, 571, 574, 575–578
– glutamate, 571, 573–581
– glutamine, 571, 573–580
- Ammonia, 204, 215, 222, 223, 225, 227, 228
- γ -Amino butyric acid, *See* GABA
- γ -Aminobutyric acid (GABA) receptor, 248
- γ -Aminobutyric acid, 590, 591, 603
- 6-Aminonicotinamide, 45
- Aminophospholipids, 406, 409–411, 417, 420
- 5'-AMP-activated protein kinase (AMPK)
– activation of glucose uptake by, 496, 503, 504
– activation of glycolysis by, 506, 507
– and activation of 6-phosphofructo-2-kinase (PFK2), 508
– nitric oxide-mediated activation of, 492, 493
- AMP-activated protein kinase (AMPK), 642, 651, 654
- Amyloid, 890, 898
- Amyotrophic Lateral Sclerosis (ALS), 538, 890, 902, 905, 906
- Anaerobic glucose metabolism, 28
- Analysis, 890, 892, 901, 903, 904
- Analytic procedures, brain lipids
– for acyl-CoA, 407
– gas chromatography and mass spectroscopy (not found)
– high energy microwaving, importance, 404
– positional selectivity fatty acids, 406
– quantitative autoradiography, 403, 404
– subfractionation, 403, 404
- Analytical (issues), 893, 896, 901, 907
- Anaplerosis, 183–192, 203, 208, 209, 213, 222
– definition of, 184
– function of, 184–186
- Anaerobic glycolysis, 772
- Anesthesia (effect on CO₂ fixation), 190
- Angiogenesis, 120
- Anoxia, 20, 23, 25
– effects on synaptic transmission, 26–28
- Antioxidant, 307, 312, 313, 706, 709, 710, 712, 721, 723
– mitochondrially targeted, 525, 534
- APO-E, 898
- Apoptosis, 531, 534, 536, 538, 668, 669, 673, 681, 684, 687
– caspases in, 714, 715, 721
– death receptor pathway of, 715–717
– in brain development, 715
– in neurodegenerative diseases, 713
– intrinsic mitochondrial pathway of, 715, 716
– regulation by Bcl-2 family proteins, 716–720
– role of cytochrome c in, 705, 707–709
- Apoptosis inducing factor (AIF), 532, 536, 715
- Arachidonic acid
– cascade, 407, 419
– concentration, brain, 409
– conversion to arachidonoyl-CoA, 407
– conversion to eicosanoids by COX-1 and COX-2, 407
– half-life, in brain phospholipids, 408

- in ischemia, release and recycling, 405
- inhibition by NSAIDs, 419
- release by phospholipase A₂, 418, 419
- toxicity at high concentrations, 417
- turnover (recycling), in brain phospholipids, 407
- ARD1, 777, 778
- ARNT2, 775
- ARNT3, 775
- Artificial cerebrospinal fluid (ACSF), 244
- Arylhydrocarbon receptor nuclear translocator (ARNT), 775
- Asparaginyl hydroxylase, 777
- Aspartate, 590, 591, 598, 599, 601, 602, 605–610
- Assembly factors, 128
- Assembly of respiratory complexes
 - factors of, 109
 - intermediates of, 103, 104, 108
 - pathway of, 108
- Astrocytes, 64–67, 71, 74, 75, 79, 80, 83, 85, 86, 184–192, 199–204, 206–230, 502–504, 531, 688, 689, 774, 778, 780, 881, 882, 884
 - biosynthesis of nitric oxide by, 488–490
 - and lactate dehydrogenase (LDH), 143, 148, 149, 152, 153
 - functional properties, 363
 - glycolytic capacity, 365, 368, 369, 389
 - metabolic properties, 363, 368
 - monocarboxylate transporters in, 144, 164, 169
 - oxidative capacity, 363, 365, 366, 368, 388, 392
- Astrocyte-Neuron Lactate Shuttle Hypothesis (ANLSH hypothesis), 148–154, 168, 881, 884
- Astrocytic-neuronal trafficking in cataplerosis, 189
- ATP, 5–11, 13, 14, 185–187, 189, 191, 430–442, 444–452, 454, 457, 520, 531, 535, 537, 538, 550, 557–562
 - consumption, 403, 405–420
 - by brain, 403, 406, 419, 420
 - by *de novo* synthesis, 416, 420
 - ether phospholipids, 406, 407, 414–416, 420
 - by fatty acid turnover in phospholipids, 407
 - increased, during recovery from ischemia, 418
 - by Na⁺/K⁺-ATPase pump, 402
 - for maintaining aminophospholipid asymmetries, 420
 - phosphatidylinositol, 411, 413
 - by phosphatidylinositol cycle, 402, 411, 412, 413
 - by phospholipid metabolism, 402, 405, 407, 418
 - homeostasis during activation, 370–371
 - hydrolysis, 122–124, 126–127
 - rotation, 120, 122–124
 - central rotor, 125
 - central stalk, 124–126
 - cross-linking, 122–124, 128
 - lateral stalk, 125, 126, 128
 - nucleotide binding, 123, 124
 - optical microscopy, 123
 - PARAP, 123
 - peripheral stalk, 121
 - rotary motor, 121, 125
 - rotor element, 126
 - single molecule experiments, 124, 126
 - stator, 121, 125–127
 - stator, 121, 125–127
 - subunit c rotation, 126
 - substeps, 123
 - subunit c rotation, 126
 - synthesis, 120, 123, 124, 127
 - aminophospholipid asymmetries, 417
 - cell death, 407
 - debt, 407, 418, 419
 - depletion, effect on, 417
 - excitotoxicity, 417
 - fatty acids, 417
 - glutamate release, 417
 - production rate, 406
 - by brain, 403, 406
 - coupled to, 406
 - glucose and oxygen consumption, 405, 406
 - human brain, 405, 406
 - fatty acid oxidation, 406
 - P/O ratio, 405, 406
 - phosphatidylinositol, 411, 413
 - rat brain, 406
- ATP supercomplex, 120
- ATP synthase, 706, 708, 714, 879, 881
- ATP/ADP carrier = Adenine Nucleotide Transporter (not found)
- ATP-sensitive potassium (K_{ATP}) channel, 642
- Autoradiography, 64, 73, 74, 79
- Batten disease, 899
- Bax
 - activation of, 717, 720
 - inhibitors, 722
- Bcl family proteins, 525
- Bcl-2 family proteins
 - anti-apoptotic, 717, 720, 722, 723
 - BH3-only subgroup of, 719
 - classification of, 718
 - in neurodegenerative diseases, 718
 - mitochondrial mechanisms of action, 716
 - pro-apoptotic, 717, 720
 - role in mitochondrial apoptotic pathway, 715, 716, 721
- Beckman LS 6500 scintillation spectrophotometer, 244
- BH3-only proteins, 705, 717, 719, 720, 721
- bHLH-PAS transcription factor, 775
- Bicarbonate
 - in propionyl-CoA carboxylation, 190
 - in pyruvate carboxylation, 189, 190
- Biliverdin reductase, 53
- Biochemical Systems Theory (BST), 868, 869, 871
- Biogenesis, 128, 129
- Biomarkers, 899, 905, 906
- Biotin, 186, 187, 191, 192
 - deficiency of, 192
 - in biotin-dependent carboxylases, 192
 - metabolizing enzymes and their deficiency, 192
- Blood flow
 - regulation of
 - nitric oxide, 380, 382, 383
 - potassium, 382, 383
 - prostanoids, 380, 383
- Blood-brain barrier (BBB)
 - expression of MCT1 in, during development, 145, 166
- Blood-brain barrier, 187, 189, 404
- BOLD Signal, 378–380
- Bongkrekic acid, 9
- Brain
 - activation
 - ATP homeostasis during, 384–388
 - BOLD signal changes during, 378–380
 - cellular activity during, 388
 - definition of, 349, 350
 - energy metabolism during, 371–377

- global steady-state changes during, 371, 372
- glycolysis during, 384–386
- hydrolysis of phosphocreatine during, 384
- ion homeostasis during, 370, 371
- localized changes in response to stimulation, 372, 373
- metabolic compartmentation during, 388–391
- metabolite changes during tissue, 373–377, 389
- metabolite changes during vascular, 373–377
- oxidative phosphorylation during, 386–388
- reaction potential changes during, 386
- stages of, 350, 351
- energy metabolism, 348–351
- work, 345–347
 - substrate delivery during, 377–382
- activity levels
- Brain, *See* Compartmental Model
- Brain aging, 166
- Brain development
 - and enzyme activities, 165, 166
- Brain energy metabolism
 - adult brain, 847, 848
 - creatine kinase system and ATP metabolism, 847–849
 - the developing brain, 848, 849
- Brain homogenates, 164–166
- Brain mitochondria
 - astrocytic, 287
 - axonal, 279, 280
 - dendritic, 280, 285
 - glial, 270, 272
 - neuronal, 270, 281, 283
 - oligodendrocytic, 287
 - somatic, 280
 - synaptic, 280
- Brain slices, 145, 146, 156, 158, 160, 162, 165, *See also* Hippocampal slices
 - energy utilization in, 21–23
 - inhibition of energy metabolism in, 23
 - positive and negative features of, 18, 19
- Brain, 79–81, 86, 668, 669, 671–674, 677–679, 680–682, 684, 685, 687, 689
- Brown adipose tissue (BAT), 550–556, 558–561, 563
- Buffer capacity, 472, 473, 477, 481
- Ca²⁺, 529–533, 537
- Calcium, 298, 300, 306, 307, 309, 310, 312–315, 436–443, 445, 447, 452–455, 668, 669, 671–677, 680, 681, 684–689, 708, 712, 719, 721
- Caloric or dietary restriction (CR), 899
- cAMP-response element binding protein (CREB), 657
- Cancer, 535, 782, 783
- Carbonic anhydrase, 470, 475, 479
- Cardiac energy metabolism
 - basic laws of cardiac physiology and energetics, 818, 819
 - regulation of mitochondrial respiration *in vivo*, 819, 820
 - the phenomenon of functional coupling in the creatine kinase system
 - membrane-bound creatine kinases, 822
 - mitochondrial creatine kinase, 820, 821
 - myofibrillar creatine kinase, 822
- Caspase
 - in brain development, 715
 - inhibitors, 721
 - initiator and effector, 715, 717, 721
- Catalysis
 - binding change mechanism, 122, 123
 - bi-site, 122–124
 - catalytic sites, 122–124
 - cooperative interconversion, 122
 - kinetic data, 122
 - tri-site, 122, 124
 - uni-site, 122
- Cataplerosis, 185, 189
 - definition of, 184
 - function of, 186
- Cell death, 668, 671, 673, 674, 681, 684–689
 - apoptotic, 704, 717, 719, 720, 721
 - caspase-independent, 721
 - necrotic, 704, 705, 719, 720
 - role of MPT in, 709
- Cellular activity, 388–391
- Cellular bioenergetics
 - infrastructure, 644
- Central dogma, 890
- Central Nervous System (CNS)
 - programmed cell death in, 704
- Cerebellar granule cells, 190
 - pyruvate carboxylation in, 190
- Cerebral activation, 65, 75, 79, 81, 82, 85, 86
- Cerebral cortex slices, energy metabolism of, 21
- Cerebral ischemia, 779, 780
- Chemosensitive neurons, 475, 476
- Chloramphenicol, 880
- Chloride-bicarbonate exchanger (AE), 474
- Cholesterol, 314
- 4-CIN, 159
- Citrate, 139, 162, 164
- Classification, 891, 894, 896, 898, 899, 902, 906
- Clinical (practice), 904–906
- c-Myc, 783
- CO₂ fixation, 186, 188–190
 - magnitude in brain, 189
- CO₂ sensitivity, 476
- Cobalt chloride CoCl₂, 777, 780, 782
- Cognitive impairment, 645
- COMET, 898, 905
- Compartmental Model, brain
 - arterial input function (integrated plasma specific activity), 404
 - ATP stoichiometry, 405
 - beta-oxidation, 404
 - dilution factor λ , 404
 - equations for, 404, 405
 - figure of, 404
 - fluxes, 404
 - half-life, 405
 - incorporation coefficient, 405
 - precursor pool, 404, 405
 - programmed intravenous infusion, 403
 - specific activity, 404
 - stable lipid compartments, 404
 - steady-state assumption, 404
 - turnover rate, 403–405
- Compartmentalized energy transfer, 817, 818, 820, 834, 845, 846, 848
 - description of the model, 838, 839
 - non-equilibrium state of the creatine kinase system, 839–842
 - the modeling of compartmentalized energy transfer in the cells, 837–842
- Compartmentation, 201, 208, 228–230
 - enzyme complement, 280
 - metabolism, 275, 280, 281
 - TCA cycle, 275
- Complex I, 520
- Complex I, 879, 881
- Complex III, 520, 526, 527, 530, 531, 534, 538, 539
- Complex IV, 878, 879, 881
- Complex V, 120, 128, 129

- Compound action potential (CAP)
 – and fructose, 160
 – and glutamine, 161, 162
 – and lactate, 145, 156, 159
 – and mannose, 160
 – and β -hydroxybutyrate, 165
- Connectivity theorem, 871, 880
- Control coefficient, 868–872, 878–881, 883, 884
- Conventional hypothesis of glucose utilization, 148, 149
- Coordinate response, 772
- Creatine kinase, 643
- Creatine, 5, 883
- Creatinephosphate, 5
- Culture
 – astrocyte-neuronal interactions, 570, 573
 – astrocytes, 575, 577
 – cerebellar cultures, 574
 – co-cultures, 574
 – cortical cultures, 577
 – neurons, 570, 574
- α -cyano-4-hydroxycinnamate, 35
- Cyclophilin D, 719
- Cyclosporin, 9
- Cytochrome
 – cytochrome a, 94, 95
 – cytochrome a₃, 95, 102
 – cytochrome b, 69, 70, 94, 97, 101, 102, 107, 109
 – cytochrome c₁,
- Cytochrome c, 520
 – mechanisms of release from mitochondria, 707, 708
 – role in apoptosis, 705, 707, 708
- Cytochrome c oxidase, 879, 880, 882
 – and cell signaling, 495, 496
 – in vivo regulation by nitric oxide of, 497–499
 – persistent inhibition by peroxynitrite, 494, 495
 – reversible inhibition by nitric oxide, 493
- Cytochrome c oxidase, complex IV, 526, 528–530, 536
 – inhibition by NO, 523, 528, 530, 535, 536
 – k_M of, 536
- Cytochrome oxidase, 775
 – oxidation, 361, 362
- Cytochrome P450 reductase, 53
- Dantrolene, 31
- Data collection, 893
- Definitions (very vague term)
- Delayed calcium deregulation (DCD), 532
- Deoxynucleotide diphosphates (dNDPs), 650
- Deoxyribonucleotides, 645
- Design (experimental), 893, 895, 903, 907
- Development
 – apoptosis, 286
 – proliferation, 286
- DFO, 777, 780, 782
- Diabetes, 53, 54, 155
- Dichlorofluorescein (DCF), 524, 526
- Diffusional nucleotide exchange
 – facilitated, 645, 646
 – reaction based, 646, 647
 – simple, 645
- Dihydroethidium (DHE), 524
- Dilution factor λ , 404, 408, 413, 419
 – equation for, 404, 405
 – in ischemia, 405
- Disc herniation, 904, 905
- Dopamine, 298, 300, 301, 304–306, 308–310, 312–314
- Dopaminergic, 300, 305
- DRAL/FHL-2 protein, 643, 644
- Drosophila, 248
- Dual Photon NADH Spectroscopy
 Fluorescence, 79, 85, 86
- EGLN1, 776
- EGLN2, 776
- EGLN3, 776
- Elasticity coefficients, 870, 871
- Electron transferring flavoprotein (ETF), 99, 100
- Electron transport chain (ETC), 361, 550, 557, 559, 560
- Electron transport, 877–884
 – oxidative phosphorylation, 878–883
 – respiratory chain, 881–883
- Emden-Meyerhof pathway, 772
- Endogenous fluorescence, 322–325, 335
- Endoplasmic reticulum
 – Ca²⁺ release channels, 626
 – high Ca²⁺ microdomain
 – negative feedback inhibition by Ca²⁺ of, 623, 626, 628
 – interaction with mitochondria, 618
 – phospholipid transfer, 629, 630
 – in the mitochondria associated membrane fraction, 625
 – regulation of structure by
 – Ras family GTPases, 621
- Endothelial cells, 120
- Energy, *See* ATP
- Energy metabolism
 – of cerebral cortex slices, 21
 – age related changes, 22, 23
 – effects of oxygen and glucose deprivation, 25
 – effects of temperature, 22
 – energy use rates, 23
 – coupling with neural activity, 323, 330
 – mitochondria, 324, 325
 – monitoring by fluorescence measurement, 326
 – oxygen metabolism, 324, 325
- Enolase (ENO), 773, 779
- Environment, 891, 893, 895, 898, 902, 904, 907
- Epidermal growth factor (EGF), 780
- Epilepsy, 192
- EPO, 776–780
- Excitatory postsynaptic potential (EPSP), 24
- Excitotoxicity, 451, 452, 453, 456, 557, 562, 708, 709, 718, 720, 721
- F₀F₁-ATPase, 557
- F₁
 – AMP-PNP, 122, 123
 – asymmetry, 122
 – electron microscopy, 120, 124, 125
 – F₁ $\alpha\beta\gamma$, 123
 – F₁ crystal structure, 122, 123
 – hexamer, 122, 125
- F₁F₀ ATP synthase, 120–122, 126, 128
- Facilitated diffusion, 645, 646
- F-actin, 242
- Factor inhibiting HIF-1 (FIH-1), 777
- Fasting. *See* Starvation
- Fatty acids, *See* Arachidonic acid
 – after ischemia-reperfusion, 417, 418
 – ATP consumption
 – brain oxidation, 406
 – concentrations, brain, 404
 – docosahexaenoic, 403, 406, 408, 409, 418
 – free, 163, 168
 – for measuring brain fatty acid kinetics, 412
 – half-lives brain phospholipids, 403, 408
 – intratissue injection radiotracers, 403
 – intravenous injection radiotracers, 409
 – palmitic, 406, 408, 09, 417, 418
 – polyunsaturated, 168
 – radioactive, intravenous, 407
 – recycling in phospholipids, 407–409
- Fibroblast growth factor 2 (FGF-2), 780
- Flavoprotein

- biphasic fluorescence, 324, 325
- Ca²⁺-dependence, 325, 330
- fluorescence imaging in anesthetized animals, 332
- fluorescence imaging in cortical slices, 332
- lipamide dehydrogenase, 324
- Flt-1, 779
- Fluorescent probes
 - limitations, 523
 - specificity, 523, 525
- Flux Balance Analysis (FBA), 883
- Flux, 891–893, 895, 899, 900, 904
- Fo
 - a subunit, 125–127, 129
 - A6L, 121, 126
 - ATP6, 120, 121, 129
 - b subunits, 123, 124, 126–128
 - c subunit ring, 125, 126
 - c subunit, 125–127
 - D61, 125, 126
 - deprotonation, 126
 - dimerization process, 127
 - E65, 125, 126
 - FoI-PVP(b), 121, 127
 - mitochondrial DNA, 121
 - NMR, 125
 - oligomer, 120, 126
 - OSCP, 121, 128
 - proton translocation, 120, 122, 124–126
 - protonation, 126
 - two half channels, 125, 126
- Free radicals, 307–312, 314, 315
- Friedrich's ataxia, 538, 539
- Fructose, 156, 159, 160
- Fructose-1,6-bisphosphatase(FBP), 156, 159
- Functional brain imaging
 - Ca²⁺ indicator, 323, 325
 - intrinsic signal, 323
 - optical recording, 323
 - pH Indicator, 324
 - voltage-sensitive dyes, 323
- Functional genomics, 898, 899
- Functional Magnetic Resonance Imaging, 64, 79
- G protein, 253
- GABA, 187, 190, 191, 891, 899
- GABAergic neurotransmission (not found)
- GAPDH/3-PGK, in synaptic functions
 - complex formation, 245
 - coupling to ATPases and ion channels, 248–250
 - pathophysiological implications, 252, 253
 - physiological relevance, 250–252
 - roles of, 247, 248
 - vesicular glutamate uptake, 245–247
- Gene knockouts, 797–799, 801, 804
- Genomics, 890, 893, 898, 899, 907
- GFP-based fluorescence probe, 337
- Gleevec, 900
- Glia, 590, 592–596, 600, 601, 605, 606, 607–609
 - in anaplerosis, 188–191
- Glial-derived nitric oxide, 499, 500
- Glioblastoma, 905
- Global cerebral ischemia, 780
- Glucogenic amino acids
 - in anaplerotic reactions, 184, 187, 189–191
 - serum levels of, 188
- Gluconeogenesis
 - and alanine, 159, 162
 - and aspartate, 159
 - and glutamate, 162
 - and glutamine, 162
 - and lactate, 154
- Glucose
 - and starvation, 139, 143, 145, 146, 155, 156, 162–164, 166, 167, 169
 - carbon dioxide (CO₂) production from, 151, 152
 - oxidation, 163, 164, 167–169
- Glucose metabolism, 199–212
- Glucose oxidation, 201, 202, 206–209
- Glucose uptake
 - activation by nitric oxide in astrocytes of, 502–504
 - main carriers in brain, 501, 502
- Glucose, 65, 67, 191, 298, 300–304, 307, 772–776, 779, 781, 782
 - ¹³C-labeled, 188–190
 - radiolabeled in tracer studies, 189, 190
- Glucose-6-phosphatase, 54, 158, 159
- Glucose-6-phosphate dehydrogenase, 42–44, 47–49, 54
- GLUT1, 774, 779, 781, 783
- GLUT-3, 781
- Glutamate accumulation
 - content in synaptic vesicles within synaptosomes, 244
 - release from synaptosomes, 244, 245
 - uptake into synaptic vesicles, 244
- Glutamate, 184, 188, 189, 192, 470, 473, 474, 478, 479, 480, 481, 590–611
 - drainage of TCA cycle through release, 187
 - reuptake, 190, 191
 - transport, 149, 162
- Glutamatergic neurotransmission, 66, 79–86
- Glutamine, 184, 187–192, 474, 479, 480, 590–596, 601–606, 609, 610
 - transport, 161
- Glutamine cycle, 65, 66, 80, 81, 83
- Glutamine synthetase, 184, 188, 191
- Glutamine-glutamate-cycle, 200, 213, 216, 222–228
- Glutathione (GSH)
 - peroxidase, 704, 706, 707
 - reductase, 706, 707, 710
 - oxidized (GSSG), 521
- Glutathione, 42, 49, 51
- Glyceraldehyde phosphate dehydrogenase (GAPDH), 242
- Glyceraldehyde phosphate isomerase, 242
- Glyceraldehyde-3-phosphate dehydrogenase (GAPDH), 35, 657, 772, 773, 776
 - role of nitric oxide in the regulation of, 506
- Glycogen, 772–775
 - and ATP yield, 142, 145, 146, 151, 158
 - phosphorylase, 773
 - storage in astrocytes, 156, 157
 - storage in neurons, 156, 157
 - synthesis, 142, 159, 160, 162, 652
 - synthase, 159, 160
- Glycogenolysis, 772, 774
 - and glucose release, 158, 159
 - and lactate release, 143, 146, 149, 150, 154, 155, 169
 - in astrocytes, 156, 157
- Glycolysis, 14, 202, 204, 206–208, 222, 228–230, 477, 481, 881, 883, 884, 892, 900, 903, 905
 - 6-Phosphofructo-1-kinase (PFK1) activation by nitric oxide and, 508
 - 6-Phosphofructo-2-kinase (PFK2) activation by nitric oxide and, 508
 - during activation, 384–386
 - nitric oxide in the regulation of, 506–508
 - regulation by 5'-AMP-activated protein kinase (AMPK), 508
- Glycolytic enzymes, 242, 649
- Glycolytic phosphotransfer enzymes, 643
- Glycolytic phosphotransfer system, 644
- Growth factor signaling, 534

- H^+ pump ATPase–VGLUT system, 253
 Heme oxygenase, 53, 534
 Hemodynamic responses, 335
 - comparison with fluorescence imaging, 330
 - nitric oxide, 331
 - non-invasive brain imaging, 330
 Heterogeneity of ATP and ADP
 - diffusion and compartmentation of adenine nucleotides, 835–837
 Heteroplasmy, 880
 Hexadecanol
 - tritiated, for measuring brain ether phospholipid synthesis, 416
 Hexokinase (HK), 160, 164, 358, 772, 773, 776
 HIF prolyl hydroxylases, 776
 HIF-1 α , 775, 777–780, 783
 Hif-1 α , hypoxia-inducible factor, 536–537
 HIF-1 β /ARNT1, 775
 HIF-2 α /EPAS1, 775
 HIF-3 α , 775
 Hippocampal slices, 145, 146, 155, 156, 158, 160, 165, *See also* Brain slices
 History, 900, 902, 903
 HPH1, 776
 HPH2, 776
 HPH3, 776
 HPLC, 892, 894–896, 901
 Huntington's disease (HD), 538, 890, 892, 906
 HUVEC, 120
 Hydrogen peroxide (H₂O₂), 521
 Hydrogen turnover, 75
 Hydroperoxyl radical (HO₂), 521
 β -Hydroxybutyrate
 - (3-hydroxybutyrate), *See also* Ketone bodies
 - and ATP, 165
 - and phosphocreatine, 165 β -Hydroxybutyrate dehydrogenase, 166
 3-Hydroxy-3-methylglutaryl-CoA, 52
 Hyperammonemia, 480
 Hyperinsulinemia, 560
 Hypermetabolism, 559
 Hypoglycemia, 20, 24, 28, 242, 253, 300, 301
 - and starvation, 139, 143, 145–147, 153–156
 Hypothermia, 32
 Hypothesis generation, 902, 903
 Hypoxia, 20, 32, 156–160, 162, 298, 300–302, 304–307, 309, 480, 481, 536, 537, 772, 775–782
 Hypoxia/ischemia
 - role of glial cells, 499, 500
 Hypoxia-inducible factor-1 (HIF-1), 651, 772, 775–783
 Hypoxic response element (HRE), 772, 775, 776, 778, 781, 782
 IF1
 - $\Delta\pi H^+$, 120, 127
 - anoxia, 127
 - ATP synthase dimer, 128
 - energy depletion, 128
 - histidine 49 (His49), 127
 - IF1 dimer, 128
 - IF1:F1 complex, 128
 - inhibitory action, 128
 - ischemia, 127
 - Luft's disease, 128
 - natural inhibitor protein, 127
 - neoplastic cells, 128
 - pathophysiology, 128
 - pH dependence, 127
 - pH independent binding, 128
 - pH, 127, 128
 - tumor cell growth, 128
 Immunoprecipitation technique, 243
 Import of mitochondrial proteins
 - internal targeting signal of, 107, 108
 - N-terminal cleavable presequences of, 107
 - post-translational, 94, 97, 107, 108
 - in neuronal function and energy metabolism
 Incorporation coefficient, 405
 Informatics, 895–897, 904, 907
 Inhibitors, 520, 525–528, 534, 538, 539
 Inhibitory postsynaptic potential (IPSP), 24
 Insulin-like growth factor 1 (IGF-1), 780, 782
 Insulin-like growth factor 2 (IGF-2), 780
 Integrated cellular phosphotransfer network, 644
 Intracellular energetic units, 822, 823
 Intracellular enzymatic networks
 - facilitated diffusion, 645, 646
 - ligand conduction, 647, 648
 - metabolite channeling, 646
 - reaction-diffusion, 646, 647
 - simple diffusion, 645
 Intracellular, 199, 201, 208, 215, 216, 223, 226–230
 Iodoacetate, 250, 252
 Ion channels, 535
 Ion homeostasis, 347, 348
 Ionotropic, 900
 Ischemia, 20, 145, 156–160, 480, 481, 528, 557, 561, 562
 - effects on synaptic transmission, 26–28
 - irreversible damage after, 25
 Ischemia, cerebral
 - arachidonic acid, increased incorporation on reperfusion, 417, 418
 - ATP debt, 407, 418, 419
 - release fatty acids from phospholipids by phospholipases, 417
 - therapeutic approaches, 418, 419
 Ischemic preconditioning (IPC), 534, 537, 538
 Isocitrate dehydrogenase (NADP⁺-dependent), 50
 Isotopomer, 891, 892
 K^+ _{ATP} channel, 535, 537, 538
 K^+ _{ATP} channel, 651, 652
 Ketogenic diet, 139, 145, 162, 164, 169
 3-Ketoacid-CoA transferase, 163, 166
 α -Ketoglutarate, 139, 161, 162
 Ketone bodies, 882, *See also* acetoacetate, β -hydroxybutyrate
 - and developing brain, 145, 165, 166, 168
 - and suckling stage, 154, 165, 166
 - during starvation, 166, 167, 169
 - glucose-sparing effect of, 163, 164, 169
 - metabolism of, 165
 - transport of, 164, *See also* Monocarboxylate transporters
 - utilization of, 163–169 α -KGDH, α -ketoglutarate dehydrogenase, 527, 528
 Krebs cycle, 891, 892, 903
 Krebs–Ringer buffer (KRB), 244
 Kynurenic acid, 891, 892
 Lactate, 202, 204–208, 216–219, 221–230, 590, 593–601, 607, 608, 610, 772–775, 781
 - and developing brain, 148, 154
 - and hypoglycemia, 143, 154–156, 159, 163, 164, 169
 - and long-term potentiation (LTP), 145, *See also* Synaptic plasticity
 - and paired-pulse facilitation, 145, *See also* Synaptic plasticity
 - carbon dioxide (CO₂) production from, 151, 152, 156
 - metabolism, 142, 143, 151

- shuttle, 148–151, 153, 477, 478
- transport, 144, 145, 159, 474, 477–480. *See also* Monocarboxylate transporters
- utilization, 148, 151, 169
- Lactate dehydrogenase (LDH), 242, 359, 360, 773
 - and reversible equilibrium, 143, 147, 148, 152, 153
 - LDH-1, 143, 144, 149, 151
 - LDH-5, 143, 144
- Lactate shuttle, 86, 774
- Leucine, 223–228
- Ligand conduction, 647, 648
- Lipid oxidation, 535
- Lipids and oxidant stress, 314, 315
- Liver, 157, 163, 165, 167
- L-type calcium blocker. *See* Nimodipine
- Luciferin/luciferase method, 245
- Malate, 162, 186, 188
 - equilibration with fumarate, 185, 188, 190
 - product of pyruvate carboxylation, 184, 187, 189, 190
- Malic enzyme, 188–191
 - mutation of in epilepsy, 192
 - Reaction catalyzed by, 186, 187
- Malic enzyme, 50
- Mannose, 159, 160
- Mannose-6-phosphate isomerase, 160
- MAP kinases, mitogen activated protein kinases, 537
- Mass spectrometry coupled to gas Chromatography (not found)
- Mass spectrometry (MS), 739, 746–750, 893–896, 898, 899, 901
- Massive depolarization-induced conduction block, 24
- Mathematical modeling
 - basic principles, 823–826
 - modeling reactions in intracellular medium: the problem of macromolecular crowding, 826
- Matrix processing peptidases (MPPs)
 - Pitriylsin family, 102
- M-CK gene, 652
- MCT1, 774
- Measurements
 - chemiluminescence, 524
 - end points vs. kinetics, 526
 - fluorescence, 523, 524, 526
 - of RNS, 528
 - of ROS, 524, 526
- Membrane permeability transition, 704, 708, 709, 714, 715, 719, 721, 723
 - anti-oxidant systems in, 709
 - biogenesis, 789–805
 - calcium circuit, 7–8
 - calcium uniporter, 7, 9, 13
 - carnitine-O-palmitoyl transferase, 406
 - dehydrogenases in, 706–708
 - DNA in, 270, 283
 - fission of, 265, 266, 270, 282, 285
 - fusion of, 266, 270
 - gene organization, 790
 - heteroplasmy, 791
 - inheritance, 790
 - isolation, 531
 - localization of, 268, 274
 - membrane permeability transition, 708
 - membrane potential indicators, 11, 13
 - mitochondrial NOS, 712
 - motility of, 268, 270, 276, 287
 - mtDNA, 791, 795–799, 801
 - nitric oxide and cytochrome c oxidase, 493
 - oogenesis, 791, 792
 - oxidative phosphorylation, 266, 275, 276
 - oxidative phosphorylation, 406, 417
 - permeability transition, 9
 - peroxynitrite and cytochrome c oxidase, 494, 495
 - pH gradient, 10
 - proton circuit, 6–7
 - protonophores, 14
 - reactive oxygen species generation (ROS), 706–709, 711, 713–715
 - replication, 792, 793
 - role in neuronal apoptotic death, 708
 - sodium circuit, 7–9
 - sodium/calcium exchanger, 7–9, 13
 - sodium/proton exchanger, 7–9
 - structure, 790
 - superoxide production, 706–709
 - targeted antioxidants, 525, 539
 - transcription, 793, 794
 - turnover, 269, 282
- Mitochondrial biogenesis, 563
 - ATP, 550, 557–562
 - calcium dysregulation, 557
 - electrochemical gradient, 550
 - electron transport chain (ETC), 550, 557, 559, 560
- Membrane potential ($\Delta\psi_m$), 520, 528, 531
- Membranes. *See* Aminophospholipids
 - Asymmetries, 402, 409–411, 417, 420
 - remodeling and reacylation of phospholipids, 419
 - synaptic, 420
- Metabolic compartmentation
 - during activation, 388–391
- Metabolic control analysis (MCA)
 - connectivity theorem, 880
 - control coefficient, 878–880
 - elasticity coefficient, 879
 - summation theorem
- Metabolic control analysis, MCA, 868–872
- Metabolic coupling, 79, 80, 83, 85
- Metabolic function, 531
- Metabolic perturbations, 20
- Metabolic syndrome, 651
- Metabolism, 402, 403, 405, 406, 417, 419, 420
 - anaplerosis, 571, 578
 - ATP production, 405, 406, 420
 - baseline (stages 0-1), 350
 - disruption ischemia, 417
 - elevated (stages 3-4), 350, 351
 - human, compared with rat, 406
 - malate, 571, 575, 580
 - normal (default), 350, 351
 - oxygen consumption, 405, 406
 - P/O ratio, 405, 406
 - resting (stage 2), 350
 - succinate, 574, 575, 578
 - transamination, 571, 578, 579
 - tricarboxylic acid cycle, 574, 576–578
- Metabolite channeling, 646
- Metabolite cycling, 368
- Metabolites, 23
- Metabolome, 893, 895, 898–901
- Metabolomics society, 907
- Metabolomics, 889–907
- Metabotropic, 900, 904
- Metalloproteases, 535
- Metastasis, of cancer cells, 535
- Methylmalonyl-CoA, 187
- Microglia, 139
- Microsomes
- Migration, 535
- Mitochondria, 430, 436, 441, 442, 445–448, 450, 455–457, 668–689
 - adenine nucleotide translocator, 5
 - adherens complex, in, 264, 278–279

- energy metabolism, 562, 563
- F_0F_1 -ATPase, 557
- mitochondrial membrane potential (ψ_m), 558, 560, 562
- pH gradient (ΔpH), 560
- proton electrochemical gradient (Δp), 550
- tricarboxylic acid (TCA) cycle, 559
- Mitochondrial diseases, 878, 880, 884
 - CPEO (Chronic Progressive External Ophthalmoplegia), 880
 - MELAS (Mitochondrial encephalopathy, lactic acidosis and stroke like episodes), 880
 - MERRF (Myoclonic epilepsy with ragged red fibers), 880
- Mitochondrial DNA, 880–882
 - heteroplasmy of, 109
 - homoplasmy of, 109
 - maternal inheritance of, 109
 - mutations of, 109–111
 - replicative segregation of, 109
- Mitochondrial membrane potential (ψ_m), 558, 560, 562
 - role of nitric oxide in, 496, 497
- Mitochondrial morphology
 - fusion/fission
 - adenine nucleotide translocase, 622
 - ATP microdomain between, 625
 - Ca^{2+} uniporter, regulation of metabolism by, 626, 627, 629
 - Ca^{2+} uniporter, shaping global Ca^{2+} signal by, 627
 - during apoptosis, 630
 - outer membrane, voltage dependent anion channel
 - evolution of machinery of, 618, 619, 621
 - interaction with creatine kinase, 623–625
 - interaction with hexokinase, 625
 - localization at ER-mitochondria contacts, 625, 632
 - membrane potential across, 626
 - Na^+/Ca^{2+} (mNCX) and H^+/Ca^{2+} (mHCX) exchanger, 627
 - permeability transition pore opening, during apoptosis and necrosis, 625
 - proteome, 633
 - permeabilization of, during apoptosis, 623
 - inner membrane
 - pH gradient across, 626
 - regulation by Ca^{2+} , 621, 626, 628
 - regulation by GTPases, 618, 621
 - yeast and drosophila mutants, 621
- Mitochondrial pathologies
 - 3-hydroxyglutarate, 129
 - Alzheimer's disease, 129
 - ataxia, 129
 - Batten disease, 129
 - brain, 129
 - ceroid lipofuscinosis, 129
 - excitotoxicity, 129
 - MILS, 129
 - mtDNA, 129
 - mutations, 129
 - NARP, 129
 - neurodegeneration, 129
 - neuronal degeneration, 129
 - NMDA receptor, 129
 - retinitis pigmentosa, 129
- Mitochondrial uncoupling proteins, 550
 - regulation of activity
 - free fatty acids, 551, 559
 - K_{ATP} channels, 560, 561
 - lipolysis, 559
 - lipid peroxidation, 558, 560
 - norepinephrine, 558, 559
 - ubiquinone, 557, 558, 562
 - regulation of expression
 - alternative initiation sites, 551
 - arachidonic acid, 561
 - calorie restriction, 560
 - fasting and high-fat diets, 551
 - lipopolysaccharide (LPS), 562
 - mRNA stability, 551
 - post-transcriptional
 - PPAR- γ , 561
 - translational, 551
 - involvement in systemic disease states, 560
 - obesity, 558, 560
 - physiological roles in metabolism, 558
 - thermogenesis, 550, 559–561
 - tissue distribution
 - brain, 562
 - Brown adipose tissue (BAT), 550
- Mitochondrially encoded subunits, 128
- Mitochondrial-nuclear intercommunication, 648–651
- Mitox red, 524
- Modeling
 - electron transport model, 882–884
 - NET model, 882
- Modeling of the functional coupling mechanisms in mitochondria
 - dynamic compartmentation, 826–828
 - direct transfer mechanism, 828–830
 - phenomenological models, 834
 - probability model of MtCK to ANT coupling, 830, 831
 - the main results of probability model, 831, 832
 - thermodynamically consistent model of MtCK-ANT coupling, 832–834
- Modeling the mitochondrial respiration controlled by Frank-Starling mechanism under conditions of metabolic stability
 - metabolic control analysis of the factors of regulation, 842–846
- Molecular chaperones, 632
 - role in folding of nascent polypeptides, 620, 632, 633
- Monoamine oxidase (MAO), 527, 529, 531
- Monocarboxylate transporters (MCTs), 474–480
 - in astrocytes, 164
 - and ketone bodies, 144
 - and lactate, 144, 169
 - in neurons, 164
 - MCT1, 144, 145, 164
 - MCT2, 164
 - MCT4, 164
 - and pyruvate, 145, 164
 - and starvation, 164
- MPP⁺, MPTP, 550, 562
- mRNA/protein stability, 551
- Müller cells, 145, 149
- Multiple sclerosis, 55, 538
- Muscarinic receptor loops, 311
- Muscarinic receptors, 309–312, 314
- Myo-inositol
 - deuterated, for measuring phosphatidylinositol cycle, 420
- N_2O -anesthetized brain, 21
- Na^+/K^+ -ATPase pump activity, 249
- NaCl solubilization experiments, 243, 244
- NAD(P)H
 - electron donor in oxidative metabolism, 324
 - electron donor in reductive biosynthesis, 324
 - Krebs-cycle dehydrogenase, 324
- NAD⁺, NADH, 520, 524, 527–529
- NADH balance, 85

- NADH/NAD⁺ ratio, 142, 145, 150, 155
 NADPH oxidase, 52, 53
 NADPH, 42, 44–55, 184, 187, 189
 Necrosis, 684, 687
 NET model (Non-Equilibrium Thermodynamic Model), 882
 Neural activity, *See* Synaptic transmission
 Neural plasticity
 – induction after cortical stimulation, 332
 – induction after learning, 332
 – long-term depression, 332
 – long-term potentiation, 332
 – spatial distribution of, 332
 Neurodegeneration, 538
 – apoptosis in, 717, 720, 723
 – oxidative stress in, 705
 Neurodegenerative diseases, 35, 253, 561, 645
 – Alzheimer's disease, 54, 538, 562, 704, 890–892, 902
 – Bcl-2 family proteins in, 717, 718, 719–721
 – Ischemia, 562
 – mitochondrial dysfunction in, 704, 705
 – Parkinson' disease, 529, 531, 538, 562, 717, 721, 890, 892, 902
 Neurological function, 803–805
 – fragile X syndrome, 803
 – glutamate receptor, 804
 – nitric oxide synthase, 804
 – NRF-2 and cytochrome oxidase, 804
 Neuron-glia interaction, 201, 213
 Neurons, 65, 67, 71, 72, 74, 79, 80, 83–86, 143–145, 148–159, 161, 162, 164, 165, 168, 199–230, 531, 538, 590–597, 599, 600–602, 605–609, 668, 677, 678, 685, 687, 689, 881, 882, 884
 – in anaplerosis, 186–192
 – brain, 413, 414, 420
 – cultured
 – myo-inositol exposure, 413, 414, 420
 – phosphatidylinositol cycle, rate in, 411
 – death following
 – ATP depletion, 417
 – Ischemia, 410, 418
 – functional properties, 363
 – glycolytic capacity, 369
 – and lactate dehydrogenase (LDH), 143, 144, 149–151, 153
 – monocarboxylate transporters in, 144, 164
 – metabolic properties, 363, 364
 – oxidative capacity, 365, 368
 – synapses of, 407, 408
 Neuroprotection, 562
 – anti-apoptotic strategies for, 713
 – anti-apoptotic, 563
 – antioxidant defense systems, 563
 – dopaminergic neurotoxicity, 562
 – Bcl-2 family proteins in, 720, 721
 – 1-methyl-4-phenyl-1,2,5,6 tetrahydropyridine (MPTP), 550, 562
 – mitochondria in, 721
 – role of nitric oxide in, 499
 – role of peroxynitrite in, 499, 504, 505
 Neurotoxicity
 – by nitric oxide, 499
 – by peroxynitrite, 499
 Neurotransmission, 184, 190–192
 Nimodipine, 31, 33
 Nitration, 709, 714
 Nitric oxide
 – biochemistry of, and RNS, 523, 528, 530
 – mtNOS, mitochondrial NOS, 530
 – physiology vs. pathology, 539
 – signaling, 536
 – synthase, NOS, 710, 712
 – biosynthesis of, 488
 Nitric oxide synthase (NOS)
 – endothelial isoform (eNOS or NOS3), 488, 489, 503, 504
 – inducible isoform (iNOS or NOS2), 488, 489, 492, 495, 499, 502, 504, 505
 – neuronal isoform (nNOS or NOS1), 488, 489, 497–499
 Nitric oxide synthase, 52
 Nitric oxide, 380, 382, 383, 780, 781
 Nitrosylation, 714
Nm23 gene, 650
N-methyl-D-aspartate blocker, 31
 NMRS, 73, 79189, 190, 893–897, 899–901, 904, 905
 Nomenclature, 521
 Nrf-2, nuclear respiratory factor 2, 535
 Nuclear factorκB (NFκB), 534
 Nuclear Magnetic Resonance Imaging, 74–79
 Nuclear Magnetic Resonance Spectroscopy, *See* NMRS
 Nuclear magnetic resonance, 201–207, 209, 211, 213, 217–219, 221, 222, 226, 230, 570, 577, 578
 – [¹³C]acetate, 574, 575
 – [¹³C]glucose, 570, 574–578
 – [¹³C]glutamate, 575–580
 – ¹³C spectroscopy, 570, 574, 575, 580
 Nuclear respiratory factors, 795–798
 Nuclear-coded proteins, 648
 Nuclearily encoded subunits, 128
 NXXS(T)K motif, 248
 Obesity, 558, 560
 Oda5p protein, 643
 Oligodendrocytes, 148, 165, 168
 Oligomycin, 120, 127, 244, 245, 250–252
 Optic nerve, 145, 156, 159–162, 165
 Orthodynamic and antidromic stimulation, 20
 Ouabain, 14
 2-oxoglutarate, 777
 Oxaloacetate, 142, 155, 162, 185, 187, 190
 – concentration in brain, 186
 – product of pyruvate carboxylation, 184, 189
¹⁸O-labeling technique, 648
 β-oxidation of fatty acids, 878, 883
 Oxidative
 – phosphorylation, 706, 708, 714, 723
 – stress, 705–715
 Oxidative metabolism, 65, 67, 80, 83, 85
 Oxidative phosphorylation, 878–883
 – consume of oxygen in, 94
 – during activation, 386–388
 – oxidative damage in, 94
 – reduction of oxygen in, 104
 Oxidative stress, 309, 559, 562, 563, 668, 672, 673, 679, 680, 681, 684, 685, 687, 688
 O₂^{•−} (Superoxide anion), 521, 522
 O₂, 298–301, 304, 305, 307, 308
 – as substrate for ROS, 536
 – concentration, 522
 – cytochrome oxidase, K_m for, 709, 713
 – microvascular
 – role in superoxide generation, 706
 – sensing in hypoxia, 536, 537
 – tissue tension in cerebral cortex, 709
 – regulation of, 378
 Oxygen-dependent degradation (ODD), 776, 777
 p53, 719, 720, 722
 Parkinson' disease (PD), *See* Neurodegenerative diseases
 PARP, poly ADP-ribose polymerase, 532
 PARP-1, 714, 715, 719, 721, 722
 Pasteur effect, 772, 783
 Pathways, 891–895, 898, 900, 903–905

- Pentose phosphate pathway, 42, 43, 47, 50, 51, 53–54
- Glucose-6-phosphate dehydrogenase, 505
 - regulation by nitric oxide, 504, 506
 - regulation by peroxynitrite, 504, 506
 - and sulfhydryl groups, 489, 490
 - and 3-nitro-tyrosine, 490
 - in neuroprotection, 504, 505
- PEPCK, 186, 187, 189, 190
- Peroxide, 49, 51
- Peroxisome proliferator activated receptor (PPAR), 535
- Peroxyntitrite, 521, 522, 532
- pH
- changes, 470–474
 - regulation, 474–477
 - sensitive dyes, 471, 472
 - sensitive K⁺ channels, 476
 - sensitive microelectrodes, 471
- pH gradient (Δ pH), 560
- Pharmacometabolomics, 904, 905
- PHD1, 776, 778
- PHD2, 776, 778
- PHD3, 776, 778
- Phenazine methosulfate, 48
- Phosphatidylinositol (PI) cycle
- as precursor in cultured neurons, 413
 - ATP requirement for, 411–414
 - biosynthetic pathway, 412
 - *de novo* synthesis, 411, 413, 414
 - extrapolation from platelets, 420
 - maintaining phosphorylation state
 - myo-inositol, 411–414
 - phospholipase C in, 411, 412, 414
- Phosphocreatine
- hydrolysis of
 - during activation, 384
 - kinase, 357
- Phosphocreatine kinase system, for maintaining ATP, 20
- Phosphocreatine, 883
- Phosphoenolpyruvate carboxykinase, *See* PEPCK
- Phosphofructokinase (PFK), 35, 772–774, 776
- Phosphofructokinase, 163, 164, 358
- 6-Phosphogluconate dehydrogenase, 42, 43, 45, 49
- 6-Phosphogluconolactonase, 42, 43, 45, 97, 101, 102
- cytochrome c, 94, 96, 97, 100, 102
- Phosphoglucose isomerase (PGI), 773, 776
- Phosphoglycerate kinase (PGK), 35, 773, 776
- Phosphoglycerate mutase (PGM), 773
- Phospholipases
- activated, in ischemia, 418
 - phospholipase A₂, 402, 407, 408, 417–419
 - phospholipase C, 402, 411, 412, 414
 - stereospecific selectivity, 407
- Phospholipids
- action of phospholipases on, 402, 408, 417
 - aminophospholipids, 406, 409–411, 417, 420
 - ATP stoichiometry, 405, 406, 410, 411, 415
 - *de novo* synthesis, 404, 407, 411, 411–414, 419
 - disrupted in ischemia, 417, 418
 - ether phospholipids
 - membrane asymmetries, 406, 409–411, 417, 420
 - rate equations (not found)
 - role translocase, 410
 - biosynthetic pathways, 415
 - definitions of, 414
 - synthesis and ATP consumption rates
 - microsomes, 414–416
 - phosphatidylcholine, 408
 - phosphatidylethanolamine, 408, 410–411
 - phosphatidylinositol, cycle, 411–414
 - phosphatidylserine, 410, 411, 417
 - turnover and half-lives of components, 403–405
- Phosphorylase, 158, 159, 167
- a, 157–158
 - b, 157–158
- Phosphotransfer networks, 642
- based metabolic signaling, 651–654
 - in mitochondrial-nuclear intercommunication, 648–651
 - in processing and integrating cellular information, 654–657
- Pi carrier, 879, 881
- Plasma membrane, 410, 411
- Platelet-activating factor (PAF), 417, 419
- Platelets
- extrapolation to brain, 420
 - phosphorylation of phosphatidylinositides, 412, 413
- PMF, 120
- Population spike, 19, 25–27
- Porin-bound hexokinase, 649
- Positron Emission Tomography, 73–74, 79, 85
- Postsynaptic density (PSD), 242
- Post-translational modifications, 738, 739, 741, 742, 746, 749, 760, 761
- review, 749, 754
- Potassium, 347, 348, 350, 363, 370, 380, 382, 383, 431–436
- Preconditioning, 534, 537–539
- Probability approach in description of enzymes and transporters, 849–852
- Prolyl hydroxylase domain-containing proteins, 776
- Propionic academia, 192
- Propionyl-CoA carboxylase
- deficiency of, 192
 - reaction catalyzed by, 187
- Propionyl-CoA, 187, 192
- metabolite of amino acids, 186
 - substrate in carboxylation reaction, 187
- Prostanoids, 380, 383
- Protein kinases, cell signaling, 535
- MAPKs, 534
 - PDH, pyruvate dehydrogenase, 528
 - PHD, prolyl-hydroxylase enzymes, 537
 - PKA, 527, 534
 - PKC, 534, 537
 - proton leak, 528
 - PT Pore, permeability transition pore, 523, 530, 532
- Protein phosphorylation, 247, 248
- cAMP dependent, 99
- Protein trafficking, 621
- Proteomics, 738–763, 890, 893, 899, 907
- brain metabolism, 759–761
- Proton
- concentration, 471, 472, 476
 - equilibrium potential, 471
 - gradient, 471, 476–477, 480
 - permeable channels, 476
 - sequestration, 471, 473
 - signaling, 470, 476
- Proton electrochemical gradient (Δ p), 550
- Proton pathways, 104, 105
- Proton transfer
- mechanism of, 94, 102–104
 - redox centers, 104, 106
- Purkinje neurons, 139, 149
- Pyruvate
- in carboxylation reactions, 184–187
 - pyruvate dehydrogenase complex, 361

- radiolabeled, 188, 189
- recycling, 189, 190
- Pyruvate carboxylase, 142, 155, 159, 187–191, 884
 - in astrocytes, 155, 159
 - deficiency of, 191, 192
 - reaction catalyzed by, 186
- Pyruvate carboxylation, 185, 187–191
 - relation to brain activity, 189
 - time dependence, 194 (found in reference)
- Pyruvate carrier, 879, 881
- Pyruvate compartmentation, 83, 85, 86
- Pyruvate dehydrogenase complex (PDHC), 142, 154, 155, 163, 164, 167, 168
 - and starvation, 167
- Pyruvate dehydrogenase kinase (PDH kinase), 163, 164, 167
- Pyruvate dehydrogenase phosphorylase (PDH phosphorylase), 167
- Pyruvate dehydrogenase, 714, 884
- Pyruvate kinase (PK), 242, 772, 773, 776
- Pyruvate recycling, 213, 216–222, 228, 230
- Pyruvate, 142–156, 158, 159, 162–165, 168, 201, 203–213, 216–225, 228–230, 772–774, 780
 - and long-term potentiation, 145, *See also* Synaptic plasticity
 - carboxylation, 155
 - transport, 155, 156, *See also* Monocarboxylate transporters
- Reaction potential, 386, 387
- Reactive Nitrogen Species (RNS), 520, 521, 705–709, 711, 713–715, 721
- Reactive Oxygen Species (ROS), 44, 520, 521, 527–530, 532, 533, 536
 - detoxification of, 706
 - mitochondrial generation of, 707, 708
 - toxicity, 706
- Reactive oxygen species generation, 560
 - complex I and III, 560
 - oxidative stress, 559, 562, 563
 - redox-sensitive, 560, 562
 - regulation by UCP, 560
 - superoxide, 558, 560
- Receptors, 301, 307, 309, 310, 313
- Redox signaling, 523, 533, 535, 536
- Red-ox switch/coupling, 83–86
- Regulation of weight and body composition, 558
- Release, 301, 302, 305–308
- Respiration, 6, 7, 10, 11, 14
- Respiratory chain complexes, 94, 97, 107, 108
- Respiratory chain, 881–883
 - respiratory complexes, 879–881, 884
- Respiratory complexes, 879–881, 884
- Reuptake, 301
- Ribulose-5-phosphate isomerase, 42, 43, 45
- Ribulose-5-phosphate, 42, 43, 45, 47
- Ribulose-5-phosphate-3-epimerase, 42
 - roles in glucose homeostasis in the brain
- Ryanodine receptor (RyR), 535
- Scavengers of ROS & RNS, 525
- ScCKmit isoforms, 649
- Sciatica, 904
- SDS-PAGE/Western blotting, 245, 246
- Seizure, 720, 721
- Sensitivity theory, 868
- SFRBM, 522
- Signaling, 523, 533–537
- Sodium, 431–436
- Sodium-bicarbonate cotransporter (NBC), 473, 474, 476–478
- Sodium-dependent chloride/bicarbonate exchanger (NCB), 474
- Sodium-hydrogen exchanger (NHE), 471, 474–478, 480
- Solute carrier protein 25 (SLC25), 550
- Sphingomyelin, 314
- Spinal stenosis, 905
- Stable Isotope-based Dynamic Metabolic Profiling (SIDMAP), 865–867
- Standards (data reporting), 895–897, 907
- Starvation, 143, 145, 147, 154, 155, 162–164, 166–168, *See also* Fasting
 - and hypoglycemia, 146, 153, 155, 156, 162–164
 - and ketone bodies, 163, 166
 - enzyme regulation during, 155
- Stroke, 537, 538, 710, 711, 717, 722
- Structure
 - condensed, 279
 - contact site, 264, 267, 268
 - crista junction, 264–268
 - cristae, 264–267, 275, 279, 281, 282, 286, 288
 - heterogeneity of, 262, 270, 271, 273, 275, 276, 281, 285, 286
 - inner membrane, 264–268, 270, 282–285
 - matrix, 264, 266–268, 274, 279
 - network, 265, 268
 - orthodox, 279
 - outer membrane, 264, 267, 273, 279, 280
 - tomography, 263, 264
- Subcellular compartmentation, 66, 78
- Subcellular transfer of reducing equivalents, 65, 67, 72, 85, 86
- Substrate transport
 - during activation, 377–382
 - glucose, 352, 353
 - monocarboxylic acids, 353–355
 - oxygen, 355
 - tricarboxylic acid cycle, 357
- Succinate, 162
- Suckling stage, 154, 165, 166
- Summation theorem, 878, 879, 881
- Superoxide, 550, 558, 560, 708, 709, 711–713
 - superoxide dismutase (SOD), 706, 714
- Superoxide Dismutase (SOD), 521, 522, 525
 - Copper/Zinc SOD, 521, 523, 533, 538
 - Manganese SOD, 522
- Supervised approaches, 896
- Synaptic activity, 470, 474, 478
- Synaptic plasticity
 - and lactate, 145
 - and pyruvate, 145
- Synaptic transmission, 145, 165, 242
 - effects of anoxia and ischemia, 26–28
 - and fructose, 145
 - and β -hydroxybutyrate, 165
 - and lactate, 145
 - long-term potentiation of, 20
 - and mannose, 145
 - and pyruvate, 145
 - and relation between glycolytic metabolism, 28–35
 - and relation between oxidative energy metabolism, 23–28
- Synaptic vesicle-associated glycolytic ATP-generating enzymes
 - complex formation of GAPDH and 3-PGK on synaptic vesicles, 245
 - coupling of glycolysis to ATPases and ion channels, 248–250
 - other roles of GAPDH/3-PGK, 247, 248
 - pathophysiological implications, 252, 253
 - physiological relevance, 250–252
 - preparation methods, 243–245
 - vesicular GAPDH/3-PGK-coupled glutamate uptake, 245–247

- Synaptosomes, 161, 166, 243, 244
 – treatment of, 252
- Systems biology, 861–873, 890, 895, 904
- TCA cycle intermediates, 187, 190, 191
 – products of anaplerosis, 184
 – transport across the blood brain barrier, 188, 189
- TCA cycle, 184–191, 527, 528, 529, 530, 537, 883, 884, 900, 905
- Tg2546 transgenic mice, 35
- Thapsigargin, 249
- Therapeutic strategies, 538
- Thermodynamics, 4, 5
 – ATP hydrolysis, 5
 – Gibbs free energy, 4–6
 – ion electrochemical potential difference, 6
 – mass action ratio, 4, 5
 – Nernst equation, 10
 – proton electrochemical potential, 6
 – redox potential, 5, 6
- Thermogenesis, 550, 559–561
- Thiamine, 46–47, 54, 55
- Thioredoxin reductase, 53
- Threshold
 – threshold curve, 880, 881, 883, 884
 – threshold effect, 881
- Tissue specificity, 881, 882
- TNF- α , tumor necrosis factor α , 534
- Toxicology, 897, 898
- Toxins
 – 3-nitropropionic acid (3-NPA), 570, 574
 – Aminoxyacetic acid (AOAA), 570, 578
 – Methionine sulfoximine (MSO), 570, 573, 574
 – Methyl mercury (MeHg), 570, 579
- Transaldolase, 42, 43, 46, 55
- Transcranial imaging, 337, 338
 – cortical activities in mice, 335, 336
 – genetically manipulated mice, 335
 – in awake mice, 336
 – in the auditory cortex, 335
 – in the somatosensory cortex, 335
 – in the visual cortex, 335
- Transcription factor signaling, 534, 535
- Transcription factor, 772, 775, 776, 783
- Transcriptional activators
 – acting on mitochondrial genes, 803
 – acting on nuclear genes, 797
 – ERR α , 797, 801
 – HAP, 794, 795
 – NRF-1, 795–804
 – NRF-2, 796–799, 801, 803–805
 – Sp1, 795, 799, 804
 – specificity factors, 794, 798, 803
 – Tfam, 791, 793, 794, 796–798, 801, 803
 – YY1, 797, 799
- Transcriptional coactivators
 – effects on mitochondrial biogenesis, 799–803
 – mechanism of action, 799–802
 – PGC-1 α , 799–803
 – PGC-1 β , 803
 – PRC, 802, 803
 – role in gluconeogenesis, 801
- Transcriptomics, 907
 – unsupervised approaches, 890, 893
- Transhydrogenase, 50
- Transient ischemic attacks (TIAs), 23
- Transketolase, 42, 43, 46, 54, 55
- Translational efficiency, 551
- Trauma, 717
- Tricarboxylic acid (TCA) cycle, 83–85, 199–204, 207–211, 213, 216–222, 225–230, 550, 559
- Tricarboxylic acid cycle, *See* TCA cycle
- Triose phosphate isomerase (TPI), 773, 776
- Tumor
 – and anaplerosis in brain, 192
- Two-dimensional gel electrophoresis, 739, 751, 762
- UbCKmit isoforms, 649
- Ubiquinone, 525, 527, 534, 557, 558, 562
- Ubiquitin-proteasome system, 775
- Ubisemiquinone radical, 526, 527
- UCPs, 528, 535
- Uncouplers, 525, 526, 539
- Uncoupling proteins, 707
- UQ $^{\bullet}$, 525, 527, 534
- Vectorial ligand conduction, principle of, 647, 648
- VEGF, 779, 780, 782
- Veratridine, 14
- Vesicular glutamate transporter (VGLUT), 251
- Virtual Free Radical School, 522
- Vitamin C, 777
- von Hippel-Lindau tumor suppressor gene (pVHL), 776, 777, 783
- Wernicke-Korsakoff syndrome, 54
- Western blot analysis, 243, 244
- Whatman GF/C filters, 244
- X-ray crystallographic structure
 – of complex III, 100, 104, 105, 107–110
 – of complex IV, 102
- Zinc, 442–444, 456, 457